



Concrete Construction Engineering Handbook

Edward G. Nawy, Editor-in-Chief

Second Edition



CRC Press
Taylor & Francis Group

Concrete Construction Engineering Handbook

Second Edition

Concrete Construction Engineering Handbook

Second Edition

Editor-in-Chief

Dr. Edward G. Nawy, P.E., C.Eng.

Distinguished Professor

Rutgers—The State University of New Jersey

New Brunswick, New Jersey



CRC Press

Taylor & Francis Group

Boca Raton London New York

CRC Press is an imprint of the
Taylor & Francis Group, an **informa** business

Cover Image: Veterans' 1-280 Glass City Skyway, Toledo, Ohio, 612-ft twin cable-stayed spans with 403-ft pylon. The top 196 ft of the pylon features four sides of glass enveloping LED light fixtures that allow an array of as many as 16.7 million color combinations at night. The bridge construction involved 185,000 cubic yards of concrete, 1.9 million lb of post-tensioning strands, and 32.6 million lb of mild steel reinforcement. The bridge was opened in June 2007. (Photos courtesy of Ms. Linda Figg, President and CEO, FIGG, Tallahassee, Florida. Owner: Ohio Department of Transportation. Designer: FIGG. Contractor: Fru-Con.)

CRC Press
Taylor & Francis Group
6000 Broken Sound Parkway NW, Suite 300
Boca Raton, FL 33487-2742

© 2008 by Taylor & Francis Group, LLC
CRC Press is an imprint of Taylor & Francis Group, an Informa business

No claim to original U.S. Government works
Printed in the United States of America on acid-free paper
10 9 8 7 6 5 4 3 2 1

International Standard Book Number-13: 978-0-8493-7492-0 (Hardcover)

This book contains information obtained from authentic and highly regarded sources. Reasonable efforts have been made to publish reliable data and information, but the author and publisher cannot assume responsibility for the validity of all materials or the consequences of their use. The authors and publishers have attempted to trace the copyright holders of all material reproduced in this publication and apologize to copyright holders if permission to publish in this form has not been obtained. If any copyright material has not been acknowledged please write and let us know so we may rectify in any future reprint.

Except as permitted under U.S. Copyright Law, no part of this book may be reprinted, reproduced, transmitted, or utilized in any form by any electronic, mechanical, or other means, now known or hereafter invented, including photocopying, microfilming, and recording, or in any information storage or retrieval system, without written permission from the publishers.

For permission to photocopy or use material electronically from this work, please access www.copyright.com (<http://www.copyright.com/>) or contact the Copyright Clearance Center, Inc. (CCC), 222 Rosewood Drive, Danvers, MA 01923, 978-750-8400. CCC is a not-for-profit organization that provides licenses and registration for a variety of users. For organizations that have been granted a photocopy license by the CCC, a separate system of payment has been arranged.

Trademark Notice: Product or corporate names may be trademarks or registered trademarks, and are used only for identification and explanation without intent to infringe.

Library of Congress Cataloging-in-Publication Data

Concrete construction engineering handbook / editor, Edward G. Nawy. -- 2nd ed.
p. cm.
Includes bibliographical references and index.
ISBN 978-0-8493-7492-0 (hardback : alk. paper)
1. Concrete construction--Handbooks, manuals, etc. I. Nawy, Edward G. II. Title.

TA681.C743 2008
624.1'834--dc22

2008013027

Visit the Taylor & Francis Web site at
<http://www.taylorandfrancis.com>
and the CRC Press Web site at
<http://www.crcpress.com>

Contents

Preface.....	xiii
Acknowledgments.....	xv
Editor-in-Chief.....	xvii
Contributors.....	xix
1 Concrete Constituent Materials <i>Sidney Mindess</i>	1-1
1.1 Introduction	1-1
1.2 Portland Cement.....	1-2
1.3 Modified Portland Cements.....	1-9
1.4 High-Alumina Cement.....	1-10
1.5 “Green” Cements	1-11
1.6 Performance of Different Cements in Concrete.....	1-11
1.7 Water.....	1-12
1.8 Water/Cement Ratio	1-12
1.9 Aggregates.....	1-14
1.10 Reinforcement.....	1-21
1.11 Durability Considerations.....	1-23
References	1-26
2 Mineral Admixtures <i>V.M. Malhotra</i>	2-1
2.1 Fly Ash	2-1
2.2 Blast-Furnace Slag.....	2-18
2.3 Silica Fume	2-29
2.4 Highly Reactive Metakaolin	2-38
References	2-42
3 Chemical Admixtures <i>David P. Whitney</i>	3-1
3.1 Introduction to Chemical Admixtures.....	3-1
3.2 Retarding Admixtures.....	3-2
3.3 Water-Reducing Admixtures.....	3-3
3.4 High-Range, Water-Reducing Admixtures.....	3-5
3.5 Accelerating Admixtures.....	3-7
3.6 Air-Entraining Admixtures	3-10
3.7 Antifreezing Admixtures	3-12
3.8 Antiwashout Admixtures.....	3-13
3.9 Shrinkage-Reducing Admixtures	3-14
3.10 Polymer Modifier Admixtures	3-14
3.11 Alkali–Silica Reaction Prevention Admixtures	3-18
3.12 Conclusion	3-18
References	3-18
4 Long-Term Effects and Serviceability <i>Edward G. Nawy and Hani Nassif</i>	4-1
4.1 Creep and Shrinkage Deformations in Concrete.....	4-1
4.2 Creep Deformations in Concrete	4-2
4.3 Creep Prediction	4-6
4.4 Shrinkage in Concrete	4-10
4.5 Strength and Elastic Properties of Concrete vs. Time	4-16
4.6 Serviceability Long-Term Considerations.....	4-18

4.7	Long-Term Shrinkage and Temperature Reinforcement Controlling Cracking between Joints in Walls and Slabs of Liquid-Retaining Structures	4-34
4.8	Autogenous Shrinkage in Early-Age Concrete	4-35
	Acknowledgments	4-35
	References	4-37
5	Properties and Performance of Normal-Strength and High-Strength Concrete <i>Steven H. Kosmatka</i>	5-1
5.1	Introduction	5-2
5.2	Workability, Bleeding, and Consolidation	5-2
5.3	Mixing, Transporting, and Placing Concrete.....	5-6
5.4	Permeability.....	5-10
5.5	Carbonation	5-10
5.6	Early-Age Characteristics and Strength.....	5-12
5.7	Density.....	5-16
5.8	Abrasion Resistance	5-17
5.9	Volume Change and Crack Control.....	5-20
5.10	Deformation and Creep	5-21
5.11	Concrete Ingredients	5-22
5.12	Proportioning of Concrete Mixtures.....	5-31
5.13	Hot and Cold Weather Concreting	5-32
5.14	Control Tests	5-33
5.15	Freeze–Thaw and Deicer Scaling Resistance.....	5-34
5.16	Sulfate-Resistant Concrete.....	5-35
5.17	Corrosion Protection.....	5-37
5.18	Alkali–Silica Reaction	5-39
5.19	Heat-Induced Delayed Expansion	5-42
5.20	Self-Consolidating Concrete	5-43
5.21	Related ASTM Standards.....	5-43
	References	5-44
6	Design and Placement of Concrete Mixtures	6-1
	Part A. Design of Concrete Mixtures <i>Edward G. Nawy</i>	6-2
6.1	General.....	6-2
6.2	Selection of Constituent Materials.....	6-2
6.3	Mixture Proportioning for High-Performance, Normal-Strength Concrete (Cylinder Compressive Strength Limit 6000 psi).....	6-9
6.4	Mixture Proportioning for High-Performance, High-Strength Concrete (Cylinder Compressive Strength Exceeding 6000 psi).....	6-18
	Part B. Applications and Constructability <i>Jaime Moreno and John Albinger</i>	6-30
6.5	Applications and Constructability with an Emphasis on High-Strength, High-Performance Concrete	6-30
6.6	Job-Site Control.....	6-41
6.7	Testing.....	6-41
	Acknowledgments	6-43
	References	6-43
7	Design and Construction of Concrete Formwork <i>David W. Johnston</i>	7-1
7.1	Introduction	7-2
7.2	Types of Formwork.....	7-5
7.3	Formwork Standards and Recommended Practices.....	7-17
7.4	Loads and Pressures on Formwork	7-23
7.5	Formwork Design Criteria	7-27
7.6	Formwork Design	7-35
7.7	Slab-Form Design Example	7-38
7.8	Wall-Form Design Example	7-43
	References	7-49

8	Construction Loading in High-Rise Buildings	<i>S.K. Ghosh</i>	8-1
8.1	Introduction		8-1
8.2	Construction Loads		8-1
8.3	Properties of Concrete at Early Ages		8-19
8.4	Strength Consequences of Construction Loads		8-37
8.5	Serviceability Consequences of Construction Loads		8-47
8.6	Codes and Standards		8-55
	References		8-58
9	Deflection of Concrete Members	<i>Russell S. Fling and Andrew Scanlon</i>	9-1
9.1	Introduction		9-1
9.2	Elastic Calculation Methods		9-2
9.3	Other Calculation Considerations		9-6
9.4	Factors Affecting Deflection		9-10
9.5	Reducing Deflection of Concrete Members		9-16
9.6	Allowable Deflections		9-20
	References		9-22
10	Structural Concrete Systems	<i>Scott W. McConnell</i>	10-1
10.1	Overview		10-2
10.2	Building Loads		10-3
10.3	Composite Steel–Concrete Construction		10-7
10.4	Foundations		10-10
10.5	Structural Frames		10-14
10.6	Concrete Slab and Plate Systems		10-17
10.7	Liquid-Containing Structures		10-23
10.8	Mass Concrete		10-26
10.9	On-Site Precasting and Tilt-Up Construction		10-28
10.10	Lift-Slab Construction		10-30
10.11	Slip-Form Construction		10-33
10.12	Prestressed Concrete		10-37
	Acknowledgments		10-40
	References		10-40
11	Construction of Prestressed Concrete	<i>Ben C. Gerwick, Jr.</i>	11-1
11.1	Introduction		11-2
11.2	Concrete and Its Components		11-4
11.3	Reinforcement and Prestressing Systems		11-8
11.4	Special Provisions for Prestressed Concrete Construction		11-13
11.5	Post-Tensioning Technology		11-19
11.6	Pretensioning Technology		11-24
11.7	Prestressed Concrete Buildings		11-29
11.8	Prestressed Concrete Bridges		11-33
11.9	Prestressed Concrete Piling		11-46
11.10	Tanks and Other Circular Structures		11-54
11.11	Prestressed Concrete Sleeper (Ties)		11-55
11.12	Prestressed Concrete Floating Structures		11-56
11.13	Prestressed Concrete Pavements		11-58
11.14	Maintenance, Repair, and Strengthening of Existing Prestressed Concrete Structures		11-58
11.15	Demolition of Prestressed Concrete Structures		11-60
11.16	The Future of Prestressed Concrete Construction		11-61
	Acknowledgments		11-62
	References		11-62

12	Unbonded Post-Tensioning System Technology in Building Construction <i>Florian G. Barth</i>	12-1
12.1	Developments in Unbonded Post-Tensioning.....	12-1
12.2	General Notes and Standard Details.....	12-6
12.3	Evaluation and Rehabilitation of Building Structures.....	12-22
12.4	Demolition of Post-Tensioned Structures.....	12-36
12.5	Defining Terms.....	12-42
	References.....	12-44
13	Concrete for Offshore Structures <i>George C. Hoff</i>	13-1
13.1	Introduction.....	13-1
13.2	Types of Concrete Structures.....	13-2
13.3	Concrete Quality.....	13-18
13.4	Concrete Materials.....	13-19
13.5	Concrete Properties.....	13-22
13.6	Design Considerations.....	13-24
13.7	Safety Considerations.....	13-25
13.8	Construction Practices.....	13-25
13.9	Construction Locations.....	13-26
13.10	Marine Operations.....	13-31
13.11	Cost Considerations.....	13-31
13.12	Summary.....	13-31
	References.....	13-32
14	Foundations for Concrete Structures <i>Manjriker Gunaratne</i>	14-1
14.1	Foundation Engineering.....	14-1
14.2	Site Exploration.....	14-27
14.3	Shallow Footings.....	14-32
14.4	Mat Footings.....	14-37
14.5	Retaining Walls.....	14-43
14.6	Pile Foundations.....	14-57
14.7	Caissons and Drilled Piers.....	14-76
	References.....	14-79
15	Specialized Construction Applications <i>Husam S. Najm</i>	15-1
15.1	Introduction.....	15-2
15.2	Preplaced-Aggregate Concrete.....	15-2
15.3	Underwater Concrete.....	15-6
15.4	Vacuum Processing.....	15-13
15.5	Portland Cement Plaster Construction.....	15-16
15.6	Self-Consolidating Concrete (SCC).....	15-19
15.7	Mass Concrete.....	15-22
15.8	Roller-Compacted Concrete.....	15-23
	Acknowledgment.....	15-26
	References.....	15-26
16	Structural Concrete Repair <i>Randall W. Poston</i>	16-1
16.1	Introduction.....	16-1
16.2	Limit States Design for Repair.....	16-2
16.3	Evaluation.....	16-3
16.4	Structural Implications.....	16-8
16.5	Repair Principles.....	16-10
16.6	Repair of Unbonded Post-Tensioned Concrete Structures.....	16-16
16.7	Construction Issues.....	16-19
16.8	Long-Term Repair Performance.....	16-20
16.9	Case Study.....	16-20
	References.....	16-41

17	Joints in Concrete Construction <i>Edward G. Nawy</i>	17-1
17.1	Introduction	17-1
17.2	Construction Joints.....	17-2
17.3	Contraction Joints	17-3
17.4	Expansion Joints	17-6
17.5	Joints in Slabs on Grade and Pavements	17-10
	References	17-15
18	Automation in Concrete Construction <i>Mirosław J. Skibniewski and Raghavan Kunigahalli</i>	18-1
18.1	Categories of Construction Automation.....	18-1
18.2	Automated Construction Equipment and Related Hardware	18-1
18.3	Economics and Management of Robots.....	18-7
18.4	Computer-Aided Design	18-8
18.5	Conclusions and Future Activities.....	18-16
	References	18-17
19	Equipment for Concrete Building Construction <i>Aviad Shapira</i>	19-1
19.1	Introduction	19-1
19.2	Equipment Selection.....	19-2
19.3	Concrete Equipment.....	19-12
19.4	Cranes	19-21
19.5	Truck Loaders.....	19-43
19.6	Belt Conveyors	19-45
19.7	Material Handlers	19-45
19.8	Hoists and Lifts	19-47
19.9	Mechanized Form Systems.....	19-48
	Acknowledgment.....	19-51
	References	19-51
20	Roller-Compacted Concrete <i>Ernest K. Schrader</i>	20-1
20.1	Introduction	20-1
20.2	Advantages and Disadvantages	20-7
20.3	Aggregates and Mixture Proportions	20-11
20.4	Material Properties	20-21
20.5	Design	20-40
20.6	Construction	20-54
	Defining Terms	20-70
	References	20-71
21	Nondestructive Test Methods <i>Nicholas J. Carino</i>	21-1
21.1	Introduction	21-1
21.2	Methods to Estimate In-Place Strength	21-2
21.3	Methods for Flaw Detection and Condition Assessment	21-28
21.4	Concluding Remarks	21-62
	References	21-63
22	Fiber-Reinforced Composites <i>Edward G. Nawy</i>	22-1
	Part A. Fiber-Reinforced Concrete	
22.1	Historical Development	22-2
22.2	General Characteristics.....	22-2
22.3	Mixture Proportioning.....	22-4
22.4	Mechanics of Fiber Reinforcement.....	22-5
22.5	Mechanical Properties of Fibrous Concrete Structural Elements.....	22-8
22.6	Steel-Fiber-Reinforced Cement Composites.....	22-14
22.7	Prestressed Concrete Prism Elements as the Main Composite Reinforcement in Concrete Beams.....	22-17

Part B. Fiber-Reinforced Plastic (FRP) Composites	
22.8 Historical Development	22-18
22.9 Beams and Two-Way Slabs Reinforced with GFRP Bars	22-19
22.10 Carbon Fibers and Composite Reinforcement	22-20
22.11 Fire Resistance	22-24
22.12 Summary	22-25
Acknowledgments	22-25
References	22-25
23 Bonded Concrete Overlays <i>Michael M. Sprinkel</i>	23-1
23.1 Introduction	23-1
23.2 Key Issues for Successful Bonded HCC Overlays	23-2
23.3 Other Issues	23-15
23.4 Summary	23-16
References	23-16
24 Engineered Cementitious Composite (ECC): Material, Structural, and Durability Performance <i>Victor C. Li</i>	24-1
24.1 Historical Development	24-1
24.2 General Characteristics	24-4
24.3 Mixture Proportioning, Material Processing, and Quality Control	24-8
24.4 Behavior of ECC Structural Elements	24-12
24.5 Durability of ECC and ECC Structural Elements	24-24
24.6 Concluding Remarks	24-37
Acknowledgments	24-40
References	24-40
25 Design of FRP Reinforced and Strengthened Concrete <i>Lawrence C. Bank</i>	25-1
25.1 Introduction	25-1
25.2 Design of FRP-Reinforced Concrete Members	25-2
25.3 Design of FRP-Strengthened Concrete Members	25-9
25.4 Summary	25-20
References	25-20
26 Low-Calcium, Fly-Ash-Based Geopolymer Concrete <i>B. Vijaya Rangan</i>	26-1
26.1 Introduction	26-1
26.2 Geopolymers	26-2
26.3 Constituents of Geopolymer Concrete	26-3
26.4 Mixture Proportions of Geopolymer Concrete	26-3
26.5 Mixing, Casting, and Compaction of Geopolymer Concrete	26-4
26.6 Curing of Geopolymer Concrete	26-5
26.7 Design of Geopolymer Concrete Mixtures	26-6
26.8 Short-Term Properties of Geopolymer Concrete	26-8
26.9 Long-Term Properties of Geopolymer Concrete	26-11
26.10 Reinforced Geopolymer Concrete Beams and Columns	26-14
26.11 Economic Benefits of Geopolymer Concrete	26-18
26.12 Concluding Remarks	26-18
References	26-19
27 Performance Evaluation of Structures <i>Richard A. Miller</i>	27-1
27.1 Introduction	27-1
27.2 ACI 318-05 Provisions on Strength Evaluation of Existing Structures	27-2
27.3 Pretest Planning for Reliable Structural Evaluation	27-4
27.4 Nondestructive Testing for Material and Structural Assessment	27-6
27.5 Static/Quasi-Static Load Testing	27-9
27.6 A Discussion of Instrumentation and Data Acquisition	27-13
27.7 Case Studies in Performance Evaluation of Concrete Structures	27-21
References	27-31

28	Masonry Design and Construction	<i>Jason J. Thompson</i>	28-1
28.1	Introduction		28-1
28.2	Masonry Design and Construction Codes and Standards		28-2
28.3	Definitions		28-2
28.4	Materials		28-4
28.5	Construction		28-15
28.6	Testing and Inspection		28-27
28.7	General Detailing		28-38
28.8	Project Specifications		28-39
28.9	Structural Design		28-40
28.10	Summary		28-68
	Acknowledgment		28-68
	References		28-68
29	Aesthetics in the Construction and Design of Long-Span Prestressed Concrete Bridges	<i>Linda Figg</i>	29-1
29.1	Aesthetics in Concrete Bridges		29-1
29.2	Conceptual Design		29-4
29.3	Environmental Sensitivity		29-9
29.4	Construction Methods		29-11
29.5	Concrete Bridge Shapes for Construction		29-17
29.6	Concrete Aesthetic Features		29-23
29.7	Design Details		29-28
29.8	Summary		29-31
30	Architectural Concrete	<i>Allan R. Kenney and Sidney Freedman; updated by James M. Shilstone</i>	30-1
30.1	History of Architectural Cast-in-Place Concrete		30-2
30.2	History of Architectural Precast Concrete		30-4
30.3	Applications		30-5
30.4	Planning		30-6
30.5	Materials–Mixture Design		30-12
30.6	Color and Texture		30-19
30.7	Construction: Cast-in-Place Concrete		30-32
30.8	Production and Installation of Precast Elements		30-60
30.9	Finish Cleanup		30-68
30.10	Acceptability of Appearance		30-72
30.11	Innovations		30-72
30.12	Defining Terms		30-73
	References		30-74
31	Fire Resistance and Protection of Structures	<i>Mark B. Hogan and Jason J. Thompson</i>	31-1
31.1	Introduction		31-1
31.2	Fire-Resistance Ratings		31-5
31.3	Fire Protection of Joints		31-9
31.4	Finish Treatments		31-11
31.5	Fire Resistance of Columns		31-11
31.6	Steel Columns Protected by Masonry		31-13
31.7	Fire Resistance of Lintels		31-14
	References		31-14
32	Seismic-Resisting Construction	<i>Walid M. Naja and Christopher T. Bane</i>	32-1
32.1	Fundamentals of Earthquake Ground Motion		32-2
32.2	International Building Code (IBC 2006)		32-7
32.3	Design and Construction of Concrete and Masonry Buildings		32-29
32.4	Seismic Retrofit of Existing Buildings		32-42
32.5	Seismic Analysis and Design of Bridge Structures		32-48

32.6	Retrofit of Earthquake-Damaged Bridges.....	32-56
32.7	Defining Terms.....	32-62
	References	32-62
33	Prefabricated Bridge Elements and Systems <i>Michael M. Sprinkel</i>	33-1
33.1	Practical Applications	33-1
33.2	Types of Elements.....	33-3
33.3	Construction Considerations.....	33-15
33.4	Looking Ahead	33-16
	References	33-16
34	Design of Precast Concrete Seismic Bracing Systems <i>Robert E. Englekirk</i>	34-1
34.1	Introduction	34-1
34.2	Basic Concepts	34-2
34.3	Precast Concrete Seismic Moment-Resisting Ductile Frame Systems.....	34-7
34.4	The Conceptual Design Process	34-18
34.5	Concluding Remarks	34-24
	References	34-24
35	Cracking Mitigation and Maintenance Considerations <i>Florian G. Barth</i>	35-1
35.1	Overview of Crack Mitigation	35-1
35.2	Member Selection	35-2
35.3	Crack Causes and Types.....	35-2
35.4	Crack Mitigation Measures	35-7
35.5	Crack Evaluation Summary	35-12
35.6	Maintenance	35-13
	References	35-18
36	Proportioning Concrete Structural Elements by the ACI 318-08 Code <i>Edward G. Nawy</i> ...	36-1
36.1	Material Characteristics.....	36-2
36.2	Structural Design Considerations	36-5
36.3	Strength Design of Reinforced-Concrete Members	36-10
36.4	Prestressed Concrete.....	36-31
36.5	Shear and Torsion in Prestressed Elements	36-34
36.6	Walls and Footings	36-36
	Acknowledgments	36-36
	References	36-36
	Index.....	I-1

Preface

A great need has existed for an in-depth handbook on concrete construction engineering and technology that can assist the constructor in making correct technical judgments in the various areas of constructed systems. This *Handbook* is intended to fill this very need. This edition is completely updated and includes ten new chapters written by leading experts on various topics dealing with the state of the art in several newly developed areas of concrete construction and design engineering. All chapters treat their particular subjects with extensive detail and depth of discussion, a feature that is lacking in any comparable texts. Also, each chapter provides selected references for the user to consult for further research beyond the scope of the *Handbook*. The topics covered here are state-of-the-art statements regarding what the design engineer and the constructor should know about concrete, the most versatile material of the 21st century. These topics can be grouped into five categories:

1. *Latest advances in engineered concrete materials*, including concrete constituents, high-performance concretes, the design of mixtures for both normal- and high-strength concretes, and special concrete applications such as architectural concrete
2. *Reinforced concrete construction*, including recommendations on the vast array of types of constructed facilities, long-term effects on behavior and performance such as creep and shrinkage, construction loading effects, formwork and falsework proportioning, and automation in construction
3. *Specialized construction*, such as prestressed concrete construction in buildings and transportation facilities; construction and proportioning of structures in seismic zones (including the latest provisions of the 2006 International Building Code on the design of structures in high-seismicity zones); masonry construction; heavy concrete construction, such as roller-compacted concrete; and concrete marine structures, such as offshore platforms concrete
4. *Design recommendations for high performance*, including deflection reduction in buildings, proportioning of concrete structural elements by the latest ACI 318-08 Building Code, prefabricated precasting, geotechnical and foundation engineering, nondestructive evaluation of long-term structural performance, and structural concrete repair, retrofit, and rehabilitation
5. *Specialized topics on new materials*, such as engineered concrete composites, geopolymer concrete, equipment for concrete building construction, joints in concrete structures, design of precast seismic bracing systems, detailed design of fiber-reinforced polymers (FRP), and aesthetics in long-span bridge construction

The 37 contributors to this new edition of the *Handbook* are leading authorities in the field, with a combined professional practice of at least 1200 years. All of them are national or international leaders in research, design, and construction. This *Handbook* is the only publication in this category that has in a single chapter a summary of all concrete design expressions in accordance with the latest ACI 318-08 Building Code for flexure, shear, torsion, strut-and-tie design of corbels and deep beams, compression, long-term effects, slender columns, and development of reinforcement. Both PI (in.-lb) and SI formats are provided. A design office will be able to quickly review all of the latest requirements for structural concrete. This *Handbook* should enable designers, constructors, educators, and field personnel to produce the best and most durably engineered constructed facilities. It is for these professionals that this *Handbook* was written in the hope that the wealth of the most up-to-date knowledge embodied in this comprehensive work will provide, in this dynamic century, vastly better, more efficient, and longer enduring constructed concrete.

Acknowledgments

I consider myself lucky to have had the chance to work with such outstanding world-class experts in developing this *Handbook*. My gratitude and thanks are extended to all of the authors, who, busy as they are, have shared their vast experience gained from extensive years of engineering and construction practice at the highest levels. Acknowledgment and thanks are due to the American Concrete Institute for permitting unrestricted use by the various authors of its vast technical resources of publications and to Prentice Hall/Pearson Education (Addison Wesley Longman) for permitting me to use material originally published in my three textbooks with them. Thanks are also due to Linda Figg for her input to the handsome jacket of the *Handbook* and to Christy Gray, of her staff, for developing its several versions.

Deep appreciation and gratitude are extended to the staff at Taylor & Francis for the hard work required to bring to fruition this second edition of such a major text: Nora Konopka, Publisher, who has always been considerate, decisive, and supportive throughout the lengthy development of this edition of the *Handbook* and the previous edition; Joseph Clements, Acquisitions Editor, for his valuable input and cooperation; Theresa Delforn, Production Manager, for her initial work on the manuscript; Jill Jurgensen, Production Coordinator, for her critical input; and Christine Andreasen, Project Editor, for keeping the production process on track. Thank you, too, to the compositor, Sarah Nicely Fortener, Nicely Creative Services.

Last, but not least, acknowledgment is due to my wife, Rachel, who has had enduring patience and given unlimited support while I was totally immersed in the development of the *Handbook*.

Edward G. Nawy
Rutgers University
Piscataway, New Jersey

Editor-in-Chief



Edward G. Nawy, distinguished professor, Department of Civil and Environmental Engineering, Rutgers, the State University of New Jersey, is internationally recognized for his extensive research work in the fields of reinforced and prestressed concrete, particularly in the areas of serviceability and crack control. He has practiced civil and structural engineering in excess of 50 years and has been on the faculty of Rutgers University almost as long, having served as chairman and graduate director for two terms. He also served two terms on the Board of Governors and one term on the Board of Trustees of the University.

His work has been published in technical journals worldwide and includes over 180 technical papers. He has been a keynote speaker for several international technical conferences and has been the editor of several Special Publication volumes of the American Concrete Institute since 1972. He is the author of several textbooks, including *Simplified Reinforced Concrete*, *Reinforced*

Concrete: A Fundamental Approach, and *Prestressed Concrete: A Fundamental Approach*, all published by Prentice Hall and which have been translated into Spanish, Chinese, South Korean, and Malaysian. He is also the author of *Fundamentals of High-Performance Concrete* (John Wiley & Sons) and has contributed chapters to several handbooks, including the *Handbook of Structural Concrete* (McGraw-Hill) and the *Engineering Handbook* (CRC Press).

Dr. Nawy is an honorary member (formerly Charter Fellow, 1972) of the American Concrete Institute, Fellow of the American Society of Civil Engineers, Fellow of the Institution of Civil Engineers (London), and a member of the Precast/Prestressed Concrete Institute. He has chaired several committees of the American Concrete Institute, including ACI Committee 224 on Cracking and ACI Committee 435 on Deflection of Structures. He is also a member of the ACI–ASCE Joint Committee on Slabs; ACI Committee 340 on the *Strength Design Handbook*, for which he served as the chairman of its Subcommittee on Two-Way Slabs and Plates; and the Technical Activities Committee of the Precast/Prestressed Concrete Institute.

Major awards he has received include the Henry L. Kennedy Award and the Design Practice Award of the American Concrete Institute, as well as Honorary Professorship of the Nanjing Institute of Technology, Nanjing, China. He is a licensed professional engineer in the states of New York, New Jersey, Pennsylvania, California, and Florida; a chartered civil engineer in the United Kingdom and the Commonwealth; a program evaluator for the National Accreditation Board for Engineering and Technology (ABET); a panelist for the National Science Foundation, Washington, D.C.; a university representative to the Transportation Research Board, Washington, D.C.; and a former chairman and subsequently Emeritus Honor member of the TRB Committee on Concrete Materials, National Research Council. He has been an engineering consultant to agencies throughout the United States, particularly in areas of structures and materials forensic engineering. He has been listed in *Who's Who in America* since 1967, in *Who's Who in Engineering*, and in *Who's Who in the World*, as well as in several other major standard reference works.

Contributors

John Albinger

President, T.H. Davidson and Company
Chicago, Illinois

Christopher T. Bane, S.E.

Senior Project Engineer
FBA, Inc.
Hayward, California

Lawrence C. Bank, Ph.D, P.E., FASCE

Professor, Civil and Environmental
Engineering Department
University of Wisconsin
Madison, Wisconsin

Florian G. Barth, P.E.

President, American Concrete Institute
Principal Consultant, FBA, Inc.
Hayward, California

Nicholas J. Carino, Ph.D. (retired)

Research Structural Engineer
National Institute of Standards and Technology
Gaithersburg, Maryland

Robert E. Englekirk, Ph.D., S.E.

Chairman Emeritus, Englekirk Companies
Adjunct Professor, Structural Engineering
Department
University of California
San Diego, California

Linda Figg

President (CEO)/Director
Bridge Art, Figg Engineering Group
Tallahassee, Florida

Russell S. Fling, P.E. (retired)

Consulting Structural Engineer
Columbus, Ohio

Sidney Freedman

Director, Architectural Precast Concrete Services
Precast/Prestressed Concrete Institute
Chicago, Illinois

Ben C. Gerwick, Jr., P.E., S.E. (deceased)

Senior Technical Consultant, Honorary Chairman
Ben C. Gerwick, Inc.
San Francisco, California

S.K. Ghosh, Ph.D., P.E.

President
S.K. Ghosh Associates, Inc.
Palatine, Illinois

Manjriker Gunaratne, Ph.D., P.E.

Professor, Civil Engineering Department
University of South Florida
Tampa, Florida

George C. Hoff, D.Eng., P.E.

President
Hoff Consulting, LLC
Clinton, Mississippi

Mark B. Hogan, P.E.

Vice President of Engineering
National Concrete Masonry Association
Herndon, Virginia

David W. Johnston, Ph.D., P.E.

Professor and Associate Head,
Civil, Construction, and Environmental
Engineering Department
North Carolina State University
Raleigh, North Carolina

Allan R. Kenney, P.E.

President
Precast Systems Consultants, Inc.
Venice, Florida

Steven H. Kosmatka, P.E.

Staff Vice President, Research and
Technical Services
Portland Cement Association
Skokie, Illinois

Raghavan Kunigahalli, Ph.D.

Technology Officer, Office of the CIO/CTO
American International Group
Jersey City, New Jersey

Victor C. Li, Ph.D., FASCE, FASME, FWIF

E. Benjamin Wylie Collegiate Chair Professor,
Civil and Environmental
Engineering Departments
University of Michigan
Ann Arbor, Michigan

V.M. Malhotra, D.D.L., D.Eng., P.Eng.

Scientist Emeritus
CANMET, Natural Resources Canada
Ottawa, Canada

Scott W. McConnell, P.E.

Principal and Director, Structural Department
CMX Engineers and Consultants
Manalapan, New Jersey

Richard A. Miller, Ph.D., P.E.

Professor, Civil Engineering Department
University of Cincinnati
Cincinnati, Ohio

Sidney Mindess, P.Eng.

Professor Emeritus, Civil Engineering Department
University of British Columbia
Vancouver, Canada

Jaime Moreno

President Emeritus
Cement Technology Corporation
Chicago, Illinois

Walid M. Naja, S.E.

Principal
FBA, Inc.
Hayward, California

Husam S. Najm, Ph.D., P.E.

Associate Professor, Civil and Environmental
Engineering Department
Rutgers, The State University of New Jersey
Piscataway, New Jersey

Hani Nassif, Ph.D., P.E.

Associate Professor, Civil Engineering Department
Rutgers, The State University of New Jersey
Piscataway, New Jersey

Edward G. Nawy, D.Eng., P.E., C.Eng.

Distinguished Professor, Civil Engineering
Department
Rutgers, The State University of New Jersey
Piscataway, New Jersey

Randall W. Poston, Ph.D., P.E.

Principal
WDP & Associates, Inc.
Austin, Texas

**B. Vijaya Rangan, Ph.D., FACI,
FIEAust, C.P.Eng.**

Emeritus Professor, Civil Engineering Department
Dean, Faculty of Engineering
Curtin University of Technology
Perth, Australia

Andrew Scanlon, S.E.

Professor, Civil Engineering Department
The Pennsylvania State University
Williamsport, Pennsylvania

Ernest K. Schrader, Ph.D., FACI

Consultant
Schrader Consulting Engineers
Walla Walla, Washington

Aviad Shapira, D.Sc.

Associate Professor, Construction Engineering
and Management
Technion-Israel Institute of Technology
Haifa, Israel

James M. Shilstone, Jr., FACI

President
The Shilstone Companies, Inc.
Dallas, Texas

Mirosław J. Skibniewski, Ph.D.

A. James Clark Chair Professor, Department
of Civil and Environmental Engineering
University of Maryland
College Park, Maryland

Michael M. Sprinkel, P.E.

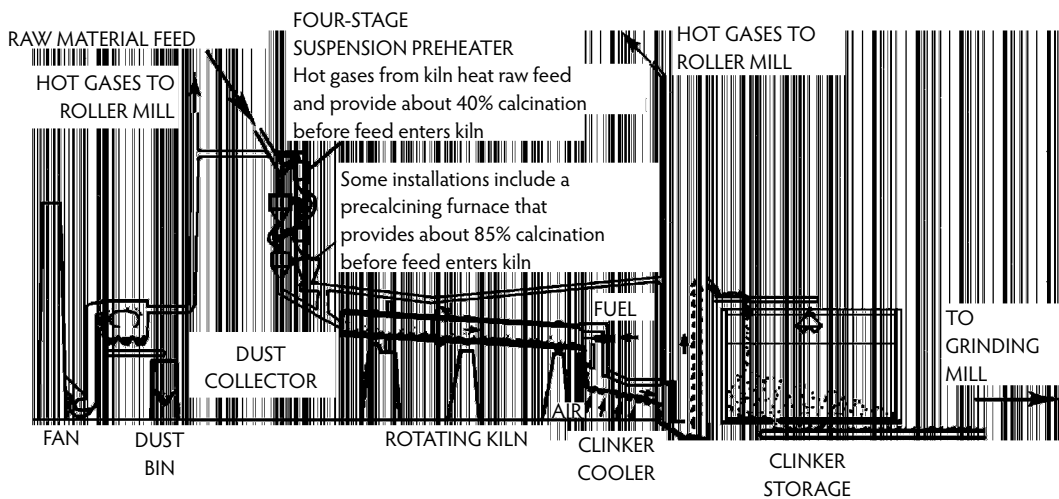
Associate Director
Virginia Transportation Research Council
Charlottesville, Virginia

Jason J. Thompson

Director of Engineering
National Concrete Masonry Association
Herndon, Virginia

David P. Whitney

Research Operations Manager and Research
Engineer
Construction Materials Research Group
The University of Texas
Austin, Texas



Schematic of Portland cement manufacturing process. (From Nawy, E.G., *Reinforced Concrete: A Fundamental Approach*, 6th ed., Prentice Hall, Upper Saddle River, NJ, 2008.)

1

Concrete Constituent Materials

Sidney Mindess, P.Eng.*

1.1	Introduction	1-1
1.2	Portland Cement	1-2
	Manufacture of Portland Cement • Hydration of Portland Cement	
1.3	Modified Portland Cements	1-9
	Portland Pozzolan Cements • Portland Blast-Furnace Slag Cements • Expansive Cements	
1.4	High-Alumina Cement	1-10
1.5	“Green” Cements	1-11
1.6	Performance of Different Cements in Concrete	1-11
1.7	Water	1-12
1.8	Water/Cement Ratio	1-12
1.9	Aggregates	1-14
	Particle Shape and Texture • Particle Grading • Aggregate Moisture Content • Lightweight Aggregates • Heavyweight Aggregates • Aggregate Durability	
1.10	Reinforcement	1-21
	General • Fiber Reinforcement • Steel Reinforcement	
1.11	Durability Considerations	1-23
	Leaching and Efflorescence • Sulfate Attack • Acid Attack	
	References	1-26

1.1 Introduction

Portland cement concrete is a composite material made by combining cement, supplementary cementing materials, aggregates, water, and chemical admixtures in suitable proportions and allowing the resulting mixture to set and harden over time. Because hardened concrete is a relatively brittle material with a low tensile strength, steel reinforcing bars and sometimes discontinuous fibers are used in structural concrete to provide some tensile load-bearing capacity and to increase the toughness of the material. In this chapter, we deal with some of the basic constituents: cements, aggregates, water, steel reinforcement, and fiber reinforcement. Chemical admixtures and supplementary cementing materials (often referred to as mineral admixtures) are covered in Chapter 2. It must be emphasized that choosing the appropriate

* Professor Emeritus, Department of Civil Engineering, University of British Columbia, Vancouver, Canada; expert in concrete materials behavior and in composites.

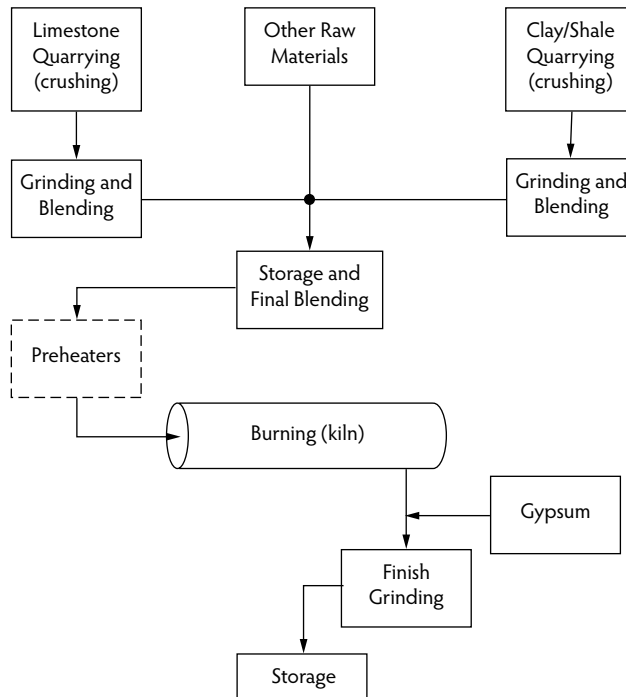


FIGURE 1.1 Schematic outline of Portland cement production.

constituent materials for a particular concrete is a necessary, but not sufficient, condition for the production of high-quality concrete. The materials must be proportioned correctly, and the concrete must then be mixed, placed, and cured properly (Chapter 6). In addition, there must be careful quality control of every part of the concrete-making process. This requires full cooperation among the materials or ready-mixed-concrete supplier, the engineer, and the contractor.

1.2 Portland Cement

Portland cement is by far the most important member of the family of **hydraulic cements**—that is, cements that harden through chemical interaction with water. The first patent for “Portland” cement was taken out in England in 1824 by Joseph Aspdin, though it was probably not a true Portland cement; the first true Portland cements were produced about 20 years later. Since then, many improvements have been made to cement production, leading to the sophisticated, though common, cements that are now so widely available.

1.2.1 Manufacture of Portland Cement

The manufacture of Portland cement is, in principle, a simple process that relies on the use of inexpensive and abundant raw materials. In short, an intimate mixture of limestone (CaCO_3) and clay or silt (iron-bearing aluminosilicates), to which a small amount of iron oxide (Fe_2O_3) and sometimes quartz (SiO_2) is added, is heated in a kiln to a temperature of between 1400 and 1600°C; in this temperature range, the materials react chemically to form calcium silicates, calcium aluminates, and calcium aluminoferrites. The cement production process is shown in Figure 1.1. The raw materials, which are ground to a fineness of less than about 75 μm , are introduced at the top end of an inclined rotary kiln, as shown in Figure 1.2. The kiln is heated by fuel (natural gas, oil, or pulverized coal) that is injected and burned at the lower end of the kiln, with the hot gases passing up through the kiln. Thus, in a period ranging from

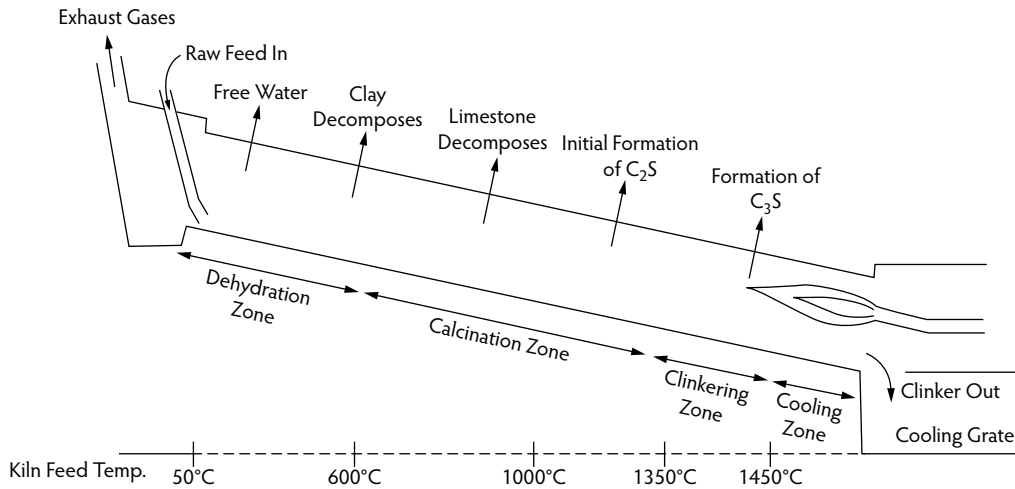


FIGURE 1.2 Schematic outline of reactions in a typical dry-process rotary cement kiln.

about 20 minutes to 2.5 hours, depending on the kiln design, the raw ingredients are subjected to increasingly higher temperatures as they pass through the kiln, and a complex series of chemical reactions takes place. The high-temperature reactions for the formation of cement **clinker** have been described as follows (Bentur, 2002):

- Decomposition of the clay minerals (~ 500 to 800°C)
- Decomposition of the calcite (~ 700 to 900°C)
- Reactions of the calcite (or lime formed from it), SiO_2 , and the decomposed clays to form $2\text{CaO}\cdot\text{SiO}_2$ (~ 1000 to 1300°C)
- Clinkering reactions at about 1300 to 1450°C to form $3\text{CaO}\cdot\text{SiO}_2$ —a melt of aluminate and ferrite is formed to act as a flux to facilitate the formation of $3\text{CaO}\cdot\text{SiO}_2$ by the reaction between CaO and $2\text{CaO}\cdot\text{SiO}_2$
- Cooling back to ambient temperature, during which time the melt crystallizes to form the ferrite and aluminate phases

As the charge in the kiln moves through the final few feet, its temperature drops rapidly, and it emerges from the kiln as clinker, dark colored nodules about 6 to 50 mm in diameter. This is then cooled and is finally interground with gypsum ($\text{CaSO}_4\cdot 2\text{H}_2\text{O}$), to a particle size of about $10\ \mu\text{m}$ or less. The gypsum is added to control the early hydration reactions of the cement. The ternary phase diagram of the $\text{CaO}\text{--}\text{Al}_2\text{O}_3\text{--}\text{SiO}_2$ system is shown in Figure 1.3 (Bentur, 2002). It may be seen that Portland cement (and, indeed, all other cementitious materials in this system) may have a considerable range of chemical compositions.

The above description of the production of Portland cement represents a considerable simplification of what really occurs, in that it overlooks several important factors:

- Because of the nature of the raw materials, about 5 to 8% impurities are present in the clinker, the exact type and amount of which depend on the particular raw material sources. These impurities include sodium and potassium oxides (from the clay), sulfates (from the fuel), magnesium (from the limestone), manganese, iron, potassium, titanium, and perhaps others as well.
- The mineral phases formed are not pure but are doped with various other ions, depending on the exact chemistry of the raw feed.
- The different mineral phases are not in the form of separate grains; each cement particle generally contains several phases.

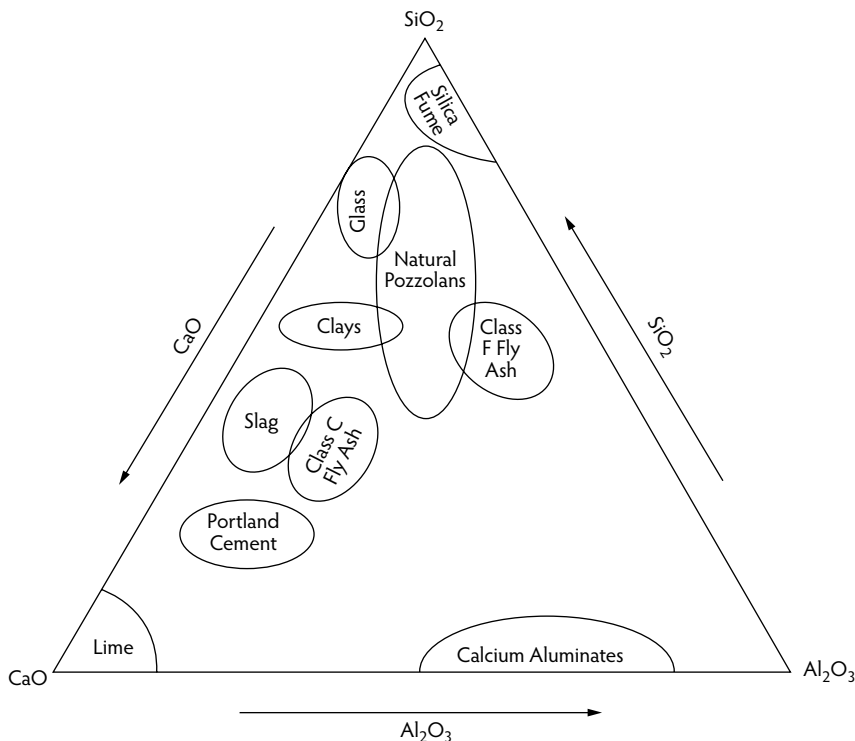


FIGURE 1.3 Ternary phase diagram of the CaO – Al_2O_3 – SiO_2 system. (Adapted from Bentur, A., *J. Mater. Civ. Eng.*, 14(1), 2–22, 2002.)

The precise details of the chemistry of cement are not particularly important for ordinary concretes, whose properties (in both the fresh and hardened states) can be predicted reasonably well based on the aggregate grading, the cement content, and the water/cement (w/c) ratio. This permits us to design normal concrete mixes with little regard to the source and composition of the particular cement being used; however, for high-performance concretes, these details can be of vital importance, as such concretes will invariably contain both mineral and chemical admixtures and in particular superplasticizers (also known as high-range water reducers). The behavior and durability of these much more complex mixtures can be greatly affected by the minor components of the cement and by the cement mineralogy and composition. The problems of cement–superplasticizer incompatibility and other adverse admixture interactions can create difficulties in finding satisfactory mix designs for concretes for some special applications.

The chemical composition of Portland cement is customarily reported in terms of the **oxides** of the various elements that are present, using the shorthand notation given in Table 1.1. Using this notation, the typical compound composition of ordinary Portland cement may be given as shown in Table 1.2. The characteristics of these compounds when cement is hydrated are indicated in Table 1.3. It can be seen that the two calcium silicates are primarily responsible for the strength that the cement will develop upon hydration. The C_3A can lead to durability problems when the concrete is in contact with soils or groundwater containing sulfates. By making relatively small changes in the relative proportions of raw materials, one can bring about relatively large changes in the relative proportions of the principal compounds of Portland cement. In North America, this has led to the specification of five types of Portland cement, as indicated in Table 1.4. It is thus possible, to a considerable degree, to tailor cements for particular applications, as long as the quantities required are sufficiently large to be economically feasible. For example, special cements have been formulated for very high-strength concretes and for particular durability considerations.

TABLE 1.1 Shorthand Notation for the Oxides in Portland Cement

Oxide	Shorthand Notation	Common Name	Typical Weight Percent in Ordinary Cement
CaO	C	Lime	63
SiO ₂	S	Silica	22
Al ₂ O ₃	A	Alumina	6
Fe ₂ O ₃	F	Ferric oxide	2.5
MgO	M	Magnesia	2.5
K ₂ O	K	Alkalis	0.6
Na ₂ O	N		0.4
SO ₃	\bar{S}	Sulfur trioxide	2.0
CO ₂	\bar{C}	Carbon dioxide	—
H ₂ O	H	Water	—

TABLE 1.2 Typical Compound Composition of Ordinary Portland Cement

Chemical Formula	Shorthand Notation	Chemical Name	Weight Percent
3CaO·SiO ₂	C ₃ S	Tricalcium silicate	50
2CaO·SiO ₂	C ₂ S	Dicalcium silicate	25
3CaO·Al ₂ O ₃	C ₃ A	Tricalcium aluminate	12
4CaO·Al ₂ O ₃ ·Fe ₂ O ₃	C ₄ AF	Tetracalcium aluminoferrite	8
CaSO ₄ ·2H ₂ O	C \bar{S} H ₂	Calcium sulfate dihydrate (gypsum)	3.5

TABLE 1.3 Contribution of Cement Compounds to the Hydration of Portland Cement

Compound	Reaction Rate	Heat Liberated	Contribution to Strength
C ₃ S	Moderate	High	High
C ₂ S	Slow	Low	Low initially; high later
C ₃ A + C \bar{S} H ₂	Fast	Very high	Low
C ₄ AF + C \bar{S} H ₂	Moderate	Moderate	Low

TABLE 1.4 Approximate Chemical Compositions of the Principal Types of Portland Cement

ASTM Designation	Common Name	Percent by Weight					Fineness ^a
		C ₃ S	C ₂ S	C ₃ A	C ₄ AF	C \bar{S} H ₂	
Type I	Ordinary	50	25	12	8	5	350
Type II	Modified	45	30	7	12	5	350
Type III	High early strength	60	15	10	8	5	450
Type IV ^b	Low heat	25	50	5	12	4	300
Type V	Sulfate resistant	40	40	4	10	4	350

^a Blaine fineness (m²/kg).^b Now rarely produced; replaced with blends of Portland cement and fly ash.

The hydration reactions of Portland cement do not involve the complete dissolution of the cement grains; rather, the reactions take place between water and the exposed surfaces of the cement particles. As a result, the fineness of the cement will have a considerable effect on its rate of reaction, as this will determine the surface area exposed to water. Clearly, more finely ground cements will hydrate more rapidly, but they give rise to higher rates of heat liberation during hydration, the consequences of which are discussed later.

1.2.2 Hydration of Portland Cement

The hydration reactions that take place between finely ground Portland cement and water are highly complex, because the individual cement grains vary in size and composition. As a consequence, the resulting hydration products are also not uniform; their chemical composition and microstructural characteristics vary not only with time but also with their location within the concrete. The basic characteristics of the hydration of Portland cement may be described as follows:

- As long as the individual cement grains remain separated from each other by water, the cement paste remains fluid.
- The products of the hydration reactions occupy a greater volume than that occupied by the original cement grains.
- As the hydration products begin to intergrow, setting occurs.
- As the hydration reactions continue, additional bonds are formed between the cement grains, leading to strengthening of the system.

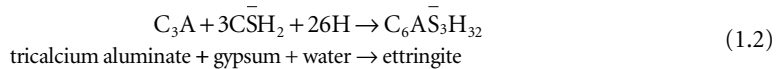
1.2.2.1 Chemistry of Hydration

The principal products of the hydration reactions, which are primarily responsible for the strength of concrete, are the calcium silicate hydrates that make up most of the hydrated cement. They are formed from the reactions between the two calcium silicates and water. Using the shorthand notation of Tables 1.1 and 1.2, these reactions may be written as:

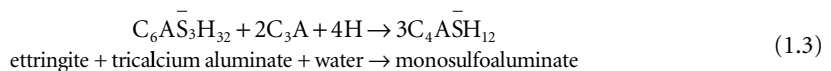


In reality, calcium silicate hydrate is a largely amorphous material that does not have the precise composition indicated in Equation 1.1. It is thus more often referred to merely as C–S–H so no specific formula is implied. The reactions of Equation 1.1 are highly exothermic. These reactions, and the others described below, occur first on the surfaces of the finely divided cement; as the surface layers react, water must diffuse through the hydration products to reach still unhydrated material for the reactions to proceed. The reactions will continue, at an ever-decreasing rate, until either all of the water available for hydration is used up or all of the space available for the hydration products is filled.

In the absence of the gypsum that is interground with the Portland cement clinker, the C_3A would react very rapidly with the water, leading to early setting (within a very few minutes) of the cement, which, of course, is highly undesirable. In the presence of gypsum, however, a layer of **ettringite** forms on the surface of the C_3A particles which slows down the subsequent hydration:

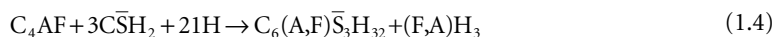


As the gypsum becomes depleted by this reaction, the ettringite and the C_3A react further:



The monosulfoaluminate is thus the stable phase in concrete.

The ferrite phase is much less reactive than the C_3A , so it does not combine with much of the gypsum. Its reaction may be written as:



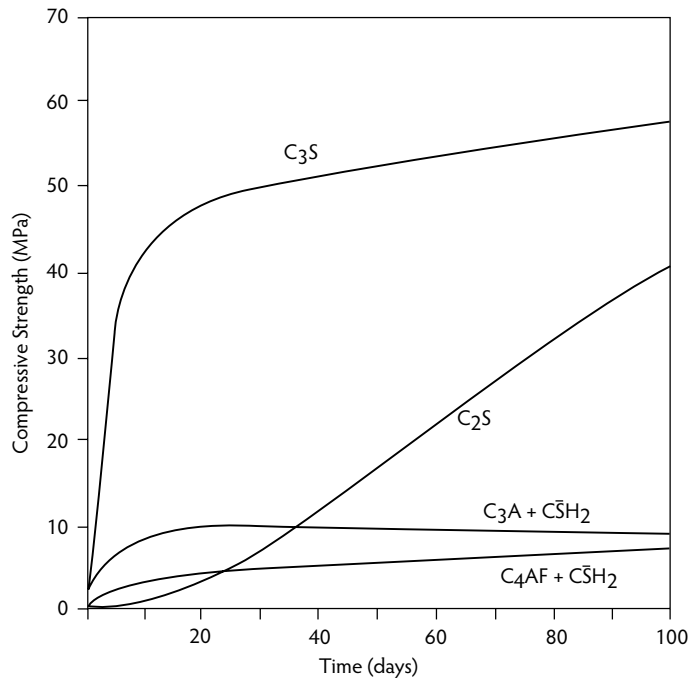


FIGURE 1.4 Compressive strength development of the pure cement compounds.

(A, F) means that A and F occur interchangeably in the so-called hexagonal hydrates, but the ratio A/F need not be the same as that in the parent compounds. These hydrates derive their name from the fact that they tend to occur in thin, hexagonal plates. The tetracalcium aluminate hydrate is structurally related to monosulfoaluminate; the ferric–alumina hydroxide is amorphous.

It must be emphasized again that the chemical formulae presented in Equations 1.1 to 1.4 are only approximate. There may be as much as 5% of various other impurities in the raw materials used to make cement (K_2O , Na_2O , MgO , etc.), and these atoms also find their way into the structure of the hydration compounds, so the pure phases represented above are rarely found in that form. In general, this has little effect on the mechanical properties of hardened cement or concrete; however, the impurities may have a considerable effect on the durability of the concrete and on interactions between the cement and modern chemical admixtures.

1.2.2.2 Development of Hydration Products

The hydration reactions described above occur at quite different rates, so the rates of strength development and the final strengths achieved by the various hydration products vary widely (Figure 1.4). Most of the strength comes from the hydration of the calcium silicates. The C_3S hydrates more rapidly than the C_2S and so is responsible for most of the early strength gain. The aluminate and ferrite phases hydrate quickly but contribute little to strength. The course of the hydration of Portland cement is best described by reference to Figure 1.5, in which the hydration process is divided into five stages on the basis of the amount of heat being liberated. The first stage lasts only a few minutes; the heat liberated is due mostly to the wetting and early dissolution of the cement grains. In the second, or induction stage, which may last for several hours, there is very little hydration activity, and the cement paste remains fluid. The beginning of the hydration of C_3S marks the start of the third stage, during which both initial set and final set occur, due to the production of the hydration products and the development of a solid microstructural skeleton. Stage four is marked by the hydration of the C_3A after depletion of the gypsum. Finally, in stage five, the rate of reaction slows as long as water is present, and the skeleton developed in stage three is filled in and densified by additional hydration products.

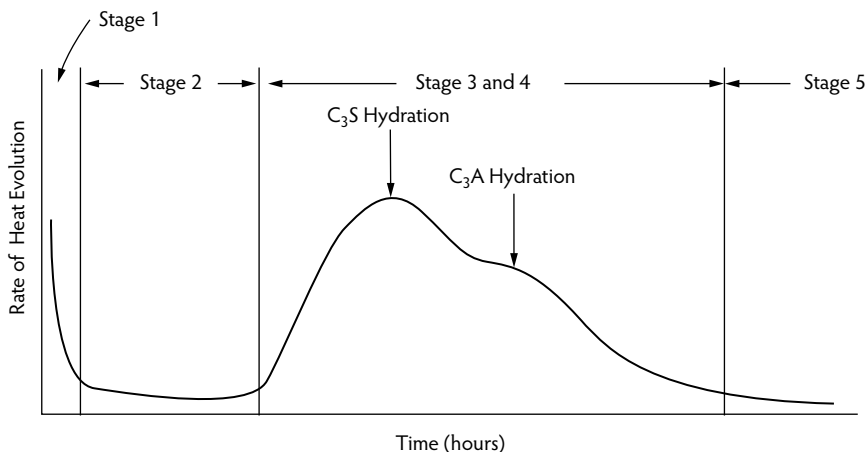


FIGURE 1.5 Rate of heat evolution during the hydration of Portland cement.

1.2.2.3 Mechanical Properties of Hydration Products

What determines the mechanical properties of the hardened cement is not so much the chemical details of the hydration reactions but the physical microstructure that is developed as a result of these reactions. As a continuous matrix of C–S–H is formed, the porosity of the system is reduced, and it is this reduction in porosity that is largely responsible for the gain in strength with an increasing degree of hydration. Of course, in addition to the C–S–H, the hardened matrix also contains the still unhydrated residues of the cement grains, relatively large crystals of calcium hydroxide, and monosulfoaluminate crystallites, but the latter two are more important for durability than for strength considerations. Here, we focus on the resultant porosity of the system. Pores may exist in hydrated Portland cement over a wide range of sizes. They may generally be classified into the following size ranges:

Micropores, which are <2.5 nm

Mesopores, which are 2.5 to 100 nm (0.1 μm)

Macropores, which are >100 nm

If, however, we adopt the simplified model of pore structure first suggested by Powers (1958), it is possible to relate the strength of the hardened paste to its porosity. Powers subdivided pores into two types. Gel pores, with a diameter of <10 nm, are an intrinsic part of the microstructure of the hardened paste, whereas capillary pores, >10 nm in diameter, represent the spaces in the hardened paste that were originally filled with mixing water and have not been completely filled by the various hydration products. The larger the amount of mixing water used, therefore, the greater the volume of capillary pores; the volume of gel pores is largely independent of the amount of mixing water. It is possible to calculate the volume fraction of the pores and the solid fraction in terms of two parameters: the original water/cement (w/c) ratio and the degree of hydration (α), which is the fraction of cement that is hydrated and ranges from 0 to 1. The following equations were originally determined empirically by Powers and are still often used:

$$\text{Volume of total hydration products} = 0.68\alpha \text{ cm}^3/\text{g of original cement (including gel pores)} \quad (1.5)$$

$$\text{Volume of unhydrated cement} = 0.32(1-\alpha) \text{ cm}^3/\text{g of original cement} \quad (1.6)$$

$$\text{Volume of capillary pores} = [w/c - 0.36\alpha] \text{ cm}^3/\text{g of original cement} \quad (1.7)$$

$$\text{Volume of gel pores} = 0.16\alpha \text{ cm}^3/\text{g of original cement} \quad (1.8)$$

$$\text{Capillary porosity (relative volume of capillary pores)} = \frac{w/c - 0.36\alpha}{w/c + 0.32} \quad (1.9)$$

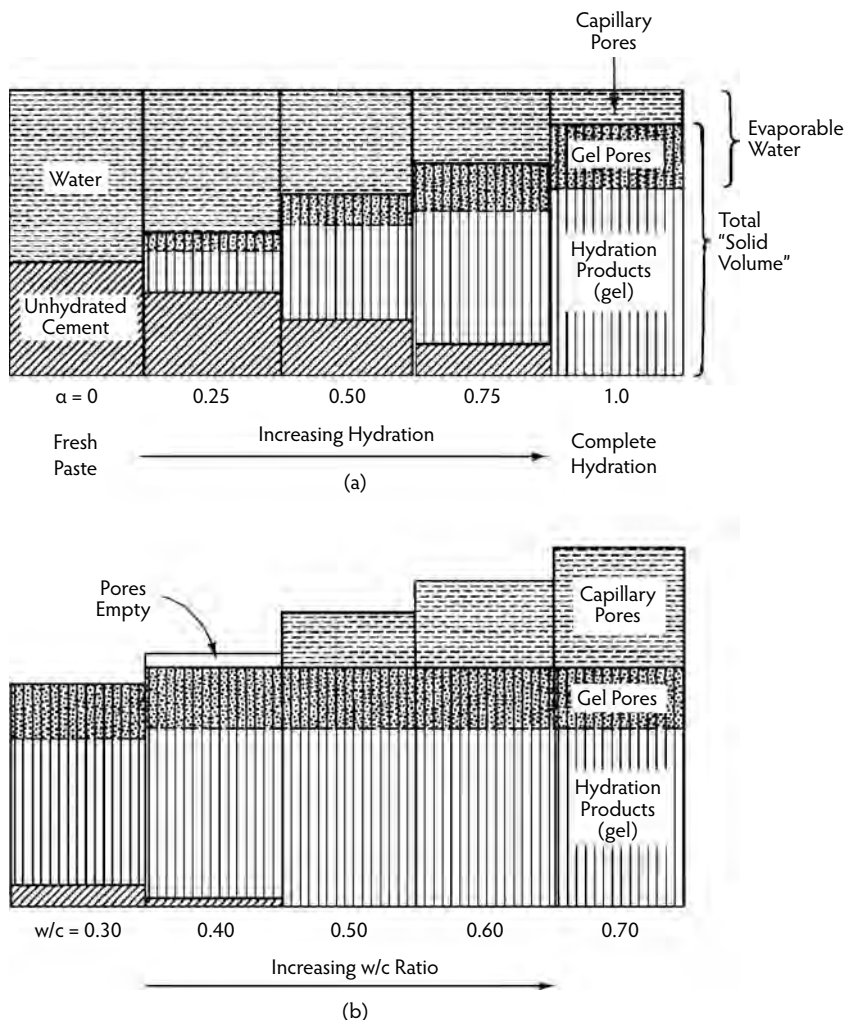


FIGURE 1.6 Volume relationships among the hydration products of hydrating Portland cement pastes: (a) constant w/c ratio = 0.50; (b) increasing w/c ratio ($\alpha = 1.0$).

These volume relationships can be seen more clearly in Figure 1.6, in terms of the degree of hydration and w/c ratio. From the above, it may be seen that the w/c ratio essentially controls the capillary porosity, which in turn controls the permeability and strength of the hardened paste. This is the basis of the w/c ratio law on which most mix design procedures are based. To produce high-strength, low-permeability concretes, it is thus necessary to use a low w/c ratio and to ensure a high degree of hydration by following proper curing procedures.

1.3 Modified Portland Cements

Increasingly, modern concretes contain a blend of Portland cement and other cementitious materials. When other materials are added to Portland cement at the time at which the concrete is batched, they are referred to as **mineral admixtures**, which are described in detail in Chapter 2; however, there are also *hydraulic cements*, which are produced either by forming other compounds during the burning process or by adding other materials to the clinker and then intergrinding them. The common types of such modified cements are described in the following sections.

1.3.1 Portland Pozzolan Cements

Portland pozzolan cements are blends of Portland cement and a pozzolanic material (see Chapter 2). The role of the pozzolan is to react slowly with the calcium hydroxide that is liberated during cement hydration. This tends to reduce the heat of hydration and the early strength but can increase the ultimate strength of the material. These cements tend to be more resistant to sulfate attack and to the alkali–aggregate reaction.

1.3.2 Portland Blast-Furnace Slag Cements

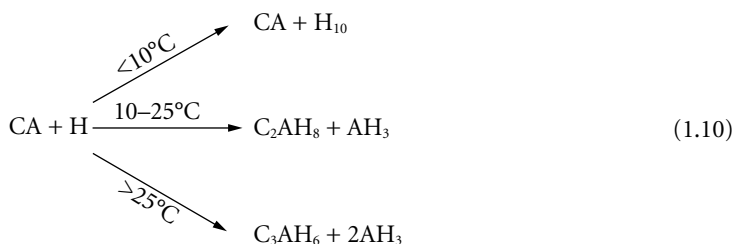
Ground granulated blast-furnace slag (GGBFS), which is a byproduct of the iron and steel industry, is composed largely of lime, silica, and alumina and thus is a potentially cementitious material. To hydrate it, however, it must be activated by the addition of other compounds. When the GGBFS is to be activated by lime, the lime is most easily supplied by the hydration of the Portland cement itself. Slags may be present in proportions ranging from 25 to 90%. They react slowly to form C–S–H, which is the same product that results from the hydration of the calcium silicates. In general, because they react more slowly than Portland cement, slag cements have both lower heats of hydration and lower rates of strength gain. On the other hand, they have an enhanced resistance to sulfate attack. When the GGBFS is to be activated with calcium sulfate (CaSO_4), together with a small amount of lime or Portland cement, the material is known as **supersulfated cement**. This cement is available mostly in Europe, where it is used for its lower heat of hydration and its resistance to sulfate attack.

1.3.3 Expansive Cements

Expansive cements were developed to try to offset the drying shrinkage that concrete undergoes. This is particularly important when the concrete is restrained against contraction or when it is to be cast against mature concrete in repair situations. In both cases, severe cracking may occur as a result of the shrinkage. Expansive cements are based on the formation of large quantities of ettringite during the first few days of hydration; however, they are little used today, in large part because it is very difficult to control (or predict) the amount of expansion that will take place for a particular concrete formulation.

1.4 High-Alumina Cement

A number of non-Portland inorganic cements are available, but by far the most important is high-alumina cement (also known as calcium–aluminate cement). It was developed originally for its sulfate-resistant properties but was subsequently used structurally because of its high rate of strength gain. Its use has been limited by structural problems due to the loss of strength that can occur in certain circumstances, which has led to several disastrous structural collapses. High-alumina cement (HAC) is about 60% CA, 10% C_2S , and 5 to 20% C_2AS (gehlenite), with 10 to 25% various minor constituents. When this material hydrates, much depends on the temperature:



These reactions take place rapidly, so HAC reaches about 75% of its ultimate strength in one day. Unfortunately, C_2AH_8 and CAH_{10} are transformed to C_3AH_6 at temperatures above 30°C , particularly in moist conditions. This leads to a considerable loss in strength, because C_3AH_6 has a smaller solid volume

TABLE 1.5 Comparison of Mix Proportions for 25-MPa Concrete

Component	Conventional Concrete		HVFA Concrete	
	By Mass (kg/m ³)	By Volume (m ³)	By Mass (kg/m ³)	By Volume (m ³)
Cement	307	0.097	154	0.049
Fly ash	—	—	154	0.063
Water	178	0.178	120	0.120
Entrapped air (2%)	—	0.020	—	0.020
Coarse aggregate	1040	0.387	1210	0.449
Fine aggregate	825	0.318	775	0.299
Total	2350	1.000	2413	1.000

Source: Adapted from Mehta, P.K., *Concrete Int.*, 24(7), 23–28, 2002.

than the other two calcium aluminate hydrates, causing a large increase in porosity. This loss in strength can be minimized if a low w/c ratio (<0.40) is used, but because of difficulties in predicting or controlling strength loss HAC is now not used structurally. Rather, it is used primarily for refractory purposes because of its good high-temperature properties.

1.5 “Green” Cements

The concrete industry is the largest user of natural resources in the world and thus has a considerable environmental impact. Each ton of Portland cement requires about 1.5 tons of raw material for its production. This industry is not only energy intensive but is also a major contributor of greenhouse gases, in the form of CO₂. Each ton of Portland cement that is produced involves the release into the atmosphere of about one ton of CO₂. Indeed, according to Mehta (1999), the cement industry is responsible for about 7% of global CO₂ emissions; thus, there is considerable interest now in developing cements that are more environmentally friendly. One such cement (CEMROC), based on blast-furnace slag, has recently been described by Gebauer et al. (2005). This cement, produced by Holcim in Europe, is reported to show close to zero CO₂ emission during its production (only about 100 pounds per ton of cement). It is similar to the supersulfated cement described above and is particularly well suited for use in structures exposed to aggressive environments. Other cements of this general type will almost certainly be developed in the future. Another (and simpler) approach is to use much greater proportions of fly ash in concrete. A great deal of development is being conducted on what is referred to as *high-performance, high-volume fly ash concrete* (Malhotra, 2002; Malhotra and Mehta, 2002). Such concretes may be defined as:

- Containing at least 50% fly ash by mass of the cementing materials
- Having a Portland cement content of less than 200 kg/m³
- Having a water content of less than 130 kg/m³
- Having a water/cementing materials ratio of less than 0.35

These concretes reach their full strength potential rather more slowly than conventional concretes, but the end result is a low-permeability, durable concrete. A comparison of the mix proportions for conventional and high-volume fly ash concretes is given in Table 1.5 (Mehta, 2002).

1.6 Performance of Different Cements in Concrete

The compositions of each of the five American Society for Testing and Materials (ASTM) types of cements may vary widely from cement to cement, due to variations in locally available raw materials, kiln design, burning conditions, and so on. Their fineness may also be quite variable. As a result, their cementitious properties may also vary widely. In some regions, for example, it may not be possible to find a commercially available cement for the production of very high-strength (>100 MPa) concrete.

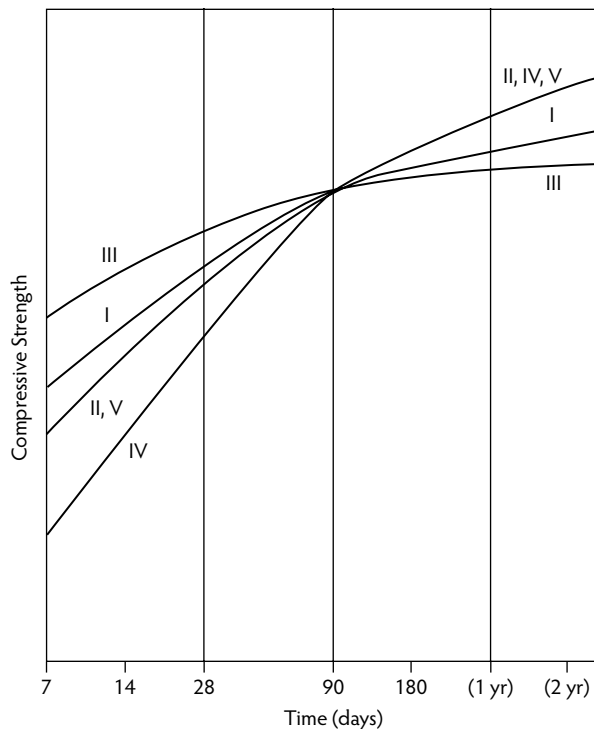


FIGURE 1.7 Relative compressive strengths of concretes made with different cements. (Adapted from U.S. Bureau of Reclamation, *Concrete Manual*, 8th ed., U.S. Bureau of Reclamation, Washington, D.C., 1975.)

Because most cements contain about 75% by weight of calcium silicates and undergo the same hydration reactions, though perhaps at different rates, their ultimate performances in concrete are similar, as shown in Figure 1.7. Here, the major differences are in the rate of strength gain and in the heat of hydration.

1.7 Water

Although the water itself is often not considered when dealing with materials that go into the production of concrete, it is an important ingredient. Typically, 150 to 200 kg/m³ of water is used. The old rule of thumb for water quality is “If you can drink it, you can use it in concrete,” although good-quality concrete can be made with water that is not really potable. Indeed, more bad concrete is made by using too much drinkable water than by using the right amount of undrinkable water. The tolerable limits for various common impurities in mixing water are given in Table 1.6. When in question, the suitability of the water is determined by comparing the strength of concrete made with the suspect water to the strength of concrete made with a known acceptable water.

1.8 Water/Cement Ratio

For brittle ceramic materials, including cementitious systems, the strength has been found to be inversely proportional to the porosity. Often, an exponential equation is used to relate strength to porosity; for example,

$$f_c = f_{c0}e^{-kp} \quad (1.11)$$

TABLE 1.6 Tolerable Levels of Some Impurities in Mixing Water

Impurity	Maximum Concentration (ppm)	Remarks
Suspended matter (turbidity)	2000	Silt, clay, organic matter
Algae	500–1000	Entrains air
Carbonates	1000	Decreases setting times
Bicarbonates	400–1000	400 ppm for bicarbonates of Ca or Mg
Sodium sulfate	10,000	May increase early strength but reduce later strength
Magnesium sulfate	40,000	
Sodium chloride	20,000	Decreases setting times, increases early strength,
Calcium chloride	50,000	reduces ultimate strength, and may lead to corrosion
Magnesium chloride	40,000	of reinforcing steel
Sugar	500	Affects setting behavior

where f_c is the strength, f_{c0} is the intrinsic strength at zero porosity, p is the porosity, and k is a constant that depends on the particular system. Equations such as this do not consider the pore-size distribution, the pore shape, and whether the pores are empty or filled with water; thus, they are a gross simplification of the true strength vs. porosity relationship. Nonetheless, for ordinary concretes for the same degree of cement hydration, the strength does indeed depend primarily on the porosity. Because the porosity, in turn, depends mostly on the original w/c ratio, mix proportioning for normal-strength concretes is based, to a large extent, on the w/c ratio law articulated by D.A. Abrams in 1919: “For given materials, the strength depends only on one factor—the ratio of water to cement.” This can be expressed as:

$$f_c = \frac{K_1}{K_2^{(w/c)}} \quad (1.12)$$

where K_1 and K_2 are constants, and w/c is the water/cement ratio by weight.

In fact, of course, given the variability in raw materials from concrete to concrete, the w/c ratio law is really a family of relationships for different mixtures. As stated by Gilkey (1961a):

For a given cement and acceptable aggregates, the strength that may be developed by a workable, properly placed mixture of cement, aggregate, and water (under the same mixing, curing, and, testing conditions) is influenced by the: (a) ratio of cement to mixing water; (b) ratio of cement to aggregate; (c) grading, surface texture, shape, strength, and stiffness of aggregate particles; and (d) maximum size of aggregate.

Thus, in some cases, simple reliance on the w/c ratio law may lead to serious errors. It should be noted that many modern concretes contain one or more mineral admixtures that are, in themselves, cementitious to a greater or lesser degree; therefore, it is becoming more common to use the term **water/cementitious material ratio** to reflect this fact rather than the simpler water/cement ratio.

For ordinary concretes, the w/c ratio law works well for a given set of raw materials, because the aggregate strength is generally much greater than the paste strength; however, the w/c ratio law is more problematic for high-strength concretes, in which the strength-limiting factor may be the aggregate strength or the strength of the interfacial zone between the cement and the aggregate. Although it is, of course, necessary to use very low w/c ratios to achieve very high strengths, the w/c ratio vs. strength relationship is not as straightforward as it is for normal concretes. Figure 1.8 shows a variety of water/cementitious material vs. strength relationships obtained by a number of different investigators. A great deal of scatter can be seen in the results. In addition, the range of strengths for a given w/c ratio increases as the w/c ratio decreases, leading to the conclusion that, for these concretes, the w/c ratio is not by itself a very good predictor of strength; a different w/c ratio “law” must be determined for each different set of materials.

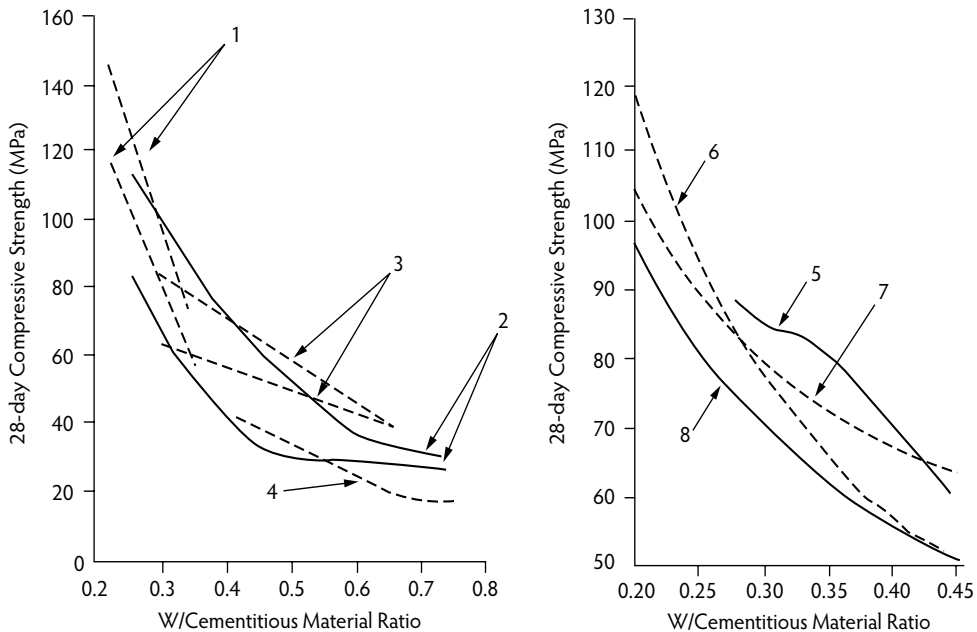


FIGURE 1.8 Water/cementitious material vs. strength relationships obtained by different investigators: (1) (Aitcin, P.-C., private communication, 1992.) (2) (Fiorato, A.E., *Concrete Int.*, 11(4), 44–50, 1989.) (3) (Cook, J.E., *Concrete Int.*, 11(10), 67–75, 1989.) (4) (CPCA, *Design and Control of Concrete Mixtures*, Canadian Portland Cement Association, Ottawa, Canada, 1991.) (5) (Addis, B.J. and Alexander, M.G., in *High-Strength Concrete, Second International Symposium*, ACI SP-121, pp. 287–308, American Concrete Institute, Farmington Hills, MI, 1990.) (6) (Hattori, K., in *Superplasticizers in Concrete*, ACI SP-62, pp. 37–66, American Concrete Institute, Farmington Hills, MI, 1979.) (7) Ordinary Portland cement. (From Suzuki, T., in *Utilization of High-Strength Concrete, Symposium Proceedings*, pp. 53–54, Tapis Publishers, Trondheim, Norway, 1987.) (8) High-early-strength cement. (From Suzuki, T., in *Utilization of High-Strength Concrete, Symposium Proceedings*, pp. 53–54, Tapis Publishers, Trondheim, Norway, 1987.)

1.9 Aggregates

Aggregates make up about 75% of the volume of concrete, so their properties have a large influence on the properties of the concrete (Alexander and Mindess, 2005). Aggregates are granular materials, most commonly natural gravels and sands or crushed stone, although occasionally synthetic materials such as slags or expanded clays or shales are used. Most aggregates have specific gravities in the range of 2.6 to 2.7, although both heavyweight and lightweight aggregates are sometimes used for special concretes, as described later. The role of the aggregate is to provide much better dimensional stability and wear resistance; without aggregates, large castings of neat cement paste would essentially self-destruct upon drying. Also, because they are less expensive than Portland cement, aggregates lead to the production of more economical concretes. In general, aggregates are much stronger than the cement paste, so their exact mechanical properties are not considered to be of much importance (except for very high-strength concretes). Similarly, they are also assumed to be completely inert in a cement matrix, although this is not always true, as will be seen in the discussion on the alkali–aggregate reaction. For ordinary concretes, the most important aggregate properties are the particle grading (or particle-size distribution), shape, and porosity, as well as possible reactivity with the cement. Of course, all aggregates should be clean—that is, free of impurities such as salt, clay, dirt, or foreign matter. As a matter of convenience, aggregates are generally divided into two size ranges: **coarse aggregate**, which is the fraction of material retained on a No. 4 (4.75-mm) sieve, and **fine aggregate**, which is the fraction passing the No. 4 sieve but retained on a No. 100 (0.15-mm) sieve.

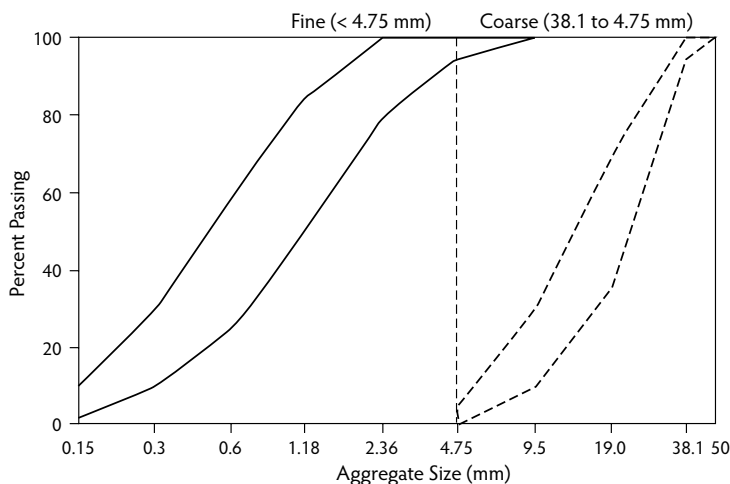


FIGURE 1.9 ASTM grading limits for fine aggregate and for coarse aggregate with a maximum particle size of 38.1 mm.

1.9.1 Particle Shape and Texture

Ideally, to minimize the amount of cement paste required to provide adequate workability of the fresh concrete, aggregate particles for ordinary concrete should be roughly equidimensional with relatively smooth surfaces, such as most natural sands and gravels. Where natural sands and gravels are unavailable, crushed stone may be used. Crushed stone tends to have a rougher surface and to be more angular in shape. As a result, it tends to require rather more cement paste for workability. Whether using natural gravels or crushed stone, however, either flat or elongated particles should be avoided, as they will lead to workability and finishing problems.

1.9.2 Particle Grading

The **particle-size distribution** in a sample of aggregate, referred to as the *grading*, is generally expressed in terms of the cumulative percentage of particles passing (or retained on) a specific series of sieves. These distributions are most commonly shown graphically as **grading curves**. Examples of such curves are given in Figure 1.9, which shows the usual North American grading limits for fine aggregate and for a particular maximum size (38.1 mm) of coarse aggregate. Such grading limits have been determined empirically. They are intended to provide a fairly dense packing of aggregate particles, again to minimize the cement paste requirement; however, no ideal aggregate grading exists that can be derived theoretically. In practice, one can provide good concrete with quite a range of aggregate gradings. Although the continuous type of grading described in Figure 1.9 is the most common, other types of grading are sometimes used for special purposes; for example, **gap grading** refers to a grading in which one or more of the intermediate size fractions is omitted. This is sometimes convenient when it is necessary to blend different aggregates to achieve a suitable grading. Such concretes are also prone to segregation of the fresh concrete. **No-fines concrete** is a special case of gap-graded concrete in which the fine aggregate (<4.75 mm) is omitted entirely to produce a porous, lighter weight concrete that, for example, may allow water to drain through it. For fine aggregates, the particle-size distribution tends to be described by a single number, the **fineness modulus** (FM), which is defined as:

$$\text{FM} = \frac{\sum (\text{cumulative \% retained on standard sieves})}{100} \quad (1.13)$$

where the standard sieve sizes are No. 100 (0.15-mm), No. 50 (0.30-mm), No. 30 (0.60-mm), No. 16 (1.18-mm), No. 8 (2.36-mm), and No. 4 (4.75-mm). An example of the calculation of the fineness

TABLE 1.7 Calculation of Fineness Modulus

Sieve Size	Weight Retained	Weight Percent Retained	Cumulative Weight Percent Retained
#4	30	3	3
#8	100	10	13
#16	195	19.5	32.5
#30	200	20	52.5
#50	260	26	78.5
#100	215	21.5	100.0
			$\Sigma = 279.5$

Note: Sample weight 1000 g; fineness modulus (FM) = $(279.5/100) = 2.80$.

modulus is shown in Table 1.7. Normally, the FM should fall between 2.3 and 3.1 (higher values imply a coarser material). The value of the FM is required for mix design purposes. (Also see Chapter 6 of this handbook, which discusses the proportioning of concrete mixtures.)

1.9.3 Aggregate Moisture Content

Aggregates can hold water in two ways: absorbed within the aggregate porosity or held on the particle surface as a moisture film. Thus, depending on the relative humidity, recent weather conditions, and location within the aggregate stockpile, aggregate particles can have a variable moisture content. For the purposes of mix proportioning, however, it is necessary to know how much water the aggregate will absorb from the mix water or how much extra water the aggregate might contribute. Figure 1.10 illustrates four different moisture states:

- *Oven-dry (OD)*—All moisture is removed by heating the aggregates in an oven at 105°C to constant weight.
- *Air-dry (AD)*—No surface moisture is present, but the pores may be partially full.
- *Saturated surface dry (SSD)*—All pores are full, but the surface is completely dry.
- *Wet*—All pores are full, and a water film is on the surface.

Of these four states, only two (OD and SSD) correspond to well-defined moisture conditions; either one can be used as a reference point for calculating the moisture contents. In the following discussion, the SSD state will be used. Now, to determine how much water the aggregate may add to or take from the mixing water, three further quantities must be defined:

- The *absorption capacity* (AC) represents the maximum amount of water the aggregates can absorb. From Figure 1.10, this is the difference between the SSD and OD states, expressed as a percentage of the OD weight:

$$AC = \frac{W_{SSD} - W_{OD}}{W_{OD}} \times 100\% \quad (1.14)$$

where W represents weight. It should be noted that, for most common aggregates, the absorption capacities are of the order of 0.5 to 2.0%. Absorption capacities greater than 2% are often an indication that the aggregates may have potential durability problems.

- The *effective absorption* (EA) refers to the amount of water required for the aggregate to go from the AD to the SSD state:

$$EA = \frac{W_{SSD} - W_{AD}}{W_{SSD}} \times 100\% \quad (1.15)$$

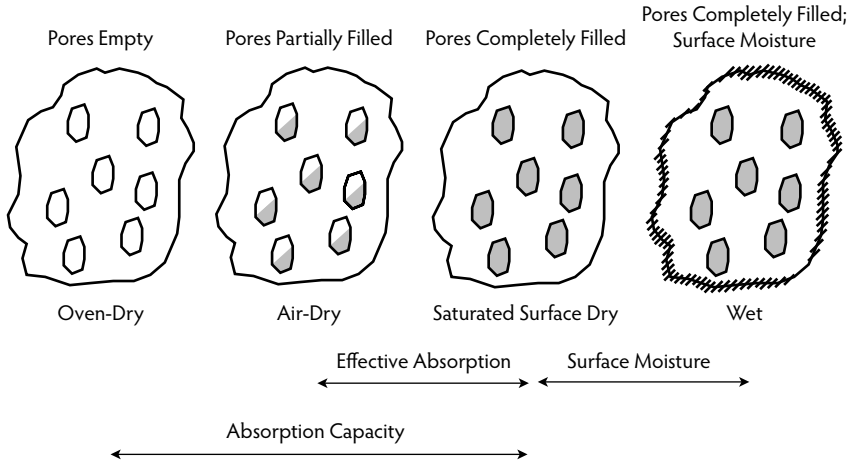


FIGURE 1.10 Moisture states of aggregates.

To calculate the weight of the water absorbed (W_{abs}) by the aggregate in the concrete mix:

$$W_{abs} = (EA)W_{agg} \quad (1.16)$$

- The *surface moisture* (SM) represents water in excess of the SSD state, held on the aggregate surface:

$$SM = \frac{W_{wet} - W_{SSD}}{W_{SSD}} \times 100\% \quad (1.17)$$

Thus, the extra water added to the concrete from the wet aggregates will be:

$$W_{add} = (SM)W_{agg} \quad (1.18)$$

1.9.4 Lightweight Aggregates

Lightweight aggregates, which can be either natural or synthetic materials, are characterized by a high internal porosity. Ordinary concrete has a unit weight of about 2300 kg/m^3 , but lightweight concretes with unit weights as low as 120 kg/m^3 can be produced, although they are accompanied by a significant decrease in concrete strength. Natural lightweight aggregates include pumice, scoria, and tuff; however, most lightweight aggregates are synthetically produced. The most common such lightweight aggregates are made from expanded clay, shale, or slate. The raw material is either crushed to the desired size or ground and then pelletized; it is then heated to 1000 to 1200°C . At these temperatures, the material **bloats** (or puffs up) due to the rapid generation of gas produced by the combustion of the small amounts of organic material that these particles generally contain. (The process is similar to that of popping popcorn.) Other materials, such as volcanic glass (perlite), calcium silicate glasses (slags), or vermiculite, can similarly be bloated. Lightweight aggregates tend to be angular and irregular in shape and can be quite variable. They will also tend to have high porosities, leading to a considerable potential for absorbing water from the mix; hence, mix design with lightweight aggregates is much more of a trial-and-error procedure than with normal-weight aggregates. Lightweight concretes made with these aggregates may be classified as shown in Figure 1.11. The properties of different types of lightweight concrete are described in Table 1.8. It should be noted that, despite the high porosity and relative weakness of the aggregate, it is not a problem to reach strengths as high as 40 MPa . To do this, lower w/c ratios are required for lightweight concretes than are required for ordinary concretes of the same strength. Although a general relationship exists between strength and density of the concrete, it can be seen in Figure 1.12 that this relationship depends on the particular aggregate used.

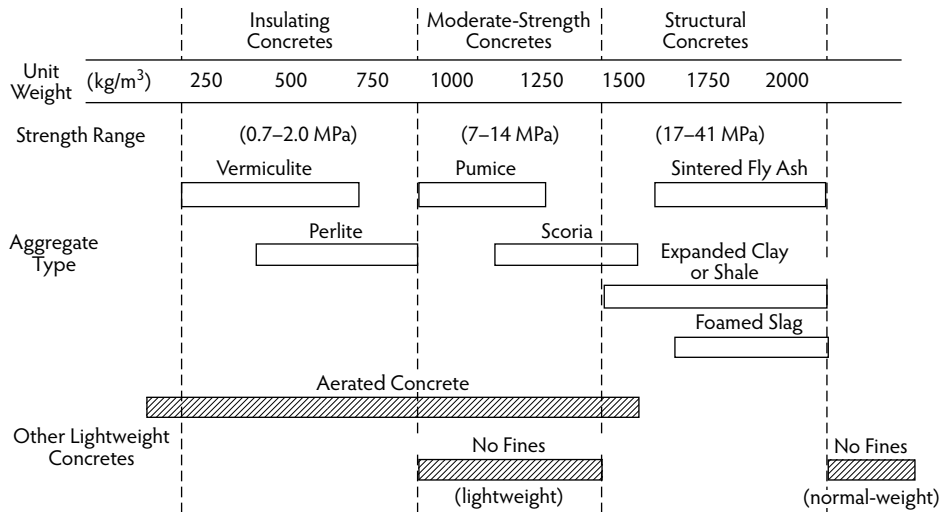


FIGURE 1.11 Classification of lightweight concretes.

TABLE 1.8 Properties of Some Lightweight Concretes

Type of Lightweight Concrete	Type of Aggregate	Aggregate Density (kg/m ³)	Concrete Density (kg/m ³)
Aerated	—	—	400–600
Partially compacted	Expanded vermiculite and perlite	5–240	400–1150
	Foamed slag	480–960	960–1500
	Sintered pulverized-fuel ash	640–960	1100–1300
	Expanded clay or shale	560–1040	950–1200
Structural lightweight aggregate concrete	Foamed slag	480–960	1650–2050
	Sintered pulverized-fuel ash	640–960	1350–1750
	Expanded clay or shale	560–1040	1350–1850

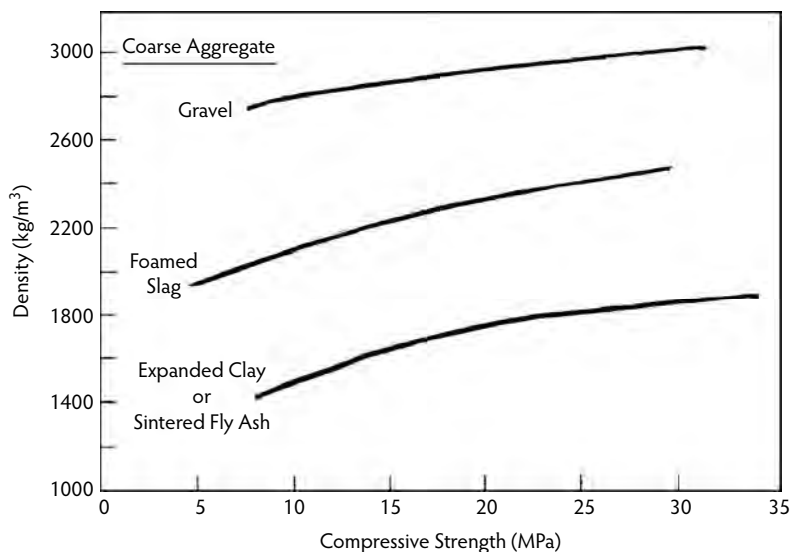
FIGURE 1.12 Average density vs. compressive strength relationships. (Adapted from Short, A. and Kinniburgh, W., *Lightweight Concrete*, 3rd ed., Applied Science Publishers, London, 1978.)

TABLE 1.9 Physical Properties of Some Heavyweight Aggregates

Material	Chemical Composition	Relative Density	Granular Bulk Density (kg/m ³)
Goethite	Fe ₂ O ₃ · H ₂ O	3.5–3.7	2100–2250
Limonite	Impure Fe ₂ O ₃	3.4–4.0	2100–2400
Barytes	BaSO ₄	4.0–4.6	2300–2550
Illmenite	FeTiO ₃	4.3–4.8	2550–2700
Magnetite	Fe ₃ O ₄	4.2–5.2	2400–3050
Hematite	Fe ₂ O ₃	4.9–5.3	2900–3200
Ferro phosphorus	Fe ₂ O ₃ · P ₂ O ₃	5.8–6.8	3200–4150
Steel	Fe (scrap iron, steel punchings)	7.8	3700–4650

1.9.5 Heavyweight Aggregates

Heavyweight aggregates are used to make heavyweight concretes, with unit weights ranging from about 2900 to 6000 kg/m³. Such concretes are used primarily for radiation shielding, but they are sometimes used to make counterweights as well. Natural heavyweight aggregates include materials such as goethite, limonite, barite, illmenite, magnetite, and hematite, with specific gravities (SGs) ranging from about 3.5 up to about 5.3, leading to concretes with unit weights up to about 4100 kg/m³. For higher unit weight concretes, synthetic materials such as ferrophosphorous (SG 5.8 to 6.8) or scrap iron and steel punchings (SG 7.8) can be used, with resulting concrete unit weights of up to 6100 kg/m³. The physical properties of some heavyweight aggregates are shown in Table 1.9. High-density aggregates are good attenuators of gamma rays and of fast neutrons, hence their use in radiation shielding. Although heavyweight concretes can be proportioned in much the same way as ordinary concretes, the aggregates tend to be harsh and have a tendency to segregate from the rest of the mix. As a result, both higher than usual cement contents and a higher ratio of fine to coarse aggregates are recommended.

1.9.6 Aggregate Durability

It is generally assumed that aggregates are inert in concrete, but this is often not true, so their durability must also be considered.

1.9.6.1 Soundness

Soundness refers to the ability of aggregates to withstand cyclic volume changes due to wetting and drying or freezing and thawing without deteriorating. Rocks that are susceptible to wetting and drying cycles are rare, so soundness generally refers to freeze–thaw resistance. Aggregates will deteriorate if high internal stresses are developed when water absorbed within the aggregate freezes. This deterioration, in turn, depends on the size, porosity, permeability, and degree of saturation of the aggregate. For most aggregates, the critical size above which unsoundness develops is greater than the maximum size normally used in concrete; however, for some sedimentary rocks (chert, graywacke, sandstone, shale, and poorly consolidated limestone), the critical size can be less than 25 mm. The most susceptible rocks are those that have a relatively high absorption (porosity), greater than 2%, combined with a very fine pore structure (low permeability) so the freezing water cannot easily be expelled from the aggregate. If aggregates are unsound, this can lead to surface pop-outs and to D-cracking in pavements and slabs.

1.9.6.2 Alkali–Aggregate Reaction

A large number of failures have resulted from expansions caused by reactions between certain types of siliceous aggregates and the alkalis (K₂O and Na₂O) contained in the cement. The types of rocks that are likely to participate in these reactions include siliceous limestones, cherts, shale, flint, volcanic glasses, opaline rocks, quartzite, sandstone, and some granites and schists. In some cases, these expansive

TABLE 1.10 The Alkali–Silica Reaction

Reaction Step	Reaction	Consequences
1	Release of alkali ions during cement hydration	Increased alkalinity of water in the pores (pore solution)
2	Initial hydrolysis of the reactive silicates in the alkaline pore solution: $K(Na)OH + SiO_2 \rightarrow K_2O(Na_2O)-SiO_2-H_2O$, amorphous alkali silicate gel	Aggregate integrity destroyed
3	Swelling of alkali silicate gel as it imbibes water	Localized cracking
4	Liquefaction of alkali silicate gel as it imbibes more moisture	Liquid gel expelled through the cracks

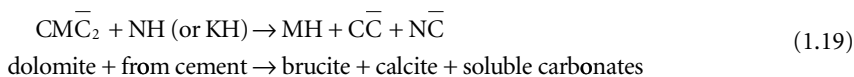
reactions, which are first manifested by extensive surface cracking, occur within a few years after the concrete has been cast. In other cases, however, damage may not appear until 15 to 20 years after construction.

The factors that control the rate and extent of the alkali–aggregate reaction are (1) the nature of the reactive silica, (2) the amount of reactive silica, (3) the particle size of the reactive material, (4) the amount of alkali available, and (5) the amount of available moisture. Regardless of the specifics of the cement and the aggregate, however, the alkali–silica reaction progresses through the steps indicated in Table 1.10. Step 1 is controlled by the alkali content of the cement. Any real control of the reaction potential must be taken at this step, either by avoiding reactive aggregates or by keeping the alkali content of the cement quite low ($Na_2O + 0.6K_2O \leq 0.60$). Step 2 depends on the exact form of the silica and determines the rate at which the reaction will take place. It is at Step 3 that the damage occurs as the alkali–silicate gel imbibes water and swells, cracking the matrix. Step 4 mostly produces the visible signs of the reaction. It should be noted that Steps 3 and 4 will not occur if the concrete is kept dry.

If low-alkali cements are not available in a particular region (because the raw materials used to produce the cement are themselves too high in alkali content), a useful strategy is often to replace some of the cement with a pozzolanic material (such as fly ash) that contains no alkalis at all, to reduce the total alkali content of the cementitious materials to an acceptable level. Although pozzolanic materials contain silica in a reactive form, the silica is very finely divided and reacts very quickly with the alkalis. Harmful expansions do not occur because the resulting alkali–silicate gel is distributed throughout the cementitious matrix, so the expansions are distributed. The worst case is to have relatively small volumes of reactive aggregates in large pieces scattered throughout the concrete; this localizes and concentrates the expansions, leading to severe cracking.

1.9.6.3 Alkali–Carbonate Reaction

Expansive reactions can also occur between the alkalis in the cement and certain dolomitic limestones ($MgCO_3/CaCO_3$) that contain some clay. Not all dolomitic limestones are subject to this reaction; those that are have the following features: (1) very small crystals of $MgCO_3$, (2) presence of considerable fine-grained calcite, (3) abundant interstitial clay, and (4) dolomite and calcite crystals uniformly distributed in the clay matrix. The expansive reaction is:



This reaction is still not fully understood. The alkali–carbonate reaction can also be controlled by keeping the alkali content of the cementitious material very low ($<0.40\%$). Unlike the case of the alkali–silica reaction, pozzolanic materials in this case cannot control the alkali–carbonate reaction.

1.10 Reinforcement

1.10.1 General

Plain concrete is a brittle material, with low tensile strength and strain capacities; hence, reinforcement has to be used to balance this deficiency. Main bar reinforcement is used in tensile zones to enhance the capacity of concrete elements so the structural beam or slab will be able to withstand high loads and deform adequately without brittle failure. Chapter 27 of this handbook details the ACI 318 design equations for proportioning reinforced concrete members. Another method that can increase the tensile capacity of plain concrete within a structural bar-reinforced section is the use of fiber reinforcement. The use of **fiber-reinforced concrete (FRC)** has steadily increased since the early 1960s, as has the use of **fiber-reinforced plastics (FRPs)**.

1.10.2 Fiber Reinforcement

The role of the fibers is not to increase strength, although modest strength increases may occur. Rather, the role of discrete, discontinuous, randomly oriented fibers is to bridge the cracks that develop in concrete either as it is subjected to environmental changes (such as drying) or as it is loaded. If the fibers are strong enough, stiff enough, and present in sufficient quantity and develop sufficient bonds with the cementitious matrix, they will serve to keep the crack widths small and will permit the FRC to withstand significant stresses over a relatively large strain capacity in the post-cracking (or strain-softening) stage. In other words, by bridging the cracks that develop, the fibers can provide a considerable amount of post-cracking ductility. This is often referred to as **toughness**. The toughness may be defined in terms of the area under the load vs. the deflection curve. The stress is transferred from the matrix to the fibers in two ways:

- At early stages of loading, the stress is transmitted from the matrix to the fibers through an elastic shear-transfer mechanism, which, however, has only a small effect on the limit of proportionality or first-crack stress of the FRC.
- After the initial cracking, and at more advanced stages of loading, debonding along the fiber–matrix interface occurs, and frictional slip becomes the process controlling the stress transfer. The degree of frictional slip affects both the ultimate strength and strain of the FRC. At this stage, the fibers may increase the strength of the FRC by transferring loads and stresses across the cracked matrix. In addition, and more importantly, they may increase the toughness of the FRC by providing energy absorption mechanisms related to the pullout processes of the fibers. Chapter 22 of this handbook gives an in-depth treatment of this subject for both FRC and FPC concretes.

1.10.3 Steel Reinforcement

Typically, steel reinforcement used in concrete has yield strengths in the range of 275 to 550 MPa (40,000 to 80,000 psi). For all these steels, the modulus of elasticity is in the range of 200×10^6 MPa (29×10^6 psi). The bar sizes in the United States range from No. 3 to No. 18 deformed bars. In slabs, the use of welded wire fabric is more prevalent. Table 1.11 and Table 1.12 give the properties of most commonly used bars for concrete reinforcement. Table 1.13 gives standard wire fabric reinforcement for one-way and two-way slabs and plates. These tables are derived from the ASTM Standards. The bar deformations shown in Figure 1.13 are in accordance with ASTM A 616.

One of the problems resulting from permeability of concrete to moisture is the corrosion of the reinforcement. Corrosion can lead to a reduction in the effective cross-sectional area of the steel and a spalling of the concrete above the steel, both of which can lead to severe damage or even failure of a structure or structural element. The mechanisms of corrosion in steel are by now well known. An isolated steel bar will rust spontaneously (Figure 1.14) because different areas of the bar may have different

TABLE 1.11 Reinforcement Grades and Strengths

1982 Standard Type	Minimum Yield Point or Yield Strength (f_y) (psi)	Ultimate Strength (f_u) (psi)
<i>Billet steel (A615)</i>		
Grade 40	40,000	70,000
Grade 60	60,000	90,000
<i>Axle steel (A617)</i>		
Grade 40	40,000	70,000
Grade 60	60,000	90,000
<i>Low-alloy steel (A706)</i>		
Grade 60	60,000	80,000
<i>Deformed wire</i>		
Reinforced	75,000	85,000
Fabric	70,000	80,000
<i>Smooth wire</i>		
Reinforced	70,000	80,000
Fabric	65,000, 56,000	75,000, 70,000

Source: Nawy, E.G., *Reinforced Concrete: A Fundamental Approach*, 6th ed., Prentice Hall, Upper Saddle River, NJ, 2008.

electrochemical potentials and thus set up anode–cathode pairs, with corrosion occurring in localized anodic areas; however, steel corrosion should not occur, even in the presence of moisture and oxygen. This is because the highly alkaline concrete (pH of about 12 to 12.5) causes a passive oxide film to form on the surface of the steel, which prevents corrosion. Only when the pH falls below 11 will the passive iron oxide layer be destroyed, permitting rusting to occur. The pH may be reduced in two ways:

- The calcium hydroxide that is responsible for the high pH can be converted to calcium carbonate by atmospheric carbonation. For good concrete, the depth of carbonation rarely exceeds 25 mm, so adequate cover (25 mm to 40 mm) over the reinforcement should provide adequate protection. For high-permeability concretes or very severe exposures, a thicker cover must be used. Of course, if there are cracks in the concrete, perhaps due to drying shrinkage, CO_2 may penetrate to the steel and initiate corrosion. It has been found empirically, however, that if the crack widths at the surface of the concrete can be kept below 0.025 mm by suitable reinforcing details, then the rate of CO_2 diffusion will be slow enough to avoid extensive corrosion.
- Chloride ions have the capacity to destroy the passive oxide layer even at high pH, and relatively little chloride is required to initiate corrosion. Chloride ions may enter concrete from CaCl_2 used as an accelerating admixture, from seawater, and from the deicing salts commonly used on bridge decks and pavements. This may be particularly severe for prestressing steel, because in this case **stress corrosion** may occur. Whatever the source of the Cl^- ions, when a critical concentration of chlorides develops at the level of the steel (0.6 to 1.2 kg Cl^- per m^3), corrosion will occur.

Several strategies to combat steel corrosion have been developed, but corrosion remains one of the principal concrete construction problems. The most common techniques at this time (apart from making more impermeable performance concrete) are the following:

- Suppression of electrochemical corrosion by using **cathodic protection**. In this technique, an electric current is applied to the rebars (which must be connected electrically) in the direction opposite that of the current flow in spontaneous corrosion. This makes the steel cathodic, preventing corrosion. This technique has been used successfully but is difficult to apply.
- Various corrosion-inhibiting admixtures are now available commercially that serve to maintain the passive oxide film.

TABLE 1.12A Weight, Area, and Perimeter of Individual Bars

Bar Designation Number	Weight per Foot (lb)	1982 Standard Nominal Dimensions		
		Diameter (d_b) (mm)	Cross-Sectional Area (A_b) (in. ²)	Perimeter (in.)
3	0.376	0.375 (9)	0.11	1.178
4	0.668	0.500 (13)	0.20	1.571
5	1.043	0.625 (16)	0.31	1.963
6	1.502	0.750 (19)	0.44	2.356
7	2.044	0.875 (22)	0.60	2.749
8	2.670	1.000 (25)	0.79	3.142
9	3.400	1.128 (28)	1.00	3.544
10	4.303	1.270 (31)	1.27	3.990
11	5.313	1.410 (33)	1.56	4.430
14	7.65	1.693 (43)	2.25	5.32
18	13.60	2.257 (56)	4.00	7.09

TABLE 1.12B ASTM Standard Metric Reinforcing Bars

Bar Size Designation Number	Nominal Dimensions		
	Mass (kg/m)	Diameter (mm)	Area (mm ²)
10 M	0.785	11.3	100
15 M	1.570	16.0	200
20 M	2.355	19.5	300
25 M	3.925	25.2	500
30 M	5.495	29.9	700
35 M	7.850	35.7	1000
45 M	11.775	43.7	1500
55 M	19.625	56.4	2500

Note: ASTM A615M Grade 300 is limited to size No. 5, 10 M through No. 20 M; otherwise, grades 400 or 500 MPa for all the sizes. Check availability with local suppliers for No. 45 M and No. 55 M.

Source: Nawy, E.G., *Reinforced Concrete: A Fundamental Approach*, 6th ed., Prentice Hall, Upper Saddle River, NJ, 2008.

- Epoxy-coated rebars have become more and more common, but this technique has two problems: (1) If the bars are scratched during handling or are bent too severely, then the epoxy coating may be damaged, exposing the steel to corrosion, and (2) the epoxy-coated bars develop substantially less bond with the concrete, and if this issue is not recognized severe structural cracking can occur. New design techniques for epoxy-coated bars are now being developed that address this reduction in bond. More efficient deformation patterns are also being developed.

1.11 Durability Considerations

If concrete is properly designed for the environment to which it is to be exposed and is properly placed and cured, it should last for many decades without costly repairs. This is particularly the case for the modern generation of high-performance concretes; however, concrete is potentially vulnerable to both chemical attack and physical attack. Several of these durability problems (alkali–aggregate reaction and corrosion of reinforcing steel) have already been discussed, while freeze–thaw durability is discussed in Chapter 4 of this handbook. Here, the major consideration is primarily chemical attack.

The single parameter that has the largest influence on durability is the porosity of the concrete (governed by the w/c ratio), because damage due to surface attack of concrete occurs slowly. A dense, well-cured concrete has a permeability similar to that of low-porosity rocks, despite the much higher porosity of the paste, because in such concretes the porosity is discontinuous. This means that, instead

TABLE 1.13 Standard Wire Reinforcement

U.S. Customary			Center-to-Center Spacing (in.²/ft of Width)								
W & D Size		Nominal Diameter (in.)	Nominal Area (in.²)	Nominal Weight (lb/ft)	2	3	4	6	8	10	12
Smooth	Deformed										
W31	D31	0.628	0.310	1.054	1.86	1.24	0.93	0.62	0.465	0.372	0.31
W30	D30	0.618	0.300	1.020	1.80	1.20	0.90	0.60	0.45	0.366	0.30
W28	D28	0.597	0.280	0.952	1.68	1.12	0.84	0.56	0.42	0.336	0.28
W26	D26	0.575	0.260	0.934	1.56	1.04	0.78	0.52	0.39	0.312	0.26
W24	D24	0.553	0.240	0.816	1.44	0.96	0.72	0.48	0.36	0.288	0.24
W22	D22	0.529	0.220	0.748	1.32	0.88	0.66	0.44	0.33	0.264	0.22
W20	D20	0.504	0.200	0.680	1.20	0.80	0.60	0.40	0.30	0.24	0.20
W18	D18	0.478	0.180	0.612	1.08	0.72	0.54	0.36	0.27	0.216	0.18
W16	D16	0.451	0.160	0.544	0.96	0.64	0.48	0.32	0.24	0.192	0.16
W14	D14	0.422	0.140	0.476	0.84	0.56	0.42	0.28	0.21	0.168	0.14
W12	D12	0.390	0.120	0.408	0.72	0.48	0.36	0.24	0.18	0.144	0.12
W11	D11	0.374	0.110	0.374	0.66	0.44	0.33	0.22	0.165	0.132	0.11
W10.5		0.366	0.105	0.357	0.63	0.42	0.315	0.21	0.157	0.126	0.105
W10	D10	0.356	0.100	0.340	0.60	0.40	0.30	0.20	0.15	0.12	0.10
W9.5		0.348	0.095	0.323	0.57	0.38	0.285	0.19	0.142	0.114	0.095
W9	D9	0.338	0.090	0.306	0.54	0.36	0.27	0.18	0.135	0.108	0.09
W8.5		0.329	0.085	0.289	0.51	0.34	0.255	0.17	0.127	0.102	0.085
W8	D8	0.319	0.080	0.272	0.48	0.32	0.24	0.16	0.12	0.096	0.08
W7.5		0.309	0.075	0.255	0.45	0.30	0.225	0.15	0.112	0.09	0.075
W7	D7	0.298	0.070	0.238	0.42	0.28	0.21	0.14	0.105	0.084	0.07
W6.5		0.288	0.065	0.221	0.39	0.26	0.195	0.13	0.097	0.078	0.065
W6	D6	0.276	0.060	0.204	0.36	0.24	0.18	0.12	0.09	0.072	0.06
W5.5		0.264	0.055	0.187	0.33	0.22	0.165	0.11	0.082	0.066	0.055
W5	D5	0.252	0.050	0.170	0.30	0.20	0.15	0.10	0.075	0.06	0.05
W4.5		0.240	0.045	0.153	0.27	0.18	0.135	0.09	0.067	0.054	0.045
W4	D4	0.225	0.040	0.136	0.24	0.16	0.12	0.08	0.06	0.048	0.04
W3.5		0.211	0.035	0.119	0.21	0.14	0.105	0.07	0.052	0.042	0.035
W3		0.195	0.030	0.102	0.18	0.12	0.09	0.06	0.045	0.036	0.03
W2.9		0.192	0.029	0.098	0.174	0.116	0.087	0.058	0.043	0.035	0.029
W2.5		0.178	0.025	0.085	0.15	0.10	0.075	0.05	0.037	0.03	0.025
W2		0.159	0.020	0.068	0.12	0.08	0.06	0.04	0.03	0.024	0.02
W1.4		0.135	0.014	0.049	0.084	0.056	0.042	0.028	0.021	0.017	0.014

Source: Nawy, E.G., *Reinforced Concrete: A Fundamental Approach*, 6th ed., Prentice Hall, Upper Saddle River, NJ, 2008.

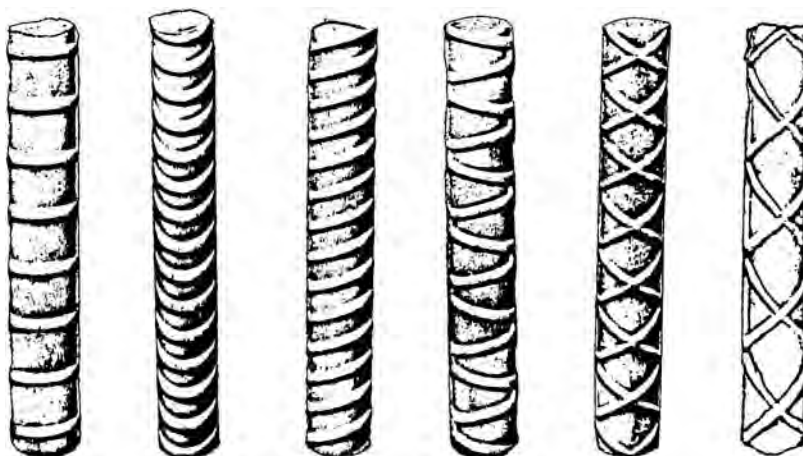


FIGURE 1.13 Various forms of ASTM-approved bars.

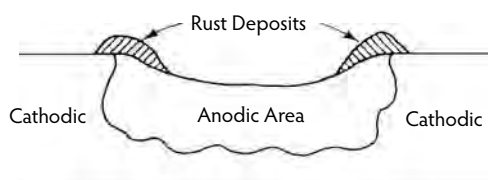


FIGURE 1.14 Schematic of rusting in reinforcing steel.

of the bulk flow that would occur through continuous capillary pores, water can flow only by a much slower molecular diffusion process through micropores. Permeability can be further reduced by the use of silica fume or blast-furnace slag which helps to create an even, more discontinuous pore structure.

1.11.1 Leaching and Efflorescence

Efflorescence consists of salts that are leached out of the concrete by water and are then crystallized on the concrete surface by the subsequent evaporation of the water. Efflorescence due to the leaching of calcium hydroxide from concrete and its subsequent carbonation (to CaCO_3) on the concrete surface is frequently seen as white deposits on the underside of floor slabs in parking garages. Efflorescence itself is primarily an aesthetic rather than a durability problem, but it does indicate substantial leaching in the concrete, which will lead to an increase in porosity and permeability.

1.11.2 Sulfate Attack

Sulfates are often present in groundwaters and in seawater. Chemical attack by sulfates occurs when sulfate ions penetrate into the concrete and react to form gypsum. This is followed by the formation of ettringite, which is accompanied by a volume expansion sufficient to cause cracking of the concrete. This process can continue to complete destruction of the concrete. The principal methods of preventing sulfate attack are to reduce the permeability of the concrete by reducing the w/c ratio or by using a slag or pozzolanic mineral admixture. The use of a sulfate-resistant cement (Type V, with $\leq 5\% \text{ C}_3\text{A}$) with a w/c ratio less than 0.45 will minimize the possibility of sulfate attack.

1.11.3 Acid Attack

Because concrete is an alkaline material ($\text{pH} \cong 12.5$), it is susceptible to attack by acids, such as might occur in industrial wastes or near some mining operations. The problem is particularly severe when the acidity is high ($\text{pH} < 4$) and water flow is present. Any acid that forms soluble calcium salts on contact

with concrete is particularly aggressive (hydrochloric, nitric, acetic, sulfuric, and lactic acids). In contrast, for acids that form an insoluble salt (phosphoric, tannic acids), the precipitation of their salts within the capillary pores will slow or even prevent further deterioration.

References

- Addis, B.J. and Alexander, M.G. 1990. A method of proportioning trial mixes for high-strength concrete. In *High-Strength Concrete, Second International Symposium*, ACI SP-121, pp. 287–308. American Concrete Institute, Farmington Hills, MI.
- Aitcin, P.C. 1992. *High-Performance Concrete from Material to Structure*. Chapman & Hall, New York.
- Alexander, M. and Mindess, S. 2005. *Aggregates in Concrete*. Taylor & Francis, New York, 435 pp.
- Bentur, A. 2002. Cementitious materials: nine millennia and a new century: past, present, and future. *J. Mater. Civ. Eng.*, 14(1), 2–22.
- Cook, J.E. 1989. 10,000 psi concrete. *Concrete Int.*, 11(10), 67–75.
- CPCA. 1991. *Design and Control of Concrete Mixtures*, 213 pp. Canadian Portland Cement Association, Ottawa, Canada.
- Fiorato, A.E. 1989. PCA research on high-strength concrete. *Concrete Int.*, 11(4), 44–50.
- Gebauer, J., Ko, S.-C., Lerat, A., and Roumain, J.-C. 2005. Experience with a new cement for special applications. In Bilek, V. and Kersner, Z., Eds., *Non-Traditional Cement & Concrete II*, Proceedings of the International Symposium, June 14–16, Brno University of Technology, Brno, Czech Republic.
- Gilkey, H.J. 1961a. Water–cement ratio versus strength: another look. *ACI J.*, 57(10), 1287–1312.
- Gilkey, H.J. 1961b. Discussion of water–cement ratio versus strength: another look. *ACI J.*, 58(6), 1851–1878.
- Hattori, K. 1979. Experiences with Mighty superplasticizer in Japan. In *Superplasticizers in Concrete*, ACI SP-62, pp. 37–66. American Concrete Institute, Farmington Hills, MI.
- Malhotra, V.M. 2002. High performance high volume fly ash concrete. *Concrete Int.*, 24(7), 30–34.
- Malhotra, V.M. and Mehta, P.K. 2002. *High-Performance, High-Volume Fly Ash Concrete*, 101 pp. Supplementary Cementing Materials for Sustainable Development, Inc., Ottawa, Canada.
- Mehta, P.K. 1999. Concrete technology for sustainable development. *Concrete Int.*, 24(7), 23–28.
- Mehta, P.K. 2002. Greening of the concrete industry for sustainable development. *Concrete Int.*, 24(7), 23–28.
- Nawy, E.G. 2008. *Reinforced Concrete: A Fundamental Approach*, 6th ed., 934 pp. Prentice Hall, Upper Saddle River, NJ.
- Powers, T.C. 1958. Structure and physical properties of hardened Portland cement paste. *J. Am. Ceram. Soc.*, 4(1), 1–6.
- Short, A. and Kinniburgh, W. 1978. *Lightweight Concrete*, 3rd ed. Applied Science Publishers, London.
- Suzuki, T. 1987. Experimental studies on high-strength superplasticized concrete. In *Utilization of High Strength Concrete, Symposium Proceedings*, pp. 53–54. Tapis Publishers, Trondheim, Norway.



(a)



(b)

(a) Society Center, Cleveland, Ohio; composite frame. (b) Scotia Plaza in Toronto, a 68-story office tower; 1000-psi silica fume concrete. (Photographs courtesy of the Portland Cement Association, Skokie, IL.)

Mineral Admixtures

V.M. Malhotra, D.D.L., D.Eng., P.Eng.*

2.1	Fly Ash.....	2-1
	Introduction • Physical, Chemical, and Mineralogical Properties of Fly Ash • Chemical and Mineralogical Composition • Proportioning Concretes Containing Fly Ash • Influence of Fly Ash on the Setting Time of Portland Cement Concrete • Effect of Fly Ash on Workability, Water Requirement, and Bleeding of Fresh Concrete • Effects of Fly Ash on Air Entrainment in Fresh Concrete • Effects of Fly Ash on Properties of Hardened Concrete • Effects of Fly Ash on the Durability of Concrete	
2.2	Blast-Furnace Slag	2-18
	Ground, Granulated, or Pelletized Blast-Furnace Slag • Mixture Proportions and Properties of Fresh Concrete Incorporating Blast-Furnace Slag • Properties of Hardened Concrete • Durability of Concrete Incorporating Blast-Furnace Slag • Carbonation	
2.3	Silica Fume.....	2-29
	Production of Silica Fume • Physical and Chemical Characteristics of Silica Fume • Physical and Chemical Mechanisms in the Cement–Silica Fume System • Properties of Fresh Concrete • Properties of Hardened Concrete • Durability Aspects	
2.4	Highly Reactive Metakaolin.....	2-38
	Chemical and Mineralogical Composition • Properties of Fresh Concrete • Mechanical Properties of Hardened Concrete • Durability Aspects of Hardened Concrete	
	References	2-42

2.1 Fly Ash

2.1.1 Introduction

Fly ash is a byproduct of the combustion of pulverized coal in thermal power plants. A dust-collection system removes the fly ash, as a fine particulate residue, from combustion gases before they are discharged into the atmosphere (Figure 2.1). The types and relative amounts of incombustible matter in the coal used determine the chemical composition of fly ash. More than 85% of most fly ashes is comprised of chemical compounds and glasses formed from the elements silicon, aluminum, iron, calcium, and

* Scientist Emeritus at CANMET, Natural Resources Canada, Ottawa, Canada; prolific author, editor, and researcher who has received many awards and honors from the ACI, ASTM, and other institutions throughout the world.

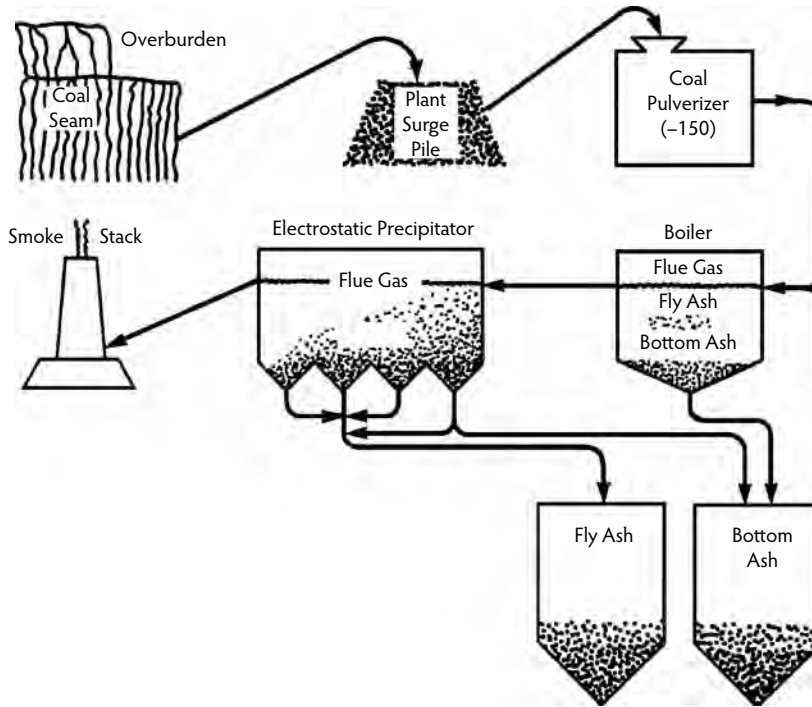


FIGURE 2.1 Schematic of a fossil-fuel plant.

magnesium. Generally, fly ash from the combustion of subbituminous coals contains more calcium and less iron than fly ash from bituminous coal; also, fly ash from subbituminous coals contains very little unburned carbon. Plants that operate only intermittently (peak-load stations) and that burn bituminous coals produce the largest percentage of unburned carbon. Fly-ash particles are typically spherical, ranging in diameter from $<1\ \mu\text{m}$ up to $150\ \mu\text{m}$.

Fly ashes exhibit pozzolanic activity. The American Society for Testing and Materials (ASTM) (ASTM, 1975) defines a pozzolan as “a siliceous or siliceous and aluminous material which in itself possesses little or no cementitious value but which will, in finely divided form and in the presence of moisture, chemically react with calcium hydroxide at ordinary temperature to form compounds possessing cementitious properties.” Fly ashes contain metastable aluminosilicates that will react with calcium ions, in the presence of moisture, to form calcium silicate hydrates.

The term *fly ash* was first used in the electrical power industry around 1930. The first comprehensive data on the use of fly ash in concrete in North America were reported by Davis et al. (1937). The first major practical application was reported in 1948 with the publication of the U.S. Bureau of Reclamation’s data on the use of fly ash in the construction of the Hungry Horse Dam. Worldwide acceptance of fly ash as a component of concrete slowly followed these early efforts, but interest was particularly noticeable in the wake of the rapid increases in energy costs (and hence cement costs) that occurred during the 1970s.

In recent years, it has become evident that fly ashes differ in significant and definable ways that reflect their combustion and, to some extent, their origin. The ASTM recognizes two general classes of fly ash:

- Class C, normally produced from lignite or subbituminous coals
- Class F, normally produced from bituminous coals

Several publications are available that discuss in detail the properties and use of fly ash in concrete (ASTM, 1978; Berry and Malhotra, 1978; Malhotra and Mehta, 1996; Malhotra and Ramezani-pour, 1994), and Table 2.1 shows the estimated production and use of coal ash in major coal-using countries (Malhotra and Ramezani-pour, 1994).

TABLE 2.1 Coal Ash Production and Use in Major Coal-Using Countries

Country	Fly Ash (kt/yr)	Coarse Ash (kt/yr)	Total Ash (kt/yr)	Use (kt/yr)	Use (%)	Year
Australia	7050	850	7900	800	10	1990
Belgium	930	160	1090	795	73	1989
Canada	3830	1420	5250	1575	30	1987
France	2200	405	2605	1300	50	1987
Germany	7480	4120	11,600	6465	56	1989
Italy	1300	135	1435	900	63	1988
Japan	3480	445	3925	1920	49	1989
Spain	7390	1305	8695	1220	14	1987
United Kingdom	9950	2590	12,540	6120	49	1989
United States	48,430	16,750	65,190	15,895	24	1989
China	—	—	62,500	16,200	26	1989
Czechoslovakia	—	—	18,100	1400	8	1989
East Germany (former GDR)	—	—	19,100	7200	38	1989
Hungary	—	—	4100	1100	27	1987
India	—	—	40,000	6750	17	1991
Poland	—	—	29,500	4500	15	1989
Romania	—	—	27,000	700	3	1989
Former Soviet Union	—	—	125,000	11,500	9	1989
Others	—	—	116,470	3660	3	1989

Note: In 2007, the total production of fly ash in China, India, and the United States exceeded 80,000, 130,000, and 70,000 kilotons a year, respectively.

Source: Malhotra, V.M. and Ramezaniapour, A.A., *Fly Ash in Concrete*, MSL 94-45(IR), Canada Center for Mineral and Energy Technology (CANMET), Ottawa, 1994.

2.1.2 Physical, Chemical, and Mineralogical Properties of Fly Ash

2.1.2.1 Physical Properties

Fly ash is a fine-grained material consisting mostly of spherical, glassy particles. Some ashes also contain irregular or angular particles. The size of particles varies depending on the sources. Some ashes may be finer or coarser than Portland cement particles. Figure 2.2 and Figure 2.3 show scanning electron



FIGURE 2.2 SEM micrograph of a subbituminous ash: backscattered electron image of a polished section of the dispersed sample. (From Malhotra, V.M. and Ramezaniapour, A.A., *Fly Ash in Concrete*, MSL 94-45(IR), Canada Center for Mineral and Energy Technology (CANMET), Ottawa, 1994.)



FIGURE 2.3 SEM micrograph of a lignite fly ash: backscattered electron image of a polished section of the dispersed sample. (From Malhotra, V.M. and Ramezaniapour, A.A., *Fly Ash in Concrete*, MSL 94-45(IR), Canada Center for Mineral and Energy Technology (CANMET), Ottawa, 1994.)

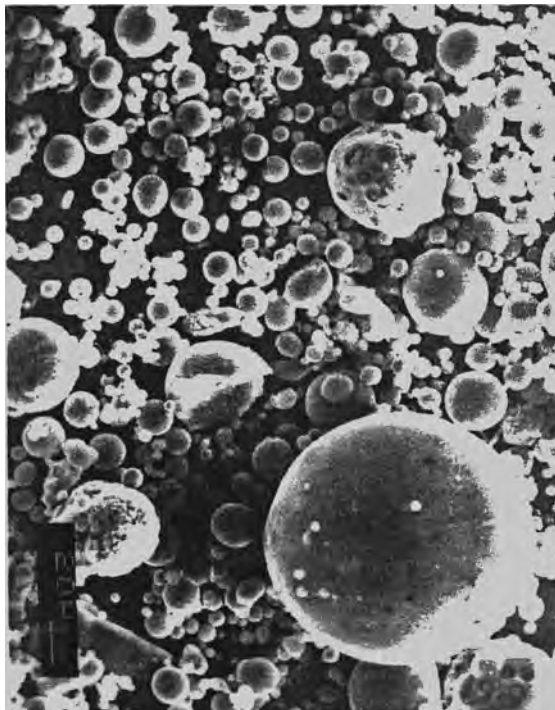


FIGURE 2.4 SEM micrograph of bituminous fly ash: secondary electron image of the sample. (From Malhotra, V.M. and Ramezaniapour, A.A., *Fly Ash in Concrete*, MSL 94-45(IR), Canada Center for Mineral and Energy Technology (CANMET), Ottawa, 1994.)

microscope (SEM) micrographs of polished sections of subbituminous and lignite fly ashes, and Figure 2.4 shows a secondary electron SEM image of bituminous fly-ash particles. Some of these particles appear to be solid, whereas other larger particles appear to be portions of thin, hollow spheres containing many smaller particles.

TABLE 2.2 Fineness of Fly Ashes

Fly Ash Source	Type of Coal ^a	Physical Properties			Blaine Specific Surface (m ² /kg)
		Specific Gravity (Le Chatelier Method)	Fineness (% Retained on 45-μm Sieve)		
			Wet Sieving ^b	Dry Sieving (Alpine Jet)	
1	B	2.53	17.3 (14.9)	12.3	289
2	B	2.58	14.7 (12.7)	10.2	312
3	B	2.88	25.2 (21.7)	18.0	127
4	B	2.96	19.2 (16.6)	14.0	198
5	B	2.38	21.2 (18.3)	16.1	448
6	B	2.22	40.7 (35.1)	30.3	303
7	SB	1.90	33.2 (28.7)	26.4	215
8	SB	2.05	19.4 (16.7)	14.3	326
9	SB	2.11	46.0 (39.7)	33.0	240
10	L	2.38	24.9 (21.5)	18.8	286
11	L	2.53	2.7 (2.4)	2.5	581

^a B, bituminous; L, lignite; SB, subbituminous.

^b Values in parentheses do not include sieve correction factor.

Source: Malhotra, V.M. and Ramezaniapour, A.A., *Fly Ash in Concrete*, MSL 94-45(IR), Canada Center for Mineral and Energy Technology (CANMET), Ottawa, 1994.

2.1.2.2 Fineness

Dry- and wet-sieving methods are commonly used to measure the fineness of fly ashes. ASTM C 311-77 recommends determining the amount of the sample retained after it is wet sieved on a 45- μ m sieve, in accordance with ASTM C 430, except that a representative sample of the fly ash or natural pozzolan is substituted for hydraulic cement in the determination. Dry sieving on a 45- μ m sieve can be performed according to a method established at the Canada Center for Mineral and Energy Technology (CANMET) (Malhotra and Wallace, 1993). Table 2.2 shows the fineness of 11 fly ashes as determined by wet and dry sieving. The particle-size distribution of fly ash can be determined by various means, such as x-ray sedigraph, laser particle-size analyzer, and Coulter counter. In some cases, agglomeration of a number of small particles may form a large particle. In most cases, fly ashes contain particles greater than 1 μ m in diameter. Mehta (1994), using an x-ray sedimentation technique, reported particle-size distribution data for several U.S. fly ashes. Mehta found that high-calcium fly ashes were finer than low-calcium fly ashes, and he related this difference to the presence of larger amounts of alkali sulfates in the high-calcium fly ashes.

2.1.2.3 Specific Surface

The specific surface of fly ash, which is the area of a unit of mass, can be measured by various techniques. The most common technique is the Blaine specific-surface method, which measures the resistance of compacted particles to air flow. ASTM C 204 describes this method for measurement of the surface area of Portland cement.

2.1.2.4 Specific Gravity

The specific gravity of hydraulic cements is determined according to ASTM C 188. This method can also be used to determine the specific gravity of fly ashes. If fly ashes contain water-soluble compounds, the use of a nonaqueous solvent, instead of water, is recommended. The specific gravity of different fly ashes varies over a wide range. In the CANMET investigation of 11 fly ashes (Carette and Malhotra, 1986), the specific gravity ranged from a low value of 1.90 for a subbituminous ash to a high value of 2.96 for an iron-rich bituminous ash. Three subbituminous ashes had a comparatively low specific gravity of ~ 2.0 , and this suggested that hollow particles, such as cenospheres or plerospheres, were present in significant proportions in the three ashes.

In general, the physical characteristics of fly ashes vary over a significant range, corresponding to their source. Attempts have been made to correlate the physical properties of different fly ashes. In one CANMET investigation, no apparent relationship was found between type of fly ash and fineness, as determined by the percentage retained on a 45- μm sieve. Fineness is probably influenced more by factors such as coal combustion and ash collection and classification than by the nature of the coal itself (Carette and Malhotra, 1986). Similarly, the type of fly ash showed no apparent influence on the specific surface as measured by the Blaine technique. Moreover, except in one or two cases, there was very little relationship between the specific surface as measured by the Blaine technique and the fineness as determined by percentage retained on a 45- μm sieve.

2.1.3 Chemical and Mineralogical Composition

2.1.3.1 Chemical Composition

Several authors have reported the chemical composition of various fly ashes produced in North America. In their study of 11 Canadian fly ashes, Carette and Malhotra (1986) reported a wide range of chemical compositions (Table 2.3). Manz et al. (1989) examined 19 North American lignite fly ashes, and their data are given in Table 2.4. The results of the CANMET investigations (Carette and Malhotra, 1986) and the data reported by Manz et al. (1989) on bituminous, subbituminous, and lignite ashes obtained from various coal-powered plants in North America show significant differences in the chemical composition of fly ashes.

2.1.3.2 Mineralogical Composition

In general, both the type and source of fly ash influence its mineralogical composition. Due to the rapid cooling of burned coal in the power plant, fly ashes consist of noncrystalline particles ($\leq 90\%$), or glass and a small amount of crystalline material. Depending on the system of burning, some unburned coal may be collected with ash particles. In addition to a substantial amount of glassy material, each fly ash may contain one or more of the four major crystalline phases: quartz, mullite, magnetite, and hematite. In subbituminous fly ashes, the crystalline phases may include C_3A , $\text{C}_4\text{A}_3\bar{\text{S}}$, calcium sulfate, and alkali sulfates (Mehta, 1989). Table 2.5 shows the mineralogical composition of some selected fly ashes. The reactivity of fly ashes is related to the noncrystalline phase or glass. The reasons for the high reactivity of high-calcium fly ashes may lie partially in the chemical composition of the glass. Mehta (1989) pointed out that the composition of glass in low-calcium fly ashes is different from that in high-calcium fly ashes.

2.1.4 Proportioning Concretes Containing Fly Ash

In most applications, the objective of using fly ash in concrete is to achieve one or more of the following benefits:

- Reducing the cement content to reduce costs
- Obtaining reduced heat of hydration
- Improving workability
- Attaining required levels of strength in concrete at ages >90 days
- Improving durability

The properties of any particular fly ash will greatly affect the properties of the concrete in which it is used. The mixture-proportioning method can minimize the effects that the inclusion of different fly ashes has on concrete performance. In practice, fly ash can be introduced into concrete in one of two ways:

- A blended cement containing fly ash may be used in place of Portland cement.
- Fly ash may be introduced as an additional component at the concrete-mixing stage.

The use of blended cement is the simpler of the two, as it is free from the complication of batching additional materials and may ensure more uniform control. The relative proportions of fly ash and cement are predetermined, and this limits the range of mixture proportions.

TABLE 2.3 Chemical Composition of Fly Ashes

Fly-Ash Source	Type of Coal ^a	Chemical Composition (wt%) ^b										Loss on Ignition (LOI) (%) ^c		
		SiO ₂	Al ₂ O ₃	Fe ₂ O ₃	CaO	MgO	Na ₂ O	K ₂ O	TiO ₂	P ₂ O ₃	MnO	BaO	SO ₃	
1	B	47.1	23.0	20.4	1.21	1.17	0.54	3.16	0.85	0.16	0.78	0.07	0.67	2.88
2	B	44.1	21.4	26.8	1.95	0.99	0.56	2.32	0.80	0.25	0.12	0.07	0.96	0.70
3	B	35.5	12.5	44.7	1.89	0.63	0.10	1.75	0.56	0.59	0.12	0.04	0.75	0.75
4	B	38.3	12.8	39.7	4.49	0.43	0.14	1.54	0.59	1.54	0.20	0.04	1.34	0.88
5	B	45.1	22.2	15.7	3.77	0.91	0.58	1.52	0.98	0.32	0.32	0.12	1.40	9.72
6	B	48.0	21.5	10.6	6.72	0.96	0.56	0.86	0.91	0.26	0.36	0.21	0.52	6.89
7	SB	55.7	20.4	4.61	10.7	1.53	4.65	1.00	0.43	0.41	0.50	0.75	0.38	0.44
8	SB	55.6	23.1	3.48	12.3	1.21	1.67	0.50	0.64	0.13	0.56	0.47	0.30	0.29
9	SB	62.1	21.4	2.99	11.0	1.76	0.30	0.72	0.65	0.10	0.69	0.33	0.16	0.70
10	L	46.3	22.1	3.10	13.3	3.11	7.30	0.78	0.78	0.44	0.13	1.18	0.80	0.65
11	L	44.5	21.1	3.38	12.9	3.10	6.25	0.80	0.94	0.66	0.17	1.22	7.81	0.82

^a B, bituminous; L, lignite; SB, subbituminous.
^b By inductively coupled argon plasma (ICAP) technique, except for Na₂O, K₂O, SO₃, and LOI.
^c 105 to 750°C.
Source: Malhotra, V.M. and Ramezaniapour, A.A., *Fly Ash in Concrete*, MSL 94-45(IR), Canada Center for Mineral and Energy Technology (CANMET), Ottawa, 1994.

TABLE 2.4 Chemical Analyses for North American Lignite Fly Ashes

Fly Ash	Bulk Chemical Analysis (wt%)							Available Alkalis	Loss on Ignition (LOI) (%)
	SiO ₂	Al ₂ O ₃	Fe ₂ O ₃	Sum	CaO	MgO	SO ₃	Na ₂ O	K ₂ O
<i>North Dakota and Montana lignite</i>									
81-271	25.7	15.0	9.2	49.9	26.8	7.2	8.8	—	—
81-560	30.2	12.5	4.6	47.3	23.6	7.9	9.6	7.3	0.6
82-179	42.1	12.0	8.1	62.2	18.5	5.0	4.1	8.0	1.2
83-275	45.6	15.5	7.3	68.4	20.3	5.0	1.9	1.0	1.7
85-352	39.6	14.0	10.7	64.3	15.9	5.7	2.6	4.4	1.4
87-139	27.9	10.7	9.9	48.5	21.6	5.5	12.3	5.4	1.5
86-305	35.2	20.3	6.3	61.8	25.0	6.8	1.1	0.2	0.5
<i>Saskatchewan lignite</i>									
85-147	50.4	21.4	3.5	75.3	11.6	3.0	0.5	6.6	0.9
86-805	46.4	24.5	4.9	75.8	13.7	4.0	0.6	0.9	1.6
87-144	47.9	21.9	4.9	74.7	13.3	2.9	1.1	6.1	1.0
<i>Texas and Louisiana lignite</i>									
87-146	50.3	20.2	5.5	76.0	14.4	4.0	0.7	0.9	1.2
87-147	57.9	26.3	3.9	88.1	9.6	2.1	0.4	0.0	0.4
87-154	62.3	20.9	2.2	85.3	6.1	0.7	0.5	4.1	2.1
87-155	52.2	18.0	10.5	80.7	11.9	2.5	1.3	0.2	0.4
87-156	55.5	18.6	4.3	78.4	7.0	0.8	0.3	0.6	0.9
87-159	57.5	20.6	7.0	85.1	9.1	2.6	0.2	0.4	1.4
87-219	62.0	20.1	2.0	84.1	6.9	1.2	0.6	0.9	0.9
87-239	48.9	18.5	21.8	89.1	7.3	2.6	0.5	0.4	0.9
87-157	52.8	23.6	8.9	85.3	9.5	2.7	0.4	1.1	0.8

Note: ASTM C 618 specification limits: Class F fly ash, SiO₂ + Al₂O₃ + Fe₂O₃ = 70%; SO₃ = 5% max.; LOI = 5% max. Class C fly ash, SiO₂ + Al₂O₃ + Fe₂O₃ = 50%; SO₃ = 5% max.; LOI = 5% max.

Source: Manz, O.E. et al., In *Proceedings of the 3rd International Conference on the Use of Fly Ash, Silica Fume, Slag, and Natural Pozzolans in Concrete* (supplementary papers), 1989, pp. 16-32.

TABLE 2.5 Mineralogical Composition of Some Selected Fly Ashes

Fly-Ash Source	Type of Coal ^a	Phase Composition (%)					Loss on Ignition (LOI) (%)
		Glass	Quartz	Mullite	Magnetite	Hematite	
1	B	72.1	4.0	12.6	6.2	1.6	3.5
4	B	70.1	3.2	3.3	17.2	4.7	1.5
5	B	55.6	6.2	19.8	5.6	3.1	9.7
6	B	54.2	8.3	23.5	4.4	2.1	7.5
7	SB	90.2	2.9	6.1	—	—	0.8
8	SB	83.9	4.1	10.2	—	1.4	0.4
9	SB	79.8	8.7	11.5	—	—	0.8
10	L	94.5	4.6	—	—	—	0.9

^a B, bituminous; L, lignite; SB, subbituminous.

Source: Carette, G.G. and Malhotra, V.M., *Characterization of Canadian Fly Ashes and Their Relative Performance in Concrete*, Report 86-6E, Canada Center for Mineral and Energy Technology (CANMET), Ottawa, 1986.

The addition of fly ash at the concrete-mixing stage is flexible and allows for more complete exploitation of the qualities of fly ash as a component of concrete. It does, however, demand that the unique properties of fly ash be considered in determining the proportions of the mixture. In current trends, fly ash plays more than one role in concrete. In freshly mixed concrete, it generally acts as a fine aggregate and to some degree may reduce the demand for water. In hardened concrete, because of the pozzolanic nature of fly ash, it becomes a component of the cementitious matrix and influences strength and durability. Thus, the use of fly ash in a concrete introduces a number of complexities regarding proportioning, if the accepted relationships among workability, strength, and the water/cement ratio are taken into account. Two common assumptions are made when selecting an approach to mixture proportioning of fly-ash concrete:

- Fly ash usually reduces the strength of concrete at early ages.
- For equal workability, concrete incorporating fly ash usually requires less water than concrete containing only Portland cement.

Neither assumption is universally true, and both are influenced by the presence of other common concrete components; however, both assumptions have strongly influenced the approach to mixture proportioning of fly-ash concrete. As with any other type of concrete, the mixture proportions for a fly-ash concrete can be selected either by reference to some standard concrete (excluding fly ash) or on the basis of the ways in which all the concrete components (including fly ash) will behave in fresh and hardened states.

Throughout the more than 40 years that fly ash has been used in concrete, common practice has been to use some plain concrete as a standard of comparison for the mixture proportions of fly-ash concretes. Similarly, the properties of both fresh and hardened concrete usually have been compared with those of a reference concrete. Thus, fly ash has generally been considered to be a replacement for cement, rather than a component that complements the functions of the cement, sand, or water. The trend now is to consider the components of fly-ash concrete as a whole and to treat it as a unique material without reference to an equivalent plain-concrete mixture.

2.1.5 Influence of Fly Ash on the Setting Time of Portland Cement Concrete

The rate at which concrete sets during the first few hours after mixing is expressed as the initial and final setting time and is determined by some form of penetrometer test. Fly ash may be expected to influence the rate of hardening of cement for a number of reasons:

- The ash may be cementitious (high calcium).
- Fly ash may contain sulfates that react with cement in the same way as the gypsum added to Portland cement does.

- The fly-ash–cement mortar may contain less water as a consequence of the presence of fly ash, and this will influence the rate of stiffening.
- The ash may absorb surface-active agents added to modify the rheology (water reducers) of concrete, and, again, this influences the stiffness of the mortar.
- Fly-ash particles may act as nuclei for crystallization of cement hydration products.

There seems to be general agreement in the literature that low-calcium fly ashes retard the setting of cement. In experiments conducted at CANMET (Carette and Malhotra, 1986), the data show that all but 2 of the 11 ashes significantly increase both the initial and final setting times.

2.1.6 Effect of Fly Ash on Workability, Water Requirement, and Bleeding of Fresh Concrete

The small size and the essentially spherical form of low-calcium fly-ash particles influence the rheological properties of cement pastes, causing a reduction in the water required or an increase in workability compared with that of an equivalent paste without fly ash. As Davis et al. (1937) noted, fly ash differs from other pozzolans that usually increase the water requirement of concrete mixtures. The improved workability allows a reduction in the amount of water used in concrete. According to Owens (1979), the major factor influencing the effects of ash on the workability of concrete is the proportion of coarse material (>45 mm) in the ash. Owens has shown, for example, that substitution of 50% by mass of the cement with fine particulate fly ash can reduce the water requirement by 25%. A similar substitution using ash with 50% of the material larger than 45 mm has no effect on the water requirement.

2.1.7 Effects of Fly Ash on Air Entrainment in Fresh Concrete

Cycles of freezing and thawing are extremely destructive to water-saturated concretes that are not properly proportioned. Concrete will be frost-resistant if it is made with sound, coarse aggregate and is properly protected until some maturity is attained. To obtain the number of correctly spaced air voids in hardened concrete necessary for frost resistance, an air-entraining admixture (AEA) is added (at a prescribed dosage) to the concrete during mixing. Two attributes are important: (1) the AEA must produce the required volume of air bubbles of the desired size and spacing in the concrete, and (2) it must do so in a manner that allows the air content to remain stable while the concrete is mixed, transported, and placed. The use of some fly ashes causes an increase in the quantity of AEA required to produce a given level of air entrainment in fresh concrete. Larson (1994), writing on the use of fly ash in air-entrained concrete and reviewing the work of other investigators, concluded that the primary effect of fly ash was on the AEA requirement rather than on the air entrainment as such.

Gebler and Klieger (1983) examined 10 different fly ashes representing a range of chemical and physical properties. Carbon content was 0.14 to 4.19%, total organics were 0.09 to 1.04%, CaO was 1.2 to 9.0%, and fineness (as a percentage retained on a 45- μ m sieve) was 11.24 to 38.45%. Concretes were proportioned by simple replacement of 25% of the cement by fly ash (by mass). All mixtures were proportioned to have 75 ± 25 -mm slump and $6 \pm 1\%$ air. Neutralized Vinsol™ resin was the only AEA used. The AEA requirement as a percentage of that for the control concrete (for 6% air content) showed the following results:

- For ashes containing >10% CaO, the range of AEA requirements was 126 to 173%.
- For ashes containing <10% CaO, the range of AEA requirements was 170 to 553%.

Gebler and Klieger (1983, p. 107) offered the following summary of the findings and conclusions relevant to air entrainment in fresh concrete:

- Generally, concretes containing Class C fly ash require less air-entraining admixture than those concretes with Class F fly ash. All concretes with fly ash required more air-entraining admixture than Portland cement concretes without fly ash.

- Plastic concretes containing Class C fly ash tended to lose less air than concretes with Class F ash.
- As the air-entraining admixture requirement increases for a concrete containing fly ash, the air loss increases.
- Air contents in plastic concrete containing Class F fly ash were reduced as much as 59%, 90 minutes after completion of mixing.
- As the organic matter content, carbon content, and loss-on-ignition of fly ash increase, the air-entraining admixture requirement increases, as does the loss of air in plastic concrete.
- Generally, as the total alkalis in fly ash increase, the air-entraining admixture requirement decreases.
- As the specific gravity of a fly ash increases, the retention of air in the concrete also increases. Concrete containing a fly ash that has a high lime content (Class C fly ash) and less organic matter tends to be less vulnerable to loss of air.
- Generally, as the SO_3 content of fly ash increases, the retained air in concrete increases.

2.1.8 Effects of Fly Ash on Properties of Hardened Concrete

2.1.8.1 Strength Development in Fly-Ash Concrete

As discussed earlier, the main factors determining strength in concrete are the amount of cement used and the water/cement ratio. In practice, these are established as a compromise between the need for workability in the freshly mixed state, strength and durability in the hardened state, and cost. The degree and manner in which fly ash affects workability are major factors in its influence on strength development. As was shown earlier, a fly ash that permits a reduction in the total water requirement in concrete will generally present no problems in selection of mixture proportions and permit any rate of strength development. Many variables influence the strength development of fly-ash concrete; the most important are the following:

- The properties of the fly ash
- Chemical composition
- Particle size
- Reactivity
- Temperature and other curing conditions

2.1.8.2 Effect of Fly-Ash Type on Concrete Strength

The first difference among fly ashes is that some are cementitious even in the absence of Portland cement; these are the so-called ASTM Class C, or high-calcium, fly ashes, usually produced at power plants that burn subbituminous or lignitic coals. In general, the rate of strength development in concretes tends to be only marginally affected by high-calcium fly ashes. Concrete incorporating high-calcium fly ashes can be made on an equal-weight or equal-volume replacement basis without any significant effect on strength at early ages. Yuan and Cook (1983) examined the strength development of concretes with and without high-calcium fly ash ($\text{CaO} = 30.3 \text{ wt\%}$). The data from their research are shown in Figure 2.5 and Figure 2.6. Using a simple replacement method of mixture proportioning (Table 2.6), they found the rate of strength development of fly-ash concrete to be comparable to that of the control concrete, with or without air entrainment. Low-calcium fly ashes, the so-called ASTM Class F fly ashes, were the first to be examined for use in concrete. Most of what has been written on the behavior of fly-ash concrete examines concretes that use Class F ashes. In addition, the ashes used in much of the early work came from older power plants and were coarse in particle size, contained unburned fuel, and were often relatively inactive pozzolans. Used in concrete and proportioned by simple replacement, these ashes showed exceptionally slow rates of strength development. This led to the erroneous view that fly ash reduces strength at all ages. Gebler and Klieger (1986) evaluated the effect of ASTM Class F and Class C fly ashes from 10 different sources on the compressive strength development of concretes under different curing conditions, including effects of low temperature and moisture availability. Their tests indicated that concrete containing fly ash had the potential to produce satisfactory compressive strength development. The influence of the class of fly ash on the long-term compressive strength of concrete was not significant. In general,

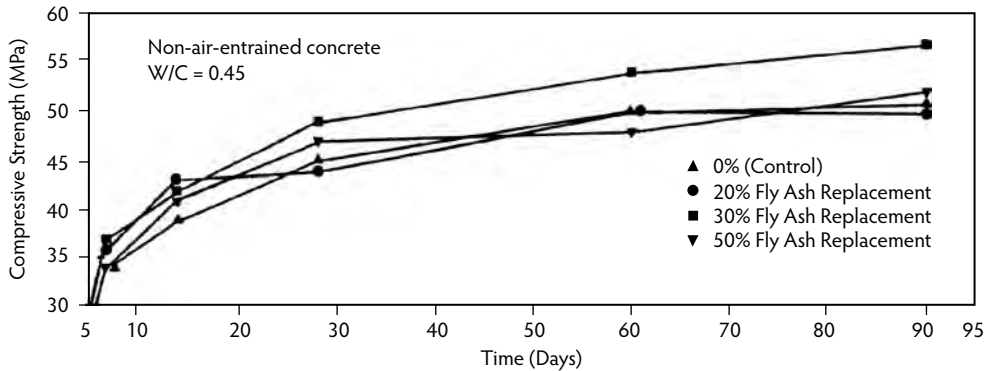


FIGURE 2.5 Compressive strength development of non-air-entrained concretes containing high-calcium fly ash. (From Yuan, R.L. and Cook, J.E., in *Fly Ash, Silica Fume, Slag, and Other Mineral Byproducts in Concrete*, Spec. Publ. SP-79, Malhotra, V.M., Ed., American Concrete Institute, Detroit, MI, 1983, pp. 307–319.)

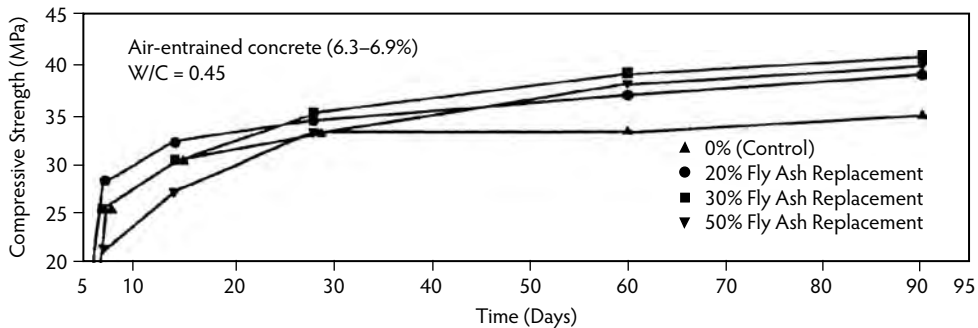


FIGURE 2.6 Compressive strength development of air-entrained concrete containing high-calcium fly ash. (From Yuan, R.L. and Cook, J.E., in *Fly Ash, Silica Fume, Slag, and Other Mineral Byproducts in Concrete*, Spec. Publ. SP-79, Malhotra, V.M., Ed., American Concrete Institute, Detroit, MI, 1983, pp. 307–319.)

compressive strength development of concretes containing Class F fly ash was more susceptible to low curing temperature than concretes with Class C fly ash or the control concretes. Gebler and Klieger concluded that Class F fly-ash concretes required more initial moist curing for long-term, air-cured compressive strength development than did concretes containing Class C fly ashes or the control concretes.

2.1.8.3 Effects of Temperature and Curing Regime on Strength Development in Fly-Ash Concretes

When concrete made with Portland cement is cured at temperatures greater than 30°C, an increase in strength occurs at early ages but a marked decrease in strength in the mature concrete. Concretes containing fly ash and control concretes behave significantly differently. Figure 2.7 shows the general way in which the temperature maintained during the early ages of curing influences the 28-day strength of concrete (Williams and Owens, 1982).

2.1.8.4 Effect of Fly-Ash on Elastic Properties of Concrete

Published data indicate that fly ash has little influence on the elastic properties of concrete. Abdun-Nur (1961) made the following observation:

The modulus of elasticity of fly ash concrete is lower at early ages and higher at later ages. In general, fly ash increases the modulus of elasticity of concrete when concretes of the same strength with and without fly ash are compared.

TABLE 2.6 Mixture Designations, Proportions, and Properties of Concrete Incorporating High-Calcium Fly Ash

	Mixture Designation			
	C1	C2	C3	C4
<i>Proportions (kg/m³)</i>				
Cement	387	309	272	196
Fly ash	0	77	117	196
Cement + fly ash	387	386	389	392
Water	145	145	146	147
Coarse aggregate	1146	1144	1153	1160
Fine aggregate	701	690	678	654
<i>Properties</i>				
Slump (cm)	3	9	12	21
Air content (%)	2.1	1.9	1.9	1.4
Unit weight (kg/m ³)	2377	2364	2364	2352
Fly ash as percentage of cement	0	20	30	50

Source: Yuan, R.L. and Cook, J.E., in *Fly Ash, Silica Fume, Slag, and Other Mineral Byproducts in Concrete*, Spec. Publ. SP-79, Malhotra, V.M., Ed., American Concrete Institute, Detroit, MI, 1983, pp. 307–319.

2.1.8.5 Effect of Fly Ash on Creep Properties of Concrete

Data on creep of fly-ash concrete are limited. Ghosh and Timusk (1981) examined bituminous fly ashes of different carbon contents and fineness values in concretes at nominal strength levels of 20, 35, and 55 MPa (water/cement ratio of 1.0, 0.4, and 0.2, respectively). Each concrete was proportioned for equivalent strength at 28 days. Fly-ash concretes showed less creep in the majority of specimens than the reference concretes. This was attributed to a relatively higher rate of strength gain after the time of loading for the fly-ash concretes than for the reference concretes. Yuan and Cook (1983) investigated creep of high-strength concrete containing a high-calcium fly ash and showed that concrete containing 30 and 50% fly ash exhibited more creep than either the control concrete or a concrete with 20% fly ash.

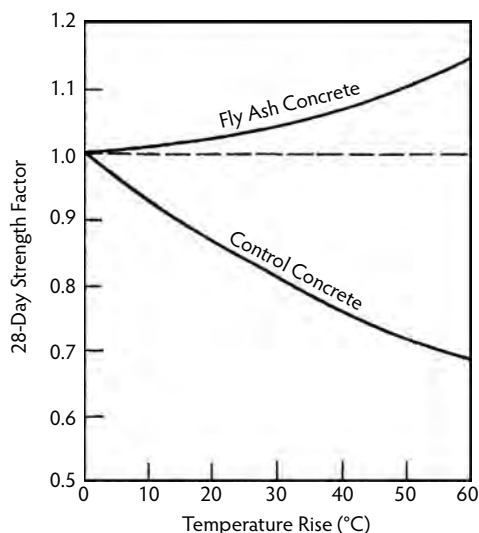


FIGURE 2.7 Effect of temperature rise during curing on the compressive strength development of concretes. (From Williams, J.T. and Owens, P.L., in *Proceedings of International Symposium on the Use of PFA in Concrete*, Cabrera, J.G. and Cusens, A.R., Eds., Department of Civil Engineering, University of Leeds, Leeds, U.K., 1982, pp. 301–313.

TABLE 2.7 Relative Permeability of Concretes with and without Fly Ash

Type	Fly Ash	W/(C + F) by Weight	Relative Permeability (%)	
	Percent (%) by Weight		28 Days	6 Months
None	—	0.75	100	26
Chicago	30	0.70	220	5
	60	0.65	1410	2
Cleveland	30	0.70	320	5
	60	0.69	1880	7

Note: W/(C + F) = water/cement + fly ash ratio.

Source: Davis, R.E., *Pozzolan Materials With Special Reference to Their Use in Concrete Pipe*, Technical Memo, American Concrete Pipe Association, Irving, TX, 1954.

2.1.8.6 Effect of Fly Ash on Volume Changes of Concrete

It has been generally reported that the use of fly ash in normal proportions does not significantly influence the drying shrinkage of concrete. Typical of the conclusions of most researchers in this area are those made by Davis et al. (1937), who commented as follows:

- For masses of ordinary thickness, such as are normally found in highway slabs and in the walls and frames of buildings, the drying shrinkage at the exposed surfaces of concrete up to the age of one year for fly-ash cements is about the same as, or somewhat less than, that for corresponding Portland cement. At a short distance from the exposed surface the drying shrinkage up to the age of one year is substantially less for concretes containing corresponding Portland cements.
- For very thin sections and for cements of normal fineness, the drying shrinkage of concretes containing finely ground high-early-strength cements may be somewhat reduced by the use of fly ash.

2.1.9 Effects of Fly Ash on the Durability of Concrete

Increasingly, concrete is being selected for use as a construction material in aggressive or potentially aggressive environments. Concrete structures have always been exposed to the action of seawater. In modern times, the demands placed on concrete in marine environments have increased greatly, as concrete structures are used in arctic, temperate, and tropical waters to contain and support the equipment, people, and products of oil and gas exploration and production. Concrete structures are used to contain nuclear reactors and must be capable of containing gases and vapors at elevated temperatures and pressures under emergency conditions. Concrete is increasingly being placed in contact with sulfate and acidic waters. In all of these instances, the use of fly ash as a concrete material plays a role, and an understanding of its effect on concrete durability is essential to its correct and economical application.

2.1.9.1 Effects of Fly Ash on Permeability of Concrete

A number of investigations have studied the influence of fly ash on the relative permeability of concrete pipes containing fly ash substituted for cement in amounts of 30 to 50%. In a study by Davis (1954), permeability tests were made on 150 × 150-mm cylinders at the ages of 28 days and 6 months. The results of these tests are shown in Table 2.7. It is clear from these data that the permeability of the concrete was directly related to the quantity of hydrated cementitious material at any given time. After 28 days of curing, at which time little pozzolanic activity would have occurred, the fly-ash concretes were more permeable than the control concretes. At 6 months, this was reversed. Considerable imperviousness had developed, presumably as a result of the pozzolanic reaction of fly ash. Short and Page (1982) reported on the diffusion of chloride ions in solution into Portland blended cement pastes and found the following values of diffusion coefficient (D_c) for different cement types:

Type of Cement	D_c Value ($\times 10^{-9}$ cm ² /s)
Normal Portland	44.7
Sulfate-resisting	100.0
Fly-ash/Portland	14.7
Slag/Portland	4.1

It was concluded from these data that slag and fly-ash cements were more effective in limiting chloride diffusion in pastes than were normal or sulfate-resisting cements.

2.1.9.2 Effects of Fly Ash on Carbonation of Concrete

In moist conditions, calcium hydroxide, and to a lesser degree, calcium silicates and aluminates in hydrated Portland cement react with carbon dioxide from the atmosphere to form calcium carbonate. The process, termed *carbonation*, occurs in all Portland cement concretes. The rate at which concrete carbonates is determined by its permeability, the degree of saturation, and the mass of calcium hydroxide available for reaction. Well-compacted and properly cured concrete, at a low water/cement ratio will be sufficiently impermeable to resist the advance of carbonation beyond the first few millimeters. If carbonation progresses into a mass of concrete, two deleterious consequences may follow: shrinkage may occur, and carbonation of concrete immediately adjacent to steel reinforcement may reduce the resistance of steel to corrosion.

Nagataki et al. (1986) reported the long-term results of experiments carried out since 1969 that investigated the depth of carbonation in concrete with and without fly ash. The authors concluded that the initial curing period affects the carbonation of concrete cured indoors; hence, it is necessary for fly-ash concrete to have a longer curing period in water at early ages. The carbonation of concrete cured outdoors is not affected by the initial curing period in water, provided it is cured in water for a period of 7 days.

2.1.9.3 Effects of Fly Ash on the Durability of Concrete Subjected to Repeated Cycles of Freezing and Thawing

It is generally accepted, other criteria also being met, that air entrainment renders concrete frost resistant. Fly ashes, in common with other finely divided mineral components in concrete, tend to cause an increase in the quantity of admixture required to obtain specified levels of entrained air in concrete. In some instances, the stability of the air or the rate of air loss from fresh concrete is also affected. In general, the observed effects of fly ash on freezing and thawing durability support the view expressed by Larson (1994):

Fly ash has no apparent ill effects on the air voids in hardened concrete. When a proper volume of air is entrained, characteristics of the void system meet generally accepted criteria.

Klieger and Gebler (1987) also evaluated the durability of concretes containing ASTM Class F and Class C fly ashes. Their test results indicated that air-entrained concretes, with or without fly ash, that were moist cured at 23°C generally showed good resistance to freezing and thawing. For specimens cured at a low temperature (4.4°C), air-entrained concretes with Class F fly ash showed slightly less resistance to freezing and thawing than similar concretes made with Class C fly ash.

Bilodeau et al. (1991), in an investigation carried out at CANMET, determined the scaling resistance of concrete incorporating fly ashes. Water/cement + fly ash ratios of 0.35, 0.45, and 0.55 were used. Concrete without fly ash and concretes containing 20 and 30% fly ash as replacement by mass for cement were made. The results of Bilodeau et al. showed that the concrete containing $\geq 30\%$ fly ash performed satisfactorily under the scaling test with minor exceptions (Table 2.8).

Carette and Langley (1990) studied the performance of fly ash concrete subjected to 50 freezing and thawing cycles in the presence of deicing salts. They concluded that the incorporation of fly ash in concrete mixtures with $\leq 30\%$ replacement of Portland cement did not show significant difference in salt-scaling resistance in the presence of a 4% calcium chloride solution when examined by visual rating of surface

TABLE 2.8 Mass of Scaling Residue after 50 Freezing and Thawing Cycles—Series I

Time of Moist Curing (days)	Time of Air Drying (weeks)	Mass of Scaling Residue (kg/m ³)								
		W/(C + F) = 0.35 (Percentage of Fly Ash)			W/(C + F) = 0.45 (Percentage of Fly Ash)			W/(C + F) = 0.55 (Percentage of Fly Ash)		
		0	20	30	0	20	30	0	20	30
3	3	0.195	0.504	0.184	0.149	0.160	0.206	0.123	0.282	0.321
	4	0.122	0.237	0.208	0.178	0.200	0.680	0.126	0.281	0.638
	5	0.076	0.128	0.143	0.091	0.243	0.634	1.131	0.734	0.354
	6	0.100	0.074	0.158	0.105	0.306	0.263	0.129	0.255	0.226
7	3	0.154	0.047	0.371	0.135	0.212	0.362	0.160	0.335	0.426
	4	0.147	0.092	0.265	0.158	0.448	0.209	0.172	0.312	0.885
	5	0.098	0.108	0.151	0.114	0.180	0.199	0.119	0.238	0.396
	6	0.192	0.038	0.223	0.169	0.268	0.177	0.118	0.370	0.562
14	3	0.139	0.670	1.094	0.188	0.264	0.409	0.517	0.895	0.705
	4	0.144	0.158	0.449	0.126	0.198	0.202	0.131	0.636	0.625
	5	0.174	0.066	0.493	0.135	0.319	0.839	0.162	0.811	0.613
	6	0.168	0.064	0.189	0.117	0.293	0.463	0.286	0.728	0.814

Note: Each value represents the average of results from two slabs.

Source: Bilodeau, A. et al., in *Proceedings of Second CANMET/ACI International Conference on Durability of Concrete*, Vol. 1, Spec. Publ. SP-126, Malhotra, V.M., Ed., American Concrete Institute, Detroit, MI, 1991, pp. 201–228.

deterioration. In the measurement of weight loss due to surface deterioration, which they believed was a meaningful way to assess surface deterioration, concretes containing fly ash showed greater weight loss than control concrete. Carette and Langley stated that the surface scaling appeared not to be sensitive to the length of time that specimens were moist cured or air dried subsequent to initial moist curing, at least within the periods investigated.

2.1.9.4 Abrasion and Erosion of Fly-Ash Concrete

Under many circumstances, concrete is subjected to wear by attrition, scraping, or the sliding action of vehicles, ice, and other objects. When water flows over concrete surfaces, erosion may occur. In general, regardless of the type of test performed, the abrasion resistance of concrete is usually found to be proportional to its compressive strength. Similarly, at constant slump, resistance to erosion improves with increased cement content and strength. It may be anticipated that fly-ash concrete that is incompletely or inadequately cured may show reduced resistance to abrasion.

Carrasquillo (1987) examined the abrasion resistance of concretes containing no fly ash, 35% ASTM Class C fly ash, or 35% ASTM Class F fly ash. Specimens tested were cast from concretes having similar strengths, air contents, and cementitious materials contents. The abrasion resistance of concrete containing Class C fly ash was greater than that of concrete containing Class F fly ash or no fly ash. The latter two exhibited approximately equal abrasion resistance; measurement was based on the depth of wear.

Naik et al. (1992) carried out an investigation of the compressive strength and abrasion resistance of concrete containing ASTM Class C fly ash. They proportioned concrete mixtures to have cement replacement in the range of 15 to 70 wt% fly ash. The water/cementitious materials ratio varied from 0.31 to 0.37. Their results showed that the abrasion resistance of concrete containing $\leq 30\%$ fly ash was similar to that of the control concrete; however, the abrasion resistance of concretes containing $>40\%$ fly ash was lower than that of control concrete without fly ash.

2.1.9.5 Effects of Fly Ash on Sulfate Resistance of Concrete

In 1967, Dikeou (1970) reported the results of sulfate-resistance studies on 30 concrete mixtures made with Portland cement, Portland fly-ash cement, or fly ash. From this work, it was concluded that all of the 12 fly ashes tested greatly improved sulfate resistance. Kalousek et al. (1972) studied the requirements of concretes for long-term service in a sulfate environment. From their study, they drew the following conclusions:

- Eighty-four percent of ASTM Types V and II cement concretes without pozzolan showed a life expectancy of <50 years.
- Certain pozzolans very significantly increased the life expectancy of concrete exposed to 2.1% sodium sulfate solution. Fly ashes meeting current specifications were prominent among the group of pozzolans showing the greatest improvements.
- Concretes for long-term survival in a sulfate environment should be made with high-quality pozzolans and a sulfate-resisting cement. The pozzolan should not increase significantly but should preferably decrease the amount of water required.
- Cement to be used in making sulfate-resisting concrete with pozzolan of proven performance should have a maximum C_3A content of 6.5% and maximum C_4AF content of 12%. Restriction of cements to those meeting present-day specifications for Type V cement does not appear justified.

The fly-ash samples examined by Dikeou (1970) and those examined by Kalousek et al. (1972) originated from bituminous coals.

Dunstan (1976) reported the results of experiments on 13 concrete mixtures made with fly ashes from lignite or subbituminous coal sources. On the basis of this work, he concluded that lignite and subbituminous fly-ash concrete generally exhibited reduced resistance to sulfate attack. The *Concrete Manual* published by the U.S. Bureau of Reclamation gives options for cementitious materials for producing sulfate-resistant concretes (Bureau of Reclamation, 1981; Pierce, 1982).

2.1.9.6 Effects of Fly Ash on Alkali–Aggregate Reactions in Concrete

Shortly after Stanton (1940) discovered that alkali–aggregate reactions (AARs) caused expansion and damage in some concretes, he reported that the effects could be reduced by adding finely ground reactive materials to the concrete mixture. Subsequently, a variety of natural and artificial pozzolans and mineral admixtures, including fly ash, were found to be effective in reducing the damage caused by AARs. The effectiveness of fly ash (and other mineral admixtures) in reducing expansion due to AARs appears to be limited to reactions involving siliceous aggregates. A form of AAR known as the alkali–carbonate reaction (Poole, 1981) is relatively unresponsive to the addition of pozzolans (Swenson and Gillott, 1960). The role of fly ashes in reducing expansion by AAR can be summarized as follows:

- Substantial published data show that low-calcium fly ashes with alkali contents of less than about 4% are effective in reducing expansion caused by alkali–silica reactions when the fly ashes are used at a replacement level in the range of 25–30%. High-volume fly ash concrete is very effective in this regard.
- The use of high-calcium ashes has received less attention; hence, the background information relevant to their use is less well developed. If they are to be used, there is some indication that effective replacement levels may be higher than those for low-calcium ashes.
- The mechanism and details of the control of expansion caused by alkali–silica reactions are not fully understood. Much research remains before a satisfactory understanding can be developed.

2.1.9.7 Effects of Fly Ash on the Corrosion of Reinforcing Steel in Concrete

Recently, an issue of concern has been the corrosion of steel reinforcement in fly-ash concrete structures exposed to chloride ions from deicing salts or seawater. If the concrete cover over steel reinforcement is sufficiently thick and impermeable, it will normally provide adequate protection against corrosion. The protective effect of the concrete cover is of both a physical and a chemical nature and functions in three ways:

- It provides an alkaline medium in the immediate vicinity of the steel surface.
- It offers a physical and chemical barrier to the ingress of moisture, oxygen, carbon dioxide, chlorides, and other aggressive agents.
- It provides an electrically resistive medium around the steel members.

Under alkaline conditions (pH higher than ~11.5), a protective oxide film will form on a steel surface, rendering it immune to further corrosion.

When concrete carbonates and the depth of carbonation reach the steel–concrete boundary, passivation may be reduced and corrosion may occur if sufficient oxygen and moisture reach the metal surface. Chlorides or other ions may also undermine the protective effect of passivation and encourage corrosion.

The *Réunion internationale des laboratoires d'essais et de recherches sur les matériaux et les constructions* (RILEM) Technical Committee on Corrosion of Steel in Concrete (1974) made the following statement, which gives perspective to this issue:

The efficiency of the (concrete) cover in preventing corrosion is dependent on many factors which collectively are referred to as its “quality.” In this context, the “quality” implies impermeability and a high reserve of alkalinity which satisfies both the physical needs and chemical requirements of the concrete cover. If the concrete is permeable to atmospheric gases or lean in cement, corrosion of the reinforcement can be anticipated and good protection should be attempted by the use of dense aggregate and a well-compacted mix with a reasonably low water/cement ratio. . . . If chloride corrosion is excepted, it is now usually agreed that carbonation of concrete cover is the essential condition for corrosion of reinforcement.

As discussed in the Effects of Fly Ash on Carbonation of Concrete section above, the issue of carbonation of fly-ash concrete has received some attention in recent years; however, it is our belief that the carbonation of fly-ash concrete is not a matter of concern, provided attention is paid to obtaining adequate impermeability in the concrete mass.

2.1.9.8 Effects of Fly Ash on Concrete Exposed to Seawater

Exposure of concrete to the marine environment subjects it to an array of severely aggressive factors, including most of those discussed in the preceding sections of this chapter. Concrete in tidal zones is the most severely attacked, subjected as it is to alternating wetting and drying, wave action, abrasion by sand and debris, frequent freezing and thawing cycles, and corrosion of reinforcement—all occurring in a chemically aggressive medium. Permanently immersed concrete is less severely affected.

Very little direct observation of fly-ash concrete in seawater has been reported in the literature, although some research in this area has been reported (Malhotra et al., 1980). In 1978, CANMET (Malhotra et al., 1988, 1992) initiated a long-term project on marine-environment performance of concretes incorporating supplementary cementing materials. Test specimens were exposed to repeated cycles of wetting and drying and up to approximately 100 freezing and thawing cycles per year. Even under exposure to severe marine conditions, concretes incorporating 25% fly ash from a bituminous source were in satisfactory condition after 15 years. The only exceptions were the specimens with a water/cement + fly ash ratio of 0.60. It was concluded that fly-ash concrete at a 25% cement replacement level (by mass) can be satisfactory under such conditions of exposure, provided the water/cementitious materials ratio is ≤ 50 .

Whereas permeability is considered to be the major factor affecting the durability of concrete in seawater, it is evident that fly ash has the potential to contribute to a number of aspects of concrete durability in the marine environment. It is clear also that this is an area of fly-ash concrete behavior that is greatly in need of research.

2.2 Blast-Furnace Slag

2.2.1 Ground, Granulated, or Pelletized Blast-Furnace Slag

Blast-furnace slag is a byproduct of iron manufacture. When it is rapidly quenched with water to a glassy state and finely ground, it develops the property of latent hydraulicity. Most of the slags so produced are, in themselves, cementitious materials to a certain degree, whereas others become so in the presence of activators such as Portland cement and calcium sulfate. Their performance in concrete,

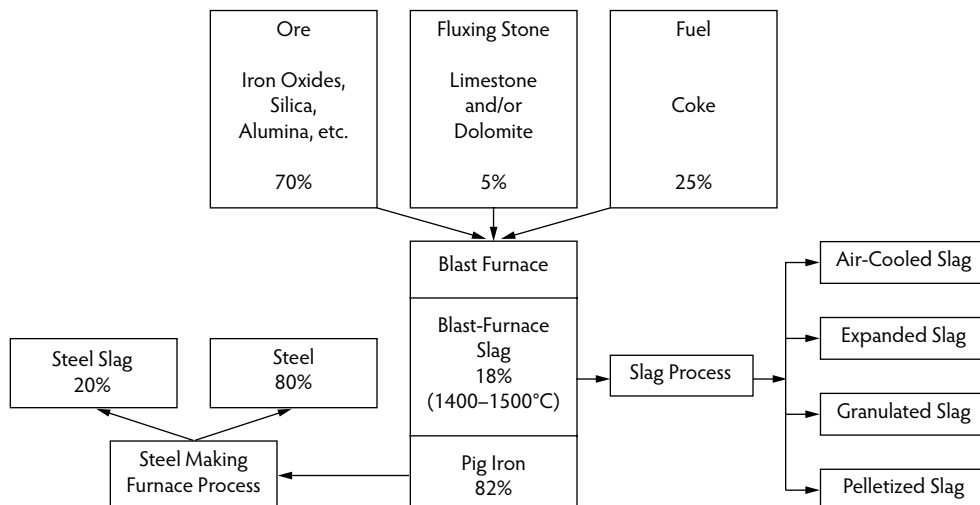


FIGURE 2.8 Flowchart showing production of pig iron and blast-furnace slag. (From Kim, C.S., *Waste and Secondary Product Utilization in Highway Construction*, M.S. thesis, McMaster University, Hamilton, Ontario, 1975.)

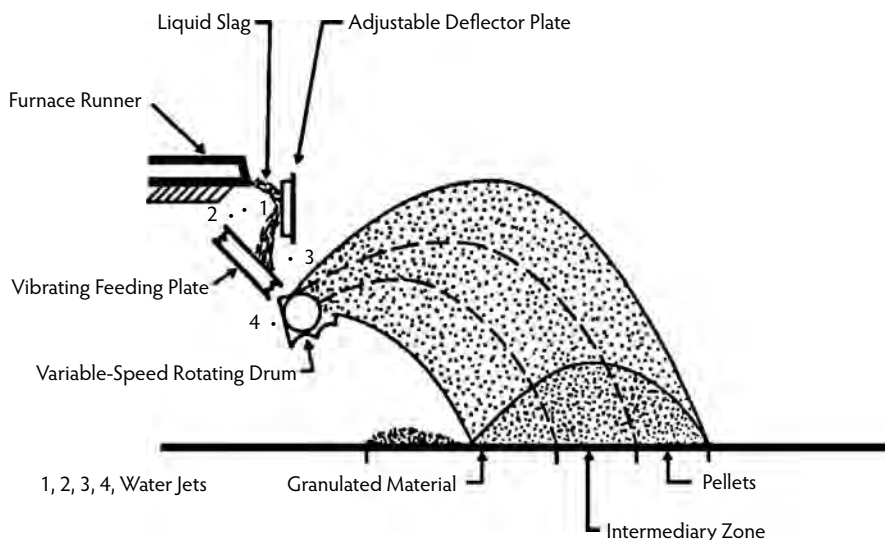


FIGURE 2.9 Diagram of a typical slag pelletizer. (From Hooton, R.D., in *Supplementary Cementing Materials*, Malhotra, V.M., Ed., Canada Center for Mineral and Energy Technology (CANMET), Ottawa, Ontario, 1987, pp. 247-330.)

however, is independent of whether they are inherently cementitious or not. Figure 2.8 shows a flow chart for the production of pig iron and blast-furnace slag (Kim, 1975). The technology for utilization of granulated blast-furnace slags in concrete is now well established worldwide. In the early 1970s, a pelletizing process to produce glassy slag was introduced in southern Ontario. This process uses considerably less water than granulation techniques. The molten slag is first expanded by treatment with water sprays, and the material is then passed over a rotating finned drum. The semimolten material is then thrown into the air for cooling and pelletization (Figure 2.9). Several pelletization plants are in operation worldwide (Hooton, 1987a).

2.2.2 Mixture Proportions and Properties of Fresh Concrete Incorporating Blast-Furnace Slag

2.2.2.1 Mixture Proportions

The proportions of ground, granulated, or ground, pelletized, blast-furnace slag* used in concrete depend on the job requirements. In normal ready-mixed concrete operations, in which the primary aim is to conserve cement, the usual proportions vary from 25 to 50% by weight of cement on a cement-replacement basis; however, if the purpose is to enhance some aspect of concrete durability (for example, sulfate resistance), then the slag content is at least 50% of the total cementitious material. As each slag has a unique chemical composition, glass content, and fineness, it is necessary to perform exploratory laboratory investigations with the cement, aggregates, and chemical admixtures to be used at a project to determine the correct percentage of slag to be incorporated into the concrete. This aspect cannot be overemphasized. The specific gravity of slags ranges from 2.85 to 2.95, compared with 3.15 for Portland cements; thus, a given replacement of cement by slag on a weight basis results in a higher volume of paste in a concrete mixture. This result is of little consequence at lower percentages of cement replacement. If, however, 50 to 75% cement replacements are being considered, this will affect the rheology of the concrete mixtures and may allow some increase in the volume of coarse aggregate to be used, especially in mixtures incorporating higher amounts of cement.

2.2.2.2 Time of Setting

The incorporation of slag as a replacement for Portland cement in concrete normally results in increased setting time. Final setting time can be delayed up to several hours depending on the ambient temperature, concrete temperature, and mixture proportions. At temperatures lower than 23°C, considerable retardation in setting time can be expected for slag concretes compared with control concrete, which has serious implications in winter concreting. At higher temperatures (>30°C), there is little or no change in the setting time of slag concrete as compared to control concrete. Data by Hogan and Meusel (1981) on initial and final setting for concrete incorporating granulated slag are shown in Table 2.9.

2.2.2.3 Bleeding

Few published data are available on the bleeding of slag concretes. Slags are generally ground to a higher fineness than normal Portland cement; therefore, a given mass of slag has a higher surface area than the corresponding mass of Portland cement. As the bleeding of concrete is governed by the ratio of the surface area of solids to the volume of water, in all likelihood the bleeding of slag concrete will be lower than that of the corresponding control concrete. The slags available in Canada and the United States have fineness, as measured by the Blaine method, greater than 4500 cm²/g, compared with that of about 3000 cm²/g for Portland cement. Thus, in concrete in which a given mass of Portland cement is replaced by an equivalent mass of slag, bleeding should not be a problem.

2.2.2.4 Dosage of Air-Entraining Admixtures

The dosage requirement of an air-entraining admixture to entrain a given volume of air in slag concrete increases with increasing amounts of slag. The increased demand for the admixture is, once again, probably due to the higher total surface area of the slag particles compared with that of the Portland cement particles. In an investigation reported by Malhotra (1979), the admixture dosage required to entrain about 5% air increased from 177 mL/m³ for the control concrete to 562 mL/m³ for a concrete mixture incorporating 65% pelletized slag. The water/cement + slag ratio was 0.30.

*Granulated slag implies that the slag is granulated by rapid-water quenching of the molten slag, whereas pelletized slag implies that the granulation is achieved by a pelletizing process. Hereafter, these are referred to either as *granulated* or *pelletized slag* or only as *slag* when reference is made to both types.

TABLE 2.9 Data on Time of Setting for Air-Entrained Concrete Incorporating Granulated Slag

Properties	Control, No Slag	Slag Content (%)			Control, No Slag	Slag Content (%)		
		40	50	65		40	50	65
Water/(cement + slag)	0.40	0.40	0.40	0.40	0.55	0.55	0.55	0.55
Cement factor (cement and slag) (kg/m ³)	413	435	419	408	272	290	245	301
Fine aggregate/coarse aggregate	33/67	33/67	33/67	33/67	46/54	46/54	46/54	46/54
Air content (%)	5.4	3.4	4.5	5.0	4.3	3.5	6.0	4.9
Unit weight (kg/m ³)	2330	2350	2320	2310	2345	2355	2310	2295
Slump (mm)	75	75	95	90	70	15	50	75
Air-entraining admixture (mL/kg cement)	4.4	4.4	9.0	9.5	8.4	4.6	8.2	8.2
Initial set at 21.1°C (70°F) (hr:min)	4:06	4:02	4:31	4:30	4:32	5:02	5:10	5:21
Final set at 21.1°C (70°F) (hr:min)	5:34	5:40	6:29	7:04	7:03	6:40	8:10	8:09
Initial set at 32.2°C (70°F) (hr:min)	3:30	—	3:45	—	—	—	—	—
Final set at 32.2°C (70°F) (hr:min)	4:30	—	4:50	—	—	—	—	—

Source: Hogan, F.J. and Meusel, J.W., *ASTM Cement, Concrete, Aggregates*, 3(1), 40–52, 1981.

2.2.2.5 Rates of Slump Loss

Meusel and Rose (1979) have shown that the rate of slump loss of concrete incorporating granulated slag at 50% cement replacement was comparable to that of the control concrete.

2.2.3 Properties of Hardened Concrete

2.2.3.1 Color

Concrete incorporating slags is generally lighter in color than normal Portland cement concrete, due to the lighter color of slags. When concrete is tested for compression or flexure, the interior of the broken specimens exhibit a deep blue–green color. After sufficient exposure to air, the color disappears. The degree of color, which results from the reaction of sulfides in the slag with other compounds in cement, depends on the percentage of slag used, curing conditions, and the rate of oxidation.

2.2.3.2 Curing

The rate and degree of hydration of cement paste, and consequently its strength, are affected significantly by lack of proper curing because of the slow formation of strength-producing hydrates. This effect becomes more pronounced when the paste incorporates high percentages of slag. To ensure proper strength and durability of concretes incorporating high percentages of slag (>30%), it is important that they be given more curing than concretes without slag. Such extended curing is especially important during winter concreting in Canada and the northern United States. The increase in curing time would depend on the ambient temperature, the concrete temperature, the type and amount of cement used, and the percentage of cement replacement.

2.2.3.3 Compressive Strength

The compressive strength development of slag concrete depends primarily on the type, fineness, activity index, and proportions of slag used in concrete mixtures. Other factors that affect the performance of slag in concrete are the water/cementitious materials ratio and the type of cement used. In general, the strength development of concrete incorporating slags is slow at 1 to 5 days, compared to that of the control concrete. Between 7 and 28 days, the strength approaches that of the control

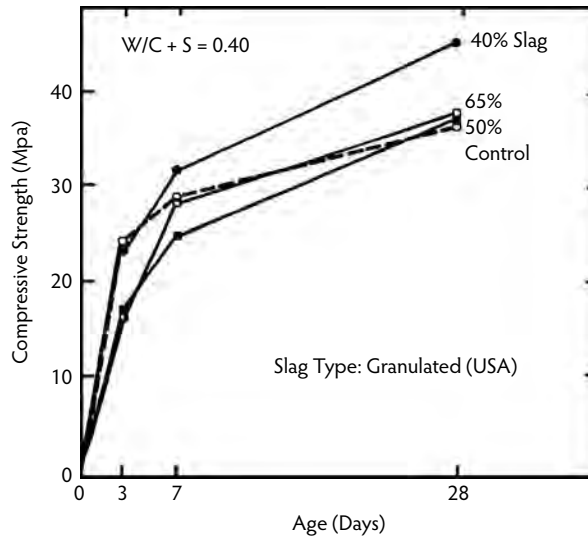


FIGURE 2.10 Age vs. compressive strength relationship for air-entrained concrete: $W/(C + S) = 0.40$. (From Hogan, F.J. and Meusel, J.W., *ASTM Cement, Concrete, Aggregates*, 3(1), 40–52, 1981.)

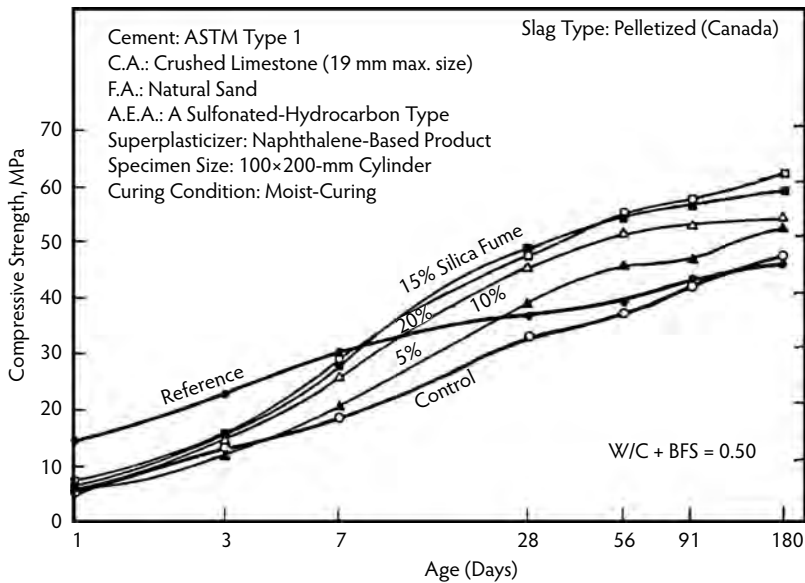


FIGURE 2.11 Age vs. compressive strength relationship for concrete incorporating condensed silica fume and pelletized slag, water/cement + blast-furnace slag ($W/(C + BFS) = 0.50$). (From Malhotra, V.M. et al., in *Proceedings of the RILEM/ACI Symposium on the Technology of Concrete When Pozzolans, Slags and Chemical Admixtures Are Used*, Monterey, Mexico, 1985, pp. 395–414.)

concrete, and beyond this period the strength of slag concrete exceeds the strength of the control concrete. Figure 2.10 and Figure 2.11 show compressive strength development with age for granulated slag concrete for water/cement + slag ratios of 0.40 and 0.55. Note that the highest strength gain at 28 days was for concrete with a slag content of 40% cement replacement.

Malhotra et al. (1985) reported investigations in which small amounts of condensed silica fume were added to pelletized slag concrete to increase the early-age strength. Figure 2.11 illustrates the strength development of concrete from 1 to 180 days. The authors concluded that:

- The low early-age strength of Portland cement concrete incorporating blast-furnace slag can be increased by the incorporation of condensed silica fume. The gain in strength is generally directly proportional to the percentage of the fume used.
- At 3 days, the increase in strength is generally marginal, especially for concrete with high W/C + blast-furnace slag (BFS) ratios. However, at the age of 14 days and beyond, with minor exceptions, the loss in compressive strength of concrete due to the incorporation of BFS can be fully compensated for with a given percentage of condensed silica fume, regardless of the W/(C + BFS). This is also true for the flexural strength.
- The continuing increase in strength at 56, 91, and 180 days of the concrete incorporating BFS and condensed silica fume indicates that sufficient lime (liberated during the hydration of Portland cement) is present at these ages for the cementitious reaction to continue.

2.2.3.4 Flexural Strength

In general, at 7 days and beyond, the flexural strength of concrete incorporating slag is comparable to, or greater than, the corresponding strength of control concrete; however, in one instance, the reverse was reported for a water/cement + slag ratio of 0.38. The increased flexural strength of slag concrete is probably due to the stronger bonds in the cement–slag–aggregate system because of the shape and surface texture of the slag particles.

2.2.3.5 Young's Modulus of Elasticity

According to Stutterheim (1960), at the same strength level, there is little, if any, difference between the modulus of elasticity of the control concrete and a concrete containing a granulated slag of South African origin. No published data are available on Young's modulus of elasticity of slags currently available in North America. Investigations performed by Nakamura et al. (1986) on a Japanese slag showed no significant difference between the values of the Young's modulus of elasticity of concrete incorporating granulated slag and that of the control concrete.

2.2.3.6 Drying Shrinkage

Hogan and Meusel (1981) showed that drying shrinkage of concrete incorporating granulated slag is more than that of control concrete. The increase in shrinkage is attributed to increased paste volume in concrete when slag is used as replacement for Portland cement on an equal weight basis because of the lower specific gravity of the slag. This finding may or may not be true for other slags, and further research is needed to confirm this. Fulton (1974) suggested that the shrinkage of concrete incorporating granulated slag can be reduced by taking advantage of improved workability to increase the aggregate/cement ratio or by reducing the water/cement ratio of concrete.

2.2.3.7 Creep

Few published data are available on creep of concrete incorporating North American slags. The available data from South Africa and Japan are conflicting (Fulton, 1974). This conflict is due primarily to the fineness of slags used, methods of tests, age of testing, humidity conditions, and the stress/strength ratio employed; for example, it has been shown that the fineness of cement significantly affects the creep strains (Fulton, 1974). Bamforth (1980) has reported limited data on creep strains for concretes with and without fly ash and granulated slags, loaded to a constant stress/strength ratio of 0.25. He found that for concretes loaded at an age greater than 24 hours, the effects of fly ash and slag significantly reduced the magnitude of the creep. Neville and Brooks (1975) showed that, when creep tests are performed at ordinary room temperature and humidity conditions (i.e., 20°C and 60% relative humidity) on test specimens that have been loaded after moist curing for 28 days, the total creep of the concrete incorporating a slag from a British source was greater than that of the control concrete, although not significantly so. The rationale for this finding may be that under such test conditions, the rate of gain of strength of the slag concrete is lower than that of the control concrete.

2.2.3.8 Permeability

The permeability of concrete depends mainly on the permeability of the cement paste, which, in turn, depends on its pore-size distribution. Using mercury-intrusion techniques, several investigators (Manmohan and Mehta, 1981; Mehta, 1983) demonstrated that incorporating granulated slags in cement paste helps transform large pores into smaller pores, resulting in decreased permeability of the matrix and, hence, of the concrete. The exact mechanism by which the pore refinement occurs in a hydrated slag–cement matrix, however, is not fully understood. Detailed data comparing the permeability of concrete with and without slags are not available, although it has been observed that granulated slag concretes incorporating slags at up to 75% cement replacement have performed satisfactorily when exposed to seawater (Wiebenga, 1980).

2.2.4 Durability of Concrete Incorporating Blast-Furnace Slag

It is believed that the increased durability of Portland cement concrete incorporating blast-furnace slag results from a finer pore structure and a reduction in easily leached calcium hydroxide in the hardened cement paste. Subsequently, the volume previously occupied by calcium hydroxide is filled in with hydration products, resulting in a less-permeable material. Permeability controls the physical and chemical processes of degradation caused by the action of migrating water; therefore, permeability to water determines the rate of deterioration.

2.2.4.1 Resistance to Sulfate Attack

Sulfates attack concrete and affect its coherence and strength. The resistance of concrete to sulfate attack is improved by partially replacing Portland cement with ground granulated blast-furnace slag. In Germany, France, and the Netherlands, cements with a high blast-furnace slag content have been used for many years and are considered appropriate for use in a high-sulfate environment (DIN 1164, 1978; NEN 3550, 1979). Hogan and Meusel (1981) carried out a study that demonstrated high resistance to sulfate attack when the granulated slag proportion exceeded 50% of the total cementitious material; ASTM Type II cements were used. Results of studies carried out by Frearsen (1986) confirmed that ordinary Portland cements and blends of both ordinary and sulfate-resisting Portland cement containing lower levels of granulated slag replacement have inferior resistance to sulfate attack. Sulfate resistance increased with granulated slag content, and a mortar with 70% slag content was found to have a resistance superior to mortars containing sulfate-resisting Portland cements alone. Also, the influence of slag content on sulfate resistance was found to be more significant than the water/cement ratio in the mixtures investigated. According to Ludwig (1989), the cements exhibiting resistance to sulfate attack are:

- Portland cement with C_3A content ≤ 3 wt%
- Portland cement with $\leq 70\%$ slag content
- Nonstandard cements such as high-alumina and supersulfated cements

Bakker (1983) found that slag concretes with a high slag content display an increased resistance to sulfates because of the low permeability of the concrete to different ions and water, as shown by the various coefficient values in Table 2.10.

Where granulated slag is used in sufficient quantities, several changes occur that improve resistance to sulfate attack. These changes include the following:

- The C_3A content of the mixture is proportionally reduced depending on the percentage of slag used; however, Lea (1970) reported that increased sulfate resistance depends not only on the C_3A content of Portland cement alone but also on the Al_2O_3 content of the granulated slag. Lea further reported that sulfate resistance increased where the alumina content of the slag is less than 11%, regardless of the C_3A content of the Portland cement when blends with 20 to 50% granulated slags were used.

TABLE 2.10 Diffusion Coefficients of Na, K, and Cl Ions in Hardened Cement Paste and Mortars Made with Portland and Blast-Furnace Cement after Different Hardening Times

Diffused Ion	Hardening Time (days)	D_m (10^{-8} cm ² /sec)			Slag Content (%)
		Water/Cement Ratio	Portland Cement	Blast-Furnace Cement	
Na ⁺	3	0.50	7.02	1.44	75
	14	0.50	2.38	0.10	75
	28	0.55	1.47	0.05	60
	28	0.60	3.18	0.05	60
	28	0.65	4.73	0.06	60
K ⁺	3	0.50	11.38	2.10	75
	14	0.50	3.58	0.21	75
Cl ⁻	28	0.55	3.57	0.12	60
	28	0.60	6.21	0.23	60
	28	0.65	8.53	0.41	60
	5	0.50	5.08	0.42	75
	103	0.50	2.96	0.04	75
	60	0.50	4.47	0.41	75

Source: Owens, P.L., *Concrete J. Concrete Soc.*, 13, 21–26, 1979.

- Through the reduction of soluble $\text{Ca}(\text{OH})_2$ in the formation of calcium silicate hydrates (CSHs), the environment for the formation of ettringite is reduced. Resistance to sulfate attack is greatly dependent on the permeability of the concrete or cement paste. The formation of CSH in pore spaces usually occupied by alkalis and $\text{Ca}(\text{OH})_2$ reduces the permeability of the paste and prevents the intrusion of aggressive sulfates.

Mehta (1981) tested pastes incorporating natural pozzolans, rice-husk ash, and granulated slag. The 28-day-old paste of the blended cement containing 70% blast-furnace slag showed excellent resistance to sulfate attack. Few large pores were present in the hydrated paste, although the total porosity (pores >45 Å) was the highest among all the cements tested. The direct relationship between sulfate resistance of a cement and the slope of its pore-size distribution plot in the range of 500 to 45 Å probably shows that the presence of a large number of fine pores is associated with improved sulfate resistance of the material (Figure 2.12). Although the total porosity of the cement containing 30% slag was considerably less than the cement containing 70% slag, the former was not found to be sulfate resistant. On the basis of the test results, Mehta proposed that the chemical resistance of blended Portland cements results mainly from the process of pore refinement, which is associated with the pozzolanic reactions involving the removal of $\text{Ca}(\text{OH})_2$.

2.2.4.2 Resistance to Seawater

The action of sulfate in seawater on concrete is rather similar to that of sulfate-bearing groundwater, but in the former case the attack is not accompanied by expansion of the concrete. The absence of expansion is partly due to the presence of a large quantity of chlorides in the seawater that inhibit the expansion; gypsum and calcium sulfoaluminate are more soluble in a chloride solution than in water, so they either do not form or are leached out by the seawater.

Regourd et al. (1977) studied mortar cubes that had been exposed to seawater since 1904 at the port of La Rochelle, France. They concluded that all Portland slag cements with a slag content $>60\%$ perform well in seawater. In the case of lower slag content, the MgSO_4 reacts with the $\text{Ca}(\text{OH})_2$ from C_3S and C_2S hydration and produces gypsum. The gypsum reacts with the aluminates to form expansive ettringite. Mehta (1989), on the other hand, proposed that the deterioration of concrete by seawater is not characterized by expansion but rather is affected by erosion or loss of the solid constituents from the mass. Mehta suggested that ettringite expansion is suppressed in environments where $(\text{OH})^-$ ions have been replaced by Cl^- ions.

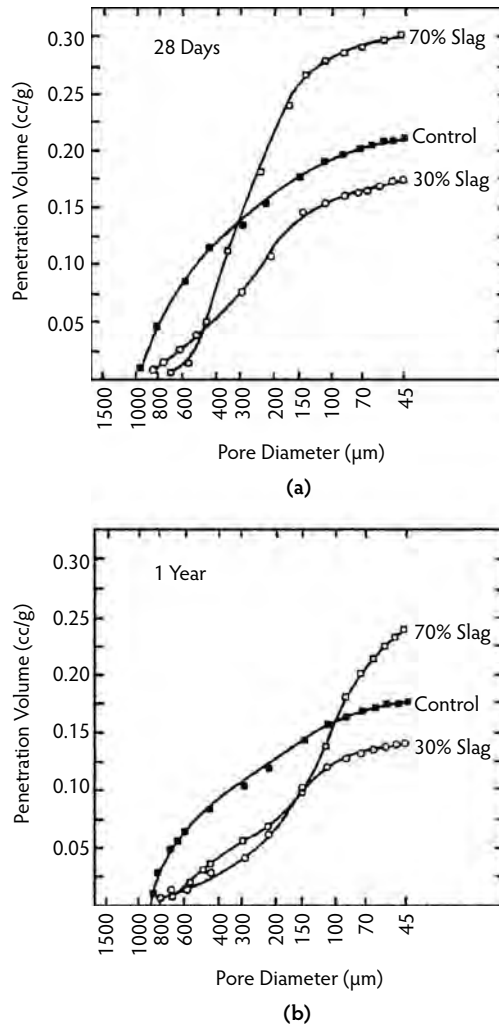


FIGURE 2.12 Pore-size distribution of hydrated cements containing 30% or 70% granulated blast-furnace slag. (From Mehta, P.K., in *Proceedings of the Fifth International Symposium on Concrete Technology*, Rivera, R., Ed., Monterey, Mexico, 1981, pp. 35–50.)

In seawater, well-cured concretes containing large amounts of granulated slag or pozzolan usually outperform reference concretes containing only Portland cement, partly because the former contain less uncombined $\text{Ca}(\text{OH})_2$ after curing. In permeable concretes, the normal amount of CO_2 present in seawater is sufficient to decompose the cementitious products. The presence of calcium silicocarbonate (thaumasite), calcium carboaluminate hydrate (hydrocalumite), and calcium carbonate (aragonite) have been reported in cement pastes derived from deteriorated concretes exposed to seawater for long periods.

2.2.4.3 Reduction of Expansion Due to Alkali–Silica Reactions

In concrete containing reactive siliceous aggregates, slag cements are preferable to Portland cements, which are rich in alkalis (Regourd, 1980). Research undertaken at the Concrete Research Institute of the Dutch Cement Industry and by other investigators (Smolczyk, 1974, 1975) confirmed that the reason for the high resistance of concretes incorporating slags to the alkali–silica reaction is the low permeability

of these concretes to various ions and to water. The low permeability is due not only to the amount of gel formed but also to the locality where the gel is precipitated; that is, the gel can block a pore when Portland cement and slag grains are close to each other. The potential alkali–aggregate reactivity for combinations of Portland cement and granulated slag was investigated by Hogan and Meusel (1981) using ASTM Test C 227; the aggregate used was Pyrex® glass, known to be highly reactive. The data indicate that the expansion of mortar bars made with slag-cement mixtures and Pyrex® glass is significantly less than for bars made with Portland cement alone. The cement used for these tests had an alkali content of 0.51% sodium oxide equivalent, which conforms to the ASTM C 150 specification for Portland cement requirement for low-alkali cement. Suppression of the alkali–aggregate reaction by the addition of slag was cited by Mather (1965), who suggested that an alkali limit for Portland slag cements, which have a performance equal to that of 0.60% Na₂O for Portland cements alone, could be as high as 1.20% Na₂O equivalent.

2.2.4.4 Resistance to Repeated Cycles of Freezing and Thawing

Many studies have been published in which granulated blast-furnace slag has been used as partial replacement for Portland cement in concrete subjected to repeated cycles of freezing and thawing (Fulton, 1974; Klieger and Isberner, 1967; Mather, 1957). Results of these studies indicated that, when mortar or concrete made with granulated slag and Portland cement were tested in comparison with Type I and Type II cements, their resistance to freezing and thawing (ASTM C 666, Procedure A) was essentially the same, provided the concrete was air entrained. Malhotra (1983b) reported results of tests performed in an automatic unit capable of performing eight freezing and thawing cycles per day (ASTM C 666, Procedure B). The percentage of slag used as replacement for normal Portland cement varied from 25 to 65 wt% of cement. Initial measurements were taken at 14 days. After about every 100 cycles, the specimens were measured, weighed, and tested by resonant frequency and by the ultrasonic-pulse velocity method. The test was terminated at 700 freezing and thawing cycles. Durability of the exposed concrete prisms was determined from weight, length, resonant frequency, and pulse velocity of the test prisms before and after the freezing and thawing cycling, and relative durability factors (ASTM C 666) were calculated. The test results (Table 2.11) indicated that, regardless of the water/cement + slag ratio and whether the concretes were air entrained or air entrained and superplasticized, these specimens performed excellently in freezing and thawing tests, with relative durability factors greater than 91%.

2.2.5 Carbonation

Concrete exposed to air will partially release its free water from the layers next to the surface. During evaporation, the pore water in the concrete is replaced by air, and reactions between the CO₂ of the atmosphere and the alkali compounds of the concrete take place. This process between the CO₂ of the atmosphere and the hydration products of the hardened cement paste is called *carbonation*. The properties of the concrete, as well its protective properties against corrosion of reinforcing steel, are affected by these reactions. In general, in well-compacted low water/cement ratio slag concrete, carbonation is not a problem; however, if the concrete incorporates a large percentage of slag, is not cured properly, and has a high water/cement + slag ratio, then the depth of carbonation will exceed that for normal Portland cement concrete. Steel in the presence of high concentrations of hydroxyl does not corrode. Bird (1969) suggested that this passivity is the result of the formation of a protective film of gamma ferric oxide on the surface of the steel. As long as this protective film is maintained by a high pH and is not disrupted by aggressive substances, complete protection of the steel against corrosion is assured. Carbonation can reduce the pH to an extent determined by the permeability of the concrete. Hamada (1968) and Meyer (1968) agreed that carbonation proceeds more rapidly in concretes incorporating slag than in those made with ordinary Portland cement; however, this finding was disputed by Schröder and Smolczyk (1968), who pointed out that comparative tests should be based on specimens of equal initial permeability rather than on specimens of equal age.

TABLE 2.11 Summary of Freeze-Thaw Test Results for Concrete Series B and D

Mix Series	W/(C + S) ^a	Type of Mix	Summary of Freeze-Thaw Test Results							
			At Zero Cycles				At Completion of 700 Cycles			
			Weight (kg)	Length (mm) ^b	Longitudinal Resonant Frequency (Hz)	Pulse Velocity (m/sec)	Weight (kg)	Length (Hz)	Longitudinal Resonant Frequency (m/sec)	Pulse Velocity (%)
B	0.38	Control + AEA	8.703	2.89	5150	4717	8.693	2.90	5200	4747
		Control + AEA + SP	8.499	2.70	5150	4684	8.486	2.72	5138	4661
		25% slag + AEA	8.697	3.00	5300	4788	8.673	3.05	5225	4788
		25% slag + AEA + SP	8.540	2.96	5125	4684	8.517	3.01	5100	4656
		65% slag + AEA	8.622	2.74	5140	4684	8.626	2.91	4950	4568
D	0.56	65% slag + AEA + SP	8.302	1.59	5025	4589	8.302	1.68	4875	4531
		Control + AEA	8.331	2.56	5000	4568	8.299	2.56	5010	4600
		Control + AEA + SP	8.443	2.76	4980	4568	8.394	2.76	4980	4504
		25% slag + AEA	8.451	2.85	5000	4573	8.416	2.88	5000	4606
		25% slag + AEA + SP	8.544	2.83	5040	4639	8.483	2.91	5050	4622
		65% slag + AEA	8.465	2.61	4950	4546	— ^c	2.88	— ^d	— ^d
		65% slag + AEA + SP	8.471	2.52	4930	4563	— ^c	2.75	— ^d	70

^a Water/(cement + slag) ratio.

^b Gauge length of 345 mm should be added to this value to arrive at the exact length.

^c Prisms failed at the end of 533 freeze-thaw cycles when the resonant frequency was 3840 Hz.

^d Prisms failed at the end of 450 freeze-thaw cycles when the resonant frequency was 4150 Hz.

Source: Malhotra, V.M., in *Fly Ash, Silica Fume, Slag, and Other Mineral Byproducts in Concrete*, Vol. 2, Spec. Publ. SP-79, Malhotra, V.M., Ed., American Concrete Institute, Detroit, MI, 1983, pp. 892–931.

2.3 Silica Fume

2.3.1 Production of Silica Fume

Silica fume is a byproduct of the manufacture of silicon or of various silicon alloys produced in submerged electric-arc furnaces. The type of alloy produced and the composition of quartz and coal, the two major components used in the submerged-electric arc furnace, greatly influence the chemical composition of silica fume (Malhotra et al., 1987). Most of the published data on the use of silica fume in cement and concrete are related to silica fume collected during the production of a silicon alloy containing at least 75% silicon.

2.3.1.1 Forms of Silica Fume

Silica fume is available commercially in several forms in both North America and Europe:

- *As-produced silica fume* is silica fume collected in dedusting systems known as *bag houses*. In this form, the material is very fine and has a bulk density of about 200 to 300 kg/m³, compared with 1500 kg/m³ for Portland cement (Malhotra et al., 1987). As-produced silica fume is available in bags or in bulk. Because of its extreme fineness, this form poses handling problems; in spite of this, the material can be and has been transported and handled like Portland cement.
- *Compacted silica fume* has a bulk density ranging from 500 to 700 kg/m³ and is considerably easier to handle than as-produced silica fume. To produce the compacted form, the as-produced silica fume is placed in a silo, and compressed air is blown in from the bottom of the silo. This causes the particles to tumble, and in doing so they agglomerate. The heavier agglomerates fall to the bottom of the silo and are removed at intervals. The air compaction of the as-produced silica fume is designed so the agglomerates produced are rather weak and quickly break down during concrete mixing. Mechanical means have also been used to produce compacted silica fume.
- *Water-based silica fume slurry* overcomes the handling and transporting problems associated with as-produced silica fume; the slurry contains about 40 to 60% solid particles. Typically, these slurries have a density of about 1300 kg/m³. Some slurries may contain chemical admixtures such as superplasticizers, water reducers, and retarders. One such product (known as Force 10,000®) has been successfully marketed in North America.

2.3.2 Physical and Chemical Characteristics of Silica Fume

2.3.2.1 Physical Characteristics of Silica Fume

Silica fume varies in color from pale to dark gray. The carbon content and, to a lesser extent, the iron content seem to have significant influence on the color of silica fume. The bulk specific weight is of the order of 200 kg/m³ and is 500 kg/m³ when compacted. The specific gravity of silica fume is about 2.20. The particles have a wide range of sizes, but they are perfectly spherical (Figure 2.13). The mean particle diameter is 0.1 μm, compared with 10 μm for particles of cement. The specific surface of silica fume ranges from 13,000 to 30,000 m²/kg as measured by the nitrogen adsorption technique; the values for Portland cement are 300 to 400 m²/kg as measured by the Blaine method. Table 2.12 gives values for the fineness, specific surface, pozzolanic activity index, and specific gravity for silica fume from the production of silicon and ferrosilicon alloys (Malhotra et al., 1987). X-ray diffractograms of samples of different types of silica fume have shown them to be vitreous. All the diffractograms exhibit a very wide scattering peak centered at about 4.4 Å, the most important peak of cristobalite (Figure 2.14). When heated to 1100°C, silica fume crystallizes in the form of cristobalite, except the FeSi-50% type, which crystallizes as enstatite, most probably due to the presence of a high amount of iron and magnesium oxide.

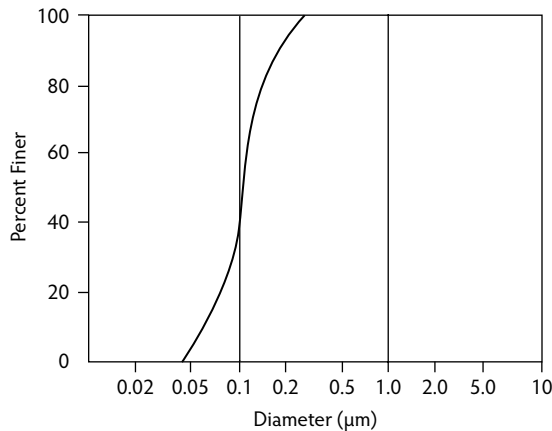


FIGURE 2.13 Typical particle size distribution of silica fume. (From Hjorth, L., in *Characterization and Performance Prediction of Cement and Concrete, Proceedings of the Second Engineering Foundation Conference*, Young, J.F., Ed., Henniker, NH, 1982, p. 165.)

TABLE 2.12 Physical Characteristics of Silica Fume

Physical Characteristics	Nebesar and Carette Results		Pistilli et al. Results	
	Si Silica Fume (24 Samples)	FeSi-75% Silica Fume (24 Samples)	Mixture of Si and FeSi-75% Silica Fume (32 Samples) ^b	FeSi-75% Silica Fume (30 Samples)
Fineness by 45 μm sieve (% passing)	94.6	98.2	94.0	96.3
Specific surface area (m ² /kg)	20,000 ^a	17,200 ^a	3750 ^b	5520 ^b
Pozzolanic activity index with Portland cement (%)	102.8	96.5	91.9	95.3
Water requirement (%)	138.8	139.2	140.1	144.5
Pozzolanic activity index with lime (MPa)	8.9	—	7.0	9.1
Specific gravity	—	—	2.27	2.26

^a Nitrogen adsorption.

^b Blaine permeability.

Source: Malhotra, V.M. et al., *Condensed Silica Fume in Concrete*, CRC Press, Boca Raton, FL, 1987. With permission.

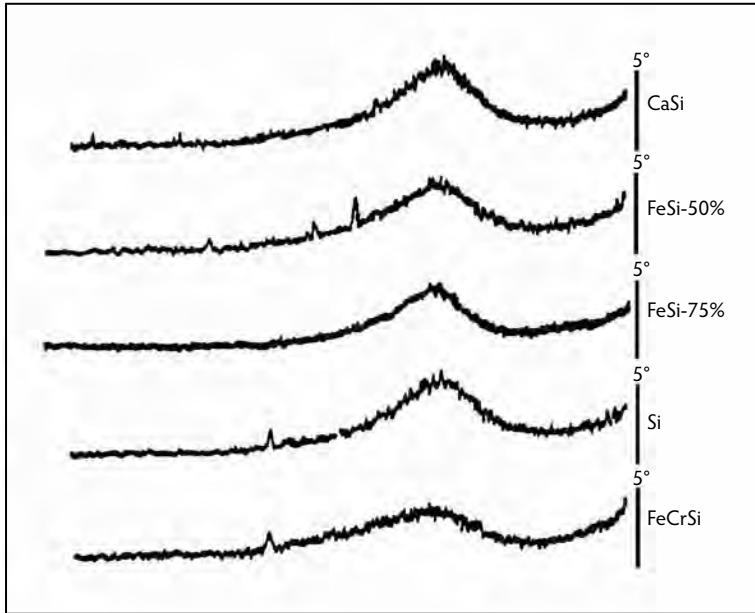
2.3.2.2 Chemical Composition of Silica Fume

The chemical composition of silica fume from different furnaces is given in Table 2.13. A change in the type of alloy manufactured may cause changes in the characteristics of the silica fume produced; therefore, it is important that concrete plants using silica fume know of any changes in the source of raw materials used for the furnace or changes in the nature of the alloy being produced by a plant.

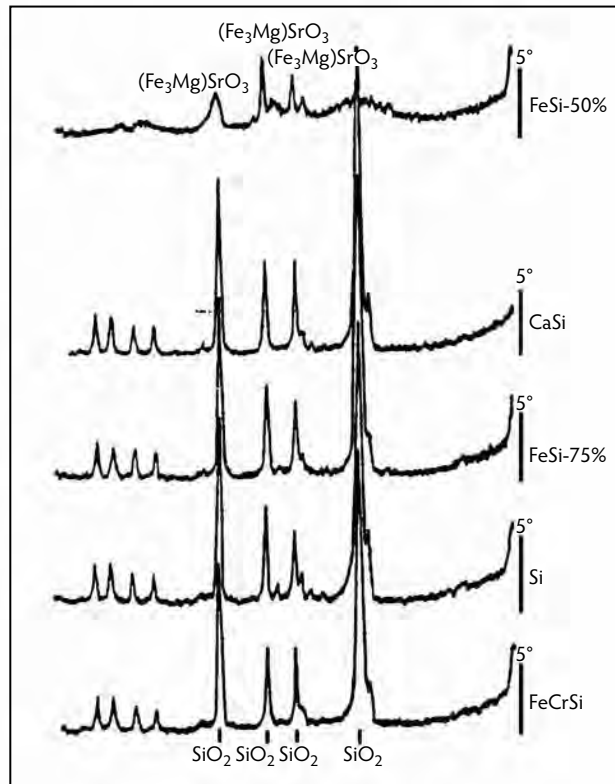
2.3.3 Physical and Chemical Mechanisms in the Cement-Silica Fume System

2.3.3.1 Physical Mechanisms

Silica fume enhances the properties of concrete by several physical mechanisms, including increasing the strength of the bond between the paste and aggregate by reducing the size of the CH crystals in the region by: (1) providing nucleation sites for the CH crystals so they are smaller and more randomly oriented, and (2) reducing the thickness of the weaker transition zone (Detwiler and Mehta, 1989; Monteiro and Mehta, 1986). Physical mechanisms also include increasing the density of the composite system due to



(a)



(b)

FIGURE 2.14 X-ray diffractograms of different types of silica fume for concrete with water/cement + silica fume ($W/(C + SF)$) of 0.64: (a) before heating; (b) after heating at 1100°C . (From Carette, G.G. and Malhotra, V.M., *ASTM J. Cement Concrete Aggregates*, 5(1), 3–13, 1983.)

TABLE 2.13 Chemical Characteristics of Silica Fume

Chemical Composition	Nebesar and Carette Results		Pistilli et al. Results	
	Si Silica Fume (24 Samples)	FeSi-75% Silica Fume (24 Samples)	Mixture of Si Silica Fume and FeSi-75% Silica Fume (32 Samples)	FeSi-75% Silica Fume (6 Samples)
SiO ₂	93.7 ^a	93.2	92.1	91.4
Al ₂ O ₃	0.28	0.3	0.25	0.57
Fe ₂ O ₃	0.58	1.1	0.79	3.86
CaO	0.27	0.44	0.38	0.73
MgO	0.25	1.08	0.35	0.44
Na ₂ O	0.02	0.10	0.17	0.20
K ₂ O	0.49	1.37	0.96	1.06
S	0.20	0.22	—	—
SO ₃	—	—	0.36	0.36 ^b
C	3.62	1.92	—	—
LOI	4.4	3.1	3.20	2.62 ^b

^a Calculated.^b Thirty samples.Source: Malhotra, V.M. et al., *Condensed Silica Fume in Concrete*, CRC Press, Boca Raton, FL, 1987. With permission.

the filler packing effect and by providing a more refined pore structure (Bache, 1981; Hjorth, 1982; Sellevold and Nilsen, 1987). For the above mechanisms to take place, it is essential that silica-fume particles be well dispersed in a concrete mixture. To achieve this, the use of high-range water reducers (superplasticizers) becomes almost mandatory.

2.3.3.2 Chemical Mechanisms and Pozzolanic Reactions

Malhotra et al. (1987) have reported extensively on the chemical reactions involved in the cement–silica fume–water system. In the presence of Portland cement, the basic reaction, known as the *pozzolanic reaction*, involves combining finely divided amorphous silica with lime to form a calcium silicate hydrate.

2.3.4 Properties of Fresh Concrete

2.3.4.1 Color

In general, the color of silica-fume concrete is darker than that of conventional concrete. This color difference is more evident on the surface of wet-hardened concrete and in fresh concrete. Also, in concretes incorporating high levels of silica fume that has high carbon content, the dark color is more pronounced. In investigations of silica-fume concrete made with dark-colored fume, it was observed that the color difference disappeared when concrete specimens were stored in the laboratory environment for extended periods. Presumably, this difference in color was neutralized by drying and perhaps by carbonation.

2.3.4.2 Water Demand

Due to its spherical, small particles, silica fume fills the pores between larger grains of cement and gives a better particle-size distribution, leading to a decrease in water demand in silica-fume concrete; however, the high specific area of the silica-fume particles tends to increase water demand, giving a net effect of increased water demand compared to Portland cement concrete with the same level of workability. Figure 2.15 shows that the increase in water demand is almost directly proportional to the amount of silica fume used in concretes that have an initial water/cement ratio of 0.64 (Carette and Malhotra, 1983). Superplasticizers or high-range water reducers can be used in silica-fume concretes to reduce the water demand. In a study using high-resolution nuclear magnetic resonance (NMR) in combination with thermal analysis (DTA/TG), Justnes et al. (1992) investigated the pozzolanicity of condensed silica fume

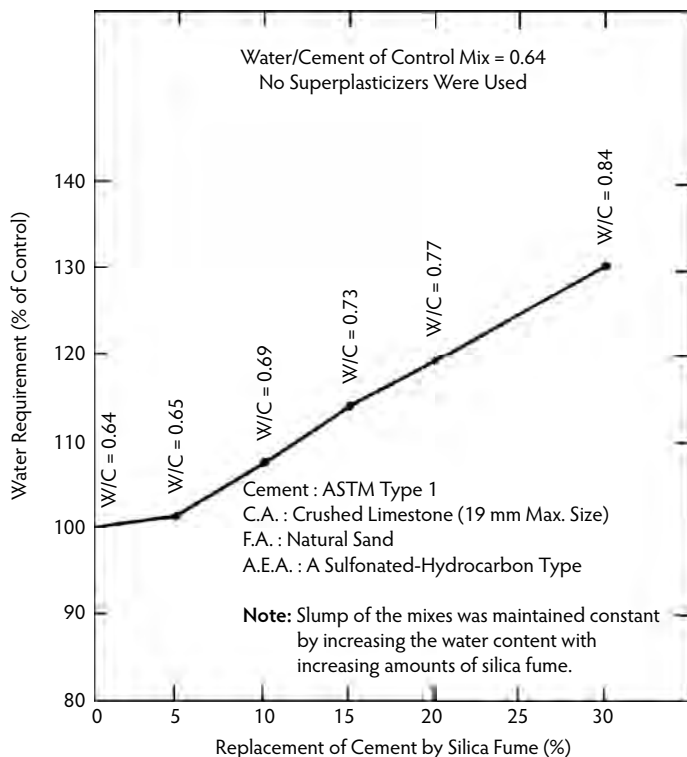


FIGURE 2.15 Relation between water requirement and dosage of silica fume for concrete with a $W/(C + SF)$ of 0.64. (From Carette, G.G. and Malhotra, V.M., *ASTM J. Cement, Concrete, Aggregates*, 5(1), 3–13, 1983.)

in cement pastes. Their results confirmed that condensed silica fume is a very reactive pozzolan. The conversion rate of condensed silica fume to hydration products after 3 days of curing was higher than for cement at the same age. In a parallel study, Sellevold and Justnes (1992) studied the decrease in relative humidity and chemical shrinkage during hydration for sealed cement pastes. The Portland cement pastes incorporated 0, 8, and 16% condensed silica fume and had water/cement + silica fume ratios of 0.2, 0.3, and 0.40, respectively. They found that the relative humidity (RH) decreased rapidly during the first 2 weeks and reached about 78% after more than a year for the pastes with the lowest water/cement + silica fume ratios; the value for the paste with the highest water/cement + silica fume ratio was about 87% RH. According to the authors, the decrease in RH is the main cause of increased cracking tendency in high-strength concretes that incorporate silica fume.

2.3.4.3 Bleeding

Bleeding of silica fume concretes is generally lower than that of plain Portland cement concrete. The extremely fine silica-fume particles attach themselves to the cement particles, reducing the channels for bleeding and leaving very little free water available in the fresh concrete.

2.3.4.4 Workability

When compared to Portland cement concrete, silica-fume concrete is more cohesive and resistant to segregation due to the increase in the number of solid-to-solid contact points. Silica-fume concrete also tends to lose slump rapidly, and a higher initial slump than that of a conventional concrete is often required. In lean concretes incorporating less than 300 kg/m^3 cement, however, workability appears to improve when silica fume is added.

2.3.4.5 Air Entrainment

Because of the extremely high surface area of the silica fume, the dosage of air-entraining admixture required to produce a certain volume of air in silica fume concretes increases considerably with increasing silica-fume dosage. The presence of carbon in the silica fume adds to the increase in air-entraining admixture demand. It has been reported that entrainment of more than 5% air is difficult in concretes that incorporate high amounts of silica fume, even in the presence of a superplasticizer (Carette and Malhotra, 1983).

2.3.4.6 Shrinkage Cracking

Shrinkage cracking occurs in fresh concrete under curing conditions that cause a net removal of water from exposed concrete surfaces, thus creating tensile stresses beyond the low early-age tensile strength capacity of concretes. As concretes containing silica fume show little or no bleeding, thus allowing very little water to rise to the surface, the risk of cracking is high in fresh concrete. Shrinkage cracking can be a very serious problem under curing conditions of elevated temperatures, low humidity, and high winds, which allow rapid evaporation of water from freshly placed concrete. Johansen (1980) and Sellevold (1984) reported that fresh concrete is most vulnerable to shrinkage cracking as it approaches initial set. To overcome this problem, the surface of concrete should be protected from evaporation by covering it with plastic sheets or wet burlap or by using curing compounds and evaporation-retarding admixtures.

2.3.4.7 Setting Time

Ordinary mixtures (with 250 to 300 kg/m³ cement) that incorporate small amounts of silica fume, up to 10% by weight of cement, exhibit no significant difference in setting times compared with conventional concretes. As silica fume is invariably used in concretes in combination with water reducers and superplasticizers, the effect of silica fume on the setting of concrete is masked by the effects of the admixtures. Investigations by Bilodeau (1985) showed that the addition of 5 to 10% silica fume to superplasticized and nonsuperplasticized concretes had a negligible effect on the setting time of concrete; however, in concrete with a water/cementitious materials ratio of 0.40 and 15% silica fume, there was a noticeable delay in setting time. The high dosage of superplasticizer used because of the high silica-fume content in the concrete could have contributed to the setting delay (Bilodeau, 1985).

2.3.5 Properties of Hardened Concrete

2.3.5.1 Compressive Strength

It is well recognized that silica fume can contribute significantly to the compressive strength development of concrete. This is because of the filler effect and the excellent pozzolanic properties of the material, which translate into a stronger transition zone at the paste–aggregate interface. The extent to which silica fume contributes to the development of compressive strength depends on various factors, such as the percentage of silica fume, the water/cement + silica fume ratio, cementitious materials content, cement composition, type and dosage of superplasticizer, temperature, curing conditions, and age.

Superplasticizing admixtures play an important role in ensuring optimum strength development of silica-fume concrete. The water demand of silica-fume concrete is directly proportional to the amount of silica fume (used as a percentage replacement for Portland cement) if the slump of concrete is to be kept constant by increasing the water content rather than by using a superplasticizer. In such instances, the increase in the strength of silica-fume concrete over that of control concrete is largely offset by the higher water demand, especially for high silica-fume content at early ages. In general, the use of superplasticizer is a prerequisite to achieving proper dispersion of the silica fume in concrete and fully utilizing the strength potential of the fume. In fact, many important applications of silica fume in concrete depend strictly upon its utilization in conjunction with superplasticizing admixtures.

Silica-fume concretes have compressive strength development patterns that are generally different from those of Portland cement concretes. The strength development characteristics of these concretes are

somewhat similar to those of fly-ash concrete, except that the results of the pozzolanic reactions of the former are evident at earlier ages. This is due to the fact that silica fume is a very fine material with a very high amorphous silica content. The main contribution of silica fume to concrete strength development at normal temperatures takes place between the ages of about 3 and 28 days. The overall strength development patterns can vary according to concrete proportions and composition and are also affected by the curing conditions.

Carette and Malhotra (1992) reported investigations dealing with the short- and long-term strength development of silica-fume concrete under conditions of both continuous water curing and dry curing after an initial moist-curing period of 7 days. Their investigations covered superplasticized concretes incorporating 0 and 10% silica fume as a replacement by weight for Portland cement and water/cement + silica fume ratios ranging between 0.25 and 0.40. As expected, the major contributions of silica fume to the strength took place prior to 28 days; the largest gains in strength of the silica-fume concrete over the control concrete were recorded at the ages of 28 and 91 days, although this gain progressively diminished with age. For concretes with water/cement + silica fume ratios of 0.30 and 0.40, the gain largely disappeared at later ages. Under air-drying conditions, the strength development pattern was found to be significantly different from that of water-cured concretes up to the age of about 91 days; thereafter, however, air drying clearly had some adverse effect on the strength development of both types of concrete. The effect was generally more severe for silica-fume concrete, where some reduction in strength was recorded between the ages of 91 days and 3.5 years, especially for concretes with water/cement + silica fume ratios of 0.30 and 0.40. These trends of strength reduction have not yet been clearly explained, but they appear to stabilize at later ages and therefore are probably of little practical significance.

Curing temperatures have also been shown to affect significantly the strength development of silica-fume concrete. This aspect has been examined in some detail by several investigators in Scandinavia. In general, these investigations have indicated that the pozzolanic reaction of silica fume is very sensitive to temperature, and elevated-temperature curing has a greater strength-accelerating effect on silica-fume concrete than on comparable Portland cement concrete. The dosage of silica fume is obviously an important parameter influencing the compressive strength of silica-fume concrete. For general construction, the optimum dosage generally varies between 7 and 10%; however, in specialized situations, up to 15% silica fume has been incorporated successfully in concrete.

2.3.5.2 Young's Modulus of Elasticity

Based on the data published by various investigators, there appears to be no significant differences between the Young's modulus of elasticity (E) of concrete with and without silica fume. Malhotra et al. (1985) reported data on the Young's modulus of elasticity of Portland cement–blast-furnace slag–silica-fume concrete. They found no significant difference between the E values obtained at 28 days, regardless of the various percentages of silica fume and water/cementitious materials ratios.

2.3.5.3 Creep

The published data on the creep strain of silica-fume concrete are sparse; Bilodeau et al. (1989) reported an investigation on the mechanical properties, creep, and drying shrinkage of high-strength concretes incorporating fly ash, slag, and silica fume. The cementitious-material content of the concretes was about 530 kg/m³, and the water/cementitious material ratio was 0.22. In addition to the reference concrete, concretes with silica fume at 7 and 12% cement replacements, fly ash at 25% cement replacement, slag at 40% cement replacement, a combination of 7% silica fume and 25% fly ash, and 7% silica fume and 40% slag were investigated. Specimens of these concretes were subjected to creep loading after 35 days of moist curing and an applied stress equivalent to 35% of the compressive strength. After one year, the creep strains of the reference, 7% silica fume, and 12% silica fume concretes were 1505×10^{-6} , 713×10^{-6} , and 836×10^{-6} , respectively. For concrete with 7% silica fume and 40% slag, the creep strain measured was the lowest at 641×10^{-6} . The pore structure and minimal quantity of free water in concrete with the highest amount of supplementary materials could have resulted in these very low creep values, about 40% of the creep of the reference concrete.

2.3.5.4 Permeability

The incorporation of supplementary cementing materials such as fly ash, slag, silica fume, and natural pozzolans in concrete results in fine pore structure and changes to the paste–aggregate interface, leading to a decrease in permeability. This decrease is much higher in concretes incorporating silica fume, due to its high pozzolanicity. The filler and pozzolanic activity of the silica fume, as well as the virtual elimination of bleeding, improve the interfacial zone through pore refinement. Plante and Bilodeau (1989) reported that the addition of 8% silica fume significantly reduced the penetration of chloride ions into concrete. With increasing cementitious materials content and decreasing water/cementitious materials ratios, the chloride-ion penetration was reduced further. At a water/cement + silica fume ratio of 0.21 and 500 kg/m³ cement and 40 kg/m³ silica fume, the chloride-ion penetration was found to be 196 coulombs at 28 days, compared to 1246 C for the reference concrete. This reduction is primarily due to the refined pore structure and increased density of the matrix.

2.3.6 Durability Aspects

2.3.6.1 Carbonation

Silica fume, like other pozzolanic materials, reduces the Ca(OH)₂ content of the concrete, and this promotes a faster rate of carbonation. On the other hand, this effect may be offset by the more impermeable nature of silica-fume concrete, which tends to impede the ingress of CO₂ into concrete. The net effect can be somewhat variable, as it depends on various factors such as silica-fume content, water/cementitious materials ratio, and curing conditions, all of which can have a determinant influence on the ultimate Ca(OH)₂ content and permeability of the concrete. Vennesland and Gjorv (1983) reported that using up to 20% silica fume as an addition to cement in concrete, in combination with the use of a plasticizer, reduced the rate of carbonation. The concrete specimens were initially moist cured for a period of 7 days prior to air storage at 60% relative humidity. Carrette and Malhotra (1992) compared the rate of carbonation of silica-fume concrete with that of reference Portland cement concrete up to the age of 3.5 years. The test specimens had been initially moist cured for 7 days before being stored under ambient room drying conditions. At a water/cementitious materials ratio of 0.25, they found that all concretes remained free of any noticeable carbonation during a 3.5-year period, whereas at a water/cement + silica fume ratio of 0.40, all specimens exhibited signs of carbonation, the effect being slightly more marked for the silica-fume concrete. In general, however, it is agreed that carbonation is not a problem in adequately cured, high-quality, low water/cement ratio concrete, and this also applies to silica-fume concrete.

2.3.6.2 Chemical Resistance

Chemical attack on concrete causes destructive expansion and decomposition of the cement paste, leading to severe deterioration. A permeating solvent as innocuous as water can result in the leaching of calcium hydroxide liberated from the hydration of cement. The ingress of chemicals and acids into concrete allows them to react with calcium hydroxide to form water-soluble salts that leach out of concrete, increasing the permeability of concrete and allowing further ingress of chemicals. Sulfates react with calcium hydroxide, forming ettringite, which causes expansion and cracking of the concrete. Silica-fume concretes have better resistance to chemicals than comparable Portland cement concretes due to the depletion of calcium hydroxide liberated during the hydration of Portland cement by means of pozzolanic reaction with silica fume, which thus reduces the amount of lime available for leaching, and also due to the decrease in permeability resulting from the refined pore structure of the mortar phase of the concrete.

Mehta (1985) compared the chemical resistance of low water/cement ratio (0.33 to 0.35) concretes exposed to solutions of 1% hydrochloric acid, 1% sulfuric acid, 1% lactic acid, 5% acetic acid, 5% ammonium sulfate, and 5% sodium sulfate. Specimens of a reference concrete, latex-modified concrete, and silica-fume concrete with 15% silica fume by weight of cement were used, and the criteria for failure

was 25% weight loss when fully submerged in the above solutions. The investigation showed that concrete incorporating silica fume better resisted chemical attacks than did the other two types of concrete. The only exception was the silica-fume concrete specimens immersed in ammonium sulfate solution which performed poorly. This was attributed to the ability of the ammonium salts to decompose the calcium silicate hydrate in the hydrated cement paste.

2.3.6.3 Freezing and Thawing Resistance

Extensive laboratory and field experience in Canada and the United States has shown that, for satisfactory performance of concrete under repeated cycles of freezing and thawing, the cement paste should be protected by incorporating air bubbles, 10 to 100 μm in size, using an air-entraining admixture. Briefly, the most important parameters concerning the entrainment of air in concrete are the air content, bubble-spacing factor, and specific surface. For satisfactory freezing and thawing resistance, it is recommended that air-entrained concrete should have bubble-spacing factor (\bar{L}) values of less than 200 μm and specific surface (α) greater than 24 mm^{-1} . Usually, fresh Portland cement concrete incorporating between 4 to 7% entrained air by volume will yield the above values of \bar{L} and α .

Several investigators have performed studies on the freezing and thawing resistance of silica-fume concrete. These include, among others, Sorensen (1983), Gjorv (1983), Carette and Malhotra (1983), Malhotra (1984), Yamato et al. (1986), Hooton (1987b), Hammer and Sellevold (1990), Virtanen (1985), Pigeon et al. (1986), and Batrakov et al. (1992). In one CANMET investigation, the freezing and thawing resistance of non-air-entrained and air-entrained concrete incorporating various percentages of silica fume was compared (Malhotra, 1984). The study led to the following conclusions:

- *Non-air-entrained concrete:* Non-air-entrained concrete, regardless of the water/cement + silica fume ratio and irrespective of the amount of condensed silica fume, shows very low durability factors and excessive expansion when tested in accordance with ASTM C 666 (Procedure A or B). The concrete appears to show somewhat increasing distress with increasing amounts of fume; therefore, the use of non-air-entrained condensed silica-fume concrete is not recommended when it is to be subjected to repeated cycles of freezing and thawing.
- *Air-entrained concrete:* Air-entrained concrete, regardless of the water/cement + silica fume ratio and containing up to 15% condensed silica fume as partial replacement for cement, performs satisfactorily when tested in accordance with ASTM C 666 (Procedures A and B). However, concrete incorporating 30% of the fume and a water/cement + silica fume ratio of 0.42 performs very poorly (durability factors less than 10), regardless of the procedure used. This is probably due to the fact that the hardened concrete has high values of \bar{L} , or it might be due to the high amount of condensed silica fume in concrete, resulting in a very dense cement matrix system that, in turn, might adversely affect the movement of water. It is difficult to entrain more than 5% air in the above type of concrete, and this amount of air may or may not provide satisfactory \bar{L} values in hardened concrete for durability purposes. The users are therefore asked to exercise caution when using high percentages of condensed silica fume as replacement for Portland cement in concretes with water/cement + silica fume ratios of the order of 0.40 if these concretes are to be subjected to repeated cycles of freezing and thawing.

2.3.6.4 Frost Resistance in the Presence of Deicing Salts

Limited published data are available on the deicing salt scaling resistance of silica-fume concrete. Gagne et al. (1990) reported that the frost resistance of concrete incorporating 6% silica fume as an addition to cement is satisfactory in the procedure of deicing salt scaling tests (ASTM C 672). This was true for both air-entrained and non-air-entrained concrete. The water/cement + silica fume ratio of the concretes ranged from 0.23 to 0.30, and the concretes were air dried for 28 days before being subjected to the deicing salt scaling test. Using the ASTM C 672 tests, Bilodeau and Carette (1989) investigated the deicing salt scaling resistance of Portland cement concrete and concretes incorporating 8% silica fume

as replacement for cement. In their investigation, superplasticized and nonsuperplasticized concretes were made, with water/cementitious materials ratios ranging from 0.40 to 0.65, all having adequate air-void parameters. They reported that, in general, all concretes performed satisfactorily under the action of deicing salts, although the silica-fume concrete exhibited a slightly inferior performance when compared to that of Portland cement concrete. In particular, silica-fume concrete with a water/cement + silica fume ratio of 0.60 showed appreciable weight loss after 50 cycles.

2.3.6.5 Role of Silica Fume in Reducing Expansion Due to Alkali-Silica Reaction

A number of laboratory investigations have indicated that silica fume, like other pozzolans, is effective in reducing the above-mentioned expansions due to alkali-silica reactions; however, the percentage of silica fume to be incorporated into concrete would depend on the type of reactive aggregate, the exposure conditions, the alkali and silica contents, the silica fume used, the type of cement used, and the water/cementitious materials ratio of the mixture. Published data indicate that the percentage replacement of cement by silica fume may range from about 10 to 15% (Durand, 1991). CANMET-funded studies have indicated that silica fume is not effective in controlling expansions due to alkali-carbonate reactions (Chen and Sunderman, 1990). At present, no significant well-documented data are available as to the long-term effectiveness of silica fume in controlling alkali-silica expansions in actual field structures. Based on current knowledge, it is recommended that those contemplating the use of silica fume to control expansion due to alkali-silica reactions perform accelerated tests in the laboratory, using the materials to be employed on a job site, to determine the percentage of silica fume to be used as replacement for cement.

2.4 Highly Reactive Metakaolin

Highly reactive metakaolin has recently become available as a very active pozzolanic material for use in concrete. Unlike fly ash, slag, or silica fume, this material is not a byproduct but is manufactured from a high-purity kaolin clay by calcination at temperatures in the region of 700 to 800°C (Caldarone et al., 1994). The material, ground to an average particle size of 1 to 2 μm , is white in color. In 1994, a plant was commissioned in Atlanta to produce the material on a commercial scale.

2.4.1 Chemical and Mineralogical Composition

Unlike silica fume, which contains more than 85% SiO_2 , highly reactive metakaolin contains equal proportions of SiO_2 and Al_2O_3 by mass. A typical oxide analysis is given below:

SiO_2	Al_2O_3	Fe_2O_3	CaO	MgO	Alkalis	Loss on Ignition
51	40	1	2	0.1	0.5	2

The highly reactive metakaolin derives its reactivity from the combination of two factors—namely, a totally noncrystalline structure and a high surface area. As far as mineralogical character is concerned, like silica fume, metakaolin is composed essentially of noncrystalline aluminosilicate (Si-Al-O) phase. Occasionally, a small amount of crystalline impurities may be present—that is, 1 to 2% of quartz, feldspar, or titania. The material has a specific surface of about 20 m^2/g and a specific gravity of 2.5.

2.4.2 Properties of Fresh Concrete

According to the limited published data, the initial and final setting time of concrete incorporating 10% of metakaolin by mass are comparable to those of control concrete and concrete incorporating

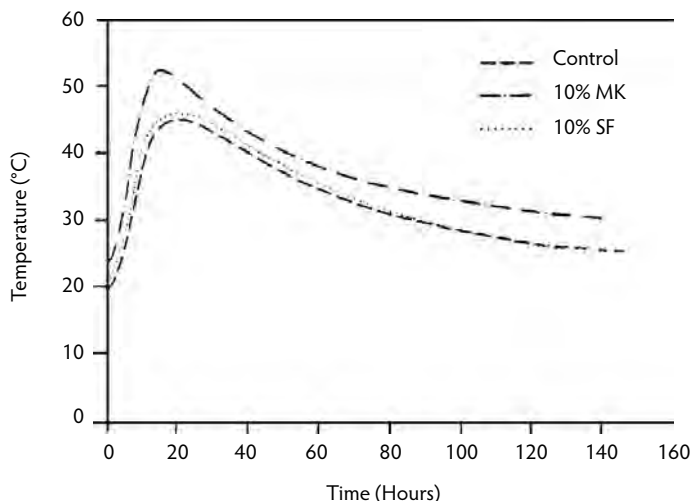


FIGURE 2.16 Autogenous temperature rise in control, silica fume, and metakaolin concretes.

10% silica fume. Also, the air-entraining admixture demand is similar to that of silica-fume concrete. Because of its very high specific surface, the bleeding of concrete incorporating metakaolin is negligible. According to the data published by Zhang and Malhotra (1995), the autogenous temperature rise of concrete made with metakaolin was higher than that of the control and silica-fume concrete at ages up to 6 days, indicating high reactivity of the material (Figure 2.16).

2.4.3 Mechanical Properties of Hardened Concrete

2.4.3.1 Strength Development

Table 2.14 gives some data on strength development and Young's modulus for concrete made with metakaolin; also, data on the control concrete and silica fume are included for comparison purposes. The faster strength development of the metakaolin concrete at early ages as compared with the silica-fume concrete is probably due to the faster rate of hydration, as discussed earlier.

2.4.3.2 Drying Shrinkage

Zhang and Malhotra (1995) investigated the drying shrinkage of concrete incorporating metakaolin; the data are shown in Figure 2.17, together with data for control and silica-fume concrete. The concretes were exposed to drying shrinkage after 7 days of initial curing in lime-saturated water. The metakaolin concrete had a lower drying shrinkage strain compared with that of the control and silica-fume concrete. After 112 days of drying at a relative humidity of 50%, the metakaolin concrete had a drying shrinkage strain of 427×10^{-6} compared with 596×10^{-6} for the control concrete.

2.4.4 Durability Aspects of Hardened Concrete

Air-entrained concrete incorporating 10% metakaolin by mass of cement has high resistance to the penetration of chloride ions and excellent durability in regard to repeated cycles of freezing and thawing. Table 2.15 and Table 2.16 show some test results on these above aspects of durability (Zhang and Malhotra, 1995). Limited data on the deicing salt scaling resistance of the metakaolin concrete indicates that its performance in the ASTM deicing salt scaling test (ASTM C 672) is comparable to that of silica-fume concrete but somewhat inferior to that of plain Portland cement concrete.

TABLE 2.14 Mechanical Properties of Hardened Concrete

Mix	MK Content (%)	Silica Fume Content (%)	W/C or W/(C + MK) or W/(C + SF)	Unit Weight (kg/m ³)	Strength (MPa)							<i>E</i> Modulus (GPa) ^d	
					Compressive ^a			Splitting- Tensile ^b	Flexura ^c				
					1 day	3 days	7 days		28 days	180 days	28 days		28 days
CO	0	0	0.40	2350	20.9	25.5	28.9	36.4	42.5	44.2	2.7	6.3	29.6
MK10	10	—	0.40	2330	25.0	32.9	37.9	39.9	43.0	46.2	3.1	7.4	32.0
SF10	—	10	0.40	2320	23.2	28.6	34.7	44.4	48.0	50.2	2.8	7.0	31.1

^a Average of three 102 × 203-mm cylinders.
^b Average of two 152 × 305-mm cylinders.
^c Average of two 102 × 76 × 406-mm prisms.
^d Average of two 152 × 305-mm cylinders.
Note: MK, metakaolin; W/C, water/cementitious material ratio; SF, silica fume.
Source: Zhang, M.H. and Malhotra, V.M., *Cement Concrete Res.*, 25(8), 1713–1725, 1995.

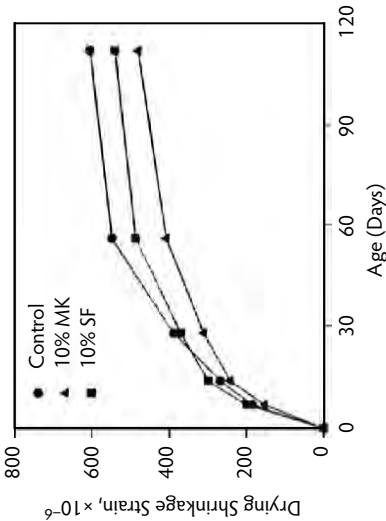


FIGURE 2.17 Drying shrinkage of control silica fume and metakaolin concrete.

TABLE 2.15 Resistance of Concrete to Chloride-Ion Penetration

Mix	Type of Concrete	W/C or W/(C + MK) or W/(C + SF)	Unit Weight (kg/m ³)	28-Day Compressive Strength (MPa)	Resistance to Chloride-Ion Penetration (coulombs)		
					28 Days	90 Days	
CO-D	Control	0.40	2320	36.5	3175	1875	
MK10-D	10% MK	0.40	2330	37.9	390	300	
SF10-D	10% SF	0.40	2310	42.8	410	360	

Note: W/C, water/cementitious materials ratio; MK, metakaolin; SF, silica fume.
Source: Zhang, M.H. and Malhotra, V.M., *Cement Concrete Res.*, 25(8), 1713–1725, 1995.

TABLE 2.16 Summary of Test Results after 300 Cycles of Freezing and Thawing

Mix	Type of Concrete	28-Day Compressive Strength (MPa)	Air Content		Specific Surface (mm ⁻¹)	Spacing Factor L (mm)	Change at the End of 300 Freezing/Thawing Cycles (%)					Durability Factor (%)	Residual Flexural Strength (%)
			Fresh Concrete (%)	Hardened Concrete (%)			W	L	PV	RF			
CO-D	Control	36.5	5.8	6.6	21.2	0.15	0.08	0.006	-0.55	-0.84	98.3	85	
MK10-D	10% MK	37.9	5.1	4.9	17.9	0.22	0.09	-0.003	0	0.16	100.3	89	
SF10-D	10% SF	42.8	5.8	5.0	22.2	0.17	0.12	0.001	0.19	0.47	100.9	96	

Note: L, length; PV, pulse velocity; RF, resonant frequency; W, weight.
Source: Zhang, M.H. and Malhotra, V.M., *Cement Concrete Res.*, 25(8), 1713–1725, 1995.

References

- Abdun-Nur, E.A. 1961. *Fly Ash in Concrete: An Evaluation*, Highway Research Bull. 284. Highway Research Board, Washington, D.C.
- ASTM. 1975. ASTM C 595. In *Annual Book of ASTM Standards*. Part 13. *Standard Specification for Blended Hydraulic Cements*. American Society for Testing and Materials, Philadelphia, PA. pp. 353.
- ASTM. 1978. *ASTM C 618-78: Specification for Fly Ash and Raw or Calcined Natural Pozzolan for Use as a Mineral Admixture in Portland Cement Concrete*. American Society for Testing and Materials, Philadelphia, PA.
- Bache, H.H. 1981. Densified Cement/Ultra-Fine Particle-Based Materials, paper presented at the Second International Conference on Superplasticizers and Other Chemical Admixtures in Concrete, June 10–12, Ottawa, Canada.
- Bakker, R.F.M. 1983. Permeability of blended cement concrete. In *Fly Ash, Silica Fume, Slag and Other Mineral Byproducts in Concrete*, Vol. 1, SP-79, Malhotra, V.M., Ed., pp. 589–605. American Concrete Institute, Farmington Hills, MI.
- Bamforth, P.B. 1980. *In-situ* measurements of the effects of partial Portland cement replacement using fly ash, ground granulated blast furnace slag, on the performance of mass concrete. *Proc. ICE*, 69(Part 2), 777–800.
- Batrakov, V.G., Kaprielov, S.S., and Sheinfeld, A.V. 1992. Influence of different types of silica fume having varying silica content on the microstructure and properties of concrete. In *Proceedings of the 4th International Conference on the Use of Fly Ash, Silica Fume, Slag, and Natural Pozzolans in Concrete*, May 3–8, Istanbul, Turkey, Malhotra, V.M., Ed., pp. 943–963. American Concrete Institute, Farmington Hills, MI.
- Berry, E.E. and Malhotra, V.M. 1978. *Fly Ash for Use in Concrete*. Part II. *A Critical Review of the Effects of Fly Ash on the Properties of Concrete*, Report 78-16. Canada Center for Mineral and Energy Technology (CANMET), Ottawa.
- Bilodeau, A. 1985. *Influence des fumées de silice sur le ressuage et le temps de prise du béton*, Report MRP/MSL 85-22(TR). Canada Center for Mineral and Energy Technology (CANMET), Ottawa, 11 pp.
- Bilodeau, A. and Carette, G.G. 1989. Resistance of condensed silica fume concrete to the combined action of freezing and thawing cycling and deicing salts. In *Fly Ash, Silica Fume, Slag and Natural Pozzolans in Concrete*, Vol. 2, SP-114, Malhotra, V.M., Ed., pp. 945–970. American Concrete Institute, Farmington Hills, MI.
- Bilodeau, A., Carette, G.G., and Malhotra, V.M. 1989. *Mechanical Properties of Non-Air-Entrained, High-Strength Concrete Incorporating Supplementary Cementing Materials*, Report MSL 89-129. Canada Center for Mineral and Energy Technology (CANMET), Ottawa, 30 pp.
- Bilodeau, A., Carette, G.G., Malhotra, V.M., and Langley, W.S. 1991. Influence of curing and drying on salt scaling resistance of fly ash concrete. In *Durability of Concrete, Second International Conference*, Montreal, Canada, Vol. 1, SP-126, Malhotra, V.M., Ed., pp. 201–228. American Concrete Institute, Farmington Hills, MI.
- Bird, C.E. 1969. Corrosion of steel in reinforced concrete in marine atmosphere. In *Concrete Technology*, Fulton, F.S., Ed. Portland Cement Institute, Johannesburg.
- Boubitsas, D. 2004. Long-term performance of concrete incorporating ground granulated blast furnace slag. In *Proceedings of the 8th International Conference on the Use of Fly Ash, Silica Fume, Slag and Natural Pozzolans in Concrete*, SP-221, Malhotra, V.M., Ed., pp. 265–280. American Concrete Institute, Farmington Hills, MI.
- Bureau of Reclamation. 1981. *Concrete Manual*, 8th ed., p. 11. U.S. Bureau of Reclamation, Denver, CO.
- Caldarone, M.A., Gruber, K.A., and Burg, R.G. 1994. High-reactivity metakaolin: a new generation mineral admixture. *ACI Concrete Int.*, 16(11), 37–40.
- Carette, G.G. and Langley, W.S. 1990. Evaluation of deicing salt scaling of fly ash concrete. In *Proceedings of International Workshop on Alkali-Aggregate Reactions in Concrete: Occurrences, Testing and Control*. Canada Center for Mineral and Energy Technology (CANMET), Ottawa.

- Carette, G.G. and Malhotra, V.M. 1983. Mechanical properties, durability and drying shrinkage of Portland cement concrete incorporating silica fume. *ASTM J. Cement, Concrete, Aggregates*, 5(1), 3–13.
- Carette, G.G. and Malhotra, V.M. 1986. *Characterization of Canadian Fly Ashes and Their Relative Performance in Concrete*, Report 86-6E. Canada Center for Mineral and Energy Technology (CANMET), Ottawa.
- Carette, G.G. and Malhotra, V.M. 1992. Long-term strength development of silica fume concrete In *Proceedings of the 4th International Conference on the Use of Fly Ash, Silica Fume, Slag, and Natural Pozzolans in Concrete*, May 3–8, Istanbul, Turkey, Malhotra, V.M., Ed., pp. 1017–1044. American Concrete Institute, Farmington Hills, MI.
- Carrasquillo, P. 1987. Durability of concrete containing fly ash for use in highway applications. In *Concrete Durability: Katharine and Bryant Mather International Conference*, Vol. 1, SP-100, Scanlon, J.M., Ed., pp. 843–861. American Concrete Institute, Farmington Hills, MI.
- Chen, H. and Suderman, R.W. 1990. *The Effectiveness of Canadian Supplementary Cementing Materials in Reducing Alkali-Aggregate Reactivity*, Final Report, DSS Contract No. 0SQ83-00215. Canada Center for Mineral and Energy Technology (CANMET), Ottawa, 245 pp.
- Collepari, M., Collepari, S., Ogoumah Olagot, J.J., and Simonelli, F. 2004. The influence of slag and fly ash on the carbonation of concrete. In *Proceedings of the Eighth CANMET/ACI International Conference on Fly Ash, Silica Fume, Slag and Natural Pozzolans in Concrete*, SP-221, Malhotra, V.M., Ed., pp. 483-494. American Concrete Institute, Farmington Hills, MI.
- Davis, R.E. 1954. *Pozzolanic Materials with Special Reference to Their Use in Concrete Pipe*, Technical Memo. American Concrete Pipe Association, Irving, TX.
- Davis, R.E., Carlson, R.W., Kelly, J.W., and Davis, H.E. 1937. Properties of cements and concretes containing fly ash. *J. Am. Concrete Inst.*, 33, 577–612.
- Detwiler, R.J. and Mehta, P.K. 1989. Chemical and physical effects of silica fume on the mechanical behaviour of concrete. *ACI Mat. J.*, 86(6), 609–614.
- Dikeou, J.T. 1970. *Fly Ash Increases Resistance of Concrete to Sulphate Attack*, Res. Report 23. U.S. Bureau of Reclamation, Denver, CO.
- DIN 1164, Part 1. 1978. *Portland, Einsenportland Hochofen und Trabzement* [Portland, Blast Furnace and Pozzolanic Cements].
- Dunstan, E.R. 1976. *Performance of Lignite and Sub-Bituminous Fly Ash in Concrete: A Progress Report*, Report REC-ERC-76-1. U.S. Bureau of Reclamation, Denver, CO.
- Durand, B. 1991. Preventive measures against alkali-aggregate reactions. In *Course Manual: Petrography and Alkali-Aggregate Reactivity*, pp. 399–489. Canada Center for Mineral and Energy Technology (CANMET), Ottawa.
- Frearsen, J.P.H. 1986. Sulfate resistance of combination of Portland cement and ground granulated blast furnace slag. In *Proceedings of the 2nd International Conference on the Use of Fly Ash, Silica Fume, Slag, and Natural Pozzolans in Concrete*, Vol. 2, SP-91, Malhotra, V.M., Ed., pp. 1495–1524. American Concrete Institute, Farmington Hills, MI.
- Fulton, F.S. 1974. *The Properties of Portland Cement Containing Milled Granulated Blast Furnace Slag*. Portland Cement Institute, Johannesburg.
- Gagne, R., Pigeon, M., and Aitcin, P.C. 1990. *Deicersalt Scaling Resistance of High Performance Concrete*, SP-122. American Concrete Institute, Farmington Hills, MI, pp. 29–44.
- Gebler, S. and Klieger, P. 1983. Effect of fly ash on the air-void stability of concrete. In *Fly Ash, Silica Fume, Slag, and Other Mineral Byproducts in Concrete*, SP-79, Malhotra, V.M., Ed., pp. 103–142. American Concrete Institute, Farmington Hills, MI.
- Gebler, S. and Klieger, P. 1986. Effect of fly ash on physical properties of concrete. In *Proceedings of the 2nd International Conference on the Use of Fly Ash, Silica Fume, Slag, and Natural Pozzolans in Concrete*, Vol. 2, SP-91, Malhotra, V.M., Ed., pp. 1–50. American Concrete Institute, Farmington Hills, MI.
- Ghosh, R.S. and Timusk, J. 1981. Creep of fly ash concrete. *J. Am. Concrete Inst.*, 78, 351–357.

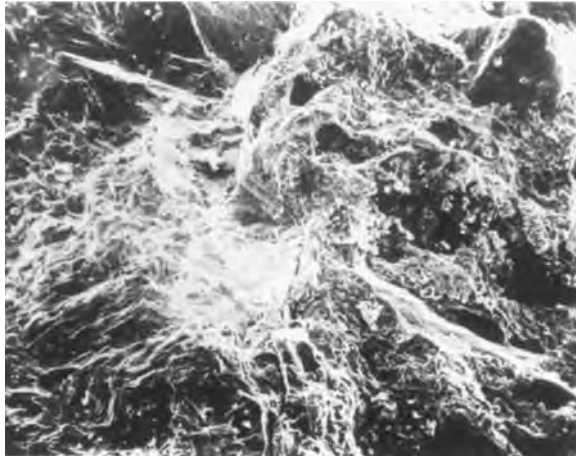
- Gjorv, O.E. 1983. Durability of concrete containing condensed silica fume. In *Fly Ash, Silica Fume, Slag, and Other Mineral Byproducts in Concrete*, SP-79, Malhotra, V.M., Ed., pp. 695–708. American Concrete Institute, Farmington Hills, MI.
- Hale, W.M., Ling, T.A., Bush Jr., T.D., and Russell, B.W. 2004. The use of high-range water-reducers in concrete containing fly ash and ground, granulated blast-furnace slag. In *Proceedings of the 8th International Conference on the Use of Fly Ash, Silica Fume, Slag and Natural Pozzolans in Concrete*, SP-221, Malhotra, V.M., Ed., pp. 217–232. American Concrete Institute, Farmington Hills, MI.
- Hamada, M. 1968. Neutralization (carbonation) of concrete and corrosion of reinforcing steel. In *Proceedings of the 5th International Symposium on the Chemistry of Cement*, Tokyo, Japan, pp. 343–369.
- Hammer, T.A. and Sellevold, E.J. 1990. Frost resistance of high-strength concrete. In *Proceedings of the Second International Symposium on High-Strength Concrete*, SP-121, pp. 457–487. American Concrete Institute, Farmington Hills, MI.
- Hjorth, L. 1982. Silica fumes as additions to concrete. In *Characterization and Performance Prediction of Cement and Concrete, Proceedings of the Second Engineering Foundation Conference*, Henniker, NH, Young, J.E., Ed., p. 165.
- Hogan, F.J. and Meusel, J.W. 1981. The evaluation for durability and strength development of ground granulated blast furnace slag. *ASTM Cement, Concrete, Aggregates*, 3(1), 40–52.
- Hooton, R.D. 1987a. The reactivity and hydration products of blast-furnace slag. In *Supplementary Cementing Materials for Concrete*, Report SP 86-8E, Malhotra, V.M., Ed., pp. 247–330. Canada Center for Mineral and Energy Technology (CANMET), Ottawa.
- Hooton, R.D. 1987b. Some Aspects of Durability with Condensed Silica Fume in Pastes, Mortars, and Concretes, paper presented at International Workshop on Condensed Silica Fume in Concrete, Montreal, May 4–5.
- Jiang, L., Zhang, M.H., and Malhotra, V.M. 2004. Evaluation of test methods for determining the resistance of concrete to chloride-ion penetration. In *Proceedings of the 8th International Conference on the Use of Fly Ash, Silica Fume, Slag and Natural Pozzolans in Concrete*, SP-221, Malhotra, V.M., Ed., pp. 1–28. American Concrete Institute, Farmington Hills, MI.
- Johansen, R. 1980. *Risistendens ved plastisk svinn*, Report STF 65 A80016, FCB/SINTEF. The Norwegian Institute of Technology, Trondheim, Norway.
- Justnes, H., Sellevold, E.J., and Lundevall, G. 1992. High-strength concrete binders. Part A. Reactivity and composition of cement pastes with and without condensed silica fume. In *Fly Ash, Silica Fume, and Natural Pozzolans in Concrete*, SP-132, Malhotra, V.M., Ed., pp. 873–889. American Concrete Institute, Farmington Hills, MI.
- Kalousek, G.L., Porter, L.C., and Benton, E.J. 1972. Concrete for long-term service in sulphate environment. *Cement Concrete Res.*, 2, 79–89.
- Kim, C.S. 1975. Waste and Secondary Product Utilization in Highway Construction, M.S. thesis. McMaster University, Hamilton, Ontario, 256 pp.
- Klieger, P. and Gebler, S. 1987. Fly ash and concrete durability. In *Concrete Durability: Katharine and Bryant Mather International Conference*, Vol. 1, SP-100, Scanlon, J.M., Ed., pp. 1043–1069. American Concrete Institute, Farmington Hills, MI.
- Klieger, P. and Isberner, A. 1967. Laboratory studies of blended cement: Portland blast furnace slag cement. *J. PCA Res. Dev. Lab.*, 9(3), 35.
- Kurgan, G.J., Tepke, D.G., Schokker, A.J., Tikalsky, P.J., and Scheetz, B.E. 2004. The effects of blended cements on concrete porosity, chloride permeability, and resistivity. In *Proceedings of the 8th International Conference on the Use of Fly Ash, Silica Fume, Slag and Natural Pozzolans in Concrete*, SP-221, Malhotra, V.M., Ed., pp. 107–134. American Concrete Institute, Farmington Hills, MI.
- Larson, T.D. 1994. Air entrainment and durability aspects of fly ash concrete. *Proc. Am. Soc. Test. Mater.*, 64, 866–886.
- Lea, F.M. 1970. *The Chemistry of Cement and Concrete*, E. Arnold, Ltd., London.

- Ludwig, U. 1989. Effects of environmental conditions on alkali–aggregate reaction and preventive measures. In *Proceedings of the 8th International Conference on Alkali–Aggregate Reaction in Concrete*, pp. 583–596. Society of Materials Science, Kyoto, Japan.
- Malhotra, V.M. 1979. Strength and durability characteristics of concrete incorporating a pelletized blast furnace slag. In *Fly Ash, Silica Fume, Slag, and Other Mineral Byproducts in Concrete*, SP-79, Malhotra, V.M., Ed., pp. 891–922. American Concrete Institute, Farmington Hills, MI.
- Malhotra, V.M., Ed. 1983a. *Fly Ash, Silica Fume, Slag, and Other Mineral Byproducts in Concrete*, SP-79. American Concrete Institute, Farmington Hills, MI, 1182 pp.
- Malhotra, V.M. 1983b. Strength and durability characteristics of concrete incorporating a pelletized blast furnace slag. In *Fly Ash, Silica Fume, Slag, and Other Mineral Byproducts in Concrete*, Vol. 2, SP-79, Malhotra, V.M., Ed., pp. 892–931. American Concrete Institute, Farmington Hills, MI.
- Malhotra, V.M. 1984. *Mechanical Properties and Freezing and Thawing Resistance of Non-Air-Entrained and Air-Entrained Condensed Silica Fume Concrete Using ASTM Test C 666 Procedure A and B*, Report MRP/MSL 84-153(OP&J). Canada Center for Mineral and Energy Technology (CANMET), Ottawa.
- Malhotra, V.M. and Mehta, P.K. 1996. *Pozzolanic and Cementitious Materials*. Gordon and Breach, Philadelphia, PA.
- Malhotra, V.M. and Ramezaniapour, A.A. 1994. *Fly Ash in Concrete*, Report MSL 94-45(IR). Canada Center for Mineral and Energy Technology (CANMET), Ottawa, 307 pp.
- Malhotra, V.M. and Wallace, G.G. 1993. *A New Method for Determining Fineness of Cement*, Mines Branch Investigation Report 63-119. Canada Center for Mineral and Energy Technology (CANMET), Ottawa.
- Malhotra, V.M., Carette, G.G., and Bremner, T.W. 1980. *Durability of Concrete Containing Granulated Blast Furnace Slag or Fly Ash or Both in Marine Environments*, Report 80-18E. Canada Center for Mineral and Energy Technology (CANMET), Ottawa.
- Malhotra, V.M., Carette, G.G., and Aitcin, P.C. 1985. Mechanical properties of Portland cement concrete incorporating blast furnace slag and condensed silica fume. In *Proceedings of RILEM/ACI Symposium on the Technology of Concrete When Pozzolans, Slags, and Chemical Admixtures Are Used*, Monterey, Mexico, pp. 395–414.
- Malhotra, V.M., Ramachandran, V.S., Feldman, R.F., and Aitcin, P.C. 1987. *Condensed Silica Fume in Concrete*. CRC Press, Boca Raton, FL.
- Malhotra, V.M., Carette, G.G., and Bremner, T.W. 1988. Current status of CANMET's studies on the durability of concrete containing supplementary cementing materials in marine environments. In *Proceedings of the 2nd CANMET/ACI International Conference on Concrete in Marine Environment*, August 21–26, Saint Andrews, New Brunswick, SP-109, Malhotra, V.M., Ed., pp. 31–72. American Concrete Institute, Farmington Hills, MI.
- Malhotra, V.M., Carette, G.G., and Bremner, T.W. 1992. *CANMET Investigations Dealing with the Performance of Concrete Containing Supplementary Cementing Materials at Treat Island, Maine*, Report MSL 744. Canada Center for Mineral and Energy Technology (CANMET), Ottawa.
- Manmohan, D. and Mehta, P.K. 1981. Influence of pozzolanic, slag, and chemical admixtures on pore size distribution and permeability of hardened cement paste. *ASTM Cement, Concrete, Aggregates*, 3(1), 63–67.
- Manz, O.E., McCarthy, G.J., Stevenson, R.J., Dockter, B.A., Hassett, D.G., and Thedchanamoorthy, A. 1989. Characterization and classification of North American lignite fly ashes for use in concrete. In *Proceedings of the 3rd International Conference on the Use of Fly Ash, Silica Fume, Slag, and Natural Pozzolans in Concrete* (supplementary papers), pp. 16–32.
- Mather, B. 1957. Laboratory test of Portland blast furnace slag cements. *J. ACI*, 54(13), 205–232.
- Mather, B. 1965. *Investigation of Portland Blast-Furnace Slag Cement*, Technical Report 6-4555 (supplementary data). U.S. Army Corps of Engineers Waterways Experimental Station, Vicksburg, MS.

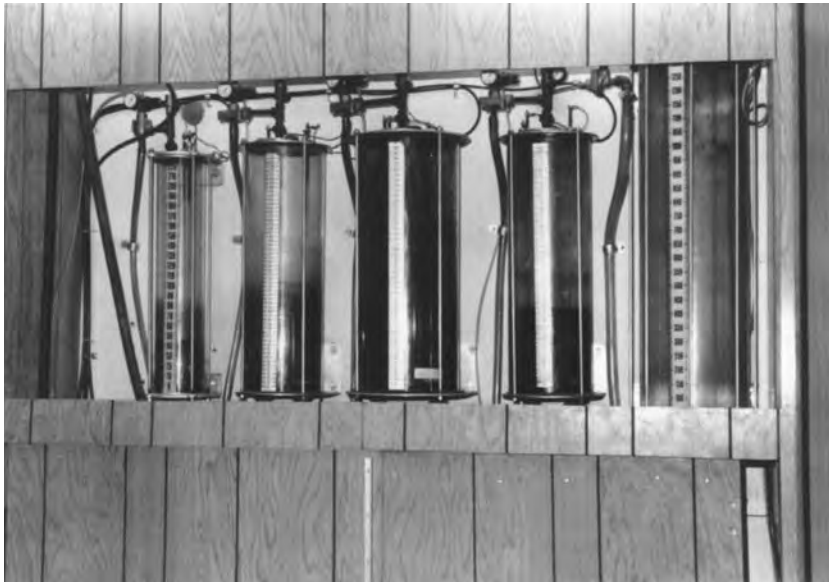
- Mehta, P.K. 1981. Sulfate resistance of blended Portland cements containing pozzolans and granulated blast furnace slag. In *Proceedings of the 5th International Symposium on Concrete Technology*, Monterey, Mexico, Rivera, R., Ed., pp. 35–50.
- Mehta, P.K. 1983. Pozzolanic and cementitious by products as mineral admixtures for concrete: a critical review. In *Fly Ash, Silica Fume, Slag, and Other Mineral Byproducts in Concrete*, Vol. 1, SP-79, Malhotra, V.M., Ed., pp. 1–46. American Concrete Institute, Farmington Hills, MI.
- Mehta, P.K. 1985. Durability of low water-to-cement ratio concretes containing latex or silica fume as admixtures. In *Proceedings of RILEM/ACI Symposium on the Technology of Concrete When Pozzolans, Slags, and Chemical Admixtures Are Used*, Monterey, Mexico, pp. 325–340.
- Mehta, P.K. 1989. Pozzolanic and cementitious by-products in concrete: another look. In *Fly Ash, Silica Fume, Slag and Natural Pozzolans in Concrete*, Vol. 2, SP 114, Malhotra, V.M., Ed., pp. 1–43. American Concrete Institute, Farmington Hills, MI.
- Mehta, P.K. 1994. *Testing and Correlation of Fly Ash Properties with Respect to Pozzolanic Behaviour*, Report CS3314. Electric Power Research Institute, Palo Alto, CA.
- Meusel, J.W. and Rose, J.H. 1979. *Production of Blast Furnace Slag at Sparrows Point and the Workability and Strength Potential of Concrete Incorporating the Slag*, ACI SP-79, Malhotra, V.M., Ed., pp. 867–890. American Concrete Institute, Farmington Hills, MI.
- Meyer, A. 1968. Investigations on the carbonation of concrete. In *Proceedings of the 5th International Symposium on the Chemistry of Cement*, Tokyo, pp. 394–401.
- Monteiro, P.J.M. and Mehta, P.K. 1986. Improvement of the aggregate-cement paste transition zone by grain refinement of hydration products. In *Proceedings of the 8th International Conference on the Chemistry of Cements*, Rio de Janeiro, pp. 433–437.
- Nagataki, S., Ohga, H., and Kim, E.K. 1986. Effect of curing on the carbonation of concrete with fly ash and the corrosion of reinforcement in long-term tests. In *Proceedings of the 2nd International Conference on the Use of Fly Ash, Silica Fume, Slag, and Natural Pozzolans in Concrete*, SP-91, Malhotra, V.M., Ed., pp. 521–540. American Concrete Institute, Farmington Hills, MI.
- Naik, T.R., Singh, S.A., and Hossein, M.M. 1992. *Abrasion Resistance of High-Volume Fly Ash Concrete Systems*. Electric Power Research Institute, Palo Alto, CA.
- Nakamura, N., Sakai, M., Koibuchi, K., and Iijima, Y. 1986. Properties of high strength concrete incorporating very finely ground granulated blast-furnace slag. In *Proceedings of the 2nd International Conference on the Use of Fly Ash, Silica Fume, Slag, and Natural Pozzolans in Concrete*, SP-91, Malhotra, V.M., Ed., pp. 1361–1380. American Concrete Institute, Farmington Hills, MI.
- Nebesar, B. and Carette, G.G. 1986. Variations in the chemical composition, surface area, fineness and pozzolanic activity of a Canadian silica fume. *ASTM Cement, Concrete, Aggregates*, 8(1), 42–46.
- NEN 3550. 1979. *Netherlands Standard for Cement*.
- Neville, A.M. and Brooks, J.J. 1975. Time dependent behaviour of Cemsave concrete. *Concrete*, 9(3), 36–39.
- Owens, P.L. 1979. Fly ash and its usage in concrete. *Concrete J. Concrete Soc.*, 13, 21–26.
- Pierce, J.S. 1982. Use of fly ash in combating sulphate attack in concrete. In *Proceedings of the 6th International Symposium on Fly Ash Utilization*, DOE/METC/82-52, pp. 208–231. U.S. Department of the Environment, Washington, D.C.
- Pigeon, M., Pleau, R., and Aitcin, P.C. 1986. Freeze–thaw durability of concrete with and without silica fume in ASTM C666 (Procedure A) test method: internal cracking versus scaling. *ASTM J. Cement, Concrete, Aggregates*, 8(2), 76–85.
- Pistilli, N.F., Rau, G., and Cechner, R. 1984. The variability of condensed silica fume from a Canadian source and its influence on the properties of Portland cement concrete. *ASTM J. Cement, Concrete, Aggregates*, 6(2), 120–124.
- Plante, P. and Bilodeau, A. 1989. Rapid chloride ion permeability test data on concretes incorporating supplementary cementing materials. In *Fly Ash, Silica Fume, Slag and Natural Pozzolans in Concrete*, Vol. 1, SP-114, Malhotra, V.M., Ed., pp. 625–644. American Concrete Institute, Farmington Hills, MI.

- Poole, A.B. 1981. Alkali-Carbonate Reactions in Concrete, paper presented at the 5th International Conference on Alkali-Aggregate Reaction in Concrete, March 30–April 3, Cape Town, South Africa.
- Radlinski, M., Olek, J., and Nantung, T.E. 2004. Evaluation of Transport Properties of Ternary (OPC/FA/SF) Concrete Mixtures Using Migration and Absorption-Type Tests. In *Proceedings of the 8th International Conference on the Use of Fly Ash, Silica Fume, Slag and Natural Pozzolans in Concrete*, SP-221, Malhotra, V.M., Ed., pp. 481–496. American Concrete Institute, Farmington Hills, MI.
- Regourd, M. 1980. Structure and behaviour of slag Portland cement hydrates. In *Proceedings of the 7th International Congress on the Chemistry of Cement*, Paris, Vol. I, Thème III-2, pp. 10–26.
- Regourd, M., Hornain, H., and Montureux, B. 1977. Résistance à l'eau de mer des ciments au laitiers. *Silicates Indust.*, 1, 19–27.
- RILEM Technical Committee 12-CRC. 1974. Corrosion of reinforcement and prestressing tendons: a state of the art report. *Matér. Const.*, 9, 187–206.
- Sagawa, Y., Matsushita, H., Maeda, Y., Chikada, T., and Kaneyasu, S. 2004. Influence of blast furnace slag on durability of high-strength concrete. In *Proceedings of the 8th International Conference on the Use of Fly Ash, Silica Fume, Slag and Natural Pozzolans in Concrete*, SP-221, Malhotra, V.M., Ed., pp. 703–720. American Concrete Institute, Farmington Hills, MI.
- Schröder, F. and Smolczyk, H.G. 1968. Carbonation and protection from steel corrosion. In *Proceedings of the 5th International Symposium on the Chemistry of Cement*, Tokyo, pp. 188–191.
- Sellevold, E.J. 1984. Review: *Microsilica in Concrete*, Project Report No. 08037-EJS TJJ. Norwegian Building Research Institute, Oslo, Norway.
- Sellevold, E.J. and Justnes, H. 1992. *High-Strength Concrete Binders*. Part B. *Non-Evaporable Water, Self-Desiccation and Porosity of Cement Pastes With and Without Condensed Silica Fume*, ACI SP-132, Malhotra, V.M., Ed., pp. 891–902. American Concrete Institute, Farmington Hills, MI.
- Sellevold, E.J. and Nilsen, T. 1987. Condensed silica fume in concrete: a world review. In *Supplementary Cementing Materials for Concrete*, Report SP 86-8E. Malhotra, V.M., Ed., pp. 167–229. Canada Center for Mineral and Energy Technology (CANMET), Ottawa.
- Short, N.R. and Page, C.L. 1982. The diffusion of chloride ions through Portland and blended cement pastes. *Silicates Indust.*, 47, 237–240.
- Smolczyk, H.G. 1974. Slag cements and alkali-reactive aggregates. In *Proceedings of the 6th International Congress on the Chemistry of Cement* (supplementary papers), Moscow, Section III.
- Smolczyk, H.G. 1975. Investigation on the Diffusion of Na Ion in Concrete, paper presented at Symposium on Alkali-Aggregate Reaction, Reykjavik.
- Sorensen, E.V. 1983. Freezing and thawing resistance of condensed silica fume (microsilica) concrete exposed to deicing salts. In *Fly Ash, Silica Fume, Slag, and Other Mineral Byproducts in Concrete*, SP-79, Malhotra, V.M., Ed., pp. 709–718. American Concrete Institute, Farmington Hills, MI.
- Stanton, T.E. 1940. Expansion of concrete through reaction between cement and aggregate. *Proc. Am. Soc. Civ. Eng.*, 66, 1781.
- Stutterheim, N. 1960. Properties and uses of high-magnesia Portland slag cement concretes. *J. ACI*, 31(10), 1027–1045.
- Swenson, E.G. and Gillott, J.E. 1960. *Characteristics of Kingston Carbonate Rock Reaction*, Bull. 275. Highway Research Board, Washington, D.C.
- Vennesland, O. and Gjorv, O.E. 1983. Silica concrete: protection against corrosion of embedded steel. In *Fly Ash, Silica Fume, Slag, and Other Mineral Byproducts in Concrete*, SP-79, Malhotra, V.M., Ed., pp. 719–729. American Concrete Institute, Farmington Hills, MI.
- Virtanen, J. 1985. *Mineral Byproducts and Freeze-Thaw Resistance of Concrete*, Publ. No. 22:85. Dansk Betonforening, Copenhagen, Denmark, pp. 231–251.
- Wiebenga, J.G. 1980. Durability of concrete structures along the North sea coast of the Netherlands. In *Performance of Concrete in Marine Environment*, SP-65, Malhotra, V.M., Ed., pp. 437–452. American Concrete Institute, Farmington Hills, MI.

- Williams, J.T. and Owens, P.L. 1982. The implications of a selected grade of United Kingdom pulverized fuel ash on the engineering design and use in structural concrete. In *Proceedings of International Symposium on the Use of PFA in Concrete*, Cabrera, J.G. and Cusens, A.R., Eds., pp. 301–313. Department of Civil Engineering, University of Leeds, Leeds, U.K.
- Yamato, T., Emoto, Y., and Soeda, M. 1986. Strength and freezing and thawing resistance of concrete incorporating condensed silica fume. In *Proceedings of the 2nd International Conference on the Use of Fly Ash, Silica Fume, Slag, and Natural Pozzolans in Concrete*, SP-91, Malhotra, V.M., Ed., pp. 1095–1117. American Concrete Institute, Farmington Hills, MI.
- Yuan, R.L. and Cook, J.E. 1983. Study of a Class C fly ash concrete. In *Fly Ash, Silica Fume, Slag, and Other Mineral Byproducts in Concrete*, SP-79, Malhotra, V.M., Ed., pp. 307–319. American Concrete Institute, Farmington Hills, MI.
- Zhang, M.H. and Malhotra, V. M. 1995. Characteristics of a thermally activated alumina-silicate pozzolanic material and its use in concrete. *Cement Concrete Res.*, 25(8), 1713–1725.



(a)



(b)

(a) Scanning electron micrograph of a polymer concrete fracture surface. (Photograph courtesy of Edward G. Nawy, Rutgers University.) (b) Chemical admixtures analysis. (Photograph courtesy of Portland Cement Association, Skokie, IL.)

3

Chemical Admixtures

David P. Whitney*

3.1	Introduction to Chemical Admixtures	3-1
3.2	Retarding Admixtures	3-2
3.3	Water-Reducing Admixtures	3-3
3.4	High-Range, Water-Reducing Admixtures	3-5
3.5	Accelerating Admixtures.....	3-7
	Accelerating Corrosion-Inhibiting Admixtures	
3.6	Air-Entraining Admixtures.....	3-10
3.7	Antifreezing Admixtures.....	3-12
3.8	Antiwashout Admixtures	3-13
3.9	Shrinkage-Reducing Admixtures.....	3-14
3.10	Polymer Modifier Admixtures.....	3-14
3.11	Alkali-Silica Reaction Prevention Admixtures.....	3-18
3.12	Conclusion	3-18
	References	3-18

3.1 Introduction to Chemical Admixtures

In recent decades, tremendous success has been achieved in the advancement of chemical admixtures for Portland cement concrete. Materials scientists, chemists, engineers, and manufacturers' technical representatives have helped the concrete industry to improve our ability to control work times, workability, strength, and durability of Portland cement concrete. Most efforts have centered on improving the properties of concrete with minimal investments by ready-mix suppliers and contractors in the way of specialized equipment or special skills and education of their labor forces. This approach has resulted in construction cost reductions and universally accepted ready-made remedies for unexpected problems during construction.

The function of each admixture focuses on a specific need, and each has been developed independently of the others. Some admixtures already have chemistry that affects more than one property of concrete, and some have simply been combined for ease of addition during the batching process. Their definitions and specifications are discussed in the American Society for Testing and Materials (ASTM) C 494 and in the American Concrete Institute (ACI) *Manual of Concrete Practice* 212.3R and 212.4R. Retarders have been developed that allow for longer working times with minimal effect on the final cure strength. These retarders provide better finishing and higher quality concrete in the heat of the summer. Accelerators have been produced that initiate the cement hydration process much earlier in lower temperatures. Air-entraining agents were developed into commercial admixtures when it was observed that air entrainment

* Research Operations Manager, Research Engineer, Construction Materials Research Group, The University of Texas at Austin; expert in construction materials with emphasis on concrete durability, polymers, and other additives.

improved the resistance of concrete to freezing and thawing. This is accomplished by the production of many well-distributed tiny bubbles that act as pressure-relief mechanisms in the matrix whenever water in the pores expands and contracts under freezing and near-freezing conditions.

Water reducers, or plasticizers, have allowed finishers to place and work the concrete with much less water and thus produce higher strengths and more durable concrete. High-range water reducers (HRWRs), or superplasticizers, were developed to adjust the plasticity of low-water concrete to a consistency that can easily be pumped up to higher elevations without compromising strength or durability. Later, organic polymers such as latex and epoxies were developed to modify the concrete matrix in such a way as to improve the bond of the cured concrete to a given substrate or to reduce permeability and internally reinforce the cured matrix. Often, a stronger matrix is also a result. Monomer systems have also been used to impregnate cured Portland cement concrete, filling the small pores, capillaries, and voids with a liquid that quickly hardens, leaving a less porous, higher modulus, and more chemical-resistant concrete.

All of these admixtures have been refined to provide concrete designers and builders with increasing options and greater adaptability to an expanding variety of applications and ambient conditions. It is estimated that one or more chemical admixtures, not including air-entraining agents, are present in 80% of the concrete placed today, and the figure rises to almost 100% when air-entraining agents are included (Whiting et al., 1994).

The most commercially important chemical admixtures are described in the *ACI Manual of Concrete Practice* (ACI Committee 212 on Admixtures for Concrete) and ASTM C 494 (Specifications for Chemical Admixtures for Concrete); in the Canadian Standards Association's admixture standards A 266.1, A 266.2 M78 (chemical admixtures), A 266.4 M78 (guidelines for the use of admixtures), 266.5 M 1981 (guidelines for use of HRWRs), and 266.6 M85 (HRWR requirements); and in the Reunion Internationale des Laboratoires d'Essais et de Recherches sur les Matériaux et les Constructions (RILEM) *Guide for Use of Admixtures in Concrete*. To better understand recommended usage for various applications of these chemical admixtures in concrete, a review of each functional category is presented. This review would be simpler if each of the admixtures worked independently in the matrix, but the performance of each is often affected by the presence of another. For this reason, known reactions and interactions are discussed wherever appropriate for specific materials.

3.2 Retarding Admixtures

Retarding admixtures are used to slow down the initial set of the concrete whenever elevated ambient temperatures shorten working times beyond the practical limitations of normal placement and finishing operations. Retarders are specified in ASTM C 494 as Type B admixtures and are used in varying proportions, often in combination with other admixtures, so that, as working temperatures increase, higher doses of the admixture may be used to obtain a uniform setting time (ACI 305R). Simple retarders typically consist of one of four relatively inexpensive materials: lignin, borax, sugars, or tartaric acids or salts. Retarders serve best to compensate for unwanted accelerations of working times due to changes in temperature or cement or due to other admixture side effects. They also are used to extend the working time required for complicated or high-volume placements and for retarding the set of concrete at a surface where an exposed aggregate finish is desired.

Retarding admixtures interfere with the critical chemical reactions of the fastest hydrating cement reactant groups, C_3A and C_3S (Colleparidi, 1984). These reactants normally initiate the hydration process in the early stages. Eventually, the hydration process accelerates due to another initially slower reaction group, and the heat of reaction allows the hydration to continue at a normal rate until completion. Typical retardation effects are significant for the first 24 to 72 hours.

The intent is for concrete in its plastic state to be affected by retarders with little or no negative effect on the hardened properties. Improvements in fresh concrete properties include extended times for workability and set, better workability with less water, frequently an increase in air content, and minimal

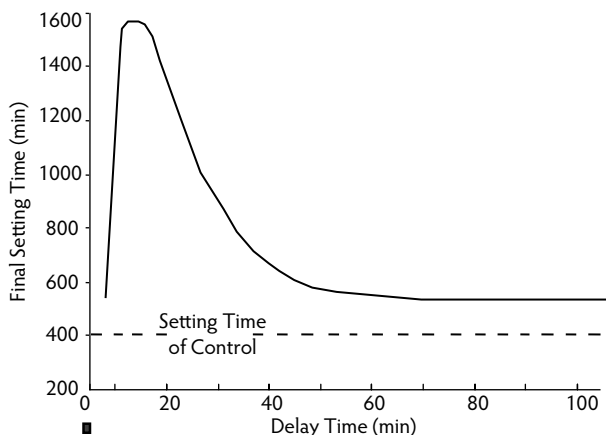


FIGURE 3.1 Effect of delayed addition of retarding admixture on its retarding power. (From Mindess, S. and Young, J.F., *Concrete*, Prentice Hall, Englewood Cliffs, NJ, 1981.)

delay in final cure time. Retarders may reduce critical physical properties when used in excess. Changes in hardened concrete properties due to retarders usually relate to delayed early strength development, which may affect early (especially plastic) shrinkage and creep (Daugherty and Kowalewski, 1976).

Dosage rates vary considerably depending on the needs of the concrete application, ambient and material temperatures, retarder type and concentration, cement type and content, and presence of other admixtures in the concrete, but it generally is best to use the least amount necessary to produce the required properties. This is typically between 2 and 7 fluid ounces per 100 pounds cement (ACI 211.1-4) added with a portion of the mixing water a few minutes after the first addition of water. This is recommended to ensure the most efficient and uniform dispersion throughout the batch (Figure 3.1). Manufacturers' recommendations are a good place to start, but trial batches under the expected field conditions followed by a complete evaluation of effects on all critical properties should be conducted.

It should be noted that retardation may be a side effect of other chemical admixtures that are specified for the adjustment of other properties in the matrix. If the retardation effect is desirable and predictable, as in many water-reducing admixtures, the material is marketed as such (e.g., water-reducing and -retarding admixtures). Because users noticed that earlier water reducers tended to retard set times, today many retarders are meant to serve double duty as water reducers. This added functionality is discussed in the next section. If the retardation side effect is predictable but not desired, the simple addition of a compatible accelerator may be all that is necessary. If, however, the retardation side effect is not desired or predictable, an incompatibility may exist between the cement or other admixtures and the corrupting admixture (Dodson and Hayden, 1989; Johnston, 1987). Every effort must be made to determine the faulty ingredient and substitute it with a more compatible choice.

3.3 Water-Reducing Admixtures

Water-reducing agents, or plasticizers, are added to provide workability in the freshly mixed concrete matrix while using significantly lower amounts of mix water, thus achieving better strength and durability. These agents provide the lubricity in coarse mixes that would normally require additional paste or more water in the paste. According to ASTM C 494, these admixtures are classified as Type A and must allow at least a 5% reduction in water without changing the consistency or reducing the strength of the control batch having the higher water content without this admixture. They often are able to reduce the water demand by 10% and as much as 15% for even greater strength and durability benefits derived from lowering the water/cement ratio (Figure 3.2). This class of admixtures is typically made from relatively inexpensive lignosulfonates, hydroxylated carboxylic acids, or carbohydrates.

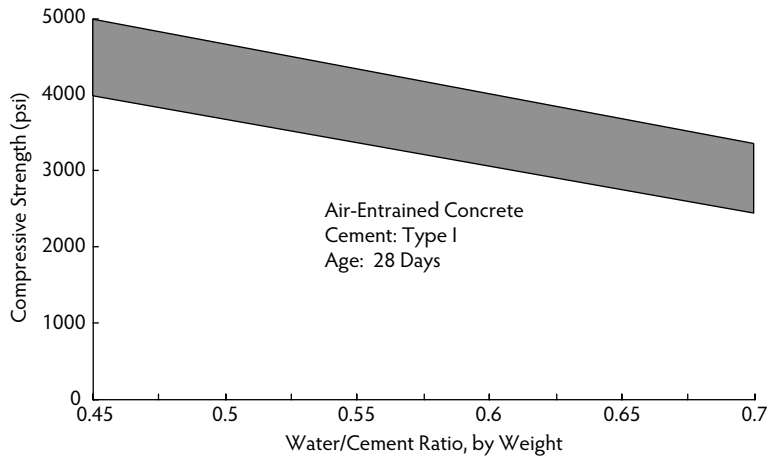


FIGURE 3.2 Typical relationship between 28-day compressive strength and water/cement ratio for a wide variety of air-entrained concretes using Type I cement. (From Kosmatka, S.H. and Panarese, W.C., *Design and Control of Concrete Mixtures*, 13th ed., Portland Cement Association, Skokie, IL, 1988.)

Several theories exist as to what mechanisms are responsible for the reduction in water demand in the plastic concrete matrix, but all agree that the improvement is mainly due to the chemical and physical effects of the water-reducing admixtures (WRAs) on the surface of the hydrating cement particles. Deflocculating and dispersion of the cement particles are the net result and allow better use of the available water for more uniform lubrication and hydration. Also, because many WRAs entrain as much as 2% air, increased lubricity is partly due to the distribution of tiny added air bubbles.

Many WRAs retard set times and are sometimes used with an accelerator for compensation. WRAs that are combined with an accelerator into one admixture are classified as Type E under ASTM C 494. Of course, retardation may be desired for higher temperature concreting conditions. Whenever the natural tendency of WRAs to retard hydration is not adequate for the desired application, additional retarders are added. Commercially available single admixtures that combine a retarder with the WRA are classified as Type D under ASTM C 494.

Many WRAs are associated with higher shrinkage rates and faster slump loss even though the water/cement ratio is reduced. Bleeding properties, too, are sometimes affected by the choice of WRA. To overcome these tendencies WRAs are often added at the batch plant along with much less of the more expensive, but more efficient, high-range (or mid-range) water reducers described in the next section.

Considerations for usage of WRAs are economically based, and strategies fall into the following three main categories (Collepari, 1984):

1. Reduce the water/cement ratio for higher strengths and improved durability while maintaining the same workability and cement content.
2. Reduce the paste portion of the matrix, water, and cement, for the purpose of reducing shrinkage and heat development in massive placements; workability, strength, and durability are maintained at a comparative level.
3. Keep water and cement the same and maintain the same strength and durability but improve flow and workability.

Efficient dosage rates vary with chemical composition of the WRA, individual batch designs, cement types, other admixtures, environmental conditions (Kosmatka and Panarese, 1988), flow and workability constraints in the job, and end-product needs. Manufacturers' guidelines typically recommend 2 to 7 fluid ounces per 100 pounds cement added into the mix water. These recommendations should be used as a starting place for several trial batches closely monitored for critical properties under field conditions in both the fresh and hardened states.

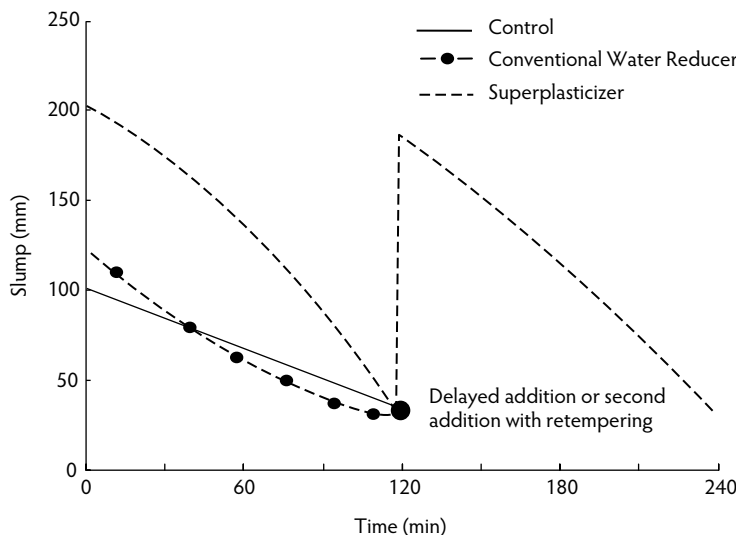


FIGURE 3.3 Effect of superplasticizers on slump loss. (From Mindess, S. and Young, J.F., *Concrete*, Prentice Hall, Englewood Cliffs, NJ, 1981.)

3.4 High-Range, Water-Reducing Admixtures

High-range water reducers (HRWRs) are also known as superplasticizers, super fluidizers, and super water reducers due to their higher efficiency than conventional WRAs in improving workability and flow of concrete mixes. They were developed for use where the amount of WRAs required to reach a desired slump or flow resulted in unacceptable reductions of other critical properties. Different chemistry enabled developers to produce an admixture that allowed contractors to place highly workable, pumpable, or even flowing concrete with higher strengths and greater durability and less shrinkage when the concrete mix was properly designed. The specifications for superplasticizers are detailed in ASTM C 494 as Type F for high-range water reduction with normal set times or Type G for high-range water reduction with retarded setting times. ASTM C 1017 specifies chemical admixtures for use in flowing concrete. HRWRs are typically one of four chemical groups: sulfonated melamine–formaldehyde condensate (SMF), sulfonated naphthalene–formaldehyde condensate (SNF), modified lignosulfonate (MLS), and others that may include sulfonic acid esters or carbohydrate esters (carboxylates). HRWRs deflocculate and disperse the cement particles in a similar manner but much more efficiently than WRAs. Superplasticizers can reduce water demand in the matrix by as much as 30%, and, because HRWRs can be added into the transit mixer at the plant and again at the jobsite, workability can continue to be customized at the site for specific application needs regardless of transit-time slump loss (Fisher, 1994) (Figure 3.3). HRWRs are often referred to as first-, second-, and third-generation superplasticizers:

1. First-generation superplasticizers are primarily anionic materials that create negative charges on the cement particles, resulting in reduced friction due to the same-charge particles repelling each other. These HRWRs have no effect on the hydration process, but using them to reduce water/cement ratios without the addition of retarders makes for quicker set times. Because of the shorter workability times, first-generation HRWRs are normally added at the jobsite. Their chemistry allows a reduction in water of 20 to 30%.
2. Second-generation superplasticizers, which are normally added at the batch plant, coat the cement particles with a thixotropic material; they lubricate the mix, allow lower water/cement ratios, and add a measure of control in the hydration process. Second-generation HRWRs can be used at higher concrete temperatures, thus reducing or eliminating the need for ice. Water demand is typically reduced 20 to 30%, and the higher workability time is extended.

3. Third-generation superplasticizers coat the cement particles and are added at the batch plant, just like the second-generation HRWRs. Third-generation superplasticizers offer the same advantages as second-generation HRWRs, plus they offer the added bonus of maintaining initial setting characteristics similar to normal concrete while producing a highly plastic mix at an extremely low water/cement ratio. Second-generation and third-generation superplasticizers are relatively expensive (typically \$5 to \$6 additional per yard of concrete), but they have proven themselves to be cost effective in such applications as hot weather concreting, wall placements, bucket and crane placements, slabs on grade, and pumped concrete (Guennewig, 1993). Modern trends are clearly moving toward the use of polycarboxylates over the older sulfonated lignins or melamine-based products, as they are so much more effective at deflocculating cement grains due to steric hindrance.

Strategies for the use of HRWRs include those listed in the WRA section above, but application-related considerations may dictate that HRWRs must be used and require decisions of which type and quantity are required to achieve the proper concrete placement. Determining optimal superplasticizer dosage can be a relatively complex task involving consideration of costs, rheology of the fresh concrete, mechanical properties at early ages, and long-term durability under expected service conditions. Optimal dosage is highly dependent on determination of the saturation concentration—the highest ratio of the mass of HRWR solids to the mass of cementitious materials over which any higher dosage will not significantly improve the workability of the paste (Gagné et al., 1996). This ratio is usually 0.8 to 1.2% and is affected by type and quality of superplasticizer, fineness of the cement, C_3A content, type and content of sulfates, and the speed and shearing action of the mixer employed (Baalbaki, 1990).

The ability of superplasticized concrete to flow through congested reinforcement and into otherwise inaccessible areas and a requirement for minimal vibration make it a natural choice in any applications presenting such problems. The ease with which it can be pumped and placed makes it a good choice for floors, structural and foundation slabs, pavements, bridges, and roof decks. Contractors and precasters prefer superplasticized concrete for its faster strength gain, improved surface details, and pigment dispersion in architectural applications. HRWRs are used in sprayed concrete applications, self-consolidating concrete, and tremie pipe placements because of the increased fluidity and higher strengths. High-performance concrete has been implemented primarily through the engineered concrete mix designs made possible by using HRWRs to reduce water/cement ratios and by adding high-surface fine materials such as silica fume and fly ash while maintaining good workability and minimal segregation. Consequently, higher and earlier strengths and increased durability are commonly expected and achieved.

Regular reporting of successful concrete applications relying on HRWRs has led to a tendency to think of HRWRs as a panacea for all concrete problems; however, good batch designs that consider the level of HRWRs to be added are critically important to avoid serious segregation, excessive bleeding, and needless extra expense. Normal mixes made flowable through the addition of HRWRs typically require an increase of approximately 5% more sand. Surface finishes can become mottled and irregular when too much HRWR is used. Water/cement ratios are critical to strength and durability, but, for even minimal workability and accounting for evaporation and substrate absorption, the practical lower water/cement ratio limits of concrete mixtures without HRWRs are well above the theoretical minimum required for complete hydration. Because HRWRs allow concrete to be made with the lowest water/cement ratios, care must be exercised to ensure that enough water is present in the matrix throughout the entire hydration process to fully hydrate all of the cement in the matrix.

As for WRAs, HRWRs tend to retard concrete setting times, but this effect may be compensated for or overridden by the addition of accelerating admixtures or the further addition of retarding admixtures. When a retarder is combined with a superplasticizer, the resulting admixture is classified by ASTM C 494 as Type G.

Slump loss is a problem of particular importance in high-slump or flowable concretes utilizing HRWRs. The rate of slump loss may be affected by the type and dosage of HRWR, other admixtures, order of addition, type and brand of cement, concrete temperature, and concrete batch design. Concrete that has

HRWRs added at the batch plant will tend to experience moderate to rapid slump loss, unless special slump-loss-control admixtures are also added. Normally, the higher dosage rates tend to slow down the rate of slump loss, and cement with higher levels of C_3A , as found in Type I and Type III cements, exhibit a more rapid rate of slump loss. Higher concrete temperatures also tend to accelerate the rate of slump loss (ACI Committee 212), but adherence to ACI Committee 305 hot-weather concreting procedures can minimize slump loss.

Entrained air content is initially increased by the addition of HRWRs, but redoing flowing concrete causes loss of entrainment with each dose. Also, air bubbles may have a tendency to be larger and coalesce in flowing concrete. Shrinkage and creep are generally as good as or better than control mixes, but flowing concrete may exhibit more shrinkage depending on water and cement content and the choice of HRWRs. Durability is generally better for concrete modified with HRWRs because strength is higher, cement particles are more uniformly dispersed and hydrated, and permeability of the hardened concrete is lower. Resistance to sulfate attack and abrasion should be better, and resistance to salt scaling and resistance to corrosion of reinforcing steel are comparable with control batches containing no superplasticizer (ACI Committee 212). As always, evaluation of trial batches cured under field conditions is highly recommended.

3.5 Accelerating Admixtures

Accelerators are commonly used to offset retardation effects from other admixtures, although overcoming weather-induced retardation due to colder temperatures at the job site is probably their primary application. Through the use of accelerators contractors can place concrete at much lower temperatures than would be practical without their use (ACI 306R). Accelerating admixtures are also commonly used to speed up normal set and cure times for purposes of earlier service than would be possible with an unaccelerated mix design. Such an application is most often the case for concrete repair mix designs and in prestressed or precast applications, where time delays cost customers or precasters significant amounts of money and inconvenience.

Accelerating admixtures should conform to ASTM C 494 Type C. These materials are predominantly calcium chloride or closely related salts because of their availability, relatively low costs, and more than a century of documented usage. Caution should be exercised, however, as the use of chloride accelerators will corrode reinforcement in concrete exposed to water. Other materials such as silicates, fluorosilicates, thiocyanates, alkali hydroxides, calcium formate, calcium nitrate, calcium thiosulfate, potassium carbonate, sodium chloride, aluminum chloride, and various organic compounds, including triethanolamine, are also used as accelerating admixtures (ACI 517.2R). Calcium nitrite is frequently recommended and commercially available as an accelerator that also inhibits corrosion of reinforcing steel wherever exposure to precipitation and salt from deicing materials or seawater is likely to initiate corrosion problems. Lignosulfonate, benzoates, phosphates, hypophosphates, chromates, fluorides, Calgon®, and alkali nitrates have also been promoted as corrosion inhibitors, too, but their effectiveness is not widely accepted.

Because of the long-term usage of calcium-chloride-based accelerating admixtures, many of their effects on concrete are well known and highly touted in manufacturers' literature. They should conform to ASTM D 98 requirements and be sampled and tested according to the procedures in ASTM D 345. Calcium chlorides are known to reduce initial and final setting times. The workability of the mix is usually improved by accelerators, and the air content of the matrix may be increased slightly with average-sized voids (Figure 3.4). Accelerators also tend to reduce the bleeding rate and bleeding capacity of concrete.

The effects of accelerators on hardened concrete are as important as they are for the fresh mix. Benefits of their use include accelerated strength development in both compression and in flexural modes, although less so in the latter. Modulus of elasticity, too, increases at a faster rate. Abrasion resistance and erosion resistance are improved with the use of accelerating admixtures, as is pore structure, due to reduced porosity. Frost resistance in concrete is better at early ages when calcium chloride accelerators are used, but performance declines with time, and resistance is actually worse at later ages. Other

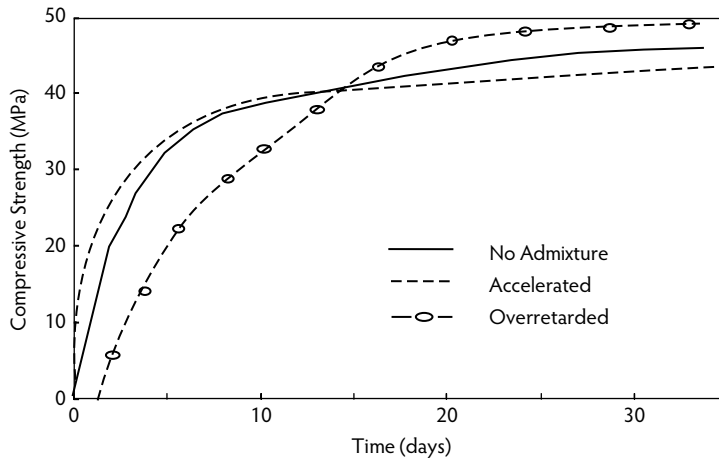


FIGURE 3.4 Effect of set-modifying admixtures on strength development of concrete. (From Mindess, S. and Young, J.F., *Concrete*, Prentice Hall, Englewood Cliffs, NJ, 1981.)

disadvantages of using common calcium chloride accelerating admixtures in concrete include slight increases in drying shrinkage and creep increases from 20 to 35%, all of which may occur because rapid strength gain is usually obtained at the expense of reduced ultimate strength (Figure 3.4). Accelerators also often increase alkali-silica reactions and decrease resistance to external sulfate attack. Additionally, they are known to increase the rate of freeze-thaw scaling and of corrosion of steel reinforcement, except for those previously mentioned accelerating admixtures known as corrosion inhibitors (i.e., calcium nitrite and sodium thiocyanate) (Nmai et al., 1994). Accelerated concrete is also usually darker in color than unaccelerated concrete.

With these effects on properties in mind, the Portland Cement Association (PCA) recommends that calcium chloride and other admixtures containing soluble chlorides should not be used under the following conditions:

- Prestressed concrete, due to potential corrosion hazards
- Concrete containing embedded aluminum, due to serious corrosion problems in humid environments
- Concrete subjected to alkali-silica reactions or exposed to soil or water containing sulfates
- Floor slabs intended to receive dry-shake metallic finishes
- Hot ambient conditions or hot constituent materials such as aggregates or water
- Massive concrete placements

The PCA also recommends caution when using calcium chloride in the following applications (Kosmatka and Panarese, 1988):

- Concrete subjected to steam curing because of possible expansion problems with delayed ettringite formation
- Concrete containing embedded dissimilar metals, especially when electrically connected to reinforcing steel
- Concrete slabs supported on galvanized steel forms

The ACI 318 Committee on Building Code Requirements for Reinforced Concrete has recommended maximum allowable levels of chloride ions for corrosion protection in steel reinforced concrete under various service exposures. These levels are shown in Table 3.1. In spite of the cautions, calcium chlorides are used on a regular basis for interior concrete with predictable performance. Recommended usage rates vary with mixture designs, temperatures, and exposure conditions. As with any admixture,

TABLE 3.1 ACI 318 Maximum Chloride-Ion Content for Corrosion Protection (ACI 318/318R Building Code and Commentary)

Type of Application	Maximum Water-Soluble Chloride Ion (Cl^-) in Concrete (Percent by Weight of Cement)
Prestressed concrete	0.06
Reinforced concrete exposed to chloride in service	0.15
Reinforced concrete that will be dry or protected from moisture in service	1.00
Other reinforced concrete construction	0.30

though, no more should be used in the batching than is necessary to accomplish its intended purpose. Even then it is not generally used at rates higher than 2% of the weight of cement (Kosmatka and Panarese, 1988), and care must be taken to ascertain complete dissolution of all of the salt into the mixing water before adding it to the rest of the matrix to avoid popouts and serious local staining problems. Laboratory evaluations of field-cured trial batches are recommended before full-scale placements are made.

3.5.1 Accelerating Corrosion-Inhibiting Admixtures

When designers have concerns about corrosion of reinforcing steel under shallow concrete cover, corrosion-inhibiting admixtures are often prescribed as a mitigation strategy. This class of materials electrochemically interferes with the galvanic corrosion process by scavenging either electrons or protons near the steel reinforcement. The three general categories of corrosion inhibitors are:

1. *Anodic* or *active* corrosion inhibitors actively interfere with the corrosion process by occupying overactive electrons oxidizing rapidly dissolving ferrous oxide ions into an insoluble protective coating of ferric oxide on their way to the surface of the anodic steel reinforcement. Calcium nitrite is the primary material in this category, although sodium nitrite, sodium benzoate, and sodium chromate are also used outside the United States.
2. *Cathodic* or *passive* corrosion inhibitors indirectly interfere with the corrosion process by slowing down the cathodic reactions by serving as proton acceptors and thus impeding the corrosion current. They are normally highly alkaline materials that render the ferrous ions at the surface of the reinforcing steel insoluble in water and unable to participate in the corrosion current. The most commonly used materials in this category are sodium hydroxide, sodium bicarbonate, and ammonium hydroxide, although the use of organic materials such as substituted forms of aniline and mercaptobenzothiazole has been reported.
3. *Mixed* or *passive-active* corrosion inhibitors might be preferable over either of the previous two types by themselves, as this type attacks the problem at both ends of the reaction, interfering more completely with the corrosion process before it can begin. These materials can be in the form of more complicated organic molecules that are attracted to and tie up both cathodic and anodic sites, forming salts as they accept either the available electrons or protons. This category may also be a physical mixture of two simpler compounds where one component reacts at the cathodic reaction site while the other reacts at the anodic site.

Corrosion inhibitors are typically used at dosage rates of 1 to 4%, based on the weight of the cement. Properties of concrete are affected by the use of corrosion-inhibiting admixtures. Inorganic salts such as calcium nitrite are known accelerators, but organic corrosion inhibitors may retard set times. Workability may be improved at levels up to 2% but begins to degenerate above that. Hardened concrete strengths are often slightly diminished, and alkali-silica reaction may be aggravated by corrosion inhibitors if reactive aggregates are present in the matrix.

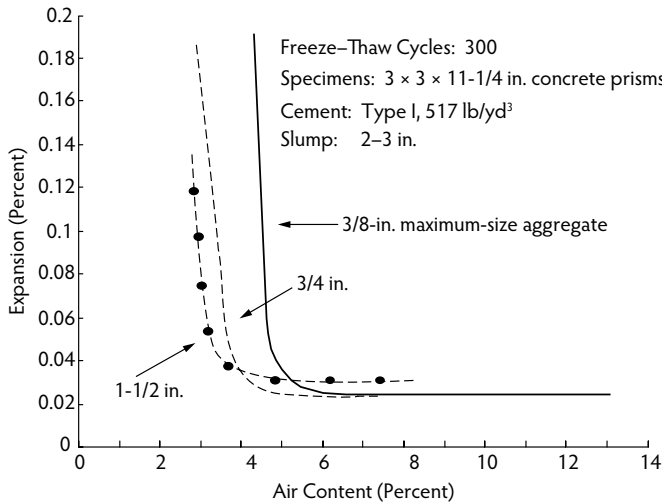


FIGURE 3.5 Relationship between air content and expansion of concrete test specimens during 300 cycles of freezing and thawing for various maximum aggregate sizes. (From Kosmatka, S.H. and Panarese, W.C., *Design and Control of Concrete Mixtures*, 13th ed., Portland Cement Association, Skokie, IL, 1988.)

3.6 Air-Entraining Admixtures

Air-entrained concrete was developed in the 1930s, and it is still recommended today for nearly every commercial application. Air-entraining agents are provided already ground into the cement (air-entrained cement) or as an admixture whose addition can be adjusted for individual batch design needs. Because air-entraining agents provide extremely small and well-dispersed air bubbles in the paste, they act as localized stress reducers in the cured matrix. This is advantageous in concrete exposed to moisture and especially to wet deicing chemicals during freezing and thawing conditions (Figure 3.5). Because the bubble voids provide room for microscopically localized expansions, resistance to damage from alkali-silica reactions and sulfate attack is enhanced as well. The trade-off is that air is compressible and not strength enhancing; therefore, some loss in strength of the concrete will result. A good rule of thumb is that every 1% increase in air content reduces the strength of a well-designed concrete 2 to 4% (Kosmatka and Panarese, 1988) (Figure 3.6). Generally, manufacturers recommend between 0.3 and 2.0 mL/kg cement depending on the specific air-entraining admixture, mineral admixtures also included in the batch, batch conditions, and the amount of air required. Manufacturers' recommendations for a specific air-entraining agent should be used as a guideline, but property evaluations should be made on several small batches before deciding on the optimum quantity required to produce the air content necessary for the batch design (Table 3.2).

Air-entraining admixtures are members of a class of chemicals known as surface-active substances or *surfactants*. These surfactants are made of molecules having a polar (water-attracted) head and a nonpolar (water-repulsed) tail. If the head is negatively charged, the surfactant is anionic, as represented by carboxylates, sulfonates, and sulfate esters. When the head is positively charged, the surfactant is cationic, as represented by substituted ammonium ion products. Nonionic surfactants are made of molecules with uncharged polar heads, and they are generally polyoxyethylenated compounds. Commercial air-entraining agents for concrete are inexpensive and have served the concrete industry well over time. They come from surfactants that can be categorized into the following seven groups (Dolch, 1984):

1. **Vinsol™** is the most widely used type of air-entraining admixture. It is the byproduct of the distillation and extraction of pine stumps for other materials. The leftover insoluble residue is neutralized in sodium hydroxide, resulting in the soluble solution used to produce entrained air in concrete.

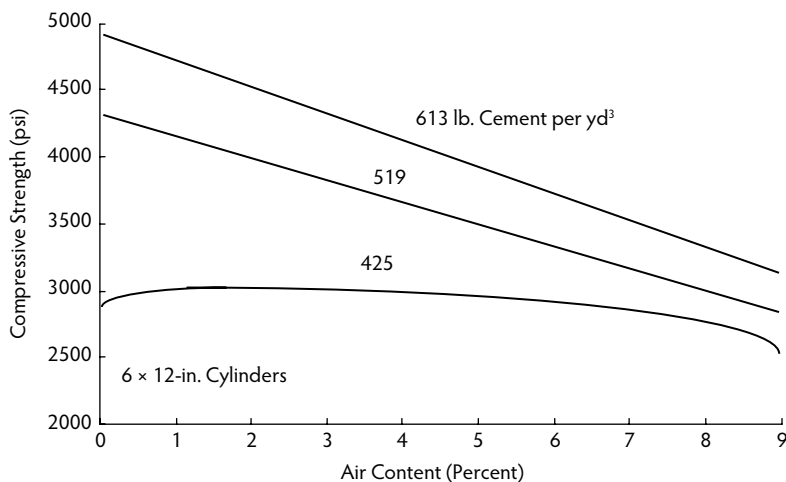


FIGURE 3.6 Relationship between air content and 28-day compressive strength for concrete at three constant cement contents. Water content was reduced with increased air content to maintain a constant slump. (From Kosmatka, S.H. and Panarese, W.C., *Design and Control of Concrete Mixtures*, 13th ed., Portland Cement Association, Skokie, IL, 1988.)

TABLE 3.2 Properties of Typical Air-Entraining Admixtures

Product	Manufacturer	Active Ingredient	Dosage	Specific Gravity
Protex® Regular	Protex Industries	Neutralized Vinsol™ resin	0.3–1.0	1.044
Darex® AEA	W.R. Grace & Co.	Organic acid salts	0.65–1.95	1.00–1.05
Airex® “D”	Mulco, Inc.	Sulfonated HC salt	1.5–1.85	1.01–1.03
Oxy-Plastair	Sider-Oxydro, Inc.	Vinsol™ resin	1.4	—
Plastade	Sternson, Ltd.	Coconut acid amide	0.6–1.9	1.0

Source: Dolch, W.L., in *Concrete Admixtures Handbook: Properties, Science, and Technology*, Ramachandran, V.S., Ed., Noyes Publications, Park Ridge, NJ, 1984, pp. 269–302. With permission.

2. **Synthetic detergents**, normally alkyl aryl sulfonates, come from petroleum-based (typically C_{12}) residues that are condensed with benzene then sulfonated and neutralized to obtain the soluble salt.
3. **Salts of sulfonated lignin** are byproducts of the paper industry. These tend to be relatively poor air-entraining agents but have been used extensively in concrete as water reducers and retarders.
4. **Salts of petroleum acids** are the leftovers from petroleum refineries. Sludge left after the extraction of white oils with sulfuric acid contains water-soluble sulfonates that are then neutralized with sodium hydroxide.
5. **Salts of proteinaceous materials** are products of animal- and hide-processing industries. They consist of salts from a complex mixture of carboxylic and amino acids. This group does not produce many commercial air-entraining admixtures.
6. **Fatty and resinous acids and their salts** are produced from various sources such as vegetable oil, coconut oil, and tall oil, another byproduct of the paper industry.
7. **Organic salts of sulfonated hydrocarbons** are the same water-soluble sulfonates described in group 4, except they are neutralized with triethanolamine instead of sodium hydroxide.

When determining air contents, an observant technician would note that even concrete without air-entraining admixtures contains some air. This air, however, is air that has become entrapped during the mixing process. Entrapped air is evident as much larger, irregularly spaced voids that do nothing to resist freeze–thaw stresses.

TABLE 3.3 Effect of Entrained Air on Concrete

Properties	Effect
<i>Plastic</i>	
Bleeding	Significant reduction of bleeding
Plastic shrinkage	Reduction
Slump	Increases (25 mm more slump/0.5–1% more air)
Unit weight	Decreases as air content increases
Water demand (for equal slump)	Decreases 3–6 kg/m ³ /1% increase in air
Workability	Increases as air increases
<i>Hardened</i>	
Abrasion	Insignificant (only as it relates to strength and modulus)
Absorption	Insignificant
Alkali–silica reactivity	Concrete expansion decreases as air increases
Bond to steel	Decreases as air increases
Compressive strength	Typically decreases strength 2–6%/1% air increase; unusually harsh or lean mixes may gain strength
Creep	Insignificant (only as it relates to strength and modulus)
Deicer scaling	Significantly more resistant as air increases
Fatigue	Insignificant (only as it relates to strength and modulus)
Flexural strength	Decreases strength 2–4%/1% increase in air
Freeze–thaw resistance	Water-saturated F-T resistance improves with added air
Heat of hydration	Insignificant
Modulus of elasticity	Decreases 724–1380 MPa (1.05×10^5 – 2.00×10^5 psi) per 1% air increase
Permeability	Minimal; if higher air means lower w/c then lower permeability results

Source: Kosmatka, S.H. and Panarese, W.C., *Design and Control of Concrete Mixtures*, 13th ed., Portland Cement Association, Skokie, IL, 1988.

Entrained air has a significant influence on many of the properties of both fresh and cured concrete. In fresh concrete, it is known to reduce water demand and the tendency toward bleeding, as well as plastic shrinkage. It increases slump and workability. In hardened concrete, entrained air improves deicer scaling resistance and resistance to freezing and thawing degradation, although small and predictable reductions in compressive, flexural, and bond strengths are to be expected (Table 3.3).

If air is determined to be excessive, very small quantities of defoaming or air-detraining agents may be used as recommended by the manufacturer. Defoaming agents are typically composed of silicones, esters of carbonic acid (water-insoluble), octyl alcohol, dibutylphthalate, or tributylphosphate. These materials are very effective, but too much may hurt concrete properties; thus, care must be taken to use only enough defoamer or detrainer to bring concrete air into the specified range. All air-entraining admixtures that are to be added at the time of mixing should conform to ASTM C 260 specifications. Air-entraining cements should conform to ASTM C 150 and ASTM C 595 with ASTM C 226 specifications for the air-entraining additives in air-entraining cements.

Typically total air content needs are dependent on anticipated exposure conditions vs. the strength and quality of the matrix mortar and coarse aggregates. Table 3.4 illustrates target air content considerations for various coarse aggregates. It should be noted that sometimes other chemical or mineral admixtures in the matrix may detrimentally reduce the anticipated volume of entrained air. Of course, trial batching to verify the effects of air-entraining admixtures on critical properties for any proposed batch design is recommended.

3.7 Antifreezing Admixtures

As the name implies, this category of admixtures is employed to allow most types of concrete construction work and precasting to take place at freezing and well below freezing temperatures. These admixtures are sometimes used in conjunction with external energy and heat sources, but they are often used without

TABLE 3.4 Total Target Air Content for Concrete

Nominal Maximum Aggregate Size (in.)	Air Content (%) ^a		
	Severe Exposure ^b	Moderate Exposure ^b	Mild Exposure ^b
3/8	7-1/2	6	4-1/2
1/2	7	5-1/2	4
3/4	6	5	3-1/2
1	6	4-1/2	3
1-1/2	5-1/2	4-1/2	2-1/2
2 ^c	5	4	2
3 ^c	4-1/2	3-1/2	1-1/2

^a Project specifications often allow the air content of the delivered concrete to be within -1 to +2 percentage points of the table target values.

^b Severe exposure is an environment in which concrete is exposed to wet freeze-thaw conditions, deicers, or other aggressive agents. Moderate exposure is an environment in which concrete is exposed to freezing but will not be continually moist, will not be exposed to water for long periods before freezing, and will not be in contact with deicers or aggressive chemicals. Mild exposure is an environment in which concrete is not exposed to freezing conditions, deicers, or aggressive agents.

^c These air contents apply to total mix, as for the preceding aggregate sizes. When testing these concretes, however, aggregate larger than 1-1/2 in. is removed by hand picking or sieving, and air content is determined on the -1-1/2 in. fraction of mix. (Tolerance on air content as delivered applies to this value.) Air content of total mix is computed from value determined on the -1-1/2 in. fraction.

Source: Kosmatka, S.H. and Panarese, W.C., *Design and Control of Concrete Mixtures*, 13th ed., Portland Cement Association, Skokie, IL, 1988.

them, even under bitterly cold environmental conditions. Antifreezing admixtures work by lowering the freezing point of the water in fresh concrete (Brook et al., 1993; Ratinov and Rosenberg, 1984). This is accomplished by dissolving salts and mixing in higher-molecular-weight alcohols, ammonia, or carbamide into the mix water. For this reason, the admixture dosage rates are based on the amount of mixing water in the given batch design. These antifreeze admixtures tend to seriously retard the set and cure properties of the matrix, as do freezing temperatures. It is obvious, then, that at the same time the water is being kept unfrozen and thus available for hydration acceleration of the hydration process is also important and must be designed to work with the antifreezing component. Thus, these two admixtures—antifreeze and accelerator—are often combined into one complex multicomponent additive. This compensating type of antifreeze typically consists of inexpensive combinations of potash and calcium-chloride-type additives. A third group of antifreeze admixture used occasionally promotes a highly accelerated hydration process and utilizes the much higher earlier exothermic temperatures in the concrete mass to push the curing process in spite of ambient temperatures that are too low to allow normal curing. Chemicals in this group include ferric sulfate and aluminum sulfate. Dosage rates for the various materials may differ significantly even for the same antifreeze admixture, because their effect is influenced by many things, including the temperature of the forms, air, aggregates, and mix water, as well as the concrete mass and geometry, mitigating construction technology, and type and brand of cement used.

3.8 Antiwashout Admixtures

This class of chemical admixture was developed as a viscosity-modifying admixture that could improve the rheological properties of the cement paste. It has proved itself in the field by significantly improving the cohesiveness of concrete being placed underwater, where the exposed matrix is in jeopardy of being diluted and segregated or washed away by the surrounding water. It is most commonly used underwater in large placements and in repairs. These admixtures are also known as viscosity-enhancing admixtures

and are sometimes used to produce self-leveling concrete or self-consolidating concrete (SCC), which is used wherever extreme congestion due to reinforcement configurations or unusual geometry of the forms requires a very fluid, cohesive concrete that resists bleeding and segregation (Khayat, 1996).

Disadvantages of antiwashout or viscosity-enhancing admixtures include the typical reductions in strength and modulus of elasticity. Depending on the base concrete batch design, water/cement ratio, and the type and dosage rate of antiwash admixture (AWA), compressive strength has been determined to be 75 to 100% of the same control mix without this admixture. Flexural strengths have been reported at 84 to 100%, and modulus of elasticity measurements are 80 to 100% of the control batch.

The two most commonly used AWAs are based on either welan gum or hydroxypropylmethylcellulose. Some AWAs are made from variations of related microbial saccharides similar to welan gum or various cellulose-based polymers such as hydroxyethylcellulose and hydroxyethylmethylcellulose. The thixotropic mechanisms that enable this admixture to work include attachment of its long molecules to water molecules. This inhibits the free displacement of the water by heavier mix constituents. The long chains can slip past each other under conditions of high shear, such as mixing and pumping and rapid flow, but when the moving concrete slows down the chains intermesh and the matrix behaves in a much more viscous state. This self-adjusting behavior minimizes segregation and bleeding. Workability is usually better, too, because the constituents of the mix are better dispersed, even with the higher additions of HRWRs.

Set time, cure time, shrinkage, and creep are not significantly affected by the presence of AWAs themselves but may be influenced by the addition of higher levels of HRWR associated with the use of AWAs. Electric current passed through cured permeability specimens is lower in concrete containing AWAs, indicating reduced chloride ion permeability. Addition levels for AWAs are totally dependent on the application needs and constraints, but the mechanism suggests that its function is based on the availability of free water. It is essential that trial batches be made and evaluated for all important properties before concrete containing AWA is placed. Known interactions include higher air-entraining admixture demand when higher levels of HRWRs are needed. Acceptable entrainment levels are easily attainable but require trial batch evaluations. Hydroxypropylmethylcellulose tends to entrap air unless a deaerating agent is added into the mixer with it; therefore, careful adherence to a specific mixing procedure may be more important than with other batch designs.

3.9 Shrinkage-Reducing Admixtures

Shrinkage-reducing or shrinkage-compensating admixtures promote expansion of the concrete at about the same volume that normal drying shrinkage is contracting it. The net change in length of the hardened concrete should be small enough to prevent shrinkage cracks. The typical materials used for shrinkage compensation in concrete are based on calcium sulfoaluminate or calcium aluminate and calcium oxide. Some losses in properties are typical with the introduction of these antishrinkage agents. Any ill effects on strength are minimized by the use of HRWRs, which provide good workability while allowing reduction of the water content. These admixtures can be used to great advantage in slabs, bridge decks, structures, and repair work where cracking can lead to steel reinforcement corrosion problems, but maintaining effective air entrainment for resistance to freezing and thawing damage can be difficult with shrinkage-reducing admixtures. Usage rates vary with batch designs and water content but typically range from 8 to 25%. ACI 223 (Standard Practice for the Use of Shrinkage-Compensating Concrete) specifies the best methods for utilization of this admixture.

3.10 Polymer Modifier Admixtures

Different types of polymers can be used in concrete as polymerizing admixtures for comatrix formation or where the hydraulic cement paste and the polymer simultaneously form into separate, but interdependent, phases in the matrix. This polymer-modified concrete (PMC) is the result of adding higher-

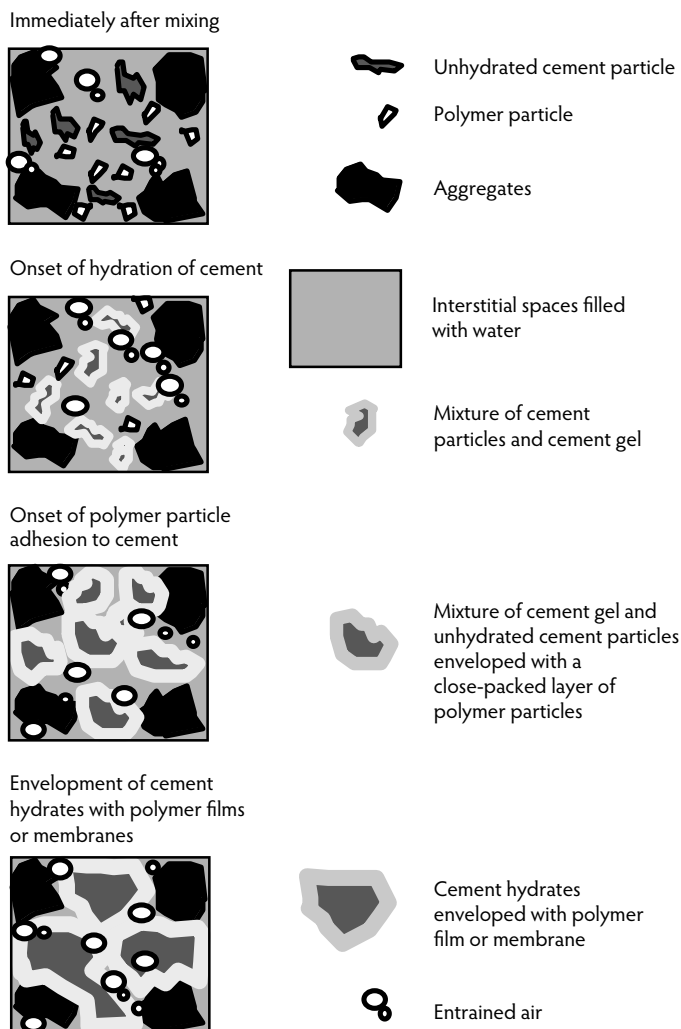


FIGURE 3.7 Simplified formation model for latex-cement co-matrix. (From Ohama, Y., in *Report of the Building Research Institute No. 65*, Building Research Institute, Tokyo, Japan, 1973.)

molecular-weight polymers to concrete batch designs for the purposes of improved adhesion, greater chemical resistance, lower permeability, lower drying shrinkage, improved tensile strength, or accelerated cure. Different chemical families and physical forms of polymers have been tried with varying degrees of success, but latex, acrylic, and epoxy additives are the most commonly used. They are available as powdered or liquid forms of resins, monomers, or emulsions, and their uses include concretes and mortars for flooring, ship decks, bridge decks overlays, repair, anticorrosive coatings, and adhesives. Improvements over the properties of normal concrete or mortar depend on the polymer phase formation and the cement hydration forming an interpenetrating network structure of polymer and hydrated cement phases. The resulting monolithic matrix exhibits properties beyond either isolated phase material.

Initially, the mixing process disperses the admixture into the fresh concrete matrix. As hydration begins and free water is lost, membrane strands of polymer begin forming either through water loss or independent polymerization. These membranes adhere to major portions of the hydrating cement particle surfaces. As the process continues, membranes interconnect and hydration progresses somewhat independently until both constituents of the matrix have cured (Figure 3.7). This modified matrix tends to arrest propagating microcracking due to local tensile or impact insults to the concrete. The mechanics

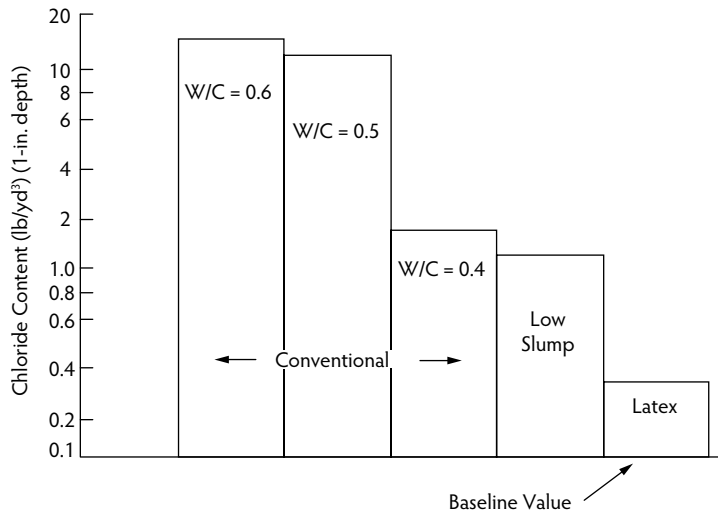


FIGURE 3.8 FHWA test results of 90-day ponding test. (Figure courtesy of Dow Chemical Company, Midland, MI.)

of this phenomenon seem to rely upon higher tensile strengths of the polymer network and the better bond to aggregates and hydration product. Additionally, higher curing shrinkage strains and resulting stresses in the polymer may post-tension the polymer phase, internally compressing the Portland cement concrete phase. Because of their significantly higher costs, these polymer modifiers are considered premium admixtures for concrete with special needs. The gains in tensile and flexural strength over normal concrete are primarily a function of the polymer/cement ratio rather than water/cement ratio.

Although mixing and placement of PMC are similar to normal concrete, there are some important differences, and finishing and curing may be very different. Normally, set times are delayed in PMC, and initial set times for PMC may be much more sensitive to ambient, substrate, and concrete constituent temperatures. Because of this sensitivity to temperature and unwanted additional air content from overmixing, latex-modified concrete is generally batched and mixed in mobile batching-plant trucks or trailers at the jobsite. With latex in particular, too much entrained air requires the addition of an antifoaming agent if it is not already included in the admixture. Initially, workability may be better than unmodified concrete, but as the polymer phase progresses and the surface begins to dry, finishing operations may tear the sticky or crusty surface due to polymer adhesion, so workers need to quickly place and finish PMC. Styrene-butadiene resin (SBR) concretes should be wet cured for 24 to 48 hours to permit concrete to gain adequate strength before the latex is allowed to cure and shrink.

Bleeding and segregation are also less in most PMCs because of the hydrophilic nature of the polymer modifiers used. Placement and finishing tools must be cleaned thoroughly and immediately after each use, and reuseable formwork must be carefully coated with a special form release that releases from latex or epoxy as well as the cement paste. All joints should be formed, including construction joints and control joints. Sawed joints for control of cracking are not recommended (ACI 548 Committee, 1992).

Changes in hardened concrete properties are important to anticipate. Shrinkage is dependent on the batch design and the choice and amount of polymer modifier. Some PMCs exhibit the same or less shrinkage, and some exhibit more than expected from normal concrete. Creep properties from SBR latex-modified concrete are typically lower than for normal concrete, but epoxy-modified concrete may be higher, depending on the polymer loading in the matrix. The coefficient of thermal expansion for PMCs is minimally affected by the polymer, as it such a small constituent in the matrix compared to the aggregates. Although significant increases in tensile strength, flexural strength, and bond strength may be expected, compressive strengths do not necessarily increase. Cured PMC typically exhibits lower water absorption and water or water vapor permeability due to larger pores being filled with polymer (Figure 3.8, Figure 3.9, and Figure 3.10); however, some polymers can re-emulsify, which may reduce the strength

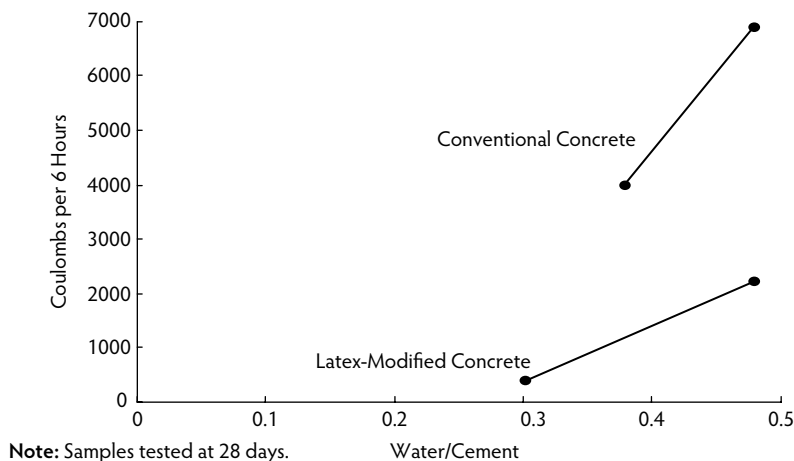


FIGURE 3.9 Permeability vs. water/cement ratio. (Figure courtesy of Dow Chemical Company, Midland, MI.)

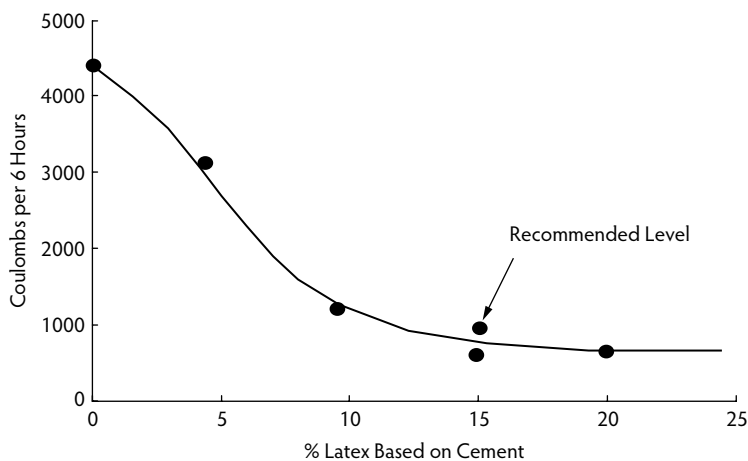


FIGURE 3.10 Effect of latex level on permeability. (Figure courtesy of Dow Chemical Company, Midland, MI.)

of the matrix at least near the surface when it is saturated with water over time. Epoxy-modified concretes are more suitable for constantly wet conditions (Popovic, 1985).

Polymer-modified concrete strengths are normally better than for conventional concrete with similar water/cement ratios at ambient temperatures below 100°F. Due to marked decreases in the polymer's modulus at polymer-specific glass transition temperatures (T_g s), usually somewhere between 100 and 120°F, the strength differences may decrease in service temperatures at or above this range. Abrasion resistance, frost resistance, chemical resistance, and bond to concrete or steel substrates are normally better in PMC than unmodified concrete.

Epoxy-modified concrete typically has a polymer/cement ratio of 20% for water-reducible resins and more than 30% for others (even more than 50% for some resins) (Ohama, 1984). This makes epoxy-modified concretes more expensive than latex-modified concretes, but all strengths are typically higher, including compressive strength, and these systems can be cured in water, whereas latex-modified concrete usually must be allowed to dry after 48 hours of moist curing.

Other commercially available polymers such as polyvinyl acetates, water-soluble unsaturated polyester resins, methylcellulose, and polyurethanes are used to modify concrete for specific applications, but latexes (particularly SBR and acrylic) and epoxies are the two that claim most of the market. PMC is used most often in protective coatings such as shotcrete (Shorn, 1985), overlays (Irvin, 1989), and large-

surface-area repairs (Smoak, 1985), because these applications can take cost-effective advantage of the better adhesion, better abrasion resistance, and lower permeability afforded the matrix through the use of polymer modifiers. Also, crews associated with these applications generally tend to be better trained for the special batching, placing, finishing, and curing requirements of PMC. Job-specific materials, usage, and batch design recommendations from polymer modifier manufacturers should be solicited and closely followed to make trial batches under field conditions which must be tested for critical properties before large-scale use of PMC is implemented.

3.11 Alkali–Silica Reaction Prevention Admixtures

In recent years, alkali–silica reaction (ASR) has been found to be responsible for much of the premature deterioration of many concrete structures in the United States and other countries throughout the world; consequently, there has been renewed interest in using lithium compounds (lithium hydroxide, lithium carbonate, and lithium nitrate) to combat this deleterious chemical reaction. The most promising of these lithium compounds is a solution of lithium nitrate. Research efforts are increasingly focused on understanding the mechanism by which lithium materials inhibit alkali–silica reaction. Furthermore, work continues toward improving the cost effectiveness of this mitigation strategy (Folliard et al., 2006).

3.12 Conclusion

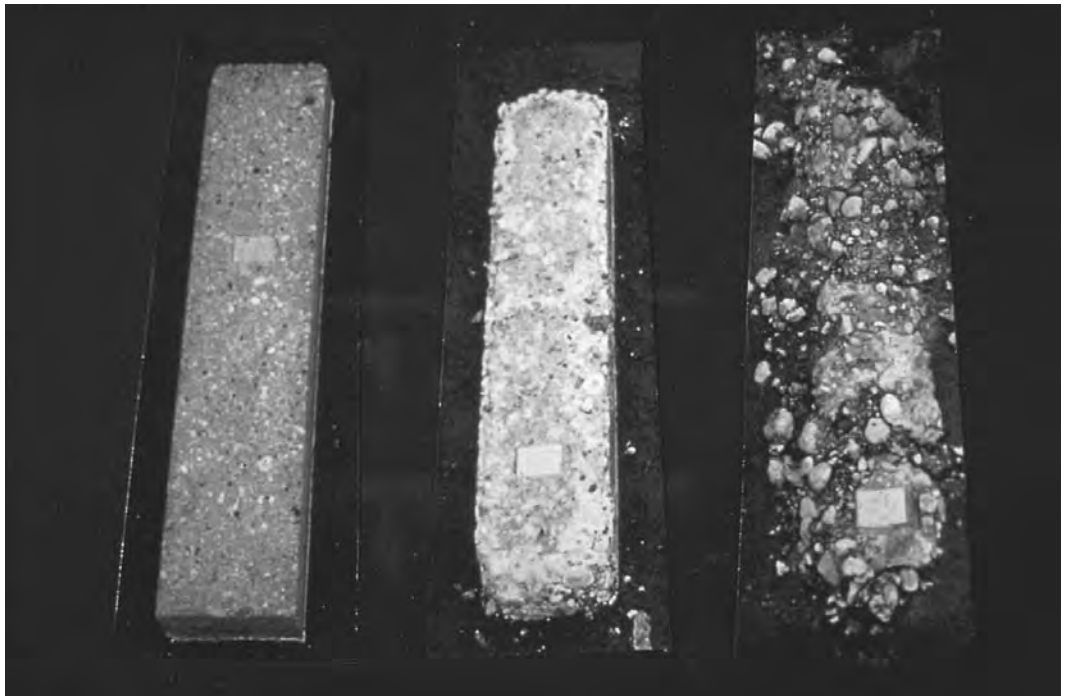
It should be noted that all of the many admixtures are intended to enhance the properties of concrete, but they are not intended to substitute for proper concrete design, batching, transport, and finishing practices. It is often more cost effective to change the mixture proportions or the aggregate than to use higher quantities of admixtures; therefore, it is recommended that a cost analysis be done on both proposed and alternative batch designs. Any change in admixtures or their quantities should be verified in trial batch evaluations for strength and any other critical properties before delivered to any jobsite. Trial batches should be mixed with all intended admixtures and cured under expected field conditions before evaluation.

References

- ACI Committee 201. 2001. *Guide to Durable Concrete*, ACI 201.2R. American Concrete Institute, Farmington Hills, MI.
- ACI Committee 211. 1991. *Standard Practice for Selecting Proportions for Normal, Heavyweight, and Mass Concrete*, ACI 211.1-91. American Concrete Institute, Farmington Hills, MI.
- ACI Committee 212. 2004a. *Chemical Admixtures for Concrete*, ACI 212.3R-04. American Concrete Institute, Farmington Hills, MI.
- ACI Committee 212. 2004b. *Guide for the Use of High-Range Water-Reducing Admixtures (Superplasticizers) in Concrete*, ACI 212.4R-04. American Concrete Institute, Farmington Hills, MI.
- ACI Committee 305. 1999. *Hot Weather Concreting*, ACI 305R-99. American Concrete Institute, Farmington Hills, MI.
- ACI Committee 306. 1988/2002. *Cold Weather Concreting*, ACI 306R-88. American Concrete Institute, Farmington Hills, MI.
- ACI Committee 318. 2005. *Building Code Requirements for Structural Concrete*, ACI 318-05 and ACI 318R-05. American Concrete Institute, Farmington Hills, MI.
- ACI Committee 517. 1987. *Accelerating Curing of Concrete at Atmospheric Pressure: State of the Art*, ACI 517.2R-87. American Concrete Institute, Farmington Hills, MI.
- ACI Committee 546. 1980. *Guide for Repair of Concrete Bridge Superstructures*, ACI 546.1R-80. American Concrete Institute, Farmington Hills, MI.

- ACI Committee 548. 1992. *Guide for Use of Polymers in Concrete*, ACI 548.1R-92. American Concrete Institute, Farmington Hills, MI.
- ACI Committee 548. 1994. *Guide for Polymer Concrete Overlays*, ACI 548.5R-94. American Concrete Institute, Farmington Hills, MI.
- ASTM C 260-94. 1999. Standard specification for air-entraining admixtures for concrete. In *Annual Book of ASTM Standards*, v. 04.02, pp. 153–155. American Society for Testing and Materials, Philadelphia, PA.
- ASTM D 345-90. 1990. Test method for sampling calcium chloride for roads and structural applications. In *Annual Book of ASTM Standards*, Vol. 4.03, pp. 63–64. American Society for Testing and Materials, Philadelphia, PA.
- ASTM C 494-92. 1992. Standard specification for chemical admixtures for concrete. In *Annual Book of ASTM Standards*, v. 04.02, pp. 251–259. American Society for Testing and Materials, Philadelphia, PA.
- ASTM C 1017-92. 1992. Standard specification for chemical admixtures for use producing flowing concrete. In *Annual Book of ASTM Standards*, v. 04.02, pp. 498–505. American Society for Testing and Materials, Philadelphia, PA.
- Baalbaki, M., 1990. Practical means for estimating superplasticizer dosage: determining the saturation point. In *Superplasticizers: Report of the Canadian Network of Center of Excellence in High Performance Concrete*, pp. 49–57. University of Sherbrooke, Quebec.
- Brook, J.W., Factor, D.F., Kinney, F.D., and Sarter, A.K. 1993. Cold weather admixture. In *Chemical Admixtures*, C-23. American Concrete Institute, Farmington Hills, MI.
- Collepardi, M. 1984. Water reducers/retarders. In *Concrete Admixtures Handbook: Properties, Science, and Technology*, Ramachandran, V.S., Ed., pp. 116–210. Noyes Publications, Park Ridge, NJ.
- Collepardi, M. 1994 Superplasticizer and air-entraining agents: state of the art and future needs. In *Proceedings of V. Mohan Malhotra Symposium*, ACI SP-144, Mehta, P.K., Ed., pp. 399–416. American Concrete Institute, Farmington Hills, MI.
- Daugherty, K.E., and Kowalewski, M.J., Jr. 1976. *Use of Admixtures Placed at High Temperatures*, 564-10-20. Transportation Research Board, Washington, D.C.
- Dodson, V.H. and Hayden, T.D. 1989. Another look at the Portland cement/chemical admixture incompatibility problem. *Cement, Concrete, Aggregates*, 11(1), 52–56.
- Dolch, W.L., 1984. Air entraining admixtures. In *Concrete Admixtures Handbook: Properties, Science, and Technology*, Ramachandran, V.S., Ed., pp. 269–302. Noyes Publications, Park Ridge, NJ.
- Dow Chemical Company. 1994. *A Handbook on Portland Cement, Concrete, and Mortar Containing Styrene/Butadiene Latex*, Dow Chemical Company, Midland, MI.
- Fisher, T.S. 1994. A contractor's guide to superplasticizers. *Concrete Construct.*, 39(7), 547–550.
- Folliard, K.J., Fournier, B., Ideker, J.H., Kurtis, K.E., and Thomas, M.D. 2006. *Interim Recommendations for the Use of Lithium to Mitigate or Prevent Alkali-Silica Reaction (ASR)*, FHWA-HRT-06-073. Office of Infrastructure Research and Development, Federal Highway Administration, Washington, D.C.
- Fowler, D.W. 1983. Polymers in concrete. In *Handbook of Structural Concrete*, Kong, F.K. et al., Eds., pp. 8.1–8.32. McGraw Hill, New York.
- Fowler, D.W. and Paul, D.R. 1975. *Polymer Impregnation of Concrete Walls*, Research Report to U.S. Army District Engineers, Walla Walla Corps of Engineers, Walla Walla, WA.
- Fowler, D.W., Houston J.T., and Paul, D.R. 1973. *Polymer-Impregnated Concrete Surface Treatment for Highway Bridge Decks*, ACI SP-40. American Concrete Institute, Farmington Hills, MI, pp. 93–117.
- Gagné, R., Boisvert, A., and Pigeon, M. 1996. Effect of superplasticizer dosage on mechanical properties, permeability, and freeze-thaw durability of high strength concrete with and without silica fume. *ACI Mater. J.*, 93(2), 111–120.
- Guennewig, T. 1993. Cost-effective use of superplasticizers. In *Chemical Admixtures*, C-53. American Concrete Institute, Farmington Hills, MI.

- Irvin, B.D. 1989. Application of styrene-butadiene latex modified Portland cement concrete overlays in parking structure repair and rehabilitation. In *Polymers in Concrete: Advances and Applications*, Mendis, P. and McClaskey, C., Eds., pp. 1–14. American Concrete Institute, Farmington Hills, MI.
- Johnston, C.D. 1987. Admixture cement incompatibility: a case history. *Concrete Int.*, 9(9), 43–51.
- Khayat, K.H. 1996. Effects of antiwashout admixtures on properties of hardened concrete. *ACI Mater. J.*, 93(2), 134–146.
- Kosmatka, S.H. and Panarese, W.C. 1988. *Design and Control of Concrete Mixtures*, 13th ed. Portland Cement Association, Skokie, IL.
- Mindess, S. and Young, J.F. 1981. *Concrete*, Prentice Hall, Englewood Cliffs, NJ.
- Nawy, E. G. 1996. *Fundamentals of High-Strength High-Performance Concrete*, Longman, London.
- Nmai, C.K., Bury, M.A., and Farzam, H. 1994. Corrosion evaluation of a sodium thiocyanate-based admixture. *Concrete Int.*, 16(4), 22–25.
- Nmai, C.K. 1995. Corrosion inhibiting admixtures: passive, passive-active versus active systems. In *Advances in Concrete Technology: Proceedings of the Second CANMET/ACI International Symposium*, Malhotra, M., Ed., pp. 565–585. American Concrete Institute, Farmington Hills, MI.
- Ohama, Y. 1973. Study on properties and mix proportioning of polymer modified mortars for buildings. In *Report of the Building Research Institute No. 65*. Building Research Institute, Tokyo, Japan.
- Ohama, Y. 1984. Polymer modified mortars and concretes. In *Concrete Admixtures Handbook: Properties, Science, and Technology*, Ramachandran, V.S., Ed., pp. 337–429. Noyes Publications, Park Ridge, NJ.
- Popovics, S. 1985. Modification of Portland cement concrete with epoxy as admixture. In *Polymer Concrete Uses, Materials, and Properties*, Dikeou, J. and Fowler, D.W., Eds., pp. 207–229. American Concrete Institute, Farmington Hills, MI.
- Ratinov, V.B. and Rosenberg, T.I. 1984. Antifreezing admixtures. In *Concrete Admixtures Handbook: Properties, Science, and Technology*, Ramachandran, V.S., Ed., pp. 430–479. Noyes Publications, Park Ridge, NJ.
- Shorn, H. 1985. Epoxy modified shotcrete. In *Polymer Concrete Uses, Materials, and Properties*, Dikeou, J. and Fowler, D.W., Eds., pp. 249–260. American Concrete Institute, Farmington Hills, MI.
- Smoak, W.G. 1985. Polymer impregnation and polymer concrete repairs at Grand Coulee Dam. In *Polymer Concrete Uses, Materials, and Properties*, Dikeou, J. and Fowler, D.W., Eds., pp. 43–49. American Concrete Institute, Farmington Hills, MI.
- Whiting, D., Nagi, M., Okamoto, P., Yu, T., Peshkin, D., Smith, K., Darter, M., Clifton, J., and Kaetzel, L. 1994. *SHRP-C-373 Optimization of Highway Technology*. Strategic Highway Research Program, National Research Council, Washington, D.C.



Laboratory test on long-term deterioration of concrete prisms. (Photograph courtesy of Portland Cement Association, Skokie, IL.)

4

Long-Term Effects and Serviceability

Edward G. Nawy, D.Eng., P.E., C.Eng.*
Hani Nassif, Ph.D., P.E.**

4.1	Creep and Shrinkage Deformations in Concrete	4-1
4.2	Creep Deformations in Concrete.....	4-2
	Creep Effects • Rheological Models	
4.3	Creep Prediction.....	4-6
	Creep Prediction for Standard Conditions • Factors Affecting Creep • Creep Prediction for Nonstandard Conditions • CEB-FIP Model Code for Creep	
4.4	Shrinkage in Concrete.....	4-10
	General Shrinkage Behavior • Shrinkage Prediction for Standard Conditions • Shrinkage Prediction for Nonstandard Conditions • Alternate Method for Shrinkage Prediction in Prestressed Concrete Elements • CEB-FIP Model Code for Shrinkage • Effects of Water and Slump on Drying Shrinkage	
4.5	Strength and Elastic Properties of Concrete vs. Time	4-16
	Cylinder Compressive Strength (f'_c) • Modulus of Rupture (f_r) and Tensile Strength (f'_t) • Modulus of Elasticity (E_c)	
4.6	Serviceability Long-Term Considerations	4-18
	Cracking Moment (M_{cr}) and Effective Moment of Inertia (I_e) • Flexural Crack Width Development	
4.7	Long-Term Shrinkage and Temperature Reinforcement Controlling Cracking between Joints in Walls and Slabs of Liquid-Retaining Structures.....	4-34
4.8	Autogenous Shrinkage in Early-Age Concrete	4-35
	Acknowledgments.....	4-35
	References	4-37

4.1 Creep and Shrinkage Deformations in Concrete

Creep, or lateral material flow, is the increase in strain with time due to sustained load. Initial deformation due to load is the **elastic strain**, while the additional strain or time-dependent deformation due to the same sustained load is the **creep strain**. Drying shrinkage, on the other hand, is the decrease in volume

* Distinguished Professor, Civil Engineering, Rutgers University, The State University of New Jersey, Piscataway, New Jersey, and ACI honorary member; expert in concrete structures, materials, and forensic engineering.

** Associate Professor, Civil and Environmental Engineering, Rutgers University, The State University of New Jersey; expert in structural concrete and cementitious materials.

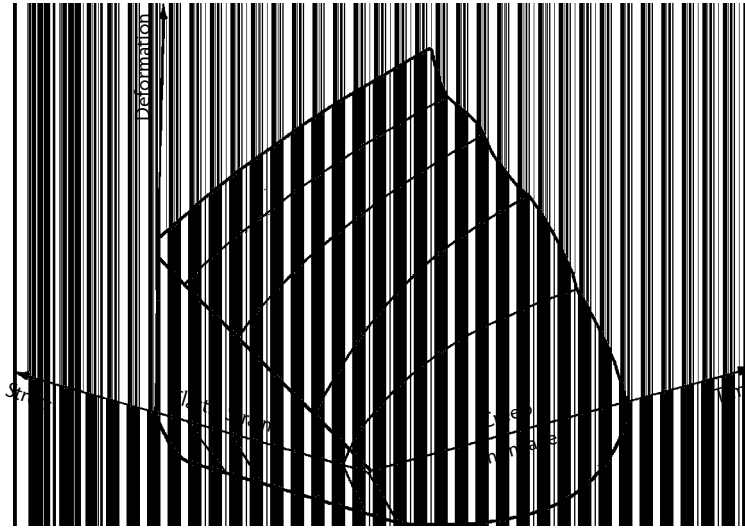


FIGURE 4.1 Three-dimensional model of time-dependent structural behavior. (From Nawy, E.G., *Reinforced Concrete: A Fundamental Approach*, 6th ed., Prentice Hall, Upper Saddle River, NJ, 2008.)

of the concrete element when it loses moisture due to evaporation. Because every infrastructure element under load will suffer this long-term deformation that has to be accounted for in a durable system, this aspect has been chosen as one of the major topics for consideration in this chapter.

If we look at the three-dimensional representation in Figure 4.1 and its two-dimensional counterpart in Figure 4.2, we can see that the nonlinear relationship in the creep and shrinkage behavior makes it difficult to come up with an exact model of prediction. This has been a challenge for researchers from the 1920s onwards and is why there are so many models of prediction (ACI 209, 1992; Bazant and Boweja, 1995a,b, 2000a,b; Bazant and Murphy, 1995; Branson, 1971, 1977; CEB-FIP, 1990; Gardner, 2000; Gardner and Lockman, 2001; Ross, 1937). Because of the incomplete reversibility of both creep and shrinkage strains, we can observe cracking, sagging of elements, and progressive deterioration as the strain continues to increase with time. Figure 4.2a shows a section of the three-dimensional model presented in Figure 4.1 parallel to the plane that contains the stress and deformation axes at time t_1 . The figure indicates that both elastic and creep strains are linearly proportional to applied stress. In a similar manner, Figure 4.2b illustrates a section parallel to the plane that contains the time and strain axes at a stress f_1 ; hence, it shows the familiar creep time and shrinkage time relationships.

The current ACI 318 code expressions due to Branson are still the acceptable general-purpose expressions for the prediction of creep and shrinkage as embodied in the ACI 209 model, and the designer can use other methods such as the CEB-FIP (1990), Bazant's B3 model (Bazant and Boweja, 1995a,b, 2000a,b), or Gardner's GL 2000 model (Gardner, 2000; Gardner and Lockman, 2001) for refined predictions (Nawy, 2006a,b, 2008). Recent work by Nassif at Rutgers (Saksawang et al., 2005), shown in Figure 4.3, indicates that the ACI 209 model seems to be a close best fit for creep prediction in high-strength, high-performance concrete; Figure 4.4 shows essentially similar characteristics for shrinkage but with lesser correlation.

4.2 Creep Deformations in Concrete

Creep or lateral material flow is the increase in strain with time due to sustained load. Initial deformation due to load is the *elastic strain*, while the additional strain due to the same sustained load is the *creep strain*. This practical assumption is quite acceptable, as the initial recorded deformation includes few time-dependent effects. Figure 4.5 illustrates the increase in creep strain with time; in the case of

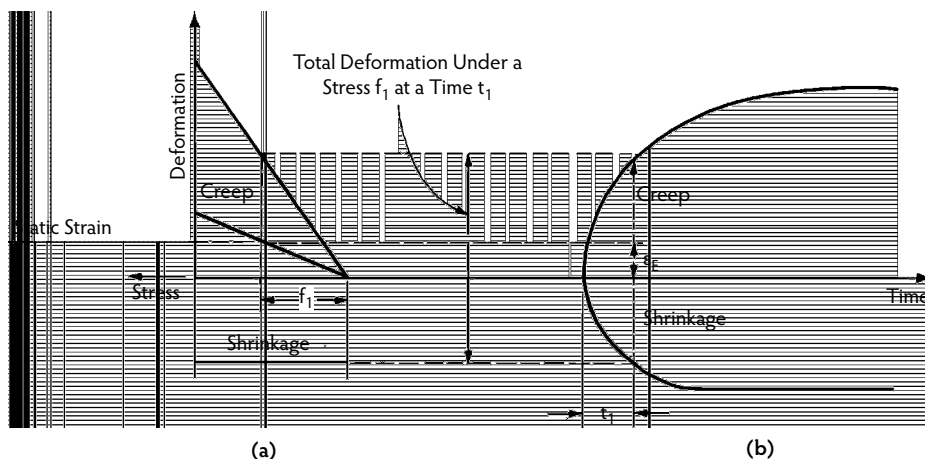


FIGURE 4.2 Two-dimensional section of deformations in Figure 4.1: (a) Section parallel to stress-deformation plane; (b) section parallel to deformation-time plane. (From Nawy, E.G., *Reinforced Concrete: A Fundamental Approach*, 6th ed., Prentice Hall, Upper Saddle River, NJ, 2008.)

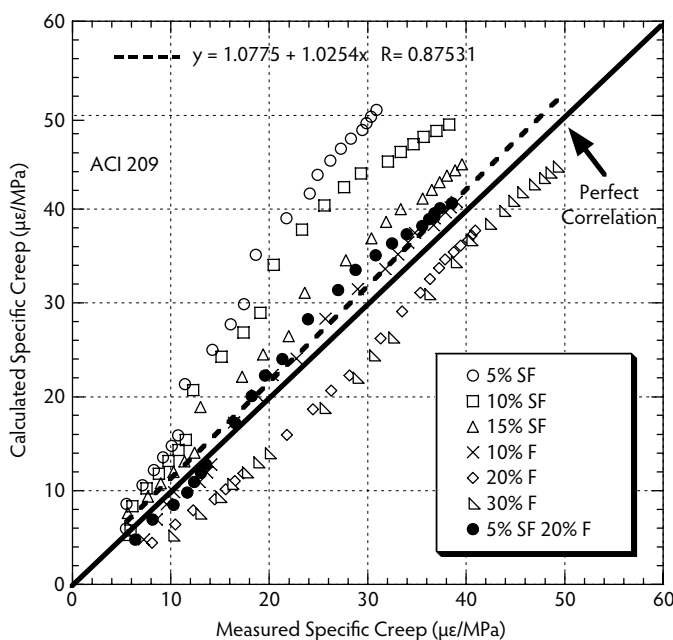


FIGURE 4.3 Comparison of measured and calculated specific creep for ACI 209 model.

shrinkage, it can be seen that the rate of creep decreases with time. Creep cannot be measured directly but is determined only by deducting elastic strain and shrinkage strain from the total deformation. Although shrinkage and creep are not independent phenomena, it can be assumed that superposition of strains is valid; hence,

$$\text{total strain } (\epsilon_t) = \text{elastic strain } (\epsilon_e) + \text{creep } (\epsilon_c) + \text{shrinkage } (\epsilon_{sh})$$

An example of the relative numerical values of strain due to elastic strain creep and to shrinkage is presented in the figure for a normal concrete specimen subjected to 900 psi in compression (Nawy, 2001; Ross, 1937). These relative values illustrate that stress-strain relationships for short-term loading in

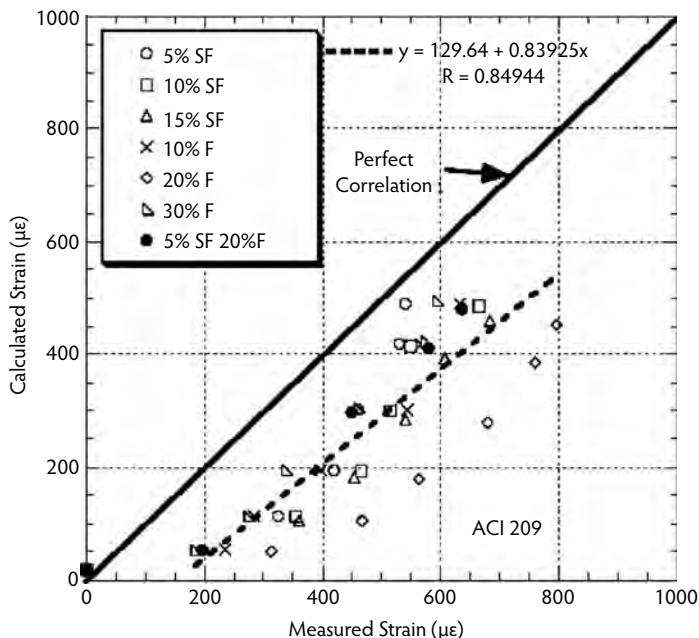


FIGURE 4.4 Comparison of measured and calculated shrinkage strain for ACI 209 model.

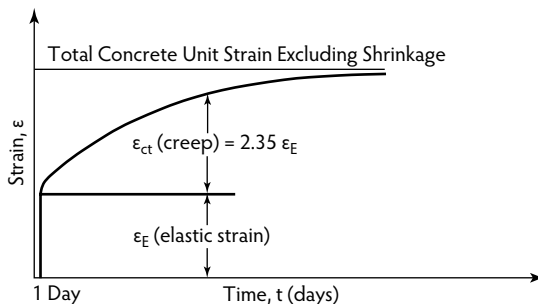


FIGURE 4.5 Long-term creep stress-time curve. (From Nawy, E.G., *Reinforced Concrete: A Fundamental Approach*, 6th ed., Prentice Hall, Upper Saddle River, NJ, 2008.)

normally reinforced or plain concrete elements lose their significance and the effects of long-term loadings become dominant on the behavior of a structure. In cases of large heavily reinforced columns in buildings, elastic strain can be a more significant component of the total strain.

Numerous tests have indicated that creep deformation is proportional to the applied stress, but the proportionality is valid only for low stress levels. The upper limit of the relationship cannot be determined accurately but can vary between 0.2 and 0.5 of the ultimate strength f'_c . This range in the limit of the proportionality is expected due to the large number of microcracks that exist at about 40% of the ultimate load.

As in the case of shrinkage, creep is not completely reversible. If a specimen is unloaded after a period of being under a sustained load, an immediate elastic recovery is obtained that is less than the strain precipitated on loading. The instantaneous recovery is followed by a gradual decrease in strain, called **creep recovery**. The extent of the recovery depends on the age of the concrete when loaded; older concretes present higher creep recoveries, while residual strains or deformations become frozen in the structural element, as shown in Figure 4.6.

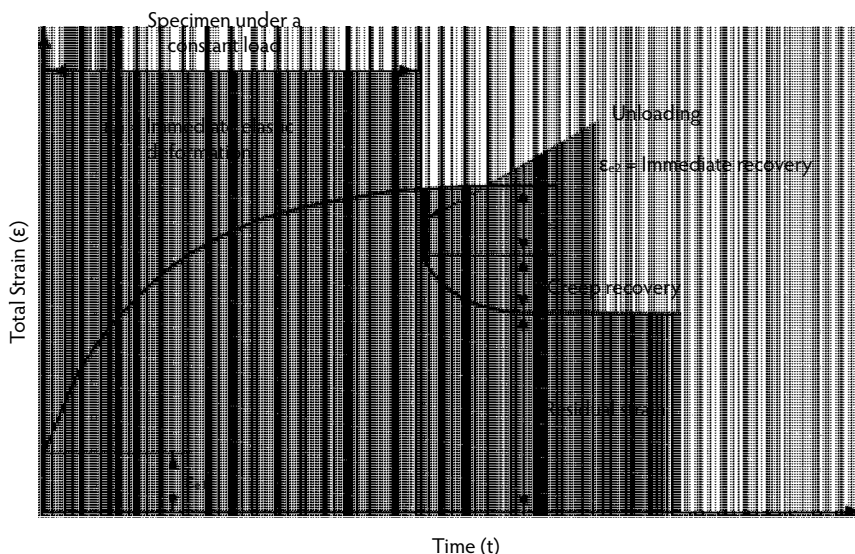


FIGURE 4.6 Creep recovery vs. time. (From Nawy, E.G., *Reinforced Concrete: A Fundamental Approach*, 6th ed., Prentice Hall, Upper Saddle River, NJ, 2008.)

4.2.1 Creep Effects

As in shrinkage, creep increases the deflection of beams and slabs and causes loss of prestress in prestressed concrete elements. In addition, the initial eccentricity of a reinforced concrete column increases with time due to creep, resulting in the transfer of the compressive load from the concrete to the steel in the concrete section. When the steel yields, additional load has to be carried by the concrete; consequently, the resisting capacity of the column is reduced, and the curvature of the column increases further, resulting in overstress in the concrete and leading to failure. Similar behavior occurs in axially loaded columns.

4.2.2 Rheological Models

Rheological models are mechanical devices that portray the general deformation behavior and flow of materials under stress. A model is basically composed of elastic springs and ideal dashpots denoting stress, elastic strain, delayed elastic strain, irrecoverable strain, and time. The springs represent the proportionality between stress and strain, and the dashpots represent the proportionality of stress to the rate of strain. A spring and a dashpot in parallel form a Kelvin unit, and in series they form a Maxwell unit.

Two rheological models are discussed here: the Burgers model and the Ross model. The Burgers model (Figure 4.7) is shown because it can approximately simulate the stress–strain–time behavior of concrete at the limit of proportionality, with some limitations. This model simulates the instantaneous recoverable strain (a), the delayed recoverable elastic strain in the spring (b), and the irrecoverable time-dependent strain in dashpots (c and d). The weakness in this model is that it continues to deform at a uniform rate as long as the load is sustained by the Maxwell dashpot—a behavior not similar to concrete, where creep reaches a limiting value with time, as shown in Figure 4.7. A modification in the form of the Ross rheological model (Ross, 1958) (Figure 4.8) can eliminate this deficiency. In this model, A represents the Hookian direct proportionality of the stress-to-strain element, D represents the Newtonian element, and B and C are the elastic springs that can transmit the applied load $P(t)$ to the enclosing cylinder walls by direct friction. Because each coil has a defined frictional resistance, only those coils whose resistance equals the applied load $P(t)$ are displaced; the others remain unstressed, symbolizing irrecoverable deformation in concrete. As the load continues to increase, it overcomes the spring resistance of unit B,

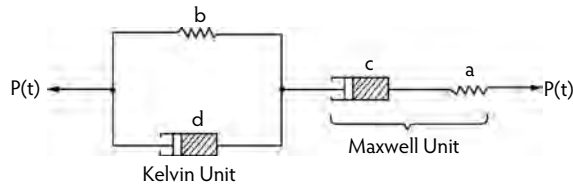


FIGURE 4.7 The Burgers rheological model. (From Nawy, E.G., *Reinforced Concrete: A Fundamental Approach*, 6th ed., Prentice Hall, Upper Saddle River, NJ, 2008.)

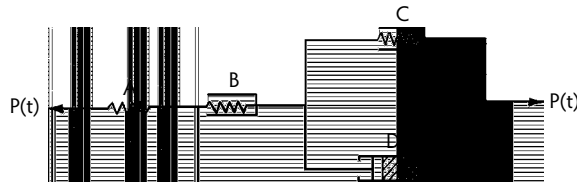


FIGURE 4.8 Ross rheological model. (From Nawy, E.G., *Reinforced Concrete: A Fundamental Approach*, 6th ed., Prentice Hall, Upper Saddle River, NJ, 2008.)

pulling the spring from the dashpot and signifying failure in a concrete element. More rigorous models have been used, such as Roll's model, to assist in predicting the creep strains. Mathematical expressions for such predictions can be very rigorous. One convenient expression from Ross defines creep (C) under load after time interval t as follows:

$$C = \frac{t}{a + bt} \quad (4.1)$$

where a and b are constants that can be determined from tests. As will be discussed in the next section, this model seems to represent the creep deformation of concrete and is the background for the ACI code equations for creep.

4.3 Creep Prediction

4.3.1 Creep Prediction for Standard Conditions

Creep and shrinkage are interrelated phenomena because of the similarity of the variables affecting both, including the forms of their strain–time curves, as seen in Figure 4.2. The ACI (ACI Committee 209, 1992) proposed a similar model for expressing both creep and shrinkage behavior. The expression for creep is as follows:

$$C_t = \frac{t^\alpha}{a + t^\alpha} C_u \quad (4.2)$$

where a and α are experimental constants and t , in days, is the duration of loading.

Work by Branson (1971, 1977) formed the basis for Equation 4.2 and Equation 4.3 in a simplified creep evaluation. The additional strain (ϵ_{cu}) due to creep can be defined as:

$$\epsilon_{cu} = \rho_u f_{ci} \quad (4.3)$$

where:

ρ_u = unit creep coefficient, generally referred to as **specific creep**.

f_{ci} = stress intensity in the structural member corresponding to initial unit strain ϵ_{cu} .

TABLE 4.1 Standard Conditions for Creep and Shrinkage Factors

Parameter		Factors	Variable Considered	Standard Conditions
Concrete (creep and shrinkage)	Concrete composition	Cement paste content	Type of cement	Type I and Type III
		Water/cement ratio	Slump	2.7 in. (70 mm)
		Mixture proportions	Air content	≤6%
		Aggregate characteristics	Fine aggregate percentage	50%
		Degree of compaction	Cement content	470 to 752 lb/yd ³ (279 to 446 kg/m ³)
	Initial curing	Length of initial curing	Moist-cured	7 days
			Steam cured	1–3 days
		Curing temperature	Moist-cured	73.4 ± 4°F (23 ± 2°C)
			Steam-cured	≤212°F (≤100°C)
		Curing humidity	Relative humidity	≥95
Member geometry and environment (creep and shrinkage)	Environment	Concrete temperature	Concrete temperature	73.4 ± 4°F (23 ± 2°C)
	Geometry	Concrete water content	Ambient relative humidity	40%
		Size and shape	Volume/surface ratio (V/S)	V/S = 1.5 in. (38 mm)
			Minimum thickness	6 in. (150 mm)
			Loading (only creep)	Loading history
Application	Steam-cured	1–3 days		
Duration	Sustained load	Sustained load		
Duration of unloading period	—	—		
Number of unloading cycles	—	—		
Stress conditions	Type of stress and distribution across the section	Compressive stress		Axial compression
				Stress/strength ratio

Source: ACI Committee 209, *Prediction of Creep, Shrinkage, and Temperature Effects in Concrete Structures*, ACI 209R-92, American Concrete Institute, Farmington Hills, MI, 1992, pp. 1–47.

$$C_u = \frac{\epsilon_{cu}}{\epsilon_{ci}} = \rho_u E_c \quad (4.4)$$

if C_u is the ultimate creep coefficient. An average value of C_u is 2.35.

Branson's model, verified by extensive tests, relates the creep coefficient (C_t) at any time to the ultimate creep coefficient for standard conditions as follows:

$$C_t = \frac{t^{0.6}}{10 + t^{0.6}} C_u \quad (4.5)$$

or, alternatively,

$$\rho_t = \frac{t^{0.6}}{10 + t^{0.6}} \quad (4.6)$$

where t is the time in days during which the load is applied. Standard conditions are summarized in Table 4.1 for both creep and shrinkage (ACI Committee 209, 1992).

4.3.2 Factors Affecting Creep

Creep is greatly affected by concrete constituents. The coarse-aggregate modulus affects the creep strain level, but the cementitious paste and its shear–friction interaction with the aggregate are constituents that significantly influence the time-dependent, load-induced strain. Other factors are environmental effects. A summary of these factors follows:

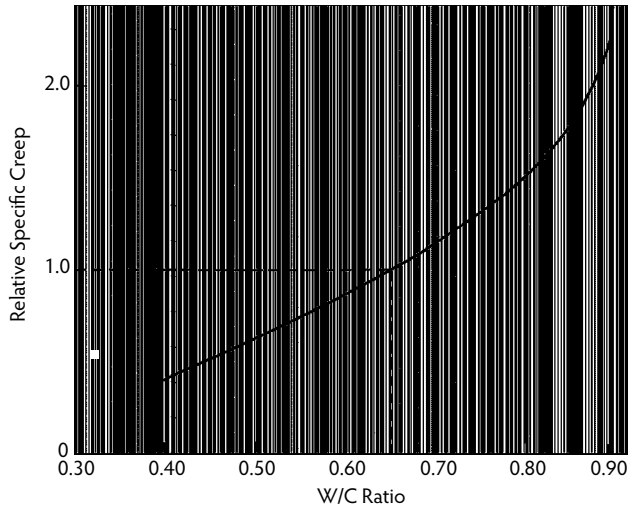


FIGURE 4.9 Water/cement ratio effect on the relative specific creep. (From Mindess, S. et al., *Concrete*, Prentice Hall, Upper Saddle River, NJ, 1999. With permission.)

- *Sustained load.* Creep as a result of sustained load is proportional to the sustained stress and is recoverable up to 30 to 50% of the ultimate strain.
- *Water/cementitious materials ratio ($w/(c + p)$ or w/cm).* The higher this ratio, the larger the creep, as seen in Figure 4.9, which relates specific creep to the $w/(c + p)$ ratio (Mindess et al., 1999).
- *Aggregate modulus and aggregate/paste ratio.* For a constant paste-volume content, an increase in aggregate volume decreases creep. As an example, an increase from 65 to 75% lowered creep by 10%. This behavior is the same whether the coarse aggregate is natural stone or lightweight artificial aggregate.
- *Age at time of loading.* The older the concrete at the time of loading, the smaller the induced creep strain for the same load level.
- *Relative humidity.* Reconditioning the concrete at a lower relative humidity before applying the sustained external load reduces the resulting creep strain. If creep is considered in two categories—drying creep and wetting creep—the creep strain develops irrespective of the direction of change (Mindess et al., 1999), provided the exposure is above 40%.
- *Temperature.* Creep increases with increase in temperature if the concrete is maintained at elevated temperatures while under sustained load. It increases in a linear manner up to a temperature of 175°F (80°C). Its value at this temperature level is almost three times the creep value at ambient temperatures.
- *Concrete member size.* Creep strain decreases with increasing thickness of the concrete member.
- *Reinforcement.* Creep effects are reduced by use of reinforcement in the compressive zones of concrete members.

4.3.3 Creep Prediction for Nonstandard Conditions

As the standard conditions for creep described in Table 4.1 change, corrective modifying multipliers have to be applied to the ultimate creep coefficient (C_u) in Equation 4.5. If the average ultimate creep C_u is 2.35 for standard conditions, it has to be adjusted by a multiplier (γ_{CR}) so:

$$C_u = 2.35\gamma_{CR} \quad (4.7a)$$

Here, γ_{CR} has component coefficients that account for the change in conditions enumerated in the preceding section. ACI Committee 209 recommends, in detailed tabular form, the various component

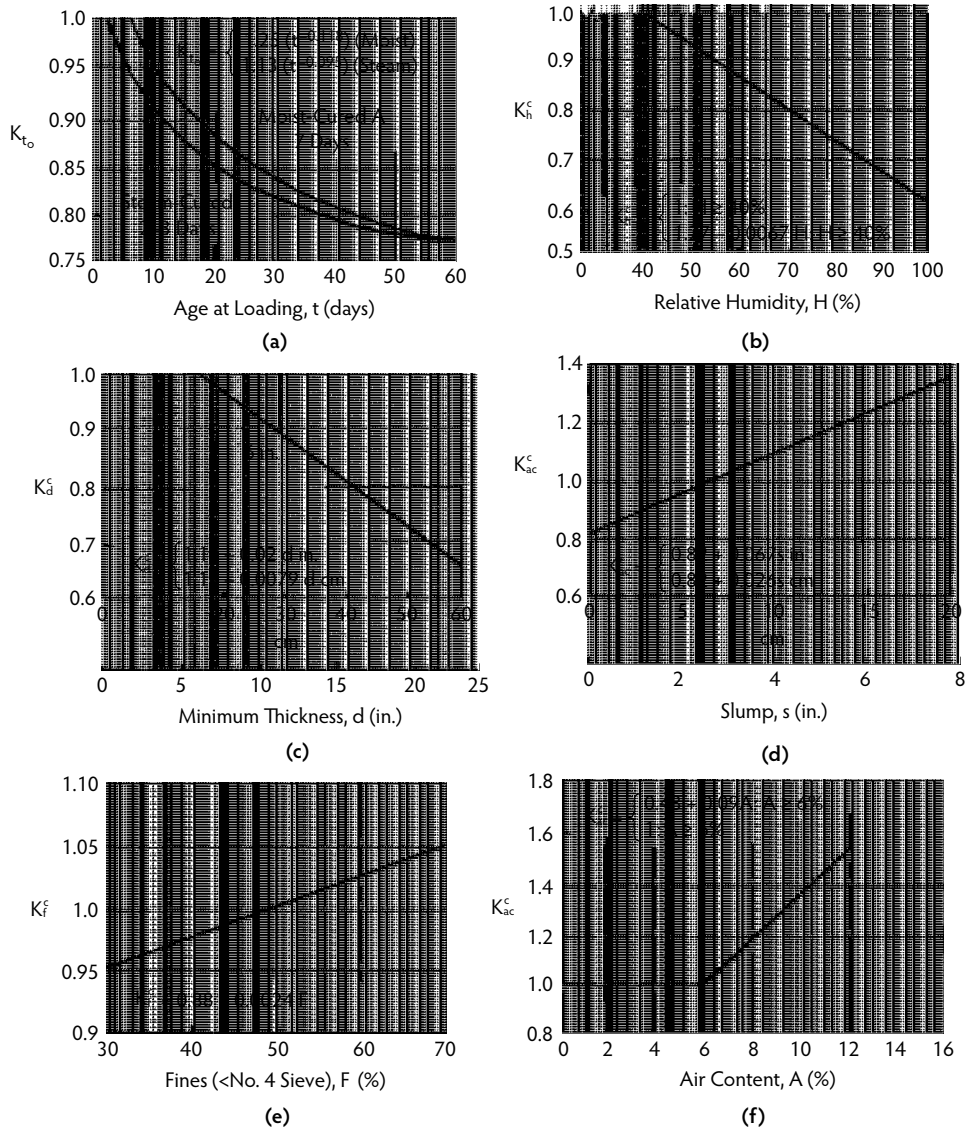


FIGURE 4.10 Creep correction factors for nonstandard conditions, ACI 209 method. (From Meyers, B.L. and Thomas, E.W., in *Handbook of Structural Concrete*, Kong, F.K. et al., Eds., McGraw-Hill, New York, 1983, pp. 11.1–11.33. With permission.)

coefficients for the γ_{CR} multiplier (ACI Committee 209, 1992). These are generally based on Branson's (1977) studies. Tabulated values are given in graphical form (ACI Committee 435, 1995; Branson, 1977; Meyers and Thomas, 1983) in Figure 4.10 for the multiplier as follows:

$$\gamma_{CR} = K_h^c K_d^c K_s^c K_f^c K_{ac}^c K_{t_0}^c \quad (4.7b)$$

where:

$\gamma_{CR} = 1$ for standard conditions.

K_h^c = relative humidity factor.

K_d^c = minimum member thickness factor.

K_s^c = concrete consistency factor.

K_f^c = fine aggregate content factor.
 K_{ac}^c = air-content factor.
 $K_{t_0}^c$ = age of concrete at load application factor.

4.3.4 CEB-FIP Model Code for Creep

The total stress-dependent strain per unit stress in the CEB-FIP 90-99 model is given by the following expression:

$$\epsilon_{CR(t,t_s)} = \frac{1}{E_{t_0}} + \frac{\phi_{(t,t_0)}}{E_{28}} \quad (4.8)$$

where:

E_{t_0} = modulus of elasticity at age of loading (MPa).
 E_{28} = modulus of elasticity at 28 days (MPa).
 $\phi_{(t,t_0)}$ = creep coefficient dependent on several factors, each defined by a separate equation relating to cement type, relative humidity, concrete strength, and age of concrete.

4.4 Shrinkage in Concrete

4.4.1 General Shrinkage Behavior

In general, the two types of shrinkage are **plastic shrinkage** and **drying shrinkage**; carbonation shrinkage is another form of shrinkage. Plastic shrinkage occurs during the first few hours after placing fresh concrete in forms. Exposed surfaces such as floor slabs are more easily affected by exposure to dry air because of their large contact surface. In such cases, moisture evaporates from the concrete surface faster than it is replaced by bleed water from the lower layers. Drying shrinkage, on the other hand, occurs after the concrete has already attained its final set and a good portion of the chemical hydration process in the cement gel has been accomplished. Drying shrinkage is the decrease in the volume of a concrete element when it loses moisture by evaporation. The opposite phenomenon—volume increase through water absorption—is termed *swelling*. In other words, shrinkage and swelling represent water movement out of or into the gel structure of a concrete specimen that is caused by the difference in humidity or saturation levels between the specimen and the surroundings, regardless of the external load.

Shrinkage is not a completely reversible process. If a concrete unit is saturated with water after having fully shrunk, it will not expand to its original volume. Figure 4.11 relates the increase in shrinkage strain

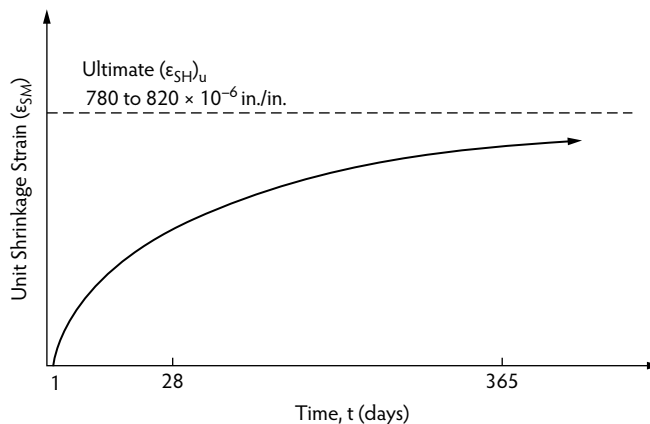


FIGURE 4.11 Concrete shrinkage vs. time curve. (From Nawy, E.G., *Reinforced Concrete: A Fundamental Approach*, 6th ed., Prentice Hall, Upper Saddle River, NJ, 2008.)

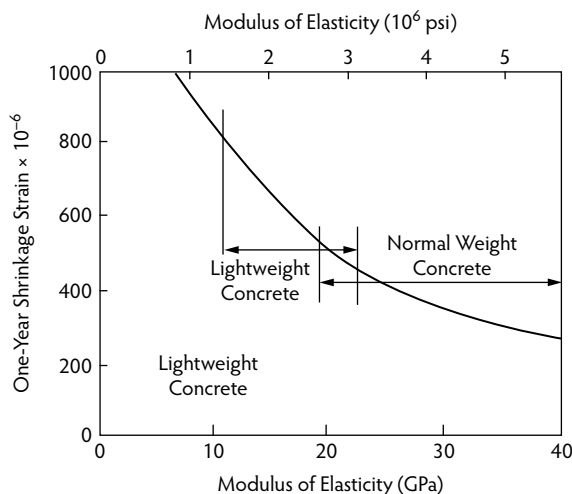


FIGURE 4.12 Aggregate modulus effect on shrinkage strain. (From Mindess, S. et al., *Concrete*, Prentice Hall, Upper Saddle River, NJ, 1999. With permission.)

(ϵ_{sh}) with time. The rate decreases with time, as older concretes are more resistant to environmental effects and consequently undergo less shrinkage, so the shrinkage strain becomes almost asymptotic with time. Several factors affect the magnitude of drying shrinkage:

- **Aggregate.** Aggregate acts to restrain the shrinkage of cement paste; hence, concretes with a high aggregate content are less vulnerable to shrinkage. In addition, the degree of restraint of a given concrete is determined by the properties of the aggregates; those with a high modulus of elasticity or with rough surfaces are more resistant to the shrinkage process (see Figure 4.12 and Figure 4.13) (Mindess et al., 1999).
- **Water/cementitious materials ratio.** Traditionally, it is accepted that the higher the water/cementitious materials ratio, the higher the shrinkage effects. Figure 4.14 is a typical plot relating shrinkage to aggregate content and, significantly, to the water/cement ratio. More recent work (Suprenant and Malisch, 2000), shown in Figure 4.15, indicates only a slight increase in average drying shrinkage with increase in water content.
- **Size of the concrete element.** Both the rate and total magnitude of shrinkage decrease with an increase in the volume of the concrete element; however, the duration of shrinkage is longer for larger members as more time is needed for drying to reach the internal regions. It is possible that 1 year may be required for the drying process to begin at a depth of 10 inches from the exposed surface and 10 years for drying to begin at 24 inches below the external surface; large members may never dry out completely.
- **Ambient conditions of the medium.** The relative humidity of the medium greatly affects the magnitude of shrinkage; the rate of shrinkage is lower at high relative humidity. Temperature is another important factor, in that shrinkage becomes stabilized at low temperatures.
- **Amount of reinforcement.** Reinforced concrete shrinks less than plain concrete; the relative difference is a function of the reinforcement percentage.
- **Admixtures.** This effect varies depending on the type of admixture. An accelerator such as calcium chloride, used to accelerate the hardening and setting of the concrete, increases the shrinkage. Pozzolans can also increase the drying shrinkage, whereas air-entraining agents have little effect.
- **Type of cement.** Rapid-hardening cement shrinks somewhat more than other types, whereas shrinkage-compensating cements minimize or eliminate shrinkage cracking when used with restraining reinforcement.

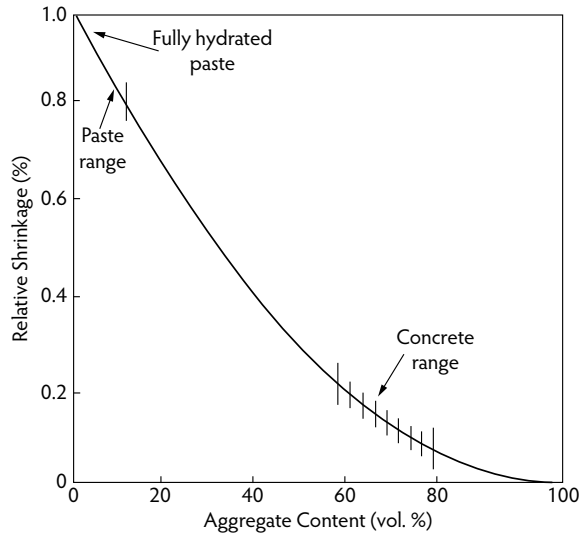


FIGURE 4.13 Aggregate content effect on drying shrinkage. (From Mindess, S. et al., *Concrete*, Prentice Hall, Upper Saddle River, NJ, 1999. With permission.)

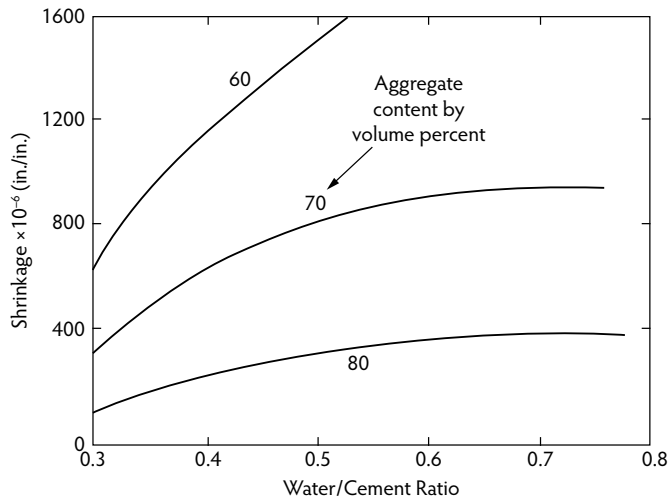


FIGURE 4.14 Water/cement ratio and aggregate content effect on shrinkage. (From Nawy, E.G., *Reinforced Concrete: A Fundamental Approach*, 6th ed., Prentice Hall, Upper Saddle River, NJ, 2008.)

- **Carbonation.** Carbonation shrinkage is caused by the reaction between carbon dioxide (CO_2) present in the atmosphere and that present in the cement paste. The amount of combined shrinkage from carbonation and drying varies according to the sequence of carbonation and drying processes. If both phenomena take place simultaneously, less shrinkage occurs. The process of carbonation, however, is dramatically reduced at relative humidity below 50%.

4.4.2 Shrinkage Prediction for Standard Conditions

The mathematical model for shrinkage prediction in Equation 4.3 as an ACI 209 model is:

$$(\epsilon_{SH})_t = \frac{t^\beta}{b + t^\beta} (\epsilon_{SH})_u \quad (4.9)$$

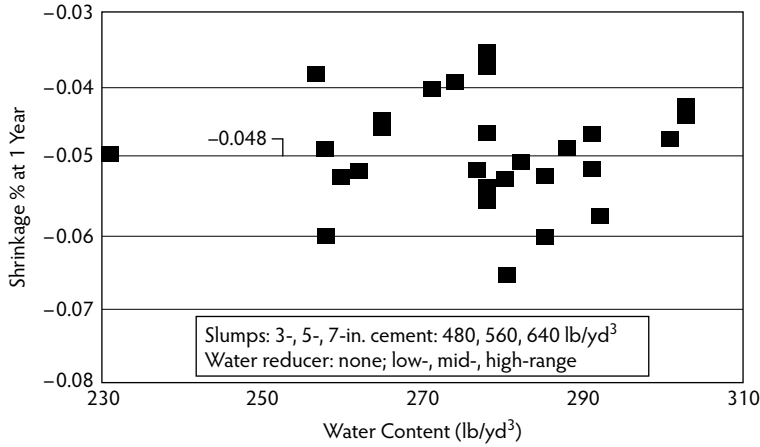


FIGURE 4.15 Effect of water content on 1-year drying shrinkage for concretes with and without water reducers. (From Suprenant, B.A. and Malisch, W. R., *A New Look at Water, Slump, and Shrinkage*, Technical Note, Paper No. C00D048, Hanley-Wood, Washington, D.C., 2000, pp. 1–6. With permission.)

where β is a constant and t , in days, is the amount of time after curing that the concrete hardened. The value of the ultimate shrinkage strain at the standard conditions defined in Table 4.1 has the following range:

$$(\epsilon_{SH})_u = 415 \times 10^{-6} \text{ to } 1070 \times 10^{-6} \text{ in./in. (mm/mm)}$$

stipulated by ACI Committee 209 (1992) is as follows:

Moist-cured for 7 days:

$$(\epsilon_{SH})_u = 800 \times 10^{-6} \text{ in./in. (mm/mm)}$$

Steam-cured for 1 to 3 days:

$$(\epsilon_{SH})_u = 730 \times 10^{-6} \text{ in./in. (mm/mm)}$$

A common sufficiently accurate average shrinkage strain in standard conditions for both moist-cured and steam-cured concretes (ACI Committee 209, 1992) is:

$$(\epsilon_{SH})_u = 780 \times 10^{-6} \text{ in./in. (mm/mm)}$$

The values of constant b in the mathematical model of Equation 4.8 are $b = 35$ for 7-day moist-cured specimens and $b = 55$ for 1- to 3-day steam-cured specimens; hence, the shrinkage-strain prediction expressions for standard conditions become:

Shrinkage after 7 days of moist curing:

$$(\epsilon_{SH})_t = \frac{t}{35+t} (\epsilon_{SH})_u \quad (4.10a)$$

where t is the age of concrete in days after curing.

Shrinkage after 1 to 3 days of steam curing:

$$(\epsilon_{SH})_t = \frac{t}{55+t} (\epsilon_{SH})_u \quad (4.10b)$$

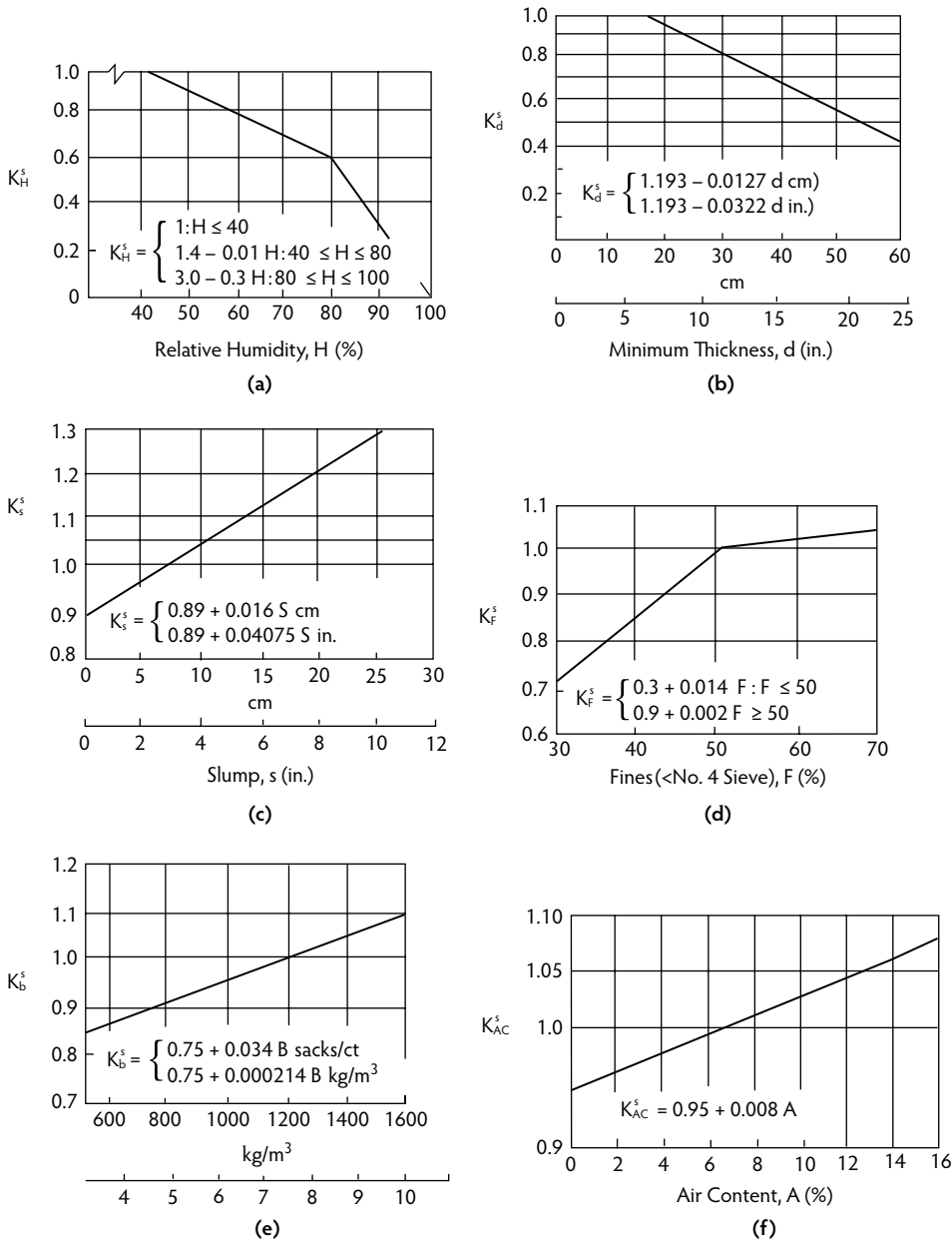


FIGURE 4.16 Shrinkage correction factors for nonstandard conditions, ACI method. (From Meyers, B.L. and Thomas, E.W., in *Handbook of Structural Concrete*, Kong, F.K. et al., Eds., McGraw-Hill, New York, 1983, pp. 11.1–11.33. With permission.)

4.4.3 Shrinkage Prediction for Nonstandard Conditions

As the standard conditions for shrinkage described in Table 4.1 change, corrective modifying multipliers have to be applied to the ultimate value of the shrinkage strain $(\epsilon_{SH})_u$ in Equations 4.10a and 4.10b. If γ_{SH} is the shrinkage-adjusting multiplier, then the average ultimate shrinkage strain for nonstandard conditions becomes:

$$(\epsilon_{SH})_u = 780 \times 10^{-6} \gamma_{SH} \quad (4.11a)$$

TABLE 4.2 Values of K_{SH} for Post-Tensioned Members

	Time from End of Moist Curing to Application of Prestress (Days)							
	1	3	5	7	10	20	30	60
K_{SH}	0.92	0.85	0.80	0.70	0.73	0.64	0.58	0.45

Source: Precast/Prestressed Concrete Institute (PCI), Chicago, IL.

or

$$(\epsilon_{SH})_{u,n} = \gamma_{SH}(\epsilon)_u \quad (4.11b)$$

where $(\epsilon_{SH})_{u,n}$ is the average ultimate strain for nonstandard conditions; hence, for nonstandard conditions, Equations 4.10a and 4.10b, respectively, become:

$$(\epsilon_{SH})_t = \frac{1}{35+t} \gamma_{SH}(\epsilon_{SH})_u \quad (4.12a)$$

and

$$(\epsilon_{SH})_t = \frac{1}{55+t} \gamma_{SH}(\epsilon_{SH})_u \quad (4.12b)$$

The multiplier γ_{SH} has component coefficients that account for the change in conditions enumerated in Section 4.4.1 (General Shrinkage Behavior). ACI Committee 435 (1995) recommends, in detailed tabular form, the various component coefficients for the γ_{SH} multiplier. These are generally based on Branson's (1977) studies. The tabulated values (ACI Committee 435, 1995; Branson, 1977; Meyers and Thomas, 1983) are given in graphical form in Figure 4.16 for:

$$\gamma_{SH} = K_H^s K_d^s K_s^s K_F^s K_B^s K_{AC}^s \quad (4.12c)$$

where values of these factors are given in Figure 4.13:

$\gamma_{SH} = 1$ for standard conditions.

K_H^s = relative humidity-factor.

K_d^s = minimum member thickness factor.

K_s^s = slump factor.

K_F^s = fine aggregate content factor.

K_B^s = cement-content factor.

K_{AC}^s = air-content factor.

4.4.4 Alternate Method for Shrinkage Prediction in Prestressed Concrete Elements

For standard conditions, the Precast/Prestressed Concrete Institute (PCI) stipulates an average value for nominal ultimate shrinkage strain $(\epsilon_{SH})_u = 820 \times 10^{-6}$ in./in. (mm/mm). If ϵ_{SH} is the shrinkage strain after adjusting for relative humidity (RH, in percent) at a volume-to-surface ratio (V/S, in inches), the shrinkage strain is:

$$\epsilon_{SH} = 8.2 \times 10^{-6} K_{SH} \left(1 - 0.06 \frac{V}{S} \right) (100 - RH) \quad (4.13)$$

where $K_{SH} = 1.0$ for pretensioned members. Table 4.2 gives the values of K_{SH} for post-tensioned members. Adjustment of shrinkage losses for standard conditions as a function of time t , in days, is made using Equations 4.10a and 4.10b for standard conditions and Equations 4.12a and 4.12b for nonstandard conditions.

4.4.5 CEB-FIP Model Code for Shrinkage

The CEB-FIP 90 model proposed by the Euro-International Concrete Committee and the International Federation for Prestressing is based on Muller and Hillsdorf (1990) and is only applicable for concrete with 28-day compressive strength in the range of 20 to 90 MPa. The input parameters of this model differ from the ACI model in terms of compressive strength and type of curing method. The strain due to shrinkage at normal temperature may be calculated from:

$$\epsilon_{SH(t,t_s)} = \epsilon_{cs0} \beta_s (t - t_s) \quad (4.14)$$

where:

ϵ_{cs0} = shrinkage coefficient.

β_s = coefficient to describe shrinkage with time.

t = age of concrete (days).

t_s = age of concrete (days) at the beginning of shrinkage.

4.4.6 Effects of Water and Slump on Drying Shrinkage

Traditionally, it has been accepted that the higher the water/cement ratio (w/c) and, correspondingly, the higher the water/cementitious materials ratio (w/cm), the higher the shrinkage effects. This concept dates back to the early days of the 1930s and is exemplified by the relationship shown in Figure 4.16, which relates shrinkage to aggregate content and, significantly, to the water/cement ratio. More recent work (Suprenant and Malisch, 2000) has produced results that bring into question the degree of influence on the drying shrinkage value by the increase in slump resulting from an increase in water content in the mix. The indicated work, monitoring the increase in drying shrinkage over a 1-year period, demonstrated that only a 5% increase in shrinkage resulted for each 2-inch increase in slump: "As a general rule of thumb, each added gallon of water per cubic yard increases slump by 1 inch" (Suprenant and Malisch, 2000). Figure 4.15 graphically illustrates that only a slight increase in average drying shrinkage results from appreciable increase in water content. The authors proposed in their investigation that, with proper inspection, jobsite water additions seldom exceed 2 gallons of water per cubic yard of concrete, or enough to increase the slump 2 inches. On this basis, the 2 gallons of water, or the extra 2 inches of slump, "might increase drying shrinkage by 4% to 5%," which is not significant over a 1-year period after placement of the concrete.

4.5 Strength and Elastic Properties of Concrete vs. Time

4.5.1 Cylinder Compressive Strength (f'_c)

Cylinder compressive strength increases with time as the cement hydration reaction progresses in the presence of water. As a function of time, the developing compressive strength is:

$$(f'_c)_t = \frac{1}{\alpha/\beta + t} (f'_c)_u \quad (4.15)$$

where:

α/β = age of concrete, in days, at which one half of the ultimate (in time) compressive strength of concrete $(f'_c)_u$ is reached.

t = age of concrete in days.

The range of α and β for normal weight, sand lightweight, and all lightweight concrete is $\alpha = 0.05$ to 9.25, and $\beta = 0.67$ to 0.98. These constants are a function of the type of cement and the type of curing applied. Typical values for α/β and the time strength ratios are given in Table 4.3.

TABLE 4.3 Values of Constant α/β and Time Strength Ratio $(f'_c)_t/(f'_c)_u$ at a Given Age

Type of Curing	Cement Type	Constant α/β	Concrete Age									Ultimate (in time)
			Days							Years		
			3	7	14	21	28	56	91	1	10	
Moist	I	4.71	0.39	0.60	0.75	0.82	0.86	0.92	0.95	0.99	1.0	1.0
	III	2.5	0.54	0.74	0.85	0.89	0.92	0.96	0.97	0.99	1.0	1.0
Steam	I	1.50	0.74	0.87	0.93	0.95	0.96	0.98	0.99	1.0	1.0	1.0
	III	0.71	0.81	0.91	0.95	0.97	0.97	0.99	0.99	1.0	1.0	1.0

Source: ACI Committee 209, *Prediction of Creep, Shrinkage, and Temperature Effects in Concrete Structures*, ACI 209R-92, American Concrete Institute, Farmington Hills, MI, 1992, pp. 1–47.

4.5.2 Modulus of Rupture (f_r) and Tensile Strength (f'_t)

The modulus of rupture (f_r) can be expressed as:

$$f_r = g_r \sqrt{w(f'_c)_t} \quad (4.16)$$

where g_r has a range of 0.6 to 1.00, with an average value of 0.65 (in SI units, this range is 0.012 to 0.021, with an average of 0.0135 MPa for f_r); w is the unit weight of the concrete in pounds per cubic foot for f_r in psi or kg/m³ for f_r in megapascals. Hence, Equation 4.16 becomes:

$$f_r \text{ (psi)} = 0.65 \sqrt{w f'_c} \quad (4.17a)$$

and

$$f_r \text{ (MPa)} = 0.013 \sqrt{w f'_c} \quad (4.17b)$$

Equation 4.17 is applicable for concrete strengths up to 12,000 psi (83 MPa). For normal weight concrete, $w = 145 \text{ lb/ft}^3$ (2320 kg/m³), and Equation 4.17 becomes:

$$f_r \text{ (psi)} = 7.5 \sqrt{f'_c} \quad (4.18a)$$

and

$$f_r \text{ (MPa)} = 0.60 \sqrt{f'_c} \quad (4.18b)$$

ACI Committee 363 (1992) on high-strength concrete (Nawy, 1996, 2001) recommends higher values for the modulus of rupture for normal weight concrete:

$$f_r \text{ (psi)} = 11.7 \sqrt{f'_c} \quad (4.19a)$$

and

$$f_r \text{ (MPa)} = 0.94 \sqrt{f'_c} \quad (4.19b)$$

The tensile splitting strength f'_t as recommended in ACI Committee 363 (1992) and ACI Committee 435 (1995) for normal weight concrete of a compressive-strength range up to 12,000 psi (83 MPa) is:

$$f'_t \text{ (psi)} = 7.4 \sqrt{f'_c} \quad (4.20a)$$

and

$$f'_t \text{ (MPa)} = 0.59 \sqrt{f'_c} \quad (4.20b)$$

4.5.3 Modulus of Elasticity (E_c)

The modulus of elasticity of concrete is strongly influenced by the concrete materials and mix proportions used. An increase in compressive strength is accompanied by an increase in the modulus, as the slope of the ascending branch of the stress–strain diagram becomes steeper. For concretes with densities in the range of 90 to 155 lb/ft³ (1440 to 2320 kg/m³), based on the secant modulus at $0.45f'_c$ intercept and compressive strength up to 6000 psi (42 MPa):

$$E_c \text{ (psi)} = 33w^{1.5} \sqrt{f'_c} \quad (4.21a)$$

and

$$E_c \text{ (MPa)} = 0.0143w_c^{1.5} \sqrt{f'_c} \quad (4.21b)$$

As the strength of the concrete increases beyond 6000 psi, the measured value of E_c increases at a slower rate such that the value expressed in Equation 4.21 underestimates the actual value of the modulus. The value of the modulus for a compressive strength range of 6000 to 12,000 psi (42 to 83 MPa) (Nilson, 1985) can be predicted by:

$$E_c \text{ (psi)} = \left(40,000 \sqrt{f'_c} + 1.0 \times 10^6 \right) \left(\frac{w_c}{145} \right)^{1.5} \quad (4.22a)$$

and

$$E_c \text{ (MPa)} = \left(3.32 \sqrt{f'_c} + 6895 \right) \left(\frac{w_c}{2320} \right)^{1.5} \quad (4.22b)$$

Figure 4.17 gives the best fit for E_c vs. f'_c for high-strength concretes. Deviations from the predicted values are highly sensitive to properties of the coarse aggregate such as size, porosity, and hardness. When very high-strength concretes (20,000 psi or 140 MPa, or higher) are used in major structures or when deformation is critical, E_c should be determined from actual field cylinder test values and the $0.45 f'_c$ intercept in the resulting stress–strain diagram. Long-term effects on the modulus of elasticity can be viewed in terms of the gain in the compressive strength $(f'_c)_t$ such that:

$$E_{ct} = E_c \sqrt{[(f'_c)_t / f'_c]} \quad (4.23)$$

where $(f'_c)_t$ is equal to compressive strength at later ages and (f'_c) is equal to the 28-day compressive strength.

4.6 Serviceability Long-Term Considerations

In concrete structural members, serviceability is evaluated by cracking and deflection behavior. Creep and shrinkage effects on cracking and deflection are well established. Both deflections and crack widths increase with time. As a section cracks, its gross moment of inertia is reduced, resulting in reduced stiffness and larger deformations and deflections. The crack width (w) and the cracking moment (M_{cr}), are the principal parameters, together with the contribution of the reinforcement (compressive reinforcement in the case of deflection), that determine the long-term behavior of structural elements and systems.

4.6.1 Cracking Moment (M_{cr}) and Effective Moment of Inertia (I_e)

4.6.1.1 Reinforced Concrete Beams

Tension cracks develop when externally imposed loads cause bending moments in excess of the cracking moment, M_{cr} . As a result, tensile stresses in the concrete at the tensile extreme fibers exceed the modulus

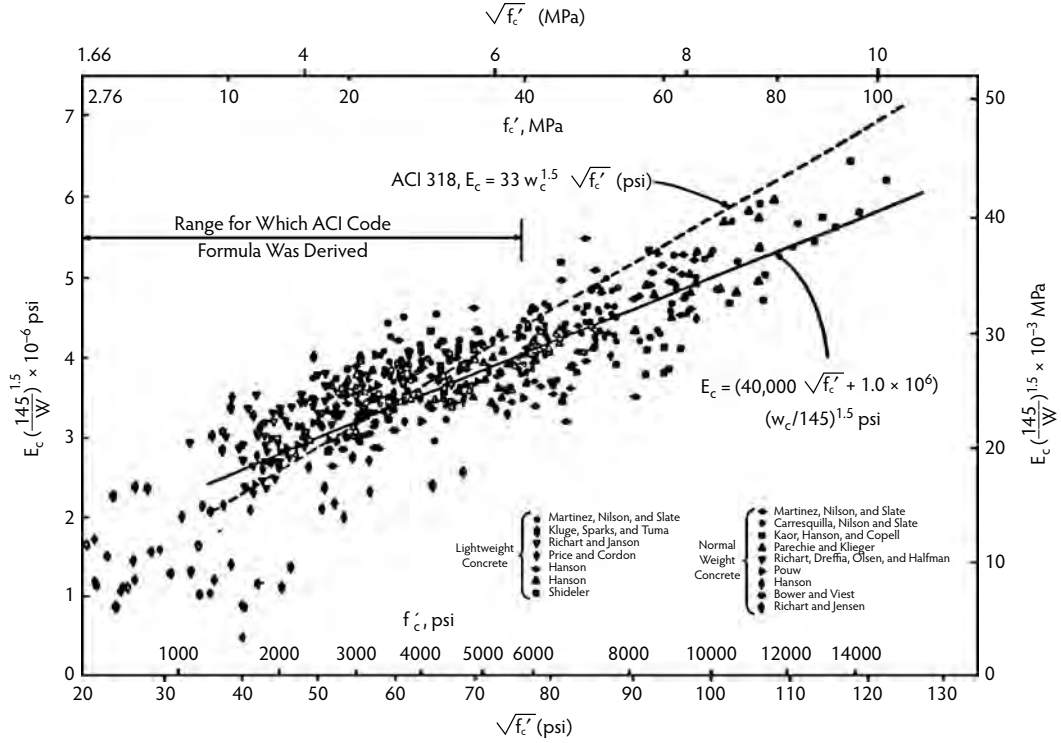


FIGURE 4.17 Modulus of elasticity vs. concrete strength. (From Nilson, A.H., *Design Implications of Current Research on High Strength Concrete*, ACI SP-87-7, American Concrete Institute, Farmington Hills, MI, 1985.)

of rupture (f_r) of the concrete. The cracking moment for an uncracked section can be computed from the basic flexural formula:

$$M_{cr} = \frac{f_y I_g}{y_t} \quad (4.24a)$$

or

$$M_{cr} = \frac{f_r}{S_t} \quad (4.24b)$$

where:

I_g = gross moment of inertia.

y_t = distance from the neutral axis to the extreme tension fibers.

f_r = modulus of rupture.

S_t = section modulus to the extreme tension fibers.

Cracks develop at several sections along a member length. At those sections where the modulus of rupture (f_r) is exceeded, cracks develop and the moment of inertia is reduced to a cracked moment (I_{cr}). At other sections where cracks do not develop, I_g is used for evaluating the stiffness of the sections.

Branson's work (1977), the basis of the ACI 318 Code, proposed using the effective moment of inertia (I_e) for cracked sections:

$$I_e = \left(\frac{M_{cr}}{M_g} \right)^3 I_g + \left[1 - \left(\frac{M_{cr}}{M_a} \right)^3 \right] I_{cr} \leq I_g \quad (4.25)$$

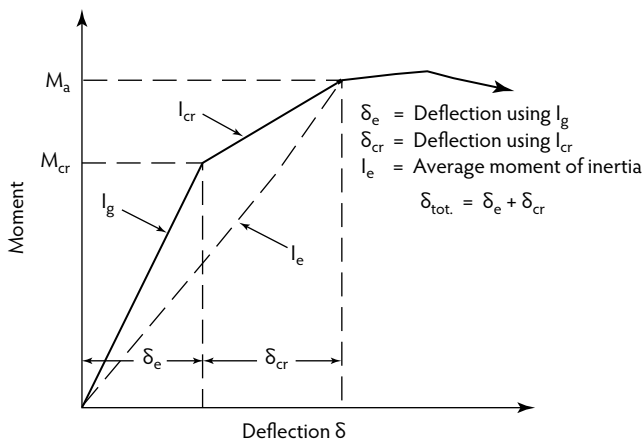


FIGURE 4.18 Bilinear moment of inertia diagram. (From ACI Committee 435, *Control of Deflection in Concrete Structures*, American Concrete Institute, Farmington Hills, MI, 1995.)

where:

M_{cr} = cracking moment.

M_a = maximum moment at the stage at which deflections are being considered.

I_g = gross moment of inertia of the section.

I_{cr} = moment of inertia of the cracked transformed section.

The two moments, I_g and I_{cr} , are based on the assumption of bilinear load-deflection behavior, as seen in Figure 4.18 (Nawy, 2008). The cracked moment of inertia (I_{cr}) is:

$$I_{cr} = nA_s d \left(1 - 1.6\sqrt{n\rho} \right) \quad (4.26)$$

where:

n = modular ratio = E_s/E_c .

ρ = A_s/bd .

d = effective depth.

Equation 4.25 can be rewritten as follows:

$$I_e = I_{cr} + \left(\frac{M_{cr}}{M_a} \right)^3 (I_g - I_{cr}) \leq I_g \quad (4.27)$$

For continuous beams, ACI 318 allows I_e to be taken as the average value obtained from Equation 4.25 or Equation 4.26 for the critical positive and negative moment sections. For prismatic sections, I_e may be taken as the value obtained at midspan for continuous spans. If the designer chooses to average the effective moments of inertia (I_e), the following expression can be used:

$$I_e = 0.5I_{e(m)} + 0.25(I_{e1} + I_{e2}) \quad (4.28)$$

where m , 1, and 2 refer to midspan and the two beam ends, respectively. Improved results for continuous prismatic members can be obtained by using a weighted average (ACI Committee 435, 1995) for beams that are continuous on both ends:

$$I_e = 0.70I_{e(m)} + 0.15(I_{e1} + I_{e2}) \quad (4.29a)$$

Or, for beams continuous on one end:

$$I_e = 0.85I_{e(m)} + 0.15(I_{e1}) \quad (4.29b)$$

4.6.1.2 Prestressed Concrete Beams

The effective moment of inertia (I_e) in Equation 4.25 and Equation 4.27 is based on different moment levels for M_{cr} and M_a in the case of prestressed concrete beams because of the initial compressive stress imposed by the prestressing force. The M_{cr}/M_a value is defined by:

$$\left(\frac{M_{cr}}{M_a} \right) = \left(1 - \frac{f_{TL} - f_r}{f_L} \right) \quad (4.30)$$

where:

$$f_r = 7.5\lambda\sqrt{f'_c}$$

Here, $\lambda = 1.0$ for normal weight concrete; $\lambda = 0.85$ for sand lightweight concrete; $\lambda = 0.75$ for all lightweight concrete, and

M_{cr} = moment due to that portion of the *unfactored live-load* moment that causes cracking.

M_a = maximum *unfactored* live-load moment.

f_{TL} = *total* calculated stress in the member.

f_L = calculated stress owing to *live load*.

In prestressed beams that are partially prestressed by the addition of mild steel reinforcement:

$$I_{cr} = \left(n_p A_{ps} d_p^2 + n_s A_s d^2 \right) \left[\left(1 - 1.6 \sqrt{n_p \rho_p + n_s \rho} \right) \right] \quad (4.31)$$

4.6.1.3 Effect of Compression Reinforcement

Compression reinforcement in reinforced flexural members and nontensioned reinforcement such as mild steel in prestressed flexural members tend to offset the movement of the neutral axis caused by creep (ACI Committee 209, 1992). A reverse movement toward the tensile fibers can thus result. A multiplier (γ) has to be used to account for increase in deflection, as required in the ACI 318 Building Code:

$$\gamma = \frac{\xi}{1 + 50\rho'} \quad (4.32)$$

where:

ξ = time-dependent factor for the long-term increase in deflection obtained from Figure 4.19 (ACI Committee 435, 1995).

$\rho' = A'_s / bd$.

A'_s = area of compression reinforcement (in square inches).

Nilson (1985) suggested that two modifying factors should be applied to Equation 4.32: the material modifier (μ_m) to be applied to ξ and the section modifier (μ_s) to be applied to ρ' . Both μ_m and μ_s have a value of 1 or less. Combining the two multipliers, without significant loss in accuracy, Equation 4.32 becomes:

$$\gamma = \frac{\mu \xi}{1 + 50\mu \rho'} \quad (4.33)$$

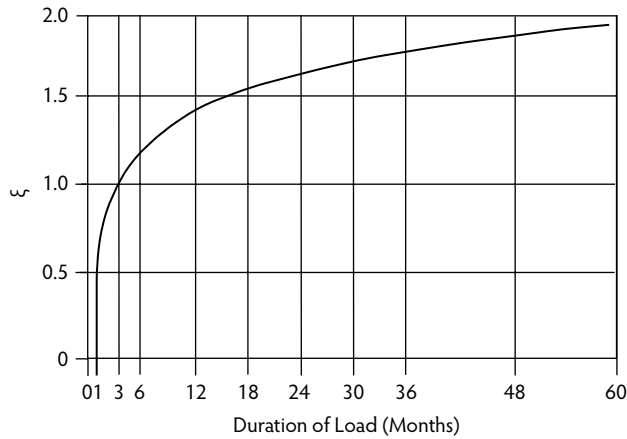


FIGURE 4.19 Multipliers for long-term deflection. (From Nawy, E.G., *Reinforced Concrete: A Fundamental Approach*, 6th ed., Prentice Hall, Upper Saddle River, NJ, 2008.)

with the range of μ values as follows within the 6000- to 9500-psi (42- to 66-MPa) compressive strength tests conducted:

$$\mu \geq 0.7 \quad (4.34a)$$

$$\mu \leq (1.3 - 0.00005f'_c) \leq 1.0$$

or, megapascals for f'_c :

$$\mu \leq (1.3 - 0.0072f'_c) \leq 1.0 \quad (4.34b)$$

Further evaluations are needed for cases where the concrete strength is higher than 12,000 psi (83 MPa).

4.6.2 Flexural Crack Width Development

External load results in direct and bending stresses, which cause flexural, bond, and diagonal tension cracks. Immediately after the tensile stress in the concrete exceeds its tensile strength at a particular location, any internal microcracks that might have formed begin to propagate into macrocracks. These cracks develop into macrocracks that propagate to the external fiber zones of the element. Immediately after full development of the first crack in a reinforced concrete element, the stress in the concrete at the cracking zone is reduced to zero and is assumed by the reinforcement (Nawy, 2001, 2008). The distribution of ultimate bond stress (μ), longitudinal stress in the concrete (f_t), and longitudinal tensile stress (f_s) in the reinforcement can be schematically represented as shown in Figure 4.20. Crack width is primarily a function of the deformation of reinforcement between the two adjacent cracks, 1 and 2 (Figure 4.20), if the small concrete tensile strain along the crack interval a_c is neglected. The crack width is thus a function of crack spacing up to the load level at which no more cracks develop, which leads to stabilization of the crack spacing, as shown in Figure 4.21. The major parameters affecting the development and characteristics of cracks are percentage of reinforcement, bond characteristics and size of bar, concrete cover, and the concrete area in tension. On this basis, one can propose the following mathematical model:

$$w = \alpha a_c^\beta \epsilon_s^\gamma \quad (4.35)$$

where w is maximum crack width and α , β , and γ are nonlinearity constants. Crack spacing (a_c) is a function of factors to be subsequently discussed and is inversely proportional to bond strength and active steel ratio (steel percentage in terms of the concrete area in tension). Here, ϵ_s is the strain in the reinforcement induced by the external load.

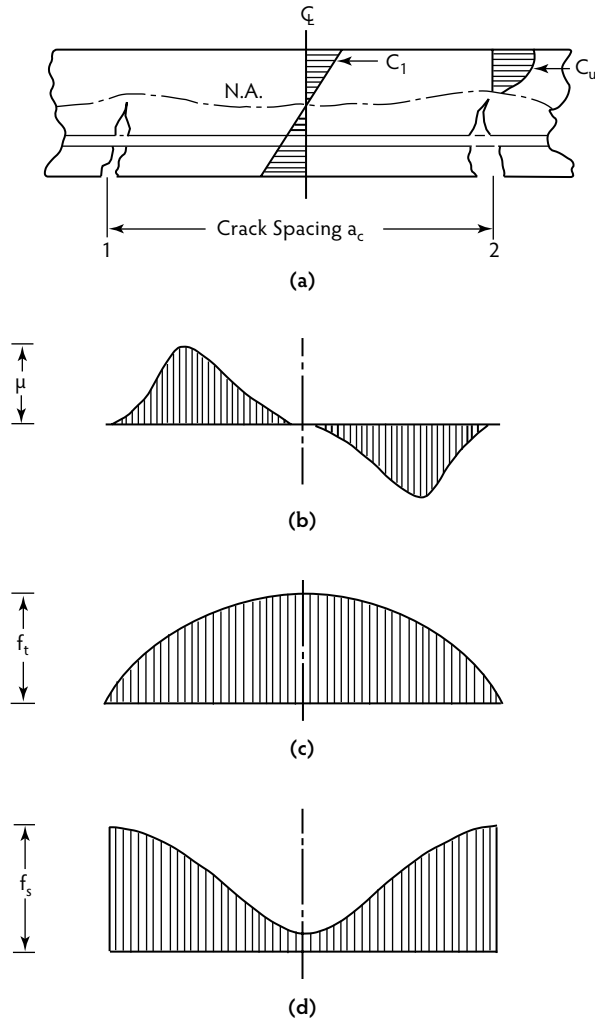


FIGURE 4.20 Schematic stress distribution between two flexural cracks. (From Nawy, E.G. and Blair, K.W., in *Cracking, Deflection, and Ultimate Load of Concrete Slab Systems*, ACI SP-30, Nawy, E.G., Ed., American Concrete Institute, Farmington Hills, MI, 1971, pp. 1–41.)

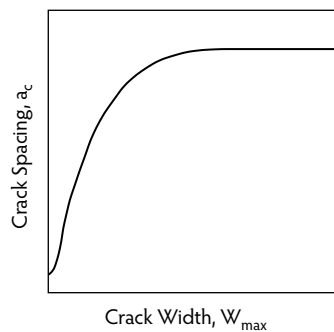


FIGURE 4.21 Schematic variation of crack width with crack spacing. (From Nawy, E.G. and Blair, K.W., in *Cracking, Deflection, and Ultimate Load of Concrete Slab Systems*, ACI SP-30, Nawy, E.G., Ed., American Concrete Institute, Farmington Hills, MI, 1971, pp. 1–41.)

The basic mathematical model (Equation 4.35), with the appropriate experimental values of the constants α , β , and γ , can be derived for a particular type of structural member. Such a member can be a one-dimensional element such as a beam, a two-dimensional structure such as a two-way slab, or a three-dimensional member such as a shell or circular tank wall. Hence, it is expected that different forms or expressions apply for evaluation of macrocracking behavior of different structural elements consistent with their fundamental structural behavior (ACI Committee 224, 2001; ACI Committee 318, 2008; CEB-FIP, 1990; Gergely and Lutz, 1968; Nawy, 1972a,b, 1994; Nawy and Blair, 1971).

4.6.2.1 Reinforced Concrete Beams and One-Way Slabs

The requirements for crack control in beams and thick one-way slabs—10 in. (250 mm) or thicker—in the ACI Building Code (ACI Committee 318, 2008) are based on the statistical analysis of maximum crack width data from a number of sources. On the basis of the analysis, the following general conclusions were reached (Gergely and Lutz, 1968; Nawy, 1972a,b, 1994; Nawy and Blair, 1971):

1. The steel stress is the most important variable.
2. The thickness of the concrete cover is an important variable.
3. The area of concrete surrounding each reinforcing bar is an important geometric variable.
4. Bar diameter is not a major variable.
5. The bottom crack width is influenced by the amount of strain gradient from the level of the steel to the tension face of the beam.

The simplified expression relating crack width to steel stress is (Gergely and Lutz, 1968):

$$w_{\max} (\text{in.}) = 0.076\beta f_s \sqrt[3]{d_c A} \times 10^{-3} \quad (4.36a)$$

where:

f_s = reinforcing steel stress (ksi).

A = area of concrete symmetrical with reinforcing steel divided by number of bars (in.^2).

d_c = thickness of concrete cover measured from extreme tension fiber to center of bar or wire closest thereto (in.).

β = h_2/h_1 , where h_1 is the distance from the neutral axis to the reinforcing steel (in.), and h_2 is the distance from the neutral axis to the extreme concrete tensile surface.

When the strain (ϵ_s) in the steel reinforcement is used instead of stress (f_s), Equation 4.36a becomes:

$$w = 2.2\beta \epsilon_s \sqrt[3]{d_c A} \quad (4.36b)$$

Equation 4.36b is valid in any system of measurement.

The cracking behavior in thick one-way slabs is similar to that in shallow beams. For one-way slabs that have a clear concrete cover in the range of 1 in. (25.4 mm), Equation 4.38 can be adequately applied if $\beta = 1.25$ to 1.35 is used.

The ACI 318 Building Code currently uses reinforcement spacing as the criteria for control of the crack width. It recommends for beams and one-way slabs the following expression:

$$s (\text{in.}) = 15 \left(\frac{40,000}{f_s} \right) - 2.5c \quad (4.37)$$

but not greater than $12(40,000/f_s)$, where:

s = spacing (in.).

f_s = calculated reinforcement stress at service level or alternatively taken as 2/3 the yield strength f_y (psi).

c = clear cover to the reinforcement (in.).

TABLE 4.4 Maximum Tolerable Flexural Crack Widths

Exposure Condition	Crack Width	
	Inch	Min.
Dry air or protective membrane	0.016	0.40
Humidity, moist air, soil	0.012	0.30
Deicing chemicals	0.007	0.18
Seawater and seawater spray; wetting and drying	0.006	0.15
Water-retaining structures (excluding nonpressure pipes)	0.004	0.10

Sources: ACI Committee 224, *Proc. ACI J.*, 20(10), 35–76, 2001; Nawy, E.G., *Reinforced Concrete: A Fundamental Approach*, 6th ed., Prentice Hall, Upper Saddle River, NJ, 2008, p. 864.

The SI expression in Equation 4.37 is:

$$s \text{ (mm)} = 380 \left(\frac{280}{f_s} \right) - 2.5c_c \quad (4.38)$$

but not to exceed $300(280/f_s)$, where f_s in usual cases is taken as 252 MPa.

It should be noted that the ACI expression is applicable to reinforced concrete beams and one-way slabs in normal environmental conditions. In aggressive environments, such as liquid-retaining sanitary structures, Equations 4.36a and 4.36b, with the appropriate limitation of tolerable crack widths listed in Table 4.4, are more appropriate in such cases.

4.6.2.2 Prestressed Concrete Beams

4.6.2.2.1 Crack Spacing

Primary cracks form in the region of maximum bending moment when the external load reaches the cracking load. Sometimes, in post-tensioned parking garage elements, cracks form in the draped region before forming at the maximum moment region. They can also form at debonded tendon locations. As loading is increased, additional cracks will form, and the number of cracks will be stabilized when the stress in the concrete no longer exceeds its tensile strength at further locations, regardless of load increase. This condition is important, as it essentially produces the absolute minimum crack spacing that can occur at high steel stresses, and is termed the **stabilized minimum crack spacing**. The maximum possible crack spacing under this stabilized condition is twice the minimum and is termed the *stabilized maximum crack spacing*. Hence, the **stabilized mean crack spacing** (a_{cs}) is deduced as the mean value of the two extremes. The total tensile force (T) transferred from the steel to the concrete over the stabilized mean crack spacing (Nawy, 1990, 1994, 1996) can be defined as:

$$T = \gamma a_{cs} \mu \sum o \quad (4.39a)$$

where:

γ = a factor reflecting the distribution of bond stress.

μ = maximum bond stress that is a function of $\sqrt{f'_c}$.

$\sum o$ = sum of reinforcing elements' circumferences.

Figure 4.22 illustrates the forces that cause the formation of the stabilized crack.

The resistance (R) of the concrete area in tension (A_c) can be defined as:

$$R = A_c f'_t \quad (4.39b)$$

where f'_t is the tensile splitting strength of the concrete.

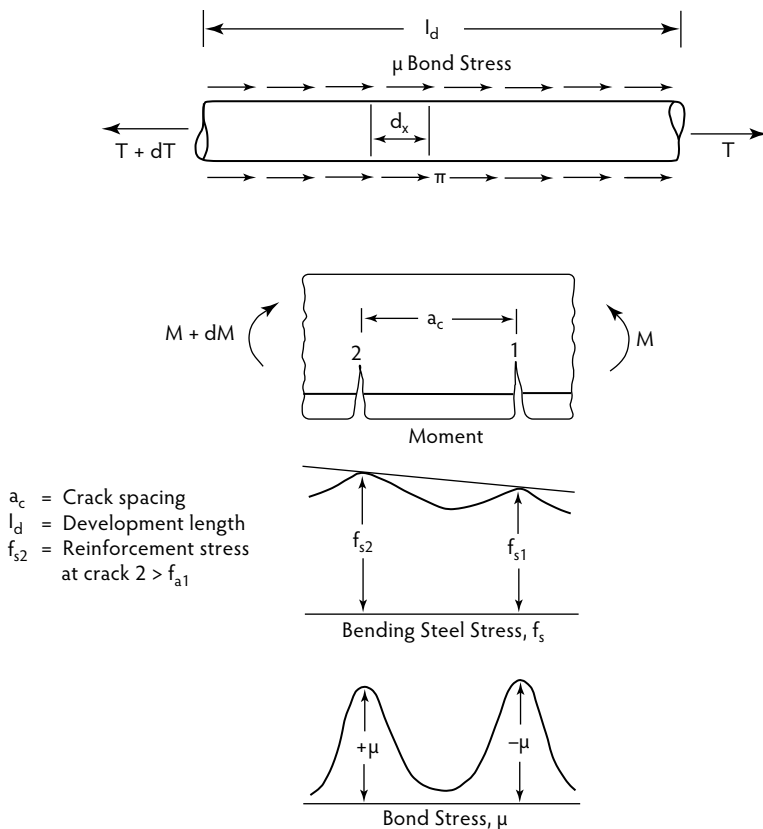


FIGURE 4.22 Force and stress distribution in stabilized crack in a prestressed beam. (From Nawy, E.G., in *Cracking in Prestressed Concrete Structures*, ACI SP-113, American Concrete Institute, Farmington Hills, MI, 1990, pp. 1–42.)

By equating Equations 4.39a and 4.39b, the following expression for a_{cs} is obtained, where c is a constant to be developed from the tests:

$$a_{cs} = c \frac{A_t f_t'}{\sum_o \sqrt{f_c'}} \quad (4.40a)$$

The concrete stretched area (namely, the concrete area A_t that is under tension for both the evenly distributed and unevenly distributed reinforcing elements) is illustrated in Figure 4.23. With a mean value of:

$$f_t' / \sqrt{f_c'} = 7.95$$

the mean stabilized crack spacing becomes:

$$a_{cs} = 1.20 \frac{A_t}{\sum_o} \quad (4.40b)$$

4.6.2.2.2 Crack Width

If Δf_s is the net stress in the prestressed tendon or the magnitude of the tensile stress in normal steel at any crack-width load level in which the decompression load (decompression here means $f_c' = 0$ at the

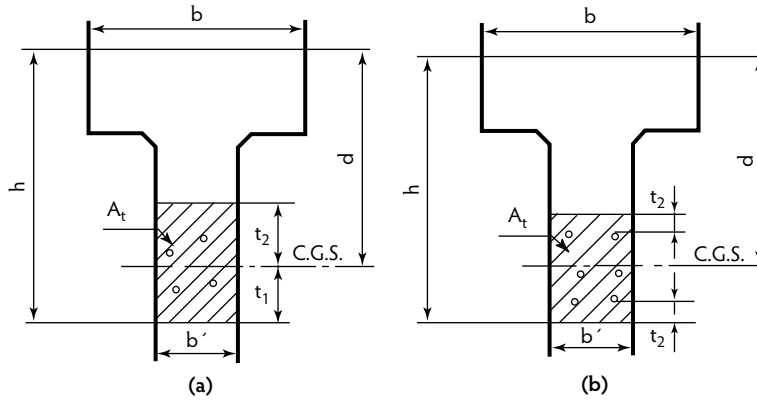


FIGURE 4.23 Effective concrete area in tension: (a) even reinforcement distribution; (b) non-even reinforcement distribution. (From Nawy, E.G., in *Cracking in Prestressed Concrete Structures*, ACI SP-113, American Concrete Institute, Farmington Hills, MI, 1990, pp. 1–42.)

level of the reinforcing steel) is taken as the reference point (Nawy, 1990, 1996), then for the prestressed tendon:

$$\Delta f_s = f_{nt} - f_d \quad (4.41)$$

where:

f_{nt} = stress in the prestressing steel at any load beyond the decompression load.

f_d = stress in the prestressing steel corresponding to the decompression load.

Unit strain $\epsilon_s = \Delta f_s / E_s$. It is logical to disregard as insignificant unit strains in the concrete caused by temperature, shrinkage, and elastic shortening effects. The maximum crack width as defined in Equation 4.35 can therefore be taken as:

$$w_{\max} = k a_{cs} \epsilon_s^\alpha \quad (4.42a)$$

or

$$w_{\max} = k' a_{cs} (\Delta f_s)^\alpha \quad (4.42b)$$

where k' is a constant in terms of constant k .

4.6.2.2.3 Expression for Pretensioned Beams

Equation 4.42b is rewritten in terms of Δf_s to give the maximum crack width at the reinforcement level as follows:

$$w_{\max} (\text{in.}) = 5.85 \times 10^{-5} \frac{A_t}{\sum o} (\Delta f_s) \quad (4.43a)$$

where A_t = square inches, $\sum o$ = inches, and Δf_s = kips/in.², and

$$w_{\max} (\text{mm}) = 8.48 \times 10^{-5} \frac{A_t}{\sum o} (\Delta f_s) \quad (4.43b)$$

where A_t = cm², $\sum o$ = cm, and Δf_s = MPa.

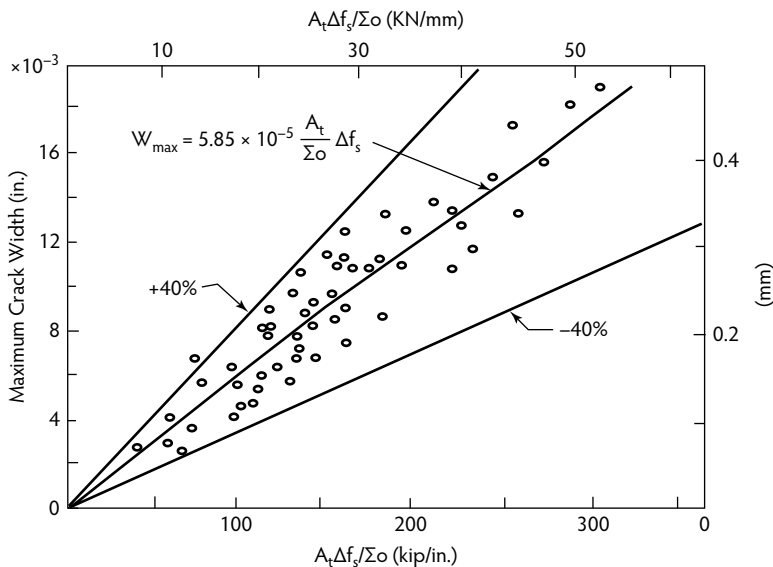


FIGURE 4.24 Linearized maximum crack width vs. $(A_t/\Sigma_o)\Delta f_s$ for pretensioned beams (Nawy, 1990, 1994, 1996, 2005).

The maximum crack width (inches) at the tensile face of the concrete is:

$$w'_{\max} = 5.85 \times 10^{-5} R_i \frac{A_t}{\sum_o} (\Delta f_s) \quad (4.43c)$$

where R_i is the distance ratio equal to h_2/h_1 , where h_2 is the distance from the neutral axis to the extreme tension fibers and h_1 is the distance from the neutral axis to the reinforcement centroid. A plot of the pretensioned beams test data and the best fit expression for Equation 4.43a is given in Figure 4.24 with a 40% spread, which is reasonable in view of the randomness of crack development.

4.6.2.2.4 Expressions for Post-Tensioned Beams

The expression developed for the crack width in post-tensioned bonded beams that contain mild steel reinforcement is:

$$w_{\max} \text{ (in.)} = 6.51 \times 10^{-5} \frac{A_t}{\sum_o} (\Delta f_s) \quad (4.44a)$$

and

$$w_{\max} \text{ (mm)} = 9.44 \times 10^{-5} \frac{A_t}{\sum_o} (\Delta f_s) \quad (4.44b)$$

for the crack width at the reinforcement level closest to the tensile face.

At the tensile face, the crack width for the post-tensioned beams becomes:

$$w_{\max} \text{ (in.)} = 6.51 \times 10^{-5} R_i \frac{A_t}{\sum_o} (\Delta f_s) \quad (4.44c)$$

For nonbonded beams, the factor 6.51 in Equations 4.44a and 4.44c becomes 6.83. A plot of the data and the best-fit expression for Equation 4.44a is given in Figure 4.25. A typical plot of the effect of the various steel percentages on the crack spacing at various stress levels (Δf_s) is given in Figure 4.26. It can be seen from this plot that crack spacing stabilizes at a net stress level range of 30 to 36 kips/in.² (207 to 248 MPa).

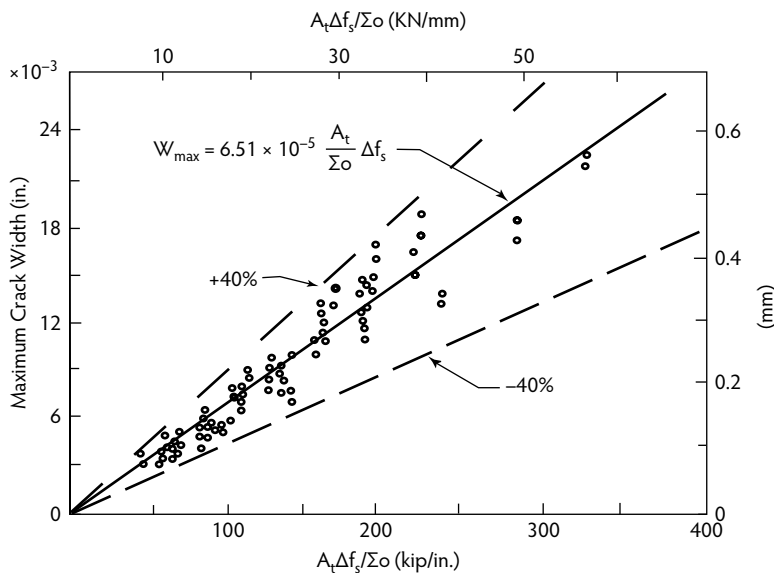


FIGURE 4.25 Linearized maximum crack width vs. $(A_t/\Sigma_o)\Delta f_s$ for post-tensioned beams (Nawy, 1990, 1994, 1996, 2005).

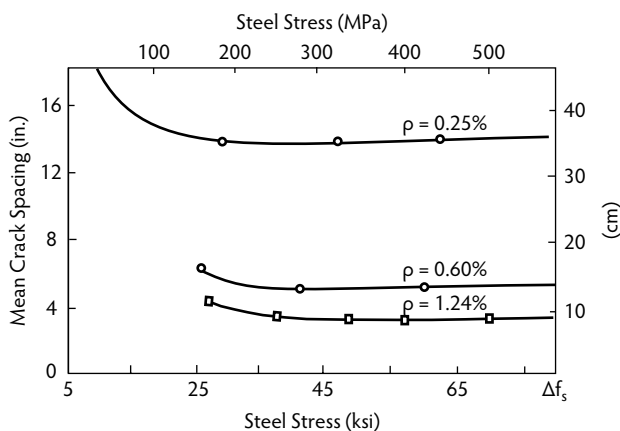


FIGURE 4.26 Effect of steel percentage on mean crack spacing in prestressed beams (Nawy, 1990, 1994, 1996, 2005).

4.6.2.2.5 Cracking of High-Strength Prestressed Beams

Analysis of continuing subsequent work by the first author on the cracking behavior of pretensioned and nonbonded post-tensioned beams having cylinder compressive strengths in the range of 10,200 to 14,200 psi (70.3 to 97.9 MPa) have resulted in the following expression for crack width at the reinforcement level of pretensioned members:

$$w_{\max} (\text{in.}) = 2.75 \times 10^{-5} \frac{A_t}{\Sigma_o} (\Delta f_s) \quad (4.45a)$$

and

$$w_{\max} (\text{mm}) = 4.0 \times 10^{-5} \frac{A_t}{\Sigma_o} (\Delta f_s) \quad (4.45b)$$

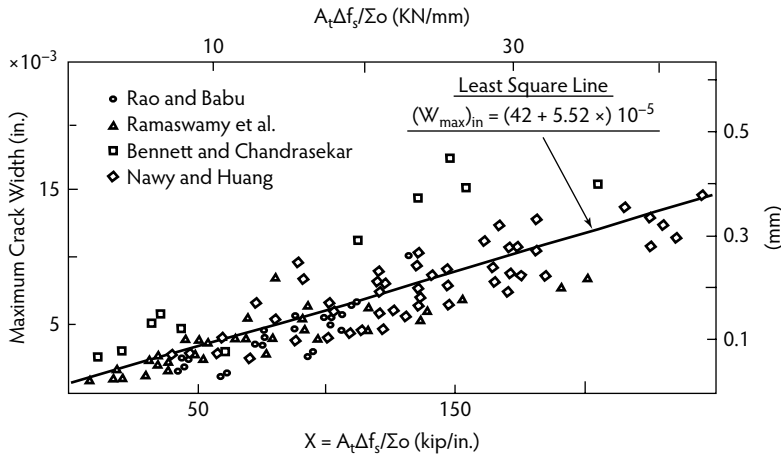


FIGURE 4.27 Reinforcement stress vs. crack width (best-fit data of several investigators). (From Nawy, E.G., in *Proceedings of CANMET International Symposium on Advances in Concrete Technology*, 2nd ed., Malhotra, V.M., Ed., Canada Center for Mineral and Energy Technology (CANMET), Ottawa, 1994, pp. 203–242.)

The factor 2.75 is an average of values from the following statistical expression (Nawy, 1994) for a reduction multiplier λ_r of w_{\max} in Equation 4.43 such that:

$$\lambda_r = \frac{2}{(0.75 + 0.06\sqrt{f'_c})\sqrt{f'_c}} \quad (4.45c)$$

This reduced crack width due to use of high-strength concrete is expected in view of the increased bond interaction between the concrete and the reinforcement.

4.6.2.2.6 Other Work on Cracking in Prestressed Concrete

After analyzing results from various investigators (Harajli and Naaman, 1989; Naaman and Siriakson, 1979), Naaman produced the following modified expression for partially prestressed pretensioned members:

$$w_{\max} (\text{in.}) = \left(42 + 5.58 \frac{A_t}{\sum o} (\Delta f_s) \right) \times 10^{-5} \quad (4.46)$$

This expression is very close to that in Equation 4.43 by Nawy. If plotted against results of the various researchers' work, it gives a best fit as shown in Figure 4.27.

4.6.2.3 Two-Way Supported Slabs and Plates

Flexural crack control is essential in structural floors, most of which are under two-way action. Cracks at service-load and overload conditions can be serious in floors such as those in office buildings, schools, parking garages, and industrial buildings and in other floors where the design service load and overload levels exceed loads in normal-size apartment building panels. Such cracks can only lead to detrimental effects on the integrity of the total structure, particularly in adverse environmental conditions.

4.6.2.3.1 Flexural Cracking Mechanism and Fracture Hypothesis

Flexural cracking behavior in concrete structural floors under two-way action is significantly different from that in one-way members. Crack control equations for beams underestimate crack widths developed in two-way slabs and plates and do not tell the designer how to space reinforcement. Cracking in two-way slabs and plates is primarily controlled by the steel stress level and the **spacing** of reinforcement in two perpendicular directions. In addition, the clear concrete cover in two-way slabs and plates is nearly

constant (3/4 in., or 20 mm, for interior exposure), whereas it is a major variable in the crack control equations for beams. Results from extensive tests on slabs and plates (Nawy, 1972a, 1994; Nawy and Blair, 1971) demonstrate this difference in behavior in a fracture hypothesis on crack development and propagation in two-way plate action. Nawy's work also conclusively demonstrated that surface deformations of individual reinforcing elements have little effect on arresting the generation of cracks or controlling crack type or width in a two-way-action slab or plate. One may also conclude that the scale effect on two-way-action cracking behavior is insignificant, as the cracking grid is a reflection of the reinforcement grid if the preferred orthogonal narrow cracking widths develop. To control cracking in two-way-action floors, then, the major parameter to be considered is the reinforcement spacing in the two perpendicular directions. Concrete cover has only a minor effect, as the cover is usually small, with a constant value of 0.75 in. (20 mm). Maximum spacing of the reinforcement in both orthogonal directions should not exceed 12 in. (30 cm) in any structural floor.

4.6.2.3.2 Crack Control Equation

The basic Equation 4.35 for relating crack width to strain in the reinforcement is:

$$w = \alpha a_c^\beta \epsilon_s^\gamma$$

The effect of the tensile strain in the concrete between the cracks is neglected as insignificant. The parameter a_c is the crack spacing, ϵ_s is the unit strain in the reinforcement, and α , β , and γ are constants evaluated by tests. The mathematical model in Equation 4.35 and statistical analysis of the data of 90 slabs tested to failure give the following equation (ACI Committee 224, 2001; Nawy and Blair, 1971) for serviceability requirements for crack control:

$$w \text{ (in.)} = K \beta f_s \sqrt{G_I} \quad (4.47)$$

Using SI units, the expression becomes:

$$w_{\max} \text{ (mm)} = 0.145 K \beta f_s \sqrt{G_I} \quad (4.48)$$

where f_s is in megapascals, and all the terms for the grid index (G_I) in Equation 4.49 are in millimeters. $G_I = d_{b1} s_2 / \rho_{t1}$ is the grid index that defines the reinforcement distribution in two-way action slabs and plates. It can be transformed in Equation 4.47 to:

$$G_I = \frac{s_1 s_2 d_c}{d_{b1}} \frac{8}{\pi} \quad (4.49)$$

where:

K = fracture coefficient, having a value of $K = 2.8 \times 10^{-5}$ for uniformly loaded restrained two-way action square slabs and plates. For concentrated loads or reactions, or when the ratio of short to long span is less than 0.75 but larger than 0.5, a value of $K = 2.1 \times 10^{-5}$ is applicable. For a span-aspect ratio of 0.5, $K = 1.6 \times 10^{-5}$. Units of coefficient K are in square inch per pound. (See also Table 4.5.)

β = ratio of the distance from the neutral axis to the tensile face of the slab to the distance from the neutral axis to the centroid of the reinforcement grid (to simplify the calculations use, $\beta = 1.25$, although it varies between 1.20 and 1.35).

f_s = actual average service load reinforcement stress level, or 40% of the design yield strength (ksi).

d_{b1} = diameter of the reinforcement in direction 1 closest to the concrete outer fibers (in.).

s_1 = spacing of the reinforcement in perpendicular direction 1 (in.), closest to the tensile face.

s_2 = spacing of the reinforcement in perpendicular direction 2 (in.).

1 = direction of the reinforcement closest to the outer concrete fibers; this is the direction for which the crack control check is to be made.

ρ_{t1} = active steel ratio in direction 1:

TABLE 4.5 Fracture Coefficients for Slabs and Plates

Loading Type ^a	Slab Shape	Boundary Condition ^b	Span Ratio (S/L) ^c	Fracture Coefficient (10 ⁻⁵ K)
A	Square	4 edges r	1.0	2.1
A	Square	4 edges s	1.0	2.1
B	Rectangular	4 edges r	0.5	1.6
B	Rectangular	4 edges r	0.7	2.2
B	Rectangular	3 edges r, 1 edge h	0.7	2.3
B	Rectangular	2 edges r, 2 edges r	0.7	2.7
B	Square	4 edges r	1.0	2.8
B	Square	3 edges r, 1 edge h	1.0	2.9
B	Square	2 edges r, 2 edges h	1.0	4.2

^a A, concentrated; B, uniformly distributed.

^b r, restrained; s, simply supported; h, hinged.

^c S, clear short span; L, clear long span.

Source: Nawy, E.G. and Blair, K.W., in *Cracking, Deflection, and Ultimate Load of Concrete Slab Systems*, ACI SP-30, Nawy, E.G., Ed., American Concrete Institute, Farmington Hills, MI, 1971, pp. 1-41.

$$\rho_{t1} = \frac{\text{Area of steel } A_s \text{ per foot width}}{12(d_{b1} + 2c_1)}$$

where c_1 is the clear concrete cover measured from the tensile face of the concrete to the nearest edge of the reinforcing bar in direction 1, and w is the crack width (in.) at the face of the concrete caused by flexural load. Subscripts 1 and 2 pertain to the directions of reinforcement. Detailed values of the fracture coefficients for various boundary conditions are given in Table 4.5. A graphical solution for Equation 4.47 is given in Figure 4.28 for $f_y = 60$ ksi (414 MPa), $f_s = 40\%$, and $f_y = 40$ ksi (165.5 MPa) for rapid determination of the reinforcement size and spacing needed for crack control.

Because cracking in two-way slabs and plates is primarily controlled by the grid intersections of the reinforcement, concrete strength is not of major consequence; hence, the value of crack width in two-way action predicted by Equation 4.47 should not be significantly affected if higher strength concretes are used in excess of 6000 psi (41.4 MPa). It has to be pointed out that in two-way normal-slab floors, the use of much higher strengths is not justified in economical terms.

4.6.2.3.3 Tolerable Crack Widths in Concrete Structures

The maximum crack width that a structural element should be permitted to develop depends on the particular function of the element and the reasonable guide to the tolerable average crack widths in concrete structures under various normally encountered environmental conditions. Its values are in close agreement with the Comité Eurointernational du Béton recommendations (CEB-FIP, 1990) foremost exposure conditions. The crack-control equation and guidelines presented are important not only for the control of corrosion in reinforcement but also for deflection control. The reduction of the stiffness (EI) of the two-way slabs or plates due to orthogonal cracking when the tolerable crack widths in Table 4.6 are exceeded can lead to both short- and long-term excessive deflection. Deflection values that are several times greater than those anticipated in the design, including deflection due to construction loading, can be reasonably controlled through camber and control of the flexural crack width in the slab or plate. Proper selection of reinforcement spacing s_1 and s_2 in the perpendicular directions, as discussed in this section, that does not exceed 12 in. (30 cm) center-to-center can maintain the good serviceability performance of a slab system under normal and reasonable overload conditions.

4.6.2.3.4 Long-Term Effects on Cracking

In most cases, the magnitude of crack widths increases in long-term exposure and long-term loading. Increase in crack width can vary considerably in cases of cyclic loading, such as in bridges; however, the crack width increases at decreasing rate with time. In most cases, a doubling of crack width after several years under sustained loading is not unusual.

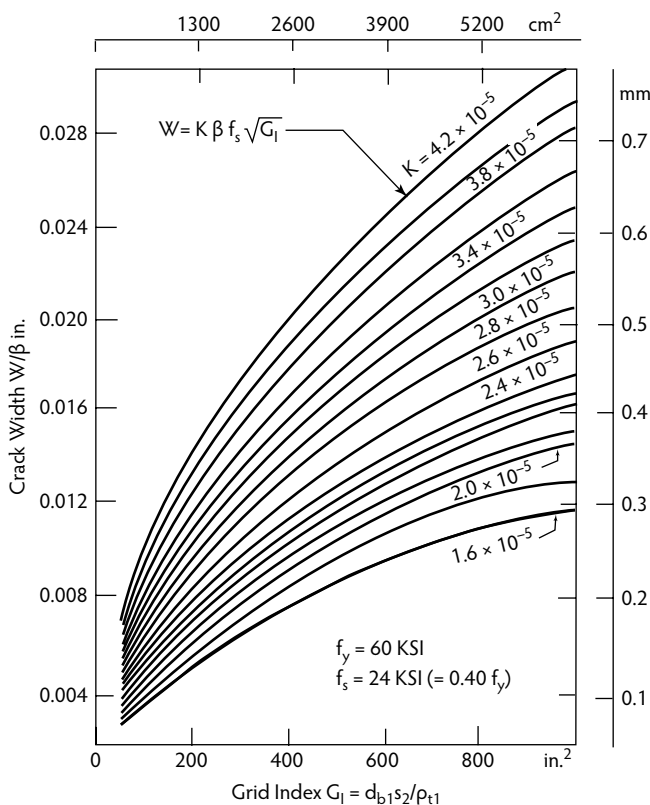


FIGURE 4.28 Crack control reinforcement distribution in two-way action slabs and plates (Nawy, 1994, 2005; Nawy and Blair, 1971).

TABLE 4.6 Minimum Shrinkage and Temperature Reinforcement

Length between Movement Joints (ft)	Minimum Temperature and Shrinkage Reinforcement Ratio	
	Grade 40	Grade 60
Less than 20	0.0030	0.0030
20 to less than 30	0.0040	0.0030
30 to less than 40	0.0050	0.0040
40 and greater	0.0060 ^a	0.0050 ^a

^a Maximum shrinkage and temperature reinforcement where movement joints are not provided.

Note: When using this table, the actual joint spacing shall be multiplied by 1.5 if no more than 50% of the reinforcement passes through the joint.

Source: ACI Committee 350, *Code Requirements for Environmental Engineering Concrete Structures*, American Concrete Institute, Farmington Hills, MI, 2001.

4.6.2.4 Cracking in Circular Prestressed Concrete Tanks

Circular prestressed tanks are cylindrical shell elements of very large diameter in relation to their height; hence, with respect to flexural cracking, it is possible to treat the wall of a tank in a manner similar to the treatment of two-way action plates. Vessey and Preston (1978) modified Nawy and Blair's (1971) expressions for two-way action slabs and plates so the maximum crack width can be defined as:

$$w_{\max} (\text{in.}) = 4.1 \times 10^{-6} \epsilon_{ct} E_{ps} \sqrt{G_I} \quad (4.50)$$

Using SI units, the expression becomes:

$$w_{\max} (\text{mm}) = 0.6 \times 10^{-6} \epsilon_{ct} E_{ps} \sqrt{G_I} \quad (4.51)$$

where, in the SI expression, E_{ps} is in MPa, the dimensions of all the parameters of the grid index G_I are in millimeters, and

ϵ_{ct} = tensile surface strain in the concrete = $(\lambda_t F_p)/(E_{ps})$.

f_p = actual stress in the steel.

f_{pi} = initial prestress before losses.

$\lambda_t = f_p/f_{pi}$.

G_I = grid index = $(s_1 s_2 d_c/d_{b1})(8/\pi)$.

d_{b1} = diameter of steel in direction 1.

s_1 = spacing of the reinforcement in direction 1 closest to the tensile face.

s_2 = spacing of the reinforcement in direction 2.

d_c = concrete cover to center of steel, inches.

Note that $w_{\max} = 0.004$ in. (0.1 mm) should be the limit of crack width for liquid-retaining tanks.

4.7 Long-Term Shrinkage and Temperature Reinforcement Controlling Cracking Between Joints in Walls and Slabs of Liquid-Retaining Structures

Cracking resulting from these unavoidable short-term and long-term strain gradients has always been a problem for the designer to consider as a significant factor in any structural design; hence, the use of joints is inevitable. It would be rare to find a structural system with total stress relievers, where if enough reinforcement is provided in the direction of the induced forces to prevent the cracks from opening then no joint would be needed. It would be economically prohibitive, as the volume of reinforcement required to perform this task would be significant. Because the induced forces are highly indeterminate, engineering judgment has to be exercised in interpreting the imprecise guidelines in codes and the literature on the type and spacing of joints to control cracking, which often render conflicting solutions.

Table 4.6 and Figure 4.29 (ACI Committee 350, 2001) stipulate the reinforcement percentages of shrinkage and temperature reinforcement for effective control of cracks that is essential to maintain between joints in liquid-retaining structures. Whereas the maximum percentage in Table 4.6 is given as 0.5% for movement joints of 40 feet, the high rigidity of the foundation slab at the wall joint to the slab renders this percentage inadequate. The relative lower flexibility of the wall as compared to the stiff foundation slab at the lower wall segment makes the connection totally rigid with a low magnitude of rotation at the joint, as the wall is almost fixed at the base and free at the top. To prevent long-term vertical cracking concentration at the lower quarter of the wall height, it might even be prudent to use almost 1.0 to 1.25% horizontal reinforcement for the lowermost segment of the wall if the wall thickness is in the range of 30 in. Details regarding the design, spacing, and construction of joints in most types of structural systems for the control of long-term cracking are covered in Chapter 17 of this *Handbook*.

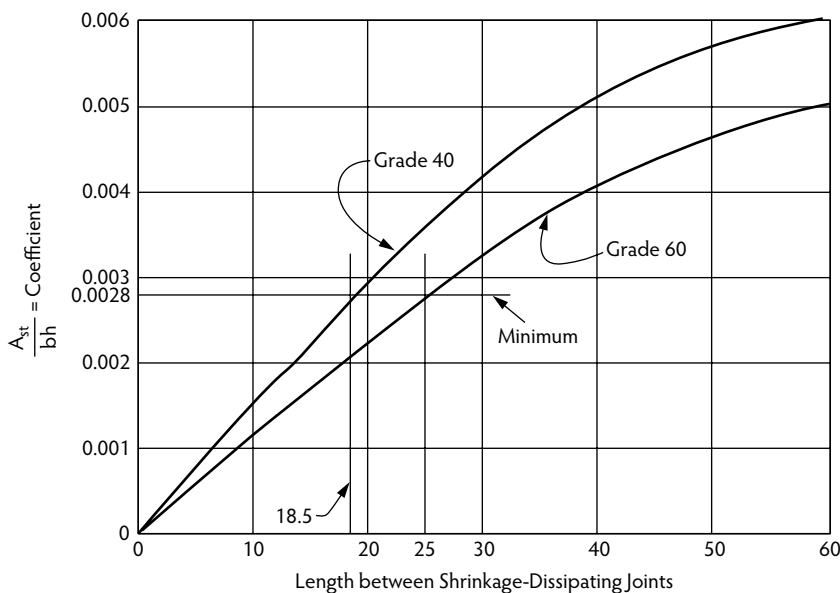


FIGURE 4.29 Shrinkage and temperature reinforcement for environmental engineering concrete structures (ACI Committee 224, 1995; ACI Committee 350, 2006).

4.8 Autogenous Shrinkage in Early-Age Concrete

Shrinkage in early-age concrete is an important aspect in determining the long-term cracking performance of concrete. The methods of curing have a significant effect on the level of shrinkage strains that develop, so it is useful to observe the different performances expected from different methods of curing and also the effect of the constituent cementitious materials on the autogenous shrinkage performance of the system. Tests by Suksawang et al. (2005) have provided a measure of differences in strains (hence, stresses) at 0 to 7 days and up to 100 days of curing. Figure 4.30a (early-age performance) and Figure 4.30b (100-day performance) indicate that, after 28 days of curing, the dry-cured specimen exhibited steeper shrinkage levels than the others due to the fact that less internally adsorbed water was available to prevent a higher increase in shrinkage strains. Figure 4.31 shows the effect of the pozzolanic content in the mixture on the autogenous shrinkage, where concrete with fly ash outperformed the others. Figure 4.32 demonstrates the significant difference between the shrinkage performance of lightweight and normal weight aggregate concrete under identical dry curing conditions and having the same water/cementitious ratio (w/cm) of 0.29. Shrinkage in the lightweight aggregate concrete was almost stabilized with minimal increase in shrinkage strain after 36 hours at a shrinkage strain of $200\ \mu\epsilon$, whereas in the case of normal weight concrete it was close to $700\ \mu\epsilon$ at the same time interval and continuing to increase at a fast rate. This behavior has been observed by many investigators and can be attributed to the fact that lightweight aggregate concrete has a higher inert moisture content; hence, as the cement hydrates, it is constantly supplied with adsorbed moisture, making the specimen, through internal curing, less susceptible to shrinkage.

Acknowledgments

This chapter is based on material appearing in the previous edition of this *Handbook*; from *Fundamentals of High-Performance Concrete*, 2nd ed., by E.G. Nawy (John Wiley & Sons, 2001); from *Reinforced Concrete: A Fundamental Approach*, 6th ed., by E.G. Nawy (Prentice Hall, 2008); from *Prestressed Concrete: A Fundamental Approach*, 5th ed., by E.G. Nawy (Prentice Hall, 2006); and from various committee reports and standards of the American Concrete Institute, Farmington Hills, MI.

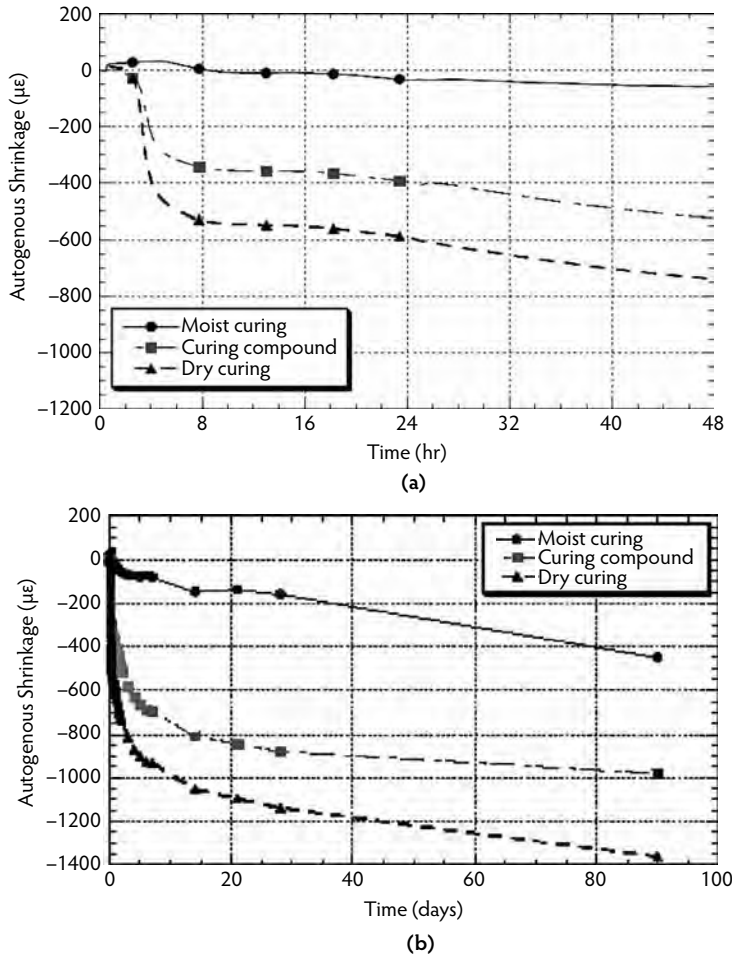


FIGURE 4.30 Effect of curing methods on concrete shrinkage: (a) early (autogenous) shrinkage; (b) long-term (drying) shrinkage.

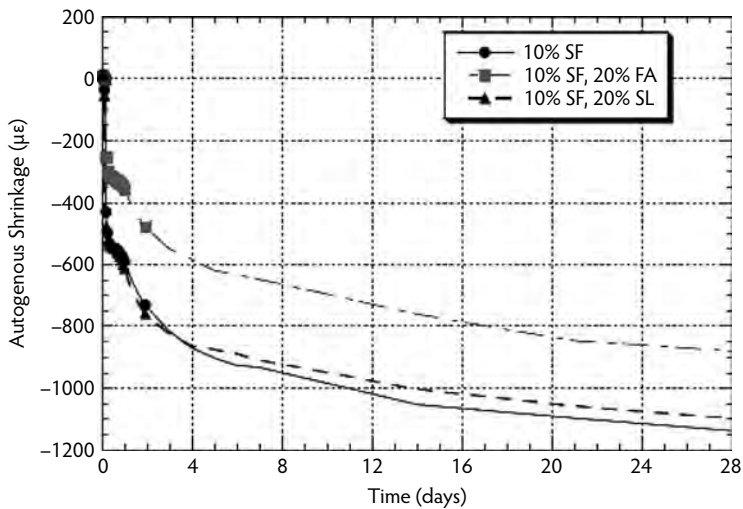


FIGURE 4.31 Effect of pozzolanic material on autogenous shrinkage of concrete.

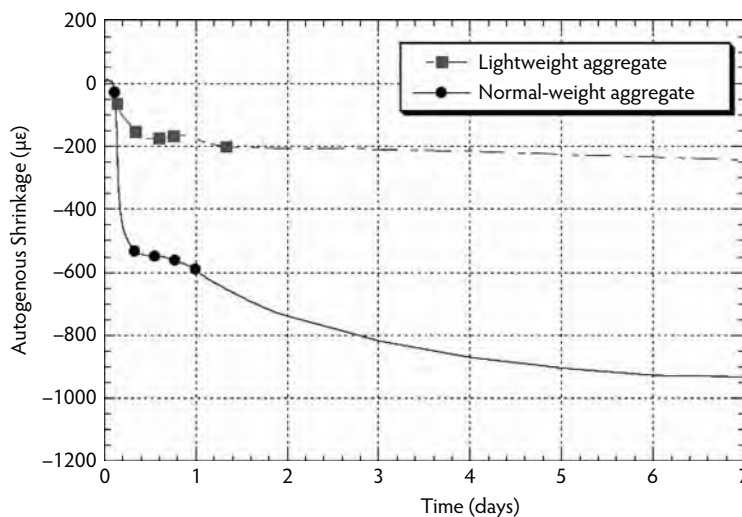


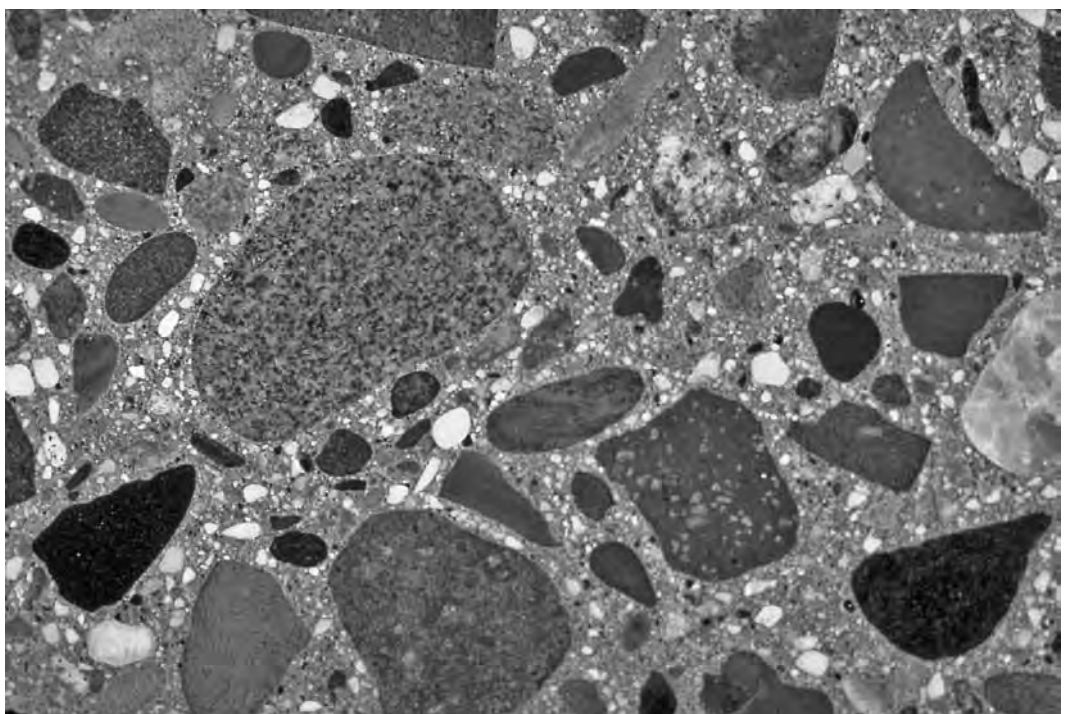
FIGURE 4.32 Effect of aggregate type on autogenous shrinkage of concrete.

References

- ACI. 2008. *Manual of Concrete Practice*, Vols. 1–5. American Concrete Institute, Farmington Hills, MI.
- ACI Committee 209. 1992. *Prediction of Creep, Shrinkage, and Temperature Effects in Concrete Structures*, ACI 209R-92. American Concrete Institute, Farmington Hills, MI, pp. 1–47.
- ACI Committee 224. 1995. *Joints in Concrete Construction*, ACI 224-3R-95. American Concrete Institute, Farmington Hills, MI, 2005, pp 1–44.
- ACI Committee 224. 2001. Control of cracking in concrete structures. *Proc. ACI J.* 20(10), 35–76.
- ACI Committee 318. 2008. *Building Code Requirements for Structural Concrete*, 318-08; *Commentary*, ACI 318R-08. American Concrete Institute, Farmington Hills, MI.
- ACI Committee 350. 2006. *Code Requirements for Environmental Engineering Concrete Structures and Commentary*, ACI 350/ACI 350R. American Concrete Institute, Farmington Hills, MI.
- ACI Committee 363. 1992. *State-of-the-Art Report on High-Strength Concrete*, ACI 363R-92. American Concrete Institute, Farmington Hills, MI, pp. 1–55.
- ACI Committee 435. 1995. *Control of Deflection in Concrete Structures*. American Concrete Institute, Farmington Hills, MI, p. 77.
- Bazant, Z.P. and Boweja, S. 1995a. Justification and refinements of model B3 for concrete and shrinkage. 1. Statistics and sensitivity. *Mater. Struct.*, 28(181), 415–430.
- Bazant, Z.P., and Boweja, S. 1995b. Justification and refinements of model B3 for concrete and shrinkage. 2. Updating and theoretical basis. *Mater. Struct.*, 28(182), 488–495.
- Bazant, Z.P. and Boweja, S., 2000a. Creep and shrinkage prediction model for analysis and design of concrete structures: model B3. In *The Adam Neville Symposium: Creep and Shrinkage—Structural Design Effects*, SP-194. American Concrete Institute, Farmington Hills, MI, pp. 1–83.
- Bazant, Z.P. and Boweja, S., 2000b. Creep and shrinkage prediction model for analysis and design of concrete structures: model B3 (short form). In *The Adam Neville Symposium: Creep and Shrinkage—Structural Design Effects*, SP-194. American Concrete Institute, Farmington Hills, MI, pp. 85–100.
- Bazant, Z.P. and Murphy, W.P. 1995. Creep and shrinkage prediction model for analysis and design of concrete structures: model B3. *Mater. Struct.*, 28(180), 357–365.
- Branson, D.E. 1971. Compression steel effects on long-term deflections, *Proc. J. Am. Concrete Inst.*, 68, 555–559.
- Branson, D.E. 1977. *Deformation of Concrete Structures*. McGraw-Hill, New York, p. 546.
- CEB-FIP. 1990. *Model Code for Concrete Structures*, Vols. 1–3. CEB-FIP, Paris.

- Gardner, N.J., 2000. Design provisions for shrinkage and creep of concrete. In *The Adam Neville Symposium: Creep and Shrinkage—Structural Design Effects*, SP-194. American Concrete Institute, Farmington Hills, MI, pp. 101–134.
- Gardner, N.J. and Lockman, M. 2001. Design provision for drying shrinkage and creep of normal-strength concrete, *ACI Mater. J.*, 98, 159–167.
- Gergely, P. and Lutz, L.A. 1968. Maximum crack width in reinforced concrete flexural members. In *Causes, Mechanism, and Control of Cracking in Concrete*, ACI SP-20, Nawy, E.G., Ed., pp. 87–117. American Concrete Institute, Farmington Hills, MI.
- Harajli, M.H. and Naaman, A.E. 1989. Cracking in partially prestressed beams under static and fatigue loading. In *Cracking in Prestressed Concrete Structures*, ACI SP-113, pp. 29–56. American Concrete Institute, Farmington Hills, MI.
- Meyers, B.L. and Thomas, E.W. 1983. Elasticity, shrinkage, creep and thermal movement of concrete. In *Handbook of Structural Concrete*, Kong, F.K. et al., Eds., pp. 11.1–11.33. McGraw-Hill, New York.
- Mindess, S., Young, J.F., and Darwin. 1999. *Concrete*. Prentice Hall, Upper Saddle River, NJ, p. 671.
- Muller, H.S. and Hillsdorf, H.K. 1990. *Evaluation of Time Dependent Behavior of Concrete*, Summary Report of General Task Force 9, *CEB Bulletin d'Information*, No. 199, p. 290.
- Naaman, A.E. and Siriakorn, A. 1979. Serviceability based design of partially prestressed beams. Part I. Analysis. *Proc. PCI J.*, 24(2), 64–89.
- Nawy, E.G. 1972a. Crack control through reinforcement distribution in two-way acting slabs and plates. *Proc. ACI J.*, 69(4), 217–219.
- Nawy, E.G. 1972b. Crack control in beams reinforcement with bundled bars. *Proc. ACI J.*, 69, 637–639.
- Nawy, E.G. 1990. Flexural cracking behavior of partially prestressed pretensioned and post-tensioned beams: state-of-the-art. In *Cracking in Prestressed Concrete Structures*, ACI SP-113, pp. 1–42. American Concrete Institute, Farmington Hills, MI.
- Nawy, E.G. 1994. Cracking of concrete: ACI and CEB approaches. In *Proceedings of the CANMET International Symposium on Advances in Concrete Technology*, 2nd ed., Malhotra, V.M., Ed., pp. 203–242. Canada Center for Mineral and Energy Technology (CANMET), Ottawa.
- Nawy, E.G. 1996. *Fundamentals of High-Strength, High-Performance Concrete*. Addison Wesley Longman, London, 350 pp.
- Nawy, E.G. 2001. *Fundamentals of High-Performance Concrete*, 2nd ed. John Wiley & Sons, New York, 440 pp.
- Nawy, E.G. 2003. *Design for Crack Control in Reinforced and Prestressed Concrete Beams, Two-Way Slabs and Circular Tanks*, ACI SP 204-1. American Concrete Institute, Farmington Hills, MI, pp. 1–42.
- Nawy, E.G. 2006a. *Concrete: The Sustainable Infrastructure Material for the 21st Century*, TRB Circular E-C103. Transportation Research Board, National Research Council, Washington, D.C., pp. 1–23.
- Nawy, E.G. 2006b. *Prestressed Concrete: A Fundamental Approach*, 5th ed. Prentice Hall, Upper Saddle River, NJ, 944 pp.
- Nawy, E.G. 2008. *Reinforced Concrete: A Fundamental Approach*, 6th ed., pp. 934. Prentice Hall, Upper Saddle River, NJ.
- Nawy, E.G. and Blair, K.W. 1971. Further studies on flexural crack control in structural slab systems. In *Cracking, Deflection, and Ultimate Load of Concrete Slab Systems*, ACI SP-30, Nawy, E.G., Ed., pp. 1–41. American Concrete Institute, Farmington Hills, MI.
- Neville, A.M. 1995. *Properties of Concrete*, 4th ed. Addison Wesley Longman, London, 844 pp.
- Nilson, A.H. 1985. *Design Implications of Current Research on High-Strength Concrete*, ACI SP-87-7. American Concrete Institute, Farmington Hills, MI, pp. 85–118.
- Ross, A.D. 1937. Creep concrete data. *Proc. Inst. Struct. Eng.*, 15, 314–326.
- Ross, A.D. 1958. The elasticity, creep and shrinkage of concrete. In *Proceedings of the Conference on Non-Metallic Brittle Materials*, pp. 157–174. Interscience, London.
- Shah, S.P. and McGarry, F.J. 1971. Griffith fracture criteria and concrete, *Proc. J. Eng. Mech. Div. ASCE*, 47(EM6), 1663–1676.

- Suksawang, N., Nassif, H., and Mohammed, A. 2005. Creep and shrinkage of high-performance/high-strength concrete. In *ACI Seventh International Symposium on Utilization of High-Strength/High-Performance Concrete*, Vol. 2, ACI SP-228, pp. 1397–1416. American Concrete Institute, Farmington Hills, MI.
- Suprenant, B.A. and Malisch, W.R., 2000. *A New Look at Water, Slump, and Shrinkage*, Technical Note, Paper No. C00D048, Hanley-Wood, Washington, D.C., pp. 1–6.
- Vessey, J.V. and Preston, R.L. 1978. *A Critical Review of Code Requirements for Circular Prestressed Concrete Reservoirs*, Federation International Precontrainte, Paris, p. 6.



Uniform distribution of ingredients in high-performance concrete. (Photograph courtesy of Portland Cement Association, Skokie, IL.)

5

Properties and Performance of Normal-Strength and High-Strength Concrete

Steven H. Kosmatka, P.E.*

5.1	Introduction	5-2
5.2	Workability, Bleeding, and Consolidation.....	5-2
5.3	Mixing, Transporting, and Placing Concrete	5-6
5.4	Permeability	5-10
5.5	Carbonation.....	5-10
5.6	Early-Age Characteristics and Strength	5-12
5.7	Density	5-16
5.8	Abrasion Resistance.....	5-17
5.9	Volume Change and Crack Control	5-20
5.10	Deformation and Creep.....	5-21
5.11	Concrete Ingredients.....	5-22
	Portland Cements • White Portland Cement • Blended Hydraulic Cements • Hydraulic Cements • Supplementary Cementing Materials	
5.12	Proportioning of Concrete Mixtures.....	5-31
5.13	Hot and Cold Weather Concreting.....	5-32
5.14	Control Tests.....	5-33
5.15	Freeze–Thaw and Deicer Scaling Resistance	5-34
5.16	Sulfate-Resistant Concrete	5-35
5.17	Corrosion Protection	5-37
5.18	Alkali–Silica Reaction.....	5-39
5.19	Heat-Induced Delayed Expansion.....	5-42
5.20	Self-Consolidating Concrete.....	5-43
5.21	Related ASTM Standards	5-43
	References	5-44

* Staff Vice President, Research and Technical Services, Portland Cement Association, Skokie, Illinois; member of American Concrete Institute, National Concrete Pavement Technology Center, Transportation Research Board, Concrete Research Council, Strategic Development Council, and ASTM committees on cement and concrete.

5.1 Introduction

Portland cement concrete is a simple material in appearance but has a very complex internal nature. Despite its internal complexity, the versatility, durability, and economy of concrete have made it the world's most used construction material. This can be seen in the variety of structures for which it is used, from highways and bridges to buildings and dams (Figure 5.1). Concrete is a mixture of Portland cement, water, and aggregates, with or without admixtures. Portland cement and water form a paste that hardens due to chemical reactions between the cement and water. The paste acts as a glue, binding the aggregates, composed of sand and gravel or crushed stone, into a solid rock-like mass. The quality of the paste and aggregates dictates the engineering properties of concrete construction. Paste qualities are directly related to the amount of water used in relation to the amount of cement. The less water used, the better the quality of the concrete. Reduced water content results in improved strength and durability and reduced permeability and shrinkage. Fine and coarse aggregates make up 60 to 75% of the total volume of the concrete (Figure 5.2); therefore, selection of aggregate is important. Aggregates must be of adequate strength, resistant to exposure conditions, and durable.

Concrete is often discussed as being of “normal strength” or “high strength.” Normal-strength concrete typically has a compressive strength of between 3000 and 6000 psi (20 to 40 MPa). In this chapter, high-strength concrete refers to concrete with a compressive strength of between 6000 and 20,000 psi (40 to 140 MPa). The distinction between normal- and high-strength concrete has changed through history as concrete technology has advanced. One hundred years ago, 4000-psi (28-MPa) concrete would have been considered a high-strength concrete. Today, concretes for special applications can achieve compressive strengths over 120,000 psi (800 MPa)—these are called *reactive powder concretes*. These very exotic materials will not be addressed due to their limited use in general construction; however, for efficiency, normal- and high-strength concretes (up to 20,000 psi) are discussed in tandem, as they use the same materials and have similar properties (Kosmatka et al., 2006; Nawy, 1996, 2008).

Normal-strength concrete is used in most construction applications. Only a small percentage of concrete structures use high-strength concrete. High-strength concrete is used for reduced weight, creep, or permeability; for improved durability; or where architectural considerations require smaller load-carrying elements. The Two Union Square building in Seattle has the highest strength concrete used in a major building—almost 20,000 psi (140 MPa) in the columns (Figure 5.3). In this case, high strength was needed to minimize creep. In other high-rise buildings, high-strength concrete helps achieve more efficient floor plans through smaller vertical members.

5.2 Workability, Bleeding, and Consolidation

Freshly mixed concrete should be plastic or in a semifluid state that can be molded by hand or by mechanical means. In a plastic concrete mixture, all the particles of sand and coarse aggregate are encased and held in suspension. The ingredients should not segregate or separate during transport or handling. A uniform distribution of aggregate particles helps control segregation. After the concrete hardens, it becomes a homogeneous mixture of all the components. Concrete of plastic consistency should not crumble but should flow sluggishly without segregation (Figure 5.4). Concrete consistency is measured by the slump test, ASTM C 143 (Figure 5.5). Slumps of 1 to 3 in. (25 to 75 mm) are used for pavements and slabs. Slumps of 3 to 5 in. (75 to 125 mm) are used for columns and walls. Higher slump concretes, made with plasticizers, are used in thin applications, in locations with large amounts of reinforcing steel, or where concrete needs to be essentially self-consolidating.

Workability reflects the ease of placing, consolidating, and finishing freshly mixed concrete. Concrete should be workable but should not segregate or bleed excessively. Normal-strength concrete usually has good workability as long as concrete ingredients are used in proper proportions and an adequate aggregate gradation is used; however, high-strength concrete is often sticky and difficult to handle and place, even with the aid of plasticizers, due to its high cement content. Concrete temperature also affects workability. Figure 5.6 illustrates that increases in temperature for an established mix reduce slump and workability,

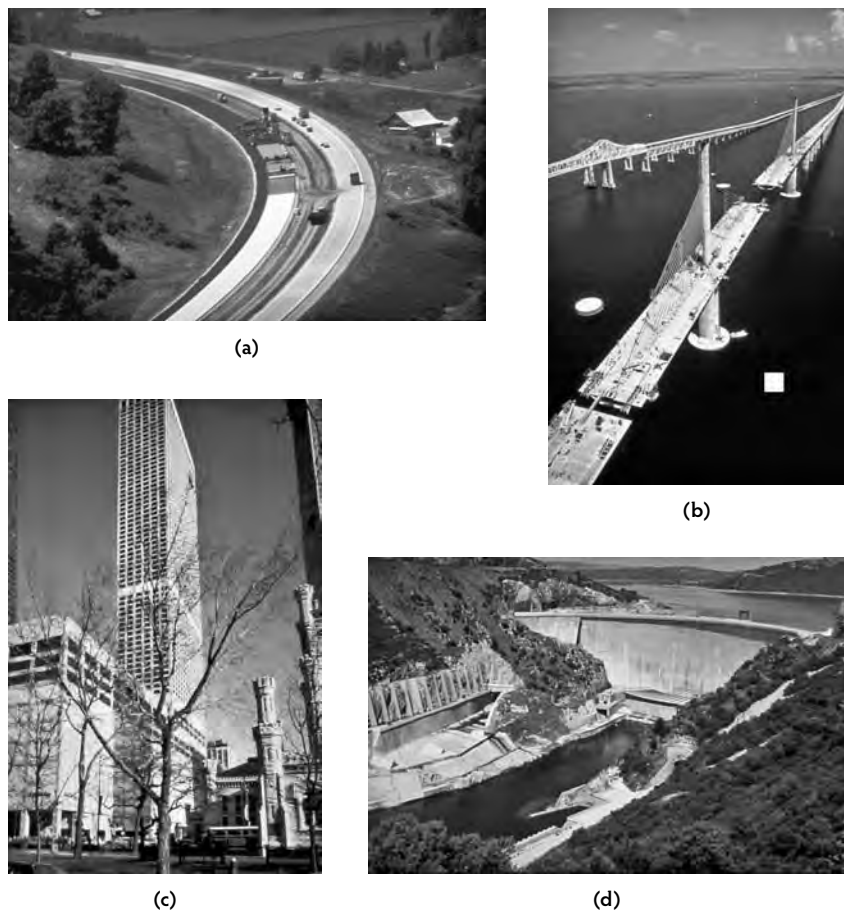


FIGURE 5.1 Concrete used in a variety of applications: (a) highways, (b) bridges, (c) buildings, and (d) dams. (Figure courtesy of the Portland Cement Association, Skokie, IL.)

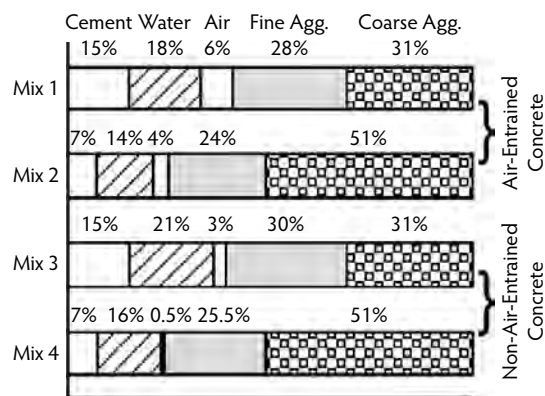


FIGURE 5.2 Range of proportions of materials used in concrete. (From Kosmatka, S.H. et al., *Design and Control of Concrete Mixtures*, EB001, Portland Cement Association, Skokie, IL, 2006.)

resulting in the need to adjust the mix for environmental conditions. As concrete mixture temperature is increased from 73°F (23°C), slump will decrease approximately 0.8 in. for each 20°F temperature increase (20 mm for each 10°C increase).

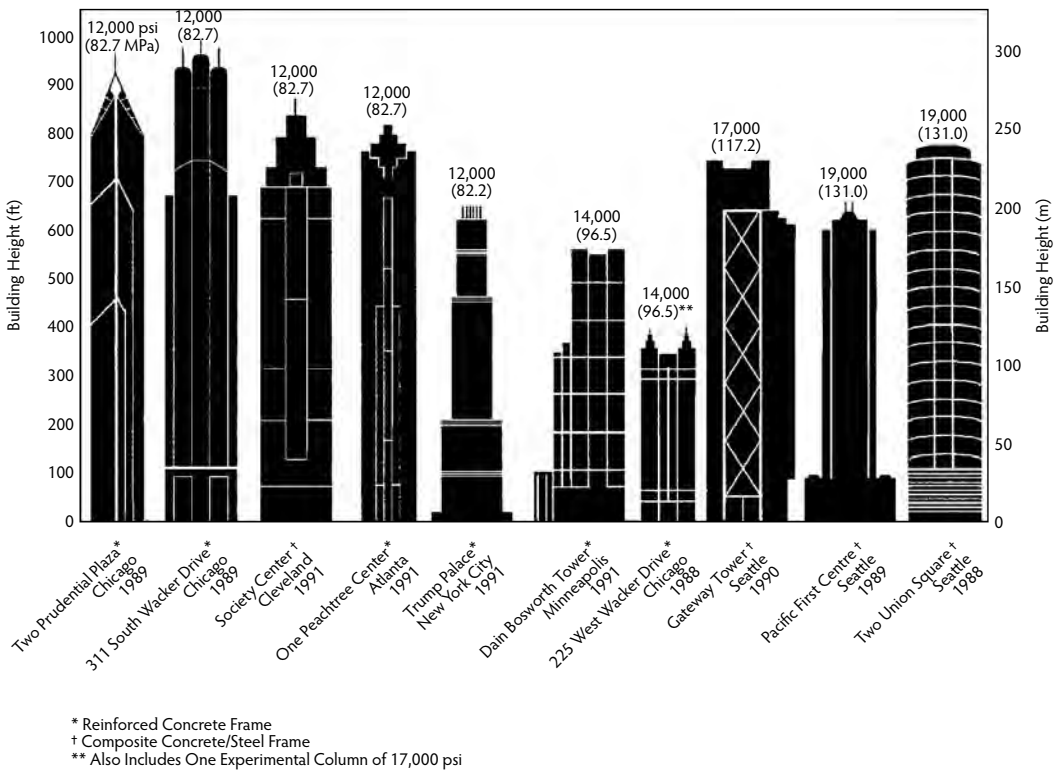


FIGURE 5.3 High-strength concrete in buildings in the 1980s and 1990s. (From Farny, J.A. and Panarese, W.C., *High-Strength Concrete*, EB114, Portland Cement Association, Skokie, IL, 1994.)



FIGURE 5.4 Workable concrete should flow sluggishly into place without segregation. (Figure courtesy of the Portland Cement Association, Skokie, IL.)



FIGURE 5.5 Consistency slump test of concrete. (Figure courtesy of the Portland Cement Association, Skokie, IL.)

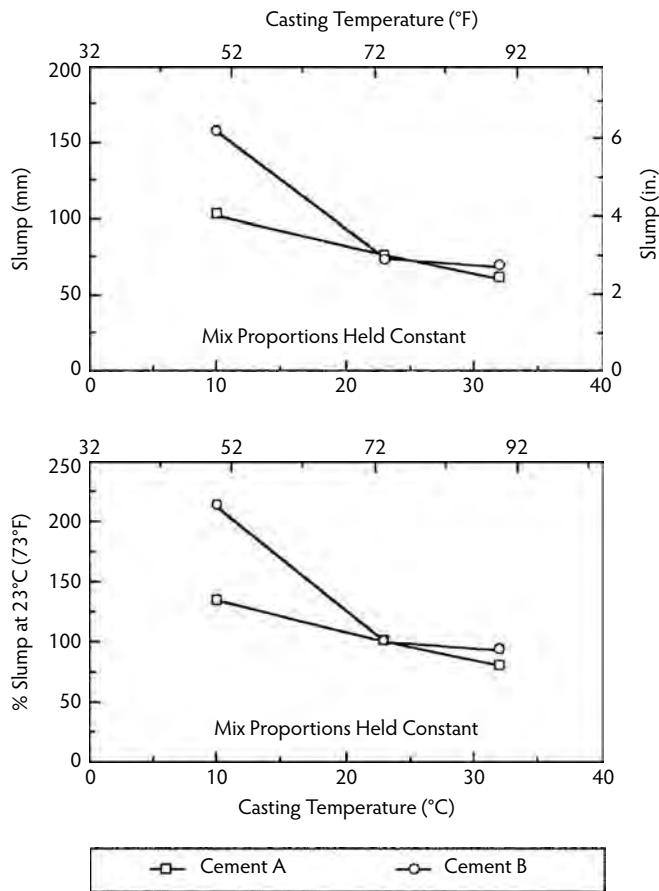


FIGURE 5.6 Slump characteristics vs. casting temperature for two different concretes. (From Burg, R.G., *The Influence of Casting and Curing Temperatures on the Properties of Fresh and Hardened Concrete*, RD113, Portland Cement Association, Skokie, IL, 1996.)

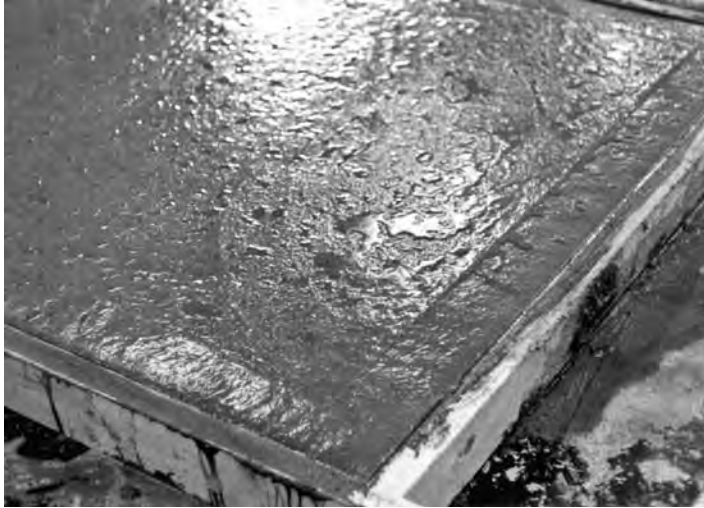


FIGURE 5.7 Bleed water on freshly placed concrete surface. (Figure courtesy of the Portland Cement Association, Skokie, IL.)

Bleeding is the development of a layer of water at the top of freshly placed concrete that is caused by settlement of solid particles of cement and aggregate and the simultaneous upward migration of water (Figure 5.7). A small amount of bleeding is normal and will not affect the durability or strength of the concrete; however, excessive bleeding can result in high water/cement ratios that can cause durability and surface-strength problems. Finishing should be performed after the presence of bleed water is gone. Use of a properly graded aggregate and a proper dosage of cementitious materials will reduce bleeding to an acceptable level. High-strength concrete essentially does not bleed due to its low water content and large amount of cementitious materials. Air-entrained concrete also has little to no bleed water. To achieve desired strength and durability, concrete must be consolidated to form a homogeneous mass without the presence of large voids. Internal and external vibration of concrete, using vibrators, allows stiff, low-slump mixtures to be properly densified. The use of mechanical vibration provides an economical, practical method to quickly consolidate concrete without detrimentally affecting its properties (Figure 5.8).

5.3 Mixing, Transporting, and Placing Concrete

All concrete should be mixed thoroughly until it is uniform in appearance and all ingredients are evenly distributed. If concrete has been adequately mixed, samples taken from different portions of a batch will have essentially the same unit weight, air content, slump, and strength. Concrete is sometimes mixed at a jobsite in a stationary mixer or paving mixer; at other times, it is mixed in central mixers at ready-mix plants. Ready-mixed concrete can be manufactured by any of the following methods:

- Centrally mixed concrete is completely mixed in a stationary mixer and then delivered in a truck agitator or in a truck mixer at agitating speed to the job site.
- Shrink-mixed concrete is partially mixed in a stationary mixer and completed in a truck mixer.
- Truck-mixed concrete is mixed completely in a truck mixer.

When concrete has been transported to a job site, it is conveyed by a variety of methods, including belt conveyors, buckets, shoots, cranes, pumps, wheelbarrows, and other equipment (Figure 5.9). Concrete should be conveyed in such a manner that it is not allowed to dry out; it should not be delayed, and it should not be allowed to segregate before it is placed. Table 5.1 describes the advantages of various methods and types of equipment for transporting and handling concrete.



FIGURE 5.8 Proper vibration facilitates concrete placement even in heavily reinforced members. (Figure courtesy of the Portland Cement Association, Skokie, IL.)



(a)



(b)

FIGURE 5.9 (a) Truck-mounted pump and boom, and (b) a conveyer belt, which can conveniently move concrete to the desired location. (Figure courtesy of the Portland Cement Association, Skokie, IL.)

Concrete should be deposited continuously as near as possible to its final position. Concrete should be placed in horizontal layers of uniform thickness, each layer being thoroughly consolidated before the next is placed. The rate of placement should be rapid enough that a layer of concrete is not yet set when a new layer is placed upon it. Drop shoots should be used to prevent segregation and spattering of mortar on reinforcement and forms in wall placements.

When the concrete has been placed in a form or layer, it should be consolidated or compacted into the mold so it forms in and around embedded items and reinforcement and removes entrapped air. Consolidation is usually accomplished by mechanical methods. Use of internal vibrators is the most common method of consolidating concrete. When concrete is vibrated, it behaves like a liquid; it settles in the forms by the action of gravity, and large entrapped air voids rise to the surface. Workers must be careful to make sure that the vibrator is inserted into the concrete at a uniform distribution within the radius of action of the vibrator to properly consolidate all of the concrete. Even highly fluid, plasticized mixes with slumps over 7-1/2 in. (190 mm) require some vibration for proper consolidation.

TABLE 5.1 Methods and Equipment for Transporting and Handling Concrete

Equipment	Type and Range of Work for Which Equipment Is Best Suited	Advantages	Points to Watch for
Mobile batcher mixers	Used for intermittent production of concrete at jobsite	Combined materials transporter and mobile batching and mixing system provides quick, precise proportioning of specified concrete; one-man operation.	Trouble-free operation requires a preventive maintenance program equipment. Materials must be identical to those in original mix design.
Nonagitating trucks	Used to transport concrete on short hauls over smooth roadways	Capital cost of nonagitating equipment is lower than that of truck agitators or mixers.	Concrete slump should be limited. Segregation is possible. Height is necessary for high lift of truck body discharge.
Pneumatic guns (shotcrete)	Used where concrete is to be placed in difficult locations and where thin sections and large areas are needed	Shotcrete is ideal for placing concrete in free-form shapes, for repairing and strengthening buildings, for protective coatings, and thin linings.	Quality of work depends on skill of those using equipment; only experienced nozzlemen should be employed.
Pumps	Used to convey concrete directly from central discharge point at jobsite to formwork or to secondary discharge point	Pipelines take up little space and can be readily extended. Pump delivers concrete in continuous stream and can move concrete both vertically and horizontally. Mobile pumps can be delivered when necessary to small or large projects. Stationary pump booms provide continuous concrete for tall building construction.	Constant supply of freshly mixed concrete with average consistency and without any tendency to segregate is necessary. Care must be taken in operating pipeline to ensure an even flow and to clean out pump at the conclusion of each operation. Pumping vertically, around bends, and through flexible hose will considerably reduce the maximum pumping distance.
Screw spreaders	Used for spreading concrete over flat areas, as in pavements	With a screw spreader, a batch concrete discharged from bucket or truck can be quickly spread over a wide area to a uniform depth. The spread concrete has good uniformity of compaction before vibration is used for final compaction.	Screw spreaders are usually used as part of a paving train. They should be used for spreading before vibration is applied.
Tremies	For placing concrete underwater	Tremies can be used to funnel concrete down through the water into the foundation or other part of the structure being cast.	Precautions are necessary to ensure that the tremie discharge end is always buried in fresh concrete so a seal is preserved between the water and concrete mass. Diameter should be 10 to 12 in. unless press is available. Concrete mixture requires more cement (700 lb/yd ³) and greater slump (6 to 9 in.) because concrete must flow and consolidate without any vibration.
Truck agitators	Used to transport concrete for all uses in pavements, structures, and buildings	Truck agitators usually operate from central mixing plants where quality concrete is produced under controlled conditions. Discharge from agitators is well controlled. Concrete is uniform and homogeneous on discharge.	Timing of deliveries must suit job organization. Haul distances must allow discharge of concrete within 1-1/2 hours, but limit may be waived under certain circumstances. Concrete crew and equipment must be ready onsite to handle concrete.

Truck mixers	Used to transport concrete for all uses in pavements, structures, and buildings	No central mixing plant is needed, only a batching plant, as concrete is completely mixed in truck mixer. Discharge is the same as for truck agitators.	Timing of deliveries must suit job organization. Haul distances must allow discharge of concrete within 1 to 1/2 hours, but limit may be waived under certain circumstances. Concrete crew and equipment must be ready onsite to handle concrete. Control of concrete quality is not as good as with central mixing. Method is slow and labor intensive.
Wheelbarrows and buggies	For short flat hauls on all types of onsite concrete construction, especially where accessibility to work area is restricted	Wheelbarrows and buggies are very versatile and therefore ideal for inside work and on jobsites where placing conditions are constantly changing.	
Belt conveyors	For conveying concrete horizontally or to a higher or lower level; usually used between main discharge point and secondary discharge point	Belt conveyors have an adjustable reach, a traveling diverter, and variable speed, both forward and reverse. They can place large volumes of concrete quickly when access is limited.	End-discharge arrangements are necessary to prevent segregation and leave no mortar on return belt. In adverse weather (hot, windy), long reaches of belt require cover.
Belt conveyors mounted on truck mixers; buckets	For conveying concrete to a lower, horizontal, or higher level; used with cranes, cableways, and helicopters for construction of buildings and dams; convey concrete directly from central discharge point to formwork or to secondary discharge point	Conveying equipment arrives with the concrete. Equipment has an adjustable reach and variable speed; allows the full versatility of cranes, cableways, and helicopters to be exploited; and has a clean discharge. Buckets offer a wide range of capacities.	End-discharge arrangements are necessary to prevent segregation and leave no mortar on return belt. Select bucket capacity to conform to the size of the concrete batch and capacity of placing equipment. Discharge should be controllable.
Chutes	For conveying concrete to lower levels, usually below ground level, on all types of concrete construction	Chutes offer low cost and are easy to maneuver. No power is required, as gravity does most of the work.	Slopes range between 1 to 2 and 1 to 3, and chutes must be adequately supported in all positions. Arrange for discharge at the end (downpipe) to prevent segregation.
Cranes	The right tool for work above ground level	Cranes can handle concrete, reinforcing steel, formwork, and sundry items in high-rise, concrete-framed buildings.	A crane has only one hook. Careful scheduling between trades and operations is necessary to keep it busy.
Dropchutes	Used for placing concrete in vertical forms of all kinds; some chutes are one piece, but others are assembled from loosely connected segments	Dropchutes direct concrete into formwork and carry it to bottom of forms without segregation. Their use avoids spillage of grout and concrete on the form sides, which is harmful when off-the-form surfaces are specified. They also will prevent segregation of coarse particles.	Dropchutes should have sufficiently large, splayed-top openings into which concrete can be discharged without spillage. The cross-section of the dropchute should be chosen to permit inserting it into the formwork without interfering with reinforcing steel.

Source: Kosmatka, S.H. et al., *Design and Control of Concrete Mixtures*, EB001, Portland Cement Association, Skokie, IL, 2006.

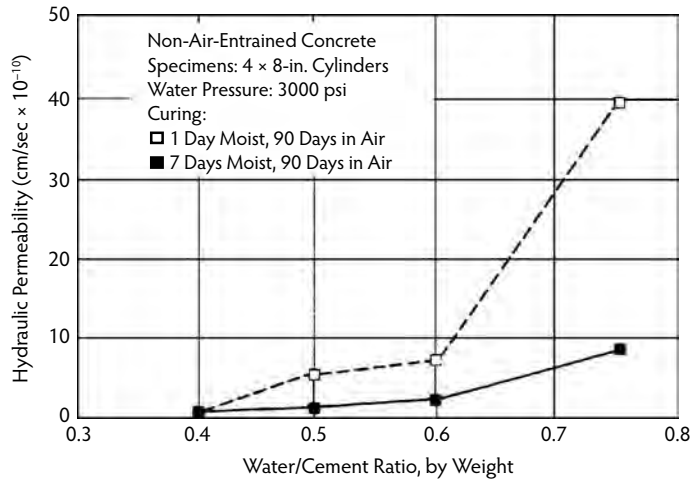


FIGURE 5.10 Water permeability of concrete as influenced by water/cement ratio and curing. (From Whiting, D., in *Permeability of Concrete*, SP108-11, American Concrete Institute, Farmington Hills, MI, 1988, pp. 195–225.)

5.4 Permeability

Concrete's durability, corrosion resistance, and resistance to chemical attack are directly related to permeability. If a substance cannot enter concrete, it cannot damage it. Concrete permeability is a function of the permeability of the paste and aggregate. Decreased permeability improves concrete's resistance to saturation, sulfate attack, chemical attack and chloride penetration. Paste permeability has the greatest influence on concrete permeability. Paste permeability is directly related to the water/cement ratio and the degree of hydration or length of moist-curing. A low water/cement ratio and an adequate moist curing period result in concrete with low permeability. The permeability of mature, good-quality, normal-strength concrete is approximately 1×10^{-10} cm/sec. Figure 5.10 illustrates the relationship between the water/cement ratio and permeability. Supplementary cementing materials such as fly ash and, especially, silica fume reduce permeability. High-strength concrete usually has very low permeability as a result of its low water/cement ratio and the common use of silica fume. High-strength concretes often have water permeability coefficients from 1×10^{-11} to 1×10^{-13} cm/sec. Low permeability and inherent resistance to chlorides make high-strength concrete ideal for structures such as bridges and parking decks that are exposed to deicers or seawater. A variety of methods are used to determine the permeability of concrete. Some of the common methods are the chloride ponding test (AASHTO T259), electrical conductance–rapid chloride permeability test (ASTM C 1202), water permeability (Army Corps CRD-C 163), air permeability (SHRP 2031), and volume of permeable voids (ASTM C 642). Table 5.2 illustrates the relationship between various permeability methods and normal- and high-strength concretes of different water/cement ratios. Table 5.3 provides conversions for various permeability units. The first step in achieving a low permeability is to specify a water/cement ratio of 0.4 or less and then consider using a supplementary cementing material or blended hydraulic cement.

5.5 Carbonation

Carbonation is related to permeability. Carbonation of Portland cement concrete paste occurs on all exposed concrete surfaces. Carbonation is a chemical reaction in which carbon dioxide in air or water reacts with compounds in the hardened cement paste to form carbonates, primarily calcium carbonate.

TABLE 5.2 Various Permeability Tests on Concrete

Mix	W/C	Cure Time (days)	RCPT (Coulombs)	90-Day Ponding (% Cl)	Permeability		Porosity (%)	Volume Permeable Voids (%)
					Hydraulic (μDarcys) ^a	Air (μDarcys) ^a		
1	0.26	1	44	0.013	— ^b	37	8.3	6.3
		7	65	0.013	— ^b	29	7.5	6.2
2	0.28	1	942	0.017	— ^b	28	9.1	8.1
		7	852	0.022	— ^b	33	8.8	8.0
3	0.4	1	3897	0.062	0.030	130	11.3	11.4
		7	3242	0.058	0.027	120	11.3	12.2
4	0.5	1	5703	0.103	0.560	120	12.4	13.0
		7	4315	0.076	0.200	170	12.5	12.7
5	0.6	1	5911	0.104	0.740	200	13.0	12.8
		7	4526	0.077	0.230	150	12.7	12.5
6	0.75	1	7065	0.112	4.100	270	13.0	14.2
		7	5915	0.085	0.860	150	13.0	13.3
Coefficient of variation (%)			7.0	12.9	20.9	14.0	2.5	2.4

^a To convert from μ Darcys to m^3 multiply by 9.87×10^{-7} .

^b Permeability too small to measure.

Note: W/C = water/cement ratio, RCPT = rapid chloride permeability test.

Source: Whiting, D., in *Permeability of Concrete*, SP108-11, American Concrete Institute, Farmington Hills, MI, 1988, pp. 195–225.

TABLE 5.3 Conversion Table for Permeability Units

Unit	Darcy	Millidarcy	cm/sec	m^3	Meinzers	ft/day
Darcy	1	1000	9.68×10^{-4}	9.87×10^{-13}	20.50	2.75
Millidarcy	10^{-3}	1	9.68×10^{-7}	9.87×10^{-16}	2.05×10^{-2}	2.75×10^{-3}
cm/sec	1.03×10^3	1.03×10^6	1	1.03×10^{-9}	2.12×10^4	2.84×10^3
m^3	1.01×10^{12}	1.01×10^{15}	9.71×10^8	1	20.7×10^{12}	2.78×10^{12}
Meinzers	4.88×10^{-2}	48.78	4.72×10^{-5}	4.83×10^{-14}	1	1.34×10^{-1}
ft/day	3.64×10^{-1}	3.64×10^2	3.52×10^{-4}	3.60×10^{-13}	7.46	1

Note: To convert from units in first column to units at the top, multiply by the indicated factor. Conversions given are appropriate for cases of saturated, steady-state flow. For units associated with diffusion processes or with relative, empirical test procedures, no direct conversions are available.

Source: Whiting, D., in *Permeability of Concrete*, SP108-11, American Concrete Institute, Farmington Hills, MI, 1988, pp. 195–225.

The reaction begins immediately upon exposure of the concrete to air. The rate of carbonation is largely a function of paste permeability, temperature, relative humidity, and the concentration of carbon dioxide in the air. Paste permeability is controlled by the water/cement ratio, amount of moist curing, and the degree of densification of the exposed surface. Carbonation increases drying shrinkage and lowers the alkalinity (pH) of concrete. The inherent high alkalinity of concrete (pH greater than 12.5) protects embedded reinforcing steel from corrosion by causing a passive and noncorroding protective oxide film to form on the steel surface. By reducing the pH, carbonation destroys the protective film and, in the presence of moisture and oxygen, allows steel to corrode. Engineers specify a certain amount of protective concrete cover over reinforcing steel, assuming that the small depth of carbonated concrete will fall far short of the steel. In effect, the designer assumes that the concrete will not carbonate down to the depth of the steel during the expected life of the structure. The depth of carbonation is usually of little importance, less than 0.5 in. (13 mm) after 10 years for good-quality Portland cement concrete, and the depth of cover required by building codes provides an adequate factor of safety against corrosion (Campbell et al., 1991; Kosmatka and Farny, 2007).

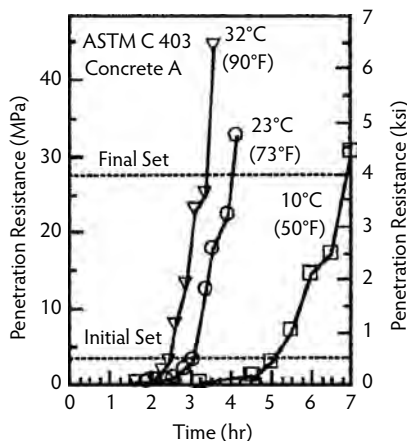


FIGURE 5.11 Temperature effect on set time. (From Burg, R.G., *The Influence of Casting and Curing Temperatures on the Properties of Fresh and Hardened Concrete*, RD113, Portland Cement Association, Skokie, IL, 1996.)

5.6 Early-Age Characteristics and Strength

Concrete is primarily known for its massive compressive strength. Concrete gains strength through the reaction between cement and water called *hydration*. Portland cement is primarily a calcium silicate cement. The calcium silicate combines with water and forms calcium silicate hydrate, which is responsible for the primary engineering properties of concrete, such as strength and dimensional stability. During the first few hours, the cement in the concrete slowly reacts with water, giving the concrete some early strength. This period of early hardening is the *setting time*. Initial set is defined as the time at which concrete has attained 500 psi (3.5 MPa); final set is defined as the time at which it reaches 4000 psi (27.6 MPa), based on penetration resistance. The contractor should be aware of the setting properties of a concrete to properly control finishing operations on slabs and pavements. Temperature has one of the greatest effects on setting time. Figure 5.11 illustrates how an increase in temperature decreases set time and a decrease in temperature increases set time. Setting time can be expected to change approximately 30% for each 10°F change (50% for each 10°C change) in temperature from a base temperature of 73°F (23°C).

The compressive strength of concrete is directly related to the water/cement ratio. A decrease in water/cement ratio results in higher strength. Table 5.4 illustrates a conservative relationship between strength and water/cement ratio, and Table 5.5 and Table 5.6 illustrate typical mix designs for concretes with

TABLE 5.4 Typical Relationship between Water/Cement Ratio and Compressive Strength of Concrete

Compressive Strength at 28 Days, psi (MPa) ^a	Water/Cement Ratio by Weight	
	Non-Air-Entrained Concrete	Air-Entrained Concrete
6000 (41)	0.41	—
5000 (34)	0.48	0.40
4000 (28)	0.57	0.48
3000 (21)	0.68	0.59
2000 (14)	0.82	0.74

^a Values are estimated average strengths for concrete.

Note: Strength is based on 6 × 12-in. cylinders moist-cured 28 days at 73.4°F ± 3°F in accordance with Section 9b of ASTM C31. Relationship assumes maximum size of aggregate of about 3/4 in. to 1 in.

TABLE 5.5 Examples of Trial Mixes for Air-Entrained Concrete of Medium Consistency, 3- to 4-in. Slump (English Units)

W/C Ratio (lb/lb)	Maximum Aggregate Size (in.)	Air Content (%)	Water (lb/yd ³ of Concrete)	Cement (lb/yd ³ of Concrete)	Aggregate with Fine Sand Fineness Modulus = 2.50			Aggregate with Coarse Sand Fineness Modulus = 2.90		
					Fine (%) Total Aggregate	Fine (lb/yd ³ of Concrete)	Coarse (lb/yd ³ of Concrete)	Fine (%) Total Aggregate	Fine (lb/yd ³ of Concrete)	Coarse (lb/yd ³ of Concrete)
0.40	3/8	7.5	340	850	50	1250	1260	54	1360	1150
	1/2	7.5	325	815	41	1060	1520	46	1180	1400
	3/4	6	300	750	35	970	1800	39	1800	1680
	1	6	285	715	32	900	1940	36	1010	1830
	1-1/2	5	265	665	29	870	2110	33	990	1990
0.45	3/8	7.5	340	755	51	1330	1260	56	1440	1150
	1/2	7.5	325	720	43	1140	1520	47	1260	1400
	3/4	6	300	665	37	1040	1800	41	1160	1680
	1	6	285	635	33	970	1940	37	1080	1830
	1-1/2	5	265	590	31	930	2110	35	1050	1990
0.50	3/8	7.5	340	680	53	1400	1260	57	1510	1150
	1/2	7.5	325	650	44	1200	1520	49	1320	1400
	3/4	6	300	600	38	1100	1800	42	1220	1680
	1	6	285	570	34	1020	1940	38	1130	1830
	1-1/2	5	265	530	33	980	2110	36	1100	1990
0.55	3/8	7.5	340	620	54	1450	1260	53	1560	1150
	1/2	7.5	325	590	45	1250	1520	49	1370	1400
	3/4	6	300	545	39	1140	1800	43	1260	1680
	1	6	285	520	35	1060	1940	39	1170	1830
	1-1/2	5	265	480	33	1030	2110	37	1150	1990
0.60	3/8	7.5	340	565	54	1490	1260	58	1600	1150
	1/2	7.5	325	540	46	1290	1520	50	1410	1400
	3/4	6	300	500	40	1180	1800	44	1300	1680
	1	6	285	475	36	1100	1940	40	1210	1830
	1-1/2	5	265	440	33	1060	2110	37	1180	1990
0.65	3/8	7.5	340	525	55	1530	1260	59	1640	1150
	1/2	7.5	325	500	47	1330	1520	51	1450	1400
	3/4	6	300	460	40	1210	1800	44	1330	1680
	1	6	285	440	37	1130	1940	40	1240	1830
	1-1/2	5	265	410	34	1090	2110	38	1210	1990
0.70	3/8	7.5	340	485	55	1560	1260	59	1670	1150
	1/2	7.5	325	465	47	1360	1520	51	1480	1400
	3/4	6	300	430	41	1240	1800	45	1360	1680
	1	6	285	405	37	1160	1940	41	1270	1830
	1-1/2	5	265	380	34	1110	2110	38	1230	1990

Source: Kosmatka, S.H. et al., *Design and Control of Concrete Mixtures*, EB001, Portland Cement Association, Skokie, IL, 2006.

TABLE 5.6 Example of Trial Mixes for Air-Entrained Concrete of Medium Consistency, 80- to 100-mm Slump (Metric Units)

W/ C Ratio (kg/kg)	Nominal Aggregate Size (mm)	Air Content (%)	Water (kg/m ³ of Concrete)	Cement (kg/m ³ of Concrete)	With Fine Sand Fineness Modulus = 2.50			With Coarse Sand Fineness Modulus = 2.90		
					Fine Aggregate (% Total Aggregate)	Fine Aggregate (kg/m ³ of Concrete)	Coarse Aggregate (kg/m ³ of Concrete)	Fine Aggregate (% Total Aggregate)	Fine Aggregate (kg/m ³ of Concrete)	Coarse Aggregate (kg/m ³ of Concrete)
0.40	10	7.5	202	505	50	744	750	54	809	684
	14	7.5	194	485	41	630	904	46	702	833
	20	6	178	446	35	577	1071	39	648	1000
	40	5	158	395	29	518	1255	33	589	1184
0.45	10	7.5	202	450	51	791	750	56	858	684
	14	7.5	194	428	43	678	904	47	750	833
	20	6	178	395	37	619	1071	41	690	1000
	40	5	158	351	31	553	1225	35	625	1184
0.50	10	7.5	202	406	53	833	750	57	898	684
	14	7.5	194	387	44	714	904	49	785	833
	20	6	178	357	38	654	1071	42	726	1000
	40	5	158	315	32	583	1225	36	654	1184
0.55	10	7.5	202	369	54	862	750	58	928	684
	14	7.5	194	351	45	744	904	49	815	833
	20	6	178	324	40	702	1071	43	750	1000
	40	5	158	286	33	613	1225	37	684	1184
0.60	10	7.5	202	336	54	886	750	58	952	684
	14	7.5	194	321	46	768	904	50	839	833
	20	6	178	298	40	720	1071	44	773	1000
	40	5	158	262	33	631	1225	37	702	1184
0.65	10	7.5	202	312	55	910	750	59	976	684
	14	7.5	194	298	47	791	904	51	863	833
	20	6	178	274	40	720	1071	44	791	1000
	40	5	158	244	34	649	1225	38	720	1184
0.70	10	7.5	202	288	55	928	750	59	994	684
	14	7.5	194	277	47	809	904	51	880	883
	20	6	178	256	41	738	1071	45	809	1000
	40	5	158	226	34	660	1225	38	732	1184

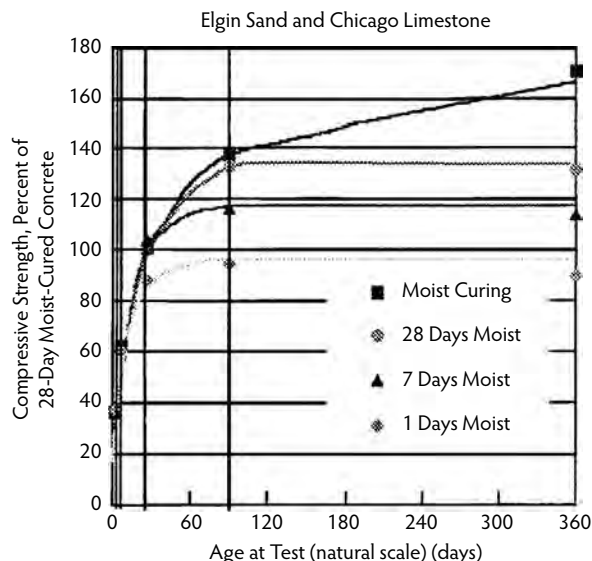


FIGURE 5.12 Increase in concrete strength with age as affected by curing moisture levels. (Figure courtesy of the Portland Cement Association, Skokie, IL.)

various water/cement ratios. The compressive strength of concrete increases with age as long as an appropriate moisture content and temperature are available (Figure 5.12 and Figure 5.13). The compressive strength of concrete at 7 days is approximately 75% of the 28-day strength for concrete cast and cured at 73°F (23°C). Later-age strength of concrete cast and cured at 50°F (10°C) often equals or exceeds that of the same concrete cast and cured at 73°F (23°C). For most concretes cast and cured at 90°F (32°C), 3-day compressive strength will be approximately 70% of 28-day compressive strength of concrete cast and cured at 90°F (32°C). The effect of casting and curing at 90°F (32°C) roughly results in a 3-day compressive strength similar to 7-day strength for concrete cast and cured at 73°F (23°C).

Outdoor concrete continues to gain strength as moisture is maintained by natural humidity or rainfall. Strength gains for various concretes under different environmental conditions are illustrated in Figure 5.14, Figure 5.15, and Figure 5.16. Figure 5.14 also illustrates the effect of water/cement ratios. Compressive strength is usually specified at the age of 28 days; however, depending on the project, ages of 3 and 7 days can also be specified. For high-strength concrete, ages of 56 or 90 days may be specified. For general-use concrete, a compressive-strength between 20 and 35 MPa (3000 psi and 6000 psi) is used. Compressive strength development of high-strength concrete is illustrated in Figure 5.17 and corresponds to the mixes in Table 5.7. The rate of strength gain for high-strength concrete vs. that of normal-strength concrete is illustrated in Figure 5.18. Compressive strength is usually determined by casting and testing 6 × 12-in. (150 × 300-mm) cylinders; however, 4 × 8-in. (100 × 200-mm) cylinders are commonly used for high-strength concrete and sometimes for normal-strength concrete. For high-strength concrete, 4 × 8-in. (100 × 200-mm) cylinders generally have strengths within about 1% of 6 × 12-in. (150 × 300-mm) cylinders.

Increase in strength with age continues as long as any unhydrated cement is still present, the relative humidity in the concrete is approximately 80% or higher, and the concrete temperature is favorable. To maintain this increase in strength, concrete must be properly cured. Curing means that not only must a favorable temperature be present but also moisture loss will not be permitted or extra water will be provided at the surface. Use of a wet burlap or plastic covering for 7 days or use of a curing compound usually provides adequate curing for normal- and high-strength concrete.

Although concrete is very strong in compression, it is weak in tensile strength. Tensile strength is about 8 to 12% of the compressive strength. Flexural strength (modulus of rupture) is 5 to 7.5 times (0.7 to 0.8 times for metric units) the square root of the compressive strength. Shear strength is about 20% of the

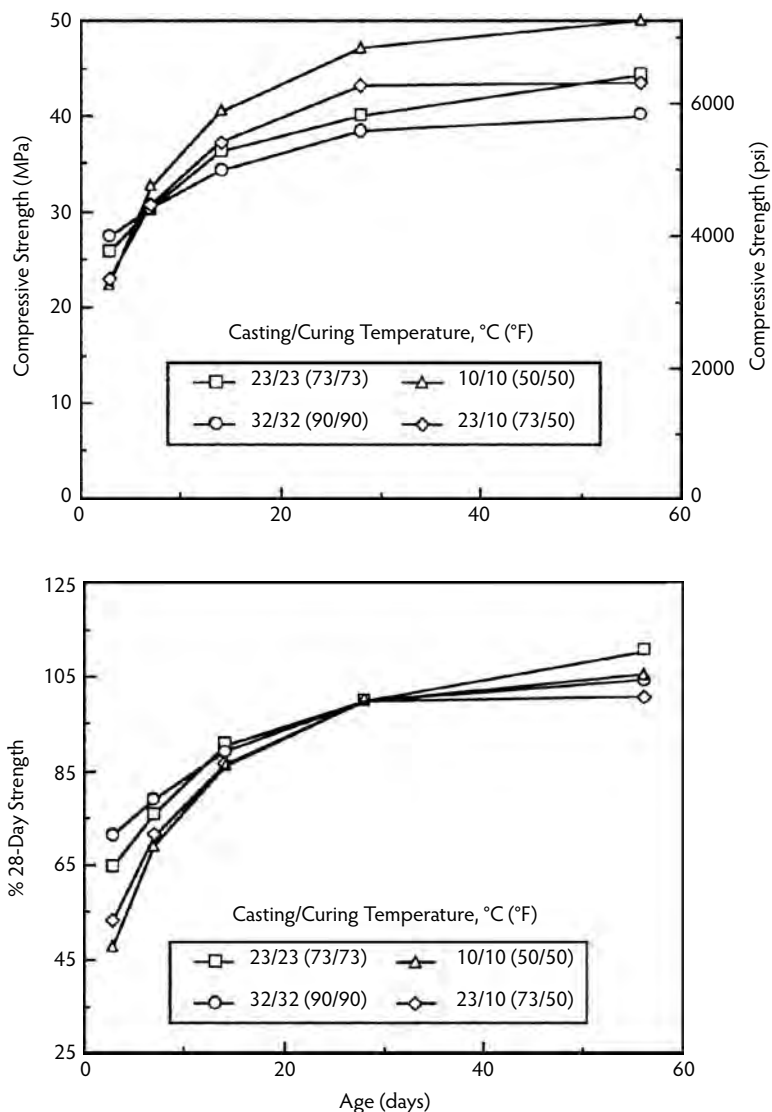


FIGURE 5.13 Strength gain vs. age for different casting and curing temperatures. (From Burg, R.G., *The Influence of Casting and Curing Temperatures on the Properties of Fresh and Hardened Concrete*, RD113, Portland Cement Association, Skokie, IL, 1996.)

compressive strength. Modulus of elasticity ranges from 2 to 6 million psi or 57,000 times the square root of the compressive strength (in English units, 14,000 to 41,000 MPa) and can be estimated as 5000 times the square root of the compressive strength in metric units. Figure 5.19, Figure 5.20, and Figure 5.21 illustrate these properties. Table 5.8 lists the flexural and tensile strengths for high-strength concretes cited in Table 5.7.

5.7 Density

Normal weight concrete, as is used in pavements and bridges, has a density of 140 to 150 lb/ft³ (2240 to 2400 kg/m³). The density of concrete varies with the relative density of the aggregate, the amount of air present in the paste, and the amount of water and cement in the mixture. The density of non-air-entrained, high-strength concrete is often over 150 lb/ft³ (2400 kg/m³). The high-strength concretes in

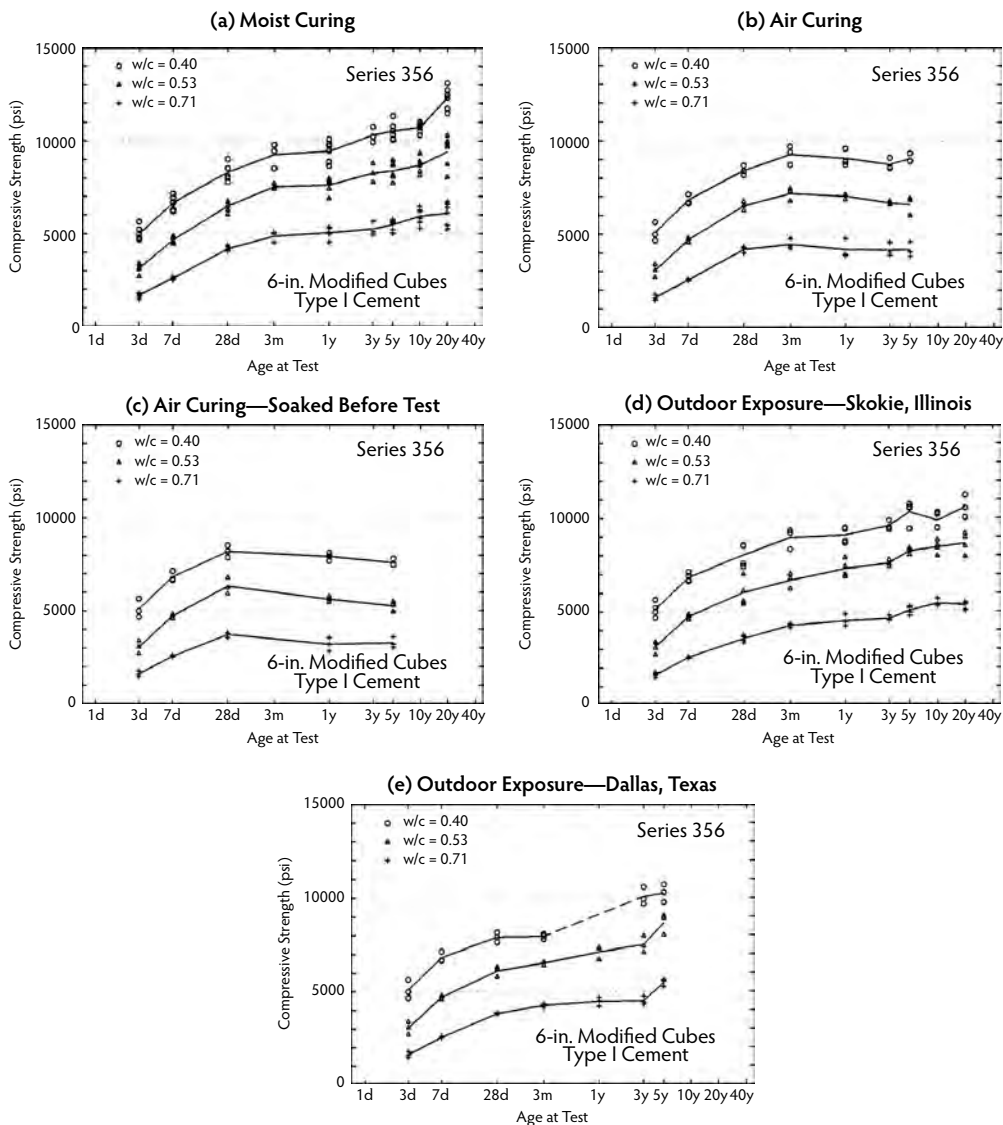


FIGURE 5.14 Variation of compressive strength with log age for different exposure conditions (all specimens received a 7-day moist curing prior to ultimate exposure). (From Wood, S.L., *Evaluation of the Long-Term Properties of Concrete*, RD102, Portland Cement Association, Skokie, IL, 1992.)

Table 5.7 use a crushed dolomite coarse aggregate and have densities ranging from 152 to 155 lb/ft³ (2430 to 2490 kg/m³) and air contents ranging from 0.7 to 1.6%. Heavyweight concretes, used for radiation shielding, can have densities approaching 400 lb/ft³ (6400 kg/m³).

5.8 Abrasion Resistance

Structures such as pavements and bridge decks are subjected to constant abrasion; therefore, concrete in these applications must have a high degree of abrasion resistance. Abrasion resistance is directly related to the compressive strength of the concrete. The type of aggregate and surface finish also have a strong influence on abrasion resistance. A hard aggregate, such as a granite, provides more abrasion resistance than a soft limestone aggregate.

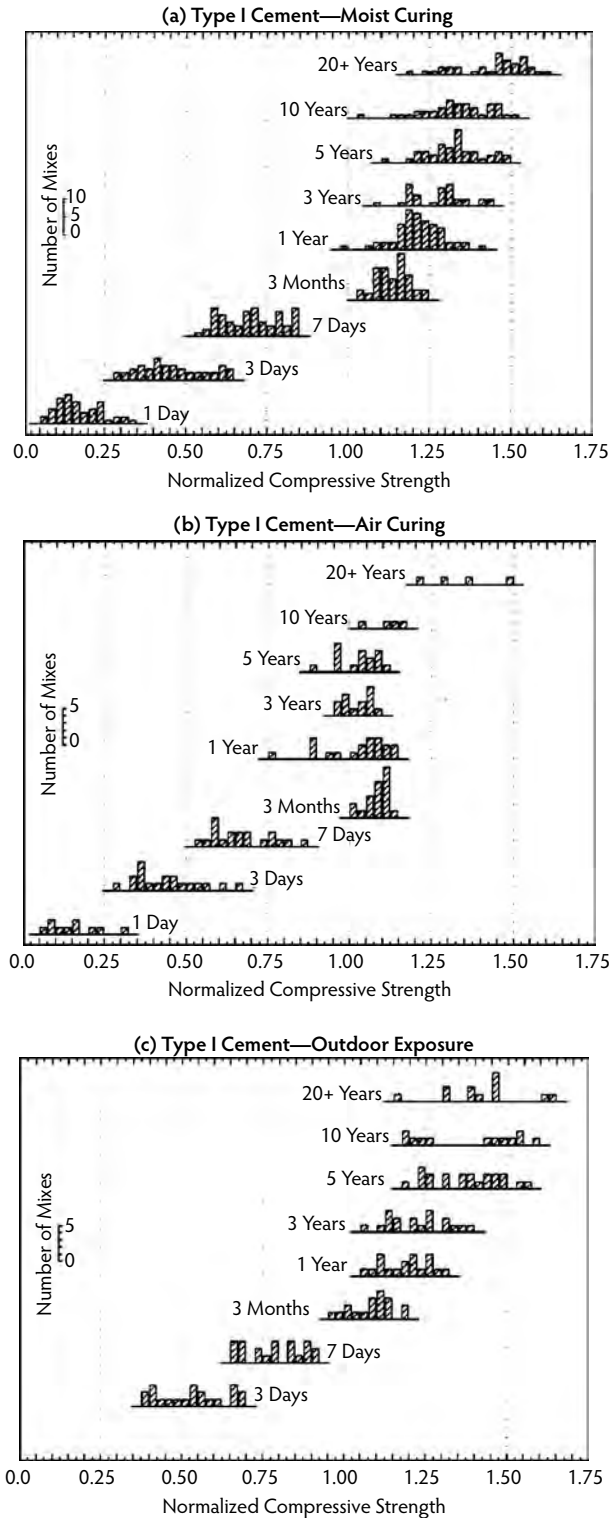


FIGURE 5.15 Distribution of compressive strength normalized to 28 days for Type I cement concrete (all specimens received a 7-day moist curing prior to ultimate exposure). (From Wood, S.L., *Evaluation of the Long-Term Properties of Concrete*, RD102, Portland Cement Association, Skokie, IL, 1992.)

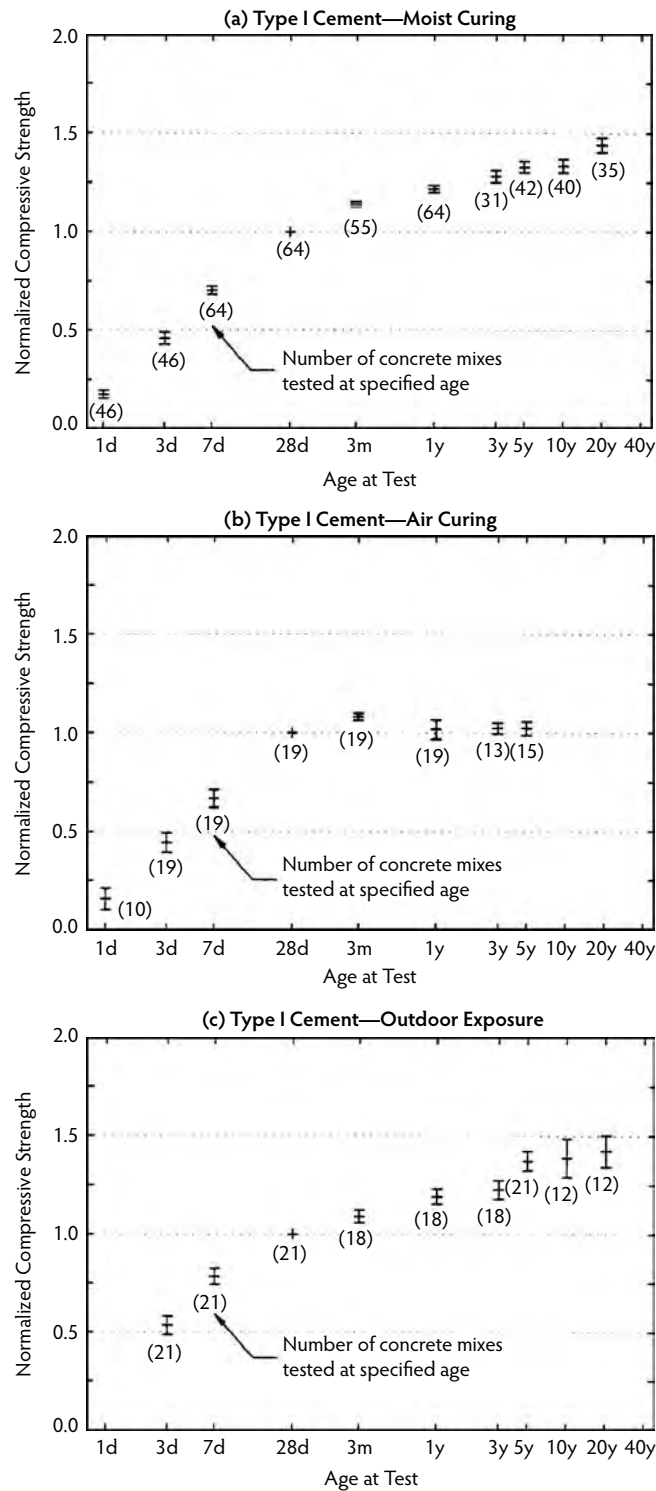


FIGURE 5.16 Ninety-five percent confidence intervals for mean normalized compressive strength of concrete made with Type I cement (7 days in moist room followed by indoor dry air exposure at 50% humidity, significantly reduced long-term strength gain). (From Wood, S.L., *Evaluation of the Long-Term Properties of Concrete*, RD102, Portland Cement Association, Skokie, IL, 1992.)

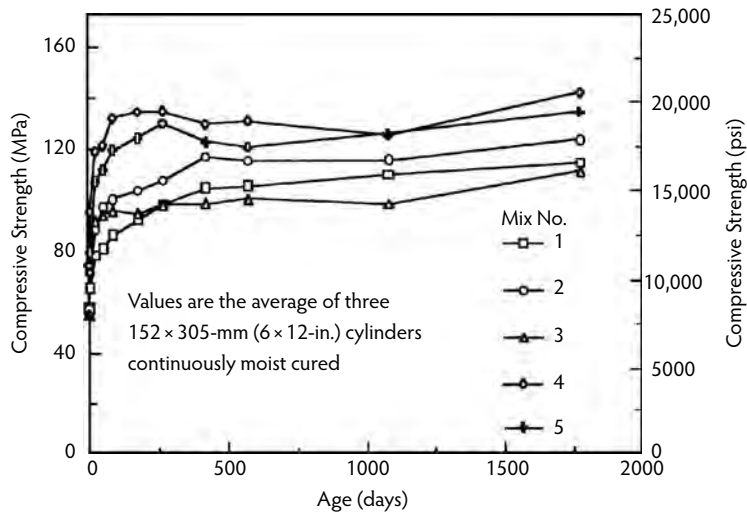


FIGURE 5.17 Strength development for five high-strength concrete mixes over a 5-year period. Mixes correspond to Table 5.7. (From Detwiler, R.J., *Concrete Technol. Today*, 17(2), 1–4, 1996 (PL962).)

TABLE 5.7 Example of High-Strength Concretes, SI (English Units)

Parameter, Units per Cubic Yard (m ³)	Mix Number ^a				
	1	2	3	4	5
Cement Type I, lb (kg)	950 (564)	800 (475)	820 (487)	950 (564)	800 (475)
Silica fume, lb ^b (kg)	—	40 (24)	80 (47)	150 (89)	125 (74)
Fly ash, lb (kg)	—	100 (59)	—	—	175 (104)
Coarse aggregate SSD, lb ^c (kg)	1800 (1068)	1800 (1068)	1800 (1068)	1800 (1068)	1800 (1068)
Fine aggregate SSD, lb (kg)	1090 (647)	1110 (659)	1140 (676)	1000 (593)	1000 (593)
HRWR type F, fl. oz. (L)	300 (11.60)	300 (11.60)	290 (11.22)	520 (20.11)	425 (16.44)
Retarder type D, fl. oz. (L)	29 (1.12)	27 (1.05)	25 (0.97)	38 (1.46)	39 (1.50)
Total water, lb ^d (kg)	267 (158)	270 (160)	262 (155)	242 (144)	254 (151)
Water/cement ratio	0.28	0.34	0.32	0.26	0.32
Water/cementitious materials ratio	0.28	0.29	0.29	0.22	0.23

^a As reported by ready-mix supplier.

^b Dry weight.

^c Maximum aggregate size 12.5 mm.

^d Mass of total water in mix including admixtures.

Note: See Figures 5.17, 5.22, 5.24, 5.26, and 5.30. SSD, saturated surface dry; HRWR, high-range water reducer.

Source: Burg, R.G. and Ost, B.W., *Engineering Properties of Commercially Available High-Strength Concretes (Including Three-Year Data)*, RD104, Portland Cement Association, Skokie, IL, 1994.

5.9 Volume Change and Crack Control

Concrete changes slightly in volume for various reasons. Understanding the nature of these changes is useful in planning concrete work and preventing cracks from forming. If concrete is free to move, normal volume changes have very little consequence, but, because concrete in service is usually restrained by foundations, subgrades, reinforcement, or connecting elements, significant stresses can develop. As the concrete shrinks, tensile stresses develop that can exceed the tensile strength of the concrete, resulting in crack formation. The primary factors affecting volume change are temperature and moisture changes. Concrete expands slightly as temperature rises and contracts as temperature falls. The average value for

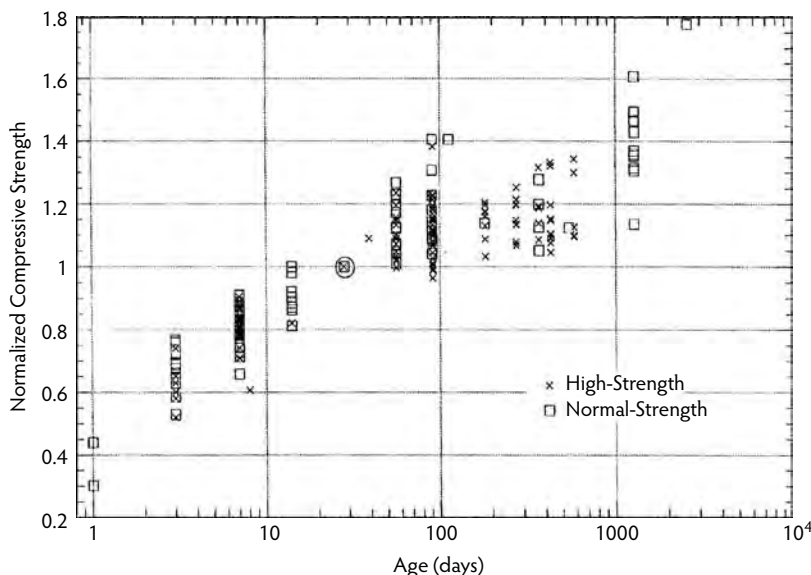


FIGURE 5.18 Compressive strength vs. time for normal and high-strength concretes cast in the 1980s and 1990s, normalized to 28-day strength. (From Lange, D.A., *Long-Term Strength Development of Concrete*, RP326, Portland Cement Association, Skokie, IL, 1994.)

the coefficient of thermal expansion of concrete is about 5.5 millionths per degree Fahrenheit (10 millionths per degree Celsius). This amounts to a length change of 0.66 in. for 100 ft (5 mm for a 10-m length) of concrete subjected to a rise or fall of 100°F (50°C). The thermal coefficient of expansion for steel is about 6.5 millionths per degree Fahrenheit (12 millionths per degree Celsius), comparable to that of concrete. The coefficient for reinforced concrete can be assumed to be 6 millionths per degree Fahrenheit (11 millionths per degree Celsius). Concrete expands slightly with a gain in moisture and contracts with a loss in moisture. The drying shrinkage of normal- and high-strength concrete specimens ranges from 400 to 800 millionths when exposed to air at 50% relative humidity. Figure 5.22 illustrates the drying-shrinkage characteristics of high-strength concretes in Table 5.7. Concrete with a unit shrinkage of 550 millionths shortens by about the same amount as a thermal contraction caused by a decrease in temperature of 100°F (55°C). The shrinkage of reinforced concrete is less than that for plain concrete due to the restraint offered by the reinforcement. Reinforced concrete structures with normal amounts of reinforcement have a drying shrinkage in the range of 200 to 300 millionths. The amount of shrinkage is directly related to the amount of water in the concrete. Higher water content results in higher shrinkage. Specimen size also has an effect. Larger specimens shrink less than small specimens. Cement type and content have little effect on drying shrinkage. Drying shrinkage can also be reduced by using aggregates that do not have high drying-shrinkage properties such as quartz, granite, or limestone. Some chemical admixtures may increase drying shrinkage. Drying shrinkage is an inherent and unavoidable property of concrete; therefore, properly positioned reinforcing steel is used to reduce crack widths, or joints are used to predetermine or control the location of cracks. Thermal stress due to fluctuations in temperature can also cause cracking, particularly at early ages.

5.10 Deformation and Creep

Concrete deforms a small amount at initial loading. When concrete is loaded, the deformation caused by the load can be divided into two parts: a deformation that occurs immediately, such as elastic strain, and a time-dependent deformation that begins immediately but continues at a decreasing rate for as long

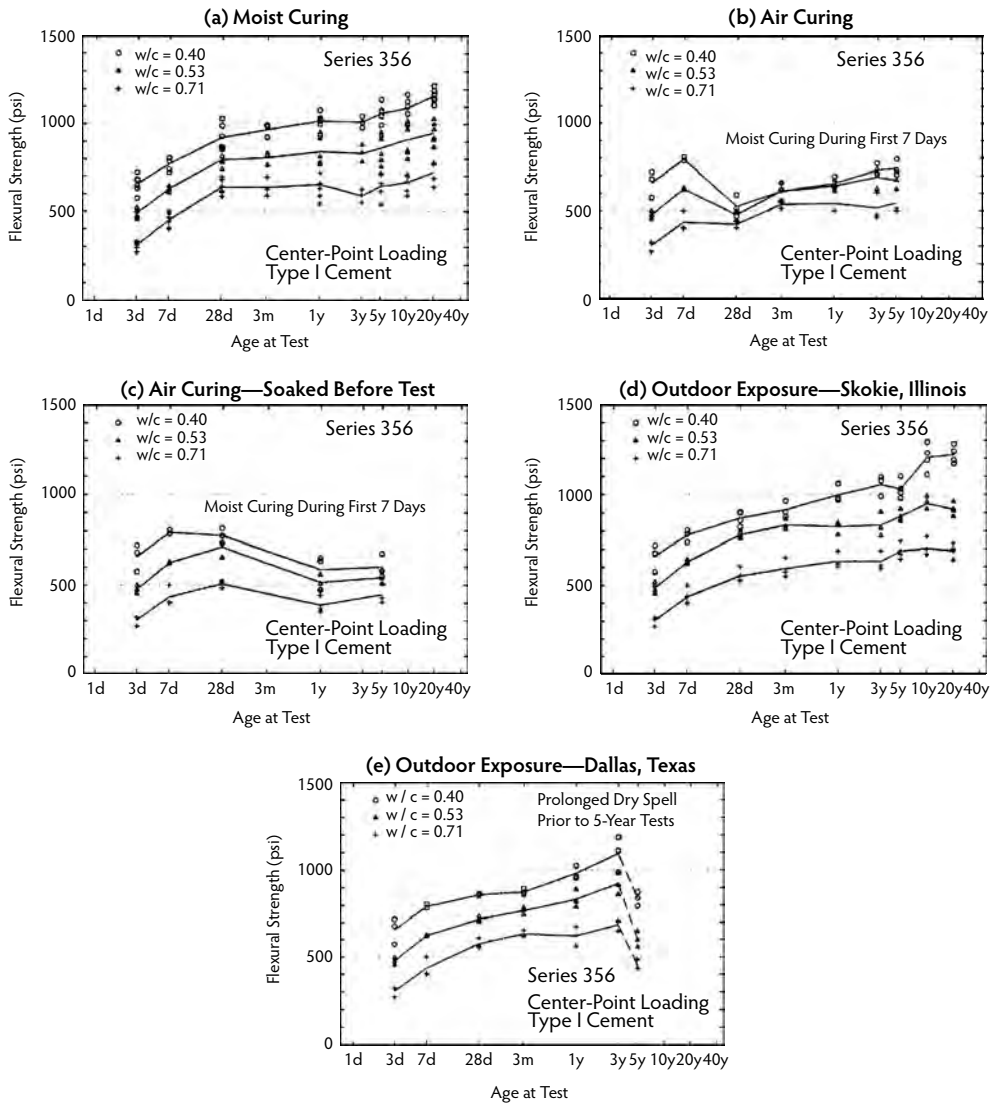


FIGURE 5.19 Variation of concrete flexural strength with log of age. (From Wood, S.L., *Evaluation of the Long-Term Properties of Concrete*, RD102, Portland Cement Association, Skokie, IL, 1992.)

as the concrete is loaded. This latter is called *creep*. The amount of creep is dependent on the magnitude of the stress, the age and strength of the concrete when the stress is applied, and the length of time the concrete is stressed. Figure 5.23 illustrates the combined effects of elastic and creep strains. Creep is of little concern for normal concrete buildings, pavements, and bridges; however, creep should be considered when designing for very tall buildings or very long bridges. High-strength concrete is sometimes used to control creep by keeping load values low. The specific creep of high-strength concretes in Table 5.7 is illustrated in Figure 5.24.

5.11 Concrete Ingredients

Normal- and high-strength concretes use a variety of cements, aggregates, mineral admixtures, and chemical admixtures. These materials are reviewed briefly in this section.

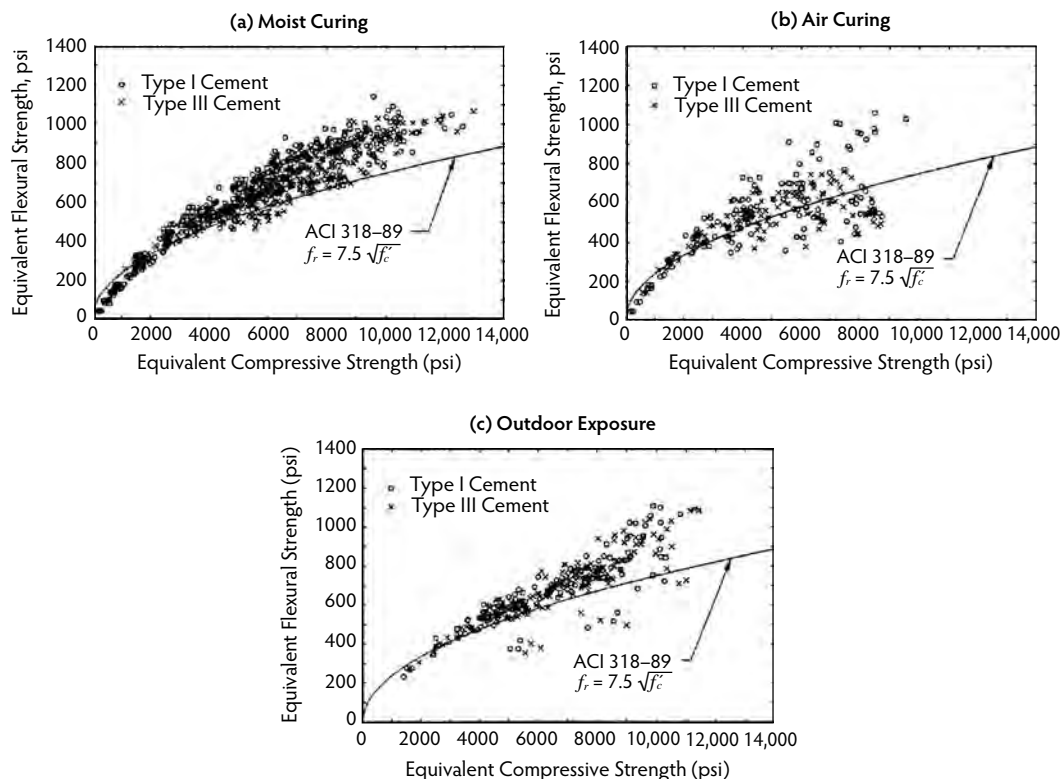


FIGURE 5.20 Flexural strength vs. compressive strength (such a relationship is often used in paving projects where cylinders are used in place of flexural beams). (From Wood, S.L., *Evaluation of the Long-Term Properties of Concrete*, RD102, Portland Cement Association, Skokie, IL, 1992.)

5.11.1 Portland Cements

Portland cements are hydraulic cements; that is, they set and harden by reacting with water. This reaction, called *hydration*, causes water and cement to combine to form a stone-like mass. Portland cement was invented in 1824 by an English mason, Joseph Aspdin, who named his product Portland cement because it produced a concrete that was of the same color as natural stone from the Isle of Portland in the English Channel. Portland cement is produced by combining appropriate proportions of lime, iron, silica, and alumina and heating them. These raw ingredients are fed into a kiln that heats the ingredients to temperatures from 2600 to 3000°F (1450 to 1650°C) and chemically changes the raw materials into cement clinker. The clinker is cooled and then pulverized. During this operation, a small amount of gypsum is added to control the setting of the cement. The finished pulverized product is Portland cement. Portland cement is essentially a calcium silicate cement. Powdered coal, oil, natural gas, or other materials are used as fuel for the kiln. A detailed discussion of cements and their chemistry is given in Chapter 1 of this *Handbook*. The American Society for Testing and Materials (ASTM) Standard C 150, Specification for Portland cement, defines the following types of Portland cement:

- Type I—general Portland cement
- Type II—moderate sulfate-resistant cement
- Type III—high-early-strength cement
- Type IV—low heat of hydration cement
- Type V—high sulfate-resistant cement

Types I, II, and III may also be designated as being air entraining.

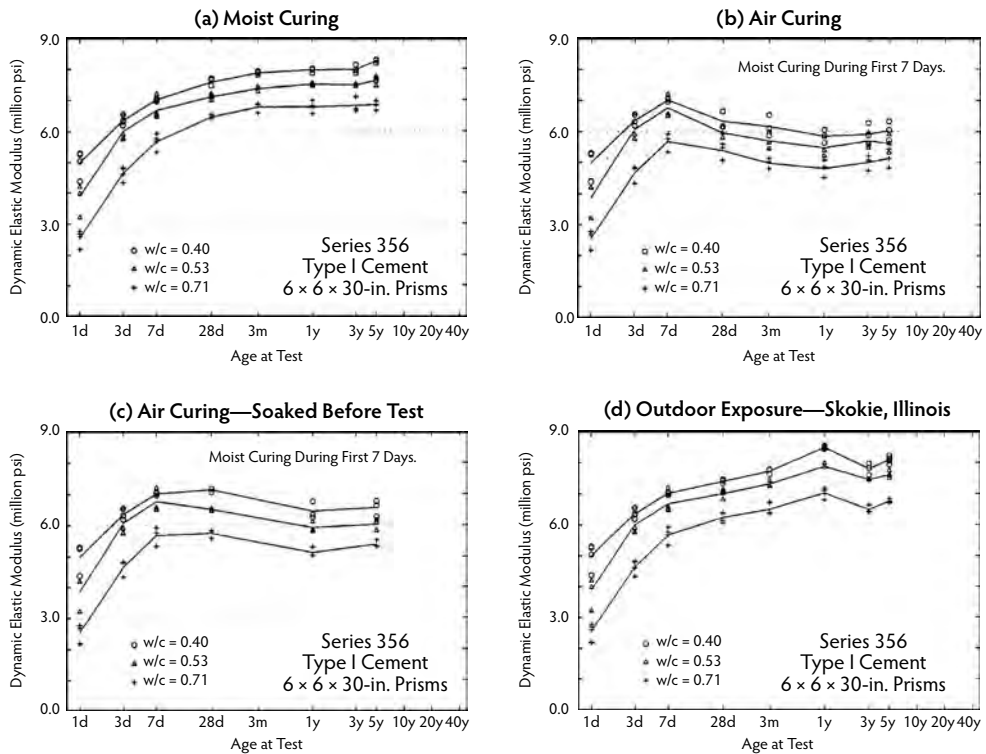


FIGURE 5.21 Dynamic modulus of elasticity of concrete vs. age. (From Wood, S.L., *Evaluation of the Long-Term Properties of Concrete*, RD102, Portland Cement Association, Skokie, IL, 1992.)

TABLE 5.8 Relative Flexural and Tensile Strengths of High-Strength Concrete at 91 Days

Mix	Cure	Modulus of Rupture (psi) ^a	Modulus of Rupture (MPa)	Tensile Strength (psi) ^b	Tensile Strength (MPa)
1	Moist	1370	9.4	925	6.4
1	Air	890	6.1	445	3.1
2	Moist	1470	10.1	860	5.9
2	Air	770	5.3	630	4.3
3	Moist	1440	9.9	720	5.0
3	Air	810	5.6	710	4.9
4	Moist	1990	13.7	1050	7.2
4	Air	980	6.8	940	6.5
5	Moist	1390	9.6	950	6.6
5	Air	940	6.5	670	4.6

^a Values are averages of three 6 × 6 × 30-in. (152 × 152 × 762-mm) specimens.

^b Values are averages of three 6 × 12-in. (152 × 305-mm) specimens.

Note: See compressive strengths in Figure 5.17 and mixes in Table 5.7.

Source: Burg, R.G. and Ost, B.W., *Engineering Properties of Commercially Available High-Strength Concretes (Including Three-Year Data)*, RD104, Portland Cement Association, Skokie, IL, 1994.

Type I Portland cement is a general cement suitable for all uses where the special properties of other cements are not required. It is commonly used in pavements, buildings, bridges, and precast concrete products. Type II Portland cement is used where precaution against moderate sulfate attack is important, as in bridge or pavement structures, or where sulfate concentrations in groundwater or soil are higher than normal but not too severe. Type II cement can also be specified to generate less heat than Type I

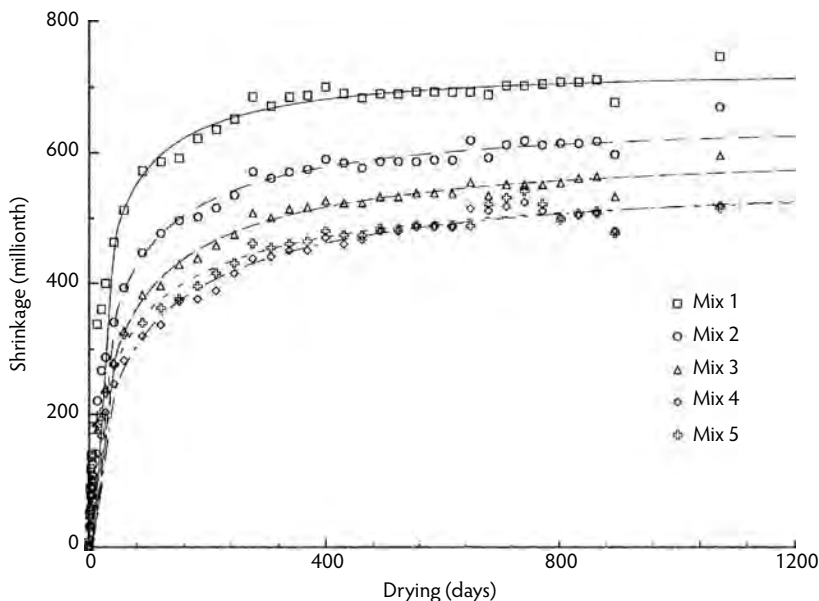


FIGURE 5.22 Drying shrinkage of $3 \times 3 \times 11.25$ -in. ($76 \times 76 \times 286$ -mm) prisms of high-strength concrete after 28-day moist curing. (From Burg, R.G. and Ost, B.W., *Engineering Properties of Commercially Available High-Strength Concretes (Including Three-Year Data)*, RD104, Portland Cement Association, Skokie, IL, 1994.)

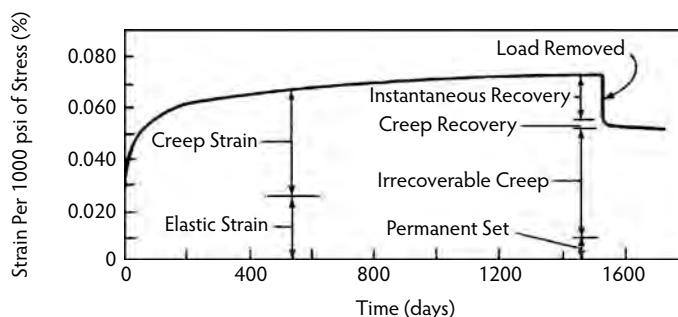


FIGURE 5.23 Combined elastic-creep strain vs. time (cylinders loaded at 8 days immediately after removal from fog room, then stored at 70°F and 5% relative humidity; applied stress = 25% compressive strength at 8 days). (From Kosmatka, S.H. et al., *Design and Control of Concrete Mixtures*, EB001, Portland Cement Association, Skokie, IL, 2006.)

cement. This moderate heat of hydration is helpful when placing massive structures such as piers, heavy abutments, and retaining walls. Type II cement may be specified when water-soluble sulfate in soil is between 0.1 and 0.2% or when the sulfate content in water is between 150 and 1500 ppm.

Type III Portland cement provides strength at an early age. Figure 5.25 illustrates the earlier strength gain of Type III cement over that of other cement types. It is chemically similar to Type I cement except that the particles are ground finer to increase the rate of hydration. It is commonly used in fast-track paving or when a concrete structure must be put into service as soon as possible, as in bridge deck repair.

Type IV Portland cement is used where the rate and amount of heat generated from hydration must be minimized. This low heat of hydration cement is intended for massive structures such as gravity dams. Type IV cement is rarely available. Type V Portland cement is used in concrete subject to very severe sulfate exposures. Type V cement is used when concrete is exposed to soil with a water-soluble sulfate content of 0.2% and higher or to water with over 1500 ppm of sulfate. The high sulfate resistance of Type V cement is attributed to its low tricalcium aluminate content.

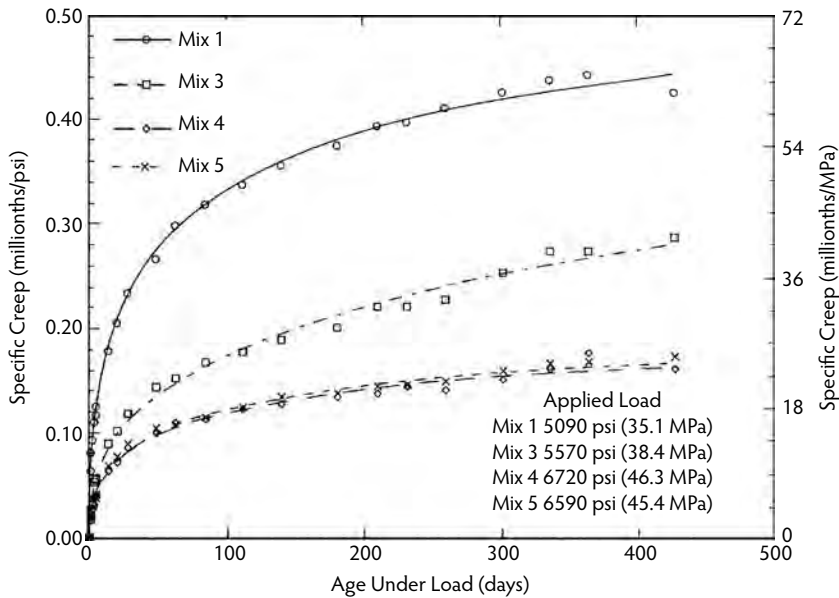


FIGURE 5.24 Specific creep of high-strength concrete in 6×12 -in. (150×300 -mm) cylinders. (From Burg, R.G. and Ost, B.W., *Engineering Properties of Commercially Available High-Strength Concretes (Including Three-Year Data)*, RD104, Portland Cement Association, Skokie, IL, 1994.)

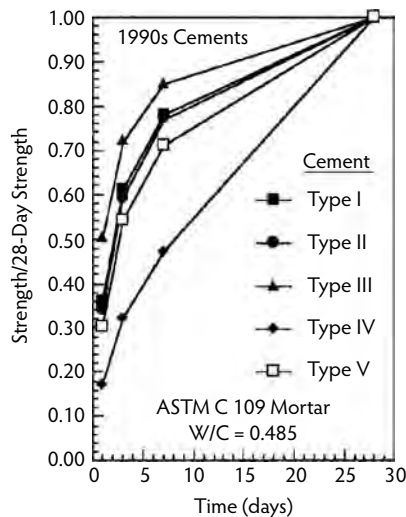


FIGURE 5.25 Strength gain curves for ASTM C 109 mortar cubes for various 1990s cement types. (From Detwiler, R.J., *Concrete Technol. Today*, 17(2), 1–4, 1996 (PL962).)

Cement Types I and II are commonly available and represent about 90% of the cement shipped in the United States, while Type III and white cement (discussed in the following section) represent only 4% of the cement produced. Type IV cement is manufactured only when specified for massive structures and is therefore not readily available. Type V is only available in specific severe sulfate environments.

5.11.2 White Portland Cement

White Portland cement has essentially the same chemistry as regular gray Portland cement except that it is white in color. White Portland cement is made of select raw materials that contain a negligible amount of iron and other dark metal oxides. White Portland cement is usually used for architectural purposes such as noise barrier walls and decorative concrete.

5.11.3 Blended Hydraulic Cements

Blended hydraulic cements are produced by blending two or more types of cementitious material. Primary blending materials are Portland cement, ground granulated blast-furnace slag, fly ash, natural pozzolans, and silica fume. These cements are commonly used in the same manner as Portland cements. Blended hydraulic cements conform to the requirements of ASTM C 595 or C 1157. ASTM C 595 cements are as follows: Type IS, Portland blast-furnace slag cement, and Type IP, Portland–pozzolan cement. The naming practice for blended cements allows adding the suffix (X) to the type designation, where (X) equals the targeted percentage of slag or pozzolan in the product expressed as a whole number by mass of the final blended product. These blended cements may also be designated as air-entraining (A), as moderate sulfate-resistant (MS), or as moderate (MH) or low (LH) heat of hydration. The United States uses a relatively small amount of blended cement compared with countries in Europe or Asia; however, this may change as consumer demands for products with specific properties and as environmental and energy concerns change.

5.11.4 Hydraulic Cements

ASTM C 1157 (Performance Specification for Hydraulic Cements) uses performance criteria, instead of constituent and prescription criteria, for blended and Portland cements. ASTM C 1157 hydraulic cements include the following: Type GU, for general construction use; Type HE, high early-strength cement; Type MS, moderate sulfate-resistant cement; Type HS, high sulfate-resistant cement; Type MH, moderate heat of hydration cement; and Type LH, low heat of hydration cement. These cements can also be designated for low reactivity (option R) with alkali-reactive aggregates. These cements may be specified as Portland cements, blended cements, or hydraulic cements. Except for the Portland designation, no restrictions are placed on the composition of the ASTM C 1157 cements. The manufacturer can optimize ingredients, such as pozzolans and slags, to optimize particular concrete properties.

5.11.5 Supplementary Cementing Materials

Supplementary cementing materials, previously called *mineral admixtures*, contribute to the properties of hardened concrete through hydraulic or pozzolanic activity. Typical examples are natural pozzolans, fly ash, ground granulated blast-furnace slag, and silica fume, which can be used individually with Portland or blended cement or in different combinations. These materials react chemically with calcium hydroxide released from the hydration of Portland cement to form cement compounds. Fly ash is a finely divided residue that results from the combustion of pulverized coal and is carried from the combustion chamber of the furnace by exhaust gases. Commercially available fly ash is a byproduct of thermal power-generating stations. Blast-furnace slag, or iron blast-furnace slag, is a nonmetallic product consisting essentially of silicates, aluminosilicates of calcium, and other compounds that form in a molten condition simultaneously with iron in the blast furnace. Silica fume, also called *condensed silica fume* and *microsilica*, is a finely divided residue resulting from the production of elemental silicon or ferrosilicon alloys that is carried from the furnace by the exhaust gases. Silica fume, with or without fly ash or slag, is usually used to make high-strength concrete. The following is a summary of the specifications and classes of supplementary cementing materials.

- Ground granulated iron blast-furnace slag (ASTM C 989)
 - Grade 80—Slags with a low activity index
 - Grade 100—Slags with a moderate activity index
 - Grade 120—Slags with a high activity index
- Fly ash and natural pozzolan (ASTM C 618)
 - Class N—Raw or calcined natural pozzolans including diatomaceous earth, opaline cherts, shales, tuffs, volcanic ashes, and some calcined clays and shales
 - Class F—Fly ash with pozzolanic properties
 - Class C—Fly ash with pozzolanic and cementitious properties
- Silica fume (ASTM C 1240)

A detailed discussion of supplementary cementitious materials is given in Chapter 2 of this *Handbook*.

5.11.5.1 Effects of Supplementary Cementing Materials on Properties of Freshly Mixed Concrete

Concrete mixes containing fly ash or slag will generally require less water, about 1 to 10%, for a given slump than concrete containing only Portland cement. Silica fume requires more water unless a water reducer is used. The amount of air-entraining admixture required to obtain a specified air content is normally greater when fly ash or silica fume is used. Class C fly ash generally requires less air-entraining admixture than Class F fly ash and tends to lose less air with mixing time. Ground slag has about the same effect as Portland cement on air-entrainment dosage. Fly ashes with high carbon contents require higher air-entraining dosages and also tend to lose more air with mixing or agitation. Fly ash and ground slag will generally improve the workability of concrete of equal slump and strength. Silica fume may reduce workability. Fly ash and ground slag can reduce the amount of heat of hydration in concrete for structures where lower heat development is required. The use of fly ash, natural pozzolans, and ground slag will generally retard the setting time of concrete. In one study, for example, fly ash caused the initial set to be retarded by 10 to 55 minutes and the final set to be retarded by 5 to 130 minutes for concrete incorporating 10 different fly ashes (Gebler and Klieger, 1986). The degree of retardation depends on the amount of Portland cement, the water requirement, the type of supplementary cementing material, and the concrete temperature. Finishability and pumping are generally improved with these materials.

Fly ash is commonly used in the United States at a dosage of 15 to 25% by mass of cementitious material. High-calcium Class C ashes have been used at higher dosages for particular situations. Ground slag commonly averages about 40% of the cementing material in the mix. Silica fume is typically used at a 5 to 10% dosage rate by weight of cementitious material. The dosage of a supplementary material depends on the particular concrete property the user is trying to improve or affect; therefore, it is very important to determine the optimal amount of the fly ash, slag, or silica fume to use. An overdose or underdose can be harmful or not have the desired effect. Also, these materials react differently with different cements.

The effects of temperature and moisture on the setting properties and strength development of concretes containing supplementary cementing materials are similar to the effects on concrete made with only Portland cement; however, the curing time may have to be longer for some materials. Relatively high dosages of silica fume can make a very cohesive concrete with very little bleeding. With little to no bleed water available at the surface for evaporation, plastic cracking can readily develop on hot days; therefore, special precautions to minimize evaporation during early curing are essential when using silica fume in concrete.

5.11.5.2 Effects on Hardened Concrete

Supplementary cementing materials contribute to the strength gain of concrete by providing additional cementitious compounds; however, the rate of strength gain of concrete containing these materials often differs from the strength gain of concrete that uses Portland cement as the only cementitious material. Due to the lower rate of hydration when using some of these materials, the early strength gain can be

lower than that of comparable concrete without such materials; yet, other materials perform in a manner very similar to Portland cement. Drying shrinkage and creep are little affected by the presence of normal dosages of supplementary cementing materials. The permeability of concrete containing supplementary cementing materials is usually reduced with adequate curing. Silica fume is frequently used in bridges to minimize chloride penetration into concrete.

5.11.5.3 Effects on Durability

The effect on durability of normal dosages of supplementary cementing materials is usually insignificant with regard to freeze–thaw resistance and deicer scaling. Depending on the dosage and the specific mineral admixture, alkali–silica reactivity and sulfate resistance may be improved, not affected, or even aggravated. These materials will usually improve the corrosion resistance of embedded steel because they reduce permeability and help keep chloride ions out of the concrete; however, some materials may slightly increase the depth of carbonation of concrete. Carbonation reduces the alkalinity of the concrete that is required to protect the embedded steel. Normal dosages of supplementary materials have an insignificant effect on carbonation.

5.11.6 Mixing Water for Concrete

Almost any natural water that is drinkable can be used as mixing water for concrete; however, some waters that are not fit for consumption may be suitable for concrete. Of particular concern are the levels of chloride, sulfate, and alkalis, as these can affect the durability of the concrete. Kosmatka et al. (2006) provide guidance concerning the use of waters containing alkali carbonates, chlorides, sulfates, acids, oils, and other materials, as well as guidance regarding allowable levels of contamination. Seawater containing salt can be suitable for nonreinforced concrete, but it should not be used for steel-reinforced concrete due to corrosion concerns. Mixing water should meet ASTM C 1602 (Specification for Mixing Water Used in the Production of Hydraulic Cement Concrete).

5.11.7 Aggregates for Concrete

The importance of using the right type and quality of aggregates cannot be overemphasized as the fine and coarse aggregates occupy between 60 and 75% of the concrete volume and strongly influence the freshly mixed and hardened properties, mix proportions, and economy of the concrete. Fine aggregates consist of natural sand or fresh stone with particles smaller than 0.2 in. (5 mm). Coarse aggregates consist of a combination of gravel or crushed aggregate with particles predominately larger than 0.2 in. (5 mm) and generally between 3/8 and 1-1/2 in. (10 and 38 mm). The most common coarse-aggregate sizes are 3/4 and 1 in. (19 and 25 mm). High-strength concrete often uses 1/2 in. (12 mm) maximum coarse aggregate. Natural gravel and sand are usually dug from pits. Crushed aggregate is produced by crushing quarry rock, boulders, or large-size gravel. Crushed air-cooled blast-furnace slag is also used as a fine or coarse aggregate. About half of the coarse aggregates used in Portland cement concrete in the United States are gravels and the remainder are crushed stone. Recycled concrete or crushed waste concrete is also a common source of aggregates and an economic necessity where good aggregates are scarce.

The most commonly used aggregates, such as gravel or crushed stone, produce a concrete with a freshly mixed unit weight of about 140 to 150 lb/ft³ (2240 to 2400 kg/m³). Special heavyweight or lightweight aggregates are also available for making concretes with a range of densities. Normal-weight aggregates should meet the requirements of ASTM C 33. This specification limits the amounts of harmful substances and states the requirements for aggregate characteristics such as grading.

Grading is the particle-size distribution of an aggregate and is determined by a sieve analysis. The 7 standard ASTM C 33 sieves for fine aggregate have openings ranging from 150 μ m to 3/8 in. (10 mm). The 13 standard sieves for coarse aggregate have openings ranging from 0.046 to 4 in. (1.18 to 100 mm). For highway construction, ASTM D 448 lists the 13 sizes in ASTM C 33 plus additional coarse aggregate sizes.

The grading and maximum size of the aggregate affect the relative aggregate proportions as well as cement and water requirements, workability, pumpability, economy, shrinkage, and durability of the concrete. Variations in grading can seriously affect the uniformity of the concrete from batch to batch. In general, aggregates that do not have a large deficiency or excess of any size and have a uniform distribution of particle sizes will produce the most satisfactory results.

The particle shape and surface texture of an aggregate influence the properties of freshly mixed concrete more than the properties of hardened concrete. Rough-textured, angular, elongated particles require more water to produce a workable concrete mixture than do smooth, rounded, compact aggregates; hence, aggregate particles that are angular require more cement to maintain the same water/cement ratio. With satisfactory gradation, both crushed and noncrushed aggregates of the same rock type generally give essentially the same strength for the same cement content and water/cement ratio.

The unit weight, also called the *unit mass* or *bulk density*, of an aggregate is the weight of aggregate required to fill a container of a specified unit volume. The volume referred to here is occupied by both the aggregate and the voids between aggregate particles. The approximate bulk density of aggregates commonly used in concrete ranges from about 70 to 110 lb/ft³ (1120 to 1760 kg/m³). Most natural aggregates have specific gravities or mass densities of between 2.4 and 2.9, with corresponding solid densities of 150 to 180 lb/ft³ (2400 to 2880 kg/m³). The density of an aggregate used in mixture-proportioning computations (not including voids between particles) is determined by multiplying the relative density (specific gravity) of the aggregate times the density of water. A value of 62.4 lb/ft³ (1000 kg/m³) is used for the density of water.

The absorption and surface moisture of aggregate should be determined according to ASTM test methods so the net water content of the concrete can be controlled and correct batch weights determined. The internal structure of an aggregate particle is made up of solid matter and voids that may or may not contain water. Following are the moisture conditions of aggregate:

- Oven dry—fully absorbent
- Air dry—dry at the particle surface but containing some interior moisture and thus still somewhat absorbent
- Saturated surface dry (SSD)—neither absorbing water nor contributing water to the concrete mixture
- Damp or wet—containing excessive moisture on the surface (free water)

The amount of water used in the concrete mixture must be adjusted for the moisture conditions of the aggregates to meet the designated water requirement. If the water content of the concrete mixture is not kept constant, the compressive strength, workability, and other properties will vary from batch to batch. Coarse and fine aggregate will generally have absorption levels in the range of 0.2 to 0.4% and 0.2 to 2%, respectively. Free-water contents will usually range from 0.5 to 2% for coarse aggregate and 2 to 6% for fine aggregate.

Harmful substances that may be present in aggregates include organic impurities, silt, clay, shale, iron oxide, coal, and certain lightweight or soft particles. In addition, certain substances and minerals such as chert may also be reactive to alkalis in the concrete. Certain aggregates such as shales will cause pop-outs at the concrete surface. Most specifications limit the permissible amounts of these substances in aggregates. Aggregates are potentially harmful if they contain compounds known to react chemically with Portland cement concrete and produce significant volume changes in the paste, aggregates, or both; interfere with the normal hydration of the cement; or otherwise have harmful byproducts. Alkali-aggregate reactivity is discussed in Section 5.18.

5.11.8 Chemical Admixtures for Concrete

Admixtures are ingredients in concrete other than Portland cement, water, and aggregates that are added to the mixture immediately before or during mixing. Common chemical admixtures include air-entraining, water-reducing, retarding, accelerating, and superplasticizing admixtures. The major reasons for

using admixtures are to reduce the cost of concrete construction, achieve certain properties in concrete more effectively than by other means, and to ensure the quality of concrete during the stages of mixing, transporting, placing, or curing in adverse weather conditions.

The most common admixtures are air-entraining admixtures. Air-entraining admixtures are used to purposely entrain microscopic air bubbles in concrete. Air entrainment will dramatically improve the durability of concrete exposed to moisture during freezing and thawing. Entrained air greatly improves the resistance of concrete to surface scaling caused by chemical deicers. The workability of fresh concrete is also improved significantly, and segregation and bleeding are reduced or eliminated. Air-entraining admixtures are commonly used to provide between 5 and 8% air content in concrete. The second most common admixture is the water-reducing admixture. Water-reducing admixtures are used to reduce the quantity of mixing water required to produce concrete of a certain slump, reduce the water/cement ratio, reduce cement content, or increase slump. Typical water reducers reduce the water content by approximately 5 to 10%. High-range water reducers reduce the water content by approximately 12 to 30%.

Retarding admixtures are used to retard the rate of setting of concrete. High temperatures of fresh concrete, around 90°F (32°C) or higher, often cause an increased rate of hardening that makes placing and finishing difficult. One of the most practical methods of counteracting this effect is to reduce the temperature of the concrete by cooling the mix water or aggregates. Retarders are sometimes used to offset the accelerating effect of hot weather on the setting of concrete, delay the initial set of concrete when difficult or unusual conditions of placement occur, or delay the set for special finishing processes, such as exposed aggregate finishes.

An accelerating admixture is used to accelerate the strength development of concrete at an early age. Calcium chloride is the most common accelerating admixture used for nonreinforced concrete. Care must be taken to make sure that the chloride content induced by the calcium chloride does not exceed the maximum chloride content allowed by local building codes. An excess of calcium chloride can cause corrosion in reinforced concrete. Besides accelerating strength gain, calcium chloride causes an increase in drying shrinkage and may slightly darken the concrete. Calcium chloride is not an antifreeze and will not reduce the freezing point of water by more than a few degrees. The amount of calcium chloride added should be no more than necessary to produce the desired results and should in no case exceed 2% by weight of cement in nonreinforced concrete. Nonchloride, noncorrosive admixtures are also available where corrosion is a concern.

Superplasticizers are high-range water reducers that are added to concrete with a low to normal slump and water/cement ratio to make high-slump flowing concrete. Flowing concrete is a highly fluid, workable concrete that can be placed with little or no vibration or compaction and yet is free of excessive bleeding or segregation. Superplasticized flowing concrete is used in thin section placements, areas of closely spaced reinforcing steel, underwater placements, and other applications where a more fluid mixture is more economically handled or placed.

All of the admixtures discussed in this section must meet the appropriate ASTM standards. When used at appropriate dosages, these materials should not adversely affect concrete properties; however, an overdose has significant effects on strength, shrinkage, and durability. In-depth details of chemical admixtures are given in Chapter 3 of this *Handbook*.

5.12 Proportioning of Concrete Mixtures

The objective in proportioning concrete mixtures is to determine the most economical and practical combination of readily available materials to produce a concrete that will satisfy the performance requirements (design) for the particular conditions of use. To fulfill these objectives, a properly proportioned concrete mix should possess these following qualities: (1) acceptable workability of freshly mixed concrete; (2) durability, strength, and uniform appearance of hardened concrete; and (3) economy. Only with proper selection of materials and mixture characteristics can the above qualities be obtained in concrete production. Concrete mixtures should be kept as simple as possible, as an excess number of ingredients can make a concrete mixture difficult to control.

The key to designing a concrete mixture is to be fully aware of the relationship between water/cement ratio and strength and durability. The specified compressive strength at 28-day and durability concerns dictate the water/cement ratio established for a concrete mixture. The water/cement ratio is simply the weight of water divided by the weight of cement. If pozzolans or slag are used, the ratio would include their weights and be referred to as the water/cementitious material ratio. The water/cement ratio can be established by a known relationship to strength or by durability requirements. For example, a concrete structure may require only 3000 psi (20 MPa) compressive strength, which would relate to a water/cement ratio of about 0.6; however, if the concrete is exposed to deicers, the maximum water/cement ratio should be 0.45. For corrosion protection or for reinforced concrete exposed to deicers, the maximum water/cement ratio should be 0.40. When designing concrete mixtures, it is important to remember that, where durability is concerned, the water/cement ratio should be as low as practical.

Aggregate grading and the nature of the particles such as shape, size, and surface texture all affect the mix design. The maximum size that can be used depends on the size and shape of the concrete member to be cast as well as on the amount of reinforcing steel present. The maximum size of coarse aggregate should not exceed one fifth of the narrowest dimension between sides of the forms or three fourths of the clear space between individual reinforcing bars.

The designer has to decide whether air entrainment is required. Entrained air must be used in all concrete that will be exposed to freezing and thawing and deicing chemicals. The typical range for the amount of entrained air depends on the size of the coarse aggregate and the degree of exposure. A typical air content for concrete would range from 5 to 8%. Concrete must also be workable and have an adequate consistency for the job placement conditions. The slump test is a measure of concrete consistency. The slump range for pavements and slabs is between 1 and 3 in. (25 and 75 mm). Slumps for wall and other applications can range from 3 to 6 in. (75 to 150 mm).

The water content of concrete is influenced by a number of factors: aggregate size and shape, slump, water/cement ratio, air content, cement content and admixtures, and environmental conditions. Increased air content and aggregate size, reduction in water/cement ratio and slump, rounded aggregates, and the use of water-reducing admixtures or fly ash all reduce water demand. On the other hand, increased temperatures, cement contents, water/cement ratio, and aggregate angularity all increase water demand. The cement content is determined from the selected water/cement ratio and water content.

Kosmatka et al. (2006) provide the Portland Concrete Association's step-by-step procedures for proportioning concrete by absolute volume methods from field or laboratory data. Farny and Panarese (1994) provide guidance for high-strength concrete. Chapter 6 of this *Handbook* presents a detailed treatment including numerical examples of the design of concrete mixtures for both normal- and high-strength concretes using the methods of the American Concrete Institute (see ACI 211 and related proportioning documents at www.concrete.org).

5.13 Hot and Cold Weather Concreting

All concrete must be properly cured. Curing is maintaining a satisfactory moisture content and temperature in concrete for some definite time period immediately following placing and finishing so the desired properties of strength and durability may develop. Concrete should be moist cured for 7 days at a temperature of between 50 and 80°F (10 to 27°C). Common methods of curing include the use of ponding, spraying, or fogging; wet covers; impervious paper; plastic sheets; or membrane-forming curing compounds, or some combination of these. These techniques will properly maintain adequate moisture in the concrete. When hot or cold weather conditions are present, temperature protection must be provided. In hot weather concreting, the concrete temperature should be less than 90°F (32°C). This can be achieved by cooling the concrete with ice, cold water, or nitrogen injection when the concrete is batched. High-strength concrete especially requires extra care to minimize plastic cracking during hot weather.

When the temperature approaches freezing, cold-weather concreting practices should be instituted. This may include methods for accelerating the early strength of the concrete such as using extra cement, a lower water/cement ratio, or an accelerator. Cold temperatures can dramatically reduce the setting rate

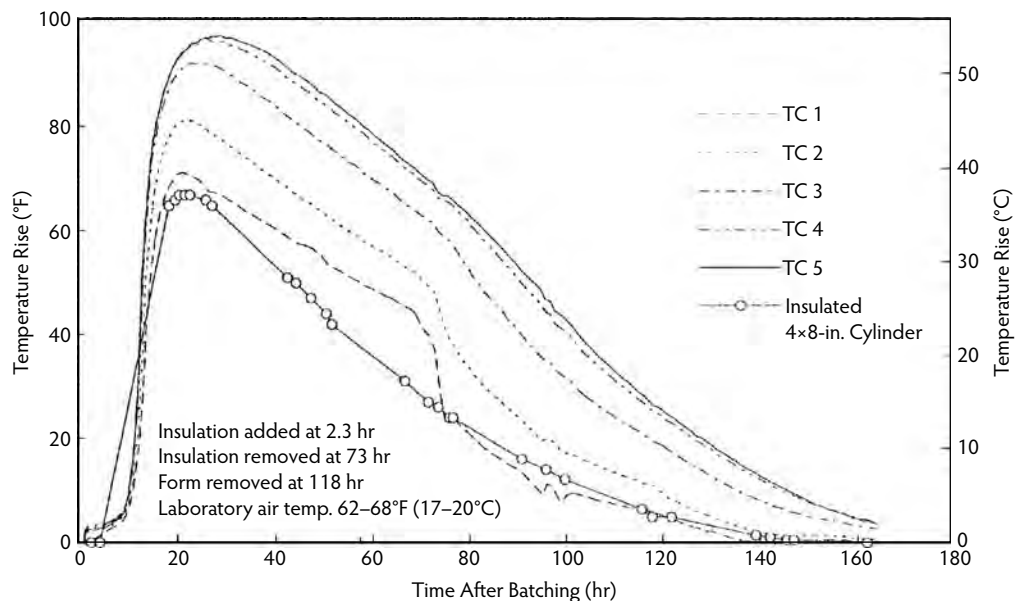


FIGURE 5.26 Temperature rise vs. time for high-strength concrete in a 4-ft (1.2-m) cube (TC1 through TC5 represent temperatures from the outside to the inside of the cube). (From Burg, R.G. and Ost, B.W., *Engineering Properties of Commercially Available High-Strength Concretes (Including Three-Year Data)*, RD104, Portland Cement Association, Skokie, IL, 1994.)

of concrete. The use of insulating blankets or temporary heated enclosures is an effective means of providing an adequate temperature for concrete. The natural temperature rise of concrete helps maintain the desired temperature. The temperature rise of high-strength concrete is illustrated in Figure 5.26. The temperature rise of high-strength concrete, being greater than that of normal-strength concrete, also leads to concern about controlling the cracking caused by extreme temperature differences. Figure 5.11 and Figure 5.13 illustrate the effects of temperature on set time and strength gain for normal-strength concrete. Concrete temperatures below freezing essentially halt hydration and strength gain. With appropriate precautions, concrete can be successfully placed in the winter (Figure 5.27).

5.14 Control Tests

Satisfactory concrete construction and performance require concrete possessing specific properties. To ensure that these properties are obtained, quality control and acceptance testing are indispensable parts of the construction process. Past experience and sound judgment must be relied on in evaluating tests and assessing their significance in the ultimate performance of concrete. The most common tests performed on concrete include the slump, strength, temperature, and air-content tests. The number of tests done depends on project conditions and specifications. Strength tests should be done every day at least and should be done no less than once for each 150 yd³ (115 m³) of concrete. A 7-day strength cylinder, along with two 28-day cylinders, is often made to provide early indications of strength development. The slump test should be performed in accordance with ASTM C 143; the temperature of concrete should be measured in accordance with ASTM C 1064; the air content should be determined in accordance with ASTM C 231, C 173, or C 138; and strength specimens should be made and cured in accordance with ASTM C 31. Traditionally, concrete cylinders 6 in. (150 mm) in diameter by 12 in. (300 mm) high were used for concretes with aggregates no larger than 2 in.; however, because most aggregates are less than 1 in. (25 mm) in size, most testing laboratories use 4 × 8-in. (100 × 200-mm) cylinders.



FIGURE 5.27 Cold-weather concreting under suitable preparation conditions. (Figure courtesy of the Portland Cement Association, Skokie, IL.)

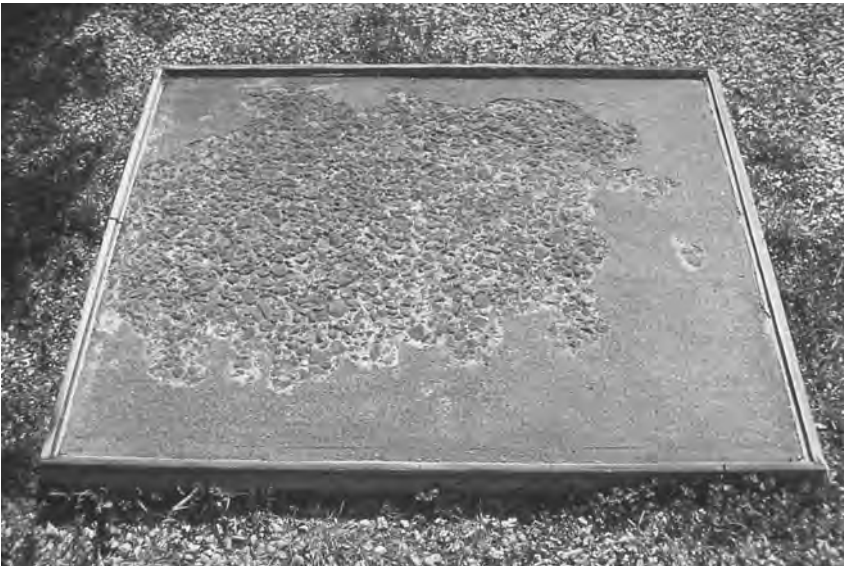


FIGURE 5.28 Frost-damaged concrete with surface scaling. (Figure courtesy of the Portland Cement Association, Skokie, IL.)

5.15 Freeze–Thaw and Deicer Scaling Resistance

As water freezes in wet concrete, it expands 9%, producing hydraulic pressures in the capillaries and pores of cement paste and aggregate. If the pressure exceeds the tensile strength of the paste or aggregate, the cavity will rupture. Accumulated effects of successive freeze–thaw cycles and disruption of the paste and aggregate eventually cause significant expansion and extensive deterioration of the concrete. The deterioration is visible in the form of cracking, scaling, and crumbling, as seen in Figure 5.28. The resistance of hardened concrete to freezing and thawing in moist conditions, with or without the presence

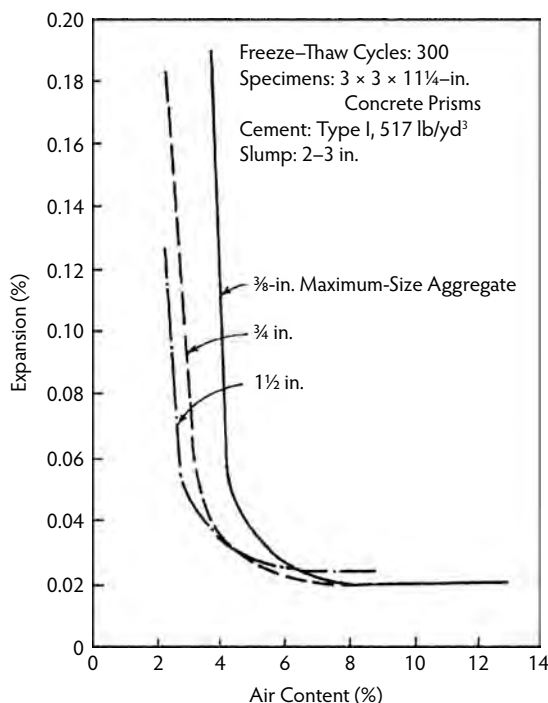


FIGURE 5.29 Air content vs. expansion of normal-strength concrete (air content above 5 to 6%, depending on aggregate size, essentially eliminates frost damage). (From Klieger, P., *Studies of the Effect of Entrained Air on the Strength and Durability of Concretes Made with Various Maximum Sizes of Aggregates*, RX040. Portland Cement Association, Skokie, IL, 1952.)

of deicers, is significantly improved by the use of entrained air. Air entrainment prevents frost damage and scaling and is required for all concretes exposed to freezing and thawing or deicer chemicals. An air content of between 5 and 8% should be specified for normal- and high-strength concrete exposed to wet freezing conditions (Figure 5.29). In the past, it was thought that high-strength concrete did not have to be air entrained because of its low permeability; however, research has shown that in most cases high-strength concrete also requires air entrainment (Figure 5.30). A good air-void system should have a spacing factor of less 0.008 in. (0.203 mm). Air-entrained concrete should be composed of durable materials and have a low water/Portland cement ratio (maximum 0.45), a minimum cement content of 564 lb/yd³ (335 kg/m³), proper finishing after bleed water has evaporated from the surface, adequate drainage, a minimum of 7-day moist curing at or above 50°F (10°C), a minimum compressive strength upon frost exposure of 4000 psi (28 MPa), and a minimum 30-day drying period after moist curing. Sealers may also be applied to provide additional protection against the effects of freezing and thawing and deicers; however, a sealer should not be necessary for properly proportioned and placed concrete.

5.16 Sulfate-Resistant Concrete

Excessive amounts of sulfates in soil or water can, over 5 to 30 years, attack and destroy concrete that is not properly designed. Sulfates attack concrete by reacting with hydrated compounds in the hardened cement paste, especially calcium aluminate hydrate. Due to crystallization, these expansive reactions can induce sufficient pressure to disrupt the cement paste, resulting in cracking and disintegration of the concrete. Furthermore, magnesium sulfate solutions can attack concrete by reacting with calcium silicate hydrate, the primary binding material in Portland cement paste. Advanced sulfate attack can turn concrete into a noncohesive mass of rubble, similar to crushed stone or gravel in appearance.

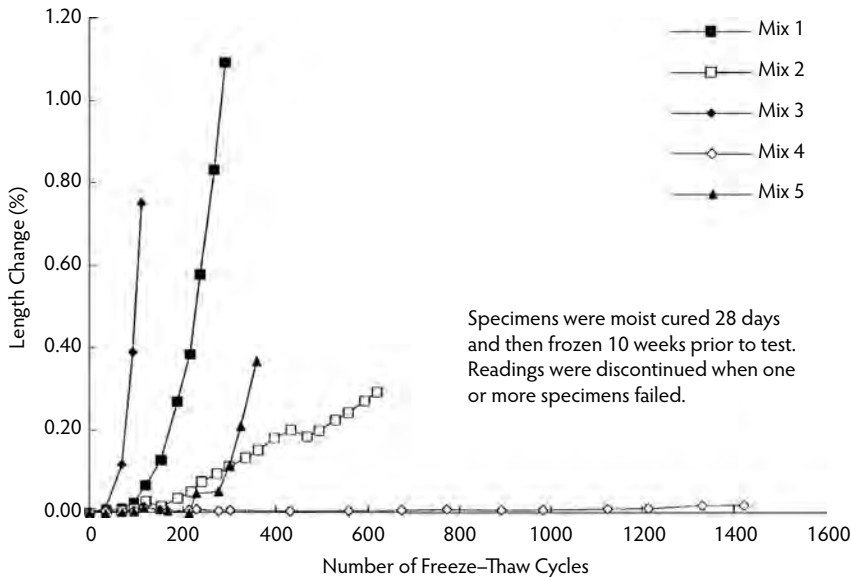


FIGURE 5.30 Length change vs. wet freeze-thaw cycles in non-air-entrained, high-strength concrete prisms (see Table 5.7). Expansions over 0.10% are considered failure; hence, most non-air-entrained, high-strength concretes are not durable under frost exposure. (From Burg, R.G. and Ost, B.W., *Engineering Properties of Commercially Available High-Strength Concretes (Including Three-Year Data)*, RD104, Portland Cement Association, Skokie, IL, 1994.)

TABLE 5.9 Requirements for Concrete Exposed to Sulfate

Sulfate Exposure	Water-Soluble Sulfate (SO ₄) in Soil (% by Mass)	Sulfate (SO ₄) in Water (ppm)	Cement Type ^a	Maximum Water/Cementing Material Ratio (by Mass)
Negligible	0.00–0.10	0–150	Use any cement	—
Moderate ^b	0.10–0.20	150–1500	II, IP (MS), IS (<70) (MS), MS	0.50
Severe	0.20–2.00	1500–10,000	V, HS	0.45
Very severe	Over 2.00	Over 10,000	V, HS	0.40

^a Cement Type II and Type V are specified in ASTM C 150, and the remaining types are specified in ASTM C 595 or ASTM C 1157. Pozzolans or slags determined by test to improve sulfate resistance may also be used.

^b Seawater.

Note: HS, high sulfate-resistant; IP, Portland–pozzolan cement; IS, Portland blast-furnace slag; MS, moderate sulfate-resistant.

The water/cement ratio (or water/cementitious materials ratio) is the most critical part of a mix design for preventing sulfate attack. The ratio should be no more than the value recommended in Table 5.9 for a particular sulfate exposure and should preferably be less than 0.4 where practical to maximize sulfate resistance. Figure 5.31 and Figure 5.32 clearly illustrate the great importance of using a low water/cementitious materials ratio to protect concrete against the ravages of sulfate attack. Air entrainment is also helpful for improving sulfate resistance when it reduces the water/cement ratio. The cement content for normal weight and lightweight concrete should be at least 564 lb/yd³ (335 kg/m³). When possible, concrete should be allowed to achieve its design strength before it is exposed to sulfate solutions.

Selection of the cement type is the second step (after selecting the water/cement ratio) in designing a sulfate-resistant concrete. Table 5.9 provides recommendations for cement types for different sulfate conditions (adapted from requirements originally established by the U.S. Bureau of Reclamation). Cement standards such as ASTM C 150 (Specification for Portland Cement), ASTM C 595 (Specification for Blended Hydraulic Cements), and ASTM C 1157 (Performance Specification for Blended Hydraulic

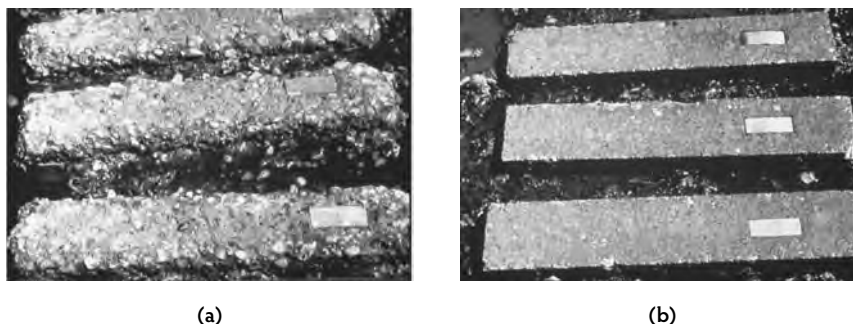


FIGURE 5.31 Sulfate attack of concrete beams placed in high-sulfate soil; 5-year performance with water/cementitious ratios of (a) 0.50 and (b) 0.39. (From Stark, D., *Durability of Concrete in Sulfate-Rich Soils*, RD097, Portland Cement Association, Skokie, IL, 1989.)

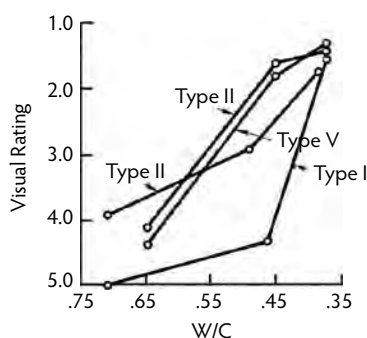


FIGURE 5.32 Sulfate resistance of concrete with various cement types and water/cement ratios; a rating of 1 is no deterioration, and a rating of 5 is severe deterioration (namely, mortar loss). (From Stark, D., *Durability of Concrete in Sulfate-Rich Soils*, RD097, Portland Cement Association, Skokie, IL, 1989.)

Cement) provide specifications for cements that are to be used in concrete exposed to sulfate conditions. Portland cements for sulfate exposures must have low amounts of tricalcium aluminate (C_3A). Type II and V ASTM C 150 cements are intended for use in moderate and severe sulfate exposures, respectively. Type II cement is usually available where needed; however, Type V and the blended cements are available only in certain areas. Supplementary cementing materials can also be used in sulfate environments, especially in low water/cement ratio concrete; however, their effects on sulfate resistance should be demonstrated by field record or test. Some supplementary cementing materials are helpful and others are detrimental. For concrete exposed to seawater, cement with a C_3A content up to 10% can be used due to the ability of chloride in seawater to inhibit expansive sulfate reactions. Usually a Type II cement is specified for use in seawater (see Table 5.9), but some Type I cements will meet this criteria. An analysis of the sulfate conditions to which concrete will be exposed and proper selection of materials, proportioning, and testing of concrete mixtures will minimize the effects of sulfate attack and ensure the long-term durability of concrete structures.

5.17 Corrosion Protection

Concrete protects embedded steel from corrosion through its highly alkaline nature. The high-pH environment (usually greater than 12.5) causes a passive and noncorroding protective oxide film to form on steel; however, carbonation or the presence of chloride ions from deicers or seawater can destroy or penetrate the film. When this happens, an electric cell is formed along the steel or between steel bars and the electrochemical process of corrosion begins. Some steel areas along the bar become anodes,

discharging current in the electric cell, and in those areas the iron goes into solution. Steel areas that receive current are cathodes, where hydroxide ions are formed. The iron and hydroxide ions form iron hydroxide (FeOH), which further oxidizes to form rust, or iron oxide. Rusting is an expansive process—rust expands to up to four times its original volume—that induces internal stress and eventual spalling in concrete over reinforcing steel. The cross-sectional area of the steel can also be significantly reduced. Once it starts, the rate of steel corrosion is influenced by the electrical resistivity of the concrete, its moisture content, and the rate at which oxygen migrates through the concrete to the steel. Chloride ions alone can also penetrate the passive film on the reinforcement and combine with iron ions to form a soluble iron chloride complex that carries the iron into the concrete, where it is later oxidized and forms rust. As little as 0.15% water-soluble chloride (about 0.2% acid-soluble) by weight of cement is sufficient to initiate corrosion of embedded steel under some conditions.

Premature deterioration of concrete bridges and parking structures can be a major concrete problem. These structures are often exposed to very severe conditions. Deicer and ocean salts, temperature and moisture changes, freezing and thawing, and abrasion all challenge the life of bridges and other structures. Of these exposure conditions, chloride salts from deicers and ocean spray in marine environments provide the greatest challenge to durability. They can corrode embedded steel, usually causing cracks, spalls, rust stains, and sometimes structural failure.

Deficient corrosion protection has resulted in millions of dollars in repairs over the last two decades. The severity of chloride-induced corrosion and the need for extra protection were not fully realized in the design, construction, and maintenance of early structures; however, field experience and extensive research in recent years have provided new insights into the mechanism of chloride-induced corrosion and methods to cope with the problem. The use of certain protective strategies to prevent or retard steel corrosion can result in bridges with long-term durability, extended structural life, and significantly reduced maintenance and repair costs. To reduce the risk of corrosion, the following protective strategies can be used individually or in combination:

- Cover thickness of 3.5 in. (90 mm) or more of concrete over the top of reinforcing steel in compression zones in bridge decks (note that excessive cover in tension zones exacerbates surface-crack width)
- Low-slump dense concrete overlay
- Latex-modified concrete overlay
- Interlayer membrane/asphaltic concrete systems
- Epoxy-coated reinforcing steel
- Corrosion-inhibiting admixtures in concrete
- Sealers with or without overlay
- Silica fume or other pozzolans that significantly reduce concrete permeability
- Low water/cement ratio superplasticized concrete, monolithic or in overlay
- Cathodic protection
- Polymer concrete overlay
- Galvanized reinforcing steel
- Polymer impregnation
- Lateral and longitudinal prestressing for crack control
- Blended cements containing silica fume or other pozzolans to reduce permeability

The purpose of most of these strategies is to delay or stop chloride ions from coming in contact with reinforcing steel. Most of the strategies can also be used alone or in combination for repair and maintenance of older structures showing signs of deterioration.

Studies of the corrosion activity of concretes made with varying water/cement ratios, calcium nitrite corrosion-inhibiting admixtures, silane and methacrylate surface treatments, epoxy-coated rebars and prestressing strands, galvanized reinforcement, and silica-fume admixtures were reported in *Protective Systems for New Prestressed and Substructure Concrete* FHWA/RD-86/193 (FHA, 1987). The 3-year

corrosion research project involved 11 protection systems. A summary of some design considerations and research conclusions from this study are as follows:

- The lowest possible water/cement ratio should be used, preferably in the range of 0.32 to 0.44. Concrete permeability and corrosion severity both decrease dramatically as the water/cement ratio is decreased. Long-term chloride permeability to the 1-in. (25-mm)-deep level in concrete was reduced in this study by about 80% and 95% when the water/cement ratio was reduced from 0.51 to 0.4 and 0.28, respectively.
- The clear concrete cover over reinforcement should be maximized—it should be as large as possible to minimize long-term penetration of water and chloride ions.
- Silica-fume admixtures and surface sealers (such as silane) both drastically reduce chloride penetration.
- Corrosion-inhibiting admixtures can significantly reduce corrosion severity.
- Epoxy-coated reinforcing bars and coated prestressing strands were found to be free of corrosion in chloride-laden concrete.

A belt-and-suspenders approach to bridge construction (using more than one protection method simultaneously) can result in significant savings in maintenance costs and produce a structure with a long trouble-free life. Examples of some double-protection systems would include the use of silica fume and a corrosion inhibitor, silica fume and cathodic protection, or latex-modified concrete and extra concrete cover over steel, assuming a low water/cement ratio in each case.

In addition, concrete surfaces must be sloped for adequate drainage, and concrete must be properly proportioned, placed, finished, and cured. Admixtures containing chlorides should be avoided, or, at least, the acid-soluble chloride content should be limited to a maximum of 0.08% and 0.20% (preferably less) by weight of cement for prestressed and reinforced concrete, respectively (ACI Committee 222, 2003; Stark, 1989b). Today, engineers can feel confident that, with the use of good design and construction practices and one or more available corrosion protection systems, a concrete structure can be built to endure even the most severe environment for many years with little maintenance.

5.18 Alkali–Silica Reaction

Most aggregates are chemically stable in hydraulic cement concrete; that is, they are without deleterious interaction with other concrete ingredients. This is not the case, however, for aggregates containing certain siliceous substances that react with alkali hydroxides in concrete. Alkali–silica reactivity (ASR) has been reported in structures throughout the world. ASR is usually first identified by surface map-pattern cracks. Very reactive aggregates can induce cracks within a year, whereas slowly reactive aggregates can take over 20 years to induce noticeable cracks (Figure 5.33). Because ASR deterioration is slow, the risk of catastrophic failure is low; however, cracking due to ASR can cause serviceability problems and can exacerbate other deterioration mechanisms such as occur in frost, deicer, or sulfate exposures. Normal-strength and high-strength concretes are both susceptible to ASR. The basic options for avoiding reactivity problems are relatively simple in concept:

- Do not use potentially reactive aggregates.
- Use fly ash, slag, silica fume, natural pozzolans, or blended hydraulic cement to control reactions.
- Reduce the level of soluble alkalis in the concrete.

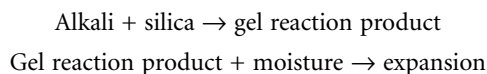
Avoiding potentially reactive aggregates is the most effective approach to solving reactivity problems; unfortunately, with a diminishing supply of proven nonreactive aggregate sources, concrete producers have no alternative but to use potentially reactive aggregate. As this is often the case, other options must be considered. Use of pozzolans, slag, or blended cement is an effective option in areas where appropriate materials are available. Reducing alkalis is commonly equated with using low-alkali cement; however, for



FIGURE 5.33 Cracking of concrete as a result of alkali-silica reactivity.

a number of reasons, low-alkali cements are not always readily available nor is reliance on a simple low-alkali cement specification always effective with highly reactive aggregates. The following provides guidance for detecting which aggregates are potentially reactive and methods of controlling ASR based on the current state of the art.

Alkali-silica reactivity is an expansive reaction between reactive forms of silica in aggregate and alkali hydroxides. The alkalis potassium and sodium come mostly from cement, although some come from aggregates, pozzolans, admixtures, and mixing water. External sources of alkali from soils, deicers, and industrial processes can also contribute to reactivity. The reaction forms an alkali-silica gel that swells as it draws water from the surrounding paste, inducing pressure, expansion, and cracking of the aggregate and surrounding paste. The reaction can be visualized as a two-step process:



The outward manifestation of the expansion often results in map-pattern cracks or longitudinal cracks. Crack patterns are affected by restraint conditions and other volume change movements.

Aggregate sources are prone to ASR if the following silica constituents are present: opal (more than 0.5%); chert and chalcedony (more than 3.0%); tridymite and cristobalite (more than 1.0%); strained or microcrystalline quartz (more than 5.0%), as found in granites, granite gneiss, graywackes, argillites, phyllites, siltstones, and natural sand and gravel; and natural volcanic glasses. The aggregate should then be evaluated for ASR in accordance with ASTM C 1260 (rapid mortar bar test) or ASTM C 1293 (concrete prism test). As with other methods, the ASTM C 1260 test is an accelerated procedure that is intended to force the potential reactions. The high alkali content and temperature are not representative of field conditions. ASTM C 1567 (a variation of ASTM C 1260) or ASTM C 1293 can be used to determine the effectiveness of pozzolans or slags to control ASR. The use of ASTM C 1293 comes from demonstrated Canadian practice. Criteria to determine if the aggregate is potentially reactive based on these physical tests follow:

- ASTM C1260—Mean expansion at 14 days, >0.10%, potentially reactive
- ASTM C1293—Expansion at 1 year, >0.04%, potentially reactive

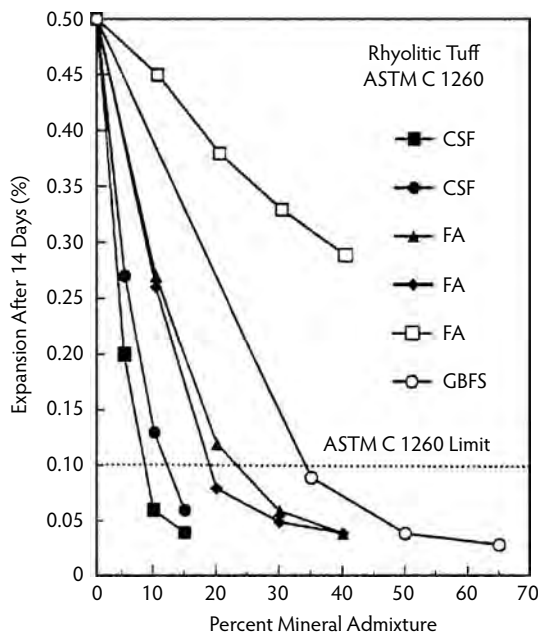


FIGURE 5.34 ASR expansion vs. dosage for silica fume (CSF), fly ash (FA), and slag (GBFS). (From Berube, M.A. and Duchesne, J., in *Fly Ash, Silica Fume, Slag, and Natural Pozzolans in Concrete*, American Concrete Institute, Farmington Hills, MI, 1992, pp. 549–575.)

After an aggregate is determined to be potentially reactive by the above tests, special precautions in mix proportioning and mix ingredient selection must be taken. ASR is avoidable by using the following approaches individually or in combination (Farny and Kerkhoff, 2007; Portland Cement Association, 2007).

5.18.1 Blended Cement

Blended hydraulic cement meeting ASTM C 595 or ASTM C 1157 can be used to control alkali–silica reactivity as long as it has been demonstrated to be effective in controlling it using ASTM C 1293 or ASTM C 1567.

5.18.2 Supplementary Cementing Materials

Supplementary cementing materials such as fly ash, slag, silica fume, and natural pozzolans can be added to concrete to control alkali–silica reactivity (Figure 5.34). The benefits of these materials come from their pozzolanic properties. Fly ash and natural pozzolans should meet ASTM C 618 requirements. Ground granulated blast-furnace slag should meet ASTM C 989. Silica fume should meet ASTM C 1240. As an incorrect dosage of supplementary cementing materials may not control ASR or can increase the potential for ASR, the optimum amount should be determined using ASTM C 1293 or ASTM C 1567. Low-alkali Class F ash is generally more effective than many Class C ashes in reducing ASR.

5.18.3 Controlling Concrete Alkali Content

The concrete alkali content can be limited to a level that has been demonstrated to be effective by the field performance of concretes with the potentially reactive aggregate. This approach assumes that concrete ingredients for future construction are the same as those materials used in the past where detrimental alkali–silica reactivity did not occur. Specifications in the United States have traditionally limited the alkali content in concrete through the use of low-alkali Portland cement. ASTM C 150 defines low-alkali

cement as having a maximum alkali content of 0.60% equivalent sodium oxide; however, higher alkali limits have been safely used with certain moderately reactive aggregates. Low-alkali cements are not available in many areas, and deleterious reactivity has been observed with certain glassy volcanic aggregates, especially andesite and rhyolite rocks, even when low-alkali cements (alkali contents of 0.35 to 0.6%) were used (Farny and Kerkhoff, 2007). Thus, the use of local cements in combination with one or more of the above alternatives is the preferable approach to controlling ASR.

The methods outlined to evaluate the potential for aggregate reaction provide estimates based on accelerated laboratory tests. Although these methods are often the only approach available, the best indicator of potential aggregate performance is field history under conditions similar to the intended application. If a proven service record can be documented, the comfort level regarding potential performance is increased dramatically. Complete documentation of service history should include condition evaluations of several structures, preferably at least 15 years old, exposed to moisture in service, and made with concrete containing the aggregates in question and cement having an alkali content at least as high (equivalent sodium oxide) as the cement intended for the new construction. Condition evaluations should include petrographic examination of the concrete by ASTM C 856. Requirements for reactivity are:

- A potentially reactive aggregate
- Sufficiently available alkali
- Sufficiently available moisture

If any of the three requirements is missing, deleterious reactivity will not occur. The approaches listed above for avoiding reactivity focus on the first two requirements; however, the moisture requirement, while difficult to control, should not be ignored. Of particular importance are wetting and drying exposures, as they can concentrate alkalis near the drying surface, inducing reactivity. Design considerations should include steps to minimize available moisture and wet-dry cycles. Alkali-silica reactivity requires at least 80% relative humidity (RH) at 73°F (23°C) in the concrete to develop. In some applications, it may be possible to dry out the concrete to less than 80% RH. For example, sealed laboratory concrete with a water/cement ratio of 0.35 or less can self-desiccate to below 80% RH, which provides little opportunity for expansion due to ASR. Another environmental factor that affects reactivity is temperature. As with any chemical reaction, the rate of reactivity increases with temperature; thus, structures in warmer exposures are more susceptible to ASR than those in colder climates.

5.19 Heat-Induced Delayed Expansion

Heat-induced delayed expansion (HIDE), also called *delayed ettringite formation* (DEF), refers to a rare condition of internal sulfate attack in which mature concretes undergo expansion and cracking. Only concretes of particular chemical makeup are affected when they have achieved high temperatures—158 to 212°F (70 to 100°C)—usually after the first few hours of placement, depending on the concrete ingredients and the time the temperature is achieved after casting. This can occur because the high temperature decomposes any initial ettringite formed and holds the sulfate and alumina tightly in the calcium silicate hydrate (C–S–H) gel of the cement paste. The normal formation of ettringite is thus impeded. In the presence of moisture, sulfate desorbs from the confines of the C–S–H and reacts with calcium monosulfoaluminate to form ettringite in cooled and hardened concrete. After months or years of desorption, ettringite forms in confined locations within the paste. Such ettringite can exert crystallization pressures because it forms in a limited space under supersaturation. This paste expansion usually results in a visible separation of the paste from the aggregate. Only concretes in massive elements that retain the heat of hydration or elements exposed to very high temperatures at an early age are at risk of HIDE; of these, only a few have the chemical makeup or temperature profile to cause detrimental expansion. Normal-sized concrete elements cast and maintained near ambient temperatures cannot experience HIDE when sound materials are used. The best way to avoid HIDE is to not let concrete exceed 158°F (70°C) at an early age. Delayed ettringite formation must not be confused with the beneficial

primary ettringite formation required to help control early strength gain and harmless secondary ettringite formation, an opportunistic and nonexpansive reformation of ettringite in cracks and voids, often found in connection with frost damage, ASR, or aging in a moist environment.

5.20 Self-Consolidating Concrete

Self-consolidating concrete (SCC) is normal- or high-strength concrete that is able to flow and consolidate under its own weight. At the same time, it is cohesive enough to fill spaces of almost any size and shape without segregation or bleeding. This makes SCC particularly useful wherever placing is difficult, such as in heavily reinforced concrete members or in complicated formwork. This technology, developed in Japan in the 1980s, is based on increasing the amount of fine material (e.g., fly ash or limestone filler) without changing the water content compared to common concrete. This changes the rheological behavior of the concrete. SCC has to have a low yield value to ensure high flowability; a low water content ensures high viscosity, so the coarse aggregate can float in the mortar without segregating. To achieve a balance between deformability and stability, the total content of particles finer than the 150- μm (No. 100) sieve has to be high, usually about 520 to 560 kg/m^3 (880 to 950 lb/yd^3). High-range water reducers based on polycarboxylate ethers are typically used to plasticize the mixture. SCC is very sensitive to fluctuation in water content; therefore, stabilizers such as polysaccharides are used. Because SCC is characterized by special fresh concrete properties, many new tests have been developed to measure flowability, viscosity, blocking tendency, self-leveling, and stability of the mixture (Lange, 2007). The ASTM C 1611 slump flow test is the most common testing method for flowability. The final slump flow diameter and time to reach a spread diameter of 20 in. (50 cm) are recorded. The ASTM C 1621 J-ring test, along with the U-box and L-box test, is used to evaluate passing ability. The strength and durability of well-designed SCC are similar to conventional concrete. Without proper curing, SCC tends to have higher plastic shrinkage. It is difficult to keep SCC in the desired consistency over a long period of time; however, construction time is shorter, and the production of SCC is environmentally friendly (no noise, no vibration). Furthermore, SCC produces a good surface finish. These advantages make SCC especially valuable for use in precasting plants, but SCC is also used in cast-in-place construction.

5.21 Related ASTM Standards

ASTM C 33—Specification for Concrete Aggregates

ASTM C 150—Specification for Portland Cement

ASTM C 227—Test Method for Potential Alkali Reactivity of Cement-Aggregate Combinations (mortar bar method)

ASTM C 289—Test Method for Potential Reactivity of Aggregates (chemical method)

ASTM C 294—Descriptive Nomenclature of Constituents of Natural Mineral Aggregates

ASTM C 295—Practice for Petrographic Examination of Aggregates for Concrete

ASTM C 441—Test Method for Effectiveness of Mineral Admixtures or Ground Blast-Furnace Slag in Preventing Excessive Expansion of Concrete Due to the Alkali-Silica Reaction

ASTM C 586—Test Method for Potential Alkali Reactivity of Carbonate Rocks for Concrete Aggregates (rock cylinder method)

ASTM C 595—Specification for Blended Hydraulic Cements

ASTM C 618—Specification for Fly Ash and Raw or Calcined Natural Pozzolans for Use As a Mineral Admixture in Portland Cement Concrete

ASTM C 823—Practice for Examination and Sampling of Hardened Concrete in Construction

ASTM C 856—Practice for Petrographic Examination of Hardened Concrete

ASTM C 989—Specification for Ground Granulated Blast-Furnace Slag for Use in Concrete and Mortars

ASTM C 1105—Standard Test Method for Length of Change of Concrete Due to Alkali-Carbonate Rock Reaction

ASTM C 1157—Performance Specification for Hydraulic Cement

ASTM C 1240—Specification for Silica Fume for Use in Hydraulic-Cement Concrete and Mortar Test Method for Accelerated Detection of Potential Deleterious Expansion of Mortar Bars Due to Alkali–Silica Reaction

ASTM C 1260—Test Method for Potential Alkali Reactivity of Aggregates (mortar bar method)

ASTM C 1293—Test Method for Concrete Aggregates by Determination of Length Change of Concrete Due to Alkali–Silica Reaction

ASTM C 1567—Test Method for Determining the Potential Alkali Silica Reactivity of Combinations of Cementitious Materials and Aggregate (accelerated mortar bar method)

ASTM C 1602—Specification for Mixing Water Used in the Production of Hydraulic Cement Concrete

ASTM C 1611—Test Method for Slump Flow of Self-Consolidating Concrete

ASTM C 1621—Test Method for Passing Ability of Self-Consolidating Concrete by J-Ring

References

- ACI Committee 211. 1991. *Standard Practice for Selecting Proportions for Normal, Heavyweight, and Mass Concrete*, ACI 211.1-91, 38 pp. American Concrete Institute, Farmington Hills, MI.
- ACI Committee 222. 2003. *Design and Construction Practices to Mitigate Corrosion of Reinforcement in Concrete Structures*, ACI 3R-03, 29 pp. American Concrete Institute, Farmington Hills, MI.
- Berube, M.A. and Duchesne, J. 1992. Evaluation of testing methods used for assessing the effectiveness of mineral admixtures in suppressing expansion due to alkali–aggregate reaction. In *Fly Ash, Silica Fume, Slag, and Natural Pozzolans in Concrete*, pp. 549–575. American Concrete Institute, Farmington Hills, MI.
- Burg, R.G. 1996. *The Influence of Casting and Curing Temperatures on the Properties of Fresh and Hardened Concrete*, RD113, 20 pp. Portland Cement Association, Skokie, IL.
- Burg, R.G. and Farny, J.A. 1996. The influence of concrete casting and curing temperatures. *Concrete Technol. Today*, 12(1), 1–5 (PL963).
- Burg, R.G. and Ost, B.W. 1994. *Engineering Properties of Commercially Available High-Strength Concretes (Including Three-Year Data)*, RD104, 62 pp. Portland Cement Association, Skokie, IL.
- Campbell, D.H., Sturm, R.D., and Kosmatka, S.H. 1991. Detecting carbonation. *Concrete Technol. Today*, 12(1), 1–5.
- Detwiler, R.J. 1996. Long-term strength tests of high-strength concrete. *Concrete Technol. Today*, 17(2), 1–4 (PL962).
- Farny, J.A. and Kerkhoff, B. 2007. *Diagnosis and Control of Alkali–Aggregate Reactions in Concrete*, IS413. Portland Cement Association, Skokie, IL.
- Farny, J.A. and Panarese, W.C. 1994. *High-Strength Concrete*, EB114, 58 pp. Portland Cement Association, Skokie, IL.
- FHA. 1987. *Protective Systems for New Prestressed and Substructure Concrete*, FRWA/RD-86/193. Federal Highway Administration, Washington, D.C.
- Gebler, S.H. and Klieger, P. 1986. *Effect of Fly Ash on Some of the Physical Properties of Concrete*, RD089. Portland Cement Association, Skokie, IL.
- Klieger, P. 1952. *Studies of the Effect of Entrained Air on the Strength and Durability of Concretes Made with Various Maximum Sizes of Aggregates*, RX040. Portland Cement Association, Skokie, IL.
- Kosmatka, S.H. 2006. Bleed water. In *Significance of Tests and Properties of Concrete and Concrete-Making Materials*, STP169D, 28 pp. American Society for Testing and Materials, West Conshohocken, PA.
- Kosmatka, S.H. and Farny, J.A., 2007. *Long-Term Performance of Concrete in the PCA Outdoor Test Facility*, 28 pp. American Concrete Institute, Farmington Hills, MI.
- Kosmatka, S.H., Kerkhoff, B., and Panarese, W.C. 2006. *Design and Control of Concrete Mixtures*, EB001, 372 pp. Portland Cement Association, Skokie, IL.

- Lange, D.A. 1994. *Long-Term Strength Development of Concrete*, RP326, 36 pp. Portland Cement Association, Skokie, IL.
- Lange, D.A. 2007. *Self-Consolidating Concrete*, 42 pp. Center for Advanced Cement-Based Materials (ACBM), Evanston, IL.
- Nawy, E.G. 1996. *Fundamentals of High-Strength, High-Performance Concrete*. Addison Wesley Longman, London.
- Nawy, E.G. 2008. *Reinforced Concrete: A Fundamental Approach*, 6th ed. Prentice Hall, Upper Saddle River, NJ.
- Portland Cement Association. 1996. Portland cement: past and present characteristics. *Concrete Technol. Today*, 17(2), 1–4.
- Portland Cement Association. 2007. *Guide Specification for Concrete Subject to Alkali–Silica Reactions*, IS415, 8 pp. Portland Cement Association, Skokie, IL.
- Stark, D. 1989a. *Durability of Concrete in Sulfate-Rich Soils*, RD097, 18 pp. Portland Cement Association, Skokie, IL.
- Stark, D. 1989b. *Influence of Design and Materials on Corrosion Resistance of Steel in Concrete*, RD098, 40 pp. Portland Cement Association, Skokie, IL.
- Whiting, D. 1988. Permeability of selected concretes. In *Permeability of Concrete*, SP108-11, pp. 195–225. American Concrete Institute, Farmington Hills, MI.
- Wood, S.L. 1992. *Evaluation of the Long-Term Properties of Concrete*, RD102, 99 pp. Portland Cement Association, Skokie, IL.



(a)



(b)

(a) Hoist delivery and placement of ready-mix concrete. (b) Truck delivery of ready-mix concrete. (Photographs courtesy of Portland Cement Association, Skokie, IL.)

6

Design and Placement of Concrete Mixtures

Part A. Edward G. Nawy, D.Eng., P.E., C.Eng.*

Part B. Jaime Moreno and John Albinger*****

Part A. Design of Concrete Mixtures

- 6.1 General6-2
- 6.2 Selection of Constituent Materials6-2
 - Cement and Other Cementitious Materials • Normal Weight and Lightweight Aggregate • Workability-Enhancing and Strength-Enhancing Admixtures
- 6.3 Mixture Proportioning for High-Performance, Normal-Strength Concrete (Cylinder Compressive Strength Limit 6000 psi).....6-9
 - Example 6.1: Mixture Proportions Design for Normal-Strength Concrete • Estimating Compressive Strength of a Trial Mixture Using the Specified Compressive Strength • Recommended Proportions for Concrete Strength (f_{cr}') • Example 6.2: Calculation of Design Strength for a Trial Mixture
- 6.4 Mixture Proportioning for High-Performance, High-Strength Concrete (Cylinder Compressive Strength Exceeding 6000 psi)6-18
 - General • Strength Requirements • Selection of Ingredients • Recommended Proportions • Step-by-Step Procedure for Selecting Proportions • Example 6.3: Mixture Proportions Design for High-Strength Concrete

Part B. Applications and Constructability

- 6.5 Applications and Constructability with an Emphasis on High-Strength, High-Performance Concrete.....6-30
 - General • Constructability Preparation Process • Mixture Components • Materials Control • Mixing, Transporting, Placing, and Curing
- 6.6 Jobsite Control.....6-41

* Distinguished Professor, Civil Engineering, Rutgers University, The State University of New Jersey, Piscataway, New Jersey, and ACI honorary member; expert in concrete structures, materials, and forensic engineering.

** President Emeritus, Cement Technology Corp., Chicago; expert on cements, blending of cements, high-performance concretes, and efficient mixture proportioning.

*** President, T. H. Davidson and Company, Chicago; expert in mixture design and in high-strength, high-performance concrete.

6.7	Testing	6-41
	General • Sampling • Extent of Testing • Compressive Strength Specimens • Prequalification of Testing Laboratories and Ready-Mix Suppliers	
	Acknowledgments	6-43
	References	6-43

Part A. Design of Concrete Mixtures (E.G. Nawy)

6.1 General

The design of concrete mixtures involves choosing appropriate proportions of ingredients for particular strengths, long-term qualities, and performance of the concrete produced. Several factors determine these properties. They include the following parameters, which are summarized in Figure 6.1:

- Quality of cement
- Proportion of cement in relation to water in the mix (water/cementitious material ratio)
- Strength and cleanliness of aggregate
- Interaction or adhesion between cement paste and aggregate
- Adequate mixing of the ingredients
- Proper placing, finishing, and compaction of the fresh concrete
- Curing at a temperature not below 50°F while the placed concrete gains strength
- Chloride content not to exceed 0.15% in reinforced concrete exposed to chlorides in service and 1% in dry protected concrete

A study of these requirements shows that most control actions have to be taken prior to placing the fresh concrete. Because such control is governed by the proportions of ingredients and the mechanical ease or difficulty in handling and placing the concrete, the development of criteria based on the theory of proportioning for each mix should be studied. Most mixture design methods have become essentially only of historical and academic value. The two universally accepted methods of mixture proportioning for normal weight and lightweight concrete are the American Concrete Institute's methods of proportioning, described in their recommended practices for selecting proportions for normal weight, heavy-weight, and mass concrete, and in the recommended practice for selecting proportions for structural lightweight concrete (ACI Committee 211, 1991a,b; ASTM, 1993; Nawy, 1996).

6.2 Selection of Constituent Materials

6.2.1 Cement and Other Cementitious Materials

As discussed in Chapter 1, several types of cement are available. The most commonly used is Portland cement. Table 6.1 lists the general composition of the various types of Portland cement. Types I and III fundamentally differ in that Type III (high early cement) is considerably finer than Type I, and in 7 days achieves the strength that normal cement concrete achieves in 28 days. Other hydraulic cements include blended cements, rapid-setting cements, expansive cements (type K), very high early cements, and exotic cements such as macrodefect-free cement (MDF), densified cement (DSP), perlite cement, and alkali-activated cement.

6.2.2 Normal Weight and Lightweight Aggregate

Aggregates are those parts of the concrete that constitute the bulk of the finished product. They comprise 60 to 80% of the volume of the concrete and have to be graded so the whole mass of concrete acts as a relatively solid, homogeneous, dense combination, with the smaller particles acting as inert filler for the voids that exist between the larger particles. Aggregates are of two types:

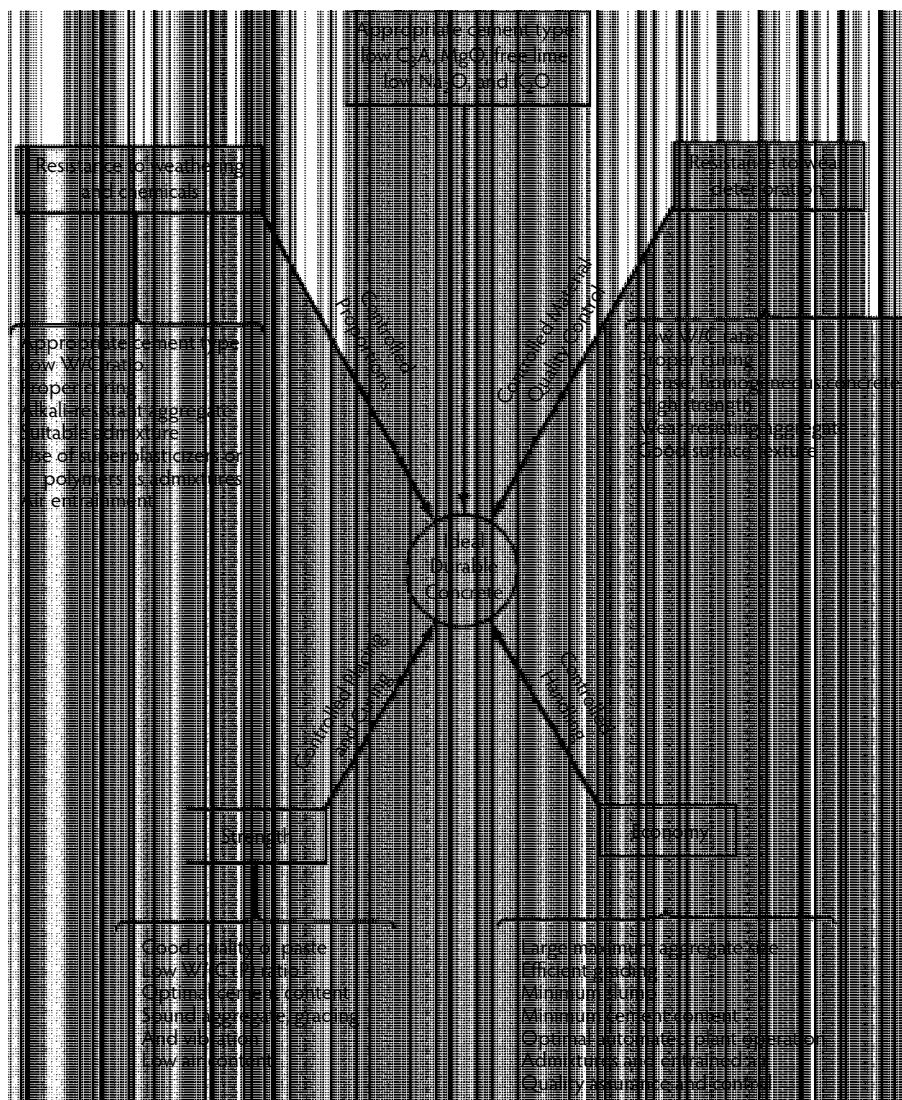


FIGURE 6.1 Principal properties of good concrete. (From Nawy, E.G., *Reinforced Concrete: A Fundamental Approach*, 6th ed., Prentice Hall, Upper Saddle River, NJ, 2008.)

- *Coarse aggregate*—gravel, crushed stone, or blast-furnace slag
- *Fine aggregate*—natural or manufactured sand

Because the aggregate constitutes the major part of the mix, the more aggregate in the mix the less expensive the concrete, provided the mix is of reasonable workability for the specific job for which it is used. Coarse aggregate is classified as such if the smallest particle is greater than 1/4 in. (6 mm). Properties of coarse aggregate affect the final strength of hardened concrete and its resistance to disintegration, weathering, and other destructive effects. Mineral coarse aggregates must be clean of organic impurities and bond well with the cement gel. Common types of coarse aggregate include:

- *Natural crushed stone* is produced by crushing natural stone or rock from quarries. The rock may be igneous, sedimentary, or metamorphic. Crushed rock gives higher concrete strength but is less workable for mixing and placing than the other types of aggregate.

TABLE 6.1 Percentage Composition of Portland Cements

Type of Cement	Component (%)							General Characteristics
	C ₃ S	C ₂ S	C ₃ A	C ₄ AF	CaSO ₄	CaO	MgO	
Normal (I)	49	25	12	8	2.9	0.8	2.4	All-purpose cement
Modified (II)	45	29	6	12	2.8	0.6	3.0	Comparatively low heat liberation; used in large structures
High early strength (III)	56	15	12	8	3.9	1.4	2.6	High strength in 3 days
Low heat (IV)	30	46	5	13	2.9	0.3	2.7	Used in mass concrete dams
Sulfate-resisting (V)	43	36	4	12	2.7	0.4	1.6	Used in sewers and structures exposed to sulfates

Source: Data from Nawy, E.G., *Reinforced Concrete: A Fundamental Approach*, 6th ed., Prentice Hall, Upper Saddle River, NJ, 2008; Nawy, E.G., *Fundamentals of High-Strength, High-Performance Concrete*, Addison Wesley Longman, London, 1996; Nawy, E.G., *Fundamentals of High-Performance Concrete*, John Wiley & Sons, New York, 2001.

- *Natural gravel* is produced by the weathering action of running water on the beds and banks of streams. It gives less strength than crushed rock but is more workable.
- *Artificial coarse aggregates* are mainly slag and expanded shale and are frequently used to produce lightweight concrete. They are byproducts of other manufacturing processes such as blast-furnace slag or expanded shale, or pumice for lightweight concrete.
- *Heavyweight and nuclear-shielding aggregates* have been produced to meet the specific demands of our atomic age and the hazards of nuclear radiation; due to the increasing number of atomic reactors and nuclear power stations, special concretes have had to be produced to shield against x-rays, gamma rays, and neutrons. In such concretes, economic and workability considerations are not of prime importance. The main heavy coarse aggregate types are steel punchings, barites, magnetites, and limonites. Whereas concrete with ordinary aggregate weighs about 144 lb/ft³, concrete made with these heavy aggregates weighs from 225 to 330 lb/ft³. The property of heavy-weight radiation shielding in concrete depends on the density of the compact product rather than on the water/cement ratio criterion. In certain cases, high density is the only consideration, whereas in others both density and strength govern.
- *Fine aggregate* is a smaller filler made of sand. It ranges in size from No. 4 to No. 100 in U.S. standard sieve sizes. A good fine aggregate should always be free of organic impurities, clay, or any deleterious material or excessive filler of size smaller than No. 100 sieve. Preferably, it should have a well-graded combination conforming to the American Society for Testing and Materials (ASTM) sieve analysis standards. For radiation-shielding concrete, fine steel shot and crushed iron ore are used as fine aggregate.

The recommended grading of coarse and fine aggregates for normal weight concrete is presented in Table 6.2 (ASTM C 33), grading requirements for lightweight aggregate (ASTM C 330) are given in Table 6.3, and Table 6.4 provides grading requirements for coarse aggregate for aggregate concrete (ASTM C 637). The unit weights of the commonly used aggregates in structural concrete are given in Table 6.5.

6.2.3 Workability-Enhancing and Strength-Enhancing Admixtures

Admixtures are materials other than water, aggregate, or hydraulic cement that are used as ingredients of concrete and that are added to the batch immediately before or during mixing. Their function is to modify the properties of concrete for strength, workability, and long-term performance. The major types of admixtures can be summarized as follows:

TABLE 6.2 Grading Requirements for Aggregates in Normal Weight Concrete (ASTM C-33)

U.S. Standard Sieve Size	Percent Passing				
	Coarse Aggregate				Fine Aggregate
	No. 4 to 2 in.	No. 4 to 1-1/2 in.	No. 4 to 1 in.	No. 4 to 3/4 in.	
2 in.	95–100	100	—	—	—
1-1/2 in.	—	95–100	100	—	—
1 in.	25–70	—	95–100	100	—
3/4 in.	—	35–70	—	90–100	—
1/2 in.	10–30	—	25–60	—	—
3/8 in.	—	10–30	—	20–55	100
No. 4	0–5	0–5	0–10	0–10	95–100
No. 8	0	0	0–5	0–5	80–100
No. 16	0	0	0	0	50–85
No. 30	0	0	0	0	25–60
No. 50	0	0	0	0	10–30
No. 100	0	0	0	0	2–10

Source: ASTM, *Annual Book of ASTM Standards*. Part 14. *Concrete and Mineral Aggregates*, American Society for Testing and Materials, Philadelphia, PA, 1993.

TABLE 6.3 Grading Requirements for Aggregates in Lightweight Structural Concrete (ASTM C-330)

Size Designation	Percentage (by weight) Passing Sieves with Square Openings								
	1 in. (25.0 mm)	3/4 in. (19.0 mm)	1/2 in. (12.5 mm)	3/8 in. (9.5 mm)	No. 4 (4.75 mm)	No. 8 (2.36 mm)	No. 16 (1.18 mm)	No. 50 (300 μm)	No. 100 (150 μm)
<i>Fine aggregate</i>									
No. 4 to 0	—	—	—	100	85–100	—	40–80	10–35	5–25
<i>Coarse aggregate</i>									
1 in. to No. 4	95–100	—	25–60	—	0–10	—	—	—	—
3/4 in. to No. 4	100	90–100	—	10–50	0–15	—	—	—	—
1/2 in. to No. 4	—	100	90–100	40–80	0–20	0–10	—	—	—
3/8 in. to No. 8	—	—	100	80–100	5–40	0–20	0–10	—	—
<i>Combined fine and coarse aggregate</i>									
1/2 in. to 0	—	100	95–100	—	50–80	—	—	5–20	2–15
3/8 in. to 0	—	—	100	90–100	65–90	35–65	—	10–25	5–15

Source: ASTM, *Annual Book of ASTM Standards*. Part 14. *Concrete and Mineral Aggregates*, American Society for Testing and Materials, Philadelphia, PA, 1993.

- Accelerating admixtures
- Air-entraining admixtures
- Water-reducing admixtures and set-controlling admixtures
- Finely divided mineral admixtures
- Admixtures for no-slump concretes
- Polymers
- Superplasticizers

Details of the various mineral and organic admixtures for strength enhancement are given in Chapter 2 and Chapter 3. The following is a brief outline of these admixtures (Nawy, 2001).

TABLE 6.4 Grading Requirements for Coarse Aggregate for Aggregate Concrete (ASTM C-637)

Sieve Size	Percentage Passing	
	Grading 1 ^a	Grading 2 ^b
<i>Coarse aggregate</i>		
2 in. (50 mm)	100	—
1-1/2 in. (37.5 mm)	95–100	100
1 in. (25.0 mm)	40–80	95–100
3/4 in. (19.0 mm)	20–45	40–80
1/2 in. (12.5 mm)	0–10	0–15
3/8 in. (9.5 mm)	0–2	0–2
<i>Fine aggregate</i>		
No. 8 (2.36 mm)	100	—
No. 16 (1.18 mm)	95–100	100
No. 30 (600 μ m)	55–80	75–95
No. 50 (300 μ m)	30–55	45–65
No. 100 (150 μ m)	10–30	20–40
No. 200 (75 μ m)	0–10	0–10
Fineness modulus	1.30–2.10	1.00–1.60

^a For 1-1/2-in. (37.5-mm) maximum-size aggregate.

^b For 3/4-in. (19.0-mm) maximum-size aggregate.

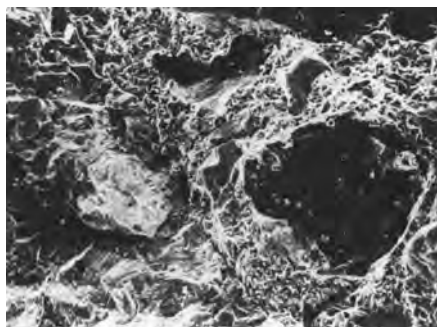
Source: ASTM, *Annual Book of ASTM Standards*. Part 14. *Concrete and Mineral Aggregates*, American Society for Testing and Materials, Philadelphia, PA, 1993.

TABLE 6.5 Unit Weight of Aggregates

Type	Unit Weight of Dry-Rodded Aggregate (lb/ft ³) ^a	Unit Weight of Concrete (lb/ft ³) ^a
Insulating concretes (perlite, vermiculite, etc.)	15–50	20–90
Structural lightweight	40–70	90–110
Normal weight	70–110	130–160
Heavyweight	>135	180–380

^a 1 lb/ft³ = 16.02 kg/m³.

Source: Data from ASTM, *Annual Book of ASTM Standards*. Part 14. *Concrete and Mineral Aggregates*, American Society for Testing and Materials, Philadelphia, PA, 1993; Nawy, E.G., *Reinforced Concrete: A Fundamental Approach*, 6th ed., Prentice Hall, Upper Saddle River, NJ, 2008; Nawy, E.G., *Fundamentals of High-Performance Concrete*, John Wiley & Sons, New York, 2001.

**PHOTO 6.1** Electron-microscope photographs of concrete. (Photograph courtesy of E.G. Nawy et al.)

6.2.3.1 Accelerating Admixtures

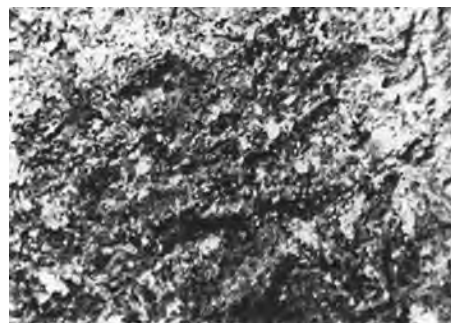
Accelerating admixtures are added to the concrete mixture to reduce the time of setting and accelerate early strength development. The best known are calcium chlorides. Other accelerating chemicals include a wide range of soluble salts such as chlorides, bromides, carbonates, and silicates, as well as other organic compounds such as triethanolamine. It must be stressed that calcium chlorides should not be used where progressive corrosion of steel reinforcement can occur. The maximum dosage recommended is 0.5% by weight of Portland cement.

6.2.3.2 Air-Entraining Admixtures

Air-entraining admixtures form minute bubbles that are 1 mm in diameter or smaller in concrete or mortar during mixing; they are used to increase both the workability of the mix during placing and the frost resistance of the finished product. Most air-entraining admixtures are in liquid form, although a few are powders, flakes, or semisolids. The amount of admixture required to obtain a given air content depends on the shape and grading of the aggregate used. The finer the aggregate, the larger the percentage of admixture needed. The amount required is also governed by several other factors, such as type and condition of the mixer, use of fly ash or other pozzolans, and degree of agitation of the mix. It can be expected that air entrainment reduces the strength of the concrete. Maintaining cement content and workability, however, offsets the partial reduction of strength because of the resulting reduction in the water/cement ratio.



(a)



(b)

PHOTO 6.2 Fracture surface in tensile splitting test: (a) mortar failure, $f'_t = 450$ psi, 3.1 MPa; (b) aggregate failure, $f'_t = 1550$ psi, 10.7 MPa. (From Nawy, E.G., *Fundamentals of High-Performance Concrete*, John Wiley & Sons, 2001.)



(a)



(b)

PHOTO 6.3 Slump test of fresh concrete. (Photograph courtesy of E.G. Nawy et al.)

6.2.3.3 Water-Reducing and Set-Controlling Admixtures

Water-reducing and set-controlling admixtures increase the strength of the concrete. They also enable reduction of cement content in proportion to the reduction of water content. Most admixtures of the water-reducing type are water soluble. The water they contain becomes part of the mixing water in the concrete and is added to the total weight of water in the design of the mix. It has to be emphasized that the proportion of mortar to coarse aggregate should always remain the same. Changes in the water content, air content, or cement content are compensated for by changes in the fine-aggregate content so the volume of the mortar remains the same.

6.2.3.4 Finely Divided Admixtures

Finely divided admixtures are mineral admixtures used to rectify deficiencies in concrete mixes by providing missing fines from the fine aggregate, improving one or more qualities of the concrete (such as reducing permeability or expansion), and reducing the cost of concrete-making materials. Such admixtures include hydraulic lime, slag cement, fly ash, and raw or calcined natural pozzolans.

6.2.3.5 Admixtures for No-Slump Concrete

No-slump concrete is defined as a concrete with a slump of 1 in. (25 mm) or less immediately after mixing. The choice of admixture depends on the desired properties of the finished product such as plasticity, setting time and strength development, freeze–thaw effects, strength, and cost.

6.2.3.6 Polymers

Polymer admixtures allow production of concretes of very high strength up to a compressive strength of 15,000 psi or higher and a splitting tensile strength of 1500 psi or higher. Such concretes are generally produced using a polymerizing material through: (1) modification of the concrete property by water reduction in the field, or (2) impregnation and irradiation under elevated temperature in a laboratory environment. Polymer concrete (PC) is concrete made through the addition of resin and hardener as admixtures. The principle is to replace part of the mixing water with the polymer to attain a high compressive strength and other desired qualities. The optimum polymer/concrete ratio by weight to achieve such high compressive strengths seems to lie within the range of 0.3 to 0.45.

6.2.3.7 Superplasticizers

Superplasticizers can be termed *high-range water-reducing chemical admixtures*. The types of plasticizers include:

- *Sulfonated melamine formaldehyde* (SMF) condensates, with a chloride content of 0.005%
- *Sulfonated naphthalene formaldehyde* (SNF) condensates, with negligible chloride content
- *Modified lignosulfonates*, which contain no chlorides

These plasticizers are made from organic sulfonates and are considered superplasticizers in view of their considerable ability to facilitate reduction of water content in a concrete mix while simultaneously increasing the slump up to 8 in. (206 mm) or more. A dosage of 1 to 2% by weight of cement is advisable; higher dosages can result in a reduction in compressive strength. Other superplasticizers include *sulfonic acid esters* or other *carbohydrate esters*. A dosage of 1 to 2-1/2% by weight of cement is advisable; higher dosages can result in a reduction in compressive strength unless the cement content is increased to balance the reduction. It should be noted that superplasticizers exert their action by decreasing the surface tension of water and by equidirectional charging of cement particles. These properties, coupled with the addition of silica fume, help achieve high strength and water reduction in concrete without loss of workability.

6.2.3.8 Silica Fume Admixture Use in High-Strength Concrete

Silica fume is generally accepted as an efficient mineral admixture for high-strength concrete mixes. It is a pozzolanic material that has received considerable attention in both research and application. Silica

fume is a byproduct resulting from the use of high-purity quartz with coal in electric-arc furnaces during production of silicon and ferrosilicon alloys. Its main constituent, fine spherical particles of silicon dioxide, makes it an ideal cement replacement and simultaneously raises concrete strength. As it is a waste product that is relatively easy to collect compared to fly ash or slag, silica fume is used extensively worldwide. Proportions of silica fume in concrete mixes vary from 5 to 30% by weight of the cement, depending on strength and workability requirements. Water demand is greatly increased as the proportion of silica fume is increased, and high-range water reducers are essential to keep the water/cementitious material ratio low to produce higher strength yet workable concrete. Silica fume seems to reach a high early strength in about 3 to 7 days with relatively less increase in strength at 28 days. The strength-development pattern of flexural and splitting tensile strengths is similar to that of compressive-strength gain for silica-fume-added concrete. The addition of silica fume to the mixture can produce significant increases in strength in excess of 20,000 psi, increased modulus of elasticity, and increased flexural strength.

6.3 Mixture Proportioning for High-Performance, Normal-Strength Concrete (Cylinder Compressive Strength Limit 6000 psi)

The ACI method of designing mixtures for normal weight concrete is summarized in Figure 6.2, based on water slump values selected from Table 6.6, Table 6.7, and Table 6.8. One aim of the mixture design is to produce workable concrete that is easy to place in forms. A measure of the degree of consistency and extent of workability is the **slump**. In the slump test, a plastic concrete specimen is formed into a conical metal mold, as described in ASTM C 143. The mold is lifted, leaving the concrete to slump—that is, to spread or drop in height. This drop in height is the slump measure of the degree of workability of the mixture.

6.3.1 Example 6.1: Mixture Proportions Design for Normal-Strength Concrete

Design a concrete mixture using the following details:

- Required strength—4000 psi (27.6 MPa)
- Type of structure—beam
- Maximum size of aggregate—3/4 in. (18 mm)
- Fineness modulus of sand—2.6
- Dry-rodded weight of coarse aggregate—100 lb/ft³
- Moisture absorption—3% for coarse aggregate and 2% for fine aggregate

Solution

- Required slump for beams (Table 6.6) is 3 in.
- Maximum aggregate size (given) is 3/4 in.
- For a slump between 3 and 4 in. and a maximum aggregate size of 3/4 in., the weight of water required per cubic yard of concrete (Table 6.7) is 340 lb/yd³.

For the specified compression strength (4000 psi), the water/cement ratio (Table 6.8) is 0.57. Table 6.9 is also required if volumes instead of weights are used in the mix design calculations. Therefore, the amount of cement required per cubic yard of concrete is $340/0.57 = 596.5$ lb/yd³.

Using a sand fineness value of 2.6 and Table 6.9, the volume of coarse aggregate is 0.64 yd³. Using the dry-rodded weight of 100 lb/ft³ for coarse aggregate, the weight of coarse aggregate is $(0.64) \times (27 \text{ ft/yd}^3) \times 100 = 1728$ lb/yd³. The estimated weight of fresh concrete for aggregate of 3/4 in. is as follows:

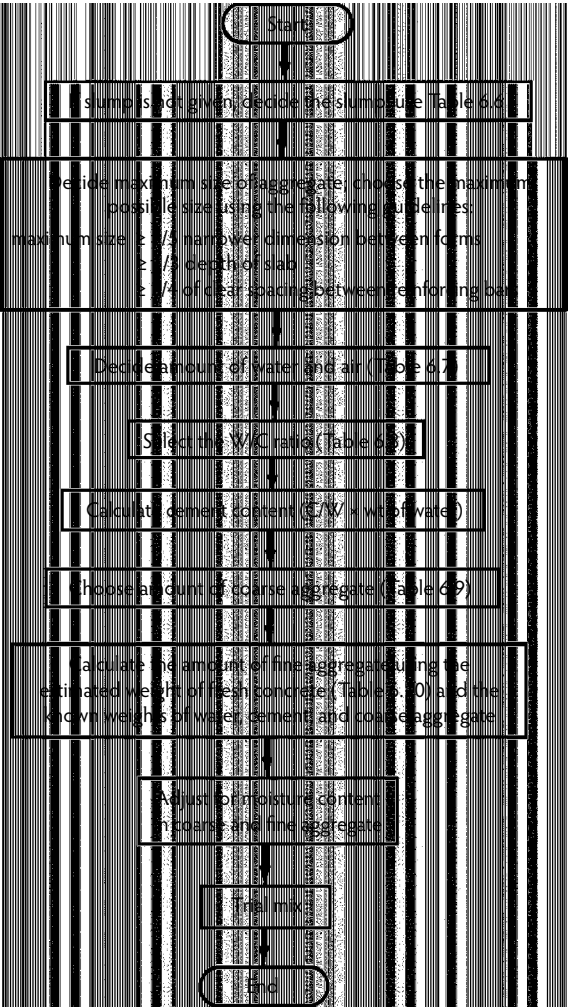


FIGURE 6.2 Flow chart for normal weight concrete mixture design. (From Nawy, E.G., *Reinforced Concrete: A Fundamental Approach*, 6th ed., Prentice Hall, Upper Saddle River, NJ, 2008.)

TABLE 6.6 Recommended Slumps for Various Types of Construction

Types of Construction	Slump (in.) ^a	
	Maximum ^b	Minimum
Reinforced foundation walls and footings	3	1
Plain footings, caissons, and substructure walls	3	1
Beams and reinforced walls	4	1
Building columns	4	1
Pavements and slabs	3	1
Mass concrete	2	1

^a 1 in. = 25.4 mm.
^b May be increased 1 in. for methods of consolidation other than vibration.
Source: Data from ACI Committee 211, *Standard Practice for Selecting Proportions for Normal, Heavyweight, and Mass Concrete*, ACI 211.1-91, American Concrete Institute, Farmington Hills, MI, 1991; Nawy, E.G., *Reinforced Concrete: A Fundamental Approach*, 6th ed., Prentice Hall, Upper Saddle River, NJ, 2008.

TABLE 6.7 Approximate Mixing Water and Air Content Requirements for Different Slumps and Nominal Maximum Sizes of Aggregates

Slump (in.)	Water (lb/yd ³ of Concrete for Indicated Nominal Maximum Sizes of Aggregate)							
	3/8 in. ^a	1/2 in. ^a	3/4 in. ^a	1 in. ^a	1-1/2 in. ^a	2 in. ^{a,b}	3 in. ^{b,c}	6 in. ^{b,c}
<i>Non-air-entrained concrete</i>								
1 to 2	350	335	315	300	275	260	220	190
3 to 4	385	365	340	325	300	285	245	210
6 to 7	410	385	360	340	315	300	270	—
Approximate amount of entrapped air in non-air-entrained concrete (%)	3	2.5	2	1.5	1	0.5	0.3	0.2
<i>Air-entrained concrete</i>								
1 to 2	305	295	280	270	250	240	205	180
3 to 4	340	325	305	295	275	265	225	200
6 to 7	365	345	325	310	290	280	260	—
<i>Recommended average total air content^d (percent for level of exposure)</i>								
Mild exposure	4.5	4.0	3.5	3.0	2.5	2.0	1.5 ^{e,f}	1.0 ^{e,f}
Moderate exposure	6.0	5.5	5.0	4.5	4.5	4.0	3.5 ^{e,f}	3.0 ^{e,f}
Extreme exposure ^g	7.5	7.0	6.0	6.0	5.5	5.0	4.5 ^{e,f}	4.0 ^{e,f}

^a These quantities of mixing water are for use in computing cement factors for trial batches. They are maximal for reasonably well-shaped angular coarse aggregates graded within limits of accepted specifications.

^b The slump values for concrete containing aggregate larger than 1-1/2 in. are based on slump tests made after removal of particles larger than 1-1/2 in. by wet screening.

^c These quantities of mixing water are for use in computing cement factors for trial batches when 3-in. or 6-in. nominal maximum-size aggregate is used. They are average for reasonably well-shaped coarse aggregates, well graded from coarse to fine.

^d Additional recommendations for air content and necessary tolerances on air content for control in the field are given in a number of ACI documents, including ACI 201, 345, 318, 301, and 302. ASTM C 94 for ready-mixed concrete also gives air-content limits. The requirements in other documents may not always agree exactly, so in proportioning concrete consideration must be given to selecting an air content that will meet the needs of the job and also meet the applicable specifications.

^e For concrete containing large aggregates that will be wet screened over the 1-1/2-in. sieve prior to testing for air content, the percentage of air expected in the 1-1/2-in. material should be tabulated in the 1-1/2-in. column; however, initial proportioning calculations should include the air content as a percent of the whole.

^f When using large aggregate in low-cement-factor concrete, air entrainment need not be detrimental to strength. In most cases, the mixing water requirement is reduced sufficiently to improve the water/cement ratio and thus to compensate for the strength-reducing effect of entrained-air concrete. Generally, therefore, for these large maximum sizes of aggregate, air contents recommended for extreme exposure should be considered even though there may be little or no exposure to moisture and freezing.

^g These values are based on the criteria that 9% air is needed in the mortar phase of the concrete. If the mortar volume will be substantially different from that determined in this recommended practice, it may be desirable to calculate the needed air content by taking 9% of the actual mortar volume.

Source: Data from ACI Committee 211, *Standard Practice for Selecting Proportions for Normal, Heavyweight, and Mass Concrete*, ACI 211.1-91, American Concrete Institute, Farmington Hills, MI, 1991; Nawy, E.G., *Reinforced Concrete: A Fundamental Approach*, 6th ed., Prentice Hall, Upper Saddle River, NJ, 2008.

- Maximum size (Table 6.10) = 3960 lb/yd³.
- Weight of sand = weight of fresh concrete – weight of water – weight of cement – weight of coarse aggregate:

$$3960 - 340 - 596.5 - 1728 = 1295.5 \text{ lb}$$

- Net weight of sand to be taken (moisture absorption 2%) = $1.02 \times 1295.5 = 1321.41 \text{ lb}$.

TABLE 6.8 Relationship between Water/Cement Ratio and Compressive Strength of Concrete

Compressive Strength at 28 Days (psi)	Water/Cement Ratio (by weight)	
	Non-Air-Entrained Concrete	Air-Entrained Concrete
6000	0.41	—
5000	0.48	0.40
4000	0.57	0.48
3000	0.68	0.59
2000	0.82	0.74

Note: 1000 psi = 6.9 MPa. Values are estimated average strengths for concrete containing not more than the percentage of air shown in Table 6.7. For a constant water/cement ratio, the strength of concrete is reduced as the air content is increased. Strength is based on 6×12 -in. cylinders moist-cured 28 days at $73.4 \pm 3^\circ\text{F}$ ($23 \pm 1.7^\circ\text{C}$) in accordance with Section 9(b) of ASTM C 31 (Making and Curing Concrete Compression and Flexure Test Specimens in the Field). Relationship assumes maximum size of aggregate about j to 1 in.; for a given source, strength produced for a given water/cement ratio will increase as maximum size of aggregate decreases.

Source: Data from ACI Committee 211, *Standard Practice for Selecting Proportions for Normal, Heavyweight, and Mass Concrete*, ACI 211.1-91, American Concrete Institute, Farmington Hills, MI, 1991; Nawy, E.G., *Reinforced Concrete: A Fundamental Approach*, 6th ed., Prentice Hall, Upper Saddle River, NJ, 2008.

TABLE 6.9 Volume of Coarse Aggregate per Unit of Volume of Concrete

Maximum Size of Aggregate (in.) ^a	Volume of Dry-Rodded Coarse Aggregate ^b per Unit Volume of Concrete for Different Fineness Moduli of Sand			
	2.40	2.60	2.80	3.00
3/8	0.50	0.48	0.46	0.44
1/2	0.59	0.57	0.55	0.53
3/4	0.66	0.64	0.62	0.60
1	0.71	0.69	0.67	0.65
1 1/2	0.75	0.73	0.71	0.69
2	0.78	0.76	0.74	0.72
3	0.82	0.80	0.78	0.76
6	0.87	0.85	0.83	0.81

^a 1 in. = 25.4 mm.

^b Volumes are based on aggregates in dry-rodded condition, as described in ASTM C 29 (Unit Weight of Aggregate). These volumes are selected from empirical relationships to produce concrete with a degree of workability suitable for usual reinforced construction. For less workable concrete, such as that required for concrete pavement construction, they may be increased about 10%. For more workable concrete, the coarse aggregate content may be decreased up to 10%, provided that the slump and water/cement ratio requirements are satisfied.

Source: Data from ASTM, *Annual Book of ASTM Standards*. Part 14. *Concrete and Mineral Aggregates*, American Society for Testing and Materials, Philadelphia, PA, 1993; ACI Committee 211, *Standard Practice for Selecting Proportions for Normal, Heavyweight, and Mass Concrete*, ACI 211.1-91, American Concrete Institute, Farmington Hills, MI, 1991; Nawy, E.G., *Reinforced Concrete: A Fundamental Approach*, 6th ed., Prentice Hall, Upper Saddle River, NJ, 2008.

- Net weight of gravel (moisture absorption 3%) = $1.03 \times 1728 = 1779.84$ lb.
- Net weight of water = $340 - (0.02 \times 1295.5) - (0.03 \times 1728) = 262.25$ lb.

For 1 yd³ of concrete:

- Cement = 596.5 lb = 600 lb (273 kg).
- Sand = 1321.41 lb = 1320 lb (600 kg).
- Gravel = 1779.84 lb = 1780 lb (810 kg).
- Water = 262.25 lb = 260 lb (120 kg).

TABLE 6.10 First Estimate of Weight of Fresh Concrete

Maximum Size of Aggregate (in.) ^a	First Estimate of Concrete Weight (lb/yd ³) ^b	
	Non-Air-Entrained Concrete	Air-Entrained Concrete
3/8	3840	3690
1/2	3890	3760
3/4	3960	3840
1	4010	3900
1-1/2	4070	3960
2	4120	4000
3	4160	4040
6	4230	4120

^a 1 in. = 25.4 mm.

^b Values calculated and presented in this table are for concrete of medium richness (550 lb of cement per cubic yard) and medium slump with aggregate specific gravity of 2.7. Water requirements are based on values for 3- to 4-in. slump in Table 5.3.2 of ASTM C 143. If desired, the estimated weight may be refined as follows if necessary information is available: For each 10-lb difference in mixing water from Table 5.3.2 values for 3- to 4-in. slump, correct the weight per cubic yard 15 lb in the opposite direction; for each 100-lb difference in cement content from 550 lb, correct the weight per cubic yard 10 lb in the same direction; for each 0.1 by which aggregate specific gravity deviates from 2.7, correct the concrete weight 100 lb in the same direction.

Source: Data from ACI Committee 211, *Standard Practice for Selecting Proportions for Normal, Heavyweight, and Mass Concrete*, ACI 211.1-91, American Concrete Institute, Farmington Hills, MI, 1991; Nawy, E.G., *Reinforced Concrete: A Fundamental Approach*, 6th ed., Prentice Hall, Upper Saddle River, NJ, 2008.

6.3.1.1 PCA Method of Design of Concrete Mixtures

The mixture design method of the Portland Cement Association (PCA) is essentially similar to the ACI method. Generally, results would be very close once trial batches are prepared in the laboratory. The PCA publication *Design and Control of Concrete Mixtures* (Kosmatka and Panarese, 1994) provides details regarding the method as well as other information on properties of the ingredients.

6.3.2 Estimating Compressive Strength of a Trial Mixture Using the Specified Compressive Strength

The compressive strength for which the trial mixture is designed is not the strength specified by the designer. The mixture should be overdesigned to ensure that the actual structure uses concrete with the specified minimum compressive strength. The extent of mixture overdesign depends on the degree of quality control available in the mixing plant. ACI Committee 318 (2008a,b) specifies a systematic way of determining the compressive strength for mixture designs using the specified compressive strength (f'_c). The procedure is presented in a self-explanatory flow-chart form in Figure 6.3. The cylinder compressive strength (f'_c) is the test result 28 days after casting normal weight concrete. Mixture design has to be based on an adjusted higher value, the adjusted cylinder compressive strength (f'_{cr}). The f'_{cr} value for which a trial mixture design is calculated depends on the extent of field data available, as shown below:

- *No cylinder test records available.* If field-strength test records for the specified class (or within 1000 psi of the specified class) of concrete are not available, the trial mixture strength can be calculated by increasing the cylinder compressive strength (f'_c) by a reasonable value, depending on the spread in values expected in the supplied concrete. Such a spread can be quantified by the standard deviation values represented by values in excess of f'_c in Table 6.11. Table 6.12 can then be used to obtain the water/cement ratio necessary for the required cylinder compressive strength value f'_c .

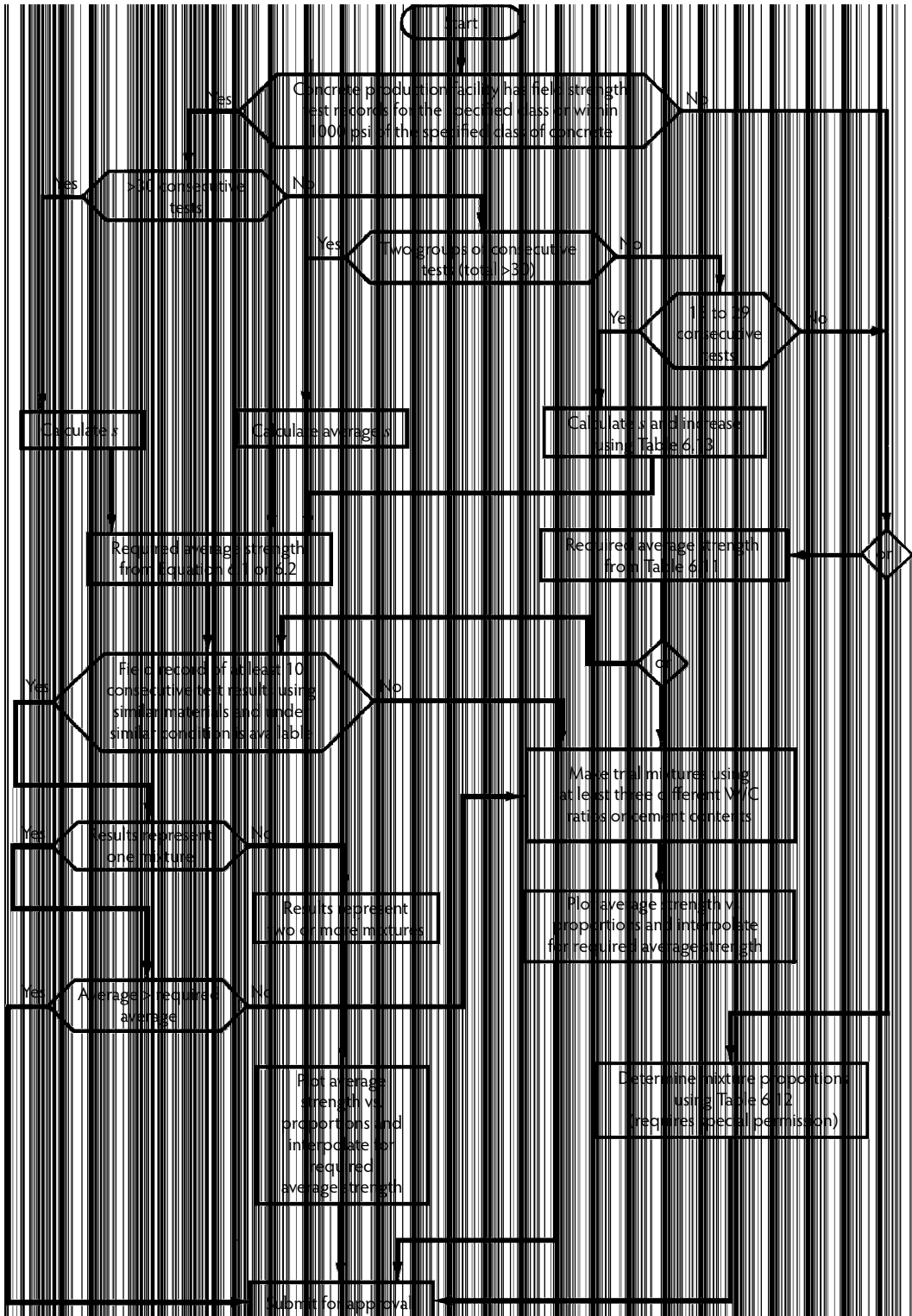


FIGURE 6.3 Flow chart of selection and documentation of concrete properties. (From Nawy, E.G., *Reinforced Concrete: A Fundamental Approach*, 6th ed., Prentice Hall, Upper Saddle River, NJ, 2008.)



PHOTO 6.4 Cylinder compressive-strength testing set-up.

TABLE 6.11 Required Average Compressive Strength When Data Are Not Available to Establish a Standard Deviation

Specified Compressive Strength (f'_c) (psi)	Required Average Compressive Strength (f'_{cr}) (psi)
Less than 3000	$f'_c + 1000$
3000–5000	$f'_c + 1200$
More than 5000	$f'_c + 1400$

Note: 1000 psi = 6.9 MPa.

Source: Data from ACI Committee 211, *Standard Practice for Selecting Proportions for Normal, Heavyweight, and Mass Concrete*, ACI 211.1-91, American Concrete Institute, Farmington Hills, MI, 1991; Nawy, E.G., *Reinforced Concrete: A Fundamental Approach*, 6th ed., Prentice Hall, Upper Saddle River, NJ, 2008.

- *Data are available on more than 30 consecutive cylinder tests.* If more than 30 consecutive test results are available, Equation 6.1, Equation 6.2, and Equation 6.3a can be used to establish the required mixture strength (f'_{cr}) from f'_c . If two groups of consecutive test results with a total of more than 30 are available, f'_{cr} can be obtained using Equation 6.1, Equation 6.2, and Equation 6.3b.
- *Data are available on fewer than 30 consecutive cylinder tests.* If the number of consecutive tests results available is fewer than 30 and more than 15, Equation 6.1, Equation 6.2, and Equation 6.3a should be used in conjunction with Table 6.13. Essentially, the designer should calculate the standard deviation (s) using Equation 6.3a, multiply the s value by the magnification factor provided in Table 6.13, and use the magnified s in Equation 6.1 and Equation 6.2. In this manner, the expected degree of spread of cylinder test values as measured by the standard deviation (s) is well accounted for.

6.3.3 Recommended Proportions for Concrete Strength (f'_{cr})

When the required average strength (f'_{cr}) for the mixture design has been determined, the actual mixture required to obtain this strength can be established using either existing field data or a basic trial mixture design:

TABLE 6.12 Maximum Permissible Water/Cement Ratios for Concrete When Strength Data from Field Experience or Trial Mixtures Are Not Available

Specified Compressive Strength (f'_c) (psi) ^a	Absolute Water/Cement Ratio by Weight	
	Non-Air-Entrained Concrete	Air-Entrained Concrete
2500	0.67	0.54
3000	0.58	0.46
3500	0.51	0.40
4000	0.44	0.35
4500	0.38	— ^b
5000	— ^b	— ^b

^a 28-day strength; with most materials, the water/cement ratios shown will provide average strengths greater than those calculated using Equation 6.1 and Equation 6.2.

^b For strengths above 4500 psi for non-air-entrained concrete and 4000 psi for air-entrained concrete, mix proportions should be established using trial mixes.

Note: 1000 psi = 6.9 MPa.

Source: Data from ACI Committee 211, *Standard Practice for Selecting Proportions for Normal, Heavyweight, and Mass Concrete*, ACI 211.1-91, American Concrete Institute, Farmington Hills, MI, 1991; Nawy, E.G., *Reinforced Concrete: A Fundamental Approach*, 6th ed., Prentice Hall, Upper Saddle River, NJ, 2008.

TABLE 6.13 Modification Factor for Standard Deviation When Fewer Than 30 Tests Are Available

Number of Tests ^a	Modification Factor for Standard Deviation ^b
Less than 15	Use Table 6.11
15	1.16
20	1.08
25	1.03
30 or more	1.00

^a Interpolate for intermediate number of tests.

^b Modified standard deviation to be used to determine required average strength f'_{cr} in Equation 6.1 and Equation 6.2.

Source: Data from ACI Committee 211, *Standard Practice for Selecting Proportions for Normal, Heavyweight, and Mass Concrete*, ACI 211.1-91, American Concrete Institute, Farmington Hills, MI, 1991; Nawy, E.G., *Reinforced Concrete: A Fundamental Approach*, 6th ed., Prentice Hall, Upper Saddle River, NJ, 2008.

- *Use of field data*—Field records of existing f'_{cr} values can be used if at least 10 consecutive test results are available. The test records should cover a period of at least 45 days. The material and conditions of the existing field mix data should be the same as those to be used in the proposed work.
- *Trial mixture design*—If field data are not available, trial mixtures should be used to establish the maximum water/cement ratio or minimum cement content necessary for designing a mix that produces a 28-day f'_{cr} value. In this procedure, the following requirements have to be met:
 1. The materials used and age at testing should be the same for the trial mixture and the concrete used in the structure.
 2. At least three water/cement ratios or three cement contents should be tried in the design of the mixture. The trial mixtures should result in the required f'_{cr} value. Three cylinders should be tested for each water/cement ratio and each cement content tried.

3. The slump and air content should be within ± 0.75 in. and 0.5% of permissible limits.
4. A plot should be constructed of the compressive strength at the designated age vs. the cement content or water/cement ratio, from which one can then choose the water/cement ratio or the cement content that will give the average f'_{cr} value required.

If field test data are available for more than 30 consecutive tests, the trial mixture should be designed for a compressive strength (f'_{cr}) calculated from:

$$f'_{cr} = f'_c + 1.34s \quad (6.1)$$

or from:

$$f'_{cr} = f'_c + 2.33s - 500 \quad (6.2)$$

where f'_c is the individual strength, and f'_{cr} is the average of the n specimens. The larger value of f'_{cr} from Equation 6.1 and Equation 6.2 should be used in designing the mixture, with the expectation that the minimum specified compressive strength will be attained. The standard deviation (s) is defined by the expression:

$$s = \left[\frac{\sum (f_i - f'_c)^2}{(n-1)} \right]^{1/2} \quad (6.3a)$$

If two test records are used to determine the average strength, the standard deviation becomes:

$$s = \left[\frac{(n_1 - 1)(s_1)^2 + (n_2 - 1)(s_2)^2}{(n_1 + n_2 - 2)} \right]^{1/2} \quad (6.3b)$$

where s_1 , s_2 are the standard deviations calculated from two test records, 1 and 2, respectively, and n_1 and n_2 are the number of tests in each test record, respectively. If the number of test results available is fewer than 30 and more than 15, the value of s used in Equation 6.1 and Equation 6.2 should be multiplied by the appropriate modification factor given in Table 6.13.

6.3.4 Example 6.2: Calculation of Design Strength for a Trial Mixture

Calculate the average compressive strengths for the design of a concrete mixture where the specified compressive strength is 5000 psi (334.5 MPa) and:

1. The standard deviation obtained using more than 30 consecutive tests is 500 psi (3.45 MPa).
2. The standard deviation obtained using 15 consecutive tests is 450 psi (3.11 MPa).
3. Records of prior cylinder test results are not available.

Solution

1. Using Equation 6.1:

$$f'_{cr} = 5000 + 1.34 \times 500 = 5670 \text{ psi}$$

Using Equation 6.2:

$$f'_{cr} = 5000 + 2.33 \times 500 = 5665 \text{ psi}$$

Hence, the required trial mix strength is 5670 psi (39.12 MPa).

2. The standard deviation is equal to 450 psi in 15 tests. From Table 6.13, the modification factor for s is 1.16; hence, the value of the standard deviation to be used in Equation 6.1 and Equation 6.2 is $1.16 \times 450 = 522$ psi (3.6 MPa). Using Equation 6.1:

$$f'_{cr} = 5000 + 1.34 \times 522 = 5700 \text{ psi}$$

Using Equation 6.2:

$$f'_{cr} = 5000 + 2.33 \times 522 = 5716 \text{ psi}$$

Hence, the required trial mixture strength is 5716 psi (39.44 MPa).

3. Records of prior test results are not available. Using Table 6.11:

$$f'_{cr} = f'_c + 1200$$

for 5000-psi concrete, so the trial mixture strength is $5000 + 1200 = 6200$ psi (42.78 MPa).

If a mixing plant keeps good records of its cylinder test results over a long period, the required trial mixture strength can be reduced as a result of quality control, thus reducing costs for the owner.

6.4 Mixture Proportioning for High-Performance, High-Strength Concrete (Cylinder Compressive Strength Exceeding 6000 psi)

6.4.1 General

By current ACI definitions, high-strength concrete covers concretes whose cylinder compressive strength exceeds 6000 psi (41.4 MPa). Proportioning concrete mixtures is more critical for high-strength concrete than for normal-strength concrete. The procedure is similar to the proportioning process for normal-strength concrete, except that adjustments have to be made for admixtures that replace part of the cement content in the mixture and it is often necessary to use smaller size aggregates in very high-strength concretes.

As discussed in Chapter 2 and Chapter 3 and in Section 6.5, there are several types of strength-modifying admixtures: high-range water reducers (superplasticizers), fly ash, polymers, silica fume, and blast-furnace slag. When mix proportioning for very high-strength concrete, however, isolating the water/cementitious materials ratio, $W/(C + P)$, from the paste/aggregate ratio because of the very low water content can be more effective for arriving at the optimum mixture with fewer trial mixtures and field trial batches. Few other methods are available today. The very low $W/(C + P)$ ratios necessary for strengths in the range of 20,000 psi (138 MPa) or higher require major modifications to the standard approach used for mixture proportioning that seems to work well for strengths up to 12,000 psi (83 MPa). The optimum mixture, chosen with minimum trials, has to produce a satisfactory concrete product in both its plastic and its hardened states.

An approach presented by ACI Committee 211 (1993) is based on the mortar volume/stone volume ratio and proportions the solids in the mortar on the basis of the ratio:

$$\frac{\text{Solid sand volume} \pm \text{cementitious solid volume}}{\text{Mortar volume}}$$

The ACI standard is well established for fly ash concrete (FAC). Ample mixture-proportioning results are available for polymers, and the same is true for silica-fume concrete (SFC) and slag concrete (SC or GGBFSC); however, they are not established in the form of a standard such as the committee reports of the *ACI Manual of Concrete Practice* (ACI, 1997). Additionally, several sections in the ACI manual list mixture proportions for the types of strength-generating admixtures that have been discussed in this chapter. The computational example in this chapter on fly ash concrete design for strengths up to 12,000 psi (83 MPa) should serve as a systematic step-by-step guide for proportioning mixtures using polymers, silica fume, and granulated blast-furnace slag within the compressive strength range of the example.

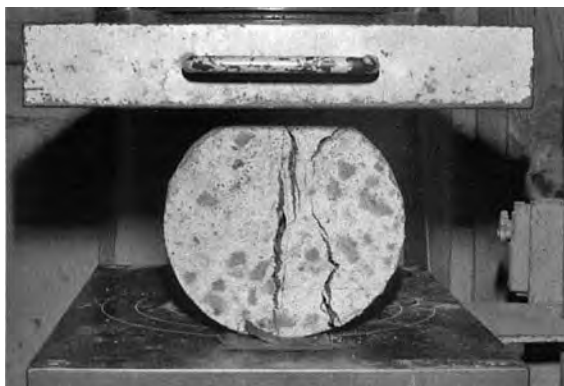


PHOTO 6.5 Splitting tensile strength test to failure.

6.4.2 Strength Requirements

The age at test is a governing criteria for selecting mixture proportions. The standard 28-day strength for normal-strength concrete penalizes high-strength concrete because the latter continues gaining strength after that age. One also has to consider that a structure is subjected to its service load at 60 to 90 days age at the earliest; consequently, in this case mixture proportioning has to be based on the latter age levels and also on either *field experience* or *laboratory batch trials*. The average compressive field-strength results should exceed the specified design compressive strength by a sufficiently high margin so as to reduce the probability of lower test results.

6.4.2.1 Mixture Proportions on the Basis of Field Experiences

If the concrete producer chooses the mixture on the basis of field experience, the required average strength f'_{cr} should be the larger of:

$$f'_{cr} = f'_c + 1.34s$$

or

$$f'_{cr} = 0.90f'_c + 2.33s$$

where f'_c is the specified design compressive strength, and s is the sample standard deviation (lb/in.²) from Equation 6.3.

6.4.2.2 Mixture Proportions on the Basis of Laboratory Trial Batches

In this case, the laboratory trial batches should give:

$$f'_{cr} = \frac{(f'_c + 1400)}{0.90} \text{ psi} \quad (6.4a)$$

or, in SI units:

$$f'_{cr} = \frac{(f'_c + 27.6)}{0.90} \text{ MPa} \quad (6.4b)$$

It is important to note that high-strength, high-performance concrete requires special attention in the selection and control of ingredients in the mixture to obtain optimum proportioning and maximum strength. To achieve this aim, care in the choice of the particular cement, admixture brand, dosage rate, mixing procedure, and quality and size of aggregate becomes paramount. Because not all of the cement hydrates, it is advisable that the cement content be kept at a minimum for optimum mixture proportioning.

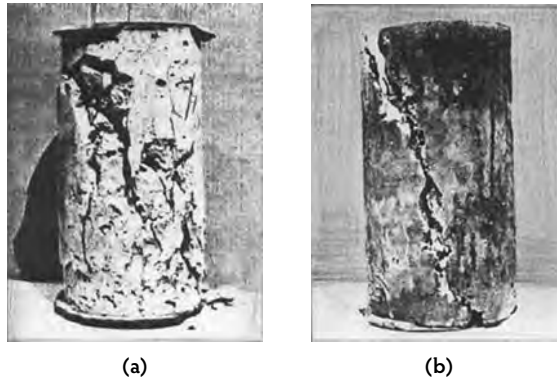


PHOTO 6.6 Cylinder compressive-strength test result: (a) normal-strength concrete; (b) higher-strength concrete. (Photographs courtesy of E.G. Nawy et al.)



PHOTO 6.7 Failure patterns of higher strength concrete compressive test. (Photograph courtesy of E.G. Nawy et al.)

6.4.3 Selection of Ingredients

6.4.3.1 Cement and Other Cementitious Ingredients

A proper selection of types and source of cement is extremely important. ASTM cement requirements are only minimum requirements, and certain brands are better than others due to variations in the physical and chemical makeup of various cements. High-strength concrete requires high cementitious materials content (namely, a low water/cementitious materials ratio), and the fineness of the cementitious materials has a major effect on the workability of the fresh mixture and the strength of the hardened concrete. They contribute to the reduction in water demand and lower the temperature of hydration; hence, a determination has to be made whether to choose Class F fly ash or Class G silica fume or granulated slag. The discussion in Chapter 2 of these cementitious materials gives guidelines for choosing ingredients.

6.4.3.2 Coarse Aggregate

Aggregates greatly influence the strength of the hardened concrete, as they comprise the largest segment of all the constituents; consequently, only hard aggregate should be used for normal weight high-strength concrete so the aggregate has at least the strength of the cement gel. As higher strength is sought, aggregate size should be decreased. It is advisable to limit aggregate size to a 3/4-in. (19-mm) maximum size for strengths up to 9000 psi (62 MPa). For higher strengths, a 1/2-in. or preferably 3/8-in. aggregate should

be used (12.7 to 9.5 mm). To achieve very high strengths in the range of 15,000 to 20,000 psi (103 to 138 MPa), higher-strength trap rock from selected quarries should be used. Beyond 20,000 to 30,000 psi, aggregate size should not exceed 3/8 in. for structural components.

6.4.3.3 Fine Aggregate

A fineness modulus (FM) in the range of 2.5 to 3.2 is recommended for high-strength concrete to facilitate workability. Lower values result in decreased workability and a higher water demand. The mixing-water demand is dependent on the void ratio in the sand. The basic void ratio is 0.35 and should be adjusted for other void ratios such that the void content (V , in percent) can be evaluated from:

$$V = \left(1 - \frac{\text{Oven-dry-rodded unit weight (lb/ft}^3\text{)}}{\text{Bulk dry specific gravity} \times 62.4} \right) 100 \quad (6.5a)$$

or, in SI units:

$$V = \left(1 - \frac{\text{Oven-dry-rodded unit weight (kg/m}^3\text{)}}{\text{Bulk dry specific gravity} \times 10^3} \right) 100 \quad (6.5b)$$

The mixing water has to be adjusted accordingly to account for the change in the basic void ratio such that the mixing-water adjustment (A) would be as follows:

$$A = 8(V - 35) \quad (6.6a)$$

where A is pounds per cubic yard. In SI units,

$$A = 4.7(V - 35) \quad (6.6b)$$

where A is kilograms per cubic meter.

6.4.3.4 Workability-Enhancing Chemical Admixtures

High-strength mixtures have a rich cementitious content that requires a high water content. Because excessive water reduces the compressive strength of the concrete and affects its long-term performance, water-reducing admixtures become mandatory. For these applications, high-range water reducers (HRWRs) are used (see Chapter 2 and Chapter 3). These are sometimes called *superplasticizers*. The dosage rate is usually based on fluid ounces per 100 pounds (45 kg) of total cementitious materials if the HRWRs are in liquid form. If the water-reducing agent is in powdered form, the dosage rate would be on a weight-ratio basis. The optimum admixture percentage should be determined on a trial-and-adjustment basis, as admixtures can reduce the water demand by almost 30 to 35% with a corresponding increase in compressive strength. A slump of 1 to 2 in. (25 to 50 mm) is considered adequate; however, if no HRWR admixtures are used, then the slump should be increased to 2 to 4 in. (50 to 100 mm). In addition, air-entraining admixtures are used if the concrete is exposed to freezing and thawing cycles in severe environmental conditions. For structural components in building systems, air entraining is unnecessary as these usually are not subjected to the type of frost action that exposed bridge decks or marine platforms endure.

6.4.4 Recommended Proportions

Table 6.14 to Table 6.22, adapted from ACI Committee 211 (1993), ACI Committee 212 (1983), ACI Committee 221 (1961), Nawy (2001), Neville (2001), and Russell (1993), recommend the necessary ingredients for proportioning mixes for high-strength concrete. Where the void content (V , in percent) is:

$$V = \left(1 - \frac{\text{Oven-dry-rodded unit weight}}{\text{Bulk dry specific gravity (dry)} \times 62.4} \right) 100$$

TABLE 6.14 Recommended Slump

With HRWR, in. (mm) ^a	Without HRWR, in. (mm)
1–2 (25–50) before adding HRWR	2–4 (50–100)

^a Adjust slump to that desired in the field by adding HRWR.

Note: HRWR, high-range water reducer.

TABLE 6.15 Required Average Compressive Strength When Data Are Not Available to Establish a Standard Deviation

Specified Strength (f'_c), psi (MPa)	Required Strength (f'_{cr}), psi (MPa)
>5000 (34.5)	$f'_c + 1400$ ($f'_c + 9.7$)

TABLE 6.16 Maximum-Size Coarse Aggregate

Required Concrete Strength (f'_c), psi (MPa)	Maximum Aggregate Size, in. (mm)
<9000 (62)	3/4–1 (19–25)
≥9000 (62)	3/8–1/2 (9.5–12.7)

TABLE 6.17 Ratio of Coarse Aggregate to Concrete Fractional Volume (Sand Fineness Modulus 2.5 to 3.2)

	Nominal Maximum Size, in. (mm)			
	0.03352	0.004701	3/4 (19)	1 (25)
Fractional volume of oven-dry rodded coarse aggregate	0.65	0.68	0.72	0.75

the mixing-water adjustment, in pounds per cubic yard, is:

$$(V - 35) \times 8$$

and in kilograms per cubic meter is:

$$(V - 35) \times 4.7$$

6.4.5 Step-by-Step Procedure for Selecting Proportions

The following are the steps necessary in the proportioning selection process:

1. Select the slump and required strength (f'_{cr}) (Table 6.14 and Table 6.15).
 - Based on field experience, select the f'_{cr} that is the larger of $f'_c + 1.34s$ or $0.9f'_{cr} + 2.33s$.
 - Based on laboratory batching, use $(f'_c + 1400)/0.9$.
2. Select the maximum size of aggregate (Table 6.16).
3. Select the optimum coarse-aggregate content (Table 6.17).
4. Estimate the mixing water and air content (Table 6.18).
5. Select the $W/(C + P)$, where C is the cement content and P is the pozzolanic content by weight (Table 6.19 and Table 6.20).
6. Compute the necessary content of the cementitious material P . This can be obtained by dividing the amount of mixing water per cubic yard or cubic meter of concrete (step 4) by the $W/(C + P)$ ratio.

TABLE 6.18 Mixing-Water Requirement and Air Content of Fresh Concrete Using Sand with 35% Void Ratio—First Trial Water Content

Slump, in. (mm)	Mixing Water, lb/yd ³ (kg/m ³)			
	Maximum-Size Coarse Aggregate, in. (mm)			
	3/8 (9.5)	1/2 (12.7)	3/4 (19)	1 (25)
1–2 (25–50)	310 (183)	295 (174)	285 (168)	280 (165)
2–3 (50–75)	320 (189)	310 (183)	295 (174)	290 (171)
3–4 (75–100)	330 (195)	320 (189)	305 (180)	300 (177)
Entrapped air (%) ^a	3 (2.5) ^b	2.5 (2.0)	2 (1.5)	1.5 (1.0)

^a Adjust mixing-water values for sand-void ratios other than 35%.

^b Mixtures using HRWR.

Note: lb/yd³ = 0.59 kg/m³.

Source: Data from Nawy, E.G., *Fundamentals of High-Performance Concrete*, John Wiley & Sons, New York, 2001; ACI Committee 211, *Guide for Selecting Proportions for High-Strength Concrete with Portland Cement and Fly Ash*, 211.4R-93, American Concrete Institute, Farmington Hills, MI, 1993.

TABLE 6.19 W/(C + P) Ratio for Concrete without High-Range Water Reducer

Field Strength f'_{cr} , psi (Pa) ^{a,b}		W/(C + P) Ratio			
		Maximum-Size Coarse Aggregate, in. (mm)			
		3/8 (9.5)	1/2 (12.7)	3/4 (19)	1 (25)
7000 (48)	28 days	0.42	0.41	0.40	0.39
	56 days	0.46	0.45	0.44	0.43
8000 (55)	28 days	0.35	0.34	0.33	0.33
	56 days	0.38	0.37	0.36	0.35
9000 (62)	28 days	0.30	0.29	0.29	0.28
	56 days	0.33	0.32	0.31	0.30
10000 (69)	28 days	0.26	0.26	0.25	0.25
	56 days	0.29	0.28	0.27	0.26

^a Here, $f'_{cr} = f'_c + 1400$ ($f'_{cr} = f'_c + 9.7$).

^b These are average field values; enter into the table 0.9 (required f'_{cr}).

- Proportion a basic mixture without the cementitious pozzolanic material P.
- Proportion a companion mixture using the cementitious pozzolanic material P such as fly ash.
- Produce a trial mix for each of the trial mix proportions designed in steps 1 to 8.
- Adjust the mixture proportions to achieve the required slump by changing the contents and adjusting the HRWR agent rate for several trial mixes.
- Select the optimum mixture.

6.4.6 Example 6.3: Mixture Proportions Design for High-Strength Concrete

Design a high-strength concrete mixture for columns in a multistory structure for a 28-day compressive strength of 10,000 psi (69 MPa). A slump of 9 in. (229 mm) is necessary for the workability required for congested reinforcement in the columns. Do not use an aggregate size exceeding 1/2 in. (12.7 mm). Use a high-range water reducer (HRWR) to obtain the 9-in. slump and a set-retarding admixture. Assume that the ready-mix producer has no prior history with high-strength concrete. Also assume the following sand properties:

TABLE 6.20 W/(C + P) Ratio for Concrete with High-Range Water Reducer

Field Strength f'_{cr} , psi (MPa) ^{a,b}		W/(C + P) Ratio			
		Maximum-Size Coarse Aggregate, in. (mm)			
		3/8 (9.5)	1/2 (12.7)	3/4 (19)	1 (25)
7000 (48)	28 days	0.50	0.48	0.45	0.43
	56 days	0.55	0.52	0.48	0.46
8000 (55)	28 days	0.44	0.42	0.40	0.38
	56 days	0.48	0.45	0.42	0.40
9000 (62)	28 days	0.38	0.36	0.335	0.34
	56 days	0.42	0.39	0.37	0.36
10,000 (69)	28 days	0.33	0.32	0.31	0.30
	56 days	0.37	0.35	0.33	0.32
11,000 (76)	28 days	0.30	0.29	0.27	0.27
	56 days	0.37	0.31	0.29	0.29
12,000 (83)	28 days	0.27	0.26	0.25	0.25
	56 days	0.30	0.28	0.27	0.26

^a Here, $f'_{cr} = f'_c + 1400$ ($f'_{cr} = f'_c + 9.7$).

^b These are average field values; enter into the table 0.9 (required f'_{cr}).

Note: A comparison of the values contained in Table 6.19 and Table 6.20 permits, in particular, the following conclusions: (1) For a given water/cementitious material ratio, the field strength of concrete is greater with the use of HRWR than without it, and this greater strength is reached within a shorter period of time. (2) With the use of HRWR, a given concrete field strength can be achieved in a given period of time using less cementitious material than would be required when not using HRWR.

- Fineness modulus (FM) = 2.90.
- Bulk specific gravity (over dry) (BSG_{dry}) = 2.59.
- Absorption based on dry weight (Abs) = 1.1%.
- Dry-rodded unit weight (DRUW) = 103 lb/ft³ (1620 kg/m³).
- Moisture content in sand = 6.4%.

Solution

1. Select the slump and required concrete strength.

Because a HRWR agent is used, choose strength on the basis of a 1- to 2-in. slump prior to the addition of HRWR. Also, because the ready-mix producer has no prior history with high-strength concrete, laboratory trial mixtures have to be designed for selection of the optimum proportions. From Equation 6.4a:

$$f'_{cr} = (f'_c + 1400)/0.90 = (10,000 + 1400)/0.90 = 12,670 \text{ psi (87 MPa)}$$

2. Select the maximum aggregate size.

A crushed limestone graded 1/2 in. (12.7 mm) maximum size is selected with $BSG_{dry} = 2.76$, Abs = 0.70, DRUW = 101 lb/ft³, and stone moisture content = 0.5%.

3. Select the optimum coarse aggregate content.

From Table 6.16, the fractional ratio is equal to 0.68. The dry weight (W_{dry}) of coarse aggregate per cubic yard of concrete is:

$$W_{dry} = (\%DRUW) \times (DRUW \times 27) = 0.68 \times 101 \times 27 = 1854 \text{ lb (841 kg)}$$

4. Estimate the mixing water and air content.

From Table 6.18, the first estimate of the required mixing water is 295 lb/yd³ (174 kg/m³) of concrete, and the entrapped air content when HRWR is used is 2.0%. From Equation 6.5a, the void content of the sand to be used is:

$$V = \left[1 - \frac{103}{2.59 \times 62.4} \right] \times 100 = 36\%$$

From Equation 6.6a, the mixing water adjustment (A) is:

$$A = 8(V - 35) = 8(36 - 35) = +8 \text{ lb/yd}^3 \text{ (4.7 kg/m}^3\text{) of concrete}$$

Hence, the total mixing water (W) is $295 + 8 = 303 \text{ lb (138 kg)}$.

5. Select the water/cementitious materials ratio, W/(C + P).

The values in Table 6.19 and Table 6.20 are average field-strength values; hence, the strength f'_{cr} for which the W/(C + P) ratio is to be found is:

$$f'_{cr} = 0.90 \times 12,670 = 11,400 \text{ psi (77 MPa)}$$

From Table 6.20, for a 1/2-in. aggregate, the desirable W/(C + P) ratio is 0.272, by interpolation.

6. Compute the content of cementitious material. From step 6, the mixing water (W) is 303 lb; hence,

$$C + P = 303/0.272 = 111 \text{ lb (505 kg)}$$

7. Proportion the basic mixture with cement only.

Volumes of all materials per cubic yard, except sand, are as follows:

- Cement = $1114/(3.15 \times 62.4) = 5.67 \text{ ft}^3$.
- Stone = $1854/(2.76 \times 62.4) = 10.77 \text{ ft}^3$.
- Water = $303/62.4 = 4.86 \text{ ft}^3$.
- Air = $0.02 \times 27 = 0.54 \text{ ft}^3$.
- Total = $21.77 \text{ ft}^3 \text{ (0.62 m}^3\text{)}$.

(Note: $1 \text{ m}^3 = 35.31 \text{ ft}^3$.) Hence, the required volume of sand per cubic yard of concrete is:

$$27 - 21.77 = 5.23 \text{ ft}^3$$

Converting the sand volume to weight:

$$\text{Sand} = 5.23 \times 62.4 \times 2.59 = 845 \text{ lb (384 kg)}$$

The mixture proportions by weight for the no-fly-ash concrete would be:

	lb/yd ³	kg/m ³
Cement	1114	661
Sand, dry	845	501
Stone, dry	1854	1100
Water (including 3 oz./cwt retarding admixture) ^a	303	180
Total	4116	2442

^a Here, cwt = 100 weight of cement.

8. Proportion companion mixtures using cement and fly ash.

In this case, use ASTM Class C fly ash (FA), which has a bulk specific gravity of 2.64. From Table 6.21, the fly ash replacement is 20 to 35%. Use four trial mixture levels: 20%, 25%, 30%, and 35%. For trial mixture 1, the silica fume is $0.20 (1114) = 223 \text{ lb}$; hence, the cement is $1114 - 223 = 891 \text{ lb}$. In a similar manner, the weights of the cementitious materials would be as shown in the following table:

Mixture	Cement, lb (kg)	Fly Ash, lb (kg)
1	891 (404)	223 (101)
2	835 (379)	279 (126)
3	780 (354)	334 (151)
4	724 (328)	390 (177)

TABLE 6.21 Fly Ash Values to Replace Part of the Cement

Type	Replacement % by Weight
ASTM Class F	15–25
ASTM Class C	20–35

TABLE 6.22 Modification Factor for Standard Deviation When Fewer Than 30 Tests Are Available

Number of Tests ^a	Modification Factor for Standard Deviation ^b
Less than 15	Use Table 6.15
15	1.16
20	1.08
25	1.03
30 or more	1.00

^a Interpolate for intermediate number of tests.

^b Modified standard deviation to be used to determine required average strength f'_{cr} in Equation 6.1 and Equation 6.2.

TABLE 6.23 Mixture Proportion in Example 6.3 without Moisture Trial Batch Adjustment

Ingredient	Basic Mix Cement Only (lb)	Cement + CFA Mixes (lb)			
		#1	#2	#3	#4
Cement	1114	891	835	780	724
Fly ash	0	223	279	334	390
Sand (dry)	845	800	790	781	773
Stone (dry)	1854	1854	1854	1854	1854
Water (plus retarder)	303	303	303	303	303
Total (lb/yd ³ concrete)	4116	4071	4061	4052	4044
Total (kg/m ³ concrete)	2428	2402	2396	2391	2386

Note: 1 lb/yd³ = 1 kg/m³. CFA, fly ash Class C.

In mixture 1, the volumes of components, except sand, per cubic yard of concrete are:

- Cement = $891 / (3.15 \times 62.4) = 4.53 \text{ ft}^3$.
- Fly ash = $223 / (2.64 \times 62.4) = 1.35$.
- Stone = 10.77 (from earlier table).
- Water (including 2.5 oz./cwt retarder) = 4.86 (from earlier table).
- Air = 0.54 (from earlier table).
- Total = 22.05 ft³.

The sand volume is $27 - 22.05 = 4.95 \text{ ft}^3 = 4.95 \times 62.4 \times 2.59 = 800 \text{ lb}$. The mixture proportions by weight for the fly-ash concrete mixture 1 would be:

	lb/yd ³	kg/m ³
Cement	891	526
Fly ash	223	132
Sand (dry)	800	472
Stone (dry)	1854	1094
Water plus retarder	303	179
Total	4071	2402

Note: 1 lb/yd³ = 0.59 kg/m³.

TABLE 6.24 Moisture-Adjusted Mixture Proportion in Example 6.3

Ingredient	Basic Mix Cement Only (lb)	Cement + CFA Mixes (lb)			
		#1	#2	#3	#4
Cement	1114	891	835	780	724
Fly ash	0	223	279	334	390
Sand (wet)	899	851	841	831	823
Stone (wet)	1863	1863	1863	1863	1863
Water (plus retarder)	262	262	262	262	262
Total (lb/yd ³ concrete)	4138	4090	4080	4070	4062
Total (kg/m ³ concrete)	2441	2413	2407	2401	2397

Note: 1 lb/yd³ = 0.89 kg/m³. CFA, fly ash Class C.

In a similar manner, the mixture proportions for 25%, 30%, and 35% fly ash content are computed to give the companion mixtures shown in Table 6.23.

9. Adjust the trial mixtures for absorbed water content in aggregate.

From before, the moisture content in sand is 6.4%, and the moisture content in stone is 0.5%. From Table 6.23, corrections in the basic mixture for the wetness of the aggregates are as follows:

$$\text{wet sand} = 845 (1 + 0.064) = 899 \text{ lb}$$

$$\text{wet stone} = 1854 (1 + 0.005) = 1863 \text{ lb}$$

From input data, the sand absorption based on dry weight is 1.1% and the stone absorption is 0.7%. Hence, the water correction is:

$$303 - 845(0.064 - 0.011) - 1854(0.005 - 0.007) = 303 - 45 + 4 = 262 \text{ lb (119 kg)}$$

Accordingly, the batch weight of water has to be corrected to account for the excess moisture contributed by:

$$\text{Aggregates} = \text{Total moisture} - \text{aggregate absorbed moisture}$$

Hence, Table 6.23 is modified to give Table 6.24.

10. Select the size of the laboratory trial mixture.

The usual size of the trial mixture is 3.0 ft³ (0.085 m³). The reduced batch weights to yield 3.0 ft³ of concrete would be 1/9 of the values tabulated in Table 6.24 to yield the values in the following table:

Ingredient	Basic Mix Cement Only (lb)	Cement + CFA Mixes (lb)			
		#1	#2	#3	#4
Cement	123.78	99.00	92.78	86.67	80.44
Fly ash	0	24.78	31.00	37.11	43.33
Sand (dry)	99.89	94.56	93.44	92.33	91.44
Stone (dry)	207.00	207.00	207.00	207.00	207.00
Water plus retarder	29.11	29.11	29.11	29.11	29.11
Total (lb/3 yd ³ concrete)	460	455	453	452	451
Total (kg/1/10 m ³ concrete)	245.3	242.7	241.6	241.1	240.5

11. Adjust the trial mixture on the basis of slump observation.

(a) *Basic mixture.* Assume that the water calculated to produce 1- to 2-in. slump (29.11 lb) was found not to be adequate and has to be increased to 30 lb per 3 ft³, including the 2.5 oz./cwt retarding admixture. The actual batch weights have to be adjusted so the actual batch weight for the basic mixture (no fly ash) becomes:

- Cement = 123.78 lb.
- Sand = 99.89 lb.
- Stone = 207.00 lb.
- Water = 30.00 lb.

These values have to be adjusted for moisture correction to the dry weight. The basic total added water is $30 \times 9 = 270 \text{ lb/yd}^3$. From before, the absorbed water in the aggregates is $45 - 4 = 41 \text{ lb}$. The actual total water content is $270 + 41 = 311 \text{ lb/yd}^3 = 34.56 \text{ lb/ft}^3$; thus,

- Cement = 123.78 lb.
- Sand = $99.89/1.064 = 93.88 \text{ lb}$.
- Stone = $207/1.005 = 205.97 \text{ lb}$.
- Batch water = $30.00 + 45/9 - 4/9 = 34.56 \text{ lb}$.

(b) *Yield of trial batch.* The actual yield of the trial mixture becomes:

- Cement = $123.78/(3.15 \times 62.4) = 0.63 \text{ lb}$.
- Sand = $93.88/(2.59 \times 62.4) = 0.58 \text{ lb}$.
- Stone = $205.97/(2.76 \times 62.4) = 1.20 \text{ lb}$.
- Water = $34.56/62.4 = 0.55 \text{ lb}$.
- Air = $0.02 \times 3 \text{ ft}^3 = 0.06 \text{ lb}$.
- Total yield volume of trial batch = 3.02 ft^3 .

The yield in pounds per cubic yard of concrete is obtained by multiplying all of the previous values by 9 and converting the volumes to weights, giving:

- Cement = $1114 \times (3.0/3.02) = 1107 \text{ lb}$.
- Sand (dry) = $845 \times (3.0/3.02) = 839 \text{ lb}$.
- Stone = $1854 \times (3.0/3.02) = 1841 \text{ lb}$.
- Water (plus retarder) = $311 \times (3.0/3.02) = 309 \text{ lb}$.

The new mixture proportions result in a water/cementitious materials ratio of:

$$W/(C + P) = 309/1107 = 0.28$$

vs. the desirable ratio of 0.272 previously obtained from Table 6.20. To maintain the 0.272 ratio, the weight of the cement should be increased to $309/0.272 = 1136 \text{ lb/yd}^3$ of concrete. The increase in volume due to the adjustment of the weight of cement is:

$$(1136 - 1107)/(3.15 \times 62.4) = 0.148 \text{ ft}^3$$

This increase in volume should be adjusted for by the removal of an equal volume of sand; hence, the weight of sand to be removed is $0.148 \times 2.59 \times 62.4 = 23.98 \text{ lb/yd}^3$, say, 18 lb/yd^3 . The resulting adjusted mixture proportions become:

- Cement = 1131 lb.
- Sand (dry) = $839 - 24 = 815$.
- Stone (dry) = 1841.
- Water + 2.5 oz./cwt retarder = 309.

(c) *Increase slump to 9 in. (229 mm).* The required slump in this example is 9 in. (229 mm). To achieve this value without the addition of water, which will reduce the strength, a high-range water reducer (namely, a plasticizer) is used. The dosage recommended by the manufacturer of the HRWR varies from

TABLE 6.25 Laboratory Final Trial Mixtures

Ingredient	Basic Mix Cement Only (lb)	Cement + CFA Mixes (lb)			
		#1 (20% CFA)	#2 (25% CFA)	#3 (30% CFA)	#4 (35% CFA)
Cement	1131	905	848	792	735
Fly ash	—	226	283	339	396
Sand (dry)	803	754	748	739	731
Stone (dry)	1841	1850	1850	1850	1850
Water (+ retarder)	309	302	298	296	295
Slump, in. (mm)	1.00 (25)	1.20 (31)	1.15 (29)	1.50 (38)	1.90 (48)
Retarder (oz./cwt)	3.5	2.5	2.0	2.5	2.0
HRWR (oz./cwt)	10.00	10.50	11.00	10.25	9.00
Slump, in. (mm)	10.00 (250)	10.75 (270)	8.75 (220)	10.50 (270)	9.25 (235)
28 day, psi (MPa)	12,600 (87)	12,400 (85)	12,550 (87)	12,750 (88)	12,250 (84)

Note: CFA, fly ash Class C; HRWR, high-range water reducer.

Source: Data from Nawy, E.G., *Fundamentals of High-Performance Concrete*, John Wiley & Sons, New York, 2001.

8 to 16 oz. per 100 lb of cementitious material. Tests performed in a laboratory with an ambient temperature of 74°F indicated the following:

- An 8-oz. dosage produced a 5-in. slump.
- An 11-oz. dosage produced 10-in. slump.
- A 16-oz. dosage produced segregation of the fresh concrete.

In all of these cases, a constant dosage rate of a retarding admixture of 2.5 oz./cwt was also added to the mixture along with the mixing water. When the HRWR was added to the mixture about 15 minutes after the initial mixing, it was determined that:

- The mixture with 10-in. (255 mm) slump had adequate workability; hence, no correction to the coarse aggregate content was necessary.
- The air content of the HRWR concrete mixture was found to be 1.9%; hence, no correction was necessary.
- The 28-day compressive strength of the No. 3 mixture was found to be 12,750 psi, satisfying the required f'_{cr} value of 12,670 psi. (Note: It is important to recognize that if additional water at this stage was required to produce the necessary slump and workability, then an additional cycle of corrections to actual batches of aggregate would have to be executed in the same manner as in the previous steps.)

12. Summary of the trial mixtures laboratory performance.

Table 6.25 provides a summary of the performance of the five mixtures: the basic no-fly-ash concrete and the four concretes with fly-ash contents of 20%, 25%, 30%, and 35% of the total cementitious material. Slump values for no-HRWR mixtures and those with HRWR were measured in the laboratory slump tests.

In addition, field trials must be done to verify the choice of laboratory trial mix. In this case, Mix 3 from Table 6.25, which gave the highest 28-day compressive strength of 12,750 psi (88 MPa), is closest to the required f'_{cr} of 12,670 psi that gives the compressive strength (f'_c) of 10,000 required in this example.

Part B. Applications and Constructability (J. Moreno and J. Albinger)

6.5 Applications and Constructability with an Emphasis on High-Strength, High-Performance Concrete

6.5.1 General

High-strength concrete (HSC) has a relative meaning according to the availability and utilization of materials and resources in each geographical area. In several parts of the country, concrete strengths of more than 112 MPa (16,000 psi) have been produced, while in other parts of the country 42 MPa (6,000 psi) is considered high. The type of market, availability of materials, and know-how are the reasons for such divergence. It should be understood that these factors are relative to the type of construction, initiative of the design engineer, commitment of the concrete producer, and quality of local materials. The permissible margin of error for high-strength concrete is smaller than for normal-strength concrete. Small variations in mixture proportions and deviations from good testing practices can have a greater effect on the strength or perceived strength of HSC than on normal-strength concrete. Preconstruction meetings are advisable to define responsibilities and avoid problems during construction.

6.5.2 Constructability Preparation Process

6.5.2.1 Preconstruction Meetings

Prior to construction, all of the project participants should meet to clarify contract requirements, discuss planned placement conditions, and review the planned inspection and testing programs of the various parties. The effects of time, temperature, placing, curing, and acceptance criteria and how those criteria will be established should be reviewed. The capabilities of the contractor's work force, the inspection staff, the testing laboratory, and the batching facilities should also be evaluated or inspected. The meeting should establish lines of communication and identify responsibilities. It is especially important to review the procedures the inspector will follow when noncompliance with contract requirements is found or suspected. This advance understanding will minimize future disputes and will give all members of the construction team an opportunity to participate in the quality process. Timely and accurate reporting are paramount. In addition to the required structural characteristics, trial production batches should take workability and placeability into consideration. It may, however, be necessary to make adjustments due to placement conditions or weather conditions when the job has started. The ready-mix concrete producer is essential to this discussion, as the producer is most familiar with and responsible for the product. Only designated individuals should have the authority to add admixtures or water or make any other mix changes on the site. No water in excess of the approved mixture proportions should be added to high-strength concrete.

6.5.2.2 Material Selection and Proportioning

Unlike more conventional, lower strength concrete, established procedures cannot always be used to determine the proportioning of high-strength concrete. As will be seen later, modifications to published procedures for mixture design of HSC must be made, although the basic principles remain. Maintaining the lowest possible water/cementitious materials ratio, for example, is not merely important but also critical (Table 6.26). The basic consideration is still the selection of a combination of materials that will produce a quality concrete with the desired workability, ease of placement, strength, and durability. Because of the innumerable types and grades of aggregate, varying chemical contents, and physical characteristic of cements, pozzolans, and chemical admixtures, and the interaction of these materials, arriving at the optimum combination often becomes a matter of producing several trial mixes. Caution must be exercised when examining the data of others, inasmuch as conclusions reached may reflect a particular set of materials unlike those in the researcher's area. For this reason, it is suggested that the following data be evaluated in a conceptual rather than quantitative manner. The slump required for pumping, placement, and consolidation normally varies with individual job conditions. If a high-range water reducer (super-plasticizer) is not part of the original design, it should be considered to facilitate placement.

TABLE 6.26 Suggested Water/Cementitious Material (W/C) Ratio

Specified Strength, psi (MPa)	Maximum W/C
6000 (41.4)	0.40
8000 (55.2)	0.36
9000 (62.1)	0.34
10,000 (69.0)	0.32
12,000 (82.8)	0.30
14,000 (96.6)	0.28

Note: For purposes of calculating the W/C of the mixture, the weight of all pozzolan should be added to the weight of the cement.

6.5.3 Mixture Components

6.5.3.1 Cement

In a study conducted by Blick et al. (1973), five cements of various types were ground and evaluated (Table 6.27). It was found that mortar cubes of Brand C, Type III, performed best at all ages (Figure 6.4). When it was used in concrete, the results were quite different (Figure 6.5). This phenomenon was further substantiated by tests conducted in the laboratory. In this study, mortar cubes were made with five different types of cement. When 20% of the cement, by mass, was replaced with fly ash, the results were quite different, as seen in Figure 6.6. The mortar containing the highest strength cement showed a loss of strength, while the mortar with the lowest strength cement showed the highest strength gain. Mortar cubes alone might not tell the whole story at the design level, but they are an important means of control after a selection has been made. Stress performance at ages up to 90 days should be evaluated. Limits of the physical properties of the cement should be established and submitted to the cement producer for compliance. The optimum cement quantity must be obtained through a series of laboratory trial mixtures. At least three cement quantities ranging from 136 to 409 kg/m³ (600 to 900 lb/yd³) should be tested. The tests should be conducted at a constant slump if a superplasticizer is not used or at a constant water/cementitious materials (W/C) ratio if a superplasticizer is used. The strength efficiency per pound of cement is influenced by all the variables that affect the strength of concrete. If the cement quantity of a mix is below optimum, higher strength may be obtained by using a larger size aggregate. If the cement quantity is above the optimum, higher strength may be achieved by using a smaller aggregate. After an optimum cement content for a given set of materials is selected, the maximum strength will not be increased by adding additional cement (Figure 6.7). Excessive cement content will also cause the concrete to become sticky and unworkable.

6.5.3.2 Fly Ash

The benefits derived from the use of fly ash vary with its class (ASTM C 618), chemical and physical properties, and quantity and compatibility with the cement. Cook (1982) and others have shown that higher strengths can be achieved using a Class C fly ash with a high calcium oxide content, as shown in Figure 6.8. Amounts of 10 to 15% of fly ash by mass of cement are common, but amounts of 25% and higher should be evaluated if Class C fly ash is being considered. The calcium hydroxide liberated during the hydration of the cement combines with the silica in the fly ash to form additional calcium silicate hydrate gel. This strength gain generally occurs after 14 days. Class F will have more of an effect on later strength, 28 to 90 days. The gains achieved with the use of fly ash cannot be attained through the use of additional cement. Additional benefit is derived mechanically from the fly ash as it acts as a filler that optimizes the particle distribution of the cementitious materials.

TABLE 6.27 Chemical and Physical Analysis of Cements for High-Strength Concrete Program

	Brand A, Type I	Brand B, Type II	Brand C, Type I	Brand C, Type II	Brand C, Type III
<i>Composition</i>					
SiO ₂ (%)	21.80	20.60	20.50	21.90	20.40
Al ₂ O ₃ (%)	5.30	6.10	5.70	4.10	5.50
Fe ₂ O ₃ (%)	2.00	3.20	2.10	2.90	2.00
CaO (%)	65.20	63.20	63.80	65.10	63.60
MgO (%)	2.50	2.80	3.60	2.70	3.50
SO ₃ (%)	2.10	2.60	2.50	2.00	3.00
Ignition loss (%)	1.10	1.10	2.00	1.00	2.10
Na ₂ O (%)	0.19	0.31	0.11	0.14	0.12
K ₂ O (%)	0.41	0.70	0.17	0.24	0.20
Na ₂ O equivalent (%)	55.00	48.00	55.00	61.00 ^a	56.00
C ₃ S (%)	21.00	23.00	17.00	17.00	17.00
C ₂ S (%)	10.60	10.70	11.50	5.90 ^a	11.20
C ₃ A (%)	6.10	9.70	6.40	8.90	6.10
C ₄ AF (%)	0.33	0.59	0.09	0.15	0.12
Blaine (air permeability)	3670	3780	3550	4220	5400
+325	4.10	8.40	5.60	2.50	0.90
N.C.	25.80	23.60	23.00	24.80	20.60
Setting time	2:35	2:15	1:35	1:55	1:45
<i>Vicat false set</i>					
H ₂ O (%)	30.00	30.00	30.00	30.00	33.00
3 min	50.00	50.00	50.00	50.00	50.00
5 min	35.00	50.00	50.00	50.00	50.00
8 min	18.00	50.00	50.00	46.00	45.00
11 min	12.00	50.00	50.00	40.00	39.00
Remix, 15 min	11.00	None	None	50.00	50.00
Air content (%)	9.10	9.50	7.60	6.60	6.20
H ₂ O (%)	69.00	68.00	68.00	68.00	71.00
<i>Comparative strength</i>					
H ₂ O (%)	50.40	49.00	48.00	47.00	51.40
Flow (%)	114.00	106.00	113.00	106.00	108.00
1-Day (psi)	1460	1400	1200	1860	2090
3-Day (psi)	2930	2870	2700	3280	4420
7-Day (psi)	4460	3980	4370	4560	6290
28-Day (psi)	6220	5730	6410	6770	7870
63-Day (psi)	6870	6320	7310	7850	8320

^a This cement does not meet Type II specifications for moderate heat of hydration. Maximum percent of C₃S + C₃A = 58%, and maximum percent of C₃A = 8% (according to ASTM C 150).

6.5.3.3 Microsilica

Microsilica, or silica fume as it is sometimes called, has been used to create high-strength concretes. Its chemistry is similar to both cement and fly ash (Table 6.28). Its super fineness of over 100,000 cm³/g, in combination with its pozzolanic reactivity, offers strengths in excess of 15,000 psi (103.4 MPa). Quantities of 5 to 15% of cement weight should be evaluated. A superplasticizer must be used in conjunction with microsilica because of the negative affect on the slump caused by the fineness of the silica. Microsilica has been used with and without fly ash. The benefit of the fly ash may be lessened when it is used with microsilica, but when attempting to produce an ultra-high-strength concrete, every benefit must be exploited (Figure 6.9).

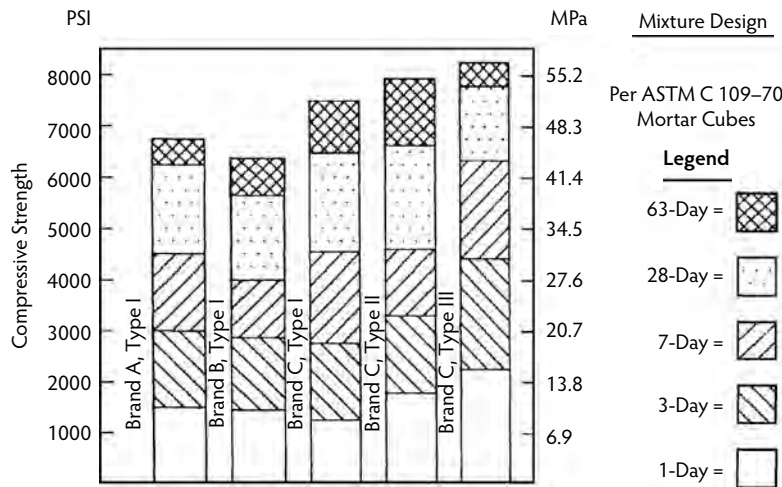


FIGURE 6.4 Effect of various cements on mortar cube compressive strength.

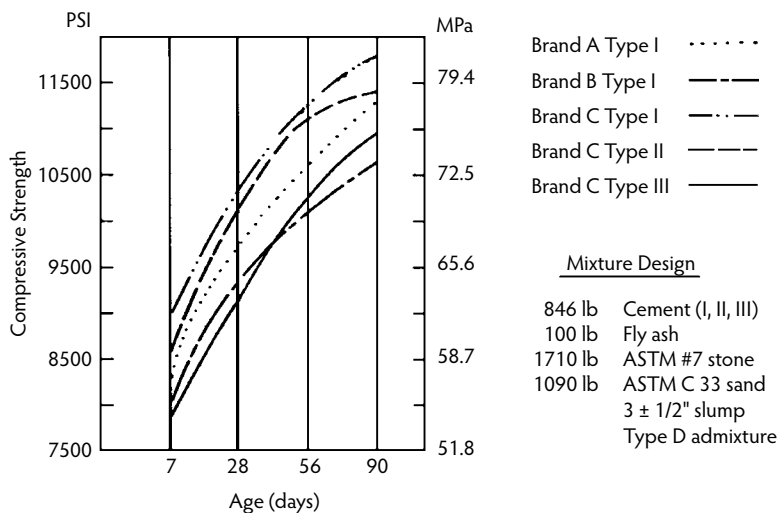


FIGURE 6.5 Effect of various cements on concrete compressive strength.

6.5.3.4 Granulated Blast-Furnace Slag

Granulated blast-furnace slag (GBFS) is a byproduct of the steel production process. It is a glassy granular material primarily consisting of aluminates, silicates, and calcium-alumina-silicates. Grinding reduces the particle size to a cement fineness typically less than 3500 cm³/g. It reacts with liberated calcium hydroxide, the same as fly ash. Its benefits are most realized when used in conjunction with fly ash and microsilica; ternary mixes further optimize particle distribution of the cementitious materials.

6.5.3.5 Chemical Admixtures

The use of a normal-set water reducer, retarding water reducer, or a combination of these becomes necessary to efficiently utilize all cementitious materials and to maintain the lowest practical water/cement ratio. Dosages higher than those recommended by the admixture manufacturer have been found to increase strength without detrimental affects (Figure 6.10). The use of an ASTM Type D retarding water reducer was found to offer strength benefits beyond 56-day strengths. Varying dosages of this material

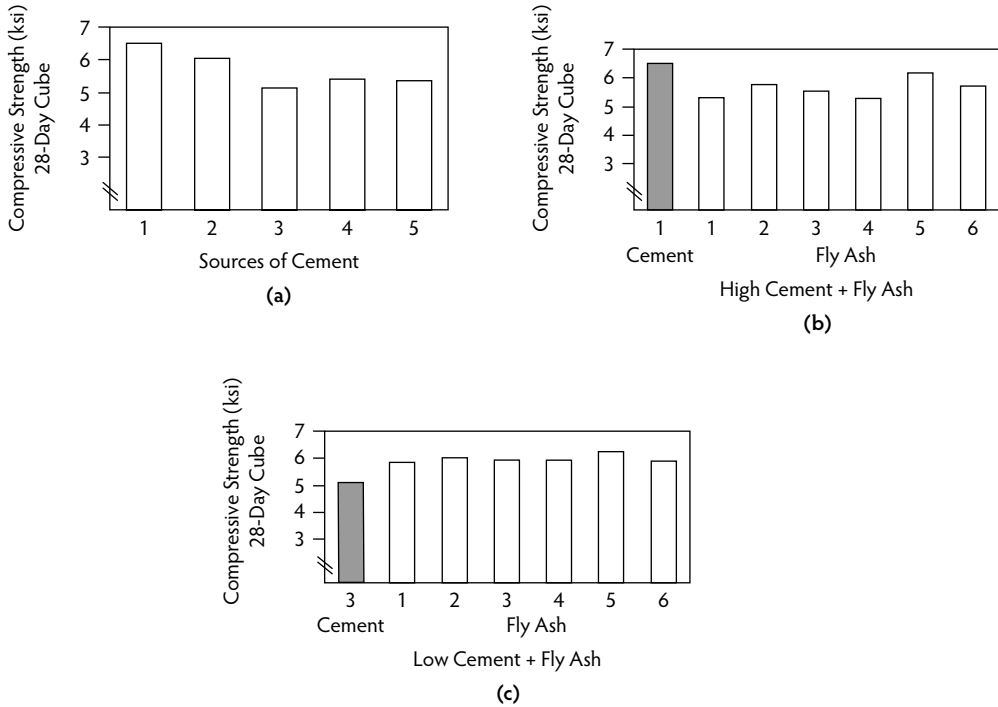


FIGURE 6.6 Effect of compressive strength on various cements and fly ash: (a) source of cement, (b) high cement content plus fly ash, and (c) low cement content plus fly ash.

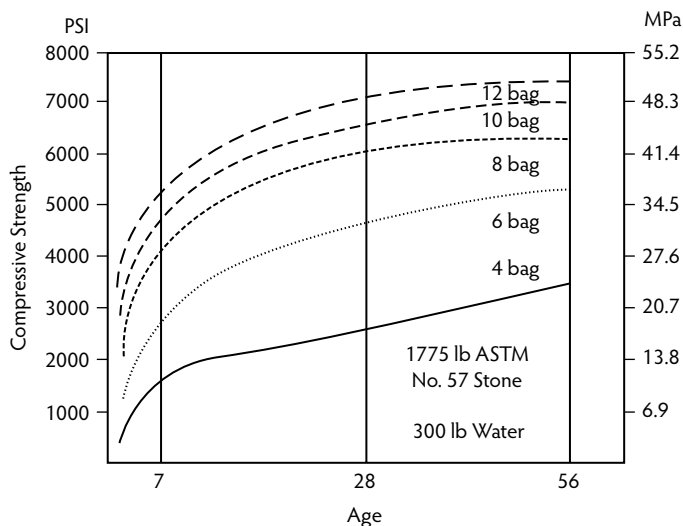


FIGURE 6.7 Cement efficiency vs. compressive strength.

help offset the rapid setting time that might be expected from a mix containing a high amount of cement. During hot weather, this type of control is imperative. The heat of hydration of this type of concrete generates quickly and if left uncontrolled will cause high early strength, lower ultimate strength, and excessive cracking. Factors to be considered when evaluating an admixture are cement and fly-ash compatibility, water reduction, setting times, workability, time of addition, and dosages.

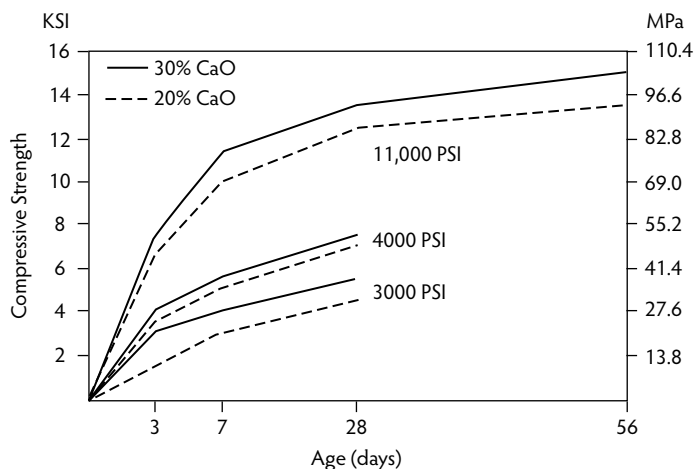


FIGURE 6.8 Effect of CaO on compressive strength (ASTM C 618, Class C fly ash).

TABLE 6.28 Chemical Analysis

	Normal Portland Cement (%)	Microsilica (%)	Fly Ash, Class F (%)	Fly Ash, Class C (%)	Slag, Type 100 (%)
Silica (SiO ₂)	20.13	94–98	49.00	40.40	27–38
Calcium oxide (CaO)	63.44	0.08–0.30	5.00	25.40	34–43
Magnesium oxide (MgO)	2.86	0.30–0.90	1.50	4.70	7–15
Ferric oxide (Fe ₂ O ₃)	2.96	0.02–0.15	6.00	5.90	.2–1.6
Aluminum oxide (Al ₂ O ₃)	5.10	0.10–0.40	26.00	17.00	7–12
Sulfur trioxide (SO ₃)	3.00	—	0.50–0.60	2.75	.15–.23
Potassium oxide (K ₂ O)	1.12	0.20–0.70	0.80–0.90	0.27	—
Sodium oxide (Na ₂ O)	0.30	0.10–0.40	0.25	1.60	.6–.9
Loss on ignition	0.80	0.80–1.50	3.50	0.43	—
Silicon carbide (SiC)	—	0.20–0.10	—	—	—
Carbon (C)	—	0.20–1.30	—	—	.78
C ₄ AF	9.00	—	—	—	8.89
C ₃ S	57.40	—	—	—	54.00
C ₂ S	14.40	—	—	—	19
C ₃ A	8.50	—	—	—	8
Blaine (cm ² /g)	3782	100,000+	—	—	5360

Superplasticizers (high-range water reducers) offer the ability to achieve higher strengths than were previously attainable. Water reductions of up to 30% are possible while still maintaining a placeable consistency (Figure 6.11). This additional water reduction was instrumental in increasing our 9000-psi mix to 11,000 psi. Superplasticizers may be used in conjunction with an ASTM Type D retarder and can successfully be added at the ready-mix plant and again at the jobsite if necessary.

Recently, superplasticizers have been developed using polycarboxylate polymers in the development of self-consolidating concrete (SCC). SCC is characterized in terms of a measured slump flow of 18 to 26 in. (ASTM C 1611-05). SCC can be described as a very flowable cohesive concrete that does not segregate. These properties make the SCC capable of being placed with little or no vibration even in the presence of dense reinforcement. Mix designs may have to be modified to produce SCC, and care should be taken not to use polycarboxylate polymers in combination with naphthalate-based HRWRs. Air-entraining agents are not generally used because of the accompanying strength loss and because the type of application normally precludes their use (i.e., caissons, interior columns, and shear walls).

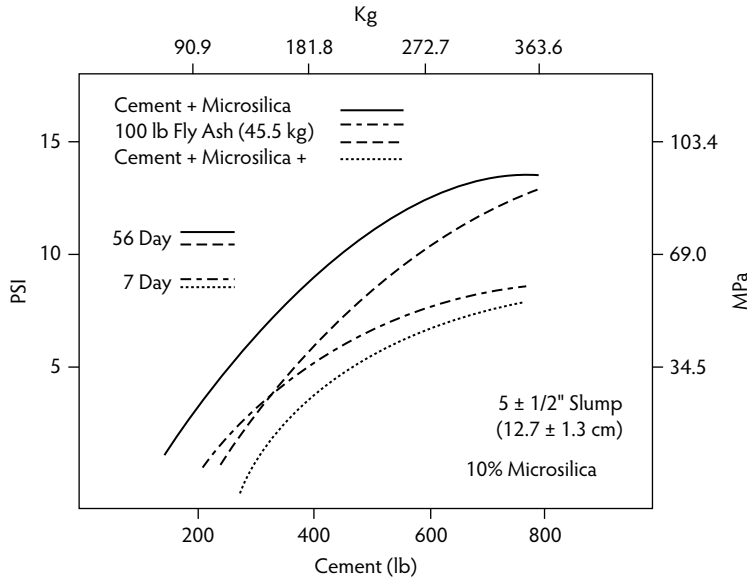


FIGURE 6.9 Benefit of fly ash when used with microsilica.

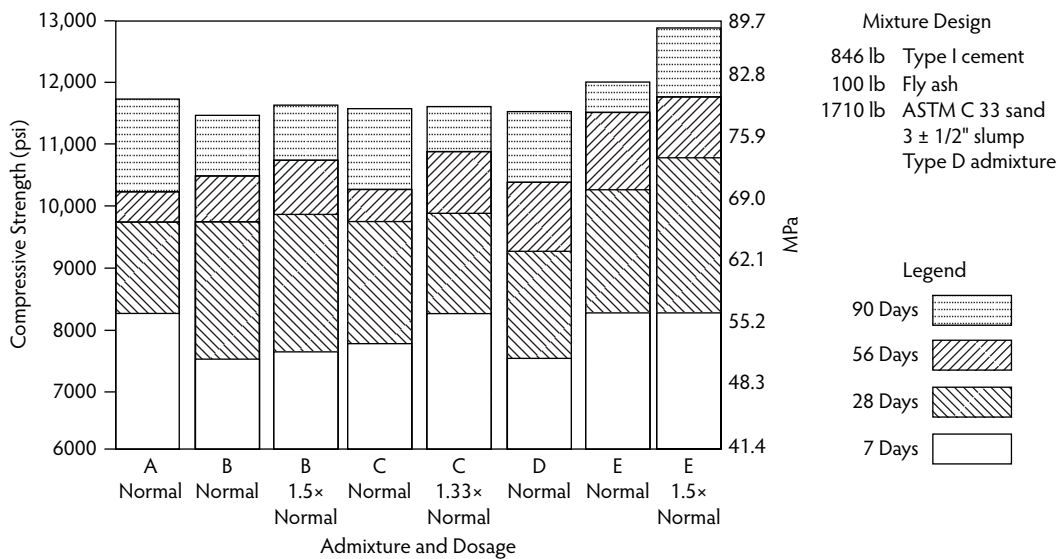


FIGURE 6.10 Effect of chemical admixtures on concrete compressive strength.

6.5.3.6 Aggregates

Careful consideration should be given to the shape, surface texture, and mineralogy of aggregates. Cubically shaped crushed stone with a rough surface texture appears to produce the highest strength. Smoother faced, uncrushed gravel may be used to produce strengths of up to about 10,000 psi, but it does not have the bond strength necessary to produce higher strengths. Tests we have conducted showed that gravels produce lower compressive strengths and moduli of elasticity when compared to the same size crushed stone with equal cement content (Figure 6.12). Each strength level will have an optimum size aggregate that will yield the greatest compressive strength. Because of the high volume of cementitious materials in high-strength concrete, the optimum aggregate surface area is necessary to provide maximum bonding. In addition to optimizing the gradation of the coarse aggregate, further benefit can

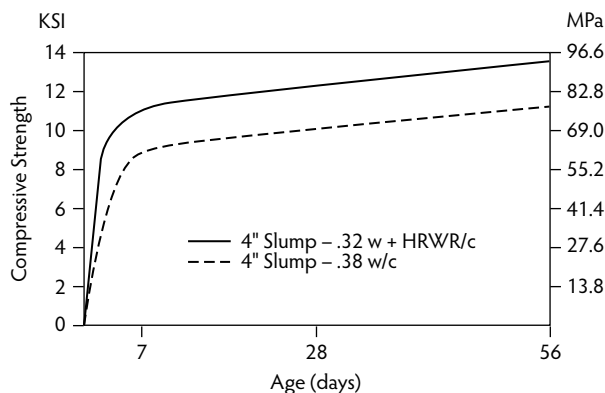


FIGURE 6.11 Compressive strength of high-strength concrete containing a high-range water reducer.

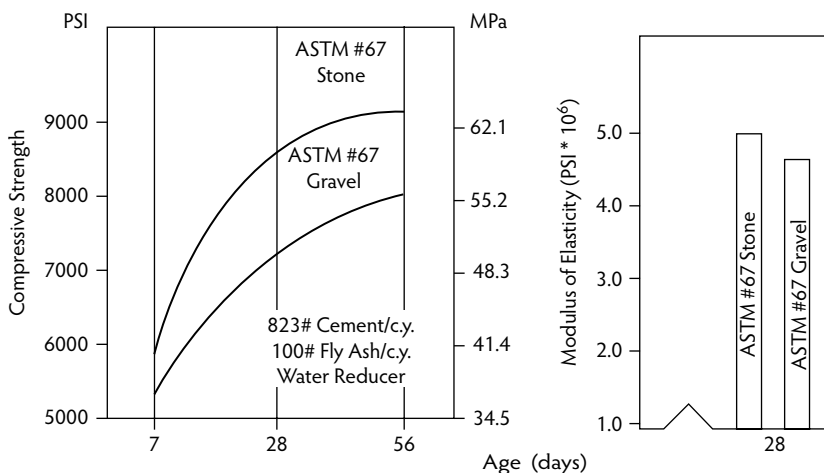


FIGURE 6.12 Compressive strength and modulus of elasticity vs. age for various sizes and types of coarse aggregate.

TABLE 6.29 Volume of Dry-Rodded Coarse Aggregate per Unit Volume of Concrete for 2.80 Fineness Modulus of Sand

Maximum Size of Aggregate (in.)	Modified for High Strength	From ACI 211.1-82
3/8	0.61	0.46
1/2	0.64	0.55
3/4	0.66	0.62
1	0.70	0.67

be derived from altering the proportions of coarse to fine aggregate. It was found that the proportions recommended by ACI 211.1-82 do not apply, as seen from the comparative values in Table 6.29. Well-graded fine aggregates that provide good finishing characteristics in regular-strength concrete are not only unnecessary but may also require more water than can be tolerated (Table 6.30). Fine aggregates, with a fineness modulus of 2.5 and under will produce concrete with a sticky consistency, less workability, and lower compressive strength. A fineness modulus of 2.75 to 3.20 appears to produce the highest strengths. As with coarse aggregates, cubically shaped particles in fine aggregate have been found to increase bonding (NCSA, 1975, 1976). Very angular manufactured sands should not be used because they increase water demand.

TABLE 6.30 Fine Aggregate for 7500-psi and above Concrete (Fineness Modulus, 2.78)

Typical Gradation		Chemical Analysis (Approximate Percentage)	
Sieve Size	% Passing		
3/8 in.	100.0	Silicon dioxide (SiO ₂)	35%
No. 4	96.5	Iron oxide (FeO ₃)	—
No. 8	81.7	Aluminum oxide (Al ₂ O ₃)	5% combined total
No. 16	70.9	Magnesium carbonate	12%
No. 30	53.5	Calcium carbonate	48%
No. 50	16.5		
No. 100	2.8		

TABLE 6.31 Required Increases in Design Strength as Coefficient of Variation Increases

	CV 7%		CV 10%		CV 13%	
	SD	DS	SD	DS	SD	DS
6000	465	6700	693	7200	943	7690
7500	581	8400	866	9010	1178	9740
9000	697	10,200	1040	10,920	1414	11,790

Note: CV, coefficient of variation; DS, design strength; SD, standard deviation; SS, specified strength.

TABLE 6.32 Material Sampling Schedule

Material	Frequency	Test
Cement	1/week	Hold for 120 days
Fly ash	1/week	Hold for 120 days
Slag	1/week	Hold for 120 days
Admixtures	Each delivery	Specific gravity
Water	As needed	—
Aggregates	1/week	Gradation 200 wash specific gravity

6.5.3.7 Water

Various sources of water have been evaluated, and it appears that the limitations listed in ASTM C 94 are adequate. Water need not be potable. ASTM C 94 states, “If it contains quantities of substances which discolor it or make it smell or taste unusual or objectionable or cause suspicion, it shall not be used unless service records of concrete made with it or other information indicates that it is not injurious to the quality of the concrete.”

6.5.4 Materials Control

After the materials are chosen, the consistency of the materials becomes imperative. If variations become excessive, the required average strength may become unattainable. As an example, if the specified strength was 9000 psi and the standard deviation was 697 psi (7% coefficient of variation), the overdesign required would be 8.4 MPa (1200 psi). On the other hand, if the standard deviation is 1414 psi (13% coefficient of variation), the overdesign would have to be nearly 21 MPa (3000 psi) (Table 6.31). A materials-sampling program should be established so the appropriate test may be run in the event of low breaks (Table 6.32). All suppliers of constituent materials should be made aware of the importance of providing consistent

TABLE 6.33 Composition of Concretes Produced in a Ready-Mix Plant

	Concrete Type				
	Reference	Silica Fume	Fly Ash	Slag + Silica Fume	
<i>Water/cementitious material ratio</i>	0.30	0.30	0.30	0.30	0.25
<i>Ingredients kg/m³ (lb/yd³):</i>					
Water	127 (214)	128 (216)	129 (217)	131 (221)	128 (216)
Cement ASTM Type II	450 (759)	425 (716)	365 (615)	228 (384)	168 (283)
Silica fume	—	45 (76)	—	45 (76)	54 (91)
Fly ash	—	—	95 (160)	—	—
Slag	—	—	—	183 (308)	320 (539)
<i>Dolomitic limestone:</i>					
Coarse aggregate	1100 (1854)	1110 (1871)	1115 (1879)	1100 (1871)	1100 (1854)
Fine aggregate	815 (1374)	810 (1365)	810 (1365)	800 (1349)	730 (1230)
Superplasticizer, L/m ³ (oz/yd ³) ^a	153 (395)	14 (362)	13 (336)	12 (310)	13 (336)
Slump after 45 min, mm (in.)	110 (4–1/4)	180 (7)	170 (6–3/4)	220 (8–3/4)	210 (8–1/4)
<i>Compressive strength:</i>					
28-day, MPa (psi)	99 (14,360)	110 (15,950)	90 (13,050)	105 (15,230)	114 (16,530)
91-day, MPa (psi)	109 (15,810)	118 (17,110)	111 (16,100)	121 (17,550)	126 (18,280)
1-year, MPa (psi)	119 (17,260)	127 (18,420)	125 (18,130)	127 (18,420)	137 (19,870)

^a Sodium salt of a naphthalene sulfonate.

materials. As the job progresses, they should also be involved in the periodic testing of the material they supply. The handling and storage of materials need not be substantially different from the procedures used for conventional concrete. Proper stockpiling of aggregates, control of moisture, and adequate segregation of cementitious materials are essential. Table 6.33 gives selected data on some HSC mixes used; however, the information tabulated is intended to serve as only an example and should not replace locally generated data.

6.5.5 Mixing, Transporting, Placing, and Curing

6.5.5.1 Mixing

High-strength concrete may be produced in manual, semiautomatic, or automatic plants. It should be noted, however, that total automation almost always improves consistency. Normal batching procedures need not be altered, but a modification in timing may help. Admixtures have been found to be most effective if they are introduced after the cement has been wetted. Caution should be exercised if the concrete is to be truck mixed. Truck mixers that are not maintained or that have worn fins and blades will not thoroughly mix the concrete and will cause unacceptable variations in all the physical characteristics of the concrete. Once in the stationary or truck mixer, the materials should be mixed as follows: 1 minute for 1 yd³ plus 0.25 minute for each additional cubic yard; for example, 3.75 m³ (5 yd³) = 2 minutes. The speed at which the concrete is mixed should be in accordance with the mixer manufacturer's recommendations. Care should be taken so the temperature of the concrete as delivered does not exceed 42°C (90°F). As with all concrete, higher temperatures mean more water. If the water demand becomes excessive or slump loss becomes rapid, increased dosages of chemical retarders or superplasticizers should be considered. If problems persist, ice or chilled aggregates may be required to lower the temperature. Maintaining a minimum temperature is normally not a problem, in that the concrete is typically used in more massive structural members where lower temperatures are beneficial. Additionally, lower concrete temperature means less total water, higher later strengths, and less cracking.

6.5.5.2 Transporting

High-strength concrete can be successfully mixed and transported in a number of ways. Quality assurance/quality control (QA/QC) personnel must be aware that prolonged mixing will cause slump loss and result in lower workability. Adequate job control must be established to prevent delays. When practical, withholding some of the high-range water-reducing admixture until the truck arrives at the jobsite or on-site addition of high-range water-reducing admixtures may be desirable. When materials are added at the site, proper mixing is required. Because of the consequences of segregation, QA/QC personnel should pay close attention to on-site mixing and verify that the mixture is uniform. The ACI 304.R Committee Report contains information on proper mixing. Truck mixers should be equipped with drum revolution counters, and their fins should be in good condition. All mixer trucks used to transport high-strength concrete should be regularly inspected and certified to comply with the National Ready Mixed Concrete Association (NRMCA) inspection requirements prior to and during their use in this capacity.

6.5.5.3 Placing

High-strength concrete is typically produced with slumps in excess of 200 mm (8 in.). Despite their fluid appearance, these mixes require thorough consolidation. All concrete should be consolidated quickly and thoroughly. Standby vibratory equipment is recommended, with at least one standby vibrator for every three vibrators required. The provisions in the ACI 309 Committee Report (1987) should be followed for proper consolidation. In construction, different strength concretes are often used within or between different members. QA/QC personnel should be aware of the exact location for each approved mixture. Often, *mushrooming* is performed over column and shear-wall locations when placing floor slabs; that is, high-strength concrete is mushroomed around those locations to form a cap prior to placing lower-strength concrete around it in the floor. QA/QC personnel should be aware of how far the cap should extend. Because cold joints between the two concretes are not allowed, the inspector should determine that the high-strength mushroom is still plastic enough to blend with the lower-strength slab concrete. When two (or more) concrete mixes are being used in the same pour, it is mandatory that sufficient control be exercised at the point of discharge from each truck to ensure that the intended concrete is placed as specified. Planning is necessary to determine the best procedures. Consideration might be given to the use of retarding admixtures.

6.5.5.4 Curing

The full potential strength and durability of high-strength concrete will be fully developed only if it is properly cured for an adequate period prior to being placed in service or subjected to construction loading. Many acceptable methods for curing are available, as presented in the ACI 308 Committee Report (1992). High-strength concretes are extremely dense and impermeable; therefore, appropriate curing methods for various structural elements should be selected in advance. For interior columns, curing is often impractical, and durability is not a problem. The period during which the forms are in place may be adequate in such instances. QA/QC personnel should verify that the accepted methods are properly employed in the work.

High-strength concretes usually do not exhibit much bleeding, and, without protection from loss of surface moisture, plastic shrinkage cracks may form on exposed surfaces. Protection methods include fog misting, use of evaporation retarders, covering concrete with polyethylene sheeting, or application of a curing compound. Water curing of high-strength concrete is recommended because of the low water/cementitious material ratios employed. Water curing of vertical members is usually impractical, and other curing methods should be employed. When forms are released or removed at very early ages, typically less than 1 day, prevention of thermal cracking by providing insulation should be considered, particularly in cold weather. Each high-strength mixture has heat evolution and dissipation characteristics in the context of its curing environment. Maximum temperature and thermal gradients and their effects on constructability and long-term design properties should be determined by preconstruction trials. Consideration might be given to computer simulation of the expected thermal history in a structure so appropriate curing and protection can be performed.

The higher cement contents of high-strength concrete generate a higher heat of hydration and, possibly, thermal gradients in excess of 20°C/m (11°F/ft), especially in uninsulated mass placements; however, studies have shown that thermal gradients are similar to those for conventional-strength concretes. Data have shown that for deep foundations, when the ultimate internal temperature developed during hydration rose to 78°C (172°F), the *in situ* strength and stiffness were not adversely affected. The architect or engineer should understand the effects of heat generation in the various structural elements and address them in-project specifications. Specifications for mass concrete often require that the temperature difference between the concrete interior and surface not exceed 20°C (36°F). The inspector should monitor and record ambient temperatures and curing temperatures at the surface and center of large concrete components so the design/construction team can effectively make any adjustments such as mixture design changes or use of insulating forms during the course of the project. Concrete delivered at temperatures exceeding specification limits should be rejected, unless alternative procedures are agreed to at the preconstruction meeting.

6.6 Jobsite Control

Coordination of delivery time between the concrete supplier and contractor is critical. Concrete should be delivered so minimal waiting is experienced. Delays on the job may result in slump loss and, subsequently, the concrete may require rettempering. Water added at the jobsite can be extremely detrimental to the structural integrity of the concrete and should not be permitted. Any adjustments made in the slump should be made with a high-range water reducer. As always, the amount of water in the admixture must also be considered in the water/cementitious material ratio. The time allowed from loading to discharge should be limited to 90 minutes. If the concrete is older but still has a placeable consistency, it may be used. Again the concern is that rettempering may be required as the concrete ages. If a high-range water reducer is being used, slumps should not be used as a basis of acceptance or rejection. The concrete should be used, regardless of the slump, as long as it is placeable or not segregated. The specified water/cement ratio should be the governing factor. The method of placement (pump, bucket, or conveyor), quantity, and spacing of reinforcement will also dictate what slump is necessary.

6.7 Testing

6.7.1 General

Measurement of mechanical properties during construction provides the basic information required to evaluate whether design considerations are met and the concrete is acceptable. Because high-strength concrete is more sensitive to testing variables than normal-strength concrete, the quality of these measurements is very important. Factors having little or no effect on 21-MPa (3000 psi) concrete can have significant effects on high-strength concrete, especially on compressive strength. Standard, established procedures such as the latest editions of ASTM C 31, ASTM C 39, and ASTM C 94 must be followed. Deviation from these procedures cannot be tolerated. Such deviations not only result in nonrepresentative tests but also introduce variations that cannot be compensated for.

6.7.2 Sampling

Statistical methods are an excellent means to evaluate high-strength concrete. For statistical procedures to be valid, the data (slump, unit weight, temperature, air content, and strength) should be derived from samples obtained by means of a random sampling plan designed to reduce the possibility that choice will be exercised by the testing technician. Random sampling means that any portion of the material being presented has an equal chance of being selected. The samples should represent the quality of concrete supplied; therefore, composite samples are taken in accordance with ASTM C 172. They should be combined and remixed to ensure uniformity prior to testing the freshly mixed concrete or casting test

specimens. These samples are representative of the quality of concrete delivered to the jobsite and may not truly represent the quality of the concrete in the structure, which may be affected by site transportation and placing methods. If additional test samples are required to check the quality of the concrete at the point of placement, as in pumped concrete, this should be established at the preconstruction meeting.

6.7.3 Extent of Testing

Tests for air content, unit weight, slump, and temperature should be made on the first truckload each day to establish that batching is adequate; thereafter, these tests should be performed on a random basis in accordance with project specifications. When visual inspection reveals inconsistent concrete, it should be rejected unless additional tests show it to be acceptable. Such test results should not be counted in the statistical evaluation of the mixture unless they are made on samples that are taken at random. The architect or engineer will generally take advantage of the fact that high-strength concrete containing fly ash or ground granulated blast-furnace slag develops considerable strength at later ages (that is, at 56 and 90 days). It is not uncommon, therefore, that more test specimens than normally required are specified. The technician should be prepared to take a large enough sample to properly accommodate the volume required to cast all test specimens. Under no circumstances should the technician use other samples to top-off test specimens. If the sample is too small, another sample should be taken; however, only a reasonable number of specimens can be made in a high-quality manner and within the correct time frame from collection of each sample. Where later ages are specified to enable the use of more economical mixes, it may be desirable to make an early assessment of potential strength by testing early-age specimens or specimens with accelerated curing.

6.7.4 Compressive Strength Specimens

Because one of the main interests in high-strength structural concrete is its strength in compression, compressive-strength measurements are of primary concern. The primary function of standard laboratory-cured specimens is to provide assurance that the concrete mix as delivered to the jobsite has the potential to meet contract-specification requirements. The potential strength and variability of the concrete can be established only by specimens made, cured, and tested under standard conditions. Cylindrical specimens used can be 150 mm (6-in.) by 300-mm long or 100 mm (4-in.) by 200 mm long. The use of the smaller cylinder is recommended, provided the test result is determined in accordance with ASTM C 39. Regardless of specimen size, the size used to determine mix proportions should be consistent with the size specified for acceptance testing and approved by the engineer of record.

6.7.4.1 Mold Type

The choice of mold material can have a significant effect on measured compressive strength. A given consolidation effort is more effective with rigidly constructed molds. Rigid single-use plastic molds with 6-mm (1/4-in.) wall thickness or greater have been used successfully for 112-MPa (16,000-psi) concrete. The mold type used for field specimens should be the same as the mold type used to develop the design mix. Molds should comply with ASTM C 470.

6.7.4.2 Testing Apparatus

The higher compressive loads carried by high-strength concrete put more demands on compression machines. Machine characteristics that may affect the measured strength include calibration accuracy, longitudinal and lateral stiffness, alignment of the machine components, type of platens, and the behavior of the platen spherical seating. Testing machines should meet the requirements of ASTM C 39. On the basis of practical experience, it is recommended that the machine have a load capacity at least 20% in excess of the expected cylinder breaking load, as premature damage and loss of calibration have been known to occur as a result of large numbers of explosive failures at high loads.

6.7.5 Prequalification of Testing Laboratories and Ready-Mix Suppliers

To prequalify a laboratory as well as a ready-mix supplier, both should be examined from two perspectives: how they have performed in the past and how well they are equipped to perform properly in the future. A review of past test data for high-strength concrete analyzed in accordance with ACI 214 will show that in-test variability is a measure of the testing consistency of the laboratory. The qualifications and experience of technicians and inspectors should be reviewed. The laboratory should be accredited or inspected for conformance to the requirement of ASTM C 1077 by a recognized agency such as the American Association for Laboratory Accreditation (AALA), AASHTO Materials Reference Laboratory (AMRL), National Voluntary Laboratory Accreditation Program (NV-LAP), Cement and Concrete Reference Laboratory (CCRL), or their equivalent. The architect or engineer should approve the testing laboratory. A comprehensive internal quality control protocol that covers test procedures; the use, care, and calibration of testing equipment; and the checking and reporting procedures to be followed provides evidence of a well-run laboratory. Depending on the results of the review of past and potential performance of the laboratory, some tests of personnel and equipment may or may not be made to conclude the prequalification examinations.

Acknowledgments

Part A of this chapter (Sections 6.1–6.4) is based on material from *Fundamentals of High-Performance Concrete*, 2nd ed., by E.G. Nawy (John Wiley & Sons, 2001); from *Reinforced Concrete: A Fundamental Approach*, 6th ed., by E.G. Nawy (Prentice Hall, 2008); from *Prestressed Concrete: A Fundamental Approach*, 5th ed., by E.G. Nawy (Prentice Hall, 2006); and from various committee reports and standards of the American Concrete Institute, Farmington Hills, MI.

References

- ACI. 1994. *ACI Manual of Concrete Practice 1994, Part I, Materials*. American Concrete Institute, Farmington Hills, MI.
- ACI. 1997–2008. *ACI Manual of Concrete Practice*, Vols. 1–5. American Concrete Institute, Farmington Hills, MI.
- ACI Committee 211. 1993. *Guide for Selecting Proportions for High-Strength Concrete with Portland Cement and Fly Ash*, 211.4R-93. American Concrete Institute, Farmington Hills, MI.
- ACI Committee 211. 1991a. *Standard Practice for Selecting Proportions for Normal, Heavyweight, and Mass Concrete*, ACI 211.1-91, 38 pp. American Concrete Institute, Farmington Hills, MI.
- ACI Committee 211. 1991b. *Standard Practice for Selecting Proportions for Structural Lightweight Concrete*, ACI 211.2-91, 14 pp. American Concrete Institute, Farmington Hills, MI.
- ACI Committee 212. 1983. Admixtures for concrete. In *ACI Manual of Concrete Practice 1983*, 212.1 R-81, 29 pp. American Concrete Institute, Farmington Hills, MI.
- ACI Committee 221. 1961. Selection and use of aggregate for concrete. *J. Am. Concrete Inst.*, 58(5), 513–542.
- ACI Committee 304. 1989. *Guide for Measuring, Mixing, Transporting and Placing Concrete*, 304-89. American Concrete Institute, Farmington Hills, MI.
- ACI Committee 308. 1992. *Standard Practice for Curing Concrete*, 308-92. American Concrete Institute, Farmington Hills, MI.
- ACI Committee 309. 1987. *Guide for Consolidation of Concrete*, 309R-87. American Concrete Institute, Farmington Hills, MI.
- ACI Committee 318. 2008a. *Building Code Requirements for Structural Concrete*, ACI Standard 318-08. American Concrete Institute, Farmington Hills, MI.
- ACI Committee 318. 2008b. *Commentary on Building Code Requirements for Structural Concrete*, ACI Standard 318-08. American Concrete Institute, Farmington Hills, MI.

- Addis, B.J. and Alexander M.G. 1990. A method of proportioning trial mixes for high strength concrete. In *Proceedings of the 2nd International Symposium on High-Strength Concrete*, ACI SP-121, pp. 287–308. American Concrete Institute, Farmington Hills, MI.
- ASTM. 1978. *Significance of Tests and Properties of Concrete and Concrete Making Materials*, Spec. Tech. Publ. 169B, 882 pp. American Society for Testing and Materials, Philadelphia, PA.
- ASTM. 1993. *Annual Book of ASTM Standards*. Part 14. *Concrete and Mineral Aggregates*, 834 pp. American Society for Testing and Materials, Philadelphia, PA.
- Cook, J.E. 1982. Research and applications of high strength concrete using Class C fly ash. *Concrete Int.*, 4(7), 72–80.
- Kosmatka, S.H. and Panarese, S.H., Eds. 1994. *Design and Control of Concrete Mixtures*, 13th ed., 212 pp. Portland Cement Association. Skokie, IL.
- NCSA. 1975. *Quality Concrete with Crushed Stone Aggregate*, CSC-3. National Crushed Stone Association, Washington, D.C.
- NCSA. 1976. *Stone Sand for Portland Cement Concrete*, National Crushed Stone Association, Washington, D.C.
- Nawy, E.G. 2001. *Fundamentals of High-Performance Concrete*, 2nd ed., 440 pp. John Wiley & Sons, Hoboken, NJ.
- Nawy, E.G. 2008. *Reinforced Concrete: A Fundamental Approach*, 6th ed., 934 pp. Prentice Hall, Upper Saddle River, NJ.
- Neville, A.M. 2001. *Properties of Concrete*, 5th ed., 844 pp. Pitman Books, London.
- Russell, H.G. 1993. Long-term properties of high-strength concretes. *Concrete Technol. Today*, 14(3), 1–4.



Framework for concrete wall. (Photograph courtesy of Portland Cement Association, Skokie, IL.)

7

Design and Construction of Concrete Formwork

David W. Johnston, P.E., Ph.D.*

7.1	Introduction	7-2
7.2	Types of Formwork.....	7-5
	Contact Surface Materials • Floor-Forming Systems • Column Forms • Wall Forms • Shoring • Bracing and Lacing • Other Forms and Components	
7.3	Formwork Standards and Recommended Practices.....	7-17
	American Concrete Institute Recommendations • OSHA Standards • American National Standards Institute • Scaffolding, Shoring, and Forming Institute Guides and Rules • American Society of Civil Engineers Standards • Information from Formwork Suppliers • General Material Design Standards	
7.4	Loads and Pressures on Formwork.....	7-23
	Vertical Loads • Lateral Pressures of Concrete • Horizontal Loads	
7.5	Formwork Design Criteria.....	7-27
	ASD Adjustment Factors for Lumber Stresses • Load Duration Factor (C_D) • Moisture Factor (CM) • Size Factor (C_F) • Flat-Use Factor (C_{fu}) • Beam-Stability Factor (C_L) • Column-Stability Factor (C_P) • Bearing-Area Factor (C_b) • Repetitive-Use Factor (C_r) • Adjustment Factors for Plywood Stresses • Manufactured Wood Products • Safety Factors for Formwork Accessories	
7.6	Formwork Design.....	7-35
	Determination of Resultants from Loads • Fundamental Relations between Resultants and Stresses • Basis of Examples	
7.7	Slab-Form Design Example.....	7-38
	Sheathing Design • Joist Design • Stringer Design • Shore Design • Bracing Design Considerations	
7.8	Wall-Form Design Example	7-43
	Sheathing Design • Stud Design • Wale Design • Tie Design • Bracing Design	
	References	7-49

* Edward I. Weisiger Distinguished Professor in Construction Engineering and Management, North Carolina State University, and Fellow of the American Concrete Institute and American Society of Civil Engineers; expert in the construction and performance of structures, formwork loadings and design, failure analysis, and bridge management systems.



FIGURE 7.1 Formwork serves as a mold to define concrete structure shape.



FIGURE 7.2 Formwork elements must support many heavy loads.

7.1 Introduction

Forms are extremely important in concrete construction. They mold the concrete to the required size and shape while controlling its position and alignment (Figure 7.1). Forms are self-supporting structures that are also sufficient to hold the dead load of the reinforcement and fresh concrete and the live load of equipment, workers, and miscellaneous materials (Figure 7.2). In building and designing formwork, three major objectives must be considered:

1. *Quality*—Forms must be designed and built with sufficient stiffness and accuracy so the size, shape, position, and finish of the cast concrete are attained within the required tolerances.
2. *Safety*—Forms must be built with sufficient strength and factors of safety so they are capable of supporting all dead and live loads without collapse or danger to workers and to the concrete structure.
3. *Economy*—Forms must be built efficiently, minimizing time and cost in the construction process and schedule for the benefit of both the contractor and the owner.



FIGURE 7.3 Large and complex placements require substantial formwork.

Economy is important because the costs of formwork often range from 35 to 60% or more of the total cost of the concrete structure. Considering the impact of formwork on total cost, it is critical that the structural engineer of the facility also design the facility structure for economy of forming, not just for economy of the materials in the finished structure.

Ideally, the builder will achieve maximum economy with no cost to either safety or specified quality. In designing formwork, the construction engineer can reduce costs by carefully considering the materials and equipment to be used; the fabrication, erection, and stripping procedures; and the reuse of forms. However, economy measures that result in either formwork failure or poor-quality products that require (often expensive) modification are self-defeating.

Correctly designed formwork will ensure that the concrete maintains the desired size and shape by having the proper dimensions and being rigid enough to hold its shape under the stresses of the concrete. It must be stable and strong to keep large sections of concrete in alignment (Figure 7.3). Finally, formwork must be substantially constructed so it can be reused and frequently handled while maintaining its shape. Formwork must remain in place until the concrete is strong enough to carry its own weight. In addition, the surface finish of the concrete is dependent on the contact material of the form.

The quality of the formwork itself has a direct impact on safety, accidents, and failures. A floor formwork system filled with wet concrete has its weight at the top and is not inherently stable. As a result, one of the most frequent causes of failure is from effects that induce lateral forces or displacement of supporting elements; therefore, inadequate cross-bracing or horizontal bracing is one of the most frequently involved factors in formwork failure. Poor bracing can make a minor failure turn into a major disaster, in what might be thought of as a domino effect or a **progressive failure**: A failure at one point in the formwork that can become an extensive collapse through chain reaction. Vibration is one factor that can trigger failure through inadequate bracing. Two other formwork problems are unstable soil under mudsills and shoring that is not plumb. Formwork is stable if adequately braced and built so all loads are carried to solid ground through vertical and bracing members.



FIGURE 7.4 Planning is required to achieve maximum overall construction efficiency.

Regardless of the quality of the formwork, premature removal of the forms or shores, often out of a wish for economy, can result in collapse or sagging. Sagging, while not an immediate problem, can lead to hairline cracks and extensive maintenance problems. Careless reshoring, often involving inadequate size, spacing, or attachment, can also cause damage or collapse. Specific related standards (e.g., OSHA, ACI, ASCE) for formwork are discussed in Section 7.3.

In addition to optimizing material in the form design process, there are three major factors to be considered when planning forms that are cost effective:

- Designing and planning for maximum reuse
- Economical form assembly
- Efficient setting and stripping

Each factor must be balanced with the other two to determine the most efficient form design.

In planning for maximum reuse, the specifications, rate of concrete strength gain, and local code requirements regarding stripping must be taken into account. The sooner a form can be stripped safely, the more practical it is to reschedule many reuses. In addition, for a minimum of cost, the least number of forms required for a smooth work schedule should be built. For example, the formwork on the outside of a spandrel beam can be stripped sooner than the formwork on the bottom; hence, fewer side forms than bottom forms must be built because they can be reused more frequently. It is also important to consider the labor involved in reuse; for example, does the form need to be disassembled and rebuilt? To create a plan for reuse, the construction engineer needs to make a detailed study of the work flow and construction sequence to determine the practical number of reuses that will result in smooth and efficient construction with the lowest total cost (Figure 7.4). When comparing designs, the construction engineer should calculate the ratio of total contact area of the formed concrete structure to the first-use form contact area for various alternatives, which is a general indication of overall reuse efficiency.

Several considerations are involved in determining an economical form construction, such as:

- Cost and feasibility of adapting materials on hand vs. cost of buying or renting new materials
- Cost of a higher grade of material vs. cost of lower grade of material plus labor to improve for required quality and use
- Selection of more expensive materials that provide greater durability and capability for reuse vs. less expensive materials that have a shorter use-life
- Building on-site vs. building in a central shop and shipping to site (this depends on the site itself and space available, the size of project, the distance of shipping, etc.)

An estimate of the cost of constructing a particular job-built form can be obtained by determining the quantity of wood materials required to make 1 square foot of contact area, while allowing for waste and rejection of some wood, and multiplying by the unit prices of lumber involved. This provides the contractor with an estimate of lumber costs for 1 square foot of contact area. In addition to lumber, the costs for labor, hardware, miscellaneous materials, handling, and clean-up must also be evaluated. The construction engineer should also consider the possibility of using prefabricated forms, either rented or purchased. The advantages of using rented prefabricated forms are reduced risk, no investment cost, and transfer of some management responsibility to the formwork supplier or subcontractor.

The last major factor, efficient setting and stripping practices, has a direct impact on the two already discussed. Reuse of a form is only fully efficient if the form can be stripped and rebuilt without too much labor time or damage to the form. The estimate for constructing a form must take into account the worker hours required to erect and dismantle the form during each reuse. When calculating time and cost for setting and stripping forms, the contractor should allow for delays from weather, equipment problems, etc., as well as cleaning and other miscellaneous expenses.

In addition to the above elements of cost, planning of formwork operations should consider the overall flow of operations, including the following:

- *Crew efficiency*—Providing a reasonable schedule creates a smooth daily repetition of the same operation so the workers can be familiar with their tasks and thus perform efficiently.
- *Concreting*—The ease and speed of pouring the concrete are directly related to the choice of design and the construction schedule.
- *Bar setting and other trades (mechanical, electrical, piping)*—Schedules of these activities must be coordinated with the concreting schedule so that all groups can work efficiently.
- *Cranes and hoists*—Plan to use appropriate cranes at times when they are not needed for other functions and reduce idle time.

7.2 Types of Formwork

Formwork components can be assembled in a wide variety of systems for casting many structural shapes. The terms **formwork** and **falsework** are often used in combination. Formwork is the total system of support for freshly placed concrete and includes the sheathing that is in contact with the concrete as well as all supporting members, hardware, and necessary bracing. Falsework is a temporary structure erected to support work in the process of construction. Falsework may be the temporary support for steel bridge girders, for precast concrete elements to be post-tensioned together, or for many other applications. When this term is used in relation to formwork, the forms are often considered to be the horizontal system of elements directly under heavier concrete placements, such as cast-in-place bridges (Figure 7.2), and the falsework includes the temporary girders, shores or vertical posts, and lateral bracing. Forms can either be job built or prefabricated. Job-built forms, frequently of wood (Figure 7.5), are most frequently selected where the shape does not conform to the constraints of commercial systems or where the economics are viable. Prefabricated forms can be purchased, rented, or rented with an option to buy. They are usually constructed substantially for the purpose of frequent reuse. These forms can either be ready made or custom made (Figure 7.6). The latter is designed for specialized use, usually on a single job, but is often reused multiple times on that project.



FIGURE 7.5 Wood column form.



FIGURE 7.6 Custom-made steel form with integrated access platforms.

7.2.1 Contact Surface Materials

The material serving as the contact face of forms is known as **sheathing** and sometimes is referred to as *lagging* or *sheeting* in specialty applications. Plywood is frequently used for sheathing, but some forms use steel sheet metal, steel plate, fiber-reinforced plastic, paperboard, wood boards, or other materials.

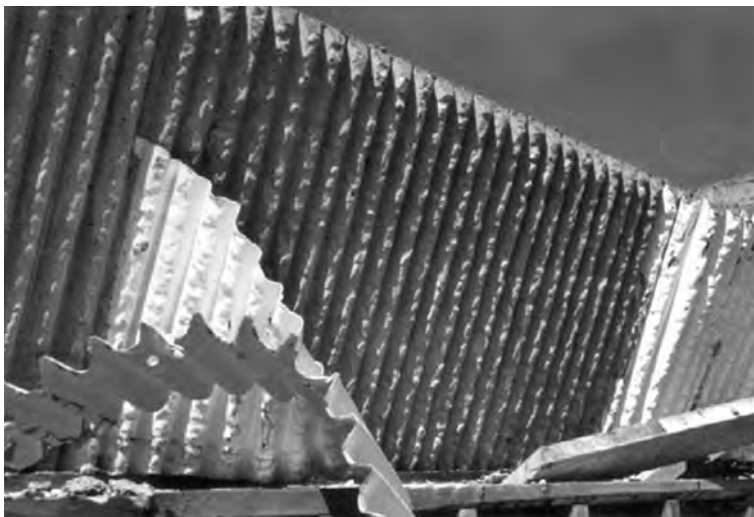


FIGURE 7.7 Plastic form liner used to create rough ribbed pattern.



FIGURE 7.8 Stay-in-place corrugated galvanized metal deck for bridge-slab form.

A primary characteristic in selection of the sheathing type and grade is the quality of surface required by the specification. For some applications, steel or high-density overlay plywood may be needed. In other cases where a decorative surface is required, the sheathing may be specially treated (wire brushing to expose wood grain, addition of rustication strips, etc.) or fitted with a commercial plastic **liner** imprinted or shaped to provide a specified design (Figure 7.7). **Permanent forms** are any form that remains in place after the concrete has developed its design strength. The form may or may not become an integral part of the structure. Metal deck forms, the most prevalent permanent form, are made of a ribbed or corrugated steel sheet, usually galvanized to reduce the potential for future rust staining, and are secured to the structure with clips or by welding. The diaphragm created by the attached deck may also contribute to the lateral stability of the supporting members during concrete placement. Metal deck forms are used in floor and roof slabs cast over steel joists or beams, in bridge decks (Figure 7.8), and over pipe trenches and other inaccessible locations where removing wood forms is impractical. Precast concrete deck forms are often used in combination with prestressed concrete bridge girders. Sometimes

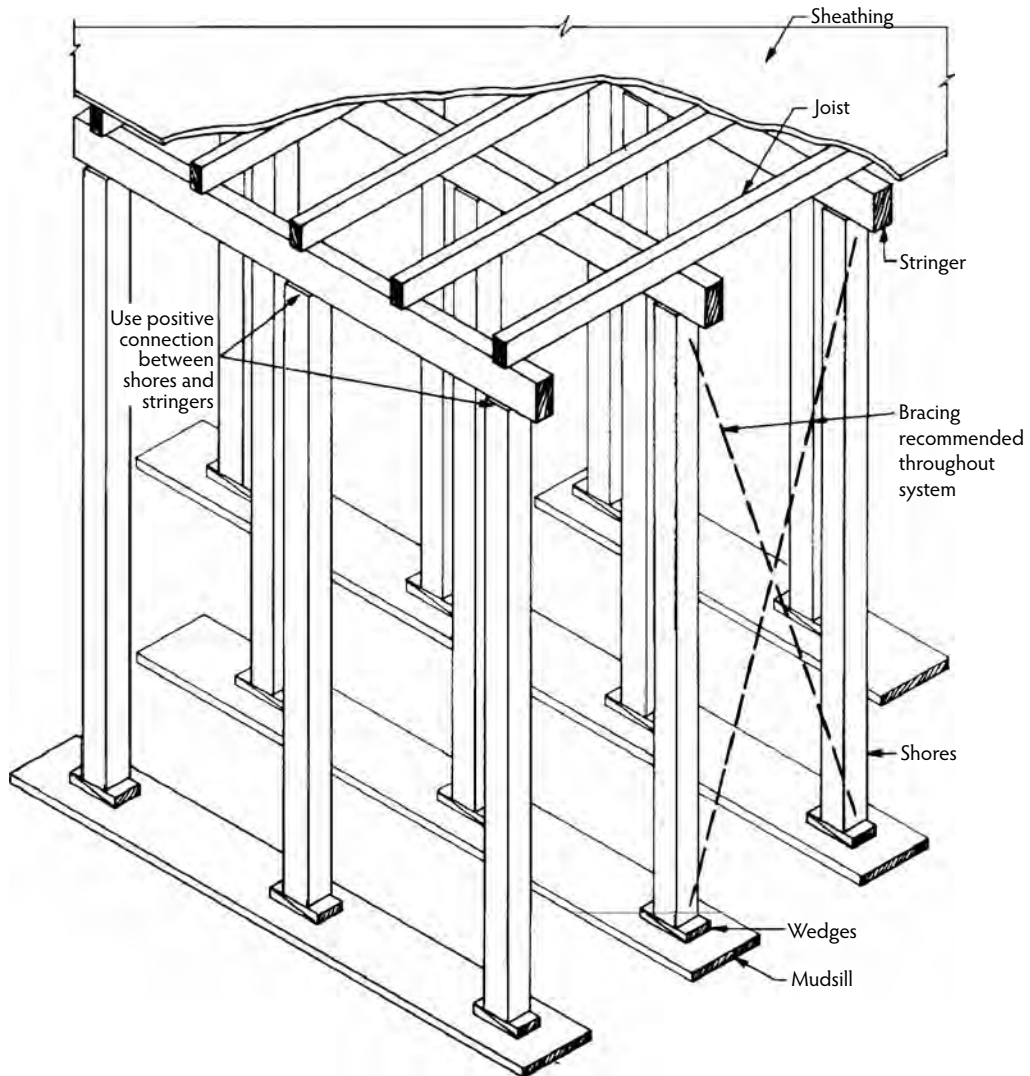


FIGURE 7.9 Typical elevated flat-slab formwork elements. (From Hurd, M.K., *Formwork for Concrete*, 7th ed., SP-4, American Concrete Institute, Farmington Hills, MI, 2005.)

the deck forms must be temporarily shored at intermediate points to support the loads applied during construction; however, deck forms of adequate section profile can often be selected to span between the permanent structural members and safely support the weights of reinforcement, fresh concrete, and construction live loads. In the latter case, the added cost of the stronger section is often offset by savings in shoring materials and labor.

7.2.2 Floor-Forming Systems

Floor-forming systems vary somewhat with the configuration of the concrete floor system being cast. Figure 7.9 illustrates the basic wood member arrangements for flat-plate floors, most areas of flat slabs, and the slab areas of slab and beam floors. The terms used to describe the members are the same in systems assembled from steel or aluminum members. The **joist** is a horizontal structural member supporting the deck-form sheathing and usually rests on stringers or ledgers. **Stringers** are horizontal structural members usually (in slab-forming) supporting joists and resting on vertical supports such as shores.



FIGURE 7.10 Fiber-reinforced plastic pan and dome molds for floor formwork.

In one-way (pan joist) and two-way (waffle) joist construction, a similar layout is usually adopted. **Pans and domes** (Figure 7.10) are used in concrete joist construction, which is a cast-in-place floor system with a thin slab integral with regularly spaced joists that span to beams and columns. In some cases, the pans or domes are placed on the plywood sheathing; in other cases, the pan or dome edges are supported on wide joists, and the sheathing is omitted. Pans are prefabricated form units, usually steel or fiberglass, used to form single-direction joists. Domes, also usually made of steel or fiberglass, are square pan forms used in two-way, or waffle, concrete joist construction.

Steel and aluminum joists and stringers are usually flanged shapes. Some aluminum extrusions have special configurations allowing easy connection and incorporating a top channel for a wood nailer. Commercial steel sections fabricated specifically for formwork systems also incorporate connection features. **Horizontal shoring** is formed by adjustable beams, trusses, or combinations of the two that support formwork over clear spans and eliminate numerous vertical supports. Metal or timber support beams are used for small spans. Telescoping shores, steel lattice, plate, or box members are used to support forms in spans of 6 to 30 feet. Heavy-duty horizontal shores (for example, trusses supporting flying-form panels) can span up to 80 feet. The disadvantage of using horizontal shoring is the potential need for special bearing plates to support the high end load on each individual shore.

Flying forms, or table forms, are large crane-handled sections of floor formwork (frequently including supporting truss, beam, or scaffolding frames) that are completely unitized. Such forms can be lowered for clearance under joists or beams, rolled out the face of the building bay, picked by a crane, and reset at the next floor level. By having a large movable unit, the costs of stripping and reassembly are reduced, particularly when a crane is available on site.

7.2.3 Column Forms

Column-form materials tend to vary with the column shape. Wood or steel is often used with square or rectangular columns (Figure 7.11). Round column forms (Figure 7.12), more typically premanufactured in a range of standard diameters, are available in steel, paperboard, and fiber-reinforced plastic. Square and rectangular forms are composed of short-span bending elements contained by external ties or clamps. Round column forms are more structurally efficient because the internal concrete pressures can be resisted by a hoop membrane tension in the form skin with little or no bending induced. Round, single-piece glass-fiber-reinforced plastic tubes with a single joint can be removed from the column without cutting. They are held together with either bolts or clamps. Round paperboard tubes are single-use forms that are stripped by unwrapping and then discarded. They can be cut to the exact length needed, and sections of the tube can be adapted to making partial column sections (e.g., half-round, quarter-round). Steel column forms have built-in bracing for short heights so the only external bracing required serves to keep the column plumb and for taller columns. Both half-round and rectangular panel units are available in various section heights that can be connected vertically to form tall columns. Round steel forms are generally used for larger columns and bridge piers and come in diameters ranging from about 14 inches to 10 feet.



FIGURE 7.11 Modular steel form for rectangular columns.



FIGURE 7.12 Steel round-column form with access scaffolding in preparation.

7.2.4 Wall Forms

Wall forms principally resist the lateral pressures generated by fresh concrete as a liquid or semi-liquid material. The pressures can be quite large, certainly many times the magnitude of live loads on permanent floors. Thus, wall form design often involves closely spaced and well-supported members, as shown in Figure 7.13. As mentioned, the contact surface of the wall form is referred to as *sheathing*. **Studs** are

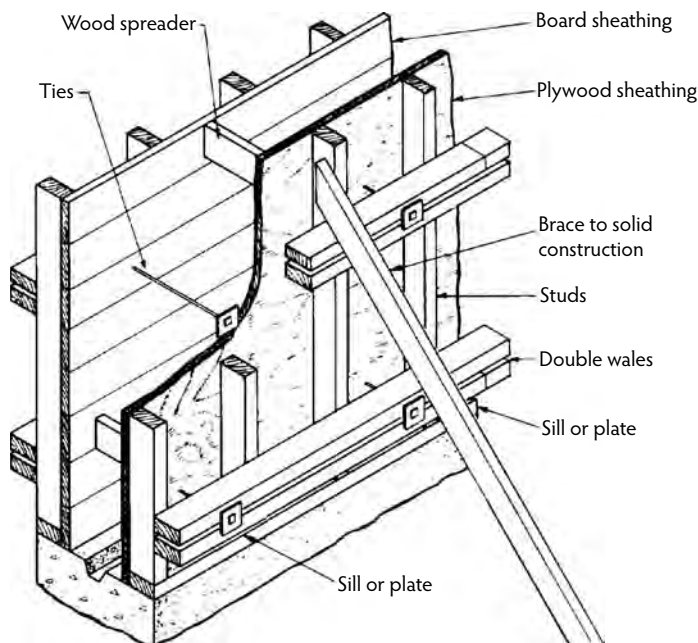


FIGURE 7.13 Typical wall form components with alternate sheathing materials illustrated. (From Hurd, M.K., *Formwork for Concrete*, 7th ed., SP-4, American Concrete Institute, Farmington Hills, MI, 2005.)

vertical supporting members to which sheathing is attached. **Wales** are long horizontal members (usually double) used to support the studs. The studs and wales are often wood, steel, or aluminum beam-like elements. Commercial form suppliers are innovative in devising elements as well as hardware for connections. The wall form members are sometimes oriented with the stud members placed horizontal rather than vertical, and the wales are run vertical.

The wales are in turn supported on washer plates or other bearing devices attached to form ties. A concrete **form tie** is a tensile unit connecting opposite sides of the form and providing a link for equilibrium. Form ties are usually steel, although some fiber-reinforced plastic ties are also available. The ties come in a wide range of types (Figure 7.14) and tension working capacities rated by the manufacturer. Snap ties, loop ties, and flat ties are single-use ties, usually of relatively low capacity (1500 to 3200 lb) that are twisted and snapped off a specified distance back from the concrete surface. Coil ties, she bolts, and he bolts are examples of ties where some parts are left embedded within the cast wall and some parts can be reused. The taper tie, a tapered rod threaded on each end, is completely removed and reused. The tension capacity of heavy ties can range upward to over 60,000 lb. Some of the ties have built-in provisions for spacing the forms a definite distance apart; this is particularly true of single-use ties if this feature is ordered. An alternative means of maintaining the correct inside distance is by means of a **spreader**, a strut (usually of wood) inserted inside the forms that can be retrieved with an attached rope or wire when the concrete placement reaches that level.

Strong-backs, frames attached to the back of a form or additional vertical wales placed outside horizontal wales, are sometimes added for strength, to improve alignment, or to assemble a ganged form. **Gang forms** (Figure 7.15) are prefabricated panels joined to make a much larger unit for convenience in erection, stripping, and reuse; they are usually braced with wales, strong-backs, or special lifting hardware. Such units require the use of a crane for stripping and resetting.

Panel forms, sections of form sheathing constructed from boards, plywood, metal, etc. that can be erected and stripped as units, are primarily used in wall construction. They may be adapted for use as slab or column forms. The four basic types of panel forms are unframed plywood, plywood in a metal frame (Figure 7.16), all-metal, and heavier steel frame. The first two are most frequently used for general light

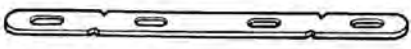
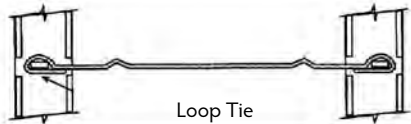

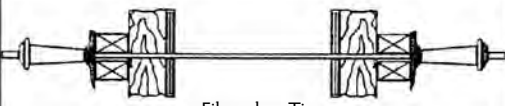

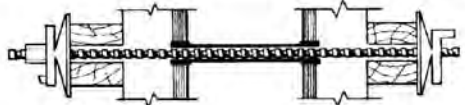

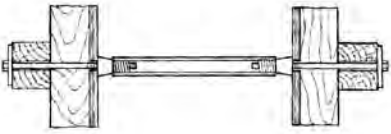
One-Piece Ties		Used to secure and space modular panel forms Available in several configurations Notched for breakback Safe Loads 1500, 2250, and 3000 lb
		Secures and spaces prefabricated modular forms Notched for a 1-in. breakback Crimp is anti-turn feature Safe Loads: 2250 and 3000 lb
		Used for job-built forms, lighter construction May have cone spreader and waterseal washer Notched for 1-in. breakback Safe Loads: 2250 and 3350 lb
		Long lengths supplied for cutting as desired on the job Custom colors available Cut off flush with surface of hardened concrete Safe Loads: 3000, 7500, and 25,000 lb
		Used where specs require or permit complete removal of tie from concrete Tie is reusable Safe Loads: 7500 to 50,000 lb
		Standard 20-ft lengths cut to meet project requirements Double nuts may be needed for higher load capacities Bar is reusable Safe Loads: 10,000 to 32,500 lb
Internally Disconnecting Ties		Heavy duty, with reusable end bolts No internal spreader, but external spreader bracket available Safe Loads: 4900 to 64,000 lb Up to 155,000 in High-Strength Steel
		Designed for medium to heavy construction With or without cone spreaders Bolts reusable Safe Loads: Two-strut, 3000 to 13,500 lb; Four-strut, 9000 to 27,000 lb

FIGURE 7.14 Examples of form ties. (From Hurd, M.K., *Formwork for Concrete*, 7th ed., SP-4, American Concrete Institute, Farmington Hills, MI, 2005.)

construction and erecting walls with heights ranging from 2 to 24 feet. Both are sometimes backed by steel braces. All-metal panel forms can be made of either steel or aluminum. The heavier steel frame panel forms are faced with either wood or plywood and are used for projects involving large pressures or loads.

Slip forms are forms that move, usually continuously, during placing of the concrete. Movement may be either horizontal or vertical. Slip-forming is like an extrusion process, with the forms acting as moving dies to shape the concrete. In wall forming, the slip form is usually moved vertically at a rate of 6 to 12 inches per hour. This method can be economical when constructing concrete cores of tall buildings, tall concrete stacks, and concrete towers.



FIGURE 7.15 Ganged forms allow movement by crane and reduce re-erection costs.

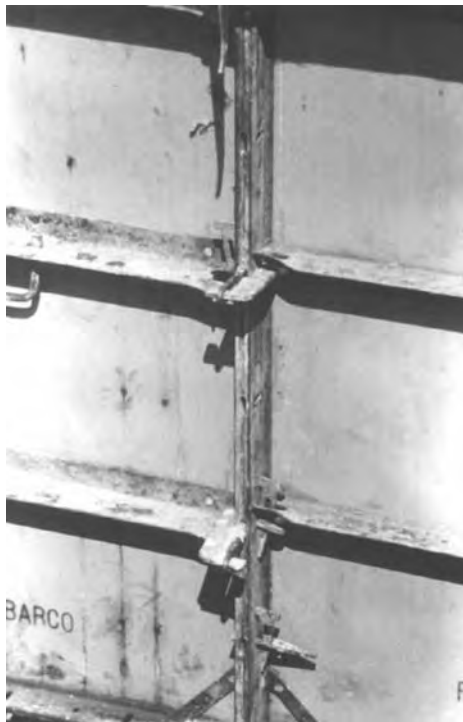


FIGURE 7.16 Steel-framed plywood panel system with integrated loop-tie anchors.

Climbing forms, or **jump forms**, are forms that are raised vertically for succeeding lifts of concrete in a given structure, usually supported by anchors embedded in the previous lift. The form is moved only after an entire lift is placed and (partially) hardened; this should not be confused with a slip form that moves during placement of the concrete. Support of the climbing form is usually provided by anchors cast in the previous placements. It is critical that the concrete strength gain at the anchors be sufficient at each stage of the operation to resist the imposed loads.

Although the use of proper support chairs for reinforcement is routinely required in horizontal construction, similar elements are sometimes neglected in wall and column forms. **Side form spacers** are devices similar to chairs that can be used to advantage in wall and column forms to attain correct cover for the reinforcement.

7.2.5 Shoring

Shores are vertical or inclined column-like compression supports for forms. Shoring systems may be made of wood or metal posts, scaffold-type frames, or various patented members. **Scaffolding** is an elevated platform to support workmen, tools, and materials. In concrete work, heavy-duty scaffolding is often adapted to double as shoring. The simplest type of vertical shore is a 4×4 or 6×6 piece of lumber with special hardware attached to the top to facilitate joining to the stringers with a minimum of nailing. Metal shore-jack fittings may be placed at the lower end of the shore to allow some adjustment for exact height. Various manufacturers sell all-metal adjustable shores, also known as **jack shores** or simply as *jacks*, in a number of designs. They are usually available in adjustable heights from 6 to 16 ft and can carry working loads ranging from 2500 to 9000 lb with a safety factor of 2.5, depending on the type and the length of the shore. A third type of vertical support is a device that attaches to a column or bearing wall of the structure. Components of this kind of shore include friction collars and shore brackets that are attached to the support with through bolts or heavy embedded anchors. These attached supports are particularly useful in supporting slab-forming systems.

Basic scaffold-type shoring is made from tubular steel frames. End frames are assembled with diagonal bracing, locking connections, and adjustable bases to create a shoring tower. These may have flat top plates, U-heads, or other upper members for attaching to supported forms. Most scaffold-type shoring has a safe working load between 4000 and 25,000 lb per leg, depending on the height, bracing, and construction of the tower (Figure 7.17). Ultra-high-load shoring frames can support up to 100,000 lb of load per leg. Scaffold-type shoring can also be made of tubular aluminum, which has the advantage of being more lightweight than a similar steel frame.

In multistory concrete building construction (Figure 7.4), a process called **shoring and reshoring** is used (ACI Committee 347, 2005). The weight of the fresh concrete, reinforcing, forms, and construction live load for an individual floor usually exceeds the design live-load capacity of the floor below. Furthermore, that floor has not gained full 28-day strength, as floors are often cast at intervals of 4 to 14 days. By interconnecting several floors with shores and reshores, the loads at the top can be distributed over several floors. When this construction process is engineered and controlled properly, the time-varying loads on all elements (floors, forms, shores, and reshores) are safely within their time-varying strengths. One or more sets of floor forms with shores may be used. After the forms and shores are stripped completely from the lowest form-supported floor, that floor and the cast floors above deflect and must share the equivalent of the support that has been removed. Reshores are then placed under the stripped floor. **Reshores** are shores placed snugly under a concrete floor so future loads imposed from construction at the highest level can be shared over sufficient floors to carry the dead and live loads safely.

In some multistory construction, this process is varied slightly. **Backshores** are shores placed snugly under a concrete slab or structural member after the original forms and shores have been removed from a small area without allowing the slab or member to deflect or support its own weight or existing construction loads from above. **Preshores** are added shores placed snugly under selected panels of a deck-forming system before any primary (original) shores are removed. Preshores and the panels they support remain in place until the remainder of the bay has been stripped and backshored, a small area at a time.

Shoring systems produced by some manufacturers include a **drophead** mechanism (Figure 7.18). The systems include panels, beams, and a shore with a top plate that is in direct contact with the concrete slab underside. When the drophead mechanism is released, the beams and panels can be lowered and removed while the shore stays in place. This allows rapid reuse of the panels and beams while the shore continues to support the early-age, low-strength slab. Overall, this approach allows rapid reuse of components, increasing speed of construction and reducing forming materials needed. Keeping the shores

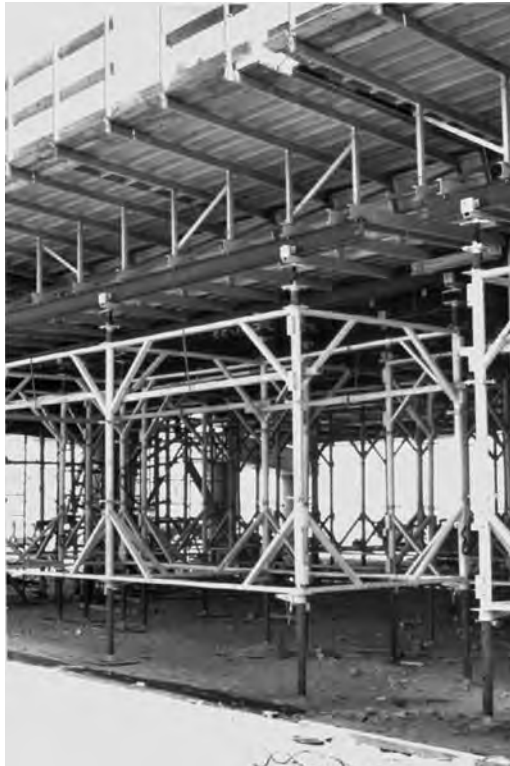


FIGURE 7.17 Shoring towers used for bridge falsework.



FIGURE 7.18 Drop-head shore allowing removal of panels and beams. (Figure courtesy of MEVA Formwork Systems, Haiterbach, Germany.)

in place longer under the most recently placed slab also increases safety. After appropriate slab strength gain to support the slab self-weight and construction loads, the slab is activated by releasing the shores and then resnugging them to act as reshores.



FIGURE 7.19 Precast concrete mudsills distribute bridge falsework load to soil.

Centering is a specialized temporary vertical support used in construction of arches, shells, and space structures where the entire temporary support is lowered (**struck** or **decentered**) as a unit to avoid introduction of injurious stresses in any part of the structure. Shores that are supported on the ground must have a temporary footing (termed, in formwork, a **mudsill**) that is of adequate strength and size (Figure 7.19). The mudsill may be a plank, wood grillage, or precast pad, depending on the loads and ground conditions.

7.2.6 Bracing and Lacing

A brace is any structural member used to support another, always designed for compression loads and sometimes for tension under special load conditions. In formwork, **diagonal bracing** is a supplementary (not horizontal or vertical) member designed to resist lateral load. Form braces are frequently made of wood or steel. Commercial steel pipe braces in various diameters and wall thicknesses and load-rated for adjustable lengths are popular. Buckling strength of braces is always a primary design consideration. **Horizontal lacing**, horizontal members attached to shores or braces to reduce their unsupported length, can thus increase the available load capacity. Both bracing and lacing must be adequately connected at each end. This can be accomplished with bolts, nails, and a variety of commercial devices, depending on the materials involved. When attaching braces to the ground, a buried or above-ground concrete mass known as a *deadman* is sometimes used (Figure 7.20).

7.2.7 Other Forms and Components

The above represents only a brief summary of some of the most typical form elements. Many other configurations must be considered in many jobs. Beam forms are somewhat like short wall forms in that lateral pressures must be resisted; however, they also involve concentrations of vertical load, requiring strong bottom forms and more shoring. The casting of footings sometimes requires forming where the concrete cannot be cast against vertical earth sides. This forming often must be braced from the outside to hold the lateral pressure of the earth if the width of the foundation is large. Supplementary forming elements such as **templates** are often incorporated in foundation forms to precisely locate anchor bolts and dowels (Figure 7.21). Where concrete elements must be subdivided into two or more placement sections, a form **bulkhead** is usually placed, either as a construction joint or as an end closure. The bulkhead, although involving short spans, must be carefully designed and connected as it must resist the same pressure magnitudes as the faces of the form.



FIGURE 7.20 Formwork brace anchored to buried concrete mass.

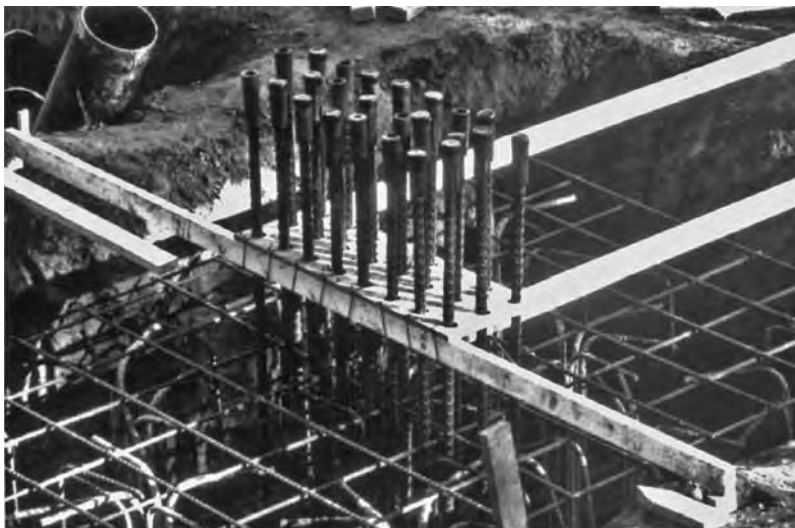


FIGURE 7.21 Plywood templates secure dowels or anchor bolts at correct position.

Forms may also incorporate a host of other features. **Chamfer strips** are triangular or curved inserts placed in the inside corner of a form to produce a rounded or beveled corner. These are often specified in rectangular columns and at outside corners of walls. **Cleanouts** are openings sometimes provided at the bottom of wall or column forms for removal of refuse before the concrete is placed to ensure a good construction joint. There must be a means of closing and supporting the cleanout door to resist concrete pressure. **Wrecking strips** are small pieces or panels fitted into a formwork assembly in such a way that they can be easily removed ahead of the main panels or sections, making it easier to strip the major form components. Various references, such as Hurd (2005) and form-supplier catalogs, provide numerous illustrations of formwork details.

7.3 Formwork Standards and Recommended Practices

Ultimately, formwork safety is dependent on the system in place on individual projects to ensure proper and safe design, fabrication, handling, erection, inspection, monitoring, and stripping of the forms and supports (Figure 7.22). As noted earlier, formwork materials and labor are roughly equal in cost to the concrete and reinforcing materials and placing labor. The loads supported by formwork



FIGURE 7.22 Guardrails and rated, well-maintained access ladders are components of a safety system.

(say, for an individual floor) are usually similar in magnitude to the loads supported by the finished structure and are sometimes much greater. Thus, it is justifiable for the design and planning of formwork to require the significant time of a professional, just as is required for design of the structure of the facility being built. Savings can accrue from a well planned and designed system. This section summarizes some of the resources available to the construction engineer to guide the planning and design of formwork. Most of the resources are in the form of guides or recommended practices. Except for some provisions of OSHA, there has previously been no uniformly mandated standard in the United States for design of temporary structures such as formwork; however, this is in the process of change, as is noted in the following sections. As in all engineering work, the construction engineer should seek the most recent edition of the following resources. Most standards are updated or reconfirmed on a cycle of 6 years or less.

7.3.1 American Concrete Institute Recommendations

Prior to about 1958, formwork was designed based on only limited data and guidance for loads. At that time, recommendations for loads and pressures for the design of formwork became available from the American Concrete Institute (ACI). These recommendations have evolved over the years and are available in three often-consulted and periodically updated ACI publications:

- *Guide to Formwork for Concrete*, ACI 347-04 (ACI Committee 347, 2004)
- *Formwork for Concrete*, 7th ed., ACI SP-4 (Hurd, 2005)
- *Guide for Shoring and Reshoring of Multistory Concrete Buildings*, ACI 347.2R (ACI Committee 347, 2005)

The first provides the recommended practice for design and construction of formwork, including recommendations for loads and pressures. The second is a manual that extensively describes systems and provides design procedures, design aids, and examples. The third provides methods for determining shore, reshore, and early-age slab loads during multistory building construction. ACI also publishes, through its journals and other monographs, numerous articles on concrete formwork as well as guides for craftspersons involved in formwork fabrication and erection. ACI Committee 347 recommendations for loads and pressures to be applied in the design of formwork are discussed more thoroughly in Section 7.4 of this chapter.



FIGURE 7.23 Fall-protection nets.



FIGURE 7.24 Work platform being installed on tall wall form.

7.3.2 OSHA Standards

By the early 1970s, legislation to establish the Occupational Health and Safety Administration (OSHA) began to have an impact on formwork. OSHA expectations not only include an adequate temporary structure but also emphasize components for worker fall protection (Figure 7.23 and Figure 7.24) and procedures for safe handling and erection of formwork. Some states have their own requirements that are different from, but cannot be less restrictive than, the federal requirements. Sections of the federal OSHA *Occupational Safety and Health Standards for the Construction Industry* (29 CFR, Part 1926) particularly affecting formwork planning, design, and execution includes the following requirements:

- Subpart L—Scaffolding
- Subpart M—Fall Protection
- Subpart Q—Concrete and Masonry Construction

Subpart Q contains sections on scope, application, and definitions; general requirements; equipment and tools; cast-in-place concrete; precast concrete; lift-slab operations; and masonry construction. Of primary interest here is the following section on cast-in-place concrete:

§ 1926.703 Requirements for cast-in-place concrete.

(a) General requirements for formwork.

(1) Formwork shall be designed, fabricated, erected, supported, braced, and maintained so that it will be capable of supporting without failure all vertical loads that may reasonably be anticipated to be applied to the formwork. Formwork which is designed, fabricated, erected, supported, braced, and maintained in conformance with the Appendix to this section will be deemed to meet the requirements of this paragraph.

(2) Drawings or plans, including all revisions, for the jack layout, formwork (including shoring equipment), working decks, and scaffolds, shall be available at the jobsite.

(b) Shoring and reshoring.

(1) All shoring equipment (including equipment used in reshoring operations) shall be inspected prior to erection to determine that the equipment meets the requirements specified in the formwork drawings.

(2) Shoring equipment found to be damaged such that its strength is reduced to less than that required by § 1926.703(a)(1) shall not be used for shoring.

(3) Erected shoring equipment shall be inspected immediately prior to, during, and immediately after concrete placement.

(4) Shoring equipment that is found to be damaged or weakened after erection, such that its strength is reduced to less than that required by § 1926.703(a)(1), shall be immediately reinforced.

(5) The sills for shoring shall be sound, rigid, and capable of carrying the maximum intended load.

(6) All base plates, shore heads, extension devices, and adjustment screws shall be in firm contact, and secured when necessary, with the foundation and the form.

(7) Eccentric loads on shore heads and similar members shall be prohibited unless these members have been designed for such loading.

(8) Whenever single post shores are used one on top of another (tiered), the employer shall comply with the following specific requirements in addition to the general requirements for formwork:

(i) The design of the shoring shall be prepared by a qualified designer and the erected shoring shall be inspected by an engineer qualified in structural design.

(ii) The single post shores shall be vertically aligned.

(iii) The single post shores shall be spliced to prevent misalignment.

(iv) The single post shores shall be adequately braced in two mutually perpendicular directions at the splice level. Each tier shall also be diagonally braced in the same two directions.

(9) Adjustment of single post shores to raise formwork shall not be made after the placement of concrete.

(10) Reshoring shall be erected, as the original forms and shores are removed, whenever the concrete is required to support loads in excess of its capacity.

(c) Vertical slip forms.

(1) The steel rods or pipes on which jacks climb or by which the forms are lifted shall be

(i) Specifically designed for that purpose; and

(ii) Adequately braced where not encased in concrete.

- (2) Forms shall be designed to prevent excessive distortion of the structure during the jacking operation.
 - (3) All vertical slip forms shall be provided with scaffolds or work platforms where employees are required to work or pass.
 - (4) Jacks and vertical supports shall be positioned in such a manner that the loads do not exceed the rated capacity of the jacks.
 - (5) The jacks or other lifting devices shall be provided with mechanical dogs or other automatic holding devices to support the slip forms whenever failure of the power supply or lifting mechanism occurs.
 - (6) The form structure shall be maintained within all design tolerances specified for plumbness during the jacking operation.
 - (7) The predetermined safe rate of lift shall not be exceeded.
- (d) Reinforcing steel.
- (1) Reinforcing steel for walls, piers, columns, and similar vertical structures shall be adequately supported to prevent overturning and to prevent collapse.
 - (2) Employers shall take measures to prevent unrolled wire mesh from recoiling. Such measures may include, but are not limited to, securing each end of the roll or turning over the roll.
- (e) Removal of formwork.
- (1) Forms and shores (except those used for slabs on grade and slip forms) shall not be removed until the employer determines that the concrete has gained sufficient strength to support its weight and superimposed loads. Such determination shall be based on compliance with one of the following:
 - (i) The plans and specifications stipulate conditions for removal of forms and shores, and such conditions have been followed, or
 - (ii) The concrete has been properly tested with an appropriate ASTM standard test method designed to indicate the concrete compressive strength, and the test results indicate that the concrete has gained sufficient strength to support its weight and superimposed loads.
 - (2) Reshoring shall not be removed until the concrete being supported has attained adequate strength to support its weight and all loads in place upon it.

APPENDIX TO § 1926.703(a)(1) General requirements for formwork. (This Appendix is non-mandatory.)

This appendix serves as a non-mandatory guideline to assist employers in complying with the formwork requirements in §1926.703(a)(1). Formwork which has been designed, fabricated, erected, braced, supported, and maintained in accordance with Sections 6 and 7 of the American National Standard for Construction and Demolition Operations—Concrete and Masonry Work, ANSI A10.9-1983, shall be deemed to be in compliance with the provision of § 1926.703(a)(1).

7.3.3 American National Standards Institute

The standard suggested in the above OSHA provisions as a means for achieving compliance is the American National Standard for Construction and Demolition Operations—Concrete and Masonry Work—Safety Requirements, ANSI A10.9-1997(R2004). Section 6, on vertical shoring, has provisions for loads and design, field practices, removal, tubular welded frame shoring, tube and coupler tower shoring, and single-post shores. Section 7, on formwork, has provisions for loads, formwork design, placing and removal of forms, vertical slip forms, flying-deck forms, and horizontal shoring beams. Most of the load and design provisions refer to the ACI Committee 347 *Guide to Formwork for Concrete* as the procedure to follow.

7.3.4 Scaffolding, Shoring, and Forming Institute Guides and Rules

This industry-supported institute publishes many relevant guides, rules, and training aids related to formwork and its support systems. Examples include the following:

- Scaffold Code of Safe Practice
- Safety Procedures for Vertical Formwork
- Flying and Handling Concrete Formwork
- The Difference Between Scaffolding and Shoring
- Wind Loads and Shoring
- Safe Practices for Erecting and Dismantling Frame Shoring
- Horizontal Shoring Beam Safety Rules
- Single Post Shore Safety Rules
- Rolling Shore Bracket Safety Rules
- Recommended Frame Shoring Erection Procedures
- Flying Deck Form Safety Rules

7.3.5 American Society of Civil Engineers Standards

A committee of the American Society of Civil Engineers has developed ASCE 37-02 *Design Loads on Structures during Construction*, a standard for loads imposed on structures during construction, including temporary structures. The standard covers many topics, including loads for formwork, falsework, and shoring. The loads and pressures imposed by concrete, construction interval winds, and other sources are defined. For wind loadings, reference for analysis method is made to ASCE 7, but ASCE 37 defines wind velocity reductions reflecting the short period of exposure during construction. As with any voluntary consensus standard, it is available for groups to specify in individual contracts, or it could be cited as the standard for use by government agencies in rule making. Although various guides and industry practices have been available for many years for the design of formwork, this standard makes available for the first time in the United States a document that defines loads in mandatory language that can be incorporated in contracts, codes, and safety laws.

7.3.6 Information from Formwork Suppliers

Formwork suppliers, of course, publish literature defining their products and limitations for their use. Data sheets indicate the load ratings of products such as form ties, shores, braces, wales, etc. for reference by form designers of job-built systems. In addition, many form manufacturers supply preengineered formwork systems (Figure 7.25) under rental or purchase arrangements for individual projects or general use. Such systems will come with rules and limitations whose implementation is required by the contractor as part of the rental or sales agreement. It is critical that these requirements be implemented as the normal procedures for use and for training workers involved with the formwork.

7.3.7 General Material Design Standards

Although they do not specifically address formwork, the same criteria used for the design of permanent structures in any particular material should also be applied to the design of formwork once the loads and safety factors appropriate for formwork have been determined. Most forms are made of wood, steel, or aluminum or some combination of these materials. The usual reference design standards for these materials are as follows:

- *National Design Specification for Wood Construction*, ASD/LRFD, ANSI/AF&PA NDS-2005, American Forest & Paper Association, Washington, D.C., 2005
- *Steel Construction Manual: Allowable Stress Design*, 13th ed., American Institute of Steel Construction, Chicago, 2005



FIGURE 7.25 Preengineered wall form system.

- *Aluminum Design Manual*, The Aluminum Association, Arlington, VA, 2005
- *Plywood Design Specification*, APA—The Engineered Wood Association, Tacoma, WA, 1997

The use of *allowable stress design* (ASD) currently dominates in the design of formwork, but use of the *load and resistance factor design* (LRFD) method is expected to gradually increase. Addresses for many of the above sources of standards and specifications are given following the references at the end of this chapter.

7.4 Loads and Pressures on Formwork

The possible loads acting on formwork are many. Vertical loads are usually associated with the dead load of the placed concrete and formwork and the live load of workers and their equipment. Internal pressures on vertical formwork result from the liquid or semi-liquid behavior of the fresh concrete. External forces such as wind exert horizontal loads on the forms, requiring bracing systems for lateral form stability.

7.4.1 Vertical Loads

Vertical loads acting on formwork (Figure 7.26) include the self-weight of the forms, the placed reinforcement, the weight of fresh concrete, the weight of the workers, and the weight of placing equipment and tools. The dead load of the concrete is usually estimated at 145 to 150 lb/ft³, including an allowance for normal amounts of reinforcement. In cases where the reinforcement appears to be heavy, the materials should be calculated separately to determine the actual unit weight. Adjustments are also made for lightweight concrete densities. An 8-in. normal weight slab thus imposes a dead load of 150 lb/ft³ × (8 in./12 in./ft), or 100 psf, on horizontal formwork. ACI Committee 347 (2004) recommends that horizontal formwork be designed for a minimum vertical live load of 50 psf to allow for workers and their incidental

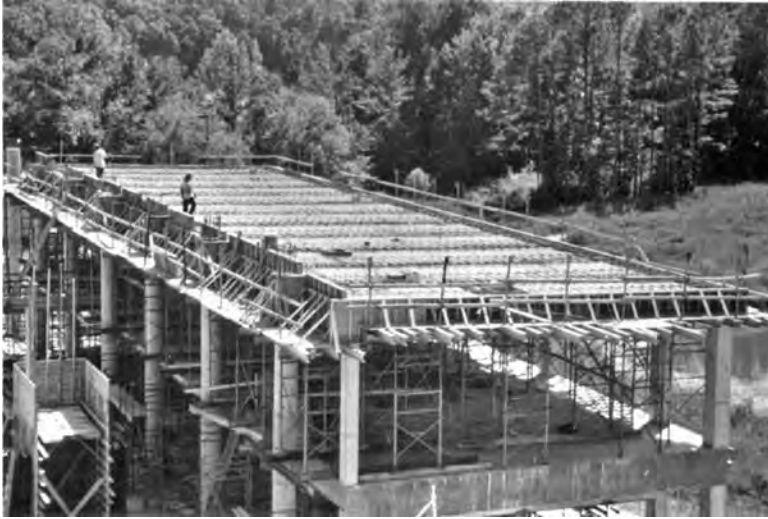


FIGURE 7.26 Weights of concrete, reinforcing, and formwork contribute to dead load.

placing tools such as screeds, vibrators, and hoses. When motorized carts or buggies are used, a minimum live load of 75 psf is recommended. Furthermore, it is recommended that the minimum combined total design dead and live load should be no less than 100 psf, or 125 psf if motorized buggies are used. Formwork self-weight can be calculated from the unit weights and sizes of the components. The weight of the formwork is often much less than the dead load of the concrete and the construction live loads; thus, during design, an allowance is frequently made for the form components as a superimposed load per square foot. Because forms often weigh 5 to 15 psf, an initial estimate is made in this range based on experience and then is verified after the members are sized.

7.4.2 Lateral Pressures of Concrete

Vertical formwork, such as that for walls and columns, is subjected to internal lateral pressure from the accumulated depth of concrete placed. In a placement, fresh concrete, at least near the top and sometimes at greater depths, behaves as a liquid during vibration and generates lateral pressures equal to the vertical liquid head. Although concrete is a granular material with internal friction, the fluidization of the concrete resulting from internal vibration at least temporarily creates a liquid state; however, many factors appear to contribute to the lateral pressures being less than a liquid head at depths below the controlled depth of vibration. If the vertical placement rate is slow, the concrete mass below may have time to begin stiffening. If the concrete is warm, this stiffening may begin earlier. Internal concrete granular friction, form friction, migration of pore water, and other factors may also reduce the resulting lateral pressures. Admixtures, different types of cements, cement substitutes, and construction practices also affect the level of lateral pressure.

Tests have indicated that the pressures often have a distribution, as indicated in Figure 7.27, starting as a liquid pressure near the top and reaching a maximum at some lower level. For simplicity, design practice usually assumes that the maximum pressure is uniform at a conservative value. ACI Committee 347 (2004) recommends that, unless certain conditions are met, calculation of the pressure magnitude vs. depth should be as a full liquid head:

$$p = wh \quad (7.1)$$

where p is the lateral pressure of concrete (lb/ft^2), w is the unit weight of fresh concrete (lb/ft^3), and h is the depth of fluid or plastic concrete from the top of the placement to the point of consideration in the form (ft).

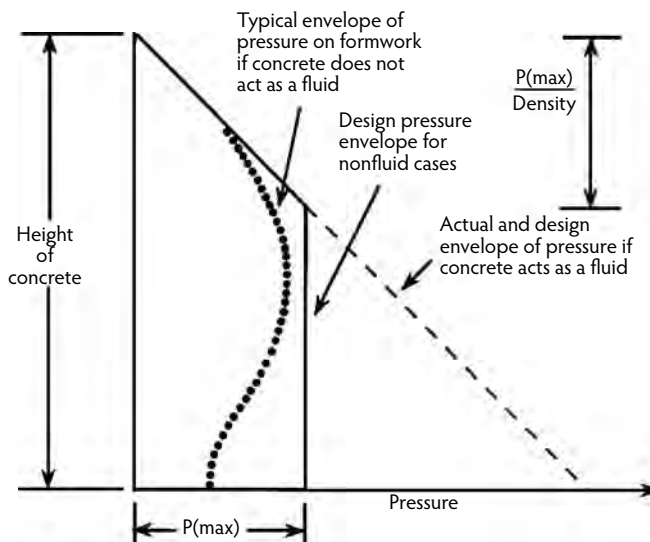


FIGURE 7.27 Typical and assumed distributions of concrete lateral pressure.

TABLE 7.1 Unit Weight Coefficient (C_W)

Unit Weight of Concrete	C_W
Less than 140 lb/ft ³	$C_W = 0.5[1 + (w/145 \text{ lb/ft}^3)]$
140 to 150 lb/ft ³	1.0
More than 150 lb/ft ³	$C_W = w/145 \text{ lb/ft}^3$

TABLE 7.2 Chemistry Coefficient (C_C)

Cement Type or Blend	C_C
Types I, II, and III without retarders ^a	1.0
Types I, II, and III with a retarder ^a	1.2
Other types or blends containing less than 70% slag or 40% fly ash without retarders ^a	1.2
Other types or blends containing less than 70% slag or 40% fly ash with a retarder ^a	1.4
Blends containing more than 70% slag or 40% fly ash	1.4

^a Retarders include any admixture, such as a retarder, retarding water reducer, retarding midrange water-reducing admixture, or high-range water-reducing admixture (superplasticizer), that delays setting of concrete.

ACI 347-04 further states, however, that for concrete having a slump no greater than 7 in. and placed with normal internal vibration to a depth of 4 ft or less, the formwork may be designed for a lateral pressure as follows, where p_{\max} is the maximum lateral pressure (psf), R is the rate of vertical placement (ft/hr), T is the temperature of concrete (°F), C_W is the unit weight coefficient per Table 7.1, and C_C is the unit weight coefficient per Table 7.2:

1. For columns:

$$p_{\max} = C_W C_C [150 + 9000R/T] \quad (7.2)$$

with a minimum of $600C_W$ psf, but in no case greater than wh .

2. For walls with rate of placement (R) less than 7 ft/hr and a placement height not exceeding 14 ft:

$$p_{\max} = C_W C_C [150 + 9000R/T] \quad (7.3)$$

with a minimum of $600C_W$ psf, but in no case greater than wh .



FIGURE 7.28 Tall wall form with internal pressures resisted by ties and wind resisted by external braces.

3. For walls with rate of placement (R) less than 7 ft/hr where placement height exceeds 14 ft and for walls with a placement rate of 7 to 15 ft/hr:

$$p_{\max} = C_w C_c [150 + 43,400/T + 2800R/T] \quad (7.4)$$

with a minimum of $600C_w$ psf but in no case greater than wh .

For the purpose of the pressure formulas, columns are defined as vertical elements with no plan dimension exceeding 6.5 ft, and walls are vertical elements with at least one plan dimension exceeding 6.5 ft.

When working with concrete mixtures using newly introduced admixtures that increase set time or increase slump characteristics, such as self-consolidating concrete, Equation 7.1 should be used until the effect on formwork pressure is understood by measurement. Caution should be used if a concrete form is filled by pumping upward from the base of the form. Not only can a liquid head be developed, but also a portion of the pump surcharge pressure is likely to be developed due to friction and drag resistance of the concrete moving upward through the form and reinforcing.

Internal concrete lateral pressures are usually resisted in wall forms by transferring the pressures through beamlike members (plywood, studs, and wales) to tension ties linking the two wall form sides (Figure 7.28). Because tension elements are the most efficient structural members, this is also the most cost-effective solution. The internal pressures in most column forms are transferred to external tie elements on adjacent faces of the form that serve as links between the opposite sides of a square or rectangular column form. Circular columns have a great forming advantage in that the column-form skin can act as a hoop, resisting the pressures in tension. Although these are effective methods of resisting internal pressures of the concrete, separate resisting elements, such as external braces, must be provided to resist external horizontal loads that tend to overturn wall, column, and slab forms.

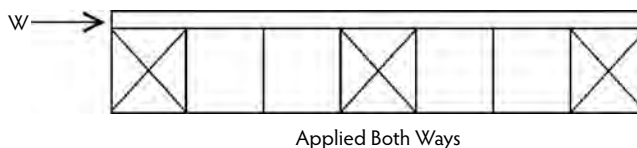


FIGURE 7.29 Schematic bracing of slab formwork.

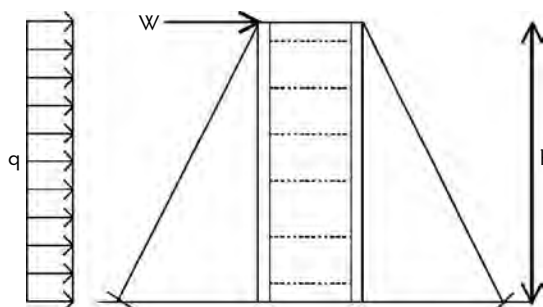


FIGURE 7.30 Schematic bracing of wall formwork.

7.4.3 Horizontal Loads

Horizontal loads from such forces as wind, seismic activity, cables, inclined supports, inclined dumping of concrete, and starting or stopping of equipment must be resisted by braces and shores. ACI Committee 347 (2004) recommends the following minimum loads for design to prevent lateral collapse of the formwork. For elevated floor formwork in building construction, the horizontal load (w) for design in any direction at each floor line should not be less than 100 lb per linear foot of floor edge or 2% of the total dead load on the form distributed as a uniform load per foot of slab edge, whichever is greater (see Figure 7.29). For wall forms, bracing should be designed to meet the minimum wind load requirements of ASCE 7-05 with wind velocity adjustment for shorter recurrence interval as provided in ASCE 37-02. If exposed to elements, the minimum wind design pressure (q) should not be less than 15 psf, and bracing should be designed for at least $w = 100$ lb per linear foot of wall, applied at the top. In Figure 7.30, the minimum lateral load (w) for design of the bracing system would be the greater of $q \times h/2$ or 100 lb/ft. The formwork designer must also be alert for other conditions such as post-tensioning operations, unusual geometry, or sequence of construction of operations that may create special loads on the forming system.

7.5 Formwork Design Criteria

Formwork components can be designed and constructed in many materials, such as plywood, wood, steel, aluminum, and fiber composites. Frequently, a mixture of materials is used (Figure 7.31). Steel, aluminum, and fiber composites are more likely to be parts of manufactured components or systems that are rated or designed by the producer and may be supplied predesigned on a rental basis for the project needs. Forms intended to be job built are often made of wood and require design by the construction engineer associated with the project or by a consultant to the contractor. The examples in this chapter illustrate the latter case for wood components designed by allowable stress methods. To understand the examples, it is necessary to provide some of the essentials of wood design. Readers undertaking the design of formwork in wood are advised to obtain and follow the more comprehensive specifications in the *National Design Specification for Wood Construction* (AFPA, 2005) and the *Plywood Design Specification* (APA, 1997).

Most of the lumber used in formwork is surfaced on four sides (S4S) to achieve its final dimensions as shown in Table 7.3. The S4S dimensions are smaller than the nominal sizes referred to in the table. Except for classification purposes, it is the actual dimensions and actual section properties that are used



FIGURE 7.31 Wood joists supported on steel beams and steel scaffolding towers.

in design. A second set of sizes known as *rough lumber* (not shown in Table 7.3) has slightly larger dimensions but is still not the full nominal size. Rough lumber sizes are sometimes used in heavy falsework-supporting forms.

Plywood is frequently used as the surface layer of the formwork in contact with the fresh concrete. Plywood has different strengths and stiffness depending on the direction of its span relative to the direction of the grain in the outer layers. The equivalent section, considering the varying elastic modulus and strength between parallel-to-grain loading and side-grain loading, is illustrated by equivalent sections in Figure 7.32. When the grain of the outer layers is parallel to the span direction, the strength and stiffness are greatest (Figure 7.33). Many types of plywood are available. Section properties for B-B Plyform, Class I, plywood, one of the most frequently selected types for moderate reuse in formwork, are given in Table 7.4. Note that, due to the alternating grain directions in the plywood veneer layers, conventional methods for calculating section properties of homogeneous, isotropic sections do not apply. The section properties given in Table 7.4 have been determined by considering the varying properties in the different layers as well as the complications of weakness induced by the tendency of fibers to roll over each other in shear lateral to the grain, or **rolling shear** (Figure 7.34). For these reasons, use the listed value of S only in bending calculations, use I only for deflection calculations, and use Ib/Q , the rolling-shear constant, for shear calculations.

The basic design values for wood and for plywood of the species, grades, sizes, and types frequently used in formwork are listed in Table 7.5. The species and grades readily available in the area of the project should always be verified. Contractors also often have stocks of form lumber for reuse from previous projects. Such lumber should always be inspected for defects as the material is assembled, and unsuitable pieces must be rejected.

7.5.1 ASD Adjustment Factors for Lumber Stresses

The AFPA-NDS (AFPA, 2005) provides for adjustment of the lumber **reference design values** (F), such as those given in Table 7.5, by a series of multipliers yielding the **allowable design values** (F') for stress as follows:

Bending:

$$F' = F_b \times C_D \times C_M \times C_L \times C_F \times C_{fu} \times C_r \times [C_t \times C_i] \quad (7.5)$$

TABLE 7.3 Example Section Properties of Standard Dressed (S4S) Sawn Lumber

Nominal Size	Standard Dressed Size (S4S) $b \times d$ (x-x) $d \times b$ (y-y) (in. \times in.)	Area of Section (A) (in. ²)	x-x Axis		y-y Axis		Approximate Weight (lb/ft) When Wood Density Equals the Following Weights		
			Section Modulus (S_{xx}) (in. ³)	Moment of Inertia (I_{xx}) (in. ⁴)	Section Modulus (S_{yy}) (in. ³)	Moment of Inertia (I_{yy}) (in. ⁴)	25 (lb/ft ³)	30 (lb/ft ³)	35 (lb/ft ³)
2 \times 4	1-1/2 \times 3-1/2	5.250	3.063	5.359	1.313	0.984	0.911	1.094	1.276
2 \times 6	1-1/2 \times 5-1/2	8.250	7.563	20.80	2.063	1.547	1.432	1.719	2.005
2 \times 8	1-1/2 \times 7-1/4	10.88	13.14	47.63	2.719	2.039	1.888	2.266	2.643
2 \times 10	1-1/2 \times 9-1/4	13.88	21.39	98.93	3.469	2.602	2.409	2.891	3.372
4 \times 4	3-1/2 \times 3-1/2	12.25	7.146	12.51	7.146	12.51	2.127	2.522	2.977
4 \times 6	3-1/2 \times 5-1/2	19.25	17.65	48.53	11.23	19.65	3.342	4.010	4.679
4 \times 8	3-1/2 \times 7-1/4	25.38	30.66	111.1	14.80	25.90	4.405	5.286	6.168

Note: Table is an abbreviated list of properties of selected sizes; see AFPA-NDS (2005) for additional data.

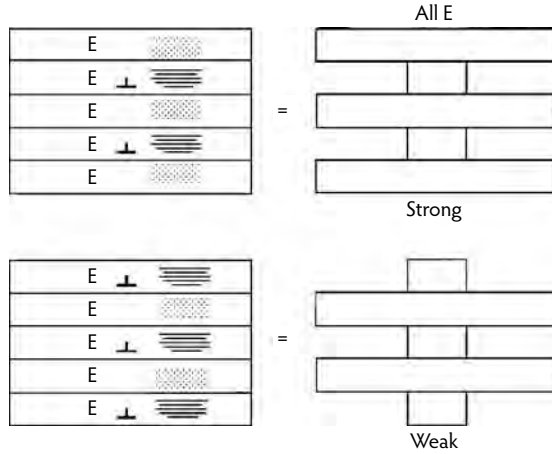


FIGURE 7.32 Plywood equivalent sections recognizing the weakness of lateral modulus.

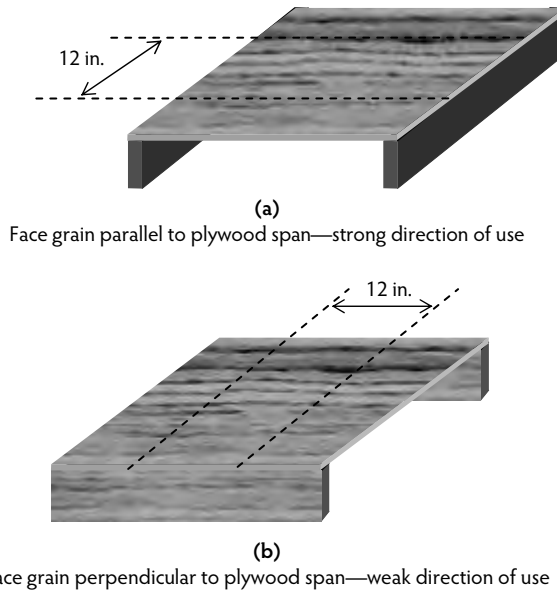


FIGURE 7.33 Plywood load capacity and stiffness varies with direction of face grain span.

Shear:

$$F'_v = F_v \times C_D \times C_M \times [C_t \times C_i] \quad (7.6)$$

Bearing:

$$F'_{c\perp} = F_{c\perp} \times C_M \times C_b \times [C_t \times C_i] \quad (7.7)$$

Compression:

$$F'_c = F_c \times C_D \times C_M \times C_F \times C_P \times [C_t \times C_i] \quad (7.8)$$

Elastic modulus:

$$E' = E \times C_M \times [C_t \times C_i] \quad (7.9a)$$

$$E'_{\min} = E_{\min} \times C_M \times [C_t \times C_i \times C_T] \quad (7.9b)$$

TABLE 7.4 Example Effective Section Properties for Plywood: 12-in. Unit Width of B-B Plyform, Class I

Plywood Net Thickness (in.)	12-in Width, Used with Face Grain Parallel to Span			12-in. Width, Used with Face Grain Perpendicular to Span			Weight (psf)
	Moment of Inertia (I) (in. ⁴)	Effective Section Modulus (S) (in. ³)	Rolling Shear Constant (Ib/Q) (in. ²)	Moment of Inertia (I) (in. ⁴)	Effective Section Modulus (S) (in. ³)	Rolling Shear Constant (Ib/Q) (in. ²)	
1/2	0.077	0.268	5.153	0.024	0.130	2.739	1.5
5/8	0.130	0.358	5.717	0.038	0.175	3.094	1.8
3/4	0.199	0.455	7.187	0.092	0.306	4.063	2.2
7/8	0.296	0.584	8.555	0.151	0.422	6.028	2.6
1	0.427	0.737	9.374	0.270	0.634	7.014	3.0

Note: Use listed S value in bending calculations and use I only in deflection calculations. Properties of B-B Plyform, Class I, are taken from APA (2004). Consult reference or manufacturer for other plywood types.

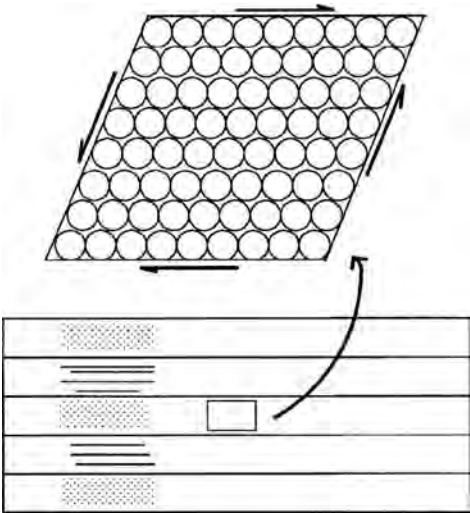


FIGURE 7.34 Grains of wood tend to roll when subjected to lateral shear.

Some of the adjustment factors (in brackets) only apply to truss members (buckling stiffness factor, C_T), when the member is incised (incising factor, C_i) or when the temperature is $>100^{\circ}\text{F}$ (temperature factor, C_t), and thus have only rare uses in formwork. The remaining factors are discussed below.

7.5.2 Load Duration Factor (C_D)

The adjustment for load duration (C_D) reflects the ability of wood to exhibit increased strength under shorter periods of loading. The following values may be applied for the indicated cumulative maximum load durations:

- $C_D = 0.9$ Load duration > 10 year
- $C_D = 1.0$ 2 months $<$ load duration ≤ 10 year
- $C_D = 1.15$ 7 days $<$ load duration ≤ 2 months
- $C_D = 1.25$ Load duration ≤ 7 days
- $C_D = 1.6$ Wind/earthquake
- $C_D = 2.0$ Impact

For most formwork, an adjustment of $C_D = 1.25$ is applied; however, when the components are reused for longer cumulative durations at maximum level, C_D should be appropriately reduced.

TABLE 7.5 Example Reference Design Values for Visually Graded Dimension Lumber at 19% Maximum Moisture and Plywood Used Wet

Species, Specific Gravity, Grade, and Size Category	Extreme Fiber Bending (F_b) (psi)	Compression \perp to Grain (F_{\perp}) (psi)	Compression \parallel to Grain, F_c (psi)	Shear \parallel to Grain (F_v) (psi)	Modulus of Elasticity	
					E (psi)	E_{min} (psi)
Douglas Fir–Larch, $G = 0.50$						
No. 2, 2–4 in. thick, 2 in. and wider	900	625	1350	180	1,600,000	580,000
Construction, 2–4 in. thick, 2–4 in. wide	1000	625	1650	180	1,500,000	550,000
Douglas Fir–South, $G = 0.49$						
No. 2, 2–4 in. thick, 2 in. and wider	850	520	1350	180	1,200,000	440,000
Construction, 2–4 in. thick, 2–4 in. wide	975	520	1650	180	1,200,000	440,000
Southern Pine, $G = 0.55$ (size-adjusted values)						
No. 2, 2–4 in. thick, 2–4 in. wide	1500	565	1650	175	1,600,000	580,000
No. 2, 2–4 in. thick, 5–6 in. wide	1250	565	1600	175	1,600,000	580,000
No. 2, 2–4 in. thick, 8 in. wide	1200	565	1550	175	1,600,000	580,000
Construction, 2–4 in. thick, 4 in. wide	1100	565	1800	175	1,500,000	550,000
Spruce–Pine–Fir, $G = 0.42$						
No. 2, 2–4 in. thick, 2 in. and wider	875	425	1150	135	1,400,000	510,000
Construction, 2–4 in. thick, 4 in. wide	1000	425	1400	135	1,300,000	470,000
Hem–Fir, $G = 0.43$						
No. 2, 2–4 in. thick, 2 in. and wider	850	405	1300	150	1,300,000	470,000
Construction, 2–4 in. thick, 2–4 in. wide	975	405	1550	150	1,300,000	470,000
Adjustment factor (C_M) for moisture content $> 19\%$ (lumber)	0.85 ^c	0.67	0.8 ^d	0.97	0.9	—
Adjustment factor (C_D) for maximum load duration 7 days or less (lumber and plywood)	1.25	—	1.25	1.25	—	—
Other applicable adjustment factors for lumber	$C_F, C_P, C_{\beta}, C_L, C_T$	C_r, C_b	C_t, C_P, C_P	C_t	C_t	C_t
Plywood sheathing used wet: B-B Plyform, Class I	1545 ^b	Face Bearing 210	—	Rolling Shear 57 ^b	1,500,000	—

^a Size adjustments apply to all lumber basic bending and compression parallel to the grain design values, except for Southern Pine. The size adjustments are already included in the Southern Pine basic design values. Consult Table 7.4 for details of size adjustments.

^b Plywood stresses include an experience factor of 1.3 recommended by the American Plywood Association.

^c When $F_b C_F \leq 1150$ psi, $C_M = 1.0$.

^d When $F_c C_F \leq 750$ psi, $C_M = 1.0$.

Note: Data are based on recommendations of the American Forest and Paper Association and American Plywood Association.

TABLE 7.6 Size and Flat-Use Adjustment Factors for Example Dimension Lumber Grades

Grade	Width (in.)	Size Factor (All Species Except Southern Pine)			Flat-Use Factor	
		Bending Stress (F_b)		Compression (F_c)	Bending Stress (F_b)	
		2 and 3 in. Thick	4 in. Thick		2 and 3 in. Thick	4 in. Thick
No. 1 and No. 2	2 and 3	1.5	1.5	1.15	1.0	—
	4	1.5	1.5	1.15	1.1	1.0
	5	1.4	1.4	1.1	1.1	1.05
	6	1.3	1.3	1.1	1.15	1.05
	8	1.2	1.3	1.05	1.15	1.05
	10	1.1	1.2	1.0	1.2	1.1
	12	1.0	1.1	1.0	1.2	1.1
	14 and wider	0.9	1.0	0.9	1.2	1.1
Construction	2 and 3	1.0	1.0	1.0	1.0	—
	4	1.0	1.0	1.0	1.1	1.0

7.5.3 Moisture Factor (C_M)

Wood gains in strength as it loses moisture in a range below the fiber saturation point (about 30% moisture content). The basic design values are established for lumber that has a moisture content of 19% or less, typical of air-dried lumber. When the exposure is such that the wood moisture content will exceed 19% for an extended period of time, the design values should be multiplied by the C_M values indicated in Table 7.5.

7.5.4 Size Factor (C_F)

Tests indicate that member overall size affects the failure stress. To account for these variations, the size factor (C_F) as shown in Table 7.6 is applied to the bending and compression basic design values. Note that the size factor does not apply to the basic design values of Southern Pine, whose basic design values in Table 7.5 are preadjusted to reflect most of the size effect.

7.5.5 Flat-Use Factor (C_{fu})

Lumber loaded on its wide face and bending about its weak axis (y - y) exhibits a slightly higher failure stress. To reflect these variations, the flat-use factor (C_{fu}) adjustments in Table 7.6 may be applied to the basic design values for bending stress.

7.5.6 Beam-Stability Factor (C_L)

The AFPA-NDS (AFPA, 2005) provides equations for determining the beam-stability factor (C_L), an adjustment less than 1.0, when the compression edge of a beam may become unstable. For sawn lumber, however, the AFPA-NDS also provides prescriptive d/b ratios, based on nominal dimensions and lateral support conditions where the member may be assumed to be stable and no reduction for C_L is needed, as follows:

- $d/b = 2$ to 1 or less, no lateral support is necessary.
- $d/b = 3$ to 1 or 4 to 1, ends shall be held in position against lateral rotation or displacement by blocking or connection to other members.
- $d/b = 5$ to 1, one edge shall be held in line for the entire length.
- $d/b = 6$ to 1, bridging, blocking, or cross-bracing shall be installed at intervals not exceeding 8 ft unless both edges are held in line.
- $d/b = 7$ to 1, both edges shall be held in line for the entire length.

7.5.7 Column-Stability Factor (C_p)

The column-stability factor (C_p) is an adjustment less than 1.0 to reduce the allowable compression stress parallel to the grain when longer column-like members such as shores or braces may fail in a buckling mode rather than by crushing. The factor is given by:

$$C_p = \frac{1 + (F_{cE} / F_c^*)}{2c} - \sqrt{\left[\frac{1 + (F_{cE} / F_c^*)}{2c} \right]^2 - \frac{F_{cE} / F_c^*}{c}} \quad (7.10)$$

where:

F_c^* = tabulated compression design value multiplied by all applicable adjustment factor except C_p

c = 0.8 (for sawn lumber).

$F_{cE} = 0.822E'_{\min} / (l_e/d)^2$, where l_e is the effective length, and l_e/d is the larger of the slenderness ratios about the possible buckling axes; the value of l_e/d shall not normally exceed 50, except for short-duration loadings during construction when it shall not exceed 75.

7.5.8 Bearing-Area Factor (C_b)

The bearing-area factor (C_b) is for the case of bearing perpendicular to the grain of the wood—that is, bearing on the side grain. The bearing factor is normally taken as 1.0; however, if the bearing area is more than 3 in. from the end of the member and less than 6 in. in length as measured along the grain, then the following increase factor may be applied:

$$C_b = \frac{l_b + 0.375}{l_b} \quad (7.11)$$

where l_b is the length of bearing (in inches) measured parallel to the grain. Note that in formwork design, unless there is certainty that the bearing area will not be within 3 in. of the end of the member, it is usually best to assume $C_b = 1.0$.

7.5.9 Repetitive-Use Factor (C_r)

The AFPA-NDS (AFPA, 2005) includes a repetitive-use factor (C_r) that may be used to increase the bending design value when there are at least three members spaced not more than 24 in. on-center, such as joists and studs, and they are joined by a load-distributing member, such as sheathing. The increase is allowed because it is unlikely that normal defects would occur in the repetitive members at the same critical location and the load could be shared if one had a defect. In formwork design, however, ACI SP-4 (Hurd, 2005) suggests that this factor should only be applied to carefully constructed panels whose components are securely nailed or bolted together. The factor values > 1.0 are listed in the AFPA-NDS.

7.5.10 Adjustment Factors for Plywood Stresses

Relative to formwork, the allowable stresses given by the APA—The Engineered Wood Association (APA, 2004) are subject to three primary adjustments: load duration, wet use, and experience factors. A load duration factor similar to the value of C_D for wood is normally applied as listed in Table 7.5. The wet use and experience factors appropriate to formwork applications have been incorporated in the allowable stresses listed for B-B Plyform, Class I, plywood in Table 7.3. The calculation of plywood deflection can be refined to include both the bending deflection and the shear deflection. In this presentation, for simplicity, only the bending deflection is considered, but the lower value of the plywood elastic modulus will be used to partially compensate for this. Consult APA (2004) for procedures for calculating the shear deflection component.

TABLE 7.7 Minimum Safety Factors of Formwork Accessories

Accessory	Safety Factor	Type of Construction
Form tie	2.0	All applications
Form anchor	2.0	Formwork supporting form weight and concrete pressures only
	3.0	Formwork supporting form weight of forms, concrete, construction live loads, and impact
Form hanger	2.0	All applications
Anchoring inserts used as form ties	2.0	Precast concrete panels when used as formwork

7.5.11 Manufactured Wood Products

Various manufactured wood products are sometimes used in formwork applications. These include not only sheathing but also structural composite lumber. **Laminated veneer lumber** (LVL) is made of wood-veneer sheet elements 1/4-in. thick or less, bonded with an exterior adhesive, with wood fibers oriented along the length of the member. **Parallel strand lumber** (PSL) is made of wood strands having a least dimension of 1/4 in. or less and an average length of at least 150 times the least dimension, bonded with exterior adhesive, and with strands oriented along the length of the member. **Laminated strand lumber** (LSL) is made of wood strands with a least dimension of about 1/32 in., approximately 12 in. long, parallel to the length of the member, and bonded with an exterior adhesive. The suitability of these materials for exposed formwork should be evaluated for each application. Design information can be obtained from the manufacturers or the APA.

7.5.12 Safety Factors for Formwork Accessories

Various accessories are used in formwork such as form ties, anchors, and hangers. Most of these devices are made of steel and are rated by the manufacturers. The ratings may be listed as either the allowable or ultimate strengths of the devices under certain types of loading. The type of rating (allowable or ultimate) should be carefully determined from the information provided. If ultimate strengths are listed, the allowable strength should be calculated by dividing by an appropriate factor of safety. ACI Committee 347 (2004) has recommended the safety factors listed in Table 7.7 for such accessories.

7.6 Formwork Design

Most components of a form system can be subdivided into members that are primarily bending elements (sheathing, joists, studs, stringers, and wales) and members that are primarily tension or compression elements (shores, braces, etc.). In addition, there are numerous details to design, such as connections (Figure 7.35), hangers, and footings or mudsills (Figure 7.36). The following sections provide example designs, in wood, of the main members of an elevated floor slab form and a vertical wall form to convey a sense of the procedures involved. After the design is complete, the formwork material specifications, member layout, member sizes, connection details, erection procedures, and use limitations should be conveyed by means of drawings with appropriate notes to the field workers who will fabricate and erect the form.

7.6.1 Determination of Resultants from Loads

The bending members of a wood form system are either single-span or continuous multiple-span elements, usually with bearing supports as illustrated in Figure 7.37. Although the members may sometimes have more than three spans, the benefits from considering more than three span conditions are very limited. Many of the member loads are uniform. In other cases, the loadings may be a series of closely spaced concentrated loads that can often be approximated as a uniform load if there is a sufficient number in a span. Figure 7.37 also provides the formulas for the maximum moments, shears, and



FIGURE 7.35 Connections at corners, braces, and bulkheads require specific design.



FIGURE 7.36 Wood timber grillage mudsill.

deflections for the uniformly loaded one-, two-, and three-span cases. It should be noted that the formulas for calculating the maximum shear force are modified to calculate the shear at a distance d from the face of the supporting member, where d is the depth of the member being designed and l_b is the length of bearing at the supporting member. In wood design, the AFPA-NDS provides that loads within a distance d of the face of the support can be neglected when designing for shear if the member is loaded on one face and supported on the opposite face or edge. However, in cases where the member is notched or connection is made in the web, as by bolting, other AFPA-NDS special provisions should be consulted which, in effect, magnify the shear force used for design.

7.6.2 Fundamental Relations between Resultants and Stresses

From mechanics of solids, the following relationships apply to the elastic design of wood elements:

Bending of beams or plywood:

$$f_b = \frac{M}{S} \quad (7.12)$$

Shear of solid rectangular beams:

$$f_v = \frac{3}{2} \frac{V}{bd} \quad (7.13)$$

Uniformly Loaded Beam Formulas for Wood Design		
One Span		$\Delta_{\max} = \frac{5}{384} \frac{wl^4}{EI}$ $M_{\max} = wl^2/8$ $V_{EM} = [0.5wl - w(d + \frac{l_b}{2})]$ (end, modified)
		$\Delta_{\max} = \frac{1}{185} \frac{wl^4}{EI}$ $M_{\max} = wl^2/8$ $V_{EM} = [0.375wl - w(d + \frac{l_b}{2})]$ $V_{IM} = [0.625wl - w(d + \frac{l_b}{2})]$ (interior, modified)
		$\Delta_{\max} = \frac{1}{145} \frac{wl^4}{EI}$ $M_{\max} = wl^2/10$ $V_{EM} = [0.4wl - w(d + \frac{l_b}{2})]$ $V_{IM} = [0.6wl - w(d + \frac{l_b}{2})]$

Design Notes: 1. If l_b is unknown, use $l_b = 0$ for shear calculations.
 2. If d is unknown when calculating shear force, either:
 a) Assume $d = 0$ in calc. and reevaluate with d determined if shear controls.
 b) Assume a likely value of d and check with an additional iteration when d is determined.

FIGURE 7.37 Beam formulas for one-, two-, and three-span conditions.

Shear of plywood:

$$f_v = \frac{VQ}{Ib} = \frac{V}{Ib/Q} \quad (7.14)$$

where Ib/Q is the rolling shear constant.

Bearing and axial compression:

$$f_{c\perp} \text{ or } f_c = \frac{P}{A} \quad (7.15)$$

When f is used in the above equations, the actual stress is sought in the calculation from the actual resultant. When F is used, the maximum allowable stress is implied and the maximum resultants are sought. Load-deflection relationships are given in Figure 7.37 as a function of the number of spans.

7.6.3 Basis of Examples

When undertaking a form design, some parameters are frequently known, and others must be calculated to meet the required strength needs and deflection limitations. For example, the spacings of members may be dictated by the geometry of the area to be formed or the modular needs of the system or plywood facing. For this case, the unknowns become the required member sizes. In another case, the contractor may have material of a given size that is desired to be used. For the latter case, the unknowns are the maximum spacings of the members required to limit the loads on each to its allowable value. In the following elevated slab form example, the spacings are assumed to be set by job conditions and the members are the unknowns. In the wall form design example, the member sizes are assumed to be predetermined by available material and the spacings are the unknowns. For both examples, the ASD procedures of the AF&PA NDS-2005 will be used.

7.7 Slab-Form Design Example

Assume that an elevated flat-plate floor slab of 8-in. thickness is to be formed with a top elevation 10 ft above the supporting surface below. The general layout of the plywood sheathing, joists, stringers, and shores is shown in Figure 7.9 and Figure 7.38. Because of the floor layout, the contractor desires to space the joists at 16 in. on-center, the stringers at 5 ft on-center under the joists, and the shores at 5 ft on-center under the stringers. The materials are B-B Plyform, Class I, plywood and No. 2 Spruce–Pine–Fir (SPF) joists, stringers, and shores. It has been determined that the strength gain of the concrete will allow the forms to be stripped in 4 days, followed by installation of reshores. The project specification requires that the formwork element deflections shall be no greater than $l/360$. The plywood will be assumed to be used wet, as it is frequently exposed for a lengthy period during rebar placement and in contact with the fresh concrete; however, the lumber elements will be assumed to be relatively sheltered and not exposed to significant moisture for lengthy periods. The plywood will be oriented with its face grain parallel to the span direction—that is, the strong way. From the earlier section on vertical loads, the distributed pressure (q) for design on a working basis is:

Dead load of 8-in. concrete slab	100 psf
Construction live load	50 psf
Formwork estimated dead load	<u>5 psf</u>
Total	155 psf

7.7.1 Sheathing Design

The plywood span is the spacing of the joists, and 8-ft-long plywood panels can typically have three or more spans. The plywood allowable stresses adjusted for load duration (see Table 7.5) are:

$$F'_b = F_b \times C_D = 1545 \text{ psi} \times 1.25 = 1931 \text{ psi}$$

$$F'_v = F_v \times C_D = 57 \text{ psi} \times 1.25 = 71 \text{ psi}$$

$$E' = E = 1,500,000 \text{ psi}$$

Considering the loading to be a uniform load (w) of 1-ft width, corresponding to the section properties of the plywood based on 12-in. width:

$$w = q \times \text{unit width} = 155 \text{ psf} \times 1.0 \text{ ft} = 155 \text{ lb/ft}$$

For the limitation of flexural bending, the maximum moment (M) is:

$$M = \frac{wl^2}{10} = \frac{155 \text{ lb/ft} \times (1.33 \text{ ft})^2}{10} = 27.5 \text{ ft-lb} = 330 \text{ in.-lb}$$

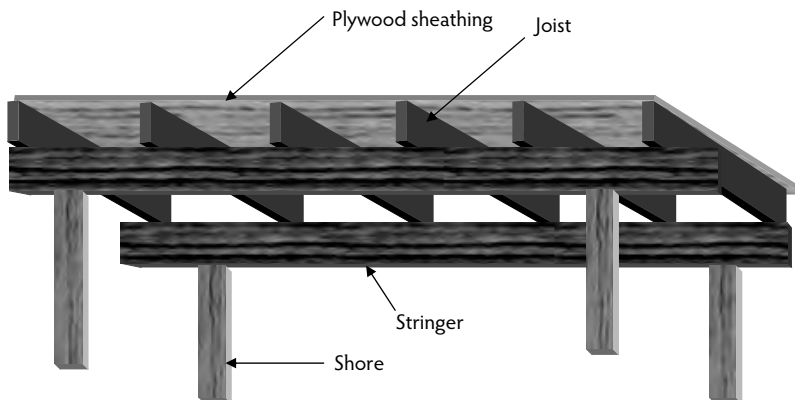


FIGURE 7.38 Slab formwork layout.

and the required section modulus (S) is given by:

$$S = \frac{M}{F'_b} = \frac{330 \text{ in.-lb}}{1931 \text{ psi}} = 0.171 \text{ in.}^2$$

For the shear limitation, the maximum shear force for design is determined at the center of the support as the support width is not yet known:

$$V = 0.62wl = 0.62(155 \text{ lb/ft})(16 \text{ in./12 in./ft}) = 124 \text{ lb}$$

$$\frac{Ib}{Q} = \frac{V}{F'_v} = \frac{124 \text{ lb}}{71 \text{ psi}} = 1.74 \text{ in.}^2$$

The deflection limit is determined from:

$$\frac{l}{360} = \frac{1}{145} \frac{wl^4}{EI}$$

$$I = \frac{360}{145} \frac{155 \text{ lb/ft}}{12 \text{ in./ft}} \frac{(16 \text{ in.})^3}{1,500,000 \text{ psi}} = 0.0876 \text{ in.}^4$$

From these requirements, 1/2-in. plywood would be adequate for bending and shear, but 5/8-in. is required for deflection. Select the plywood thickness to be 5/8 in. Because deflection controls, there is no benefit to further refining the shear calculation after the joist width is known.

7.7.2 Joist Design

The joist span is the 5-ft spacing of the stringers, and the joists can be constructed with a three-span continuous arrangement (Figure 7.9 and Figure 7.38). Lateral buckling of the joists will be restrained by nailing the sheathing to the joists. For selection of the joist reference design values (Table 7.5) and adjustment factors, assume initially that a 2 × 6 joist might work. Allowable stresses for the No. 2 SPF joist are as follows:

$$F'_b = F_b \times C_D \times C_M \times C_L \times C_M \times C_F \times C_r = 875 \text{ psi} \times 1.25 \times 1.0 \times 1.0 \times 1.3 \times 1.0 = 1421 \text{ psi}$$

$$F'_v = F_v \times C_D \times C_M = 135 \text{ psi} \times 1.25 \times 1.0 = 169 \text{ psi}$$

$$E' = E \times C_M = 1,400,000 \text{ psi} \times 1.0 = 1,400,000 \text{ psi}$$

Considering the loading to be a uniform load (w) of 16-in. tributary width corresponding to the spacing of the joists:

$$w = q \times \text{tributary width} = 155 \text{ psf} \times 1.33 \text{ ft} = 207 \text{ lb/ft}$$

For the limitation of flexural bending, the maximum moment (M) is:

$$M = \frac{wl^2}{10} = \frac{207 \text{ lb/ft} \times (5 \text{ ft})^2}{10} = 517 \text{ ft-lb} = 6210 \text{ in.-lb}$$

and the required section modulus (S) is given by:

$$S = \frac{M}{F'_b} = \frac{6210 \text{ in.-lb}}{1421 \text{ psi}} = 4.37 \text{ in.}^3$$

For the shear limitation, the maximum shear force for design is determined at d from the center of the support, as the supporting stringer width is not yet known. At the interior support,

$$V = 0.6wl - wd = 0.6(207 \text{ lb/ft}) - 207 \text{ lb/ft} \left(\frac{5.5}{12} \text{ ft} \right) = 526 \text{ lb}$$

$$bd = (3/2)(V / F'_v) = 3 \times 526 \text{ lb} / (2 \times 169 \text{ psi}) = 4.67 \text{ in.}^2$$

The deflection limit is determined from:

$$\frac{l}{360} = \frac{1}{145} \frac{wl^4}{EI}$$

$$I = \frac{360}{145} \frac{207 \text{ lb/ft}}{12 \text{ in./ft}} \frac{(60 \text{ in.})^3}{1,400,000 \text{ psi}} = 6.61 \text{ in.}^4$$

From these combined requirements, a 2×6 joist is the optimum size having the least area. The result also agrees with the size assumption for selecting the reference design values and size factor. If the size did not agree, the calculations would be repeated with an improved size assumption. In this case, there is no benefit to further refining the shear calculation after the joist width is known because shear alone is not controlling the size.

7.7.3 Stringer Design

The stringer span is the 5-ft spacing of the shores, and the stringers can be constructed with a three-span continuous arrangement. For selection of the stringer basic design values (Table 7.5), assume initially that a 4×6 stringer might work. Lateral buckling of a stringer of this size would not be a problem because $d/b \leq 2$ to 1. Allowable stresses for the No. 2 SPF stringers are as follows:

$$F'_b = F_b \times C_D \times C_M \times C_L \times C_F \times C_r = 875 \text{ psi} \times 1.25 \times 1.0 \times 1.0 \times 1.3 \times 1.0 = 1421 \text{ psi}$$

$$F'_v = F_v \times C_D \times C_M = 135 \text{ psi} \times 1.25 \times 1.0 = 169 \text{ psi}$$

$$E' = E \times C_M = 1,400,000 \text{ psi} \times 1.0 = 1,400,000 \text{ psi}$$

The stringer loading is actually a series of concentrated loads from the joists at 16 in. on-center; however, the starting position of the loads can vary in each span. Due to the complications involved in considering many possible starting positions and recognizing that loads within distance d of the support can be neglected for shear calculations, it is often the practice in formwork to assume a uniform load as being adequately similar (Hurd, 2005). This assumption works reasonably well when three or more equally

spaced concentrated loads of equal magnitude are in the span. Considering the loading to be a uniform load (w) of 5-ft tributary width corresponding to the spacing of the stringers:

$$w = q \times \text{tributary width} = 155 \text{ psf} \times 5 \text{ ft} = 775 \text{ lb/ft}$$

For the limitation of flexural bending, the maximum moment (M) is:

$$M = \frac{wl^2}{10} = \frac{775 \text{ lb/ft} \times (5 \text{ ft})^2}{10} = 1938 \text{ ft-lb} = 23,250 \text{ in.-lb}$$

and the required section modulus (S) is given by:

$$S = \frac{M}{F'_b} = \frac{23,250 \text{ in.-lb}}{1421 \text{ psi}} = 16.36 \text{ in.}^3$$

For the shear limitation, the maximum shear force for design is determined at distance d from the face of the support, assuming the shore will be at least 4×4 or have a head of equal or larger size if it is a metal shore. At the interior support where shear is greatest:

$$V = 0.6wl - w(d + l_b/2) = 0.6(775 \text{ lb/ft})(5 \text{ ft}) - 775 \text{ lb/ft} \left\{ \left[5.5/12 \right] + (3.5/2)/12 \right\} \text{ ft} = 1857 \text{ lb}$$

$$bd = (3/2)(V/F'_v) = (3/2) \times (1857 \text{ lb}/169 \text{ psi}) = 16.5 \text{ in.}^2$$

The deflection limit is determined from:

$$\frac{l}{360} = \frac{1}{145} \frac{wl^4}{EI}$$

$$I = \frac{360}{145} \frac{775 \text{ lb/ft}}{12 \text{ in./ft}} \frac{(60 \text{ in.})^3}{1,400,000 \text{ psi}} = 24.73 \text{ in.}^4$$

From these requirements, a 4×6 stringer is the optimum size meeting all the requirements and having the least area. The result also agrees with the size assumption for selecting the reference design values and size factor. If the size did not agree, the calculations would be repeated with an improved size assumption. A check is also necessary to make sure that there is adequate bearing area for the joist on the stringer.

The tributary load is:

$$P = 155 \text{ psf} \times 1.33 \text{ ft} \times 5 \text{ ft} = 1031 \text{ lb}$$

The allowable bearing stress is given by:

$$F'_{c\perp} = F_{c\perp} \times C_M \times C_b = 425 \text{ psi} \times 1.0 \times 1.0 = 425 \text{ psi}$$

and the actual stress is:

$$f_{c\perp} = \frac{P}{A} = \frac{1031 \text{ lb}}{1.5 \text{ in.} \times 3.5 \text{ in.}} = 196 \text{ psi} < 425 \text{ psi}$$

7.7.4 Shore Design

To determine the shore unbraced height, the slab thickness and depth of forming elements are subtracted from the floor-to-floor height:

$$l_e = 120 - 8 - 0.625 - 5.5 - 5.5 \text{ in.} = 100.4 \text{ in.}$$

For design purposes, the shore is assumed to be concentrically loaded, pinned at the top and the bottom and prevented from translation by an adequate overall form diagonal bracing system. The load to be supported based on the tributary area is:

$$P = 155 \text{ psf} \times 5 \text{ ft} \times 5 \text{ ft} = 3875 \text{ lb}$$

Two stress checks are necessary to size the shore: (1) the bearing perpendicular to the grain of the stringer at the upper end of the shore, and (2) the compression parallel to the grain of the shore (including the possibility of buckling). Evaluation of bearing first will establish a first trial size of the shore area. The allowable bearing stress is:

$$F'_{c\perp} = F_{c\perp} \times C_M \times C_b = 425 \text{ psi} \times 1.0 \times 1.0 = 425 \text{ psi}$$

C_b is assumed to be 1.0, because the bearing length is not yet known and the shore may sometimes be located at the end of the stringer. The required bearing area is given by:

$$A = \frac{P}{F'_{c\perp}} = \frac{3875 \text{ lb}}{425 \text{ psi}} = 9.12 \text{ in.}^2$$

A 4×4 shore is adequate for bearing perpendicular to the grain of the stringer and matches the width of the 4×6 stringer. For this 4×4 shore size, the allowable compression stress parallel to grain is:

$$F'_c = F_c \times C_D \times C_M \times C_F \times C_P = 1150 \text{ psi} \times 1.25 \times 1.0 \times 1.15 \times C_P = 1653 \text{ psi} \times C_P = F_c^* \times C_P$$

$$E'_{\min} = E_{\min} \times C_M = 510,000 \text{ psi} \times 1.0 = 510,000 \text{ psi}$$

Because the trial shore is square and braced only at the ends to resist translation, the l_e/d ratios for each buckling axis are equal; thus,

$$\frac{l_e}{d} = \frac{100.4 \text{ in.}}{3.5 \text{ in.}} = 28.68 < 50$$

and

$$F_{cE} = 0.822 E'_{\min} / (l_e/d)^2 = 0.822 \times 510,000 \text{ psi} / (28.68)^2 = 510 \text{ psi}$$

so

$$F_{cE} / F_c^* = 510 \text{ psi} / 1653 \text{ psi} = 0.308$$

and C_P from Equation 7.10 is:

$$C_P = \left[(1 + 0.308) / (2 \times 0.8) \right] - \left\{ \left[(1 + 0.308) / (2 \times 0.8) \right]^2 - (0.308 / 0.8) \right\}^{0.5} = 0.285$$

Thus, the allowable stress in compression parallel to the grain for the unbraced length is:

$$F'_c = F_c = 1653 \text{ psi} \times C_P = 1653 \text{ psi} \times 0.285 = 471 \text{ psi}$$

Because $F'_c > F'_{c\perp}$, compression perpendicular to the grain in the bearing controls the design, and the 4×4 shore is adequate.

In summary, the design requires 5/8-in. Plyform spanning the strong way, 2×6 joists at 16 in. on-center, 4×6 stringers at 5 ft on-center, and 4×4 shores at 5 ft on-center each way.

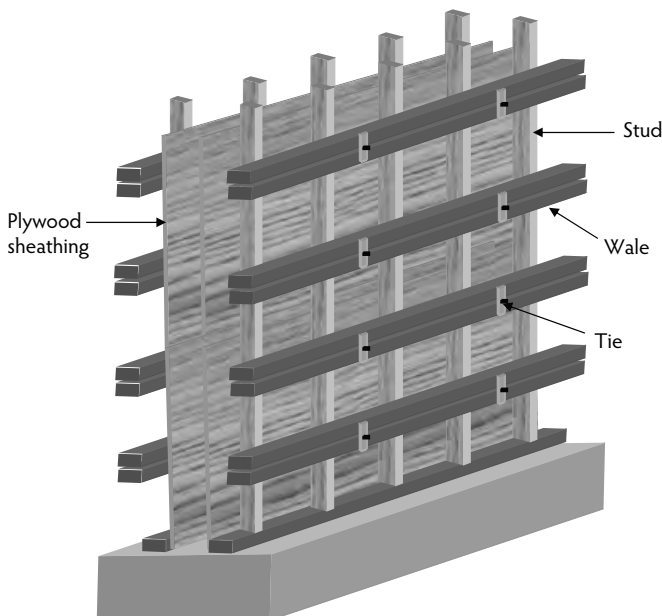


FIGURE 7.39 Wall-form components.

7.7.5 Bracing Design Considerations

The slab form must be braced, as a minimum, to resist the horizontal loads recommended by ACI 347-04. When the concrete columns have been placed prior to erection of the floor forms, the column can contribute to lateral stability if the form has an adequate horizontal diaphragm and is tied to the columns. Horizontal cross-bracing can be added to improve the diaphragm. Vertical cross-bracing in two directions at right angles, in combination with an adequate diaphragm, can also provide a workable system. The braces need not be located in the opening between every pair of shores (Figure 7.29). Often, they are located between alternate pairs of shores (and sometimes farther apart) in a well-dispersed, symmetrical pattern in each direction. The brace size is usually controlled by the buckling resistance in the compression direction of force, and the analysis and design proceed in a manner similar to that for the shore or wall form brace design. It is critical to provide a connection at the top and bottom ends of the brace that is adequate to resist the forces imposed.

7.8 Wall-Form Design Example

Assume that a form is needed for the placement of a 12-ft high wall. The general layout of the plywood sheathing, studs, and wales is shown in Figure 7.39. Because of the availability of the material from previous projects, the contractor wishes to use 3/4-in. B-B Plyform, Class I, plywood for the sheathing and No. 2 Southern Pine 2 × 4 studs and double 2 × 4 wales. Ties can be ordered to meet project needs. The project specification requires that the formwork element deflections be no greater than $l/240$. The plywood will be assumed to be used wet, as it is in contact with the fresh concrete, and the lumber elements will be assumed to be exposed to sufficient rain moisture on the job such that the wood moisture content might rise to above 19%. The normal weight 145 pcf concrete, made with Type II cement, has a slump of <7 in. and contains a set-retarding admixture. Internal vibration during placement will be controlled and limited to an immersion depth <4 ft. The rate of vertical placement (R) will be limited to 4 ft per hour, and the concrete temperature (T) is expected to be above a minimum of 80°F.

From the earlier section on lateral pressures, the maximum distributed pressure (p) for design on a working basis is given by Equation 7.2:

$$p_{\max} = C_w C_c [150 + 9000R/T] = 1.0 \times 1.2 [150 + (9000 \times 4/80)] = 720 \text{ psf}$$

The pressure is assumed to gradually increase with depth at a rate of 150 lb/ft³/ft until reaching the maximum uniform pressure at a depth of 720 psf/150 lb/ft³ or 4.8 ft. For purposes of illustrating the form design procedure, first consider the spacing of members in the uniform pressure region. Because the sizes of the members are predetermined, the unknowns are the maximum allowable spacings of their supports.

7.8.1 Sheathing Design

The plywood span is the spacing of the studs, and the 8-ft-long plywood panels can typically have three or more spans. The plywood allowable stresses adjusted for load duration (see Table 7.5) are:

$$F'_b = F_b \times C_D = 1545 \text{ psi} \times 1.25 = 1931 \text{ psi}$$

$$F'_v = F_v \times C_D = 57 \text{ psi} \times 1.25 = 71 \text{ psi}$$

$$E' = E = 1,500,000 \text{ psi}$$

Considering the loading to be a uniform load (w) of 1-ft unit width corresponding to the section properties of the plywood based on 12-in. width,

$$w = p_{\max} \times \text{unit width} = 720 \text{ psf} \times 1.0 \text{ ft} = 720 \text{ lb/ft}$$

For the limitation of flexural bending, the maximum allowable moment (M) is:

$$M = f'_b S = 1931 \text{ psi} \times 0.455 \text{ in.}^3 = 878 \text{ in.-lb} = 73.2 \text{ ft.-lb}$$

and the maximum span (l) is given by:

$$M = wl^2/10$$

$$73.2 \text{ ft.-lb} = 720 \text{ lb/ft} \times l^2/10$$

$$l = 1.01 \text{ ft} = 12.1 \text{ in.}$$

For the shear limitation, the support width is known to be 1.5 in., so the maximum shear force for design can be determined at the face of the support:

$$V = F'_v (lb/Q) = 71 \text{ psi} \times 7.187 \text{ in.}^2 = 510 \text{ lb}$$

$$V = 0.6wl - w(l_b/2)$$

$$510 \text{ lb} = 0.6(720 \text{ lb/ft})(l) - 720 [(1.5 \text{ in.}/2)/12 \text{ in./ft}]$$

$$l = 1.26 \text{ ft} = 15.4 \text{ in.}$$

For the deflection limit, the maximum span is determined from:

$$l/240 = (1/145)(wl^4/E'I)$$

$$l/240 = (1/145) \left[720 \text{ lb/ft} \times l^4 / \left(12 \text{ in./ft} \times 1,500,000 \text{ psi} \times 0.199 \text{ in.}^4 \right) \right]$$

$$l = 14.4 \text{ in.}$$

From these requirements, 12.1 in. (based on bending) is the maximum span of the plywood. Considering the 8-ft modular length of the plywood panel, provide 8 equal spans with the studs spaced at 12 in. on-center.

7.8.2 Stud Design

The stud span is the spacing of the double wales, and the studs can be constructed with a three-span continuous arrangement. Lateral buckling of the studs will be restrained by nailing the sheathing to the studs. Allowable stresses for the No. 2 Southern Pine 2 × 4 stud from Table 7.5 are as follows:

$$F'_b = F_b \times C_D \times C_M \times C_L \times C_F \times C_r = 1500 \text{ psi} \times 1.25 \times 0.85 \times 1.0 \times 1.0 \times 1.0 = 1593 \text{ psi}$$

$$F'_v = F_v \times C_D \times C_M = 175 \text{ psi} \times 1.25 \times 0.97 = 212 \text{ psi}$$

$$E' = E \times C_M = 1,600,000 \text{ psi} \times 0.9 = 1,440,000 \text{ psi}$$

Considering the loading as a uniform load (w) of 12-in. tributary width corresponding to the spacing of the studs,

$$w = q \times \text{tributary width} = 720 \text{ psf} \times 1.0 \text{ ft} = 720 \text{ lb/ft}$$

For the limitation of flexural bending, the maximum allowable moment (M) is:

$$M = F'_b S = 1593 \text{ psi} \times 3.063 \text{ in.}^3 = 4879 \text{ in.-lb} = 406.6 \text{ ft-lb}$$

and the maximum allowable span is given by:

$$M = w l^2 / 10$$

$$406.6 \text{ ft-lb} = 720 \text{ lb/ft} \times l^2 / 10$$

$$l = 2.37 \text{ ft} = 28.5 \text{ in.}$$

For the shear limitation, the maximum shear force for design is determined at distance d from the face of the support because the supporting wale width ($2 \times 1.5 \text{ in.} = 3 \text{ in.}$) is known. At the interior support where shear is greatest:

$$V = (2/3) F'_v b d = (2/3) \times 212 \text{ psi} \times 1.5 \text{ in.} \times 3.5 \text{ in} = 742 \text{ lb}$$

$$V = 0.6 w l - w(d + l_b / 2)$$

$$742 \text{ lb} = 0.6(720 \text{ lb/ft})(l) - 720 \text{ lb/ft} \left\{ \left[3.5/12 \right] + (3.0/2)/12 \right\} \text{ ft} \Big\} = 1857 \text{ lb}$$

$$l = 2.41 \text{ ft} = 28.9 \text{ in.}$$

The deflection limit is determined from:

$$l / 240 = (1/145)(w l^4 / E' T)$$

$$l / 240 = (1/145) \left[720 \text{ lb/ft} \times l^4 / \left(12 \text{ in./ft} \times 1,440,000 \text{ psi} \times 5.359 \text{ in.}^4 \right) \right]$$

$$l = 42.6 \text{ in.}$$

From these requirements, the spans for bending and shear control the maximum span, which is 28.5 in. Use 28 in. for layout convenience.

7.8.3 Wale Design

The wale span is the spacing of the form ties, and the wales can be constructed with a three-span continuous arrangement. Lateral buckling of the wale is not a problem because $d/b \leq 2$ to 1. Allowable stresses for the No. 2 Southern Pine double 2×4 wales are the same as determined above for the studs. The wale loading is actually a series of concentrated loads from the studs at 12 in. on-center; however, the starting position of the loads can vary in each span. Due to the complications involved in considering the many possible starting positions and recognizing that loads within distance d of the support can be neglected for shear calculations, it is often the practice in formwork to assume a uniform load to be adequately similar to many closely spaced equally concentrated loads (Hurd, 2005). This assumption works reasonably well when three or more equally spaced concentrated loads of equal magnitude are in the span. Considering the loading to be a uniform load (w) of 2.33-ft tributary width corresponding to the spacing of the wales,

$$w = q \times \text{tributary width} = 720 \text{ psf} \times 2.33 \text{ ft} = 1680 \text{ lb/ft}$$

For the limitation of flexural bending, the maximum allowable moment (M) is:

$$M = F_b' S = 1593 \text{ psi} \times 2 \times 3.063 \text{ in.}^3 = 9758 \text{ in.-lb} = 813 \text{ ft.-lb}$$

and the maximum allowable span is given by:

$$\begin{aligned} M &= w l^2 / 10 \\ 813 \text{ ft.-lb} &= 1680 \text{ lb/ft} \times l^2 / 10 \\ l &= 2.2 \text{ ft} = 26.4 \text{ in.} \end{aligned}$$

For the shear limitation, the maximum shear force for design is determined at distance d from the face of the support assuming that the tie-washer plate will have at least a 3-in. length of bearing. The wale interior support is examined where shear is greatest. At the interior support:

$$\begin{aligned} V &= (2/3) F_v' b d = (2/3) \times 212 \text{ psi} \times 2 \times 1.5 \text{ in.} \times 3.5 \text{ in.} = 1484 \text{ lb} \\ V &= 0.6 w l - w \left(d + l_b / 2 \right) \\ 1484 \text{ lb} &= 0.6 (1680 \text{ lb/ft}) (l) - 1680 \text{ lb/ft} \left\{ \left[(3.5/12) + (3.0/2) \right] 12 \right\} \text{ ft} \\ l &= 2.17 \text{ ft} = 26.0 \text{ in.} \end{aligned}$$

The deflection limit is determined from:

$$\begin{aligned} l / 240 &= (1/145) (w l^4 / E T) \\ l / 240 &= (1/145) \left[1680 \text{ lb/ft} \times l^4 / \left(12 \text{ in./ft} \times 1,440,000 \text{ psi} \times 5.359 \text{ in.}^4 \right) \right] \\ l &= 40.5 \text{ in.} \end{aligned}$$

From these requirements, the maximum span is 26.0 in. and is controlled by shear. Select a wale span of 24 in. so the tie spacing can be coordinated easily with the stud spacing.

A check is also needed to make sure that there is adequate bearing area for the stud on the double wale. The tributary load is:

$$P = 720 \text{ psf} \times 1.0 \text{ ft} \times 2.33 \text{ ft} = 1678 \text{ lb}$$

The allowable bearing stress is given by:

$$F_{c\perp}' = F_{c\perp} \times C_M \times C_b = 565 \text{ psi} \times 0.67 \times 1.0 = 378 \text{ psi}$$

and the actual stress is:

$$f_{c\perp} = P/A = 1678 \text{ lb} / (1.5 \text{ in.} \times 3.0 \text{ in.}) = 373 \text{ psi} < 378 \text{ psi}$$

7.8.4 Tie Design

Select the tie capacity to exceed the tie force (T) based on the tributary area supported:

$$T = p_{\max} \times \text{wale spacing} \times \text{tie spacing} = 720 \text{ psf} \times 2.33 \text{ ft} \times 2.0 \text{ ft} = 3350 \text{ lb}$$

Select a heavy snap tie with a 3350-lb working capacity, and check the bearing of the 3-in. square tie washer on the double wale (Figure 7.40):

$$f_{c\perp} = P/A = 3350 \text{ lb} / (2 \times 1.5 \text{ in.} \times 3.0 \text{ in.}) = 372 \text{ psi} < 378 \text{ psi}$$

7.8.5 Bracing Design

Braces are required to keep the form from overturning due to wind or incidental construction loads such as ladders leaning on the form or workers climbing on the form. The effects of an elevated work platform may also have to be considered in some designs. If designing for the minimum recommendations of ACI



FIGURE 7.40 Bearing of form tie bracket on double wood wale.

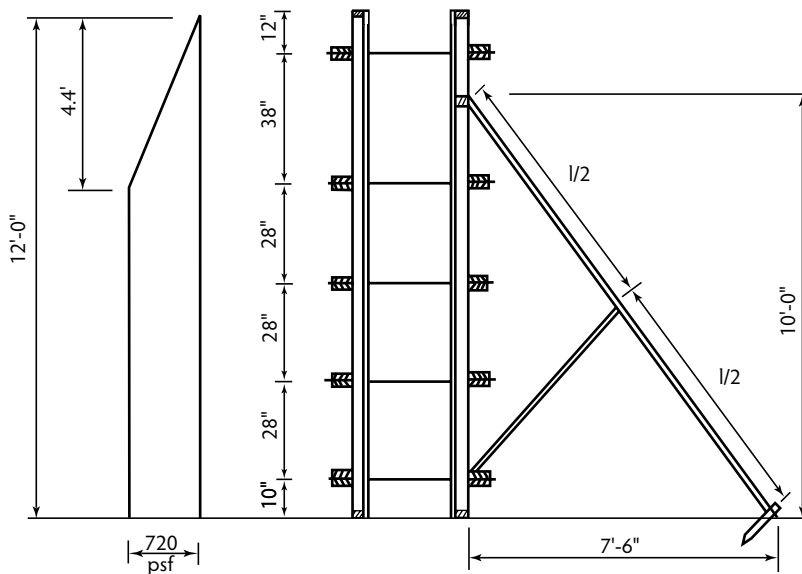


FIGURE 7.41 Layout of wall-form members.

347-04, the loadings would include a wind pressure of 15 psf or a line load of 100 lb/linear foot at the top, whichever is greater. The contractor desires to lay out the braces as shown in Figure 7.41, with the braces at 4 ft on-center, the brace attached at an elevation of 10 ft on the 12-ft form, and the brace anchored to the ground 7.5 ft from the form. This results in a brace length of 12.5 ft, including the adjustable connectors at each end. For design purposes, the brace is assumed to be concentrically loaded, pinned at the top and the bottom, and prevented from translation by the longitudinal rigidity of the form. The horizontal brace load (H) from the wind is:

$$H = 15 \text{ psf} \times 4 \text{ ft} \times 12 \text{ ft} \times 6 \text{ ft}/10 \text{ ft} = 432 \text{ lb}$$

Alternatively, the horizontal brace load from the 100 lb/ft line load is:

$$H = 100 \text{ lb/ft} \times 4 \text{ ft} \times 12 \text{ ft}/10 \text{ ft} = 480 \text{ lb}$$

The brace should be designed to resist a horizontal component of 480 lb, which results in an axial compression force (P) of:

$$P = 480 \text{ lb} \times 12.5 \text{ ft} / 7.5 \text{ ft} = 800 \text{ lb}$$

Try a No. 2 Southern Pine 2×4 brace with a bracing strut at mid-length in the weak buckling direction. For this 2×4 size, the allowable compression stress is:

$$F'_c = F_c \times C_D \times C_M \times C_F \times C_p = 1650 \text{ psi} \times 1.25 \times 0.8 \times 1.0 \times C_p = 1650 \text{ psi} \times C_p = F_c^* \times C_p$$

$$E'_{\min} = E_{\min} \times C_M = 580,000 \text{ psi} \times 0.8 = 464,000 \text{ psi}$$

Because the trial brace is rectangular, check the l_e/d ratios for each buckling axis:

$$\frac{l_1}{d_1} = \frac{150 \text{ in.}}{3.5 \text{ in.}} = 42.8 \leq 50$$

$$\frac{l_2}{d_2} = \frac{75 \text{ in.}}{1.5 \text{ in.}} = 50.0 \leq 50$$

For this short-term construction period loading, a l_e/d limit of 75 might also be considered if necessary. Thus, the weak axis controls, and $l_e/d = 50$. Substituting to determine C_p :

$$F_{cE} = 0.822 E'_{\min} / (l_e/d)^2 = 0.822 \times 464,000 \text{ psi} / (50.0)^2 = 152 \text{ psi}$$

so

$$F_{cE}/F_c^* = 152 \text{ psi} / 1650 \text{ psi} = 0.092$$

and C_p from Equation 7.10 is:

$$C_p = \left[(1 + 0.092) / (2 \times 0.8) \right] - \left\{ \left[(1 + 0.092) / (2 \times 0.8) \right]^2 - (0.092 / 0.8) \right\}^{0.5} = 0.090$$

Thus, the allowable stress in compression parallel to the grain for the unbraced length is:

$$F'_c = F_c^* \times C_p = 1650 \text{ psi} \times C_p = 1650 \text{ psi} \times 0.090 = 149 \text{ psi}$$

$$f_c = P/A = 800 \text{ lb} / 5.25 \text{ in.}^2 = 153 \text{ psi} > 149 \text{ psi (not adequate)}$$

The 2×4 brace with the mid-length strut is slightly less than the needed section. Increase to a 2×6 brace with a mid-length strut, which will be adequate based on the increased area. Alternatively, a steel-pipe brace rated for the load at the extended length of 12.5 ft could be used. Appropriate connection, adequate for a tension or compression of 800 lb, must be made at the top and bottom ends of the brace by bolting, nailing, or use of a rated commercial hardware device, without inducing significant eccentricities.

A possible layout for the wall form is shown in Figure 7.41. The top and bottom extensions of the studs beyond the wales are usually about 1/3 of the adjacent span up to perhaps 12 in. At the top of the form, where the pressures are lower, the span of the studs can be investigated with ramp loading, and the wale spacing can often be increased, sometimes eliminating a level of wales and ties in comparison to the number required for a constant spacing. Careful consideration of all design details, communicating these requirements to the form craftspersons, and providing knowledgeable verification of execution can lead to safe and economical support of concrete during construction.

References

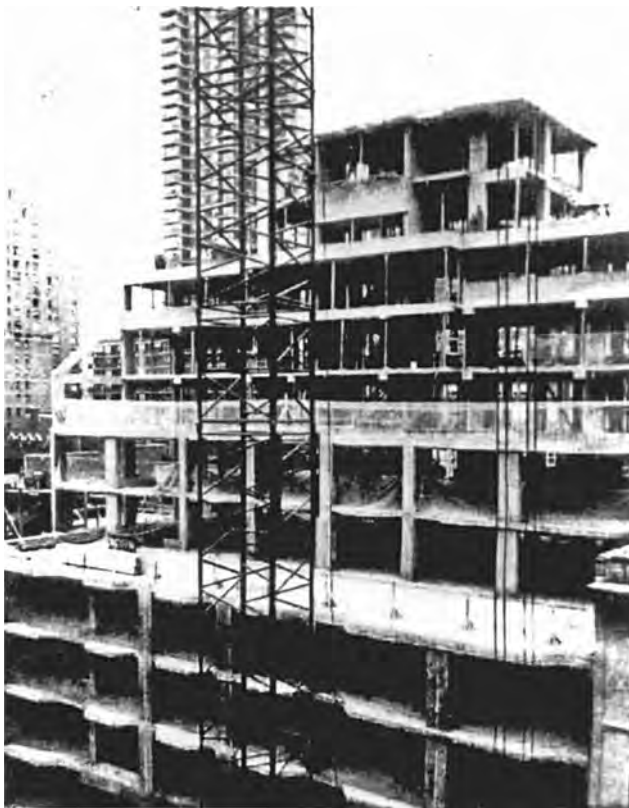
- ACI Committee 347. 2004. *Guide to Formwork for Concrete*, ACI 347-04, 34 pp. American Concrete Institute, Farmington Hills, MI.
- ACI Committee 347, 2005. *Guide to Shoring and Reshoring of Multistory Concrete Buildings*, ACI 347.2R-05, 18 pp. American Concrete Institute, Farmington Hills, MI.
- AFPA. 2005. *National Design Specification for Wood Construction ASD/LRFD*, ANSI/AF&PA NDS-2005. American Forest and Paper Association, Washington, D.C.
- APA. 1997. *Plywood Design Specification*, 31 pp. APA—The Engineered Wood Association, Tacoma, WA.
- APA. 2004. *Concrete Forming*, 27 pp. APA—The Engineered Wood Association, Tacoma, WA.
- ASCE. 2002. *Design Loads on Structures during Construction*, ASCE/SEI 37-02. American Society of Civil Engineers, Reston, VA.
- Hurd, M.K. 2005. *Formwork for Concrete*, 7th ed., SP-4. American Concrete Institute, Farmington Hills, MI.

Further Information

- Aluminum Association, 1525 Wilson Boulevard, Suite 600, Arlington, VA 22209, www.aluminum.org.
- American Concrete Institute, P.O. Box 9094, Farmington Hills, MI 48333-9094, www.concrete.org.
- American Forest and Paper Association/American Wood Council, 1111 19th Street, Suite 800, Washington, D.C. 20036, www.awc.org.
- American National Standards Institute, 11 West 42 Street, New York, NY 10036, www.ansi.org.
- American Society of Civil Engineers, 1801 Alexander Bell Drive, Reston, VA 20191-4400, www.asce.org.
- APA—The Engineered Wood Association, 7011 S. 19th Street, Tacoma, WA 98466, www.apawood.org.
- Scaffolding, Shoring and Forming Institute, Inc., 1300 Sumner Avenue, Cleveland, OH 44115-2851, www.ssf.org.



(a)



(b)

(a) Construction loading in high-rise buildings. (Photograph courtesy of Portland Cement Association, Skokie, IL.)
(b) Ronald McDonald House under construction in New York. (Photograph courtesy of *New York Construction News* and Edward G. Nawy, Rutgers University.)

8

Construction Loading in High-Rise Buildings

S.K. Ghosh, Ph.D., P.E.*

8.1	Introduction	8-1
8.2	Construction Loads.....	8-1
	Design Considerations • Field Verification • Refined Analysis	
8.3	Properties of Concrete at Early Ages	8-19
	Compressive Strength • Tensile Strength and Bond Strength • Punching Shear Strength • Modulus of Elasticity • Shrinkage of Unreinforced (Plain) Concrete • Creep of Unreinforced (Plain) Concrete • Effects of Drying on Flexural Cracking	
8.4	Strength Consequences of Construction Loads.....	8-37
	Safety Analysis • Refined Safety Analysis	
8.5	Serviceability Consequences of Construction Loads.....	8-47
	Causes of Excessive Deflections • Components of Long-Term Deflection • Experimental Investigation • Control of Slab Deflections	
8.6	Codes and Standards.....	8-55
	References	8-55

8.1 Introduction

Structural formwork and its support system must be given careful consideration in two different respects: (1) loads that are applied to the formwork and its supports, and (2) loads that the formwork and its supports apply to the structure. The first is the subject of Chapter 7 on formwork and falsework; the second is the subject of this chapter.

8.2 Construction Loads

8.2.1 Design Considerations

In the construction of multistory buildings with reinforced concrete floor slabs, a step-by-step sequence of operations is employed. The sequence is comprised of the steps of setting up shoring on the most recently poured floor, forming the next floor, setting up reinforcement, and concreting the slab. Because the floor below the one being concreted is usually only a few days old, it is common practice to leave

* President, S.K. Ghosh Associates, Inc., Palatine, Illinois, and Fellow of the American Concrete Institute; specializes in structural design, including wind- and earthquake-resistant design.

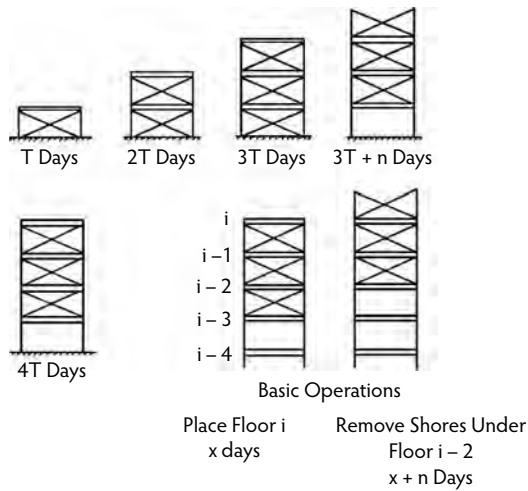


FIGURE 8.1 Construction sequence using three levels of shores.

formwork supports in place between that floor and a small number of floors below it. A typical construction cycle using three levels of shores is illustrated in Figure 8.1.

In discussing construction loads, it is convenient to express them as a factor times the sum of the self-weight of the floor and the dead load of the formwork. The term **floor loading ratio** is used for this factor. Progressive slab deflections that had been causing problems in Sweden in the early 1950s led to the first study by Nielsen (1952) of a rational approach to stripping formwork for floors. Nielsen gave a detailed analysis of the distribution of load between a system of connected shores and floor slabs. The method considered the deformation characteristics of both the slabs and the shores. The maximum load ratio obtained by Nielsen on a slab assuming three levels of shores was 2.56. Grundy and Kabaila (1963) developed a simplified method of analysis for floor loads based on the following assumptions:

1. The slabs behave elastically.
2. Initially, the slabs are supported from a completely rigid foundation.
3. The shores supporting the slabs and formwork may be regarded as a continuous uniform elastic support, the elastic properties of which may be expressed by a coefficient K , where K is the load intensity that produces unit deformation of the support.
4. Any added load is distributed among the supporting slabs in proportion to their relative flexural stiffnesses.

Grundy and Kabaila assumed that K was infinite and carried out their analyses assuming a constant flexural stiffness for all connected slabs, as well as a flexural stiffness increasing with age. It was found that the error introduced by assuming equal relative stiffnesses for the floors is not appreciable.

Figure 8.2 represents the construction of a multifloor building using three levels of shores (and forms) for a 7-day casting cycle, with stripping in 5 days. The loads carried by the slabs and the shores, in terms of the loading ratio, are indicated on the figure adjacent to the element concerned. Floors 1, 2, and 3, supported from the ground by stiff shores, cannot deflect and therefore carry no load; all the load is carried by the shores directly to the foundation. At the age of 26 days, the lowest level of shores is removed, allowing all three slabs to deflect and carry their self-weight. The removed shores are placed on the third floor slab and the fourth floor is poured. As all three supporting slabs have equal stiffness, the weight of the newly poured slab is carried equally by the three lower slabs. The absolute maximum load ratio occurs when the shores connecting the supporting assembly with the ground level are removed; however, the load ratio converges for upper floor levels. For the same structure considered by Nielsen, Grundy

3 Levels of Shoring
Construction Cycle Time, $T = 7$ Days
Time of Removal of Lowest Level of Shores
from Concreting of Top Floor, $m = 5$ Days

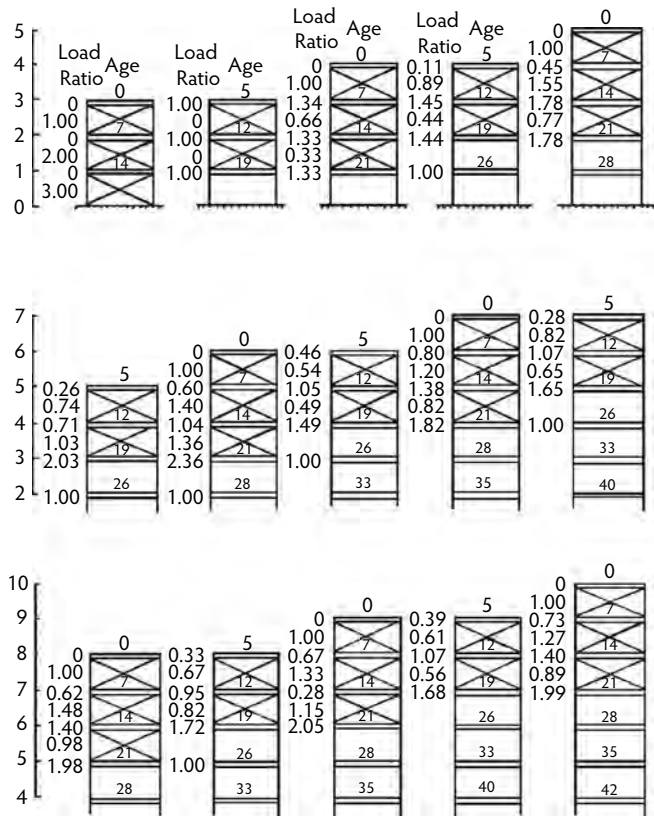


FIGURE 8.2 Load ratio vs. time for three levels of shores.

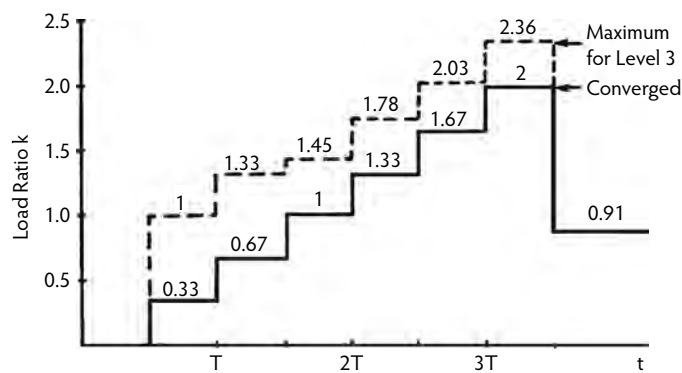


FIGURE 8.3 Load-ratio history for three levels of shores.

and Kabaila obtained an absolute maximum load ratio of 2.36, while the converged value for upper floor levels was 2.00 (Figure 8.2). The most heavily loaded slab is always the last slab that is supported directly from the foundation. The load time histories of the third floor slab and a typical slab are shown in Figure 8.3. Altering the number of shored levels has little effect on the maximum load ratio value; however, by

TABLE 8.1 Floor-Loading Ratio

Author	Maximum Value (Converged Values in Brackets)				Comment
	$m = 2$	$m = 3$	$m = 4$	$m = 5$	
Nielsen (1952)	2.17 2.0Δ	2.28× 2.56+	—	—	Values for floor level 2 only; ×, timber props; +, steel props ($n = 1$); Δ, observed
Grundy and Kabaila (1963)	2.25 (2.00)	2.36 (2.00)	2.43 (2.00)	—	$n = 5$
Beresford (1964)	2.25	(2.00)* (2.06)* 2.35 (2.32)	2.45	2.50	* Obtained for rapid hardening, normal and slow maturing concretes, respectively ($n = 5$)
Blakey and Beresford (1965)	2.25 2.25+	2.3	—	—	+, Stepwise construction
Beresford (1971)	—	2.2 1.5Δ	—	—	$n = 4$; Δ, observed

Note: Here m = number of levels of shoring used and n = time in days for removal of lowest levels of shores after concreting top floor.

Source: Adapted from Wheen, R.J., *Concrete Int.*, 4(5), 56–62, 1982.

decreasing the number of shored levels, the age of the slab at which the maximum ratio occurs also decreases. Beresford (1964) used infinite as well as various finite values of K (see assumption 3 above) and found that the results of floor-load analysis were not appreciably affected.

In addition to variations in moduli of elasticity due to concrete age, cracking of slabs occurring during construction affects the distribution of loads among slabs in the supporting assembly. Sbarounis (1984) reported that incorporating the effects of cracking into the load distribution factors for the supporting slabs reduced the previously calculated maximum load ratios by approximately 10%. Blakey and Beresford (1965) recommended a stepped sequence of construction in a system of floors and shores as a means of controlling the construction loads imposed on both the slabs and the shores. The advantage of this method lies in the fact that a young slab is given more time to develop adequate strength before the application of construction load from the casting of a new slab directly above. Table 8.1, adapted from Wheen (1982), shows clearly that all writers on the subject agree that floor loading ratios during construction usually exceed values of 2.

The sequence of construction illustrated in Figure 8.1 uses three sets of forms. Economic considerations usually necessitate the removal of formwork as soon as possible for reuse. This necessity has given rise to the widespread practice of *reshoring*. The reshoring technique typically involves using only one level of forms or shores and several levels of reshores. Basically, the forms or shores are removed from beneath a slab, allowing it to deflect and carry its own weight; reshores are then installed, allowing the load during subsequent concrete placement to be shared between the various slabs in the supporting assembly. At the time of installation, reshores carry no significant load. Figure 8.4 illustrates a construction scheme with two levels of shoring and one level of reshoring.

Agarwal and Gardner (1974) in Canada and Marosszeky (1972) in Australia analyzed the loads imposed on slabs using the shoring/reshoring method of construction and utilizing the same simplifying assumptions as used earlier by Grundy and Kabaila (1963). The slab loads when using two levels of shores and one level of reshores are calculated as shown in Figure 8.5. The time history of slab loads using two levels of shores and one level of reshores is shown in Figure 8.6.

Taylor (1967) suggested a technique of stripping formwork to reduce the loads imposed on a slab during construction. By slackening and tightening adjustable shores before each new slab is cast, the loads distributed to the shores and slabs are reduced considerably. With this method, all shores at one level must be slackened simultaneously; thus, it requires greater supervision and inspection. Taylor reported that the maximum load ratio was reduced from the 2.36 obtained by Grundy and Kabaila to a

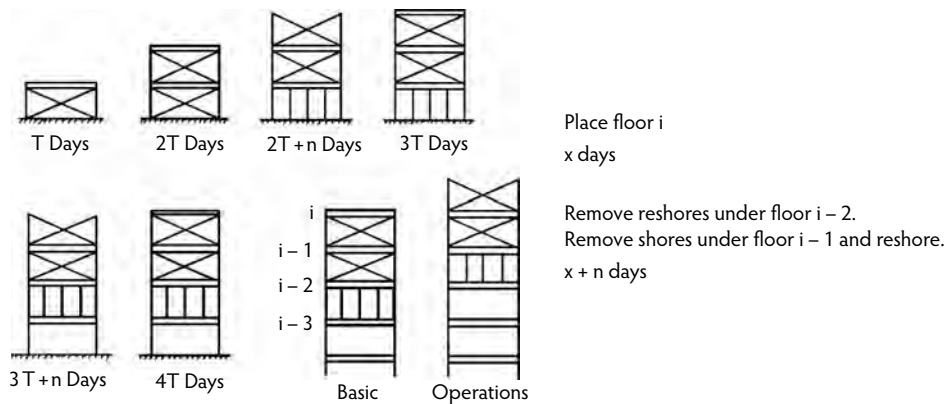


FIGURE 8.4 Construction sequence using two levels of shores and one level of reshores.

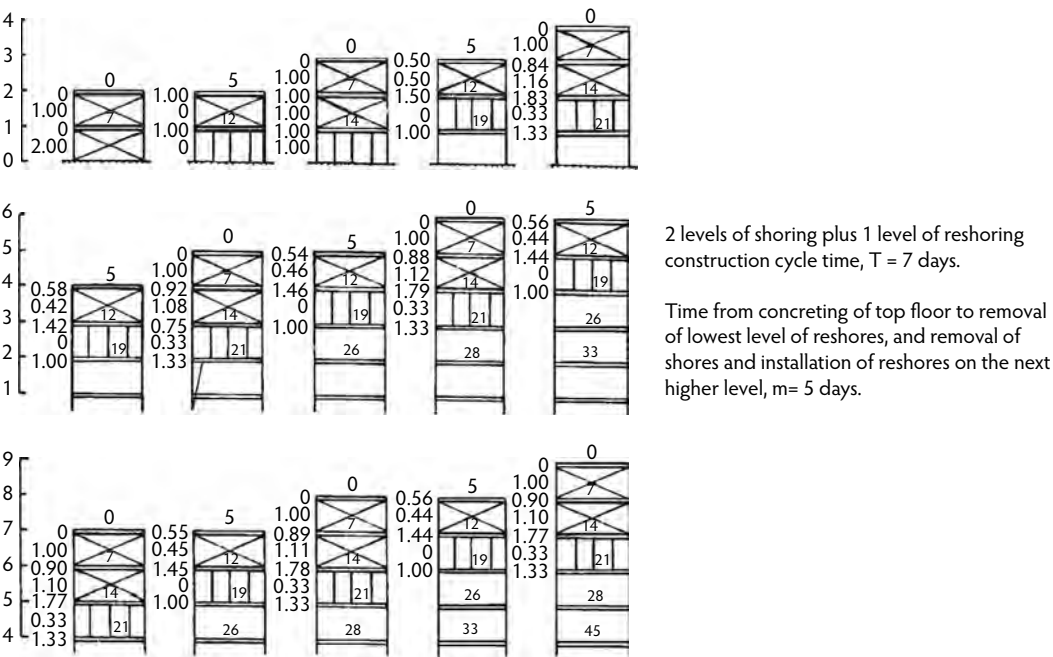


FIGURE 8.5 Load ratio vs. time for two levels of shores and one level of reshores.

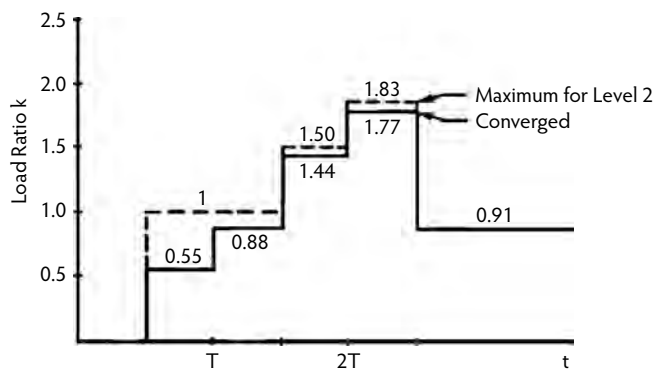


FIGURE 8.6 Load-ratio history for two levels of shores and one level of reshores.

TABLE 8.2 Theoretical Maximum Load Ratios on Floor and Prop for Various Shore/Reshore Combinations

Shore + Reshore	Absolute Maximum Load Ratio		Converged Maximum Load Ratio	
	On Floor Slab	On Prop	On Floor Slab	On Prop
1 + 1	1.50	1.0	1.50	1.0
1 + 2	1.34	1.0	1.34	1.0
1 + 3	1.25	1.0	1.25	1.0
1 + 4	1.20	1.0	1.20	1.0
1 + 5	1.17	1.0	1.17	1.0
2 + 0	2.25	2.0	2.00	1.0
2 + 1	1.83	2.0	1.78	1.11
2 + 2	1.75	2.0	1.67	1.17
2 + 3	1.61	2.0	1.60	1.21
2 + 4	1.60	2.0	1.56	1.25
2 + 5	1.55	2.0	1.53	1.24
3 + 0	2.36	3.0	2.00	1.34
3 + 1	2.10	3.0	1.87	1.37
3 + 2	1.97	3.0	1.80	1.40
3 + 3	1.84	3.0	1.76	1.42
3 + 4	1.77	3.0	1.72	1.43
3 + 5	1.77	3.0	1.70	1.43

Source: Lasisi, M.Y. and Ng, S.F., *Concrete Int.*, 1(2), 24–29, 1979.

value of 1.44. Taylor's method is the same in principle as stripping and immediate reshoring of a slab. Marosszeczy (1972) described complete release and reshoring of a floor slab such that the floor carried its own dead weight at a time $(T - 1)$ days, where T is the construction cycle of floors. This reshoring technique produces less construction load on the supporting slabs and props when compared with using undisturbed shores.

Although the load ratios previously defined reflect the slab-plus-formwork dead weights, a construction live load is also present. Whereas the dead load can be estimated with reasonable certainty, the live loads can vary significantly depending on the construction method used to place concrete. ACI Committee 347 (2004) recommends that the design live load should be at least 50 psf (2.4 kPa) of the horizontal projection. A comprehensive study (Fattal, 1983) on construction loads in concrete buildings indicated that, when concrete is placed by a bucket, the live load may be as high as 40 to 50 psf (1.9 to 2.4 kPa). On the other hand, the American National Standards Institute (ANSI) Standard A10.9 (1997) does not provide a numerical value and leaves the determination of live load to the formwork designer; however, the standard does list factors to be considered in estimating the design load, such as the weight of workers, equipment, runways, and impact of concrete.

Hurd (2005) has suggested a minimum construction live load of 50 psf (2.4 kPa) for designing forms. Lasisi and Ng (1979) presented a method to include the live-load effect. For a typical flat-plate structure, assuming a supporting assembly of two shore levels plus one reshore level, a construction live load of 50 psf (2.4 kPa) removed after the casting day, and a constant modulus of elasticity for the connected slabs, the absolute maximum load ratio would increase 9% over that predicted by Grundy and Kabaila (1963). Both Agarwal and Gardner (1974) and Sbarounis (1984) accounted for the construction live-load effect by increasing the maximum load carried by the lowest slab in the supporting assembly. Sbarounis recommended additional loads, due to a 50-psf (2.4-kPa) live load, of $55/N$ and $35/N$ psf ($2.6/N$ and $1.7/N$ kPa) for uncracked and cracked slabs, respectively, with N representing the total number of levels in the supporting assembly.

Table 8.2 shows absolute maximum and converged maximum load ratios on slabs and supporting props for various combinations of levels of shores and reshores. Table 8.2 and Figure 8.6 indicate that the use of two levels of shoring and one level of reshoring, rather than three levels of shores, reduces the

TABLE 8.3 Comparison of Construction Loads with Service Loads

Construction Loads (psf)		Service Loads (psf)	
8-in. slab	100	8-in. slab	100
Formwork	10	Ceiling and mechanical	15
Subtotal	110	Partitions	20
		Live load	50
		Total (after 28 days)	185
Load Ratio			
3 Level of Shores		2 Levels of Shores Plus 1 Level of Reshores	
1.00 at 5 days	110	1.00 at 5 days	110
1.34 at 7 days	147	1.00 at 7 days	110
1.45 at 12 days	160	1.50 at 12 days ^b	165
1.78 at 14 days	196	1.83 at 14 days	201
2.03 at 19 days	223 ^a	1.00 at 19 days	110
2.36 at 21 days	260		
1.00 at 26 days	110		

^a Deflection not restrained beyond 19 days.

^b Allowed to deflect under these construction loads at 12 days. Further deflections partly restrained for the next 7 days.

absolute maximum load ratio from 2.00 to 1.78. This is advantageous in most situations, although with reshoring the maximum load ratios come into play at an earlier age than with shoring, as should be apparent from Figure 8.2 and Figure 8.5. Table 8.3 presents construction loads for floor 3, which experiences the absolute maximum load ratio. The construction loads are compared with the design service loads in the table. It is clear that the construction loads are more critical than the design loads. Also important, construction loads act on concrete that has not attained the age at which it is supposed to experience design service loads.

8.2.2 Field Verification

Agarwal and Gardner (1974) used field measurements to check the accuracy of various analysis methods for estimating the shore and slab load distribution. Their investigation consisted of directly measuring the load ratios applied to shores and reshores during construction and determining the loads carried by the floor slabs at different stages of construction. The shore and reshore loads for two buildings were measured: Alta Vista Towers in Ottawa, Ontario, Canada, and Place du Portage in Hull, Quebec, Canada. Steel shores were used for both structures. Three levels of shores and four levels of reshores were used to temporarily support the flat-slab floors in the construction of the 22-story Alta Vista Towers. Measurement of the shore and reshore loads, for the shore and reshore arrangements shown in Figure 8.7, was limited to the 7th through the 13th stories. Three levels of shores and no reshores were used in the construction of the 27-story Place du Portage structure, which is a flat-slab office building. The shoring arrangement is shown in Figure 8.8. Measurements were taken from the 19th through the 22nd stories.

According to Liu et al. (1985a), three factors concerning the field measurement data should be noted:

1. Field measurements were not taken from the ground level, so the actual slab and shore loads of the entire system during construction were not available.
2. Typical shores and reshores chosen for instrumentation were located in the central portions of the slabs (Figure 8.7 and Figure 8.8); thus, the influence of the surrounding boundary beams and columns was less pronounced. From the measured data reported in Agarwal and Gardner (1974),

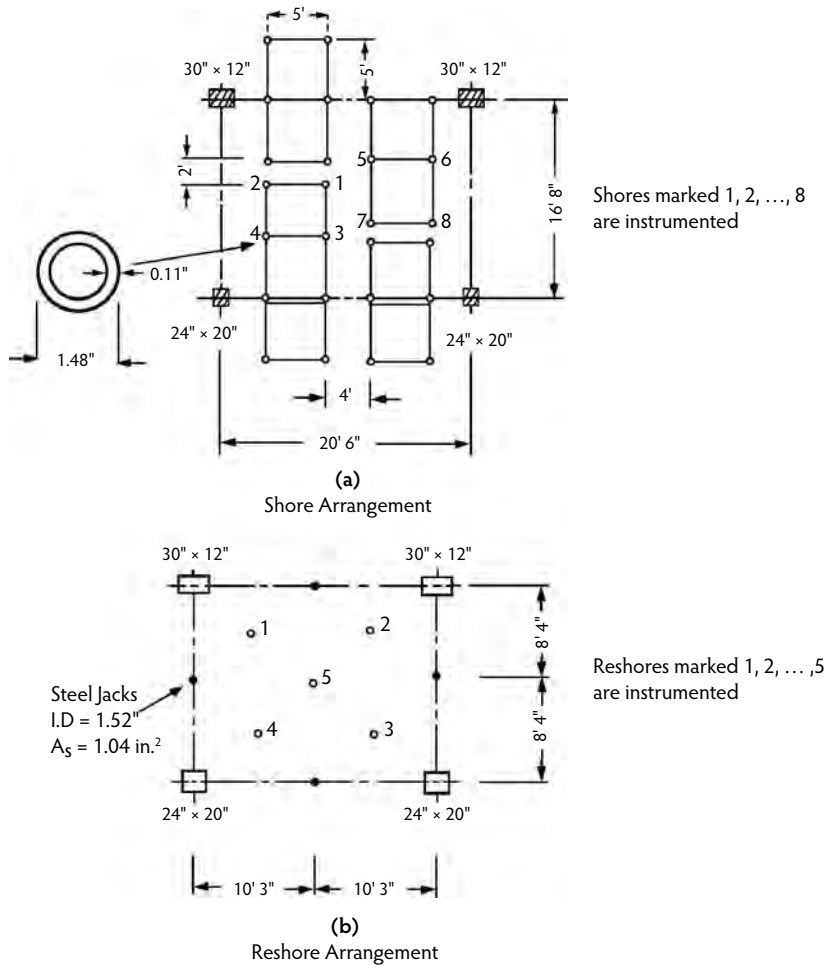


FIGURE 8.7 (a) Shore and (b) reshore arrangements for Alta Vista Towers. (From Agarwal, R.K. and Gardner, N.J., *ACI J.*, 71(11), 559–569, 1974.)

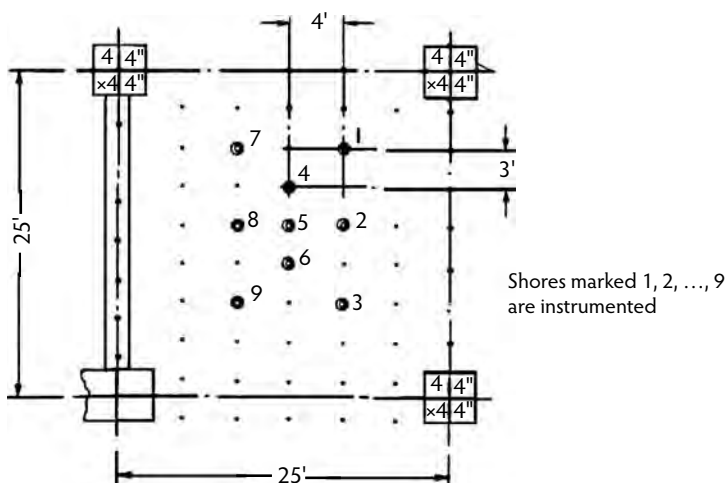


FIGURE 8.8 Shoring arrangements for Place du Portage. (From Agarwal, R.K. and Gardner, N.J., *ACI J.*, 71(11), 559–569, 1974.)

the coefficient of variation of the shore axial force varied from 0.04 to 0.23, depending on the distance of the shore from the boundary line.

3. The values of the modulus of elasticity of concrete (E_c) and the shore height were not reported in Agarwal and Gardner (1974). Without these, it is not possible to use the measured shore-load data to check other methods further.

Comparisons between field measurements for both buildings and the slab and shore loads given by the simplified analysis of Grundy and Kabaila (1963) are reported in Agarwal and Gardner (1974). To check the assumptions of equal slab stiffness originally used by Grundy and Kabaila, the slab shore loads were calculated by both using equal slab stiffnesses and varying the slab stiffness for each floor to account for an increase in E_c with age. Table 8.4 shows the comparison of field measurements for each story in both buildings to the calculated maximum slab and shore loads.

Good agreement between the predictions of simplified analysis and the field measurements was generally observed. Uses of variable slab stiffnesses in the simplified analysis produced closer agreement: The maximum discrepancy for variable slab stiffness was less than 10%, but for constant slab stiffness it was as high as 16%. Further, it was shown in Agarwal and Gardner (1974) that the calculated results based on either constant or variable slab stiffnesses consistently predicted the correct construction step and the location of the maximum shore and slab loads.

Lasisi and Ng (1979) carried out measurements on 5 regular floors to investigate peak construction loads on slabs, shores, and reshores in a 15-story flat-slab office building in Ottawa, Canada. One level of shores and two levels of reshores were utilized in construction. The period between the casting of a slab section and the next slab directly above was 10 days on average. The forms were supported on tubular steel shores. Reshores were made of telescopic steel jacks. The average stripping time for a slab in the instrumented section of the building was 5 days. Measurement on this building was commenced during concreting of the 7th-floor slab and continued until after the stripping of the 11th floor. An interior bay of a section of the building was instrumented. Load cells were installed beneath a shore or a reshore at the chosen location; the instrumented reshore on each level was vertically below the load cell placed underneath the scaffold shore.

Shore and reshore loads were calculated by Lasisi and Ng (1979) using Grundy and Kabaila's simplified analysis, taking into consideration the presence of 50 psf (2.4 kPa) of construction live load during concrete placement. As can be seen from Table 8.5, there was reasonably close agreement between measured and theoretical maximum shore loads; however, the loads measured on the reshores were found to be on average considerably less than the corresponding theoretical values.

8.2.3 Refined Analysis

Liu et al. (1985a) carried out refined analysis to determine shore and slab load distribution, considering the actual rigidity of shores and the time-dependent variation in slab stiffness due to concrete maturity. Their refined analysis technique treated the shore-slab interaction as a two-dimensional problem and was based on the following assumptions:

1. The slabs behave elastically and their stiffnesses are time-dependent.
2. The shores and reshores behave as continuous uniform elastic supports, and their axial stiffnesses are finite and time-independent.
3. The foundation is rigid.
4. The joints between the shores and slabs are pinned connections.
5. The slab edges are either fixed or simply supported.

Comparison of maximum loads computed by the simplified Grundy-Kabaila method (1963) with those predicted by the refined method indicated that the maximum relative differences in the two methods varied between -5 and +9%. Because the effect of shore stiffness was not considered, the calculated results using the simplified method showed larger errors (deviations from field measurements) than the results

TABLE 8.4 A Comparison between Field Measurements and Calculated Maximum Slab and Shore Loads

Building	Level	Maximum Slab Load ÷ Slab Weight			Maximum Shore Load ÷ Slab Weight						
		Field Measurement (1)	Calculation with E_c Constant (2)	Calculation with E_c Variable (3)	Field Measurement (4)	Calculation with E_c Constant (5)	Calculation with E_c Variable (6)	Comparisons			
								(2)/(1)	(3)/(1)	(4)/(5)	(4)/(6)
Alta Vista Towers	7	1.88	1.72	1.83	0.91	0.97	1.65	1.40	1.58	0.85	0.96
	8	1.93	1.70	1.85	0.88	0.96	1.51	1.46	1.57	0.97	1.04
	9	1.91	1.72	1.74	0.90	0.91	1.70	1.42	1.58	0.84	0.93
	10	2.02	1.72	1.99	0.85	0.99	1.37	1.43	1.46	1.04	1.07
	11	1.07	1.13	0.99	1.06	0.93	1.68	1.44	1.62	0.89	1.00
	12						1.64	1.43	1.61	0.87	0.98
Standard deviation	Mean				0.92	0.95				0.90	1.00
					0.08	0.03				0.09	0.05
Place du Portage	19	2.11		2.11		1.00	1.48		1.41		0.95
	20	1.34		1.30		0.97	1.44		1.44		1.00
	21						1.45		1.41		0.97
Standard deviation	Mean					0.99					0.97
						0.02					0.03

Source: Taylor, P.J., *Australian Civil Eng. Const.*, 8(2), 31–35, 1967.

TABLE 8.5 Measured Construction Loads on Shores and Reshores

Shore or Reshore Resting on Level	Construction Operation		Imposed Loads		
	A (Concreting)	B (After Stripping and Reshoring)	psf	Load Ratios	Theoretical Load Ratios
4	A-7R	—	50.1	0.40	0.47
5	A-7R	—	77.0	0.62	0.93
	—	B-7R	5.0	0.04	0
6	A-8R	—	13.4	0.11	0.47
	A-7S	—	154.0	1.23	1.40
	—	B-7	—	—	—
	A-8R	—	97.3	0.78	0.93
	—	B-8R	8.9	0.07	0
7	A-9R	—	17.6	0.14	0.47
	A-8S	—	188.8	1.51	1.40
	—	B-8	—	—	—
	A-9R	—	106.4	0.85	0.93
	—	B-9R	21.1	0.17	0
8	A-10R	—	40.1	0.32	0.47
	A-9S	—	209.5	1.68	1.40
	—	B-9	—	—	—
	A-10R	—	110.9	0.89	0.93
	—	B-10R	9.4	0.08	0
9	A-11R	—	28.2	0.23	0.47
	A-10S	—	135.6	1.09	1.40
	—	B-10	—	—	—
	A-11R	—	59.9	0.48	0.93
	—	B-11R	23.3	0.19	0
10	A-11S	—	182.5	1.46	1.40
	—	B-11	—	—	—

Note: S, shore; R, reshore.

Source: Lasisi, M.Y. and Ng, S.F., *Concrete Int.*, 1(2), 24–29, 1979.

predicted using the refined method. The simplified Grundy–Kabaila method reliably predicted the construction step and location where the maximum slab and shore loads would occur but generally underestimated the actual load ratios; consequently, the maximum slab and shore loads predicted by the simplified method could be corrected using a modification coefficient. Liu et al. (1985a) recommended that the value of the modification coefficient for the simplified method vary from 1.05 to 1.10 for design purposes.

Liu et al. (1985b) also used a more realistic three-dimensional (3-D) model to check the approximation of the Grundy–Kabaila simplified method and the two-dimensional (2-D) refined method (Liu et al., 1985a). A number of simplifying assumptions were made when they conducted the refined 3-day analysis. First, the reinforced concrete slabs were assumed to behave elastically; their stiffnesses were taken as time dependent; slab edges were either free or rotationally fixed (but free to deflect). Second, the vertical deflections of the slabs at the slab–column joints were neglected. Third, the weight and structural details of each floor were assumed to be similar. Fourth, the shores and reshores were presumed to be continuous ideal elastic supports with equal axial stiffnesses; the joints between the shores and the slabs were assumed to be pin-ended connections. Finally, the foundation was assumed to be rigid and unyielding. The influences of foundation rigidity, column deformation, and slab aspect ratio were examined using the 3-day model.

On the basis of the various factors examined for the 3-day model, the following conclusions and observations were made:

1. The maximum slab loads given by the 2-day refined analysis and the 3-day refined analysis were nearly identical. The maximum shore load increased slightly for the 3-day refined analysis.
2. Variations of the foundation rigidity affected slab displacements more than the maximum shore loads and slab moments. When the rigidity of the foundation decreased, the maximum slab moments and the maximum shore loads decreased.
3. The vertical deformation of columns could be neglected when computing the maximum shore loads and slab moments.
4. A change in the slab aspect ratio produced very little increment in the maximum shore load for slabs with free edges. For a slab with fixed edges, the total increment of the maximum shore load was 3% for the aspect ratios examined (between 0.6 and 1.0).

In all cases examined, a modification coefficient that varied from 1.05 to 1.10 could be used to conservatively correct the results of the Grundy–Kabaila simplified method. It was found that nonuniform distribution of shore stiffnesses did not change the prediction of the construction step and location where the maximum slab moments and shore loads occurred.

Stivaros and Halvorsen (1990) questioned the good agreement mentioned earlier between the simplified Grundy–Kabaila method and existing field measurements. They pointed out that, in actual building cases investigated (Agarwal and Gardner, 1974; Lasisi and Ng, 1979), steel shoring systems had been used, justifying the Grundy–Kabaila assumption of infinite shoring system stiffness. The fact that the field measurements were observations around the center of the slab and thus ignored the influence of structural continuity contributed to the good agreement between field data and the theoretical values. Another important fact was that field measurements were not taken from the ground level, so the complete loading–unloading construction cycle was not recorded.

Stivaros and Halvorsen (1991) also pointed out that most practical methods for analyzing construction loads have employed single-bay idealizations of frames. This is a definite limitation to the proper evaluation of the punching shear forces that are the critical load effect in most flat-slab systems. A single-bay structural idealization cannot fully assess the maximum shear force effects at the columns from both direct shear forces and unbalanced moments; therefore, a practical and simple method that took into account the continuity of concrete structures over several bays, as well as the interaction of the floor slabs and the shoring system over several stories, was thought to be needed.

The *equivalent frame method* (EFM) of analysis was found by Stivaros and Halvorsen (1990) to be a reasonable procedure for accomplishing the preceding goal. The EFM was first developed as a viable procedure for analyzing reinforced concrete slab systems, particularly for the effects of gravity loads. It has been applied to lateral load analysis of slab systems, as well. A computer program was developed for the study to determine the construction load distribution among the slabs and the shoring system during the construction of multistory buildings. A multistory building under construction is modeled according to the assumptions of the equivalent frame method as described in ACI Committee 318 (2005). A schematic representation of an idealized structure is shown in Figure 8.9. The shores and reshores are replaced by an equal number of elastic supports, each having a stiffness equal to the total stiffness of the corresponding shores. It is assumed that the reshores carry no load at the time of installation. The load of the freshly cast concrete is applied to the top-floor shores as concentrated loads. The load is shared among the shores according to their tributary areas. The connection between the shores or reshores and the floor slabs can be reasonably assumed to be pin-jointed. At ground level, shores and reshores are assumed to be supported on a rigid foundation. The EFM concepts are applied to determine the frame member stiffness coefficients. The idealized two-dimensional frame is then analyzed elastically using conventional stiffness analysis procedures to determine the member forces, including the axial load on the shoring system.

A typical floor plan of the equivalent frame used by Stivaros and Halvorsen (1990) for parametric studies is shown in Figure 8.10. The shores and reshores are idealized as series of vertical truss-type elements, each with a stiffness equivalent to the total stiffness of the shores or reshores on the row it

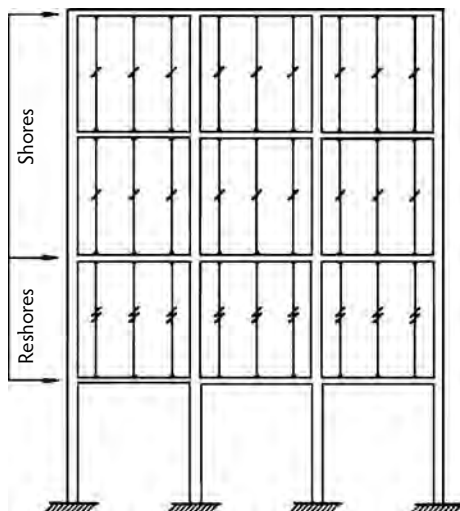


FIGURE 8.9 Structural idealization. (From Stivaros, P.C. and Halvorsen, G.T., *Concrete Int.*, 13(8), 57–62, 1991.)

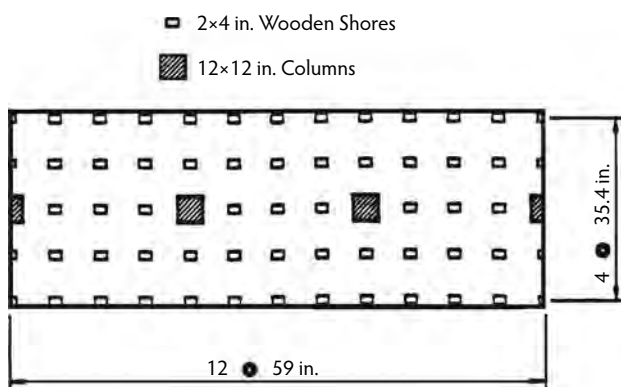


FIGURE 8.10 Typical plan of equivalent frame studied by Stivaros and Halvorsen. (From Stivaros, P.C. and Halvorsen, G.T., *ACI Struct. J.*, 87(5), 589–596, 1990.)

represents. Two levels of shores and one level of reshores were assumed, with a construction rate of one floor per week. Only the slab dead load was considered in analysis. The loads in slabs were normalized to the self-weight of each slab, and the loads on shores were normalized to the weight of the slab supported by the shores. The construction operations were denoted with a set of two numbers. The first number represented the number of the floor level under construction, and the second indicated the phase of construction (Figure 8.11). The numeral 1 indicated casting of the top floor, 2 denoted the removal of lower level of reshores, and 3 indicated the removal of the lower level shores; for example, “Operation 3–2” referred to the maximum slab or shore loads during removal of the lower level of reshores after casting the third floor. The maximum slab loads evaluated using the EFM, both multi-bay and single-bay models, along with the corresponding results of the simplified Grundy–Kabaila method and results by Liu et al., are plotted in Figure 8.12 with respect to the sequential construction operations. The results reported for the EFM multi-bay model are those for an interior bay.

Figure 8.13 and Figure 8.14 show the variation of the maximum slab load with respect to the number of reshored levels for both the equivalent frame model and the simplified method for one level and two levels of shoring, respectively. As the figures show, the EFM and the simplified method diverge as the number of reshored levels increases. As the number of shored levels increases (comparing both figures), the diversion of the EFM from the simplified method slows. Figure 8.14 shows that the combination of

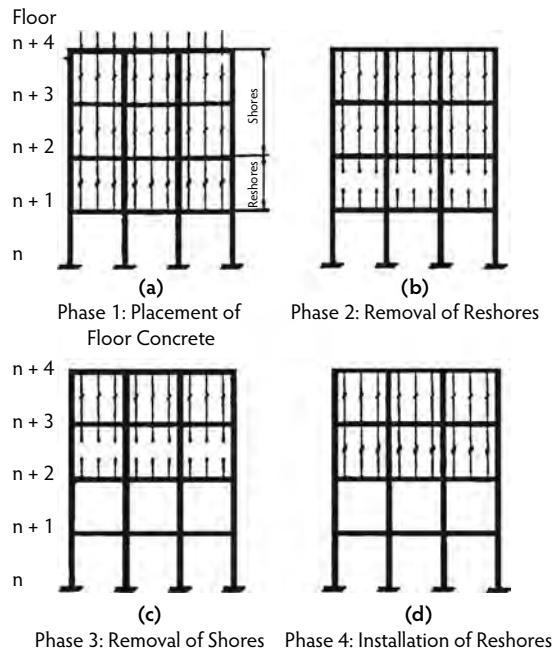


FIGURE 8.11 Construction phases. (From Stivaros, P.C. and Halvorsen, G.T., *Concrete Int.*, 14(8), 27–32, 1992.)

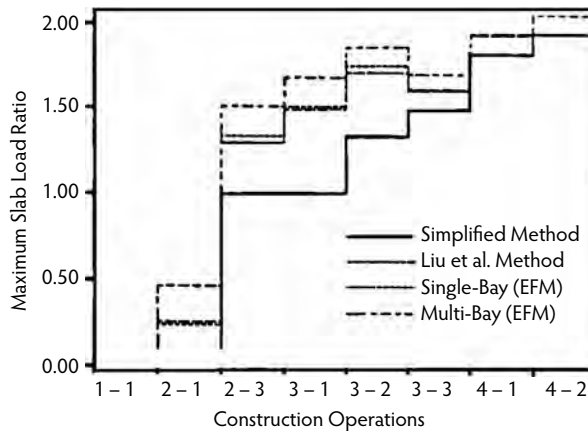


FIGURE 8.12 Comparison of methods of construction load analysis. (From Stivaros, P.C. and Halvorsen, G.T., *ACI Struct. J.*, 87(5), 589–596, 1990.)

two shored levels and one reshored level (the combination used by Liu et al.) is a case where the EFM and the simplified method converge with a difference of about 5%. The difference increases as the number of reshored levels increases, approaching 15% when three reshored levels are used. Considering the case of the one-shore scheme with four reshored levels from Figure 8.13, the difference between the two methods is about 30%.

Figure 8.15 shows the variation of the maximum slab load with respect to the number of reshored levels for one level of shoring and for both the single-bay and multi-bay models. As can be seen, the two methods diverge as the number of reshored levels increases. The multi-bay model always predicts higher maximum slab loads than the single-bay model, with differences as great as 14% in the case of three reshored levels.

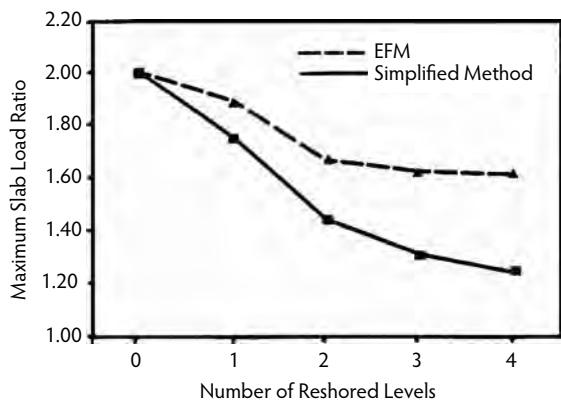


FIGURE 8.13 Comparison of EFM and simplified method: one shored level. (From Stivaros, P.C. and Halvorsen, G.T., *ACI Struct. J.*, 87(5), 589–596, 1990.)

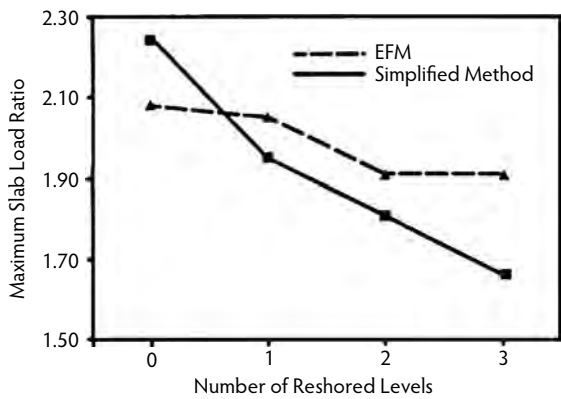


FIGURE 8.14 Comparison of EFM and simplified method: two shored levels. (From Stivaros, P.C. and Halvorsen, G.T., *ACI Struct. J.*, 87(5), 589–596, 1990.)

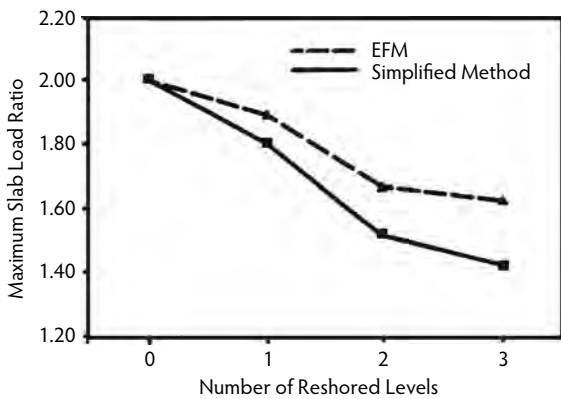


FIGURE 8.15 Comparison of single-bay and multi-bay models: one shored level. (From Stivaros, P.C. and Halvorsen, G.T., *ACI Struct. J.*, 87(5), 589–596, 1990.)

The stiffness of the shoring system affects the behavior of both the single-bay and multi-bay models. Figure 8.16 shows the variation of the maximum slab load of the first floor during the casting of the third floor with respect to the shoring system stiffness for both models. The stiffness of the shoring system varies

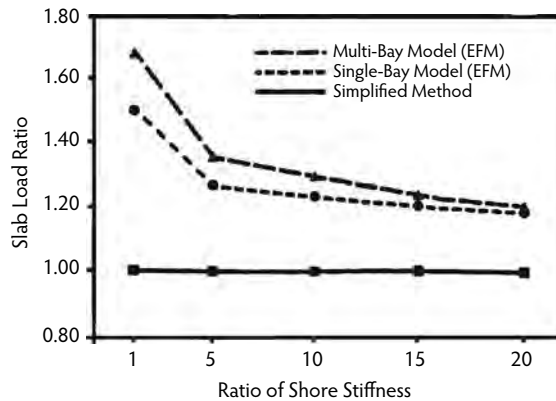


FIGURE 8.16 Comparison of analytical models based on shoring system stiffness. (From Stivaros, P.C. and Halvorsen, G.T., *ACI Struct. J.*, 87(5), 589–596, 1990.)

in five increments from the actual value to 20 times the actual value. As the figure shows, the multi-bay model predicts higher values than the single-bay model. As the stiffness of the shoring system increases, both methods tend to converge. When the stiffness reaches a relatively infinite value, both methods produce almost identical results approaching the simplified method. The multi-bay model is more advantageous than the single-bay model because it represents the concrete structure as a more realistic monolithic continuous frame. Furthermore, it can provide information about the total shear force (due to the gravity load and the unbalanced moments) applied to slab–column joints. Considering the advantages that multi-bay analysis offers, it is preferable to apply the more realistic continuous multi-bay model when possible.

To investigate the influence of slab stiffness, the construction example was analyzed for two construction cycles of 3 and 7 days. The percentages of the 28-day concrete strength for the 3- and 7-day cycles were determined using the maturity concept. The age of the slab at which the maximum load occurred differed for the two construction schedules. Figure 8.17 shows the maximum slab loads with respect to the slab age in days for the 3- and 7-day construction rates. Despite the fact that both schedules predict almost identical maximum slab loads, the ages of the slabs under these loads are different. The maximum load of 2.08 times the slab self-weight for the 3-day schedule occurred on a 7-day-old slab, whereas the maximum load of 2.06 times the slab self-weight for the 7-day schedule occurred on a 19-day-old slab.

The presence of drop panels around the columns or beams between columns can significantly increase the stiffness of slabs and columns. To determine the influence of drop panels and beams, the construction example was analyzed for two additional conditions. The first condition assumes beams spanning between columns in both directions, with an overall depth of 20 in. (510 mm) and width of 12 in. (300 mm). The second condition assumes a type of flat-slab construction with square drop panels around columns with depth equal to half the slab thickness of 7.1 in. (180 mm) and length equal to one third the 236-in. (6000-mm) span. Figure 8.18 compares the results of the cases with and without beams or drop panels. The slabs with beams or drop panels share higher loads than the flat-plate slab because the beams and the drop panels increase the stiffness of the slab. A similar construction load distribution occurs when the slab thickness and, consequently, the slab stiffness are increased. The degree of influence of beams, drop panels, or the slab thickness on the construction load distribution is totally dependent on the size of these structural members relative to the global size of the equivalent frame as well as on the stiffness of the shoring system. If the stiffness of the shoring system is infinite relative to the stiffness of the supported slabs, the effect of the slab stiffness variation on the load distribution will be minimal.

To determine the influence of the axial shore stiffness on the load distribution, the construction example was investigated by increasing the shoring system stiffness by 5 increments up to 20 times the actual value. The slab stiffness and the number of shores or reshores per bay were kept constant for this analysis, the results of which are shown in Figure 8.19. As can be seen, the shoring stiffness has a

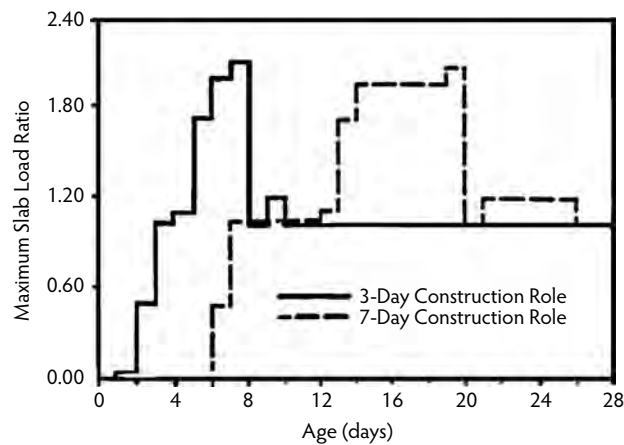


FIGURE 8.17 Comparison of construction rates. (From Stivaros, P.C. and Halvorsen, G.T., *ACI Struct. J.*, 87(5), 589–596, 1990.)

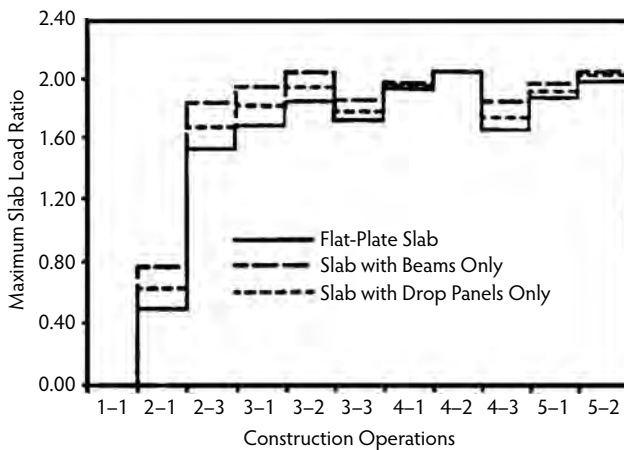


FIGURE 8.18 Comparison of slab types. (From Stivaros, P.C. and Halvorsen, G.T., *ACI Struct. J.*, 87(5), 589–596, 1990.)

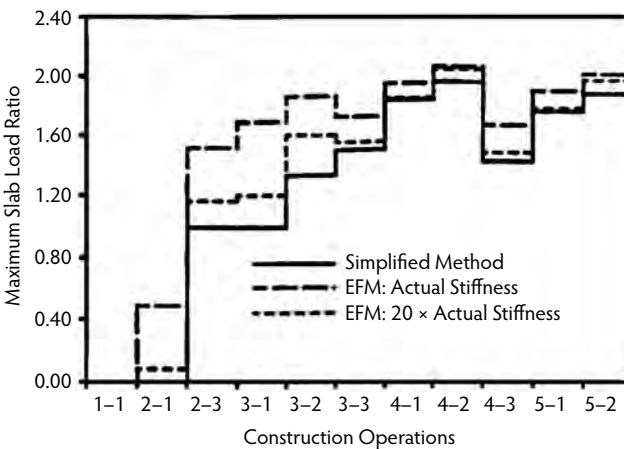


FIGURE 8.19 Comparison of shoring system stiffnesses. (From Stivaros, P.C. and Halvorsen, G.T., *ACI Struct. J.*, 87(5), 589–596, 1990.)

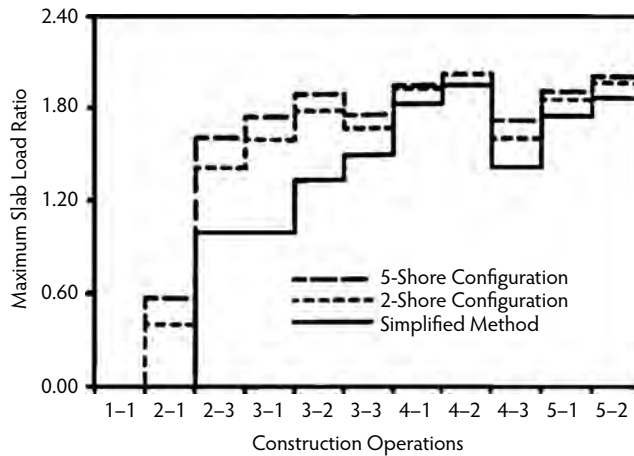


FIGURE 8.20 Comparison of shoring configuration types. (From Stivaros, P.C. and Halvorsen, G.T., *ACI Struct. J.*, 87(5), 589–596, 1990.)

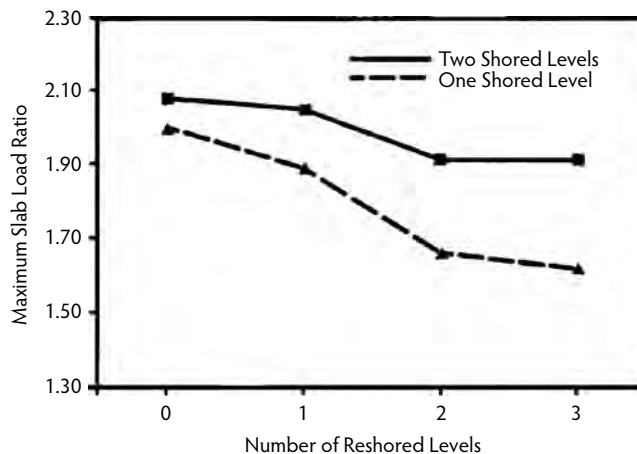


FIGURE 8.21 Influence of the number of reshored levels on the maximum slab load. (From Stivaros, P.C. and Halvorsen, G.T., *ACI Struct. J.*, 87(5), 589–596, 1990.)

considerable influence on the construction load distribution. The difference in the slab load, for example, is up to 40% during Operation 3-1. Figure 8.19 also incorporates the values predicted by the simplified method and illustrates how the shoring system stiffness affects the slab load during construction. An important observation from Figure 8.19 is that, as the stiffness of the shoring system approaches infinity, the predicted maximum slab loads using the EFM draw near the loads predicted by the simplified method. This clearly shows that the differences of the equivalent frame method and the simplified method are very much due to the shoring system stiffness.

It has been common practice to consider the shores to be spaced closely enough that shore reactions can be treated as uniformly distributed. This may not be true when a flying-truss forming system is used. To determine the effects of various shoring systems, the construction example was investigated using two, three, four, and five shores in each bay. The total stiffness of shores and reshores in each bay was kept constant for all cases and was evenly distributed among the shores and reshores. The slab stiffness was also kept constant. As can be seen from Figure 8.20, the two-shore-per-bay configuration predicts lower values than the five-shore configuration throughout the construction, despite the fact that the total stiffness of the shoring system is the same for both cases. The fewer the number of shores per bay, the

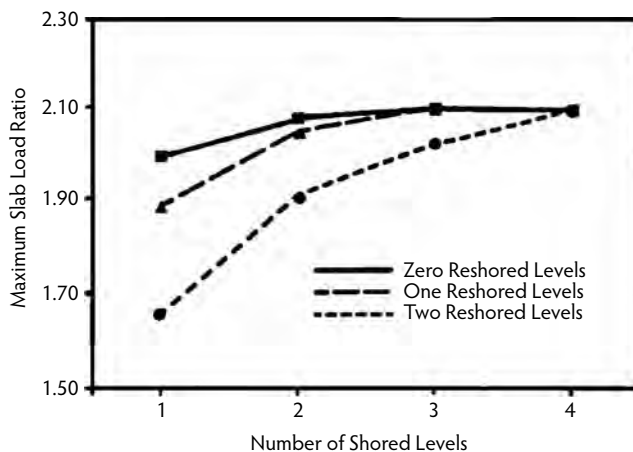


FIGURE 8.22 Influence of the number of shored levels on the maximum slab load. (From Stivaros, P.C. and Halvorsen, G.T., *ACI Struct. J.*, 87(5), 589–596, 1990.)

lower the construction load the floor slabs share. A comparison between the two-shore and five-shore configurations and the simplified method shows that the two-shore configuration is closer to the simplified method. Thus, the simplified method is more suitable for cases with fewer concentrated reaction-type shores per bay. The simplified method underestimates the construction slab loads during the early stages of construction, when a more dense shoring system is used. Figure 8.21 shows how the maximum slab load changes with respect to the number of reshored levels for combinations with one and two levels of shoring. The maximum slab load decreases at a decreasing rate as the number of reshored levels increases.

According to the simplified method, any applied construction load is distributed equally among the interconnected slabs or in proportion to their relative stiffnesses. As the number of slabs in the shoring system increases, the amount of load that each slab shares decreases; however, when compressible shores or reshores are used, the uppermost floor slabs carry most of the applied construction load, leaving the lower slabs without much load to share. This makes the additional reshored levels redundant and ineffective. Figure 8.22 shows the relationship between the number of shored levels, along with various combinations of reshores, and the maximum slab load. The figure shows that as the number of the shored levels increases, the maximum slab load also increases. Although this is true, the maximum slab load occurs on an older slab, which has more strength, when more shored levels are used. During the design of the shoring system, it is important to determine the minimum number of shored levels required so the maximum applied load will occur on a slab that is old enough to have developed the necessary strength to withstand this load. Either the number of shored levels or the construction rate can be controlled. It is also interesting to observe from Figure 8.22 that all reshore combinations, from zero to three reshored levels, tend to converge as the number of shored levels increases; therefore, it is important to determine the maximum number of reshored levels that can cause an appreciable change in the maximum applied construction loads.

8.3 Properties of Concrete at Early Ages

As discussed in detail in Section 8.2, when the usual shore/reshore method of construction is used for multistory buildings, high early-age, short-duration loads are imposed on the slabs. These loads can be comparable in magnitude to, or even exceed, the design service loads. Also, they are applied to concrete slabs that have not achieved their specified concrete strength. The consequences may very well be structural failure, unless adequate precautions are taken during construction, based on proper evaluation of the construction loads and sound knowledge of the early-age properties of concrete. Structural failures

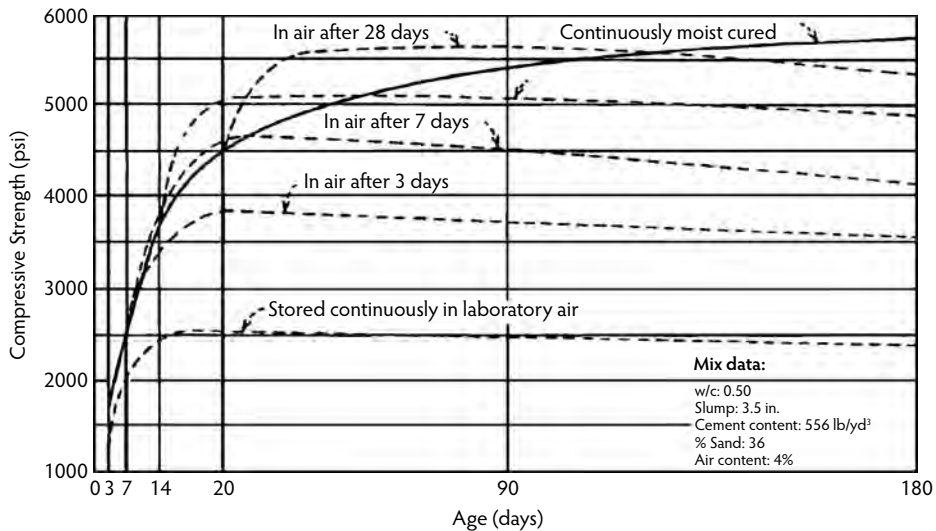


FIGURE 8.23 Compressive strength of concrete dried in laboratory air after preliminary moist curing. (From Price, W.H., *ACI J.*, 22(6), 417–432, 1951.)

may be associated with collapse of a structure or part of a structure or structural member, or they may be associated with structural distress that causes a significant reduction in the capability of a structure to function in the way originally intended. The former may be classed as *strength* failures, while the latter may be referred to as *serviceability* failures. Strength failures occur relatively infrequently but can be catastrophic, sometimes leading to loss of life. Serviceability failures occur more frequently and, although not usually catastrophic or life threatening, may result in significant financial losses. Objectionable cracking or excessive floor-slab deflections are examples of serviceability failure.

Heavy construction loads applied to slabs at early ages may be a major contributing factor to strength failures as well as serviceability failures. To understand the strength-related consequences, which may be due to deficiencies of flexural-axial loading strength, shear strength, or bond strength, a knowledge of the compressive strength, tensile strength, shear strength, and bond strength of concrete is necessary. For an understanding of the serviceability related consequences, a knowledge of the modulus of elasticity, shrinkage, and creep of concrete at early ages is essential.

8.3.1 Compressive Strength

Price (1951) and Klieger (1958) generated considerable information on the development of the compressive strength of concrete under varying temperature and moisture conditions. Temperature and moisture have pronounced effects on the strength development of concrete. Figure 8.23 (Price, 1951) shows that the development of strength stops at an early age when a concrete specimen is exposed to dry air with no previous moist curing. Concrete exposed to dry air from the time it is placed is about 42% as strong at 6 months as concrete that was continuously moist cured. Specimens cured in water at 70°F were found to be stronger at 28 days than those cured in a fog room at 100% relative humidity. The richer mixes showed up to better advantage than the leaner ones under water curing. The strength of the water-cured specimens was about 10% higher than that of the fog-cured specimens for concrete having water/cement ratios of 0.55 by weight.

Curing temperatures have a marked effect on the strength development of concrete. Test results were obtained by casting and curing concrete specimens at different temperatures, and under such treatment the highest temperatures developed the highest 28-day strength. Other concrete specimens were cured at 70°F after holding the specimens at different casting temperatures for 2 hours. Such treatment produced

opposite results, as the specimens made at the lower temperatures produced the highest 28-day strength. It was speculated that concrete cast at high temperatures is weakened by rapid setting, which is not overcome by subsequent curing at 70°F. Continued curing at higher temperatures for the full 28-day period, as was done for some of the first sets of specimens, accelerated the strength development sufficiently to produce the highest strength for the highest temperature. At later ages, however, the specimens made and cured at higher temperatures had lower strengths than those made and cured at lower temperatures.

In Klieger's (1958) investigation, concretes were mixed and placed at temperatures of 40, 55, 73, 90, 105, and 120°F. Specimens were tested at ages 1, 3, 7, and 28 days; 3 months; and 1 year. ASTM Type I, II, and III cements were used. Concretes were made both with and without calcium chloride as an accelerator. An air-entraining agent was added at the mixer to entrain a prescribed amount of air in all of the concretes. In Part I (73°F and lower), all specimens were continuously moist cured (100% relative humidity) at the mixing and placing temperature for 28 days or less, depending on the test age. After the initial 28-day period, half of the remaining specimens for tests at 3 months and 1 year, were stored at 73°F and 100% relative humidity and the other half at 73°F and 50% relative humidity. Additional concretes were mixed and placed at 40°F, and, immediately after placing, the specimens in their molds were stored at 25°F. All surfaces were kept continuously moist (prior to and following removal from the molds at 1 day of age) for 28 days or less, depending on test age. After 28 days, specimens kept for tests at 3 months and 1 year were treated like those stored at other temperatures.

In Part II (73°F and higher), half of the specimens were moist cured for 7 days at the fabrication temperature, and the remainder of the specimens were moist cured for 28 days at the fabrication temperature. At the end of the 7- and 28-day preliminary curing periods, each half was divided into two groups, one cured at 73°F and 100% relative humidity and the other at 73°F and 50% relative humidity. For concretes mixed at 40 and 73°F, the net water/cement ratio was held at the value determined to produce the target slump at 55°F. In Part II, the net water/cement ratio for each concrete was such as to produce a certain target slump at a concrete temperature of 90°F. Continuity between Parts I and II was provided by a repetition of the tests for all the concretes at 73°F; a small difference in net water/cement ratio between the concretes in Parts I and II was found.

Two 6 × 6 × 30-in. beam specimens were cast for each test age and curing condition. Beams were tested in flexure with load applied at the third points of an 18-in. span. Two flexural breaks were obtained for each beam. The two beam ends were tested for compression as 6-in. modified cubes. (For the particular aggregate, the ratio of 6 × 12-in. cylinder strength to 6-in. modified cube strength was taken as 0.93.) For each test age, concrete mix, and curing procedure, two beams were tested, yielding four flexural and four compressive test results for averaging. All strength tests were made at a concrete temperature of 73°F. Specimens stored at temperatures other than 73°F were placed in the 73°F moist room for temperature conditioning 1/2 hour before testing.

Figure 8.24 shows all the compressive strength data for three types of cement with and without accelerator, expressed as percentages of the strengths developed at 73°F for each test age. This figure shows the accelerating effect of temperatures above 73°F on the early-age strengths, with a sacrifice, however, in strength at later ages. On the other hand, concretes placed and cured at temperatures below 73°F, while showing lower strengths at the early ages, show strengths at the later ages in excess of those developed at 73°F. This was true even for concretes mixed and cast at 40°F and stored immediately after casting at 25°F for the first 28 days. For concretes cured initially at low temperatures followed by curing at 73°F, 1-year strengths close to or exceeding those for the concretes cured continuously moist at 73°F were attained only when moist curing was employed. Air drying during this subsequent 73°F period generally resulted in lower strengths, particularly for concretes made with Type I and Type II cements.

The data in Figure 8.24 are for concretes moist cured the first 28 days. In Part II, a 7-day moist-curing period at the fabrication temperature was included for comparison with the 28-day moist-curing period at the fabrication temperature. The qualitative interpretation of results for this 7-day group was similar to that for the 28-day group. The following conclusions were drawn by Klieger (1958):

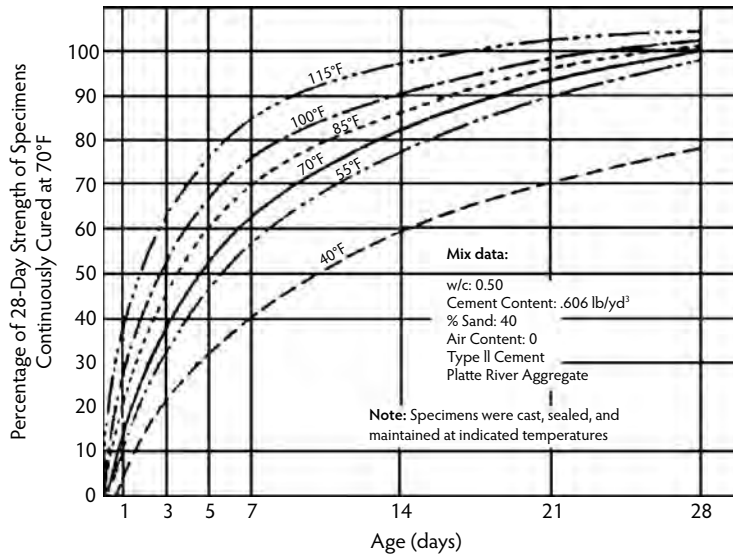


FIGURE 8.24 Effect of temperature on compressive strength of concretes made with different types of cement with and without an accelerator. (From Klieger, P., *ACI J.*, 29(12), 1063–1081, 1958.)

1. At 1, 3, and 7 days, concrete compressive strengths increase with an increase in the initial and curing temperatures of the concrete.
2. Increasing the initial and curing temperatures results in considerably lower compressive strengths at 3 months and 1 year.
3. Compressive strengths of concretes made with the three cement types used were influenced in a like manner by temperature; differences were in degree only.
4. These tests indicated that there is a temperature during the early life of concrete that may be considered optimum with regard to strength at later ages or, more strictly, at comparable degrees of hydration. This temperature is influenced somewhat by cement type. For Types I and II, this temperature appears to be 55°F; for Type III, 40°F.
5. For concretes with calcium chloride added, compressive strength increases due to the accelerator were proportionately greater at early ages and lower temperatures.

ACI Committee 209 (1971) has recommended the following expression for the time-dependent strength of moist-cured (as distinct from steam-cured) concrete using Type I cement:

$$f'_a = \frac{t}{4.00 + 0.85t} f'_c \quad (8.1)$$

where t is the time in days from casting up to loading and f'_c is the 28-day compressive strength of concrete.

The validity of Equation 8.1 at very early ages needs to be examined in view of the data reported above and a significant volume of European data that is also available (Byfors, 1980; RILEM Commission 42-CEA, 1981).

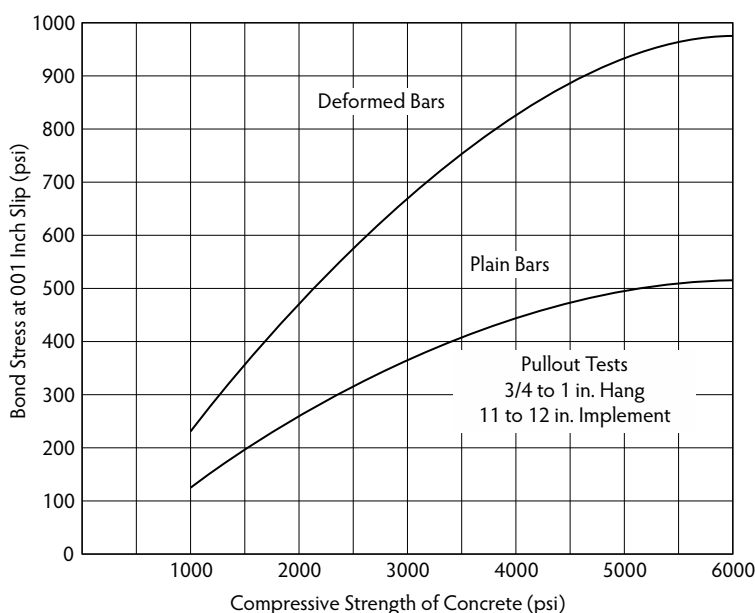
8.3.2 Tensile Strength and Bond Strength

Price (1951) reported data (Table 8.6) from tests at the Portland Cement Association showing relationships among the compressive strength, the tensile strength, and the flexural strength (modulus of rupture) of concrete. It was not stated, but may probably be assumed, that the tensile strength reported was the splitting tensile strength: “The ratio of tensile to compressive strength decreases as the compressive strength increases and approaches a constant of about 7% for higher compressive strength. Other published data

TABLE 8.6 Comparison of Compressive, Flexural and Tensile Strength of Plain Concrete

Strength of Plain Concrete (psi)			Ratio (%)		
Compressive	Modulus of Rupture	Tensile	Modulus of Rupture to Compressive Strength	Tensile Strength to Compressive Strength	Tensile Strength to Modulus of Rupture
1000	230	110	23.0	11.0	48
2000	375	200	18.8	10.0	53
3000	485	275	16.2	9.2	57
4000	580	340	14.5	8.5	59
5000	675	400	13.5	8.0	59
6000	765	460	12.8	7.7	60
7000	855	520	12.2	7.4	61
8000	930	580	11.6	7.2	62
9000	1010	630	11.2	7.0	63

Source: Price, W.H., *ACI J. Proc.*, 22(6), 417–432, 1951.

**FIGURE 8.25** Variation of bond with strength of concrete. (From Price, W.H., *ACI J.*, 22(6), 417–432, 1951.)

indicate that the ratio of tensile to compressive strength decreases as the age of concrete increases to the same constant value of 7%” (Price, 1951). Figure 8.25 shows in a qualitative way the relationship between bond strength and compressive strength of concrete for plain and deformed bars. The ratio of bond strength to compressive strength decreases as compressive strength increases. The bond strength of the deformed bars is 24% of the compressive strength for 2000-psi concrete and 18% of the compressive strength for 5000-psi concrete. “The relationship of bond to compressive strength apparently is not changed materially by air entrained in the proportions recommended” (Price, 1951).

Klieger’s (1958) flexural strength data for the same concretes as were tested for Figure 8.24 showed that the discussion about compressive strength data in the previous section applies equally to the flexural strength data. Flexural strengths at early ages increased with increase in temperature. At later ages, the effect of temperature was reversed. Concretes made and cured at lower temperatures showed the highest flexural strengths at 1 year. The optimum temperatures for flexural strength development appeared to be the same as those for compressive strength. The use of calcium chloride frequently resulted in flexural

strengths at later ages that were somewhat lower than for comparable concretes without calcium chlorides. Maximum reductions noted were on the order of 10%.

In a significant investigation by Gardner and Poon (1976), six series of specimens were cast: three using Type I and three using Type III cement concretes. The specimens for each series were cast from a single batch of ready-mixed concrete. Two series of tests, one made with Type I cement concrete and one with Type III cement concrete, were carried out with the concrete continuously moist cured at 72°F (22°C). Two series of specimens, one made using Type I cement concrete and one with Type III cement concrete, were subjected to extended curing under wet burlap at a steady temperature of 55°F (13°C). The remaining two series were subjected to extended curing under wet burlap at a steady temperature of 35°F (2°C). All specimens were cast at 72°F (22°C). To examine the effect of time on the concrete, specimens were cured at 72°F (22°C) for different periods before exposing them to low temperatures. One third of the specimens of each series were cured for 1 day, one third were cured for 3 days, and the remainder were cured for 7 days at 72°F (22°C) before being transferred to the cooler environment.

Each series involved the casting of 160 standard 6 × 12-in. (150 × 300-mm) cylinders and 80 bond specimens. Five specimens were tested for compressive strength, 5 for tensile strength, and 5 for bond strength at 1, 3, 7, 14, and 28 days and at 3 months for each of the 14 curing schedules. All concretes had a specified cylinder strength of 4000 psi (28 MPa) and a water/cement ratio of approximately 0.5. Compressive and tensile strengths were determined by the standard compressive strength test and the split-cylinder test, respectively, on 6 × 12-in. (150 × 300-mm) cylinders. Bond specimens were made by casting a #6 reinforcing bar into a 6 × 6-in. (150 × 150-mm) cylindrical block of concrete to closely approximate the ASTM standard specimen, which is a 6-in. (150-mm) concrete cube or a 6 × 6 × 12-in. (150 × 150 × 300-mm) block of concrete. Concrete strengths are plotted against the log of time in Figure 8.26 for concretes made with Type I cement and subjected to extended curing at 35°F (2°C). Figure 8.26 was typical of all six batches of concrete. The following conclusions were drawn:

1. Temperature influences the tensile and bond strength development of concrete in much the same manner as it does compressive strength development. Compressive strength, tensile strength, and bond strength are all related, and an increase in one is reflected in the others.
2. The compressive strength, tensile strength, and bond strength of concrete at early ages increases with increased curing temperature. The lower the initial curing temperature the greater the eventual ultimate strength of the concrete, provided curing is continuous.
3. Bond strength and tensile strength are proportional to the 0.8 power of the cylinder strength at the appropriate age. Neither extended curing at temperatures of 35°F (2°C) and 55°F (13°C) nor type of cement appears to have any significant effect on the interrelationship of bond strength or tensile strength and cylinder strength.
4. With respect to construction schedules, there is a 5 to 9% gain in the 7-day and in the 14-day strengths due to casting and curing Type I cement concretes for 3 days and 7 days, respectively, at 72°F (22°C), compared to casting and curing for 1 day at 72°F (22°C).
5. Type III cement concretes exhibited a small strength gain due to prolonged initial curing at 72°F (22°C) when subjected to extended curing at 35°F (2°C) but no strength gain for prolonged initial curing at 72°F (22°C) when subjected to extended curing at 55°F (13°C).

Lew and Reichard (1978) performed three types of tests:

1. Compressive strength tests of cylindrical specimens
2. Splitting tensile tests of cylindrical specimens
3. Bond-strength tests using cylindrical pullout specimens

All three types of tests were made on specimens cured at different temperatures—35°F (2°C), 55°F (13°C), and 73°F (22°C)—and tested at nine ages (1, 2, 3, 5, 7, 14, 21, 28, and 42 days).

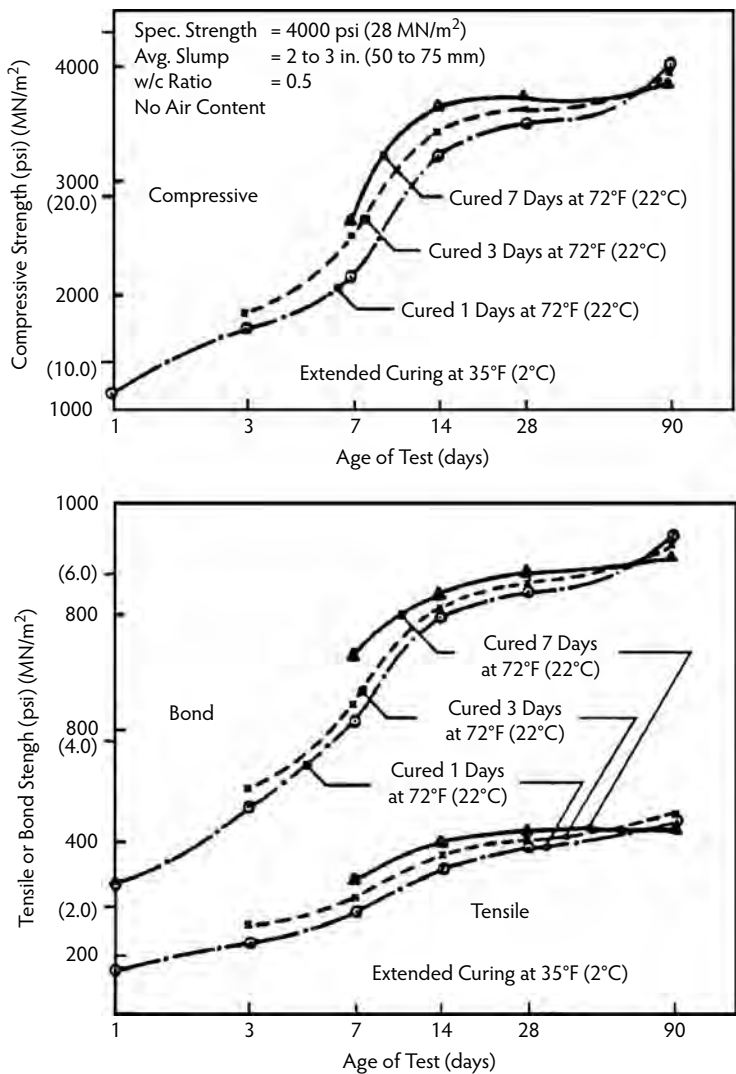


FIGURE 8.26 Variation of concrete strength with temperature for Type I cement concrete cured at 35°F (2°C). (From Gardner, N.J. and Poon, S.M., *ACI J.*, 73(7), 405–409, 1976.)

The combined effect of temperature and time, or *maturity*, usually expressed in degree-days (or hours), may be defined as the sum of the product of the increment of age of cure and the difference between curing and some temperature below which no strength gain takes place. The definition can be written as:

$$M = \sum (T - T_0) \Delta t \tag{8.2}$$

where T is temperature of the concrete at any time, T_0 is a datum temperature below which no strength gain of concrete takes place, and Δt is the increment of time. Taking $T_0 = 10^\circ\text{F}$ (-12°C) on the basis of prior tests, Equation 8.2 can be rewritten as:

$$M = \sum (T - 10) \Delta t \tag{8.3}$$

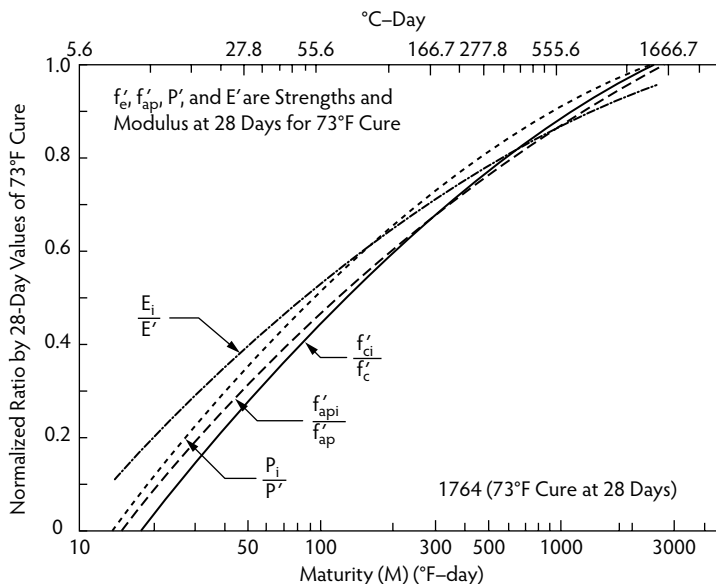


FIGURE 8.27 Mechanical properties normalized with respect to 28-day values vs. maturity. (From Lew, H.S. and Reichard, T.W., *ACI J.*, 75(10), 533–542, 1978.)

where T is in degrees Fahrenheit. Analysis of Lew and Reichard's test data showed that the compressive strength of concrete can be related to maturity expressed in terms of concrete temperature and age of cure. When related to maturity, the elastic modulus data and the splitting tensile strength data of specimens cured at various temperatures could be treated as being from a single group. The pullout strength, when not governed by the yielding of the bar, could be expressed in terms of maturity, thus allowing the specimens cured at various ages to be treated as a single group as well. Figure 8.27 (Lew and Reichard, 1978) shows that, at early ages, the rate of increase in the splitting tensile strength is about the same as that of the compression strength, whereas the rate of increase in the pullout bond strength and the modulus are slightly greater than that of the compressive strength.

Carino and Lew (1982) performed a series of statistical analyses on published data of Gardner and Poon (1976), on published data from the National Bureau of Standards (NBS) (Lew and Reichard, 1978), and on previously unpublished data from the NBS. These data were used to determine the best relationship between the splitting tensile strength and the compressive strength of normal weight concrete, which was then compared with a larger group of published data. The unpublished data were from tests of specimens made with concretes similar to those reported in Lew and Reichard (1978) but which were allowed to cure under ambient, outdoor conditions. Three replicate specimens were tested at ages ranging from 1 to 37 days.

This study clearly indicated that the assumed proportionality of splitting tensile strength to the square root of compressive strength is not the most precise relationship when dealing with a wide range of compressive strengths. The square-root relationship was originally formulated on the basis of tests on mature concrete with strengths generally greater than 2500 psi (17.2 MPa). For low compressive strength, the current ACI formula overestimates splitting tensile strength and underestimates it for high compressive strength. A simple power law of the form $f'_{sp} = (f'_c)^b$ was found to be a more precise representation of data over the full range of concrete strengths. For the Gardner–Poon data and data from the two series of NBS tests mentioned above, the best-fit estimate of b was found to be 0.73. When additional data from four different published references and from other unpublished work at NBS were added to the mix, $f'_{sp} = (f'_c)^{(0.71)}$ seemed to be appropriate for estimating the average expected splitting tensile strength. The function $f'_{sp} = (f'_c)^{(0.71)}$ appeared to give a reasonable lower bound estimate, overestimating about 10% of the data.

8.3.3 Punching Shear Strength

According to Nilson (1991) (who was discussing mature concretes), a reasonable estimate for the split-cylinder strength (f'_{sp}) is 6 to 7 times the square root of f'_c for normal weight concretes. The true tensile strength (f'_t) is on the order of 0.5 to 0.7 times f'_{sp} (3 to $5\sqrt{f'_c}$), and the flexural tension strength (f'_r) (modulus of rupture) varies from 1.25 to 1.75 times f'_{sp} (7.5 to $12\sqrt{f'_c}$). The smaller of the foregoing factors apply to higher strength concretes and the larger to lower strength concretes. The modulus of rupture controls the behavior of flexural members subject to large bending moments and small shear forces; for large shear forces, the concern becomes safety against premature failure due to diagonal tension in the concrete, resulting from combined shear and longitudinal flexural stresses. In flexural members subject to large shear forces and small bending moments, *web-shear* cracks can be expected to form when the diagonal tension stress in the vicinity of the neutral axis becomes equal to the tension strength of the concrete (3 to $5\sqrt{f'_c}$). In members subject to large shear forces as well as large bending moments, *flexure-shear* cracks form when the diagonal tension stress at the tip of one or more flexural cracks exceeds the tensile strength of the concrete.

The information presented on the early-age modulus of rupture and split-cylinder strength of concrete in the previous section is directly relevant to the flexural and diagonal tension failure of beams and one-way slabs; however, as noted, one of the common causes of failure of flat-plate structures during construction is insufficient early-age punching shear strength under relatively high construction loads. Direct knowledge of early-age punching shear strength was thus thought to be desirable and was investigated by Gardner (1960). A relatively large number of circular flat plates were made and subjected to a centrally applied load through a circular steel plate. All steel was located on the tension side of the slabs, and steel ratios ranged from .5 to 5%. Concrete strengths ranged from 2000 to nearly 8000 psi (14 to 56 MPa). Slab thicknesses were 2, 4, and 6 in. (50, 100, and 150 mm). An initial set of experiments was undertaken to determine how punch diameter relates to slab thickness, slab outer diameter, and slab support diameter.

For punching shear failure to occur, at least three slab thicknesses are necessary between the punch and the slab support. Further, the slab outer diameter must be sufficient to enable the slab steel to develop any necessary stress; otherwise, the slab will fail in bond, separating at the reinforcement level. All specimens with zero steel or steel ratios less than .5% failed in flexure. A few conclusions, given below, were drawn.

1. The steel ratio in the region 3 dia from the column should be of the order of 0.5% in each direction, and the spacing should be similar to the effective depth.
2. In all cases, slabs should be detailed so some of the top (negative-moment tension) steel passes through the column.
3. The cube-root relationship between shear strength and concrete strength is preferable to the square-root relationship currently used by ACI Committee 318 (1995).
4. If the punching shear strength is in doubt, the shear perimeter should be increased by using larger columns or column capitals.

8.3.4 Modulus of Elasticity

Figure 8.28 (Byfors, 1980) provides an idea of how the stress–strain relationship of concrete in compression changes with age. The stress and the strain are related to the compressive strength and the corresponding strain, respectively. The arrows in the figure indicate possible unloading. The relationship is practically a straight-line curve at a very early age (5.0 hours). It can be seen that the strain is mainly inelastic. At this early stage, concrete shows properties that are similar to those of a claylike material. A few hours later (7.9 hours), the stress–strain relationship has a completely different character. One can see a clear transition from the elastic to the inelastic part. After 15.8 hours, the curve begins to get the appearance that normally characterizes concrete. The continued changes in the appearance of the stress–strain relationship are not, however, as radical any longer. Expressed in absolute values, the changes are nevertheless large.

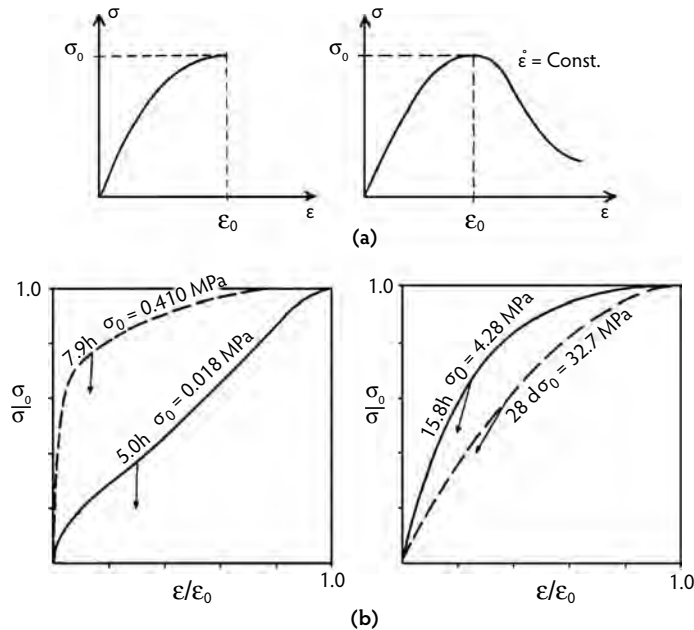


FIGURE 8.28 (a) Basic appearance of the compressive stress–strain relationship under constant stress rate (left) and constant deformation rate (right). (b) Change of shape of compressive stress–strain relationship at early ages. (From Byfors, J., *Plain Concrete at Early Ages*, Fo. 3, No. 80, Swedish Cement and Concrete Research Institute, Stockholm, Sweden, 1980.)

The modulus of elasticity, also referred to as elastic modulus, Young's modulus, and Young's modulus of elasticity, may be defined in general terms as the ratio of normal stress to corresponding strain for tensile or compressive stress below the proportional limit of the material. Few materials, however, conform to Hooke's law throughout the entire range of stress–strain relations; deviations there from are caused by inelastic behavior. If the deviations are significant, the slope of the tangent to the stress–strain curve at the origin, the slope of the tangent to the stress–strain curve at any given stress, the slope of the secant drawn from the origin to any specified point on the stress–strain curve, or the slope of the chord connecting any two specified points on the stress–strain curve may be considered to be the modulus. In such cases, the modulus is designated as the initial tangent modulus, the tangent modulus, the secant modulus, or the chord modulus, respectively, and the stress is stated. Normally, the static modulus of elasticity of concrete is determined as the secant modulus based on short-term experiments but with a certain number of repeated loadings at a low stress level. The stress level for the secant's intersection is normally 30 to 50% of strength. Studies leading to the expression for modulus of elasticity of concrete in ACI Committee 318 are summarized in Pauw (1960), where E_c was defined as the slope of the line drawn from a stress of zero to a compressive stress of $0.45f'_c$.

According to ACI Committee 209 (1971), the effect of age of concrete at the time of loading on the modulus of elasticity of concrete is accounted for when strength of concrete at the time of loading, rather than at 28 days, is inserted into the modulus of elasticity expression given in ACI Committee 318 (1995):

$$E_{ct} = 33w^{1.5} \sqrt{f'_{ct}} \quad (8.4)$$

where E_{ct} is the time-dependent modulus of elasticity of concrete in pounds per square inch, w is the unit weight of concrete in pounds per cubic feet, and f'_{ct} is the time-dependent concrete strength in pounds per square inch.

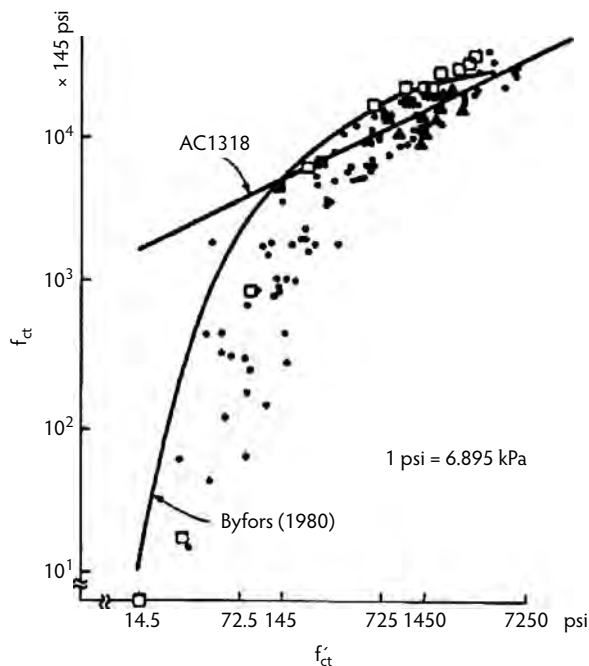


FIGURE 8.29 Modulus of elasticity of concrete at early ages. (From Fintel, M. et al., *Column Shortening in Tall Structures: Prediction and Compensation*, EB108-01D, Portland Cement Association, Skokie, IL, 1987.)

Equation 8.4 for normal weight concrete, when converted to SI units and rounded off, becomes:

$$E_{ct} = 5000\sqrt{f'_{ct}} \quad (8.5)$$

where E_{ct} and f'_{ct} are in megapascals. Figure 8.29 shows a comparison of Equation 8.5 with the experimental information currently available on the modulus of elasticity of concrete at early ages (RILEM Commission 42-CEA, 1981). Concrete strengths of 1 MPa (145 psi) and less are encountered only during the first few hours after concrete is poured and are not of interest here. In the range of practical interest, the ACI equation relating modulus of elasticity and strength agrees quite favorably with the trend of experimental results.

8.3.5 Shrinkage of Unreinforced (Plain) Concrete

Shrinkage of concrete is caused by the evaporation of moisture from the surface. The rate of shrinkage is high at early ages and decreases with an increase in age until the curve becomes asymptotic to the final value of shrinkage. The rate and amount of evaporation and consequently of shrinkage depend greatly upon the relative humidity of the environment, size of the member, and mix proportions of the concrete. In a dry atmosphere, moderate-size members (24-in. or 600-mm diameter) may undergo up to half of their ultimate shrinkage within 2 to 4 months, whereas identical members kept in water may exhibit growth instead of shrinkage. In moderate-size members, the inside relative humidity has been measured at 80% after 4 years of storage in a laboratory at 50% relative humidity.

8.3.5.1 Basic Value of Shrinkage

Let e_s denote the ultimate shrinkage of 6-in. (150-mm)-diameter standard cylinders (volume-to-surface or $v:s$ ratio = 1.5 in. or 38 mm) moist-cured for 7 days and then exposed to 40% ambient relative humidity. If concrete has been cured for less than 7 days, multiply e_s by a factor linearly varying from

1.2 for 1 days of curing to 1.0 for 7 days of curing (ACI Committee 209, 1971). Attempts have been made in the past to correlate e_s with parameters such as concrete strength. In view of available experimental data (Russell and Corley, 1977), it appears that no such correlation may in fact exist. The only possible correlation is probably that between e_s and the water content of a concrete mix (Troxell et al., 1968). In the absence of specific shrinkage data for concretes to be used in a particular structure, the value of e_s may be taken as between 500×10^{-6} in./in. (mm/mm) (low value) and 800×10^{-6} in./in. (mm/mm) (high value) (Fintel et al., 1987). The latter value has been recommended by the ACI Committee 209 (1971).

8.3.5.2 Effect of Member Size

Because evaporation occurs from the surface of members, the volume-to-surface ratio of a member has a pronounced effect on the amount of its shrinkage. The amount of shrinkage decreases as the size of the specimen increases. For shrinkage of members having volume-to-surface ratios different from 1.5, e_s must be multiplied by the following factor:

$$SH_{v:s} = \frac{0.037(v:s) + 0.944}{0.177(v:s) + 0.734} \quad (8.6a)$$

where $v:s$ is the volume-to-surface ratio in inches. The metric equivalent of Equation 8.6a is:

$$SH_{v:s} = \frac{0.015(v:s) + 0.944}{0.070(v:s) + 0.734} \quad (8.6b)$$

where $v:s$ is the volume-to-surface ratio in millimeters. As indicated in Fintel et al. (1987), Equation 8.6 is based on laboratory data (Hansen and Mattock, 1966) and European recommendations (CEB, 1964, 1972). Much of the shrinkage data available in the literature were obtained from tests on prisms of a 3×3 -in. (75×75 -mm) section ($v:s = 0.75$ in. or 19 mm). According to Equation 8.6, the size coefficient for prisms of that size is 1.12. Thus, shrinkage measured on a prism of a 3×3 -in. (75×75 -mm) section must be divided by 1.12 before the size coefficient given by Equation 8.6 is applied. It should be cautioned, however, that as the specimen size becomes smaller, the extrapolation to full-size members becomes less accurate.

8.3.5.3 Effect of Relative Humidity

The rate and amount of shrinkage greatly depend upon the relative humidity of the environment. If ambient relative humidity is substantially greater than 40%, then e_s must be multiplied by:

$$SH_H = \begin{cases} 1.40 - 0.010H & \text{for } 40 \leq H \leq 80 \\ 3.00 - 0.030H & \text{for } 80 \leq H \leq 100 \end{cases} \quad (8.7)$$

where H is the relative humidity in percent. Average annual values of H should probably be used. Maps giving average annual relative humidities for locations around the United States are available (Fintel et al., 1987). If locally measured humidity data are available, however, they are likely to be more accurate than information such as that included in Fintel et al. (1987) and should be used in conjunction with Equation 8.7, which is based on ACI Committee 209 (1971) recommendations. A comparison with European recommendations is shown in Fintel et al. (1987). If shrinkage specimens are stored under job-site conditions rather than under standard laboratory conditions, the correction for humidity, as given by Equation 8.7, should be eliminated.

8.3.5.4 Progress of Shrinkage with Time

Hansen and Mattock (1966) established that the size of a member influences not only the final value of shrinkage but also the rate of shrinkage, which appears to be only logical. Their expression giving the progress of shrinkage with time is:

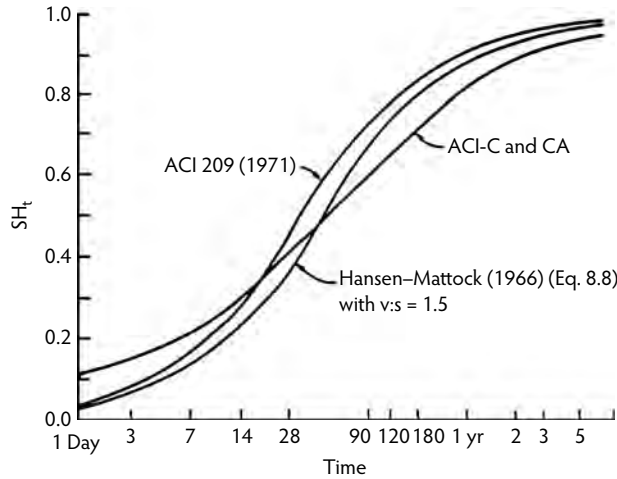


FIGURE 8.30 Progress of shrinkage with time. (From Fintel, M. et al., *Column Shortening in Tall Structures: Prediction and Compensation*, EB108-01D, Portland Cement Association, Skokie, IL, 1987.)

$$SH_t = \frac{\epsilon_{st}}{\epsilon_s} = \frac{t}{26.0e^{0.36(v:s)} + t} \quad (8.8)$$

where ϵ_{st} and ϵ_s are shrinkage strains up to time t and time infinity, respectively, and t is measured from the end of moist curing. Equation 8.8 is compared in Figure 8.30 with the progress of shrinkage curve from the *Recommendations for an International Code of Practice for Reinforced Concrete* (CBE, 1964). Also shown in Figure 8.30 is a comparison of Equation 8.8 with the progress of shrinkage relationship recommended by ACI Committee 209 (1971). It should be noted that both the ACI and Cement and Concrete Association (C&CA) (CBE, 1964) and the ACI Committee 209 (1971) relationships are independent of the volume-to-surface ratio.

8.3.6 Creep of Unreinforced (Plain) Concrete

Creep is a time-dependent increment of the strain of a stressed element that continues for many years. The basic phenomenon of creep is not yet conclusively explained. During the initial period following the loading of a structural member, the rate of creep is significant. The rate diminishes as time progresses until it eventually approaches zero. Creep consists of two components:

1. Basic (or true) creep occurs under conditions of hygral equilibrium, which means that no moisture movement occurs to or from the ambient medium. In the laboratory, basic creep can be reproduced by sealing a specimen in copper foil or by keeping it in a fog room.
2. Drying creep results from an exchange of moisture between the stressed member and its environment. Drying creep has its effect only during the initial period under load.

Creep of concrete is very nearly a linear function of stress up to stresses that are about 40% of the ultimate strength. This includes all practical ranges of stresses in columns and walls. Beyond this level, creep becomes a nonlinear function of stress. For structural engineering practice, it is convenient to consider specific creep, which is defined as the ultimate creep strain per unit of sustained stress.

8.3.6.1 Value of Specific Creep

Specific creep values can be obtained by extrapolating results from a number of laboratory tests performed on samples prepared from the actual mix to be used in a structure. It is obvious that sufficient time for such tests must be allowed prior to the start of construction, as reliability of the prediction improves

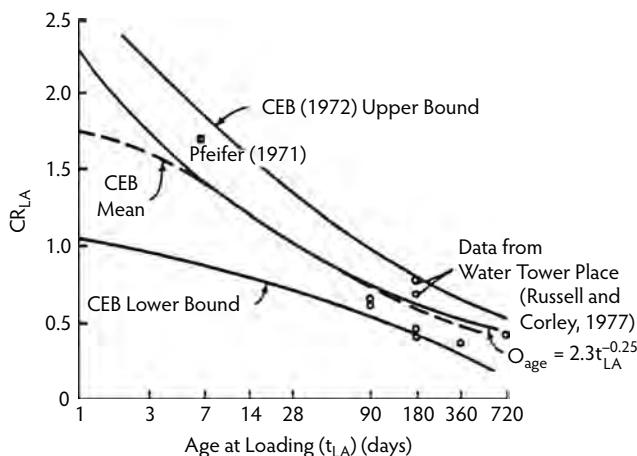


FIGURE 8.31 Creep vs. age of concrete at time of loading. (From Fintel, M. et al., *Column Shortening in Tall Structures: Prediction and Compensation*, EB108-01D, Portland Cement Association, Skokie, IL, 1987.)

with the length of time over which creep is actually measured. A way of predicting basic specific creep (excluding drying creep), without testing, from the modulus of elasticity of concrete at the time of loading was proposed by Hickey (1968) on the basis of long-term creep studies at the Bureau of Reclamation in Denver. A simpler suggestion was made in Fintel et al. (1987), as described below:

Let ϵ_c denote the specific creep (basic plus drying) of 6-in. (150-mm)-diameter standard cylinders ($v:s = 1.5$ in. or 38 mm) exposed to 40% relative humidity following about 7 days of moist curing and loaded at the age of 28 days. In the absence of specific creep data for concretes to be used in a particular structure, the following likely values of ϵ_c may be used:

$$\epsilon_c = 0.003/f'_c \text{ (low value) to } 0.005/f'_c \text{ (high value)} \quad (8.9a)$$

where ϵ_c is in inch per inch per kips per square inch if f'_c is in kips per square inch, or in inch per inch per pounds per square inch if f'_c is in pounds per square inch. The metric equivalent of Equation 8.9a is:

$$\epsilon_c = 0.000435/f'_c \text{ (low value) to } 0.000725/f'_c \text{ (high value)} \quad (8.9b)$$

where ϵ_c is in millimeter per millimeter per megapascal if f'_c is in megapascal, or in millimeter per millimeter per kilopascal if f'_c is in kilopascal. The lower end of the proposed range is in accord with specific creep values suggested by Neville (1981). The upper end agrees with laboratory data obtained by testing the concretes used in Water Tower Place in Chicago (Russell and Corley, 1977).

8.3.6.2 Effect of Age of Concrete at Loading

For a given mix of concrete, the amount of creep depends not only on the stress level but also to a great extent on the age of the concrete at the time of loading. Figure 8.31 shows the relationship between creep and age at loading as developed by Comité Européen du Béton (CEB, 1972), using available information from many tests. The coefficient CR_{LA} relates the creep for any age at loading to the creep of a specimen loaded at the age of 28 days. The 28-day creep is used as a basis of comparison, the corresponding CR_{LA} being equal to 1.0. Figure 8.31 also depicts the following suggested relationship (Fintel et al., 1987) between creep and age at loading:

$$CR_{LA} = 2.3t_{LA}^{-0.25} \quad (8.10)$$

where t_{LA} is the age of concrete at the time of loading, in days. The form of Equation 8.10 is as suggested by the ACI Committee 209 (1971). Equation 8.10 gives better correlation with the CEB mean curve than the corresponding equation suggested by the ACI Committee 209. Figure 8.31 also provides comparison with a few experimental results (Lew and Reichard, 1978; Pfeifer et al., 1971). According to Equation 8.10, the creep of concrete loaded at 7 days of age is 41% higher than that of concrete loaded at 28 days.

8.3.6.3 Effect of Member Size

Creep is less sensitive to member size than shrinkage, as only the drying-creep component of the total creep is affected by the size and shape of members, whereas basic creep is independent of size and shape. For members with volume-to-surface ratios different from 1.5 in. or 38 mm, ϵ_c should be multiplied by:

$$CR_{v:s} = \frac{0.044(v:s) + 0.934}{0.1(v:s) + 0.85} \quad (8.11a)$$

where $v:s$ is the volume-to-surface ratio in inches. The metric equivalent of Equation 8.11a is:

$$CR_{v:s} = \frac{0.017(v:s) + 0.934}{0.039(v:s) + 0.85} \quad (8.11b)$$

where $v:s$ is the volume-to-surface ratio in millimeters. As indicated in Fintel et al. (1987), Equation 8.11 is based on laboratory data (Hansen and Mattock, 1966) and European recommendations (CEB, 1964, 1972). Much of the creep data available in the literature were obtained by testing 6-in. (150-mm)-diameter standard cylinders wrapped in foil. The wrapped specimens simulated very large columns. Equation 8.11 yields a value of $CR_{v:s}$ equal to 0.49 for $v:s = 100$. Thus, it is suggested that creep data obtained from sealed specimen tests should be multiplied by $2(1/0.49 \approx 2)$ before the modification factor given by Equation 8.11 is applied to such data.

8.3.6.4 Effect of Relative Humidity

For an ambient relative humidity greater than 40%, ϵ_c should be multiplied by the following factor, as suggested by ACI Committee 209 (1971):

$$CR_H = 1.40 - 0.01H \quad (8.12)$$

where H is the relative humidity in percent. Again, it is suggested that the average annual value of H be used.

8.3.6.5 Progress of Creep with Time

The progress of creep relationship recommended by ACI Committee 209 (1971) is given by the following expression:

$$CR_t = \frac{\epsilon_{ct}}{\epsilon_c} = \frac{t^{0.6}}{10 + t^{0.6}} \quad (8.13)$$

where ϵ_{ct} is the creep strain per unit stress up to time t , and t is measured from the time of loading. This relationship is plotted in Figure 8.32, where it compares well with the creep-vs.-time curve suggested in European recommendations (CEB, 1964).

8.3.6.6 Irreversible Nature of Creep

Another important aspect of creep of concrete must be addressed. Figure 8.33 shows the strain history of a concrete specimen that was stored in air at near 100% relative humidity to eliminate shrinkage and subjected to a sustained axial stress that was removed at 120 days from the time of loading. The instantaneous recovery is followed by a gradual decrease in strain, called *creep recovery*. The shape of the creep-

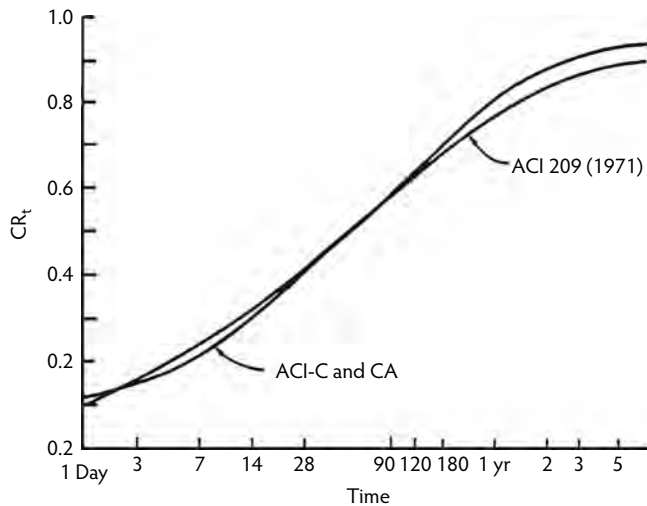


FIGURE 8.32 Progress of creep with time. (From Fintel, M. et al., *Column Shortening in Tall Structures: Prediction and Compensation*, EB108-01D, Portland Cement Association, Skokie, IL, 1987.)

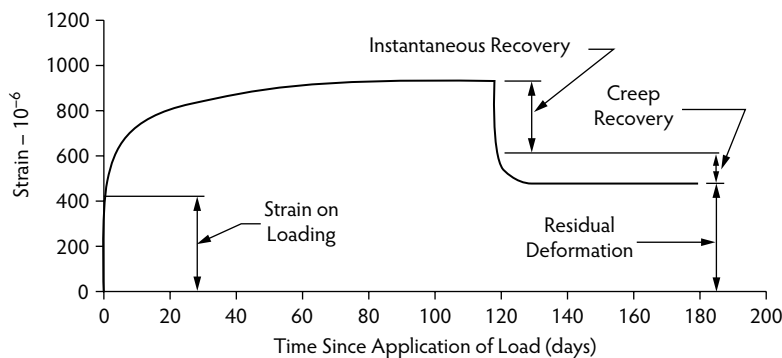


FIGURE 8.33 Creep strain vs. time when part of sustained load is removed at a certain time after application. (From Fintel, M. et al., *Column Shortening in Tall Structures: Prediction and Compensation*, EB108-01D, Portland Cement Association, Skokie, IL, 1987.)

recovery curve is similar to that of the creep curve, but the recovery approaches its maximum value much more rapidly. The reversal of creep is not complete, so any sustained application of load, even over only a day, results in a residual deformation (Neville, 1981).

8.3.7 Effects of Drying on Flexural Cracking

Hover (1988) pointed out that the resistance to flexural cracking in beams and slabs decreases sharply during periods in which the surface of the concrete is drying, such as the period that immediately follows the removal of forms. Hover considered a 6-in. (150-mm)-thick reinforced concrete slab with a concrete compression strength of 4000 psi (28 MPa). The solid lines in Figure 8.34a show the increase in the allowable superimposed live load as a function of the amount of reinforcing steel for continuous spans of 14 to 18 ft (4.2 to 5.4 m). The allowable load was determined by subtracting the factored dead load from the ultimate load and dividing the result by an appropriate load factor. The dotted lines in Figure 8.34a indicate the superimposed live load that caused cracking of the same slabs. Note that, for lightly reinforced slabs, the cracking load is actually greater than the safe allowable load. This means that cracking will be avoided by complying with the load limitations imposed on the basis of strength calculations. Whereas the allowable

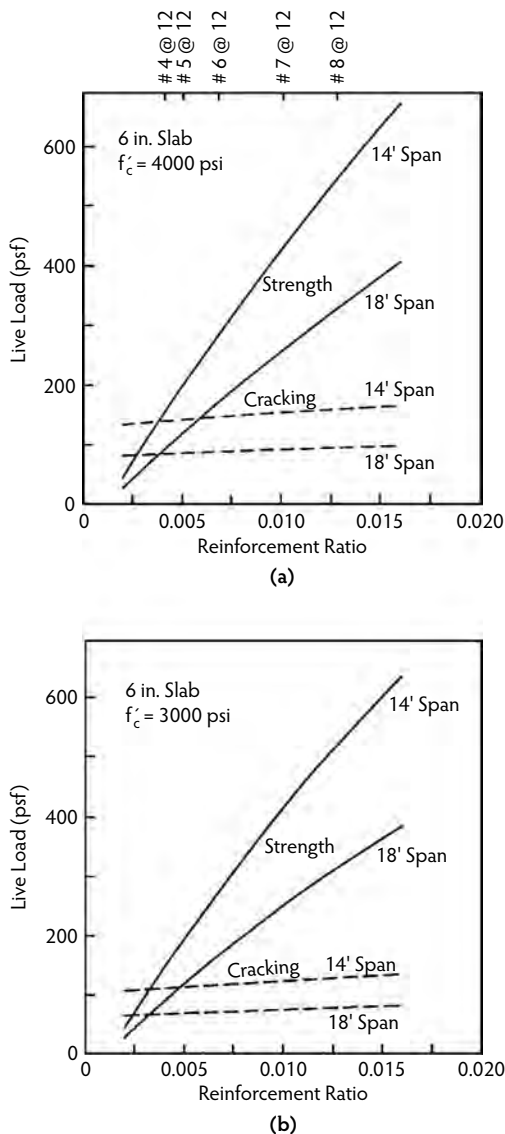


FIGURE 8.34 Allowable live load calculated on the basis of strength vs. cracking live load: (a) $f'_c = 4000$ psi (28 MPa); (b) $f'_c = 3000$ psi (21 MPa). (From Hover, K.C., in *Forming Economical Concrete Buildings: Proceedings of the Third International Conference*, SP107, American Concrete Institute, Farmington Hills, MI, 1988, pp. 169–184.)

load on the basis of strength considerations increases dramatically with an increasing amount of reinforcing steel, the cracking load increases by only 25% or so for an 8-fold increase in the amount of reinforcing steel. For members with the maximum allowable amount of reinforcing steel, the safe load on the basis of strength exceeds the cracking load by a factor of four. One would therefore expect heavily reinforced slabs and beams to crack at loads well below the safe or allowable load calculated on the basis of strength.

In Figure 8.34b, it is assumed that the same slabs have a compressive strength of only 3000 psi (21 MPa) at the time of load application. Note that this case corresponds to the above 4000-psi (28-MPa) concrete about 7 days after casting, when the concrete has attained approximately 75% of its expected 28-day strength. Comparison of Figure 8.34a with Figure 8.34b shows an approximate 6% decrease in the allowable load on the basis of strength and an approximate 20% decrease in the cracking load for a compression strength decrease from 4000 psi to 3000 psi (28 MPa to 21 MPa). Thus, low concrete

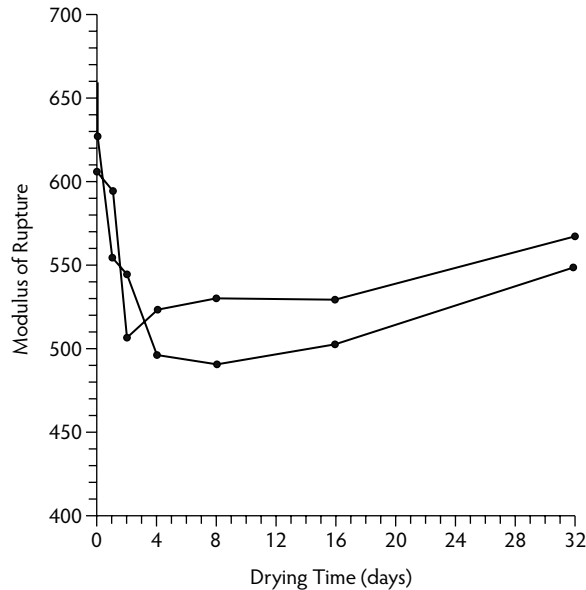


FIGURE 8.35 Data presented by Walker and Bloem (1957b) concerning the influence of drying on the flexural strength of concrete. (From Hover, K.C., in *Forming Economical Concrete Buildings: Proceedings of the Third International Conference*, SP107, American Concrete Institute, Farmington Hills, MI, 1988, pp. 169–184.)

compressive strength has a more significant effect on resistance to cracking than on the strength of the slabs considered in these examples.

Calculation of the cracking load in the above example was done using $f_r = 7.5 \sqrt{f'_c}$ as in ACI Committee 318 (2005). Walker and Bloem (1957a,b) and Hover (1984) studied the influence of surface drying on flexural tension strength. The essential results are shown in Figure 8.35, in which the modulus of rupture (MOR) is shown as a function of the time during which the concrete test specimen is exposed to air drying. The modulus of rupture of wet concrete is seen to decrease immediately upon exposure to air. This decrease continues for several days of air drying until a minimum is reached after 3 to 6 days, followed by a slow restoration of the original wet MOR. Continued slow drying eventually leads to a modulus of rupture that is greater than the original wet-tested value. It was found that the MOR could vary from a high of $16 \sqrt{f'_c}$ to an apparent lower limit of approximately $4 \sqrt{f'_c}$, depending entirely on moisture conditions at the time of testing. Critically, during the first few days and hours of surface drying, the actual modulus of rupture (and therefore the actual cracking resistance) could be as little as 55% of the commonly expected value ($4 \sqrt{f'_c}$ rather than $7.5 \sqrt{f'_c}$).

The surface of concrete beams and slabs begins to dry immediately upon the removal of the formwork and the subsequent exposure to dry, moving air. While this surface drying is taking place, the removal of shoring and further construction operations load the members. The removal of forms and shores from flexural members is therefore a delicate issue, not only because of the strength development of early-age concrete but also because the surface drying, which is an almost unavoidable consequence of form removal, can decrease the cracking resistance by almost 50%.

To further investigate the phenomenon, beam specimens were cast in forms with steel sides and oiled plywood bottoms. Four days after casting, the forms were removed from three beams, which were then permitted to dry for 4 hours in laboratory air. Three other beams were removed from their forms one at a time and immediately tested so as to avoid appreciable air drying. The average MOR of the beams that were tested immediately upon form removal was 573 psi (4.0 MPa), and the average MOR of the beams that had dried for 4 hours was 450 psi (3.1 MPa), representing a 25% decrease in cracking resistance due to short-term drying.

It is not unreasonable to envision a situation in which the conditions of this experiment are realized on the jobsite, where the removal of beam sides may precede the removal of the beam bottom and supporting shoring by several hours. In that case, the self-weight of the slab or beam would be applied during this critical drying period. Similarly, in the case of rapid construction where the weight of falsework, materials, flying forms, etc. is applied to the top of a recently stripped beam or slab, it is likely that superimposed load would be applied during the critical drying period during which the cracking resistance is substantially reduced.

As part of a related experiment, flexural specimens were cast against steel forms with oiled plywood bottoms, with companion specimens cast in similar forms that had been lined with polyethylene. From tests conducted at 4 hours, 2 hours, and immediately after removal of forms, the modulus of rupture of the beams with the plastic-lined forms was on an average 25% greater than for the beams cast in steel and wood forms. When companion specimens were tested after 28 days of drying in laboratory air, the results for the two types of forms were statistically indistinguishable. It was concluded that the influence of the form surface on the cracking resistance was primarily due to the effects of moisture conditions at early ages. It was pointed out that timing the removal of forms and shores so as not to load a member while the concrete surface is drying can reduce the incidence of flexural cracking or can increase the applied load necessary to initiate such cracking. The use of smooth form surfaces or nonabsorptive form liners may be beneficial in reducing flexural cracking.

8.4 Strength Consequences of Construction Loads

It would be instructive to begin this section with the following four paragraph reproduced, with only minor paraphrasing, from Kaminetzky and Stivaros (1994):

Throughout the history of concrete construction, numerous construction failures have occurred. Many statistical surveys point out that failures and total collapses occur more frequently during construction than during the service life of a structure. Also, it has been well documented that failure of concrete structures during construction most often occur as a result of formwork failure, concrete member failure due to overloading, or lack of concrete strength.

The most common and often devastating failures are punching shear failures. These are triggered by a localized failure around a single column at an upper-level floor, resulting in progressive collapse going all the way down to the lowest level. Such a domino-effect failure can be stopped by localizing it to a single level. Because punching shear is the weakest link in the chain, the use of large-size columns coupled with continuous reinforcing bars running through the column periphery at both the top and the bottom of the slab will minimize the possibility of progressive collapse.

The most devastating and well-known collapses, during construction, resulting from punching shear, are those that occurred at Bailey's Crossroads, Virginia (Skyline Plaza) (Leyendecker and Fattal, 1977), Commonwealth Avenue, Boston, Massachusetts (1971); and Cocoa Beach, Florida (Harbour Cay Condominiums) (Lew et al., 1982a,b). All of these multistory flat-plate buildings in late stages of construction collapsed vertically in a progressive manner to the ground. The triggering cause was typical: localized punching shear failure at the slab-column connection. Premature removal of formwork coupled with insufficient concrete strength at the time of the collapse were partially blamed for these disasters. The maturity of concrete was affected by the low temperatures that prevailed during the construction of these projects.

Although the Cocoa Beach collapse was mainly attributed to design and construction errors and not directly to concrete strength, procedures for concrete strength determination prior to the removal of forms were flawed. Construction records showed that laboratory-cured cylinders were used in order to determine the actual field strength of the slabs prior to stripping, where proper procedures and common sense dictated testing of field-cured cylinders.

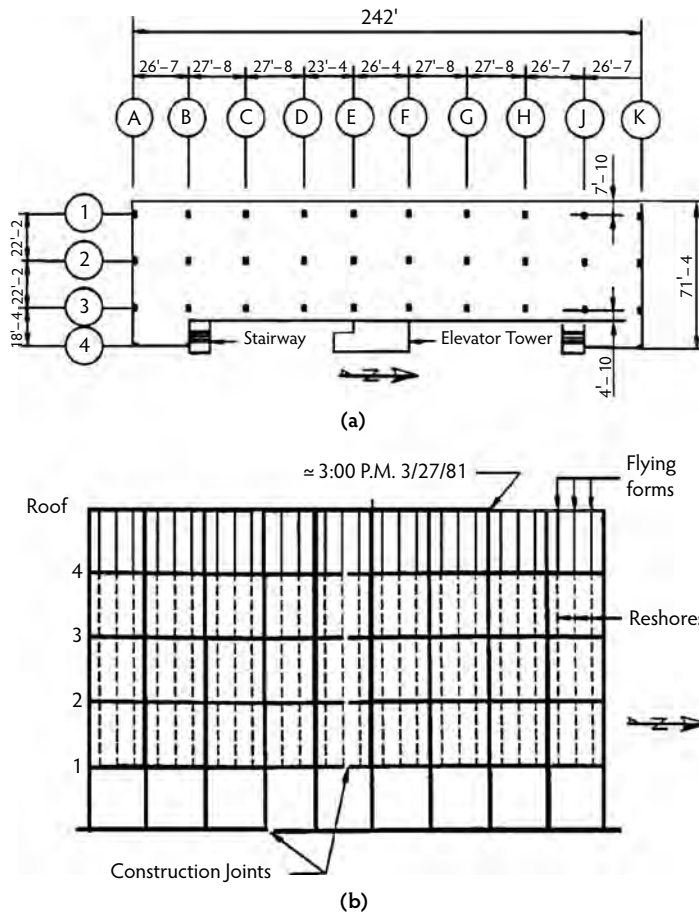


FIGURE 8.36 (a) Typical floor plan of the Harbour Cay Condominium, and (b) assumed state of construction at the time of collapse. (From Stivaros, P.C. and Halvorsen, G.T., *Concrete Int.*, 13(8), 57–62, 1991.)

A reexamination of the Harbour Cay Condominium failure later attributed it more directly to deficiency of punching shear strength (Stivaros and Halvorsen, 1992). The Harbour Cay was a five-story flat-plate concrete building. A typical floor framing plan is shown in Figure 8.36. At the time of collapse, flying forms on the fifth floor supported the fresh concrete roof slab. Three levels of wood reshores rested below. Figure 8.36 shows the flying form and reshore layout and indicates the portion of the roof believed to have been in place at the time of collapse.

National Institute of Standards and Technology (NIST) investigators (Lew et al., 1982a) used the ICES-STRU DL II finite-element program to analyze the Harbour Cay structure. The finite-element model consisted of rectangular plate bending elements for the columns and three-dimensional truss elements for the shoring system. The distribution of loads from the shoring and reshoring procedure was examined by means of the Grundy–Kabaila simplified method. The analysis indicated that, when all the floors were reshored to the ground, the removal of the flying forms at the topmost level completely relieved the forces in the reshores. The existing slabs always supported their own dead load and did not share in supporting a portion of the load of the newly cast floor. Only after the first-story reshores were removed, thus removing a direct load path to the ground, did the existing floor slabs share the load of a newly cast slab. These observations stem from Grundy–Kabaila’s basic assumption of an infinitely stiff shoring system.

As a result of the above observations, to determine the state of load distribution at the time of collapse, NIST investigators studied two separate load cases (Figure 8.37). In the first, the structure without reshores

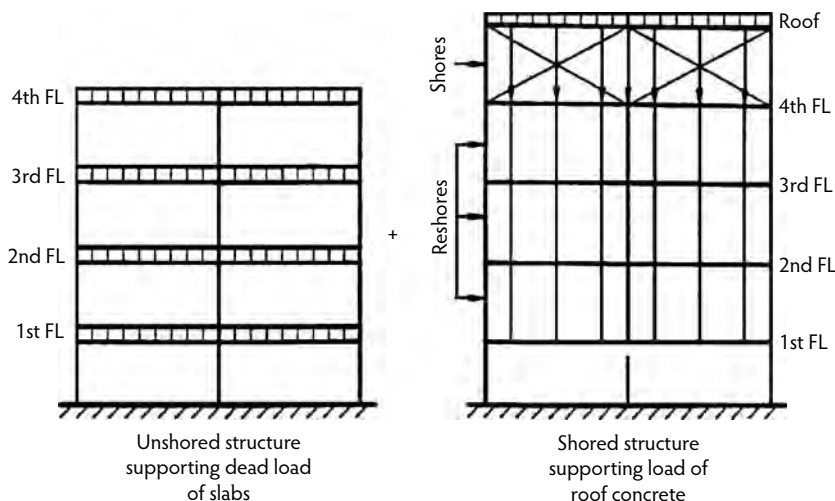


FIGURE 8.37 Two load cases considered in NIST analysis of Harbour Cay Condominium. (From Stivaros, P.C. and Halvorsen, G.T., *Concrete Int.*, 13(8), 57–62, 1991.)

was analyzed under the dead load of the slabs. In the second, the reshored structure was analyzed under the load of the fresh concrete and the formwork. The final result was obtained by superimposing the results of the two analyses. Given in Figure 8.38a are the combined punching shear forces, in kips, for the slab-column connections along column line 2 of the building.

Stivaros and Halvorsen (1992) carried out a preliminary equivalent frame analysis of the Harbour Cay failure, using the same structural data and loading conditions as those used by NIST investigators. The preliminary analysis used the plane frame capabilities of ICES-STRUDL II. The results of this analysis are shown in Figure 8.38a in square brackets. After the preliminary analysis indicated reasonable results, Stivaros and Halvorsen developed their special-purpose computer program [Stivaros and Halvorsen, 1990] that recognized time-dependent material properties and time in the construction process. This program was applied to the construction-load distribution of the Harbour Cay Condominium failure in two different ways. First, the structure was analyzed according to the two loading cases and structural details identified by Lew et al. (1982a). The results of this first analysis are shown in parentheses in Figure 8.38a.

An alternative approach assumed more realistic construction-loading conditions. Grundy–Kabaila’s simplified method, as mentioned, assumes an infinitely stiff shoring system; however, the Harbour Cay Condominium used compressible wooden reshores. In the course of the alternative analysis, the program built the structure from the first floor to the roof and considered the effects of all the cycles of loading and unloading as the construction progressed upward. Thus, the effect of compressible reshores could be assessed. Variations in concrete maturity, strength, and stiffness are also incorporated. The punching shear forces at slab-column joints along the height of column stack C-2 are shown in Figure 8.38b. The results of the alternative analysis, which considered the two separate loading cases, are shown in parentheses.

The accuracy of the Grundy–Kabaila simplified method was tested against observations of the Harbour Cay Condominium collapse. Figure 8.38c shows the punching shear forces at every slab–column joint along the height of column stack C-2. The first number indicates the force obtained by the alternative equivalent multi-bay frame, the second number (in parentheses) represents the force obtained by the alternative method using a single-bay model, and the third number (in square brackets) represents the force obtained from the simplified method that invariably uses a single-bay model. A comparison shows that the alternative equivalent single-bay model and the simplified method underestimate the punching shear forces along column stack C-2 on the top floor by 13 and 21%, respectively, as compared to the results of the equivalent multi-bay frame model. On the floors below, both the simplified method and the equivalent single-bay frame model differ by smaller percentages from the equivalent multi-bay frame model.

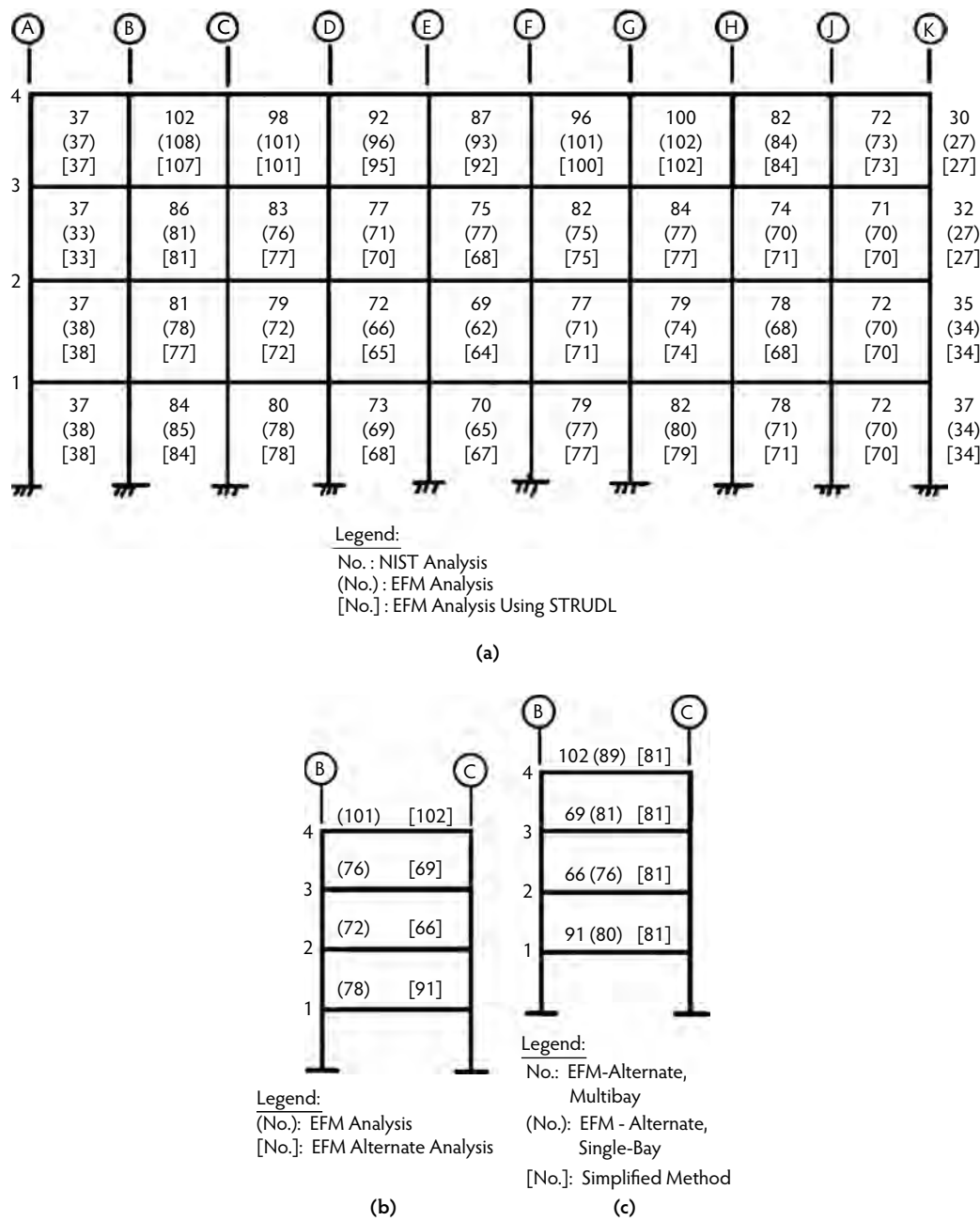


FIGURE 8.38 (a) Punching shear forces along column line 2 (kips); (b) slab loads on bay B-C from multi-bay EFM analysis (kips); (c) slab loads on bay B-C from EFM and simplified method (kips), Harbour Cay Condominium analysis. (From Stivaros, P.C. and Halvorsen, G.T., *Concrete Int.*, 13(8), 57–62, 1991.)

Based on the simplified method and the equivalent single-bay frame analysis, punching shear force at the top slab–column joint along column stack C-2 was within the punching shear strength of that joint; however, analysis based on the equivalent multi-bay frame model indicated that the available punching shear strength was exceeded at the same joint. According to Stivaros and Halvorsen (1992), “Here is exactly where the significance of the EFM multi-bay model lies....”

TABLE 8.7 Development of Tensile/Bond/Shear Strength, Percent of 28-day, 73°F (22.8°C) Value

Aged (day)	Type I Cement Temperature			Type III Cement Temperature		
	73°F (22.8°C)	55°F (12.8°C)	40°F (4.4°C)	73°F (22.8°C)	55°F (12.8°C)	40°F (4.4°C)
1	0.31 ^a	0.15 ^a	0.03 ^a	0.54 ^a	0.33 ^a	0.11 ^a
2	0.47	0.28	0.11	0.65	0.50	0.30
3	0.59 ^a	0.40 ^a	0.18 ^a	0.74 ^a	0.62 ^a	0.43 ^a
4	0.66	0.49	0.24	0.78	0.66	0.54
5	0.72	0.57	0.32	0.81	0.70	0.63
6	0.76	0.63	0.39	0.83	0.73	0.70
7	0.79 ^a	0.68 ^a	0.44 ^a	0.85 ^a	0.75 ^a	0.77 ^a
8	0.81	0.72	0.48	0.86	0.77	0.80
9	0.83	0.75	0.52	0.88	0.79	0.82
10	0.85	0.77	0.56	0.89	0.81	0.84
11	0.86	0.80	0.59	0.90	0.82	0.86
12	0.88	0.82	0.62	0.91	0.84	0.88
13	0.89	0.84	0.64	0.92	0.85	0.89
14	0.90	0.86	0.67	0.92	0.86	0.90
21	0.96	0.94	0.80	0.97	0.93	0.99
28	1.00 ^a	1.02 ^a	0.88 ^a	1.00 ^a	0.96 ^a	1.07 ^a

^a Klieger's (1958) original data.Source: Gardner, N.J., *Concrete Int.*, 7(4), 28–34, 1985.

8.4.1 Safety Analysis

Gardner (1985) was the first to attempt a systematic safety analysis of construction (shoring/reshoring) schemes for multistory buildings, as described in this section. The strength of a reinforced concrete slab is a function of the design (factored) load, age of the slab, and the critical mode of behavior of the slab: flexure, bond, or shear. The required strength for various live-load/dead-load ratios, in terms of dead load, can be calculated from ACI 318-05 (ACI Committee 318, 2005) Appendix C as follows:

$$U = 1.4D + 1.7L = D \left[1.4 + 1.7 \frac{L}{D} \right] \quad (8.14)$$

Design strength (nominal strength reduced by the appropriate strength-reduction factor) must equal or exceed the required strength and was assumed by Gardner to equal the required strength. It should be noted that, in U.S. design practice, the design strength is assumed to be available at 28 days of age. The strength available at the early age at which a slab experiences construction loads is, of course, lower than the 28-day design strength. Gardner and Poon (1976) had concluded earlier that the tensile and bond strengths of concrete were proportional to the compressive cylinder strength raised to the power 0.8. As shear is governed by tensile strength, it was assumed that shear strength was also related to compressive strength the same way. Data in Table 8.7 were prepared by Gardner (1985) from Klieger's (1958) data, using the 0.8-power criterion to estimate early-age strength as a fraction of the 28-day, 73°F cylinder strength for both Type I normal Portland cement and Type III high-early-strength cement concretes. Gardner (1985) noted that no existing design code specifies a construction load factor. ANSI A10.9-1997 (ANSI, 1997) recommends a load factor of 1.3 for both dead and live construction loads. Kaminetzky and Stivaros (1994) indicated preference for the more conservative load factors required by ACI 318 Appendix C for service conditions—that is, 1.4 and 1.7 for construction dead and live loads, respectively. Gardner used a construction load factor of 1.4 and assumed that the forms have self-weights equal to 10% of the slab self-weight and that the simplified Grundy–Kabaila method is approximately 10% in error. This yielded a factored construction load combination (required strength) of:

TABLE 8.8 Factored Construction Loads on Slabs with Two Shores and Two Reshores

Slab	Age of Slab (Cycles after Casting)							
	1		2		3		4	
	a	b	a	b	a	b	a	b
1	0 ^a	0 ^a	1.54 ^a	1.54 ^a	1.54 ^a	1.54 ^a	1.94	2.37
2	1.54 ^a	1.69 ^a	2.31 ^a	2.31 ^a	1.94	2.37	1.94	2.37
3	0.77 ^a	0.77 ^a	2.37	2.79	1.94	2.37	1.94	2.37
4	1.52	1.94	2.79	3.21	1.94	2.37	1.94	2.37
5	1.10	1.52	2.60	3.01	1.94	2.37	1.94	2.37

^a Slab supported on grade so construction live load transmission is directly to the ground.

Note: Operation a is removal of lowest level of shores and reshores; operation b is casting of next slab.

Source: Gardner, N.J., *Concrete Int.*, 7(4), 28–34, 1985.

$$U = \left[\underset{(a)}{1.1} \times \underset{(b)}{1.1} \times \underset{(c)}{1.4} \times \underset{(d)}{\text{load ratio}} + \underset{(e)}{\frac{1}{N}} \right] \text{dead load} \quad (8.15)$$

where (a) is error in simplified method, (b) is the weight of the formwork, (c) is the load factor, (d) is the calculated load ratio (Table 8.2), and (e) is an allowance for the construction live load where N is the total number of shore and reshore levels. Using Equation 8.15, the factored construction loads at various stages of construction are shown in Table 8.8 for two levels of shoring and two levels of reshoring. A complete version of Table 8.8 for other combinations of shore and reshore levels is shown in Table 8.9. Gardner (1985) provided the following three examples of safety analysis.

8.4.1.1 Example 8.1

Determine if a flat-slab structure designed for a live-load/dead-load ratio of 1.00 by ACI 318 can be constructed using a two-shore/two-reshore system with a seven-day casting cycle and form stripping one day before casting. Assume an ambient temperature of 73°F and Type I Portland cement concrete:

$$U = D \left[1.4 + 1.7 \frac{L}{D} \right] = 3.1D$$

Assuming that the 28-day design strength is equal to the required strength U , the strengths available at various ages of interest are as follows:

Age (days)	Strength Available
6	$0.76 \times 3.1D = 2.36D$
7	$0.79 \times 3.1D = 2.45D$
13	$0.89 \times 3.1D = 2.76D$
14	$0.90 \times 3.1D = 2.79D$
20	$0.96 \times 3.1D = 2.98D$
27	$1.00 \times 3.1D = 3.1D$
28	$1.00 \times 3.1D = 3.1D$

Using the load data from Table 8.8, the adequacy can be checked for every slab at every stage of construction. The results of the check are shown in Table 8.10. It can be seen that the proposed construction scheme overloads slab 4 at ages 13 and 14 days and slab 5 at 14 days. Thus, it cannot be used without modification.

8.4.1.2 Example 8.2

Determine the construction cycle for a slab designed for a live-load/dead-load ratio of 0.5, using one shore plus five reshore levels at a temperature of 55°F. Assume Type I Portland cement concrete and a specified concrete strength of 4000 psi. From Table 8.8, for one level of shores and five levels of reshores, the factored construction loads are $1.86D$ at stripping and $2.15D$ at casting of the next slab. The required strength is:

$$U = D \left[1.4 + 1.7 \frac{L}{D} \right] = 2.25D$$

Assuming that the 28-day, 73°F design strength is equal to the required strength U , the concrete strength at casting at 55°F needs to be $2.15/2.25 = 96\%$ of the 28-day strength, which occurs at approximately 23 days. The concrete strength at stripping has to be $1.86D/2.25D = 83\%$, which occurs at 13 days. In most cases, a 23-day cycle would not be economically acceptable.

8.4.1.3 Example 8.3

Redo the above example to achieve a 7-day placing cycle. The strength of the slab required at casting (7 days) is $0.96 \times 4000 \text{ psi} = 3840 \text{ psi}$; the strength of the slab required at stripping (6 days) is $0.83 \times 4000 \text{ psi} = 3320 \text{ psi}$. To obtain a concrete strength of 3840 psi at 7 days, either the concrete mix must be redesigned or heat must be supplied to accelerate the hydration process. It should be noted that this safety analysis is probably flawed if punching shear governs safety, as it usually does for slab systems without column-line beams. This is for two important reasons. First, as mentioned earlier, simplified Grundy–Kabaila-type analysis cannot lead to accurate estimates of punching shear forces at slab–column joints. Second, the assumption that punching shear strength varies with the 28-day compressive cylinder strength of concrete raised to the power 0.8 was not verified in later tests by Gardner (1960), who found punching shear strength to vary with the cube root of the 28-day compressive cylinder strength.

8.4.2 Refined Safety Analysis

A more refined safety analysis was carried out by Kaminetzky and Stivaros (1994) on a test multistory flat-plate office building (Figure 8.39), assumed to have been designed according to ACI 318 with a 50-psf (2.4 kPa) live load and an additional superimposed partition load of 30 psf (1.5 kPa). This example assumed one level of shores and three levels of reshores with a construction rate of two floors per week. It is also assumed that the shores and reshores were removed and relocated a day before casting the top slab. A 50-psf (2.4 kPa) construction live load was assumed to be present only during the placement of concrete in the top slabs. The *in situ* concrete strength can be estimated by testing field-cured cylinders in combination with other available nondestructive methods. Figure 8.40 shows the assumed compressive strength–time relationship for two different construction temperatures: 55 and 73°F.

Stivaros' computer program (Stivaros and Halvorsen, 1990), based on the equivalent frame method of analysis, was employed to evaluate the construction load distribution between the shoring system and the concrete frame. The program, as mentioned earlier, builds the structure from the first floor to the roof and evaluates the loads on each floor slab and the support system for every construction stage. The punching shear stresses due to applied loads are also computed at each column location for every construction step. The program provides the available load-carrying capacities of the slabs and the available punching shear strengths of slab–column connections at the time of application of the construction loads; thus, a safety comparison can be made. The load-carrying capacities are based on flexural considerations, accounting for partially developed concrete compressive strength. A key assumption is that the load factors and strength-reduction factors used for the design of the slabs for service conditions are the same for the construction stage as well. The available punching shear strength is evaluated according to ACI 318 (ACI Committee 318, 2005) and is equal to $\sqrt{F_{ct}}$, where $\phi = 0.85$, and F_{ct} is the available concrete strength at the time the load is applied. The results of the construction load analysis are shown in Figure 8.41 and Figure 8.42. The figures show the maximum factored slab loads (normalized

to the self-weight of the slab) and punching shear stresses that occurred on the floor slabs during construction. Also shown in the figures are the load-carrying capacities (allowable loads) and allowable punching shear stresses of the concrete slabs at two temperature conditions: 55 and 73°F. Figure 8.41 shows that the maximum applied factored load, which occurred on 4-day-old slabs, exceeded the allowable loads

TABLE 8.10 Comparison of Strength and Factored Load for Worked Example

Age After Casting	Strength Available	Load Applied				
		Slab 1	Slab 2	Slab 3	Slab 4	Slab 5
6	2.36	0	1.54	0.77	1.52	1.10
7	2.45	0	1.69	0.77	1.94	1.52
13	2.76	1.54	2.31	2.37	2.79	2.60
14	2.79	1.54	2.31	2.79	3.21	3.01
20	2.98	1.54	1.94	1.94	1.94	1.94
21	2.98	1.54	2.37	2.37	2.37	2.37
27	3.10	1.94	1.94	1.94	1.94	1.94
28	3.10	2.37	2.37	2.37	2.37	2.37

Source: Gardner, N.J., *Concrete Int.*, 7(4), 28–34, 1985.

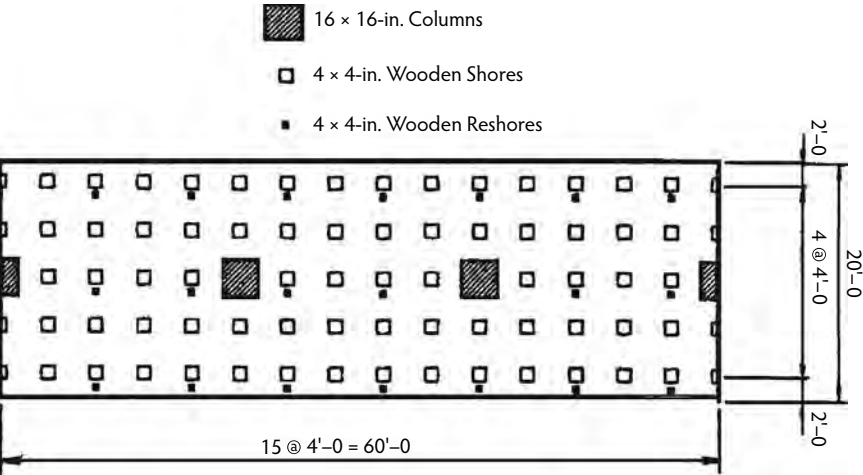


FIGURE 8.39 Typical floor plan of construction example studied by Kaminetzky (1994).

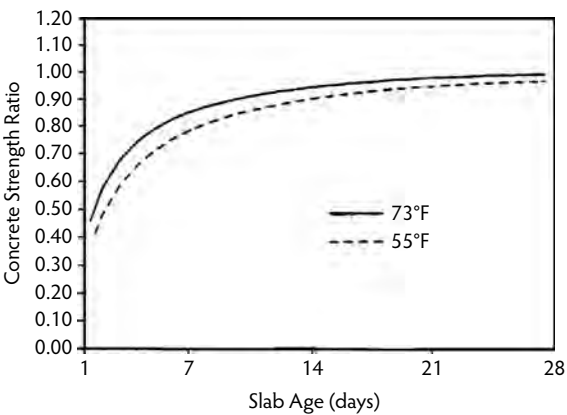


FIGURE 8.40 Compressive strength development vs. time assumed by Kaminetzky (1994).

for both temperature conditions. This means that the proposed construction scheme cannot be safely executed. Similar unsafe construction conditions are shown in Figure 8.42, where the punching shear stresses due to the applied loads exceeded the allowable stresses. For this particular example, the available strengths in both flexure and shear have been exceeded; however, because of the possibility of inelastic redistribution of bending moments and because of the improbabilities of any redistribution of punching shear stresses, a sudden shear failure is likely to occur prior to flexural failure. Kaminetzky and Stivaros (1994) pointed out that had some floors of the above building been designed for an additional live load of 20 psf (1.0 kPa), the slabs would have been flexurally adequate to carry the construction loads for the 73°F temperature condition at a rate of two floors per week (Figure 8.43). Also, a construction rate of one floor per week would have been safe even for the 55°F temperature condition; however, the construction operation still could not proceed safely because of the punching shear deficiency of the slabs.

8.5 Serviceability Consequences of Construction Loads

Floors in residential as well as office buildings are often made of thin, solid concrete slabs with two-way reinforcement. The trend in recent years has been toward a progressive decrease in the ratio of the thickness of slab to length of span. This obviously causes a corresponding reduction in the flexural rigidity

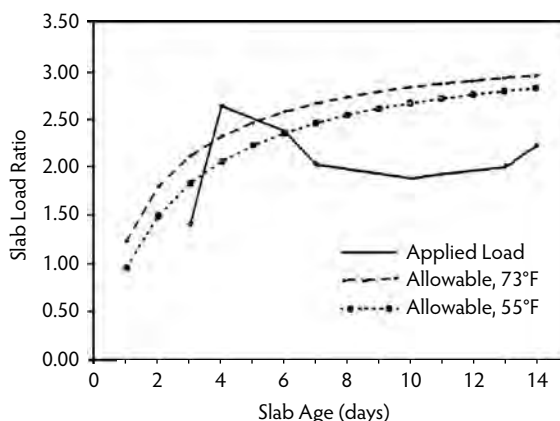


FIGURE 8.41 Allowable and applied slab loads from Kaminetzky's (1994) analysis (live load = 50 psf).

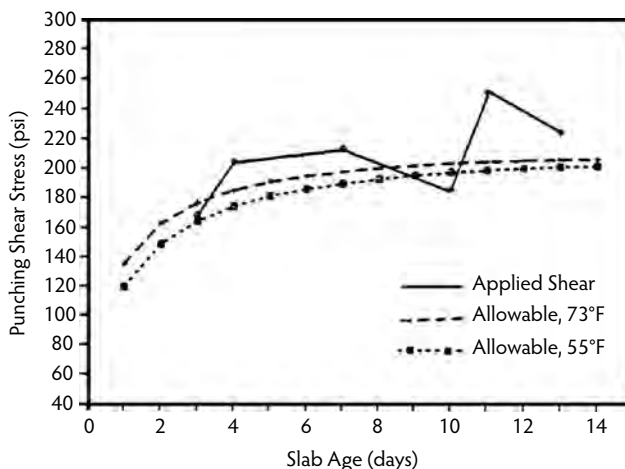


FIGURE 8.42 Allowable and applied punching shear stress from Kaminetzky's (1994) analysis.

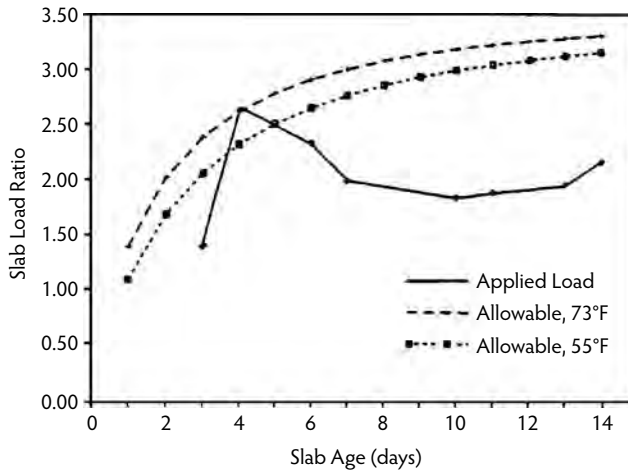


FIGURE 8.43 Allowable and applied slab loads from Kaminetzky's (1994) analysis (live load = 70 psf).

of slabs. The consequent deformations have not always received as much attention as preventing collapse. Large permanent deformations of floor slabs have sometimes resulted. Whereas such deformations are often aesthetically unacceptable, their effects may also be seriously disturbing from a practical point of view. Cracking of brick partitions, jamming of doors, and cracking of windows have not been uncommon. At least in one reported case, long-term deflection of an interior span of a floor caused an adjacent balcony to slope inward. Rain falling on the balcony ran inward under the doorway and formed a pool in the middle of the floor, damaging carpets. Excessive long-term deflections of slabs are clearly to be avoided.

8.5.1 Causes of Excessive Deflections

Excessive deflections can sometimes be attributed to a single cause. More commonly, however, the problem may be traced to a combination of several contributing factors. Potential problem areas include design, construction, materials, environmental conditions, and change in occupancy (Scanlon, 1987).

8.5.1.1 Design

The single most common cause of large deflections associated with design is the selection of a slab thickness that is too small for the spans used. Another common problem is inadequate flexural reinforcement; as a result, premature yielding may occur, causing a substantial loss of flexural stiffness and leading to excessive deflection.

8.5.1.2 Materials

Higher than normal creep and shrinkage characteristics have been identified as contributing factors in cases of large deflections reported in Australia. While achieving high concrete strengths, high-shrinkage characteristics have sometimes been produced; the increase in slab warping has more than offset the benefits obtained from the increase in the modulus of elasticity of the concrete. In post-tensioned slabs, higher than normal prestress losses may lead to unanticipated deflections. Alkali-aggregate reactions produced by certain types of aggregate and cement may cause cracking that can adversely affect flexural stiffness.

8.5.1.3 Environmental Conditions

For slab surfaces exposed to daily or seasonal temperature fluctuations, temperature gradients set up through the member thickness may lead to unanticipated deflections.

8.5.1.4 Change in Occupancy

Slabs adequately designed and constructed for the original design loading may suffer deflection problems if the occupancy changes and if the change involves an increase in the sustained load applied to the slab.

8.5.1.5 Construction

The following is a list of factors, as compiled by Taylor and Heiman (1977), that contribute to excessive long-term slab deflections:

1. Formwork has not been cambered in cantilevers and large interior panels, so even early deflections are obvious.
2. Slabs have been supported by props bearing on sole plates that were of inadequate size to prevent appreciable settlement into the ground surface and hence induced slab deformation before stripping.
3. Construction loading from propping or the storage of materials during the early life of the slabs has been severe enough to cause extensive slab cracking and hence loss of stiffness.
4. Top reinforcement at supporting elements has been pushed down during slab construction, substantially reducing its effective depth and hence reducing the contribution made to slab stiffness by continuity at supports.
5. Curing has in many instances been inadequate and has sometimes led to insufficient strength development and excessive shrinkage cracking.

Item 4 above is a surprisingly common occurrence. Quite often, the top steel over supports is not securely held in place and is displaced toward the neutral axis, greatly reducing the stiffness over the support. If the effective depth is 7 in. instead of 8 in., as has been observed, the stiffness is reduced by 23%, and the member tends to behave as if it were simply reinforced.

Discussion here obviously needs to focus on the very important item 3 above. As noted earlier, when the shore/reshore method of multistory building construction is used, high-early-age, short-duration loads are imposed on the floor slabs. These loads can be comparable in magnitude to, or even exceed, the design service loads and are applied to concrete slabs that have not achieved their specified concrete strength. Because the slab concrete is immature with a reduced modulus of elasticity (see preceding section), the immediate deflections due to the construction loads are relatively large. Creep effects may be looked upon as being dependent upon the magnitude of the applied stress relative to the developed concrete strength; hence, creep deflections due to construction loads are also large. Deflection due to concrete shrinkage must also be considered.

8.5.2 Components of Long-Term Deflection

Shrinkage and creep are the two primary contributors to long-term deflections of reinforced concrete members. Shrinkage produces a shortening of the concrete in a member that is resisted by the reinforcing steel. The magnitude of shrinkage curvature (Figure 8.44b) depends on the amount of nonsymmetry of reinforcement and on the relative areas of concrete and steel in a reinforced concrete member. These shrinkage curvatures, which are the greatest for beams with tension reinforcement only, generally have the same sign as those due to moments produced by transverse loads, and thus they magnify the deflection due to load.

Considering creep alone, the increase in strain with time will be as shown by line B in Figure 8.45b, while line A indicates the strain distribution immediately on application of the load. Strain at the extreme fiber in compression increases considerably, while the strain at the level of the steel changes very little. As this occurs, the compressive stresses in the concrete are reduced (Figure 8.45c) because the neutral axis moves toward the reinforcement, and the steel stresses increase because the internal lever arm shortens. It can be seen from Figure 8.45b that the relative increase in curvature caused by creep is less than the relative increase in strain due to creep. Thus, the relative increase in deflection is also less than the increase in strain due to creep.

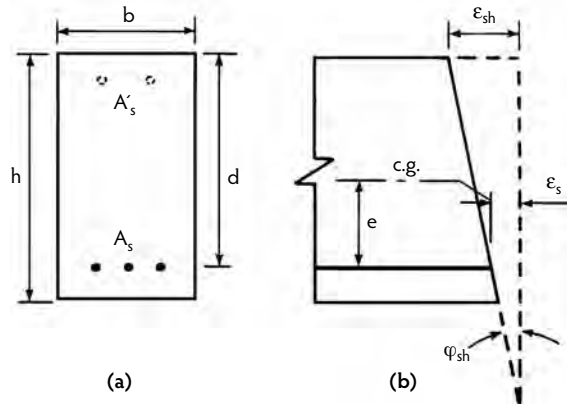


FIGURE 8.44 Shrinkage curvature of a section of a reinforced concrete flexural member.

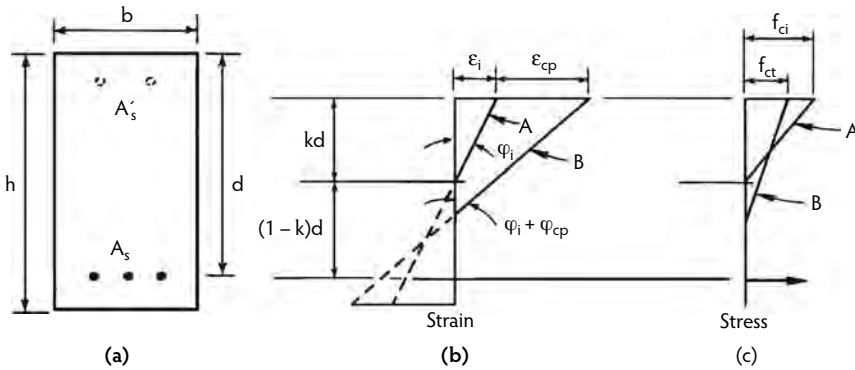


FIGURE 8.45 Strain and stress distribution and curvature due to initial and creep deformation in a section of a reinforced concrete flexural member.

In addition to the difficulty of determining the creep-time history of a particular concrete under constant, uniformly distributed sustained stress, a reinforced concrete flexural member is subjected to a nonuniform stress distribution and often a variable load history. A detailed analysis of the effects of a variable stress history, even for uniformly loaded members, is usually not feasible, and shorter, more appropriate methods are used. One such method uses a reduced or effective modulus called the *sustained modulus of elasticity*, which refers to concrete under a constant sustained stress:

$$E_{ct} = \frac{\sigma_{\text{constant}}}{\epsilon_{\text{initial}} + \epsilon_{\text{creep},t}} = \frac{\sigma_{\text{constant}}}{(1 + C_t) \epsilon_{\text{initial}}} = \frac{E}{1 + C_t} \quad (8.16)$$

where $C_t = \epsilon_{\text{creep}} / \epsilon_{\text{initial}}$ is the creep coefficient at time t , the ultimate value of which may be denoted by C_u . It may be parenthetically noted that in considering creep deformations, use of the specific creep strain δ_t (creep per unit stress) or creep coefficient C_t (ratio of creep strain to initial strain) yields the same results (ACI Committee 209, 1971), as:

$$C_t = \delta_t E_{ci} \quad (8.17)$$

This can be seen from the following relations: creep strain at time $t = (\sigma_{\text{constant}}) \delta_t = (\epsilon_{\text{initial}}) C_t$, and $E_{ci} = \sigma_{\text{constant}} / \epsilon_{\text{initial}}$. The choice of δ_t or C_t is a matter of convenience, depending on whether applying the creep factor to stress or strain is desired.

With reference to Figure 8.45 and the earlier discussion on that figure,

$$\frac{\Delta_{\text{creep},t}}{\Delta_{\text{initial}}} = \frac{\phi_{\text{creep},t}}{\phi_{\text{initial}}} = k_{rc} \frac{\epsilon_{\text{creep},t}}{\epsilon_{\text{initial}}} = k_{rc} C_t \quad (8.18)$$

provided that the same moment of inertia is used in the computation of short- and long-term deflections. The factor k_{rc} accounts for the effect of compression steel and the offsetting effects of a downward movement of the neutral axis due to creep strain distribution and upward movement of the neutral axis due to progressive cracking under creep loading (plus the small effect, if any, of repeated live-load cycles). These offsetting effects normally appear to result in a downward movement of the neutral axis, such that k_{rc} is less than unity.

Because shrinkage and creep deflections are additive, their combined value is often estimated in approximate calculations with a single time-dependent factor applied to the initial deflection:

$$\Delta_t = k_r T_t \Delta_{\text{initial}} \quad (8.19)$$

where T_t is a multiplier for additional long-term deflections due to creep and shrinkage, the ultimate value of which may be denoted by T_u . The factor k_r in Equation 8.19 and the factor k_{rc} in Equation 8.18 serve largely the same purpose. The following values have been suggested for the two factors (ACI Committee 209, 1971):

$$k_{rc} = 0.85 - 0.45(A'_s / A_s) \geq 0.40 \quad (8.20)$$

$$k_r = 1.00 - 0.60(A'_s / A_s) \geq 0.40 \quad (8.21)$$

ACI 318 (ACI Committee 318, 2005) basically takes the Equation 8.19 approach to estimating long-term deflections.

The opportunity usually does not arise for temperature to influence deflections of floor systems, as these are usually protected from large temperature changes soon after casting. In slabs that are not so protected, temperature changes can be important. Because the thermal coefficients of steel and concrete are roughly the same, little if any curvature results from temperature changes that are uniform across a section of a member. With regard to differential temperatures (such as inside vs. outside temperatures of heated or cooled buildings), the deformation of reinforced concrete members is similar to or opposite that due to shrinkage; for example, the deflection would be downward in the case of roofs of heated buildings and upward in the case of roofs of air-conditioned buildings (Branson, 1977).

Because shrinkage is independent of load, it appears illogical for deflection directly caused by shrinkage to be related to load via the initial deflection; there is, however, an indirect way in which shrinkage can influence deflection. The stiffness of a cracked reinforced concrete section is usually less—sometimes much less—than the stiffness of the surrounding gross concrete section. It would appear that this change from an uncracked to a cracked section, which may be brought about and extended over a considerable period by shrinkage (plus creep and thermal) effects, offers the potential for a corresponding continuing increase in deflection. Branson (1987) cited laboratory tests by others to indicate that the formation of new cracks during sustained loading depends on the development of earlier cracks during the initial loading stage. For example, in beams with a low 0.60% steel and a steel stress $f_s = 20$ ksi at initial loading, about half the cracks occurred upon initial loading and the remainder during the sustained loading. In beams with the same low steel percentage but $f_s = 30$ ksi, almost all cracks occurred upon initial loading. In beams with a higher 2.0% steel, cracks appeared rather early, with little additional cracking occurring during the sustained loading. According to Branson, this effect, which would seem to require the use of a $k_r > 1$ in Equation 8.19, is for most practical purposes taken into account through the use of a suitable effective moment of inertia in initial deflection calculations and through the use of the k_r factor as given by Equation 8.21.

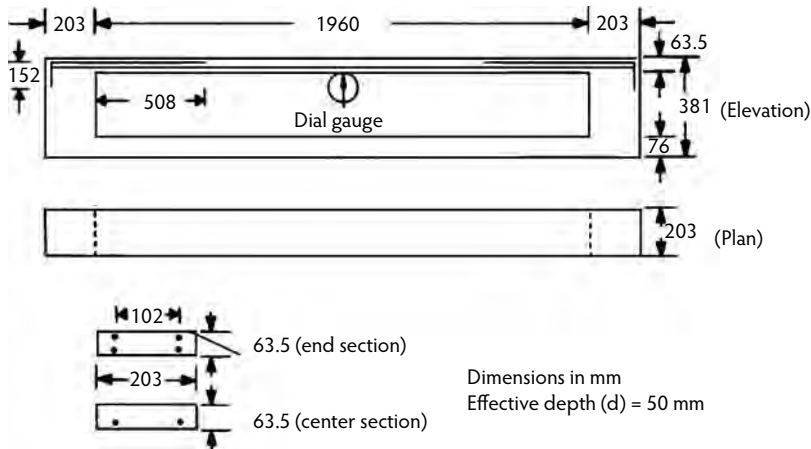


FIGURE 8.46 Details of one-way slab models tested by Fu and Gardner. (From Fu, H.C. and Gardner, N.J., in *Properties of Concrete at Early Ages*, SP-95, American Concrete Institute, Farmington Hills, MI, 1986, pp. 173–200.)

8.5.3 Experimental Investigation

Fu and Gardner (1986) fabricated five nominally identical single-span one-way slabs. All of the slabs (Figure 8.46) were 8 in. (203 mm) wide and 2.5 in. (64 mm) deep, spanned 77 in. (1960 mm), were reinforced with 5-mm diameter wires in one direction, and were cast from the same mix. Ready-mixed concrete with a target 28-day strength of 4000 psi (28 MPa) was used. Only the midspan deflections of the five one-way slabs were measured under load. After the formwork was stripped, measurements were made every day for the first month and then weekly afterward. In addition, shrinkage of four concrete prisms, compressive strength, and modulus of elasticity of the concrete were also measured. The five slabs were subjected to different load histories during the first 28 days after casting. Slabs 1 and 2 were subjected to simplified load histories, while slabs 3, 4, and 5 were subjected to load histories typical of one shore plus two reshores, one shore plus two levels of preshores (this term is discussed later), and three levels of shores. The load histories are given in Figure 8.47. The measured deflections are given in Figure 8.48a for the first 28 days and Figure 8.48b for the first 489 days. An examination of the deflection curves in Figure 8.48a reveals that the slopes of all these curves were virtually the same after day 28; subsequent deflections after removal of the construction loads seemed to be independent of prior loading. In other words, the additional deflections due to creep and shrinkage of concrete during the first 28 days of loading could not be recovered despite removal of the construction loads and even though identical loads were sustained on the slabs afterward. The net deflections after 28 days, taken as the sum of deflections due to loading (plus) and unloading (minus) alone and excluding deflections due to creep and shrinkage, were measured to be 0.60, 0.63, 0.62, 0.60, and 0.58 mm for slabs 1 to 5, respectively. It is equally interesting to note that the increases in deflections from day 28 to the end of the observation period (say, 489 days) for all five slabs were very close indeed: 1.60, 1.41, 1.49, 1.50, and 1.57 mm for slabs 1 to 5, respectively. However, due to the distinct loading histories in the initial stages, the corresponding final deflections after 489 days were 3.26, 4.13, 3.32, 3.51, and 4.31 mm, giving ratios of final deflection to net deflection at 28 days of 5.43, 6.56, 5.35, 5.85, and 7.43.

8.5.4 Control of Slab Deflections

The state of the art for control of two-way slab deflections was reviewed in ACI Committee 435 (1995). The methods of calculating slab deflections were presented, and the effects of two-way action, cracking, creep, shrinkage, and construction loads were considered. Probably the surest way to control deflections is to carefully sequence the operations of shore removal and reshoring. With a column layout like the one shown in Figure 8.49, stringers would normally be run in the short direction at about 4 ft on-center,

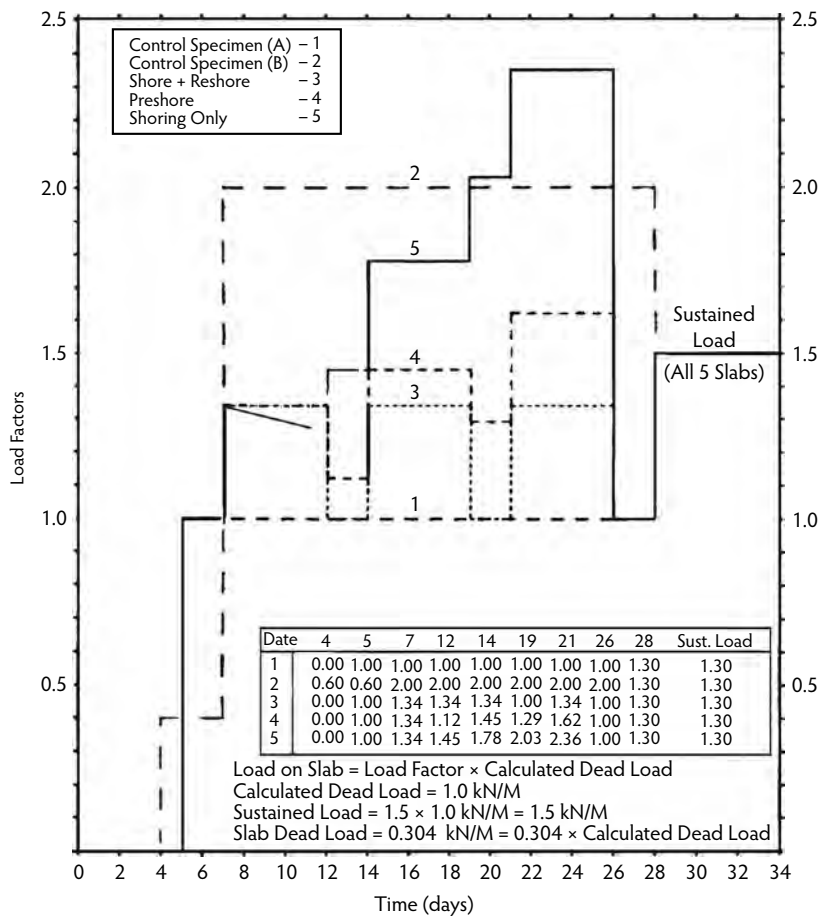


FIGURE 8.47 Loading histories on slab models tested by Fu and Gardner. (From Fu, H.C. and Gardner, N.J., in *Properties of Concrete at Early Ages*, SP-95, American Concrete Institute, Farmington Hills, MI, 1986, pp. 173–200.)

supported on shores. Ribs or purlins would then be run in the orthogonal direction, also at about 4 ft on-center, supported on the stringers. Finally, the 4 ft \times 8-ft plywood sheets would be supported on the ribs. It has been suggested (Cantor and Rizzi, 1982), on the basis of successful experience with flat-plate buildings in the New York area, that alternate plywood sheets in both the long and the short direction (shown shaded in Figure 8.49) should be supported directly by extra shores (indicated by x in Figure 8.49). These latter shores (attached to the plywood rather than to the stringers as the other shores are), also called *preshores* or permanent shores, may be installed at the time the other shores are installed or just before shore removal. When the time comes for removal of formwork, a day or two after casting or when concrete strength reaches a certain minimum value, the regular shores, the stringers, the purlins, and the plywood sheets that are not directly held by the extra shores can all be removed. Before the extra shores and the plywood sheets held by them are removed, however, reshores should be installed at about 8 ft on-center directly to the concrete slab. The extra shores or preshores should be removed only after the reshores have been installed.

The above scheme of removing the shores and installing the reshores does not permit more than 8 ft of slab span to be left unsupported at any time until the slab is sufficiently mature. With such short unsupported slab spans, slab deflections under usual circumstances cannot assume disturbing proportions, however high the loading may be during construction and however immature the slab may be when it is called upon to support those loads.

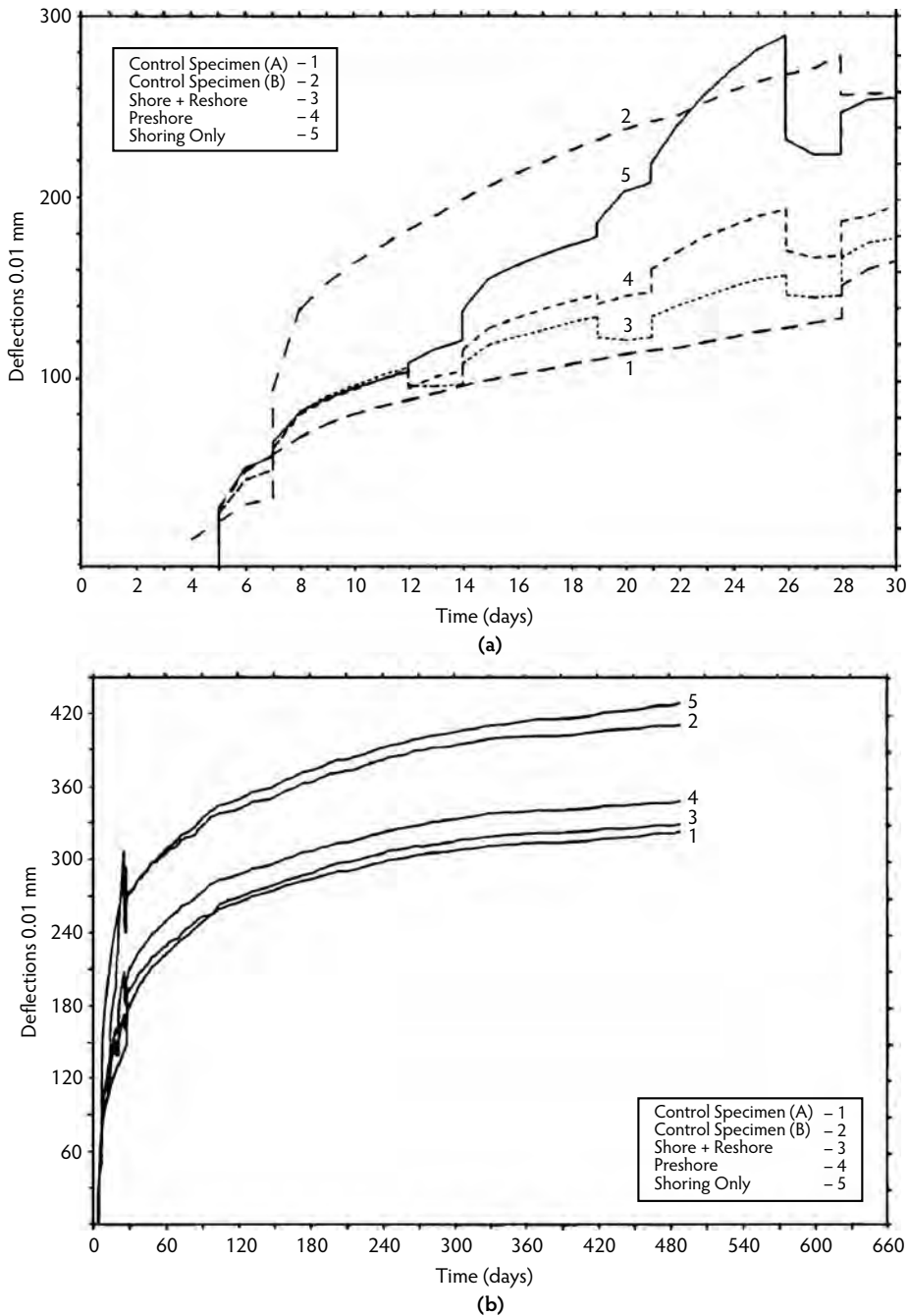


FIGURE 8.48 Deflections due to construction loads measured in slab models tested by Fu and Gardner. (From Fu, H.C. and Gardner, N.J., in *Properties of Concrete at Early Ages*, SP-95, American Concrete Institute, Farmington Hills, MI, 1986, pp. 173–200.)

The above consideration applies for the use of flying forms also. Figure 8.50 shows a reinforced concrete slab supported on reinforced concrete columns spaced at 20 ft on-center in both directions. With such a column layout, an 18-ft-wide form table would normally be used; however, in that case, as soon as the

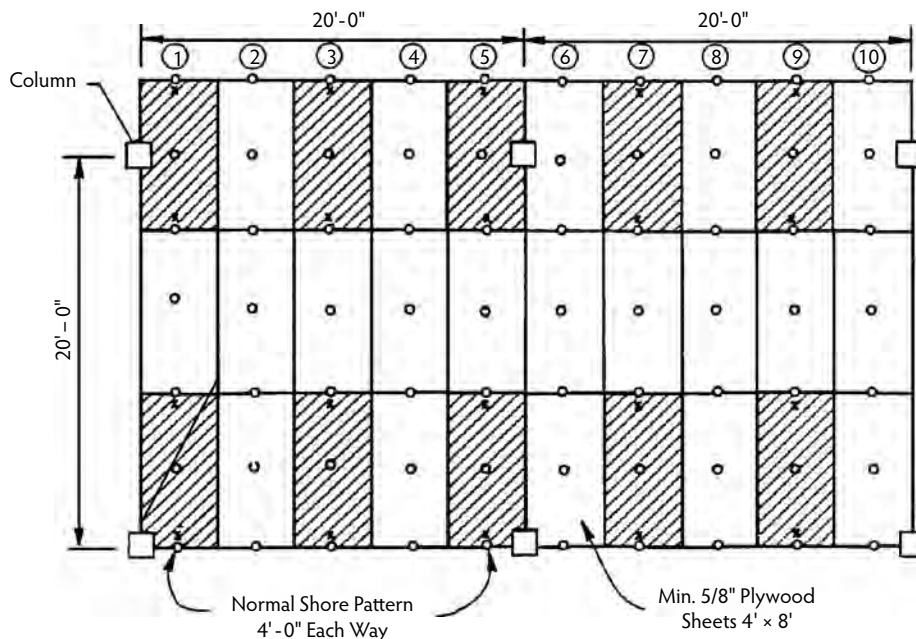


FIGURE 8.49 Sequence of shore removal and reshoring that restricts the slab span left unsupported at an early age. (From Cantor, I.G. and Rizzi, A.V., in *Proceedings of the First International Conference on Forming Economical Concrete Buildings*, Lincolnshire, IL, November 8–10, Portland Cement Association, Skokie, IL, 1982, pp. 18.1–18.12.)

flying form is removed 18 ft of slab span would be left unsupported. If deflections are of concern, two 8-ft-wide form tables, with a filler strip of formwork in between, may be used instead. With the narrower form tables, even when they are removed no more than 8 ft of slab span would be left unsupported. Admittedly, two 8-ft-wide form tables with a filler strip of formwork are significantly more expensive than a single 18-ft-wide form table. The added expense has to be weighed carefully against any advantage that is to be gained in terms of reduced deflections.

8.6 Codes and Standards

The following documents have been mentioned in this chapter:

1. *Guide to Formwork for Concrete*, ACI 347-04 (American Concrete Institute, Farmington Hills, MI)
2. *American National Standard for Construction and Demolition Operation—Concrete and Masonry Work—Safety Requirements*, ANSI A10.9-1997 (American National Standards Institute, New York)

The first of the items is an ACI committee report, and the second is an ANSI standard. Neither of the two is adopted into the International Building Code (IBC), the model code that increasingly forms the basis of the legal codes of various local jurisdictions (cities, counties, and states) within the United States. The latest edition of the IBC, dated 2006, adopts the 2005 edition of ACI Committee 318 *Building Code Requirements for Structural Concrete* for regulations concerning concrete design and construction. This edition of the standard contains interesting and important provisions related to the loading imposed on a concrete structure during construction. These provisions are discussed below. It should also be mentioned that the ASCE Standards Committee on Design Loads during Construction has issued a relatively new standard, ASCE/SEI 37-02 (*Design Loads on Structures during Construction*).

For the first time, the 1995 edition of the ACI 318 standard contained the following requirements, which have remained unchanged through the 2005 edition and are directly quoted from the standard:

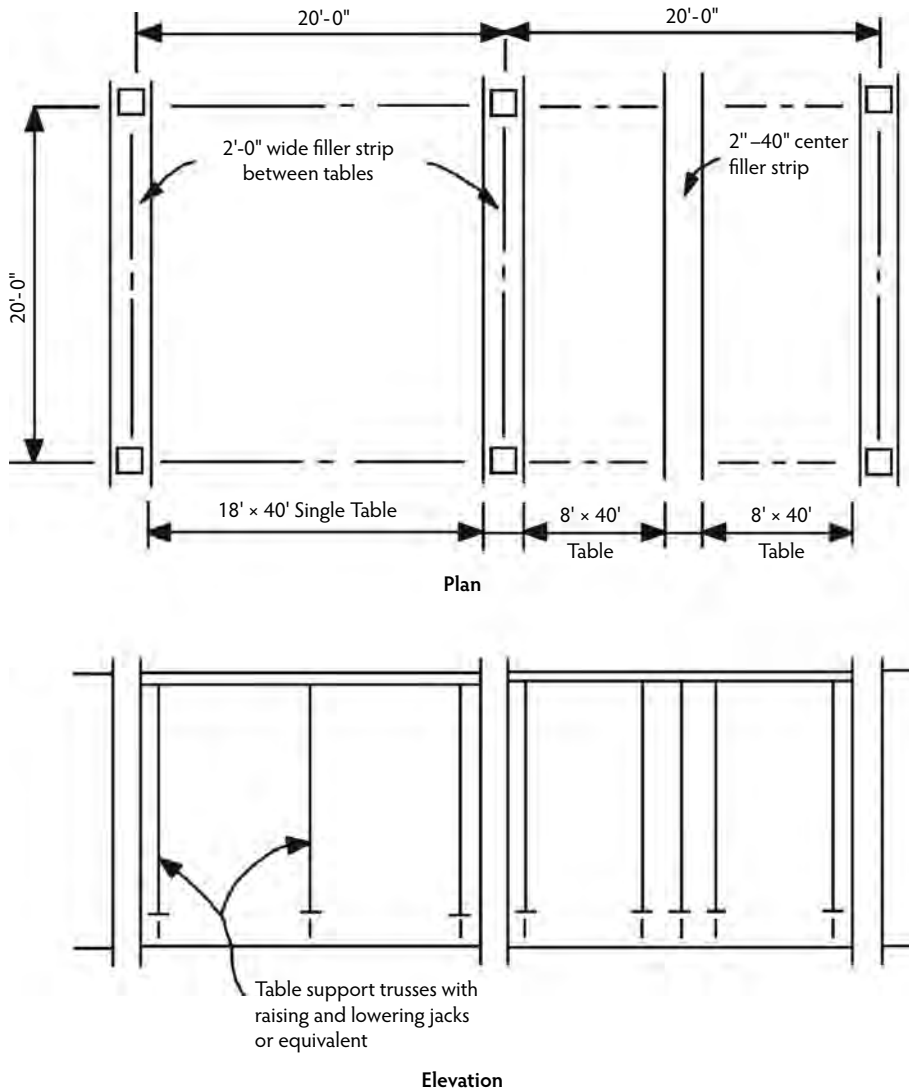


FIGURE 8.50 Restriction on slab span left unsupported at an early age with the use of flying forms. (From Cantor, I.G. and Rizzi, A.V., in *Proceedings of the First International Conference on Forming Economical Concrete Buildings*, Lincolnshire, IL, November 8–10, Portland Cement Association, Skokie, IL, 1982, pp. 18.1–18.12.)

ACI 318 §6.2. Removal of forms, shores, and reshoring

ACI 318 §6.2.1. Removal of forms

Forms shall be removed in such a manner as not to impair safety and serviceability of the structure. Concrete to be exposed by form removal shall have sufficient strength not to be damaged by removal operation.

ACI 318 §6.2.2. Removal of shores and reshoring

The provisions of ACI 6.2.2.1 through ACI 6.2.2.3 shall apply to slabs and beams except where cast on the ground.

ACI 318 §6.2.2.1. Before starting construction, the contractor shall develop a procedure and schedule for removal of shores and installation of reshores and for calculating the loads transferred to the structure during the process.

- (a) The structural analysis and concrete strength data used in planning and implementing form removal and shoring shall be furnished by the contractor to the building official when so requested;
- (b) No construction loads shall be supported on, nor any shoring removed from, any part of the structure under construction except when that portion of the structure in combination with remaining forming and shoring system has sufficient strength to support safely its weight and loads placed thereupon;
- (c) Sufficient strength shall be demonstrated by structural analysis considering proposed loads, strength of forming and shoring system, and concrete strength data. Concrete strength data shall be based on tests of field-cured cylinders or, when approved by the building official, on other procedures to evaluate concrete strengths.

ACI 318 §6.2.2.2. No construction loads exceeding the combination of superimposed dead load plus specified live load shall be supported on any unshored portion of the structure under construction, unless analysis indicates adequate strength to support such additional loads.

ACI 318 §6.2.2.3. Form supports for prestressed concrete members shall not be removed until sufficient prestressing has been applied to enable prestressed members to carry their dead load and anticipated construction loads.

The ACI 318 Commentary explains that in determining the time for removal of forms, consideration should be given to the construction loads and to the possibility of deflections. The construction loads are frequently at least as great as the specified live loads. At early ages, a structure may be adequate to support the applied loads but may deflect sufficiently to cause permanent damage. It is further stated in the commentary that:

The removal of formwork for multistory construction should be a part of a planned procedure considering the temporary support of the whole structure as well as that of each individual member. Such a procedure should be worked out prior to construction and should be based on a structural analysis taking into account the following items, as a minimum:

- (a) the structural system that exists at the various stages of construction and the construction loads corresponding to those stages;
- (b) the strength of the concrete at the various ages during construction;
- (c) the influence of deformations of the structure and shoring system on the distribution of dead loads and construction loads during the various stages of construction;
- (d) the strength and spacing of shores or shoring systems used, as well as the method of shoring, bracing, shore removal, and reshoring including the minimum time intervals between the various operations; and
- (e) Any other loading or condition that affects the safety or serviceability of the structure during construction.

For multistory construction, the strength of the concrete during the various stages of construction should be substantiated by field-cured test specimens or other approved methods.

It should be noted that the above requirements of ACI 318 and the accompanying suggestions in the commentary, while fairly comprehensive and meaningful, do not necessarily reflect current practice. It is also of interest to note here that prescriptive detailing requirements for structural integrity were added for the first time to the 1989 edition of the ACI 318 standard for cast-in-place concrete structures. Similar requirements were added to ACI 318-95 for precast concrete structures. The requirements were prompted by experience showing that the overall integrity of a structure can be substantially enhanced by minor changes in the detailing of reinforcement. It is the intent of Section 7.13 of ACI 318-95 (requirements for structural integrity) to improve the redundancy and ductility in structures so that, in the event of damage to a major supporting element or an abnormal loading event, the resulting damage may be confined to a relatively small area and the structure may have a better chance to maintain overall stability. Specifically for flat-plate and flat-slab construction, ACI 318-89 required that at least two of the column

strip bottom bars or wires in each direction should be made continuous, pass within the column core, and be anchored at exterior supports. Since its 1995 edition, ACI 318 has contained the following expanded requirements for flat plates or flat slabs:

ACI 318 §13.3.8.5. All bottom bars or wires within the column strip, in each direction, shall be continuous or spliced with Class A splices...At least two of the column strip bottom bars or wires in each direction shall pass within the column core and shall be anchored at exterior supports. The continuous column strip bottom reinforcement provides the slab with some residual ability to span to the adjacent supports, should a single support be damaged. A structural integrity provision has now also been added for other two-way slabs without beams:

ACI 318 §13.3.8.6. In slabs with shearheads and in lift-slab construction..., at least two bonded bottom bars or wires in each direction shall pass through the shearhead or lifting collar as close to the column as practicable and be continuous or spliced with a Class A splice. At exterior columns, the reinforcement shall be anchored at the shearhead or lifting collar.

References

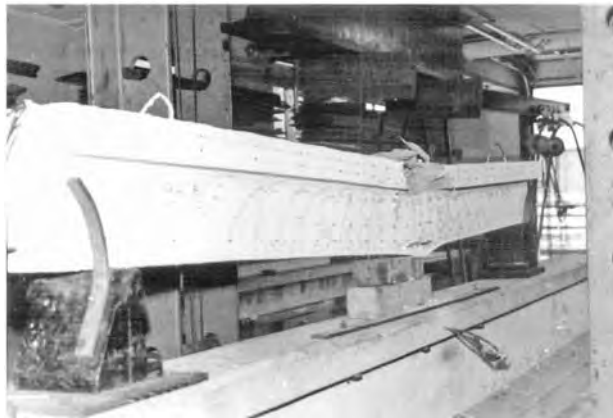
- ACI Committee 209. 1971. Prediction of creep, shrinkage and temperature effects in concrete structures. In *Designing for Creep, Shrinkage, and Temperature in Concrete Structures*, SP-27, pp. 51–93. American Concrete Institute, Farmington Hills, MI.
- ACI Committee 318. 1995. *Building Code Requirements for Structural Concrete and Commentary*. ACI 318-95 and ACI 318R-95, 370 pp. American Concrete Institute, Farmington Hills, MI.
- ACI Committee 318. 2005. *Building Code Requirements for Structural Concrete and Commentary*. ACI 318-05 and ACI 318R-05, 430 pp. American Concrete Institute, Farmington Hills, MI.
- ACI Committee 347. 2004. *Guide to Formwork for Concrete*, ACI 347-04, 32 pp. American Concrete Institute, Farmington Hills, MI.
- ACI Committee 435. 1995. *State-of-the-Art Report on Control of Two-Way Slab Deflections*, ACI 435-9R-95 (reapproved 2000), 14 pp. American Concrete Institute, Farmington Hills, MI.
- Agarwal, R.K. and Gardner, N.J. 1974. Form and shore requirements for multistory flat slab type buildings. *ACI J. Proc.*, 71(11): 559–569.
- ANSI. 1997. *American National Standard for Construction and Demolition Operation—Concrete and Masonry Work—Safety Requirements*, ANSI A10.9-1997, 22 pp. American National Standards Institute, Washington, D.C.
- Beresford, F.D. 1964. An analytical examination of propped floors in multistory flat plate construction. *Construct. Rev.*, 37(11), 16–20.
- Beresford, F.D. 1971. Shoring and reshoring of floors in multistory buildings. In *Symposium on Formwork*, pp. 559–569. Concrete Institute of Australia, North Sydney.
- Blakey, F.A. and Beresford, F.D. 1965. Stripping of formwork for concrete in buildings in relation to structural design. *Civil Eng. Trans. Inst. Eng. Australia*, 7(2), 92–96.
- Branson, D.E. 1977. *Deformation of Concrete Structures*. McGraw-Hill, New York.
- Byfors, J. 1980. *Plain Concrete at Early Ages*, Fo. 3, No. 80, 566 pp. Swedish Cement and Concrete Research Institute, Stockholm, Sweden.
- Cantor, I.G. and Rizzi, A.V. 1982. Shore and reshore procedures for flat slabs. In *Proceedings of the First International Conference on Forming Economical Concrete Buildings*, Lincolnshire, IL, November 8–10, pp. 18.1–18.12. Portland Cement Association, Skokie, IL.
- Carino, N.J. and Lew, H.S. 1982. Re-examination of the relation between splitting tensile and compressive strength of normal weight concrete. *ACI J. Proc.*, 79(3), 214–219.
- CEB. 1964. *Recommendations for an International Code of Practice for Reinforced Concrete*. Bulletin D'Information, No. 80, Comité Européen du Béton (CEB), Paris.
- CEB. 1972. *Manual: Structural Effects of Time-Dependent Behavior of Concrete*. Bulletin D'Information, No. 80, Comité Européen du Béton (CEB), Paris.

- City of Boston. 1971. *The Building Collapse of 2000 Commonwealth Avenue, Boston, Massachusetts*, Report, Mayor's Investigating Commission, 159 pp. Boston, MA.
- Fattal, S.G. 1983. *Evaluation of Construction Loads in Multistory Concrete Buildings*. NBS Building Science Series No. 146, 130 pp. National Bureau of Standards, Washington, D.C.
- Fintel, M. Iyengar, S.H., and Ghosh, S.K. 1987. *Column Shortening in Tall Structures: Prediction and Compensation*, EB108-01D. Portland Cement Association, Skokie, IL.
- Fu, H.C. and Gardner, N.J. 1986. Effect of high early-age construction loads on the long term behavior of slab structures. In *Properties of Concrete at Early Ages*, SP-95, pp. 173–200. American Concrete Institute, Farmington Hills, MI.
- Gardner, N.J. 1960. Relationship of the punching shear capacity of reinforced concrete slabs with concrete strength. *ACI J. Proc.*, 87(1), 66–71.
- Gardner, N.J. 1985. Shoring, reshoring, and safety. *Concrete Int.*, 7(4), 28–34.
- Gardner, N.J. and Poon, S.M. 1976. Time and temperature effects on tensile, bond and compressive strengths. *ACI J. Proc.*, 73(7), 405–409.
- Grundy, P. and Kabaila, A. 1963. Construction loads on slabs with shored formwork in multistory buildings. *ACI J. Proc.*, 60(12), 1729–1738.
- Hansen, T.C. and Mattock, A.H. 1966. Influence of size and shape of member on the shrinkage and creep of concrete. *ACI J. Proc.*, 63(2), 267–289.
- Hickey, K.B. 1968. *Creep of Concrete Predicted from Elastic Modulus Tests*, Report No. C-1242. U.S. Department of the Interior, Bureau of Reclamation, Denver, CO.
- Hover, K.C. 1984. The Effects of Moisture on the Physical Properties of Hardened Concrete and Mortar, Ph.D. thesis. Cornell University, Ithaca, NY.
- Hover, K.C. 1988. The effects of drying and form and shore removal on flexural cracking in beams and slabs. In *Forming Economical Concrete Buildings: Proceedings of the Third International Conference*, SP107, pp. 169–184. American Concrete Institute, Farmington Hills, MI.
- Hurd, M.K. 2005. *Formwork for Concrete*, 7th ed., SP-4, 500 pp. American Concrete Institute, Farmington Hills, MI.
- Kaminetzky, D. and Stivaros, P.C. 1994. Early-age concrete: construction loads, behavior and failures. *Concrete Int.*, 16(1), 58–63.
- Klieger, P. 1958. Effect of mixing and curing temperature on concrete strength. *ACI J. Proc.*, 29(12), 1063–1081.
- Lasisi, M.Y. and Ng, S.F. 1979. Construction loads imposed on high-rise floor slabs. *Concrete Int.*, 1(2), 24–29.
- Lew, H.S. 1985. Construction loads and load effects in concrete building construction. *Concrete Int.*, 7(4), 20–23.
- Lew, H.S. and Reichard, T.W. 1978. Mechanical properties of concrete at early ages. *ACI J. Proc.*, 75(10), 533–542.
- Lew, H.S., Carino, N.J., Fattal, S.G., and Batts, M.E. 1982a. *Investigation of the Construction Failure of Harbour Cay Condominium in Cocoa Beach, FL*. NBS Building Science Series No. 145. National Bureau of Standards, Washington, D.C.
- Lew, H.S., Carino, N.J., and Fattal, S.G. 1982b. Cause of the condominium collapse in Cocoa Beach, FL. *Concrete Int.*, 4(8), 64–73.
- Leyendecker, E.V. and Fattal, S.G. 1977. *Investigation of the Skyline Plaza Collapse in Fairfax County, Virginia*, Building Science Series No. 94, 88 pp. National Bureau of Standards, Washington, D.C.
- Liu, X.-L., Chen, W.-F., and Bowman, M.D. 1985a. Construction loads on supporting floors. *Concrete Int.*, 7(12), 21–26.
- Liu, X., Chen, W.-F., and Bowman, M.D. 1985b. Construction load analysis for concrete structures. *J. Struct. Eng. ASCE*, 111(5), 1019–1036.
- Marosszeky, M. 1972. Construction loads in multistory structures. *Civil Eng. Trans. Inst. Eng. Australia*, 14(1), 91–93.
- Nawy, E.G. 2008. *Reinforced Concrete: A Fundamental Approach*, 6th ed., 934 pp. Prentice Hall, Upper Saddle River, NJ.
- Neville, A.M. 1995. *Properties of Concrete*, 4th ed., 844 pp. Longman, London.

- Nielsen, K.E.C. 1952. *Loads on Reinforced Concrete Floor Slabs and Their Deformations during Construction*. Proc. No. 15, 113 pp. Swedish Cement and Concrete Research Institute, Stockholm.
- Pauw, A. 1960. Static modulus of elasticity of concrete as affected by density. *ACI J. Proc.*, 57(6), 679–687.
- Pfeifer, D.W., Magura, D.D., Russell, H.G., and Corley, W.G. 1971. Time-dependent deformations in a 70-story structure. In *Designing for Creep, Shrinkage, and Temperature in Concrete Structures*, SP-27, pp. 159–185. American Concrete Institute, Farmington Hills, MI.
- Price, W.H. 1951. Factors influencing concrete strength. *ACI J. Proc.*, 22(6), 417–432.
- RILEM Commission 42-CEA. 1981. Properties of set concrete at early ages: state-of-the-art report. *Mater. Struct.*, 14(84), 399–450.
- Russell, H.G. and Corley, W.G. 1977. *Time-Dependent Behavior of Columns in Water Tower Place*, RD025B, 10 pp. Portland Cement Association, Skokie, IL.
- Sbarounis, J.A. 1984. Multistory flat plate buildings: construction loads and immediate deflections. *Concrete Int.*, 6(2), 70–77.
- Scanlon, A. 1987. Excessive slab deflection: a serviceability failure. *J. Forensic Eng.*, 1(2), 21–29.
- Stivaros, P.C. and Halvorsen, G.T. 1990. Shoring/reshoring operations for multistory buildings. *ACI Struct. J.*, 87(5), 589–596.
- Stivaros, P.C. and Halvorsen, G.T. 1991. Equivalent frame analysis of concrete buildings during construction. *Concrete Int.*, 13(8), 57–62.
- Stivaros, P.C. and Halvorsen, G.T. 1992. Construction load analysis of slabs and shores using microcomputers. *Concrete Int.*, 14(8), 27–32.
- Taylor, P.J. 1967. Effects of formwork stripping time on deflections of flat slabs and plates. *Australian Civil Eng. Const.*, 8(2), 31–35.
- Taylor, P.J. and Heiman, J.L. 1977. Long-term deflections of reinforced concrete flat slabs and plates. *ACI J. Proc.*, 74(11), 556–561.
- Troxell, G. E. Davis, H.E., and Kelly, J.W. 1968. *Composition and Properties of Concrete*, 2nd ed. McGraw-Hill, New York.
- Walker, S. and Bloem, D.L. 1957a. Effects of curing and moisture distribution on measured strength of concrete. *Highway Res. Rec.*, 36, 334–346.
- Walker, S. and Bloem, D.L. 1957b. Studies of flexural strength of concrete. Part 3. Effects of variations in testing procedures. *Proc. Am. Soc. Test. Mater.*, 57, 1122–1142.
- Wheen, R.J. 1982. An invention to control construction floor loads in tall concrete buildings. *Concrete Int.*, 4(5), 56–62.
- Winter, G. and Nilson, A.H. 1991. *Design of Concrete Structures*, 11th ed. McGraw-Hill, New York.



(a)



(b)

(a) Deflection test of a prestressed beam. (Photograph courtesy of Portland Cement Association, Skokie, IL.) (b) Deflection of a prestressed concrete beam prior to failure. (Photograph courtesy of Edward G. Nawy, Rutgers University.)

Deflection of Concrete Members

Russell S. Fling, P.E.*
Andrew Scanlon, S.E.**

9.1	Introduction	9-1
9.2	Elastic Calculation Methods	9-2
	Selection of Methods • Indirect Method (Minimum-Thickness Tables) • Simplified Method (Use of Graphs to Estimate Stiffnesses) • Normal Method • Extended Method	
9.3	Other Calculation Considerations	9-6
	Long-Term Deflection • Continuous Members • Two-Way Construction • Prestressed Members • Torsional Deflection • Temperature Deflection	
9.4	Factors Affecting Deflection	9-10
	Computational Errors • Loading • Flexural Stiffness • Factors Affecting Fixity • Construction Variations • Creep and Shrinkage	
9.5	Reducing Deflection of Concrete Members	9-16
	Design Techniques • Construction Techniques • Materials Selection	
9.6	Allowable Deflections	9-20
	Sensory Acceptability • Serviceability of the Structure • Effect on Nonstructural Elements • Effect on Structural Elements	
	References	9-22

9.1 Introduction

When applying strength design procedures, engineers can obtain building structures that have adequate strength but unsatisfactory serviceability; that is, they exhibit excessive deflection. Thus, the size of many flexural members is determined by deflection response rather than by strength. The purpose of this chapter is to outline efficient procedures for estimating deflection, discuss factors affecting the variability of deflections, suggest procedures for use in the design process to reduce the expected deflection, and enable design engineers to proportion building structures closer to both strength and

* Practicing consulting structural engineer who has served on many technical committees of the American Concrete Institute and as President of the Institute in 1976.

** Professor of Civil Engineering, Penn State University, who has served on several technical committees of the American Concrete Institute, including serving as Chair of ACI Committee 435 (Deflections).

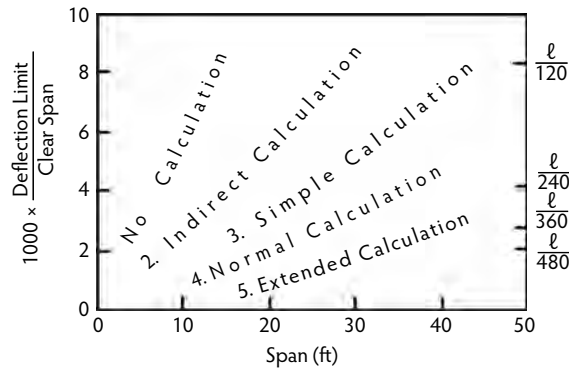


FIGURE 9.1 Recommended calculation procedures.

serviceability requirements. The result could be more economical structures compared to those designed too conservatively because of concerns about deflection or those designed without adequate deflection control resulting in expensive repair costs. Throughout this chapter, the discussion assumes that a competent design is prepared according to ACI 318 Building Code (ACI Committee 318, 2005) and that construction follows good practices. It should be noted that the ACI Code provides minimum requirements for design. The engineer should determine (in consultation with the owner) whether these minimum requirements are adequate for the project in question; for example, certain types of brittle partitions such as unreinforced masonry may require smaller deflection limits, and certain types of sensitive equipment may require more stringent limits than those given in the code.

9.2 Elastic Calculation Methods

9.2.1 Selection of Methods

Perhaps the most important step in computing deflection is to sketch the deflected shape of the structure, especially if its geometry or loading is somewhat complicated. Computations of deflection magnitude will be meaningless if the engineer has the wrong concept of deflection response. Horizontal members can deflect upward as well as downward, and vertical members can deflect in either direction. Sometimes a member is in double curvature and deflects in both directions. One load may cause a member to deflect in one direction, and another load may cause the same member to deflect in the opposite direction. If an engineer has difficulty visualizing the direction of deflection, experimentation with a simple model of heavy paper, balsa wood, plastic, or other flexible material should clarify the deflection response. The labor in preparing deflection calculations can be considerably reduced by the judicious selection of a few critical members in a structure for which deflection calculations will be made and disregarding all other members. The success of this approach depends on the skill of the engineer in selecting critical members. Labor in preparing deflection calculations can also be reduced by first deciding the reason for limiting the deflection (see Section 9.6) and directing the calculations to that end. Finally, deflection calculations can be minimized by determining the deflection limit and span and then selecting an appropriate calculation method by referring to Figure 9.1. There are no precise lines of demarcation between methods. Experienced engineers will consider computation time available, the importance of the member and its deflection response, and the importance that owners and users of the structure will assign to proper deflection behavior before selecting a calculation method. Some details of the normal or extended calculation methods can be used in a simpler method as the situation warrants. For these reasons, an engineer may want to start with the simplest calculation method and extend it if results of the first calculation indicate a potential deflection problem.

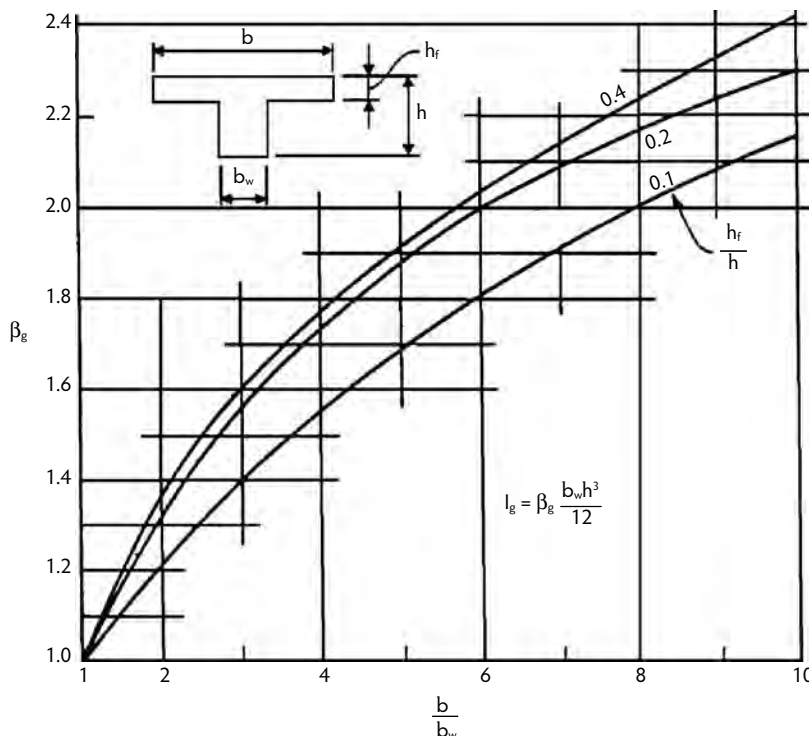


FIGURE 9.2 Moment of inertia (I_g) of uncracked T-beams (in.⁴).

9.2.2 Indirect Method (Minimum-Thickness Tables)

Deflection can be limited indirectly by limiting the span-to-depth ratio of a member or by limiting the stress level. For beams and one-way slabs, deflection need not be further calculated if the minimum thickness given in the ACI Code is met and if members do not support and are not attached to partitions or other construction likely to be damaged by large deflections. This is an important qualification as many members do support or are attached to fragile building elements. Likewise, deflection of flat slabs and flat plates need not be calculated if the thickness is limited to values given in the ACI Code. A satisfactory deflection response can normally be expected if the superimposed load is small in relation to the self-weight of the concrete, as is usually the case with buildings intended for human residence. Alternatively, experience indicates that flexural members remaining essentially uncracked at service loads will generally not have excessive deflection. This condition can be easily checked using structural mechanics; that is, $f_r \leq M_{cr}/S$. The section modulus (S) of T-beams can be approximated by increasing the section modulus by half as much as the moment of inertia is increased by the flanges for tensile stress at the bottom of the stem [$1 + (\beta_g - 1)/2$] and increasing the section modulus twice as much as the moment of inertia for tensile stress at the top of the flange [$1 + 2(\beta_g - 1)$]. The factor β_g can be taken from Figure 9.2. The error introduced by this approximation is normally less than 10%. Use of indirect methods should be limited to members with a span no more than about 25 or 30 ft, usual loading conditions, and normal allowable deflections. Reasons for these limitations are further discussed in Sections 9.4 and 9.6.

9.2.3 Simplified Method (Use of Graphs to Estimate Stiffnesses)

For a quick estimate of deflection, use the midspan moment at service loads as calculated for strength design (or maximum moment in cantilevers). If only factored moment is available, divide it by the estimated average load factor to obtain the service moment. Alternatively, service moments may be

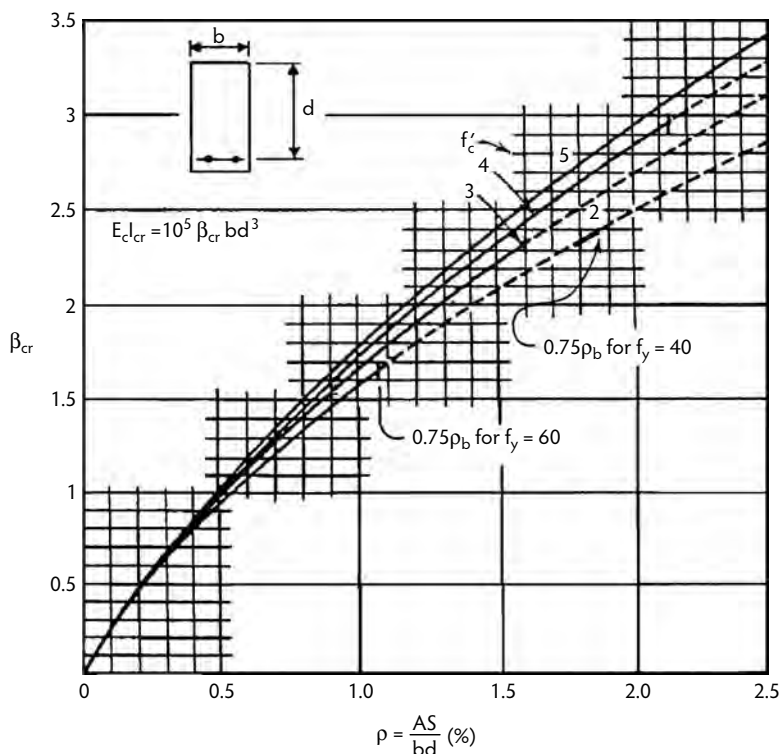


FIGURE 9.3 Flexural stiffness $E_c I_{cr}$ of cracked beams (lb/in.²).

computed directly. If concentrated loads or variable uniform loads are present, use an average uniform load, taking care to make due allowance for loads concentrated near the center of the span. If end moments are not equal to zero or to fixed end moments, use an appropriate moment coefficient from standard references. Estimate whether or not the beam is cracked at midspan by using Equation 9.1 and calculate either $E_c I_g$ or $E_c I_{cr}$. Use Figure 9.2 to assist in calculating I_g and Figure 9.3 to assist in calculating $E_c I_{cr}$. Do not include the effects of compression reinforcement. Use the appropriate flexural stiffness in the usual equations for deflection of indeterminate structures to determine the immediate deflection:

$$M_{cr} = f_r I_g / y_t \quad (9.1)$$

where M_{cr} , f_r , I_g , E_c , I_{cr} , and y_t are defined in the ACI Code. Estimate the additional long-term deflection due to creep and shrinkage by multiplying the immediate deflection by a factor λ taken from Figure 9.4. Do not calculate incremental deflection. Incremental deflection is that portion of the total deflection that occurs after the installation of deflection-sensitive elements of construction and continues until these elements are removed.

9.2.4 Normal Method

For a more careful estimate of deflection, use actual service loads and moments and calculate deflection using normal methods of structural mechanics. Calculate I_g using the normal procedures of structural mechanics, then calculate the cracking moment for the midspan section. If service moment M_a is less than the cracking moment, use I_g in the deflection calculations. If the service moment is more than the cracking moment, calculate I_{cr} and I_e , and use the latter in the calculations. Computation of I_g , I_{cr} , and I_e is developed in Chapter 4 and Chapter 27 of this *Handbook*, and the resulting equations are given below.

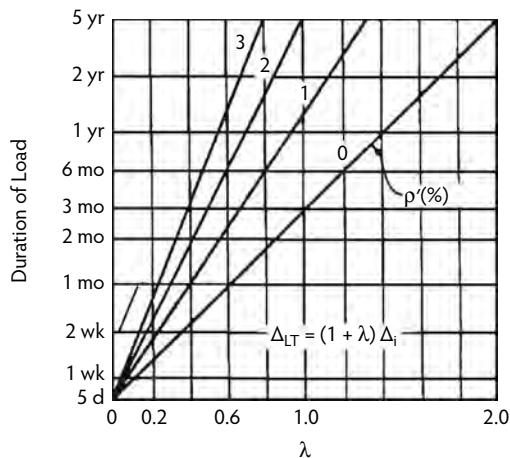


FIGURE 9.4 Values of multiplier λ for sustained load.

Neglecting compression reinforcement (and tension reinforcement in the gross section) will meet ACI Code requirements. For the cracked moment of inertia I_{cr} , use Equation 9.2a:

$$I_{cr} = nA_s(1-k)jd^2 \quad (9.2a)$$

Alternatively, for the cracked flexural stiffness $E_c I_{cr}$ use Equation 9.2b:

$$E_c I_{cr} = E_s A_s(1-k)jd^2 \quad (9.2b)$$

where the depth of compression block kd by elastic theory is computed using:

$$k = \left[(\rho n)^2 + 2\rho n \right]^{0.5} - \rho n \quad (9.3)$$

and the internal lever arm by elastic theory jd is computed using:

$$j = (1 - k/3) \quad (9.4)$$

For the effective moment of inertia I_e , use Equation 9.5:

$$I_e = I_{cr} + \left(M_{cr}/M_a \right)^3 (I_g - I_{cr}) \quad (9.5)$$

The labor in making these calculations can be considerably eased, and the chance for error reduced, by using a spreadsheet program prepared by the user. Deflection of concrete increases with time; see Section 9.3.1, Chapter 8 of Fling (1987) and Fling (1996). Incremental deflection that is less than the total long-term deflection may have to be compared to the allowable deflection; see Section 9.6 for a discussion of incremental deflection.

9.2.5 Extended Method

Extended methods involve consideration of all relevant factors affecting deflection as listed in Section 9.4. By carefully allowing for each relevant factor, an engineer can significantly improve the accuracy of deflection calculations. Extended calculations may result in better estimates of deflection, but they do not necessarily meet ACI Code requirements.

TABLE 9.1 Variations in Creep Coefficient from Standard Conditions

Parameter	Standard Conditions	Variations (%) ^a
Age at loading	7 days	–23
Relative humidity	40%	–40
Minimum thickness	6 in.	–38
Slump	3 in.	+36
Cement content	7 bags/y ³	+5
Fines content	50% passing No. 4 sieve	+56

^a Variations in the ultimate creep coefficient. A positive variation indicates deflection would be increased, and a negative variation indicates deflection would be decreased.

Source: ACI Committee 435, *Control of Deflection in Concrete Structures*, ACI 435-95, American Concrete Institute, Farmington Hills, MI, 1995.

9.3 Other Calculation Considerations

9.3.1 Long-Term Deflection

The ACI Code procedures using a single multiplier for additional long-term deflection may be used for simplified-method and normal-method calculation procedures. The initial deflection is multiplied by a single factor that depends only on the duration of the load and the quantity of compressive reinforcement. No other factor, such as ambient conditions, materials, or construction conditions, need be considered, yet these and many other factors do affect long-term deflection. This observation alone should raise a warning flag about the accuracy of the procedure under all possible conditions. When more accurate deflection estimates are needed, using extended method procedures, consider the six parameters that affect the magnitude of the creep coefficient and shrinkage strain, listed by Branson and Christiason (1971), ACI Committee 209 (1992), and ACI Committee 435 (1995). The numerical values they assigned to each factor for potential variations from standard conditions for the creep coefficient are summarized in Table 9.1. In addition, it is known that temperature, coarse aggregate, and the stress/strength ratio affect creep (ACI Committee 209, 1992; Smadi et al., 1987).

The volume/surface (v/s) ratio has an important effect on the modulus of rupture (f_r). In thin members (small v/s ratio), excess mixing water has a shorter average distance to the surface, where it can evaporate, leaving the concrete more prone to shrinkage and a lower flexural strength. Conversely, thicker members (large v/s ratio) take longer to dry out, maintaining the flexural strength as the concrete gains strength with time. Experience indicates that thin members with a v/s ratio of 2 may have a flexural strength of only $5(f'_c)^{0.5}$, whereas thick members with a v/s ratio of 6 or more may have a flexural strength of $10(f'_c)^{0.5}$. Whereas this is only a one third variation from the ACI Code value for flexural strength, the effect on deflection can be more dramatic because it may determine whether a member is cracked in flexure or not and to what extent it is cracked. When flanges are a significant part of a member, they should be included in the v/s calculation.

Current computation procedures do not consider the amount and location of tensile reinforcement or the location of compressive reinforcement with respect to the centroid of the gross concrete section, even though it is likely that location of reinforcement has some affect on shrinkage warping and long-term creep. Indeed, experience indicates that ribbed slabs do deflect more than thicker beams that are loaded to the same stress level and have the same span as the slabs. This can be attributed to thin flanges with potentially higher creep and shrinkage due to their lower volume/surface ratio and to flange location as far as possible from tensile reinforcement. The distance from tension steel to the centroid of the compression zone in ribbed slabs is often 0.8 to 0.9 times the total depth, whereas in rectangular beams it is usually about 0.6 to 0.7 times the depth. The factors for additional long-term deflection contained in the ACI Code make no distinction between members that are fully cracked and those that are

uncracked. If a beam is **uncracked**, the creep deflection should be proportional to the creep coefficient. If, however, a beam is **cracked**, it is more likely that creep deflection is proportional to some fraction of the creep coefficient.

The long-term creep factors given in the ACI Code and illustrated graphically in Figure 9.4 normally give satisfactory results. This may be because most concrete flexural members are partially cracked and the ultimate creep coefficient is normally about 2.0, rather than because the procedure is valid over a wide range of conditions. For conditions other than “normal,” the procedure may be flawed and contribute to erratic fluctuation in the ratio of calculated to measured deflection.

9.3.2 Continuous Members

For continuous members, it is essential that an accurate assessment of the distribution of moments be used in calculating deflection. Use of inaccurate moment values is the largest single source of error (Fling, 1996). Deflection calculations may proceed in the normal manner for structural mechanics; however, most continuous members are not prismatic if flexural cracking occurs somewhere in the span. Thus, the most important decision is what flexural stiffness value EI to use. For simplified or normal calculation methods (see Section 9.2), it is satisfactory to use the midspan flexural stiffness because it has the greatest effect on deflection. For greater accuracy, an average of midspan and end-region flexural stiffness can be used, taking care to give greater weight to the midspan stiffness than to the end-region stiffnesses. Guidance on averaging the stiffnesses is given in ACI Committee 435 (1995). For cantilevers, flexural stiffness at the end support should be used for calculations.

9.3.3 Two-Way Construction

When two-way construction consists of beams and slabs of normal proportions, deflection is considered for each direction (beams or slabs) independently of the other. When two-way slab systems, with or without beams in one or both directions, fall into the limitations of Chapter 13 of the ACI Code (ACI Committee 318, 2005), deflection can still be considered for each direction independently of the other, but deflection of that portion of the slab on the column line (column strip) will be greater than that portion spanning in midbay (middle strip). Appropriate allowance for this phenomenon can be made by adjusting the moments used in the deflection calculations in proportion to the positive moments used for design of the slab system. The procedure is known as the *crossing-beam method* and is discussed in ACI Committee 435 (1995). For all types of two-way construction, the maximum deflection at midbay will be the sum of the deflections in the two directions.

9.3.4 Prestressed Members

Normally, prestressing tends to balance the dead load. With perfect balance, there would be no immediate deflection under dead loads and no long-term deflection. Only live-load deflections would occur. Such balance can rarely be achieved because of construction tolerances and the difficulty of placing tendons in the theoretically correct location. Also, prestressing cannot simultaneously balance concrete self-weight, superimposed dead loads, and semipermanent live loads. The engineer must make a choice of which loads to balance. Nevertheless, prestressed members can generally be made thinner with lower deflection than nonprestressed members under similar conditions. Chapter 3 of the latest ACI Committee 435 report (1995) gives extensive guidance on calculation of deflection of prestressed members.

9.3.5 Torsional Deflection

Sometimes it is necessary to calculate the rotation of a member with torsional moment or the deflection of an element supported by the member but eccentric to its center of gravity. In such cases, the twist q over a length l_t of a member can be calculated as:

$$\theta = \Sigma T / GK \quad (9.6)$$

where:

Σt = summation of the service torsional moment along length ℓ_t of the member (see Figure 9.5).

GK = torsional stiffness similar to the flexural stiffness EL .

For an uncracked member, it is sufficiently accurate to take:

$$\begin{aligned} G &= 0.3E_c \\ K_g &= \Sigma x^3 y / 3 \\ GK_g &= 0.1E_c \Sigma x^3 y \end{aligned} \quad (9.7)$$

where:

x = shorter overall dimension of the rectangular part of the cross-section.

y = longer overall dimension of the rectangular part of the cross-section.

Component rectangles of flanged sections should be selected to yield the largest value of $\Sigma x^3 y$ as in strength design for torsion.

For a torsionally cracked member, it is sufficiently accurate to use an equation developed by Lampert (1973):

$$GK_{cr} = \frac{E_s (x_0 y_0)^2 A_n (1+m)}{2(x_0 + y_0)s} \quad (9.8)$$

where:

E_s = modulus of elasticity of steel.

x_0 and y_0 = shorter and longer dimension, respectively, between longitudinal corner bars.

s = stirrup spacing.

A_n = area of one stirrup leg:

$$m = \frac{(A_s + A'_s)s}{2A_n(x_0 + y_0)}$$

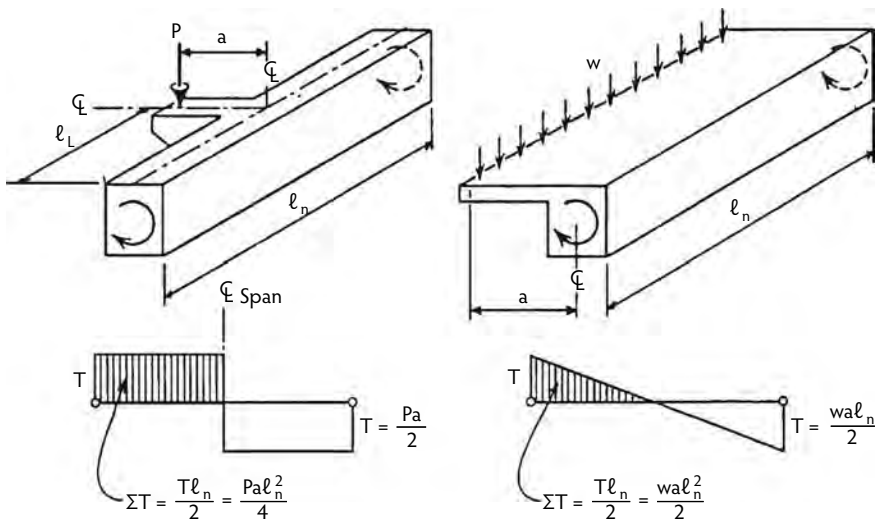


FIGURE 9.5 Twist on an isolated beam due to eccentric loads.

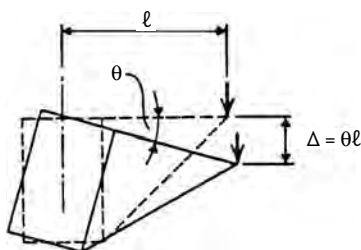


FIGURE 9.6 Deflection due to beam rotation.

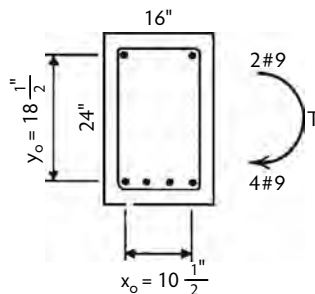


FIGURE 9.7 Beam subject to rotation.

where:

A_s = area of longitudinal tension steel.

A'_s = area of longitudinal compression steel.

Deflection of an element supported by a twisting member can be calculated by multiplying the angle of twist in the member at the element by the distance from the center of gravity of the member to the point in question (see Figure 9.6).

For most cases in which twist or deflection due to twisting members is significant, the member will be at least partially torsionally cracked, and torsional stiffness given by Equation 9.8 should be used, as it will give an upper bound to the deflection. Torsional stiffness of an uncracked member is usually much larger than that of the same member torsionally cracked, but little research is available to indicate the proper transition from uncracked to cracked stiffnesses. Procedures for calculating torsional rotation are not intended for application to moment-distribution procedures.

9.3.5.1 Example 9.1

What is the twist in an 11-ft length of a rectangular beam 16 in. wide by 24 in. deep with a uniform service torsional moment of 50 ft-kips? The beam is reinforced with four No. 9 bottom and two No. 9 top bars, as shown in Figure 9.7. Shear reinforcement is No. 4 bars at 5 in. center-to-center. Assume that $f'_c = 3$ ksi.

Solution. Using Equation 9.8, $2(x_o + y_o) = 2(10.5 + 18.5) = 58$, and cracked torsional stiffness is:

$$GK_{cr} = \frac{29 \times 10^6 (10.5 \times 18.5)^2 \times 0.20}{58 \times 5} \times \left(1 + \frac{6.00 \times 5}{0.2 \times 58} \right) = 2.7 \times 10^9 \text{ psi}$$

Using Equation 9.6, torsional rotation or twist is:

$$\theta = \frac{50 \times 10^3 \times 12 \times (11 \times 12)}{2.7 \times 10^9} = 2.9 \times 10^{-2} \text{ rad} \approx 1.7^\circ$$

Actual twist may be less than that calculated if the beam remains partially uncracked.

9.3.6 Temperature Deflection

When there is a temperature gradient across a flexural member from one side to the other, temperature warping will result. In most structures, the temperature gradient is small, so the movement is small. In some structures, such as the top level of a parking garage, the gradient may be large, but the resulting movement is inconsequential because it does not affect either the serviceability of the structure or nonstructural elements. Occasionally, a structure will have large thermal gradients, and serviceability or nonstructural elements will be affected; for example, tall buildings with exposed exterior columns may

TABLE 9.2 Parameters Affecting Deflection: Known before Construction

1	<i>Loading</i>
1.1	Specified maximum live loads
1.2	Dead load based on assumed unit weights and specified sizes
1.3	Location and arrangement of loads
2	<i>Flexural Stiffness</i>
2.1	Member sizes (including flange width) and bar placement
2.2	Presence of compression and tension bars in uncracked concrete
2.3	Tolerances on concrete outlines and bar locations
2.4	Relation of steel reinforcement to centroid of concrete section
2.5	Location of compression reinforcement at end sections, midspan, and in columns
2.6	Specified concrete compressive strength f'_c , flexural strength f_r , and modulus of elasticity E_c
2.7	Modulus of rupture f_r based on specified minimum compressive strength f'_c vs. the actual average f'_c
3	<i>Moment Distribution</i>
3.1	Frame completion before loads are applied
3.2	Homogeneous, isotropic, monolithic material
3.3	Rigid joints
3.4	Pattern loading
4	<i>Time-Dependent Factors</i>
4.1	Multiplier based on Yu and Winter's (1960) work that ignores relevant parameters such as cracked vs. uncracked sections, volume/surface ratio (V/S), absolute size of member, and shape of member (e.g., T-beam vs. rectangular beam)
4.2	Creep coefficient and shrinkage coefficient
4.3	Properties of concrete proportional to its compressive strength (or its square root); relationships assumed constant for all ages and not interrelated (e.g., shrinkage is assumed not to affect effective modulus of rupture f_r)
4.4	Constant normal ambient conditions of humidity and temperature
4.5	Calculations not separated for creep deflection using reduced E_c and shrinkage warping
5	<i>Criteria for Deflection Limits</i> (considering only span/deflection ratios and ignoring other relevant parameters such as the following)
5.1	Spans over 30 ft or under 10 ft
5.2	Absolute values of deflection limits
5.3	Dynamic (vibration) characteristics

experience thermal lengthening and shortening relative to internal columns that are at a nearly constant temperature. Thin precast wall-cladding panels may also be susceptible to temperature deflection, particularly if they span more than one story. An exposed roof may deflect up and down with seasonal or daily changes in temperature and affect partitions and ceilings below. In such cases, ACI Committee 435 (1995) offers guidance on temperature deflection.

9.4 Factors Affecting Deflection

To properly assess the variability of deflections, it is important to understand and consider all parameters that have an effect on the variability. Table 9.2 lists most of the parameters that are known or that might be determined before construction starts. Table 9.3 lists parameters that, by their very nature, cannot be known before construction starts. Parameters are separated between Table 9.2 and Table 9.3 to illustrate the difficulties facing a design engineer attempting to make a precise estimate of deflection. The values of the parameters that have the largest effect on the actual deflection of a structure are unknown at the time of design (those in Table 9.3); indeed, they *cannot* be known. Although it is theoretically possible to determine the value of parameters in Table 9.2 before construction starts, it is frequently impractical to obtain all necessary information; thus, an even higher proportion of variables cannot be determined

TABLE 9.3 Parameters Affecting Deflection: Not Known before Construction

1	<i>Loading</i>
1.1	Actual live load
1.2	Actual superimposed dead loads
1.3	Concrete dead load due to actual dimensions and weight of concrete
1.4	Construction loads due to shoring and reshoring procedures
1.5	Loading history: magnitude, duration, and frequency of application
1.6	Arching of masonry and fabricated walls, thus reducing load on supporting beams
2	<i>Flexural Stiffness</i>
2.1	Bar sizes and quantities actually installed
2.2	In-tolerance and out-of-tolerance construction of member sizes and bar placement
2.3	Actual concrete properties f'_c , f_r , E_c
3	<i>Moment Distribution</i>
3.1	Moment redistribution due to incomplete frame (e.g., upper columns or adjacent beams not yet constructed)
3.2	Moment redistribution due to creep and shrinkage
3.3	Moment distribution due to nonprismatic members (prismatic outlines may become nonprismatic members because of cracking and location of reinforcement)
3.4	Moment redistribution due to construction overloads
3.5	Cracking of supporting columns, especially those with light reinforcement and low axial load levels
3.6	Transverse (deflection) and torsional (rotation) movements of supporting girders
3.7	Joint stiffness less than infinite
4	<i>Time-Dependent Factors</i>
4.1	Actual shrinkage coefficient and its time variation
4.2	Actual creep coefficient and its time variation
4.3	Stress/strength ratio f_c/f'_c ratio at time of loading
4.4	History of actual ambient conditions of humidity and temperature
4.5	Location of compression reinforcement with respect to centroid of section
5	<i>Criteria for Deflection Limits</i>
5.1	Changed or refined criteria

by the design engineer before construction. When the parameters that can be anticipated before construction are separated from the parameters that cannot be anticipated, the effect of unanticipated variations can be more than four times the effect of anticipated variations.

Design engineers attempting to accurately assess probable deflection should consider all parameters affecting deflection and assign realistic values to each parameter, not conservative values as is done for strength design; that is, in computing deflections, loads should not be higher and concrete strength lower than expected. The potential variability of deflection can be estimated by computing deflections using realistic maximum and minimum values for parameters. Although the length of the lists in the tables may seem daunting, design engineers can increase the accuracy of their computations by carefully selecting the values of parameters used in the calculations.

It is unlikely that the actual deflection would reach either the extreme minimum or extreme maximum computed deflection, assuming the maximum variation is in the same direction for all parameters. For example, if the probability of reaching one of the extreme values in each of nine steps is 20%, the probability of the actual deflection reaching either extreme of the computed deflections is less than one chance in a million. Note, however, that the probability of variation in some parameters could be higher than 20% in actual practice. Furthermore, the probability that actual deflection will be less than computed is about the same as the probability that it will be more than computed, even though the latter event gets more attention in actual construction. Factors considered in more precise calculations can be categorized under computational errors, loading, flexural stiffness, fixity, creep and shrinkage, and construction variations.

9.4.1 Computational Errors

Because computations are usually made by humans, computational errors become a significant source of discrepancy between the calculated and actual values of deflection. Some of these computational errors are outlined below:

- There are many steps in the calculation of deflection. If the probability of error in each step is 1%, then the probability of error in the final calculation could be almost 10%. If the probability of error in each step increases to 5%, then the probability of error in the final calculation could be as much as 40%. The magnitude and type of individual errors are such that even an experienced engineer might not notice errors of 1 to 5% on casual inspection. Calculation errors of 25 to 50% are not uncommon.
- The length and intricacy of deflection computations can be alleviated and the chances of error minimized if a computer program is used. The program should be capable of taking into account most of the known parameters affecting deflection. The program, no matter how sophisticated, should credibly predict the deflection of actual structures (not just laboratory specimens) with reasonable accuracy over a wide range of conditions. These are high standards, and whether such a program exists is open to question. Practicing design engineers should make a habit of comparing deflection performance with calculated deflection and thereby sharpen their judgment skills.
- Factored moments or loads determined in the design for strength might be inadvertently used in deflection computations instead of the actual service moments or loads.
- Maximum moments from pattern loading or from moment coefficients might be used rather than actual moments for the loading condition under consideration. Unrealistically large moments result in unrealistically large computed deflections.

9.4.2 Loading

- Consider the loading history, including the age at loading and unloading for each increment, as it will affect the immediate deflection because concrete strength and modulus of elasticity may be different at different ages. The degree of cracking could affect the flexural stiffness under first, partial loading but this is usually not a factor in multistoried buildings because construction loading frequently equals or even exceeds design loading and should therefore be used to determine the effective moment of inertia under subsequent loading.
- Use actual loads rather than those assumed in strength design. It is not unusual to find that live loads specified by the building code having jurisdiction are never reached in the actual structure. On the other hand, numerous studies indicate that reshoring loads on lower floors in multistoried buildings can be as much as twice the self-weight of the floor construction. Concrete dead load is frequently more than the specified live load plus superimposed dead load.
- Consider the proportion of long-term vs. transient loading. Permanent live load will cause more creep deflection than will transient live load because creep occurs only under loads lasting for some time. Some live loads may remain in place for significant periods of time and contribute to creep deflection, while others are in place such a short time that they have no measurable effect on long-term deflection.
- Correctly assess the live load. If actual service live load is smaller than the design live load, the ratio of the applied service moment (M_a) to the cracking moment (M_{cr}) is lower, probably resulting in a higher effective moment of inertia (I_e). Thus both dead-load as well as live-load deflection would be lower.
- Consider redundancy; for example, walls may arch from end to end of beams and carry their own weight. Also, concrete members transverse to the main span might carry some load, thus reducing the moment and hence the deflection of the member under consideration.
- Calculate the service load moments separately for live and dead loads rather than proportion the moments at critical sections for every loading stage to the moments at the final loading stage. For

many beams, dead load moments will be nearly equal to moments in a fixed-end beam, but with live load on just one of the spans (pattern loading) live-load moments compared to fixed-end moments are proportionally larger at midspan and smaller at the ends. If deflections are calculated using separate moments for dead and live loads, the computed total long-term deflection and the computed incremental deflection may differ 5 to 10% from those calculated using the same moment pattern. A separate distribution of moments for dead and live loads may not be justified for simplified and normal calculation methods but should be considered for extended-method calculations.

- Consider the support that members transverse to the span may provide. Such support has the effect of reducing the load; for example, slabs nominally designed as spanning one way may actually receive some support from parallel side members.

9.4.3 Flexural Stiffness

- Use the actual, measured modulus of elasticity of concrete (E_c), if available.
- Even if preconstruction tests are required, use the measured modulus of rupture of concrete (f_r) because it is one of the more important parameters affecting deflection. The ACI Code specifies a ratio of $f_r/(f'_c)^{0.5} = 7.5$, whereas research indicates the ratio usually varies from a low value of 7.5 to a high of about 10. A one third increase in f_r (and, hence, M_{cr}) will increase the effective moment of inertia (I_e) by as much as 75%.* The ACI Code value is conservative, which means the actual deflection will frequently be less than the computed deflection. On the other hand, if there is significant restraint to shortening of flexural members by shrinkage, the resulting tensile stresses may reduce the effective or apparent modulus of rupture (f_r). Shrinkage restraint can result from a number of factors, including embedded reinforcing bars, stiff supporting elements such as walls, adjacent portions of slabs placed at different times, and nonuniform shrinkage through the thickness of the member. The effect is more significant in lightly loaded slabs with low reinforcement ratios than more heavily reinforced beams. For members with reinforcement ratios greater than about 1%, the effective moment of inertia rapidly approaches the cracked moment of inertia and is not sensitive to the actual cracking moment. When interpreting the results of tests for modulus of rupture, make allowance for the relative humidity of ambient conditions around the test specimen and for its size. See the discussion in Section 9.3.1.
- If construction loads are not allowed to crack the concrete prematurely, consider the effective moment of inertia at every loading stage based on the amount of cracking at that stage. If the maximum load on a structure occurs during construction, only one cracking condition need be considered and one flexural stiffness calculation need be made—that is, for the amount of cracking that occurs at full load. This assumption results in simpler calculations and is usually justified by the field observation that the most severe loading condition frequently occurs during construction when material stockpiles, shoring loads from the floor above, and other construction loads are on the structure. Many papers have been published on this subject (e.g., see Grundy and Kabaila, 1963; Sbarounis, 1984).
- For investigation of completed structures, use the actual location of reinforcement as built, especially if there is significant deviation from the specified location.
- Use the amount and location of compression reinforcement in computing I_g and I_{cr} . The transformed area of the steel can contribute significantly to the flexural stiffness of the cross section, even though it is not part of the ACI Code requirements.
- Use the amount and location of tension reinforcement in computing I_g . As with compression reinforcement, it can contribute significantly to the gross flexural stiffness. For cracked-section flexural stiffness, tension reinforcement is specifically considered in the calculation.

* For example, assume that $I_{cr}/I_g = 0.25$. When $M_{cr}/M_a = 7.5/10 = 0.75$, $I_e = (0.75)^3 I_g + [1 - (0.75)^3] 0.25 I_g = 0.57 I_g$ and $1/0.57 = 1.76$.

- For deflection calculations based on curvature along the span, use variation in flexural stiffness EI along the span due to change in cross-section, change in amount of reinforcement, and degree of cracking.
- Include the effect of flanges, even though they may be small. If a rectangular beam instead of a T-beam (flanges are usually present) is used in computations, both the cracked and uncracked (or gross) moments of inertia will be unrealistically low and the computed deflection unrealistically high. For more than 50 years, the ACI Code (currently Section 8.10) has specified essentially the same criteria for determining the width of the flange. Although the rationale for these criteria may be lost, the criteria have served well for strength design because few, if any, failures due to inadequate flange width have been reported. For deflection computations, the situation is not so good. The design engineer is concerned with an accurate estimate of deflection, neither high nor low, as contrasted with an effort to estimate minimum strength, not necessarily the actual strength. ACI Code T-beam procedures are inconsistent and probably conservative.
- Make a realistic assessment of the contribution of end-region stiffness to the overall stiffness rather than a simple averaging of end and midspan region stiffnesses. A simple average gives far more weight to the end-region stiffnesses than is justified. Using midspan stiffness is satisfactory for simple and normal calculation procedures, but accuracy can be increased somewhat for extended procedures by including the effect of stiffness in the end regions. For beams continuous on two ends, ACI 435 recommends the following:

$$I_e = 0.70I_{e(m)} + 0.15(I_{e(1)} + I_{e(2)}) \quad (9.9a)$$

For beams continuous on one end only:

$$I_e = 0.85I_{e(m)} + 0.15(I_{e(1)}) \quad (9.9b)$$

where subscript (m) indicates a midspan location, and subscripts (1) and (2) indicate locations at ends one and two.

9.4.4 Factors Affecting Fixity

- Consider the support rotation for cantilevers because movement due to support rotation at the end of the cantilever could be greater than the flexural deflection of the member itself. Furthermore, rotation could result in the end rising or lowering, depending on the back-span dimensions and loading.
- Consider the restraint that nearby, unloaded, parallel members provide through the torsional stiffness of supporting beams. In a load test of a large beam and slab roof, it was found that parallel members as far as 200 ft away helped restrain end rotation of a loaded member (Fling, 1996). Of course, this is a consideration primarily when individual members are loaded; if the entire structure is loaded simultaneously, restraint from parallel members will be minimized.
- Base the moment distribution on actual conditions of loading and stiffness of members rather than on assumed prismatic members. Until the advent of computers, such a consideration was beyond the capacity of manual computations. Depending on the physical conditions, a moment analysis based on nonprismatic members may give small to significant results for deflection considerations.
- Make allowance for the stiffness of joints if they are weak or have inadequately anchored reinforcement. The effect will be similar to rotation of the support for cantilevers. At present, no satisfactory analytical tools are available to deal with this consideration.
- Analyze end spans carefully, because they are especially sensitive to assumptions of moment at critical sections. The less stiffness the end support is assumed to have, the higher the positive moment in the end span and the higher the computed deflection, even though more positive-

moment steel is provided to resist the higher moment. For this reason, an engineer might use wider beams and more reinforcement in end spans simply to control deflection rather than as a necessary requirement for strength. Edge columns in the upper stories of multistoried buildings are frequently cracked from the high moment induced by the beams framing into them. Thus, their stiffnesses will be less than that for the gross uncracked section assumed in the moment analysis.

- Carefully control shoring and reshoring procedures, because moment distribution has the largest effect on deflection variability. Unsuitable procedures, especially near construction joints, may impose moments during construction that are more adverse than those assumed in design.

9.4.5 Construction Variations

In design, an engineer can do little about construction variations beyond taking care to specify reasonable tolerances and procedures. One might also make a study of the effect certain tolerable variations have on the deflection of a critical member. Of course, in an investigation of an existing member, some construction variations can be measured and allowance made in the deflection calculations. ACI Committee 117 (1990) recommended tolerances on concrete outlines, steel placement, and material properties that are considered reasonable and achievable. If deflection is computed using the maximum variation in one direction, the effect on deflection can be dramatic (Fling, 1992). Fortunately, variations tend to cancel each other, but if a number of variables each affected deflection in the same direction, the effect could be significant. Following is a list of the most serious variations:

- Tolerances on concrete outlines may result in a larger or smaller member than specified.
- Concrete cover on bottom bars may be smaller than specified due to gravity. The increase in effective depth will increase the cracked moment of inertia. Likewise, the cover on the top bars may be greater than specified with a reduction in effective depth and moment of inertia, but end-region stiffness has a much smaller effect on deflection than does the midspan stiffness.
- Concrete modulus of rupture is more variable than compressive strength; however, variability could be along the length of a member and thus tend to reach an average in its effect on deflection. There are few studies on this variation.
- Concrete compressive strength may average 15% higher than the specified strength, with a consequent increase in the modulus of elasticity (E_c) of 7%. Depending on job conditions, the average could diverge from the specified strength even more than 15%. When a structure is loaded before it has reached its design strength, the adverse effects on deflection may be even more severe than indicated by a lower compressive strength because the creep coefficient can be up to 50% higher for stress/strength ratios f_c/f_c' greater than 0.50 than for f_c/f_c' less than 0.5. For this reason, engineers should specify procedures that avoid loading deflection-sensitive structures before concrete reaches its design strength.
- Concrete modulus of elasticity (E_c) depends on many parameters other than compressive strength, such as, for example, the aggregates. Lightweight aggregates in the concrete will generally result in a lower modulus. The ACI Code gives an average value, but specific aggregates could vary significantly. In addition, certain very hard aggregates could result in a much higher modulus than assumed for the strength of the concrete.
- If the number of bottom tension bars is more than or less than specified, the effect on deflection will be proportional, if the section is cracked.

9.4.6 Creep and Shrinkage

Factors affecting creep and shrinkage have been discussed by ACI Committee 209 (1992) and some are noted in Section 9.3.1. These factors include age at loading, relative humidity, minimum thickness, volume/surface ratio, slump, cement content, air content, aggregates, admixtures, and ambient temperature.

9.5 Reducing Deflection of Concrete Members

The size of flexural members is in many cases determined by deflection response rather than by strength. This section gives design procedures for reducing the expected deflection that will enable design engineers to proportion building structures to meet both strength and serviceability requirements. The result could be more economical structures compared to those designed with unnecessarily conservative deflection response or those exhibiting deflection problems requiring costly repairs. The discussion assumes that a competent design is prepared in accordance with the ACI Code and construction follows good practices. To properly evaluate options for reducing deflection, a design engineer must know the level of stress in the member under consideration. That is, is the member uncracked, partially cracked, or fully cracked, and does light or heavy reinforcement indicate low or high stresses? Heavily reinforced members tend to be fully cracked because they are highly stressed. This chapter considers only two limiting conditions: uncracked members and fully cracked members. For the purposes of this chapter, if the applied moment in the positive region is more than twice the cracking moment, considering the effect of flanges, the member may be considered to be fully cracked. Frequently, a member is only partially cracked ($M_{cr} < M_a < 2M_{cr}$), and the statements about both limiting conditions are not strictly applicable. Instead, engineers must use their judgment or make appropriate calculations to interpolate between the limiting conditions. See Section 9.2.4 for methods to compute the degree of cracking in a member. In addition to the stress conditions, there may be physical or nonstructural constraints on the use of some options, such as limits on increasing concrete outlines. For all options, the financial implications must be evaluated for each situation. Some options may increase the cost, some may have offsetting considerations that reduce the cost, and still others may have little effect on cost. Except as noted, only non-prestressed, reinforced concrete members are discussed below. For each option presented, the discussion includes the effect of implementation on deflection, the approximate range of potential reduction of deflection, and appropriate situations in which the option should be considered. Options are arranged in three groups: design techniques, construction techniques, and materials selection.

9.5.1 Design Techniques

9.5.1.1 Option 1: Make the Member Deeper

While increasing the depth may not be possible after schematic design of the building has been established because it affects the architectural and mechanical work, there are many instances where beam depth can be increased. The reduction in deflection is approximately equal to the square of the ratio of effective depths d for cracked sections* and approximately equal to the cube of the ratio of total concrete depths for uncracked sections.** For example, if an 18-in.-deep, rectangular beam with an effective depth of 15.5 in. is increased to 20 in. deep, and all other parameters are kept the same, the cracked stiffness will increase by $(17.5/15.5)^2 = 1.27$, and the uncracked stiffness will increase by $(20/18)^3 = 1.37$. For heavily reinforced members, if the amount of steel is reduced when the depth is increased, the cracked stiffness is increased only in proportion to the increase in depth, or by 13% for this example.*** The increase in stiffness of an uncracked T-beam when it is made deeper will be less than that for a rectangular beam because the flanges do not change. Flanges tend to have a fixed influence rather than a proportional influence on uncracked stiffness. If, by increasing the depth, the concrete tensile stress in a member is reduced sufficiently so it changes from a cracked, or partially cracked, to an uncracked member, the stiffness could increase dramatically. The uncracked stiffness can be as much as three times the partially cracked stiffness (Grossman, 1981).

* $I = nA_s(1 - k)jd^2$, $I \approx d^3$.

** $I = bh^3/12$, $I \approx h^3$.

*** $A_s = M/f_sjd$, $I \approx d$.

9.5.1.2 Option 2: Make the Member Wider

This option is not applicable to slabs or other members with physical constraints on their width; however, where beams cannot be made deeper because of floor-to-floor height limitations but can be made wider, the increase in stiffness is proportional to the increase in width if the member is uncracked. If the member is cracked and remains cracked after increasing the width, the increase in stiffness is very small; however, if a cracked member will be uncracked after the width is increased, the stiffness will increase dramatically, possibly by as much as a factor of three (Grossman, 1981).

9.5.1.3 Option 3: Add Compression Reinforcement

Using ACI Code procedures, compression reinforcement has no effect on immediate deflection but can reduce additional long-term or incremental deflection by a factor of up to about 50% (Branson, 1971). The effect on total deflection is somewhat less; for example, if immediate deflection is 0.50 in. and additional long-term deflection is 1.00 in., then the total deflection is 1.50 in. The addition of 2% compression reinforcement reduces the additional long-term deflection to 0.50 in., or by 50%, and the total deflection to 1.00 in., or by 33%. Long-term deflection has two components: creep deflection and shrinkage warping. Compression reinforcement reduces deflection because concrete creep tends to transfer the compression force to the compression steel, which does not itself creep. The closer the steel is to the compression face of the member, the more effective the steel is in reducing long-term creep deflection; thus, compression steel will be more effective in deeper beams than in shallower beams or slabs if concrete cover to the compression face is a constant value. Indeed, in some very shallow members, due to the requirements of minimum bar cover, compression steel could be at or near the neutral axis and almost totally ineffective in reducing long-term creep deflection. Shrinkage warping occurs where the centroids of steel and concrete do not coincide and the shrinkage of concrete, combined with the dimensional stability of steel, warps the member, similar to a piece of bimetal subject to temperature variations. Compression steel reduces shrinkage warping because it brings the centroid of all reinforcement (tension plus compression) closer to the concrete neutral axis. Although this is true of all flexural members, compression steel is especially effective for T-beams where the neutral axis is close to the compression face and far from the tension steel. If the T-beam has a thin slab subject to higher than normal shrinkage because of its high surface/volume ratio, then compression reinforcement will be more effective than for a rectangular beam. This will be true for ribbed slabs or joist systems as well.

9.5.1.4 Option 4: Add Tension Reinforcement

For uncracked members, the addition of tension steel has hardly any effect on deflection. For fully cracked members, the addition of tension steel will reduce both immediate and long-term deflection almost in proportion to the increase in steel.* For example, if the total deflection of a cracked member is 1.50 in., as in the example above, increasing the tension steel by 50% will reduce the deflection to about 1.10 in. Of course, the increased steel area should still be less than the maximum permitted by the ACI Code or $0.75\rho_b$ (rho balanced). This option is most useful for lightly reinforced solid and ribbed slabs. The option of adding more tension reinforcement is not available or is limited for heavily reinforced beams unless compression reinforcement is also added to balance the increase in tension-bar area in excess of $0.75\rho_b$. If this option is selected, excessive bar congestion may result.

9.5.1.5 Option 5: Add or Increase Prestressing

Many prestressed members are designed for load balancing; that is, the upward reaction of the prestressing tendons approximately equals the downward force of dead and other sustained loads. Deflection due to live-load and other transient loads will be the same as for an ordinary reinforced concrete member, subject to two qualifications. If prestressing keeps the member in an uncracked state, whereas otherwise it would

* The moment of inertia of cracked sections $I = nA_s(1 - k)jd^2$ and $I \approx 0.9A_s$, because $(1 - k)j$ does not vary much with changes in A_s .

be cracked, the live-load deflection will be smaller. On the other hand, if the member size is reduced to take advantage of the prestressing, the live-load deflection could be larger. For this reason, the span/depth ratio is usually limited to 48 for floor slabs with light live loads and 52 for roof slabs. See the ACI Code Commentary, Section R18.12.3 (ACI Committee 318, 1995). If the member has a high ratio of live load to dead load, the span/depth ratio must be proportionally smaller to give satisfactory deflection performance. If the sole purpose of prestressing a member is to achieve satisfactory deflection response, then prestressing to achieve full dead-load balancing is not necessary. Only a prestressing force sufficient to produce satisfactory deflection response is required. In this situation, the member may be partially cracked.

9.5.1.6 Option 6: Revise Structure Geometry

Common solutions include increasing the number of columns to reduce the length of the spans, adding cross members to create two-way systems, and increasing the size of columns to provide more end restraint to flexural members (this is especially effective for end spans).

9.5.1.7 Option 7: Revise Deflection Limit Criteria

If deflection of a member is excessive, the deflection limits may be reexamined to determine if they are unnecessarily tight. If experience or analysis indicates that the limits (see Section 9.6) can be loosened, then other action might not be required. Many building codes do not set absolute restrictions on deflection. An engineer might decide that the building occupancy or construction conditions such as a sloping roof do not require the normal deflection limits.

9.5.2 Construction Techniques

9.5.2.1 Option 8: Cure the Concrete to Allow It to Gain Strength

Deflection response is determined by concrete strength at first loading, not by its final strength. If the construction schedule makes early loading of the concrete likely or desirable, then measures to ensure high strength at first loading can be effective. For example, if design compressive strength f'_c is 4 ksi, if the member would be uncracked as designed, and if it is loaded when concrete strength is 2.5 ksi, it could be highly cracked due to a lower modulus of rupture even though its load-carrying ability is satisfactory. A cracked member will deflect several times as much as the same member in an uncracked state. Furthermore, the modulus of elasticity of 4-ksi concrete is higher than that of 2.5-ksi concrete. See the discussion in Option 19 and Option 20 for the effect of these parameters on deflection.

9.5.2.2 Option 9: Cure the Concrete to Reduce Shrinkage and Creep

Good curing will not affect the immediate deflection, but additional long-term deflection will be reduced. Assuming that the long-term component of deflection is evenly split between shrinkage and creep, if shrinkage is reduced 20% by good curing, the additional long-term deflection due to shrinkage will be reduced by 10%. The effect will be most pronounced on members subject to high shrinkage such as those with a low volume/surface ratio (small members), those with thin flanges, structures in arid atmospheres, or members that are restrained. The effect of good curing on creep is similar to the effect on shrinkage.

9.5.2.3 Option 10: Control Shoring and Reshoring Procedures

Many studies indicate that the shoring load on floors of multistoried buildings can be up to two times the dead weight of the concrete slab itself (Sbarounis, 1984). Because the design superimposed load is frequently less than the concrete dead load, the slab may be seriously overstressed and cracked due to shoring loads instead of remaining uncracked as assumed by calculations based on design loads. Thus, the flexural stiffness could be reduced to as little as one third of the value calculated by assuming design loads only. Furthermore, the shoring loads may be imposed on the floor slabs before the concrete has reached its design strength. See the discussion in Option 8. Construction of formwork and shoring should ensure that a sag or negative camber is not built into the slab. Experience indicates that frequently the

apparent deflection varies widely between slabs of identical design and construction. Some reasons for this may be that such slabs were not all built level or at specified grade or that the method and timing of form stripping were not uniformly applied. Also, construction loads may not have been applied uniformly. Soil conditions for shoring supported at ground level should be checked to ensure that the formwork does not sag under the weight of freshly placed concrete due to soil settlement.

9.5.2.4 Option 11: Delay the First Loading

This allows the concrete to gain more strength than specified or helps ensure that it reaches its design strength. Both the modulus of elasticity (E_c) and the modulus of rupture (f_r) will be increased. An increase in E_c will increase the flexural stiffness as noted in Option 19. An increase in f_r will reduce the amount of cracking or even allow the member to remain uncracked with an increase in flexural stiffness EI as noted in Option 20. Creep deflection will also be reduced by delaying first loading.

9.5.2.5 Option 12: Delay Installation of Deflection-Sensitive Elements or Equipment

Such delay will have no effect on immediate or total deflection, except as noted in Option 11, but incremental deflection (that occurring from the time a deflection-sensitive component is installed until it is removed or deflection reaches its final value) will be reduced. For example, if the additional long-term deflection is 1.00 in. and installation of partitions is delayed for 3 months, then the incremental deflection will be approximately 0.50 in. or one half as much as the total (see Section 9.5.2.5 of the ACI Code).

9.5.2.6 Option 13: Locate Deflection-Sensitive Equipment to Avoid Deflection Problems

Printing presses, scientific equipment, and other equipment that must remain level should be located at midspan where the change in slope is very small with an increase in deflection. On the other hand, because the amplitude of vibration is highest at midspan, vibration-sensitive equipment may be best located near the supports.

9.5.2.7 Option 14: Provide Architectural Details to Accommodate the Expected Deflection

Partitions that abut columns may show the effect of deflection by separating horizontally from the column near the top, even though the partition is not cracked or otherwise damaged. Architectural details should accommodate such movements. Likewise, windows, walls, partitions, and other nonstructural elements supported by or located under deflecting concrete members can be provided with slip joints to accommodate the expected deflections or differential deflections between concrete members above and below the nonstructural elements.

9.5.2.8 Option 15: Build Camber into the Floor Slab

Camber will have no effect on computed deflection of the slab, after deflection takes place, for installation of partitions and equipment. For best results, deflection must be carefully calculated (not overestimated), the pattern of cambering specified (not just a single value), results monitored during construction, and procedures revised as necessary for slabs constructed later.

9.5.2.9 Option 16: Ensure That Top Bars Are Not Displaced Downward

Downward displacement will always reduce strength. The effect on deflection in uncracked members will be minimal. The effect on cracked members (those that are heavily loaded) is in proportion to the square of the ratio of change in effective depths for cantilevers but much less for continuous spans because the flexural stiffness (and resulting deflection) of the member is determined primarily by member stiffness at the midspan section. Thus, the deflection of cantilevers is especially sensitive to misplacement of the top bars. In continuous members, if the reduction in strength at negative moment regions results in redistribution of moments, then deflection could be increased.

9.5.3 Materials Selection

9.5.3.1 Option 17: Select Materials That Reduce Shrinkage and Creep or Increase the Moduli of Elasticity and Rupture

Materials having an effect on these properties include aggregates, cement, silica fume, and admixtures. See Options 19 and 20.

9.5.3.2 Option 18: Use a Mix Design That Will Reduce Shrinkage and Creep or Increase the Moduli of Elasticity and Rupture

For example, use a lower water/cement ratio or a lower slump or change the proportions of materials. See Options 9, 19, and 20 for a discussion of the effects of these properties on deflection.

9.5.3.3 Option 19: Use a Concrete with a Higher Modulus of Elasticity

Using ACI Code procedures, the stiffness of an uncracked member will increase in proportion to the elastic modulus or in proportion to the square root of the cylinder strength (see ACI Code Sections 9.5.2.2 and 8.5). The stiffness of a cracked section is affected very little by a change in modulus of elasticity. Highly cracked members will not be affected.

9.5.3.4 Option 20: Use Concrete with a Higher Modulus of Rupture

Stiffness of partially cracked members will increase because the degree of cracking will be reduced. The increase in stiffness (decrease in deflection) will depend on steel percentage, the increase in the modulus of rupture, and magnitude of applied moment.

9.5.3.5 Option 21: Add Short Discrete Fibers to the Concrete Mix

The effect is to reduce shrinkage (see Option 9) and increase the cracking strength (see Option 20), both of which will reduce deflection, but the increase in cost may be substantial.

Table 9.4 summarizes some of the preventive measures required to reduce or control deflection. This table can serve as a general guide for the design engineer but is not all inclusive, and engineering judgment has to be exercised in the choice of the most effective parameters to control deflection behavior.

9.6 Allowable Deflections

Allowable deflection is the other side of the equation to which computed deflection should be compared. If there are no deflection limits, then the computed deflection is irrelevant. When the computed deflection is more than the presumed allowable deflection, it is appropriate to carefully consider the reason for limiting deflection. In some cases, the deflection limit might be increased while in other cases, it might be tightened. Incremental deflection is that portion of the total deflection that occurs after the construction or installation of a part of the facility until it is removed. In many cases, incremental deflection controls the design, not the live-load deflection or the total deflection. As spans exceed 25 to 30 ft, the absolute deflection becomes more critical than the span/deflection ratio; for example, a span/deflection ratio of 360 for a 30-ft span is 1 in. Deflections of this amount and greater can be seen with the naked eye, and many owners and users will object. Also, standard tolerances for many construction components have stated or assumed values that do not exceed about 1 in. Deflection limitations can be categorized into four groups: sensory acceptability, serviceability of the structure, effect on nonstructural elements, and effect on structural elements. Each group is discussed below. For a more complete discussion, see ACI Committee 435 (1984a,b).

9.6.1 Sensory Acceptability

Droopy cantilevers and excessive sag in long-span beams may be unacceptable to the public. The total deflection is relevant. Cambering can alleviate this concern almost regardless of the amount of deflection. Floors that vibrate can distress occupants. The rate of change in the acceleration is the relevant parameter,

TABLE 9.4 Deflection-Reducing Options

Description	Effect on Stiffness of Section	
	Uncracked	Cracked
<i>Design Techniques</i>		
1 Deeper members	$(h^*/h)^3$ for rectangular beams less for T-beams	$(d^*/d)^2$ or (d^*/d) if change to uncracked section, up to 300%
2 Wider members	(b^*/b)	Small, or change to uncracked section
3 Add A'_s	Up to 50% for D_{LT} No effect for D_i	Up to 50% for D_{LT} No effect for D_i
4 Add A_s	No effect	A'_s/A_s
5 Add prestress	Reduces dead load deflection to nearly zero	Reduces dead load deflection to nearly zero and changes member to uncracked
6 Structure geometry	Large effect	Large effect
7 Revise criteria	See text	See text
<i>Construction Techniques</i>		
8 Cure: f'_c	Same as higher E_c and f_r	Same as higher E_c and f_r and could change to uncracked section
9 Cure: ϵ_{sh} and ϵ_{cr}	For long-term deflection, $(\epsilon_{sh}^*/\epsilon_{sh})$ and $(\epsilon_{cr}^*/\epsilon_{cr})$	For long-term deflection, $(\epsilon_{sh}^*/\epsilon_{sh})$ and $(\epsilon_{cr}^*/\epsilon_{cr})$
10 Shoring	Large effect, see text	Large effect, see text
11 Delay first loading	Similar to Options 19 and 20	Similar to Options 19 and 20
12 Delay installation	Up to 50%+, depending on time delay	Up to 50%+, depending on time delay
13 Locate equipment	See text	See text
14 Architectural details	See text	See text
15 Camber	See text	See text
16 Top bars	No effect	Up to $(d^*/d)^2$ for cantilevers
<i>Materials</i>		
17 Materials	See Options 19 and 20	See Options 19 and 20
18 Mix design	See Options 9, 19, and 20	See Options 9, 19, and 20
19 Higher E_c	(E_c^*/E_c) or $(f_c^*/f_c')^{0.5}$	Small
20 Higher f_r	None	Significant
21 Use fiber reinforcement	See Options 9 and 20	See Options 9 and 20

but live-load deflection is commonly used to judge the acceptability of floors. More sophisticated analyses consider amplitude, frequency, and damping of vibration. Although vibration is not a problem for most structures, it should be considered if the structure supports, for example, vibration-sensitive laboratory equipment or for a long-span open floor in an important public building.

9.6.2 Serviceability of the Structure

Roofs and outdoor decks that should drain water must do so. The total deflection is relevant. Cambering and other construction such as topping fills or tapering insulation must also be considered. Tolerances on the levelness of floor-finishing generally require a slope of 1% or greater to ensure complete water drainage. Floors for gymnasias and bowling alleys must remain plane and level. Both total deflection and incremental deflection are relevant. Cambering may compensate for some of the total deflection, but it is difficult to build in most structures. Incremental deflection occurring after the floor has been installed should be limited to an acceptable amount for the anticipated use. Members supporting sensitive equipment such as printing presses and certain building mechanical equipment must not deflect more than the amount permitted for the equipment. The incremental deflection occurring after the equipment has been installed is relevant. In some cases, deflection between two points on the span, not the ends, is relevant and limits can be measured in thousandths of an inch.

9.6.3 Effect on Nonstructural Elements

Partition walls built of brittle materials such as masonry and plaster cannot tolerate large deflections. Even an incremental deflection of span/360 after installation of the partition may not be tolerable. More forgiving materials such as a gypsum wallboard partitions (drywall) can tolerate larger incremental deflections. Prefabricated metal partitions may not be damaged by incremental deflections, but the total deflection may cause problems if the partitions are set to a laser-leveled ceiling and must meet a floor that is not level. Most ceilings installed today are not damaged by deflections that are acceptable by other criteria. Curtain walls, windows, doors, and certain other nonstructural building elements can be damaged by incremental deflection that exceeds the tolerance built into the element in question. In some cases, such as windows or cabinetwork that must fit between concrete floors above and below, the total deflection must be limited. In such cases, tolerances and perhaps other construction details must also be considered.

9.6.4 Effect on Structural Elements

Occasionally, deflections can cause instability of the primary structure, such as arches, shells, and long columns, for example. Deflection can cause higher stresses in another element, such as, for example, in masonry supporting a beam that rotates at the support. Mutually perpendicular cantilevers meeting at their tips must have the same deflection but may have different deflection properties. Thus deflection becomes a problem in moment analysis. In other cases, a slab supported on a deflecting beam may rest at the other end on an unyielding support, thus causing a moment pattern in the slab that is different from that computed using two unyielding supports. Engineers should be alert to special situations of this type that may distress the structure as well as cause damage to nonstructural elements.

References

- ACI Committee 117. 1990. Standard tolerances for concrete construction and materials (ACI 117-90). *Concrete Int. Design Construct.*, 2(8), 38–46.
- ACI Committee 209. 1992. Effects of concrete constituents, environment, and stress on creep and shrinkage of concrete. In *Designing for Effects of Creep, Shrinkage, Temperature in Concrete Structures*, SP-27, pp. 1–42. American Concrete Institute, Farmington Hills, MI.
- ACI Committee 318. 2005. *Building Code Requirements for Structural Concrete*, ACI 318-05; *Commentary*, ACI 318R-05. American Concrete Institute, Farmington Hills, MI.
- ACI Committee 435. 1984a. Allowable deflections (ACI 435.3R-68). *ACI J. Proc.*, 65(6), 433–444.
- ACI Committee 435. 1984b. Deflections of continuous concrete beams (ACI 435.5R-73). *ACI J. Proc.*, 70(12), 784–789.
- ACI Committee 435. 1995. *Control of Deflection in Concrete Structures*, ACI 435-95, pp. 1–77. American Concrete Institute, Farmington Hills, MI.
- Branson, D.E. 1971. Compression steel effect on long-term deflections. *ACI J. Proc.*, 68(8), 555–559.
- Branson, D.E. and Christiason, M.L. 1971. Time-dependent concrete properties related to design-strength and elastic properties, creep, and shrinkage. In *Designing for Effects of Creep, Shrinkage, Temperature in Concrete Structures*, SP-27, pp. 257–278. American Concrete Institute, Farmington Hills, MI.
- Fling, R.S. 1987. *Practical Design of Reinforced Concrete*. John Wiley & Sons, New York.
- Fling, R.S. 1992. Practical consideration in computing deflection of reinforced concrete. In *Designing Concrete Structures for Serviceability and Safety*, SP-133. American Concrete Institute, Farmington Hills, MI.
- Fling, R.S. 1996. Deflection of a concrete beam and slab roof. In *Recent Developments in Deflection Evaluation of Concrete*, SP-161, Nawy, E. G., Ed., pp. 1–24. American Concrete Institute, Farmington Hills, MI.

- Grossman, J.S. 1981. Simplified computations for effective moment of inertia, I_e and minimum thickness to avoid deflection computations. *ACI J. Proc.*, 78(6), 423–439.
- Grundy, P. and Kabaila, A. 1963. Construction loads on slabs with shored formwork in multi-story buildings. *J. Am. Concrete Inst. Proc.*, 60(12), 1729–1738.
- Lampert, P. 1973. Postcracking stiffness of reinforced concrete beams in torsion and bending. In *Analysis of Structural Systems for Torsion*, SP-35, pp. 385–433. American Concrete Institute, Farmington Hills, MI.
- Sbarounis, J.A. 1984. Multistory flat plate buildings: effects of construction loads on long-term deflections. *Concrete Int. Design Construct.*, 6(4), 62–70.
- Smadi, M.M., Slate, F.O., and Nilson, A.H. 1987. Shrinkage and creep of high-, medium-, and low-strength concretes, including overloads. *ACI Mater. J.*, 84(3), 224–234.
- Yu, W.W. and Winter, G. 1960. Instantaneous and long-term deflections of reinforced concrete beams under working loads. *ACI J. Proc.*, 57(1), 29–50.



(a)



(b)

(a) Preload prestressing system for concrete liquid containers. (Photograph courtesy of Preload Corporation, New York, NY.) (b) Structural concrete high-rise system. (Photograph courtesy of Portland Cement Association, Skokie, IL.)

10

Structural Concrete Systems

Scott W. McConnell, P.E.*

10.1	Overview	10-2
	Introduction • Durability • Constructability • Appearance	
10.2	Building Loads.....	10-3
	Introduction • Gravity Live Loads • Lateral Live Loads	
10.3	Composite Steel–Concrete Construction	10-7
	Introduction • Advantages and Disadvantages • Other Considerations • Composite Action • Unshored vs. Shored Construction • Composite Columns	
10.4	Foundations	10-10
	Shallow Foundations • Deep Foundations	
10.5	Structural Frames.....	10-14
	Rigid Frames • Braced and Unbraced Frames • Column Proportioning • Beam Proportioning • Beam–Column Joints • Construction Considerations	
10.6	Concrete Slab and Plate Systems.....	10-17
	One-Way Beam–Slab Systems • Flat Plates and Flat Slabs	
10.7	Liquid-Containing Structures	10-23
	Introduction • Circular Tanks • Rectangular Tanks	
10.8	Mass Concrete	10-26
	Introduction • Materials for Mass Concrete • Concrete Mixture Design • Quality Control	
10.9	On-Site Precasting and Tilt-Up Construction	10-28
10.10	Lift-Slab Construction	10-30
	Introduction • Foundations • Columns • Supported Slabs • Lifting Collars • Lifting Jacks • Critical Component Design • Applications	
10.11	Slip-Form Construction	10-33
	Introduction • Materials and Methods • Advantages and Disadvantages • Economy	
10.12	Prestressed Concrete	10-37
	Introduction • Pretensioned (Precast) Concrete • Post-Tensioned Concrete	
	Acknowledgments.....	10-40
	References	10-40

* Principal and Director, Structural Department of CMX (formerly Schoor DePalma, Engineers and Consultants), Manalapan, New Jersey; registered engineer in several states and practicing engineering for more than 15 years.

10.1 Overview

10.1.1 Introduction

Concrete structural systems must be durable, constructable, economical, and functional. The system selected must be strong and in many cases aesthetically pleasing. The system must have deflections that are within acceptable limits and, in seismic areas, must have the ability to absorb the large amounts of energy generated by seismic events. Selection of a structural system can sometimes be a difficult process. In many cases, structural steel is the more economical system to use. In general, when the system is to be hidden by architectural finishes, concrete systems are not the systems of choice. When the structure itself becomes an architectural expression, concrete is often the material of choice. In most cases, the formwork for the concrete system selected represents almost half of the total expense of the structure. Obviously, repetitive systems that reduce the cost of formwork relative to the cost of the concrete and reinforcing are candidates for concrete systems. In fact, under certain conditions concrete systems may be the structural systems of choice, even when the concrete is not exposed or architectural. The plastic nature of the material provides an effective structural solution to any unusual requirements. In such cases, structural steel systems cannot provide the freedom of design that concrete provides.

10.1.2 Durability

Properly proportioned concrete, when placed, finished, and cured in accordance with established standards, provides a durability that is virtually maintenance free and seldom matched by structural steel systems. The weathering steels, often used in bridge design, are the closest rivals to a good dense concrete with proper air entrainment. The problems associated with rust staining have largely limited the use of steel structural systems to bridge structures. The durability of concrete is directly related to the quality of the concrete. Dense, well-consolidated concrete with a low water/cement ratio and proper amounts of entrained air will be durable in all but the most hostile environments. Varying cement types, additives, and surface treatments are effective in extending the durability of concrete subjected to less than desirable conditions.

10.1.3 Constructability

The choice of the structural system must be based on the availability of skilled labor to accomplish the design requirements. Concrete construction, unlike steel, is somewhat regional with respect to accepted and common practices. For example, the use of high-strength concrete (f'_c in excess of 5000 psi) is more prevalent in metropolitan areas of the United States. Experience with the construction of ductile moment frames is more widespread in geographic areas traditionally considered to be seismically active. Bridges, highways, water treatment facilities, and buildings each have their own special sets of design requirements, specialized techniques, and selection of materials developed to address these needs. Localized labor practices and costs have a major influence on the degree to which concrete structural systems are utilized. Cast-in-place concrete is considerably more labor intensive than the fabrication of precast concrete. Conversely, transportation and erection of precast systems are obviously more expensive than those of cast-in-place systems. In theory, the optimum reinforcement for reinforced concrete would be an extremely large number of very small reinforcing bars to provide a uniform distribution of tensile reinforcing. The reality is that one is forced to use the least number of reinforcing bars and to use large bars to keep the labor costs within reason. Local union agreements, in many cases, place restrictions on which bars may be cut and fabricated in the field vs. which may be shop cut and fabricated. Obviously, shop fabrication is more desirable, because the equipment available and the controlled work environment generally result in a better product.

The cost of formwork constitutes a major portion of the cost of concrete structures. It is not uncommon for the cost of the formwork to represent 50% of the total cost of the in-place concrete. Systems that require simple, straightforward, reusable forms have a significant cost advantage over systems requiring

more complex forms. Many times the effort to reduce the complexity of formwork leads to simpler configurations that, unfortunately, require additional concrete along with additional loads, which must be carried by the foundation system. Whenever formwork can be reused, more complex configurations can be utilized. The ability to quickly strip and re-erect forms is a major cost savings in that overall construction time and general condition-related costs are reduced. For a structure under construction, the use of concrete or masonry usually results in the greatest time exposure to the elements. Given this significant length of exposure, the geographic location and the time of year that construction takes place can have a major impact on the costs of concrete construction. Obviously, some steps can be taken to allow concreting operations to continue during weather extremes, but this invariably results in additional job costs. An added concern during periods of weather extremes is quality control.

10.1.4 Appearance

In many cases, concrete is called upon to perform several functions. In addition to providing strength for a structure, it also acts as cladding, it must be durable and weather resistant, and it must have a pleasing appearance. The design of the exposed finish may require a simple rubbed surface to remove minor surface blemishes and form marks or a considerably more expensive architectural surface finish. Great care must be taken to successfully achieve consistent architectural finishes. Elements that must be considered include:

- A workable concrete mix to facilitate placing and finishing activities
- Consistent, controlled water content in the mix
- Use of cement from a single batch, as ASTM C 150 allows for a wide variation in the coarseness and thus color of the cement powder
- Accurate batching of the components of the cement
- Leak-free formwork to eliminate bleed marks due to loss of paste
- Proper placing techniques to avoid segregation of the mix and cold joints
- Consideration of varying weather conditions
- Proper curing
- Careful formwork removal
- Protection of the concrete from damage and staining during subsequent construction operations

Failure to successfully accomplish all of the above will almost certainly lead to less than satisfactory finishes, placing the designer and owner in the unenviable position of deciding to accept blemished concrete or delaying the project while the defective concrete is removed and replaced. Repaired honeycombing of exposed surfaces invariably deteriorates with time (at least with respect to appearance) and is a major contributor to unsightly concrete. In some instances, surface coatings are the only way to obtain an acceptable surface finish. Structural concrete not required to meet the visual requirements of architectural concrete must nevertheless be durable and weather resistant. The placing and curing requirements above should still be required. The color variations resulting from use of cement from varying batches and manufacturers and some relaxation of moisture control may be acceptable for the application.

10.2 Building Loads

10.2.1 Introduction

Design loads dictated by model building codes reflect the statistically probable maximum loads that can be expected to act upon a structural system. These loads are typically quoted as service loads, meaning that they have not been factored upward. Load factors are employed to account for inconsistencies in material properties, construction and fabrication practices, and the predictability of the load itself. They are, in essence, safety factors. In addition, load factors are employed to conduct analysis of the structural system in the ultimate stress range, as opposed to the service stress range.

Typically, the yield point of commonly used construction materials, such as steel and concrete, is well established; therefore, it is possible to design to the ultimate performance range of these materials. It is not desirable, however, to design structures so they perform in the ultimate range under typical loading conditions. This would not leave a sufficient factor of safety in the event of anomalies in the design assumptions. For this reason, the service loads quoted by the model building codes are intended to be applied to materials within their elastic stress ranges. If the designer wishes to analyze a structure by considering the ultimate performance of the materials, then load factors must be applied to the service loads.

As noted above, load factors are the product of both materials analysis and probabilistic theory concerning the construction and fabrication processes. Concrete design per ACI 318-05 employs load factors of 1.2 for dead loads and 1.6 for live loads acting simultaneously. Other combinations of load factors are employed depending on the code being used and the effect of one or more loads being applied at the same time. The distinction between these values is primarily based on the lack of predictability of how live loads will be applied to a structure. How to classify a dead load and a live load is a question to be addressed by the designer; however, certain truisms should be considered.

Material weights are generally predictable and can be specifically calculated as they apply to a given structural member. The weights of large, immovable objects, such as mechanical equipment, permanent shelving or storage racks, or planters are also fairly predictable. These elements can be classified as dead loads with little risk of inaccuracy.

Human occupancy, furniture, and transient storage that fluctuate in volume and intensity are among the items that are less predictable and thus subject to a higher load factor. In addition, external loads that act on structures are equally unpredictable. Wind, seismic, hydrostatic, and earth loads must be factored as live loads to consider their inherent unpredictable nature.

Maximum load combinations, such as live plus dead plus wind, have the statistical tendency to occur so infrequently that the various model building codes and material-design manuals permit reductions in the overall load applied to the structural system. The reduction factors differ according to the codes and manuals, so the designer should check the applicable references for the particular project.

Model building codes determine the load factor combinations that must be used. Individual jurisdictions must adopt the provisions of a model building code for it to be the governing code. Jurisdictions might consist of municipalities, counties, or whole states. Jurisdictions may adopt only certain provisions of a model code and not others. They might supplement the model code with additional design information that is specifically applicable to a given region.

The designer is cautioned to fully understand the applicable building code where his or her project is to be built. It is the location of the structure that dictates the governing code, not the location of the designer, client, or reviewing agency. The designer must also be aware of local provisions that supersede the model code; for example, municipalities located close to hurricane zones may adopt more stringent wind loads than are dictated by the adopted model code.

Finally, third-party sources assemble construction data pertaining to loads and material performance. These resources, such as Factory Mutual and Underwriters Laboratories, often develop their data to assist insurance companies in establishing rate structures for coverage. As such, they tend to be slightly more conservative in their statement of loads than the model building codes. The designer is obligated to follow these design guidelines only if the jurisdiction has adopted them into the local building code or if the building owner, for whom the designer is producing the design, dictates that the more stringent design standard be used. If these resources are used, specific attention should be paid to the treatment of snow and wind loading and to the fire rating of structural assemblies.

The most frequently referenced model building code in the United States is the International Building Code (IBC), which is used by 47 states and Washington, D.C. Adopted code editions and supplements might vary with each jurisdiction. It is incumbent on the designer to make certain which model code and what code amendments and provisions have been adopted for the location of the project. For the purposes of the following discussion, the IBC 2006 edition is referenced.

10.2.2 Gravity Live Loads

Analytically, design loads can be divided into two primary groups: gravity loads, which predominantly act vertically on the structure, and lateral loads, which predominantly act horizontally on the structure. Gravity loads account for all dead loads and those live loads associated with occupancy of the structure. The designer can refer to several sources for information to provide weight data regarding various building materials. Manufacturers provide tabulated load data for proprietary building materials. Nonproprietary material weights, such as concrete, asphalt, and roofing and flooring materials, can be found in the American Society of Civil Engineers' publication ASCE 7 (*Minimum Design Loads for Buildings and Other Structures*, Tables C3-1 and C3-2). Live-load data are developed with respect to the use and occupancy of a given structure. IBC Chapter 16, Section 1607, is devoted to establishing the intensity of various live loads as they relate to various uses and types of structures. IBC Tables 1607.1 and 1607.6 provide a breakdown of the maximum anticipated design live loads for a wide variety of use conditions. The designer should refer to these tables and the subsections of Section 1607 to establish the design live load for the use that most closely matches the anticipated use of the given structure. Local building codes do not generally permit interpolation between specified live loads; therefore, larger, multiuse facilities may require subdivision into several analytical pieces for design purposes. It is both permissible and recommended that different live loads be applied to the structural model, as required to satisfy the variety of intended uses. An example of this is the application of a 100-psf load near public means of exit, although the remainder of the building requires only a 50-psf live load to satisfy an office-use criteria. The designer is reminded that the IBC live load data for use and occupancy are quoted as service loads. Appropriate load factors must be applied to permit analysis of the ultimate material stress range.

10.2.3 Lateral Live Loads

The second group of live loads that must be considered by the designer are lateral loads, which are frequently the least predictable live loads. Such loads include wind, seismic, hydrostatic, and earth loads. Per IBC 2006, wind loads are determined in accordance with Chapter 6 of ASCE 7. The designer must first establish the applicable basic wind speed for the locale of the given structure. The basic wind speed is defined as the fastest 3-second gust speed in miles per hour for a given locale associated with an annual probability of 0.02 (50-year mean recurrence interval) and measured at a point 33 feet above the ground in Exposure C. The next design task is to determine the applicable exposure for the given structure. The exposure classifications differentiate between sites that are subjected to high, direct wind forces due to terrain characteristics and those that do not experience such wind forces due to shielding effects, building or forest density, or other terrain irregularities. Because subsequent adjustment factors are determined based on the exposure classification, it is crucial that the designer make a thoughtful selection. The designer is cautioned that wind forces are notoriously unpredictable. Large, concentrated forces can accumulate due to irregular building geometry or aerodynamic effects around canopies, roofs, balconies, or multiple-story structures. Consequently, it is not recommended that liberties be taken with the exposure classification in an attempt to refine the load analysis. The most prominent physical features of the terrain, surrounding buildings, the given structure, and potential changes over the life span of the structure should be considered when selecting the exposure group. The design wind pressure is determined by applying several modification factors to the basic wind pressure. These factors consider gust effects, the windward or leeward face of the building, the type of structure involved, and the slope of the roof. Special factors are provided for chimney, tower, sign, and flagpole structures. When determining the wind force on an entire structure, the designer is reminded that the combination of both windward and leeward forces must be considered. ASCE 7 distinguishes between *main wind force-resisting systems* and *components and cladding*. This distinction is based on the acknowledgment that, although the combination of windward and leeward forces acts only upon a primary system, components often experience intense concentrated forces due to surface irregularities of the building. Consequently, determining forces and gusts acting on components requires that the designer consider both the size and the position of the component in question relative to the entire building.

In practical application, buildings with multiple roof heights and articulated facades often require the development of a wind-pressure chart superimposed over each elevation of the building. This exercise permits the designer to account for major component features on the building exterior. In addition, because the design industry has moved progressively further away from requiring individual structural engineering consultants to shoulder the entire design responsibility for all building components, the development of a wind-force chart by the primary structural engineer provides appropriate information for subconsultants to design cladding systems and canopies.

Application of wind loads to a structural model is generally considered to occur at the slab-column joints for each floor level. This mode of application addresses the usual facade configuration in which the cladding is connected to the structure at each floor diaphragm. Where the facade treatment attaches to the structure in a different fashion, the designer must follow the load path from the cladding to the framing to determine the most accurate mode of application of wind loads. The designer is reminded that the wind-load data provided in the IBC and ASCE 7 are service loads and must be factored upward by the appropriate load factor in order to work in the ultimate material stress range.

The second form of lateral load to be considered is seismic load. Seismic load is generated from the movement of the ground and thus acts on the structure in a very different manner than wind loads. Seismic forces are transferred to the structure through the foundation elements. The influence on the supported floors occurs as a function of the weight of each floor. The acceleration of the ground thus causes the mass of each floor to accelerate, resulting in a seismic force in each diaphragm.

A delay occurs between the initial seismic force impact at the foundation level and the influence on the supported floors. Depending on the configuration of the structural components and the distribution of stiffness, the frequency and period of motion of the structure will vary. These variables—frequency and period—play an important role in establishing the design loads to be applied to the structural system. The stiffer the lateral load resisting system, the shorter the period of motion and the greater the frequency. Ductile systems tend to absorb load rather than transfer it through to the other structural members. Thus ductile systems result in longer periods of motion and lower frequencies of vibration. The detailing of reinforcement and the degree of confinement to increase ductility is of major importance. Sufficient reinforcement at the locations of large stress concentrations have to be provided. Beam-or slab-column connections are particularly susceptible to stress concentrations due to the large differences in stiffness between the members. In addition, re-entrant corners, edges near shear walls, and openings for stairs and elevators must be carefully detailed to avoid cracking problems. Chapter 21 of the ACI 318 Building Code (ACI Committee 318, 2005) covers the provisions for seismic proportioning of members and their detailing. The reader is referred to Chapter 26 of this *Handbook* for details of design and proportioning of seismic-resistant concrete structures, their shear-wall components, and the latest provisions on this subject.

It is important to highlight some of the major factors in the context of this general discussion. Typically, shear-wall systems provide satisfactory resistance to seismic loads due to their unique performance characteristics. Shear walls tend to be very stiff at the base but gradually become more flexible as they increase in height. At extensions above approximately 120 feet, shear walls tend to deflect more than $h/300$, where h represents the height of the structure. It is advisable that the deflection level does not exceed $h/400$.

For high-rise construction, a dual system is recommended that employs a combination of both shear-wall elements and moment-resisting frame elements. Frames are flexible throughout but tend to deflect in a regular and predictable manner throughout their height. Thus, at lower elevations on the structure, the shear walls act to restrain the frames, while at higher elevations in the structure the frames act to restrain the deflection of the shear walls. The designer should note that a dual system employing ordinary moment-resisting frames and concrete shear walls provides better resistance than either an independent shear-wall system or an independent ordinary moment-resisting frame system.

Finally, when considering deflections of structures subjected to seismic loads, the designer must acknowledge that the building codes are developed to prevent catastrophic collapses. This should be understood to mean that conformance with the provisions of the model codes will not ensure that a

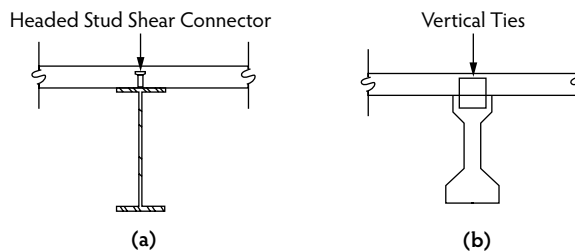


FIGURE 10.1 Composite beam systems: (a) composite steel beam, and (b) composite precast prestressed concrete beam.

structure will survive seismic activity unharmed. It can be expected that cracking and possibly spalling of concrete near high-stress-concentration zones may occur. In addition, peak deflections due to maximum anticipated seismic ground accelerations can be more than 10 times greater than those that will be generated using the design seismic base shear; however, adherence to code provisions will dramatically improve the potential for a structure to survive seismic activity. Localized repairs are preferable to the complete demolition of a structure.

10.3 Composite Steel–Concrete Construction

10.3.1 Introduction

Composite construction is the use of two or more building materials or systems that are bonded or interlocked to act as a single unit. In most common building systems, composite construction involves the use of concrete and steel. These materials work extremely well together for beam construction due to the high compression resistance and stability provided by concrete combined with the good tension-resisting attributes of steel. In the early part of the twentieth century, composite beam construction existed primarily as a result of fire protection needs, the end result of complete concrete encasement of steel I-shaped beams. In most cases, the composite action of the two building materials was not realized and was completely neglected in design. The composite action existed due to chemical bonding and friction at the material interface and by the shear strength of the concrete along the shortest failure plane. Although this type of construction and design is still permitted, it is very rarely used. With the development of welding techniques, a more solid mechanical interlock could be developed to resist the horizontal shear that develops during bending. The use of a mechanical interlock to develop this composite action was first utilized in bridge construction beginning in the 1930s. Economics prevented the widespread use of composite construction of this nature in buildings until the 1960s. Today, composite construction has been used worldwide in both bridge and building construction. Figure 10.1 illustrates two composite beam–slab systems.

10.3.2 Advantages and Disadvantages

Several advantages can be realized with the use of composite construction. As a rule of thumb, composite action becomes most efficient when loads are heavy, the beams are spaced as far apart as practical, and spans are relatively long. Typically, a 20 to 30% reduction in steel weight can be gained, providing better economy and, in many instances, shallower beam depths. Shallower beam depths may result in substantial savings in high rises, where floor-to-floor depths can be reduced. Lower floor-to-floor depths result in smaller overall building heights, generating savings from reduced wall materials and reduced lengths of mechanical, electrical, and plumbing risers. Compared with a noncomposite floor system, the stiffness and overload strength of a composite floor system are considerably greater. This is because the concrete slab acts as a large cover plate, shifting the neutral axis upward and allowing more efficient use of the two materials. This often allows a section that works as a noncomposite member to be used like a

composite member for longer spans without creating deflection concerns. Although composite construction does have some disadvantages, the advantages and overall economy favor its use. The cost of providing and placing mechanical shear connectors has significantly decreased over the years but should be considered, particularly on small jobs where mobilization of additional trades may completely offset the savings provided by reduced steel weight. In some cases, although smaller beam sizes may theoretically work as composite members, their use is not practical. Beams with flange thickness less than 1/4 inch require careful shear-stud placement to guard against burn-through failure during welding. The use of projecting shear connectors also increases safety hazards by keeping workmen from walking on the beams; for that reason, the installation of the shear connectors is often delayed until the deck forms or metal decking is installed.

10.3.3 Other Considerations

The advantages of composite action are largely unrealized in continuous-beam or frame construction due to the limited continuity in areas of negative bending. Because concrete is unable to effectively resist tension, continuity in these areas is limited to that which is provided by bar reinforcement and is usually neglected. Because the negative moment at a support often exceeds the positive midspan moment, composite action will have little effect other than to reduce midspan deflections. End reactions for composite beams are almost always larger than those for noncomposite beams of the same size. Engineers and fabricators often design connections based on uniformly loaded, noncomposite beam capacity. Such a practice potentially understates the shear loads and should not be used for composite construction. Long-term creep deflections are usually small enough to be neglected in composite beams but may warrant special consideration where heavy, sustained loading situations are encountered and when deflection criteria are more stringent.

10.3.4 Composite Action

Composite steel beam and concrete-slab systems behave in a similar manner to reinforced concrete T-beams. The analysis procedure is based on a standard transformed-section methodology. For detailed information on the design of composite members, the designer is referred to AISC Specification Chapter I. For buildings, AISC limits the portion of the slab that can be considered to participate as a flange for beam action. The AISC limits are very similar in nature to the T-beam construction requirements of the ACI 318 Code. The effective flange width on each side of the beam centerline for an interior beam is taken as the smaller value of 1/8 the beam span, 1/2 the distance to the nearest adjacent beam, and the distance to the edge of the slab. The slab thickness criteria of ACI 318 Section 8.10 are not considered in the AISC specification. Although composite construction using steel and concrete has only been discussed thus far, it should be noted that conventional slabs are sometimes designed to act compositely with precast, prestressed concrete beams. In such cases, the T-beam requirements of the ACI 318 Building Code should be followed.

The computation of section properties is based on the principle of transforming all components into a single, homogenous member. This is done on the basis of the ratio of the moduli of elasticity of the two materials. If a steel beam is used, the concrete slab is converted into an equivalent width of steel by dividing the effective flange width by the modular ratio $n = E_s/E_c$. The calculations necessary for composite design are similar to those for a built-up beam. The composite section must be proportioned to resist the loads, and the shear connectors must be adequate to ensure that the section acts as a solid, single member. The design of the shear connectors between the slab and the beam is based on the total horizontal shear that exists at the interface. The shear flow is the force per unit length that must be resisted at the interface to achieve composite action. Shear flow is given as:

$$f = \frac{VQ}{I}$$

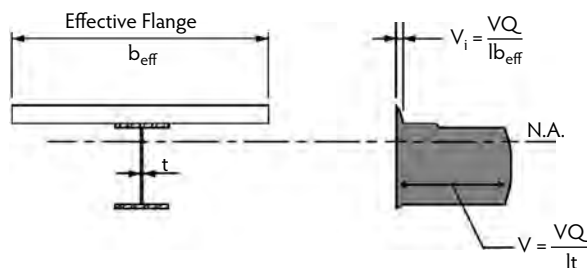


FIGURE 10.2 Shear-stress distribution across a composite section.

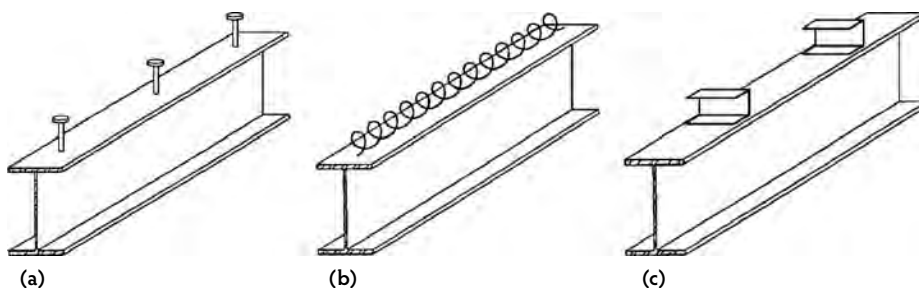


FIGURE 10.3 Types of shear connectors: (a) headed stud, (b) spirals, and (c) channels.

where V is the shear force, Q is the first moment of the effective area above the interface with respect to the neutral axis, and I is the moment of inertia of the composite section. If a given connector has a shear capacity of q , the maximum spacing can then be determined as:

$$s \leq \frac{q}{f}$$

In Figure 10.2, the shear flow at the steel–concrete interface is $v_i b_{\text{eff}}$. Numerous types of shear connectors have been utilized over the years. They include headed studs, spiral rods, channels, angles, and L-shaped connectors. Figure 10.3 illustrates some of these connectors. In building construction, composite sections usually involve using steel deck as a slab form. When composite metal decking is used, AISC only allows the use of welded studs. The minimum stud length is equal to the rib height of the deck plus 1-1/2 in. A minimum of 1/2 in. of concrete cover is required above the top of the installed studs. The shear studs are commonly fastened in the field with special stud-welding guns. This is done to prevent damage to the connectors during transportation and to allow easier steel erection and deck placement. It should be noted that shear connectors must be capable of resisting both horizontal and vertical forces. Because of the tendency of the slab to separate vertically from the beam, it is good practice to limit the connector spacing to around 2 ft. AISC limits the maximum stud connector spacing to eight times the total slab thickness. The reader is referred to the AISC Code for specifics regarding the use of form deck for composite construction.

10.3.5 Unshored vs. Shored Construction

For unshored construction, the beam member must be capable of supporting its own self-weight plus the weight of the wet slab concrete. Once the slab concrete attains about 75% of its 28-day compressive strength, the beam and slab are considered to act as composites. The composite section must then be capable of resisting the live loads and any additional superimposed dead loads. For unshored construction, the compressive stresses in the concrete slab will seldom be critical. For unshored construction, the service-load stresses can be computed as:

$$f = \frac{M_c}{S_d} + \frac{M_s}{S_c}$$

where M_c is the moment due to construction loads, M_s is the moment due to superimposed loads after slab curing, S_b is the section modulus of the beam, and S_c is the section modulus of the *composite member*. When shored construction is used, the working stresses are computed as follows:

$$f = \frac{M_c M_s}{S_c}$$

Although shored construction is usually more costly, dead-load deflections can be significantly reduced. Shored construction also results in higher concrete compressive stresses.

10.3.6 Composite Columns

Composite-column construction usually combines the use of concrete and steel. The two primary forms of composite column construction are (1) concrete-encased steel sections, and (2) steel-encased concrete members. It is important to realize that composite construction implies that there is a shear transfer between the concrete and steel. Simply filling a steel pipe or tube column with concrete will not create a composite member. Section 10.16.3 of the ACI 318-05 Code requires that any axial load assumed to be resisted by the concrete must be transferred to the concrete via lugs or brackets in direct bearing. Similarly, all axial load strength not taken by the concrete must be developed by a direct bearing or shear connection to the structural steel member. The capacity of a composite column is computed on the basis of the same requirements as a conventionally reinforced concrete column. For structural-steel-encased concrete sections, the thickness of the wall jacket must be sufficient to reach longitudinal yield stress before buckling outward. To ensure this, ACI 318 Section 10.16.6.1 stipulates minimum wall thicknesses for both rectangular and circular sections. For concrete-encased structural steel members, ACI 318 Section 10.16.7 sets limits on the compressive strength of the concrete and the design yield strength of the structural steel for members with a spirally reinforced steel core. The radial confining pressure provided by the spiral results in sufficient composite action between the concrete, reinforcing bars, and steel core such that the reinforcing bars assist in both stiffening and strengthening the member. ACI therefore permits the inclusion of the longitudinal bars when computing the area and moment of inertia of the steel core for evaluation of slenderness effects. For structural steel cores confined by tie reinforcement, it is likely that there will not be complete interaction between the concrete, steel, and reinforcing bars; therefore, use of the longitudinal reinforcing bars is permitted for computing the moment of inertia of the steel core because they assist in strengthening the section but do not effectively stiffen it. The tie-spacing requirements are similar to the spacing requirements of ACI 318 Section 7.10.5, with the exception that tie spacing for composite columns may not exceed one half the smallest side dimension of the member. This increased spacing requirement is intended to help maintain the concrete core, which may separate from the smooth surfaces of the structural steel. ACI 318 Section 10.16.8 defines the requirements for concrete-encased steel sections with transverse tie reinforcement.

10.4 Foundations

10.4.1 Shallow Foundations

Foundation systems are commonly referred to as *shallow* or *deep*, depending on the depths to which they extend to achieve adequate bearing capacity. Shallow foundations are those foundations that transfer column loads either directly or through relatively short piers, pilasters, or walls to the supporting soil below. The most common types of shallow foundations are strip or wall footings, spread footings, and combined footings. Strip footings are commonly used beneath walls and rely on one-way action as they

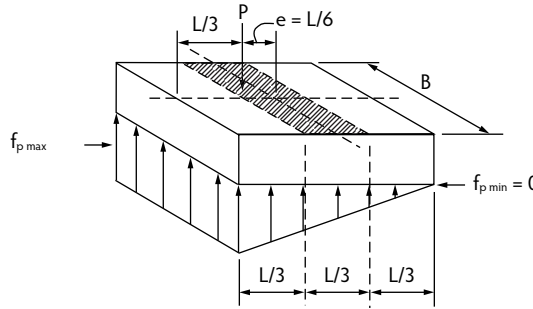


FIGURE 10.4 Footings with resultant vertical reaction of the middle third of the footing.

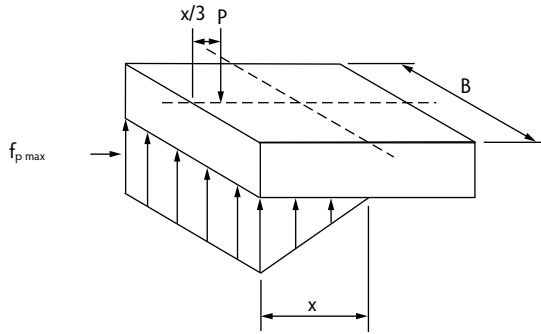


FIGURE 10.5 Footings with resultant vertical reaction outside the middle third of the footing.

cantilever a short distance on either side of the wall. Spread footings are usually square or rectangular pads that act to distribute individual column loads over a soil area large enough to support imposed loads. Combined footings act to distribute loads from two or more columns to the soil. Spread and combined footings rely on two-way distribution of the loads to the soil. In general, these footings are subjected to axial loads, shears, and moments from above that mobilize resisting soil pressures that can be determined by one of the following formulas. For those footings in which the resultant vertical reaction occurs in the middle third of the footing (Figure 10.4):

$$f_{p \max} = \frac{P}{A} \left(1 + \frac{6e}{L} \right) \quad (10.1)$$

For those footings in which the resultant vertical reaction occurs outside the middle third of the footing (Figure 10.5), equilibrium requires that the total resisting force equal the imposed force. Assuming a triangular pressure distribution:

$$P = f_{p \max} \frac{Bx}{2} - 5pt \quad (10.2)$$

where:

$$x = 3 \left(\frac{L}{2} - e \right), \quad f_{p \max} = \frac{4P}{3A(L - 2e)}, \quad f_{p \min} = 0 \quad (10.3)$$

where:

f_p = soil pressure (kips/ft²).

P = vertical load (kips).

e = eccentricity of the vertical load (ft).

A = contact area of the footing in square feet.

L = length of footing, perpendicular to axis of the moment (eP) in feet.

B = width of footing, parallel to axis of the moment (eP) in feet.

The design of a shallow footing must consider resistance to flexural and shear forces. ACI 318, Chapter 15, outlines the code requirements for the design of isolated column footings. Section 10.5.4 states that the minimum reinforcement for structural footings must meet the shrinkage and temperature requirements for steel given in Section 7.12. For grade-60 reinforcement, the minimum area of the temperature flexural reinforcement becomes:

$$A_{s(\min)} = 0.0018(bh) \quad (10.4)$$

where b is the width, and h is the thickness of the footing. The maximum spacing of footing reinforcement must not exceed the smaller of $5h$ or 18 in.

The thickness of a footing is usually governed by shear. This is because it is generally less expensive and easier to increase the depth of a footing than to try to provide web reinforcement in the form of stirrups. The standard requirements of ACI 318, Chapter 11, are used for shear design. For spread footings, both one-way shear based on beam action and two-way punching shear must be checked. The critical section for one-way shear is located at a distance d from the face of the concrete column or halfway between the face of the column and edge of the base plate for steel columns.

Another form of shallow foundation is a mat foundation, which becomes viable in locations with relatively low bearing conditions and potential water conditions. If the sum of the footing areas exceeds one half of the total building areas, it is usually preferable to combine the footings into a mat (also referred to as a *raft*) foundation. Because mat foundations may be used at locations where the bearing capacity can be marginal, it is important to recognize that the excess loads (above those acting on the natural deposit prior to construction) imposed upon the soil are significant. Excess loads can be reduced by increasing the basement depth. This increases the factor of safety with respect to bearing and also reduces settlement.

It should be recognized that the seat of settlement of a mat foundation extends deeper than conventional isolated footings; thus, consideration should be given to compressible layers within the depths of concern. Because of the random distribution of compressible zones in subsoil, combined with the stiffening effect of the mat and the superstructure frame, it can safely be assumed that the differential settlement of a mat foundation (per total inches of maximum settlement) will not be more than 0.5 of the corresponding value for buildings supported on isolated footings.

Prior to the advent of sophisticated computer-aided analyses, the analysis of mat foundations involved several simplifying assumptions. As a result, it has been common practice to use twice as much reinforcing as the analysis indicated. If different portions of the mat carry significantly different loadings, it is advisable to use control joints. Irregular shapes such as narrow appendages cause problems and must be carefully designed if they cannot be avoided; otherwise, cracking and rotation will occur in the vicinity of the junction of the appendage and the main segment of the mat.

10.4.2 Deep Foundations

As the depth to reach suitable support conditions increases, alternative systems must be considered, such as drilled piers, caissons, and piles. These systems may receive support from end bearing on high-capacity geological strata such as bedrock or other dense strata, or they may develop their capacity through skin friction with the surrounding soil. Because these systems have significant surface areas exposed to the surrounding soil, their capacity may be reduced as the surrounding soil consolidates. Clusters of friction piles tend to act as a unit rather than as isolated individual members.

Deep foundations are somewhat specialized and require considerable design input from the geotechnical engineer. The selection of a system is usually dictated by geotechnical considerations. Timber and steel piles that support pile caps are the most commonly used deep foundations. The capacities of the

piles in these foundations range from relatively low 10-ton values for timber piles to values in excess of 200 tons for steel piles. Piles with 40-ton capacities are the most commonly used steel piles because most building codes require load tests for capacities in excess of 40 tons. The load tests are costly and time consuming. The capacity of piles not subjected to load tests is determined by any of a number of empirical formulas.

Steel wide-flange members and open-ended pipe piles, which, when used, have relatively small steel cross-sections and displace very little soil as they are driven, are thus suitable for driving through soils with dense strata. Closed-end pipe piles displace soil and densify the soil in the immediate vicinity of the member. As clusters of these pipe piles are driven, the soil contained within the pile array becomes relatively dense and causes the entire cluster to act as a monolithic unit. The structural capacity of closed-end piles may be increased by filling the pile with concrete; however, in many cases, the capacity of the pile will be dictated by geotechnical considerations rather than its internal structural capacity. Filling piles with concrete adds considerable stiffness to the member. In cases where concrete fill is used to stiffen the member, proper reinforcement must be provided and the interior of the pile must be cleaned prior to concreting.

Precast prestressed concrete piles are somewhat less commonly used than steel and timber piles in the United States but are popular abroad. When precast piles are used in the United States, they are usually high-capacity, hollow, cylindrical piles with large diameters. The diameters are usually considerably larger than steel-pipe piles. Bridges and piers are candidates for this type of pile. The large diameter helps develop a stiff member, which makes placement easier, especially when underwater placement through considerable distances and soft material is involved. As mentioned, although not especially popular in the United States, solid precast prestressed piles are used. These piles usually have cross-sectional dimensions that more closely approximate steel piles.

The stresses resulting from driving must be carefully controlled with precast piles. The hammer introduces a compressive wave that travels down the pile and reflects back as a tension wave. The precompression supplied by the prestressing strands must be adequate to prevent damage to the pile due to tensile driving stresses. The prestressing tends to close any cracks that develop during the life of the pile. If the pile can be maintained in a crack-free condition, its stiffness is greatly increased. Prestressed piles are sometimes coated for protection. Obviously, any coating is susceptible to damage during driving and should not be depended upon solely for the longevity of the pile. Coatings in general extend the useful life of both steel and concrete used in marine environments, as the most hostile environment is in the splash zone, an area in which the coating is less likely to be damaged by the driving operations.

Lateral load resistance of pile foundations requires careful consideration. In a limited number of conditions, the lateral resistance of the pile foundation is developed by soil pressures reacting against the vertical face of the pile cap. A standard technique is battering the piles to utilize the vertical loads available to provide a horizontal component that resists the applied lateral loads. In lightly loaded structures with batter piles, uplift forces may develop as a result of the lateral loads. In many cases, the geotechnical engineer can determine a *point of fixity* at which the pile can be considered to have a rigid support. This enables the structural engineer to investigate the feasibility of developing lateral resistance using the flexural capacity of the piles. Flexural stresses introduced into the pile caps must be considered when the cantilever approach is used. Special consideration must be given to the proper anchorage of an uplift pile into the pile cap. The problem arises because of the relatively limited depth of penetration of the pile into the bottom of the pile cap. The problem is not as pronounced with respect to steel piles as it is with timber piles. Load-resisting lugs can easily be welded onto steel piles. Timber piles have potential problems due to the parallel orientation of the grain with limited edge distance. In addition to the traditional reinforcing rod inserted through holes drilled through the pile, several anchors are commercially available.

Drilled piers and caissons are concrete foundation elements that may or may not be permanently cased or reinforced. Usually, the decision to case or not is driven by the surrounding soil conditions. Unless the soil has the ability to maintain a vertical cut, casing is usually called for. If any clean-out, bottom preparation, or inspection is required, casing is almost certainly required, even if it is removed as the

concrete is placed. Because most drilled piers and caissons are high-capacity members, verification of the bearing capacity is a must. If verification requires that personnel be lowered into the hole, a minimum diameter of 30 in. should be considered. Verification may include a relatively simple visual confirmation that conditions are as expected or it may entail drilling into the rock to confirm the anticipated properties.

Auger cast piles might be considered for sites where noise, vibrations caused by pile driving, and disturbance of adjacent structures are a concern. An auger cast pile is constructed by drilling into the ground with a hollow-stemmed continuous flight auger. As the auger is withdrawn, a high-slump concrete is pumped down the stem of the auger. Reinforcement placed by hand is generally limited to 20 feet in depth. Reinforcement can be placed at higher depths by a vibrator or prior to concrete placement if specialized drilling equipment is used.

As seismic requirements continue to be refined for almost all geographic regions, there is generally a recognition that lateral loads may be greater than previously anticipated, and the ability to absorb large amounts of seismically generated energy is of paramount structural importance. Batter piles, the most common method for resisting lateral loads, depend on axial transfer of the loads from the structure to the support strata and may experience excessively large loads in a seismic event. It is probable that the design community will move to flexural-resisting elements for substructures as well as superstructures. This will result in large flexural and shear stresses, requiring considerable reinforcing to provide required strength and ductility. Traditionally, piers and caissons have been minimally reinforced, with the reinforcing frequently located in the upper portion of the member to ensure adequate connection to the supported structure. The designer should not be surprised to encounter some resistance from contractors with regard to the amount and detail of the reinforcing required in areas previously considered safe from earthquakes.

Differential settlements must be considered with respect to the type of superstructures supported by the foundations. Simple post-and-beam construction has more tolerance to movement than structures with shear walls or moment frames. Shear-wall structures usually have several isolated, very stiff elements. Excessive differential settlement may cause damage immediately adjacent to the shear walls, as rotations and displacements tend to be concentrated at the perimeter of the shear elements. Although moment frames have the inherent ability to accommodate considerable movement, the permanent stresses introduced into the structure must also be considered in the design of overstress during extreme loading events such as seismic activity, which may cause overload and failure.

In most cases, foundations can tolerate minor cracking; thus, standard ultimate-load analyses are commonly used. Thickness of the members is frequently governed by shear considerations. This is especially true of pile-cap design, which requires that large concentrated loads be safely transferred to the support piles. For those structures that cannot tolerate cracking, thickness of the members must also be checked to ensure that flexural stresses will be below the modulus of rupture.

For these cases, stresses related to volume changes must also be considered. Because foundations should be placed at elevations where the support soil is not subjected to seasonal (or annual) volume changes, there is the potential that the foundations may be placed at or below water level. The construction documents must clearly define requirements to ensure that the concrete is properly placed in these conditions. This is especially true of concrete-placing operations for deep-foundation systems. Consideration must be given to material selection and foundation protection for construction in aggressive soils (such as acid and acid-producing soils) that attack and deteriorate concrete. Chapter 14 in this *Handbook* details the geotechnical engineering of foundations in all their categories.

10.5 Structural Frames

10.5.1 Rigid Frames

It is common in the design of concrete structures to design members as an isolated entity. When the overall structural system and layout have been determined, a structural analysis is performed to determine the moments, shears, and axial forces in each of the structural members. The individual members are

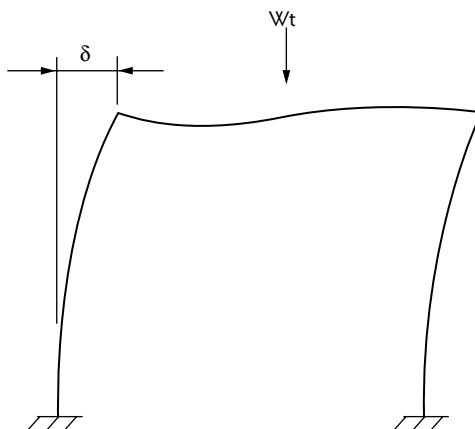


FIGURE 10.6 Sway of portal frame.

then proportioned to resist these forces. A structural building frame system relies on continuity between beam and column members to distribute and resist shears and moments induced by various loadings. As a building material, concrete naturally lends itself to frame-type construction, as it can easily be shaped, via formwork, to resist the applied loads in an optimal manner. Continuity is achieved, in part, by providing longitudinal reinforcement through the joint. For a concrete frame system to perform as intended, particular attention must be given to the design and detailing of the beam–column joints and to proper construction procedures and placement sequences. Frame connections and construction issues are discussed later in this section.

10.5.2 Braced and Unbraced Frames

Building-frame systems can be divided into two categories: (1) nonsway or braced frames, and (2) sway or unbraced frames. The majority of concrete building structures fall into the braced-frame category. In most cases, the bracing for frames is accomplished with structural walls placed at stairwells, or elevator shafts, where they serve the secondary purpose of providing a certain level of fire protection. In a general sense, a braced frame is defined as a frame in which the majority of side-sway buckling is prevented by diagonals, shear walls, or other bracing members relative to the restraint provided by the frame itself. To better develop an understanding of frame behavior, one must first consider the unbraced frame. Stability in an unbraced frame is dependent on the internal stiffness of the beam and column members that comprise the frame system. Lateral deflection in an unbraced frame consists of a displacement component resulting directly from horizontal loads as well as a component caused by unsymmetrical gravity loads, member properties, or frame geometry. When a building deflects laterally, the weight of the structure acts at an eccentricity to the support locations, introducing secondary bending moments in the beam and column members. This phenomena is known as the *P-delta effect*. Figure 10.6 demonstrates the *P-delta* effects in a typical unbraced frame. In braced frames, *P-delta* effects are generally small enough to be neglected.

10.5.3 Column Proportioning

A major factor affecting the design of unbraced frames is the reduction in axial capacity as a result of *slenderness effects*. For concrete frames, ACI considers a column to be slender if the column experiences more than a 5% reduction in its axial load capacity due to moments resulting from *P-delta* effects. Elastic stability of a column exists until a critical load, corresponding to the Euler buckling load, is reached. This critical load is greatly affected by rotational end restraints and lateral bracing, which alter the length and number of half-sine waves in the deflected shape of the column. To account for various end and bracing

restraints, most codes have adopted the concept of *effective length*. The effective length is the actual length of the column multiplied by a modification factor (k) necessary to produce a column with pinned-end restraints having the same buckling-load capacity.

Lateral drift of columns results in an increase in column moments which reduces the axial capacity of the column. Provided that the axial load is below the critical value, the structure will stabilize with increasing lateral deflection as the load becomes greater. The resulting load-vs.-moment curve is nonlinear, with a stability convergence process that can be described with a second-order differential equation. As a result, the additional forces and moments that result from material nonlinearity, cracking, and P-delta effects are generally considered in what is known as a *second-order analysis*. The 2005 ACI Code allows the use of such nonlinear, second-order analysis and provides a simplified design method for approximating these slenderness effects. The simplified design combines the forces based on a first-order, elastic analysis with a moment-magnifier approach.

To utilize the moment-magnifier design method, one must first establish whether a column is designated as a sway or nonsway column. Usually, this is readily evident by inspection, provided the column is located within a building level where lateral deflection is limited by stiff bracing members such as shear walls. If there is any doubt, ACI Section 10.11.4.1 permits a column to be considered nonsway if there is less than a 5% end-moment increase in the elastic moments due to second-order effects. Having established the type of frame that the column is a part of, the engineer can then design for the magnified moments given by the approximate equations and methods found in ACI Section 10.12 for nonsway columns or in Section 10.13 for sway columns.

10.5.4 Beam Proportioning

Frames and continuous beams are statically indeterminate members. With the faster and more powerful microcomputers available today, moments and shears in such members can be determined using any one of several frame analysis programs. For smaller, less complex structures, other procedures such as traditional elastic analyses (e.g., moment-area, slope-deflection, moment-distribution), plastic analyses, or approximate methods (such as the portal or cantilever methods) can be employed.

The greatest moments in a frame often result because of pattern loadings, also referred to as *skip live-loading* or *checkerboard loading*. Influence lines based on the Mueller–Breslau principle are often used to determine which spans should and should not be loaded to produce the worst-case design moments or shears. An influence line is a graphical representation of a design parameter at a particular point due to a unit load that moves across the structure. To account for the effects of pattern loadings, ACI 318 Section 8.9.2 requires that continuous-beam members must be proportioned to resist loads produced by two cases: (1) the dead load placed on all spans with the live load placed on two adjacent spans, a condition that produces the largest negative moment at the support as well as the worst-case shear force; or (2) the dead load placed on all spans with the live load positioned on alternate spans, a loading that results in the maximum and minimum positive moments at midspan and the maximum negative moment at the exterior support.

For smaller size structures where computer modeling is not warranted, the hand calculations required to produce the moment envelopes for the various loading patterns become quite tedious. To simplify design, the ACI has developed the use of moment and shear coefficients that can be used to approximate actual member forces. The approximate analyses permitted by ACI 318 Code Section 8.3 apply only to braced frames where significant moments due to lateral loads do not exist. The following criteria must be met for the simplified moment and shear coefficients to be valid:

1. There must be two or more spans of approximately equal lengths.
2. The larger of two adjacent spans must not exceed the shorter span by more than 20%.
3. Loads must be uniformly distributed.
4. Unfactored live load must not exceed three times the unfactored dead load.
5. The members must be prismatic.

Provided that the above criteria are met, the approximate equations give slightly conservative design moments and shears. Chapter 35 in this *Handbook* outlines the procedures and presents the equations governing the analysis and design of concrete structural members.

10.5.5 Beam–Column Joints

Considering that joints are often the weakest link in a structural system, considerable research on beam–column and slab–column connections has been conducted that led to the development of the ACI Committee 352 (2002) recommendations for design of monolithic connections. There are several parameters that interact to influence the mechanics of a joint. These parameters include joint shear–stress level, joint confinement, and the bond between the reinforcement and the concrete. ACI Committee 352 has provided design recommendations for ensuring adequate development length and horizontal joint reinforcement and also has set limits on the horizontal shear capacity of the joint, depending on the type and classification. The importance of adequate joint detailing has become increasingly evident in recent years due to research and better understanding of seismic failure modes. Concrete confinement in the form of transverse closed-tie reinforcement can greatly improve the ductility of concrete, which is a highly brittle material.

10.5.6 Construction Considerations

An increased behavioral understanding of reinforced concrete has resulted in more stringent reinforcement-detailing requirements that often make construction more difficult, particularly at beam–column joints where significant rebar congestion occurs. For exterior and knee joints, where the primary longitudinal reinforcement cannot be run continuously through the joint, hooked-bar anchorages must be used. This further increases joint congestion and may prevent adequate concrete placement. Many times, geometric limitations prevent the use of larger diameter reinforcing bars due to lengthy hook extensions and large bend diameters. In such cases, designers must be cognizant of the construction implications that their designs may have. Even with proper design and detailing attention, improper construction techniques can significantly affect the performance of individual members or affect the continuity between them. The concrete placement sequence has significant importance on the behavior of frames. ACI 318 Section 6.4.6 dictates that the column concrete must be placed and allowed to set prior to placing any concrete in the floor supported by those columns. This is to ensure that any settlement or bleeding of the column concrete while in the plastic state occurs beforehand, thus preventing any gaps or cracking at the beam–slab and column interface.

10.6 Concrete Slab and Plate Systems

10.6.1 One-Way Beam–Slab Systems

The selection of a beam–slab structural system is most frequently driven by the geometry of a given column bay. Rectangular bays, with an aspect ratio exceeding 2:1, will function to distribute nearly 100% of the shear and moments in the short direction. Configuring beams in the long-span direction only, with slabs spanning one way, perpendicular to the beams, creates a structural system that maximizes the benefits of each element. In addition, the continuity created by casting the slab system integrally across each beam support allows the framing system to redistribute load between the positive and negative moment zones so as to provide redundancy at the ultimate load state. Finally, deflections are minimized due to the continuity of the system. Under standard loading conditions (see Section 10.2), slabs can be kept thin (see Table 10.1), with reinforcing steel provided primarily in one direction only. Nominal transverse temperature and shrinkage reinforcement must always be provided to prevent cracking. It is important to stress that it is more effective to use smaller diameter bars at closer spacing than larger diameter bars at larger spacing. The former is essential to controlling cracking development in the slabs.

TABLE 10.1 Minimum Thickness h of Nonprestressed One-Way Slabs

Loading Condition	h
Simply supported	$L_n/20$
One end continuous	$L_n/24$
Both ends continuous	$L_n/28$
Cantilever	$L_n/10$

Note: L_n = effective span or cantilever arm.

The distribution pattern of the primary reinforcing steel closely follows the pattern of the bending-moment diagram (see Figure 10.7). Where negative moments are greatest (over the beam supports), top-reinforcing steel is provided. The cutoff point for the top steel occurs where the concrete no longer requires steel to resist tension stresses. The ACI Code requires that reinforcement must extend beyond this point a distance equal to the greater of the effective depth of the slab or $12d_b$, the diameter of the bar. Also, at least 1/3 of the total tension reinforcing provided for negative moment must be extended beyond the point of inflection not less than the effective depth of the slab, $12d_b$, or 1/16 the clear span, whichever is greater. Chapter 12 of the ACI Code gives the expressions for determining the development length required for the various conditions and categories. In practice, the ACI criteria result in extensions of the top reinforcing steel for distances of 1/3 (span) beyond each side of the support (see Figure 10.8). Using the guidelines established in Table 10.1, the resulting slab thicknesses will be sufficiently proportioned to resist shear stresses from typical loadings. Where extremely heavy loads (exceeding 250 psf) are experienced, the slab shear capacity should be checked. In accordance with Chapter 11 of the ACI 318 Code, the critical shear plane is located at a dimension d away from the face of the support for one-way slabs.

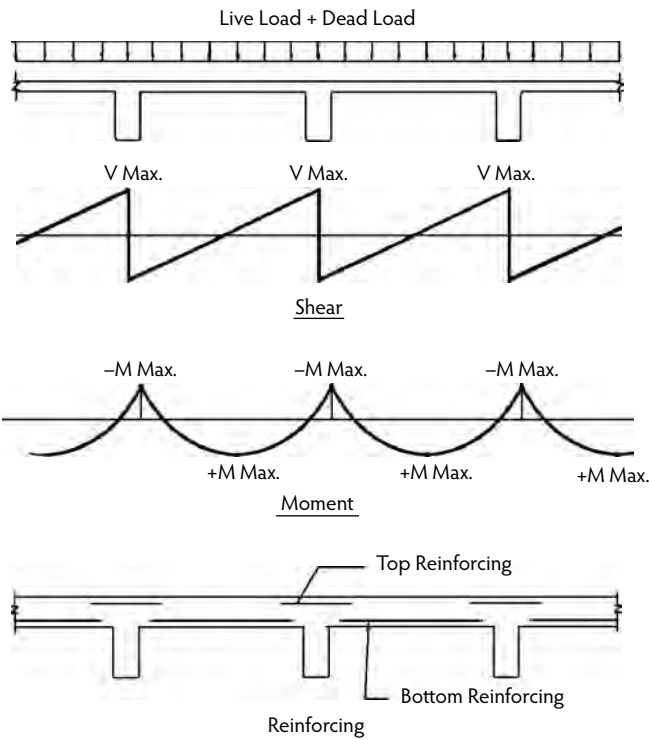


FIGURE 10.7 Moments and reinforcement locations in continuous beams.

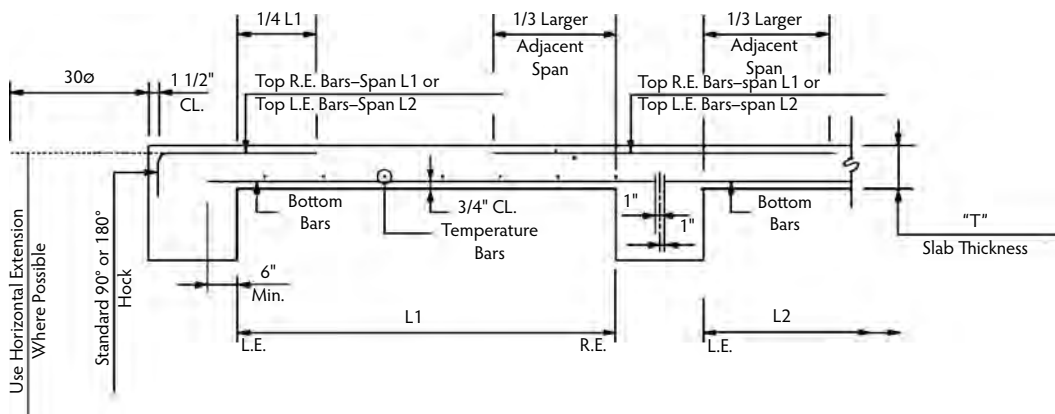


FIGURE 10.8 One-way slab bar bending and placing detail.

Special detailing requirements are limited in scope for one-way slab design. As long as the load path to the supporting beam element is maintained, the structure will perform as intended. Thus, openings parallel to the slab span are easily accommodated by providing internally reinforced headers along the short edges of the openings. The designer should strive to orient all major openings in a one-way system such that the long dimension is parallel to the span of the slab. No special detailing at columns is required, as the beam element is intended to carry 100% of the load from the slab to the column. One-way slab systems have the following advantages:

- Long-span capability of the beam elements permits wide column spacings and frame elements for lateral resistance.
- Predictable slab thicknesses, reinforcing requirements, and deflection performance allow the designer to concentrate design efforts elsewhere.
- Reinforcing detailing and placement are prioritized in one direction only, reducing complication at the construction site.

One-way concrete-slab systems are frequently used in parking structures, where the predictable traffic patterns require long open-column bays in one direction but permit shorter bays in the other direction.

10.6.2 Flat Plates and Flat Slabs

Where the designer is presented with a fairly regular, essentially square column bay, the most economical concrete structural system available is the two-way column-supported slab. As a monolithic material, the placed concrete naturally spans in two directions. By taking advantage of this natural tendency, the designer can achieve significant economy while maintaining desired deflection control and lateral resistance. Flat plates are distinguished from flat slabs by the treatment at the columns. Both systems are entirely beam free; however, flat slabs employ drop caps or column capitals to assist with shear transfer at columns. Flat plates are flat on their underside, and shear transfer is accomplished by proper proportioning of the concrete plate with the appropriate design and use of shear-moment transfer reinforcement.

Two-way column-supported slabs derive redundancy from the fact that 100% of the applied loads must be carried by the structure in each of the two orthogonal directions. Thus, for a column bay of widths I_a and I_b , the structure is proportioned and designed such that 100% of the load can at any time be carried in either the I_a or the I_b direction. Load transfer in a two-way system is accomplished by effective widths of slab that serve as shallow beams. For analytical purposes, these effective widths are divided into column strips and middle strips. By definition, column strips are widths of slab centered on the column grid line, in both grid directions. The ACI Code specifies that column strips should extend

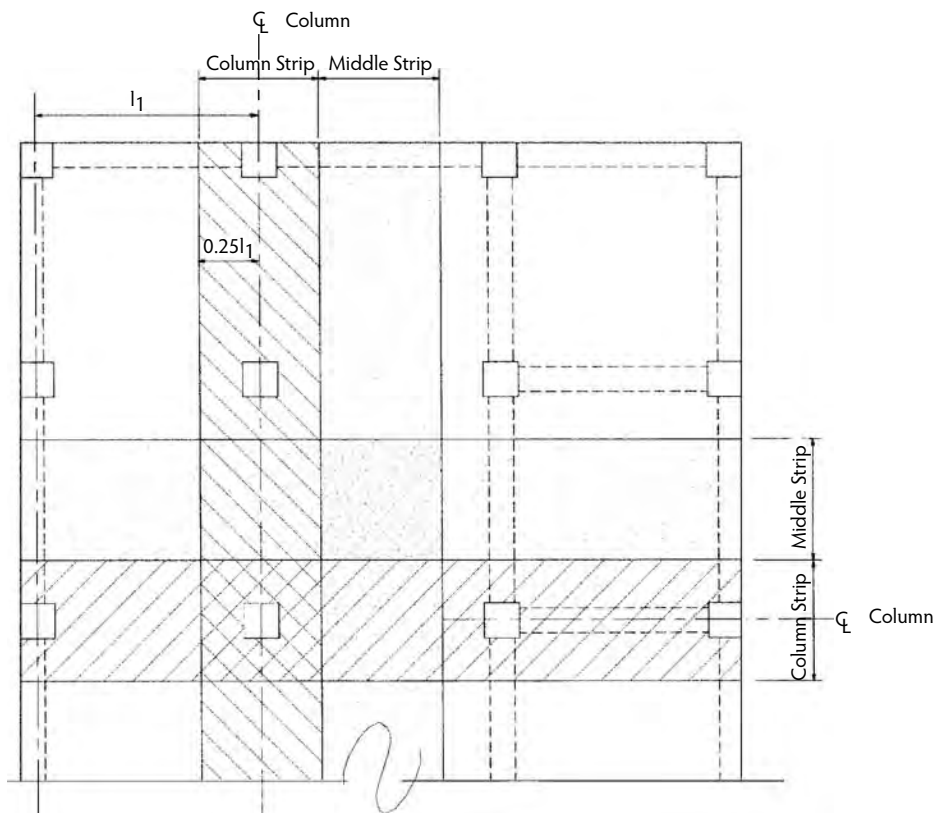


FIGURE 10.9 Column and middle strips in two-way slabs and plates.

$0.25L_1$ or $0.25L_2$ on each side of the column, whichever is less, where L_1 and L_2 are the adjacent slab spans. Middle strips occupy the region between the column strips, at the centers of the column bays, in both directions, as shown in Figure 10.9.

Chapter 13 of the ACI 318 Code addresses the design of two-way slab systems. The code allows that design may be made by any procedure satisfying conditions of equilibrium and geometric compatibility. The code then describes two alternative design approaches: the direct-design method and the equivalent-frame method. The direct-design method is an empirical method developed essentially from the elastic theory of the distribution of moments in continuous slabs. Strict conformance to the limitations must be maintained or the reliability of the method will be compromised. The slab system must operate within the following constraints if the direct-design method is used:

- There shall be a minimum of three continuous spans in each direction.
- Panels shall be rectangular, with a ratio of longer to shorter span, center-to-center of supports, not greater than 2.
- Successive span lengths center-to-center of supports in each direction shall not differ by more than one third the longer span.
- Offset of columns by a maximum of 10% of the span (in the direction of the offset) from either axis between center lines of successive columns shall be permitted.
- All loads shall be due to gravity only and uniformly distributed over the entire panel. Live load shall not exceed two times the dead load.
- For a panel with beams between supports on all sides, the relative stiffness of beams in two perpendicular directions shall not be less than 0.2 or greater than 5.0.

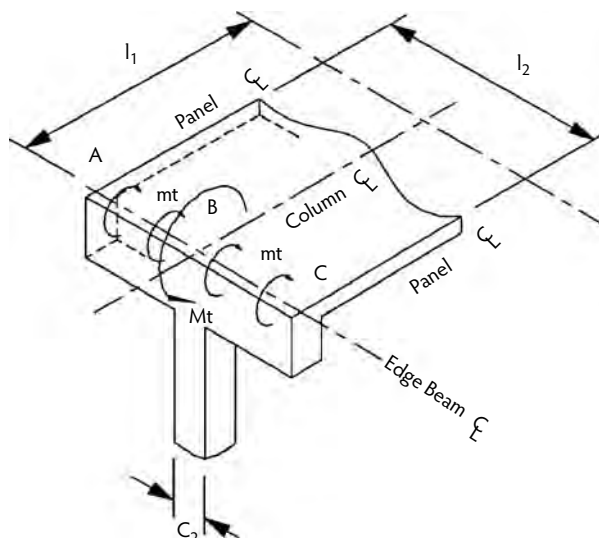


FIGURE 10.10 Torsional beam element in two-way action.

Using factors provided in the ACI 318 Code, Chapter 13, the total gravity load acting on the slab system is distributed into the column strip and middle strip zones. This method acknowledges that the summation of the negative and positive moments for any given span must equal the simple beam moment for a corresponding span. Consequently, the total static moment acting on any panel is denoted M_o , and the positive and negative moment distribution factors sum to $1.0M_o$. For interior spans, the total static moment (M_o) is distributed 65% to the negative moment and 35% to the positive moment. End-span conditions require reference to the tabular information provided in the ACI Code. After the moment-distribution factor is derived, additional factors are employed to proportion the moments between the column strips and the middle strips.

The equivalent-frame method is also essentially based on elastic theory. The slab is divided into frames comprised of the column grid and the slab on each side, extending to the middle of the panel. Each slab-column frame can be designed separately at each floor level, assuming that the columns are fixed at the floors above and below. Using stiffness coefficients for the various intersecting components at the column junction, inclusive of the stiffness of the torsional beam, a moment distribution is performed. Figure 10.10 illustrates the torsional moment transferred to the slab from the torsional beam. The moment of inertia may be calculated using the gross area of concrete. Determining the distribution of moment through the slabs and columns resolves the flexural phase of the design. The second and perhaps more critical aspect in the design of flat plates or slabs by either method is the shear transfer at the column junction. Because neither the flat-plate system nor the flat-slab system has beams that can transfer load into the columns, all of the load carried by the column strips must be transferred through the slab thickness. In a flat-slab system, drop caps and column capitals can be used to supplement the shear capacity of the slab concrete alone. The designer must consider two forms of shear transfer.

As seen in Figure 10.11, a portion of the unbalanced moment is transferred to the column by a vertical balancing couple in the form of vertical shear acting at the face of the column, while another portion is transferred by a horizontal force couple (flexure) occurring within the slab depth. ACI 318, Chapter 11, indicates that approximately 60% of the unbalanced moment is transferred by flexure, with the balance transferred by shear. These percentages have to be calculated for each case. The designer must remember that the vertical reaction due to gravity loads in the slab must be added to the unbalanced moment forces to gain a complete picture of the slab–column interface.

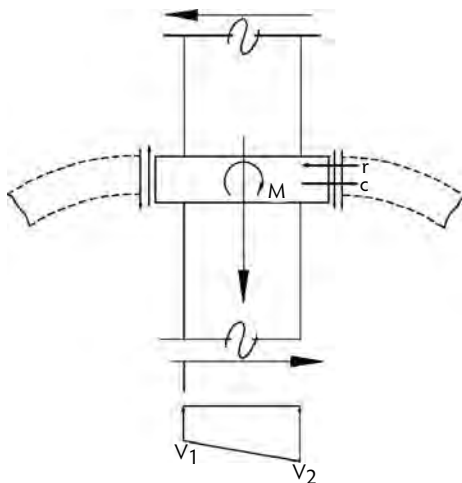


FIGURE 10.11 Shear-moment transfer mechanism.

For columns that are essentially square in cross-section, such shear failure typically governs the proportioning of the plate or column cap. The shear-failure plane occurs as a 45° crack that forms around the full perimeter of the column. The failure plane is angled upward from the bottom of the column. The critical shear zone for analysis is considered to be a distance $d/2$ from the face of the column, where d is the effective depth of concrete above the reinforcing.

Where the applied shear forces greatly exceed the concrete-slab shear strength, the designer has two primary options. One is to provide additional concrete in a region slightly wider than the critical shear zone; this is accomplished by adding a flat drop cap consisting of several additional inches of concrete. Alternatively, a column capital, shaped like an inverted cone, can be provided to widen the critical shear zone and to thicken the concrete in the zone, thereby increasing the concrete shear capacity. Chapter 35 of this *Handbook* lists the maximum allowable shear capacity (V_c) that can be used in the design for two-way action to determine the thickness of the plate or slab as governed by shear. The other alternative is the use of special steel reinforcing assemblies. Commonly referred to as *shear heads*, these assemblies can consist of steel beams or channels welded in a cross shape, placed on top of the column, and poured monolithically with the slab. Other shear-head assemblies consist of flat steel bars with welded-head shear studs. These assemblies are placed so they overlap the column and extend outward, thus increasing the critical shear zone.

Where significant shear-head reinforcing is required, the slab is proportioned too thin for the applied loads or the tributary areas. Shear failure is a sudden failure mode. The designer must exhibit extreme caution in analyzing shear transfer. Although not in favor for many architectural designs due to infringement of the ceiling plenum space, drop caps provide the designer with a simple but effective means of increasing slab capacities without resorting to complicated reinforcing schemes that are ultimately only as reliable as the installation method. The designer is encouraged to analyze the perimetric punching shear transfer as early in the design process as possible.

A final means of increasing the slab shear capacity, if the other two alternatives are not economically justifiable, is increasing the size of the columns. In practice, this method is only effective when the differential between the applied shear force and the slab capacity is within 20%. In this case, a 4-in. increase in the column dimensions will increase the slab shear capacity sufficiently to support the shear transfer.

As noted earlier, perimetric shear is typically the governing shear condition for design purposes; however, where rectangular columns with an aspect ratio in excess of 2:1 are provided, one-way beam shear can govern the slab thickness. Where applied shear forces exceed the concrete capacity, drop caps can be employed to increase the critical shear zone and the thickness of the concrete. Column capitals are not used for rectangular columns. The designer may find more success in increasing the long dimension of the column, if this option is available.

10.6.2.1 Post-Tensioned Two-Way Plates

Prestressed, post-tensioned, two-way floors are frequently used today, particularly in apartment buildings. The primary advantages of post-tensioning are the ability to use thinner slabs, the crack control derived from the presence of a significant precompression force in the concrete, greater shear capacity as a result of the precompression force, and greater deflection control as a function of reverse cambering. The designer is cautioned that the advantages realized from post-tensioning in the slab elements can quickly be lost in the column elements. The extremely high compression forces generated by the tensioning strands cause large unbalanced moments in exterior columns. To adequately reinforce the columns to resist these forces, much of the available room for shear reinforcing and negative flexural steel is occupied. The designer must carefully detail these conditions to ensure that no conflicts exist among the different types of required reinforcement that could jeopardize the design once it is under construction. The final aspect of two-way column-supported slab design considered here is the transfer of lateral moments between the slab–diaphragm system and the columns. Under uniform gravity loading, flexural stresses are essentially balanced at interior columns, and shear transfer is accomplished via independent analysis. Where unbalanced moments are to be transferred into the columns, the analysis of shear and flexure becomes combined. Analysis of this moment transfer requires calculation of the polar moment of inertia for the column element. Then, by applying the standard stress analysis theory of shear stress and bending stress, the proportion of the slab or drop cap at the column head can be checked. The designer is cautioned that the analysis of punching shear as a function of unbalanced moment transfer is of utmost importance and should be addressed as early in the design process as possible to allow for changes in the structural approach, if necessary. Because slabs tend to be thinner in post-tensioned systems, the analysis of punching shear and unbalanced moment transfer at the columns takes on even greater significance.

10.7 Liquid-Containing Structures

10.7.1 Introduction

Concrete structures for liquid containment consist mainly of water-treatment plants, wastewater-treatment facilities, tanks, and reservoirs. The concrete used for these facilities should be watertight and should be protected against contamination from groundwater. In addition, exposed concrete structures require protection against freeze–thaw damage and environmental effects. In containment concrete, low water permeability and low shrinkage are essential to prevent damage and cracking of concrete. Although proper design, such as specifying proper control joints and reinforcing steel, is important, the most effective way of controlling shrinkage and minimizing water permeability is by designing good-quality concrete mixes. In addition, proper concrete quality, concrete batching, delivery to the site, and placing are essential factors for good quality containment concrete.

The compressive strength of concrete used for containment structures should be a minimum of 4000 psi at 28 days of age. The air content should be $6 \pm 1\%$. The amount of mixing water should be enough to produce a slump of 2 to 3 in. The minimum cement content for a 4000-psi concrete should be 560 lb/yd³. Containment concrete should have a maximum water/cement ratio of 0.45 lb/lb.

The use of a water-reducing admixture generally helps reduce the amount of mixing water used. The use of high-range water reducers may also be used to reduce the amount of mixing water and increase the slump, easing the placement. Slump after the addition of superplasticizers should not exceed 7 in. In warm weather, a high-range water reducer and retarder may be used to prevent quick setting of the cement. For more information on admixture types and their functions, ASTM C 494 as well as reputable admixture manufacturers may be consulted.

To further reduce permeability and increase the density and durability of concrete, the addition of microsilica to the concrete mix may be considered. In general, the addition of 5% microsilica by weight of Portland cement reduces the permeability of concrete considerably. Microsilica-containing concrete is widely used for parking garage floors to reduce chloride infiltration into the slabs.

The size and amount of coarse aggregate used in concrete are also governing factors in controlling the shrinkage and cracking of concrete. The size of aggregate should not exceed 1-1/2 in. (ASTM C33, size #57). The amount of coarse aggregate should be between 1750 and 1850 lb/yd³. The higher the amount of coarse aggregate, the lower the amount of sand, which is a factor in controlling shrinkage. All other concreting practices such as placement techniques, finishing procedures, and curing should be done as per the ACI specifications. The joint type and spacing as well as the reinforcing percentage and the other design details of the project should be designed by the structural engineer.

The most important aspect of concrete tanks is that they must be leak free. This requires that careful consideration must be given to the analysis, detailing, and construction of tanks. The requirement that the tanks be free of leaks leads to the rather obvious conclusion that the stresses in the tank must be must be below the modulus of rupture. Because reinforcing becomes effective at strains near those that cause cracking in concrete, reinforcing is present in the tanks to resist the tensile stresses if the concrete ruptures, thus averting a catastrophic failure. The thickness of the walls is therefore selected to keep shear and flexural stresses below the cracking point. The ideal configuration for tanks is the circular shape. Resisting loads with tensile members is more efficient than doing so with flexural members. Most of the loads generated by the contents of a circular tank are very efficiently resisted by circumferential tensile forces. When space or process constraints must be considered, rectangular tanks may be the proper choice.

10.7.2 Circular Tanks

The analysis and design procedures for circular liquid-containing tanks are not complicated. They follow the elastic theory of shells (Billington, 1982; Nawy, 2003). The method basically consists of a membrane analysis of the tank with the introduction of shears and moments to account for boundary conditions that are noncompliant with the membrane theory. The Portland Cement Association (PCA) publication *Circular Concrete Tanks Without Prestressing* (PCA, 1992) provides procedures and examples for the design of circular tanks. Much of the information and formulas contained herein are extracted from the PCA pamphlet. There are also computer programs that can analyze these tanks. From a practical standpoint, it should be noted that the base slabs for most tanks are relatively thick for several reasons and the nominal amounts of steel to control volumetric changes of the concrete result in capacities greater than those required by the analysis.

The basic approach to design of a circular tank is to select a wall thickness that is strong enough that the stresses in the wall will always be less than the modulus of rupture of the concrete. Circumferential reinforcing is provided to carry all of the ring tension should the concrete crack. Vertical reinforcing is selected to resist the flexural stresses caused by the support conditions. It is interesting to note that using reduced allowable stresses in the reinforcing steel causes higher stresses in the concrete. The area of reinforcing steel required to resist the ring tension (T) is:

$$A_s = \frac{T}{f_s} \quad (10.5)$$

where A_s is the area of steel required, and f_s is the design stress for the reinforcing steel. The stress in the concrete can be expressed as:

$$f_c = \frac{(CE_s A_s + T)}{(A_c + nA_s)} \quad (10.6)$$

where f_c is the stress in the concrete, C is the thermal coefficient of expansion, A_s is the cross-sectional area of the steel, A_c is the cross-sectional area of the concrete, $n = E_s/E_c$, and E_c and E_s are the moduli of elasticity of concrete and steel, respectively. Inserting varying design stresses for the reinforcing confirms that as the steel design stresses decrease the stresses in the concrete increase. Of interest is the revelation that, as the design stress of reinforcing approaches infinity, A_s approaches zero and the stress in the concrete approaches T/A_c . In other words, the effects of thermal stresses disappear.

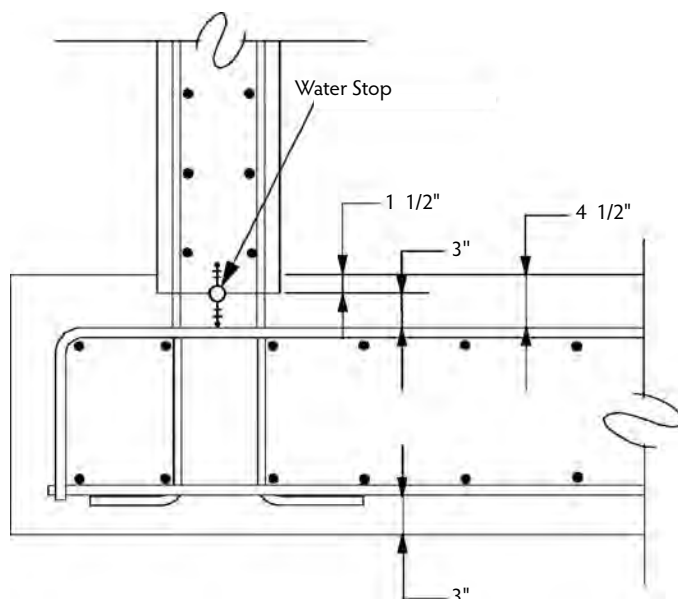


FIGURE 10.12 Detailing of wall–base intersection.

Because volumetric changes cause tensile stresses in the concrete, efforts should be made to control shrinkage. Construction joints should be specified on the construction documents. Joint spacings in excess of 30 ft will almost invariably lead to shrinkage cracking. A closer spacing should be considered for relatively low walls because of the circumferential fixity at the base and the unrestrained top surface of the wall. Expansive concrete is an option used by several designers. An alternative to expansive concrete is to attempt to limit those components contributing to shrinkage in the concrete matrix. By limiting the amount of cement, sand, and water in the concrete, major contributors to shrinkage are reduced. The reduction in paste results in reduced workability, which can, at least in part, be addressed by the use of superplasticizing admixtures in the mix. Prestressing is an option for reducing or eliminating tensile stresses in the concrete.

Attention to details is an important part of producing leak-free tanks. In general, it is better to use smaller reinforcing rods with their greater specific area for developing bond, shorter lap splices, and smaller bend radii. Conversely, it is important that the bar spacing allow for effective concrete placement to avoid honeycombing and inadequately consolidated concrete. Most leaks in concrete tanks occur at joints. Acknowledgment of difficulties in placing concrete should be reflected in the design details; for example, to ensure proper water stop installation at the slab–wall intersection, consider lowering the top layer of reinforcing as shown in Figure 10.12. Also, consideration must be given to joint details that do not utilize starter walls as a part of the slab. This is because effective consolidation of concrete, necessary for a leak-free joint, is difficult for these cases. Reinforcing congestion at joints makes proper placement of the concrete difficult and may contribute to honeycombing and leaks.

Prestressed concrete tanks, both pretensioned and post-tensioned, are probably the most efficient leak-proof circular containment vessels. The principles of the shell theory for cylindrical shells applies equally. The design factors used are similar to those for the reinforced concrete already discussed. Two types of prestressing systems are used: (1) circular strand wire-wrapped, such as the preload system used extensively worldwide, and (2) post-tensioned, both horizontally and vertically. Reports by ACI Committees 372 (2003) and 373 (1997) give detailed requirements for maximum allowable stresses and other pertinent provisions for design. Nawy (2003) presents a detailed chapter on the design of prestressed circular tanks of both types, with examples, as well as the design of the cylindrical shell roof of a typical circular tank.

10.7.3 Rectangular Tanks

Performance criteria for rectangular reinforced concrete tanks are usually similar to those of circular tanks—namely, no leakage. The wall thickness of relatively shallow tanks is dictated by the need to keep flexural stresses below the modulus of rupture. The wall thicknesses of deep tanks, such as those associated with pump stations, are often dictated by shear stresses; flexural stresses are usually less than the modulus of rupture cracking stresses. The Portland Cement Association's *Rectangular Concrete Tanks* (PCA, 1998) provides guidelines and design procedures. Extensive additional information is available in the literature (see, for example, Timoshenko and Woinowsky-Krieger, 1959; Young, 1989). The corners of rectangular tanks tend to be subjected to large stresses; hence, considerable attention should be devoted to detailing and joint placement to limit cracking to an acceptable minimum. Construction joint locations must be incorporated into the design documents to limit the effects of volume changes. As the horizontal dimensions of the tanks increase, the effects of the corners diminish, and the wall behaves more like a cantilevered retaining wall. Introduction of counterforts reintroduces two-dimensional behavior and should be considered in long walls. This technique can also be utilized for large-diameter circular reinforced concrete tanks in which the circumferential stresses become exceedingly large. Buried rectangular tanks present a special problem at wall corners. Slabs at the corners of rectangular tanks tend to curl upward; thus, the corners must be properly attached to the walls. Because diagonal cracks occur at the corners, additional diagonal reinforcing steel is usually provided.

10.8 Mass Concrete

10.8.1 Introduction

Large structures such as dams, bridge foundations, mat foundations, nuclear plants, and large-span deep beams require the placement of large quantities of concrete that are required to act in a monolithic manner. The successful placement of mass concrete requires careful planning, mixture design, placement, and consolidation. Quality mass concrete, like other concrete, begins with the proper mixture for the job. Volume changes within the concrete can cause internal cracking, with its attendant reduction in strength and degree of watertightness. To keep shrinkage to a minimum, factors that are major contributors to shrinkage must be controlled. Successful placement of mass concrete requires the prevention of early setting of the cement and shrinkage of the concrete. During the placement of concrete, the temperature increases due to the hydration of the cement; therefore, minimizing the increase of heat of hydration is essential to prevent shrinkage and cracking of the concrete. The publication *Control of Cracking in Concrete Structures* (ACI Committee 224, 2001) deals with the preventive measures necessary to control internal temperature in mass concrete. Concrete used for various large structures has to have excellent control of early setting to prevent shrinkage, cracking, and problems associated with placement and workability of concrete. Among the factors to be considered for mass concrete are the following:

- Engineering design details of mass concrete (this phase of the work requires considerable knowledge and experience of structural engineering)
- Selection of materials and proportioning of concrete mixes
- Control of concrete quality during batching and placement

10.8.2 Materials for Mass Concrete

The following materials are appropriate for mass concrete:

- *Portland cement with low heat of hydration.* It is common to use Type II or Type IV Portland cement (ASTM C 150). The minimum amount of Portland cement should be used to achieve the design strength.
- *Pozzolans* (ASTM C 311 and ASTM C 618). Addition of a pozzolan such as fly ash in the range of 20 to 25% by weight of cement will assist in reducing the heat of hydration and improving workability and long-term strength gain.

- *Aggregates* (ASTM C33). Both fine and coarse aggregates should meet ASTM C 33 requirements. For dams, the coarse aggregate should preferably be size No. 1. In case of structural mass concrete for beams, coarse aggregate should have a nominal size of 1 to 1-1/2 in. The amount of coarse aggregate should be high, approximately 1900 lb/yd³ of concrete. Especially in concrete dams, the ratio of fine aggregate to total aggregate by absolute volume should be low—approximately 25%.
- *Mixing water*. The amount of mixing water to be used should be low to provide a slump of 2 to 3 in.
- *Admixtures*. Admixtures should be used to entrain air and reduce the water/cement ratio. The water reducer should preferably be a Type D water-reducing and retarding admixture, as specified in ASTM C 494.
- *High-range water-reducing (HRWR) admixtures*. Mass concrete to be pumped should be treated with either an HRWR admixture (Type F) or an HRWR and retarding admixture (Type G) as specified in ASTM C 494. The slump before the addition of the superplasticizer should be 2 to 3 in.; after the addition of superplasticizer, the slump should be 5 to 7 in.
- *Coolants*. The temperature of mass concrete for dams should be controlled to be between 40 and 50°F, especially in hot weather conditions. Finely chipped ice may be added to concrete to control the temperature. Other methods of cooling the aggregates, such as keeping them damp and under shaded conditions, will reduce the temperature. When steel forms are used, they should be sprayed with cold water if necessary. Curing the concrete with cold water also will help in controlling the temperature of cast concrete. The maximum temperature for mass structural concrete, such as beams, should be 70°F. In this case also, the use of chipped ice may be considered to lower the concrete temperature.

10.8.3 Concrete Mixture Design

Concrete mixtures used for mass concrete should be proportioned in a qualified laboratory in accordance with ACI Committee 211.1-91 (*Standard Practice for Selecting Proportions for Normal, Heavyweight and Mass Concrete*; reapproved 2002). The materials used in concrete mix designs should be the same materials intended for use in the project. The compressive strength of concrete used for dams generally is low, 3000 psi to 3500 psi. The full design compressive strength is achieved 6 to 12 months after placement. In the case of mass structural concrete, the design compressive strengths are generally between 4000 and 6000 psi. The design strength is based on 28-day age.

10.8.4 Quality Control

Thorough quality control and quality assurance are essential for the proper execution of a mass concrete project. The selection and quality of ingredients to be used, batching, and placing of the concrete should be observed, and the necessary tests should be performed as per the applicable ACI and ASTM specifications. Equipment that allows rapid placement of large concrete quantities should be used to reduce the possibility of cold joints. The typical low-water, low-slump concrete used for mass concreting must be properly consolidated to eliminate cold joints and honeycombing. Segregation of aggregates must be avoided. Large-volume delivery systems are less susceptible to segregation than smaller volume systems. With minimum handling, there is less potential for segregation. Large-volume buckets with their wide discharge openings are effective means of delivering large quantities with minimum segregation. When it has been placed, the concrete must be properly vibrated to knit successive layers together in a joint-free matrix. Transportation of concrete using vibrators should not be done because of the potential for segregation. Preplacement planning must include the involvement of the concrete supplier to resolve potential problems such as truck breakdowns or the opposite—a backup of trucks leading to excessive mix time. Effective communication is an absolute must. Proper equipment maintenance greatly reduces the potential for breakdown. If a pump-delivery system is utilized, consider having a spare unit on-site to ensure an uninterrupted delivery to the point of placement.

10.9 On-Site Precasting and Tilt-Up Construction

On-site precasting is used in lift-slab, tilt-up, and miscellaneous general construction. Lift-slab on-site precasting consists of casting the floor and roof slabs on top of one another so they can be lifted into place once the columns and jacking equipment are in place. Section 10.10 discusses the lift-slab system in more detail, so specifics of the system are not discussed here. Site-casting of the slabs provides economies resulting from:

- Reduced formwork costs, as only edge forms are required and these are reused several times
- Reduced placing costs, as all of the concrete placement is at ground level
- Reduced curing and protection costs due to the limited surface area exposed to the elements
- Reduced reinforcing costs due to the considerable repetition from floor to floor and because the materials do not have to be hoisted to elevated floors
- Uniformly flat soffits of the slabs, thus simplifying design and installation of mechanical and electrical systems
- Favorable fire-resistance ratings that may be obtained without the application of fireproofing to the underside of the slabs

Several of these advantages can also be realized by site-casting specific structural members. In the northeastern portion of the United States, it is not unusual to site-cast concrete columns to be used with structural steel roof systems. The concrete columns provide favorable fire protection ratings while also providing high-capacity concrete members at a price that compares very favorably with structural steel columns. The site-cast columns can be made as durable as steel columns with respect to impact damage from material-handling equipment. The majority of site-cast concrete is used in tilt-up construction. In addition to many of the potential cost savings listed above, tilt-up construction can replace exterior structural steel with concrete bearing walls that can be architecturally treated at a relatively low cost. Figure 10.13 shows the various components and their arrangement along a bearing wall of a tilt-up building. Basically, the system consists of the following steps:

- Prepare the site and cast the footings.
- Cast the slab on grade, omitting a strip several feet wide around the perimeter of the building and erosion-control measures such as draping plastic sheeting over the exposed soil at the perimeter of the building between the exterior footings and the edge of the slab on grade.
- Place edge forms for the wall panels directly on top of the slab on grade.
- Patch any blemishes on the surface of the slab on grade, and temporarily patch all joints occurring within the area of the wall panels as these will read through onto the wall panels.
- Apply a high-quality bond breaker to the slab on the grade surface.
- Apply any architectural finishes that will be exposed on the surface cast against the slab on grade.
- Place reinforcing and tilt-up hardware, such as lift and bracing inserts, and place the concrete, using care to avoid shifting reinforcing, inserts, or architectural finishes.
- Apply curing compound or moist cure wall panels.
- Install bracing inserts in the slab on grade if they have not been previously placed.
- Place leveling pads on footings, and mark for transverse and longitudinal alignment.
- Tilt up wall panels and lift into position using a suitably sized rubber-tired moving crane.
- Brace wall panels to slab on grade using a system of pipe braces and dimensional lumber attached to the wall and slab at the appropriate inserts.
- Stabilize the base of the wall using concrete infill at the oversized shear key in the footing.
- Erect the structural steel; when the entire structure is plumbed and square, weld structure to tilt-up wall panels.
- Backfill around the exterior and interior of the perimeter footings.
- Extend the slab connection reinforcing from the wall panels and place the perimeter strip between the wall and edge of slab on grade.

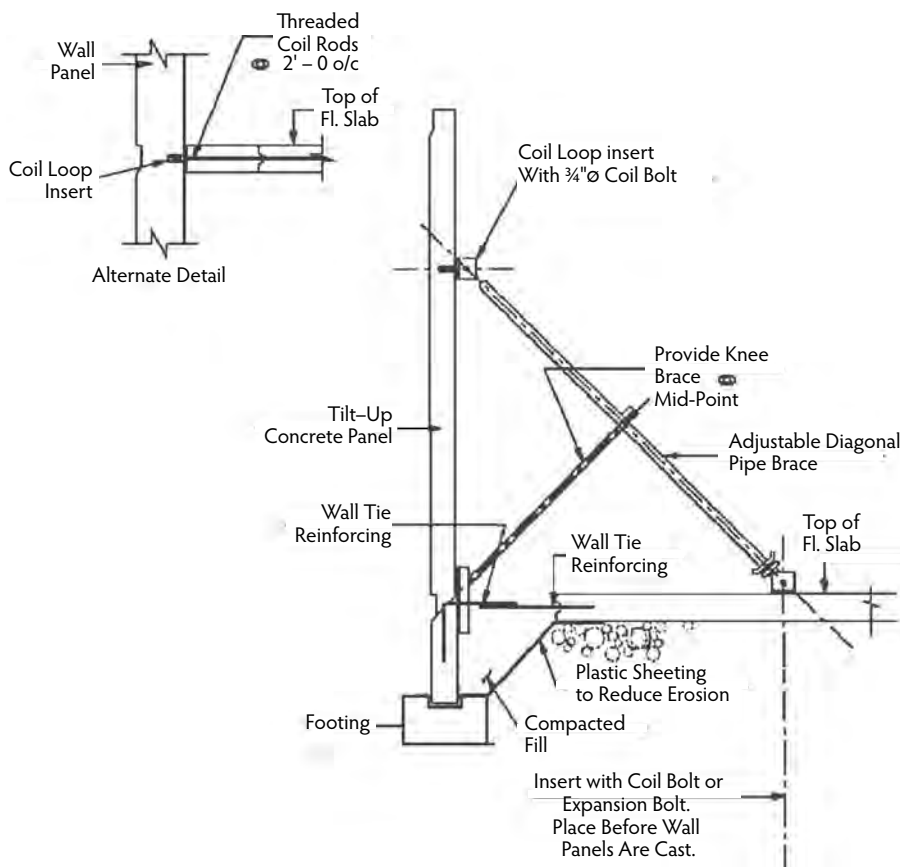


FIGURE 10.13 Typical panel bracing.

Although greater economies can be realized by using the system for bearing-wall construction, the system also deserves consideration when nonbearing walls are contemplated. The system usually becomes economical when the floor area is 40,000 ft² or more. Obviously, this threshold area will vary from region to region. The important requirement is to have adequate room to precast the panels on the floor slab. Local labor rates and work rules will also affect the viability of the system. In northern regions, it would not be prudent to begin a tilt-up project at the onset of winter or other anticipated extended periods of inclement weather. It is especially important not to leave a slab on grade that is exposed to freezing weather unprotected because of the possibility of the slab heaving. Irregularities in the slab such as this are difficult to remove and will read through to the wall panels. Typically the wall panels are cast so that when lifted the exterior panel face is cast against the slab or facing upward. Tilt-up panels are also cast on concrete site paving in addition to the interior slab on grade. Another option is to use temporary site casting beds or to stack cast the panels.

The exterior face-down casting position provides an opportunity to economically treat the exterior face of the panel if desired. Because the contact surface of the floor slab will in all probability contain blemishes, treatment of the wall panels may be more effective than the elimination of floor blemishes that might very well be acceptable for the intended floor use. Typical finishes for the panels include graphics formed into the surface, accents, aggregate finishes, or combinations thereof. Accent strips are constructed using inexpensive dimensional lumber. The exposed aggregates are placed on a layer of treated sand that is bounded by the accent strips. Prior to placing the surface aggregate the sand receives two applications of bond breaker to prevent the concrete from adhering to the sand or the aggregate. After the sand has been sprayed, the aggregates are carefully spread over the areas to receive the finish.

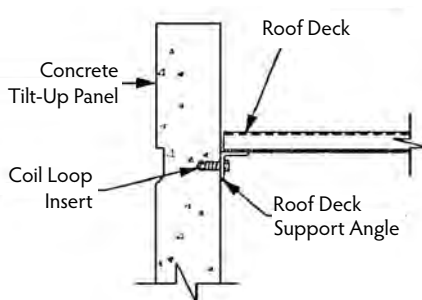


FIGURE 10.14 Alternative detail of transfer of lateral loads.

Care must be exercised during the placing operations to avoid displacement of the aggregates. Stainless-steel reinforcing accessories must also be utilized, or rust staining of the surface will occur. During the design, reducing thickness to accommodate the surface treatment of the panels must be considered.

Footings supporting the wall panels may either be continuous or discrete. If continuous footings are not utilized, additional horizontal reinforcement near the bottom of the panels must be provided to ensure adequate flexural capacity to enable the panel to span from footing to footing. In many cases, use of continuous footings is an option that results in ease of construction and reduction of potential for differential settlement.

Panel thicknesses are determined by the economics of reduced concrete and panel lift weight vs. additional reinforcing. Panel thickness is also related to the number and arrangement of lift inserts necessary to ensure that the flexural stresses are kept below the cracking level. Allowance for an increase in stress resulting from partial adhesion of the panel to the slab on grade, if a sand or aggregate layer is not used, should also be incorporated into the design. The panels will almost certainly be considered to be slender compression elements, requiring that the effects of panel deflection (P-delta) under lateral loads be considered in the analysis, in addition to global effects as a result of the diaphragm deflection. If the structural framing for the roof utilizes steel joists, the connection of the joist bottom chord to the panels should be avoided as the deflection of the joists will introduce a potentially large moment into the panels through the fixity of the top and bottom chords. It is more economical to consider the additional unsupported height in the design of the panel. If possible, seat the joists at or near the mid-depth of the panels to reduce the eccentricity of the loads supported by the panels.

Lateral loads can be resisted through horizontal diaphragm action in the roof structure. The lateral loads can effectively be transferred from the roof deck to the wall panels as shown in Figure 10.14. The angle is also a cost-effective replacement for a joist placed adjacent to the panel and simplifies roofing details through its zero displacement. Panels at corners should always be connected across the corner joint to ensure alignment. Panel joint connections elsewhere are a function of the need to engage more than one or more panels for overturning shear wall action. In addition, in high seismic areas, the continuous diaphragm chord is typically accomplished by connecting continuous rebar along the top of the panels across the joints.

10.10 Lift-Slab Construction

10.10.1 Introduction

The lift-slab method of construction was first introduced in the 1950s by Phillip N. Youtz, who later joined Thomas B. Slick to refine the design concept and construction techniques of his system. From this research, the original concept of lift-slab construction was introduced. The structural components of lift-slab buildings are no different from conventionally constructed buildings. The difference is how the building is erected. The procedure is to cast the concrete floor slabs, one on top of the other, on the slab on grade and lift them to their final elevation with hydraulic jacks (Russillo, 1988). Lift-slab concrete

construction is seldom used any more, so the following discussion is provided more as a historical reference. The first step is to prepare the site for construction and install the foundation system for the building, using normal construction techniques. The first level of columns is then erected on the foundation with the steel lifting collars in place. The columns are usually two stories high for economy. When all of the columns are in place, the concrete slab on grade is placed, allowed to set, and coated with a separating material. The first steel shear collar is then slid down the column and is aligned on the slab on grade. The slab reinforcing is installed, along with embedded electrical conduit and plumbing lines directly on the slab surface. The edge of the slab is formed, and finally the concrete is placed. The above procedure is repeated for each of the supported floors plus the roof. When the roof slab is completed, it is loaded with the upper column sections and the slab-lifting equipment. The lifting jacks are placed atop each of the columns and are connected to the roof-lifting collar by threaded rods. The roof slab is then lifted to the top of the column section and temporarily secured. With the roof slab in this position, the tops of the columns are braced and the column capacity is increased for the successive lifts. The upper level slabs are then lifted to the underside of the roof and are temporarily secured. The lower level slabs are lifted and are permanently attached to the column sections at their designated elevations. The lifting jacks are removed and the next column sections are erected. The jacks are then placed on top of the next column section, and the lifting sequence is repeated until all the floor and roof slabs are in their final position. When all of the slabs are secured to the columns, the exterior facade can be constructed, and the floors are ready to be fitted out.

10.10.2 Foundations

The process of lifting the precast concrete slabs does not impose any loads on the foundation system that are different from the design service loads. No special foundation requirements are necessary for this type of construction. The foundation type is selected and proportioned based on the geotechnical characteristics of the project site and the dead loads and service live loads anticipated for the occupancy of the building. The concrete slab on grade is to be placed and finished based on the requirements of its end use. Note that the finish of the slab will be reflected on the ceiling above. Any depressions in the slab on grade for floor finishes can be filled with lean concrete to prevent them from being reflected on the ceilings above.

10.10.3 Columns

The columns for lift-slab buildings are usually steel wide-flange shapes, but precast and cast-in-place concrete columns have also been used. Our discussion here is limited to steel wide-flange shapes, although concrete columns are similarly erected. The length of the column sections is usually two stories high and is limited by the design column section and the length of the lifting rods supplied by the contractor. No limiting column-spacing requirements are imposed by the lift-slab process. It is controlled by architectural layout, span of the slabs, and the loads supported by the slab. The lift-slab contractor may, however, limit the total area to be lifted at a time, thus dividing the slab into sections. This is determined by the number of jacks and support equipment available to the contractor. The boundary between two adjacent slabs is known as a *pour strip*. After the slabs are lifted into place, these areas are formed and concrete is placed to complete the floor system.

10.10.4 Supported Slabs

The concrete slabs used at the inception were conventionally reinforced two-way flat slabs. These slabs worked well, were easy to construct, and were sized to eliminate drop panels. This limits formwork to blockouts for the mechanical chases and perimeter-slab edge. The major drawbacks with conventional two-way slabs are that they are thick and heavy and their spans are relatively short. Today, most slabs are two-way flat plates that are post-tensioned. Post-tensioned slabs are thinner for the same loading conditions or have greater capacity for the same span and slab thickness. The slabs are generally the

same, whether the building is lift-slab or conventionally constructed. The advantage is obtained by casting all the slabs at grade level, one on top of the other. It is not necessary for large cranes to hoist material to the elevated floors, a man lift is not required, the time required to move material is reduced, and the fall hazard for the workmen is nearly eliminated.

10.10.5 Lifting Collars

Lifting collars, threaded onto the columns prior to erection, are centered on each column and cast into each of the supported slabs. The original steel castings were found to be expensive and had limited lift capacity. Today, lift collars are exclusively steel sections that are welded with full-penetration welds. The purpose of the lift collar is threefold: It connects the slab to the lifting jack via a threaded rod, attaches the slabs to the columns for load transfer, and acts as shear reinforcement in the slabs (shear heads) to eliminate drop panels in the thinner post-tensioned slabs.

10.10.6 Lifting Jacks

The lifting jacks used to raise the slabs are mounted to the top of each of the columns and are attached to the slab by two threaded rods. The jacks are hydraulic and are driven in such a manner that they lift in unison at a rate of 4 to 10 feet per hour. This is to eliminate damage to the slabs as they are being lifted.

10.10.7 Critical Component Design

The design of the structural components of a lift-slab building is, for the most part, the same as for a conventionally constructed building. The differences occur in the critical components such as the lifting collar, the slab at the column connection, and the columns, which need to be checked for all conditions and end restraints during construction.

10.10.7.1 Columns

The columns of a building utilizing the lift-slab method of construction serve a dual purpose in that they support the building in its final position, braced at each floor by the slab, and they are used to support the lifting jacks during positioning of the slabs. The columns require analysis for all the load cases proscribed by local building codes as well as for construction loads. During jacking of the roof slab, the columns are freestanding, with base fixity achieved by the base plate detail and encasement of the columns by the slab on grade. The stage during which the roof slab is lifted up along the freestanding columns is the most critical condition. The column sections must be sized for this condition as well as for conditions during successive lifts. The first load condition is best checked using Euler's column formula for columns fixed at the base and free at the top:

$$P_{(all)} = \frac{\pi^2 EI}{4L^2 (F.S.)}$$

where:

- $P_{(all)}$ = allowable load (kips).
- E = modules of elasticity (kips/in.²).
- I = moment of inertia (in.⁴).
- L = column height (in.).
- F.S. = factor of safety.

When the roof slab is at the top of the column section and has been secured (temporarily or permanently), the slab connects all of the columns together and fixes the top of the column section. The column condition now becomes fixed at the bottom and fixed against rotation at the top but is allowed to translate laterally. This condition reacts the same way as columns that are pinned at both ends and is analyzed using the following column expression:

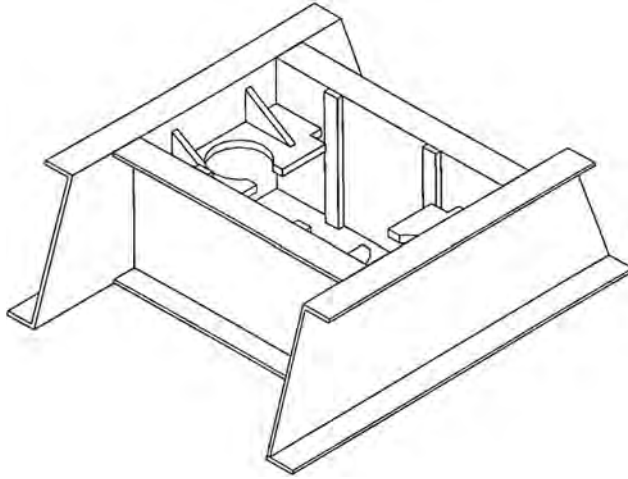


FIGURE 10.15 Lift collar in lift-slab construction.

$$P_{\text{(all)}} = \frac{\pi^2 EI}{L^2 (\text{F.S.})}$$

The capacity of the columns at this stage quadruples. This extra capacity in the columns may allow a number of slabs to be lifted simultaneously.

10.10.7.2 Lift Collar

Lift collars (see Figure 10.15) must be designed to perform adequately for multiple purposes. The collar is sized to transfer the construction loads imposed on the slabs to the lifting jacks and all of the service loads to the column. Finally, the collar must be sized to reinforce the slab to keep the diagonal tension stresses in the slab below the allowable stress dictated by the building code. The design of the collar also depends on the forces to be transferred from the slab to the column. Depending on the designers assumptions, the forces could be shear only, shear with partial-moment transfer, or shear with full-moment transfer. The design of the lift collar is the responsibility of the lift-slab contractor. The design engineer should note the type of collar desired and anticipated design forces on the design documents.

10.10.8 Applications

The lift-slab method of construction is best suited for buildings whose column layout is ideal for two-way post-tensioned concrete slabs. Although higher structures have been lifted, up to 20-story buildings are the best candidates. The exterior facade does not affect the decision as to whether this system should or should not be used. Constricted construction sites warrant investigation of the lift-slab method because large track-mounted tower cranes are not required. When construction of the superstructure is scheduled to occur during cold seasons, this approach becomes economical in that when the foundation is completed and the columns have been erected a shelter can be constructed and heated to provide a protected work area.

10.11 Slip-Form Construction

10.11.1 Introduction

Vertical slip-form construction is a process of placing concrete continuously with a single form that is constructed on the ground and raised as the concrete is cast. Casting is done at a rate that prevents the formation of a cold joint in previously placed concrete. The result is a continuous placing sequence

resulting in a monolithically erected wall with no visible joints. This construction process utilizes lifting jacks located on the ground or on the working platform that elevates the form and the workers' scaffolding attached with smooth rods or pipes. These rods or pipes are embedded in the hardened concrete. The construction technique is similar to an extrusion process.

The die (slip form) moves upward as it extrudes the concrete wall. The rate of the extrusion process is controlled by the setting time of the concrete and the crew's ability to prepare the wall for the pour. The average time of lift for any project is 6 to 8 in./hr, placing approximately 4- to 10-in. layers of concrete per lift; however, the time varies anywhere from 2 to 4 in./hr for the lower levels of a nuclear reactor containment structure to 20 to 50 in./hr for an underground shaft lining. The project foreman looks for zero slump from the 4- to 10-in. layer below the layer being placed.

It is important to note that, when this construction procedure is utilized, the concrete wall being slipped through supports only its own weight. The jacking rods located in the wall support the weight of the slip-form structure. The concrete keeps the jacking rods from buckling. In some cases, the jacking rods become part of the permanent structure. The other alternative is to have the jacking rods slip through a thin pipe sleeve as the form slips upward. Engineers designing these walls should not rely on the steel rods for reinforcement due to lack of bond between the bars and the concrete.

Slip-form construction, even though in a state of continuous motion, can be interrupted by weekends and evenings simply by extruding the form away from the poured wall as it sets. The form should never be allowed to adhere to the concrete. Slip-form construction is used for various applications, such as bridge piers, building cores, apartment-house shear walls, chimneys, communication towers, cooling towers, and silos, among many other applications. In many cases, the procedure can be used to erect a structure in half the time of conventionally formed work. In addition, the working platforms rise with the form and reduce the labor costs of dismantling and re-erecting scaffolds at each floor. Close inspection of the concrete must be performed at all times to ensure elimination of blowout (concrete plastic state) or bonding of concrete to the slip form during the construction process.

10.11.2 Materials and Methods

The major components of a slip-form assembly consist of lifting jacks and rods, yokes, wales, sheathing, a working platform, and suspended scaffolding (see Figure 10.16). All components, with the exception of the lifting jacks and concrete, climb integrally when the form is elevated. The lateral loads of the form are transferred through the sheathing and wales, which are supported by the yokes. The vertical loads of the scaffolding and platforms, in addition to live loads (equipment), are carried by the wales and transmitted to the yokes and into the jacking rods embedded in the concrete. The weight of the concrete acts as a lateral support to the rods.

The **lifting jacks** provide the forces that lift the forms upward. The three types of jacks are screw, hydraulic, and pneumatic, with hydraulic being the most common. Hydraulic jacks range anywhere from 3 to 25 tons/jack in uplift force. Care must be taken to properly position the jacks. The dead and live loads dictate the size and number of lifting jacks required for the application. All jacks must lift equal weight; otherwise, distortions in the wall will result in excessive stress to the yokes at certain locations. Operations must include quality control to avoid excessive live loads concentrated in an area of the working platform.

Jacking rods require careful design as well. These rods provide the required support of the slip-form structure and are located in the poured concrete wall. If they remain in the wall, they have reduced or minimal bond strength and should not be designed as a typical reinforcing rod. The rods can be salvaged by sliding them through a thin metal sleeve attached to the yoke. The rods must be vertical at all times when placed in the walls. This will prevent buckling of the rods in the concrete as the form rises.

The **yokes** are connected to the lifting jacks and consist of a horizontal member and two yoke legs. Depending on the design of the wall, the yoke should be engineered to compensate for the loads that will be applied to it. The yoke acts as a clamp holding the wales and sheathing in place, and it transfers the weight of the entire slip-form assembly directly onto the vertical jacking rods. In addition, the

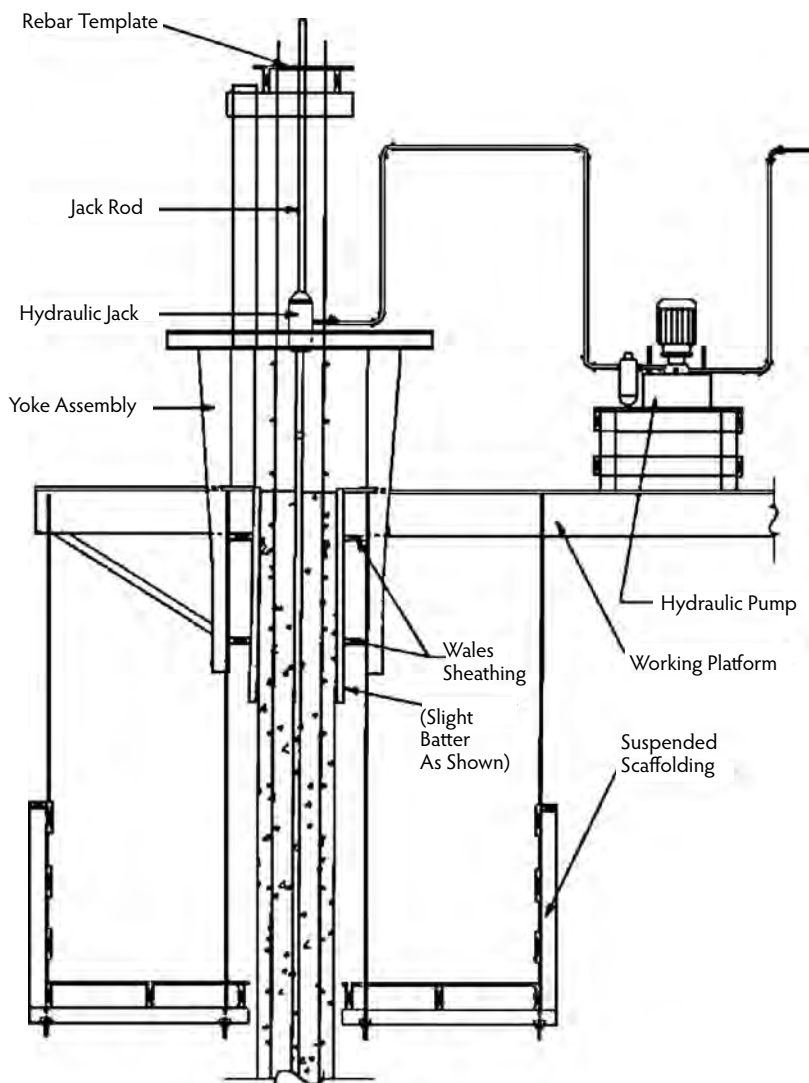


FIGURE 10.16 Lifting jack assembly.

yokes support the reinforcing steel of the concrete wall. The yoke has to support the lateral pressure of concrete as per the ACI standard, which is described in the following formula:

$$p = 100 + \frac{6000R}{T}$$

where:

p = maximum lateral pressure (lb/ft²).

R = rate of concrete placement (ft/hr).

T = temperature of concrete forms (°F).

Additional frames or false yokes are sometimes located between the yokes. The primary difference between the two is that the false yokes do not transfer the vertical loads onto the jacking rods; instead, the false yokes only support the lateral loads transmitted through the wales.

The **wales** are the longitudinal supports for the sheathing. An upper and a lower wale are usually located on each side of the concrete wall. More wales should be provided if the form height warrants the additional support. Normally, this is a height exceeding 4 ft. The wales resist the loads and transfer these loads directly to the yokes. The wales must be engineered to withstand the ACI lateral pressure requirement as indicated previously. In addition, ACI Committee 347 (2005) also requires that tolerances be maintained for the finished structure. The variation of wall thickness cannot be greater than $\pm 3/8$ in. for walls up to 8 in. thick or $\pm 1/2$ in. for walls thicker than 8 in.; therefore, good engineering practice must be applied in the design of these forms. As per ACI SP-4, timber wales should be a minimum of two- or three-ply lumber or at least one ply of 2-in. material; when the span between jacks approaches 10 ft, the wales should be braced to act as a truss in the vertical plane between yokes. For curved walls, the minimum depth of segmental wales should be 4-1/2 in. at the center after cutting. Peurifoy (1995) discusses in depth the formwork for concrete structures.

The **sheathing** is the vertical support in direct contact with the concrete. Swelling of sheathing must be controlled because the sheathing is in continuous contact with moist concrete for the duration of the construction. Protecting sheathing prior to construction should be accomplished either by presoaking lumber or with a waterproofing preparation. In many cases, a nonabsorbent surface that can withstand moisture and temperature conditions is selected. Sheathing should be higher on the exterior face of the form to avoid splashing materials onto workers on the scaffolding below. As per ACI SP-4, forms should be constructed of at least 1-in. board, 3/4-in. plywood, 10-gauge steel sheet, or other approved material. The sheathing, when constructed, should have a slight batter to it. This will enable the forms to self-clear. The batter should be tapered inward at the top of the form and tapered outward at the bottom of the form. The middle area of the sheathing is the finished dimension of the concrete wall. The height of the form is usually 4 ft. The sheathing is kept well oiled as it rises to eliminate excessive drag forces. The construction engineer should compensate for this additional vertical load in the design.

The **working platform** houses all of the construction equipment necessary for the form to advance. The platform also keeps the poured walls square. Care should be taken in the design of the platform. A minimum of 75 psf is recommended for design. In addition, concentrated buggy loads must be considered. **Suspended scaffolds** are located below and on either side of the form. They provide a work area that enables work crews to finish the concrete wall that has been placed. Because the concrete is still wet, it is workable.

10.11.3 Advantages and Disadvantages

One disadvantage is that the monolithic pour precludes the placement of floors during the extrusion process. Horizontal reinforcing protruding through the walls cannot be placed until the slip form passes through the wall. Provisions can be incorporated to prepare for floors, corbels, or openings (see Figure 10.17). This is accomplished by blockouts. The crews provide openings or pockets by creating forms within the form. Quality control is of considerable importance. Care must be taken to lift the form at the right time. As a result, the construction procedure requires skilled laborers and experienced project management. Placing concrete too quickly can result in a blowout and too slowly can cause the concrete to adhere to the form, which could damage the wall as well as the form. Construction engineering is an important aspect of the overall procedure. Careful preparation and analysis should be undertaken prior to construction. Temperature and climatic conditions are all factors that must be incorporated in the design of slip-form construction. All of the above incur additional costs for the project as opposed to using conventional forms. Another disadvantage is the difficulty of inspecting the wall, as steel is placed only a few feet above prior to the pour. The advantage of slip-form construction is the speed at which a wall can be erected. A slip-formed wall can eliminate up to 3 months of construction, compared to conventionally formed work, and the wall is free of horizontal joints. The taller the building, the more cost effective the system can be. The level of safety is greatly increased when utilizing the slip-form process. Preparation for the process must be carefully carried out by well-trained and skilled individuals. As a result, all staging is eliminated and the working areas only have to be built once.

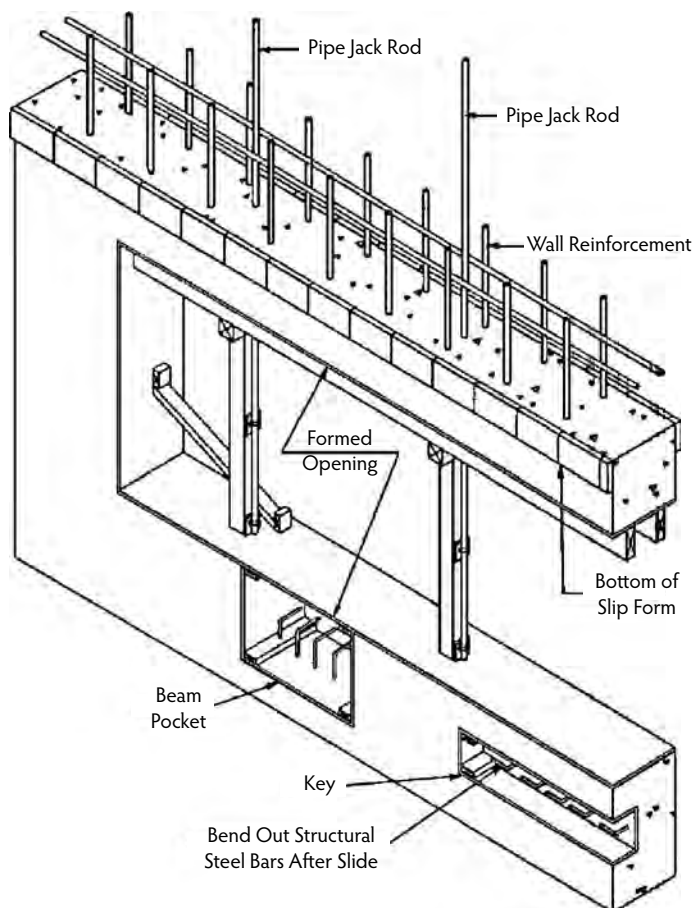


FIGURE 10.17 Blockouts for floors, corbels, and openings.

10.11.4 Economy

Slip-forming tall cores (in excess of 12 stories) can greatly reduce the cost of construction. Only one form has to be built which can often be reused for every level to the top. The cost of forms per contact area is greatly reduced. The overall question of cost, however, is difficult to address due to varying costs with regional conditions, available skilled labor, and the complexity of the project. This issue must be evaluated by the conditions that dictate the design and the location of the site.

10.12 Prestressed Concrete

10.12.1 Introduction

When gravity loads are applied to a flatwork element (slab or beam), moments and shears are created within the element. Applied moments are resisted by the development of a force couple within the element section. The couple consists of a tension and a compression force, each occurring on opposite sides of the neutral axis within the section. Shears are resisted by the effective concrete area of the section; at times, supplemental resistance is provided by shear-reinforcing steel.

In conventional concrete design, the moment-resisting couple is essentially the only resistance to bending moments; thus, the proportioning of the section dimensions, in association with the sizing of adequate reinforcing steel, must be sufficient to resist the applied moments, with tension stresses often

being the limiting design criterion. By designing so tension stresses are resisted by mild steel reinforcement, the failure mode of an element will be ductile and gradual, giving ample warning of precipitating failure. This is ensured by designing all beams, slabs, and plates as under-reinforced; that is, the reinforcement percentage does not exceed 75% of the balanced condition—in most cases, not more than 50% to prevent congestion of reinforcement.

Pretensioned (precast) and post-tensioned concrete design, generally grouped as prestressed design, involves an additional form of resistance to the applied moments and shears. By externally applying a compressive force to the element, the stress distribution over the section is dramatically altered. The compressive force acting on the section reduces the tensile stresses at the tension zones, thereby preventing cracking and also increasing considerably the diagonal capacity of the section. This permits the section size to be reduced while keeping the total resulting stress within the allowable range. Chapter 35 of this *Handbook* gives the basic expressions for the stresses and diagrams of stress distribution across the depth of a prestressed beam as affected by the external compressive prestressing force (see also Nawy, 2003, for details regarding the design of prestressed concrete structures).

The use of prestressing methods can allow the designer to reduce section proportions while carrying the same or larger load as a conventionally reinforced concrete section, which results in a corresponding reduction in cost in terms of the gross volume of concrete. The designer must acknowledge that the prestressing equipment, materials, and installation can, in some circumstances, cause the total construction cost to exceed that of conventionally reinforced concrete. Preliminary cost/benefit analysis is advisable before deciding to use a prestressing system, provided that other requirements of span and load might necessitate the use of a prestressed concrete design.

10.12.2 Pretensioned (Precast) Concrete

Prestressed concrete generally falls into two groups: pretensioned or precast concrete and post-tensioned concrete. Precast concrete usually is made in off-site casting plants and may or may not include prestressing. Construction elements ranging from hollow core slabs to T sections to architectural wall panels are regularly precast. Precasting offers the controlled environment of a plant, which results in very consistent production in terms of quality and delivery speed. Precast plants work with heated, steel form beds with polished form surfaces. The quality of the concrete is controlled and is usually 5000 psi or higher. The color, consistency, and dimensions of precast elements are usually of better quality than can be produced in the field. Concrete admixtures, to achieve rapid set and also to gain durability advantages, are frequently added to produce higher quality concrete.

As noted earlier, precast concrete can be either prestressed or not. Conventionally reinforced precast concrete is most frequent in wall panels, columns, and miscellaneous elements such as highway dividers. Prestressed elements are most frequently produced for structures carrying high loads, bridging long spans, or subjected to harsh environments. In these cases, the precompression force improves both load-carrying performance by reducing tension stresses and durability by closing surface cracks on the tension face that might allow the intrusion of corrosive salts or chemicals.

Where prestressing is used in precast applications, bonded prestressing is usually used. Bonded prestressing consists of placing high-tensile-strength (270-ksi) wire strands, or bundles, in the setting beds prior to pouring the concrete. The strands are then tensioned by jacking them tight against a rigid frame at the head and foot of the setting bed. When the required jacking force has been introduced to the strands, fresh concrete is poured into the bed in direct contact with the strands. As the concrete sets, the strands become bonded to the concrete.

The initial jacking force introduced to the strand is released into the precast element via the bond between the strand and the concrete. This produces a fairly even distribution of compressive stress along the length of the member. In addition, because the bond is continuous along the length of the member, a bonded precast element can be cut into smaller pieces without losing the precompression force.

The designer is cautioned that the latter characteristic of precast concrete is only applicable where the strand drape is flat, thus producing an even precompression force over the entire length of the element.

Where the strand drape is not flat (discussed further below), the influence of the jacking process will be to introduce both a precompression force and an internal moment into the element. In such a case, cutting the element could result in the loss of the internal moment, as it would not be resolved by the balancing remainder of the element that has been cut away. In practice, hollow-core plank is frequently cast in long lengths, with an essentially flat strand. The plank is then cut to the appropriate length for project needs. Some forms of wall panel are also produced in this fashion; however, where strict quality control is required to ensure proper architectural appearance, each precast member is usually cast alone.

When designing precast concrete sections, the designer must be cognizant of several forces that act on the member during its life. It is not sufficient to simply analyze the service loads to be applied once the member is situated in its final position. Because concrete cures over a period of time, the relative strength of a concrete member changes as the concrete strength increases; thus, loads that are applied to a member shortly after casting could cause stresses that exceed the capacity of the member at that specific moment in its life.

The designer must therefore consider three types of loads that act on every precast member at some point. First are stripping stresses, created when the casting forms are released. This action causes suction forces that can induce large, concentrated tensile stresses in the concrete. Second are transport stresses, created from lifting and stacking the members for transport around the casting yard and to the job site. Lifting lugs are frequently cast into the precast members to provide a location for the attachment of lifting equipment. The use of strategically located lifting lugs allows the designer to anticipate and design for the stresses that result from moving the members. Last are service stresses, which occur as a result of the design loads that are expected to act on the structure, determined by its use classification. These are the traditional design loads that must always be addressed.

When precast elements arrive at the job site, they are erected piece by piece and bearing pads are used to separate the elements. Precast concrete shop drawings specifically detail all of the connections between the precast pieces and any other structural members. Local stress concentrations must be taken into consideration during the design process to address conditions where ledges or corbels will support adjoining members.

In certain applications of precast concrete, a final cast-in-place concrete topping is applied when the precast superstructure has been erected. This is typical in precast plank or double-tee construction, where a consistent, durable wearing surface is required. The topping course (typically, 2 to 3 in. thick) is sometimes reinforced with welded wire fabric, thus providing catenary reinforcement, which aids in the distribution of loads over the entire floor system.

10.12.3 Post-Tensioned Concrete

While pretensioning is generally conducted in a plant setting, post-tensioning is mostly conducted in the field. The “post” term is something of a misnomer, as the precompression force introduced into the concrete is added prior to the introduction of any load on the structural system. The term has evolved, however, because the procedures occur at the construction site rather than at a precasting plant and thus are “post” because the members are not brought to the site ready to install. Post-tensioning design follows the same procedures and expressions used in the design of pretensioned elements except for prestress losses. By introducing a precompression force into the concrete section, the maximum tensile stress is reduced by the compressive stress, thereby permitting the use of smaller sections that support the same loads as conventionally reinforced concrete members. Construction procedures can be considered an extension of those used in traditional cast-in-place (*situ*-cast) concrete. Formwork must be erected to support the fresh, poured concrete; mild reinforcing steel must be placed to provide system ductility; and site curing procedures must be followed to ensure that quality, final concrete is produced. The concrete stresses permissible in flexural prestressed members occur at three load levels: stresses occurring immediately after prestress transfer, stresses at service load, and stresses at the ultimate load level. Section 18.4 of the ACI 318-05 Code presents the permissible stresses at the extreme fibers of the members for these loading stages. Also, Chapter 11 and Chapter 12 in this *Handbook* and *Prestressed Concrete: A*

Fundamental Approach by Nawy (2003) address most of the design and construction aspects pertinent to pretensioning and post-tensioning beams and one-way and two-way slabs and plates. It is important to recognize that, in two-way slab design, attention must be given to re-entrant corners, large openings, L-shaped plan configurations, balconies, repetitive perimeter openings, or steps in slab elevations. Each of these conditions poses a difficult design problem if conventionally reinforced concrete is used. The problems are multiplied when the system is precompressed and compelled to shorten. Cracks can rapidly develop at corners, and localized crushing of concrete can occur, particularly due to stress concentration at these locations. To counter this condition, significant mild steel reinforcement has to be provided to prevent cracking propagation at the early stages of post-tensioning or loading.

Acknowledgments

This is a revised and updated version of the original text, which was authored by the late Terry O. Blackburn, P.E., Ph.D., former Principal and Director, Structural Department of Schoor DePalma, Engineers and Consultants, Manalapan, New Jersey. The author wishes to extend deep appreciation to D. Matthew Stuart, P.E., S.E., F. ASCE, SECB, and Delcho Palechev for their contributions to updating the chapter and to all of the author's coworkers at the Structural Department of CMX, Inc.

References

- ACI Committee 224. 2001. *Control of Cracking in Concrete Structures*, ACI 224R. American Concrete Institute, Farmington Hills, MI.
- ACI Committee 318. 2005. *Building Code Requirements for Structural Concrete*, ACI 318-05 and ACI 318R-05. American Concrete Institute, Farmington Hills, MI.
- ACI Committee 347. 2005. *Formwork for Concrete Handbook*, 7th ed., SP-4. American Concrete Institute, Farmington Hills, MI.
- ACI Committee 352. 2002. *Recommendations for Design of Beam–Column Connections in Monolithic Reinforced Concrete Structures*, ACI 352R. American Concrete Institute, Farmington Hills, MI.
- ACI Committee 372. 2003. *Design and Construction of Circular Wire- and Strand-Wrapped Prestressed Concrete Structures*, ACI 372R. American Concrete Institute, Farmington Hills, MI.
- ACI Committee 373. 1997. *Design and Construction of Circular Prestressed Concrete Structures with Circumferential Tendons*, ACI 373R. American Concrete Institute, Farmington Hills, MI.
- AISC. 2005. *Steel Construction Manual*, 13th ed. American Institute of Steel Construction, Chicago.
- ASCE. 2005. *Minimum Design Loads for Buildings and Other Structures*, SEI/ASCE 7-05. American Society of Civil Engineers, Reston, VA.
- ASTM. ASTM Standards C33, C150, C311, C494, C618 (referred to in the text). American Society for Testing and Materials, Philadelphia, PA.
- Billington, D.P. 1982. *Thin Shell Concrete Structures*. McGraw-Hill, New York.
- ICC. 2006. *2006 International Building Code*. International Code Council, Washington, D.C.
- Nawy, E.G. 2003. *Prestressed Concrete: A Fundamental Approach*, 4th ed. Prentice Hall, Upper Saddle River, NJ.
- Peurifoy, R.L. 1995. *Formwork for Concrete Structures*, 3rd ed. McGraw-Hill, New York.
- PCA. 1992. *Circular Concrete Tanks Without Prestressing*. Portland Cement Association, Skokie, IL.
- PCA. 1998. *Rectangular Tanks*. Portland Cement Association, Skokie, IL.
- Russillo, M.A. 1988. Forming economical concrete buildings: lift-slab construction—its history, methodology, economics, and applications. In *Proceedings of the Third International Conference*. ACI/ASCE/TMS, Farmington Hills, MI.
- Timoshenko, S. and Woinowsky-Krieger, S. 1959. *Theory of Plates and Shells*. McGraw-Hill, New York.
- Young, W.C. 1989. *Roark's Formulas for Stress and Strain*. McGraw-Hill, New York.



(a)



(b)

(a) Float-in dam segment for Braddock Dam on the Monongahela River upstream of Pittsburgh, Pennsylvania. (Photograph courtesy of U.S. Army Corps of Engineers.) (b) Segment erection for the new San Francisco Bay Bridge Skyway Segment. (Photograph courtesy of KFM Constructors Joint Venture.)

11

Construction of Prestressed Concrete

Ben C. Gerwick, Jr., P.E., S.E.*

In Memoriam

Professor Ben C. Gerwick, Jr., a world authority and pioneer in prestressed concrete, died December 25, 2006, a month after he so graciously expanded, upgraded, and completed the revision to this chapter which he originally wrote for the previous edition of the *Handbook*. He is fondly remembered as a prolific author of papers and books and as a foremost expert in the innovational designs of offshore-prestressed concrete structures.

11.1	Introduction	11-1
11.2	Concrete and Its Components	11-4
	Aggregates • Cementitious Materials • Admixtures • Water • Batching of Concrete • Mixing of Concrete • Transporting and Placing • Consolidation • Curing • Testing	
11.3	Reinforcement and Prestressing Systems	11-8
	Reinforcing Steel • Prestressing Tendons and Assemblies • Anchorages and Splices • Ducts	
11.4	Special Provisions for Prestressed Concrete Construction	11-13
	Concreting in Congested Areas • Special Reinforcement at Location of Curvature of Prestressing • Tendons • Special Reinforcement to Distribute Anchorage Zone Strains • Embedments • High-Performance Concrete • Lightweight Concrete • Modified-Density Concrete • Composite Construction • Architectural Prestressed Concrete	
11.5	Post-Tensioning Technology	11-19
	Principles • Storage of Tendons and Anchorages • Installation of Ducts and Anchorage Bearing Plates • Installing and Stressing Tendons • Scaffolding and Falsework for Post-Tensioned Cast-in-Place • Construction • Corrosion Protection of Tendons • External Tendons	
11.6	Pretensioning Technology	11-24
	General • Description of Process • Tendon Installation and Stressing • Forms • Concreting • Curing • Release of Prestress • Cycle • Tendon Profile	

* Professor Ben Gerwick was Chairman of Ben C. Gerwick, Inc., San Francisco, California; Professor of Construction Engineering at the University of California, Berkeley; Past President of the International Association of Prestressed Concrete (FIP); and Honorary Member of the American Concrete Institute.

11.7	Prestressed Concrete Buildings	11-29
	General • Precast Pretensioned Concrete • Cast-in-Place Post-Tensioned Buildings	
11.8	Prestressed Concrete Bridges	11-33
	General • Precast Pretensioned Bridge Girders • Post-Tensioned Girders, Cast-in-Place on Falsework • Post-Tensioned Precast Segmental Bridges • Cast-in-Place Cantilever Segmental Bridge Construction • Precast Cantilevered Segmental Construction • Incremental Launching • Lift-In and Float-In Erection • External Tendons for Bridges	
11.9	Prestressed Concrete Piling	11-46
	General • Durability of Piles • Manufacture • Pile Installation	
11.10	Tanks and Other Circular Structures	11-54
11.11	Prestressed Concrete Sleepers (Ties)	11-55
11.12	Prestressed Concrete Floating Structures	11-56
11.13	Prestressed Concrete Pavements	11-58
11.14	Maintenance, Repair, and Strengthening of Existing Prestressed Concrete Structures	11-58
	Maintenance • Repairs • Strengthening Existing Structures	
11.15	Demolition of Prestressed Concrete Structures	11-60
11.16	The Future of Prestressed Concrete Construction	11-61
	Acknowledgments	11-62
	References	11-62

11.1 Introduction

The effective construction of prestressed concrete structures requires the practical application and implementation of sophisticated engineering technology in a safe and reliable manner under the constraints of time, budget, and the external environment. It incorporates the assembly of materials, equipment, and personnel and the execution of the work so as to attain the results envisioned in the design. The key elements in prestressed concrete construction are the following:

- The production of concrete that has stable, predictable properties, not only of strength but also of creep, shrinkage, elastic modulus, and durability (high strength is essential to attaining efficiency of structural performance)
- The forming (molding) of concrete into the design shape and within the specified tolerances
- The incorporation of mild steel reinforcement, accurately placed and held during concreting
- The placement of high-strength steel wires, strands, or bars to fit the design profile and the stressing and anchoring and corrosion protection of such elements
- Installation of the composite structural elements or assemblages described above, in their final positions, whether they are cast in place or prefabricated

During construction, prestressed concrete passes through a number of steps or stages, each of which must be considered. Then, after attaining the designed state, it undergoes a lifetime of relatively subtle but cumulatively important changes. Although conventional reinforced concrete passes through a similar life history, the changes and the importance of the stages are generally far less dramatic, and the consequences of oversights are not as severe; hence, in this chapter, the emphasis is on the practical attainment of safety and stability. We are working with an active, rather than a passive, structural system.

Environmental conditions are given considerable emphasis. Important prestressed concrete structures have been completed and now serve in Arctic, temperate, and tropical zones. They are successfully employed in the ocean, in the urban environments of large cities, and in remote deserts. Prestressed



FIGURE 11.1 Prestressed concrete cantilever segmental bridge over the Columbia River Bridge on I-5.



FIGURE 11.2 Statfjord B offshore platform with prestressed concrete shafts. (From Gerwick, B.C., Jr., *Construction of Prestressed Concrete Structures*, John Wiley & Sons, New York, 1996. With permission.)

concrete is used in buildings; bridges (Figure 11.1); offshore platforms (Figure 11.2); liquefied natural gas (LNG) import facility floating structures; towers; poles; tanks; wind, wave, and current energy structures; and railroad sleepers. Each of these uses has its own special criteria and practices. Each has its own constraints and limitations. The reliable performance of prestressed concrete (that is, its durability) throughout its design life requires careful consideration during design and construction. The requirements for such widespread use can be summed up in a few key words:

- Reliable, stable material properties
- Full consideration of the stages of construction of a prestressed concrete structure
- Durability with regard to long-term performance and serviceability

Various authorities have issued their precepts or commandments. These generally include the following:

- When prestress is applied, the concrete element must be allowed to shorten in the direction of the prestress. If the structure is restrained from shortening, it will not be prestressed.
- When the prestressing tendon is curved, it exerts a radial shear force.
- Prestressing applied to concrete too soon after casting, before it has gained strength and maturity, will lead to excessive creep. Prestress applied too late after concreting may result in extensive shrinkage cracks.
- Prestressing eccentric to the centroid of the concrete section produces bending. This bending (e.g., camber) tends to grow with age due to creep.
- The energy and hence force induced in a prestressing tendon by stressing are very large and result in a temporarily dangerous missile; safety precautions are essential.

11.2 Concrete and Its Components

The concrete material components must meet the general requirements for construction of reinforced concrete structures and, in addition, must usually conform to more stringent requirements to attain the design objectives.

11.2.1 Aggregates

Coarse aggregates are usually siliceous or limestone. Both gravels from riverine deposits and crushed rock are used. Desirable properties are hardness, soundness, nonreactivity, surface roughness, cubic as opposed to plate cleavage, low water absorption, and impermeability. Slightly reactive aggregates may often be utilized in specific applications if the proper chemistry of the cementitious materials is selected. Some limestones are not only porous but also permeable; their use in marine structures requires special actions to preserve durability. Lightweight (ceramic) aggregates are used extensively. Those of high strength, low creep, and low absorption are most appropriate to prestressed concrete application. Fine aggregates may be from natural deposits or they may be crushed from coarse aggregate. In any event, screening will be necessary to ensure a proper proportion of coarse sands and a suitable grading curve, preferably with a low percentage of the fine fractions, as a mix rich in cementitious material will fill the interstices while an excessive percentage of very fine particles will have a high water demand. The aggregates must be clean and free from salt and dirt. They should be properly stored above ground and protected from snow and ice and from excessive heat. Shielding from the sun may be provided by portable sheets of galvanized metal on temporary posts in the aggregate pile. To a large degree, cooling of aggregates may be accomplished by evaporation. A water soaker hose may be effective. Conversely, aggregates should be above freezing when batched. They may be heated by steam. Care must be taken to avoid accumulation of ice in the aggregate, whether by snow or the freezing of condensate, as ice particles may be unintentionally weighed and batched as coarse aggregate. Aggregates, both fine and coarse, should not contain or be encrusted with salts and silt. Washing is usually required, preferably with fresh water; but, if fresh water is not available, even brackish water can be used to remove the condensed salt crystals and silt.

11.2.2 Cementitious Materials

The practical construction of prestressed concrete is based on the use of Portland cement as the principal cementing agent. American Society for Testing and Materials (ASTM) cement Types I, II, and III are used. Type I can be used in geographical areas and applications where sulfate attack is not a problem. Type II, with closer control over the constituent compounds, especially tricalcium aluminate (C_3A), is widely employed where durability is a concern. Fly ash and metakaolin are pozzolanic materials that gain strength over a longer period of time than cement. They can be substituted for up to 20% or more of the cement. The silica of the fly ash binds up the soluble calcium hydroxide, substantially increasing impermeability. It also provides resistance to sulfate attack and alkali-aggregate reactivity while lowering

the heat of hydration and reducing thermal strains. Fly ash requires a separate silo and should be weighed separately from the cement. In some areas, fly ash is interground with the cement. For proper strength gain, continuous moisture is essential over an extended period of up to 30 days. This is usually best obtained by wet curing for 3 days followed by sealing with one or two coats of membrane-sealing compound. Finely ground blast-furnace slag (BFS) can be used with a limited portion of Portland cement to act as an efficient cementitious material with low heat of hydration and low permeability. Mix proportions of BFS to cement range from 50–50% to 70–30%.

11.2.3 Admixtures

Many revolutionary new admixtures are commercially available. The most important are water-reducing agents, especially high-range water reducers (superplasticizers), air-entraining agents, and microsilica, called *silica fume*. Corrosion-inhibiting admixtures, retarding admixtures, pumping aids, and viscosity admixtures are also available. Tests mixes are essential to ensure that the admixtures selected are compatible with the particular cement and other admixtures. The use of high-range water reducers (superplasticizers) is the best way to achieve the low water/cementitious material ratios essential for high-performance concrete. The usable life of high-range, water-reducing admixtures is typically 1-1/2 hours after mixing, so the concrete must be placed and consolidated within that period to prevent sudden premature stiffening. This life can be extended by adding retarders. Some high-range, water-reducing admixtures incorporate a retarder and hence have an extended slump life.

Air entrainment creates tiny air bubbles of proper distribution throughout the concrete, thus enabling the structure to resist a large number of freeze–thaw cycles. Its use is essential in cold regions. Its efficacy is dependent on in-place characteristics. Unfortunately, these can only be verified by microscopic examination of hardened concrete specimens, although other real-time tests give valuable indications as to the entrained air and can be used for control when they have been properly calibrated by a petrographic inspection. Day-to-day control can be exercised by use of a meter that measures the total air content (entrapped plus entrained air) in the fresh concrete mix. Microsilica or silica fume consists of very small particles of silica about 1/100 the size of cement grains which combine with gypsum to produce high early strength, very low permeability, improved bond, and enhanced fatigue endurance. Microsilica also increases electrical resistivity. It is used in percentages (by weight of cement) of 3 to 10%. More than 6% makes the concrete quite sticky and difficult to place and consolidate; however, this property of added cohesiveness can be beneficially used for concrete placed underwater. Microsilica can be introduced as a powder or in a slurry, or, in some cases, can be ground with the cement. If introduced as powder, it must be well mixed. Although most commercially available microsilica is a mineral byproduct of silicon production, rice-husk ash has recently been used as a source, with similar and possibly enhanced properties. Use of high-range, water-reducing admixtures is essential to the incorporation of microsilica in the mix.

Proprietary corrosion-preventing admixtures, based on calcium nitrite, are available. Similar admixtures that reduce the diffusion of chlorides in concrete are commercially available but are relatively expensive. Other thixotropic (viscosity-control) agents are available that promote the initial flow of concrete and self-leveling but gel when movement ceases, thus preventing bleed. They are often used for underwater concreting and for grouting post-tensioning ducts.

11.2.4 Water

Water for prestressed concrete is required to have no more than 650 ppm of chlorides and 1000 ppm of sulfate ion, although in many specifications, the latter is increased to 1300 ppm. Water furnishes the essential electrolyte that initiates the chemical reactions and promotes fluidity (workability) by coating the particles; however, excess water is inimical to strength and durability. For this reason, the water/cementitious materials ratio (w/cm) should be limited to a maximum of 0.42 and preferably 0.40. In practice, w/cm ratios of 0.32 for precast elements and 0.37 for cast-in-place concrete are attainable. In hot weather, ice may be added to the mix in place of water to lower the temperature of the fresh concrete. Alternatively, liquid nitrogen may be injected.

11.2.5 Batching of Concrete

Concrete is weigh-batched in the same manner as in conventional reinforced concrete practice except that in prestressed concrete construction, there are usually more dry components (e.g., cement, coarse aggregate, fine aggregate, fly ash, blast-furnace slag, microsilica) and more wet components in the form of admixtures, each of which must be accurately dosed. The moisture content of the aggregates must be ascertained from free-moisture meters in the bins and corrections made to the amount of water added.

11.2.6 Mixing of Concrete

It is obvious that mixing must be very thorough to blend the many components. For this reason, turbine mixers and shear mixers are favored. Even when the concrete is subsequently transported in ready-mix trucks, premixing at the plant is desirable. The order in which admixtures are added to the mix is important—particularly for air-entrainment agents and superplasticizers, as the latter may inhibit the proper development of entrained air. Adding half the dosage and then mixing for a brief period before adding the remainder can solve the problem in some cases.

11.2.7 Transporting and Placing

Transporting and placing follows conventional practice; ready-mix trucks, concrete pumps, buckets, and conveyors are used. For discharge of stiff mixes from the trucks, screw conveyors may be used. In some high-rise construction using slip forms, where the required rate of concreting at any one location is low, buckets have been used to raise the concrete to elevated hoppers, from which the concrete has been distributed by buggies running on runways. The loss of slump and of entrained air content when pumping concrete to high elevations must be considered.

11.2.8 Consolidation

Internal high-frequency vibration is the typical means of consolidation for cast-in-place concrete. It should also be used to supplement external vibration in all precast concrete elements except very thin (150-mm or 6-in. or less) members, as external vibratory energy is not effective at depth. Self-consolidating concrete (so-called *flowing concrete*) is now being used in thin and congested sections.

11.2.9 Curing

Membrane curing (curing compound) is generally considered to be the most reliable for vertical surfaces. For horizontal surfaces, wet curing is best, although sealing with polyethylene sheets is also widely practiced. Concrete containing fly ash, and especially that containing microsilica, requires special attention to curing to prevent surface crazing. For precast elements and occasionally for cast-in-place segments, steam curing is used to accelerate gain in strength. Steam curing at atmospheric pressure provides both moisture and heat and results in generally superior concrete; however, certain practical precautions are required with steam curing (see PCI, 1999):

- Concrete should have its initial set 3 to 4 hours before the temperature is elevated; otherwise, it may be damaged as it expands.
- The maximum curing temperature should be limited to 60°C (140°F) to prevent long-term development of delayed ettringite.
- Steel forms expand before concrete; hence, changes in section must be detailed to accommodate length change so as not to crack the concrete. Soft rubber gaskets may be used between flanges of forms to absorb their early expansion.
- Concrete, once cured, should not be exposed to cold, drying winds until it has cooled to within about 10 to 15°C (20 to 30°F) above ambient. It is important not only to prevent sudden cooling of the outer surface while the inner core is still hot but also to prevent rapid evaporation of



FIGURE 11.3 Spreading rubberized nylon tarpaulins in preparation for steam curing. (From Gerwick, B.C., Jr., *Construction of Prestressed Concrete Structures*, John Wiley & Sons, New York, 1996. With permission.)

moisture. The latter may require supplemental water or membrane curing. Membrane-curing compounds evaporate with heat; hence, in hot weather a second coat may be required.

In cold weather, and especially with dry winds, the concrete must be protected by insulated forms or blankets (tarpaulins) until the surface temperature is no more than 15°C (30°F) above that of the core (Figure 11.3); otherwise, cracking will occur due to the early contraction of the outer layer.

11.2.10 Testing

Testing of high-strength and high-performance concrete is a demanding technology, requiring trained personnel and sophisticated equipment. Specimens must be taken and prepared carefully if the results are to be meaningful. Cylinders should be vibrated with a pencil vibrator in steel molds, because plastic and cardboard molds will give erroneously low results. The cylinders should be subjected to the same temperature regime as the structural element—for example, placed under the steam hood near each end and at the center of the bed. When removed, cylinders should be placed in a water bath containing lime and kept at 20°C (70°F) until one day before the test. They should then be removed to dry out before testing. Ends of the cylinders should be rubbed smooth to remove any surface irregularities. Numbers should never be etched in the top surface! Cylinders should be carefully capped with new capping compound or ground smooth to test without capping. Similarly, cubes, where used, should be ground and tested without capping. Be sure there is a strong screen around the testing machine, as high-strength concrete fails explosively. Testing of other properties is even more complex. Air-entrainment characteristics are determined by microscopic petrographic examination of thin slices cut from a core in the hardened concrete. Impermeability is very difficult to measure at the upper limits associated with high-performance concrete. The validity of the rapid chloride permeability tests of both ASTM and British Standards has recently been questioned. On many important projects involving prestressed concrete, various properties are specified. These include permeability and determination of the extent of microcracking. In practice, some of the values specified have proven to be extremely difficult to attain in the field. The contractor should therefore start the mix development and testing program at the earliest possible moment, working in cooperation with the engineer and technicians so as to avoid delays and rejections.



FIGURE 11.4 T-headed bars lock against reinforcing steel to provide high shear capacity and confinement.

11.3 Reinforcement and Prestressing Systems

11.3.1 Reinforcing Steel

Because in prestressed concrete structures the role of primary reinforcement has largely been replaced by prestressing steel, an unfortunate tendency has been to denigrate the importance of supplementary conventional reinforcing. Conventional reinforcement fulfills the essential functions of distribution and resistance in the orthogonal directions to the prestressing, most typically in the transverse direction. It serves to augment prestressing steel in critical areas of concentrated stress. It serves as confinement, resisting the bursting and delamination stresses due to prestressing itself (Figure 11.4). It also resists punching shear under concentrated loads.

The role of reinforcing steel is secondary to the structural behavior and is concerned with stress distribution and crack prevention, so close spacing with small bars is preferable to large, widely spaced bars. Confining reinforcement usually consists of spirals, although hoops (welded rings) perform best under ultimate loads. Mechanically headed bars (Figure 11.5) have been used on a number of recent major structures. Subject to the design engineer's approval, bundling of bars may be acceptable, especially in cast-in-drilled shafts and columns. This clustering of bars together often facilitates concrete placement. For splices, mechanical splices are best, although lap splices may be used.

Reinforcing bars typically develop anchorage by having an embedment length that extends beyond the location of high stress, preferably terminating in a confined zone or core. Bends, such as those of stirrups, are only about 70% effective in ultimate capacity, as the concrete under the bend crushes at high stress. Headed bars typically anchor the bar, develop its full strength, and permit the use of larger bars or those with higher yield strength. They are much easier to install than stirrups and reduce congestion of steel bars. It is a serious mistake by both designer and constructor to reduce anchorage lengths to the absolute minimum permitted by code or specifications, as practicable placement tolerances frequently result in inadequate length for anchorage. A typical concern arises with the provision of *cover*—that is, the thickness of concrete outside the reinforcing bars. Because cover is a major factor in durability, as well as in mechanical behavior, it is normally specified to a tolerance of -6 mm ($-1/4$ in.).

Main bars should be tied with wire at every intersection. Stirrups or hoops must be tied to the longitudinal bars at three intersections so as to prevent displacement along the bars during concreting (a typical problem in concreting that has serious consequences). Lap splices in reinforcement are another



FIGURE 11.5 Mechanically headed bars used to replace conventional closed stirrups.

source of difficulty. These can be more easily achieved if the bar is a little longer than the minimum required by code. The designer or the code should specify whether or not the overlapping bars must be tied together with soft iron wire. In general, this is good practice. Compression splices are rendered most efficient by being well tied together at both ends; otherwise, the concrete may locally crush under one or both bar ends. Lap splices, especially those in tension, must be confined on both orthogonal axes, transverse and through thickness.

Reinforcing bars require support. Both concrete dobie blocks and plastic chairs are used and are left in place in the completed concrete structure. Reinforcing bars are frequently epoxy coated to protect against corrosion. The electrostatic fusion process is most widely used. Problems sometimes occur with insufficient thickness of epoxy over the lugs of the deformations. Regardless of the method of manufacture or whether the bars are bent before coating or bent afterward, there will be some scratches and some “holidays” due to handling and placement. Fiber slings and pads must be used. Abraded areas must be touched up in the field after placing. Special care must be taken to ensure that the reinforcing steel is stored in a salt-free area before concreting—that is, where seawater chlorides cannot be carried by fog or spray to contaminate bars. In critical areas and special applications, corrosion-resistant or stainless-steel reinforcement is utilized, enabling a reduction in cover and providing long-term durability.

11.3.2 Prestressing Tendons and Assemblies

Prestressing tendons are made of cold-drawn wire, both parallel and stranded, or rods of high-yield strength steel. Bars and rods consist of heat-treated alloys, which have been prestretched beyond yield and tempered in the manufacturing process. They are rolled with spiral threads, either cut in upset ends or continuously rolled so the threads also act as deformations. Cold-drawn wire is typically low alloy that has been tempered. Wires are generally wound into seven-wire strands and prestretched. The seven-wire strand, with an outside strand diameter of 12 to 15 mm (0.5 to 0.6 in.) is most typical for both the pretensioning and post-tensioning systems discussed in Sections 11.5 and 11.6. For pretensioning, the strands are directly embedded in the concrete, gaining anchorage by bond on the twisted surface. For special applications, such as railroad ties (sleepers), a wire with a deformation is stranded into one outer layer of the strand to shorten the stress transfer length. For post-tensioning, anchorages are locked to a socket by serrated wedges, locking into a female sleeve. High-strength bars are used primarily for short

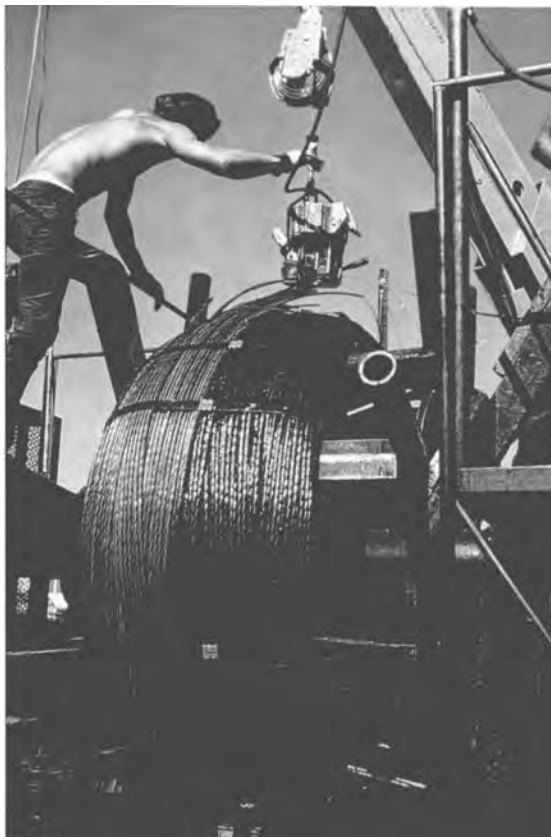


FIGURE 11.6 Seven-wire prestressing strand is shipped in coils to the precast concrete plant or jobsite. (Photograph courtesy of VSL Corporation, Campbell, CA.)

tendons. Wedges can be used to anchor bars although threaded connections are more often employed. These permit restressing to counter the set typical of wedge anchors.

Bars, wires, and strands are usually left *black*, or uncoated. They may be galvanized for corrosion protection; hot-dip process galvanizing appears to be most reliable. A chromate wash applied at the end of the galvanizing process will passivate the zinc and inhibit the liberation of individual hydrogen atoms that results from reaction with the alkali cement. Evidence indicates, however, that the protection resulting from galvanizing has a limited life of 10 to 15 years in seawater. Individual strands that are sheathed in plastic are now available. They are then bundled into tendons for post-tensioning application. Epoxy coating is occasionally applied to steel strands. Sand is dusted on while the epoxy is still wet to improve bond.

Prestressing steels, which are under high sustained stress, are subject to a long-term plastic rearrangement of molecules known as *stress relaxation*. This can produce long-term losses in prestress of the member up to 13%. By a special tempering process, the stress relaxation may be reduced significantly, to about 6%. Seven-wire strand has approximately 30% voids as compared to a solid bar of the same external diameter. *Compact strand* is available, in which the wires are shaped so they fit tightly together. This allows an approximately 15% increase in total force to be obtained within the same external dimensions and is a valuable technique for solving space problems in highly stressed members and in repairs. Prestressing wire and strand are shipped in coils that are wrapped with heavy, water-resistant paper (Figure 11.6). If the cover is torn, the entire coil may be corroded at regular intervals. Bars and rods are similarly shipped in bundles, wrapped for protection from moisture. For protection against corrosion, vapor-phase-inhibiting crystals may be inserted in the package. More frequently, however, the tendons are coated with water-soluble oil.

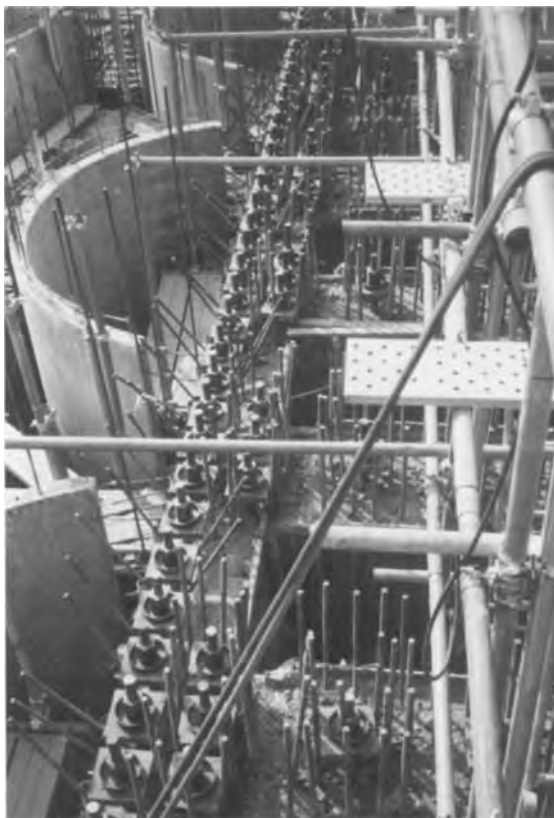


FIGURE 11.7 High-strength alloy steel bars are used to prestress this wall to enable it to resist the pressures of Arctic sea ice. (From Gerwick, B.C., Jr., *Construction of Prestressed Concrete Structures*, John Wiley & Sons, New York, 1996. With permission.)

11.3.3 Anchorages and Splices

The anchorages and splice hardware for prestressing systems consist of cast alloy steels, machined to accurate dimensions with very close tolerances to provide a positive grip to the tendons under high forces (Figure 11.7). The anchorage includes, either separately or monolithically, a bearing plate that transfers force to the concrete. The concrete at the anchorage, being under a force that is typically several times its uniaxial compressive strength, must be confined, either by a ring integral with the anchorage or by hoops or spiral. The anchorage may also include the socket and wedges for gripping the tendon. Anchorages must be transported, stored, and handled with extreme care. Some European specifications require storage in a heated, dehumidified, warehouse. Anchorage assemblies must be clean and free from foreign material, except the grease specified by the system manufacturer. Damaged or visually defective anchorages should never be used. A failure may result in the other anchorage and the tendon being ejected at high velocity. Splices of prestressing tendons are similar to anchorages in that they anchor to both ends of the tendons. It is fundamental that the splice be free so as to allow the tendon to elongate upon stressing; thus, a recess or opening must be temporarily left in the concrete at the splice location. Post-tensioned anchorages are either encased or recessed for reasons of durability, fire protection, and appearance. A recessed pocket is formed in the end block with protruding steel ties that are temporarily bent aside. The surfaces of the pocket or recess are coated with bonding epoxy or latex, then a fine (small coarse aggregate) concrete is placed in a manner so as to eliminate a shrinkage and bleed pocket at the top. After the form is stripped, the joint may be sealed with a penetrant epoxy.

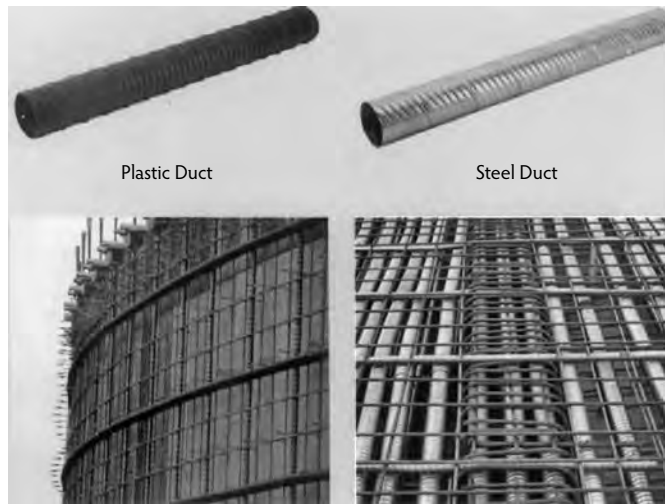


FIGURE 11.8 Ducts for post-tensioning may be of steel or plastic. (Photograph courtesy of VSL Corporation, Campbell, CA.)

11.3.4 Ducts

For post-tensioning, ducts are used to preform holes in the concrete structure during casting so that later, after the concrete has hardened, tendons may be inserted and stressed. Several types of ducts have been used, including steel pipe, semirigid steel ducting made of strips spirally wound to lock to each other, thin flexible metal tubular ducting, and plastic (Figure 11.8). Ducts are usually circular in cross-section, although flat ducts with a rectangular cross-section are used where the concrete cross-section and crossing bars or tendons constrict the available space.

Flexible metal ducts, made of thin corrugated steel and usually galvanized for temporary corrosion protection, are used for tendons of sharp or reversing curvature. These ducts are readily wound in coils and can be spliced by a short overlapping sleeve of similar material. These ducts are very flexible, so that they develop unwanted local curvature, called “wobble.” This can be prevented by insertion of a mandrel of smaller diameter, for example, electrical conduit. After the concrete has been placed, the mandrel is drawn forward and backward to prevent any bond with mortar that may have leaked into the duct, and then removed.

Semirigid metal ducts are bright steel strip, wound spirally with crimped overlaps (Figure 11.9). This ducting has less wobble but still requires use of a mandrel in those applications where even slight deviations have serious consequences. This material is normally furnished in straight lengths but can still be deviated over large-radius curves, depending on the sheet thickness used. Semirigid and flexible ducts are neither watertight nor mortar tight. If a mandrel is not used, a wire or single strand should be run back and forth to clean out any mortar leaking in from the concreting operation. For long, straight runs, especially long vertical runs, thin-walled pipe with screwed splice fittings is employed. Wall thicknesses of 1 to 2 mm are typically used. Splicing of metallic ducts is done by sleeving, with an adequate overlap of at least two diameters and taping with waterproof tape; however, the latter has not proven to be fully reliable. Heat-shrink tape is now preferred.

Steel ducts may be epoxy coated externally where used in zones vulnerable to corrosion, such as transverse post-tensioning of bridge decks in geographical areas where salts are applied to prevent icing. Plastic ducts of polyethylene or polystyrene, with corrugations inside and out, are increasingly employed because they are watertight and grout tight, have controllable flexibility, and give long-term corrosion protection to the tendons. They can readily be fabricated to exact length and can be spliced, either by fusion or by use of sleeves and glue or heat-shrink tape. Plastic ducts should have a minimum thickness of 2 mm; plastic ducts are available both as circular tubes and as rectangular flat ducts.



FIGURE 11.9 Both longitudinal and transverse ducts in place to receive tendons after concrete has been placed and cured.

When a plastic duct is installed on a profile or plan that is curved and wires or strands are later pushed in, the duct may be cut by abrasion, resulting in subsequent grout leakage. Ribbed ducts, in which the strand or wire will bear on enlarged ribs, have been used successfully to overcome this problem, as has lubrication with water-soluble oil. The ribs or corrugations enhance the bond between a plastic duct and the surrounding concrete. Use of 3- to 4-mm-thick plastic duct and pulling-in of the tendon as a bundle with a protective nose-piece (“Chinese finger”) will also minimize the problem of abrasive cutting.

The integrity of ducts, after installation in the concrete, is critical to the successful completion of prestressing. The duct location and the tolerances determine the subsequent profile of the tendon. Any blockage, as by in-leakage of mortar during concreting or out-leakage and crossover of grout from one duct to an adjacent one, will prove very costly, time consuming, and, in some cases, impracticable to correct.

11.4 Special Provisions for Prestressed Concrete Construction

11.4.1 Concreting in Congested Areas

It is typical of much prestressed concrete construction that certain zones, such as the ends of girders and locations of deviation of prestress, are heavily congested (Figure 11.10). Such areas may include, for example, zones in which post-tensioning anchorages, trumpets, spiral confinement, and transverse and vertical reinforcing steel bars compete for the limited space available. At the same time, such zones may make the highest demand on the concrete for compressive and tensile strength. Placing concrete of the required quality, without any voids, honeycomb, or segregation requires one or more of the following techniques:

- Bundling of reinforcing steel bars, especially stirrups, or substitution of headed reinforcement to give more clearance for the concrete
- Changing the concrete mix to reduce the maximum size of the coarse aggregate (e.g., to 10 mm), while increasing the cement content as necessary to obtain the required strength
- Use of flowing concrete
- Prior to concreting, marking the location of reinforcing steel on the forms to enable subsequent insertion of the vibrator



FIGURE 11.10 Congestion of conventional reinforcement and multi-axial prestressing ducts creates problems for concrete placement. (From Gerwick, B.C., Jr., *Construction of Prestressed Concrete Structures*, John Wiley & Sons, New York, 1996. With permission.)

- Prior to concreting, insertion of tremie tubes through the reinforcement, gradually withdrawing these as the concrete is placed
- Prior to concreting, inserting the vibrator within a tube that penetrates through reinforcement (Figure 11.11), gradually withdrawing the tube as the concrete is placed, allowing the vibrator to consolidate concrete below the tube
- In extreme cases, precasting of the end block in the horizontal position, then setting the end block in the forms and joining it to the cast-in-place concrete by protruding reinforcing dowels and the axial post-tensioning

11.4.2 Special Reinforcement at Location of Curvature of Prestressing Tendons

At locations where the centroid of prestressing deviates sharply in relation to the centroid of the concrete section, high radial stresses are introduced. These may cause cracking or, in extreme cases, actual pullout of the concrete in punching shear. It is important to tie this zone to the main concrete section. Typical zones where this phenomenon occurs and has led to damage in the past are at intermediate anchorages, especially where the anchorages are in bolsters or blisters protruding from the concrete section, and at deviation points for deflected-strand pretensioning. Similar conditions exist where external post-tensioning is constructed alongside an existing concrete section but is eccentric to it. In all of the above cases, U-stirrups or the equivalent are required. Their legs must be anchored deeply within the concrete core, preferably in a compressive zone.

11.4.3 Special Reinforcement to Distribute Anchorage Zone Strains

It has long been recognized that the concentrated forces at anchorages of post-tensioning tendons creates radial bursting forces that lead to cracking in the immediately surrounding concrete. All commercial producers of prestressing systems include appropriate confining reinforcement. Not so well recognized is that in the zone between two anchorages, or between the ends of two groups of pretensioned strands, splitting tension is developed. This requires distributed reinforcement to prevent detrimental cracking. When prestressing tendons are anchored at locations other than the ends of the member (e.g., the intermediate anchorages of continuity tendons or dead-end anchorages), the concrete behind the anchorage is subject to tension as the concrete in front of the anchorage tries to shorten. Either adjacent



FIGURE 11.11 Vibrating concrete in order to ensure thorough consolidation below ducts. (From Gerwick, B.C., Jr., *Construction of Prestressed Concrete Structures*, John Wiley & Sons, New York, 1996. With permission.)

prestressing tendons or conventional reinforcing bars are required to distribute these stresses back into the body of the concrete behind.

In vertical walls and webs, looped U-tendons are often used to provide prestress against shear. These situations occur in the vertical walls of silos, offshore platforms, and bridge piers and in the web of deep girders. Adjacent U's must overlap at the bottom; if the adjacent U's are separated, then high-tensile strains exist between them that can lead to cracking. Orthogonal reinforcing steel bars are needed. Additional bars for the above cases should be well distributed over the zone where the potential crack will initiate. The number and size of bars, while calculable by finite-element methods, are often determined on an empirical basis—for example, by provision of enough conventional reinforcement to transfer 50% of the prestress force to the zone behind. Failure to counter the tensile forces and strains can lead not only to cracking but also to a serious reduction in shear capacity.

It can be argued that the above problems are the responsibility of the design engineer; however, the counter-argument is that these local strains are associated with the anchorages of the prestressing system, which are typically selected by the contractor or a subcontractor and, hence, to some degree, are their responsibility. In any event, the occurrence of the cracking, etc. described above may initially be blamed on the constructor and may have serious cost consequences. Conversely, the extra reinforcing required is minimal compared with the overall project; therefore, it appears prudent for the constructor to ensure that it is provided. The matter should be resolved before the concrete is cast.

11.4.4 Embedments

Steel embedment plates are frequently installed in the sides or surfaces of prestressed concrete members. Frequently, these are square plates. As a result of at least three phenomena, cracks often originate at the corners:

- *Steam curing*—The steel plate expands rapidly as the temperature rises, before the concrete expands and before it gains strength.
- *Concrete shrinkage*—The concrete surrounding the embedment is subject to both setting and drying shrinkage.
- *Strains at sharp corners*—Such strains arise due to prestress.



FIGURE 11.12 Sylhan Viaduct in the French Alps combines high performance, high-strength concrete truss members with external tendons inside trussed extension. (Photograph courtesy of Bouygues, Paris, France.)

Solutions that will prevent or minimize such cracks are as follows:

- Place soft wood or a neoprene strip around the embedment, which will later be removed and filled with epoxy, latex, cement mortar, or an equivalent material.
- Round the corners of embedment plates.
- Install short diagonal bars across corners.

11.4.5 High-Performance Concrete

The criteria for high-quality concrete has been presented in general terms in Section 11.2. High performance, above the range normally associated with high-quality reinforced concrete, is often required for prestressed concrete members (Figure 11.12). Typical high-performance requirements specify very high strength (above 60 MPa, or 8700 psi), enhanced impermeability (less than 10^{-10} m/sec), special requirements limiting microcracks, high abrasion resistance, and high tensile strength (above 4 MPa, or 600 psi). The attainment of these requires advanced concrete technology and strict control of field construction practices, including:

- Rescreening and rewashing of aggregates
- Selection of aggregates with surface roughness (e.g., crushed rock and crushed sand)
- Smaller coarse aggregate sizes
- Higher sand content
- Higher cement content
- Replacement or addition of fly ash
- Alternatively, use of blast-furnace-slag cement
- Addition of silica fume (microsilica)
- Use of a high-range, water-reducing agent or higher than normal doses of conventional water-reduction agents
- Special admixtures related to specific properties desired
- Precooling of concrete mix
- Curing practices



FIGURE 11.13 Prestressed lightweight concrete girder being prepared for shipment by rail. (From Gerwick, B.C., Jr., *Construction of Prestressed Concrete Structures*, John Wiley & Sons, New York, 1996. With permission.)

As stated in Section 11.2.3, development, testing, and approval of special mixture designs take time and therefore should be initiated as early as possible. Extensive treatment of this subject is given in Chapter 2.

11.4.6 Lightweight Concrete

Prestressed lightweight concrete has a substantial history of very satisfactory performance in highly demanding structures, including bridge girders (Figure 11.13) and offshore structures. In several important cases, beneficial properties other than light weight have been the rationale for selection. These properties include:

- Durability
- Insulation
- Fire resistance
- In conjunction with silica fume, enhanced fatigue resistance

Structural lightweight concrete has often been selected to reduce the inertial mass of structures in seismic regions and to reduce draft of floating structures. The performance of lightweight concrete is highly dependent on the specific aggregates selected, which in turn depends on the raw materials (clay or shale), the manufacturing process, and the temperature and duration at which they are fired in the kiln. Unfortunately, because of the previous widespread use of low-quality, lightweight aggregates for less-demanding applications, such as fireproofing, and because of the wide range of properties covering lightweight aggregates, most current codes require increased allowances for creep and shrinkage. It should be noted, however, that careful selection of the highest quality lightweight aggregates and the use of some natural sand can keep creep and shrinkage within the same ranges as with natural stone aggregates. Some properties of these high-quality lightweight concretes are inherently less than those of hard-rock (conventional) concrete of the same strength; these include modulus of elasticity, shear strength, and tensile strength. High-performance lightweight concrete has a unit weight of only 75 to 80% of conventional hard-rock concrete; however, compressive strengths of up to 62 MPa (9000 psi) can be obtained by the use of natural sand for the fine aggregate and the addition of microsilica. Microsilica is especially beneficial to lightweight concrete because it chemically bonds with aggregate particles which in turn gives better fatigue endurance under cyclic loads.

11.4.7 Modified-Density Concrete

By using natural sand to replace the lightweight fine aggregate in part or whole and using 50 to 60% of hard-rock coarse aggregate (by volume), a concrete having about 85 to 90% of the density of all-hard-rock concrete can be produced that has almost the same properties, including modulus, shear, and tensile strength as the comparable all-hard-rock concrete. This mixture has been used on a number of offshore structures where weight was critical for draft and stability.

11.4.8 Composite Construction

Composite steel–concrete construction is widely used for high-speed-railroad bridges in Germany, as well as for major bridges elsewhere. Composite construction has also been proposed for offshore structures where the membrane characteristic of the steel plate and its two-dimensional tensile reinforcement properties can be combined with the shell action of the concrete to resist concentrated forces. Connectors used to ensure shear transfer have included welded studs, shear rings, and special shear ribs. Prestressing has been suggested as a potentially synergistic way in which to utilize composite properties, as the steel is kept from local buckling if it is properly anchored to the concrete. The shear on the connectors that is created by the prestressing must be considered. The tendons must be located with consideration of the various moduli of elasticity. Composite construction using half-depth precast prestressed slabs and beams with structural concrete topping has been widely utilized for floor slabs of buildings and for decks of short-span bridges. Shear transfer may be accomplished by the roughened concrete surface alone in the case of light live loads or by means of reinforcing ties. Cleanliness of the surfaces and proper preparation (e.g., saturated or surface damp) are important to ensure bond. The constructor must ensure that the specified degree of roughness of the lower slab or beam is attained. Steel ties are very effective. Typically, the precast member is longitudinally pretensioned. Conventional reinforcing in the topping slab is used to distribute forces transversely and to provide live-load continuity, although in certain instances, especially bridge and wharf decks, the composite system has also been post-tensioned transversely. The designer of such a transversely post-tensioned structure must have adequately considered the effects of differences in moduli and the inherent eccentricity of two orthogonal layouts of tendons. In areas where significant eccentricity is unavoidable, use of steel ties will prevent delamination.

11.4.9 Architectural Prestressed Concrete

Many applications of prestressed concrete have a criterion for architectural and esthetic appearance. Prestressing can be used to help attain the criterion by preventing cracking. One- and two-way prestressing has been utilized for this purpose (Figure 11.14). Care must be taken that neither the ends of pretensioned strands nor the anchorages of post-tensioned tendons can rust and stain the surface. Pretensioned strands can be cut back by a small flame torch or by a welding rod and then plugged with latex cement mortar or a light colored epoxy mortar. Post-tensioned anchors should be recessed and later filled with concrete or mortar. In some cases, epoxy mortar is used. These plugs should be tied to the parent concrete by steel ties; otherwise, cracks may occur around the plugs and allow corrosion products to leach out. Alternatively, in some architectural applications, the architect has elected to emphasize the anchorage, in which case, heavy galvanizing or epoxy coating has been pre-applied.

Some architectural panels incorporate ceramic tiles as facing elements with a backing of concrete. Prestressing locks the ceramics in place and prevents cracking, which otherwise might reflect through the face. Great care must be taken in locating the tendons to offset the difference in modulus of the facing from that of the backing. Some architectural treatments of concrete involve processes that are corrosive to prestressing steel. Acid washing or etching is especially dangerous as residue may remain in ducts and recesses. Joints between segments require special attention if they are to be blended into the overall members. Any epoxy residue must be removed. Use of white cement as part of the mortar mix will help to prevent discoloration, as patches tend to be darker than the surrounding concrete. Steam curing may adversely affect colored concrete; condensation may drip onto colored concrete and leave unsightly marks.



FIGURE 11.14 Two-way pretensioned concrete wall units serve both structural and architectural purposes in the construction of new university building.

Microsilica or antibleed admixtures can be used to prevent unsightly bleed holes. Fly ash or microsilica can be used to prevent efflorescence. These can also be used to reduce permeability and thus minimize the unsightly fungus growth that occurs in semitropical and humid environments.

11.5 Post-Tensioning Technology

11.5.1 Principles

With post-tensioning, the concrete sections are cast first with all conventional passive reinforcement, then, after the concrete has gained sufficient strength, tendons are placed, usually through holes formed by ducts. These tendons are stressed so as to react against the concrete and precompress it. The concrete must be free to shorten under the precompression. The tendons are then anchored, and corrosion protection, such as grout or grease, is installed. There are many variations on the above procedures, of which the most common and important are described here.

11.5.2 Storage of Tendons and Anchorages

Tendons and anchorages are high-strength steel, accurately made to very close tolerances. As such, they are subject to corrosion in storage or, even more insidious, to contamination that will lead to hidden long-term corrosion. Tendons and anchorages should be stored in a covered area, fully protected from the weather and raised off the ground. Some specifications require that the storage facility be dehumidified.

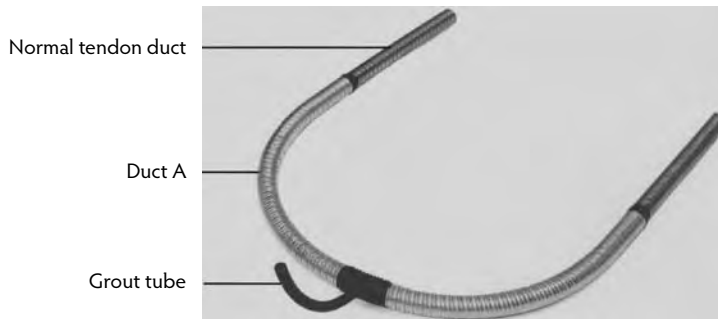


FIGURE 11.15 U-duct is specially fabricated to hold vertical tendons in webs of bridge girders. (Photograph courtesy of VSL Corporation, Campbell, CA.)

Usually, heat is applied to keep the relative humidity well below 50%. In some countries, including the United States and Canada, open storage is acceptable, provided the material is up off the ground and dry. Among the many cases of corrosion of tendons due to inadequate storage are the following:

- Tendons were stored in mud adjacent to a roadway on which salt was applied to prevent icing.
- Tendons were stored on a beach and subject to immersion at high tide.

11.5.3 Installation of Ducts and Anchorage Bearing Plates

Ducts, whether of steel strip or plastic, must be carefully placed to true profile and rigidly held so as not to be displaced during concreting. Their location and alignment determine the position of the tendons that are later installed. Ducts must be kept free from dents and flattening; otherwise, they will not permit the free installation of the tendons. Dents, bulges, and burred ends must not be allowed to occur during the subsequent placing of reinforcement, and care must be taken in the use of the vibrator when consolidating the concrete. Preferably, ducts should be supported on saddles of plastic or steel, rather than bearing directly on the reinforcing steel, which may dent the duct when the load of fresh concrete impinges on it. It is particularly difficult to align ducts accurately across splices. A temporary internal mandrel may be used to ensure proper alignment across splices. Sleeves, overlapping at least two diameters on each end, should be sealed with heat-shrink tape. Screw fittings can be used on ducts comprised of pipe. Although waterproof tape and epoxy have been used to seal overlapping sleeves, tests and experience have shown that these are not as reliable as the heat-shrink tape. The duct cross-section should be about twice the gross cross-section of the tendons and should allow 6-mm (1/4-in.) clearance all around to permit proper encasement in grout. The preferred anchorage for post-tensioning tendons is a recess pocket formed in the end of the concrete member. This is boxed out with forms attached to the end form.

When the duct is placed, the trumpet and bearing plate are attached by screws and sealed to prevent mortar inflow. This rigid attachment serves to ensure that the bearing plate is truly normal to the design tendon axis. Vent tubes and grout tubes must be properly affixed to the duct and taped securely to prevent rupture or leakage. Vents are installed at the high points of upward-curving tendons or at about 20-m intervals on near-horizontal ducts. A tube is also installed at each end just behind the bearing plate to act as an inlet when injecting grout and as a vent at the far end. Drains are used at low points in the tendon profile. They should be used at the bottom of U-ducts installed vertically, such as, for example, in the webs of girders (Figure 11.15 and Figure 11.16). The drain tube may also function as an intermediate grout tube. For the primary prestressing of major structures, such as bridge girders, provision of at least one extra longitudinal duct on each side will facilitate corrective action in case of excessive creep or blockage of a duct. Ducts should preferably be delivered to the job site with plastic covers already fitted. If not, covers should be fitted during installation to keep foreign material, including rain, from entering the duct.

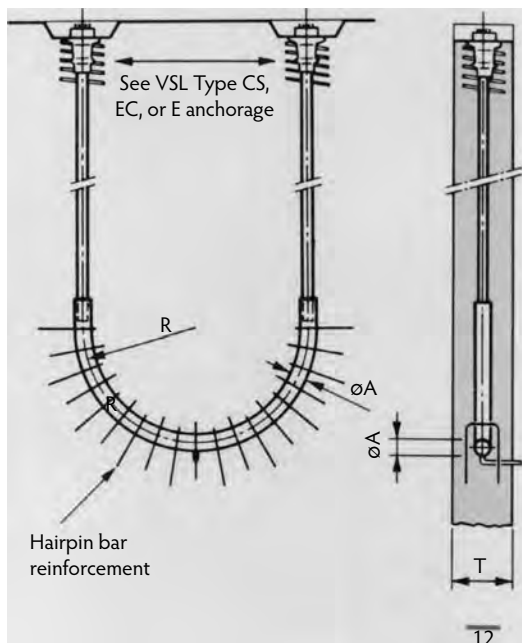


FIGURE 11.16 Duct, tendons, and anchorages for vertical prestress of deep webs of long-span bridges. (Photograph courtesy of VSL Corporation, Campbell, CA.)

11.5.4 Installing and Stressing Tendons

Groups of steel strands and bundles of steel wires can be preassembled with a nose-piece attached. A pull-wire is fed through the duct; one means to feed it through the duct is to blow it by compressed air acting on a rubber ball. A line is attached to the ball which can then be used to pull in the pull wire. The nose-piece is often a Chinese finger grip of spirally wound wire. The bundle is then pulled through the duct. It is usually more efficient, however, to push strands through one at a time, using a pushing feeder of mechanically driven rolls. The end of the strand is fused together by a torch so the individual wires do not separate. Water-soluble oil is brushed onto the strand as it enters the duct. When all of the strands have been pushed through the duct and through holes in the anchorages, they are pulled to a nominal tension by a single-strand jack and temporarily wedged. This ensures that all strands are of the same length. See Figure 11.17 for a graphic representations of the sequence. A multistrand jack is then fitted so as to extend the tendons to their designed stressing level, which is usually about 72% of the ultimate strength. The wedges are hydraulically pushed home (Figure 11.18). When there is considerable curvature in the tendon, the tendon is stressed from both ends. Cycling it by pulling from first one jack and then the other reduces frictional loss. Final stress in the tendon should match theoretical elongation, using calculations based on the modulus of elasticity as furnished by the manufacturer. The modulus varies with the lay of the strand. Allowable tolerance is usually set at 5%. Where this value is exceeded, the cause should be determined. It may be excessive friction, in which case adding water-soluble oil and cycling can help, or the cause may be in the assumed modulus. These data are recorded for each tendon. After the jack is removed, the ends should now be protected from rain and spray by a covering of polyethylene or similar material.

11.5.5 Scaffolding and Falsework for Post-Tensioned Cast-in-Place Construction

A great many building and bridge structures are constructed on scaffolding and falsework. After the cast-in-place concrete has gained strength, the structure is post-tensioned. This prestressing redistributes the dead loads, typically raising the span off of the central scaffolding and transferring it to the end supports.

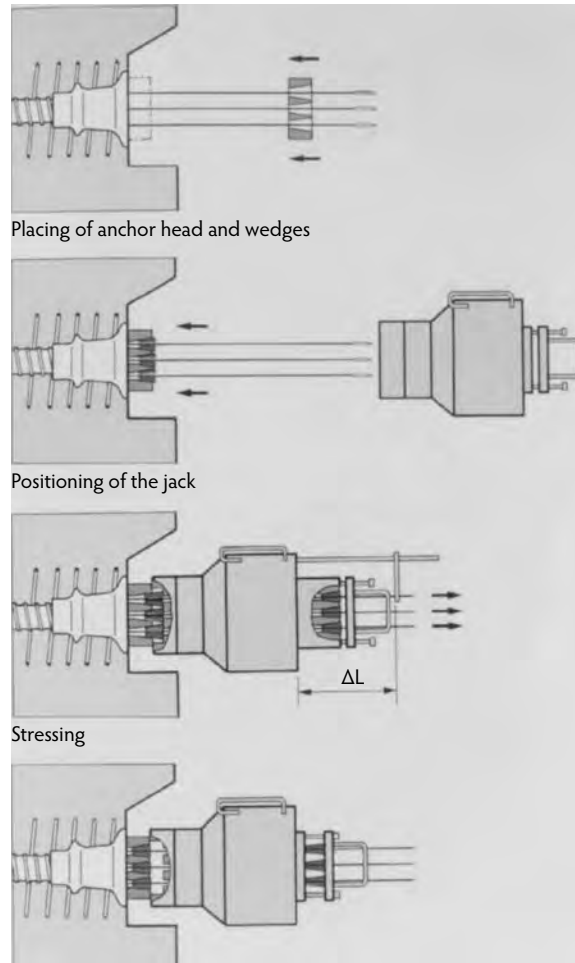


FIGURE 11.17 Sequence for stressing post-tensioning tendon. (Photograph courtesy of VSL Corporation, Campbell, CA.)



FIGURE 11.18 The stressing operation. (Photograph courtesy of VSL Corporation, Campbell, CA.)

In the typical case, this redistribution and induced camber are beneficial to the construction process, making it easier to remove the scaffolding; however, the constructor must ensure that any temporary supports at the reaction points are capable of taking the increased dead load and lateral forces imposed on them. Prestressing also shortens the span. If one end is on neoprene bearing pads it will be free to move. The intermediate scaffolding will be distorted by the shortening but is usually able to accommodate this because of its height and flexibility; however, this should be verified in each case. If the ends are fixed, then the act of prestressing pulls the supports toward each other. The stiffer support will take most of the force and in turn will counter the prestressing, reducing its efficacy. Because of creep, the problem gets more severe as time goes on. This situation has unfortunately arisen on a substantial number of building projects where the effects were not adequately foreseen, resulting in spalling at the edges of bearing seats and, in at least one case, splitting of a stiff column. If a permanent connection must be made at both ends, and the supports do not have adequate flexibility to accommodate the shortening with only small opposing force, then it is best to temporarily place one end on a neoprene pad or sliding bearing, then fix it after the elastic shortening and early creep have taken place. Of course, long-term creep may still cause problems, but its magnitude will be less. Neoprene strips should be used at the edges of the bearing surface to allow minor rotation and to minimize the tendency to spall.

11.5.6 Corrosion Protection of Tendons

The standard method of providing corrosion protection of tendons is by injection of cement grout. If properly done, this encapsulates the strands and penetrates between the wires of the strands. In the case of ducts no larger than two times the gross area of the tendon, cement and water are the principal components of the grout. Sand or other fines are incorporated only in the rare cases of very large ducts. Water-reducing admixtures are necessary for corrosion protection. Fly ash may be used to replace up to 20% of the cement. Thixotropic admixtures are very valuable in reducing bleed, which leads to voids at high spots in the profile. Thixotropic grouts require a positive-displacement pump for injection. Special grouting admixtures have proven very successful for promoting full filling of ducts and preventing bleed pockets. Expansive admixtures, such as aluminum powder have been used but have sometimes created problems with excessive pressure and with the control of expansion. A thixotropic antibleed admixture is believed to be more effective.

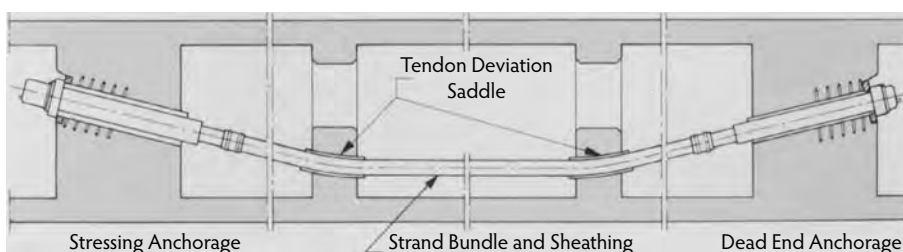
The grout should be injected from one end. The first grout ejected from a vent is dark due to the water-soluble oil. Grout should be wasted until the ejected material has the same color and consistency as the grout to be injected. When the grout ejected from the first vent is deemed satisfactory, that vent is closed. When the end vent is discharging satisfactory grout, that vent is closed. This forces the grout through the tendon anchorages and seals the strands at these critical locations.

Vertical ducts present a special problem in that the strands act as wicks, promoting bleed. Use of a thixotropic admixture helps but is not always 100% effective. One solution is to have an extra hole in the top anchorage plate, through which a tube leads to a small tank above. This tank or receptacle is filled during grouting; the grout then can feed down to fill the duct as the column of grout subsides. Silica fume, as an admixture, also reduces bleed; however, the combination of silica fume and thixotropic or anti-washout admixture is frequently too viscous for effective injection. The anchorage pockets then must be completed. Preferably, small-sized bars have been placed that can be bent down into the pocket. The anchorage pockets should be filled with a fine concrete—that is, one made with small-size coarse aggregate, say 8 to 10 mm (pea gravel)—and a mix rich in cement. Silica fume may be added to minimize bleed. Frequently, the surface of the anchor and the pocket is coated with bonding epoxy. In other cases, latex-modified concrete is used to improve bond.

Shrinkage should be prevented by using the window-box technique, in which the concrete is filled to an elevation higher than the pocket, so if bleed occurs the grout will feed down into the space. Any excess concrete can be easily chipped off after a day or so. The joint around the pocket may be painted with an epoxy that has high capillarity and can be sucked into any shrinkage crack.



VSL External Post-Tensioning System Components

**FIGURE 11.19** External tendons. (Photograph courtesy of VSL Corporation, Campbell, CA.)

In a number of cases, especially nuclear reactor containments, the tendons and the anchorages are encapsulated in grease instead of cement grout. The grease is injected in much the same manner as grout and periodically examined; also, where necessary, additional grease is injected. This technology is now giving way to an advanced system in which each strand of the tendon is sheathed in polyethylene and grease is injected so the strand is free to move within the sheath. This protection is very positive. A cluster of such sheathed strands is fed into a duct. They are then stressed and the duct is grouted or grease is injected, thus achieving a multiple protection system. The critical zone in such a system is at the anchorage, where the strands must be bared for the wedges to grip them. Caps with grease or grout fittings are provided that screw onto the anchorage so they too may be injected after stressing.

11.5.7 External Tendons

The term *external tendons* is used to describe post-tensioning tendons that are not directly incorporated into ducts in the concrete. Usually, these tendons are placed inside the box of a trapezoidal box girder, but they may also be outside. External tendons are unbonded. They are anchored at blisters or bolsters, usually near the ends of the member, and may be deviated at intermediate points along the profile. The tendons are typically encased in a heavy polyethylene sheath. At deviation points, a steel sleeve may be used to prevent the tendon from cutting into the polyethylene. The polyethylene sheath may be continued through the steel sleeve. The steel sleeve is preformed to the design radius. It should have belled ends to prevent stress concentrations (Figure 11.19). Large radial forces at the deviators must be resisted by proper reinforcing details. Deviators must be adequately anchored to the webs or flanges. One problem frequently encountered with external tendons is the failure to leave enough space at the anchorages in which to place a large multistrand jack on the prescribed angle. This must be considered in the working drawings.

11.6 Pretensioning Technology

11.6.1 General

Pretensioning denotes the process by which tensioned high-strength steel wires or strands are incorporated in a concrete segment. The process is relatively simple in concept, economical, and technically efficient; however, it requires a major plant facility that is able to temporarily restrain the forces in the tensioned



FIGURE 11.20 Stretching strands down pretensioning bed.

tendons until the concrete cast around them has gained sufficient strength to effectively bond the tendons and transfer their force to the concrete. The process lends itself to prefabrication—that is, precasting. Most precast pretensioned concrete is produced in permanent plants; however, for large projects, especially in remote areas, contractors have found it practical to set up job-site plants. Although the process is adaptable to a wide range of shapes and configurations, economy favors the use of standardized members fabricated on a repetitive process with a fixed cycle. The principal standardized members produced are piles, bridge girders, building floor slabs, roof slabs, wall panels, railroad ties (sleepers), and poles. Nonstandardized but repetitive segments that lend themselves to pretensioning include stadium seats.

11.6.2 Description of Process

In its simplest form, the pretensioning facility consists of a casting slab or bed on which the segments will be fabricated, reaction frames or stands at the end to temporarily resist the tendon forces, hydraulic jacks for tensioning, tarpaulins or hoods to cover the segments during curing, and lifting equipment to remove the completed segments for storage and shipment.

11.6.3 Tendon Installation and Stressing

The tendons most commonly employed are seven-wire strands with a nominal diameter of 15 mm (0.6 in.), an ultimate tensile strength of 1900 MPa (270,000 psi), and a 0.2% offset yield strength, which is 80% of ultimate. These strands are spaced apart to develop bond for stress transfer and are arranged in appropriate patterns to develop the design compressive stress in the concrete cross-section. Multi-wedge strand anchors are used to temporarily grip the ends of each strand so the jacks can impart the desired force and elongation. Both single-strand and multistrand jacks are used. After the strands are properly stretched, they are anchored to the stands at each end of the bed (Figure 11.20 and Figure 11.21). When



FIGURE 11.21 Fully extended jacks impart prestress to pretensioning strands. (From Gerwick, B.C., Jr., *Construction of Prestressed Concrete Structures*, John Wiley & Sons, New York, 1996. With permission.)

strands are stretched with a multiple jack, very large forces are stored. To prevent serious accidents, nuts should be progressively run up on the extension arms of the jack to limit travel in the event of a loss of hydraulic pressure. The achievement of the proper prestress can be determined both by gauge pressure readings of calibrated jacks and by the elongation. Most specifications require that these deviate not more than 5%. Variations are caused by difference in moduli of the strands or by frictional restraint at the ends and intermediate supports. It is important to keep foreign materials such as oil and grease off of the strands. Welding should never be permitted on or near the tendons as it will destroy the special properties that have been induced by cold drawing of the wires. Unstressed reinforcing steel can usually be most easily placed after the strands are tensioned. The entire reinforcing assembly can then be held in proper position by tying it to the strands or by using plastic chairs and dobie block or by hanging it from overhead spreader bars with plastic wires.

11.6.4 Forms

The forms for concrete segments are typically made of steel. Because the forms are standardized members, they minimize the effort and time required to set them in place and subsequently strip them. For some configurations, the forms may be fixed and tapered so the segment can be removed without moving the forms. For other shapes, mechanical means may be used to close and open the forms. The end gates of the forms are especially critical, as they must allow the strands, and perhaps some reinforcing bars, to pass through without leakage; hence, they may have to be made up in small pieces. Rubber gaskets can be used to seal around the strands and at the sides. For some products, such as piles, it is important that the head be normal, or square, to the longitudinal axis. This can best be achieved by making the end gates up in pairs, spread apart and rigidly held in a frame.

11.6.5 Concreting

The concrete mix is designed to gain strength rapidly so the tendons may be released, transferring their force into the concrete; the segment is then removed to storage. The strength required for release is controlled by two factors: (1) adequate bond strength to limit the transfer length at the ends of the member, and (2) adequate strength to minimize the creep under sustained stress. Typical release strengths



FIGURE 11.22 Concreting and finishing operations.

range from 20 to 30 MPa (3000 to 4300 psi). Concreting follows normal practices of placement (Figure 11.22). External vibrators are often used; they may be moved progressively to brackets on the steel form or permanently mounted on them. They produce excellent consolidation and drive water and air bubbles from the outer exterior 100 to 150 mm (4 to 6 in.) of concrete thickness. For members thicker than about 200 mm (8 in.), internal vibration is also required, even with so-called flowing concrete; otherwise, in densely reinforced and congested zones, such as the end blocks of girders and the heads and tips of piles, honeycomb and rock pockets may occur.

11.6.6 Curing

To gain strength rapidly, accelerated curing is usually applied, which provides heat and moisture. Most commonly, such curing will consist of low-pressure steam. Ideally, adequate strength will be gained in 8 to 12 hours, enabling a daily cycle of production. Forms must be free when the tendons are released, as the concrete will shorten. If the forms are locked to the concrete (for example, by a change in the cross-section), then they also will be forced to shorten. A variety of means are used to prevent damage to the forms. Safe removal can be effected by lifting, sliding, or hinging. If tapered and smooth, of constant cross-section, and sufficiently rugged, then the concrete member may partially slide in the form. Multiple short forms may be designed to slide on the bed.

11.6.7 Release of Prestress

After curing is complete, the tendons are released from the stands, transferring force into the concrete. The concrete shortens under compressive stress. To ensure behavior as a prestressed concrete member, the shortening must not be restrained. In practice, when heavy segments are cast, the friction between the segment and the soffit of the forms may restrict the shortening. In many cases, this problem may be overcome by initially lifting one end of the segment before the other, thus allowing the member to shorten and become prestressed before the full load is realized. Any discontinuity in the cross-section, whether inherent in the design or accidental, such as a fin due to leakage from the forms, may prevent shortening. At this early stage the concrete segment is subject to drying shrinkage and thermal shrinkage, so cracks may occur. Also, steel forms expand under steam or heat curing more rapidly than concrete, forcing a crack. To prevent cracks at changes in cross-section, soft neoprene or rubber gaskets may be installed to

accommodate the dimensional changes. Covering and insulation of the surfaces after curing will postpone drying and thermal shrinkage strains until the concrete has more tensile strength.

Release of the pretensioning into the segments is preferably accomplished by use of a hydraulic jack. This requires reinstalling the jack, exerting a slight additional pull to loosen the wedges, then slowly backing down on the force, allowing the strands to slacken. Even then the friction of heavy concrete segments on the bed or in the forms may prevent their movement and prevent release of prestress into the individual segments. The release then is accomplished by burning the strands. This should be done in a balanced pattern, using low heat (yellow flame) and then cutting with the blue flame. The intention is to reduce the stress gradually. A sudden shock release increases the development length over which the prestress force is transferred to the concrete.

Over this transfer length, particularly near the ends of the segment, the prestress compression is not uniform over the concrete cross-section. Tension develops between strands and especially between groups of strands. Orthogonal reinforcement, in the form of short bars or mesh, is often needed at the ends to prevent splitting cracks. Although this supplemental reinforcement should be part of the design, in practice it is often left up to the fabricator and thus must be considered when preparing shop drawings for fabrication.

11.6.8 Cycle

The typical cycle in precast pretensioned fabrication is as follows:

- 4:00 a.m. Terminate steam-curing cycle.
- 5:00 a.m. Remove test cylinders from under the tarpaulins for testing; replace tarpaulins.
- 6:00 a.m. Test cylinders, and verify that the required release strength has been obtained.
- 6:30 a.m. Remove tarpaulins.
- 7:00 a.m. Detension tendons, and cut strands between segments.
- 8:00 a.m. Lift products out to storage, and store on timber sleepers at correct points to minimize deflection due to creep.
- 8:30 a.m. Clean forms.
- 9:00 a.m. Stretch new strand tendons the length of the bed.
- 10:00 a.m. Equalize lengths with single-strand jack.
- 10:30 a.m. Stress strands.
- 11:00 a.m. Place reinforcing steel, and place end stops or gates.
- 1:00 p.m. Place concrete, consolidate, and finish.
- 2:00 p.m. Cover progressively to prevent premature drying out.
- 6:00 p.m. Turn on low-pressure steam, raising temperature 1°C every 2 minutes to 60°C (140°F).
Hold temperature constant until 4 a.m.

Obviously, times and operations have to be adjusted to fit individual products and reinforcing steel patterns.

11.6.9 Tendon Profile

The efficient design of many segments, such as slabs, beams, and girders, requires that the profile of the tendons follow a path other than a straight line. This means that the strands must be deflected. Deflection has been accomplished in a number of ingenious ways. One such way is described in the following. Strands are initially stressed to a precalculated reduced stress. They are then pulled down or up at specific points, forcing the strands into a series of chords approximating the design path (Figure 11.23). This, of course, raises the stress in the strands to near the desired value. The jack then brings the stress to the design level. By this method, frictional losses and variations of stresses between segments are minimized. Another method is to pull the tendons over a series of rollers, set at selected deviation points; unfortunately, the frictional losses with this method are cumulative and result in unequal tendon stresses in the several segments.



FIGURE 11.23 Deflecting pretensioned strands with special hold-down devices. (Photograph courtesy of Ben C. Gerwick, Inc., San Francisco, CA.)

The hardware at the deviation points can be likened to the arrow in a stretched bow; thus, they are points of danger to personnel during placement of reinforcement and subsequent concreting until the concrete has at least reached final set. These points should be clearly marked with red paint on the tops of the forms, and all personnel must be kept clear. This is especially important for the vibrator operator.

The release of a member made with deflected strands requires special consideration. If the deflected strands are released first, the pull-down devices hold the segment tightly against the casting bed, preventing shortening and effective transfer of prestress. Conversely, if the deviation points are released first, the resulting upward force in an unstressed member could break it. For this reason, the first method is used—that is, first releasing the longitudinal strands and then releasing the pull-downs at the deviation points. In some advanced installations, provisions have been incorporated to allow limited longitudinal movement at the deviation points.

11.7 Prestressed Concrete Buildings

11.7.1 General

Buildings represent perhaps the largest overall use of prestressed concrete and certainly the most diversified use of precast pretensioned concrete segments. Standardized modular configurations have been extensively employed for roof slabs, floor panels, beams, and wall panels. Cast-in-place post-tensioned concrete has been widely used for floor slabs, especially of lift-slab construction and for heavy beams and girders. Post-tensioning permits the full integration of slabs, beams, and girders. Similar monolithic construction is attained with precast pretensioned construction by jointing and cast-in-place infill and topping. Because the construction process differs significantly between the two processes, they are treated separately in the following sections; however, the two systems may be combined in any particular building.

11.7.2 Precast Pretensioned Concrete

The most widely employed precast concrete segment is the double-tee (Figure 11.24). It is used for roof slabs and wall panels. In combination with cast-in-place topping, double-tees are used for floor slabs. Widths are modular; in the United States, this means either 4 or 8 ft (1.22 or 2.44 m).



FIGURE 11.24 Double-tee precast, pretensioned concrete slab. (From Gerwick, B.C., Jr., *Construction of Prestressed Concrete Structures*, John Wiley & Sons, New York, 1996. With permission.)

11.7.2.1 Manufacture

The precast segments are cast in steel forms with tapered legs. The taper plus the slight flexibility of the steel forms permit the segments to be lifted out, or stripped, without adjustment to the forms. Inserts can be placed in the bottom of the legs to reduce their depth for shorter spans. Straight strands are employed for short spans, and deflected strands are employed for longer and more heavily loaded spans. Because the typical deflecting forces are low, much less than with bridge girders, the system of pushing up at the ends while holding down at the middle or third points is commonly employed. Shear reinforcement may be in the form of bent reinforcing bars or welded wire mesh. A few widely spaced strands may be run in the top slab to prevent shrinkage cracking. Transverse bars or diagonal bars will provide cross-slab reinforcement and can anchor embedments for connection between flanges of adjacent slabs. Where topping is to be placed for composite behavior, the top surface is roughened with a transverse broom finish. When double-tee segments are employed for walkways and small bridges, the legs are usually wider and deeper to accommodate the necessary strands and shear reinforcement. For longer spans, single tees with deeper and thicker stems are used (Figure 11.25). Another form of slab, the hollow-core slab (Figure 11.26), is made by several proprietary processes, resulting in a flat top and bottom with multiple longitudinal holes. Both lightweight and conventional concrete are used in manufacture. For lightweight concrete, the replacement of part or all of the fines with natural sand will reduce problems of creep and shrinkage.

11.7.2.2 Erection

Precast segments are typically transported by truck and erected by a large truck crane with extended outriggers. Proper procedures and safety practices must be followed to ensure safe and efficient operations. The Prestressed Concrete Institute has published a manual, *Erection Safety for Precast and Prestressed Concrete* (PCI, 1995), that includes sections on the following important aspects:

- Preplanning of the erection
- Site conditions
- Cranes
- Equipment
- Rigging



FIGURE 11.25 Single-tee slab for longer spans.



FIGURE 11.26 Hollow-core floor slabs.

- Tools
- Unloading
- Lifting
- Fall protection
- Setting/connecting/releasing

Preplanning of the erection is proving especially valuable to contractors, who use it to determine access for cranes and trucks, the swing of the crane and segment in three-dimensional space, and the sequence of erection and means for accurate positioning. Temporary bracing and staying may be required. Marking the exact seats of segments beforehand saves valuable time in the final positioning. Connecting or jointing details are quite critical. Tolerances must be considered, both relative to adjacent segments and cumulative. Details of embedment of strands or reinforcing or welding and bolting have proved to be very important, especially when the structures are subjected to dynamic loads such as earthquake, hurricane, and tornado.



FIGURE 11.27 Erecting a tapered double-tee floor slab in circular parking garage.

Large truck cranes with outriggers are the most commonly used means of erection (Figure 11.27). It is essential that the outriggers be properly supported by timber mats or the equivalent to prevent settlement during the swing of the load. Care must be taken to ensure that neither the boom nor the rigging swing into already erected elements. Adequate room must be available for the counterweight during swing. Tower cranes are also employed; the weight of the units determines their capacity and reach.

Because of the large number of relatively light segments that are typically erected in a building, attention must be given to the detailing and construction of the lifting inserts. These must be compatible with the hooks and slings employed by the rigger, and they must be properly anchored into the member to resist inclined as well as vertical forces. Local pullout can cause a serious accident. Adequate factors of safety must be provided to take care of the dynamic amplification of lifting and minor accidental lateral impact.

When a cast-in-place concrete topping slab is placed on top of precast pretensioned slabs, the latter often require temporary shoring to sustain the dead load of the fresh concrete without excessive deflection (Figure 11.28). This shoring is typically made tight and the grade adjusted by the use of either wedges or screw jacks. These must be set in such a manner that they do not become loose or tip while the top concrete is being placed. The shores react against a lower slab, which may have been placed only a week before, in which case the topping may not have adequate strength. Serious progressive collapses have occurred when the shoring has not been carried far enough or was not strong enough to carry the accumulated loads. Other serious collapses have occurred when the shoring was removed too early. The in-place strength of concrete should be ascertained by companion cylinders stored alongside or through nondestructive testing (e.g., Schmidt hammer). Particular care must be taken during winter when low temperatures delay the strength gain.

Creep must be considered by both the designer and erector, as lengths and camber will change with time. For that reason, it is desirable to let the precast segments mature a reasonable length of time before erection (e.g., 1 to 3 months). Rigid welded connections at both ends are to be avoided. Bearing slabs must be of adequate length and adequately reinforced. Neoprene bearing pads will allow minor rotation and shortening. Shear at the ends of slabs becomes increasingly critical with time due to the tensile stresses induced by creep and the increase in the transfer length of pretensioned strands with time. The erector needs to consider this when preparing the shop drawings.

Camber is affected by a number of factors, including eccentricities of prestressing, the modulus of elasticity of the concrete, creep, differential temperature from top side to bottom, and differential moisture. The cumulative effect of these factors and of various tolerances may create difficulties, especially in

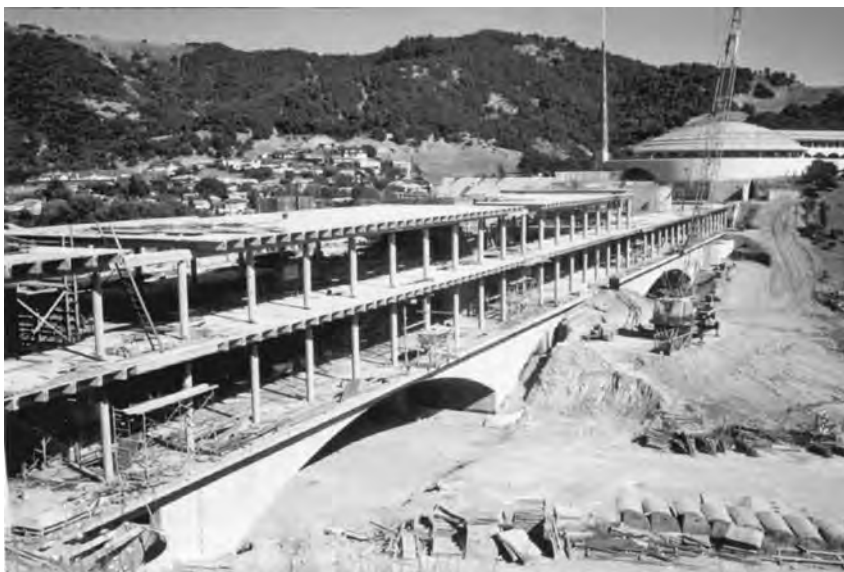


FIGURE 11.28 All precast, pretensioned building of the Marin County Civic Center in California nears completion.

thin, highly stressed slabs such as those most often employed in roofs. These difficulties may in turn cause problems in waterproofing. In extreme cases, loss of camber may lead to ponding of rainwater, which in turn increases downward deflection and ponding of more water, leading to progressive collapse. The camber of adjacent segments may not fully match. Adjacent sections usually can be pulled to match with minimal force, provided the differences in camber and the stiffness of the members are not too great. Where excessive force is required, typically more than 100 kg (220 lb), the design engineer should be consulted. Excessive camber may be reduced by tensioning of embedded polyethylene-sheathed and greased strands installed for this contingency.

11.7.3 Cast-in-Place Post-Tensioned Buildings

Both bonded and unbonded tendons are employed for cast-in-place post-tensioned buildings. Unbonded tendons are extensively used in flat slabs, both lift slabs and cast-in-place slabs. The advent of polyethylene-sheathed and greased strands has made this process reliable and durable. The details of this type of construction are presented in Chapter 10 and Chapter 12. Conventional post-tensioning in ducts, with subsequent encasement of the strands in grout, is typically employed for deep beams and girders. In parking garages, this method is often employed for the ramp (Figure 11.29). For lift-slab construction and wherever precast columns are used, post-tensioning through the columns is desirable to ensure shear friction transfer from the slab, so as to offset subsequent shrinkage. A key detail in post-tensioned building construction is the protection of anchorages to prevent moisture in leakage and to safeguard against fire. Both conventional and polyethylene-sheathed tendons have bare strands through anchorage zones; thus, this is the most vulnerable area for potential corrosion. Recessed anchorages, filled with concrete and tied to the structural slab, are the most reliable.

11.8 Prestressed Concrete Bridges

11.8.1 General

Prestressed concrete has been quite successfully used in the field of bridges, ranging from low- to medium-span precast pretensioned bridges to post-tensioned girder spans 250 m (820 ft) in length and, beyond that, to cable-stayed concrete bridges 600 m (2000 ft) long (which are a derivative form of post-tensioning).

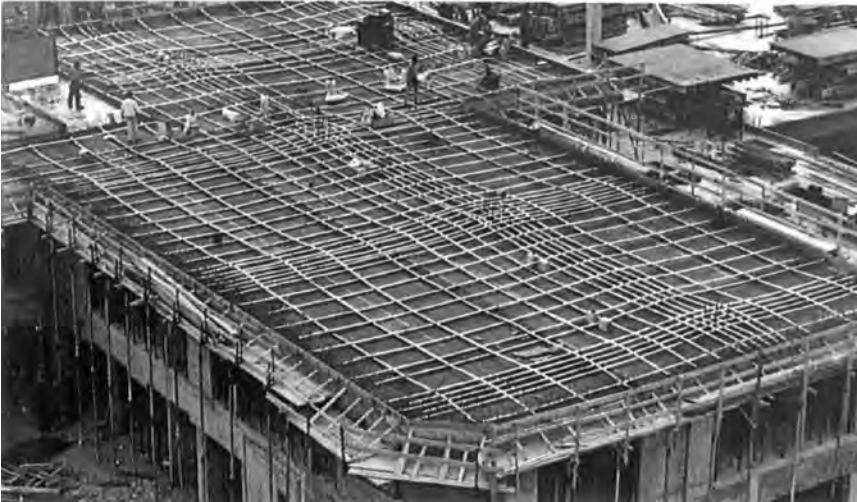


FIGURE 11.29 Cast-in-place concrete floor slab will be post-tensioned in both directions. (Photograph courtesy of VSL Corporation, Campbell, CA.)

Prestressed concrete bridges are now used worldwide in remote developing countries as well as in the urban centers of highly developed countries. Prestressing has proven very versatile in its application and can be used to solve many complex problems of curvature and skewness. It has become the standard by which alternative materials and systems are measured. This success, however, has not come without some problems. Some of these are common to all reinforced concrete—for example, the corrosion of steel in bridge decks on which salts are applied to prevent icing. Many of the problems peculiar to prestressing are due to the widespread adoption of this new technology, sometimes without proper attention to details of design and workmanship. Although in most cases these problems were resolved on the site, they have proven costly and cause delays to the constructor. Fortunately, most problems are now in the past, in that we understand their causes and have adequate solutions available.

11.8.2 Precast Pretensioned Bridge Girders

The precast, pretensioned I-beam girder is widely used for trestle-type bridges, viaducts, and overcrossings (Figure 11.30). This element has proven to be adaptable to mass production, with resultant economies and reductions in cost. The girders are manufactured on long-line pretensioning beds, with deflected strands as described in Section 11.6. They are then transported, principally by truck and dolly, so the support is within 1 m (3 ft) of each end. Long and deep-webbed girders are hog-rodged to prevent buckling during transport.

Girders must be positively restrained against tipping. At this stage, there is no additional dead load from the slab acting; hence, the girder stresses are usually within safe limits only when they are near vertical. If tipped too far, they may fail explosively due to overcompression in the top flange. Blocking and chaining are used to prevent tipping. (Note that wire rope stretches under sustained and repeated loads, so chains or structural members are the only safe means for providing restraint.)

The girders are usually erected by crane. When one crane is used, slings leading at 45° to the horizontal or more (60° is preferable) are employed. This limits the height to which the girders can be lifted. These slings develop a horizontal thrust due to their angle, which may overload the compression flange of the girder, especially because of the low buckling resistance of the girder in the y - y (transverse) direction. To overcome this problem, a spreader beam with vertical slings from the girder to the beam is often used (Figure 11.31). The axial compression of the spreader is then utilized to resist that imposed by the inclined slings. A pipe strut is usually used for the spreader beam, but trusses are employed for very long girders.

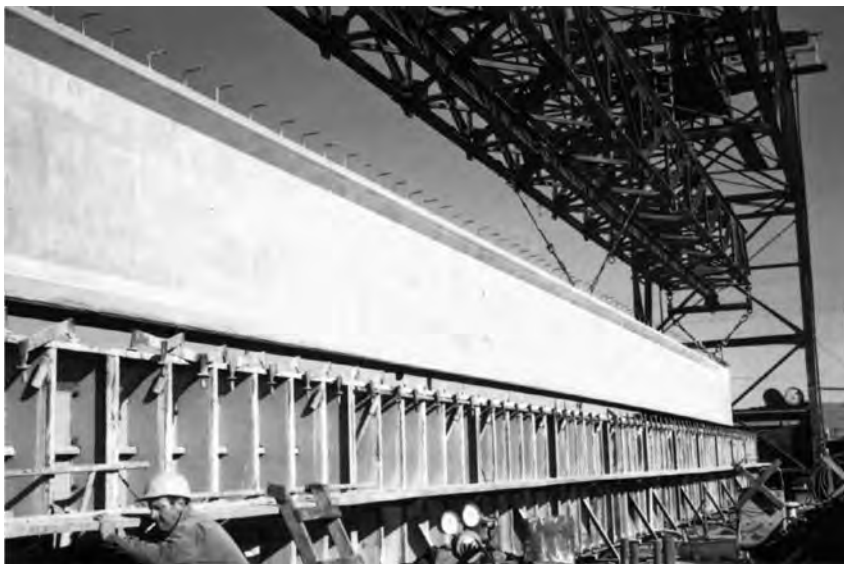


FIGURE 11.30 Precast, pretensioned I-girder for high-level bridge across the Napa River in California.



FIGURE 11.31 Erecting precast girder using trussed spreader beam. (From Gerwick, B.C., Jr., *Construction of Prestressed Concrete Structures*, John Wiley & Sons, New York, 1996. With permission.)

The process of lifting and setting precast girders is a demanding one due to the dynamic forces caused by inertia and swinging, as well as to long and high lifts. Most erection is carried out by crawler and truck cranes; the latter use their outriggers for stability.

The picking inserts in the girders must be properly anchored deep into a compressive zone and must be capable of taking the force at an angle. Slings must be properly designed to meet the amplified load due to angle. Both must be adequate for the dynamics of inertia force and acceleration. The latter is especially critical when floating equipment is used for lifting due to the potential dynamic motion of the barge hull. The rules of crane and rigging safety must be carefully followed.

When bridge girders are erected, they are initially vulnerable to tipping. Tipping may be caused by girders being set on a superelevation, by wind, or by contact with a line from a second girder while it is being lifted. For this reason, long and deep I-beam girders should be braced as soon as they are set. Cast-in-place decks are designed to act compositely with the precast girders. To ensure full transfer of horizontal and vertical shear across the joint, the top flange of the precast girder is roughened and multiple stirrups are employed to tie the girder and deck together. Transverse diaphragms are cast between the end blocks of the girders and sometimes at intermediate locations, although the latter have proven to be less prevalent than was necessary in the early years of this new technology. Experience and tests have shown that the deck slab provides adequate transfer in most cases.

Girders are usually set on neoprene bearing pads. To facilitate accurate and rapid setting, it is helpful to mark a line on the pad for the planned ends of the girder, so no further measurements in either direction need to be made. The cantilever suspended span concept has been used to extend the span of precast prestressed girders. The two side spans are continued over the main piers and are haunched and prestressed for negative moment. Either pretensioning or post-tensioning may be used to provide the required moment capacity. The suspended span, designed for simple span behavior, is then installed. At the interim stage, when the side spans are set but do not have the relieving load of the suspended span, they may be overstressed by the prestressing. This can be countered by the addition of mild steel reinforcement at the bottom of the haunch or by the use of temporary counter prestress.

In the typical bridge, the deck acts as the compressive flange, while the web transmits the shear to the bottom flange. The bottom flange has to have enough prestress to resist both superimposed dead load and design live loads. The top flange has to be large enough to accommodate the tendons necessary to sustain the dead-load compression. In longer girders, this frequently results in temporary excessive precompression in the bottom flange. Enlarging the bottom flange results in a *bulb tee*, which has the desired stress characteristics at all stages and provides the necessary room for the prestressing tendons. Other cross-sectional shapes have been employed for shorter span bridges. These include the double-tee and the triple-tee, or M shape. The typical double-tee used in buildings has a rather narrow web, which may not provide adequate cover for durability or adequate strength for shear. Special forms with a wider web may be used.

Precast prestressed slabs are also employed for short spans and have the advantage of minimum depth and a flat underside. For slightly longer spans, hollow cores may be formed to reduce weight. These slabs may also have a cast-in-place composite topping. To temporarily support the load of fresh concrete, the precast member may require shoring at its midspan or third points.

11.8.3 Post-Tensioned Girders, Cast-in-Place on Falsework

This is a widespread application of prestressed concrete. Falsework shoring is set up, is adequately supported on the ground (or on the new foundations or on piling), and is capable of resisting the dead load of the concrete with minimal deflection. Provision should be made to offset the calculated deflection, whether it be elastic bending of falsework beams or elastoplastic deformations of the ground support. It is important that the shores be adequately braced for both transverse and longitudinal movement during casting of the concrete (Figure 11.32) and subsequent stressing.

For continuous structures, the concrete is usually cast in progression from the center of the span to each end, so as to reach its deflected profile prior to casting the concrete over the piers, thus preventing cracking in the negative moment zone. As the cast-in-place sections are prepared, the ducts are placed to the required profile and alignment. At vertical construction joints, the sections are spliced. Because splices and construction joints are a principal source of problems that occurred in the early years of this technology, attention must be paid to the details, as described in Section 11.3.4. This includes accurate prolongation of the profile across the joint (e.g., by the use of mandrels), the application of heat-shrink tape to the ends of splice sleeves, and proper preparation of the construction joint surfaces (Figure 11.33).

In the negative moment zone, over the piers, the design often calls for several ducts with their tendons lined up one above the other in groups of two, three, or more. Space between these ducts may be very



FIGURE 11.32 Structural steel falsework supports high-level cast-in-place post-tensioned bridge (Ma Wan Viaduct, Hong Kong).

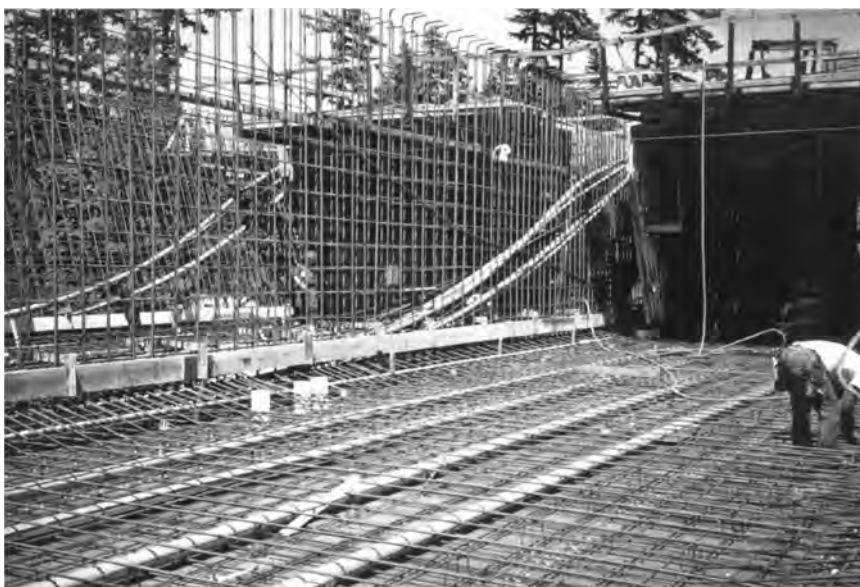


FIGURE 11.33 Draping ducts for cast-in-place post-tensioned bridge (I-205 north approach, Columbia River Bridge between Washington and Oregon). (From Gerwick, B.C., Jr., *Construction of Prestressed Concrete Structures*, John Wiley & Sons, New York, 1996. With permission.)

limited, so the potential exists for an upper duct to pull through into the one below. To prevent this, small reinforcing bar hairpins may be placed transversely, between each pair of ducts. In extreme cases, the lower tendon must be stressed first and grouted, then the second tendon is stressed and grouted, and so on. It generally proves economical and practicable to space the tendons so the shear strength (in double shear) of the concrete and the dowel effect of the transverse bar are adequate to resist the radial component of the tendon force.

As cautioned in Section 11.4.9, the design of supporting falsework must consider not only the stage when the concrete is cast, and hence imposes its dead load on the supports, but also the stage when the prestressing force has transferred the dead load, distributing it with concentrated forces under the zones of concave curvature downward while relieving the load on the zones of convex curvature.

The cumulative effect of shortening between joints of multispan continuous girders must be considered. Intermediate supports must be able to accept the curvature imposed by this shortening or, better, be temporarily freed from it by temporary devices that allow the girders to move the short increment of prestress deformation. Stressing from each end will minimize the actual movements over the intermediate piers. Some very important bridges of moderate span have been cast-in-place and post-tensioned with temporary support on a steel deck truss. When the span is post-tensioned, it rises up off the truss so it is independently supported directly on the piers. The truss can now be slid forward past the pier to the adjacent pier and the process repeated for the adjacent span. This results in a series of simple spans that can subsequently be made continuous for live load by post-tensioning for negative moment over the supports. To facilitate the sliding of the truss from one span to the next, the pier must have an appropriate configuration, such as a division into two shafts between which the truss slides or the provision of steps on the outside of the piers on which individual trusses may be slid forward.

Transverse post-tensioning of the deck is increasingly employed, especially for box girders with cantilevered deck flanges. Because space is limited, ducts must be kept small. Rectangular ducts encasing four side-by-side strands are frequently employed. Tendons may have a dead-end anchorage in the concrete at one end and a stressing anchorage in a pocket at the other end. To provide additional corrosion protection, plastic ducts may be used. In other cases, plastic-sheathed and greased strands are employed with special care being taken to protect the anchorages.

The primary longitudinal post-tensioning tendons are located in the upper flange in the negative moment region near the piers. This means that the transverse tendons should go over them above the webs and under them near the transverse centerline. This is a three-dimensional problem of location, and some eccentricity is unavoidable. To prevent delamination, hairpin dowels at 600-mm (24-in.) spacing may suffice.

11.8.4 Post-Tensioned Precast Segmental Bridges

The concept here is that short segments of the full cross-section of the bridge are cast in a prefabrication site or casting yard. These segments are then transported to the site and erected on falsework or on a truss, as described in the previous section. The segments are then jointed and post-tensioned. Because the segments are cast as relatively small, discrete units, it is possible to obtain close tolerances for reinforcing and duct placement, as well as for finished concrete dimensions. The ability to obtain high-strength and high-performance concrete is enhanced. At the same time, segments are kept to a reasonable size for transport and erection. After erection, segments are carefully aligned to the correct profile; thus, dead-load deflection is taken care of prior to stressing.

Joints may be constructed by a variety of means. Cast-in-place joints, typically 500 to 1500 mm (1.6 to 5 ft) in width, can be constructed in which the reinforcing steel is made continuous by lap splices, welded splices, or couplers. Ducts can be readily spliced by sleeves and sealed by heat-shrink tape. Thin grouted joints, typically 75 mm (3 in.) in thickness, were used in the past but have not proven to be successful because of difficulty with duct continuity.

Vertical joints usually require shear keys. In the past, trapezoidal keys were widely used, but experience has shown them to be subject to diagonal cracking at the corners. Installing a short diagonal bar across the potential crack is one solution. More recently, curved shear keys, corrugated on a large pitch, have been used for both cast-in-place and precast concrete segments.

Dry joints have been used for many bridges in which the precast concrete deck girder segments have been match cast. Match casting consists of constructing each successive segment with its trailing edge cast against the leading edge of the preceding segment (Figure 11.34 and Figure 11.35); thus, a perfect fit is ensured. Ducts are extended from the first segment to the second by use of a mandrel.



FIGURE 11.34 Precast concrete segments are match-cast in elevated cells to facilitate their alignment and movement.



FIGURE 11.35 Precast match-cast segment for viaduct in Riyadh, Saudi Arabia. Note shear keys and anchor blocks (blisters). (Photograph courtesy of CCC Group, Athens, Greece.)

Some problems with fit have occurred with match casting when steam curing has been employed. The segments tend to warp in unequal fashion with the heat. To prevent this, it is best to steam cure the first and second segments together, prior to separation. A bond breaker must be used on the common joint surface. After separation, a light sand blasting, wire brushing, or water-jet blasting can be employed to clean the mating surface.

With dry joints, a thin O-ring seal can be placed in a recess around each duct to seal against grout leakage and cross-over of grout between ducts. Alternatively, thorough swabbing of the duct may suffice but the results need to be verified. Dry or match-cast joints have been greatly improved by the use of epoxy glue on the mating surfaces. Typically, during erection, the second segment of the joint is raised. It is positioned by the use of two mating dowels, either cast in the segment or temporarily affixed to the top. After verifying proper fit, the segments are moved apart and epoxy glue is applied with a gloved



FIGURE 11.36 Cast-in-place cantilever segmental construction for the I-205 Columbia River Bridge.

hand. Because epoxy is incompatible with free moisture, the surface must be protected from rain, etc. during this process. The second segment is again pulled into contact with the first and a temporary precompression is applied by stressing bars at the top, bottom, and both sides. The precompression on the concrete surface of the joint should be 0.3 MPa (44 psi). The epoxy sets under the applied pressure. Many such matings have been successfully made using only epoxy glue to seal the ducts at the joint; however, use of a thin O-ring gasket is believed to be a conservative and justified step to prevent inadvertent blockages in later grouting.

Assembly of complete and multiple spans has been successfully carried out both by erection on falsework and by lifting up a completed span with one or two crane barges. In some instances, the full span, less the two pier-head segments, has been assembled, jointed, and prestressed on a barge, then lifted up from the preset pier heads. Prestressing such an assembly on a barge requires the consideration of the extreme loads imposed on the barge deck at the girder ends due to the post-tensioning. Additional posting or support of the deck may be required.

11.8.5 Cast-in-Place Cantilever Segmental Bridge Construction

This process has been successfully employed on spans up to 200 m (660 ft) and more (Figure 11.36). With cable-stayed concrete segmental bridges that employ the external tendon principle, much longer spans—500 m (1600 ft) and longer—have been attained. The concept is to cast two segments, one on each side of a pier. The casting is followed by prestressing the segments over the pier to resist the negative moment in cantilever. Two more segments can then be cast and post-tensioned, and so on. Each stage must be carefully analyzed to ensure adequate prestressing for the dead load of that segment plus the forms and the weight of the next segment during its casting. Because it is generally not feasible to cast two segments simultaneously, one on each side of the pier, the pier shaft must be adequately reinforced to withstand, out of balance, the temporary bending that is induced. These cantilevered decks are typically extended to near midspan. After a waiting period, to allow as much of the creep as practical to take place, the two extended arms are locked together and a closure pour is made.

At the initial stage of this process, a pier-cap segment is first constructed which is temporarily locked by vertical post-tensioned bars to the pier shaft. A small skid derrick is then erected on the pier-cap segment. The derrick lifts up a prefabricated form for the first cantilevered segment. Reinforcing steel and ducts are placed and the segment concreted. The concrete mix is designed to attain adequate strength

for prestressing within 1 to 3 days. This segment is then post-tensioned to the pier cap segment, and the skid derrick is moved out onto it and temporarily bolted to the deck. This leaves room on the pier cap to install a second small skid derrick headed in the other direction. It now raises the forms and constructs and stresses its cantilevered segment. Now the process can proceed in parallel on each arm of the deck. A typical cycle requires 4 to 7 days for each pair of segments. In many designs for continuous bridges, a hinge is required near the quarter point. To permit the cantilever segmental process to continue past the hinge, it is temporarily locked with removable post-tensioning bars. In other designs, a hinge is placed at midspan. To prevent undesirable movements as heavy live loads cross the hinge, complex devices that transfer shear but no moment are installed.

The cantilever segmental process is very demanding for the contractor; accurate and thorough quality control are essential. Prestressing ducts must be accurately placed to close tolerances and rigidly held in position so as not to be displaced during subsequent concreting and vibrating. At the ends of each segment, the ducts are held in exact location by the end bulkhead of the form. To ensure that the profile of a duct is continuous across the joint, without a small, sharp bend, a pipe mandrel should be inserted which can be extended into the duct in the next segment when it is formed. Pipe mandrels also serve the secondary purpose of ensuring that the duct remains clear and open when adjacent tendons are grouted. Each time a form is extended from the preceding segment, it is purposely set sufficiently high at its leading end to counter the deflection under the weight of the fresh concrete. Concrete placement should proceed from the outer end back toward the previously completed segment.

Segments are typically very congested by conventional reinforcement in three directions and longitudinal and transverse post-tensioning tendons. Near the piers, vertical post-tensioning tendons are often installed as well. This congestion makes concreting difficult. Fortunately, the use of high-range, water-reducing admixtures (superplasticizers) makes obtaining a very workable mix feasible while still achieving high early strength and high long-term strength.

Because of the congestion in the deck near the pier, the horizontal section through the middle of the top deck may have a greatly diminished concrete section; the area is largely occupied by closely spaced longitudinal and transverse ducts. Thus, horizontal shear transfer across this section is diminished and may result in laminar cracking due to the unavoidable eccentricities in the prestressing centroid in the two directions. This problem has been successfully prevented in a number of cases by provision of small-diameter hairpin stirrups in the deck at a nominal spacing of about 0.6 m (24 in.) in each direction. Whereas laminar cracking should be considered for design, it should also be considered by the contractor because laminar cracking is not readily apparent at early ages and repairs are very difficult, usually requiring stitch bolting. Creep and shrinkage, as well as elastic deformations, affect the profile of the completed bridge; thus, it is necessary to take accurate readings at the same time each day, preferably early in the morning before the heat of the sun distorts the structure. This allows corrections to be calculated by the engineer and implemented on the next segment.

In lieu of the temporary support of forms by a small skid derrick or overhead frame, a gantry may be used, extending over at least 1-1/2 spans. This gantry is moved forward after the two cantilever arms are completed on one pier. When its leading edge reaches the next pier, temporary supports are placed, allowing the gantry to move forward one half span farther. The rear end of the gantry, now over the first pier, is locked to it by post-tensioning bars. The gantry can now support the forms and the fresh concrete of the cantilever segments as they are constructed.

Earlier, the installation of near-vertical tendons in the webs was mentioned. These tendons resist the high shear forces near the piers. Frequently, these are installed in U-shaped ducts, with the two anchors in the deck slab. During construction, these ducts must be covered to prevent rain and curing water from entering as well as to protect them from being clogged by debris. Even soda bottles have been found wedged in the U at duct bottoms! Grouting of these vertical ducts must employ the special procedures discussed in Section 11.5 to ensure complete filling of the duct.

Continuity tendons are installed after the closure has been completed. They are designed to provide positive moment capacity over the mid-portion of the span. Typically, their anchorages are in bolsters (blisters) on the webs or bottom flange and the tendons are installed in the bottom flange. Anchorage



FIGURE 11.37 Erecting precast match-cast segment in cantilever construction.

bolsters should be staggered in balanced pairs, with adequate longitudinal spacing and reinforcing to distribute the tensile strains behind them. Proper reinforcing details are also required to resist the pullout forces of the sharp curvature at these anchorages.

11.8.6 Precast Cantilevered Segmental Construction

In this type of construction, the segments are prefabricated in a casting yard, using the match-cast process. They may be cast as individual segments (short-line-process) that are subsequently placed against their partner for concreting or by the long-line method, where the entire girder is cast with segments separated by a bond breaker. Care is taken to ensure the correct positioning of the longitudinal ducts and their extension into the next segment through the use of pipe mandrels (Figure 11.37). The erection process in the field may proceed in a manner similar to that described for cast-in-place segments. In this case, the skid derricks or frames must lift a segment that is positioned directly underneath and raise it into position. Epoxy glue is then applied to the faces of the segments. The tendons are then installed and stressed. The process is inherently very rapid, in that a pair of segments can be completed each day. In some cases, using multiple shifts, two pairs of segments have been completed per day.

The gantry scheme of erection is especially well adapted for this concept. The precast segments can be transported along the completed deck, oriented at right angles to their final position. They can be lifted by the rear end of the gantry and run forward to their final location, where they are turned 90° for erection. Usually, a longer gantry is used, extending over 2-1/2 or even 3 spans. This enables the work to proceed further ahead while previous spans are being post-tensioned and grouted and closures are being effected. If the gantry has adequate capacity, several segments may be suspended from it, thus minimizing the amount of post-tensioning required. If the gantry is of adequate length and strength so it can support the entire double cantilever midspan to midspan, then the required post-tensioning will be reduced to that required for the permanent structure. Because the segments are precast and the concrete has attained greater maturity, the creep and shrinkage are reduced. Nevertheless, the profile and alignment have to be checked daily. Minor corrections can be made as needed by the insertion of wire mesh shims. Alternatively, corrections may be accomplished by additional post-tensioning. A few more strands may be inserted in an existing duct, compact strands may be used, or an additional tendon may be placed in a spare duct.

One significant disadvantage of precast segmental construction is the lack of mild steel reinforcement across the joints, which would minimize crack width under ultimate load conditions as well as improve

stress distribution. This is especially needed at the ends of transversely cantilevered deck flanges, where shear lag may reduce the effective prestress. The latter problem can be resolved by including a high-strength bar in the end of each flange that is stressed at each segment. Couplers can be used to extend the bar from one segment to the next.

Perhaps the best means of providing the desired monolithic behavior and ductility is to include additional ducts, spaced out over the contact surfaces where no primary tendons cross, and to install unstressed strands and grout them so as to provide a nominal steel area across the joint, which is adequate to ensure that if the joint does open the steel, both stressed and passive, is not elongated beyond yield strain. Another method is to provide mild steel dowels in slots or holes across each joint that are subsequently grouted.

11.8.7 Incremental Launching

The incremental launching method is suitable for straight bridges (on a tangent) and for bridges of a constant circular alignment and superelevation; unfortunately, it is unsuitable in its current state of development for constructing spirals. The bridge may be on a straight-line profile or a constant vertical curve. With this process, all work is carried out from one end, in a job-site facility. A segment, typically 6 m (20 ft) long, is cast to its full cross-section. A second segment is then cast immediately behind and post-tensioned to the first. Both segments are seated on bearing plates of stainless steel that slide on Teflon® with a friction coefficient of 0.03 to 0.05. Large hydraulic jacks are installed below the first segments and arranged so they can pull the two segments forward.

As each succeeding segment is cast, it is post-tensioned to the preceding assemblage, and they are pulled forward as a group. Obviously, because the leading segments overhang the abutment, they must be counterbalanced by the segments still at the casting site. A trussed steel nose extension is attached to the leading segment. When the nose reaches the next pier, it is guided onto Teflon® and stainless-steel bearings. The nose is slightly tapered so it can engage the sliding bearings. Despite the elastic downward deflection, the nose raises the bridge to grade as it progressively slides past the second pier. Side guides should be provided at each pier bearing to prevent the bridge from creeping laterally. This is especially important when the bridge is superelevated or on a curved alignment. Because all work is carried out at one location, it is feasible to provide an enclosure so work can be carried out regardless of weather conditions.

Stage post-tensioning is critical to this method. During launching, because the girders are alternating between positive and negative moment, the post-tensioning must be more or less concentric. For the final service condition, after the bridge is in final position, the centroid of prestress must be raised over the piers and deflected downward over the central portion. To physically accomplish this, several methods have been employed. Through the use of external tendons located inside the box of a box girder, the tendons are jacked to their required profile, then secured to the webs with stirrups and concreted in place. This requires an accurate computation of the increase in the stress due to deflection. The process is conceptually similar to the deflection of pretensioned strands. Additional prestressing tendons with exaggerated profile are added to move the centroid of the total prestress to the desired location. These additional tendons can be internal tendons (i.e., in preplaced ducts) or external tendons inside the central opening of the box girder.

11.8.8 Lift-In and Float-In Erection

Lift-in and float-in erection are processes in which the span is **preassembled** and post-tensioned, either on a barge or on shore, then transported to the specific site and positioned beneath the piers. For the lift-in process, heavy lift jacks can be placed on the pier caps so as to raise the complete span. When the span is to be erected one girder at a time, the lifts may be made by skid derricks on top or by floating cranes below. On overland projects, the bridge span may be constructed at ground level and then raised by lift jacks to the pier tops, then a cast-in-place closure is constructed. This closure should incorporate



FIGURE 11.38 Full-width, full-length bridge span for the Great Belt Western Bridge in Denmark is prefabricated on land.



FIGURE 11.39 Erecting one of the 124 spans of the Great Belt Western Bridge in Denmark; each is 100 m long and weighs 7000 t.

a shear key or keys. The lifted-in span is connected to the pier caps by post-tensioning through the pier cap. Float-in spans are similar, except that in this case, the tide plus ballasting or deballasting may be used to place the span onto the pier caps. This concept is most suitable for low-level bridges and trestles. Float-in may also be used with a large crane on a catamaran-type barge (see Figure 11.39). The crane picks the girder, and the barge then moves to straddle the pier. The crane then lowers the girder onto its bearing. This process has been used for very large spans over 100 m in length and up to 8000 t in weight (Figure 11.38 through Figure 11.41).



FIGURE 11.40 Construction of one of the five bridges of the King Fahd Causeway connecting Bahrain to Saudi Arabia.



FIGURE 11.41 Prestressed concrete girders being erected at Prince Edward Island Bridge in eastern Canada.

11.8.9 External Tendons for Bridges

This relatively new technology was introduced in Section 11.5.7. External tendons are located outside the concrete cross-section of the bridge girder, although they may be inside the box of a box girder. External tendons may constitute the entire primary post-tensioning or a portion of the total, the remainder being internal, grouted tendons. The external tendons are anchored at or near the ends in typical recessed pockets. The tendons themselves are multistrand cables encased in a polyethylene sheath. At several locations along the span, either at third or quarter points, the tendons are deviated to the correct profile by structural concrete deviators—that is, partial diaphragms anchored to the webs. Because the forces on these deviators are concentrated, the deviators must be heavily reinforced themselves as must their ties to the concrete webs.

The bending at the deviator must be over a curve of substantial radius to minimize the normal bearing stress on the strands that acts concurrently with the axial elongation changes under varying live load. A steel sleeve with belled ends is used, which is pre-bent to the required radius. The polyethylene duct may be spliced to the steel section or run through this sleeve. Steps to minimize cutting of the plastic when pulling in the strands must be taken. These include pulling as a bundle with protective nose piece, pulling slowly, and use of a thicker plastic duct. The strands are grouted in the duct. The duct is usually left free in the steel sleeve.

One of the advantages of using external tendons in bridges is the ability to remove and replace one or two tendons at a time. This is feasible only if the anchorages are accessible for removal and subsequent replacement and restressing. Anchorages may have screwed-on, grease-filled caps. Although such replacement is frequently a design criterion for bridges that will be treated with salts in the winter to prevent icing, and therefore exposed to a very corrosive environment, the protection afforded by polyethylene sleeves and caps plus grout is believed to be essentially permanent. The use of external tendons has also been applied to concrete truss spans, in which the truss members can be used as the deviators. In this case, because the tendons are exposed to daylight, the polyethylene should be pigmented to minimize ultraviolet degradation of the polyethylene.

11.9 Prestressed Concrete Piling

11.9.1 General

Prestressed concrete piling are used on a very large scale as bearing piles for building foundations, as bridge superstructures, and as support for wharves and quays and tanks and towers. They have been used for offshore terminals and for fender piles and sheet piles for quays and bridge piers (Figure 11.42, Figure 11.43, and Figure 11.44). Piles up to 600 mm (24 in.) in cross-section and, occasionally, to 800 mm (36 in.) are typically pretensioned, using standard pretensioning practices as described in Section 11.6. Further specifics for manufacture of piles will be given later in this section. Cylinder piles, 800 to 1650 mm (36 to 66 in.) in diameter have been produced both by pretensioning and by post-tensioning, the latter again using standard post-tensioning processes. Fender piles and sheet piles are usually pretensioned. Sheet piles may incorporate sheathed and greased tendons arranged in a vertical profile to suit the final service conditions. They are stressed from the top only after the sheet pile is at final grade.

11.9.2 Durability of Piles

Piling for most land foundations, such as for the support buildings, are generally fully embedded in a benign environment of soil below the water table with little oxygen; hence, corrosion of steel has not been a problem. Exceptions may arise when piles are driven through garbage dumps or highly corrosive soils. For piling that extends above the permanent water table, durability must be considered. At sites up to 70 km (42 miles) from the sea and especially in arid zones, chlorides pose a threat to the steel. Corrosion has occurred in serious amounts in the Middle East for piles in both water and land foundations. Preventing corrosion of prestressing steels and conventional reinforcing in marine environments requires



FIGURE 11.42 Prestressed concrete cylinder pile for pier of Napa River Bridge in California. (From Gerwick, B.C., Jr., *Construction of Prestressed Concrete Structures*, John Wiley & Sons, New York, 1996. With permission.)



FIGURE 11.43 Spreading spirals along tensioned strands of prestressed concrete piling.

a dense, highly impermeable mix of at least 350 kg/m^3 (600 lbs/yd^3) of cement containing at least 5 to 10% C3A, with a low water/cementitious materials ratio, preferably less than 0.43. Fly ash may be used to replace 15 to 20% of the cement. In marine installations subject to freezing, the problems of freeze–thaw



FIGURE 11.44 Placing inserts for lifting piles in pretensioned concrete piles.

attack may be especially severe. High tide and waves saturate the concrete, while low air temperatures cause the concrete to freeze during low tide. Some sections of the pile may see two cycles of freeze–thaw a day throughout the depth of winter. Substantial air entrainment is required, with the proper spacing factor and specific surface, as shown by petrographic analysis of hardened specimens or cores. Coatings other than those that breathe water vapor can be counterproductive, as the moisture migrates to the cold face and is trapped behind the impermeable coating, where it then freezes, popping the cover off. Thus, high strength, high impermeability, minimum water absorption by aggregates, low water/cementitious materials ratios, and adequate air entrainment are all required for this environment.

11.9.3 Manufacture

The manufacture of pretensioned piling is a mass-production process, typically involving a small number of standardized cross-sections; hence, economy of production is of great importance. Forms may be double or quadruple so that two to four lines can be manufactured simultaneously. Preferably, the forms are designed so as to require minimal effort for setting and release. Flexible steel side panels may be held in position during concreting by intermittent straps across the top which are easily removed to lift out the hardened pile. Or, the side forms may be stiff enough to hold the fresh concrete without significant deflection yet be tapered so the member may be lifted out directly. A draft of 1 on 50 is usually adequate for steel forms of moderate stiffness. For hollow-core and cylinder piles, the two upper sloping surfaces may be formed by portable panels that clamp to the fixed form and use a neoprene gasket between (Figure 11.45). Alternatively, the upper sloping forms may be hinged.

The internal voids of hollow-core and cylinder piles have been formed in many ways. All of the methods used face the problem of keeping the void form accurately centered so it will not float up when the concrete is vibrated. One method that has proven capable of consistently producing high-quality cylinder piles is to use an internal steel form that is collapsible. A form segment is typically half the length of a pile, so after lift-out of the completed pile each half-length segment may be retracted.

In a typical manufacturing sequence, the internal void forms are set up in the lower half of the fixed outer form and are then blocked up. Coiled spreading spirals of an appropriate amount are then set at the ends of the piles (Figure 11.43). The strands are pulled down the bed, through the coiled spiral but outside the inner void form. The strands are now properly spaced around the circle and tensioned with a single-strand jack. They may be fully tensioned to the desired value (70 to 75% of ultimate) or only



FIGURE 11.45 Closing up forms during manufacture of pretensioned cylinder piles.

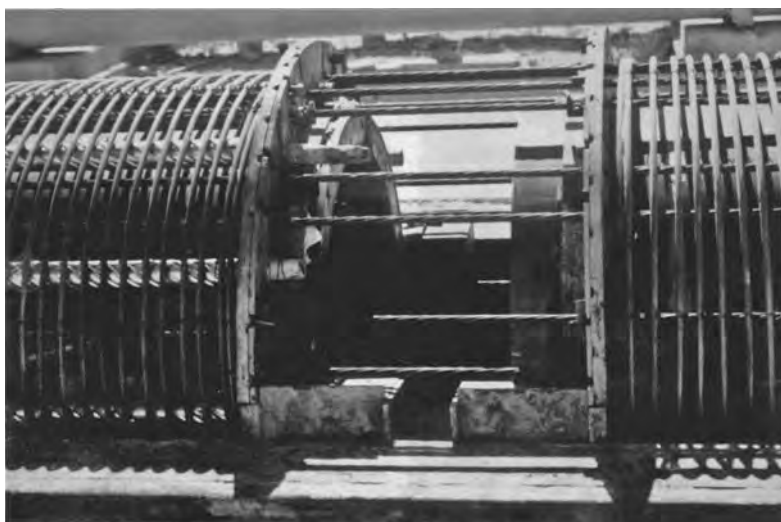


FIGURE 11.46 View of end-gates separating piles during manufacture. Note heavy spiral to resist driving stresses as well as plastic hinging during earthquakes.

partially tensioned, with the remaining tension applied by a large jack. The spirals are then distributed to their correct spacing and tied to the strand as needed.

At appropriate stages, end forms (end gates) are set in place; these are usually fabricated in several segments. Rubber or plastic stops are used to seal against mortar leakage where the strands penetrate the end gates (Figure 11.46). The upper side forms are set in place and the pile is ready for concrete. In a properly designed pile, the spirals or hoops will be very closely spaced at the head and tip. Additional longitudinal bars or tubes may also be inserted at the pile head. The head and tip are zones where the highest concrete quality is essential, so vibration must be thorough. To permit this, the spirals may be bunched and a pencil vibrator used to penetrate between them.

After the piles in a line have been cast and cured, the upper forms are laid back, the strand tension is released, and the strands are cut between piles. This is an especially critical time for cylinder piles, as well as for all large piles, in that the upper surface of the pile is now exposed to both rapid drying

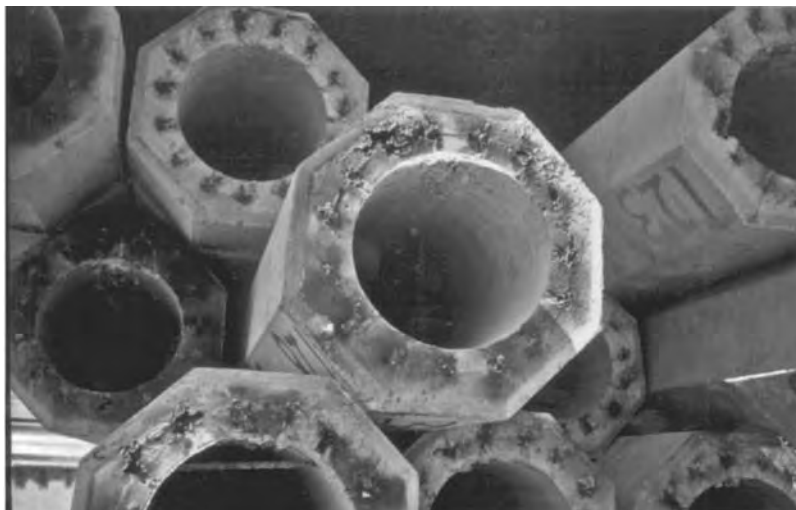


FIGURE 11.47 Pretensioned hollow-core piles in storage.

shrinkage and thermal shrinkage as the top cools off while the warm bottom half and inside is still protected by the forms. Application of membrane-curing compounds and blanketing the pile will prevent the longitudinal cracks that often occur, especially in winter and on windy days.

Cylinder piles are also manufactured by sliding a long internal mandrel along the bed to form the void. The mandrel may be coated so it slides with minimal friction. The rate of progress is matched by the stiffening of the concrete to prevent slumping of the top as the tail end of the mandrel passes. Internal heat has been used to accelerate the rate of stiffening. During the main part of the mandrel slide or slip, the cement paste from the concrete will lubricate the mandrel, but at the beginning it is necessary to coat the mandrel with fluid paste or at least to wet it. Particular attention has to be given to the ends of the piles to prevent the drag of the mandrel from causing cracks or spalls. Slumping of the top and displacement of the strands will cause eccentricity in the cross-section and even delamination, which may then lead to breakage or spalling during driving, as well as reduce the performance of the piles under lateral loads. The bottom strands must be supported in such a way as to maintain their cover. Also, cylinder piles are manufactured by the assembly of short concrete pipe segments. Jointing can be by epoxy or by a 200-mm-wide cast-in-place joint. The pile is then tensioned by running strands through preformed holes, and the tendons are grouted. This process has been used for cylinder piles from 1 m to 3.5 m in diameter.

Piles are lifted from the forms by one of several means. Except in the splash and tidal zone of marine piles (and to a lesser extent the submerged zone), lifting inserts or bundled loops of strand may be used (Figure 11.44). Lifting inserts must be adequately embedded in the pile. Spacing of these inserts may be designed to minimize negative bending moments. Because these negative moments peak at the lifting points and the load is augmented by friction in the forms for large and heavy piles, short lengths of mild-steel bars may be incorporated in the top of the pile.

Where inserts are not permitted, a thin band may be preplaced in the forms, enabling the pile to be raised a short distance by a jacking frame so it can be progressively blocked about 50 mm (2 in.) above the soffit. A lifting wire rope choker can then be inserted so slings from an overhead gantry or crane can lift the pile clear. Piles should be blocked at the same picking points while they are in storage to prevent development of a sweep due to creep. While in storage, the projecting ends of the strands, especially those at the pile head, should be burnt back into the concrete (Figure 11.47). A daub of epoxy mortar may be applied if desired. During load-out and transport, piles should be supported so they do not develop a net tension in the concrete (Figure 11.48). For truck transport, the dynamic amplification must be considered, especially for the overhanging ends.



FIGURE 11.48 Loading heavy prestressed cylinder piles on barge by rolling.



FIGURE 11.49 Pretensioned hollow-core piles driven to support new pier in San Francisco Bay.

11.9.4 Pile Installation

Although one of the primary benefits of prestressing for piles is that they can be driven in a wide range of soil conditions and achieve the required penetrations, even though this requires prolonged hard driving, a number of very specific steps can be taken to prevent pile damage or breakage. Lofting the pile (that is, lifting it from the horizontal to the vertical) typically requires two or more lifting points (Figure 11.49). The slings or lines to these points will typically be at an angle, and this angle will vary during the lift. This means that the vertical components of the force in the lines will be different; thus, the situation differs from that in the manufacturing yard where all lifting forces are normal to the pile. Fortunately, it turns out that in most cases the maximum moments in the pile occur during initial lofting, so the calculation of angles and resultant moments and stresses is relatively



FIGURE 11.50 Lifting prestressed concrete pile into position for driving.

simple. A dynamic amplification factor should be applied to the dead load of the pile. For very long piles, the moments and stresses should be checked through the several stages of lofting from horizontal to vertical.

Most cases of damage to prestressed concrete piles occur during the initial and early phases of driving. This is a consequence of the fact that the tension capacity of the pile is limited to the sum of the precompression due to prestress and the tensile strength of the concrete; the latter is less than 10% of the compressive strength. High tensile stresses during driving are due to a rebound wave of the pile hammer blow from the pile tip in soft driving, when the tip has little or no resistance. Consider the following three typical cases. First consider a pile driven by a diesel hammer (Figure 11.50). Initially, the pile tip is in soft clay or mud. To start the diesel hammer, it has to be raised to almost full stroke, typically about 2-1/2 m (8 ft). Thereafter, in soft driving, the diesel hammer automatically delivers soft blows, but that first blow at full stroke is the one that cracks the pile. The tensile rebound wave is greater than the tension capacity of the pile. This cracking may or may not be noticed, so driving continues. Eventually, the pile encounters hard driving, and the hammer delivers maximum compressive stresses across the cracks. This leads to local crushing at the crack and eventually to fatigue of the strands. Finally, the pile plunges, obviously broken somewhere below ground. Typically, the hard driving is blamed, but the initial damage was done on the first blow (Figure 11.51).

A second case arises when the pile is driven through compacted soil that overlies softer materials such as mud. The pile is subjected to hard driving when in the compacted soils. Then it suddenly breaks through and plunges 3 m (10 ft) or more. The single hammer blow, with little tip resistance, is what has caused the cracking. A somewhat similar situation arises when the pile is required to penetrate a



FIGURE 11.51 Driving long prestressed concrete piling for major naval facility in Puget Sound, Washington.

hard stratum. The contractor employs jetting to reduce the end bearing. Prolonged jetting erodes a hole. The pile drives through with relative ease due to the low tip resistance. In this case, the tension is exacerbated by the fact that the pile is gripped by skin friction along its sides while there is essentially no resistance at the tip, so the compressive wave from the hammer blow is literally driving the end off. In all of these cases, the actual breakage may not occur until there is subsequent sustained hard driving. Prevention of damage due to tensile rebound stresses begins with placing a cushion block on top of the concrete pile. This block is contained within the driving head or helmet on which the pile hammer ram delivers its blow. The material and thickness of this pile cushion block is selected so as to attenuate the peak compressive force, which lasts only a few milliseconds during each blow. When properly selected, this cushion block can actually aid penetration by lengthening the period of application of compressive force while reducing its peak. The best material, after thousands of trials, has proven to be softwood, such as pine or spruce, laminated in multiple layers. To hold this softwood block together, plywood sheets may be nailed top and bottom and inserted in between every third or fourth lamination. The required thickness varies with the pile, the soil, and the hammer. Thicknesses of 150 to 350 mm (6 to 14 in.) are typical. The cushion block compresses during driving. Except when it breaks into pieces and falls out or catches fire and burns up, it is not necessary to replace the block during the driving of any one pile. Exceptions occur for piles in highly stratified ground, where soft soils lie below hard soils. A new cushion block should be used for each pile. Even if the cushion block appears undamaged, its attenuating compressibility has been greatly reduced. For the typical case of a diesel hammer driving a pile whose tip is in soft mud, the pile may be driven down to moderate tip resistance by using the diesel hammer as a drop hammer—that is, raising the ram half distance and dropping it to prevent the damage resulting from a high starting blow. For the second case, predrilling through the fill is indicated. In both cases, the pile may be pulled down through the soft soil by a line rigged to the hoist engine.

The third case is more complex, especially where penetration of the intermediate hard stratum proves difficult and requires extensive jetting. Steps that may be used are as follows:

- Increase prestress; however, this is costly and piles may have already been cast.
- Limit the jetting at the tip but increase the jetting higher up along the sides to reduce skin friction.
- Install a new, thick cushion block when driving through the hard stratum and before re-driving the pile.
- Prebore by jet or auger to break up the hard stratum.

Hundreds of thousands of prestressed concrete piles have been driven successfully without breakage, provided they had the required design and a suitable cushion block was used.

The design prestress should ensure that, if a crack does occur for any reason, the steel strand will not be stressed beyond yield. Cracking will occur when the residual prestress in the concrete (after losses that have occurred to that date) plus the effective tensile strength of the concrete exceed the yield strength of the strand. To prevent this requires an adequate area of steel strand plus any supplemental reinforcement.

Values of 5 MPa (725 psi) have been successfully used for hundreds of thousands of prestressed concrete piles driven in normal soils, where moderate to hard resistances were encountered throughout the driving cycle. Values of 7 to 8 MPa (1000 to 1160 psi) have been used for piles subject to potentially severe tensile rebound stresses; however, the calculated value is extremely sensitive to the assumed tensile strength of the concrete, which is progressively degraded by repeated hammer blows in soft soil. Prestress as high as 10 MPa (1450 psi) may be employed for sensitive conditions and piles with high importance, for instance, large-diameter cylinder piles.

Driving of a concrete pile produces high axial compression, which is additive to the prestress. The Poisson effect develops high transverse (circumferential) strain, typically about 0.22 that of the axial compression. Because this often exceeds the tensile strain capacity of the concrete, longitudinal cracks develop. These can be resisted by spirals or hoops. The matter is complicated by the cover, so the confining reinforcement has to bond to the concrete cover (e.g., through adhesion); thus, epoxy-coated spirals, if used, must have sand embedded in the epoxy.

To prevent the pile head from spalling, additional spiral confinement should be placed close to the head. This can be a circular hoop placed just beneath the chamfer at the corners of the head, perhaps 50 mm from the head, and of adequate diameter to extend to the sides, as cover is not normally a requirement at this location. The tip of the pile should be square, not pointed or wedge shaped, because these shapes tend to wedge the pile out of vertical and, in the case of batter piles, out of proper inclination. Extra spiral, similar to that for the pile head, will prevent local spalling when rip-rap or boulders may be encountered.

11.10 Tanks and Other Circular Structures

The first application of prestressing technology was circular tanks, for which circumferential wrapping with high-strength wire under tension was used to create precompression in the walls of the tank. Walls were cast in place using jump forms or slip forms. When cast-in-place walls are employed, concrete construction may be by slip forms. Flowing, self-consolidating concrete may be more readily placed, especially in thin, heavily-congested walls. Today, such walls are often made of precast concrete staves, set vertically and joined by grout infill or, with wider openings, concrete infill. The wires or strands are then wound under tension. These are then encased by mortar, usually applied pneumatically by a wet shotcrete process. Placing and tensioning of the wires are almost always performed by a specialist contractor using a proprietary process. Both black and galvanized wires are used. In this section, only those elements of work performed by the general contractor are discussed.

The circular wall is usually set on neoprene pads to permit inward deformation under prestressing and hence the development of a state of prestress in the concrete at the base. In seismic regions, special shear keys or restrainer strands connect the base slab and the walls. The details must be executed with great care, not only to ensure safety during earthquakes but also to ensure proper performance and leak

tightness under normal service conditions. When precast staves are used, they are erected to true position and verticality and temporarily supported by tilt-up braces. By marking the location of each stave or panel beforehand, minor errors in position will be minimized and prevented from accumulating.

Tanks may also be prestressed by internal post-tensioning. If the joints between panels are relatively wide, 200 mm or more, they may be treated like similar joints between bridge segments, with overlapping reinforcing and sleeving of ducts so that they may be internally post-tensioned. Anchorages are in blisters spaced at 120° , so each tendon covers 240° and alternate tendons overlap. Blisters must be adequately tied to the wall by stirrups to resist the radial stresses. Tendons are usually stressed from both ends to offset the friction due to curvature.

The joints between panels are filled with high-strength grout or concrete. This grouting is very critical as it must fill the complete joint with a high-strength material that will be able to withstand 70% or so of the ultimate strength of the wall panels, applied within a short period after grouting. The encasement with wet shotcrete is then applied, first by washing the wall with fresh water to remove any contaminants, such as wire-drawing lubricant or water-soluble oil, then by applying a flash coat of neat cement grout, and finally by placing several coats of shotcrete. Where the tanks are to be backfilled (i.e., buried tanks), a coating of epoxy asphalt is also applied. The long-term performance of shotcrete is determined by its impermeability and is dependent to a large degree on the expertise of the nozzle man, who must direct his spray at a slight angle so rebound is not entrapped.

A critical location in tank construction lies at the top of the wall, where any small crack, even a microcrack, between wall concrete and shotcrete can result in progressive corrosion due to moisture infiltration and freeze-thaw attack. This location should be covered by monolithic concrete or epoxy asphalt, as specified or approved by the design engineer. The walls of tanks that will contain sewage or organic materials, hot chemicals, etc. must be free from cracks such as those due to drying shrinkage or thermal strains. Coating the interior surface with a suitable polyurethane material, durable to the contained fluids and able to span minor cracks, should be considered. Where a circular structure such as a penstock is in contact with the soil, or backfilled, epoxy asphalt coatings may provide protection against contamination and penetration of salts from the soil. In freeze-thaw or deep-freeze environments, a special problem arises from the fact that the concrete is saturated and the freeze front will form in the middle of the wall. This can lead to delamination and the spalling of the exterior concrete. An internal coating or membrane appears to be essential.

Containments for nuclear power reactors and for high-temperature gas reactors are usually thick-walled structures with either internal post-tensioning or exterior wrapping. The construction of these structures is similar to that of tanks, but the walls are much thicker and of higher strength concrete, the reinforcing is much denser and more complex, and the post-tensioning ducts and anchorages are very thickly congested. A thin ductile steel liner or membrane must be attached. Because thermal strains in the thick concrete wall have to be minimized, the fresh concrete mix should be precooled using ice or liquid nitrogen, and walls should be protected or insulated after the forms are stripped.

Prestressed concrete tanks may be used as primary or secondary barriers for containment of cryogenic liquids such as liquefied petroleum gas and liquefied natural gas. These applications are highly specialized, especially in providing critical design details for base and roof connections adequate to accommodate the thermal shortening; hence, they require specialty contractors.

11.11 Prestressed Concrete Sleepers (Ties)

Sleepers are a mass-produced element made complex by the need to anchor prestress in a short length, to vary the prestress profile to match the moments, to affix the rail, and to develop adequate electrical resistivity (Figure 11.52). Pretensioned concrete sleepers have been used for the Amtrak from Boston to Richmond as well as on heavy-rail coal railroads in the Southwest and Metro systems nationwide. Their heavy weight is of benefit to anchor welded rail. They must be durable under conditions of freeze-thaw and saltwater dripping from refrigerated cars. Chemistry of the cement and concrete requires careful control because some problems have occurred when durability was not adequately considered. Microsilica

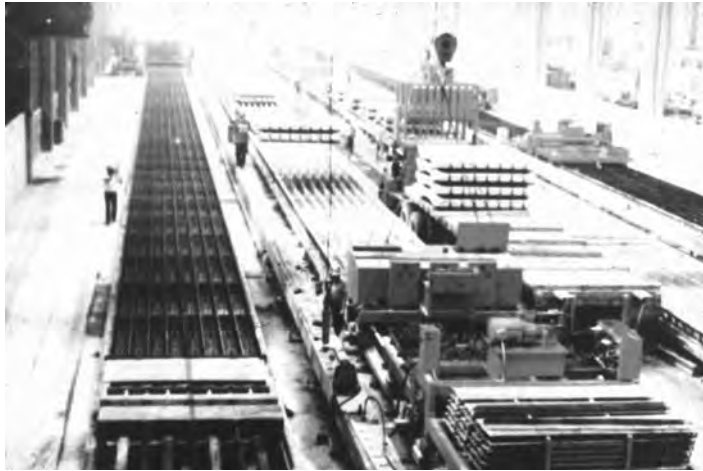


FIGURE 11.52 Pretensioned concrete sleepers (“ties”) being fabricated.



FIGURE 11.53 Offshore LNG Import Terminal under construction; it will be towed to the Adriatic and be seated as a gravity-based structure (GBS). (Photograph courtesy of Exxon-Mobil, Irving, TX.)

(silica fume) has been used to provide the necessary high strength, bond strength, and impermeability as well as electrical resistivity. To provide adequate bond, the lay of the strand may be shortened or deformations provided in the strand during manufacture. Any corrosion-protection oil must be soluble. Sleepers can also be manufactured by post-tensioning.

11.12 Prestressed Concrete Floating Structures

Concrete has been utilized for floating structures ever since World War I, initially prompted by war-time shortages of steel but subsequently used for reasons of economy and performance, the latter being primarily structures that do not require mobility. It especially lends itself to offsite prefabrication of bridge piers, offshore platforms, floating bridges, and, most recently, river navigation structures (Figure 11.53, Figure 11.54, Figure 11.55). Permanently floating concrete structures include barges for support of construction operations, floating breakwaters, floating oil storage, and floating marine terminals. The U.S. Navy is currently testing a half-scale floating pier module in San Diego Bay. The benefits of prestressing have been



FIGURE 11.54 Arco Sakti Ardjuna en route to Java Sea.



FIGURE 11.55 Temporary post-tensioned segment of the Oresund Tunnel exiting assembly basin. (Photograph courtesy of Oresundbro Konsortiet, Copenhagen, Denmark.)

the ability to resist the cyclic bending, shear, and torsional stresses in the hull due to the waves. Other benefits are the minimization of cracking, the resistance to fatigue, and the resistance to thermal strains. Prestressing is used to connect prefabricated elements and subassemblies. In recent years, renewed interest is being exhibited in mobile vessels, either towed or self-propelled. The main deterrent to such use has been the much greater weight compared to steel vessels. With the advent of high- and ultra-high-performance concretes and corrosion-resistant tendons and reinforced concrete, vessels can be constructed with thinner sections, hence less weight and smaller draft.

11.13 Prestressed Concrete Pavements

Prestressed concrete pavements have been used for major airport runways, taxiways, heavy industrial floors, container terminal yards, etc., especially where it is desirable to minimize irregularities and provide a truly level surface during service. Post-tensioning is usually employed and is centered in the concrete cross-section. Because the pavement is subject to water collection, major changes in temperature, etc., providing a crack-free structure is important. Cracks prior to stressing must be avoided by such means as precooling the mix, placing concrete at night, and covering the concrete for several days with ponding, wet burlap, or polyethylene. To permit shortening under prestress, the slab is usually placed on a bed of sand 50 mm (2 in.) thick that is covered by a polyethylene sheet. Splices in post-tensioning ducts and couplers in bar tendons are made at the longitudinal joints. These construction joints are an obvious location of leakage and subsequent corrosion and so must be made with great care. The edges of slabs tend to warp upward due to thermal strains. Many designs incorporate an edge beam so the weight of the concrete offsets the thermal strains and any design eccentricities in the centroid of prestressing.

11.14 Maintenance, Repair, and Strengthening of Existing Prestressed Concrete Structures

11.14.1 Maintenance

Although prestressed concrete structures, properly designed and constructed, have proven highly durable in a wide range of environments, in numerous cases corrosion has seriously damaged both the conventional reinforcing steel and the prestressing tendons. The most prevalent cases are the following:

- Decks of prestressed concrete bridges to which deicing salts have been applied during winter
- Decks of parking structures where tires have carried salts from the adjoining streets
- Piling and the underside of wharf decks of coastal marine structures in tidal and splash zones
- Unbonded tendons, wrapped in paper and bitumastic, in an area near the seacoast where chlorides are present in the fog
- Walls of graving docks that are intermittently flooded by seawater and then dewatered for extended periods of time

In the above microenvironments, chloride contamination is the principal cause of corrosion. Chloride ions penetrate the concrete to the reinforcing and prestressing steel and depassivate it. With the presence of water and the permeation of oxygen, electrochemical corrosion proceeds. Carbonation from CO_2 in the atmosphere can cause similar corrosion attacks but the penetration is slower and more easily prevented. Prevention of these attacks must be primarily focused on initial design and construction, where steps can be implemented to make the concrete more impermeable, to give adequate cover over the steel, and to limit cracking.

The lives of existing prestressed concrete structures that have not been significantly damaged may be prolonged by a rigorous maintenance program. The following program may serve as a checklist:

- Wash down concrete surfaces on which salt has been deposited by spray, accident, or intention.
- Periodically treat the surfaces with silane to render them relatively impermeable to water that contains chlorides.
- Seal static cracks with epoxy injection or coatings.
- Seal active cracks with flexible membranes, such as polyurethane, which have crack-spanning ability.
- Where feasible, reduce the relative humidity in enclosures to below 50%; this is applicable to such structures as seawater pump rooms.
- Apply penetrating corrosion inhibitors; these are a relatively new development that may work in special cases, particularly where the concrete can be dried so water in the pores does not impede penetration of the corrosion inhibitor.



FIGURE 11.56 Attaching plastic sleeve to repair damaged prestressed concrete pile.

- Where applicable, keep the structure flooded with water, even seawater, to maintain the concrete fully saturated. The oxygen content of seawater is only a few percent of the oxygen content in the atmosphere, and oxygen does not penetrate saturated concrete very rapidly. This applies to prestressed concrete penstocks, conduits, sewers, and piping, especially during the period between completion of construction and initiation of service.
- Repair and seal laminar cracks by stitch bolting and epoxy injection.
- Where freeze-thaw attack is eroding the cover of concrete over the reinforcement, provide insulation and coating or covering.
- Install a cathodic protection system, connected to both the reinforcing steel and the prestressing steel. This step is normally instituted after serious corrosion of the reinforcement or prestressing has developed but can be provided for by bonding of the steel and by installing studs for future electrical connection if needed.

11.14.2 Repairs

In many cases, serious damage to a prestressed concrete structure will have only penetrated to the conventional mild steel, causing delamination, spalling, and cracking; thus, conventional repairs can be instituted. These include removal of the damaged concrete, cleaning of existing rebar, replacement of badly corroded rebar, and patching with new concrete or mortar. The problem that often arises is that the new salt-free concrete becomes cathodic to the adjoining chloride-contaminated concrete, leading to accelerated corrosion at the periphery of the patch. Various techniques have been developed to prevent or minimize this process, such as fastening zinc bracelets to the ends of the rebar or coating of the bars by zinc silicate. For concrete piles that are suffering visible deterioration to the concrete cover in the tidal and splash zones, it is necessary to shut off further ingress of seawater with its dissolved ions of sulfate and chloride. Although coatings and jackets have been used in the past with marginal results, the current state of the art is encasement in a sleeve of high-density polyethylene (HDPE) with an inner wrap of felt impregnated with a petrolatum jelly that blocks all further inflow of seawater and air (see Figure 11.56). The following section primarily addresses the repair of those structures in which the prestressing tendons have become corroded.

Prior to undertaking repairs, the existing structure should be adequately shored. The shores must extend down to firm and adequate support. In cases where the damage is due to corrosion, after the structural situation is rectified cathodic protection may be applied to prevent further corrosion. In the case of exposed beams, new external tendons can be installed on each side. They are tied to the existing beam by drilled and grouted dowels and then encased in new concrete.

Bolting steel plates on the bottom and sides of existing beams or gluing on carbon-fiber sheets provides external strengthening sufficient to offset the loss of prestress. The structure then becomes essentially a reinforced concrete structure instead of a prestressed concrete structure. The current state of the art is to affix carbon-fiber strips by epoxy glue.

For temporary repairs to badly corroded structures, structural steel beams may be placed to provide additional support in critical areas. Wedging or shimming may be used to ensure contact and predeflect the steel. Cathodic protection or coatings may be applied for corrosion protection of the steel. Overlays of concrete with new tendons, such as polyethylene-encased and greased strands, may be used in certain cases. In cases where the damage to the tendons is localized, new short tendons, such as bars, may be placed in adjacent slots cut in the concrete, anchored at the ends, and stressed at the center by special center-pull jacks. Where tendons in a deck are corroded but the concrete is still sound, slots may be cut and new tendons installed, stressed, and encased in concrete one at a time. Existing tanks may be repaired by additional circumferential prestressing, followed by shotcrete to give corrosion protection to the new tendons. Righthand–lefthand threaded coupler sleeves may be used to splice the bars.

11.14.3 Strengthening Existing Structures

This is the arena where prestressing has a major role to play, as it is ideally adapted to providing greater strength and correcting unacceptable deflections. Post-tensioning by means of external tendons has been used to correct excessive sag in long-span bridges and to provide additional load capacity. It has been used to transversely tie cantilevered additions to existing bridges to widen them. When new structural elements are added adjacent to existing structures, post-tensioning can tie them so both new and old deform together, sharing the load. In these cases, post-tensioning has been applied either by drilling holes through the existing structure or by placing external tendons. The external tendons must be adequately tied to the existing concrete by dowels. Post-tensioning is extensively employed to strengthen existing buildings and bridges for earthquake resistance. It has been used effectively to transfer the loads from existing columns to new underpinning. Construction follows the general guidelines for post-tensioning with the following special provisions:

- Seats for anchorages must be carefully prepared by mortar or grout to ensure that the anchor plates can be fully seated on a plane normal to the trajectory of the tendon. The concrete beneath must have the ability to accept high compressive stress without bursting or cracking due to the concentrated load; thus, it may be necessary to remove and replace defective concrete. Adequate confining reinforcement is essential.
- Where external tendons are placed and are to be bonded to the existing concrete, the surface should be roughened and cleaned and a bonding epoxy applied.
- Adequate corrosion protection and, where applicable, fireproofing must be provided for the anchorages.
- In planning for strengthening, consideration must be given to access for the jacks and bearings for them to react against.
- The retrofitted structure must be able to accommodate the elastic and plastic shortening due to prestress.

11.15 Demolition of Prestressed Concrete Structures

Buildings and bridges must eventually be demolished and removed to make room for larger structures or other uses. Such demolition can be piecemeal, using the time-honored methods of headache ball, concrete saw, drill, and burning torch, or by more modern approaches that use diamond saws, hydraulic jacks (feathers) or controlled explosives that can topple the entire structure within a matter of seconds, turning it into rubble. Prestressed concrete structures require special considerations, due to the fact that tremendous amounts of energy are stored in the stressed tendons. Sudden release can produce a missile

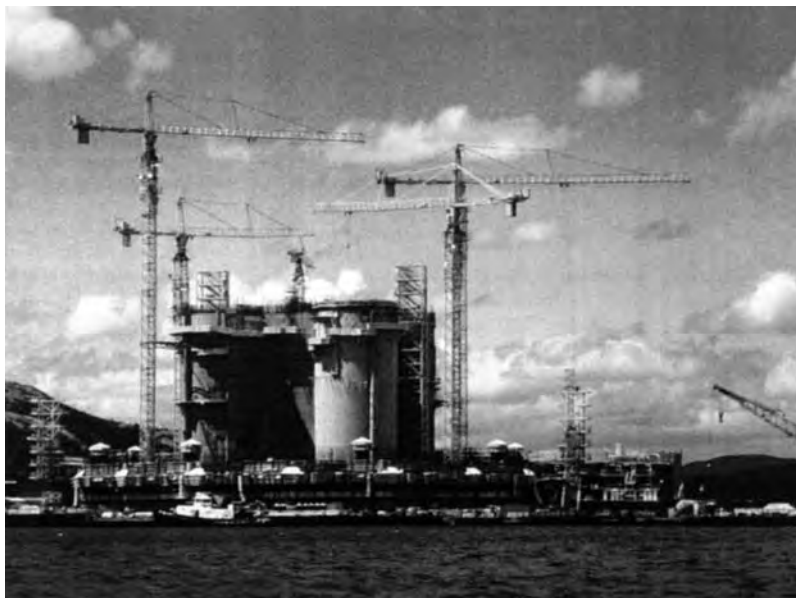


FIGURE 11.57 Heidrun is the world's first permanently floating semi-submersible offshore oil platform; it is shown here under construction in Norway.

that can fly 100 m or more with a velocity sufficient to penetrate a board fence. More serious is the potential for injury to workmen or the public.

When removing a structure in stages, it is usually necessary to shore under the span being demolished to prevent its collapse. The shores should be wedged up to fit tightly against the member to prevent erratic loading as the tension is released. Heavy timbers or blasting mats should be placed behind the end anchorages to absorb impact energy. Post-tensioned tendons and especially unbonded tendons must be destressed gradually. One method is to heat the tendon with the yellow flame of a burning torch, allowing it to slowly elongate. The other, applicable to large post-tensioning tendons, is to cut one wire at a time. Controlled heating is the most reliable method.

When the precompression in the structural element is fully released, the element will transfer its load onto the shores, so they must be designed to take the resultant loads. Bonded, post-tensioning, multi-strand tendons are more difficult to release. Because their transfer length is typically short, they have to be cut at frequent intervals, but the projectile phenomenon is not as great a factor. When demolishing by explosives, millisecond delays should be used to ensure that unbonded tendons are cut close behind the anchorages prior to the release of the main spans. Demolition of a small area to repair a damaged zone should follow isolation of the concrete by a saw cut, so spalling, etc. will not extend farther than intended. Stitch bolts through the thickness may be installed around the periphery. The concrete can then be removed by a small chipping gun or jet blast of water, taking care not to seriously damage the tendons. The tendons may be clamped at their ends or bonded by epoxy injection if they have not already been bonded by grout. They are then heated to relieve tension and cut for splicing or other remedial repair.

11.16 The Future of Prestressed Concrete Construction

Prestressed concrete is now accepted for a wide range of applications such as those described in the preceding chapters. It not only enhances the tensile capacity of the structural elements but also enables the control of deformations and service performance. It prevents cracking, thus enhancing durability (Figure 11.57 and Figure 11.58). In the future, it will give an expanding capability to the architect and his structural engineer. Magnificent buildings and bridges will be translated from creative ideas into



FIGURE 11.58 Rion-Antirion cable-stayed bridge across Gulf of Corinth, Greece.

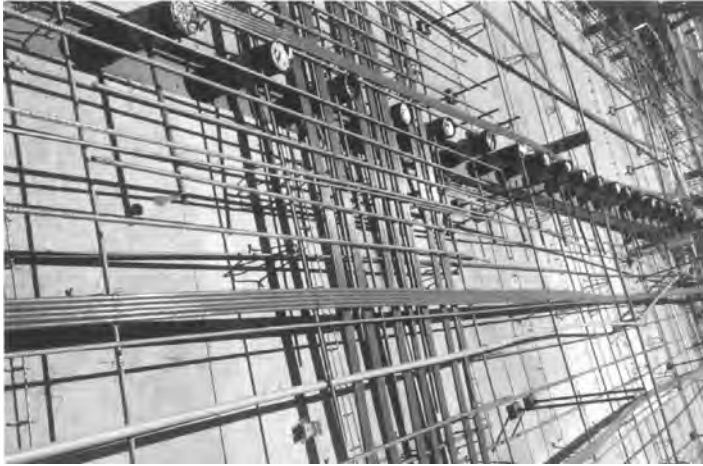
realities. Mass production of prefabricated elements, both prestressed by themselves and prestressed to create a monolithic whole, will be even more widely employed. The continued creative imagination and innovation of designers, and constructors will allow the horizon to expand exponentially.

Acknowledgments

Many of the pictures of post-tensioning operations were made available by VSL Corporation. The author's firm, Ben C. Gerwick, Inc., provided many pictures of prestressed concrete manufacture and erection.

References

- Gerwick, B.C., Jr. 1996. *Construction of Prestressed Concrete Structures*, 2nd ed. John Wiley & Sons, New York.
- Libby, J.R. 1990. *Modern Prestressed Concrete*, 3rd ed. Van Nostrand-Reinhold, New York.
- Nawy, E.G. 2001. *Fundamentals of High-Performance Concrete*. John Wiley & Sons, New York.
- Nawy, E.G. 2006. *Prestressed Concrete: A Fundamental Approach*, 5th ed., Prentice Hall, Upper Saddle River, NJ.
- PCI. 1995. *Erection Safety for Precast and Prestressed Concrete*, MNL-132. Precast/Prestressed Concrete Institute, Chicago.
- PCI. 1999. *Quality Control of Prestressed and Precast Concrete*, MNL-116. Precast/Prestressed Concrete Institute, Chicago.
- Podolny, W., Jr., and Muller, J. 1982. *Construction and Design of Prestressed Concrete Segmental Bridges*. John Wiley & Sons, New York.



(a)



(b)

(a) Unbonded post-tensioning reinforcement. (Photograph courtesy of FBA, Inc., Belmont, California.) (b) High-rise building with prestressed post-tensioned floors. (Photograph courtesy of Portland Cement Association, Skokie, IL.)

12

Unbonded Post-Tensioning System Technology in Building Construction

Florian G. Barth, P.E.*

12.1	Developments in Unbonded Post-Tensioning	12-1
	Introduction • Unbonded Post-Tensioning System Technology • Durability of Unbonded Tendons	
12.2	General Notes and Standard Details.....	12-6
	General Notes • Standard Details • Typical Field Shortcomings: Problems and Solutions	
12.3	Evaluation and Rehabilitation of Building Structures.....	12-22
	Evaluation • Repair • Retrofitting Concrete Structures Using Unbonded Post-Tensioning	
12.4	Demolition of Post-Tensioned Structures	12-36
	Introduction • Structural Evaluation • Deconstruction Analysis • Methods of Demolition • Other Considerations	
12.5	Defining Terms	12-42
	References	12-44

12.1 Developments in Unbonded Post-Tensioning

12.1.1 Introduction

During the last three decades, unbonded post-tensioning has progressively become the predominant construction choice for commercial concrete buildings in the United States. The utilization of unbonded tendons is now standard practice for concrete structures. Because of their excellent performance record and their economical and versatile application, the total use of unbonded tendons increased from approximately 7500 tons in 1976 to over 180,000 tons of prestressing steel in 2005, adding up to over 1 billion square feet of slab constructed with unbonded post-tensioning. Early applications of unbonded tendons and their limitations in design and construction were soon succeeded by well-established analysis, design, detailing, and field procedures. Driven by durability considerations, post-tensioning

* Principal Consultant, FBA, Inc., Hayward, California, and Vice President of the American Concrete Institute; expert in analysis, design, evaluation, and retrofit of post-tensioned concrete structures.

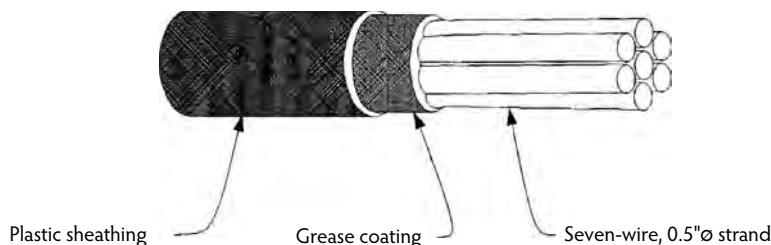


FIGURE 12.1 Unbonded monostrand tendon.

manufacturers have implemented product improvements for corrosive environments. The most meaningful testimony for unbonded post-tensioned construction is the successful performance of over 1 billion square feet of concrete construction.

The four common types of tendon systems are monostrand tendons, single-bar tendons, multistrand tendons, and multiwire tendons. During the 1960s and early 1970s, several proprietary tendon systems were used for concrete building structures. Unbonded single-strand or monostrand (1/2-in.-diameter, seven-wire) tendons with various types of sheathing applications were used predominantly over construction using unbonded single-bar tendons in plastic (or metal) ducts and unbonded button-head wire tendon. The application of unbonded monostrand tendons offers an economical and versatile application for post-tensioning thin slabs and narrow beams. Together with the small tendon diameter, positioning monostrand tendons horizontally, side by side (maximum bundle of four), provides the maximum possible offset from the neutral axis (eccentricity) within a member cross-section. In addition, the monostrand post-tensioning system utilizes compact anchorage devices and anchor recess pocket formers, together with small, lightweight stressing jacks, thus permitting the stressing operation to be executed with hand-carried equipment. The relatively simple components of unbonded tendons, their proven performance, and the economical advantages they offer positioned unbonded post-tensioning to record an average annual growth of over 8.5% between 1986 and 2004, according to the *Post-Tensioning Manual*, 6th ed., hereafter referred to as the PTI Manual of the Tensioning Institute (PTI, 2006).

The use of 5/8-in.-diameter single-bar tendons (smooth rods) was discontinued due to the labor and material costs involved in splicing the standard bar length. In contrast, unbonded multiwire tendons (button-head wire tendons) were used until the mid-1970s for beams and transfer girders, which required large localized forces. The economical application of multistrand tendons has continued until today. Multistrand tendons originally intended as bonded tendons but kept ungrouted for surveillance (nuclear) are specifically excluded and not part of this review.

12.1.2 Unbonded Post-Tensioning System Technology

In the United States, the first unbonded monostrand tendons were used in the mid-1950s for building construction using greased and paper-wrapped seven-wire strand. The spirally applied continuous paper strip was intended to be a bond breaker between the strand and concrete, and the grease coating assumed the role of corrosion protection. Plastic sheathing introduced during the mid- to late 1960s assumed the roles of (1) bond breaker, (2) protection against damage by mechanical handling, and (3) providing a barrier against intrusion of moisture and chemicals. The strand coating, commonly referred to as *grease*, reduces the friction between the strand and the sheathing and provides protection against corrosion (Figure 12.1). Three principal polyethylene coating applications were used for several years—namely, a plastic tube into which the grease-coated strands were pushed (stuffed or push-through tendons); a continuous polyethylene strip positioned parallel with the strand, wrapped around the coated strand, and sealed with a seam along the longitudinal axis of the strand (heat sealed); and the extrusion of polyethylene over the coated strand. Primarily used in Canada until approximately 1990, the stuffed or push-through tendons were discontinued during the early 1970s in the United States. Heat-sealed

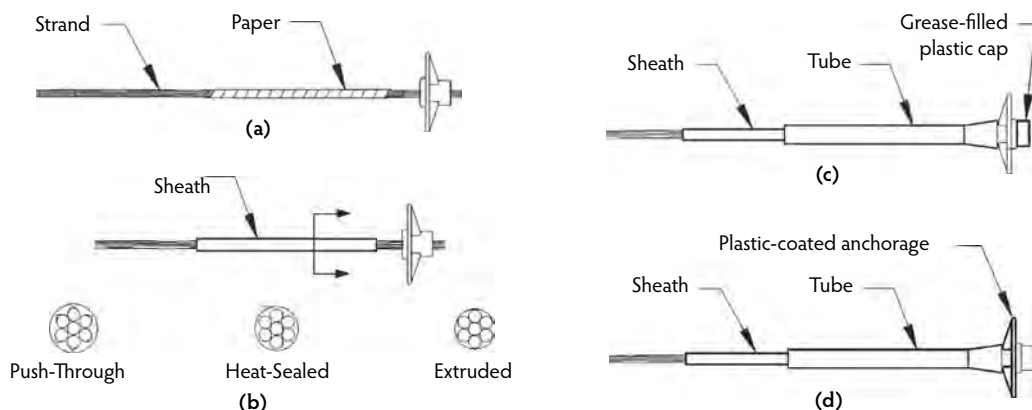


FIGURE 12.2 Unbonded tendon evolution: (a) paper-wrapped, (b) plastic sheath types, (c) encapsulated system, and (d) electrically isolated tendon.

fabrication of monostrand sheathing was supplied until the early to mid-1990s. In corrosive environments, stuffed and heat-sealed tendons have the inherent shortcoming of either trapping or allowing access of corrosive substances in the oversized sheathing. Extruded polyethylene sheathing has demonstrated excellent performance since its first introduction in 1969. The extrusion process applies the sheathing, eliminating voids between the sheathing and the grease coating. The extrusion sheathing application, with encapsulation of anchor zones for corrosive environments, has been used almost exclusively in the United States since the latter part of the 1990s until today. Again, the sheathing progression for most parts of the United States was paper-wrapped, stuffed or push-through, heat-sealed, extruded, encapsulated, and, for special applications, electrically isolated sheathing (Figure 12.2). Electrically isolated monostrand tendons have had limited application (Schupack, 1980).

12.1.2.1 Material Specifications

12.1.2.1.1 Prestressing Steel

Prestressing steel properties have essentially remained unchanged, conforming to ASTM A 416 Grade 250 or 270. The seven-wire low-relaxation strand, with a nominal diameter of 0.5 in. and a specified tensile strength of 270 ksi, is typically anchored near 70% of its ultimate strength. The material should be packaged at the source in a manner that prevents physical damage to the strand during transportation and protects the material from deleterious corrosion during transit and storage.

12.1.2.1.2 Anchorages

Tendon anchorages and couplings should be designed to develop the static and fatigue strength requirements of Section 2.2.1.1 and Section 2.2.1.2 of the Post-Tensioning Institute's *Specification for Unbonded Single-Strand Tendons* (PTI, 2000) and Section 4.1 of *Acceptance Standards for Post-Tensioning Systems* (PTI, 1998). Castings should be nonporous and free of sand, blow holes, voids, and other defects. The average compressive concrete bearing stress of anchorages should not exceed the limits set forth in Section 2.2.1.3 of the referenced specifications. For wedge-type anchorages, the wedge grippers should be designed to preclude premature failure of the prestressing steel due to notch or pinching effects under the static or dynamic test load conditions stipulated under Section 2.2.3 (PTI, 2000) and Section 4.1 (PTI, 1998), for both stress-relieved and low-relaxation prestressing steel materials. Anchors intended for use in corrosive environments should include design features permitting a watertight connection of the sheathing to the anchorage and a watertight closing of the wedge cavity for stressing and nonstressing (fixed) anchorages. Intermediate stressing anchorages should be designed to permit complete watertight encapsulation of the unbonded tendon.

12.1.2.1.3 Sheathing

Sheathing for unbonded single-strand tendons should be made of a material with the following properties:

- Sufficient strength to withstand unrepairable damage during fabrication, transport, installation, concrete placement, and tensioning
- Watertightness over the entire sheathing length
- Chemical stability, without embrittlement or softening over the anticipated exposure temperature range and the service life of the structure
- Nonreactivity with concrete, steel, and the tendon corrosion-preventive coating

Minimum thickness of the sheathing used in all environments and all applications other than ground-supported post-tensioned slabs for residential and light commercial construction should be 0.050 in. for polyethylene or polypropylene with a minimum density of 0.034 lb/in.³, or equivalent if other materials are used. Minimum thickness of sheathing used in ground-supported post-tensioned slabs for residential and light commercial construction should be 0.040 in. for polyethylene or polypropylene with a minimum density of 0.034 lb/in.³, or equivalent if other materials are used (Section 2.3.2.1 in PTI, 2000).

12.1.2.1.4 Corrosion-Preventive Coating

The corrosion-preventive coating material should have the following functions and properties:

- Provide corrosion protection to the prestressing steel.
- Provide lubrication between the strand and the sheathing.
- Resist flow within the anticipated temperature range of exposure.
- Provide continuous nonbrittle coating at lowest anticipated temperature of exposure.
- Be chemically stable and nonreactive with prestressing steel, sheathing material, and concrete.

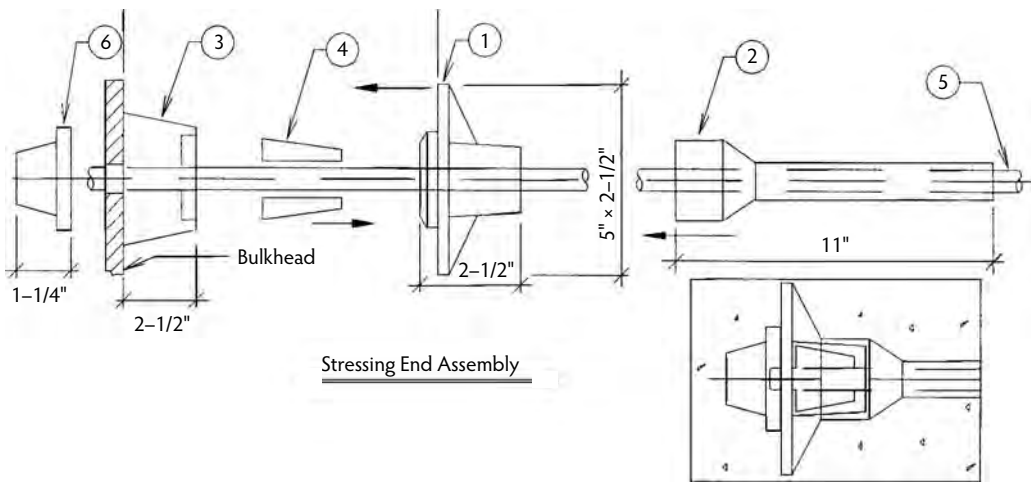
The film should be an organic coating with appropriate polar, moisture-displacing, and corrosion-preventive additives. According to Section 2.4.3 of *Specification for Unbonded Single-Strand Tendons* (PTI, 2000), the minimum weight of post-tensioned coating material on the prestressing strand should be not less than 2.5 lb per 100 ft for 0.5-in.-diameter strand and 3.0 lb per 100 ft for 0.6-in.-diameter strand. The amount of coating material used should be sufficient to ensure essentially complete filling of the annular space between the strand and the sheathing. The coating should extend over the entire tendon length.

12.1.3 Durability of Unbonded Tendons

Post-tensioned concrete members inherently provide enhanced durability due to the limitation of cracks that provide access to reinforcement for corrosive agents. The use of post-tensioning typically eliminates most slab joints, which, if not eliminated, may give corrosive agents access to beams and columns. The excellent durability performance of existing concrete structures in corrosive environments reflects the potential of unbonded monostrand tendons. Most of these structures were built without specific durability design and construction considerations. The visual inspection of a 15-year-old parking structure in Baltimore, Maryland, following demolition confirmed that no significant corrosion had occurred on the unbonded tendons over the 15-year service life (Suarez and Posten, 1990).

The distinguishing characteristic of an unbonded tendon is that, by design, it does not form a bond along its length with the surrounding concrete. The axial force in the stressed tendon is transferred to the concrete primarily by the anchors provided at each end. Because the force of an unbonded tendon is primarily resisted by the anchors at each end, the long-term integrity of tendons and anchors throughout the service life of an unbonded tendon are of concern.

The Post-Tensioning Institute originally published *Specification for Unbonded Single-Strand Tendons* in 1993; the second edition, published in 2000, includes special durability requirements for tendons used in structures exposed to aggressive environments. These specifications provide for watertight encapsulation of the strand within the tendon sheathing over its entire length, including watertight



Notes:

1. Locate anchor at bulkhead per project plans.
2. Install grommet flush between bulkhead and anchor for tight seal.
3. Slide sleeve tight against anchor. Be sure no bare strand is exposed. Tape if necessary.
4. After pouring, at time of stressing, remove grommet and insert wedges.
5. After stressing, cut strand to within 1/8" of end of end cap and grease end cap prior to inserting it tight against anchor.
6. Patch stressing pocket per project plans.

Item	Description
1	Anchorage
2	Protection sleeve
3	Grommet
4	Monowedges type 1.5
5	Strand (greased and coated)
6	End cap

FIGURE 12.3 Encapsulated system for tendons in corrosive environments (stressing end).

enclosure of the tendon anchorage device (Figure 12.3). The specifications further require the use of a specially formulated corrosion-inhibiting grease and include many other secondary provisions to ensure enhanced durability.

Nevertheless, some buildings constructed with unbonded tendons have suffered durability shortcomings. A survey of 215 concrete structures in Toronto, Ottawa, and Montreal concluded the following: “The evidence indicates that durable structures can be built, and that poor performance must be attributed to design and construction practices whose effectiveness falls short of that required by the environment” (Litvan and Bickley, 1987). A map that divides the United States into five principal environmental zones is available to help with understanding and evaluating environmental considerations when selecting appropriate unbonded tendon systems. The selection of zones was in part based on the geographical use of deicing salts and presence of airborne salts from oceans. Detailed information on the zoning requirements and related system recommendations can be found in Walker (1990).

To improve the quality and consistency of unbonded post-tensioned tendons, the Post-Tensioning Institute developed plant certification requirements and issued in 1998 *Acceptance Standards for Post-Tensioning Systems*. To further a better understanding of the durability aspect, the Post-Tensioning Institute issued the second edition of *Specification for Unbonded Single-Strand Tendons* in 2000. The specifications provide for tendons in both normal and aggressive environments.

12.2 General Notes and Standard Details

12.2.1 General Notes

This section is intended to offer a sample layout of general notes for the construction of an unbonded post-tensioned concrete structure, typically outlined on structural drawings. The sample notes are limited to the post-tensioning activity of the concrete frame or member only. The notes are neither considered complete nor applicable for every project that includes the construction of unbonded post-tensioned members; however, with minor revisions and additions and deletions, the notes have been used by the author on over 500 concrete structures. The design engineer should be aware that the concrete frame may develop cracking as a result of concrete creep, shrinkage, temperature deformation, and elastic shortening on members that are partially or fully restrained from movement. For this reason, notes should be added on the drawings that disclose the likelihood of potential concrete cracking and allow for a funding mechanism for crack repair in the form of a postconstruction material maintenance allowance.

12.2.1.1 General

Material, installation, stressing, and finishing specifications. The tendon shall meet the requirements set forth in *Specification for Unbonded Single-Strand Tendons* (PTI, 2000).

Marking of tendon location. If desired by the owner, the tendons may be marked using the dye-transfer method or by paint marking the formwork along the tendon lines just prior to placement of concrete. The paint transfers to the concrete soffit to permanently locate tendons (Section 6.4, PTI, 2006).

Power-driven fasteners. No power-driven fasteners or inserts shall be shot or drilled into the post-tensioned slab after concrete is placed without the written authorization of the engineer.

Openings. All openings, penetrations, and inserts shall be preplanned to the fullest extent possible. No changes shall be made in the field without prior approval of the engineer.

Formwork. For multilevel structures, the formwork shall extend beyond the slab edge, or scaffolding shall be provided to allow adequate room for the stressing operation.

Shop drawings. The contractor shall submit shop drawings showing tendon layout, dead-end and stressing-end locations, and tendon support layouts with details necessary for installation to the engineer for approval. The contractor shall supply the engineer with two sets of shop drawings a minimum of three weeks prior to fabrication. The review of shop drawings by the engineer is only for general compliance with the structural drawings and specifications. A set of approved shop drawings must be filed with the city engineer by the contractor.

Post-tensioned slab review. The tendon and mild reinforcement layout of a post-tensioned slab shall be reviewed by the engineer or the engineer's designated representative prior to concrete pour. The engineer shall be notified at least 48 hours in advance.

Field foreman. The field foreman responsible for the placement, stressing, and finishing of all break post-tensioning material shall have a minimum of five (5) years of specialized experience in this capacity for this type of construction.

12.2.1.2 Materials

Strand quality. One sample of each reel or heat shall be tested by an approved laboratory. Test results or mill certificates shall be submitted to the engineer before stressing of tendons. Post-tensioning tendons shall be stress relieved or be of low-relaxation quality and shall conform to the following:

PT hardware quality. All anchorages, couplers, and miscellaneous hardware shall be standard products and approved by governing agencies and the engineer.

Tendons. Unbonded strands shall be encased in slippage sheathing that shall consist of a sealed durable waterproof plastic tubing (minimum thickness as specified by PTI) capable of preventing the penetration of moisture and cement paste and that will contain a rust-inhibiting grease coating.

Tears in the sheathing shall be repaired to restore the watertightness of the sheathing. The sheathing application shall be limited to the extrusion process. Tendons shall be secured during shipping and supported during handling to avoid damage to the tendon sheathing. During shipping and storage, the tendons shall be covered or protected to avoid moisture access to post-tensioning material.

12.2.1.3 Installation

Installation of unbonded tendons. If the post-tensioning supplier does not install the material supplied, detailed instructions for the installation and stressing of tendons shall be furnished. The contractor responsible for hiring the independent post-tensioning placer shall ensure that the installation crew meets the standards set forth above. The supplier shall provide technical assistance necessary to properly install, stress, and finish all post-tensioning material.

Tendons. Tendons shall be shop fabricated with preassembled fixed-end anchorages. Anchor casting with plastic pocket formers shall be used at all stressing ends to recess the anchor in enough concrete to achieve required cover.

Banded layout. The banded tendon placement layout shall be used for two-way post-tensioned slabs.

Tendon placement. Care shall be taken that tendons are located and held in their designated positions. Tolerances for the location of the prestressing steel shall not be more than $\pm 1/8$ in. vertically, except as noted or approved by the engineer. Access to stressing ends shall be maintained where shown.

Strand bundles. The maximum allowable number of strands per bundle is four (4) for slabs and six (6) for beams.

Tendons over columns. For two-way slab construction, a minimum of two (2) tendons in each orthogonal direction shall be placed directly over the supporting column.

Tendon adjustments. Small deviations in the horizontal spacing of the slab tendons will be permitted when required to avoid openings, inserts, and dowels with specific locations. Where locations of tendons seem to interfere with each other, one tendon may be moved horizontally to avoid the interference.

Twisting. Twisting or entwining of individual wires or strands within a bundle or a beam shall not be permitted.

Vertical profiles. Profiles shall conform to controlling points shown on the drawings and should be in approximate parabolic drape between supports, unless noted otherwise. Low points are at midspan unless noted otherwise. Harped tendons shall be straight between high and low point controls.

Horizontal profiles. Should the tendons be horizontally curved to miss an opening or other obstructions, tendon bundles shall be flared with a minimum distance of 2 in. between each individual tendon while horizontally curved. In addition, #3 hairpins at 12 in. on-center for each tendon shall be installed, transferring the horizontal radial force via the hairpin mild reinforcing to the concrete.

Prestress cover. All dimensions showing the location of prestressing tendons are to the center of gravity (CGS) of the tendon unless noted otherwise.

Minimum chairing. Tendons shall be secured to a sufficient number of positioning devices to ensure correct location during and after the placing of concrete and shall be supported at a maximum of 3 ft, 6 in. on-center. Chairs greater than 2.5 in. shall be stapled to the formwork.

Support bars. Support bars located at the face of drop panels shall be #6 or greater. Drop panels greater than 4 ft in width shall have additional #6 or greater support bars at the center, with a maximum support bar spacing of 4 ft for larger panels. All other support bars shall be minimum #4 bars. Continuous support bar lap splices shall be 24 in. minimum.

Anchors. Anchorages shall be recessed a minimum of two (2) in. Place two (2) #4 bars continuous behind all anchorages unless otherwise noted. Splices shall be 24 in. minimum and staggered. Special anchorage zone reinforcement shall be provided for groups of six or more anchors for 1/2-diameter strand tendons spaced at 12 in. or less on center.

Blockouts. All pockets or blockouts required for anchorage shall be adequately reinforced so as not to decrease the strength of the structure. All pockets should be waterproofed to eliminate water leakage through or into the pocket.

Pipes and conduits. Plastic or metal conduits may be embedded in the slab providing that the following criteria are met:

- A. Plumbing pipe and electrical conduit layout proposed to be within the slab cross-section must be specifically approved by the engineer of record.
- B. Maximum pipe or conduit size shall be 1.5-in. diameter (O.D.), located within the middle third of the slab cross-section, and supported independently from all reinforcement.
- C. Center-to-center spacing of conduits shall not be less than three (3) times the diameter of the largest conduit.
- D. No aluminum pipes, conduit, or embedment shall be permitted in post-tensioned concrete slabs.
- E. Conduits must not interrupt the post-tensioned tendon layout or profile.
- F. No pipe or conduit may be placed within the column shear cone.
- G. It is undesirable to have excess amounts of conduit entering the slab from one location. If this condition exists, the conduits must be fanned out immediately.

Penetrations. Penetrations shall not be permitted in beams or drop caps unless permitted on post-tensioning drawings or typical details.

12.2.1.4 Concrete Placement

Concrete consolidation. The contractor shall take precautions to ensure complete consolidation and densification of concrete behind all post-tensioning anchorages.

Concrete placement. When concrete is placed in post-tensioned slabs, special care shall be taken at all column drop caps (panels). Insert the pump hose into the column drop panel below reinforcement and fill until concrete reaches the top reinforcing layer. Monitor concrete elevation to avoid flotation of top reinforcing. After the drop panel is full of concrete, place concrete over the top reinforcing layer to specified slab thickness. Vibrate adequately in and around column drop panels.

Pumped concrete. If concrete is placed by the pump method, horses shall be provided to support the hose. The hose shall not be allowed to ride on the tendons.

Chlorides. Grout or concrete containing chlorides shall not be permitted.

12.2.1.5 Stressing of Tendons

Tendon stresses. Such stresses shall conform to the following:

- Maximum tendon jacking stress, 216 ksi
- Maximum tendon stress at anchorage immediately after prestress transfer, 189 ksi

Effective force. Forces shown on structural drawings are effective forces after all losses. All losses (short- and long-term losses) due to creep, shrinkage, tendon relaxation, and elastic shortening, including friction losses and losses due to wedge seating, may be assumed as 14 ksi. Thus, the effective force per tendon may be assumed to be 24.8 kips for stress-relieved tendons and 26.8 kips for low-relaxation tendons, when tendon length is less than 100 feet. For variance from this value or for tendons over 100 feet, the post-tensioning supplier shall provide friction and long-term loss calculations for the engineer's approval. Friction losses may not be averaged or assumed to redistribute along the tendon length. The available effective force shall be established at a location along the tendon length where the force demand meets the minimum effective tendon force.

Concrete strength at stressing. Prior to transfer of prestress, concrete shall reach a minimum compressive strength of $f'_c = 3000$ psi. Minimum concrete strength shall be established by breaking concrete test cylinders. The stressing shall not commence until concrete reaches the specified strength; however, tendons shall be stressed within 72 hours after concrete reaches the minimum specified strength to mitigate early-age concrete cracking. This may not apply to stage stressing of transfer floor or mat foundations.

Calibration. The ram and attendant gauge used shall have been calibrated within sixty (60) days of use.

Tendon stressing. The stressing operation shall be done by jacking under the immediate control of a person experienced in this type of work. Continuous inspection and recording of elongations are required during all stressing operations.

Stressing sequence. In general, uniformly distributed tendons shall be stressed before concentrated beam strip (banded) tendons, and slab tendons shall be stressed before beam tendons. Additional stressing sequence requirements shall be as specified below.

Two-Way Slab Sequence

1. Stress continuous distributed tendons
2. Stress continuous banded tendons
3. Stress added distributed tendons
4. Stress added distributed tendons
5. Stress added slab tendons

One-Way Slab and Beam Sequence

1. Stress temperature tendons
2. Stress continuous slab tendons
3. Stress beam tendons
4. Stress transfer girder tendons

Elongation. Individual tendon field readings of elongations and/or stressing forces shall not vary by more than $\pm 7\%$ from the calculated required values shown on the shop drawings. If the measured elongations vary from calculated values by more than $\pm 7\%$, the contractor shall provide friction calculations and/or other justification, to the satisfaction of the engineer, for the discrepancies.

Member forces. The post-tensioned force provided in the field for each structural member shall not be less than the values noted on the structural drawings. In this context, structural members are beams or slabs, whether with banded or distributed tendons, each serving its respective tributary area.

Tendon ends. Do not burn off tendon ends until the entire floor system has been satisfactorily stressed and the engineer's approval is obtained.

Anchor protection. The stressing end anchors and wedges shall be spray-painted with rust-inhibiting paint or a similar coating for corrosion protection prior to grouting of recess pockets. Install grease caps within 24 hours after cutting tendon tails.

Grouting of stressing pockets. Stressing pockets shall be filled with nonshrink grout after stressing, tendon end cutting, painting, and grease capping to stop moisture access to the strand.

Deshoring. Slabs or beams may be deshored when all tendons have been satisfactorily stressed and the engineer's approval is obtained, unless shoring is required to carry floors of multiple levels (reshoring). In areas supporting a partial span, such as near a pour strip or construction joint, the shoring in the partial span and immediate back span shall stay in place until the remaining section of the span has been poured and stressed or cured.

Inspection for prestressing steel. Continuous special inspection shall be provided during placement of reinforcing steel, tendon supports, and prestressing steel. Tendon location and integrity of the protective wrapping for post-tensioned tendons shall be inspected prior to placement of concrete. During stressing of post-tensioned tendons, the special inspection shall include recording of field-measured elongation and jacking force for each tendon.

Admixtures. No admixtures shall be added to the concrete mix without the approval of the engineer, unless noted otherwise. Admixtures concrete containing chlorides shall not be used in post-tensioned slabs.

Special notes to the owner. Under normal conditions, and for conventional buildings, reinforced concrete as well as post-tensioned concrete develops cracks. The cracks are due to inherent shrinkage of concrete, creep, and the restraining effects of walls and other structural elements to which the beams/slabs are tied. The early-age concrete cracks that may develop are usually of a cosmetic nature. The slab typically retains its serviceability and strength capability. Due to special features of unbonded post-tensioning, it is possible that a number of hair cracks, which would normally spread over a wide area, will integrate into a single crack with a width exceeding 0.01 in. It is emphasized that, although special efforts are made to reduce the potential causes and number of such cracks, it is not practical to provide total articulation between

the floor system and its supports and thereby achieve complete inhibition of all cracks. Most early-age cracks develop during the first two (2) years after construction of the floor system is complete. Cracks that are wider than 0.01 in. may have to be pressure epoxied. Refer to the notes under the Material Allowances section. The objective of providing joints is to allow movement. Movements due to creep and shrinkage may be noticeable at joints for up to two (2) years after construction, beyond which movements due to variations in temperature will persist. In aggressive environments, cracks should be repaired at the time they are first noticed.

12.2.1.6 Material Allowances

The contractor shall include in the project budget material allowance for the engineer to use at the engineer's discretion during construction to address unforeseen conflicts. Any materials not used by the engineer shall be credited back to the individual (owner, developer) funding such allowances.

Reinforcement allowance. The contractor shall provide an amount of reinforcement as specified by the engineer of record for the engineer to use at the engineer's discretion during construction. (Example: The contractor shall provide 2000 lb plus 0.05 lb per square foot of elevated concrete slab of reinforcement for the engineer to use at the engineer's discretion during construction.)

Post-tensioning allowance. The contractor shall provide an amount of post-tensioning material as specified by the engineer of record for the engineer to use at the engineer's discretion during construction. (Example: The contractor shall provide 1000 lb plus 0.02 lb per square foot of elevated concrete slab of post-tensioning material for the engineer to use at the engineer's discretion during construction.)

Pressure epoxy allowance. The contractor shall include an amount for pressure epoxy injection of cracks that may develop in the structure during the first two (2) years. (Example: The contractor shall include the cost of \$0.10 per square foot of elevated concrete slab for pressure epoxy injection of cracks that may develop in the structure during the first 2 years.)

12.2.2 Standard Details

In accordance with standard industry procedures for most construction-related work, details for unbonded post-tensioned members are first developed by the design engineer or architect. The details typically show the member geometry, reinforcing layout (location of tendons and mild reinforcing), and other embedments. After the construction contract is awarded, the post-tensioning supplier commonly prepares more project-specific drawings, called *shop drawings*. The shop drawings for post-tensioning materials are normally prepared in much more detail than the design drawings. Typically, they are submitted for review and approval to the design engineer or agency before fabrication of the tendons is initiated. It is essential that details of the post-tensioning tendons, nonprestressed reinforcement, ducting for electrical or mechanical service, and other embedment items be reviewed and coordinated during the detailing stage. It is not uncommon for final details for different material trades to be shown on different shop drawings, indicating incompatible or conflicting layout. In most cases, details can be rather easily adjusted at the shop-drawing stage to accommodate all embedded items. When conflicts do arise during the development of shop drawings or during construction, the tendon layout should govern over other elements or embedments conflicts. Many specialized structural details have been developed for the construction of unbonded post-tensioned members. The following selected details illustrate typical design and detailing practices for most common applications of unbonded post-tensioning in building construction.

12.2.2.1 Tendon Anchorage Zone

The anchorage zone, probably the most critical concrete region, has to retain the tension force of unbonded tendons during the service life of the post-tensioned structure. Figure 12.4 shows typical details of stressing and dead ends. Unless otherwise detailed on the design or post-tensioning installation drawings, banded tendon anchorage zones in normal weight concrete for groups of six or more 1/2-in.-diameter single-strand tendons with anchor spacing of 12 in. or less should be reinforced in accordance

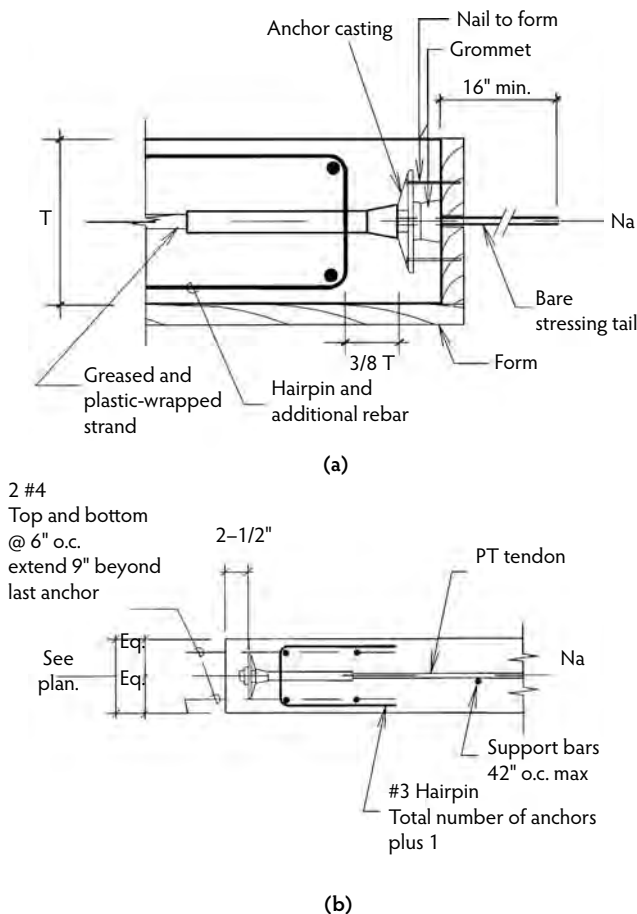


FIGURE 12.4 Stressing and dead ends: (a) stressing end anchor for banded tendon in a corrosive environment, and (b) dead end at banded tendons in a corrosive environment.

with Figure 12.4b. For restriction of anchorage zone embedments, see Figure 12.14. The flaring of tendon bundles near anchorage zones, in the horizontal plane of the concrete member, and fixed-end tendon staggering requirements are suggested in Figure 12.5.

12.2.2.2 Two-Way Slab Tendons over Column Supports

The congested mild-reinforcing arrangement and tendon layout of banded and uniform tendons over column supports must be detailed so the field personnel can understand the various layers of top reinforcement and their support system. Figure 12.6 and Figure 12.7 indicate a typical two-way slab tendon layout over interior and exterior columns. The layout of tendon groups is arranged so, except for the bundle of uniform tendons (minimum two tendons) directly above the supporting column, all tendons in both directions have essentially the same eccentricity within the proposed slab section in the negative moment region. A detailed account of all layers can be found in Figure 12.8.

12.2.2.3 Beams

A number of field problems can be eliminated if simple installation recommendations are considered during installation of the beam reinforcement. Figure 12.9 and Figure 12.10 show typical beam-column joints and beam sections with detailed information on tendon and mild reinforcement layout. In addition to showing a detailed bar layout for mild reinforcing, the tendon support system is very critical. The

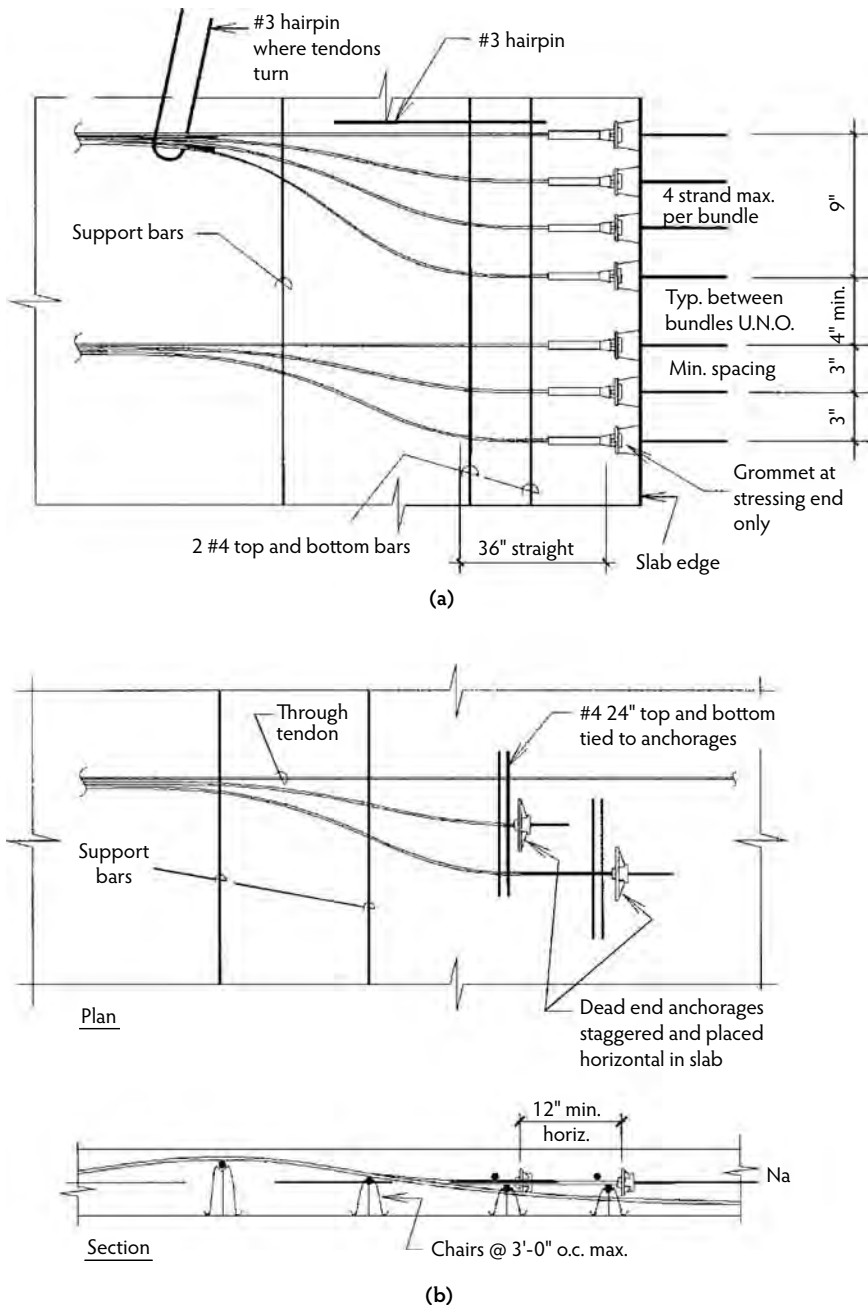


FIGURE 12.5 Flaring of tendon bundles and fixed-end tendon staggering: (a) flaring of banded tendons at the slab edge in a corrosive environment, and (b) placement of added tendons.

tendon support bars must be stable and properly secured to ensure a firm tendon profile during the concrete pour. Also, large tendon bundles, such as multiple bundles of six tendons, that are not properly spaced and layered may result in tendons bunching up at locations of curvature (high and low points) and developing splitting forces in the concrete beam. The use of tendon support bars, which guide the installation crew in the appropriate spacing of tendon bundles, has successfully addressed this concern (Figure 12.11).

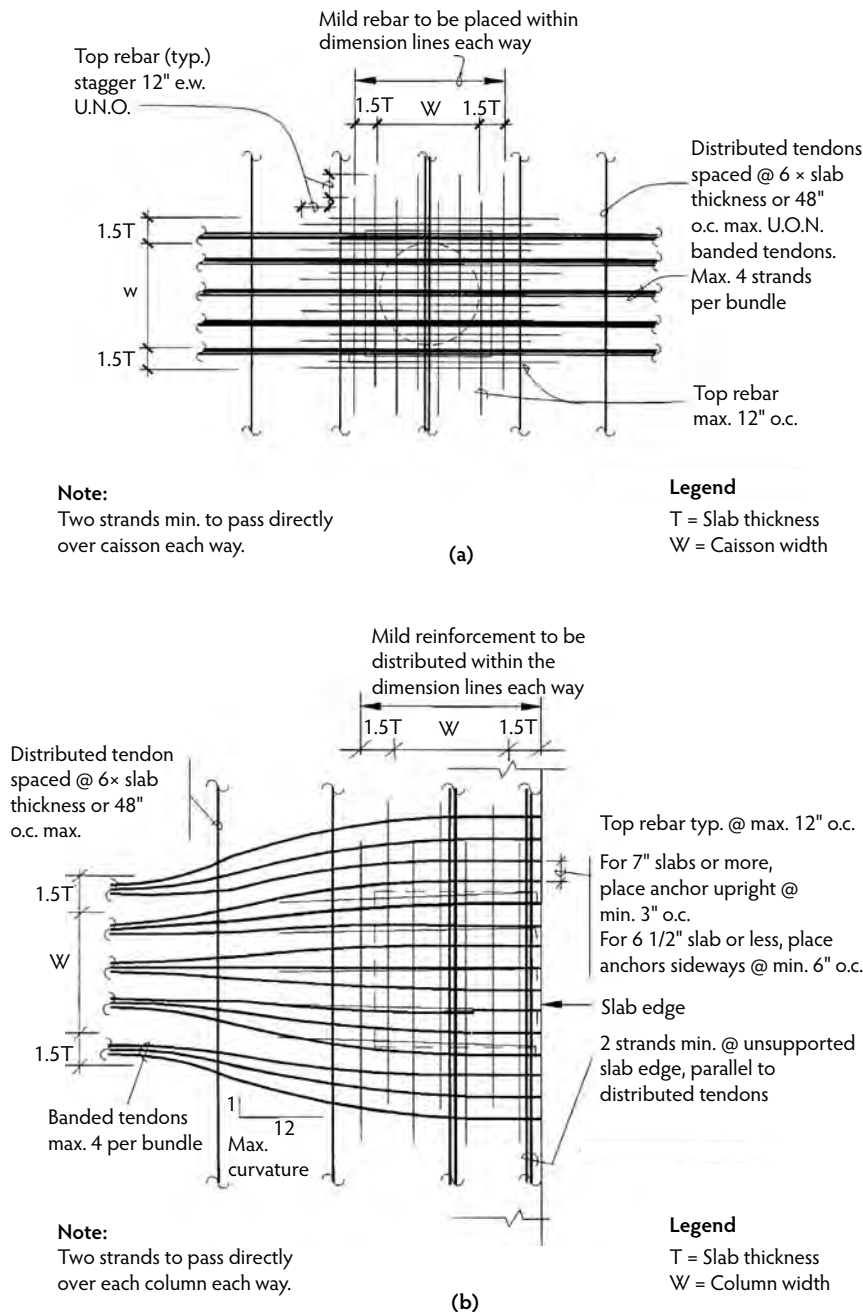
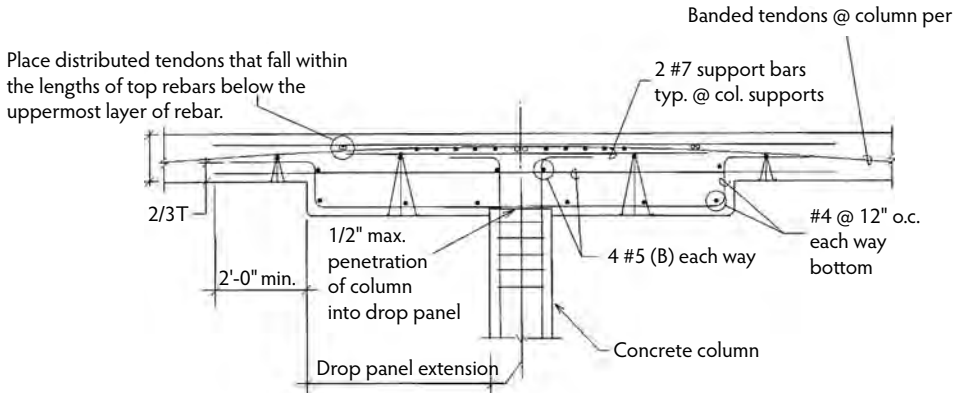


FIGURE 12.6 Typical two-way slab tendon layout: (a) top reinforcement at interior columns, and (b) top reinforcement at exterior columns.

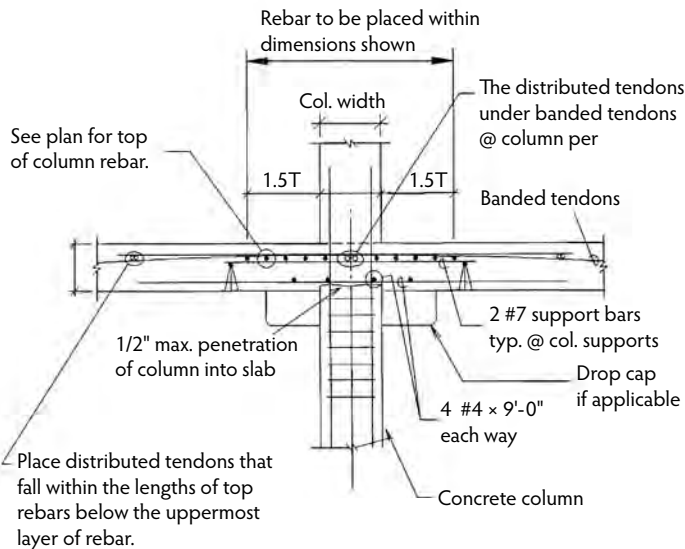
12.2.2.4 Joints

Section 12.3 discusses in detail the types and optimum locations for joints to mitigate the restraint effects of post-tensioned members. In addition to restraint considerations, joints may have to be located to limit concrete pour size (Figure 12.12a) or allow for intermediate stressing (Figure 12.12b). The selection of pour-strip location and duration of pour-strip opening shall be based on a numerical shortening evaluation of the structure. A sample reinforcing layout for a typical interior stressing blockout and a 3-foot-wide



Note: A minimum of two tendons shall be placed in each direction directly over column.

(a)



Note: A minimum of two tendons shall be placed in each direction directly over column.

(b)

FIGURE 12.7 Typical two-way slab tendon layout: (a) typical interior column, and (b) typical drop-panel section.

pour strip is shown in Figure 12.13. The preceding discussion emphasizes that the successful performance of an unbonded post-tensioned structure is directly related to the understanding and extent of detailing of specific performance considerations.

12.2.3 Typical Field Shortcomings: Problems and Solutions

12.2.3.1 Preventing the Most Frequent Problems

Prior to placing the concrete, the post-tensioning installation should be checked for the following. The area behind the anchors (18 in. behind the anchor at 45° angles on each side, as shown in Figure 12.14) should be free of sleeves, blockouts, large conduit, or any other voids or congestion that could

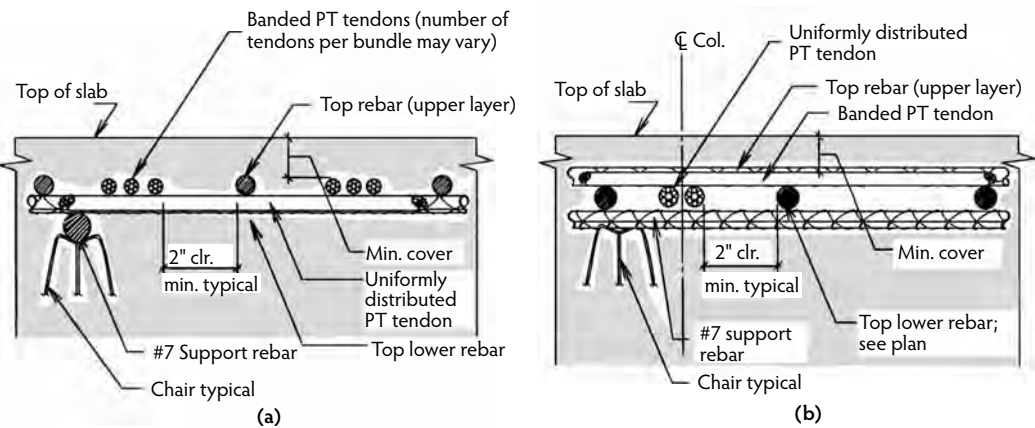


FIGURE 12.8 Layers in typical two-way slab tendon layout: (a) section through banded tendon at column, and (b) section through distributed tendon at column.

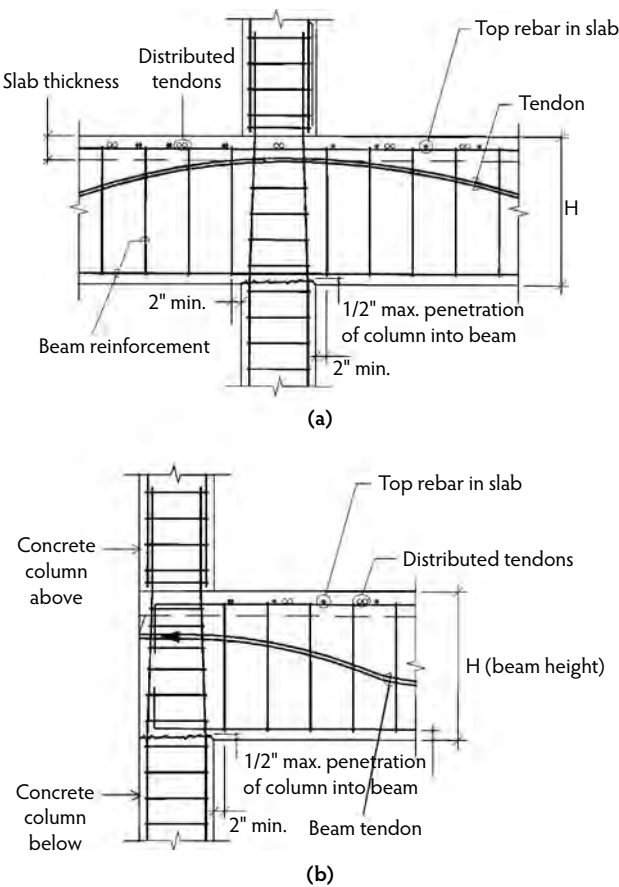


FIGURE 12.9 Typical column-beam joints: (a) typical column-beam section; (b) exterior beam-column connection.

allow the concrete to crush or form a void in this high-stress zone. If penetrations must be positioned within the 45° region, steel pipe inserts must be used as specified by the engineer. Frequently, the electrical, mechanical, and plumbing contractors place their sleeves just before the pour, after the

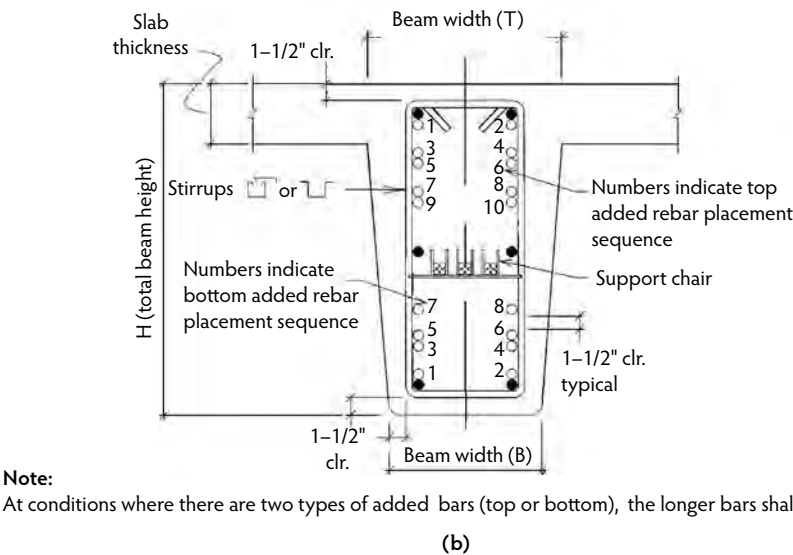
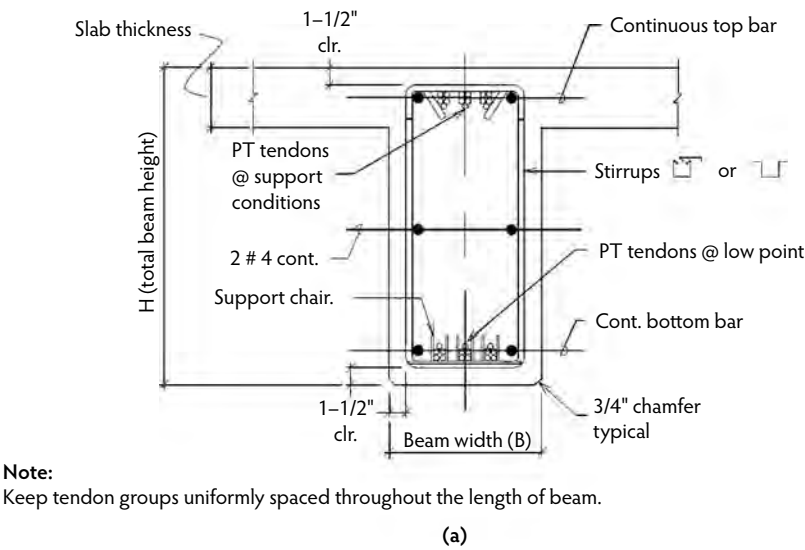


FIGURE 12.10 Typical beam sections: (a) placement of tendons in beam, and (b) placement of reinforcement in beams.

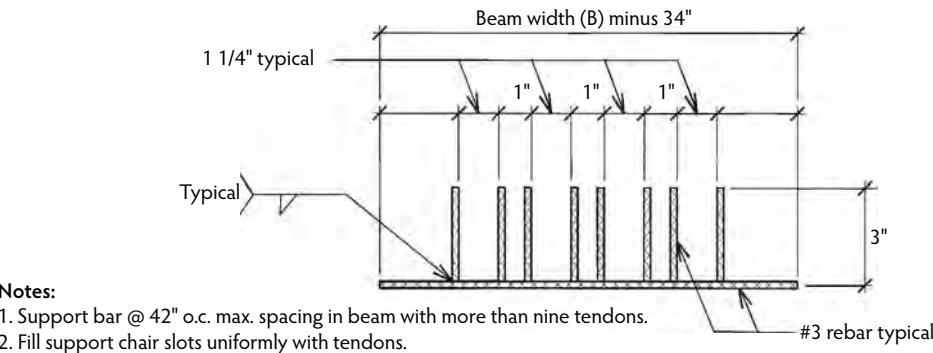


FIGURE 12.11 Tendon support bar.

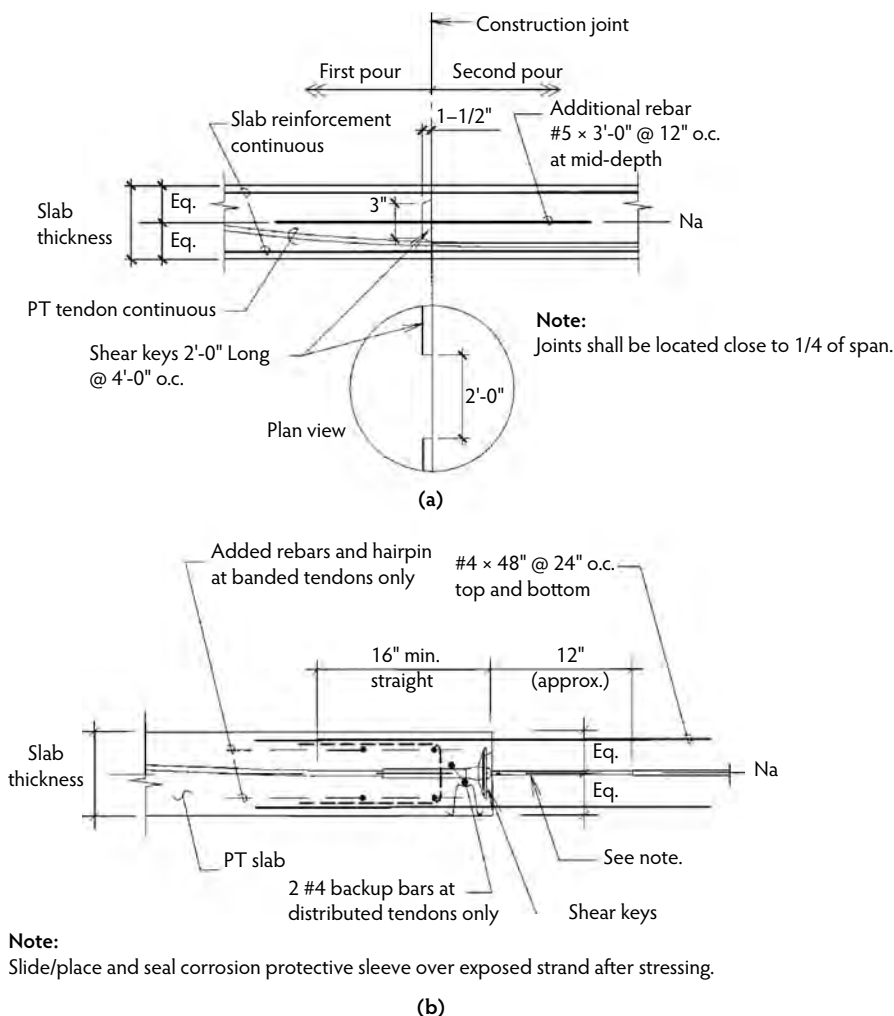
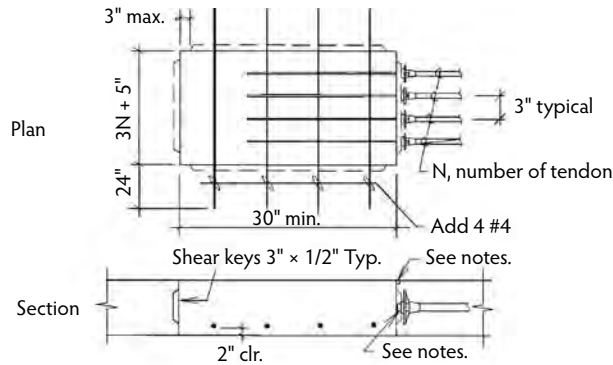


FIGURE 12.12 Joint locations: (a) construction joint with no intermediate stressing, and (b) construction joint with intermediate stressing in a corrosive environment.

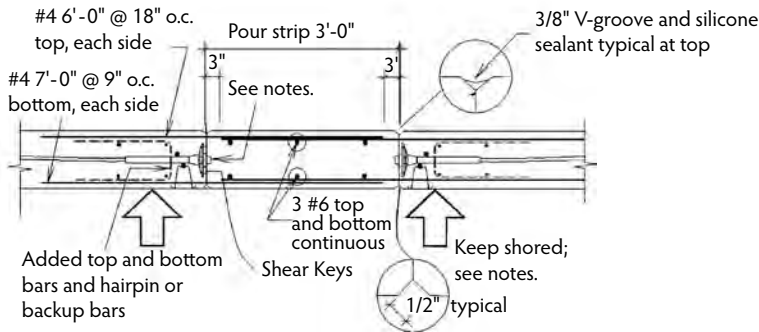
tendon-placement inspection. While checking the anchor zones, make sure a sufficient strand tail extension is protruding through the edge form. It is typically much easier to adjust the tendon by a few inches prior to placing the concrete than it is to use splices and special equipment to stress a short tendon later.

For an encapsulated system, the sheathing should be connected to the anchor according to the manufacturer's recommendation to ensure that there will be no exposed strand and to provide continuous protection. In normal environments, however, because there is no connection between the anchor and the sheathing, special care should be taken to minimize the length of greased strand behind the anchor. The maximum length of greased strand should not exceed 1 in. If concrete is cast against unsheathed strand, the rifling pattern of the strand will be cast in the concrete, forming spiral grooves that twist the strand when stressed. The spiraling of the strand will cause the stressing jack to spin at the end of the stressing cycle and could injure the person operating the stressing equipment or break the hydraulic supply hoses on the jack. Even if no one is harmed, the twisting motion of the strand through the jack grippers causes premature wear. It is important to tape wrap exposed strands before the concrete pour, as the fix is costly once the concrete has hardened.



- Notes:** 1. Cut stressed strands; grease and place end cap.
2. Continue all interrupted bars shown in plans through the blockout.
3. Fill blockout with nonshrink concrete of same strength as slab, minimum.

(a)



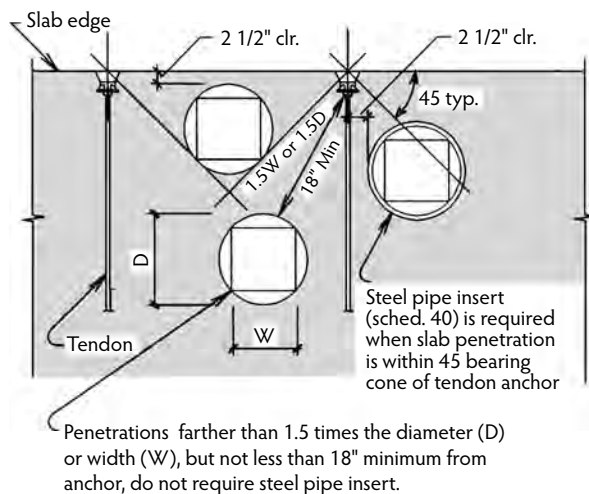
- Notes:** 1. Retain shoring until closure concrete reaches slab's design strength or 14 days.
2. Closure strip to be poured with non-shrink concrete not less than \times days after stressing.
3. Roughen & clean joints & wet prior to placing concrete.
4. Eliminate accidental misalignment between edge of slabs that are to be joined with a closure strip. Use mechanical methods such as jacking, if necessary.
5. Raise edge of slab 1/4" @ closure to allow for settlement.
6. Provide waterproofing membrane if required for water-tightness.
7. Cut stressed strand tails; grease and place end cap.

(b)

FIGURE 12.13 Sample reinforcing layouts: (a) stressing blockout and (b) closure strip in a corrosive environment.

If more than 1 in. is exposed, repair the sheathing right up to the back of the anchors. If this area is difficult to access due to bursting steel or other obstructions, make a circular cut on the sheathing 18 to 24 in. back from the anchor, slide the sheathing forward until it touches the anchor, and then repair the bare spot at a location away from the congestion. The second option has the advantage of leaving the most critical area (that zone 12 in. behind the anchor) covered with good sheathing.

The quality of the installation can be jeopardized by people walking on the placed cable before a pour. The pocket former must be held tight against the anchors so concrete slurry does not leak into the anchor cavity. This can happen if the concrete vibrator bounces the edge form and separates the pocket former from the anchors. There is no substitute for having the anchors tightly attached. If a small amount of post-tensioning coating is applied to the tip of the pocket former before inserting it in the anchor cavity, it will make a seal between the two pieces that will keep concrete slurry out even if a small gap develops.



- Notes:** 1. Penetrations with dimensions greater than 12" require trim reinforcement.
 2. Sweat PT tendons (where possible) to avoid conflict between PT anchors and openings.

FIGURE 12.14 Openings at post-tensioning anchorage.



(a)



(b)

FIGURE 12.15 Split troubleshooting anchor.

12.2.3.2 Slipping Strand and Jack Hang-Up

When wedges fail to hold the strand, the most common cause is concrete slurry in the wedge seat of the anchor cavity. If a separation between the pocket former and the anchor occurs, concrete slurry can flow into the anchor cavity and set up in the form of a ring around the strand at the back of the anchor. This will stop the wedges from penetrating into the anchor the proper distance and result in strand slippage. If the elongation requires more than one cycle of the stressing equipment, it can cause the jack to become locked onto the tendon. On the first cycle, the wedges usually hold because they do not have to be fully seated and the pressure is low. On the second cycle, the wedges bottom out on the concrete slurry and the strand will be free to slide back into the concrete, stripping the teeth on the wedges and hanging up the jack. Several different methods can be used to detension the tendon, thereby releasing the jack, depending on individual site conditions as follows. A second jack should not be used on the back of the one that is hung up to detension it. Once the jack is hung up, a troubleshooting split anchor (Figure 12.15) must be inserted behind the nosepiece of the jack bearing on the anchor cast in the concrete but in front of the gripper block of the jack to free up the jack.

During this procedure, do not exceed the recommended gauge stressing pressure. Open the jack just enough to insert the troubleshooting split anchor on the strand. Insert the wedges in the troubleshooting anchor and slowly release the pressure on the jack until the stress in the strand is taken up by the troubleshooting anchor. Continue closing the jack until the jack grippers in the jack gripper block are released from strand. Extend the jack fully and then retract the jack approximately 2 in. Engage the jack grippers and extend the jack to stress the strand again and release the wedges in the troubleshooting anchor. (Applying a thin coat of Never-Seez® or a similar product on the back of the wedges will make them easier to remove during this step.) Slowly release the pressure in the jack and let the strand slide back into the concrete slab until fully relaxed. (If the jack bottoms out before the strand is relaxed, simply repeat all the steps of the sequence.) When the jack is fully released, remove it and the wedges from the anchor in the slab. It is not uncommon to find that the wedge seating was either restricted by a small film of concrete slurry around the tapered sides of the anchor cavity or a ring of concrete formed around the strand at the back of the anchor. If necessary, remove the debris by scraping or chipping the slurry out of the anchor. Because the area is very congested, a small screwdriver may be the proper tool for this procedure. After removal of all debris, clean the wedge seat of loose materials and dust using compressed air. Insert a new pair of wedges and stress the tendon.

12.2.3.3 Honeycomb in Concrete

Rock pockets, sand pockets, or voids should be repaired prior to the stressing operation. Remove all loose material and dust prior to repair. Wet the concrete surface before repair. When patching, use a high-strength, nonshrink concrete grout mix with an epoxy binder. Grout strength should equal or exceed specified concrete strength. *Do not* use grout that contains calcium chloride or other materials containing chloride. When the patch has attained proper strength, the stressing operation may proceed. It is essential to repair honeycomb in anchorage zones to avoid blowouts. After detensioning of tendons, all loose material and dust should be removed until sound concrete surfaces are encountered. Stress tendons after the repaired area reaches the minimum concrete compressive strength specified. Prior to stressing, check the quality of the patch by tapping it with a hammer to sound for voids. A hollow sound indicates a poor patch that is not suitable for stressing.

12.2.3.4 Splicing Tendons

Tendons are sometimes too short to reach an edge form because of misplacement or misfabrication. If the tendon is in one pour only and not continuous, every effort should be made to replace the short tendon with a tendon of proper length instead of using couplers. If tendons are continuous from another pour, thus making tendon couplers necessary, the engineer of record and the post-tensioning material supplier should be notified. The coupler location should be determined by the post-tensioning material supplier such that the coupler is centered in the member and not at a point of tendon curvature. Couplers should not be located side by side. If more than one tendon requires splicing, couplers should be staggered at half-bay increments per tendon group.

A PVC pipe of sufficient inside diameter to hold the coupler and of sufficient length to allow for subsequent elongation movement should be used. Also, an additional piece of sheathed strand of sufficient length to reach the edge form is required, along with two pocket formers. Post-tensioning coating should be used to fill the void in the PVC pipe. The tapered tip of the pocket former that normally fits inside the anchor cavity can be cut off when being used for splicing, thereby reducing the length of the PVC pipe needed. The original strand is first cut with a saw or abrasive plate at the coupler location, and one pocket former is placed on the strand. The strand should be marked before coupling to make certain that the proper length of strand has been fully inserted into the coupler. The coupler is then coupled to the original strand. The PVC pipe is placed over the coupler. The second pocket former is placed over the new strand (the strand is marked) and inserted into the coupler. A pocket former is taped to one end of the PVC pipe, which is then packed tightly with post-tensioning coating, allowing no air voids. The second pocket former is affixed to the PVC pipe, completing a tightly sealed coupler.

The tendon coupler's location within the PVC pipe must permit the coupler to move the required elongation amount in the direction of stressing. Allowance for movement in both directions must be provided when the tendon is to be stressed from both ends. Conservatively, a minimum of 1.5 times the total expected elongation at the splice location should be allowed for. A dark crayon or paint mark on the deck will facilitate locating the coupler after the pour, should that become necessary if the above procedure was not properly followed.

12.2.3.5 Tendons Too Short to Stress Using Normal Stressing Procedure

Short tendons can result from an incorrect tendon-fabrication cutting list, misfabrication, misplacement, or a job-site mistake such as cutting tendons off prior to stressing. During stressing, most conditions may be addressed with special equipment that can be obtained from the post-tensioning material supplier. If a tendon is too short to be stressed using a standard jack, in some cases a short tendon can be stressed by simply removing the nose piece and using jack feet. When using jack feet, care should be taken to center the jack with the tendon before applying pressure. If the tendon is stressed without being centered on the anchor, it will rub on the side of the anchor, and inserting one of the wedges may be impossible. This will cause the other wedge to be drawn all the way to the back of the anchor cavity, breaking or damaging the strand. Without the hydraulic-seating attachment, the wedges will have to be inserted and seated using a hand-seating tool and a hammer. Tendons that are too short for the above procedure will have to be stressed using a coupler with a short piece of strand fixed on one end of the coupler. Tendons that were cut with a torch prior to stressing have lost some of the temper in the steel due to the heat. If the jack grippers or the coupler grip near the previously heated area, the tendon may slip at a very low pressure. If this condition exists, make the first pull as short as possible (so the stressing pressure is kept low), install the wedges in the anchor, and regrip the tendon farther away from the end that was heated.

12.2.3.6 Lift-Off Procedures

The purpose of a lift-off is to verify the force of a tendon after it has been stressed. A lift-off may be required when the recorded elongation is out of code-recommended tolerance. Project specification may call for a selected force verification using the lift-off method. A lift-off test may be conducted by use of the standard hydraulic stressing jack on previously stressed and anchored monostrand post-tensioning tendons to determine the residual effective force in the tendon at the anchorage. The lift-off test is preferable and most easily done before the stressing tails of the tendons have been cut off. While it may be possible to conduct a lift-off test after the stressing tails have been cut off, this possibility is determined by the length of tendon protruding beyond the wedges in the stressing pocket as well as the possibility of connecting the hydraulic jack to this length of tendon (this may be dangerous). When the tendon is initially stressed and anchored, the wedge seating that occurs develops a mechanical-friction force between the strand, wedges, and anchorage casting. During the lift-off test, it is necessary to stress the tendon in excess of the residual effective tendon force at the anchorage by an amount equivalent to this mechanical-friction force to break the wedges loose and determine the force remaining in the tendon. This process will be reflected during the lift-off test by stressing to a level (reflected on the gauge attached to the ram) sufficient to break the wedges loose and a subsequent reduction in the gauge pressure to reflect the residual force in the tendon. It should be understood that the lift-off test determines the residual force in the tendon at the anchorage. Determination of the force level in the tendon at other locations requires detailed consideration of friction and wedge-seating effects.

12.2.3.7 Cracked Wedges

Hairline cracks may appear in the case-hardened surface of wedges due to deformation of the wedges around the strand at the time of seating. These cracks do not affect the integrity of the post-tensioning system.

12.2.3.8 Shooting Power-Driven Fasteners

The structural designer of an unbonded post-tensioned member should offer detailed information regarding the limited application of power-driven fasteners that may be used on a particular project

member. Frequently, developers are concerned about damage to tendons if future plumbing penetrations are added. This problem can be solved for structures in which changes are anticipated. The dye-transfer technique relies on the dye color marked on the forms to transfer to the concrete soffit after the member is poured. Alternatively, markers may be installed to visually mark the location of each band and tendon bundle.

12.2.3.9 “Hazardous” Statement

The procedures described in this part of Section 12.2.3 may be hazardous. Only qualified experienced personnel, with a minimum of 5 years of specialized experience in the installation and repair of unbonded post-tensioned systems, should attempt these procedures.

12.3 Evaluation and Rehabilitation of Building Structures

12.3.1 Evaluation

Even though concrete is considered to be one of the most durable construction materials, building structures must be evaluated during their useful life for various reasons. Some of the more common reasons may include deterioration (serviceability shortcomings, loss of strength), change in loading of a structure, building modification, overloading (disaster), or simply as an assurance evaluation. The evaluation of an existing unbonded post-tensioned elevated floor system may be divided into three principal activities: (1) examination of the existing floor system and structure (conditional survey), (2) diagnosis, and (3) prognosis or findings. All three steps are necessary before a repair or retrofit can be outlined. The level of evaluation may vary from simple nondestructive examinations and preliminary calculations for initial reporting to rigorous destructive testing with detailed analytical diagnosis of the structure.

12.3.1.1 Examination of an Existing Unbonded Post-Tensioned Floor System

As part of the structural assessment, the engineer should initially complete a detailed survey of the structural floor framing system, geometry, and the “as-is” condition of the structure, including environmental impact. This stage includes the collection of existing information about the structure, surveying the floor system for signs of distress, and establishing a listing of proposed nondestructive and destructive testing based on the distress observed and information gathered. To establish as-built data, the examination should consider the material properties and the detailed survey of the condition of each material and the material configuration or quantity.

The physical testing of concrete may include verification of the concrete compressive strength, material uniformity, mix properties, permeability, and aggregate type. In addition, chemical testing may be performed to establish the concrete constituents, which are used in the evaluation of concrete reactivity or concrete resistivity. The tests should determine the amount of chloride, sulfate, or other materials that may result in a chemical attack on the concrete section of concern. Properties such as the tensile strength of the mild steel and post-tensioning strands may be of interest. Should the tendon anchorage zones be of concern, it may be necessary to test individual elements of the anchorage system.

The material-condition survey of the examination may focus on locations of primary distress but should extend to the comparative performance of the entire structure. Concrete voids (consolidation), delamination, spalling, discolored concrete, chemical attack, excessive air voids, and cracking should be investigated to determine the extent, formation, and amount of concrete damage within the distressed concrete area. In addition to selectively locating the position and amount of reinforcing steel and post-tensioning, the level of deterioration, as a result of corrosion, should be assessed. Specifically, post-tensioned slab edges should be surveyed for exiting tendons or loose grout plugs at stressing ends. The removal of grout plugs at tendon-stressing ends may allow visual assessment of the anchorage zone. Along the tendon length, removal of the tendon sheathing may be necessary to view the condition of the high-strength strand wires at high and low points.

In addition to the factual material-condition review of structural members, the survey should include a performance survey. Besides the typical serviceability considerations, this would include the performance review of joints, hinges, attachments, locations of movement, and locations of restraint. As part of the material-condition survey, each distress location should be assessed using time as one of the evaluating parameters.

12.3.1.2 Diagnosis

After all project documents have been collected and reviewed and after detailed inspection and testing of the floor system of the structure have been performed, the formal process of analytically assessing the existing unbonded post-tensioned floor member takes place. First, the floor framing system should be checked for adequate strength. The selected modeling must accurately represent the actual geometry and boundary conditions using the two-dimensional simple beam frame or the equivalent frame slab strip for a two-way slab. The calculated elastic factored-load moments may be increased by the code-permissible plastification, commonly referred to as *redistribution of moments*. The elastic support moments may be raised or lowered to the maximum percent of the code-permissible redistribution for each respective support. This band of the factored-load moment demand yields a range of acceptable solutions.

After establishing the band of acceptable moment-demand solutions, determine the capacity of the existing structure at critical points. Select a redistribution based on the capacities of the existing structure and the permissible percentages computed, and, finally, establish whether or not the redistribution made on the basis of the existing capacities falls within the permissible range. The demand-vs.-capacity check should include consideration of possible strength loss due to distressed member cross-sections. For conditions where the demand design strength exceeds the capacity of the member, refer to Section 12.3.3, below. For unbonded post-tensioned slabs in particular, extensive destructive testing should be conducted to confirm that calculated member capacity is based on the observed quality and quantity of the tendon.

Serviceability of the unbonded floor system should then be reviewed. Sectional stress checks at critical locations and immediate and long-term deflections should be calculated. The observed distress may reveal a direct relationship to the original design, material sections, construction, or applied loads and maintenance. In most cases, serviceability limitations, such as durability or deferred maintenance shortcomings, initiate concerns that are typically answered by evaluations. The more common serviceability shortcomings include corrosion of strands and anchorage zones, as well as broken strand wires and tendon concrete cover at high and low points.

12.3.1.3 Findings

Assessing a post-tensioned member, particularly one showing signs of distress, is not simply a matter of conservatively selecting the desired material properties and load flow path, as is the case for a newly designed member. After an analytical model representing the unbonded post-tensioned member has been developed, it should be used to perform a detailed review. The objective is to explore the consequences of variation in tested material properties, assumed loading and load distribution, boundary conditions, extent of distress, and rate of material deterioration. As part of a member evaluation process, it is common to apply various modeling techniques in the process of understanding how the structure behaves and where hidden strength reserves may be available. After the diagnosis of the structural element is completed, the engineer should have developed a clear understanding of how the structure behaves and be clear on the causation of distress, including future behavior, considering time and site-specific adverse environmental conditions as additional dimensions. Based on the preceding description, it is obvious that the prognosis is based on a multitude of variables that may only be understood by a reviewer with extensive experience in the evaluation of unbonded post-tensioned concrete structures. In closing, it should be noted that the review or evaluation of an existing post-tensioned member requires the highest degree of professional expertise, knowledge, and integrity from the assessing engineer.

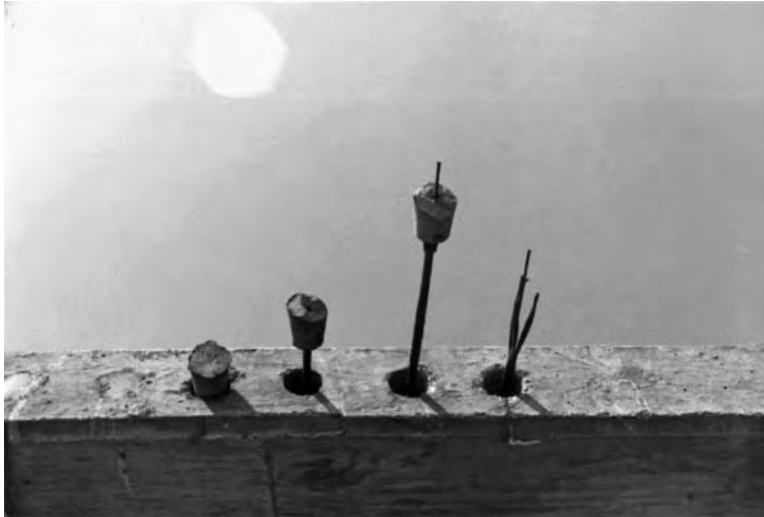


FIGURE 12.16 Tendon exiting at slab edges.

12.3.2 Repair

Unbonded post-tensioned concrete members are considered one of the more difficult structural members to assess for repair or retrofit. It is not uncommon for engineers who are not experienced with unbonded post-tensioning to misinterpret the distress observed. The author frequently encounters assessment reports of crack development that conclude that cracks may have developed as a result of member strength deficiency, where, in fact, the cracks may have developed as a result of reverse tendon-profile curvature or restraint member effects. Even if the assessing engineer correctly found the cause of concrete cracking of the post-tensioned member, the effects that the distress has on the structure and its repair may be grossly misjudged. For this reason, it is not uncommon for proposal requests for evaluation and repair to require the contractors to have a minimum of 5 years of specialized experience in designing, analyzing, and repairing unbonded post-tensioned members. This is a fundamental consideration before assessing the repair of a member. The common repairs outlined below may be used to address distress resulting from poor detailing or construction execution and deterioration of the materials.

12.3.2.1 Blowout

The sudden exiting of a tendon at the slab edge or at tendon profile high or low points, during or after stressing, is typically referred to as *tendon blowout*. In contrast, if the concentrated precompression force behind tendon anchors or the reverse tendon-profile curve causes the sudden disintegration of a localized concrete pocket, it is typically referred to as *concrete blowout*.

12.3.2.1.1 Typical Examples of Tendon Blowout

Tendon blowouts are typically recorded either at the slab edge or on the slab surface or soffit. During the installation of mechanical, electrical, or structural elements, should the contractor partially rupture or cut the unbonded tendon, the tendon tail may eject from the slab edge. The amount of existing slab edge is primarily related to the type of sheathing that was supplied. Extruded tendon should typically result in minimal tendon exiting (up to 3 ft) at slab edges (Figure 12.16). If unbonded tendons are used with a stuffed or heat-sealed sheathing application, the tendon exiting during a sudden release of stored energy may be unpredictable. The minimal void between the sheathing and the creased strand (of stuffed or heat-sealed tendons) limits the internal friction, allowing the stored energy to travel past the existing location. During a sudden release of the entire tendon force, the strand may exit vertically (also known as *vertical tendon blowout*) at locations of minimal concrete cover, typically the high and low points of



FIGURE 12.17 Vertical loop resulting from exit of seven-wire strand.



FIGURE 12.18 Tendon blowout resulting from strands riding on each other.

profiled tendons, due to the vertical component of the draped profile. The seven-wire strand may exit, resulting in a 1- to 3-ft vertical strand loop (Figure 12.17). Conditions noted above may be a result of the accidental cutting of a strand or due to deterioration of the member. *Horizontal tendon blowouts* are typically found where horizontal tendon curves around openings are not detailed and executed correctly. Tendons are typically installed side by side in groups of two to four unbonded tendons. The tension force allows the strands to ride on each other in the horizontal radial plane, creating a splitting force that can result in a tendon blowout (Figure 12.18). Tendon groups should be reduced and limited to groups of two maximum over the length of the horizontal curvature. In addition, adequate reinforcing steel (U-pins) should be added to account for and tie back the centrifugal forces.



FIGURE 12.19 Pulverized concrete behind tendon anchor due to low concrete strength.



FIGURE 12.20 Pulverized concrete behind tendon anchor due to voids.

12.3.2.1.2 Typical Examples of Concrete Blowout

Concrete blowouts are most frequently recognized during the tendon-stressing operation. The anchoring of tendon forces tests the compressive strength of the concrete pocket immediately behind the tendon anchorage. A simple void, rock pocket, low concrete strength, or lack of reinforcing behind the tendon anchor may cause the concrete to pulverize, resulting in a concrete blowout. Figure 12.19 and Figure 12.20 show pulverized concrete behind the tendon anchor due to low concrete strength and voids, respectively. Most concrete blowouts are recognized during the stressing operation or within several months of stressing the tendons. In addition, tendons that are stretched over a longer distance near the concrete surface (i.e., with minimal concrete cover) and that have a reverse tendon-profile curvature may split the concrete section over the distance of reverse curvature to allow the tendon to straighten. This may take place during the stressing operation or at a later date if the concrete section experiences additional concrete stresses due to loading.

12.3.2.1.3 How to Repair Concrete Blowout

Depending on the location and severity of the blowout, adjacent tendons may have to be detensioned before concrete removal can begin. After detensioning (as necessary), the damaged concrete is removed in sufficient amounts to expose any damaged strands and allow the resetting of the anchorages. In some cases, it may be necessary to use couplers in the repair to increase tendon length due to strand damage. It is important that the back side of the opening be cut square and perpendicular to the tendon to avoid slippage of the concrete patch during stressing. Remove all loose debris and clean the surface of dust. Make sure all the anchor zone reinforcements have been replaced, and fill the area to be repaired with a high-strength, nonshrink concrete grout mix. *Do not* use grout that contains calcium chloride or other materials containing chlorides. Stress the tendons only after the grout patch has attained the required design strength as approved by the engineer of record.

12.3.2.2 Tendon Rupture

Tendons may rupture partially if only one wire is damaged or totally when several wires are damaged, causing the remaining wires to fail under sustained tension load. The cause of tendon rupture for tendons should be determined. One of the most critical actions for unbonded post-tensioned structures is to immediately determine the extent of damage. If corrosion is the leading cause of the damage, several tendons should be spot checked to establish the extent of damage to each tendon and the slab area or beams in which damage has been recorded. If preliminary calculation indicates that the loss of the ruptured tendons affects the strength of the unbonded post-tensioned member, the member should immediately be shored. Destructive testing to recover representative strand samples should be considered to record the tendon location, wire condition at the location of rupture, concrete cover, type of sheathing, condition of the crease, remaining cross-sectional area of the seven-wire strand, and other project-specific conditions. When the extent of damage and type of tendon sheathing have been identified, strand replacement or splicing of tendons may be considered.

Strand rupture or breakage can also occur from misalignment of wedges, the anchor to the strand not being perpendicular, overstressing, or internal damage to the tendon. Misalignment of wedges occurs when the two or three parts of the wedges are offset prior to stressing. The wedges can pinch one or more wires due to different circumstances. Internal damage to the tendon could be caused by nicks in the strand or heating of the strand due to torch cutting of adjacent objects prior to concrete placement. Damage can be caused after concrete placement by drilling, saw cutting, or shooting power-actuated studs into the concrete.

If a strand does not hold, remove the wedges, clean the cavity, install new wedges, and restress. Overstressing of a tendon can occur by misreading the pressure gauge or using a jack and gauge that are out of calibration or that are not a matched set. The strand may either break or be stressed beyond yield. If the strand breaks, the engineer of record will determine how the structure is affected and whether replacement is necessary. If the wedges hold and the strand does not break, it is usually preferable to leave the tendon in the overstressed condition. Attempts to detension the tendon may damage tendon or break it necessitating replacement of the strand.

Prior to replacement of existing strands, adjacent strands may have to be detensioned. After exposing stressing and dead ends, it may be advantageous to weld a 1/4-in. wire rope to the existing damaged strand tail, allowing repulling of the new strand. If the existing strand is ruptured, not allowing the rethreading of a wire, the new strand may have to be pushed into the sheathing void by hand. Strand replacement can be effectively executed for unbonded monostrand tendons with heat-sealed or stuffed sheathing. The slightly oversized sheathing typically can accommodate new strands. For long tendons or tendons with extruded sheathing, a smaller size strand, such as 7/16- or 3/8-in.-diameter strands, may be selected. Strand replacement for tendons with paper-wrapped sheathing is nearly impossible. For all strand replacement, adequate creasing application should take place as part of the strand installation procedure.

The substitution of the original 1/2-in.-diameter strand with a smaller strand may be acceptable for the following reasons. Most older structures used stress-relieved type strands that are typically replaced by new low-relaxation strands. Strain tempering is very effective in improving the stress-strain characteristics and has the additional advantage of substantially reducing time-dependent losses due to



FIGURE 12.21 Beam cracking due to incorrect tendon profile high point placement.

relaxation of the strand. Stress-relieved type strands may experience over 10% more loss in stresses due to relaxation than do low-relaxation strands. The stress loss due to concrete shortening may not have to be compensated for.

12.3.2.3 Cracking of Concrete Members

12.3.2.3.1 Crack Development

The most frequent crack development is typically due to restraint of adjoining members. This phenomenon is extensively covered in Chapter 35 of this book. Crack development due to the incorrect installation of the tendon profile or anchors and overbalancing of the member self-weight is in most cases misinterpreted. The incorrect placement of an unbonded tendon profile high point near the quarter span of a beam instead of over the column support has resulted in notable beam cracking approximately two beam depths away from the support (Figure 12.21). In this case, even though the inspection reports and survey of the installation crew confirmed correct placement of the tendons, destructive testing revealed the misaligned tendon profile (Figure 12.22). A simple realignment of the tendon profile reconditioned the beam for its intended life cycle. The layout of unbonded tendons should incorporate appropriate locations for the dead ends and stressing ends of the tendon. The localized concrete zone surrounding groups of added tendons may be subjected to high-tension stresses, which, if combined with flexural stresses, may result in crack development. Figure 12.23 illustrates a significant crack that developed in a post-tensioned beam at the location of added tendon dead ends. The dead ends were not staggered, allowing a load distribution as called for in the standard details.

12.3.2.3.2 Repair of Cracks

The objectives of crack repair on structures with cracks caused by restraint effects tendon profiles or for cracks in anchorage zones, which were surveyed by the author, served the following purposes:

- In most cases, repair was conducted as a precautionary measure to eliminate the exposure of reinforcements and post-tensioning to weather and moisture. In some cases, it was performed to stop leakage.
- It was rarely necessary to carry out repairs to restore structural strength.
- Occasionally, repairs were conducted for aesthetic reasons.

Which cracks should be repaired? Cracks that are determined to be of structural significance should be repaired regardless of width and location. Most such cracks are due to poor design, deficient detailing, or bad workmanship. Cracks that affect the serviceability of a structure, such as deflection and local distress,



FIGURE 12.22 Misaligned tendon revealed by destructive testing.



FIGURE 12.23 Crack in a post-tensioned beam where tendon dead ends were added.

may be left unrepaired if the diminished serviceability is acceptable and the repair is not cost effective. Under normal conditions of service, shortcomings due to deterioration may be encountered if cracks exceed 0.01 in. in width. Such cracks should be sealed to prevent intrusion of moisture and possible oxidization, loss of steel area, and possible spalling. Cracks in structures exposed to especially adverse conditions should be sealed, even if they are less than 0.01 in. in width. Also, cracks that show rust stain should be sealed.

When should cracks be repaired? Restraint cracks are best repaired after the shrinkage and creep shortenings are essentially complete. Generally, a lapse of approximately 2 years after construction is adequate, after which cracks may be repaired. A time delay in sealing of cracks is only justifiable if corrosion considerations permit. Cracks caused by reverse tendon profile should not be repaired until the reverse profile is relieved, neutralizing the cause of cracking.

How should cracks be repaired? Among the numerous reports on methods for sealing cracks in prestressed concrete structures, the most common and effective procedure is the injection of an epoxy resin compound under pressure into the cracks to fill in the crack voids. For details, consult the

manufacturer's literature. For cracks that are nonworking (that is, they no longer move), the best sealing method is to inject the cracks with an epoxy resin of low viscosity. This is done in such a manner that the cracks filled with the resin and the concrete on each side of the cracks are reunited by the gluing action of the resin. Another method is to rout a groove along the crack throughout its entire length and fill the groove with an epoxy compound. The latter scheme is not recommended in highly corrosive environments. Cracks that are working (that is, they open and close as a result of loads, temperature, etc.) cannot normally be successfully sealed with epoxy compounds but must be sealed with flexible sealant that can withstand the movements to which the cracks are subjected.

12.3.3 Retrofitting Concrete Structures Using Unbonded Post-Tensioning

From the mid-1980s to the mid-1990s, a series of natural disasters tested the performance of existing structures on the west and east coasts of the United States. As a result, building-code revisions addressed improved strength and serviceability considerations. The perception of building performance during recent disasters, the ever-changing building codes, and the gradual deterioration of existing structures have sparked increased public interest in the retrofitting of structures. The objective of retrofitting a structure is to modify or improve the strength and serviceability of the existing member. The options of strengthening an existing concrete floor system for gravity loads include the following:

- Adding drop caps, drop panels, or beams at the slab soffit
- Slab overlay that supports the existing slab dead load
- Increase in or jacketing of existing beams, girders, and columns
- Adding columns or remove and replace existing columns
- Adding a gridwork of beams at the slab soffit
- Attaching externally applied metal plates to the existing concrete slab
- External prostrating

The options outlined in the following sections are limited to members being retrofitted with unbonded post-tensioning. It is understood that other elements or connections may have to be strengthened (columns, walls, and foundations and their connections) within the structure as a result of the external tendon retrofit application. The application of external prestressing for nonprestressed or prestressed floors is a widely used retrofit option for gravity-load strengthening and serviceability. The following section differentiates between gravity-load strengthening and serviceability considerations.

12.3.3.1 External Prestressing for Gravity-Load Strengthening

A strength requirement ensures that all elements of the building provide an adequate factor of safety against injury or material damage in the event of a code-specified overload. Slabs with inadequate strength or slabs that are subject to overload initially exhibit significant crack formation in tandem with noticeable deflections. If a thorough evaluation indicates inadequate member capacity for code-predicted factored load demand, the member should be subject to strength retrofit. Using an external unbonded post-tensioning retrofit scheme, the author has used two principal approaches to compensate for the strength shortfall of the existing structure—namely, direct-member strengthening (for one-way slabs and beams) and indirect-member strengthening (for two-way slabs).

Direct-member strengthening is typically used for one-way members such as one-way slabs and beams. First, the engineer should establish the capacity of the existing member and scale the strength shortfall by comparing the established capacity with the load demand. The strength-shortfall compensation may be readily supplied by attaching externally stressed unbonded tendons on each side of a beam. The tendons should be profiled (typically, harped with one or two deviators) so as to uplift or unload the beam equal to or more than the amount of load that the existing capacity cannot safely sustain. The external tendons are only intended to supplement the existing capacity. It may be difficult to establish the capacity of damaged structures or members with highly deteriorated reinforcing. In such cases, the

external post-tensioning may be considered to take all loads. Where anchors are attached to columns or beams, the applied load is retained in the form of precompression in the existing member. The installation of deviators (deflector saddles) or anchors should miss all main member reinforcing.

Indirect-member strengthening, typically used for two-way slabs, takes advantage of the possibility of alternate load passes by using the capacity of the existing structure. Initially, a two-way member may be examined, using code-factored loading, to establish the as-is failure mechanism and locations of hinge formation. The objective is to search for and select an alternative failure mechanism that is capable of safely sustaining the factored loading. Through the addition of external applied post-tensioning upward forces, the failure mechanism may be altered to accomplish this objective. External prestressing, if used to supplement the strength of the member, should be encased in fire-retardant material that meets the fire-resistivity or rating requirements for the particular application.

12.3.3.2 External Prestressing for Serviceability

Serviceability describes the in-service functionality of a building for its users. Excessive out-of-level floors, inadequate drainage, perceived vibration, perceived sagging of ceiling lines, exposure of reinforcement to corrosive elements due to excessive crack widths, and unsightly cracks are the primary serviceability considerations. Serviceability may be influenced by original design, material selection, construction, applied loads, and maintenance. When a structure reflects signs of serviceability shortcomings, such as excessive deflections or cracking, external prestressing has been effective as a corrective retrofit. For example, the installation of tendons at the underside of a slab or at each side of a beam, profiled to result in upward forces where desired, may be an effective and economical retrofit solution. For cracks or deterioration of members, additional work may be required beyond the application of external post-tensioning. The retrofitting of nonprestressed members, using external forces to counteract excessive elastic deflection and plastic deformation, may have to be analyzed using specialized software to model the time-dependent creep deformation. If the application of external tendons is used solely for the purpose of improving serviceability shortcomings in a structure with adequate strength to sustain the code-predicted factored loading, then the tendons may not require corrosion protection if they are aesthetically acceptable.

12.3.3.3 Retrofit Application of External Unbonded Post-Tensioning

The principal considerations for the selection of a retrofit scheme are performance, durability, economy, and appearance. The performance records of external prestressing on hundreds of retrofitted structures across the United States and its versatile and economical application have resulted in today's frequent use of this system. External tendons may be threaded through existing concrete members (such as walls or beams), directly attached to existing elements, or routed over deflector supports. When selecting a particular tendon layout support system, access, available space, fire protection requirements, and aesthetics must be considered. The following section is intended to offer selected examples of the external prestressing installation application. The information on member selection and connections, shown in the details, offers project-specific design information prepared by the author which may not be applicable to other retrofit projects.

12.3.3.3.1 Beam Retrofit

During the course of evaluating the nonprestressed beams of a private parking structure in Woodland Hills, California, excessive post-elastic deformation and concrete cracking were recorded. The use of bundled unbonded tendons on each side of the beam, with one deviator at midspan, was selected to utilize the upward force component to instantly neutralize elastic deflection and to remove the postconstruction plastic deformation (creep) to near zero within a 10-year period after the retrofit was successfully installed. A time-dependent analysis was performed to establish the deformation of the nonprestressed beams during their predicted useful life. A typical elevation and details of tendon attachments are shown in Figure 12.24 and Figure 12.25. An alternative connection of external unbonded tendons is shown in Figure 12.26.

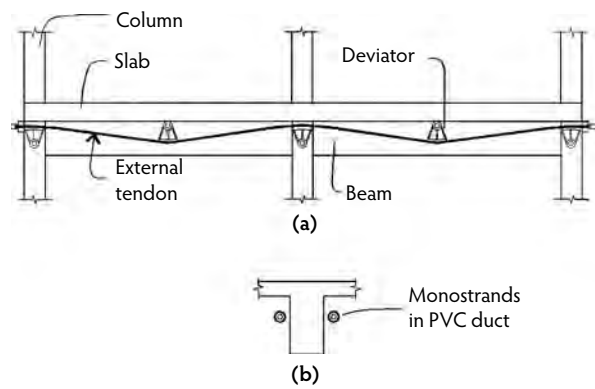


FIGURE 12.24 Schematic of external tendons profiled on each side of the beam: (a) typical elevation, and (b) section.

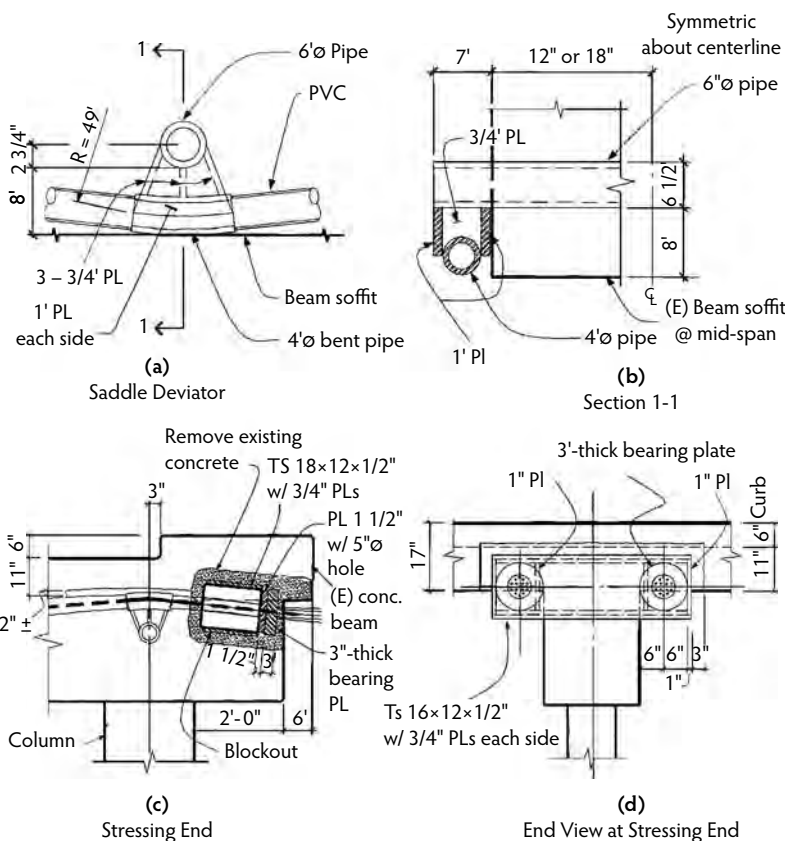


FIGURE 12.25 Retrofit details.

12.3.3.3.2 Slab Retrofit

During the final construction stages of a hybrid structure (a three-story residential wood framing over a one-story concrete garage) located in Glendale, California, excessive deflection and cracking of the elevated concrete slab were recorded. An initial document review revealed that inadequate reinforcement was specified in the original design. The nonprestressed cast-in-place concrete slab was supported on an array of orthogonally spaced concrete columns. The first-mode failure mechanism of parallel hinge line formation was altered by the introduction of external upward forces along said hinge line (Figure 12.27).



FIGURE 12.26 Alternative connection of external unbonded tendons.

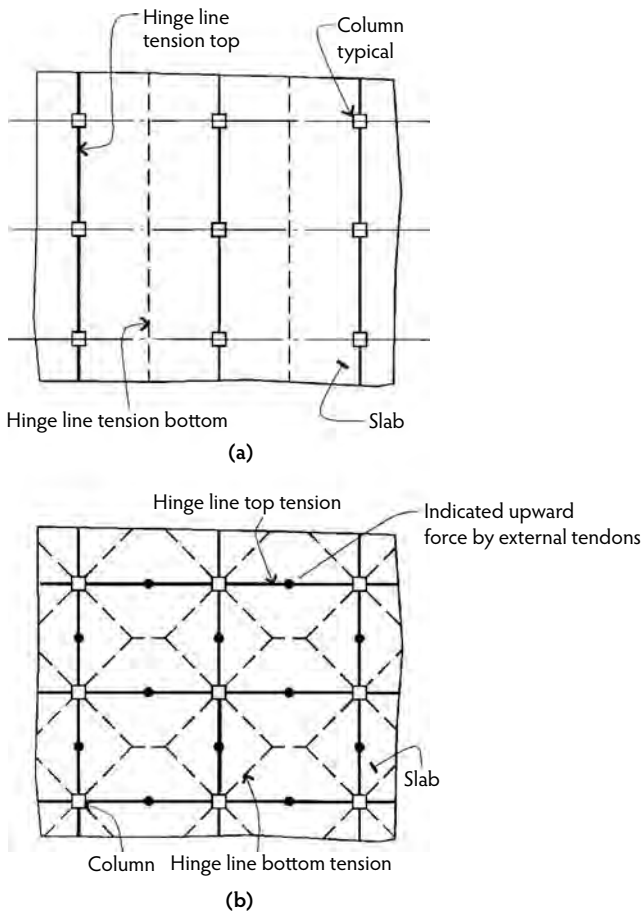


FIGURE 12.27 Simplified failure mechanisms of column-supported slabs: (a) failure mechanism as constructed, and (b) new failure mechanism after retrofitting the slab.

The upward force was calculated, utilizing the existing slab’s capacity, allowing for an alternative failure mechanism with a significantly higher capacity limit. Three principal external tendon layout support systems were proposed.

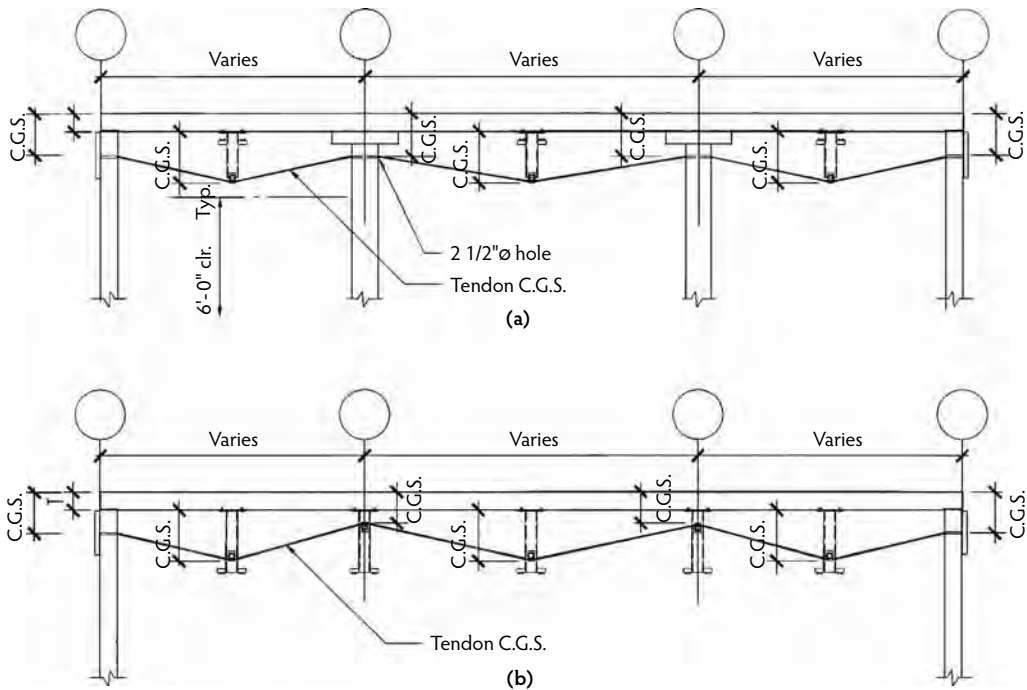


FIGURE 12.28 External tendon layout support systems: (a) typical harped tendon layout at column lines, and (b) typical harped tendon layout at midspan.

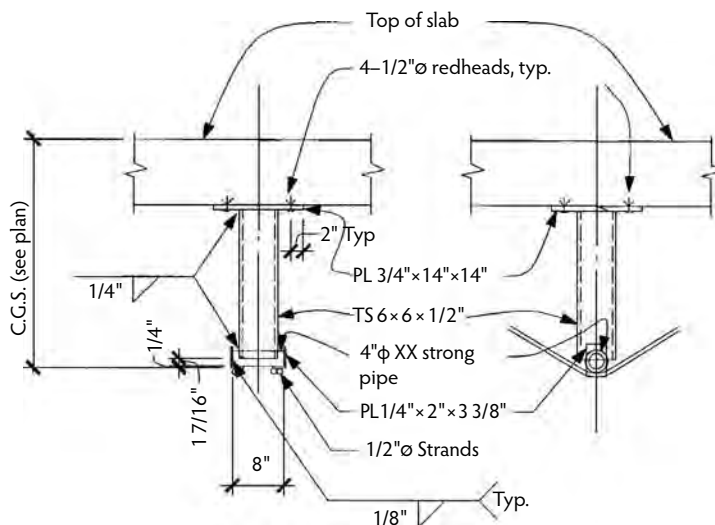


FIGURE 12.29 Typical saddle detail.

The first system consists of simple steel tube deviator or saddle supports anchored at each end of the structure (Figure 12.28 and Figure 12.29). The fabrication and application of this externally applied system can be readily installed around utility pipes and other obstructions. This layout should be considered if adequate headroom is available, allowing for large harped-profile shapes; however, short spans may result in large tendon angular changes over the deviator, which may result in localized damage to the tendons. Aesthetics considerations may be difficult to satisfy, especially if the entire system requires fire-protection coating (Figure 12.30).



FIGURE 12.30 Fire-protection coating.

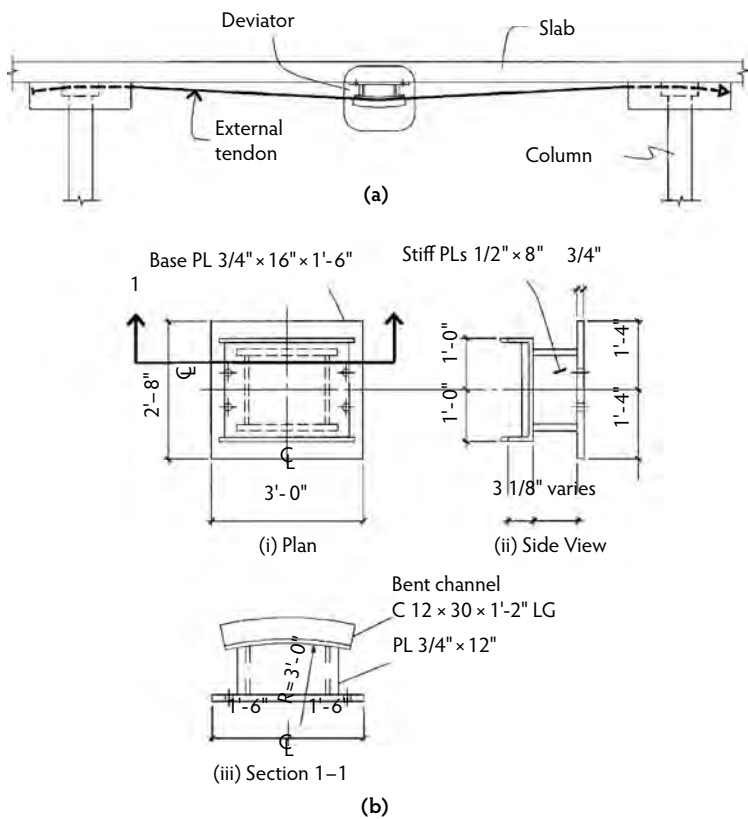


FIGURE 12.31 Schematic of external tendon at column line: (a) typical elevation, and (b) typical tendon deviator detail.

The second option may allow for using more tendons with a less vertically harped profile and tendons anchored in added drop panels at columns (Figure 12.31). The advantage of this option is that tendons may be discontinued at column lines for localized application, and it may be installed in areas with limited headroom. The concrete for the added column capitals may have to be poured through access holes from above the slab. A fire-protective coating must be applied if external tendons are required to supplement strength shortcomings.

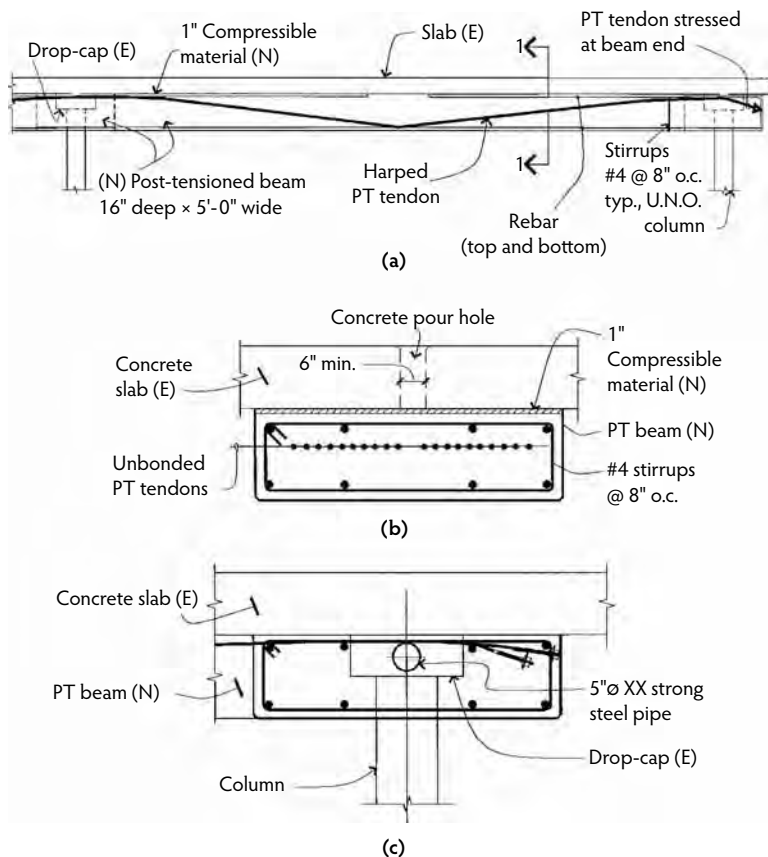


FIGURE 12.32 Retrofit beam and details: (a) typical beam elevation, (b) section 1-1, and (c) rebar through beam.

The third option was added to address fire protection and aesthetic considerations. The objective of this option is to install additional unbonded tendons without the structure retrofitting becoming visible. The tendons are installed within a reinforcing cage reflecting the intended vertical profile (Figure 12.32 to Figure 12.34). A concrete beam is poured at each column grid line to encase the tendons, offering fire protection and concealing the retrofit approach in concrete, hiding the afterthought even to a trained eye. Enough tendons must be selected to balance the dead load of the added concrete beam in addition to achieving the required upward force. The beams are isolated from the existing slab with contact at midspan for upward load transfer. The concrete for the added beams may have to be poured through access holes from above the slab. As this option addresses the durability and aesthetics of the retrofit effectively, the economic penalty of adding a grid of concrete beams may not be of great significance.

12.4 Demolition of Post-Tensioned Structures

12.4.1 Introduction

The purpose of this section is to address the concerns of the industry, primarily contractors and engineers, regarding the unique properties of prestressed concrete that must be addressed to safely demolish structures that contain unbonded prestressing systems and devices. The scope of this section is limited to the structural engineering considerations that must be made to properly evaluate prestressed structures for demolition and not for the purpose of mandating regulatory requirements.

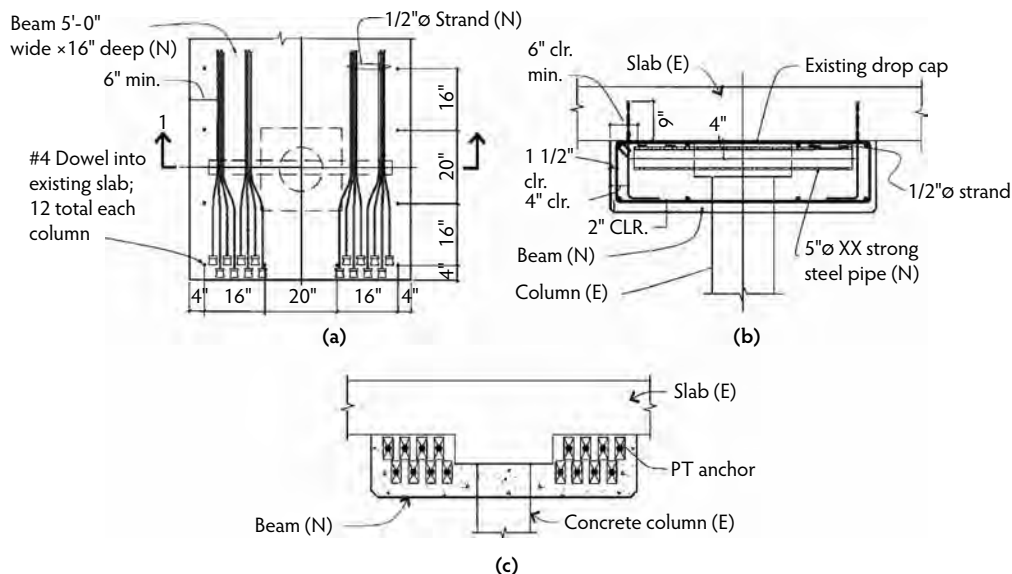


FIGURE 12.33 Details of retrofit using external tendons: (a) plan, (b) section 1-1, and (c) post-tensioning anchor orientation.



FIGURE 12.34 Tendons installed within a reinforcing cage.

The reader is advised to refer to those publications prepared by OSHA (promulgates rules and regulations regarding health and safety in the workplace) and the American National Standards Institute (provides standards for safety during construction and demolition operations). In addition, the National Association of Demolition Contractors' publication *Demolition Safety Manual* covers the use of demolition equipment and safety procedures to be followed for all forms of structures to be demolished including precast and prestressed concrete structures. The recommendations are presented for the guidance and information of professional engineers, who must add their engineering judgment to the application of these recommendations.

12.4.2 Structural Evaluation

The demolition of an unbonded post-tensioned structure should be carefully evaluated by an engineer to ensure safety during all phases of the demolition operation. Shoring that is to be used to support the structure during all phases of demolition, including tendon destressing, should be designed to accommodate vertical loads and horizontal loads, including any associated structural deflections. It is important to account for the loss of strength in multiple spans (over the tendon length) when detensioning unbonded tendons. It is important to secure the slab edge, as the release of energy stored in each tendon can result in sudden exiting of the strand at stressing ends.

12.4.2.1 Material Considerations

Wood and steel structures allow the demolition contractor to stage the demolition sequence and procedures based on the member strength and configuration. Concrete structures have inherent uncertainties with regard to the location, size, splice, prestressing force, and quantity of tensile reinforcing beyond the information provided by original construction documents. The layout and amount of mild and prestressed reinforcing in the continuous beams of frames must be reviewed, accounting for the altered modeling of a span by a span-demolition sequence.

12.4.2.2 Identification of Structural System Used

It is necessary to review available records relating to the design and construction of the building or structure to be demolished. These include design drawings, shop drawings, project specifications, field reports, repair records, job photographs, and correspondence. These records should be retained by the building owner; they may also be available from the engineer or architect of record or the contractor and should be on file with the local building department.

12.4.2.3 Condition Survey of Building or Structure

Prior to demolition operations, an engineering condition survey of the premises should be performed to determine the type and condition of the structural elements to prevent a collapse of any portion of the structure. This survey should include adjacent structures, overhead and underground utilities, and sidewalk vaults that may be affected by the demolition operations. All necessary permits and notices to adjacent owners and utilities should be obtained. The condition survey should include intrusive probes of the slab, girder, and column connections of critical elements to verify both their presence and their condition.

12.4.2.4 Determination of the Condition of Critical Elements

All structural elements reviewed should be to ensure that sufficient load-carrying capacity and stability is maintained for each stage of demolition. Strength capacity may be affected when adjacent supports and lateral load-resisting elements such as shear walls are removed. Strength reduction may already be diminished due to previous damage from fire, corrosion, age, and improper and undocumented alterations to the structure. All structural elements reviewed should be for the controlled release of stored energy in cutting tendons, especially the unbonded tendons. The location and direction of the anchor wedge seating of the intermediate anchors and splices may be of great interest to avoid a progressive collapse in a multi-frame structure. Stability requirements for each stage of demolition should be evaluated. Locations of stair and elevator towers may be isolated from the primary structure and may require special attention. A structural analysis may be required to determine unbalanced post-tensioning thrusts on framed elements, shear forces on wall systems, cantilever construction, continuously designed floor elements, and locations of critical tensile stresses in post-tensioned concrete elements due to temporary loading and unloading conditions. The presence of wind forces and other environmental effects should be considered in the analysis, including temporary crane and equipment loads that may be supported on the structure. The prime concern to be addressed in all demolition of post-tensioned concrete buildings and prestressed elements is the sudden release of stored energy caused by either removing the adjacent concrete cover or

cutting or burning the stressed tendon strands, either intentionally or accidentally, which may cause a sudden uncontrolled collapse to occur. In addition, the possibility exists that anchors and tendons may be released suddenly, resulting in steel ejection at slab edges or blowouts along the tendon length.

12.4.2.5 Preparation of Demolition Plan

A written plan for controlled demolition operations should be prepared that includes the following:

- Identification of anchorage layout within the structure
- Site protection and barriers
- Sequence of dismantling structural elements and demolition of entire assemblies
- Location of all temporary shores and supports
- Location of all equipment loads
- Sequence of cutting strands
- Sequence of cutting partial structural elements
- Control of other site operations
- Preparation of demolition sequence and procedural drawings
- Predemolition survey

12.4.3 Deconstruction Analysis

Mass concrete demolition prior to the mid-1980s was typically executed by positioning equipment such as the crane and impact ball outside the collapse envelope of a structure. This was considered nonengineered demolition or removal of concrete. The demolition contractor's survey of available documents and field conditions were the primary basis for equipment selection and the removal sequence or procedure.

Engineered demolition involves the analytical evaluation of a concrete structure during all stages of demolition to verify the adequacy of its strength and stability. The deconstruction analysis is essentially the reverse process of the original construction of a structure, with revised partial framing and alternative load patterns. Engineered demolition is mandatory for post-tensioned structures if the operator is on the structure or is within the collapse envelope of the structure to be demolished. The contractor should seek experienced engineering advice. The process of engineered demolition should, at a minimum, include a thorough review of the existing condition of a structure, its proximity to other structures, any utilities above and below grade, the preparation of the demolition sequence, the procedures, the assignment of equipment to be used, an analysis of all actual altered structural models, and a stability analysis of the structure considering the member demand (all demolition-load combinations) and the member capacity (remaining concrete cross-section, tendon profile, tendon layout, and location of anchors). Absent design guidelines for engineered demolition of concrete structures, several state agencies have agreed on minimum considerations. The following guidelines have been used on over 50 major engineered demolition projects since 1990.

The intent of the stability analysis is to confirm that the structure to be demolished has the capacity during all stages of demolition to safely support the weight of equipment or other demolition-related loading such as debris loading. The analysis is limited to a strength review only; no serviceability stress checks are considered. Strength-reduction factors are employed as recommended for new construction. Concrete configuration, reinforcing quantity, size of bars, splice locations, and prestressing forces are obtained from the as-built drawings. To calculate the demand or required strength (U), live loads are magnified by a load factor of 1.3 ($U = 1.0D + 1.3L$), except as noted below. The live-load factor is assumed to include an adequate increase for impact loading as the equipment live load is a well-defined load. Where supporting members show minor visual damage such as cracking at beam-column joints or questionable rebar configuration, the live-load factor is increased to 2.0. For damaged sections of the structure, shoring should be considered and installed to support the dead and live load of its respective tributary area. Minimum temporary lateral-load capacity of the structures to be demolished is defined as a horizontal

force, applied at the center of mass of a section, equal to 2% of its own weight. Pinned joints of supporting elements may require lateral bracing during demolition. Adequacy of the structure or a member of a structure to be demolished is established when the capacity/demand ratio is equal to or exceeds 1.0.

12.4.4 Methods of Demolition

The following demolition methods may be used on prestressed concrete structures where applicable and permitted by local regulations.

12.4.4.1 Ball and Crane

The method requires the controlled swing (choking) or dropping of a steel headache ball from a crane. The chief advantage is that the workers are outside of the building collapse envelope during this work. A disadvantage is that it cannot be used on tall structures and on those structures that are close to adjacent ones or in congested urban areas.

12.4.4.2 Explosives

Explosives require experienced personnel to detonate critical building elements to effect a proper controlled collapse of the structure. The chief advantage is that this is a fast method of demolition. Disadvantages include ground and air vibration effects that may damage adjacent facilities. Users of this method should consider the stored energy effects of prestressed concrete when determining the charge levels of the explosives being used. Due to the sudden stored-energy release of unbonded tendons, explosives have limited application for purposes of demolition.

12.4.4.3 Pressure Bursting

This method utilizes hydraulic bursters, gas expansion bursters, and hydraulic jacks to break the concrete into sections. This method is not frequently used and is limited to mass concrete, areas of limited direct access, and other unique conditions.

12.4.4.4 Thermal Lance

This method uses a steel rod in conjunction with oxygen or acetylene to melt concrete aggregates to form a series of boreholes that permit further demolition by other methods such as pressure bursting or the use of hand tools.

12.4.4.5 Torch

Typically, an acetylene torch is used to cut strands by heating the strands, resulting in a yielding behavior of the steel section. This tool is also frequently used to cut reinforcement during demolition as it may interfere with demolition equipment access. Acetylene torches are an effective tool to cut steel embeds and structural steel section connected to the concrete structure.

12.4.4.6 Diamond Saws and Drills

Using diamond plate saws is an effective way to cut a large concrete slab into smaller sections that can be removed and transported. The most common application is to sever concrete to be removed from slab sections that will remain. Line drilling by using cores can be used in slabs and beams.

12.4.4.7 Hand-Held Percussion Tools

These are typically operated from a compressor and are used locally to remove concrete from tendons and reinforcing steel to permit access for torches and other saws to cut the reinforcement.

12.4.4.8 Pneumatic and Hydraulic Breakers

These are large pieces of equipment, such as excavators, special pulverizers, and shear or hammer attachments. They can extract and demolish thick floors with a maximum boom reach of up to 85 ft. Hydraulic crushers are used extensively because the pulverizer separates and processes the base materials during the demolition of a floor or wall.

12.4.4.9 Water Jetting

High-pressure water cuts and removes aggregate from concrete. Very high pressures can cut steel. The disadvantage is that large volumes of water are required during the demolition.

12.4.4.10 Other Methods

Other methods include chemical reactions, cutting by lasers, plasma-arc thermal cutting, and variations of methods previously described.

12.4.5 Other Considerations

12.4.5.1 Type of Construction

The type of original framing and erection should be investigated, as lift-slab framing or other types of unique erection require special attention. Multistory buildings must be shored to allow the dead load of the uppermost slab (slab to be removed) to be distributed to several levels below using reshoring. The deconstruction of a post-tensioned building must consider the reverse construction sequence and reverse removal of structural members of the original construction.

12.4.5.2 Proximity to Other Buildings

Adjacent buildings and structures must be protected during all phases of the demolition. Adequate dust and noise control should be addressed. Adequate limits can be selected for dust and noise and be monitored to satisfy other property owners in densely populated areas. If applicable, vibration measurements should be taken.

12.4.5.3 Accessibility of the Exterior Slab Edge and Beam Ends

Exterior wall assemblies, cladding, or other facades should be safely removed to provide access to exterior slab edge strips and beam ends.

12.4.5.4 Interior Closure Strips

These strips should be carefully opened to release tendon stresses, if applicable. Controlled cutting of one side of the closure strip at a time is required so as not to adversely affect the adjacent concrete slab area of the other side of the closure strip. Adequate shoring of both sides of the closure strip may be required before any cutting proceeds when structural drawings and shop drawings are not available.

12.4.5.5 Intermediate Stressing Joints or Construction Joints

Intermediate stressing joints can be an advantage during the deconstruction of a building. When tendons are severed, the loss of strength may be limited to an area before or after the intermediate stressing joint location. It is imperative for the engineer to understand the location and direction of the intermediate stressing anchor to confirm the direction in which the strength of the slab is retained during detensioning. (See also the description of interior closure strips in Section 12.4.5.4.)

12.4.5.6 Height of Structure

Special consideration for high-rise construction containing prestressed elements may be necessary. Any and all interferences (e.g., power lines), adjacent buildings, and debris disposal during demolition must be carefully considered. It is not uncommon for high-rise structures to be removed in small sections, level by level, similar to a reverse sequence or operation of the original building construction. Any and all elements must be secured during the removal process to minimize the effects of falling debris.

12.4.5.7 Condition of Concrete

A strength evaluation of the *in situ* concrete is advisable to determine the stability of remaining elements of the structure and to determine limits of possible deterioration that has occurred within the structure.

12.4.5.8 Condition of Reinforcement

A strength evaluation of floor systems may be required where severe deterioration of reinforcement has occurred. The designer may use a load test or other methods outlined in Chapter 20 of *Building Code Requirements for Structural Concrete* (ACI Committee 318, 2008).

12.4.5.9 Shoring Requirements

Adequate shoring is required for all phases of demolition. The design of shoring and reshoring is one of the most critical aspects of a demolition plan. A detailed sequence of shoring installation and removal must be offered to give guidance to the contractor and to retain structural stability during all phases of demolition. The shoring plan and installation and removal sequence must be submitted to the local building officials for approval.

12.4.5.10 Protection of Personnel and Public

Adequate site supervision, sidewalk bridges, barriers, and other protective devices should be employed. It is advisable to retain a safety officer on site at all times during the demolition of a concrete structure. Due to the large potential variation between actual construction and old as-built drawings, the engineer (or designated representative) designing the deconstruction of a post-tensioned building should consider remaining on-site at all times to confirm compliance with the removal and demolition sequence. This allows the engineer to verify that as-built conditions match assumptions made on a continuous basis.

12.4.5.11 Partial Demolition

Where a structure is to undergo partial demolition to alter or maintain adjacent parts, special consideration to demolition procedures is required. Lack of consideration for impact loads and sudden stress release may damage existing concrete. The reduction of mechanical energy from pneumatic hammers in areas to be preserved may be limited to 1200 ft-lb or less so as not to fracture sound concrete unnecessarily.

12.5 Defining Terms

Added tendons—Tendons, usually short in length, placed in specific locations, such as end bays, to increase the structural capacity at that location without having to use full-length tendons.

Anchor, trouble-shooting—See troubleshooting anchor.

Anchorage—A mechanical device comprised of all components required to anchor the prestressing steel and permanently transmit the prestressing force to the concrete.

Anchorage, dead-end—See dead-end anchorage.

Anchorage, intermediate—See intermediate anchorage.

Anchorage, live end—See live-end anchorage.

Anchorage zone—The region in the concrete adjacent to the anchorage subjected to stresses (forces) resulting from the prestressing force.

Anchor—For monostrand tendons, normally a ductile iron casting that houses the wedges and is used to transfer the prestressing force to the concrete.

Back-up bars—Reinforcing steel used to control the tensile splitting forces in the concrete resulting from the concentrated anchor force developed by the stressed tendons.

Bearing plate—A metal plate that bears directly against concrete and is part of an overall anchorage system.

Blowout—A blowout is a concrete failure that occurs during or after stressing; a blowout may be explosive in character.

Bonded tendon—A tendon in which the annular spaces around the prestressing steel (strands) are grouted after stressing, thereby bonding the tendon to the concrete section.

Bulkhead—See edge form.

Bursting steel—Reinforcing steel used to control the tensile bursting forces developed at the bearing side of the anchor as the concentrated anchor force from the stressed tendon spreads out in all directions.

Cantilever—Any rigid horizontal structural member projecting beyond its vertical support.

Casting—See anchor.

Chair—Hardware used to support or hold prestressing tendons in their proper position to prevent displacement before and during concrete placement.

Chuck, single-use splice—See coupler.

Coating—Material used to protect against corrosion and reduce the friction of the prestressing steel.

Coupler—A device, normally spring loaded, for connecting two strand ends together, thereby transferring the prestressing force from end to end of the tendon.

Creep—The time-dependent deformation (shortening) of prestressing steel or concrete under sustained stress (load).

Dead-end anchorage—The anchorage at the end of the tendon that is usually installed before the tendon arrives at the project site and that is not used for field stressing of the tendon.

Detensioning—A means of releasing the prestressing force from the tendon.

Edge form—Formwork used to limit the horizontal spread of fresh concrete on flat surfaces such as floors.

Effective prestress—The prestressing force at a specific location in a prestressed concrete member after all prestress losses have occurred.

Elastic shortening—The shortening of a member that occurs immediately after the application of the prestressing force.

Elongation—Increase in the length of the prestressing steel (strand) under the applied prestressing force.

Encapsulated system—A system that provides watertight connections at all stressing, intermediate, and dead ends and that has the wedge-cavity side of the anchorage covered by a watertight cap filled with a corrosion-protective coating material.

Fixed-end anchorage—See dead-end anchorage.

Friction loss—The stress (force) loss in a prestressing tendon resulting from friction created between the strand and sheathing due to the wobble or profile of the tendon during stressing.

Friction, wobble—See wobble friction.

Hand-seating tool—A small, hand-held device used to properly align (seat) the wedges in the anchor prior to attaching the jack to the strand for stressing.

Initial prestress—The stress (force) in the tendon immediately after transferring the prestressing force to the concrete. This occurs after the wedges have been seated in the anchor.

Installation drawings—Drawings furnished by the post-tensioning material supplier showing information such as the number, size, length, marking, location, elongation, and profile of each tendon to be placed.

Intermediate anchorage—An anchorage, located at any point along the tendon length, that can be used to stress a given length of tendon without the need to cut the tendon; normally used at concrete pour breaks to facilitate the early stressing and removal of formwork.

Jack—A mechanical device (normally hydraulic) used for applying force to the prestressing tendon.

Jack-gripper plates—Steel plates designed to hold the jack grippers in place in the jack.

Jack grippers—Wedges used in the jack to hold the strand during the stressing operation.

Jacking force—The maximum temporary force exerted by the jack while introducing the prestressing force into the concrete through the tendon.

Kip—One kip = 1000 lb force.

Live end—See stressing end.

Live-end anchorage—The anchorage at the end of a tendon that is used to stress the prestressing steel (strand).

Monostrand—A single strand.

Multiuse splice chuck—A coupler that uses three-piece wedges and is made of heavier material for repeated use.

Nosepiece—The front part of the jacking device that fits into the stressing pocket to align the jack with the anchor.

Split donut—See troubleshooting anchor.

Split pocket former—A temporary device used at the intermediate end during casting of concrete to provide an opening in the concrete for access by the installer and the stressing equipment to the anchorage area.

Stage stressing—Sequential stressing of tendons in separate steps or stages in lieu of stressing all the tendons during the same stressing operation.

Strand—High-strength steel wires twisted around a center wire. For unbonded tendons, seven-wire strand conforming to ASTM A 416 is used almost exclusively.

Stresses—Internal forces acting on adjacent parts of a body.

Stressing end—The end of the tendon at which the prestressing force is applied.

Stressing equipment—Consists normally of a jack, pump, hoses, and a pressure gauge.

Stressing force—See jacking force.

Tendon—A complete assembly consisting of anchorages, prestressing steel (strand), protective coating, and sheathing; the tendon imparts the prestressing force to the concrete.

Tendon, bonded—See bonded tendon.

Tendon, unbonded—See unbonded tendon.

Tensile stresses—Internal forces directed away from the part of a body on which they act.

Tension—The effect of tensile forces on a body.

Trouble-shooting anchor—A special anchor used for structural modification or repair of existing tendons. The anchor consists of a removable segment that allows it to slide onto an existing strand; the segment is then returned and tightened by a screw or bolt.

Unbonded tendon—A tendon in which the prestressing steel (strand) is prevented from bonding to the concrete and thus is free to move relative to the concrete; therefore, the prestressing force is permanently transferred to the concrete by the anchorage only.

Wedge set—The relative movement of the wedges into the anchor cavity during the transfer of the prestressing force to the anchorage, resulting in some loss of prestressing force.

Wedges—Pieces of tapered metal with teeth that bite into the prestressing steel (strand) during transfer of the prestressing force. The teeth are beveled at the front end to ensure gradual development of the tendon force over the length of the wedge. Two-piece wedges are normally used for monostrand tendons.

Wobble friction—The friction caused by the unintended horizontal deviation of the tendon.

Note: Local practices, customs, and usage may employ terminology, jargon, and nicknames different from the terms and definitions set forth in this chapter. Check with the local engineering community or other qualified person to clarify terms and definitions.

References

-
- Aalami, B.O. and Barth, F.B. 1988. *Restraint Cracks and Their Mitigation in Unbonded Post-Tensioned Building Structures*. Post-Tensioning Institute, Phoenix, AZ.
- Aalami, B.O. 1990. Developments in post-tensioned floors in buildings, paper presented at FIP XIth International Congress on Prestressed Concrete, June 4–9, Hamburg, Germany.
- Aalami, B.O. 1994a. *Strength Evaluation of Existing Post-Tensioned Beams and Slabs*, PTI Technical Notes Issue 4. Post-Tensioning Institute, Phoenix, AZ.
- Aalami, B.O. 1994b. *Unbonded and Bonded Post-Tensioning Systems in Building Construction*, PTI Technical Notes Issue 5. Post-Tensioning Institute, Phoenix, AZ.
- Aalami, B.O. and Chegini, M. 1995. Structural retrofitting of cast-in-place concrete parking structures, paper presented at the Third National Concrete and Masonry Engineering Conference, June 15–17, San Francisco, CA.
- ACI. 2008. *Manual of Concrete Practice*. American Concrete Institute, Farmington Hills, MI.
- ACI Committee 318. 2008. *Building Code Requirements for Structural Concrete and Commentary*, ACI 318-08. American Concrete Institute, Farmington Hills, MI, 465 pp.

- Barth, F.G. 1993. Engineered demolition of earthquake-damaged bridge structure. *Concrete Constr.*, 38(7), 480–486.
- Barth, F.G. and Aalami B.O. 1992. *Controlled Demolition of an Unbonded Post-Tensioned Concrete Slab*. Post-Tensioning Institute, Phoenix, AZ.
- Buchner, S.H. and Lindsell, P. 1987. Testing of prestressed concrete structures during demolition. In *Proc. 1st Struct. E/BRE Sem. Struct. Assess. Based on Full and Large Scale Testing*, pp. 46–51.
- Buchner, S.H., Lindsell, P., and Robinson, S. 1985. Monitoring of prestressed concrete structures during demolition. In *Proc. EDA/RILEM Conference on Demo-Recycling*, May 31–June 3, Rotterdam.
- Collins, M.P. and Mitchell, D. 1991. *Prestressed Concrete Structures*. Prentice Hall, Englewood Cliffs, NJ.
- FIP. 1982. *Guide to Good Practice: Demolition of Reinforced and Prestressed Concrete Structures*. Federation Internationale de la Precontrainte, London.
- Hom, S. and Kost, G. 1983. Investigation and repair of post-tensioned concrete slabs: a case study. *Concrete Int.*, 44–49.
- Libby, J.R. 1984. *Modern Prestressed Concrete*. Van Nostrand Reinhold, New York.
- Litvan, G. and Bickley, J. 1987. *Durability of Parking Structures: Analysis of Field Survey*, ACI SP 100-76. American Concrete Institute, Farmington Hills, MI.
- Nawy, E.G. 2006. *Prestressed Concrete: A Fundamental Approach*, 5th ed., 944 pp. Prentice Hall, Upper Saddle River, NJ.
- NFDC. 1975. *The Demolition of Prestressed Concrete Structures*, report of Joint Liaison Committee, National Federation of Demolition Contractors, Leicester, U.K.
- Ojha, S. 1986. Rehabilitation of a parking structure. *Concrete Int.*, 24–28.
- PCI. 2004. *PCI Design Handbook for Precast and Prestressed Concrete*, 6th ed. Prestressed Concrete Institute, Chicago, IL.
- Podolny, W., Jr. 1986. The cause of cracking in post-tensioned concrete box girder bridges and retrofit procedures. *Portland Concrete J.*, 30(2), 82–139.
- PTI. 1989. *Manual for Certification of Plants Producing Unbonded Single-Strand Tendons*. Post-Tensioning Institute, Phoenix, AZ.
- PTI. 2000. *Field Procedure Manual for Unbonded Single Strand Tendons*, 3rd ed. Post-Tensioning Institute. Phoenix, AZ.
- PTI. 1998. *Acceptance Standards for Post-Tensioning Systems*. Post-Tensioning Institute, Phoenix, AZ.
- PTI. 2000. *Specification for Unbonded Single Strand Tendons*, 2nd ed. Post-Tensioning Institute, Phoenix, AZ.
- PTI. 2006. *Post-Tensioning Manual*, 6th ed. Post-Tensioning Institute, Phoenix, AZ.
- Price, W.I.J., Lindsell, P., and Buchner, S.H. 1987. Monitoring of a post-tensioned bridge during demolition. In *IABSE Colloquium: Monitoring of Large Structures and Assessment of Their Safety*, IABSE Report, Vol. 56, pp. 357–365. International Association for Bridge and Structural Engineering, Zurich.
- Richardson, M.G. 1987. Cracking in reinforced concrete buildings. *Concrete Int.*, 21–23.
- RILEM Commission DRC 37. 1985. *Demolition Techniques*. RILEM/European Demolition Association, Bagneux, France.
- Schupack, M. et al. 1980. Electrically Isolated Reinforcing Tendon Assembly and Method, U.S. Patent No. 4,348,844.
- Schupack M. 1989. Unbonded performance. *Civil Eng.* ASCE, 59(10), 75–77.
- Suarez, M.G. and Posten, R.W. 1990. *Evaluation of the Condition of a Post-Tensioned Concrete Parking Structure After 15 Years of Service*. Post-Tensioning Institute, Phoenix, AZ.
- Tanaka, Y. et al. 1989. *Ten Years Marine Atmosphere Exposure Test of Unbonded Prestressed Concrete Prisms*. Post-Tensioning Institute, Phoenix, AZ.
- Walker, C.H. 1990. *Durability Systems for Concrete Parking Structures*. Carl Walker Engineers, Inc., Kalamazoo, MI.



Hibernia offshore oil platform constructed in Newfoundland. (Figure courtesy of Hoff Consulting LLC, Clinton, MS.)

13

Concrete for Offshore Structures

George C. Hoff, D.Eng., P.E.*

13.1	Introduction	13-1
13.2	Types of Concrete Structures	13-2
	Bottom-Founded Structures • Floating Structures • Other Structures	
13.3	Concrete Quality	13-18
13.4	Concrete Materials	13-19
13.5	Concrete Properties.....	13-22
13.6	Design Considerations.....	13-24
13.7	Safety Considerations.....	13-25
13.8	Construction Practices.....	13-25
13.9	Construction Locations	13-26
	Dry-Dock Construction • Construction on Barges • Skid-Way Construction • Site Limitations	
13.10	Marine Operations	13-31
13.11	Cost Considerations	13-31
13.12	Summary.....	13-31
	References	13-32

13.1 Introduction

Concrete has a long history and a significant and successful presence in offshore and marine applications. Throughout this chapter, reference will be made to things that are onshore, inshore, and offshore. *Onshore* is connected to the land, such as a pier or bridge might be. *Inshore* means that the location is away from the land but is close enough to the shore to be in protected waters with respect to the open sea. *Offshore* means that it is located in the open sea. The term *owner* is also used. The owner of an offshore, inshore, or onshore structure can be a single company, a collection of companies who retain varying percentages of the operation but who have designated a single company to operate and maintain the facility, or some level of government ownership.

Offshore concrete structures are generally understood to be those structures exposed to an open-sea environment (ACI Committee 357, 1989; FIP, 1985). They are designed to remain permanently or semi-permanently fixed to the seabed by gravity, piles, or anchors or to remain afloat and moored. They are

* President, Hoff Consulting LLC, Clinton, Mississippi; past-president, American Concrete Institute; past chairman, Commission 10 (Construction), Fédération Internationale du Béton(fib); past chairman, Materials Directorate of ASCE; expert on offshore concrete platforms and marine structures and on concrete behavior under severe conditions.

often associated with the exploration and production of hydrocarbons but may have many other specialized uses. Inshore concrete structures are also exposed to seawater but are not necessarily exposed to the harsh environmental loads experienced by offshore structures. They also are designed to remain permanently or semipermanently fixed to the seabed by gravity, piles, or anchors or to remain afloat and moored. Onshore concrete structures may or may not be exposed to seawater. They are commonly referred to as *marine structures* and include berthing and mooring structures for marine transportation, seawater crossings for inland transportation, structures for marine navigation, facilities for shipbuilding and ship repair, shore protection and recreational facilities, wave attenuation structures, floating plants and pump stations, and other special structures. Most of these structures have a direct connection to the land. Marine structures on rivers have the same or similar design and structural requirements as marine structures in contact with the sea but generally do not require as strict durability considerations depending on the environmental exposure.

Like most other types of concretes, those for use in offshore structures are usually made with local materials by local labor in conformance to local guidelines or specifications; thus, they can vary widely in quality. Depending on the particular application, their strengths can vary from 25 to 65 MPa (3600 to 9500 psi). All such concretes must be extremely durable. Once in service, maintenance becomes very difficult due to the hostile environment and is very expensive. Some offshore concrete platforms have design lives of 50 to 70 years.

The use of concrete in marine structures dates back to the ancient Greeks and Romans, and remains of some of their constructions still exist. The first use of reinforced concrete in a floating vessel is attributed to Lambot who, in 1848, constructed a boat by applying sand-cement mortar over a framework of iron bars and mesh. One of Lambot's boats survives today in a museum in France. The use of concrete as a hull construction material for commercial vessels began at the end of the 19th century (Harrington, 1987). Initial applications were generally used worldwide and consisted of concrete barges and pontoons. The first reinforced concrete seagoing ship was the *Namsenfjord*, constructed in Norway in 1917 by N.K. Fougner. Fougner went on to build several larger self-propelled reinforced concrete vessels. The first concrete platform for oil and gas production in the Gulf of Mexico was installed in 1950. Since that time, more than 1000 functionally similar concrete structures have been built in that area (Norwegian Contractors, 1991a). The first concrete gravity-base structure in U.S. waters was installed in 1978 (Huntman et al., 1979). The first large offshore concrete platform for the North Sea (Ekofisk Tank) was installed in 1973. Three concrete caisson structures, functionally similar to the Ekofisk Tank, were built in Brazil in 1977 and 1978 for South American offshore waters (Anon., 1988a). In recent years, similar offshore concrete structures have been built for use in Germany, the Netherlands, Australia, the Philippines, Nigeria, Russia, Italy, and Canada. Significant offshore and inshore floating concrete structures have been built for use in Japan, Indonesia, and the Congo.

13.2 Types of Concrete Structures

Offshore, inshore, and onshore structures can generally be either bottom founded or floating. Many of the bottom-founded structures are also required to float at various stages of their life. The following descriptions of various types of platforms are very brief but are meant to give the reader a feeling for the enormous versatility that can be realized when concrete is used.

13.2.1 Bottom-Founded Structures

Bottom-founded structures can be further identified as:

- Gravity-base structures
- Concrete cylinder pile-supported structures
- Floatable/bottom-founded concrete-hull structures

Examples of each are shown in Figure 13.1, Figure 13.2, and Figure 13.3.



FIGURE 13.1 Typical gravity-base structure.

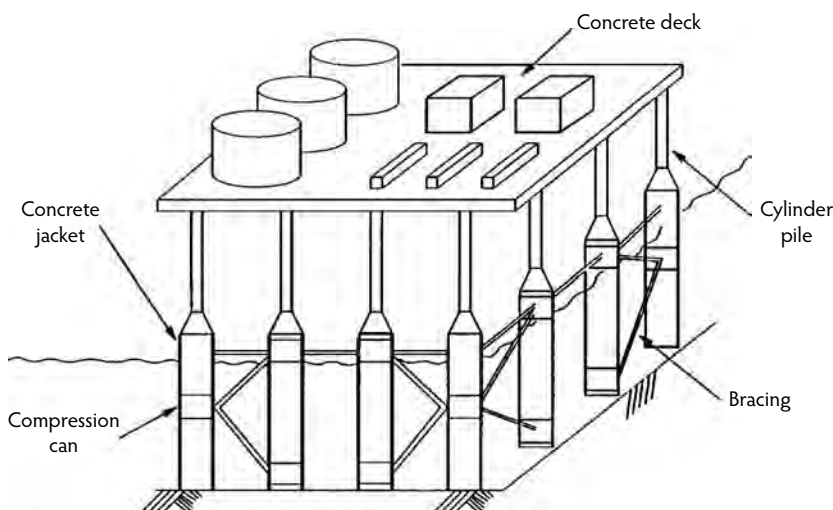


FIGURE 13.2 Typical cylinder-pile-supported platform.

The gravity-base structure (GBS) (Figure 13.1) maintains its position on the sea bottom because of its very large weight. The sliding force and over-turning moment due to the maximum environmental loads are resisted by the weight of the concrete, the operating weights on the structure, and any additional ballast weight that is contained within the structure. This type of structure is common for hydrocarbon exploration and production. The produced oil must be temporarily stored before being removed to a tanker or pipeline. The practical range of water depths for these platforms is 40 to 350 m (130 to 1150 ft). These structures are built at onshore or inshore locations and floated out to their final location. They can also be refloated

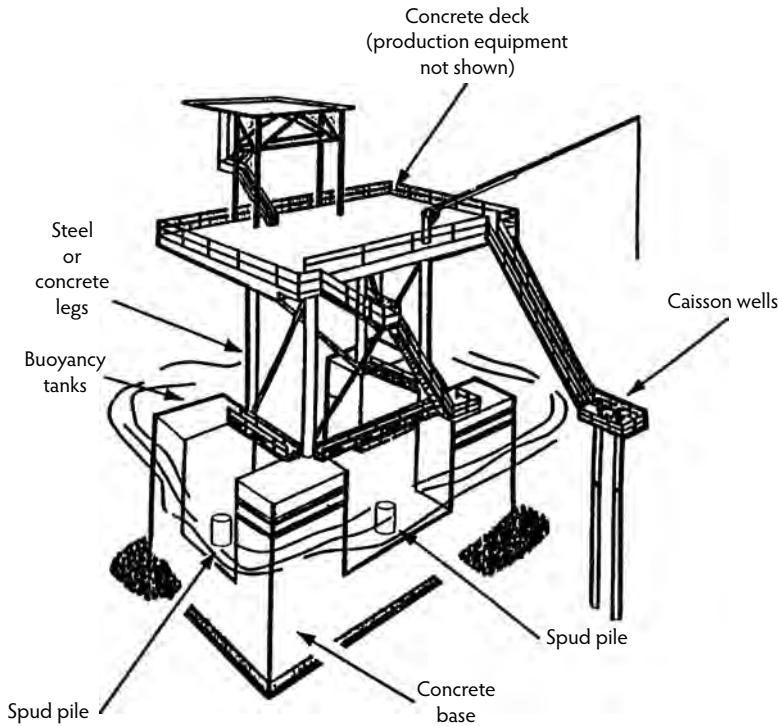


FIGURE 13.3 Floatable/bottom-founded structure. (Figure courtesy of Production Management Structural Systems, New Orleans, LA.)

when platform removal is required (Anon., 1990a). More detailed descriptions of these types of platforms can be found in ACI Committee 357 (1989, 1990) and FIP (1985). Figure 13.4 shows the wide variety of offshore concrete platforms that were built in Hinna, Norway, using a construction dry dock and a deep-water fjord for multistage construction.

Concrete-cylinder-piled structures (Figure 13.2) were the earliest type of concrete offshore platform used. The first platform of this type in the Gulf of Mexico was installed in 1950. More than 1000 of these platforms have been installed in Lake Maracaibo in Venezuela (Norwegian Contractors, 1991a). They consist of an array of prestressed concrete piles that are driven into the seabed. The piles are arranged so a prefabricated template deck can be placed over the array to form the working surface of the platform. The decks can be made of concrete or any other suitable construction material. Concrete jackets are often placed around the piles in the splash zone and boat-impact region of the platform. Steel cross bracing between piles may also be used to stiffen the overall arrangement when the piles become fairly long. The practical range of water depths for these platforms is from 5 to 20 m (16 to 65 ft). The use of concrete cylinder piles is also common for the support of docks, wharves, bridges, and roadways over water.

Floatable/bottom-founded concrete hull platforms generally consist of a barge-like concrete hull that is designed to float. Extending upward from the hull are posts or columns that act as the support frame for the platform (Figure 13.3 and Figure 13.5). These posts or columns can be made of concrete or steel. The hull is floated to its desired location and then water-ballasted down until it sits on the seabed. It is then pinned to the seabed by spud piles around its perimeter. These piles maintain the position of the platform and help resist sliding and overturning, as the platform does not have sufficient on-bottom weight by itself. Once the hull is piled into position, the topsides deck and equipment are usually added using a crane barge. This type of platform has many variations. It can accommodate some subsea storage of oil in the hull. The practical range of water depths for these platforms is from 4 to 30 m (13 to 98 ft).

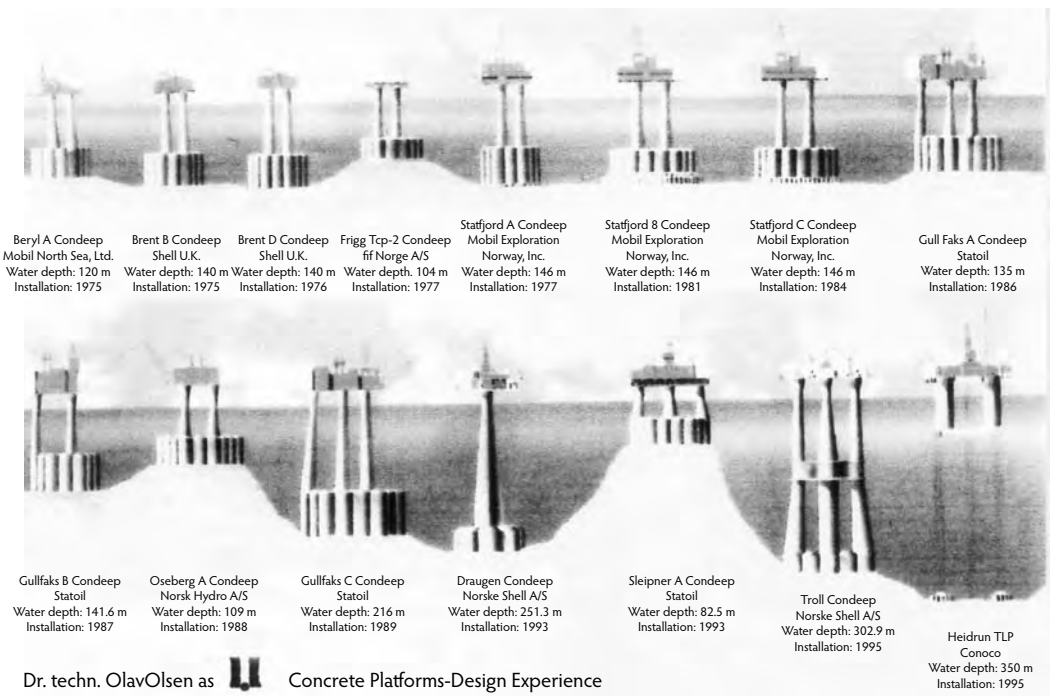


FIGURE 13.4 Concrete structures constructed at Hinna, Norway. (Figure courtesy of Dr. techn. Olav Olsen, Lysaker, Norway.)



FIGURE 13.5 Eighteen-year-old floatable/bottom-founded platform after refloating and relocation to wet dock for equipment modifications.

Platforms of this type that are in use in the Gulf of Mexico have, on numerous occasions, been refloated and reused at different locations. Table 13.1 provides a listing of this type of structure constructed by one firm for the Gulf of Mexico and shows typical concrete hull dimensions, and Table 13.2 provides a summary of larger platforms built in various locations around the world.

In the 1990s, there was considerable interest around the world in developing offshore reinforced concrete liquefied natural gas (LNG) receiving terminals. These terminals are bottom-founded structures that would allow the berthing of ocean-going LNG carriers and subsequent off-loading of the LNG into the concrete terminal. The LNG would then be re-gasified on the structure and sent through pipelines

TABLE 13.1 Summary of Floatable/Bottom-Founded Concrete Hull Structures for the Gulf of Mexico Constructed by One Contractor between 1984 and 1989

Year Installed	Location	Water Depth		Hull Dimensions (width × length × height)	
		m	ft	(m × m × m)	(ft × ft × ft)
1984	Eugene Island, Block 45	6.1	20	17.7 × 17.7 × 3.7	58 × 58 × 12
	Bayou Sorrel	2.4	8	9.4 × 11.0 × 3.7	31 × 36 × 12
	Cox Bay North	2.1	7	19.5 × 46.9 × 3.0	64 × 154 × 10
	Cox Bay South	2.1	7	19.5 × 33.5 × 3.0	64 × 110 × 10
	Vermilion Block 72	7.0	23	17.7 × 17.7 × 3.7	58 × 58 × 12
	Eugene Island, Block 45	7.0	23	18.3 × 18.3 × 3.7	60 × 60 × 12
1985	Brenton Sound, ^a Block 1	2.7	9	18.3 × 26.8 × 3.7	60 × 88 × 12
	Lease Platform	NK	NK	8.5 × 30.5 × 3.7	28 × 100 × 12
	Eugene Island, Block 44	6.4	21	17.7 × 17.7 × 3.7	58 × 58 × 12
	South Pass	2.4	8	21.9 × 49.4 × 3.7	72 × 162 × 12
1986	Gordon Island Bay	NA	NA	10.7 × 19.8 × 3.7	35 × 65 × 12
	Lease Platform	NK	NK	8.5 × 30.5 × 3.7	28 × 100 × 12
	Brenton Sound, ^b Block 2	3.7	12	18.3 × 24.4 × 3.7	60 × 80 × 12
	Quarantine Bay	NK	NK	21.3 × 38.7 × 3.7	70 × 127 × 12
1987	Delta Dock	NA	NA	12.2 × 30.5 × 3.7	40 × 100 × 12
	Pt. Ala Hache	NK	NK	21.3 × 40.8 × 3.4	70 × 134 × 11
	Pt. Ala Hache	NK	NK	28.0 × 32.9 × 3.4	59 × 108 × 11
	W. Lake Verret	NK	NK	15.2 × 29.9 × 3.7	50 × 98 × 12
1988	Chandeleur Sound	NA	NA	4.6 × 7.6 × 3.0	15 × 25 × 10
	Atchsduya Bay ^c	NA	NA	15.5 × 15.5 × 4.3	51 × 51 × 14
	S. Marsh Island, Block 253	NK	NK	18.3 × 18.3 × 3.4	60 × 60 × 11
1989	Main Pass, Block 69	NA	NA	12.2 × 18.3 × 3.7	40 × 60 × 12
	Eugene Island, Block 30	4.3	14	21.9 × 25.0 × 4.0	72 × 82 × 13
	West Bay	NK	NK	21.9 × 42.7 × 3.7	72 × 140 × 12

^a Designed for 5000 bbl of storage.

^b Designed for 4500 bbl of storage.

^c Designed for 2500 bbl of storage.

Note: NK, not known; NA, not applicable.

Source: Norwegian Contractors, *Durability of Concrete in the Gulf of Mexico: Experience from Existing Marine Concrete Structures*, prepared by Ben C. Gerwick, Inc., San Francisco, CA, for Norwegian Contractors, Joint Industry Project on Concrete for Gulf of Mexico, Floating Production Platforms, 1991.

to shore, where it would be introduced into various distribution or end-use systems. The use of an offshore terminal eliminated the need for deep-water harbor facility and satisfied many concerns of the general public about having a terminal near their homes. Various concepts were proposed; some had the LNG contained in tanks or membranes within the reinforced concrete structure, others had the LNG stored in the concrete in direct contact with the concrete, and some had LNG tanks partially contained in a concrete barge with the top of the tanks extending above the barge. The LNG, at a temperature of -167°C (-269°F), could be placed against the concrete with no adverse effects. Onshore LNG storage tanks with the LNG in direct contact with the concrete walls have been built in Philadelphia, Pennsylvania, and in Spain in the 1970s and have provided excellent service to date. Figure 13.6 shows an artist's concept of a proposed offshore reinforced concrete LNG terminal. Figure 13.7 and Figure 13.8 show the Isola di Porto Levante LNG terminal that will be located approximately 17 km (10.6 miles) off the coast of Italy in the North Adriatic Sea in 30 m (98 ft) of water. The structure was built in Spain and towed to the project site and is expected to begin operation in 2008.

TABLE 13.2 The Major Offshore Concrete Structures for the Oil and Gas Industry

	Operator	Field/Installation	Platform Type	Depth		Year
				(m)	(ft)	
1	Phillips	Ekofisk	Concrete tank, Jarlan wall	70	230	1973
2	Atlantic Richfield	Ardjuna Field	LPG barge	43	141	1974
3	Mobil	Beryl A	Condeep, 3 shafts	118	387	1975
4	Shell	Brent B	Condeep, 3 shafts	140	459	1975
5	Elf	Frigg CDP1	Concrete caisson, Jarlan wall	98	322	1975
6	Shell	Brent D	Condeep, 3 shafts	140	459	1976
7	Elf	Frigg TP1	CGS, 2 shafts	104	341	1976
8	Elf	Frigg MCP-01	Concrete caisson, Jarlan wall	94	308	1976
9	Petrobras	Ubaranna-Pub 3	Concrete caisson	15	49	1977
10	Shell	Dunlin A	Andoc, 4 shafts	153	502	1977
11	Elf	Frigg TCP2	Condeep, 3 shafts	104	341	1977
12	Mobil	Statfjord A	Condeep, 3 shafts	145	476	1977
13	Petrobras	Ubaranna-Pub 2	Concrete caisson	15	49	1978
14	Petrobras	Ubaranna-Pag 2	Concrete caisson	15	49	1978
15	Shell	Cormorant A	CGS, 4 shafts	149	489	1978
16	Chevron	Ninian Central	CGS Jarlan wall	136	446	1978
17	Shell	Brent C	CGS, 4 shafts	141	463	1978
18	Mobil	Statfjord B	Condeep, 4 shafts	145	476	1981
19	Dome Petroleum	Tarsuit	Arctic platform	26	85	1981
20	Texaco	Schwedeneck A	4 shafts	25	82	1981
21	Texaco	Schwedeneck B	4 shafts	16	53	1981
22	Phillips	Maureen ALC	Gravity-base articulated column	92	302	1982
23	Mobil	Statfjord C	Condeep, 4 shafts	145	476	1984
24	Global Marine	Beaufort Sea, Alaska (now Sakhalin, Russia)	CGS arctic platform	16	53	1984
25	Statoil	Gullfaks A	Condeep, 4 shafts	135	443	1986
26	Statoil	Gullfaks B	Condeep, 3 shafts	141	463	1987
27	Norsk Hydro	Oseberg A	Condeep, 4 shafts	109	358	1988
28	Statoil	Gullfaks C	Condeep – 4 shafts	216	709	1989
29	Hamilton Brothers	North Ravensburn	CGS, 3 shafts	42	138	1989
30	Phillips	Ekofisk P.B.	CGS protection ring	75	246	1989
31	Elf Congo	N’Kossa	Concrete barge	170	558	1989
32	Shell	NAM F3-FB	CGS	43	141	1992
33	Saga	Snorre CFT	3-cell suction anchors	310	1017	1992
34	Statoil	Sleipner A	Condeep, 4 shafts	82	269	1993
35	Shell	Draugen	Condeep monotower	251	824	1993
36	Conoco	Heidrun Foundation	19-cell suction anchors	350	1148	1994
37	BP	Harding	CGS foundation tank	106	348	1995
38	Shell	Troll A	Condeep, 4 shafts	303	994	1995
39	Conoco	Heidrun TLP	Concrete TLP	350	1148	1995
40	Norsk Hydro	Troll B	Concrete semisubmersible	340	1115	1995
41	Esso	West Tuna	CGS, 3 shafts	61	200	1995
42	Esso	Bream B	CGS, 1 shaft	61	200	1995
43	Ampolex	Wandoo B	CGS, 4 shafts	54	177	1996
44	Elf Congo	N’Kossa	LPG process barge	170	558	1996
45	Mobil	Hibernia	Ice wall; CGS, 4 shafts	80	262	1997
46	Amarada Hess	South Arne	CGS, 1 shaft	60	197	1999
47	Shell	Malampaya	CGS, 4 shafts	43	141	2000
48	SEIC	Lunskoye A (LUN-A)	CGS arctic platform	50	164	2005
49	SEIC	Piltun Astokhskoye (PA-B)	CGS arctic platform	30	98	2005
50	ExxonMobil	Northern Adriatic LNG	LNG import terminal	29	95	2008
51	MPU	MPU HL	Heavy lift vessel	n/a	n/a	2008

Sources: Olsen, T.O., in *Proc. of the Terence C. Holland Symposium on Advances in Concrete Technology*, 9th CANMET/ACI International Symposium on Fly Ash, Silica Fume, Slag, and Natural Pozzolans in Concrete, Warsaw, Poland, 2007; FIB Task Group 1.5, *The Merits of Concrete Structures for Oil and Gas Fields in Hostile Marine Environments*, Revision 19.12.2006.

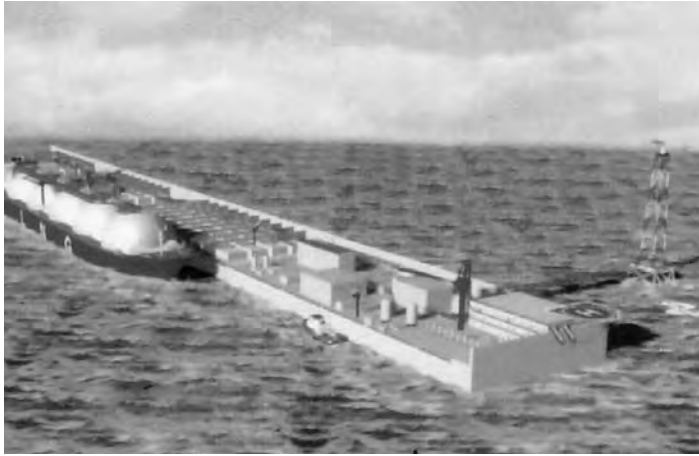


FIGURE 13.6 Artist's concept of reinforced concrete offshore LNG receiving terminal with three storage modules. (Figure courtesy of Hoff Consulting LLC, Clinton, MS.)

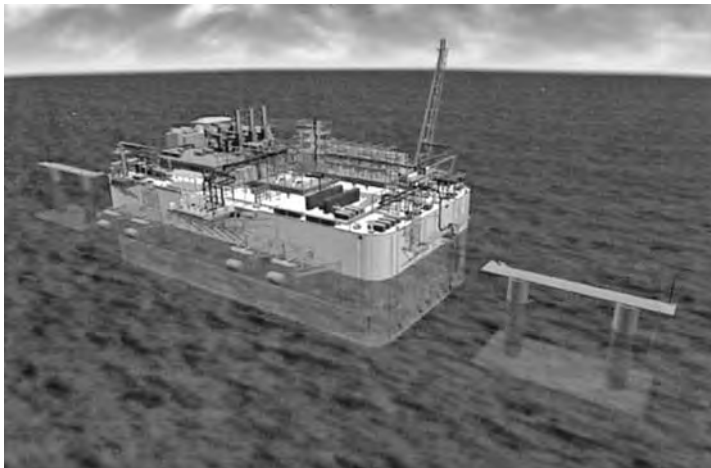


FIGURE 13.7 Isola di Porto Levante LNG terminal for the Northern Adriatic Sea, Italy.



FIGURE 13.8 Dry-dock construction of the reinforced concrete Isola di Porto Levante LNG terminal. (Photograph courtesy of Aker Kvaerner, Lysaker, Norway.)

Other types of bottom-founded concrete structures that are fabricated elsewhere and floated to their final location before installation include bridge piers, sea walls, river navigation structures, dams, and marine caissons. These precast structures are usually thin-shell floating structures with internal ballasting compartments. The innovative methods used for these types of structures offer substantial benefits in cost, construction time, risk reduction, and facility utilization while reducing environmental impact.

13.2.2 Floating Structures

Floating structures are those structures that will perform their operational function while in a floating mode. These structures require a permanent mooring system. In general, the current family of floating concrete structures includes:

- Concrete tension-leg platforms (TLPs)
- Deep-draft concrete floaters (DDCFs)
- Industrial plantships
- Floating bridges
- Floating piers and docks

Examples of each are shown in Figure 13.9 through Figure 13.17. Large concrete buoy-type floating structures have also been conceptualized.

Concrete tension-leg platforms (TLPs) (Figure 13.9) derive their name from the fact that they are fastened to large anchors on the seabed by long tethers that have a predetermined amount of tension in them. These tethers, which originate at the corners of the platform, keep the floating platform in a very precise position. The platform itself can have various configurations but generally resembles the semisubmersible drilling rigs that are common throughout the offshore petroleum industry. It consists of an

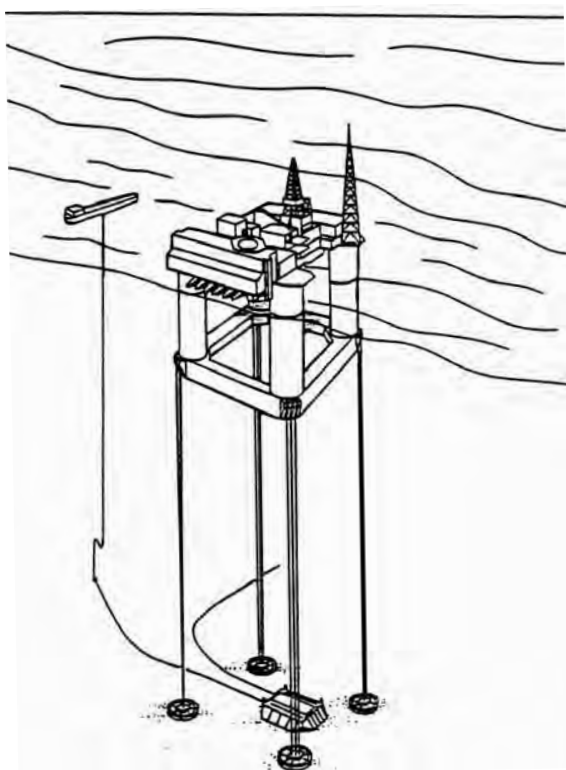


FIGURE 13.9 Concrete tension leg platform (TLP).

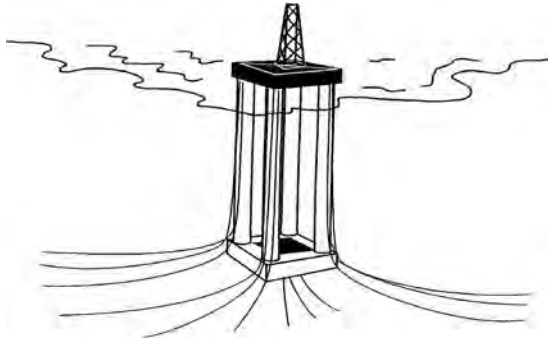


FIGURE 13.10 Deep-draft concrete floater (DDCF).

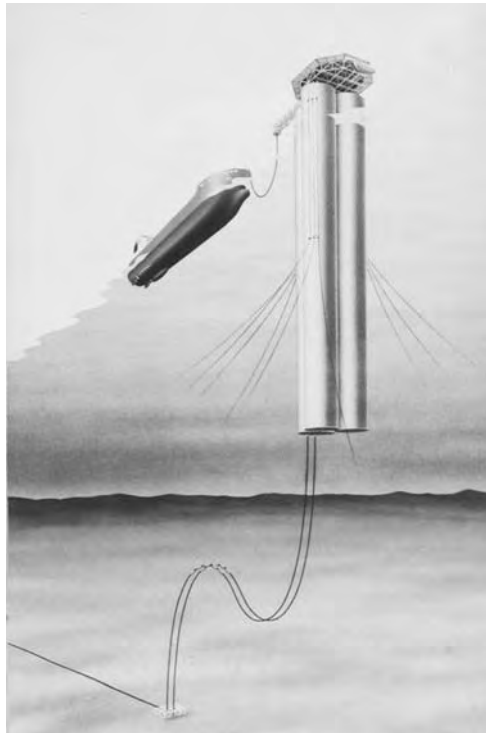


FIGURE 13.11 Spar buoy platform. (Figure courtesy of Norwegian Contractors, Stabekk, Norway.)

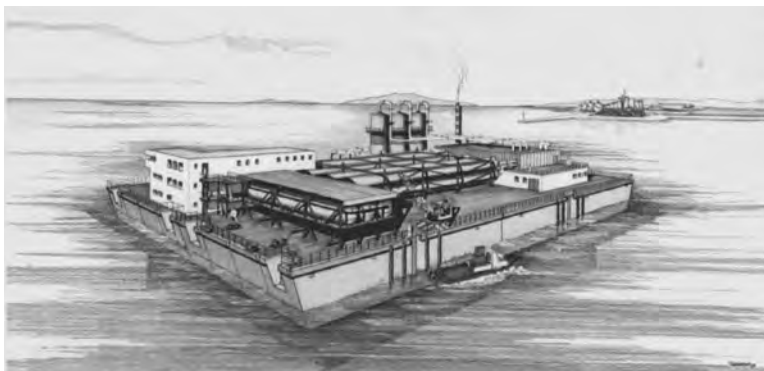
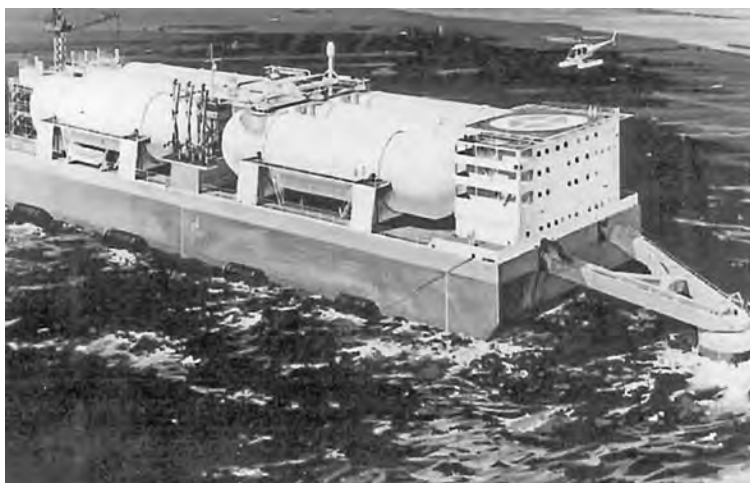
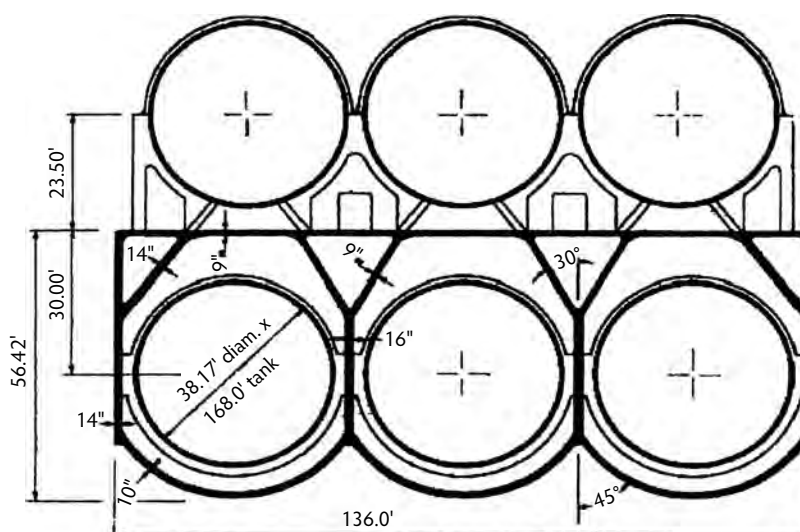


FIGURE 13.12 Concrete production barge. (Figure courtesy of Ed. Züblin AG, Stuttgart, Germany.)



(a)



(b)

FIGURE 13.13 (a) Processing and storage facility and (b) cross-section of Ardjuna Sakti LPG.

arrangement of base pontoons, shafts, or columns that extend upward from the pontoons and a deck that sits on top of the shafts or columns. The entire hull (pontoons and shafts) and the deck can be made in concrete. The practical water depth for use of this type of platform is from 300 to 1500 m (1000 to 5000 ft). The size of the TLP is generally dictated by the amount of operational weight to be carried. Current designs have ranged as high as 50,000 tonnes (55,000 tons).

The deep-draft concrete floater (DDCF) (Figure 13.10) is similar in principle to the TLP but uses a conventional mooring system rather than tension tethers. It maintains its position during operations because of its extremely deep draft, greater than 130 m (425 ft); large weight; low center of gravity; and mooring from the lower portions of the hull. These factors tend to make the structure relatively insensitive to the motions of the sea. Like the TLP, its configuration can have many variations, but in general it resembles a TLP but with a very deep hull. The pontoons, columns, deck, and any bracing can be made in concrete. The practical water depth for use of a DDCF is from 300 to 900 m (1000 to 3000 ft). Like the TLP, the size of the DDCF is generally dictated by the amount of operational weight

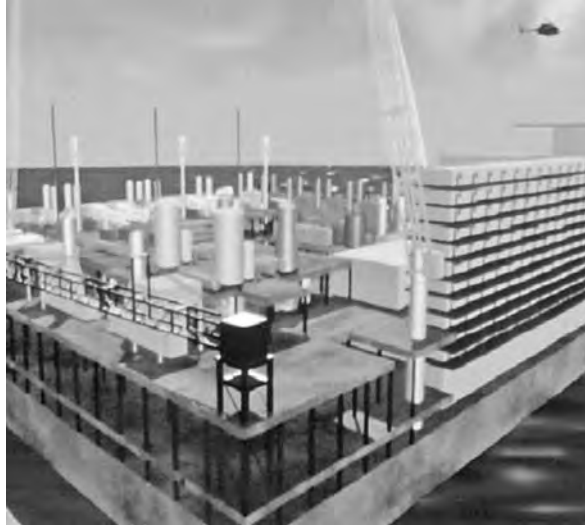


FIGURE 13.14 Floating LNG production, storage, and off-loading plantship.



FIGURE 13.15 Hood Canal floating concrete bridge.



FIGURE 13.16 Ford Island (Admiral Clarey) Bridge, with the precast prestressed floating drawspan being retracted under fixed bridge spans.



(a)



(b)

FIGURE 13.17 (a) Floating concrete-pontoon-supported bridge in Norway; (b) floating concrete pontoon construction in the dry dock. (Photographs courtesy of Aas Jakobsen, Stabekk, Norway.)

to be carried. Current designs have ranged as high as 50,000 tonnes (55,000 tons). A variation of the DDCF is the spar buoy platform (Figure 13.11). Because of the low center of gravity and heavy weight of the concrete, it is relatively insensitive to the motion of the sea. The spar buoy platform can accommodate crude storage, if desired. It also requires a mooring system (Anon., 1991).

Industrial plantships (Figure 13.12) are custom-built prestressed concrete barges that provide a support surface for the processing equipment, work and storage areas, and living quarters necessary for offshore oil and gas production or for any other industrial applications. Process applications for reinforced concrete plantships include fertilizer production, manufacturing plants, refineries, desalinization plants, electrical power stations, chemical treatment facilities, tidal power generation facilities, and liquefied natural gas (LNG) and liquefied petroleum gas (LPG) terminals.

For hydrocarbon production, drilling is usually not done from these barges but is done from special drilling vessels or jack-up rigs. The production wells are usually located on a nearby unmanned fixed platform. The entire barge or selected portions of the barge can be built in concrete. A mooring system must be provided for the barge. Produced oil and other partially processed fluids can be accommodated in the barge; large floating concrete oil-storage facilities have been built in Japan. The size of the barges

is influenced by the sea states in which they must operate and the amount of working area they must provide. The water depth in which a barge can operate is a function of the draft of the barge and the operational sea states. A notable production/storage concrete barge is the Ardjuna Sakti LPG barge currently on station in the Java Sea (Figure 13.13) (Anderson, 1977). A thoroughly developed concept for the production of LNG is shown in Figure 13.14. For this structure, the gas wells are drilled from the floating reinforced-concrete barge. The vapor gas is then processed into liquid form and stored in the reinforced concrete hull until it can be off-loaded into LNG tankers that moor adjacent to the barge. More detailed information on concrete barge-like structures and concrete hulls can be found in ACI Committee 357 (1988, 1989) and Harrington (1987).

The concept of floating bridges goes back to ancient times, when river crossings were frequently accomplished by adjoining rafts of floating timber or by placing a hard surface over boats or pontoons that were in contact with each other from one side of the river to the other. These generally were temporary, seasonal structures. The use of floating concrete elements in modern times for water crossings has provided an optimum and cost-effective solution for some difficult sites and for special applications.

In the United States, two well-known examples of floating bridges are the Hood Canal Bridge (Abrahams and Belvedere, 1984; Nichols, 1964) and the Ford Island Bridge (Abrahams and Wildon 1998). The Hood Canal floating bridge crosses Puget Sound in Washington (Figure 13.15). The structure was originally opened for traffic in 1960 and was modified from 1979 to 1982, with portions being reconstructed and replaced. The bridge is 2347 m (7863 ft) long, including approach ramps. The floating concrete portion is 1973 m (6471 ft) long and consists of normal weight, prestressed concrete pontoons having a compressive strength at 10 days age of 21 MPa (3000 psi). The pontoons were built in a graving dock in Seattle and towed to the site in 1959 (Anon., 1983).

The Ford Island Bridge, across Pearl Harbor to connect Ford Island and the island of Oahu in Hawaii, was completed and opened in 1998. The bridge includes a causeway 305 m (1000 ft) long, a 1219-m (4000-ft) fixed trestle, and a movable section 315 m (1035 ft) long. The moveable section consists of two steel transition spans and a 284-m (930-ft) floating drawspan with its two ends extending under the transition spans. The floating drawspan is made up of three floating concrete modules, each 94.5 m (310 ft) long, 15.2 m (50 ft) wide, and 5.3 m (17.5 ft) deep. The pontoon modules were constructed with a combination of precast and cast-in-place concrete. Each pontoon was post-tensioned longitudinally. The three pontoons were tied together with high-strength bolts to provide the entire drawspan. Figure 13.16 shows the precast prestressed floating drawspan being retracted under the bridge spans so a large Navy vessel can pass through. The floating section was fabricated in Tacoma, Washington, and towed to Hawaii for on-site assembly and installation.

Another example is the use of floating concrete pontoons in the very deep fjords of Norway. The width and depth of the fjords often make it too expensive to use typical bridge piers to support the bridge deck or long-span bridge elements. Figure 13.17a shows the Norhordland Bridge across the Salhus fjord in Western Norway. It is a combined floating bridge and cable-stayed bridge that was opened in 1994. The total length of the bridge is 1616 m (5302 ft), with a floating portion that is 1246 m (4088 ft) long. The superstructure is supported by 10 floating concrete pontoons designed in lightweight aggregate concrete (LWAC) with a density of 1900 kg/m³ (118.6 lb/ft³) and a concrete cube strength of 70 MPa (10150 psi). The pontoons are 42.0 m (13.8 ft) long and 20.5 m (67 ft) wide, with each side curved with a radius of 10.25 m (33.6 ft); each pontoon has nine compartments. Figure 13.17b shows construction of the pontoons in a dry dock. They were floated from the dry dock to the bridge site for installation.

Numerous concrete floating piers, docks, and quays exist throughout the world. They vary in size from small fishing boat docks to very large docks for container ships, ferry boats, and cruise ships. They typically are moored in such a manner that allows them to move up and down with tidal fluctuations or seasonal changes in water level. One example is a precast, prestressed concrete container dock at Valdez, Alaska (Figure 13.18) (PCI, 1982). The dock is 30 m wide, 210 m long, and 9 m deep (100 × 700 × 30 ft) with a mooring system to hold it in place and a fender system that protects both the dock and the ships during berthing operations. The segments of the dock were fabricated in Tacoma, Washington, and towed to Valdez, where they were joined together on-site.



FIGURE 13.18 Valdez, Alaska, floating container pier.

Another example is the twin ferry terminals on either side of Burrard Inlet in Vancouver, British Columbia, Canada (ABAM, 1986b). Each terminal is E-shaped in plan and consists of four cellular concrete modules post-tensioned together to form a single integrated unit. The concrete modules were cast in a graving dock and post-tensioned together prior to floating them out. While they were afloat, the decking of the individual modules was completed. The completed modules were joined together by post-tensioning through the cast-in-place joints. Normal weight concrete with a 28-day design compressive strength of 48 MPa (7000 psi) was used throughout.

Figure 13.19 shows the floating pier that was installed at the entrance to the Harbor at Monaco on the Mediterranean Sea. This very large structure was built in Spain and towed to its present site. In addition to providing a berth for ships, it also includes car parking in the structure.

13.2.3 Other Structures

Concrete subsea oil-storage tanks (Anon., 1984, 1986, 1988b) (Figure 13.20) have been proposed for use in water depths ranging from 20 to over 400 m (65 to over 1300 ft). These tanks can be built like the base of a GBS but are fully submerged to the seabed, where they function as a gravity-base structure. Concrete wall caissons (Figure 13.21) have been used to provide retaining walls for earth-filled islands. These islands provide the working surface for oil and gas exploration and production. The caissons are built as floating units, towed to location, joined into a unit, and then ballasted to the seafloor. The framework of the caissons then forms the perimeter of an island. A hydraulic fill is usually used to fill the interior. When the use of the caisson-retained island is complete, the caissons can be refloated and disassembled, and nature is allowed to reclaim the island. A notable application was the Tarsuit Caisson Retained Island (Fitzpatrick and Stenning, 1983), where the caisson was made of lightweight aggregate concrete. Concrete caissons for an artificial island were a strong contender for development of the Wytch Farm prospect in the offshore southern United Kingdom (Anon., 1990b). The use of caissons for artificial islands is generally limited to water depths of less than 15 m (50 ft). Reinforced concrete segments were used to construct an underwater tunnel to connect Amsterdam with surrounding areas (Gimsing and Iversen, 2001). The reinforced concrete segments were constructed in a dry dock and assembled into units 135 m (440 ft) long that were then floated to the tunnel site. The Oresund Crossing, a fixed traffic link between Denmark and Sweden, used 20 precast concrete segments to form a 4050-m (13,290-ft) immersed tunnel. The tunnel segments were fabricated in a casting yard in the Copenhagen North Harbor and towed approximately 16 km (10 miles) to the project site for immersion. Figure 13.22a shows the Bjorvika project in Oslo, Norway, that used a submerged concrete tunnel to connect two existing rock tunnels (Maage et al., 2007). The immersed tunnel, which is 675 m (2215 ft) long, is divided into six segments that were produced in a dry dock on the West coast of Norway (Figure 13.22b). After floating from the dry dock, they were then towed approximately 800 km (500 miles) to the project site.



(a)



(b)

FIGURE 13.19 (a) Installation of floating pier in Monaco Harbor; (b) Monaco floating pier in service. (Photographs courtesy of Saipem Energies, Milan, Italy.)

Concrete has been used for the base of flare towers and offshore loading buoys. An entire flare boom tower made of concrete was proposed for the Sliepner platform in Norway, and concrete anchors for the Snorre TLP have been built (Anon., 1990c). The Maureen offshore development uses a concrete offloading buoy. Oseberg II in the North Sea utilizes concrete subsea wellhead protectors (Norwegian Contractors, 1990). The potential for concrete use is great and is limited only by the ingenuity of the concrete designer and constructor.



FIGURE 13.20 Concrete subsea storage tank.



FIGURE 13.21 Concrete retaining-wall caissons. (From Anon., *Ocean Industry*, 21(8), 32, 1986.)

As many oil and gas fields are depleted, it is necessary to remove offshore steel platforms due to the OSPAR Convention. For the North Sea alone, this represents a market value of some \$US10 billion. This market potential initiated the development of a robust, inexpensive reinforced concrete heavy lifter (MPU Heavy Lifter) (Maage and Olsen, 2000; Olsen, 2000; www.mpu.no). It is a concrete, U-shaped semisubmersible that utilizes the simple principle of Archimedes to lift straight up (Figure 13.23). Construction of the Heavy Lifter was begun in 2007.



(a)



(b)

FIGURE 13.22 (a) Overview of Bjørvika immersed road system in Oslo, Norway; (b) construction in graving dock of Bjørvika immersed tunnel segment. (From Maage, M. et al., in *Proc. of the Terence C. Holland Symposium on Advances in Concrete Technology*, 9th CANMET/ACI International Symposium on Fly Ash, Silica Fume, Slag and Natural Pozzolans in Concrete, Warsaw, Poland, 2007.)

13.3 Concrete Quality

There is a perception that all concrete used in offshore and inshore platforms is something unique and special and requires a technology that is beyond normal practice for concrete construction. If *normal practice* means the practice applied to residential construction, then this perception is correct. If *normal practice* means practices applied to any major civil-engineering structure such as a building or bridge, then this perception is wrong. There is nothing unique or special in the application of proper batching, delivery, consolidation, and curing of properly proportioned concrete mixtures. In general, the recommended practices for concrete construction, including materials selection and mixture proportioning, that exist in the various building codes, specifications, and standard practices of most developed countries

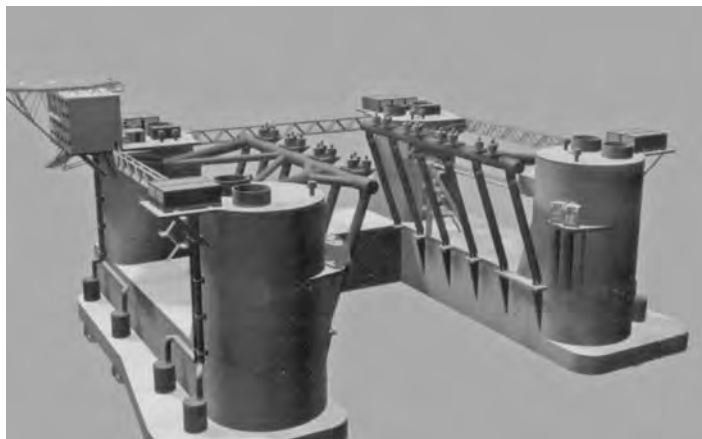


FIGURE 13.23 Reinforced concrete MPU Heavy Lifter. (Figure courtesy of Dr. techn. Olav Olsen, Lysaker, Norway.)

are entirely sufficient for use in the offshore concrete industry. Somewhat different values for the water/cementitious materials ratio, cementing material content, and concrete cover over reinforcing bars may be required because of marine exposure, but these values are well documented. Examples are given in Table 13.3 and Table 13.4.

The concrete provided for offshore North Sea platforms has seen a gradual evolution of cube compressive strength from 50 to 70 MPa (7200 to 10100 psi) (Moksnes, 1989). Table 13.5 shows the strength development for platforms built by one North Sea contractor. The unique environment in which this concrete is used demands such high quality of concrete. The Ravenspurn North platform (Jackson and Bell, 1990; Roberts, 1990) was built in a more moderate environment in the southern part of the North Sea and required only 50-MPa (7250-psi) concrete, which was delivered from local ready-mix suppliers. The early concrete platforms made in the Gulf of Mexico used concrete with cylinder compressive strengths from 25 to 35 MPa (3600 to 5000 psi). Samples from some 33-year-old platforms in the Gulf of Mexico showed an increase in strength from 50 to 69 MPa (7200 to 10,000 psi) over the life of the structure (Hoff, 1991a; Tate and Core, 1989). The actual strength required for a given structure depends on a large number of factors but is significantly influenced by environmental and operating loads. When these loads are small, the strength of the concrete can usually be consistent with that commonly made in the region of the construction.

13.4 Concrete Materials

As noted in Section 13.1, the constituents of the concrete can be local materials. They must be evaluated, however, to ensure that they have the proper concrete-making characteristics and that they will be durable in the environment in which they are used. Most offshore concrete platforms have a service life of 20 years or more. Because of their offshore location, they are not easily accessible for remedial work when problems occur. To eliminate the high cost of future offshore repair work, the materials used and the resulting concrete must be virtually maintenance free for the service life of the structure.

The durability of offshore and marine Portland cement concrete is generally defined as its ability to resist weathering action, chemical attack, abrasion, or any other process of deterioration while still retaining its original form, quality, and serviceability when exposed to its environment. This includes resistance to deterioration from freezing and thawing action; chemical attack by the constituents of the seawater; physical abrasion due to wave action, floating or suspended solids and debris, and floating ice; corrosion of steel or other metals imbedded in the concrete; and chemical reactions associated with aggregates in the concrete (Tate and Core, 1989). When considering these deteriorating actions collectively, it can be easily deduced that the most aggressive exposure that a concrete can

TABLE 13.3 Summary of Relevant Code Requirements for Water/Cement Ratio, Cement Content, and Compressive Strength

Codes ^a	Exposure Zones		
	Submerged	Splash	Atmospheric
<i>ACI 357</i>			
Maximum water/cement ratio	0.45	0.40	0.40
Minimum cement content, kg/m ³ (lb/yd ³)	356 (600)	356 (600)	356 (600)
Maximum cement content, kg/m ³ (lb/yd ³)	415 (700)	415 (700)	415 (700)
Minimum 28-day cylinder compressive strength, MPa (psi)	35 (5000)	35 (5000) 42 (6100) ^b	35 (5000)
<i>CSA S474</i>			
Maximum water/cement ratio	0.45	0.40	0.40
Minimum quantity of cementing material, kg/m ³ (lb/yd ³)	360 (610)	400 (675)	400 (675)
Minimum quantity of Portland cement, kg/m ³ (lb/yd ³)	300 (510)	300 (510)	300 (510)
Minimum cylinder compressive strength, MPa (psi)			
28-day	30 (4350)	40 (5800)	40 (5800)
91-day	35 (5000)	45 (6500)	45 (6500)
<i>FIP</i>			
Maximum water cement ratio	45 (less than or equal to 0.40 preferred)		
Minimum cement content, kg/m ³ (lb/yd ³)	320 to 360 ^c (540 to 610)	400 (675)	320 to 360 ^c (540 to 610)
Maximum cement content, kg/m ³ (lb/yd ³)	500 (845)	500 (845)	500 (845)
Minimum 28-day cylinder compressive strength, MPa (psi)	32 (4650)	32 (4650) 40 (5800) ^b	32 (4650)
<i>DnV</i>			
Maximum water/cement ratio	0.45 (≤ 0.40 preferred)		
Minimum cement content, kg/m ³ (lb/yd ³)	300 (510)	400 (675)	300 (510)
Maximum cement content, kg/m ³ (lb/yd ³)	—	—	—
Minimum 28-day cylinder compressive strength, MPa (psi)	—	—	—
<i>BS 6235</i>			
Maximum water/cement ratio	0.40	0.40	0.40
Minimum cement content, kg/m ³ (lb/yd ³)	320 to 360 ^c (540 to 610)	400 (675)	400 (675)
Maximum cement content, kg/m ³ (lb/yd ³)	—	—	—
Minimum 28-day cylinder compressive strength, MPa (psi)	32 (4650)	32 (4650) 40 (5800) ^b	32 (4650)

^a See Table 13.6.^b If subject to abrasion.^c 320 kg/m³ (540 lb/yd³) for a maximum aggregate size of 40 mm (1.57 in.); 360 kg/m³ (610 lb/yd³) for a maximum aggregate size of 20 mm (0.78 in.). Cylinder strength is assumed to be 80% of specified cube strength.

routinely experience is in a tidal zone in freezing weather. For most offshore structures, the most prevalent of the destructive mechanisms is the corrosion of reinforcing bars associated with ingress into the concrete of chlorides from the seawater.

Portland cements should have as low a tricalcium aluminate (C_3A) content as is practical with the local cement production. This helps to reduce the possibility of attacks from sulfates. The total alkali of the cement, calculated as sodium oxide, should not exceed 0.60% to minimize any potential for reactivity with the aggregates. The cement should have some finely divided siliceous material added to it (Hoff, 1991a). This includes natural pozzolans, fly ash, granulated slag, or condensed silica fume. These products contribute to the formation of a dense binder that inhibits the migration of the seawater into the concrete. They also combine with the alkalis to reduce the amount of available alkalis.

TABLE 13.4 Summary of Relevant Code Requirements for Minimum Concrete Cover

Codes ^a	Exposure	
	Splash or External Atmospheric	Other
ACI 357		
Untreated reinforcing bars	65 mm (2.6 in.)	50 mm (2.0 in.)
Prestressing tendons	90 mm (3.5 in.)	75 mm (3.0 in.)
Cover of stirrups	13 mm (0.5 in.)	Less than above
CSA S474		
Untreated reinforcing bars	65 mm (2.6 in.)	50 mm (2.0 in.)
Epoxy-coated reinforcing bars	50 mm (2.0 in.)	35 mm (1.4 in.)
Prestressing tendons	90 mm (3.5 in.)	75 mm (3.0 in.)
	A cover of 75 mm (3.0 in.) may be used in atmospheric zone	
Cover of stirrups	15 mm (0.6 in.)	Less than above
FIP		
Untreated reinforcing bars	65 mm (2.6 in.)	50 mm (2.0 in.)
Prestressing tendons	90 mm (3.5 in.)	75 mm (3.0 in.)
DnV		
Untreated reinforcing bars	50 mm (2.0 in.)	40 mm (1.6 in.)
Prestressing tendons	100 mm (4.0 in.)	80 mm (3.2 in.)
BS 6235		
Untreated reinforcing bars	75 mm (3.0 in.)	60 mm (2.4 in.)
Prestressing tendons	100 mm (4.0 in.)	75 mm (3.0 in.)

^a See Table 13.6.

TABLE 13.5 Strength Developments for North Sea Offshore Concrete Structures

Platform (Year)	Concrete in Cell Walls, m ³ (yd ³) ^a	Specified Concrete Grade	Obtained 28-Day Cube Strength, MPa (psi)	Typical Slump, mm (in)
Ekofisk I (1972)	—	C40 ^a	45 ^a (6530)	100 (3.9)
Beryl A (1974)	17,100 (22.370)	C45	55.0 (7980)	120 (4.7)
Brent B (1974)	40,600 (53.100)	C45	53.0 (7690)	120 (4.7)
Brent D (1975)	34,000 (44.470)	C50	54.2 (7860)	120 (4.7)
Statfjord A (1975)	47,400 (62.000)	C50	54.6 (7920)	120 (4.7)
Statfjord B (1979)	56,700 (74.160)	C55	62.5 (9070)	160 (6.3)
Statfjord C (1982)	63,700 (83.320)	C55	67.5 (9790)	210 (8.3)
Gullfaks A (1984)	63,400 (82.930)	C55	65.2 (9460)	220 (8.7)
Gullfaks B (1985)	45,000 (58.860)	C55	80.8 (11,720)	220 (8.7)
Oseberg A (1986)	43,000 (56.240)	C60	76.7 (11,120)	230 (9.1)
Gullfaks C skirts (1986)	17,400 (22.760)	C70	83.8 (12,150)	240 (9.4)
Gullfaks C (1989)	115,000 (150.420)	C65	79.0 (11,460)	230 (9.1)

^a Only slipformed concrete in the cell walls, except where noted. Does not represent the total concrete in the structure.

Source: Norwegian Contractors, *NC News*, pp. 6–7, 23, 1990.

Coarse aggregates can be either normal-density gravel or crushed stone or good-quality lightweight aggregate. The aggregates should be evaluated with respect to their potential for reactivity with the alkalis in the cement. Those aggregates that are potentially reactive should not be used. Aggregates from areas in close proximity to the sea should be checked for concentrations of sea salts. These salts

must be washed from the aggregate before it is used. Fine aggregates can be either natural or manufactured sands. They, too, must be nonreactive and free from deleterious materials. In no instance should seawater or brackish water be used to make the concrete. All mixing water should be potable. Washing of aggregates should also be done with potable water.

Chemical admixtures are essential for the production of durable marine concrete. Air entrainment is necessary when cycles of freezing and thawing can occur. High-range, water-reducing admixtures (HRWRAs), commonly called *superplasticizers*, are required for both consolidation assistance and for improved durability. A HRWRA will allow mixing water reductions of up to 30% without sacrificing workability. This water reduction significantly reduces the permeability of the concrete and contributes to a densification of the binder fraction of the concrete.

13.5 Concrete Properties

Of importance to structural designers are the properties of construction materials at an age when appreciable loads are applied to the structure. For most offshore structures, maximum loadings occur when the structure is put into service. This can vary from 1 to 5 years from the start of construction, depending on the size and complexity of the structure and its ultimate use. The properties of hardened concrete that are used by the designers of offshore concrete platforms include:

- Compressive strength
- Tensile strength
- Modulus of rupture
- Modulus of elasticity
- Poisson's ratio
- Stress-strain relationships
- Fatigue strength
- Absorption
- Shear strength
- Creep and shrinkage
- Shear-friction capacity
- Bearing strength
- Thermal properties such as the coefficient of thermal expansion, thermal conductivity, specific heat, and diffusivity

The numerical value of each of these properties is generally not critical because the design process can usually use whatever values the selected concrete produces. The specific properties, however, may not always be complementary; for example, a very high compressive strength concrete (e.g., 65 MPa, or 9400 psi) may allow compressive structural members to be reduced in cross-section for a given loading. If, however, the corresponding increase in the modulus of elasticity of that concrete allows cracking to occur at lower strain levels, then additional reinforcement may be required to reduce the cracking. Because the cross-section has now been reduced, the additional reinforcing steel adds to the congestion within the wall and makes concrete placement more difficult. The cost of the in-place reinforcing steel may also be more than the reduction in cost due to using less concrete. Trade-offs between the various properties of the concrete should be attempted, where possible, to achieve the most efficient and cost-effective design.

All of the hardened concrete properties should be determined at advanced ages for the specific concrete to be used in an offshore structure. Unfortunately, this is not always possible, and early-age properties (e.g., at 28 days) are often used. This gives the design a conservative flavor, but it may add substantial costs to the structure. There is a risk associated with extrapolating early-age data, particularly with high-strength concretes, because the improvement of concrete properties with age may not always follow assumed trends. Other properties of the concrete that are of concern to the constructor rather than the designer include:

- Workability
- Pumpability
- Unit weight
- Air content
- Consolidation
- Thermal gradients
- Finishing

The interrelationship of these properties is a complex problem. Of utmost importance is the unit weight of the concrete. For a structure of given dimensions and configuration that may also be required to carry a fixed amount of dead load while floating, variations in the concrete unit weight may adversely affect the floating stability of the structure, causing it to sink or overturn. The in-place unit weight, in turn, is affected by the mixture ingredients, their proportions, and the void content, which is both a function of the entrained air content and the entrapped air or voids remaining after consolidation. A mixture that does not have adequate workability to surround the high levels of reinforcing bars that may occur could result in additional voids in the concrete. The absorption values determined on the hardened concrete are applied to the hardened density of the concrete to establish what the concrete density is when the structure is in the water. If the actual density varies significantly, so will the actual absorption values, which will be different from those used in the design process.

As described later, the typical structural members in an offshore structure and in some inshore structures are quite thick. Because most offshore codes require fairly high cement contents (see Table 13.3) for durability purposes, the possibility of significant heat development within the concrete exists. Limiting values for the maximum placing temperature and the maximum heat rise are contained in the codes. Even when meeting these requirements, care must be exercised to minimize thermal gradients so thermal cracking of the structural members does not occur.

The finish of the concrete surface of an offshore structure may seem like a noncritical item, but a poor finish can have several undesirable effects besides poor appearance. For most offshore structures, the governing design load is caused by the forces from sea waves acting on the surface of the structure. Rough surfaces tend to gather more wave forces and thus reduce the factor of safety planned for a structure. In cold climates, an initially rough surface tends to degrade faster when subjected to cycles of freezing and thawing because there are receptacles in the surface of the concrete where water can collect and freeze. In ice-congested waters, ice moving against and past a structure tends to abrade rough surfaces faster than smooth surfaces (Hoff, 1991a).

Other properties of the concrete that are usually not of concern to either the designer or the constructor are durability properties. These are of concern to the owner, as the offshore structure is usually part of a profit-making venture that has a prescribed lifetime. Some of the durability aspects of the concrete, such as freezing and thawing resistance, are addressed in the code requirements. Matters such as the air-void system in hardened concrete as defined by the spacing factor, the specific surface, and voids per millimeter (inch) have specific requirements that must be met. Guidance is also provided in the codes to prevent or mitigate such deleterious effects as sulfate attack and alkali-aggregate reactivity through proper materials selection.

Chloride-ion permeability of the concrete should also be evaluated to ensure that a satisfactory concrete is being provided to resist reinforcing-bar corrosion. Although minimum concrete cover over the reinforcing bars is specified for a given exposure zone (see Table 13.4), this may have to be increased if the concrete to be used in the platform does not have adequate resistance to chloride-ion penetration.

The abrasion resistance of the concrete to waterborne sediments, debris, floating objects, and ice is usually not specified as it is a rather site-specific phenomenon. In offshore areas where significant abrasion can occur, such as in ice-congested waters, the resistance of the concrete to the abrading medium must be evaluated and loss rates for the concrete surface determined (Hoff, 1988). Once these rates are known, measures to accommodate or eliminate the losses, such as additional concrete cover or steel plates in the abrasion zone, respectively, can be implemented.

TABLE 13.6 Summary of Relevant Codes for Offshore Concrete Structures

American Concrete Institute, Farmington Hills, Michigan
<i>Guide for the Design and Construction of Fixed Offshore Concrete Structures</i> , ACI 357R-84 (reaffirmed 1997)
<i>Design and Construction of Concrete Structures for the Containment of Refrigerated Liquefied Gases (RLG) and Commentary. Appendix B. Offshore Concrete Terminals</i> , ACI 376-08
American Bureau of Shipping (ABS), <i>Rules for Building and Classing Offshore Installations</i> , 1983, New York
American Bureau of Shipping (ABS), <i>Guide for Building and Classing Offshore LNG Terminals</i> , September, 2003, New York
Lloyd's Register, <i>Classification and Certification of Offshore Gravity-Based Liquefied Gas Terminals: Guide Notes</i> , April, 2004, London
Canadian Standards Association (CSA), <i>Code for the Design, Construction, and Installation of Fixed Offshore Structures</i> :
S471-04. General Requirements, Design Criteria, the Environment, and Loads
S474-04. Concrete Structures
S472-04. Foundations
S475-03. Sea Operations
ISO 19900-06, <i>Petroleum and Natural Gas Industries: General Requirements for Offshore Structures</i> , 2002
ISO 19901-6, <i>Petroleum and Natural Gas Industries: Specific Requirements for Offshore Structures. Part 6. Marine Operations</i>
Fédération Internationale de la Précontrainte (FIP), The Institution of Structural Engineers, London
<i>Design and Construction of Concrete Sea Structures</i> , 4th ed., 1985
<i>Design and Construction of Concrete Ships</i> , 1986
Det norske Veritas (DnV), Hovik, Norway
DnV-OS-C502. Offshore Concrete Structures, 2004-07
DnV-OS-C503. Concrete LNG Terminal Structures and Containment Systems
DnV-OSS-102. Rules for Classification of Floating Production and Storage Units
DnV-OSS-103. Rules for Classification of LNG/LPG Floating Production and Storage Units of Installations
British Standards Institution, London, England
BS 6235. Code of Practice for Fixed Offshore Structures, 1982
BS ISO 19903. Petroleum and Natural Gas Industries, Fixed Concrete Offshore Structures, 2006
American Petroleum Institute (API), Washington, D.C.
API RP 2A. <i>Recommended Practice for Planning, Designing and Constructing Fixed Offshore Structures</i> , 1993
ANSI/API 2N. <i>Recommended Practice for Planning, Designing, and Constructing Structures and Pipelines for Arctic Conditions</i> , 1995

An evaluation of all of the above concrete properties for a specific concrete for a specific structure is the ideal situation, but it has not often been done. When actual numerical values are not available, conservative approximations are chosen, and these result in a satisfactory, but not necessarily cost efficient, design. One study that addressed most of the properties noted above was performed on high-strength lightweight aggregate for use in offshore Arctic structures and is described in ABAM (1983, 1984, 1986a).

13.6 Design Considerations

As noted in Section 13.2, concrete offshore structures can be bottom founded or floating. With the exception of a structure that has a base made entirely from prestressed concrete piles, most of the other bottom-founded structures are in a floating mode at some time in their early life. These structures must then include design provisions for both bottom-founded operational loads and those loads associated with the behavior of the structure as a ship. Design codes and guidelines for offshore concrete structures have been developed by various regulatory agencies and standards groups. A listing of some of the major codes and regulations is given in Table 13.6. These are constantly being upgraded as technology advances. In general, detail design of the individual elements of an offshore concrete structure for such things as shear, tension, flexure, compression, eccentric loads, etc. is not significantly different than for any other type of concrete structure. It is only the types of loads, their frequency and duration, and their magnitude that differ from ordinary civil-engineering structures.

The principal loads the offshore structure encounters are permanent loads, variable functional loads, environmental loads, accidental loads, and deformation loads. These various loads are combined in a realistic way to determine their net effect. Permanent loads include the weight of the structure, any permanent equipment, ballast that will not be removed, and the external hydrostatic seawater up to mean sea level. Variable functional loads are the loads associated with the normal operation of the structure. Loads in this category that are unique to offshore structures include variable ballast, installation and drilling loads, vessel impact, fendering and mooring, weight of petroleum products temporarily stored in the platform, helicopter loads, and crane operations. Environmental loads include waves, wind, current, ice and snow, and earthquake. Accidental loads include fire, explosion, ship impact, unintentional flooding, unintentional ballast distribution, and changes in presupposed pressure differences. Examples of deformation loads include prestressing, concrete shrinkage, and thermal gradients.

The geotechnical considerations offshore are much more complex than onshore. For bottom-founded structures, this is an extremely critical area of design. The anchors and moorings of floating structures are also significantly influenced by the subsea soil conditions. Seismically active areas warrant special consideration. Specialists in subsea foundation problems, not onshore foundation specialists, should always be chosen to work on this part of the design problem.

For the first structure in countries or regions that have never used offshore concrete structures before, initially it is best to use the design expertise of companies or firms that have prior experience with these structures. Such firms exist in North America, Europe, Scandinavia, the United Kingdom, and Japan. By involving local design firms in partnerships with these experienced firms, the philosophy and mechanics of the design process can be transferred to the local regions.

13.7 Safety Considerations

Modern offshore concrete platforms are designed with sufficient redundancy to resist major accidental loads. Concrete has exceptionally good impact resistance, and only a few isolated instances of structural damage due to ship impact have been reported. Sufficient ductility can be designed into structural concrete elements to eliminate the problem of progressive collapse. The fire resistance of concrete is well known, with concrete often being used to protect steel from fires in many major structures. A summary of the service record of concrete platforms in the North Sea can be found in Hoff (1986). Floating concrete structures are designed for one-compartment damage stability, which means that any local damage that causes leakage of the sea into the hull will not cause the floating structure to be at risk. Similar criteria are applied to bottom-founded structures so they are not at risk while in their floating mode. Bottom-founded structures, such as that shown in Figure 13.1, have the unique capability of having each of their shafts or towers operate independently of the others. All living quarters and other major personnel areas can be isolated on top of one shaft and kept removed from the more dangerous areas where drilling and processing of hydrocarbons take place. All areas can be connected by bridges. This is a significant advantage over a structure where most of the supporting structural members are tied together in some fashion and collectively support all of the operations of the platform. In the event of a major fire or explosion in or on shafts where hydrocarbons are present, living quarters would not be affected, and successful evacuation of the GBS-type platform could take place.

13.8 Construction Practices

No unique construction practices are required to build structures such as those described above. The good practices employed for any major civil-engineering project are sufficient for building an offshore, inshore, or onshore concrete platform. This gives the owner flexibility in selecting construction contractors. The large offshore concrete platforms of the North Sea have been constructed using predominantly slipforming (Moksnes et al., 1987). It has been demonstrated that North Sea slipforming techniques can be satisfactorily applied to offshore concrete construction in the hotter climate of the Gulf of Mexico

(Norwegian Contractors, 1991b). The small barge-like platforms in the Gulf of Mexico are cast in place (Harrington, 1987). The Hibernia platform (Michel, 1989) for the east coast of Canada, which was completed in 1996, was originally planned to be jump formed but was ultimately slipformed. Precast elements have been used in some structures (Yee et al., 1984). The method of construction can be anything that works and should be left to the discretion of the contractor.

The concrete can be delivered to the form by pump, boom, conveyor, bucket, buggy, barrow, or, again, anything that works. Sophisticated distribution systems normally are not needed. The distribution of the concrete into the slipforms used on North Sea structures has been by wheelbarrow. Proper and sufficient consolidation of the concrete is essential. The equipment and procedures to do this already exist. Adequate curing must be provided. This includes protection from early freezing in regions where this is a possibility.

Two items of offshore concrete construction that differ from most onshore concrete construction are the thickness of the concrete elements and the amount of reinforcing steel that is used. The thinnest concrete walls are usually 350 mm (13 in.). The thickest walls can be several meters (more than 6 ft) thick. Typical wall thicknesses are 500 to 600 mm (20 to 24 in.). Temperature control of the concrete in these thick walls is essential to eliminate thermal cracking problems. Reinforcement densities typically average 400 kg/m³ (676 lb/yd³). Extremes in critical areas have been as great as 1100 kg/m³ (1859 lb/yd³). The proportioning of the concrete and the consolidation methods must be tailored to ensure that the reinforcing steel is completely encapsulated by the concrete. In general, the maximum size aggregates used in these structures has been 19 mm (3/4 in.) or less to allow the concrete to move around the large amounts of reinforcing bars. The use of high-range water reducers (superplasticizers) is a necessity. Prestressing is also used in almost every structure. This is to ensure watertightness of the concrete. The amounts of prestressing are structure and location specific. Standard prestressing materials and practices can be used for these structures, keeping in mind that the work will be done in a marine environment. Special care must be taken to protect the end anchorages of the prestressing from the corrosive environment of the sea.

13.9 Construction Locations

Bottom-founded and floating offshore concrete structures can be constructed, either partially or completely:

- In dry docks or graving docks
- On submersible barges
- On skid ways
- In precast facilities onshore

Precast facilities are used principally for the precast concrete piles and template decks. These facilities can also be used to prefabricate substantial portions of a structure. The prefabricated elements are then transported to and assembled at other locations. For construction of the concrete Arctic drilling structure Glomar Beaufort Sea I, also known as the CIDS (concrete island drilling system), most of its interior concrete elements were made in a prefabrication facility (Yee et al., 1984). The actual method selected depends greatly on the existing site facilities where construction is planned and on the economics of the project.

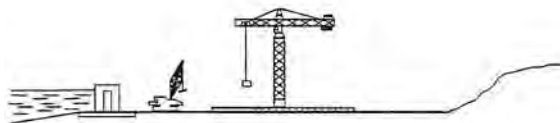
13.9.1 Dry-Dock Construction

The principal method of construction used for large North Sea concrete platforms is to begin the construction in a dry dock or graving dock. Figure 13.24 shows the construction sequence. When the base of the structure has become stiff enough and has sufficient buoyancy, the dock is flooded and the base is allowed to float. It is then towed from the graving dock to a deeper water location where it is temporarily moored. Construction then continues at that location. Depending on available water depths, this location can be close to the shore or a great distance away. If the structure is located close enough to shore to be reached by a floating or fixed bridge, materials and personnel can reach the structure directly from the shore. Office facilities and concrete production facilities can remain onshore. If the

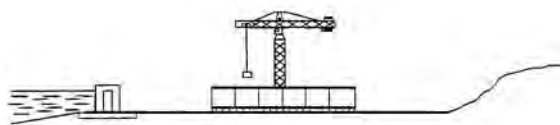
1. Excavation of construction area



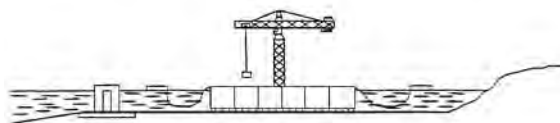
2. Construction of subbase or base slab of platform



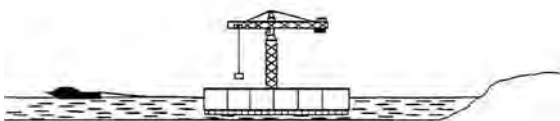
3. Construction of concrete platform to sufficient height for tow-out



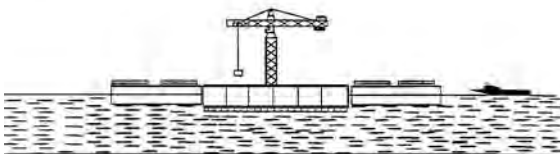
4. Flooding of dry rock



5. Tow-out of platform to deeper water construction site



6. Continuation of construction of floating base from floating work barges



7. Continued construction until base is complete

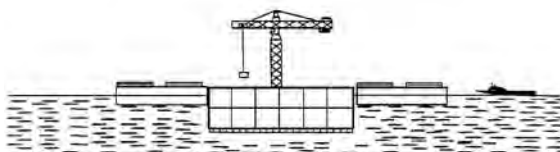


FIGURE 13.24 Dry-dock construction scenario.

structure is located some distance away from the shore, it will be necessary to have adjoining barges that support offices, materials lay-down areas, concrete batching plants, and other essential equipment. Concrete materials are obtained directly from supporting ships. Work crews are shuttled back and forth from the shore by crew ships. Figure 13.8 shows partial concrete construction of the Isola di Porto Levante LNG terminal built in a dry dock in Spain. When the concrete construction is complete, the structure may be moved to an even deeper water location, where it is mated with the topsides equipment and hook-up of the equipment begins.

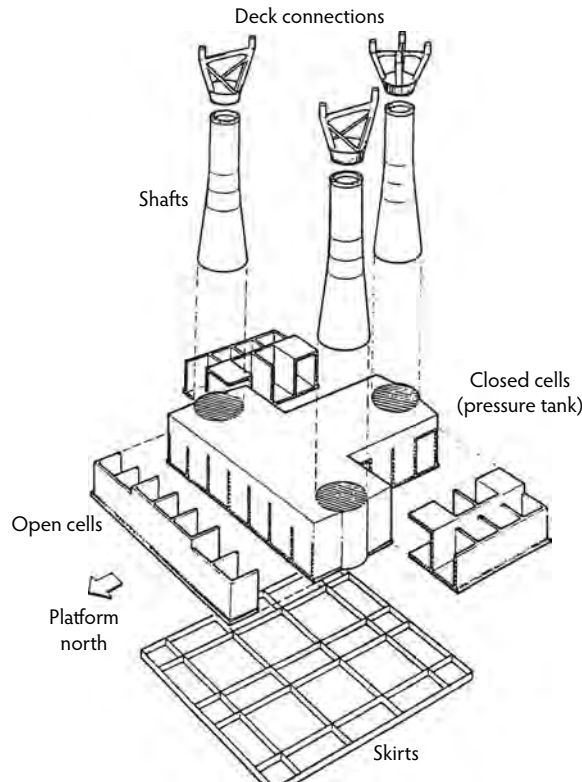


FIGURE 13.25 Principal components of the Ravenspurn North concrete platform. (Figure courtesy of Ove Arup & Partners, London.)

It generally costs less to construct a GBS entirely in a dry dock rather than partially in the dry dock, at a wet dock, or at a jetty mooring. Productivity is generally higher in the dry dock, and specialized equipment is minimized. Construction risk is usually lower. For smaller concrete platforms, the platform can be built entirely in the dry dock with sufficient buoyancy to be floated out and towed to the final location. The Ravenspurn North platform (Moksnes, 1989; Roberts, 1990) and all the barge-like platforms (see Figure 13.3 and Figure 13.5) built for the Gulf of Mexico have been constructed in this manner. Figure 13.25 shows an exploded view of various components of the Ravenspurn North platform (Ove Arup & Partners, 1990). It has been reported (Anon., 1989) that, in Europe, concrete GBSs for water depths from 100 to 150 m (330 to 490 ft) can be constructed entirely in a dry dock. The limit is governed by a combination of gate width and sill draft. As noted above, the total support for complete dry dock construction is land based, and the process is very similar to constructing a concrete building. Very large platforms can also be built in this manner but require the use of auxiliary buoyancy compartments for flotation. These compartments can be designed to be removed after platform installation or can be left in place. Some small platforms have also used additional buoyancy compartments to satisfy installation requirements.

A major expense in the construction of a concrete platform is the development of a dry dock if one does not exist or the modification of existing dry dock facilities to accommodate the construction. This expense can include land procurement; excavation, cofferdam construction; dewatering systems; dredging of channels for float out; construction of supporting quays, docks, and wharves; and overall infrastructure upgrades to improve project support (e.g., roads, bridges, power supply, water supply, sewage treatment). These costs can easily reach 80% of the project cost in remote areas.

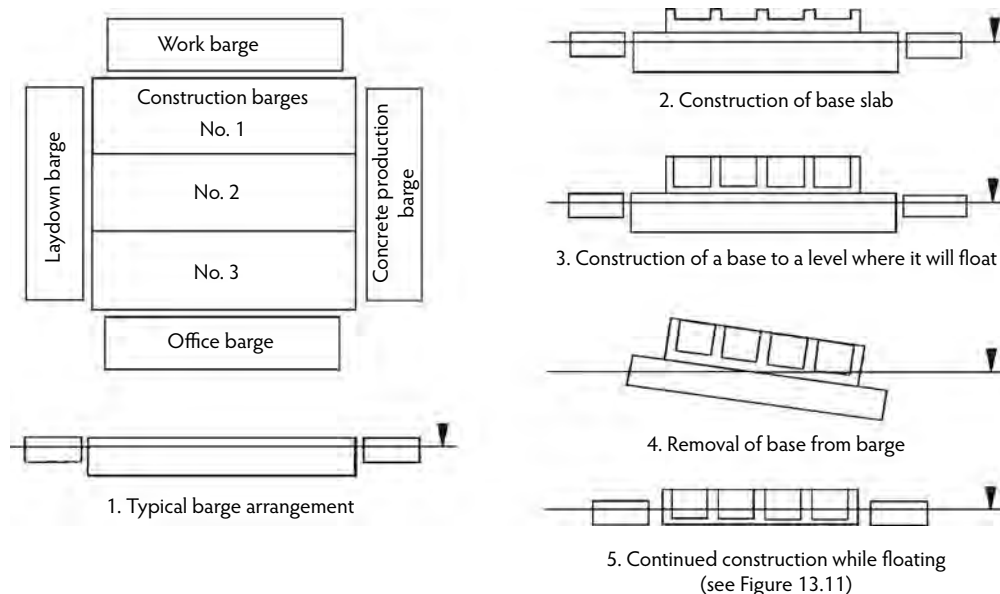


FIGURE 13.26 Barge construction scenario.

13.9.2 Construction on Barges

To eliminate much of the costs associated with the construction of a dry dock, the construction of some or all of the platform on submersible barges is a practical solution. Such an approach eliminates the need for a dry dock and thus greatly expands the potential number of construction-site locations. Figure 13.26 shows a typical barge construction scenario. Any location with sufficient water depth for barge and supply-ship operation is a possible construction site. Preferably, this site should be in sheltered waters and not subject to severe seas. The number of barges required will depend on the size of the structure and the capacity of the barges. Specially built barges are always a solution, but it may be more economical to weld together a sufficient number of smaller, standard-size barges to accomplish the same objective. When the barges have been assembled to provide the working platform, construction then proceeds on the barges as it would on land. Construction support will depend on the water depths available. Initially, construction can probably begin with the barges moored adjacent to the shore so all construction support can come directly from the land. Figure 13.27 shows the concrete tether anchors for the Snorre tension-leg platform (TLP), which were constructed entirely on barges with direct land support. If the platform is small, the entire platform can be built on the barges at one location. If the platform is large, only a portion would be built on the barges. That portion would be floated off the barges and temporarily moored, and construction would be completed while the portion is in a floating mode.

13.9.3 Skid-Way Construction

Skid ways exist in almost all marine fabrication yards. A skid way is basically a structural slab having a small slope that extends from a construction area down into the sea. Structures that are built on the skid way can be gravity assisted as they are moved down the slope and into the sea. The structures can be self-floating or can be skidded onto barges. Skid ways can be gravity assisted as they are moved down the slope and into the sea. The structures can be self-floating or can be skidded onto barges. For a concrete GBS, the structure can be built either in part or in its entirety on the skid way (Ben C. Gerwick, Inc., 1989). Small structures (Figure 13.28) are the most likely candidate for this type of construction. Because the weight of a complete large concrete structure is so great, there is probably an upper limit where any

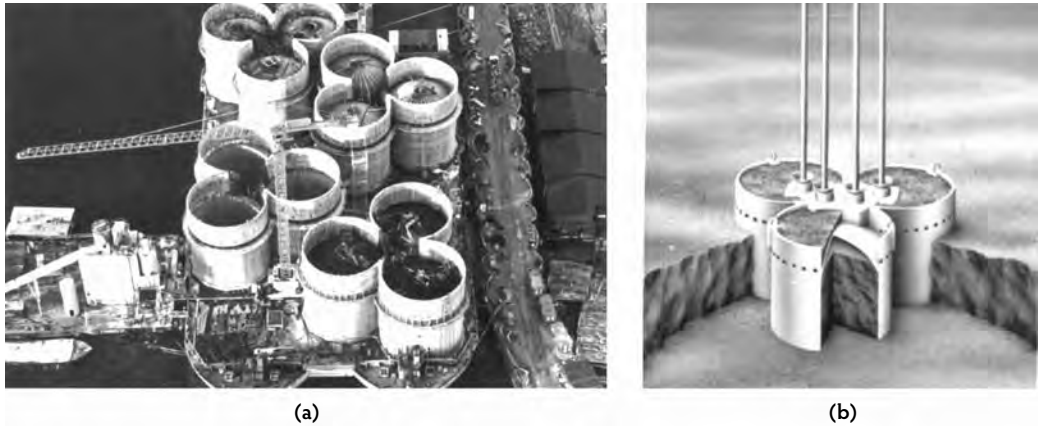


FIGURE 13.27 Snorre TLP foundation anchors. (Figure courtesy of Norwegian Contractors, Stabekk, Norway.)

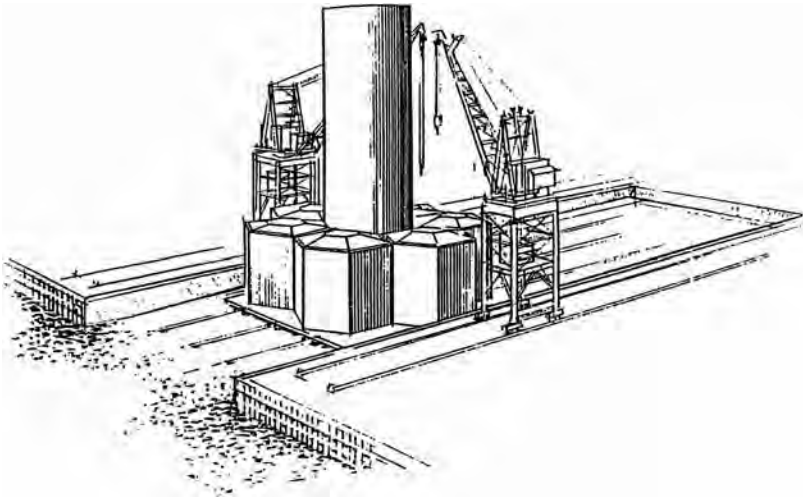


FIGURE 13.28 Skid-way construction. (Figure courtesy of Ben C. Gerwick, Inc., San Francisco, CA.)

given skid way could not be used without significant structural upgrading. This upgrading may not be cost effective but does warrant consideration. The base of most concrete structures can probably be constructed on a skid way to a level where the structure would be self-floating. It can then be skidded into a floating mode and towed to a deeper water site for mooring and completion.

13.9.4 Site Limitations

The principal limitation for any construction site is access to the open sea or to maintained ship channels. As most of the structures will float at some time during their construction and installation phases, water of sufficient depth for them to float and be towed to their final location must exist in close proximity to the construction site. Dredging of new channels is very expensive and may not be possible due to physical, environmental, or political reasons. Most large structures with deep drafts have been completed while in a floating mode. When this is done, the deep-water requirement is further constrained because the deep-water location must be in a relatively mild environment with respect to wind, waves, and current. It is also desirable to have the deep-water location close enough to shore that materials supply and construction crew changes can be made without having to stockpile large amounts of material offshore or provide temporary offshore quarters for personnel. Both of these aspects of construction can add

greatly to the cost of the project. If a dry dock is required and must be built, the supporting infrastructure must be carefully studied before a site is selected. If the site is not convenient to major population areas, the site development will have to include such things as accommodations for work crews, dining facilities, water supply, sewage disposal, recreation facilities, communication facilities, transportation, and all the other things required for a small city. As noted above, the existence of skid ways in operating shipyards does not necessarily mean they can be used for concrete structures because they may be undersized or structurally inadequate. Dredged channels leading away from skid ways most likely will not be of sufficient depth for the draft of larger concrete platforms, and some additional dredging may be required.

13.10 Marine Operations

The subject of marine operations is outside the scope of this chapter, but it should be noted that offshore development and marine operations go hand in hand. The construction and installation of any type of offshore concrete platform will involve significant marine operations (FIP, 1991). The structure itself must float, be towed, and perhaps be submerged for final installation. The structure may have its topside equipment installed in a mating operation. In this operation, the structure is ballasted down until it is almost submerged. The assembled topside equipment is then floated over the submerged structure. Deballasting is initiated, and as the structure rises it picks the topside up off the barges. Deballasting is continued until the structure reaches its final draft for towing operations. Hook-up of the topside to the structure is then performed. This mating is a critical marine operation. Marine operations are expensive and may require special vessels. Fortunately, many good specialist firms or consultants with offshore structure installation experience exist around the world, and they should be consulted for this aspect of the use of concrete platforms.

13.11 Cost Considerations

The costs of an offshore structure are usually dictated by the complexity of the structure, the location where it will be built, and the methods of construction used. These structures have the potential for low capital costs because the materials are local and the labor skill level usually does not have to be high. When properly made, concrete can be virtually maintenance free, thus producing an attractive life-cycle cost. Detailed cost discussions are beyond the scope of this chapter, but a cost philosophy for these structures is described in des Desert and Gifford (1989) and Hoff (1991b).

13.12 Summary

The information presented in this chapter is intended to provide a general overview of what is required in the use of concrete for offshore structures. A significant amount of information on the subject is distributed throughout the literature but has not yet been assembled in a useful textbook form. Concrete is the material of choice for permanent constructions in all regions of the world. It can be produced with local labor and local materials. The potential exists for its use in the offshore oil and gas industry in developing regions of the world and in existing offshore regions where steel structures have been predominately used before. The use of concrete for these structures generally must be sold to owners or developers who are used to dealing with steel structures. Concrete technology is well established for use in offshore structures. No special materials are required, the concrete quality is not unusual, design requirements are well established, competent offshore concrete design firms exist in many regions of the world, no special construction practices are required, flexibility exists in construction-site selection, capital costs can be low, and life-cycle costs can be very attractive. Because of the severe environment that exists offshore, durability aspects of concrete will require special attention. The potential for the use of concrete in offshore structures is great and is limited only by the ingenuity of the concrete designer and constructor and their ability to sell their ideas to the owners.

References

- ABAM. 1983. *Developmental Design and Testing of High-Strength Lightweight Concretes for Marine Arctic Structures*, Program Phase I, Joint Industry Project Report, AOGA Project No. 198. ABAM Engineers, Inc., Federal Way, WA.
- ABAM. 1984. *Developmental Design and Testing of High-Strength Lightweight Concretes for Marine Arctic Structures*, Program Phase II, Joint Industry Project Report, AOGA Project No. 230. ABAM Engineers, Inc., Federal Way, WA.
- ABAM. 1986a. *Developmental Design and Testing of High-Strength Lightweight Concretes for Marine Arctic Structures*, Program Phase III, Joint Industry Project Report, AOGA Project No. 230. ABAM Engineers, Inc., Federal Way, WA.
- ABAM. 1986b. *Floating Ferry Terminals, Burrard Inlet, Vancouver, B.C.* ABAM Engineers, Inc., Federal Way, WA.
- Abrahams, M.J. and Belvedere, J.A. 1984. Hood Canal Bridge. In *Proceedings of the American Concrete Institute Symposium on Offshore Structures*, October, New York.
- Abrahams, M. and Wilson, G. 1998. Precast prestressed segmental floating drawspan for Admiral Clarey Bridge, *Precast Concrete Inst. J.*, 43(4), 60–79.
- ACI Committee 357. 1988. *State-of-the-Art Report on Barge-Like Concrete Structures*, ACI 357.2R-88, 89 pp. American Concrete Institute, Farmington Hills, MI.
- ACI Committee 357. 1989. *Guide for the Design and Construction of Fixed Offshore Concrete Structures*, ACI 357R-89, 23 pp. American Concrete Institute, Farmington Hills, MI.
- ACI Committee 357. 1990. *State-of-the-Art Report on Offshore Concrete Structures for the Arctic*, ACI 357.1R-90, 117 pp. American Concrete Institute, Farmington Hills, MI.
- Anderson, A.R. 1977. World's largest prestressed LPG floating vessel. *J. Prestressed Concrete Inst.*, 22(1), 21.
- Anon. 1983. Bridge pontoons as cast singly in tight order, *Eng. News-Record*, September 29, p. 70.
- Anon. 1984. New idea for tanker loading and crude storage for remote areas. *Ocean Industry*, 19(6), 55.
- Anon. 1986. Concrete seabed storage. *Ocean Industry*, 21(8), 32.
- Anon. 1988a. Concrete work for Petrobras provides unique work experience. *Offshore*, 48(5), 84–87.
- Anon. 1988b. Field storage moves to seabed. *Offshore*, 48(4), 88–89.
- Anon. 1989. Concrete advantages in shallow water marginals. *Offshore Eng.*, February, pp. 143–144.
- Anon. 1990a. Anatomy of a concrete platform removal. *Offshore Eng.*, March, pp. 28 and 33.
- Anon. 1990b. Artificial island finds favour at Wytch Farm. *Offshore Eng.*, July, p. 19.
- Anon. 1990c. Concrete gravity foundations. *Offshore Eng.*, August, p. 42.
- Anon. 1991. Concrete FPS (floating production system) targets deepwater, marginal fields. *Ocean Industry*, 26(3), 78.
- Ben C. Gerwick, Inc. 1989. *Segmental Construction of Steel-Concrete Composite Base Rafts for Concrete Gravity-Base Structures*. Ben C. Gerwick, Inc., San Francisco, CA.
- des Desert, L. and Gifford, L.C. 1989. Minimum concrete platform for medium-depth waters. *Ocean Industry*, 24(8), 43–48.
- Fédération Internationale de la Précontrainte (FIP). 1985. *FIP Recommendations for the Design and Construction of Concrete Sea Structures*, 4th ed., 29 pp. Thomas Telford, London.
- Fédération Internationale de la Précontrainte (FIP). 1991. *Marine Practice for Large Offshore Structures*, Cement and Concrete Association, London.
- Fitzpatrick, J. and Stenning, D.G. 1983. Design and construction of Tarsuit Island in the Canadian Beaufort Sea. In *Proceedings of the Offshore Technology Conference*, Houston, TX, OTC Paper 4517.
- Gimsing, N.J. and Iversen, C. 2001. *The Tunnel*. Øresund Technical Publications, Copenhagen.
- Harrington, K. 1987. Concrete as a Fabrication Material for Simple Hulls: A Marine Innovation Study, Ph.D. dissertation, 454 pp. Sunderland Polytechnic, London.
- Hoff, G.C. 1986. The service record of concrete offshore platforms in the North Sea. In *Proceedings of the International Conference on Concrete in Marine Environments*, pp. 131–142. Concrete Society, London.

- Hoff, G.C. 1988. Resistance of concrete to ice abrasion: a review. In *Proceedings of the 2nd International Conference on Concrete in Marine Environments*, ACI SP-109, Malhotra, V.M., Ed., pp. 427–455. American Concrete Institute, Farmington Hills, MI.
- Hoff, G.C. 1991a. Durability of offshore and marine concrete structures. In *Proceedings of the 2nd CANMET/ACI International Conference on the Durability of Concrete*, Vol. 1, ACI SP-126, Malhotra, V.M., Ed., pp. 33–64. American Concrete Institute, Farmington Hills, MI.
- Hoff, G.C. 1991b. Considerations in the use of concrete for offshore structures. In *Proceedings of the International Conference on the Evaluation and Rehabilitation of Concrete Structures and Innovation in Design*, Vol. 2, ACI SP-128, Malhotra, V.M., Ed., pp. 749–788. American Concrete Institute, Farmington Hills, MI.
- Huntman, J.E., Anastasio, Jr., F.L., and Deshazer, W.A. 1979. Concrete gravity platform in shallow offshore Louisiana water. In *Proceedings of the Offshore Technology Conference*, Houston, TX, OTC Paper 3473.
- Jackson, G. and Bell, T.A. 1990. The design of the Ravenspurn North concrete gravity substructure: an innovative application of conventional technology. In *Proceedings of the Offshore Technology Conference*, Houston, TX, OTC Paper 6394.
- Jakobsen, S.E. 2000. The use of LWAC in the pontoons of the Nordhordland and floating bridge, Norway. In *Proceedings of the Second International Symposium on Structural Lightweight Aggregate Concrete*, Kristiansand, Norway, pp. 73–78.
- Maage M. and Olsen, T.O. 2000. LETTKON: a major joint Norwegian research programme on lightweight aggregate concrete. In *Proceedings of the Second International Symposium on Structural Lightweight Aggregate Concrete*, Kristiansand, Norway, pp. 261–270.
- Maage, M., Smeplass, S., and Bjøntegård, Ø. 2007. Fly ash cement in a mass concrete structure. In *Proceedings of the Terence C. Holland Symposium on Advances in Concrete Technology*, 9th CANMET/ACI International Symposium on Fly Ash, Silica Fume, Slag, and Natural Pozzolans in Concrete, Warsaw, Poland.
- Michel, D. 1989. Severe environmental loading challenges Hibernia designers. *Offshore*, 49(8), 73–74.
- Moksnes, J. 1989. Oil and gas concrete platforms in the North Sea: reflections on two decades of experience. In *Proceedings of the International Experience with Durability of Concrete in Marine Environments*, Mehta, P.K., Ed., pp. 127–146. University of California, Berkeley.
- Moksnes, J., Haug, A.K., Modeer, M., and Beravam, T. 1987. Concrete quality in Norwegian offshore structures: 15 years of laboratory and *in situ* testing of high-strength concrete. In *Proceedings of the International Symposium on Utilization of High-Strength/High-Performance Concrete*, Holand I. and Sellevold, E.J., Eds., pp. 405–416. Norwegian Concrete Association, Stabekk, Norway.
- Nichols, C.C. 1964. Construction and performance of the Hood Canal Floating Bridge. In *Proceedings of the Symposium on Concrete Construction in Aqueous Environments*, SP-8, pp. 97–106. American Concrete Institute, Farmington Hills, MI.
- Norwegian Contractors. 1990. Concrete subsea structures: well templates. *NC News*, pp. 6–7, 23.
- Norwegian Contractors. 1991a. *Durability of Concrete in the Gulf of Mexico: Experience from Existing Marine Concrete Structures*, prepared by Ben C. Gerwick, Inc., San Francisco, CA, for Norwegian Contractors, Joint Industry Project on Concrete for Gulf of Mexico, Floating Production Platforms.
- Norwegian Contractors. 1991b. *Concrete for Gulf of Mexico Floating Production Platforms*, Joint Industry Study Report No. 948, Vols. 1 and 2. Norwegian Contractors, Stabekk, Norway.
- Olsen, T. O. 2000. Heavy-duty floating unit for the offshore industry. In *Proceedings of the Second International Symposium on Structural Lightweight Aggregate Concrete*, Kristiansand, Norway.
- Olsen, T.O. 2007a. Why we need good concrete: the offshore experience from a design point of view. In *Proceedings of the Terence C. Holland Symposium on Advances in Concrete Technology*, 9th CANMET/ACI International Symposium on Fly Ash, Silica Fume, Slag, and Natural Pozzolans in Concrete, Warsaw, Poland.

- Ove Arup & Partners. 1990. *The Ravenspurn North Concrete Gravity Substructure (CGS)*. Ove Arup & Partners, London.
- Prestressed Concrete Institute (PCI). 1982. Floating container terminal, Valdez, Alaska, *J. Prestressed Concrete Inst.*, 27(4), 9 pp.
- Roberts, J. 1990. Innovation in concrete gravity substructures: the Ravenspurn North platform and beyond. In *Proceedings of the Offshore Technology Conference*, Houston, TX, OTC Paper 6347.
- Tate, S.H. and Core, J.A. 1989. Eugene Island 126 concrete refurbishment. In *Proceedings of the Offshore Technology Conference*, Houston, TX, OTC Paper 6146.
- Yee, A.A., Masuda, F.R., Kim, C.N., Doi, D.A., and Daly, L.A. 1984. Concrete module for the global marine concrete island drilling system. In *Proceedings of the FIP/CPCI Symposium*. Vol. 2. *Concrete Sea Structures in Arctic Regions*, August 25–31, Calgary, Canada, pp. 23–30.



Foundation preparation for high-rise building. (Photograph courtesy of Portland Cement Association, Skokie, IL.)

14

Foundations for Concrete Structures

Manjriker Gunaratne, Ph.D., P.E.*

14.1	Foundation Engineering	14-1
	Soil Classification • Strength of Soils • Compressibility and Settlement • Groundwater and Seepage • Dewatering of Excavations • Environmental Geotechnology • Design of Landfill Liners	
14.2	Site Exploration	14-27
	Plate Load Tests	
14.3	Shallow Footings	14-32
	Bearing Capacity of Shallow Footings • Footings with Eccentricity • Presumptive Load-Bearing Capacity	
14.4	Mat Footings.....	14-37
	Design of Rigid Mat Footings • Design of Flexible Mat Footings	
14.5	Retaining Walls	14-43
	Determination of Earth Pressures • Design of Concrete Retaining Walls • Effect of Water Table • Reinforced Walls • Sheet Pile Walls • Braced Excavations • Soil Nail Systems • Drainage Considerations	
14.6	Pile Foundations.....	14-57
	Advantages of Concrete Piles • Types of Concrete Piles • Estimation of Pile Capacity• Computation of Pile Settlement • Pile Groups • Verification of Pile Capacity	
14.7	Caissons and Drilled Piers.....	14-76
	Estimation of Bearing Capacity	
	References	14-79

14.1 Foundation Engineering

Geotechnical engineering is a branch of civil engineering in which technology is applied to the design and construction of structures involving earthen materials, and there are many branches of geotechnical engineering. Surficial earthen material consists of soil and rock; soil and rock mechanics are fundamental studies of the properties and mechanics of soil and rock. Foundation engineering is the application of

* Professor of Civil Engineering at University of South Florida, Tampa; expert in various areas of geotechnical engineering, including foundation design, numerical modeling, and soil stabilization.

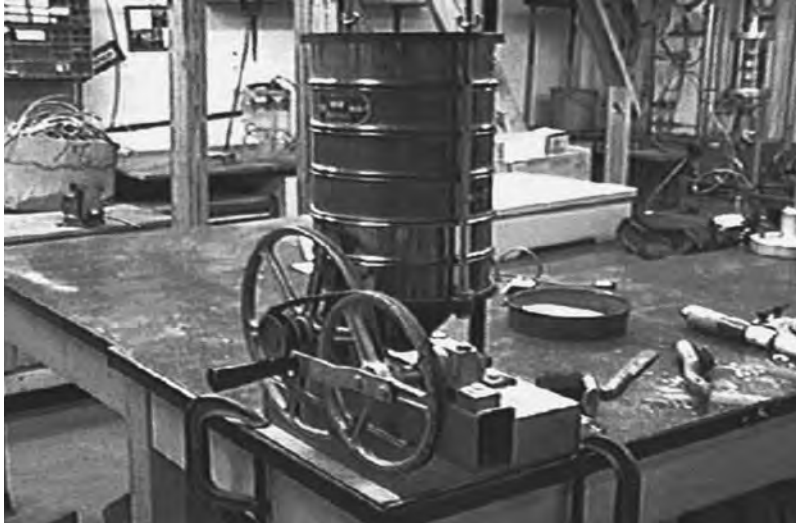


FIGURE 14.1 Equipment for sieve analysis.

the principles of soil mechanics, rock mechanics, and structural engineering to the design of structures associated with earthen materials. It is generally observed that most common foundation types supported by intact bedrock present no compressibility problems; hence, when designing common foundation types, the foundation engineer's primary concerns are the strength and compressibility of the subsurface soil and, whenever applicable, the strength of bedrock.

14.1.1 Soil Classification

14.1.1.1 Mechanical Analysis

According to texture or the feel, two different soil types can be identified: (1) coarse-grained soil (gravel and sand), and (2) fine-grained soil (silt and clay). Whereas the engineering properties (primarily strength and compressibility) of coarse-grained soils depend on the size of individual soil particles, the properties of fine-grained soils are mostly governed by moisture content. Hence, it is important to identify the type of soil at a given construction site, because effective construction procedures invariably depend on the soil type. Soil engineers use a universal format called the *unified soil classification system* (USCS) to identify and label soil. The system is based on the results of common laboratory tests of mechanical analysis and Atterberg limits (Bowles, 1986). To classify a given soil sample, mechanical analysis is conducted in two stages: (1) sieve analysis for the coarse fraction (gravel and sand), and (2) hydrometer analysis for the fine fraction (silt and clay). Of these, sieve analysis is conducted according to ASTM D 421 and D 422 procedures, using a set of U.S. standard sieves (Figure 14.1). The most commonly used sieves are numbers 20, 40, 60, 80, 100, 140, and 200, corresponding to sieve openings of 0.85, 0.425, 0.25, 0.18, 0.15, 0.106, and 0.075 mm, respectively.

During the test, the percentage (by weight) of the soil sample retained on each sieve is recorded, from which the percentage (R%) passing (or finer than) a given sieve size (D) is determined. On the other hand, if a substantial portion of the soil sample consists of fine-grained soils ($D < 0.075$ mm), then sieve analysis has to be followed by hydrometer analysis (Figure 14.2). This is performed by first treating the fine fraction with a deflocculating agent such as sodium hexametaphosphate (Calgon®) or sodium silicate (water glass) for about half a day and then allowing the suspension to settle in a hydrometer jar kept at a constant temperature. As the heavier particles settle, followed by the lighter ones, a calibrated ASTM 152H hydrometer is used to estimate the fraction (R%) still settling above the hydrometer bottom at any

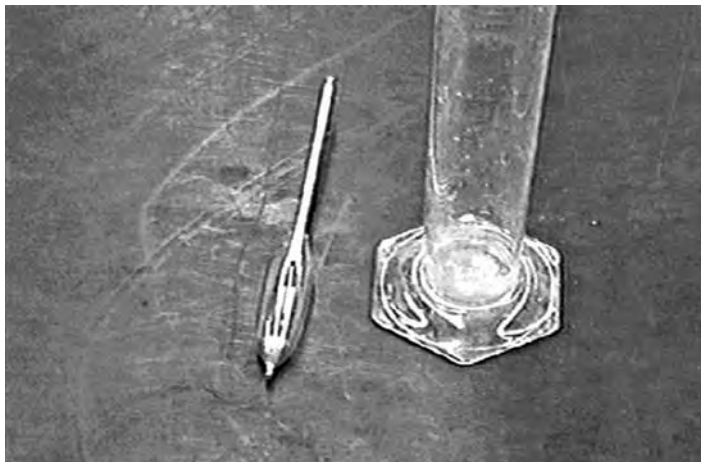


FIGURE 14.2 Equipment for hydrometer analysis.

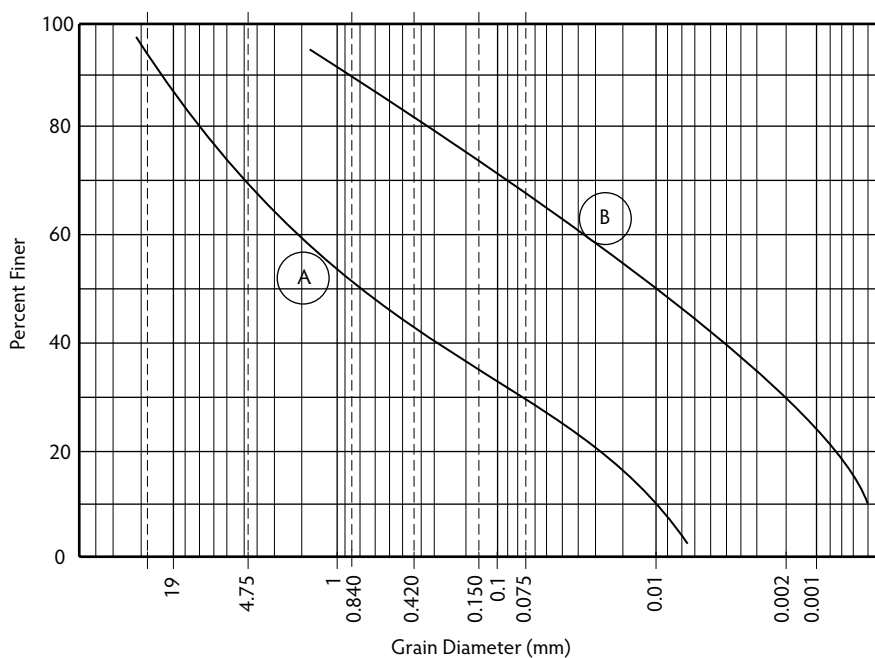


FIGURE 14.3 Grain-size distribution curves.

given stage. Further, the particle size (D) that has settled past the hydrometer bottom at that stage in time can be estimated from Stokes' law. It can be seen that $R\%$ is the weight percentage of soil finer than D .

Complete details of the above tests are provided in Bowles (1986). For soil samples that have significant coarse and fine fractions, the sieve and hydrometer analysis results ($R\%$ and D) can be logically combined to generate grain (particle) size distribution curves such as those indicated in Figure 14.3. From Figure 14.3, it can be seen that 30% of soil type A is finer than 0.075 mm. (U.S. No. 200 sieve), with $R\% = 30$ and $D = 0.075$ mm being the last pair of results obtained from the sieve analysis. In combining sieve analysis data with hydrometer analysis data, one has to convert the $R\%$ (based on the fine fraction only) and D obtained from hydrometer analysis to $R\%$ based on the weight of the entire sample to ensure continuity of the curve.

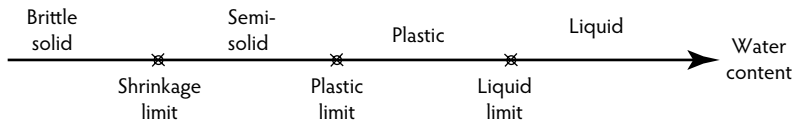


FIGURE 14.4 Variation of the fine-grained soil properties with water content.

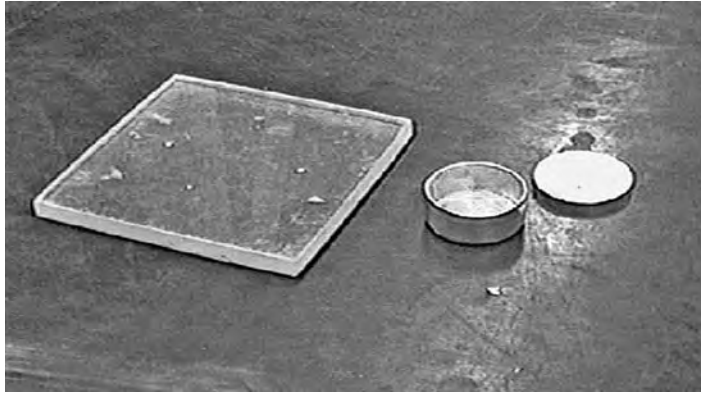


FIGURE 14.5 Equipment for the plastic limit test.

As an example, let the results from one hydrometer reading of soil sample A be $R\% = 90$ and $D = 0.05$ mm. To plot the curve, one needs the percentage of the entire sample finer than 0.05 mm. Because what is finer than 0.05 mm is 90% of the fine fraction (30%) used for hydrometer analysis, the converted $R\%$ for the final plot can be obtained by multiplying 90% by the fine fraction of 30%. Hence, the converted data used in Figure 14.3 are $R\% = 27$ and $D = 0.05$ mm.

14.1.1.2 Atterberg Limits

As mentioned earlier, properties of fine-grained soils are governed by water; hence, the effect of water on fine-grained soils has to be considered in soil classification. This is achieved by employing the Atterberg limits or consistency limits. The physical state of a fine-grained soil changes with increasing water content, as shown in Figure 14.4, from a brittle to a liquid state. Theoretically, the plastic limit (PL) is defined as the water content at which the soil changes from *semisolid* to *plastic* (Figure 14.4). For a given soil sample, this is an inherent property that can be determined by rolling a plastic soil sample into a worm shape to gradually reduce its water content by exposing more and more of an area until the soil becomes semisolid. This change can be detected by the appearance of cracks on the sample. According to ASTM 4318, the plastic limit is the water content at which cracks develop on a rolled soil sample at a diameter of 3 mm; thus, the procedure is one of trial and error. The apparatus (ground glass plate and moisture cans) used for the test is shown in Figure 14.5, but the reader is also referred to Bowles (1986) and Wray (1986) for details.

On the other hand, the liquid limit (LL), which is visualized as the water content at which the state of a soil changes from *plastic* to *liquid* with increasing water content, is determined in the laboratory using Casagrande's liquid limit device (Figure 14.6). This device is specially designed with a standard brass cup where a standard-sized soil paste is laid during testing. In addition, the soil paste is grooved in the middle by a standard grooving tool, thereby creating a gap with standard dimensions. The brass cup is then made to drop through a distance of 1 cm on a hard rubber base. The number of drops (blows) required to close the above gap along a distance of 1/2 in. is counted. Details of the test procedure can be found in Bowles (1986). ASTM 4318 specifies the liquid limit as the water content at which closing of the standard-sized gap is achieved in 25 drops of the cup; therefore, one has to repeat the experiment for different trial water contents, each time recording the number of blows required to close the above

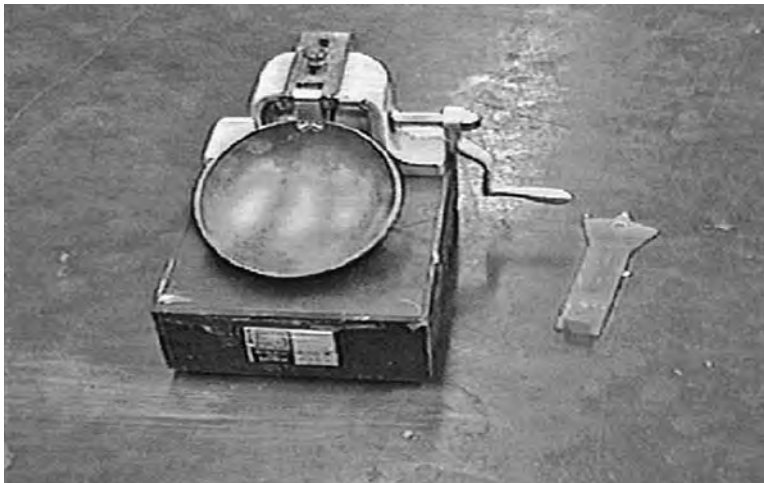


FIGURE 14.6 Equipment for the liquid limit test.

standard-sized gap. Finally, the water content corresponding to 25 blows can be interpolated from the data obtained from all of the trials. The plasticity index (PI) is defined as follows:

$$PI = LL - PL$$

14.1.1.3 Unified Soil Classification System

In the commonly adopted unified soil classification system (USCS) shown in Table 14.1, the aforementioned soil properties are effectively used to classify soils. Example 14.1 below illustrates the classification of the two soil samples shown in Figure 14.3. Defining the following two curve parameters is necessary to accomplish the classification:

Coefficient of uniformity: $C_u = D_{60}/D_{10}$

Coefficient of curvature: $C_c = (D_{30})^2/(D_{60} \times D_{10})$

where D_i is the diameter corresponding to the i th percentage on the grain-size distribution curve.

Example 14.1

Soil A. The percentage of coarse-grained soil is equal to 70%; hence, soil A is a coarse-grained soil. The percentage of sand in the coarse fraction is equal to $(70 - 30)/70 \times 100 = 57\%$. Thus, according to the USCS (Table 14.1), soil A is a sand. If one assumes clean sand, then:

$C_c = (0.075)^2/(2 \times 0.013) = 0.21$ does not meet criterion for SW.

$C_u = 2/0.013 = 153.85$ meets criterion for SW.

Hence, soil A is a poorly graded sand (SP).

Soil B. The percentage of coarse-grained soil is equal to 32%; hence, soil B is a fine-grained soil. Assuming that LL is equal to 45 and PL is equal to 35 (then PI is equal to 10) and using Casagrande's plasticity chart (Table 14.1), it can be concluded that soil B is a silty sand with clay (ML).

14.1.2 Strength of Soils

The two most important properties of a soil that a foundation engineer must be concerned with are strength and compressibility. Because earthen structures are not designed to sustain tensile loads, the most common mode of soil failure is shear; hence, the shear strength of the foundation medium constitutes a direct input to the design of concrete structures associated with the ground.

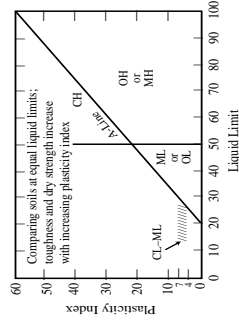
TABLE 14.1 Unified Soil Classification System

Major Divisions				Group Symbols (τ)		Typical Names		Laboratory Classification Criteria			
1		2		3		4		6			
Coarse-grained soils: More than half of the material is larger than No. 200 (75 μm) sieve size	(Particles smaller than the No. 200 sieve cannot be seen with the naked eye.)	Gravels: More than half of gravel fraction is larger than No. 4 (4.75 mm) sieve size	(For visual classification, 5-mm may be used as equivalent to the No. 4 sieve size.)	Clean gravels (few or no fines)	GW	Well-graded gravels, gravel-sand mixtures, few or no fines	Determine percentage of gravel and sand from grain size curve. Depending on percentages of fines (fraction smaller than No. 200 sieve size), coarse-grained soils are classified as follows: More than 12%, GM, GC, SM, SC Less than 5%, GW, GP, SW, SP 5–12%, Borderline cases requiring use of dual symbols	C _u = D ₆₀ /D ₁₀ greater than 4 C _c = (D ₃₀) ² /(D ₁₀ × D ₆₀) between 1 and 3 (see Section 2.5)		Not meeting all gradation requirements for GW	
					GP	Poorly graded gravels, gravel-sand mixtures, few or no fines					
		Sands: More than half of coarse fraction is smaller than No. 4 (4.75 mm) sieve size	Gravels with fines (appreciable amount of fines)	GM	Silty gravels, gravel-sand-silt mixtures	Above A-line with PI values between 4 and 7 are borderline cases requiring use of dual symbols					
				GC	Clayey gravels, gravel-sand-clay mixtures						
Fine-grained soils: More than half of material is smaller than No. 200 (75 μm) sieve size	(Particles smaller than the No. 200 sieve cannot be seen with the naked eye.)	Sands with fines (appreciable amount of fines)	(For visual classification, 5-mm may be used as equivalent to the No. 4 sieve size.)	Clean sands (few or no fines)	SW	Well-graded sands, gravelly sands, few or no fines	Determine percentage of gravel and sand from grain size curve. Depending on percentages of fines (fraction smaller than No. 200 sieve size), coarse-grained soils are classified as follows: More than 12%, GM, GC, SM, SC Less than 5%, GW, GP, SW, SP 5–12%, Borderline cases requiring use of dual symbols	C _u = D ₆₀ /D ₁₀ greater than 6 C _c = (D ₃₀) ² /(D ₁₀ × D ₆₀) between 1 and 3 (see Section 2.5)		Not meeting all gradation requirements for SW	
					SP	Poorly graded sands, gravelly sands, few or no fines					
					SM	Silty sands, sand-silt mixtures		Limits plotting in hatched zone with PI values between 4 and 7 are borderline cases requiring use of dual symbols.			
					SC	Clayey sands, sand-clay mixtures					
		Silty and clays; liquid limit less than 50	(For visual classification, 5-mm may be used as equivalent to the No. 4 sieve size.)	Sands with fines (appreciable amount of fines)	(For visual classification, 5-mm may be used as equivalent to the No. 4 sieve size.)	Clean sands (few or no fines)	ML	Inorganic silts and very fine sands, rock flour, silty or clayey fine sands or clayey silts with slight plasticity	Limits plotting in hatched zone with PI values between 4 and 7 are borderline cases requiring use of dual symbols.		
							CL	Inorganic clays of low to medium plasticity, gravelly clays, sandy clays, silty clays, lean clays			
							OL	Organic silts and organic silty clays of low plasticity			
							MH	Inorganic silts, micaceous or diatomaceous fine sandy or silty soils, elastic silts			
Silty and clays; liquid limit greater than 50	(For visual classification, 5-mm may be used as equivalent to the No. 4 sieve size.)	Gravels with fines (appreciable amount of fines)	(For visual classification, 5-mm may be used as equivalent to the No. 4 sieve size.)	Clean gravels (few or no fines)	CH	Inorganic clays of high plasticity, fat clays	Limits plotting in hatched zone with PI values between 4 and 7 are borderline cases requiring use of dual symbols.				
					OH	Organic clays of medium to high plasticity, organic silts					
					Pt	Peat and other highly organic soils					

Plasticity Chart for Laboratory Classification of Fine-Grained Soils

Comparing soils at equal liquid limits; toughness and dry strength increase with increasing plasticity index

Plasticity Chart for Laboratory Classification of Fine-Grained Soils



Source: Holtz, R.D. and Kovacs, W.D., *An Introduction to Geotechnical Engineering*, Prentice Hall, Englewood Cliffs, NJ, 1981. With permission.

14.1.2.1 Effective Stress Concept

Pores (or voids) within the soil skeleton contain fluids such as air, water, or other contaminants. Any load applied on a soil is partly carried by such pore fluids in addition to being borne by the soil grains; therefore, the total stress at any given location within a soil mass can be expressed as the summation of the stress contributions from the soil skeleton and the pore fluids as:

$$\sigma = \sigma' + u_p \quad (14.1)$$

where:

- σ = total stress (above atmospheric pressure).
- σ' = stress in soil skeleton (above atmospheric pressure).
- u_p = pore (fluid) pressure (above atmospheric pressure).

The stress in the soil skeleton, or the intergranular stress, is also known as the *effective stress*, as it indicates that proportion of the total stress carried by grain-to-grain contacts.

In the case of **dry soils** in which the pore fluid is primarily air, if one assumes that all pores anywhere within the soil are open to the atmosphere through interporous connectivity, then from Equation 14.1 the effective stress would be the same as the total stress:

$$\sigma' = \sigma \quad (14.2)$$

On the other hand, in completely wet (**saturated**) soils, the pore fluid is mostly water, and the effective stress is completely dependent on the *pore water pressure* (u_w). Then, from Equation 14.2:

$$\sigma' = \sigma - u_w \quad (14.3a)$$

Using the unit weights of soil (γ) and water (γ_w), Equation 14.3a can be modified to a more useful form as shown in Equation 14.3b:

$$\sigma'_{v0} = \gamma z - \gamma_w d_w \quad (14.3b)$$

where:

- z = depth of the location from the ground surface.
- d_w = depth of the location from the groundwater table.

Finally, in **partly saturated soils**, the effective stress is governed by both the pore water and pore air pressures (u_a). For unsaturated soils that contain both air and water with a high degree of saturation (85% or above), Bishop and Blight (1963) showed that:

$$\sigma = \sigma' + u_a - \chi(u_a - u_w) \quad (14.4)$$

where ($u_a - u_w$) is the soil matrix suction that depends on the surface tension of water and χ is a parameter in the range of 0 to 1.0 that depends on the degree of saturation. One can verify the applicability of Equation 14.3a for saturated soils based on Equation 14.4, as $\chi = 1$ for completely saturated soils.

14.1.2.2 Determination of Shear Strength

The shear strength of soils is assumed to originate from the strength properties of cohesion (c) and internal friction (ϕ). Using the basic Coulomb's friction principle, the shear strength of a soil can be expressed as:

$$\tau_f = c + \sigma \tan \phi \quad (14.5)$$

However, it is also known that the magnitudes of the soil shear strength properties vary with prevailing drainage conditions and to a minor extent with the stress level; hence, it is important to characterize the strength properties in terms of the drainage condition (drained or undrained) employed during testing. A wide variety of laboratory and field methods are used to determine the shear strength parameters c and ϕ of soils. The triaxial test, the standard penetration test (SPT), and the static cone penetration tests (CPTs) are the most common ones used in foundation engineering.

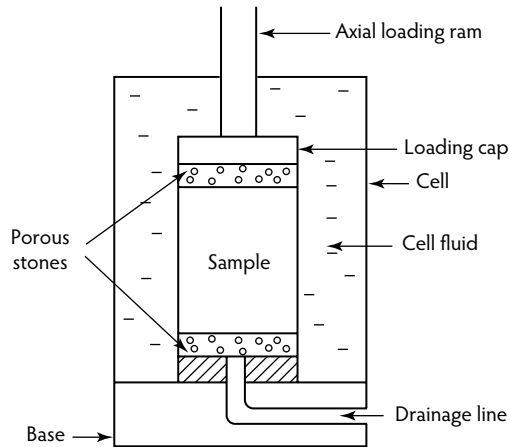


FIGURE 14.7 Schematic diagram of triaxial cell.

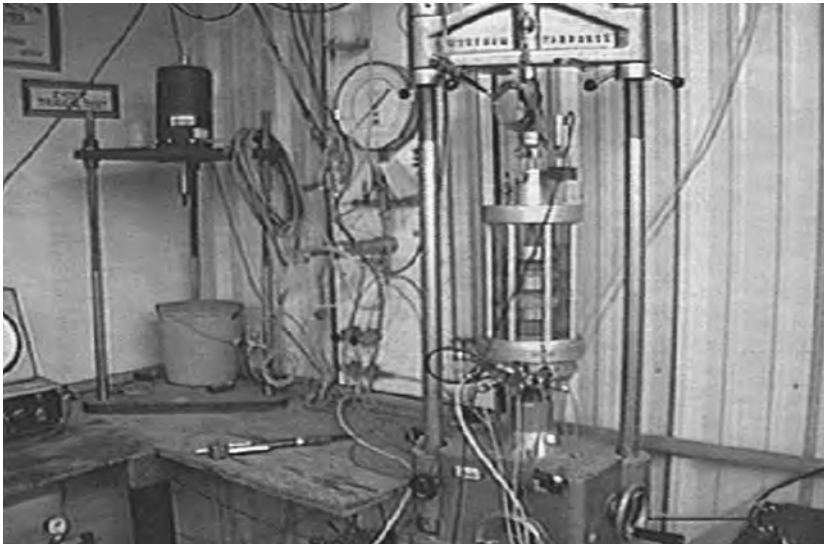


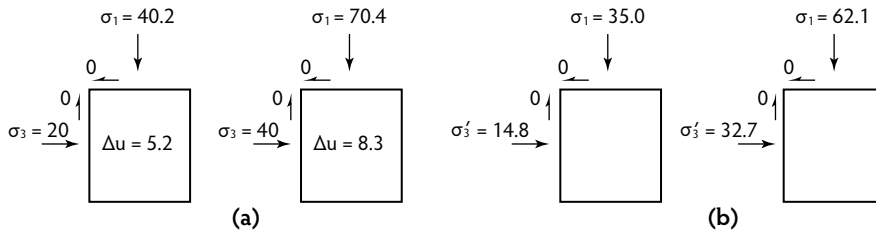
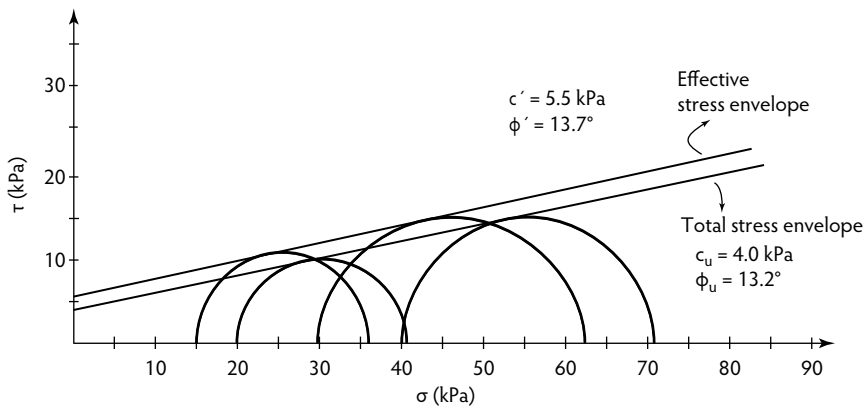
FIGURE 14.8 Triaxial testing apparatus.

14.1.2.3 Triaxial Tests

In this test, a sample of undisturbed soil retrieved from a site is tested under a range of pressures that encompass the expected field stress conditions due to the building. Figure 14.7 is a schematic diagram of the important elements of a triaxial setup, and the actual testing apparatus is shown in Figure 14.8. From the discussion of soil strength, it can be seen that the type of soil and the field-loading rate have a bearing on selection of the laboratory drainage conditions and hence the loading rate. Accordingly, three types of triaxial tests are commonly conducted: (1) consolidated drained (CD) tests, (2) consolidated undrained (CU) tests, and (3) unconsolidated undrained (UU) tests. In CU and CD tests, the pressure exerted on the cell fluid is used to consolidate the soil sample back up to the *in situ* stress state before applying the axial compression. On the other hand, in UU tests, the cell pressure is applied with no accompanying consolidation merely to provide a confining pressure. Computations involving CU and UU tests are given in Example 14.2 and Example 14.3, and the reader is referred to Holtz and Kovacs (1981) for more details regarding the testing procedure.

TABLE 14.2 Measured CU Triaxial Test Data

Test	Cell Pressure (kPa)	Deviator Stress at Failure (kPa)	Pore Pressure (kPa)
1	20	20.2	5.2
2	40	30.4	8.3

**FIGURE 14.9** Stress states at failure: (a) total stresses (kPa); (b) effective stresses (kPa).**FIGURE 14.10** Mohr circle diagram for a consolidated undrained (CU) test.**Example 14.2**

Assume that one conducts two CU triaxial tests on a sandy clay sample from a tentative site to determine the strength properties. The applied cell pressures, deviator stresses, and measured pore pressures at failure are given in Table 14.2. The strength parameters can be easily estimated using the Mohr circle method as follows:

- *Total strength parameters.* The total stresses (σ_1 and σ_3) acting on both test samples at failure are indicated in Figure 14.9a. Accordingly, the Mohr circles for the two stress states can be drawn as in Figure 14.10. Then, the total strength parameters (sometimes referred to as the *undrained strength parameters*) can be evaluated from the slope of the direct common tangent, which is the Coulomb envelope (Equation 14.5) plotted on the Mohr circle diagram:

$$c_u = 4.0 \text{ kPa and } \phi_u = 13.2^\circ$$

It is obvious that the generated pore pressure has been ignored in the above solution.

- *Effective strength parameters.* The effective stresses (σ'_1 and σ'_3) on both test samples at failure, computed by subtracting the pore pressure from the total stress, are indicated in Figure 14.9b. The Mohr circles corresponding to the two stress states are drawn in Figure 14.10. The effective

TABLE 14.3 Measured UU Triaxial Test Data

Test	Cell Pressure (kPa)	Deviator Stress at Failure (kPa)	Pore Pressure (kPa)
1	40	102.2	N/A
2	60	101.4	N/A

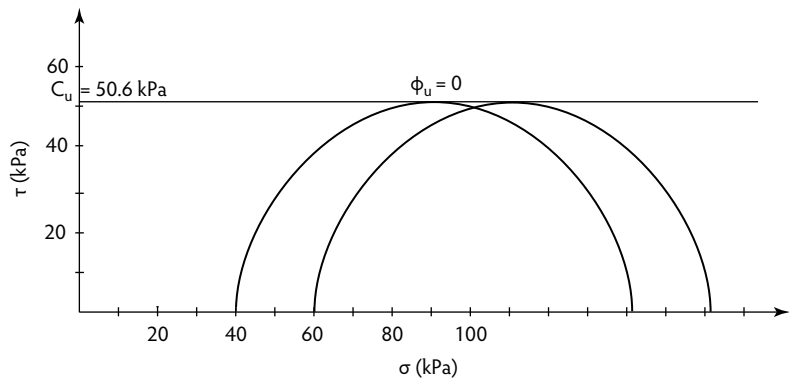


FIGURE 14.11 Mohr circle diagram for an unconsolidated undrained (UU) test.

strength parameters (sometimes referred to as the *drained strength parameters*) can be found from the slope of the Coulomb envelope for effective stresses plotted on the Mohr circle diagram:

$c' = 5.5 \text{ kPa}$ and $\phi' = 13.7^\circ$

Example 14.3

Assume that one wishes to determine the strength properties of a medium stiff clayey foundation under short-term (undrained) conditions. An effective method for achieving this is to conduct a UU (quick) test. For the results presented in Table 14.3, the undrained strength parameters have to be estimated. Because the pore pressure generation is not monitored in these tests, only the total stresses can be plotted, as in Figure 14.11. It can be seen that the deviator stress at failure does not change with the changing cell pressure during this type of test. This is because the soil samples are not consolidated to the corresponding cell pressures during UU (unconsolidated undrained) tests; therefore, the soil structure is unaffected by the change in cell pressure. Hence, the following strength parameters can be obtained from Figure 14.11:

$c_u = 50.6 \text{ kPa}$ and $\phi_u = 0^\circ$

The reader should note that the subscripts *u* are used to distinguish the UU test parameters.

14.1.2.2.1 Selection of Triaxial Test Type Based on the Construction Situation

The CD strength is critical for consideration of long-term stability. Examples of such situations include:

- Slowly constructed embankment on a soft clay deposit
- Earth dam under steady-state seepage
- Excavation of natural slopes in clay

On the other hand, CU strength is more relevant for the following construction conditions:

- Raising of an embankment subsequent to consolidation under its original height
- Rapid drawdown of a reservoir of an earthen dam previously under steady-state seepage
- Rapid construction of an embankment on a natural slope



FIGURE 14.12 Standard penetration test hammer.

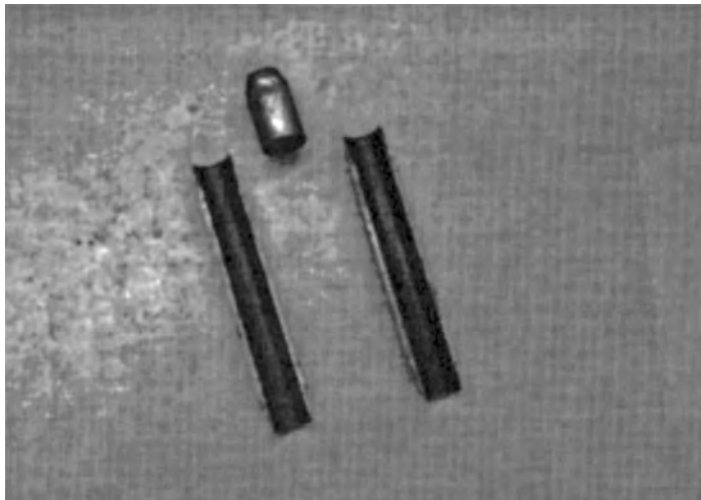


FIGURE 14.13 Split spoon sampler.

Finally, the UU strength is applicable under the following conditions:

- Rapid construction of an embankment over a soft clay
- Large dam constructed with no change in water content in the clay core
- Footing placed rapidly on a clay deposit

14.1.2.4 Standard Penetration Test

The standard penetration test (SPT) is the most common field test used to estimate the *in situ* shear strength of foundation soil. In this test, a 140-lb hammer (Figure 14.12) that falls 30 in. is used to drive a standard split spoon sampler (Figure 14.13) 18 in. into the ground. The number of hammer blows necessary to achieve the last 12 in. of penetration is recorded as the blow count (N). Although it is relatively easy to perform, SPT suffers because it is crude and not repeatable. The basic principle underlying the SPT test is the relation between the penetration resistance and shear strength of the soil, which can be visualized as a unique relationship. Because the penetration resistance is obviously affected by the overburden, the following correction is applied before determining the soil properties:

TABLE 14.4 Relation between SPT Blow Count and Friction Angle of Granular Soils

Description	Very Loose	Loose	Medium	Dense	Very Dense
Relative density (D_r)	0	0.15	0.35	0.65	0.85
SPT N'_{70}					
Fine	1–2	3–6	7–15	16–30	?
Medium	2–3	4–7	8–20	21–40	>40
Coarse	3–6	5–9	10–25	26–45	>45
ϕ					
Fine	26–28	28–30	30–34	33–38	—
Medium	27–28	30–32	32–36	36–42	<50
Coarse	28–30	30–34	33–40	40–50	—
γ_{wet} (kN/m ³)	11–16 ^a	14–18	17–20	17–22	20–23

^a Excavated soil or material dumped from a truck has a unit weight of 11 to 14 kN/m³ and must be quite dense to weigh much over 21 kN/m³. No existing soil has a $D_r = 0.00$ nor a value of 1.00. Common ranges are from 0.3 to 0.7.

Note: Empirical values for ϕ and D_r and unit weight of granular soils are based on a normally consolidated (approximately, $\phi = 28^\circ + 15^\circ D_r, \pm 2^\circ$) SPT at about 6-m depth.

Source: Bowles, J.E., *Foundation Analysis and Design*, McGraw-Hill, New York, 1995. With permission.

TABLE 14.5 Relation between SPT Blow Count and Unconfined Compression Strength of Clay

Consistency of Saturated Cohesive Soils ^a		N'_{70}	q_u (kPa)	Remarks
Very soft	<div style="display: flex; align-items: center; justify-content: center;"> <div style="writing-mode: vertical-rl; transform: rotate(180deg);">Increasing OCR</div> <div style="text-align: center; margin: 0 10px;"> <div style="border-left: 1px solid black; border-right: 1px solid black; height: 100px; position: relative;"> <div style="position: absolute; top: 0; left: 0; right: 0; border-bottom: 1px solid black;"></div> </div> </div> <div style="writing-mode: vertical-rl; transform: rotate(180deg);">Young clay</div> </div>	0–2	<25	Squishes between fingers when squeezed
Soft		3–5	25–50	Very easily deformed by squeezing
Medium		6–9	50–100	?
Stiff		10–16	100–200	Difficult to deform by hand squeezing
Very stiff		17–30	200–400	Very difficult to deform by hand squeezing
Hard	<div style="display: flex; align-items: center; justify-content: center;"> <div style="writing-mode: vertical-rl; transform: rotate(180deg);">Increasing OCR</div> <div style="text-align: center; margin: 0 10px;"> <div style="border-left: 1px solid black; border-right: 1px solid black; height: 100px; position: relative;"> <div style="position: absolute; top: 0; left: 0; right: 0; border-bottom: 1px solid black;"></div> </div> </div> <div style="writing-mode: vertical-rl; transform: rotate(180deg);">Aged/cemented</div> </div>	>30	>400	Nearly impossible to deform by hand

^a Blow counts and OCR division serve as a guide; in clay, exceptions to the rule are very common.

Source: Bowles, J.E., *Foundation Analysis and Design*, McGraw-Hill, New York, 1995. With permission.

$$N' = \sqrt{\frac{1}{\sigma'_v}} N \quad (14.6)$$

where σ'_v is the effective overburden stress (in tons per square feet) computed as follows:

$$\sigma'_v = \gamma z - \gamma_w d_w \quad (14.7)$$

where:

γ = unit weight of soil.

z = depth of test location.

γ_w = unit weight of water.

d_w = depth of test location from the groundwater table.

Once the corrected blow count (N'_{70}) is determined, one can find the strength parameters based on the empirical correlations shown in Table 14.4 and Table 14.5. The subscript 70 indicates 70% efficiency in energy transfer from the hammer to the sampler. This value has been shown to be relevant for the North American practice of SPT. It should be noted that the undrained strength (c_u) of a saturated clay is one half the unconfined compression strength (q_u).

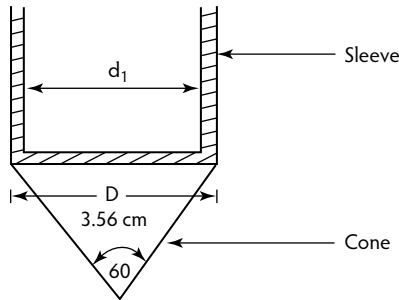


FIGURE 14.14 Cone and sleeve.



FIGURE 14.15 Cone penetration test equipment. (From Stinnette, P., Geotechnical Data Management and Analysis System for Organic Soils, Ph.D. dissertation, University of South Florida, Tampa, 1996.)

14.1.2.5 Static Cone Penetration Test

The cone penetration test (CPT) has been gaining popularity as a more reliable and repeatable alternative to SPT. In this test, a standard cone and a sleeve (Figure 14.14) are advanced at a steady rate (1 cm/sec) into the ground while the cone resistance (q_c) and the sleeve friction (f_s) are electronically measured. The entire cone apparatus and the associated computing facilities are usually trunk mounted, as shown in Figure 14.15. A typical cone profile obtained from a University of South Florida organic soil research site is shown in Figure 14.16. Because it measures the two parameters q_c and f_s , CPT is a useful tool for identifying soil type as well as for evaluating soil properties. A convenient parameter termed the *friction ratio* (F_R) is defined for this purpose as:

$$F_R = \frac{f_s}{q_c} \quad (14.8)$$

Figure 14.17 shows a simple chart that can be used for soil classification using CPT data. Currently, it is commonplace to have cone tips fitted with transducers that can produce a continuous record of the ground pore pressures at various depths. Using CPT data, the undrained strength of a clay can be obtained as:

$$s_u = \frac{qt - p_0}{N_{KT}} \quad (14.9)$$

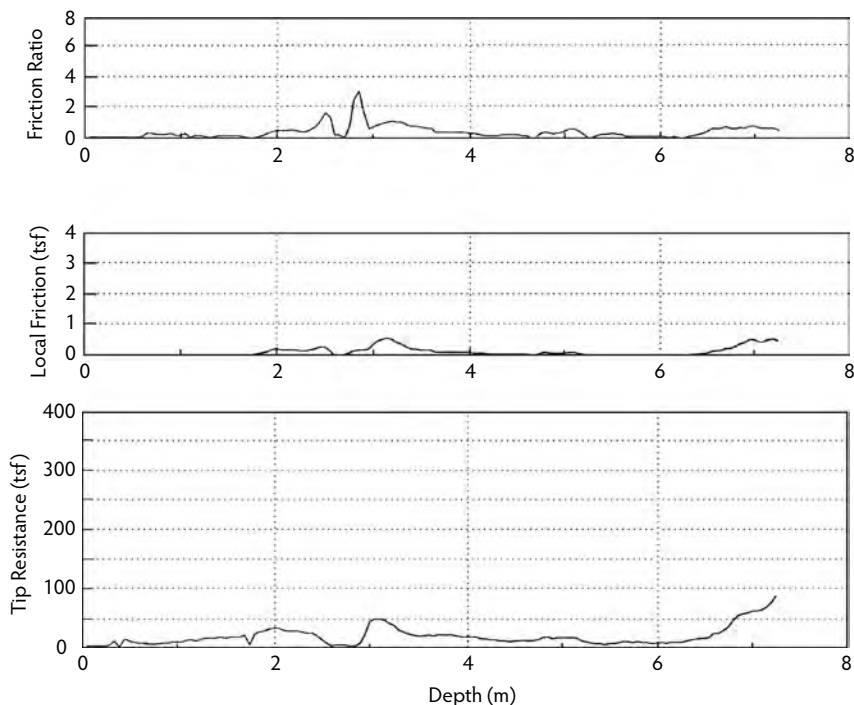


FIGURE 14.16 A typical cone profile. (From Mullins, A.G., Field Characterization of Dynamic Replacement of Florida Soils, Ph.D. dissertation, University of South Florida, Tampa, 1996.)

where:

$$q_T = q_c + u_c(1-a) \quad (14.10)$$

$$N_{mT} = 13 + \frac{5.5}{50} PI \quad (14.11)$$

and p_o and u_c are the effective overburden pressure and the pore pressure, respectively, measured in the same units as s_u and q_c ; a is taken as the approximate diameter ratio $(d_1/D)^2$ (Figure 14.14).

On the other hand, the friction angle of a granular soil can be obtained from q_c (in megapascals) based on the following approximate expression:

$$\phi = 29 + \sqrt{q_c} \quad (14.12)$$

For gravel and silty sand, corrections of $+5^\circ$ and -5° , respectively, have to be made.

14.1.3 Compressibility and Settlement

Soils, like any other material, deform under loads; hence, even if the integrity of a structure is satisfied, soil supporting the structure can undergo compression, leading to structural settlement. For most dry soils, this settlement will cease almost immediately after the particles readjust to attain an equilibrium with the structural load. This immediate settlement is evaluated using the theory of elasticity; however, if the ground material is wet, fine-grained (low permeability) soil, then the settlement will continue for a long period of time with slow drainage of water until the excess pore water pressure completely dissipates. This is usually evaluated by Terzaghi's consolidation theory. In some situations involving very fine clays and organic soils, settlement continues to occur even after the pore water pressure in the foundation vicinity comes to an equilibrium with that of the far field. Secondary compression concepts are required to estimate this secondary settlement.

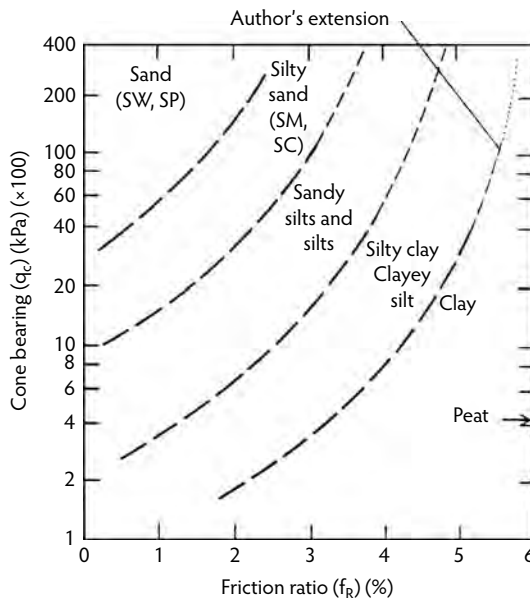


FIGURE 14.17 Soil classification using CPT data. (From Bowles, J.E., *Foundation Analysis and Design*, McGraw-Hill, New York, 1995. With permission.)

14.1.3.1 Estimation of Foundation Settlement in Granular Soils

Very often, settlement of footings founded on granular soils is determined based on the plate load tests discussed in Section 14.2. The most commonly adopted analytical methods for settlement evaluation in granular soils are based on the elastic theory; however, one must realize that reliable estimates of elastic moduli and Poisson's ratio values for soils are not easily obtained. This is mainly because of the sampling difficulty and, particularly, the dependency of the elastic modulus on the stress state. Reliable field methods for obtaining elastic moduli are also scarce. The following expressions can be used to find the immediate settlement:

$$s_e = f \frac{B_{q_0}}{E_s} (1 - \mu_s^2) \frac{\alpha}{2} \quad (14.13)$$

where:

s_e = immediate (elastic) settlement.

f = 0.5 or 1.0 (depending on whether s_e is at the corner of the foundation).

B = width of foundation.

q_0 = contact pressure (P/BL , where L is the length of the foundation).

E_s = elastic modulus.

α = a factor to be determined from Figure 14.18.

Another widely used method for computing granular soil settlements is the Schmertmann and Hartman (1978) method based on the elastic theory:

$$s_e = C_1 C_2 (\bar{q} - q) \sum_0^z \frac{I_z}{E_s} \Delta z \quad (14.14)$$

where:

C_1 = foundation depth correction factor = $1 - 0.5[q/\bar{q} - q]$.

C_2 = correction factor for creep of soil = $1 + 0.2 \log(\text{time in years}/0.1)$.

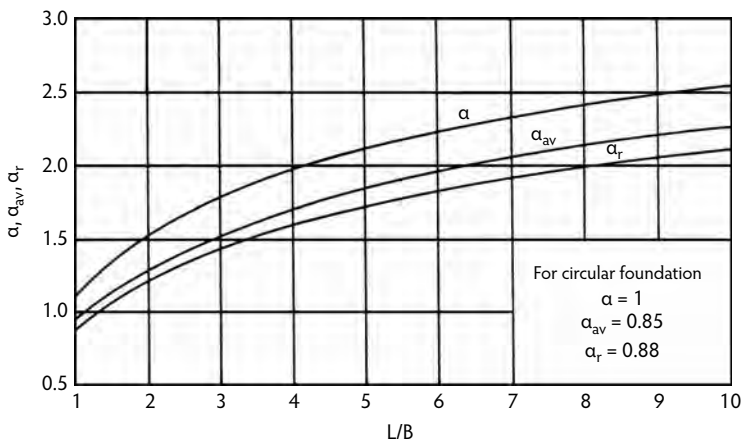


FIGURE 14.18 Chart for obtaining α factor. (From Das, B.M., *Principles of Foundation Engineering*, PWS Publishing, Boston, MA, 1995. With permission.)

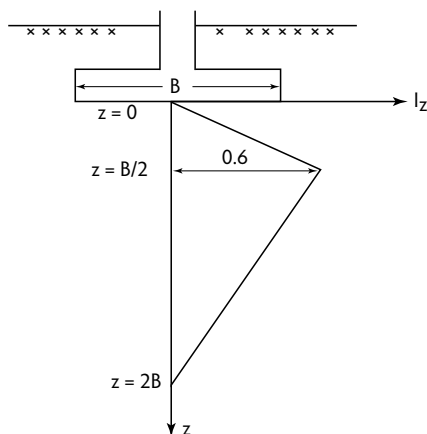


FIGURE 14.19 Strain influence factor. (From Schmertmann J.H. and Hartman, J.P., *J. Geotech. Eng. Div., Am. Soc. Civ. Eng.*, 104(GT8), 1131–1135, 1978. Reprinted with permission of ASCE.)

\bar{q} = stress at foundation level.

q = overburden stress.

I_z = strain influence factor in Figure 14.19.

The elastic properties necessary to manipulate the above expressions are provided in Table 14.6 and Table 14.7. Furthermore, some useful relationships that can provide the elastic properties from *in situ* test results are given below:

$$E_s \text{ (tsf)} = 8N \quad (14.15)$$

and

$$E_s = 2q_c \quad (14.16)$$

A comprehensive example illustrating the use of the above relations is provided in Example 14.4.

14.1.3.2 Estimation of Foundation Settlement in Saturated Clays

The load applied on a saturated fine-grained soil foundation is immediately acquired by the pore water, as illustrated in Figure 14.20a; however, with the dissipation of pore pressure resulting from drainage of water, the applied stress (total stress) is gradually transferred to the soil skeleton as an effective stress

TABLE 14.6 Elastic Properties of Geomaterials

Soil	E_s (MPa)
<i>Clay:</i>	
Very soft	2–15
Soft	5–25
Medium	15–50
Hard	50–100
Sandy	25–250
<i>Glacial till:</i>	
Loose	10–150
Dense	150–720
Very dense	500–1440
Loess	15–60
<i>Sand:</i>	
Silty	5–20
Loose	10–25
Dense	50–81
<i>Sand and gravel:</i>	
Loose	50–150
Dense	100–200
Shale	150–5000
Silt	2–20

Note: Value range for the static stress-strain modulus E_s for selected soils (see also Table 5.6). The value range is too large to use an “average” value for design. Field values depend on stress history, water content, density, and age of deposit.

Source: Bowles, J.E., *Foundation Analysis and Design*, McGraw-Hill, New York, 1995. With permission.

TABLE 14.7 Poisson Ratios for Geomaterials

Type of Soil	μ
Clay, saturated	0.4–0.5
Clay, unsaturated	0.1–0.3
Sandy clay	0.2–0.3
Silt	0.3–0.35
Sand, gravelly sand commonly used	–0.1–1.00, 0.3–0.4
Rock	0.1–0.4 (depends somewhat on type of rock)
Loess	0.1–0.3
Ice	0.36
Concrete	0.15
Steel	0.33

Source: Bowles, J.E., *Foundation Analysis and Design*, McGraw-Hill, New York, 1995. With permission.

(Figure 14.20b). The long-term soil skeleton rearrangement taking place during this process is termed the *consolidation settlement*. The soil properties required for estimation of the magnitude and rate of consolidation settlement can be obtained from the laboratory one-dimensional (1-D) consolidation test. Figure 14.21 shows the consolidometer apparatus where a saturated sample (2.5-in. diameter and 1.0-in. height) is subjected to a constant load while the deformation and sometimes the pore pressure are

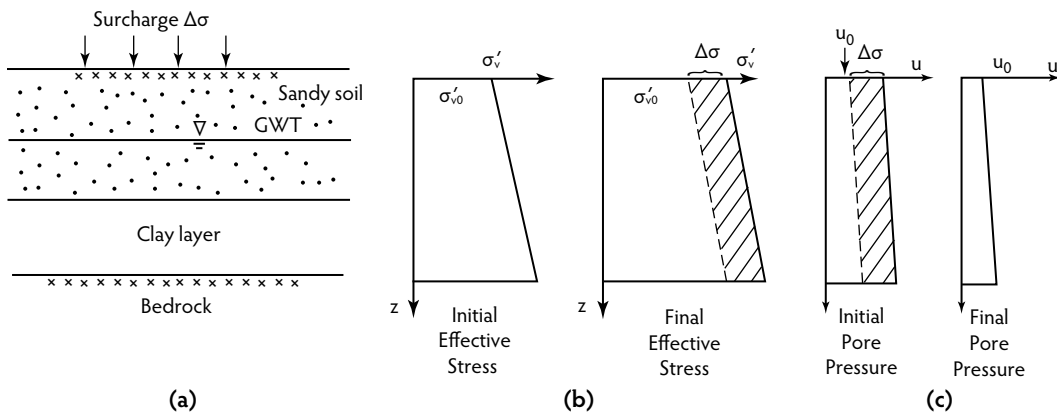


FIGURE 14.20 Illustration of consolidation settlement: (a) subsurface profile, (b) effective stress distribution, and (c) pore pressure distribution.



FIGURE 14.21 Laboratory consolidometer apparatus. (Figure courtesy of the University of South Florida, Tampa.)

monitored until consolidation is complete. A detailed description of this procedure can be found in Bowles (1986). The sample is tested in this manner for a wide range of stresses that encompass the expected foundation pressure. Using Terzaghi's 1-D consolidation theory, the relationship shown in Table 14.8 between the degree of consolidation U (settlement at any time t as a percentage of the ultimate settlement) and the time factor T can be derived for a clay layer subjected to a constant pressure increment throughout its depth.

Figure 14.22 shows the results of a consolidation test conducted on an organic soil sample. The coefficient of consolidation (C_v) for the soil can be obtained from these results using Casagrande's logarithm-of-time method (Holtz and Kovacs, 1981). Using this method, from Figure 14.22 one can estimate the time for 90% consolidation as 200 sec. Then, by using the following expression for the time factor, one can estimate C_v as 2.5×10^{-4} in.²/sec, because $U = 90\%$ when $t = 200$ sec:

$$T = \frac{C_v t}{H_{dr}^2} \quad (14.17)$$

TABLE 14.8 Degree of Consolidation vs. Time Factor

U_{avg}	T
0.1	0.008
0.2	0.031
0.3	0.071
0.4	0.126
0.5	0.197
0.6	0.287
0.7	0.403
0.8	0.567
0.9	0.848
0.95	1.163
1.0	∞

where H_{dr} is the longest drainage path in the consolidating soil layer. It should be noted that the water in the laboratory soil sample drains through both sides during consolidation, so $H_{dr} = 0.5$ in.

When the above consolidation test is repeated for several other pressure increments, doubling the pressure each time, variation of the post-consolidation (equilibrium) void ratio e with pressure p can be observed using the following relation between e and the sample strain computed from the monitored sample deformation:

$$\frac{\Delta e}{1 + e_0} = \frac{\Delta H}{H} \quad (14.18)$$

where e_0 and H are the initial void ratio and the sample height, and ΔH and Δe are their respective changes. A typical laboratory consolidation curve (e vs. $\log p$) for a clayey soil sample is shown in Figure 14.23. The following important parameters can be obtained from Figure 14.23:

Recompression index (C_r) = $(1.095 - 1.045)/(\log 60 - \log 10) = 0.064$.

Compression index (C_c) = $(1.045 - 0.93)/(\log 120 - \log 60) = 0.382$.

Preconsolidation pressure (p_c) = 60 kPa.

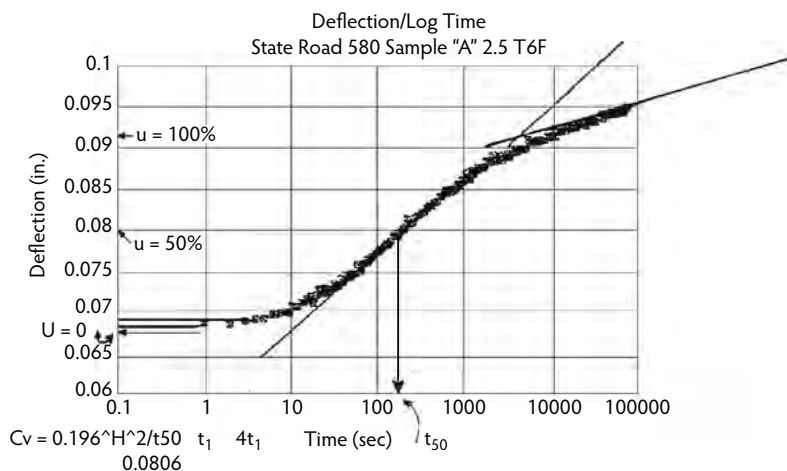


FIGURE 14.22 Settlement vs. logarithm-of-time curve. (From Stinnette, P., Engineering Properties of Florida Organic Soils, Master's project, University of South Florida, Tampa, 1992.)

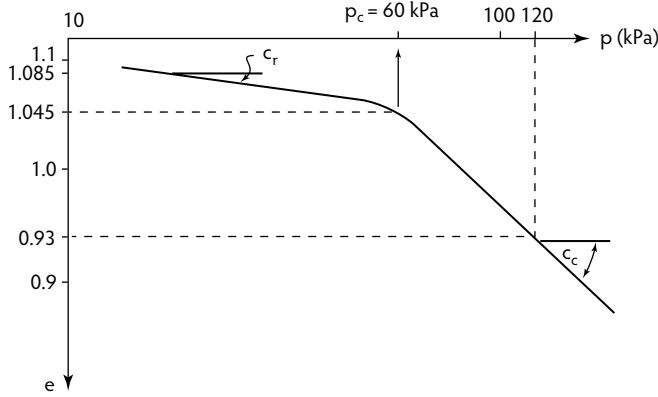


FIGURE 14.23 Laboratory consolidation curve (e vs. $\log p$).

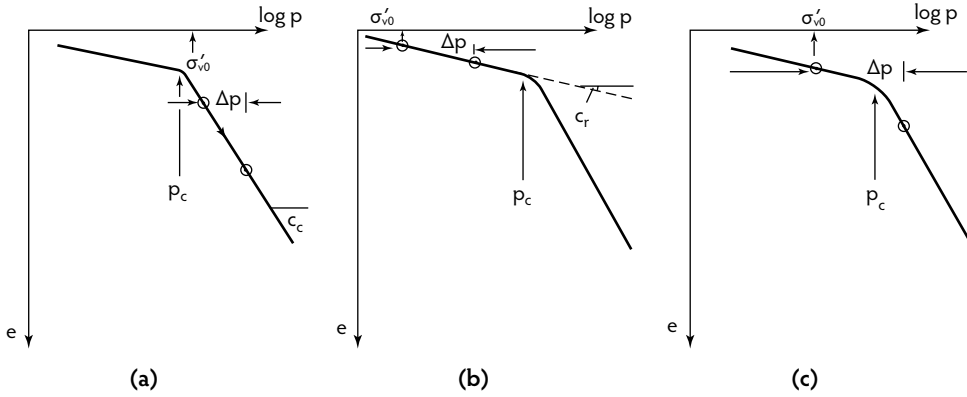


FIGURE 14.24 Illustration of the use of the consolidation equation: (a) case 1, (b) case 2, and (c) case 3.

All of the above information can be used to estimate the ultimate consolidation settlement of a saturated clay layer (of thickness H) due to an average pressure increase of Δp . The ultimate consolidation settlement (s_{con}) can be expressed by the following, depending on the individual case, as illustrated in Figure 14.24:

Case 1 ($\sigma'_{v0} > p_c$):

$$s_{\text{con}} = \frac{C_r H}{1 + e_0} \log \frac{\sigma'_{v0} + \Delta p}{\sigma'_{v0}} \quad (14.19)$$

Case 2 ($\sigma'_{v0} + \Delta p < p_c$):

$$s_{\text{con}} = \frac{C_r H}{1 + e_0} \log \frac{\sigma'_{v0} + \Delta p}{\sigma'_{v0}} \quad (14.20)$$

Case 3 ($\sigma'_{v0} + \Delta p > p_c$):

$$s_{\text{con}} = \frac{C_r H}{1 + e_0} \log \frac{p_c}{\sigma'_{v0}} + \frac{C_c H}{1 + e_0} \log \frac{\sigma'_{v0} + \Delta p}{p_c} \quad (14.21)$$

The average pressure increase in the clay layer can be accurately determined by using Newmark's chart, shown in Figure 14.25. When the footing is drawn on the chart to a scale of $OQ = d_c$ (the depth of the midplane of the clay layer from the footing bottom), Δp can be evaluated by:

$$\Delta p = qIM \quad (14.22)$$

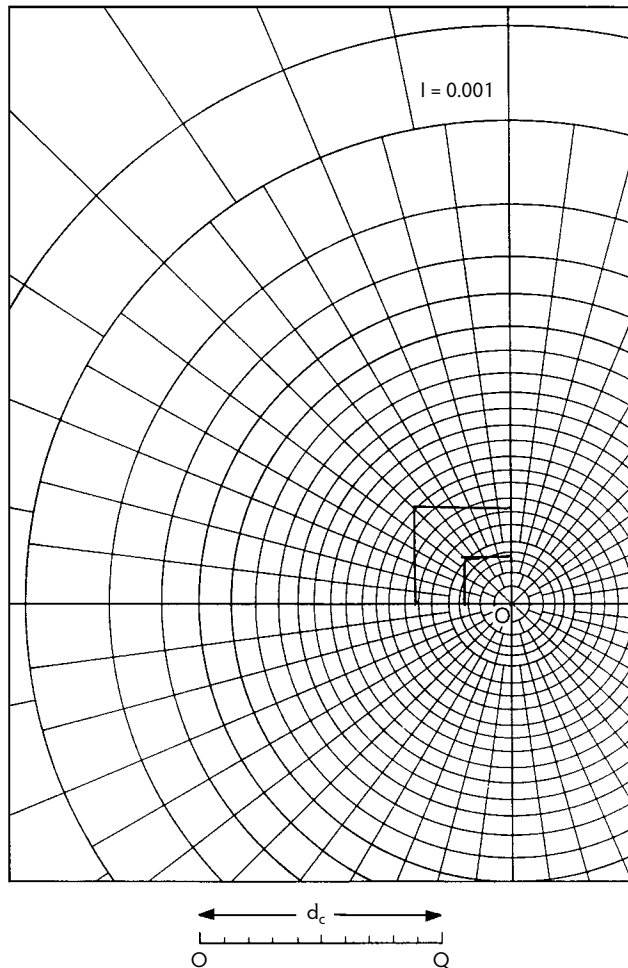


FIGURE 14.25 Newmark's chart. (From Holtz R.D. and Kovacs W.D., *An Introduction to Geotechnical Engineering*, Prentice Hall, Englewood Cliffs, NJ, 1981. With permission.)

where q , I , and M are the contact pressure, the influence factor (specific to the diagram), and the number of elements of the chart covered by the drawn footing, respectively.

Example 14.4

Assume that it is necessary to compute the maximum differential settlement of the foundation shown in Figure 14.26, which also shows the SPT, elastic moduli (using Equation 14.15 for sands and 33% of the estimate for clay), and unit weight profiles as well as the strain influence factor plot. For the above data:

Contact pressure (\bar{q}) = $200/(1.5)^2$ kPa = 88.89 kPa.

Overburden pressure at footing depth (q) = 16.5×1.0 kPa = 16.5 kPa.

Immediate Settlement. Areas of the strain-influence diagram covered by different elastic moduli are:

$$A_1 = 0.5(0.75 \times 0.6) + 0.5(0.25)(0.533 + 0.6) = 0.367 \text{ m}$$

$$A_2 = 0.5(1.5)(0.533 + 0.133) = 0.5 \text{ m}$$

$$A_3 = 0.5(0.5)(0.133) = 0.033 \text{ m}$$

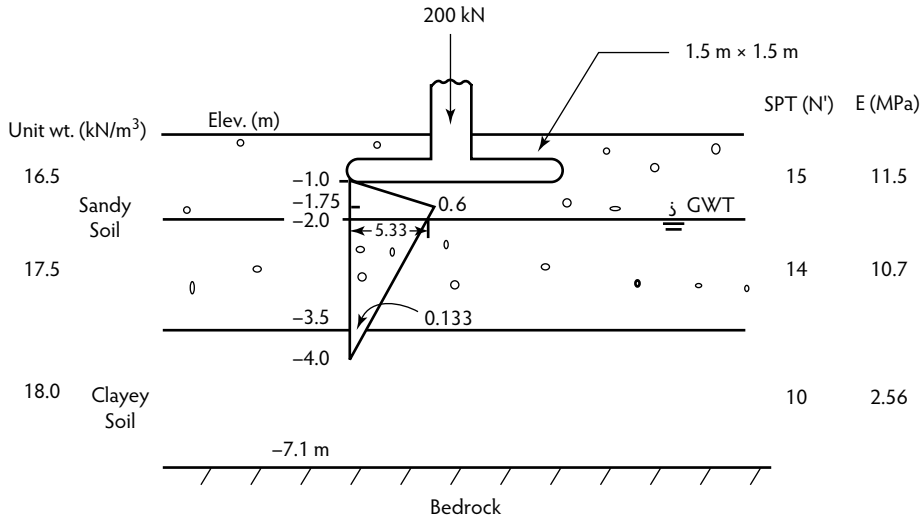


FIGURE 14.26 Settlement computation.

Then, by applying Equation 14.14, one obtains the immediate settlement as:

$$S_{\text{center}} = \left[1 - 0.5 \left\{ 16.5 / (88.89 - 16.5) \right\} \right] \left[1.0 \right] \left[88.89 - 16.5 \right] \left[0.367(1.0) / (11.5 \times 10^3) + 0.5 / (10.7 \times 10^3) + 0.033 / (2.57 \times 10^3) \right] = 5.87 \text{ mm}$$

From Equation 14.13, s_{corner} can be deduced as $0.5(5.87) = 2.94 \text{ mm}$.

Consolidation Settlement. As for the consolidation settlement, the average stress increase in clay can be obtained as:

$$\Delta p_{\text{center}} = 4 \times 19 \times 88.89 \times 0.001 = 6.75 \text{ kPa}$$

$$\Delta p_{\text{corner}} = 58 \times 88.89 \times 0.001 = 5.2 \text{ kPa}$$

On the other hand, the average overburden pressure at the clay layer is found from Equation 14.3b as:

$$\sigma'_{v0} = 16.5(2) + 17.5(1.5) + 18.0(1.0) - 9.8(2.75) = 54.8 \text{ kPa}$$

From Figure 14.24, one observes that the relevant expression for this situation is Equation 14.21, and by using the above estimates the consolidation settlement is found as:

$$s_{\text{center}} = \left[0.064 / (1 + 1.06) \right] (2.5) \log(60 / 54.8) + \left[0.382 / (1 + 1.06) \right] (2.5) \log \left[(54 + 6.75) / 60 \right] = 0.0819 \text{ m} = 8.19 \text{ mm}$$

As for the corner, the applicable expression from Figure 14.24 is Equation 14.20; hence,

$$s_{\text{corner}} = \left[0.064 / (1 + 1.06) \right] (2.5) \log(54.8 + 5.2 / 54.8) = 3.06 \text{ mm}$$

Therefore, the total settlement at the center of the footing will be 30.39 mm (1.12 in.), while that at the corner will be 6.0 mm (0.24 in.).

Total Settlement Check. Most building codes stipulate the maximum allowable total settlement to be 1.0 in., so the above value is unacceptable.

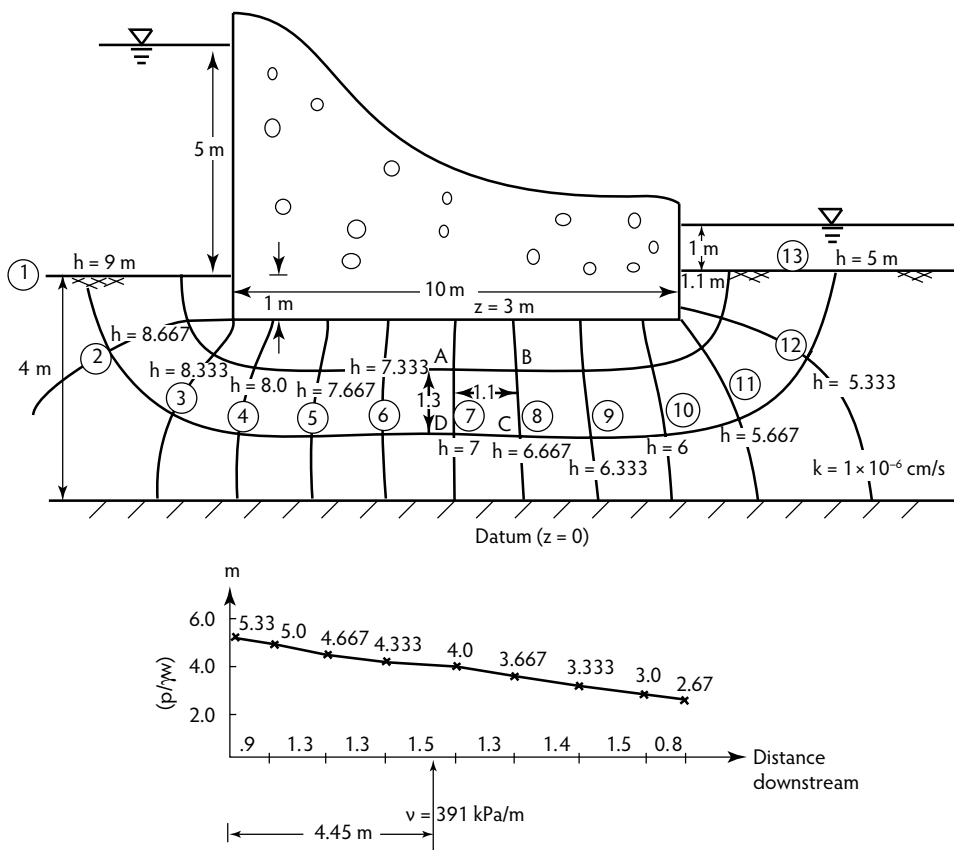


FIGURE 14.27 Seepage under a concrete dam.

Differential Settlement Check. The differential settlement is equal to $(s_{\text{center}} - s_{\text{corner}})$ distance from center to corner, or $(30.39 - 6.00)/1.06 \times 1000 = 0.023$. According to most building codes, the maximum allowable differential settlement to prevent structural cracks in concrete is 0.013; hence, the above design fails the differential settlement criterion.

14.1.4 Groundwater and Seepage

Stability analysis of water-retaining concrete structures requires that the uplift forces exerted on them be evaluated. These structures often exist in groundwater flow regimes caused by differential hydraulic heads; hence, an analysis of groundwater seepage has to be performed invariably when estimating the uplift forces. The most common and the simplest means of seepage analysis is the method of *flownets*. In this method, two orthogonal families of equipotential and flow lines are sketched in the flow domain (Figure 14.27) using the following basic principles. A *flow line* is an identified or a visualized flow conduit boundary in the flow domain. On the other hand, an *equipotential line* is an imaginary line in which the total energy head is the same.

14.1.4.1 Rules Governing the Construction of a FLOWNET

1. Equipotential lines do not intersect each other.
2. Flow lines do not intersect each other.
3. Equipotential lines and flow lines form two orthogonal families.
4. To ensure equal flow in the drawn flow conduits and equal head drop between adjacent equipotential lines, individual flow elements formed by adjacent equipotential lines and flow lines bear the same height/width ratio (typically 1.0).

With seepage velocities being generally very low, the pressure (p) exerted by seeping water contributes along with the potential energy to the total head (energy/unit weight) of water as:

$$h = \frac{p}{\gamma_w} + z \quad (14.23)$$

The quantity of groundwater flow at any location in a porous medium such as soil can be expressed by D'Arcy's law as:

$$q = kiA \quad (14.24)$$

where k is the coefficient of permeability (or hydraulic conductivity) at that location, and i , the hydraulic gradient, can be expressed by:

$$i = \frac{dh}{dx} \quad (14.25)$$

The following example illustrates the flownet method of seepage analysis and evaluation of uplift pressures. For more accurate and rigorous methods, the reader is referred to Harr (1962).

Example 14.5

Assume that it is necessary to establish the pressure distribution on the bottom of the dam shown in Figure 14.27 and the seepage under the dam shown in Figure 14.27. As the first step in the solution, a flownet has been drawn to scale, following the rules above. Using the bedrock as the datum for the elevation head, total heads have been assigned using Equation 14.23 for all of the equipotential lines as shown. It is noted that the head drop between two adjacent equipotential lines is:

$$(9 \text{ m} - 5 \text{ m})/12 = 0.333 \text{ m}$$

Then, by applying Equation 14.23 to the points where the equipotential lines and the dam bottom (B_i) intersect, the following expression can be obtained for the pressure distribution, which is plotted in Figure 14.27:

$$p = \gamma_w(h - 3.0)$$

Then, the total upthrust can be computed from the area of the pressure distribution as .34 kPa/m acting at a distance of .45 m downstream.

By applying Equation 14.25 to the element ABCD, one obtains:

$$i = (5.333 - 5.0)/1.1 = 0.302$$

Because $k = 1 \times 10^{-6}$ cm/s, one can apply Equation 14.24 to obtain the quantity of seepage through ABCD as:

$$q_1 = 1s(10^{-9})(0.302)(1.3)(1) \text{ m}^3/\text{s}/\text{m} \text{ (because AD = 1.3 m)}$$

Because all of the conduits must carry equal flow (see rule 4 of the flownet construction):

$$q = 3 \times (10^{-9})(0.302)(1.3)(1) \text{ m}^3/\text{s}/\text{m} = 1.18 \times 10^{-9} \text{ m}^3/\text{s}/\text{m}$$

Note the following important assumptions made in the above analysis:

1. The subgrade soil is homogeneous.
2. The bedrock and concrete dam are intact.
3. There is no free flow under the dam due to **piping** (or erosion).

Thus, the design and installation of an adequate pore-pressure monitoring system that can verify the analytical results are essential. A piezometer with a geomembrane/sand filter that can be used for monitoring pore pressures is shown in Figure 14.28.



FIGURE 14.28 Piezometer probes. (From Thilakasiri, H.S., Numerical Simulation of Dynamic Replacement of Florida Organic Soils, Ph.D. dissertation, University of South Florida, Tampa, 1996.)

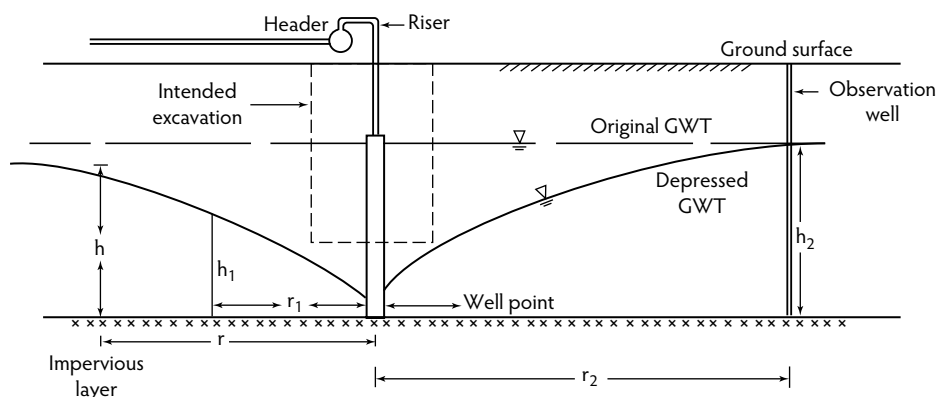


FIGURE 14.29 Dewatering of excavations.

14.1.5 Dewatering of Excavations

Construction in areas of shallow groundwater requires dewatering prior to excavation. Although contractors specialized in such work determine the details of the dewatering program depending on the field performance, a preliminary idea of equipment requirements and feasibility can be obtained by a simplified analysis. Figure 14.29 shows the schematic diagram for such a program and the elevations of the depressed water table at various distances from the center of the well. Observation wells (or bore holes) can be placed at any location, such as those shown at distances of r_1 and r_2 , to monitor the water table depression. When analyzing a seepage situation like this, Dupuit (Harr, 1962) assumed that: (1) for a small inclination of the line of seepage, the flow lines are horizontal, and (2) the hydraulic gradient is equal to the slope of the free surface and is invariant with depth. For discharge through any general section such as an

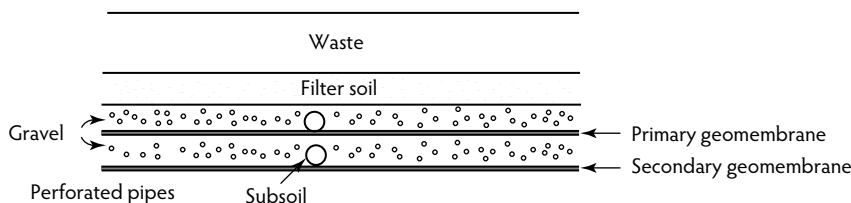


FIGURE 14.30 Typical cross-section of a geomembrane-lined landfill. (From Koerner, R.M., *Designing with Geosynthetics*, 3rd ed., Prentice Hall, Upper Saddle River, NJ, 1994. With permission.)

observation well, one can write the following expression for the flow by combining Equation 14.24 and Equation 14.25:

$$q = k \left(-\frac{dh}{dx} \right) h \quad (14.26)$$

Noting that q and k are constants throughout the flow regime considered, Equation 14.26 can be integrated between distances of r_1 and r_2 to obtain:

$$q = \frac{\pi k (h_1^2 - h_2^2)}{\ln(r_1 / r_2)} \quad (14.27)$$

By defining the extent of dewatering, using parameters r_1 , r_2 , h_1 , and h_2 , one can utilize the above expression to determine the capacity requirement of the pump.

14.1.6 Environmental Geotechnology

The amount of solid waste generated in the United States was expected to exceed 510M tons by the year 2000 (Koerner, 1994); thus, the immediate need for construction of adequate landfills cannot be over-emphasized. Although the construction of landfills involves political and legal issues, properly designed, constructed, and maintained landfills have proven to be secure, especially if they are provided with lined facilities. These are installed on the bottom or sides of a landfill to control groundwater pollution by the liquid mixture (**leachate**) formed by the interaction of rainwater or snowmelt with waste material. Types of liners for leachate containment are basically: (1) clay liners, (2) geomembranes, and (3) composite liners consisting of geomembranes and clay liners. Of these, until recently, the most frequently used liners were clay liners, which minimized leachate migration by achieving permeability values as low as 5×10^{-8} to 5×10^{-9} cm/sec; however, due to the large thickness requirement (0.6 to 2 m) and chemical activity in the presence of organic-solvent leachates, geomembranes have been increasingly utilized for landfills.

14.1.7 Design of Landfill Liners

As shown in Figure 14.30 and Figure 14.31, the important components of a solid material containment system include: (1) a leachate collection/removal system, (2) a primary leachate barrier, (3) a leachate detection/removal system, (4) a secondary leachate barrier, and (5) a filter above the collection system to prevent clogging. Some of the design criteria are as follows (Koerner, 1994):

- The leachate collection system should be capable of maintaining a leachate head of less than 30 cm.
- Both collection and detection systems should have 30-cm-thick granular drainage layers that are chemically resistant to waste and leachate and that have a permeability coefficient of not less than 1×10^{-2} cm/sec or an equivalent synthetic drainage material.
- The minimum bottom slope of the facility should be 2%.

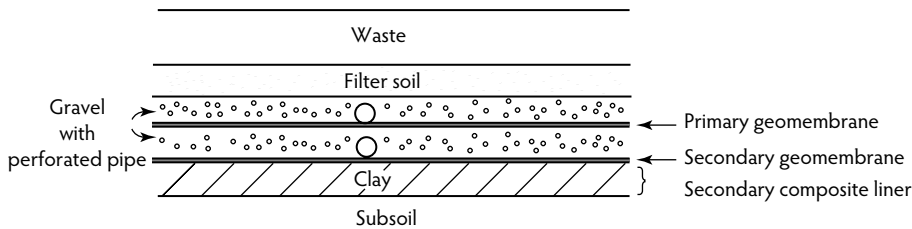


FIGURE 14.31 Typical cross-section of a clay/geomembrane-lined landfill. (From Koerner, R.M., *Designing with Geosynthetics*, 3rd ed., Prentice Hall, Englewood Cliffs, NJ, 1994. With permission.)

4.1.7.1 Design Considerations for Clay Liners

In the case of clay liners, the U.S. Environmental Protection Agency (EPA) requires that the coefficient of permeability be less than 10^{-7} cm/sec. This can be achieved by meeting the following classification criteria:

- The soil should have at least 20% fines (see Section 14.1.1.1, Mechanical Analysis).
- The plasticity index should be greater than 10 (see Section 14.1.1.2, Atterberg Limits).
- The soil should not have more than 10% gravel-size (>4.75 mm) particles.
- The soil should not contain any particles or chunks of rock larger than 50 mm.

It is realized that liner criteria can be satisfied by blending available soils with clay minerals such as sodium bentonite.

4.1.7.2 Design Considerations for Geomembrane Liners

Geomembranes are mainly used in geotechnical engineering to perform the functions of: (1) separation, (2) filtration, and (3) stabilization. In this application of geotextiles, the functions of separation and, to a lesser extent, filtration are utilized. Due to the extreme variation of solid-waste leachate composition from landfill to landfill, the candidate liner should be tested for permeability with the actual or synthesized leachate. In addition to the permeability criterion, other criteria also play a role in geomembrane material selection. They are as follows:

- Resistance to stress cracking induced by the soil/waste overburden
- Different thermal expansion properties in relation to subgrade soil
- Coefficient of friction developed with the waste material that governs slope stability criteria
- Axisymmetry in tensile elongation when the material is installed in a landfill that is founded on compressible subgrade soils

In selecting a geomembrane material for a liner, serious consideration should also be given to its durability, which is determined by the possibility of leachate reaction with the geomembrane and premature degradation of the geomembrane. For more details on geomembrane durability and relevant testing, the reader is referred to Koerner (1994). According to U.S. EPA regulations, the required minimum thickness of a geomembrane liner for a hazardous waste pond is 0.75 mm.

14.2 Site Exploration

In addition to screening possible sites, a thorough site study can reveal plenty of vital information regarding the soil and groundwater conditions at a tentative site, leading to more efficient selection of foundation depth and type as well as other construction details; hence, a site investigation that includes a subsurface exploration can certainly aid in economizing the time and cost involved in foundation construction projects. An exhaustive site study can be separated into two distinct phases: (1) preliminary investigation, and (2) detailed investigation. In the preliminary investigation, one would attempt to obtain

TABLE 14.9 Approximate Spacing of Boreholes

Type of Project	Spacing (m)
Multistory	10–30
One-story industrial plants	20–60
Highways	250–500
Residential subdivisions	250–500
Dams and dikes	40–80

as much valuable information about the site as possible at the least expense. Useful information regarding the site can often be obtained from the following sources:

- Local department of transportation (DOT) soil manuals
- Local U.S. Geological Survey (USGS) soil maps
- Local U.S. Army Corps of Engineers hydrological data
- U.S. Department of Agriculture (USDA) agronomy maps
- Local university research publications

A preliminary investigation also involves site visits (or reconnaissance surveys) where one can observe such site details as topography, accessibility, groundwater conditions, and nearby structures (especially in the case of expected pile driving or dynamic ground modification). Firsthand inspection of the performance of existing buildings can also add to this information. A preliminary investigation can be an effective tool for screening all alternative sites for a given installation. A detailed investigation has to be conducted at a given site only when that site has been chosen for the construction, as the cost of such an investigation is enormous. This stage of the investigation invariably involves heavy equipment for boring; therefore, at first, it is important to set up a definitive plan for the investigation, especially in terms of the bore hole layout and the depth of boring at each location. Generally, there are rough guidelines for bore hole spacing, as indicated in Table 14.9.

In addition to planning boring locations, it is also prudent on the part of the engineer to search for any subsurface anomalies or possible weak layers that can undermine construction. As for the depth of boring, one can use the following criteria:

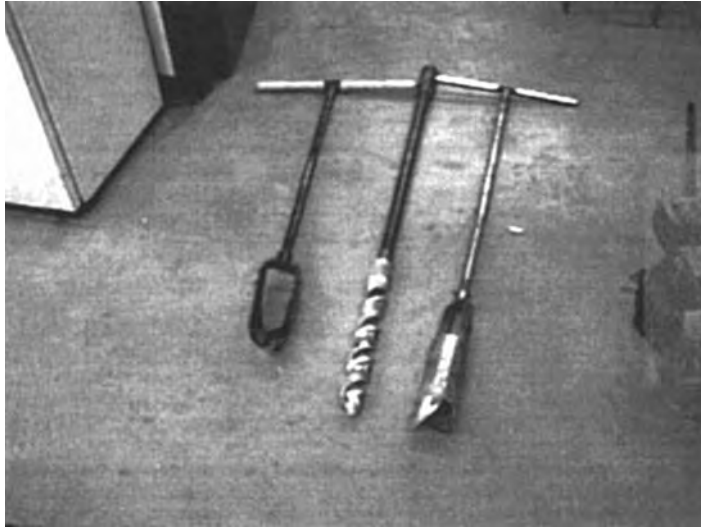
1. If bedrock is in the vicinity, continue boring until sound bedrock is reached, as verified from rock core samples.
2. If bedrock is unreachable, one can seek depth guidelines for specific buildings such as those given by the following expressions (Das, 1995):

$$D = 3S^{0.7} \text{ (for light steel and narrow concrete buildings).}$$

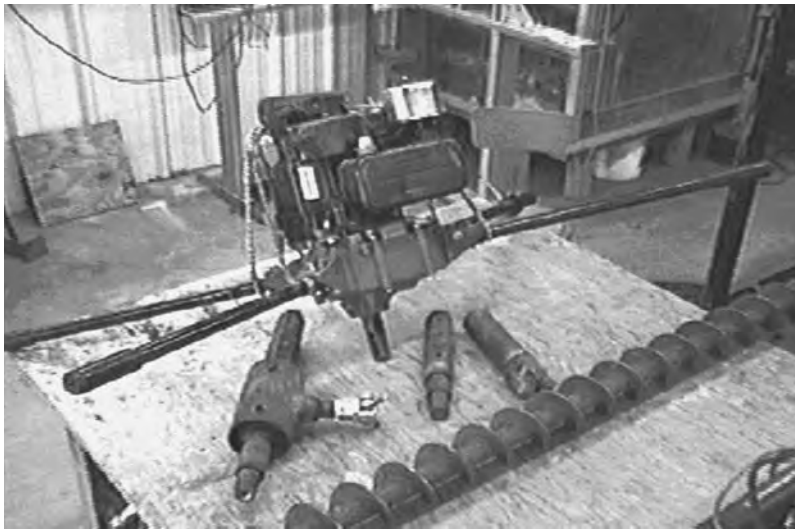
$$D = 6S^{0.7} \text{ (for heavy steel and wide concrete buildings).}$$

3. If none of the above conditions is applicable, then one can explore up to a depth at which the foundation stress attenuation reduces the applied stress by 90% ($\Delta p/\sigma'_{v0} = 0.1$ in Example 14.4). This generally occurs around a depth of $2B$, where B is the minimum foundation dimension.

Hand augers and continuous flight augers (Figure 14.32a) can be used for boring up to a depth of about 3 m in loose to moderately dense soil. For extreme depths, a mechanized auger (Figure 14.32b) can be used in loose to medium dense sands or soft clays. When the cut soil is brought to the surface, a technically qualified person should observe the texture, color, and type of soil found at various depths and prepare a bore-hole log identifying the soil types at the different depths. This type of boring is called **dry sample boring** (DSB). On the other hand, if relatively hard strata are encountered, investigators have to resort to a technique known as **wash boring**. Wash boring is carried out using a mechanized auger and a water-circulation system that aids in cutting and drawing the cut material to the surface. A schematic diagram of the wash-boring apparatus is shown in Figure 14.33, and the Florida Department of Transportation drill rig, which utilizes the above technique, is shown in Figure 14.34.



(a)



(b)

FIGURE 14.32 Drilling equipment: (a) hand-auger, and (b) mechanized auger. (Figure courtesy of the University of South Florida, Tampa.)

In addition to visual classification, one has to obtain soil type and strength and deformation properties for a foundation design; hence, the soil at various depths has to be sampled as the bore holes advance. Easily obtained disturbed samples suffice for classification, index, and compaction properties, while triaxial, and consolidation tests require carefully obtained undisturbed samples (samples with minimum disturbance). Disturbed granular or clayey samples can be obtained by attaching a standard split spoon sampler (Figure 14.13) to the drill rods. An undisturbed clay sample can be obtained by carefully advancing and retrieving a Shelby tube (Figure 14.35) into a clay layer; however, if one needs to evaluate a granular material for strength, settlement, or permeability, then *in situ* tests have to be performed due to the difficulty in obtaining undisturbed samples in such soils. In this regard, the reader is referred to the *in situ* tests shown in Table 14.10. A description of the plate load test is presented in Section 14.2.1.

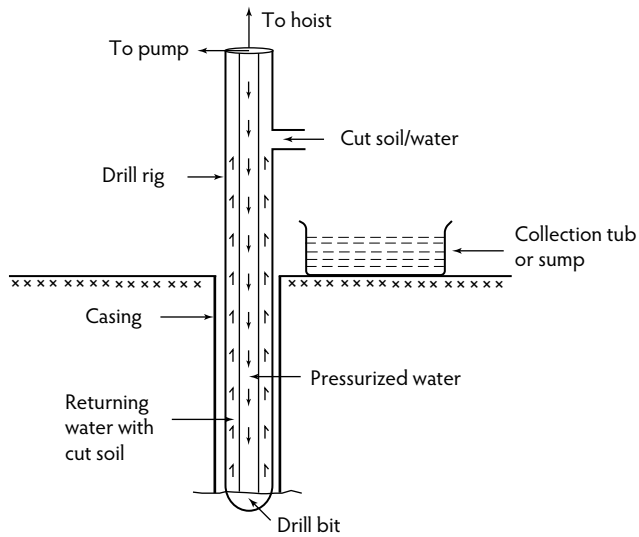


FIGURE 14.33 Schematic diagram of wash boring.



FIGURE 14.34 Florida Department of Transportation's CME-75 drill rig.



FIGURE 14.35 Shelby tubes.

TABLE 14.10 Recommended *In Situ* Tests

Evaluation Parameter	Test
Permeability	Field pumping test ^a
Settlement	Plate load test ^b
Shear strength	SPT or CPT ^c

^a In Section 14.1.5, Dewatering of Excavations.^b In Section 14.2.1, Plate Load Tests.^c In Section 14.1.2, Strength of Soils.

14.2.1 Plate Load Tests

Plate load apparatus consists of a set of steel plates of standard diameters (12 in., 18 in., etc.), a hydraulic loading and recording mechanism, a reaction frame, and a deflection gauge (Figure 14.36). During the test, the plate is laid at the tentative foundation depth and gradually loaded while the magnitude of the load and plate deflection at different stages is recorded. Figure 14.37 shows a typical plot of plate load results on a sand deposit. When one scrutinizes Figure 14.37, it can be seen that the ultimate bearing capacity of the plate can be estimated from the change in gradient of the load–deflection curve; hence, the bearing capacity and the settlement of a tentative foundation can be predicted in the following manner, based on the results of a plate load test performed on that location. In the following expressions, the subscripts f and p refer to the foundation and the plate, respectively.

Ultimate bearing capacity in clayey soils:

$$q_{u(f)} = q_{u(p)} \quad (14.28)$$

Ultimate bearing capacity in sandy soils:

$$q_{u(f)} = q_{u(p)} \left(\frac{B_f}{B_p} \right) \quad (14.29)$$

where B_p and B_f refer to the plate diameter and the minimum foundation dimension, respectively.

One can deduce the above expressions based on the basic expression for the bearing capacity of shallow footings (Section 14.3, Equation 14.32) when one realizes that predominant contributions for bearing capacity in clay and sand are made by the terms involving B_c and N_γ terms of Equation 14.32, respectively.



FIGURE 14.36 Plate load test.

Settlement of a footing under a given contact pressure (q) can be estimated by the corresponding plate settlement (s_p) (Figure 14.37) using the following expressions:

Immediate settlement in clayey soils:

$$s_f = s_p \left(\frac{B_f}{B_p} \right) \quad (14.30)$$

Immediate settlement in sandy soils:

$$s_f = s_p \left(\frac{2B_f}{B_f + B_p} \right)^2 \quad (14.31)$$

14.3 Shallow Footings

A shallow spread footing must be designed for a building column to transmit the column load to the ground without exceeding the bearing capacity of the ground and causing an excessive settlement (Figure 14.38). Plate-load test results clearly demonstrate the existence of a maximum stress (approximately 10 psi in Figure 14.37) that can be imposed on a plate without causing excessive settlement. This maximum stress is termed the *bearing capacity* of a foundation.

14.3.1 Bearing Capacity of Shallow Footings

To avoid catastrophic bearing failures, shallow footings are proportioned based on the bearing-capacity criterion. Two expressions extensively used to evaluate the ground bearing capacity are provided below.

14.3.1.1 Terzaghi's Expression

$$q_{ult} = s_c c N_c + q N_q + s_\gamma (0.5 B \gamma) N_\gamma \quad (14.32)$$

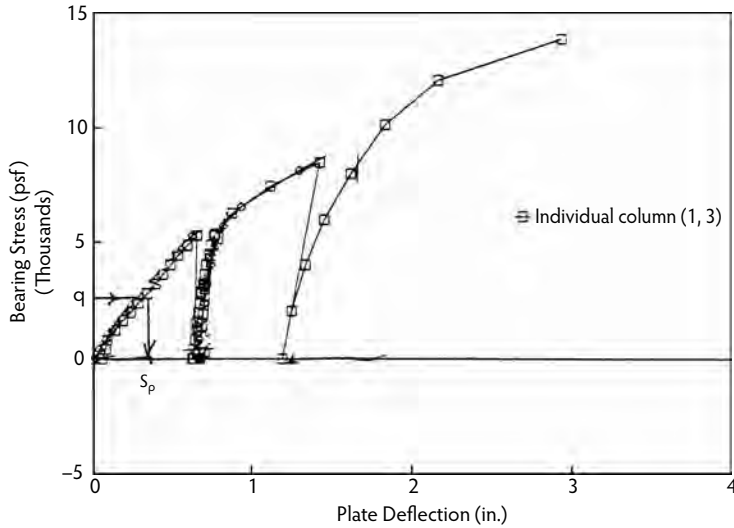


FIGURE 14.37 Typical plate load test results. (From A.G. Mullins, A.G., Field Characterization of Dynamic Replacement of Florida Organic Soils, Ph.D. dissertation, University of South Florida, Tampa, 1996.)

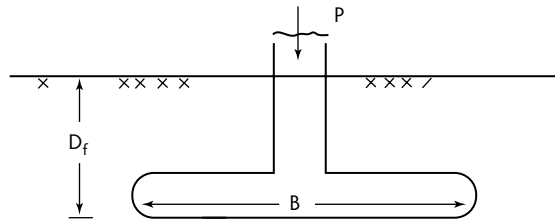


FIGURE 14.38 Schematic diagram of a shallow footing.

14.3.1.2 Hansen's Expression

$$q_{ult} = s_c d_c i_c c N_c + s_q d_q i_q q N_q + s_\gamma d_\gamma i_\gamma 0.5 B \gamma N_\gamma \quad (14.33)$$

where:

N_c , N_q , and N_γ are bearing capacity factors (Table 14.11).

s coefficients are shape factors based on B/L (Table 14.12).

d coefficient are depth factors based on D_f/B (Table 14.12).

i coefficients are inclination factors based on load inclination ϕ (Table 14.12).

γ is the unit weight of soil in the footing influence zone.

c and ϕ are the shear strength parameters of the soil.

Thus, to avoid bearing-capacity failure:

$$\frac{q_{n,ult}}{F} > \frac{P}{A} \quad (14.34)$$

where:

$q_{n,ult}$ = net ultimate bearing capacity based on Equation 14.35.

P = structural load.

A = footing area.

F = safety factor.

$$q_{n,ult} = q_{ult} - q \quad (14.35)$$

TABLE 14.11 Bearing Capacity Factors

Terzaghi's Expression				Hansen's Expression		
ϕ	N_c	N_q	N_γ	N_c	N_q	N_γ
0	5.7	1.0	0.0	5.14	1.0	0.0
5	7.3	1.6	0.5	6.49	1.6	0.1
10	9.6	2.7	1.2	8.34	2.5	0.4
15	12.9	4.4	2.5	11.0	3.9	1.2
20	17.7	7.4	5.0	14.8	6.4	2.9
25	25.1	12.7	9.7	20.7	10.7	6.8
30	37.2	22.5	19.7	30.1	18.4	15.1
35	57.8	41.4	42.4	46.4	33.5	34.4
40	95.7	81.3	100.4	75.25	64.1	79.4
45	172.3	173.3	297.5	133.5	134.7	200.5

TABLE 14.12 Shape, Depth, and Inclination Factors

	Hansen's Expression	Terzaghi's Expression
	$S_q = 1 + (B/L) \tan\phi$ $S_\gamma = 1 - 0.4(B/L)$	1.0 for strip footings 0.6 for circular footings 0.8 for square footings
Depth	For $D_f/B < 1$: $d_c = 1 + 0.4(D_f/B)$ $d_q = 1 + 2\tan\phi(1 - \sin\phi)^2(D_f/B)$ $d_\gamma = 1$ For $D_f/B > 1$: $d_c = 1 + 0.4\tan^{-1}(D_f/B)$ $d_q = 1 + 2\tan\phi(1 - \sin\phi)^2\tan^{-1}(D_f/B)$ $d_\gamma = 1$	
Inclination	$i_c = i_q = (1 - \beta/90^\circ)^{2a}$ $i_\gamma = (1 - \beta/\phi)^{2a}$	

^a Here, β is the load inclination to the vertical.

Example 14.6

Proportion a suitable footing for a 1000-kN vertical column load on a sandy ground where the SPT results are as indicated below. Assume that the groundwater table is at a depth of 0.5 m below the ground surface.

Elevation (m)	N
1.0	5
2.0	7
3.0	10
4.0	12
5.0	12

An average N value has to be determined from the above data within the influence zone of the footing. For this, one has to assume a footing size, as the influence zone depends on the size of the footing, so assume a circular footing of diameter 1.5 m placed at a depth of 1 m from the ground surface. As indicated in Figure 14.39, the influence zone extends from $0.5D_f$ above the footing (i.e., elevation -0.5 m) to $2B$

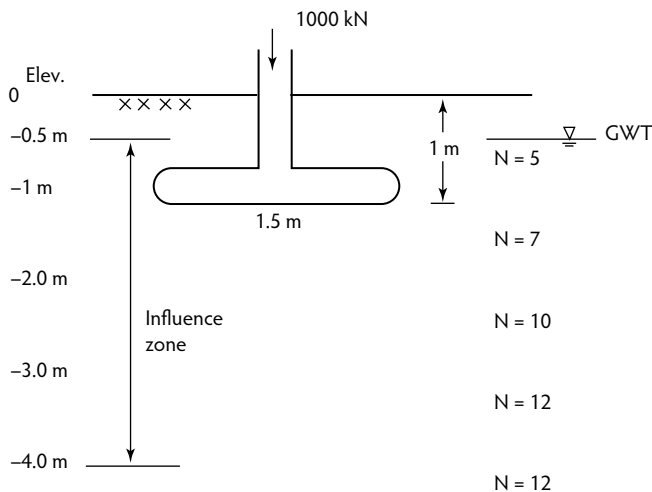


FIGURE 14.39 Foundation influence zone.

below the footing (i.e., -4.0 m). Then, by averaging the corrected N values within this range, one can obtain the average N' as worked out in the table below:

Elevation (m)	N	σ'_v (kPa)	C_N	N'
1.0	5	12.1	2.81	14
2.0	7	19.3	2.23	15.6
3.0	10	26.5	1.9	19
4.0	12	33.7	1.69	20.3

Note: Average $N' = [14(1.0) + 15.6(1.0) + 19(1.0) + 20.3(0.5)]/3.5 = 17$.

Note that the vertical effective stresses (σ'_v) are obtained using Equation 14.3 and assuming unit weights of 17.0 kN/m^3 and 9.8 kN/m^3 , respectively, for sand and water, while C_N is obtained using Equation 14.6.

Then, from Table 14.4, a ϕ of 37° can be found. This yields interpolated values $N_c = 60$, $N_q = 49$, and $N_\gamma = 57$ from Table 14.11 (Hansen's factors). The following factors can also be evaluated from Table 14.12:

$$s_c = 1.816, \quad s_q = 1.657, \quad s_\gamma = 0.6$$

$$d_c = 1.266, \quad d_q = 1.176, \quad d_\gamma = 1.0$$

$$i_c = 1.0, \quad i_q = 1.0, \quad i_\gamma = 1.0 \text{ (because the load is applied vertically)}$$

The following quantities are also needed for Equation 14.35:

$$q = \sigma'_v \text{ at the foundation level} = 12.1 \text{ kPa}$$

$$\gamma = \gamma' \text{ (because the foundation is fully submerged)} = 17.0 - 9.8 = 7.2 \text{ kN/m}^3$$

Finally, by substituting the above values in Equation 14.33, one obtains the ultimate bearing capacity as:

$$q_{n,ult} = (1.657)(1.176)(12.1)(49 - 1) + (0.5)(0.6)(1.0)(1.5)(7.2)(57) = 1316.7 \text{ kPa}$$

Note that the cohesion term is dropped due to negligible cohesion in sandy soils. Then, using Equation 14.34, one obtains a safety factor of $1316.7(1000/1.5/1.5) = 2.96$, which provides an adequate design; hence, a 1.5×1.5 -m footing at a depth of 1.0 m would suffice. Note that, if the groundwater table was well below the footing (usually greater than $2B$), then one would revise the following quantities as:

$$q = \sigma_v' \text{ at foundation level} = 17 \text{ kPa}$$

$$\gamma = \text{kN/m}^3$$

If the groundwater table was below the footing but still near it (a distance of d below), one can use the following approximation to evaluate the γ term:

$$\gamma = \gamma' + \frac{(\gamma_{\text{dry}} - \gamma')d}{2B} \quad (14.36)$$

As an example, if the groundwater table was 2.0 m below the ground, one can assume a γ_{dry} of 16.5 kN/m³ to modify the above two quantities as:

$$q = \sigma_v' \text{ at foundation level} = 16.5 \text{ kPa}$$

$$\gamma = 7.2 + (16.5 - 7.2)(1.0)/2(1.5) = 10.3 \text{ kN/m}^3$$

14.3.2 Footings with Eccentricity

If a footing has to be designed for a column that carries an axial load (P) as well as a moment (M), or an eccentric axial load, the resulting contact pressure distribution is as shown in Figure 14.40a. One realizes, however, that this is statically equivalent to the uniform distribution shown in Figure 14.40b; hence, a simple method of computing the bearing capacity is to assume that only the portion of the footing containing the column at its center contributes to bearing capacity. When designing such a footing, modified dimensions (B' and L') have to be used in Equation 14.32 or Equation 14.33, where B' and L' are defined as follows:

$$B' = B - 2e_x$$

$$L' = L - 2e_y$$

Example 14.7

Check the adequacy of the footing shown in Figure 14.41 for the soil data obtained from the UU test in Example 14.3 ($c_u = 50.6 \text{ kPa}$). From Figure 14.41:

$$e_x = M_x/P = 50.0 \text{ kNm}/250.0 \text{ kN} = 0.2 \text{ m}$$

$$e_y = M_y/P = 62.5 \text{ kNm}/250.0 \text{ kN} = 0.25 \text{ m}$$

Then, $B' = 1.1$ and $L' = 1.1$. Because $\phi = 0^\circ$, one obtains $N_c = 5.14$, $N_q = 1.0$, and $N_\gamma = 0.0$ from Table 14.11; hence, the only significant term in Equation 14.33 is the cohesion term, and only the relevant factors are computed as follows:

$$S_c = 1 + 1.0/5.14 = 1.195$$

$$d_c = 1 + 0.4(1.0/1.5) = 1.267$$

$$i_c = 1.0$$

$$q_{ult} = 1.195(1.267)(50.6)(5.14) = 393.78 \text{ kPa}$$

Finally, the safety factor can be computed as:

$$F = (393.78)(1.1)(1.0)/250 = 1.733$$

Because the safety factor has to be more than 2.5, this is not a safe design. This factor can be improved by increasing the dimensions to about $2.0 \times 2.0 \text{ m}$, depending on the available space.

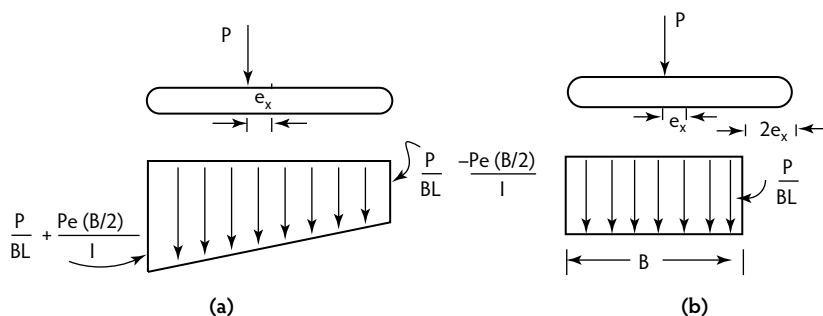


FIGURE 14.40 Simplistic design of an eccentric footing: (a) pressure distribution due to an eccentric load, and (b) equivalent pressure distribution.

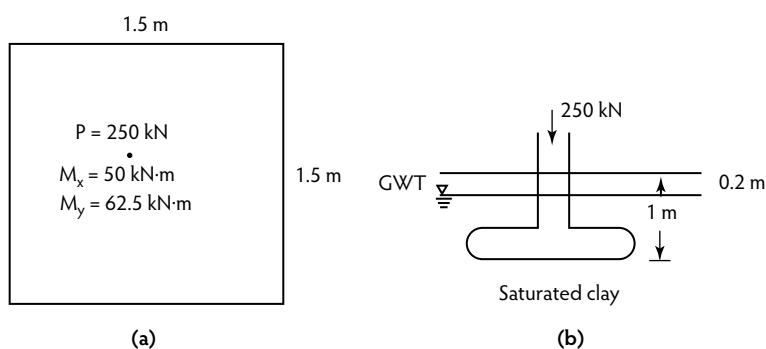


FIGURE 14.41 Design of an eccentric footing: (a) plan, and (b) elevation.

14.3.3 Presumptive Load-Bearing Capacity

The building codes of some cities suggest bearing capacities for a certain building site based on the classification of the predominant soil type at the site. Table 14.13 presents a comprehensive list of presumptive bearing capacities for various soil types; however, it should be noted that these values do not reflect the foundation shape, depth, load inclination, location of the water table, and settlements that are associated with the sites. For this reason, the use of these bearing capacities is primarily advocated in situations where a preliminary idea of the potential foundation size is needed for the subsequent site investigation.

14.4 Mat Footings

Because mat footings are larger in dimension than isolated spread footings, they are commonly used for transferring multiple column loads to the ground to prevent bearing-capacity failures. Thus, an ideal application of a mat footing would be on relatively weak ground. However, if the ground has sufficient strength to produce adequate bearing for isolated spread footings, a mat footing will be an economical alternative only if the combined area of the spread footings is less than 50% of the entire building plan area.

14.4.1 Design of Rigid Mat Footings

14.4.1.1 Bearing Capacity of a Mat Footing

One can use Equation 14.32 or Equation 14.33 to proportion a mat footing if the strength parameters of the ground are known. However, because the most easily obtained ground strength parameter is the standard penetration blow count (N), an expression is available that uses N to obtain the bearing capacity of a mat footing on a granular subgrade. This is expressed as follows:

TABLE 14.13 Presumptive Bearing Capacities

Soil Description	Presumptive Bearing Capacities from Indicated Building Codes (kPa)			
	National Board of Fire			
	Chicago (1995)	Underwriters (1976)	BOCA (1993) ^a	Uniform Building Code (1991) ^b
Clay, very soft	25	—	—	—
Clay, soft	75	100	100	100
Clay, ordinary	125	—	—	—
Clay, medium stiff	175	100	—	100
Clay, stiff	210	—	140	—
Clay, hard	300	—	—	—
Sand, compact and clean	240	—	140	200
Sand, compact and silty	100	—	—	—
Inorganic silt, compact	125	—	—	—
Sand, loose and fine	—	—	140	210
Sand, loose and coarse; sand–gravel mixture; compact and fine	—	140–400	240	300
Gravel, loose and compact; coarse sand	300	—	240	300
Sand-gravel, compact	—	—	240	300
Hardpan; cemented sand; cemented gravel	600	950	340	—
Soft rock	—	—	—	—
Sedimentary layered rock (hard shale, sandstone, siltstone)	—	—	6000	1400
Bedrock	9600	9600	6000	9600

^a Building Officials and Code Administrators International, Inc.

^b Bowles (1995) interpretation.

Note: Values converted from pounds per square foot to kilopascals and rounded. Soil descriptions vary widely between codes; table represents author's interpretations.

Source: Bowles, J.E., *Foundation Analysis and Design*, McGraw-Hill, New York, 1995. With permission.

$$q_{n,\text{all}} = \frac{N}{0.08} \left(1 + \frac{1}{3.28B} \right)^2 \left(1 + \frac{0.33D_f}{B} \right) \left(\frac{s}{25.4} \right) \quad (14.37)$$

where:

$q_{n,\text{all}}$ = net allowable bearing capacity (kPa).

B = width of footing.

s = settlement (mm).

D_f = depth of footing (mm).

Then, the following condition has to be satisfied to avoid bearing failure:

$$q_{n,\text{all}} > \frac{P}{A} \quad (14.38)$$

in which the use of a safety factor is precluded by employing an allowable bearing capacity.

Example 14.8

Figure 14.42 shows the plan of a column setup where each column is 0.5×0.5 m in section. Design an adequate footing if the corrected average SPT blow count of the subsurface is 10 and if the allowable settlement is 25.4 mm (1 in.). Assume a foundation depth of 0.5 m. The bearing capacity can then be computed from Equation 14.37 as:

$$q_{n,\text{all}} = 10 \left[1 + 0.33(0.5)/5.0 \right] \left[1 + 0.3/5.0 \right] / (0.08) = 136.87 \text{ kPa}$$

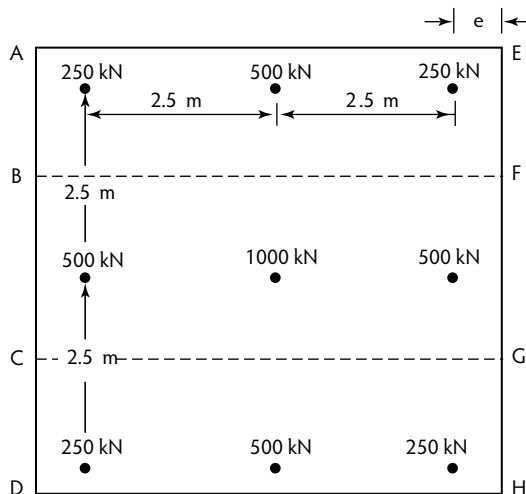


FIGURE 14.42 Illustration of a mat footing.

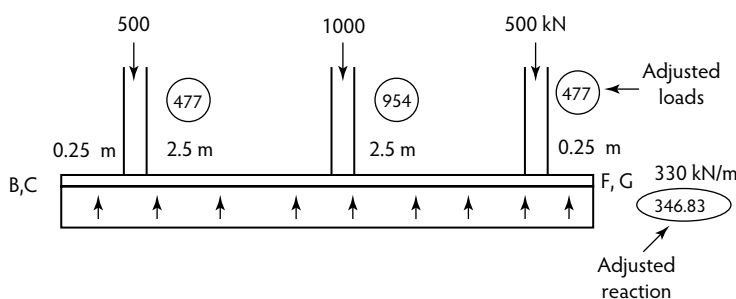


FIGURE 14.43 Free-body diagram for strip BCGF (Figure 14.42).

By applying Equation 14.38:

$$4000 / (5.0 + 2e)^2 < 136.87$$

$$e > 0.2029 \text{ m}$$

Hence, the mat can be designed with a 0.25-m edge space as shown in Figure 14.42.

For the reinforcement design, one can follow the simple procedure of separating the slab into a number of strips as shown in Figure 14.42. Each strip (BCGF in Figure 14.42) can be considered as a beam. The uniform soil reaction per unit length (w) can be computed as $(4000)(2.5)/[(5.5)(5.5)] = 330.5 \text{ kN/m}$. Figure 14.43 indicates the free-body diagram of the strip BCGF (Figure 14.42). It can be seen from the free-body diagram that the vertical equilibrium of each strip is not satisfied because the resultant downward load is 2000 kN, as opposed to the resultant upward load of 1815 kN. This discrepancy results from the arbitrary separation of strips at the midplane between the loads where nonzero shear forces exist. In fact, one realizes that the resultant upward shear at the boundaries BF and CG (Figure 14.42) account for the difference—that is, 185 kN. To obtain shear and moment diagrams of the strip BCGF, one can add this to modify them as indicated in the figure. This was achieved by reducing the loads by a factor of 0.954 and increasing the reaction by a factor of 1.051. The two factors were determined as follows:

For the loads, $[(2000 + 1815)/2]/2000 = 0.954$

For the reaction, $[(2000 + 1815)/2]/1815 = 1.051$

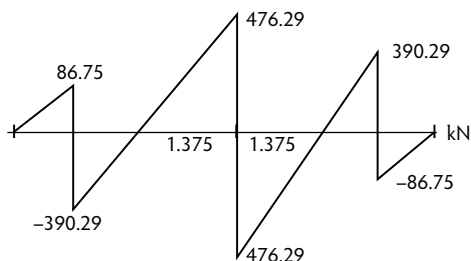


FIGURE 14.44 Distribution of shear on strip BCGF (Figure 14.42).

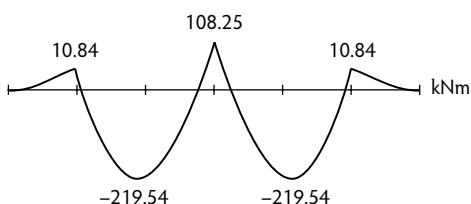


FIGURE 14.45 Distribution of moment on strip BCGF (Figure 14.42).

The resulting shear and moment diagrams are indicated in Figure 14.44 and Figure 14.45. Now, using Figure 14.44 and Figure 14.45, we can determine the steel reinforcements as well as the mat thickness. This estimation is not repeated here as it can be found in other chapters of this book.

14.4.1.2 Settlement of Mat Footings

The settlement of mat footings can also be found using the methods that were outlined in Section 14.1.3 (Compressibility and Settlement), assuming that they impart stresses on the ground in a manner similar to that of spread footings.

14.4.2 Design of Flexible Mat Footings

Flexible mat footings are designed based on the principle of slabs on elastic foundations. Because of their finite size and relatively large thickness, one can expect building foundation mats to generally exhibit rigid footing behavior; therefore, applications of flexible footings are limited to concrete slabs used for highway or runway construction. The most significant parameter associated with the design of beams on elastic foundations is the radius of relative stiffness ($1/\beta$) given by the following expression:

$$\frac{1}{\beta} = 4 \sqrt{\frac{Eh^3}{12(1-\mu^2)k}} \quad (14.39)$$

where:

E = elastic modulus of concrete.

μ = Poisson's ratio of concrete.

k = coefficient of subgrade reaction of the foundation soil usually determined from the plate load test (Section 14.2.1) or Equation 14.40.

h = slab thickness.

$$k = \frac{E_s}{B(1-\mu_s^2)} \quad (14.40)$$

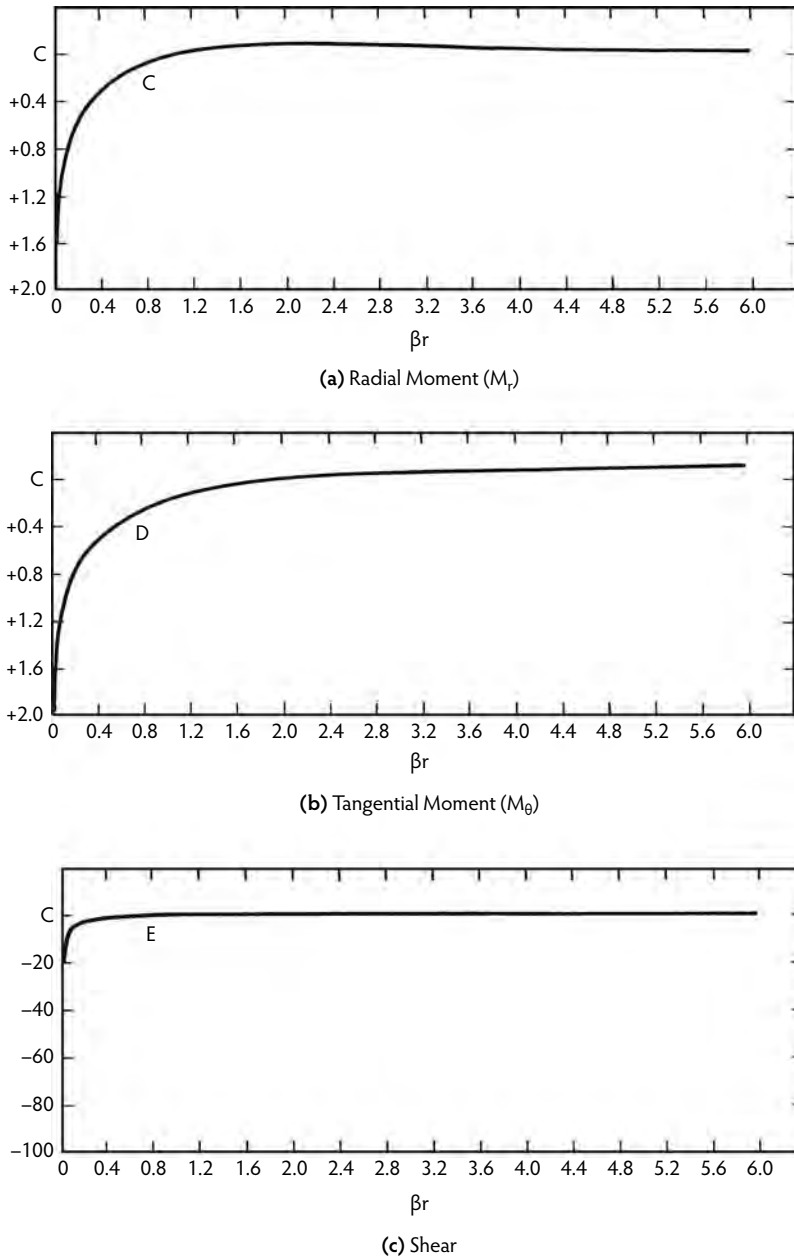


FIGURE 14.46 Radial and tangential moments and shear coefficients in a slab under point load. (From Scott, R.F., *Foundation Analysis*, Prentice Hall, Englewood Cliffs, NJ, 1981. With permission.)

where:

E_s = elastic modulus of subgrade soil.

μ_s = Poisson's ratio of subgrade soil.

When β has been evaluated for a particular mat, the shear, moment, and reinforcing requirements can be determined from nondimensional charts that are based on the solution for a concentrated load (P) applied to a slab on an elastic foundation. The following expressions can be used, along with Figure 14.46, for the evaluation:

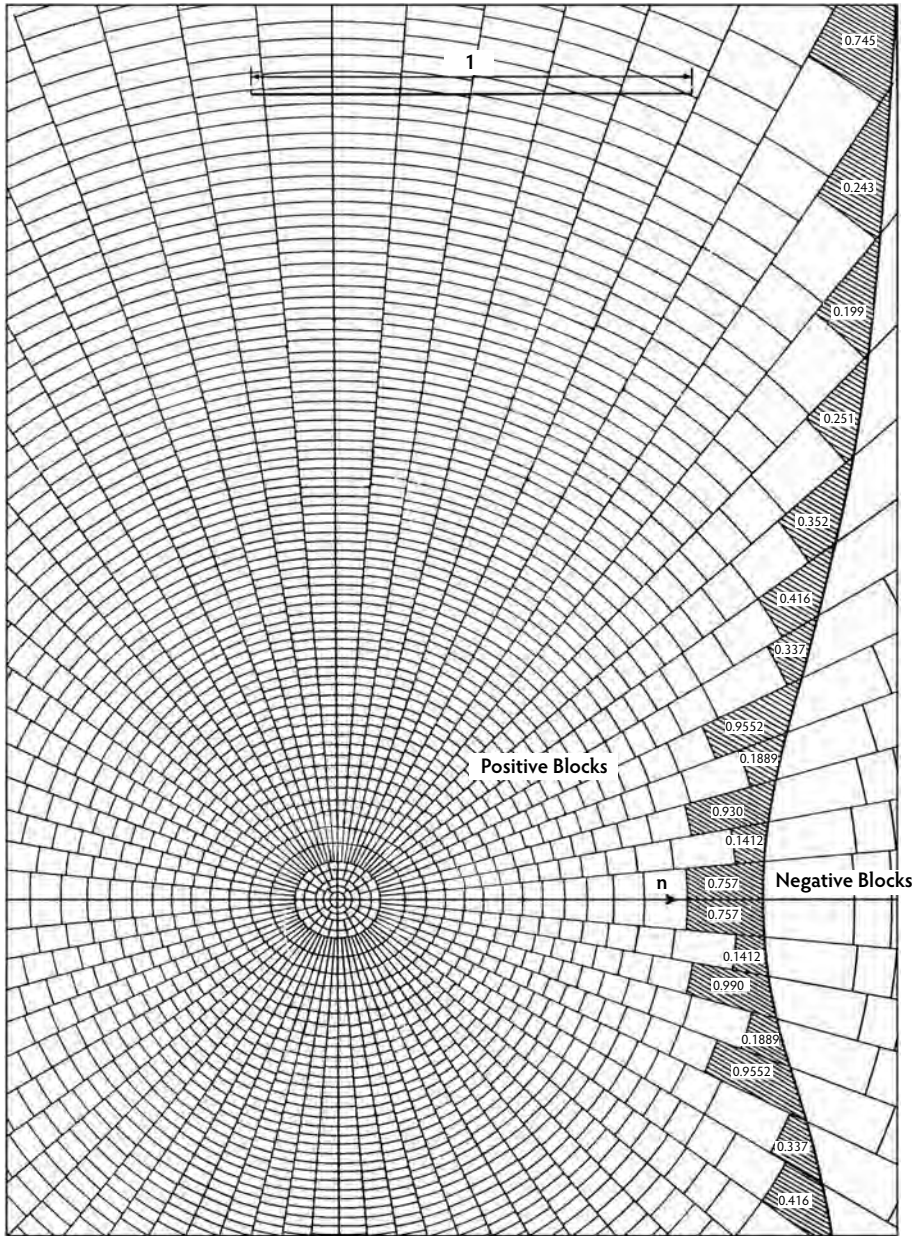


FIGURE 14.47 Influence chart for determining moment at the edge of a slab. (From Pickett, G. and Ray, G.K., *Am. Soc. Civ. Eng. Trans.*, 116(2425), 49-73, 1951.)

$$M_r = -\frac{P}{4}C \quad (14.41a)$$

$$M_\theta = \frac{P}{4}D \quad (14.41b)$$

$$V = -\frac{P\beta}{4}E \quad (14.42)$$

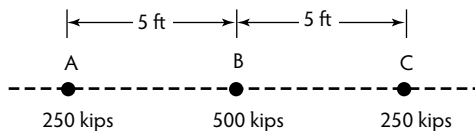


FIGURE 14.48 Illustration of an infinite flexible slab.

TABLE 14.14 Flexible Footing Moments

Distance from A (ft)	C Coefficient for Load at A	C Coefficient for Load at B	C Coefficient for Load at C	Moment (kip-ft)
0.0	1.6	0.18	0.0	122.5
1.0	0.8	0.25	0.02	32.25
2.0	0.5	0.4	0.05	84.38
3.0	0.4	0.5	0.08	92.5
4.0	0.25	0.8	0.1	121.88
5.0	0.18	1.6	0.18	222.5
6.0	0.1	0.8	0.25	121.88
7.0	0.08	0.5	0.4	92.5
8.0	0.05	0.4	0.5	84.38
9.0	0.02	0.25	0.8	32.25
10.0	0.0	0.18	1.6	122.5

The moment due to a distributed load can be obtained by drawing the contact area on an influence chart, such as the one shown in Figure 14.47, and then using Equation 14.43. It should be noted that the scale for the drawing should be selected such that $1/\beta$ is represented by the distance l shown in Figure 14.47:

$$M = \frac{P(1/\beta)^2 N}{10,000} \quad (14.43)$$

where:

P = distributed load.

N = number of elements covered by the loading area drawn.

Example 14.9

Plot the shear and moment distribution along the columns A, B, and C of the infinite slab of 8-in. thickness shown in Figure 14.48. Consider it to be a flexible footing. Assume a coefficient of subgrade reaction of 2600 lb/ft³. Because $E_c = 5.76 \times 10^8$ psf and $\mu_c = 0.15$, then one can apply Equation 14.39 to obtain $\beta = 0.1156$ ft⁻¹. Using the above results, Figure 14.46a, and Equation 14.41a, Table 14.14 can be developed for the radial moment (the moment on a cross-section perpendicular to the line ABC in Figure 14.48). These moment values are plotted in Figure 14.49.

14.5 Retaining Walls

When designing a retaining structure, one must ascertain that its structural capacity is adequate to withstand any potential instability that can be caused by the lateral earth pressures of the retained backfill; hence, a major step in the design of a retaining structure is the evaluation of the magnitude, direction, and the line of action of the lateral force. Most of the methods available for analyzing lateral earth pressures assume a yielding soil mass in the vicinity of the retaining structure, so the solutions are based on the limit equilibrium. The magnitude of the lateral force depends on the soil failure mechanism. The mechanism in which the backfill yields with the outward movement of the wall is known as the *active*

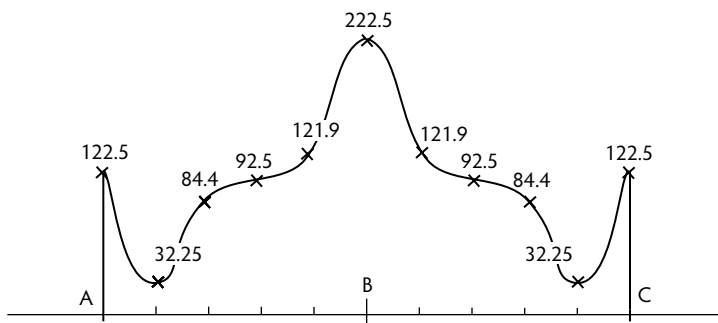


FIGURE 14.49 Moment distribution on a flexible slab (in kip-ft).

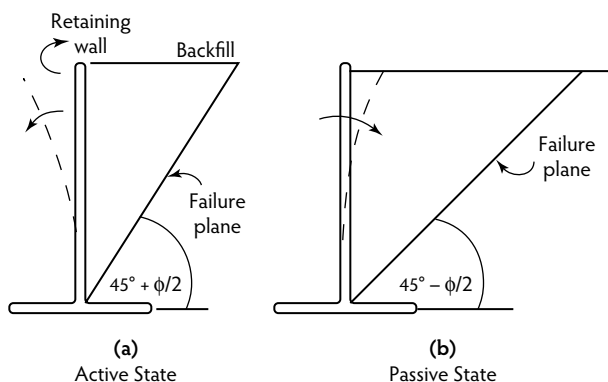


FIGURE 14.50 Illustration of (a) active and (b) passive states.

failure mechanism (Figure 14.50a), while the yielding of soil due to inward wall movement is termed the *passive failure mechanism* (Figure 14.50b). Also indicated on Figure 14.50 is the orientation of the failure planes for each condition in the case of a smooth, vertical wall supporting a horizontal backfill. The two most widely used analytical methods are illustrated below.

14.5.1 Determination of Earth Pressures

14.5.1.1 Rankine Method

The Rankine method of analysis can be employed for the relatively simple case of a smooth, vertical wall supporting a homogeneous backfill. A modified form of Rankine's original analysis allows one to obtain the active and passive earth pressure distributions by using the following expressions:

$$\sigma'_a = \sigma'_v K_a - 2c \sqrt{K_a} \quad (14.44)$$

and

$$\sigma'_p = \sigma'_v K_p - 2c \sqrt{K_p} \quad (14.45)$$

where the subscripts *a* and *p* stand for active and passive states, respectively, and the coefficients of earth pressure K_a and K_p can be determined from the following expressions:

$$K_a = \cos \beta \frac{\cos \beta - \sqrt{\cos^2 \beta - \cos^2 \phi}}{\cos \beta + \sqrt{\cos^2 \beta - \cos^2 \phi}} \quad (14.46)$$

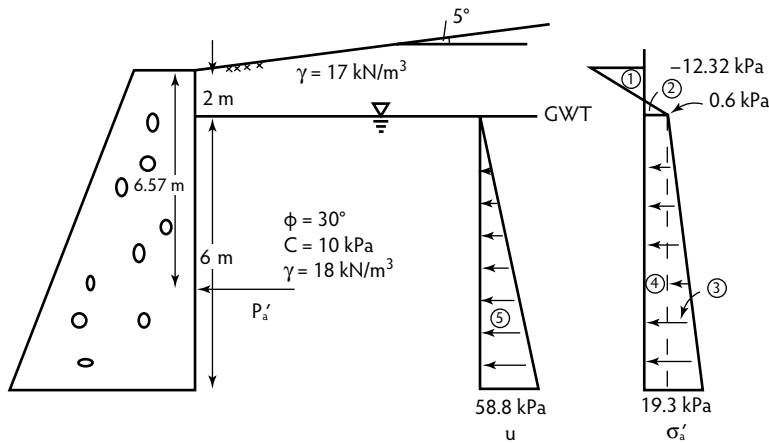


FIGURE 14.51 Illustration of the Earth's pressure distribution.

and

$$K_p = \cos\beta \frac{\cos\beta + \sqrt{\cos^2\beta - \cos^2\phi}}{\cos\beta - \sqrt{\cos^2\beta - \cos^2\phi}} \quad (14.47)$$

where:

β = inclination of the backfill.

c, ϕ = soil strength parameters.

The direction of the resultant lateral pressure and the line of action are indicated on Figure 14.51.

Example 14.10

Determine the lateral pressure on the retaining wall shown in Figure 14.51. Assume active conditions. By using Equations 14.46, one obtains $K_a = 0.38$. Then, by using Equation 14.44,

At $z = 0.0$ m, $\sigma'_a = -2(10)(0.616) = -12.32$ kPa.

At $z = 2.0$ m, $\sigma'_a = 0.6$ kPa.

At $z = 8.0$ m, $\sigma'_a = 19.3$ kPa.

The line of action of the effective force can be found by discretizing the pressure diagram into five segments as shown in Figure 14.51:

Segment	Area (A)	Centroidal Distance (z)	Az
1	-11.77	0.64	-7.49
2	0.027	1.97	0.053
3	112.2	6.0	673.2
4	3.6	5.0	18.0

Hence,

$$z = (-7.49 + 0.053 + 673.2 + 18.0) / (-11.77 + 0.027 + 112.2 + 3.6) = 6.57 \text{ m}$$

In obtaining the total force on the wall, one should remember to include the water pressure in segment 5 in addition to the effective force.

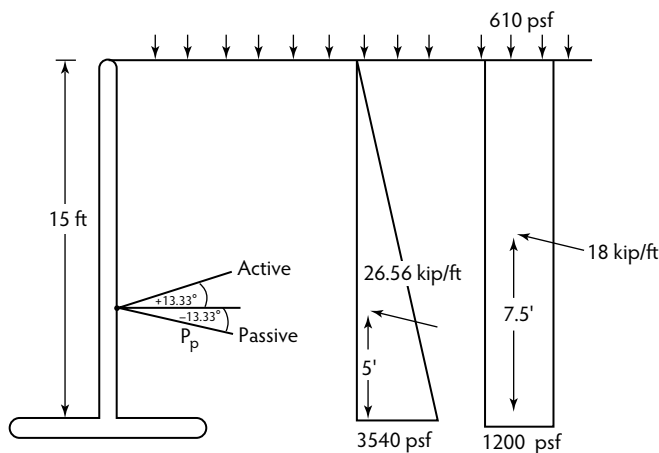


FIGURE 14.52 Illustration of the application of Coulomb's analysis.

14.5.1.2 Coulomb Method

The Coulomb method of analysis is an attractive alternative to the Rankine method due to its ability to handle more complex cases involving rough, nonvertical retaining walls. The relevant equations for lateral earth pressure coefficients are given below:

$$K_a = \frac{\sin^2(\alpha + \phi)}{\sin^2 \alpha \sin(\alpha - \delta) \left[1 + \frac{\sin(\phi + \delta) \sin(\phi - \beta)}{\sin(\alpha - \delta) \sin(\alpha + \beta)} \right]^2} \quad (14.48)$$

$$K_p = \frac{\sin^2(\alpha - \phi)}{\sin^2 \alpha \sin(\alpha + \delta) \left[1 + \frac{\sin(\phi + \delta) \sin(\phi + \beta)}{\sin(\alpha + \delta) \sin(\alpha + \beta)} \right]^2} \quad (14.49)$$

where α and δ are the inclination of the wall face to the horizontal and the angle of wall friction, respectively. As illustrated in Figure 14.52, the direction of the resultant lateral force changes when conditions change from active to passive states, with the line of action remaining on the generators of the friction cone. The above coefficients can be used in conjunction with Equation 14.44 and Equation 14.45.

On the other hand, if $\alpha = 90^\circ$, and $\beta = \delta = 0^\circ$, it can be easily shown that Equation 14.48 and Equation 14.46 reduce to:

$$K_a = \frac{1 - \sin \phi}{1 + \sin \phi} \quad (14.50)$$

Hence one can see that Rankine's and Coulomb's analytical predictions agree only when earth pressures are predicted on smooth, vertical walls supporting horizontal backfills. In this case, the direction of the lateral force is horizontal.

Example 14.11

Use the Coulomb method to determine the lateral earth pressure on the wall shown; assume passive conditions. Because the angle of wall friction (δ) is not specified in this problem, it would be adequate to assume that $\delta = (2/3)\phi = 13.33^\circ$. Substituting $\alpha = 70^\circ$, $\phi = 20^\circ$, $\delta = 13.33^\circ$, and $\beta = 0^\circ$ in Equation 14.49, one would obtain $K_p = 1.968$. With $c = 0.0$, and a surcharge of q , Equation 14.45 reduces to the following:

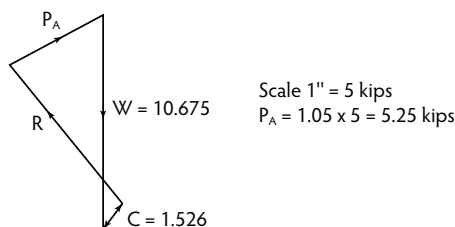


FIGURE 14.54 Force polygon.

- Step 6. Repeat the above procedure for a number of different trial failure planes. Estimate the minimum lateral force to be the actual P_a and consider the corresponding trial failure plane to be the actual failure plane.
- Step 7. If G is the centroid of the actual failure wedge, obtain the line of action of P_a from the point Q on the wall such that QG is parallel to the failure surface OC .

14.5.2 Design of Concrete Retaining Walls

The two basic types of concrete retaining walls are the *gravity* type and the *cantilever* type. The following conditions must be satisfied when designing a concrete retaining wall:

- Stability against overturning due to earth pressure
- Stability against base sliding due to earth pressure
- Prevention of any possible tensile stresses in the base soil

In addition to these design criteria, the design must also provide for a good drainage system and adequate bearing (see Section 14.3.1, Bearing Capacity of Shallow Footings) and no excessive settlements (see Section 14.1.3, Compressibility and Settlement).

14.5.2.1 Design of a Cantilever Retaining Wall

The basic design of a cantilever retaining wall is illustrated by the following example.

Example 14.13

Design a suitable cantilever retaining wall to support the backfill shown in Figure 14.55. Bowles (1995) recommended the tentative dimensions shown in Figure 14.56 for a cantilever retaining wall. Based on Bowle's recommendations, the dimensions shown in Figure 14.55 are assumed for the retaining wall. In computing the lateral pressure on the wall, it is usually assumed that the wall section starts at the cross-section CG shown in Figure 14.56; hence, the active wall pressure can be evaluated, using either of the described methods, as 4.496 kips/ft at a height 5 ft from the base. Despite the passive force due to the soil berm on the toe, practitioners generally neglect it for a conservative design. The weights of the different retaining wall components are computed as follows:

$$\begin{aligned}w_1 &= (5.0 \times 13.5 \times 120)/1,000 = 8.1 \text{ kips/ft} \\w_2 &= (9.0 \times 1.5 \times 150)/1,000 = 2.025 \text{ kips/ft} \\w_3 &= (1.0 \times 13.5 \times 150)/1,000 = 2.025 \text{ kips/ft} \\w_4 &= (0.5 \times 0.5 \times 13.5 \times 150)/1,000 = 0.506 \text{ kips/ft}\end{aligned}$$

The locations of the respective centroids from the toe are indicated below:

Element	Weight (w_i)	Centroidal Distance (x_i)	$w_i x_i$
1	8.1	6.5	52.65
2	2.025	4.5	9.11
3	2.025	3.5	7.09
4	0.506	2.83	1.43

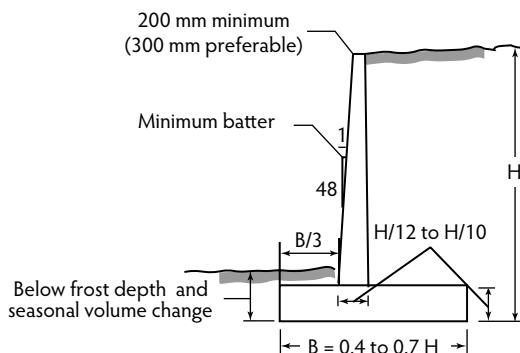


FIGURE 14.55 Tentative design dimensions for a cantilever retaining wall. (From Bowles, J.E., *Foundation Analysis and Design*, McGraw-Hill, New York, 1995. With permission.)

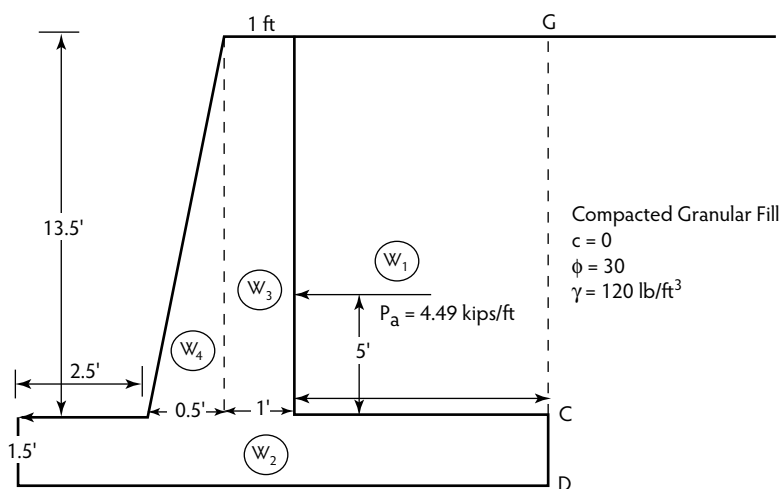


FIGURE 14.56 Cantilever retaining wall design.

Stability Against Overturning. The factor of safety against overturning can be computed as:

$$F_1 = \frac{\text{Stabilizing moment}}{\text{Overturning moment}} = \frac{(52.65 + 9.11 + 7.09 + 1.43)}{4.496 \times 5} = 3.13$$

This is adequate, as it is greater than 1.5.

Stability Against Sliding. The normal reaction on the base is equal to $\Sigma w_i = 12.656$. Thus, the maximum frictional force on the base is equal to $12.656(\tan\phi) = 6.449$ kips/ft. Then, the safety factor against sliding can be computed as:

$$F_2 = \frac{\text{Stabilizing force}}{\text{Sliding force}} = \frac{6.449}{4.496} = 1.43$$

This is also acceptable, as it is greater than 1.25.

Check for Tension in the Base Soil. The eccentricity on the base produced by the above forces is equal to $0.5(8.1 \times 2.0 - 2.025 \times -0.506 \times 1.67 - 4.496 \times 5)/(12.656) = e = -0.723$ m. For tension not to develop in the base soil, $e < B/6$. Because $B/6.0 = 1.5$, the base tension criterion is also satisfied by this design (Figure 14.57).

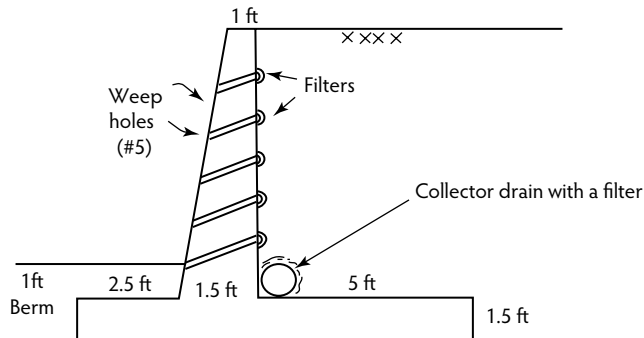


FIGURE 14.57 Design details.

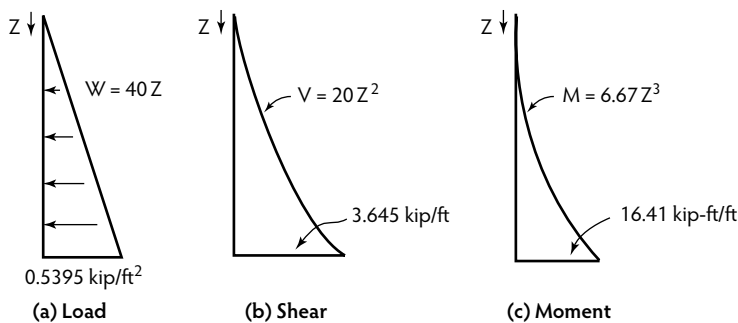


FIGURE 14.58 Load, shear, and moment diagrams for the retaining wall stem.

Reinforcement Requirements. To determine reinforcement requirements, the shear and bending moment diagrams can be drawn separately for the stem and the base (Figures 14.58 and 14.59). It should be noted that the maximum shear and moment in the stem occurs at its base and are 3.045 kips/ft and 16.412 kip-ft/ft, respectively. The reader should note that, when obtaining the shear and moment diagrams for the base, the base soil pressure is represented by a uniform distribution within a distance of B' (equal to $B - 2e$), as this is statically equivalent to an eccentric force of 12.656 kips/ft. A maximum shear force of 3.743 kips/ft is produced at the base. The reader should also note that in the moment diagram, within the stem area of the base, an unbalanced stem moment of 16.512 kips/ft (Figure 14.58) is gradually transferred to the base. Further, the heel of the base will have a moment of 4.2 kip-ft/ft due to the earth pressure distribution on the base thickness as shown in the load distribution diagram (Figure 14.59a). This information can be utilized for reinforcement design.

Drainage Design. The interested reader is referred to Bowles (1995) for further design details; however, one should remember the following preliminary guidelines:

- Provide a compacted free-draining soil layer adjacent to the retaining wall if the backfill material is clayey in nature.
- Provide a perforated collector drain with an appropriate soil or geomembrane filter at the base of the retaining wall.
- Make provisions for drainage outlets known as **weep holes** in the stem with a soil or geomembrane filter at the wall face to prevent clogging.

14.5.3 Effect of Water Table

In many instances, the soil behind an earth-retaining structure is submerged. Examples include seawalls, sheet pile walls in dewatering projects, and offshore structures. Another reason for saturation of backfill material is poor drainage, which leads to an undesirable buildup of water pressure behind the retaining

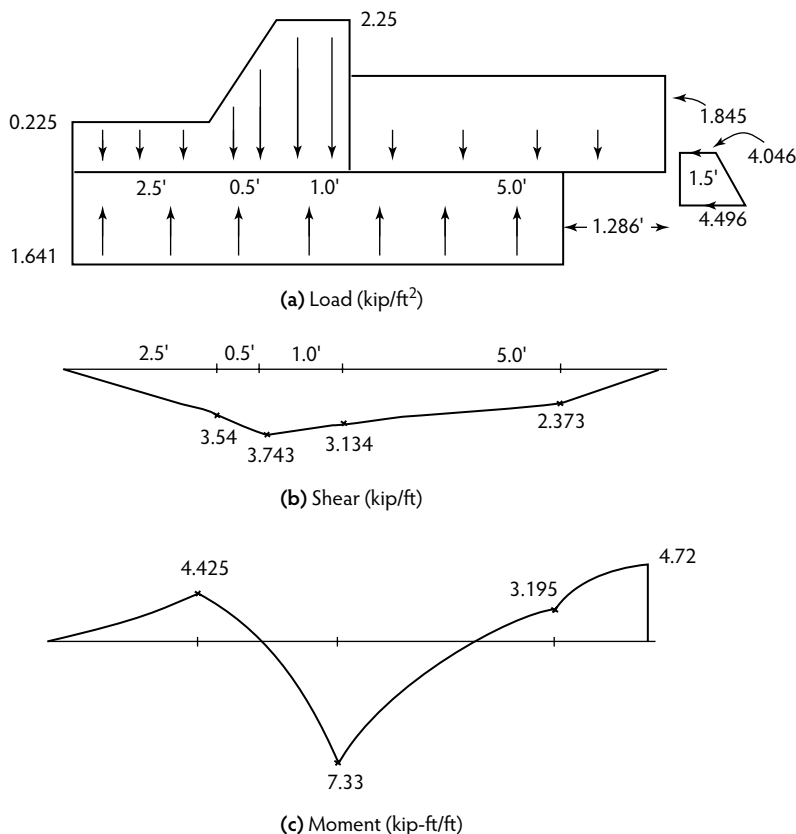


FIGURE 14.59 (a) Load, (b) shear, and (c) moment diagrams for the retaining wall base.

wall. Drainage failure often results in subsequent failure and collapse of the earth-retaining structure. In cases where the design considers the presence of a water table, the lateral earth pressure is calculated from the effective soil stress. Oddly enough, this leads to a *reduction* in effective horizontal earth pressure, as the effective stresses are lower than their total counterpart; however, the total stresses on the wall increase due to the presence of the hydrostatic water pressure. In other words, while the effective horizontal stress decreases, the total horizontal stress increases.

14.5.4 Reinforced Walls

14.5.4.1 Geogrid-Reinforced Walls

With the increased availability of high-strength geogrid materials in the 1990s, geogrid-reinforced walls were introduced as an alternative to metallic strip reinforcement. They provide increased interface area (because the coverage area can be continuous), better interlocking with the backfill (due to the geometry of the openings), resistance to corrosive environments, and lower cost. The most common type of geogrids used in earth reinforcement is the uniaxial type, due to its high strength and stiffness in the main direction. Facing panel units may be connected to the geogrid using a steel bar interwoven into the grid (known as a Bodkin connector) or, more recently, through special plastic clamps that tie into a geogrid section embedded in the concrete panel.

Among the concerns associated with the use of geogrids in heavily loaded walls (such as bridge abutments) are the time-dependent stress relaxation (creep deformation), installation damage, and chemical degradation. It is, therefore, crucial to determine the design strength of the geogrid considering the various reduction factors due to creep, installation damage, chemical degradation, and biological

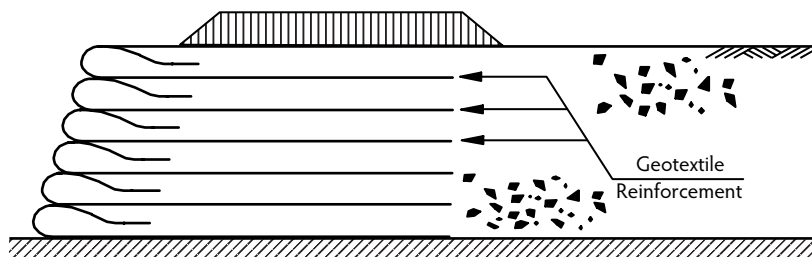


FIGURE 14.60 Geotextile-reinforced wall with wrapped-around facing.

degradation (Gunaratne, 2006). In addition, it is extremely important to ensure that the geogrid is fully stretched during installation and compaction of the subsequent soil layer; otherwise, significant deformation is required before tensile stresses and interface friction are mobilized. A closely related problem that has been identified is the difficulty in keeping the facing elements plumb during installation, especially when close tolerance is required in tall walls.

Design and construction procedures for geogrid reinforced walls are almost identical to reinforced earth walls. One distinct exception is that the strength of the geogrid is expressed in terms of force per unit length, and the associated horizontal spacing (s_h) is taken as a unit length in all calculations. Another difference is that, because of the effective interlocking of the soil particles within the geogrid openings, the interface friction angle is usually equal to the internal friction angle of the soil.

14.5.4.2 Geotextile-Reinforced Walls

Unlike metallic and geogrid reinforcement, typical geotextile-reinforced wall designs do not require facing elements. Instead, the geotextile layer is wrapped around the compacted soil at the front to form the facing (Figure 14.60). The finished wall must be covered with shotcrete, bitumen, or gunite to prevent ultraviolet radiation from reaching and damaging the geotextile. Such walls are usually constructed as temporary structures or where aesthetics are not of prime importance; however, it is possible to cover the wall with a permanent faux finish that blends with the surrounding environment. The design procedures for geotextile-reinforced walls are also identical to those described earlier for steel and geogrid reinforcement. The interface friction angle between the soil and the geotextile sheet is typically equal to $1/2$ to $2/3\phi$. In addition, the overlap length (L_o) must be determined from the following equation:

$$L_o = \frac{s_v \times \sigma_{h,z}}{2\sigma_{v,z} \times \tan \phi_i} \times FS_{\text{overlap}} \quad (14.53)$$

where s_v is the vertical spacing of the geotextile and z is any given depth. The minimum acceptable overlap length is 1 m.

14.5.5 Sheet Pile Walls

14.5.5.1 Cantilever Sheet Piles

A conceptual representation of the lateral earth pressure acting on a cantilever sheet pile is shown in Figure 14.61. Only active pressure is present on side A, from the ground surface to the depth of excavation. Below the excavation depth, passive conditions are assumed to act on side B of the sheet pile, while active conditions persist on side A, up to point O, where a reversal of conditions occurs. Point O can be viewed roughly as the point of rotation of the sheet pile in the ground. Such rotation is necessary to achieve static equilibrium of the system. Below point O, active conditions develop on side B while passive earth pressures are present on side A. Cantilever sheet pile design typically involves the determination of the embedment depth (D), given other geometric constraints of the problem as well as soil properties. Therefore, the first step is to calculate the magnitude of the horizontal stresses

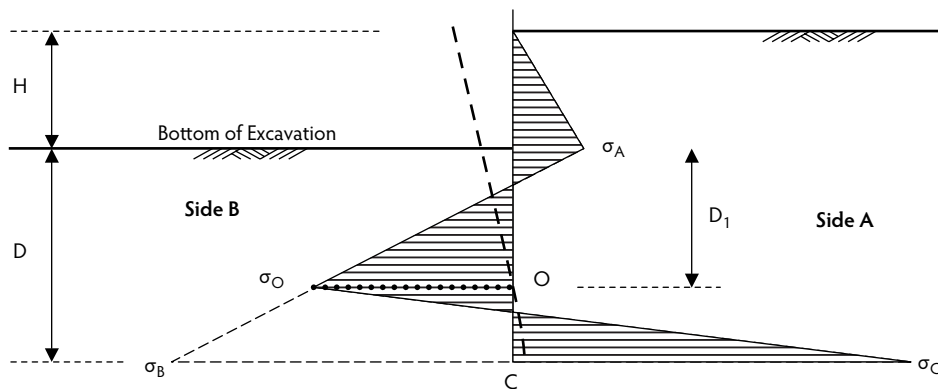


FIGURE 14.61 Conceptual representation of lateral earth pressure on a cantilever sheet pile wall.

σ_A , σ_B , and σ_C . The value of σ_A is readily calculated as the active earth pressure acting at depth H . The magnitudes of σ_O and σ_B must be calculated as a function of the embedment depth (D) and the depth to the rotation point (D_1), both of which are unknown. The value of σ_O is calculated assuming passive conditions on side B and active conditions on side A. Similarly, σ_B is calculated with passive earth pressure on side A and active earth pressure on side B. Two equilibrium conditions are to be satisfied: The sum of the horizontal forces and the sum of the moments in the system must be equal to zero. By solving both equilibrium equations, the two unknowns, D and D_1 , can be determined. As force and moment calculations become complex, it is often convenient to determine the value of σ_C , which is the hypothetical lateral earth pressure at depth D that corresponds to passive earth pressure on Side B and active earth pressure on Side A.

14.5.5.2 Anchored Sheet Piles

For large excavation depths, the inclusion of an anchor tie rod is necessary to reduce the moment on the sheet pile wall; otherwise, unreasonably large cross-sections may be required to resist the moment. Anchored sheet piles may be analyzed using either the free earth support or the fixed earth support method. Under free earth support conditions, the tip of the sheet pile (Figure 14.62) is assumed to be free to displace and rotate in the ground. Only active earth pressures develop on the tie-back side, while passive pressures act on the other side. No stress reversal or rotation points exist down the embedded depth of the sheet pile. In contrast, the tip of fixed-earth support sheet piles is assumed to be restricted from rotation. Stress reversal occurs down the embedded depth, and the sheet pile is analyzed as a statically indeterminate structure.

To design free earth support sheet piles, typically the depth of the anchor tie rod must be known. Equilibrium conditions are checked in terms of horizontal forces and moments, and the force in the tie rod as well as the depth of embedment are calculated accordingly. Alternatively, the maximum allowable force in the tie rod may be given, while the depth of the tie rod and the embedment depth of the sheet pile are unknowns. It is usually convenient to sum the system moments about the connection of the tie rod with the sheet pile to eliminate the tensile force in the tie rod from the equation.

The necessary anchor resistance in the tie rod is supplied through an anchor plate or deadman located at the far end of the tie rod (Figure 14.62a). To ensure stability, the anchor plate must be located outside the active wedge behind the sheet pile, which is delineated by line AB from the tip. In addition, this active wedge must not interfere with the passive wedge through which the tension in the tie rod is mobilized, which is bounded by the ground surface and line BC. Therefore, the length of the tie rod (L_t) is calculated from:

$$L_t = (H + D) \tan(45 - \phi/2) + D_1 \tan(45 + \phi/2)$$

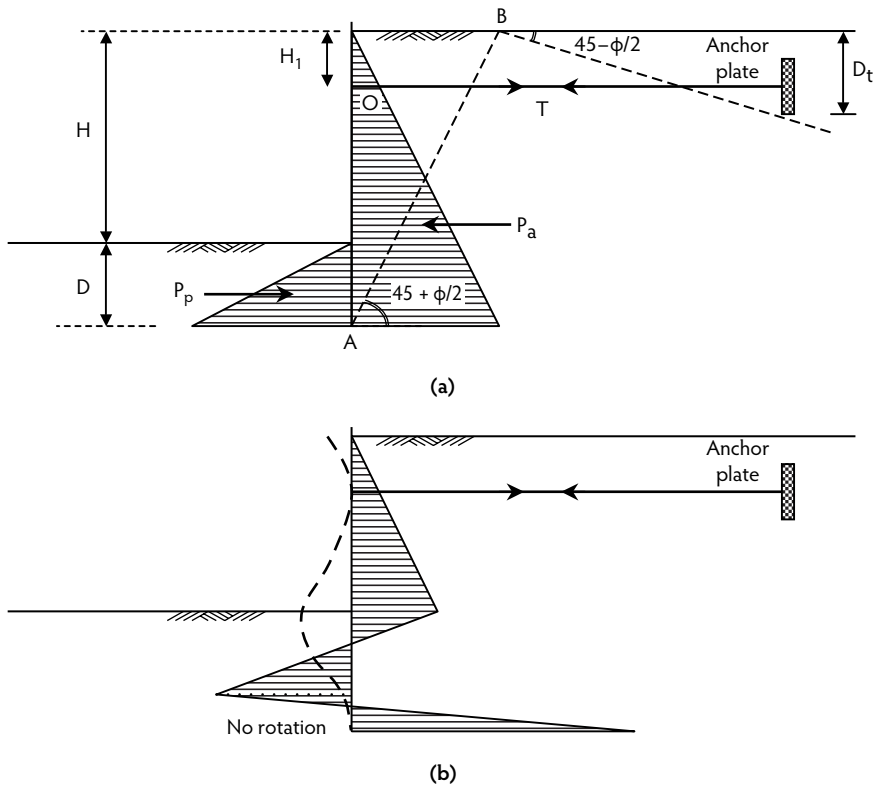


FIGURE 14.62 Conceptual representation of lateral earth pressure on tie-rod-anchored sheet pile walls: (a) free earth support; (b) fixed earth support.

Example 14.14

For the sheet pile wall shown in Figure 14.62a, determine the depth of embedment (D) and the force in the tie rod. The soil on both sides of the sheet pile is well-graded sand, with a unit weight $\gamma = 19 \text{ kN/m}^3$ and an internal friction angle of 34° . The tie rods are spaced at 3 m horizontally and are embedded at a depth $H_1 = 1 \text{ m}$. The height of the excavation $H = 15 \text{ m}$.

Solution

The active force (P_a) on the right side is calculated from:

$$P_a = \frac{1}{2} K_a \gamma (H + D) = \frac{1}{2} \times 0.283 \times 19 \times (15 + D) = 40.328 + 2.689D$$

The passive force (P_p) on the right side is calculated from:

$$P_p = \frac{1}{2} K_p \gamma D = \frac{1}{2} \times 3.537 \times 19 \times D = 33.60D$$

The sum of the moments about point O is:

$$(40.328 + 2.689D) \left(\frac{2}{3} \{15 + D\} - 1 \right) - (33.60D) \left(15 + \frac{2}{3} D \right) = 0$$

Solving for D , we obtain:

$$D = 0.77 \text{ m}$$

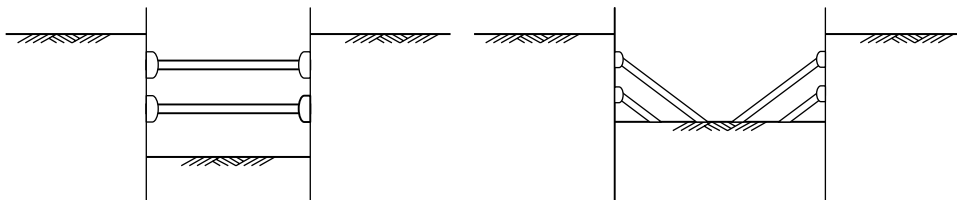


FIGURE 14.63 Examples of braced excavations.

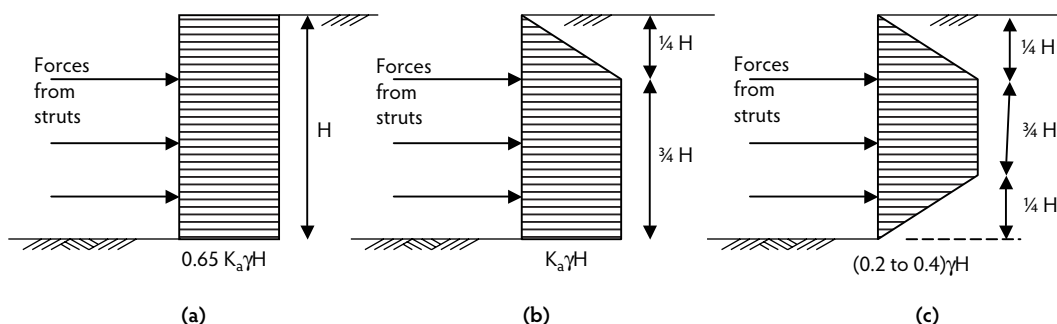


FIGURE 14.64 Approximate earth pressure diagrams for use in designing braced excavations: (a) sand; (b) soft to medium clay; and (c) stiff fissured clay.

The tension in the tie rods per meter width of the sheet pile wall is then calculated from the equilibrium of the horizontal forces:

$$T(\text{per m}) = (40.328 + 2.689 \times 0.77) - (33.60 \times 0.77) = 16.3 \text{ kN/m}$$

The force in each tie rod is calculated by multiplying the result by the horizontal spacing:

$$T = 3 \times 16.53 = 50 \text{ kN}$$

Theoretical depth D is multiplied by a safety factor of 1.2, thereby giving a total embedment depth of 0.92 m, which is rounded to 1.0 m.

14.5.6 Braced Excavations

Excavations in urban environments are constrained by the lack of adjacent space for installing tie rods or ground anchors. Where cantilever sheet piles are impractical, it becomes imperative to provide support to the sheet piles through internal bracing and struts. Examples of typical braced excavations are shown in Figure 14.63. It is important to ensure that the bracing system is stiff enough to prevent or minimize adjacent ground movement and strong enough to resist the earth pressure associated with such restricted deformations. Construction is usually initiated by driving the sheet piles or lateral support system, then excavating gradually from the ground level down. Rows of bracing or lateral support are installed as the excavation progresses down. The earth pressure developing in the case of braced excavations is different from the theoretical linear increase with depth described earlier for conventional retaining walls. In braced excavations, the lateral earth pressure is dictated by the sequence of excavation, soil type, stiffness of the wall and struts, and movement allowed prior to installing the struts. Although accurate determination of the distribution of earth pressure in braced cuts is almost impossible, Terzaghi et al. (1996) provided approximate methods based on actual observations for use in strut design (Figure 14.64). In the case of sands, the envelope of the apparent earth pressure is constant and equal to $0.65 K_a \gamma H$, where H is the depth of the excavation. In the case of soft/medium clays and stiff fissured clays, the diagrams shown in Figure 14.64b and Figure 14.64c are used, respectively. It is

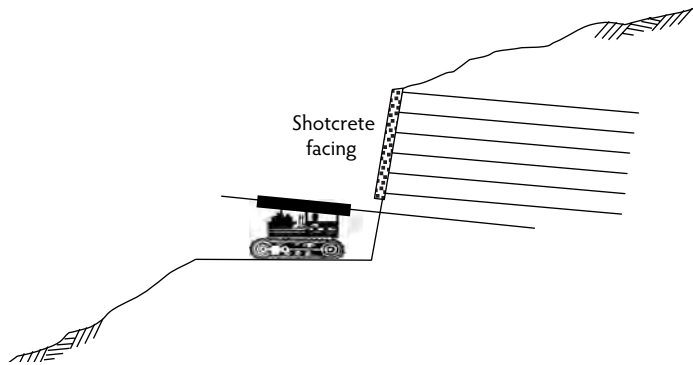


FIGURE 14.65 Construction of soil-nailed wall.

imperative, however, to monitor the development of forces in the struts and deformations along the depth of the braced cut during construction. Forces in the struts and deformations must be continuously adjusted to comply with design specifications.

14.5.7 Soil Nail Systems

Soil nailing is a technique for stabilizing steep slopes and vertical cuts. The technique relies on driving soil nails, which are steel rods 25 to 50 mm in diameter, into a vertical or steep cut at a 15° angle as excavation proceeds (Figure 14.65). Alternatively, the soil nails may be installed through drilling and grouting. Conceptually, the method differs from tie-back anchored walls in that no prior driving or installation of an earth retaining wall (sheet pile, soldier piles, or slurry wall) is conducted. Instead, the exposed soil surface is kept from caving in by installing a wire mesh on which the soil nails are connected through face plates. The technique works best in cohesive soils, as significant unraveling may occur in sandy soils. The wire mesh is then covered with shotcrete, and excavation proceeds to the next level. Soil nail walls are typically used as temporary earth-retaining systems, although they have been used successfully as permanent structures. When analyzing soil nail systems, global stability is considered. Conventional methods for slope stability analysis are used, with the tension in the soil nails contributing to the stability of the slope. Typically, the method of slices is chosen, and the forces acting on each slice, including the tensile resistance of the soil nail, are included. The global stability of the reinforced soil mass is then assessed, and a factor of safety is calculated. The length of the soil nails is determined accordingly, so as to satisfy equilibrium of the slope or vertical cut.

14.5.8 Drainage Considerations

Proper drainage of backfill materials is a crucial component of retaining wall design. In general, cohesive backfills are highly undesirable because of their poor drainage, loss of strength and increase in density upon wetting, and high coefficient of active earth pressure. This is particularly important in the case of mechanically stabilized earth (MSE) walls, where only select backfill material may be used. Acceptable soil types for such purpose are SW (well-graded sand), GW (well-graded gravel), and SP (poorly graded sand). The vast majority of current design codes prohibit the use of cohesive materials as backfill in MSE walls. In addition, proper drainage provisions must be included in the design. This entails the inclusion of drains and filters in the cross-section, such as those shown in Figure 14.66. While graded sand constituted the majority of filters and drains in the past, geosynthetics (geotextiles, geonets, and geocomposites) are used in almost all projects today. To select the proper filter material, the acceptable apparent opening size (O_{95}) of the geosynthetic must be first determined. Current guidelines require that O_{95} be smaller than $2.5D_{85}$, where D_{85} is the grain size corresponding to the 85th percentile of the grain size distribution of the soil. Geonets selected for drainage must have a maximum flow rate that is greater than the anticipated flow rate in the structure.

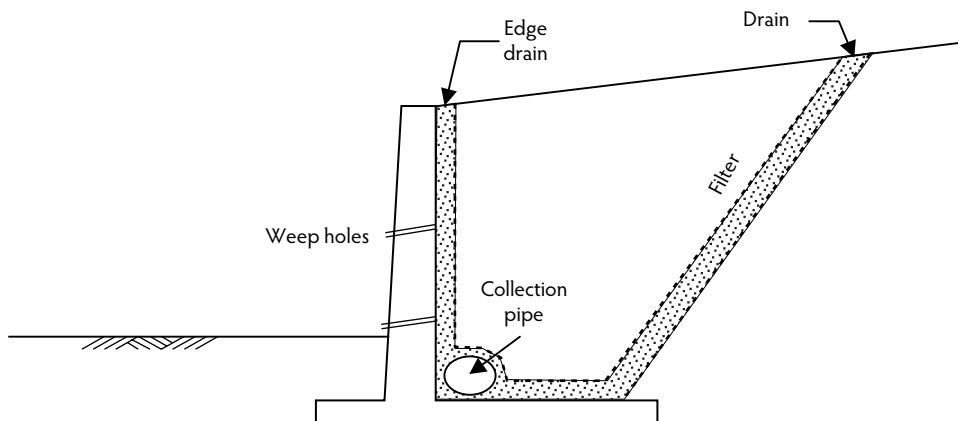


FIGURE 14.66 Drainage provisions in cantilever retaining wall.

14.6 Pile Foundations

A pile foundation can be employed to transfer superstructure loads to stronger soil layers deep underground; hence, it is a viable technique for foundation construction in the presence of undesirable soil conditions near the ground surface. However, due to the high cost involved in piling, this method is only utilized after other less costly alternatives, such as combined footings and ground modification, have been considered and ruled out for the particular application. On the other hand, piles may be the only possible foundation construction technique in the case of subgrades that are prone to erosion and in offshore construction.

14.6.1 Advantages of Concrete Piles

Depending on applicability, one of the three different pile types: timber, concrete, or steel, is selected for a given construction situation. Concrete piles are selected for foundation construction under the following circumstances:

- Heavy loads must be supported in maritime areas where steel piles can easily corrode.
- Stronger soil types are located at a relatively shallower depth that are easily accessible to concrete piles.
- Bridge piers and caissons require large-diameter piles.
- A large pile group is needed to support a heavy extensive structure so the total expense can be minimized.
- Minipiles are necessary to support a residential building on a weak and compressible soil.

The disadvantages of concrete piles are that they are damaged by acidic environments (organic soils) and undergo abrasion due to wave action when used to construct offshore structures.

14.6.2 Types of Concrete Piles

The two most common types of concrete piles are precast and cast *in situ*. Of these, precast piles may be constructed to specifications at a casting yard or at the site itself if a large number of piles is needed for the particular construction. In any case, handling and transportation can cause intolerable tensile stresses in precast concrete piles; hence, one should be cautious in handling them so as to minimize bending moments in the pile. Cast *in situ* piles are of two classes: (1) cased type, which are piles that are cast inside a steel casing that is driven into the ground, and (2) uncased type, which are piles that are formed by pouring concrete into a drilled hole or into a driven casing before the casing is gradually withdrawn.

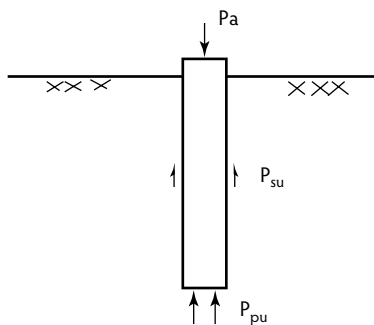


FIGURE 14.67 Load-bearing capacity of a pile.

14.6.3 Estimation of Pile Capacity

The pile designer should be aware of the capacity of a pile under normal working conditions (**static**) and when it is driven (**dynamic**).

14.6.3.1 Static Pile Capacity

The ultimate working load that can be applied to a given pile depends on the resistance that the pile can produce in terms of side friction and point bearing (Figure 14.67); hence, the expression for the allowable load on a pile will take the following form:

$$P_a = \frac{P_{pu} + P_{su}}{F} \quad (14.54)$$

where:

P_{pu} = ultimate point capacity.

P_{su} = ultimate side friction.

F = safety factor.

The ultimate point capacity component in Equation 14.54 corresponds to the bearing capacity of a shallow footing expressed by Equation 14.55, which is a modified form of Equation 14.32:

$$P_{pu} = A_p \left[cN_c^* + q(N_q^* - 1) \right] \quad (14.55)$$

where:

A_p = area of the pile cross-section.

q = vertical effective stress at the pile tip.

c = cohesion of the bearing layer.

N_c^*, N_q^* = bearing capacity factors modified for deep foundations (and a B/L ratio of 1.0).

The bearing capacity factors for deep foundations can be found in Figure 14.68. Using the above bearing capacity factors is more involved than in the case of shallow footings because, in the case of deep foundations, the mobilization of shear strength also depends on the extent of the penetration of the pile into the bearing layer. In granular soils, the depth ratio at which the maximum strength is mobilized is called the **critical depth ratio** $(L_b/D)_{cr}$. Figure 14.69 shows $(L_b/D)_{cr}$ for the mobilization of N_c^* and N_q^* for different values of ϕ . According to Meyerhoff (1976), the maximum values of N_c^* and N_q^* are usually mobilized at depth ratios of $0.5(L_b/D)_{cr}$. An interpolation process must be followed to evaluate the bearing capacity factors if the depth ratio is less than $0.5(L_b/D)_{cr}$. This is illustrated in Example 14.15.

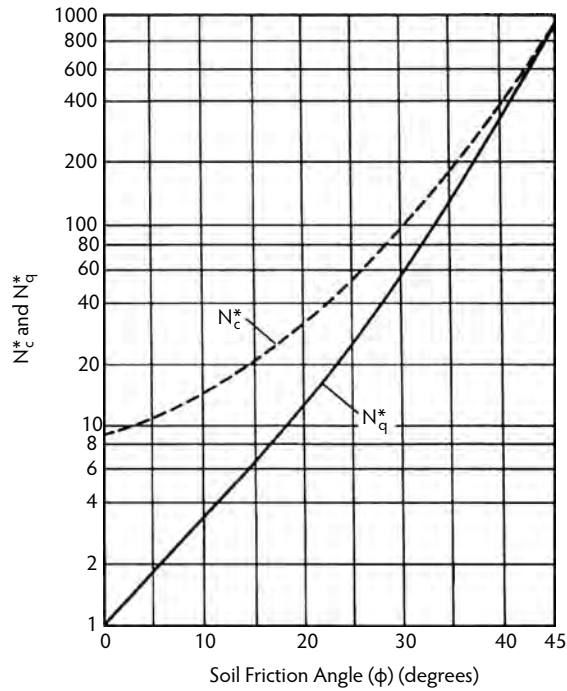


FIGURE 14.68 Bearing capacity factors for deep foundations. (From Das, B.M., *Principles of Foundation Engineering*, PWS Publishing, Boston, MA, 1995. With permission.)

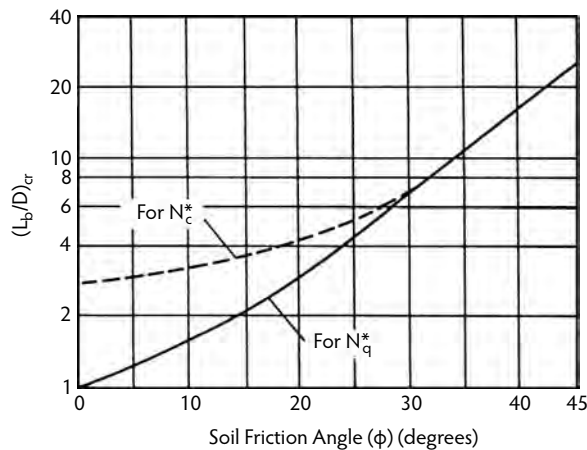


FIGURE 14.69 Variation of critical depth ratio with ϕ . (From Das, B.M., *Principles of Foundation Engineering*, PWS Publishing, Boston, MA, 1995. With permission.)

Point Capacity in Sands. In the case of sandy soils where the cohesive resistance is negligible, Equation 14.55 can be reduced to:

$$P_{pu} = A_p q (N_q^* - 1) \quad (14.56)$$

where the limiting point resistance is:

$$P_{pu_{max}} = A_p 50 N_q^* \tan \phi \text{ (kN)}; P_{pu_{max}} = A_p N_q^* \tan \phi \text{ (kips)} \quad (14.57)$$

Point Capacity in Clays. The most critical design condition in clayey soils is the undrained condition where the apparent angle of internal friction is zero. Under these conditions, it can be seen that Equation 14.55 reduces to:

$$P_{pu} = A_p (9.0c_u) \quad (14.58)$$

where c_u is the undrained strength.

Skin-Friction Capacity of Piles. The skin-friction capacity of piles can be evaluated by means of the following expression:

$$P_{sf} = \int_0^L p f dz \quad (14.59)$$

where:

- p = perimeter of the pile section.
- z = coordinate axis along the depth direction.
- f = unit skin-friction at any depth z .
- L = length of the pile.

Unit Skin Friction in Sandy Soils. Because skin friction in granular soils is due to the frictional interaction between piles and granular material, the unit skin friction can be expressed as:

$$f = K \sigma'_v \tan \delta \quad (14.60)$$

where:

- K = earth pressure coefficient (K_0 for bored piles and $1.4K_0$ for driven piles).
- δ = angle of friction between the soil and pile material (usually assumed to be $2/3\phi$).
- σ'_v = vertical effective stress at the point of interest.

It can be seen from the above expression that the unit skin friction can increase linearly with depth; however, practically, a depth of $15B$ (where B is the cross-sectional dimension) has been found to be the limiting depth for this increase.

Skin Friction in Clayey Soils. In clayey soils, on the other hand, skin friction results from adhesion between soil particles and the pile; hence, the unit skin friction can be simply expressed by:

$$f = \alpha c_u \quad (14.61)$$

where **adhesion factor** α can be obtained from Figure 14.70.

Example 14.15

Estimate the maximum allowable static load on the 200-mm-square driven pile shown in Figure 14.71. From Table 14.14 and Table 14.15, the following strength parameters can be obtained, based on the SPT data given:

Soil Layer	Representative N'	Cohesion (c) (kPa)	Friction (ϕ) ($^\circ$)
Loose sand	5	0.0	28
Clay	8	40.0	0
Medium dense sand	20	0.0	38

Computation of Skin Friction in Loose Sand. Applying Equation 14.60, one would obtain:

$$f = 1.4K_0(17.0)z \tan \delta$$

up to a depth of -30 m (i.e., 15.0×0.2) and constant thereafter. Assuming $\delta = 2/3(\phi) = 19^\circ$ and $K_0 = (1 - \sin \phi) \text{OCR} = 0.574$, because the overconsolidation ratio (OCR) = 1.0 for normally consolidated soils, one obtains:

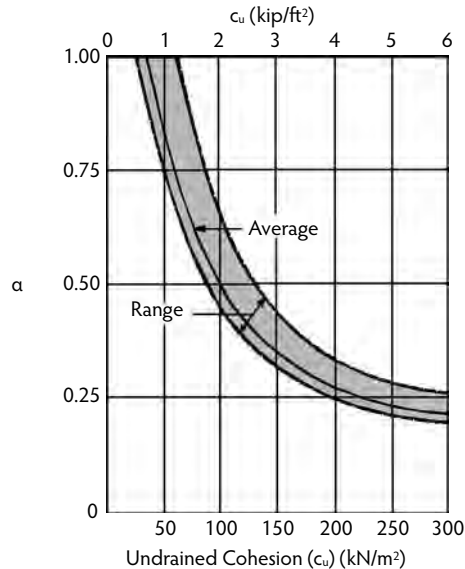


FIGURE 14.70 Variation of α with undrained strength. (From Das, B.M., *Principles of Foundation Engineering*, PWS Publishing, Boston, MA, 1995. With permission.)

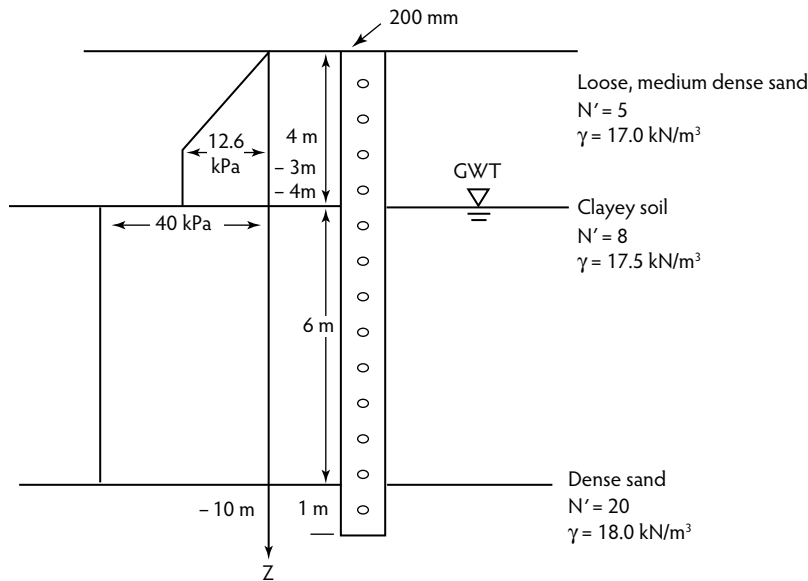


FIGURE 14.71 Illustration of the computation of pile capacity.

TABLE 14.15 Comparison between Maintained Load and Quick Load Tests

Test Parameter	Maintained Load Test	Quick Load Test
Test load	200% of design load	300% of design load or up to failure
Load increment	25% of the design load	10–15% of the design load
Load duration	Up to a settlement rate of 0.001 ft/hr or 2 hr, whichever occurs first	2.5 min
Test duration	48 hr	3–5 hr

$$f = 4.203z \text{ kPa, for } z < 3 \text{ m} \quad \text{and} \quad f = 12.6z \text{ kPa, for } z > 3 \text{ m}$$

Computation of Skin Friction in Clay. Applying Equation 14.61, one obtains:

$$f = \alpha(40)$$

where $\alpha = 1.0$ from Figure 14.70, so:

$$f = 40 \text{ kPa}$$

The dense sand layer can be treated as an end-bearing layer, so its skin-frictional contribution cannot be included. Because the pile perimeter is constant throughout the depth, the total skin-frictional force (Equation 14.59) can be computed by multiplying the area of the skin-friction distribution shown in Figure 14.68 by the pile perimeter of 0.8 m. Hence,

$$P_{sf}(0.8) \left[0.5(3)(12.6) + 12.6(1) + 40(6) \right] = 217.2 \text{ kN}$$

Computation of the Point Resistance in Dense Sand. From Figure 14.69, $(L/D)_{cr} = 15$ for $\phi = 30^\circ$. For the current problem, $L/D = 1/0.2 = 5$. Because, in this case, $L/D < 0.5(L/D)_{cr}$, N_q^* can be prorated from the maximum N_q^* values given in Figure 14.68. Thus,

$$N_q = \left[(L/D) / 0.5(L/D)_{cr} \right] (N_q^*) = 5/7.5 \times 300 = 208$$

Note that $N_q^* = 300$ was obtained from Figure 14.68. Also,

$$A_p = 0.2 \times 0.2 = 0.04 \text{ m}^2$$

$$q = \sigma'_v = 17.0(4) + (17.5 - 9.8)(6) + (18.0 - 9.8)(1) = 122.4 \text{ kPa}$$

Then, by substituting in Equation 14.56:

$$P_{pu} = 0.04(208 - 1)(122.4) \text{ kN} = 974.3 \text{ kN}$$

but

$$P_{pu\max} = 0.04(5)(208) \tan 38^\circ = 271.8 \text{ kN} \quad \therefore P_{pu} = 271.8 \text{ kN}$$

Finally, by applying Equation 14.55, one can determine the maximum allowable load as:

$$P_{all} = (271.8 + 217.2)/4 = 122.3 \text{ kN}$$

14.6.4 Computation of Pile Settlement

In contrast to shallow footings, a pile foundation settles not only because of the compression the tip load causes on the underlying soil layers but also because of the compression caused by the skin friction on the surrounding layers. The elastic shortening of the pile itself is another source of settlement. In addition, if an underlying saturated soft clay layer is stressed by the pile, the issue of consolidation settlement will also have to be addressed. In this section, only the immediate settlement will be analytically treated, as a computation of consolidation settlement of a pile group is provided in Example 14.16. According to Poulos and Davis (1990), the immediate settlement of a single pile can be estimated from the following expressions:

$$s = \frac{PI}{E_s d} \quad (14.62)$$

and

$$I = I_o R_k R_h R_v \quad (14.63)$$

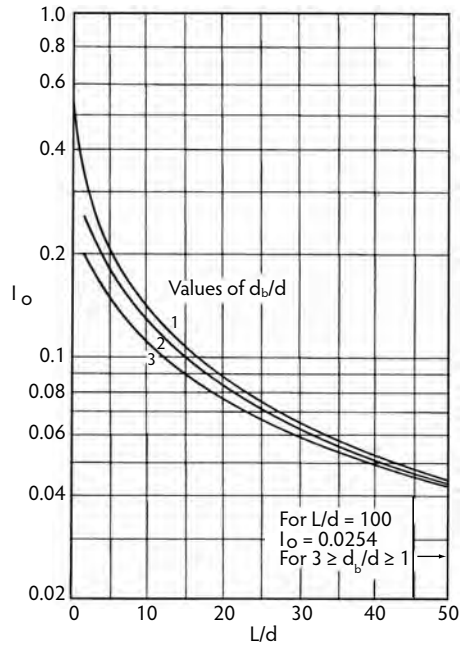


FIGURE 14.72 Influence factor I_o . (From Poulos, H.G. and Davis, E.H., *Pile Foundation Analysis and Design*, Krieger, Melbourne, FL, 1990. With permission.)

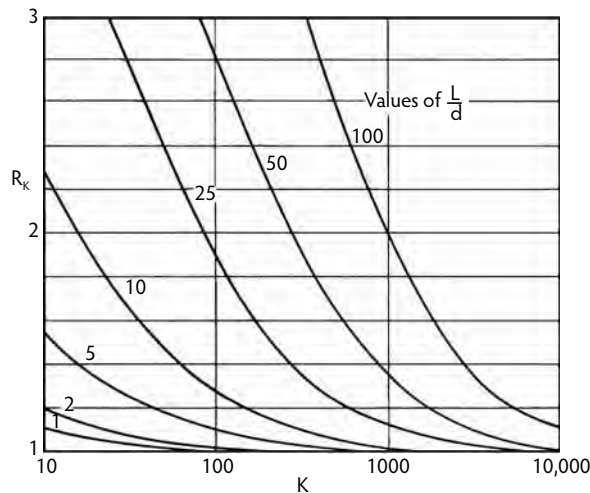


FIGURE 14.73 Correction factor for pile compressibility. (From Poulos, H.G. and Davis, E.H., *Pile Foundation Analysis and Design*, Krieger, Melbourne, FL, 1990. With permission.)

where:

I_o = influence factor for an incompressible pile in a semi-infinite medium with $\nu_s = 0.5$ (Figure 14.72).

R_k = correction factor for pile compressibility k ($= E_p/E_s$) (Figure 14.73).

R_h = correction factor for a finite medium of thickness h (Figure 14.74).

R_v = correction factor for the Poisson's ratio (ν_s) of soil (Figure 14.75).

E_s = elastic modulus of soil.

E_p = elastic modulus of pile material.

d = minimum pile dimension (pile diameter).

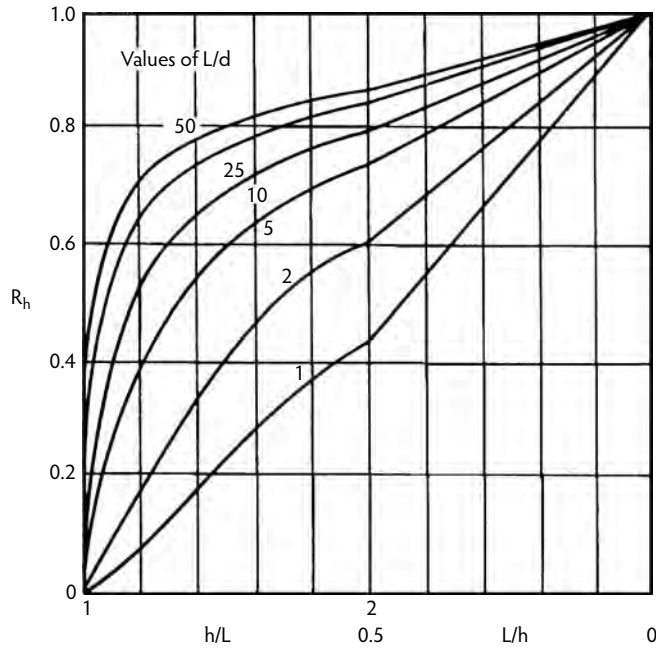


FIGURE 14.74 Correction factor for layer thickness. (From Poulos, H.G. and Davis, E.H., *Pile Foundation Analysis and Design*, Krieger, Melbourne, FL, 1990. With permission.)

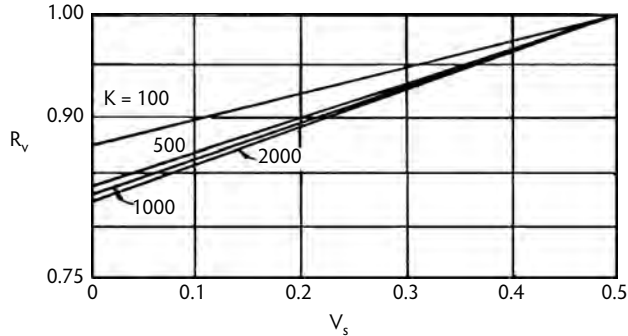


FIGURE 14.75 Correction factor for Poisson ratio. (From Poulos, H.G. and Davis, E.H., *Pile Foundation Analysis and Design*, Krieger, Melbourne, FL, 1990. With permission.)

14.6.5 Pile Groups

For purposes of stability, pile foundations are usually constructed of pile groups that transmit the structural load through a pile cap, as shown in Figure 14.76. If the individual piles in a group are not ideally placed, the individual influence zones will overlap, as shown in Figure 14.76. This will be manifested in the following group effects, which have to be considered when designing a pile group:

- The bearing capacity of the pile group will be different (generally lower) than the sum of the individual capacities, due to the above interaction.
- The group settlement will also be different from individual pile settlement due to additional stresses induced on the piles by the neighboring piles.

Both topics are discussed in the following sections, and illustrative examples are provided.

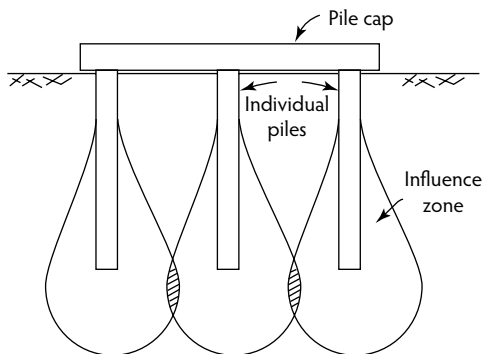


FIGURE 14.76 Illustration of the group effect.

14.6.5.2 Bearing Capacity of Pile Groups

The efficiency of a pile group is defined as:

$$\eta = \frac{\text{Ultimate capacity of the pile group } (P_{g(u)})}{\text{Sum of individual ultimate } (\sum P_{(u)i})} \quad (14.64)$$

where η is the group efficiency. Due to the complexity of individual pile interaction, the literature does not indicate any definitive methodology for determining the group efficiency in a given situation other than the following common Converse–Labarre equation, which is applied for clayey soils:

$$\eta = 1 - \frac{\xi}{90} \left[\frac{(n-1)m + (m-1)n}{mn} \right] \quad (14.65)$$

where:

$\xi = \tan^{-1}$ (diameter/spacing ratio).

n = number of rows in the group.

m = number of columns in the group.

Although the above expression indicates that the maximum possible efficiency is about 90%, reached at a spacing/diameter ratio of 5, the results from experimental studies (Bowles, 1995; Das, 1995; Poulos and Davis, 1990) have shown group efficiency values of well over 100% under certain conditions, especially in dense sand. This may be explained by possible densification accompanied by pile driving in medium-dense sands. Computation of group capacity is illustrated in Example 14.16.

14.6.5.3 Settlement of Pile Groups

One method for determining the immediate settlement of a pile group is by evaluating the interaction factor (α_F), defined as follows:

$$\alpha_F = \frac{\text{Additional settlement caused by adjacent pile}}{\text{Settlement of pile under its own load}} \quad (14.66)$$

The settlement of individual piles can be determined on the basis of the method described in Section 14.6.4. Then, once α_F is estimated from Figure 14.77, one can easily compute the settlement of each pile in a group configuration. At this point, the issue of the flexibility of the pile cap has to be considered. This is because if the pile cap is rigid (thick and relatively small in area), it will ensure equal settlements throughout the group by redistributing the load to accommodate equal settlements. On the other hand, if the cap is flexible (thin and relatively extensive in area), all of the piles will be equally loaded, which results in different settlements.

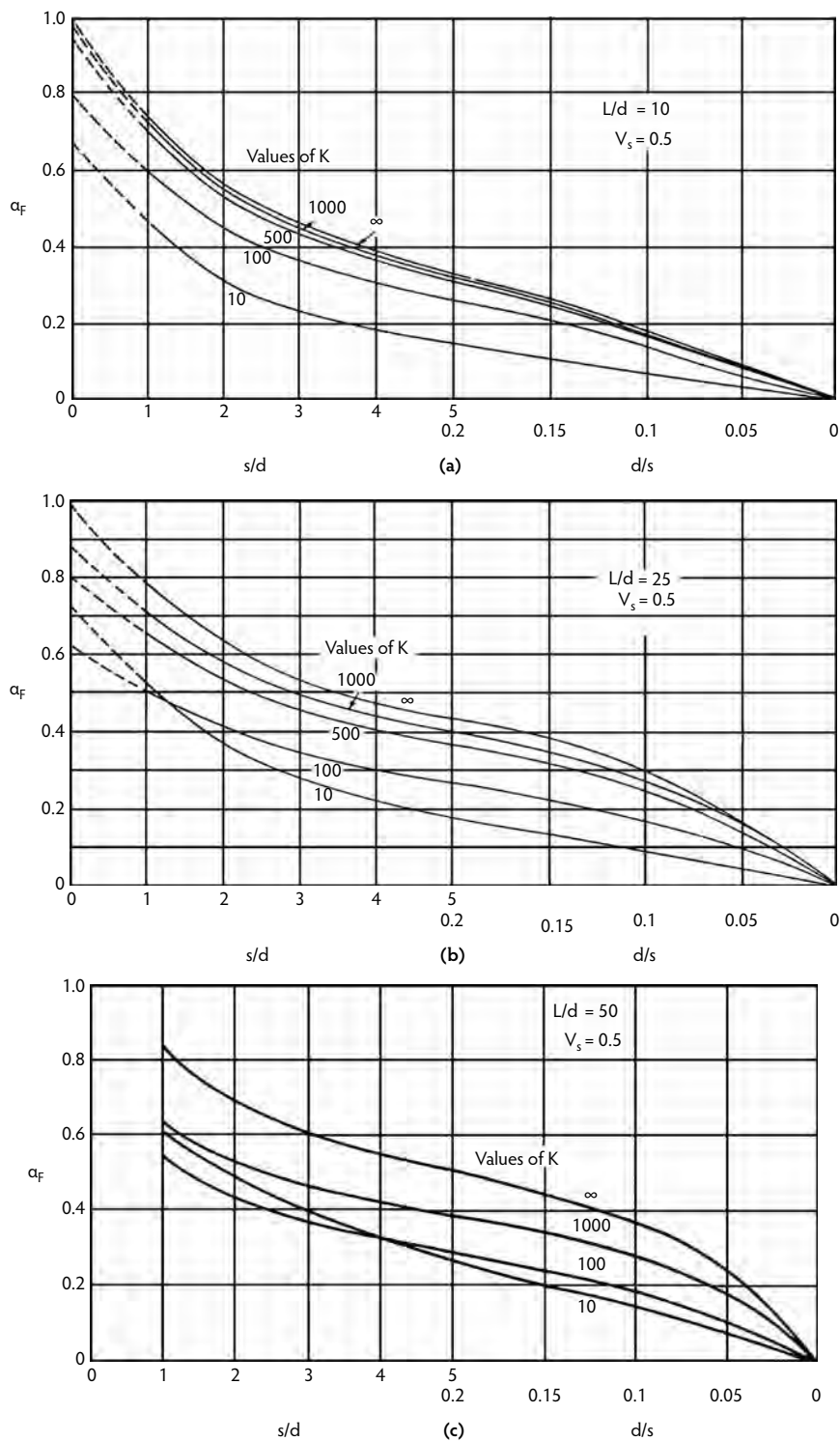


FIGURE 14.77 Determination of α_F factor for (a) $L/D = 10$, (b) for $L/D = 25$, and (c) for $L/D = 50$. L = pile length; D = pile diameter; k and v_s are as defined in Equation 14.58. (From Poulos, H.G. and Davis, E.H., *Pile Foundation Analysis and Design*, Krieger, Melbourne, FL, 1990. With permission.)

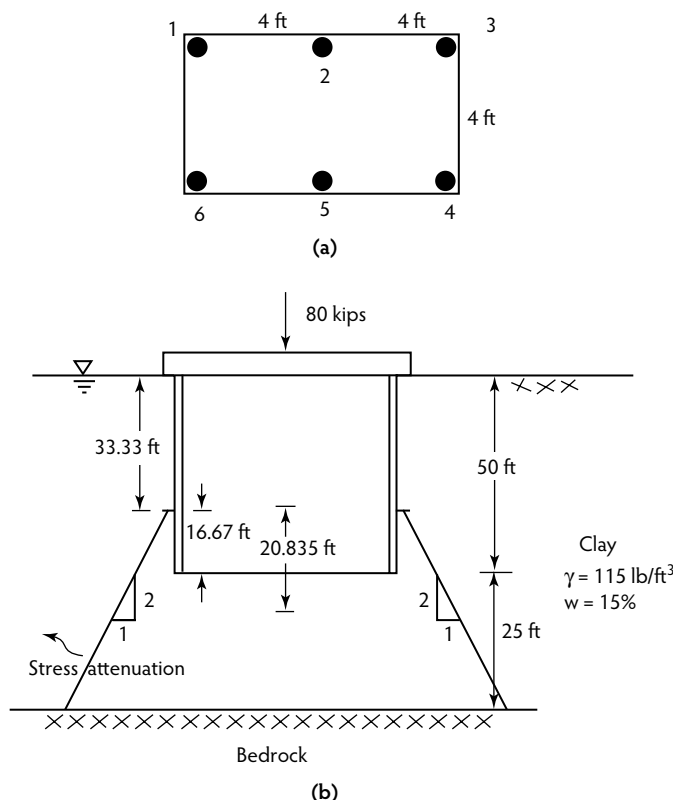


FIGURE 14.78 Illustration of pile group load attenuation: (a) plan, and (b) elevation.

Under conditions that require the estimation of consolidation settlement under a pile group, one can assume that the pile group acts as a large single footing and use the principles discussed in Section 14.1.3 (Compressibility and Settlement). However, the difference in load attenuation between a shallow footing and a rigid pile group with substantial skin friction is accounted for by assuming that the load attenuation originates from the lower middle-third of the pile length, as shown in Figure 14.78b.

Example 14.16

The pile group (six 1×1 -ft piles) shown in Figure 14.78 is subjected to a load of 80 kips. A compression test performed on a representative clay sample at the site yielded an unconfined compression strength of 3 psi and an elastic modulus of 8000 psi; a consolidation test indicated no significant overconsolidation, with a compression index of 0.3 and a water content of 15%. Estimate the safety of the pile foundation and its settlement. The undrained strength is 0.5 (unconfined compression strength) = 1.5 psi = 216 psf.

Computation of Skin Friction of a Single Pile. Using Equation 14.61, $f = 1.0(216)$ psf. From Equation 14.60, the resultant skin-frictional force = $216(4)(50) = 43.2$ kips.

Computation of End-Bearing of a Single Pile. Using Equation 14.58, $P_{pu} = (1)(9)(216) = 1.944$ kips (in fact, one could have easily expected the insignificance of this contribution due to the frictional nature of the pile). Thus, the ultimate capacity of the pile is 45.14 kips.

Estimation of Group Efficiency. Using Equation 14.65), $\eta = 1 - [(3 - 1)(2) + (2 - 1)(3)](\zeta)/[90(3)(2)] = 0.8$. Then, using Equation 14.64, the group capacity can be obtained as $0.8(45.14)(6) = 216$ kips; hence, the safety factor is 2.7.

Estimation of Single Pile Immediate Settlement. The relative stiffness factor for a rigid pile (K) is $E_{\text{concrete}}/E_s = 4,000,000/8000 = 500L/D = 50/1 = 50$.

From Figure 14.72, $I_o = 0.045$.

From Figure 14.73, $R_k = 1.85$.

From Figure 14.74, $R_h = 1.00$.

From Figure 14.75, $R_v = 1.00$ (undrained $v = 0.5$).

Substituting in Equation 14.62:

$$s = P(0.045)(1.85)(0.8)(1.00)/(8000 \times 12) = 0.032 \times 10^{-5}P \text{ in.}$$

where P is the load on a single pile in kips.

Analysis of Group Settlement. If the cap is assumed to be rigid, then the total settlement of all six piles must be identical. The total settlement consists of both immediate settlement and consolidation settlement; however, only an average consolidation settlement can be computed for the entire pile group based on the stress attenuation method (Figure 14.78) assuming equal consolidation settlement. Thus, one has to assume equal immediate settlements as well. Because of their positions with respect to the applied load, it can be seen that piles 1, 3, 4, and 6 can be considered as one type of pile (type 1) carrying identical loads, while piles 2 and 5 can be categorized as type 2. Thus, it will be sufficient to analyze the behavior of pile types 1 and 2 only. Assume that the loads carried by type 1 and 2 piles are P_1 and P_2 , respectively. Then, for vertical equilibrium:

$$4P_1 + 2P_2 = 80 \text{ kips} \quad (14.67)$$

Using Figure 14.78a, the interaction factors for pile types 1 and 2 due to other piles can be obtained as follows:

Pile Type 1		
Pile i	s/d for Pile i	α_F from Pile i
1	0	—
2	4	0.4
3	8	0.3
4	8.94	0.25
5	5.67	0.35
6	4	0.4
$\alpha = 1.7$		
Pile Type 2		
Pile i	s/d for Pile i	α_F from Pile i
1	4	0.4
2	0	—
3	4	0.4
4	5.67	0.35
5	4	0.4
6	5.67	0.35
$\alpha = 1.9$		

Then, using Equation 14.66, the total settlement of pile type 1 is estimated as $(1 + 1.7)P_1(0.032 \times 10^{-5})$, and the total settlement of pile type 2 would be $(1 + 1.9)P_2(0.032 \times 10^{-5})$. By equating the settlement of pile types 1 and 2 (for equal immediate), one obtains:

$$2.7P_1 = 2.9P_2 \quad (14.68)$$

$$P_1 = 1.074P_2$$

By substituting in Equation 14.67,

$$2(1.074P_2) + P_2 = 40$$

$$P_2 = 12.706 \text{ kips}$$

$$P_1 = 13.646 \text{ kips}$$

Hence, immediate settlement of the pile group is equal to $2.9(0.032)(10^{-5})(12.706)(10^3) = 0.012 \text{ in.}$

Computation of Consolidation Settlement. On the basis of the stress attenuation shown in Figure 14.78b, the stress increase on the midplane of the wet clay layer induced by the pile group can be found as:

$$\Delta\sigma = 80,000/[(8 + 20.835)(4 + 20.835)] = 111.71 \text{ psf}$$

The initial effective stress at the above point is equal to $(115 - 62.4)(54.165) = 2849 \text{ psf}$. From basic soil mechanics, for a saturated soil sample $e = \omega G_s = 0.15 \times 2.65 = 0.4$, assuming that the solid specific gravity (G_s) is 2.65. Then, by applying Equation 14.19, one obtains the consolidation settlement as:

$$s_{ult} = (0.3)(41.67)(1/1 + 0.4)\log[1 + 111.71/2849] = 0.149 \text{ ft} = 1.7889 \text{ in.}$$

Hence, in this case the consolidation settlement is predominant.

14.6.6 Verification of Pile Capacity

Several methods are available to determine the load capacity of piles. The commonly used methods include: (1) the use of pile-driving equations, (2) the use of the wave equation, and (3) full-scale load tests. A brief description of the first two methods is provided in the next two sections.

14.6.6.1 Use of Pile-Driving Equations

In the case of driven piles, one of the very first methods used to determine the load capacity was using numerous pile-driving equations. Of these equations, one of the more popular is the Engineering News-Record (ENR) equation, which expresses the pile capacity as follows:

$$P_u = \frac{EW_h h}{S + C} \frac{W_h + n^2 W_p}{S + CW_h + W_p} \quad (14.69)$$

where:

n = coefficient of restitution between the hammer and the pile (<0.5 and >0.25).

W_h = weight of the hammer.

W_p = weight of the pile.

S = pile set per blow (in inches).

C = 0.1 in.

h = hammer fall.

E = hammer efficiency (usually estimated by monitoring the free fall).

It can be seen how one can easily compute the instant capacity developed at any given stage of driving by knowing the pile set (S), which is usually computed by the reciprocal of the number of blows per inch of driving. To avoid damage to the pile and the equipment, it should be noted that, when driving has reached a stage where more than 10 blows are needed for a penetration of 1 in. ($S = 0.1$ or refusal), further driving is not recommended.

14.6.6.2 Use of the Wave Equation

With the advent of modern computers, use of the wave equation method for pile analysis, as introduced by Smith (1960), became popular. Smith's idealization of a driven pile is elaborated in Figure 14.79. The governing equation for wave propagation can be written as follows:

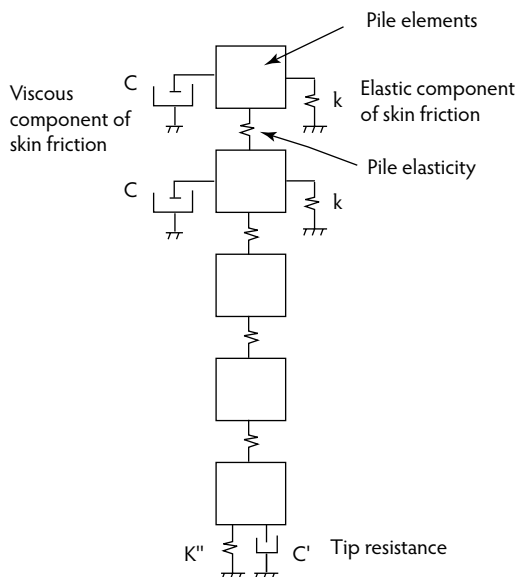


FIGURE 14.79 Idealization of a driven pile.

$$\rho A \frac{\partial^2 u}{\partial t^2} dz = AE \frac{\partial^2 u}{\partial z^2} dz - R(z) \quad (14.70)$$

where:

- ρ = mass density of pile.
- A = area of cross-section of pile.
- u = particle displacement.
- t = time.
- z = coordinate axis along the pile.
- $R(z)$ = resistance offered by any pile slice (dz).

The above equation can be transformed into the finite-difference form to express the displacement, the force, and the velocity, respectively, of a pile element i at time t as follows:

$$D(i, t) = D(i, t - \Delta t) + V(i, t - \Delta t) \quad (14.71)$$

$$F(i, t) = [D(i, t) - D(i+1, t)]K \quad (14.72)$$

$$V(i, t) = V(i, t - \Delta t) + \frac{\Delta t g}{\omega(i)} [F(i-1, t) - F(i, t) - R(i, t)] \quad (14.73)$$

where:

- $K = EA/\Delta x$.
- $\omega = \rho \Delta x A$.
- Δt = selected time interval at which computations are made.

Idealization of Soil Resistance. In Smith's model, the point resistance and the skin friction of the pile are assumed to be viscoelastic and perfectly plastic in nature; therefore, the separate resistances can be expressed by the following equations:

$$P_p = P_{pD} (1 + JV_p) \quad (14.74)$$

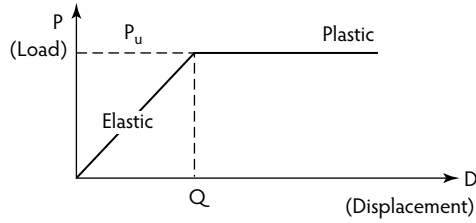


FIGURE 14.80 Assumed viscoelastic perfectly plastic behavior of soil resistance.

and

$$P_s = P_{sD} (1 + J' V_p) \quad (14.75)$$

where:

P_{pD}, P_{sD} = resistances at a displacement of D .

V_p = velocity of the pile.

J and J' = damping factors.

The assumed elastic, perfectly plastic behavior for P_{pD} and P_{sD} are illustrated in Figure 14.80. When implementing this method, the user must assume a value of total resistance (P_u), a suitable distribution of the resistance between the skin friction and point resistance (P_{pD} and P_{sD}), the quake (Q in Figure 14.80), and damping factors J and J' . Then, by using Equations 14.71 to 14.73, the pile set S can be determined. By repeating this procedure, a useful curve between P_u and S , which can eventually be used to determine the resistance at any given set S , can be obtained.

Example 14.17

For simplicity, assume that a model pile is driven into the ground using a 1000-lb hammer dropping 1 ft, as shown in Figure 14.81. Assuming the following data, predict the velocity and the displacement of the pile tip after three time steps.

$$J = 0.0 \text{ s/ft}, J' = 0.0 \text{ s/ft.}$$

$$Q = 0.1 \text{ in.}$$

$$\Delta t = 1/4000 \text{ sec.}$$

$$R_{pu} = R_{su} = 50 \text{ kips.}$$

$$k = 2 \times 10^6 \text{ lb/in.}$$

As shown in Figure 14.81, assume the pile consists of two segments ($i = 2$ and 3) and the time step to be $1/4000$ sec. Then, the following boundary conditions can be written:

$$D(1,0) = D(2,0) = D(3,0) = 0$$

$$F(1,0) = F(2,0) = F(3,0) = 0$$

$$V(1,0) = (2gh)^{1/2} = 96.6 \text{ in./sec}$$

After the First Time Step. From Equation 14.71,

$$D(1,1) = D(1,0) + V(1,0)\Delta t = 1 + 8.0498(1/4000) = 0.024 \text{ in.}$$

$$D(2,1) = D(3,1) = 0$$

From Equation 14.72,

$$F(1,1) = [(D(1,1) - D(2,1))k] = (0.024 - 0)(2)(106) = 48 \times 103 \text{ lb/in.}$$

$$F(2,1) = F(3,1) = 0$$

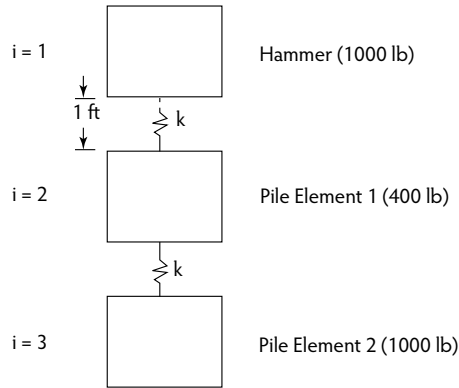


FIGURE 14.81 Application of the wave equation.

From Equation 14.73,

$$V(1,1) = V(1,0) + (1/4000)(388.8)(0 - 48,000)/1000 = 91.93 \text{ in./sec}$$

$$V(2,1) = 0 + (1/4000)(388.8)[48,000 - 0 - R(1,1)]/400 = 11.664 \text{ in./sec}$$

$$V(3,1) = 0.0$$

After the Second Time Step. By repeating the above procedure, one obtains the following results:

$$D(1,2) = D(1,1) + V(1,1)\Delta t = 0.024 + 91.93(1/4000) = 0.047 \text{ in.}$$

$$D(2,2) = D(2,1) + V(2,1)\Delta t = 0 + 11.664(1/4000) = 0.0029 \text{ in.}$$

$$D(3,2) = 0$$

$$F(1,2) = [D(1,2) - D(2,2)](2)(10^6) = 88,200 \text{ lb/in.}$$

$$F(2,2) = [D(2,2) - D(3,2)](2)(10^6) = 5900 \text{ lb/in.}$$

$$F(3,2) = [D(3,2) - D(4,2)](2)(10^6) = 0$$

$$V(1,2) = V(1,1) + 9.72(10^{-5})[F(0,2) - F(1,2)] = 91.93 + 9.72(10^{-5})(0 - 88,200) = 83.35 \text{ in./sec}$$

$$V(2,2) = V(2,1) + 24.3(10^{-5})(88,200 - 5900 - 1450) = 31.3 \text{ in./sec}$$

$$V(3,2) = 0 + 9.72(10^{-5})(5900 - 0 - 0) = 0.56 \text{ in./sec}$$

After the Third Time Step. By repeating the above steps, one obtains the following results:

$$D(1,3) = D(1,2) + V(1,2)\Delta t = 0.047 + 83.35(1/4000) = 0.0678 \text{ in.}$$

$$D(2,3) = D(2,2) + V(2,2)\Delta t = 0.0029 + 31.3(1/4000) = 0.0078 \text{ in.}$$

$$D(3,3) = 0 + 0.56(1/4000) = 0.00014 \text{ in.}$$

$$F(1,3) = [D(1,3) - D(2,3)](2)(10^6) = 120,000 \text{ lb/in.}$$

$$F(2,3) = [D(2,3) - D(3,3)](2)(10^6) = 15,320 \text{ lb/in.}$$

$$F(3,3) = [D(3,3) - D(4,3)](2)(10^6) = 280 \text{ lb/in.}$$

$$V(1,3) = V(1,2) + 9.72(10^{-5})[F(0,3) - F(1,3) - R(1,3)] = 71.69 \text{ in./sec}$$

$$V(2,3) = V(2,2) + 24.3(10^{-5})(210,000 - 15,320 - 3900) = 55.79 \text{ in./sec}$$

$$V(3,3) = 0.56 + 9.72(10^{-5})(15,320 - 70 - 70) = 2.04 \text{ in./sec}$$

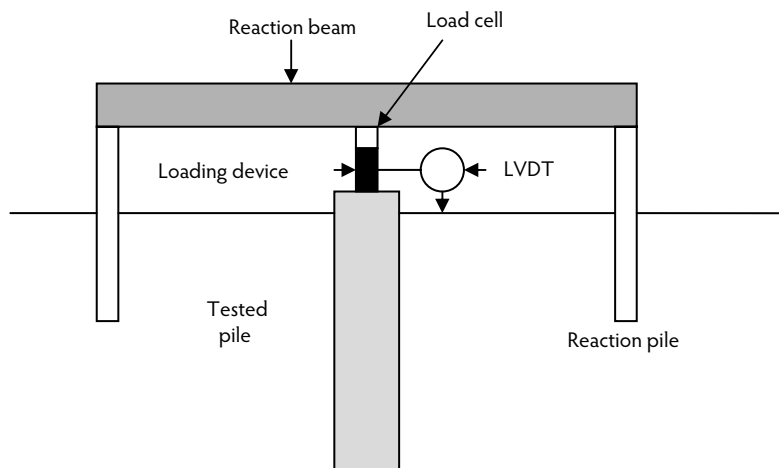


FIGURE 14.82 Schematic of pile load test set-up.

This computational procedure must be repeated on the computer until the bottom pile segment does not move during a given time step and the velocities of all of the pile segments become zero.

14.6.6.3 Pile Load Tests

The most reliable method of verifying the capacity of a driven or a bored pile is a full-scale load test. In a load test, a prototype pile is driven at the construction site and gradually loaded while the load and the corresponding deflections up to failure are monitored. Because this is an expensive test, it is usually justified on a few test piles when a pile group is to be installed under similar soil conditions.

The static pile load test is the most common method for testing the capacity of a pile, and it is also considered to be the best measure of foundation suitability to resist anticipated design loads. Procedures for conducting axial compressive load tests on piles are presented in ASTM D 1143 (Standard Test Method for Piles Under Axial Compressive Load). The most common tests are the *maintained load test* and the *quick load test*; a third test, the *constant rate of penetration test*, is generally performed only on friction piles. These tests involve the application of a load capable of displacing the foundation and determining its capacity from its response. Various approaches have been devised to obtain this information. When comparing these approaches, they can be sorted from simplest to most complex in the following order: static load test, rapid load test, and dynamic load test. These categories can be delineated by comparing the duration of the loading event with respect to the axial natural period of the foundation ($2L/C$), where L represents the foundation length and C represents the strain wave velocity. Tests with a duration between $10L/C$ and $1000L/C$ are denoted as rapid load tests. Although there are various set-ups for this test, the basic principle is the same, in that a pile is loaded beyond the desired strength of the pile (Figure 14.82). There must be an anchored reaction system of some sort that allows a hydraulic jack to apply a load to the pile to be tested. Ideally, a test pile should be loaded to failure, so the actual *in situ* load is known. The load is added to the pile incrementally over a long period of time (a few hours), and the deflection is measured using a laser sighting system. The pile can be instrumented with load cells at varied depths along the pile to evaluate the pile performance at a specific location. Instrumentation of the pile load cells, strain gauges, etc. can provide a great deal of information. All of the data, including time, are collected by a data acquisition unit for processing with software.

If a load test is performed on a pile immediately after installation, irrespective of the surrounding soil type, such a test would underestimate the long-term ultimate carrying capacity of the pile; therefore, a sufficient time period should be allowed before a load test is performed on a pile. Moreover, the additional capacity due to the long-term strength gain allows the designer to use a factor of safety on the lower side of the normal range used. Establishing a trend in the strength gain of driven piles with time will boost

the confidence of the designer to consider such an increase in the capacity during design and specifying the wait period required from the time the pile is installed before performing a pile load test. Although the above procedures are generally applicable for pile tension tests, additional loading procedures are found in ASTM Standard D 3689 (Standard Method of Testing Individual Piles Under Static Axial Tensile Load) for the pile tension test.

Two methods of pile load test interpretation are discussed in this *Handbook*: (1) Davisson's offset limit method, and (2) De Beer's method. In Davisson's method, the failure load is identified as corresponding to the movement that exceeds the elastic compression of the pile, when considered as a free column, by a value of 0.15 in. plus a factor depending in the diameter of the pile. This critical movement can be expressed as follows:

For piles of 600 mm or less in diameter or width,

$$S_f = S + (3.81 + 0.008D) \quad (14.76)$$

where:

S_f = movement of pile head (in mm).

S = elastic deformation of total pile length (in mm).

D = pile diameter or width (in mm).

For pile greater than 600 mm or less in diameter or width,

$$S_f = S + (0.033D) \quad (14.77)$$

In De Beer's method, the load and the movement are plotted on a double logarithmic scale, where the values can be shown to fall on two distinct straight lines. The intersection of the lines corresponds to the failure load.

The elastic displacement of a pile can be expressed as:

$$\delta = \frac{1}{EA_p} \int_0^L P(z) dz \quad (14.78)$$

It is apparent that determination of elastic settlement can be cumbersome even if one has knowledge of the elastic properties of the subsurface soil. This is because the actual axial load distribution mechanism or the load transfer mechanism is difficult to determine. Generally, one can instrument the pile with a number of strain gauges to observe the variation of the axial load along the pile length and hence determine the load transfer. If the reading on the i th strain gauge is ϵ_i , then the axial load at the strain gauge location can be expressed as:

$$P_i = EA\epsilon_i \quad (14.79)$$

where:

E = elastic modulus of the pile material.

A_p = cross-sectional area of the pile.

Hence, the elastic displacement of the pile can be approximated by:

$$s = \sum \epsilon_i (\Delta L) \quad (14.80)$$

where ΔL is the interval at which the strain gauges are installed.

Example 14.18

A static compression load test was performed on a 450-mm-square prestressed concrete pile embedded 20 m below the ground surface in a sand deposit (Figure 14.83). The test pile was equipped with two telltales extending to 0.3 m from the pile tip. A summary of data from the load test is provided in Table

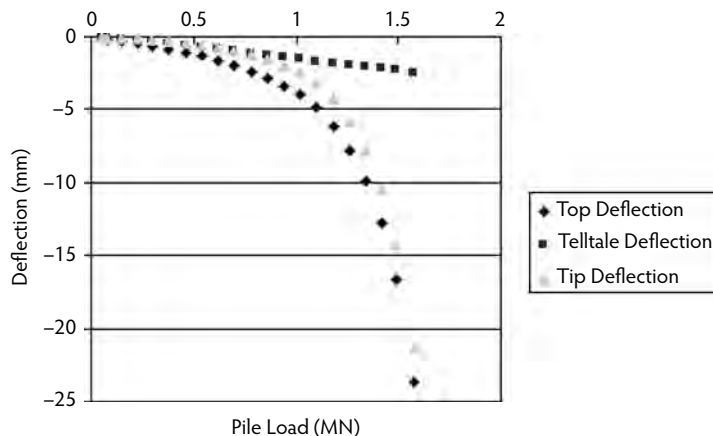


FIGURE 14.83 Pile load test results (Example 14.18).

TABLE 14.16 Load Test Data for Example 14.18

Time (h:m)	Load (MN)	Top Δ (mm)	Telltale Δ (mm)	Tip Δ (mm)
12:55	0.0	0.0	0.0	0.0
13:00	0.05798	0.1016	0.0508	0.0508
13:05	0.082064	0.2032	0.1016	0.1016
13:10	0.146288	0.3048	0.2032	0.1016
13:15	0.22746	0.4572	0.3048	0.1524
13:19	0.299712	0.635	0.4064	0.2286
13:24	0.379992	0.8636	0.5334	0.3302
13:29	0.45938	1.0668	0.6604	0.4064
13:33	0.543228	1.3462	0.762	0.5842
13:38	0.619048	1.651	0.9144	0.7366
13:43	0.698436	2.0066	1.016	0.9906
13:48	0.781392	2.413	1.1684	1.2446
13:53	0.86524	2.8448	1.3208	1.524
13:57	0.940168	3.4036	1.4478	1.9558
14:02	1.015988	4.0132	1.5748	2.4384
14:07	1.09716	4.8768	1.7272	3.1496
14:11	1.184576	6.1214	1.8796	4.2418
14:16	1.263964	7.8232	1.9558	5.8674
14:21	1.340676	9.906	2.0828	7.8232
14:26	1.416496	12.7254	2.2352	10.4902
14:31	1.491424	16.6116	2.3622	14.2494
14:36	1.575272	23.7236	2.4892	21.2344

14.16. Determine the failure load and the corresponding side friction and end-bearing. Based on Davisson's method (Figure 14.84), the failure load can be determined as 1.3 MN. Based on De Beer's method (Figure 14.85), the failure load can be determined as 1.1 MN.

Another frequently used, nondestructive experimental method for estimating the capacity of a pile is the pile-driving analyzer (PDA) method. In this method, an accelerometer and a strain gauge are attached to the top of the driven pile to monitor the particle velocity and longitudinal stress during shock wave propagation following a hammer blow. By analyzing these records using the wave equation method (Section 14.6.6.2), one can closely predict the resistance mobilized during a given stage of driving. Details of this method can be found in Rausche et al. (1972).

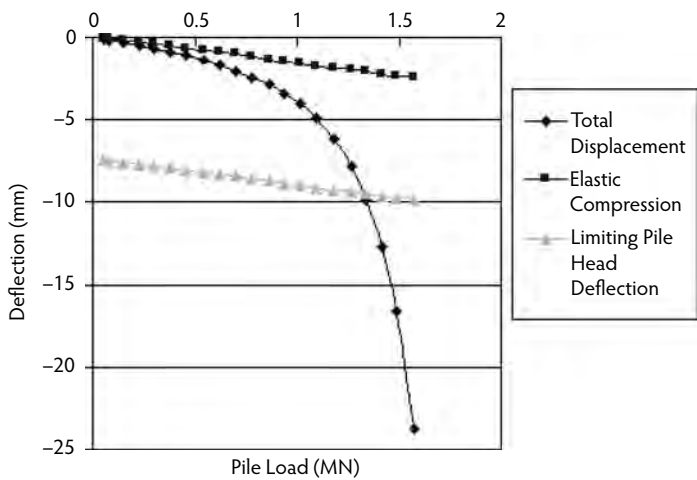


FIGURE 14.84 Determination of pile capacity, Davisson's method.

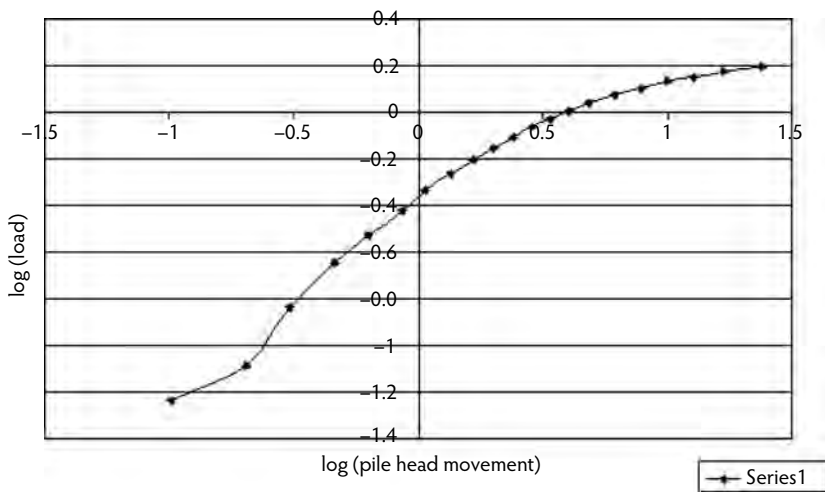


FIGURE 14.85 Determination of pile capacity, De Beer's method.

14.7 Caissons and Drilled Piers

Both caissons and drilled piers are very large-diameter concrete bored piles that can be used in lieu of pile groups to transmit structural loads to bedrock. The term *caisson* is reserved for drilled piers involving a waterway. Construction of caissons and drilled piers is more easily accomplished than driving a group of piles in stiff soils such as dense sands and stiff clays. An added advantage is that installation of drilled piers and caissons precludes disturbance to nearby structures and ground movement. On the other hand, construction of caissons and drilled piers may involve ground loss and consequent settlements that require careful monitoring and supervision.

14.7.1 Estimation of Bearing Capacity

In rare situations when drilled piers are founded on stiff sand or clay, the bearing capacity of the pier can be estimated based on the procedure outlined in Section 14.6.3; however, the bearing capacity factors for drilled piers should be somewhat lower than those for driven piles due to the fact that it is more difficult for bored piles to mobilize the ultimate shear strength. This is especially the case for drilled piers

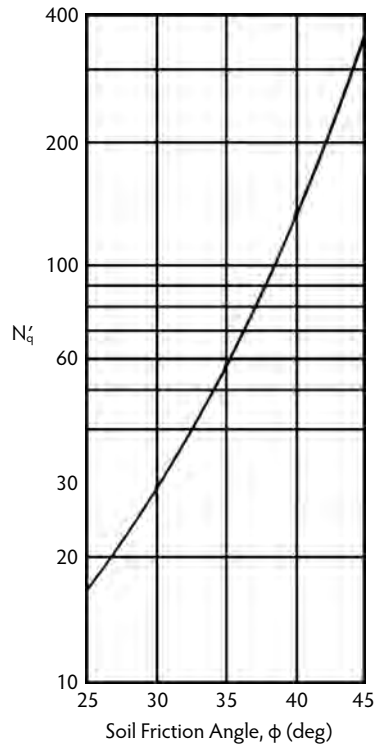


FIGURE 14.86 Vesic's bearing capacity factor N'_q for deep foundations. (From Das, B.M., *Principles of Foundation Engineering*, PWS Publishing, Boston, MA, 1995. With permission.)

founded on sand where Equation 14.55 is applicable. Das (1995) suggested using Vesic's N'_q values, given in Figure 14.86, for computing the bearing capacity using Equation 14.55. In most cases however, drilled piers and caissons are embedded in sound bedrock, so the load bearing capacity criteria have to be adjusted accordingly. The following stepwise procedure can be utilized for drilled pier design in rock.

14.7.1.1 Selection of Diameter

The pier diameter can be estimated using the compressive strength (f'_c) of concrete as:

$$\beta f'_c = \frac{P_o}{\pi \frac{D^2}{4}} \quad (14.81)$$

where:

- β = strength reduction factor (code recommended value is 0.25).
- P_o = allowable (working) load.
- D = pier diameter.

14.7.1.2 Maximum Embedment Length

The maximum length of embedment (L_{\max}) can be estimated by assuming that the overlying soil exerts negligible friction and the pile tip carries zero load. Thus,

$$L_{\max} = \frac{P_o}{\pi D \tau_{\text{all}}} \quad (14.82)$$

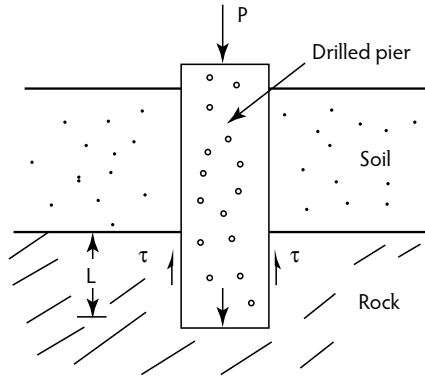


FIGURE 14.87 Drilled pier/rock interface.

where:

L_{\max} = maximum required length of embedment.

τ_{all} = allowable shear stress between pile and rock.

The allowable shear stress on the concrete–rock interface can be expressed as (Goodman, 1980):

$$\tau_{\text{all}} = \frac{q_u}{20F} \quad (14.83)$$

where:

q_u = minimum of the unconfined compression strengths of rock and concrete.

F = safety factor.

Check for Rock-Bearing Capacity. The normal stress at a depth of z in a concrete pier embedded in rock (Figure 14.87) can be obtained from the following expression (Das, 1995):

$$\sigma_z = \frac{P_w}{(\pi/4)D^2} \exp \left[-\frac{2\mu_c \tan \delta}{1 - \mu_c + (1 + \mu_r) \frac{E_c}{E_r}} \frac{2z}{D} \right] \quad (14.84)$$

where:

δ = angle of friction between rock and concrete.

μ_c and μ_r = Poisson's ratios of concrete and rock.

E_c/E_r = moduli ratio of concrete to rock.

For z , one can assume any design embedment depth L ($< L_{\max}$) and compare the normal stress at the tip of the pier with the maximum allowable bearing capacity of rock.

Check for Adequate Shear. One can estimate the average shear stress induced in the pier–rock interface by assuming a uniform shear stress distribution (τ). Then it can be seen that:

$$\tau = \left(P_w - \sigma_z (\pi/4) D^2 \right) \frac{1}{\pi D L} \quad (14.85)$$

Finally, τ can be compared with τ_{all} in Equation 14.83.

Example 14.19

Design a suitable drilled pier to carry a load of 1000 tons with the following data:

Moduli ratio of concrete–rock = 1.5.

Friction angle at concrete–rock interface = 35° .

Allowable compressive strength of rock = 0.65 kips/in.².

Allowable compressive strength of concrete = 3 kips/in.².

Unconfined compression strength of rock = 4.3 kips/in.².

Determine the Pier Diameter. From Equation 14.81,

$$\pi D^2/4 = 1000(2000)/(0.25)/(3 \times 1000)$$

$$D = 4.85 \text{ ft}$$

Determine Maximum Pier Length. From Equation 14.83,

$$\tau_{\text{all}} = 4.3/20/3 = 0.072 \text{ kips/in.}^2 \text{ (assuming } F = 3.0)$$

Then, from Equation 14.82,

$$L_{\text{max}} = 2000(2000)/[\pi(4.85 \times 12)(.072 \times 1000)] = 12.66 \text{ ft}$$

Check for Bearing on Rock. Assume an embedment depth of 7 ft and Poisson's ratios of rock and concrete to be 0.3 and 0.15, respectively. Then, by applying Equation 14.84,

$$\sigma_z = 44.78 \text{ tons/ft}^2 = 0.62 \text{ kips/in.}^2 < 0.35 \text{ kips/in.}^2$$

The bearing is adequate.

Check for Shear. Shear force on the shaft = $1000 - 44.78(\pi)(D)^2/4 = 173$ tons. Average shear stress = $173/(\pi)(D)(7) = 1.622 \text{ tons/ft}^2 = 0.0225 \text{ kips/in.}^2 < 0.072 \text{ kips/in.}^2$. Thus, design a pier of 4.85 ft in diameter embedded to 7.0 ft.

References

-
- Bishop, A.W. and Blight, G.E. 1963. Some aspects of effective stress in saturated and partly saturated soils. *Geotechnique*, 13(3), 177–197.
- Bowles, J.E. 1986. *Engineering Properties of Soils and Their Measurements*. McGraw-Hill, New York.
- Bowles, J.E. 1995. *Foundation Analysis and Design*. McGraw-Hill, New York.
- Das, B.M. 1995. *Principles of Foundation Engineering*. PWS Publishing, Boston, MA.
- Goodman, R.E. 1980. *Introduction to Rock Mechanics*. John Wiley & Sons, New York.
- Gunaratne, M., 2006. *Foundation Engineering Handbook*, Taylor & Francis, Boca Raton, FL.
- Harr, M. 1962. *Groundwater and Seepage*. McGraw-Hill, New York.
- Holtz R.D. and Kovacs W.D. 1981. *An Introduction to Geotechnical Engineering*. Prentice Hall, Englewood Cliffs, NJ.
- Koerner, R. 1994. *Designing with Geosynthetics*. Prentice Hall, Englewood Cliffs, NJ.
- Meyerhoff, C.G. 1976. Bearing capacity settlement of pile foundations. *J. Geotech. Eng. Div. ASCE*, 102(GT3), 197–228.
- Mullins, A.G. 1996. Field Characterization of Dynamic Replacement of Florida Organic Soils, Ph.D. dissertation. University of South Florida, Tampa.
- Pickett, G. and Ray, G.K. 1951. Influence charts for concrete pavements. *Am. Soc. Civ. Eng. Trans.*, 116(2425), 49–73.
- Poulos H.G. and Davis, E.H. 1990. *Pile Foundation Analysis and Design*. Krieger, Melbourne, FL.

- Rausche, F., Moses, F., and Goble, G.G. 1972. Soil resistance predictions from pile dynamics. *J. Soil Mech. Found. Div. Am. Soc. Civ. Eng.*, 98(SM9), 917–937.
- Schmertmann J.H. and Hartman, J.P. 1978. Improved strain influence factor diagrams. *J. Geotech. Eng. Div. Am. Soc. Civ. Eng.*, 104(GT8), 1131–1135.
- Scott, R.F. 1981. *Foundation Analysis*. Prentice Hall, Englewood Cliffs, NJ.
- Smith, E.A.L. 1960. Pile-driving analysis by the wave equation. *J. Soil Mech. Found. Div. Am. Soc. Civ. Eng.*, 86(EM4), 35–51.
- Stinnette, P. 1992. Engineering Properties of Florida Organic Soils, Master's project. University of South Florida, Tampa.
- Stinnette, P. 1996. Geotechnical Data Management and Analysis System for Organic Soils, Ph.D. dissertation. University of South Florida, Tampa.
- Terzaghi, K., Peck, R.B., and Mesri, G. 1996. *Soil Mechanics in Engineering Practice*, 3rd ed. Wiley Interscience, New York, 549 pp.
- Thilakasiri, H.S. 1996. Numerical Simulation of Dynamic Replacement of Florida Organic Soils, Ph.D. dissertation. University of South Florida.
- Wray, W. 1986. *Measurement of Engineering Properties of Soil*, Prentice Hall, Englewood Cliffs, NJ.



Sydney Opera House, Sydney, Australia. (Photograph courtesy of the Australian Information Service.)

15

Specialized Construction Applications

Husam S. Najm, Ph.D., P.E.*

15.1	Introduction	15-2
15.2	Preplaced-Aggregate Concrete.....	15-2
	General • Applications • Materials and Proportioning • Preplacing Aggregate • Contaminated Water • Preparation of Underwater Foundation • Pumping • Joint Construction • Grouting Procedure • Finishing Unformed Surfaces	
15.3	Underwater Concrete.....	15-6
	General • Structures Conducive to Underwater Placement • Available Methods • Bucket Placement • Tremie • Basic Tremie Methods • Mixtures for Underwater Placements • Use of Antiwashout Admixtures • Characteristics of Antiwashout Underwater Concrete • Characteristics of the Hardened Concrete • Characteristics of the Horizontal Flow Time of Nondispersible Underwater Concrete • Principal Considerations • Summary	
15.4	Vacuum Processing	15-13
	General • Concrete Mixtures • Early Equipment • New Equipment • Procedure • Conclusions	
15.5	Portland Cement Plaster Construction	15-16
	General • Most Frequently Found Problems • Technical Aspects of Portland Cement Plaster • Portland Cement Plaster Materials • Proportioning • Mixing • Bases for Plaster • Weather Barrier Backing • Sample Panels • Surface Preparation • Application of Plaster • Types of Application	
15.6	Self-Consolidating Concrete (SCC).....	15-19
	Introduction • Mix Design • Testing Methods and Specifications • Applications	
15.7	Mass Concrete	15-22
	Introduction • Methods of Controlling Temperatures	
15.8	Roller-Compacted Concrete	15-23
	Introduction • Mix Design, Placement, and Curing • Testing Methods for RCC	
	Acknowledgment	15-26
	References	15-26

* Associate Professor, Department of Civil and Environmental Engineering, Rutgers, The State University of New Jersey, Piscataway, New Jersey; expert in the design of steel and concrete structures and concrete material research.

15.1 Introduction

Specialized construction applications are considered to be those that contain materials that are not routinely used in conventional structural or mass concrete (ACI 116R, 1990), those that are not proportioned using procedures given in the American Concrete Institute Standard Practice 211.1 (ACI 211.1, 1991), or those that are placed with equipment or by methods that require additional attention from the contractor to ensure the required quality is achieved. The techniques of mixing, batching, transporting, consolidating, protecting, and placing concrete have drastically changed during the past few decades. The reasons for these drastic changes include the following:

- Owners demanded that cost escalation of new construction must be kept under control.
- These demands required the development of accelerated construction techniques and new materials.
- Governmental agencies initiated regulations that required better protection of the environment.
- Construction had to be accomplished with fewer workers; consequently, new techniques being developed had to use innovative equipment and materials.

Some of the more successful specialized construction techniques, primarily relating to the use of hydraulic-cement concrete, that are covered in this chapter include:

- Preplaced-aggregate concrete
- Underwater concreting
- Conveying concrete by pumping
- Vacuum processing
- Cement mortar and plastering
- Self-consolidating concrete (SCC)
- Mass concrete
- Roller-compacted concrete (RCC)

Research has resulted in many new types of equipment, materials, admixtures, and improvements in older types, thereby permitting concrete construction to be accomplished more quickly and, consequently, more economically, with better control and superior quality. The use of admixtures, both mineral and chemical, has greatly expanded the utilization of concrete in new construction techniques, has extended the life of freshly mixed concrete for as long as the user desires, and has allowed concrete to be dropped through water without segregating or separating. Admixtures have allowed concrete to be used in corrosive environments without corrosion of the reinforcing steel and to be used in freezing and thawing environments without the previously experienced rapid deterioration. They have also allowed concrete to attain much greater compressive strength with higher moduli of elasticity for use in high-rise concrete structures. These vastly improved capabilities have been accomplished to keep hydraulic-cement concrete competitive as a primary construction material. This competitiveness has to be maintained for concrete to remain the most cost-effective construction material in the world. Without the progress of concrete technology, the industry will flounder and more exotic construction materials will be developed as alternatives.

15.2 Preplaced-Aggregate Concrete

15.2.1 General

Preplaced-aggregate concrete (PA) (ACI 116R, 1990) is concrete produced by placing coarse aggregate in a form and later injecting a hydraulic cement, sand, and fly-ash grout, usually with chemical admixtures, to fill the voids. Smaller-size coarse aggregate (less than 1/2 in.) is not used in the mixture to facilitate grout injection (ASTM C 926, 2006). Much of the information presented on preplaced-aggregate concrete has been taken from the U.S. Army Corps of Engineers' *Standard Practice for Concrete for Civil Works Structures* (U.S. Army Corps of Engineers, 1994).

One of the primary advantages claimed for PA concrete is that it can easily be placed in locations where conventional concrete would be extremely difficult to place. The primary use of PA concrete is in the repair of existing concrete structures. PA concrete may be particularly suitable for underwater construction, for placements in areas with closely spaced reinforcing steel and cavities where overhead contact is necessary, and in areas where low-volume change of the hardened concrete is desired. PA differs from conventional concrete in that it contains a higher percentage of coarse aggregate, as the coarse aggregate is placed directly into the forms, with coarse aggregate having point-to-point contact rather than being contained in a flowable plastic mixture.

Hardened PA concrete properties are greatly dependent on the properties of the coarse aggregate. Drying shrinkage of PA concrete may be less than 50% that of conventional concrete, which partially accounts for the excellent bond between PA concrete and existing roughened concrete. The compressive strength of PA concrete is dependent on the quality, proportioning, and handling of materials but is generally comparable to that achieved with conventional concrete. The frost resistance of PA concrete is also comparable to conventional air-entrained concrete, assuming that the grout mixture has air content, as determined by ASTM C 231 (2004), of approximately 9%.

Preplaced-aggregate concrete may be particularly applicable to underwater repair of old structures and new underwater construction where dewatering may be difficult, expensive, or impractical. Bridge piers and abutments are typical of applications for underwater PA concrete construction or repair. ACI 304R (1989) provides an excellent discussion of PA concrete.

15.2.2 Applications

Preplaced-aggregate concrete has been used successfully on various types of projects, including those in the following construction categories:

- Underwater construction of and/or repair of bridge piers
- Resurfacing of lock chambers and guide walls
- Massive fills in permanent sheet-piling piers and cofferdams
- Construction of atomic-reactor shields
- Resurfacing of dam spillways

Preplaced-aggregate concrete is not used frequently, perhaps due to concern on the part of the construction industry that the technology exceeds the industry's normal capabilities; however, successful PA projects can be accomplished by any construction entity that has a knowledgeable concrete technologist on staff.

15.2.3 Materials and Proportioning

Intrusion grout mixtures should be proportioned in accordance with ASTM C 938 (2002) to obtain the specified consistency, air content, and compressive strength. The grout mixture should also be proportioned such that the maximum water/cement ratio complies with the same ratio that conventional concrete would be required to have for the same environmental exposure and placing requirements. Compressive-strength specimens should be made in accordance with ASTM C 943 (2002). Compressive-strength testing of the grout alone should not be used to estimate the PA concrete strength because it does not reveal the weakening effect of bleeding; however, such testing may provide useful information on the potential suitability of grout mixtures.

The ratio of cementitious materials to fine aggregate will usually range from about 1 for structural preplaced-aggregate concrete to 0.67 for massive concrete sections. A grout fluidifier meeting the requirements of ASTM C 937 (2002) is commonly used in the intrusion grout mixtures to offset bleeding, to reduce the water/cement ratio while still providing a given consistency, and to retard stiffening so handling times can be extended. Grout fluidifiers typically contain a water-reducing additive or admixture, a suspending agent, aluminum powder, and a chemical buffer to ensure timed reaction of the aluminum powder with the alkalis in the hydraulic cement.

Products proposed for use as fluidifiers that have no prior record of successful use in PA concrete can normally be accepted based on successful field use. ASTM C 937 (2002) requires that intrusion grout, made as prescribed for acceptance testing of fluidifiers, have an expansion within certain specified limits that may be dependent on the alkali content of the cement used in the test. Experience has shown, however, that because of differences in mixing time and other factors, expansion of the field-mixed grout ordinarily will range from 3 to 5%. If, under field conditions, expansion of less than 2% or more than 6% occurs, adjustments to the fluidifier should be made to bring the expansion to within these limits. The fluidifier should be tested under field conditions with job materials and equipment as soon as practicable so sufficient time is available to make adjustments to the fluidifier, if necessary. If the aggregates are potentially reactive, the total alkali content of the hydraulic cement plus fluidifier added to increase expansion should not exceed 0.60%, calculated as equivalent sodium oxide by mass of cement. The grout submitted for use may exhibit excess bleeding if the ratio of its cementitious material to fine aggregates is different from that of the grout mixture used to evaluate the fluidifier. Expansion of the grout should exceed bleeding, as desired, at the expected in-place temperature. Grouts should be placed in an environment where the temperature will rise above 40°F, as expansion caused by the fluidifier ceases at temperatures below 40°F.

This condition is normally readily obtainable when preplaced-aggregate concrete is placed in massive sections or placements are enclosed by timber forms. When an air-entraining admixture is used in the PA concrete, adjustments in the grout mixture proportions may be necessary to compensate for the significant strength reduction caused by the combined effects of entrained air and the hydrogen generated by the aluminum powder in the fluidifier; however, these adjustments must not reduce the air content of the mixture to a level that compromises its frost resistance. The largest practical nominal maximum size aggregate (NMSA) should be used to increase the economy of the PA concrete. A 1.5-in. NMSA will typically be used in most PA concrete, although provisions are made for the use of 3-in. NMSA when it is considered appropriate. It is not expected that many situations will arise where the use of aggregate larger than 2 in. will be practical and economical. Pozzolan is usually specified to increase flowability of the grout.

15.2.4 Preplacing Aggregate

Because excessive breakage and objectionable segregation are to be avoided, it is necessary to preplace the coarse aggregate in the placement with extreme care. The difficulties are magnified as the nominal maximum size of the aggregate increases, particularly when two or more sizes are blended; therefore, proposed methods of placing aggregate should be carefully established to ensure that satisfactory results will be attained. Coarse aggregate must be prewashed, screened, and saturated immediately prior to placement to remove dust and dirt and to eliminate coatings and undersized particles. Washing aggregate in forms should never be permitted because fines may accumulate at the bottom.

15.2.5 Contaminated Water

Contaminated water is a matter of concern when PA concrete is placed underwater. Contaminants present in the water may coat the aggregate and adversely affect setting of the cement or bonding of the mortar to the coarse aggregate. If contaminants in the water are suspected, the water should be tested before construction begins. If contaminants are present in such quantity or of such character that the harmful effects cannot be eliminated or controlled, or if the construction schedule imposes a long delay between aggregate placement and grout injection, then PA concrete should not be used.

15.2.6 Preparation of Underwater Foundation

The cleanup of foundations in underwater construction when the foundation material is glacial till or similar material is always difficult. The difficulty develops when, as a result of prior operations, an appreciable quantity of loose, fine material is left on the foundation or in heavy suspension just above

the foundation. The fine material is displaced upward into the aggregate as it is being placed. The dispersed fine material coats the aggregate or settles and becomes concentrated in void spaces in the aggregate just above the foundation, thus precluding proper intrusion and bond. Care must therefore be exercised to ensure that as much loose, fine material is removed as possible before placement of the aggregate.

15.2.7 Pumping

Pumping of grout should be as continuous as practical; however, minor stoppages are permissible and ordinarily will not present any difficulties when proper precautions are taken to avoid plugging of grout lines. The rate of grout rise within the aggregate should be controlled to eliminate cascading of grout and to avoid form pressures greater than those for which the forms were designed. For a particular application, the grout injection rate will depend on form configuration, aggregate grading, and grout fluidity.

15.2.8 Joint Construction

A cold joint is formed in PA concrete when pumping is stopped for longer than the time it takes for the grout to harden. When delays in grouting occur, the insert pipes should be pulled to just above the grout surface before the grout stiffens and then rodded clear. When pumping is ready to resume, the pipes should be worked back to near contact with the hardened grout surface, and then pumping should be resumed slowly for a few minutes. Construction joints are formed similarly by stopping grout rise approximately 12 in. below the aggregate surface. Care must be taken to prevent dirt and debris from collecting on the aggregate surface or filtering down to the grout surface.

15.2.9 Grouting Procedure

The two patterns for grout injection are the horizontal layer and the advancing slope. Regardless of the system used, grouting should start from the lowest point in the form.

- *Horizontal layer.* In this method, grout is injected through an insert pipe that raises the grout until it flows from the next insert hole, 3 to 4 ft above the point of injection. Grout is then injected into the next horizontally adjacent hole, 4 or 5 ft away, and the procedure is repeated sequentially around the member until a layer of coarse aggregate is grouted. Successive layers of aggregate are grouted until all aggregate in the form has been grouted.
- *Advancing slope.* The horizontal-layer method is not practical for construction of slabs having large horizontal dimensions. In such situations, it becomes necessary to use an advancing-slope method of injecting grout. In this method, intrusion is begun at one end of the form and pumping is continued until the grout emerges on the top of the aggregate for the full width of the form and assumes a slope that is advanced and maintained by pumping grout through successive rows of intrusion pipes until the entire mass is grouted. In advancing the slope, the pumping pattern is begun first in the row of holes nearest the toe of the slope and continued row by row up the slope (opposite to the direction of advance of slope) to the final row of pipes. This process is repeated, moving ahead one row of pipes at a time as the intrusion is completed.
- *Grout insert pipes and sounding devices.* The number, location, and arrangement of grout insert pipes will depend on the size and shape of the work being constructed. For most work, grout insert pipes will consist of pipes arranged vertically and at various inclinations to suit the configurations of the work. Grout pipes are generally either 3/4, 1, or 1-1/2 in. Normally, either a 3/4- or 1-in. diameter would be necessary for structural concrete having a maximum size aggregate of 1-1/2 in. or less. If the preplaced aggregate has a maximum size larger than 1-1/2 in., then the grout insert pipes should have a diameter of 1-1/2 in.

Intrusion points should be spaced about 6 ft apart; however, spacing wider than 6 ft may be permissible under some circumstances, and spacing closer than 6 ft will be necessary in some situations. Normally, one sounding device should be provided for every four intrusion points, but fewer sounding devices

may be permissible under some circumstances. There should always be enough sounding devices, and these should be so arranged that the level of the grout at all locations can be accurately determined at all times during construction. Accurate knowledge of the grout level is essential to accomplish the following tasks:

- Check the rate of intrusion.
- Avoid getting the grout too close to the level of the top of the aggregate when placement of the aggregate and intrusion are progressing simultaneously.
- Avoid damage to the work that would occur if a plugged intrusion line was washed out while the end of the line was within the grout zone.

Sounding devices usually consist of wells (slotted pipes) through which the level of the grout maybe readily and accurately determined. If sounding devices other than wells are considered, conclusive demonstrations should be performed to verify that such devices will readily and accurately indicate the level of the grout at all times.

15.2.10 Finishing Unformed Surfaces

If a screeded or troweled finish is required, the grout should be brought up to flood the aggregate surface, and any diluted grout should be removed. A thin layer of pea gravel or 3/8- to 1/2-in. crushed stone should then be worked into the surface by raking and tamping. After the surface has stiffened sufficiently, it may be finished as required. A finished surface may also be obtained on PA concrete by adding a bonded layer of conventional concrete of the prescribed thickness to the surface. The surface should be adequately prepared prior to applying the topping.

15.3 Underwater Concrete

15.3.1 General

(See ASTM C 150, 2007; ASTM C 231, 2004; ASTM C 943-02, 2002.) Until recently, underwater concreting was defined as tremie concrete only, but now, due to research in the use of admixtures, new procedures have been developed so freshly mixed concrete can now be placed by dropping it through water without the use of a tremie. Although this system is discussed here, it is recommended that, unless absolutely necessary, the concrete should be deposited through a tremie or possibly a pump line.

Placement of concrete underwater requires conveying freshly mixed concrete from the surface of a liquid environment to a location underneath that surface in such a way that the concrete is not damaged by segregation or separation. During administration of the U.S. Army Corps of Engineers' Repair, Evaluation, Maintenance and Rehabilitation (REMR) research program (Scanlon et al., 1983), it was discovered that the cost of dewatering an underwater area to be repaired increased the cost of the repair by 100% when compared to making the same repair in dry conditions.

Generally, many organizations avoid placing concrete underwater, as the probability of major problems occurring is excessive. Also, many owners desire to actually see the concrete that has been placed so they have a better understanding of the appearance and quality. Underwater concreting normally cannot be observed due to the water. Underwater concreting can be a very successful operation, but it is absolutely necessary for the contractor to pay close attention to details.

At times it is physically or economically impracticable to expose a foundation prior to concrete placement. At such times, suitable underwater placing procedures such as pumping or use of tremies or special concrete buckets should be employed. Research has provided techniques for placing freshly mixed concrete through water without the use of a pump line, tremie, or bucket, and innovative antiwashout chemical admixtures have been developed that permit freshly mixed concrete to be dropped through water without segregation or separation (see Figure 15.1). Although these are proprietary admixtures, practically all of the chemical admixture companies provide versions to the industry.



FIGURE 15.1 Clearness of underwater concreting.

15.3.2 Structures Conducive to Underwater Placement

Underwater concreting is appropriate for all types of structures: massive sections, walls, slabs, foundations, piers, caissons, stilling basins, cofferdams, conduits, and many others. It is obvious that underwater concreting is most advantageous for relatively large structures such as bridge piers, cofferdams, thick walls, and large foundations. In this chapter, we discuss the use of tremies, buckets, pumps, aqua valves, and, of course, antiwashout admixtures.

15.3.3 Available Methods

Use of the tremie is currently the most often utilized technique for placing concrete under water. A tremie is defined by the American Concrete Institute in ACI 116R (1990) as a pipe or tube through which concrete is deposited under water, having at its upper end a hopper for filling and a bail for moving the assemblage, as shown in Figure 15.2. Underwater bucket placing consists of lowering a special bucket



FIGURE 15.2 Tremie concreting operation.

containing freshly mixed concrete to the bottom of the foundation and opening the bucket slowly to permit the concrete to flow out gently without causing turbulence or mixing with the water. One of the most troublesome problems associated with using a tremie is controlling the head pressure on concrete in the tremie pipe so the pipe does not empty itself too quickly and allow water to enter the pipe from the bottom. Fortunately, a concrete pump can be used to overcome this problem. A concrete pump permits the pump line to remain full at all times, and the end of the pump line can remain very deep in the fresh concrete, preventing the intrusion of water into the pump line. We will now discuss underwater placement techniques in greater detail.

15.3.4 Bucket Placement

The buckets used for underwater placement of freshly mixed concrete should have drop-bottom or roller-gate openings. The gates should be able to be opened from above water. If air is used to open the bucket, the air should discharge through a line to the surface to prevent water disturbance. The top of the bucket must be covered to prevent water from washing the surface of the freshly mixed concrete. One way is to cover the top with canvas or plastic sheets; the covering should be as watertight as possible. Special buckets designed for the underwater placement of concrete have sloping tops that minimize the water surge. The first bucket of concrete should be slowly lowered to the bottom of the foundation and allowed to rest on the bottom. The gates should be opened slowly to permit the concrete to flow out gently, without causing turbulence or mixing with the water. Additional buckets should land on the previously placed concrete and slightly penetrate the surface so opening the gates and releasing the fresh concrete will result in even less turbulence. The operation is continued until all of the concrete has been placed. An example of concrete placed underwater with buckets is the foundation for the San Francisco–Oakland Bay Bridge, which has a 240-ft-deep foundation.

15.3.5 Tremie

The tremie process is the underwater placing technique used most frequently by contractors. Figure 15.2 depicts a conveyor being used to feed concrete to the tremie hopper for distribution down the tremie pipe in a massive placement. The tremie consists of a vertical pipe through which concrete is placed. The concrete flows from the bottom of the tremie pipe. After the original placement, the end of the tremie pipe is kept submerged in the fresh concrete at all times. The first concrete placed is the concrete that will most likely end up on top of the placement in small-diameter placements. It has been observed that, in a 36-in. caisson, the first cubic yard of grout placed ends up on top of the placement and then is allowed to overflow the top of the caisson until the caisson is filled with concrete. This assures the contractor that there will be no voids in the placement, and when the tremie pipe is removed slowly a good job is almost guaranteed. The discharge end of the pipe should always remain buried in the freshly placed concrete after the initial placement. A tremie pipe should be made of heavy-gauge steel to withstand all stresses induced by the handling operation. The pipes should have a diameter large enough to ensure that aggregate bridging will not occur. Normally, pipes should be between 8 and 12 in. in diameter for concrete containing up to 2 in. NMSA. Pipe sections in increments of 10 ft should be used; for deep placements, the tremie should be fabricated in sections with joints that permit the upper sections to be removed as the placement progresses; otherwise, the hopper will become too elevated for efficient discharge from a ready-mix truck. The joints between sections of pipe must be watertight and capable of being disconnected rapidly so no major interruptions occur during placement of the concrete.

15.3.6 Basic Tremie Methods

The two basic methods of initiating concrete placement when using the tremie method underwater are the **wet-pipe** and **dry-pipe** methods. The wet-pipe method refers to initiating placement with the open-ended tremie pipe on the bottom and with the pipe filled with water. To keep the concrete being delivered from being washed out by the water in the pipe, a plug or go-devil is placed at the upper level of the

water in the pipe before the concrete is discharged into the tremie. When the concrete is discharged into the tremie, the plug or go-devil is between the water and the fresh concrete, preventing the fresh concrete from being washed out.

The weight of the concrete (approximately 140 lb/ft³) pushes the water, which weighs approximately 64 lb/ft³, down the tremie pipe. When the concrete, which has never been in contact with the water, arrives at the bottom, it pushes the plug or go-devil out of the pipe, and the concrete is deposited on the bottom of the placement. Many go-devils are designed so they are lighter than water and float to the top to be used at a later time. When the fresh concrete begins to flow from the end of the tremie, the end of the pipe should stay submerged in the concrete. Continuing to deposit fresh concrete into the tremie hopper causes the concrete to continue flowing through the pipe. The end of the tremie pipe should be kept at a depth in the freshly deposited concrete that permits the concrete to flow at a slow speed through the pipe.

If the concrete flows out of the pipe so the concrete load in the pipe is less than the water load outside the pipe, and if the pipe is not adequately embedded in the freshly placed concrete, then water may refill the pipe. This will not happen if the end of the tremie pipe is adequately embedded in the freshly placed concrete. If the crane operator holding the tremie and hopper feels that the fresh concrete is being completely discharged onto the bottom, the operator should immediately drop the pipe so it will be more deeply embedded. This may prevent the water from getting into the empty pipe. If water does not get into the empty pipe, concrete placement can continue, but if water does get into the pipe it will be necessary to restart the placement by reinserting the plug or go-devil as during initiation of the placement. An ideal tremie placement is one where the initial concrete placed is the concrete that ends up on top. This will only occur when the placement area is relatively small (say, 4 ft²). The dry-pipe method requires a tremie pipe that is watertight, including the sectional pipe joints. In this method, a pressure-seal plate is attached to the bottom of the tremie pipe in such a way that the water pressure makes the end completely watertight and the interior of the pipe is completely empty and free of any water. Such a method requires that the walls of the pipe be heavy enough to overcome the buoyancy of the water; otherwise, it would be impossible to lower the tremie pipe to the bottom of the placement.

When the end of the tremie pipe with a pressure-seal plate is placed on the bottom, freshly mixed concrete can be introduced into the pipe. After the pipe is sufficiently filled with concrete, the pipe can be slowly raised, which releases the pressure-seal plate due to the weight of the concrete. After the initial discharge of fresh concrete on the bottom, the placement continues exactly as in the wet-pipe method. One drawback to the dry-pipe method is that the pressure-seal plate has to be left in the placement; however, it can be retrieved if a rope or cable is attached in such a way that the cable is on the outside of the tremie pipe. Another technical drawback is that, should the tremie seal be lost (water gets into the pipe), a plug or go-devil would be required to reinitiate the start of the placement.

15.3.7 Mixtures for Underwater Placements

Concrete must be proportioned for very workable concrete if it is to be placed underwater. The slump should be controlled at approximately 7 in. Normally, the hydraulic-cement content should be around seven bags per cubic yard. The maximum size aggregate should be 1-1/2 to 2 in., and the fine aggregate (fine) content should be around 45% of the total aggregate content. The concrete should be air entrained at about 6 to 7%. Any application that improves the workability of concrete should be considered. This includes pozzolans, natural aggregates in lieu of crushed stone, and use of chemical admixtures to extend the setting time and permit additional water reduction.

15.3.8 Use of Antiwashout Admixtures

(See ACI 304.1, 1995; ACI 524R, 1992; ASTM C 937, 2002; ASTM C 938, 2002; Neeley, 1988.) Many of the companies dealing with the manufacture of concrete construction materials have developed admixtures for use in concrete that permit the concrete to be placed underwater without the use of a tremie.

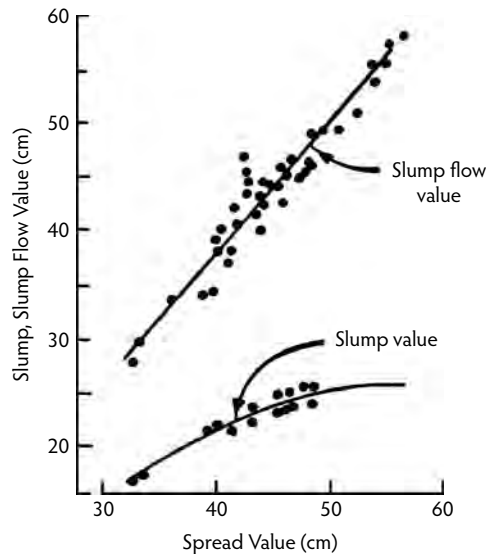


FIGURE 15.3 Relationship of slump, slump-flow value, and spread value.

These materials are referred to as *antiwashout admixtures*. Japan has been a leader in this new concrete technology, although it is believed that Japan obtained its knowledge from a product that was originally used in Germany. Figure 15.1 depicts the clearness with which concrete containing an antiwashout admixture can be discharged under water. Other terms for this type of concrete are *nondispersible concrete* and *colloidal underwater concrete*. The admixture that provides the clearness of this special concrete is known as a nondispersible underwater concrete admixture, but in the United States it is referred to as an antiwashout admixture. This innovative admixture was developed in West Germany around 1981. The admixture is intended to prevent washout of cementitious material and dispersion of aggregate during underwater placement of concrete. The admixture serves to increase the viscosity and the water retention of the concrete matrix. The antiwashout admixtures currently being marketed in Japan use cellulose or acrylic as the primary ingredient. Admixtures containing acrylic use a polyacrylamide polymer as the primary ingredient. Admixtures containing cellulose use a nonionic water-soluble cellulose ether, which has a hydroxide ion (OH) base and is almost like water. Hydroxyethylcellulose (HEC), hydroxyethylmethylcellulose (HEMC), and hydroxypropylmethylcellulose (HPMC) are among the various admixtures used. When dissolved, their viscosities differ considerably according to polymerization, molecular weight, and type of substituent. They dissolve in water rapidly when placed in a high-pH environment such as concrete. They are also not susceptible to chemical changes within concrete-like reactions, gelation, or decomposition.

15.3.9 Characteristics of Antiwashout Underwater Concrete

Antiwashout underwater concretes have slightly different properties than ordinary hydraulic cement concrete because of the effect of the admixture. Fresh antiwashout concrete can be characterized by the following properties.

15.3.9.1 Flowability

Because of the increased viscosity of antiwashout underwater concrete, the slump transformation takes place over several minutes. The slump is ultimately 8 to 10 in. To have a better understanding of the flowability of this type of concrete, a slump-flow value or a spread value determined by the German Standard DIN 1048 is more suitable than a slump value. The relationship of these values is demonstrated in Figure 15.3. Table 15.1 provides criteria for the relationship between flowability and conditions of execution.

TABLE 15.1 Criteria of Relationship Between Flowability and Conditions of Execution

Slump Flow Value (cm)	Softness	Conditions for Applications	Conditions for Execution
40	Hard consistency	When it is desired to keep the flow small, such as the execution of a slanted path	Concrete pump pressure transmission boundary
45	Medium consistency	General case	Less than 50-m concrete pump pressure transmission distance
50	Medium soft consistency	When excellent filling capability is needed	Concrete pump pressure transmission distance of 50–200 m
55	Soft consistency (plastic concrete) Supersoft consistency	When excellent flowability is especially needed, such as in reinforced concrete members of dense fiber and filler for narrow and deep supersoft consistency holes	

15.3.9.2 Air Content

Mortar and concrete mixed with cellulose ether have greatly increased air content; therefore, such antiwashout admixtures contain an air-detraining admixture to reduce the air content of the concrete to between 3 and 5%. From a petrographic standpoint, the bubble-spacing factor of concrete containing the antiwashout admixture is about the same as concrete without the admixture, but the freezing and thawing resistance tends to be somewhat low.

15.3.9.3 Bleeding

Concrete containing the antiwashout admixture retains more of the mixing water. Because the normal amount of admixture used is more than double the amount required to prevent bleeding, very little, if any, bleeding occurs in antiwashout underwater concrete. This lack of bleeding is responsible for the small reduction in quality of the concrete and increases the need for reinforcing steel.

15.3.9.4 Setting Time

The use of antiwashout cellulose admixtures affects the setting time of underwater concrete. When a cellulose antiwashout admixture is used, the setting time (ASTM C 191, 2007) is greatly extended; therefore, the antiwashout admixture contains an accelerating admixture. The most common accelerating admixture amounts are adjusted to result in a final setting time of from 5 to 12 hours. Antiwashout admixtures containing acrylic have no effect on the setting time. When an air-entraining, water-reducing admixture is added to the antiwashout admixture, the setting time is slightly extended, but the increase in setting time for the normal admixture amounts is less than 5 hours. Specialty admixtures can extend the setting time for underwater antiwashout concrete by 30 hours or more.

15.3.9.5 Underwater Dispersion Resistance

The dispersion resistance of concrete during an underwater placement operation is evaluated by such tests as the cementitious materials outflow rate, the change of water permeation rate, the turbidity of the water, the change of pH value, and the change of composition. The rate of dispersion is decreased as the quantity of antiwashout admixture in the underwater concrete is increased.

15.3.10 Characteristics of the Hardened Concrete

15.3.10.1 Compressive Strength

The relationship between the compressive strength of concrete containing no antiwashout admixture and concretes containing various amounts of cellulose antiwashout admixture is shown in Figure 15.4. Generally, the compressive strength of a test specimen fabricated in air is lowered by an increase in the

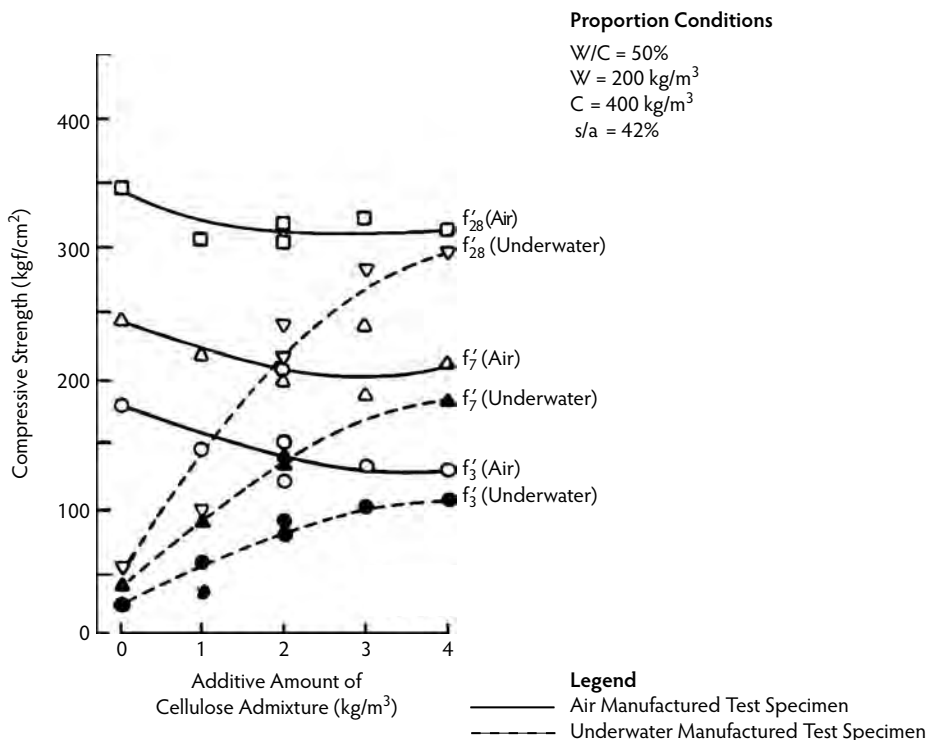


FIGURE 15.4 Relationship of quantity of cellulose admixture and concrete compressive strength.

quantity of admixture, but in some instances the compressive strength has increased slightly. Test specimens fabricated underwater are made by placing concrete into water that is 12 to 20 in. deep. The compressive strength of such specimens increases with an increase in the quantity of antiwashout admixture used; consequently, the compression strength ratio of test specimens made underwater increases compared to those made in air as the quantity of admixture increases. The amount of admixture to be used is determined by the flowability required, depth of the underwater placement, horizontal flow distance, desired water cementitious materials ratio, and, of course, the quantity of cementitious materials to be used. In general, the compressive strength ratio referenced above can be expected to range from 0.8 to 0.9.

15.3.10.2 Miscellaneous Strength and Other Characteristics

The ratio of tensile strength and flexural strength to compressive strength of an underwater fabricated test specimen is identical to that of specimens fabricated in ordinary dry concrete. The modulus of elasticity is the same or slightly less than that of ordinary concrete. The unit volume of water in antiwashout underwater concrete is much greater than that of ordinary concrete. Because water retention is so high, drying shrinkage is large at 20 to 35%. Also, creep in air appears to be somewhat greater than in ordinary concrete.

15.3.11 Characteristics of the Horizontal Flow Time of Nondispersible Underwater Concrete

Qualitative changes in antiwashout underwater concrete can be made by adding a water-reducing admixture, which causes the concrete to flow longer distances. Underwater concrete with water-reducing admixtures has been shown to have a slump flow of 50 to 60 cm, a cement content of 364 to 430 kg/m³, and a water/cement ratio of 0.48 to 0.60. The final flow gradient was 1/125 to 1/500. Even though the

TABLE 15.2 Combinations of Antiwashout and Water-Reducing Admixtures

Antiwashout Admixtures	Water-Reducing Admixtures
Cellulose	Melamine sulfonate (triazine)
Acrylic	Naphthalene sulfonate
	Melamine sulfonate (triazine)
	Acrylic
	Polycarbonic acid

concrete surface was virtually horizontal, qualitative changes were recognizable when the flow distance exceeded 10 m. The area near the edge of the concrete may suffer a drop in unit weight and modulus of elasticity as well as in compressive strength because the quantity of aggregate declines. The greatest flow distance is best determined by fully considering proportions and placement conditions.

15.3.12 Principal Considerations

Because antiwashout underwater concrete has a high viscosity, the mixer load is increased by 25 to 50%, so the capability of the mixer and the quantity of materials mixed must be considered. Use of a water-reducing admixture causes a decline in dispersion resistance and some extension of the time of setting. In some instances, a specific flowability cannot be obtained by combining the water-reducing admixture and the antiwashout admixture; therefore, the types of water-reducing admixture and their recommended dosages must be considered. Table 15.2 illustrates the various combinations of types of antiwashout admixtures and water-reducing admixtures ordinarily used. Because the dispersion resistance is high, blockage will occur in pump lines only if problems are encountered within the pressure transmission tube during the pumping pressure period. Qualitative changes in the concrete should not occur before or after the pressure is transmitted. Due to high viscosity, however, pressure transmission resistance is 2 to 4 times that of ordinary concrete. It has been reported that the pressure transmission capacity of the squeeze-type pumps is inferior to that of the piston-type pumps, an aspect that must be considered.

15.3.13 Summary

Antiwashout underwater concrete is being considered for use in many underwater structures and other large-scale projects. Under current conditions, several problems remain, such as: (1) differences in performance of the more than ten kinds of admixtures currently being marketed, (2) differences in mixing methods and placement methods used by various contractors, and (3) inappropriateness of the antiwashout concrete for use in above-water structures due to its drying shrinkage and poor resistance to freezing and thawing. It is recommended, therefore, that the engineer and contractor fully understand the quality of the antiwashout underwater concrete and the procedures involved in the placement of this relatively new and innovative material.

15.4 Vacuum Processing

15.4.1 General

The ACI report 116R (1990) defines vacuum concrete as concrete from which excess water and entrapped air are extracted by a vacuum process before hardening occurs. This process is administered by applying a vacuum to formed or unformed surfaces of ordinary concrete immediately or very soon after the concrete is placed. Additional compaction of the concrete is the primary result of vacuum processing. As the water and entrapped air are removed, the mortar is subjected to consolidation; the

concrete becomes denser because approximately 40% of the water close to the surface has been removed. Entrapped air is also removed, resulting in a concrete surface that is more resistant to freezing and thawing, especially if the concrete originally contained entrained air of at least 9% of the paste fraction. The air, being noncontinuous, is removed from the surface and not from the interior. The depth of water extracted and the amount of water removed depend on the coarseness of the mixture, mixture proportions, and the number of surfaces to which the vacuum is applied. The depth of water extraction can, under good conditions, extend to 12 in., and the amount of water extracted a few inches below the surface can be equal to one third of the mixing water. Removal of an average of 20% of the water down to a depth of 6 in. from the surface is common. The best results from vacuum processing occur when (1) the mixture contains a minimum amount of fines, (2) the vacuum can be applied promptly while the concrete is still plastic, and (3) the concrete near the vacuum panel can be vibrated during the first few minutes of the vacuum treatment. Vacuum procedures result in concrete with higher strength and greater durability. The Bureau of Reclamation (1992) found that vacuum processing increased the 3-day strength of one concrete from 800 psi to 1800 psi. Although vacuum processing improves the surface of hardened concretes, the improved appearance is normally not adequate justification for use of the process. Vacuum processing improves durability, but this should not be used as justification not to use air entrainment. Vacuum treatment has been used to increase the resistance of concrete surfaces to high-velocity liquid flow, but its use should not justify reduced efforts to perfect alignment of flow lines.

15.4.2 Concrete Mixtures

It is not absolutely necessary that special concrete mixtures be used when vacuum processing of the concrete surface is planned. This is not to say that slight changes in the normal mixtures should not be considered. The best results are obtained when the fines are at a minimum; in other words, vacuum processing seems to work best when the mixture is relatively lean and contains a minimum amount of fine aggregate (sand) that is on the coarse side of the grading. Sticky mixtures with an excess of fines do not respond well to vacuum treatment. The treatment is also more effective at low ambient temperatures. One of the primary goals of concrete construction is to place concrete in a uniform fashion so the finished results will be uniform. The vacuum should be applied soon after placing the concrete while the concrete is still plastic. The concrete should be highly workable, and during the first few minutes of the vacuuming process the concrete should be slightly vibrated, permitting the small channels left by the water removal to close, thus improving the watertightness.

15.4.3 Early Equipment

During early use of the vacuum process, the vacuum was applied to the concrete surface by vacuum hoses attached to special vacuum mats or form panels. The mats for unformed surfaces were usually reinforced plywood faced with two layers of screen wire covered by muslin. For unformed curved surfaces, such as the buckets of dams, flexible steel that could adapt to the curved surface was used in lieu of plywood. Sometimes, a fiberglass cloth without screen backing was used for the lining of steel forms for concrete pipe. The equipment was very cumbersome and required much preparation time. In addition, it was expensive and complicated. As a result, use of the equipment was not very inviting, and very little use was made of the process.

15.4.4 New Equipment

Vacuum equipment has since been simplified, and its use, especially in Europe, has greatly increased. The vacuum process is now being used more frequently in the United States. The panels have been replaced by vacuum pads that are flexible, light, and easy to handle (see Figure 15.5). This newer system greatly improves the handling, and the system is much more efficient and cost effective.



FIGURE 15.5 Distribution of vacuum pads on newly placed concrete slab.



FIGURE 15.6 Vacuum pump used in vacuum processing.

15.4.5 Procedure

After the concrete slab is vibrated, the surface is immediately covered with a base filter pad and a suction mat connected to a vacuum pump. The pump (see Figure 15.6) creates a vacuum under the pad. The vacuum causes the atmospheric pressure to compress the concrete, and the water is extracted. The base pad is designed to distribute the vacuum under the entire surface evenly and permit water to pass through. The vacuum is applied for approximately 4 minutes for each inch of slab thickness. After the pads and mats are removed, the surface is normally firm enough to walk on, and finishing is then performed with specially designed, low-amplitude, high-frequency disk floats. Following finishing, the slabs are preferably cured with water, but practically any method that prevents the concrete from additional drying can be used. Because internal water has been removed from the concrete, it is best to ensure that adequate water is available for hydration of the cement; consequently, water curing is best.

15.4.6 Conclusions

For attaining a highly impervious concrete floor, vacuum processing is a viable method, but, just as for all processing methods, options such as using low water/cement ratios and adequately air-entrained concrete and incorporating proper curing and protection techniques must be considered during construction. Do not depend 100% on vacuum processing to provide the high-quality, low-permeability, smooth floor that is desired; quality concrete materials must be used, and proven mixing, transporting, placing, finishing, curing, and protection procedures also have to be followed.

15.5 Portland Cement Plaster Construction

15.5.1 General

Portland cement plaster construction, commonly referred to as *stucco*, has been around for many years, but it has normally been considered an art rather than a science. The knowledge necessary to apply Portland cement plaster was previously acquired by learning from others and not from technical literature. ACI Report 524R, *Guide to Portland Cement Plastering*, was developed in 1992. Before then, little information was available to engineers who wished to include this subject in project specifications; consequently, the U.S. Army Corps of Engineers initiated worldwide studies to identify the problems associated with defective concretes and Portland cement plaster construction.

15.5.2 Most Frequently Found Problems

During visits to the various sites around the world, numerous installations were inspected where the design and the workmanship for stucco were excellent. The recurring problems that were found can be separated into three categories:

- Questionable design
- Incomplete specifications or specifications lacking in detail
- Inadequate inspection and poor workmanship

The following general procedures must be fully considered when contemplating a Portland cement plaster construction project:

- Quality plaster is essential to any successful installation. The plaster must develop adequate tensile strength to resist imposed stress and have sufficient resiliency to accommodate expansion and contraction. Consistency in the batching operation is as important to the development of quality plaster as the ingredients and quantities.
- The most important ingredient is the aggregate. Aggregate should conform to specifications. The physical properties of aggregate that have the most pronounced effect on plaster are grading, shape and denseness of the particles, and particle surface characteristics (roughness and porosity).
- Curing procedures play a vital role in reducing shrinkage cracking by permitting the plaster to dry slowly and uniformly. Fog curing requires the application of a fine mist at intervals related to job conditions. The purpose of curing is to maintain enough water within the plaster to keep the interior relative humidity above 80% during the specified curing period.
- It is acceptable to place a second coat of plaster as soon as the first coat is strong enough to withstand the pressure of the second application. When plaster is applied to a solid backing such as block, concrete, or wire lath backed with rigid sheathing, both base coats can be applied in one day and the finish coat on the following day. Or, successive coats can be applied on consecutive days.

15.5.3 Technical Aspects of Portland Cement Plaster

The desirable properties of fresh Portland cement plaster can be summarized by the following properties:

- *The ability to stick to the particular substrate*—The primary concerns in this area relate to the influence of the aggregate, the water/cement ratio, and the absorptive characteristics of the substrate or base.
- *The ability of the fresh plaster to stick to itself*—The plaster should not sag, slough, or separate (delaminate).
- *The ability to be placed, shaped, floated, and tooled*—The plaster should already have the first two properties; plaster without these abilities is generally incorrectly proportioned or possibly incorrectly mixed.

Hardened Portland cement plaster should have excellent durability against weathering, should be highly impermeable, and should be resistant to temperature changes. Such plaster should also be highly resistant to the action of freezing and thawing. Plaster should be air entrained for better freeze–thaw resistance and better impermeability, which provides protection from acid rain and aggressive chemicals. Hardened Portland cement plaster should also be proportioned for high tensile strength. Properly proportioned plasters that have been properly cured should have acceptable tensile strength.

15.5.4 Portland Cement Plaster Materials

The cement used in Portland cement plaster may be practically any type or class of cementitious materials conforming to the various ASTM Standards, such as:

- Portland cement (ASTM C 150, 2007)
- Blended cements (ASTM C 595, 2007)
- Masonry cement (ASTM C 91, 2007)
- Plastic cement (ASTM C 926, 2006)

Should the aggregates be potentially reactive, low-alkali cements should be used, and air-entraining cements should be used, when possible. Lime conforming to the requirements of Type S, ASTM C 206 (2003) or ASTM C 207 (2006) should be used along with an air-entraining admixture when possible. Lime is necessary only when regular cement is used.

The aggregates should be either natural or manufactured fine aggregate (sand) complying with the requirements of ASTM C 897 (2005). Lightweight aggregates such as perlite or vermiculite may be used but should not be used in base courses when conventional-weight aggregate plaster is to be applied as a finish coat. Perlite or vermiculite aggregates have low resistance to freezing and thawing. Sand should be washed clean; should be free of organic matter, clay, and loam; and should be well graded.

The water used should be as good as water used in hydraulic-cement concrete. Drinking water is normally all right to use. The water should comply with the requirements of ASTM C 191 (2007) for setting time and ASTM C 109 (2007) for strength. Calcium chloride should not be used in Portland cement plaster because of the embedded metals. Should chemical admixtures be considered for use, be sure they do not contain chlorides and they are not corrosive. Accelerating admixtures that do not contain chlorides or other corrosive materials are available and could be used.

15.5.5 Proportioning

As stated earlier, Portland cement plastering (stucco) is thought of as an art and not a science. The industry does not seem to want to join the 21st century, as materials are still proportioned by shovel. Measurement of sand is accomplished by counting the number of shovels of sand per bag of cement and seven No. 2 shovels are equated to one cubic foot of sand. The quantity of water is determined by the

appearance of the plaster in the mixer. Some project specifications require the use of a cone for measuring the slump; the cone is 6 in. high by 4 in. in diameter at the bottom and 2 in. in diameter at the top. Many specifications permit a slump of 1-1/2 to 3 in. for either hand- or gun-applied plaster. Plasticizers are also normally required, and again the quantity is determined by the appearance. When plastic or masonry cements are used, the addition of plasticizers is not necessary. When Portland or blended cements are used, it may be necessary to add plasticizer to up to 20% by weight of the cementitious material. Avoid sloppy and overwatered mixtures, as they tend to cause segregation and separation of materials. Proportioning Portland cement plaster drastically affects the final quality and serviceability of the hardened plaster. Proportions of the ingredients should be in accordance with project specifications, local building codes, and ASTM C 926 (2006).

15.5.6 Mixing

Experience dictates that a particular sequence for mixing should be followed: The water should be added first, followed by 50% of the sand, the cement and any admixtures, and finally the remaining 50% of the sand. Normal mixing time is approximately 3 to 10 minutes. Excessive mixing should be avoided because it could be detrimental to the quality of the plaster.

15.5.7 Bases for Plaster

Metal plaster bases come in three types. One type is woven-wire plaster base, which is fabricated galvanized steel wire that is reverse twisted into a hexagonal mesh pattern and normally comes in rolls or sheets. Expanded-metal diamond mesh lath is fabricated from coils of steel that are slit and then expanded to form a diamond pattern (chicken wire). The third type is welded-wire lath, which is fabricated from at least 15-gauge copper-bearing, cold-drawn galvanized steel wire.

15.5.8 Weather Barrier Backing

Several materials are being used as weather barrier backing, including waterproof paper or felt meeting the requirements of Federal Specifications UU-B-790, Type II, Class D. The paper should be free of holes and breaks and should weigh at least 14 lb per 108-ft² roll. A large number of accessories are required to obtain a proper plaster job. Accessories establish plaster grounds and transfer stresses in critical areas of plaster elements. Portland cement plaster should not be considered to be part of the load-bearing members; the plastering project should be designed so the plaster is not placed under stress. To construct a successful plaster project, all locations—corners and joints (expansion and contraction)—must contain the correct accessories to prevent the plaster from experiencing the normal stress that would occur at these locations. Special accessories are made for corners; they may be expanded flange corner beads, welded or woven wire, vinyl bead, or expanded-metal corner lath. The corner reinforcement must be designed so plaster can be applied without hollow areas. Inside corner joints must have accessories designed to provide stress relief at internal angles. Casing beads, often called *plaster stops*, should be installed wherever plaster terminates or joins a dissimilar material. Plaster screeds are used to establish the thickness of the plaster or to create decorative motifs. Ventilating screeds contain perforated webs that permit air to pass freely from the outside. Additional screeds include drip screeds that are installed on outside plaster ceilings to prevent the water that runs down the face of the structure from penetrating the plaster soffits and the ceiling. Weep screeds are normally installed at the foundation plate line and function as a plaster stop, permitting trapped moisture to escape from the space between the backing paper and the plaster.

15.5.9 Sample Panels

Sample panels or mock-ups should always be constructed, especially on large jobs where all the plastering will not be performed by one crew of plasterers. These panels or mock-ups should include examples of all joints, windows, doors, corners, and, in general, all conditions to which the plaster will be exposed.

Sample panels should be constructed until the results describe the desired quality and appearance expected of the structure. The panels should be kept close to the project so workers and supervisors can verify that the previously approved results are being obtained.

15.5.10 Surface Preparation

Concrete surfaces to which plaster will be applied should be straight, true to line, and plane. Concrete surfaces should be cleaned or roughened to increase the likelihood of a good chemical and mechanical bond. The concrete surface should be cleaned with a cleaning agent to remove most surface contaminants. Other methods of cleaning might include the use of wire brushes, hammers or chisels, water blasting, or light sandblasting.

15.5.11 Application of Plaster

Prior to beginning to apply plaster, the substrate must be prepared as described above. It is also necessary to verify that the lath and backup paper have been installed along with the necessary accessories. After the required substrate treatment has been verified, proper application procedures must be followed. The project specifications will normally require or allow the plaster to be applied by hand or by machine. When hand application is permitted, the plasterer applies the plaster to the surface using a trowel. The plasterer determines the amount of water required to obtain the desired consistency of the plaster. Plaster pumps are sometimes required for plaster application. In this case, batches of plaster are prepared in a mixer, and the individual performing the mixing operation is responsible for batching the correct quantities of cement, sand, and water. The quantity of water is determined by the mixer operator. The plaster is placed in a hopper and pumped onto the surface through a hose and nozzle. The nozzle operator controls the spray pattern by adjusting the air jet, air pressure, and nozzle orifice.

15.5.12 Types of Application

Portland cement plaster is normally applied in either two or three coats. The three coats are referred to as the *scratch coat*, *brown coat*, and *finish coat*. The scratch coat should be thick enough to result in a good bond to the substrate; on substrates containing metal laths, this coat should fully cover the lath. The scratch coat should be scored horizontally so mechanical bonding is improved. When the specification requires a delay between application of the scratch coat and the brown coat, it is necessary to cure the scratch coat by moist curing. If no delay is required, then the brown coat should be applied as soon as possible to secure a good bond. The brown coat should be applied when the scratch coat is rigid enough to receive the brown coat without cracking. The brown coat normally contains more sand than the scratch coat. The required thicknesses are established either in the local specifications or by construction codes. In some cases, the brown coat is the finish coat. Where a finish coat is specifically required, it is normally proportioned to provide a particular texture, color, or appearance. Prior to applying the finish coat, the brown coat must be moist cured for at least 2 days. Finish coats can be applied and finished in numerous aesthetically pleasing patterns. Smooth troweled surfaces are not recommended because of their tendency to crack. Finish coats must not be burnished; burnishing will almost always induce cracking. Moist curing is an absolute necessity.

15.6 Self-Consolidating Concrete (SCC)

15.6.1 Introduction

Self-compacting concrete (SCC) or self-consolidating concrete, as it is referred to by ASTM Subcommittee C09.47, can be defined as concrete that does not require compaction or vibration. Because of its high viscosity, SCC can flow freely without segregation. SCC is able to flow under its own self-weight into corners of formwork and through closely spaced reinforcement with little or no vibration or compaction.

This leads to lower energy cost, lower stress on the formwork, reduced labor costs, and elimination of potential human error in the consolidation of the concrete. The concrete becomes more consistent, as the cementitious paste and aggregates are equally dispersed. As a result, both SCC mechanical properties and durability are improved over normal or conventional concrete, and it has enjoyed increased popularity in Europe and Japan (Okamura, 1997); however, the use of SCC in the United State remains limited. Part of the reason is because of the limited knowledge and experience regarding its use, as well as its high initial cost. Nevertheless, the Federal Highway Administration (FHWA) is leading an effort to promote the use of SCC in transportation structures in the United States, and SCC has been used by several state departments of transportation, such as those in New York, New Jersey, and Virginia.

The proper use of SCC requires: (1) good understanding and knowledge of the new generation of superplasticizers and chemical admixtures, (2) control of the constituent materials and water content of the concrete, (3) familiarity with and understanding of the acceptance of fresh and hardened concrete, (4) documentation of properties and durability, (5) use and implementation of proper casting methods, (6) control of pressure on the formwork, and (7) contingency plans for repair of defects and for interrupted casting (Suksawang et al., 2005).

15.6.2 Mix Design

Fresh concrete can easily attain high flowability by simply increasing the water-to-binder (w/b) ratio; however, increasing the w/b ratio alone could lead to concrete segregation and less durability. Thus, to successfully develop SCC, mineral and chemical admixtures, such as pozzolans, limestone filler, superplasticizer, and viscosity-modifying admixtures (VMAs), must be added to the mix design to prevent segregation and enhance the durability of SCC. In addition, the absolute volume of coarse aggregates also must be limited to reduce interparticle friction and allow the SCC to flow under its self-weight without segregation (Okamura, 1997). Also, a reduction in the volume of coarse aggregate would have to be balanced by an increase in the volume of cement paste, which would result in higher material costs and an increase in the capillary pores. One solution to decreasing the paste volume is to use a VMA that reduces interparticle friction and increases flowability, so the volume of coarse aggregates could be increased. Despite this solution, concrete producers and owners still have questions regarding the use of VMAs because little information on its long-term effects and the effects of various chemical admixtures on SCC is available. An alternative solution is to use pozzolans, such as fly ash or dust powder, to replace the cement content (Persson, 2001; Zhu and Bartos, 2003). The pozzolanic materials not only reduce the cement content but also fill the capillary pores, thus making the concrete denser and increasing its durability. Moreover, some pozzolans, such as fly ash and slag, can also increase the flowability of concrete, which reduces the amount of superplasticizers required and lowers production costs. However, any decrease in the volume of coarse aggregate and any increase in the volume of cementitious paste will greatly affect the mechanical properties of SCC. Also, most of these mix designs are based on Japanese and European experiences. SCC mix designs using raw materials in the United State are limited. The cementitious materials typically consist of ordinary Portland cement (OPC), silica fume (SF), fly ash, and slag. Fine and coarse aggregates consist of river sand and crushed aggregates. The size and type of coarse aggregates influence concrete consolidation and distribution. In addition, several admixtures such as high-range, water-reducing agents and air-entraining agents (AEAs) are also used in SCC mix designs. Viscosity-modifying admixtures can also be used to increase flowability without segregation, which allows the volume of coarse aggregates to be increased.

15.6.3 Testing Methods and Specifications

For SCC to become a standard concrete mixture, acceptance tests on fresh and hardened SCC to evaluate its physical and mechanical properties must be established to ensure a level of comfort for the contractors, designers, and owners (Persson, 2001). As mentioned earlier, SCC does not require compaction; therefore, the rheological characteristics of SCC are very important, as its consolidation depends on its rheological performance. In ordinary concrete, adequate slump in conjunction with good consolidation practice will

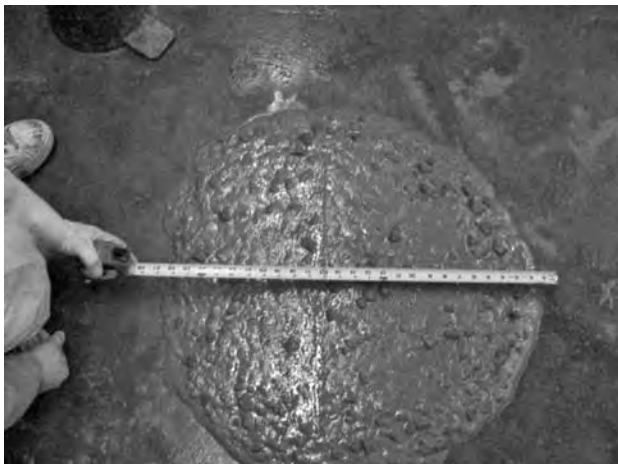


FIGURE 15.7 Self-consolidating concrete (SCC) spread test.



FIGURE 15.8 J-ring test for SCC.

yield a dense concrete structure with few air voids. The external forces due to vibration compensate for the variations in plastic concrete, so the rheology of concrete can be ignored; hence, only the slump test is performed for testing fresh ordinary concrete. In SCC, however, the rheological characteristic cannot be ignored, because the concrete must meet certain rheological requirements. The plastic concrete is generally described as a Bingham fluid, where the concrete behavior is characterized by its shear yield stress and plastic viscosity. For SCC, the shear yield stress has to be lower than ordinary concrete for the concrete to self-compact (Khayat, 1999). The rheology of concrete could be measured using a concrete rheometer, which measures the shear yield stress and viscosity of concrete. The problem with doing so is that the device is very expensive, and the test is impractical to perform at a job site, so other practical fresh concrete testing methods similar to the slump test of ordinary concrete have been developed. These tests include: (1) the spread test, (2) the L-shaped or U-shaped box, (3) the V-funnel (4) the J-ring, and (5) sieve stability. Figure 15.7, Figure 15.8, and Figure 15.9 illustrate the various tests for fresh SCC (Suksawang et al., 2005, 2006). It must be noted, however, that these tests do not measure the rheology of concrete but instead are used to simulate actual environment and field conditions. Furthermore, not

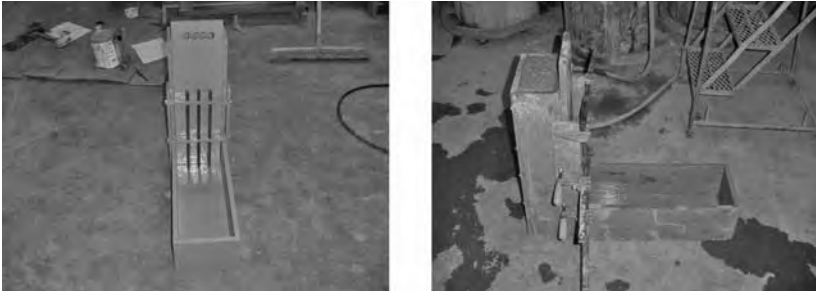


FIGURE 15.9 L-box test for SCC.



FIGURE 15.10 SCC in drilled shafts.

enough data are available to correlate these tests with the rheology of concrete, especially for mix designs that use raw materials available in the United States. Hardened SCC is subjected to the same tests used for normal concrete, such as compressive strength, elastic modulus, shrinkage, freeze–thaw, rapid chloride permeability, and scaling, among others.

15.6.4 Applications

Because of its ability to flow easily in highly congested areas, SCC is now being considered for structural members with high volumes of steel reinforcement. In addition, SCC is become more attractive because it offers accelerated construction schedules, reduced noise levels, and smooth surface finishes. The first SCC application in Japan was in buildings in 1990. Since then, it has been used in bridge towers, bridge girders, bridge decks, box culverts, anchorages, and immersed tunnels. Lightweight SCC was also used in bridge girders (Okamura and Ouchi, 2003). In the United States, SCC has been used in nonstructural elements such as noise walls and parapets. The New York State Department of Transportation is already using SCC in bridge decks, and the New Jersey Department of Transportation is using SCC in drilled shafts. Figure 15.10 shows SCC pours in drilled shafts. Durability issues in SCC and its mechanical properties compared to those of normal concrete are being evaluated by many researchers; however, these studies are still limited and do not address all of the durability issues for highway structures. In addition, current prediction equations for the mechanical properties of normal or conventional concrete still must be validated for their applicability and accuracy in predicting properties of SCC mixes.

15.7 Mass Concrete

15.7.1 Introduction

Mass concrete is defined in ACI Committee 116 (1990) as “any concrete with dimensions large enough to require that measures be taken to cope with generation of heat from hydration of the cement and attendant volume change to minimize cracking.” Mass concrete according to the Portland Cement Association (PCA,

1987) can be any placement of normal concrete that has minimum dimension equal to or greater than 3 ft. Many structural elements require the use of large amounts of concrete, such as abutments, shear walls, tanks, mat foundations, large-diameter drilled shafts, footings, transfer girders, and dams. The biggest concerns with mass concrete are the maximum temperatures generated and the maximum temperature differentials. Several factors influence temperature changes, including the size of the component, the amount of reinforcement, the ambient temperature, the initial temperature of the concrete at time of placement, and the curing program. To minimize the effects of high thermal loads in mass concrete, engineers use various methods to apply mass concrete. These methods include refining concrete mix proportions, protecting exposed surfaces and formwork from extreme environmental factors, using aggregates with desirable thermal properties, precooling the concrete constituent materials prior to mixing, using internal pipes to cool the concrete itself after placement, and placing the concrete in several lifts or pours.

15.7.2 Methods of Controlling Temperatures

Some mix designs for mass concrete include supplementary cementitious materials in the mix, including slag cement or fly ash. The Slag Cement Association offers some guidance on specifying slag cement for mass concrete. The American Coal Ash Association also offers information on the benefits and specification of fly ash. Many state departments of transportation specify 35°F (19°C) as the maximum differential temperature between the core and the surface and 135°F (57°C) as the maximum concrete temperature (Gajda and Alsamsam, 2006). This is difficult to achieve unless other measures are used to control the heat of hydration. Many argue that this limit is arbitrary and should not be put in the specifications; rather, the maximum differential temperature should be calculated using ACI guidelines given in ACI 207.2R (Anon., 2001). Using less cement content and adding fly ash or ground granulated blast-furnace slag to replace some of the cement or using aggregates with low coefficient of thermal expansion can help reduce the rise in temperature and the temperature differential in mass concrete. In addition to controlling the mix design, other temperature control methods include precooling the concrete mix using shading and sprinkling of the aggregates, using cold water in the mix, and post-cooling of concrete using cooling pipes (Gajda and Alsamsam, 2006). Placing concrete in several lifts has also been used, but precautions should be taken to avoid cold joints. Slag and fly ash should be used with caution, but slag and fly ash can be useful for small mass concrete pours with temperature control.

Modeled temperatures in a 10-ft slab with 600 lb/yd³ of cementitious materials made up of 65% Type II cement and 35% fly ash Type F are shown in Figure 15.11. The figure shows the variations in temperature vs. time for different locations in the slab as well as variations in the differential temperatures in the concrete with time (Gajda and Alsamsam, 2006). Figure 15.12 shows the temperature change with time for the massive footing shown in Figure 15.13. For this massive concrete pour, an optimal mix design was used along with cooling pipes to cool the concrete after the pour (Gajda, 2003).

15.8 Roller-Compacted Concrete

15.8.1 Introduction

Roller-compacted concrete (RCC) is a type of concrete that exhibits zero slump and requires no vibration or forms; paving machines and compaction rollers compact the concrete after placement. Newer generations of paving machines, however, can achieve compaction of RCC during placement without the need for any additional compaction (see http://www.cement.org/pavements/pv_rcc_pcc.asp). Applications of this type of concrete include pavements, dams, and industrial sites with large areas, such as maintenance yards, military fields, container and truck distribution areas, and precast yards. RCC is an attractive material because of its easy preparation and placement, speed of construction, reduced labor requirements, and high strength. With its low water/cement ratio and high density, RCC has high strength and good durability; however, it requires special equipment for placement and lacks a smooth surface finish. The material was developed in the mid-1970s by Canadian builders for the logging industry. Today, RCC is a competitive material that is widely used in many projects all over the world.

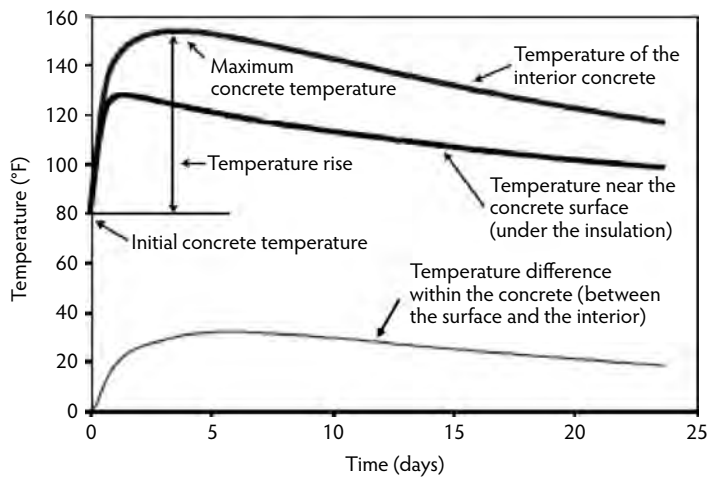


FIGURE 5.11 Modeled temperatures for 10-ft slab with 600 lb of cement materials per cubic yard (65% Type II OPC and 35% fly ash). (From Gajda, J. and Alsamsam, E., *Engineering Mass Concrete Structures*, Seminar Development Series, Portland Cement Association, Skokie, IL, 2006.)

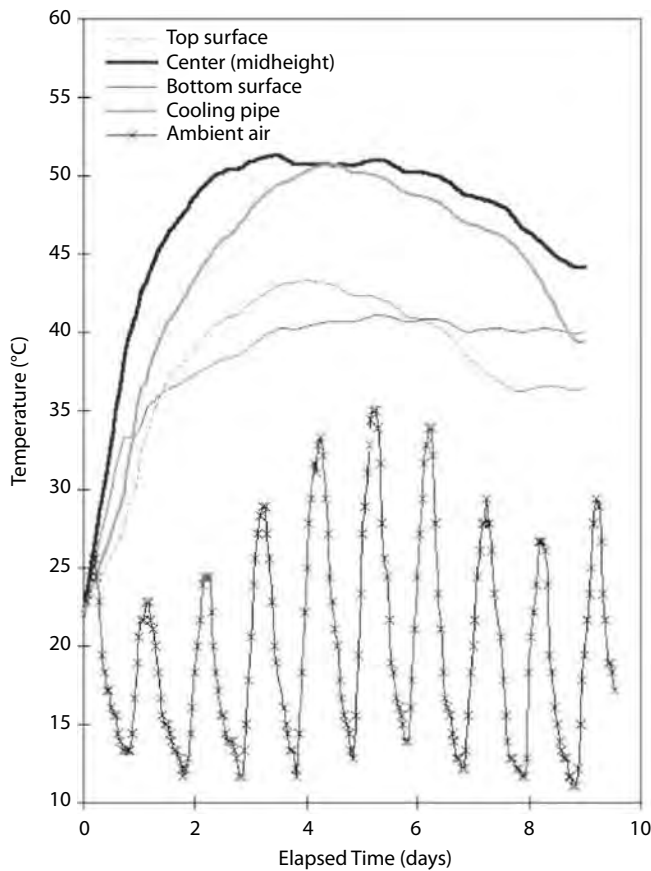


FIGURE 15.12 Measurement of concrete temperature in footing. (From Gajda, J., *Concrete Technol. Today*, 24(3), 34–37, 2003.)



FIGURE 15.13 Overview of footing and pier prior to footing placement. (From Gajda, J., *Concrete Technol. Today*, 24(3), 34–37, 2003.)

15.8.2 Mix Design, Placement, and Curing

Mix design for RCC uses a low water-to-binder ratio, making it a dry mix with zero slump. The aggregates are a blend of various sizes chosen to achieve a well-graded aggregate mix. Typical maximum coarse aggregate size is 3/4 in. Aggregate sizes larger than 3/4 in. could result in segregation and less density. Gravel aggregates or crushed stone are typically used for coarse aggregates, and natural sand or river sand is used for fine aggregates (PCA, 2000). RCC is placed in various thicknesses and various widths. Thicknesses can be as thin as 5 in. and as thick as 12 in. for slabs; the width depends on the paving machine used. Placement can also be achieved by spreading the RCC mix and then applying compaction; however, care must be taken to ensure that the spread is continuous and the compaction process is uniform. Precaution should be taken when placing RCC in hot weather—when the temperature increases, the mix tends to lose more moisture. Contractors should maintain the required moisture of the mix by either increasing the moisture content in the mix or delaying the moisture loss by using admixtures or cooling methods. Like regular concrete, RCC should be cured. Improper curing could lead to severe dryness and incomplete hydration of cement, resulting in weaker RCC and cracking. Curing is typically applied for 7 days after placement. Plastic sheets and wet burlap can be used similar to regular concrete (PCA, 2000).

15.8.3 Testing Methods for RCC

The moisture content and densities of RCC are important properties that must be verified for acceptance. ASTM Subcommittee C09.45 is in charge of developing standard test procedures for measuring RCC properties. ASTM Subcommittee C09.45 developed ASTM Standard C 1170 (2006), a test method for determining the consistency of concrete using a vibrating table and a surcharge and determining the density of the consolidated concrete specimen. They also developed ASTM Standard C 1040 (2005), a standard test method for in-place density of unhardened and hardened concrete, including roller-compacted concrete, by nuclear methods using gamma radiation.

Acknowledgment

This chapter is adapted from the original text by the late John M. Scanlon, Senior Consultant, Wiss, Janney, Elstner Associates and formerly Chief, Concrete Technology Division, U.S. Army Water Experiment Station, Vicksburg, MS.

References

- ACI 116R. 1990. *Cement and Concrete Terminology*. American Concrete Institute, Farmington Hills, MI.
- ACI 211.1. 1991. *Standard Practice for Selecting Proportions for Normal, Heavyweight, and Mass Concrete*. American Concrete Institute, Farmington Hills, MI.
- ACI 304.1. 1989. *Guide for the Use of Preplaced Aggregate Concrete for Structural and Mass Concrete Applications*. American Concrete Institute, Farmington Hills, MI.
- ACI 304R. 1989. *Guide for Measuring, Mixing, Transporting, and Placing Concrete*. American Concrete Institute, Farmington Hills, MI.
- ACI 524R. 1992. *Guide to Portland Cement Plastering*. American Concrete Institute, Farmington Hills, MI.
- Anon. 2001. Are temperature requirements in mass concrete specifications reasonable? *Concrete Construct. Mag.*, October, pp. 68–70.
- ASTM C 91. 2005. *Specifications for Masonry Cement*. American Society for Testing and Materials, Philadelphia, PA.
- ASTM C 109. 2007. *Test Method for Compressive Strength of Hydraulic Cement Mortars Using 2-in Cube Specimens*. American Society for Testing and Materials, Philadelphia, PA.
- ASTM C 150. 2007. *Specifications for Portland Cement*. American Society for Testing and Materials, Philadelphia, PA.
- ASTM C191. 1992. *Test Method for Time of Setting of Portland Cement by Vicat Needle*. American Society for Testing and Materials, Philadelphia, PA.
- ASTM C 206. 2003. *Specification for Finishing Hydraulic Lime*. American Society for Testing and Materials, Philadelphia, PA.
- ASTM C 207. 2006. *Specifications for Hydraulic Lime for Masonry Purposes*. American Society for Testing and Materials, Philadelphia, PA.
- ASTM C 231. 2004. *Test Method for Air Content of Freshly Mixed Concrete by the Pressure Method*. American Society for Testing and Materials, Philadelphia, PA.
- ASTM C 595. 2007. *Specifications for Blended Hydraulic Cement*. American Society for Testing and Materials, Philadelphia, PA.
- ASTM C 897. 2005. *Aggregate for Job-Mixed Portland Cement-Based Plasters*. American Society for Testing and Materials, Philadelphia, PA.
- ASTM C 926. 2006. *Specifications for Application of Portland Cement-Based Plaster*. American Society for Testing and Materials, Philadelphia, PA.
- ASTM C 937. 2002. *Specifications for Grout Fluidifiers for Preplaced-Aggregate Concrete*. American Society for Testing and Materials, Philadelphia, PA.
- ASTM C 938. 2002. *Practice for Proportioning Grout Mixtures for Preplaced-Aggregate Concrete*. American Society for Testing and Materials, Philadelphia, PA.
- ASTM C 943-02. 2002. *Practice for Making Test Cylinders and Prisms for Determining Strength and Density of Preplaced-Aggregate Concrete in the Laboratory*. American Society for Testing and Materials, Philadelphia, PA.
- ASTM C 1040. 2005. *Standard Test Methods for In-Place Density of Unhardened and Hardened Concrete, Including Roller-Compacted Concrete, by Nuclear Methods*, Vol. 04.02. American Society for Testing and Materials, Philadelphia, PA.
- ASTM C 1170. 2006. *Standard Test Method for Determining Consistency and Density of Roller-Compacted Concrete Using a Vibrating Table*, Vol. 04.02. American Society for Testing and Materials, Philadelphia, PA.

- Bureau of Reclamation. 1992. *Concrete Manual: A Manual for the Control of Concrete Construction*, 9th ed. U.S. Department of the Interior, Washington, D.C.
- Gajda, J., Save time and money on concrete construction. *Concrete Technol. Today*, 24(3), 34–37.
- Gajda, J. and Alsamsam, E. 2006. *Engineering Mass Concrete Structures*, Seminar Development Series, Portland Cement Association, Skokie, IL.
- Gerwick, B.C. 1988. *Review of the State of the Art for Underwater Repair Using Abrasion-Resistant Concrete*, Technical Report REMR-CS-19, prepared for U.S. Army Engineer Waterways Experiment Station, Vicksburg, MS. University of California, Berkeley.
- Kawai, T. 1988. Special underwater concrete admixtures. *Concrete J.*, 26(3), 45–49.
- Khayat, K. 1999. Workability, testing and performance of self-consolidating concrete. *ACI Materials Journal*, 96(3), 346–353.
- Khayat, K. and Hester, W. 1991. *Underwater Repair of Concrete Slab*, Technical Report REMR-CS-13X. University of California, Berkeley.
- Neeley, B.D. 1988. *Evaluation of Concrete Mixtures for Use in Underwater Repairs*, Technical Report REMR-CS-18. U.S. Army Waterways Experiment Station, Vicksburg, MS.
- Neeley, B.D. 1989. *Antiwashout Admixtures for Use in Underwater Concrete Placement*, Video Report REMR-CS-3. U.S. Army Engineer Waterways Experiment Station, Vicksburg, MS.
- Neeley, B.D. and Saucier, K.L. 1990. *Laboratory Evaluation of Concrete Mixtures and Techniques for Underwater Repairs*, Technical Report REMR-CS-34. U.S. Army Engineer Waterways Experiment Station, Vicksburg, MS.
- Okamura, H. 1997. Self-compacting high-performance concrete. *Concrete Int.*, 19(7), 50–54.
- Okamura, H. and Ouchi, M. 2003. Self-compacting high-performance concrete. *J. Advanced Concrete Technol. Jpn. Concrete Inst.*, 1(1), 5–15.
- PCA. 1987. *Concrete for Massive Structures*. Portland Cement Association, Skokie, IL.
- PCA. 2000. *Guide for Developing RCC Specifications and Commentary: Roller-Compacted Concrete for Embankment Armoring and Spillway Projects*. Portland Cement Association, Skokie, IL.
- Persson, B. 2001. A comparison between mechanical properties of self-compacting concrete and the corresponding properties of normal concrete. *Cement Concrete Res.*, 31, 193–198.
- Rail, R.D. and Haynes, H.H. 1991. *Underwater Stilling Basin Repair Techniques Using Precast or Prefabricated Elements*, Technical Report REMR-CS-118. Naval Civil Engineering Laboratory, Port Hueneme, CA, and Haynes and Associates, Oakland, CA.
- Ribar, J.W. and Scanlon, J.M. 1984. *How to Avoid Deficiencies in Portland Cement Plaster Construction*, Technical Report SL-84-10. U.S. Army Corps of Engineers. Washington, D.C.
- Scanlon, J.M., McDonald, J.E., McAnear, C.L., Hart, E.D., Whalin, R.W., Williamson G.R., and Mahloch, J.L. 1983. *REMR Research Program Development Report*, prepared for Chief of Engineers, U.S. Army, Washington, D.C.
- Suksawang, N., Nassif, H., and Najm, H. 2005. Durability of self-consolidating concrete (SCC) with pozzolanic materials. In *Proceedings of the SCC Second North American Conference and Fourth RILEM International Conference*, October 20–November 2, Chicago, IL.
- Suksawang, N., Nassif, H., and Najm, H. 2006. Evaluation of mechanical properties of self-consolidating, normal, and high-performance concrete. *Transport. Res. Record, J. Transport. Res. Board*, No. 1799, Transportation Research Board of the National Academies, Washington, D.C., pp. 36–45.
- U.S. Army Corps of Engineers. 1994. *Standard Practice for Concrete for Civil Works Structures*, EM 1110-2-2000. U.S. Government Printing Office, Washington, D.C.
- Waddell, J.J. and Dobrowolski, J.A. 1993. Preplaced-aggregate concrete. In *Concrete Construction Handbook*, 3rd ed., Dobrowolski, J.A. and Waddell, J.J., Eds., pp. 38.1–38.7. McGraw-Hill, New York.
- Zhu, W. and Bartos, P. (2003) Permeation properties of self-compacting concrete. *Cement Concrete Res.*, 33(6), 921–926.



(a)



(b)

- (a) Repair of deteriorated beam underside. (Photograph courtesy of Portland Cement Association, Skokie, IL.)
(b) Repair of deteriorated bridge element. (Photograph courtesy of Randall W. Poston.)

16

Structural Concrete Repair

Randall W. Poston, Ph.D., P.E.*

16.1	Introduction	16-1
16.2	Limit States Design for Repair	16-2
16.3	Evaluation	16-3
	Information Gathering • Visual Inspection • Testing	
16.4	Structural Implications	16-8
16.5	Repair Principles	16-10
	Material Selection • Preparation • Cleaning and Protecting Reinforcement • Curing • Crack Repair • Corrosion Protection • Strengthening	
16.6	Repair of Unbonded Post-Tensioned Concrete Structures.....	16-16
	Do Nothing • Tendon Splice or Replacement	
16.7	Construction Issues.....	16-19
16.8	Long-Term Repair Performance.....	16-20
16.9	Case Study.....	16-20
	Background • Repair Strategy • Life-Cycle Cost Analysis • Impact-Echo to Assess Deterioration • Reliability in Assessing Deterioration • Cathodic Protection • Structural Analysis • Life Safety Implications • Cost Savings • Conclusions • Reports, Standards, and Guidelines	
	References	16-41

16.1 Introduction

Concrete has been used as a construction material in a wide variety of structures ranging from buildings and parking structures to bridges, dams, earth-retaining structures, pressure vessels, tanks, boats, and offshore platforms. Today, it is the most widely used construction material. As with other forms of infrastructure, there is an ever-increasing need to evaluate and repair concrete structures. Repairs may be required for a variety of reasons, ranging from a change in the space requirements of the structure to the deterioration of concrete and corrosion of the steel reinforcement. Although most concrete structures have good long-term performance records, deterioration problems have occurred because of poor construction practices, poor design, lack of quality materials, and aggressive environmental exposure. Perhaps the most-cited statistic in the technical concrete literature concerns the extent of deterioration of this

* Principal of WDP & Associates, Inc., Austin, Texas, and chairman, ACI Committee 318; expert in structural design both in reinforced and prestressed concrete and in retrofit of concrete structures.

country's roads and bridges, often referred to as the nation's highway infrastructure. The American Association of State Highway and Transportation Officials (AASHTO) rates 40% of U.S. highways as below minimum standards of engineering. According to the U.S. Department of Transportation, 230,000 out of the 575,000 bridges on primary and secondary roads are structurally deficient or functionally obsolete. It has been estimated that between \$18 billion and \$21 billion is spent by owners for repair, protection, and strengthening (Strategic Development Council, 1996). The value of the concrete-based infrastructure in the United States is estimated to be \$8 trillion. And, as was so simply put in a Smithsonian article, "a lot of that concrete needs fixing" (Wolkomir, 1994).

Repair of structural concrete—that is, repair of structures in which concrete is the principal load-carrying material—can be classified into three major categories: *rehabilitation*, where repairs are conducted to extend the service life of the structure; *restoration*, where repairs are effected to upgrade the functionality or change the use of the structure; and *strengthening*, to restore the intended load capacity of the structure or perhaps, as in the case of restoration, increase its capacity because of an anticipated change in use. As can be surmised, the boundaries between rehabilitation, restoration, and strengthening of concrete structures often overlap. The principal objectives of a repair are to ensure safety and structural integrity, extend useful life, improve aesthetics, change use, or to improve serviceability. The design of repairs must, therefore, address strength, durability, and serviceability analogous to the limit states considered in the design of a new structure.

It is not the intent of this chapter to present a comprehensive treatise of all aspects of the repair of concrete structures. Detailed information is available in the literature with regard to concrete preparation, repair materials, and execution of repair construction. Rather, the objective is to present the structural concepts concerning concrete repair that include evaluation procedures and general design concepts. The structural guidelines presented are generally applicable to all types of concrete structures, including bridges, buildings, water-containing structures, parking garages, and special structures. A detailed case study of an infrastructure repair project is presented to demonstrate the importance of proper evaluation within the context of a repair project. This comprehensive case study also illustrates the various structural analysis and design techniques that are sometimes necessary to ensure a cost-effective solution in a large-scale infrastructure repair project.

16.2 Limit States Design for Repair

To repair a concrete structure, it is important to understand what has "failed." Perhaps one of the simplest definitions of what might constitute failure of a structure can be inferred from the definition of limit states given by the structural sage, Professor J.G. MacGregor (1976), who stated: "When a structure becomes unfit for its intended use, it is said to have reached a limit state." Thus, the inference is that when a structure can no longer perform in its intended function this, in essence, constitutes failure. The three generally recognized limit states for concrete structures are:

- Serviceability limit state
- Ultimate limit state
- Durability limit state

Although concrete building codes such as ACI 318-08 (ACI Committee 318, 2008) may not have code provisions and standards that explicitly guard against failure for all of these limit state categories, they do so implicitly. When concrete structures suffer from premature deterioration caused by steel reinforcement corrosion, this is generally thought to affect their durability. A concrete structure designed for an intended life of 40 years could be considered to reach the durability limit state if severe corrosion and attendant distress were manifested, for example, in only 15 years. But, as conceptually illustrated in Figure 16.1, it is difficult to separate the pernicious effects of corrosion on durability, serviceability, and strength because the deterioration that results from corrosion not only compromises durability but clearly can

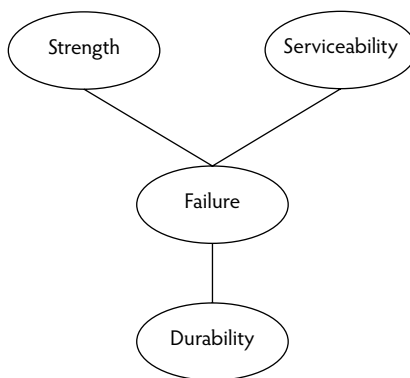


FIGURE 16.1 Limit states in structural concrete repair.

also impair the serviceability and strength of the structure. In fact, there is a confluence of limit states with regard to the effects of deterioration in structural concrete. It is therefore necessary to design concrete repairs to satisfy all three limit states.

16.3 Evaluation

Prior to undertaking repairs to concrete structures, a condition assessment to determine the existing conditions and nature and causes of observed distress must be conducted; otherwise, the absence of this information could lead to a high risk of failure of the repair. The extent of the condition assessment depends largely on the objectives of the repairs. The factors that affect the repair objectives include safety and structural integrity, the desired service-life extension, change in intended use or loading requirements, serviceability, aesthetics, and cost. Internationally recognized organizations, such as the American Society of Civil Engineers (ASCE) and the American Concrete Institute (ACI), have published guidelines for condition assessment of structures (ASCE, 2000).

The Strategic Highway Research Program (SHRP) was established in 1987 by Congress to improve the performance and durability of the nation's highway systems (TRB, 1986). As part of this effort, a number of nondestructive evaluation (NDE) tools were developed that have been implemented by states and local government agencies, by industry, and by private sectors. Some of the methods developed by SHRP include alkali-silica reactivity (ASR) test methods and a rapid method for determining chloride content and the rate of corrosion of steel reinforcement in hardened concrete. These, along with other existing and emerging NDE techniques, have aided in diagnosing problems, specifying repairs, and quantifying the extent of adverse conditions and deterioration.

A condition assessment of a concrete structure may be necessary even if repairs are not contemplated. In some cases, condition assessment is required for determining the load rating of a structure. Moreover, a condition assessment may be conducted in an ongoing inspection program simply to show that a structure is structurally sound. In fact, the Federal Highway Administration (FHWA) has mandated biennial inspections for bridges since 1968. Traditionally, a condition assessment of a concrete structure generally meant a visual examination of the structure along with select coring of various concrete elements for compressive strength testing, perhaps a petrographic analysis, and sounding by chain drag. Although these techniques are still helpful and largely necessary, over the past two decades other very valuable and practical nondestructive evaluation methods have been developed. These newer generation nondestructive methods greatly improve and increase the efficiency of the condition assessment process for concrete structures. Some of these recently developed nondestructive evaluation technologies allow for relatively rapid inspection of damage and deterioration of concrete structures.

The objectives of this section are to summarize selected nondestructive evaluation methods that can be used as an aid in conducting condition assessment of concrete structures, highlight some of the more recently developed methods, and discuss the relative merits of various NDE methods. For our purposes, NDE is defined as any test or method that yields information regarding the quality of a structure or portion thereof that does not impair the serviceability of the element or structure. Destructive testing in the sense of removing samples from a structure or element, such as coring, is considered a nondestructive test for the purposes of this discussion. The techniques and methods discussed are generally applicable to all types of concrete structures.

16.3.1 Information Gathering

Prior to the field-investigation component of the evaluation, it is important to gather as much information as possible related to the original design and construction. This includes gathering structural and shop drawings, project specifications, and construction records. Records such as concrete batch tickets, test reports, and weather and daily logs can be particularly useful if there is observed deterioration, cracking, or other types of service-performance problems. These types of original construction documents should be perused to ascertain if existing conditions are related to original construction problems or perhaps to design deficiencies.

16.3.2 Visual Inspection

Despite the advances in nondestructive evaluation methods, visual inspection is still an integral part of a condition assessment and, in fact, is the most widely used form of NDE. It is always the first step in condition assessment of a structure. The forms of distress and deterioration that should be recorded in the field evaluation and some of the associated causes are summarized in Table 16.1. In some select cases, the evaluation may be concluded with a simple visual inspection; however, in more cases than not, some form of nondestructive testing (NDT) is required to determine the cause of the observed deterioration, assess its implications and the extent to which it affects structural integrity, and develop appropriate repair and maintenance strategies to meet the client's budget.

16.3.3 Testing

The types, location, and size of material samples should be consistent with the size of the structure so the results are statistically meaningful; for example, determining chloride-ion content at only one or two locations in a bridge deck will not provide sufficient data to draw statistically significant conclusions. Table 16.2 summarizes some methods of field and laboratory testing that may be conducted to aid in the condition assessment of a concrete structure. Selection of the appropriate test method to determine a particular characteristic depends on several factors, including desired sensitivity and cost. At a minimum, the concrete strength and condition and location of the reinforcement should be assessed to generally characterize the strength, safety, and integrity of the structure. Other testing is then conducted to determine the extent of deterioration and to establish causes. Establishing the cause of deterioration is an important element in developing appropriate repair strategies within prescribed budget limitations. The test methods for evaluating concrete structures described in Table 16.2 are well documented in the literature (e.g., ACI 228.2R). Because of their relative virtues and effectiveness, two of the test methods—impact-echo and surface-penetrating radar (SPR)—are briefly described to illustrate the power and versatility of selected nondestructive testing technologies for evaluating structural concrete.

16.3.3.1 Impact-Echo

In the impact-echo technique, a transient stress pulse is introduced into a test object by mechanical impact on the surface as illustrated in Figure 16.2. The stress pulse propagates into the object along spherical wave fronts as P- and S-waves and along the surface of the object along a circular wave front as an R-wave. The P- and S-waves are reflected by internal cracks or interfaces and by the external

TABLE 16.1 Forms of Concrete Distress and Deterioration Noted in a Visual Condition Assessment

Description	Typical Causes
Cracking	Plastic shrinkage Drying shrinkage Restraint Subgrade support deficiencies Absence or location of vapor barrier Expansion Corrosion of reinforcing steel/prestressing steel or other embedded metal Components Thermal loading Vehicular impact Overloading Aggregate reaction
Scaling	Inadequate air content Finishing problems Freeze-thaw cycling Chemical deicers
Spalling	Aggregate reaction Corrosion Freeze-thaw cycling Construction Poor preparation of construction joints Early-age loading
Disintegration	Frozen concrete Freeze-thaw cycling Low strength Chemical attack Sulfate attack
Honeycombing and surface voids	Poor placement Poor consolidation Congested reinforcement
Discoloration and staining	Different cement production Different water-cement ratios Corrosion Aggregates Use of calcium chloride Curing Finishing Nonuniform absorption of forms
Efflorescence	Calcium carbonate and other mineral deposits caused by leakage

boundaries of the object. The arrival of these reflected waves at the surface where the impact was generated produces displacements that are monitored by a transducer. If the transducer is placed close to the impact point, the waveform is dominated by displacements caused by P-wave arrivals.

Because it is difficult and time consuming to analyze time-domain waveforms to determine the arrival times of reflected waves and thereby calculate the depth of reflecting interfaces, waveforms are transformed into the frequency domain using the fast Fourier transform (FFT) technique (Sansalone and Carino, 1986, 1988). The resulting amplitude spectrum is used to identify the dominant frequencies present in the waveform. Because these frequencies are produced by multiple wave reflections between interfaces, they can be used to determine if a structure is solid or if flaws exist within the structure. Each type of structure—plate (bridge deck, slab), bar (beam, column), hollow cylinder (pipe, shaft line), etc.—exhibits a characteristic frequency response when subjected to impact. The presence of a flaw affects this response.

TABLE 16.2 Selected Tests for Condition Assessment of Concrete Structures

Mechanical/Physical/ Chemical Property	Test Type	Reason for Test
Compressive strength	Swiss hammer (ASTM 805) Windsor probe (ASTM C 803) Core for compression testing (ASTM C 42) Ultrasonic pulse velocity (UPV) (ASTM 597)	Strength of in-place concrete; comparison of concrete strength in different locations (UPV and Swiss hammer provide relative differences in strength only)
Reinforcement location	Pachometer Radiography Radar (ASTM D 4748)	Steel location and distribution; concrete cover
Corrosion potentials	Half-cell potential (ASTM C 876) Linear polarization (SHRP S-330)	Identification of location of active reinforcement corrosion; corrosion rate
Chloride ion content	Acid-soluble, by titration (ASTM C 1152)	Susceptibility of steel reinforcement to chloride-induced corrosion
pH	Phenolphthalein; direct measurement with pH meter	Assess corrosion protection value of concrete with depth and susceptibility of steel reinforcement to corrosion; depth of carbonation
Air content; cement and aggregate properties; scaling	Petrographic examination of concrete core removed from structure (ASTM C 856)	Assist in determination of cause(s) of distress; degree of damage; quality of concrete when originally cast
Alkali-silica reactivity; freeze-thaw susceptibility	(ASTM C 457)	—
Permeability	Electrical indication of concretes Ability to resist chloride ion penetration (ASTM C 1202) (AASHTO T277) Resistance of concrete to chloride ion penetration (90-day ponding test) (AASHTO T259) Absorption test (ASTM C 642)	Establish relative susceptibility of concrete to chloride ion intrusion; assess effectiveness of chemical sealers, membranes, and overlays in repair

In a plate, the impact-echo is dominated by reflections between the top and bottom surface of the plate or from a defect if one exists. Knowing the P-wave speed (to determine the P-wave speed, a test must be carried out over a portion of the test object of known thickness) in the test object (C_p), the depth (T) to a reflecting interface can be calculated as:

$$T = \frac{C_p}{2f_p} \quad (16.1)$$

where f_p is the frequency of P-wave reflections from the interface. In plates, wave reflections from the side boundaries do not have a significant effect on the response.

An impact-echo test system is composed of three components: an impact source, a receiving transducer, and a waveform analyzer or a portable computer with a data acquisition card that can sample at a frequency of at least 500 kHz. The duration of the impact determines the frequency content of the stress waves generated by the impact. Impacts with shorter durations contain higher frequency (shorter wavelength) components, which are required for testing thinner structures or detecting smaller or shallow flaws. Hardened steel spheres on spring steel rods are used as impact sources. The impact durations produced by impactors generally range from about 10 to 80 μ s.

Figure 16.3 shows the impact-echo test results from a 20,000-ft² industrial concrete overlay delaminated from a structural slab at an industrial facility. Impact-echo was used to identify the delaminated repairs,

TABLE 16.2 (cont.) Selected Tests for Condition Assessment of Concrete Structures

Mechanical/Physical/ Chemical Property	Test Type	Reason for Test
Alkali-silica reactivity	SHRP rapid test (SHRP-C/FR-91-101)	Establish in field if observed deterioration is due to alkali-silica reactivity
Location of delaminations, voids, and other hidden defects	Limited information of shallow defects from sounding (ASTM D 4580), impact-echo, infrared thermography (ASTM D 4788), pulse echo, surface-penetrating radar (ASTM D 4748), impulse response	Assessment of reduced structural properties; extent and location of unobserved damage and defects
Steel area reduction; defect identification	Invasive probing	Observe and measure rust and area reduction in steel; observe corrosion of embedded post-tensioning components; verify location and extent of deterioration; provide more certainty in capacity calculations
Concrete component thickness	Impact-echo radar (ASTM D 4748); invasive probing	Verify thickness of concrete; provide more certainty in capacity calculations
Local or global strength and behavior	Load test; strain measurements; acceleration; deformation; displacement measurements	Uncertainty in integrity and behavior; ascertain acceptability without repair or strengthening; determine accurate load rating
Tensile strength	Pull-off tests (ASTM C 1583) Splitting tests (ASTM C 496) Tension tests	Assess tensile strength of concrete and steel; relative quality of material
Material property determination	Density (ASTM C 642) Moisture content (ASTM C 642) Shrinkage (ASTM C 341) Dynamic modulus (ASTM C 215) Modulus of elasticity (ASTM C 469)	Determine mechanical properties of materials and volumetric properties

Note: ASTM, American Society for Testing and Materials Testing Standards; AASHTO, American Association of State Highway and Transportation Officials Testing Standards; SHRP, test methods developed as part of the Strategic Highway Research Program.

which appear as dark areas in the map. The test results facilitated the selective removal of the delaminated areas, lowering the cost of the repair work. Chapter 19 provides more detailed information regarding the impact-echo testing system.

16.3.3.2 Surface-Penetrating Radar

Surface-penetrating radar (SPR) is a nondestructive evaluation technique that utilizes electromagnetic energy to locate objects, subsurface flaws, or interfaces within a material. The system utilizes a high-frequency dipole antenna to transmit a train of discrete amplitude modulation (AM) radiowave pulses. A second antenna, housed next to the transmitting antenna, is used to receive the scattered pulses as they return to the surface of the material. The radar unit detects back-scattered radiation that is reflected at the boundary between differing dielectric media. By measuring the time it takes to receive the reflected signal, the depth of an embedded object or interface may be determined. A real-time visual display of the material cross-section is recorded as the antennae are moved along the surface. The output is fed to sampling circuitry before being digitally processed by a computer. The color and intensity of the patterns in the output are related to the amplitude of the reflected signals. Figure 16.4 illustrates SPR scanning and sample signal output. The bands of alternating light and dark areas that appear in the remainder of the output correspond to the positive and negative reflections of the input wave from subsurface objects. Reflections from a lower dielectric media to a higher one, such as from concrete to steel, will undergo a phase inversion, or reversal, and the boundary will show up as a bright signal (assuming the input wave

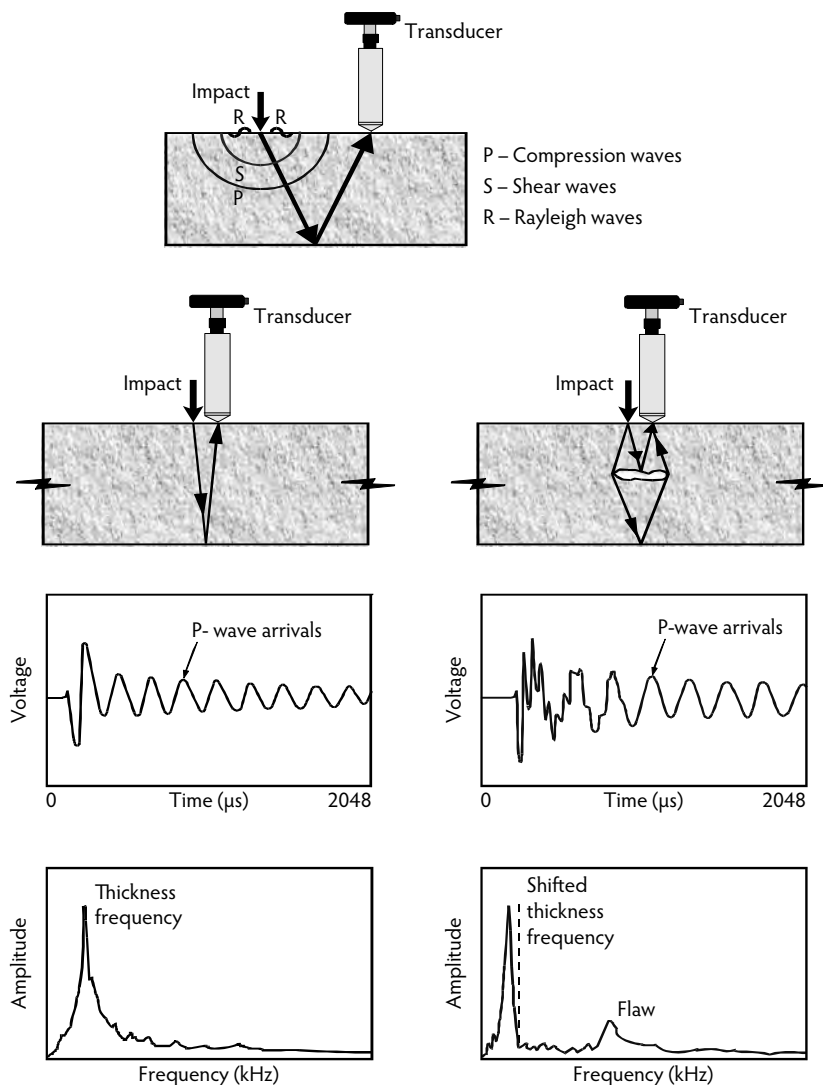


FIGURE 16.2 Schematic of the impact-echo technique applied to a concrete structure.

is dark). Conversely, the boundary from concrete to air (higher dielectric to lower) will show up as a dark signal. SPR antennae are specifically tuned to detect cylindrical objects, such as rebar, conduit, pipes, etc. These types of features show up as hyperbolas, or arch shapes, on the data record, as seen in Figure 16.4. Steel shows up more distinctly than other media due to the high reflective property of electrically conductive materials, and, as a result, SPR is particularly well suited for locating mild reinforcing steel in concrete.

16.4 Structural Implications

Results from field and laboratory observations and testing must be assessed to determine the cause of the observed deterioration. In addition, findings from the investigation results must be assimilated to determine their effects on strength, serviceability, and durability of the structure. As previously discussed, each of these factors must be considered for a successful concrete repair. The strength and integrity of

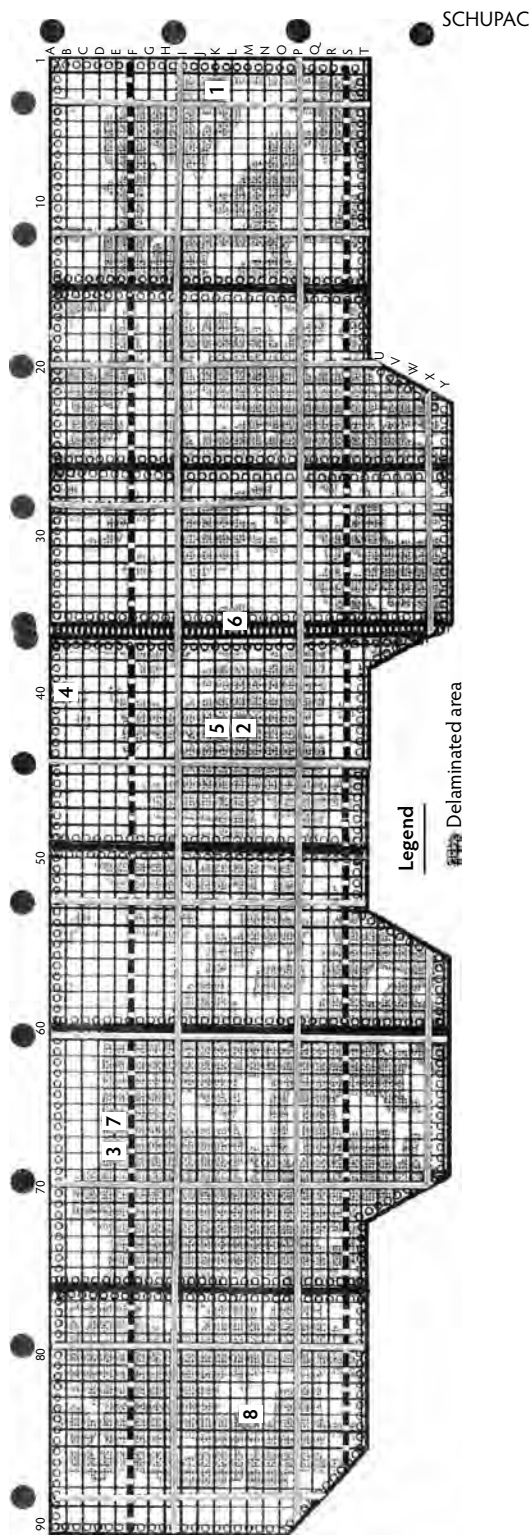


FIGURE 16.3 Results from impact-echo testing on an industrial lab showing areas of delamination.

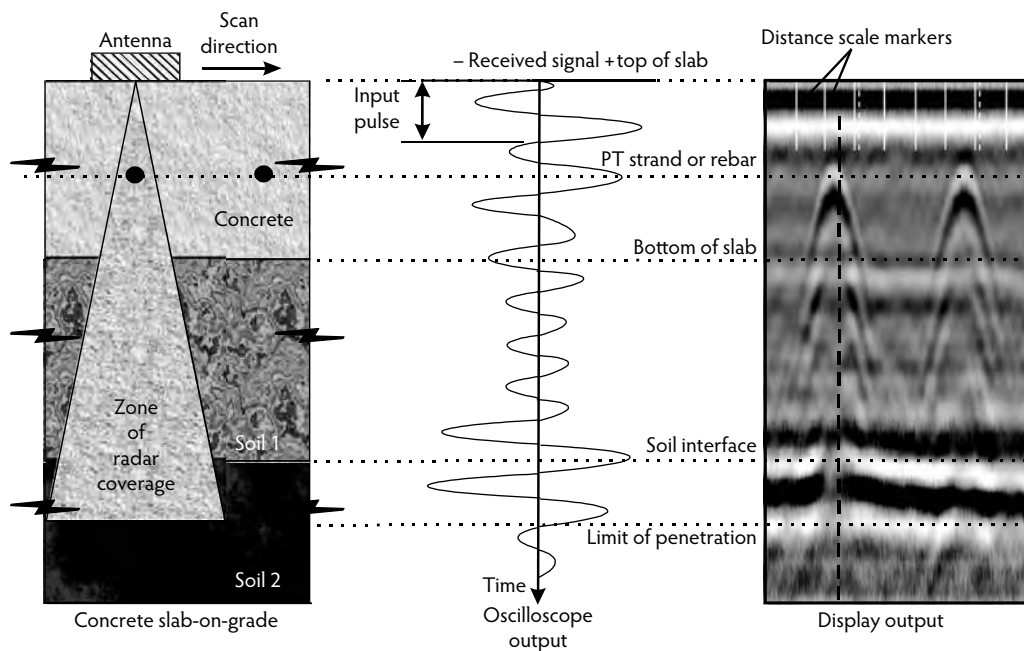


FIGURE 16.4 Schematic of surface penetrating radar technique applied to a concrete structure.

concrete structures suffering from deterioration can be assessed using conventional analysis techniques for concrete structures utilizing quantitative assessments of reduced material properties as determined in the investigation. This requires some judgment about the extent of deterioration. It is prudent to reduce the capacity-reduction (ϕ) factors in the ACI Building Code (ACI Committee 318, 2008), as they were calibrated for material variations that occur in new concrete construction. Several technical committees within ACI are examining this issue of ϕ -factor selection for repair and strengthening designs. Depending on the conditions and factors involved, a ϕ factor as low as 0.5 may not be unreasonable. In extreme cases, where analysis of a structure with reduced properties may be inappropriate or produces questionable results concerning integrity and safety, load testing of the structure is an option. Load testing can be expensive and must be conducted with extreme caution, particularly on deteriorated and suspected grossly deficient structures. In some cases, however, it may be the only viable alternative for demonstrating the integrity of a repaired structure (Poston and Irshad, 1996).

16.5 Repair Principles

Various organizations such as the American Concrete Institute (ACI) and the International Concrete Repair Institute (ICRI) have developed guidelines for the repair of concrete structures. These include technical and construction-related guidelines for, among other things, preparing the surfaces of deteriorated concrete and selecting and specifying materials for repair. These are valuable resources that describe in detail the proper construction-preparation techniques for good concrete repair. The reader is referred to the ICRI documents listed at the end of this chapter and the *Concrete Repair Manual* (ACI, 2002) for additional information on these construction-related aspects of concrete repair. The principles presented in this section are generally applicable for all structural concrete, including conventionally reinforced, prestressed, or partially prestressed structures; however, some of the more unique aspects of repairing unbonded post-tensioned concrete structures are presented in Section 16.6.

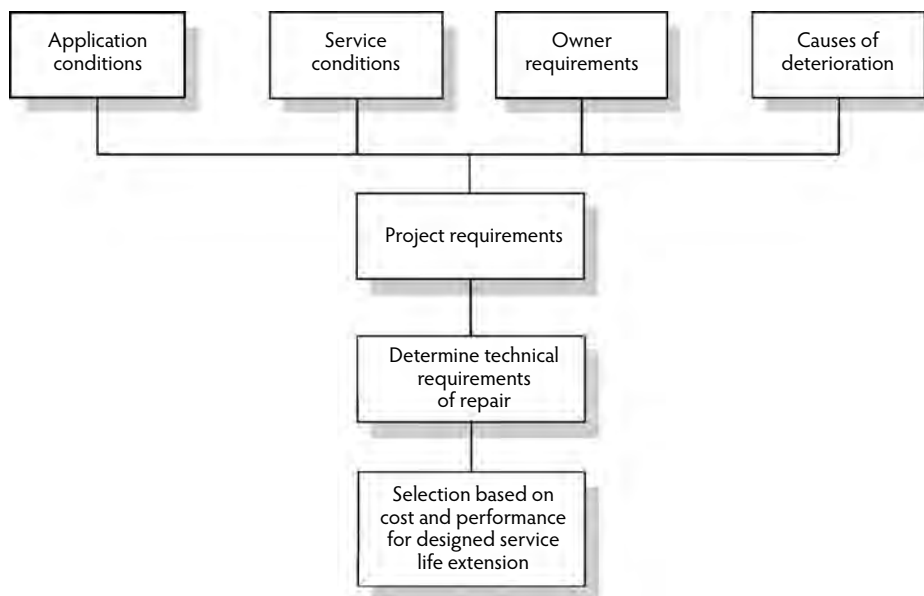


FIGURE 16.5 Representation of material selection process.

16.5.1 Material Selection

A general axiom in the repair of concrete structures is to use a material of physical and mechanical characteristics similar to those of the existing parent material. One of the most important mechanical properties to match, but which is often overlooked, is the coefficient of thermal expansion. As an example, epoxy concrete used in a repair exposed to large temperature differentials, such as on a parking garage deck, is not appropriate, as deformation of the epoxy is much greater than that for concrete. As shown in Figure 16.5, the process of selecting concrete materials for repair must include identification of the causes of deterioration, service conditions, owner requirements, and the application conditions. Thus, this somewhat complex selection process must consider constructability and service issues guided by the owner's needs and the engineering requirements of the repair. The final selection of a repair material is based on the relationship between cost and performance. ICRI Guideline No. 03733 (ICRI, 1996) provides in-depth information for the process of selecting repair materials.

16.5.1.1 Bond Strength

In almost all cases, one of the most important properties for repair is the bond strength (see Figure 16.6) between the repair material and the existing concrete substrate. Bond failures are generally a result of dimensional incompatibility between the repair material and the existing substrate, such as from drying shrinkage (McDonald et al., 2002). The failure is generally not a direct result of lack of bond strength. The relative dimensional changes that can occur, such as those illustrated in Figure 16.7, can affect the repair. Bond can be reduced and shrinkage cracks can appear; thus, the durability of the repair is compromised (McDonald et al., 2002).

16.5.1.2 Dimensional Compatibility

Drying shrinkage of the repair concrete is one of the important factors that influence the dimensional behavior. The existing concrete substrate has already experienced most of its time-dependent effects such as drying shrinkage and creep. The repair concrete that is then added must also undergo its shrinkage; consequently, it is very important to identify and select a low-shrinkage material. The time required for

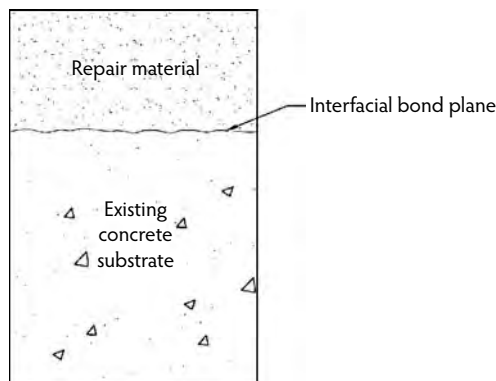


FIGURE 16.6 Bond strength, an important property for the success of break repair.

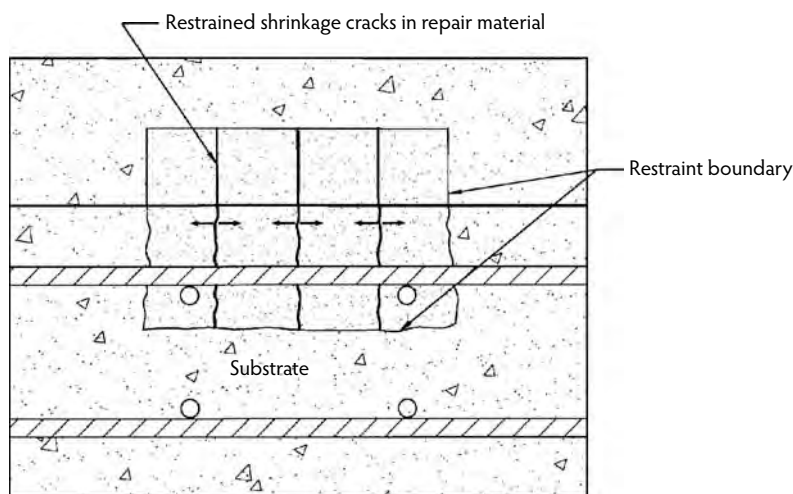


FIGURE 16.7 Dimensional changes in repair material that have resulted in restrained shrinkage cracks.

a material to achieve dimensional stability is dependent primarily on the ambient temperature and humidity. It is important to adequately cure the repair to mitigate shrinkage cracking. It is recommended that the repair concrete material be limited to less than 0.05% shrinkage at 28 days as measured by ASTM C 157 (McDonald et al., 2002). Other properties of the repair material that are important in achieving dimensional compatibility include the coefficient of thermal expansion, modulus of elasticity, and creep, both compressive and tensile. In general, these properties in the repair material should reasonably match those of the existing concrete to achieve dimensional compatibility. By matching these properties, cracking in the repair will be mitigated. This will help ensure long-term durability of the repair.

16.5.1.3 Durability Considerations

The durability of the concrete repair is its ability to resist structural loading and environmental conditions without degradation and deterioration. The environmental conditions that may affect durability include weathering, temperature changes, chemical attack, and abrasion, among others. It is essential that the cause and extent of deterioration of an existing concrete structure be identified. Based on this information, a strategy can be identified to satisfy the durability limit state of the repair.

Material properties that can affect the durability of a repair include permeability, water-vapor transmission, freeze-thaw resistance, scaling resistance, sulfate resistance, abrasion resistance, and alkali-silica reaction. Permeability is the rate of transmission of a liquid through the concrete. In general, the lower

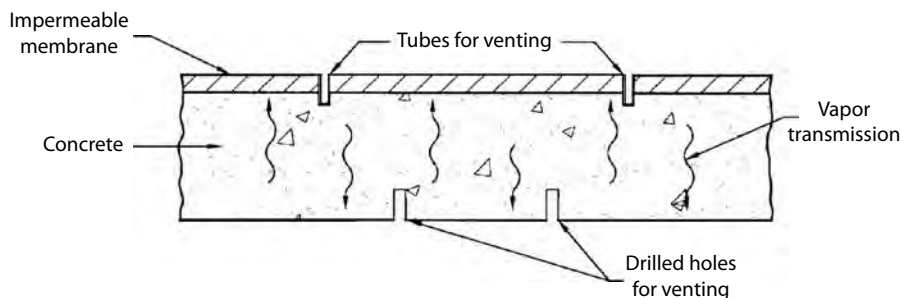


FIGURE 16.8 Provision for vapor transmission in repair.

the permeability, the better the protection against the ingress of aggressive elements such as chloride ions from chemical deicers and from diffusion of carbon dioxide leading to carbonation. Water-vapor transmission can lead to failure of a repair that uses an impermeable barrier. The movement of vapor in the concrete can become trapped at the interface of a permeable concrete and an impermeable barrier, such as a membrane, leading to debonding. As shown in Figure 16.8, the repair must make provision for this vapor transmission, such as by adding vents to allow the vapor to escape or by providing materials that allow vapor transmission such as chemical sealers or silicone-based coatings. The selected repair material must have adequate freeze–thaw resistance to ensure long-term durability. The cyclic freezing and thawing of concrete that is critically saturated leads to a deterioration of the paste matrix. Repair materials that have entrained air or that have been proven through laboratory testing to provide freeze–thaw resistance should be specified. In industrial applications, abrasion resistance is an important durability consideration. The resistance to abrasion is governed principally by the hardness, quality, and strength of the aggregate.

16.5.1.4 Mechanical Properties

Repair materials must be capable of resisting the internal stresses generated by loading and volume changes. The mechanical properties of the repair material are generally selected to match those of the existing concrete. This ensures compatibility of strains under load. The principal mechanical properties that should be examined in the repair design include compressive strength, tensile strength, modulus of elasticity, and coefficient of thermal expansion. In some circumstances, Poisson's ratio and flexural strength are also important mechanical properties for repair design.

16.5.1.5 Placement

The placement of the repair material and field conditions can greatly affect the type of repair procedure and material selection. Characteristics such as slump, pumpability, rate of strength gain, heat of hydration, set time, and characteristics in hot or cold weather can affect material selection. Conventional ready-mixed or machine-mixed concrete is the repair material of choice for existing-concrete deterioration that goes through, or mostly through, the structural element and beyond the reinforcement, or if the area to be repaired is large. Affected areas should be excavated until there is no question as to the soundness of the concrete. The excavation and repair area should avoid sharp angles that produce stress concentrations. Forms should maintain their shape during casting and maintain existing lines of the structure. For small repair areas that are relatively deep, rodding a very stiff, low water/cement ratio, dry-pack mortar is the method of choice. The rodding should be done in thin lifts, rodding the dry pack between successful lifts. If large volumes of repair are required in tight places, preplacing aggregate followed by pumping of grout is a good repair method. This usually requires specialized equipment and experience. For large-quantity shallow overhead and vertical repairs, shotcrete is an excellent choice. It bonds very well and is capable of supporting itself without a form. The nozzlemen must have good experience to control rebound that can lead to pockets of sandy layers. Mobilization costs require the repair project to be of reasonable size to justify using shotcrete. Repair of shallow areas of limited size are well suited for proprietary prepackaged

repair materials. These prepackaged materials often contain polymers to enhance the bond of the material to the existing concrete substrate; however, it has been observed that some prepackaged repair materials have excessive shrinkage characteristics and thus are dimensionally incompatible with concrete.

16.5.2 Preparation

In general, deteriorated concrete should be removed to sound concrete substrate. Partial-depth repairs are desirable because less demolition is required, no formwork is required for horizontal repairs, and they are generally less costly; however, if repair is required on two sides of a slab or wall, then full-depth removal is preferable. Saw cuts around the perimeter of the repair are advisable, particularly in the case of slabs to eliminate feather edges. After deteriorated concrete is removed, the surfaces to be bonded should be thoroughly cleaned, such as by wet sandblasting, then all loose particles should be vacuumed or pressure blown from the repair area. The surface should be thoroughly wet. The repair material should be placed when the surface has no standing water. A bonding agent such as a cement slurry coat or epoxy is normally not necessary but should be utilized if the manufacturer of a prepackaged material recommends their use.

16.5.3 Cleaning and Protecting Reinforcement

Prior to placing the repair material, steel reinforcement and other metal components should be cleaned of corrosion and other scale. Mechanical abrasion can be used, although sandblasting is preferable if environmental conditions permit. There are various components on the market for coating the reinforcement. These include epoxy, zinc-rich compounds, and cement-based coatings. Epoxy and some of the zinc-rich compounds can act as bond breakers and therefore, must be applied carefully. Recent findings regarding epoxy have raised questions about the appropriateness of its use. It has been speculated that the application of epoxy on reinforcing steel in an area under repair results in accelerated corrosion in surrounding areas, sometimes referred to as the *anodic ring effect*.

16.5.4 Curing

All concrete repairs must be properly cured to ensure hydration of the cement and strength gain and to minimize shrinkage and cracking. Curing should follow the same good practices as for new construction.

16.5.5 Crack Repair

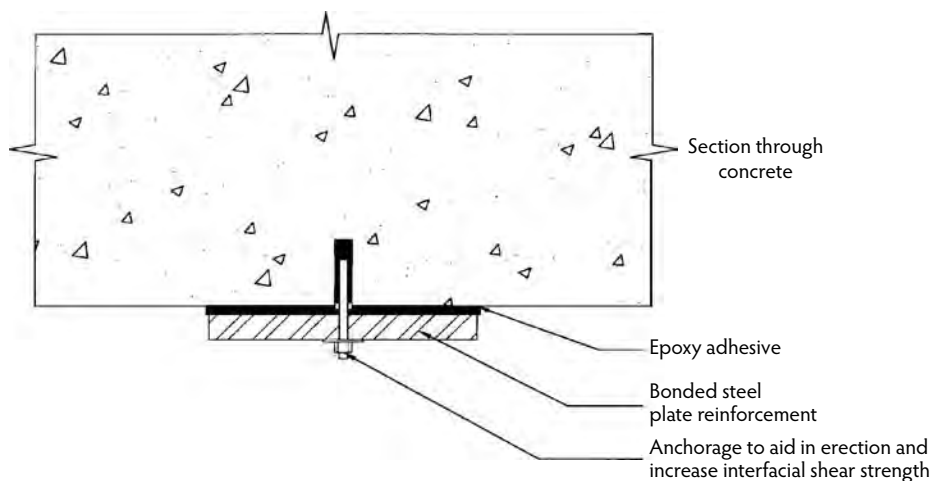
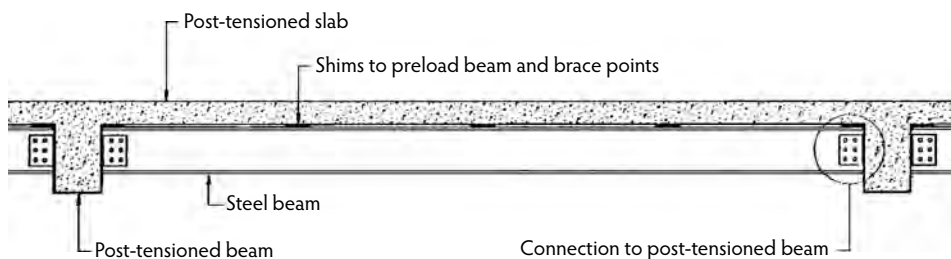
Whether a crack in concrete should be repaired to restore structural integrity or merely sealed is dependent on the nature of the structure and the cause of the crack and on its location and extent. If the stresses that caused the crack have been relieved by its occurrence, the structural integrity can be restored with some expectation of permanency. In the case of working or moving cracks, such as cracks that open and close because of temperature changes, the only satisfactory solution is to seal them with a flexible or extensible material. ACI 224.1R (ACI Committee 224, 1998) provides comprehensive information on crack repair. Cleaning of the crack is essential before any treatment takes place. All loose particles and foreign material must be removed. The method of cleaning is dependent on the size of the crack and the nature of the contaminants. It may include compressed air, sandblasting, or routing. Restoration of cracks without restoration of structural integrity requires the use of materials and techniques similar to those used in sealing joints. Typically, the cracks are routed and a urethane sealant is applied. A bond breaker should be used on the bottom of the routed crack so bonding occurs on only two sides.

16.5.6 Corrosion Protection

Various corrosion protection strategies are being used in repair and new construction projects. Their selection depends on the type of structural system, exposure conditions, service life, and, naturally, costs. Selected corrosion protection strategies are summarized in Table 16.3.

TABLE 16.3 Selected Corrosion Protection Strategies for Concrete Structures

Strategy	Selected Types of Materials	Range of Additional Unit Costs
Reinforcing steel coatings	Epoxy	\$0.25–\$0.75/lb of steel
Corrosion inhibitors	Admixed in concrete	\$10.00–\$20.00/yd ³ concrete
Chemical sealers	Methacrylate, silane	\$0.50–\$1.00/ft ² of concrete surface
Elastomeric membranes	Urethane, neoprene	\$2.50–\$3.50/ft ² of concrete surface
Low-permeability concrete overlays	Fly ash and microsilica	\$6.00–\$8.00/ft ²
Cathodic protection	Impressed current	\$10.00–\$15.00/ft ² of concrete surface
Low-permeability polymer overlays	Epoxy, methacrylate	\$2.00–\$3.00/ft ² of concrete surface

**FIGURE 16.9** Strengthening using bolted and epoxied steel plates.**FIGURE 16.10** Strengthening using steel subframing.

16.5.7 Strengthening

A repair that has been conducted for understrength concrete structures resulting from deterioration or upgrading of load capacity is the addition of auxiliary bonded reinforcement or addition of members. The strengthening may take one of the following forms: wire mesh or reinforcing bars added to the understrength area and bonded to existing concrete using shotcrete, latex-modified concrete, or other means; structural steel plates epoxied and bolted through deficient structural concrete to increase capacity, as shown in Figure 16.9; the addition of supplemental steel subframing, as shown in Figure 16.10; the use of external post-tensioning, as shown in Figure 16.11; or the use of bonded carbon fiber applied to the concrete surface. Depending on conditions, there may be a need for corrosion protection and fireproofing. The requirements for engaging all or some of the superimposed loads on the structure must be carefully reviewed. Generally, it is preferable to preload the structural member being strengthened to

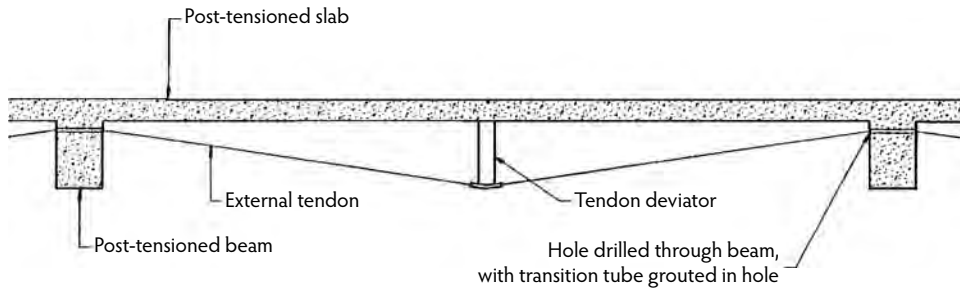


FIGURE 16.11 Strengthening using external post-tensioning.

some degree. The amount of preloading depends on whether the deficiency is under service or ultimate loads or both. In some cases, no preloading is required and the strengthening is only effected to ensure that the structural element can achieve ultimate strength.

16.6 Repair of Unbonded Post-Tensioned Concrete Structures

Prestressed concrete is a type of reinforced concrete construction in which steel reinforcement is tensioned so permanent internal compressive stresses in the concrete improve the response of a member of structure to loading. Compared to conventionally reinforced concrete, prestressed members typically have greater load capacity or deflect less for the same load. Two different procedures are used for prestressing concrete structures. In pretensioned concrete, the general repair principles presented in Section 16.5 are applicable. Figure 16.12 illustrates post-tensioning, where the steel is tensioned after the concrete has been cast and gains strength. Metal or plastic ducts are used to prevent bond with multistrand tendons, whereas for single-strand tendons plastic sheathing is used. The prestressing force is transmitted to the concrete through bearing at mechanical anchorages. Tendons are usually stressed from one anchorage, known as the live end, or from both end anchorages if stress losses due to friction and curvature are significant. Pockets for stressing anchors are usually grouted to protect the hardware. If the duct is filled with a conventional grout, then bonding or partial bonding of the steel to the concrete is achieved. This is referred to as *bonded post-tensioned concrete*. In unbonded post-tensioned concrete, the duct remains unfilled after anchoring so the steel is not bonded to the concrete and is permanently free to move. Unbonded post-tensioning systems are more common in North America. Unbonded post-tensioning is used for applications ranging from buildings, bridges, and parking structures to pressure vessels, tanks, and earth-retaining structures. Steel used for unbonded applications includes high-strength wires, strands, and threaded bars. The most commonly used unbonded tendon is the monostrand system, which has a seven-wire, 0.5- or 0.6-in.-diameter, 270-ksi strand, as shown in Figure 16.13. The steel is covered with a corrosion-inhibiting grease or other coating and enclosed in a plastic sheath or a plastic or metal duct.

More than 2.0 billion square feet of unbonded post-tensioned concrete structures have been constructed in the United States since the mid-1960s. There is an ever-increasing need to repair and strengthen these structures to extend their service lives and to restore structural integrity. The need for repair and strengthening is primarily due to one or more of the following reasons: the strand is unintentionally damaged or cut, such as when coring concrete to install a mechanical pipe; there is a change in load or the space requirements of a structure, such as adding a stairwell; improper design or construction resulting in inadequate structural capacity; and corrosion of the prestressing strand or mechanical anchorages.

Prior to repairing an unbonded post-tensioned concrete structure, it is important to conduct a comprehensive engineering evaluation using the techniques previously discussed to determine the causes of observed problems. Because of the potential for tendon release, caution must be exercised during the evaluation and repair phases. The methods for assessing an existing unbonded post-tensioned concrete

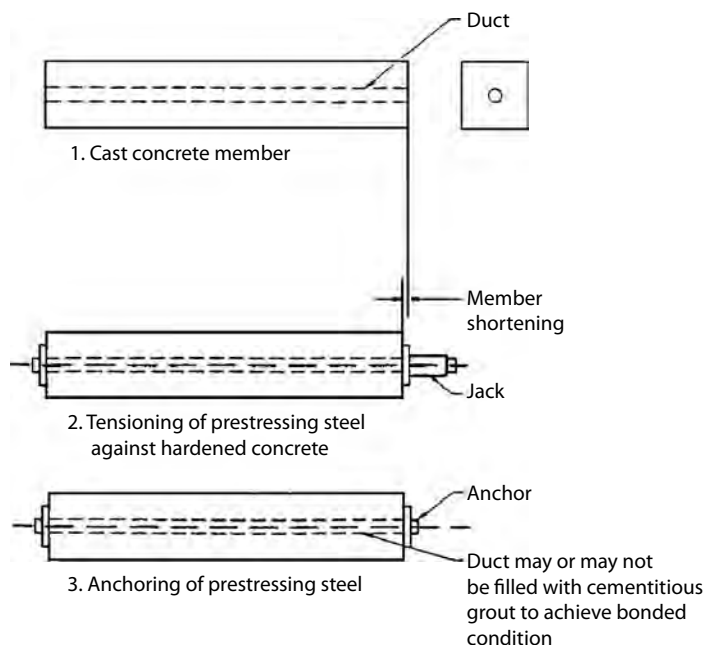


FIGURE 16.12 Post-tensioned concrete.

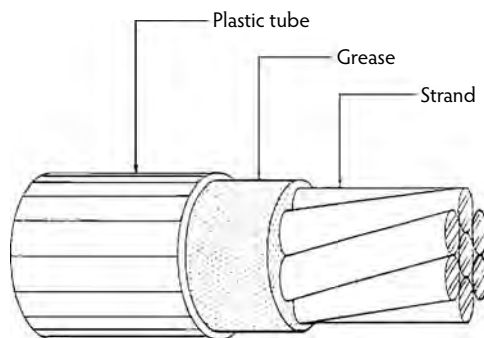


FIGURE 16.13 Plastic sheath filled with grease containing unbonded monostrand.

structure are, for the most part, the same as for a concrete structure constructed with mild steel reinforcement; however, the repair of existing unbonded post-tensioned structures is different in many respects.

The repair of unbonded post-tensioned concrete structures cannot be easily divided into categories where a certain type of repair is best for a certain type of problem. The type of repair depends on the expected cost of the repair, cause of the problem, the need to maintain service of the structure, whether the repair is to a beam, slab or other structural member, and many other factors. Moreover, once repairs begin, the owner, engineer, and repair contractor must be able to adapt to unobserved latent defects and changed conditions. The most important axiom in the repair of unbonded post-tensioned structures is to expect the unexpected. The general types of repair of unbonded post-tensioning are classified as (1) do nothing, (2) tendon splice or replacement, and (3) strengthening by adding bonded reinforcement, structural members, or external post-tensioning to improve or increase structural capacity. If the repair is due to a corrosion problem, it is likely that other concrete repairs will be necessary because of the deterioration that is generally attendant with corrosion. As with all types of concrete repair, extreme caution should be exercised by all individuals during the investigation, demolition, and repair. The need for shoring and the sequence of repair should be thoroughly thought out prior to starting any work.

16.6.1 Do Nothing

On some occasions nothing needs to be done for a failed post-tensioned strand. If it is known unequivocally that one strand or possibly two have been accidentally severed, then these strands can be pulled out and not replaced. Section 18.20.4 of the ACI Building Code (ACI Committee 318, 2005) allows the total loss of prestress due to unreplaced broken tendons that does not exceed 2% of the total prestress. Thus, for example, in the case of a post-tensioned slab structure that might contain hundreds of tendons in a single floor, the loss of one strand without replacement would be acceptable and would not be considered to have a significant impact on structural integrity.

16.6.2 Tendon Splice or Replacement

Tendon splice or replacement is the most common form of repair to an unbonded concrete structure. This type of repair is generally cost effective when the number of tendons to be spliced or replaced is limited, although there have been several notable examples where the tendons in an entire structure have been replaced (Aalami and Swanson, 1988). Tendon replacement may include replacement of the strand or one or more of the anchorages, depending on access for retensioning and anchorage condition. This option is the repair method of choice if the strand has been severed or if corrosion is localized. The cost of tendon splicing or replacement can range between \$1500 and \$5000 per strand, depending on the difficulty of the repair and the number of strands required. If the strand to be spliced or replaced is already severed, then the repair is somewhat simplified. If the strand is still tensioned, then the following procedure is required:

- Choose a point in the structure in which the tendon is more accessible. If the location of the problem and thus the splice point is known, then choose that point. Locate the tendon by use of a pachometer. In more complicated repairs, radiography or SPR may be warranted.
- Make a shallow saw cut in the concrete surrounding the tendon that defines the limits of the concrete to be removed.
- Remove the concrete around the tendon by light chipping hammer or jackhammer.
- If the strand is to be respliced, it is preferable to install a temporary anchorage. After placing the temporary anchorage, the strand may then be cut using a grinder. If a temporary anchorage is impractical, then, exercising extreme caution by making sure no one is in the area of the entire tendon length, the strand may be cut using a grinder. After cutting through just two wires of a seven-wire strand, the strand will yield and then fracture, with an attendant loud noise from the energy release. In some cases, controlled heating of the strand over a length of several feet may be preferred. This is the case when sudden detensioning can push out wedges at inaccessible anchorages, making restressing of the tendons impossible. Heating can result in less shock and more control in the detensioning process.
- If the existing strand is to be replaced or partially replaced, the strand piece to be removed can now be pulled from the anchorage. A new strand, coated with a corrosion-inhibiting grease, can then be threaded through the existing duct. A special type of splicing hardware allows for retensioning at the point of splice. This is beneficial when access to the end anchorages does not allow the use of a standard hydraulic stressing jack.

When stressing has been completed, the concrete can be recast in the excavation. As previously discussed, it is generally preferred to use a concrete of similar strength and modulus as the existing concrete. Exposed reinforcing steel should be cleaned and coated for corrosion protection. Exposed concrete surfaces should be sprayed with water prior to casting concrete. Curing should follow established good practices. In some cases, the entire post-tensioning strand may have to be replaced because of corrosion. In other cases, such as in buildings where access for splicing may be difficult, anchorages at the edge of a member can become the splice point. If the existing anchorage is not easily accessible for jacking, then a new anchorage can be added for ease of constructability.



FIGURE 16.14 New anchorages and bursting steel.

It is important to emphasize that if the strands are still tensioned and the anchorages are still engaged, do not try to release the stress by jack-hammering around the anchorage. This is very dangerous. Instead, as previously noted in the procedure for splicing, cut a slot in the concrete away from the anchorage zone. Making sure that no one is in the way of the tendon trajectory at the ends of the structure or above or below, the strands can be detensioned using a grinder or by heating at the control point. Again, expect a loud noise when several of the wires of the seven-wire strand have been cut. Removal of the anchorages can begin by first placing a shallow saw cut around the boundary of the anchorage zone. The concrete can then be removed by light chipping. The anchorages and strand can then be removed.

Figure 16.14 shows an arrangement of new corrosion-protected anchorages in place. Note that new mild reinforcement for control of anchorage zone bursting stresses has been placed just in front of the anchorages. In this case, the replacement anchorages are epoxy coated, and the plastic transition trumpets are attached integrally to the anchorages and the extruded sheathing to prevent water intrusion. The trumpet is filled with a corrosion-resistant grease. To expedite retensioning of the replaced tendons, a high-early-strength concrete may be used. In no circumstances should it contain calcium chloride as an accelerator. Many of these high-early-strength concrete materials can gain enough strength (>4000 psi) in 24 hours to allow retensioning the next day.

16.7 Construction Issues

The disruption caused by repairs to an existing structure depends on the degree of deterioration, the type of the structure being repaired, time of day when the construction is being done, expertise of the selected contractor, and other factors. Disruption to the owners and users of the structure is virtually unavoidable. Disruption, however, can be minimized with a carefully thought out and detailed schedule that is issued by the contractor to the affected parties. Generally, by breaking the project into workable units that are taken out of service one at a time, completed, then brought back into service is preferable to taking all of the affected areas out of service. Repairs of this nature cost more but allow for continued use of at least a portion of the structure. Historically, the knowledge level of repair contractors was not what might have been expected, but today many more competent and knowledgeable contractors are available for conducting specialized concrete repairs. This has resulted in high-quality, cost-competitive structural concrete repairs.

16.8 Long-Term Repair Performance

The question most often asked by owners relates to the anticipated long-term performance of repair alternatives. If this question can be answered with certainty and repair and maintenance costs are known, then it is a relatively simple matter to conduct a benefit/cost analysis. Of course, how long something will last depends on numerous variables, such as quality of repair, exposure conditions, maintenance, and a host of other factors, most of which are difficult to define. As part of a repair program, costs for a return after the first year to conduct an engineering inspection of the repairs should be included. If the budget permits, embedded sensors, such as wires to measure half-cell potentials, and a corrosion-rate probe should be included to monitor the repairs. All structures require maintenance. This is even more true with a repaired structure. Depending on the nature of the effected repairs, annual maintenance costs on the order of 1 to 5% of the repair costs may be appropriate for maintaining the repaired structure.

16.9 Case Study

To illustrate some of the general principles involved in structural concrete repair, a detailed case study of a large infrastructure rehabilitation project is presented here. This case study of an existing seawall clearly shows the value of conducting an informed evaluation prior to undertaking the repair design. It demonstrates the necessity of determining the cause of deterioration and selecting a multifaceted repair approach to meet the expressed objective of extending the service life for 30 more years. Utilizing a comprehensive approach in this infrastructure repair project ultimately saved the funding public agencies \$6 million on a \$15 million project.

16.9.1 Background

The 7.5-mile Marina del Rey Seawall was constructed in western Los Angeles, California, during the late 1950s and early 1960s as a means of reclaiming a low-lying swamp area for dry-land uses. Over \$5 billion of infrastructure has developed in and around this area. The original construction was high quality for the time. The vertical flexural reinforcement in the cantilevered wall has been subjected to aggressive saltwater exposure, principally through a construction joint located near the base of the wall (see Figure 16.15). The long-term exposure to seawater has led to chloride-induced corrosion of the reinforcing steel crossing the construction joint and attendant concrete deterioration on the hidden (land) side of the wall. Because of the nonredundant nature of the cantilever wall system, loss of primary vertical reinforcement at the wall base by corrosion results in a loss of overall structural integrity. In February 1986, a failure mechanism (see Figure 16.16) that resulted from severe corrosion of the vertical reinforcement occurred when an isolated 60-ft wall panel collapsed. An engineering investigation into the collapse concluded that the failure was caused by corrosion of the reinforcing steel due to exposure to natural seawater. No other factors were identified as having contributed to the collapse. To address concerns about the integrity of the seawall panels, a restoration program with three distinct focuses was developed by various public agencies:

- Utilize an impressed current cathodic protection system to mitigate active corrosion of the seawall reinforcing steel.
- Utilize a drilled caisson strong-back system to reduce reliance on the vertical reinforcing steel that had been subjected to corrosion and to upgrade the seismic behavior of the system. The strong-back concept was successfully installed during a trial repair in the marina.
- Conduct nondestructive impact-echo testing to locate areas where corrosion damage had occurred. This would allow for categorization of repairs based on the extent of delamination and concerns for life safety in areas of high public exposure. The impact-echo technique had been proven to be successful in locating corrosion-deteriorated areas in the seawall.

Figure 16.17 shows a schematic representation of the multifaceted seawall rehabilitation strategy. Each of the three distinct focuses of the restoration program is represented in this figure.

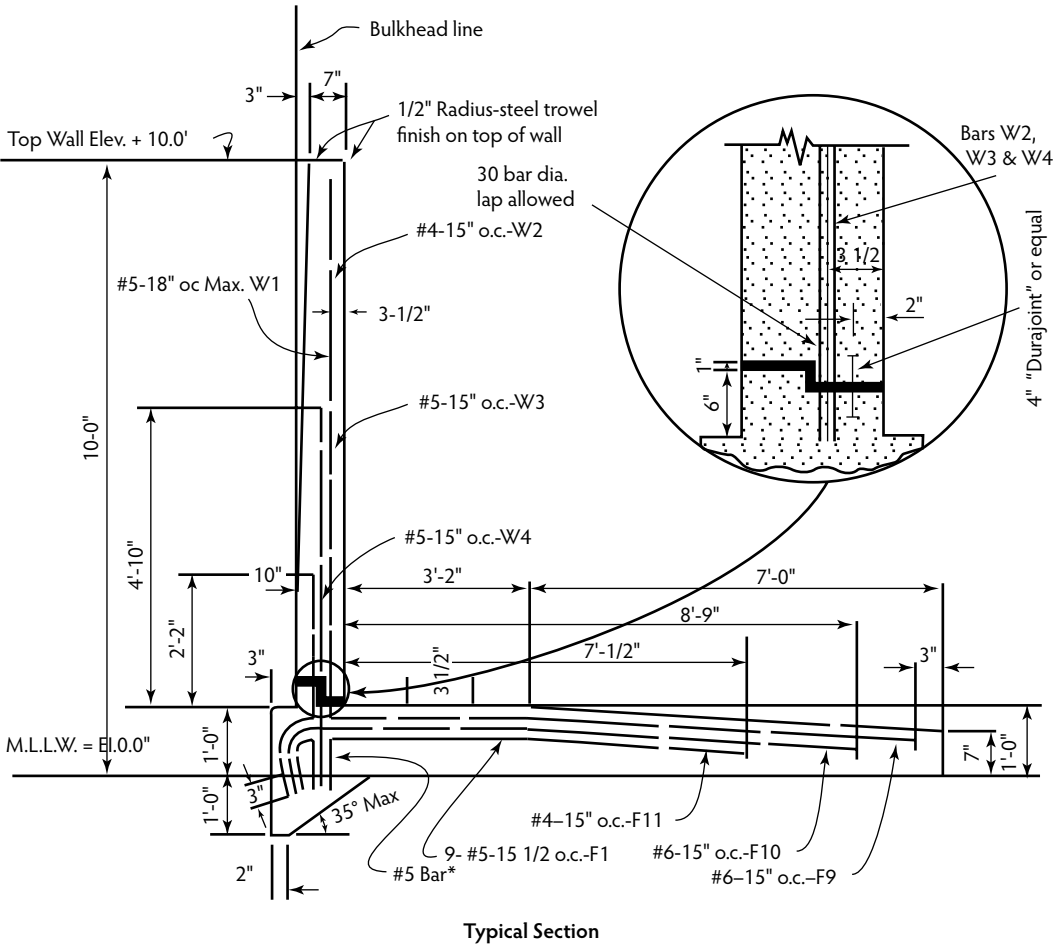


FIGURE 16.15 Typical reinforcing details of Marina del Rey Seawall. (From the original project drawings, October 1959.)



FIGURE 16.16 Failure of an isolated 60-ft wall panel due to corrosion.

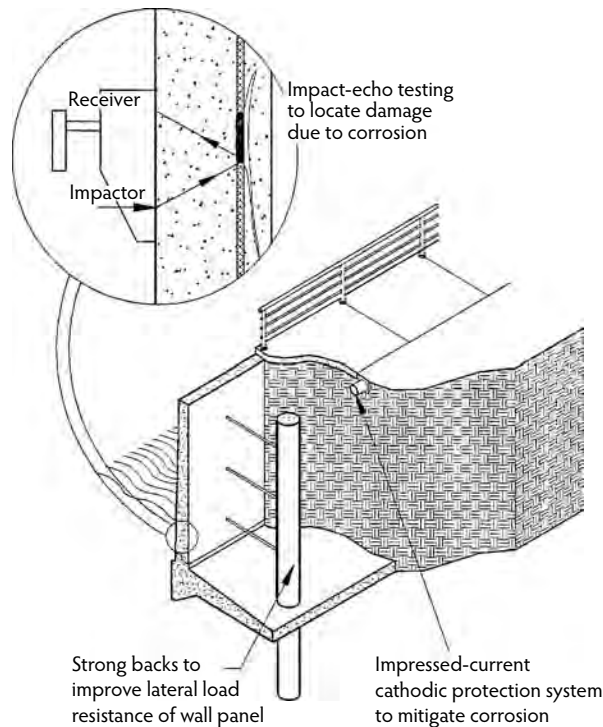


FIGURE 16.17 Schematic representation of proposed rehabilitation strategy for Marina del Rey Seawall.

16.9.2 Repair Strategy

Prior to development of the strong-back concept, several repair strategies were considered. The repair strategies included utilization of rip-rap ballast on the sea side of the wall, installation of precast panels anchored to caissons, and the use of soil tie backs. These preliminary designs were abandoned because they were cost prohibitive or failed to adequately address the seismic upgrading of the wall. As part of the strategic planning, it was decided that the rehabilitation must address the need to prevent additional corrosion damage along the base of the seawall, to upgrade the capacity of the seawall due to the loss of strength caused by the corrosion of the primary vertical reinforcing steel, and to provide seismic resistance that was not originally considered in the seawall design.

16.9.2.1 Full Damage along the Base of the Seawall

On the basis of the results of preliminary impact-echo testing and select concrete coring, significant reinforcing steel corrosion and attendant concrete deterioration were found to be present along the base of the seawall. Corrosion of reinforcing steel along the base of the seawall was determined to be the cause of the isolated seawall panel collapse in 1986. Because of these factors, all repair strategies had to assume that the vertical reinforcing steel at the vulnerable construction joint had lost capacity to carry tension if corrosion deterioration was found to be present; therefore, under a fully repaired condition, the connection between the wall and the footing was assumed to be hinged and only capable of transmitting shear across the joint.

16.9.2.2 Service Life of Repairs

The Marina del Rey Seawall had been in service for over 30 years. This was consistent with the expected design life of concrete structures. Much of this nation's concrete infrastructure is now routinely being rehabilitated because replacement is becoming more and more cost prohibitive. At the time of the evaluation, the seawall concrete was not showing any significant signs of visible deterioration due to abrasion, sulfate attack, or other mechanisms. Previous testing had shown levels of chloride-ion penetration

sufficient to cause chloride-induced corrosion; however, it was strongly believed that an effective rehabilitation strategy implemented in a timely fashion would extend the life of the seawall by another 30 years or more. To ensure a minimum 30-year life extension of the seawall, the repair strategy had to mitigate corrosion of the vertical reinforcing steel and provide a load path for forces originally carried by the deteriorated reinforcing steel. Corrosion engineers had indicated that the impressed current cathodic protection system would fully mitigate the corrosion of the vertical reinforcing steel. In essence, it was indicated that the corrosion would virtually stop and the corrosion rate would be essentially zero. The strong-back repair system had been shown to be effective in carrying loads in a panel with existing deterioration along the wall base. With the implementation of these rehabilitation measures, the service life of the seawall could clearly be extended by 30 years or more.

16.9.2.3 Strategic Ordering of Repairs

Because of life safety concerns and budget constraints, a strategic ordering of repairs was developed. This logical ordering of repairs was developed to ensure that areas of high public access, such as parks, were given high priority in the ordering of repair to address life safety concerns. Because only a portion of the needed funding was in place at the time, the repairs were categorized to address budget constraints. Impact-echo test results were evaluated to locate wall panels with significant deterioration that would be categorized as the highest priority.

16.9.3 Life-Cycle Cost Analysis

Because of the complex interaction of concrete corrosion and repair issues, life safety considerations in the marina area, and the budget constraints of the various municipal and state agencies involved, a life-cycle cost analysis of the marina seawall refurbishment project was requested. The principal objective of this analysis was to consider and prioritize various facets of the seawall refurbishment project so critical decisions could be made with due consideration of the concerns of all agencies and with respect to a logical and strategic ordering of the repairs. Figure 16.18 shows a schematic representation of the interaction of issues that were considered in the Marina del Rey Seawall rehabilitation project.

16.9.3.1 Life Safety Issues

The Marina del Rey area serves as a mixed-use residential and recreational area. Present in the marina are boat yards, restaurants, parks, and residential areas. It was anticipated that the areas of public exposure would be of high priority in the seawall repairs. Use of impact-echo testing in these areas further prioritized the repair sequencing on the basis of the amount of damage detected in panels in public areas. Significant damage detected in areas of high public exposure were naturally categorized as higher priority.

16.9.3.2 Seismic Upgrade

In addition to considering the corrosion-induced deterioration, the engineering design for the Marina del Rey Seawall refurbishment project mandated upgrading the seismic capacity of the seawall. The original design did not consider seismic loading. Development of the seismic retrofit included consideration of the degree of corrosion-induced deterioration as determined by impact-echo testing. This deterioration was modeled as a loss of vertical reinforcing steel capacity at the base of the seawall. As the degree of deterioration increased, additional caissons (strong-backs) were required to upgrade the capacity of the seawall. The wall was upgraded to survive the maximum credible seismic event even though damage would be expected. The proposed strong-back repair strategy minimized the risk of wall collapse during the maximum credible earthquake.

16.9.3.3 Sequence and Ordering of Testing

To provide information on the deterioration level at various locations in the marina, a sequence of impact-echo testing was developed. The sequence and ordering prescribed that a small number of panels should initially be tested in all basins. The preliminary testing provided an initial deterioration assessment for the various structural engineering tasks.

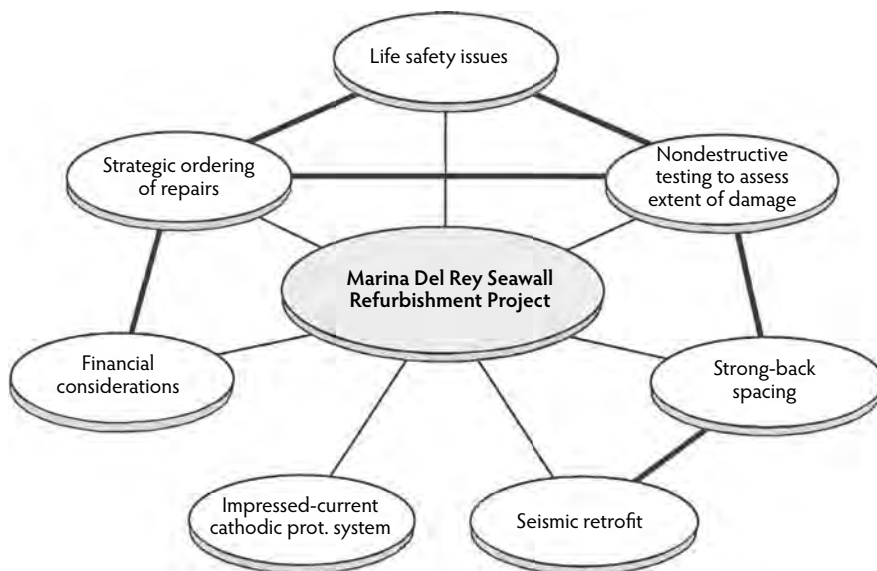


FIGURE 16.18 Interaction of issues being considered in the Marina del Rey Seawall refurbishment project.

16.9.3.4 Deterioration Ratings

Impact-echo testing was used to locate areas where physical manifestations of corrosion damage were present. This information was used to develop deterioration ratings that correlated to the number of caissons required. Both the effects of continuous damage and isolated damage were considered. Using corrosion damage models, ratings were developed to distinguish the number of caissons required at varying levels of deterioration. The models were based on estimated lengths of continuous or intermittent damage along the construction joint. As impact-echo testing results became available, modifications were made to the preliminary damage models. Using the corrosion-damage models previously discussed, caisson spacing parameters were developed. The parameters delineated when additional caissons were required due to the extent of corrosion damage and to minimize the risk of collapse during the maximum credible earthquake.

16.9.3.5 Design Guidelines

The following criteria were agreed upon by the various public agencies involved for developing the life-cycle cost analysis:

- Maximum credible seismic event—0.5-g lateral acceleration
- Surcharge loading—2 ft of soil
- Design life for all rehabilitation measures—30 years

No guidelines were established for a serviceability-level seismic event. In essence, the seismic retrofit strategy was to minimize the risk of collapse during the maximum credible seismic event. Damage to the wall during the maximum credible earthquake would be expected and acceptable. After completion of the life-cycle analysis, the parameters were modified to reflect further refinement and development of the analysis models based on the results obtained from the geotechnical investigation and impact-echo testing.

16.9.4 Impact-Echo to Assess Deterioration

Various studies were conducted as part of the strategic planning of the Marina del Rey Seawall refurbishment project. Numerous nondestructive test methods were reviewed as candidates for assessing deterioration of the seawall due to corrosion-induced delaminations. The majority of nondestructive

testing techniques for assessing reinforcing steel corrosion, such as measurement of half-cell corrosion potentials and chloride-ion content, provide only limited, indirect information about whether or not corrosion is occurring. These testing measures do not provide an assessment of the amount of corrosion damage or the degree of concrete deterioration present.

Stress-wave propagation methods known as *pulse-echo* and *pitch-catch* were reviewed as candidates for detecting damage on the soil side of the wall in the vicinity of the construction joint. These methods had limitations that made them impractical for use on the seawall as constructed. During the project development, the transient stress-wave method known as impact-echo was examined as a possible candidate for nondestructively determining the location of corrosion-induced deterioration. This method was determined to be well suited for finding flaws in concrete. The reader is referred to Section 16.3.3.1 for a description of the impact-echo method.

It is important to note that, although impact-echo is effective for finding flaws in concrete structures, such as the corrosion-induced delaminations on the soil side of the wall near the level of the construction joint at the base of the wall, it cannot assess the amount of deterioration in terms of degree of steel-reinforcement corrosion. In this case, impact-echo was used to locate the manifestation of corrosion—that is, the attendant delamination of the concrete caused by reinforcing steel corrosion—but it was not used to assess the degree of corrosion. This implies that, when using the impact-echo method, if a delamination or defect is found it is assumed that the reinforcing steel at this location is in essence completely corroded. There could have been some measure of steel area that was still effective, but for condition-assessment purposes, the steel was assumed to be ineffective for developing a tension force and thus incapable of carrying moment at the base of the wall. This was a conservative assumption in the context of the rehabilitation design.

16.9.5 Reliability in Assessing Deterioration

16.9.5.1 Previous Trial Studies on the Seawall

It is generally beneficial in larger projects to conduct trial testing and, in some cases, repairs to prove the veracity of the methods. This approach provides confidence for all parties concerned prior to spending large sums of money. In the case of the seawall project, previous studies that assessed the efficiency of using impact-echo to detect corrosion-induced deterioration on the unobservable soil side of the seawall clearly indicated the veracity of the method. Concrete coring at select locations of delaminations located by the impact-echo method demonstrated the reliability of the procedure for detecting damage.

16.9.5.2 Test Locations

A visual examination in a trial study that sliced a piece of the wall clearly showed that the damage caused by corrosion of the vertical reinforcing was in the range of about 10 to 20 cm (4 to 8 in.) above the construction joint. The average of this range was 6 in., which was used to define the height of impact-echo testing in the field-test program. It is also important to note that a trial study indicated that the corrosion appeared isolated to the local region near the construction joint. All seawall panels were tested about 6 in. above the construction joint as part of the field evaluation; however, select panels were tested on a two-way horizontal and vertical grid to confirm that the damage was generally confined to the region near the construction joint. Figure 16.19 presents a schematic representation of the approximate area of influence during impact-echo testing for the geometry of the wall and assumed type of corrosion-induced delamination. Note that the influence area is on the order of 27 in.; thus, testing on 25-in. centers provided for about a 2-in. overlap. Based on generalized stress-wave propagation principles, there was assurance that most delaminations were located and that finding the delaminations was independent of whether the test was conducted directly over a reinforcing bar. The 25-in. spacing used in the evaluation program was determined to be sufficient to detect most of the damage that was present.

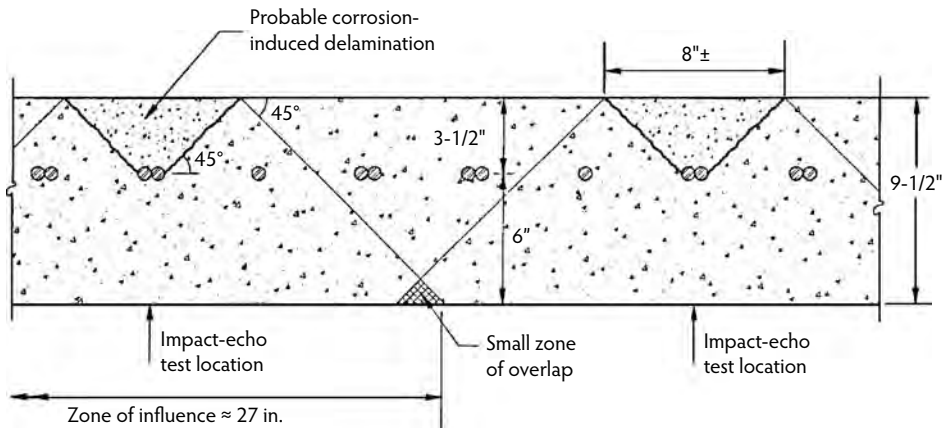


FIGURE 16.19 Influence area of impact-echo test on seawall for anticipated corrosion-induced break delamination.

16.9.6 Cathodic Protection

The galvanic corrosion of reinforcing steel in concrete is an electrochemical process in which the reinforcing steel reacts with water and oxygen to form iron-oxide products (rust). For galvanic corrosion to occur, four elements must be present. The elements are anodes (locations where corrosion activity occurs), cathodes (areas that are protected by the corrosion activity at anodes), a metallic path between the anodes and cathodes, and an electrolyte. The metallic path is provided by the horizontal and vertical reinforcing steel mat. Moisture in the soil backfill, seawater, and moist concrete all serve as the electrolyte. The corrosion cell is driven by the differences in electrical potential that exist between the anodic and cathodic areas. Figure 16.20 shows a schematic representation of the electrochemical process of corrosion of reinforcing steel.

Cathodic protection (CP) is an electrochemical technique in which external anodes are added to the electrochemical cell present in the seawall. The addition of external anodes to the seawall structure resulted in the shift of electrical potentials at the reinforcing steel from anodic (actively corroding) to cathodic values (noncorroding). Figure 16.21 shows a schematic representation of both sacrificial anode and impressed current cathodic protection systems. Two types of cathodic protection systems were considered for the Marina del Rey Seawall. A galvanic or sacrificial anode system utilizes metal (typically zinc) anodes attached directly to the reinforcing steel grid. When connected to the reinforcing steel grid, the sacrificial anodes corrode instead of the reinforcing steel. Corrosion of the sacrificial anode results in electrons traveling to the reinforcing steel, which further prevents corrosion of the seawall reinforcing steel. Sacrificial anode systems are best suited to areas of low electrical resistivity or to submerged areas. An impressed current cathodic protection system is similar to a sacrificial anode system, except that an external power supply is used to provide the electrical potential that drives the corrosion cell.

The seawall rehabilitation concept required that the horizontal (temperature and shrinkage) reinforcing steel carry the redistributed moments resulting from the caisson installation. This required protecting both the horizontal and vertical reinforcing steel from long-term corrosion. An impressed current cathodic protection system was determined to be better suited for long-term corrosion control. This was because of the location of the seawall above the mean low water level and the measured soil resistivities. A successful application of an impressed current cathodic protection system must ensure the electrical continuity of all protected areas. Reinforcing steel in both the horizontal and vertical directions was tested to ensure connectivity.

After installation of an impressed current cathodic protection system, the rate of reinforcing steel corrosion is effectively reduced to zero. This has been proven time and again in actual field applications. To mitigate corrosion, cathodic protection must have an electrolyte present. In the seawall, the seawater below the water table and the moist soil acted as the electrolyte. An electrolyte allows the flow of the

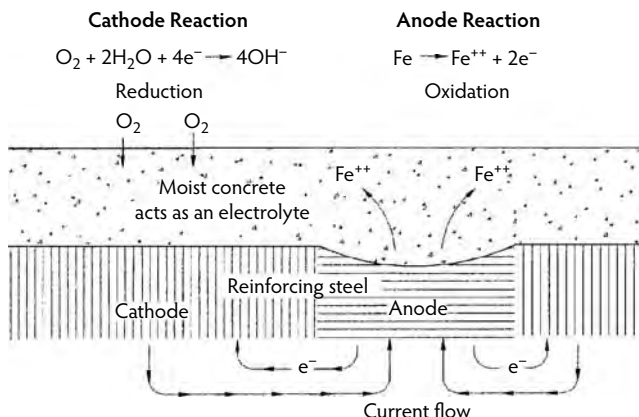


FIGURE 16.20 Schematic of electrochemical corrosion of reinforcing steel in concrete.

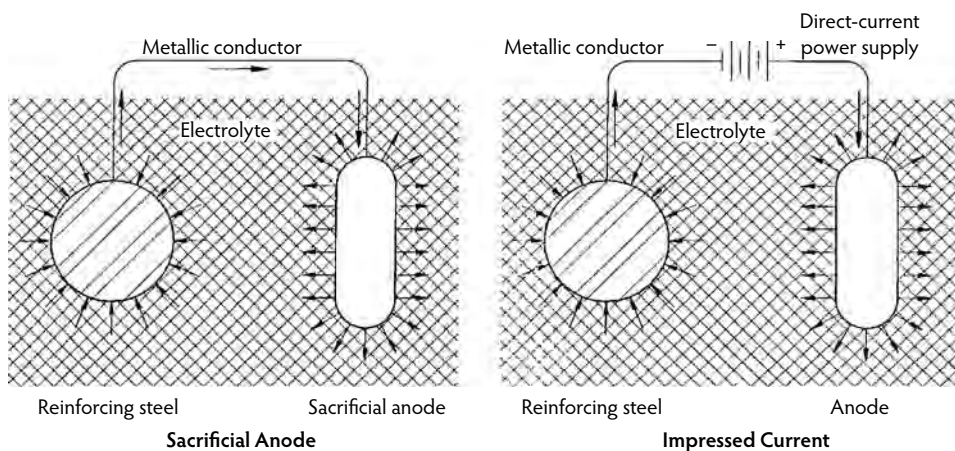


FIGURE 16.21 Schematic representation of cathodic protection systems.

impressed current from the sacrificial anode to the reinforcing steel in the seawall. In areas where concrete delaminations have occurred due to corrosion, the cathodic protection system will protect the existing reinforcing steel if sufficient electrolyte is present at these locations. The cathodic protection system cannot protect areas where an air gap is present between delaminated concrete and the reinforcing steel; however, this condition was not considered likely to be present to any significant degree.

The Marina del Rey Seawall refurbishment project was designed to provide a minimum 30-year life extension to the seawall. Accordingly, all facets of the rehabilitation strategy were designed for the ultimate serviceability and durability limit state to reflect a minimum 30-year life cycle. After installation of the cathodic protection system, no further reinforcing steel corrosion was expected to occur; thus, the 30-year service life was clearly attainable. The steel was, in essence, kept in its existing condition without further corrosion.

16.9.7 Structural Analysis

This section summarizes the results from various structural analyses that were conducted on a typical 60-ft wall panel. Analyses were conducted to assess the integrity of the existing wall without the strong-back system in place for various postulated damage models. Parametric analyses were then conducted for a typical seawall panel that incorporated different combinations of strong-backs (caissons) for postulated damage models and included the loads resulting from the assumed maximum credible seismic event.

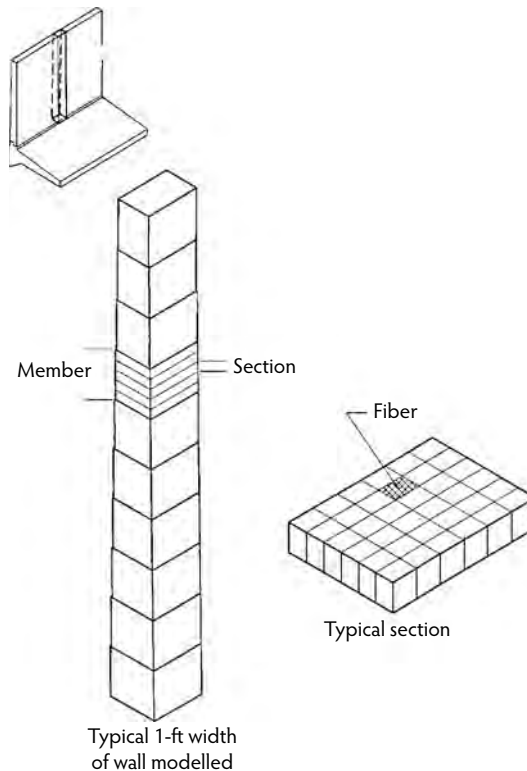


FIGURE 16.22 Representation of the nonlinear model used for analysis of a typical seawall panel.

16.9.7.1 Integrity of the Typical Existing Panel

Analyses were conducted to assess the integrity of a typical 60-ft wall panel in its current condition for various assumed damage models. The threshold damage in terms of the degree of corrosion necessary to cause collapse of a typical wall panel was then established by examining the results of these analyses:

- *Nonlinear analysis model.* To assess the integrity of a typical 60-ft seawall panel, as constructed for various assessed-damage models, a nonlinear analysis of the typical wall section was undertaken. The analytical model used a tangent stiffness formulation. Incremental loads were applied to the structure, then the incremental displacements and forces were calculated and added to the previous displacements and forces to obtain the new displacements and forces. The stiffness method is used to calculate incremental displacements from applied loads, and incremental forces are then computed from the displacements. The model uses a linear formulation that has been modified to include various nonlinear effects. The nonlinearities include second-order deflection effects (P-delta), geometric nonlinearity, and material nonlinearity. Analytically, failure occurs when defined material strength limits are exceeded or by the instability of the structure. Because the seawall was originally designed principally as a cantilever retaining wall, only a typical 1-ft width of wall was required to represent its behavior under lateral load. Figure 16.22 shows a schematic representation of the nonlinear model used for the wall. The reinforcing steel was terminated (cut off) at the appropriate wall height location as indicated in Figure 16.15. The wall taper was also duly accounted for in this analysis. The base of the wall was assumed to be fixed.
- *Loading.* Figure 16.23 summarizes the load conditions for which a typical seawall panel was analyzed under anticipated actual operating service load conditions. Note that these were not

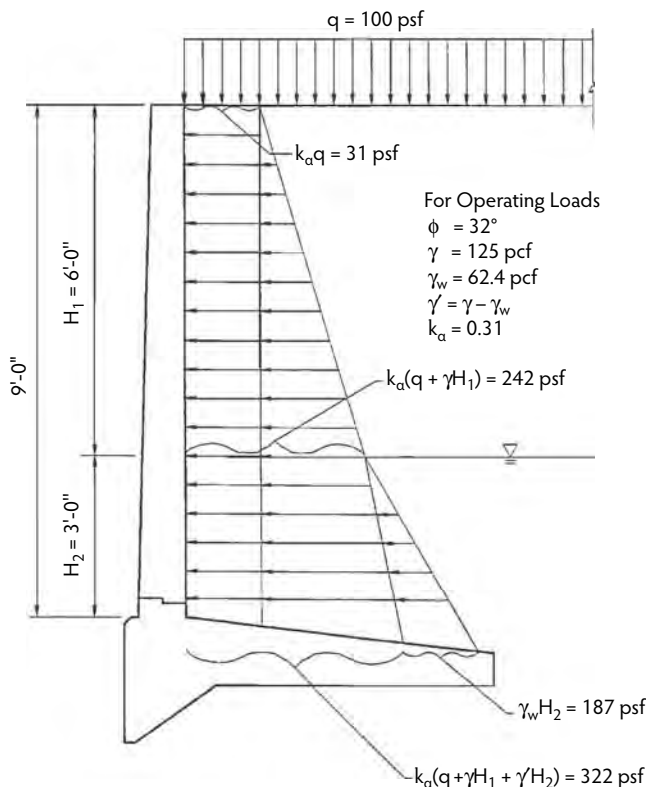


FIGURE 16.23 Estimated operating service wall loads.

design loads—they represented an assessment of the probable operating loads on the wall as might exist on a typical existing wall panel. For purposes of this analysis, no earthquake loading was considered.

- *Effect of reinforcing steel loss.* Analyses were conducted for the typical seawall panel assuming an average net section loss of reinforcing steel at the construction joint due to corrosion. Incremental lateral loads were applied to the wall for various cases of assumed reinforcing steel loss until a failure occurred. The loads due to the surcharge and water table were applied first, then the lateral earth pressure was incrementally applied until failure occurred. The parameters of interest in this type of analysis are the load necessary to cause failure compared to the probable in-service lateral earth pressure (see Figure 16.23) and the expected horizontal deflection at the tip of wall before collapse occurs (see Figure 16.24).

Table 16.4 summarizes the results of the nonlinear analysis of the wall for various postulated scenarios of the degree of corrosion of the vertical steel at the construction joint. The results of the analysis of the wall as constructed (0% loss of the reinforcing steel) indicated that the wall had adequate integrity for the probable existing operating loads if seismic loads were not considered. This suggested that, for wall panels determined to have little or no damage as established by impact-echo testing, some measure of strengthening to upgrade the wall for seismic loading was still needed. The analyses clearly revealed that, as the percentage loss of reinforcing steel due to corrosion increases, the load to cause failure and the associated horizontal wall deflection at the top of the wall at failure decreases. Further, the analysis results indicated that an average of about 60% (actual value, 62%) of the reinforcing steel at the construction joint must be lost to corrosion for failure of the wall to occur under current probable operating-load conditions.

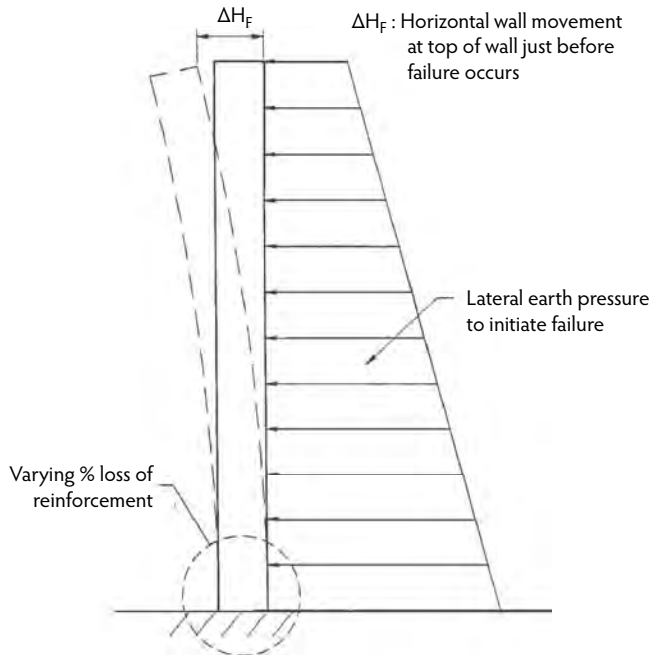


FIGURE 16.24 Horizontal deflection of wall just before failure.

This model assumes that the corrosion damage is uniformly distributed along the wall, which may not be the case. Contiguous damage would be even more detrimental than the uniform damage implicit in this analysis. This suggests that if impact-echo testing revealed that the wall along the construction joint indicated evidence of randomly distributed corrosion-induced delaminations (say, to about the 40% level), then the panel could be approaching collapse conditions and would naturally be of the highest priority in terms of repair sequencing.

The nonlinear analysis results also clearly indicated that there would be very little visual evidence of distress before failure occurred. Table 16.4 indicates that the horizontal deflection at the top of the wall is about 3/4 in. just before failure, assuming no corrosion damage; however, for the case of 62% average loss of reinforcement due to corrosion, the calculated horizontal movement at the top of the wall is only about 3/8 in. just before collapse occurs. This small amount of relative movement between adjacent wall panels over time would likely not be perceptible due to the observed construction tolerances and to wall rotations that may have occurred because of differential soil settlement. This analysis clearly indicated that there would be very little warning before failure.

TABLE 16.4 Summary of Nonlinear Analysis of Typical Wall Panel in Service

Assumed Percent Loss of Steel Reinforcement Due to Corrosion of Construction Joint	Ratio of Failure Load to Probable In-Service Lateral Earth Pressure	Horizontal Deflection at Top of Wall before Collapse (in.)
0	2.8	0.74 \approx 3/4
20	2.4	0.74 \approx 3/4
50	1.5	0.45 \approx 1/2
62	1.0	0.41 \approx 3/8
80	0.5 ^a	0.24 \approx 1/4

^a Indicates section fails at about one half of the present estimated operating service loads.

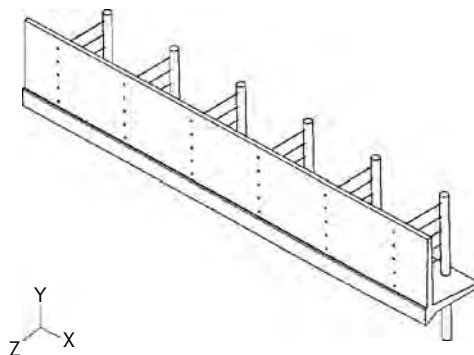


FIGURE 16.25 Seawall with strong-back retrofit.

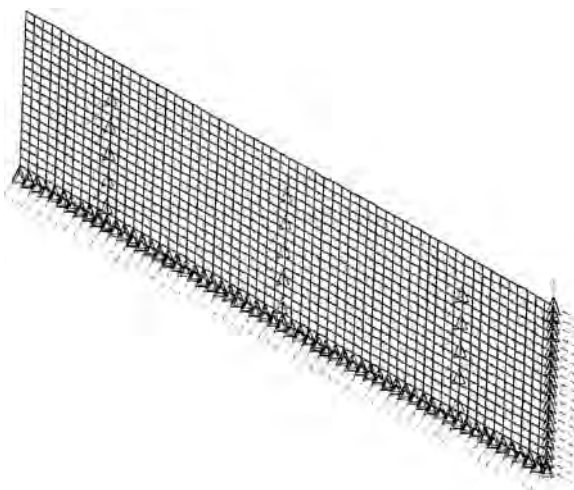


FIGURE 16.26 Finite-element model of a typical wall panel for a case with six caissons.

16.9.7.2 Finite-Element Analysis of the Wall With and Without a Strong-Back System

To evaluate the capacity of a typical 60-ft seawall panel for various reinforcing steel corrosion damage models and to assess the effect of strong-back spacing, a parametric study was conducted using linear elastic finite-element analysis techniques.

16.9.7.2.1 Model

A typical 60-ft seawall panel with the proposed strong-back retrofit is shown in Figure 16.25. To evaluate the effects of reinforcing steel corrosion and strong-back spacing on the seawall stem, a finite-element model was developed for the stem using four node isotropic plate elements. A finite-element model with six caissons installed is shown in Figure 16.26. It should be noted that the finite-element model took advantage of geometric symmetry about the centerline of the 60-ft seawall panel. For this analysis, it was assumed that loading, strong-back spacing, and reinforcing steel corrosion damage were symmetrical about the centerline of the seawall. For simplicity, only one half of the seawall was modeled for the parametric study using appropriate boundary conditions at the plane of symmetry. For comparison, a typical horizontal moment dithering for the half-model using symmetry and for a model of the full 60-ft seawall panel is shown in Figure 16.27. Note that the computed moments are identical, indicating the validity of the symmetry model. A 6×6 -in. element grid was used for the model. Element thickness varies to correspond with the taper in the face of the seawall.

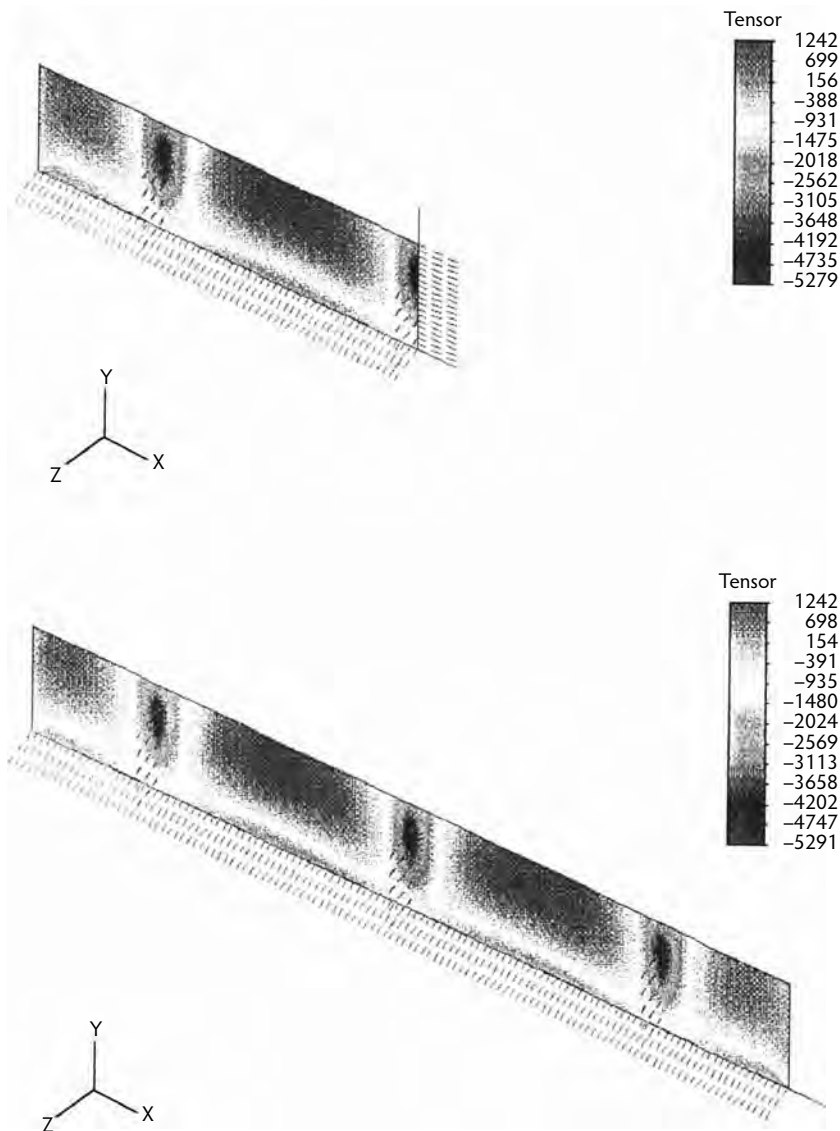


FIGURE 16.27 Horizontal moments from the full and symmetric models (ft-lb/ft).

Because the capacity of a typical seawall panel is dependent on the strength of the stem, it was not necessary to model the seawall footing. Instead, boundary elements were used to model the interface between the seawall stem and footing. To model the condition of no loss of reinforcing steel at a particular node, a boundary condition constraining translation and rotation about the three axes was assumed. To model the condition of total loss of reinforcing steel at a particular node, a boundary condition constraining translation, but not rotation, about the three axes was assumed. Also, the interface between the seawall and the strong-back system was modeled using translational boundary elements with an assumed spring constant. For this analysis, explicit modeling of the caisson was not necessary. A tie-back spring constant was assumed to connect the wall to a rigid element (the caisson). A spring constant of 200 kips/in. was assumed. Five tie backs were assumed for each caisson location, spaced 1 ft, 6 in. on-center starting 2 ft from the top of the wall.

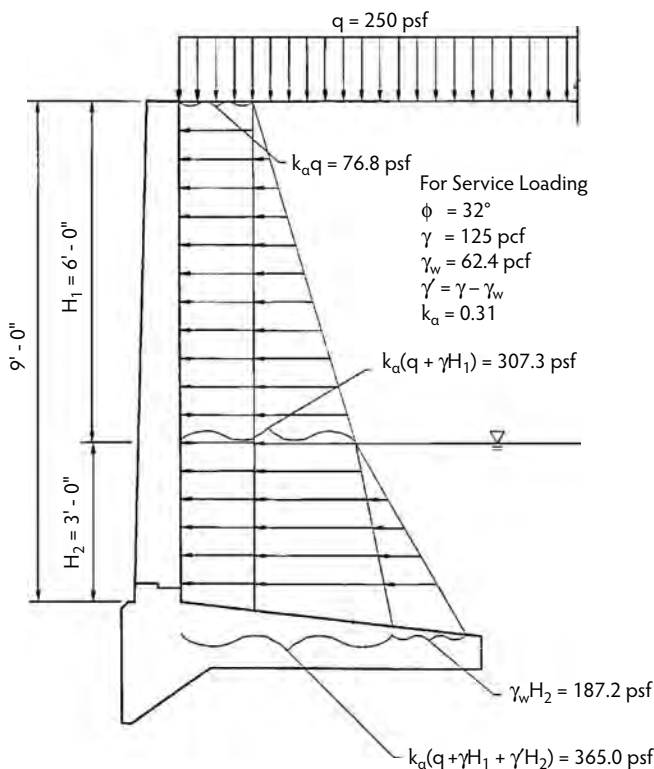


FIGURE 16.28 Preliminary design earth-pressure loads.

16.9.7.2.2 Loading

The loads imposed on the stem of the seawall are primarily due to lateral earth pressure. Using Rankine theory, the active lateral earth pressure diagram shown in Figure 16.28 was developed, using the following parameters derived from a comprehensive geotechnical investigation:

- Soil friction angle (ϕ) = 32
- Unit weight of soil (γ) = 125 pcf
- Unit weight of water (γ_w) = 62.4 pcf
- Active pressure coefficient (K_A) = 0.31
- 2-ft soil surcharge load

To determine earthquake loads, a seismic analysis was performed using a procedure by Mononobe and Okabe, as described in the AASHTO Specifications (1992). This procedure, which uses an equivalent static loading, replaces the active soil coefficient (K_A) with a seismic active soil coefficient (K_{AE}). Using a horizontal acceleration of 0.5 g based on a geoseismic study of the area, K_{AE} was calculated to be 0.62. The following design load combinations were calculated in accordance with Appendix C of the ACI Building Code (ACI Committee 318, 2005):

$$U = 1.7H \quad (16.2)$$

$$U = 0.75(1.7H + 1.7(1.1E)) \quad (16.3)$$

where:

- U = required strength to resist factored loads.
- H = earth pressure.
- E = lateral earth pressure due to earthquake loading.

TABLE 16.5 Moment and Shear Capacities of a Typical Undamaged Wall Panel

Inches	Vertical Moment		Horizontal Moment		Shear (lb/ft)
	Negative (ft-lb/ft)	Positive (ft-lb/ft)	Negative (ft-lb/ft)	Positive (ft-lb/ft)	
0	-12,229	6292	-3636	2534	4190
6	-11899	6292	-3531	2534	3230
12	-11569	6292	-3426	2534	3980
18	-7133	6292	-3321	2534	3870
24	-6928	6292	-3216	2534	3760
30	-6723	4058	-3111	2534	3660
36	-6518	4058	-3006	2534	3550
42	-6313	4058	-2901	2534	3440
48	-2442	4058	-2796	2534	3330
54	-2362	1642	-2691	2534	3230
60	-2282	1642	-2586	2534	3120
66	-2202	1642	-2481	2534	3010
72	-2122	1642	-2376	2534	2900
78	-2042	1642	-2271	2534	2800
84	-1962	1642	-2166	2534	2690
90	-1882	1642	-2061	2534	2580
96	-1802	1642	-1956	2534	2470
102	-1722	1642	-1851	2534	2370
108	-1642	1642	-1746	2534	2260

The seismic load combination in Equation 16.3 resulted in forces approximately 60% larger than the load combination in Equation 16.2, which considers only the static lateral earth pressure. Thus, the load combination in Equation 16.3 governed the analysis. The appropriate load combinations were used in conjunction with the lateral earth pressure diagram shown in Figure 16.28 to determine the pressure loads used in the finite-element analysis.

16.9.7.2.3 Wall Capacities

Moment and shear capacities were calculated for the stem of the seawall in accordance with the ACI Building Code and are summarized in Table 16.5. These capacities were calculated using the reinforcing steel details shown on the original plans, and $f' = 4000$ psi and $f_y = 40,000$ psi. Review of the original construction records indicated a concrete strength of 3000 psi as used in the original seawall design. The results of compressive-strength tests conducted during the field investigation indicated an average compressive strength of 4400 psi for the concrete at the time of the evaluation some 35 years later. These test results justified the use of 4000 psi as the *in situ* concrete compressive strength for the repair design.

16.9.7.2.4 Analysis Results

Various combinations of reinforcing steel corrosion damage scenarios and strong-back spacing were analyzed using the finite-element model and load combinations previously discussed. A summary of the cases analyzed is presented in Table 16.6. The results of each analysis case were examined and compared with the moment and shear capacities listed in Table 16.5. Vertical and horizontal shears and moments were examined separately, similar to the ACI analysis procedures used for two-way slab design. Sample outputs of horizontal and vertical moments are shown in Figure 16.29 and Figure 16.30, respectively, for Case 8 (six strong-backs, 100% corrosion of vertical reinforcing steel, and load combination (Equation 16.2)).

Negative horizontal moments that occur at strong-back locations were redistributed, as allowed by Section 8.4 of the ACI Building Code. A maximum redistribution limit of 40% was also examined in lieu of the more restrictive 20% limit imposed by ACI. With the lower reinforcement ratio of the horizontal reinforcing steel, it was believed that the wall would exhibit adequate ductility to allow this larger redistribution limit with the caissons in place. For the final design, a detailed moment-curvature analysis of the wall ductility generally confirmed this assumption.

TABLE 16.6 Summary of Finite-Element Analysis Cases

Case Number	Corrosion of Vertical Steel at Construction Joint (%)	Load Combination	Number of Strong-Backs
1	0	1	None
2	0	2	None
3	0	2	2
4	0	2	3
5	0	2	4
6	100	2	4
7	100	2	5
8	100	2	6
9	100	2	7
10	8	2	4
	(5 ft at one end)		
11	17	2	4
	(5 ft between strong-backs)		
12	17	— ^a	None
	(10 ft at one end)		
13	17	— ^a	None
	(8 ft at one end)		

^a Anticipated actual operating service-load conditions.

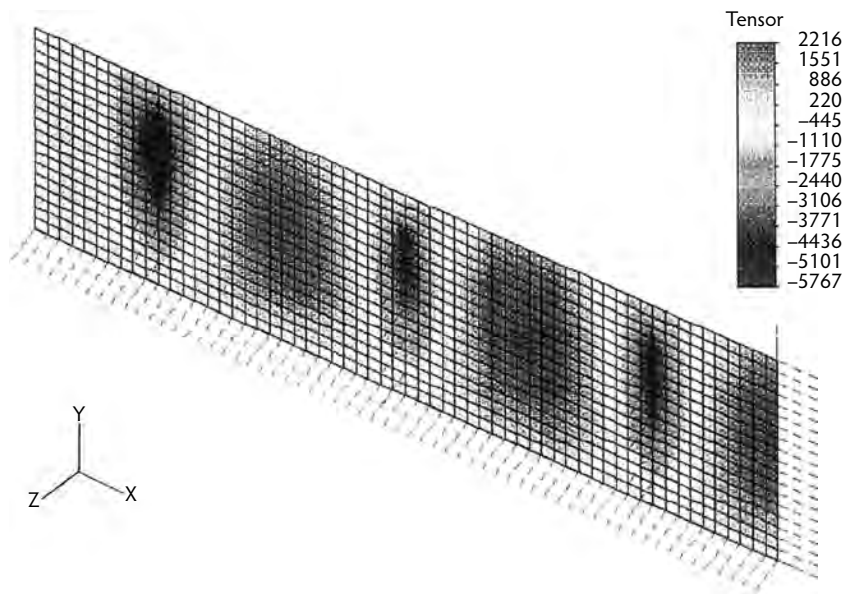


FIGURE 16.29 Horizontal moments for case 8 (ft-lb/ft).

- *Case 1.* The Case 1 analysis examined a typical seawall panel with no corrosion of vertical reinforcing steel, no strong-backs, and no earthquake loading. The average vertical moments were typically slightly below the calculated capacities; however, an 8.5% overstress occurred at the interface with the footing, and a 17% overstress occurred 1 ft, 6 in. above the footing. Considering that a larger value of compressive strength was used for the analysis than was originally specified, the overstress indicated that either the load assumptions or the design procedures used for the analysis were more conservative than those used for the original design. Hand calculations were also done for this case and were used to verify the results of the finite-element analysis.

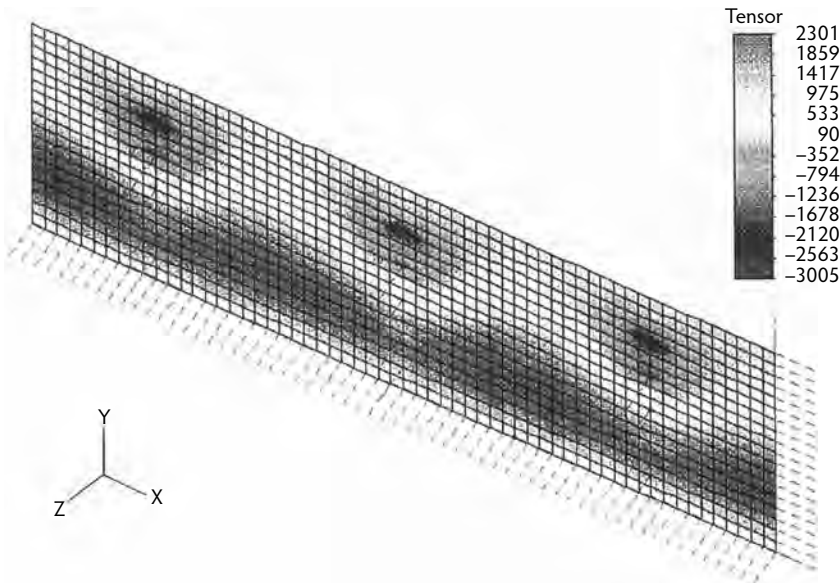


FIGURE 16.30 Vertical moments for case 8 (ft-lb/ft).

- *Case 2.* The Case 2 analysis examined a typical seawall panel with no corrosion of vertical reinforcing steel and no strong-backs for earthquake loading. The average vertical moments were larger than the wall capacity from the intersection with the footing to a height of 5 ft, 6 in. above the footing. The overstress at the interface of the footing was 71%. The results of this analysis indicated the need for a retrofit to address earthquake loading even if there was no corrosion damage.

Using the strong-back retrofit concept, the next three cases were used to determine the minimum number of strong-backs required for earthquake loading, assuming no corrosion of vertical reinforcing steel:

- *Case 3.* The Case 3 analysis examined a typical seawall panel for earthquake loading assuming no corrosion of vertical reinforcing steel and strong-backs placed 15 ft from each end. By inspection of the horizontal and vertical moments, it was clear that two strong-backs would be ineffective for reducing the vertical movement to an acceptable level.
- *Case 4.* The Case 4 analysis examined a typical seawall panel for earthquake loading assuming no corrosion of vertical reinforcing steel and three strong-backs placed at a spacing of 20 ft. The average vertical moment at the base of the seawall for a middle strip equal to half the distance between strong-backs was 13,840 ft-lb/ft, which was 13% larger than capacity. In addition, considering a 40% moment redistribution, the average positive and negative moments for the top 4.5 ft of the seawall were 2710 ft-lb/ft and -2460 ft-lb/ft, respectively, resulting in overstresses of 7% and 11%. A more detailed analysis of earthquake loading, soil properties, and surcharge loading provided justification for reducing the load level, thus it was determined that three strong-backs would provide the required lateral-load resistance.
- *Case 5.* The Case 5 analysis examined a typical seawall panel for earthquake loading assuming no corrosion of vertical reinforcing steel and four strong-backs placed at a spacing of 15 ft. The average vertical moment at the base of the seawall for a middle strip equal to half the distance between strong-backs was 13,220 ft-lb/ft, which was 8% larger than capacity. However, considering a 35% moment redistribution, the average positive and negative moments for the top 4 ft, 6 in. of the seawall were 2430 ft-lb/ft and -2250 ft-lb/ft, respectively, both less than the average capacities for

these regions. Although the vertical moment at the base is slightly overstressed, the horizontal moment capacity was considered adequate when considering a 35% moment redistribution. Based on analysis of the results for Case 5, the installation of a minimum of four strong-backs at each typical panel would be required for the assumed earthquake loading.

The next four cases were used to determine the maximum number of strong-backs required for earthquake loading assuming 100% corrosion of the vertical reinforcing steel:

- *Case 6.* The Case 6 analysis examined a typical seawall panel for earthquake loading assuming 100% corrosion of the vertical reinforcing steel and four strong-backs placed with a spacing of 15 ft. By inspection of the positive and negative horizontal moments, it was clear that both were significantly overstressed.
- *Case 7.* The Case 7 analysis examined a typical seawall panel for earthquake loading assuming 100% corrosion of the vertical reinforcing steel and five strong-backs placed at a spacing of 12 ft. As with Case 6, inspection of the positive and negative horizontal moments made it clear that both were significantly overstressed.
- *Case 8.* The Case 8 analysis examined a typical seawall panel for earthquake loading assuming 100% corrosion of the vertical reinforcing steel and six strong-backs placed at a spacing of 10 ft. The average positive and negative moments for the top 4 ft, 6 in. of the seawall assuming a 40% redistribution were 3500 ft-lb/ft and -2340 ft-lb/ft, respectively, resulting in overstresses of 38% and 6%. Considering the level of overstress of both the horizontal positive and negative moments, the installation of six strong-backs would not be sufficient to resist the loadings assumed in the preliminary study. Again, it was later determined that six strong-backs was the maximum number required for a given 60-ft seawall panel when more refined soil parameters became available.
- *Case 9.* The Case 9 analysis examined a typical seawall for earthquake loading assuming 100% corrosion of the vertical reinforcing steel and seven strong-backs placed at a spacing of 8 ft, 6 in. The average positive and negative moments for the top 4 ft, 6 in. of the seawall using a 35% redistribution were 2480 ft-lb/ft and -2000 ft-lb/ft, respectively, both less than the average capacities for these regions.

Based on analysis of the results for Case 9, a maximum number of seven strong-backs would be required for the assumed earthquake loading; therefore, it was determined that for the loading conditions each seawall panel required the installation of seven strong-backs, depending on the amount of vertical reinforcing steel corrosion. This requirement was relaxed to three to six caissons on the basis of the results from the soil investigation and refinements in the seismic and surcharge loadings. Case 10 and Case 11 examined the effect of a continuous strip of reinforcing steel corrosion damage on strong-back spacing:

- *Case 10.* The Case 10 analysis examined a typical seawall panel for earthquake loading assuming 5 ft of continuous (8%) corrosion of the vertical reinforcing steel at the end of a panel and four strong-backs placed at a spacing of 15 ft. Based on the analysis of this case, 5 ft of continuous corrosion of the vertical steel at the end of a panel required an additional strong-back.
- *Case 11.* The Case 11 analysis examined a typical seawall panel for earthquake loading assuming 5 ft of continuous (8%) corrosion of the vertical reinforcing steel, centered between two strong-backs, assuming four strong-backs placed at a spacing of 15 ft. The average positive and negative moments for the top 4 ft, 6 in. of the seawall using a 40% redistribution were 3850 ft-lb/ft and -2380 ft-lb/ft, respectively, resulting in overstresses of 52% and 7%. Considering this level of overstress of both the horizontal positive and negative moments, it was determined that 5 ft of continuous damage between strong-backs required a strong-back spacing of less than 15 ft.

The Case 12 and Case 13 analyses examined a typical seawall panel with no strong-backs using the anticipated actual operating service load conditions to determine the amount of continuous vertical

reinforcing steel damage at one end that would lead to a failure (“unzipping”) of the panel. In this case, failure would occur by progressive yielding of the noncorroded vertical reinforcing adjacent to the damaged area that continued to the opposite end of the panel.

- *Case 12.* The Case 12 analysis examined 10 ft of continuous damage from one end. On the basis of the results of this analysis, it was determined that continuous damage of 10 ft or more was sufficient to cause a progressive failure of the seawall panel.
- *Case 13.* The Case 13 analysis used the same assumption as Case 12, except that continuous damage of 8 ft from one end was examined. On the basis of the results of this analysis, it was determined that continuous damage of less than 8 ft would not cause a progressive failure of the seawall panel.

16.9.8 Life Safety Implications

To address life safety concerns, a multifaceted restoration program was developed by various local and state agencies. The plan utilized an impressed current cathodic protection system to mitigate active corrosion of the reinforcing steel. A strong-back system was developed to upgrade the seismic behavior of the seawall and the integrity lost by corrosion of the reinforcing steel. A minimum of three caissons was determined to be necessary to upgrade the seismic capacity of the seawall to satisfy current building-code requirements. The number of additional caissons was directly proportional to the extent of corrosion damage along the base of the seawall. For the case of full damage along the seawall (worst-case scenario), analysis indicated that six caissons were required to provide satisfactory capacity. To determine the extent of the corrosion damage along the base of the seawall, a program of nondestructive impact-echo testing was conducted. Because of budget constraints of the various municipal and state agencies involved, guidelines for prioritization of the repairs were needed. These guidelines helped to ensure that life safety considerations were of paramount importance with respect to the prioritization of repairs.

The budget constraints of the municipal and state agencies involved in the Marina del Rey Seawall restoration program required a prioritization of repairs based on two criteria: (1) the extent of damage along the base of the seawall panel, and (2) the degree of public exposure of an individual seawall panel. To simplify the categorization of public exposure, use of two categories was proposed. A public exposure categorized as high was limited to areas where a seawall panel collapse would result in a high probability of personal injury. All other areas were categorized as low exposures.

Analysis indicated that a 60% loss of reinforcing steel might result in the collapse of the seawall panel at its actual operating service load levels. This was based on the assumption of uniformly distributed corrosion damage across the base of the seawall. Analysis also indicated that contiguous damage from the end of a seawall panel was more severe in nature than uniform damage. For the purposes of categorizing the extent of damage, the adoption of a dual-criteria classification was proposed. The classification assigned the panels to one of three categories, as described in Table 16.7. Wall panels were placed into the appropriate damage category if either criteria in Table 16.7 was satisfied. The use of 40% of total wall damage was recommended as the maximum allowable to provide some additional measure of conservatism. During the impact-echo testing, panels classified in the high-damage category were immediately brought to the attention of the public agencies involved.

Due to the financial considerations, a phased construction schedule was proposed. To minimize public exposure to the potential collapse of a seawall panel, repairs in areas of high public exposure with high priority and intermediate damage levels were classified as the highest priority. Other areas were categorized into two additional groups based on public exposure and degree of deterioration. Table 16.8 specifies the repair prioritization groupings that were made.

16.9.9 Cost Savings

Structural analysis of the Marina del Rey Seawall indicated that the number of caissons required to upgrade the capacity of the seawall for seismic loads was directly related to the amount of corrosion

TABLE 16.7 Prioritization Based on Degree of Wall-Panel Damage

Percent of Total Wall Damage	Number of Feet of Continuous Damage	Corrosion Damage Category
>40	>8	High
20–40	4–8	Intermediate
<20	<4	Little or no damage (seismic upgrade required)

TABLE 16.8 Repair Priority

Damage Category	Public Exposure	
	High	Low
High	Highest priority	High priority
Intermediate	Highest priority	High priority
Little or no damage (seismic upgrade required)	Priority	Priority

TABLE 16.9 Caisson Requirements Based on Degree of Damage

Degree of Damage	Number of Caissons Required
High	6
Intermediate–high	5
Intermediate–low	4
Little or no damage (seismic upgrade only)	3

TABLE 16.10 Cost Savings Resulting from Impact-Echo Testing

Caissons required, assuming 100% damage	3971
Caissons required utilizing impact-echo testing results	2473
Caissons saved as a result of impact-echo testing	1498
Estimated construction cost per caisson	\$3900
Construction savings resulting from impact-echo testing	\$5,842,000

damage present at the construction joint. This indicated that a categorization of seawall panels into logical groupings, based upon the extent of damage detected by impact-echo, could provide a significant cost savings during the construction phase of the project.

Based on the extent of damage detected during impact-echo testing, the seawall panels were placed into three categories: high damage level, intermediate damage level, and little or no damage present (only seismic upgrade required). The number of caissons required for panels in the high-damage and little-to-no-damage categories was fairly well established. In the intermediate-damage category, a further breakdown of the category was possible. The division of the intermediate-damage category into two groups resulted in four families of repairs, categorized in terms of the number of caissons required to provide the upgraded seismic capacity and to address the loss of strength due to corrosion. The categories, or families, of repair are summarized in Table 16.9. Panels at the intermediate-damage level were placed into separate categories based on the results of impact-echo testing and further structural analysis that examined the effects of localized corrosion damage and distribution of damage on the repaired system. After completion of the seawall testing and extensive structural analysis, a construction cost savings estimate was made. This estimate is shown in Table 16.10. The cost savings were based on comparing the number of caissons required to strengthen the walls, assuming 100% corrosion damage, to the number of caissons used in the repair scheme. A savings of \$5.8 million was realized by conducting impact-echo testing. On an economic basis, the merits of using nondestructive testing in this infrastructure repair project are clearly seen.

16.9.10 Conclusions

The Marina del Rey Seawall had been in service as a mixed-use residential and recreational area for over 30 years, and \$5 billion of infrastructure had been built around the area. To ensure its continuing service for at least another 30 years or more, an extensive restoration program was developed to mitigate the ongoing corrosion of the seawall reinforcing steel, to upgrade the seismic capacity of the seawall, and to restore the integrity of seawall panels that had been lost due to corrosion. The following are the more salient conclusions from the presentation of this case study:

- Analysis of the seawall indicated that, with increasing levels of reinforcing steel corrosion, the ductility of the wall decreased. At an assumed 60% loss of reinforcing steel due to corrosion at the seawall base, a failure was possible at the operating service load levels on the seawall. The horizontal deflection of the top of the wall prior to failure was determined to be approximately 3/8 in. for the case of 60% reinforcing steel loss. This would provide little warning of pending failure.
- The finite-element analysis clearly indicated the need for strong-back installation to seismically upgrade the seawall panels; however, the number of caissons required beyond the number necessary for seismic resistance increased as the amount of corrosion damage increased. Between three and six caissons were required to provide adequate lateral load resistance depending on the degree of corrosion damage detected.
- Threshold criteria were established to prioritize the repairs. The categorization was based primarily on life safety concerns in areas of high public exposure. Seawall panels that were determined to have a high degree of deterioration and that were located in areas of high public exposure were classified as the highest priority.
- On the basis of the cost estimate for caisson installation and the estimated number of panels that required only seismic-capacity upgrades, a substantial cost savings was realized with the performance of nondestructive impact-echo testing. Some \$5.8 million was saved by conducting this testing.

16.9.11 Reports, Standards, and Guidelines

16.9.11.1 American Concrete Institute (ACI) Reports

ACI 224.1R-93 Causes, Evaluation and Repair of Cracks in Concrete Structures (reapproved 1998)

ACI 228.2R-98 Nondestructive Test Methods for Evaluation of Concrete in Structures

ACI 364.1R-94 Guide for Evaluation of Concrete Structures Prior to Rehabilitation (reapproved 1999)

16.9.11.2 American Society for Testing and Materials (ASTM) Standards

ASTM C 39 Test Method for Compressive Strength of Cylindrical Concrete Specimens

ASTM C 42 Test Method for Obtaining and Testing Drilled Cores and Sawed Beams of Concrete

ASTM C 157 Test Method for Length Change of Hardened Hydraulic Cement Mortar and Concrete

ASTM C 805 Test Method for Rebound Number in Concrete

ASTM C 803 Test Method for Penetration Resistance of Hardened Concrete

ASTM C 597 Test Method for Pulse Velocity Through Concrete

ASTM C 876 Test Method for Half-Cell Potentials of Uncoated Reinforcing Steel in Concrete

ASTM C 856 Standard Practice for Petrographic Examination of Hardened Concrete

ASTM C 457 Test Method for Microscopical Determination of Parameters of the Air-Void System in Hardened Concrete

ASTM C 1084 Test Method for Portland Cement Content of Hardened Hydraulic-Cement Concrete

ASTM C 642 Test Method for Density, Absorption, and Voids in Hardened Concrete

ASTM C 496 Test Method for Splitting Tensile Strength of Cylindrical Concrete Specimens

ASTM C 215 Test Method for Fundamental Transverse, Longitudinal, and Torsional Frequencies of Concrete Specimens

ASTM C 469	Test Method for Static Modulus of Elasticity and Poisson's Ratio of Concrete in Compression
ASTM C 341	Test Method for Length Change of Drilled or Sawed Specimens of Hydraulic-Cement Mortar and Concrete
ASTM C 1152	Test Method for Acid-Soluble Chloride in Mortar and Concrete
ASTM C 1583	Test Method for Tensile Strength of Concrete Surfaces and the Bond or Tensile Strength of Concrete Repair and Overlay Materials by Direct Tension (Pull-Off Method)
ASTM C 1202	Test Method for Electrical Indication of Concrete's Ability to Resist Chloride Ion Penetration
ASTM D 4748	Test Method for Determining the Thickness of Bound Pavement Layers Using Short-Pulse Radar
ASTM D 4580	Practice for Measuring Delaminations in Concrete Bridge Decks by Sounding
ASTM D 4788	Test Method for Deflecting Delaminations in Bridge Decks Using Infrared Thermography

16.9.11.3 International Concrete Repair Institute (ICRI) Documents

Guideline No. 03730	Surface Preparation for the Repair of Deteriorated Concrete Resulting from Reinforcing Steel Corrosion
Guideline No. 03732	Guide for Selecting and Specifying Surface Preparation for Sealers, Coatings, and Polymer Overlays
Guideline No. 03733	Guide for Selecting and Specifying Materials for Repair Of Concrete Surfaces
Guideline No. 03734	Guide for Verifying Field Performance of Epoxy Injection of Concrete Cracks

16.9.11.4 Strategic Highway Research Program (SHRP) Documents

SHRP-C/FR-91-101	Handbook for the Identification of Alkali-Silica Reactivity in Highway Structures
SHRP-S-330	Condition Evaluation of Concrete Bridges Relative to Reinforcement Corrosion, Volume 8, Procedure Manual
SHRP-S-324	Condition Evaluation of Concrete Bridges Relative to Reinforcement Corrosion, Volume 2, Method for Measuring the Corrosion Rate of Reinforcing Steel
SHRP-S/FR-92-108	Condition Evaluation of Concrete Bridges Relative to Reinforcement Corrosion, Volume 6, Method for Field Determination of Total Chloride Content

16.9.11.5 Repair, Evaluation, Maintenance, and Rehabilitation (REMR) Research Program Reports

These reports can be purchased from <http://www.ntis.gov/>.

REMR-CS-47	Performance Criteria for Concrete Repair Materials, Phase I
REMR-CS-57	Performance Criteria for Concrete Repair Materials, Phase II Laboratory Results
REMR-CS-60	Performance Criteria for Concrete Repair Materials, Phase II Field Studies
REMR-CS-61	An Evaluation of Equipment and Procedures for Tensile Bond Testing of Concrete Repairs
REMR-CS-62	Performance Criteria for Concrete Repair Materials, Phase II Summary Report

References

-
- Aalami, B.O. and Swanson, D.T. 1988. Innovative rehabilitation of a parking structure. *Concrete Int.* 10(2), 30–35.
- AASHTO. 1992. *Standard Specification for Highway Bridges*, 15th ed. American Association of State Highway and Transportation Officials, Washington, D.C.
- ACI. 2002. *Concrete Repair Manual*, 2nd ed. American Concrete Institute, Farmington Hills, MI.
- ACI Committee 224. 1998. *Causes, Evaluation, and Repair of Cracks in Concrete Structures*, ACI 224.1R-93. American Concrete Institute, Farmington Hills, MI.

- ACI Committee 318. 2005. *Building Code Requirements for Reinforced Concrete*, ACI 318-05; *Commentary*, ACI 318R-05. American Concrete Institute, Farmington Hills, MI.
- ACI Committee 318. 2008. *Building Code Requirements for Structural Concrete*, ACI 318-08. American Concrete Institute, Farmington Hills, MI.
- ASCE. 2000. *Guideline for Structural Assessment of Existing Buildings*, SEI/ASCE 11-99. American Society of Civil Engineers, Reston, VA.
- Emmons, P.H. 1994. *Concrete Repair and Maintenance Illustrated*, 295 pp. R.S. Means, Kingston, MA.
- Emmons, P.H., Vaysburd, A.M., and McDonald, J.E. 1994. Concrete repair in the future turn of the century: any problems? *Concrete Int.*, 16(3), 42–49.
- ICRI. 1996. *Guide for Selecting and Specifying Materials for Repair of Concrete Surfaces*, ICRI Technical Guidelines No. 03733. International Concrete Repair Institute, Des Plaines, IL.
- MacGregor, J.G. 1976. Safety and limit states design for reinforced concrete. *Can. J. Civ. Eng.*, 3(4), 484–513.
- McDonald, J.E., Vaysburd, A.M., Emmons, P.H., Poston, R.W., and Kesner, K.E. 2002. Selecting durable repair materials: performance criteria summary. *Concrete Int.*, 24(1), 37–44.
- Natesaiyer, K. and Hover, K.C. 1988. *In situ* identification of ASR products in concrete. *Cement Concrete Res.*, 18, 455–463.
- Natesaiyer, K. and Hover, K.C. 1989. Some field strategies of the new *in situ* method for identification of alkali–silica reaction products in concrete. *Cement Concrete Res.*, 19, 770–778.
- Poston, R.W. and Irshad, M. 1996a. Load tests: externally post-tensioned bridge girders, Parts I and II. *Concrete Int.*, 18(8), 39–43.
- Sansalone, M. and Carino, N.J. 1986. *Impact-Echo: A Method for Flow Detection in Concrete Using Transient Stress Waves*, NBSIR 86–3452, 222 pp. National Bureau of Standards, Gaithersburg, MD.
- Sansalone, M. and Carino, N.J. 1988. Impact-echo method: detecting honeycombing, the depth of surface-opening cracks, and ungrouted ducts. *Concrete Int.*, 10(4), 38–46.
- Strategic Development Council. 1996. *Vision 2020: A Vision for the Concrete Repair Protection and Strengthening Industry*, http://www.concretesdc.org/projects/focaltopics_current.htm.
- TRB. 1986. *Strategic Highway Program Research Plans*, final report, NCHRP Project 20-20, TRA 4-1–TRA 4-60. Transportation Research Board, Washington, D.C.
- Wolkomir, R. 1994. Inside the lab and out, concrete is more than it's cracked up to be. *Smithsonian*, 24(10), 22–31.



Panoramic view of high-rise buildings at the shoreline in San Diego, California, that embody joints in the various categories. (Photograph courtesy of Edward G. Nawy.)

17

Joints in Concrete Construction

Edward G. Nawy, D.Eng., P.E., C.Eng.*

17.1	Introduction	17-1
17.2	Construction Joints.....	17-2
17.3	Contraction Joints.....	17-3
	Formed Contraction Joints • Tooled Joints • Sawed Joints • Contraction Joint Effectiveness	
17.4	Expansion Joints.....	17-6
	Structural Response • Expansion Joint Width • Expansion Joint Details • Expansion Joints in Environmental Concrete Structures and Minimum Reinforcement Requirements • Seismic Joints	
17.5	Joints in Slabs on Grade and Pavements.....	17-10
	Slabs on Grade • Pavements	
	References	17-15

17.1 Introduction

Restrained volumetric changes result in strains and ensuing stresses that lead to cracking. For a concrete system to be viable long term, it is essential to reduce the magnitude and extent of cracking by imposing artificial crack locations through the use of joints that relieve the stress levels and sometimes reduce them to a negligible magnitude. In essence, such joints can be viewed as artificial cracks. This chapter utilizes American Concrete Institute (ACI) committee reports and standards on this subject as a background, particularly ACI 224.3R, *Joints in Concrete Construction* (ACI Committee 224, 1995), and ACI 350, *Environmental Engineering Concrete Structures* (ACI Committee 350, 2006). Informational discussions on this subject are also utilized from the references provided at the end of the chapter.

It is important to note that the type of joint utilized depends on the function it must serve. As a general classification, the following are the types of joints commonly used today:

- *Construction joints*
- *Contraction joints* (secondary movement joints)
- *Expansion joints* (principal movement joints; sometimes referred to as *isolation joints*)

Drying shrinkage, carbonation, irreversible creep, fluctuating ambient temperature changes, and externally imposed loads are all factors that induce tensile stress conditions exceeding the modulus of rupture

* Distinguished Professor, Civil Engineering, Rutgers University, The State University of New Jersey, Piscataway, New Jersey, and ACI honorary member; expert in concrete structures, materials, and forensic engineering.

of concrete, resulting in cracking. An example of the magnitude of strains developed by direct elastic strains from external loads and the resulting volumetric changes for a normal concrete specimen subjected to 900-psi (6.2-MPa) compression is presented below (Nawy, 2008):

$$\text{Immediate elastic strain:} \quad \epsilon_e = 250 \times 10^{-6} \text{ in./in.}$$

$$\text{Shrinkage strain after one year:} \quad \epsilon_{sh} = 500 \times 10^{-6} \text{ in./in.}$$

$$\text{Creep strain after one year:} \quad \epsilon_{cr} = 750 \times 10^{-6} \text{ in./in.}$$

$$\text{Total strain:} \quad \epsilon_T = 1500 \times 10^{-6} \text{ in./in.}$$

If the element is 12 ft (3.65 m) long, the resulting dimensional change is $1500 \times 10^{-6} (12 \times 12) = 0.22$ in. A rise in temperature of 65°F results in an additional change of $65(5.5 \times 10^{-6} \text{ in./in.})(12 \times 12) = 0.05$ in. to give a total dimensional change of $0.22 + 0.05 = 0.27$ in. If the element is restrained as part of a monolithic concrete structure, as is usually the case, this element will be subjected to a significant tensile force that will cause extensive cracking or even failure. Some of these cracks can be prevented from opening by providing continuous horizontal and vertical reinforcement in the structure that would resist the tensile forces in the orthogonal directions.

Cracking resulting from these unavoidable strain gradients has always been a significant factor that the designer must consider in any structural design; hence, the use of joints is inevitable. It would be rare to find a structural system of reasonable size that is constructed without the use of construction joints, contraction (control) joints, expansion (isolation) joints, and shrinkage strips—separately or in combination (Fintel, 1974). If, apart from construction joints, other types of joints are to serve as stress relievers, it can be assumed that if enough reinforcement is provided in the direction of the induced forces to prevent the cracks from opening, then no joint would be needed; however, it would be economically prohibitive to do so as the volume of reinforcement required to perform this task would be significant.

Because the induced forces are highly indeterminate, engineering judgment has to be exercised in interpreting the imprecise guidelines in codes and the literature which often render conflicting solutions. This chapter attempts to synthesize in a compact manner the generally accepted industry approaches for the design of joints in concrete.

17.2 Construction Joints

For many structures, construction joints are required to accommodate the construction sequence for placement of concrete. The amount of concrete that can practically be placed in any operation is a function of the batching and mixing capacity and the time available for placing the concrete in the particular segment that is placed. The construction joint is the separating plane between the old (parent) concrete and the new concrete batch. As a result, the spacing of the construction joints must not interfere with flexural and shear continuity through the interface between the parent concrete and the concrete that is placed thereafter. To achieve this continuity, the hardened concrete must be clean and free of laitance if even a few hours elapse between successive placements. The ACI 318 Building Code stipulates that existing concrete should be moistened thoroughly before placement of the fresh concrete so the parent and the new concrete can achieve full monolithic behavior (ACI Committee 224, 1995; ACI Committee 318, 2008). Because the spacing of the construction joints is determined by the volume of the batch, it is often advisable in large area walls to have the construction joint coincide with the contraction (movement) joint. A spacing of 20 to 30 ft (6.1 to 9.1 m) for contraction joints in reinforced concrete continuous walls is often chosen. It is thus logical to use the contraction joint as a construction joint, with a spacing of 20 to 30 ft, depending on the number of openings in the wall. Figure 17.1 shows two types of construction joints: a butt joint in structural slabs and a tongue-and-groove joint with the option of a water stop for use in a liquid-retaining structure.

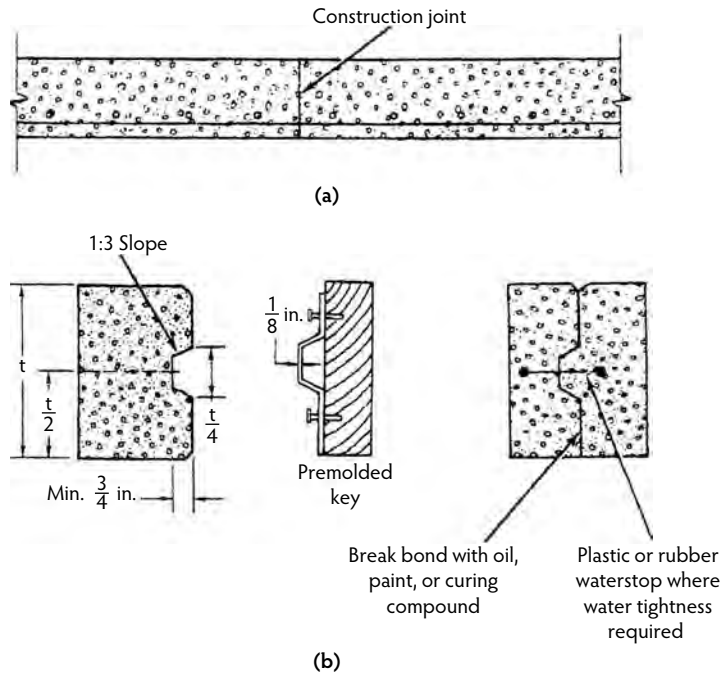


FIGURE 17.1 Typical construction joint assembly: (a) butt joint, (b) tongue-and-groove joint.

17.3 Contraction Joints

Tensile stresses result from drying shrinkage and ambient temperature drops in restrained concrete elements that are prevented from contracting. These tensile stresses resulting from the incipient volumetric change can be reduced to tolerable levels through the use of contraction joints, sometimes referred to as *control joints*. Typically, four methods are commonly used to create contraction joints in concrete surfaces: forming, tooling, sawing, and placement of joint formers (ACI Committee 224, 1995). To form a plane of weakness at the designed spacing, the joints are imposed during concrete placement by tacking rubber, plastic, wooden, or metal strips or caps to the inner faces of the forms to create notches, such as those shown in Figure 17.2.

17.3.1 Formed Contraction Joints

Joint formers can be used to create contraction joints as well as expansion (isolation) joints. Expansion joints usually have removable caps over the expansion joint material. After the concrete hardens, the cap is removed and the void space is caulked and sealed. Joint formers can be either rigid or flexible. Contraction joints are not meant to be isolation joints but are merely made by forming a weakened plane in the concrete with a rigid plastic strip. These strips are essentially T-shaped elements that are inserted to a proper depth into the freshly placed concrete, usually with a bar cutter. The cap must be pulled out prior to bullfloating or troweling the concrete surface. When such joints are formed at construction joint locations in concrete slabs and walls, they serve both as construction and contraction control joints. Tongue-and-groove joints can be made with preformed metal or plastic strips or built to job requirements. The strips have to be securely fastened so they cannot be dislodged during the process of concrete placement and consolidation. Prefabricated circular forms can be used as column isolation joints; these one-piece elements are left in place.

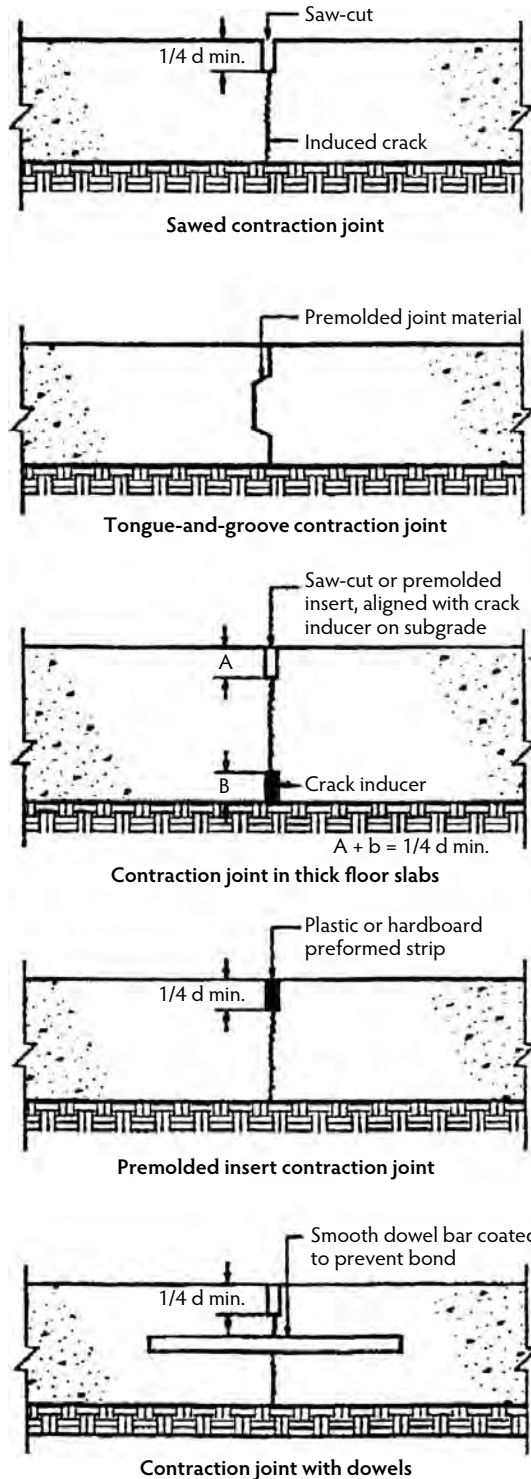


FIGURE 17.2 Contraction joint types. (From ACI Committee 224, *Joints in Concrete Construction*, ACI 224.3R-95, American Concrete Institute, Farmington Hills, MI, 1995, pp. 1–44; ACI Committee 302, *Guide for Concrete Floor and Slab Construction*, ACI 302.1R-89, American Concrete Institute, Farmington Hills, MI, 1989.)

TABLE 17.1 Contraction Joint Spacings

Author	Spacing
Merrill (1943)	20 ft (6 m) for walls with frequent openings 25 ft (7.5 m) for solid walls
Fintel (1974)	15–20 ft (4.5–6 m) for walls and slabs on grade; recommends joint placement at abrupt changes in plan and at changes in building height to account for potential stress concentrations
Wood (1981)	20–30 ft (6 to 9 m) for walls
PCA (1982)	20–25 ft (6 to 7.5 m) for walls depending on number of openings
ACI 302.1R (1989)	15–20 ft (4.5–6 m) recommended until 302.1R-89, then changed to 24 to 36 times slab thickness
ACI 350R (1983)	30 ft (9 m) in sanitary structures
ACI 350 (2006)	Joint spacing varies with amount and grade of shrinkage and temperature reinforcement
ACI 224R (1992)	One to three times the height of the wall in solid walls

Source: Data from ACI Committee 224, *Joints in Concrete Construction*, ACI 224.3R-95, American Concrete Institute, Farmington Hills, MI, 1995, pp. 1–44.

17.3.2 Tooled Joints

These contraction joints are tooled into the concrete surface during the finishing operations. A groove is formed to cause a weakened plane, which controls the location of the developing crack. Grooving tools with blades 1-1/2 to 2 in. (40 to 50 mm) in depth are used. The groove should be at least the thickness of the concrete. Cracks may develop within such a groove, although they also can occur at adjacent locations. At a tooled contraction joint, reinforcement in the concrete element should be reduced to *at least* 50% of the designed steel reinforcement or discontinued altogether (ACI Committee 350, 2006). As the distance between tooled joints increases, the volume of steel reinforcement not crossing the joint should be increased to control the tensile stresses that are developed. Often, tooled joints are of insufficient depth to function properly.

17.3.3 Sawed Joints

Sawed joints can reduce the intensity of labor required during the finishing process, but the necessary work and power equipment has to be available within a short period of time after the concrete hardens—namely, as soon as practicable. The most favorable time is when the generated heat of hydration renders the concrete temperature at its peak, but the concrete has to be hardened enough that the surface is not damaged during the cutting operation. As with tooled joints, saw-cut grooves should be made at least 1/4 the depth of the member. Various types of sawing equipment and techniques are available, including diamond-studded blades and abrasive blades. If abrasive blades are used, it is important to set a limit on the magnitude of wear that is acceptable for blade replacement. A drawback to the use of sawed joints is the large equipment clearance required; for example, it is difficult to place the saw at a slab edge where it abuts a wall. Based on industry experience a contraction joint spacing not to exceed 25 ft (7.5 m) is advisable; however, guidelines on joint spacing are diverse and conflicting. Table 17.1 summarizes various recommendations for contraction joint spacing. The focus should be on what spacing will result in an as narrow and aesthetically acceptable crack width and appearance as possible.

17.3.4 Contraction Joint Effectiveness

The effectiveness of a contraction joint is governed by whether any reinforcement passes through it. ACI 318 and ACI 350 consider a contraction joint to be fully effective when no reinforcing bars traverse the joint. For a partially effective contraction joint, a maximum 50% of the design reinforcement is allowed. Any reinforcement exceeding this limit would render the joint useless in controlling the volumetric change cracking in the structural system. It is therefore essential to provide a complete break in the reinforcement

TABLE 17.2 Expansion Joint Spacings

Author	Spacings
Lewerenz (1907)	75 ft (23 m) for walls
Hunter (1953)	80 ft (25 m) for walls and insulated roofs 30–40 ft (9–12 m) for uninsulated walls
Billig (1960)	100 ft (30 m) maximum building length without joints; recommends joint placement at abrupt changes in plan and at changes in building heights to account for potential stress concentrations
Wood (1981)	100–120 ft (30–35 m) for walls
Indian Standards Institution (1964)	148 ft (45 m) maximum building length between joints
PCA (1982)	200 ft (60 m) maximum building length without expansion joint
Kaminetsky (2001)	100 ft (30 m) maximum in environmental structures (see also Table 17.5)

Source: Data from ACI Committee 224, *Joints in Concrete Construction*, ACI 224.3R-95, American Concrete Institute, Farmington Hills, MI, 1995, pp. 1–44.

at the joint. It is recommended that bars should be stopped at 1-1/2 to 2 in. (3-1/2 to 5 cm) away from the joint at both sides of the joint line. A bond breaker should be placed between successive placements at contraction and construction joints, similar to expansion joints, and should pass through the entire structure in one plane. If the joints are not aligned, movement at a joint could induce cracking in an unjoined portion of the structure until the crack intercepts another joint (ACI Committee 224, 1995).

17.4 Expansion Joints

17.4.1 Structural Response

Expansion joints are effective isolation joints that divide a structure, including its foundation, into separate isolated units. This becomes necessary in large structural systems where continuity restraint induces significant stresses and large forces due to temperature changes, including ambient temperature variations, during a 24-hour period. The resulting cracking becomes considerably magnified at the lower segment of a wall if it is highly restrained by monolithic attachment to the stiff foundation slab, particularly in liquid-retaining structures. Such structures usually have high walls and stiff thick foundation slabs and cannot tolerate seepage caused by wide cracks that can be avoided. Expansion joints serve to isolate segments that are affected by large dimensional changes due to expansion, contraction, and differential settlement and also prevent cracking when walls change in direction. As an example, the contraction or elongation of a 190-ft (58-m) long wall in an environmental structure subjected to an ambient temperature change of 60°F (34°C) using a concrete coefficient of expansion of $5.5 \times 10^{-6}/^{\circ}\text{F}$ ($9.9 \times 10^{-6}/^{\circ}\text{C}$) would undergo a dimensional change equal to $5.5 \times 10^{-6} \times 60(190 \times 12) = 0.75$ in. (19 mm). Because the wall is monolithically cast with the stiff foundation slab, the lower wall segment will develop severe vertical cracking, as the upper segments are less restrained and can move relatively more freely. To avoid such long-term failure, expansion joints are vital. The joint width should be sufficient to prevent portions of the structure on either side of the joint from coming in contact.

17.4.2 Expansion Joint Width

The width of expansion joints can vary between 1 and 6 inches (25 and 150 mm), with 2 in. (50 mm) being typical. Such joints also serve an additional function as construction joints. As discussed in the case of contraction joints, no definitive standards are available that address the necessary spacing of expansion joints. A rule-of-thumb approach and good engineering judgment should be relied upon when specifying joint widths. Table 17.2 provides general guidelines for recommended spacings in various systems under different conditions.

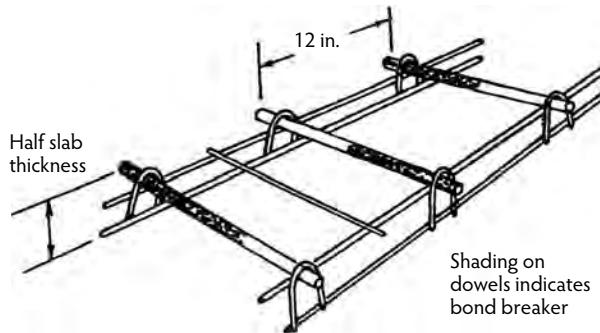


FIGURE 17.3 Example of a dowel bar assembly. (From ACI Committee 224, *Joints in Concrete Construction*, ACI 224.3R-95, American Concrete Institute, Farmington Hills, MI, 1995, pp. 1–44.)

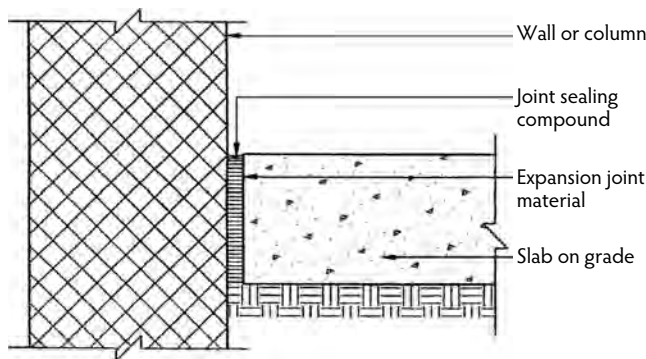


FIGURE 17.4 Isolation joint between a supported floor and a wall. (From ACI Committee 224, *Joints in Concrete Construction*, ACI 224.3R-95, American Concrete Institute, Farmington Hills, MI, 1995, pp. 1–44; PCA, *Building Movements and Joints*, Portland Cement Association, Skokie, IL, 1982.)

17.4.3 Expansion Joint Details

It is important to stress that the joint should extend through the entire height of the structure and through its foundation slab. Column footings should preferably not be placed at a joint. As in the case of construction joints, no reinforcement bars should pass through the joint but should terminate 2 in. (50 mm) from both faces of the joint. Dowels with breakers can be used to maintain plane (Fintel, 1974). The expansion joint can be covered, filled with a mastic filler, or left open. In the case of liquid-retaining structures, appropriate water stops have to be well designed, detailed, and properly installed to ensure complete liquid-tightness throughout the life of the structure. The water stops should also be suitable for minor foundation adjustments. Figure 17.3 shows a dowel assembly for an expansion joint, and Figure 17.4 illustrates an isolation joint between a supported slab and a wall.

17.4.4 Expansion Joints in Environmental Concrete Structures and Minimum Reinforcement Requirements

17.4.4.1 Expansion Joint Spacing

As previously discussed, expansion joints are isolation joints that divide a long structure into two segments joined by a resilient water stop and sealants. The water stop is designed to allow for anticipated movements in the structure. ACI 350R (ACI Committee 350, 2006) stipulates that “in general, expansion joint spacing preferably should not be greater than 120 ft (36 m)”;

however, engineering practice over the decades and effluent leakage failures have revealed that this spacing limit is too excessive. A modification of the ACI

TABLE 17.3 Recommended Joint Width and Spacing

Temperature Range	Spacing Between Expansion Joints			
	12 m (40 ft) cm (in.)	18 m (60 ft) cm (in.)	24 m (80 ft) cm (in.)	30 m (100 ft) cm (in.)
Underground, 4.44°C (40°F)	1.27 (1/2)	1.50 (3/4)	2.22 (7/8)	2.54 (1)
Partly protected, above ground, 26.7°C (80°F)	1.90 (3/4)	2.22 (7/8)	2.54 (1)	— ^a
Unprotected, exposed roof slabs, 48.9°C (120°F)	2.22 (7/8)	2.54 (1)	— ^a	— ^a

^a Not recommended

Source: Kaminsky, D., in *ICJCRR: Repair and Rehabilitation: A Compilation from The Indian Concrete Journal*, Research & Consultancy Directorate, Thane, India, 2001.

350 standard given in Table 17.3 recommends joint spacings and widths, with a maximum spacing of 100 ft (30 m); otherwise, wide liquid-leaking cracks could develop that would render the structure ineffective for retaining treated effluent. Even so, current engineering practice, given the reinforcement percentage values set in ACI 350, often specifies an expansion joint spacing not to exceed 80 ft (24 m). It should be emphasized that the actual width of the joint should be at least *twice* the expected movement.

17.4.4.2 Reinforcement

Prevention of liquid leakage is a major factor to be considered when designing liquid-retaining structures such as water tanks and towers, water-treatment facilities, aeration tanks, and biofords, among others. Such structures are designed for both strength and long-term serviceability. Service stress levels in the concrete and the steel reinforcement are kept low—for example, 20,000 psi (138 MPa) in the reinforcement. The volumetric change reinforcement percentage to be used in such structures has to be higher than in non-liquid-retaining structures. The shrinkage and temperature reinforcement in such specialized structures stipulated by ACI 350 is shown in Figure 17.5 and tabulated in Table 17.4, based on provision of full contraction joints in the walls and the slab foundation. If partial contraction joints as described in Section 17.3 are used, a maximum 50% of wall reinforcement is permitted to cross the contraction joint (ACI Committee 350, 2006). The spacing of these joints is permitted to be up to 30 ft by ACI 350; yet, it is preferable not to exceed 20- to 25-ft spacing to reduce the width and extent of volumetric change cracking. Although the maximum percentage in Figure 17.5 and Table 17.4 is given as 0.5% for 40-ft movement joints, the high rigidity of the foundation slab at the wall joint renders this percentage inadequate. The relative lower flexibility of the wall as compared to the stiff foundation slab at the lower wall segment renders the joint totally rigid with a low magnitude of rotation at the joint, because the wall is almost fixed at the base and free at the top. As a result, vertical cracking, and wide cracks develop, and the liquid-retaining structure becomes heavily permeable. To prevent vertical cracking at the lower quarter segment of the wall, more than 0.5% reinforcement would be needed for walls with expansion joints spaced in excess of 40 to 50 ft. It is the opinion of the author that a percentage ratio in the range of 1.0 to 1.25% for horizontal reinforcement at the lower 15 to 20% of the wall height is necessary to prevent the often excessive cracking at lower segments of a wall. This need arises because the flexible wall element is rigidly held by its monolithically supporting rigid foundation, so as to eliminate the consequent leakage of the retained liquid and its environmentally hazardous effects.

17.4.4.3 Expansion Joint Stops and Fillers

Liquid-tightness is vitally necessary in environmental structures to maintain their long-term integrity. A joint sealant at the liquid face and a suitable water stop made of high-quality rubber or plastic is necessary. As described in ACI 224 (ACI Committee 224, 1995), liquid stops and sealants can be chosen from a variety of alternatives. Rubber water stops allow more joint movement than polyvinylchloride (PVC) water stops. Either type should be at least 9 in. (225 mm) wide to provide adequate concrete embedment, and they should be 3/8 to 1/2 in. (9 to 12 mm) thick. To allow movement at the joint, a preformed joint filler should ideally be able to compress to half of its original width and be able to re-expand to fill the

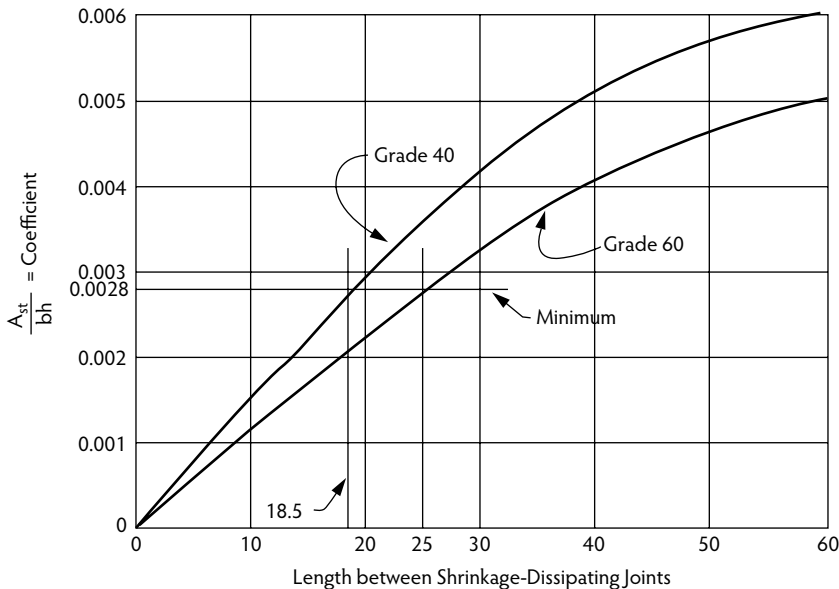


FIGURE 17.5 Shrinkage and temperature reinforcement for environmental engineering concrete structures. (From ACI Committee 224, *Joints in Concrete Construction*, ACI 224.3R-95, American Concrete Institute, Farmington Hills, MI, 1995, pp. 1–44; ACI Committee 350, *Code Requirements for Environmental Engineering Concrete Structures and Commentary*, ACI 350, American Concrete Institute, Farmington Hills, MI, 2006.)

TABLE 17.4 Minimum Shrinkage and Temperature Reinforcement

Length between Movement Joints (ft)	Minimum Temperature and Shrinkage Reinforcement Ratio	
	Grade 40	Grade 60
Less than 20	0.0030	0.0030
20 to less than 30	0.0040	0.0030
30 to less than 40	0.0050	0.0040
40 and greater	0.0060 ^a	0.0050 ^a

^a Maximum shrinkage and temperature reinforcement where movement joints are not provided.

Note: When using this table, the actual joint spacing should be multiplied by 1.5 if no more than 50% of the reinforcement passes through the joint.

Source: Data from ACI Committee 350, *Code Requirements for Environmental Engineering Concrete Structures and Commentary*, ACI 350, American Concrete Institute, Farmington Hills, MI, 2006.

joint as the joint enlarges. According to ASTM Standards D 994, D 1751, and D 1752, cork, rubber, foam, and other products conforming to these standards should perform satisfactorily in permitting such levels of movement. Figure 17.6 presents optimal expansion joint water stop detail and illustrates a typical expansion joint for a non-liquid-retaining structure.

17.4.5 Seismic Joints

Seismic joints are wide expansion joints intended to separate portions of buildings that are dissimilar in mass and stiffness. They are designed to allow adjacent units to respond to a seismic wave without the structural units banging against each other. The width of the joint should be equal to the sum of the total displacement at the particular affected level from the base of the two adjacent units, but no less

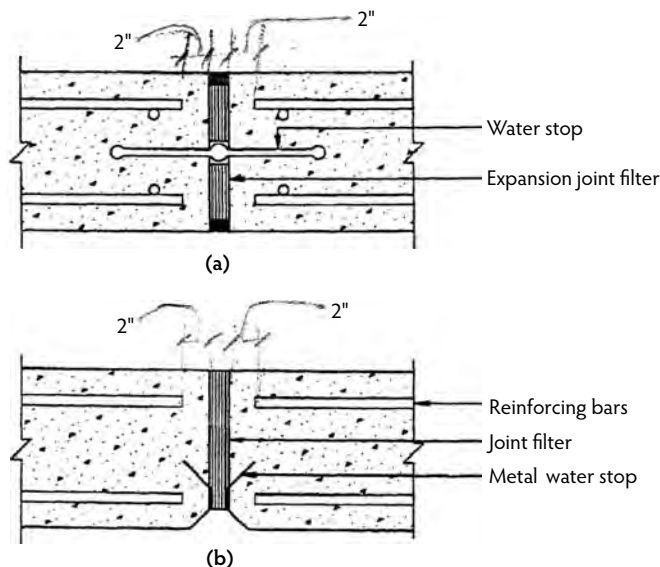


FIGURE 17.6 Expansion joint details: (a) liquid-retaining structures, (b) non-liquid-retaining structures. (From ACI Committee 224, *Joints in Concrete Construction*, ACI 224.3R-95, American Concrete Institute, Farmington Hills, MI, 1995, pp. 1–44; ACI Committee 302, *Guide for Concrete Floor and Slab Construction*, ACI 302.1R-89, American Concrete Institute, Farmington Hills, MI, 1989.)

than 1 in. for the first 20 ft of height and 1/2 in. for each additional 10 ft of height. The details of the joint should permit a doubling of the joint opening as a minimum when subjected to the seismic wave (Fintel, 1974). Because a seismic joint as a separation joint is normally wider than 2 in. (50 mm), it has to be adequately and aesthetically covered. Figure 17.7 provides suggested configurations for the plate closure at the floor and at the wall–slab separation.

17.5 Joints in Slabs on Grade and Pavements

17.5.1 Slabs on Grade

Slab movements are the result of four actions: volumetric change due to drying or shrinkage, temperature changes, stresses due to applied stationary or moving loads, and slab settlement. When movement is restrained, the slab will have to crack when the tensile stress in the concrete exceeds its modulus of rupture. The ensuing cracks may appear at any time and at any location; hence, joints become necessary to ensure that cracks form at the imposed, prescribed locations. A slab on grade with the minimum initial construction cost is unreinforced and with closely spaced joints, but unreinforced concrete may not be economical over the long term and would often require a larger thickness of the slab. Yet, joint construction and maintenance usually increase costs and must be considered in the design of joint spacing. It is always important to consider the relationship between initial construction costs and recurring costs, including slab reinforcement, use of shrinkage-compensating cement in the concrete, post-tensioning, and special-use considerations of the finished slab, such as flat slabs (ACI Committee 224, 1995). Typical placement of joints in slabs on grade in a typical structure with columns is shown in Figure 17.8 and discussed in the following sections.

17.5.1.1 Contraction Joints

Contraction joints should be provided in slabs on grade to accommodate shrinkage and temperature expansion and contraction, as well as to relieve the resulting internal stresses. As discussed in ACI Committee 224 (1995), a concrete slab on grade does not dry uniformly throughout its depth because

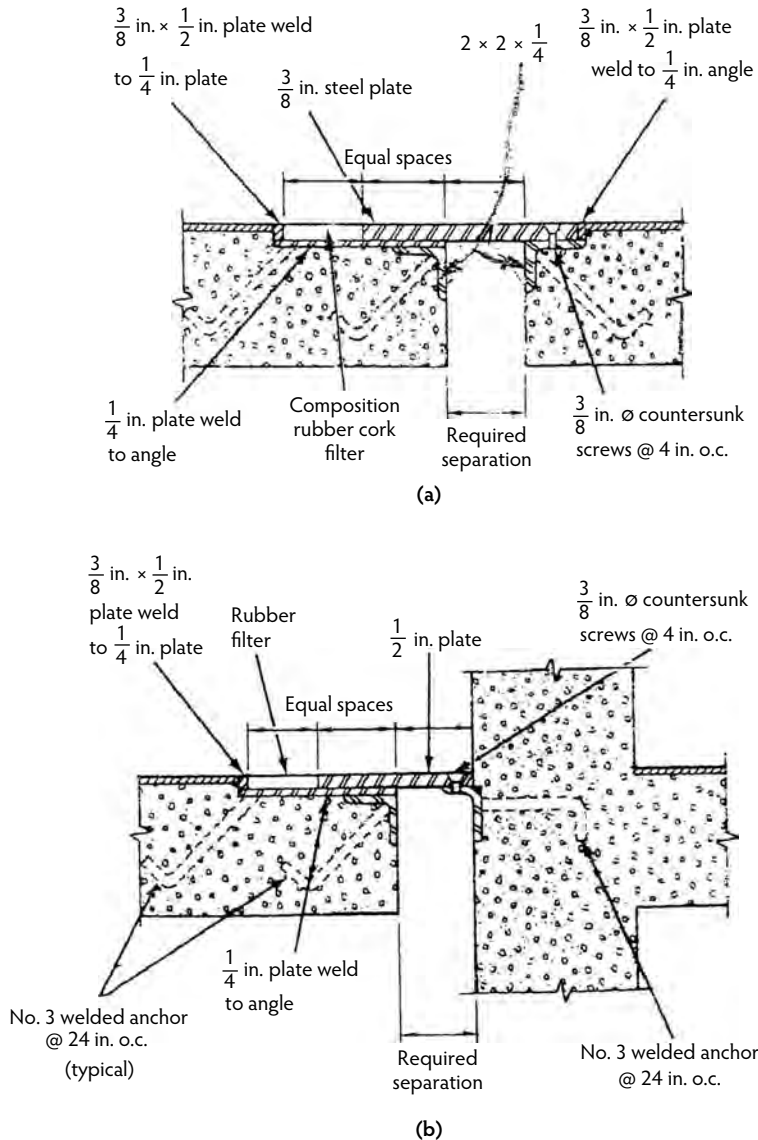


FIGURE 17.7 Seismic separation joints in concrete structures: (a) isolated floor plate closure, (b) building separation floor plate closure at the structure wall. (Adapted from Fintel, M., Ed., *Handbook of Concrete Engineering*, Van Nostrand Reinhold, New York, 1974, pp. 94–110.)

the temperature gradient is different at the slab top and bottom surfaces. The top surface of the slab dries faster than the lower surface, resulting in warping of the slab and intense curling at corners and at some joint boundaries. Use of dowelled joints, proper distribution and an adequate percentage of reinforcement, or thickening of the slab edges can reduce the level of deformation and possibly eliminate cracking in the slab on grade. Additionally, it is advisable to provide contraction joints at locations of change in subgrade slab support to reduce the possibility of cracking in those transition areas, in addition to providing contraction joints at column lines. It is recommended that joints be spaced in such a manner that the slab on grade is divided into small rectangular areas, preferably squares, but the recommended ratio of the long to short side should not exceed a value of 1.25 to 1.5. As a general guideline, the spacing of contraction joints in slabs on grade should be 24 to 36 times the slab thickness in both directions

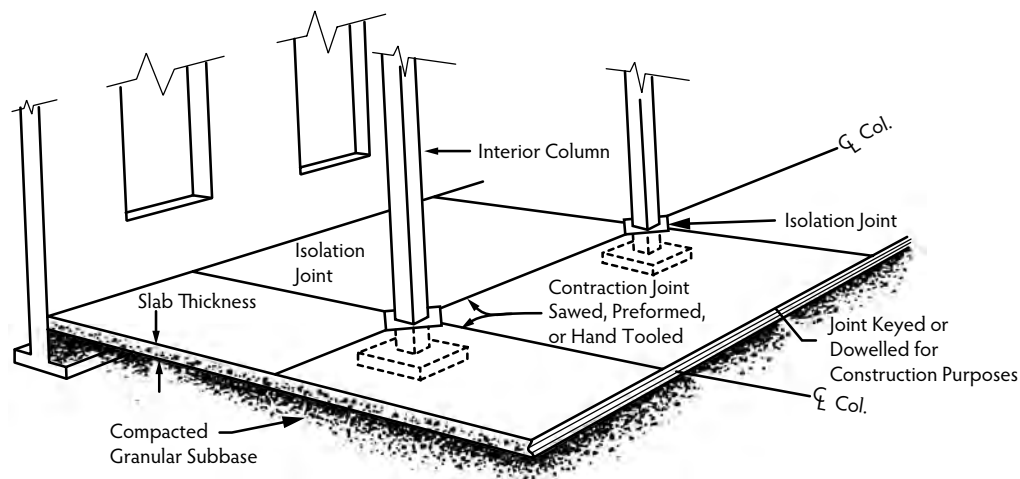


FIGURE 17.8 Location of types of joints in slabs on grade. (From ACI Committee 224, *Joints in Concrete Construction*, ACI 224.3R-95, American Concrete Institute, Farmington Hills, MI, 1995, pp. 1–44; ACI Committee 350, *Code Requirements for Environmental Engineering Concrete Structures and Commentary*, ACI 350, American Concrete Institute, Farmington Hills, MI, 2006.)

unless intermediate cracks are acceptable (ACI Committee 302, 1989). A greater spacing is permitted for low-slump concrete with aggregate size larger than 3/4 in. (20 mm).

Several types of contraction joints can be used, such as sawed joints, hand-tooled or preformed joints, keyed joints, or dowelled joints. Figure 17.2 illustrates these types of joints. Sawed joints are the most common method of making contraction joints in slabs on grade by saw-cutting the hardened concrete. Hand-tooled joints are produced by hand-tooling or by inserting plastic strips before finishing. If floor slabs are so thick that insertion of preformed strips or hand tooling becomes cumbersome, premolded inserts can be placed at the bottom of the slab. Sometimes it is preferable to use keyed joints to ensure full load transfer. In such cases, a full-depth premolded joint can be inserted in the slab on grade. This process is required in cases where movement between sections of the slab exceeds the level of movement chosen for adequate load transfer through aggregate interlock. Load transfer in keyed joints can also be accomplished through the insertion of full-depth preformed keys at the time of concrete placement so the slab will have a tongue-and-groove joint when the concrete is cast on both sides of the joint. The keyway can be formed through the use of beveled wood strips with premolded keys or the use of metal forms. Keyed contraction joints should not be used for slabs on grade less than 6 in. (150 mm) thick (ACI Committee 224, 1995).

Dowelled joints are used in heavily loaded slabs on grade with a high percentage of reinforcement for adequate load resistance and crack control requirement. Load transfer at the contraction joint is accomplished through the use of steel dowels, such as the dowel assembly shown in Figure 17.3. The dowels have to be centered at the joint and must not bond to the concrete on at least one side to enable horizontal movement. Greasing the dowels or coating them with a bond-breaker plastic will prevent them from bonding with the concrete. Table 17.5 gives recommended dowel spacing.

17.5.1.2 Expansion Joints

Expansion joints are isolation joints that allow horizontal and vertical movement between slabs and adjoining structures (e.g., walls, columns, footings) or in especially loaded areas such as heavy machinery foundations. Movement of the structural elements supported by or adjoining the slabs on grade differs from that of the slab itself because of differences in support conditions, in environmental effects, and in the way the stresses develop due to loading, particularly the rigid connections at column and wall joints. Lack of adequate isolation or separation joints in these areas of stress concentration result in cracking. The joints in their different categories separate the reinforcement, mechanical connection, or keyways

TABLE 17.5 Dowel Length and Spacing for Slabs on Grade

Slab Thickness		Dowel Diameter		Total Dowel Length ^a	
in.	mm	in.	mm	in.	mm
5	125	3/4	20	16	400
6	150	3/4	20	16	400
7	175	1	25	18	450
8	200	1	25	18	450
9	225	1-1/4	30	18	450
10	250	1-1/4	30	18	450
11	275	1-1/4	30	18	450

^a Allowance made for joint openings and minor errors in positioning dowels.

Note: Recommended dowel spacing is 12 in. (300 mm) on-center. Dowels must be carefully aligned and supported during concreting operations. Misaligned dowels cause cracking.

Source: Data from ACI Committee 224, *Joints in Concrete Construction*, ACI 224.3R-95, American Concrete Institute, Farmington Hills, MI, 1995, pp. 1–44; ACI Committee 302, *Guide for Concrete Floor and Slab Construction*, ACI 302.1R-89, American Concrete Institute, Farmington Hills, MI, 1989.

across the entire joint and ensure that no bond interaction between adjacent segments is present. An example of a dowel bar assembly for isolation joints is shown in Figure 17.3, and a typical isolation (or, more correctly, expansion joint) is shown in Figure 17.4. The isolation material filling the joint between the slab on grade and the adjoining structural element has to be wide enough to permit both vertical and horizontal movement (ACI Committee 224, 1995; PCA, 1982). It is important to emphasize that joints have to be adequately sealed to improve joint performance. Sealing joints prevents water and deleterious materials from entering the joints and causing damage through corrosion of reinforcement or freezing, for example. ACI 302.1R (ACI Committee 302, 1989) stipulates that joints in industrial and flat floors subject to hard-wheeled traffic have to be adequately filled with a durable hard material such as epoxy to give adequate support for the joint and provide good resistance to wear and tear. The joint material should have an elongation of at least 6% and should be applied in joint locations where further movements are unlikely. It is recommended that the filling epoxy be applied from 3 to 6 months after slab placement (ACI Committee 224, 1995). In summary, it is extremely important for the subgrade to be stable and that soils such as silts and clays are removed to sufficient depths before a stabilized subgrade is placed; otherwise, failure of joints develops and accelerates with time.

17.5.1.3 Special Considerations

17.5.1.3.1 Shrinkage-Compensating Cement Concrete

Concrete made with shrinkage-compensating cement is sometimes used in large slab areas or slabs on grade with a reduced number and enlarged spacing of joints. The use of such a concrete could significantly improve the performance of these slabs by offsetting shrinkage through expansion of the concrete. Gulyas (1984) noted that the use of shrinkage-compensating cement causes greater expansion in the top half of the slab depth than in the bottom half. As a result, less curling is noticed as compared to slabs constructed of normal Portland cement concrete. This difference in shrinkage level between the top and bottom of the slab concrete section seems to be caused by differences in the restraint imposed by the subgrade on the lower surface of the slab. The reduced curling leads to better long-term performance of slabs on grade; in such cases, the additional costs incurred by the use of shrinkage-compensating cement would be justified over the long term.

17.5.1.3.2 Post-Tensioning

Post-tensioning is a technique that can eliminate cracking of slabs on grade or significantly control the extent of cracking caused by restrained drying shrinkage and temperature variations normally occurring during the initial few days after concrete placement. This technique is used for the construction of large areas of slabs without any joints—for example, 100 to 250 ft (30 to 60 m) of slab length without separation

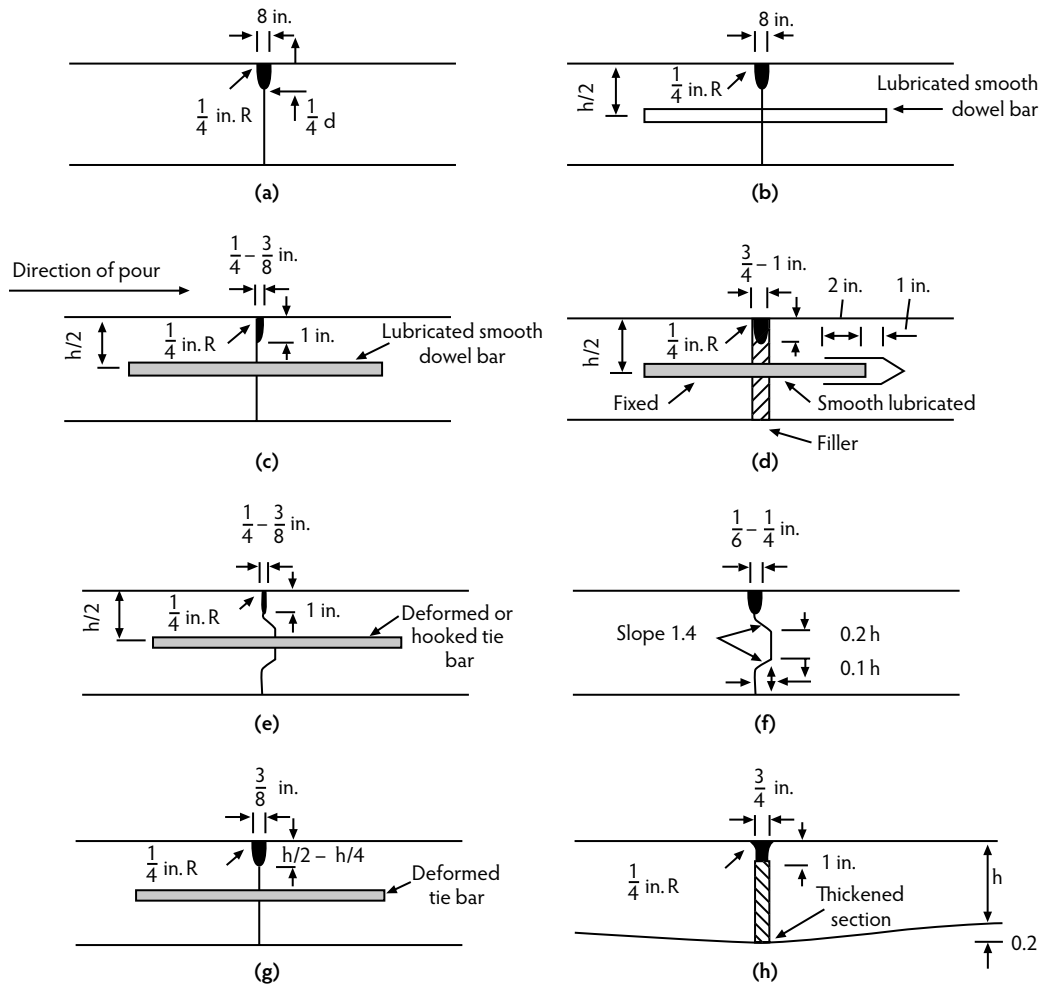


FIGURE 17.9 Various types of pavement joints. (From ACI Committee 224, *Joints in Concrete Construction*, ACI 224.3R-95, American Concrete Institute, Farmington Hills, MI, 1995, pp. 1–44.)

joints. Prestressing induces large compressive forces in the longitudinal direction and prevents any developing cracks from opening. The construction joints in such slabs on grade will open wider than slabs reinforced with conventional steel reinforcement.

17.5.2 Pavements

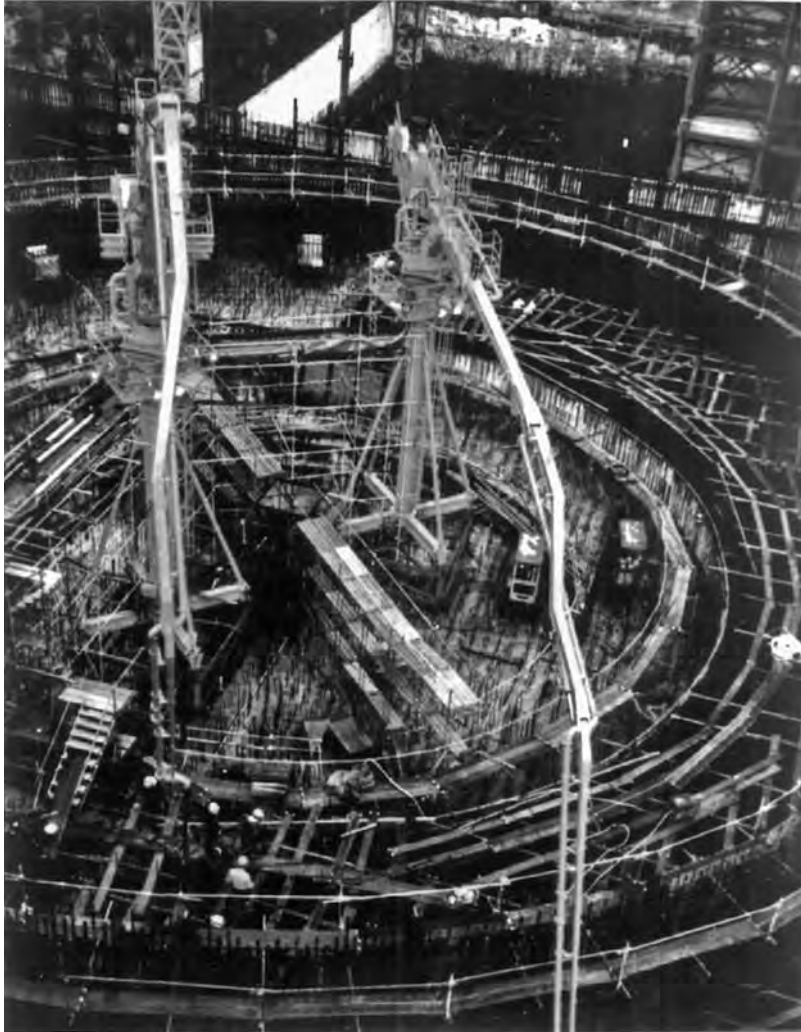
Pavements are usually thick rigid slabs that have to carry heavy vehicular loads. As in the case of slabs on grade, cracks in pavements are generated as a result of restrained drying shrinkage and temperature variation. They also occur primarily during the first few days after the concrete is placed, namely while the initial curing is taking place. Sometime, blow-ups can occur if the open joint is full of debris and traffic loads are present. The differential temperature gradient through the slab thickness and the restraint imposed by the subgrade on the bottom surface of the slab result in curling of the slab, particularly at the joint. The weight of the pavement slab itself can cause the slab to be subjected to tensile stresses at its lower face that are magnified by additional tensile stresses due to vehicular traffic loads. Such tensile stresses are expected to result in transverse and longitudinal cracks that generate from the lower surface of the slab in contact with the yielding subgrade, with longitudinal cracks developing from warping, curling, ambient temperature changes, and moisture loss (ACI Committee 224, 1995).

To minimize cracking in rigid pavements, it becomes necessary to use both transverse and longitudinal joints in reinforced as well as unreinforced concrete slab pavements. The joints should be designed to transfer loads between adjacent segments and to systematically open and close. Also, all joints have to be properly sealed, as for slabs on grade, to prevent liquids and deleterious materials from entering the joint and corroding the reinforcement; trapped water could freeze in cold temperatures and result in continuous deterioration of the pavement and its ultimate failure. It is important for contraction and expansion (isolation) joints to be well designed so they can help maintain the integrity of the pavement. Figure 17.9 gives recommended pavement joints (ACI Committee 224, 2005). As in the case of slabs on grade, contraction joints have to be provided, as shown in Figure 17.9, with a groove of at least 1/4 to 1/3 the slab thickness. For cut grooves, concrete should be sawed as soon as possible after hardening. The load transfer in Figure 17.9a is accomplished by aggregate interlock of the cracked lower portion of the slab. When dowel bars are used for joint interlock, they are usually spaced at 12 in. (300 mm) mid-depth in the pavement slab, as shown in Figure 17.9c. The dowels can be coated with paraffin-based lubricant, asphalt emulsions, form oil, or grease to prevent bonding of the concrete. Expansion joints, on the other hand, are constructed with a clean break as a total separation through the entire depth of the pavement slab (Figure 17.9d). Sometimes, the slab is thickened at the expansion joint as shown in Figure 17.9h. When keyed construction joints are used (Figures 17.9e,f), it is recommended that be placed in alternative lanes. Again, it should be emphasized that all joints in pavement slabs must be sealed with appropriate filler material as described in Section 17.5.1 for slabs on grade.

References

- ACI Committee 224. 1995. *Joints in Concrete Construction*, ACI 224-3R-95. American Concrete Institute, Farmington Hills, MI, 2005, pp 1–44.
- ACI Committee 302. 1989. *Guide for Concrete Floor and Slab Construction*, ACI 302.1R-89. American Concrete Institute, Farmington Hills, MI, 1989, 45 pp.
- ACI Committee 318. 2008. *Building Code Requirements for Structural Concrete and Commentary*, ACI 318-08/ACI 318R-08. American Concrete Institute, Farmington Hills, MI, 430 pp.
- ACI Committee 350. 2006. *Code Requirements for Environmental Engineering Concrete Structures and Commentary*, ACI 350/ACI 350R, American Concrete Institute, Farmington Hills, MI.
- Billig, K. 1960. Expansion joints. In *Structural Concrete*, Macmillan, London, pp. 962–965.
- Fintel, M., Ed. 1974. *Handbook of Concrete Engineering*. Van Nostrand Reinhold, New York, 1974, pp. 94–110.
- Gray, D.C. and Darwin, D. 1984. *Expansion and Contraction Joints in Reinforced Concrete Buildings: An Annotated Bibliography*, SM Report No. 14. University of Kansas Center for Concrete Research, Lawrence.
- Gulyas, R.J. 1984. Discussion of ‘Warping of Reinforced Concrete Slabs Due to Shrinkage’ by H.M.S. Abdul-Wahab and A.S. Jaffer, *Proc. ACI J.*, 81(1), 100–102.
- Gustaferro, A.H. 1980. How to plan and specify floors on grade. *Plant Eng.*, 34(2), 73–78.
- Hunter, L.E. 1953. Construction and expansion joints for concrete. *Civil Eng. Public Works Rev.*, 48(560), 157–158; 48(561), 263–265.
- Indian Standards Institution. 1964. *Code of Practice for Plain and Reinforced Concrete*, 2nd rev. Indian Standards Institution, New Delhi.
- Kaminetsky, D. 2001. Cracking and repair of environmental concrete structures. In *ICJCRR: Repair and Rehabilitation: A Compilation from The Indian Concrete Journal*. Research & Consultancy Directorate, Thane, India.
- Lewerenz, A.C. 1907. Notes on expansion and contraction of concrete structures, *Eng. News*, 57(19), 512–514.
- Mann, O.C. 1970. Expansion–contraction joint locations in concrete structures. In *Proceedings of Symposium on Designing for the Effect of Creep, Shrinkage, and Temperature in Concrete Structures*, SP-27, pp. 301–322. American Concrete Institute, Farmington Hills, MI.

- Martin, I. 1970. Effect of environmental conditions on thermal variations and shrinkage of concrete structures in the United States. In *Proceedings of Symposium on Designing for the Effect of Creep, Shrinkage, and Temperature in Concrete Structures*, SP-27, pp. 279–300. American Concrete Institute, Farmington Hills, MI.
- Merrill, W.S. 1943. Prevention and control of cracking in reinforced concrete buildings. *Eng. News-Record*, 131(23), 91–93.
- Nawy, E.G. 2002. *Fundamentals of High-Performance Concrete*, 2nd ed. John Wiley & Sons, New York, 2002, 442 pp.
- Nawy, E.G. 2008. *Reinforced Concrete: A Fundamental Approach*, 6th ed. Prentice Hall, Upper Saddle River, NJ, 934 pp.
- PCA. (1982). *Building Movements and Joints*, Portland Cement Association, Skokie, IL, 64 pp.
- PCA. (1992). *Joint Design for Concrete Highways and Street Pavements*. Portland Cement Association, Skokie, IL, 13 pp.
- Reynolds, C.E. 1960. *Reinforced Concrete Designer's Handbook*, 6th ed. Concrete Publications, London.
- Schrader, E.K. 1987. A solution to cracking and stresses caused by dowels and tie bars, *Concrete Int.*, 13(7), 40–45.
- Wood, R.H. 1981. Joints in sanitary engineering structures. *Concrete Int.*, 3(4), 53–56.



Automation in placement of concrete wall. (Photograph courtesy of Portland Cement Association, Skokie, IL.)

18

Automation in Concrete Construction

Mirosław J. Skibniewski, Ph.D.*
Raghavan Kunigahalli, Ph.D.**

18.1	Categories of Construction Automation.....	18-1
18.2	Automated Construction Equipment and Related Hardware.....	18-1
18.3	Economics and Management of Robots	18-7
18.4	Computer-Aided Design.....	18-8
	Traditional Architectural CAD Modeling • Solid Geometric Modeling • Solid Modeling of Reinforcing Elements • Computerized Engineering Model	
18.5	Conclusions and Future Activities	18-16
	References	18-17

18.1 Categories of Construction Automation

Concrete construction automation is a broadly defined planning and technical endeavor that includes two distinct areas. The first is development of programmable (i.e., robotic) hardware for the execution of construction work tasks; significant progress has been achieved in equipment navigation, locomotion systems, and concrete-placement systems. The second is development of computer-based tools for efficient and optimal planning, design, construction, and operation of concrete structures. Of particular importance is the development and practical application of tools for design visualization, quantity takeoff and cost estimation, generation of work schedules and job cost reports, design–construction integration, construction task planning, optimal resource management, and design for constructability and maintainability of concrete structures.

18.2 Automated Construction Equipment and Related Hardware

Construction robotics are now beyond the initial design and academic discourse stages, which was not the case throughout the 1980s and early 1990s (Skibniewski, 1988, 1996). A number of institutions worldwide have developed prototype hardware for various applications that are now in field testing or

* A. James Clark Chair Professor, Department of Civil & Environmental Engineering, University of Maryland, College Park; expert in construction automation, e-construction, and technology management.

** Chief Technology Officer, SBA Technologies, Inc., New York; expert in computer-aided engineering and information technology.

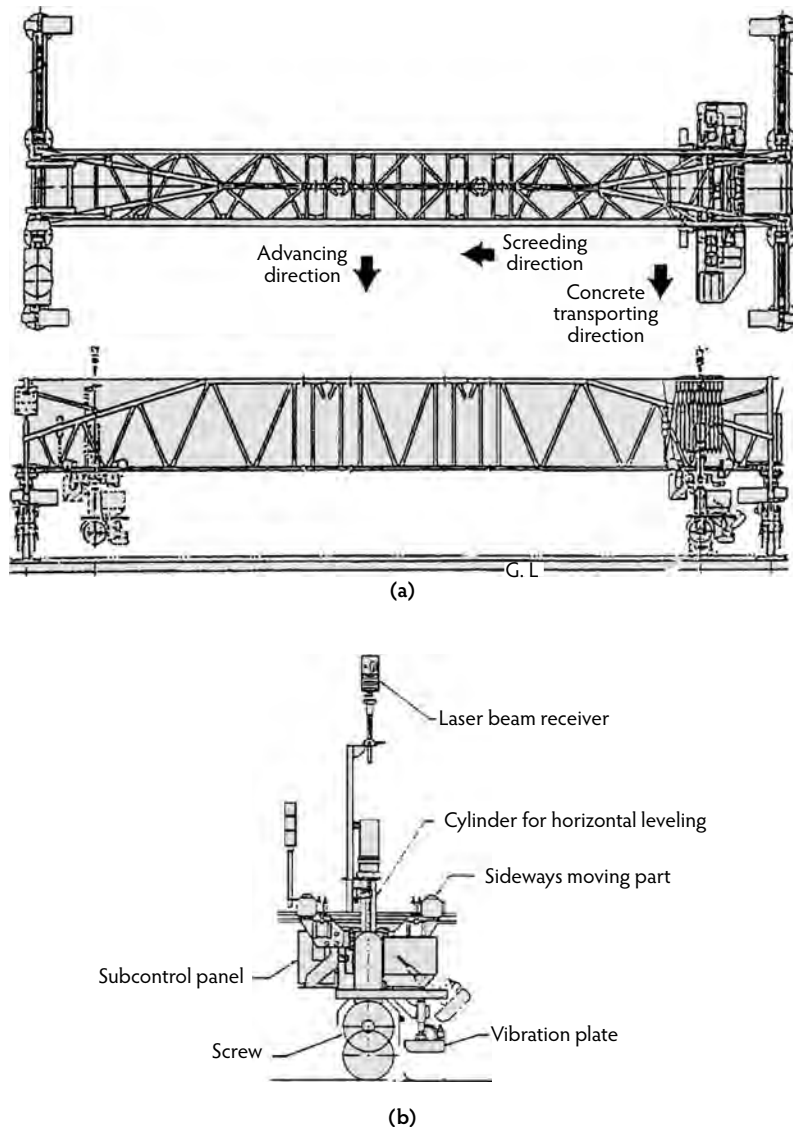


FIGURE 18.1 Takenaka Corp. concrete screeder: (a) top and side views; (b) detail.

initial implementation stages. Currently, the most mature applications of robotics in concrete construction include concrete screeding, surface finishing, scrubbing, and cleaning. Japanese construction firms that have developed their own prototypes of such machines include Obayashi Corp., Taisei Corp., Takenaka Corp., and Shimizu Corp.

An automatic concrete screeder has been developed by Takenaka Corp. (see Figure 18.1). The girder-mounted machine has an automatically controlled screeding tool that operates sequentially along a girder running over a self-shifting rail. When the tool reaches the edge of the rail, the rail is shifted forward automatically after invoking the rail-shifting function on the machine controller. The entire screeder has a modular design and can be manually assembled on the construction site. Assembly and disassembly can be accomplished by two or three workers in about 4 hours. The screeding tool includes a screw to perform concrete leveling by transporting surplus concrete to the side. This is done using a vibrating board that ensures an adequately horizontal surface when the concrete is shifted to the side. The maximum weight of the screeding tool is approximately 130 kg. The girder support structure for the trowel is also

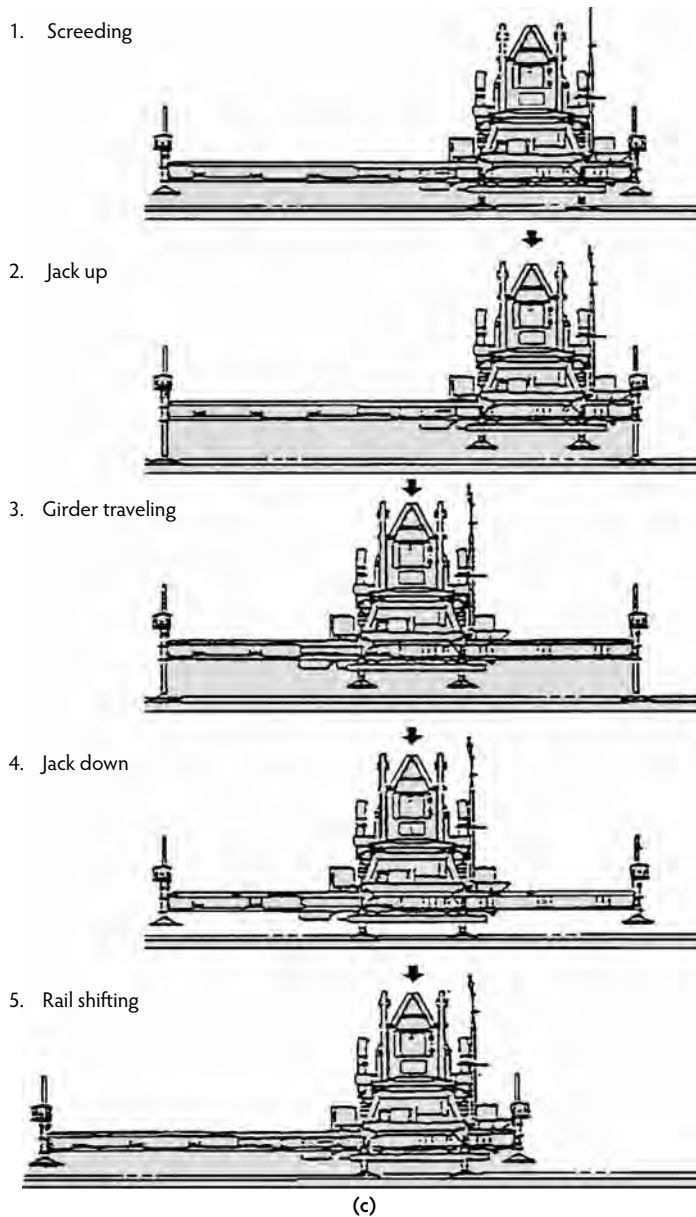


FIGURE 18.1 (cont.) Takenaka Corp. concrete screeder: (c) operational steps.

modular, with parts ranging from 2 to 3 m in width. The traveling saddle for the trowels is located under the girder. The maximum weight of the girder components is approximately 50 kg. The control system for the screeder includes an inclinometer, a laser leveling device, and a rotary encoder (Okuda et al., 1992). The screeding capacity of the machine is approximately 350 m² of a slab area per hour, or 35 m³ of fresh concrete mix per hour on a slab with a thickness of 18 cm.

An example of a concrete surface finishing robot, the *Flatkin* by Shimizu Corp., is shown in Figure 18.2. The Flatkin consists of travel rollers, a power trowel, a controller, and a guard frame. A pair of travel rollers is attached at the bottom of the main body of the robot. The robot can move back and forth or left and right, using DC motors to drive the rollers. The power-trowel mechanism has three supporting arms. Each arm has a rotating trowel assembly with three trowels each. A gasoline engine is

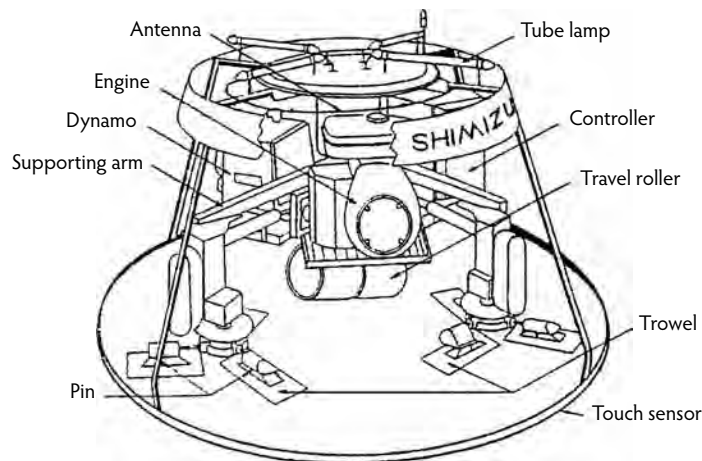


FIGURE 18.2 Concrete surface finishing robot by Shimizu Corp.

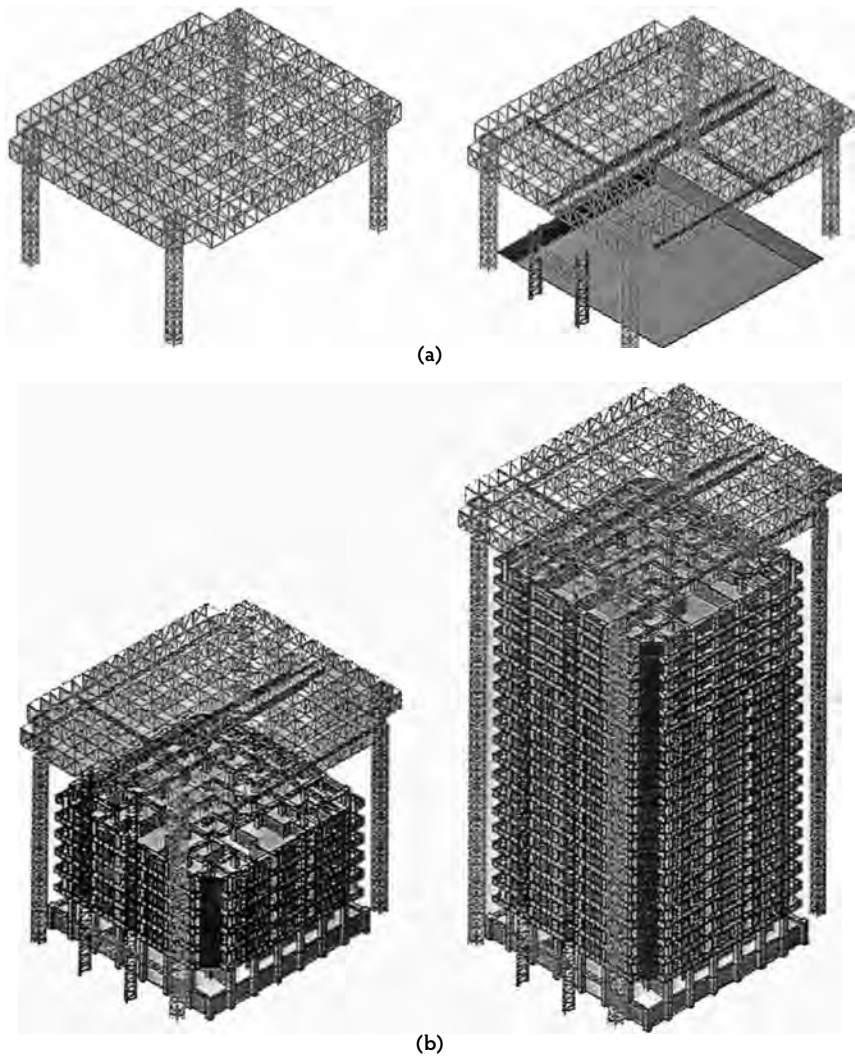
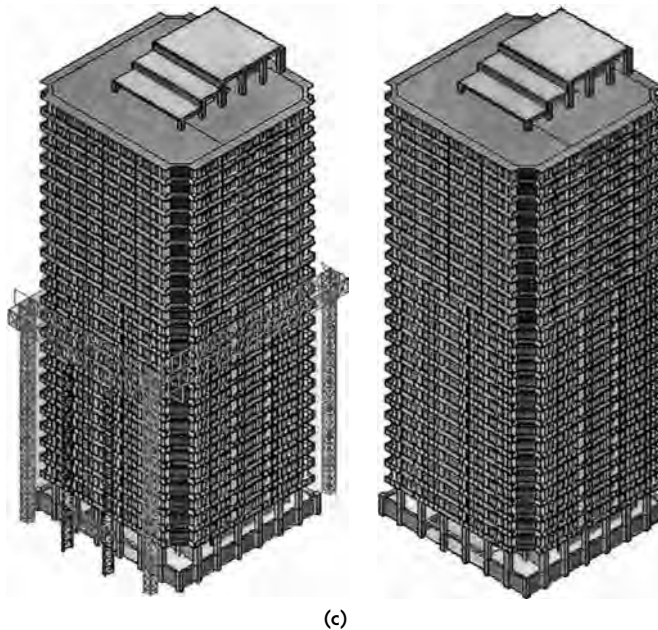


FIGURE 18.3 High-rise building automation by Obayashi Corp.



(c)

FIGURE 18.3 (cont.) High-rise building automation by Obayashi Corp.

used as a power unit to drive the trowel assemblies, so the trowel assemblies rotate around the axis and simultaneously rotate around the entire traveling device. The ratio of the rotation speed of the trowels to the revolution speed of the robot around its own axis is approximately 10 and above. The angle between the concrete surface and the trowel can be adjusted by a cam mechanism. This angle is usually changed depending on the hardness of the concrete surface to be finished. The robot is equipped with a guard frame with a touch sensor mounted as a safety device. In addition to the engine for the trowel, the robot has a small generator that enables the elimination of electric power cables, thereby increasing its mobility. The Flatkin can be operated by radio remote control, which is a useful feature for changing the trowel blade positions depending on the hardness of concrete encountered in a given work area. The robot work output is approximately 600 to 700 m² of concrete surface area per day, utilizing two operators in the process. The productivity of the robot is four to five times higher than that of human workers utilizing mechanized walk-behind trowels and manual tools (Ueno et al., 1988).

A partially automated overhead construction factory system for high-rise reinforced concrete frame buildings had been developed by Obayashi Corp. Their *Big Canopy* system integrates a synchronously climbing canopy that houses semiautomated overhead cranes, prefabricated concrete paneling components, computerized management of storage and retrieval of materials on-site, and a semiautomated structural assembly (see Figure 18.3). The canopy covers the entire story of the building being erected to protect workers from severe weather and to produce a safer work environment. Tower crane posts are used as four columns that support the canopy. Raising of the canopy is performed by the climbing facility of the tower cranes. Safety of motion is maintained by synchronized control. A high-speed construction lift and three hoist cranes are combined to deliver the structural components and materials for assembly. The material is raised to the working floor by the lift and passed to the hoist on the delivery girder. The movement of the hoist is fully automated for maximum work efficiency. Upon completion of the building construction, the canopy is disassembled on the top of the building. The external frame is then lowered and then safely disassembled on the ground.

Among the automated surveying technologies relevant to concrete construction, the Consortium for Advanced Positioning Systems (CAPS) has engineered an application of a laser-based positioning device called Odyssey™, developed by Spatial Positioning Systems, Inc. (SPSi) (Figure 18.4). The system has two primary components: transmitters and receivers. At least two transmitters are required to provide

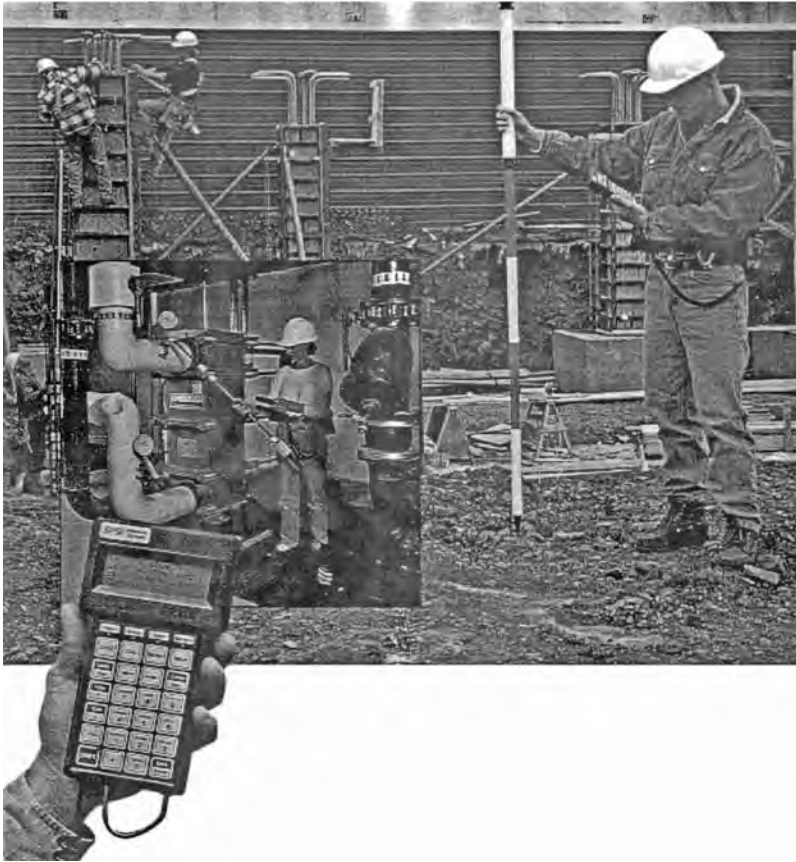


FIGURE 18.4 Laser-based positioning system. (Photograph courtesy of Spatial Positioning Systems, Inc., Blacksburg, VA.)

positioning signals to a receiver; however, any number of receivers can utilize the positioning signals simultaneously. The transmitters can be set up at convenient locations and generally aimed at the work site. Existing benchmarks are used to calibrate the system using any local coordinate system. Each receiver is composed of two lenses mounted on a pole, a processor, a data entry and retrieval system, and a power supply.

The two lenses form a line, and the position of the lenses and the known geometry of the pole allow the point of position measurement to be projected to the end of the pole. Because the position of the tip of the pole does not change if the pole is slanted, rotated, turned upside down, or sideways, the position of any point that the user touches with the receiver is accurately and instantly measured. SPSi system software provides basic functions such as distance between two points, areas, volumes, or angles, although the integrated site positioning system combines real-time coordinate data from the Odyssey™ system with computer-aided design (CAD) design data. The combination of real-time coordinate measurement and CAD representation allows field position and graphical design data to be provided simultaneously to the user. A variety of applications for this system exist in new construction as well as in retrofit projects; for example, in facility characterization, the comparison of as-designed with as-built physical parameters is a large application area in itself. Other applications include industrial plant outage planning and simulation, modular planning, fabrication and construction, consistent site control during construction, providing plant database baselines, and real-time position feedback for automated construction equipment (Beliveau, 1996).

18.3 Economics and Management of Robots

The most decisive factor when considering using a robotic application in construction is its impact on the overall cost of the concrete construction process (Skibniewski, 1988). The promising areas of application are in tasks where the work volume, high repetition, and simple control requirements result in promising robot automation potential. Such tasks include concrete surface treatment (e.g., cleaning, painting, sandblasting), inspection (e.g., nondestructive testing of concrete and reinforcement steel and assessment of ceramic tile adhesion to concrete surfaces), and concrete placement.

Robot-related costs to be reconciled during the analysis include capital costs and operating costs. The capital costs include research and development expenditures (hardware and software, work-system engineering, calibration, and field hardening). Operating costs include energy, maintenance, downtime, repair, tooling, setup, dismantling, transportation, operator, and other related expenditures. Robot-related benefits include construction labor and material savings, improved work quality, extension of work activity into additional locations and time periods, and possibly improved productivity. Details of the economic analysis of construction surface finishing tasks can be found in Skibniewski (1988).

As can be expected from the conditions under which the construction industry operates, the most important decision factor for robot implementation will be a short-term profit potential resulting from labor savings through productivity improvement and possibly through increased construction quality. Most conservative construction firms will be unlikely to invest in robot research and development and will rely on robotics technology developed by commercial robotic systems houses. Such robots will then be either sold or leased by commercial vendors operating in the construction equipment market.

A major difficulty that construction firms will initially face is estimating the robot costs and benefits, as outlined above. The estimation process will improve as more experience with particular robot applications is gained. Detailed information on the cost and benefit items for various robot applications in typical job-site settings can accelerate the pace of robotization if it is made available to all interested construction firms. Future construction robot equipment vendors will be well positioned to fulfill this function in cooperation with robot system developers and manufacturers. When more robotics become available for use on construction sites, significant challenges to both management and technical staff will emerge. For the reasons outlined above, robots must be managed wisely and perform at a high quality level to ensure maximum economic benefits for the contractor's firm.

Despite a number of advantages over traditional methods of performing construction tasks, robots are currently, and will continue to be in the near future, in short supply in comparison to other construction equipment. Thus, robots should be regarded as a scarce resource and their use should be maximized to their full operating potential. By maximizing robot capabilities on as many construction projects as possible, the economic benefits of robot use can be easier to attain; consequently, robot development costs can be recovered faster, and robot use can spread to other applications and types of construction tasks. A hypertext-based optimization program called the *Construction Robotics Management System* (CREMS) has been developed for that purpose. As shown in Figure 18.5, it consists of four modules: Construction Task Analysis, Robot Capability Analysis, Robot Economic Evaluation, and Robot Implementation Logistics (Skibniewski and Russell, 1991).

Automation in construction still constitutes a difficult technical and managerial challenge; however, potential benefits may be significant in this industry. Due to the lack of investment in research and development by construction firms in most industrialized countries except Japan, in combination with other factors, the industry has been experiencing difficulties in introducing and adopting new technologies at the project site level. To facilitate a more comprehensive impact of automation on the construction industry in the future, further research and development are essential. In particular, more attention should be focused on the redesign of construction sitework environments to enable direct technology transfer from other industries to construction, rather than on development of customized automated construction equipment that would closely resemble the humanlike performance of traditional construction tasks (Skibniewski and Nof, 1989). Sound methodologies for systematic technology transfer and

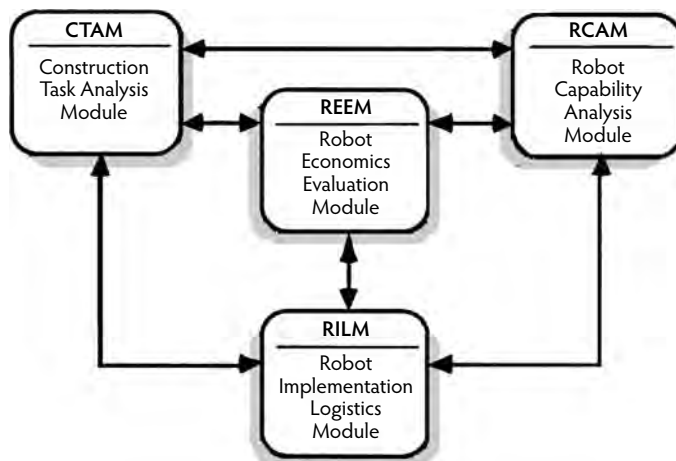


FIGURE 18.5 Construction robotics equipment management system.

evaluation are also necessary (Gaultney et al., 1989), particularly those utilizing the recent advances in computing technologies (Hijazi and Skibniewski, 1989). Better quality constructed products will increase the competitiveness of concrete construction firms involved and can ultimately lead to greater demand for their services. As research and development of construction robotics systems continue, the latest developments are regularly reported in annual symposia on automation and robotics in construction (see, for example, Cho et al., 2006) and in *Automation in Construction*, a bimonthly international research journal published since 1994.

18.4 Computer-Aided Design

18.4.1 Traditional Architectural CAD Modeling

Reinforced concrete (RC) structural facility delivery processes include the design and drafting of various sectional views, on drawing sheets, as two-dimensional drawings. Even a small design modification requires time-consuming redrawing of various sectional views, along with detailed rebar specifications. The emergence of traditional computer-aided design (CAD) systems changed the time-consuming manual design and drafting process into a series of keystrokes and mouse drags-and-clicks on a computer. As basic operations such as drawing and erasing a line, arc, etc. are much faster on a computer, traditional CAD systems reduced the costs of redrawing that resulted from design modifications. Traditional CAD systems require manual interpretation of the information pertaining to a given RC structural facility; for example, a given RC structural component such as beam is represented by several projections along with a set of symbols. This representation process requires manual interpretation not only during the design stage, which provides input of geometric and symbolic information, but also during the construction stage, which reproduces the exact shapes and configurations intended during the design stage. Further, the shapes and configurations are manually interpreted during the design and construction stages by different sets of people with widely varying knowledge and skills. In cases of complex reinforcement configurations—resulting from either the shape of the structure or special requirements such as earthquake resistance—total misinterpretation of shapes and configurations is possible during the construction stage, resulting in costly redesigns and rework. More advanced solid-modeling approaches, currently not prevalent in the RC structure domain, employ specialized representation schemes that would facilitate the interpretation process by capturing the shape information pertaining to a given design object. A brief discussion of various solid-modeling approaches is provided below.

18.4.2 Solid Geometric Modeling

A solid geometric model is an unambiguous and informationally complete mathematical representation of the physical shape of an object in a form that a computer can easily process (Mortenson, 1985). Topology and algebraic geometry provide the mathematical foundation for solid modeling. Computational aspects of solid modeling include data structures and algorithms from computer science and application considerations from the design and construction of engineering projects. The following techniques are available for the solid modeling of civil engineering facilities (Requicha, 1980):

- Primitive instancing
- Cell decompositions
- Spatial occupancy enumeration (SOE)
- Constructive solid geometry (CSG)
- Sweep representations
- Boundary representation (B-Rep)

18.4.2.1 Primitive Instancing

The primitive instancing modeling technique consists of an independent approach to solid-object representation in the context of the group technology (GT) paradigm. The modeling approach is based on the notion of families of objects, each member of the family being distinguishable by a few parameters. Columns, beams, and slabs can be grouped as separate families in the case of general buildings. Each object family is called a **generic primitive**, and individual objects within a family are called **primitive instances** (Requicha, 1980).

18.4.2.2 Cell Decompositions

Cell decompositions are generalizations of triangulations. Using the cell decomposition modeling technique, a solid may be represented by decomposing it into cells and representing each cell in the decomposition. This modeling technique can be used for the analysis of trusses and frames in industrial and general buildings, bridges, and other civil-engineering structures. In fact, the cell decomposition technique is the basis for finite-element modeling (Mortenson, 1985).

18.4.2.3 Spatial Occupancy Enumeration

The spatial occupancy enumeration (SOE) technique is a special case of the cell decomposition technique. A solid in the SOE scheme is represented using a list of spatial cells occupied by the solid. The spatial cells, called **voxels**, are cubes of a fixed size that lie in a fixed spatial grid. Each cell may be represented by the coordinates of its centroid. Cell size determines the maximum resolution. This modeling technique requires large memory space, thereby leading to inefficient space complexity; however, this technique may be used for motion planning of automated construction equipment under the complete information model (Requicha, 1980).

18.4.2.4 Constructive Solid Geometry

Constructive solid geometry (CSG), often referred to as **building-block geometry**, is a modeling technique that defines complex solids as a composition of simpler primitives. Boolean operators are used to execute the composition. CSG concepts include regularized Boolean operators, primitives, boundary-evaluation procedures, and point membership classification. CSG representations are ordered binary trees. Operators, which may consist of rigid motion, regularized union, intersection, or difference, are represented by nonterminal nodes. Terminal nodes are either primitive leaves, which represent subsets of three-dimensional (3D) Euclidean space, or transformation leaves, which contain the defining arguments of rigid motions. Each subtree that is not a transformation leaf represents a set resulting from applying the motional and combinational operators to the sets represented by the primitive leaves. The CSG modeling technique can be adopted to develop computer-aided design and drafting (CADD) systems for civil-engineering structures. It can be combined with primitive instancing that incorporates the group

technology paradigm to assist the designer. Although the CSG technique is most suitable for design-engineering applications, it is not suitable for construction-engineering applications as it does not store the topological relationships required for construction process planning (Requicha, 1980).

18.4.2.5 Sweep Representation

The sweep representation technique is based on the idea of moving a point, curve, or surface along a given path. The locus of points generated by this process results in one-dimensional, two-dimensional, and three-dimensional objects, respectively. Two basic ingredients are required for sweep representation: an object to be moved and a trajectory to move it along. The object can be a curve, surface, or solid. The trajectory is always an analytically definable path. The two major types of trajectories are translational and rotational (Mortenson, 1985).

18.4.2.6 Boundary Representation (B-Rep)

The boundary-representation modeling technique involves representing the boundary of a solid by decomposing it into a set of faces. Each face is then represented by its bounding edges and the surface on which it lies. Edges are often defined in the two-dimensional parametric space of the surface as segments of piecewise polynomial curves. A simple enumeration of the faces of a solid is sufficient to unambiguously separate the solid from its complement; however, most boundary-representation schemes store additional information to aid feature extraction and determine topological relationships. The additional information enables intelligent evaluation of CAD models for construction process planning and the automated equipment path planning required in computer-aided design/computer-aided construction (CAD/CAC) systems (Kunigahalli and Russell, 1995a; Kunigahalli et al., 1995; Requicha and Rossignac, 1992). A boundary-representation technique that stores topological relationships among geometric entities is most suitable for computer-aided generation of construction process plans. Primitive instancing, sweep representation, and CSG techniques are useful in developing user-friendly CAD software systems for design of civil-engineering structures. CAD systems that incorporate CSG or the primitive instancing technique during the interactive design process and that employ the boundary-representation technique for internal storage of design information are efficient for use in CAD/CAC systems (Kunigahalli and Russell, 1995b).

18.4.3 Solid Modeling of Reinforcing Elements

18.4.3.1 General

The shape of the boundary of a reinforcing element corresponds to a solid cylindrical primitive. A solid cylindrical primitive consists of three faces, three edges, and two vertices. A boundary-representation scheme must account for storage and manipulation of these topological entities. A boundary-representation scheme, the rectangle adjacency graph (RAG), supports solid modeling of reinforcing elements for various structural components such as beams, columns, and slabs. A brief description of the RAG modeling approach for reinforcement detail is described next. A more detailed description can be found in Kunigahalli (1997).

18.4.3.2 Description of RAG Scheme for Reinforcement Detail

18.4.3.2.1 Beam (or Column) Components

An RC beam or a column component consists of longitudinal bars to resist bending moment and stirrups or ties to resist shear force. The portion of a beam or column having the same configuration of longitudinal reinforcement is called a **region**. The geometric and topological information regarding reinforcement detail in a given region of a beam or column component is stored in a structure known as a **Beam_Column_Region**. The information regarding the boundary and reinforcement detail of a beam or column component and the connectivity of a beam or column component to its adjoining structural joints is stored in a structure known as the **Beam_Column_Component**.

The **Beam_Column_Component** structure contains a beam identification number, pointers to two adjacent structural joints, a pointer to a **Face_Table** structure that stores the boundary representation

(B-rep) of a beam or column component itself, and a pointer to a list of *Beam_Column_Region* structures. A parent pointer included in the *Beam_Column_Region* structure enables faster identification of the relative location of a region with respect to a complete RC-framed structure. **Long_Circular_List** and **Loop_List** store geometric and topological information pertaining to longitudinal reinforcement and stirrup or tie reinforcement, respectively.

The geometric and topological information regarding an individual reinforcing bar in a given region i is stored using an **Edge_Face** structure that contains a pointer to the parent region and an enumerated type to uniquely identify an individual longitudinal bar in a given region. Geometric and topological information pertaining to lap-spliced bars are stored using a separate structure known as the **Splicing_Rebar**. The **Edge_Face** structures of longitudinal bars in a given region i are stored in a circular list. A specification for the ordering of the circular list and labeling of longitudinal bars using the enumerated types has been provided to ensure an unambiguous representation.

There can be more than one loop of stirrup/ties to resist the shear force at a given cross-section of a beam or column component. The spacing of loops, and in some cases configurations of the loops of stirrups or tie bars themselves, may vary along the length of a given region. Geometric information pertaining to the vertices and faces is stored using floating point numbers. The information regarding the identified edge of a stirrup or tie reinforcing bar is stored using a pointer to an **Edge_Type** structure. The edge-to-edge and edge-to-contact-vertex topological relationships between a stirrup or tie bar and a longitudinal bar at the location of a standard hook can also be stored using a tailored structure designed specifically for storing hook information.

18.4.3.2.2 Slab Component

The RAG scheme supports solid modeling of reinforcement detail pertaining to a slab component, designed using one-way and two-way slab theories, that consists of longitudinal reinforcing bars to resist positive bending moment, negative bending moment, and torsion at the four corners. The reinforcement for positive bending moment and torsion are typically provided in two layers of bars—namely, upper and lower—that are placed along the two principal orthogonal directions x and y . There exists a boundary edge-to-edge contact between a given longitudinal bar and every other longitudinal bar placed in the other (orthogonal) direction. Negative bending moment reinforcement for a slab normally results in edge-to-edge contacts with longitudinal bars near the top faces of the beams enclosing the slab.

The geometric and topological information pertaining to a reinforcing bar in a slab component can be stored using an **Edge_Face_Slab** structure in the RAG scheme that stores the bar as an enumerated type. The enumerated bar type enables identification of appropriate topological relationships that must be stored. The direction of a given longitudinal bar is also stored using another enumerated type. As only two types of boundary edge-to-edge relationships occur in the case of slab-reinforcing elements, an array of only two elements that contain self-pointers is provided to maintain edge-to-edge topological relationships. The structures of longitudinal bars in a slab are arranged as lists ordered in the two principal directions x and y . Two such lists in orthogonal directions, which are confined within the boundary of a slab component, give rise to a rectangular grid structure. Thus, positive bending moment and torsional reinforcement in a slab component results in a total of five grid structures. Negative bending moment reinforcement for a slab component forms four lists, two in the x -direction and two in the y -direction, respectively.

18.4.4 Computerized Engineering Model

Although solid modeling approaches try to capture the shape of a given design object, the focus still remains on the geometric and topological information pertaining to the design object. A true engineering model, however, must also account for project-specific information pertinent to the model, the semantic relationships between various components of the model, and context-specific information associated with a given engineering domain. This requirement gave birth to a whole new concept that utilizes the object-oriented paradigm to allow incorporation of domain-specific expertise into a CAD application (BSI, 1996).

18.4.4.1 Object-Oriented CAD Modeling

An engineering facility-delivery process involves various participants such as owners, architects, structural designers, and construction contractors. These participants often work on different hardware and operating systems. In large engineering organizations, it is not uncommon for different groups using different hardware and operating systems to work on a single engineering project. Successful implementation of computer-integrated construction (CIC) concepts requires that the CAD data originating in one environment must be usable in any other environment without translation. Further, to support CIC concepts, a CAD system must archive a model in such a way that it can be reactivated after years or decades—for operation and maintenance or renovation purposes—without depending on the hardware or operating systems used during the model-creation process. Such a capability would facilitate smooth progression of users to more cost-effective hardware and operating systems of the future. An object-oriented CAD system that supports CIC concepts must also be capable of handling large datasets. Further, information pertaining to objects (e.g., a beam) present in a project model must be in a consistent state at all times during a CAD session. This is achieved by making sure that the beam information is always accessed and modified by the schema that defined and created the beam object.

The horizontally fragmented nature of the architecture design/engineering/construction (A/E/C) industry requires simultaneous sharing of a given project model by many users for different purposes. For example, let us consider a single beam in a project model. A structural designer may need to modify model information such as the depth of a beam, diameter and spacing of stirrups, and diameter and number of longitudinal bars at the soffit. On the other hand, a rebar subcontractor needs only to query the number and diameter of longitudinal bars, diameter and spacing of stirrups, and grade of concrete and steel. Further, a formwork subcontractor would typically be interested in a query related to the surface area that results from the beam dimension. Apart from allowing tailored intelligent views for different project participants, an object-oriented CEM that supports CIC concepts must ensure that modifications to a project model are properly coordinated and the model is kept in a consistent state at all times during the facility-delivery process. A concrete engineering project typically involves collaboration between experts in several domains such as design, rebar detailing, formwork installation, rebar placement, and concrete placement. An object-oriented CEM must facilitate integration of the information created by each of the domains and allow easy and consistent access by users in other domains (e.g., HVAC, electrical, and mechanical systems). Hence, it should be possible for one schema to reference information defined and maintained by another schema within a given project model that includes schemas that support several disciplines such as architecture, structure, HVAC, construction, and operation and maintenance.

18.4.4.2 Example Object-Oriented CAD System

Objective MicroStation is an example system that addresses the requirements of an object-oriented CAD system and supports the concepts of computer-integrated construction. It includes a schema implementation language called *ProActiveM*, which is an object-oriented programming language that allows the engineering application developers to include domain-specific expertise by creating schemas tailored to model domain-specific information. A rebar design and detailing application, for instance, can focus on modeling domain-specific information such as spacing, hook location and type, grade of steel, and lap splicing.

18.4.4.3 Internet CAD

Downloading standard formwork components from a formwork vendor's website and attaching them to an existing CAD model to check if readily available formwork components fit the designed model geometry is not far from reality with the availability of an Internet CAD system such as MicroStation. Internet CAD supports an Internet programming environment that is simple, is active (i.e., works on all platforms), and possesses web-distribution functionality (Bentley, 1996). Java is an Internet programming language that was developed by Sun Microsystems. The Java programming language allowed inline sound and animation in a web page for the first time. Java is not just a Web browser with special features but is also a programming language for distributed application. Java allows adding new types of content and

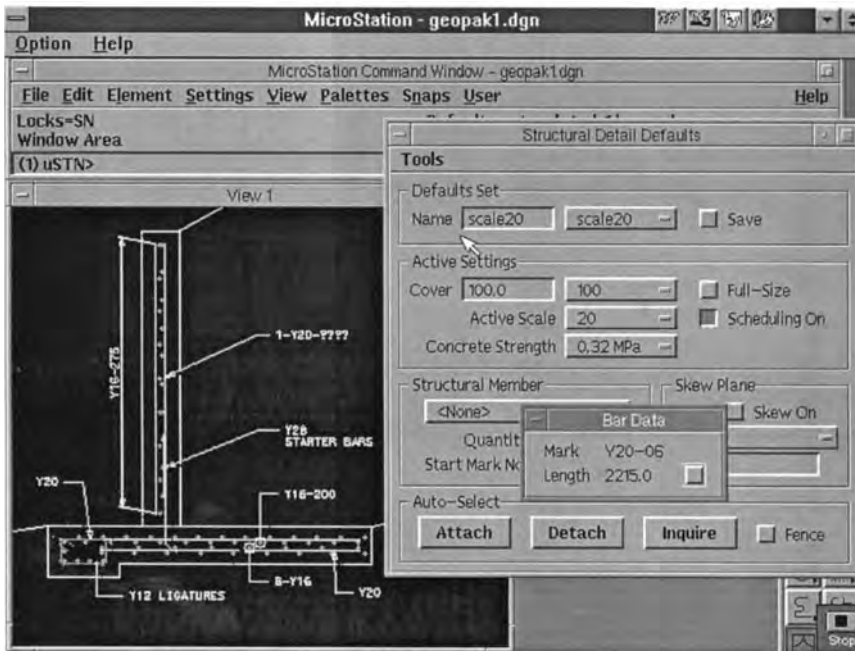


FIGURE 18.6 Geopak® rebar modeling.

the codes necessary to interact with that content; however, Java does not allow two aspects necessary for web-based manipulation of CAD models: maintaining active CAD models and automatic transaction management. ProActiveM, developed by Bentley Systems, Inc., includes all the functionalities of Java programming language and supports automatic transaction management and maintenance of active CAD models. By augmenting CAD systems, such as MicroStation, with an Internet programming language, such as ProActiveM, civil engineers can create **desktop sites** to work with active CAD models of a given project located at a remote **geographic site** (Bentley, 1996).

18.4.4.4 Example Rebar Modeling Systems

Geopak® rebar transforms the MicroStation CAD system into a rebar design and detailing system for reinforced concrete structures. Modeling of any regular or irregular reinforcement arrangements that include many configurations of rebar such as straight bars, stirrups, circular and spiral ties, and radial reinforcement is supported. Geopak provides the tight coupling of a given structural component with the rebar model used to reinforce the structural component. For example, a modification to the model that changes the overall dimension of a structural component will result in an automatic update in the arrangement, spacing, and clearance for the reinforcing steel bars. Automatic scheduling of bar lengths and bar quantities and monitoring of bar marks and shapes is supported for several national reinforced concrete design codes and specifications. Geopak exploits the graphical user interface (GUI) capabilities of MicroStation to provide a large range of specialized touch-click-and-drag editing functions to move, copy, or stretch an instance of a reinforcing-bar object. Figure 18.6 and Figure 18.7 show example screens from the Geopak rebar modeling system (Geopak, 1996). *ArtifexPlus* is a rebar and formwork planning software that specializes in complex compound units. Automatic prefabricated generation of completely reinforced structural modules such as staircases and foundations is supported. Reinforcement planning supports the import and export of reinforced areas, thereby enabling complete or partial reuse of reinforcement models for other projects. The mesh-reinforcement program supported by the reinforcement-planning package provides useful routines for laying single meshes or groups of meshes. Detailed

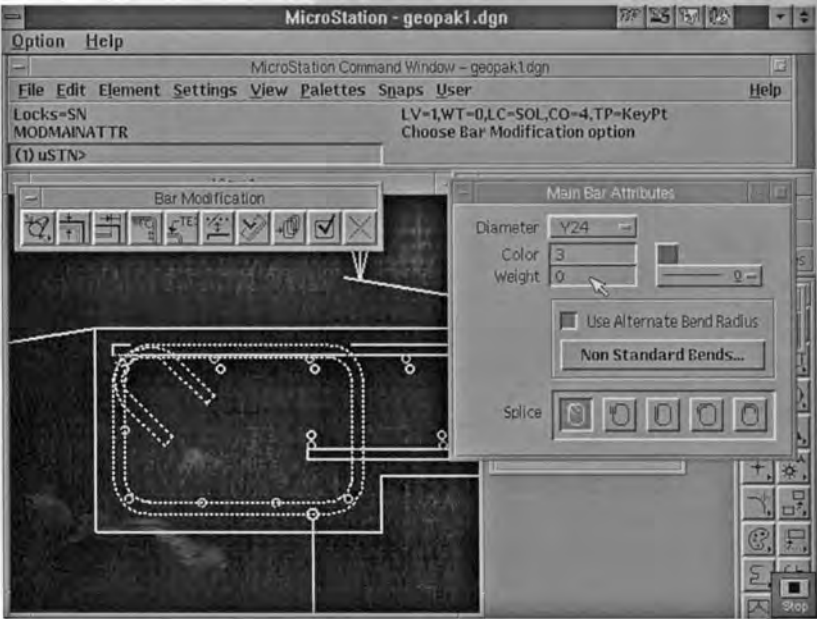


FIGURE 18.7 Geopak® rebar modeling detail.

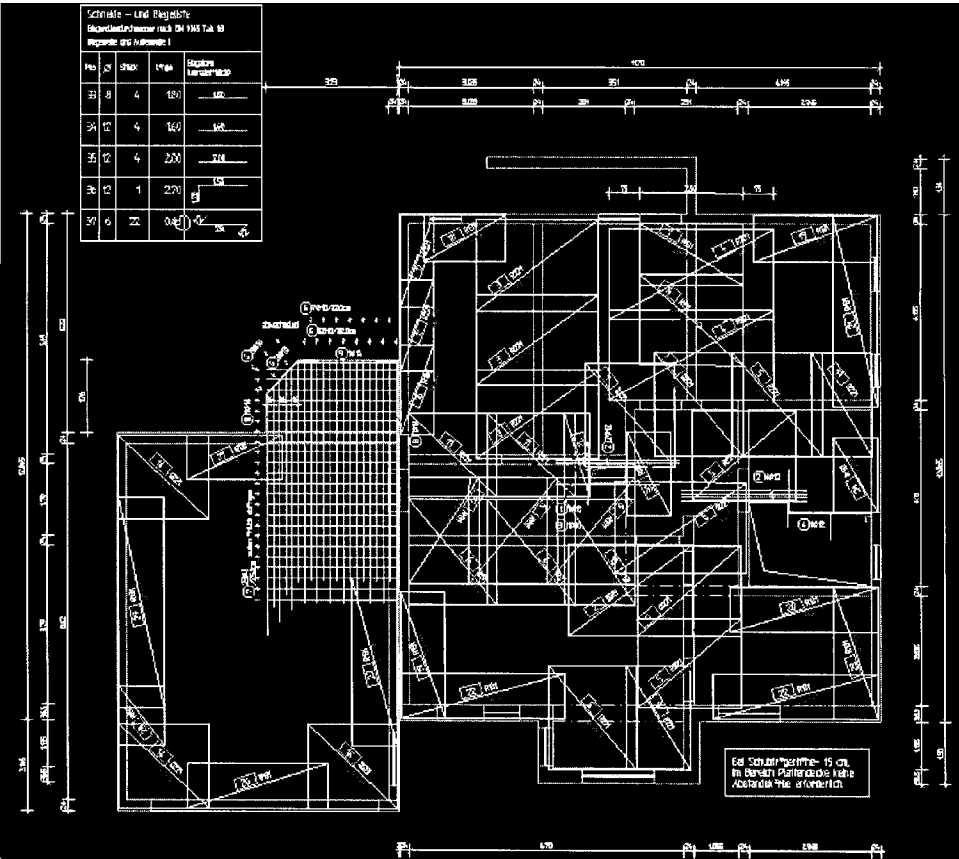


FIGURE 18.8 ArtifexPlus application.

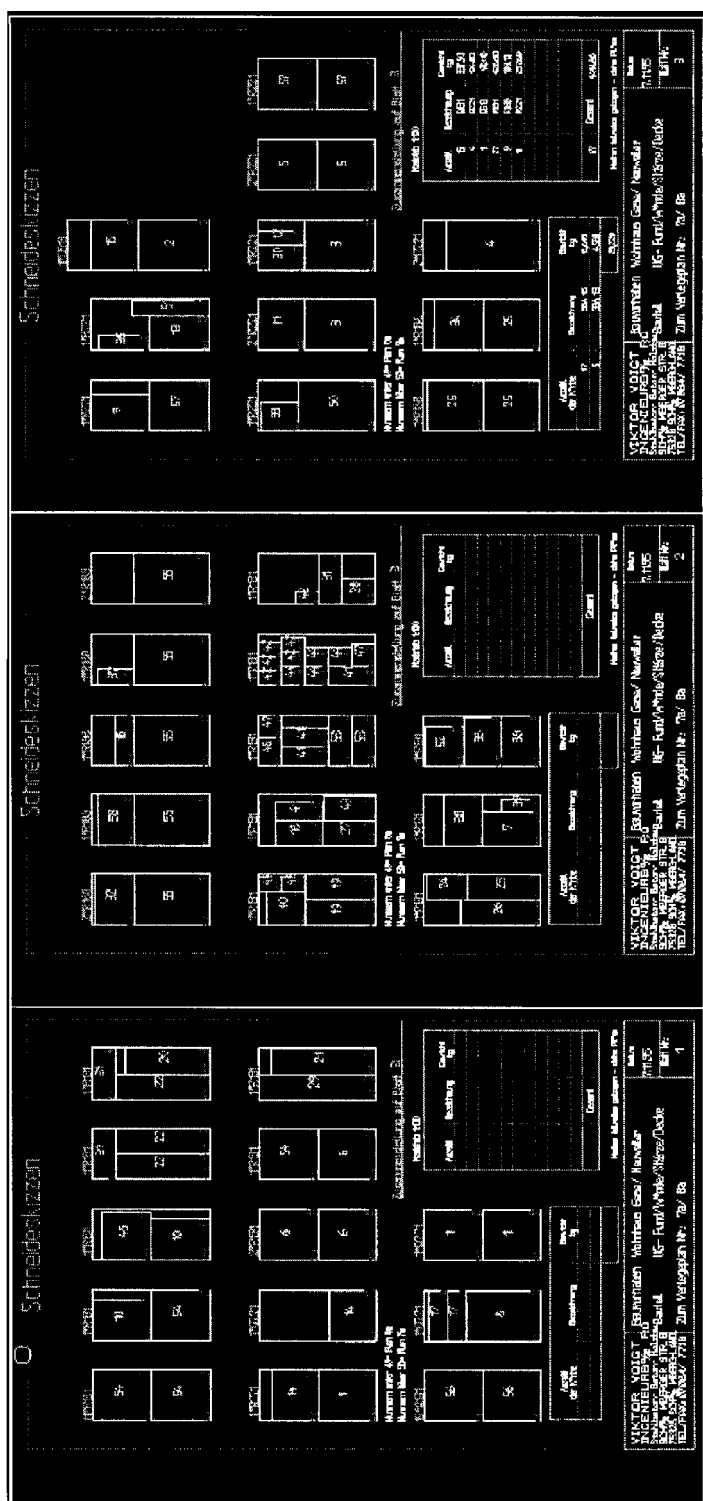


FIGURE 18.9 ArtifexPlus application, cross-sectional sketches.

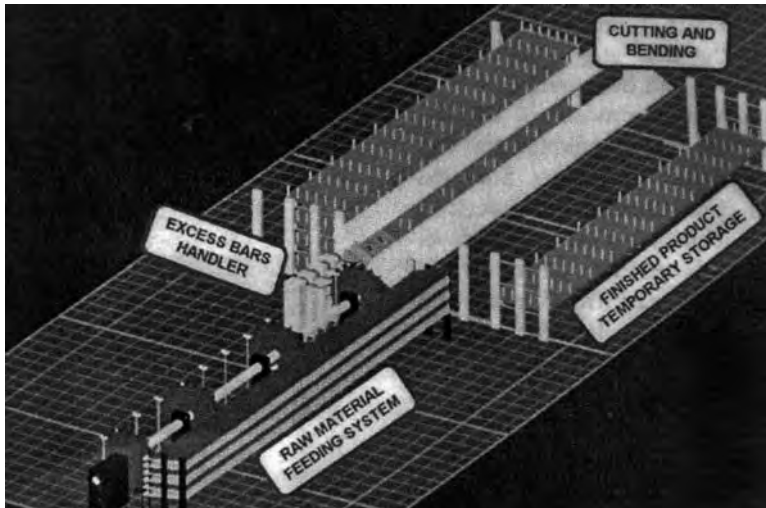


FIGURE 18.10 Rebar cutting and bending machine: general view. (From Navon, R. et al., *Automat. Construct.*, 4(3), 239–253, 1995.)

representation of the single and double bars of meshes can be created easily, and the weight of all meshes is automatically determined and saved. ArtifexPlus supports creation of formwork drawings based on architectural drawings. Figure 18.8 and Figure 18.9 show example screens from an ArtifexPlus application (Computer Unterstützt, 1996).

18.4.4.5 Automated Manufacturing of Reinforcement Bars

Concrete construction shows a trend toward integrating the achievements of automated design and construction capabilities, at least in off-site production. One example of this trend is the development of an automated rebar manufacturing machine (Navon et al., 1995). This machine produces bars larger than 16 mm in diameter. The machine receives the raw steel bar in a discrete manner, automatically inputs the bars for processing, cuts and bends the bars, and disposes of the excess material. In addition, the machine deals with the temporary storage of the finished product (see Figure 18.10). The machine was designed and developed with the aid of the *ROBCAD* graphical simulation system. This made it possible to check, in a three-dimensional environment, the logic of the material flow, the production methodology, relative location of the subsystems, interference between parts of the machine and the product, and the productivity of the process. The developers of this machine claim a 30% higher productivity compared to traditional rebar-bending machines.

18.5 Conclusions and Future Activities

Research and development of core technologies for automated construction equipment continues to make remarkable progress; however, much remains to be accomplished to bring about the successful automation of today's concrete construction and related work tasks. Concerns for short-term profits, fierce competition among contractors, and lack of top management commitment to technological change are often cited as primary obstacles to the rapid introduction of automation and robotics technology among construction firms. To date, the primary motivation for the robotization of on-site work was to remove humans from safety and health hazards. Eventually, with shortages of skilled construction labor becoming more acute, the scope of tasks considered for automation will be enlarged to include the simple, high-volume, and repetitive tasks that could be effectively automated. More emphasis on the development of new construction systems will be put on the redesign of traditional work tasks to better match the limited capabilities of automation and robot technologies. Automation of design and planning of reinforced

concrete structures at A/E/C firms has become, to a large extent, a reality. The most recent developments in the automation of design–construction integration are taking advantage of the existence of the information superhighway, allowing company professionals to communicate and transfer data instantly not only within their own organization, but also to clients, subcontractors, and other parties that may be located worldwide. This trend, independent of on-site work automation, is likely to continue.

References

- Beliveau, Y. 1996. What can real-time positioning do for construction? *Automat. Construct.*, 5(2), 79–89.
- Bentley, K. 1996. *Engineering for the Year 2000*, keynote presentation at the AEC Systems® Conference, June 18–20, Anaheim, CA.
- BSI. 1996. *Objective MicroStation*, technical abstract. BSI Group, Exton, PA.
- Cho, K.-H., Kim, H.-J., Kim, M.-K., Han, S.-H., and Park, S.-H. 2006. Identifying the demand for innovative future construction technology. In *Proceedings of the 23rd International Symposium on Automation and Robotics in Construction*, Tokyo, Japan. International Association for Automation and Robotics in Construction and Japan Robot Association, Tokyo.
- Computer Unterstützt. 1996. *ArtifexPlus*, technical description. Computer Unterstützt, Berlin, Germany.
- Gaultney, L., Skibniewski, M., and Salvendy, G. 1989. A systematic approach to industrial technology transfer: a conceptual framework and a proposed methodology. *J. Inform. Technol.*, 4(1), 7–16.
- Geopak. 1996. *Geopak® Rebar*, technical description. Geopak, North Miami Beach, FL.
- Hijazi, A. and Skibniewski, M. 1989. Computer simulation of concrete placement operations. *J. Eng. Comput. Appl.*, 4(1), 19–25.
- Kunigahalli, R. 1996. Geometric and topological representation of reinforcement detail for reinforced concrete framed structures. In *Proceedings of the 13th International Symposium on Automation and Robotics in Construction*, pp. 521–530. Japan Robot Association, Tokyo.
- Kunigahalli, R. 1997. 3-D modeling for computer-integrated construction of R.C. structures. *ASCE J. Comput. Civ. Eng.*, 11(2), 92–101.
- Kunigahalli, R. and Russell, J.S. 1995a. Framework for development of CAD/CAC systems. *Int. J. Automat. Construct.*, 4(3), 327–340.
- Kunigahalli, R. and Russell, J.S. 1995b. Sequencing for concrete placement using RAG: a CAD data structure. *ASCE J. Comput. Civ. Eng.*, 9(3), 216–225.
- Kunigahalli, R., Russell, J.S., and Veeramani, D. 1995. Extracting topological relationships from a wire-frame CAD model. *ASCE J. Comput. Civ. Eng.*, 9(1), 29–42.
- Mortenson, M.E. 1985. *Geometric Modeling*. John Wiley & Sons, New York.
- Navon, R., Rubinovitz, Y., and Coffler, M. 1995. Development of a fully automated rebar manufacturing machine. *Automat. Construct.*, 4(3), 239–253.
- Okuda, K., Yanagawa, Y., Kawamura, T., Ochiai, M., and Aoyagi, H. 1992. Development of the automatic screeding machine mounted on a girder for concrete placing work. In *Proceedings of the 9th International Symposium on Automation and Robotics in Construction*. Japan Robot Association, Tokyo.
- Requicha, A.A.G. 1980. Representation for rigid solids: theory, methods, and systems. *ACM Comput. Surv.*, 12, 439–465.
- Requicha, A.A.G. and Rossignac, J.R. 1992. Solid modeling and beyond. *IEEE Comput. Graphics Appl.*, 12, 31–44.
- Skibniewski, M. 1988. *Robotics in Civil Engineering*. Van Nostrand Reinhold, New York.
- Skibniewski, M. 1996. State of the art in construction automation R&D in the USA. In *Proceedings of the 13th International Symposium on Automation and Robotics in Construction*. Japan Robot Association, Tokyo.
- Skibniewski, M. and Nof, S. 1989. A framework for programmable and flexible construction systems. *Robot. Automat. Syst.*, 5, 135–150.
- Skibniewski, M. and Russell, J. 1989. Robotics application in construction. *AACE Cost Eng. J.*, 31(6), 10–18.

- Skibniewski, M. and Russell, J. 1991. Construction robot fleet management system prototype. *ASCE J. Comp. Civ. Eng.*, 5(4), 444–463.
- Skibniewski, M., Arciszewski, T., and Lueprasert, K. 1997. Constructability analysis: a machine learning approach. *ASCE J. Comput. Civ. Eng.*, 11(1), 8–18.
- Ueno, T., Kajioka, Y., Sato, H., Maeda, J., and Okuyama, N. 1988. Research and development of robotic systems for assembly and finishing work. In *Proceedings of the 8th International Symposium on Robotics in Construction*. Japan Industrial Robot Association, Tokyo.



The construction of the Allianz Arena, a 70,000-capacity stadium in Munich, Germany, makes a fine example of a multi-crane site. Nearly 20 tower cranes, as well as several mobile cranes, were in use when this photograph was taken in September of 2003. (Photograph courtesy of Israel Mizrahi, Israel.)

19

Equipment for Concrete Building Construction

Aviad Shapira, D.Sc.*

19.1	Introduction	19-1
19.2	Equipment Selection	19-2
	General • Example • Soft Considerations	
19.3	Concrete Equipment	19-12
	Concrete Mixers • Concrete Pumps • Power Trowels	
19.4	Cranes	19-21
	Tower Cranes • Mobile Cranes • Cranes in the Electronic Age	
19.5	Truck Loaders	19-43
19.6	Belt Conveyors.....	19-45
19.7	Material Handlers.....	19-45
19.8	Hoists and Lifts	19-47
19.9	Mechanized Form Systems	19-48
	Acknowledgment	19-51
	References	19-51

19.1 Introduction

Today's building construction projects are highly mechanized. With the growing industrialization of construction and the gradual shift to offsite prefabrication of structural and finishing elements that are then assembled (rather than produced) on site, production equipment is increasingly making room for *transportation* equipment. Thus, material handling and lifting equipment dominates construction sites as an essential resource, constituting a major part of the project's construction cost.

The typical concrete-construction building site will employ several or all of the following equipment types: (1) cranes, (2) material handlers, (3) concrete pumps, (4) hoists and lifts, and (5) forming systems. Concrete is commonly produced on-site only in the case of large projects requiring high concrete volumes or transportation distances that are too great for the supply of ready-mixed concrete. Earthmoving equipment is used for the initial, substructure phase of construction and often during final landscape development work but is hardly seen on the jobsite throughout construction of the structure itself (unless construction progress at various parts of the project is sequenced such that one part of the project is already above ground while another may still be under ground).

* Associate Professor of Construction Engineering and Management, Technion—Israel Institute of Technology, Haifa, Israel; specializes in construction equipment selection, operation, management, productivity, economics, and safety. Unless otherwise noted, all photographs in this chapter were taken by the author.

Of the above-listed equipment types, *cranes* are the most conspicuous machines on-site, not only because of their size but also because of the vital role they have in transporting materials and building components vertically and horizontally. When selecting equipment for the project, cranes are the centerpiece of the process, and decisions made on the selection and location of cranes commonly govern the selection of other equipment; therefore, cranes are discussed throughout this chapter in greater detail than other equipment types. The North American construction industry has traditionally been a *mobile-crane* culture (Shapira and Glascock, 1996); the number of mobile cranes in the United States is far greater than the number of *tower cranes*, which are the epitome of construction in Europe and the industrialized Far East. Tower cranes, however, have been increasing their presence in the United States since the early 2000s. Whereas mobile cranes are still by and large the backbone of the U.S. construction industry, the demand for tower cranes is on the rise. American contractors now favor tower cranes to a growing degree, and crane rental companies are responding to the demand by increasing the share of tower cranes in their fleets (Bishop, 2000; Shiffler, 2006b). High-rise construction has always been predominated by tower cranes, but now these machines are often seen on mid-rise and low-rise projects, as well, particularly for concrete construction of buildings, given the type of work and long service durations involved, as well as the all too often constricted sites that cannot accommodate mobile cranes.

Equipment offered and used for building construction has seen other changes in recent years. Most notable is the abundance of telescopic machines used for moving materials and workers about the jobsite. Modern *telehandlers* now replace the traditional forklifts. Coming with a variety of front-end attachments, these machines are gradually taking over other equipment as well, such as backhoe-loaders and small rough-terrain mobile cranes. Telescopic aerial work platforms and scissor-type lifts are often used on works for which conventional scaffolds commonly had to be erected. Sometimes a great number of these and other light, versatile, and mobile units may be seen on just one construction site.

This chapter focuses on equipment typically used for concrete construction on today's *building* sites. Forming systems, also undergoing significant modernization in recent years, are an integral component of today's on-site equipment for concrete building construction. Formwork design and forming systems in general are treated elsewhere in this book (see Chapter 7), but this chapter, in its last section, addresses mechanized form systems for building construction.

19.2 Equipment Selection

19.2.1 General

Selection of equipment (often termed *equipment planning*) for a construction project is one of the major functions and decision-making processes carried out by the construction company planning the construction of the project. This is due to the key role in the success of the project played by the selection of the appropriate equipment. Simple, "regular" projects, especially if similar to projects the company has previously built, may not pose a challenge in terms of equipment selection; however, when the project is no longer "regular," and definitely in the case of complex and large-scale projects, equipment selection also becomes very complex and challenging. This is due mainly to the following reasons, which should also serve as general guidelines for conducting the selection process:

- A great variety of makes and models is available for each type of equipment which, by itself, generates a great number of alternatives.
- For many equipment types, and particularly for cranes, selection also means the consideration of various location alternatives, within the overall site layout planning.
- For most equipment types, selection cannot be carried out separately for each type because they are interrelated (e.g., cranes, concrete pumps, and forming systems).
- The consideration of equipment alternatives is often interrelated with the consideration of construction methods (e.g., cast-in-place vs. precast concrete elements), thus the circle of options widens further.

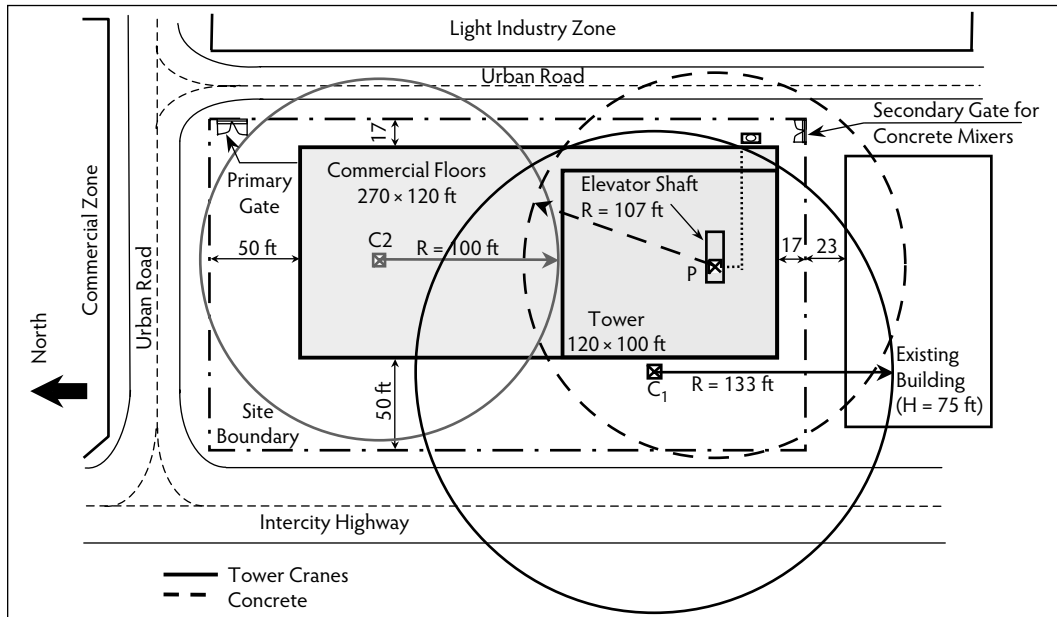


FIGURE 19.1 Example site layout (Alternative 1).

- Constructing a building is a dynamic process that continues to change throughout the project life. Equally variable are the equipment requirements. With the high level of uncertainty typically inherent in construction projects, equipment planning is frequently reexamined and occasionally even revised during construction.
- Construction companies commonly build several projects concurrently, each requiring its own equipment planning, and individual equipment plans that look into utilizing equipment owned by the company must be in concert with each other.
- Feasible equipment alternatives are primarily evaluated and compared on the basis of costs; however, a great many qualitative and intangible factors that are difficult or impossible to quantize must be considered systematically to ensure the selection of a “good” alternative (Shapira and Goldenberg, 2005).

The following example demonstrates these issues (Goldenberg and Shapira, 2007).

19.2.2 Example

Figure 19.1 is a site layout drawing for the construction of a 42-floor, 470-ft-high residential and office tower sitting above a 60-ft-high podium of commercial space. The building is set in a confined site, located within a busy urban area and in proximity to congested thoroughways; the entire area is occasionally subject to strong winds. The structural frame of the building is cast-in-place concrete, but the contractor is free to convert the external walls of the tower into precast elements. Construction progress for the concrete work for the tower is scheduled at one floor per week, and overall construction time is set at 24 months.

19.2.2.1 Alternatives

As shown in Figure 19.1, major equipment for the project (Alternative 1) includes two tower cranes (C_1 and C_2) and a concrete pump with a placing boom (P). Not shown in the drawing is a self-climbing wall system for the forming of all tower walls (external and core walls). With placing of concrete for all tower elements carried out by the pump and climbing boom and with the crane-free operation of the automatic climbing form system, only one crane (C_1) satisfies all other required lifting services for the tower (mainly

rebar, slab forms, and various finish materials). This is a full-height (520 ft) external crane, whose mast is braced to the west façade of the tower. The second tower crane (C_2) is a much shorter (100-ft), freestanding crane that serves the lower structure (commercial floors); this crane is located inside the building in openings left in the floors. The stationary concrete pump is located outside the southeast corner of the building, in close proximity to a gate for the entrance of ready-mixed concrete trucks. The placing boom and concrete supply pipeline climb inside the elevator shaft. Other equipment on the site, not shown in the drawing, includes a passenger lift serving the tower, as well as a telehandler serving the lower structure (but also the entire site as a multipurpose utility machine).

Each one of these equipment types offers a great variety of options in terms of specific makes and models entailing various dimensions, capacities, and other important work parameters. Related to these factors are locations of the equipment. For example, if the tower crane serving the high-rise structure (C_1) were placed inside the building in a climbing configuration, a shorter jib would suffice to secure full coverage of the high-rise building, and only a small portion of the sections currently making up the external crane mast would be required. On the other hand, dismantling an internal climbing crane is a much more complicated and costlier operation than that for an external tower crane.

Decisions on each major equipment type affect the entire equipment array on site. For example, another lifting solution (Alternative 2) would be two full-height external tower cranes, one on each side of the high-rise building (east and west façades). Concrete placing can then be accomplished with the cranes, eliminating the need for a concrete pump. The costly automatic climbing wall-form system may also be relinquished, but at the likely cost of extended work hours due to crane time overload. The cranes will also have to provide partial lifting services to the lower structure, within their reach and lifting capacity limits; otherwise, lifting for the lower structure would be done by the telehandler. Concrete for the lower structure is to be placed in this alternative by a truck-mounted pump and placing boom. The pump can be stationed in various locations along the north and west façades.

The interrelation between equipment selection and construction methods can be exemplified by the possible conversion of the tower's external walls from cast-in-place to precast concrete. Drawn from Alternative 1, the current case is likely to have the tower crane servicing the high-rise structure located inside the structure as an internal climbing crane. This way, the crane can handle the heavy precast elements along the circumference of the tower with a shorter jib; by moving the crane from the façade of the tower inside, the problem of installing precast wall panels at close proximity to the mast of the crane is also avoided. In this alternative, no forming of the external walls is required, and the use of the automatic climbing system is reduced to the core of the tower only.

Note that, in some cases, not only are equipment selection and construction methods interrelated such that the latter affect the former, but also *vice versa*. This brings into the picture the concept of *constructability*, where, among other things, equipment planning may begin as early as the design of the building. In such cases, the major equipment to be used on the project is taken into account in the course of design; alternatively, the initial design is revised. An example is the reorientation of a large set of wide-span precast concrete beams whose placement in the building according to the original orientation designed would not be possible with the crane already purchased for the project by the owner.

Alternatives 1 and 2 are merely two alternatives among several possible for this project. The *feasibility* of each alternative, in terms of satisfying all lifting and other logistics requirements, must be investigated and guaranteed before any cost comparison is conducted. The main parameters considered for each equipment type in the course of generating alternatives and investigating feasibility are mentioned separately for each equipment type in the subsequent sections of this chapter.

Cost estimates of each alternative examined will be affected by procurement patterns of the various machines. Procurement, in turn, essentially a matter of company policy (to own or rent equipment), is often dictated by the availability of existing company-owned equipment not engaged on any of the company's other projects. This could apply to whole machines or part of a machine; for example, even if the company owns the two tower cranes required for Alternative 2, it might still have to rent a portion of the mast sections for the two exceptionally high external cranes.

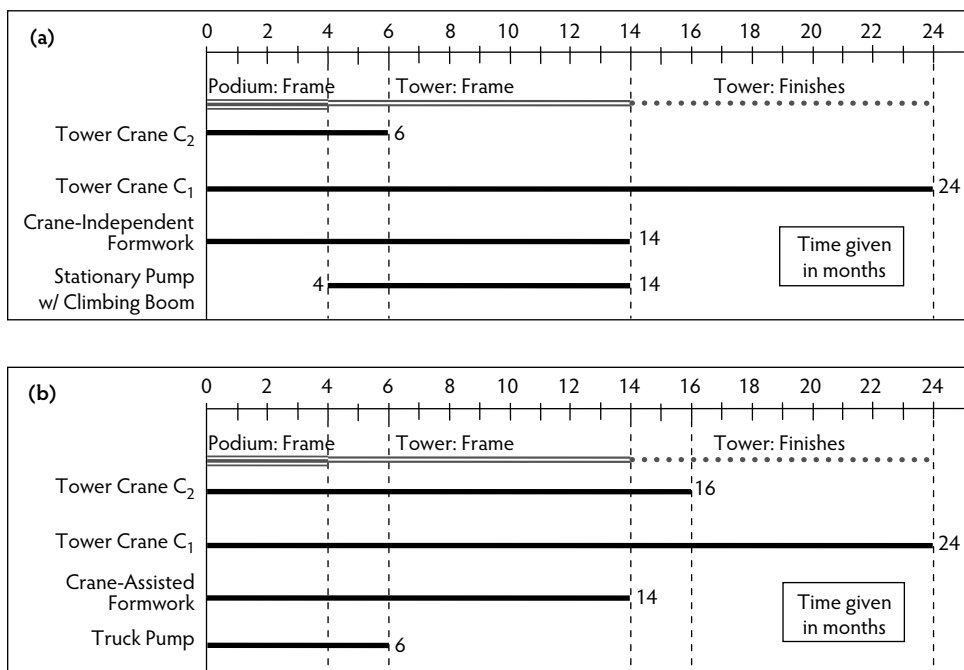


FIGURE 19.2 Example scheduling of equipment service: (a) Alternative 1; (b) Alternative 2.

Cost estimates must also take into account on-site service durations of each individual equipment unit, as derived from the schedule developed for each alternative. These schedules, in turn, must conform to the required construction progress and the overall construction time specified for the project. Figure 19.2 shows the schedules developed for major equipment in Alternatives 1 and 2.

19.2.2.2 Employment Times

Service durations of the various equipment units are closely associated with the planning of *daily crane employment*. Such planning is necessary to ensure the feasibility of each alternative. Table 19.1 is an example of crane employment times, as compared for the two equipment alternatives demonstrated in this section, focusing on the high-rise tower. Employment times are estimated on the basis of daily quantities of materials to be lifted and considering the predicted lift-cycle durations. Predicted lift-cycle durations should not be averaged but rather must correspond to the specific work conditions, as well as to the specific equipment reviewed. For example, the unit duration of 7.5 min per cu yd, as shown in Table 19.1 for concrete placement in slabs, corresponds to production rates of 8 cu yd per hr. Arithmetically, this could be achieved, for example, by the use of a 1.0-cu yd concrete bucket completing 8 cycles per hr (namely, 7.5 min per cycle), or by the use of a 2.0-cu yd bucket completing 4 cycles per hr (namely, a 15-min actual cycle time). Because bucket size virtually does not affect travel time, larger buckets would commonly be desirable, as they save crane time and entail overall higher productivity. (Note, though, that an increased concrete placing rate may require larger placing crews.) Here, however, enters another factor, which is the lifting capacity of the crane at the desired concrete placing location. A fully loaded 1.0-cu yd bucket weighs about 4800 lb (including self-weight); the respective weight of a 2.0-cu yd bucket is 9200 lb, or 4.6 tons. This is more than the maximum lifting capacity offered by many tower crane models at the jib end. For this reason, preparation of a crane employment table, such as Table 19.1, must relate, among other things, to the specific crane model and bucket size designated for the project.

TABLE 19.1 Example Daily Crane Employment Requirement

Material/Element	Unit	Quantity	Lift Cycle Duration per Unit (min)	Total Duration, Cranes Only (min)	
				Alternative 1	Alternative 2
Concrete for slabs	cu yd	80	7.5	Concrete pump	600
Concrete for walls and columns	cu yd	50	9.6	Concrete pump	480
Reinforcement steel	ton	5	24	120	120
Slab forms	Complete work	1	100	100	100
Core forms	Complete work	1	100	Automatic climbing system	100
External wall forms	Complete work	1	100	Automatic climbing system	100
Finish materials (estimated)				100	100
			Total	320	1600
			15% idling time	48	240
			Total time	368	1840
Required work shifts of cranes (10-hr, 600-min shifts)				One day shift	Three shifts: two parallel day shifts, one night shift

Another factor—in addition to bucket size and crane lifting capacity—that must be taken into account when actual *cycle times* are estimated is vertical travel distances. The values entered in Table 19.1 correspond to a building height of about 450 ft—namely, the top floors of the tower structure in Figure 19.1. Vertical travel times take up a major portion of the overall cycle time in such lifting heights, depending on the specific *hoisting* speed of the crane model. (Note that, to increase speed, hoisting motors may usually be replaced by more powerful ones, for any given crane model, whether new or used.) Thus, if a crane employment table were to be prepared for a low-rise building, then travel times would be almost ignored, as they virtually play no role in lifting heights of up to 60 ft. In these cases, crane cycle times are governed mostly by loading and unloading (or rigging and unrigging) times and by the fine maneuvering time required for the lifting hook of the crane to approach the exact loading/unloading point (Rosenfeld and Shapira, 1998). It can be concluded, then, that for the lower floors of the tower structure, lift-cycle durations are likely to be much shorter, resulting in shorter overall crane employment times.

According to the total-time results given in Table 19.1, the one crane serving the high-rise tower in Alternative 1 is underemployed. Note that 15% idling time was added to the computed service durations. In Alternative 2, on the other hand, the two cranes serving the tower are overloaded; therefore, one of them has to continue its work into a full night shift.

Preparing the crane employment table, which essentially takes into account other major equipment as well, is necessary to ensure feasibility, to obtain overall service durations of the equipment on-site, and to serve as the basis for the cost estimates of the various equipment alternatives. The study of employment times required for the project often involves refinement of more general decisions made when equipment alternatives were generated and checked for feasibility. Finally, calculation of work time exposes tradeoffs between type and quantity of equipment, overall size of labor crews, and workday duration, as exhibited by the various equipment alternatives.

19.2.2.3 Cost Estimates

Table 19.2 is an example of cost estimates worked out for major equipment in Alternatives 1 and 2. Costs were estimated based on total service durations of the cranes, pump, and wall-forming system, as shown in Figure 19.2. The extended work hours and night shifts revealed by the crane employment analysis shown in Table 19.1 for Alternative 2 incur higher wages for equipment operators and other labor crews.

TABLE 19.2 Example Cost Estimates of Equipment Alternatives

Equipment	Cost Factor	Cost Estimate (\$)	
		Alternative 1	Alternative 2
Tower crane (C ₁)	Capital cost (of owned equipment) or rental	377,000	310,000
	Maintenance	78,000	74,000
	Insurance, taxes, license	54,000	52,000
	Transportation, erecting, dismantling	44,000	44,000
	Ties, climbing device	102,000	102,000
	Operator wages	160,000	160,000
	Operating (energy)	24,000	24,000
	Climbing	6000	6000
Tower crane (C ₂)	Capital cost (of owned equipment) or rental	(–)	278,000
	Maintenance	14,000	49,000
	Insurance, taxes, license	8000	35,000
	Transportation, erecting, dismantling	33,000	44,000
	Ties, climbing device	(–)	53,000
	Operator wages	40,000	213,000
	Operating (energy)	4000	32,000
	Climbing	(–)	6000
Concrete pump	Capital cost (of owned equipment) or rental	96,000	51,000
	Maintenance	31,000	(–)
	Insurance, taxes, license	11,000	(–)
	Transportation, erecting, dismantling	(–)	(–)
	Operator wages	51,000	(–)
	Operating (energy)	9000	(–)
	Climbing	38,000	(–)
	Telescopic material handler	(–)	28,000
Forming systems	Capital cost (of owned equipment) or rental	682,000	(–)
	Maintenance	46,000	9000
	Insurance, taxes, license	38,000	(–)
	Transportation, erecting, dismantling	(Marginal)	(Marginal)
	Operating (energy)	(Marginal)	(–)
	Labor wages for vertical elements	498,000	1,692,000
Total cost for alternative		2,444,000	3,262,000

Direct costs of all equipment include capital costs (in case of owning) or rental costs, maintenance, insurance and licensing of owned equipment, deployment (transportation to the site and erection) and dismantling, climbing operations of cranes and placing booms (including work required to close openings left in slabs), operating costs (energy), and operator wages where applicable (always for owned equipment and, depending on the contracting base, “bare rental” or “all-included,” for rented equipment). For tower cranes, costs entailed by the specific crane configuration should be added (e.g., bracing to the structure and climbing mechanism for high cranes). Earthworks and foundations for the cranes, where applicable, are included in erection costs. There are *time-dependent* cost items (e.g., capital cost or rental), *production-dependent* cost items (e.g., operating costs), and *fixed* cost items (e.g., deployment). The values for all these, as shown in Table 19.2, are computed using the basics of engineering economics and common assumptions with respect to useful life, interest rate, maintenance rates, residual (resale) value of owned equipment, etc. These computations are beyond the scope of the current chapter; the interested reader should refer to Peurifoy et al. (2006) or any other similar book addressing the economics of construction equipment.

Indirect equipment costs in this example, with respect to major equipment, include auxiliary equipment (e.g., a telehandler for the low structure in Alternative 1) and labor wages in formwork. Note how the latter may constitute the largest single cost item (Alternative 2). Passenger lifts serve the high-rise tower equally in the two alternatives and are not included in Table 19.2. It should be noted that cost estimation

is much more than merely technical calculations; critical, big-picture decisions, on the one hand, and a great many fine details, on the other hand, are equally embedded in the process and mirrored in its results.

With respect to specific project and company data that are behind the numbers appearing in Table 19.2, the following should be noted as examples of parameters affecting cost estimation of equipment alternatives, in addition to those mentioned above:

- *General*—Capital costs and rentals reflect a specific given situation, in which part of the equipment is owned by the company and part is rented. Additionally, part of the owned equipment may have already exceeded its nominal useful life (and therefore no longer incurs capital costs). Note that “equipment” in this respect is not necessarily the complete machine as configured for the specific project; for example, the company may own a tower crane but not enough mast sections. Similarly, it may have to rent a climbing device for its owned crane. This is a rather common situation with equipment (such as mobile and tower cranes) that is modular in terms of its use and therefore also in terms of its manufacturing and procurement; manufacturers and dealers of such equipment cater this way to the great variety of different and changing requirements. On the other hand, other types of equipment (mainly when viewed by the company as being more of specialized equipment, given the company’s line of project types) are commonly procured in the complete configuration required for a particular use. An example could be a climbing concrete placing boom system, which would include the climbing mast, climbing gear, the placing boom, and all other accessories.
- *Climbing the cranes*—For the external cranes (C_1 in Alternative 1, C_1 and C_2 in Alternative 2), the cost of climbing depends only on the number of climbing steps, as no completion works are entailed in the floors (as would be with an internal crane). The number of climbing steps depends on the freestanding height of the crane, as specified by the manufacturer, and on the height to which the crane was erected initially. The higher these two are, the fewer the climbing steps required. If any of these cranes were in an internal-climbing configuration, a much higher overall climbing cost would result, due to (1) higher cost of each climbing step, (2) greater number of climbing steps, and (3) completion works in the floors. The cost for climbing the concrete placing boom in Alternative 1, an operation similar to that of climbing an internal crane, reflects these differences. The short crane installed inside the lower commercial structure (C_2 in Alternative 1) is initially erected to its full-required height, which does not change during construction. Hence, climbing costs in this case are incurred only by completion works of the lower structure’s floors, and these are marginal.
- *Location of concrete placing boom*—As shown in Figure 19.1, and also mentioned above, the placing boom transporting concrete from the stationary pump is located inside the elevator shaft. Elevator shafts, as well as stairwells, are commonly part of the structural core of the building. As such, they are a natural choice for the location of climbing booms and cranes, in terms of transferring loads imposed by the equipment. Indeed, when such equipment is located elsewhere inside the building, it usually requires temporary vertical shoring of the floors and sometimes additional bracing of the permanent structure being constructed. However, from the viewpoint of the construction process and progress, there are at least two disadvantages to locating climbing equipment in the elevator shaft: (1) it delays the installation of the building’s permanent elevators; and (2) it may interfere with, and therefore limit the choice of, forming systems for the walls of the core. As a compromise, the boom can climb elsewhere in the core, rather than in the elevator shaft. Stairwells should likewise be left free so as not to interfere with the installation of the stairs, as these serve workers moving between the floors during construction.
- *Ties and climbing device*—The device used to climb an external crane, whether it is a freestanding crane or a crane braced to the building, is modular equipment, often referred to as a *climbing cage*. A company owning several tower cranes may be able to climb them using a smaller number of climbing cages (owned or rented), depending on compatibility (due to make and model and to the cross-section of the mast). This is a desired situation, given the high price of these devices.

The ties and climbing device costs appearing in Table 19.2 reflect a similar situation, where one climbing cage can climb both external cranes in Alternative 2. Hence, the procurement cost of the cage in Alternative 2 was taken into account only once (C_1). The corresponding cost for the second crane (C_2) is essentially that of the ties to the building, with a small addition for moving the cage between the two cranes (as mentioned above, the number of climbing steps in this case is small). No climbing device costs appear in Table 19.2 for the concrete placing boom, as these were computed within the concrete pump's rental costs.

- *Deployment of cranes*—No fundamental difference in erection costs exists between the external crane (C_1) and the freestanding crane (C_2) in Alternative 1. Both are erected to their full, or nearly full, freestanding height, an operation that requires an erecting mobile crane. With similar jib lengths of the two tower cranes and pending comparable accessibility conditions to the site, a same-size mobile crane can be used, and the entire operation is similar in terms of other resources as well (erection team, duration). Deployment costs, however, do differ between the two cranes due to the much costlier transportation of all mast sections required for the high external crane. Another difference is in the crane foundations. Even if the two cranes are similar in terms of jib length and lifting capacity, a larger foundation is required for the high external crane due to its much higher weight (due mainly to the much greater number of mast sections but also to the likely larger and more robust cross-section of the mast). There is no fundamental difference in deployment costs between the two cranes in Alternative 2.
- *Dismantling of cranes*—Whereas crane erection is similar for both cranes in Alternative 1, the cranes that have to be dismantled at the end of construction are different. The same mobile crane that erected the external tower crane (C_1) can also dismantle it. The freestanding tower crane (C_2), however, now inside a 60-ft-high building from where it has to be pulled out, would require a larger mobile crane to dismantle it than the one needed to set it up. On the other hand, dismantling the external tower crane by a mobile crane must be preceded by climbing the tower crane down, in a process opposite that used for climbing it up (or else a much larger mobile crane would be required for dismantling). Thus, the overall cost of taking down the two cranes would still be similar, and the overall cost difference in deployment and dismantling could be attributed mainly to transportation and foundations. Note that lowering the external crane prior to dismantling it with a mobile crane is possible only as long as the jib of the crane can be aligned such that it does not make contact with the building. In some cases, the building geometry will not allow it, a constraint that must be borne in mind when crane location alternatives are considered.
- *Concrete pumps*—Three separate systems are combined together in Table 19.2 under the “concrete pump” category for Alternative 1: (1) stationary pump, (2) pipeline, and (3) climbing placing boom. This is specialized equipment commonly procured on a rental basis. In this case, transportation to the site, as well as erection and dismantling, were incorporated by the pump rental company within the monthly rate. The pump is brought to the site and the climbing boom system is installed in the building only after the first floors have been completed (see Figure 19.2). Thus, erection is assisted by the tower crane already on-site and so is dismantling. The service of the truck-mounted pump in Alternative 2 is procured on a quantity basis, but other rate systems are available. In the quantity-based rate system, there is commonly a fixed pumping rate for an initial concrete quantity plus a rate for each additional volume unit (cu yd). To estimate costs, therefore, the number of times the pump will be needed on site and the average concrete placing quantity on each time are assessed.
- *Forming systems*—As clearly evidenced from the costs in Table 19.2, the crane-independent automatic climbing wall-forming system used in Alternative 1 symbolizes industrialization more than any other single equipment used in the example project. Not only does it save precious crane time (which, together with the concrete pump, allows for the use of one crane only on the high-rise structure), but it also makes an enormous difference in terms of labor power needed on the project. The high cost of labor in Alternative 2 is due mainly to the much lower production rates achieved with manual forming as compared to the automatic system in Alternative 1, but

TABLE 19.3 Typical Soft Equipment Selection Factors

Factor	Explanation/Examples
Company policy toward own vs. rent	“Own” policy may result in purchasing equipment that, with a view to future projects, exceeds the requirements of a particular project, whereas “rent” policy is likely to produce a solution catering to the exact needs of that project only. Similarly, preference may be given to the use of owned, currently unemployed equipment (e.g., two small cranes) over rented equipment (e.g., one large crane), even if the latter would have otherwise been the optimal solution. Companies would generally look first into using their own equipment before other options are considered, even if cost comparisons would point to a rental-based solution.
Company project forecast	This factor influences current purchase vs. rent decisions and thus may affect the equipment selected for a particular project under discussion. It has a bearing on costs through the value given to the predicted return period in economic calculations.
Commercial considerations	The desire to start operating part of the constructed facility (in case of a cash-flow-producing asset) earlier than the rest of it may affect equipment selection (e.g., refraining from locating tower crane in underground parking of an office building if it may interfere with the early operation of the parking as a public facility before the main building was completed).
Procurement method and subcontracting	Quite often, the client/owner dictates certain requirements that affect equipment selection (e.g., using the client’s given equipment, providing craning services to other contractors on the same project, or forbidding the use of certain zones for locations of equipment). Another case example is of a joint venture project where the two construction companies decide to have identical equipment on site to simplify accounting between them (e.g., two cranes), even if another solution (e.g., a crane and a concrete pump) may otherwise be favored.
Company project specialization	A company may specialize in certain categories of construction (e.g., high-rise buildings, precast structures). This is reflected in the equipment it owns and operates and can have direct implications on the equipment available for a new project. It also influences the type, experience, and size of the company’s equipment maintenance department, which, in turn, affects cost estimates.
Dependence on outsourcing	Outsourcing increases dependence on factors outside the site management control, chances of mishaps, and uncertainty in general. Avoiding it may lead, for example, to favoring on-site plant for the fabrication of precast elements over ordering them externally.
Shifting responsibility to external party	Favoring ready-mixed concrete over on-site concrete production or favoring the ordering of precast elements over on-site fabrication has an advantage in terms of quality assurance of the product as well as contractual liability to this quality.
Working night shifts	Night shifts commonly result from either a tight schedule or traffic-induced difficulties in transporting concrete/precast elements to the site during the daytime. It may affect site management and is also an additional cause for safety concerns. Obviously, it incurs higher wages, which are reflected in the cost estimates.

also to the need to work at night, when wages are much higher. The forms rental company that provides the automatic system and supervises its erection includes transportation costs for most parts of the system in the monthly rate. Erection and dismantling are carried out by the construction company workforce and their costs are included in labor wages. As for the forms used in Alternative 2, they are owned by the construction company and have exceeded their nominal useful life.

19.2.3 Soft Considerations

If equipment alternatives were compared based on costs only, then, for example, Alternative 1, considerably less costly than Alternative 2, would be the one selected for the above-exemplified project. As mentioned earlier, however, the great variety of qualitative and intangible factors, if considered, may

TABLE 19.3 (cont.) Typical Soft Equipment Selection Factors

Factor	Explanation/Examples
Tradition, previous experience	The types of equipment selected for the project may be heavily affected by experience and by tradition, whether on the market level (availability of technical support), company level (culture), or site management level (personal preferences). The same applies for the location of equipment (e.g., internal climbing crane or climbing placing boom located in the elevator shaft or elsewhere in the floor through openings in the slabs).
Redundancy of equipment	The need to have backup for contingencies (e.g., breakup of a machine) so as to avoid work stoppage may give advantage to using multipurpose equipment or excess equipment.
Obstacles on site	Obstacles commonly include overhead power lines and adjacent structures, which can affect productivity and safety. Fixed (rather than mobile) equipment may have an advantage; specialized operator aids may be required.
Labor availability	Labor shortage increases the attractiveness of higher mechanization in general and automated systems in particular. This goes beyond the need to pay higher wages, which should be taken fully into account in the cost estimates. Temporary unavailability of skilled laborers may impede work progress severely.
Noise levels	Give preferences to electric over diesel powered equipment; noise levels may also exclude night work.
Site accessibility	Narrow roads may limit the size of precast concrete elements or steel trusses transported to the site, which in turn may affect equipment size requirements (e.g., a greater number of smaller machines).
Heavy traffic	For projects located in urban areas near congested roads, heavy reliability on a continuous external supply (e.g., of ready-mixed concrete in large volumes overall) may be abandoned in favor of on-site production, even if the latter is much costlier (e.g., if the constructed facility takes up the entire area of the site, necessitating relocation of an on-site concrete production plant several times during construction). Night work is another solution (but it may have been reserved for supply of other materials/elements, such as precast panels).
Strong winds	In areas given to strong winds, tower cranes may be preferred over mobile cranes. Additionally, the use of forming systems that climb automatically without crane assistance may be considered to avoid craning of large forms that act like a sail.
Equipment age and reliability	Technological advantages aside, newer equipment is likely to encounter fewer operational problems and less downtime, thus offering better service overall.
Overlapping of crane work envelopes	Overlapping tower cranes often are unavoidable, whether because of reach limits or daily schedule demands. Careful work and designation of forbidden zones helps in coping with safety hazards, but work may be slowed down. The use of (costly) anticollision systems may be considered.
Obstruction of crane operator view	Even with signal persons, this could become a major safety hazard (lower productivity is another result), and hence should be taken into account when equipment selection and location alternatives are considered. Operator vision aids (e.g., crane-mounted cameras) offer a partial solution.

point to the solution offered by Alternative 2, which otherwise is costlier. Alternatively, these factors may consolidate the selection of Alternative 1, as was made on economic grounds only. Certainly, if Alternatives 1 and 2 showed near enough the same costs, then the decision as to which one to select would depend entirely on adequate assessment of these qualitative and intangible factors. Table 19.3 offers a list of typical such “soft” factors, as these are usually termed (Shapira and Goldenberg, 2007). The following points are common to most soft factors:

- They are strongly connected to local cultures and traditions, as well as to the physical, organizational, and market environment. They express the uncertainty and intuition rooted in construction decision making, as well as the subjective judgment that is likely in the background of many seemingly pure technical calculations. Their consideration draws from the experience accumulated by the individuals who participate in the decision-making process and in the construction company.

- If they are measurable, they exhibit a great variety of measurement units, which makes it difficult or even impossible to compare them on a common quantitative basis. Only seldom can they be expressed in monetary terms; primarily, they are altogether immeasurable.
- Often the particular decision arrived at by the consideration of one factor is in conflict with that arrived at by another. See, for example, in Table 19.3, “Dependence on outsourcing” and “Heavy traffic” vs. “Shifting responsibility to an external party.” Another example is using mobile cranes owned and readily available by the company vs. using rented tower cranes with which the site superintendent has good experience.
- They affect the initial decision-making process when they are considered, usually intuitively and at times even unconsciously, in the course of the alternative generation phase, alongside hard factors. In many cases, they have a bearing on costs and are taken into account in the cost estimation phase (e.g., see “Company project forecast” and “Company project specialization” in Table 19.3).
- Veteran project managers and other functionaries involved in equipment planning (e.g., equipment managers) may have the rich experience, professional skills, and tacit knowledge it takes to detect all soft factors relevant to the project and to consider them successfully, especially if they operate in a well-developed planning environment. However, the lack of practical tools for the systematic evaluation and consideration of soft factors often results in equipment solutions that eventually are found to be inappropriate or costlier than initially estimated.

It is all these points, and particularly the lack of practical methods and tools to integrate the consideration of soft factors within the entire selection process in a structured and systematic manner, that contribute to the complexity of equipment planning and to the potential realization of inadequate solutions.

A method presented by Shapira and Goldenberg (2005) to deal with this problem is based on a widely accepted multi-attribute decision-making technique referred to as the *analytic hierarchy process* (AHP). AHP, introduced by Thomas Saaty (1980), was developed to assist in the making of decisions that are characterized by a great number of interrelated and often contending factors. To make such decisions, the relative importance of the factors involved must be properly assessed to allow tradeoffs among them. The main feature of AHP is its inherent capability of systematically dealing with a vast number of intangible and nonquantifiable attributes, as well as with tangible and objective factors. AHP allows for incorporation into the decision-making process of subjective judgments and user intuition by producing a common formal and numeric basis for solution.

Recent implementation of the AHP-based equipment selection method to evaluate soft factors and to assess their impact *vis-à-vis* the results of cost comparisons, in a rational process that leads to the selection of a “good” equipment alternative for the project, is demonstrated in detail by Goldenberg and Shapira (2007). The method was examined and tested in real-life settings to satisfying results. The interested reader is referred to Shapira and Goldenberg (2005) to learn about the fundamentals and concepts of the method, and to Goldenberg and Shapira (2007) for an elaborate case study.

19.3 Concrete Equipment

The use of concrete as a building material involves equipment throughout production: from batching and mixing, through transporting and placing, to consolidating and finishing. This section focuses on major equipment commonly used for these operations.

19.3.1 Concrete Mixers

Concrete can be centrally *mixed* in a “wet” plant—a plant that has a built-in mixer—and transported to the site in truckmixers operating at agitating speed, centrally *batched* in a “dry” plant, and mixed in the truckmixer itself, which then drives to the site at agitating speed, or it can be produced on-site. On-site production is a viable solution mainly in case of exceptionally large concrete amounts or if the site is located remotely such that transport distances from the closest plant are too great. The view of a compact



(a)



(b)

FIGURE 19.3 Truckmixers: (a) rear-discharge truckmixer; (b) front-discharge truckmixer.

mobile mixing plant on a small construction site in some parts of the world (e.g., Europe) is not rare; today, this equipment is highly automated, among other things, to ensure high concrete quality control. Where high concrete volumes are required, larger mixing plants with higher outputs are sometimes used on-site—for example, in dense urban areas with access difficulties due to traffic-congested roads. The great majority of today's building sites, however, use ready-mixed concrete delivered to the site from the dry or wet central plant in **truckmixers**, also called *ready-mixed trucks*.

Truckmixers the world over are of the *rear-discharge* type (Figure 19.3a), but in North America, *front-discharge* truckmixers are used as well (Figure 19.3b). The drum in the front-discharge mixer is more elongated. This shape of the drum and the overall configuration of the truck result in a better weight distribution, which allows these trucks to meet road and bridge load restrictions better than the rear-discharge truckmixers. The front-discharge truckmixer allows the driver a more convenient approach to the discharge location; the driver's ability to control the operation from the cab without leaving the cab is an additional advantage in bad weather. This carrier truck, however, is specialized equipment, unlike the standard carrier truck of the rear-discharge mixer, and therefore more costly.



FIGURE 19.4 Truckmixers lined up on the street, awaiting their turn to enter the restricted site and position themselves at the concrete pump.

The drum in the ready-mixed concrete truck, both of the rear- and front-discharge type, is a *freelfall*-type mixer. Freefall mixers blend concrete by lifting the ingredients with the aid of fixed blades inside the rotating drum (in the case of a truckmixer, the blades are spiral) and then letting them drop by gravitation (hence, the term *gravity mixer* is also used for freefall mixers). This is unlike *power* mixers, which blend the concrete by rapid rotary motion of paddles, making them particularly suitable for dry mixes. The drum of the truckmixer is rotated in one direction for loading and in the opposite direction for mixing or agitating (i.e., it is a reversible-type freefall mixer).

When planning a pour with ready-mixed concrete, several points should be considered. The rate of concrete delivery is affected by the size of the truck (namely, the effective intake volume of the drum), distance from the plant to the site, the number of truckmixers allocated by the plant for the specific operation, and possible delays that may be caused by heavy traffic. In terms of site organization, maneuvering space must be ensured for the large and heavy trucks, as well as proper ground conditions for travel. If the site is too restricted to allow free truck movement, as is often the case in mid-city construction sites, provisions should be made to allow for the nearby waiting of trucks. Such operations require thorough planning, workers designated for traffic control, and communication means. Often, one traffic lane would have to be blocked for the duration of the pour, after coordination with the local authorities (Figure 19.4).

Truckmixers come in sizes up to 20 cu yd, with 8 to 12 cu yd being the most common size range. The most popular size appears to be gradually increasing, although it has stabilized at 11 cu yd for several years now. Truckmixers are sometimes equipped with a boom pump or belt conveyor (see below), which gives them greater operational flexibility and independence and can be particularly useful for small jobs (e.g., house renovation) requiring small amounts of concrete.

In Europe, the use of another type of concrete mixing equipment is quite common. This is the **self-propelled mobile mixer**. The compact rough-terrain wheeled carrier, similar to that of the telehandler (see below), carries a self-loading drum-mixer with high-discharge capabilities. Mixer volumes in current models are in the range of 1 to 6 cu yd. Concrete can commonly be discharged with chutes up to 30 ft horizontally and at heights of 3 to 7 ft; with a special hydraulically elevated drum, height discharge can be up to 10 ft. Not used much on building construction sites, this self-contained machine is particularly useful on spread-out, low-rise civil projects, such as long concrete walls, utility lines, or small repair works on airfields, where relatively small quantities of concrete are required at different locations. If aggregates and cement are stored near these locations, the self-loading mixer can travel between them and carry out concrete placing as well. Quite often, such projects are remotely located and are inaccessible to truckmixers. Under such conditions, the use of one machine that offers a solution for aggregate loading and concrete mixing, transporting, and placing is even more attractive.

19.3.2 Concrete Pumps

19.3.2.1 Uses and Outputs

Concrete pumps transport concrete by moving it through a pipeline at high placing rates. As such, a concrete pump is a single-purpose machine—namely, it cannot be the only material transportation equipment on the site (unless concrete is the only or primary material requiring transportation, such as in the construction of culverts and retaining walls or at the foundation phase of the building). Hence, concrete pumps are commonly used on building construction sites generally serviced by cranes, for one or more of the following reasons: (1) the crane is engaged in other lifting services, (2) a high placing output is required (typically for large pours), or (3) the location of the cast element is outside the reach of the crane. Concrete pumps are often also seen on sites where their ability to deliver the concrete while bypassing obstructions becomes useful, such as inside low-roofed spaces (e.g., tunnels), for renovation work on existing buildings, and on sites located such that access of any other transportation means is impossible (e.g., in old cities with narrow lanes). The effective pumping distance of common concrete pumps is 300 to 1000 ft horizontally and 100 to 300 ft vertically (although special pumps have moved concrete for much greater distances). The maximum theoretical output of commonly used pumps is 80 to 200 cu yd/hr, or even up to 300 cu yd/hr for the largest pumps available today, but these rates are rarely realized. Placing rates are determined in practice by the type and dimensions of the cast element, the size of the concrete placing crew, and the rate at which the concrete is fed into the intake hopper of the pump (an intake hopper can be seen in Figure 19.6b), the latter being dictated most commonly by gross truckmixer discharge cycle time. Effective outputs, in a properly organized placing operation and under normal conditions, are as follows:

- Common building elements of regular dimensions, 40 cu yd/hr
- Thick slabs and similar elements, 60 cu yd/hr
- Mass concreting of large elements (e.g., raft foundations), 80 cu yd/hr

19.3.2.2 Types and Configurations

The three main configurations of concrete pumping equipment are (1) a pump-and-boom combination, (2) a pump with a separate pipeline, and (3) a pump and pipeline with a separate, tower-mounted boom. The first of these is particularly efficient and cost-effective in saving labor and eliminating the need for pipelines to transport the concrete. The last of these, used mostly in high-rise construction, combines elements from the former two and is a less common configuration. The following description of these three configurations was adapted in part from Peurifoy et al. (2006).

19.3.2.2.1 Pump-and-Boom Combination

In this configuration (Figure 19.5), also termed a *boom pump*, the pump is mounted on a truck and equipped with a slewing boom to which a fixed-length delivery line is connected. The line is made of a



(a)



(b)

FIGURE 19.5 Pump and boom combination (boom pump): (a) arriving at site, with folded boom; (b) in operation, with extended boom.

steel pipe, commonly 5 in. in diameter. The free end of the line has a flexible rubber pipe (end hose), 9 to 12 ft long, connected to it. The end hose eases the task of the worker who holds it and can also be used to slightly extend the boom's reach.

Booms come in lengths of 60 to 210 ft, but the more commonly used booms are in the range of 80 to 140 ft. Hydraulically operated and articulated, booms in most truck-mounted pump models have four or five sections, but three sections for short booms and six sections for the longest ones are available, too. For a given boom length, a greater number of sections provides the boom with greater maneuverability, which may be an advantage in confined areas. Note that boom length is a nominal length and not the effective length of the boom. It indicates the maximum vertical reach of the boom, measured

from the ground, which includes the dead length from the ground to the first boom joint. Because this dead part is around 13 ft for most makes and models of truck-mounted pumps, the maximum horizontal reach of the boom, measured from the slewing axis of the boom, is always shorter by about 13 ft from the nominal boom length. Effective horizontal reach is even shorter, as loss of distance measured from the slewing axis to the front of the truck or to the truck side must be taken into account. Depending on truck make and size, the extended outriggers, by which the truck is stabilized while in operation, may also contribute to the shortening of the effective horizontal reach.

Truck-mounted pumps use one of two types of booms that differ from each other in their articulation mode. One type of boom extends convexly, but the other extends in a Z-like mode. Z-booms are particularly suitable for jobs with height restrictions (e.g., working under obstacles) and for confined spaces with low overhead, such as inside tunnels.

Because the reach of boom pumps is limited, these pumps use ready-mixed concrete, with the truck-mounted pump optimally positioned to enable maximum coverage of the concreting area for each concreting operation. If coverage from one location is not possible, the truck is relocated in the course of the operation. Relocation, however, interrupts work continuity and may cause delays, depending on the time it takes to fold the boom, retract the outriggers, move the truck, extend the outriggers, and unfold the boom to continue concrete placing. If the relocation was not planned, a line of waiting ready-mixed trucks may result as well.

Truck-mounted booms are available in two additional equipment configurations: as separate trailer placing booms and in combination with a trailer-type pump (see below). The trailer boom uses a two-wheel carriage with counterweights to help balance the extended boom. When combined with a trailer pump, the pump serves as a partial counterweight. In both configurations, the equipment is stabilized on outriggers when in operation. Booms in both cases are shorter than truck-mounted booms, and their maximum operation range is around 60 ft.

19.3.2.2.2 Pump with a Pipeline

In this configuration, also termed a *line pump*, the pipeline is a separate system that must be assembled and connected to the pump before pumping operations begin. The pipeline is laid from the location of the pump to the concrete casting area. The pump is located such that the ready-mixed concrete trucks have good access to it. In the case of on-site-mixed concrete, the pump would be placed with the hopper just under the discharge opening of the mixer. On spread-out projects, sizeable floor-area buildings, or high-rise projects comprised of more than one building, several pipelines can be stretched from one pump to various project zones, thus eliminating the need to relocate the pipeline with each change in casting location. A special pipeline gate is used to control which line is being used to any given pumping operation. Another option is to prepare several pipelines and relocate the pump according to the placement location. This latter option requires the use of truck-delivered ready-mixed concrete. In terms of its mobility, the pump is a stationary pump, trailer pump, or truck pump (not to be confused with the truck-mounted pump-and-boom combination). Figure 19.6 shows a truck pump being fed by truckmixers. Two mixers position themselves at the pump and feed it alternately such that concrete supply for the pump is continuous and a higher placing rate is achieved. Pipelines for concrete transportation use pipe diameters of 3 to 8 in. (with 5 and 6 in. being the most common sizes). The pipeline is assembled of straight and curved steel pipe sections connected to each other by quick couplings. Similar to the boom pump, here, too, the free end of the line has a 10- to 30-ft long flexible rubber pipe connected to it for better control of the concrete discharge location and for easier handling by the workers who have to direct the spreading of the concrete. To help with the difficult work of holding and moving the end of the concrete-filled pipe, a special lightweight distribution (or placing) boom can be used and crane-lifted for relocation as the concreting progresses.

19.3.2.2.3 Pump with a Pipeline and Tower-Mounted Boom

Given their limited boom length, boom pumps cannot provide solutions for high-rise buildings. Even the longest boom available, nominally 210 ft long, can practically place concrete in buildings no higher



(a)



(b)

FIGURE 19.6 Truck pump being fed by ready-mixed concrete trucks.

than 14 floors. The solution is, then, to use the basic pump-and-pipeline configuration, render it with climbing capability similar to that of the internal-climbing tower crane, and enhance horizontal distribution reach and convenience by use of a boom-pump-type hydraulic articulated placing boom (Figure 19.7). This configuration, used above in the selection example (19.2.2), is today the preferred solution for concrete placing in high-rise structures. Depending on the size of the floor in the constructed building,



FIGURE 19.7 Climbing placing booms.

two such systems may be used concurrently (with one or two pumps). In this case, either two booms are used (as seen in Figure 19.7) or one detachable boom, with a quick boom–mast connection, is transferred as required between the two climbing masts. The hollow-section or lattice-type climbing mast on which the boom is mounted and the pipeline running from the pump to the boom are located next to each other inside the building. However, an external climbing mast, similar to the mast of a top-slewing tower crane, can also be used.

19.3.3 Power Trowels

The final operations in the production of concrete elements that involve equipment are consolidating and finishing. Immediately following placement, concrete has to be consolidated by the use of vibrators (see Chapter 30). Finishing may actually be required only in the form-free faces of the cast element. Typical faces are the upper surfaces in floor slabs, where finishing to a smooth face—if required—is attained by the use of power trowels (Figure 19.8).

The main part of the power trowel is the rotating blade system, commonly termed *rotor* or *spider*. When the blades rotate at high speed, frictionally engaging the concrete surface, they improve the density of the upper concrete layer, seal plastic cracks, and polish the surface to obtain a smooth and hardened



(a)



(b)



(c)

FIGURE 19.8 Finishing of concrete floor by troweling: (a) walk-behind single trowel; (b) ride-on double trowel; (c) ride-on triple trowel.

concrete face. Maximum rotating speed is in the range of 90 to 180 rpm. Several steps are involved in troweling (the first step of which is termed *floating*), and with each step and successive troweling cycle the blades are slightly angled. Power trowels come in various rotor sizes (diameters). Large-size rotors are advantageous in large open areas, where high production rates can be realized; in tight spaces and mainly for finishing around various obstructions, small-size rotors or small troweling discs (see Figure 19.8a) must be used.

Powered by electric motors or by diesel or gasoline engines, trowels come in either a walk-behind or a ride-on configuration. In terms of number of rotors, the most common are single-rotor (Figure 19.8a) and double-rotor (Figure 19.8b) trowels, but triple-rotor trowels are also available (Figure 19.8c). Single-rotor trowels are of the walk-behind type, and the two others are of the ride-on type. Rotor diameter varies from 2 to 5 ft, and the number of blades per rotor varies from four to six.

Power trowels can be quite heavy, ranging from 100 to 300 lb for the single-rotor trowels and up to 500 to 3000 lb for double-rotor and triple-rotor trowels; the two latter owe their additional weight to the extra rotors, riding engine, and operator deck. To be crane-lifted around the jobsite and for loading and unloading, the lighter weight machines are fitted with a lifting hook, whereas the heavier machines have a robust lifting system. The latter are often moved around the workplace on transport dollies and transported between sites on trailers.

19.4 Cranes

Construction cranes are classified into two major families: tower cranes and mobile cranes. In some regions, including North America, the term *mobile cranes* is often used to refer to truck-mounted mobile cranes only, and track-mounted mobile cranes are considered a separate family, referred to as *crawler cranes*. This chapter adheres to the two-family classification. Some machine types are almost equally tower and mobile cranes. They are listed in this chapter under the family of their origin. Use of the word *family* in this chapter implies that a great many different equipment types and configurations fall under each one of the two terms *tower cranes* and *mobile cranes*. This chapter presents the main types and equipment in use today, with a focus on cranes that typically serve on building construction projects. The lack of universally accepted classification and taxonomy for cranes attests, too, to the great variety of both very different and quite similar crane types and models available. Because the various types of cranes can be confusing, an effort has been made in this chapter to be consistent in the use of these terms and to clarify such confusions.

19.4.1 Tower Cranes

19.4.1.1 Introduction

Tower cranes, essentially in the same configuration as we know them today, became visible in the late 1940s when they helped rebuild Europe after World War II. The tower crane was a small-footprint machine suitable for tight urban construction sites for both low-rise and high-rise structures, and it was powered electrically for noiseless operation. Over the years, the tower crane has seen enormous developments in terms of reach and lifting capacity, as well as deployment and operation convenience, suitability to a wide range of work assignments and site conditions, and responsiveness to the great variety of needs and preferences of construction firms and crane rental companies. Its operating and control systems have undergone major changes in parallel with the technological developments of our times, as has its safety features. Although the electrically powered tower crane is still the most common one, diesel-powered models are available and used as well, particularly in North America.

In high-rise construction, tower cranes essentially provide the only solution for lifting materials other than concrete, which can also be, and often is, pumped up. In many parts of the world, however, particularly in Europe, tower cranes are widely used for all kinds of building projects, urban and rural, as well as on infrastructure projects such as bridges, utilities, and landscaping. Lightweight, fast-erecting models are the machines of choice for the construction of low-rise residential and commercial structures, and even one-story houses, in France, Italy, Germany, and Switzerland, to name but a few. In recent years, these lighter models have begun to show a modest but growing and noticeable presence in North America as well, on a variety of projects having traditionally employed mobile cranes (Bishop, 2004; Shiffler, 2006a).

Tower crane “forests” have been conspicuous these past years in, among other places, the renewal of unified Berlin as Germany’s new capital in the late 1990s; the Chinese cities of Shanghai and Beijing, which is preparing for the 2008 Olympic Games; and the unprecedented surge of office, condominium, and hotel complexes in the United Arab Emirates in the mid 2000s. Yet, in the United States, as well, the increasing use of tower cranes has recently led to many cities being dubbed “Crane City”; for example, 300 tower cranes were estimated to have been working in Miami alone at one point in 2006 (Shiffler, 2006b).

Because tower cranes can be mounted on rails, a *traveling* tower crane had traditionally been a common way to obtain a larger work envelope and better site coverage whenever site conditions allowed installing a railway. This solution allowed saving at least one additional crane, as long as lifting requirements in terms of service time could be accommodated by one crane only. This, however, is not the situation for today’s typical construction sites. The competitive construction atmosphere and the high priority given to meeting tight deadlines practically dwarf the costs of additional cranes on site. Furthermore, with the increasing industrialization of construction sites, cranes are now busy providing a variety of lift services and in frequencies far surpassing yesterday’s requirements, thus demand on crane time has increased manifold. Consequently, cranes are often utilized to their full daytime capacity (and, in many instances, their nighttime capacity also) to meet all lifting requirements within their work envelope, but in many cases one crane cannot provide all of the lifting services required within its own reach within the time allotted. The result is a growing number of multi-crane sites, as well as a greater extent of shared work zones created by overlapping crane envelopes. This, in turn, has driven other developments in recent years; these developments, such as the increased use of *flat-top* tower cranes and the growing demand for advanced anticollision systems, are addressed later on in this chapter. The photograph appearing at the beginning of this chapter is an example of a multi-crane site (also see Figure 19.13).

19.4.1.2 Types and Configurations

The two main types of tower cranes are *top-slewing* and *bottom-slewing*. The major differences between these two types are reflected in erection and dismantling operations of the cranes and in their maximum height. Erection and dismantling of bottom-slewing cranes are relatively simple and rapid, earning these cranes the nicknames of *self-erecting* and *fast-erecting* (the latter, however, should not be confused with the same term often used by manufacturers to describe certain models of top-slewing cranes). This, however, comes at the expense of their limited height. Top-slewing cranes, on the other hand, take much longer to erect and dismantle when more complicated and costly operations are involved, but their height is practically unlimited. For these reasons, bottom-slewing tower cranes are suitable mainly for short-term service durations on low-rise projects, while top-slewing tower cranes are suitable primarily for mid-rise and high-rise projects requiring long service periods. A 6-month cut-off time is often cited in the industry when referring to the service durations of these two crane types, but this approximation should clearly be used, if at all, for general indication only.

19.4.1.3 Top-Slewing Tower Cranes

19.4.1.3.1 Structure and Configuration

The main parts of a typical top-slewing tower crane (Figure 19.9) are as follows:

- *Undercarriage*. These cranes are usually stationary, and crane stability is accomplished in one of two ways: (1) the mast is anchored directly into an engineered concrete foundation in a no-undercarriage configuration using fixing angles (see Figure 19.10), or (2) a base frame is ballasted by modular concrete blocks. In a traveling configuration, stability is attained by a concrete-block ballasted undercarriage mounted on rails. Rail-mounted undercarriages are sometimes placed on short rails for stationary, nontraveling use if the crane was originally procured in this configuration. Assisting in maintaining the stability in each of these configurations are the



FIGURE 19.9 Top-slewing saddle-jib tower crane.



(a)



(b)

FIGURE 19.10 Anchoring the first mast section of a top-slewing tower crane into an engineered concrete foundation.



(a)



(b)

FIGURE 19.11 Top-slewing tower crane climbing itself by the addition of new sections (Trump Tower, Chicago).

counterweights installed on the counter-jib of the crane which is the most recognizable feature of top-slewing tower cranes. The undercarriage of a traveling crane also carries the traveling motors for the crane.

- *Mast.* Often termed *tower*, the mast is assembled of modular lattice-type sections (hence, the term *sectional tower crane*, which is also used for top-slewing cranes). When being erected, always by another piece of equipment, the crane will rise, section after section, to a certain initial height. Later on, it can climb itself with the addition of more sections. A hydraulically operated telescopic climbing frame (or climbing cage) is used to raise the upper part of the crane, thereby making room for the insertion of a new section, which is lifted and moved into place by the crane itself (Figure 19.11). In that regard, then, the crane has no height limit. Typical section lengths are 10 to 15 ft, but various other lengths exist, including exceptionally long sections (e.g., 40 ft) for city cranes, where speed of erection (determined, among other things, by the number of sections) is of the essence. (Note that the term *city crane* is not exclusive for tower cranes, as it is also used for certain types of mobile cranes.)



(a)



(b)

FIGURE 19.12 Top-slewing flat-top tower crane. Note the modern design operator cab with large window area.

- *Operator cab.* Located at the top of the mast, above the slewing ring, is the operator cab. It is either located co-centrally on the mast (as in Figure 19.9) or is attached to it on the side (as in Figure 19.12). Because tower cranes can rise to great heights, some crane models can optionally be equipped with a small elevator for the operator. In some European countries (e.g., Sweden and the Netherlands), such elevators, or similar means (e.g., a climbing operator cab), have recently become mandatory for cranes exceeding climbing heights of around 100 ft. (Note that the climbing height would be the full crane height in the case of a freestanding crane only; for taller cranes, braced to the constructed building, climbing begins at the top of the building or near its top, where a temporary bridge connects the building and the crane.) Today's operator cabs feature a comfortable and ergonomic work environment. Cabs are optionally fitted with air conditioning and similar other comforts to support a safer and more productive work environment; in particular, the window area has been increased (see Figure 19.12) to allow better vision of the site and greater control of rigging and hook movement.
- *Slewing ring.* This is the slewing (rotating) mechanism of the crane, located at the top of the mast right below the jib. It allows the entire upper part of the crane, which includes the jib and the operator cab, to slew while leaving the mast stationary. This is essentially what allows the mast to be braced to a permanent structure, thereby rising to any desirable height.
- *Jib.* There are several jib configurations for top-slewing tower cranes. The most common configuration is the horizontal *saddle jib*, also known as *hammerhead* (see Figure 19.9). It has a counter-jib, which carries, in addition to counterweights, the main motors, controls, and cable drum of



FIGURE 19.13 A cluster of flat-top tower cranes on a commercial building project in Budapest, Hungary. The photograph was taken in January 2007, when the site was inoperative, as is apparent from the weathervaning cranes. (Photograph courtesy Meir Simcha, Israel.)

the crane. The jib and the counter-jib are held by pendants (tie bars) connected to the top part of the crane, called the *cathead* or *A-frame*. A trolley moving along the jib (in a motion called *trolleying*) carries the lift cables and hook block. Similar to the mast, the lattice-type jib is modular, with several length options available within the maximum length prescribed for the given crane model. *Flat-top* cranes, also nicknamed *topless*, have a pendant-free, cantilever jib connected only to the mast (Figure 19.12). Sparing the use of a cathead, these cranes are particularly suitable for a shared-zone, multi-crane environment, where overlapping cranes must be set up to different heights (Figure 19.13). Because safety clearance must be maintained between the uppermost part of the lower crane and the jib-bottom of the higher crane, the entire length of the cathead frame, which could be as much as 40 ft, is gained in crane height when using flat-top cranes. This is also an advantage in situations with height restrictions, such as near airports. Flat-top cranes, however, have become very popular regardless of the above constraints due, for example, to their ease of set-up, and they now constitute a growing share of crane fleets in America. Another popular jib configuration is the *luffing jib* (Figure 19.14). Top-slewing cranes of this type, nicknamed *luffers*, do not use trolleys but rather change their operating radius by raising and lowering the jib. Many luffing-jib crane models feature a very short counter-jib; along with the luffing capability, it may be an advantage when the crane operates in proximity to other cranes or obstacles (such as nearby buildings). These cranes, therefore, are often seen in high-dense urban construction. A *moving-counterweight system* for luffing-jib cranes, first introduced several decades ago, appears to have regained some interest recently. This mechanism increases the distance between the counterweight and the mast as the jib is lowered and thereby causes less stress to be placed on the crane's structure. However, the moving-counterweight system has thus far had only limited use. (The two luffers in Figure 19.14 are fitted with moving counterweights.)

Top-slewing tower cranes are engineered to withstand high winds. This becomes particularly important at the heights these cranes often operate and is one of the advantages tower cranes have over mobile cranes. To ensure crane stability when the crane is unattended, tower cranes are left to slew freely with the wind, or to *weathervane* (see Figure 19.13).



FIGURE 19.14 Top-slewing luffing-jib tower cranes.

19.4.1.3.2 Transportation, Erection, and Dismantling

Top-slewing cranes, disassembled to their basic parts, are transported by any number of large trucks to the worksite. Preferably, the site would have adequate space to store these parts for later connection to larger assemblies using a smaller mobile crane than the one needed later to erect the tower crane. These larger assemblies would then be lifted up by a bigger mobile crane for assembly and erection of the tower crane (Figure 19.15a). When no such storage space is available, the tower crane may have to be erected directly off of the transporting trucks. For an urban site on a busy street, just-in-time delivery of crane parts may be required to minimize street closures. As mentioned above, a top-slewing tower crane requires another crane to erect it. The erecting crane is almost always a mobile crane, often two mobile cranes, unless the site is to have two or more overlapping tower cranes located close enough to each other such that the big cranes can be erected first and then used to erect some of the others. Dismantling the tower crane when its service is no longer needed is essentially the same process in reverse (Figure 19.15b), except that it may become more complicated because a building is now standing where there had been an empty space when the tower crane was originally erected. Quite often, a larger mobile crane will be required for dismantling than the one used for erection. These processes take from a few days up to a few weeks, depending on the size of the crane erected or dismantled, its location with regard to the constructed building, and accessibility of the erecting or dismantling crane. Bad weather, particularly winds, may be a delaying factor. Earthwork and foundation work, when required, add to setup time. Dismantling a crane climbing inside the building is a particularly complicated, long, and costly process. It is addressed separately in the next section.

19.4.1.3.3 Operation Modes

The common operation modes of top-slewing tower cranes are freestanding, externally braced, internal climbing, and traveling:

- *Freestanding.* If the model-specific maximum freestanding height of the crane, as specified by the manufacturer, satisfies the requirements of the project, this would be the most economic solution. Top-slewing cranes can now stand free of braces to heights in the range of 200 to 400 ft, much higher than before. One of several advantages of freestanding cranes is the freedom to place them virtually anywhere in the site.



FIGURE 19.15 Erecting and dismantling a top-slewing tower crane using a mobile crane: (a) erecting; (b) dismantling. Note the lane closure and interruption to traffic.

- *Externally braced.* If lifting service is required to heights greater than those possible with a free-standing crane, the crane must be braced to the constructed building, either as a full-height external climbing crane or as an internal climbing crane. To be braced externally to the building, the crane must be placed as close as possible to the façade of the building. Braces (or ties) to the building, commonly spaced 30 to 100 ft apart, are expensive additions to the cost of the crane. These braces are made of steel and are engineered to stabilize the crane and prevent mast buckling while absorbing horizontal motions of the mast. The cost of these braces sharply increases with the distance from the façade. One other issue associated with an external braced crane is completion of the façade after the crane has been dismantled.
- *Internal climbing.* The pros and cons of an internal vs. external climbing crane were mentioned earlier, as were those of climbing the crane in the elevator shaft or through openings in the slabs (see Section 19.2.2). A major issue with regard to an internal climbing crane is dismantling it at the top of the high-rise host building at the end of construction. In the case of more than one internal climbing crane servicing the building, the contractor should opt for taking down all cranes, but one, with each other. Sometimes, a high-rise building is serviced by two climbing cranes, one external and one internal, in which case the former may be able to dismantle the latter. In such cases, careful consideration of dismantling issues at the equipment-planning phase may affect crane location, lift capacity (i.e., greater than might otherwise be needed), and jib length (i.e., longer than might otherwise be needed). In most cases, if the use of an external tower crane for dismantling is not an option, then climbing cranes can be dismantled by one of two means: a mobile crane or a derrick. The mobile-crane option is faster and less complicated; however, it is an option only if two conditions are satisfied: (1) a mobile crane with the required vertical and horizontal reach is available, and (2) the vicinity of the building allows for setup of the mobile crane. It would be advantageous if the internal crane climbed near the façade of the host building

alongside which the dismantling mobile crane would be set up. If a mobile crane is not an option, which is always the case in the construction of ultra-high-rise buildings, then the tower crane to be dismantled can erect a derrick (Shapiro et al. 2000), which can then dismantle the tower crane and, in turn, be dismantled manually and taken down in small parts using the building elevator. Similarly, a custom-made hoisting apparatus may be used instead of a derrick. Another option, though seldom used, is the use of a helicopter.

- *Traveling.* As mentioned earlier, the crane in this operation mode is essentially freestanding. The railway can be either straight or curved. Preparatory earthwork is required, and the crane manufacturer typically specifies the maximum grade allowed (commonly 1%).

19.4.1.4 Bottom-Slewing Tower Cranes

19.4.1.4.1 Structure and Configuration

The main parts of a typical bottom-slewing tower crane (Figure 19.16 and Figure 19.17) include:

- *Undercarriage.* Unlike top-slewing cranes, which are often configured without an undercarriage, bottom-slewing cranes would always have an undercarriage to connect between the ground or any other supporting surface and the slewing crane. The undercarriage is commonly either stationary (Figures 19.16a and Figure 19.17b) or rail-mounted. Light models may have a wheeled undercarriage, but this is used only for infrequent crane relocations on the jobsite, without loads, and not for operation. In truck-mounted tower cranes (see below), the truck replaces the conventional undercarriage. Another configuration, seen mainly in Europe, is that of a crawler undercarriage (Figure 19.16b). Whenever it is not in motion, the crane is stabilized by outriggers.
- *Slewing ring.* The slewing ring of the top-slewing crane is located near the top of the crane, but the slewing ring of a bottom-slewing crane is located near its base, such that practically the entire crane—slewing platform, mast, and jib—can slew. For this reason, the mast cannot be braced to the building for increased stability, and its height is limited.
- *Slewing platform.* The slewing platform carries, in addition to the mast, the entire ballast of the crane, as well as the motors. To balance the crane, the ballast blocks are located at the rear of the platform, always opposite the jib. To be most effective, the greatest possible distance between the ballast and the mast would be desired. On the other hand, the smallest possible projection of the rear end of the platform from the footprint of the crane (as determined by the undercarriage) is desired to allow crane setup in close proximity to the building and for increased safety. Newer models, therefore, have a compact platform, compensated for by a high stack of ballasting concrete blocks.
- *Mast.* Earning the bottom-slewing tower crane the name *telescopic tower crane* (to distinguish from the sectional top-slewing crane), the mast of this crane is made of two to three telescoping parts. This type of structure is in line with the limited height of the crane and, even more so, with its rapid self-erecting concept. The operator cab is traditionally located at the top of the mast, or the crane can be operated from a control post at the lower part of the mast. Many new models now offer a climbing cab that can move along the mast for optimal view (Figure 19.17b). Wireless radio remote control of these cranes is now offered on most models. Masts are either lattice (Figure 19.16) or hollow section (Figure 19.17). Hollow-section masts used to be common only on smaller models but are increasingly being seen on larger models, as well. In smaller models, this hollow-section mast is often foldable instead of telescopic.
- *Jib.* The lattice-type jib is similar to the main jib (i.e., no counter-jib) and trolley system of the top-slewing crane; however, it is foldable for fast erection and dismantling and, in many models for a shorter jib work option. Some models feature a telescoping jib. Unlike top-slewing cranes, where the horizontal jib and the luffing jib are two different crane configurations altogether, the jib of the common bottom-slewing crane can usually be raised, though not in a sharp angle (commonly up to 30°), while maintaining trolley movement. This grants the initially height-limited crane an additional lifting height. Some models have an articulated jib, in which the part closer to the mast is horizontal and the outer part can be angled upward.



(a)



(b)

FIGURE 19.16 Bottom-slewing tower crane, lattice-type mast (two-part telescope): (a) general view, stationary undercarriage; (b) slewing platform and ballast, crawler undercarriage. Note the operator standing post.



(a)



(b)

FIGURE 19.17 Bottom-slewing tower crane, hollow-section mast (three-part telescope): (a) general view; (b) slewing platform and ballast, stationary undercarriage. Note the climbing operator cab.



FIGURE 19.18 Bottom-slewing tower crane in towing position. Note the concrete ballast blocks, at the right of the picture, to be carried by the towing truck.

19.4.1.4.2 Transportation, Erection, and Dismantling

Convenient transport, erection, and dismantling are the main features of these cranes. Towable by a truck or a semitrailer for transportation between jobsites, they are usually mounted on a designated wheeled undercarriage in a fully folded position (Figure 19.18). For relocation on the jobsite, partial folding suffices. Erection and dismantling are performed by the crane itself, using its own motors. Light models may be erected and dismantled within an hour, but heavier models may take up to one day.

19.4.1.4.3 Operation Modes

Operation modes of bottom-slewing tower cranes, as dictated by the means of their mobility, are stationary, rail-mounted, crawler-mounted, and truck-mounted:

- *Stationary.* The crane is stabilized by outriggers. It is folded partially or fully for relocation on the site, but light models can be towed in an upright position. Some models are self-propelled (for relocation only); moving on wheels, they require a hardened surface, usually with a maximum ground gradient as specified by the manufacturer. By no means is the crane allowed to move with a load.
- *Rail-mounted.* Same as with top-slewing cranes, this type of crane can travel with its load, assuming a work envelope whose size is limited only by the length of the railway.
- *Crawler-mounted.* This mode is suitable for operation in rough and sloping terrains. Bottom-slewing cranes of this type can accommodate both longitudinal and transverse gradients and are commonly equipped with a balancing mechanism. For lifted loads or ground slopes exceeding certain specified values, the crane must work on its outriggers.
- *Truck-mounted.* This is an old concept that has seen a renaissance in recent years. Essentially a hybrid configuration combining a mobile crane and a tower crane, it combines some key features of these two crane types—mainly, the mobility of the truck crane with the height and reach of the tower crane where lifting requirements do not call for a larger crane.

19.4.1.5 Technical Data

The major technical data relevant to selection of tower cranes, top-slewing and bottom-slewing alike, are (1) jib length, (2) lifting capacity, and (3) lifting height. These data determine the work options and ranges of a crane, as well as the crane's suitability for a given project or for a specific type of projects. Many other pertinent data, such as footprint dimensions, mast cross-section, motors power, and speeds,

are decisively dictated by these three parameters. Tower cranes are manufactured in a great variety of models in terms of jib length, lifting capacity, and lifting height, to cater for the great variety of building dimensions and construction methods. The broad range of tower cranes offered on the market can be classified into four classes by their size and designation:

- *Light cranes* are designated for maintenance and renovation works in buildings up to about four stories and for the construction of one- to two-story structures. These kinds of projects are characterized by material batches of 1000- to 2000-lb maximum weight and a relatively short duration of the crane on the jobsite; therefore, this class of cranes is manufactured as bottom-slewing cranes only.
- *Medium cranes* are designated for the construction of cast-in-place concrete structures using conventional or industrialized methods (e.g., using large form panels), with the possible combining of certain precast elements (e.g., flights of stairs). This category of structures is characterized by material batches of 2000- to 5000-lb maximum weight, varying crane service durations on-site (depending mostly on the height of the constructed building), and a broad range of building heights. Cranes in this class are manufactured both as bottom-slewing cranes, suitable mainly for structures up to eight stories high, and as top-slewing cranes, suitable mainly for structures six stories or taller. Because this kind of building constitutes the majority of buildings, these are also the most widely used tower cranes.
- *Heavy cranes* are designated for the construction of structures using precast methods or other methods that combine heavy elements. The central attribute of these structures is building components weighing 5000 to 13,000 lb. Cranes in this class are mostly top-slewing cranes; the small number of bottom-slewing models in this class fall in the lower part of this weight range.
- *Special-application cranes* are designated for the construction of unusual structures in terms of their size, weight of elements, or site conditions (e.g., nuclear plants, dams). These cranes, exceptionally large in jib length, lifting capacity, or lifting height, are always manufactured as top-slewing cranes.

Table 19.4 presents typical technical data for tower cranes by the classes listed above. Following are some explanations with regard to the headings in Table 19.4, as well as several other technical features of tower cranes.

Jib length is the maximum working radius, measured from the centerline of the mast to the centerline of the trolley at the jib end. It is the maximum length offered with any specific crane model; however, as mentioned above, most crane models can be configured with shorter jibs. The *lifting capacity* of the crane changes with the work (or lifting) radius, as determined by the distance of the trolley from the mast. The crane can lift its heaviest load (*maximum lifting capacity*) at a certain model-specific radius (often termed *minimum radius*), after which lifting capacity decreases gradually until it reaches its minimum at the end of the jib (*jib-end lifting capacity* in Table 19.4 but often referred to as *maximum lifting capacity at maximum radius* or *tip capacity*, for short). No heavier loads can be lifted at radii smaller than that minimum radius. Maximum lifting capacity at the end of the jib is governed by the structure and overall stability of the crane. Maximum lifting capacity at *minimum* radius, however, is additionally governed by the strength of the lifting cables. Most tower cranes can use either a single cable (*two-part line*) or a double cable (*four-part line*). With a double cable, maximum lifting capacity at minimum radius is doubled (though at the expense of a 50% reduction in hoisting speed). As for maximum lifting capacity at maximum radius, not only is it unchanged with a double cable but it also drops somewhat compared to a single cable, as the extra cable weight reduces the net lifting capacity.

Tower cranes are occasionally denoted by their *lifting moment*, commonly computed by multiplying the maximum jib length by the end-of-jib maximum lifting capacity. Note, though, that although it provides some indication of the size of the crane, this parameter discloses no information with regard to jib length or lifting capacity. *Lifting height* of a crane denotes the maximum height to which the lifting hook can be raised, which is slightly lower than the bottom of the jib. The maximum allowable height of a building to be serviced by a crane is at least 20 ft lower than the lifting height of the crane.

TABLE 19.4 Technical Data for Tower Cranes

Properties	Class and Crane Type					
	Light Cranes	Medium Cranes		Heavy Cranes		Special Cranes ^b
	Bottom-Slewing	Bottom-Slewing	Top-Slewing	Bottom-Slewing	Top-Slewing	Top-Slewing
Jib length (ft)	50–80	80–150	100–150	150–180	150–250	250–330
Jib-end lifting capacity (lb)	1000–2000	2000–5000	2000–5000	4000–7000	4000–13,000	7000–100,000
Maximum lifting capacity (lb)	2000–5000	5000–18,000	5000–20,000	10,000–20,000	15,000–80,000	50,000–350,000
Lifting moment (ton-ft)	35–80	80–250	140–300	300–600	350–1200	1000–15,000
Maximum freestanding height ^a (ft)	50–70	70–110	110–200	100–130	150–250	200–450

^a For rail-mounted traveling cranes: 100 ft for bottom-slewing, 230 ft for top-slewing, excluding special cranes.

^b Data provided do not include cranes at the far extreme of this range. The largest tower crane model known to have ever been manufactured, the K-10,000, can lift 220,000 lb at the end of its 330-ft long jib (i.e., 36,000 ton-ft lifting moment). About one dozen of these cranes have been manufactured (by the Danish manufacturer Krøll) and are known to be still operating at this time.

Crane cycle time and work output are largely determined by the speed of the crane's various motions, as has already been demonstrated above (see Section 19.2.2.2). Common speeds are as follows:

Hoisting (vertical), 150 to 500 ft/min

Trolleying (radial), 100 to 350 ft/min for top-slewing, 60–200 ft/min for bottom-slewing

Slewing (circular), 0.6 to 1.0 rpm (0.8 for most makes and models) for top-slewing, 0.8 rpm for bottom-slewing

Traveling (horizontal), 65 to 100 ft/min

When estimating cycle-time durations, due attention should be given to the normal mode of operation in which the crane operator exercises two, sometimes even three, motions simultaneously. Additionally, loading and unloading times have to be considered; in low-rise building, they constitute the major part of the cycle time. Unloading can be particularly long when accurate placing of elements such as flying forms or precast panels is required.

19.4.2 Mobile Cranes

19.4.2.1 Introduction

Unlike the tower crane, which essentially is a stationary machine even when it has acquired some mobility capabilities, the mobile crane is what its name implies—a self-propelled mobile machine, capable of moving freely about the jobsite and between jobsites, as well. Contrary to the silhouette of the tower crane as a vertical mast with a horizontal jib at its top, the jib of the mobile crane—termed *boom*—is inclined and connected directly to the carriage of the machine. The variety of tower crane types, as presented above, may appear to be wide, but the mobile crane itself features a great many more types and models, and it can range in size from small machines that fit in the wagon of a pickup truck to gigantic machines that dwarf almost any other construction equipment.

Mobile cranes owe their extensive use in North America to the ambitious heavy civil and infrastructure projects this country has launched since the early 20th century. In part, this is also due to the developed agricultural machinery industry, thought to be the motivated power behind the birth of heavy construction equipment in the United States. Among other things, this has contributed to the great versatility of



FIGURE 19.19 Mobile cranes on a mid-rise concrete building construction project.

mobile cranes, which until merely a decade ago were equally associated with non-building operations, such as excavation, pile driving, and demolition, and with building construction per se. Even today, these machines find their main use in a great variety of civil engineering projects other than building construction. Some mobile crane types, however, show great presence on building construction sites, whether for short-term tasks or throughout most of construction (Figure 19.19). If for no other use, they are the machines that set up the tower cranes at the onset of construction and dismantle them at the conclusion of their service on site. This is a classic demonstration of the mobile crane's main features: its capacity to handle heavy loads and its rapid deployment. A relatively small mobile crane has a lifting capacity equal to that of a heavy tower crane. The high-end mobile cranes can lift hundreds of tons.

While the major types of mobile cranes are mentioned in what follows, the focus in this chapter is on the types used in building construction. It should be stressed that concrete building construction involves a great extent of *duty-cycle* work, namely, work in which the crane is engaged in repetitive lifts of relatively short cycle time. Handling a bucket for concrete placing is a typical example of such work. While tower cranes inherently are suitable for duty-cycle work, mobile cranes are not so. Because loads involved in cast-in-place concrete building construction are relatively low, mobile cranes—of various types—that are fitted for duty-cycle work are commonly of the small- to mid-size models.

19.4.2.2 Types and Configurations

Mobile cranes are characterized and distinguished from each other mainly by two parameters: their undercarriage (or carrier) and their boom. The two types of undercarriage are *wheeled* and *crawler*, and the two types of boom are *lattice* and *telescopic*. Combinations of these two parameters yield four different machine types; however, other parameters, such as mobility, accommodation of varying ground surfaces, and rigging mechanisms, add more types to the large class of mobile cranes. Common to all of these types is their suitability to meet lifting requirements in which they have an advantage over tower cranes: handling of heavy loads, short-term lifting services, and various transportation works requiring frequent relocation of the crane on the jobsite. These characterize the kinds of construction projects where the capabilities of mobile cranes are maximized.

19.4.2.2.1 Boom Configurations

The *lattice boom* is made of lattice-type steel sections, similar to the mast sections of tower cranes. The number of sections varies according to the desirable boom length. There are always two pyramid-shaped

end sections. The length of the boom is fixed and cannot be changed in the course of work, unless the boom is lowered and sections are added or taken out, thus work height and radius change due to changes in the inclination angle of the boom. An auxiliary boom (boom extension), known as a *fly jib*, can be fitted angularly to the end of the main boom, giving the crane farther reach for better building coverage (see Figure 19.19). In larger crane models, this boom extension is often longer than the main boom of the crane. The *telescopic boom* is made of telescoping sections. It is operated hydraulically, allowing boom length and inclination to change in the course of work. A short, straight, lattice-type extension boom can be connected to the end of the telescopic boom. When not in use, this extension boom is stowed next to the telescopic boom such that its connection is convenient and rapid (see Figure 19.21). Additionally, a short auxiliary boom, commonly of the hollow-section type, can be fitted to the end of the extension boom. A lattice-type fly jib, same as with the lattice main boom mentioned above, is also very common (see Figure 19.15a).

The main advantage of the lattice boom is its simple structure and, consequently, its lower cost. It is also the preferable boom for cranes with exceptionally high loading capacities. The telescopic boom, on the other hand, offers two important advantages that account for the growing popularity of this type of boom: (1) more efficient crane use due to the continuous adjustment of boom length in the course of work, and (2) much faster crane deployment, as compared to complicated rigging and unrigging of the lattice boom, which often requires the assistance of other lifting means and separate transportation.

The lifting capacity of the crane, whether equipped with a lattice or telescopic boom, changes with the boom's length and inclination angle. The minimum working radius is attained at the shortest boom length and the most upright possible boom position (i.e., minimum inclination angle when measured from the vertical). Although varying with crane configuration and model, this minimum radius is commonly taken as 10 ft nominally. This is important because mobile cranes are often denoted by their maximum lifting capacity at this nominal minimum working radius, although no standard universal rating system exists. For example, a 100-ton crane is likely to have a maximum lifting capacity of 100 tons, effective at a 10-ft radius, which corresponds to a lifting moment of 1000 ton-ft.

19.4.2.2.2 *Truck Cranes*

Truck cranes are suitable mainly for short-term lifting assignments; this is not the kind of a crane seen working for extended durations on construction sites. The superstructure of this crane, which includes the boom (lattice or telescopic), engine, counterweight, and operator cab, is mounted on a specialized carrier truck. Connecting the two is a slewing ring ("turntable") allowing a full 360° rotation. The crane travels the public road system (with a retracted telescopic boom or partial lattice boom) essentially like any other truck but can also travel on rough roads. To utilize its maximum lifting capacity, the crane must be leveled and stabilized on its outriggers while in operation; it can operate while on its wheels to only partial capacity. Because of the high loads these machines transfer to the ground through the outriggers, mats of various sizes must be used to spread the load, as depends on the soil-bearing capacity. Together with the extended outriggers, these mats increase the overall width of the vehicle, which should be taken into account when planning the lift and the crane's exact location.

Lattice-boom truck cranes are gradually making room for telescopic-boom truck cranes, given the greater flexibility of the latter in moving between jobsites. This trend has been observed, initially in Europe and in recent years in North America, with regard to truck cranes in general, due to the growing popularity of *all-terrain cranes* (see below). However, truck cranes—both lattice-boom and telescopic-boom—appear to be maintaining their standing as a viable option when no particularly rough-terrain site conditions have to be accommodated, due mainly to their lower cost compared to all-terrain cranes.

A different style of truck crane has recently appeared on the market. Nicknamed the *city crane* and featuring a compact design, lower boom mounting, and a single dual-purpose (truck and crane) operator cab, it is designated mainly for urban work and travel. Often confused with truck cranes are **truck-mounted cranes**. The main difference is the carrier vehicle—a standard-type truck in the truck-mounted crane, a specialized truck in the truck crane; truck cranes also have, in general, higher lifting capacity. Truck cranes are manufactured as an integral (though often modular) unit by the same manufacturer, but different manufacturers supply the truck and the crane components for truck-mounted cranes.



FIGURE 19.20 Crawler crane.

19.4.2.2.3 Crawler Cranes

The revolving superstructure of the crawler crane is similar to the superstructure of the truck crane but is mounted on a crawler undercarriage. This change from the truck crane has several implications, in that the crawler crane has better maneuverability and offers outrigger-free work with rapid relocation within the jobsite but requires longer transfers between sites, including loading it on a haul truck. Given these qualities, crawler cranes (Figure 19.20) are particularly suitable for jobs with difficult ground conditions and for projects requiring frequent crane movement. Due to the usually long on-site service, the importance of convenient transfer between sites is reduced, and the majority of crawler cranes have traditionally been equipped with lattice booms. For some uses, however, a crawler crane with a telescopic boom might appear an appropriate option. For this reason, in addition to the growing attractiveness of telescopic booms in general, smaller crawler telescopic-boom crane models have recently begun appearing on the market. One application of such a crane would be on urban projects in areas where contact pressure with the street surface is restricted due to underground facilities. Wheeled or outriggered undercarriages may not be suitable under these conditions, but a rubber crawler telescopic-boom crane that can travel on pavement would be. A crawler undercarriage also serves as a platform for what is known as the *American-type tower crane*, which is a crawler crane rigged with a tower attachment made up of a vertical lattice boom fitted at its top with a luffing boom. In essence, this is a more robust version of the crawler-mounted bottom-slewing crane, exclusive of trolleying capability.

19.4.2.2.4 Rough-Terrain Cranes

Arguably the most visible mobile crane on a great variety of construction sites the world over, the smaller models of rough-terrain cranes are often used as high-mobility auxiliary equipment on building sites that employ tower cranes as the central lifting services providers. As implied by its name, the crane is designated mainly for lifting works on sites with rough terrain conditions and frequent relocation on the jobsite. The high-ground-clearance, wheeled undercarriage of this crane (Figure 19.21) has two closely spaced axles and large wheels. With a retracted boom, the crane has the ability to move on steep slopes; some models can manage grades up to 70% (35°). At the same time, the crane can travel the public road system, although commonly in speeds not exceeding 25 mph and in low driving comfort, which is why it is often hauled on a low-bed truck between jobsites. The operator cab is either a fixed part of the undercarriage or is part of the superstructure and rotates with the slewing of the boom (see Figure 19.21a). Usually equipped with a telescopic boom, it can also use a



(a)



(b)

FIGURE 19.21 Rough-terrain crane: (a) in operation; (b) in stowed position.

quick-fitting, lattice-type extension boom to which an additional auxiliary boom can be added. Extension and auxiliary booms, stowed alongside the main boom, can be seen in Figure 19.21b, and the auxiliary boom is shown in Figure 19.21a. The rough-terrain crane can be utilized to its full lifting capacity when operating on its outriggers; however, because it is designated to provide lifting services requiring constant movement on the jobsite, it can carry loads while on its wheels and in motion, though to partial capacity only, depending on ground conditions, speed, working radius, and type of tires. In any case, moving with a load can be carried out only when the boom is oriented along the longitudinal axis of the crane. Model-specific allowable load ratings under various conditions are provided by crane manufacturers.



FIGURE 19.22 All-terrain crane.

19.4.2.2.5 All-Terrain Cranes

Relatively new to North America, all-terrain cranes (Figure 19.22) combine the best of truck cranes and rough-terrain cranes. The number of models offered by manufacturers is constantly growing in response to the increasing demand for these telescopic-boom cranes worldwide. These cranes cannot accommodate ground slopes as steep as those manageable by rough-terrain cranes but their maneuverability is better than that of truck cranes. At the same time, they can travel public roads at much higher speeds and with greater comfort compared to rough-terrain cranes. Boom configuration and extension options are similar to those of rough-terrain cranes. Tilting operator cabs have become standard (Figure 19.23); they improve



FIGURE 19.23 Tilting operator cab on an all-terrain crane superstructure.

operator view and increase operation efficiency while preventing neck strain. In terms of technology and features, all-terrain cranes are perhaps the most advanced and sophisticated mobile cranes offered today, as reflected in their high price and the high lifting cost per unit tonnage for these cranes.

19.4.2.2.6 Specialized Cranes

This class of mobile cranes includes a variety of enhanced lifting capacity machines only seldom used on concrete building construction sites. They usually feature a lattice boom stabilized by a rear mast and mounted on specialized trucks or crawlers, often with various other counterweight-carrying assemblies. These machines are perhaps the largest and most powerful of any construction equipment manufactured; their maximum lifting capacity now approaches 2000 tons. Accordingly, their transportation, setup, and dismantling are exceptionally complicated.

19.4.2.3 Technical Data

Table 19.5 presents typical technical data for mobile cranes.

19.4.3 Cranes in the Electronic Age

Developments in computerization and communication have not overlooked the world of construction equipment. Today's novel crane models are electronically loaded with regard to their drives, controls, monitoring, and communication. Whether standard or optional, various advanced-technology features are aimed, among other things, at enhancing crane work productivity and safety. A multitude of auxiliary systems is offered by both crane manufacturers and the crane peripheral industry to support crane selection and operation, as well as equipment maintenance and fleet management. Many of the systems are integral part of new cranes only, while others can be fitted on used cranes as well, thereby upgrading their operation. Only three types of developments are mentioned here as examples of the abundance of systems available on the market:

- *Selection software.* These advanced graphics software packages are helpful in dealing with the “hard” technical and engineering aspects of crane selection and location, as well as lift planning. As a minimum, they serve as structured checklists of all site and machine parameters that have to be considered; however, their main asset lies in their facility to check a great number of alternatives instantly. Some of the packages offer crane databases containing built-in dimensions and capacities of common equipment models by various manufacturers. Most packages available on the market handle mobile cranes only, but some of them accommodate tower cranes as well (Meehan, 2005).
- *Camera systems.* Lifting operations involving concealment of the work zone or travel path from the operator's eyes, often termed *blind lifts*, are very common in crane work, for both tower and mobile cranes. The use of signalers is the common solution the world over; no safe blind lift can be performed without a signaler—or several of them—using hand signs or radio communication, or both. In many countries, the presence of at least one signaler on a site using a crane is mandatory by law. Many crane-related accidents have been attributed, wholly or partly, to faulty signaling for various reasons (such as high worker turnover, inadequate signaler training, and language barriers, to name but a few). Crane-mounted video camera systems (Figure 19.24), available for both tower and mobile cranes, help overcome most of the safety problems associated with blind lifts. They also have the potential to increase crane work productivity due to speedier work and shorter cycle times. The camera, installed on the trolley of the tower crane or the boom end of the mobile crane, is permanently directed downward at the work scene, with the lifting hook constantly located at the center of the image. The video image is processed and the picture of the load and its immediate surrounds is transmitted, via wireless communication, to a monitor located in the operator cab (Howes, 2005; Shapira et al., 2008).
- *Anticollision systems.* Combining hardware and software, these systems are devised to prevent collisions of tower cranes operating in shared zones, a common safety hazard on construction sites employing more than one tower crane. The systems use wireless and various other advanced

TABLE 19.5 Technical Data of Mobile Cranes

Maximum Lifting Capacity (ton)	Telescopic-Boom Truck Crane			Lattice-Boom Truck Crane			Lattice-Boom Crawler Crane			Rough-Terrain Crane	
	Length of Main Boom (ft)	Maximum Hook Height with Fly Jib (ft)		Length of Main Boom (ft)	Length of Fly Jib (ft)	Maximum Hook Height with Fly Jib (ft)	Length of Main Boom (ft)	Length of Fly Jib (ft)	Maximum Hook Height with Fly Jib (ft)	Length of Main Boom (ft)	Maximum Hook Height with Fly Jib (ft)
10	—	—	—	—	—	—	—	—	—	20–70	90
20	25–80	100	—	30–110	13	110	30–100	30	100	25–80	100
40	35–100	150	—	40–170	50	170	40–140	40	140	35–100	150
60	40–120	170	—	40–190	60	190	40–170	50	180	40–130	170
80	40–130	190	—	40–200	60	230	40–180	60	200	40–150	190
100	40–140	210	—	50–200	60	240	50–230	80	260	40–170	210
150	—	—	—	50–300	60	330	60–270	100	310	—	—
250	—	—	—	50–330	100	370	60–330	150	400	—	—
450	—	—	—	—	—	—	60–330	260	450	—	—
700	—	—	—	—	—	—	60–400	300	530	—	—
1000	—	—	—	—	—	—	60–400	300	600	—	—

Note: Common ranges for all-terrain cranes (largest machines in parentheses): maximum lifting capacity, 40–300 (1300) ton; length of main boom, 100–200 (330) ft; maximum hook height with fly jib, 140–350 (560) ft.



(a)



(b)

FIGURE 19.24 Video camera system mounted on a tower crane: (a) moving unit (camera case, batteries, solar panel) mounted on the service balcony of the jib's trolley; (b) stationary unit (monitor, video decoder, controls) inside operator cab. (Photograph courtesy of Yehiel Rosenfeld, Technion, Israel.)

technologies to monitor the movements of the crane in real time; warnings are followed by automatically slowing down the crane motion and, eventually, by completely stopping the crane. Most anticollision systems are designed to prevent collisions with adjacent buildings and other obstacles, such as power lines, as well as slewing and trolleying over areas defined as prohibited zones, such as busy streets and public buildings. These added features make the systems useful on single-crane sites, as well. Due to the fairly high price of these systems and the tendency of construction firms to adhere to old, traditional solutions, the use of these system so far has been limited primarily to multi-crane projects. Today, though, they have come to be appreciated by a growing number of construction firms that are opting to use them on sites with a small number of cranes, as well.

19.5 Truck Loaders

The truck loader, also known as a *crane truck* or *boom truck*, is a payload truck fitted with a crane, thus making up a combined hauling and loading self-contained unit. A subclass of the telescopic-boom truck crane and often confused with the similar truck-mounted crane (see Section 19.4.2.2.2), this type of equipment is listed here separately because the concept is completely different. Whereas the truck crane and truck-mounted crane are first and foremost cranes mounted on a wheeled carrier for mobility, the truck loader is initially a hauling truck that is then equipped with a loading crane (hence, the term *loader crane* is also used for this equipment). Several differences between truck loaders and truck cranes or truck-mounted cranes can be identified:

- The truck loader uses a standard commercial truck chassis, while the truck crane uses a specialized carrier (although the truck-mounted crane also uses a standard chassis).
- The truck loader transports its own payload, although it often provides lifting services other than to do with its hauled loads. Truck cranes and truck-mounted cranes have no cargo-hauling capacity whatsoever.
- Truck loaders are smaller than truck cranes, and their lifting capacity is reduced compared to that of truck cranes.
- The truck crane often requires special permits and provisions to travel public roads and city streets, but the truck loader is a regular vehicle in that regard.
- Truck cranes are commonly owned by crane rental companies (but sometimes by sufficiently large construction companies), whereas the truck loader is usually owned by its operator.
- Truck cranes may stay on-site for long hours or days, but truck loaders commonly provide short-term services, often staying on-site less than one hour and visiting several sites on the same day (hence, the terms *taxi crane* and *service crane* are often used for this equipment).

Truck loaders are characterized mainly by the type of boom: a *knuckle-boom* truck loader has an articulated folding boom; a *stiff-boom* truck loader has a straight telescopic boom. The end section of the knuckle boom can also extend telescopically. Some booms feature a basic folding configuration with a stiff-boom end section.

The use of knuckle-boom truck loaders (Figure 19.25) is more widespread, and the number of models of this type offered on the market is considerably greater than that of straight-boom truck loaders. The booms of both types are commonly mounted directly behind the truck cab, facing rearward. This way, most of the truck bed is left free for cargo. A newer and less common configuration is of a rear-mounted boom, leaving smaller space for cargo but allowing for increased lifting capacity, as the boom is supported directly on the rear axles. Featuring a slewing upper-structure resembling that of the truck-mounted crane, these rear-mounted boom models allow operation from a seat, often enclosed in a cab. This is in contrast to the regular truck loaders, which are operated from a stand-up station (most models have two such stations, one on each side of the truck, or even more). This makes a big difference in terms of operation convenience, particularly in bad weather. Typical dimensions and capacities of truck loaders are given in Table 19.6.



FIGURE 19.25 Knuckle-boom truck loader in form-assembly work.

TABLE 19.6 Technical Data of Truck Loaders

Properties	Boom Type			
	Articulated Boom		Straight Boom	
	Common Range	Largest Machines	Common Range	Largest Machines
Lifting moment (ton-ft)	10–200	500	5–70	200
Maximum lifting capacity (lb)	2000–40,000	60,000	2000–20,000	40,000
Maximum radius (horizontal reach) ^a (ft)	20–80	130	10–40	80
Maximum lifting capacity at maximum radius (lb)	1000–5000	20,000	500–3000	10,000

^a Maximum vertical reach above ground is 3 to 6 ft more than maximum horizontal reach in the smaller model and 10 to 14 ft more in the larger models. Most truck-loader models feature below-ground reach, as well.

On the construction site, truck loaders offer advantages in both of their service modes. As independent hauling and loading equipment, they can save crane time by self-unloading their cargo (or picking up cargo from the site), as well as by lifting it directly to where it is needed, within the reach limit of the boom. They also have an advantage in being able to drop off or pick up cargo outside the work envelope of cranes at the site. Their hourly operation costs are lower than those of on-site trucks or rough-terrain cranes which is why, on some low- to mid-rise building projects as well as many non-building project types, there is a preference to use truck loaders quite frequently on an on-demand basis, rather than maintaining a resident crane on-site (see Figure 19.25).



FIGURE 19.26 Truck-mounted telescopic belt conveyor.

19.6 Belt Conveyors

Placing concrete by belt conveyors had been popular in North America, particularly for high-volume, fast-rate pours. Belt conveyors, available in a variety of configurations, are still used but not as commonly as before, having been replaced gradually by the more popular concrete pump. One advantage of belt conveyors over concrete pumps is their ability to transport other bulk materials, such as sand and gravel, as well as concrete. Another advantage is their ability to transport coarse aggregate concrete and dry concretes, which a concrete pump cannot do.

Belt conveyors used in the mining industry, quarries, and central mixing plants are stationary and can be quite long; however, the use of belt conveyors for construction requires high mobility and, consequently, relatively short conveyors. Belt conveyors for placing concrete are either stand-alone portable units or equipment fitted onto a host carrier, such as a truck, mobile crane, or truckmixer. To be fed by a truckmixer, the feeder hopper of the conveyor must be adequately low. The concrete is then conveyed upward, either directly to its discharge location or to additional conveyor segments moving it further horizontally, upward, or downward to the final placement location.

A popular configuration is that of the truck-mounted telescopic conveyor (Figure 19.26), resembling a truck-mounted boom pump. The boom can rotate a full circle, and the truck can set up and operate under heights as low as 15 ft. Typical dimensions and capacities of this equipment are as follows:

- Maximum horizontal reach, 50 to 125 ft
- Maximum upward angle, 30°
- Maximum horizontal reach at maximum upward angle, 40 to 110 ft
- Maximum discharge height above ground, 30 to 70 ft
- Maximum downward angle, -10° to -15°
- Maximum discharge height below ground, 5 to 25 ft

A different belt-conveyor type, used mainly on civil-engineering projects requiring long conveying distances, is the series conveyor. It is composed of modular segments and typically conveys concrete up to 600 ft away from the feeding truckmixer.

19.7 Material Handlers

Telescopic-boom material handlers, known as *telehandlers*, first appeared in the early 1980s and have grown constantly in popularity ever since. They are today's classic multi-purpose equipment on construction sites, due to their high mobility, versatility, and reach (both horizontal and vertical). The



(a)



(b)

FIGURE 19.27 Telehandlers: (a) as a forklift, stowed boom; (b) in concrete placing.

increased popularity of telehandlers can be attributed to their usefulness on industrial, agricultural, and construction sites alike, as well as to the increasing use of materials packed and delivered to the site for forklifting on pallets. A variety of front-end attachments can easily and quickly be interchanged, so telehandlers can be configured not only as forklifts but also as cranes, front loaders, concrete buckets, access platforms, and more. Telehandlers (Figure 19.27) are wheel based and can commonly travel at up to 25 mph. They feature good site maneuverability on various ground surfaces due to their two axles and high ground clearance, as well as their advanced drive, steering, and lateral-balancing capabilities. To fully utilize their lifting capacity with an extended boom, most telehandler models operate on outriggers (often termed *stabilizers* with this equipment). Some telehandler models have performance enhancements such as a fully rotating upper structure (*slewing handlers*), forward horizontal boom motion at any height from the chassis, elevating forks, carriage side shift, and a tilting operator cab. The rapidly evolving telehandler market offers a great many models with ever-growing reach and capacity

ranges. The telehandlers of the 1980s were able to serve up to three-story buildings, but telehandlers today can reach up to the ninth story. Some of the largest machines available today are not much different in size and capacity from small rough-terrain cranes. Typical dimensions and capacities are as follows:

- Maximum load capacity, 6000 to 20,000 lb
- Maximum vertical reach, 20 to 80 ft
- Maximum load capacity at maximum vertical reach, 2000 to 10,000 lb
- Maximum horizontal reach, 10 to 60 ft
- Maximum load capacity at maximum horizontal reach, 1000 to 4000 lb

19.8 Hoists and Lifts

The three main types of personnel lifts used on building construction sites are the mast-climbing passenger hoist, scissor lift, and aerial work platform. **Mast-climbing passenger hoists**, also used as material hoists, are the only personnel-movement solution for high-rise construction. No high-rise building is constructed anywhere in the world without using this type of hoist; on some buildings, several units are used. As construction progresses and the building rises, the constructor has to decide when to install the hoist; until it is installed, workers and other personnel must use the stairs (permanent or temporary). Typically, buildings ten stories and higher use passenger hoists; on taller buildings, the hoist may be installed early on, before the building reaches that height. When construction has reached the top and the permanent lifts have been installed, the hoist can be dismantled, although it often stays in service almost to the end of construction. The mast is erected outside the building next to the façade to which it is braced. After it is dismantled, some finishing work may have to be done where the ties were anchored to the building.

The climbing passenger hoist is a heavy-duty, old-concept machine that excels in safe performance. On the site, it is probably the first machine to begin running in the morning and the last one to shut down at the end of the workday; in between, it hardly ever stops. There are single-car and twin-car hoists (a twin-car hoist is shown in Figure 19.30). Car size varies from small 2×3 -ft cars, which can take one or two passengers in addition to the operator, to large 7×15 -ft cars capable of carrying a great many passengers. Maximum typical payloads vary from 1000 lb for the small car to 7000 lb for the large car. Electrically powered (by in-car motors), various hoist models operate at speeds up to 100 to 400 ft per min. The large-car high-speed models, capable of hoisting up to 40 passengers, are designated for service on ultra-high-rise buildings.

For a climbing hoist to be used, a landing deck and gate must be installed at each floor of the building. As a safety feature, the car would not start moving until the gate has been closed. No gate at any floor can open while the car is in motion. A gate opens only after the car has reached that floor and come to a stop at the exact level of the gate. Next to each door is a buzzer or call button that is used to call the hoist for service. Radio communication is frequently used, as well. Modern hoists now feature advanced-technology control systems; for example, with the twin-car hoist, the system can store all calls from the floors and send the car that is nearest to the floor to pick up passengers, thus reducing waiting times.

Probably the most widely used form of powered access, self-propelled **scissor lifts** for construction sites (Figure 19.28) were developed from similar industrial lifts. These four-wheel-mounted lifts can be used on smooth concrete or similar solid surfaces or as rough-terrain equipment. Operated from the upper deck or ground, the lift serves the worker using it by also hauling tools and materials, depending on the kind of work performed (e.g., lifting plywood boards for slab formwork) (see Figure 19.28). The platform may be raised only vertically, but most models offer a slide-out platform extension for increased access capability, as well as removable guardrails for easier loading and unloading of materials. Scissor lifts are used where less reach and height but greater workspace and lifting capacity are required. They are designed to provide larger platform work areas and generally to allow for heavier loads than aerial work platforms of the boom type. Common platform height is in the range of 20 to 60 ft, and lifting capacity is in the range of 500 to 2500 lb.



FIGURE 19.28 Scissor lift in slab deck formwork.

Self-propelled **aerial work platforms** (often termed *boom lifts*) come in two main boom configurations: telescopic (straight) boom (Figure 19.29a) and articulated (knuckle) boom (Figure 19.29b). Reach is the main size identifier of these units; common maximum vertical reach is in the range of 30 to 120 ft, but some telescopic models extend as high as 150 ft. Common maximum horizontal reach is 20 to 60 ft; 80 ft maximum for the largest-size models. Lifting capacity of most models is 500 lb. Other than reach, machines also differ from each other in terms of maneuverability on various surface conditions and slopes, dimensions and their ability to move through narrow paths and operate in confined spaces, self-weight *vis-à-vis* load limits of the surface upon which they move and work, and platform size. Manufacturers offer a variety of standard and optional features that are likely to be used by workers performing their jobs from the platform. Examples include electrical outlets and air lines on the platform, as well as integrated generators with electric, air, and water lines running through the boom to the platform to power all kinds of tools (Hindman, 2005).

The articulated aerial platform is useful mainly for reaching up and over obstacles mounted on the floor and for reaching other elevated positions not easily approached by a straight boom. The telescopic, straight boom platform is especially useful for applications that require high reach capability. Booms of both types can be raised or lowered from vertical to below horizontal (although better under-reach can be attained with the articulated boom) and can be extended while the platform itself remains horizontal and stable. Articulated booms can often telescope their bottom or front section. In both boom-type machines, the operator can maneuver and steer the machine from the work platform even when it is fully extended and elevated.

19.9 Mechanized Form Systems

Mechanized cast-in-place concrete forming systems for specialized uses such as in bridge and tunnel construction have been in use for many years, and they are also widely used in the precast concrete construction industry; however, form systems for building construction, though increasingly industrialized and modernized, have not been mechanized for the most part. In fact, the classification of form systems as construction equipment, similar to other construction machines (such as cranes and pumps), is not taken for granted by many.



(a)



(b)

FIGURE 19.29 Aerial work platforms: (a) straight boom; (b) articulated boom.

Two exceptions of long-standing mechanized form systems used in building construction are hydraulic *tunnel* forms for the combined forming of walls and slabs, and vertical slipforms. Dating many years back and originating in Europe, tunnel forms are three-dimensional room-size systems suitable for the construction of orthogonal spaces in buildings that are designed in a repetitive pattern. Hotels and office buildings are typical examples, although tunnel forms have also been widely used in America since the 1990s in apartment-building construction. After the pour, when it is time to strike the forms, they are trapped in hardened concrete at the sides (walls) and above (ceiling slab). The hydraulic mechanism of the form is then actuated to retract the forms forcefully inward from the encapsulating concrete to allow their removal. Unlike tunnel forms, *slipforms* were not originally devised for building construction but rather for silos, chimneys, and similar vertical structures characterized by minimal horizontal projections interfering with the continuous vertical movement of the form. Slipforms, however, soon found use as



FIGURE 19.30 Crane-independent self-climbing forming system (Trump Tower, Chicago).

well in the forming of elevator and utility cores in high-rise buildings. Slipforming is covered in Chapter 10. The remainder of this section describes a newer mechanized form system for walls and other vertical building elements. Interchangeably termed a *self-climbing* or *automatic climbing* system, it is essentially a crane-independent system that uses hydraulics to raise itself from one floor of the building to the next (Figure 19.30). Unlike the slipform, which is attached to the fresh concrete throughout the process, the self-climbing form retracts from the hardened concrete wall before climbing to the next level. The climbing rails and other load-carrying components of the hydraulic mechanism are supported on the hardened walls of the lower level. Two main differences between this system and a slipform that relate directly to the system's primary designation as an automatic climbing system for use on buildings are that (1) it climbs by building floors, not continuously; and (2) it can accommodate horizontal elements, such as connecting slabs. Often nicknamed a *vertical plant*, it is perhaps the building form system closest to being considered equipment or a machine. Moving upward is a fully integrated, self-contained, three- or four-deck assembly, carrying a complete two-sided wall formwork system, climbing machinery, worker access platforms, material storage and reinforcing steel areas, weather protection and safety systems, and various worker utilities. Also available are provisions for concreting walls and slabs in one-pouring steps. These systems are not limited to building cores only and are often used for the entire vertical enclosure of the floors, offering integral solutions for column and beam formwork that are customizable for almost any façade design. If a climbing concrete placing boom is used, its climbing mast and running pipeline can be integrated in the climbing system, as well.

The climbing system is composed of several sections, termed *platforms*, depending on the size and layout of the system and the building elements formed by it (e.g., core walls only or entire building enclosure). Some climbing systems offer a central hydraulic system and climbing control such that the entire system can climb together. Other systems allow each platform to climb independently (as seen in Figure 19.30). Typically, these platforms carry 40 to 80 tons each; thus, the overall weight of the complete assembly carried up by the hydraulic mechanisms and supported by the host building can reach several hundred tons. The main advantages of these systems include: (1) savings in crane time required, (2) operability in bad weather and strong winds, (3) high production rates and fast progress, and (4) increased safety. Because of the considerable acquisition costs of these systems, they are viable solutions primarily for ultra-high-rise buildings (and other tall structures), where many reuses can be realized. A lower limit of 25 to 30 stories is the general rule of thumb; however, the economics of any specific use should be investigated by assessing the suitability of a particular system to the proposed architectural design, structural design, finishes requirements, use of other major equipment, weather, and more.

Acknowledgment

This chapter was written during the author's sabbatical as a Visiting Professor at the University of Wisconsin–Madison. The author is grateful for the hospitality of the UW Department of Civil and Environmental Engineering. Some of the technical information on certain equipment types was compiled from commercial manufacturer material available for free public use on the Internet. This availability is thankfully acknowledged.

References

- Bishop, P. 2000. Reborn in the USA: tower cranes. *Cranes Today*, 304, 21–23.
- Bishop, P. 2004. An unfolding market: self erectors. *Cranes Today*, 360, 16–18.
- Goldenberg, M. and Shapira, A. 2007. Systematic evaluation of construction alternatives: case study. *J. Construct. Eng. Manage.*, 133(1), 72–85.
- Hindman, W. 2005. Selecting an aerial lift. *Vertikal Conexpo*, 46 (www.vertikal.net).
- Howes, R. 2005. An eye in the sky: cameras. *Cranes Today*, 370, 48–50.
- Meehan, J. 2005. Computerize to organize: lift planning. *Cranes Today*, 369, 50.
- Peurifoy, R.L., Schexnayder, C.J., and Shapira, A. 2006. *Construction Planning, Equipment, and Methods*, 7th ed. McGraw-Hill, Boston.
- Rosenfeld, Y. and Shapira, A. 1998. Automation of existing tower cranes: economic and technological feasibility. *Automat. Construct.*, 7(4), 285–298.
- Saaty, T.L. 1980. *The Analytic Hierarchy Process*. McGraw-Hill, London.
- Shapira, A. and Glascock, J.D. 1996. Culture of using mobile cranes for building construction. *J. Construct. Eng. Manage.*, 122(4), 298–307.
- Shapira, A. and Goldenberg, M. 2005. AHP-based equipment selection model for construction projects. *J. Construct. Eng. Manage.*, 131(12), 1263–1273.
- Shapira, A. and Goldenberg, M. 2007. 'Soft' considerations in equipment selection for building construction projects. *J. Construct. Eng. Manage.*, 133(10), 749–760.
- Shapira, A., Rosenfeld, Y., and Mizrahi, I. 2008. Vision system for tower cranes. *J. Construct. Eng. Manage.*, 134(5), 320–332.
- Shiffler, D.A. 2006a. Seeing is believing: self-erecting tower cranes. *Am. Cranes Transport*, 2(10), 28–29.
- Shiffler, D.A. 2006b. Crane city: tower cranes. *Am. Cranes Transport*, 2(12), 21–25.

Bibliography

The following books offer additional reading on construction equipment and related topics:

- Harris, F. and McCaffer, R. 2001. *Modern Construction Management*, 5th ed. Blackwell, London.
- Illingworth, J.R. 2000. *Construction Methods and Planning*, 2nd ed. E & FN Spon, London.
- Nunnally, S.W. 2000. *Managing Construction Equipment*, 2nd ed., Prentice Hall, Upper Saddle River, NJ.
- Peurifoy, R.L., Schexnayder, C.J., and Shapira, A. 2006. *Construction Planning, Equipment, and Methods*, 7th ed. McGraw-Hill, Boston.
- Schaufelberger, J.E. 1999. *Construction Equipment Management*. Prentice Hall, Upper Saddle River, NJ.
- Shapiro, H.I., Shapiro, J.P., and Shapiro, L.K. 2000. *Cranes and Derricks*, 3rd ed. McGraw-Hill, New York.

Websites

In addition to information offered on the Internet by equipment manufacturers, the following websites are useful sources of current construction equipment industry and market information:

- www.aem.org (Association of Equipment Manufacturers)
- www.constructionequipment.com (*Construction Equipment*)
- www.cranestodaymagazine.com (*Cranes Today*)

www.enr.com (*Engineering News Record*)

www.hoistmagazine.com (*Hoist*)

www.khl.com (KHL Group, including the following journals: *Access International*, *American Cranes & Transport*, *International Construction*, *International Cranes and Specialized Transport*)

www.liftlink.com (*Lift Applications & Equipment*)

www.mhia.org (Material Handling Industry of America)

www.scranet.org (Specialized Carriers and Rigging Association)

www.vertical.net (VerticalNet, including *Cranes & Access*)



Placing RCC at 500 cu yd/hr, Paradise (Burnett River) Dam in Australia. (Photograph courtesy of Ernest K. Schrader.)

20

Roller-Compacted Concrete

Ernest K. Schrader, Ph.D., FACI*

20.1	Introduction	20-1
	What Is RCC? • History	
20.2	Advantages and Disadvantages.....	20-7
	General • Cost • Schedule • Equipment, Materials, and Manpower • Weather	
20.3	Aggregates and Mixture Proportions.....	20-11
	Aggregates • Mixture Types and Designations • Fresh Mixture Consistency • Water/Cement Ratio and Optimum Water Content • Approaches to Mixture Design and Proportions • Chemical Admixtures and Grout-Enriched RCC	
20.4	Material Properties.....	20-21
	Density and Air Content • Coefficient of Thermal Expansion • Thermal Diffusivity and Conductivity • Poisson's Ratio • Autogenous Volume Change • Freeze–Thaw Resistance • Cavitation and Erosion Resistance • Compressive Strength • Tensile Strength	
20.5	Design	20-40
	General • Overdesign Strength Requirements • Design Section Options • Upstream and Vertical Face Options • Downstream and Sloping Face Options • Thermal Considerations	
20.6	Construction.....	20-54
	General • Aggregate • Mixing • Delivery • Placing and Spreading • Compaction • Joint Treatment and Inspection • Curing and Weather Protection	
	Defining Terms.....	20-70
	References	20-71

20.1 Introduction

Roller-compacted concrete (RCC) has rapidly become a commonly used material for dams and massive structures. It is also used for overtopping and erosion protection of embankments and for heavy-duty pavements. This chapter concentrates on mass applications of RCC, primarily for dams; however, many of the concepts, from testing to material properties and mix designs, apply to all uses of RCC. In a sense, RCC dams can be thought of as a series of bonded pavements or parking lots stacked on top of each

* Consultant, Schrader Consulting Engineers, Walla Walla, Washington; expert in the theory and application of roller-compacted concrete, including planning, design, and construction of more than 100 international projects.



FIGURE 20.1 Placing RCC with 110 lb of cement and 54 lb of fly ash per cubic yard using a 24-in. conveyor at Rompepicos Dam, Mexico. (Photograph courtesy of Ernest K. Schrader.)

other. This chapter provides an explanation of what RCC is, how it differs from conventional concrete, what its special properties are, and how to use it effectively. The chapter covers specific technical and construction issues, including aggregates and mixture proportioning, laboratory testing, properties, engineering and design, cost, and construction. Emphasis is placed on areas of controversy and significant interest, such as cost savings, mixture proportions, material properties, watertightness, lift-joint quality, and design options.

20.1.1 What Is RCC?

Roller-compacted concrete is concrete, but it is placed by nontraditional methods. It requires a drier or stiffer consistency than conventional concrete. RCC can have a much broader range of material properties than conventionally placed concrete. It can use aggregates not meeting normal requirements, it can be placed at very high production rates, and it can be much less expensive. By definition (ACI Committee 207.5R, 1999), RCC is concrete that has a consistency that allows it to be compacted with a vibratory roller. Usually a 10-ton vibratory roller intended for compaction of asphalt and granular base is used because of its high compactive energy with high-frequency and low-amplitude vibration. RCC is often mixed in a continuous process rather than in batches. It is delivered with dump trucks or conveyors, spread in layers using a bulldozer, and given final compaction with a vibratory roller. Figure 20.1 shows a typical application of mass RCC on a medium-sized dam, using a 24-in. conveyor delivery system. A condensed summary of the RCC process has been described in earlier literature (Schrader, 1988; Schrader and Namikas, 1988). More thorough summaries have also been published (ACI Committee 207.5R, 1999; Hansen and Reinhardt, 1991; ICOLD, 1989; Jansen, 1989; Schrader, 1994, 1995c,d, 2002, 2003a). Freshly mixed uncompacted RCC generally looks like damp gravel that might be used for a road base, although some mixtures that have a wetter consistency look more like a conventional no-slump concrete. Not until the cement has reached a point near final setting or until the hydrated interior is exposed does RCC have the visual appearance of normal concrete. Portland cement is normally the primary cementing medium, although fly ash or natural **pozzolan** is often used for a major portion of the cementing material. Slag cement has also been used. Low-cement-content mixtures typically use natural nonplastic fines or rock dust as a filler to compensate for the lack of **paste** that would otherwise exist. At times, the fines have cementing abilities.

20.1.2 History

The rapid worldwide acceptance of RCC dams is a result of need, success, and economics. Materials used occasionally 30 to 40 years ago, in hindsight, could be considered to be RCC. These applications were typically stabilized gravel fills, and the material was not viewed as an engineered concrete. In the 1960s, a high-production, no-slump mixture that could be spread with bulldozers was used at Alpe Gere Dam in Italy (Gentile, 1964) and at Manicougan I in Canada (Wallingford, 1970). A similar process was used as late as the 1980s at Burdekin Falls Dam in Australia. These mixtures were almost RCC, but they were consolidated with groups of large internal vibrators mounted on backhoes or bulldozers, a procedure that is currently used at times with conventional low-slump mass concrete—for example, at the Tekeze Arch Dam in Ethiopia.

During the 1970s, a number of organizations were involved with trials, laboratory evaluations, and the development of various philosophies concerning mass RCC. A number of RCC applications for portions of dams and spillways, for temporary structures, and for noncritical uses were completed during this first decade of significant RCC development, including the placement of more than 1 million cubic yards of RCC at Tarbela Dam. In 1974, a preliminary design with extensive laboratory testing was completed by the U.S. Army Corps of Engineers for the Zintel Canyon Dam. This would have been the world's first RCC dam, but because of funding issues the dam was not actually constructed until 1992.

The work with RCC in the 1970s formed the basis for RCC dams as they began to appear in the 1980s. Growth and acceptance of this new process was dramatic. In 1983, only one major all-RCC dam existed in the world (Willow Creek in Colorado) (Schrader 1982a,b). About the same time, Shimijagawa Dam, a rolled-concrete dam (RCD) was completed in Japan. RCDs typically use RCC for the interior portions. By 1996, just 13 years after completion of the first all-RCC dam, about 200 large RCC dams worldwide were completed, under construction, or under design. There are now too many to keep track of, with many hundreds of projects being documented. In the United States alone, about 300 documented uses of RCC in dams can be found, including 46 dams higher than 50 feet, more than 30 dams lower than 50 feet, 126 uses of RCC to allow overtopping of embankment dams, more than 10 uses of RCC for added support of existing concrete dams, several for raising the height of existing dams, and several uses for earth-dam rehabilitation applications, among the many miscellaneous uses.

Although the United States initially had the greatest number of RCC dams, they are now more prevalent in countries such as China, Spain, and Brazil, and their popularity is increasing in Vietnam, India, and elsewhere in Asia and Southeast Asia. RCC dams can be found on every continent except Antarctica. RCC dams are in use, under design, or in the planning stages in countries that have climates ranging from arctic to tropical and are at elevations ranging from sea level to very high mountain regions. Figure 20.2 through Figure 20.9 show examples of completed RCC dams of various mixes, sizes, and locations.

Rolled-concrete dams are now being used extensively in Japan, where over 30 projects have been completed, are under construction, or are in various stages of planning and design; however, RCD has not become popular outside of Japan. The process uses a relatively low-cement-content RCC for the interior portion of the dam, but typically encases the entire mass of RCC with at least 10 ft of conventional concrete. This includes the upstream and downstream faces, the foundation, and the upper portion of the dam, although the current trend seems to use more RCC and less conventional concrete. **Monolith** joint spacings are typically the same as those used for conventional concrete dams. The result is a very attractive dam that looks and behaves like a traditional concrete dam, but the RCD procedure tends to compromise the substantial cost savings and reduction in schedules possible with dams that are almost entirely RCC. The trend in the United States has moved from using RCC primarily for new dams to using it more for rehabilitation and support or the buttressing of existing dams, for raising the height of existing dams, and for providing emergency spillway capacity over existing embankment dams. This trend is expected to develop in other countries as they begin to realize the benefits and additional uses of RCC. Figure 20.10 shows the use of RCC to provide a buttress and an overtopping spillway at the Tongue River embankment dam in Montana.



FIGURE 20.2 Willow Creek Dam in Colorado, which was the world's first major all RCC dam and used mostly 80 lb of cement and 32 lb of ash per cubic yard. (Photograph courtesy of Ernest K. Schrader.)



FIGURE 20.3 Urugua-I Dam in Argentina, which used 105 lb of cement per cubic yard (no ash). (Photograph courtesy of Ernest K. Schrader.)



FIGURE 20.4 Balambano Dam in Indonesia, which used 121 lb of cement and 81 lb of fly ash per cubic yard. (Photograph courtesy of Ernest K. Schrader.)



FIGURE 20.5 Miel I Dam in Colombia, which is 620 ft high and used low to medium cement content mixes and no ash. (Photograph courtesy of Ingetec S.A., Colombia.)



FIGURE 20.6 Burnett River (Paradise) Dam in Australia, which used 106 lb of cement per cubic yard (no ash). (Photograph courtesy of Ernest K. Schrader.)



FIGURE 20.7 Mujib Dam in Jordan, which primarily used 143 lb of cement per cubic yard (no ash). (Photograph courtesy of Lahmeyer International, Bad Vilbel, Germany.)



FIGURE 20.8 Saluda Dam in South Carolina, which was built downstream of an existing unstable embankment dam using 150 lb of cement and 150 lb of dumped waste ash per cubic yard. (Photograph courtesy Paul C. Rizzo Associates; Monroeville, PA.)



FIGURE 20.9 Rompepicos Dam in Mexico, which is 350 feet high; mostly used 73 lb of cement and 54 lb of waste ash per cubic yard. (Photograph courtesy of Ernest K. Schrader.)



FIGURE 20.10 RCC used to provide a buttress and overtopping spillway for the Tongue River embankment dam in Montana. The mix primarily used 150 lb of cement (no ash) with surface layers of the stilling basin having higher cement content.

As with conventional concrete, there is no known limit to the size or height of dams that can be designed and constructed with RCC. Currently, dams on the order of 300 ft high are common, and dams about 600 ft high are not unusual, such as the 620-ft Miel I dam in Colombia. Very large dams such as Longtan in China and Gibe III in Ethiopia are beginning to emerge. Dams up to about 900 ft high, with nearly 20 million cubic yards of RCC are also being designed, such as Diamer Basha in Pakistan. The performance of RCC dams has been very good, although like other dams some projects have had issues with regard to cracking and seepage (Schrader, 1988, 1994, 1995a,c,d, 2002, 2003a; Schrader and Namikas, 1988). These two specific issues are discussed later in more detail.

20.2 Advantages and Disadvantages

20.2.1 General

The list of RCC dam advantages is extensive, but some disadvantages should be recognized. Some of the potential advantages can only be realized with certain types of RCC mixtures, structural designs, production methods, weather, or other conditions. Likewise, some disadvantages only apply to certain conditions and types of mixtures. One condition that remains constant with RCC is that each job must be thoroughly evaluated on its own. What is advantageous for one project with a given set of conditions may not be advantageous for a different project, and what is a problem at one location may actually be a benefit at another location. No single design, mixture, or construction method is ideal for all projects. Although it is almost routine for efficiently designed RCC dams to be the least costly alternative when compared to other types of dams, in some circumstances RCC may be more costly. A situation in which RCC may not be appropriate is when aggregate material is not reasonably available but an abundance of good material is available for impervious fill. When a large spillway capacity is necessary, RCC dams usually are the most economical because the spillway can be placed over the dam, and the non-overflow portion of the dam can be allowed to overtop in an emergency. Fill and embankment dams typically require a separate, very expensive spillway excavated into an abutment and, because they cannot be allowed to overtop, they usually have added height to ensure that overtopping is avoided.

20.2.2 Cost

Typical reasons for using RCC are the reduced cost and time it offers. Savings can be dramatic, sometimes in excess of 50%; however, in reality, some projects lacking the proper planning, equipment, and supervision have not saved any time, and the potential cost savings have been lost. Some projects have experienced added costs because of design decisions by the engineer or owner that resulted in expensive or time-consuming options—for example, architectural concrete, nonessential extra nonessential galleries, excess conventional facing concrete, elaborate spillways added to the face of the dam after finishing the RCC, and arbitrary decisions to use imported or excessive cementitious materials and expensive aggregates when they really were not necessary. Each project must be evaluated on its own. A trade-off in appearance and other characteristics that may be associated with high costs must be acceptable to the owner and compatible with technical requirements.

It is difficult to obtain final actual cost data for RCC dams, although bid price data for various portions of the RCC are abundant, and several reasonable summaries of approximate overall costs are available in various references (Forbes, 1988; Hansen and Reinhardt, 1991; Schrader, 1988, 1995c,d; Schrader and Namikas, 1988). Apparent discrepancies in costs reported in publications and in costs discussed at various meetings exist for two primary reasons: First, the work and materials included in the costs can be very inclusive (e.g., mobilization, joints, engineering, facings, diversion, spillway, forming, galleries, drains, foundation preparation), or the costs may include only the very basic costs of RCC production (aggregate, cement, mixing, and placing). Second, costs are sometimes based on unit bid prices, which can be unbalanced and not the true prices and do not include subsequent added costs for claims, litigation, time extensions, modifications, and overruns.

TABLE 20.1 Typical RCC Prices (1996 U.S. Dollars)

Volume (yd ³)	Price per yd ³
1000–6000	\$42–94
30,000–100,000	\$34–42
250,000–500,000	\$23–34
1,000,000–7,500,000	\$22–29

Note: Prices include RCC, facings, conventional concrete, and miscellaneous items.

Because of the many interrelated aspects of RCC, a fair way to compare the costs of various designs and projects is to consider the volume and combined cost of applicable mobilization; access and haul roads for RCC and related activities; cement; pozzolan; aggregate; admixtures; mixing; delivery; placing; compaction; grout-enriched or bedding mixtures; lift-surface cleaning; curing and protection; upstream and downstream facings; watertightness; spillways; joints; detailed work at the top of the dam; foundation preparation, including leveling the concrete if used; galleries; drainage; and cooling or crack mitigation, if required. Consideration should also be given to the required quantity of excavation, as well as the length of diversion and outlet structures.

The reason for this comprehensive comparison is that misunderstandings have occurred without it. An example is when comparing a more massive lower strength design to a less massive higher strength design. The low-strength design may have significantly lower RCC unit costs, but high dams may require greater volume, more excavation, and longer conduits. Lower unit costs are usually the result of greater volume, lower strengths, and reduced aggregate, cement, pozzolan, and admixture requirements. High-strength designs typically have greater unit costs. They may also have significantly more foundation treatment, **gallery** requirements, lift-joint requirements, leveling concrete, monolith joints or crack control, and cooling requirements. Another example is a design that requires more costly and complex RCC placing methods but has the benefit of less costly spillway and facing work, whereas a different design may have very simple RCC placing that then requires time-consuming and costly spillway or facing construction.

Even with these problems, general price guidelines can be provided. Typically, the final price of RCC (all ingredients, mixing, delivery, and placing, including joint treatment, drains, cure, facings, and other directly related items) varies from about \$22/yd³ to \$94/yd³ (1996 U.S. dollars), depending on the size of the project, strength, and complexity. Table 20.1 provides typical price ranges for different sizes of dams based on historical records of completed projects and estimates for future projects. The table excludes projects in France, where RCC tends to be more expensive than elsewhere (but still locally competitive). Another exception is the relatively high final cost of the high-cementitious-content RCC at Upper Stillwater Dam (Parker, 1992). Exceptions at the other end of the spectrum are Zintel Canyon Dam and Willow Creek Dam, where uncomplicated projects resulted in final real costs less than the range indicated in Table 20.1.

Table 20.2 provides a typical price breakdown (1996 U.S. dollars), showing where the more expensive aspects of RCC typically lie—namely, in aggregate and **ementitious** materials. The table also demonstrates the increased unit cost of RCC with a higher cementitious content, but also the typical lower volume required for a high-cementitious-content dam compared to a low-cementitious-content dam. Historically, and in estimates of future projects, the final cost of an entire dam with all related construction such as outlets, spillway crests and gates, access, foundations, diversion, instrumentation, valves, finishing, and environmental restoration is usually about 1.5 to 2.5 times the cost of the RCC. The reasons are different from job to job, but the range stays the same. Simple designs with unformed faces and more massive sections tend to be less, while more complex designs and smaller sections tend to be more.

A big part of the savings of RCC dams compared to embankment dams comes from incorporating the spillway into the dam rather than having a separate major excavation and structure. Additional major

TABLE 20.2 Example RCC Price Breakdown (1996 U.S. Dollars)

Item	Lower Strength, More Massive (\$/yd ³)	Higher Strength, Less Massive (\$/yd ³)
Aggregate	11.45	13.20
Cement + pozzolan	7.25	12.75
Delivery	2.80	3.00
Mixing	1.50	1.60
Cooling	.20	1.40
Place-spread-compact	.55	.60
Cure and protection	.20	.15
Bedding and special mixes	.40	.05
Cleaning and surface prep	.25	.10
Survey, joints, drains, gallery, miscellaneous	.20	.40
Total	24.80	33.25
RCC volume (yd ³)	1,000,000	850,000
RCC cost for dam	\$24,800,000	\$28,262,000
Total dam	\$28.60	\$38.60
Total volume (yd ³)	1,030,000	880,000
Total concrete	\$29,461,000	\$33,968,000

savings are related to the speed of construction. Often, the dam can be raised in one dry season, thereby greatly reducing the diversion and cofferdam costs when compared to the costs of providing protection during the wet season for other designs. When a large project can be completed with RCC sooner than the completion date for an alternative type of dam or design, the savings resulting from lower interest payments for borrowed money during construction can also be significant. The additional income from earlier completion and earlier water storage can be extraordinary for large hydroelectric and irrigation projects. On the other hand, due to weather, lack of availability of cementing materials, funding limitations, or, more frequently, inappropriate equipment, some RCC projects have finished well after the originally projected completion date. If, however, the factors that impacted RCC production occur with an alternative design, the outcome for the alternative can usually be shown to be even worse than it might have been for the RCC dam.

20.2.3 Schedule

In addition to the cofferdam and diversion benefits, being able to schedule RCC placement for dry seasons improves the efficiency of construction. RCC can occasionally remove the dam portion of a large project with tunnels and powerhouses from the critical path and can allow a delay in the start of dam construction, thereby saving interest on that portion of the work. Typical placing rates for projects having RCC volumes on the order of 10,000 to 25,000 yd³ are about 50 to 200 yd³/hr. Medium-sized projects of about 50,000 to 200,000 yd³ generally achieve rates of about 150 to 400 yd³/hr. Large projects of about 400,000 to 2,000,000 yd³ or more can be expected to achieve about 500 to 1000 yd³/hr. In most cases, especially with medium-sized projects, the time required to mobilize, produce aggregates, and prepare foundations exceeds the time required to place the RCC. Emergency projects have benefited from the speed of RCC construction. Kerrville Dam in Texas utilized RCC for the rapid construction of a new dam downstream of an embankment dam that was in imminent danger of failure due to overtopping; the design and construction were accomplished in a matter of weeks. Concepcion Dam in Honduras used RCC to build a water-supply project after declaration of a national emergency in the capitol city of Tegucigalpa (Giovagnoli et al., 1991, 1992). Burton Gorge Dam was essentially investigated, planned, designed, constructed, and put into operation in less than 1 year (Schrader, 1999b).

20.2.4 Equipment, Materials, and Manpower

The construction equipment required for RCC is usually available, including appropriate mixers and conveyors, which are the more difficult pieces of equipment to locate and may have to be imported. Depending on the approach taken in the design and location of the project, materials required for RCC may be difficult or very simple to procure. For example, the design of Concepcion Dam took into account the poor quality of the aggregate, cement, and pozzolan so local materials and a low-strength mixture could be used for economical construction without delays (Gaekel and Schrader, 1992; Giovagnoli et al., 1992, 1992). These materials could not meet normal requirements for conventional concrete or for RCC requiring medium to high strengths. If the design had not been adapted to materials that were readily available, a much more expensive RCC dam would have resulted that utilized specially produced cement and pozzolan and very expensive aggregates that would have been hauled a long distance. A similar situation developed at Mujib Dam in Jordan, where the original design with higher quality aggregate and imported fly ash was changed to eliminate the need for imported fly ash (or any purchased pozzolan) and to allow for the use of more economical dirty basalt aggregate (Schrader et al., 2002, 2003a). A similar approach was also used at the Burnett River Dam in Australia (Herweynen et al., 2004; Lopez et al., 2005). The redesign of Rompepicos Dam in Mexico also used this approach with regard to both cementitious content and aggregates (Schrader and Bali, 2003). Other examples are discussed in Section 20.3.1.

Roller-compacted concrete dams can be built by labor-intensive methods with reduced equipment requirements, but this should only be considered for smaller projects where economics and political reasons justify it and where relaxed quality can be tolerated. RCC is best suited to high production with large equipment and a small labor force. Even where labor is inexpensive and readily available, experience has shown that it is best to use a small work force. It is essential for supervisory staff to understand RCC as well as the type of dam construction to be used. Laborers do not require special skills other than those found in the general heavy-construction industry, but they should be given an orientation for special concerns when handling RCC. It is common for contractors new to RCC to use the services of a specialist familiar with RCC to assist at the start of placing.

20.2.5 Weather

Rain and hot weather are arguably the biggest problems in RCC production, but they are not insurmountable. For a variety of reasons, including the impact of weather on production or hauling, aggregate supply and the reliable delivery of cementitious materials have also been factors in slowing or stopping RCC production on some projects. Many major RCC projects are located in tropical and desert climates. Hot weather causes higher internal peak temperatures, but if the environment remains warm and does not have a severe cold season, thermal cracking can usually be avoided without extraordinary cooling measures for the mix, at least for mixes designed to have relatively low cementitious contents. Hot weather also reduces the allowable time before the concrete must be delivered, spread, and compacted, as well as the time that a lift surface can be exposed before it starts to suffer a significant loss of quality. Rain can be a significant problem if it is heavy or if equipment drives across the concrete surface when it is wet. Light rain will not significantly damage a compacted surface if conveyor delivery is used and hauling equipment is not driving over and disturbing the surface, but it can be a major problem if haul vehicles are used to deliver RCC on a damp lift surface. Rain problems are minimized by scheduling RCC placing during the dry season, avoiding placing during hours when rains are common, providing rain protection when appropriate, and using very high production rates with high-speed conveyor delivery. Table 20.3, developed by the author based on actual production records of different types of RCC dams in various climates, provides general guidance concerning the probable amount of time that an RCC project will be down as a result of rain. As shown in Table 20.3, downtime is a function of rain intensity and duration as well as the method of delivery. If trucks are used for delivery and they must operate on the RCC surface, rain is a much more significant problem compared to when an all-conveyor delivery system is used. This is because tire traffic on a wet surface causes the surface to develop a slurry that then must be removed before placing the next layer, or the dam must be designed with consideration for the decreased lift-joint quality if adequate cleaning is not done.

TABLE 20.3 Shifts Lost Because of Rain

Method	Peak Rain Intensity (in./hr)				
	0	0 < 0.04	0.04 < 0.08	0.08 < 0.20	<0.20
Haul vehicles on dam	0	0 ^a	1 ^a	1 ^a	2
All-conveyor delivery	0	0	0	0 ^a	1 ^a

^a Add one more lost shift if rain duration is greater than 8 hr.

Note: Assumes a two-shift/day work schedule.

20.3 Aggregates and Mixture Proportions

20.3.1 Aggregates

With respect to grading and other properties, aggregates similar to those used in conventional concrete can be used for RCC; however, materials and gradations that would normally be considered totally unacceptable for conventional concrete have been used very successfully in RCC dam construction and can actually be advantageous. Although aggregates meeting normal concrete requirements can be used, they are not necessary in RCC dam construction. Because there were no economical options, Concepcion Dam, discussed earlier in Section 20.2.4, has the unique honor of successfully using probably the worst quality materials in a major concrete dam. Monksville and Copperfield Dams used unwashed gravels with minimal processing. The aggregate included friable particles of decomposed granite in the sand sizes. Middle Fork Dam used marlstone oil shale with a specific gravity of about 2.2, a high Los Angeles abrasion loss, and absorption of 12 to 20%. In this case, an unlimited supply of this rock was available at the dam, whereas the nearest aggregate that met traditional criteria for concrete was expensive and required a long haul, all up steep grades. The marlstone required a slightly increased dam section and volume, but the overall result was a large savings.

Willow Creek Dam was the first of many projects to use dirty overburden and dirty quarry materials that normally would be wasted or require extensive washing. As discussed earlier, the fines that normally would be washed out of traditional concrete aggregate are actually needed to achieve a low cementitious content in the RCC mix. Each project must be evaluated separately to find out how to best use the available aggregate materials. In some cases, such as where a poor foundation controls the design section, a low density may actually be beneficial. In most cases, fines are beneficial, especially if they tend to be pozzolanic and well graded. The fines should be nonplastic. Some low-strength aggregates may produce a low but tolerable strength along with a desirable high creep and high strain capacity. High Los Angeles abrasion losses can usually be accepted because of service conditions, the mixing and compacting equipment, and the typical RCC grading.

Roller-compacted concrete mixtures are less affected by particle shape than are conventional concrete mixtures because of the mixing and delivery equipment used and the typical grading. The presence of flat and elongated particles is still undesirable, but amounts up to about 40% on any sieve size with an average below about 30% for all sieve sizes have been acceptable. Both crushed and rounded materials work well, but the ideal combination appears to be angular crushed coarse particles with natural rounded sand. When steep unformed slopes are to be constructed, crushed material becomes more important.

Alkali-aggregate reaction in RCC is a subject in itself. A few comments are made here. Potentially reactive aggregates have been used in RCC without problems for various reasons, including low cement contents and high pozzolan contents in some mixtures and the use of low-alkali cements when available. A nontraditional concept to consider is that a slight expansion due to the alkali-aggregate reaction can actually be beneficial if it offsets thermal contraction.

The key to controlling segregation, minimizing cement contents, and providing a good compactable mixture begins with a grading that is more uniform and contains more material passing the No. 4 sieve than would be common in conventional concrete. Using concepts from conventional mass concrete,

TABLE 20.4 Typical Aggregate Gradations for RCC

Sieve Size	Earlier RCC Projects							Typical Current Practice
	Willow Creek	Upper Stillwater	Christian Siegrist	Zintel Canyon	Stage-coach	Concepcion	Elk Creek	
4 in.	—	—	—	—	—	100	—	—
3 in.	100	—	—	—	—	99	100	—
2.5 in.	—	—	—	100	—	—	96	100
2.0 in.	90	100	—	98	100	94	86	98–100
1.5 in.	80	95	100	91	95	90	76	92–100
1.0 in.	62	—	99	77	82	80	64	76–88
3/4 in.	54	66	91	70	69	72	58	65–79
1/2 in.	—	—	—	—	—	—	—	56–68
3/8 in.	42	45	60	50	52	56	51	47–59
No. 4	30	35	49	39	40	43	41	36–47
No. 8	23	26	38	25	32	33	34	28–38
No. 16	17	21	23	18	25	25	31	20–30
No. 30	13	17	14	15	15	19	21	15–23
No. 50	9	10	10	12	10	15	15	10–16
No. 100	7	2	6	11	8	9	10	7–12
No. 200	5	0	5	9	5	6	7	3–7 ^a
Cement+pozzolan (lb/yd ³)	80 + 32	134 + 291	100 + 70	125 + 0	120 + 130	135	118 + 56	—
Total paste volume (%) ^b	20	21	19	21	—	21 ^c	21	21–23
Workability	Poor	Excellent	Excellent	Excellent	Good	Excellent	Excellent	Excellent

^a Adjust the maximum and minimum percent passing the No. 200 sieve on a combined gradation as follows: up 1% if the cement plus ash content of the RCC is less than 120 lb/yd³; down 1% if the cement plus ash content of the RCC is more than 240 lb/yd³.

^b Total paste is all materials in the full mixture with a particle size smaller than the No. 200 sieve (see text).

^c Total cementitious materials consists of pozzolanic cement having approximately 15% natural pozzolan.

earlier projects tended to use 3-in. maximum size aggregate (MSA), but the recent trend has been to use smaller MSA, on the order of about 1-1/2 to 2 in. This reduces segregation, improves lift-joint quality, and reduces equipment maintenance. The reduced MSA arguably can cause a minor reduction in strength, but such a reduction is minimal and not as significant as would be expected in conventional concrete.

It is inappropriate to provide a single set of upper and lower gradation limits that could be considered correct for all RCC. A wide range of gradations has been used successfully. Table 20.4 shows some example gradations that have been used in RCC. The mixture-proportioning concept that uses a low cementitious content and requires fines in the mixture ideally has a grading similar to an impervious gravel with nonplastic fines. Mixes with lower cementitious content generally require more fines. The maximum amount of fines that can be added without a reduction in strength, and without causing the RCC to become too sticky to mix, spread, and compact, depends on the plasticity of the fines. Plasticity can be defined in terms of soil mechanics by the liquid limit (LL) and plastic index (PI). Based on the LL and PI, Table 20.5 has been developed and used over the past 30 years as a guide for the maximum amount of fines that can be included for most RCC mixtures.

20.3.2 Mixture Types and Designations

Roller-compacted concrete suitable for use in dams can be made with very low cementitious contents, on the order of 85 to 150 lb/yd³, or it can be made with very high cementitious contents, on the order of 200 to 425 lb/yd³. Both options, plus intermediate cementitious contents, have been used quite successfully on low and high dams, both options continue to be popular, and both are expected to be used in the future (Schrader 1994, 1995c,d, 2002, 2004). The decision-making process for selecting the type of mix is not very dependent on the size or height of the dam. Unfortunately, it is often more related

TABLE 20.5 Maximum Fines Content

Liquid Limit	Plastic Index	Maximum Percent Passing No. 200 Sieve (%)
0–25	0–5	8.0
	5–10	6.5
	10–15	5.0
	15–20	3.0
	20–25	2.0
25–35	0–5	7.0
	5–10	6.0
	10–15	4.5
	15–20	3.0
	20–25	1.5
35–45	0–5	6.0
	5–10	4.0
	10–15	3.5
	15–20	2.0
	20–25	1.5
45–55	0–5	4.0
	5–10	3.0
	10–15	2.0
	15–20	1.5
	20–25	1.0

TABLE 20.6 Roller-Compacted Concrete Mixture Designations

Designation	Cement + Pozzolan (lb/yd ³)	Strength (psi)
Low	85–150	700–2100
Medium	140–210	1600–3000
High	200–425	2500–4500

to the simple issue of what the designer or owner has used in the past. The decision should be based on factual information related to foundation quality, the degree of reliable inspection expected, facing techniques, climate, cooling and thermal issues, the age at which the reservoir will be filled, and available materials with their associated costs and quality. The best overall option might be a higher strength, high-cementitious-content mix with less mass in one situation, but it could be a lower strength, low-cementitious-content mix in another situation.

Dams designed with higher cementitious content mixes may have slightly less volume but typically have a much higher unit cost and more stringent cooling and quality-control requirements. Lower cementitious content mixtures typically have lower unit costs and less stringent quality control but may require more mass. They also may require special attention to achieve watertightness along lift joints. Costs and watertightness are discussed elsewhere in this chapter. Higher cementitious content mixtures tend to result in good cement efficiencies (strength per unit of cementitious material) when compared to conventional concrete, but lower cementitious content mixtures tend to have even greater efficiencies, on the order of about 10 to 20 psi/lb of cementitious material in a cubic yard of RCC. Efficiencies on the order of 10 psi/lb are typical for excellent quality conventional concrete.

The American Concrete Institute's subcommittee on RCC has recently completed its proposed latest major update on RCC for massive structures. The new report is intended to identify low-, medium-, and high-cementitious-content mixes by a combination of cementitious content and strength ranges that are consistent with other publications. There is a deliberate overlap for the different cementitious content designations, allowing flexibility in judgment with regard to whether the aggregate fines provide some cementitious or pozzolanic value. Nonetheless, the designations, shown in Table 20.6, provide useful guidance.

TABLE 20.7 Types of RCC Mixtures: Typical Extremes

	Dry, Low Cementitious		Wet, High Cementitious	
	lb/yd ³	ft ³	lb/yd ³	ft ³
Cement	100	0.51	150	0.76
Pozzolan (ash)	0	0.00	250	1.60
Water	185	2.96	180	2.88
Air (0.5%)	0	0.14	0	0.14
Aggregate fines (8%)	280	1.80	0	0.00
Total paste	565	5.41	580	5.38
Percent paste	14%	20%	14%	20%

Note: Pozzolans and fines may or may not be cementitious in RCC.

At times, terminology has referred to RCC as being high or low *paste content* rather than having high or low *cementitious content*. This is an inaccurate description of the different types of RCC mixes (Schrader, 1994, 1995c,d, 2002, 2003a, 2004). Although RCC mixtures have high, medium, and low cementitious contents, they should not have high and low paste contents. All RCC mixtures should have at least 20% paste by volume (about 14% paste by weight), with the recent tendency being toward paste contents on the order of about 21 to 23% by volume. Paste is considered to be all of the materials that constitute the pasty portion of the mix. This includes everything smaller than 75 μm —small air bubbles, water, admixtures, pozzolans, cement, and aggregate fines.

If low-cementitious-content RCC is used, aggregate fines are necessary to supplement the otherwise deficient paste content. If a high-cementitious-content RCC is used, clean aggregates are required to keep the paste content from being too high. If the paste content is too low, low strengths, excess water demands, and segregation can be expected. If the paste content is too high, inefficient use of cementitious materials can be expected (i.e., less strength per pound of cementitious material). Mixes with too much paste can also result in lift surfaces with excess paste and laitance at the lift surface after compaction, thereby requiring lift-joint cleaning similar to that used for conventional concrete. Table 20.4 and Table 20.7 demonstrate the concept of constant paste contents for all types of RCC. They compare two extreme examples of RCC mix types and consistency. These examples are from two early RCC projects that used mixes near the extremes: (1) the very dry, lean Willow Creek Dam, and (2) a mix similar to one of the very high-cementitious-content, wet-consistency mixes at Upper Stillwater Dam.

Roller-compacted concrete mixtures can have low or high pozzolan contents. Current use ranges from 0 to about 80% pozzolan. There is no universal optimum. In some cases (such as for Stagecoach Dam), using 100% cement resulted in lower strengths than using essentially the same total cementitious content (cement plus pozzolan) but with 50% of it being pozzolan. In other more common cases, adding pozzolan while keeping the cement constant has actually caused a reduction in strength or no significant strength change. Some examples are the Burnett Dam (renamed Paradise dam) (Herweynen et al., 2004; Lopez et al., 2005), the Mujib Dam (Schrader et al., 2003a), the 358-ft high Rompepicos Dam (Schrader and Bali, 2003), and the recently completed mix studies for Dong Nai 3 Dam in Vietnam. In each case, an initial arbitrary decision had been made that a mix with high pozzolan content would be best and worth the extra cost; however, when the cost and difficulty of obtaining good-quality pozzolan were finally appreciated, tests without pozzolan were done that showed that not only was the use of pozzolan costly and unnecessarily complicated but the pozzolan also caused a reduction in strength compared to some mixes with the same cement content but no pozzolan.

The long-term strength gain of RCC is not necessarily determined by the amount of pozzolan that is used, as would normally be expected with traditional concrete. For example, a lean RCC mix at one project using only 92 lb of cement per cubic yard and no pozzolan resulted in 1-year strengths that were 380% greater than the 28-day strengths, while other mixes with pozzolan at other projects have achieved strength gains of only about 150% over the same time period. Figure 20.11 and Figure 20.12 show the global range of values that have been experienced for different pozzolans with different RCC mixtures.

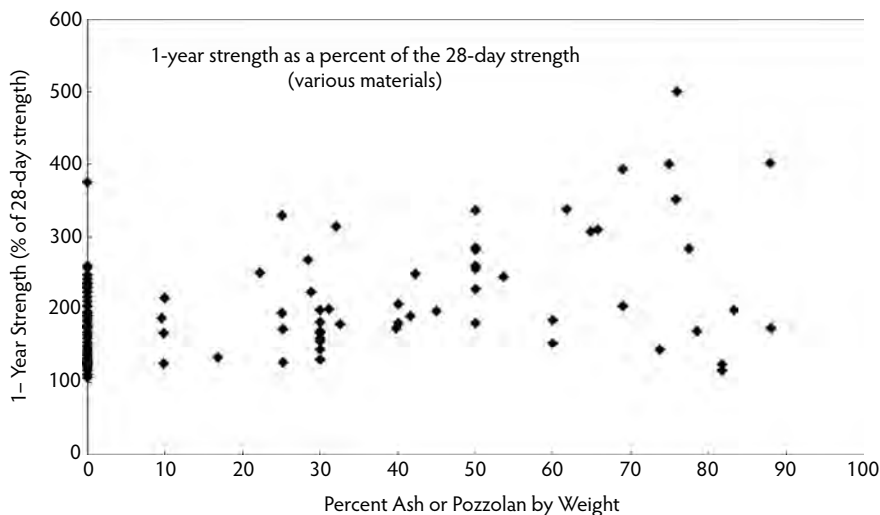


FIGURE 20.11 Efficiency of cementitious material as a function of pozzolan.

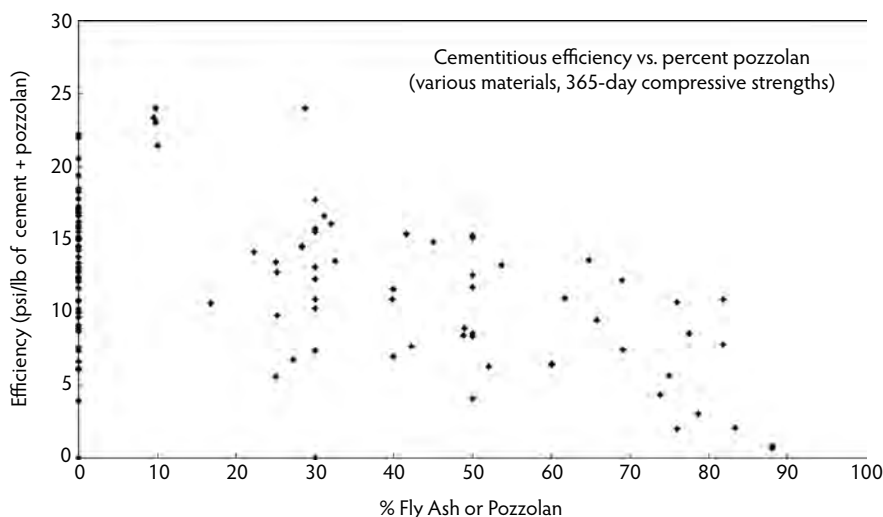


FIGURE 20.12 Long-term strength increase as a function of pozzolan.

Another observation concerning RCC is that some projects have required a minimum cementitious content of about 50 to 100 lb/yd³ to gain good strength efficiency (strength per pound of cementitious material), whereas at other projects the efficiency has been relatively constant from 0 to about 150 pounds of cement per cubic yard of RCC. Overall, strength efficiency typically tends to decrease at high cementitious contents for the same aggregates and materials at any given project, as shown in Figure 20.13. Strength as a function of total cementitious content is shown in Figure 20.14.

The important point is that RCC does not follow the same rules and trends as conventional concrete with regard to optimum cementitious and pozzolan content. Each project should be evaluated on its own merits, with its own materials, and with a wide range of options during the initial investigations. Open mindedness on the part of decision makers is essential. They should not be misled by old traditional concrete experience or guidelines or experience with only one type of RCC.

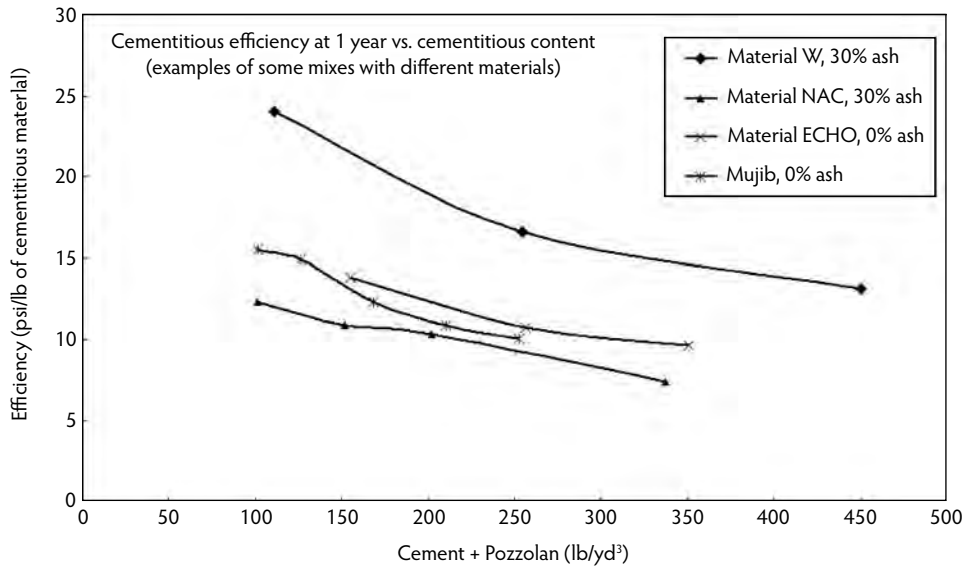


FIGURE 20.13 Reduced strength efficiency as a function of increased cementitious content.

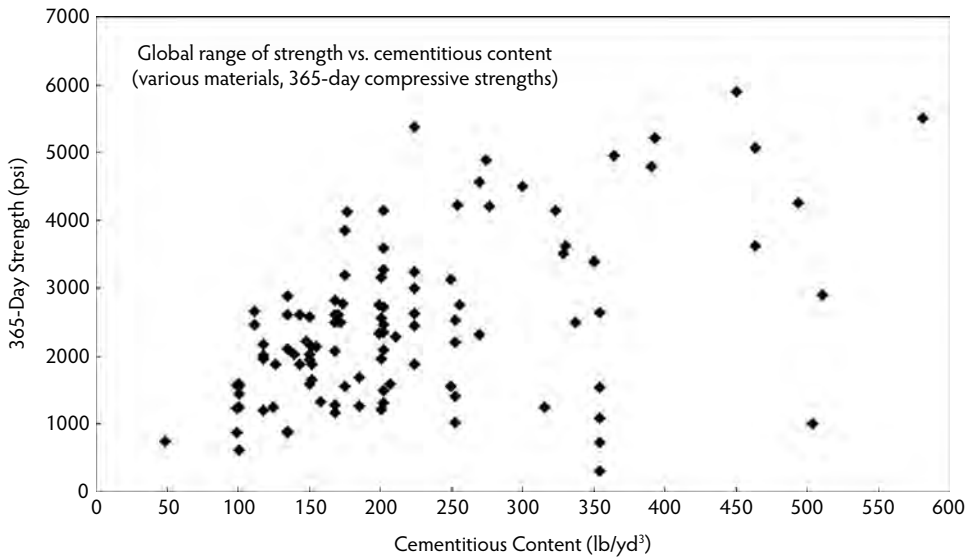


FIGURE 20.14 Example effect of moisture content.

20.3.3 Fresh Mixture Consistency

The terms *wet* and *dry mixture consistency* can be a source of confusion. RCC mixtures have no slump. They must be stiff enough to support a large vibratory roller. By traditional concrete standards, all RCC has a dry consistency; however, within the RCC community, mixtures are referred to as being wet or dry on the basis of their appearance and how they behave in the fresh state during and after compaction. Roller-compacted concrete mixtures that are considered to be wet generally produce a weaving effect or surface waviness as rollers and trucks drive across the freshly compacted RCC. This is due to an excess of moisture or the use of more water than necessary to fill all of the void space. Internal pore pressure develops in the fresh mixture, similar to what occurs in some soils. By contrast, mixtures that are considered to have a dry consistency generally do not weave under traffic after compaction. The terms

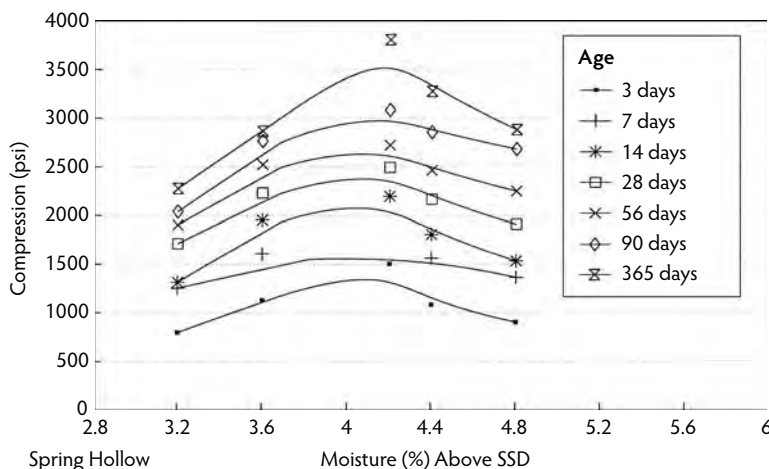


FIGURE 20.15 Example effect of moisture content.

wet and *dry* reasonably describe the behavior of the mixture, but they do not indicate whether the actual water content is high or low. Because of differences in aggregate (texture, shape, and grading) and in cements and pozzolans, the effects of fines when they are included, and the influences of temperature and humidity, a mixture with a higher water content can actually be drier in appearance than another mixture with a lower water content and *vice versa*. This is true when considering water in excess of the water absorbed by the aggregate, and it can be even more exaggerated when total water contents based on oven-dry aggregates are considered. Table 20.7 contains an example.

20.3.4 Water/Cement Ratio and Optimum Water Content

Although it is a somewhat controversial issue, the well-known water/cement ratio rule for traditional concrete does not necessarily apply to RCC. In fact, if what appears to be an excessively high water/cement ratio in a lean mix is decreased too much by simply reducing the water content, it will result in decreased strengths and poor-quality material resulting from inadequate moisture for compaction. As with embankment materials and soils, there is an optimum moisture, as shown in Figure 20.15. At this optimum, both strength and density are maximized. The shapes of the moisture vs. density and moisture vs. strength curves help establish the probable type of mix for a project. If the curve is fairly flat, adding more water will have little harmful effect on the strength of the RCC mass while improving the more important lift-joint quality. In this case, the wetter mix is desirable. If the curve drops off sharply at moisture contents above optimum, a drier-consistency mix is probably best.

For other reasons, the designer may stipulate in advance that a wet or a dry consistency mix is desired. Typically, dry-consistency mixtures are at or near optimum moisture. They typically have modified Vebe times (ASTM C 1170) in excess of 30 sec when that test is used for workability with a surcharge weight. These mixes have very little, if any, deformation under truck and tire traffic after rolling; however, the freshly compacted surface of these mixes can be damaged by truck traffic due to abrasion and turning of the tires. This damage typically can be removed by blowing with an air hose. Dry mixes typically do not have any bleeding problems and are essentially impervious to rain when they are compacted. Rain will simply collect on the surface. If there is any vehicular traffic or other surface disturbance, however, free water on the lift will begin to seriously damage the lift.

Typically, wet-consistency mixtures have modified Vebe times, on the order of about 10 to 15 sec, and they are much wetter than the optimum moisture content. Because they have more moisture than needed for maximum density, there is an excess of water within the compacted RCC. This water has no place to go, so it tends to develop a slight amount of free surface moisture at the lift surface. This can leave a pasty material and surface laitance that requires cleaning. These mixes easily weave under the roller because of



FIGURE 20.16 Surface damage caused by truck tires on wet-mix RCC.



FIGURE 20.17 Interior damage caused by truck traffic on wet-mix RCC.

internal pore pressure caused by the extra water. They also weave under truck or other vehicular traffic until the mix sets sufficiently to support the traffic. A serious issue is when trucks are used to deliver the RCC and must drive across wet mixes, because for a period of time when the mix is between initial and final set when the cement is hydrating and beginning to harden it has insufficient strength to support truck traffic. The result is that the cement paste is disrupted and damaged as it deforms under tire traffic while it is trying to set. This shears and breaks the mortar matrix. The strength loss cannot be regained. The problem can be apparent at times due to cracking at the lift surface next to tire ruts, as shown in Figure 20.16. The more significant problem of internal damage to the RCC can only be seen by saw cutting into the mass afterwards to expose the internal damage as shown in Figure 20.17 (Schrader, 2002).

Because the optimum moisture for RCC is established primarily by the aggregates (there is little or no change in optimum moisture as the cementitious content is adjusted up or down), any major change in water/cement ratio can only be accomplished by increasing or decreasing the cementitious content,

TABLE 20.8 Water/Cement Ratio Examples for Dry-Consistency Roller-Compacted Concrete

Maximum Size Aggregate (in.)	Cement + Fines (lb/yd ³)	Water (% above saturated surface dry)	W/(C + F)	W/C ^a
3	80 + 32	4.4	1.63	1.47
3	175 + 00	4.5	1.06	1.06
3	175 + 80	4.5	0.73	0.65
1-1/2	315 + 135	4.8	0.44	0.39

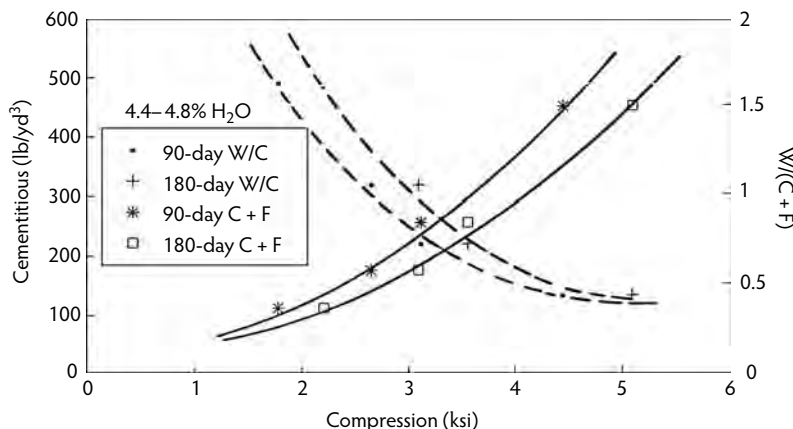
^a Water/equivalent cement ratio if the ash volume was cement.

as shown in Table 20.8. When nonapplicable experience from conventional concrete is used to arbitrarily apply a low water/cement ratio requirement to the RCC, the result will be higher cementitious contents with associated higher costs, increased heat and thermal stresses, and a more brittle **elastic modulus** with less stress relaxation due to creep. Attempts to change the water/cement ratio by changing the water content have only minor effects on the water/cement ratio, and such changes can alter the mix consistency and cause deviations from the optimum or desired moisture content and compactability. If the cementitious content is low, the water/cement ratio must be high. Values on the order of 1.0 to 2.0 are common in RCC. This is a major deviation from traditional water/cement ratios in conventional concrete that are more on the order of 0.4 to 0.6. This high water/cement ratio with lean RCC is normal. It does not imply low-quality concrete. It implies a low cementitious content rather than a high water content and wet mix consistency.

Data have been reported implying that a high water/cement ratio automatically causes a major reduction in RCC strength. This erroneous conclusion is the result of incompletely reporting all of the data. As the water/cement ratio decreases, strengths were shown to go up dramatically, but this was primarily because the water/cement ratio was decreased by increasing the cementitious content while keeping the water and mix consistency essentially constant. Figure 20.18 shows the complete picture, with the strength shown as both a function of water/cementitious ratio and as a function of cementitious content.

20.3.5 Approaches to Mixture Design and Proportions

Roller-compacted concrete mixture proportions should follow the convention used in traditional concrete—that is, identifying the mass of each ingredient contained in a compacted unit volume (cubic yard) of the mixture based on saturated surface dry (SSD) aggregate conditions. Moisture contents are then typically converted to a percentage of water above SSD aggregate conditions divided by the compacted

**FIGURE 20.18** Strength vs. water/cementitious ratio and cementitious content.

density of the total RCC mixture. Confusion has occurred when some publications and engineers have based the water content on the oven-dry aggregate mass, as done for soils, or on some other parameter. Care should be exercised when reviewing the literature. Mixture proportioning for some earlier projects relied on making many mortar cubes with varying cement, pozzolan, water, and admixture contents in an effort to optimize the mixture without making cylinders of the full mixture. This approach can be very misleading. Experience at several projects has shown that mortar cubes do not necessarily indicate how the full RCC mixture will perform. In some cases, mortar cubes have actually indicated the opposite of what ultimately happened with the full RCC mixture (Gaekel and Schrader, 1992).

Mix designs for RCC can be approached in many ways (ACI Committee 207.5R, 1999; Herweynen et al., 2004; Lopez et al., 2003a,b; Rizzo et al 2003; Schrader, 1994, 1995d; Schrader et al., 2003b; Tatro and Hinds, 1992); see Schrader (2004) for a comprehensive summary. One procedure is based on the concept of water/cement ratio. Another procedure uses a series of lab mixtures to pinpoint the optimum cementitious and pozzolan contents for a given set of aggregates. Other procedures are basically variations of these two themes. No single approach to mix design is best for all situations. All approaches to mix designs ultimately require full-scale job trials and tests, with adjustments based on the results of those tests.

The term *soils approach* has been erroneously used by others to describe a mix-design method developed by the author. This method has nothing to do with soils, and the term is misleading. All methods of RCC mix design, including the one mislabeled as the soils approach, treat the material as a no-slump concrete. They all use a suitable controlled gradation aggregate. They all intend to optimize the amount of pozzolan (if used). They all produce a consistency suitable for RCC construction. They all determine basic concrete material properties such as density and strength.

Whichever procedure is used for mix designs, the method of making test samples must be suitable for the type of mixes that will be made. Some methods, such as the vibrating table, are suitable only for wetter and higher paste mixes, whereas the pneumatic tamper and Kango or Hilti hammer are suited to drier and lower paste mixes. Some laboratories have concluded that a drier or leaner mix is not suitable for a particular project when in reality the mixes were actually quite suitable but the lab had made the samples with the wrong equipment (Schrader, 2003b).

20.3.6 Chemical Admixtures and Grout-Enriched RCC

Chemical admixtures have not been very effective in low-cementitious-content and dry RCC mixes that do not exhibit a fluid paste when subjected to vibration under full consolidation (Gaekel and Schrader, 1992; Schrader, 1984). If enough water is added to cause a fluid paste, retarders have been useful and water reducers have worked, but this may require very high admixture dosages on the order of 3 to 12 times the normal rate. The benefit of retarders and water reducers must be balanced against the cost, the complication of an additional ingredient, and any strength reduction associated with additional water required to provide the necessary wetter paste consistency. Most wetter consistency and higher cementitious content mixes depend on both the high cementitious content and a retarded set time to achieve good lift-joint quality and impermeability for the design. In this case, when the next layer of RCC has to be placed before the previous layer sets, a wetter consistency mix with high doses of retarder and a usually high pozzolan content is usually unavoidable.

As discussed further in Section 20.4.6, field experience has shown good or tolerable resistance to most natural freeze–thaw exposure conditions of mass RCC without air entrainment, but the option of using entrained air has now been achieved with some mixtures. Again, the benefits should be balanced against the disadvantages and cost for each application. Air entraining has been difficult to accomplish with RCC on a routine and consistent basis, but it has been done in the United States using special admixtures such as synthetic air, and it has been accomplished in China (Chengqian and Chusheng, 1991).

Many efforts have been made to consistently entrain air in RCC at facings by using grout-enriched RCC (GERCC). After the mix has been spread, a fluid grout is added to the RCC, with the intent being for the grout to mix uniformly throughout the RCC and turn it into a more fluid mix with higher cementitious content. The result is a zone of material (usually against a form at the face of the dam) that

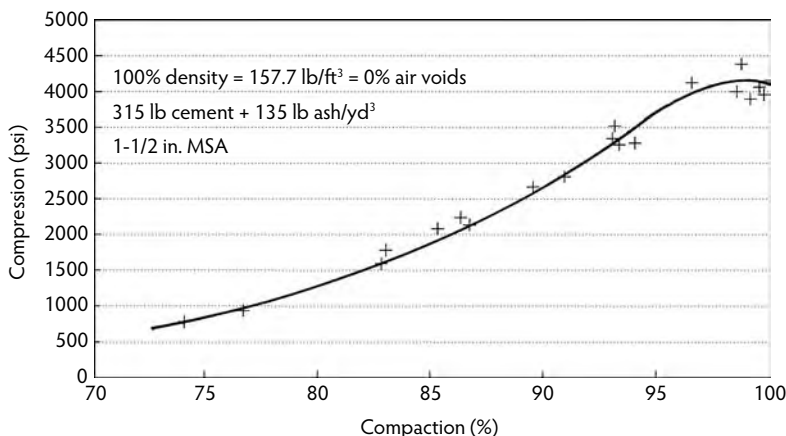


FIGURE 20.19 Twenty-eight-day strength vs. percent compaction.

will have properties and appearance similar to conventional concrete. Various procedures have been used, from simply pouring a hand-mixed grout onto the surface and using an internal poker vibrator to mix and consolidate the RCC with the grout to using sophisticated grout pumps that then inject the grout uniformly throughout the depth of the layer of RCC. Although some results have been promising by including a high dose of air entrainment in the grout, the results are more typically sporadic, with much of the air entrainment being lost by the time the mix is consolidated and sets. Tests and experience, however, have shown that the traditional amounts of air entrainment necessary for good freeze–thaw resistance are not typically required for RCC. Air entrainment is still essential, but a good-quality paste with just a few percent of entrained air has shown itself to be very effective at times (Schrader et al., 2003b).

20.4 Material Properties

20.4.1 Density and Air Content

The density and natural air void content (not entrained air) of RCC depend on the specific gravity of the aggregate, the grading, the moisture content, and the degree of compaction. Fully compacted RCC will typically have less air content and less water than conventional concrete, so its density will be slightly higher. Because RCC has been made with aggregates having a wide range of specific gravities, the specific densities of compacted RCC at different projects varies greatly from about 2.1 to 2.9. Fully compacted RCC with reasonable mixture proportions typically has an air content on the order of 0.5 to 1.5%. Specifications commonly require that field densities must obtain an average of 98% of the maximum practical achievable density (MPAD) at each test location, which is often considered to be 97% of the theoretical air-free (TAF) density, providing that no density at any level within a lift of RCC is less than about 93% of the TAF density. The average density is based on measurements taken at the top, middle, and bottom thirds of the lift. Air contents can be obtained in the laboratory using the pressure method for material compacted by tamping or by the vibrating table method, whichever is appropriate for the mixture consistency. Some of the first RCC projects required greater densities than suggested above, with the thought that densities representing 98 to 100% of the TAF would result in significant increases in strength. This is not correct. Unfortunately, some older specifications and concepts continue to be copied. As shown in Figure 20.19, it is important to achieve a reasonably well-compacted mix with a density of at least 95 to 96% of the TAF, but greater densities provide essentially no increase in strength. Excessive compactive effort can actually be harmful. Excessive compaction can cause a reduction in strength if it begins to break the aggregate particles, and, as with most gravel and sands, overcompaction of RCC can also begin to loosen the material and reduce density.

20.4.2 Coefficient of Thermal Expansion

The coefficient of thermal expansion of RCC tends to be slightly higher than the thermal expansion coefficient of the aggregate and slightly less than that for a conventional concrete made with the same aggregate but more cement paste. Because of the wide range of aggregate materials that can be used in RCC, the range of thermal expansion coefficients is much wider than would be expected for traditional concrete. Traditional concrete typically has an expansion coefficient somewhere between 4 and 8 millionths per degree Fahrenheit. Measured expansion coefficients for RCC have varied from about 3 to about 18 millionths per degree Fahrenheit.

20.4.3 Thermal Diffusivity and Conductivity

Thermal diffusivity and conductivity of RCC mixes tend to be similar to the values obtained for the aggregate by itself and similar to conventional mass concrete made with that aggregate.

20.4.4 Poisson's Ratio

Poisson's ratio for RCC tends to be similar to values for conventional mass concrete; typical values are on the order of 0.18 to 0.24, depending on the concrete age, aggregate, and strength. At very early ages and very low strengths and for mixtures with soft aggregates or very high contents of noncementitious fines, Poisson's ratio can be much higher. Under these conditions, some RCC mixes have had Poisson's ratio values on the order of 0.3 to 0.5.

20.4.5 Autogenous Volume Change

Autogenous volume change (the increase or decrease in size with no applied load or environmental change) cannot be reliably estimated in conventional mass concrete without at least some test data. This is true of RCC also, especially for mixtures that have peculiar cement, pozzolan, and aggregate. In some cases, there has been early expansion followed by a later period of contraction, or *vice versa*. Typically, the amount of change is minimal and of little consequence, but the potential for expansion or contraction can be important to large mass structures and should be investigated for large projects and for dam projects that use unusual materials. Autogenous volume changes should be considered when determining strain and creep properties and when performing a cracking analysis of large RCC structures.

20.4.6 Freeze–Thaw Resistance

(See also Section 20.3.6.) Resistance to freezing and thawing of non-air-entrained RCC subjected to natural exposure has usually been reasonably good, even when these materials had performed badly in laboratory tests. Examples include projects such as Winchester and Willow Creek Dams, which have unformed and uncompacted downstream faces of exposed RCC with cementitious material contents for the exposed face of 175 and 255 lb/yd³, respectively. Monksville Dam is another project with an unformed downstream face but with a cement content of only 105 lb/yd³ (no fly ash or pozzolan). Initially it performed well in freeze–thaw exposure, but after many years it began to show areas of deterioration. Some of this was localized, and attributable to issues during construction, but overall the severe environment has had an effect. Each of these projects receives almost daily cycles of freezing and thawing during much of the winter. Monksville and Willow Creek also have saturation from lift-joint seepage. After more than 25 years, Willow Creek and Winchester have not shown any significant change in the downstream face. Other projects, such as Middle Fork, located in severe climates where temperatures can reach –40°F and that used about 1 ft of conventional concrete facing, have also shown no distress.

Based on test data and observations, the following typical deterioration rates have been developed by the author. These estimates are for cementitious material contents in the range of 85 to 250 lb/yd³. The deterioration rate for unformed and uncompacted surfaces subjected to freeze–thaw cycles that penetrate about 1 inch is 1 inch of erosion per 100 to 250 cycles of freeze–thaw. Compacted interior RCC is estimated to deteriorate at about 1000 to 2000 cycles per inch of erosion.

As discussed in the sections on aggregates, chemical admixtures, and mix proportions, some projects have been able to achieve sufficient air entrainment to provide good freeze–thaw **durability** even in severe laboratory tests. Early RCC studies indicated that this might be possible only with high-cementitious-content mixtures with very wet consistencies; however, some lower and medium cementitious content mixtures with a relatively dry consistency have also achieved adequate air entrainment and durability using some admixtures. Synthetic air-entraining admixtures seem to offer the best promise, but traditional admixtures have also worked at times. A clear understanding of which admixture will work best is not achieved until after comprehensive testing for each RCC mix and set of materials. A recent example is the set of initial mix studies for the Tongue River project, which is exposed to temperatures ranging from about -40°F to $+120^{\circ}\text{F}$. Another recent series of interesting tests was done for the proposed Nordlingaalda Dam in Iceland, where very good freeze–thaw resistance was achieved with a normal air-entraining admixture and medium cementitious content at a relatively low entrained-air content (Schrader et al., 2003b).

20.4.7 Cavitation and Erosion Resistance

Cavitation and erosion resistance of RCC have been surprisingly good, and a historical summary has been published (Schrader and Stefanakos, 1995). Very early evaluations of erosion resistance, including full-scale tests at velocities on the order of about 100 ft/sec, were documented by the U.S. Army Corps of Engineers (1981). Based on available data, including two high-velocity and high-head, full-scale trials for a limited duration as well as laboratory and other tests, cavitation and erosion rates have been developed and used with caution to justify exposed RCC spillway surfaces. Assuming good-quality mixtures with cementitious-material contents on the order of 170 to 300 lb/yd³, an erosion rate of 0.002 lb per square foot of surface per hour of exposure has been extrapolated for a rolled surface and 0.05 lb per square foot of surface per hour of exposure for a rough surface. Field experience confirms that these numbers are either reasonable or conservative.

20.4.8 Compressive Strength

The compressive strength of RCC depends on a variety of factors, including the aggregate, quantity and quality of fines, quantity and quality of cementitious material, degree of compaction, and moisture content. The efficiency, or strength per pound of cement in a cubic yard of RCC, has been discussed in Section 20.3. The wide range of strengths that has been experienced with different RCC mixes having different aggregate, cements, and pozzolans was shown in Figure 20.14. Section 20.3 also included general information about the wide disparity of pozzolan (including fly ash) performance in RCC and the effect of moisture on compressive strength. The relationship between compressive strength and density or air voids content was discussed earlier in Section 20.4.1.

Care must be used when reviewing RCC literature that is based only on one set of site-specific aggregates, pozzolans, mixture proportions, moisture contents, and gradations. Publications occasionally offer misleading global statements about RCC strength when, in fact, the experience used as a basis for those statements has included only one project, one set of materials, and one type of RCC mixture. Because of the wide range of materials and mixture proportions that can be used in RCC, it is very difficult to develop global or general statements or rules about RCC strength relationships. Figure 20.11 through Figure 20.14 show examples of the wide range of strengths, different rates of strength gain, and the wide range in strength performance that can occur with RCC mixes containing fly ash or other pozzolans.

Traditional thinking would limit the amount of fines (material passing the No. 200 sieve) in the aggregate to very small amounts, based on the accepted traditional concept that clean washed aggregates with no fines are best. However, as discussed in Section 20.3, natural or manmade fines are essential in low cementitious RCC mixtures to provide adequate paste and to fill void spaces for control of segregation and for compaction. Nonplastic fines typically increase the strength of low-cementitious-content mixtures. The reasons for this are not entirely clear. In some cases, it is probable that the fines are providing

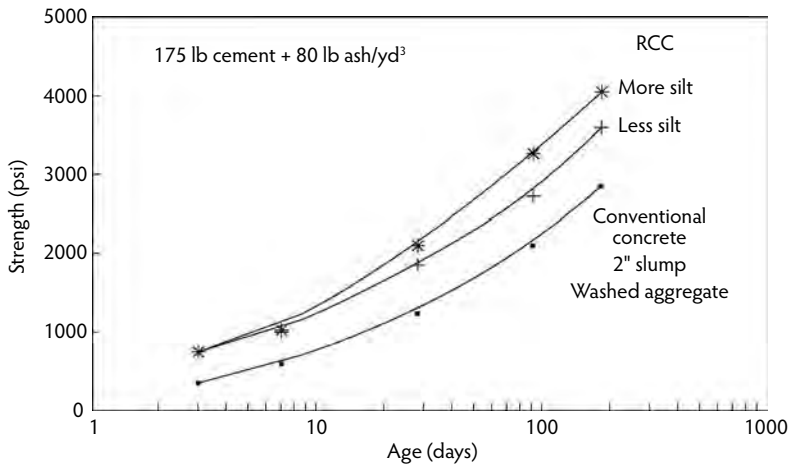


FIGURE 20.20 Effect of fines on strength (Willow Creek Dam).

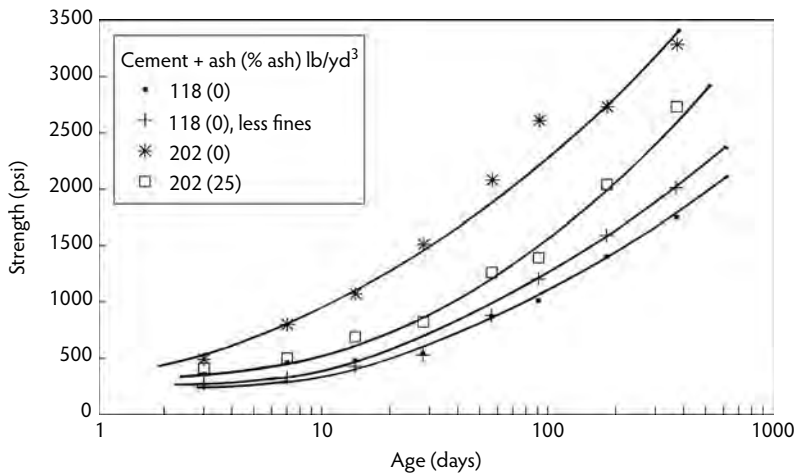


FIGURE 20.21 Effect of fines on compressive strength (Agos Dam).

some degree of pozzolanic strength gain, but it also appears that mechanical benefit is also being provided. Because the fines have substantial surface area and they are used primarily in low cementitious content mixes, the traditional thought that sufficient cementitious material is needed to coat all of the aggregate surfaces obviously does not apply to RCC.

Figure 20.20 shows a case where the addition of fines caused an increase in strength in a medium cementitious content mix. In this situation, the optimum fines content was about 5 to 6%. A slight increase in fines to about 8% resulted in minimal additional strength. At even higher fines contents, the strength could be expected to decrease. The fines were a natural silt with very little plasticity. Figure 20.20 also shows much lower strengths at every age when the aggregate was washed to eliminate all fines, screened to an ideal traditional gradation, and used to make low-slump conventional concrete. Additionally, it shows the strength achieved when the dirty RCC aggregate was washed and sorted to an ideal conventional aggregate gradation. The mix made with this gradation was an excellent quality 2-in. slump mix with a water-reducing admixture. At all ages, the strength of the conventional concrete was substantially less than the RCC concrete made with the same basic aggregate without the expensive washing.

Figure 20.21 shows another project demonstrating nontypical behavior where an increased fines content of a low cementitious content mix caused a slight reduction in strength. The only way this was

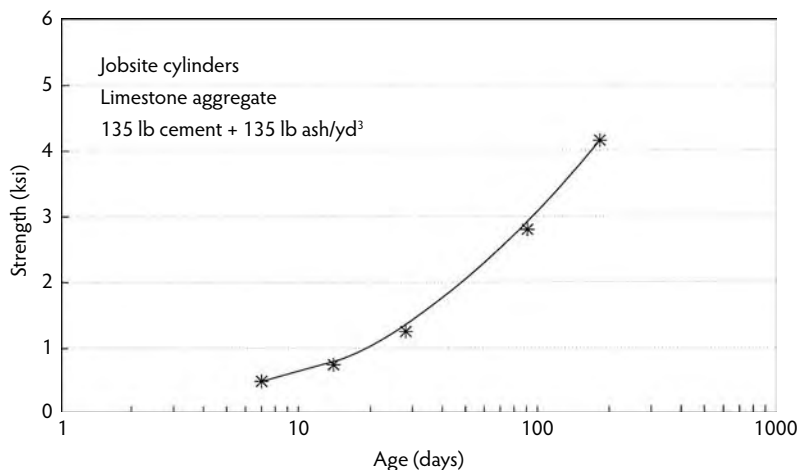


FIGURE 20.22 Compressive strengths (Salt Lick Dam). (Data courtesy of Gannett Fleming Engineers, Harrisburg, PA.)

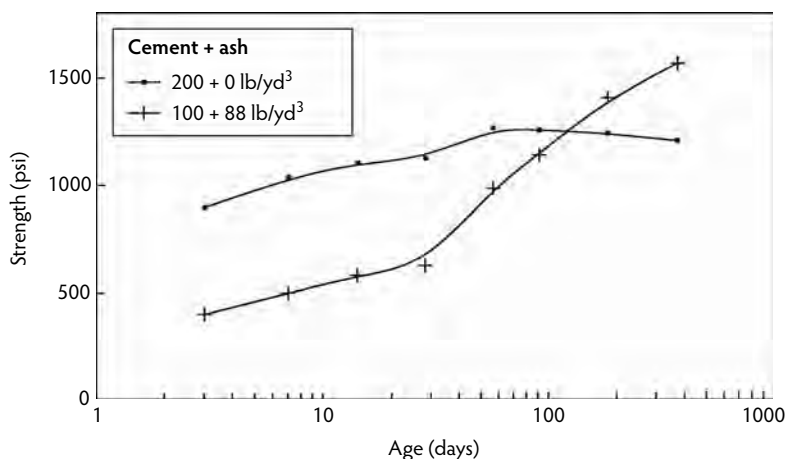


FIGURE 20.23 Strength vs. time (Stagecoach Dam).

detected was by tests. In this case, the fines were siliceous and expected to add substantially to, rather than decrease, the strength. Figure 20.22 shows very good strength gain for a mixture that was used in an application where durability and traditional strength levels of about 4000 psi were important. This was achieved with only 270 lb of cement per cubic yard (135 lb of cement and 135 lb of fly ash). The aggregate was limestone, including the beneficial rock dust which, in the case of limestone, was expected to react somewhat with the siliceous fly ash. Figure 20.23 shows the benefit of fly ash in a low-strength mass RCC made with lower quality aggregates at Stagecoach Dam. In this case, evaluation of the comparative mixtures at ages up to 28 days indicated that fly ash was not beneficial; however, after 28 days the ash performed extremely well, ultimately achieving a strength greater than the mix made with cementitious material that was 100% Portland cement with no ash. In this case, the aggregates were lower quality and the efficiency of the cementitious material was relatively low by RCC standards.

Although Figure 20.22 and Figure 20.23 suggest that fly ash is very beneficial in RCC and can even be better than adding more Portland cement, this is not always the case. Figure 20.21 and Figure 20.24 show mixtures where adding fly ash increased the cost and complexity of the mix while doing essentially nothing for strength. Figure 20.21 shows that when a mix with 202 lb of cement per cubic yard used fly ash for 25% of the cementitious material the strength was reduced by about 25% at all ages, including

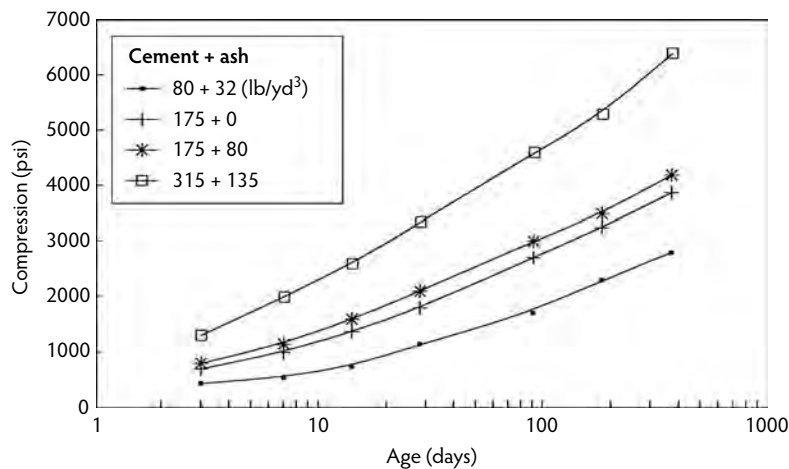


FIGURE 20.24 Strength vs. time (Willow Creek Dam).

the long-term ages up to 1 year. Figure 20.24 indicates that a mix with 175 lb of cement per cubic yard had no significant change in strength when 80 lb of ash per cubic yard was added. In this case, adding silty fines to the mix was found to have the same or better effect as adding fly ash. Figure 20.22 and Figure 20.24 show RCC mixes that achieved relatively high strengths on the order of 4000 and 6000 psi, respectively. This is comparable to very good quality traditional concrete, but the strength was achieved with cementitious contents that are about half that used in traditional concrete. Figure 20.20 through Figure 20.24 represent a wide variety of RCC mixtures, with different aggregate types and gradations, different cementitious and fly ash contents, and different maximum aggregate sizes. In all the examples, the individual data points have been plotted to show that, although the strength gain trends can be different from mix to mix, the strength gain trend for any given RCC mix plots vary predictably with an incredibly small amount of data dispersion. RCC is a reliable engineering material with predictable and dependable properties once a mix design program has been undertaken.

Figure 20.20 through Figure 20.24 plot strength vs. time. Another very useful way to present the data is by plotting strength vs. cementitious content, with different lines representing different ages, as shown in Figure 20.25. From the family of curves shown, the required cementitious content can then be selected

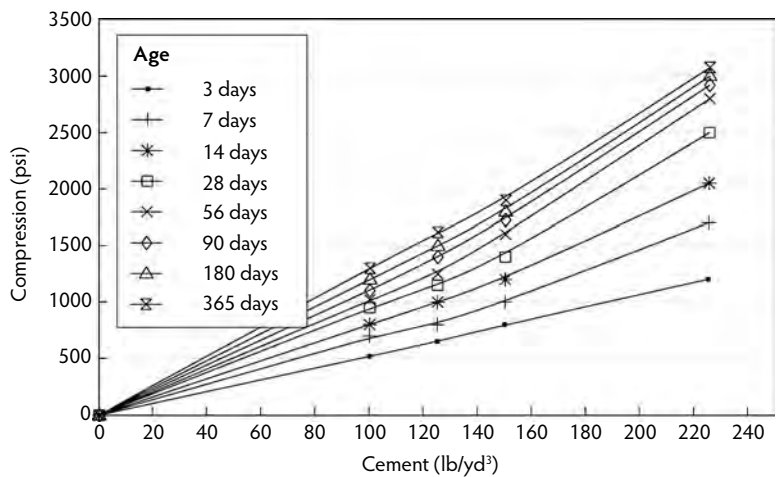


FIGURE 20.25 Compression vs. cement content.

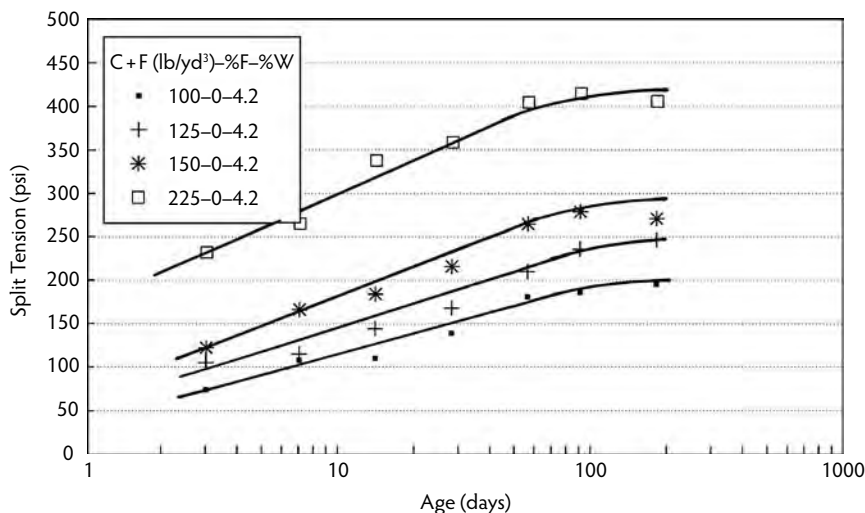


FIGURE 20.26 Split tension vs. time for different cement contents (Big Haynes).

to achieve any strength at any age. The shape of these curves is of particular interest. Figure 20.25 shows a generally linear relationship between strength and cementitious content from 0 to 230 lb of cement per cubic yard; however, other RCC mixes have shown no significant strength gain beyond a certain cementitious content. In other cases, no significant strength was achieved until some minimal amount of cementitious material was used.

The strength data and charts are for projects that range from the start of RCC dams 30 years ago to projects just now being built. Throughout the history of RCC to the present, some projects simply have not benefited from using pozzolan but others have. By relying on an all-encompassing, open-minded approach to mix design studies on both high and low cementitious contents with both high and low pozzolan contents, a project manager can properly evaluate whether or not it is advisable to use pozzolan and how much to use (Schrader, 2004).

20.4.9 Tensile Strength

As with compressive strength, the tensile strength of RCC can vary greatly from mixture to mixture. Cementitious material content is a principal influencing factor, but moisture content and aggregates are also important. Higher cementitious material contents, lower moisture, and crushed coarse aggregates tend to increase tensile strength; however, the tensile *strain* capacity, discussed below, may be more important than the tensile *strength*. A highly deformable mixture with a low elastic modulus can be more desirable than a stronger mixture that is much more brittle and cracks earlier under the same amount of deformation.

The Brazilian split-cylinder test (ASTM C 496) is a simple and economical indirect method of obtaining an indication of the direct tensile strength of concrete. It is frequently used for RCC, but care must be taken when deriving the probable direct tensile strength from indirect split-tension results. This applies to traditional concrete as well, but it is more important for RCC where the relationship of direct to indirect strength can vary from project to project as well as within the range of compressive strengths that might be considered for a particular project. Figure 20.26 and Figure 20.27 show examples of the development of split tensile strength with time for a crushed gneiss aggregate with and without fly ash. The mix designations used in the figures indicate the total amount of cement plus fly ash (in pounds per cubic yard), followed by the percentage of cementitious material that is fly ash, followed by the moisture content as a percentage of the full mix.

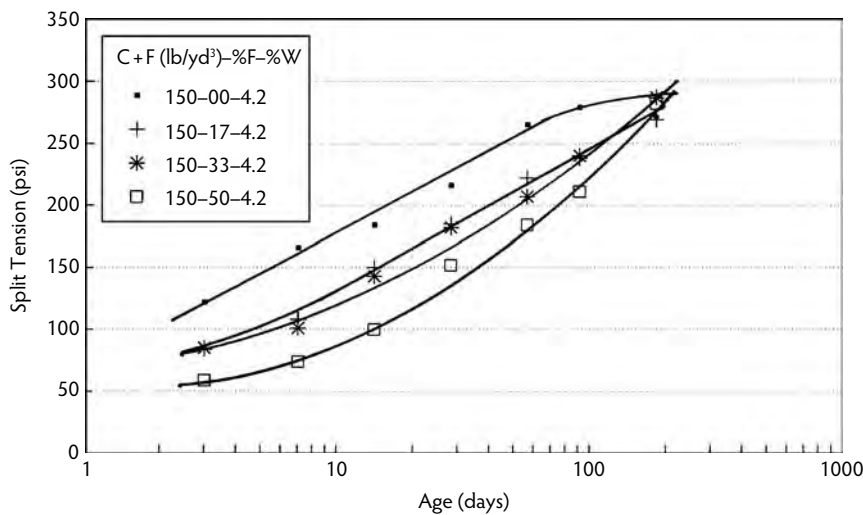


FIGURE 20.27 Split tension vs. percent fly ash (Big Haynes).

The split tensile strength of RCC mixtures with higher cementitious material contents and higher compressive strengths is typically a lower percentage of the compressive strength than what occurs with low-strength mixtures. Some examples of the ratio of split tension to compression strength for various mixes and tests at different projects are 4 to 7% for Upper Stillwater, 7 to 12% for Willow Creek, 9 to 13% for Monksville, 10 to 18%, 13% for Burnett (Paradise), 10 to 18% for Uruguay-I, 12 to 17% for Concepcion, 14 to 15% for Mujib, and 13 to 19% for Middle Fork. These have been listed in order from the highest to lowest average strength.

When converting split tensile strengths to direct tensile strengths, a factor should be taken into account based on the compressive strength. Figure 20.28 shows this factor as a function of the logarithm of the compressive strength (Schrader, 1995b). The factor is almost the same when converting from flexural strengths of beams to direct tensile strength and when converting from split tensile strengths to direct tensile strengths. The factor has recently been updated with additional test data (Schrader et al., 2003a). The factor for a particular compressive strength is multiplied by the split-cylinder strength to obtain the derived direct tensile strength.

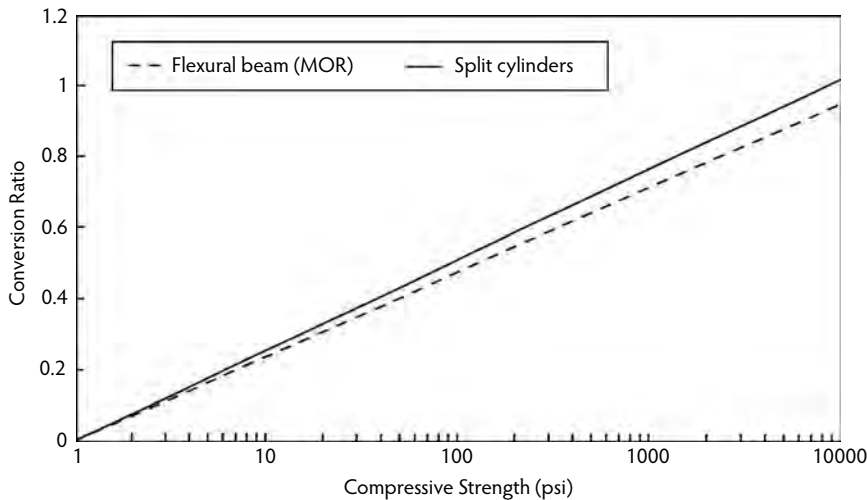


FIGURE 20.28 Tensile strength conversion.

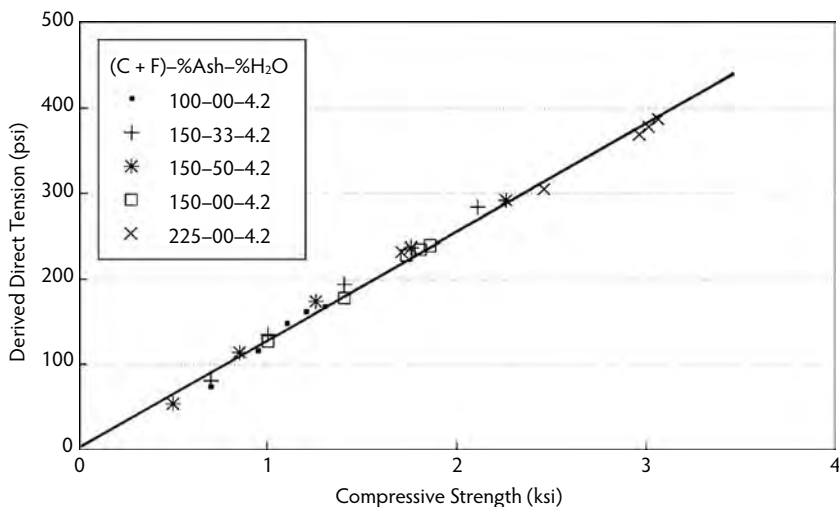


FIGURE 20.29 Derived direct tension vs. compression (Big Haynes).

For metric units in mega-pascals, the updated conversion is:

$$\text{Direct tensile strength} = [0.3 \log(10 \times \text{compressive strength})] \times (\text{split tensile strength})$$

For units in PSI the updated conversion is:

$$\text{Direct tensile strength} = [0.2 \log(\text{compressive strength})] \times (\text{split tensile strength})$$

When all of the adjusting factors are taken into consideration, the final ratio of direct tensile strength to compressive strength typically is nearly a direct linear relationship, as indicated in Figure 20.29.

20.4.10 Modulus of Elasticity

The modulus of elasticity and creep for RCC can have an extraordinary range of values. Mixtures with large amounts of cementitious materials and mixtures made by the water/cementitious materials ratio approach to mixture proportioning usually produce long-term values for the static and sustained elastic modulus and creep similar to conventional mass concrete—namely, modulus values on the order of 3 to 4 million psi and creep values on the order 0.02 to 0.05 ln (time) for loading ages of about 28 to 90 days. Mixtures made with very high pozzolan contents can usually be expected to have lower early-age values of static modulus but higher later-age values.

Low-cementitious-content mixtures can have very low elastic modulus values and high creep rates. The decrease in modulus and increase in creep tends to be exponentially proportional to decreases in strength below about 1500 psi. Each incremental decrease in cement content has much more effect than the previous incremental decrease, but each mixture and aggregate can perform differently. Static modulus values on the order of 0.1 to 1.5 million psi are reasonable for cementitious material contents on the order of 100 to 125 lb/yd³ at ages of 3 to 90 days. Corresponding ultimate values could be on the order of 0.8 to 2.5 million psi. At Burton Gorge Dam, ultimate elastic moduli were on the order of only 0.15 to 0.30 million psi. This was a quality designed into the mixture. It is attributed mostly to the gradation and use of what might normally be considered lower quality aggregates. A deformable concrete was desired to avoid thermal stress and because the foundation condition had a low and varying mass modulus that could not be accurately predefined. Figure 20.30 shows the typical range of the modulus of elasticity for traditional concrete and extreme values that have occurred with RCC. Although it is an extreme example, it is important to note the substantial increase of modulus (increased stiffness) at later ages for the Agos mix studies. This is attributed to the pozzolanic activity of the added fly ash, plus some

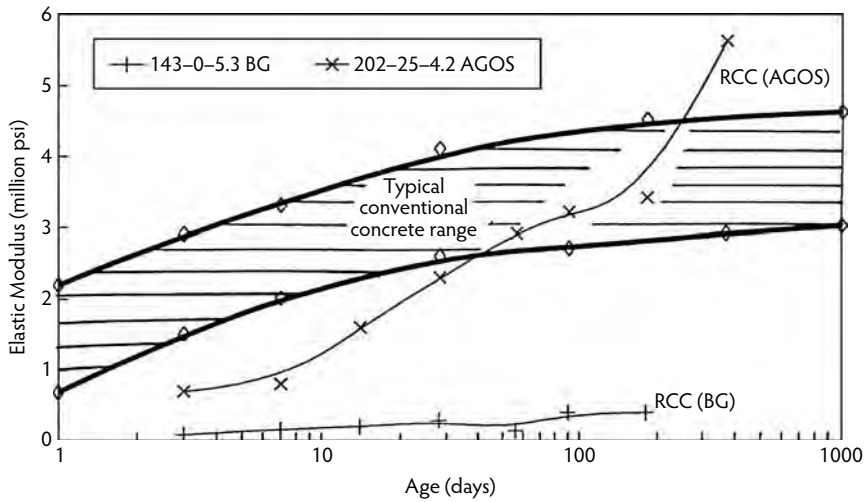


FIGURE 20.30 Modulus of elasticity, typical range.

suspected pozzolanic activity from the natural fines. In this case, a similar increase in strength did not develop; that is, the stiffness increased substantially with time while strength increased at a slower rate. The same occurred for some mixes at the La Miel I project. In both cases, the addition of fly ash caused no noticeable strength gain, although it did cause the RCC to become much more brittle; consequently, the mix in these cases was more susceptible to cracking due to pozzolans.

Figure 20.31 shows the derivation of a new and useful value referred to as the **ultimate modulus**, which is the slope of the secant drawn from the origin to the average peak compressive strength of companion cylinders at failure (Schrader, 1995b; Schrader and Rashed, 2002). It is clear in this typical example that it takes much more deformation and substantial energy to cause the lower strength RCC mixture to fail compared to the higher strength mixture. The mixes were made with identical aggregates and moisture contents and the same source of cement. The only difference was the increased cement content from 100 lb/yd³ to 225 lb/yd³. A lower ultimate modulus is associated with more deformation before cracking.

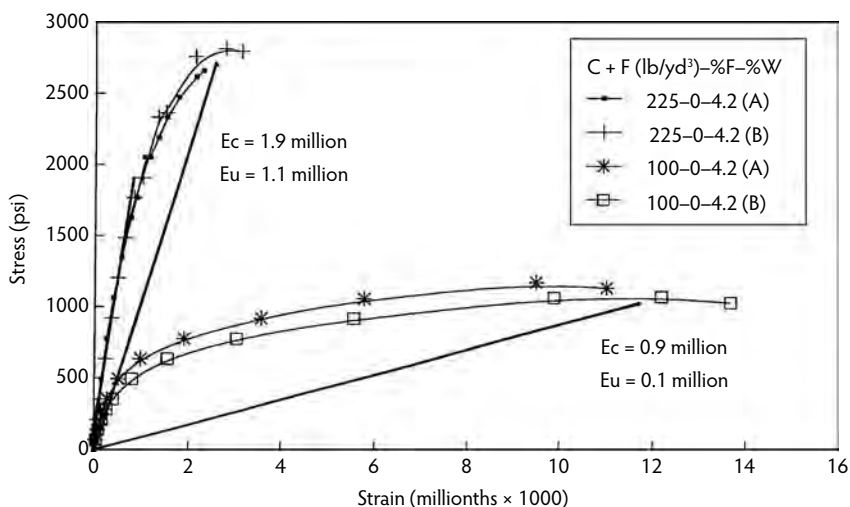


FIGURE 20.31 Modulus of elasticity, elastic and ultimate.

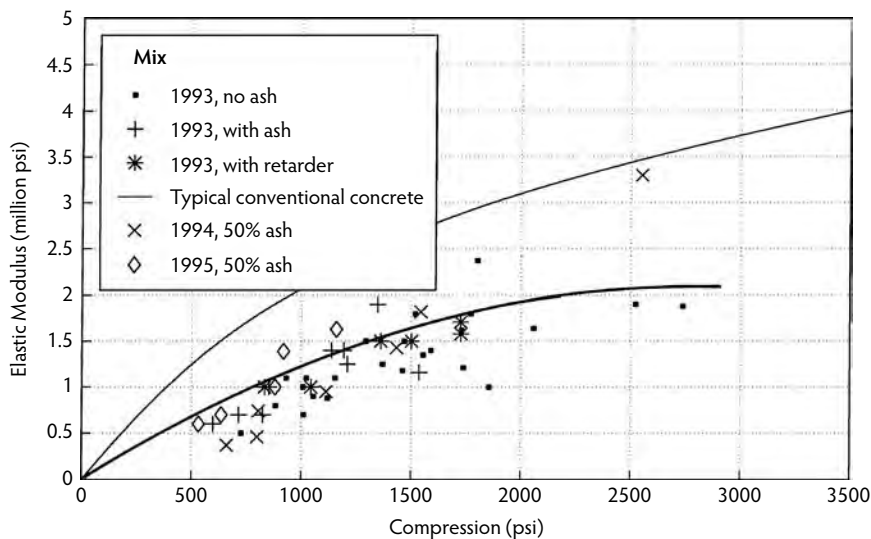


FIGURE 20.32 Elastic modulus at 25% of ultimate load vs. compression.

This is highly desired in a mass structure but may be a detriment in more traditional structures such as bridges. In a cracking analysis of mass concrete, it is the ultimate condition that is critical and that should be studied, not just the elastic condition. As the mix becomes stronger, the elastic and ultimate modulus come closer to the same value, so it is not as important with higher strength mixtures. With lower strength mixtures that are typical of mass placements, using the elastic modulus alone in the cracking analysis can be an extraordinarily conservative approach. The ultimate modulus in compression is a reasonable indicator of the ultimate modulus in tension (Schrader and Rashed, 2002). Figure 20.32 shows the relationship between elastic modulus and compressive strength for a typical RCC mixture with reasonable quality aggregates and about 5% fines. Figure 20.33 shows the relationship between ultimate modulus and compression for the same RCC.

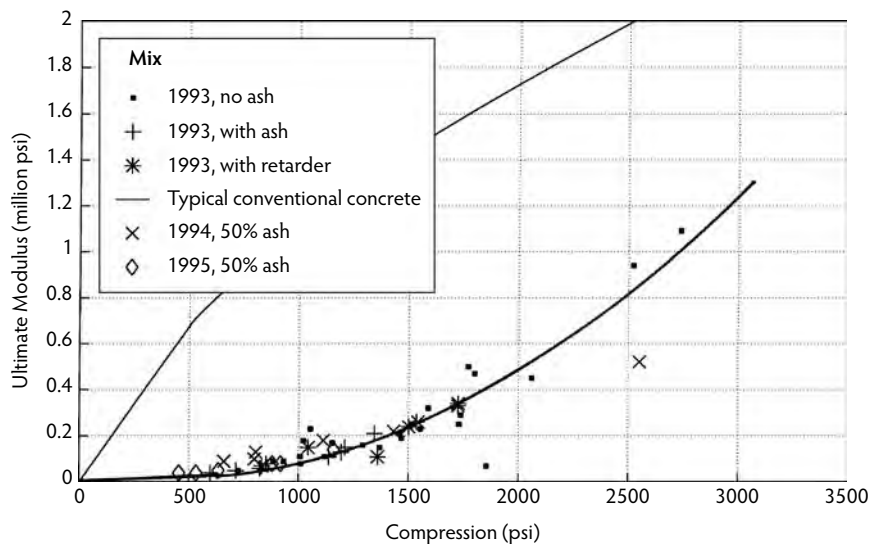


FIGURE 20.33 Ultimate modulus at 100% of ultimate load vs. compression.

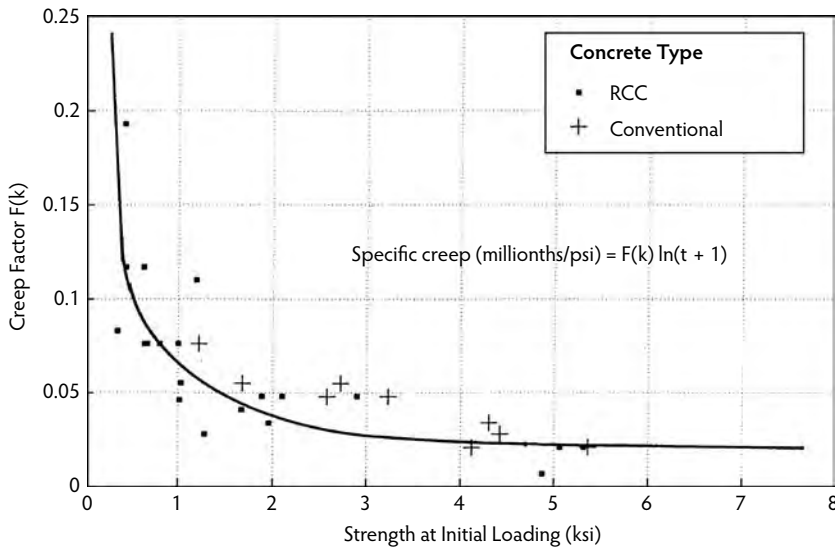


FIGURE 20.34 Specific creep.

20.4.11 Creep

Creep can be thought of in two ways. First, it is the increase in deflection or strain over time due to a sustained load. Second, it is the relaxation of stress over time while maintaining constant deformation or strain. A very high creep rate with associated dramatic reductions in stress over time is possible with low-cementitious-content RCC mixtures. When combined with the initial elastic modulus, creep reduces the **sustained modulus** that is effective over a long time period, thereby improving the crack resistance of massive placements subjected to thermal stresses (Tatro and Schrader, 1992). Figure 20.34 shows the relationship between strength at the time of initial loading and creep. The amount of creep over a selected period of time is the creep factor $F(k)$ multiplied by the natural log of the age in days plus 1 day.

20.4.12 Tensile-Strain Capacity and Toughness

Tensile-strain capacity is related to the modulus of elasticity and tensile strength. Fast-load strain capacities (maximum deformability without apparent cracking) are obtained when the load is applied over a time span of seconds or minutes. However, in dams and other massive structures, the primary concern is for slow-load strain capacity, where the strain due to external forces and internal thermal cooling develops over a long period of time. Because of creep, a dam can usually undergo more deformation without cracking if it is slowly stretched vs. when it is suddenly deformed; therefore, mixtures, with a low elastic modulus during the period of loading and a high creep rate, such as occurs with low-cementitious-material-content RCC mixtures, can have good slow-load strain properties despite low strengths.

Typical slow-load strain capacities for RCC dam mixtures are on the order of about 90 to 150 microstrain ($\text{in./in.} \times 10^{-6}$), but values outside of this range are possible. Each mixture should be evaluated, if not by direct slow-load strain capacity tests then indirectly by extrapolation from static modulus of elasticity and creep studies that can be combined to get a sustained modulus value. The tensile strength divided by the sustained modulus will provide a dependable estimate of the slow-load strain capacity over the period of time in question (Ditchy and Schrader, 1988; Tatro and Schrader, 1992; USACE, 1997). The problem with extrapolation is that it assumes that the creep rate in tension will be similar to compression (as tested). This can be conservative, especially for mixtures that contain a relatively large amount of coarse aggregate. Aggregate-to-aggregate contact can decrease creep in compression.

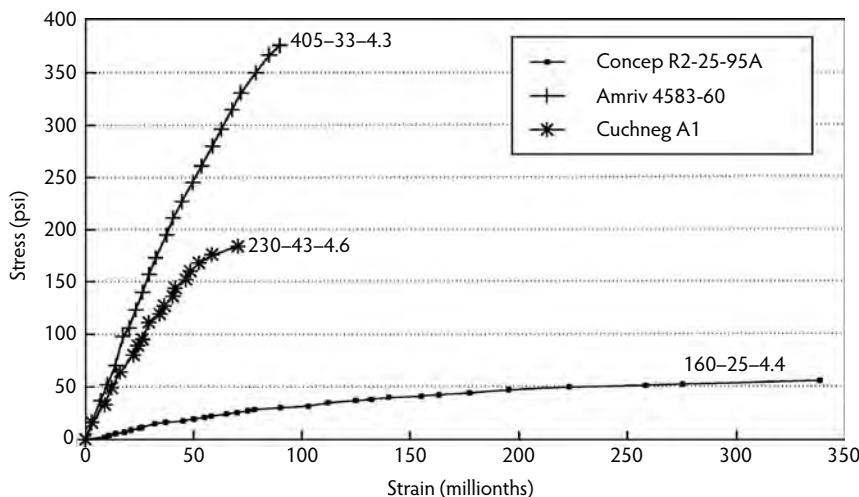


FIGURE 20.35 Tensile-strain capacity and RCC examples.

Because of the low modulus associated with RCC mixtures having lower strength and lower cementitious contents, decreasing rather than increasing the cementitious content and strength of a mixture can actually increase rather than decrease the tensile-strain capacity. This occurs when a decrease in cementitious content results in a greater decrease in modulus than the associated decrease in tensile strength. The ultimate example is the mix that has no cementitious content and insufficient stiffness to define a crack. Obviously, this would also result in an RCC with virtually no strength. Adequate cementitious material is necessary to resist the applied loads, but additional strength does not necessarily mean more crack resistance. Additional strength could result in more cracking. Figure 20.35 is an example of tensile-strain capacity and the tensile modulus of elasticity for mixes with different strengths. The mix numbers next to each tensile stress-strain curve represent the mixture that was used; the first number is the cementitious content, the second number is the percentage of fly ash or pozzolan, and the third number is the moisture content of the fresh mix. In this case, the mix with a cementitious content of 405 lb/yd³ (with 33% of that being fly ash) had a tensile-strain capacity of about 90 millionths of an inch per inch of length. The mix with only 160 lb/yd³ of cementitious material also used a very poor-quality aggregate. Its tensile strength was a low 55 psi, but its tensile-strain capacity was very high at about 340 millionths. The structure built with this mix, Concepcion Dam, has been in service for over 8 years with no cracking or distress. Because of the strain capacity of the mix, it was constructed with no cooling to control thermal stresses and contraction.

A very important consideration with lower-strength RCC mixtures is their demonstrated tensile toughness. This is related to ultimate tensile-strain capacity. Substantial toughness is not apparent in higher strength RCC or most conventional concrete. The indication of substantial toughness in lower strength mixtures is a relatively new discovery being demonstrated with time, experience, and assemblage of data. Such toughness can contribute to considerable benefits in dam performance and should be considered as an influencing factor in new dam designs and analyses. Eventually, it may lead to more efficient and economical dams that consider fracture toughness in the design. Toughness can be thought of as the ability to absorb energy. Another way to consider it is as a material property that results in the need for substantial energy to be added to cause the concrete to fail after it has been stressed beyond its elastic range.

20.4.13 Adiabatic Temperature Rise

Major decisions concerning schedule, cost, construction controls, and cracking potential are based on the expected adiabatic temperature rise of the RCC. This should be determined by careful testing using large samples and an experienced laboratory for any large or critical project. Determinations of adiabatic temperature rise based on calculations from the **heat of hydration** of the cementitious materials and the

properties of the aggregates have been reasonably accurate for some RCC mixes and quite inaccurate for others. There does not appear to be any good indicator of when they will be reliable. The only way to ensure the proper knowledge of potential peak temperatures as well as the rate of temperature rise for RCC is by proper testing of the full mixture with large samples that have a volume on the order of about 10 ft³. Companion tests of the heat of hydration of the cement by itself and the heat of hydration of the cement with pozzolan (if used) are useful for later reference.

A review of adiabatic rise for various RCC projects, typically using Type II moderate-heat cement, shows ranges (in degrees Fahrenheit rise per pound of cementitious material in each cubic yard of RCC) of 0.0 to 0.10°F at 1 day, 0.09 to 0.18°F at 7 day, and 0.13 to 0.21°F at 28 day. The adiabatic rise for RCC mixtures, especially those with large proportions of fly ash should also be determined through later ages of 56 to 90 days or more. The assumption that RCC, and other mass concrete, does not produce heat past an age of 7 or 28 days is simply not correct. Exothermic chemical reactions from hydration continue long term, even through one year. The rate of heat generation decreases with time, but it is still there. Also, the thought that fly ash does not produce heat simply is not correct. Depending on its chemistry and reaction with the cement and aggregate fines, this may be a very small amount of heat, or it may be substantial. Proper detailed tests with site-specific materials are necessary to accurately establish just how much heat is produced and when it is produced. Mixtures with lower cement contents tend to produce higher temperature rises per unit of cement. This is even more evident if pozzolan is included.

20.4.14 Thermal Stress Coefficients

Thermal stress coefficients establish how much internal tensile stress will develop in a given mixture for each degree of temperature drop over a specified period of time, assuming the RCC is restrained. RCC can have a broad range of values depending on the mixture proportions and aggregate. It is influenced by creep, coefficient of thermal expansion, and the elastic modulus. Stronger mixtures typically have much higher stress coefficients. For a time period of 28 to 365 days, typical values for low-strength mixtures (800 to 1800 psi) with low cementitious material contents are on the order of 4 to 6 psi/°F. Higher strength mixtures (2000 to 4000 psi) have stress coefficients on the order of 8 to 14 psi/°F.

20.4.15 Shear Strength and Lift-Joint Quality

The shear strength of an unjointed RCC mass, of RCC containing joints with strengths similar to the mass and of RCC with the principal load normal to the joints will generally be 10 to 20% of the compressive strength for strengths in excess of 2500 psi, about 15 to 25% for strengths on the order of 2000 psi, and about 25 to 30% for strengths on the order of 1000 psi. Lift joints, or the layer-to-layer interfaces, are the weakest part of RCC structures. Special treatments such as a bedding or mortar mix or high cementitious content mixtures can improve this problem considerably, but these techniques are expensive and time consuming. Lift-joint quality as it relates to shear strength is elaborated below; lift-joint quality as it relates to watertightness is discussed in Section 20.4.16.

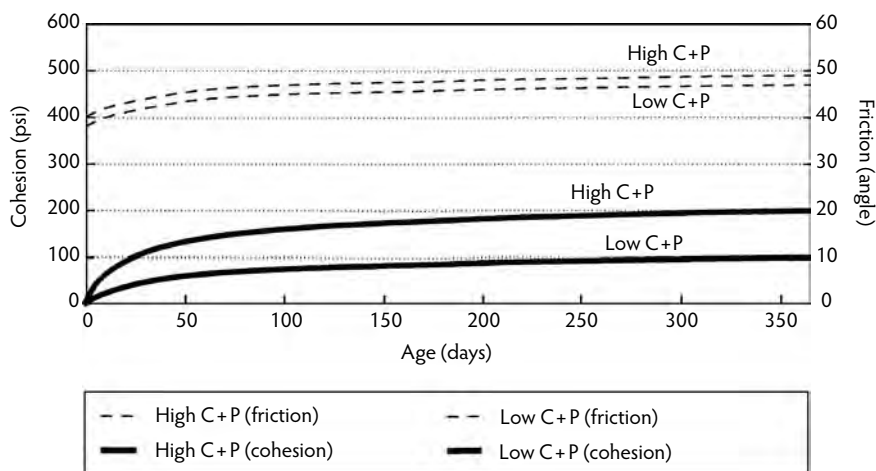
The strength of RCC lift joints is primarily dependent on the consistency of the fresh mixture, aggregate characteristics, degree of compaction at the lift surface, cementitious-material content, maturity of the lift surface when it is covered with the next lift, effectiveness of retarding admixtures, condition of the lift surface, and lift-surface treatments. A detailed procedure for assessing lift-joint quality in the field, taking into account the many factors that affect the probable lift-joint strength, has been developed (Schrader, 1995c,d, 1999a). On the basis of clearly defined criteria, the procedure establishes a numerical value (plus or minus) for each of the following factors that influence the *in situ* shear strength: surface segregation, rain, cure, maturity, surface tightness and condition, surface flatness, method of RCC delivery, and miscellaneous factors. The sum of the numerical points assigned in each category is referred to as the **lift-joint quality index (LJQI)**. The basis of design corresponds to a LJQI of 0.0. Any positive value implies a slight improvement in quality above the basis of design. A negative value indicates a quality less than the basis of design. A graph provided with the procedure indicates the percentage of the design values for **cohesion** and the percentage of the design value for friction that is associated with

various values for the LJQI (Schrader, 1995c,d, Schrader 1999a). As a matter of inspection and field control, the contractor may be penalized for slightly negative but tolerable LJQI work, with a cut-off point at about -4 , below which the structure would not perform acceptably and the work is not accepted.

A wide range of possible RCC joint strengths exists, depending on the mix and the above variables, with extremes ranging from about 0 to 400 psi for cohesion and 30 to 60° for friction angles; for example, one early summary of strengths for 35 tests that included 5 projects, 10 mixtures, 8 joint conditions, and 5 aggregate types demonstrated an average cohesion of 155 psi and a friction angle of 50° (Schrader, 1986). Each project should be carefully examined and preferably tested to determine the shear capacity of its joints. Well-proportioned, dry, low-cementitious-content mixtures with reasonable aggregates and construction controls can be expected to produce friction angles on the order of 45°, with cohesion values on the order of 40 to 110 psi. High cementitious content wetter mixtures typically have similar or slightly lower friction angles and cohesion values that may range from about 110 to 300 psi. The reduction of friction with increasing cementitious contents is usually minimal, but it tends to routinely occur when tested. The residual friction after sliding also seems to decrease for higher cementitious content mixes (Schrader, 1995c,d, 1999a, 2003d). The reason appears to be that the fine paste has less friction than the aggregate that it is replacing.

Substantial testing of lift joints reported for a variety of projects provides useful data for those specific mixtures and conditions (ACI Committee 207.5R, 1999; Boggs and Richardson, 1985; Cannon, 1985; Dolen and Tayabji, 1988; Dunstan, 1981; Gaekel and Schrader, 1992; Hansen and Reinhardt, 1991; McLean and Pierce, 1988; Oberholtzer et al., 1988; Schrader, 1982a,b, 1984, 1986, 1994, 1995b,c,d, 1999a, 2003d; Schrader and Rizzo, 2003; Tayabji and Okamoto, 1987). The most comprehensive series of tests on full-scale samples, with emphasis on shear resistance of cracked or debonded lift joints and residual strength after sliding, was done for the Saluda Dam (Schrader and Rizzo, 2003). Care must be exercised not to use one publication or one set of results that is based on one set of conditions at one project as an absolute basis for what will occur at another project. A general idea can be developed based on a compilation of information from other projects and a knowledge of the mixture and materials proposed for a new project, but absolute values should come from testing the specific mixture and conditions in question.

Every job may have its own peculiarities, but generalized observations typical of most RCC follow: Shear strength increases with age. A wetter consistency at the same cementitious material content can slightly decrease the cohesion. Higher cementitious content mixtures achieve higher potential cohesion, but the friction is essentially unaffected. Lift-joint exposure maturity (exposure time \times surface temperature) is a major influencing factor in lift-joint quality or strength. Figure 20.36 shows the general trend



Typical trends (approximately 25% ash)
Not retarded, Type I joint

FIGURE 20.36 Friction or cohesion, effect of age.

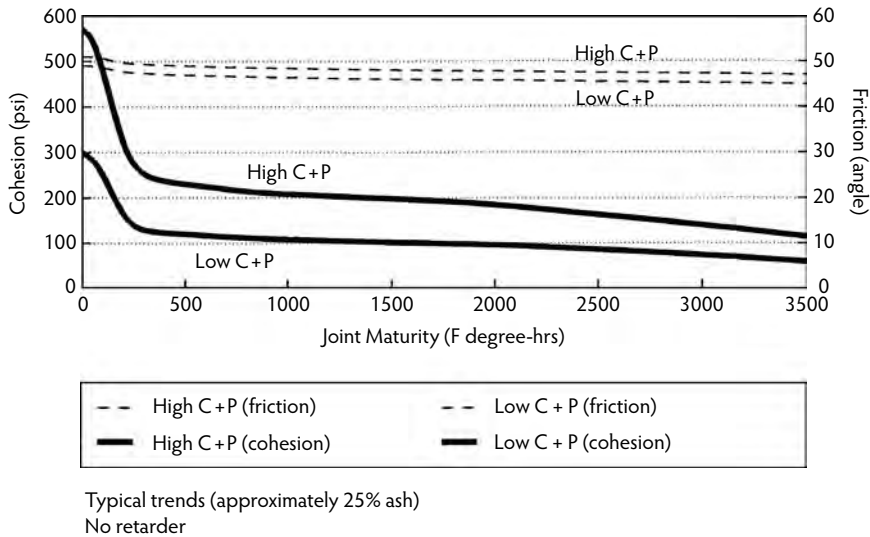


FIGURE 20.37 Friction or cohesion, effect of joint maturity.

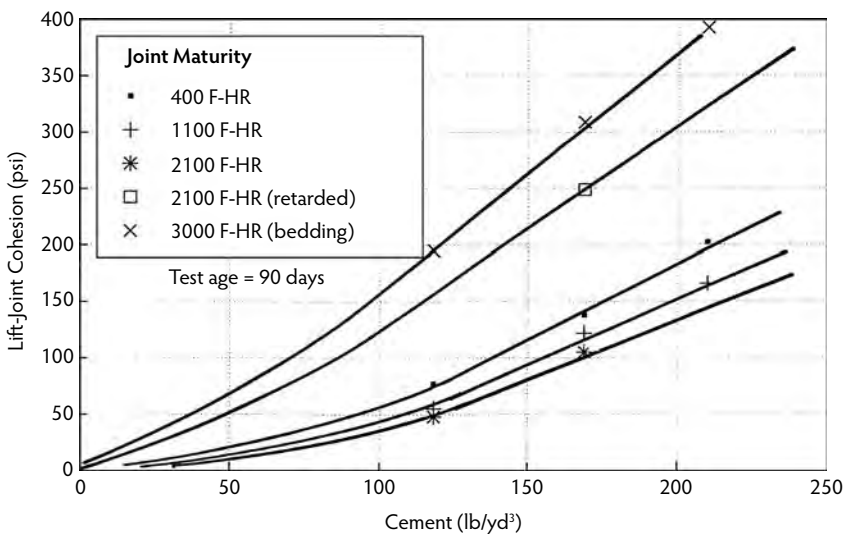


FIGURE 20.38 Miel I lift-joint cohesion vs. cement.

or effect of age on cohesion and friction for mixes with both high and low contents of cement plus pozzolan. Figure 20.37 shows the general trend for lift-joint maturity on cohesion and friction for mixes with both high and low cement and pozzolan content. These figures are intended to show typical or general trends; they should not be used as a basis for design without further consideration for the peculiarities of the RCC specific to each project.

Figure 20.38 is an example of site-specific tests for the Miel I project. The effect of cement content, maturity, admixture, and bedding mix on cohesion is clearly defined for these materials. The mix used only cement, with no fly ash or pozzolan, but it did contain approximately 6% aggregate fines. The bedding mix consisted of a 3/4-in.-thick layer of high-slump traditional concrete with about 45% sand and a high cement content. It was spread just prior to placing the RCC, and the RCC was then compacted over the bedding. Figure 20.39 shows that the friction angle is essentially independent of

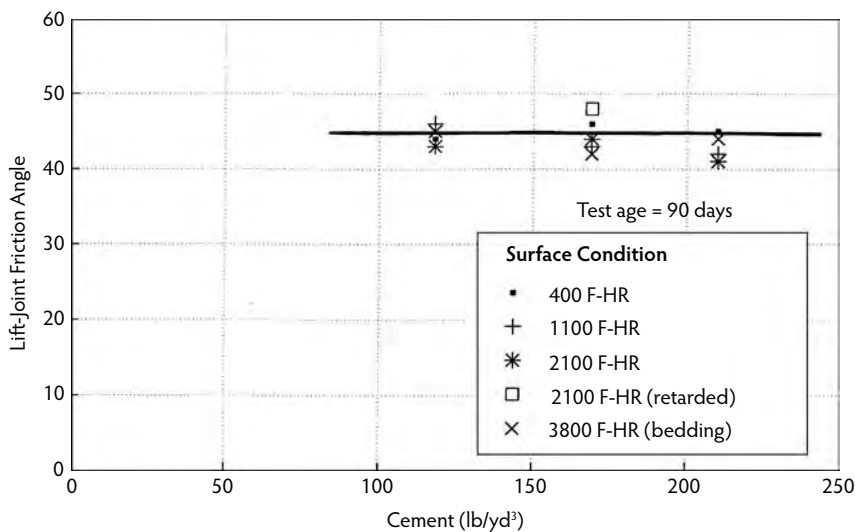


FIGURE 20.39 Miel I lift-joint friction vs. cement.

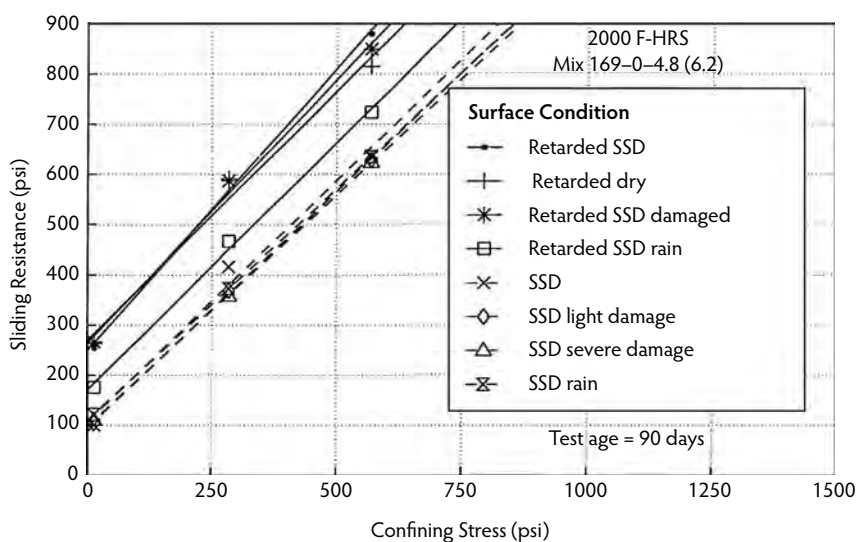


FIGURE 20.40 Miel I lift-joint shear.

maturity, cement content, admixtures, and bedding. It is almost entirely a function of the physical aggregate characteristics.

Figure 20.40 shows a typical plot of total shear stress resistance as a function of the confining stress applied normal to the lift-joint surface. These tests were performed on large blocks saw-cut from the full RCC mix. The mix contained 169 lb/yd³ of cement with no fly ash or pozzolan. It had a relatively dry consistency with 4.8% moisture and 6.2% aggregate fines. A surprising result, similar to those of full-scale tests at other projects with other materials, is that allowing the surface to dry just prior to placing the next layer of RCC had virtually no negative effect on the joint strength. This is contrary to traditional practice for conventional concrete. In the field, allowing the surface to dry just prior to placing the next layer allows efficient and very effective cleaning by blowing the surface with compressed air, thereby achieving an even better joint quality.

20.4.16 Seepage, Permeability, and Watertightness

At the time of early RCC projects, confusion developed concerning permeability and seepage in RCC dams because they were sometimes discussed or presented and compared using data that had a very different basis. Any one, or any combination, of the following was used: pressure tests and water-loss results from drill holes in dams; recordings of seepage collected from drain holes drilled into dams that may or may not have included holes that extended into the foundation or abutments; recordings of discharges from galleries or stilling basins that may have included water from any combination of sources such as foundation drains, drilled drains in the dam, cracks, monolith joints, local runoff, drains in the RCC, and water from construction activities; tests of cores that may or may not have contained joints that may or may not be oriented with or against the flow path; and permeability tests of laboratory prepared cylinders.

Another problem in reporting seepage data is the lack of a full grasp of the details of internal drains, their construction, their purpose, and how they function; for example, the design for the Urugua-I Dam originally had a grid of face drains behind the upstream membrane so seepage through the membrane could be detected and isolated if it occurred. Because of the 100% effectiveness of liner systems at other dams and confidence that the liner would have no seepage, this was deleted from the work. Only a single drain line was installed. It was located behind the membrane, just above the foundation. Seepage from this drain has been reported as being due to membrane seepage when, in the opinion of the designers and those who were responsible for construction, the seepage is primarily due to two other causes and not the membrane. One cause is poor detail where the membrane is connected to the foundation; water comes under the foundation contact and up behind the membrane to the drain. The other cause is seepage through a portion of the abutment that had questionable grouting; water probably came into the abutment and then traveled to the dam, where some of it migrated upstream to the drain line. When seepage is present, it typically diminishes naturally with time for both conventional concrete and RCC dams. The reduction is especially dramatic with low-cementitious-content RCC dams, where seepage is primarily along lift joints. Typical reductions are on the order of about 85 to 95% within about 1 to 2 years.

Unlike low-cementitious-content RCC, which typically experiences initial seepage along lift joints that do not have special treatment, high-cementitious-content RCC behaves similarly to conventional concrete dams, which typically have negligible seepage along the lift joints. As is the case, for example, with Dworshak Dam (conventional mass concrete) and Upper Stillwater Dam (high-cementitious-content RCC), watertightness problems with these types of dams are more related to leaking monolith joints or leaking cracks. Water loss occurs as high flows or leakage concentrations at fewer isolated locations in high-cementitious-content concrete dams, whereas in the lean RCC dams (without watertight facings or special lift treatment) the unit seepage is smaller but the area of seepage is greater. Two years after their respective reservoirs were raised, leakage through one of the cracks at the very high-cementitious-content Upper Stillwater Dam was greater than all of the seepage from all sources, including foundation drains, local runoff, and lift joints at the very low-cementitious-content Willow Creek Dam (it has no monolith joints or through cracks). This is not to say that all high-cementitious-content RCC dams will have cracks and joint seepage nor that all low-cementitious-content RCC dams will have seepage of lift joints. It is meant to point out general differences and where the emphasis should be placed during design for seepage control with different types of mixtures.

Some projects have been designed to allow seepage and let it pass through the structure without being collected or drained away. Seepage in these projects was the most sensible, economical, and appropriate design. Seepage was not a result of a failed design. On the contrary, the design worked. Going back to one of the first RCC dams, the U.S. Army Corps of Engineers' *Willow Creek Design Memorandum* (USACE, 1981) included a discussion of seepage that could be initially anticipated. Performance of the dam has been almost exactly as predicted. The section or mass of the dam was increased as part of the design to offset uplift pressures along lift joints that were allowed to seep without benefit of an internal uplift reduction drain system. The seepage has reduced naturally over time to about 10% of the initial value. Extensive coring soon after construction and again after years of steady seepage has shown no detrimental

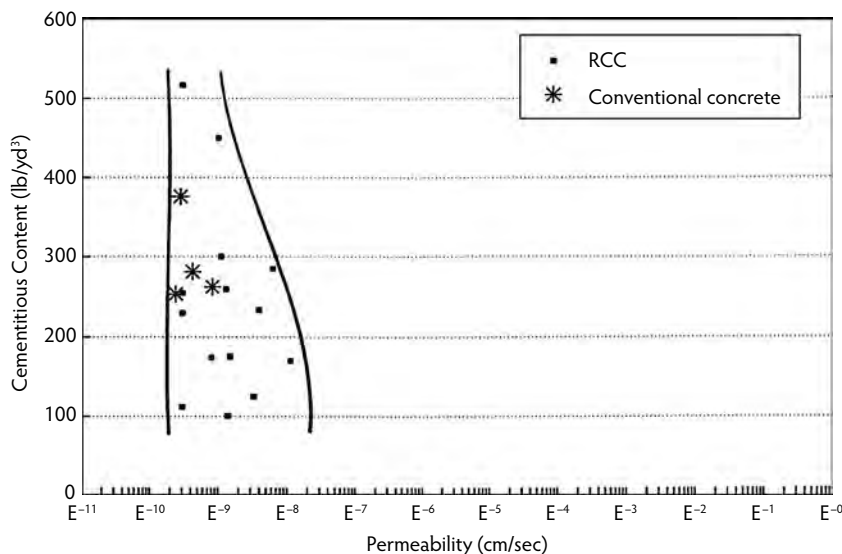


FIGURE 20.41 Sample permeabilities.

effects. This includes tests of joint strength (tension, cohesion, and friction), compression, density, tension, and appearance despite aggressive reservoir water.

Figure 20.41 illustrates essentially no change in RCC permeability (excluding joints) with changing cementitious contents, including very low cementitious contents of only 100 lb/yd³. The data represent the average permeability values primarily for test samples of RCC actually used on completed dams. For comparison, the figure also shows sample permeability values from tests of conventional mass concrete. The results of the latter are similar to RCC. All of the mixtures have permeability values suitable for dam construction. Table 20.9 shows specific average test results for various RCC mixtures listed in ascending order of cementitious-material content. It is clear from comparing the cementitious-material content to the permeability values that no defined relationship exists between cementitious-material content and permeability within the range of 100 to 450 lb/yd³. It is also clear from the table that no defined relationship exists between permeability and the proportion of cementitious material that is pozzolan.

Confusion about seepage can be easily clarified and summarized as follows. Properly designed RCC mixtures all have low permeabilities that are similar to conventional mass concrete, about 1 to 10×10^9

TABLE 20.9 Roller-Compacted Concrete Permeability: Average of Cores

Project	Cement + Pozzolan (lb/yd ³)	Permeability (cm/sec $\times 10^{-9}$)
Urugua-I	101 + 0 = 101	1.4
Willow	80 + 32 = 112	0.3
Zintel	125 + 0 = 125	3.3
Lost Creek	94 + 76 = 170	11.3
Elk Creek	118 + 56 = 174	0.8
Willow	175 + 0 = 175	1.5
Cuchillo Negro	130 + 100 = 230	0.3
Lost Creek	234 + 0 = 234	3.9
Willow	175 + 80 = 255	0.3
Lost Creek	120 + 140 = 260	1.3
Zintel	300 + 0 = 300	1.1
Willow	315 + 135 = 450	1.0
WES	517 + 0 = 517	0.3

cm/sec, regardless of cement and pozzolan content (this statement applies to the compacted mass without joints). A key aspect of properly designed RCC mixtures is that they contain at least 20% by volume of material finer than 75 μm . This includes all materials (water, small air bubbles, pozzolan, admixtures, slag, aggregate fines, and cement). If a low-cementitious-content RCC is made without adding fines to keep the paste volume greater than about 20%, the mixture is poorly proportioned and greater permeability can be expected.

Along with these strong statements about the permeability of unjointed RCC mass, a companion statement is also necessary. If special precautions (such as bedding mixture, upstream membrane, or fast lift placement) are not used, low-cementitious-content RCC dams with a dry consistency will have lift joints that seep. The joints can still achieve good friction and cohesion properties, reasonable tensile strengths, and even look tight, but they will seep. The total quantity of seepage through the joints may be low, but the unit seepage rate along the thin lift joint can be on the order of 1×10^{-3} cm/sec. If this seepage is allowed to penetrate through the dam instead of being intercepted by drains, it may cause uplift and cause the entire mass to look like it is seeping. In numerous applications this condition is tolerable and may be the best overall design, but in other applications special precautions to control seepage or a different type of design are appropriate. If a higher cementitious-content mixture with a wetter consistency is used, lift-joint seepage problems will be similar to those encountered with traditional concrete.

A few clarifications are appropriate. Bedding mixture (a retarded sanded grout or high-slump small-aggregate conventional concrete) will provide watertightness if the bedding mixture extends downstream from the upstream face a distance approximately equal to at least 8% of the hydraulic height above the joint. In the process, the bedding mixture will also provide improved tensile and shear strength. This assumes that the bedding is always placed correctly. In practice, it is reasonable to expect that there will be some less-than-perfect placement of the bedding mixture in any large project; consequently, it is reasonable to assume that some lift joints may have some seepage, just as occurs with traditionally placed mass concrete or high-cementitious-content RCC. This is usually minimal; it can be picked up by drains and will reduce substantially with time. Adding to the width of bedding provides some additional protection, but because of interference with other aspects of the construction it also makes placement of the bedding and achieving good quality more difficult. If total watertightness is desired, regardless of cracks, joints, failed water stops, poor-quality lift joints, or low-cementitious-content mixtures, the impervious upstream membrane system discussed in the next section should be considered.

20.5 Design

20.5.1 General

Efficient RCC designs require balancing considerations including stability of the structure and foundation, stresses from applied loads and dead loads, thermal stresses, construction methods and rates of placement, and mixture proportions including their material properties. Because of the low cost of RCC, the wide range of material properties possible (including properties not possible with conventional concrete), and the ability to use marginal or normally unsuitable materials if necessary, the designer needs to evaluate many more possibilities than would be necessary for conventional concrete. Also, it is necessary to pay more attention to the interrelationship of design with what might otherwise be considered inconsequential decisions with regard to construction. Examples that relate to positioning supports for RCC delivery conveyors and to leveling concrete are discussed in Section 20.6.1. The designer has a more complex task, but he also has greater opportunity to save time and money for the project and maximize the use of available resources and materials.

Roller-compacted concrete has been used for a variety of mass applications. An old example is the base on which structural concrete was placed at the Bellefonte Nuclear Plant, the base on which hydroelectric power plants were constructed at the Tarbela project, and the base under a number of large spillways. Other examples of mass applications are large buttresses or supporting walls for potentially large landslides, as was done along flood channels in El Paso and as was done for the mountainside at

the Platanovryssi Dam. Still other mass applications involve erosion protection for enormous plunge pools and stilling basins that would otherwise erode from extreme water flows at both low and high velocity (Schrader and Stefanakos, 1995). The most complex massive RCC structures, and the most common applications, are dams. The remainder of this section on design concentrates on RCC dams, but much of the content applies to other massive applications such as walls and buttresses.

Foundations that are suitable for traditional concrete dams and massive structures are also suitable for RCC dams and massive structures; however, RCC can also use foundations that would normally not be considered acceptable for concrete structures. Because RCC is less expensive than conventional concrete, it is often possible to widen the base or foundation and contact area to reduce bearing pressure and provide added sliding stability. Also, by using a low-modulus RCC, irregularities in geometry and properties of the underlying materials can often be tolerated. A detailed discussion of foundation issues as they relate to RCC is beyond the scope of this chapter, but the topic is well discussed in the literature (Schrader, 2006a,b). Some examples of RCC dams on otherwise unacceptable foundations are Conception, Big Haynes, Burton Gorge, Rompepicos, and Buckhorn (Giovagnoli et al., 1991, 1992; Schrader, 1999b, 2002, 2006a,b; Schrader and Bali, 2003).

Structural design of RCC dams uses the same basic criteria and procedures used for conventional concrete dams. After the RCC has hardened in place, it is concrete. The concrete is just placed by a more efficient method than has historically been used, and it may have a design section and material properties that are outside the normal range of conventionally placed concrete structures. These attributes, plus the rapid rate of placement and the minimization or elimination of monolith joints, may require a more in-depth study of the structure. General discussions of structural design of RCC dams can be found in ACI Committee 207 (1989), Jansen (1989) and the U.S. Army Corps of Engineers (1995). Stress analysis of RCC dams, with specific example, has been published by Schrader and Rashed (2002). Recent developments have allowed for three-dimensional analyses of RCC structures that simultaneously consider time-dependent material properties, stress-dependent material properties such as the modulus, different mixes used at different locations in the structure, different times of placement for each layer or group of RCC layers, time-dependent development of thermal stresses, dead and applied loads, and seismic loads (Angulo et al., 1995).

As discussed in Section 20.4.10, RCC mixes can have substantial strain softening. The modulus (stiffness) typically decreases at high levels of loading. This phenomenon begins to occur at stresses as low as about 25% of the ultimate strength for lower cementitious content mixes, whereas it may not be seen until greater levels of load at about 75% of ultimate strength for higher cementitious content mixes. As discussed in Section 20.4.10, the reduction in stiffness can be substantial. This can be very advantageous to RCC dams, and it should be taken into account during design. It can cause localized areas of high stress, such as at the toe and heel of a dam, to redistribute much of the load to adjacent areas of lower stress, thereby reducing what would otherwise be higher peak stresses. This phenomenon can be evaluated using a software program or analysis method that allows the nonlinear stress-strain behavior associated with strain softening to be defined as part of the input. Another way to do this is by using an iterative process that first determines the stresses without strain softening. Then, based on stresses from the first iteration, the modulus is adjusted downward for areas of higher stress, using the actual secant modulus for that area and level of stress. The process is repeated. Usually about four iterations are required before the stresses and associated modulus values are balanced and the true stress distribution evolves (Schrader and Rashed, 2002).

Design should also consider probable uplift and its distribution within the dam. The main issue is uplift pressure due to seepage along lift joints. If seepage can migrate along lift joints to the downstream face but not exit or escape at the face—for example, due to a continuous conventional reinforced concrete face slab at a spillway—then allowance must be made for this trapped uplift or drains will be required under the slab to relieve the pressure.

Seepage and uplift can be reduced at the upstream face by improved lift-joint quality, either by providing a better mix with better binding characteristics or by adding a bedding mix between layers. In theory, this will prevent uplift, but in practice there still will be at least a few lift joints that allow seepage.

Unlike conventional mass concrete, which generally has about 1 lift joint per 2 m of height and special attention is given to every lift joint, RCC typically has about 7 lift joints per 2 m of height, and less time is available to ensure that each joint is carefully cleaned. Consequently, the lift joints typically receive less attention and treatment than do conventional concrete dams, there are many more joints, and there is a greater likelihood of a seeping lift joint regardless of the type of mix and treatment. In addition, even the best of conventional concrete dams usually have the occasional lift joint with seepage. Because the locations where this might occur are not known, uplift should be considered at each joint.

Uplift reduction (usually taken to be $2/3$) can be accomplished at a series of drilled drains within the dam, as is done in conventional concrete. As discussed in Section 20.5.4, a common and reliable method of providing watertightness and uplift reduction immediately at the upstream face is to use an impervious upstream synthetic membrane or a properly designed concrete facing, with integral face drains immediately behind the membrane (Scuero and Vaschetti, 2003). Until a reliable track record of field performance under many conditions was established, earlier designs considered that the membrane or facing would provide effective watertightness but that some seepage and resulting uplift could still develop. Based on excellent performance and the concept in the U.S. Army Corps of Engineers manual (USACE, 1995), which suggests that watertightness and uplift assumptions should be based on the site-specific procedure being used and its performance, recent practice has been to consider a proper membrane system to provide essentially total uplift control at the upstream face, providing that it also has a drain system to relieve pressure from any small penetrations that may develop. A conservative design approach is to allow 50 to 75% uplift reduction at the upstream face, with an additional $2/3$ reduction at the drilled drains (if used). The impact of this uplift reduction on stresses and the required strength can be very significant (Schrader and Rashed, 2002).

Roller-compacted concrete dams have been constructed with axes that are straight or curved, with two intersecting straight axes, and with a combination of a curved axis with straight tangent axes. Both vertical and sloped upstream faces have been used. The downstream face can be vertical or at any slope. Within a given section, the downstream slope can be infinitely adjusted, curved, or parabolically shaped. Extensions of the toe, deeper excavations, and keys have been used to provide stability over poor rock and bad foundation conditions. RCC dams can be any height, ranging, for example, from 6 ft (Ferris) to 25 ft (Kerrville), 47 ft (Winchester), 125 ft (Copperfield), 160 ft (Monksville), 170 ft (Aulouz), 210 ft (Concepcion), 270 ft (Urugua-I), 300 ft (Trigomil, Rompepicos, and many others), 620 ft (Miel I), 660 ft (Longtan), and approximately 900 ft (Diamer Basah). The primary areas requiring special attention in RCC dams are overdesign strength requirements for variability, design section options, upstream and downstream facings (facings apply also to rooms in RCC masses, facings of RCC walls, and other non-dam applications), and thermal stresses.

20.5.2 Overdesign Strength Requirements

Overdesign average strength requirements for variability are required by most codes for general conventional concrete construction. Sometimes the overdesign is achieved through an arbitrary extra factor of safety applied to the required design strength, but, more appropriately, specific statistical procedures such as those outlined by the American Society for Testing and Materials (ASTM) or the American Concrete Institute (ACI) are used. European practice accomplishes the same thing as ASTM and ACI by using a specified characteristic strength, which is the strength below which not more than a certain percentage of individual strength tests is allowed. Until recently, it was not common to apply these statistical procedures to dam construction. In the earlier days of concrete dam design and construction, various arbitrary methods were employed to provide a reasonable overdesign in dams, or only an average strength was used and nothing was done for overdesign that accounted for variability.

Overdesign is an increase in the average strength requirement to account for the fact that not all cylinders will test at exactly the design strength level. Some will be higher and some will probably be lower. The overdesign factor is a method of limiting the probable number of low strengths to acceptable levels. Special care is necessary when applying overdesign factors in mass concrete, including RCC, because any extra cement used to increase the average strength may result in an unacceptable increase

in thermal stresses as well as cooling costs. Also, in high-production RCC where the results of final long-term cylinder tests are not available until the structure is essentially complete, testing of variability in the fresh mixture being placed has developed as a practical method of immediate control rather than using cylinder strengths, which are more for a matter of historical record. The overdesign requirement and its early application to RCC dams are discussed in the early literature (Schrader, 1987). Current recommendations and practice are discussed in detail in recent literature (Schrader, 2007).

Current practice for structural concrete (e.g., in an important beam or column) is to require an average strength sufficiently high so more than a limited number of test samples (typically 1, 5, or 9%) fall below the design strength. ACI Report 214R (ACI Committee 214, 2002) allows different percentages to be used based on the criticality of the incidence of an area of low strength in the structure. Using ACI 214R guidance, traditional accepted practice for mass concrete dams, and a sensible approach, it is reasonable to require the average strength of mass concrete to be sufficiently above the design strength to statistically ensure that not more than 20% of the test samples will fall below the design value. This makes good sense because an area of low strength that represents, for example, 20% of a lift or placement will not normally have a critical impact. Mass concrete dams are typically designed to have a factor of safety of about 3 built into the stress analysis, so being 20% below the design strength is still about 2.5 times more than the applied stress for the normal load condition. More importantly, stresses in an area of low strength (or a void with no strength) will redistribute around that area to adjacent areas of higher strength.

The importance of taking a reasonable approach to overdesign for variability in mass concrete, including RCC, is often overlooked. Requiring a higher average strength requires using additional cementitious materials. Doing so increases costs, but, more importantly, it also increases heat, thermal stress, stiffness of the mix (modulus), and therefore thermal cracking stresses. Arbitrarily increasing the average strength may seem like it would result in a better dam, but the reality is that it can result in a more expensive dam that cracks, rather than a less expensive dam with adequate strength that does not crack.

20.5.3 Design Section Options

Design sections and facing options for large and small RCC dams are summarized in the literature (Schrader, 1993). The variety of basic cross-section options that are generally available for RCC dams are shown in Figure 20.42 and Figure 20.43. The same options could be applied to conventional concrete, but the cost and construction methods used in conventional construction make most of them impractical. Figure 20.42 is a typical section for a low dam or a dam on a gravel foundation. The extra effort and costs required for a formed vertical upstream face usually are not worth the effort in a low RCC dam. It is easier, less expensive, and faster to simply overbuild the dam at the upstream face without forms. In addition to simpler construction, the extra mass provides additional safety within the RCC and may allow less stringent specifications or inspection. It may also justify using mix designs based on the designers' judgment without prior testing and local pit-run aggregate.

Compressive and shear stresses in a low RCC dam are so small they are almost meaningless. If the structure is subjected to overtopping, a reasonable level of bond between the top lift joints is necessary. This can be accomplished by applying a bedding mix between the top several RCC layers. Cement contents for very small dams are usually dictated by exposure conditions, mix workability, gradation of the available

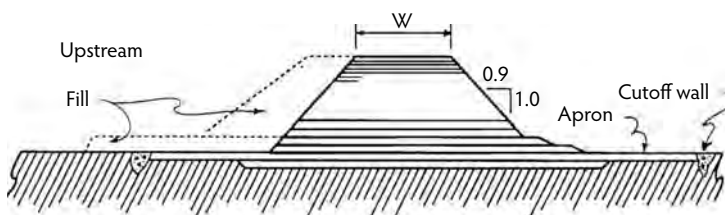


FIGURE 20.42 Small dam section options.

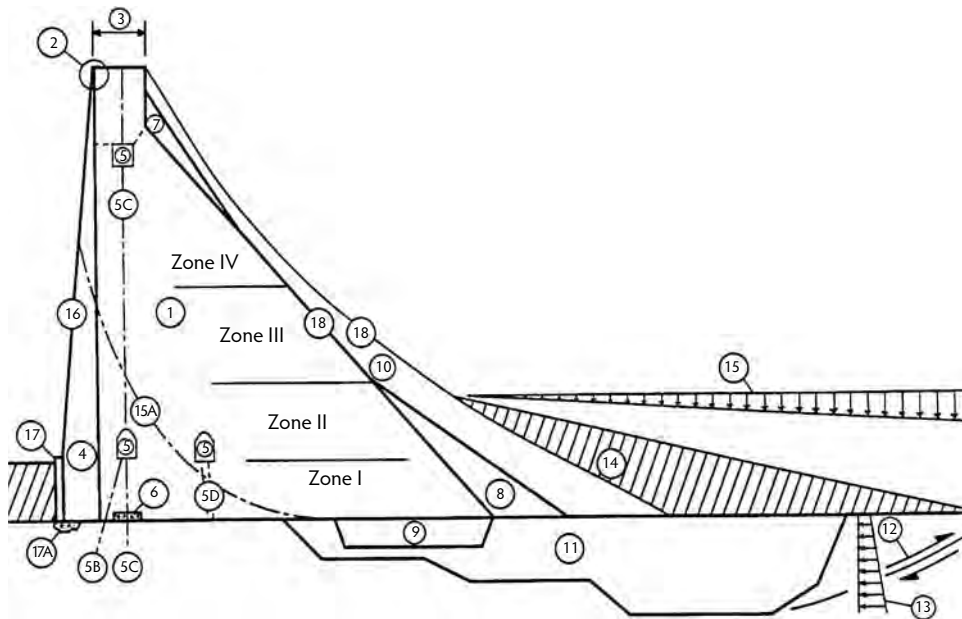


FIGURE 20.43 Large dam section options.

aggregate, quality of the mixing equipment, and degree of inspection. Small dams that may require a cement content on the order of only 50 lb/yd³ for structural loads should have higher cement contents, usually on the order of 150 to 300 lb/yd³, to account for these factors. For small dams with volumes on the order of several thousand cubic yards, the cost for the extra cement is insignificant. Extra cement is helpful when placing in cold weather due to the heat it generates. Thermal cracking in a structure of this size and shape normally is not a structural problem. When necessary, watertightness can be provided by using fast construction, a high-cementitious-content wet-mix consistency, an upstream membrane, or a bedding mix between layers at the upstream face. Some structures do not require watertightness.

A downstream slope of 0.9:1.0 (0.9 horizontal distance to 1.0 vertical distance) or flatter is suggested for low dams because it is easy to build with any RCC mix. The extra RCC material involved is negligible. The top width should be selected as the minimum that allows reasonable construction with equipment typical of small projects. The contractor should be allowed to overbuild for his convenience at no additional cost to the owner. A suggested absolute minimum width is 12 ft. Two concerns are required access (if any) after construction and minimum widths for compliance with applicable safety regulations. Fill material can be used at the upstream (or downstream) face of the dam to steepen the slope, narrow the top width of RCC, and save volume if this becomes economical or if the topography requires it. When placed at the downstream face, the fill hides minor seepage and protects the RCC from exposure. If impervious fill is used at the upstream face, it can provide improved watertightness. When fill is used to steepen the RCC slopes of a dam on a non-rock foundation, consideration should be given to the increase in bearing pressure and sliding that will result at the base of the dam.

Small RCC dams on pervious foundations may require a cutoff or grouting for foundation stability or seepage control, but usually it is faster, less expensive, and easier to spread the foundation of the dam out through wider lower lifts and to use apron slabs of RCC. Settlement studies and a slab/beam analysis of the lower lifts establish how far the extension can go without the slab or apron breaking off. The flow path will also influence the apron width. A simple cutoff wall placed into an excavation without forms is recommended. The downstream cutoff and apron normally should have drain holes.

Figure 20.43 illustrates many of the options or variations for a typical gravity dam section that are practical with RCC for larger projects. Variations and options are labeled 1 through 17 in the figure. The basic gravity section with a vertical upstream face, constant downstream slope, and a vertical downstream

face at the top of the dam has been used for many RCC dams; however, the low cost of RCC often makes it reasonable to flatten the downstream slope and add more mass than conventional concrete allows. This reduces foundation stress, RCC strength requirements, and lift-joint concerns. Reductions in cement content with related reductions in unit cost and in thermal stresses result. The possibility of using higher cementitious contents with higher strengths should also be investigated if the thermal stresses can be tolerated and the volume reduction offsets the increase in costs due to higher unit costs of the RCC. Influencing factors are the length of diversion, the cost and availability of cement and pozzolan, the quality and production costs of the aggregates, and foundation quality.

A parapet wall (2) can reduce costs by reducing the quantity of RCC. The wall can also act as a personnel barrier and curb. Added height, or *freeboard*, for overtopping waves is not necessary with RCC. Also, by curving the top of the parapet outward, it can return waves by directing them back to the reservoir. The wall can be a continuation of upstream precast panels if that option is used to form the upstream face of the dam. A breakaway parapet (fuse plug) designed to fail during overtopping can be designed. One reason to do this is so water flows over one side of the dam while any downstream powerhouse or access road on the other side remains protected.

The width of the dam (3) should be established after considering a number of factors, such as the cost of additional RCC and downstream vertical facing; the required (not just “nice to have”) width for access during operation and construction; inertia (seismic loading) of the laterally unsupported top section of the dam; the effect of the mass on sliding stability due to the added confining load; the effect of the mass on the location of the resultant force for the entire section; the distribution of foundation stresses; and the possibility of causing tensile stress across downstream lift joints for a high dam in the reservoir empty condition.

Adding mass and width to the dam at the base by using a sloped upstream face (4) may efficiently improve stability. An extra benefit is the downward vertical component of the reservoir load on the horizontal projection of the dam face. A condition to check is whether this causes tensile forces to develop or to become unacceptable at the upstream face in both the foundation and lower RCC lifts. Slopes up to about 0.10 (H):1.00 (V) can be practically built in most RCC dams without noticeable effect on the cost, schedule, or construction practicality.

Tension at the upstream face of both RCC and conventional concrete gravity sections is a controversial issue. Each project should be evaluated for its own set of conditions. What may be acceptable for one location and type of mix may be unacceptable for a different location or mix. The majority of designers and regulating codes in most countries consider that gravity sections should have little or no tension at the upstream face in the normal reservoir or normal operating condition. Minor tension is occasionally allowed for severe flood conditions; however, it is reasonable to provide high-cementitious-content mixes or bedding mixes across lift joints near the upstream face to accommodate the need for small but sustained tensile stresses on the order of a few percent of the compressive strength for the normal operating condition, if this is necessary to achieve an economical design in high dams. Allowing for softening of the foundation with a lower tensile mass modulus at the heel of the dam will also reduce this tensile stress. It is reasonable to allow minor tensile stress for flood conditions at isolated areas of good inspection or special construction treatment when necessary. For seismic conditions, tensile stress is usually unavoidable and allowed up to 150% of the expected static tensile strength to account for the increased tensile strength under very fast loading. This increase is referred as the *dynamic increase factor* (DIF). With this allowed stress, a factor of safety just greater than 1.0 is typically accepted under earthquake conditions, with higher factors of safety for flood and normal load conditions. Table 20.10 provides a simplified summary of the required safety factors and allowed stresses for various load conditions under different code or agency requirements.

Galleries (5) in RCC dams should be minimized. There has been a tendency to extend galleries beyond where they are actually needed. This causes higher costs, slower production, and lower overall RCC quality. In large open areas, such as at the base of a high dam section, galleries typically slow production by about 15% for the uncemented fill method of construction. Conventional forming slows production even more. In the upper portions of the dam, where there is less room, the decrease in production at the area of a gallery can be 50% or more, and the quality of placement may decline significantly. Where

TABLE 20.10 Concrete Dam Factor of Safety Examples

Agency	Usual		Unusual		Extreme	
<i>Sliding within the dam and at the foundation contact</i>						
Corps (1995)	2.0		1.7		1.3	
USBR	3.0		2.0		1.0	
FERC (general)	3.0		2.0		1.10	
FERC (low hazard)	2.0		1.25		1.0	
DIN/DVWK	—		1.35		1.2	
<i>Sliding within the foundation</i>						
Corps (limit equilibrium)	2.0		1.7		1.3	
USBR (shear friction)	4.0		2.7		1.3	
USBR (small dams)	4.0		—		1.5	
USBR (small, minimal risk)	2		—		1.25	
FERC (general)	3.0		2.0		1.0	
FERC (low hazard)	2.0		1.25		1.0	
DIN/DVWK	2.0		1.5		1.2	
<i>Resultant location at base</i>						
Corps (1995)	Middle 1/3		Middle 1/2		Within base	
USBR	Middle 1/3		Middle 1/3		Within base	
FERC (general)	Middle 1/3		Middle 1/3		Middle 1/2	
DIN/DVWK	Middle 1/3		Middle 1/2		Within base	
<i>Maximum stress within the dam</i>						
	Comp.	Tension	Comp.	Tension	Comp.	Tension
Corps (1995)	$0.3f'_c$	0	$0.5f'_c$	$0.6f_c'^{2/3}$	$0.9f_c$	$1.5f_c'^{2/3}$
USBR ^a	$0.33f'_c$	— ^a	$0.5f'_c$	— ^a	$1.0f_c$	— ^a
FERC (general)	$0.33f'_c$	$0.10f'_c$	$0.5f'_c$	$0.10f'_c$	$1.0f_c$	$0.10f'_c$
FERC (low hazard)	$0.5f'_c$	$0.10f'_c$	$0.8f'_c$	$0.10f'_c$	$1.0f_c$	$0.10f'_c$
DIN/DVWK	—	0	—	Yes		Yes
<i>Maximum stress at the foundation contact</i>						
Corps (1995)	Allowable bearing	—	Allowable bearing	—	$1.33 \times$ allowable bearing	—
USBR factor of safety (FS) ^a	4.0	—	2.7	—	1.3	—
FERC (general)	$0.33 \times$ ultimate bearing	0	$0.5 \times$ ultimate bearing	0	Ultimate bearing	0
FERC (low hazard)	$0.5 \times$ ultimate bearing	0	$0.8 \times$ ultimate bearing	0	Ultimate bearing	0
DIN/DVWK	—	0	May open	—	May open	—

^a Maximum $f'_c < 1500$ psi (usual) < 2250 psi (unusual). USBR allows f'_t and allows cracked sections for extreme load.

Note: The information shown applies to general conditions. Exceptions may apply or be allowed for special conditions based on the amount of investigation, field conditions, extent of analysis or design, hazard potential or risk, and whether the dam is new or existing. Corps, U.S. Army Corps of Engineers; DIN/DVWK, European standards; FERC, Federal Energy Regulatory Commission; USBR, U.S. Bureau of Reclamation.

a gallery is actually needed high in a dam for uplift, an open graded rock drain of coarse aggregate should be considered (6). If placed about four lifts high, it is possible to excavate the drain for access if necessary in the future. The vertical distance between galleries is usually determined by the accuracy with which equipment can drill from the floor of the top gallery to intersect the roof of the gallery below. This typically is about 100 feet for a gallery 6 feet wide, using rotary percussion drilling equipment operating from the floor of the upper gallery. In addition to interfering with construction, a gallery high up in a dam can also be a point of weakness in a seismic event (7). Designers of low- and medium-height dams

should consider simply overbuilding the dam enough so galleries and drains are not even necessary. The unit cost of the RCC decreases, and construction, operation, and maintenance are simplified. An example of this is Winchester Dam. Using a bedding mix between lifts or a high-cementitious-content RCC is suggested upstream of galleries and between the first three layers in the area above and below the gallery floor and ceiling. This provides watertightness, bond against uplift below the floor, and added sliding resistance against reservoir pressure at the upstream gallery wall.

A **grout curtain** (5B) can be installed prior to the RCC or can be installed afterward from a gallery. The gallery should be large enough to accommodate suitable production equipment, especially at interior corners and intersections. Internal drains (5C) can be easily drilled with track-mounted rotary percussion equipment. Nominal 3-in. holes at spacings of 10 to 15 ft are adequate. These holes can be drilled at high production rates with an accuracy on the order of ± 3 ft in about 120 ft. A very efficient way to drill these holes is immediately after placing the RCC lift that is the gallery floor. When a long gallery with holes beginning at the same elevation is called for, it is effective to stop RCC for a day while several track drills drive onto the lift and drill the holes. The area is then cleaned, treated as a cold joint, and the RCC placing resumes. High dams, dams with wide bases, dams with high heat (due to high cement contents, use of high-heat cement, or hot placing conditions), and dams with high elastic modulus values may require longitudinal joints (5D) that can be grouted from a gallery or from outside of the dam. A practical way to make this joint is to simply place open-graded coarse aggregate at the joint location as each RCC lift is spread. The RCC is then compacted with the aggregate (5D). Grout tubes are installed in the aggregate as it is placed. Before raising the reservoir but after sufficient cooling of the mass, the joint is pressure grouted from the bottom up with expansive grout. A continuous monolithic concrete mass results instead of two masses connected by a thin grout line.

Using a **fillet** (7) in the upper part of the dam at the downstream face provides additional weight that improves sliding stability and offsets some uplift pressures. On a high dam, it moves the resultant force of the entire dam section slightly upstream, whereas on a low dam it shifts the force downstream. The distribution of stress under the dam, the amount or existence of tensile stress, and the maximum compressive stress are slightly affected. The fillet also reduces the height of the section at the top of the dam. A downstream toe extension (8) can provide additional stability for a high dam where sliding stresses increase significantly with a minor addition in height. It adds both weight and total cohesion, but only in the bottom portion of the dam, which is usually where it is needed. The fillet (7) increases the mass across the full length of the dam, including the upper portions of the foundation where it usually is not needed. The fillet also adds to foundation bearing and RCC compressive stresses, whereas the toe extension reduces the bearing and maximum RCC stresses. The extended toe requires extra excavation and foundation preparation but only in the deepest section of the dam and not for much of its length. It is possible that an extended toe in a high dam will result in tension across downstream lift-joint areas at the maximum height for an empty reservoir condition. This can be overcome by an early partial reservoir filling.

A **key** (9) is an effective way of providing additional sliding stability when it is needed in the foundation but not in the RCC. Although adding the key near the upstream face may seem like a good idea because of its potential to act as a cutoff, the downstream location will typically be better. If analyzed for local stresses, an upstream key of a high dam may have tensile forces that could negate sliding friction resistance because there will be little or no vertical stress at the key and a full reservoir. A downstream location has the benefit of maximum vertical confining stresses and the resulting friction. To minimize the width of the key (upstream–downstream) and to ensure that the required load is transferred to the foundation without slippage across a weak RCC lift surface, bedding mix should be placed between RCC layers in the key or a high-paste-content mix should be considered. The key provides added foundation stability by extending the foundation failure plane (12) and by the related horizontal component of the downstream foundation-bearing capacity (13). A relatively simple consolidation grouting program in the area downstream of the key may significantly improve stability. A key is usually required only in the deeper portion of a high dam (if it is on medium- to poor-quality rock), at isolated locations where the foundation condition is bad, or for a medium-height dam on an unsuitable foundation.

When the bearing and sliding strengths of a foundation are poor, a conventional concrete dam usually is not economical, but RCC can be a viable option. Using a low-strength and low-cost RCC with a parabolically curved downstream face (10) is one approach. At the PC-1 project, a preliminary design with this concept was prepared for a tailings dam on a clay and weathered-rock foundation. The dam was composed of large monoliths that could undergo significant independent movements caused by time-dependent consolidation of the foundations. Each monolith sat on its own excavated foundation, with steps in the foundation matching the location of monolith joints. The abutments were tied in with embankments that would undergo deformation as required. The foundation for this project was so poor that a massive key was required to provide sliding resistance and to lower the bearing pressure. Because **foundation restraint** is minimal for this type of foundation and cement contents are low due to the low strength requirements, thermal stresses are minimized; however, the thickness of the key (distance from the downstream surface to the foundation under the key) should be analyzed as a cantilevered beam to ensure that it will not break from the rest of the dam. If bearing pressures under the key can accept the added weight (15), then a fill (14) can be placed over a portion of the toe to offset some of the cantilever forces. The fill also provides extra sliding stability if it is extended downstream beyond the RCC key. Regardless of which option is used to widen a dam base, a reduction in bearing pressure and maximum stress occurs in the RCC. Reduced strength requirements lead to less cement being used, lower costs, and less thermal stress. Stresses at the lower levels are closer to stresses higher up in the dam, so fewer zones requiring different quality RCC at different heights are necessary.

Although structural requirements for strength reduce to zero at the top of a dam, some minimum strength is needed for erosion and weathering protection, impermeability, and making the mix cohesive enough to be placed and compacted. The minimum RCC strength should be based on factors such as exposure conditions, function of the dam, risk level, and economics. What is appropriate for one project, owner, and location may not be appropriate for another project, owner, and location. There is some disagreement, but minimum strengths at 1-year values of about 1000 psi have been considered acceptable for the mass. Early RCC dams used higher strength mixes for the upstream and downstream regions and lower strength RCC at the interior. This proved to be a more serious construction and inspection problem than anticipated. The practice is now generally avoided. In addition, other factors have influenced this trend, including the good field performance of low-strength RCC exposed at the downstream face under severe weather. If needed, RCC can be protected at the upstream face by constant immersion in the reservoir, by an unbonded impervious membrane (with or without protective precast facing panels), and by conventional concrete placed using one of many possible techniques. The downstream surface can also be protected.

It is usually best to use one mix throughout an entire section for small- and medium-sized dams up to about 120 ft in height. Due to thermal and economic considerations, higher dams are usually separated into horizontal zones, with higher strength mixes being used in the lower part of the structure. Generally, these zones are on the order of 30 to 60 ft thick, with increases in strength of about 100 to 500 psi per zone. Initial planning for the 340-ft-high Binongan Dam used four zones. The design for the 620-ft-high Miel I dam used eight zones. In addition to the higher compressive strengths required for higher **principal stresses** in the lower portion of high dams, stronger mixes in the lower zones also provide additional lift-joint tensile strength, added cohesion, and usually a slight increase in friction.

When a mix in a lower zone has adequate strength for compression but not for sliding stability, several options are available. Increasing the mass or weight of the dam and widening the base have been discussed. Increasing the paste content of the mixes is another option, if it is economical and does not cause thermal cracking due to added heat from hydration or a higher elastic modulus. Another option uses bedding between RCC layers. As discussed in Section 20.4, this dramatically increases cohesion and moderately increases friction. This technique is especially useful when cold joints occur in low-paste mixes. Contract drawings can simply show where bedding mix is necessary for both cold joint conditions and, in some cases, with weak RCC mixes for fresh joints (15A).

20.5.4 Upstream and Vertical Face Options

Design options for the upstream face are detailed in the various sections of Figure 20.44 labeled 16A through 16M. If the upstream face is sloped (16A), the unformed face may be left exposed when it is aesthetically acceptable and when lift-joint seepage is either tolerable or controlled with bedding or higher cementitious content RCC. If total watertightness is required and special mixes with rigorous lift-joint inspection are not utilized, a flexible geomembrane can be placed over the sloping face (16B) (Schrader, 1999b). Where the membrane is exposed, it can be protected from removal by vandals by hanging a chain link fencing over it or by other methods. Below grade, it has been protected from damage by a layer of sand.

Reinforced conventional concrete placed after the RCC (16C) uses the same design concept as an upstream face on a rockfill dam. If the wall is thick enough, it is feasible to construct it ahead of the RCC with traditional slipformed or jump-formed construction. This allows the RCC to be placed rapidly as a trailing activity, with the RCC placed directly against the wall. There is no forming to delay the RCC operation. The wall is the form. It also acts as a thermal shock protection for the RCC. The wall will provide an attractive and watertight facing when properly designed and constructed. This requires slabs with water stops in the vertical and horizontal joints. A *plinth*, or watertight tie-in to the foundation and abutments, is required. Two-way reinforcing distributes shrinkage cracks throughout the slab so cracks are small and closely spaced. By limiting the crack width to about 0.006 inches, the cracks will be essentially watertight and typically undergo autogenous healing or calcification with time, even under hydraulic head. A drain system is necessary between the slabs and the RCC. Anchors are required to hold the slabs to the dam. These should be designed for the force due to horizontal acceleration in an earthquake. It is possible but difficult to position the anchors in the RCC when it is placed; drilling and grouting them afterward is the alternative. This concrete-facing method is often considered but is seldom designed or used. An extension of the concrete-faced option (16D) includes a second facing of porous concrete that acts as a total drain between the RCC and the upstream face. This also isolates the RCC from shrinkage and potential cracking or joint requirements in the facing, and it acts as thermal insulation to reduce gradients near the face. It was included as an option for the RCC design option at Kapachira Dam.

Roller-compacted concrete can be placed directly against conventional forms, but without a conventional concrete bedding or facing the degree of compaction and appearance will be compromised. Threaded anchors to the forms can be compacted into the RCC. After the RCC has been placed high enough so the next form panel can be positioned and anchored, the lower form can be slid out along the anchor and away from the RCC mass (16E). The void between the RCC and form can then be filled with conventional concrete that bonds to the young RCC and is mechanically held by the anchor. Instrumentation has shown that, by controlling the rate of placement and set time of the concrete with this type of procedure, form pressures can be developed that will stress the anchors and prestress the face in place.

Precast panels (16F) make an attractive, economical, and crack-free facing, but the panel joints are not watertight. Anchors are minimal, usually about 75 ft² of panel per in.² of steel anchor area. Watertightness can be provided with a flexible PVC membrane (about 0.08 in. thick with welded field seams) attached to the back of the panel. A nut and washer tightened against the membrane with epoxy provides a watertight seal where the anchor penetrates the membrane. This procedure has been very successful in construction, operation, and tests to a head of 600 ft. A small amount of bedding is recommended between the membrane and RCC. Drains should be provided behind the membrane to collect seepage if it occurs and to provide additional stability by creating extra uplift reductions.

Roller-compacted concrete can also be placed against a conventional form that is later removed. A small amount of bedding against the form has helped to seat the form and provide a better surface. When done properly, this will result in a conventional concrete appearance, with RCC immediately behind the face; however, it requires a mix and technique that not everyone has been able to accomplish with total success. At times, difficulties have been encountered when the bedding has not squeezed up the form face, resulting in a boney look to the RCC at the exposed face. Another way to accomplish the appearance of a conventional concrete face is to use grout-enriched RCC (GERCC), with or without an air-entraining admixture as discussed in Section 20.3.6.

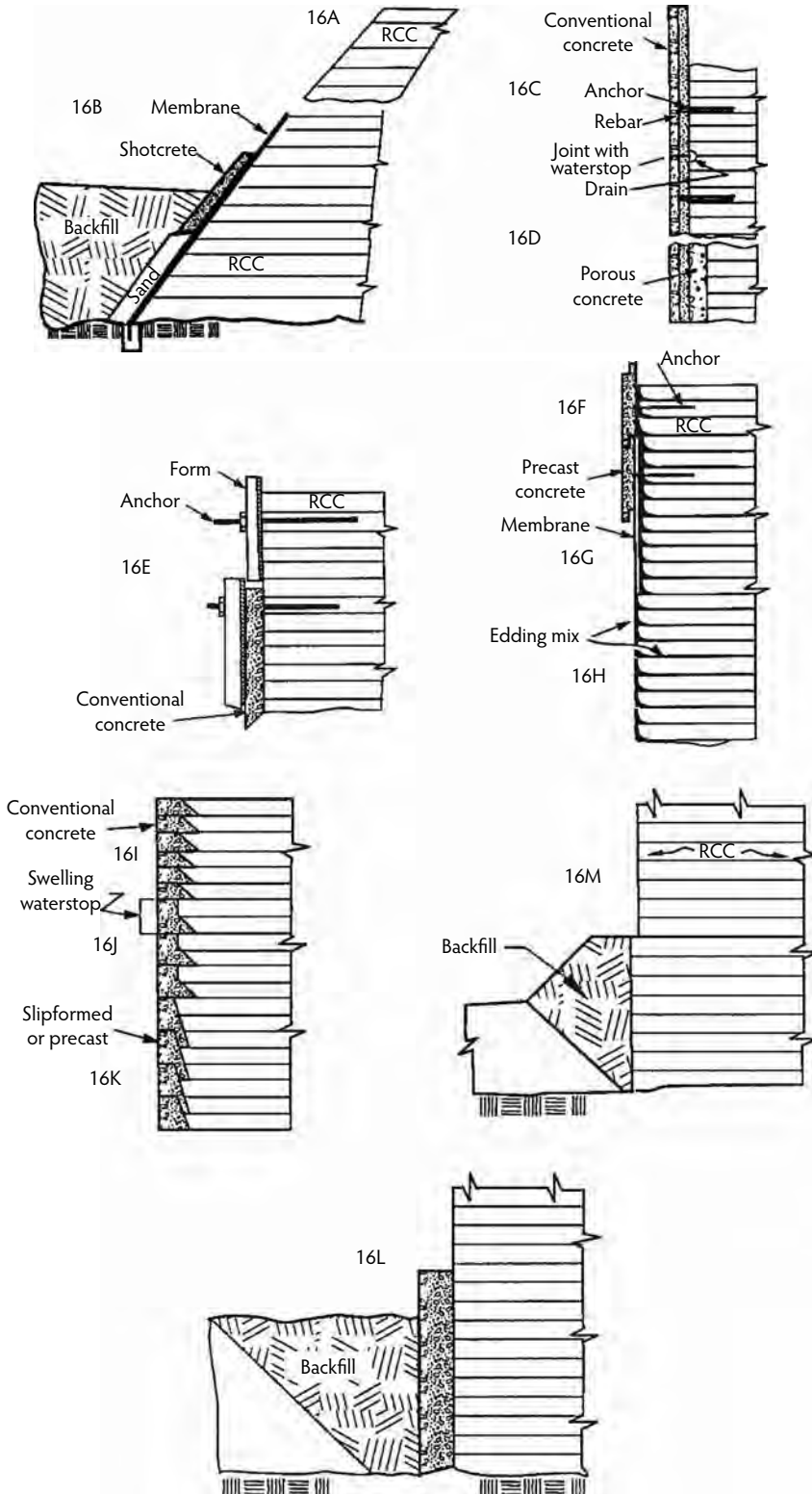


FIGURE 20.44 Upstream face options.

Watertightness can be established with an exposed polyvinylchloride (PVC) membrane placed directly against the dam face (16G) (see Section 20.4.16). The membrane requires an anchored but unbonded procedure specifically developed for concrete dam facings. A variety of synthetic membranes was used in earlier projects, either with drains or without drains. These systems worked satisfactorily, but were not entirely successful. A specially formulated PVC membrane produced and installed by the Carpi company was then adapted to RCC, using technology and proven performance from its application to provide watertightness at older conventional concrete dams with seepage and permeability problems. This membrane has routinely provided total watertightness at the upstream face. The installations include a face drain system. The Carpi exposed-membrane system has been installed with 100% success for more than 20 years on a number of RCC dams and for much longer in the rehabilitation of leaking old conventional concrete (Scuero and Vaschetti, 2003). Drains between the membrane and RCC improve stability through additional uplift reduction, as discussed in Section 20.4.16. Simply extending the bedding mix downstream along the lift joint (16H) for a distance equal to at least 8% of the hydraulic height will provide watertightness if it is done 100% correctly 100% of the time. In practice, this is not possible. Normal construction with good inspection results in about a 95% reduction in seepage; this may be technically but not aesthetically adequate.

A number of RCC dams, and the facings of rooms and walls on other RCC mass applications, have been built that using the procedure labeled 16I in Figure 20.44. The procedure results in an attractive conventional concrete face that is completed with the RCC. Usually, the facing has no anchors to the RCC and no reinforcing bars. If a low-water/low-cement/low-shrinkage conventional concrete mix containing a high-range water reducer is carefully used and controlled, a virtually crack-free facing can result—even without vertical joints. The mix should not be thicker (horizontal dimension) than about 1 ft, or thermal and shrinkage cracks will probably result. Excellent curing must be provided. Without these precautions, tight cracks at spacings of about 4 to 10 ft can be expected. Normal construction with a reasonable mix will be crack free if joints are provided in the facing about 25 ft apart. The problem with joints in a facing is that it is very difficult to install water stops. Various projects that have attempted this have had less than watertight joints. The facing does not make the horizontal lifts watertight. If placing proceeds very quickly (about four to six lifts per day), the fact that the successive layers are placed before the previous layer has fully set will improve watertightness of these joints.

A modified procedure (16J) uses a temporary blockout near the upstream face at every other RCC lift. The blockout is removed prior to placing conventional facing and the next RCC lift. Each face placement covers two RCC lifts. Added watertightness can be achieved by using a simple *swelling-strip* water stop that is impregnated with chemical grout and laid along the facing mix lift surface. If seepage penetrates the lift joint, moisture causes the strip to swell, thus creating watertight pressure against the adjacent lift surfaces.

Interlocking upstream-facing elements (16K) have been precast and slipformed. As precast pieces, the upstream area covered by each piece is only about 10 ft² of exposed surface area, so production and placing becomes labor intensive and slow. The small area is a result of the weight of the thick and overlapping shape. The joints are not watertight, and there is some concern regarding the stability of the facing if it is not anchored to the RCC. Horizontally slipformed facing can slow production of RCC on dams with a short axis, but the procedure and equipment are better suited to long dams with a large volume of RCC per lift. Careful control of the mix and its delivery is critical, and the facing will develop small shrinkage cracks. RCC can be placed against the facing the same day it is slipped. Consideration should be given to the bond between the unanchored facing and RCC. This may require a high-paste RCC mix against the slipformed facing. Sandblasting may be necessary to achieve a bond if the facing is old before the RCC is placed against it. The possibility and consequences of saturation and freezing at the bond line should be evaluated.

Dams in steep canyons, and some large projects, can benefit from an upstream wall (16L) placed across the valley. Such a wall acts as an upstream form for the RCC or as a starting wall for concrete facing and membrane systems. It protects the foundation by containing water and debris, and it allows fill to be placed against the upstream side of the wall, thereby creating a practical work area that extends to the

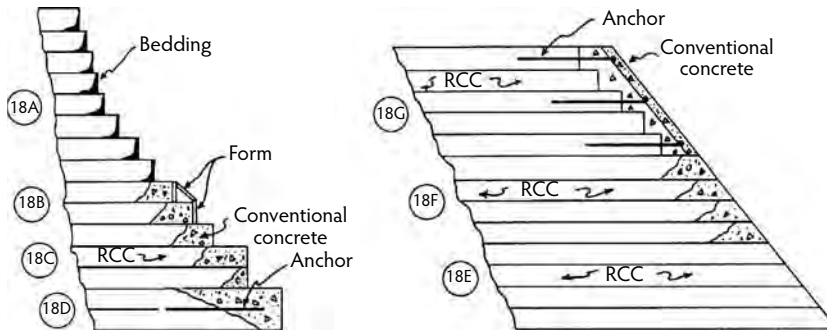


FIGURE 20.45 Downstream face options.

face of the dam. Projects such as Copperfield have saved time and money by placing backfill lift by lift with the RCC to create a vertical upstream face without forms (16M). This is fast and effective and provides a long level surface upon which subsequent forms can be set when the maximum practical height of backfill is reached. Regardless of what procedure is used for watertightness, a tight contact is essential at the interface between the upstream face and foundation. Details regarding this contact and how it varies from one upstream facing or water barrier method to another are beyond the scope of this chapter.

20.5.5 Downstream and Sloping Face Options

The downstream face of the dam, or any other sloping face, can be designed using any one of the many options shown in Figure 20.45 and labeled 18A through 18G, as well as with GERCC as discussed in Section 20.3.6. A common, economical, and practical method uses steps with a small amount of bedding placed against reusable-form panels (18A). The panels are one to three lifts high, moveable without equipment, and held by simple methods such as pins hammered into the RCC after compaction. By changing the width of the steps, any average or changing downstream slope can be achieved. If a conventional concrete appearance or protection from weather is desired, conventional concrete can be used for the facing (18B). Larger steps (e.g., if needed in a spillway) can be built with variations of this method (18C and 18D). Reinforcing steel and anchors are not required with a monolithic construction procedure, but with low-cementitious-content mixes it is essential that the conventional concrete be placed first with a mix that will have lost its slump but not reached initial set by the time the RCC is spread against it and compacted down into it. If the RCC is placed first, the result will look good at the surface, but there will be no reliable contact or interface between the two mixes. Anchorage is then necessary and the RCC should first be compacted at the edge (18D). Smooth spillways and downstream sloped surfaces have been designed and constructed using no treatment except for hand trimming (18E), unreinforced and unanchored conventional concrete facings with about a 1-ft minimum width (18F), and slipformed concrete with anchors and two-way reinforcement placed after completion of the RCC and after substantial chipping or preparation of the RCC (18G).

20.5.6 Thermal Considerations

Concrete produces heat when it hydrates and hardens. This is of little consequence to small placements, but it is of major concern to massive placements. If heat from hydration is trapped within the mass, the internal portion of the mass will harden and stiffen at an elevated temperature. Later, as this heat slowly escapes, the mass will try to contract as it cools. If the mass is restrained (e.g., by being bonded to a rock foundation), it is prevented from contracting. The attempted thermal strain is therefore converted into tensile stress. If the thermal stress is greater than the tensile strength, cracking will occur. Because massive structures typically have little, if any, reinforcement, the stability of the structure usually depends on an uncracked section with internal tensile stresses less than the cracking strength of the concrete.

Roller-compacted concrete provides several opportunities to reduce internally developed thermal stress. Its lower cement content reduces the total hydration heat in almost a direct proportion to the cement reduction. If the mix has a very low cementitious content, the stiffness or brittleness (modulus) of the concrete can be low, and substantial stress relaxation due to creep can occur. Although it can be done, it is not very practical or economical to provide forced post-cooling; some of the traditional methods of precooling, as with ice and chilled water, are also not very economical or effective. Producing aggregates in cold winter months and storing them in large stockpiles until they are used in warmer months has resulted in reduced placing temperatures. This has the same overall impact as using a submerged chilled wet belt or cold air to precool the aggregate, but it is essentially free, and it applies to both fine and coarse aggregate, whereas submerged wet belts can only be used on the coarse aggregate. In addition to controls on aggregate production, the rate of placing, hours of placing (night vs. day), and the schedule for starting and finishing placing are critical factors for thermal stress analysis. The designer must pay attention to these details and consider them in the thermal evaluation.

Thermal evaluations for RCC mass placements require much more attention to detail than is necessary with traditional mass concrete. There are several reasons for this, but the most important is the large exposed surface area for each thin layer of RCC mass that is placed in each lift. Conventional concrete uses a much smaller exposed surface area with a thick layer of concrete mass for each lift. The heat transfer, either by heat lost to the atmosphere or by heat gained from exposure to the sun, is consequently a much more critical aspect of RCC thermal studies. The time of placement of each layer or lift of RCC can also be a very significant factor, whereas the time of day for placement of conventional concrete is not as important. A low-cement-content RCC mixture may have an adiabatic temperature rise that is less than the heat absorbed from the sun before the layer is covered with the next layer of RCC. In this case, placing at a faster rate can result in lower temperatures—exactly opposite of what would occur with normal placing of conventional mass concrete. Details of thermal analyses are beyond the scope of this chapter. Various references contain examples and suggested methods for analysis (Ditchy and Schrader, 1988; Hirose et al., 1988; Tatro and Schrader, 1985, 1992; USACE, 1997).

When properly accomplished with detailed input of the time-dependent construction schedule, finite-element method (FEM) temperature analysis can accurately predict the temperatures of any RCC mix at any location in a structure at any time. This usually requires consideration of the time of day for placement of each layer of RCC, the variable temperature throughout the day, the movement of air across the lift surface, and an accurate determination of the adiabatic temperature rise of each mix. It also requires knowing the physical thermal properties of the materials, considering the type of cure and evaporative cooling, and considering probable interruptions to the placing schedule.

Thermal FEM studies can be simplified by using one-dimensional, heat-flow studies for the more massive sections of a structure, with two-dimensional analysis being reserved for areas of smaller dimensions on the order of about 20 ft wide. The results of the individual studies can then be combined to create a three-dimensional time-dependent result. Using multiple one-dimensional heat-flow analysis where possible can actually be better using than two- and three-dimensional studies because it allows better detailing of the FEM mesh, with nodes at the interface of every lift. This typically is every 12 in. throughout a structure that extends hundreds of feet in each direction. The exact time of placement of each lift can then be taken into account. Large two- and three-dimensional models that are suited to traditional concrete placements with a large mass being placed only every few days typically have much larger node spacings and are unable to account for the detailed placing of RCC in 1 ft layers every 3 to 16 hr.

Figure 20.46 provides a conceptual approach to using one- and two-dimensional models to properly study a large RCC mass. Figure 20.47 shows the results of a study performed with this methodology and gives an idea of the temperature distributions within a structure that used RCC ranging from very lean cement contents in the center of the structure to higher cement contents in the outer 9 ft of the dam. The thermal contours are based on actual field measurements. The temperatures in square boxes indicate the predicted temperature for that mix, location, and time. Predictions were within a degree or two of the actual conditions.

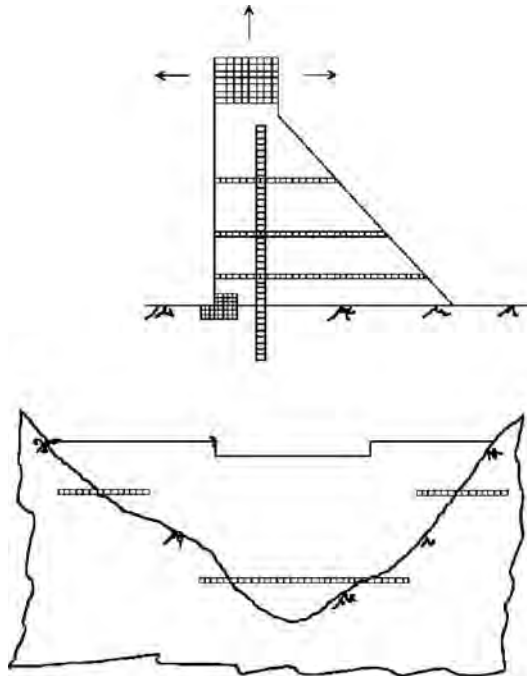


FIGURE 20.46 Sample finite-element method (FEM) mesh for thermal studies.

20.6 Construction

20.6.1 General

Construction is discussed in general in ACI Committee 207 (1989), Oury and Schrader (1992), and Schrader (1991, 1992, 1995a,c,d, 1999b, 2002). There are many examples in the literature of RCC construction methods used at specific projects and their interrelationship with RCC design issues at, for example, the Burton Gorge, Rompepicos, and Burnett dams (Schrader, 1999b; Schrader and Bali, 2003, Lopez et al., 2005). Because of the interrelationship between mix designs, structural design, material properties, and construction, many aspects of construction have been discussed, at least in part, in the previous sections of this chapter. It is important for the contractor to understand that construction equipment and methods have a direct effect on design and that some procedures, production rates, and equipment may not provide the quality or characteristics required for a particular design. What is acceptable for one design and set of conditions may not be acceptable for a different design or set of conditions. Some examples of the interrelationship of design and what may seem like simple construction decisions follow with regard to positioning of supports in the dam for RCC conveyors and how RCC is started at the foundation.

Many RCC dams are constructed using an all-conveyor system, with the conveyor being supported on posts within the dam. The posts are pulled up and raised as the dam is built. Before sufficient RCC has been placed to support the posts, they require a substantial footing. Without proper design considerations, these footings represent fixed rigid blocks protruding into the dam with vertical faces that could initiate cracking both from the perspectives of restraint to thermal contraction and the tendency for the formed vertical face to propagate into the RCC as a crack.

One way to deal with the restraint from objects such as these is to place them at the center of monoliths, or so one face of the footing is flush with a monolith joint. Because thermal contraction is toward the center of the monolith, movement will be from the free face of the monolith joint toward the center, which is already the position of maximum restraint. Footings located here should be bonded to the adjacent RCC. Ideally, footings near the middle of a monolith should be circular, without corners. If the

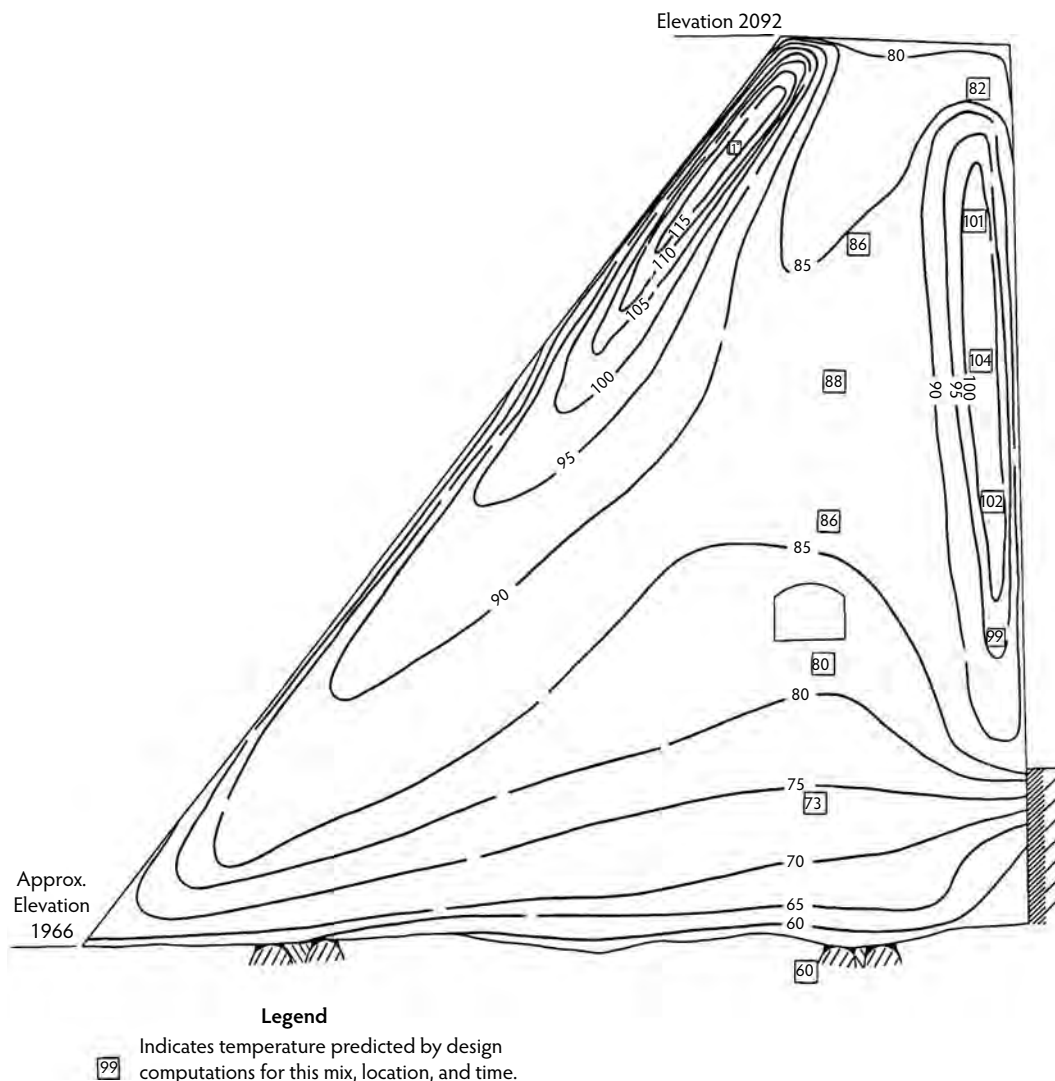


FIGURE 20.47 Predicted vs. actual internal temperatures.

footings have corners, they should be rounded or chamfered. In addition, consideration should be given to reinforcing the RCC in front of corners by dropping bars into these lifts as they are placed. If the footings are located at monolith joints, square footings can be used. In this case, the faces of the footings should be debonded from the RCC (e.g., with curing compound) so the monolith can contract away from the fixed rigid restraint of the footing.

A much preferred approach to footings above the foundation is to avoid them by setting the posts into the foundation. This can be done by drilling large-diameter holes into which the posts are placed. Another procedure that has been used is excavating into the foundation with careful blasting or hydraulic hammer excavation and then filling the hole with dental concrete. The top of the dental concrete is finished flush with the top of the surrounding foundation. The dental concrete block becomes part of the foundation. The post is embedded within the dental concrete. Because this approach eliminates the problem of a rigid block protruding into the foundation, it allows placing the posts at almost any location, with a general guide that they should not be closer than about 2 m from a monolith joint. The posts jack-up out of the foundation as RCC is placed.

Similar to the issue with massive footings above the foundation, concrete (including RCC) ramps should also be avoided within the RCC, unless their impact on design, including thermal restraint and potential for propagation of a ramp face as a crack into the RCC, is adequately addressed. If ramps are to be constructed and left in place, they should use RCC of similar quality to the RCC in the dam, and the position of the ramp should usually be toward the middle of a monolith. Because of restraint, ramps on the foundation require more attention than ramps that are within the RCC, above the foundation.

Some RCC projects have used leveling concrete to cover the foundation and provide a smooth base from which to start RCC, whereas other projects start with RCC directly on the foundation. There are arguments for each approach. Considerations for and against the use of leveling follow. Leveling concrete simplifies the start of RCC placing and its initial production rate, but it requires considerable time to construct, and it uses concrete that is more expensive than RCC, with different properties than the RCC. If the RCC or foundation has a high tensile mass modulus similar to conventional concrete, the leveling concrete will simply be another material with properties similar to what is above or below it, so this is of less concern. If conventional concrete is used for leveling on a foundation with substantial undulations and slopes, it will be very thick in most locations. This will require thermal controls that usually involve forced cooling of the leveling mix. If the project already has ice capability for other purposes, the problem is not difficult to overcome, but if no cooling capability would otherwise be necessary then this becomes a major expense. In addition to thermal cracking, consideration should be given to drying shrinkage. This requires the leveling mix to be continually cured until it is covered with RCC.

Formed vertical and clearly defined joints should be avoided in leveling concrete unless they coincide with contraction joints in the RCC. This applies to both the transverse and longitudinal directions. A formed joint represents the start of a crack off the foundation and a stress riser (restraint) where thermal stresses are usually maximum. Some projects that have used leveling concrete and could not avoid extra joints due to concrete plant and placing capacity issues have later injected the joints with epoxy after they opened and before placing the RCC. Leveling concrete typically has long-term stiffness (modulus) values on the order of 20 to 35 GPa (3 to 5 million psi) with low creep. If this concrete is placed on a foundation with lower tensile mass modulus, it creates added restraint and therefore higher thermal stresses.

Any type of RCC mix can be placed directly onto foundation rock without leveling concrete. This is accomplished by first spreading a thin layer of high-slump bedding mix (with or without coarse aggregate) onto the rock and then spreading the RCC over the bedding and compacting it while the bedding is still fresh. This has been one of the most common procedures for placing RCC on foundations, and it has been very successful. The RCC compacts into the bedding so the two materials become one concrete, while the grout and mortar portion of the bedding conforms to the rock and provides total glued contact to it. No distinctly different material lies between the foundation and the RCC, which avoids the separate leveling mix and its concerns.

If the foundation is relatively poor and it would deteriorate from exposure prior to placing the RCC, it is common to use shotcrete or a thin mud mat of high-slump concrete to seal and protect it. The shotcrete typically is on the order of 50 to 100 mm (2 to 4 in.) thick, and the mud mat is 100 to 150 mm (4 to 6 inches) thick. Clearly defined formed edges should be avoided. The material will be subject to some cracking, but the cracks will be random. By keeping the mud mat thin, cracks will likely mirror the joints in the foundation rock and not propagate up into the RCC. Where shotcrete is placed against abutments and there is a tendency for the foundation underneath to still deteriorate or where the abutment could not be cleaned to sound material before shotcreting, grout pipes have been used to ensure a seal between the shotcrete and foundation. Each grout pipe should be an individual line, usually PVC, that is routed through the dam to a convenient location such as the downstream face for later grouting. It is imperative to maintain identification of each pipe so they can be grouted in a planned pattern after the RCC has been placed to a substantial height above the location. The pipes should not be interconnected.

Rapid construction is important to quality, simplicity, and profit in RCC projects. It is more difficult to produce quality construction at low production capacity than at high production rates. In general, RCC mixtures that do not contain a retarder should be delivered within 10 minutes of when mixing started, spread within 10 minutes of when they are delivered, and compacted within 10 minutes of when

they are spread. Typical specifications require that the elapsed time from the start of mixing until the end of compaction should not exceed 40 minutes. The exposed edge of RCC lifts should also be compacted or advanced within about 40 minutes of when the material was mixed. These time limits are good guides, but consideration should be given to the particular characteristics of each mixture, the temperature, whether the mix is placed in a critical part of the structure, and the practicality of construction.

A common characteristic of profitable and technically successful RCC dams is good communication between the contractor and designer, with decisions being made promptly and with authority in the field. Interruptions and slowdowns result in reduced joint and RCC quality as well as increased costs. Interruptions to a continuous RCC construction operation are bad for both the engineer and the contractor. Direct communications and procedures for on-site problem resolution are essential, without excess personnel, management, or administration. This sounds basic and simple, but it is amazing how many projects have suffered from insufficient authority, responsibility, and responsiveness in the field—from both the contractor and engineers. When problems develop at the placing area, they must be resolved quickly. In RCC construction, there usually are no alternative monolith blocks where work can progress while the problem is studied. When contingency plans for added monolith joints are approved in advance, it may be possible to raise a portion of a structure or massive placement ahead of the rest of the structure, but this can result in placing difficulties and the design implications must be considered.

Profitable and efficient RCC construction is machine intensive, with minimal labor per cubic yard of placed RCC. Equipment should do the majority of the work, not labor, even for smaller projects. The rare exceptions are special projects designed to be labor intensive in developing countries with the intent of employing a large unskilled labor force at low wages. Fueling, form work, and assembly of embedded items should all be scheduled and planned so the majority of this work is accomplished off the lifts and during shift changes or scheduled downtime. All unnecessary vehicles and personnel (including visitors and inspector trucks) should be kept out of the placing areas and equipment paths. It is essential for all materials, access, embedded parts, foundation excavation and preparation, and similar work to be planned and readied well ahead of time.

20.6.2 Aggregate

The location, size, and withdrawal of aggregate from stockpiles must be coordinated with the RCC plant location and method of feed to minimize segregation and variability. At the very high production rates possible with RCC, several loaders or a conveyor system may be required to keep feed bins full. The length of haul and size of turnarounds must be considered so loading equipment can operate rapidly, efficiently, and safely. Aggregate stockpiles and the concrete plant location can be even more important than in the production of conventional concrete. Typically, very large stockpiles that could easily be half the material needed for a season of placement are provided prior to starting RCC placement. Some of the reasons for this are as follows:

- Technical design requirements may require producing aggregate during the winter so it can be stockpiled in the cold for later use. At Middle Fork and Monksville Dams, winter stockpiling resulted in aggregates that still had occasional frozen areas when the material was withdrawn during the summer, although ambient temperatures exceeded 80°F. At Burton Gorge Dam, instrumentation showed that producing RCC aggregate at night resulted in a 10°F lower aggregate stockpile temperature than producing similar aggregates during the day.
- It may be relatively easy to mobilize aggregate production to full operation while work for the rest of the project is just beginning. It is customary to pay for aggregate in a stockpile at the job site if it is tested and found to be acceptable. Payment should be based on an appropriate percentage of the in-place cost of RCC, including some profit.
- The rate of aggregate use during RCC placing may exceed the aggregate production capacity. With large stockpiles, material that occasionally is produced out of specifications may be spread throughout the acceptable material to produce a blend that is within specification. Larger aggregate stockpiles also have the benefit of more stable moisture contents which reduces fluctuation in RCC consistency.



FIGURE 20.48 A large “all-in” aggregate stockpile with no segregation at Burnett Dam.

Although many RCC dams have been constructed with numerous aggregate size groups and stockpiles, many others have been very successfully constructed with just two size groups. Usually this is $+3/4$ in. and $-3/4$ in. Some projects have used a single, all-in size group. Figure 20.48 shows an all-in, 2-in. MSA aggregate pile at Burnett River Dam. As cost and production benefits are demonstrated on more and more projects, with excellent control of moisture and variability, minimizing stockpiles is becoming more popular. Fewer size groups mean less area for storage and less equipment for loading and transportation. Fewer aggregate bins are required, and less complicated mix designs are possible. A major benefit that is often overlooked is what happens if an aggregate feed bin malfunctions. If a plant has four bins and each bin carries a separate material, production stops if one bin malfunctions. If the same four-bin plant is used to carry only two size groups, at least one of the size groups would be fed with more than one bin. When a bin malfunctions, production can proceed, though at a slower pace, with the operating bins while repairs are made to the bin that is down.

When low-cementitious-content RCC mixes are used, it is necessary to include nonplastic fines (passing $75\text{-}\mu\text{m}$ or No. 200 sieve) to compensate for the otherwise low paste content. When fines are included with a size group of $-3/4$ in., the material is similar to a road base. It has minimal tendency to segregate, especially if it is damp. Also, the moisture content in the pile tends to stay very uniform because the material is not free draining. This is not the case with traditional washed concrete aggregates. Very large and high stockpiles of $-3/4$ -in. RCC aggregate containing nonplastic fines have been built in layers. The aggregate is later removed without segregation by a front end loader. A potential disadvantage of handling an RCC aggregate with nonplastic fines is its tendency to compact in bins and bridge small gate openings unless special precautions are taken.

20.6.3 Mixing

A comprehensive discussion of RCC mixing and delivery philosophies and specific concerns about handling RCC is available in Oury and Schrader (1992). This reference also includes details and experiences, beyond the scope of this chapter, that are pertinent to a wide range of RCC mixing and delivery equipment types. The concrete plant location should be selected to minimize energy requirements and be appropriate for the terrain, whether the RCC is transported by conveyor or haul vehicle. It should be selected to minimize overall haul distances, vertical lift, and exposure of the fresh mixture to sun and

weather. The plant should be located on a raised area so spillage and wash water drain away without creating a muddy area, especially if vehicular haul is used. The plant location for dams will generally be in the future reservoir area just upstream of the dam and above the cofferdam level or on one of the abutments. The plant should have a bypass or belt discharge that allows wasting rejected RCC without first delivering it onto the dam. This bypass can also be used for sampling, for delivery to trial sections, and for other construction uses.

Both continuous mixers and batch mixers have been used to produce RCC; continuous **pugmill** mixers are the most common. Batch operations with drum mixers tend to cause the most difficulties and concerns. They should not be used. For the same space requirements, continuous mixers generally provide greater capacity than batch-type plants. Continuous pugmill mix plants specifically intended for RCC and properly operated and maintained routinely achieve good production rates and uniformity. This applies to plants that operate with volumetric controls as well as to those that operate on weight controls.

Although some RCC has been successfully produced with conventional batch-type plants having drum mixers, problems with low production, bulking, sensitivity to the charging sequence, mixture variability, slow discharge, and buildup in the mixer have been common. This does not mean that acceptable RCC cannot be produced by batch methods and drum mixing, but special attention is needed and low productivity can be expected. Equipment that is well suited to normal high-production conventional concrete is not necessarily suitable for all RCC mixtures and the typically higher production rates.

Roller-compacted concrete mixtures can be very harsh, and some can cause the buildup of fines. Drums should be designed or coated to resist buildup that tends to result from the high fines content of some RCC mixtures. Even with these precautions, experience has shown that substantial buildup can develop in drum mixers. If the buildup is not removed, a loss in mixer effectiveness results. Except for special small applications with higher cementitious contents, clean conventional-type aggregates, and aggregate sizes limited to about 3/4 in., transit trucks and mobile batch plants should be avoided. Even with these types of mixtures, slow discharge and high mixture variability should be anticipated.

Pugmill mixers that were originally intended for cement-treated base, asphalt, or moisture conditioning of soils have presented difficulties with maintenance and variability when they have been used to construct RCC dams; however, pugmill mixers of both the batch and continuous-mix type have performed well when they are specifically designed and intended for RCC. Typical individual plant capacities range from about 150 to over 400 compact cubic meters per hour. It is generally better to have multiple smaller plants than a single larger plant. If one plant is down, the others can usually continue placing while repairs are made. Also, it is easier to find subsequent uses for smaller plants than for very large specialized plants.

The theoretical or rated peak capacity of the plant should be well above the desired average production. As a general guide, the average sustained placing rate usually does not exceed about 65 to 70% of the peak or rated plant capacity when haul vehicles are used for delivery on the dam and 75% when an all-conveyor delivery system is used. These values tend to be lower on smaller projects and higher on uncomplicated larger projects. Table 20.11 shows the average efficiency that can be expected throughout each placement shift for different work schedules and methods of delivery with a properly managed project. These values have increased only a slight amount in recent years compared to early RCC projects.

Mixers for RCC must accomplish two basic functions: They should provide sufficient capacity for the high placing rates typical in RCC, and they should thoroughly blend all ingredients. Typical average placing rates are on the order of about 50 to 150 yd³/hr for small projects, 200 to 500 yd³/hr for medium projects, and 500 to 1000 yd³/hr for large projects. The mixer should operate with little or no downtime. Scheduled maintenance must not be neglected, and repairs should be accomplished rapidly.

Variations in the free-moisture content of the aggregates can be particularly troublesome when the plant starts up. Some plant operators make the error of overestimating free moisture and provide too little water in the initial mixtures. This is particularly undesirable because most initial mixtures will be used for covering construction joints or foundation areas where the RCC should be slightly on the wet side for improved bond. It is better to start on the high side for moisture and subsequently reduce it to the desired consistency than to start with a mixture that is too dry.

TABLE 20.11 Probable Average Sustained Production through Full Shifts

Shifts Worked	Days Worked	All-Conveyor Delivery (%)	Haul on Dam (%)
Two, 10-hour	6 on, 1 off <i>or</i> 12 on, 2 off	76	66
Two, 8-hour			
Three, 8-hour	6 on, 1 off <i>or</i> 12 on, 2 off	73	63
Two, 12-hour			
Three, 8-hour	Continuous up to 28 days	70	61
Two, 10-hour			
Two, 12-hour			
Three, 8-hour	Continuous over 28 days	65	55
Two, 10-hour			
Two, 12-hour			

Note: Assumes Aran continuous pugmill and Rotec or equal proven conveyor. Reduce efficiency by 10% if multiple shifts per day do not overlap. Although Rotec conveyors and Aran mixers (or proven equivalent) may be capable of 80 to 90% efficiency by themselves, the above efficiencies are realistic overall shift values when total maintenance, all types of other equipment breakdowns, aggregate feeding/delivery, raising and moving forms or facings, and slowdowns at abutments are considered.

Mixture uniformity must be maintained for all the production rates used. Continuous mixers typically work efficiently above a minimum production rate and up to production levels that are two to four times that of the minimum rate. A consistently uniform mixture must still be provided even when slowing production by, say, 50% near abutments and when increasing it again after leaving confined areas. Large projects with multiple mixers can simply shut down one or two mixers until the higher production rate is needed again. On smaller projects with one mixer, the mixer must be capable of uniform production at varying outputs. Mixture variability is discussed in more detail in Schrader (1987, 1988, 2003a). Table 20.12 provides a summary of what can be expected with regard to the variability of RCC mixtures at different levels of quality control.

Accurate and consistent control of cement and pozzolan feed is particularly important with continuous-mix plants. This is especially true at lower cement-feed rates. Feeders designed to operate at the high cement-feed rates typical of soil cement or conventional concrete usually do not operate well at the low cement rates required for some RCC mixes. Maintaining sufficient head in the silos, using air fluffers, and using vane feeders or positive-displacement cleated belt feeders have been necessary to provide accurate feed. Proper ribboning or sequencing and feed rates of the aggregates and cementitious material as they are fed into the mixer are critical to minimizing mixing time. Each plant and RCC mixture seems to have its own peculiar requirements that can only be determined by trial and error. Properly designed pugmills have handled 3 in. and larger nominal maximum size aggregate (NMSA), but experience has shown that the amount of material larger than 2 in. should never exceed about 8%, and the maximum size should not exceed 4 in. The preferred NMSA for most mass applications of RCC is 2 in.

Accurately introducing the correct quantities of materials into a mixer is only one part of the mixing process. Uniformly distributing and thoroughly blending them throughout the mixture and then discharging them in a continuous and uniform manner comprise the other part of the process. This can be more troublesome with some RCC mixtures than with conventional concrete mixtures. The accuracy of the concrete plant and methods for control of the mixture during production should be studied for cost effectiveness. If exacting quality control and low variability are necessary, they can be provided in RCC mixtures. Typical coefficients of variation for RCC compression tests are shown in Table 20.12.

20.6.4 Delivery

The volume of material to be placed, access to the placement area, availability of rental or lease equipment, capital cost for new equipment, and design parameters generally are the controlling factors for selection of equipment and procedures to be used for transporting RCC from the mixing location to the placing area. Essentially, the three methods for transporting RCC are by batch, continuously, or

TABLE 20.12 Quality Based on Variability for Roller-Compacted Concrete

Description		Coefficient of Variation				
		Excellent	Very Good	Good	Fair	Poor
Overall	General construction, sampled from the placement	0–11	11–14	14–18	18–23	>23
Within batch	General construction	0–4	4–6	6–8	8–10	>10
Within batch	Lab trial batches	0–3	3–5	5–7	7–9	>9

Source: Schrader, E.K. et al., in *Roller Compacted Concrete Dams*, Berga, L. et al., Eds., Swets & Zeitlinger, Lisse, 2003, pp. 355–362. With permission.

using a combination of both—typically, via a continuous conveyor feed to a hopper on the dam from which vehicles take batches for final delivery to the spreading area. To some extent, transportation may be influenced by the type of mixing equipment used; however, with proper controls and accessories, such as holding hoppers designed to control segregation, continuous mixers can be used with batch transportation and batch mixers can be used with continuous-flow transportation equipment.

The type of transporting equipment used to move RCC from the mixing plant to the placement area will also be influenced by the largest aggregate size in the mixture. Experience indicates that 1.5-in. NMSA concrete can be transported and placed in nonagitating haul units designed for aggregate hauling and earth moving without substantial uncontrollable segregation. Mixtures with large 3-in. NMSA aggregate have more of a tendency to segregate when they are dumped from this type of equipment onto hard surfaces, but with care and proper procedures these mixtures can be hauled and dumped successfully. Problems with segregation during the transportation and placing of 6-in. NMSA mixtures have been severe. Typical current practice is to require that 100% of the aggregate be smaller than 3 in., with only 1 or 2% allowed above 2 in., and allowing 100% to pass 1.5 in.

The entire system of mixing, transporting, spreading, and compacting should be accomplished as rapidly as possible and with as little rehandling as possible. The time lapse between the start of mixing and completion of compaction should be considerably less than the initial set time of the mixture under the conditions in which it is used. A general rule for nonretarded mixtures with little or no pozzolan is that placing (depositing), spreading, and compacting should be accomplished within 40 minutes of mixing, preferably, within 30 minutes of mixing. This time limit is applicable at mix and ambient temperatures of about 70°F. It can be extended for colder weather and should be reduced in warmer weather. It also can be extended for mixtures that are proven to have extended set times because of high pozzolan contents, slags, or effective admixtures with wet RCC consistencies. A simple test to establish the tolerable time for any particular mix and temperature is to compact two cylinders from the same batch every 15 minutes, beginning immediately after mixing. The cylinders are all tested for compressive strength at the same age, at about 14 or 28 days. A plot of strength vs. time of compaction will quickly indicate the age at which compressive strength becomes seriously affected. Tests have shown that tensile strength and the modulus of elasticity will begin to decrease at about the same time and at the same rate as compressive strength.

The two primary methods of transporting RCC are by conveyor and hauling vehicle. Transport by bucket or dinky has been used, but this slows the rate of production and is more prone to cause segregation; however, if such a system is already available or necessary for large volumes of conventional concrete, it can also be used for the RCC. Pipe delivery has been tried on a few projects with varying degrees of success. If pipe delivery is considered, it should be designed specifically for the mix to be used and potential pressures, it must have a steep slope, the technical issues of moisture loss and temperature gain must be addressed, the length of time in the pipe and its effect on the age of the RCC when compacted must be considered, and sustained satisfactory operation should be proven in full-scale trials.

Transporting RCC by continuous high-speed conveyors directly to the dam is generally preferred. The overall economics, including all direct and indirect costs of alternative delivery systems as well as reliability, the final quality, and schedule should be considered when deciding whether to use or require an

all-conveyor delivery system. All aspects of the conveyor system should be specifically designed for RCC of the type used on the project. The advice of personnel experienced with the type of mixture and equipment proposed should be solicited. Conveyor systems that may work well with conventional structural concrete, aggregates, coal, or other materials may not work well with RCC. Conveyor systems that work well with a high-cementitious-content, wetter, small-aggregate, or no-fines RCC may not work well with a low-cementitious-content, drier, larger aggregate, or high-fines RCC. Clogged transfers, segregation at the discharge, severe wear at transfers, segregation over rollers, slow belts, not being able to start or stop a loaded belt, drying, loss of paste, and contamination of the RCC lift surface by material dropping off the return side of belts are the most common problems. A detailed discussion of conveyor equipment and methods can be found in the literature (Oury and Schrader, 1992).

Where equipment is readily available for lease or rent, an all-conveyor system can be as economical and practical for small projects as it is for larger projects. The 4000-yd³ Echo Lake Dam in California is an example. The project utilized a highway-mobile, all-conveyor delivery system that was driven to the job site and erected in one day. It was used the next two days for RCC placement where haul units could not possibly work and was then driven off to the next project. It was fed from an equally mobile RCC continuous-mix pugmill.

A written agreement stating that the schedule and design are based on a required predeveloped conveyor delivery system is an approach that can be used at the time of the design so the engineer can confidently base the design on the better quality, cleaner, and faster lifts placed by specialized RCC conveyors, rather than relying upon the slower production and lower quality lift surfaces typical when haul vehicles are used on the surface. The supplier guarantees availability of the equipment, the required production capability, “not to exceed” reasonable downtimes, and availability of field technicians to assist the contractor. The supplier also guarantees a “not to exceed” price that will be quoted to all qualified bidders. The agreement should address an appropriate allowance for downtime and on-site spare parts.

Allowance is made for contractors to submit a more elaborate conveyor system, whereby, at their option, their costs may be greater but they purchase rather than lease the equipment or they achieve faster production rates. This approach has been used on public projects in at least two countries, with legal documents being created that satisfy all public entities as well as the designer, supplier, and contractors. This approach has proven to be good for owners, designers, and contractors. It reduces risk, ensures a low, preestablished cost, guarantees placement methods that are compatible with design, and helps maintain the planned construction schedule.

All-conveyor delivery systems can be supported and arranged in several ways. One approach that has been used for many years, including on projects such as the Cuchillo Negro Dam, Lake Robertson Dam, Loyalty Road Dam, and others, utilizes vertical posts embedded in, and raised with, the dam to support and raise the conveyors. Conveyors reach from the posts to essentially anywhere on the dam surface. Seigrist and Spring Hollow Dams are examples where conveyors were used that were supported from smaller pipe posts anchored to the upstream face of the dam with a long conveyor that extended the full length of the upstream face of the dam and that raised with the dam. This approach was successful, but the procedure has not become popular because other methods have been more effective and adaptable to changing field conditions. The conveyor feeds a tripper that runs along the main belt at the upstream face to feed a crawler-mounted mobile conveyor placer on the lift surface. The crawler placer can drive on the surface, extend or retract its conveyor, lift it, or swing it similar to the boom on a hydraulic crane. This allows the operator to deposit the RCC in a layer at its final location. Smoothing the layer with a bulldozer and compaction can follow immediately after the RCC has been deposited from the conveyor. A similar procedure was used for much of the San Rafael Dam in Mexico. The crawler placer, with a different setup for the conveyors that fed to it, was used at Concepcion Dam in Honduras and is being used at the Pangué Dam in Chile and other RCC dams.

For Echo Lake and Big Haynes Dams, wheel-mounted conveyors, called *creter cranes*, and swingers reached from outside the dam to the lift surface to deposit the RCC in layers; however, this method is only suitable for small dams or for the smaller upper abutment portions of larger dams, as was done at Burnett River Dam. Burton Gorge Dam in Australia utilized a partial conveyor system with a belt feeding



FIGURE 20.49 Tower belt with 320-ft reach at Miel I dam in Colombia.

continuously from a pugmill mixer to a hopper on the dam. Trucks then hauled the RCC from the hopper to the placing area. Problems with this type of system include continual raising of the hopper, segregation at the edges of each load dumped into and out of the trucks, damage to the surface caused by the truck tires, and insufficient room at the top of the dam for the hopper and trucks.

Large dams now typically use a *tower belt*. The largest towers may stand more than 200 ft above the surface of the dam and raise with it. They also can reach as high as 300 ft. The tower supports a horizontal boom with a line and hook that virtually hang a large conveyor out in space, or it can be used to lift very large loads at long reaches when used as a traditional crane. The tower itself can also be rigged to support connected segments of conveyor belt in space, leaving the crane available for other tasks. The conveyor belts typically feed a large *crawler placer*. This equipment is essentially a crawler-mounted crane with another belt for a boom. The belt can extend in or out, swing left or right, and angle up or down to deposit RCC in even windrows at essentially any location on the dam. Within a couple minutes of mixing, fresh RCC is typically delivered and placed on the dam with this type of system at rates ranging from about 200 to 1000 yd³/hr. The Miel I dam in Colombia is one example (Figure 20.49). Exposure time on conveyors should be as short as practical, with a maximum typically of about 5 minutes. Belt speeds should be on the order of about 10 to 30 ft/sec. Covering the conveyor to protect the mixture from drying and from rain should be required for all long sections and preferably for the entire system.

A well-designed conveyor system can also be capable of handling conventional concretes concurrently with RCC; however, this may complicate the placing operation unless separate parallel conveyors for the RCC and conventional concrete are provided. On the Elk Creek project, a larger belt was used for RCC while a parallel smaller one was used for conventional concrete, bedding mixes, facing mixes, and grout. It is especially important that conveyors do not allow RCC or other material to fall onto the compacted RCC surface along the conveyor path. Because of the rapid rise of RCC dams, conveyor systems should

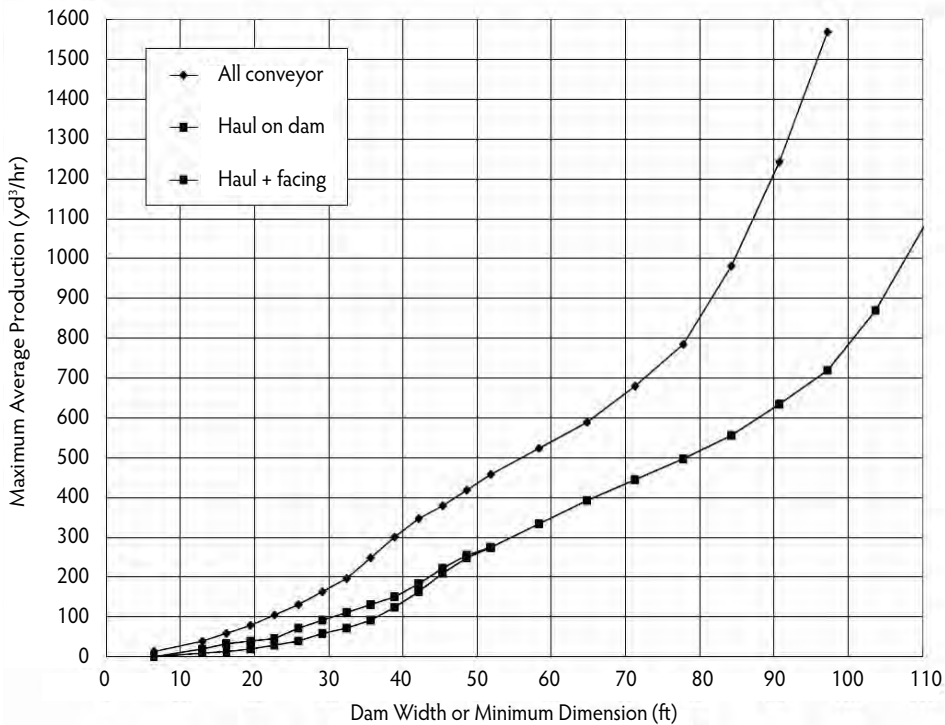


FIGURE 20.50 RCC production in confined work areas.

be designed to be raised quickly. When conveyors are located above the lift surface, provision must be made for clearance of equipment operating under them.

As with conventional mass-concrete conveyor systems, special attention should be given to belt widths, speed, protection, maintenance, incline angles, backup systems, and spare parts. Belt scrapers should be provided to clean return belts, which typically require frequent attention for adjustment and wear. Special attention is necessary to prevent segregation at transfer points and at any interim hoppers or bins.

A continuous belt running from the mixer to the final placement area can substantially increase placing rates and significantly reduce other equipment needs and their related labor requirements. Figure 20.50 compares typical average achievable productivities for reduced dam widths when delivery is totally by conveyor and when haul vehicles are used on the dam. Without a conveyor, productivity decreases to very low rates in narrow sections such as at the top of a dam. Figure 20.50 is based on a compilation of actual data at various projects and from computed round-trip delivery times at other projects.

In addition to the benefits of full-conveyor delivery (no hoppers, fast delivery, less congestion, no haul roads, less maintenance, less labor, elimination of lift-surface damage from haul vehicles, and improved productivity), the conveyor can also serve as an access walkway and as a support for lights, water, air, and electric lines to the placement area. A plan has even been developed to use the conveyor as a support for a roof or enclosure to protect the placement area from rain, sun, and wind.

When haul units are used to distribute RCC that is conveyed to the lift surface, a hopper arrangement that continuously loads them will be necessary at the end of the main conveyor. The objective is to allow the mixers and conveyors to operate and discharge without interruption or waiting for haul vehicles. The recommended minimum size of the hopper is at least twice the size of the haul vehicle. Because of the relatively high unit weight of freshly mixed RCC compared to the loose unit weight of soil, rock, or gravel normally hauled in these vehicles, weight rather than volume normally controls the amount of material hauled per trip. Bottom-dump trailers and scrapers minimize segregation, spreading requirements, and the distance the RCC drops, but they are difficult to use near abutments and obstructions. Scrapers have

better mobility than bottom-dump trailers of the highway type. Scrapers and bottom-dumps trailers have the advantage of depositing material in the layer to be spread as they are moving. This was common method of placement in some early RCC projects, but it has lost favor to large articulated trucks with special tailgates that minimize segregation or to all-conveyor delivery.

Front-end loaders have been used to deliver RCC from a central feed point on the placement to the location where it is spread. This is generally not suitable and should not be done on large projects or in critical areas. The method has resulted in problems with contamination of joint surfaces, limited productivity, and segregation. In special cases, however, where the mixture is not susceptible to segregation, spillage can be avoided, and tire tracking is not a problem, this method may result in the most economical situation that is also technically acceptable. Principle candidates for this approach are smaller dams in tight canyons where the distance for loader travel is minimal. Also, the projects should preferably have a smaller maximum size aggregate, excellent gradation, and a tendency for a higher paste and cementitious content. In addition, each layer should be placed and compacted before the set time of the previous layer. Extra cleaning or special grout or bedding mixtures may be appropriate between layers when they are not placed and compacted before the previous layer reaches its final set. If vehicles are to be used for transporting RCC, a thorough study should be made of the haul route. Problems that may prevent hauling by road include steep and rough terrain, availability of road-building material, plant location, schedule, and environmental considerations. If the concrete plant is located upstream of a dam, it may not be practical to bring the road through or over the upstream face system. Raising the roads to keep up with the rate of rise of the dam may require so much time that it becomes an inefficient system at higher elevations. To avoid slowing down the mixing and placing operations, raising the roads during a 2- to 4-hr/day shutdown period while maintenance and other work is being done should be considered. Roads must be kept at slopes consistent with the capabilities and safety requirements of the equipment.

Haul roads should make the transition onto the lift surface at a shallow angle if possible (plan view) so turning and damage by tires are minimized. If an immediate right-angle turn is necessary (from roads that enter directly onto the dam perpendicular to the face), significant scuffing and lift-surface damage will result. Operators should move slowly while turning and use the largest turning radius possible. The road should be constructed with clean, free-draining rock or gravels, if possible.

The last portion of the road prior to entering the lift should be surfaced with large aggregate or clean rock material that minimizes contamination of the RCC surface from truck tires. Simply extending the RCC onto the road will not provide cleaning action. To prevent lift contamination, it may be necessary to use water sprays to wash vehicle wheels before they are allowed on the lift surface, but excess water dripping from the truck and its tires can become a problem. To minimize adverse effects on the surface, hauling equipment should not travel in a concentrated path on the lift. Even with all of the above precautions, experience, including observation and cores, has shown that damaged lift surfaces should be expected where haul roads onto the dam are used.

When the RCC is hauled to the placing location and dumped, it should generally be deposited on previously spread but uncompacted material and pushed forward onto the compacted lift surface. This provides remixing action and minimizes clusters of coarse aggregate that otherwise would tend to occur at the lift interface. When RCC is dumped in large piles, larger aggregates tend to roll down the outside of the piles and create clusters. A general rule is to limit the height of a pile to 5 ft. Correcting this kind of segregation is nearly impossible if the rock has already rolled onto a previously compacted lift. Where this condition occurs, the segregated large aggregate must be removed, broadcast onto the RCC layer being spread, or wasted.

20.6.5 Placing and Spreading

A preferred technique for placing RCC is to advance each lift from one abutment to the other. An exception is where the distance from abutment to abutment is smaller than the distance from the upstream to the downstream face, such as at the bottom of dams in narrow canyons. In this case, placing can begin by working in the upstream–downstream direction. Large dams, where the distance from abutment to

abutment is long and where all of the foundation may not be ready at the time RCC placement starts, can benefit from placing between forms within any group of monolith blocks if the area is large enough for efficient production. This will also reduce the time of exposure of each lift, thereby improving lift-joint quality. The practice from embankment construction of limiting the direction in which rolling equipment can operate does not apply to RCC.

Some early RCC projects considered, recommended, approved, or required placing RCC in paving lanes, typically going from abutment to abutment. This initially seemed like a logical approach, but the practice is now discouraged or prohibited. The problems with it are more serious with low-cementitious-content, dry-consistency, and large aggregate mixtures. Although they may work well with paving mixtures and paving operations, spreader boxes attached to dump trucks, Jersey spreaders attached to dozer equipment, and paving machines lack mobility and occupy important space in narrow areas of the dam. They can be difficult to maneuver at the abutments. Paving lanes tend to leave segregation along the edge of the lanes with dam mixtures. The edges can also become too old to be well mixed and compacted into RCC of the adjacent lane by the time the adjacent lane is placed. The edge also tends to dry out while exposed prior to placing the adjacent lane. This has resulted in concerns over poor quality and weakened or permeable planes through the dam at the interface of paving lanes. For a high-cementitious-content mix with smaller aggregate, a wetter consistency, and a retarded set time, concerns about placing using pavement lanes are reduced.

Tracked dozer equipment has proven to be best for spreading RCC. It is fast and sufficiently accurate and contributes to uniformly compacted RCC. By careful spreading, a bulldozer can remix RCC and minimize segregation that results from dumping. Careful attention should be given to ensure that remixing is occurring and that the dozer is not simply burying segregated material. At Elk Creek Dam, retarded RCC mixtures with a Vebe time of 15 to 25 sec were end dumped in piles at least 35 ft from the advancing face. Dozers knocked down the piles and spread the RCC forward into thin, unsegregated, 6-in.-thick layers until a full lift thickness of 24 in. was reached. The entire surface of each layer was traversed by at least two passes of the dozer tracks. This dozer action produced an average density of 147 pcf. Only the top of the 24-in. full thickness of the lift then required additional compaction by the roller. Similar results have been achieved with other RCC mixtures having a wet mixture consistency. At Nickajack Dam, wet-consistency, air-entrained RCC was spread in two 12-in.-thick layers, with the second layer following behind the first layer. The second layer was compacted before the first reached initial set. The advancing layer was about 100 ft in front of the following layer.

At Burton Gorge Dam in Australia, 100% compaction was achieved using a small dozer in the top portion of the dam by modifying the mixture with retarder, using a wetter consistency, placing rapidly (one lift every 1 to 4 hours), and rigorously tracking the 12-in.-thick layers as they were spread. This resulted in densities that reached the theoretical air-free density of the mixture. Thorough dozer tracking the same mixture at a dry consistency and without retarder, but while the mixture was less than about 30 minutes old, achieved densities on the order of about 96% of the theoretical air-free values. This was followed by roller compaction to achieve a higher final density.

Typically, two rollers and one D6 dozer with a backup smaller dozer can spread and roll nonretarded RCC at a rate of about 300 to 500 yd³/hr in 12-in.-thick layers. The dozer should operate on fresh RCC that has not been compacted. All turning and crabbing should be done on uncompacted material. Operating the dozer on a compacted surface will damage the surface, unless the dozer is equipped with rubber tracks and the operator uses special care. Recently a device has been developed with rubber tires that attaches to the dozer. The device is lowered to lift the tracks off the surface so the dozer can drive across the RCC from one end to the other without causing damage. When it is necessary for the dozer without this device to drive onto compacted RCC, the operator should limit the movement to straight back-and-forth travel. Track marks made prior to the mixture reaching initial set can be recompacted by the vibratory roller without significant loss of joint quality; however, damaged surfaces that are recompacted after the mixture has set or if it has dried will have little or no strength, even though they may have acceptable surface appearance. Damaged material can be easily removed by blowing with an air jet, even many hours later. Material that is recompacted early enough will remain cemented in place if blown with an air jet.

A relatively recent development in RCC spreading is the *slope-layer method*. Starting from a previous level lift surface, the RCC layer is placed on a slope of about 10 (H):1 (V), more or less. The first layer is then just a small fillet of RCC. A second layer is immediately placed over this at the same slope followed by a third, fourth, and subsequent layers, until the vertical depth of the multiple layers at the high end is some preestablished height on the order of about 6 ft, more or less. This becomes the total lift height for the multiple layers. Because of the slope of the layers, the length of each layer is minimized. In the case of a 10 (H):1 (V) slope and 6-ft lift depth, the distance is only 60 ft. This allows each layer to be placed before the subsequent layer approaches its setting time. Lift-joint cleaning is not really required except when contamination is an issue, and the layers will bond together in one mass without noticeable layer joints lines. The final top surface requires special attention afterward for cleanup before starting the next lift of multiple layers. The procedure must be coordinated with forming and form supports, so it has places where it is beneficial and places where it is not advantageous.

Spreading equipment should leave a flat or plane surface of the proper thickness before the roller does its compaction. The roller should not bridge over high points and miss providing full compaction at low points of freshly spread lift surface. Depending on the workability of the mixture, ridges or steps between adjacent passes of the dozer blade can result in uneven compactive efforts and variable quality in the RCC. As a general rule, having a flat surface ready to roll in the least amount of time is more important than having an exact grade with delayed rolling. Typical tolerances for lift thicknesses are on the order of ± 2 in., except for the exposed final lift surface in a structure, which typically has a much smaller tolerance.

Where special mixtures are specified (e.g., at the upstream or downstream face), special procedures are required. If conventional concrete is used against a formed face with a dry-consistency RCC mass behind it, the conventional mixture should be placed first and the RCC immediately spread against and on top of the sloping unformed face of the conventional concrete. The conventional mixture should be designed to lose slump rapidly but not set rapidly. This allows the RCC to be compacted into the conventional concrete before either mixture sets. If the conventional concrete does not lose slump soon enough, the roller will sink into it resulting in a variety of construction problems. If rolling is delayed while waiting for the conventional mixture to stiffen, the RCC can become too old for proper compaction. If the roller operator simply stays back from the conventional concrete far enough to avoid sinking into it or shoving it up, the two mixtures will not adequately compact or join together. Using more of the conventional concrete makes the problem worse. Usually, only 12 in. of conventional concrete is used, but some projects have been successful with only a few inches of facing. If the facing concrete is wider than about 18 in., the mixture is usually consolidated with immersion-type vibrators while the adjacent RCC is rolled.

If the RCC has a wetter consistency, and especially if it has a delayed set, it is possible to place the conventional concrete mixture after the RCC. The facing concrete still needs to have a relatively low slump when RCC compaction is performed, but it can still be possible to immersion vibrate the interface region of the RCC and conventional concrete. With this procedure, the width of conventional concrete has typically been wider than when conventional facing mixtures are used with drier consistency RCC; however, experience, coring, and internal destructive investigations have shown that a poor interface of the two mixtures has often resulted with this procedure, even when the two mixtures appeared to respond well to immersion vibration and the exposed top surface of the layers looked well consolidated.

The most common compacted lift thickness has been 12 in. Typically, large, dual-drum vibratory rollers can develop full compaction of this thickness with only four to five passes. A factor influencing lift thickness is the maximum allowed exposure time before covering one lift with the subsequent lift. Each project should be studied to optimize the benefits of thicker or thinner lifts. Thicker lifts mean longer exposure times but fewer lift joints and fewer potential seepage paths. Thinner lifts result in more potential joints but allow the joints to be covered sooner with better bonds.

At the start of extremely rough foundations and where the foundation has deep holes that have not been filled with dental or leveling concrete, a front-end loader or excavator bucket can sometimes be used to reach the placement site to deposit material. This is a slow operation but may be the only practical

solution for some locations. The problem is eliminated with the all-conveyor delivery system or with mobile conveyors that reach across and into areas of rough terrain.

The equivalent of a Cat D-4 Case 550 rubber track or a JD-450 is required to start the foundation and for tight conditions. With an all-conveyor delivery system, a Cat D-4 is generally capable of spreading RCC at a rate of about 300 yd³/hr. Dozers should have hydraulic tilt and angle capability. It is common to underestimate the value of good spreading equipment and operators. Graders have been used on some RCC projects, but they generally are not necessary and can actually become a problem. They are difficult to maneuver in small areas, and the tires can damage otherwise good compacted surfaces. There also is a tendency to overwork and rework the surface as if it were soil instead of concrete with a limited working time.

20.6.6 Compaction

Maneuverability, compactive force, drum size, frequency, amplitude, operating speed, and required maintenance are all parameters to be considered in the selection of a roller. The compactive output in volume of concrete per hour obviously increases with the physical size and speed of the roller, but larger size rollers do not necessarily give the same or better density and compactive effort as smaller rollers with a greater dynamic force per unit of drum width. Job size, workability, lift depth, the extent of consolidation due to dozer action, and space limitations will usually dictate roller selection. Large rollers cannot operate closer than about 6 in. to vertical formwork or obstacles, so smaller hand-guided compaction equipment is usually required to compact RCC in these areas. If a slipformed or precast facing system that has an interior face sloping away from the RCC is used, the large rollers can operate all the way to the facing.

The dynamic force per unit of drum width or per area of impact on tampers is the primary factor that establishes effectiveness of the compaction equipment. Most experience has also shown that rollers with a higher frequency and lower amplitude compact RCC better than rollers with high amplitude and lower frequency, although suitable results have been achieved on some projects using rollers with both high frequency and amplitude. The typical compactor is a 10-ton double- or single-drum roller with a dynamic force of at least 475 lb of force per inch of drum width. These rollers are typically used for asphalt and roadway compaction. Larger 15- and 20-ton rollers of greater mass and size, typically used with rockfill construction, have been used with RCC, but they usually have larger amplitudes and lower frequency and are less suited to the aggregate gradings used in RCC. Achieving density and a good lift-joint interface is more difficult with these larger rollers.

In tight areas such as adjacent to forms and next to rock outcrops, large tamping foot-type compactors are most suitable. They are mobile and can provide high-impact energy to produce good density; however, they usually do not leave a smooth surface and they can sink when tamping RCC that has been placed over an excessive thickness of wet bedding mixture, when tamping RCC with excess water, or when tamping next to a conventional concrete mixture that has not lost its slump. One-man vibrating plate compactors intended for sands are not very effective, but the more recent massive plate compactors intended for deep lifts of gravel are effective, although they may require multiple passes. Walk-behind rollers are not very effective in most cases unless they can produce a dynamic force on the order of about 250 lb/in. of drum width. Four to six passes of this type roller on fresh RCC not deeper than 12 in. usually results in suitable compaction for tight areas, with densities about 98% of those achieved with the large roller. This reduced density is often considered acceptable, except for special areas that are identified as critical and truly in need of greater compaction.

The appearance of fully compacted RCC is dependent on the mixture proportions. Mixtures of wetter consistency usually exhibit a discernible pressure wave in front of the roller. If the paste content is equal to or less than the volume required to fill all the aggregate voids, rock-to-rock aggregate contact occurs and a pressure wave may not be apparent. This can also occur if the mixture is simply too dry to develop internal pore pressure under the dynamic effect of the roller. Mixtures that have more paste than necessary to fill aggregate voids and a wetter consistency will result in visible paste at the surface that may pick up

on the roller drum, depending on the constituents and plasticity of the paste. The fresh mixture surface should be spread in such a way that the roller drum produces a consistent compactive pressure under the entire width of the drum. If the uncompacted lift surface is not reasonably smooth, the drum may overcompact high spots and undercompact low spots.

Minor damage from scuff marks and unavoidable dozer tears in the surface of a freshly compacted lift can usually be immediately rolled down with the vibratory drum in a static mode or with a rubber tire roller. If the mixture was sufficiently fresh and moist when rerolled, a suitable rehabilitation of the damage will result. If the mixture is too old, severely damaged, etc., the rerolled RCC may look acceptable, but it can and should be easily blown off by an air hose used for general cleanup of loose debris on the lift. For sliding stability, joint tension, or watertightness, designs usually require clean and relatively fresh joint surfaces with good bond. This is typically achieved by the use of a suitable large vacuum truck or air blowing. Some tests have shown sandblasting at 24 and 72 hr can actually reduce bond.

20.6.7 Joint Treatment and Inspection

Lift-joint damage from free surface water (rain or overcuring) was discussed in Section 20.3.4 as it relates to the different types of RCC mixes (i.e., wetter or drier consistency and inspection). Lift joints should be kept from drying or freezing continuously, 24 hr per day, 7 days per week, prior to the next layer of RCC. Tests and experience have shown, however, that allowing the surface to dry back to just under an SSD condition, as indicated by a change in color from darker to lighter, will greatly facilitate cleaning by air blowing and will not reduce joint quality for most RCC. Some tests have even shown a slight increase in joint strength. Rewetting the surface after final cleaning and just prior to spreading RCC over it is considered prudent. In addition to the benefit of cure, keeping the surface from drying out provides evaporative surface cooling, thus reducing internal temperatures and providing a lower joint maturity value. If the surface is more than about 2 days old and it has become sufficiently hard, water washing may be necessary if air blowing alone does not adequately clean off any damage, contamination, and general laitance that may be present. Water washing can only be used after the surface has hardened. Sandblasting is generally not advised or necessary.

Roller-compacted concrete mixtures generally do not bleed or develop laitance at the surface. An exception is very wet mixtures and some cases of dry mixtures after days of moist cure. If there is no weak laitance or other contamination at the surface, the lift-joint cleaning typically required with conventional concrete is not necessary. Although it is the subject of some debate, minor intermittent laitance that may occur in some situations is generally not removed.

If the construction joint is less than about 1500°F degree-hr old and if it has been kept clean and moist throughout its exposure, no joint treatment is required under most conditions. If the surface has been contaminated by dirt, mud, or other foreign elements, the contamination should be removed. The degree-hr maturity is the sum of the temperatures of the lift surface measured every hour during the time that it is exposed. If the surface has been allowed to dry out, exceed about 1500°F degree-hr of maturity, or became damaged, it should be cleaned and may require a full or partial bedding mixture prior to placement of RCC. The 1500°F degree-hr used here is an example. It may be 900 at one project and 2100 at another. These variables make specifications for RCC lift surfaces difficult to write, and they leave inspection of this most critical item to the judgment of both the designer and contractor.

20.6.8 Curing and Weather Protection

After the RCC has been placed and compacted, the lift surface must be cured and protected, just as for concrete placed by conventional methods. The surface must be maintained in a moist condition, or at least so moisture does not escape. It should also be protected from temperature extremes and freezing until it gains sufficient strength. When haul vehicles are used on the lift surface, RCC placement typically must immediately stop with even the slightest rainfall; otherwise, the tires will turn the surface into a soft damaged material that then will require waiting for the RCC to harden so extensive cleanup can be

undertaken. When conveyors are used for delivery and little or no vehicular traffic is required on the RCC, construction can continue in slight rainfall. This may require a gradual and very slight decrease in the amount of mixture water used because of the higher humidity and lack of surface drying. Table 20.3, based on data covering various types of mixes and delivery methods throughout the world over the past 15 years, provides guidance with regard to the effect of rain on RCC placing operations. Immediately after an RCC lift has been compacted, it is essentially impermeable and will not become damaged by light to moderate rain if there is no hauling or traffic on the surface. After a rain, hauling on the lift can resume only after the surface has begun to dry naturally to a SSD condition. A slightly sloped surface will aid in draining free water and speed resumption of placing operations.

Cure during construction has been accomplished with modified water trucks on larger projects and with hand-held hoses for all size projects. Trucks should be equipped with fog nozzles that apply a fine mist that does not wash or erode the surface. Trucks can be augmented with hand-held hoses that reach areas that are inaccessible to the water truck. Provision must be made for maintaining the damp surface while the trucks are fueled, maintained, and refilled with water. Care should be exercised that the trucks do a minimum amount of turning and minimally disrupt the surface. Maintaining access on and off every lift during construction can be a problem that makes trucks impractical; consequently, the recent trend has been to use hand-held hoses rather than water trucks.

The final lift of RCC should be cured for an appropriate time, generally in excess of 14 days. Curing compound is unsuitable because of the difficulty in achieving 100% coverage on the relatively rough surface, the probable damage to the surface from construction activity, the low initial moisture in the mixture, and the loss of beneficial surface temperature control that is associated with moist curing. Unformed sloping surfaces such as the downstream face of a dam are very difficult to compact and can be considered sacrificial and unnecessary to cure provided this has been incorporated into the design. Uncompacted exposed RCC will be subject to raveling. Whereas the outside several inches will be incapable of achieving any significant strength or quality, they will serve as protection and a moisture barrier for the curing of the interior RCC.

Defining Terms

Abutment—The foundation along the sides of the valley or gorge against which a dam is constructed.

Autogenous volume change—The change in volume produced by continued hydration of concrete exclusive of effects external forces, water changes, and temperature changes.

Cementitious material—The fine solid-particle material in concrete that reacts in solution with water and at times other fine solid particles to create a hardened concrete with strength; Portland cement, sometimes with pozzolan, is usually used.

Coefficient of thermal expansion—The change in linear dimension per unit length divided by the temperature change.

Cohesion—The adhesion of concrete or mortar to other concrete, rock, and other materials.

Creep—Deformation over a long period of time under a continuous sustained load; also, the relaxation or reduction of stress over a long period of time under a sustained deformation.

Durability—The ability of concrete to resist weathering action, chemical attack, abrasion, and other service conditions.

Gallery—A long, narrow passage in a dam or concrete mass used for access, inspection, grouting, drilling drain holes, and collecting seepage.

Grout curtain—A row of holes filled with grout under pressure near the heel of a dam to control seepage under the dam.

Heat of hydration—Heat generated by chemical reactions of cementitious materials with water, such as the heat evolved during setting and hardening of Portland cement.

Lift-joint quality index (LJQI)—A numerical designation indicating the quality of a concrete lift joint, derived from evaluation of the factors affecting the quality of the joint.

Modulus of elasticity (elastic modulus)—The ratio of stress to strain in the elastic region of behavior prior to development of nonrecoverable microfracturing.

Monolith—A section or block of a large structure such as a dam that is bounded by free faces or contraction joints.

Paste—That portion of a fresh concrete mixture that is composed of a mixture of all particles that will pass through a No. 200 or 75- μm sieve (namely, cement, pozzolan or fly ash, water, small air bubbles, admixtures, and aggregate fines).

Permeability—The rate of flow of water through a unit cross-sectional area under a unit hydrostatic gradient.

Poisson's ratio—The ratio of transverse strain to axial strain resulting from a uniformly distributed axial stress.

Pozzolan—A finely divided powder that is composed of siliceous and other minerals that react with the byproducts of Portland cement hydration to form additional cementitious materials.

Principal stress—Maximum and minimum stress occurring at right angles to a principal plane of stress.

Pugmill—A mixing chamber usually composed of two horizontal rotating shafts to which mixing paddles are attached.

Restraint—Internal or external restriction of free movement of concrete in one or more directions.

Roller-compacted concrete (RCC)—A relatively dry concrete mixture that can be compacted by vibratory rolling, usually by a 10-ton roller.

Sustained modulus of elasticity—The modulus of elasticity of concrete that occurs under constant sustained load, including the effects of creep.

Theoretical air-free density—The density corresponding to a concrete that has been compacted to 100% solids with no air.

Ultimate modulus—The ratio of stress to strain that occurs at the maximum load beyond which concrete loses strength and fails.

References

-
- ACI Committee 116. 2000. *Cement and Concrete Terminology*, ACI 116R-2000. American Concrete Institute, Farmington Hills, MI.
- ACI Committee 207.5R. 1999. *Roller Compacted Mass Concrete*, ACI 207.5R-99. American Concrete Institute, Farmington Hills, MI.
- ACI Committee 214. 2002. *Evaluation of Strength Tests of Concrete*, ACI 214R. American Concrete Institute, Farmington Hills, MI.
- Angulo, C., Schrader, E.K., Santana, H., Castro, G., Salazar, H., and Lopez, J. 1995. Miel I dam. In *Proceedings, International Symposium on Roller Compacted Concrete Dams*, October 2–4, Santander, Spain, pp. 443–456.
- Boggs, H.L. and Richardson, A.T. 1985. USBR design considerations for roller-compacted concrete dams. In *Roller-Compacted Concrete*, Hansen, K.D., Ed. American Society of Civil Engineers, New York.
- Cannon, R.W. 1985. Design considerations for roller-compacted concrete and rollcrete in dams. *Concrete Int.*, 7(12), pp. 50–58.
- Chengqian, L. and Chusheng, C. 1991. A small naked freeze-resistant RCC dam. In *Proceedings, International Symposium on Roller-Compacted Concrete Dams*, Zheren, D., Ed. Chinese Society for Hydroelectric Engineering, Beijing, China.
- Ditchy, E. and Schrader, E.K. 1988. Monksville Dam temperature studies. In *Proceedings of ICOLD 16th Congress*, Vol. III, Q62, pp. 379–396. International Commission on Large Dams, Paris.
- Dolen, T.P. and Tayabji, S.D. 1988. Bond strength of roller compacted concrete. In *Roller Compacted Concrete II*, Hansen, K.D. and Guice, L.K., Eds., pp. 170–186. American Society of Civil Engineers, New York.

- Dunstan, M.R.H. 1981. *Rolled Concrete for Dams: A Laboratory Study of the Properties of High Fly Ash Content Concrete*, Technical Note 105. Construction Industry Research and Information Association, London.
- Forbes, B.A. 1988. RCC in dams in Australia. In *Roller Compacted Concrete II*, Hansen, K.D. and Guice, L.K., Eds., pp. 323–339. American Society of Civil Engineers, New York.
- Gaekel, L. and Schrader, E.K. 1992. RCC mixes and properties using poor quality materials: Concepcion dam. In *Roller Compacted Concrete II*, Hansen, K.D. and Guice, L.K., Eds., pp. 340–357. American Society of Civil Engineers, New York.
- Gentile, G. 1964. Study, preparation, and placement of low cement concrete, with special regard to its use in solid gravity dams. In *Transactions of the Eighth International Congress on Large Dams*, R16 Q 30. International Commission on Large Dams, Paris.
- Giovagnoli, M., Schrader, E.K., and Ercoli, F. 1991. Design and construction of Concepcion Dam. In *Proceedings of International Symposium on Roller Compacted Concrete Dams*, September, Beijing, pp. 49–56.
- Giovagnoli M., Ercoli, F., and Schrader, E.K. 1992. Concepcion Dam design and construction. In *Roller-Compacted Concrete III*, Hansen, K.D. and McLean, F.G., Eds., pp. 198–213. American Society of Civil Engineers, New York.
- Hansen, K. and Reinhardt, W. 1991. *Roller-Compacted Concrete Dams*. McGraw-Hill, New York.
- Herweynen, R., Griggs, T., Schrader, E., and Starr, D. 2004. Burnett RCC Dam design: an innovative approach to site-specific conditions. In *Proceedings of ANCOLD Conference on Dams*, November 13–17, Melbourne, Australia.
- Hirose, T., Nagayama, I., Takemura, K., and Sato, H. 1988. A study of control of temperature cracks in large roller compacted concrete dams. In *Transactions of the 16th International Congress on Large Dams*, June, San Francisco, CA, pp. 119–135.
- ICOLD. 1989. *Roller-Compacted Concrete for Gravity Dams: State of the Art*, Bulletin 75. International Commission on Large Dams, Paris.
- Jansen, R.B. 1989. *Advanced Dam Engineering for Design, Construction, and Rehabilitation*. Van Nostrand Reinhold, New York.
- Lopez, J., Castro, G., and Schrader, E. 2003a. RCC mix and thermal behavior of Miel I dam: design stage. In *Roller Compacted Concrete Dams*, Berga, L., Buil, J., Jofré, C., and Chonggang, S., Eds., pp. 789–798. Swets & Zeitlinger, Lisse.
- Lopez, J., Aridah, M., and Schrader, E. 2003b. RCC quality control for Mujib dam. In *Roller Compacted Concrete Dams*, Berga, L., Buil, J., Jofré, C., and Chonggang, S., Eds., pp. 983–994. Swets & Zeitlinger, Lisse.
- Lopez, J., Griggs, T., Montalvo, R., Herweynen, R., and Schrader, E. 2005. RCC construction and quality control for Burnett Dam. In *Proceedings of the ANCOLD Conference on Dams*, November 21–22, Fremantle, Australia.
- McLean, F.G. and Pierce, J.S. 1988. Comparison of joint strengths for conventional and roller-compacted concrete. In *Roller Compacted Concrete II*, Hansen, K.D. and Guice, L.K., Eds. American Society of Civil Engineers, New York.
- Oberholtzer, G. L., Lorenzo, A., and Schrader, E.K. 1988. Roller-compacted concrete design for Uruguay I Dam. In *Roller Compacted Concrete II*, Hansen, K.D. and Guice, L.K., Eds. American Society of Civil Engineers, New York.
- Oury R. and Schrader, E.K. 1992. Mixing and delivery of roller compacted concrete. In *Roller-Compacted Concrete III*, Hansen, K.D. and McLean, F.G., Eds. American Society of Civil Engineers, New York.
- Parker, J.W. 1992. Economic factors in roller compacted concrete dam construction. In *Roller-Compacted Concrete III*, Hansen, K.D. and McLean, F.G., Eds., pp. 227–242. American Society of Civil Engineers, New York.
- Rizzo, P., Schrader, E., Gaekel, L., and Osterle, J. 2003. Saluda Dam mix design program. In *Roller Compacted Concrete Dams*, Berga, L., Buil, J., Jofré, C., and Chonggang, S., Eds., pp. 177–186. Swets & Zeitlinger, Lisse.

- Schrader, E.K. 1982a. The first concrete gravity dam designed and built for roller-compacted construction methods. *Concrete Int.*, October, pp. 15–24.
- Schrader, E.K. 1982b. World's first all-rollcrete dam. *Civil Eng. ASCE*, 52(4), 45–48.
- Schrader, E.K. 1984. *Willow Creek Dam Concrete Report*, Vols. 1 and 2, final update. U.S. Army Corps of Engineers, Walla Walla, WA.
- Schrader, E.K. 1986. Discussion of the article 'Design Considerations for Roller Compacted Concrete Rollcrete Dams,' by R. Cannon. *Concrete Int.*, pp. 63–64.
- Schrader, E.K. 1987. Design for strength variability: testing and effects on cracking in RCC and conventional concretes. In *Lewis H. Tuthill International Symposium on Concrete Construction*, ACI SP-104, Halvorsen, G.T., Ed., pp. 1–25. American Concrete Institute, Farmington Hills, MI.
- Schrader, E.K. 1988. Behavior of completed RCC dams. In *Roller Compacted Concrete II*, Hansen, K.D. and Guice, L.K., Eds., pp. 76–91. American Society of Civil Engineers, New York.
- Schrader, E.K. 1993. Design and facing options for RCC on various foundations. *Water Power Dam Construct.*, 45(2), 33–38.
- Schrader, E.K. 1994. Roller compacted concrete for dams: the state of the art. In *Advances in Concrete Technology*, 2nd ed., Malhotra, V.M., Ed., pp. 371–417. American Concrete Institute, Farmington Hills, MI.
- Schrader, E.K. 1995a. Seepage, permeability, uplift, and upstream facings for RCC dams. In *Supplemental Papers, Proceedings of the Second CANMET/ACI International Symposium on Advances in Concrete Technology*, June 11–14, Las Vegas, pp. 27–43.
- Schrader, E.K. 1995b. Strain, cracking, and failure described by an ultimate modulus. In *Proceedings of the Second CANMET/ACI International Symposium on Advances in Concrete Technology*, June 11–14, Las Vegas, pp. 419–437.
- Schrader, E.K. 1995c. General report: construction of roller compacted concrete dams. In *Proceedings, International Symposium on Roller Compacted Concrete Dams*, October 2–4, Santander, Spain, pp. 1263–1295.
- Schrader, E.K. 1995d. RCC: current practice, controversies, and options. In *Proceedings of the ICOLD Conference*, July 6, Oslo, Norway, pp. 433–452.
- Schrader, E.K., 1999a. Shear strength and lift joint quality of RCC. *Hydropower & Dams*, 1, 46–55.
- Schrader, E.K., 1999b. Design, construction, and performance of Burton Gorge RCC dam. *Hydropower & Dams*, 1, 63–72.
- Schrader, E.K. 2002. Experiences and lessons learned in 30 years of design, testing, construction and performance of RCC dams. *U.S. Soc. Dams*, 127, 8–14.
- Schrader, E.K. 2003a. Performance of roller compacted concrete (RCC) dams: an honest assessment, keynote lecture. In *Roller Compacted Concrete Dams*, Berga, L., Buil, J., Jofré, C., and Chonggang, S., Eds., pp. 91–102. Swets & Zeitlinger, Lisse.
- Schrader, E.K. 2003b. Appropriate laboratory compaction methods for different types of roller compacted concrete (RCC). In *Roller Compacted Concrete Dams*, Berga, L., Buil, J., Jofré, C., and Chonggang, S., Eds., pp. 1037–1044. Swets & Zeitlinger, Lisse.
- Schrader, E.K. 2004. Roller-compacted concrete: understanding the mix. *Hydro Rev. Worldwide*, 12(6), 26–29.
- Schrader, E.K. 2006a. Building roller-compacted-concrete dams on unique foundations. *Hydro Rev. Worldwide*, 14(1), 28–33.
- Schrader, E.K. 2006b. Building roller-compacted-concrete dams on difficult foundations: practical examples. *Hydro Rev. Worldwide*, 1–1.
- Schrader, E.K. 2007. Statistical acceptance criteria for strength of mass concrete. *Concrete Int.*, 29(6), 61–65.
- Schrader, E.K. and Bali, J.A. 2003. Presa Rompepicos: a 109 meter high RCC dam at Corral des Palmas with final design during construction. In *Roller Compacted Concrete Dams*, Berga, L., Buil, J., Jofré, C., and Chonggang, S., Eds., pp. 859–864. Swets & Zeitlinger, Lisse.

- Schrader, E.K. and Namikas, D. 1988. Performance of roller compacted concrete dams. In *Proceedings of ICOLD 16th Congress*, Vol. III, Q62, pp. 339–364. International Commission on Large Dams, Paris.
- Schrader E.K. and Rashed, A. 2002. Benefits of non-linear stress-strain properties and membranes for RCC dams stresses. In *Proceedings of the International Conference on Roller Compacted Concrete Dam Construction in the Middle East*, Jordan University of Science and Technology, Irbid, Jordan, pp. 331–344.
- Schrader, E.K. and Rizzo, P.C. 2003. Extensive shear testing for Saluda dam roller compacted concrete. In *Roller Compacted Concrete Dams*, Berga, L., Buil, J., Jofré, C., and Chonggang, S., Eds., pp. 1045–1056. Swets & Zeitlinger, Lisse.
- Schrader, E.K. and Stefanakos, J. 1995. RCC cavitation and erosion resistance. In *Proceedings, International Symposium on Roller Compacted Concrete Dams*, October 2–4, Santander, Spain, pp. 1175–1188.
- Schrader, E.K., Lopez, J., and Aridah, M. 2003a. Mix design and properties of RCC at Mujib dam: high and low cementitious contents. In *Roller Compacted Concrete Dams*, Berga, L., Buil, J., Jofré, C., and Chonggang, S., Eds., pp. 859–864. Swets & Zeitlinger, Lisse.
- Schrader, E.K., Kristjansdoittir, U., Skulason, J., and Sveinbjornsson, S. 2003b. Design and mix studies with high and low cementitious content RCC for Nordlingaalda dam in Iceland. In *Roller Compacted Concrete Dams*, Berga, L., Buil, J., Jofré, C., and Chonggang, S., Eds., pp. 355–362. Swets & Zeitlinger, Lisse.
- Scuero, A. and Vaschetti, G. 2003. Synthetic geomembranes in RCC dams: since 1984, a reliable cost effective way to stop leakage. In *Roller Compacted Concrete Dams*, Berga, L., Buil, J., Jofré, C., and Chonggang, S., Eds., pp. 519–530. Swets & Zeitlinger, Lisse.
- Tatro, S.B. and Hinds, J.K. 1992. Roller compacted concrete mix design. In *Roller-Compacted Concrete III*, Hansen, K.D. and McLean, F.G., Eds. American Society of Civil Engineers, New York.
- Tatro, S.B. and Schrader, E.K. 1985. Thermal considerations for roller-compacted concrete. *J. Am. Concrete Inst.*, 119–128.
- Tatro, S.B. and Schrader, E.K. 1992. Thermal analysis for RCC: a practical approach. In *Roller-Compacted Concrete III*, Hansen, K.D. and McLean, F.G., Eds. American Society of Civil Engineers, New York.
- Tayabji, S.D. and Okamoto, A.S. 1987. *Bonding of Successive Layers of Roller Compacted Concrete*. Construction Technology Laboratories, Skokie, IL.
- USACE. 1981. *Willow Creek Design Memorandum*, Suppl. 1 to GDM 2, Phase 2. U.S. Army Corps of Engineers, Walla Walla, WA.
- USACE. 1995. *Gravity Dam Design*, Engineering Manual 1110-2-2200. U.S. Army Corps of Engineers, Walla Walla, WA.
- USACE. 1997. *Thermal Studies of Mass Concrete Structures*, Engineering Manual 1110-2-542. U.S. Army Corps of Engineers, Walla Walla, WA.
- Wallingford, V.M. 1970. Proposed new techniques for construction of concrete gravity dams. In *Proceedings of the Tenth International Congress on Large Dams*, June 1–5, Montreal, pp. 439–452.



(a)



(b)



(c)

(a) Impact testing to determine the stress-wave speed in concrete; (b) polarization resistance testing to determine the corrosion rate of reinforcing steel in concrete; and (c) testing for internal voids in concrete pipe by the impact-echo method. (Photographs courtesy of Germann Instruments, Inc.)

21

Nondestructive Test Methods

Nicholas J. Carino, Ph.D., FACI, FASTM*

21.1	Introduction	21-1
21.2	Methods to Estimate In-Place Strength.....	21-2
	Historical Background • Rebound Hammer • Ultrasonic Pulse Velocity • Probe Penetration • Pullout Test • Break-Off Test • Maturity Method • Statistical Methods	
21.3	Methods for Flaw Detection and Condition Assessment.....	21-28
	Introduction • Visual Inspection • Stress-Wave Propagation Methods • Infrared Thermography • Ground-Penetrating Radar • Electrical and Magnetic Methods for Reinforcement • Nuclear (Radioactive) Methods	
21.4	Concluding Remarks.....	21-62
	References	21-63

21.1 Introduction

Concrete differs from other construction materials in that it can be made from an infinite combination of suitable materials, and its final properties depend on the treatment it undergoes after it arrives at the job site. The efficiency of the consolidation and the effectiveness of curing procedures are critical for attaining the full potential of a concrete mixture. Although concrete is known for its durability, it is susceptible to a range of environmental degradation factors that can limit its service life. There has always been a need for test methods to measure the in-place properties of concrete for quality assurance and for evaluation of existing conditions. Ideally, these methods should be nondestructive so they do not impair the function of the structure and also permit retesting at the same locations to evaluate changes in properties with time.

Compared with the development of nondestructive test (NDT) methods for steel structures, the development of NDT methods for concrete has progressed at a slower pace, because concrete is inherently more difficult to test than steel. Concrete is highly heterogeneous, it is electrically nonconductive but usually contains significant amounts of steel reinforcement, and it is often used in thick members. Thus, it has not been easy to transfer NDT technologies developed for steel to the evaluation of concrete. In addition, there has been little interest among those from the traditional NDT community (physicists, electrical engineers, mechanical engineers) to develop test methods for concrete. Since the 1980s, however, advances have

* Concrete materials consultant and retired research structural engineer, National Institute of Standards and Technology, Gaithersburg, Maryland; expert in nondestructive test methods for concrete structural systems.

TABLE 21.1 Nondestructive and In-Place Tests

In-Place Tests to Estimate Strength	Nondestructive Tests for Integrity
Rebound hammer	Visual inspection
Ultrasonic pulse velocity	Stress wave propagation methods
Probe penetration	Ground penetrating radar
Pullout	Electrical/magnetic methods
Break-off	Nuclear methods
Maturity method	Infrared thermography

occurred as a result of the microcomputer revolution and the development of powerful signal-processing techniques. No standard definition exists for **nondestructive test** as applied to concrete. For some people, it is any test that does not alter the concrete. For others, it is a test that does not impair the function of a structure, in which case the drilling of cores is considered to be a NDT test. For still others, it is a test that does less damage to the structure than does drilling of cores. This chapter deals with methods that either do not alter the concrete or that result in only superficial local damage. The author prefers to divide the various methods into two groups: (1) those whose main purpose is to **estimate in-place strength**, and (2) those whose main purpose is to evaluate conditions other than strength—that is, to **evaluate integrity**. It will be shown that the most reliable tests for strength are those that result in superficial local damage, and the author prefers the term **in-place tests** for this group. The integrity tests, on the other hand, are truly nondestructive.

The purpose of this chapter is to provide an introduction to commonly used NDT methods for concrete. Table 21.1 lists the various test methods that are considered here. Emphasis is placed on the principles underlying the various methods so the reader may understand their advantages and inherent limitations. Additional information on the application of these methods is available in ACI 228.1R (ACI Committee 228, 2003), ACI 228.2R (ACI Committee 228, 1998), Malhotra and Carino (2004), and Bungey and Millard (1996). Portions of this chapter are based on previously published works of the author (Carino, 1992a, 1994).

21.2 Methods to Estimate In-Place Strength

21.2.1 Historical Background

Some of the first methods to evaluate the in-place strength of concrete were adaptations of the Brinell hardness* test for metals, which involves pushing a high-strength steel ball into the test piece under a given force and measuring the area of the indentation. In the metals test, the load is applied by an hydraulic loading system. Modifications were required to use this type of test on a concrete structure. In 1934, Professor K. Gaede in Germany reported on the use of a spring-driven impactor to supply the force to drive a steel ball into the concrete (Malhotra, 1976). A nonlinear, empirical relationship was obtained between cube compressive strength and indentation diameter. In 1936, J.P. Williams in England reported on a spring-loaded, pistol-shaped device in which a 4-mm ball was attached to a plunger (Malhotra, 1976). The spring was compressed by turning a screw, a trigger released the compressed spring, and the plunger was propelled toward the concrete. The diameter of the indentation produced by the ball was measured with a magnifying glass and scale.

In 1938, a landmark paper by D.G. Skramtajev, of the Central Institute for Industrial Building Research in Moscow, summarized 14 different techniques for estimating the in-place strength of concrete, 10 of which were developed in the Soviet Union (Skramtajev, 1938). This paper should be read by every student

* The term *hardness* is used routinely in the description of a series of tests of metals and concrete, yet this is not a readily quantified mechanical property. If one considers the nature of the hardness test methods that have been developed for metals, it can be concluded that these tests measure the amount of penetration caused by a specific indenter under a specific load. Therefore, a more descriptive term for these methods might be *indentation* tests.

of nondestructive testing for its historical content. Skramtajev divided the test methods into two groups: (1) those that required installation of test hardware prior to placement of concrete, and (2) those that did not require preinstallation of hardware. The methods described by Skramtajev included the following:

- Molds placed in the structure to form in-place test specimens
- Pullout tests of embedded bars
- An in-place punching shear test
- An in-place fracture test using a pincer device
- Penetration with a chisel driven by hammer blows
- Guns that fired indenters into the concrete
- Penetration with a ball powered by a spring-driven apparatus

Readers who are familiar with modern in-place test methods (to be discussed later) will recognize that many of them are variations of methods suggested more than 70 years ago. Skramtajev also commented on the need for in-place testing. For example, he noted that (Skramtajev, 1938):

- The curing conditions of standard test specimens are not representative of the concrete in the structure.
- The number of standard test specimens is insufficient to ensure the adequacy of all members in a structure.
- Standard test specimens that are tested at an age of 1 month provide no information on the later-age strength of concrete in the structure.
- Surface tests may not provide an indication of the actual concrete strength due to the effects of carbonation, laitance, and moisture condition.
- Methods requiring preplacement of hardware tend to provide more precise estimates of strength than those that do not require preplacement of hardware, but they lack flexibility for use at any desired location in an existing structure.

It is interesting to note that the same arguments and limitations are quoted today in relation to in-place testing (ACI Committee 228, 2003).

21.2.2 Rebound Hammer

In 1984, Ernst Schmidt, a Swiss engineer, developed a device for testing concrete based on the rebound principle (Malhotra, 1976, 2004). As was the case with earlier indentation tests, the motivation for this new device came from tests developed to measure the hardness of metals. In this case, the new device was an outgrowth of the Scleroscope* test, which involves measuring the rebound height of a diamond-tipped hammer, or mass, that is dropped from a fixed height above the test surface. As noted by Kolek (1958), when concrete is struck by a hammer, the degree of rebound is an indicator of the hardness of the concrete. Schmidt standardized the hammer blow by developing a spring-loaded hammer and devised a method to measure the rebound of the hammer. Several different models of the device were built (Greene, 1954), and Figure 21.1 provides a schematic of the model that was eventually adopted for field use. The essential parts of the Schmidt rebound hammer are the outer body, the hammer, the plunger, the spring, and the slide indicator. To perform the test, the plunger is extended from the body of the instrument, which causes a latch mechanism to grab hold of the hammer (Figure 21.1a). The body of the instrument is then pushed toward the concrete surface which stretches the spring attached to the hammer and the body (Figure 21.1b). When the body is pushed to the limit, the latch is released and the hammer is propelled toward the concrete by a combination of gravity and spring forces (Figure 21.1c). The hammer strikes the shoulder of the plunger and it rebounds (Figure 21.1d). The rebound distance is measured on a scale by a slide indicator. The rebound distance is expressed as a *rebound*

* In Greek, the word *sklero* means “hard.”

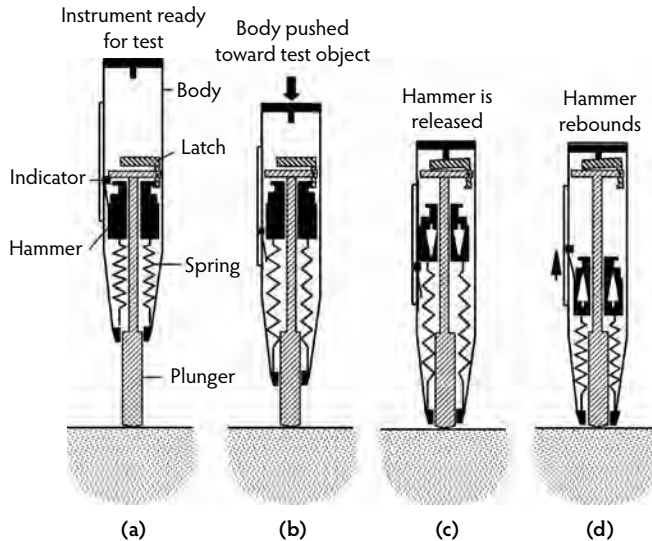


FIGURE 21.1 Schematic cross-sectional view of rebound hammer showing principle of operation.

number, which is the percentage of the initial extension of the spring (Kolek, 1958). Currently, the various models of the instrument that are available differ in the mass of the hammer and the stiffness of the spring; thus, different impact energies can be used for different materials.

Due to its simplicity and low cost, the Schmidt rebound hammer is by far the most widely used nondestructive test device for concrete. Although the test appears simple, there is no simple relationship between the rebound number and the strength of concrete. In principle, the rebound is affected by the small penetration (elastic and inelastic) of the end of the plunger in contact with the concrete. The more the end of the plunger penetrates, the lower is the rebound; thus, the rebound number is likely to be influenced by the elastic stiffness and the strength of the concrete. Because the rebound number is indicative of the near-surface properties of the concrete, it may not be indicative of the bulk concrete in a structural member. The report of ACI Committee 228 (2003) outlines some of the factors that may result in rebound numbers that are not representative of the bulk concrete. They include:

- The moisture condition of the surface concrete affects the rebound number; a dry surface results in a higher rebound number.
- The presence of a surface layer of carbonation increases the rebound number.
- The surface texture affects the rebound number, with smooth hard-troweled surfaces giving higher values than rough-textured surfaces.
- The rebound number is affected by the orientation of the instrument in relation to the direction of gravity (approximate correction factors are available).

Because the rebound number is affected by the near-surface conditions, erratic results may occur if the plunger is located directly over a coarse aggregate particle or a subsurface air void. To account for these possibilities, ASTM C 805 (ASTM, 2002b) requires that ten rebound numbers be taken for a test. If a reading differs by more than six units from the average, that reading should be discarded and a new average should be computed based on the remaining readings. If more than two readings differ from the average by six units, the entire set of readings is discarded.

The rebound hammer was constructed and tested extensively at the Swiss Federal Materials Testing and Experimental Institute in Zurich. A correlation was developed between the compressive strength of standard cubes and the rebound number, and this correlation was provided with the instrument. As other investigators began to develop correlations between strength and rebound number, it became evident that a unique relationship did not exist between strength and rebound number (Kolek, 1958).

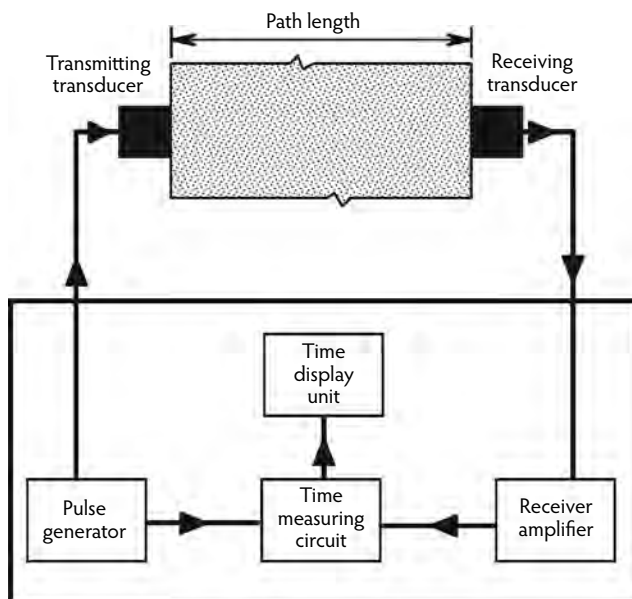


FIGURE 21.2 Schematic of ultrasonic pulse velocity method.

The current recommended practice (ACI Committee 228, 2003) is to develop the strength relationship using the same concrete and forming materials as will be used in construction. Without such a correlation, the rebound hammer is useful only for detecting gross changes in concrete quality throughout a structure.

In summary, the rebound number method is recognized as a useful tool for performing quick surveys to assess the uniformity of concrete. Because of the many factors besides concrete strength than can affect rebound number, the author does not recommended this method where reliable strength estimates are needed.

21.2.3 Ultrasonic Pulse Velocity

The ultrasonic pulse velocity method is a stress wave propagation method based on measuring the travel time, over a known path length, of a pulse of ultrasonic compressional waves (stress waves associated with normal stress). The pulses are introduced into the concrete by a piezoelectric transducer, and a similar transducer acts as receiver to monitor the surface vibration caused by the arrival of the pulse. A grease or gel is applied to the faces of the transducers to ensure good coupling with the surfaces. A timing circuit is used to measure the time it takes for the pulse to travel from the transmitter to the receiver. Figure 21.2 provides a schematic of the ultrasonic pulse velocity technique. The speed of compressional waves in a solid is related to the elastic constants (modulus of elasticity and Poisson's ratio) and the density (see Equation 21.15). By conducting tests at various points on a structure, lower quality concrete can be identified by its lower pulse velocity. Naik et al. (2004) provide additional information on the development and application of this method for estimating concrete strength.

The development of a field instrument to measure the pulse velocity occurred nearly simultaneously in Canada and in England (Whitehurst, 1967). These developments were outgrowths of earlier successful work by the U.S. Army Corps of Engineers to measure the speed of a mechanical stress pulse through concrete (Long et al., 1945). The Army Corps of Engineers approach involved attaching two receivers to the concrete surface. A horizontal hammer blow was applied in line with the receivers, and a specially designed electronic interval timer measured the time for the pulse to travel from the first to the second receiver. The major purpose of this technique was to calculate the in-place modulus of elasticity. As will be seen in Section 21.3.3.3, a similar method is still being used to extract information about elastic properties in a layered system.

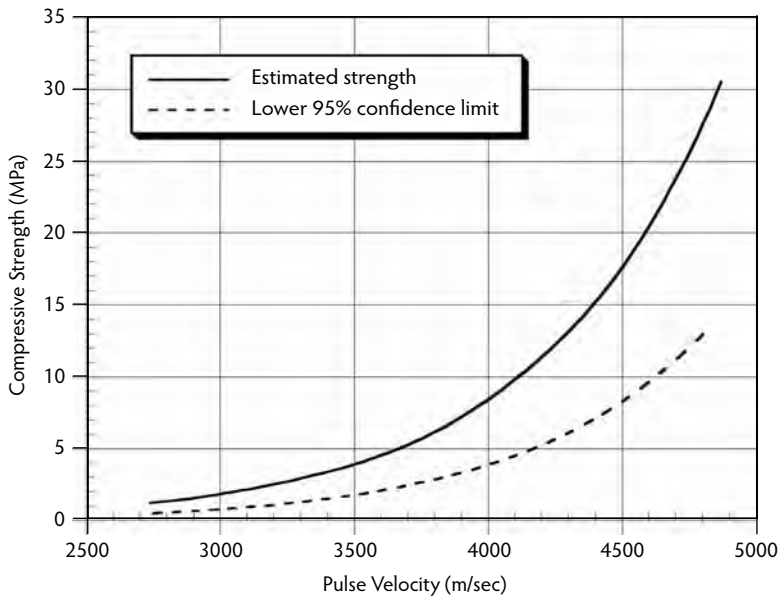


FIGURE 21.3 Compressive strength vs. pulse velocity relationship based upon 46 mixtures made with the same aggregate. (Adapted from Parker, W.E., *Proc. ASTM*, 53, 1033–1042, 1953.)

In 1946 and 1947, engineers at the Hydro-Electric Power Commission of Ontario (Ontario Hydro) worked on the development of a device to investigate the extent of cracking in dams (Leslie and Cheesman, 1949). The device developed to do so was called the *Soniscope*. It had a 20-kHz transmitting transducer, was capable of penetrating up to 15 m of concrete, and could measure the travel time with an accuracy of 3%. The stated purposes of the *Soniscope* were to identify the presence of internal cracking, determine the depth of surface-opening cracks, and determine the dynamic modulus of concrete (Leslie and Cheesman, 1949). It was further stated that the fundamental measurement was the travel time. The amplitude of the received signal was said to be of secondary importance because the transfer of energy between the transducers and the concrete could not be controlled. It was also emphasized that interpretation of results required knowledge of the history of the structure being investigated.

Early uses of the *Soniscope* on mass concrete emphasized measuring the pulse velocity rather than estimating strength or calculating the modulus of elasticity (Parker, 1953). Based on velocity readings on a grid marked on the surface, the presence of distressed concrete could be easily detected. Parker (1953) reported Ontario Hydro's early attempts to develop relationships between pulse velocity and compressive strength. They investigated 46 mixtures involving the same aggregate, different cement types, and different admixtures. The results indicated no significant differences in the velocity–strength relationships for the different mixtures; therefore, the results were treated as one group, and the best-fit relationship was determined. Figure 21.3 shows the relationship between estimated strength and pulse velocity and the lower 95% confidence limit for estimated strength. Because of the large scatter, the lower confidence limit was about 45% of the mean strength; thus, the inherent uncertainty in using pulse velocity to estimate strength was recognized very early. Figure 21.3 also shows that the change in pulse velocity per unit change in strength decreases with increasing strength. This means that pulse velocity is relatively insensitive to strength for mature concrete.

While work on the *Soniscope* was in progress in Canada, R. Jones and coworkers at the Road Research Laboratory (RRL) in England were involved in independent research to develop an ultrasonic testing apparatus (Jones, 1949a). The RRL researchers were interested in testing the quality of concrete pavements, which involved shorter path lengths compared with the work at Ontario Hydro. As a result, the apparatus that was developed operated at a higher frequency than the *Soniscope*, and it was called the

ultrasonic concrete tester. Transducers with resonant frequencies from 60 to 200 kHz were used, depending on the desired penetration (Jones, 1953). In addition to using a different operating frequency, the RRL device used a different approach than the Soniscope to measure travel time. This was necessary because of the shorter path lengths in the RRL work. It was reported that the ultrasonic concrete tester could measure travel times to within $\pm 2 \mu\text{s}$.

Jones (1949b) reviewed the research carried out with the newly developed ultrasonic concrete tester. Among these studies were the following:

- An investigation into the variations in pulse velocity with height in standard cube specimens and with depth in slabs was one of the first to document the “top-to-bottom” effect that is often mentioned as a problem when planning and interpreting in-place tests (ACI Committee 228, 2003).
- An investigation into the influence of water–cement ratio, aggregate type, and aggregate content on pulse velocity demonstrated the importance of aggregate type and aggregate content on pulse velocity.
- An investigation of the relationships between pulse velocity and compressive strength demonstrated that, for a given mixture under uniform conditions, there was good correlation between strength and pulse velocity.

Thus, Jones revealed the problems inherent in using pulse velocity to estimate concrete strength. Despite these early findings, numerous researchers sought to establish correlations between pulse velocity and strength, and many reached the same conclusions as Jones (Sturrupe et al., 1984).

In the United States, a Soniscope was developed in 1947 at the Portland Cement Association in cooperation with Ontario Hydro, and field applications were reported by Whitehurst (1951). In his summary of the industry’s experience in the United States, Whitehurst published the following tentative classification for using pulse velocity as an indicator of quality:

Pulse Velocity (m/s)	Condition
Above 4570	Excellent
3660–4570	Generally good
3050–3660	Questionable
2130–3050	Generally poor
Below 2130	Very poor

This table was quoted by others in many subsequent publications. Whitehurst warned, however, that these values were established on the basis of tests of normal concrete having a density of about 2400 kg/m^3 and that the boundaries between the conditions could not be sharply drawn. He mentioned that, rather than using these limits, a better approach would be to compare velocities with the velocity in a portion of the structure that is known to be of acceptable quality. Nevertheless, inexperienced investigators often used the above table as the sole basis for interpreting test results.

After the publication of these landmark papers in the late 1940s and early 1950s, a flurry of activity occurred worldwide, and efforts were begun to develop standard test methods. In the United States, a proposed ASTM test method was published in 1955 by Leslie (1955), but it was not until 1967 that it was adopted as a tentative test method (ASTM, 2002a). In Europe, the International Union of Testing and Research Laboratories for Materials and Structures (RILEM) organized a working group to study nondestructive testing (R. Jones was appointed chairman). In 1969, draft recommendations for testing concrete by the ultrasonic pulse method were published (Jones and Făcăoaru, 1969). In Eastern Europe, the method was used extensively as a quality control tool in precast concrete plants.

During the 1960s and 1970s, considerable attention was devoted to gaining more knowledge about the effects of different factors on pulse velocity. Researchers continued to explore the relationship between compressive strength and pulse velocity. They appear, however, to have reached a consensus that there is no unique relationship. Numerous studies showed that the type and quantity of aggregate have major

effects on pulse velocity but not on strength. Significant effort was also devoted to examining whether or not attenuation measurements could provide additional information about concrete strength. These results were, in general, found to be impractical in field situations because of difficulties in achieving consistent coupling of the transducers, which is critical for measuring attenuation.

Perhaps the most significant advances during the 1960s and 1970s were in the development of improved field instrumentation. Due to advances in microelectronic circuitry, the cumbersome instruments developed in the 1940s and 1950s gave way to compact portable devices. In the late 1960s, TNO (Netherlands Organization for Applied Scientific Research) in Delft, Netherlands, developed a portable, battery-operated pulse velocity device that incorporated a digital display of the travel time. In the earlier devices, travel time was measured by examination of oscilloscope displays, which was a time-consuming process. The portable instrument had a resolution of 1 μs , which resulted in low accuracy for short path lengths, and it had limited penetrating ability (Făcăoaru, 1969). At about the same time, R.H. Elvery of University College, London, developed a similar portable device named the *PUNDIT* (Portable Ultrasonic Nondestructive Digital Indicating Tester). It weighed 3.2 kg, had a resolution of 0.5 μs , and could be powered by rechargeable batteries (Malhotra, 1976). These and other relatively low-cost, portable devices simplified testing and resulted in a worldwide increase in the number of consultants and researchers who could perform this type of testing. Later models of these devices had resolutions of 0.1 μs , and some provided an optional output channel to allow the received signal to be displayed on an oscilloscope.

In summary, the ultrasonic pulse velocity test method is a relatively simple test to perform on-site provided it is possible to gain access to both sides of the member. Although tests can be performed with the transducers placed on the same surface, the results are not easy to interpret, and this method of measurement is not recommended. Care must be exercised to ensure that good and consistent coupling with the concrete surfaces is achieved. Other important factors, besides concrete strength, that can affect the measured ultrasonic pulse velocity and that should be considered are discussed in the report of ACI Committee 228 (2003). These factors include:

- Moisture content—An increase in moisture content increases the pulse velocity.
- Presence of reinforcement oriented parallel to the pulse propagation direction—The pulse may propagate through the bars and result in an apparent pulse velocity that is higher than that propagating through concrete.
- Presence of cracks and voids—Cracks and voids can increase the length of the travel path and result in a longer travel time.

Because of these factors, only experienced individuals should use the ultrasonic pulse velocity method for estimating concrete strength. Like the rebound number test, the pulse velocity method is useful for assessing the uniformity of concrete in a structure. It is often used to locate regions in a structure where other tests should be performed or where cores should be drilled.

21.2.4 Probe Penetration

The probe penetration method involves using a gun to drive a hardened steel rod, or probe, into the concrete and measuring the exposed length of the probe. In principle, as the strength of the concrete increases, the exposed probe length also increases; by means of a suitable correlation, the exposed length can be used to estimate compressive strength. Skramtajev mentioned a similar concept in his 1938 summary paper, and Malhotra (1976) noted that similar techniques were reported in 1954. Malhotra and Carette (2004) have provided an in-depth summary of this technique.

Development of the probe penetration test system began in about 1964 as a joint undertaking by T.R. Cantor of the Port of New York Authority and R. Kopf of the Windsor Machinery Company (Arni, 1972). The test system that was eventually commercialized became known as the *Windsor probe*. The apparatus is supplied with a table that relates exposed probe length to compressive strength for various coarse aggregates, which are distinguished by their hardness as measured by the Mohs hardness

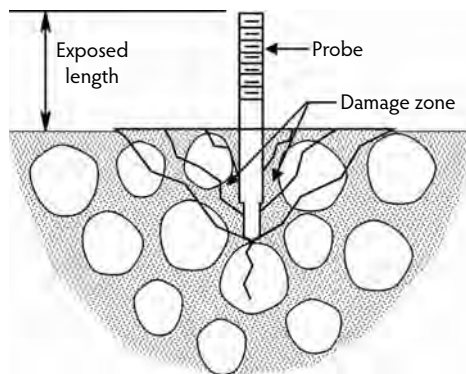


FIGURE 21.4 Schematic of conical failure zone during probe penetration test.

scale* of minerals. The basis for the values in the tables and their uncertainty were never published (Arni, 1972). In the late 1960s, independent investigations of the reliability of the Windsor probe system were carried out by the National Ready-Mixed Concrete Association (Gaynor, 1969), the Federal Highway Administration (FHWA) (Arni, 1972), and the Canadian Department of Energy, Mines, and Resources (Malhotra, 1974). In general, it was found that the probe penetration system had acceptable within-test variability. Scatter in the correlation between compressive strength and probe penetration, however, led to high uncertainties in the estimated strength. All investigators cautioned against reliance on the manufacturer's correlation tables.

Arni's (1972) study of the uncertainties of the probe penetration and rebound hammer tests is interesting and worth summarizing. He calculated the number of tests required to detect a strength difference of 1.4 MPa using test cylinders, probe penetration, or rebound number. These estimates were based on the variability of test results and slopes of the correlation equations developed in the FHWA study. For 90% confidence levels, the results were as follows:

Test Method	Number of Tests
Cylinders	8
Rebound number	120
Probe penetration	85

Note that these numbers apply for specific data used by Arni. Nevertheless, they point out the inherent inability of in-place tests to detect small differences in concrete strength unless large numbers of tests are performed. This important concept has been largely ignored.

The probe penetration test method was adopted as a tentative ASTM standard (C 803) in 1975. In 1990, the standard was modified to include the use of a pin penetration device, in which a small pin is forced into the concrete using a spring-loaded driver (ACI Committee 228, 2003; Malhotra and Carrette, 2004; Nasser and Al-Manseer, 1987a,b).

The report of ACI Committee 228 (2003) provides an explanation of the factors affecting probe penetration into concrete. Figure 21.4 is a schematic of the failure zone produced during probe penetration. The probe penetrates until its initial kinetic energy is absorbed by friction and the fracture of the mortar and aggregate. Hence, the strength properties of the aggregate affect the penetration depth. As a result, the strength relationship depends on the aggregate type. For equal concrete strength, probe penetration would be deeper in a concrete with a soft aggregate than in a concrete with a hard aggregate. See Malhotra (1976), Bungey and Millard (1996), and Malhotra and Carrette (2004) for additional information on the effects of

* A qualitative scale in which the hardness of a mineral is determined by its ability to scratch, or be scratched by, another mineral. The hardest mineral is diamond and the softest is talc.

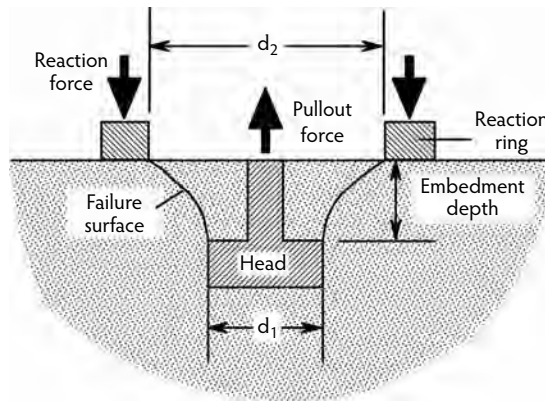


FIGURE 21.5 Schematic of cast-in-place pullout test.

aggregate type. Probe penetration is not strongly affected by the near-surface conditions and is therefore not as sensitive to surface conditions as the rebound number method. The direction of penetration is not important provided that the probe is fired perpendicular to the surface. Care must be exercised when testing reinforced concrete to ensure that tests are not carried out in the vicinity of the reinforcing steel, especially if the concrete cover is low. In practice, probe penetration tests should not be used to investigate low standard cylinder test results unless a correlation is developed for the specific concrete mixture.

21.2.5 Pullout Test

The cast-in-place pullout test is one of the most reliable techniques for estimating the in-place strength of concrete during construction. In this method, an insert with an enlarged head is cast in the concrete. The insert and the accompanying conical fragment of concrete are extracted by using a tension-loading device reacting against a bearing ring that is concentric with the insert (Figure 21.5). The force required to pull out the insert is an indicator of concrete strength. A comprehensive review of the history and theory of the pullout test is available (Carino, 2004b), and only a brief summary is provided here.

21.2.5.1 History

Ideas for pullout tests apparently originated in the Soviet Union (Skramtajev, 1938). Tremper (1944) was the first American to report on the correlation between pullout force and companion cylinder strength. The insert developed by Volf (of the Soviet Union) and the one used by Tremper are shown in Figure 21.6a and Figure 21.6b, respectively. In both cases, the reaction to the pullout force was applied sufficiently far from the insert that there was negligible interaction between the failure surface and the reaction system. As a result, failure was controlled primarily by the tensile strength of the concrete. This explains why Tremper found that the correlation between pullout force and compressive strength was nonlinear.

Despite Tremper's encouraging results, no additional documented work on the pullout test was carried out until 1962, when a comprehensive study was begun in Denmark (Kierkegaard-Hansen, 1975). The objective was to find the optimum geometry for a field test system that would have a high correlation between pullout load and the compressive strength of concrete. Kierkegaard-Hansen found that the correlation could be improved by constraining the failure surface to follow a predefined path by using a relatively small-diameter reaction ring. The study resulted in the pullout test configuration shown in Figure 21.6c, which was eventually incorporated into the Lok-Test[®] system, which is the most widely used commercial pullout test system.

* As explained by Kierkegaard-Hansen (1975), failure when a small reaction ring is used can be considered a punching type of failure. The Danish word for "punching" is *lokning*, so the term *lok-strength* was used to describe the strength measured by the test.

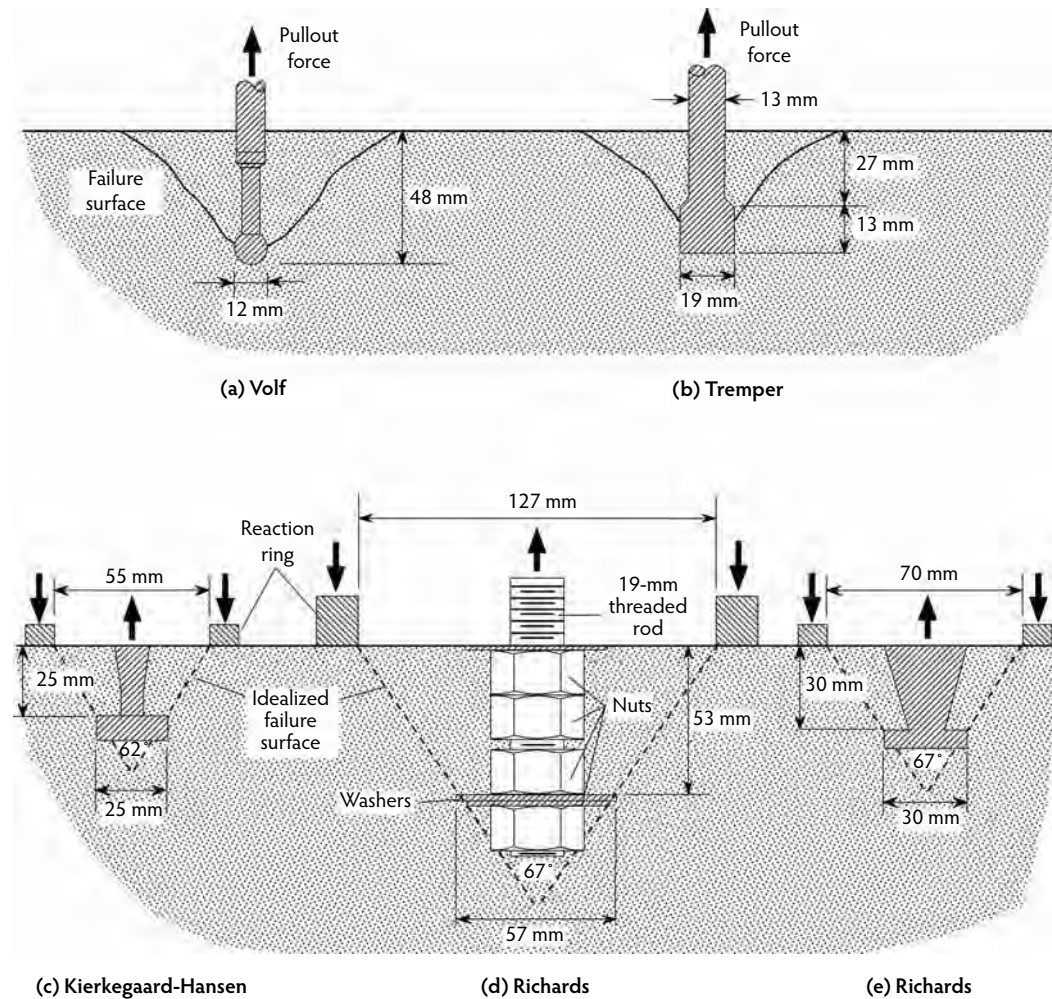


FIGURE 21.6 Various pullout test configurations.

Owen Richards, a materials consultant in the United States, carried out independent studies of a pullout test in the late 1960s and early 1970s (Richards, 1977). The early version of Richards' pullout test configuration was larger than that developed in Denmark. The inserts were manufactured from 19-mm threaded rods, and washers were used to provide the enlarged head. Nuts were used to add rigidity to the washers and to fix the embedment depth of the washers. The test geometry, which is shown in Figure 21.6d, resulted in an idealized failure surface with an area approximately equal to the area of a standard 152-mm-diameter cylinder. Richards preferred to divide the pullout force by the nominal area of the idealized failure to obtain pullout strength, which is a fictitious quantity because the pullout force is inclined to the surface area.

The first reported pullout tests using Richards' early system were performed at the Bureau of Reclamation (Rutenbeck, 1973). Strong correlation was obtained between pullout tests performed on slabs and the compressive strength of companion cylinders. Good correlation between pullout strength and compressive strength was also obtained when the inserts were placed in shotcrete panels and compressive strength test specimens were cut from the panels. In 1975, Malhotra also reported on the applicability of Richards' pullout test (Malhotra, 1975). It was found that the coefficient of variation for three replicate tests was less than 5%, which was very encouraging. In a later study (Malhotra and Carette, 1980), it was noted that similar correlations were obtained in different investigations of Richards' system.

Richards' pullout system produced encouraging results, but the large size of the insert required heavy testing equipment and produced significant surface damage. In 1977, a smaller version of the test system was introduced (Richards, 1977), as shown in Figure 21.6e. The apex angle of the conic frustum was maintained at 67° , but the insert was constructed from one piece of steel. The enlarged end of the shank accommodated a pull-rod that passed through a center-hole tension ram. In the early 1960s, investigations of the pullout test were also conducted in Great Britain (Te'eni, 1970), but the work was apparently never carried to the stage of a practical field test system. A novel feature of the British work was the use of a power function for the correlation equation, rather than a straight line as had been used in Denmark, the United States, and Canada. The usefulness of the pullout test for estimating early-age strength was quickly recognized. In 1978, ASTM adopted a tentative test method for the pullout test (ASTM C 900; see ASTM, 2006c). In North America, J. Bickley became an early advocate of the pullout test method as a tool for accelerating construction schedules without compromising safety (Bickley, 1982a).

21.2.5.2 Failure Mechanism

Ever since the pullout test was first described by Skramtajev (1938), its failure mechanism has not been completely understood. Skramtajev correctly noted that the test subjects the concrete to a combination of tensile and shearing stresses. Kierkegaard-Hansen (1975), the inventor of the widely used Lok-Test system, tried to relate the shape of the extracted conical fragment to the intact cones often observed at the ends of cylinders tested in compression. Jensen and Braestrup (1976) used plasticity theory to relate the ultimate pullout force to the compressive strength of the concrete. Malhotra and Carette (1980) proposed that the pullout strength was related to the direct shear strength of concrete. In the 1980s and 1990s, experimental and analytical studies tried to gain a better understanding of the failure process during the pullout test (Ballarini et al., 1986; Hellier et al., 1987; Krenchel and Bickley, 1987; Krenchel and Shah, 1985; Ottosen, 1981; Stone and Carino, 1983; Yener, 1994). From these independent analytical and experimental studies, it is now understood that the pullout test subjects the concrete to a nonuniform, three-dimensional state of stress. It also has been demonstrated that the failure process involves two circumferential crack systems: (1) a stable system that starts at the insert head at about one third of the ultimate load, propagates into the concrete at a large apex angle, and is arrested as it reaches a tension-free region; and (2) a system that propagates with increasing load and eventually defines the shape of the extracted cone. Figure 21.7 shows these cracking systems as predicted by Hellier et al. (1987), who used a discrete cracking, finite-element model based on nonlinear fracture mechanics.

Despite general agreement on the cracking process prior to the attainment of ultimate pullout load, no consensus has been reached on the failure mechanism at the ultimate load. Some researchers maintain that ultimate load occurs as a result of compressive failure along a strut running from the bottom of the bearing ring to the insert head (Krenchel and Bickley, 1987; Krenchel and Shah, 1985; Ottosen, 1981). This mechanism has been used to explain the good correlation between pullout strength and compressive strength. Others maintain that ultimate failure is governed by aggregate interlock across the secondary crack system, and the ultimate load is reached when sufficient aggregate particles have been pulled out of the mortar matrix (Hellier et al., 1987; Stone and Carino, 1983). In this case, it is argued that there is correlation between pullout strength and compressive strength because both properties are controlled by the tensile strength of the mortar. In the compression test, the ultimate load is associated with the formation and growth of microcracks through the mortar.

Although there is no agreement on the exact failure mechanism of the pullout test, it has been shown that the pullout strength has strong correlation with the compressive strength of concrete and that the test has good repeatability. In a review of published data, ACI Committee 228 (2003) recommended a coefficient of variation (standard deviation divided by the mean) of 8% for the pullout test. The current version of ASTM C 900 (ASTM, 2006) requires at least five individual pullout tests for each 115 m^3 of concrete in a given placement. For tests of the same concrete, the precision statement of ASTM C 900 states that the acceptable range of five replicate tests is 31% of the average. If the range should exceed this value in the field, a closer examination is required to understand the underlying reason for the greater than expected scatter.

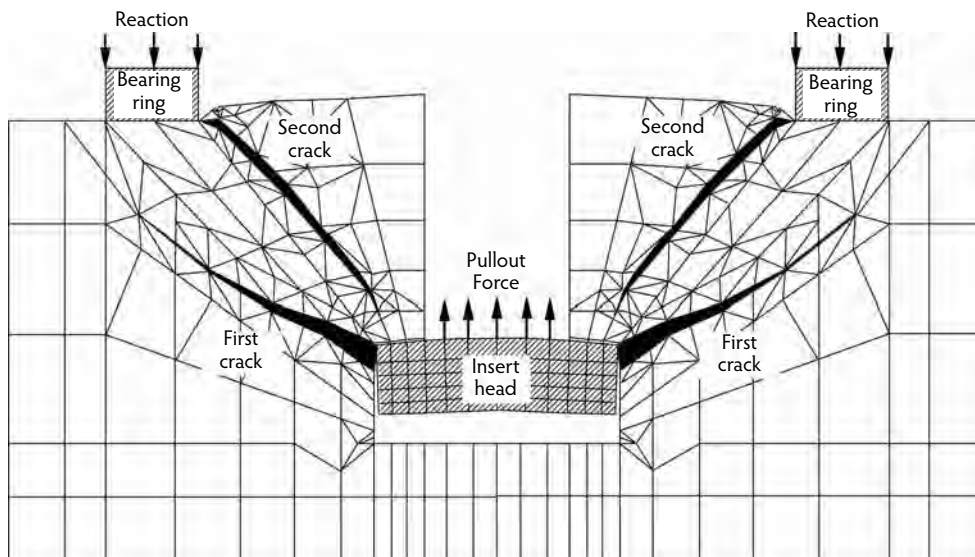


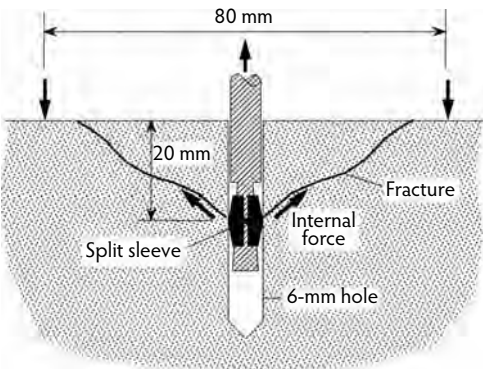
FIGURE 21.7 Crack systems formed during pullout test based on fracture analysis using the finite-element method. (From Hellier, A.K. et al., *J. Cement Concrete Aggregates*, 9(1),20–29, 1987.)

21.2.5.3 Post-Installed Tests

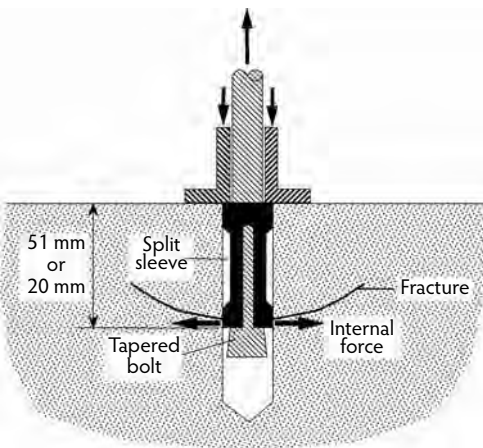
A drawback of the cast-in-place (CIP) pullout test is that the locations of the inserts have to be planned in advance of concrete placement, and the inserts must be fastened to the formwork. This limits the applicability of the CIP method to new construction. In an effort to extend the application of pullout testing to existing structures, various techniques for performing post-installed pullout tests have been investigated. Some of these approaches are shown in Figure 21.8.

During the 1970s, a need arose in the United Kingdom for in-place tests to evaluate distressed concrete structures built with high-alumina cement. Researchers at the Building Research Establishment (BRE) developed a pullout technique using commercial anchor bolts, as shown in Figure 21.8a (Chabowski and Bryden-Smith, 1980). A 6-mm-diameter hole is drilled into the concrete, and an anchor bolt is inserted so the split-sleeve is at a depth of 20 mm. After applying an initial load to expand and engage the sleeve, the bolt is pulled out, and the maximum load during the extraction is recorded. Because of the shallow embedment, failure occurs by concrete fracture. Reaction to the pullout load is provided by three reaction points located along the perimeter of a 80-mm-diameter ring. As the bolt is pulled, the sleeve imparts longitudinal and transverse forces to the concrete. Hence, the fracture surface differs from that in the cast-in-place pullout test, and the test has been referred to as an *internal fracture test* rather than a pullout test. The correlation between ultimate load and compressive strength was found to have a pronounced nonlinearity, indicating that the failure mechanism was probably related to the tensile strength of the concrete. Within-test variability was found to be greater than the CIP pullout test, and the 95% confidence limits of the correlation relationship were found to range between $\pm 30\%$ of the mean curve (Chabowski and Bryden-Smith, 1980). The relatively low precision of the internal fracture test has been attributed to two principal causes (Bungey and Millard, 1996): (1) variability in the hole drilling and test preparation, and (2) the influence of aggregate particles on the load-transfer mechanism and the failure-initiation load.

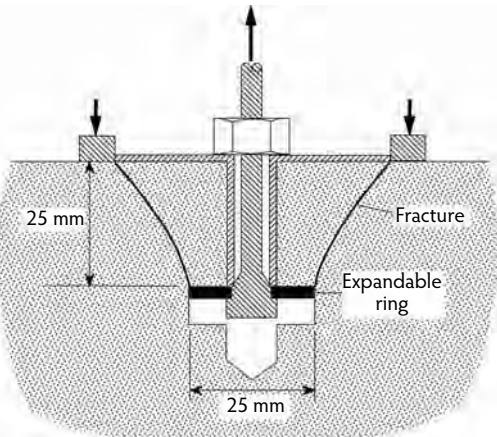
Mailhot et al. (1979) also investigated the feasibility of several post-installed pullout tests. One of these used a split-sleeve and a tapered bolt assembly that was placed in a 19-mm-diameter hole drilled into the concrete. As shown in Figure 21.8b, the details differ from the BRE method because the reaction to the pulling force acts through a specially designed high-strength, split-sleeve assembly. The force transmitted to the concrete is predominantly in the lateral direction because the tapered bolt forces the sleeve to expand laterally. It is likely that failure occurs by indirect tensile splitting, similar to that in a standard



(a) BRE Internal Fracture Test



(b) Expanding Sleeve Test



(c) CAPO Test

FIGURE 21.8 Examples of post-installed pullout tests.

splitting-tension test. As with the BRE test, the variability of this test was reported to be rather high. Another successful method involved epoxy grouting a 16-mm-diameter threaded rod into a 19-mm hole to a depth of 38 mm. After the epoxy had cured, the rod was pulled using a tension jack reacting against a bearing ring. This method was also reported to have high variability. The study concluded that these

two methods had the potential for assessing the strength in existing construction. Additional research was recommended, however, to enhance their reliability.

Domone and Castro (1986) also developed a technique similar to the expanding sleeve method shown in Figure 21.8b; however, a torque meter was used to apply the load, and the embedment was 20 mm, as in the BRE method. On the basis of a limited number of tests, it was concluded that this method gave better correlations than the BRE method.

Another method developed by the manufacturer of the Lok-Test^{*} system is referred to as the **CAPO** (Cut and Pullout) test (Petersen, 1984). The method involves drilling an 18-mm-diameter hole into the concrete and using a special milling tool to undercut a 25-mm-diameter slot at a depth of 25 mm. An expandable ring is placed in the hole, and the ring is expanded using special hardware. Figure 21.8c shows the ring after expansion. The entire assembly used to expand the ring is pulled out of the concrete using the same loading system as for a CIP pullout test. Unlike the methods discussed above, the CAPO test subjects the concrete to a similar state of stress as the CIP pullout test. The performance of the CAPO test in laboratory evaluations has been reported to be similar to that for the Lok-Test (Petersen, 1984). Early users of the CAPO test noted that the test was cumbersome to perform and care must be taken to control the variability (Read et al., 1991). The current apparatus has been refined to make it easier to prepare a test surface that is flat and perpendicular to the drilled hole. In 1999, ASTM C 900 was revised to include post-installed pullout tests based on the CAPO procedure. The ASTM procedures require that care be exercised to ensure properly aligned hardware and a properly seated reaction ring. Criteria are provided for acceptable failure geometries when the conic frustum is extracted.

21.2.6 Break-Off Test

This test measures the force required to break off a cylindrical core from the concrete mass. The method was developed in the early 1970s by R. Johansen at the Cement and Concrete Research Institute in Norway. In cooperation with contractors, Johansen sought a simple, inexpensive, and robust method to measure in-place strength (Johansen, 1977, 1979). The test method was standardized by ASTM in 1990 (ASTM C 1150; see ASTM, 1996). Naik et al. (2004) have provided a comprehensive review of research results.

Figure 21.9 provides a schematic of the break-off test. For new construction, the core is formed by inserting a special plastic mold into the fresh concrete. The mold results in a core specimen with a recessed annular void at the surface. When the in-place strength is to be estimated, the mold is removed, and a special, hand-operated, hydraulic loading jack is placed into the annular space. The jack applies a force to the top of the core until it ruptures from the concrete mass. The hydraulic fluid pressure in the jack is monitored with a pressure gauge, and the maximum pressure gauge reading in units of bar (1 bar = 0.1 MPa) is referred to as the *break-off number* of the concrete. For new construction, the molds are inserted into the top surface of the member after the concrete has been leveled. Alternatively, the molds can be attached to the sides of the formwork and filled during concrete placement. For existing construction, a special drill bit can be used to cut the core and the annular space to accept the loading the system.

For ease of mold insertion into the fresh concrete, the concrete must be workable. In addition, to minimize interference, the maximum aggregate size should be limited to a fraction of the mold diameter, which is 55 mm. The break-off test is not recommended for concrete having a maximum nominal aggregate size greater than 25 mm. Mold insertion must be performed carefully to ensure good compaction around the mold and a minimum of disturbance at the base of the formed core. Some problems have been reported with keeping the molds from floating out of very fluid concrete mixtures (Naik et al., 1987).

The break-off test subjects the concrete to a slowly applied force and measures a static strength property of the concrete. The core is loaded as a cantilever, and the concrete at the base of the core is subjected to a combination of bending and shearing stresses. In early work (Johansen, 1977, 1979), break-off

^{*} Certain trade names and company products are mentioned to identify specific test equipment. In no case does such identification imply recommendation or endorsement by the author, nor does it imply that the products are necessarily the best available for the purpose.

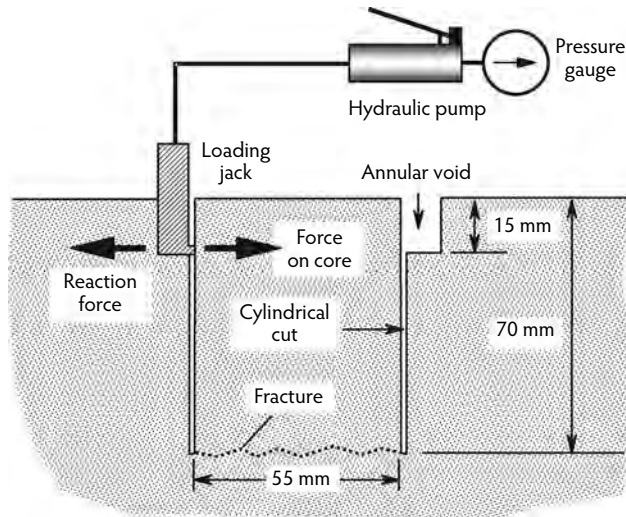


FIGURE 21.9 Schematic of break-off test.

strength was reported as the calculated flexural stress at the base of the core corresponding to the rupture force. In later applications (see review by Naik, 2004), the flexural strength was not computed, and the break-off number (pressure gauge reading) was related directly to compressive strength. This approach simplifies data analysis. Calibration of the test instrument is critical to ensure that gauge readings correspond to actual forces applied to the test specimen.

The correlations between break-off strength and compressive strength have been found to be nonlinear (Barker and Ramirez, 1988; Johansen, 1977, 1979), which is in accordance with the usual practice of relating the modulus of rupture of concrete to the square root of compressive strength. It has also been found that the correlation between break-off strength and modulus of rupture may be more uncertain than that between break-off strength and compressive strength (Barker and Ramirez, 1988).

Failure during the break-off test occurs by fracture at the base of the 55-mm-diameter core. The crack initiates at the most highly stressed point. It then propagates through the mortar and, in most cases, around coarse aggregate particles located at the base of the core. The particular arrangement of aggregate particles within the failure region would be expected to affect the ultimate load in each test. Because of the relatively small size of the core and the heterogeneous nature of concrete, the distribution of aggregate particles will be different at each test location. Hence, one would expect the within-test variability of the break-off test to be higher than that of other standard strength tests that involve larger test specimens. One would also expect that the variability might be affected by maximum aggregate size and aggregate shape. The developer of the break-off test reported a within-test coefficient of variation of about 9% (Johansen, 1979). This value has, in general, been confirmed by other investigators (Carino, 1992a).

In 2002, ASTM Committee C09 voted to withdraw ASTM C 1150. The break-off test was not being used in practice and testing equipment was no longer available commercially. This is unfortunate because the author feels that the break-off test could have become a good method for estimating in-place strength in existing structures.

21.2.7 Maturity Method

The maturity method is a technique for estimating the early strength development of concrete during its curing period by measuring the temperature history of the concrete. Carino (2004a) provides a comprehensive review of the history of the method and some of its applications. Historically, the maturity method was not classified as a nondestructive test method, but it is now regarded as a useful technique for estimating in-place strength. Its origin can be traced to a series of papers from England dealing with

accelerated steam curing methods (McIntosh, 1949; Nurse, 1949; Saul, 1951). There was a need for a procedure to account for the combined effects of time and temperature on strength development for different elevated-temperature curing processes. It was proposed that the product of time and temperature could be used for this purpose. These ideas led to the famous **Nurse–Saul maturity function**:

$$M = \sum_0^t (T - T_0) \Delta t \quad (21.1)$$

where:

M = maturity index, degree Celsius-hour (or degree Celsius-day).

T = average concrete temperature (degree Celsius) during the time interval Δt .

T_0 = datum temperature (usually taken to be 10°C).

Δt = time interval (hour or day).

The index computed by Equation 21.1 was referred to as the *maturity*; however, the current terminology is the *temperature–time factor* (ASTM C 1074; see ASTM, 2004a). Saul (1951) presented the following principle, which has become known as the **maturity rule**:

Concrete of the same mix at the same maturity (reckoned in temperature–time) has approximately the same strength whatever combination of temperature and time go to make up that maturity.

Equation 21.1 is based on the assumption that the initial rate of strength gain (during the acceleratory period following setting) is a linear function of temperature. It was soon realized, however, that this approximation may not be valid when curing temperatures vary over a wide range. As a result, a series of alternatives to the Nurse–Saul function were proposed by other researchers (Malhotra, 1971). None of the alternatives, however, received widespread acceptance, and the Nurse–Saul function was used worldwide until an improved function was proposed in the 1970s.

In 1977, a new function was proposed to compute a maturity index from the recorded temperature history of the concrete (Freiesleben Hansen and Pedersen, 1977). This function was based on the Arrhenius equation (Brown and LeMay, 1988), which is used to describe the effect of temperature on the initial rate of a chemical reaction. The new function allowed the computation of the equivalent age of concrete at a reference temperature as follows:

$$t_e = \sum_0^t e^{\frac{-E}{R} \left(\frac{1}{T} - \frac{1}{T_r} \right)} \Delta t \quad (21.2)$$

where:

t_e = equivalent age at the reference temperature (hour or day).

E = apparent activation energy (J/mol).

R = universal gas constant = 8.314 J/mol-K.

T = average absolute temperature of the concrete during interval Δt (degrees Kelvin).

T_r = absolute reference temperature (degrees Kelvin).

By using Equation 21.2, the actual age of the concrete is converted to its equivalent age, in terms of strength gain, at the reference temperature. In European practice, the reference temperature is usually taken to be 20°C, whereas in North American practice it is usually taken to be 23°C. The introduction of this function overcame one of the main limitations of the Nurse–Saul function (Equation 21.1) because it allowed for a nonlinear relationship between the initial rate of strength development and curing temperature. This temperature dependence is described by the value of the apparent activation energy. Comparative studies in the early 1980s showed that this new maturity function was superior to the Nurse–Saul function (Byfors, 1980; Carino, 1982).

21.2.7.1 Effect of Temperature on Strength Gain

The key parameter in Equation 21.2 is the “activation energy,” which describes the effect of temperature on the initial rate of strength development. In the early 1980s, the author began a series of studies to gain a better understanding of the maturity method (Carino, 1984). From this work, a procedure was developed to obtain the activation energy of a given cementitious mixture. The procedure is based on determining the effect of curing temperature on the rate constant for strength development. The rate constant is related to the curing time required to reach a certain fraction of the long-term strength, and it is obtained by fitting an appropriate equation to the strength-vs.-age data acquired under constant temperature (isothermal) curing. The procedure to determine the activation energy consists of the following steps:

- Cure mortar specimens at different constant temperatures.
- Determine compressive strengths at regularly spaced ages.
- Determine the value of the rate constant at each temperature by fitting a strength–age relationship to each set of strength–age data.
- Determine the best-fit Arrhenius equation (to be explained) to represent the variation of the rate constant with the temperature.

By using the above procedure, the activation energy was determined for concrete and mortar specimens made with different cementitious materials (Carino and Tank, 1992; Tank and Carino, 1991). It was found that for concrete with a water–cement ratio (w/c) of 0.45, the activation energy ranged from 30 to 64 kJ/mol; for a w/c of 0.60, it ranged from 31 to 56 kJ/mol, depending on the type of cementitious materials and admixtures.

The significance of the activation energy is explained further here. In Equation 21.2, the exponential term within the summation sign converts increments of actual curing time at the concrete temperature to equivalent increments at the reference temperature. Thus, the exponential term can be considered as an **age conversion factor** (γ):

$$\gamma = e^{\frac{-E}{R} \left(\frac{1}{T} - \frac{1}{T_r} \right)} \quad (21.3)$$

Figure 21.10 shows how the age conversion factor varies with curing temperature for different values of the activation energy. The reference temperature is taken as 23°C. It is seen that for an activation energy of 30 kJ/mol, the age conversion factor is nearly a linear function of temperature. In this case, the Nurse–Saul equation would be a reasonably accurate maturity function to account for the combined effects of time and temperature, because the Nurse–Saul function assumes that the rate constant varies linearly with temperature (Carino, 1984). For an activation energy of 60 kJ/mol, the age conversion factor is a highly nonlinear function of the curing temperature. In this case, the Nurse–Saul function would be an inaccurate maturity function if the temperature were to vary over a wide range. In summary, Figure 21.10 shows the nature of the error in an age conversion factor if the incorrect value of activation energy were used for a particular concrete mixture. The magnitude of the error in the computed maturity index would increase with increasing difference of the curing temperature from the reference temperature.

The reader will have noticed that the term *activation energy* was introduced with quotation marks. This is because the E -value that is determined when the rate constant is plotted as a function of the curing temperature is not truly the activation energy as implied by the Arrhenius equation. The following discussion is provided for those unfamiliar with the concept of activation energy or the origin of the Arrhenius equation.

The idea of activation energy was proposed by Svante Arrhenius in 1888 to explain why chemical reactions do not occur instantaneously when reactants are brought together, even though the reaction products are at a lower energy state (Brown and LeMay, 1988). Arrhenius proposed that, before the lower energy state is achieved, the reactants must have sufficient energy to overcome an energy barrier that separates the unreacted state from the reacted state. A physical analogy is a brick standing upright. The

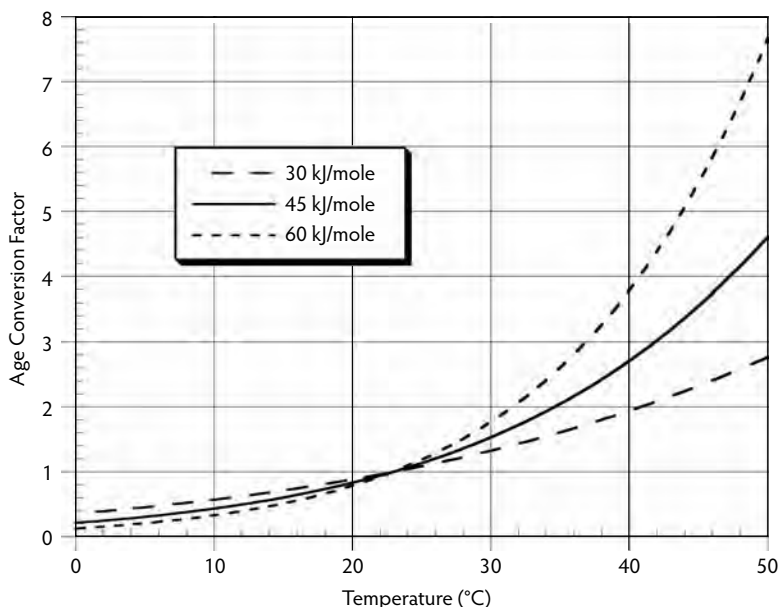


FIGURE 21.10 Effect of activation energy value on the age conversion factor.

brick will not instantaneously tip over to its lower energy state, which is the brick lying in a horizontal position. It must be pushed from the higher to the lower energy state. The energy required to push the brick from its upright position to the point of instability, after which the brick falls on its own, is the activation energy for this process.

For molecular systems, the reactant molecules are in constant motion and energy is transferred between them as they collide (Brown and LeMay, 1988). A certain number of molecules will acquire sufficient energy in these collisions to surmount the energy barrier and form the lower energy reaction product. As the system is heated, the kinetic energy of the molecules increases and more molecules will surmount the barrier; thus, the rate of reaction increases with increasing temperature. Arrhenius observed that the rate constant k of many reactions increased with temperature according to an exponential function, which has since been called the *Arrhenius equation*, as follows:

$$k = Ae^{\frac{-E}{RT}} \quad (21.4)$$

The term A is the frequency factor and is related to the frequency of collisions and the probability that the molecules will be favorably oriented for reaction (Brown and LeMay, 1988). It can be seen that the age conversion factor given by Equation 21.2 is simply the ratio of the rate constants at two different temperatures:

$$\gamma = \frac{k}{k_r} = \frac{e^{\frac{-E}{RT}}}{e^{\frac{-E}{RT_r}}} = e^{\frac{-E}{R} \left(\frac{1}{T} - \frac{1}{T_r} \right)} \quad (21.5)$$

The Arrhenius equation was derived empirically from observations of homogeneous chemical systems undergoing a single reaction. Roy and Idorn (1982) noted that researchers "... have cautioned that since cement is a multiphase material and also the process of cement hydration is not a simple reaction, homogeneous reaction kinetics cannot be applied." Thus, the activation energy obtained from strength-gain data or degree of hydration data is not a true activation energy as originally proposed by Arrhenius.

The author believes that the Arrhenius equation happens to be one of several equations that can be used to describe the nonlinear variation of the rate constant for strength gain (or degree of hydration) with curing temperature. This has been the motivation for proposing a simpler exponential function than Equation 21.2 to compute equivalent age (Carino, 1982; Carino and Tank, 1992; Tank and Carino, 1991). It has been suggested that the temperature dependence of the rate constant for strength gain can be represented by the following:

$$k = A_0 e^{BT} \quad (21.6)$$

where:

- A_0 = value of the rate constant at 0°C.
- B = temperature sensitivity factor (1/°C).
- T = concrete temperature (°C).

Based on Equation 21.6, the equation for equivalent age at the reference temperature T_r is as follows:

$$t_e = \sum_0^t e^{B(T-T_r)} \Delta t \quad (21.7)$$

where:

- B = temperature sensitivity factor (1/°C).
- T = average concrete temperature during time interval Δt (°C).
- T_r = reference temperature (°C).

It has been shown that Equation 21.2 and Equation 21.7 would result in similar values of equivalent age (Carino, 1992a) for a given temperature history. The author believes Equation 21.7 has the following advantages over Equation 21.2:

- The temperature sensitivity factor (B) has more physical significance compared with the apparent activation energy; for each temperature increment of $1/B$, the rate constant for strength development increases by a factor of approximately 2.7.
- Temperatures do not have to be converted to the absolute scale.
- Equation 21.7 is a simpler equation.

21.2.7.2 Strength Development Relationships

The key to developing an accurate maturity function for a particular concrete mixture is to determine the variation of the rate constant with curing temperature. Strictly speaking, a rate constant represents the rate at which a chemical reaction occurs at a given temperature. In the context of this discussion, however, the rate constant is related to the initial rate of strength gain at a constant temperature, and it can be obtained from the equation of strength vs. age. Thus, it is necessary to consider some of the relationships that have been used to represent the isothermal strength development of concrete. The author has successfully used the following hyperbolic equation to represent strength gain at constant curing temperature up to equivalent ages at 23°C of about 28 days:

$$S = S_u \frac{k(t-t_0)}{1+k(t-t_0)} \quad (21.8)$$

where:

- S = strength at age t (MPa).
- t = age of concrete (days).
- S_u = "limiting" strength.
- k = rate constant (1/day).
- t_0 = age at start of strength development (days).

The basis of this equation has been explained elsewhere (Carino, 1984; Knudsen, 1980). This equation assumes that strength development begins instantaneously at age t_0 ; thus, the gradual strength development during the setting period is not considered. The parameters S_u , k , and t_0 are obtained by least-squares curve fitting to the strength-vs.-age data. The limiting strength (S_u) is the asymptotic value of the strength for the hyperbolic function that fits the data. As will be discussed, the best-fit value for S_u does not necessarily represent the actual long-term strength of the concrete, and that is why the quotation marks were used in the definition following Equation 21.8. For the hyperbolic equation, the rate constant has the following property: When the age beyond t_0 is equal to $1/k$, the strength equals 50% of the limiting strength, or $0.5(S_u)$.

An equation similar to Equation 21.8 was also used by Knudsen (1980) and Geiker (1983) to represent the degree of hydration and development of chemical shrinkage as a function of age. Geiker (1983) noted, however, that Equation 21.8 gave a poor fit for certain cementitious systems. It was found that the following version of the hyperbolic equation gave a better fit to certain data than Equation 21.8 (Knudsen, 1984):

$$S = S_u \frac{\sqrt{k(t-t_0)}}{1 + \sqrt{k(t-t_0)}} \quad (21.9)$$

Knudsen explained the differences between Equation 21.8 and Equation 21.9 in terms of the hydration kinetics of individual cement particles. Equation 21.8 is based on **linear kinetics**, which means that the degree of hydration of an individual cement particle is a linear function of the product of time and the rate constant. Equation 21.9 is based on **parabolic kinetics**, which means that the degree of hydration is a function of the square root of the product of time and the rate constant. Thus, Equation 21.8 and Equation 21.9 are called the *linear hyperbolic model* and *parabolic hyperbolic model*, respectively.

Freiesleben Hansen and Pedersen (1985) proposed the following exponential equation to represent the strength development of concrete:

$$S = S_u e^{-\left(\frac{\tau}{t}\right)^\alpha} \quad (21.10)$$

where:

τ = a time constant.

α = a shape parameter.

This equation can model the gradual strength development occurring during the setting period, and it is also asymptotic to a limiting strength. The time constant τ represents the age at which the strength has reached $0.37(S_u)$; thus, the value of $1/\tau$ can be considered as the rate constant for this equation. The shape parameter α affects the slope of the curve during the acceleratory period (following the induction period*), and it affects the rate at which the strength approaches the limiting strength.

Figure 21.11 illustrates the performance of these equations in representing actual strength development data. Figure 21.11a shows strength data for mortar cubes cured at room temperature and tested at ages from 0.4 to 56 days. Figure 21.11b shows data for standard-cured concrete cylinders tested at ages from 7 days to 3.5 years (Carette and Malhotra, 1991). The curves are the best-fit curves for Equation 21.8, Equation 21.9, and Equation 21.10. For the mortar data, the linear hyperbolic function and the exponential function fit the data well, and these curves are nearly indistinguishable in Figure 21.11a. For the longer term concrete data, the parabolic hyperbolic function and the exponential function fit the data better than the linear hyperbolic function, and the curves based on these two functions cannot be distinguished in Figure 21.11b.

* After cement and water are mixed together, there is a time delay before strength development begins. This period is referred to as the *induction period*. After the induction period, strength development is rapid, and this is known as the *acceleratory period*.

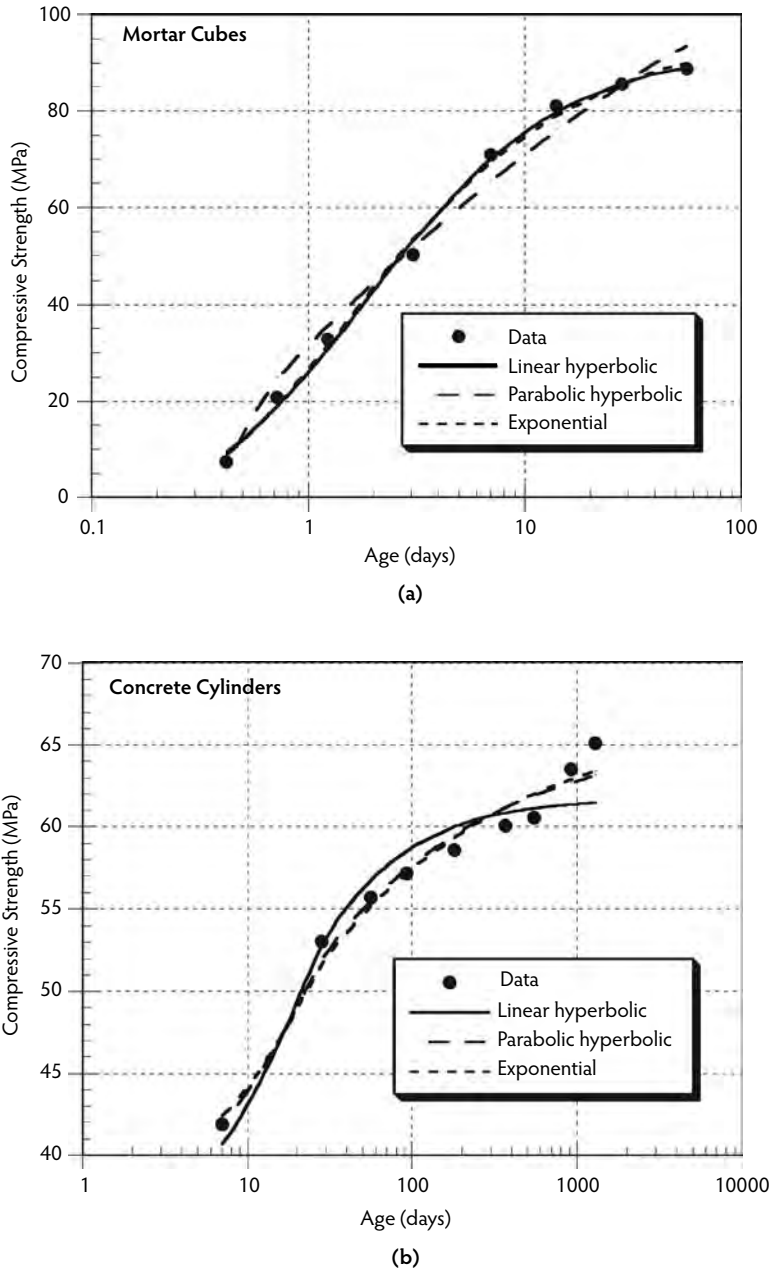


FIGURE 21.11 Fit of strength–age models to experimental data: (a) mortar cubes, and (b) concrete cylinders.

The results shown in Figure 21.11 highlight the capabilities of the various strength–age functions. The linear hyperbolic function appears to be a good model for strength development up to about 28 days (equivalent age) but not for later ages. The parabolic hyperbolic function appears to be better suited for modeling later age strength gain. The exponential model appears to be capable of modeling strength gain over the full spectrum of ages.

The inherent limitation of the linear hyperbolic function can be understood by considering the ratio of the limiting strength to the 28-day strength. If the t_0 term in Equation 21.8 is neglected, the following equation is obtained for this ratio:

$$\frac{S_u}{S_{28}} = \beta = 1 + \frac{1}{28k} \quad (21.11)$$

Thus, the value of β (the ratio of limiting strength to 28-day strength) is directly related to the rate constant. A higher value of k results in a lower value of β , which means a smaller difference between the limiting strength and the 28-day strength. The rate constant, in turn, is controlled primarily by the initial rate of strength development. The fact is that the ratio of the actual long-term strength of concrete to the 28-day strength does not obey Equation 21.11. This means that values of S_u obtained by fitting the linear hyperbolic model to strength–age data will be lower than the actual long-term strength of concrete if it is allowed to cure for a long time.

On the basis of the above discussion, one might conclude that the exponential model given by Equation 21.10 is the best model to use for determining the rate constant at a particular curing temperature. This would be correct if shape parameter α were independent of the curing temperature; however, test results show that this is not always the case (Carino et al., 1992). Thus, a maturity function based solely on the variation of the rate constant ($1/\tau$) with temperature would not be able to account accurately for the combined effects of time and temperature on strength development.

Which strength-gain function should be used? The maturity method is typically used to monitor strength development during construction; therefore, it is not necessary to accurately model the strength gain at later ages. Thus, the author believes that the linear hyperbolic function can be used to analyze strength data, up to an equivalent age of 28 days, to determine the variation of the rate constant with curing temperature. Knudsen (1985) suggested that the linear hyperbolic function is suitable up to a degree of hydration of 85%. The suitability of the linear hyperbolic function was also demonstrated in a study on the applicability of the maturity method to mortar mixtures with low ratios of water to cementitious materials, typical of those in high-performance concrete (Carino et al., 1992).

21.2.7.3 Estimating Strength

The final discussion deals with estimating strength by the maturity method. The maturity method is generally used to estimate the in-place strength of concrete by using the in-place maturity index and a previously established relationship between maturity index and strength. This assumes that a given concrete possesses a unique relationship between strength and the maturity index. This assumption would be acceptable if the long-term strength of concrete were independent of the curing temperature, but this is not the case. It is known that the long-term strength is affected by the initial temperature of the concrete. Thus, if the same concrete mixture were used for a cold-weather placement and a hot-weather placement, the strength would not be the same for a given maturity index. It has been proposed that the correct application of the maturity method is to estimate **relative strength**. Tank and Carino (1991) proposed the following **rate constant model** of relative strength development in terms of equivalent age:

$$\frac{S}{S_u} = \frac{k_r(t_e - t_{0r})}{1 + k_r(t - t_{0r})} \quad (21.12)$$

where:

k_r = value of the rate constant at the reference temperature.

t_{0r} = age at start of strength development at the reference temperature.

The previous discussion has shown that, for the linear hyperbolic function, the ratio S/S_u may not indicate the true fraction of the long-term strength because the calculated value of S_u may not be the actual long-term strength. This deficiency can be overcome by expressing relative strength as a fraction of the strength at an equivalent age of 28 days. By using the definition of β in Equation 21.11, the relative strength gain equation would be as follows:

$$\frac{S}{S_{28}} = \beta \frac{k_r(t_e - t_{0r})}{1 + k_r(t - t_{0r})} \quad (21.13)$$

The value of β would be obtained by fitting Equation 21.8 to data of strength vs. equivalent age. Then, the value of S_u is divided by the estimated strength, from the best-fit curve, at an equivalent age of 28 days.

To summarize, the following points represent the author's ideas about the maturity method:

- No single maturity function is applicable to all concrete mixtures. The applicable maturity function for a given concrete can be obtained by determining the variation of the rate constant with the curing temperature.
- The linear hyperbolic function can be used to analyze strength–age data to obtain the rate constants at different curing temperatures.
- Equation 21.6 can be used to represent the variation of the rate constant with curing temperature. The temperature-sensitivity factor governs the rate at which the rate constant increases with temperature and is analogous to the activation energy in the Arrhenius equation.
- The equivalent age can be calculated from the temperature history using Equation 21.7.
- The maturity method is more reliable for estimating relative strength development than for estimating absolute strength.

21.2.7.4 Maturity and Other Properties

The development of mechanical and transport properties of concrete is related to the degree of hydration of the cementitious materials; thus, it would be expected that the early development of other properties besides compressive strength could be related to a maturity index. Lew and Reichard (1978) showed that the development of modulus of elasticity, splitting tensile strength, and pullout bond strength could be related to the temperature–time factor. More recently, Dellate et al. (2000) related the development of splitting tensile strength and tensile bond strength of concrete overlays to the temperature–time factor. Yu and Ansari (1996) studied the development of fracture energy under different curing temperatures and found that the activation energy for development of fracture toughness was the same as for development of compressive strength. The values of fracture energy measured under different curing temperatures fell on the same curve when plotted as a function of equivalent age. Dilly and Zollinger (1998) also related the development of fracture strength to equivalent age. Pinto et al. (2001) found that the development of compressional wave speed under different curing temperatures could be related to equivalent age.

Pinto and Hover (1999) investigated whether the maturity method was applicable to the setting time of concrete measured in accordance with ASTM C 403/C 403M (see ASTM, 2006d). They found that the setting time at different temperatures could be used to obtain an apparent activation energy to represent the temperature dependence of setting time. The inverses of the setting times were used as rate constants, and the natural logarithms of the rate constants were plotted as a function of the inverse of absolute temperature. They found that the activation energy based on setting time was similar to the value recommended in ASTM C 1074 (ASTM, 2004a) for concrete made with Type I cement. Thus, by measuring setting times at two extreme temperatures, it is possible to estimate setting time for any temperature within the extremes.

21.2.7.5 Highway Applications

In 2000, the Pennsylvania Transportation Institute conducted a survey of state departments of transportation to establish progress in the adoption of the maturity method (Tikalsky et al., 2001). Of the 44 states that responded to the survey, 32 indicated that they had conducted or were conducting research on implementing the method. The reported uses of the maturity method included determination of formwork removal times, determination of joint sawing times, and determination of opening times for pavements. Some states, such as Texas (TDOT, 2002), South Dakota (SDDOT, 1999), Iowa (IDOT, 2002),

and Indiana (INDOT, 1999), developed their own test methods, based essentially on ASTM C 1074. Some of these methods were developed for estimating in-place flexural strength and others were applicable to either flexural or compressive strengths. All protocols use the temperature–time factor (Equation 21.1) as the maturity function. State department of transportation protocols include procedures for verifying during construction that previously established strength–maturity relationships are valid. Texas, for example, requires monitoring the temperature–time factor of selected specimens molded from samples of field concrete. At a preestablished level of maturity, the specimens are tested for strength. The measured strengths are compared with the estimated strength based on the strength–maturity relationship. If the difference between measured and estimated strengths is greater than 10%, a new strength–maturity relationship must be established for the project. The Texas protocol also requires enhanced batch plant inspection when the maturity method is used to estimate in-place strength.

21.2.8 Statistical Methods

In 1983, ACI Committee 318 recognized in-place test methods as alternatives to testing field-cured cylinders for assessing concrete strength during construction. The following sentence was added to Section 6.2.1.1 of ACI 318-83, dealing with evaluation of in-place strength before form removal: “Concrete strength data may be based on tests of field-cured cylinders or, when approved by the Building Official, on other procedures to evaluate concrete strength.” The Commentary to ACI 318-03 listed acceptable alternative procedures and further stated that these alternative methods “require sufficient data using job materials to demonstrate correlation of measurements on the structure with compressive-strength of molded cylinders or drilled cores.” Thus, to use the alternative methods, an empirical relationship has to be developed to convert in-place test results to estimated compressive-strength values. In addition, a procedure is required to analyze in-place test results so compressive strength can be estimated with a high degree of confidence. The latter issue is not mentioned in ACI 318. The report of ACI Committee 228 (2003) provides information on developing the **strength relationship**^{*} and how it should be used to estimate the in-place strength. Basically, the procedure is to perform in-place tests (X values) and standard compressive strength tests (Y values) on companion specimens at different levels of strength and use regression analysis to determine a best-fit curve ($Y = f(X)$) to the data. The relationship that is obtained and the results of in-place tests on the structure are used to estimate the concrete strength in the structure. To obtain a reliable estimate of the in-place strength, statistical methods are necessary to account for the various sources of uncertainty. The procedures that can be used for this purpose are reviewed in this section after a brief review of recent developments related to statistical analysis.

21.2.8.1 Background

During the 1960s and 1970s, the traditional method of ordinary least squares (OLS) analysis was used to analyze correlation data and establish the best-fit equation for the strength relationship and its confidence limits (Natrella, 1963). In the 1980s, simple procedures were used to estimate lower confidence limits of estimated in-place strength (Bickley, 1982b; Hindo and Bergstrom, 1985). It was recognized that the existing methods were not statistically rigorous and the stated confidence levels were not accurate (Stone et al., 1986). One of the deficiencies inherent in using OLS to establish the strength relationship is that OLS assumes that the X variable (the in-place test result) has no measurement error. In fact, the within-test coefficient of variation of in-place tests can be two to three times greater than those of compression tests of cores or cylinders. To overcome these deficiencies, a study was undertaken at the National Institute of Standards and Technology (NIST) to develop a rigorous method for obtaining the strength relationship and for estimating the lower confidence limit of the in-place strength (Stone and Reeve, 1986). The procedure that was developed used a method for least-squares fitting that accounted for error in the X variable (Mandel, 1984). The rigorous method was discussed in the original report of

^{*} The term *strength relationship* refers to the empirical equation, obtained from a correlation testing program, that relates the compressive strength (or other measure of strength) of concrete to the quantity measured by the in-place test.

ACI Committee 228 (1989), but it found little use due to its complexity. Subsequently, a simplification of the rigorous method was proposed that could be implemented by using a computerized spreadsheet (Carino, 1993). This simplified method was incorporated into the 1995 revision of the ACI Committee 228 report and is retained in the current version. A step-by-step procedure for implementing the method is included in the appendices to the report. That procedure was later incorporated into a stand-alone computer program (Chang and Carino, 1998).

During the late 1980s and early 1990s, A. Leshchinsky published a series of papers on statistical methods for in-place tests that were based largely on work at the Institute for Research of Building Structures in Kiev. These papers compared practices in different countries with those in the former Soviet Union, which had a long history in using in-place methods for quality control in precast concrete plants. In a review of various national standards, Leshchinsky (1990) concluded that:

- Greater numbers of in-place tests are required compared with tests of standard specimens, which makes in-place testing economically unattractive.
- The number of test specimens necessary to establish the strength relationship and the number of in-place tests on the structure have been established arbitrarily, based on the experiences of those writing the standards.
- The number of replicate tests to establish the strength relationship differs from the replications at a test location in a structure.

Leshchinsky presented procedures for selecting in-place tests based on consideration of cost and reliability of the estimated strength, as well as recommendations for reducing the cost of in-place testing.

In another paper, procedures for developing correlations were discussed and criteria were suggested for verifying the correlation at periodic intervals (Leshchinsky and Leshchinsky, 1991). The notion of a **stable correlation** was introduced. This refers to a strength relationship that is affected little by changes in concrete composition and the construction process. It was noted that methods that have a close connection between concrete strength and the quantity measured by the in-place test tend to have more stable correlations, but they also tend to be more costly than the methods that do not have this close connection. Pullout, break-off, and pull-off tests were identified as possessing stable correlations. It was also shown that the correlations may be affected by the location on the test specimens (top, middle, bottom) where the in-place test is performed (Leshchinsky, 1991a). Leshchinsky also discussed factors to consider when deciding whether or not combined methods are justified (Leshchinsky, 1991b). In addition, the following situations were identified where the combined use of a reliable, expensive method could be combined with a less expensive but less reliable method to achieve an overall cost savings in testing:

- The more reliable method is used to calibrate the strength relationship of the less reliable method; a correction factor is determined and applied to the strength estimated by the less reliable method.
- The less reliable method is used to identify areas of lower quality concrete where the more reliable tests should be performed.
- For new construction, a less reliable method is used to determine when tests by the more reliable method should be performed.

An example of such a combined approach is the use of inexpensive disposable maturity meters in combination with pullout tests. The maturity meter is used as an estimator of when the in-place concrete has reached target strength, and pullout tests are then done to confirm that the target strength has in fact been attained.

In a few instances in North America in-place testing has been used for acceptance testing. The major barrier is the lack of a consensus-based, statistical procedure for this application. Leshchinsky (1992) discussed some of the considerations for using in-place testing for acceptance testing. Because the strength of the actual concrete in the structure is measured, the acceptable in-place strength could be less than the design strength. Leshchinsky also reviewed provisions in existing national standards that allow acceptance based on in-place tests. In some of these standards, the required in-place strength depends

on the number of tests and the variability of the in-place results. For high variability, the required in-place strength might exceed the design strength. ACI Committee 228 (2003) provided the following proposal for acceptance of concrete based on in-place testing:

The concrete in a structure is acceptable if the estimated average, in-place, compressive strength based on a reliable in-place test procedure equals at least 85 percent of f'_c and no test result estimates the compressive strength to be less than 75 percent of f'_c .

These criteria are based on the ACI 318 acceptance criteria for core strengths. The ACI Committee 228 report stated that the implementation of such criteria requires a consensus-based standard practice for statistical analysis of in-place test results.

21.2.8.2 Correlation Testing

The following is a summary of the guidelines provided in the ACI Committee 228 (2003) report for establishing the strength relationship for a specific job. The procedure differs depending on whether in-place testing will be used to estimate strength during construction or in an existing structure. For new construction, the strength relationship is established from a laboratory testing program performed before using the in-place test method in the field. Companion test specimens are made using the same concreting materials to be used in construction. At regular intervals, measurements are made using the in-place test methods, and the corresponding compressive strengths of standard specimens are also measured. The number of strength levels has a significant effect on the confidence limits of the strength relationship. It is recommended that at least six strength levels be used to establish the strength relationship. More than about nine strength levels may not be economically justified. The strength levels should be evenly spaced to obtain an unbiased estimate of the strength relationship. The range of strengths in the correlation testing must include the range of strengths that are to be estimated in the structure.

For some techniques, such as rebound number and pulse velocity, it is possible to perform the in-place test on standard specimens without damaging them, and the same specimens can be tested subsequently for compressive strength. For other methods that result in local damage, in-place tests are carried out on separate specimens. It is important for the in-place tests and standard tests to be performed on specimens having similar compaction and that companion tests be performed at the same maturities. Curing companion test specimens in the same water bath is a convenient way to obtain similar temperature histories. Alternatively, internal temperatures can be recorded and test ages can be adjusted so in-place tests and standard tests are performed at the same maturity index for each strength level.

For existing construction, the strength relationship is established by performing in-place tests on the structure and determining the compressive strength from cores taken at adjacent locations. To obtain a wide range of strengths, a rebound hammer or pulse velocity survey may be performed first to identify locations with apparently different quality. At each test location, at least two cores should be taken to evaluate the compressive strength. Thus, the proper application of in-place testing for existing construction requires taking at least 12 cores to establish the strength relationship. As a result, the use of in-place testing may be economical only when large volumes of concrete are to be evaluated.

Additional information on the number of replicate in-place tests and the companion test specimens to use for different test methods may be found in the ACI Committee 228 report (2003). After paired values of average in-place test results and average compressive strengths are obtained, regression analysis is used to establish the equation of the strength relationship. The ACI 228 report recommends that linear regression be done using the natural logarithms of the test results so the following equation is fitted:

$$\ln C = a + b \ln I \quad (21.14)$$

where:

- $\ln C$ = average of natural logarithms of compressive strengths.
- $\ln I$ = average of natural logarithms of in-place test results.
- a = intercept of line.
- b = slope of line.

The report also recommends that the regression analysis to determine the values of a and b be performed using a procedure that accounts for the error in the X variable (in-place test results). This procedure is explained in detail in the appendix of ACI 228.1R. Basically, the ratio of the variances of the in-place test results and compressive strength results is used to define a parameter (λ), which is applied to the equations of ordinary least-squares regression to obtain the slope and intercept. This approach results in a more reliable estimate of the uncertainty of the strength relationship.

21.2.8.3 In-Place Strength Estimate

When making estimates of the in-place strength, the user should consider several important points:

- Where should the in-place tests be performed?
- How many in-place tests should be performed?
- How should the data be analyzed to obtain a reliable estimate of in-place strength?

These points are also covered in ACI 228.1R. In the case of new construction, a preconstruction meeting should be held to establish where and how many in-place tests should be performed. ACI 228.1R provides guidelines that can be used as a starting point to arrive at these decisions. For existing construction, a pretesting meeting should be held among all parties who share an interest in the test results. Agreement should be reached on the procedures for obtaining, analyzing, and interpreting the test results.

After the in-place test results have been obtained, statistical analysis is used to arrive at a reliable estimate of the in-place concrete strength. The term *reliable estimate* means that there should be a high likelihood that the actual in-place strength exceeds the estimated strength. The statistical procedure that is used should account for the following principal sources of uncertainty or variability:

- The uncertainty of the strength relationship
- The variability of the in-place test results
- The variability of the in-place concrete strength

ACI 228.1R includes several approaches that may be used for this purpose. One of these is based on the simplification by Carino (1993) of the rigorous procedure developed earlier by National Institute of Standards and Technology (NIST) researchers (Stone and Reeve, 1986). The underlying steps of this simplified procedure are illustrated in Figure 21.12. The average of the in-place test results is used to estimate the average concrete strength using a strength relationship. Next, the lower confidence limit of the average concrete strength is obtained by taking into account the uncertainty of the estimate from the strength relationship. This uncertainty includes a component based on the correlation testing and a component based on the variability of the in-place test results. Finally, the variability of the in-place concrete strength is used to obtain the tenth-percentile strength—that is, the strength expected to be exceeded by 90% of the concrete in the structure. This latter variability is estimated using the assumption that the ratio of the standard deviation of compressive strength tests to the standard deviation of in-place test results has the same value in the field as was obtained during the correlation testing (Stone and Reeve, 1986). The details for applying this procedure are given in ACI 228.1R (ACI Committee 228, 2003), and additional background information may be found in Carino (1993). This procedure has been implemented in a Windows-based computer program (Chang and Carino, 1998) that may be obtained by contacting the author of this chapter.

21.3 Methods for Flaw Detection and Condition Assessment*

21.3.1 Introduction

Other types of NDT methods are those used for flaw detection and condition assessment. In this context the term *flaw* include voids, honeycombing, delaminations, cracks, lack of sub-base support, and so forth. Since the 1980s, research and development efforts for these methods have exceeded those for methods

* Some of text in this section is based on a draft prepared by the author for the report on NDT methods subsequently developed by ACI Committee 228 (1998).

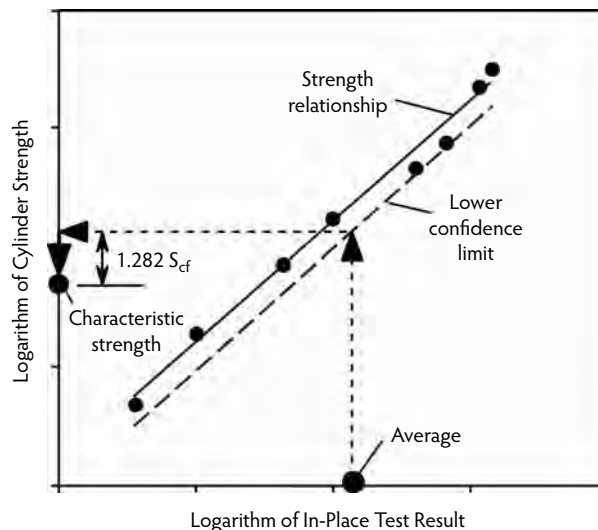


FIGURE 21.12 Schematic of statistical procedure for reliable estimate of in-place compressive strength. (From Carino, N.J., in *New Concrete Technology: Robert E. Philleo Symposium*, ACI SP-141, American Concrete Institute, Farmington Hills, MI, 1993, pp. 39–64.)

to estimate strength. The research impetus has come primarily from the transportation industry, because much of the highway infrastructure is in need of repair as a result of natural aging or the damage resulting from corrosion of reinforcing steel or deterioration of concrete. The techniques for flaw detection are based generally on the following simple principle: The presence of an internal anomaly interferes with the propagation of certain types of waves. By monitoring the response of the test object when it is subjected to these waves, the presence of the anomaly can be inferred. The interpretation of the results of these types of NDT methods usually requires an individual who is knowledgeable both in concrete technology and in the physics governing the wave propagation. This section of the chapter reviews the following techniques:

- Visual inspection
- Stress-wave propagation methods
- Infrared thermography
- Ground-penetrating radar
- Electrical/magnetic methods
- Nuclear methods

Emphasis is placed on explaining the underlying principles of the methods, and the reader may find additional information in the ACI Committee 228 report (1998), Malhotra and Carino (2004), and Bungey and Millard (1996).

21.3.2 Visual Inspection

Visual inspection is one of the most versatile and powerful of the NDT methods, and it is typically one of the first steps in the evaluation of a concrete structure (Perenchio, 1989). Visual inspection can provide a wealth of information that may lead to positive identification of the cause of observed distress. Its effectiveness depends, however, on the knowledge and experience of the investigator. Broad knowledge in structural engineering, concrete materials, and construction methods is required to extract the most information from visual inspection. Useful guides are available to assist less experienced individuals in recognizing different types of damage and determining the probable cause of the distress (ACI Committee 201, 1992; ACI Committee 207, 1994; ACI Committee 224, 2007; ACI Committee 362, 1997).

Before performing a detailed visual inspection, the investigator should develop and follow a definite plan to maximize the quality of the recorded data. Various ACI documents should be consulted for additional guidance on planning and carrying out the complete investigation (ACI Committee 207, 1994; ACI Committee 224, 2007; ACI Committee 362, 1997; ACI Committee 437, 2003). A typical investigation might involve the following activities:

- Perform a walk-through visual inspection to become familiar with the structure.
- Gather background documents and information on the design, construction, maintenance, and operation of the structure.
- Plan the complete investigation.
- Perform a detailed visual inspection.
- Perform any necessary sampling or in-place tests.

21.3.2.1 Supplemental Tools

Visual inspection has the obvious limitation that only visible surfaces can be inspected. Internal defects go unnoticed, and no quantitative information is obtained about the properties of the concrete. For these reasons, a visual inspection is usually supplemented by one or more of the other NDT methods discussed in this chapter. The inspector should consider other useful tools that can enhance the power of a visual inspection. Optical magnification allows a more detailed view of local areas of distress. Available instruments range from simple magnifying lenses to more expensive hand-held microscopes. Some fundamental principles of optical magnification can help in selecting the correct tool. The focal length decreases with increasing magnifying power, which means that the primary lens must be placed closer to the surface being inspected. The field of view also decreases with increasing magnification, making it tedious to inspect a large area at high magnification. The depth of field is the maximum difference in elevation of points on rough textured surface that are simultaneously in focus; this also decreases with increasing magnification of the instrument. To ensure that the “hills” and “valleys” are in focus simultaneously, the depth of field has to be greater than the elevation differences in the texture of the surface that is being viewed. Finally, the illumination required to see clearly increases with magnification level, and artificial lighting may be required at high magnification.

A very useful tool for crack inspection is a small hand-held magnifier with a built-in measuring scale on the lens closest to the surface being viewed (ACI Committee 224, 2007). With such a crack comparator, the width of surface opening cracks can be measured accurately. A stereo microscope includes two viewing lenses that provide a three-dimensional view of the surface. By calibrating the focus-adjustment screw, the investigator can estimate the elevation differences in surface features.

Fiberscopes and borescopes allow inspection of regions that are otherwise inaccessible to the naked eye. A fiberscope is composed of a flexible bundle of optical fibers and a lens system, and it allows cavities within a structure to be viewed by means of small access holes. The fiberscope is designed so some fibers transmit light to illuminate the cavity. In some systems, the operator can rotate the viewing head to allow a wide viewing angle from a single access hole. A borescope is composed of a rigid tube with mirrors and lenses and is designed to view straight ahead or at right angles to the tube. The image is clearer using a borescope, but the fiberscope offers more flexibility in the field of view. Use of these scopes requires drilling small holes if other access channels are absent, and the holes must intercept the cavity to be inspected. Some methods discussed in the remainder of the chapter may be used to locate these cavities; hence, the fiberscope or borescope may be used to verify the results of other NDT methods without removing cores.

A recent development that expands the flexibility of visual inspection is the small digital video camera. These are used in a manner similar to borescopes, but they offer the advantage of a video output that can be displayed on a monitor or stored on appropriate recording media. These charge-coupled device (CCD) cameras come in a variety of sizes, resolutions, and focal lengths. Miniature versions as small as 12 mm in diameter, with a resolution of 460 scan lines, are available. They can be inserted into holes drilled into the structure for views of internal cavities, or they can be mounted on robotic devices for inspections in pipes or areas with biological hazards.

In summary, visual inspection is a powerful NDT method. Its efficiency, however, is governed largely by the experience and knowledge of the investigator. A broad knowledge of structural behavior, materials, and construction methods is desirable. Visual inspection is typically one aspect of the total evaluation plan, which will often be supplemented by a series of other NDT methods or invasive procedures.

21.3.3 Stress-Wave Propagation Methods

Tapping an object with a hammer or steel rod (sounding) is one of the oldest forms of nondestructive testing based on stress-wave propagation. Depending on whether the response is a high-pitched **ringing** sound or a low-frequency **rattling** sound, the integrity of the member can be assessed. The method is subjective, as it depends on the experience of the operator, and it is limited to detecting near-surface defects. Despite these inherent limitations, **sounding** is a useful method for detecting near-surface delaminations, and it has been standardized by ASTM (Test Method D 4580; see ASTM, 2003a).

In NDT of metals, the **ultrasonic pulse-echo** (UP-E) method is a reliable method for locating small cracks and other defects. The principle of UP-E is similar to sonar. An electromechanical transducer is used to generate a short pulse of ultrasonic stress waves that propagates into the object being inspected. Reflection of the stress pulse occurs at boundaries separating materials with different densities and elastic properties (these determine the acoustic impedance of a material). The reflected pulse travels back to the transducer, which also acts as a receiver. The received signal is displayed on an oscilloscope or other display device, and the round-trip travel time of the pulse is measured electronically. By knowing the speed of the stress waves, the distance to the reflecting interface can be determined. In the absence of an internal defect, the opposite face of the test object is detected.

Early attempts to use UP-E equipment designed for metal inspection to test concrete were unsuccessful because of the heterogeneous nature of concrete. The presence of paste–aggregate interfaces, air voids, and reinforcing steel result in a multitude of echoes that obscure those from real defects. In the late 1990s and early 2000s, however, significant progress was made in using special ultrasonic transducers and a signal-processing method known as the *synthetic aperture focusing technique* (SAFT) to reconstruct internal images of concrete test objects (Kozlov et al., 2006; Krause et al., 2006; Schickert et al., 2003).

Beginning in the 1980s, considerable progress has been made in the development of usable techniques based on the propagation of impact-generated stress waves. This section reviews the basic concepts of stress-wave propagation due to impact and reviews the principles of some of the more promising impact-based methods. A more comprehensive review is provided by Carino (2004c).

21.3.3.1 Basic Relationships

When a disturbance (stress or displacement) is applied suddenly at a point on the surface of a solid, such as by impact, the disturbance propagates through the solid as three different waves: a P-wave, an S-wave, and an R-wave. The P-wave and S-wave propagate into the solid along spherical wavefronts. The P-wave is associated with the propagation of normal stress, and the S-wave is associated with shear stress. In addition, an R-wave travels away from the disturbance along the surface. In an infinite isotropic, elastic solid, the P-wave speed (C_p) is related to the Young's modulus of elasticity (E), Poisson's ratio (ν), and the density (ρ) as follows (Krautkrämer and Krautkrämer, 1990):

$$C_p = \sqrt{\frac{E(1-\nu)}{\rho(1+\nu)(1-2\nu)}} \quad (21.15)$$

The S-wave propagates at a slower speed (C_s) given by:

$$C_s = \sqrt{\frac{G}{\rho}} = \sqrt{\frac{E}{\rho 2(1+\nu)}} \quad (21.16)$$

where G is the shear modulus of elasticity.

The ratio of S-wave speed to P-wave speed depends on Poisson's ratio, as follows:

$$\frac{C_S}{C_P} = \sqrt{\frac{1-2\nu}{2(1-\nu)}} \quad (21.17)$$

For a Poisson's ratio of 0.2, which is typical of concrete, this ratio equals 0.61. The ratio of the R-wave speed (C_R) to the S-wave speed is given by the following approximate formula:

$$\frac{C_R}{C_S} = \frac{0.87+1.12\nu}{1+\nu} \quad (21.18)$$

For Poisson's ratio equal to 0.2, the R-wave travels at 92% of the S-wave speed.

In the case of bounded solids, the wave speed is also affected by the geometry of the solid. For rod-like solids, the P-wave speed is independent of Poisson's ratio and is given by the following:

$$C_P = \sqrt{\frac{E}{\rho}} \quad (21.19)$$

Thus, for $\nu = 0.2$, the wave speed in a slender rod is about 5% slower than in a large solid.

When a stress wave traveling through material 1 is incident on the interface between a dissimilar material 2, a portion of the incident wave is reflected. The amplitude of the reflection is a function of the angle of incidence and is a maximum when this angle is 90° (normal incidence). For normal incidence, the reflection coefficient, R , is given by the following:

$$R = \frac{Z_2 - Z_1}{Z_2 + Z_1} \quad (21.20)$$

where:

Z_2 = specific acoustic impedance of material 2.

Z_1 = specific acoustic impedance of material 1.

The specific acoustic impedance is the product of the wave speed and density of the material. The following are approximate Z values for P-wave reflection in some materials (Carino, 2004c):

Material	Specific Acoustic Impedance, kg/(m ² s)
Air	0.4
Water	1.5×10^6
Soil	$0.3 \text{ to } 4 \times 10^6$
Concrete	$7 \text{ to } 10 \times 10^6$
Steel	47×10^6

Thus, it can be shown that when a stress wave traveling through concrete encounters an interface with air, there is almost total reflection at the interface. This is why NDT methods based on stress-wave propagation have proven to be successful for locating defects within concrete.

21.3.3.2 Impact Methods

The greatest success in the practical application of stress-wave methods for testing concrete has been to use mechanical impact to generate the stress pulse. Impact causes a high-energy pulse that results in high penetration of the stress waves. Several techniques have been developed that are similar in principle but differ in the specific instrumentation and signal-processing methods that are used (Davis and Dunn, 1974; Davis and Hertlein, 1991; Higgs, 1979; Nazarian and Stokoe, 1986a; Sansalone and Carino, 1986; Stain, 1982; Steinbach and Vey, 1975).

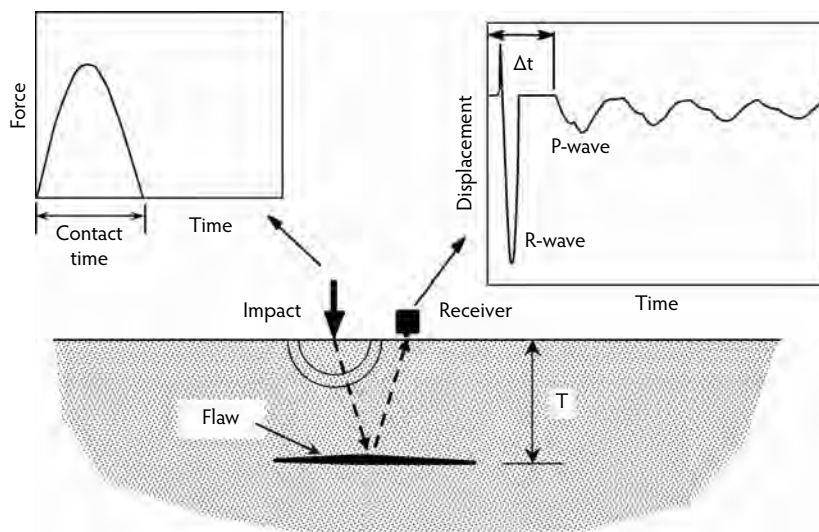


FIGURE 21.13 Schematic of test using impact to generate stress waves.

Figure 21.13 provides a schematic of an impact test. The principle is analogous to other echo methods that have been discussed. Impact on the surface produces a disturbance that travels into the object along spherical wavefronts as P- and S-waves. In addition, a surface wave (R-wave) travels away from the impact point. The P- and S-waves are reflected by internal defects (difference in elastic constants and density) or external boundaries. When the reflected waves, or echoes, return to the surface, they produce displacements that are measured by a receiving transducer. If the transducer is placed close to the impact point, the response is dominated by P-wave echoes (Sansalone and Carino, 1986). Using **time-domain** analysis, the time from the start of the impact to the arrival of the P-wave echo is measured, and the depth of the reflecting interface can be determined if the P-wave speed is known. The first successful applications of time-domain impact methods were in the field of geotechnical engineering to evaluate the integrity of concrete piles and caissons (Davis and Dunn, 1974; Steinbach and Vey, 1975). The technique is known as the *sonic-echo* or *seismic-echo* method. The long length of foundation structures allows sufficient time separation between the generation of the impact and the echo arrival, and determination of round-trip travel times is relatively simple (Lin et al., 1991b; Olson and Church, 1986).

The impact response of thin concrete members, such as slabs and walls, is more complicated than that of long slender members. Work by Sansalone and Carino (1986) led to the development of a successful technique for flaw detection in relatively thin concrete structures. The technique is known as the *impact-echo* method (Sansalone and Street, 1997). A key development leading to the success of the impact-echo method was the use of **frequency analysis**, instead of time-domain analysis, of the recorded waveforms (Carino et al., 1986; Sansalone, 1997). The principle of frequency analysis is as follows: The P-wave produced by the impact undergoes multiple reflections between the testing surface and the reflecting interface. Each time the P-wave arrives at the testing surface, it causes a characteristic displacement. Thus, the recorded waveform has a periodic pattern that depends on the frequency (f) of the P-wave arrival, which is given by:

$$f = \frac{C_p}{2D} \quad (21.21)$$

where C_p is the P-wave speed* and D is the depth of the reflecting interface. This frequency is termed the *thickness frequency*.

* Studies by Sansalone et al. (1997a) have shown that the P-wave speed in impact-echo testing of plate-like structures is approximately 96% of the P-wave speed in an infinite solid.

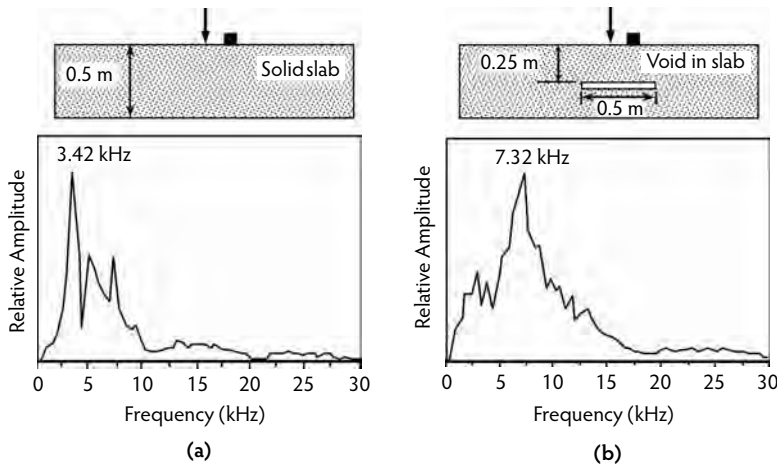


FIGURE 21.14 Examples of amplitude spectra from impact-echo test of concrete slab: (a) solid slab, and (b) slab with void.

To apply frequency analysis, the recorded waveform is transformed into the frequency domain by using the fast Fourier transform technique (Bracewell, 1978). The computed amplitude spectrum shows the frequency components in the waveform. For plate-like structures, the thickness frequency will usually be the dominant peak in the spectrum. The frequency value of the peak in the amplitude spectrum can be used to determine the depth of the reflecting interface by expressing Equation 21.21 as follows:

$$D = \frac{C_p}{2f} \quad (21.22)$$

Figure 21.14 illustrates the use of frequency analysis to interpret impact-echo tests. Figure 21.14a shows the amplitude spectrum from a test over a solid portion of a 0.5-m-thick concrete slab. There is a frequency peak at 3.42 kHz, which corresponds to multiple P-wave reflections between the bottom and top surfaces of the slab. Using Equation 21.21 or Equation 21.22 and solving for C_p , the P-wave speed is calculated to be 3420 m/s. Figure 21.14b shows the amplitude spectrum from a test over a portion of the slab containing an artificial disk-shaped void (Carino and Sansalone, 1989b). The peak at 7.32 kHz results from multiple reflections between the top of the slab and the void. Using Equation 21.21, the calculated depth of the void is $3420/(2 \times 7320) = 0.23$ m, which compares favorably with the planned distance of 0.25 m.

In the initial work leading to the impact-echo method (Sansalone and Carino, 1986), it was noted that the duration of the impact was critical to determining the success of the method. As shown in Figure 21.13, the force–time relationship for the impact may be approximated as a half-cycle sine curve, and the duration of the impact is the **contact time**. The contact time determines the frequency content of the stress pulse generated by the impact (Carino et al., 1986). As an approximation, the highest frequency component of significant amplitude equals the inverse of the contact time. To accurately locate shallow defects, the stress pulse must have frequency components greater than the frequency corresponding to the flaw depth (Equation 21.21). For example, for a P-wave speed of 4000 m/s, a pulse with a contact time shorter than 100 μ s is needed to measure the depth of defects shallower than about 0.2 m. Various impact sources have been used for impact testing. In evaluation of piles, hammers can be used to produce energetic impacts with long contact times (on the order of 1 ms). Such impacts are acceptable for testing long, slender structures but not for slabs or walls. For testing slabs from 0.15 to 0.5 m thick, steel balls and spring-loaded spherically tipped impactors have been used successfully. Steel balls are convenient impact sources because the contact time is proportional to the diameter of the ball (Goldsmith, 1965).

The impact-echo method has been successful in detecting a variety of defects (Carino, 2004c; Sansalone, 1997; Sansalone and Street, 1997). These defects include voids and honeycombed concrete in members, delaminations in bare and overlaid slabs, and voids in tendon ducts (Carino and Sansalone, 1992; Jaeger et al., 1996; Sansalone and Carino, 1986, 1988, 1989a,b). Experimental studies have been supplemented with analytical studies to gain a better understanding of the propagation of transient waves in bounded solids with and without flaws (Cheng and Sansalone, 1993a,b, 1995a,b; Lin et al., 1991a,b; Sansalone and Carino, 1987). Application of the impact-echo method has been extended to prismatic members, such as columns and beams (Lin and Sansalone, 1992a,b,c). It has been found that reflections from the perimeter of these members cause complex modes of vibration. As a result, the amplitude spectra have many peaks, and the depth of the member is not related to the dominant frequency in the spectrum according to Equation 21.21. Nevertheless, it has been shown that defects can be detected within beams and columns, and a successful field application has been reported (Sansalone and Poston, 1992). The impact-echo method has also been applied to evaluate the quality of the bond between an overlay and base concrete (Lin and Sansalone, 1996a,b). The method has also been found applicable to masonry walls (Williams et al., 1997).

As with most methods for flaw detection in concrete, experience is required to interpret stress-wave test results. To assist users in the interpretation of impact-echo results from tests of plate-like structures, an artificial intelligence technique known as a *neural network* (Sansalone et al., 1991) was investigated. In this technique, a computer program is **trained** to recognize amplitude spectra associated with flawed and unflawed structures. After this training, the program can be used to classify the results of tests on a structure under investigation. This technique was incorporated into the first commercial impact-echo test system (Pratt and Sansalone, 1992). It was found, however, that this “black box” approach was not successful because users relied blindly on the results of the neural network analysis without considering the validity of the recorded waveforms. Invalid waveforms can result from poor coupling of the receiver or an improper impact. Visual inspection of recorded waveforms by a trained operator will reveal invalid waveforms, which should be discarded, and a new test should be performed at that point.

In 1998, ASTM adopted a test method on the use of the impact-echo method to measure the thickness of plate-like concrete members (Carino, 2004c). For the purpose of this test method, a *plate* is defined as a structure or portion of a structure in which the lateral dimensions are at least six times the thickness. ASTM Test Method C 1383 (ASTM, 2004b) includes two procedures. Procedure A is used to measure the P-wave speed in the concrete. This measurement is based on measuring the travel time of the P-wave between two transducers a known distance apart. The background research for this technique is provided in Sansalone et al. (1997a,b) and Lin and Sansalone (1997). Procedure B determines the thickness frequency using the impact-echo method from which the plate thickness is calculated using the measured P-wave speed and Equation 21.22. As explained by Sansalone et al. (1997a), the P-wave speed obtained by Procedure A is multiplied by 0.96 when Equation 21.22 is used to calculate thickness. The data analysis procedure in ASTM C 1383 considers the systematic errors associated with the digital nature of the data in Procedures A and B. The thickness is reported with an uncertainty that is related to the sampling interval in Procedure A and the duration of the recorded signal in Procedure B (Sansalone et al., 1997a,b). Limited comparisons with the length of drilled cores demonstrated that pavement thickness based on impact-echo results were within 3% of core lengths (Sansalone and Streett, 1997; Sansalone et al., 1997a).

In the 2000s, extensive investigations to improve the capabilities of the impact-echo method were carried out in different countries. These studies have focused on developing scanning systems to increase the speed of impact-echo testing and exploring different signal analysis techniques to improve data presentation and interpretation. In a 2006 conference on NDT in civil engineering, 12 papers dealt with various aspects of impact-echo testing (Al-Qadi and Washer, 2006). The main themes of these papers were signal analysis, thickness measurement, and detection of voids in grouted tendon ducts.

Another type of impact method is known as *impulse–response*, *transient dynamic response*, or *impedance testing* (Davis and Dunn, 1974; Davis and Hertlein, 1991; Higgs, 1979; Olson and Wright, 1990; Stain,

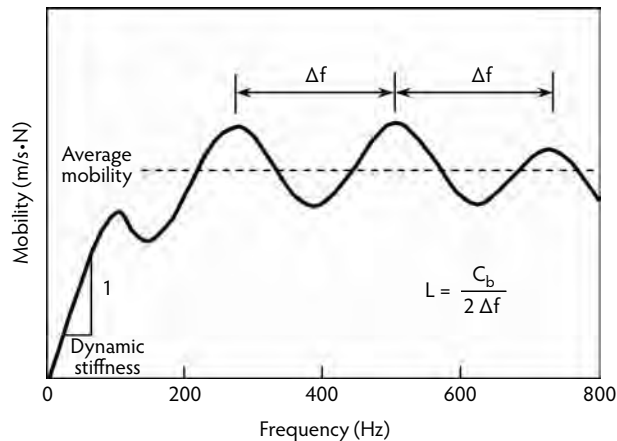


FIGURE 21.15 Idealized mobility plot of a pile in soil. (Adapted from Davis, A.G. and Dunn, C., *Proc. Inst. Civ. Eng.*, 57(Part 2), 571–593, 1974.)

1982). In this approach, the force history of the impact and the response of the structure are measured. Through a signal-processing technique, the measured response and force history are used to compute the characteristic impulse response spectrum of the structure (Carino, 2004c). The impulse–response spectrum of a structure depends on its geometry, the support conditions, and the existence of flaws or cracks.

Depending on the measured quantity of the structural response (displacement, velocity, or acceleration), the impulse–response spectrum has different meanings. Typically, velocity is measured and the resulting impulse–response spectrum has the units of velocity/force, which is referred to as *mobility*. The spectrum of mobility vs. frequency is called a *mobility plot*. Figure 21.15 is an idealized mobility plot for a pile embedded in soil (Davis and Dunn, 1974). At frequency values corresponding to resonant frequencies of the structure, mobility values are maximum. The series of peaks represents the fundamental and higher longitudinal modes of vibration. The difference between any two adjacent peaks (Δf) is equal to the fundamental longitudinal resonant frequency (Higgs, 1979). The length of the pile can be calculated by using Δf in place of f in Equation 21.22.

In addition to length, other information can be obtained from impulse–response tests on pile structures (Davis and Dunn, 1974; Finno and Gassman, 1998). At low frequencies, the pile and soil vibrate together, and the mobility plot provides information on the dynamic stiffness of the soil–pile structure (Davis and Dunn 1974; Stain, 1982). In this low-frequency range, the mobility plot is approximately a straight line, and the inverse of the slope of the straight line represents the dynamic stiffness of the pile head. Thus, mobility plots with steeper initial slopes correspond to less dynamic stiffness of the pile head. The pile head stiffness is a function of the dynamic stiffness of the pile itself and the properties of the surrounding soil.

Application of the impulse–response method has been extended to testing of plate-like structures such as pavements, floor slabs, walls, concrete tanks, and various type of cladding materials (Davis, 2003; Davis and Hertlein, 1987, 1990; Davis et al., 1997; Nazarian and Reddy, 1996; Nazarian et al., 1994). The following indices obtained from mobility plots have been found to correlate with different conditions:

- *Average mobility from 100 to 800 Hz*—The average mobility is affected by the stiffness of the concrete, the thickness of the plate, and the support conditions.
- *Mobility slope from 100 to 800 Hz*—The mobility slope, which is obtained from the slope of the best-fit line to the mobility values between 100 and 800 Hz, has been found to be related to the degree of consolidation of the concrete. For well-consolidated concrete, the mobility has a nearly constant value over this frequency range (Nazarian and Reddy, 1996). Poorly consolidated concrete, on the other hand, shows increasing mobility with frequency. These different behaviors are illustrated in Figure 21.16a.

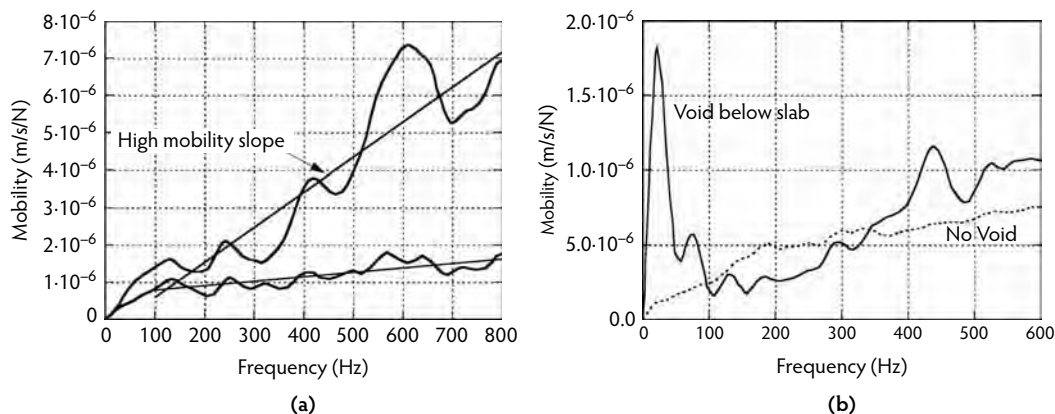


FIGURE 21.16 Examples of mobility plots from impulse-response tests of plate-like structures: (a) high mobility slope indicative of poor consolidation, and (b) high peak at low frequency indicative of a delamination or void below slab on ground. (Adapted from Germann Instruments, Inc., *NDT Systems*, Catalog NDT-2007, www.germann.org.)

- *Ratio of peak mobility to average mobility from 100 to 800 Hz*—When there is a delamination or local loss of support for a slab on ground, there will be a high mobility at low frequency. This corresponds to high amplitude flexural vibration of a plate supported at its edges. Thus, a high ratio of the peak mobility to the average mobility in the range of 100 to 800 Hz can be used as an indication of a delamination or loss of subgrade support (Davis and Hertlein, 1987). This behavior is illustrated in Figure 21.16b.

For plate-like structures, impulse-response testing is done at points on a grid laid out on the exposed surface. The results are analyzed on a comparative basis by using contour plots of one or more of the above indices. Anomalous regions in the contour plots are indicators of locations that require more in depth investigation. Impulse-response testing is more rapid than manual impact-echo testing, so the two methods are usually used in combination for cost-effective investigations of the plate-like structures. Impulse-response testing is done at a coarse grid spacing to identify potentially anomalous regions, which may be investigated further using impact-echo testing.

21.3.3.3 Spectral Analysis of Surface Waves

In the late 1950s and early 1960s, Jones (1955, 1962) reported on the use of **surface waves** to determine the thickness and elastic stiffness of pavement slabs and the underlying layers. The method involved determining the relationship between the wavelength and velocity of surface waves as the vibration frequency was varied. Apart from the studies by Jones, there seems to have been little use of this technique for testing concrete pavements. In the early 1980s, however, researchers at The University of Texas at Austin began studies of a surface-wave technique that involved an impactor instead of a steady-state vibrator. Digital signal processing was used to develop the relationship between wavelength and velocity. The technique is referred to as *spectral analysis of surface waves* (SASW) (Heisey et al., 1982; Nazarian et al., 1983). Figure 21.17 shows the configuration for SASW testing (Nazarian and Stokoe, 1986a). Two receivers are used to monitor the movement of the surface due to the R-wave produced by the impact. The received signals are processed, and a back-calculation scheme is used to infer the stiffnesses of the underlying layers.

Just as an impact is composed of a range of frequency components, the R-wave produced by a given impact also contains a range of components of different frequencies or wavelengths. (Note that the product of frequency and wavelength equals wave speed.) This range depends on the contact time of the impact; a shorter contact time results in a broader range. The lower frequency (longer wavelength)

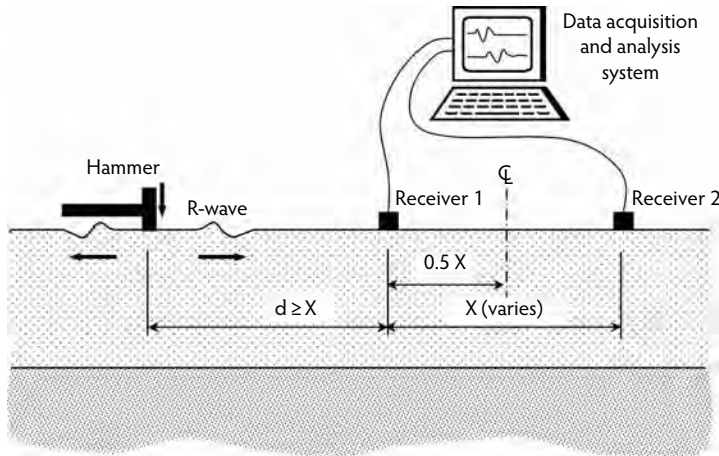


FIGURE 21.17 Schematic of testing configuration for spectral analysis of surface waves (SASW) technique.

components penetrate more deeply, and this is the key to using the R-wave to gain information about the properties of the underlying layers (Rix and Stokoe, 1989). In a layered system, the speed of these different wavelength components is affected by the wave speed in the layers through which the components travel. A layered system is a **dispersive** medium for R-waves, which means that different frequency components in the R-wave travel at different speeds, which are called *phase velocities* (Krstulovic-Opara et al., 1996).

In the SASW method, phase velocities are calculated by determining the time it takes for each frequency (or wavelength) component to travel between the two receivers. These travel times are determined from the phase difference of the frequency components arriving at the receivers (Nazarian and Stokoe, 1986b; Carino, 2004c). The phase differences are obtained by computing the **cross-power spectrum** of the signals recorded by the two receivers. The phase portion of the cross-power spectrum gives phase differences (in degrees) as a function of frequency. A schematic of such a phase spectrum is shown on the left side of Figure 21.18.* The phase velocities are determined as follows:

$$C_{R(f)} = X \frac{360}{\phi_f} f \quad (21.23)$$

where:

$C_{R(f)}$ = surface wave speed of component with frequency f .

X = distance between receivers (see Figure 21.17).

ϕ_f = phase angle of component with frequency f (degrees).

The wavelength (λ_f) corresponding to a component frequency is calculated using the following relationship:

$$\lambda_f = X \frac{360}{\phi_f} \quad (21.24)$$

By repeating the calculations given by Equation 21.23 and Equation 21.24 for each component frequency, one obtains a plot of wavelength vs. phase velocity. Such a plot is called a **dispersion curve** and is shown on the right side of Figure 21.18.

* A phase spectrum is usually plotted so the phase angle axis ranges from -180° to 180° ; hence, the spectrum folds over when the phase angle reaches -180° , giving the phase spectrum a sawtooth pattern.

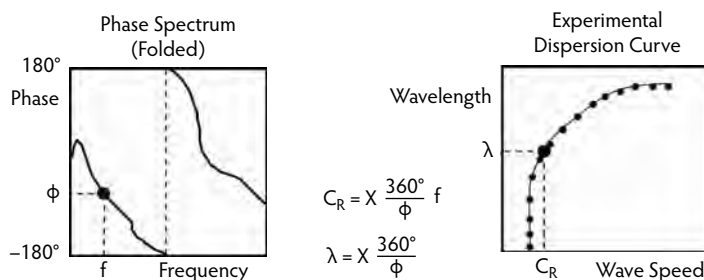


FIGURE 21.18 Schematic of phase spectrum (left) obtained from cross-power spectrum of the receiver waveforms in SASW testing and the dispersion curve (right) relating wavelength and wave speed.

After the experimental dispersion curve is obtained, a process called *inversion* is used to obtain the stiffness profile at the test site (Krstulovic-Opara et al., 1996; Nazarian and Desai, 1993; Nazarian and Stokoe, 1986b; Yuan and Nazarian, 1993). The site is modeled as layers of varying thickness. Each layer is assigned a density and elastic constants (shear modulus and Poisson's ratio). Using these assumed properties, the surface motion at the location of the receivers is calculated using numerical simulation of surface-wave propagation. The calculated responses are subjected to the same signal-processing technique as that used for the test data, and a theoretical dispersion curve is obtained. The theoretical and experimental dispersion curves are compared. If the curves match, the problem is solved, and the assumed stiffness profile is correct. If significant discrepancies are found, the properties of the assumed layered system are changed, and a new theoretical dispersion curve is calculated. This process is repeated until there is agreement between the theoretical and experimental dispersion curves. The user should be experienced in selecting plausible starting values of the elastic constants and should be able to recognize whether the final values are reasonable. Convergence cannot be assumed to indicate that the correct values have been determined, because it is possible for different combinations of layer thicknesses and elastic moduli to result in similar dispersion curves.

The general configuration for SASW testing was shown in Figure 21.17. For reliable results, tests are repeated with different receiver spacings (Nazarian and Stokoe, 1986a). The receivers are first located close together, and the spacing is increased by a factor of two for subsequent tests. As a check on the measured phase information for each receiver spacing, a second series of tests is carried out by reversing the position of the source. Typically, five receiver spacings are used at each test site. For tests of concrete pavements, the closest spacing is usually about 150 mm. The SASW method has been used to determine the stiffness profiles of soil sites and of flexible and rigid pavement systems (Nazarian and Stokoe, 1986b; Rix and Stokoe, 1989), and the method has been extended to the measurement of changes in the elastic properties of concrete slabs during curing (Rix et al., 1990).

21.3.3.4 Summary

The impact techniques discussed in this section offer great potential as reliable methods for flaw detection. Although they appear similar in terms of the physical test procedure, different information about the test object can be obtained by using the correct instrumentation and signal-processing methods. Each method is best suited for particular applications. Persons interested in using NDT methods based on stress-wave propagation should develop the ability to use all the methods, so the most appropriate one can be used for a particular situation.

21.3.4 Infrared Thermography

Infrared thermography is a technique for locating near-surface defects by measuring surface temperature. It is based on two principles. The first principle is that a surface emits electromagnetic radiation with an intensity that depends on its temperature; at about room temperature, the radiation is in the infrared

region of the electromagnetic spectrum. The second principle is that the presence of an anomaly having a lower thermal conductivity than the surrounding material will interfere with the flow of heat and alter the surface-temperature distribution. As a result, the surface temperature will not be uniform; thus, by measuring the surface temperature at different points, the presence of the defect can be inferred. In practice, the surface temperature is measured with an infrared scanner that works in a manner similar to a video camera (Manning and Holt, 1980). The output of the scanner is a **thermographic image** of temperature differences.

The following are values of thermal-conductivity for different materials (Halliday and Resnik, 1978):

Material	Thermal Conductivity (J/s·m·°C)
Steel	46
Ice	1.7
Concrete	0.8
Air	0.024

It can be seen that air has a much lower thermal conductivity than concrete, and this explains why the presence of air voids within concrete can affect the surface-temperature distribution when there is heat flow through concrete.

In civil-engineering applications, infrared thermography has been used primarily to detect corrosion-induced delaminations in reinforced-concrete bridge decks. In North America, early research on this application was performed independently in the late 1970s by the Virginia Highway and Transportation Research Council (Clemeña and McKeel, 1978) and by the Ontario Ministry of Transportation and Communication (Manning and Holt, 1983). Initial studies involved hand-held scanners and photographic cameras to record the thermographic images. This was followed by scanning from a boom attached to a truck and by airborne scanning using a helicopter. Although infrared thermography allowed more rapid surveys than the chain-drag technique (ASTM D 4580) (ASTM, 2003a), it was not as accurate as chain dragging for determining the extent of delaminations (Manning and Holt, 1983). In 1988, ASTM published a standard test method (ASTM D 4788) (ASTM, 2003b) on the use of infrared thermography to locate delaminations in exposed and overlaid concrete bridge decks. Additional information on considerations for performing an infrared survey and representative case histories are provided by Weil (2004).

The principle of infrared thermography is illustrated in Figure 21.19. The presence of a void in the concrete slab has a local insulating effect that disrupts the heat flow through the slab and affects the surface temperature. When heat flows into the slab, the area above the void is warmer than the surrounding area, and when heat flows out of the slab, the area above the void is cooler. By measuring the surface temperature distribution, one can infer the presence of the void; hence, the application of infrared thermography requires a heat-flow condition through the test object and a means for measuring small differences in surface temperature. The required heat-flow condition can be created artificially by using heating lamps, or it can occur naturally through solar heating (heat flow into the structure) and nighttime cooling (heat flow out of the structure). The latter approach is obviously more economical. The best time for doing infrared surveys is 2 to 3 hours after sunrise or after sunset (Weil, 2004). Heat flow decreases and surface temperatures become uniform with time after sunrise or sunset.

Even with the proper heat-flow conditions, not all delaminations are detectable. Maser and Roddis (1990) performed analytical studies to gain an understanding of the factors affecting the differences in the surface temperature of a solid concrete slab and a slab with a delamination. It was found that the maximum differential surface temperature decreased as the depth of the delamination increased and as the width decreased. Also, a water-filled delamination resulted in nearly identical surface temperatures as a solid slab.

In infrared thermography, differences in surface temperature are measured by using an imaging infrared scanner, a device similar to a video camera which measures the amount of infrared radiation emitted by a surface. As mentioned, the underlying principle of this measurement method is that an object at a temperature above absolute zero emits electromagnetic radiation, the wavelength of which depends on the temperature. As the temperature increases, wavelengths become shorter, and, at a sufficiently high

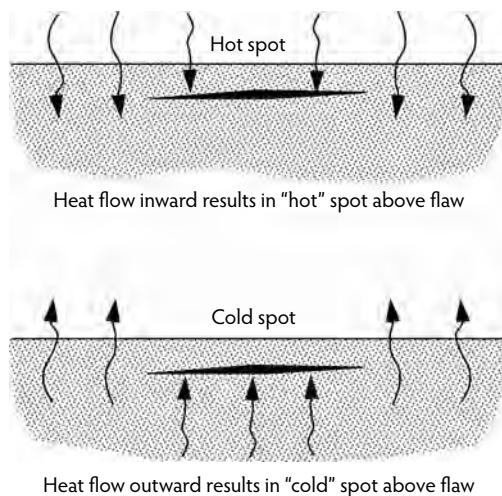


FIGURE 21.19 Effect of a void on the heat flow through a concrete slab.

temperature, the radiation is in the visible spectrum. This is the operating principle of incandescent light bulbs. At room temperature range, the wavelength of the radiation emitted by surfaces is on the order of $10\text{ }\mu\text{m}$, which is in the infrared region of the spectrum. This radiation cannot be detected by the naked eye. The infrared scanner has a detector that senses the infrared radiation. The detector output is related to the amount of incident radiant energy.

The energy emitted by a surface is related to its temperature according to the Stefan–Boltzman law (Halliday and Resnik, 1978):

$$R = e\sigma T^4 \quad (21.25)$$

where:

R = rate of energy radiation per unit area of surface (W/m^2).

e = emissivity of the surface.

σ = Stefan–Boltzman constant, $5.67 \times 10^{-8}\text{ W}/(\text{m}^2 \cdot \text{K}^4)$.

T = absolute temperature of the surface (degrees Kelvin).

With calibration, the output from the infrared sensor can be converted to a temperature. The emissivity is characteristic of the material and surface texture and has a value ranging from 0 to 1. Because the rate of energy radiation depends on temperature and emissivity, care must be exercised in interpreting thermographic images to ensure that apparent temperature differences are not caused by differences in emissivity. The emissivity of bridge deck surfaces can be affected by the type of texturing, oil spots, tire marks, paint, and loose debris.

Equipment for performing a thermographic survey includes an infrared scanner with associated hardware capable of producing a video image of the temperature distribution of the scanned surface; a conventional video camera to provide a visual record for comparison with the infrared record; video recorders to record infrared and conventional video images; analog-to-digital converters to transform the video images into digital data; a computer system and software for data storage and signal enhancement; and a distance-referencing system to correlate the infrared scan with position on the bridge deck (Kunz and Eales, 1985; Weil, 2004). The equipment is contained typically in a mobile van that travels along the roadway while data are recorded. The resolution of some infrared scanners is improved by lowering the temperature; therefore, a liquid nitrogen cooling system is used to cool the sensors. Modern infrared thermography systems do not require such cooling, making them simpler to use. Available equipment allows resolution of differences in surface temperature as low as 0.1°C .

The following is a summary of the procedure given in ASTM D 4788 for performing an infrared thermographic survey to detect delaminations in bridge decks:

- Remove debris from the surface.
- Allow the surface to dry for at least 24 hr before testing.
- Be sure there is at least a 0.5°C difference between the surface temperatures in areas above delaminations and in sound concrete. At least 3 hr of direct sunlight are generally sufficient to establish this temperature difference. A contact thermometer with a resolution of at least 0.1°C is used to determine whether the minimum temperature difference has been established.
- Do not test when the wind speed exceeds 50 km/hr because the surface temperature will be affected.
- Do not test when the ambient air temperature is less than 0°C because ice in delaminations will give false indications of sound concrete. As a guide, an ambient temperature rise of 10°C, 4 hr of sunshine, and a wind speed below 25 km/hr should result in accurate data on bare concrete surfaces during winter. For asphalt-covered concrete, at least 6 hr of sunshine are necessary during winter.
- Collect data with the van moving at speeds not greater than 15 km/hr.

The results of the inspection are usually reported in terms of delaminated area and percentage of total area that is delaminated. After the delaminated areas are identified in the infrared images, the visible video images should be compared to ensure that apparent temperature differences were not due to emissivity changes (Kunz and Eales, 1985). The ASTM standard states that 80 to 90% of the delaminations in a bare bridge deck can be located with this method. It has also been found that inspection of the same deck by four different operators resulted in a variation of $\pm 5\%$ of the known delaminated area.

A more recent development has been the use of infrared thermography to evaluate structural repairs made using bonded fiber-reinforced polymer (FRP) sheets. These repairs are made by bonding laminates of fiber cloth on the outside of a member. After the adhesive has cured, the FRP acts as external reinforcement. It is important to achieve good bonding with the concrete substrate and between the plies of FRP. It has been shown that active infrared thermography, in which heating lamps are used to create a transient heat-flow condition, is effective in locating voids that may exist between FRP plies or at the FRP-concrete interface (Levar and Hamilton, 2003; Starnes and Carino, 2003; Starnes et al., 2003).

In summary, instrumentation and computer software have been developed so inspection of bridge decks by infrared thermography is a fairly routine procedure (Kunz and Eales, 1985). Trained individuals are required to ensure that meaningful data are collected and that data are correctly interpreted. Infrared thermography is a **global** inspection method that permits large surface areas to be scanned in a short period of time, which is an advantage over other point-by-point methods that have been discussed.

21.3.5 Ground-Penetrating Radar

Radar is analogous to the ultrasonic pulse-echo technique previously discussed, except that pulses of electromagnetic waves (short radiowaves or microwaves) are used instead of stress waves. Early uses of the technique were for military applications, but radar techniques are now used in a variety of fields, such as weather, aerial mapping, and civil-engineering applications. The earliest civil-engineering applications for radar were probing into soil to detect buried pipelines and tanks. This was followed by studies to detect cavities below airfield pavements and more recently for determining concrete thickness, locating voids and reinforcing bars, and identifying deterioration (Alongi et al., 1982; Bungey and Millard, 1993; Cantor, 1984; Cantor and Kneeter, 1982; Carter et al., 1986; Clemeña, 1983; Kunz and Eales, 1985; Maser, 1986; Maser and Roddis, 1990; Steinway et al., 1981; Ulriksen, 1983). Clemeña (2004) provides a review of the applications of radar to concrete.

In civil-engineering applications, relatively short distances are involved compared with other uses of radar; thus, devices for these applications emit very short pulses of electromagnetic waves (microwaves). For this reason, the technique is often called *short-pulse radar* or *impulse radar*. Others refer to it as *ground-penetrating radar* (GPR), which is the term used in this chapter. This section discusses the principles of GPR, the instrumentation that is used, and some of the inherent difficulties in using the method.

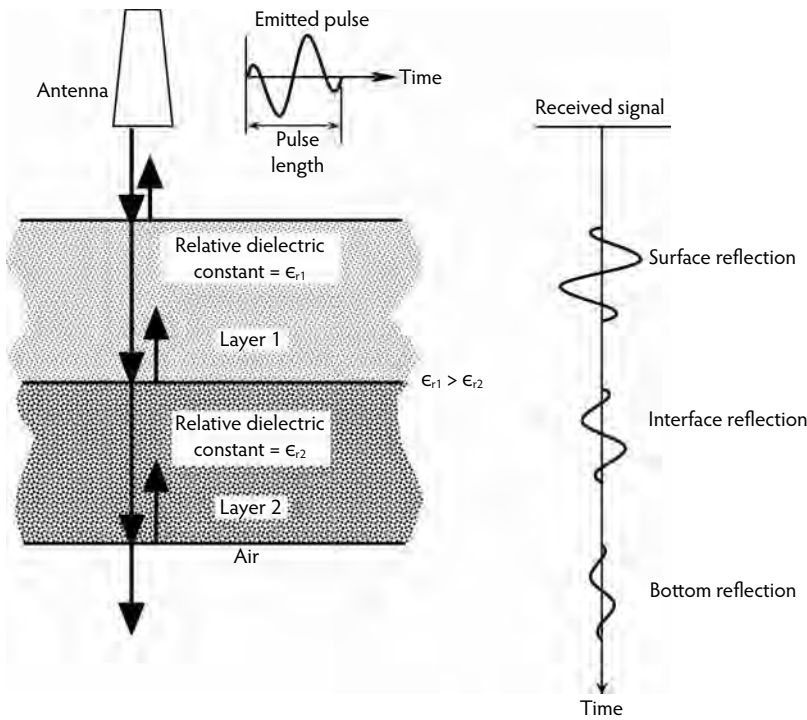


FIGURE 21.20 Reflection of electromagnetic pulse at interfaces between materials with different relative dielectric constants and antenna signal (right) caused by arrival of echoes.

Propagation of electromagnetic waves is a complex phenomenon. The following presentation is simplified based on assumptions suitable for civil-engineering applications. More detailed treatments are available (Daniels et al., 1988; Halabe et al., 1993, 1995). The operating principle of GPR is illustrated in Figure 21.20. An antenna above the test object sends out a short-duration pulse (on the order of nanoseconds) of electromagnetic waves. Some of the energy in the pulse travels through the test object, and when the pulse encounters an interface between dissimilar materials a fraction of the energy is reflected back toward the antenna as an *echo*. The antenna receives the echo and generates an output signal, as shown to the right in Figure 21.20. By measuring the time from the start of the pulse until the reception of the echo, one can determine the depth of the interface if the propagation speed through the material is known. This time-domain approach is analogous to the seismic-echo method based on stress-wave propagation.

The fraction of the incident pulse that is reflected at an interface depends on the difference between the relative dielectric constants* of the two materials and is given by the following equation (Bungey and Millard, 1993; Clemená, 2004):

$$\rho_{1,2} = \frac{\sqrt{\epsilon_{r1}} - \sqrt{\epsilon_{r2}}}{\sqrt{\epsilon_{r1}} + \sqrt{\epsilon_{r2}}} \quad (21.26)$$

where:

- $\rho_{1,2}$ = reflection coefficient.
- ϵ_{r1} = relative dielectric constant of material 1.
- ϵ_{r2} = relative dielectric constant of material 2.

Note the similarity of Equation 21.26 to Equation 21.20 for reflection of stress waves.

* The relative dielectric constant is related to the alignment of charges that occurs in an insulating material when placed in an electric field.

By definition, the relative dielectric constant of air equals 1, and typical values from ASTM D 4748 (ASTM, 2006a) for other materials are as follows:

Material	Range of Relative Dielectric Constant
Portland cement concrete	6 to 11
Asphalt–cement concrete	3 to 5
Gravel	5 to 9
Sand	2 to 6
Rock	6 to 12
Water	8

The relative dielectric constants for materials such as concrete and soil depend on the moisture content and ionic concentrations (Morey, 1974). Note that the dielectric constant of water is much higher than the other listed materials. This makes water the most significant dielectric contributor to construction materials and explains why radar is highly sensitive to moisture. As the moisture content increases, the dielectric constant of the material, such as concrete, also increases. Equation 21.26 shows that when the value of ϵ_r of material 2 is greater than that of material 1, the reflection coefficient is negative. This signifies a phase reversal in the reflected wave, which means that the positive part of the wave is reflected as a negative part. At a metal interface, such as between concrete and steel reinforcement, there is complete reflection and the reflected wave has reversed polarity. This makes GPR very effective for locating metallic embedments. On the other hand, strong reflections from embedded metals can obscure weaker reflections from other reflecting interfaces that may be present, and reflections from reinforcing bars may mask reflections from greater depths.

An important difference between GPR and stress-wave methods, such as the impact-echo method, is the amplitude of the reflections at a concrete–air interface. For stress waves, the reflection is almost 100% because the acoustic impedance of air is negligible compared with concrete. On the other hand, the mismatch in dielectric constants at a concrete–air interface is not as drastic, and only about 50% of the incident energy is reflected at a concrete–air interface. This results in two significant differences between GPR and stress-wave methods. GPR is not as sensitive to the detection of concrete–air interfaces as are stress-wave methods; however, because not all the energy is reflected at a concrete–air interface, GPR is able to penetrate beyond such an interface and detect features below the interface.

The depth of the reflecting interface is obtained from the measured round-trip travel time and the speed of the electromagnetic wave (C), which depends on the relative dielectric constant:

$$C = \frac{C_0}{\sqrt{\epsilon_r}} \quad (21.27)$$

where:

C_0 = speed of light in air (3×10^8 m/s).

ϵ_r = relative dielectric constant.

If the round trip travel time is Δt , then depth D would be:

$$D = C \frac{\Delta t}{2} \quad (21.28)$$

Equation 21.26 through Equation 21.28 form the basis for using GPR to inspect concrete structures.

Typical instrumentation for GPR includes the following main components: an antenna unit, a control unit, a display device, and a storage device. The antenna emits the electromagnetic pulse and receives the echoes. The length of the pulse is largely controlled by the antenna design. Longer pulses are associated with longer wavelengths (or lower frequency) and have greater penetrating ability but poorer resolution (poorer ability to detect small objects) than shorter pulses. Typically, an antenna with a predominant

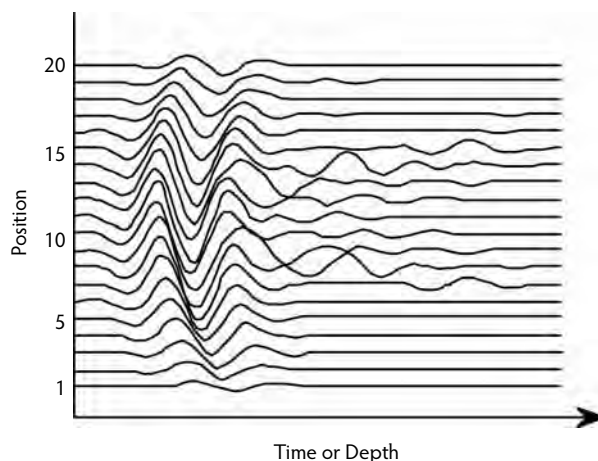


FIGURE 21.21 Waterfall plot of radar waveforms as an antenna is scanned across the surface of the test object. (Adapted from Cantor, T.R., in *In Situ/Nondestructive Testing of Concrete*, Malhotra, V.M., Ed., ACI SP-82, American Concrete Institute, Farmington Hills, MI, 1984, pp. 581–601.)

frequency of about 1 GHz is used to inspect pavements and bridge decks, and the pulse length is about 1 ns. In air, such a pulse is about 0.3 m long, and in concrete the length would depend on the value of ϵ_r . For $\epsilon_r = 6$, the pulse length would be about 120 mm. To be able to measure depths accurately, the echo must arrive after the initial pulse has ceased; therefore the round-trip travel path must exceed the pulse length. For $\epsilon_r = 6$, the minimum depth that can be measured accurately is about 60 mm. As ϵ_r increases, the minimum measurable depth decreases.

The pulse is attenuated as it travels through the test object, and there is a limit to the thickness that can be inspected. For concrete, the depth of penetration would depend on the characteristics of the GPR system, the moisture content, and the amount of reinforcement. With increasing moisture content and amount of reinforcement, penetration decreases. For dry unreinforced concrete, the maximum penetration of the pulse produced by a 1-GHz antenna is about 0.6 m (Clemeña, 2004). Figure 21.20 shows a horn antenna that is not in direct contact with the test object. In this case, the received signal includes an echo from the concrete surface. It is also possible to use a contact, or ground-coupled, dipole antenna that rests directly on the testing surface. In this case, the pulse emitted by the transmitting part of the antenna is picked up immediately by the receiving part.

The control unit is the heart of a GPR system. It controls the repetition frequency of the pulse, provides the power to emit the pulse, acquires and amplifies the received signal, and provides output to a display device. Data are usually stored and played back for later analysis and signal interpretation.

Older types of display devices include oscillographs, which plot the recorded waveforms as a **waterfall plot**, or graphic-facsimile recorders, which provide a cross-sectional view of the test object. As an example, Figure 21.21 shows a waterfall plot obtained by plotting the received waveforms next to each other. The plot takes on a topographic appearance, and changes in the pattern of the received signals are relatively easy to identify (Cantor, 1984). Computer software is also available that permits sophisticated signal processing of the data to aid in interpretation.

The operation of the graphic recorder is discussed further here because it was commonly used in the field and the same principles are applicable to modern computer displays. Figure 21.22a shows a ground-coupled, dipole antenna emitting a radar pulse into a test object containing a void. The shape of the emitted pulse is sketched above the antenna. Figure 21.22b shows the waveform from the receiving side of the antenna. The vertical axis represents time, or it can be transformed to depth by knowing ϵ_r and using Equation 21.28. The received signal at the start of the waveform represents the transmitted pulse, which is picked up directly by the receiving side of the antenna. The second received signal is the echo from the void, and the third is the echo from the bottom boundary of the test object.

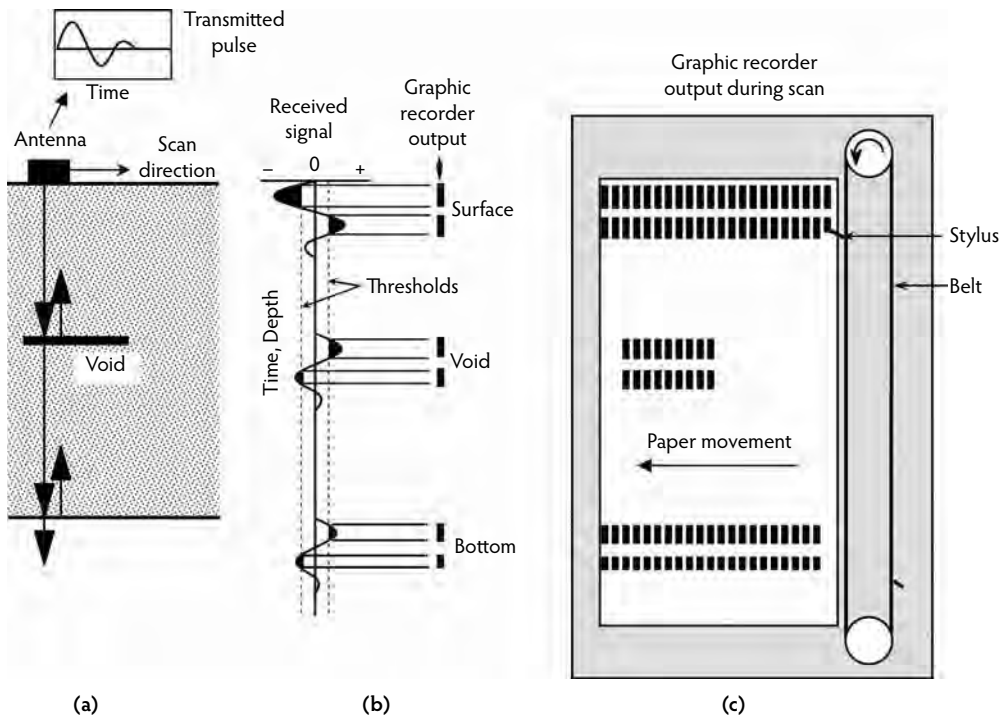


FIGURE 21.22 Schematic to illustrate peak-plotting technique used with graphic recorder: (a) reflections of electromagnetic pulse in test object; (b) received waveform and threshold limits; (c) graphic recorder output during surface scan of test object.

The output displayed by the graphic recorder is obtained by a technique known as *peak plotting*, which is illustrated in Figure 21.22b. First, the operator selects a threshold voltage range. When the amplitude of the received signal goes beyond the threshold range, the pen of the graphic recorder plots a solid line on recording paper. The line is plotted in varying shades of gray, depending on the amplitude of the signal. Thus, the antenna output is represented on the graphic recorder as a series of dashes, as shown in Figure 21.22b. Note that each echo is associated with two dashes. The actual number of dashes depends on the number of cycles in the emitted pulse and the threshold level. This is an important point to understand for proper interpretation of GPR results. As the antenna is moved along the surface, the output is displayed on the graphic recorder. The paper on the recorder moves at a constant speed that is independent of the speed of the antenna motion. The resulting display on the graphic recorder represents a cross-sectional view of the test object, as illustrated in Figure 21.22c. The test equipment provides a means for correlating the position of the antenna during the scan with the location on the paper record or computer display, so it is possible to determine the depth and approximate length (along the scan direction) of the reflecting interface.

As was mentioned, metals are strong reflectors of electromagnetic waves. This makes GPR very effective for locating buried metal objects such as reinforcing bars and conduit. Reinforcing bars result in characteristic patterns in the graphic-recorder output, which make them relatively easy to locate. There are two main factors leading to these patterns, which are discussed here with the aid of Figure 21.23. First of all, an antenna behaves like a flashlight in that the beam of radiation has a conical shape, so a reinforcing bar produces echoes before the antenna passes directly over the bar; however, the apparent depth of the bar will be larger than the actual cover because of the longer inclined travel path. Second, the pulse undergoes multiple reflections, or reverberations, between the reinforcing bar and the surface, and the output will show multiple echoes from the same bar. The resulting characteristic pattern is shown on the right side of Figure 21.23. The top of the bar is associated with the uppermost part of the arched bands.

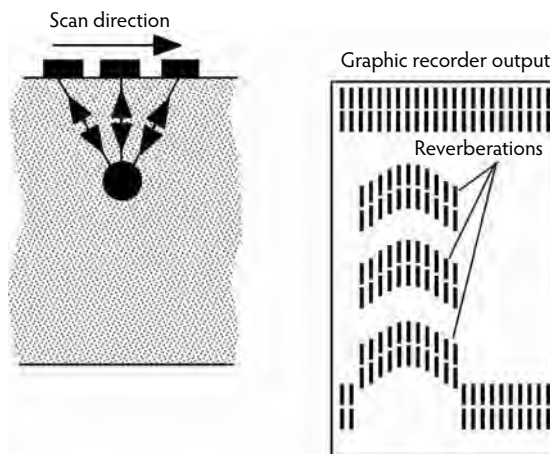


FIGURE 21.23 Schematic to illustrate characteristic pattern from ground-penetrating radar (GPR) scan over a reinforcing bar.

When multiple reinforcing bars are present, multiple arch patterns will be obtained. As the distance between bars decreases, the arch patterns overlap. At less than a critical spacing, the individual bars can no longer be discerned, and the echo pattern is similar to the case of a solid embedded steel plate. The ability to discern individual bars depends on bar size, bar spacing, cover depth, and configuration of the antenna (Bungey et al., 1994). Closely spaced bars will also prevent detection of features below the layer of reinforcement. This masking effect depends on the wavelength of the electromagnetic waves, the bar size, and cover depth. It has been found that for the 1-GHz, hand-held antenna, 32-mm-diameter bars at cover depths of 25 to 50 mm will prevent detection of underlying features when bar spacing is less than 200 mm (Bungey et al., 1994).

Simple methods do not exist to determine bar size from GPR output. Researchers have attempted to better understand the interactions of GPR with cracks, voids, and reinforcing bars (Mast et al., 1990). The objective of these studies is to develop procedures to use the recorded data to construct an image of the interior of the concrete. Some advances in this direction have occurred in France, where a prototype system has been developed that uses tomographic techniques to reconstruct the two-dimensional layout of reinforcement in concrete (Pichot and Trouillet, 1990). In the United States, successful three-dimensional reconstruction of artificial defects and reinforcement embedded in a concrete slab has been demonstrated (Mast and Johansson, 1994). These imaging methods rely on an antenna array to make multiple measurements and require extensive computational time to reconstruct the internal image.

The detection of delaminations in reinforced bridge decks using GPR is not straightforward. In studies by Maser and Roddis (1990), it was found that a 3-mm air gap in concrete produced little noticeable effect in the received waveform, but the addition of moisture to the simulated crack resulted in stronger reflections that were noticeable in the waveform. It was also found that the presence of chlorides in moist concrete resulted in high attenuation because of the increased conductivity. Thus, the ability to detect delaminations will depend on the *in situ* conditions at the time of testing. In addition, the reflections from reinforcing bars are much stronger than from a delamination, making it difficult to detect the delamination.

Within ASTM, two standards have been developed on the use of GPR in highway applications. Test Method D 4748 (ASTM, 2006a) can be used to measure the thickness of the upper layer of a multilayer pavement system. Basically, the technique involves measuring the transit time of the pulse through the pavement layer and using relationships similar to Equation 21.27 and Equation 21.28 to calculate the layer thickness. The procedure is based on using a non-contact horn antenna, so some modifications are required for measurements with a contact antenna. The calculated depth depends on the value of the relative dielectric constant. Errors in the assumed value of the relative dielectric constant can lead to

substantial inaccuracies in depth estimations (Bungey et al., 1994). For data obtained with a horn antenna, the relative dielectric constant of the concrete can be computed directly from the radar signals. For data obtained using a contact antenna, it is necessary to take occasional cores to determine the appropriate value for the pavement materials. The user is cautioned against using the method on saturated concrete because of the high attenuation and limited penetration of the pulse. In ASTM D 4748, it is stated that interoperator testing of the same materials resulted in thickness measurements within ± 5 mm of the actual thickness. Finally, it is noted that reliable interpretation of received signals can only be performed by an experienced data analyst. Test Method D 6087 (ASTM, 2007b) was originally developed in 1997 to provide a standard procedure for using GPR to evaluate the presence of delaminations due to corrosion of the top layer of reinforcement in concrete bridge decks.

Although the majority of GPR applications have dealt with locating reinforcing bars in structures, locating delaminations in bridge decks, and measuring the thickness of pavement layers, there are other potential uses. Because the dielectric properties of a material such as concrete depend strongly on the moisture content, microwave measurements can be used to monitor the progress of hydration (Clemeña, 2004; Otto et al., 1990). This is made possible because the relative dielectric constant of free water is much higher than that of chemically bound water. Clemeña (2004) has also reported on potential applications of microwave measurements to determine water content of fresh concrete. In addition, microwave sensors are used in ready-mixed concrete plants to measure the moisture content of aggregates stored in bins.

21.3.6 Electrical and Magnetic Methods for Reinforcement

Information about the quantity, location, and condition of reinforcement is needed to evaluate the strength of reinforced concrete members. This section discusses some of the magnetic and electrical methods that are used to gain information about embedded-steel reinforcement. Additional information may be found in ACI 228.2R (ACI Committee 228, 1998), Bungey and Millard (1996), Carino (2004d), Lauer (2004), and Malhotra (1976).

21.3.6.1 Covermeters

Devices to locate reinforcing bars and estimate the diameter and depth of cover are known as *covermeters*. These devices are based on interactions between the bars and low-frequency electromagnetic fields. The physical principle that is employed is that of **electromagnetic induction**, whereby an alternating magnetic field induces an electrical potential in an electrical circuit intersected by the field. Commercial covermeters can be divided into two classes: those based on the principle of **magnetic reluctance** and those based on **eddy currents**. These differences are summarized below (Carino, 1992b).

21.3.6.2 Magnetic-Reluctance Meters

When current exists in an electrical coil, a magnetic field is created and magnetic flux lines are created between the magnetic poles. This leads to a magnetic circuit, in which the magnetic flux between poles is analogous to the current in an electrical circuit (Fitzgerald et al., 1967). The resistance to creation of magnetic flux is called *reluctance*, which is analogous to the resistance to flow of charge in an electrical circuit. Figure 21.24 provides a schematic of a covermeter that is based on changes in the reluctance of a magnetic circuit caused by the presence or absence of a steel bar within the vicinity of the search head. The search head is composed of a ferromagnetic U-shaped core (yoke), an excitation coil, and a sensing coil. When alternating current (less than 100 Hz) is applied to the excitation coil, an alternating magnetic field is created, and a magnetic flux is established between the poles of the yoke. In the absence of a bar (Figure 21.24a), the magnetic circuit, composed of the yoke and the concrete between the ends of the yoke, has high reluctance, and the alternating magnetic flux in the magnetic circuit will be small. The alternating flux induces a small, secondary current in the sensing coil. If a ferromagnetic bar is present (Figure 21.24b), the reluctance decreases, the magnetic flux amplitude increases, and the sensing-coil current increases. Thus, the presence of the bar is indicated by a change in the output from the sensing

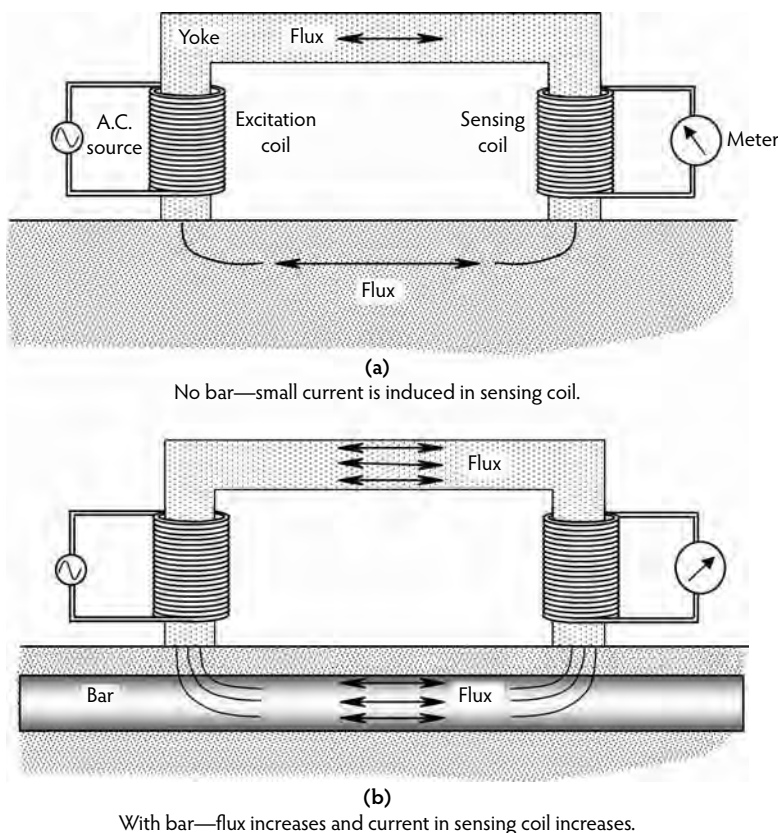


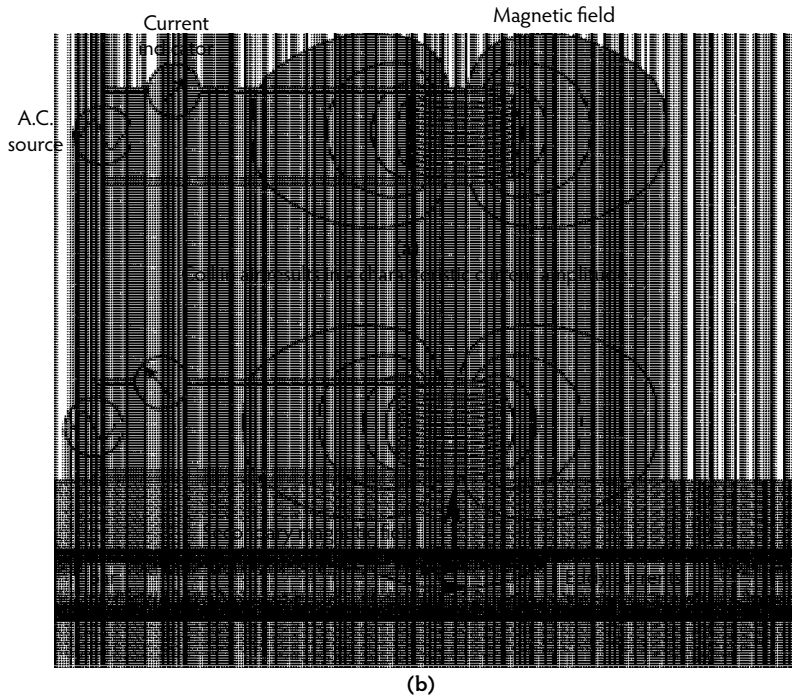
FIGURE 21.24 Covermeter based on the principle of magnetic reluctance. (Adapted from Carino, N.J., *Performance of Electromagnetic Covermeters for Nondestructive Assessment of Steel Reinforcement*, NISTIR 4988, National Institute of Standards and Technology, Gaithersburg, MD, 1992.)

coil. For a given reinforcing bar, the reluctance of the magnetic circuit depends strongly on the distance between the bar and the poles of the yoke. An increase in concrete cover increases the reluctance and reduces the current in the sensing coil. If the meter output were plotted as a function of the cover, a relationship would be established that could be used to measure the cover. Because the size of the bar affects the reluctance of the magnetic circuit, there would be a separate relationship for each bar size.

21.3.6.3 Eddy-Current Meters

If a coil carrying an alternating current is brought near an electrical conductor, the changing magnetic field induces circulating currents in the conductor. These are known as *eddy currents*. Because any current gives rise to a magnetic field, eddy currents produce a secondary magnetic field that interacts with the field of the coil. The second class of covermeters is based on monitoring the effects of the eddy currents induced in a reinforcing bar. Figure 21.25 provides a schematic of a continuous eddy-current covermeter. In the absence of a reinforcing bar, the magnitude of the alternating current (usually at about 1 kHz) in the coil depends on the coil impedance.* If the coil is brought near a reinforcing bar, alternating eddy currents are established within the surface of the bar. The eddy currents give rise to an alternating

* When direct current is applied to a circuit, the current amplitude equals the voltage divided by the electrical resistance of the circuit. When alternating current is applied to a coil, the current amplitude is governed by the value of the applied voltage, the resistance, and another quantity called **inductance**. The vector sum of resistance and inductance defines the **impedance** of the coil.



Presence of reinforcing bar causes changes in coil impedance and current amplitude.

FIGURE 21.25 Covermeter based on eddy-current principle. (Adapted from Carino, N.J., *Performance of Electromagnetic Covermeters for Nondestructive Assessment of Steel Reinforcement*, NISTIR 4988, National Institute of Standards and Technology, Gaithersburg, MD, 1992.)

secondary magnetic field that induces a secondary current in the coil. In accordance with Lenz's law (Serway, 1983), the secondary current opposes the primary current. As a result, the net current flowing through the coil is reduced, and the apparent impedance of the coil increases (Hagemaijer, 1990); thus, the presence of the bar is inferred by monitoring the change in current flowing through the coil.

Covermeters based on continuous excitation are relatively inexpensive but are not stable. An improvement is provided by covermeters based on pulsed excitation, as illustrated in Figure 21.26. A repetitive current pulse is applied to the coils. There is a period of dead time between the end of one pulse and the start of the next pulse. Measurements to infer the presence of reinforcement are made during this dead time. When the pulse is applied, current increases gradually, but then the current is turned off rapidly. The sudden end of the pulse causes a sudden collapse in the magnetic field of the coils, which induces eddy currents in a bar located below the coils. As the eddy currents decay, a decaying magnetic field induces a secondary current in the coils. The amplitude of the induced current depends on the depth and size of the bar; thus, by measuring the amplitude of the induced current during the dead time, information about the bar can be inferred. Note that in this case the search head includes two coils, which make it directional—that is, the output is largest when the coils are aligned with the bar (Carino, 1992b).

21.3.6.4 Covermeter Characteristics

A reinforcing bar is detected by a covermeter when the bar lies within the **zone of influence** of the search head (yoke or coil). The response is maximum when the search head lies directly above the reinforcing bar. An important characteristic of a covermeter is the relationship between meter amplitude and the horizontal distance from the longitudinal axis of the bar to the axis of the search head. The variation has approximately the same shape as the bell-shaped curve of a normal probability distribution. The width of the curve defines the zone of influence of the search head. A search head with a smaller zone of

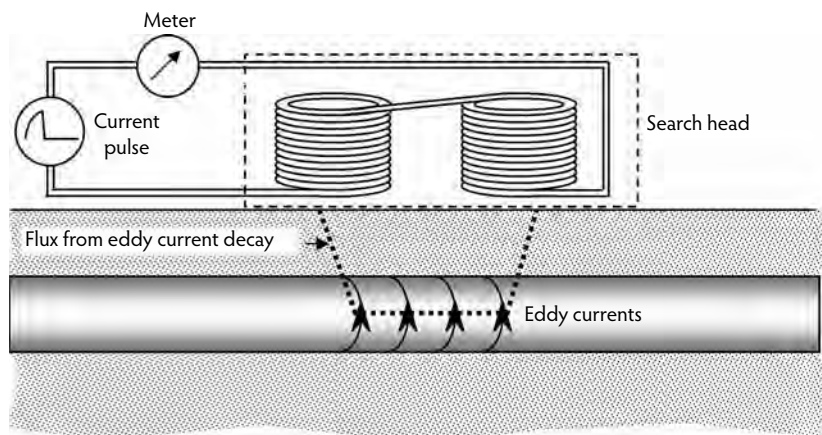


FIGURE 21.26 Covermeter based on pulsed-induction principle. (Adapted from Carino, N.J., *Performance of Electromagnetic Covermeters for Nondestructive Assessment of Steel Reinforcement*, NISTIR 4988, National Institute of Standards and Technology, Gaithersburg, MD, 1992.)

influence is better able to discern individual bars when they are closely spaced compared with a search head with a wider zone of influence, but focused search heads generally have less penetrating ability. The influence zone of the search head also affects the accuracy when trying to detect the end of a reinforcing bar (Carino, 1992b).

An important distinction between covermeters is the directionality characteristics of the search heads. Because of the shape of the yoke, a magnetic-reluctance meter is directional compared with a continuous eddy-current meter with a symmetrical coil. Maximum response occurs when the yoke is aligned with the axis of the bar. This directionality can be used to advantage when testing a structure with an orthogonal grid of reinforcing bars (Tam et al., 1977). As stated above, a pulsed excitation covermeter with two coils in the search head is also directional.

For a given covermeter, unique relationships exist between meter amplitude and depth of cover for different bar sizes. Figure 21.27 shows these relationships for a magnetic reluctance and for an eddy-current meter. These relationships illustrate a basic limitation of covermeters. Because the amplitude is a function of bar diameter and depth of cover, one cannot determine both parameters from a single measurement. As

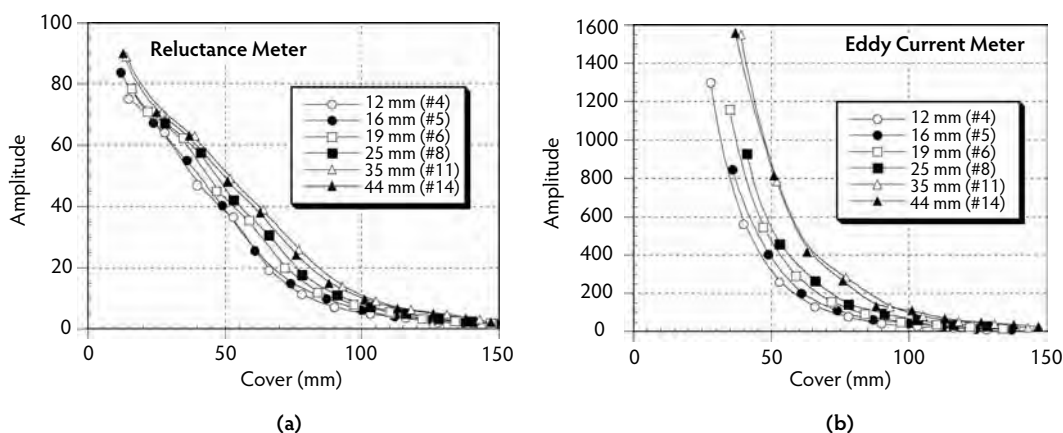


FIGURE 21.27 Amplitude vs. cover: (a) for a magnetic reluctance meter, and (b) for eddy-current meter. (Adapted from Carino, N.J., *Performance of Electromagnetic Covermeters for Nondestructive Assessment of Steel Reinforcement*, NISTIR 4988, National Institute of Standards and Technology, Gaithersburg, MD, 1992.)

a result, dual measurements are necessary to estimate both depth of cover and diameter (BSI, 1988; Das Gupta and Tam, 1983). This is done by first recording the meter amplitude with the search head in contact with the concrete and then recording the amplitude when the search head is located a known distance above the concrete. The difference in amplitudes and the amplitude–cover relationships are used to estimate the cover and bar diameter. The accuracy of this spacer technique depends on how distinct the amplitude–cover relationships are for the different bar sizes. Because these relationships are generally similar for adjacent bar sizes, it is generally only possible to estimate bar diameter within two sizes (Bungey and Millard, 1996).

The single-bar, amplitude–cover relationships are only valid when the bars are sufficiently far apart so there is little interference by adjacent bars. For multiple, closely spaced bars, the amplitude may exceed the amplitude for a single bar at the same cover depth. If they are closer than a critical amount, the individual bars cannot be discerned. The critical spacing depends on the type of covermeter and the cover depth. In general, as cover increases, the critical spacing also increases (Carino, 1992b). Because the response of a covermeter to the presence of multiple, closely spaced bars depends on its design, the user should follow the manufacturer's recommendations regarding minimum bar spacing.

The presence of two layers of reinforcement within the zone of influence cannot generally be identified with ordinary covermeters (Bungey and Millard, 1996; Carino, 1992b). The upper layer produces a much stronger signal than the deeper second layer so the presence of the second layer cannot be discerned. It has been shown, however, that it may be possible to determine lap length when bars are in contact (Carino, 1992b).

In summary, covermeters are effective for locating individual bars, provided that the spacing exceeds a critical value that depends on the meter design and the cover depth. By using multiple measurement methods, bar diameter can generally be estimated to within two adjacent bar sizes if the spacing exceeds certain limits that also depend on the particular meter. Meters are available that can estimate bar diameter without using spacers to make multiple measurements. Again, the accuracy of these estimates decreases as bar spacing decreases. To obtain reliable measurements, it is advisable to prepare mock-ups of the expected reinforcement configuration to establish whether the desired accuracy is feasible. These mock-ups can be made without using concrete (BSI, 1988; Carino, 1992b), provided the in-place concrete does not contain significant amounts of iron-bearing aggregates.

21.3.6.5 Corrosion Activity

Electrical methods are used to evaluate corrosion activity of steel reinforcement. As is the case with other NDT methods, an understanding of the underlying principles of these electrical methods is needed to obtain meaningful results. In addition, an understanding of the factors involved in the corrosion mechanism is essential for reliable interpretation of data. The subsequent sections provide basic information about these methods. Because of the complex interaction of factors, a corrosion specialist should be consulted when planning an investigation. Refer to Carino (2004d) for a more comprehensive review of methods to monitor corrosion activity.

Corrosion is an electrochemical process involving the flow of charges (electrons and ions). At active sites on the bar, called *anodes*, iron atoms lose electrons and move into the surrounding concrete as ferrous ions. This process is referred to as a *half-cell oxidation reaction*, or the *anodic reaction*, and is represented as follows:



The electrons remain in the bar and flow to sites, called *cathodes*, where they combine with water and oxygen that are present in the concrete. The reaction at the cathode is the *half-cell reduction reaction* and is represented as follows:



To maintain electrical neutrality, the ferrous ions migrate through the concrete to these cathodic sites, where they combine with water and oxygen to form hydrated iron oxide, or rust; thus, when the bar is

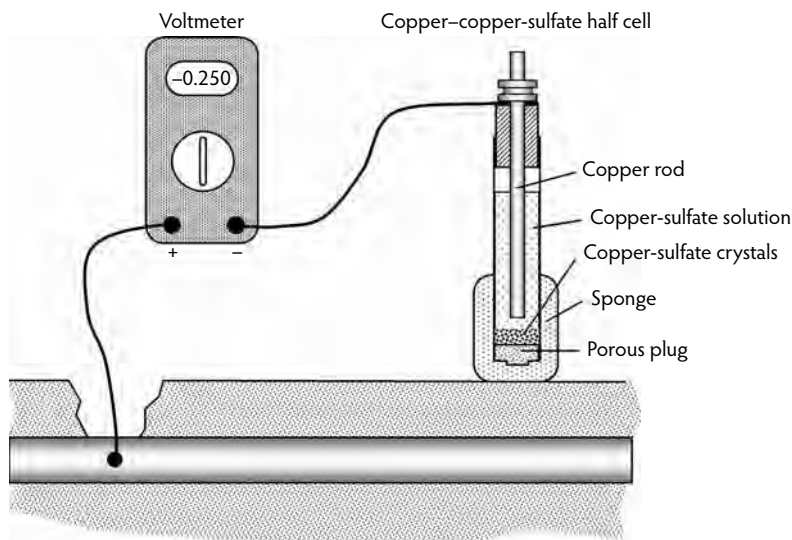


FIGURE 21.28 Apparatus for half-cell potential method described in ASTM C 876.

corroding, electrons are flowing through the bar and ions are flowing through the concrete. When the bar is not corroding, there is no flow of electrons and ions. As the ferrous ions move into the surrounding concrete, the electrons that are left behind in the bar give the bar a negative charge and lead to an electric potential field in the concrete. The **half-cell potential method** is used to measure this potential field and thereby provide an indication of corrosion activity.

21.3.6.6 Half-Cell Potential Method

Figure 21.28 provides a schematic of the half-cell potential apparatus given in ASTM C 876 (ASTM, 1991), which includes a copper–copper-sulfate half cell,* connecting wires, and a high-impedance voltmeter. The positive terminal of the voltmeter is attached to the reinforcement, and the negative terminal is attached to the copper–copper-sulfate half cell. A high-impedance voltmeter is used so very little current exists in the circuit. The half cell makes electrical contact with the concrete by means of a porous plug and a sponge that is moistened with a wetting solution (such as liquid detergent).

If the bar is corroding, electrons would tend to flow from the bar to the half cell. At the half cell, the electrons are consumed in a reduction reaction that transforms copper ions in the copper-sulfate solution into copper atoms deposited on the rod. Because of the way the terminals of the voltmeter are connected, the voltmeter would indicate a negative value. The more negative the voltage reading, the higher the likelihood that the bar is corroding. The half-cell potential is also called the *corrosion potential*, and it is an open-circuit potential because it is measured under the condition of no current in the measuring circuit (ASTM, 2007a).

The half-cell potential readings are indicative of the probability of corrosion activity of reinforcement located beneath the reference half cell; however, this is true only if all of the reinforcement is electrically connected. To ensure that this condition exists, electrical resistance measurements between widely separated reinforcing bars should be carried out (ASTM, 1991). This means that access to the reinforcement has to be provided. The method cannot be applied to concrete with epoxy-coated reinforcement.

*This half-cell is composed of a copper bar immersed in a saturated copper-sulfate solution. It is one of many half cells that can be used as a reference to measure the electrical potential of embedded bars. The measured voltage depends on the type of half cell, and conversion factors are available to convert readings obtained with other reference cells to an equivalent readings for a copper–copper-sulfate half cell.

A key aspect of the test is ensuring that the concrete is sufficiently moist. If the measured potential at a test point does not change by more than ± 20 mV within a 5-minute period (ASTM, 1991), then the concrete is sufficiently moist. If this condition is not satisfied, the concrete surface must be wetted. According to ASTM C 876, two techniques can be used to evaluate the results: (1) the **numeric** technique, or (2) the **potential-difference** technique. In the numeric technique, the value of the potential is used as an indicator of the likelihood of corrosion activity. If the potential is more positive than -200 mV, there is a high likelihood that no corrosion is occurring at the time of the measurement. If the potential is more negative than -350 mV, there is a high likelihood that active corrosion is present. Corrosion activity is uncertain when the voltage is in the range of -200 to -350 mV. ASTM C 876 also states that, unless there is positive evidence to suggest their applicability, these numeric criteria should not be used under the following conditions:

- When carbonation extends to the level of the reinforcement
- When evaluating indoor concrete that has not been subjected to frequent wetting
- When comparing corrosion activity in outdoor concrete with highly variable moisture or oxygen content
- When formulating conclusions about changes in corrosion activity due to repairs that changed the moisture or oxygen content at the level of the steel

In the potential-difference technique, areas of active corrosion are identified on the basis of half-cell potential gradients. An equipotential contour map is created by plotting the test locations on a scaled plan view of the test area. The half-cell voltage readings at each test point are marked on the plan, and contours of equal voltage values are determined. Regions of corrosion activity are indicated by closely spaced contours or large potential gradients.

As has been stated, valid potential readings are possible only if the concrete is sufficiently moist, and the user must understand how to recognize when there is insufficient moisture. Because of the factors involved in corrosion testing, a corrosion specialist is recommended to properly interpret half-cell potential surveys under the following conditions (ASTM, 1991):

- The concrete is saturated with water.
- The concrete is carbonated to the depth of the reinforcement.
- The steel is coated (galvanized).

In addition, potential surveys should be supplemented with tests for carbonation and water-soluble chloride content. A major limitation of the half-cell potential method is that *it does not measure the rate of corrosion*. It only provides an indication of the **likelihood** of corrosion activity at the time the measurement is made.

21.3.6.7 Concrete Resistivity

The corrosion rate of reinforcement depends on the availability of oxygen for the cathodic reaction. It also depends on the electrical resistance of the concrete, which controls the ease with which ions can move through the concrete in the presence of a potential field. The electrical resistance of concrete depends on the microstructure of the paste and the moisture content of the concrete; thus, a useful test in conjunction with a half-cell potential survey is the measurement of the resistivity of the concrete.

The resistivity of a material is numerically equal to the electrical resistance of a unit cube of the material and has units of resistance (in ohms) times length (Millard et al., 1989). The resistance (R) of a conductor of area A and length L is related to the resistivity (ρ) as follows:

$$R = \rho \frac{L}{A} \quad (21.31)$$

No ASTM test method has been proposed for measuring the in-place resistivity of concrete; however, one technique that has been used successfully is shown in Figure 21.29 (Bungey and Millard, 1996). This

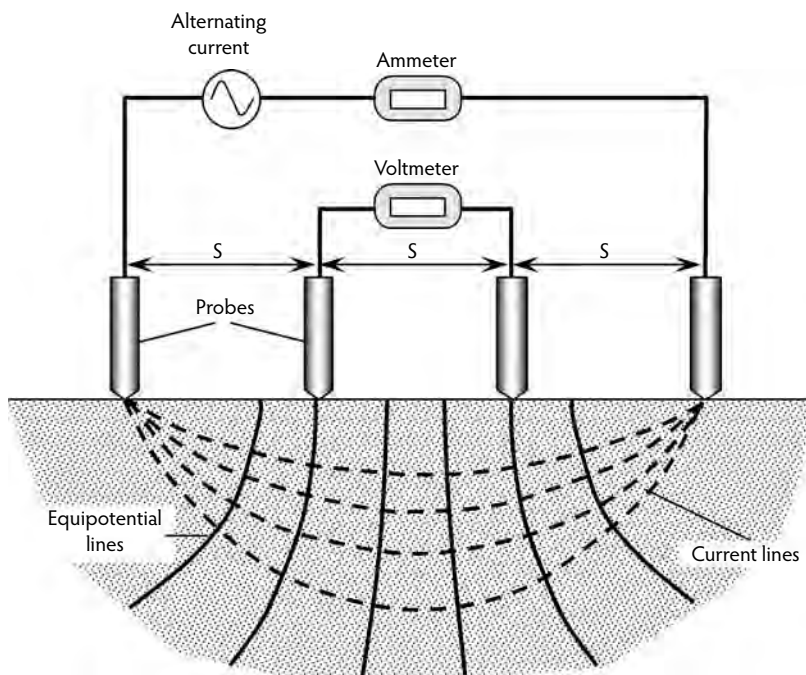


FIGURE 21.29 Four-probe, Wenner method to measure concrete resistivity.

approach is based on the classical four-electrode technique described by Wenner in 1915 which has been incorporated into ASTM G 57, a standard test method for measuring soil resistivity (ASTM, 2006b). The four equally spaced electrodes are electrically connected to the concrete surface. The outer electrodes are connected to a source of alternating current, and the inner electrodes are connected to a voltmeter. The “apparent” resistivity is given by the following expression (Wenner, 1915):

$$\rho = \frac{2\pi s V}{I} \quad (21.32)$$

where:

- s = electrode spacing.
- V = measured voltage.
- I = measured current.

The word *apparent* is used because Wenner derived Equation 21.32 under the assumption that the material is semi-infinite and homogeneous; thus, the relationship gives the correct measure of resistivity when these assumptions are satisfied. Deviations from Wenner’s assumptions lead to differences between the calculated apparent resistivity and the true resistivity of the material (Millard et al., 1990). Experimental and analytical studies have been carried out to establish the magnitudes of the errors between the apparent and true resistivity when Equation 21.32 is applied to a finite-sized concrete member (Millard et al., 1990). An important variable is the minimum electrode spacing that can be used. Because concrete is made of paste and aggregates, which have different resistivities, the spacing should be large enough so a representative average resistivity of the concrete is measured. The spacing determines the depth of the material that affects the measurements. The greater the spacing, the greater is the depth of concrete that contributes to the measurements. If the member is too shallow relative to the electrode spacing, boundary effects occur and Equation 21.32 is not a good approximation.

Based on their work, Millard et al. (1990) suggested that an electrode spacing of 50 mm is sufficient for typical concrete mixtures, and the width and depth of the member should be at least four times the electrode spacing. In addition, the edge distance should not be less than twice the electrode spacing. When these minimum dimensions are not satisfied, the apparent resistivity calculated by Equation 21.32 will exceed the true resistivity. Other factors that affect the calculated resistivity are the presence of a thin surface layer of low-resistivity concrete and the presence of reinforcing bars. Both of these conditions will result in an apparent resistivity that is lower than the true value at the level of the reinforcement. The effect of reinforcing bars is related strongly to the depth of cover and less so to the bar diameter (Millard et al., 1990). If possible, resistivity measurements should be conducted midway between two bars. When depth of cover is low and bar spacing is small, it may be possible to apply a correction factor if the diameter and location of the reinforcement are known (Millard et al., 1990).

Another technique for measuring resistivity is incorporated into one of the linear polarization devices to be described in the next section (Broomfield, 1996). In this case, the resistance measurement is affected by the concrete between the reinforcing bar and the point on the surface where a special probe is located. The author is not aware of comparisons of resistivities measured by the four-electrode device, and this single-probe device.

As noted by Carino (2004d), recommendations have been provided for relating values of concrete resistivity to the risk of corrosion (Bungey and Millard, 1996; Feliú et al., 1996). These recommended values are, however, not the same, which emphasizes the need for a better understanding of the relationship between concrete resistivity and corrosion risk when reinforcement loses its passivity.

In summary, concrete resistivity provides additional information to assist in assessing the likelihood of different levels of corrosion activity. It serves as a useful supplement to a half-cell potential survey. A high resistivity indicates that, even if the potential survey shows a high likelihood of active corrosion, the corrosion rate may be low. The resistivity of concrete is related to the ease with which ions can migrate through the concrete under the action of the potential field surrounding anodes and cathodes. The resistivity increases as the capillary pore space in the paste is reduced. This explains why concrete with low capillary porosity is vital for long service life under corrosion-inducing conditions.

21.3.6.8 Linear Polarization

The limitations of the half-cell potential method led to the development of several techniques to measure the rate of corrosion (Rodríguez et al., 1994). This section provides an overview of the **linear polarization method**, the approach used most frequently in the field (Cady and Gannon, 1992; Flis et al., 1992).

In the field of corrosion science, the term *polarization* refers to the change in the open-circuit potential as a result of the passage of current (ASTM, 2007a). In the polarization resistance test, the impressed current to cause a small change in the value of the half-cell potential of the corroding bar is measured. For a small perturbation about the open-circuit potential, a linear relationship exists between the change in voltage (ΔE) and the change in **current per unit area** of bar surface (Δi). This ratio is called the *polarization resistance* (R_p):

$$R_p = \frac{\Delta E}{\Delta i} \quad (21.33)$$

Because the current is expressed per unit surface area of bar that is polarized, the units of R_p are ohms times area. It has been pointed out that R_p is not a resistance in the usual sense of the term (Stern and Roth, 1957), but the term is widely used (ASTM, 2007a). The underlying relationships between the corrosion rate of the bar and the polarization resistance were established by Stern and Geary (1957). No attempt is made to explain these relationships, but in simple terms the corrosion rate is inversely related to the polarization resistance. The corrosion rate is usually expressed as a corrosion current per unit area of bar, and it is determined as follows:

$$i_{\text{corr}} = \frac{B}{R_p} \quad (21.34)$$

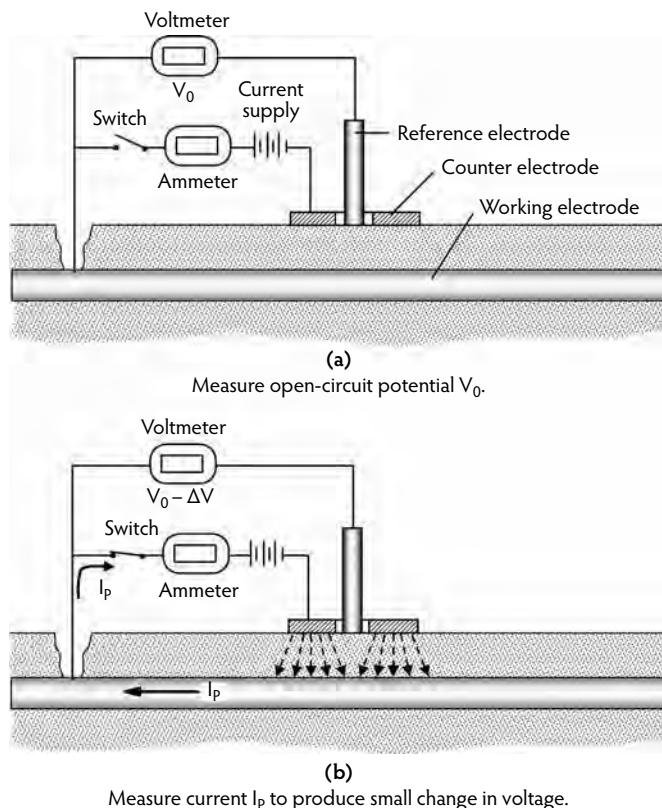


FIGURE 21.30 Three-electrode, linear polarization method to measure corrosion current.

where:

i_{corr} = corrosion rate (ampere per square centimeter).

B = a constant (volts).

R_p = polarization resistance (ohms per square centimeter).

The constant B is a characteristic of the corrosion system, and a value of 0.026 V is commonly used for corrosion of steel in concrete (Feliú et al., 1989). This value, however, is appropriate for actively corroding bars, and a value of 0.050 V is more accurate under less active conditions (Broomfield, 1996; Feliú et al., 1996). Thus, there is inherent uncertainty of a factor of 2 in corrosion rate measurements based on Equation 21.34 if a fixed value of B is used.

It is possible to convert the corrosion rate into the thickness of steel that corrodes per unit of time. Based on Faraday's second law of electrolysis, a corrosion current density of $1 \mu\text{A}/\text{cm}^2$ corresponds to a loss of about 0.012 mm/year of steel (Andrade and Alonso, 2004). This assumes that corrosion occurs uniformly over the bar, but pitting rates can be up to 10 times greater than the uniform rate.

Figure 21.30 provides a schematic of basic apparatus for measuring the polarization resistance (Clear, 1989; Escalante, 1989). It is composed of three electrodes. One electrode is a *reference half cell*. The reinforcement is the second electrode, referred to as the *working electrode*. The third electrode, the *counter electrode*, surrounds the reference electrode and supplies the polarization current to the bar. Supplementary instrumentation measures the voltages and currents during different stages of the test. Such a device can be operated in the **potentiostatic** mode, in which the current is varied to maintain constant potential of the working electrode, or it can be operated in the **galvanostatic** mode, in which the potential is varied to maintain constant current from the counter electrode to the working electrode.

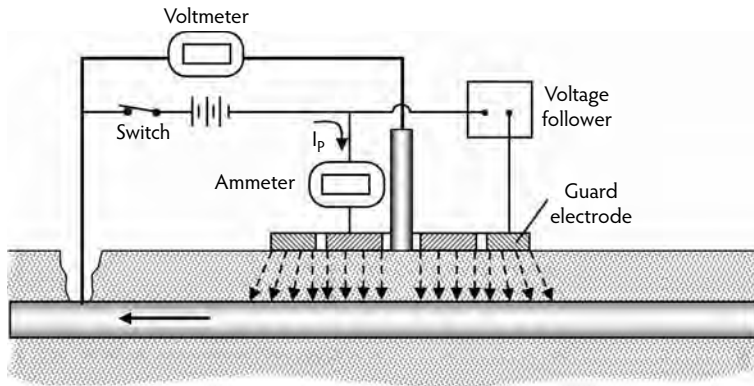


FIGURE 21.31 Linear polarization method using a guard electrode to confine polarization current.

The procedure for using such a three-electrode device to obtain the polarization resistance was provided by Cady and Gannon (1992). The basic steps are as follows:

- Locate the reinforcing-steel grid with a covermeter and mark it on the concrete surface.
- Make an electrical connection to the reinforcement (the working electrode).
- Locate the bar for which the corrosion rate is to be measured, wet the surface, and position the device over the center of the bar.
- Measure the half-cell potential of the reinforcement relative to the reference electrode (Figure 21.30a).
- Measure the current from the counter electrode to the working electrode that is necessary to produce a -4 -mV change in the potential of the working electrode (Figure 21.30b).
- Repeat the previous step for values of potential of -8 and -12 mV beyond the corrosion potential.
- Determine the surface area of bar that is affected by the measurement (perimeter of bar multiplied by the length below the counter electrode).
- Plot the potential vs. the current per unit surface area of the bar, and determine the slope of the best-fit straight line. This is the polarization resistance.

A major uncertainty in obtaining the polarization resistance is the area of the steel bar that is affected by the polarization current. In the application of the three-electrode device, it is assumed that electrons flow in straight lines perpendicular to the bar (working electrode) and the counter electrode. The bar area affected during the test is the bar circumference multiplied by the length of the bar below the counter electrode. Numerical simulations of the polarization resistance test show that the above assumption is incorrect and that the current lines are not confined to the region directly below the counter electrode (Feliú et al., 1989; Flis et al., 1992). In an effort to better control the current path from the counter electrode to the bar, a device has been developed that includes a fourth electrode, called a *guard* or *auxiliary electrode*, that surrounds the counter electrode (Feliú et al., 1990a,b). Figure 21.31 provides a schematic showing the guard electrode outside the counter electrode. The guard electrode is maintained at the same potential as the counter electrode, and, as a result, the current from the counter electrode to the working electrode is confined to the region below the counter electrode.

A drawback of the above method to measure polarization resistance is the time required for data collection. For each increment in polarization current, sufficient time is necessary to reach a steady-state condition. The duration of current application to obtain a valid measurement may vary from 30 to 100 s, depending on whether there is active or less active corrosion, respectively (Andrade and Alonso, 2004). Typically the current is applied for 100 s and it takes from 3 to 5 minutes to complete a polarization resistance measurement at each test point (Tang, 2002).

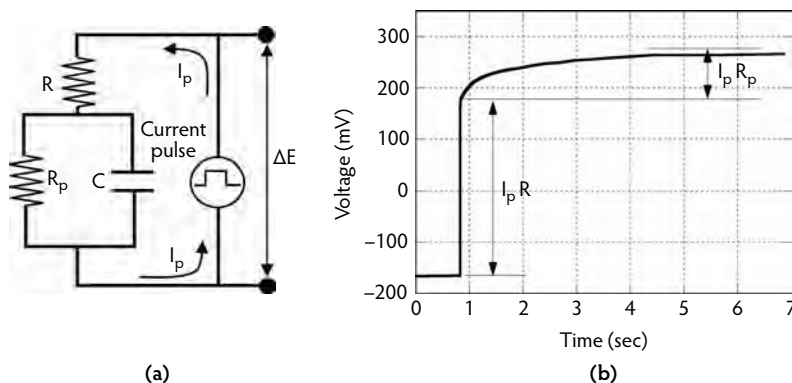


FIGURE 21.32 Galvanostatic pulse method: (a) Randles' circuit model to represent polarization of steel reinforcement; (b) change in voltage due to application of current pulse.

Another approach is to determine polarization resistance from measuring the response during the application of a short-duration current pulse. This is called the *galvanostatic pulse method* (Frølund et al., 2002). The instrumentation is similar to that shown in Figure 21.31, except that the voltage response to the applied current is measured over a short period of time (e.g., 10 s). The polarization resistance is obtained from the assumption that the polarization of the bar can be modeled by a simple electrical circuit, known as *Randles' circuit*, as shown in Figure 21.32a (Andrade and Alonso, 2004). When current is applied to this circuit, the voltage–time history across the circuit is given by the following:

$$\Delta E = I_p \left[R + R_p \left(1 - e^{\frac{-t}{R_p C}} \right) \right] \quad (21.35)$$

where:

ΔE = voltage change (V).

I_p = applied polarization current (A).

R = electrical resistance of concrete between counter electrode and bar (Ω).

R_p = polarization resistance (Ω).

C = capacitance of double layer and concrete–bar interface (F).

Figure 21.32b shows an example of a measured voltage history for an applied current pulse (Frølund et al., 2002). By means of regression analysis, Equation 21.35 is fitted to the measured voltage–time data, and the best-fit values of the three components of the equivalent Randles' circuit are obtained. In this way, the polarization resistance is determined, and, after multiplying by the polarized area of the bar, Equation 21.34 is used to determine the corrosion rate.

The pulse technique has the advantage of reducing the measurement time; however, the value of the calculated polarization resistance increases as the pulse duration (and duration of data acquisition) increases (Tang, 2002). This means that the corrosion rate will be overestimated for short pulses. It has also been found, however, that a well-defined relationship exists between polarization duration and polarization resistance, and procedures have been developed for converting measurements made at short durations to measurements made over a longer duration (Tang, 2002).

The corrosion rate based on measuring the polarization resistance represents the corrosion rate at the time of the test. The corrosion rate at a particular point in a structure is expected to depend on several factors, such as the moisture content of the concrete, the availability of oxygen, and the temperature. For this reason, the corrosion rate at any point in an exposed structure would be expected to have seasonal variations. Such variations were observed during multiple measurements that extended over a period of more than a year (Clemeña et al., 1992). A single corrosion rate measurement is unsuitable for predicting

future corrosion behavior (So et al., 2006). To project the amount of corrosion that would occur after an extended period, it is necessary to repeat the corrosion-rate measurements at different times of the year to obtain an estimate of the average rate.

No standard methods are available for interpreting corrosion-rate measurements obtained with different devices. A qualified corrosion specialist should be consulted when planning and interpreting a corrosion-rate survey; for example, based on years of experience in the laboratory and from field testing, Clear (1989) developed guidelines for interpreting measurements obtained with a specific corrosion-rate device. Additional information is provided in the comprehensive review of corrosion rate test methods prepared by Andrade and Alonso (2004).

Other limitations that should be considered when planning corrosion-rate testing have been outlined by Cady and Gannon (1992):

- The concrete surface has to be smooth (not cracked, scarred, or uneven).
- The concrete surface has to be free of water-impermeable coatings or overlays.
- The cover depth has to be less than 100 mm.
- The reinforcing steel cannot be epoxy coated or galvanized.
- The steel to be monitored has to be in direct contact with the concrete.
- The reinforcement cannot be cathodically protected.
- The reinforced concrete must not be near areas of stray electric currents or strong magnetic fields.
- The ambient temperature must be between 5 and 40°C.
- The concrete surface at the test location must be free of visible moisture.
- Test locations must not be closer than 300 mm to discontinuities, such as edges and joints.

21.3.7 Nuclear (Radioactive) Methods

Nuclear (or radioactive) methods for nondestructive evaluation of concrete involve the use of high-energy electromagnetic radiation to gain information about the internal structure of the test object. These methods involve a source of penetrating electromagnetic radiation and a sensor to measure the intensity of the radiation after it has traveled through the object. If the sensor is in the form of special photographic film, the technique is called *radiography*. If the sensor is an electronic device that converts the incident radiation into electrical pulses, the technique is called *radiometry*. A review of the early developments in the use of nuclear methods was presented by Malhotra (1976), and more recent developments have been reviewed by Mitchell (2004). Initial work in the late 1940s focused on the use of x-rays to produce radiographs of the internal structure of concrete elements, but in the 1950s attention turned to the use of gamma rays. The fundamental differences between these two forms of penetrating radiation are the sources used to generate them and their penetrating ability. X-rays are produced by high-voltage electronic devices, and gamma rays are produced by the byproducts of the decay of radioactive isotopes. The penetrating ability of gamma rays depends on the radioactive isotope and its age, but the penetration of x-rays depends on the voltage used by the generating instrument. Some of the earliest reported work using gamma rays was at Ontario Hydro (de Hass, 1954). Slabs were constructed with artificial flaws, a pipe containing a radioactive isotope of cobalt was placed beneath the slab, and a Geiger–Müller tube was placed on the top surface of the slab to measure the intensity of radiation. Other early efforts at using gamma-ray methods took place in Great Britain during the 1950s, where they were used to locate reinforcing bars, measure density, and locate voids in grouted post-tensioning tendons (Forrester, 1970). Eastern Europe and the Soviet Union also conducted early studies that eventually led to the development of portable density meters for concrete and soil.

21.3.7.1 Radiometric Methods

Two basic radiometric methods use x-rays and gamma rays for the nondestructive testing of concrete. In the **transmission** method, the amplitude of the radiation passing through a member is measured. As radiation passes through a member, the attenuation depends on the density of the material and the path length through the material. Direct transmission techniques can be used to detect reinforcement. The

main use of the technique, however, is to measure the in-place density of fresh or hardened concrete. Structures of high density and roller-compacted concretes are cases where this method is of particular value. For such applications, the radioactive source is contained in a tube that is pushed into the fresh concrete, and the detector is set on the surface of the concrete. The density meter developed at the Technical University of Brno (Czechoslovakia) is an example of such a device (Honig, 1984). The source can be lowered up to a depth of 200 mm into a hollow steel needle that is pushed into the fresh concrete. A spherical lead shield suppresses the radiation when the source is in its retracted position. Detectors are located beneath the treads used to push the needle into the concrete. It is claimed that the instrument has a resolution of 10 kg/m^3 (Honig, 1984). ASTM C 1040 (ASTM, 2005) provides procedures for using nuclear methods to measure the in-place density of fresh or hardened concrete. The key element of the procedure is development of the calibration curve for the instrument. This is accomplished by making test specimens of different densities and determining the gauge output for each specimen. The gauge output is plotted as a function of the density, and a best-fit curve is determined.

In the **backscatter** method, a radioactive source is used to supply gamma rays, and a detector close to the source is used to measure the backscattered rays. The scattered rays are of lower energy than the transmitted rays and are produced when a photon collides with an electron in an atom. Part of the photon energy is imparted to the electron, and a new photon emerges, traveling in a new direction with lower energy. This process is known as *Compton scattering* (Mitchell, 2004). Backscatter techniques are particularly suitable for applications where a large number of *in situ* measurements are required. Because backscatter measurements are affected by the top 40 to 100 mm, the method is best suited for measurement of the surface zone of a concrete element. A good example of the use of this method is monitoring the density of bridge deck overlays. Non-contacting equipment has been developed that is used for continuous monitoring of concrete pavement density during slip-form operations (Mitchell et al., 1979).

Procedures for using backscatter methods to measure concrete density are given in ASTM C 1040 (ASTM, 2005). As is the case with direct transmission measurements, it is necessary to establish a calibration curve before using a nuclear backscatter gauge to measure in-place density. The inherent precision of backscatter density gauges is less than that of direct transmission devices. ASTM C 1040 requires that a suitable backscatter gauge for density measurement result in a standard deviation of less than 16 kg/m^3 , whereas the standard deviation should be less than 8 kg/m^3 for a direct-transmission gauge. According to ASTM C 1040, backscatter gauges are influenced typically by the top 75 to 125 mm of material. The top 25 mm determines 50 to 70% of the count rate, and the top 50 mm determines 80 to 95% of the count rate.

21.3.7.2 Radiographic Methods

Radiography provides a radiation-based photograph of the interior of concrete from which the location of reinforcement, voids in concrete, or voids in grouted post-tensioning tendons can be identified. A radiation source is placed on one side of the test object, and a beam of radiation is emitted. As the radiation passes through the member, it is attenuated by different amounts, depending on the density and thickness of the material that is traversed. The radiation that emerges from the opposite side of the object strikes a special photographic film that is exposed in proportion to the intensity of the incident radiation. When the film is developed, a two-dimensional visualization (a photograph) of the interior structure of the object is obtained. The presence of high-density material, such as reinforcement, is shown on the developed film as a light area, and a region of low density, such as a void, is shown as a dark area.

The British Standards Institution has adopted a standard for radiographic testing of concrete (BS 1881, Part 205, Recommendations for Radiography of Concrete). The standard provides recommendations for investigators considering radiographic examinations of concrete (Mitchell, 2004). In x-radiography, the radiation is produced by an x-ray tube. The penetrating ability of the x-rays depends on the operating voltage of the x-ray tube. In gamma radiography, a radioactive isotope is used as the radiation source. The selection of a source depends on the density and thickness of the test object and on the exposure time that can be tolerated. The most intense source is cobalt-60, which can be used to penetrate up to 500 mm of concrete. For members with thickness of 150 mm or less, iridium-192 or cesium-137 can be used

(Mitchell, 2004). The film type will depend on the thickness and density of the member being tested. Most field applications have used radioactive sources because of their greater penetrating ability (higher energy radiation) compared with x-rays; however, a system known as Scorpion II was developed in France that uses a linear accelerator to produce very high-energy x-rays than can penetrate up to 1 m of concrete. This system was developed for the inspection of prestressed members to establish the condition and location of prestressing strands and to determine the quality of grouting in tendon ducts (Mitchell, 2004).

21.3.7.3 Summary

Whereas nuclear methods have the ability to see into concrete, they are cumbersome and require trained and licensed personnel (Mitchell, 2004.). Testing across the full thickness of a concrete element is particularly hazardous and requires extensive precautions, skilled personnel, and highly specialized equipment. Radiographic procedures are costly and require evacuation of the structure by persons not involved in the actual testing. The use of x-ray equipment poses an additional danger due to the high voltages that are used. There are limits on the thicknesses of the members that can be tested by radiographic methods. For gamma-ray radiography, the maximum thickness is about 500 mm, because thick members require unacceptably long exposure times. Radiography is not very useful for locating crack planes perpendicular to the radiation beam. Because of these major drawbacks, radiographic methods are not used routinely for flaw detection; however, in some situations the ability to see the internal structure of the member surpasses these drawbacks.

21.4 Concluding Remarks

This chapter has summarized the available nondestructive techniques for assessing the properties or condition of concrete in structures. The techniques have been divided into two groups:

- Those used for estimating the in-place strength, and
- Those used for flaw detection and condition assessment.

Emphasis has been placed on describing their underlying principles and highlighting some of their inherent limitations. The user is referred to applicable publications of the American Concrete Institute and relevant ASTM standards for additional information on using these methods.

The key feature of the methods for estimating in-place strength is the strength relationship that correlates concrete strength to the results of the in-place tests. The strength relationship should be developed experimentally before using the test method to estimate in-place strength. For new construction, test specimens should be made of concrete similar to what will be used in the structure. Care must be exercised to ensure that the companion in-place tests and standard strength tests are carried out on specimens of the same maturity at each strength level. For existing construction, it is necessary to perform in-place tests and obtain cores at different locations so a wide range of concrete strengths can be used to develop the strength relationship. After the strength relationship has been established, in-place tests are done on the structure, and statistical methods are used to convert the average in-place test result to a reliable estimate of in-place strength. Generally, in-place test methods that result in local failure of the concrete are more reliable than those that are totally nondestructive.

A variety of methods are available for flaw detection and condition assessment. Most of these methods are based on monitoring the response of the structure when it is subjected to some type of disturbance. Two broad classes of nondestructive methods are those based on stress-wave propagation and those based on electromagnetic-wave propagation. Except for visual inspection, these methods generally require sophisticated instrumentation. All nondestructive test methods have inherent strengths and weaknesses. It is often advantageous to use more than one method to make the assessment. Methods based on stress-wave propagation are suited for identifying the presence of internal concrete–air interfaces, such as those due to cracking or voids. An understanding of the basics of stress-wave propagation is essential for proper interpretation of test results. Electrical methods are well suited for gaining information about embedded

reinforcement, such as location, approximate size, and whether active corrosion exists. Radar is appropriate for finding deep metallic embedments and is also sensitive to the presence of moisture. Radar has the added advantage that large portions of a structure can be scanned in a short time.

The importance of having qualified operators cannot be overemphasized. Nondestructive tests are indirect methods by which the property or characteristic of primary interest is inferred by measuring other properties or characteristics. A lack of understanding of the underlying principles and the interferences associated with the method can lead to incorrect assessments of the concrete. When used by properly trained operators, nondestructive test methods offer technical and economic advantages compared with other invasive sampling techniques.

References

- ACI Committee 201. 1992. *Guide for Making a Condition Survey of Concrete in Service*, ACI 201.1R. American Concrete Institute, Farmington Hills, MI.
- ACI Committee 207. 1994. *Practices for Evaluation of Concrete in Existing Massive Structures for Service Conditions*, ACI 207.3R. American Concrete Institute, Farmington Hills, MI.
- ACI Committee 224. 2007. *Causes, Evaluation and Repair of Cracks in Concrete Structures*, ACI 224.1R. American Concrete Institute, Farmington Hills, MI.
- ACI Committee 228. 1989. *In-Place Methods for Determination of Strength of Concrete*, ACI 228.1R. American Concrete Institute, Farmington Hills, MI.
- ACI Committee 228. 1998. *Nondestructive Test Methods for Evaluation of Concrete in Structures*, ACI 228.2R. American Concrete Institute, Farmington Hills, MI.
- ACI Committee 228. 2003. *In-Place Methods to Estimate Concrete Strength*, ACI 228.1R. American Concrete Institute, Farmington Hills, MI.
- ACI Committee 318. 2005. *Building Code Requirements for Structural Concrete*, ACI 318/318R. American Concrete Institute, Farmington Hills, MI.
- ACI Committee 362. 1997. *Guide for the Design of Durable Parking Structures*, ACI 362.1R. American Concrete Institute, Farmington Hills, MI.
- ACI Committee 437. 2003. *Strength Evaluation of Existing Concrete Buildings*, ACI 437R. American Concrete Institute, Farmington Hills, MI.
- Alongi, A.V., Cantor, T.R., Kneeter, C.P., and Alongi, Jr., A. 1982. Concrete evaluation by radar theoretical analysis. In *Transportation Research Record No. 853*, pp. 31–37. Transportation Research Board, Washington, D.C.
- Al-Qadi, I. and Washer, G., Eds. 2006. *Proceedings of the NDE Conference on Civil Engineering*, August 14–18, St. Louis, MO. American Society for Nondestructive Testing, Columbus, OH.
- Andrade, C. and Alonso, C. 1996. Corrosion rate monitoring in the laboratory and on-site, *Construct. Build. Mater.*, 10(5), 315.
- Andrade, C. and Alonso, C. 2004. Test methods for on-site corrosion rate measurement of steel reinforcement in concrete by means of the polarization resistance method. *Mater. Struct.*, 37, 623–643.
- Arni, H.T. 1972. Impact and penetration tests of Portland cement concrete. In *Highway Research Record* 378, pp. 55–67. Highway Research Board, Washington, D.C.
- ASTM. 1991. *Standard Test Method for Half-Cell Potential of Uncoated Reinforcing Steel in Concrete*, ASTM C 876. ASTM International, West Conshohocken, PA.
- ASTM. 1996. *Standard Test Method for the Break-Off Number of Concrete*, ASTM C 1150. ASTM International, West Conshohocken, PA (withdrawn in 2002).
- ASTM. 2002a. *Standard Test Method for Pulse Velocity Through Concrete*, ASTM C 597. ASTM International, West Conshohocken, PA.
- ASTM. 2002b. *Standard Test Method for Rebound Number of Hardened Concrete*, ASTM C 805. ASTM International, West Conshohocken, PA.
- ASTM. 2003a. *Standard Practice for Measuring Delaminations in Concrete Bridge Decks by Sounding*, ASTM D 4580. ASTM International, West Conshohocken, PA.

- ASTM. 2003b. *Standard Test Method for Detecting Delaminations in Bridge Decks Using Infrared Thermography*, ASTM D 4788. ASTM International, West Conshohocken, PA.
- ASTM. 2003c. *Standard Test Method for Penetration Resistance of Hardened Concrete*, ASTM C 803/803M. ASTM International, West Conshohocken, PA.
- ASTM. 2004a. *Standard Practice for Estimating Concrete Strength by the Maturity Method*, ASTM C 1074. ASTM International, West Conshohocken, PA.
- ASTM. 2004b. *Standard Test Method for Measuring the P-Wave Speed and the Thickness of Concrete Plates Using the Impact-Echo Method*, ASTM C 1383. ASTM International, West Conshohocken, PA.
- ASTM. 2005. *Standard Test Methods for Density of Unhardened and Hardened Concrete in Place by Nuclear Methods*, ASTM C 1040. ASTM International, West Conshohocken, PA.
- ASTM. 2006a. *Standard Test Method for Determining the Thickness of Bound Pavement Layers Using Short-Pulse Radar*, ASTM D 4748. ASTM International, West Conshohocken, PA.
- ASTM. 2006b. *Standard Test Method for Field Measurement of Soil Resistivity Using the Wenner Four-Electrode Method*, ASTM G 57. ASTM International, West Conshohocken, PA.
- ASTM. 2006c. *Standard Test Method for Pullout Strength of Hardened Concrete*, ASTM C 900. ASTM International, West Conshohocken, PA.
- ASTM. 2006d. *Standard Test Method for Time of Setting of Concrete Mixtures by Penetration Resistance*, ASTM C 403/C 403M. ASTM International, West Conshohocken, PA.
- ASTM. 2007a. *Standard Terminology Relating to Corrosion and Corrosion Testing*, ASTM G 15. ASTM International, West Conshohocken, PA.
- ASTM. 2007b. *Standard Test Method for Evaluating Asphalt-Covered Concrete Bridge Decks Using Ground-Penetrating Radar*, ASTM D 6087. ASTM International, West Conshohocken, PA.
- Ballarini, R., Shah, S.P., and Keer, L.M. 1986. Failure characteristics of short anchor bolts embedded in a brittle material. *Proc. R. Soc. Lond.*, A404, 35–54.
- Barker, M.G. and Ramirez, J.A. 1988. Determination of concrete strengths using the break-off tester. *ACI Mater. J.*, 82(6), 221–228.
- Bickley, J.A. 1982a. Concrete optimization. *Concrete Int.*, 4(6), 38–41.
- Bickley, J.A. 1982b. Variability of pullout tests and in-place concrete strength. *Concrete Int.*, 4(4), 44–51.
- Bracewell, R. 1978. *The Fourier Transform and Its Applications*, 2nd ed., 444 pp. McGraw-Hill, New York.
- Broomfield, J. 1996. Field measurement of the corrosion rate of steel in concrete using a microprocessor controlled unit with a monitored guard ring for signal confinement. In *Techniques to Assess the Corrosion Activity of Steel Reinforced Concrete Structures*, ASTM STP 1276, Berke, N.S., Escalante, E., Nmai, C., and Whiting, D., Eds., p. 91. ASTM International, West Conshohocken, PA.
- Brown, T.L. and LeMay, H.E. 1988. *Chemistry: The Central Science*, 4th ed., pp. 494–498. Prentice Hall, Upper Saddle River, NJ.
- BSI. 1988. *Recommendations on the Use of Electromagnetic Covermeters*, BS 1881, Part 204. British Standards Institution, London.
- Bungey, J.H. 1981. Concrete strength determination by pull-out tests on wedge anchor bolts. *Proc. Inst. Civ. Eng.*, 71(Part 2), 379–394.
- Bungey, J.H. and Millard, S.G. 1993. Radar inspection of structures. *Proc. Inst. Civ. Eng. Struct. Build. J.*, 99, 173–186.
- Bungey, J.H. and Millard, S.G. 1996. *Testing of Concrete in Structures*, 3rd ed., 286 pp. Chapman & Hall, London.
- Bungey, J.H., Millard, S.G., and Shaw, M.R. 1994. The influence of reinforcing steel on radar surveys of structural concrete. *Construct. Build. Mater.*, 8(2), 119–126.
- Byfors, J. 1980. *Plain Concrete at Early Ages*, Report 3-80, 464 pp. Swedish Cement and Concrete Research Institute, Stockholm, Sweden.
- Cady, P.D. and Gannon, E.J. 1992. *Condition Evaluation of Concrete Bridges Relative to Reinforcement Corrosion*. Vol. 8. *Procedure Manual*, SHRP-S/FR-92-110, 124 pp. Strategic Highway Research Program, National Research Council, Washington, D.C.

- Cantor, T.R. 1984. Review of penetrating radar as applied to nondestructive evaluation of concrete. In *In Situ/Nondestructive Testing of Concrete*, Malhotra, V.M., Ed., ACI SP-82, pp. 581–601. American Concrete Institute, Farmington Hills, MI.
- Cantor, T. and Kneeter, C. 1982. Radar as applied to evaluation of bridge decks. In *Transportation Research Record No. 853*, pp. 37–42. Transportation Research Board, Washington, D.C.
- Carette, G.G. and Malhotra, V.M. 1991. Long-Term Strength Development of Silica Fume Concrete, paper presented at CANMET/ACI International Workshop on the Use of Silica Fume. April 7–9, Washington, D.C.
- Carino, N.J. 1982. Maturity functions for concrete. In *Proceedings of RILEM International Conference on Concrete at Early Ages (Paris)*, Vol. I, pp. 123–128. Ecole Nationale des Ponts et Chausses. Paris.
- Carino, N.J. 1984. The maturity method: theory and application. *ASTM J. Cement Concrete Aggregates*, 6(2), 61–73.
- Carino, N.J. 1992a. Recent developments in nondestructive testing of concrete. In *Advances in Concrete Technology*, Malhotra, V.M., Ed., MSL 92-6(R), pp. 281–328. Energy, Mines and Resources, Ottawa.
- Carino, N.J. 1992b. *Performance of Electromagnetic Covermeters for Nondestructive Assessment of Steel Reinforcement*, NISTIR 4988, 130 pp. National Institute of Standards and Technology, Gaithersburg, MD.
- Carino, N.J. 1993. Statistical methods to evaluate in-place test results. In *New Concrete Technology: Robert E. Philleo Symposium*, ACI SP-141, pp. 39–64. American Concrete Institute, Farmington Hills, MI.
- Carino, N.J. 1994. Nondestructive testing of concrete: history and challenges. In *Concrete Technology Past, Present, and Future: Proceedings of V. Mohan Malhotra Symposium*, ACI SP-144, pp. 623–678. American Concrete Institute, Farmington Hills, MI.
- Carino, N.J. 2004a. The maturity method. In *Handbook on Nondestructive Testing of Concrete*, 2nd ed., Malhotra, V.M. and Carino, N.J., Eds., pp. 5-1–5-48. CRC Press, Boca Raton, FL.
- Carino, N.J. 2004b. Pullout test. In *Handbook on Nondestructive Testing of Concrete*, 2nd ed., Malhotra, V.M. and Carino, N.J., Eds., pp. 3-1–3-38. CRC Press, Boca Raton, FL.
- Carino, N.J. 2004c. Stress wave propagation methods. In *Handbook on Nondestructive Testing of Concrete*, 2nd ed., Malhotra, V.M. and Carino, N.J., Eds., pp. 14-1–14-30. CRC Press, Boca Raton, FL.
- Carino, N.J. 2004d. Methods to evaluate corrosion of reinforcement. In *Handbook on Nondestructive Testing of Concrete*, 2nd ed., Malhotra, V.M. and Carino, N.J., Eds., pp. 11-1–11-22. CRC Press, Boca Raton, FL.
- Carino, N.J. and Sansalone, M. 1992. Detecting voids in metal tendon ducts using the impact-echo method. *ACI Mater. J.*, 89(3), 296–303.
- Carino, N.J. and Tank, R.C. 1992. Maturity functions for concrete made with various cements and admixtures. *ACI Mater. J.*, 89(2), 188–196.
- Carino, N.J., Sansalone, M., and Hsu, N.N. 1986. Flaw detection in concrete by frequency spectrum analysis of impact-echo waveforms. In *International Advances in Nondestructive Testing*, McGonagle, W.J., Ed., pp. 117–146. Gordon & Breach, New York.
- Carino, N.J., Knab, L.I., and Clifton, J.R. 1992. *Applicability to the Maturity Method to High-Performance Concrete*, NISTIR-4819, 64 pp. National Institute of Standards and Technology, Springfield, VA.
- Carter, C.R., Chung T., Holt, F.B., and Manning D. 1986. An automated signal processing system for the signature analysis of radar waveforms from bridge decks. *Can. Electr. Eng. J.*, 11(3), 128–137.
- Chabowski, A.J. and Bryden-Smith, D.W. 1980. Assessing the strength of concrete of *in situ* Portland cement concrete by internal fracture tests. *Mag. Concrete Res.*, 32(112), 164–172.
- Chang, L. M. and Carino, N. J. 1998. Analyzing in-place concrete tests by computer, *Concrete Int.*, 20(12), 34–39.
- Cheng, C. and Sansalone, M. 1993a. The impact-echo response of concrete plates containing delaminations: numerical, experimental, and field studies. *Mater. Struct.*, 26(159), 274–285.
- Cheng, C. and Sansalone, M. 1993b. Effects on impact-echo signals caused by steel reinforcing bars and voids around bars. *ACI Mater. J.*, 90(5), 421–434.

- Cheng, C. and Sansalone, M. 1995a. Determining the minimum crack width that can be detected using the impact-echo method. Part 1. Experimental study. *Mater. Struct.*, 28(176), 74–82.
- Cheng, C. and Sansalone, M. 1995b. Determining the minimum crack width that can be detected using the impact-echo method. Part 2. Numerical fracture analyses. *Mater. Struct.*, 28(177), 125–132.
- Clear, K.C. 1989. Measuring rate of corrosion of steel in field concrete structures. In *Transportation Research Record 1211*, pp. 28–37. Transportation Research Board, Washington, D.C.
- Clemeña, G.G. 1983. Nondestructive inspection of overlaid bridge decks with ground-penetrating radar. In *Transportation Research Record No. 899*, pp. 21–32. Transportation Research Board, Washington, D.C.
- Clemeña, G.G. 2004. Short-pulse radar methods. In *Handbook on Nondestructive Testing of Concrete*, 2nd ed., Malhotra, V.M. and Carino, N.J., Eds., pp. 13-1–13-20. CRC Press, Boca Raton, FL.
- Clemeña, G.G. and McKeel, Jr., W.T. 1978. Detection of delamination in bridge decks with infrared thermography. In *Transportation Research Record No. 664*, pp. 180–182. Transportation Research Board, Washington, D.C.
- Clemeña, G.G., Jackson, D.R., and Crawford, G.C. 1992. Inclusion of rebar corrosion rate measurements in condition surveys of concrete bridge decks. In *Transportation Research Record 1347*, pp. 37–45. Transportation Research Board, Washington, D.C.
- Daniels, D.J., Gunton, D.J., and Scott, H.F. 1988. Introduction to subsurface radar. *Proc. Inst. Electr. Eng.*, 135(Part F, 4), 278–320.
- Das Gupta, N.C. and Tam, C.T. 1983. Non-destructive technique for simultaneous detection of size and cover of embedded reinforcement. *Br. J. Non-Destructive Test.*, 25(6), 301–304.
- Davis, A.G. and Dunn, C. 1974. From theory to field experience with the nondestructive vibration testing of piles. *Proc. Inst. Civ. Eng.*, 57(Part 2), 571–593.
- Davis, A.G. and Hertlein, B.H. 1987. Nondestructive testing of concrete pavement slabs and floors with the transient dynamic response method. In *Proceedings of 3rd International Conference on Structural Faults and Repairs*, July, London, Vol. 2, pp. 429–433.
- Davis, A.G. and Hertlein, B.H. 1990. Assessment of bridge deck repairs by a nondestructive technique. In *Proceedings of NATO Advanced Research Workshop on Bridge Evaluation, Repair, and Rehabilitation*, April 30–May 2, Baltimore, MD, Nowak, A.J., Ed., p. 229. Kluwer, Boston, MA.
- Davis, A.G. and Hertlein, B.H. 1991. Developments of nondestructive small-strain methods for testing deep foundations: a review. In *Transportation Research Record No. 1331*, pp. 15–20. Transportation Research Board, Washington, D.C.
- Davis, A.G., Evans, J.G., and Hertlein, B.H. 1997. Nondestructive evaluation of concrete radioactive waste tanks. *J. Perform. Construct. Facil. ASCE*, 11(4), 161.
- de Hass, E. 1954. Letter to editor. *J. Am. Concrete Inst.*, 25(10), 890–891.
- Delatte, N.J., Williamson, M.S., and Fowler, D.W. 2000. Bond strength development with maturity of high-early-strength bonded concrete overlays. *ACI Mater. J.*, 97(2), 201.
- Dilly, R.L. and Zollinger, D.G. 1998. Mode I fracture strength based on pullout force and equivalent age. *ACI Mater. J.*, 95(3), 304.
- Domone, P.L. and Castro, P.F. 1986. An expandable sleeve test for in-situ concrete strength evaluation. *Concrete*, 20(3), 24–25.
- Escalante, E. 1989. Elimination of IR error in measurements of corrosion in concrete. In *The Measurement and Correction of Electrolyte Resistance in Electrochemical Tests*, Scribner, L.L. and Taylor, S.R., Eds., ASTM STP 1056, pp. 180–190. ASTM International, West Conshohocken, PA.
- Făcăoaru, I. 1969. Chairman's Report: Meeting of RILEM TC on Non-Destructive Testing of Concrete, Varna, September, 1968. *Mater. Struct.*, 2(10), 253–267.
- Feliú, S., González, J.A., Andrade, C., and Feliu, V. 1989. Polarization resistance measurements in large concrete specimens: mathematical solution for unidirectional current distribution. *Mater. Struct. Res. Test.*, 22(129), 199–205.
- Feliú, S., González, J.A., Feliu, Jr., S., and Andrade, M.C. 1990a. Confinement of the electrical signal for *in situ* measurement of polarization resistance in reinforced concrete. *ACI Mater. J.*, 87(5), 457–460.

- Feliú, S., González, J.A., Escudero, M.L., Feliú, Jr., S., and Andrade, M.C. 1990b. Possibilities of the guard ring for electrical signal confinement in the polarization measurements of reinforcements. *J. Sci. Eng. Corrosion*, 46(12), 1015–1020.
- Finno, R.J. and Gassman, S.L. 1998. Impulse response evaluation of drilled shafts, *J. Geotech. Geoenviron. Eng.*, 124(10), 965.
- Fitzgerald, A.E., Higginbotham, D.E., and Grabel, A. 1967. *Basic Electrical Engineering*. McGraw-Hill, New York.
- Flis, J., Sehgal, A., Li, D., Kho, Y.T., Sabol, S., Pickering, H., Osseo-Asare, K., and Cady, P.P. 1992. *Condition Evaluation of Concrete Bridges Relative to Reinforcement Corrosion*. Vol. 2. *Method for Measuring the Corrosion Rate of Reinforcing Steel*, SHRP-S/FR-92-104, 105 pp. Strategic Highway Research Program, National Research Council, Washington, D.C.
- Forrester, J.A. 1970. Gamma radiography of concrete. In *Proceedings of Symposium on Non-Destructive Testing of Concrete and Timber*, pp. 13–17. Institution of Civil Engineers, London.
- Freiesleben Hansen, P. and Pedersen J. 1977. Maturity computer for controlled curing and hardening of concrete. *Nordisk Betong*, 1, 19–34.
- Freiesleben Hansen, P. and Pedersen, J. 1985. *Curing of Concrete Structures*, CEB Bull. d'Inf. 166, 42 pp. International du Beton, Lausanne, Switzerland.
- Frølund, T., Jensen, F.M., and Bassler, R. 2002. Determination of reinforcement corrosion rate by means of the galvanostatic pulse technique. In *Proceedings of First International Conference on Bridge Maintenance, Safety, and Management (IABMAS)*, July 14–17, Barcelona, 8 pp.
- Gaynor, R.D. 1969. *In-Place Strength of Concrete: A Comparison of Two Test Systems*, NRMCA Technical Information Letter No. 272. National Ready Mixed Concrete Association, Silver Spring, MD.
- Geiker, M. 1983. Studies of Portland Cement Hydration by Measurements of Chemical Shrinkage and Systematic Evaluation of Hydration Curves by Means of the Dispersion Model, Ph.D. dissertation, 259 pp. Technical University of Denmark, Lyngby, Denmark.
- Germann Instruments, Inc. 2007. *NDT Systems*, Catalog NDT-2007, www.germann.org.
- Goldsmith, W. 1965. *Impact: The Theory and Physical Behavior of Colliding Solids*, pp. 24–50. Edward Arnold Press, London.
- Greene, G.W. 1954. Test hammer provides new method of evaluating hardened concrete. *J. Am. Concrete Inst.*, 26(3), 249–256.
- Hagemaijer, D.J. 1990. *Fundamentals of Eddy Current Testing*. American Society for Nondestructive Testing, Columbus, OH.
- Halabe, U.B., Sotoodehnia, A., Maser, K.R., and Kausel, E.A. 1993. Modeling the electromagnetic properties of concrete. *ACI Mater. J.*, 90(6), 552–563.
- Halabe, U.B., Maser, K.R., and Kausel, E.A. 1995. Condition assessment of reinforced concrete structures using electromagnetic waves. *ACI Mater. J.*, 92(5), 511–523.
- Halliday, D. and Resnick, R. 1978. *Physics*, 3rd ed. John Wiley & Sons, New York.
- Heisey, J.S., Stokoe II, K.H., and Meyer, A.H. 1982. Moduli of pavement systems from spectral analysis of surface waves. In *Transportation Research Record No. 853*, pp. 22–31. Transportation Research Board, Washington, D.C.
- Hellier, A.K., Sansalone, M., Carino, N.J., Stone, W.C., and Ingraffea, A.R. 1987. Finite-element analysis of the pullout test using a nonlinear discrete cracking approach. *J. Cement Concrete Aggregates*, 9(1), 20–29.
- Higgs, J. 1979. Integrity testing of piles by the shock method. *Concrete*, 13(10), 31–33.
- Hindo, K.R. and Bergstrom, W.R. 1985. Statistical evaluation of the in-place strength of concrete. *Concrete Int.*, 7(2), 44–48.
- Holt, F.B. and Eales, J.W. 1987. Nondestructive evaluation of pavements. *Concrete Int.*, 9(6), 41–45.
- Honig, A. 1984. Radiometric determination of the density of fresh shielding concrete *in situ*. In *In Situ/Nondestructive Testing of Concrete*, Malhotra, V.M., Ed., ACI SP-82, pp. 603–618. American Concrete Institute, Farmington Hills, MI.
- IDOT. 2002. *Method of Testing the Strength of Portland Cement Concrete Using the Maturity Method*, IM 383. Office of Materials, Iowa Department of Transportation, Ames.

- INDOT. 1999. *Strength of Portland Cement Concrete Pavement (PCCP) Using the Maturity Method*, ITM 402-99T. Materials & Tests Division, Indiana Department of Transportation, Indianapolis.
- Jaeger, B.J., Sansalone, M.J., and Poston, R.W. 1996. Detecting voids in grouted tendon ducts of post-tensioned concrete structures using the impact-echo method. *ACI Struct. J.*, 93(4), 462–472.
- Jensen, B.C. and Braestrup, M.W. 1976. Lok-Tests determine the compressive strength of concrete. *Nordisk Betong*, 2, 9–11.
- Johansen, R. 1977. A new method for the determination of in-place concrete strength at form removal. In *Proceedings of RILEM Symposium on In Situ Testing of Concrete Structures*, Part II, September 12–15, Budapest, pp. 276–288. Institut des Sciences de la Construction, Budapest.
- Johansen, R. 1979. *In situ* strength evaluation of concrete: the break-off method. *Concrete Int.*, 1(9), 45–51.
- Jones, R. 1949a. Measurement of the thickness of concrete pavements by dynamic methods: a survey of the difficulties. *Mag. Concrete Res.*, 1, 31–34.
- Jones, R. 1949b. The non-destructive testing of concrete. *Mag. Concrete Res.*, 2, 67–78.
- Jones, R. 1953. Testing of concrete by ultrasonic-pulse technique. In *Proceedings of the Highway Research Board No. 32*, pp. 259–275. National Research Council, Washington, D.C.
- Jones, R. 1955. A vibration method for measuring the thickness of concrete road slabs *in situ*. *Mag. Concrete Res.*, 7(20), 97–102.
- Jones, R. 1962. Surface wave technique for measuring the elastic properties and thickness of roads: theoretical development. *Br. J. Appl. Phys.*, 13, 21–29.
- Jones, R. and Făcăoaru, I. 1969. Recommendations for testing concrete by the ultrasonic pulse method. *Mater. Struct.*, 2(10), 275–284.
- Kierkegaard-Hansen, P. 1975. Lok-strength. *Nordisk Betong*, 3, 19–28.
- Kolek, J. 1958. An appreciation of the Schmidt rebound hammer. *Mag. Concrete Res.*, 10(28), 27–36.
- Knudsen, T. 1980. On particle size distribution in cement hydration. In *Proceedings of the 7th International Congress on the Chemistry of Cement (Paris)*, Vol. II, I-170–I-175. Editions Septima, Paris.
- Knudsen, T. 1984. The dispersion model for hydration of Portland cement. I. General concepts. *Cement Concrete Res.*, 14, 622–630.
- Knudsen, T. (1985). Personal communication. Technical University of Denmark, Kongens Lyngby.
- Kozlov, V.N., Samokrutov, A.A., and Shevaldykin, V.J. 2006. Ultrasonic equipment for evaluation of concrete structures based on transducers with dry point contact. In *Proceedings of NDE Conference on Civil Engineering*, August 14–18, St. Louis, MO, Al-Qadi, I. and Washer, G., Eds. American Society for Nondestructive Testing, Columbus, OH.
- Krause, M., Mielentz, F., Milmann, B., Streicher, D. and Mayer, K. 2006. Ultrasonic reflection properties at interfaces between concrete steel and air: imaging and modelling. In *Proceedings of NDE Conference on Civil Engineering*, August 14–18, Louis, MO, Al-Qadi, I. and Washer, G., Eds. American Society for Nondestructive Testing, Columbus, OH.
- Krautkrämer, J. and Krautkrämer, H. 1990. *Ultrasonic Testing of Materials*, 4th ed. Springer-Verlag, New York.
- Krenchel, H. and Bickley, J.A. 1987. Pullout testing of concrete: historical background and scientific level today. *Nordisk Betong*, 6, 155–168.
- Krenchel, H. and Shah, S.P. 1985. Fracture analysis of the pullout test. *Mater. Struct.*, 18(108), 439–446.
- Krstulovic-Opara, N., Woods, R.D., and Al-Shayea, N. 1996. Nondestructive testing of concrete structures using the Rayleigh wave dispersion method. *ACI Mater. J.*, 93(1), 75–86.
- Kunz, J.T. and Eales, J.W. 1985. Remote sensing techniques applied to bridge deck evaluation. In *Strength Evaluation of Existing Concrete Bridges*, Liu, T.C., Ed., ACI SP-88, pp. 237–258. American Concrete Institute, Farmington Hills, MI.
- Lauer, K.R. 2004. Magnetic/electrical methods. In *Handbook on Nondestructive Testing of Concrete*, 2nd ed., Malhotra, V.M. and Carino, N.J., Eds., CRC Press, Boca Raton, FL.
- Leshchinsky, A.M. 1990. Determination of concrete strength by nondestructive methods. *ASTM J. Cement Concrete Aggregates*, 12(2), 107–113.

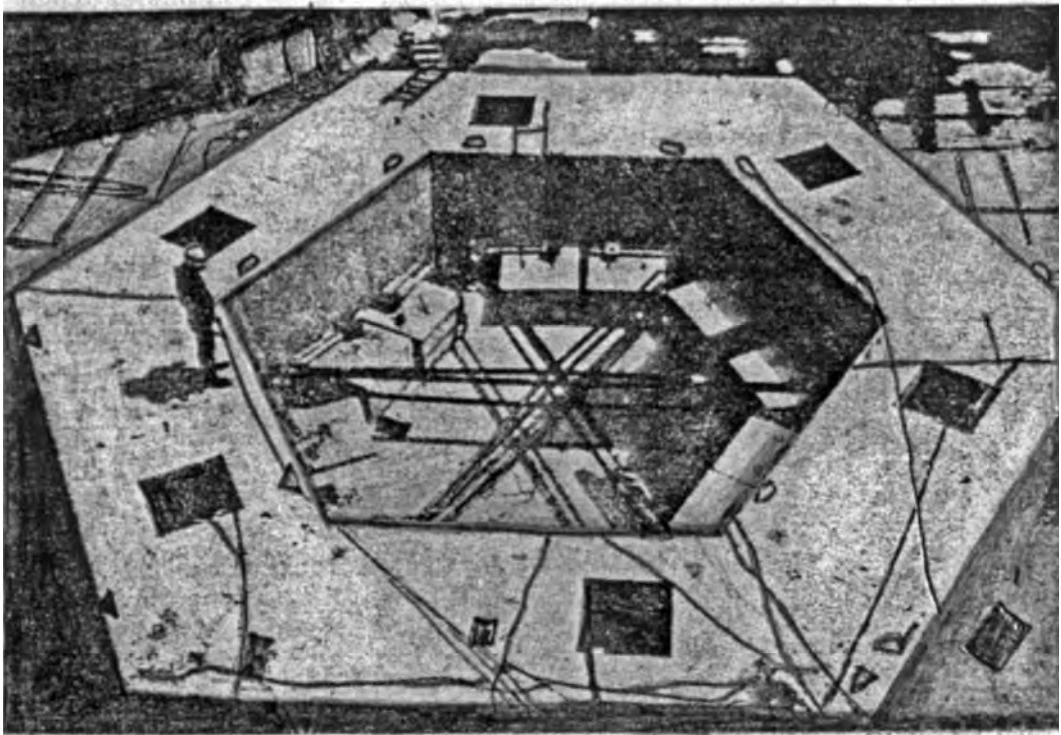
- Leshchinsky, A.M. 1991a. Correlation of concrete strength and non-destructive tests. *Indian Concrete J.*, 65(4), 184–190.
- Leshchinsky, A.M. 1991b. Combined methods of determining control measures of concrete quality. *Mater. Struct.*, 24(141), 177–184.
- Leshchinsky, A.M. 1992. Non-destructive testing of concrete strength: statistical control. *Mater. Struct.*, 25(146), 70–78.
- Leshchinsky, A.M. and Leshchinsky, M. Yu. 1991. Correlation formulae in nondestructive testing for concrete strength. *J. Struct. Eng.*, 18(3), 99–113.
- Leslie, J.R. 1955. Proposed tentative method of test for the measurement of the pulse velocity of propagation of elastic waves in concrete. *ASTM Bull.*, 204, 19–22.
- Leslie, J.R. and Cheesman, W.J. 1949. An ultrasonic method of studying deterioration and cracking in concrete structures. *J. Am. Concrete Inst.*, 21(1), 17–36.
- Levar, J.M. and Hamilton, H.R., 2003. Nondestructive evaluation of carbon fiber-reinforced polymer-concrete bond using infrared thermography. *ACI Mater. J.*, 100(1), 63–72.
- Lew, H.S. and Reichard, T.W. 1978. Mechanical properties of concrete at early ages, *J. Am. Concrete Inst.*, 75(10), 533.
- Lin, Y. and Sansalone, M.J. 1992a. Detecting flaws in concrete beams and columns using the impact-echo method. *ACI Mater. J.*, 89(4), 394–405.
- Lin, Y. and Sansalone, M.J. 1992b. Transient response of thick circular and square bars subjected to transverse elastic impact. *J. Acoust. Soc. Am.*, 91(2), 885–893.
- Lin, Y. and Sansalone, M.J. 1992c. Transient response of thick rectangular bars subjected to transverse elastic impact. *J. Acoust. Soc. Am.*, 91(5), 2674–2685.
- Lin, J.M. and Sansalone, M.J. 1996a. Impact-echo studies of interfacial bond quality in concrete. Part I. Effects of unbonded fraction of area. *ACI Mater. J.*, 93(3), 223–232.
- Lin, J.M. and Sansalone, M.J. 1996b. Impact-echo studies of interfacial bond quality in concrete. Part II. Effects of bond tensile strength. *ACI Mater. J.*, 93(4), 318–326.
- Lin, J.M. and Sansalone, M.J. 1997. A procedure for determining P-wave speed in concrete for use in impact echo testing using a Rayleigh wave speed measurement technique. In *Innovations in Non-destructive Testing*, Pessiki, S. and Olson, L., Eds., SP 168. American Concrete Institute, Farmington Hills, MI.
- Lin, Y., Sansalone, M.J., and Carino, N.J. 1991a. Finite element studies of the impact-echo response of plates containing thin layers and voids. *J. Nondestructive Eval.*, 9(1), 27–47.
- Lin, Y., Sansalone, M.J., and Carino, N.J. 1991b. Impact-echo response of concrete shafts. *ASTM Geotech. Testing J.*, 14(2), 121–137.
- Long, B.G., Kurtz, H.J., and Sandenaw, T.A. 1945. An instrument and a technique for field determination of elasticity, and flexural strength of concrete (pavements). *J. Am. Concrete Inst.*, 16(3), 217–231.
- Mailhot, G., Bisailon, G., Carette, G.G., and Malhotra, V.M. 1979. In-place concrete strength: new pullout methods. *ACI J.*, 76(12), 1267–1282.
- Malhotra, V.M. 1971. *Maturity Concept and the Estimation of Concrete Strength*, IC 277, 43 pp. Department of Energy, Mines, and Resources, Canada.
- Malhotra, V.M. 1974. Evaluation of the Windsor probe test for estimating compressive strength of concrete. *Mater. Struct.*, 7(37), 3–15.
- Malhotra, V.M. 1975. Evaluation of the pull-out tests to determine strength of *in situ* concrete, *Mater. Struct.*, 8(43), 19–31.
- Malhotra, V.M. 1976. *Testing Hardened Concrete: Nondestructive Methods*, ACI Monograph No. 9. Iowa State University Press, Ames.
- Malhotra, V.M. 2004. Surface hardness methods. In *Handbook on Nondestructive Testing of Concrete*, 2nd ed., Malhotra, V.M. and Carino, N.J., Eds. CRC Press, Boca Raton, FL.
- Malhotra, V.M. and Carette, G.G. 1980. Comparison of pullout strength of concrete with compression strength of cylinders and cores, pulse velocity, and rebound number. *ACI J.*, 77(3), 17–31.

- Malhotra, V.M. and Carette, G.G. 2004. Penetration resistance methods. In *Handbook on Nondestructive Testing of Concrete*, 2nd ed., Malhotra, V.M. and Carino, N.J., Eds. CRC Press, Boca Raton, FL.
- Malhotra, V.M. and Carino, N.J., Eds. 2004. *Handbook on Nondestructive Testing of Concrete*, 2nd ed. CRC Press, Boca Raton, FL.
- Mandel, J. 1984. Fitting straight lines when both variables are subject to error. *J. Qual. Technol.*, 16(1), 1–14.
- Manning, D.G. and Holt, F.B. 1980. Detecting deterioration in concrete bridge decks. *Concrete Int.*, 2(11), 34–41.
- Manning, D.G. and Holt, F.B. 1983. *Detecting Deterioration in Asphalt-Covered Bridge Decks*, Transportation Research Record No. 899, pp. 10–20. Transportation Research Board, Washington, D.C.
- Maser, K.R. 1986. Detection of progressive deterioration in bridge decks using ground-penetrating radar. In *Experimental Assessment of the Performance of Bridges: Proceedings of ASCE/EM Division Specialty Conference*, October, Boston, MA, pp. 42–57.
- Maser, K.R. and Roddis, W.M.K. 1990. Principles of thermography and radar for bridge deck assessment. *J. Transport. Eng.*, 116(5), 583–601.
- Mast, J.E. and Johansson, E.M. 1994. Three-dimensional ground-penetrating radar imaging using multi-frequency diffraction tomography. In *Proceedings of SPIE Conference on Advanced Microwave and Millimeter Wave Detectors*, July 25–26, San Diego, CA, Udupa, S.S. and Han, H.C., Eds., Vol. 2275, pp. 196–204.
- Mast, J.E., Lee, H., Chew, C., and Murtha, J. 1990. Pulse-echo holographic techniques for microwave subsurface NDE. In *Proceedings of NSF Conference on Nondestructive Evaluation of Civil Structures and Materials*, October 15–17, Boulder, CO, pp. 177–191.
- McIntosh, J. D. 1949. Electrical curing of concrete, *Mag. Concrete Res.*, 1(1), 21–28.
- Millard, S.G., Harrison, J.A., and Edwards, A.J. 1989. Measurement of the electrical resistivity of reinforced concrete structures for the assessment of corrosion risk. *Br. J. NDT*, 31(11), 617.
- Mitchell, T.W. 2004. Radioactive/nuclear methods. In *Handbook on Nondestructive Testing of Concrete*, 2nd ed., Malhotra, V.M. and Carino, N.J., Eds. CRC Press, Boca Raton, FL.
- Mitchell, T.M., Lee, P.L., and Eggert, G.J. 1979. The CMD: a device for the continuous monitoring of the consolidation of plastic concrete. *Public Roads*, 42(148).
- Morey, R.M. 1974. Continuous subsurface profiling by impulse radar. In *Proceedings of Engineering Foundation Conference on Subsurface Exploration for Underground Excavation and Heavy Construction*. American Society of Civil Engineering, New York.
- Naik, T.R. 1991. The break-off test method. In *Handbook on Nondestructive Testing of Concrete*, 2nd ed., Malhotra, V.M. and Carino, N.J., Eds. CRC Press, Boca Raton, FL.
- Naik, T.R., Salameh, Z., and Hassaballah, A. 1987. *Evaluation of In-Place Strength of Concrete by the Break-Off Method*. Department of Civil Engineering and Mechanics, University of Wisconsin, Milwaukee.
- Naik, T.R., Malhotra, V.M., and Popovics, J.S. 2004. The ultrasonic pulse velocity method. In *Handbook on Nondestructive Testing of Concrete*, 2nd ed., Malhotra, V.M. and Carino, N.J., Eds. CRC Press, Boca Raton, FL.
- Nasser, K.W. and Al-Manseer, A.A. 1987a. A new nondestructive test. *Concrete Int.*, 9(1), 41–44.
- Nasser, K.W. and Al-Manseer, A.A. 1987b. Comparison of nondestructive testers of hardened concrete. *ACI Mater. J.*, 84(5), 374–380.
- Natrella, M.G. 1963. *Experimental Statistics*, Chapter 5, Handbook 91. National Bureau of Standards, Washington, D.C.
- Nazarian, S. and Desai, M.R. 1993. Automated surface wave method: field testing. *ASCE J. Geotech. Eng.*, 119(7), 1094–1111.
- Nazarian, S. and Reddy, S. 1996. Study of parameters affecting impulse response method, *ASCE J. Transport. Eng.*, 122(4), 308–315.
- Nazarian, S. and Stokoe II, K.H. 1986a. *In Situ Determination of Elastic Moduli of Pavement Systems by Spectral-Analysis-of-Surface-Waves Method (Practical Aspects)*, Research Report 368-1F. Center for Transportation Research, University of Texas, Austin.

- Nazarian, S. and Stokoe II, K.H. 1986b. *In Situ Determination of Elastic Moduli of Pavement Systems by Spectral-Analysis-of-Surface-Waves Method (Theoretical Aspects)*, Research Report 437-2. Center for Transportation Research, University of Texas, Austin.
- Nazarian, S., Stokoe II, K.H., and Hudson W.R. 1983. *Use of Spectral Analysis of Surface Waves Method for Determination of Moduli and Thickness of Pavement Systems*, Transportation Research Record. No. 930. Transportation Research Board, Washington, D.C.
- Nazarian, S., Reddy, S., and Baker, M. 1994. Determination of voids under rigid pavements using impulse response method. In *Nondestructive Testing of Pavements and Backcalculation of Moduli*, Vol. 2, Von Quintas, H.L., Bush, A.J., and Baladi, G.Y., Eds., ASTM STP 1198. ASTM International, West Conshohocken, PA.
- Nurse, R. W. 1949. Steam curing of concrete. *Mag. Concrete Res.*, 1(2), 79–88.
- Olson, L. and Church, E. 1986. Survey of nondestructive wave propagation testing methods for the construction industry. In *Proceedings of the 37th Annual Highway Geology Symposium*, August, Helena, MT.
- Olson, L.D. and Wright, C.C. 1990. Seismic, sonic, and vibration methods for quality assurance and forensic investigation of geotechnical, pavement, and structural systems. In *Proceedings of Conference on Nondestructive Testing and Evaluation for Manufacturing and Construction*, dos Reis, H.L.M., Ed., pp. 263–277. Hemisphere Publishing, New York.
- Otto, G., Chew, W.C., and Young, J.F. 1990. A large open-ended coaxial probe for dielectric measurements of cements and concretes. In *Proceedings of NSF Conference on Nondestructive Evaluation of Civil Structures and Materials*, October 15–17, Boulder, CO, pp. 193–209.
- Ottosen, N.S. 1981. Nonlinear finite element analysis of pullout test. *J. Struct. Div. ASCE*, 107(ST4), 591–603.
- Parker, W.E. 1953. Pulse velocity testing of concrete. *Proc. ASTM*, 53, 1033–1042.
- Perenchio, W.F. 1989. The condition survey. *Concrete Int.*, 11(1), 59–62.
- Petersen, C.G. 1984. Lok-Test and CAPO-test development and their applications. *Proc. Inst. Civ. Eng.*, 16(Part I), 539–549.
- Pichot, C. and Trouillet, P. 1990. Diagnosis of reinforced structures: an active microwave imaging system. In *Proceedings, NATO Advanced Research Workshop on Bridge Evaluation, Repair and Rehabilitation*, Nowak, A.S., Ed., pp. 201–215. Kluwer Academic, New York.
- Pinto, R.C.A. and Hover, K.C., 1999. Application of maturity approach to setting times, *ACI Mater. J.*, 96(6), 686.
- Pinto, R.C.A., Hobbs, S.V., and Hover, K.C. 2001. The maturity approach in concrete technology: going beyond compressive strength. In *Proceedings of the Fifth CANMET/ACI International Conference on Recent Advances in Concrete Technology*, Malhotra, V.M., Ed., ACI SP 200. American Concrete Institute, Farmington Hills, MI.
- Pratt, D. and Sansalone, M. 1992. Impact-echo signal interpretation using artificial intelligence. *ACI Mater. J.*, 89(2), 178–187.
- Read, P.H., Bickley, J.A., and Omran, R. 1991. *Simulated Field Trials*, draft report, Contract 88-C204. Strategic Highway Research Program (SHRP), Washington, D.C.
- Richards, O. 1977. Pullout strength of concrete. In *Reproducibility and Accuracy of Mechanical Tests*, ASTM SP 626, pp. 32–40. ASTM International, West Conshohocken, PA.
- Rix, G.J., Bay, J.A., and Stokoe, K.H. 1990. *Assessing in Situ Stiffness of Curing Portland Cement Concrete with Seismic Tests*, Transportation Research Record 1284. Transportation Research Board, Washington, D.C.
- Rix, G.J. and Stokoe, K.H. 1989. *Stiffness Profiling of Pavement Subgrades*, Transportation Research Record 1235. Transportation Research Board, Washington, D.C.
- Rodríguez, P., Ramírez, E., and González, J.A., 1994. Methods for studying corrosion in reinforced concrete. *Mag. Concrete Res.*, 46(167), 81–90.
- Roy, D.M. and Idorn, G.M. 1982. Hydration, structure, and properties of blast furnace slag cements, mortars and concrete. *J. Am. Concrete Inst.*, 79(6), 444–457.

- Rutenbeck, T. 1973. New developments in-place testing of concrete. In *Use of Shotcrete for Underground Structural Support*, ACI SP-45, pp. 246–262. American Concrete Institute, Farmington Hills, MI.
- Sansalone, M. 1997. Impact-echo: the complete story. *ACI Struct. J.*, 94(6), 777.
- Sansalone, M. and Carino, N.J. 1986. *Impact-Echo: A Method for Flaw Detection in Concrete Using Transient Stress Waves*, NBSIR 86-3452. National Bureau of Standards, Washington, D.C.
- Sansalone, M. and Carino, N.J. 1987. Transient impact response of plates containing flaws. *J. Res. NBS*, 92(6), 369–381.
- Sansalone, M. and Carino, N.J. 1988. Impact-echo method: detecting honeycombing, the depth of surface-opening cracks, and ungrouted ducts. *Concrete Int.*, 10(4), 38–46.
- Sansalone, M. and Carino, N.J. 1989a. Laboratory and field study of the impact-echo method for flaw detection in concrete. In *Nondestructive Testing of Concrete*, Lew, H.S., Ed., ACI SP-112, pp. 1–20. American Concrete Institute, Farmington Hills, MI.
- Sansalone, M. and Carino, N.J. 1989b. Detecting delaminations in concrete slabs with and without overlays using the impact-echo method. *J. Am. Concrete Inst.*, 86(2), 175–184.
- Sansalone, M. and Poston, R. 1992. Detecting cracks in the beams and columns of a post-tensioned parking garage structure using the impact-echo method. In *Proceedings of NSF Conference on Nondestructive Evaluation of Civil Structures and Materials*, October 15–17, Boulder, CO, pp. 129–143.
- Sansalone, M. and Streett, W.B. 1997. *Impact-Echo: Nondestructive Testing of Concrete and Masonry*. Bullbrier Press, Jersey Shore, PA.
- Sansalone, M., Lin, Y., Pratt, D., and Cheng, C. 1991. Advancements and new applications in impact-echo testing. In *Proceedings, ACI International Conference on Evaluation and Rehabilitation of Concrete Structures and Innovations in Design*, Hong Kong, Malhotra, V.M., Ed., ACI SP-128, pp. 135–150. American Concrete Institute, Farmington Hills, MI.
- Sansalone, M., Lin, J.M., and Streett, W.B. 1997a. A procedure for determining P-wave speed in concrete for use in impact-echo testing using a P-wave speed measurement technique, *ACI Mater. J.*, 94(6), 531.
- Sansalone, M., Lin, J.M., and Streett, W.B. 1997b. A procedure for determining concrete pavement thickness using P-wave speed measurements and the impact-echo method. In *Innovations in Nondestructive Testing*, SP-168, Pessiki, S. and Olson, L., Eds., American Concrete Institute, Farmington Hills, MI.
- Saul, A.G.A. 1951. Principles underlying the steam curing of concrete at atmospheric pressure. *Mag. Concrete Res.*, 2(6), 127–140.
- SDDOT. 1999. *Procedure for Estimating Concrete Strength by Maturity Method*, SD407, Section 400: *Concrete*. South Dakota Department of Transportation, Pierre.
- Serway, R.A. 1983. *Physics for Scientists and Engineers with Modern Physics*. Saunders College Publishing, Philadelphia, PA.
- Schickert, M., Krause, M., and Müller, W. 2003. Ultrasonic imaging of concrete elements using reconstruction by synthetic aperture focusing techniques, *ASCE J. Mater. Civ. Eng.*, 15(3), 235–246.
- Skramtajeve, B.G. 1938. Determining concrete strength for control of concrete in structures. *J. Am. Concrete Inst.*, 34, 285–303.
- So, H.S., Millard, S.G., and Law, D.W. 2006. Environmental influences on corrosion rate measurements of steel in reinforced concrete. In *NDE Conference on Civil Engineering*, August 14–18, St. Louis, MO, Al-Qadi, I. and Washer, G., Eds. American Society for Nondestructive Testing, Columbus, OH.
- Stain, R.T. 1982. Integrity testing. *Civ. Eng.*, April, 53–59.
- Starnes, M.A. and Carino, N.J. 2003. *Infrared Thermography for Nondestructive Evaluation of Fiber Reinforced Polymer Composites Bonded to Concrete*, NISTIR 6949. National Institute of Standards and Technology, Washington, D.C.
- Starnes, M.A., Carino, N.J. and Kausel, E.A. 2003. Preliminary thermography studies for quality control of concrete structures strengthened with FRP composites. *ASCE J. Mater. Civ. Eng.*, 15(3), 266–273.

- Stehno, G. and Mall, G. 1977. The tear-off method: a new way to determine the quality of concrete in structures on site. In *Proceeding. RILEM Symposium on Testing In Situ of Concrete Structures*, Part II, September 12–15, Budapest, pp. 276–288. Institut des Sciences de la Construction, Budapest.
- Steinbach, J. and Vey, E. 1975. Caisson evaluation by stress wave propagation method. *ASCE J. Geotech.*, 101(GT4), 361–378.
- Steinway, W.J., Echard, J.D., and Luke, C.M. 1981. *Locating Voids Beneath Pavements Using Pulsed Electromagnetic Waves*, NCHRP Report 237, 40 pp. Transportation Research Board, Washington, D.C.
- Stern, M. and Geary, A.L. 1957. Electrochemical polarization. I. A theoretical analysis of the shape of polarization curves. *J. Electrochem. Soc.*, 104(1), 56–63.
- Stern, M. and Roth, R.M. 1957. Anodic behavior of iron in acid solutions. *J. Electrochem. Soc.*, 104(6), 390–392.
- Stone, W.C. and Carino, N.J. 1983. Deformation and failure in large-scale pullout tests. *ACI J.*, 80(6), 501–513.
- Stone, W.C. and Reeve, C.P. 1986. A new statistical method for prediction of concrete strength from in-place tests. *ASTM J. Cement Concrete Aggregates*, 8(1), 3–12.
- Stone, W.C., Carino, N.J., and Reeve, C.P. 1986. Statistical methods for in-place strength predictions by the pullout test. *ACI J.*, 83(5), 745–756.
- Sturup, V.R., Vecchio, F.J., and Caratin, H. 1984. Pulse velocity as a measure of concrete compressive strength. In *In Situ/Nondestructive Testing of Concrete*, Malhotra, V.M., Ed., ACI SP-82, pp. 201–227. American Concrete Institute, Farmington Hills, MI.
- Tam, C.T., Lai, L.H., and Lam, P.W. 1977. Orthogonal detection technique for determination of size and cover of embedded reinforcement. *J. Inst. Eng.*, 22, 6–16.
- Tang, L. 2002. *Calibration of the Electrochemical Methods for the Corrosion Rate Measurement of Steel in Concrete: NORDTEST Project No. 1531-01*, SP Report 2002:25, SP Swedish National Testing and Research Institute, www.nordicinnovation.net/nordtestfiler/tec521.pdf.
- Tank, R.C. and Carino, N.J. 1991. Rate constant functions for strength development of concrete. *ACI Mater. J.*, 88(1), 74–83.
- TDOT. 2002. *Estimating Concrete Strength by the Maturity Method*, Tex-426-A. Texas Department of Transportation, Austin.
- Te'eni, M. 1970. Discussion of Session B. In *Proceedings of Symposium on Non-Destructive Testing of Concrete and Timber*, pp. 33–35. Institution of Civil Engineers.
- Tikalsky, P.J., Scheetz, B.F., and Tepke, D.G., 2001. *Using the Concrete Maturity Meter for QA/QC*, Report PA-2000-0126+97-04(22), Pennsylvania Transportation Institute, University Park, PA.
- Tremper, B. 1944. The measurement of concrete strength by embedded pull-out bars. *Proc. ASTM*, 44, 880–887.
- Ulriksen, C.P.F. 1983. Application of Impulse Radar to Civil Engineering, Ph.D. thesis, Department of Engineering Geology, Lund University, Sweden. Geophysical Survey Systems, Salem, NH.
- Weil, G.J. 2004. Infrared thermographic techniques. In *Handbook on Nondestructive Testing of Concrete*, 2nd ed., Malhotra, V.M. and Carino, N.J., Eds. CRC Press, Boca Raton, FL.
- Wenner, F. 1915. A method of measuring earth resistivity. *Bull. Bur. Standards*, 12(4), 469–478.
- Whitehurst, E.A. 1951. Soniscope tests concrete structures. *J. Am. Concrete Inst. Proc.*, 47(6), 433–448.
- Whitehurst, E.A. 1967. *Evaluation of Concrete Properties from Sonic Tests*. ACI Monograph, No. 2. Iowa State University Press, Ames.
- Williams, T.J., Sansalone, M., Streett, W.B., Poston, R., and Whitlock, R. 1997. Nondestructive evaluation of masonry structures using the impact-echo method. *TMS J.*, 15(1), 47.
- Yener, M. 1994. Overview, and progressive finite element analysis of pullout tests. *ACI Struct. J.*, 91(1), 49–58.
- Yu, B.J. and Ansari, F. 1996. Method and theory for nondestructive determination of fracture energy in concrete structures. *ACI Struct. J.*, 93(5), 602.
- Yuan, D. and Nazarian, S. 1993. Automated surface wave method: inversion technique. *ASCE J. Geotech. Eng.*, 119(7), 1112–1126.



Hexagon marine structure in Kanagawa, Japan, comprised of concrete floating block reinforced with glass-fiber-reinforced plastic (GFRP) tendons. The tendons consist of nine multi-cables, each made of eight 0.3-in. (8-mm) diameter GFRP rods. The concrete floating blocks were connected by post-tensioning GFRP tendons, and the anchorage was provided by using multi-type anchor heads and wedges. Construction was completed in 1993. (Photograph courtesy of American Concrete Institute, Farmington Hills, MI.)

22

Fiber-Reinforced Composites

Edward G. Nawy, D.Eng., P.E., C.Eng.*

Part A. Fiber-Reinforced Concrete

22.1	Historical Development.....	22-2
22.2	General Characteristics	22-2
22.3	Mixture Proportioning	22-4
22.4	Mechanics of Fiber Reinforcement.....	22-5
	First Cracking Load • Critical Fiber Length: Length Factor •	
	Critical Fiber Spacing: Space Factor • Fiber Orientation: Fiber	
	Efficiency Factor • Static Flexural Strength Prediction: Beams	
	with Fibers Only	
22.5	Mechanical Properties of Fibrous	
	Concrete Structural Elements	22-8
	Controlling Factors • Strength in Compression • Strength in	
	Direct Tension • Flexural Strength • Shear Strength •	
	Environmental Effects • Dynamic Loading Performance	
22.6	Steel-Fiber-Reinforced Cement Composites	22-14
	General Characteristics • Slurry-Infiltrated Fiber Concrete •	
	DSP and CRC Cement Composites • Carbon-Fiber-Reinforced	
	Cement-Based Composites • Super-Strength Reactive-Powder	
	Concretes	
22.7	Prestressed Concrete Prism Elements as the Main	
	Composite Reinforcement in Concrete Beams.....	22-17

Part B. Fiber-Reinforced Plastic (FRP) Composites

22.8	Historical Development.....	22-18
22.9	Beams and Two-Way Slabs Reinforced	
	with GFRP Bars.....	22-19
22.10	Carbon Fibers and Composite Reinforcement	22-20
	Carbon Fibers • Hybrid GFRP and CFRP Reinforcement for	
	Bridges and Other Structural Systems • Use as Internal	
	Prestressing Reinforcement • Use as External Reinforcement	
22.11	Fire Resistance	22-16
22.12	Summary.....	22-25
	Acknowledgments.....	22-25
	References	22-25

* Distinguished Professor, Civil Engineering, Rutgers University, The State University of New Jersey, Piscataway, New Jersey, and ACI honorary member; expert in concrete structures, materials, and forensic engineering.

Part A. Fiber-Reinforced Concrete

22.1 Historical Development

Fibers have been used to reinforce brittle materials from time immemorial, dating back to the Egyptian and Babylonian eras, if not earlier. Straws were used to reinforce sun-baked bricks and mud-hut walls, horse hair was used to reinforce plaster, and asbestos fibers have been used to reinforce Portland cement mortars. Research in the late 1950s and early 1960s by Romualdi and Batson (1963) and Romualdi and Mandel (1964) on closely spaced random fibers, primarily steel fibers, heralded the era of using the fiber composite concretes we know today. In addition, Shah and Rangan (1971), Swamy (1975), and several other researchers in the United States, United Kingdom, Japan, and Russia embarked on extensive investigations in this area, exploring other fibers in addition to steel. By the 1960s, steel-fiber concrete began to be used in pavements, in particular. Other developments using bundled fiberglass as the main composite reinforcement in concrete beams and slabs were introduced by Nawy et al. (1971) and Nawy and Neuwerth (1977), as discussed in Section 22.8 of this chapter. From the 1970s to the present, the use of steel fibers has been well established as a complementary reinforcement to increase cracking resistance, flexural and shear strength, and impact resistance of reinforced concrete elements both *in situ* cast and precast.

22.2 General Characteristics

Concrete is weak in tension. Microcracks begin to generate in the matrix of a structural element at about 10 to 15% of the ultimate load, propagating into macrocracks at 25 to 30% of the ultimate load. Consequently, plain concrete members cannot be expected to sustain large transverse loading without the addition of continuous-bar reinforcing elements in the tensile zone of supported members such as beams or slabs. The developing microcracking and macrocracking, however, still cannot be arrested or slowed by the sole use of continuous reinforcement. The function of such reinforcement is to replace the function of the tensile zone of a section and assume the tension equilibrium force in the section. The addition of randomly spaced discontinuous fiber elements should aid in arresting the development or propagation of the microcracks that are known to generate at the early stages of loading history. Although fibers have been used to reinforce brittle materials such as concrete since time immemorial, newly developed fibers have been used extensively worldwide in the past three decades. Different types are commercially available, such as steel, glass, polypropylene, or graphite. They have proven that they can improve the mechanical properties of the concrete, both as a structure and a material, not as a replacement for continuous-bar reinforcement when it is needed but in addition to it.

Concrete fiber composites are concrete elements made from a mixture comprised of hydraulic cements, fine and coarse aggregates, pozzolanic cementitious materials, admixtures commonly used with conventional concrete, and a dispersion of discontinuous, small fibers made from steel, glass, organic polymers, or graphites. The fibers could also be vegetable fibers such as sisal or jute. Generally, if the fibers are made from steel, the fiber length varies from 0.5 to 2.5 in. (12.7 to 63.5 mm). They can be round, produced by cutting or chopping wire, or they can be flat, typically having cross-sections 0.006 to 0.016 in. (0.15 to 0.41 mm) in thickness and 0.01 to 0.035 in. (0.25–0.90 mm) in width and produced by shearing sheets or flattening wire. The most common diameters of the round wires are in the range of 0.017 to 0.040 in. (0.45 to 1.0 mm) (ACI Committee 544, 1988, 1993, 1996). The wires are usually crimped or deformed or have small heads on them for better bond within the matrix, and some are crescent shaped in cross-section.

The fiber content in a mixture where steel fibers are used usually varies from .25 to 2% by volume—namely, from 33 to 265 lb/yd³ (20 to 165 kg/m³). A fiber content of 50 to 60 lb/yd³ is common in lightly loaded slabs on grade, precast elements, and composite steel deck topping. The upper end of the range, more difficult to apply, is used for security applications such as vaults, safes, and impact-resisting structures.

TABLE 22.1 Typical Properties of Fibers

Type of Fiber (1)	Diameter, in. $\times 10^3$ (mm) (2)	Specific Gravity ^a (3)	Tensile Strength, psi $\times 10^3$ (GPa) (4)	Young's Modulus, psi $\times 10^6$ (GPa) (5)	Ultimate Elongation (%) (6)
Acrylic	0.6–0.13 (0.02–0.35)	1.1	30–60 (0.2–0.4)	0.3 (2)	1.1
Asbestos	0.05–0.80 (0.0015–0.02)	3.2	80–140 (0.6–1.0)	12–20 (83–138)	1–2
Cotton	6–24 (0.2–0.6)	1.5	60–100 (0.4–0.7)	0.7 (4.8)	3–10
Glass	0.2–0.6 (0.005–0.15)	2.5	150–380 (1.0–2.6)	10–11.5 (70–80)	1.5–3.5
Graphite	0.3–0.36 (0.008–0.009)	1.9	190–380 (1.0–2.6)	34–60 (230–415)	0.5–1.0
Kevlar®	0.4 (0.010)	1.45	505–520 (3.5–3.6)	9.4 (65–133)	2.1–4.0
Nylon (high-tenacity)	0.6–16 (0.02–0.40)	1.1	110–120 (0.76–0.82)	0.6 (4.1)	16–20
Polyester (high-tenacity)	0.6–16 (0.02–0.40)	1.4	105–125 (0.72–0.86)	1.2 (8.3)	11–13
Polypropylene	0.6–16 (0.02–0.40)	0.95	80–110 (0.55–0.76)	0.5 (3.5)	15–25
Rayon (high-tenacity)	0.8–15 (0.02–0.38)	1.5	60–90 (0.4–0.6)	1.0 (6.9)	10–25
Rock wool (Scandinavian)	0.5–30 (0.01–0.8)	2.7	70–110 (0.5–0.76)	~0.6	0.5–0.7
Sisal	0.4–4 (0.01–0.10)	1.5	115 (0.8)	—	3.0
Steel	4–40 (0.1–1.0)	7.84	50–300 (0.3–2.0)	29.0 (200)	0.5–3.5
Cement matrix	—	1.5–2.5	0.4–1.0 (0.003–0.007)	1.5–6.5 (10–45)	0.02

^a Density = Col. 3 $\times 62.4$ lb/ft³ = Col. 3 $\times 10^3$ kg/m³.

Note: GPa $\times 0.145$ = 10⁶ psi.

Source: Nawy, E.G., *Fundamentals of High-Strength, High-Performance Concrete*, Addison Wesley Longman, Reading, MA, 1996, p. 350.

The introduction of fiber additions to concrete in the early 1900s was aimed primarily at enhancing the tensile strength of concrete. As is well known, the tensile strength is 8 to 14% of the compressive strength of normal concretes with resulting cracking at low stress levels. Such a weakness is partially overcome by the addition of reinforcing bars, which can be either steel or fiberglass, as **main continuous reinforcement** in beams and one-way and two-way structural slabs or slabs on grade (Nawy and Neuwerth, 1977; Nawy et al., 1971). As indicated earlier, the continuous reinforcing elements cannot stop the development of microcracks. Fibers, on the other hand, are discontinuous and randomly distributed in the matrix, in both the tensile and compressive zones of a structural element. They are able to add to the stiffness and crack-control performance by preventing the microcracks from propagating and widening and also by increasing ductility due to their energy-absorption capacity. Common applications of fiber-reinforced concrete include overlays in bridge decks, industrial floors, shotcrete applications, highway and airport pavements, thin-shell structures, seismic- and explosion-resisting structures, super flat surface slabs on grade in warehouses, and for the reduction of expansion joints. Table 22.1 describes the geometry and mechanical properties of various types of fibers that can be used as randomly dispersed filaments in a concrete matrix. Because of the wide range of properties for each type of fiber, the designer should be guided by the manufacturer's data on each particular product and experience with it before a fiber type is selected.

TABLE 22.2 Typical Proportions for Normal Weight Fiber-Reinforced Concrete

Material	Range
Cement	550–950 lb/yd ³
W/C ratio	0.4–0.6
Percentage of sand to aggregate	50–100%
Maximum aggregate	3/8 in.
Air content	6–9%
Fiber content	0.5–2.5% by volume of mix (steel, 1% = 132 lb/yd ³ ; glass, 1% = 42 lb/yd ³ ; nylon, 1% = 19 lb/yd ³)

Note: 1 lb/yd³ = 0.5933 kg/m³; 1 in. = 2.54 cm.

Source: ACI Committee 544, *Fiber-Reinforced Concrete*, ACI 544.1R, American Concrete Institute, Farmington Hills, MI, 1996.

TABLE 22.3 Typical Fly-Ash Fibrous Concrete Mix

Material	Quantity
Cement	490 lb/yd ³
Fly ash	225 lb/yd ³
W/C ratio	0.54
Percentage of sand to aggregate	50%
Maximum size of coarse aggregate	3/8 in.
Steel fiber content (0.010 × 0.022 × 1.0 in.)	1.5% by volume
Air-entraining agent	Manufacturer's recommendation
Water-reducing agent	Manufacturer's recommendation
Slump	5 to 6 in.

Note: 1 lb/yd³ = 0.5933 kg/m³; 1 in. = 2.54 cm.

Source: ACI Committee 544, *Fiber-Reinforced Concrete*, ACI 544.1R, American Concrete Institute, Farmington Hills, MI, 1996.

22.3 Mixture Proportioning

Mixing the fibers with the other mix constituents can be done by several methods. The method selected—plant batching, ready-mixed concrete, or hand mixing in the laboratory—depends on the facilities available and the job requirements. The most important factor is to ensure **uniform dispersion** of the fibers and to prevent segregation or balling of the fibers during mixing. Segregation or balling during mixing is affected by many factors, which can be summarized as follows:

- Aspect ratio (ℓ/d_f), which is most important
- Volume percentage of the fiber
- Coarse aggregate size, gradation, and quantity
- Water/cementitious materials ratio and method of mixing

A maximum aspect ratio of ℓ/d_f and a steel fiber content in excess of 2% by volume make it difficult to achieve a uniform mix. Although conventional mixing procedures can be used, it is advisable to use a 3/8-in. (9.7-mm) maximum aggregate size. The water requirement will vary from that of concrete without fibers depending on the type of cement replacement cementitious pozzolans used and their percent by volume of the matrix. Table 22.2 and Table 22.3 give typical mixture proportions for normal weight fibrous reinforced concrete and fly-ash fibrous concrete mixes, respectively. A workable method for mixing in a step-by-step chronological procedure can be summarized as follows:

- Blend part of the fiber and aggregate before charging into the mixer.
- Blend the fine and coarse aggregate in the mixer, add more fibers at mixing speed, then add cement and water simultaneously or add the cement immediately followed by water and additives.

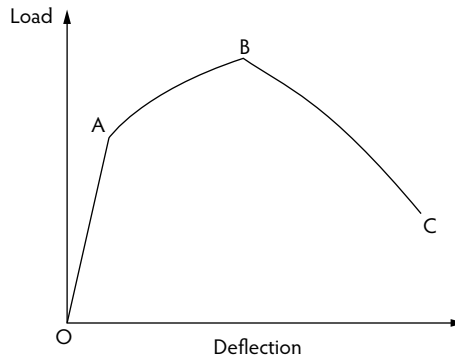


FIGURE 22.1 Schematic load–deflection relationship of fiber-reinforced concrete.

- Add the balance of the fiber to the previously charged constituents, and add the remaining cementitious materials and water.
- Continue mixing as required by normal practice.
- Place the fibrous concrete in the forms. Use of fibers requires more vibrating than required in nonfibrous concrete; although internal vibration is acceptable if carefully applied, external vibration of the formwork and the surface is preferable to prevent segregation of the fibers.

22.4 Mechanics of Fiber Reinforcement

22.4.1 First Cracking Load

Fiber-reinforced concrete in flexure essentially undergoes a trilinear deformation behavior as shown in Figure 22.1. Point A on the load-deflection diagram represents the first cracking load, which can be termed the *first-crack strength* (Mindess and Young, 1981). Normally, this is the same load level at which a nonreinforced element cracks; hence, segment OA in the diagram would be the same and essentially have the same slope for both plain and fiber-reinforced concrete. Once the matrix is cracked, the applied load is transferred to the fibers that bridge and tie the crack to keep it from opening further. As the fibers deform, additional narrow cracks develop, and continued cracking of the matrix takes place until the maximum load reaches point B of the load-deflection diagram. During this stage, debonding and pullout of some of the fibers occur, but the yield strength in most of the fibers is not reached. In the falling branch, BC, of the load-deflection diagram, matrix cracking and fiber pullout continue. If the fibers are long enough to maintain their bond with the surrounding gel, they may fail by yielding or by fracture of the fiber element, depending on their size and spacing.

22.4.2 Critical Fiber Length: Length Factor

If l_c is the critical length of a fiber above which the fiber fractures instead of pulling out when the crack intersects the fiber at its midpoint, it can be approximated by (Mindess and Young, 1981):

$$\ell_c = \frac{d_f}{2\nu_b} \sigma_f \quad (22.1)$$

where:

- d_f = fiber diameter.
- ν_b = interfacial bond strength.
- σ_f = fiber strength.

Bentur and Mindess (1990) developed an expression to relate the average pullout work and the fiber matrix interfacial bond strength in terms of the critical fiber length, demonstrating that the strength of

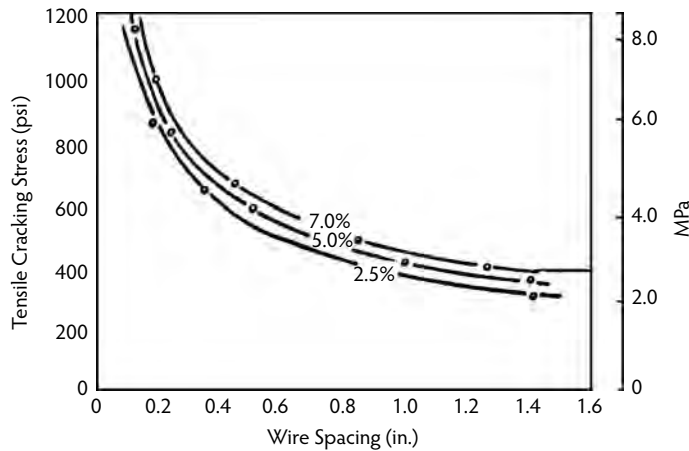


FIGURE 22.2 Effect of steel-fiber spacing on the tensile cracking stress in fibrous concrete for $\rho = 2.5, 5.9$, and 7.5% . (From Romualdi, J.P. and Batson, G.B., *Proc. ASCE Eng. Mech. J.*, 89(EM3), 147–168, 1963.)

a composite increases continuously with the fiber length. This is of significance as it indicates that pullout work may go through a maximum and then decreases as bond strength increases over a critical value. This loss of pullout work would be reduced to a typical range of $\ell = 10$ mm in the cement-based composites discussed in Section 22.6. If a critical v_b value of 1.0 MPa and a small-diameter fiber (e.g., $d_f = 20$ μm) are chosen, then an increase in bond may result in reduced toughness.

22.4.3 Critical Fiber Spacing: Space Factor

The spacing of the fibers considerably affects cracking development in the matrix. The closer the spacing, the higher the first cracking load of the matrix. This is due to the fact that the fibers reduce the stress-intensity factor that controls fracture. The approach taken by Romualdi and Batson (1963) to increase the tensile strength of the mortar was to increase the stress-intensity factor by decreasing the spacing of the fibers acting as crack arresters. Figure 22.2 relates the tensile cracking stress to the spacing of the fibers for various volumetric percentages. Figure 22.3 compares the theoretical and experimental values of the ratio of the first cracking load to the cracking strength of plain concrete (strength ratio). Both diagrams demonstrate that the strength ratio increases as the spacing of the fibers is reduced; that is, the tensile strength of the concrete increases up to the practical workability and cost-effectiveness limits. Various shapes and sizes of steel fibers are shown in Figure 22.4.

Several expressions to define the spacing of the fibers have been developed. If s is the spacing of the fibers, one expression from Romualdi and Batson (1963) gives:

$$s = 13.8d_f \sqrt{\frac{1.0}{\rho}} \quad (22.2)$$

where:

d_f = diameter of the fiber.

ρ = fiber percent by volume of the matrix.

Another expression due to McKee (1969) gives:

$$s = 3 \sqrt{\frac{V}{\rho}} \quad (22.3)$$

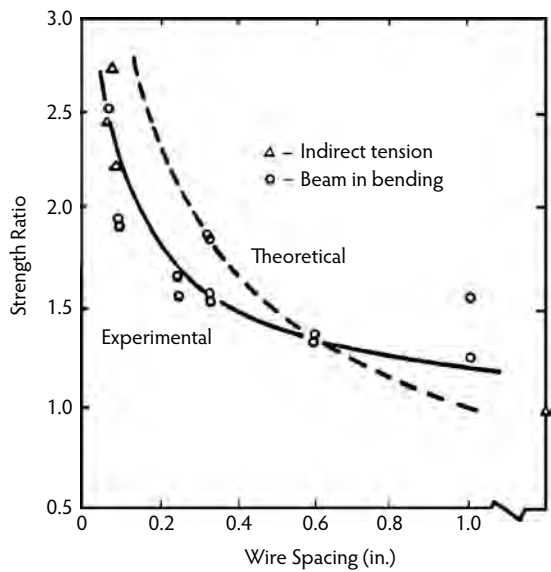


FIGURE 22.3 Effect of fiber spacing on the strength ratio. Ratio equals first cracking load of fibrous concrete divided by strength of plain concrete. (From Romualdi, J.P. and Mandel, J.A., *Proc. ACI J.*, 61(6), 657–671, 1964.)

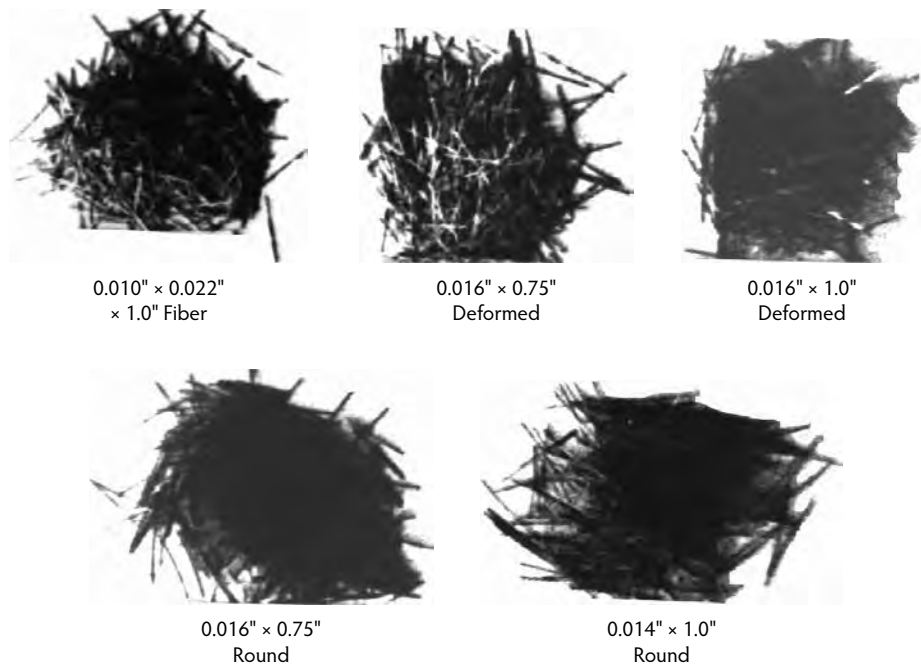


FIGURE 22.4 Various shapes and sizes of steel fibers.

where V is the volume of one fiber element. An expression that also takes into account the length of the fiber gives (Mindess and Young, 1981):

$$s = 13.8d_f \frac{\sqrt{\ell}}{\rho} \tag{22.4}$$

22.4.4 Fiber Orientation: Fiber Efficiency Factor

The orientation of the fibers with respect to load determines the efficiency with which the randomly oriented fibers can resist the tensile forces in their directions. This observation is synonymous with the contribution of bent bars and vertical shear stirrups provided in beams to resist the inclined diagonal tension stress. If one assumes perfect randomness, the efficiency factor is $0.41l$, but it can vary between $0.33l$ and $0.65l$ close to the surface of the specimen, as trowling or leveling can modify the orientation of the fibers (Mindess and Young, 1981).

22.4.5 Static Flexural Strength Prediction: Beams with Fibers Only

To predict flexural strength, several methods could be applied depending on the type of fiber, the type of matrix, whether empirical data from laboratory experiments are used, or whether the design is based on the bonded area of the fiber or the law of mixtures. An empirical expression for the composite flexural strength based on a composite-material approach is (Bentur and Mindess, 1990):

$$\sigma_c = A\sigma_m(1 - V_f) + BV_f \frac{\ell}{d} \quad (22.5)$$

where:

- σ_c = composite flexural strength.
- σ_m = ultimate strength of the matrix.
- V_f = volume fraction of the fibers adjusted for the effect of randomness.
- A, B = constants.
- ℓ/d = aspect ratio of the fiber, where l is the length and d is the diameter of the fiber.

The constants A and B were obtained from $4 \times 4 \times 12$ -in. ($100 \times 100 \times 305$ -mm) model beam tests by Swamy et al. (1974) and were adopted by ACI Committee 544 (1993). These constants lead to the following expressions:

First crack composite flexural strength (psi):

$$\sigma_f = 0.843f_r V_m + 425V_f \frac{\ell}{d_f} \quad (22.6)$$

where:

- f_r = stress in the matrix (modulus of rupture of the plane mortar or concrete) (lb/in.²).
- V_m = volume fraction of the matrix = $1 - V_f$.
- V_f = volume fraction of the fibers = $1 - V_m$.
- ℓ/d_f = ratio of length to diameter of the fibers (i.e., the aspect ratio).

Ultimate composite flexural strength (psi):

$$\sigma_{cu} = 0.97f_r V_m + 494V_f \frac{\ell}{d_f} \quad (22.7)$$

22.5 Mechanical Properties of Fibrous Concrete Structural Elements

22.5.1 Controlling Factors

From Section 22.4, it can be seen that the mechanical properties of fiber-reinforced concretes are influenced by several factors:

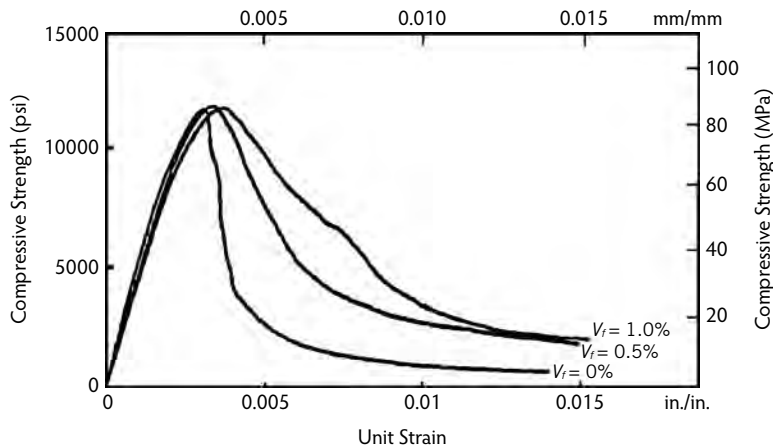


FIGURE 22.5 Influence of volume fraction of steel fibers on stress–strain behavior for 13,000-psi concrete. (From Shah, S.P. and Rangan, B.V., *Proc. ACI J.*, 68(2), 126–134, 1971.)

- Type of fiber (i.e., the fiber material and its shape)
- Aspect ratio ℓ/d_f (i.e., the ratio of fiber length to nominal diameter)
- Amount of fiber in percentage by volume (ρ)
- Spacing of the fiber (s)
- Strength of the concrete or mortar matrix
- Size, shape, and preparation of the specimen

Hence, it is important to conduct laboratory tests to failure on the mixtures using specimen models similar in form to the elements being designed. As the fibers affect the performance of the end product in all material-resistance capacities such as in flexure, shear, direct tension, and impact, it is important to evaluate the test specimen performance with regard to those parameters.

The contribution of the fiber to tensile strength, as discussed in Section 22.3, is due to its ability to act as reinforcement and assume the stress from the matrix when it cracks through the interface shear friction interlock between the fiber and the matrix. This phenomenon is analogous to the shear friction interlock hypothesis presented in Nawy (1996) in his discussion on the mechanism of shear friction interlock. Deformed or crimped fibers have a greater influence than smooth and straight ones. The pullout resistance in zone AB of Figure 22.1 is proportional to the interfacial surface area (ACI Committee 544, 1993). The non-round fiber cross-sections and the smaller diameter round fibers induce a larger resistance per unit volume than the larger diameter fibers. This is also analogous to the crack-control behavior in traditionally reinforced structural members, where a larger number of smaller diameter bars that are more closely spaced is more effective than a smaller number of large diameter bars for the same reinforcement volume percentage (Nawy and Blair, 1971). One reason for this is the larger surface interaction area between the fibers and the surrounding matrix, resulting in a higher bond and shear friction resistance.

22.5.2 Strength in Compression

The effect of the contribution of the fibers to the compressive strength of the concrete seems to be minor, as seen in Figure 22.5 (Hsu and Hsu, 1994) for tests using steel fibers; however, the ductility and toughness are considerably enhanced as a function of the increase in the volume fractions and aspect ratios of the fibers used. Figure 22.5 shows the effect of an increase in volume fraction on the stress–strain relationship of the fibrous concrete resulting from an increase in the fiber volume from 0 to 1.5% for concretes having a compressive strength of 13,100 psi (90.3 MPa). Figure 22.6 and Figure 22.7 depict a similar trend with

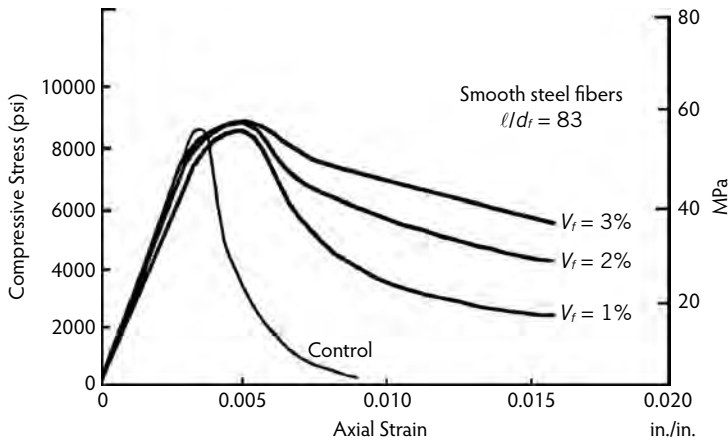


FIGURE 22.6 Influence of volume fraction of steel fibers on stress–strain behavior for 9000 psi concrete. (From Fanella, D.A. and Naaman, A.E., *ACI J.*, 82(4), 475–483, 1985.)

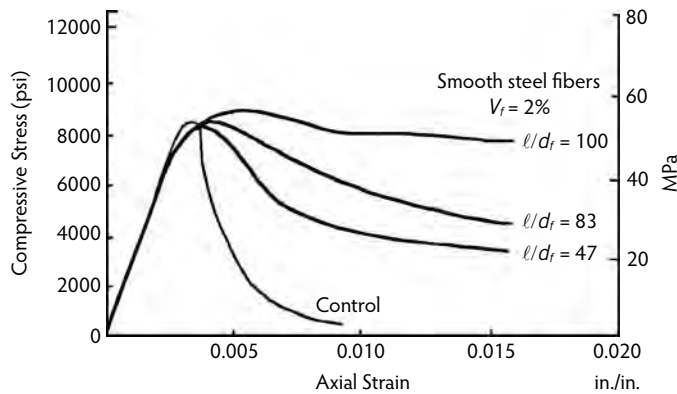


FIGURE 22.7 Influence of aspect ratio of steel fibers on stress–strain behavior. (From Fanella, D.A. and Naaman, A.E., *ACI J.*, 82(4), 475–483, 1985.)

respect to both a volume fraction ratio up to 3% and an aspect ratio in the range of 47 to 100. Figure 22.8 also demonstrates the influence of the increase in fiber content on the relative toughness of reinforced concrete members.

Toughness is a measure of the ability to absorb energy during deformation. It can be estimated from the area under the stress–strain or load–deformation diagrams. A toughness index (TI) expression proposed by Hsu and Hsu (1994) follows:

$$TI = 1.421RI + 1.035 \quad (22.8)$$

where:

RI = reinforcing index = $V_f(\ell/d_f)$.

V_f = volume fraction.

ℓ/d_f = aspect ratio.

Figure 22.9 illustrates the relationship of the toughness index to the reinforcing index of fibrous high-strength concretes within the limitations of the type, aspect ratio, and volume fractions of the steel fibers used in those tests. In short, by increasing the volume fraction, both ductility and toughness have been shown to increase significantly within the practical limits of workable volume content of fiber in a concrete mix.

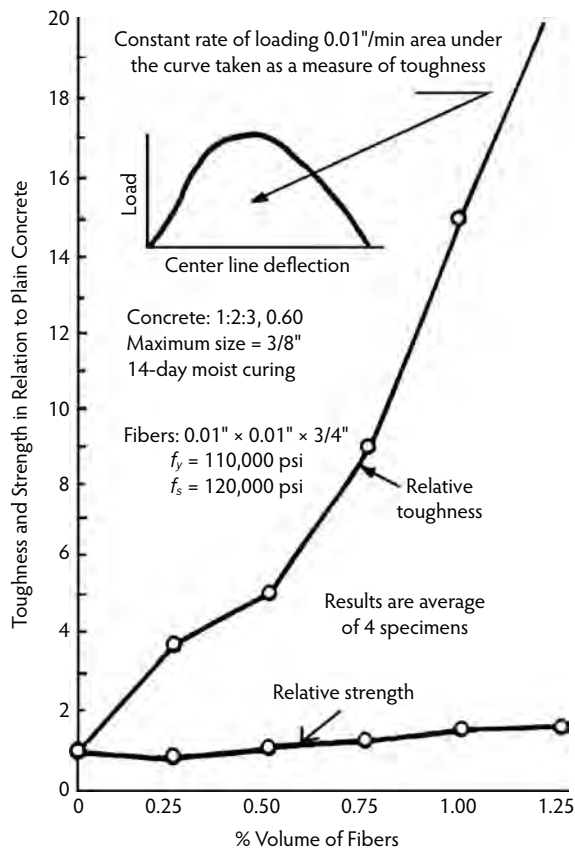


FIGURE 22.8 Relative toughness and strength vs. fiber volume ratio. (From Shah, S.P. and Rangan, B.V., *Proc. ACI J.*, 68(2), 126–134, 1971.)

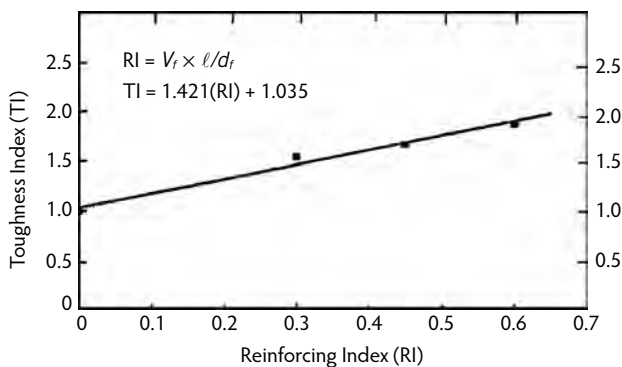


FIGURE 22.9 Toughness index vs. reinforcing index of fibrous concrete. (From Shah, S.P. and Rangan, B.V., *Proc. ACI J.*, 68(2), 126–134, 1971.)

22.5.3 Strength in Direct Tension

The effect of different shapes of the fiber filaments on the tensile stress behavior of steel-fiber-reinforced mortars in direct tension is demonstrated in Figure 22.10. The descending portion of the plots show that the fibers reinforced with better anchorage quality increase the tensile resistance of the fiber-reinforced concrete beyond the first cracking load.

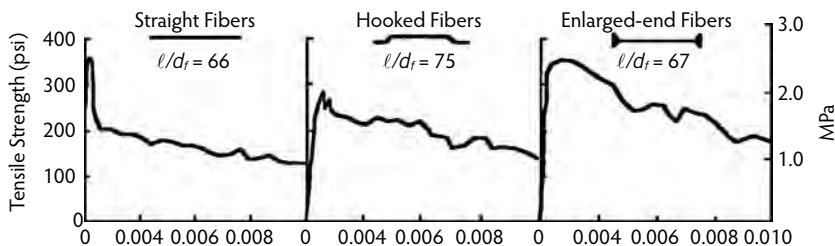


FIGURE 22.10 Effect of the shape of steel fibers on tensile stress in mortar specimens loaded in direct tension. (From Shah, S.P. and Rangan, B.V., *Proc. ACI J.*, 68(2), 126–134, 1971.)

22.5.4 Flexural Strength

Fibers seem to affect the magnitude of flexural strength in concrete and mortar elements to a much greater extent than they affect the strength of comparable elements subjected to direct tension or compression (ACI Committee 544, 1993). Two stages of loading portray the behavior. The first controlling stage is the **first cracking load stage** in the load-deflection diagram, and the second controlling stage is the ultimate load stage. Both the first cracking load and the ultimate flexural capacity are affected as a function of the product of the fiber volume concentration (ρ) and the aspect ratio (ℓ/d_f). Fiber concentrations less than .5% of the volume of the matrix and with an aspect ratio less 50 seem to have a small effect on the flexural strength, although they can still have a pronounced effect on the toughness of the concrete element, as seen in Figure 22.8. The flexural strength of plain concrete beams containing steel fibers was defined in Equation 22.6 and Equation 22.7. For structural beams reinforced with both normal reinforcing bars and fibers added to the matrix, a modification of the standard expression for nominal moment strength, $M_n = A_s f_y (d - a/2)$, must be made to account for the shear friction interaction of the fibers in preventing the flexural macrocracks from opening and propagating in the tensile zone of the concrete section, as seen in Figure 22.11 (Henager and Doherty, 1976). In this diagram, the area of concrete in the tensile zone is neglected and an additional equilibrium tensile force (T_{fc}) is added to the section. This moves the neutral axis down, leading to a higher nominal moment strength (M_n). The resulting expression for M_n becomes (Henager and Doherty, 1976):

$$M_n = A_s f_y \left(d - \frac{a}{2} \right) + \sigma_t b (h - e) \left(\frac{h}{2} + \frac{e}{2} - \frac{a}{2} \right) \quad (22.9)$$

$$e = \left[\epsilon(\text{fibers}) + 0.003 \right] \frac{c}{0.003} \quad (22.10)$$

$$\sigma_t \text{ (psi)} = \frac{1.12 \ell}{d_f \rho_f F_{be}} \quad (22.11a)$$

$$\sigma_t \text{ (MPa)} = \frac{0.00772 \ell}{d_f \rho_f F_{be}} \quad (22.11b)$$

where:

ℓ = fiber length.

d_f = fiber diameter.

ρ_f = percent by volume of the fibers.

F_{be} = bond efficiency of the steel fiber depending on its characteristics (varies from 1.0 to 1.2).

a = depth of the equivalent rectangular block.

b = width of beam.

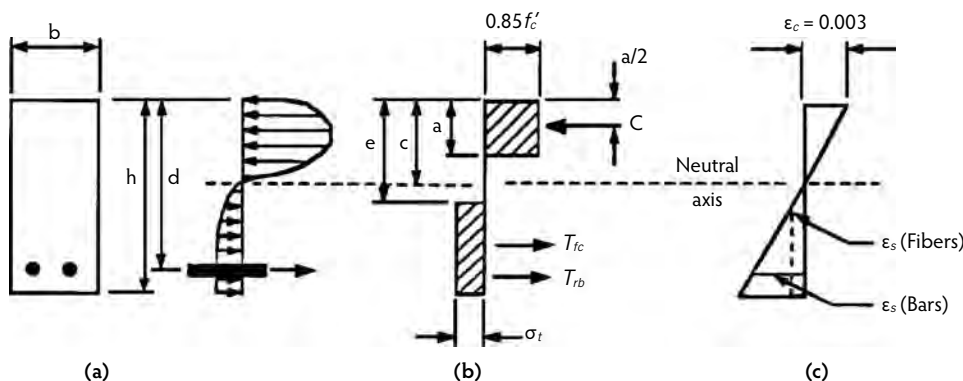


FIGURE 22.11 Stress and strain distribution across depth of singly reinforced fibrous concrete beams: (a) assumed stress distribution, (b) equivalent stress block distribution, and (c) strain distribution.

c = depth to the neutral axis.

d = effective depth of the beam to the center of the main tensile bar reinforcement.

e = distance from the extreme compression fibers to the top of the tensile stress block of the fibrous concrete.

ϵ_s = f_y/E_s of the bar reinforcement.

ϵ_f = σ_f/E_c of the fibers developed at pullout at a dynamic bond stress of 333 psi.

σ_t = tensile yield stress in the fiber.

T_{fc} = tensile yield of the fibrous concrete in Figure 22.11 = $\sigma_t b(h - e)$.

T_{rb} = tensile yield force of the bar reinforcement in Figure 22.11 = $A_s f_y$.

22.5.5 Shear Strength

A combination of vertical stirrups and randomly distributed fibers in the matrix enhances the diagonal tension capacity of concrete beams. The degree of increase in the diagonal tension capacity is a function of the shear span/depth ratio of a beam. This ratio determines the mode of failure in normal beams that do not fall in the category of deep beams and brackets as detailed by Nawy (2008). Williamson (1978) found that when 1.66% by volume of straight steel fibers are used instead of stirrups, the shear capacity increased by 45% over beams without stirrups. When steel fibers with deformed ends were used at a volume ratio of 1.1%, the shear capacity increased by 45 to 67% and the beams failed by flexure. Using crimped-end fibers increased the shear capacity by almost 100%.

In general, as the shear span/depth ratio (a/d) decreases and the fiber volume increases, the shear strength increases proportionally. Tests by Sharama (1986) resulted in the following expression for the average shear stress (v_c) for beams in which steel fibers were added (ACI Committee 544, 1993):

$$v_{cf} = \frac{2}{3} f'_t \left(\frac{d}{a} \right)^{\frac{1}{4}} \quad (22.12)$$

where:

f'_t = tensile splitting strength.

d = effective depth of a beam.

a = shear span, equal to the distance from the point of application of the load to the face of the support when concentrated loads are acting or equal to the clear beam span when distributed loads are acting.

22.5.6 Environmental Effects

22.5.6.1 Freezing and Thawing

The addition of fibers to a matrix does not seem to result in an appreciable improvement in the freezing and thawing performance of concrete, as its resistance to such an environmental effect is controlled by permeability, void ratio, and freeze–thaw cycles. Fibers, however, tend to hold the scaling concrete pieces together, thereby reducing the extent of apparent scaling.

22.5.6.2 Shrinkage and Creep

No appreciable improvement in the shrinkage and creep performance of concrete results from the addition of fibers, but a slight decrease in shrinkage can result due to the need to add more paste mortar in the mixture when fibers are used. Cracking due to drying shrinkage in restrained elements can be slightly improved, as the cracks are kept from generating because of the bridging effect of the randomly distributed fibers.

22.5.7 Dynamic Loading Performance

The cracking behavior of fibrous concrete elements under dynamic loading seems to be three to ten times better than that of plain concrete. Also, the total energy absorbed by the steel fibrous concrete beams can be 40 to 100 times that for plain concrete beams, depending on the type, deformed shape, and percent volume of the fibers (ACI Committee 544, 1993).

22.6 Steel-Fiber-Reinforced Cement Composites

22.6.1 General Characteristics

Fiber-reinforced concretes are designed to contain a maximum 2% by volume of fibers, using the same mixture design procedures and placement as nonfibrous concretes. Fiber-reinforced cement composites, on the other hand, could contain a volume fraction, namely, a fiber content by volume, as high as 8 to 25%. Consequently, neither the design of the mixture nor the constituent materials in the matrix can be similar to those of conventional fibrous or nonfibrous concretes. Either cement only or cement with sand is used in the mixture, with no coarse aggregate, to achieve the high strength, ductility, and high performance expected from such composites. The 1980s saw the development of **macrodefect-free** (MDF) cements, which have a high Young's modulus and flexural strengths up to almost 30,000 psi (~200 MPa), as well as **densified small-particle** (DSP) cements, which have a particle size less than 1/20 that of Portland cement (0.5 μm). The void content in any matrix can be reduced to a negligible percentage with the addition of pozzolans such as silica fume. With these developments as a background, the following are the types of cement-based composites being studied today:

- Slurry-infiltrated fiber concrete (SIFCON) and a composite for refractory use (SIFCA®)
- Densified small-particle (DSP) systems
- Compact reinforced composite (CRC)
- Carbon-fiber-reinforced cement-based composites
- Super-strength reactive powder concrete (RPC).

These cement-based composites can achieve a compressive strength in excess of 44,000 psi (300 MPa) in compression and an energy absorption capacity (i.e., ductility) that can be up to 1000 times that of plain concrete (Reinhardt and Naaman, 1992).

22.6.2 Slurry-Infiltrated Fiber Concrete

Because of the high volume fraction of steel fibers (8 to 25%), the mixture for a structural member is formulated by sprinkling the fiber into the formwork or over a substratum. Either the substratum is stacked with fibers to a prescribed height or the form is completely or partially filled with the fibers,

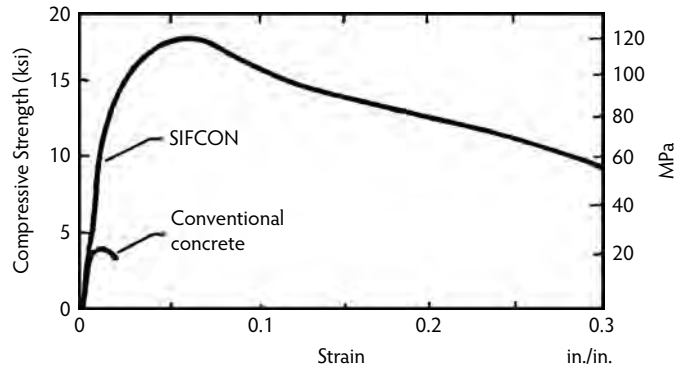


FIGURE 22.12 Stress–strain relationship of SIFCON with rupture strain in the range of 0.45 in./in. (From Naaman, A.E., in *Proceedings of the International RILEM/ACI Workshop*, Reinhardt, H.W. and Naaman, A.E., Eds., Chapman & Hall, New York, 1992, pp. 18–38.)

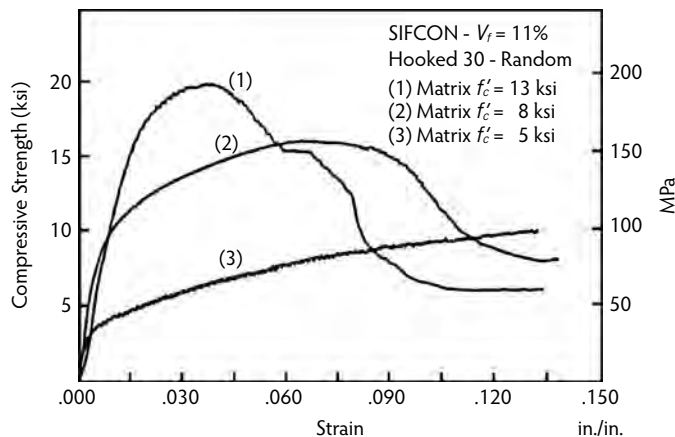


FIGURE 22.13 Influence of matrix compressive strength on the stress–strain response of SIFCON in compression. (From Naaman, A.E., in *Proceedings of the International RILEM/ACI Workshop*, Reinhardt, H.W. and Naaman, A.E., Eds., Chapman & Hall, New York, 1992, pp. 18–38.)

depending on the requirement of the design. After the fibers are placed, a low-viscosity cement slurry is poured or pumped into the fiber bed or into the formwork, infiltrating into the spaces between the fibers. Typical cement/fly-ash/sand proportions can vary from 90/10/0 to 30/20/50 by weight (Schneider, 1992). The water/cementitious ratio, $W/(C + F)$, can range between 0.45 and 0.20 by weight, with a plasticizer content of 10 to 40 oz. per 100 lb of the total cementitious weight ($C + F$). Batch trials of the slurry mix have to be carefully made with regard to the $W/(C + F)$ ratio to arrive at a workable slurry mix that can fully penetrate the depth of the fibers. Figure 22.12 provides a stress–strain diagram for a SIFCON mixture (Naaman, 1992) with a compressive strength close to 18,000 psi but with a very large strain capability in the falling branch of the diagram. Figure 22.13 illustrates the influence of the matrix compressive strength on the stress–strain response of SIFCON in compression (Schneider, 1992). A fiber content (V_f) of 11% resulted in total uniaxial strain in excess of 10%.

22.6.3 DSP and CRC Cement Composites

Densified small-particle (DSP) systems and compact reinforced composite (CRC) gain super high strength depending largely on the type of compact-density cements that are used for the cement-based composites and the proportioning used to considerably reduce or practically eliminate most of the voids in the paste. Figure 22.14 illustrates the fracture surface of a steel-fiber-reinforced concrete specimen.



FIGURE 22.14 Fracture surface of steel-fiber-reinforced concrete. (Photograph courtesy of the American Concrete Institute, Farmington Hills, MI.)

22.6.4 Carbon-Fiber-Reinforced Cement-Based Composites

Petroleum-pitch-based carbon fibers have recently been developed for use as reinforcement for cement-based composites. Their diameters vary from 0.0004 to 0.0007 in. (10 to 18 μm), and their lengths vary from 1/8 to 1/2 in. (3 to 12 mm). Their tensile strength typically ranges from 60 to 110 ksi (400 to 750 MPa). They are incorporated in the cement-based composites in essentially the same manner as steel fibers are in concrete, and they are uniformly distributed and randomly oriented. Because of the very small size of the carbon fibers and their small diameter, a high fiber count is attained in the cementitious matrix at a typical volume fraction of 0.5 to 3% (Bayasi, 1992). The spacing between the fibers is approximately 0.004 in. (0.1 mm) at a 3% fiber volume fraction. The function of the carbon fibers function is similar to that of the steel fibers in preventing microcracks from propagating and opening.

22.6.5 Super-Strength Reactive-Powder Concretes

Super-strength reactive powder concrete (RPC) has a compressive strength ranging from 30,000 to 120,000 psi (200 to 800 MPa). The lower range is used today for the construction of structural elements. The higher ranges are used in nonstructural applications such as flooring, safes, and storage compartments for nuclear waste. Concretes in the higher ranges are termed *super-high-strength concretes* and possess the very high ductility necessary for applications in structural systems. The principal characteristic of such concretes is the use of a powder concrete in which aggregates and traditional sand are replaced by ground quartz less than 300 μm in size (Richard and Cheyrezy, 1994). In this manner, the homogeneity of the mixture is greatly improved, and the distribution in the size of the particles is consequently reduced by almost two orders of magnitude. A major improvement in the properties of the hardened concrete is an increase in the Young's modulus value of the paste by almost a factor of three so its value can reach to 6 to 11 $\times 10^{-6}$ psi (55 to 75 GPa), thereby reducing the effects of incompatibility between the moduli of the paste and the quartz powder. Richard and Cheyrezy (1994) developed the following mechanical characteristics of RPC concrete:

- Improved homogeneity resulting in a Young's modulus up to 11 $\times 10^{-6}$ psi (75 GPa)
- Increase in dry compact density of the dry solids (although silica fume, with its small particle size of 0.1 to 0.5 μm and an optimum mix content of 25% cement by weight, gives excellent dry compact density, additional amounts of precipitated silica further improve the dry compact density)

TABLE 22.4 Mixture Composition and Concrete Mechanical Properties of Super-High-Strength Reactive Powder Concrete

Mixture Constituents	RPC 200 Concrete lb/yd ³ (MPa)	RPC 800 Concrete lb/yd ³ (MPa)
Portland cement, Type V	1614 (955)	1690 (1000)
Fine sand (150–400 μm)	1775 (1051)	845 (500)
Ground quartz (4 μm)	—	659 (390)
Silica fume (18 m ³ /g)	387 (229)	389 (230)
Precipitated silica (35 m ³ /g)	16.9 (10)	—
Superplasticizer (polyacrylate)	22.0 (13)	30.4 (18)
Steel fibers	323 (191)	1065 (630)
Total water	31.2 gal/yd ³ (153 L/m ³)	36.7 gal/yd ³ (180 L/m ³)
Cylinder compressive strength	24–33 (170–230)	71–99 (490–680)
Flexural strength	3.6–8.7 (25–60)	6.5–14.8 (45–102)
Fracture energy	15,000–40,000 J/m ³	1200–2000 J/m ³
Young's modulus	7.8–8.7 $\times 10^3$ (54–60 GPa)	9.8–10.9 $\times 10^3$ (65–75 GPa)

Note: 1 L/m³ = 0.2 gal/yd³ = 1.69 lb/yd³; 1 L (water) = 2.204 lb = 0.264 gal; 1000 psi = 6.895 MPa; 1 kg/m³ = 1.69 lb/yd³. Resistant type V cement was used in all the mixtures.

Source: Richard, P. and Cheyrezy, M.H., in *Proceedings, V.M. Malhotra Symposium on Concrete Technology: Past, Present and Future*, Mehta, P.K., Ed., ACI SP-144, American Concrete Institute, Farmington Hills, MI, 1994, pp. 507–518.

- Increase in the density of concrete by maintaining the fresh concrete under pressure at the placement stage and during setting, which results in the removal of air bubbles, expulsion of excess water, and partial reduction of the plastic shrinkage during final set
- Improvement in microstructure by hot curing for 2 days at 194°F (90°C) to speed the activation of the pozzolanic reaction of the silica fume, resulting in a 30% gain in compressive strength
- Increase in ductile behavior through the addition of an adequate volume fraction of steel microfibers.

Table 22.4 gives the mix proportions for Type 200 and Type 800 RPC concretes. It also lists the major mechanical properties of these concretes.

22.7 Prestressed Concrete Prism Elements as the Main Composite Reinforcement in Concrete Beams

Composite concrete that uses precast pretensioned prisms as its main tension reinforcement has shown promise for the effective control of cracking and deflection in structural concrete elements, particularly in the negative moment regions of reinforced concrete bridge decks. Most of the earlier studies on this subject were limited to experimental laboratory work (Chen and Nawy, 1994). Introducing highly precompressed prisms as the main reinforcement in the beam tension zone can increase ductility, control and delay the formation and propagation of cracking, reduce deflection, and improve the high-performance characteristics of environmentally exposed structural components, as reported by Chen and Nawy (1994). Their work involved several patterns of composite beams and a concrete strength of 14,000 psi (97 MPa), as shown in Figure 22.15. All evaluations were based on test-to-failure results. Fiberoptic Bragg grating sensors developed for this work were used to monitor strains, deformations, and crack widths in the 10-ft (3.3-m) simple, continuous beams that were tested. The relative mild steel and prestressed prism contents of the beams affected the behavior of these composite members (Chen and Nawy, 1994; Nawy and Chen, 1997). To account for this influence, a combined reinforcement index (ω) was used in the design of a prism-reinforced structural concrete beam. This index value was obtained from the following expression:

$$\omega = \frac{A_{ps}f_{ps} + A_s m f_y - A'_s f'_y}{b d_p f'_c} \quad (22.13)$$

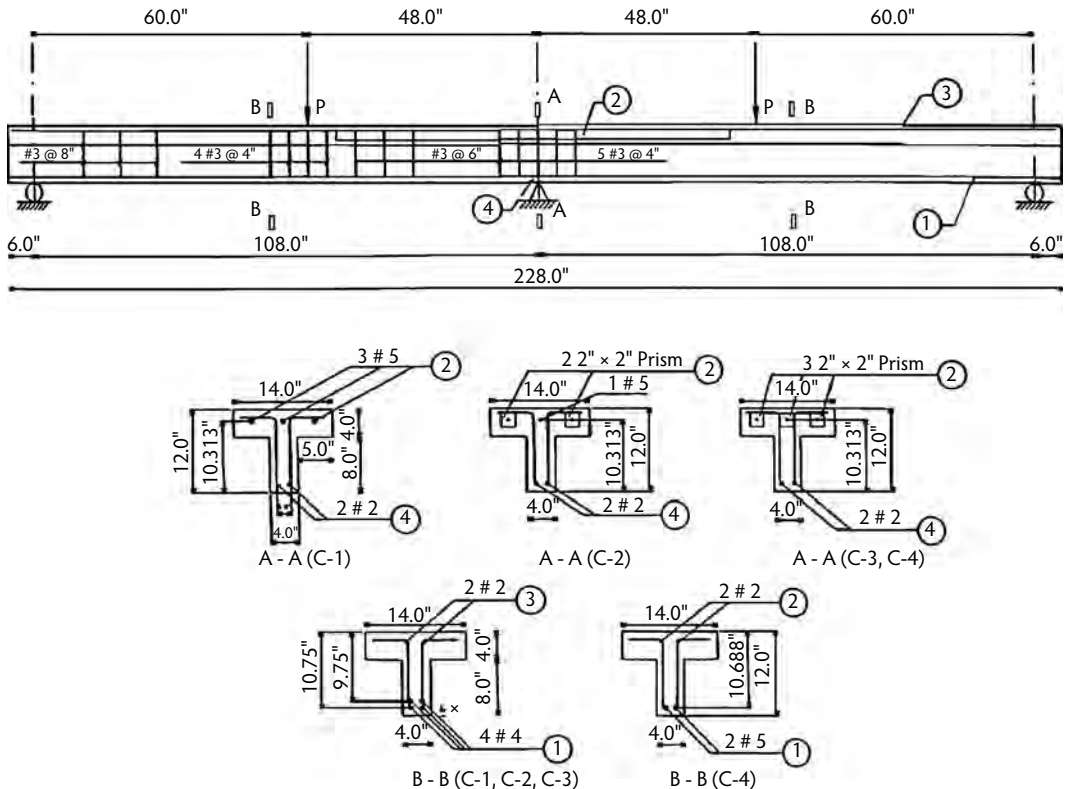


FIGURE 22.15 Prism composite reinforcement geometry. (From Nawy, E.G. and Chen, B., in *Proceedings, Transportation Research Board*. National Research Council, Washington, D.C., 1998.)

where A_{ps} , A_s , and A'_s are the areas of prestressing and nonprestressing reinforcement, f_{ps} is the design stress in the prestressing reinforcement at ultimate load, f_y and f'_y are the yield strengths of deformed bars in tension and in compression, b is the width of the compression face of the member or flange in the case of a T-section, and d_p is the effective depth of the beam cross-section.

Other systems of composites can also improve the performance of reinforced concrete beams through the use of two-layer systems, one of which is made out of normal- or high-strength concrete and the layer above or below is made of high-strength polymer concrete. In such cases, the beam cross-section is built in two layers, in a manner similar to that of the SIFCON two-layer system. Several investigations have demonstrated that the shear friction interaction of the interface between the two layers of different strength concretes, one of which is a polymer concrete, has a resistance to slip superior to the interlock between two layers made from concrete only (Nawy et al., 1992).

Part B. Fiber-Reinforced Plastic (FRP) Composites

22.8 Historical Development

Use of nonmetallic fibers, particularly fiberglass elements, bundled into continuous reinforcing elements has been considered since the 1950s for prestressing reinforcement (ACI Committee 440, 1996; Nawy, 1996; Rubinsky and Rubinsky, 1954). Advances were made in polymer development by using polymer-impregnated bundled fiberglass fibers as rods for anchorages in tunneling. In the mid-1960s, Nawy et al. (ACI Committee 440, 1996; Nawy and Neuwerth, 1977; Nawy et al., 1971) conducted extensive work on the use of bundled and resin-impregnated glass fibers formed into deformed bars as the main

reinforcement in structural elements. Except for cases where magnetic fields in supporting structures had to be avoided, commercial application of bundled and resin-impregnated reinforcement in structural concrete elements was not recognized until the late 1970s. It is important to state at this juncture that the term *plastic* could be misleading; hence, there is general consensus at this time to define FRP as *fiber-reinforced polymer* composites.

In the 1980s, an increased interest in and use of such glass-fiber-reinforced polymer (GFRP) reinforcing bars was developing. This was particularly overdue and important for reinforced concrete surrounding or supporting magnetic resonance imaging (MRI) medical equipment. Such equipment includes sensitive magnets and cannot tolerate the presence of any steel reinforcement. Also, where environmental and chemical attacks are present, GFRP reinforcement is more durable and efficient as concrete reinforcement. As stated in ACI Committee 440 (1996), composite rebars have more recently been used in the construction of seawalls, industrial roof decks, base pads for electrical and reactor equipment, and concrete floor slabs in aggressive chemical environments. In 1986, Germany built the world's first highway bridge using composite reinforcement (ACI Committee 440, 1996).

In the United States, significant funds have been expended on product evaluation and further development, and at least nine major companies have been actively marketing this product since the early 1990s. Additionally, considerable progress has been made in using glass fiber filaments as a supplement to concrete matrices to improve the mechanical properties of concrete, but not as a replacement for the main bar reinforcement in supporting structural components. Glass fibers that are alkali resistant are also gaining wide use. These normally contain zirconium (ZrO_2) to minimize or eliminate the alkaline corrosive attack on glass present in the cement paste.

Synthetic fibers made from nylon or polypropylene, both loose and woven into geotextile form, have recently begun to be utilized due to the availability of information on their mechanical performance in the matrix and a better understanding of their structural contribution to crack resistance. Although the use of other types of nonmetallic fibers has been explored, interest has grown primarily in the use of carbon fibers as the main reinforcement apart from its use in cement-based composites. It is safe to state now that the science of fibrous concrete and composites has advanced to an extent that justifies its extended use in the years to come.

22.9 Beams and Two-Way Slabs Reinforced with GFRP Bars

In the late 1960s and early 1970s, Nawy and his team at Rutgers University (Nawy and Neuwerth, 1977; Nawy et al., 1971) researched the use of glass-fiber-reinforced plastic bars as a substitute for mild steel reinforcement. Those investigations involved testing to failure a total of 30 beams and 12 two-way slabs. The slabs had an average thickness of 2-1/2 in. and an overall dimension of 7×7 ft. The slab panels had 5.5×5.5 -ft effective spans and were fully restrained along all four boundaries. The GFRP reinforcement was spaced at 3 to 8 in. In the various slabs the reinforcement area varied from 0.196 in.²/ft to 0.074 in.²/ft in each direction, giving reinforcement percentages of 0.769% and 0.290%, respectively. The beams were either simply supported or continuous over two spans. The centerline span was 9 ft, 11 in. The reinforcement percentages in the beams ranged from 1.045 to 0.696%.

These original tests and analyses indicated that both the fiberglass-reinforced slabs and the beams behaved similarly in cracking, deflections, and ultimate load to steel-reinforced beams. The large number of well-distributed cracks in the GFRP-reinforced beams and slabs indicated that a good mechanical bond developed between the GFRP bar and the surrounding concrete. The research also demonstrated that the equations for flexure accurately predicted the flexural behavior of GFRP-reinforced members with the same accuracy as for the mild steel reinforced beams. A typical stress-strain diagram of the reinforcement is shown in Figure 22.16. This research led to investigations by Larralde et al., Satoh et al., Goodspeed et al., Ehsani et al., Zia et al., Bank and Xi, Porter et al., Faza and GangaRao, and Nanni (1993). A summary of their work and publications as well as details of the original Nawy (1971) work are given in the ACI Committee 440 report (1996). Table 22.5 provides a relative comparison of the mechanical properties of GFRP and steel reinforcement.

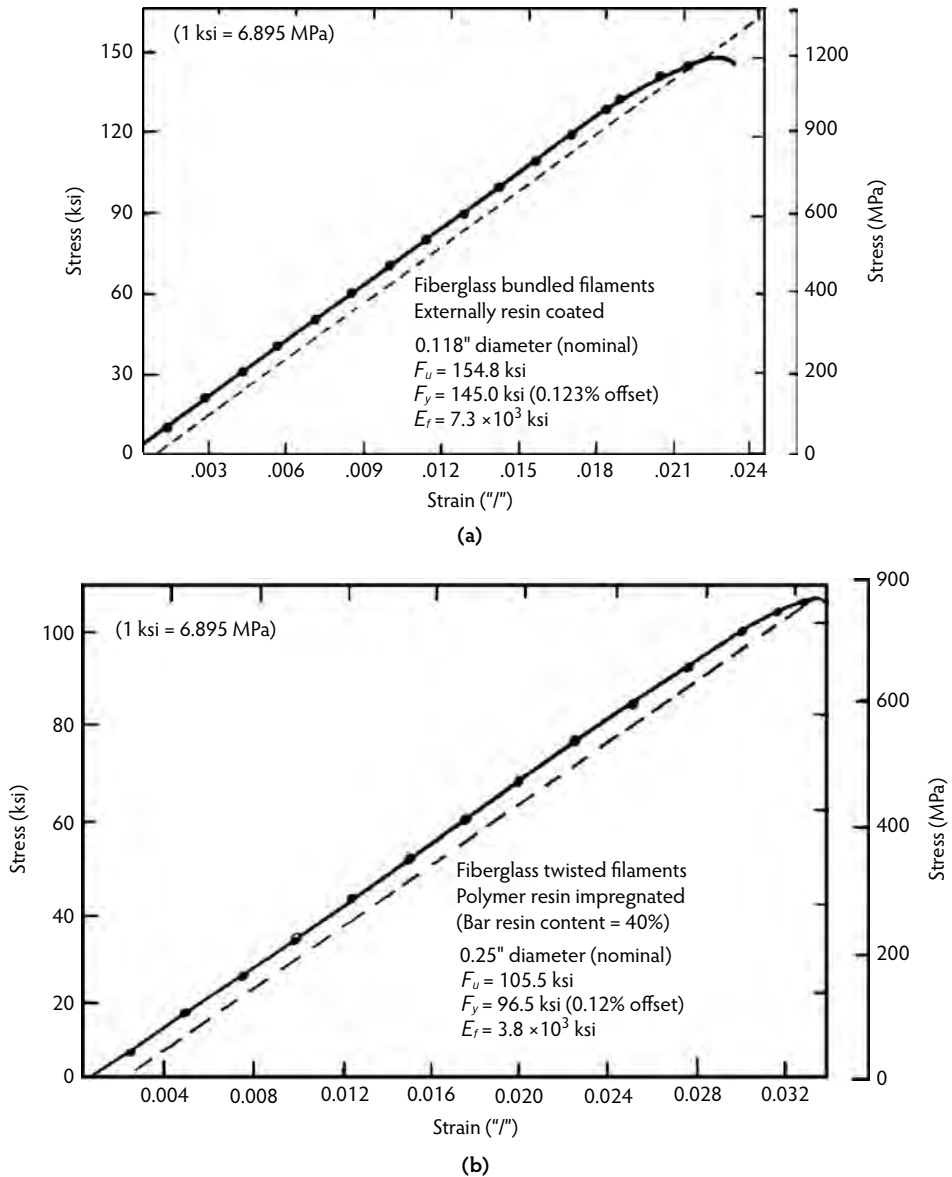


FIGURE 22.16 Typical stress-strain relationship of fiberglass composite bar reinforcement: (a) Coated filaments. (From Nawy, E.G. and Neuwerth, G.E., *Proc. ASCE J. Struct. Div.*, 103(ST2), 421–440, 1977.) (b) Impregnated filaments. (From Nawy, E.G. et al., *Proc. ASCE J. Struct. Div.*, 97(ST9), 2203–2215, 1971.)

22.10 Carbon Fibers and Composite Reinforcement

22.10.1 Carbon Fibers

Essentially, the two types of carbon fibers are high-modulus Type I and high-strength Type II. The fundamental difference between their properties is the result of the differences in their microstructures, which depend on the arrangement of the hexagonal graphine-layer networks in the graphite (ACI Committee 440, 1996). To attain a modulus of 30×10^6 psi (200 GPa), the graphine layers of high-modulus Type I carbon fibers are aligned approximately parallel to the axis of the fibers. Examples are

TABLE 22.5 Comparison of Mechanical Properties of GFRP and Steel Reinforcement

Property	Steel Rebar	Prestressing Steel Tendon	GFRP Bar	GFRP Tendon	CFRP Tendon
<i>Tensile strength</i>					
MPa	483–690	1379–1862	517–1207	1379–1724	1665–2068
ksi	70–100	200–270	75–175	200–250	240–300
<i>Yield strength</i>					
MPa	276–414	—	—	—	—
ksi	40–80	—	—	—	—
<i>Tensile modulus</i>					
GPa	200	200	414–552	48–62	152–165
ksi $\times 10^{-3}$	29	29	6–8	7–9	22–24
<i>Compressive strength</i>					
MPa	276–414	—	310–482	—	—
ksi	40–80	—	45–70	—	—
<i>Coefficient of thermal expansion</i>					
($\times 10^{-6}$)/°C	11.7	11.7	9.9	9.9	0
($\times 10^{-6}$)/°F	6.5	6.5	5.5	5.5	0
<i>Specific gravity</i>	7.9	7.9	1.5–2.0	2.4	1.7

Note: All strengths are in the longitudinal direction.

Source: ACI Committee 440, *State-of-the-Art Report on Fiber-Reinforced Plastic Reinforcement for Concrete Structures*, ACI 440R, American Concrete Institute, Farmington Hills, MI, 1996.

Kevlar® 49 by DuPont and Twaron® 1055 by Akzo Nobel. Ultra-high-modulus-fiber Kevlar® 149 and Twaron® 2000 are also available. Table 22.6 lists the minimum average strength values of Kevlar® and Twaron® reinforcing fibers. Additionally, hybrid composites made from carbon–glass–polyester are available with a strength of up to 115,000 psi (790 MPa), a modulus of 18×10^6 psi (124 MPa), and a density in the range of 0.060 to 0.069 lb/in³. It is important to state that, because of the low ductility of carbon fiber in comparison with steel, it is unlikely that it would be used as composite main bar reinforcement. Economically, it would be cost prohibitive; however, it can be used and is being used as prestressing reinforcement and as fabric reinforcement because of its high strength and high modulus, as seen in Table 22.6.

22.10.2 Hybrid GFRP and CFRP Reinforcement for Bridges and Other Structural Systems

Fiber-reinforced plastics have become widely popular in Japan, where it was originally initiated, as well as in the United States and elsewhere. They have been utilized in such transportation structures as bridge decks and in column encasements in earthquake retrofit construction, particularly hybrid GFRP bars. Figure 22.17 shows essentially negligible deflection at service load, even up to the ultimate load, with the

TABLE 22.6 Properties of Kevlar® and Twaron® Reinforcing Fibers

Property	Kevlar® 49	Twaron® 1055
Tensile strength, psi (MPa)	525,000 (3,620)	522,000 (3600)
Modulus, psi (MPa)	18×10^6 (124,000)	18.4×10^6 (127,000)
Elongation at break (%)	2.9	2.5
Density, lb/in ³ (g/cm ³)	0.052 (1.44)	0.52 (1.45)

Source: ACI Committee 440, *State-of-the-Art Report on Fiber-Reinforced Plastic Reinforcement for Concrete Structures*, ACI 440R, American Concrete Institute, Farmington Hills, MI, 1996.

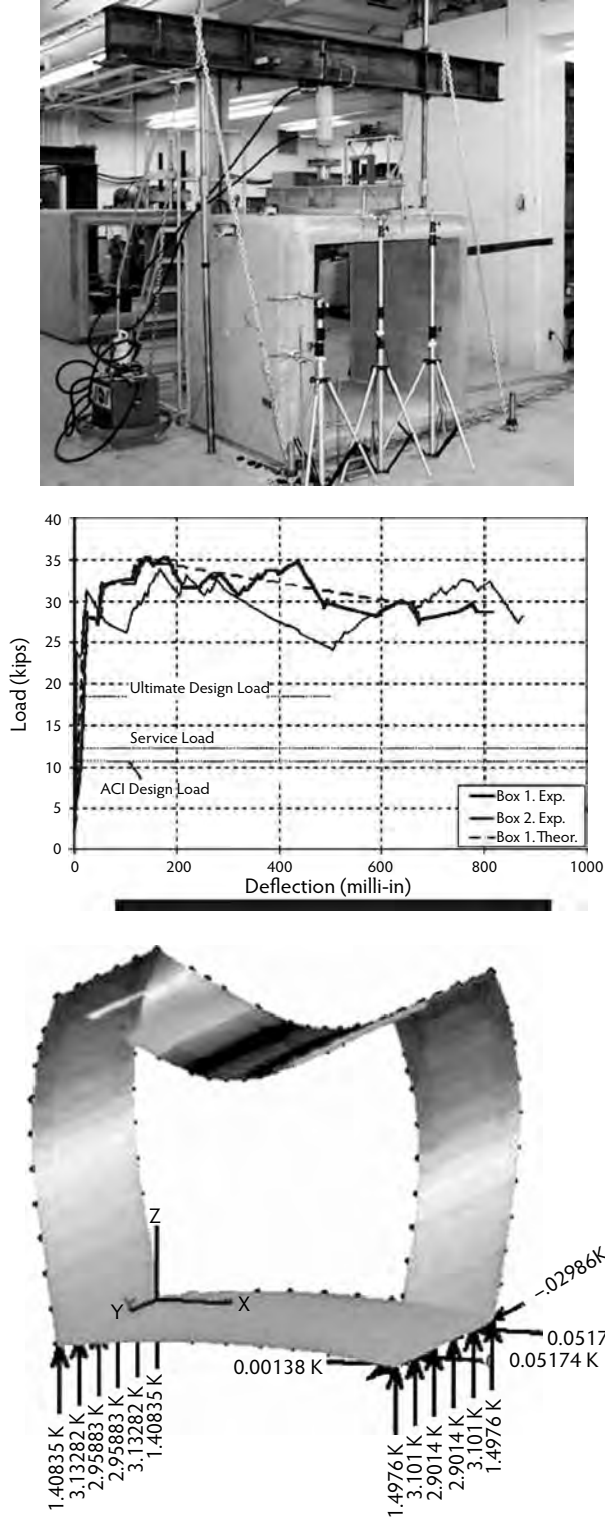


FIGURE 22.17 Deflection-load relationship of hybrid GFRP concrete box culvert analysis and laboratory testing. (From Nawy, E.G., *Concrete: The Sustainable Infrastructure Material for the 21st Century*, Circular E-C103, Transportation Research Board, Washington, D.C., 2006, pp. 1–24. Courtesy of Dr. A. Nanni.)



FIGURE 22.18 Composite technology evaluation. (From Nawy, E.G., *Concrete: The Sustainable Infrastructure Material for the 21st Century*, Circular E-C103, Transportation Research Board, Washington, D.C., 2006, pp. 1–24. Courtesy of Dr. A. Nanni.)



FIGURE 22.19 Upgrade of telecom building using hybrid GFRP-reinforced concrete in beams and joists. (From Nawy, E.G., *Concrete: The Sustainable Infrastructure Material for the 21st Century*, Circular E-C103, Transportation Research Board, Washington, D.C., 2006, pp. 1–24. Courtesy of Dr. A. Nanni.)

reserve deflection control capacity being almost twice that at the theoretical ultimate load. Figure 22.18 shows the deck of the hybrid GFRP-reinforced bridge deck in Bettendorf, Iowa, as an example. Figure 22.19 shows the use of this reinforcing system in beams in the super structure of a typical parking garage. Laminates of carbon-fiber-reinforced polymer (CFRP) can also be effectively used for mounting or wrapping concrete elements, such as damaged beam surfaces. Also, CFRP resin-impregnated strands can be spirally wound onto the surface of an existing concrete element, such as a bridge pier or structural building column. Due to the confinement imposed on the member, shear capacity and ductility are improved. CFRP plates are mounted on deteriorated surfaces using high bonding epoxies (Nawy, 2001). Table 22.7 lists the common properties of strengthening laminates. Such innovations can eliminate problems with durability and reinforcement corrosion that often plague bridge structures, garages, and deteriorated beam and slab elements in buildings.

TABLE 22.7 Properties of Strengthening Laminates

Property	Strengthening System				
	I	II	III	IV	V
Type of fibers	CFRP	CFRP	GFRP	GFRP	CFRP
Fiber orientation	Unidirectional	Unidirectional	Unidirectional	Bidirectional (x) (y)	Unidirectional
Tensile strength, MPa (ksi)	2937 (426)	758 (110)	413 (60)	482 (70) 310 (45)	2399 (348)
Modulus of elasticity, GPa ($\times 10^3$ ksi)	230 (33.4)	62 (9.0)	21 (3.0)	14 (2.1) 11 (1.6)	149 (21.7)
Failure strain (%)	1.2	1.2	2.0	3.0	1.4
Thickness, mm ($\times 10^{-1}$), in.	5 (0.02)	13 (0.05)	10 (0.04)	13 (0.05)	13 (0.05)

Sources: Nawy, E.G., *High-Performance Concrete*, John Wiley & Sons, New York, 2001, p. 440; Grace, N.F. et al., Strengthening reinforced concrete beams using fiber-reinforced polymer (FRP) laminates, *ACI Struct. J.*, 96(5), 865–874, 1999.

22.10.3 Use as Internal Prestressing Reinforcement

Fiber-reinforced-plastic carbon tendons made with fiber elements 0.125 to 0.157 in. (3 to 4 mm) in diameter are used for prestressing. Their ultimate strength is comparable to prestressing strands, ranging between 270,000 and 300,000 psi (1866 and 2070 MPa).

22.10.4 Use as External Reinforcement

Unidirectional FRP sheets made of carbon (CFRP) or glass fiber (GFRP) bonded with polymer matrix (epoxy, polyester, vinyl, or ester) are being used to provide protection against corrosion, and they eliminate the need for joints because of the unlimited length of the composite sheets (ACI Committee 440, 1996). They are useful in increasing the flexural and shear strength of concrete members when these composite plates are epoxy bonded to the exterior facing of the elements. They are also of particular use in the retrofit of deteriorating concrete structures and in retrofitting columns in seismic zones. Several techniques for wrapping concrete elements with CFRP sheets have been developed (ACI Committee 440, 1996; Nanni, 1993). CFRP resin-impregnated strands can be spirally wound onto the surface of an existing concrete element such as a bridge pier or a structural building column. In this manner, due to the confinement imposed on the member, shear capacity and ductility are improved. Nanni's (1993) work on the effect of wrapping conventional concrete demonstrated that significant enhancement can be achieved in the strength and ductility of the wrapped concrete element.

22.11 Fire Resistance

The resistance of fiber-reinforced polymer composites is relatively lower than that of other systems, as degradation of the polymer resin content under heat and ultraviolet light can lead to some long-term durability problems. The carbon and glass fibers and the fabrics used in the FRP can withstand normal fire exposure and are durable under ultraviolet light, but the weak link is the organic polymers used to prepare the fiberglass or carbon used as reinforcing elements through impregnation or wrapping. One way to address this deficiency is to substitute an inorganic resin for the organic polymer (Foden et al., 1996). An inorganic resin can be an alkali aluminosilicate that can set at moderate temperatures and be able to withstand up to 1000°C. The system is highly impermeable so it can protect the carbon filaments from oxidation. Tests conducted on carbon, silicon carbide, and glass composites under tension, bending, shear, and fatigue loading indicated that the mechanical properties of the nonorganic composites used are comparable to those of organic polymer composites while having the advantage of relatively higher fire resistance (Foden et al., 1996).

22.12 Summary

The concretes described in this chapter have demonstrated that the strength, ductility, and performance of concretes and cement-based composites have and will continue to achieve higher plateaus. A new era in construction materials technology has commenced that promises to have a revolutionary impact on constructed systems in the 21st century. Considerable work must be done to enhance the practicability of these materials and make them cost effective. It is only with simplicity and practicability in application and the achievement of a cost-effective competitive end product that these developments in the science of materials technology can gain universal acceptance and large-scale application.

Acknowledgments

This chapter is based on material taken with permission from *Fundamentals of High-Strength, High-Performance Concrete*, by E.G. Nawy (Addison Wesley Longman, 1996); *High-Performance Concrete*, by E.G. Nawy (John Wiley & Sons, 2001); *Reinforced Concrete: A Fundamental Approach*, 6th ed., by E.G. Nawy (Prentice Hall, 2008); *Prestressed Concrete: A Fundamental Approach*, 5th ed., by E.G. Nawy (Prentice Hall, 2006); and from various committee reports and standards of the American Concrete Institute, Farmington Hills, MI.

References

- ACI Committee 440. 1996. *State-of-the-Art on Fiber Reinforced Plastic Reinforcement for Concrete Structures*, ACI 440R. American Concrete Institute, Farmington Hills, MI.
- ACI Committee 544. 1988. *Design Considerations for Steel Fiber Reinforced Concrete*, ACI 544.4R. American Concrete Institute, Farmington Hills, MI.
- ACI Committee 544. 1989. *Measurement of Properties of Fiber Reinforced Concrete*, ACI 544.2R. American Concrete Institute, Farmington Hills, MI.
- ACI Committee 544. 1993. *Guide for Specifying, Proportioning, Mixing, Placing, and Finishing Steel Fiber Reinforced Concrete*, ACI 544.3R. American Concrete Institute, Farmington Hills, MI.
- ACI Committee 544. 1996. *Fiber Reinforced Concrete*, ACI 544.1R. American Concrete Institute, Farmington Hills, MI.
- Bayasi, M.Z. 1992. Application of carbon fiber reinforced mortar in composite slab construction. In *Proceedings of the International RILEM/ACI Workshop*, Reinhardt, H.W. and Naaman, A.E., Eds., pp. 507–517. Chapman & Hall, New York.
- Bentur, A. and Mindess, S. 1990. *Fiber Reinforced Cementitious Deposits*. Elsevier, London.
- Chen, B. and Nawy, E.G. 1994. Structural behavior evaluation of high strength concrete beams reinforced with prestressed prisms using fiber optic sensors. *ACI Struct. J.*, 91(6), 708–718.
- Di Ludovico, M., Nanni, A., Prota, A., and Cosenza, E. 2005. Repair of bridge girders with composites: experimental and analytical validation. *ACI Struct. J.*, 102(5), 639–648.
- Fanella, D.A. and Naaman, A.E. 1985. Stress–strain properties of fiber reinforced concrete in compression. *ACI J.*, 82(4), 475–483.
- Foden, A., Lyon, R., and Balaguru, P. 1996. A high temperature inorganic resin for use in fiber reinforced composites, paper presented at First International NSF Conference on Composites in Infrastructures, January 15–17, Tucson, AZ.
- Grace, N.K., Abdel-Sayed, G., Soliman, A.K., and Saleh, K.R. 1999. Strengthening reinforced concrete beams using fiber reinforced polymer (FRP) laminates, *ACI Struct. J.*, 96(5), 865–874.
- Henager, C.H. and Doherty, T.J. 1976. Analysis of fibrous reinforced concrete beams. *J. Struct. Div. ASCE*, 102, 177–188.
- Hsu, L.S. and Hsu, T.C.T. 1994. Stress–strain behavior of steel-fiber high-strength concrete under compression. *Proc. ACI Struct. J.*, 91(4), 448–457.

- Lopez, A. and Nanni, A. 2006. Composite technology evaluation. *Concrete Int. Design Construct.*, 28(1), 74–80.
- McKee, D.C. 1969. The Properties of Expansive Cement Mortar Reinforced with Random Wire Fibres, Ph.D. thesis, University of Illinois, Urbana.
- Naaman, A.E. 1992. SIFCON: tailored properties for structural performance. In *Proceedings of the International RILEM/ACI Workshop*, Reinhardt, H.W. and Naaman, A.E., Eds., pp. 18–38. Chapman & Hall, New York.
- Nanni, A. 1993. Flexural behavior and design of RC members using FRP reinforcement. *ASCE J. Struct. Eng.*, 119(11), 3344–3359.
- Nawy, E.G. 1996. *Fundamentals of High-Strength, High-Performance Concrete*. Addison Wesley Longman, London.
- Nawy, E. G. 2001. *Fundamentals of High-Performance Concrete*. John Wiley & Sons, New York.
- Nawy, E, G. 2006a. *Concrete: The Sustainable Infrastructure Material for the 21st Century*, Circular E-C103. Transportation Research Board, Washington, D.C.
- Nawy, E.G. 2006b. *Prestressed Concrete: A Fundamental Approach*, 5th ed. Prentice Hall, Upper Saddle River, NJ.
- Nawy, E.G. 2008. *Reinforced Concrete: A Fundamental Approach*, 6th ed. Prentice Hall, Upper Saddle River, NJ, 934 pp.
- Nawy, E.G. and Blair, K. 1971. Further studies on flexural crack control in structural slab systems. In *Proceedings of the International Symposium on Cracking, Deflection, and Ultimate Load of Concrete Slab Systems*, Nawy, E.G., Ed., ACI SP-30, pp. 1-30–1-42. American Concrete Institute, Farmington Hills, MI.
- Nawy, E.G. and Chen, B. 1998. Fiber optic sensing of the behavior of prestressed prism-reinforced continuous composite concrete beams for bridge deck application. In *Proceedings, Transportation Research Board*. National Research Council, Washington, D.C.
- Nawy, E.G. and Neuwerth, G.E. 1977. Fiber glass reinforced concrete slabs and beams. *J. Struct. Div. ASCE*, 103, 421–440.
- Nawy, E.G., Neuwerth, G.E., and Phillips, C.J. 1971. Behavior of fiber glass reinforced concrete beams. *J. Struct. Div. ASCE*, 97, 2203–2215.
- Nawy, E.G., Ukadike, M.M., and Balaguru, P.N. 1992. Investigation of concrete PMC composite. *J. Struct. Div. ASCE*, 108, 1049–1063.
- Parretti, R. and A. Nanni. 2004. Strengthening of RC members using near-surface mounted FRP composites: design overview. *Adv. Struct. Eng. Int. J.*, 7(6), 469–483.
- Reinhardt, H.W. and Naaman, A.E., Eds. 1992. High performance fiber reinforced cement composite. In *Proceedings of the International RILEM/ACI Workshop*, p. 565. Chapman & Hall, New York.
- Richard, P. and Cheyrezy, M.H. 1994. Reactive powder concretes with high ductility and 200–800 MPa compressive strength. In *Proceedings, V.M. Malhotra Symposium on Concrete Technology: Past, Present, and Future*, Mehta, P.K., Ed., ACI SP-144, pp. 507–518. American Concrete Institute, Farmington Hills, MI.
- Romualdi, J.P. and Batson, G.B. 1963. Mechanics of crack arrest in concrete. *Proc. ASCE Eng. Mech. J.*, 89(EM3), 147–168.
- Romualdi, J.P. and Mandel, J.A. 1964. Tensile strength of concrete affected by uniformly distributed closely spaced short lengths of wire reinforcement. *J. ACI*, 61(6), 657–671.
- Rubinsky, I.A. and Rubinsky A. 1954. An investigation into the use of fiber-glass for prestressed concrete. *Mag. Concr. Res.*, Vol. 6.
- Schneider, B. 1992. Development of SIFCON through application. In *Proceedings of the International RILEM/ACI Workshop*, Reinhardt, H.W. and Naaman, A.E., Eds., pp. 177–194. Chapman & Hall, New York.
- Shah, S.P. 1983. Fiber reinforced concrete. In *Handbook of Structural Concrete*, Kong, F.K. et al., Eds., pp. 6-1–6-14. McGraw-Hill, New York.
- Shah, S.P. and Rangan, B.V. 1971. Fiber reinforced concrete properties. *ACI J. Proc.*, 68(2), 126–135.

- Sharama, A.K. 1986. Shear strength of steel fiber reinforced concrete beam. *ACI J. Proc.*, 83(4), 624–628.
- Swamy, R.N. 1975. Fiber reinforcement of cement and concrete. *J. Mater. Struct.*, 8(45), 235–254.
- Swamy, R.N., Mangat, P.S., and Rao, C.V. 1974. The mechanics of fiber reinforcement of cement matrices. In *Fiber Reinforced Concrete*, ACI SP-44, pp. 1–28. American Concrete Institute, Farmington Hills, MI.
- Williamson, G.R. 1978. Steel fibers as web reinforcement in reinforced concrete. *Proc. U.S. Army Service Conf.*, 3, 363–377.



(a)



(b)



(c)

Bonded concrete overlays extend the life of bridge decks. (a) Bay Bridge in Maryland receives LMC overlay; (b) LMC overlay is placed in Virginia; (c) silica fume overlay is placed in Virginia.

23

Bonded Concrete Overlays

Michael M. Sprinkel, P.E.*

23.1	Introduction	23-1
23.2	Key Issues for Successful Bonded HCC Overlays	23-2
	Contractor Performance • Overlay Material Properties • Overlay Bond Strength • Overlay Thickness • Overlay Surface Characteristics • Overlay Protection Characteristics	
23.3	Other Issues	23-15
	Rapid Construction of Overlays • Cost • HCC Pavement Overlays • Service Life of HCC Overlays	
23.4	Summary.....	23-16
	References	23-16

23.1 Introduction

Overlays are usually placed on bridge decks to reduce the infiltration of water and chloride ions and to improve the skid resistance, ride quality, drainage, and appearance of the surface. The protection provided by the overlay can extend the life of the deck. Three types are typically used: asphalt overlays on membranes, polymer concrete overlays, and hydraulic cement concrete (HCC) overlays. Asphalt overlays on membranes and polymer overlays have been successfully used on decks that are in good condition but require a skid-resistant surface and protection against chloride intrusion (AASHTO, 1995b; NCHRP, 1995). HCC overlays have been used successfully on similar decks, as well as on decks that require a significant amount of concrete removal and rehabilitation. Overlays are placed on pavements to increase the stiffness and to improve the skid resistance, ride quality, drainage, and appearance of the surface. Both asphalt and concrete overlays are used on both asphalt and concrete pavements. HCC pavement overlays that are thicker than 4 in. are typically unbonded, and HCC overlays that are ≤ 4 in. thick are typically bonded. The overlays can extend the life of pavements. This chapter deals only with bonded HCC overlays placed on concrete bridge decks and concrete pavements; however, the designs, specifications, materials, and construction techniques should be applicable to concrete decks in buildings, parking garages, and similar concrete structures.

* Associate Director, Virginia Transportation Research Council, Charlottesville, Virginia, and Section Head, Transportation Research Board; expert in materials and construction, particularly public works.

23.2 Key Issues for Successful Bonded HCC Overlays

Properly constructed, HCC overlays can last 30 years or more. Although effective long-lasting overlays have been constructed, some overlays have cracked and delaminated and have had to be replaced before the bridge was opened to traffic. Key issues for long-lasting overlays are the contractor performance, material properties, bond strength, thickness, surface characteristics, and protection characteristics of the overlay. Many failures have been caused by placing too much emphasis on material compressive strength and protection properties and too little emphasis on the other, typically more important properties. Factors that often contribute to premature delamination of the overlay include poor surface preparation, use of mixture proportions with high shrinkage, and early shrinkage cracking in the overlay. Some other factors include the use of construction joints, use of thick overlays, and creep and shrinkage of newly constructed superstructures. Design, specification, material, and construction requirements and construction procedures that can be used to provide long-lasting HCC overlays follow.

23.2.1 Contractor Performance

Overlays are difficult to construct. Obtaining and maintaining the high bond strengths for long-lasting overlays requires that appropriate construction decisions be made with respect to the selection and use of concrete removal and surface preparation equipment and procedures, mixture proportions, and placement and curing procedures. A properly equipped and experienced overlay contractor is more likely to perform well and less likely to have problems with the construction. Use of performance-based end-result specifications in which the contractor is rewarded for the quality of the final product rather than being compensated for following a prescription specification encourages good performance.

23.2.2 Overlay Material Properties

23.2.2.1 Overlay Mixture Proportions

Materials that have been successfully used for bridge deck overlays include Type I/II Portland cement with 15% styrene-butadiene latex by weight of cement, referred to as *latex-modified concrete* (LMC); low water/cement ratio hydraulic cement concrete mixtures; and Portland cement mixtures in which silica fume (SF), fly ash, or slag is substituted for a portion of the Portland cement (Sprinkel, 1984, 1992b; Sprinkel and Ozyildirim, 1999b; Tyson and Sprinkel, 1975).

For situations in which traffic must be placed on the overlay after a curing time of 24 hours or less, successful overlays include LMC constructed with Type III Portland cement (LMC-HE), Type II Portland cement and 7% silica fume, and LMC overlays constructed with calcium sulfoaluminate and dicalcium silicate cement, referred to as *LMC very early strength* (LMC-VE) overlays. Traffic can be placed on the LMC-VE overlays after only 3 hours of curing at concrete curing temperatures of 50°F and above (Sprinkel, 1998b, 1999). At temperatures of 80°F and above, a citric acid admixture must be added to retard the mixture. Typical mixture proportions are shown in Table 23.1 (Sprinkel, 1988, 1998b, 2001;

TABLE 23.1 Typical Mixture Proportions

Mixture	LMC	Silica Fume	Fly Ash	Slag	LMC-HE	LMC-VE
Type I/II cement (lb/yd ³)	658	658	526	395	815	658
Type cement	I/II	I/II	I/II	I/II	III	Rapid-set
Silica fume (lb/yd ³)	—	46	33	33	—	—
Fly ash (lb/yd ³)	—	—	99	—	—	—
Slag (lb/yd ³)	—	—	—	230	—	—
Fine aggregates (lb/yd ³)	1552	1269	1351	1369	1402	1552
Coarse aggregates (lb/yd ³)	1187	1516	1510	1510	1142	1187
Water (lb/yd ³)	146	282	254	254	164	146
Air (%)	5	7	7	7	5	5
Admixtures	Latex	HRWR	HRWR	HRWR	Latex	Latex

TABLE 23.2 Average Compressive Strength vs. Age

Age	LMC (psi)	Silica Fume (psi)	Fly Ash (psi)	Slag (psi)	LMC-HE (psi)	LMC-VE (psi)
3 hours	—	—	—	—	—	3510
4 hours	—	—	—	—	—	3810
5 hours	—	—	—	—	—	4070
24 hours	1810	2960	3100	3400	3750	5440
7 days	3360	5140	5050	5330	5280	6290
28 days	4630	6980	6820	7180	6340	6710

Sprinkel and Moen, 1999; Sprinkel and Ozyildirim, 1999b). The latex admixture is typically a 48% solids solution that is added to the mixture at the dosage of 3.5 gallons per bag of cement. High-range water-reducing (HRWR) admixtures (ASTM, 2008) are typically added to mixtures with silica fume to help disperse the silica fume and to provide the desired workability. Air-entraining admixtures are used with all but the LMC mixtures. The latex tends to provide air voids in LMC mixtures, and an air-detaining admixture has to be added when the air content is too high.

Aggregates used in overlays typically meet the requirements of ASTM C 33 (ASTM, 2007) and the coarse aggregate is typically a No. 7 or No. 8. The LMC is batched and mixed at the point of discharge using calibrated mobile concrete mix trucks. The trucks have compartments in which the ingredients are stored separately until conveyed to a mixer on the back of the truck. Other mixtures are typically batched at a ready-mix plant and delivered to the discharge point in ready-mix trucks. Although the overlay mixtures in Table 23.1 can be used on pavements, typically the less costly mixtures are used. These include Portland cement concrete with fly ash or slag (Sprinkel and Ozyildirim, 1999a). Even the less costly mixtures are more expensive than asphalt overlays on pavements; however, in some situations, because of rutting of available asphalt mixtures, structural requirements for the composite pavement, and the availability of suitable asphalt and concrete paving materials and paving contractors, bonded concrete overlays can be economical on a life-cycle cost basis.

23.2.2.2 Compressive Strength

Overlay mixtures are typically specified to meet a minimum compressive strength (ASTM, 2005). A typical minimum compressive strength for opening an overlay to traffic is 3000 psi. Other values have been ranging from 2500 to 5000 psi depending on the requirements for the deck and the overlay mixture (VDOT, 2002). The minimum compressive strength provides an indication that acceptable concrete was provided. More importantly, it provides an indication that the overlay can have acceptable bond strength when opened to traffic. Bond strength is discussed in more detail later. Compressive strength data for typical overlay mixtures described in Table 23.1 are shown in Table 23.2 (Sprinkel, 1988, 1998b; Sprinkel and Moen, 1999; Sprinkel and Ozyildirim, 1999b). The 4-in.-diameter by 8-in.-long cylinders were typically moist cured prior to testing, with the exception that LMC specimens were typically air cured in the lab after 2 days of moist curing. The numbers are average values obtained from several deck overlay projects.

23.2.2.3 Permeability

In recent years overlay mixtures have been specified to meet a maximum permeability (AASHTO, 1995b). The maximum permeability provides an indication that the overlay will be resistant to the penetration of chloride ions and therefore can protect the reinforcing steel in the deck from corrosion for the life of the overlay. The maximum permeability is typically 1500 coulombs (C) at 28 days. Other values have been specified, ranging from 1000 to 2000 C at 28 days. Because the permeability typically decreases with age and because the early age permeability is affected by the ingredients and curing conditions, the permeability at 28 days of age does not typically provide a good indication of the permeability at later age. A procedure that accelerates the curing of the specimens by storing them at 100°F is being used to provide a better indication of later age permeability using 28-day test results (VDOT, 2006). Permeability is discussed in more detail in the section on protection.

TABLE 23.3 Permeability (AASHTO T277)

Age	LMC (C)	Silica Fume (C)	Fly Ash (C)	Slag (C)	LMC-HE (C)	LMC-VE (C)
28 days	1500–2560	950–2330	1000–1160	1040–1390	1320–2850	300–1400
1 year	200–2060	590–1280	290–300	570–820	320–1280	0–10
3 year	300–710	520–1460	300–360	500–590	—	—
5 year	450–500	780–910	—	—	510	—
9 year	100–400	—	—	—	—	0–60

Permeability data for typical overlay mixtures described in Table 23.1 are shown in Table 23.3 (Sprinkel, 1988, 1998b, 2000; Sprinkel and Moen, 1999; Sprinkel and Ozyildirim, 1999b, 2000b). The data are typically based on tests of 4-in.-diameter by 2-in.-thick slices cut from the tops of cores taken from the overlays. The numbers are maximum and minimum values obtained from several deck overlay projects. The range is often large because the overlay thickness and overlay ingredients varied from project to project. Some projects had 2-in.-thick overlays, and others had 1.5- to 2-in.-thick overlays, so as much as 0.5 in. of the bottom of the slice could be deck concrete with a higher permeability. A permeability of <100 C is negligible, 100 to <1000 C is very low, and 1000 to 2000 C is low (AASHTO, 1995). Whereas the permeability at 28 days is typically low for the mixtures, over time the permeability generally drops to the very low range. The permeability of the LMC-VE mixture drops to the negligible range over time.

23.2.2.4 Shrinkage

In the years ahead, it is anticipated that overlay materials will be required to meet a maximum shrinkage requirement to minimize or help eliminate cracks in overlays. Cracks are typically caused by a combination of factors that include plastic, autogenous, and drying shrinkage. To minimize cracks in overlays caused by autogenous shrinkage and drying shrinkage, a maximum length change after 28 days of drying of less than 0.04% is a desirable goal. To account for autogenous shrinkage, the test procedure must be

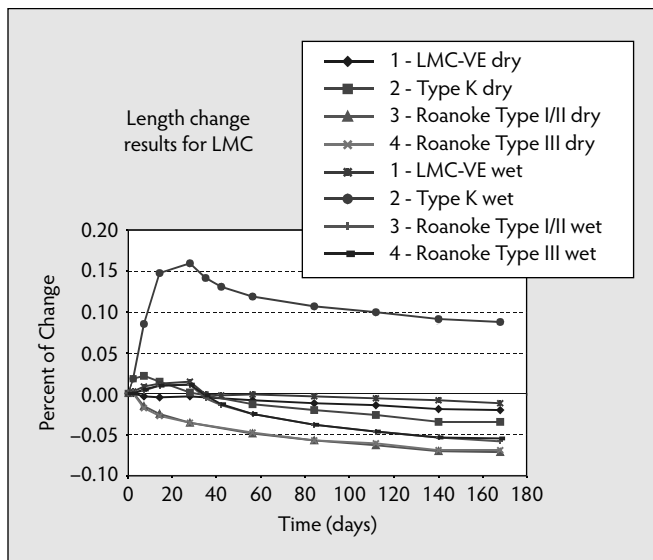


FIGURE 23.1 Length change of four LMC mixtures. (From Sprinkel, M.M., *Latex-Modified Concrete Overlay Containing Type K Cement*, VTRC 05-R26, Virginia Transportation Research Council, Charlottesville, 2005.)

modified to include an initial measurement at the time the concrete sets rather than at 24 hours of age as specified by ASTM C 157 (ASTM, 2006). Figure 23.1 shows the length change of four LMC mixtures (Sprinkel, 2005): LMC, LMC-HE, LMC-VE, and LMC mixtures made with Type K expansive cement (ASTM, 2004b). Six specimens were made from each of the four mixtures. Three specimens from each mixture were moist cured for 28 days (wet cure), and three were wet cured for the typical 2-day period and allowed to dry in the air in the laboratory after 2 days (dry cure). Each curve in Figure 23.1 is based on the average of the measurements on three specimens, 3 × 3-in. by 11 in. long. The curves indicate that the LMC and LMC-HE mixtures have a 28-day drying length change of approximately 0.04%, and the long-term length change is approximately 0.08%. Some overlays made with these mixtures have few cracks, but these mixtures are prone to plastic shrinkage cracking, and drying shrinkage causes the cracks to be wider. The curves indicate that the LMC-VE and LMC Type K cement mixtures have less length change than the LMC and LMC-HE mixtures and should be less prone to cracking. Specimens from the LMC Type K cement mixture that were moist cured for 28 days showed a significant increase in length. This increase could cause the overlay to delaminate from expansion rather than from shrinkage; however, because LMC overlays are typically moist cured for 2 days, excessive expansion typically should not be a problem. Shrinkage is discussed in more detail in the section on protection.

23.2.3 Overlay Bond Strength

The service life of an overlay is usually controlled by a failure in the vicinity of the bond interface between the overlay and the deck. The failure may be at the bond interface, in the base concrete just below the bond interface, in the overlay just above the bond interface, or at a combination of these failure locations. For convenience, unless otherwise indicated, a failure in the vicinity of the bond interface will be referred to as a *bond failure*. Factors that contribute to high bond strength include the following:

- The deck concrete is in good condition.
- Surface damage from concrete removal from the deck surface is minimal.
- Deck preparation provides a sound, clean, textured and damp surface.
- Overlay concrete is properly consolidated and cured.

Bond strength is a function of the strength of the deck concrete, surface preparation, placement of the overlay concrete, curing of the overlay concrete, and the strength of the overlay concrete. Overlay bond strength cannot be higher than the strength of the concrete in the deck and overlay.

23.2.3.1 Deck Concrete Is in Good Condition

Factors that provide an indication that the deck concrete is in good condition include the following:

- The concrete has adequate strength and few cracks.
- The reinforcement is not corroding.
- The concrete is properly air entrained and not deteriorating from alkali-silica reaction, freeze-thaw action, or other progressing material distress.

Properly prepared 4000-lb/in.² compressive strength concrete surfaces can provide tensile bond strengths of approximately 280 lb/in.² (Sprinkel, 2003b). Most overlays will have a compressive strength that exceeds 4000 lb/in.² which is more than adequate for most situations. Cracks in the deck will typically reflect through the overlay and may cause a reduction in bond strength in the vicinity of the crack. The exception can be dormant shrinkage cracks that are not moving and may not reflect. Corroding reinforcement can cause cracks in the concrete around the reinforcement and will eventually cause a reduction in bond strength. Concrete that is salt contaminated or failing because of distress from freezing and thawing or alkali-silica reaction should be removed prior to placing an overlay. Overlays should not be used to cover concrete that should be removed.

TABLE 23.4 Concrete Removal Options and Practical Removal Depths

Concrete Removal Option	Practical Removal Depth
Grit blast	<2 mm
Shot blast	<6 mm
Diamond grind	<Rebar depth
Scarification (milling)	<Rebar depth
Hydro demolition	1 mm to half depth
Pneumatic hammers	12 mm to full depth

23.2.3.2 Minimal Damage from Concrete Removal

Overlay construction typically begins with the removal of chloride-contaminated concrete and other deteriorated concrete from the deck. The depth of removal depends on the depth of deterioration and typically varies across the deck. Removal may range from as little as surface texturing to as much as full-depth removal. Deep areas should be patched prior to placing the overlay, although on occasion small areas are sometimes patched as the overlay is placed. In some situations, particularly new decks, it is not necessary to remove a considerable depth of concrete, as simple surface cleaning can provide adequate bond strengths. Concrete can be removed to greater depths to improve the grade or surface profile prior to placing the overlay or to allow for a thicker overlay to be placed. On older bridge decks, concrete may be deteriorated to the point where major concrete removal is required. Concrete removal options and typical removal depths are shown in Table 23.4. In situations in which surface cleaning and texturing are all that is required, the preferred methods are grit blast, shot blast (Figure 23.2), and hydro demolition. When concrete must be removed to greater depths, the grit blast and shot blast methods are not practical. Scarification works well to remove concrete to just above the rebar but care must be exercised not to hit the rebar. Also, follow-up removal by grit blast, shot blast, or hydro demolition is recommended to remove fractured concrete. Fine milling heads, as shown in Figure 23.3, are being used to minimize damage to the milled surface. Hydro demolition can be used to remove concrete around reinforcing steel as shown in Figure 23.4. When reinforcement is exposed, concrete removal should continue to a depth that is at least 1 in. below the reinforcement so the bond interface is not located in the reinforcement. Scarification followed by hydro demolition works well for removing the top half of the deck. The hydro demolition equipment abrades the deck surface with water at nozzle pressures that are typically about 26,000 lb/in.². The cuttings and water are usually collected and vacuumed from the surface. Large self-contained units are used for applications ranging from surface texturing to full depth removal of concrete. Large pneumatic hammers are practical for full-depth removal. A variety of methods may be used to remove deteriorated concrete. Impact methods such as hammers and scarification may fracture the concrete left in place, whereas hydro demolition does not. When impact methods are used, additional removal with other methods should be done to remove damaged and fractured concrete. Following concrete removal and patching the surface must be cleaned and textured to get good bond strengths (Sprinkel, 1997).

23.2.3.3 Surface Preparation Provides a Sound, Clean, Textured, and Damp Surface

A specification that, when enforced, should provide a properly prepared surface states: "Clean surface by shot blasting and other approved cleaning practices to remove asphalt, oils, dirt, rubber, curing compounds, paint, carbonation, laitance, weak surface mortar, and other detrimental materials that may interfere with the bonding or curing of the overlay" (VDOT, 2001). Techniques that can be used typically include a combination of the following: grit blast, shot blast, hydro demolition, power washing, and air blast. The quality of a grit blast depends on the skill of the person doing the blasting and the time devoted to the effort. Shot blasting, as shown in Figure 23.2, is a more mechanized way to prepare concrete surfaces to achieve high bond strengths. The shot blaster abrades the deck surface with shot and vacuums up the shot and concrete cuttings. The shot does not leave fractures in the prepared concrete surface. By monitoring the speed and number of passes of the shot blaster, proper surface preparation can be



FIGURE 23.2 Shot blast provides for good bond strength by cleaning and texturing the concrete surface.



FIGURE 23.3 Fine milling heads spaced ≤ 8 mm apart as shown are being used to minimize damage to the milled surface.



FIGURE 23.4 Hydro demolition can be used to remove concrete around reinforcing steel.



FIGURE 23.5 Metal disks or plates are bonded to the surface and pulled in tension.

achieved. The shot blaster typically removes up to 1/8 in. of the surface, and larger shot blasters can remove up to 1/4 in. of the surface. Hydro demolition equipment can also be used to prepare concrete surfaces to achieve high bond strengths. A low-pressure water blast is used for the final cleaning of the surface prior to placing the concrete overlay. The saturated concrete deck that results from the hydro blasting provides for a good cure of the overlay concrete.

When it may not be clear what is required for acceptable surface preparation, the test method prescribed in ACI 503R (ACI Committee 503, 1993) or ASTM C 1583 (ASTM, 2004a) can be used to determine the cleaning and texturing practice necessary to provide a tensile bond strength in test patches or a tensile surface strength in prepared surfaces greater than or equal to some minimum value (AASHTO, 1995b; ACI Committee 503, 1993; ASTM, 2004a; Sprinkel, 1997). A minimum value of 250 psi has been used (VDOT, 2001). A lower quality limit of 150 psi was used in a performance specification in which the contractor was paid for the percent of tests that were within the specification limits (Sprinkel, 2004b). A bond strength test result is usually based on the average of three individual tests. A failure at a depth of 0.25 in. or more into the base concrete is preferred (AASHTO, 1995b; VDOT, 2001).

As shown in Figure 23.5, metal disks or plates can be bonded to the prepared surface and pulled in tension to provide an indication of the tensile strength of the prepared surface. A rapid-setting acrylic adhesive can be used to bond the test disks or plates to the surface. The advantage of testing the prepared surface is that results are obtained in approximately an hour, and surface preparation activities can be adjusted as needed with negligible delay to the project. The disadvantage is that the bond strength of the HCC overlay is likely to be less than that of the acrylic adhesive used to bond the disks or plates. Also, bond problems resulting from the overlay mixture and placement are not identified ahead of time (Sprinkel, 2003b).

As shown in Figure 23.6, on larger jobs it may be practical to construct HCC overlay test patches with one or more overlay mixtures and different surface preparation procedures. Overlay mixtures and surface preparation procedures that give the desired results can be specified. Although days or weeks may be required for the overlay concrete to cure sufficiently to get tensile bond strength test results, any problems associated with the deck concrete, surface preparation, and placement and curing of the overlay can be identified ahead of time and appropriate adjustments made prior to placing the overlay. On very large jobs and where time permits, a full-width bridge deck section can be placed and tested with the concrete mixture and procedures that gave good results for the test patch.

When the acceptable cleaning and texturing practice has been determined, it is necessary to ensure that the practice is carried out over the entire deck surface. This is accomplished by determining the macro texture of the prepared surfaces upon which the acceptable bond tests were done (the macro



FIGURE 23.6 An overlay test patch is tested for bond strength.



FIGURE 23.7 Macrotexture depth measurement to ensure surface preparation (ASTM E 965).

texture is usually determined prior to construction of the test patches or test sections) and monitoring the macro texture of the prepared deck surface to ensure that the surface macro texture is the same or heavier than that on which the bond tests were performed (Sprinkel, 1997).

Two methods can be used to monitor the macro texture of the prepared deck surface (Sprinkel, 1997, 1998a). As shown in Figure 23.7, a quantitative macro texture result for the prepared surface can be determined by measuring the macro texture using the procedure specified in ASTM E 965 (ASTM, 1996). A qualitative indication of the macro texture of the prepared surface can be determined by using the International Concrete Repair Institute (ICRI) molded standards shown in Figure 23.8 (ICRI, 1997). The texture of the prepared surface is compared to the texture of the ICRI molded standard determined to best represent the prepared surface upon which acceptable bond tests were determined. A result for the macro texture measurement is based on the average of ten sand patch tests. Use of the ICRI nine molded standards requires less effort, but the owner and contractor must be able to agree on the qualitative assessment. Recent research indicates a strong correlation between laser surface macro texture measurements and the ASTM E 965 procedure (Stroup-Gardiner and Brown, 2000). Laser measurements to monitor surface preparation are a third option that will likely see greater use in the future.

Minimum macro texture values based on ASTM E 965 that have been specified in contracts include 0.06 in. and 0.08 in. (Sprinkel, 1997; Sprinkel and Ozyildirim, 1999b). Whereas 0.06 in. is often an acceptable minimum value, more or less cleaning may be required to obtain high bond strengths. Typically more cleaning and therefore texturing are necessary for old concrete surfaces than for new

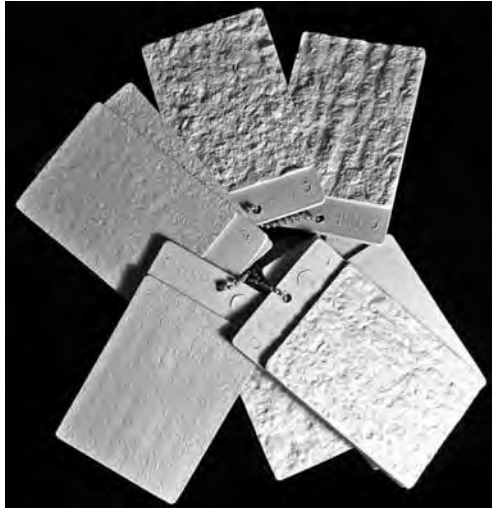


FIGURE 23.8 ICRI molded standards ensure proper surface preparation. (From ICRI, *Selecting and Specifying Concrete Surface Preparation for Sealers, Coatings, and Polymer Overlays*, Guideline No. 03732, International Concrete Repair Institute, Sterling, VA, 1997.)

ones. Also, the type and size of the aggregates in the deck can affect the optimum minimum texture value. For the same blasting effort, decks with lightweight aggregates will typically have a higher texture than decks with hard, dense aggregates because the aggregates abrade away in the lightweight decks and the mortar abrades away in the decks with hard aggregate. The minimum texture that provides good bond strength will depend on the materials in the deck, the condition of the deck, and the cleaning technique used.

As the surface is prepared, the screed is set to the proper elevation. A trial run of the screed is made with a spacer block attached to the bottom of the screed to ensure that proper cover between the screed and top reinforcement and the required minimum overlay thickness are obtained. After the screed is set and cleaning and texturing of the surface are complete, the prepared surface is wetted with potable water and covered with a polyethylene sheet to protect the prepared surface until the sheet is removed minutes prior to placing the overlay concrete. Any contamination of the prepared surface prior to placing the overlay must be removed, and dry surfaces should be rewetted so the surface is damp but has no standing water where the overlay concrete is being placed.

23.2.3.4 Overlay Concrete Is Properly Placed and Consolidated

Figure 23.9 shows the typical concrete placement procedure which is as follows:

- Deposit the overlay concrete onto the prepared surface.
- Broom mortar from the overlay concrete onto the prepared surface, and discard the excess coarse aggregate from the mortar.
- Consolidate and strike-off the concrete using a screed that vibrates.
- Finish the surface using a float that is typically attached to the back of the screed.

Some hand-finishing is typically required along the edges of the placement. Proper consolidation of the concrete at the bond interface is required for high bond strength. The vibrating pan on the front of a screed, vibrating rollers, and a vibrating strike-off bar can consolidate overlays <2.5 in. thick. The frequency of vibration can be adjusted, and care should be taken to ensure that the screed is providing adequate consolidation. Surface vibration decreases with the distance from the surface and typically fails to properly consolidate the concrete at depths greater than approximately 2.5 in. Internal vibrators are used to consolidate areas that are deeper than 2.5 in.



FIGURE 23.9 Screed strikes off and consolidates the overlay concrete.



FIGURE 23.10 Wet burlap is placed on the overlay surface as soon as possible to prevent plastic shrinkage cracks.

Some recent experience indicates that, with proper consolidation of the overlay at the bond interface, the use of brooms to apply mortar from the overlay or from separate containers does not contribute to bond strength; therefore, this step can be eliminated. Moreover, it is a step that, when done incorrectly, can cause lower bond strengths. Incorrect applications include the mortar drying before the overlay concrete is placed, retempering of a separate container of bonding mortar that results in a low strength layer of mortar, or placement of bonding mortar on a prepared surface that has a texture so heavy that a thin and uniform layer of bonding mortar cannot be placed.

23.2.3.5 Overlay Concrete Is Properly Cured

The overlay concrete must be properly cured to achieve high bond strengths. The bond strength cannot be higher than the strength of the overlay concrete, and the strength of the overlay concrete is a function of the quality and completeness of the curing. As can be seen in Figure 23.10, from the time the overlay concrete is deposited on the prepared surface until the curing materials are applied, water evaporates from the surface of the overlay concrete. The evaporation rate can be estimated using a nomograph that



FIGURE 23.11 Polyethylene sheeting covers wet burlap for the curing period.

takes as input data the air temperature, relative humidity, concrete temperature, and wind speed. When evaporation rates are high, the contractor can take steps to reduce the rate. Special precautions are typically followed when evaporation rates exceed $0.1 \text{ lb/ft}^2/\text{hr}$. These include fogging the air over the surface of the overlay to increase the relative humidity, batching the concrete at a lower temperature, and installing wind breaks to reduce the wind speed over the surface of the overlay.

Regardless of the evaporation rate, the wet burlap curing material should be placed on the finished concrete surface as soon as possible to stop further evaporation and to prevent plastic shrinkage cracking. As shown in Figure 23.11, polyethylene is placed on the wet burlap as soon as practical to help keep the burlap wet. Soaker hoses can be placed under the polyethylene to maintain the burlap in a wet condition during the curing period. The burlap should not be allowed to dry, as dry burlap can remove water from the overlay that is necessary for curing. LMC is typically moist cured for 2 days and other HCC overlays for 3 to 7 days. Longer curing periods are beneficial for the quality of the concrete but often not practical because of the need to accelerate construction and to open the overlay to traffic. LMC-VE overlays are cured for 3 hours or until opened to traffic.

23.2.3.6 Minimal Full-Depth Cracks

Plastic shrinkage cracks can occur when water evaporates from the overlay concrete because there is no water on the surface to protect the concrete from evaporation. These cracks are often fine and shallow but typically become wider, as shown in Figure 23.12, because of drying shrinkage. The cracks can penetrate the full thickness of the overlay either initially or at a later age because of drying shrinkage. Shrinkage of the overlay can stress the bond interface because the overlay is trying to shorten relative to the deck. These stresses are the highest around the perimeter of the overlay, along construction joints, and along full-depth cracks in the overlay. These stresses can cause delamination of the overlay, and the area of delamination can increase with time. Although cracks compromise the protection provided by the overlay, cracks that are full depth can increase the risk of delamination of the overlay along the cracks. The overlay concrete must also be properly cured to help prevent full-depth cracks.

23.2.3.7 Joints

To accommodate traffic, overlays are often constructed one lane at a time with traffic in the adjacent lane which results in longitudinal construction joints. These joints are like full-depth cracks in the overlay and should be avoided because they can cause premature delamination of the overlay. When possible, overlays should be placed over the entire width and length of the deck span and without any joints. Joints often control the time to repair or replace properly constructed overlays. Bridge decks with more than

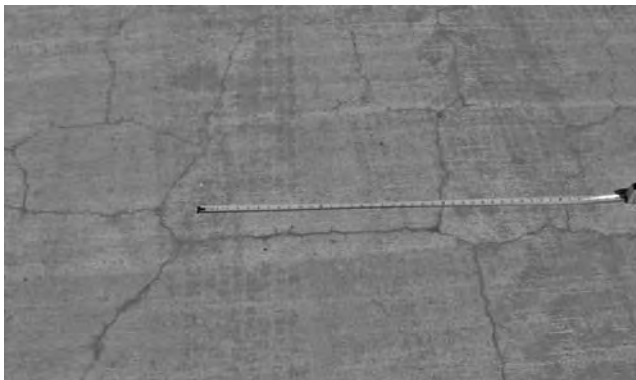


FIGURE 23.12 Shrinkage cracks are apparent in an overlay placed on a bridge deck.

one span may have expansion joints to allow for movement between the spans. The overlay should not be placed over the joints because the overlay will crack and delaminate along the joints. Joints must be constructed in the overlay directly above the joints in the deck. Typically, the joints in the overlay are similar to and replace the joints in the deck. In some situations, the construction of an overlay provides the opportunity to replace leaking joints with joints that will perform better. Either new joints or forms for new joints are placed directly above the joints in the deck, and the overlay concrete is placed against the joints or forms. When forms are used, they should be constructed with a compressible layer of material to minimize compression stresses in the overlay and shear stresses at the bond interface that may be caused by expansion of the adjacent deck spans. Also, the forms should be removed shortly after the concrete sets so the joint in the overlay can allow for movement between the adjacent deck spans (Sprinkel and Ozyildirim, 1999b). The open joint must be filled with a suitable joint material in accordance with recommended practice.

23.2.4 Overlay Thickness

Bonded concrete overlays for bridge decks are typically designed to have a nominal 1.5-in. thickness. The minimum thickness is 1.25 in., and the installed thickness typically ranges from 1.25 to 2 in. A mixture with No. 7 or No 8 coarse aggregate works well for these overlays. In situations in which the minimum thickness of the overlay is greater than 2 in., the typical overlay mixture should be redesigned to reduce shrinkage by increasing the maximum size of the coarse aggregate and if practical to reduce the cement materials content. The optimum concrete mixture has a maximum coarse aggregate size that is one third the minimum thickness; for example, No. 67 aggregate should be used in 2.25- to 3-in.-thick overlays, and No 57 aggregate should be used in 3- to 4-in.-thick overlays. Bonded concrete overlays are typically not designed to be thicker than 4 in., but thicker overlays are sometimes constructed to provide a suitable grade and profile for the surface. The thickness of an overlay is often varied over the deck surface to improve the drainage, surface profile or ride quality and to fill areas not patched prior to placing the overlay; however, the overlay is typically designed for the thinnest areas. When practical, the mixture should be changed to accommodate the thicker areas.

The thickness of an overlay is a factor in performance. Mortar rather than concrete is used for overlays that are thinner than 1.25 in. The mortar typically has higher shrinkage and therefore is more prone to cracking than concrete. The cracking can cause delamination of the overlay. Shrinkage of the overlay can stress the bond interface because the overlay is trying to shorten relative to the deck. The stress increases as the thickness of the overlay increases; therefore, overlays thicker than 2 in. are more prone to delamination. The stress can be reduced by changing the mixture to reduce shrinkage. Overlays have delaminated before being opened to traffic when a concrete mixture designed for a 1.5-in.-thick overlay was placed 4 in. thick. The optimum nominal thickness for a bonded concrete overlay is 1.5 in.

23.2.5 Overlay Surface Characteristics

Obtaining overlays with desirable surface characteristics, including good skid resistance, ride quality, drainage, and surface appearance, is typically not a problem. These factors are easily achieved with good design and construction practices. The overlay must be designed and the screed must be set to provide a final grade that provides for good ride quality and good drainage. The surface of the plastic concrete must be struck off and finished to the final grade shown on the plans. Good skid resistance is obtained by tining the plastic overlay concrete or by saw-cutting grooves into the hardened concrete surface. Tined valleys and saw-cut grooves are typically 1/8 in. wide, 1/8 in. deep and spaced 3/4 in. apart (VDOT, 2002).

23.2.6 Overlay Protection Characteristics

The protection provided by an overlay is a function of its thickness, permeability, diffusion constant, shrinkage, and cracks. Construction joints, like cracks, can affect the level of protection provided. The thicker the overlay, the greater the cover over the reinforcement and therefore the greater the protection provided. As mentioned earlier, however, overlays thicker than 2 in. are more likely to delaminate. Many HCC overlay mixtures can provide low permeability. Use of styrene–butadiene latex or supplemental cement materials, such as silica fume, fly ash, and slag, and good concreting practices easily provide for overlay concretes with a low permeability (<1000 C) (AASHTO, 1995b). Permeability values for typical overlays are shown in Table 23.3 (Sprinkel, 1988, 1998b, 2000; Sprinkel and Moen, 1999; Sprinkel and Ozyildirim, 1999b, 2000). The diffusion constant for the overlay concrete can be calculated using Fick's second law of diffusion. It provides an indication of the rate at which chloride moves through the overlay. The lower the constant, the longer it takes for chloride to penetrate the overlay. Concretes with a low permeability typically have a low diffusion constant.

Cracks compromise the protection provided by the overlay by allowing chlorides and water to bypass the low-permeability overlay concrete and travel directly to the reinforcement. Shrinkage can cause cracks in the overlay. The lower the shrinkage, the less prone the overlay is to cracking and delamination. Construction joints, like cracks, can allow for the penetration of chlorides. In addition to shrinkage, cracks can be caused by thermal contraction when overlay concrete is placed that has a much higher temperature than the deck. Cracks can be caused by cracks in the deck reflecting through the overlay, by superstructure creep and shrinkage when overlays are placed on newly constructed structures, and by traffic when the traffic loading causes tensile stress in the surface of the overlay. Most cracks in overlays originate as plastic shrinkage cracks and widen because of one or more of the other causes. Typically, a relatively crack-free overlay can be obtained when a low-shrinkage mixture is properly placed and protected from plastic shrinkage cracking.

Gravity-fill polymers can be placed in shrinkage cracks to help seal them. Products that have been successfully used include high-molecular-weight methacrylate, epoxy, and urethane (Sprinkel, 1992a, 1995). Typically the overlay surface is flooded with the monomer, and brooms are used to work the liquid into the cracks. Cracks that are not close enough to justify flooding the surface can be treated individually. Silane can also be used to seal cracks. The silane is easy to apply and makes the surface of the crack hydrophobic so it repels water. Although an overlay with sealed cracks cannot be expected to perform as well as an overlay with no cracks, application of the gravity-fill polymer or silane sealer is the only practical way to reduce the penetration of chlorides and water through the cracks.

Because the cracks will likely widen with age, it is best to wait as long as practical to seal them. The best time is a function of the shrinkage of the concrete and the use of the structure. Most of the shrinkage has occurred in approximately 3 months for a typical HCC overlay. The shrinkage may occur faster in the summer than in the winter. As much as approximately 25% additional shrinkage may occur after 3 months, so waiting 6 months to a year or more before sealing the cracks is desirable but often not practical. Another option is to seal the cracks once at an early age before opening the deck to traffic and again after 2 years after most shrinkage has occurred. Very early strength materials may be effectively sealed at an earlier age.

23.3 Other Issues

23.3.1 Rapid Construction of Overlays

In the past, most bridge decks and pavements were closed to traffic for the construction of an overlay. As traffic volumes have continued to increase, it has become difficult if not virtually impossible to close many structures for overlay construction. Overlays are typically placed one lane at a time with traffic in adjacent lanes. In the most heavily congested situations, lanes are only closed for short periods of time, such as weekends or nights, and short segments of overlay are placed during each lane closure. The sequence of construction steps for the construction of LMC-VE overlays follows:

Phase 1

- Close lane at 9 p.m.
- Mill deck surface.
- Patch deck.
- Cure patches.
- Open lane at 5 a.m.

Phase 2

- Close lane at 9 p.m.
- Shot blast surface.
- Wet surface.
- Place overlay.
- Cure overlay 3 hours.
- Open lane at 5 a.m.

Although this sequence has been used successfully, weekend lane closures are preferred for the construction of LMC-VE overlays and are required for the construction of SF and LMC-HE overlays (Sprinkel, 2006).

23.3.2 Cost

The cost of an overlay is a function of the cost of materials, surface preparation, labor, equipment, overhead, and traffic control. Cost data based on a review of bid tabulations obtained from the Virginia Department of Transportation bridge office for the period of 1994 and 1995 indicated the following average total costs per square yard for overlays: LMC and SF, \$130; LMC-HE, \$92; and LMC-VE, \$96 (Sprinkel, 1999). The rapid overlays cost less than the conventional overlay. Traffic control costs are high for conventional overlays because of the requirements for concrete barricades, removing and installing permanent and temporary pavement markings, and longer construction time. The rapid overlays are installed in a short time using cones for delineation and without the need to replace pavement markings, so the traffic control costs are less. The LMC-VE costs more than the LMC-HE because of the higher cost of the cement.

23.3.3 HCC Pavement Overlays

Bonded pavement overlays are similar to bonded bridge deck overlays, and the concrete mixtures and construction procedures are similar. One difference is that a slip-form concrete paving machine is used for pavement overlays and a bridge deck vibrating screed is used for bridge deck overlays. The slump of the overlay concrete used on pavements is typically 1 to 4 in., and the slump of the overlay concrete used on decks is typically 4 to 7 in. Overlays on decks can increase the stiffness of the deck, but the increase is typically not a significant factor in the performance of the deck. On the other hand, overlays are often placed on pavements to increase the stiffness of the pavement which should extend the life of the pavement. Deflections were reduced by 33 and 36%, respectively, after 2- and 4-in.-thick overlays were placed on 8-in.-thick continuously reinforced pavements in Virginia (Mokarem et al., 2007; Sprinkel and Ozyildirim, 1999a, 2000a). The increased stiffness has been maintained for 10 years, and it is anticipated that the overlays will perform well for 20 years or more.

23.3.4 Service Life of HCC Overlays

The service life of an overlay is usually controlled by a failure in the vicinity of the bond interface between the overlay and the deck or pavement surface. The service life of a well-bonded overlay is usually reduced by cracks and construction joints. Joints and full-depth cracks increase the probability of delamination of the overlay in the vicinity of joints and cracks. The delaminations often spread to other areas. Joints and cracks may control the time to repair of properly constructed overlays. Other common causes of failure are due to the overlay being placed on deck or pavement concrete that is deteriorating or on deck concrete that is salt contaminated and the reinforcement is corroding.

The service life of a well-bonded deck overlay with no full-depth cracks and joints placed on concrete in good condition should be controlled by the time it takes for the overlay to allow chlorides to reach the reinforcement in the deck and cause corrosion-induced spalling; however, many years are required for chlorides to penetrate the low-permeability overlays, and this type of failure is unlikely (Sprinkel, 2003a, 2004a). Also, loss of skid resistance or loss of ride quality rarely controls the life of a hydraulic cement concrete overlay. The exception is when ride quality is affected by the presence of spalling caused by low bond strength or corrosion or by reinforcement in situations where the reinforcement was corroding when the overlay was placed. It is reasonable to expect that the service life of overlays will increase with an increase in bond strength, with a decrease in the incidence of cracking and construction joints, with a decrease in permeability, and with a decrease in chloride at the level of the deck reinforcement.

The probability that long-lasting HCC overlays will be constructed increases with the use of low-shrinkage concrete mixtures; the use of good surface preparation procedures; proper consolidation of the overlay; placement of overlays when evaporation rates are low; good curing of the overlay; the construction of 1.25- to 2.0-in.-thick overlays; use of no construction joints; and the construction of overlays on bridges that are rigid and subject to low creep or pavements that have adequate stiffness, good drainage, and good base materials.

23.4 Summary

Properly constructed, HCC overlays can last 30 years or more. The six key issues for long-lasting overlays are contractor performance, material properties, bond strength, thickness, surface characteristics, and protection characteristics of the overlay. HCC overlay properties that support long-lasting overlays include adequate bond strength, low shrinkage, low permeability, and few cracks and construction joints. A sound and stable substrate and good surface preparation are required to obtain adequate bond strength. Quality mixture proportions that provide low shrinkage, low permeability, and few cracks are required to protect the deck from chlorides and moisture. Proper placement that includes adequate consolidation, strike off, and finishing is required to obtain good bond strength and low permeability. Good curing that minimizes cracking and premature loading is required for long-lasting protection of the deck. Other factors include construction of overlays with a thickness of 1.25 to 2 in. and using as few construction joints as possible. Finally, the contractor must construct an overlay that satisfies the requirements of a good specification.

References

- AASHTO. 1995a. *Guide Specifications for Polymer Concrete Bridge Deck Overlays*. American Association of State Highway and Transportation Officials, Washington, D.C.
- AASHTO. 1995b. *Standard Method of Test for Electrical Indication of Concrete's Ability to Resist Chloride Ion Penetration*, AASHTO T 277. American Association of State Highway and Transportation Officials, Washington, D.C.
- ACI Committee 503. 1993. *Use of Epoxy Compounds with Concrete*, ACI 503R. American Concrete Institute, Farmington Hills, MI.
- ASTM. 1996. *Standard Test Method for Measuring the Macrotexture Depth Using a Volumetric Technique*, ASTM E 965. American Society for Testing and Materials, West Conshohocken, PA.

- ASTM. 2004a. *Standard Test Method for Tensile Strength of Concrete Surfaces and the Bond Strength or Tensile Strength of Concrete Repair and Overlay Materials by Direct Tension (Pull-Off Method)*, ASTM C 1583. American Society for Testing and Materials, West Conshohocken, PA.
- ASTM. 2004b. *Standard Specification for Expansive Hydraulic Cement*, ASTM C 845. American Society for Testing and Materials, West Conshohocken, PA.
- ASTM. 2005. *Standard Test Method for Compressive Strength of Cylindrical Concrete Specimens*, ASTM C 39/C 39M. American Society for Testing and Materials, West Conshohocken, PA.
- ASTM. 2006. *Standard Test Method for Length Change of Hardened Hydraulic-Cement Mortar and Concrete*, ASTM C 157/C 157M. American Society for Testing and Materials, West Conshohocken, PA.
- ASTM. 2007. *Standard Specification for Concrete Aggregates*, ASTM C 33. American Society for Testing and Materials, West Conshohocken, PA.
- ASTM. 2008. *Standard Specification for Chemical Admixtures for Concrete*, ASTM C 494/C 494M. American Society for Testing and Materials, West Conshohocken, PA.
- ICRI. 1997. *Selecting and Specifying Concrete Surface Preparation for Sealers, Coatings, and Polymer Overlays*, Guideline No. 03732. International Concrete Repair Institute, Sterling, VA.
- Mokarem, D.W., Galal Khaled, A., and Sprinkel, M.M. 2007. *Performance Evaluation of Bonded Concrete Pavement Overlays after Eleven Years*. Transportation Research Board, Washington, D.C.
- NCHRP. 1995. *Waterproofing Membranes for Concrete Bridge Decks*, Synthesis 220, p. 69. National Cooperative Highway Research Program, Washington, D.C.
- Sprinkel, M.M. 1984. *Overview of Latex Modified Concrete Overlays*, VHTRC 85-R1. Virginia Transportation Research Council, Charlottesville.
- Sprinkel, M.M. 1988. *High Early Strength Latex Modified Concrete Overlay*, VTRC 88-R12. Virginia Transportation Research Council, Charlottesville.
- Sprinkel, M.M. 1992a. *Use of High Molecular Weight Methacrylate Monomers to Seal Cracks in Bridge Decks, Retard Alkali-Silica Aggregate Reactions and Prime Bridge Surfaces for Overlays*. Transportation Research Board, Washington, D.C.
- Sprinkel, M.M. 1992b. *Twenty-Year Performance of Latex-Modified Concrete Overlays*. Transportation Research Board, Washington, D.C.
- Sprinkel, M.M. 1995. *Gravity-Fill Polymer Crack Sealers*. Transportation Research Board, Washington, D.C.
- Sprinkel, M.M. 1997. Preparing bridge decks for overlays. *Concrete Repair Dig.*, 8(5), 242–247.
- Sprinkel, M.M. 1998a. Surface preparation for overlays. *Concrete Int.*, 20(5), 43–46.
- Sprinkel, M.M. 1998b. *Very Early Strength Latex-Modified Concrete Overlays*, VTRC 99-TAR3, Virginia Transportation Research Council, Charlottesville.
- Sprinkel, M.M. 1999. *Very-Early-Strength Latex-Modified Concrete Overlay*. Transportation Research Board, Washington, D.C.
- Sprinkel, M.M. 2000. *Evaluation of Latex-Modified and Silica Fume Concrete Overlays Placed on Six Bridges in Virginia*, VTRC 01-R3. Virginia Transportation Research Council, Charlottesville.
- Sprinkel, M.M. 2001. High-performance concrete overlays on Route 60 over Lynnhaven Inlet in Virginia. In *Proceedings of the PCI/FHWA International Symposium on High-Performance Concrete*, September 9–13, Orlando, FL.
- Sprinkel, M.M. 2003a. Deck protection systems for post-tensioned segmental concrete bridges. In *Abstracts and Summaries of 2003 Convention Presentations*, November 3–4, Dallas, TX. American Segmental Bridge Institute, Phoenix, AZ.
- Sprinkel, M.M. 2003b. High-performance concrete overlays for bridges. In *Proceedings of the PCI/FHWA International Symposium on High-Performance Concrete*, October 19–22, Orlando, FL.
- Sprinkel, M.M. 2004a. Deck protection systems for precast prestressed bridge deck panels. In *Proceedings of the PCI/FHWA International Symposium on High-Performance Concrete*, October 17–20, Atlanta, GA.
- Sprinkel, M.M. 2004b. *Performance Specification for High-Performance Concrete Overlays on Bridges*, VTRC 05-R2, Virginia Transportation Research Council, Charlottesville.

- Sprinkel, M.M. 2005. *Latex-Modified Concrete Overlay Containing Type K Cement*, VTRC 05-R26. Virginia Transportation Research Council, Charlottesville.
- Sprinkel, M.M. 2006. Very-early-strength latex-modified concrete bridge overlays research pays off. *TR News*, 247, 34–35.
- Sprinkel, M.M. and Moen, C.D. 1999. *Evaluation of Installation and Initial Condition of Latex-Modified and Silica Fume Concrete Overlays Placed on Six Bridges in Virginia*, VTRC 99-IR2. Virginia Transportation Research Council, Charlottesville.
- Sprinkel, M.M. and Ozyildirim, C. 1999a. *Evaluation of Installation and Initial Condition of Hydraulic Cement Concrete Overlays Placed on Three Pavements in Virginia*, VTRC 99-IR3. Virginia Transportation Research Council, Charlottesville.
- Sprinkel, M.M. and Ozyildirim, C. 1999b. *Evaluation of Installation and Initial Condition of High-Performance Concrete Overlays Placed on Route 60 over Lynnhaven Inlet in Virginia*, VTRC 99-IR4. Virginia Transportation Research Council, Charlottesville.
- Sprinkel, M.M. and Ozyildirim, C. 2000a. *Evaluation of Hydraulic Cement Concrete Overlays Placed on Three Pavements in Virginia*, VTRC 01-R2. Virginia Transportation Research Council, Charlottesville.
- Sprinkel, M.M. and Ozyildirim, C. 2000b. *Evaluation of High-Performance Concrete Overlays Placed on Route 60 Over Lynn Haven Inlet in Virginia*, VTRC 01-R1. Virginia Transportation Research Council, Charlottesville.
- Stroup-Gardiner, M. and Brown, E.R. 2000. *Segregation in Hot-Mix Asphalt Pavements*, NCHRP Report 441. National Cooperative Highway Research Program, Washington, D.C., p. 13.
- Tyson, S.S. and Sprinkel, M.M. 1975. *Two-Course Bonded Concrete Bridge Deck Construction*, Interim Report No. 1, VHTRC 76-R13. Virginia Transportation Research Council, Charlottesville.
- VDOT. 2001. *Special Provision for Epoxy Concrete Overlay*. Virginia Department of Transportation, Richmond.
- VDOT. 2002. *Road and Bridge Specifications*. Virginia Department of Transportation, Richmond.
- VDOT. 2006. *Electrical Indication of Concretes Ability to Resist Chloride Penetration*, VTM 112. Virginia Department of Transportation, Richmond.



Nabeaura Tower in Yokohoma, Japan, with precast ECC coupling beams in the building core for seismic resistance; the 41-story building was completed in 2007.

24

Engineered Cementitious Composite (ECC): Material, Structural, and Durability Performance

Victor C. Li, Ph.D., FASCE, FASME, FWIF*

24.1	Historical Development	24-1
24.2	General Characteristics	24-4
	The Family of ECC Materials • Tensile Characteristics • ECC Material Design Considerations • Compressive and Flexural Characteristics	
24.3	Mixture Proportioning, Material Processing, and Quality Control	24-8
24.4	Behavior of ECC Structural Elements	24-12
	Structural Response of R/ECC Elements • Insights from R/ECC Element Response	
24.5	Durability of ECC and ECC Structural Elements	24-24
	Material and Element Durability • ECC Durability under Various Environments • Durability of R/ECC • Long-Term Performance	
24.6	Concluding Remarks	24-37
	Acknowledgments	24-40
	References	24-40

24.1 Historical Development

The development of fiber-reinforced concrete material has undergone a number of phases. In the 1960s, research by Romualdi and coworkers (Romualdi and Batson, 1963; Romualdi and Mandel, 1964) demonstrated the effectiveness of short steel fibers in reducing the brittleness of concrete. This development has continued with expansion to a variety of other fibers, such as glass, carbon, synthetics, natural fibers, and, in recent years, hybrids that combine either different fiber types or fiber lengths. The continuously enhanced knowledge of fiber-reinforcement effectiveness has resulted in structural design recommendations by RILEM TC 162-TDF (Vandewalle et al., 2003). This document focuses on fiber-reinforced

* E. Benjamin Wylie Collegiate Chair Professor, Department of Civil and Environmental Engineering, University of Michigan, Ann Arbor; expert on high-performance fiber-reinforced cementitious composites, inventor of engineered cementitious composites.

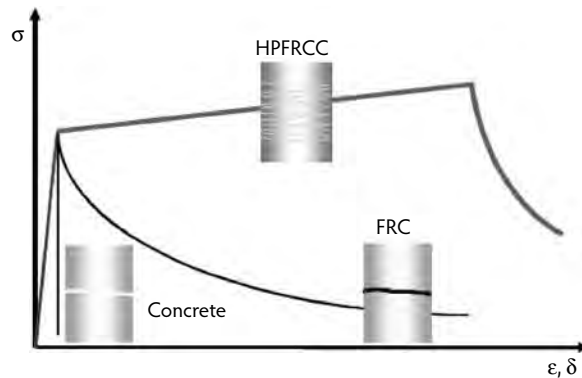


FIGURE 24.1 Uniaxial tensile stress–deformation relation of concrete, FRC, and HPFRCC. For FRC, deformation after a crack is formed is associated with crack opening δ . Tensile load capacity drops as a single crack enlarges during tension softening. For HPFRCC, deformation during the elastic and strain-hardening stages is properly described as straining. Tensile load capacity continues to rise during multiple microcracking and continued increase in strain. The strain capacity of HPFRCC is defined as the strain value at which peak tensile load is reached.

concrete (FRC) that possesses a tension-softening, quasi-brittle response (Figure 24.1). Apart from the gradual expanded use of the tension-softening branch of FRC in structural property enhancements, fibers in small quantities have been successfully used in controlling restrained drying shrinkage cracks. The subject of FRC is treated in detail in Chapter 22 of this book.

Beginning as early as the 1980s, interest in creating a fiber-reinforced concrete material with tensile ductility has been gaining ground. Within FRC, the toughness of the material is increased but no change in ductility is attained. Ductility is a measure of tensile deformation (strain) capacity typically associated with ductile steel, for example, but not with concrete material. Attempts to achieve tensile ductility in concrete material are exemplified by the early efforts of Aveston et al. (1971) and later Krenchel and Stang (1989), who demonstrated that, with continuous aligned fibers, high tensile ductility hundreds of times that of normal concrete can be attained. The modern-day version of continuous fiber reinforcement is represented by textile-reinforced concrete materials that may be prestressed (Curbach and Jesse, 1999; Reinhardt et al., 2003). Research on pultruded continuous fiber-reinforced concrete was pioneered by Mobasher et al. (2006). In parallel, research into the use of discontinuous fibers at high dosage (4 to 20%), such as in cement laminates (Allen, 1971) and in slurry-infiltrated fiber concrete (SIFCON) (Lankard, 1986; Naaman, 1992), has resulted in concrete composite materials that attain higher tensile strength than normal concrete and are not as brittle, but which have much less ductility than their continuous-fiber and textile-reinforced counterparts.

These materials may be considered a class of materials separate from FRC in that different degrees of tensile ductility are achieved, often accompanied by a strain-hardening response distinct from the tension-softening response of FRC. Naaman and Reinhardt (2003) classified such material as *high-performance fiber-reinforced cementitious composites* (HPFRCC) (Figure 24.1). It should be noted that most members of this class of material have a matrix that does not contain coarse aggregates and should therefore be regarded as fiber-reinforced cement pastes or mortars; however, in keeping with the broadened meaning used in the literature, we shall use the term *concrete material* in this chapter to include concrete, mortar, and cement paste.

Figure 24.1 illustrates the differences between the tensile response of normal concrete, FRC, and HPFRCC, such as obtained from a uniaxial tension test. This figure emphasizes the transition from brittle concrete to quasi-brittle FRC (tension softening) to ductile HPFRCC (strain hardening). Specifically, during tension softening, deformation is localized onto a single fracture plane, most appropriately described in terms of crack opening. During strain hardening, deformation is composed of the opening of multiple subparallel fine cracks and elastic stretching of the material between these cracks. Over a

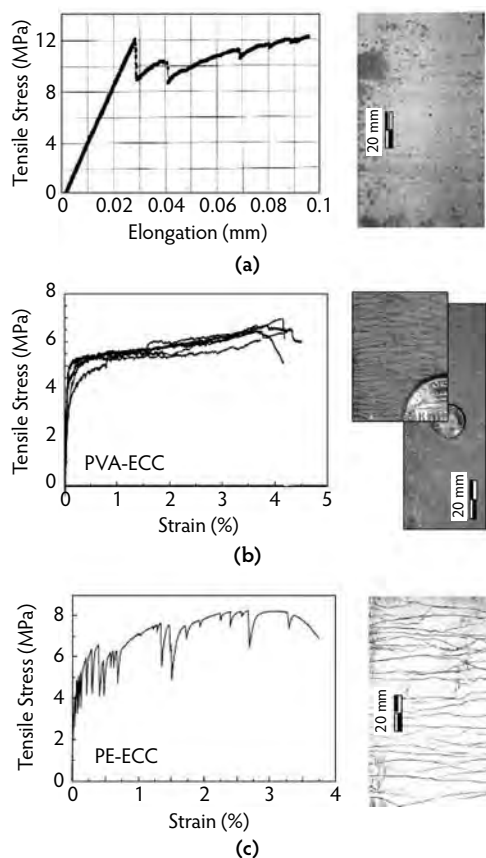


FIGURE 24.2 Two classes of HPFRCCs: (a) Tensile stress-elongation relationship for high-strength Ductal® based on prism specimen $70 \times 70 \times 160$ mm with 150-mm gauge length. (Adapted from Chanvillard, G. and Rigaud, S., in *Proceedings of High-Performance Fiber-Reinforced Cement Composites (HPFRCC 4)*, Naaman, A.E. and Reinhardt, H.W., Eds., RILEM, Paris, 2003, pp. 21–34.) (b, c) Tensile stress-strain relationship for ductile ECC, based on coupon specimen $76 \times 13 \times 305$ mm with 180-mm gauge length. (Adapted from Fischer, G. et al., in *Seventh International Symposium on Brittle Matrix Composites*, October 13–15, Warsaw, Poland, 2003, pp. 29–36; Li, V.C. and Wang, S., *ACI Mater. J.*, 99(1), 11–21, 2002.)

length scale that includes many such cracks, the deformation may be considered tensile strain smeared over a representative volume of material. As will be seen in the following sections, these distinctions between FRC and HPFRCC have significant ramifications in terms of load capacity and structural durability.

Whereas the HPFRCC materials mentioned above embody the highly desired tensile properties lacking in normal concrete or in FRC, until recently they have mostly been limited to academic research laboratories or specialized applications. This is due to additional demands in industrial projects, particularly in on-site construction, such as economical feasibility and constructability. These two demands are difficult to meet when either continuous fibers or high fiber content are used in the composites.

In recent years, two new classes of HPFRCC have emerged. Ductal® has a high tensile strength of 12 MPa and a ductility of 0.02 to 0.06% (Chanvillard and Rigaud, 2003). Engineered cementitious composite (ECC), originally developed at the University of Michigan, has a typical moderate tensile strength of 4 to 6 MPa and a higher ductility of 3 to 5% (Fischer et al., 2003; Li, 1993). The tensile stress-strain curves of these two types of HPFRCCs are illustrated in Figure 24.2. The development approach for these two classes of materials is quite different. For Ductal®, which can be traced back to the work of Bache (1981),

the approach is to employ a tightly packed dense matrix to increase both tensile and compressive strength of the material. Fiber is added to counteract the resulting high brittleness of the densified matrix. The dense matrix allows a strong bond with the fiber that results in a high post-cracking strength as long as a fiber with high strength is utilized. For ECC, the approach is to create synergistic interactions between the fiber, matrix, and interface to maximize the tensile ductility through development of closely spaced multiple microcracks while minimizing the fiber content (generally 2% or less by volume). This approach is detailed in Section 24.2.3. Ductal® is designed for use in the elastic stage, so the fiber action becomes effective only when the structural ultimate limit state (ULS) is approached. ECC is generally designed for use in the elastic and strain-hardening (inelastic) stages, so fiber action becomes effective even under normal service loads. The development of ECC is still evolving, even though a number of full-scale structural applications have already appeared in Japan, Europe, and the United States. This chapter summarizes some basic knowledge of ECC. In the following, the fundamental characteristics of ECC are described. This is followed by a section on structural behavior of steel-reinforced ECC elements (R/ECC) and a section on the durability behavior of ECC material and R/ECC.

The literature on ECC is rapidly expanding with contributions from academic research and industrial organizations around the world. Some good sources of references include recent workshop or conference proceedings on this subject, such as HPFRCC in Structural Applications (Fischer and Li, 2006), FraMCoS-6 (Carpinteri et al., 2007), and HPFRCC 5 (Reinhardt and Naaman, 2007). These documents contain a number of papers on ECC and related subjects. To assist in the transition to broader industrial use, the Japan Society of Civil Engineers has published a design guideline (JSCE, 2007; Rokugo et al., 2007), and the RILEM TC HFC technical committee will be publishing two state-of-the-art reports on this subject. To aid the reader in maneuvering this literature, some clarification on semantics will be helpful. The name *engineered cementitious composite* (ECC) was adopted by the original developers (Li, 1993) to emphasize the micromechanics basis behind the design of this material. Micromechanics serves as a powerful tool to guide materials design for targeted composite properties and enables meaningful linkage between materials engineering and structure performance design (Li, 2007). In 2006, the RILEM TC HFC technical committee decided to emphasize the unique tensile strain-hardening response of this material (Figure 24.1) as a constitutive law for structural engineering design and gave the more descriptive name *strain-hardening cementitious composite* (SHCC) to this class of materials. The Japan Society of Civil Engineers, however, prefers to emphasize the multiple fine cracking (and associated durability; see Section 24.5), thus they refer to the material as *multiple fine cracking fiber-reinforced cementitious composite*. In essence, all of these materials are designed using micromechanical tools and represent identical material technology.

24.2 General Characteristics

24.2.1 The Family of ECC Materials

Engineered cementitious composite can be regarded as a family of materials with a range of tensile strengths and ductilities that can be adjusted depending on the demands of a particular structure. ECC also represents a family of materials with different functionalities in addition to the common characteristics of high tensile ductility and fine multiple cracking. Self-consolidating ECC (e.g., ECC M45 and its variants) is designed for large-scale, on-site construction applications (Kong et al., 2003; Lepech and Li, 2007). High-early-strength ECC (HES-ECC) is designed for applications that require rapid strength gain, such as transportation infrastructure that must be quickly reopened to the motorist public (Wang and Li, 2006a). Lightweight ECC (LW-ECC) is designed for applications where the dead load of structural members must be minimized (Wang and Li, 2003). Green ECC (G-ECC) is designed to maximize material greenness and infrastructure sustainability (Lepech et al., 2007; Li et al., 2004b). Self-healing ECC (SH-ECC) emphasizes the functionality of recovering transport and mechanical properties after experiencing damage (Li and Yang, 2007; Yang et al., 2005).

TABLE 24.1 Major Physical Properties of ECC

Compressive Strength (MPa)	First Crack Strength (MPa)	Ultimate Tensile Strength (MPa)	Ultimate Tensile Strain (%)	Young's Modulus (GPa)	Flexural Strength (MPa)	Density (g/cc)
20–95	3–7	4–12	1–8	18–34	10–30	0.95–2.3

Engineered cementitious composite using local material ingredients has been successfully produced in various countries, including Japan (Kanda et al., 2006a,b), Europe (Mechtcherine and Schulze, 2006), and South Africa (Boshoff and van Zijl, 2007), in addition to the United States. To successfully develop local versions of ECC, a good understanding of the underlying design approach is helpful (Kanda and Li, 1999; Li, 1993). A synopsis of the ECC design approach is given in Section 24.2.3.

A summary of major physical properties of ECC is given in Table 24.1. It should be emphasized that ECC properties can be tailored by the use of micromechanics tools. Even broader ranges of properties beyond those in this table can be expected in the future as the need arises. The very high strength and modulus version was attained by Kamal et al. (2007). The very high tensile ductility version was reported in Li et al. (1996). The super lightweight version was described in Wang and Li (2003). The common characteristic of these ECC materials is that they have tensile ductility orders of magnitude higher than those in typical concrete or FRC materials.

It should be noted that, although a large body of literature has developed around ECC based on polyvinyl alcohol fiber, commonly referred to as PVA-ECC, other fibers have been successfully utilized. These include high-modulus polyethylene (PE) fibers (Kamal et al., 2007; Li, 1993; Li and Wang, 2002) and polypropylene (PP) fibers (Takashima et al., 2003; Yang and Li, 2008). The principle behind the design of ECC, as discussed in Section 24.2.3, does not depend on a particular fiber. Fibers with certain properties, however, may meet the criteria for tensile strain hardening at a lower volume fraction. Decisions on what fibers to use will depend on their natural characteristics, including mechanical characteristics, diameter ranges, and surface characteristics; on the resulting ECC mechanical, durability, and sustainability performance; and on economics.

24.2.2 Tensile Characteristics

As indicated earlier, the most important characteristic of ECC is the high tensile ductility represented by a uniaxial tensile stress–strain curve with strain capacity as high as 5% (Figure 24.2b,c and Figure 24.3). This metal-like behavior shows a characteristic *yield point* at the end of the elastic stage when the first

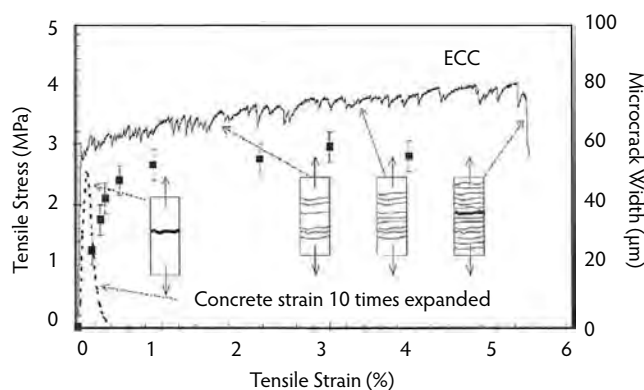


FIGURE 24.3 A tensile stress–strain curve of an ECC, showing also the crack width development (square symbols) as a function of imposed tensile strain.

microcrack appears on the specimen. Subsequent increase in load results in a strain-hardening response—that is, a rise in tensile deformation (volumetric straining in the form of multiple microcracking as opposed to localized crack opening) accompanied by a rise in load. Final failure of the specimen occurs when one of the multiple cracks forms a fracture plane. Beyond this peak load, ECC is no different than normal FRC, showing a tension-softening response. The high tensile ductility is of great value in enhancing the structural ultimate limit state (ULS) in terms of structural load and deformation capacity as well as energy absorption. In this manner, ECC can offer structural safety improvements. This contribution of ECC to structural response enhancement is discussed further in Section 24.4.

The formation of multiple microcracking is necessary to achieve high composite tensile ductility. Between first cracking strain (about 0.01%) and 1% strain, the microcrack opening increases from 0 to about 60 μm . Further loading beyond 1% causes more multiple cracks to form, but with no additional crack opening beyond the steady-state value of 60 μm (Figure 24.3). Governed by the mechanics of the fiber–matrix interaction within ECC, this unique characteristic is critically important for durability (see Section 24.5) of both material and structure. Unlike concrete or FRC, the steady-state crack width is an intrinsic material property, independent of loading (tension, bending, or shear), structure size and geometry, and steel reinforcement type and amount. This observation has important implications in service life, maximum member size, economics, and architectural aesthetics. In short, where steel reinforcement is used to control crack width in concrete, such steel reinforcement can be completely eliminated in ECC. By suppressing cracks with large crack width even in the presence of large imposed structural deformations, ECC can offer structural durability improvements in addition to watertightness and other serviceability enhancements. Although Figure 24.3 shows a particular example of ECC with steady-state crack width at 60 μm , even tighter crack widths, as low as 20 μm , have been achieved (Yang et al., 2007).

24.2.3 ECC Material Design Considerations

To attain high tensile ductility and tight microcrack width while keeping the fiber content low (2% or less by volume), ECC has been optimized through the use of micromechanics (Li, 1993; Li and Leung, 1992). Micromechanics is a branch of mechanics applied at the material constituent level that captures the mechanical interactions among the fiber, mortar matrix, and fiber–matrix interface. Typically, fibers are of the order of millimeters in length and tens of microns in diameter, and they may have a surface coating on the nanometer scale. Matrix heterogeneities in ECC, including defects, sand particles, cement grains, and mineral admixture particles, have size ranges from nano- to millimeter scale. Ideally, the micromechanics model should capture all of the deformation mechanisms at the millimeter, micrometer, and nanometer scales; however, simplifying assumptions have been made to make the model equations tractable, and the resulting conditions (in closed-form solution) for strain hardening can be used as guidelines for material component tailoring. These conditions are expressed in strength and energy terms, as shown in Equation 24.1:

Strength criterion

$$\sigma_0 \geq \sigma_{cs} \quad (24.1a)$$

Energy criterion

$$J'_b \equiv \sigma_0 \delta_0 - \int_0^{\delta_0} \sigma(\delta) d\delta \geq J_{tip} \approx \frac{K_m^2}{E_m} \quad (24.1b)$$

where σ_{cs} and σ_0 are the cracking strength and maximum fiber bridging capacity on each potential crack plane; δ_0 is the crack opening corresponding to σ_0 in the fiber bridging relationship $\sigma(\delta)$, which goes through a maximum; J_{tip} and J'_b are the crack tip matrix toughness and the complementary energy of the fiber bridging relation, respectively; and K_m and E_m are the matrix fracture toughness and Young's modulus, respectively. For derivation of Equation 24.1, see Li (1993). Physically, the strength criterion (Equation

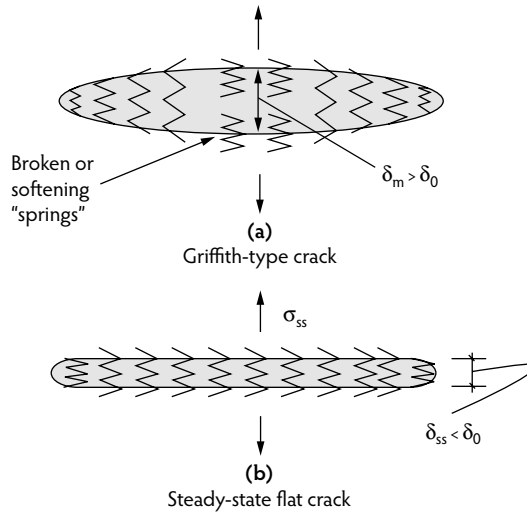


FIGURE 24.4 Illustration of the energy criterion for multiple cracking: (a) When Equation 24.1b is not satisfied, the common Griffith-type crack propagation results. Crack opening at the middle δ_m will exceed δ_0 , causing spring failure and subsequent tension softening. (b) When Equation 24.1b is satisfied, the steady-state flat crack propagation mode prevails, with δ_{ss} staying below δ_0 .

24.1a) ensures the initiation of microcracks from initial flaw sites in the composite before the tensile load exceeds the maximum fiber bridging capacity. The left-hand side of Equation 24.1a can be thought of as the maximum tensile load carried by a line of springs with tensile strength determined by the bridging fibers. Failure of the fiber springs is associated with fiber rupture, slippage, or pullout. Ensuring that the maximum fiber bridging capacities on existing crack planes remain higher than the matrix cracking strength of potential new crack planes allows additional cracks to form; otherwise, saturated multiple cracking would not be attained, and sparsely spaced cracks will result, limiting the tensile ductility.

The energy criterion (Equation 24.1b) prescribes the mode of crack propagation once initiated. The normal form of Griffith cracking is not favorable to multiple cracking. This is because the crack opening in Griffith-type cracks, especially at the midpoint of the crack line (δ_m), always increases with the length of the crack, and failure of the bridging fiber invariably results, either in the form of fiber pullout or breakage beginning at this widest point when δ_m exceeds δ_0 . The only means of preventing this is by altering the Griffith crack propagation mode to a flat crack propagation mode whereby the crack extends while the crack opening remains constant at any location (apart from a small bridging zone near the crack tip) regardless of the length of the crack. In this manner, δ_m stays below δ_0 along the entire crack line. During flat crack propagation, energy is exchanged between work input (from applied loading) and energy absorbed by the fiber bridging process in the opening of the crack near the crack tip (and only near the crack tip), as well as matrix material breakdown at the crack tip. The enforcement of energy balance results in Equation 24.1b. Violation of Equation 24.1b results in fracture localization, as in the case of FRC, and terminates the multiple cracking process. The energy criterion is illustrated in Figure 24.4.

It should be noted that both parts of Equation 24.1 have been arranged so the left-hand sides of the inequality sign contain terms that pertain to fiber and interface properties, while the right-hand sides contain terms that pertain to matrix properties, all of which are measurable physical properties. This observation emphasizes the usefulness of Equation 24.1 to aid in the fiber, matrix, and interface selection or tailoring process to arrive at viable compositions of ECCs. As an example, this approach has been adopted for tailoring of the surface coating on PVA fibers (Li et al., 2002) and for the deliberate introduction of matrix defects in lightweight ECC (Wang and Li, 2003) and high-early-strength ECC (Wang and Li, 2006a). The equality signs in Equation 24.1 are based on the assumption that initial defect size and fiber volume fraction are uniform throughout the composite. In reality, variability of these

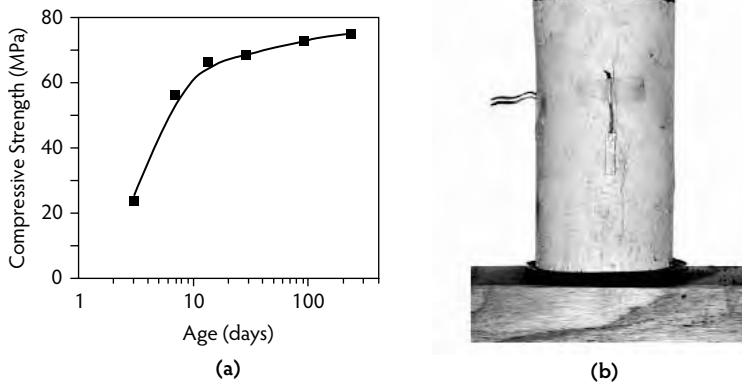


FIGURE 24.5 (a) Compressive strength development of ECC (M45), and (b) ECC specimen after compressive strength test. (From Wang, S. and Li, V.C., in *Proceedings, High-Performance Fiber-Reinforced Cementitious Composites (HPFRCC) in Structural Applications*, Fischer, G. and Li, V.C., Eds., RILEM, Paris, 2006, pp. 65–73.)

parameters must exist and depends on the mix composition as well as mixing procedure. This variability creates the need for a wider margin between the left- and right-hand sides of Equation 24.1 and explains the use of the inequality signs. Kanda and Li (2006) specifically studied the necessary margin to create robust tensile properties.

24.2.4 Compressive and Flexural Characteristics

The compressive properties of ECC are not significantly different from normal- to high-strength concrete. Compressive strengths of ECC range from 20 to 95 MPa. The elastic modulus of 15 to 34 GPa is typically lower than that for concrete due to the absence of coarse aggregates. The compressive strain capacity of ECC is slightly higher, around 0.45 to 0.65%. Figure 24.5a shows a strength development curve for an ECC (M45) compressive cylinder. The post-peak behavior of ECC under compression tends to descend more gently than high-strength concrete, accompanied by a gradual bulging of the specimen (Figure 24.5b) rather than explosive crushing failure. The flexural response of ECC reflects its tensile ductility (Kunieda and Rokugo, 2006a; Maalej and Li, 1994; Wang, 2005; Wang and Li, 2006). Under bending, multiple microcracking forms at the base of the beam, allowing it to undergo a large curvature development, a phenomenon that has resulted in the popular name of *bendable concrete*. A flexural strength (modulus of rupture, or MOR) of 10 to 15 MPa is easily achievable and is accompanied by a significant deflection-hardening regime (Figure 24.6a). Deflection hardening is an intrinsic property of ECC that does not depend on geometry. This is not the case for tension-softening FRC, for which deflection hardening becomes more difficult to attain as beam height increases (Stang and Li, 2004). A highly deformed ECC beam and fine multiple cracking on the tensile side of the beam are shown in Figure 24.6b,c (Wang, 2005; Wang and Li, 2006b). Engineered cementitious composite has significant improvements in fatigue response over normal concrete and FRC. Suthiwarapirak et al. (2002) conducted flexural fatigue tests on ECC and demonstrated higher ductility and fatigue life compared with polymer cement mortars commonly used in repair applications.

24.3 Mixture Proportioning, Material Processing, and Quality Control

Table 24.2 gives a typical mix design for ECC (ECC-M45) with self-consolidating casting properties. All proportions are given with materials in the dry state. The ingredients and mix proportions have been optimized to satisfy the multiple cracking criteria (Equation 24.1). Specifically, the type, size, and amount of fiber and matrix ingredients, along with interface characteristics, are tailored for multiple cracking

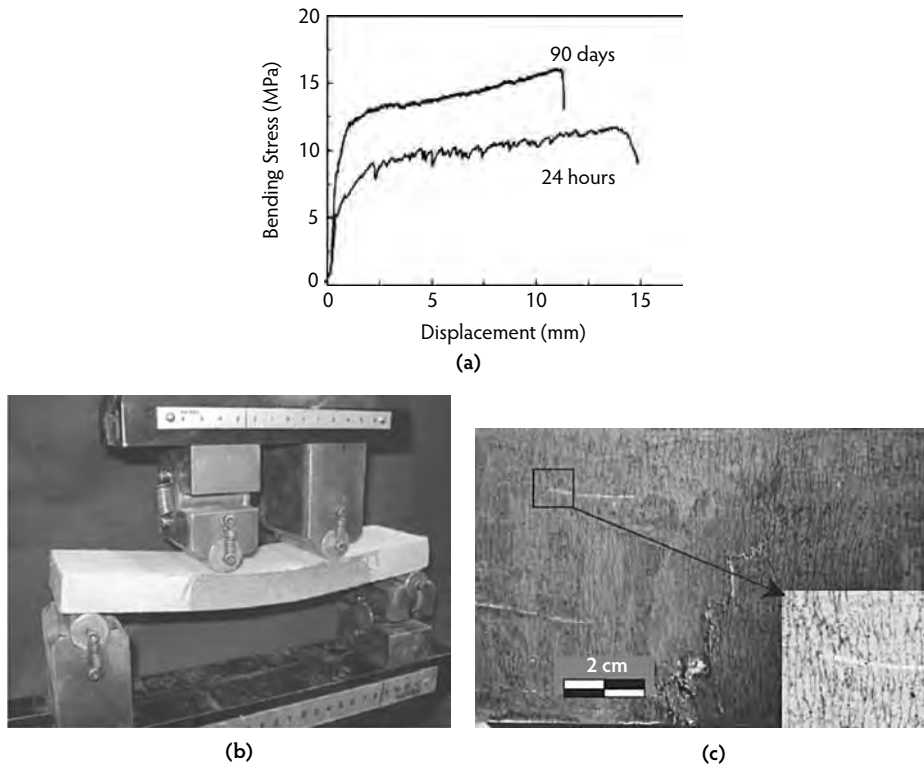


FIGURE 24.6 (a) Flexural load–deflection curve of an ECC, (b) ECC flexural specimen showing large deflection, and (c) fine multiple cracking on the tensile side of beam 304 mm (length) \times 76.2 mm (width) \times 25.4 mm (depth). (Adapted from Wang, S. and Li, V.C., in *Proceedings, High-Performance Fiber-Reinforced Cementitious Composites (HPRCC) in Structural Applications*, Fischer, G. and Li, V.C., Eds., RILEM, Paris, 2006, pp. 65–73.)

and controlled crack width. ECC incorporates fine silica sand with a sand/binder ratio (S/B) of 0.36 to maintain adequate stiffness and volume stability. ECC-M45 has a water/binder (w/b) ratio of 0.26 to attain a good balance of fresh and hardened properties. The binder system is defined as the total amount of cementitious material (i.e., cement and fly ash, Type F) in ECC. The silica sand has a maximum grain size of 250 μm and a mean size of 110 μm . The aggregated particle size of all matrix components should be properly graded to achieve self-consolidating fresh properties (Fischer et al., 2003).

Various fiber types have been used in the production of ECC, but ECC-M45, which currently has the largest experimental dataset, uses polyvinyl alcohol (PVA) fiber 12 mm in length and 39 μm in diameter. The nominal tensile strength, stiffness, and density of the fiber are 1600 MPa, 40 GPa, and 1300 kg/m^3 , respectively. The PVA fiber is surface coated by a proprietary oiling agent (1.2% by weight) to reduce the fiber–matrix interfacial bonding. To account for material heterogeneity, a fiber content of 2% by volume, which is greater than the calculated critical fiber content required to achieve strain hardening, is typically used in the mix design. The mix design described above has been experimentally demonstrated in a broad range of investigations to consistently produce good ECC fresh and hardened properties. A high-range

TABLE 24.2 Engineered Cementitious Composite Mix Design Proportions by Weight for ECC-M45

Mix Designation	Cement	Fly Ash	Sand	Water	High-Range Water Reducer (HRWR)	Fiber (Vol. %)
M45	1.0	1.2	0.8	0.56	0.012	0.02

TABLE 24.3 Material Charging Sequence into Ready-Mix Trucks

Activity No.	Activity	Elapsed Time (min)
1	Charge all sand.	2
2	Charge approximately 90–95% of mixing water, all HRWR, all hydration stabilizer.	2
3	Charge all fly ash.	2
4	Charge all cement.	2
5	Charge remaining mixing water to wash drum fins.	4
6	Mix at high RPM for 5 minutes or until material is homogenous.	5
7	Charge fibers.	2
8	Mix at high RPM for 5 minutes or until material is homogenous.	5
<i>Total</i>		24

water-reducing (HRWR) admixture containing a polycarboxylate chemical composition has been found to be most effective in maintaining the desired fresh property during mixing and placing. Adaptations of this reference mix have been used in various construction projects. Full-scale production of ECC was carried out in Japan (Kunieda and Rokugo, 2006b) and in the United States (Lepech and Li, 2007). Experience in concrete ready-mix plants suggests the charging sequence of raw material shown in Table 24.3.

The properly mixed ECC material should have a creamy texture, as shown in Figure 24.7. To ensure good self-consolidation behavior, the deformability of ECC in the fresh state should be checked at the construction site. To perform this check, a standard concrete slump cone is filled with fresh ECC material and emptied onto a level Plexiglas® or glass plate. The flowable ECC material flattens into a large pancake-shaped mass (Figure 24.8a). Two orthogonal diameters of this “pancake” are measured, and a characteristic deformability factor, denoted by Γ , is calculated:

$$\Gamma = \frac{(D_1 - D_0)}{D_0} \quad (24.2)$$

where D_1 is the average of two orthogonal diameter measurements after slump cone removal, and D_0 is the diameter of the bottom of the slump cone. For good self-consolidation, Γ should have a minimum value of 2.75 (Lepech and Li, 2007). Excessively large values of Γ , however, may indicate improper mix proportions, may potentially result in component segregation, and must be avoided. Typically, the



FIGURE 24.7 Creamy texture appearance of fresh ECC in mixing drum of a ready-mix truck. (From Lepech, M.D. and Li, V.C., *ACI Mater. J.*, 2008.)



(a)



(b)

FIGURE 24.8 (a) Slump cone test of ECC flowability; (b) Marsh cone flow rate test.

deformability value decreases over time during mixing and transport in the ready-mix concrete truck. The use of a hydration stabilizer has been found effective in maintaining good deformability without negatively affecting the hardened properties. To minimize the danger of early-age cracking, wet curing for a minimum of 7 days and nighttime casting of field applications are recommended for ECC when the air temperature is above 50°F.

Care must be taken to ensure good fiber dispersion in the mix. Yang et al. (2007) found that an effective means of controlling fiber dispersion is to ensure good mortar viscosity via a Marsh flow cone test. In the Marsh cone flow test, the funnel is filled completely with mortar (ECC mortar without fibers), and the bottom outlet is then opened, allowing the mortar to flow (Figure 24.8b). The Marsh cone flow time of mortar is the elapsed time in seconds between the opening of the bottom outlet and the time when light becomes visible at the bottom, when observed from the top.

In addition to the standard compression cylinder test typically applied to concrete quality control on job sites, the tensile coupon test should also be carried out to ensure that the tensile properties specified in design documents are met. These compression and tensile tests should be conducted at the ages of 4

days, 7 days, 14 days, and 28 days to observe property development over time. It is recognized that uniaxial tension tests are difficult to carry out on a routine quality control basis. As a result, a simpler bending test accompanied by inversion schemes to obtain material tensile properties is being developed (Kanakubo, 2006; Qian and Li, 2007).

Apart from ready-mix and self-consolidating casting, special versions of ECC have also been developed for extrusion (Stang and Li, 1999) and shotcreting (Kanda et al., 2001; Kim et al., 2003; Kojima et al., 2004). Precasting of ECC structural elements has been utilized for coupling beams in high-rise buildings in Japan (Kanda et al., 2006a,b). Kanda et al. concluded that full-scale production in a precast plant of ECC with high mechanical performance and excellent fluidity is achievable in practice. Figure 24.9 shows the various methods of ECC material processing. Although these ECC materials all carry the same hardened material characteristics described in Section 24.2, they exhibit significantly different fresh properties to meet different processing requirements. The relatively small amount of fibers used in ECC allows such versatility in processing methods.

24.4 Behavior of ECC Structural Elements

A variety of experiment programs have been performed to assess the performance of ECC at the structural element level for both seismic and non-seismic structural applications (Table 24.4). These experiments provide insight into how unique ECC material properties elevate the response performance of the structure. Within this section, we describe some observed responses of elements subjected to monotonic and fatigue flexural loading, cyclic shear loading, and steel–ECC interactions. Fundamental knowledge will then be drawn from these studies.

24.4.1 Structural Response of R/ECC Elements

24.4.1.1 Flexural Elements

Fischer and Li (2002a) studied the behavior of R/ECC flexural elements under reversed cyclic loading. The test setup is shown in Figure 24.10, and the specimen configuration is shown in Figure 24.11. A regular reinforced-concrete (R/C) beam was also tested as control. Figure 24.12 shows the substantial difference in hysteretic response for the R/ECC and the R/C control column specimens. A significantly fuller hysteretic loop with larger energy dissipation was achieved by the R/ECC beam despite the fact that no shear stirrups were used at the base of the flexural element. The damage experienced by these elements at 10% interstory drift is compared in Figure 24.13. Even at this high drift level, no spalling of the ECC was observed. In contrast, the R/C column lost all concrete cover near the fixed end subsequent to bond splitting and spalling. Clearly, the R/ECC element demonstrated significant damage tolerance under severe loading.

The high cycle fatigue response of R/ECC flexural elements was studied by Kim et al. (2004) in conjunction with a bridge deck link slab application. The full-thickness slab test configuration is provided in Figure 24.14, which shows the steel girder (anchored to the slab by steel studs) on top for convenience of testing. Over 100,000 cycles, no degradation in stiffness was observed in the R/ECC or in the R/C control beam; however, the cracks in the R/C beam grew continuously to 0.6 mm at the end of the test, while the microcracks in R/ECC beam remained at approximately 50 μm (Figure 24.15).

Motivated by the need to increase the stiffness and to reduce the tendency for fatigue cracking in steel bridge decks, a steel/ECC composite beam was studied by Walter et al. (2004) under monotonic flexural loading (Figure 24.16). For control, a steel/FRC and a steel/FRD composite beam were also tested in the same configuration. FRD is a fiber-reinforced Densit® material, a very high strength and dense concrete reinforced with steel fibers similar to Ductal®. All concrete materials were cast onto the steel plate and bonded only by adhesion to the roughened steel surface. The load-deflection response captured in Figure 24.17 demonstrates a much higher load capacity in the case of the steel/ECC beam, which showed multiple microcracking during testing, suppressing the formation of a brittle fracture that limits the capacity of the steel/concrete beam. The single fracture in the FRC and FRD beams led to their immediate debonding from the steel plate.



(a)



(b)



(c)



(d)

FIGURE 24.9 Various processing methods of ECC: (a) self-consolidating casting, (b) extrusion, (c) spraying, (d) precast mixing (photograph courtesy of S. Staniski) and precasted element.

TABLE 24.4 A Summary of Various R/ECC Structural Elements Previously Studied

Structural Element Type	Type of Loading (Type of Reinforcement) ^a	Refs.
Flexural elements	Reversed cyclic Monotonic (GFRP) Reversed cyclic (CFRP) Fatigue	Fischer and Li (2002a) Li and Wang (2002) Fischer and Li (2003a) Kim et al. (2004)
Column elements	Reversed cyclic	Fukuyama et al. (2000)
Shear beam elements	Reversed cyclic Reversed cyclic Monotonic Monotonic	Kanda et al. (1998) Fukuyama et al. (2000) Shimizu et al. (2006) Kabele and Kanakubo (2007)
Beam–column connections	Reversed cyclic	Parra-Montesinos and Wight (2000)
Wall elements	Repeated shear Reversed cyclic Reversed cyclic	Kanda et al. (1998) Kesner and Billington (2005) Fukuyama et al. (2006)
Frames	Reversed cyclic (steel and CFRP)	Fischer and Li (2003b)
Steel/ECC interactions	Monotonic flexure (plate/ECC) Monotonic shear (stud/ECC) Monotonic tension (anchor/ECC)	Walter et al. (2004) Qian and Li (2006) Leung et al. (2006); Qian (2007)

^a Steel reinforcement unless specified.

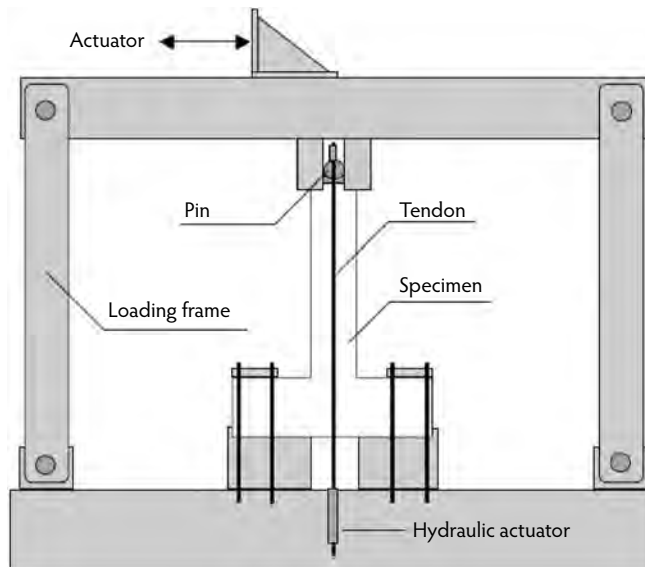


FIGURE 24.10 Test setup for full reversed loading of flexural elements. (From Fischer, G. and Li, V.C., *ACI Struct. J.*, 99(6), 781–790, 2002.)

24.4.1.2 Shear Element

Fukuyama et al. (2000) studied the behavior of R/ECC shear elements under reversed cyclic loading. The specimen configuration is shown in Figure 24.18, and the hysteretic loops for R/ECC and R/C are shown in Figure 24.19. Again, the hysteretic loops for R/ECC showed much greater stability and ability to dissipate energy. The R/C specimen suffered extensive bond splitting and loss of cover, accompanied by large diagonal cracks. In contrast, the damage experienced by the R/ECC shear element was significantly lower (Figure 24.20). No bond splitting or cover loss was observed, and microcracks continued to carry

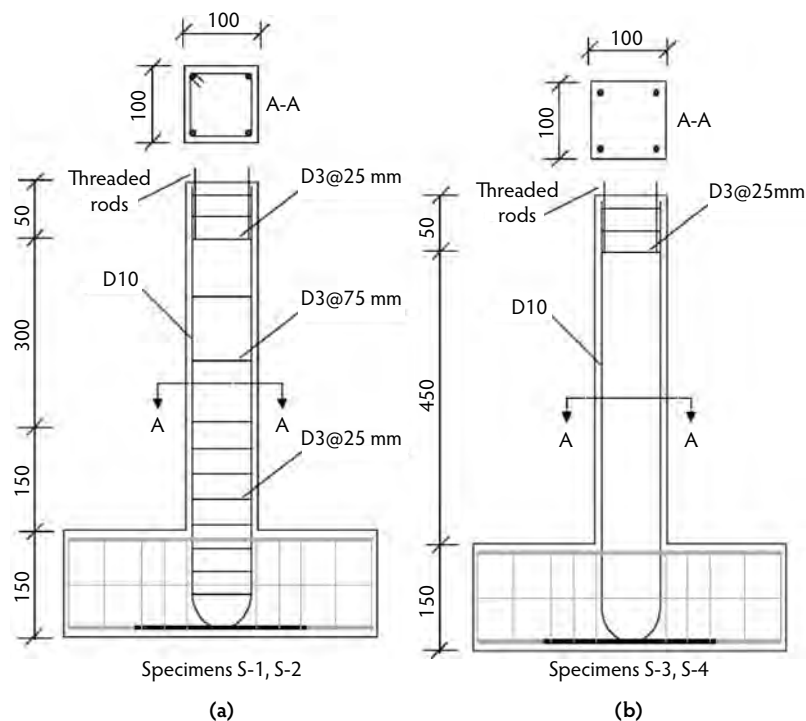


FIGURE 24.11 Specimen configurations of flexural elements: (a) R/C; (b) R/ECC with no stirrups in shear zone. (From Fischer, G. and Li, V.C., *ACI Struct. J.*, 99(6), 781–790, 2002.)

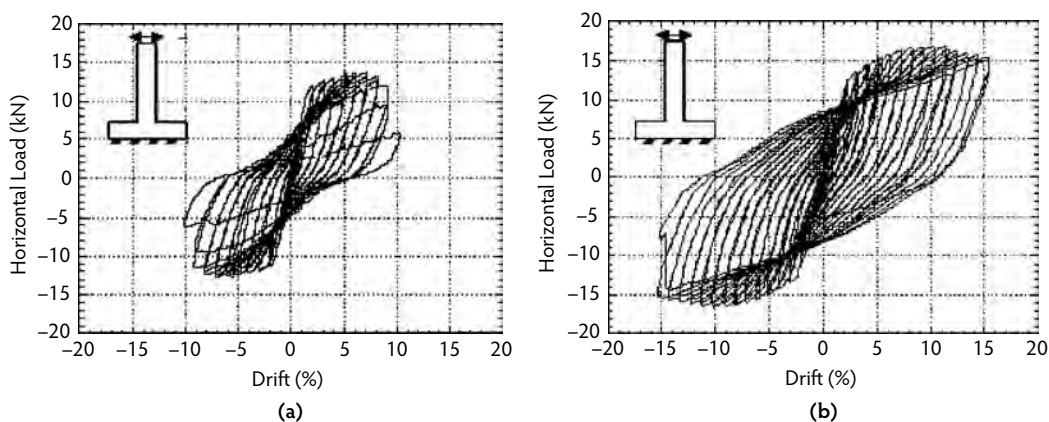


FIGURE 24.12 Hysteretic behavior of flexural members under fully reversed cyclic loading for (a) R/C with stirrups, and (b) R/ECC without stirrups. (From Fischer, G. and Li, V.C., *ACI Struct. J.*, 99(6), 781–790, 2002.)

loads up to a 5% rad deflection angle. The shear capacity of a R/ECC beam can be estimated from a linear superposition of the contributions of the ECC material and the shear and axial steel reinforcements due to the compatible deformation of the two materials even after steel yields. This approach was suggested to be reasonably accurate and conservative (Rokugo et al., 2007); however, numerical analysis combined with experimental data (Kabele and Kanakubo, 2007) suggested that only a fraction of the tensile strength and strain capacity of ECC might be utilized in the shear element due to possible damage of bridging fibers on sliding crack surfaces.

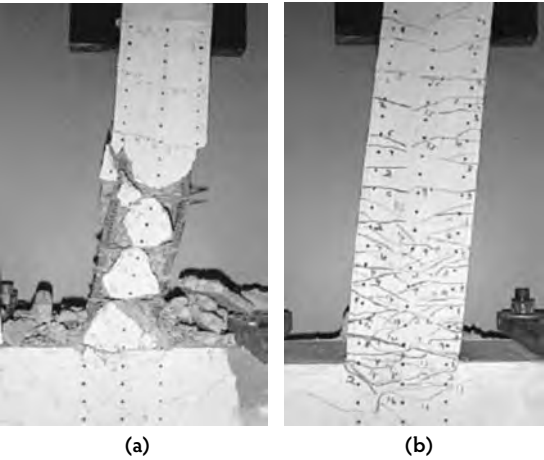


FIGURE 24.13 Damage behavior of (a) R/C and (b) R/ECC without stirrups, shown at 10% drift. (From Fischer, G. and Li, V.C., *ACI Struct. J.*, 99(6), 781–790, 2002.)

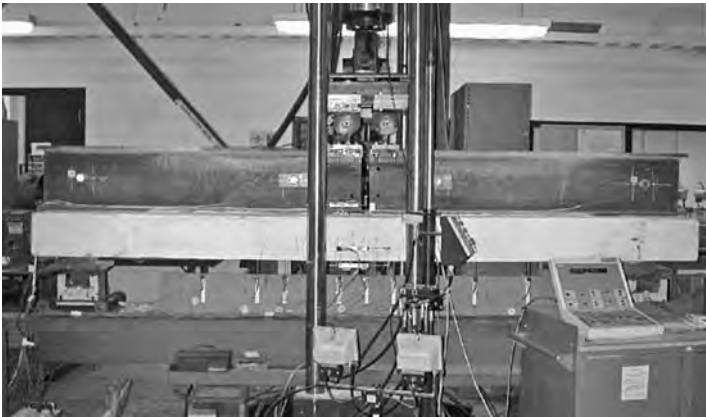


FIGURE 24.14 Flexural fatigue testing of ECC link-slab element. (From Kim, Y.Y. et al., *ACI Struct. J.*, 101(6), 792–801, 2004.)

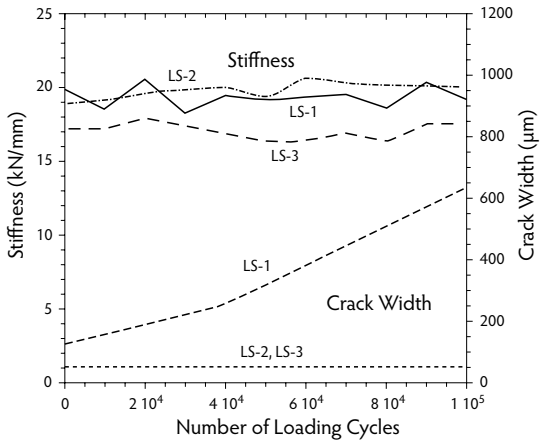


FIGURE 24.15 Stiffness and crack width change as a function of load cycles. LS-1 is the control R/C specimen; LS-2 and LS-3 are both R/ECC specimens with different reinforcement details to represent new and retrofit construction conditions. (From Kim, Y.Y. et al., *ACI Struct. J.*, 101(6), 792–801, 2004.)

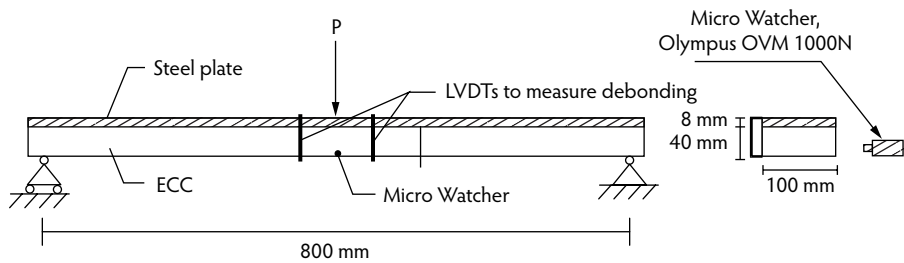


FIGURE 24.16 Composite steel/ECC beam test setup. (From Walter, R. et al., in *Proceedings of the 5th International PhD Symposium in Civil Engineering*, June 17–19, Delft, the Netherlands, 2004, pp. 477–484.)

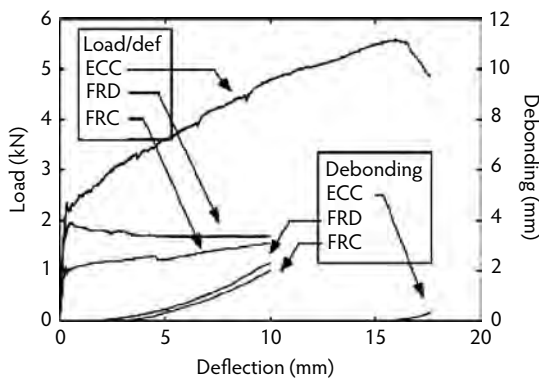


FIGURE 24.17 Load and debonding as a function of composite beam deflection. A significant increase in load capacity and a delay in debonding were achieved in the steel/ECC beam vs. the steel/FRC and steel/FRD beams. (From Walter, R. et al., in *Proceedings of the 5th International PhD Symposium in Civil Engineering*, June 17–19, Delft, the Netherlands, 2004, pp. 477–484.)

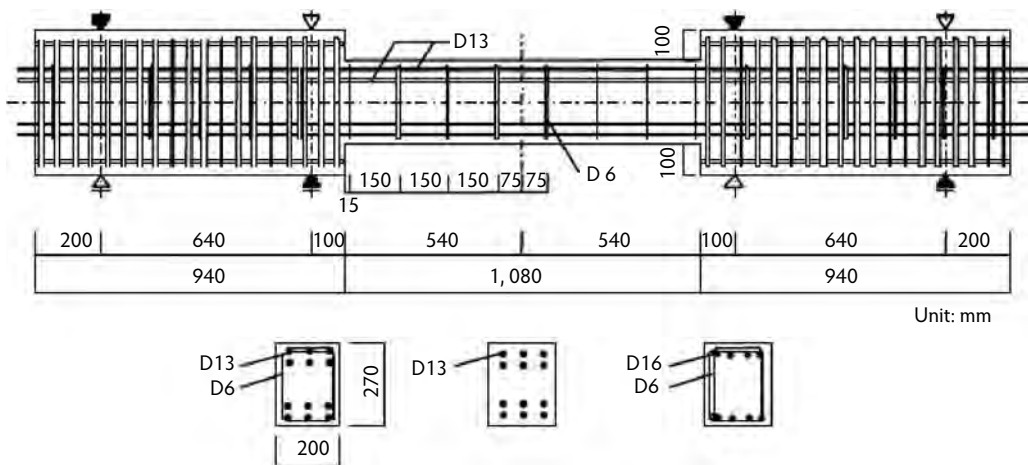


FIGURE 24.18 Fully reversed Ohno shear test setup. (From Fukuyama, H. et al., in *Proceedings of the 6th ASCCS International Conference on Steel–Concrete Composite Structures*, March 22–24, Los Angeles, CA, pp. 969–976.)

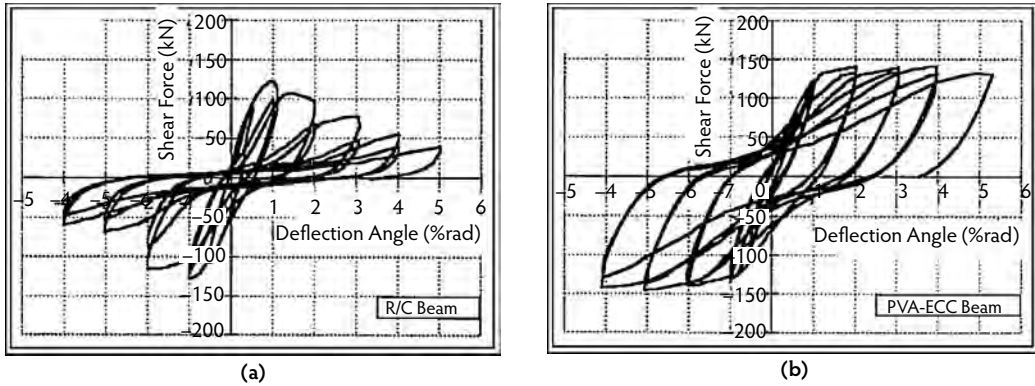


FIGURE 24.19 Hysteretic loops for Ohno shear beams under fully reversed cyclic loading for (a) R/C and (b) R/ECC. (From Fukuyama, H. et al., in *Proceedings of the 6th ASCCS International Conference on Steel–Concrete Composite Structures*, March 22–24, Los Angeles, CA, pp. 969–976.)

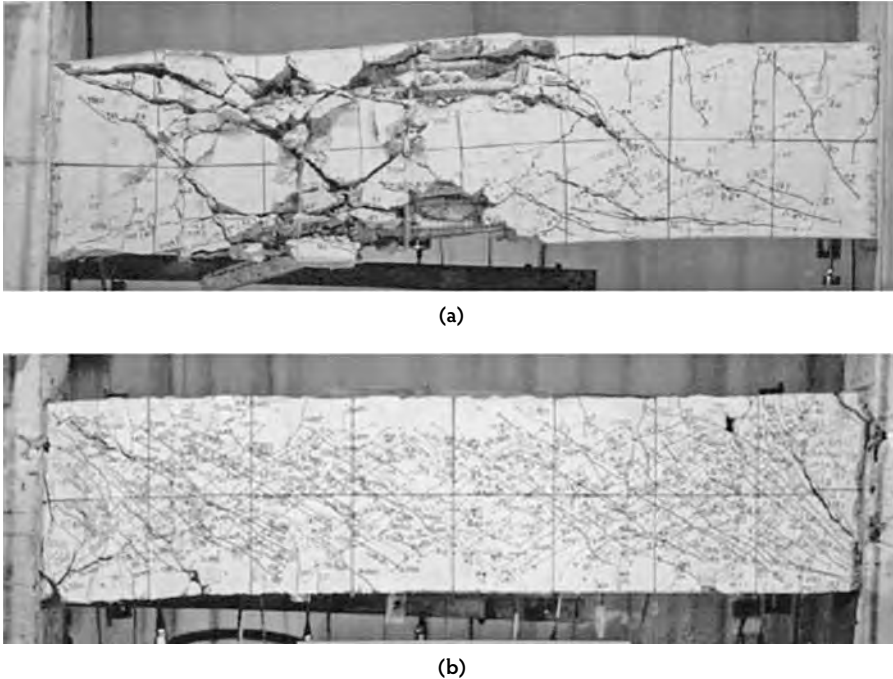


FIGURE 24.20 Damage pattern in Ohno shear beams: (a) R/C, and (b) R/ECC. (From Fukuyama, H. et al., in *Proceedings of the 6th ASCCS International Conference on Steel–Concrete Composite Structures*, March 22–24, Los Angeles, CA, pp. 969–976.)

24.4.1.3 Column Element

The response of R/ECC and R/C columns under fully reversed cyclic loading was studied by Fukuyama et al. (2000). These columns were tested under the antisymmetrical moment condition. The axial force applied to the column was 20% of the axial compressive strength of the column, calculated without the contribution of the steel reinforcements. The hysteretic behavior in terms of stability and energy dissipation was improved in the R/ECC column over the R/C column in a manner similar to that for flexural and shear elements (Figure 24.21). Large bond splitting cracks were observed in the R/C column, which

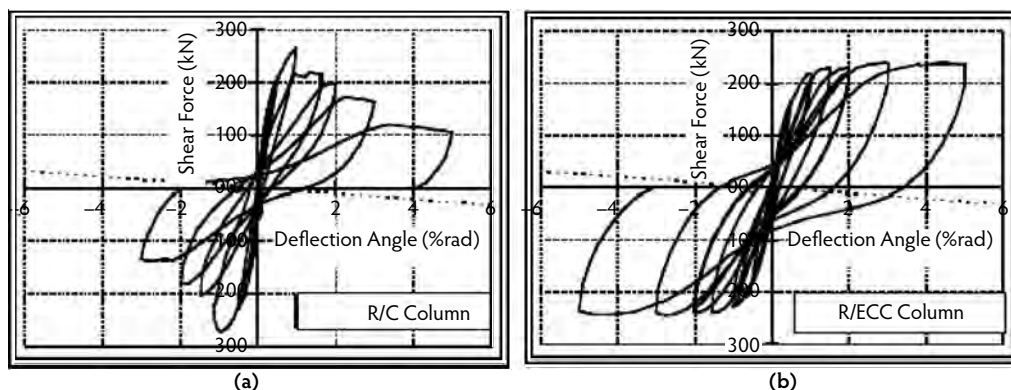


FIGURE 24.21 Hysteretic behavior of columns under fully reversed cyclic loading for (a) R/C and (b) R/ECC. (From Fukuyama, H. et al., in *Proceedings of the 6th ASCCS International Conference on Steel–Concrete Composite Structures*, March 22–24, Los Angeles, CA, pp. 969–976.)

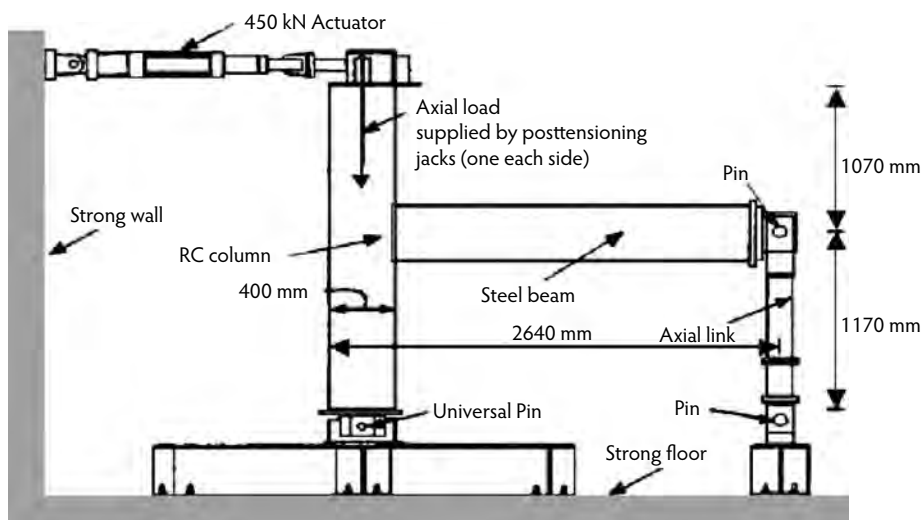


FIGURE 24.22 Test setup for beam–column connection. (From Parra-Montesinos, G. and Wight, J.K., *ASCE J. Struct. Eng.*, 126(10), 1113–1121, 2000.)

failed by shear without yielding of the longitudinal reinforcements; subsequently, the resistant shear force in the envelope curve of shear force–deflection angle relationship decreased with increase of deflection angle. On the other hand, the R/ECC column did not fail by shear or bond splitting. Instead, it maintained a ductile response up to the end of the test with fine cracks revealed on the specimen surface.

24.4.1.4 Beam–Column Connection Element

Beam–column connection was studied by Parra-Montesinos and Wight (2000), using the test setup shown in Figure 24.22. The hysteretic response for the R/ECC shear panel was substantially improved over the R/C (Figure 24.23), even when all shear stirrups were removed in the R/ECC shear panel. Under fully reversed cyclic loading, a set of orthogonal cracks formed in both specimens (Figure 24.24). Although the orthogonal cracks in R/ECC were much more closely spaced, they did not lead to surface spalling as is often observed in R/C specimens after large load reversals. In addition, edge spalling was revealed in the R/C specimen, associated with the bearing of the steel beam on the brittle concrete. This was not found in the R/ECC specimen.

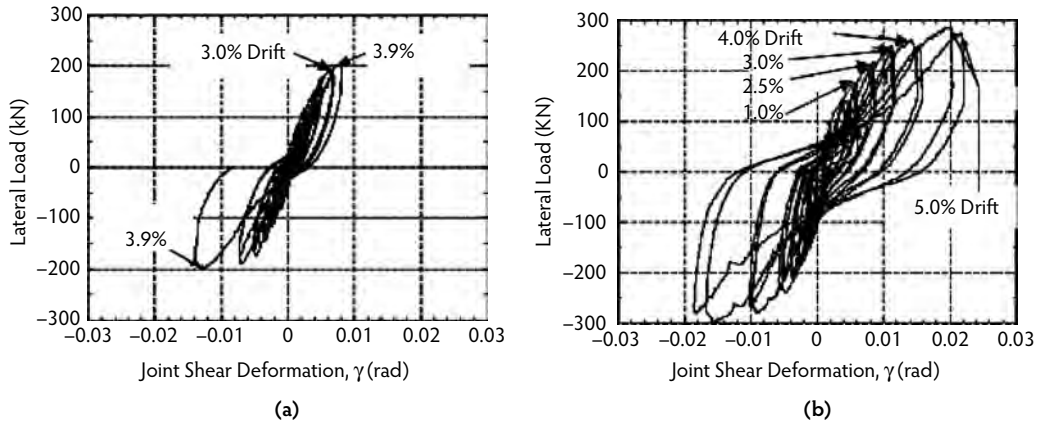


FIGURE 24.23 Hysteretic loops of fully reversed cyclic test on beam–column connections for (a) R/C with stirrups and (b) R/ECC without stirrups (From Parra-Montesinos, G. and Wight, J.K., *ASCE J. Struct. Eng.*, 126(10), 1113–1121, 2000.)

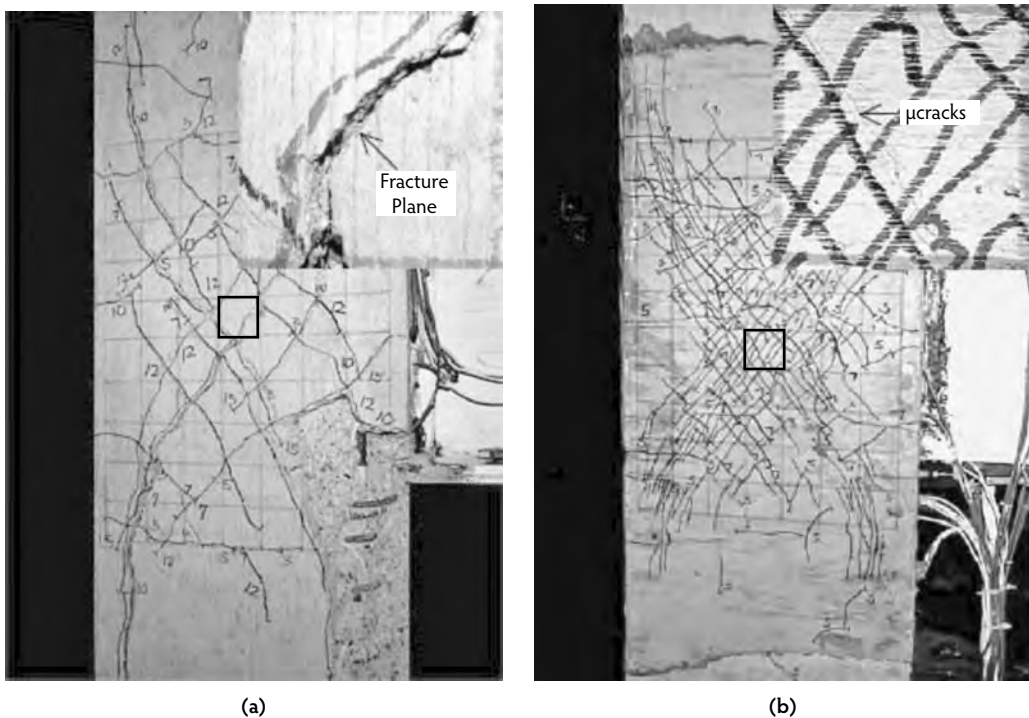


FIGURE 24.24 Damage behavior of the shear panel of a hybrid connection after cyclic loading. The enlarged inserts provide easier viewing of the cracks in (a) R/C and (b) R/ECC. (Adapted from Parra-Montesinos, G. and Wight, J.K., *ASCE J. Struct. Eng.*, 126(10), 1113–1121, 2000.)

24.4.1.5 Wall Panel Element

Wall panel elements were studied by Kesner and Billington (2005) under fully reversed cyclic loading, using the test setup shown in Figure 24.25. These tests confirmed that the R/ECC wall panels outperformed the R/C wall panels in hysteretic loop stability, peak load, and energy dissipation (Figure 24.26).

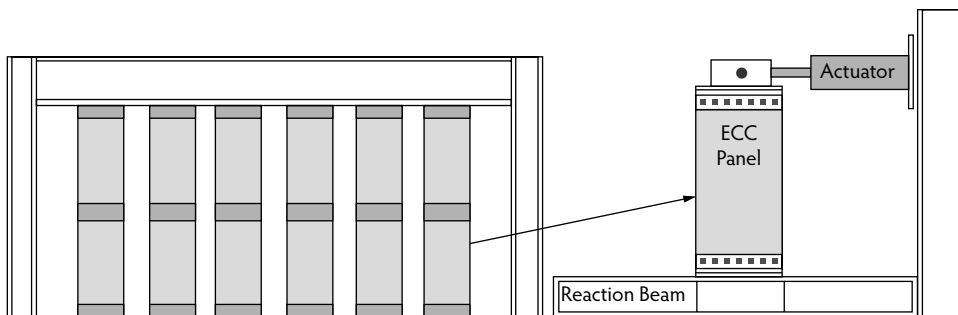


FIGURE 24.25 Wall panel test setup. (From Kesner, K.E. and Billington, S.L., *ASCE J. Struct. Eng.*, 131(11), 712–720, 2005.)

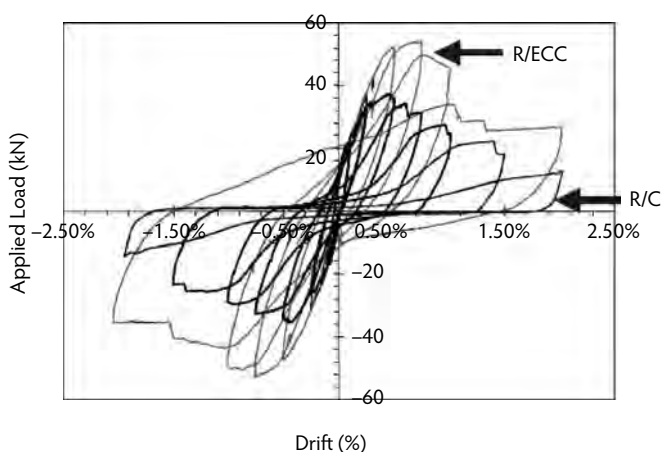


FIGURE 24.26 Hysteretic loops of shear wall. (Adapted from Kesner, K.E. and Billington, S.L., *ASCE J. Struct. Eng.*, 131(11), 712–720, 2005.)

24.4.2 Insights from R/ECC Element Response

The structural element experimental testing results briefly summarized in Section 24.4.1 share the common features of enhanced element load and deformation capacity, hysteretic loop stability, and energy dissipation. Further, structural damage is limited to microcracking while large fractures in the form of bond splitting and spalling are suppressed. A number of helpful insights for structural use of ECC can be drawn from the above studies. These are summarized below.

24.4.2.1 Potential for Reduction or Elimination of Shear Reinforcement

Through the formation of multiple cracks and delay of fracture localization, the ductility of R/ECC elements can be maintained with little or no conventional shear reinforcement. This is best demonstrated in the flexural element (Fischer and Li, 2002a) (Figure 24.11) and beam–column connection (Parra-Montesinos and Wight, 2000) studies highlighted in the previous section, where shear stirrups were completely eliminated. Additional evidence can be found in a study by Li and Wang (2002), who experimentally demonstrated that ECC beams without shear reinforcement exhibited superior performance compared to high-strength concrete beams with closely spaced steel stirrups. Experiments on the cyclic response of unbonded post-tensioned precast columns with ECC hinge zones (Billington and Yoon, 2004) also confirmed that column integrity could be better maintained when concrete is replaced by ECC without any seismic shear detailing.

24.4.2.2 Damage Tolerance

Damage tolerance is a measure of the residual strength of a material or structure when damage is introduced. The damage tolerance of ECC derives from the fact that fracture or real cracks are suppressed in favor of plastic yielding of ECC in the form of multiple microcracks. Such microcracks are not real cracks (Li, 2000) in the sense that an increasing amount of load can be carried across them during ECC strain hardening. Cracks in normal concrete or even in standard fiber-reinforced concrete are accompanied by tension softening, and load-carrying capacity drops as the crack enlarges. As a result, a reliance on steel reinforcement to maintain structural integrity becomes critical. Where no steel reinforcement exists (e.g., in the concrete cover), surface spalling results. Such failure modes are fully eliminated in R/ECC elements, as can be observed in Figure 24.13, Figure 24.20, and Figure 24.24. In these elements, the shear stiffness and the peak load at each load cycle are better maintained than in R/C due to the high damage tolerance of ECC. In structural elements loaded beyond first crack, it is reasonable to expect equal or even higher structural stiffness in R/ECC elements compared to R/C elements, despite the lower elastic modulus of ECC as compared to concrete. This is due to the capability of ECC to continue to share the load-carrying function with steel reinforcements, long after the first crack appears. This concept was verified in an analytic study of cracked reinforced beams by Szerszen et al. (2006). Fukuyama et al. (2007) regarded such damage tolerance functionality of ECC as a significant benefit to society, given the enormous economic cost of repair and reconstruction of infrastructures after a major seismic event that strikes an urban area.

24.4.2.3 Compatible Deformation between ECC and Reinforcement

In R/ECC members with steel reinforcement, both the steel and the ECC can be considered elastic–plastic materials capable of sustaining deformation up to several percent strain. As a result, the two materials remain compatible in deformation even as both steel and ECC yield. Compatible deformation implies that no shear lag exists between the steel and the ECC, resulting in a very low level of shear stress at the steel rebar to ECC material interface. This phenomenon is unique to R/ECC members. As a result of this low interfacial stress between steel and the ECC, the bond between the ECC and reinforcement is not as critical as in normal R/C elements, as stress can be transmitted directly through the ECC material (via bridging fibers) even after microcracking. In contrast, within R/C members stress must be transferred via the rebar–concrete interface to the concrete away from the crack site. After concrete cracks in an R/C element, the concrete unloads elastically near the crack site, while the steel takes over the additional load shed by the concrete. This leads to incompatible deformation and high interface shear stress responsible for the commonly observed failure modes such as bond splitting or spalling of concrete cover. Figure 24.27a shows the stress flow in the composite, before and after matrix cracking, in R/C and R/ECC. The compatible deformation between ECC and reinforcement has been experimentally confirmed (Fischer and Li, 2002b). Figure 24.27b shows the contrasting behavior of R/ECC and R/C near the interface, revealed in a cross-sectional cut of tension-stiffening specimens. In structural elements subjected to large loads such as earthquakes, steel yielding may be expected. In R/C elements, steel yielding may be concentrated at locations where the rebar crosses the concrete cracks due to the large incompatible deformations between the steel and fractured concrete. In R/ECC elements, steel yielding can spread to a much larger volume. As a result, the distributed microcracking in ECC allows for more efficient utilization of steel reinforcement for element energy dissipation. This explains the formation of fuller hysteretic loops observed in the ECC elements discussed in Section 24.4.1 (see Figure 24.12, Figure 24.19, Figure 24.21, Figure 24.23, and Figure 24.26).

24.4.2.4 Tight Crack Width Control and Elimination of Crack Control Reinforcement

A common observation in the structural element tests described is that the cracks generated in the R/ECC have very small crack widths (see Figure 24.13, Figure 24.15, Figure 24.20, and Figure 24.24). This is because crack widths in ECC are self-controlled (Section 24.2.2). Although the presence of steel reinforcement further limits the crack width, ECC material can be easily designed to have crack widths less than 100 μm without depending on steel reinforcement. This small crack width is important with

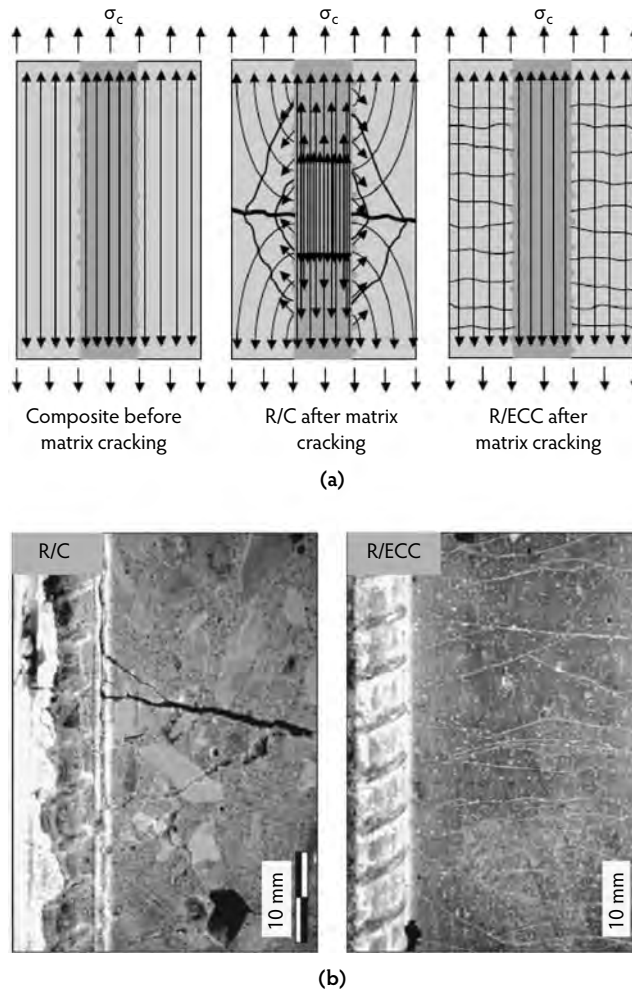


FIGURE 24.27 (a) Stress flow before and after matrix cracking. (b) On the left, brittle fracture of concrete in normal R/C causes unloading of concrete near crack, and a jump in tensile strength, straining the steel locally and resulting in high interfacial shear and bond breakage. On the right, in contrast, compatible deformation occurs between ECC and steel reinforcement with no shear lag, thus maintaining integrity of the interfacial bond. (From Fischer, G. and Li, V.C., *ACI Struct. J.*, 99(1), 104–111, 2002.)

respect to the durability of the structure (Section 24.5) and can be decisive in determining whether a structure requires repair after a major loading event (Fukuyama et al., 2007).

24.4.2.5 Transforming Material Ductility into Structural Strength

Once again, the unique feature of ECC is its ultra-high ductility. This implies that structural failure by fracture is significantly less likely in comparison to normal concrete or FRC. In traditional R/C structural design, the most common and most important material parameter of concrete is compressive strength. For this reason, structural strength (and, more generally, structural performance) is often perceived to be governed by material strength. Essentially, higher material strength (usually referred to as *compressive strength* in the concrete literature) is expected to lead to higher structural strength. This concept is valid only if the material strength property truly governs the failure mode; however, if tensile fracture failure occurs, a high-strength material does not necessarily mean higher structural strength. Instead, a high toughness material, and in the extreme, a ductile material such as ECC can lead to higher structural strength.

A number of experimental observations (Fukuyama et al., 2000; Kanda et al. 1998; Kesner and Billington, 2005; Lim and Li, 1997) provide support for the above reasoning. For example, the shear beam elements tested by Fukuyama et al. (2000) (Figure 24.18) have compressive strengths of 58.3 MPa and 52.5 MPa for concrete and ECC, respectively; however, the structural load capacity was 120 kN vs. 140 kN for the R/C and R/ECC elements, respectively (Figure 24.19). As another example, the precast in-fill wall panels (Figure 24.25) tested by Kesner and Billington (2005) for seismic retrofitting of buildings revealed that a panel with a concrete of compressive strength of 50 MPa attained a structural (shear) strength of 38 kN, while a similar panel made with ECC material of lower compressive strength (41 MPa) achieved a much higher structural strength of 56 kN (Figure 24.26). The over 35% structural strength gain in the R/ECC panel can be attributed to the material ductility of the ECC which prolonged integrity of the panel to a larger drift level. Similarly, detailed numerical analysis (Kabele, 2001) of a wall panel made with ECC demonstrated a structural strength three times that of the panel made with FRC, despite the fact that both materials had the same tensile and compressive strengths.

24.5 Durability of ECC and ECC Structural Elements

24.5.1 Material and Element Durability

As a new construction material, it is not enough to have excellent mechanical performance compared with conventional concrete or FRC. It is also important to verify the durability of the ECC material itself in various environments typical of where such materials are expected to be used. In addition, the influence of this material on structural durability performance of R/ECC must also be confirmed. In most cases, laboratory studies are performed under accelerated conditions; however, long-term performance in the field is most valuable even though it is difficult to obtain, especially for a relatively new material.

Because the greatest value of ECC lies in its superior tensile ductility, this material will likely be used in structures that impose large deformations on the material. This implies that the structure must remain serviceable even if the material undergoes tensile strain hardening accompanied by multiple microcracking. For this reason, the examination of ECC material durability should be carried out in the deformed cracked state; that is, the ECC specimen should undergo preloading to varying strain levels to deliberately create microcrack damage, prior to accelerated exposure tests. Experimental data thus determined from preloaded specimens may be considered as material durability properties under combined mechanical and environmental load. It should be noted, however, that most of these experiments were undertaken with cracked specimens in the unloaded state for experimental testing convenience. On unloading, crack widths in ECC tend to reduce by 10 to 20% from the loaded state. This reduced crack width is used in all experimental data reported. This difference from field conditions where cracks are typically under load is not expected to have a significant impact on the measured durability of ECC material or R/ECC structures but should be verified in future studies.

As will become clear in the following subsections, the durability of ECC and especially of ECC structures can be sensitive to the width of the microcracks. Microcrack widths are therefore designed to be small, typically less than 100 μm for ECC, and potentially much lower. These cracks remain small under fatigue loading, as indicated in Section 24.4.1.1; however, a recent study by Boshoff and van Zijl (2007) indicates that crack width may open wider under sustained loading due to creep mechanisms. Care must be taken for the long-term durability of a structure under combined conditions of sustained loading, deformation to the strain-hardening stage, and exposure to an aggressive environment.

In Section 24.5.2, current knowledge of ECC durability under various environments is summarized. In Section 24.5.3, the durability of R/ECC under chloride exposure is presented. This discussion is followed in Section 24.5.4 by highlights of limited long-term performance data on ECC materials already in structures exposed to the natural environment and (in one case) in combination with mechanical loads. Additional studies of ECC under various environmental or loading conditions can be found in the references in Table 24.5. Most of the durability studies covered here are for ECC reinforced with PVA fibers. The durability of PVA fiber itself has been summarized by Horikoshi et al. (2006).

TABLE 24.5 Studies of ECC Durability under Various Environments/
Loading Conditions

Environments/ Loading Conditions	Refs.
Long-term aging	Li and Lepech (2004)
Freeze–thaw cycles	Li et al. (2003)
Tropical climate exposure	Li et al. (2004)
Chloride immersion	Li et al. (2007)
Deicing salt exposure	Sahmaran and Li (2007a)
Alkali–silica reaction	Sahmaran and Li (2007b)
Fatigue	Suthiwarapirak et al. (2002)
Creep under constant load	Boshoff and van Zijl (2007)
Wheel load abrasion	Li and Lepech (2004)
Restrained drying shrinkage	Li and Stang (2005); Wang and Li (2006)
Calcium leaching	Nemecek et al. (2006)

24.5.2 ECC Durability under Various Environments

In this section, current knowledge on long-term strain capacity, as well as ECC exposed to various commonly encountered environments is summarized. These environments include freeze–thaw cycles, hot–wet cycles, chloride immersion, deicing salt exposure, and alkali–silica reaction (ASR) resistance.

24.5.2.1 Long-Term Tensile Strain Capacity

For a construction material to be considered truly durable, its mechanical properties must not degrade over time and fall below minimum design specifications. To validate ECC long-term effectiveness, a series of tensile tests were performed to determine long-term strain capacity. Due to the continued hydration process typical of cementitious materials and the delicate balance of the cement matrix, fiber, and matrix–fiber interface properties in ECC, the strain capacity of ECC evolves with age during maturing (Li and Lepech, 2004). This is exhibited in a plot of ECC strain capacity vs. age (Figure 24.28). Roughly 10 days after casting, peak strain capacity is achieved when an optimal balance of the matrix, fiber, and matrix–fiber interface properties is attained for highly saturated multiple cracking. As hydration continues, the increasing matrix toughness leads to a reduced composite ductility. Maturity of matrix and matrix–fiber properties eventually results in an ECC long-term steady strain capacity of 3%, far above

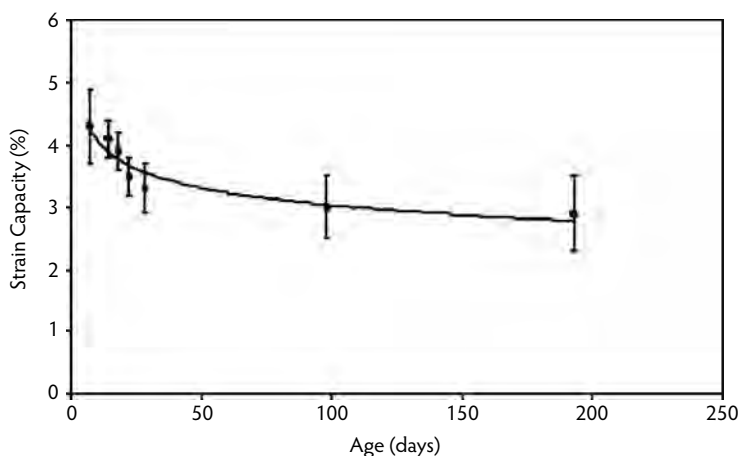


FIGURE 24.28 Tensile strain capacity of ECC as a function of age after casting. (From Li, V.C. and Lepech, M., in *Proceedings of the Transportation Research Board 83rd Annual Meeting*, Compendium of Papers CD ROM, Paper 04-4680, Transportation Research Board, Washington, D.C., 2004.)

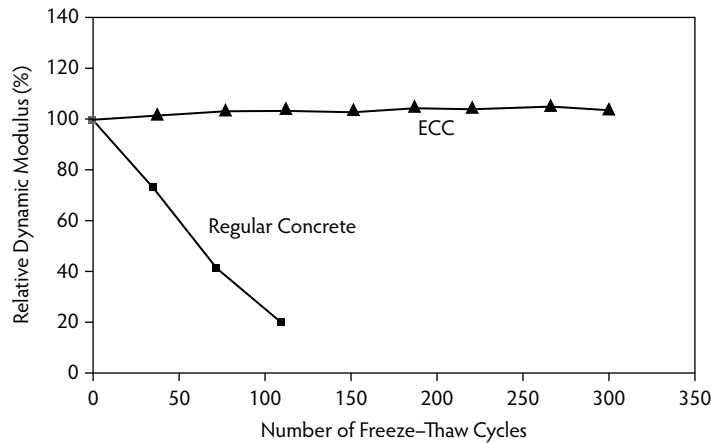


FIGURE 24.29 Relative dynamic modulus of normal concrete and three versions of ECC, all without air entrainment. (From Li, V.C. et al., *Durable Link Slabs for Jointless Bridge Decks Based on Strain-Hardening Cementitious Composites*, RC-1438, Michigan Department of Transportation, Lansing, 2003.)

the deformation demand imposed by many structural applications but significantly less than the 5% capacity seen at early age. Although long-term tests have only been carried out to 180 days, the long-term strain capacity is expected to remain at approximately 3%. The strain capacity–age curve can be seen as analogous to the compressive strength development curve in normal concrete; however, because it is not monotonically rising, the long-term value should be used for design purposes. For simplicity, 90% of the 28-day strain capacity value that approaches asymptotically to the long-term behavior may be adopted as the design strain capacity. This simplifies the design process, as the same 28-day value is used for compressive strength specification.

24.5.2.2 Freeze–Thaw Durability

Durability of non-air-entrained ECC specimens was tested by exposure to cycles of freezing and thawing, in accordance with ASTM C 666 (ASTM, 2003a). Non-air-entrained concrete specimens were also tested as reference specimens. Testing of ECC and concrete prism specimens was conducted concurrently over 14 weeks (Li et al., 2003). After 5 weeks (110 cycles), the concrete specimens had severely deteriorated, requiring removal from the freeze–thaw machine, as mandated by the testing standard; however, all ECC specimens survived the test duration of 300 cycles with no degradation of dynamic modulus (Figure 24.29). This performance resulted in a durability factor of 10 for concrete compared to 100 for ECC, as computed according to ASTM C 666. In uniaxial tension tests performed on wet-cured- and freeze–thaw-exposed ECC tensile coupons at the same age, no significant drop in strain capacity was experienced after 300 cycles. Both wet-cured and freeze–thaw specimens exhibited a strain capacity of roughly 3%.

24.5.2.3 Tropical Climate Exposure

In contrast to the freeze–thaw tests discussed above, which are designed to simulate temperature changes in winter conditions, hot-water immersion tests were conducted to simulate the long-term effects of hot and humid environments. To examine the effects of environmental exposure, hot-water immersion was performed on individual fibers, single fibers embedded in ECC matrix, and composite ECC material specimens (Li et al., 2004a). Specimens for both individual fiber pullout and composite ECC material were cured for 28 days at room temperature prior to immersion in hot water at 60°C for up to 26 weeks. After this exposure, little change was seen in fiber properties such as fiber strength, fiber elastic modulus, and elongation; however, the strain capacity of the ECC did drop from 4.5% at early age to 2.75%. Whereas the accelerated hot weather testing resulted in lower strain capacity of ECC, the 2.75% strain capacity (over 250 times that of normal concrete) seen after 26 weeks and equivalent to 70 years of natural weathering (Proctor et al., 1982) remains acceptable for most infrastructure applications.

24.5.2.4 Chloride Immersion

When ECC material is exposed to environments with high chloride concentrations, such as marine structures or for pavements and bridge decks subjected to deicing salt applications, chloride ions may alter the fiber–matrix interface and therefore the composite properties. To examine these effects, ECC coupon specimens were first preloaded under uniaxial tension to various strain levels, then exposed to a 3% NaCl solution at room temperature for 1, 2, and 3 months; they were then subsequently reloaded up to failure (Li et al., 2007). Figure 24.30 shows the data for the three sets of specimens preloaded to 0% (virgin), 0.5%, and 1.5% tensile strain. In all cases, the reloaded specimens retained multiple microcracking behavior and tensile strain capacity of more than 3%, although the average crack width increased from 40 μm to 100 μm and the tensile strength was reduced by about 10%. The wider crack width and lower tensile strength may be a result of a reduction in chemical bonding at the fiber–matrix interface, as suggested by single fiber pullout test data by Kabele et al. (2007).

24.5.2.5 Deicing Salt Exposure

Sahmaran and Li (2007) studied the durability performance of non-air-entrained ECC when subjected to mechanical loading and freezing and thawing cycles in the presence of deicing salts. After 50 exposure cycles, the surface condition visual rating and total mass of the scaling residue of ECC remained within acceptable limits according to ASTM C 672 (ASTM, 2003b) (Figure 24.31a). This level of durability held true even for specimens preloaded to cracking at high deformation levels. Non-air-entrained mortar specimens were used as reference specimens. As expected, these mortar prisms under identical testing conditions deteriorated severely. Preloaded and virgin (no preloading) ECC coupon specimens were also exposed to freezing and thawing cycles in the presence of deicing salts for 25 and 50 cycles to determine their residual tensile behavior. The reloaded specimens showed negligible loss of ductility but retained multiple microcracking behavior and a tensile strain capacity of more than 3% (Figure 24.31b). It was also found that multiple microcracks due to mechanical loading healed sufficiently under freezing and thawing cycles in the presence of salt solutions and restored the specimens to nearly the original stiffness. These results confirm that ECC, both virgin and microcracked, remains durable despite exposure to freezing and thawing cycles in the presence of deicing salts.

24.5.2.6 Alkali–Silicate Reaction Resistance

Sahmaran and Li (2008a) studied the resistance of ECC to alkali–silica reaction (ASR). ECC bar specimens were immersed in alkali solution at 80°C in accordance with ASTM C 1260 (ASTM, 2007) to determine their length change due to alkali silica reaction. The ECC bar specimens containing either Class F or Class C fly ash did not show any significant expansion at the end of a 30-day soaking period (Figure 24.32). Although very fine silica sand is used in ECC, the crystalline nature of these sand particles suppresses the reactivity in an alkaline environment. Further, the presence of a high volume of fly ash decreases the pH value due to the pozzolanic reaction, making alkali–silica reaction even less likely. Finally, the presence of the PVA microfibers tends to reduce any expansion that may occur. These studies show that ECC material will not exhibit degradation due to ASR.

24.5.3 Durability of R/ECC

Increased durability of reinforced concrete is typically associated with a dense concrete matrix—that is, a very compact microstructure expected to lower permeability and reduce transport of corrosives to the steel (Beeldens and Vandewalle, 2001; Oh et al., 2002). This can be achieved with a well-graded particle size distribution, fly ash and silica fume, or low W/C ratios. These concepts, however, rely upon the concrete remaining uncracked within a structure throughout its expected service life and resisting the transport of water, chloride ions, oxygen, etc. In this presumed uncracked state, numerous concrete materials have shown promising durability in laboratory tests (Mora et al., 2003; Weiss and Shah, 2002).

In reality, however, reinforced concrete members crack due to applied structural loads, shrinkage, chemical attack, and thermal deformations, which are practically inevitable and often anticipated in

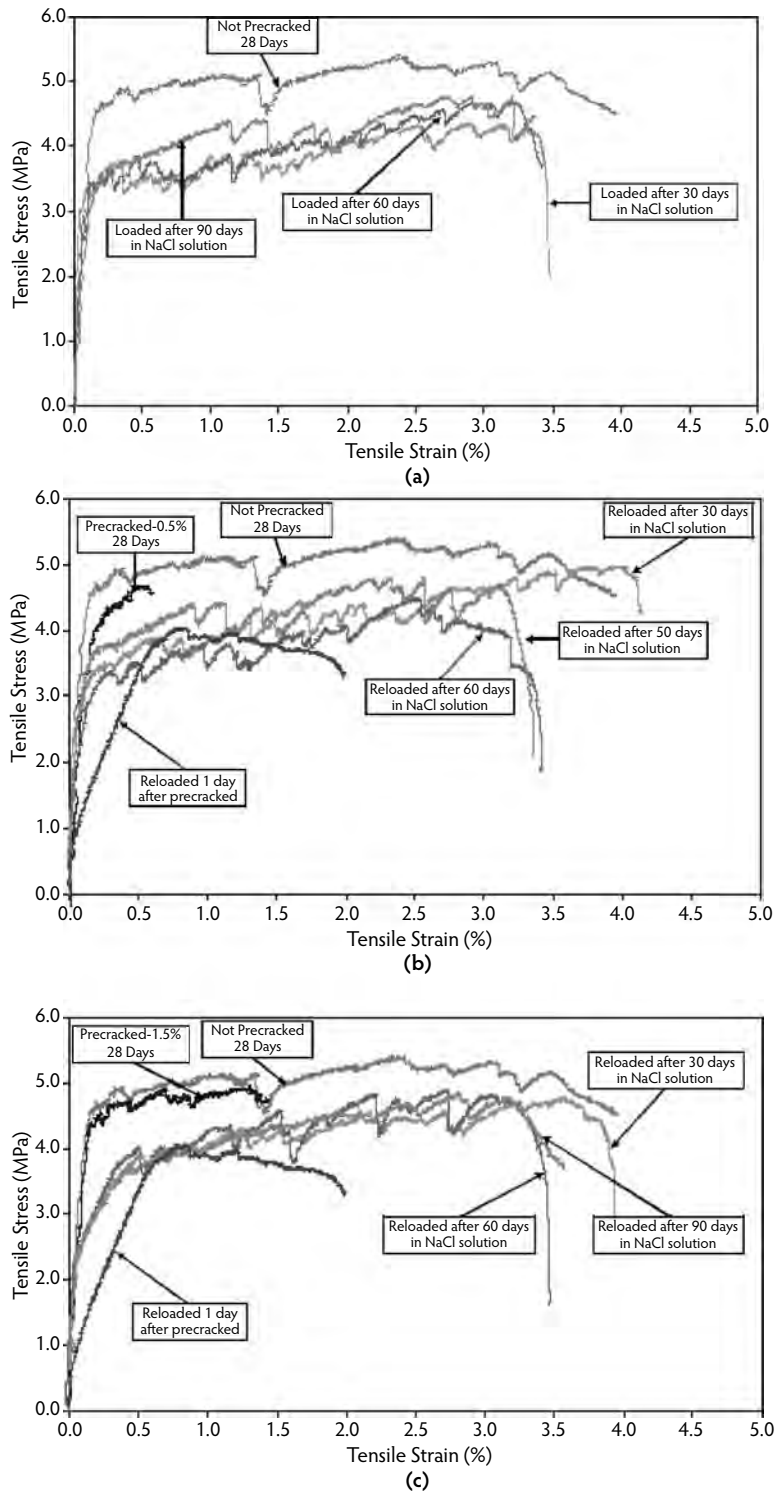


FIGURE 24.30 Tensile stress–strain curves of ECC: (a) virgin coupon specimens, (b) precracked (to 0.5%) specimens, and (c) precracked (to 1.5%) specimens, before and after being subjected to 3% NaCl solution exposure. (From Li, M. et al., in *Proceedings of the Fifth International RILEM Workshop on High-Performance Fiber-Reinforced Cement Composites (HPFRCC 5)*, Reinhardt, H.W. and Naaman, A.E., Eds., RILEM, Paris, 2007, pp. 313–322.)

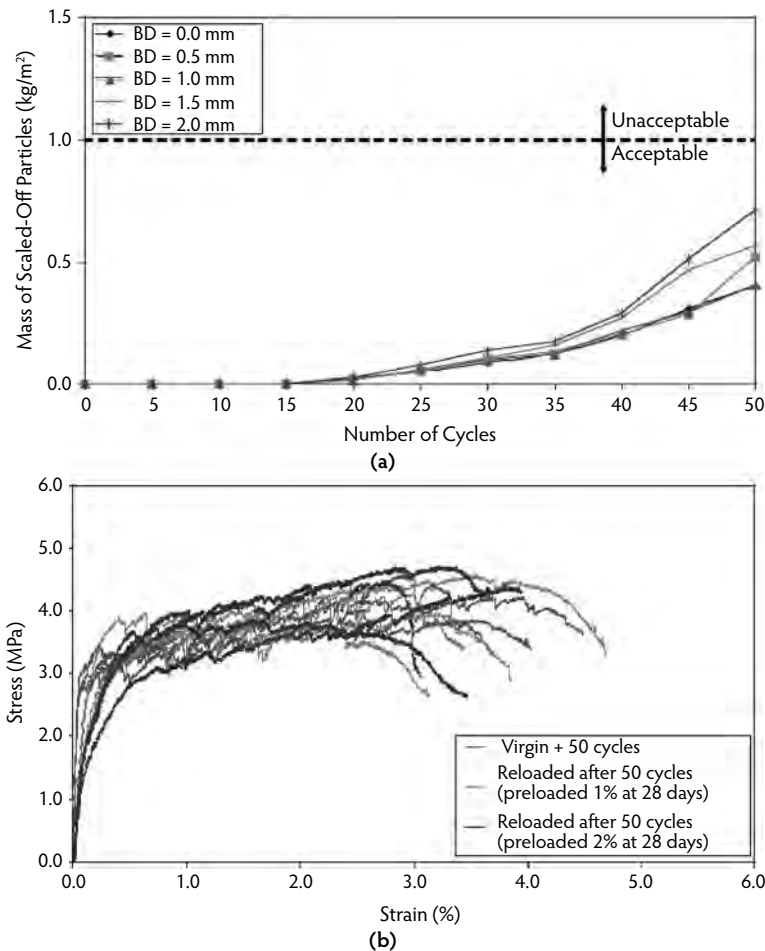


FIGURE 24.31 Effect of freeze-thaw cycles in the presence of deicing salts for (a) beams preloaded to different bending deformation (BD) levels, showing mass of scaled-off particles, and (b) coupon specimens preloaded to different levels, showing uniaxial tensile stress-strain curves after 50 cycles of exposure. (From Sahmaran, M. and Li, V.C., *J. Cement Concrete Res.*, 37, 1035–1046, 2007.)

restrained conditions (Mihashi and De Leite, 2004; Wittmann, 2002). The durability of concrete is intimately related to its transport properties—that is, the rate at which corrosives and water are able to penetrate the concrete. This is because concrete is susceptible to degradation through leaching, corrosion, sulfate attack, freezing-and-thawing damage, and other mechanisms that depend on the ingress of water. Because cracks significantly modify the transport properties of concrete, their presence greatly accelerates the deterioration process. To solve this serious problem, a fundamental solution that reduces the brittle nature of concrete is needed.

The use of ECC to replace normal concrete in steel-reinforced concrete structures has a number of implications in terms of structural durability, including:

- Alteration of transport properties in the concrete or ECC cover, thereby delaying contact of aggressive agents with steel reinforcements through the intrinsic tight crack width control of ECC
- Alteration of the nature of steel corrosion with potentials for avoiding pitting and slowing the rate of corrosion through dispersed microcracking over a region of the steel reinforcement rather than concentrating at the base of a large crack and by its resistance to cover spalling via the tensile ductility of ECC

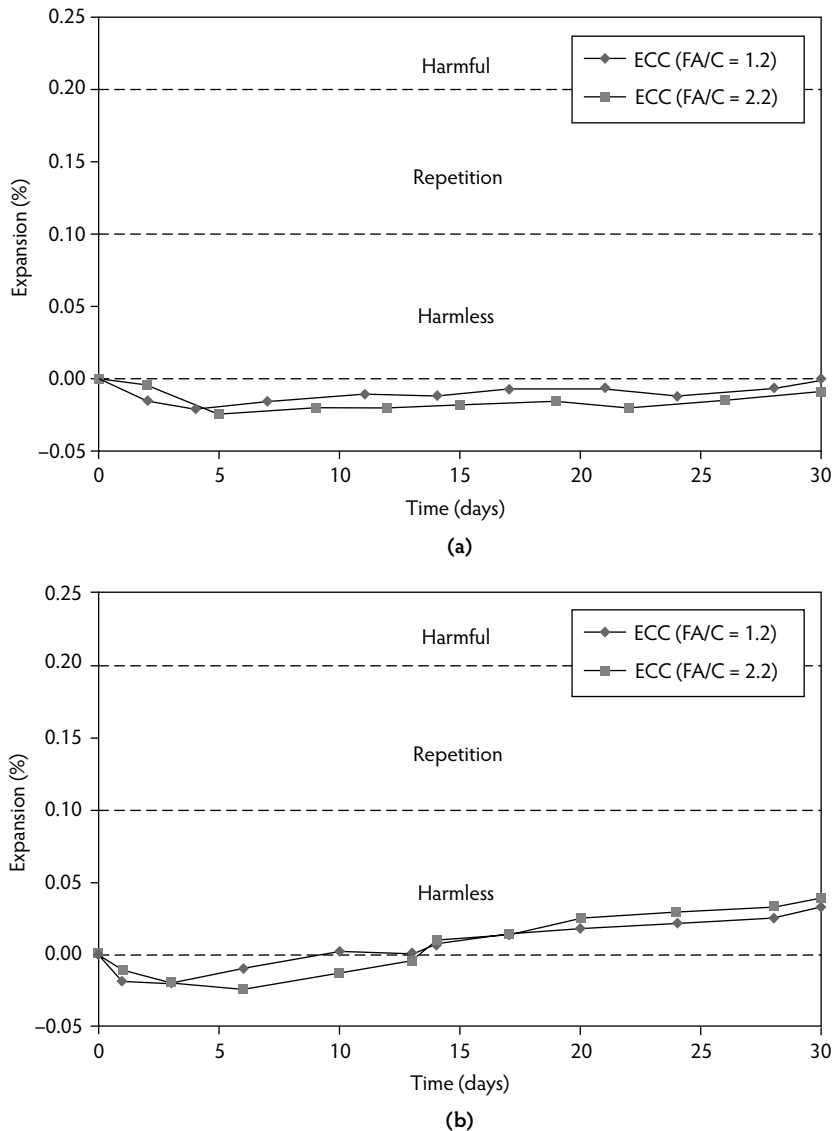


FIGURE 24.32 Length change of ECC mix with (a) Class F fly ash and (b) Class C fly ash subjected to alkali-silica reaction tests. (From Sahmaran, M. and Li, V.C., *J. Cement Concrete Composites*, 2008.)

These two alterations lead to expected improvements in structural durability due to a delay in the initiation phase of steel corrosion, and they dramatically slow the steel corrosion propagation phase. A number of experimental research efforts have been conducted that focus on the transport properties of ECC, especially when it is already in the strain-hardening stage with the presence of multiple microcracks, as well as on the behavior of steel-reinforced ECC elements in accelerated testing environments. Major findings of these two aspects are summarized in the following subsections. Recommendations for the design of R/ECC structures to protect against carbonation and chloride-ion-induced steel corrosion can be found in Rokugo et al. (2007).

24.5.3.1 Transport Properties of ECC

The most important transport properties of ECC include:

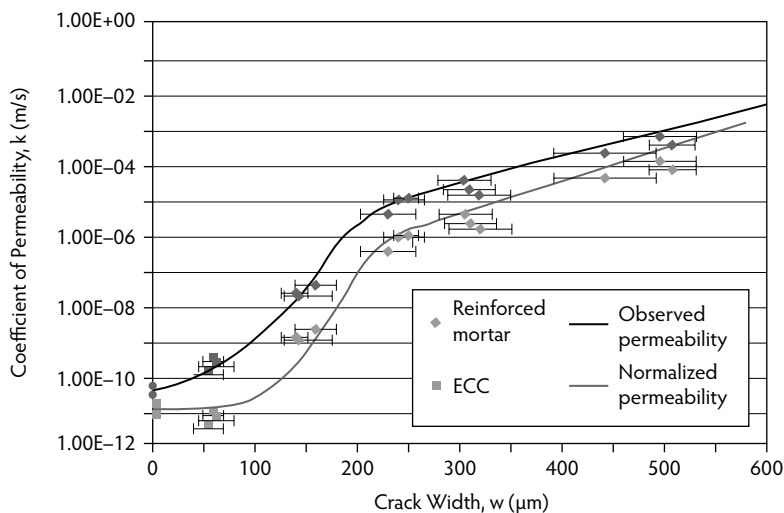


FIGURE 24.33 Permeability of precracked ECC and reinforced mortar measured as a function of crack width. (Adapted from Lepech, M.D. and Li, V.C., in *Proceedings of the 11th International Conference on Fracture (ICF XI)*, March 20–25, Torino, Italy, 2005.)

- Permeation in the presence of a hydraulic pressure, such as the condition in liquid containers and reservoir dams
- Diffusion in the presence of a ion concentration gradient, such as the condition on bridge decks, salt tanks, and marine environments
- Capillary suction induced by surface tension, of particular importance in ECC when crack width becomes very tight

All transport property tests described below were conducted at 28 days of age.

24.5.3.1.1 Water Permeation

Lepech and Li (2005a) found that cracked ECC exhibited nearly the same water permeability ($k \sim 5 \times 10^{-11}$ m/sec) as sound concrete, even when strained in tension to several percentage points (Figure 24.33). Within this study, both ECC and reinforced mortar specimens were pretensioned up to 1.5% deformation, resulting in a variety of crack widths and number of cracks among the various specimens. The permeability of these cracked materials was then determined under a hydraulic head. The dramatic rise in permeability with increasing crack width can be seen in the figure. For the ECC specimens, the crack width was intrinsically limited to about 60 μm (Section 24.2.2), regardless of the tensile deformation imposed; thus, the measured permeability was correspondingly low. Further, when normalized by number of cracks within the specimen, the comparable permeability of cracked ECC with sound material became even more apparent.

24.5.3.1.2 Chloride Diffusion

Chloride diffusion coefficients for ECC were examined by Sahmaran et al. (2007). Beam specimens were ponded in saltwater solution with 3% NaCl, according to AASHTO T259 (AASHTO, 2002). These measured values should really be regarded as the *effective chloride diffusion coefficient*, as the actual transport process is likely more complex than diffusion in a homogeneous medium without cracks. Based on tests on uncracked beams, the chloride diffusion coefficient for ECC was found to be 6.75×10^{-12} m²/sec, compared with 10.58×10^{-12} m²/sec based on tests on steel-reinforced mortar beams used as a control. Under high imposed bending deformation, preloaded ECC beam specimens revealed microcracks less than 50 μm and an effective diffusion coefficient significantly lower than that of similarly preloaded reinforced mortar control beams due to the tight crack widths inherent in ECC. In contrast, cracks larger than 150 μm were often produced under the same imposed deformation levels for the reinforced mortar

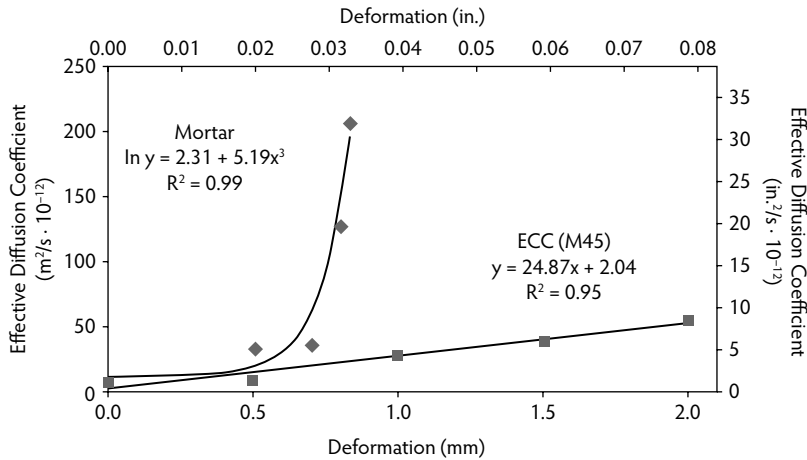


FIGURE 24.34 Diffusion coefficient vs. preloading deformation level for ECC and mortar. (From Sahmaran, M. et al., *ACI Mater. J.*, 104(6), 604–611, 2007.)

beams. Figure 24.34 shows the measured effective diffusion coefficient vs. preloading deformation level for ECC and mortar. It is revealed that the diffusion coefficient of ECC varies linearly with the number of cracks (with crack width being intrinsically constant even as beam deformation increases), whereas the diffusion coefficient of reinforced mortar is proportional to the square of the crack width. Chloride diffusion was also studied by Oh and Shin (2006) for specimens subjected up to 100,000 cycles of flexural loading. They found that the chloride diffusion coefficient did not increase significantly despite the increase number of cracks, and attribute this finding to the very fine crack width.

24.5.3.1.3 Capillary Suction

Sahmaran and Li (2008b) analyzed the water absorption and sorptivity properties of preloaded ECC, based on ASTM C 642 (ASTM, 2006) and ASTM C 1585 (ASTM, 2004) test procedures. Water absorption testing measures the mass of absorbed water per unit mass of the predried concrete material, after complete immersion in water until saturation is reached. Water absorption is expressed in terms of the volume percent of permeable pores. The sorptivity test measured the increase in mass of predried specimens at given intervals of time when permitted to absorb water by capillary suction in one direction, and it is quantified by the sorptivity index.

Figure 24.35 summarizes the findings of Sahmaran and Li which emphasized the impacts of the presence of microcracking and the water-repellent admixture on water absorption and sorptivity. From this figure, it can be seen that the presence of microcracks in ECC composites without water-repellent admixtures can lead to an exponential increase of the sorptivity index with the number of microcracks. However, sorptivity index values of cracked ECC are not particularly high when compared with those of normal concrete, probably due to the higher amount of cementitious materials, lower water/cementitious materials ratio, and high-volume fly ash content. For the ECC mixture with water-repellent admixtures, the presence of microcracks and their number had little or no effect on the sorptivity index. The water-repellent agent based on water-soluble silicon was very effective in reducing the sorptivity index of cracked ECC. ECC mixtures with water-repellent admixtures also showed lower percentages of permeable pores compared to the ECC mixtures without water-repellent admixture. In contrast to the sorptivity index, there was no significant influence of the number of cracks on the volume of permeable pores among the same ECC mixtures.

According to Neville (1995), the typical sorptivity index is $0.09 \text{ mm}/\text{min}^{1/2}$ for normal concrete with a W/C ratio of 0.4. Some other research studies suggested that ordinary Portland cement concrete with a W/C ratio of 0.4 to 0.5 would have a sorptivity index of about $0.23 \text{ mm}/\text{min}^{1/2}$ (Mehta and Monteiro, 2006). The sorptivity index for these cracked and virgin ECC specimens at a W/C ratio of 0.27 (especially

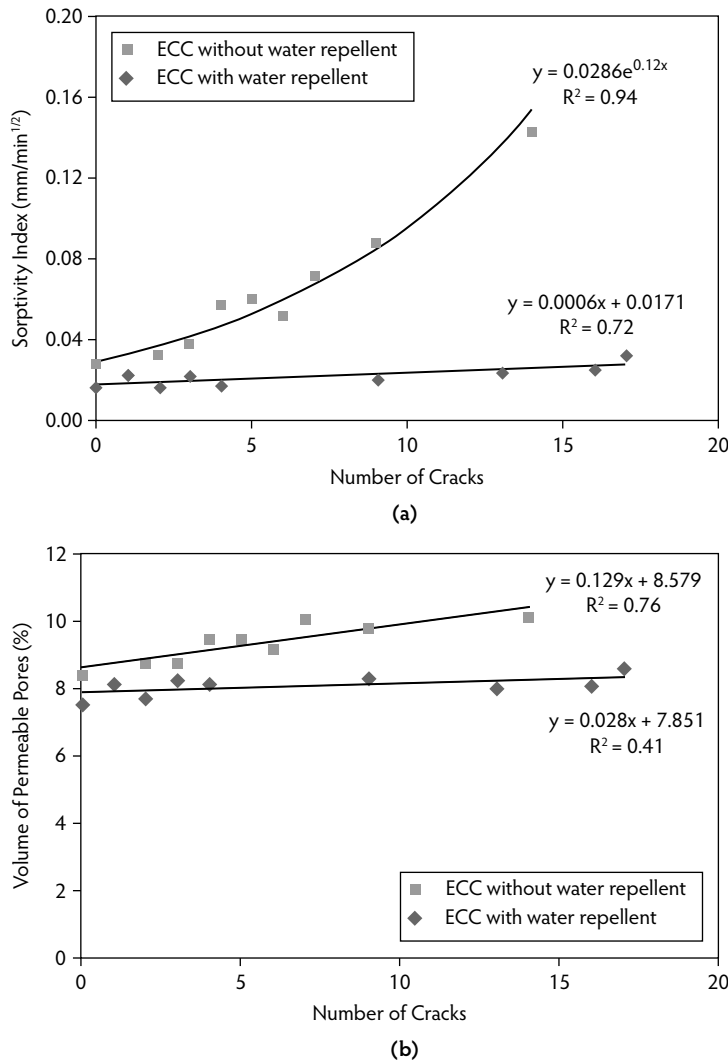


FIGURE 24.35 Capillary transport properties measured for preloaded ECC beams, showing the effects of water repellent on (a) sorptivity index and (b) volume of permeable pores as a function of the number of cracks. (From Sahmaran, M. and Li, V.C., *RILEM J. Mater. Struct.*, 2008.)

for those containing water-repellent admixtures, at about 0.02 to 0.03 mm/min^{1/2}) was significantly lower than that for conventional concrete. Water absorption tests by Mechtcherine and Lieboldt (2007) also confirmed that ECC strained to between 0.5 and 1% showed water-retardant ability. The findings by Sahmaran and Li (2008b), together with those of Mechtcherine and Lieboldt, confirm that capillary suction does not pose a danger to the durability of ECC structures despite the expected presence of fine cracks. This risk is further reduced by the use of water-repellent admixtures. These conclusions are consistent with the findings of Martinola et al. (2004).

24.5.3.2 Corrosion Resistance in R/ECC

From the discussions presented in Section 24.5.3.1, the transport properties of ECC associated with permeation under hydraulic gradient, diffusion under ion concentration gradient, or sorption and absorption under capillary suction, all show the tendency to improve over concrete and especially cracked concrete. Given that concrete structures are designed to allow some tensile cracking and that these cracks

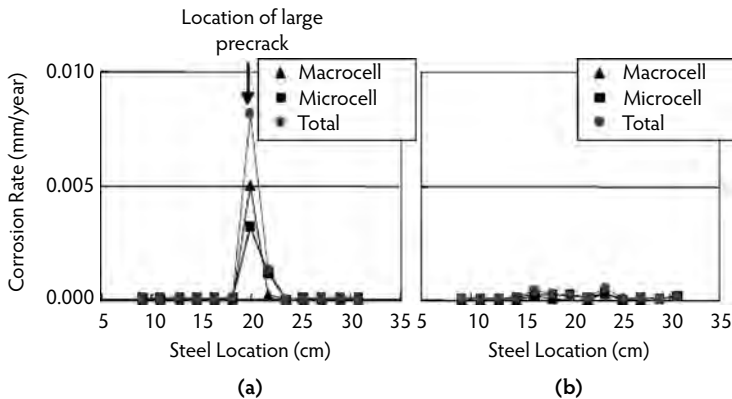


FIGURE 24.36 Measured corrosion rate along the steel rebar for preloaded (a) R/C and (b) R/ECC. (Adapted from Miyazato S. and Hiraishi, Y., in *Proceedings of the 11th International Conference on Fracture (ICF XI)*, March 20–25, Torino, Italy, 2005.)

within reinforced concrete are typically the source of corrosion due to the increased transport of water and corrosives, there is substantial potential for ECC to improve the durability of R/C structures by acting as a quality cover where all transport mechanisms are substantially inhibited. The interaction between ECC and steel reinforcement from the viewpoint of corrosion resistance has been examined. The nature and rate of steel corrosion in ECC and the spall resistance of ECC when specimens are subjected to accelerated testing conditions are presented below.

24.5.3.2.1 Nature of Steel Corrosion

A study on chloride penetration rate and corrosion rate of steel reinforcement was carried out by Miyazato and Hiraishi (2005). Preloaded R/ECC and R/C beams were exposed to a 28-day accelerated chloride environment with wet cycles (saltwater shower, 90% relative humidity, 2 days) and dry cycles (60% relative humidity, 5 days). They found that chloride penetration reached 0 to 20 mm and 80 to 100 mm in the R/ECC and the R/C beams, respectively. The total (macro- and microcell) steel rebar corrosion rate was measured to be less than 0.0004 mm/year in the R/ECC but exceeded 0.008 mm/year in the R/C beams (Figure 24.36). The observed smaller chloride penetration depth is consistent with the smaller effective diffusion coefficient found by Sahmaran et al. (2007b) discussed in Section 24.5.3.1.2. The nature of corrosion in R/ECC is decidedly different from that in R/C. Microcell currents formed between the closely spaced microcracks in the R/ECC dominate macrocell currents so a greater length of steel reinforcement experiences corrosion in the R/ECC. The much higher rebar corrosion rate concentrated at the location of the concrete crack in the R/C specimen suggests a higher tendency for pitting corrosion of the steel reinforcement to occur.

24.5.3.2.2 Corrosion Propagation and Spall Resistance

Given the tensile ductility of ECC, the ability for the cover to remain intact despite steel corrosion serves as a possibility to further prolong the service life of R/ECC structures. Sahmaran et al. (2006a) investigated R/ECC beams subjected to accelerated corrosion by electrochemical method in studies designed to induce different degrees of corrosion into the reinforcement (a single steel rebar) embedded in ECC prismatic specimens. These experiments examined the spall resistance of R/ECC cover, the influence of an intact cover on the corrosion process in the corrosion propagation phase, the rate of loss of steel by corrosion, and the residual load capacity of R/ECC elements.

The corrosion-induced crack width of mortar specimens increased with time as corrosion activity progressed. Larger crack widths, up to 2 mm wide, were obtained at higher levels of corrosion. On the other hand, crack widths of ECC remained nearly constant (~0.1 mm) with time as corrosion activity progressed, while the number of cracks on the surface of the specimen increased. The results of this study

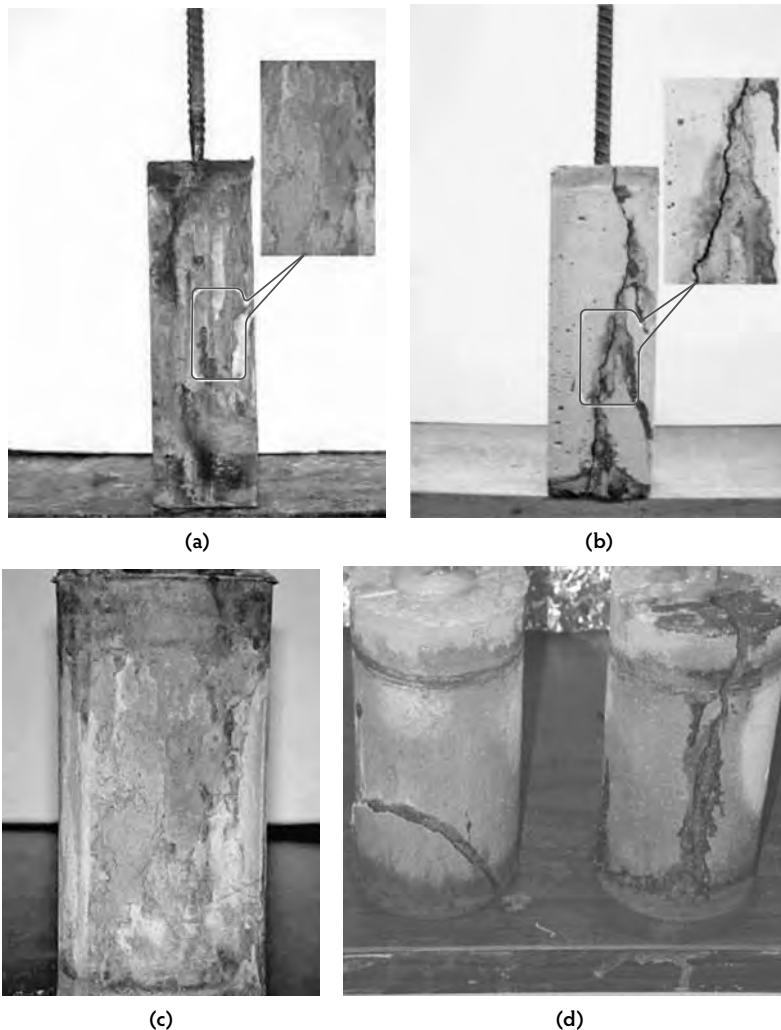


FIGURE 24.37 ECC and mortar specimens after accelerated corrosion test: (a) ECC prismatic specimen after 300 hours accelerated corrosion, (b) mortar prismatic specimen after 75 hours of accelerated corrosion, (c) ECC cylindrical specimen after 350 hours of accelerated corrosion, and (d) mortar cylindrical specimen after 95 hours of accelerated corrosion. (From Sahmaran, M. et al., *ACI Mater. J.*, 2008.)

also showed that ECC has significant anti-spalling capability as compared to conventional mortar (Figure 24.37). If a crack width of 0.3 mm, as specified by AASHTO (2004) for the maximum crack width limit for outdoor exposures, were used to represent the serviceability limit of reinforced concrete structures, the service life of reinforced ECC would be at least 15 times that of the reinforced mortar.

Reinforcement corrosion in mortar specimens resulted in a marked reduction in stiffness and flexural load capacity. After 25 hours of accelerated corrosion exposure, the flexural strength reduced to about 34% of the original flexural capacity of the control mortar beam. In contrast, the ECC specimens after 50 hours of accelerated corrosion exposure retained almost 100% of the original flexural capacity of the control specimens. Beyond 50 hours, the flexural capacity decreased but retained over 45% that of the control specimens even after 300 hours of accelerated corrosion exposure. Longitudinal cracks due to expansion of the corrosion products also affected the failure mode of the reinforced mortar under a four-point bend load (Figure 24.38). On the other hand, ECC deterioration due to the corrosion of reinforcement did not modify the type of failure in ECC beams.

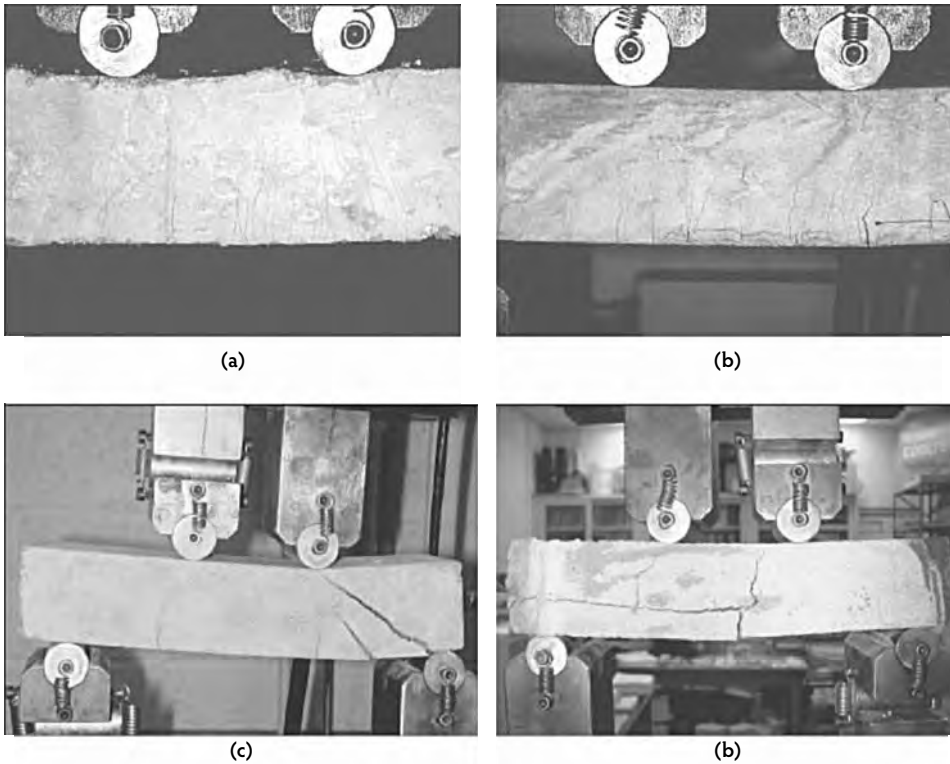


FIGURE 24.38 Types of failure of reinforced mortar and ECC beams under four-point bending test for (a) ECC before accelerated corrosion, (b) ECC after 150 hours of accelerated corrosion, (c) mortar before accelerated corrosion, and (d) mortar after 50 hours of accelerated corrosion. (Adapted from Sahmaran, M. et al., *ACI Mater. J.*, 2008.)

The loss in load-carrying capacity is related to the mass loss of the steel reinforcement due to corrosion. The percentage of steel mass losses within the ECC and mortar beams throughout the accelerated corrosion process is presented in Figure 24.39. The average percentage of mass loss of steel reinforcing bars embedded in the mortar specimens were 2.5%, 5.3%, and 11.7% at the end of 25, 50, and 75 hours of accelerated corrosion tests, respectively. On the other hand, there was nearly no mass loss of steel reinforcing bars embedded in ECC specimens after up to 50 hours of accelerated corrosion testing, and the average percentage of mass loss of reinforcing bars embedded in ECC was 17.5% at the end of 300 hours of accelerated corrosion testing. The observed superior corrosion performance of ECC compared to mortar in terms of corrosion propagation time, tight crack width, lower weight loss, and higher retention of stiffness and flexural strength is attributable to the high tensile strain capacity, strain-hardening performance, and multiple cracking behavior of ECC. Overall, the experimental results from this study suggest that the propagation period of corrosion could be safely included in estimating the service life of a structure when concrete is replaced by ECC.

24.5.4 Long-Term Performance

The long-term performance of ECC in full-scale structures has not been fully established given the relatively recent development of this material; however, at least two field demonstration studies provide limited data supporting the contention that ECC can be durable under actual field conditions. One study (Rokugo et al., 2005) involves the use of ECC for repair of a concrete gravity earth-retaining wall (18 m wide by 5 m tall) that had been damaged by alkali-silica reaction (ASR) cracking. The decision to use ECC for the 50-

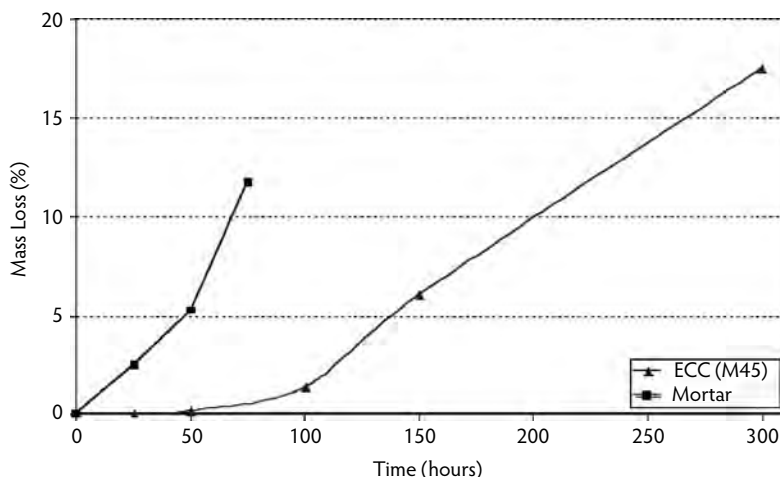


FIGURE 24.39 Mass loss vs. time for ECC and mortar corrosion specimens. (From Sahmaran, M. et al., *ACI Mater. J.*, 2008.)

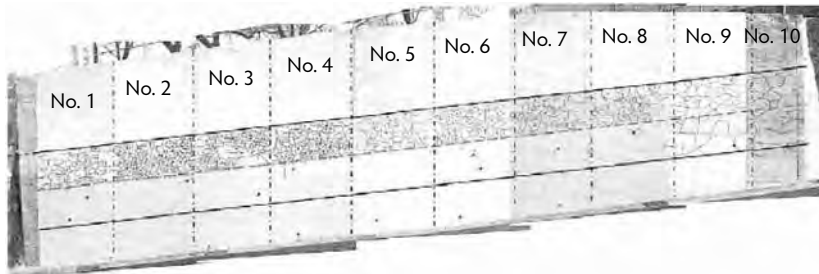
to 70-mm-thick repair overlay was based on the need to prevent cracks in the substrate concrete from reflecting onto the repair layer. Such reflection was anticipated had normal concrete been used in this repair given continued ASR expansion. For demonstration, the wall was divided into nine repair blocks while a tenth block was left unrepaired. For the repaired blocks, two types of ECC—one containing 1.5% hybrid PVA and PE fibers (blocks 1 to 4) and another containing 2.1% PVA fibers (blocks 5 to 8)—were applied. In each block, welded wire mesh reinforcement, expanded metal reinforcement, or no reinforcement was used. For control, a welded wire mesh reinforced repair mortar was applied to block 9. Since 2003, when the repair took place, this wall has been continuously monitored. No cracking in the overlay was observed until 7 months after repair by ECC, while cracking was visually observed on the blocks repaired with normal mortar just 1 month after repair. The crack widths in the ECC repair blocks were less than 50 μm and 120 μm at 10 and 24 months, respectively. In contrast, the crack widths in the normal repair mortar block were 200 μm and 300 μm at 10 and 24 months, respectively. The crack patterns at 12 months and 24 months are shown in Figure 24.40. Another long-term performance verification is a small ECC patch repair placed on the bridge deck of Curtis Road over M-14 in Southern Michigan in 2002, in collaboration with the Michigan Department of Transportation (MDOT). A complete summary of this work has been outlined by Li and Lepech (2004). During this work, one section of a deteriorated bridge deck was repaired with ECC, while the remaining portion was repaired with a commercial concrete patching material commonly used by MDOT (Figure 24.41a). This repair scenario allowed for a unique comparison of ECC and concrete because both were subjected to identical environmental and traffic loads. (This road is used frequently by 11-axle trucks heavily loaded with aggregates, although it has a relatively low average daily traffic rate of 3000 vehicles/day.) The concrete repair material used was a prepackaged mixture of Portland cement and plaster of Paris. At this writing, the repaired bridge deck has experienced more than six complete Michigan winter cycles of freezing and thawing, in addition to live loads. The monitored crack width development is shown in Figure 24.41b. The ECC patch repair has survived this combined loading state with minor microcracking limited to less than 50 μm , but the concrete repair portion experienced cracking in excess of 3.5 mm and was repaired again in 2005.

24.6 Concluding Remarks

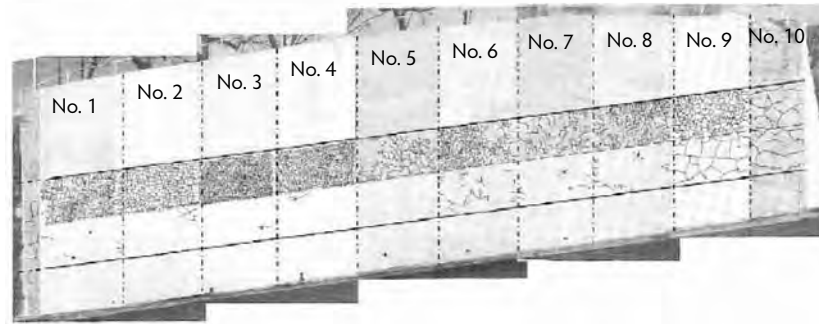
Engineered cementitious composite has a number of attractive properties. Most unique is the high tensile ductility several hundred times that of concrete with compressive strengths similar to concrete or high-strength concrete. The metal-like behavior of ECC is achieved without depending on high fiber content,



(a)



(b)



(c)

FIGURE 24.40 Cracking behavior of patched earth retaining wall: (a) Before repair, showing ASR damage; (b) after repair at 12 months; (c) after repair at 24 months. Blocks 1 to 8 used ECC, block 9 used a normal repair mortar, and block 10 was left unrepaired. (From Rokugo, K. et al., in *Proceedings of ConMat'05*, August 22–24, Vancouver, Canada, 2005.)

thus breaking the conventional wisdom of the need for a high fiber volume fraction to achieve high material performance. The moderate fiber content (2% or less by volume) makes ECC easily adaptable to construction project execution in the field or to precast plant structural element production. Indeed, ECC has demonstrated flexibility in processing routes, including on-site self-consolidating casting, and spraying, as well as off-site precasting and extrusion. Maintaining a moderately low fiber content is obviously important also for economic reasons (Li, 2004).

The large tensile ductility of ECC allows it to deform compatibly and creates a synergistic load-sharing capability with steel reinforcement in structural members. As a result, steel reinforcements in R/ECC members are better utilized in enhancing structural performance. Simultaneously, the tight crack width of ECC protects the steel reinforcement from typical corrosive processes, resulting in improved structural durability.

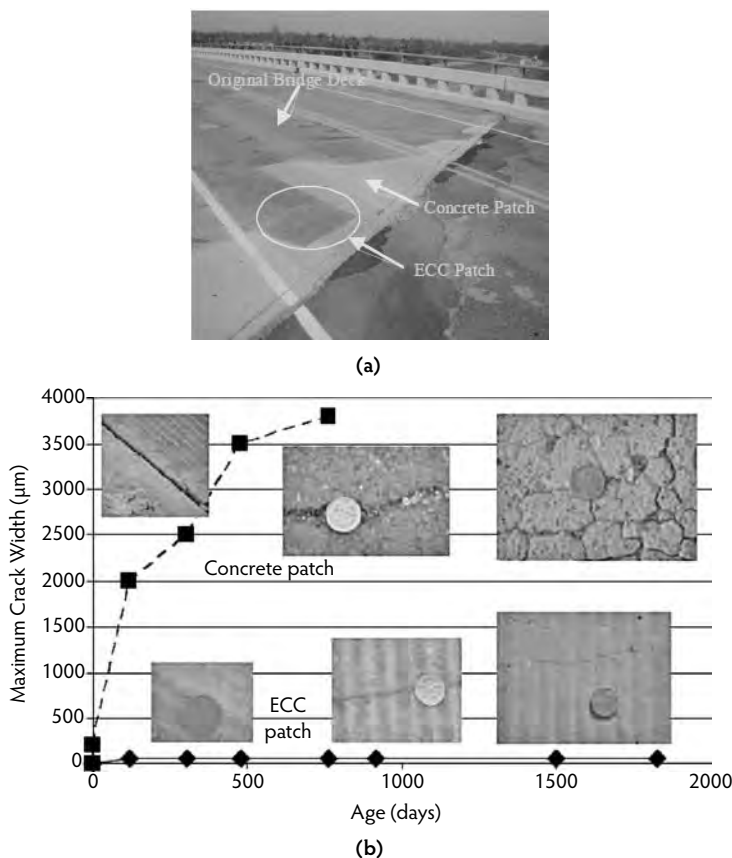


FIGURE 24.41 (a) ECC and concrete patches on the Curtis Road, Ann Arbor, MI, bridge deck; (b) maximum crack width development over time for the two materials. The concrete patch was re-repaired at about 1000 days.

In recent years, a number of full-scale applications of ECC have been carried out in various countries. Foremost among these is the use of ECC in precast R/ECC coupling beams in the core of two high-rises in Japan (Kunieda and Rokugo, 2006b; Maruta et al., 2005). This application exploits the high energy absorption capability of R/ECC to aid in the seismic resistance of these tall buildings. Other notable applications include cast-in-place ECC link slabs on bridge decks (Kim et al., 2004; Lepech and Li, 2005b) in the United States and Italy, a composite ECC/steel bridge deck in Japan (Mitamura et al., 2005), sprayed ECC tunnel linings in South Korea (Wonha, 2004), repair of the Mitaka Dam in Japan (Kojima et al., 2004), an irrigation channel repair in Japan (Kunieda and Rokugo, 2006b), and prototype pipe extrusion in Australia. Several projects in the housing and energy industries employing ECC are in various planning stages. Despite the advanced stage of development of ECC and its application readiness, a great deal of research and experimentation remain to be done. Indeed, the transformation of brittle concrete to ductile ECC offers enormous opportunities in structural innovations not possible previously.

Although safety and durability are critically important in any successful engineering project, concerns for infrastructure sustainability are growing due to greater recognition of the impact of the built environment on the natural environment. Green ECC employing industrial byproducts as components is being developed (Lepech and Li, 2008; Li et al., 2004b; Yang et al., 2007). Combined with the greater durability of ECC, such advancements offer a way to reduce environment burdens due to transportation infrastructures such as bridges and pavements (Keoleian et al., 2005; Lepech, 2006; Li et al., 2008). Sustainable infrastructures are critical to sustainable economic development in developed and developing countries. Materials technological advancements must contribute to this worldwide effort.

Acknowledgments

The author would like to acknowledge the research support of the National Science Foundation (the Biocomplexity, the Cyberinfrastructure, and the Civil, Mechanical and Manufacturing Innovation programs) and the Michigan Department of Transportation. Many former and current students, postdoctorates, and colleagues at the University of Michigan contributed to this work. Their devotion to advancing infrastructure materials is greatly appreciated. Knowledge on ECC has been greatly expanded by the intense research activities of many academic and industrial groups around the world in the last several years. Special thanks are extended to Dr. M. Lepech who reviewed a draft of this manuscript and provided helpful suggestions for improvements.

References

- AASHTO. 2002. *Standard Method of Test for Resistance of Concrete to Chloride Ion Penetration*, AASHTO T 259. American Association of State Highway and Transportation Officials, Washington, D.C.
- AASHTO. 2004. *LRFD Bridge Design Specifications*. American Association of State Highway and Transportation Officials, Washington, D.C.
- Allen, H.G. 1971. Stiffness and strength of two glass-fiber reinforced cement laminates. *J. Composite Mater.*, 5(2), 194–207.
- ASTM. 2003a. *Standard Test Method for Resistance of Concrete to Rapid Freezing and Thawing*, ASTM C 666/C 666M. American Society for Testing and Materials, Philadelphia, PA.
- ASTM. 2003b. *Standard Test Method for Scaling Resistance of Concrete Surfaces Exposed to Deicing Chemicals*, ASTM C 672/C 672M. American Society for Testing and Materials, Philadelphia, PA.
- ASTM. 2004. *Standard Test Method for Measurement of Rate of Absorption of Water by Hydraulic-Cement Concretes*, ASTM C 1585. American Society for Testing and Materials, Philadelphia, PA.
- ASTM. 2006. *Standard Test Method for Density, Absorption, and Voids in Hardened Concrete*, ASTM C 642. American Society for Testing and Materials, Philadelphia, PA.
- ASTM. 2007. *Standard Test Method for Potential Alkali Reactivity of Aggregates (Mortar-Bar Method)*, ASTM C 1260. American Society for Testing and Materials, Philadelphia, PA.
- Aveston, J., Cooper, G.A., and Kelly, A. 1971. Single and multiple fracture. In *The Properties of Fiber Composites, Conference Proceedings*, pp. 15–24. IPC Science and Technology Press, Guildford, U.K.
- Bache, H. 1981. *Densified Cement/Ultra-Fine Particle-Based Materials*, CBL Report No. 40. Aalborg Portland, Denmark.
- Beeldens, A. and Vandewalle, L. 2001. Durability of high strength concrete for highway pavement restoration. In *Proceedings of Third International Conference on Concrete Under Severe Conditions (CONSEC'01)*, June 18–20, Vancouver, Canada, pp. 1230–1238.
- Billington, S.L. and Yoon, J.K. 2004. Cyclic response of precast bridge columns with ductile fiber-reinforced concrete. *ASCE J. Bridge Eng.*, 9(4), 353–363.
- Boshoff, W.P. and van Zijl, G.P.A.G. 2007. Tensile creep of SHCC. In *Proceedings of the Fifth International RILEM Workshop on High-Performance Fiber-Reinforced Cement Composites (HPFRCC 5)*, Reinhardt, H.W. and Naaman, A.E., Eds., pp. 87–96. RILEM, Paris.
- Carpinteri, A., Gamarova, P., Ferro, G., and Plizzari, G., Eds. 2007. *Proceedings of 6th International Conference on Fracture Mechanics of Concrete and Concrete Structures (FraMCoS-6)*, June 17–22, Catania, Italy. Taylor & Francis, New York.
- Chanvillard, G. and Rigaud, S. 2003. Complete characterization of tensile properties of ductal UHPFRC according to the French recommendations. In *Proceedings of the Fourth International RILEM Workshop on High-Performance Fiber-Reinforced Cement Composites (HPFRCC 4)*, Naaman, A.E. and Reinhardt, H.W., Eds., pp. 21–34. RILEM, Paris.
- Curbach, M. and Jesse, F. 1999. High-performance textile-reinforced concrete. *Struct. Eng. Int.*, 9(4), 289–291.

- Fischer, G. and Li, V.C. 2002a. Effect of matrix ductility on deformation behavior of steel reinforced ECC flexural members under reversed cyclic loading conditions. *ACI Struct. J.*, 99 (6), 781–790.
- Fischer, G. and Li, V.C. 2002b. Influence of matrix ductility on the tension-stiffening behavior of steel reinforced engineered cementitious composites (ECC). *ACI Struct. J.*, 99(1), 104–111.
- Fischer, G. and Li, V.C. 2003a. Deformation behavior of fiber-reinforced polymer reinforced engineered cementitious composite (ECC) flexural members under reversed cyclic loading conditions. *ACI Struct. J.*, 100(1), 25–35.
- Fischer, G. and Li, V.C. 2003b. Intrinsic response control of moment resisting frames utilizing advanced composite materials and structural elements. *ACI Struct. J.*, 100(2), 166–176.
- Fischer, G. and Li, V.C., Eds. 2006. *Proceedings, High-Performance Fiber-Reinforced Cementitious Composites (HPFRCC) in Structural Applications*. RILEM, Paris.
- Fischer, G., Wang, S., and Li, V.C. 2003. Design of engineered cementitious composites for processing and workability requirements. In *Proceedings of the Seventh International Symposium on Brittle Matrix Composites*, October 13–15, Warsaw, Poland, pp. 29–36.
- Fukuyama, H., Iso, M., Ogawa, A., and Suwada, H. 2007. Mitigation of damage due to crack of RC elements utilizing high-performance fiber-reinforced cementitious composites. In *Proceedings of the Fifth International RILEM Workshop on High-Performance Fiber-Reinforced Cement Composites (HPFRCC 5)*, Reinhardt, H.W. and Naaman, A.E., Eds., pp. 427–435. RILEM, Paris.
- Fukuyama, H., Matsuzaki, Y., Nakano, K., and Sato, Y. 1999. Structural performance of beam elements with PVA-ECC. In *Proceedings of the Third International RILEM Workshop on High-Performance Fiber-Reinforced Cement Composites (HPFRCC 3)*, Reinhardt, H.W. and Naaman, A.E., Eds., pp. 531–542. Chapman & Hall, London.
- Fukuyama, H., Matsuzaki, Y., Sato, Y., Iso, M., and Suwada, H. 2000. Structural performance of engineered cementitious composite elements. In *Proceedings of the 6th ASCCS International Conference on Steel-Concrete Composite Structures*, March 22–24, Los Angeles, CA.
- Fukuyama, H., Suwada, H., and Mukai, T. 2006. Test on high-performance wall elements with HPFRCC. In *Proceedings, High-Performance Fiber-Reinforced Cementitious Composites (HPFRCC) in Structural Applications*, Fischer, G. and Li, V.C., Eds., pp. 365–374. RILEM, Paris.
- Horikoshi, T., Ogawa, A., Saito, T., and Hoshiro, H. 2006. Properties of polyvinylalcohol fiber as reinforcing materials for cementitious composites. In *Proceedings, High-Performance Fiber-Reinforced Cementitious Composites (HPFRCC) in Structural Applications*, Fischer, G. and Li, V.C., Eds., pp. 145–153. RILEM, Paris.
- JSCE. 2007. *Recommendations for Design and Construction of High-Performance Fiber-Reinforced Cement Composite with Multiple Fine Cracks (Draft)*, Japan Society of Civil Engineers, Tokyo [in Japanese].
- Kabele, P., 2001. *Assessment of Structural Performance of Engineered Cementitious Composites by Computer Simulation*, CTU Reports No. 4, Vol. 5. Czech Technical University, Prague.
- Kabele, P. and Kanakubo, T. 2007. Experimental and numerical investigation of shear behavior of PVA-ECC in structural elements. In *Proceedings of the Fifth International RILEM Workshop on High-Performance Fiber-Reinforced Cement Composites (HPFRCC 5)*, Reinhardt, H.W. and Naaman, A.E., Eds., pp. 137–146. RILEM, Paris.
- Kabele, P., Novak, L., Nemecek, J., and Pekar, J. 2007. Multiscale experimental investigation of deterioration of fiber-cementitious composites in aggressive environment. In *Proc. MHM 2007: International Conference on Modelling of Heterogeneous Materials with Applications in Construction and Biomedical Engineering*, June 25–27, Prague, Jirasek, M., Bittnar, Z., and Mang, H., Eds., pp. 270–271.
- Kamal, A., Kunieda, M., Ueda, N., and Nakamura, H. 2007. Assessment of crack elongation performance in RC beam repaired by UHP-SHCC. In *Proceedings of the Ninth International JSCE Summer Symposium*, September 18, Yokohama National University, Japan.
- Kanakubo, T. 2006. Tensile characteristics: evaluation method for DFRCC. *J. Adv. Concrete Technol.*, 4(1), 3–17.
- Kanda, T. and Li, V.C. 1999. A new micromechanics design theory for pseudo strain hardening cementitious composite. *ASCE J. Eng. Mech.*, 125(4), 373–381.

- Kanda, T. and Li, V.C. 2006. Practical design criteria for saturated pseudo strain hardening behavior in ECC. *J. Adv. Concrete Technol.*, 4(1), 59–72.
- Kanda, T., Watanabe, S., and Li, V.C. 1998. Application of pseudo strain hardening cementitious composites to shear resistant structural elements. In *Fracture Mechanics of Concrete Structures: Proceedings FramCoS-3*, pp. 1477–1490. AEDIFICATIO Publishers, Freiberg, Germany.
- Kanda, T., Saito, T., Sakat, N., and Hiraishi, H. 2001. Basic properties of sprayed repair material based on a highly ductile FRC with PVA fiber. *Proc. Annu. Meet. JCI*, 25(1), 475–480.
- Kanda, T., Kanakubo, T., Nagai, S., and Maruta, M. 2006a. Technical consideration in producing ECC pre-cast structural elements. In *Proceedings, High-Performance Fiber-Reinforced Cementitious Composites (HPFRCC) in Structural Applications*, Fischer, G. and Li, V.C., Eds., pp. 229–242. RILEM, Paris.
- Kanda, T., Tomoe, S., Nagai, S., Maruta, M., Kanakubo, T., and Shimizu, K. 2006b. Full-scale processing investigation for ECC pre-cast structural elements. *J. Asian Architect. Build. Eng.*, 5(2), 333–340.
- Keoleian, G.A., Kendall, A., Dettling, J.E., Smith, V.M., Chandler, R., Lepech, M.D., and Li, V.C. 2005. Life cycle modeling of concrete bridge design: comparison of engineered cementitious composite link slabs and conventional steel expansion joints. *ASCE J. Infrastructure Syst.*, 11(1), 51–60.
- Kesner, K.E. and Billington, S.L. 2005. Investigation of infill panels made from engineered cementitious composites for seismic strengthening and retrofit. *ASCE J. Struct. Eng.*, 131(11), 712–720.
- Kim, Y.Y., Kong, H.J., and Li, V.C. 2003. Design of engineered cementitious composite (ECC) suitable for wet-mix shotcreting. *ACI Mater. J.*, 100(6), 511–518.
- Kim, Y.Y., Fischer, G., and Li, V.C. 2004. Performance of bridge deck link slabs designed with ductile ECC. *ACI Struct. J.*, 101(6), 792–801.
- Kojima, S., Sakat, N., Kanda, T., and Hiraishi, T. 2004. Application of direct sprayed ECC for retrofitting dam structure surface: application for Mitaka Dam. *Concrete J.*, 42(5), 35–39 [in Japanese].
- Kong, H.J., Bike, S., and Li, V.C. 2003. Development of a self-compacting engineered cementitious composite employing electrosteric dispersion/stabilization. *J. Cement Concrete Comp.*, 25(3), 301–309.
- Krenchel, H. and Stang, H. 1989. Stable microcracking in cementitious materials. In *Brittle Matrix Composites 2*, Brandt, A.M. and Marshall, J.H., Eds., pp. 20–33. Elsevier, Amsterdam.
- Kunieda, M. and Rokugo, K. 2006a. Measurement of crack opening behavior within ECC under bending moment. In *Proceedings, High-Performance Fiber-Reinforced Cementitious Composites (HPFRCC) in Structural Applications*, Fischer, G. and Li, V.C., Eds., pp. 313–322. RILEM, Paris.
- Kunieda, M. and Rokugo, K. 2006b. Recent progress on HPFRCC in Japan: required performance and applications. *J. Adv. Concrete Technol.*, 4(1), 19–33.
- Lankard, D.R. 1986. Preparation, properties and applications of cement based composites containing 5–20 percent steel fiber reinforcement. In *Steel Fiber Concrete*, Shah, S.P. and Skarendahl, A., Eds. Elsevier, Amsterdam.
- Lepech, M.D. 2006. A Paradigm for Integrated Structures and Materials Design for Sustainable Transportation Infrastructure, Ph.D. thesis. University of Michigan, Ann Arbor.
- Lepech, M.D. and Li, V.C. 2005a. Water permeability of cracked cementitious composites. In *Proceedings of the 11th International Conference on Fracture (ICF XI)*, March 20–25, Torino, Italy.
- Lepech, M.D. and Li, V.C. 2005b. Design and field demonstration of ECC link slabs for jointless bridge decks. In *Proceedings of ConMat'05*, August 22–24, Vancouver, Canada.
- Lepech, M.D. and Li, V.C. 2008. Large scale processing of engineered cementitious composites. *ACI Mater. J.*, accepted.
- Lepech, M.D., Li, V.C., Robertson, R.E., and Keoleian, G.A. 2007. Design of ductile engineered cementitious composites for improved sustainability. *ACI Mater. J.*, submitted.
- Leung, C.K.Y., Cheung, A.K.F., and Zhang, X. 2006. Partial use of pseudo-ductile cementitious composites in concrete components to resist concentrated stress, *Key Eng. Mater.*, 312, 319–324.

- Li, M., Sahmaran, M., and Li, V.C. 2007. Effect of cracking and healing on durability of engineered cementitious composites under marine environment. In *Proceedings of the Fifth International RILEM Workshop on High-Performance Fiber-Reinforced Cement Composites (HPFRCC 5)*, Reinhardt, H.W. and Naaman, A.E., Eds., pp. 313–322. RILEM, Paris.
- Li, V.C. 1993. From micromechanics to structural engineering: the design of cementitious composites for civil engineering applications. *JSCE J. Struct. Mech. Earthquake Eng.*, 10(2), 37–48.
- Li, V.C. 2000. When a crack is not a crack. In *Proceedings of BMC6*, Brandt, A., Marshall, I., and Li, V.C., Eds., pp. 173–185.
- Li, V.C. 2004. Strategies for high-performance fiber-reinforced cementitious composites development. In *Fiber-Reinforced Concrete: From Theory to Practice: Proceedings of the North American/European Workshop on Advances in Fiber-Reinforced Concrete*, Ahmad, S., di Prisco, M., Meyer, C., Plizzari, G.A., and Shah, S., Eds., pp. 93–98. Starrylink Editrice, Brescia, Italy.
- Li, V.C. 2007. Integrated structures and materials design. *RILEM J. Mater. Struct.*, 40(4), 387–396.
- Li, V.C. and Lepech, M. 2004. Crack-resistant concrete material for transportation construction. In *Proceedings of the Transportation Research Board 83rd Annual Meeting*, Compendium of Papers CD-ROM, Paper 04-4680. Transportation Research Board, Washington, D.C.
- Li, V.C. and Leung, C.K.Y. 1992. Steady-state and multiple cracking of short random fiber composites. *ASCE J. Eng. Mech.*, 118 (11), 2246–2264.
- Li, V.C., and Stang, H. 2004. Elevating FRC material ductility to infrastructure durability. In *Fiber-Reinforced Concretes (BEFIB'2004)*, di Prisco, M., Felicetti, R., and Plizzari, G.A., Eds., pp. 171–186. RILEM, Paris.
- Li, V.C. and Wang, S. 2002. Failure mode and structural ductility of GFRP reinforced engineered cementitious composite beams. *ACI Mater. J.*, 99(1), 11–21.
- Li, V.C. and Wang, S. 2006. Microstructure variability and macroscopic composite properties of high-performance fiber-reinforced cementitious composites. *J. Probabil. Eng. Mech.*, 21(3), 201–206.
- Li, V.C. and Yang, E.H. 2007. Self-healing in concrete materials. In *Self-Healing Materials: An Alternative Approach to 20 Centuries of Materials Science*, van der Zwaag, S., Ed., pp. 161–193. Springer, New York.
- Li, V.C., Wu, H.C., and Chan, Y.W. 1996. Effect of plasma treatment of polyethylene fibers on interface and cementitious composite properties. *J. Am. Ceram. Soc.*, 79(3), 700–704.
- Li, V.C., Wu, C., Wang, S., Ogawa, A., and Saito, T. 2002. Interface tailoring for strain-hardening PVA-ECC. *ACI Mater. J.*, 99(5), 463–472.
- Li, V.C., Fischer, G., Kim, Y.Y., Lepech, M., Qian, S., Weimann, M., and Wang, S. 2003. *Durable Link Slabs for Jointless Bridge Decks Based on Strain-Hardening Cementitious Composites*, RC-1438. Michigan Department of Transportation, Lansing.
- Li, V.C., Horikoshi, T., Ogawa, A., Torigoe, S., and Saito, T. 2004a. Micromechanics-based durability study of polyvinyl alcohol-engineered cementitious composite (PVA-ECC). *ACI Mater. J.*, 101(3), 242–248.
- Li, V.C., Lepech, M., Wang, S., Weimann, M., and Keoleian, G. 2004b. Development of green ECC for sustainable infrastructure systems. In *Proceedings of the International Workshop on Sustainable Development and Concrete Technology*, May 20–21, Beijing, China, Wang, K., Ed., pp. 181–192.
- Li, V.C., Qian, S., Zhang, H., and Keoleian, G.A. 2008. Sustainable Infrastructure with Durable Fiber Concrete Material, paper presented at the Seventh International Congress—Concrete: Construction's Sustainable Option, July 8–10, Dundee, Scotland.
- Lim, Y.M. and Li, V.C. 1997. Durable repair of aged infrastructures using trapping mechanism of engineered cementitious composites. *J. Cement Concrete Compos.*, 19(4), 373–385.
- Maalej, M. and Li, V.C. 1994. Flexural/tensile strength ratio in engineered cementitious composites. *ASCE J. Mater. Civil Eng.*, 6(4), 513–528.
- Maalej, M. and Li, V.C. 1995. Introduction of strain hardening engineered cementitious composites in the design of reinforced concrete flexural members for improved durability. *ACI Struct. J.*, 92(2), 167–176.
- Maruta, M., Kanda T., Nagai S., and Yamamoto, Y. 2005. New high-rise RC structure using pre-cast ECC coupling beam. *Concrete J.*, 43(11), 18–26.

- Martinola, G., Baeuml, M.F., and Wittmann, F.H. 2004. Modified ECC by means of internal impregnation. *J. Adv. Concrete Technol.*, 2(2), 207–212.
- Mechtcherine, V. and Lieboldt, M. 2007. Effect of cracking on air-permeability and water absorption of strain hardening cement-based composites. In *Proceedings of the Fifth International RILEM Workshop on High-Performance Fiber-Reinforced Cement Composites (HPFRCC 5)*, Reinhardt, H.W. and Naaman, A.E., Eds., pp. 305–312. RILEM, Paris.
- Mechtcherine, V. and Schulze, J. 2006. Testing the behavior of strain hardening cementitious composites in tension. In *Proceedings, High-Performance Fiber-Reinforced Cementitious Composites (HPFRCC) in Structural Applications*, Fischer, G. and Li, V.C., Eds., pp. 37–46. RILEM, Paris.
- Mehta, P.K. and Monteiro, P.J.M. 2006. *Concrete: Structure, Properties, and Materials*, 3rd ed. McGraw-Hill, New York.
- Mihashi, H. and De Leite, J.P.B. 2004. State-of-the-art report on control of cracking in early age concrete. *Adv. Concrete Technol.*, 2(2), 141–154.
- Mitamura, H., Sakata, N., Shakushiro, K., Suda, K., and Hiraishi, T. 2005. Application of overlay reinforcement method on steel deck utilizing engineering cementitious composites: Mihara Bridge. *Bridge Foundation Eng.*, 39(8), 88–91.
- Miyazato S. and Hiraishi, Y. 2005. Transport properties and steel corrosion in ductile fiber reinforced cement composites. In *Proceedings of the 11th International Conference on Fracture (ICFXI)*, March 20–25, Torino, Italy.
- Mobasher, B., Peled, A., and Pahilajani, J. 2006. Distributed cracking and stiffness degradation in fabric-cement composites. *Mater. Struct.*, 39, 317–331.
- Mora, J., Aguado, A., and Gettu, R. 2003. The influence of shrinkage reducing admixtures on plastic shrinkage. *Materiales de Construcción*, 53(271–272), 71–80.
- Naaman, A.E. 1992. SIFCON: tailored properties for structural performance. In *High-Performance Fiber-Reinforced Cement Composites*, Reinhardt, H.W. and Naaman, A.E., Eds., pp. 18–38. E&FN Spon, London.
- Naaman, A.E. and Reinhardt, H.W. 2003. Setting the stage: toward performance-based classification of FRC composites. In *Proceedings of the Fourth International RILEM Workshop on High-Performance Fiber-Reinforced Cement Composites (HPFRCC 4)*, Naaman, A.E. and Reinhardt, H.W., Eds. RILEM, Paris.
- Nemecek, J., Kabele, P., Kopecky, L., and Bittnar, Z. 2006. Leached engineered cementitious composites. In *Proceedings, High-Performance Fiber-Reinforced Cementitious Composites (HPFRCC) in Structural Applications*, Fischer, G. and Li, V.C., Eds., pp. 205–212. RILEM, Paris.
- Neville, A.M. 1995. *Properties of Concrete*. 4th ed. Longman, London.
- Oh, B.H. and Shin, K.J. 2006. Cracking, ductility and durability characteristics of HPFRCC with various mixture proportions and fibers. In *Proceedings, High-Performance Fiber-Reinforced Cementitious Composites (HPFRCC) in Structural Applications*, Fischer, G. and Li, V.C., Eds., pp. 213–222. RILEM, Paris.
- Oh, B.H., Cha, S.W., Jang, B.S., and Jang, S.Y. 2002. Development of high-performance concrete having high resistance to chloride penetration. *Nuclear Eng. Design (Switzerland)*, 212(1–3), 221–231.
- Parra-Montesinos, G. and Wight, J.K. 2000. Seismic response of exterior RC column-to-steel beam connections. *ASCE J. Struct. Eng.*, 126(10), 1113–1121.
- Proctor, B.A., Oakley, D.R., and Litherland, K.L., 1982. Developments in the assessment and performance of GRC over 10 years. *Composites*, 13, 173–179.
- Qian, S. 2007. Influence of Concrete Material Ductility on the Behavior of High Stress Concentration Zones, Ph.D. thesis. University of Michigan, Ann Arbor.
- Qian, S. and Li, V.C. 2006. Influence of concrete material ductility on the shear response of stud connection. *ACI Mater. J.*, 103(1), 60–66.
- Qian, S. and Li, V.C. 2007. Simplified inverse method for determining the tensile strain capacity of strain hardening cementitious composites. *J. Adv. Concrete Technol.*, 5(2), 235–246.

- Reinhardt, H. and Naaman, A.E., Eds. 2007. *Proceedings of the Fifth International RILEM Workshop on High-Performance Fiber-Reinforced Cement Composites (HPFRCC 5)*. RILEM, Paris.
- Reinhardt, H.W., Krüger, M., and Große, C.U. 2003. Concrete prestressed with textile fabric. *J. Adv. Concrete Technol.*, 1(3), 231–239.
- Rokugo, K., Kunieda, M., and Lim, S.C. 2005. Patching repair with ECC on cracked concrete surface. In *Proceedings of ConMat'05*, August 22–24, Vancouver, Canada.
- Rokugo, K., Kanda, T., Yokota, H., and Sakata, N. 2007. Outline of JSCE recommendation for design and construction of multiple fine cracking type fiber reinforced cementitious composite (HPFRCC). In *Proceedings of the Fifth International RILEM Workshop on High-Performance Fiber-Reinforced Cement Composites (HPFRCC 5)*, Reinhardt, H.W. and Naaman, A.E., Eds., pp. 203–212. RILEM, Paris.
- Romualdi, N.P. and Batson, G.B. 1963. Mechanics of crack arrest in concrete. *Proc. ASCE Eng. Mech. J.*, 89(EM3), 147–168.
- Romualdi, J.P. and Mandel, J.A. 1964. Tensile strength of concrete affected by uniformly distributed closely spaced short lengths of wire reinforcement. *Proc. ACI J.*, 61(6), 657–671.
- Sahmaran, M. and Li, V.C. 2007. De-icing salt scaling resistance of mechanically loaded engineered cementitious composites. *J. Cement Concrete Res.*, 37, 1035–1046.
- Sahmaran, M. and Li, V.C. 2008a. Durability of mechanically loaded engineered cementitious composites under high alkaline environment. *J. Cement Concrete Compos.*, in print.
- Sahmaran, M. and Li, V.C. 2008b. Influence of microcracking on water absorption and sorptivity of ECC. *RILEM J. Mater. Struct.*, submitted.
- Sahmaran, M., Li, M., and Li, V.C. 2007. Transport properties of engineered cementitious composites under chloride exposure. *ACI Mater. J.*, 104(6), 604–611.
- Sahmaran, M., Li, V.C., and Andrade, C. 2008. Corrosion resistance performance of steel-reinforced engineered cementitious composites beams. *ACI Mater. J.*, in print.
- Shimizu, K., Kanakubo, T., Kanda, T., and Nagai, S. 2006. In *Proceedings, High-Performance Fiber-Reinforced Cementitious Composites (HPFRCC) in Structural Applications*, Fischer, G. and Li, V.C., Eds., pp. 443–451. RILEM, Paris.
- Stang, H. and Li, V.C. 1999. Extrusion of ECC-Material. In *Proceedings of the Third International RILEM Workshop on High-Performance Fiber-Reinforced Cement Composites (HPFRCC3)*, Reinhardt, H.W. and Naaman, A.E., Eds., pp. 203–212. Chapman & Hall, London.
- Stang, H. and Li, V.C. 2004. Classification of fiber-reinforced cementitious materials for structural applications. In *Fiber-Reinforced Concretes (BEFIB'2004)*, di Prisco, M., Felicetti, R., and Plizzari, G.A., Eds., pp. 197–218. RILEM, Paris.
- Suthiwarapirak, P., Matsumoto, T., and Kanda, T., 2002. Flexural fatigue failure characteristics of an engineered cementitious composite and polymer cement mortars. *JSCE J. Mater. Conc. Struct. Pavements*, 718(57), 121–134.
- Szerszen, M.M., Szwed, A., and Li, V.C. 2006. Flexural response of reinforced beam with high ductility concrete material. In *Brittle Matrix Composites 8*, Brandt, A.M., Li, V.C., and Marshall, I.H., Eds., pp. 263–274. Woodhead, Warsaw.
- Takashima, H., Miyagai, K., Hashida, T., and Li, V.C. 2003. A design approach for the mechanical properties of polypropylene discontinuous fiber reinforced cementitious composites by extrusion molding. *J. Eng. Fracture Mech.*, 70(7–8), 853–870.
- Vandewalle, L. et al. 2003. RILEM TC 162-TDF: test and design methods for steel fibre reinforced concrete: sigma-epsilon-design method—final recommendation. *Mater. Struct.*, 36(262), 560–567.
- Walter, R., Li, V.C., and Stang, H. 2004. Comparison of FRC and ECC in a composite bridge deck. In *Proceedings of the 5th International PhD Symposium in Civil Engineering*, June 17–19, Delft, the Netherlands, pp. 477–484.
- Wang, S. 2005. Micromechanics-Based Matrix Design for Engineered Cementitious Composites, Ph.D. thesis, University of Michigan, Ann Arbor.

- Wang, S. and Li, V.C. 2003. Materials design of lightweight PVA-ECC. In *Proceedings of the Fourth International RILEM Workshop on High-Performance Fiber-Reinforced Cement Composites (HPFRCC 4)*, Naaman, A.E. and Reinhardt, H.W., Eds., pp. 379–390. RILEM, Paris.
- Wang, S. and Li, V.C. 2006a. High early strength engineered cementitious composites. *ACI Mater. J.*, 103(2), 97–105.
- Wang, S. and Li, V.C. 2006b. Polyvinyl alcohol fiber-reinforced engineered cementitious composites: material design and performances. In *Proceedings, High-Performance Fiber-Reinforced Cementitious Composites (HPFRCC) in Structural Applications*, Fischer, G. and Li, V.C., Eds., pp. 65–73. RILEM, Paris.
- Weiss, W.J. and Shah, S.P. 2002. Restrained shrinkage cracking: the role of shrinkage reducing admixtures and specimen geometry. *Mater. Struct.*, 35(246), 85–91.
- Wittmann, F.H. 2002. Crack formation and fracture energy of normal and high strength concrete. *Sadhana*, 27(4), 413–423.
- Wonha Co., Ltd., S. Korea. 2004. Personal communication.
- Yang, E.H. and Li, V.C. 2008. Strain-hardening fiber cement optimization and component tailoring by means of a micromechanical model. *J. Construct. Build. Mater.*, in print.
- Yang, E.H., Yang, Y., and Li, V.C. 2007. Use of high volumes of fly ash to improve ECC mechanical properties and material greenness. *ACI Mater. J.*, 104(6), 620–628.
- Yang, Y., Lepech, M., and Li, V.C. 2005. Self-healing of engineered cementitious composites under cyclic wetting and drying. In *Proceedings of the International Workshop on the Durability of Reinforced Concrete Under Combined Mechanical and Climatic Loads (CMCL)*, October 27–28, Qingdao, China, pp. 231–242.



Typical FRP reinforcing bars for concrete members.

25

Design of FRP Reinforced and Strengthened Concrete

Lawrence C. Bank, Ph.D., P.E., FASCE*

25.1	Introduction	25-1
25.2	Design of FRP-Reinforced Concrete Members.....	25-2
	Introduction • Properties of FRP Reinforcing Bars •	
	Design Basis for FRP-Reinforced Concrete • Design of	
	Flexural Members with FRP Reinforcing Bars	
25.3	Design of FRP-Strengthened Concrete Members.....	25-9
	Introduction • Properties of FRP Strengthening Systems •	
	Design Basis for FRP Strengthening Systems for Concrete	
	Members • Design of FRP Flexural Strengthening Systems •	
	Design of FRP Shear Strengthening Systems • Design of FRP	
	Axial Strengthening Systems	
25.4	Summary.....	25-20
	References	25-20

25.1 Introduction

The design of concrete members either reinforced with FRP reinforcing bars or strengthened with strips or sheets of FRP laminates or fabrics is discussed in this chapter. The discussion in this chapter follows the design recommendations of the most current versions of the design guidelines published by the American Concrete Institute (ACI) that are used to design these concrete structures in the United States. The material presented is an updated and expanded version of portions of the chapter Fiber-Reinforced Polymer Composites, which appeared in the *Handbook of Structural Engineering* (Bank, 2004) and was based on ACI design guidelines in 2003. In addition, this chapter is intended to provide a brief overview of topics covered in greater detail and accompanied by illustrative examples in *Composites for Construction: Structural Design with FRP Materials* (Bank, 2006.) Research in the use of FRP reinforcements and FRP strengthening systems for concrete structures has been the focus of intense international research activity since the late 1980s. A biannual series of symposia entitled *Fiber-Reinforced Plastics in Reinforced Concrete Structures* (FRPRCS) has been the leading venue for reporting and disseminating these research results. The most recent symposium, the seventh in the series dating back to 1993, was held in Patras, Greece, in 2007 (Triantitillou, 2007).

* Professor, Civil and Environmental Engineering, at the University of Wisconsin, Madison; expert in the mechanics and design of composite material structures with an emphasis on applications to civil engineering.

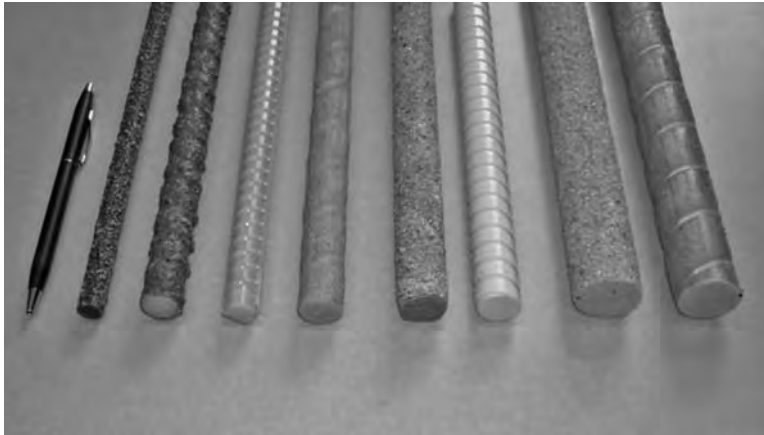


FIGURE 25.1 Typical FRP reinforcing bars for concrete members.

25.2 Design of FRP-Reinforced Concrete Members

25.2.1 Introduction

Fiber-reinforced polymer (FRP) reinforcing bars and grids have been commercially produced for reinforcing concrete structures for over 30 years (ACI Committee 440, 1996; Bank, 2006; Nanni, 1993). FRP reinforcing bars have been developed for prestressed and non-prestressed (conventional) concrete reinforcement. This section considers only non-prestressed reinforcement for concrete structures and follows the procedures of ACI 440.1R-06, *Guide for the Design and Construction of Structural Concrete Reinforced with FRP Bars* (ACI Committee 440, 2006). Note that ACI 440.1R-06 does not cover reinforcing with prefabricated FRP grids and mats. Recommendations for the design of prestressed FRP-reinforced concrete can be found in ACI 440.4R-04, *Prestressing Concrete with FRP Tendons* (ACI Committee 440, 2004b). Current FRP reinforcing bars (referred to as FRP rebars in what follows) are commercially produced using thermosetting polymer resins (commonly, polyester and vinylester) and glass, carbon, or aramid reinforcing fibers. The most common bars produced today are glass-fiber-reinforced vinylester bars. These are recommended for use in reinforcing applications for load-bearing concrete structures. The bars are primarily longitudinally reinforced with volume fractions of fibers in the range of 50 to 60%. FRP reinforcing bars are usually produced by a process similar to pultrusion (Starr, 2000) and have a surface deformation or texture to develop the bond to concrete. More information on the historical development, constituent materials, and manufacturing processes of FRP rebars can be found in Bank (2006). A photograph of some typical FRP reinforcing bars is provided in Figure 25.1. In addition to the ACI design guidelines, a number of other design guides have been published for FRP-reinforced concrete. These include Japanese (BRI, 1995; JSCE, 1997) and Canadian (ISIS, 2001; CSA, 2002) guides.

25.2.2 Properties of FRP Reinforcing Bars

Glass-fiber-reinforced vinylester bars are available from a number of manufacturers in the United States, Europe, and Asia. Bars are typically produced in sizes ranging from 3/8 in. in diameter to 1-1/4 in. in diameter (i.e., #3 to #10 bars.) FRP bars have a non-smooth surface, which is required for bond to the concrete (see Figure 25.1) and is typically produced by a sand-coated external layer, molded deformations, machined ribs, or a spiral wind. The properties of FRP rebars are intended to be measured and reported by FRP rebar manufacturers in accordance with ACI 440.3R-04, *Guide Test Methods for Fiber-Reinforced Polymers (FRP) for Reinforcing or Strengthening Concrete Structures* (ACI Committee 440, 2004a). A standard product specification for FRP rebars has recently been approved for publication by the Canadian Standards Organization (ISIS, 2006). The ACI is currently preparing a standard specification

TABLE 25.1 Properties of Typical Commercially Produced FRP Reinforcing Bars

	Glass-Reinforced Vinylester Bar ^{a,b,c} (0.5-in. Diameter)	Glass-Reinforced Vinylester Bar ^a (1-in. Diameter)	Carbon-Reinforced Vinylester Bar ^a (0.375-in. Diameter)	Carbon-Reinforced Epoxy Bar (0.5-in. Diameter)
Fiber volume (estimated)	50–60	50–60	50–60	50–60
Fiber architecture	Unidirectional	Unidirectional	Unidirectional	Unidirectional
<i>Strength</i> ($\times 10^3$ psi)				
Tensile, longitudinal	90–100	80	300	327
Compressive, longitudinal	NR	NR	NR	NR
Bond strength	1.7	1.7	1.3	NR
Shear, out-of-plane	22–27	22	NR	NR
<i>Stiffness</i> ($\times 10^6$ psi)				
Tensile, longitudinal	5.9–6.1	5.9	18	21.3
Compressive, longitudinal	NR	NR	NR	NR
CTE, longitudinal ($10^{-6}/^{\circ}\text{F}$)	3.7–4.9	3.7	–4.0–0	0.38
CTE, transverse ($10^{-6}/^{\circ}\text{F}$)	12.2–18.7	18.7	41–58	NR
Barcol hardness	60	60	48–55	NR
24-hour water absorption (% max.)	NR	NR	NR	NR
Density (lb/in. ³)	0.072	0.072	NR	0.058

^a Data for Aslan® (Hughes Brothers, Seward, Nebraska).

^b Data for V-Rod™ (Pultrall, Quebec, Canada).

^c Data for Leadline® (Mitsubishi, Tokyo, Japan).

Note: CTE, coefficient of thermal expansion; NR, not reported by the manufacturer.

for FRP bars. For design, the key mechanical properties of interest are the longitudinal tensile strength and longitudinal tensile modulus of the bar. Most FRP bars are brittle and exhibit strongly linear and elastic axial stress–strain or axial load–deformation characteristics up to their failure loads. They do not yield and have no plastic deformation capacity as do steel rebars. It is also important to note that, unlike steel rebars, the longitudinal strength (but not the longitudinal modulus) of FRP rebars decreases with the diameter of the bar. This is attributed to the relatively low in-plane shear modulus of FRP rebars (leading to shear lag effects), the additives used to produce larger diameter bars, and a statistical size effect in brittle glass fibers. Designers should always consult the manufacturer’s published properties for use in design. Typical properties for glass-fiber FRP rebars and carbon-fiber FRP bars are provided in Table 25.1. It should be noted that the carbon-fiber bars are typically used as prestressing tendons or *near-surface-mounted* (NSM) strengthening rods and not as conventional reinforcing bars due to cost considerations.

Fiber-reinforced polymer rebars are considered to be transversely isotropic from a mechanics perspective (Bank, 1993). Theoretical equations are available to predict the mechanical and physical properties of the FRP rebars from the properties of the fiber and resin constituents; however, for design purposes, measured properties of the as-produced bars must be used. At this time, theoretical methods are not yet available to predict the bond properties and the long-term durability characteristics of FRP rebars. Test methods for determining and reporting the alkali resistance, creep, and fatigue characteristics of FRP rebars are provided in ACI 440.3R-04 (ACI Committee 440, 2004a). FRP rebars containing glass fibers can fail catastrophically under sustained loads at stresses lower than their tensile strengths, a phenomenon known as *creep rupture* or *static fatigue*. Design guides therefore limit the amount of sustained load on concrete structures reinforced with FRP rebars.

Fiber-reinforced polymer rebars should only be used at service temperatures below the glass transition temperature (T_g) of the polymer resin system used in the bar. For typical vinylester polymers, this is around 200°F. The bond properties have been shown to be highly dependent on the glass transition temperature of the polymer. In addition, it is important to note that the coefficients of thermal expansion of FRP rebars are not the same in the transverse (radial) direction as in the longitudinal direction. The coefficient of thermal expansion may be close to an order of magnitude higher in the transverse direction

of the bar due to its anisotropic properties (see typical properties in Table 25.1). This may cause longitudinal splitting in the concrete due to temperature and shrinkage effects if sufficient cover is not provided.

Fiber-reinforced polymer reinforcing bars made of thermosetting polymers cannot be bent in the field and must be produced by the FRP rebar manufacturer with bends for anchorages or for stirrups. The strength of the FRP rebar at the bend is substantially reduced and must be considered in the design. According to ACI 440.1R-06, FRP rebars should not be used for carrying compressive stress in concrete members (i.e., compression reinforcement in beams or columns) as this time, as insufficient research has been conducted on this topic. Where FRP bars are used in the compression zone they should be suitably confined to prevent local instability.

25.2.3 Design Basis for FRP-Reinforced Concrete

The *load and resistance factor design* (LRFD) basis is stipulated by ACI 440.1R-06, which provides the resistance factors (ϕ , or phi factors) for use with FRP rebars that are calibrated for the load factors required for use in design with conventionally reinforced concrete structures by ACI 318-05 (e.g., 1.2 for dead load and 1.6 for live load) (ACI Committee 318, 2005). For the design of flexural members reinforced with FRP rebars, ACI 440.1R-06 provides the following resistance factors:

Flexural capacity (tensile reinforcement only):

$\phi = 0.55$ for an under-reinforced beam section ($\rho_f < \rho_{fb}$).

$\phi = 0.65$ for a substantially over-reinforced beam section ($\rho_f > 1.4\rho_{fb}$).

$\phi = 0.3 + 0.25\rho_f/\rho_{fb}$ for a lightly over-reinforced beam section ($\rho_{fb} < \rho < 1.4\rho_{fb}$).

Shear capacity (FRP shear reinforcement in the form of stirrups):

$\phi = 0.75$ per ACI 318-05.

where ρ_f is the FRP reinforcement ratio and ρ_{fb} is the balanced FRP reinforcement ratio. The FRP reinforcement ratio for an FRP-reinforced rectangular beam section (where the subscript f is used to indicate FRP reinforcement to distinguish it from conventional reinforcement) is given as:

$$\rho_f = \frac{A_f}{bd} \quad (25.1)$$

and the balanced FRP reinforcement ratio is given as:

$$\rho_{fb} = 0.85\beta_1 \frac{f'_c}{f_{fu}} \frac{E_f \epsilon_{cu}}{E_f \epsilon_{cu} + f_{fu}} \quad (25.2)$$

where A_f is the area of FRP reinforcement, b is the beam width, d is the effective depth, β_1 is a factor that depends on concrete strength (e.g., 0.85 for 4000-psi concrete), f'_c is the cylinder compressive strength of the concrete, E_f is the longitudinal modulus of the FRP rebar, ϵ_{cu} is the nominal ultimate compressive strain in the concrete (taken as 0.003), and f_{fu} is the longitudinal design strength of the FRP rebar. Figure 25.2 shows the distribution of strains, stresses, and forces at the service condition and at the ultimate condition for an FRP reinforced section.

The design strength (f_{fu}) and design failure strain (ϵ_{fu}) are obtained from the manufacturer-reported guaranteed strength and guaranteed failure strain by multiplying them by an *environmental reduction factor* (C_E), which depends on the fiber type in the bar and the type of intended service of the structure. For example, for glass FRP rebars, C_E is 0.7 for exterior concrete and 0.8 for interior concrete. The guaranteed strength and guaranteed strain to failure of FRP rebars are defined as the mean minus 3 standard deviations of a minimum of 25 test samples (ACI Committee 440, 2006).

In addition to the strength criteria described above, the design basis for FRP-reinforced concrete members also includes stipulations on the behavior and appearance of the FRP-reinforced member under service

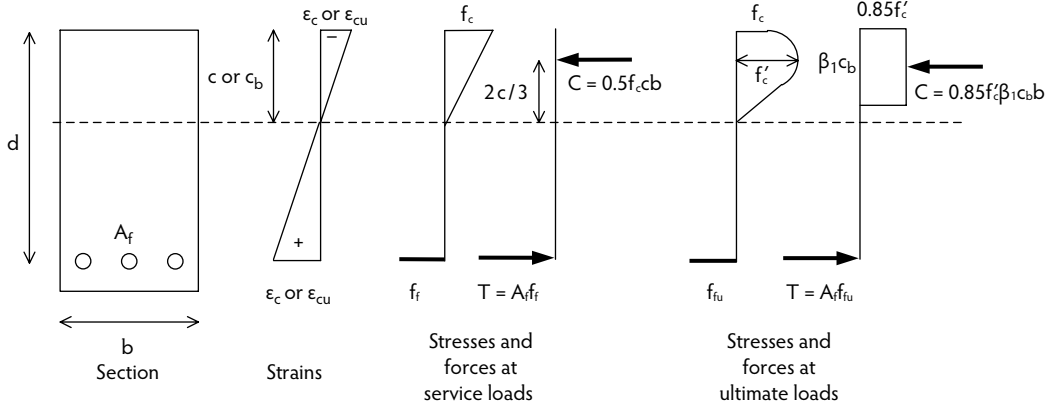


FIGURE 25.2 Strains, stresses, and forces in the FRP-reinforced section at service and ultimate loads.

loads. Maximum flexural crack widths are limited to 0.20 and 0.28 mils for exterior and interiors exposure, and the stress in the main FRP reinforcing bars is limited to $0.2f_{fu}$, $0.3f_{fu}$, and $0.55f_{fu}$ for glass, aramid, and carbon bars, respectively, to prevent failure under sustained loads due to creep rupture or due to fatigue. Because FRP rebars typically have a lower modulus than steel rebars, the serviceability criteria (typically, deflections and crack widths) can often control the design of FRP-reinforced concrete sections.

25.2.4 Design of Flexural Members with FRP Reinforcing Bars

25.2.4.1 Flexural Capacity with FRP Main Tension Bars

The nominal moment (or flexural) capacity of an FRP-reinforced concrete member (such as a beam or a slab) is determined in a manner similar to that of a steel-reinforced section. However, because FRP rebars do not yield, the ultimate strength of the bar replaces the yield strength of the steel rebar in the traditional concrete beam design formula based on strain compatibility (assuming plane sections remain plane and bars are perfectly bonded to the concrete) and equilibrium of forces. Both under-reinforced section design and over-reinforced section design are permitted; however, due to serviceability limits (primarily long-term deflections and crack widths), most glass FRP-reinforced flexural members will be over-reinforced.

When $\rho_f > \rho_{fb}$, the over-reinforced section will fail due to concrete crushing, and the nominal moment capacity is given in a manner similar to that for a section reinforced with steel rebars (where the rebar has not reached its yield stress). The stress in the rebar therefore must be calculated to determine the capacity of the section. The nominal moment capacity is given as:

$$M_n = A_f f_f \left(d - \frac{a}{2} \right) \quad (25.3)$$

where:

$$a = \frac{A_f f_f}{0.85 f'_c b} \quad (25.4)$$

$$f_f = \left(\sqrt{\frac{(E_f \epsilon_{cu})^2}{4} + \frac{0.85 \beta_1 f'_c}{\rho_f} E_f \epsilon_{cu}} - 0.5 E_f \epsilon_{cu} \right) \quad (25.5)$$

where f_f is the stress in the FRP rebar at concrete compressive failure, and a is the depth of the equivalent rectangular (Whitney) stress block in the concrete.

When $\rho_f < \rho_{fb}$, the under-reinforced section will fail due to rupture of the FRP rebars in tension. Because the FRP reinforcement will not yield prior to its failure, the moment capacity of the section cannot be calculated assuming the concrete crushes when the bar ruptures (as in the case of a steel under-reinforced section). For this reason, the section capacity should be calculated using appropriate non-linear stress-strain relations of the concrete; however, this requires an iterative solution procedure, which is not suited to design calculations. To overcome this situation, ACI 440.1R-06 recommends computing the approximate (and conservative) nominal flexural capacity as:

$$M_n = A_f f_{fu} \left(d - \frac{\beta_1 c_b}{2} \right) \quad (25.6)$$

where c_b is the depth of the neutral axis at the balanced reinforcement ratio, given as:

$$c_b = \left(\frac{\epsilon_{cu}}{\epsilon_{cu} + \epsilon_{fu}} \right) d \quad (25.7)$$

A minimum amount of flexural reinforcement should be provided when the FRP-reinforced beam is designed to fail by FRP bar rupture to prevent failure at concrete cracking. The amount is given as:

$$A_{f,min} = \frac{4.9 \sqrt{f'_c}}{f_{fu}} b d \geq \frac{330}{f_{fu}} b d \quad (25.8)$$

25.2.4.2 Shear Capacity with FRP Main Tension Bars and FRP Shear Reinforcement

The nominal shear capacity of an FRP-reinforced concrete member loaded in flexure is influenced by the mechanical properties of the FRP main tension reinforcing bars and by FRP shear reinforcement, which is typically supplied in the form premanufactured stirrups. The lower modulus of the FRP main bars (assuming glass fibers) leads to a shallower compression zone and larger deflections at flexural failure of FRP-reinforced flexural members than would be obtained in the same section reinforced with steel bars. In addition, the strain in the FRP stirrups is limited to prevent large shear cracks from developing in the FRP-reinforced concrete member. Added to this, the strength of the FRP bar is reduced when it is bent to form a stirrup due to the linear elastic material properties and the manufacturing process used to manufacture bent FRP bars.

The nominal shear capacity (V_n) of an FRP-reinforced concrete beam is:

$$V_n = V_c + V_f \quad (25.9)$$

where V_c is the nominal shear capacity of the concrete with FRP rebars used as main tension reinforcement and is given as:

$$V_c = 5 \sqrt{f'_c} b_w c \quad (25.10)$$

where b_w is the width of the beam web, and c is the depth of the neutral axis in the cracked elastic section as defined for the serviceability calculations and is given as:

$$c = k d \quad (25.11)$$

$$k = \sqrt{(\rho_f \eta_f)^2 + 2 \rho_f \eta_f} - \rho_f \eta_f \quad (25.12)$$

$$\eta_f = \frac{E_f}{E_c} \quad (25.13)$$

where η_f is the modular ratio, k is the depth ratio, and V_f is the nominal shear capacity provided by the FRP stirrups. For vertical FRP shear stirrups, it is given as:

$$V_f = \frac{A_{fv} f_{fv} d}{s} \quad (25.14)$$

where A_{fv} is the total area of the stirrups that cross the shear crack, and f_{fv} is the strength of the FRP stirrup, which is limited by the smaller of:

$$f_{fv} = 0.004 E_f \quad (25.15)$$

and the strength of the FRP rebar at its bend:

$$f_{fb} = \left(0.05 \frac{r_b}{d_b} + 0.3 \right) f_{fu} \quad (25.16)$$

where f_{fb} is the strength of the FRP rebar at its bend, r_b is the inside radius of the bend, and d_b is the diameter of the FRP rebar. Standard bend radii are reported by manufacturers and range from 4.25 to 6 in. for typical FRP rebars. The ratio of r_b/d_b may not be less than 3.

25.2.4.3 Design for Serviceability

For serviceability design of concrete members with FRP bars three criteria, all calculated with respect to the service loads on the member (with no load factors applied), must be checked against code-stipulated limits provided in ACI 440.1R-06: (1) maximum crack widths due to all loads, (2) maximum short-term and long-term deflections due to all loads accounting for long-term creep effects, and (3) maximum stresses in the FRP bars due exclusively to sustained loads and fatigue. The width of a flexural crack in an FRP-reinforced member is calculated from:

$$w = 2 \frac{f_f}{E_f} \beta k_b \sqrt{d_c^2 + \left(\frac{s}{2} \right)^2} \quad (25.17)$$

where w is the crack width (in inches), f_f is the service load stress in the FRP reinforcement (in ksi), E_f is the modulus of the FRP rebars (in ksi), β is the ratio of the distance between the neutral axis and the bottom of the section (i.e., the tension surface) and the distance between the neutral axis and the centroid of reinforcement, d_c is the thickness of the concrete cover from the tension face to center of the closest bar (in inches), s is the center-to-center bar spacing of the main FRP bars (in inches), and k_b is a bond-related coefficient. k_b is taken as 1.4 for commercially produced FRP rebars. β is determined from:

$$\beta = \frac{h - kd}{d(1 - k)} \quad (25.18)$$

where h is the section depth and d is the effective section depth. The stress in the FRP bar at service loads can be calculated from:

$$f_{f,s} = \frac{m_s \eta_f d (1 - k)}{I_{cr}} \quad (25.19)$$

where m_s is the service load moment.

To calculate maximum short-term and long-term deflections under service loads, a modified form of the Branson equation is used:

$$I_e = \left(\frac{M_{cr}}{M_a} \right)^3 \beta_d I_g + \left[1 - \left(\frac{M_{cr}}{M_a} \right)^3 \right] I_{cr} \leq I_g \quad (25.20)$$

where I_e is the effective second moment of area of the cracked section, I_g is the second moment of the gross section, M_{cr} is the moment at cracking, M_a is the applied service load moment, and β_d is a reduction coefficient for FRP reinforced beams that is given as:

$$\beta_d = \frac{1}{5} \left(\frac{\rho_f}{\rho_{fb}} \right) \leq 1.0 \quad (25.21)$$

As in conventional steel-reinforced concrete, the cracked (transformed to concrete) second moment of the section is given as:

$$I_{cr} = \frac{bd^3}{3} k^3 + \eta_f A_f d^2 (1-k)^2 \quad (25.22)$$

The long-term deflections, including the effects of creep and shrinkage of the concrete under the sustained long-term service loads (i.e., the dead load and the sustained live load), can be calculated as:

$$\Delta_{(cp+sh)} = 0.6\xi(\Delta_i)_{sus} \quad (25.23)$$

where $(\Delta_i)_{sus}$ is the short-term (or instantaneous) deflection due to the sustained loads only and is calculated using the modified Branson formula; $\xi = 2.0$ for sustained loads with a duration of 5 years or more as per ACI 318-05 (ACI Committee 318, 2005).

All FRP-reinforced concrete beams must be checked for possible failure due to creep rupture or fatigue under service loads. Creep rupture is checked with respect to all sustained service loads, whereas fatigue is checked with respect to all sustained loads plus the maximum moment induced in a fatigue loading cycle:

$$f_{f, \text{ creep rupture}} = \frac{m_{sus} \eta_f d (1-k)}{I_{cr}} \quad (25.24)$$

where m_{sus} is the moment due to the sustained service loads.

25.2.4.4 Detailing of FRP Reinforcements

The development length of an FRP rebar is different from the development length of a conventional steel rebar. In addition, a beam reinforced with FRP bars can potentially fail due to splitting bond failure between the FRP bar and the concrete due to the high tensile stress that can be developed in FRP bars. The required development length (ℓ_d) for a straight FRP bar is given as:

$$\ell_d = \frac{\alpha \frac{f_{fr}}{\sqrt{f'_c}} - 340}{13.6 + \frac{C}{d_b}} (d_b) \quad (25.25)$$

where f_{fr} is the stress in the FRP bar at failure which is the lesser of (1) the design strength of the bar for under-reinforced beams (f_{fu}), (2) the actual stress in the bar for over-reinforced sections (f_f), or (3) the effective bond critical design stress in the bar for both over and under-reinforced sections (f_{fe}), which is given as:

$$f_{fe} = \frac{\sqrt{f'_c}}{\alpha} \left(13.6 \frac{\ell_e}{d_b} + \frac{C}{d_b} \frac{\ell_e}{d_b} + 340 \right) \leq f_{fu} \quad (25.26)$$

where C is the lesser of (1) the distance from the center of the bar to the nearest outer concrete surface in the tension zone, or (2) half the on-center spacing of the bars (side-by-side); α is the bar location factor, which is taken as 1.0 for bars that are in the bottom 12 in. of the formwork when the concrete is cast and as 1.5 when the bars are more than 12 in. above the bottom of formwork when the beam is cast (known as *top-bars*). ACI 440.1R-06 further recommends that the term C/d_b not be taken as larger than 3.5 and that the minimum embedment length (ℓ_e) be at least 20 bar diameters, or $20d_b$.

For hooked bars, the development length of the portion extending beyond the bend (the tail length) is given as a function of the FRP rebar design strength. For FRP rebars with design strengths in the range of 75 to 150 ksi (typical of glass FRP rebars), the length of the hook (l_{bhf}) is given as:

$$l_{bhf} = \frac{f_{fu}}{37.5} \frac{d_b}{\sqrt{f'_c}} \quad (25.27)$$

It should not be less than $12d_b$ or 9 in. Tension lap splices for FRP rebars are based on recommendations for steel rebars and limited test data. For Class A and Class B lap splices, the recommended develop lengths are $1.3l_{df}$ and $1.6l_{df}$, respectively. FRP stirrups can be spaced at a maximum of $d/2$ (or 24 in.) and should have a minimum r_b/d_b ratio of 3. The tail length of 90° hooks in the stirrups must be at least $12d_b$.

25.3 Design of FRP-Strengthened Concrete Members

25.3.1 Introduction

Fiber-reinforced polymer reinforcing systems for strengthening structurally deficient concrete structural members and for repairing damaged or deteriorated concrete structures have been used since the mid-1980s (Bank, 2006). This section provides guidance for the design of FRP strengthening systems according to the procedures of ACI 440.2R-02, *Guide to the Design and Construction of Externally Bonded FRP Systems for Strengthening Concrete Structures* (ACI Committee 440, 2002). This guide is used for the design of most FRP strengthening systems currently designed in the United States. This guide is still based on ACI 318-99 load factors (e.g., 1.4 for dead loads and 1.7 for live loads). It is currently under revision and, in addition to other changes, the next edition will be compatible with ACI 318-05 load factors (e.g., 1.2 for dead loads and 1.6 for live loads). The reader is advised to consult the new version of this guide when it is released in 2008.

The first FRP-strengthened concrete structures were beams strengthened to increase their flexural capacity using high-strength, lightweight, carbon-fiber-reinforced epoxy laminates that were bonded to the undersides of the beams. The method is a modification of one where epoxy-bonded steel plates are used to strengthen concrete beams which has been in use since the mid-1960s. The FRP systems were shown to provide significant benefits in constructability and durability over the steel plates. Thereafter, significant work was conducted on strengthening of concrete columns to enhance their axial capacity, shear capacity, and ductility, primarily for seismic loadings. This method is a modification of one using steel jackets to strengthen concrete columns. This was followed closely by work on shear strengthening of beams. A review of the state of the art on the subject can be found Teng et al. (2001), Hollaway and Head (2001), and Bank (2006). The method has also been used to strengthen masonry and timber structures; however, applications of this type are not discussed in this chapter.

Current FRP strengthening systems for concrete fall into two popular types: *precured* and *formed-in-place* systems. The precured systems consist of factory manufactured laminates (known as *strips* or *plates*) of carbon-or glass-reinforced thermosetting polymers (typically epoxy or vinylester) that are bonded to the surface of the concrete using an epoxy adhesive. The manufactured precured laminates typically have

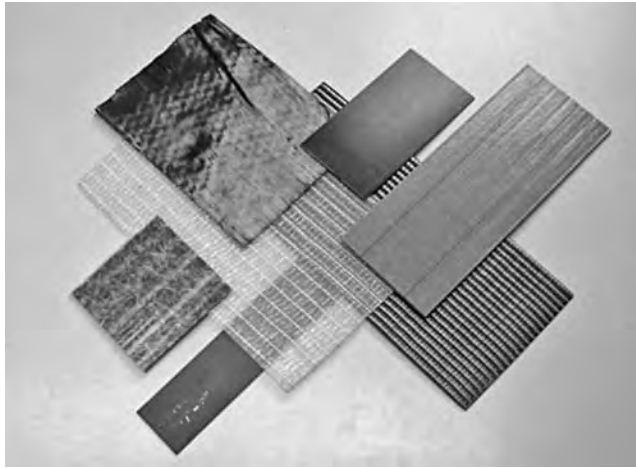


FIGURE 25.3 Typical FRP strengthening systems for concrete members.

a volume fraction of fibers in the range of 55 to 65% and are cured at high temperatures ($>300^{\circ}\text{F}$) but are bonded in the field at ambient temperatures. The formed-in-place systems consist of layers of unidirectional sheets or woven or stitched fabrics of dry fibers (usually glass, carbon, or aramid) that are saturated in the field with a thermosetting polymer (e.g., epoxy or vinylester) which simultaneously produces and bonds the FRP material to the concrete. The process is often referred to as *lay-up*. The formed-in-place FRP systems typically have a fiber volume fraction of between 20 and 40% and are cured at ambient temperatures in the field. Figure 25.3 shows a number of currently produced FRP strengthening systems.

A number of design guides and national standards are currently published that provide recommendations for the analysis, design, and construction of concrete structures strengthened with FRP materials (Concrete Society, 2004; CSA, 2002; FIB, 2001; ICC Evaluation Service, 1997; JSCE, 2001). In addition, manufacturers of FRP strengthening systems for concrete typically provide their own design and installation guides for their proprietary systems. Because the performance of the FRP strengthening system is highly dependent on the adhesive or saturating polymer used, the preparation of the concrete surface prior to application of the FRP strengthening system, and the field installation and construction procedures, manufacturers frequently certify *approved contractors* to ensure that their systems are designed and installed correctly. Guidance to ensure that FRP strengthening systems are appropriately installed, monitored, and inspected is provided in a number of guides (Concrete Society, 2003; ICC Evaluation Service, 2001; TRB, 2004).

25.3.2 Properties of FRP Strengthening Systems

Carbon-fiber-reinforced epoxy laminates (or strips) are the most commonly used of the precured FRP strengthening systems. Depending on the type of carbon fiber used in the strip, different longitudinal strengths and stiffness are produced. Strips are typically thin (less than 0.100 in.) and are available in a variety of widths (typically 2 to 4 in.). Because the strips are reinforced with unidirectional fibers, they are highly orthotropic with very low properties in the transverse and through the thickness directions. Manufacturers typically only report properties in the longitudinal directions and report very little data on physical properties. The strips are bonded to the concrete with an adhesive that is supplied by the strip manufacturer. Typical properties of strips are shown in Table 25.2. It is important to note that the properties shown for the strips are properties of the FRP composite and not the properties of the fibers alone.

In the formed-in-place FRP strengthening systems, a greater array of products is available depending on fiber type and sheet or fabric architecture. In this group of products, a unidirectional, highly orthotropic carbon-fiber *tow sheet* is produced by a number of manufacturers and is often used in strengthening

TABLE 25.2 Properties of Typical Commercially Produced FRP Strengthening Strips

	Standard-Modulus Carbon-Reinforced Epoxy Strip ^{a,b,c}	High-Modulus Carbon-Reinforced Epoxy Strip ^a	Glass-Reinforced Epoxy Strip ^b	Carbon-Reinforced Vinylester Strip ^d
Fiber volume (estimated)	65–70	65–70	65–70	60
Fiber architecture	Unidirectional	Unidirectional	Unidirectional	Unidirectional
Nominal thickness (in.)	0.047–0.075	0.047	0.055–0.075	0.079
Width (in.)	2–4	2–4	2–4	0.63
<i>Strength</i> ($\times 10^3$ psi)				
Tensile, longitudinal	390–406	188	130	300
<i>Rupture strain</i> (%)				
Tensile, longitudinal	1.8	NR	2.2	1.7
<i>Stiffness</i> ($\times 10^6$ psi)				
Tensile, longitudinal	22.5–23.9	43.5	6.0	19.0
CTE, longitudinal ($10^{-6}/^{\circ}\text{F}$)	NR	NR	NR	–4.0–0.0
CTE, transverse ($10^{-6}/^{\circ}\text{F}$)	NR	NR	NR	41–58
Barcol hardness	NR	NR	NR	48–55

^a Data for CarboDur® (Sika Group; Zurich, Switzerland).

^b Data for Tyfo® (Fyfe; San Diego, California).

^c Data for MBrace® (BASF Construction Chemicals; Seven Hills, New South Wales, Australia).

^d Data for Aslan® (Hughes Brothers; Seward, Nebraska).

Note: CTE, coefficient of thermal expansion; NR, not reported by the manufacturer. All strips must be bonded with manufacturer-supplied compatible adhesives.

applications. The individual carbon tows in the sheet are held together by a polymeric binder (or a light stitching). The sheet is often supplied on a wax paper backing. Sheets are typically 10 to 40 inches wide and can be applied in multiple layers with different orientations. The common fabric materials in the formed-in-place group are woven or stitched fiber fabrics having an areal density of 12 to 32 oz/yd². Carbon-fiber fabrics and hybrid fabrics (with more than one fiber type) are also available. Fabrics are typically much thicker than tow sheets. They are also used in multiple layers. Because of the wide variety of products available and their different thicknesses, it is not easy to compare their properties directly. In addition, the fibers must be used with a compatible resin system applied at a controlled volume fraction to achieve a FRP composite with desirable properties. In the case of sheet and fabric materials, manufacturers typically report the mechanical properties of the dry fibers and the thickness (or area) of the fibers. It is important to note that when reported in this fashion the properties are not the properties of the FRP composite but of the fibers alone. Properties of some commonly available fiber sheet and fabric materials are listed in Table 25.3.

The performance of the FRP strengthening system is highly influenced by the properties of the adhesive layer in the case of the precured systems and by the properties of the saturating polymeric resin in the case of formed-in-place systems. The interface between the FRP composite and the concrete substrate transfers the loads from the concrete to the FRP composite. In the case of flexural and shear (or axial tensile) strengthening, this load transfer is primarily in shear, and the strength and stiffness of the interface layer between the FRP composite and the concrete are critical. Such applications are termed *bond critical*. In the case of axial compressive strengthening or lateral displacement ductility enhancement of columns, the role of the strengthening system is to confine the lateral expansion of the cracked concrete. In this case, the interface bond is not as critical as long as the FRP system is in close contact with the concrete and is wrapped around the concrete continuously so as to provide a confining pressure with appropriate hoop stiffness and strength. Such applications are termed *contact critical*.

The FRP strengthening systems described above all depend on curing of the polymer adhesives or the saturating resins at ambient temperature in the field; therefore, the glass transition temperature (T_g) of these systems is typically quite low (120 to 180°F). The stiffness of the FRP strengthening system is decreased

TABLE 25.3 Properties of Typical Commercially Produced FRP Sheet-Strengthening Materials

	Standard-Modulus Carbon Fiber Tow Sheet ^{a,b,c}	High-Modulus Carbon Fiber Tow Sheet ^{a,b}	Glass Fiber Roving Sheet ^{a,b}
Thickness (in.)	0.0065–0.013	0.0065	0.014
Typical width (in.)	24	24	24
Fiber architecture	Unidirectional	Unidirectional	Unidirectional
<i>Strength</i> ($\times 10^3$ psi)			
Fiber tensile, longitudinal	550	510	220–470
<i>Rupture strain</i> (%)			
Fiber tensile, longitudinal	1.67–1.7	0.94	2.1–4.5
<i>Stiffness</i> ($\times 10^6$ psi)			
Fiber tensile, longitudinal	33.0–33.4	54.0	10.5

^a Data for MBrace® (BASF Construction Chemicals, Seven Hills, New South Wales, Australia).

^b Data for Tyfo® (Fyfe, San Diego, California).

^c Replark™ (Mitsubishi, Tokyo, Japan).

when the operating temperature approaches (and exceeds) the glass transition temperature. Designers should always be aware of the glass transition temperature of the FRP composite or adhesive they are using in a design. In the event of a fire (at temperatures higher than the T_g in the range of 750°F), the FRP material will decompose (pyrolyze), and its strength and stiffness may be severely compromised in a short time.

25.3.3 Design Basis for FRP Strengthening Systems for Concrete Members

The *load and resistance factor design* (LRFD) basis is stipulated by ACI 440.2R-02 (ACI Committee 440, 2002). Currently, resistance factors are not probabilistically based, and the load factors stipulated for use with this guide are those recommended by ACI 318-99 (e.g., 1.4 for dead loads and 1.7 for live loads) (ACI Committee 318, 1999). (The revised version of the guide, due out in 2008, will have probabilistically based resistance factors and will be compatible with ACI 318-05.) For the design of concrete members with FRP strengthening systems the ACI recommends the following resistance factors (ϕ) and FRP material reduction factors, (ψ_f):

For flexural capacity:

$\phi = 0.9$ for ductile failure of the member following steel yielding ($\epsilon_s > 0.005$).

$\phi = 0.7$ for a brittle failure when the member fails prior to steel yielding ($\epsilon_s < \epsilon_{sy}$).

$\phi = 0.7$ to 0.9 for an intermediate region ($\epsilon_{sy} < \epsilon_s < 0.005$).

$\psi_f = 0.85$ for FRP bond-critical strengths (applied in addition to ϕ factors).

For shear capacity:

$\phi = 0.85$, per ACI 318-99.

$\psi_f = 0.85$ for FRP bond-critical strengths (applied in addition to ϕ factor).

$\psi_f = 0.95$ for FRP contact-critical strengths (applied in addition to ϕ factor).

For axial capacity:

$\phi = 0.75$, per ACI 318-99, for spiral steel column reinforcement.

$\phi = 0.70$, per ACI 318-99, for tied steel column reinforcement.

$\psi_f = 0.95$ for FRP contact-critical strengths (in addition to ϕ factors).

Guaranteed strengths and strains to failure of FRP composite materials for strengthening are defined as the mean minus 3 standard deviations of a minimum of 20 test samples tested in accordance with ACI 440.3R-04 (ACI Committee 440, 2004a). The design strength (f_{fu}) and design failure strain (ϵ_{fu}) are

obtained from the manufacturer-reported guaranteed strength and failure strain by multiplying them by an *environmental reduction factor* (C_E), which depends on the fiber type in the FRP strengthening system and the type of intended service of the structure. For example, for weather-exposed concrete with a glass-reinforced epoxy FRP strengthening system, C_E is 0.65 (ACI Committee 440, 2002). Note that the environmental reduction factors for FRP strengthening systems are not the same as the environmental reduction factors for FRP reinforcing bars (even though the same symbol is used for both.)

Even though flexural strength increases of over 100% of the original strength of a concrete member can be obtained using FRP strengthening systems, the ACI limits the amount of strengthening to prevent catastrophic failure of the concrete member in the event of loss of, or damage to, the strengthening system (due to vandalism or environmental degradation). The ACI recommends that the strengthened member still have sufficient original factored capacity (i.e., discounting the additional strengthening system) to resist a substantial portion of the increased (new) factored load for which the strengthened member is designed. This limit is given as:

$$1.2D + 0.85L \quad (25.28)$$

where D represents the new dead load effect, and L the new live load effect, such as bending moment, shear force, or axial load or their products (stress and strain). To account for environments where the FRP may be exposed to fire, additional restrictions are placed on the factored capacity of the FRP-strengthened structure:

$$1.0D + 1.0L \quad (25.29)$$

Fire protection systems are available to protect FRP strengthening systems to increase their fire ratings to building code required ratings (such as 1- or 2-hour ratings). When a concrete member is strengthened to increase its capacity in a selected mode (e.g., flexure), the member must be checked to ensure that the capacities in other failure modes (e.g., shear) are not exceeded. If this is the case, the strengthening should be decreased or the secondary capacity must be enhanced with its own strengthening system.

For serviceability design, the ACI 440.2R-02 guide limits the stress in the steel at service loads to 80% of the steel yield stress and limits the sustained plus cyclic stress in the FRP strengthening system to account for creep rupture and fatigue, depending on the fiber system. For carbon FRP strengthening systems, this limit is 55% of the ultimate strength. At this time, ACI 440.2R-02 does not provide special recommendations for the determination of deflections or crack widths for FRP-strengthened members. Flexural deflections in the service range can be estimated by use of an effective second moment of area (I_e) analysis, where the tensile contribution of the FRP is added to the contribution of the steel reinforcing. For deflections in flexural members where stresses are in the service load range, the contribution of the FRP strengthening system is typically small. In the inelastic range (after the primary reinforcing steel has yielded), the contribution of the FRP strengthening to the post-yield stiffness can be quite considerable and should be accounted for in inelastic analysis (Bank, 2006).

It is extremely important to note that the method of determining the tensile force resultant in an FRP strengthening system depends on the type of system used. In the bonded, precured strip, the ultimate force is obtained from the strength of the FRP composite (see Table 25.2) and the gross cross-sectional area of the strip. In formed-in-place systems, the ultimate force is obtained from the strength of the fibers and the net area of the fibers (see Table 25.3). The designer must know if the reported strength (and stiffness) of an FRP strengthening system is for the FRP composite (gross composite cross-section) or for the fibers alone (net fiber cross-section). Both methods of calculation are permitted by ACI 440.2R-02.

25.3.4 Design of FRP Flexural Strengthening Systems

Flexural strengthening is achieved by attaching an FRP strengthening system (precured strip or formed-in-place fabric) to the underside of a flexural member to increase the effective tensile force resultant in the member and thereby increase the moment capacity of the member. This is analogous to adding steel strengthening strips (or plates) to the underside of a member; however, two fundamental differences

exist. First, the FRP strengthening system behaves in a linear elastic fashion and does not yield, and, second, the FRP strengthening system is more susceptible to detachment (debonding or delamination) failures than steel plate systems that are anchored with steel bolts in addition to the epoxy bonding. Because the steel plates themselves will yield at a similar strain to the internal steel reinforcing, the stress level in the steel strengthening system is limited. In the case of FRP strengthening with FRP systems having ultimate tensile strengths exceeding 300 ksi (see Table 25.2 and Table 25.3), the stress level in the FRP can be significantly higher than that in steel strengthening systems. In the event that the internal steel reinforcing yields before the FRP strengthening system fails (the desired failure mode), the concrete member will undergo large deflections and cracking. All of these factors lead to the greater likelihood that the FRP strengthening system will debond from the concrete before it achieves its ultimate (longitudinal) tensile strength.

Strengthening of members in flexure can only be achieved if there is sufficient additional compressive capacity in the concrete to allow for the increase in internal moment; therefore, flexural strengthening is most suitable for concrete members that are lightly to moderately reinforced, having steel reinforcement in the range of 20 to 40% of the balanced ratio. This is not uncommon in reinforced concrete members. The existing tensile strain in the concrete at the location of the applied FRP strengthening system due to sustained loads when the FRP strengthening system is applied should be accounted for in design calculations if a shoring system is not used.

The key to flexural strengthening with FRP strengthening systems is to understand the failure modes of the system. These include rupture of the FRP strengthening system, debonding of the FRP strengthening system, or compressive failure of the concrete. All of these modes can occur either before or after the internal steel has yielded. The desired mode of failure is concrete compressive failure after the internal steel has yielded with the FRP strengthening system still attached. The FRP strengthening system can debond in a number of modes. The FRP system can delaminate from the concrete substrate (due to failure in the concrete, the adhesive layer, or in the FRP laminate itself) either at the ends (due to high peeling and shear stresses) or in the interior of the beam due to flexural and shear cracks in the beam at large deflections. For a detailed discussion on debonding failure modes, see Teng et al (2001). Analytical methods to predict the various debonding failure modes are still not fully developed, and ACI 440.2R-02 limits the tensile strain level in the FRP strengthening system to prevent debonding failure by use of an empirically obtained, bond-dependent coefficient (κ_m) that is a function of the unit stiffness of the FRP system and is defined as:

$$\kappa_m = \begin{cases} \frac{1}{60\epsilon_{fu}} \left(1 - \frac{nE_f t_f}{2,000,000} \right) \leq 0.90 & \text{for } nE_f t_f \leq 1,000,000 \text{ lb/in.} \\ \frac{1}{60\epsilon_{fu}} \left(1 - \frac{500,000}{nE_f t_f} \right) \leq 0.90 & \text{for } nE_f t_f > 1,000,000 \text{ lb/in.} \end{cases} \quad (25.30)$$

where ϵ_{fu} is the ultimate strain the FRP; n is the number of layers of FRP strips, sheets, or fabrics; E_f is the longitudinal tensile modulus of the FRP composite in the case of strips or the longitudinal modulus of the fibers in the strengthening direction in the case of sheets or fabrics; and t_f is the thickness of an individual strip in the case of FRP strips or the net thickness of the fibers in a single sheet or fabric in the case of sheets or fabrics.

The strain level in the FRP strengthening system is limited by the strain in the concrete or the ultimate strain in the FRP system and is given as:

$$\epsilon_{fe} = \epsilon_{cu} \left(\frac{h-c}{c} \right) - \epsilon_{bi} \leq \kappa_m \epsilon_{fu} \quad (25.31)$$

where ϵ_{fe} is the effective ultimate strain in the FRP at failure, ϵ_{cu} is the ultimate compressive strain in the concrete (0.003), c is the depth of the neutral axis, h is the depth of the section, and ϵ_{bi} is the existing tensile strain in the concrete substrate at the location of the FRP strengthening system when the FRP system is applied.

The effective stress (f_{fe}) in the FRP is the ultimate strength of the FRP that can be achieved at failure and is linearly related to the ultimate strain as:

$$f_{fe} = E_f \epsilon_{fe} \quad (25.32)$$

The nominal moment capacity (M_n) of the strengthened section (with an existing layer of tensile steel reinforcement) is given as:

$$M_n = A_s f_s \left(d - \frac{\beta_1 c}{2} \right) + \psi_f A_f f_{fe} \left(h - \frac{\beta_1 c}{2} \right) \quad (25.33)$$

with:

$$c = \frac{A_s f_s + A_f f_{fe}}{\gamma'_c \beta_1 b} \quad (25.34)$$

and:

$$f_s = E_s \epsilon_s = E_s \left(\epsilon_{fe} + \epsilon_{bi} \right) \left(\frac{d-c}{h-c} \right) \leq f_y \quad (25.35)$$

where A_s is the area of the tensile steel, f_s is the stress in the steel at failure, d is the depth of the steel reinforcing, β_1 is the depth ratio of the equivalent Whitney stress block, A_f is the area of the FRP strip or the fibers only in a formed-in-place system, γ is the concrete stress resultant factor (0.85 when concrete compressive failure governs), b is the width of the section, and f_y is the yield stress in the reinforcing steel.

The solution to the above equations is typically found by a *trial-and-error* method by assuming a number of layers of a specific strengthening system and calculating the resulting nominal moment. Alternatively, a failure mode can be assumed *a priori* and the stresses in the materials checked using closed-form equations, as described in Bank (2006). According to ACI 440.2R-02, the four currently admissible failure modes are FRP debonding either before or after the internal steel yields or concrete compressive crushing either before or after the internal steel yields. The stress distribution in the concrete at failure of the strengthened member will depend on the failure mode of the strengthened member. If the FRP debonds when the concrete strain is still low (less than 0.002), the failure is controlled by the FRP, and a nonlinear stress distribution in the concrete should be used in determining the compressive force in the section (Bank, 2006). This is not conducive to design calculations, however, and it is typically assumed that the concrete stress can be represented by the Whitney stress block at failure even in this case. Figure 25.4 shows the strains, stresses, and forces in an FRP-strengthened section at the ultimate state according to this assumption. This assumption is felt to be reasonable because in an appropriately designed strengthening system the steel will yield before the FRP debonds or ruptures and the strain in the concrete will be larger than 0.002.

As with a conventional reinforced concrete section, a balanced reinforcement ratio can be defined that includes the effect of the internal steel reinforcing and the externally applied FRP system (Bank, 2006). The balanced ratio can be defined for failure of the section either prior to the internal steel yielding or after the internal steel has yielded, although as mentioned previously the latter is preferable. The balanced reinforcement ratio can be a useful tool in design but is not as important a parameter as in the design of conventional reinforced concrete design (either steel or FRP reinforcement), because a strengthening design depends on the properties of an existing section and it may not be always possible to achieve a balanced condition in the strengthened section. The stresses in the steel and the FRP strengthening system

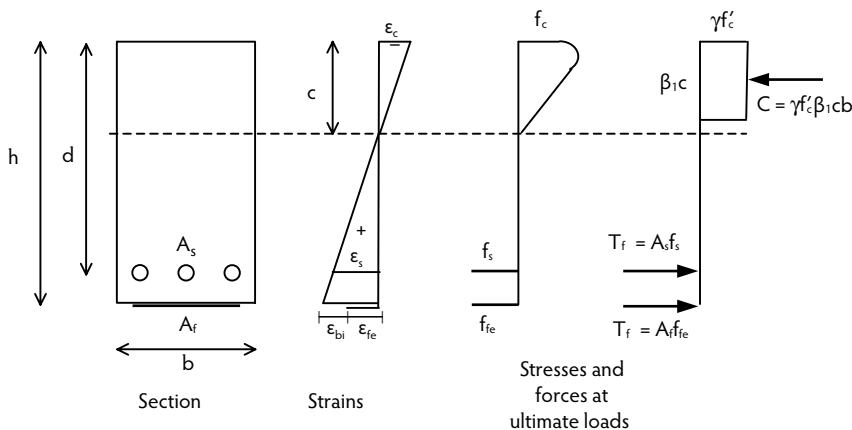


FIGURE 25.4 Strains, stresses, and forces in an FRP-strengthened section at ultimate loads.

at service loads should be determined using an elastic cracked section and checked against appropriate stress limits for sustained loads on FRP strengthened structures according to ACI 440.2R-02. Mechanical anchorages or FRP wraps can be used to enhance the attachment of the FRP strengthening system to the concrete beam, especially at the ends of the FRP strengthening system. Design guidance is not provided by the ACI 440.2R-02 for this, although the use of such a system is recommended by many manufacturers to prevent debonding failures.

25.3.5 Design of FRP Shear Strengthening Systems

Fiber-reinforced polymer strengthening systems can be used to increase the shear capacity of concrete beams and columns. FRP strengthening systems are applied to the webs of beams (or columns) and function in an analogous fashion to internal steel shear reinforcement. Because FRP shear strengthening systems are applied to concrete members that are often constructed monolithically with other continuous members (such as floors and walls) it is not always possible wrap the FRP strengthening system completely around the member (which is the desirable condition.) The FRP strengthening system must therefore be terminated at the top of the web (a *three-sided U-wrap*) or terminated at both the top and the bottom on the web (a *two-sided wrap*). The non-fully wrapped systems are susceptible to debonding failures (similar to flexural strengthening), and their strains are limited by a shear bond-reduction coefficient (κ_v), which is a function of the concrete strength, the wrapping type used, and the stiffness of the FRP strengthening system. It is given by ACI 440.2R-02 (in U.S. units) as:

$$\kappa_v = \frac{k_1 k_2 L_e}{468 \epsilon_{fu}} \leq 0.75 \quad (25.36)$$

where L_e is the active bond length over which the shear stress is transferred between the FRP and the concrete. It has been shown that it is this finite length that limits the maximum force that can be transferred between the two materials regardless of the bonded length of the FRP strip. It is given as:

$$L_e = \frac{2500}{(n t_f E_f)^{0.58}} \quad (25.37)$$

The coefficients k_1 and k_2 are given as:

$$k_1 = \left(\frac{f'_c}{4000} \right)^{2/3} \quad (25.38)$$

For three-sided shear strengthening systems:

$$k_2 = \frac{d_f - L_e}{d_f} \quad (25.39)$$

For two-sided shear strengthening systems:

$$k_2 = \frac{d_f - 2L_e}{d_f} \quad (25.40)$$

where d_f is the effective depth of the FRP shear strengthening system. For fully wrapped sections, it is equal to the full depth (h) of the section, but for two- and three-sided wraps it is the vertical distance from the top of the FRP system to the main tensile reinforcing bars in the beam and is less than h .

The nominal shear capacity of an FRP strengthened concrete member with existing steel shear reinforcing is determined by adding the contribution of the FRP strengthening system to the existing shear capacity and is given as:

$$V_n = V_c + V_s + \psi_f V_f \quad (25.41)$$

where:

$$V_f = \frac{A_{fv} f_{fe} (\sin \alpha + \cos \alpha) d_f}{s_f} \quad (25.42)$$

$$A_{fv} = 2nt_f w_f \quad (25.43)$$

$$f_{fe} = E_f \epsilon_{fe} \quad (25.44)$$

where V_c is the shear capacity of the concrete, V_s is the shear capacity of the existing steel shear reinforcement, and V_f is the shear capacity of the FRP strengthening system. The FRP material reduction factor (ψ_f) is taken as 0.95 for completely wrapped *contact-critical* sections and as 0.85 for *bond-critical* two- or three-sided wrapped sections. A_{fv} is the area of the FRP shear strengthening system, f_{fe} is the effective tensile stress in the FRP at ultimate, α is the inclination of the fiber in the FRP strengthening system to the longitudinal axis of the member, s_f is the center-to-center spacing of the FRP shear strengthening strips, and w_f is the width of the FRP shear strengthening strip. (For a continuous FRP shear strengthening sheet or fabric, $s_f = w_f$). E_f is the longitudinal modulus of the FRP strengthening system, and ϵ_{fe} is the effective longitudinal strain in the FRP strengthening system.

The effective strain in the FRP shear strengthening system is limited to prevent debonding failures and to maintain the integrity of the concrete aggregate interlock in the concrete member. For completely wrapped FRP shear strengthening systems, the maximum effective strain in the FRP strengthening system at failure is limited to:

$$\epsilon_{fe} = 0.004 \leq 0.75 \epsilon_{fu} \quad (25.45)$$

For two- or three-sided shear strengthening, the effective shear strain in the FRP strengthening system at failure is limited to:

$$\epsilon_{fe} = \kappa_v \epsilon_{fu} \leq 0.004 \quad (25.46)$$

Mechanical anchorages can be used to anchor two- or three-sided wraps in the compression zone of the web; however, design guidance is not provided by ACI 440.2R-02.

When FRP shear strengthening is added to the conventional steel shear reinforcement, the shear reinforcement limit for conventional concrete members must hold for both types of reinforcement:

$$V_s + V_f \leq 8\sqrt{f'_c}b_wd \quad (25.47)$$

When intermittent strips are used, a maximum spacing between the strips is mandated so every shear crack will be covered by sufficient strip width. The following maximum spacing of intermittent strips is required:

$$s_f^{\max} = \frac{d_f}{4} + w_f \quad (25.48)$$

25.3.6 Design of FRP Axial Strengthening Systems

Concrete compression members can be strengthened to increase their axial load carrying capacity, their shear capacity, their steel rebar lap splice capacity, and their lateral load carrying deformation capacity (which is related to the ductility of the member). FRP strengthening of columns is most effective when applied to circular columns and must always consist of complete wrapping to obtain confinement of the concrete. FRP strengthening systems for confinement of columns are classified as *contact-critical* applications. It is also important to note that FRP axial strengthening systems are regarded as *passive* systems; that is, they are not effective (or active) until the concrete reaches its transverse cracking strain and begins to dilate, thus placing hoop stress on the FRP wrap. This is in contrast to the FRP flexural and shear strengthening systems that must be active at all load levels.

For a non-slender, non-prestressed, normal weight concrete column reinforced with steel *spiral reinforcement*, the nominal axial capacity is given as:

$$P_n = 0.85 \left(0.85 \psi_f f'_{cc} (A_g - A_{st}) + f_y A_{st} \right) \quad (25.49)$$

and for steel *tied reinforcement*, the nominal axial capacity is given as:

$$P_n = 0.80 \left(0.85 \psi_f f'_{cc} (A_g - A_{st}) + f_y A_{st} \right) \quad (25.50)$$

The confined compressive strength (f'_{cc}) is given in ACI 440.2R-02 as:

$$f'_{cc} = f'_c \left(2.25 \sqrt{1 + 7.9 \frac{f_l}{f'_c}} - 2 \frac{f_l}{f'_c} - 1.25 \right) \quad (25.51)$$

where f_l is the confining pressure provided by the FRP wrap and is given as:

$$f_l = \frac{\kappa_a \rho_f E_f \epsilon_{fe}}{2} \quad (25.52)$$

where A_g is the gross area of the concrete; A_{st} is the area of the existing longitudinal steel; f_y is the yield stress in the steel bars; f'_c is the unconfined (existing) concrete compressive strength; ψ_f is the FRP material reduction factor taken as 0.95 for this contact-critical application; κ_a is an efficiency factor that depends on the shape of the column; ρ_f is the reinforcement ratio of the FRP system; E_f is the modulus of the FRP system in the hoop direction; and ϵ_{fe} is the effective strain the FRP system in the hoop direction.

For circular columns, κ_a is 1.0 and the reinforcement ratio is given as:

$$\rho_f = \frac{A_f}{A_g} = \frac{4nt_f}{h} \quad (25.53)$$

where h is the diameter of the circular column. It is important to note that the fiber layers must all be oriented in the hoop direction around the column (or, if they are not, the effective properties of the FRP system in the hoop direction must be used). If layers are also oriented in the longitudinal direction (e.g., for flexural strengthening), these layers should not be considered to contribute to the axial strengthening. For noncircular columns, FRP strengthening to increase axial capacity is much less effective due to stress concentrations at the corners (even when chamfered) and the nonuniform confining pressure developed by the wrap. See Teng et al. (2001) for more discussion and proposed equations to address this topic.

Limits are placed on the amount of FRP axial strengthening to ensure that the concrete does not approach its transverse cracking strain nor the steel its yield strain in the service range. ACI 440.2R-02 limits the service load stress in the concrete to $0.65f'_c$ and the service load stress in the longitudinal steel to $0.60f_y$. The stresses in the concrete ($f_{c,s}$) and the steel ($f_{s,s}$) at service loads are found using traditional mechanics of materials formulae:

$$f_{c,s} = p_s \left(\frac{E_c}{A_c E_c + A_{st} E_s} \right) \quad (25.54)$$

and

$$f_{s,s} = p_s \left(\frac{E_s}{A_c E_c + A_{st} E_s} \right) \quad (25.55)$$

where p_s is the axial load at service conditions in the FRP-strengthened column.

25.3.6.1 Ductility Enhancement

The lateral displacement capacity, which is related to the ductility of a concrete column, can also be increased by confining it with FRP strengthening wraps. The determination of the lateral displacement capacity is beyond the scope of ACI 440.2R-02 and is addressed in a number of texts related to the seismic capacity of concrete structures (Paulay and Priestley, 1992; Priestley et al., 1996). One of the key parameters used in determining the lateral displacement capacity of a concrete column is the maximum confined concrete compressive strain (ϵ'_{cc}), which is the failure strain in the concrete in the large-deformation, inelastic range. The maximum concrete compressive strain is typically greater than ϵ_{cu} , which is the assumed nominal concrete strain at failure (based on standard unreinforced cylinder tests), and is stipulated by the ACI as 0.003. This is due to the fact that the concrete in the compression zone in a member is confined by the transverse reinforcing steel (stirrups, ties, hoops or spirals). By using an FRP wrap on the exterior of the member, the concrete in the compression zone can be confined in a similar manner and the maximum concrete strain at ultimate can be increased to a confined compressive strain (ϵ'_{cc}). The equation provided by ACI 440.2R-02 for the maximum confined concrete compressive strain of an FRP wrapped column is:

$$\epsilon'_{cc} = \frac{1.71(5f'_{cc} - 4f'_c)}{E_c} \quad (25.56)$$

where E_c is the elastic modulus of the concrete and f'_{cc} is as defined previously. This equation is valid for both circular and rectangular columns. To use the equation for rectangular columns, the efficiency factor (κ_a) is calculated from:

$$\kappa_a = 1 - \frac{(b - 2r)^2 + (h - 2r)^2}{3bh(1 - \rho_g)} \quad (25.57)$$

where h and b are the depth and breadth of the rectangular concrete column, r is the corner radius, and $\rho_g = A_{st}/A_g$ is the steel reinforcement ratio. This equation is only applicable when $h/b \leq 1.5$ and when

both b and h are less than 36 in., as it has been shown that ductility enhancement in rectangular columns with larger aspect ratios and longer sides is negligible. The FRP reinforcement ratio for a rectangular FRP confined column is given as:

$$\rho_f = \frac{2nt_f(b+h)}{bh} \quad (25.58)$$

It is important to recognize that, even though a confined compressive strength for a rectangular column is calculated as an intermediate step to calculating the confined compressive strain, this confined strength should not be used to determine any strength increase in the column.

25.4 Summary

The fundamental considerations and the basic equations that are used to design FRP-reinforced and FRP-strengthened concrete members have been presented in this chapter. The design procedures presented are those promulgated in design guides published by the American Concrete Institute, but it is important to note that these guides are often updated as new research is conducted in this rapidly evolving area of concrete structures. Readers are therefore advised to make sure to obtain the current versions of these guides when designing FRP-reinforced and FRP-strengthened concrete members. Even though the equations and the factors may change in forthcoming versions of these guides, the fundamental concepts presented in this chapter will remain the basis for the design procedures provided. At this time, the properties of the FRP materials for use with the equations presented in this chapter and with the ACI guides must be obtained from the manufacturers of the FRP products being used. Efforts are underway at a number of organizations to develop standard specifications for FRP-reinforcing and FRP-strengthening materials for use in concrete structures.

References

- ACI Committee 318. 1999. *Building Code Requirements for Structural Concrete and Commentary*, ACI 318-99, American Concrete Institute, Farmington Hills, MI.
- ACI Committee 318. 2005. *Building Code Requirements for Structural Concrete and Commentary*, ACI 318-05/ACI 318R-05. American Concrete Institute, Farmington Hills, MI.
- ACI Committee 440. 1996. *State-of-the-Art Report on Fiber-Reinforced Plastic (FRP) Reinforcement for Concrete Structures*, ACI 440R-96. American Concrete Institute, Farmington Hills, MI.
- ACI Committee 440. 2002. *Guide to the Design and Construction of Externally Bonded FRP Systems for Strengthening Concrete Structures*, ACI 440.2R-02. American Concrete Institute, Farmington Hills, MI.
- ACI Committee 440. 2004a. *Guide Test Methods for Fiber Reinforced Polymers (FRP) for Reinforcing or Strengthening Concrete Structures*, ACI 440.3R-04, American Concrete Institute, Farmington Hills, MI.
- ACI Committee 440. 2004b. *Prestressing Concrete with FRP Tendons*, ACI 440.4R-04, American Concrete Institute, Farmington Hills, MI.
- ACI Committee 440. 2006. *Guide for the Design and Construction of Structural Concrete Reinforced with FRP Bars*, ACI 440.1R-06. American Concrete Institute, Farmington Hills, MI.
- Bank, L.C. 1993. FRP reinforcements for concrete. In *Fiber-Reinforced Plastic (FRP) for Concrete Structures: Properties and Applications*, Nanni, A., Ed., pp. 59–86. Elsevier, New York.
- Bank, L.C. 2004. Fiber reinforced polymer composites. In *Handbook of Structural Engineering*, 2nd ed., Chen, W.F. and Liu, E., Eds. CRC Press, Boca Raton, FL.
- Bank, L.C. 2006. *Composites for Construction: Structural Design with FRP Materials*. John Wiley & Sons, New York.
- BRI. 1995. *Guidelines for Structural Design of FRP Reinforced Concrete Building Structures*. Building Research Institute, Tokyo; see also Sonobe, Y. et al. 1997. Design guidelines of FRP-reinforced concrete building structures, *J. Composites Construct.*, 1(3), 90–115.

- Concrete Society. 2003. *Strengthening Concrete Structures with Fibre Composite Materials: Acceptance, Inspection and Monitoring*, TR57. The Concrete Society, London.
- Concrete Society. 2004. *Design Guidance for Strengthening Concrete Structures Using Fibre Composite Materials*, TR55. The Concrete Society, London.
- CSA. 2002. *Design and Construction of Building Components with Fibre-Reinforced Polymers*, S806-02. Canadian Standards Association, Toronto.
- FIB. 2001. *Externally Bonded FRP Reinforcement for RC Structures*, International Federation for Structural Concrete, Switzerland.
- Hollaway, L.C. and Head, P.R. 2001. *Advanced Polymer Composites and Polymers in the Civil Infrastructure*. Elsevier, London.
- ICC Evaluation Service. 1997. *Interim Criteria for Concrete and Reinforced and Unreinforced Masonry Strengthening Using Fiber-Reinforced Polymer (FRP) Composite Systems*, AC 125, ICC Evaluation Service, Whittier, CA.
- ICC Evaluation Service. 2001. *Interim Criteria for Inspection and Verification of Concrete and Reinforced and Unreinforced Masonry Strengthening Using Fiber-Reinforced Polymer (FRP) Composite Systems*, AC 187, ICC Evaluation Service, Whittier, CA.
- ISIS. 2001. *Reinforcing Concrete with Fibre Reinforced Polymers*. ISIS Canada, Manitoba.
- ISIS. 2006. *Specifications for Product Certification of FRPs as Internal Reinforcement in Concrete Structures*. ISIS Canada, Manitoba.
- JSCE. 1997. *Recommendation for Design and Construction of Concrete Structures Using Continuous Fiber Reinforcing Materials*, Concrete Engineering Series 23. Japan Society of Civil Engineers, Tokyo.
- JSCE. 2001. *Recommendation for Upgrading of Concrete Structures with use of Continuous Fiber Sheets*, Concrete Engineering Series 41. Japan Society of Civil Engineers, Tokyo.
- Nanni, A., Ed. 1993. *Fiber-Reinforced Plastic (FRP) for Concrete Structures: Properties and Applications*, Elsevier, New York.
- Paulay, T. and Priestley, M.J.N. 1992. *Seismic Design of Reinforced Concrete and Masonry Buildings*, John Wiley & Sons, New York.
- Priestley, M.J.N., Seible, F., and Calvi, G.M. 1996. *Seismic Design and Retrofit of Bridges*, John Wiley & Sons, New York.
- Starr, T., Ed. 2000. *Pultrusion for Engineers*. CRC Press, Boca Raton, FL.
- Teng, J.G., Chen, J.F., Smith, S.T., and Lam, L. 2001. *FRP Strengthened RC Structures*, John Wiley & Sons, New York.
- TRB. 2004. *Bonded Repair and Retrofit of Concrete Structures Using FRP Composites: Recommended Construction Specifications and Process Control Manual*, NCHRP Report No. 514. National Cooperative Highway Research Program, Transportation Research Board, Washington, D.C.
- Triantifillou, T., Ed. 2007. *Proceedings of the 8th International Symposium on Fiber-Reinforced (FRP) Polymer Reinforcement for Concrete Structures*, July 16–18, Patras, Greece.



Failure mode of reinforced geopolymer concrete columns. (From Sumajouw, M.D.J. and Rangan, B.V., *Low-Calcium Fly-Ash-Based Geopolymer Concrete: Reinforced Beams and Columns*, Research Report GC3, Faculty of Engineering, Curtin University of Technology, Perth, 2006.)

26

Low-Calcium, Fly-Ash-Based Geopolymer Concrete

B. Vijaya Rangan, Ph.D., FACI, FIEAust, C.P.Eng.*

26.1	Introduction	26-1
26.2	Geopolymers.....	26-2
26.3	Constituents of Geopolymer Concrete.....	26-3
26.4	Mixture Proportions of Geopolymer Concrete	26-3
26.5	Mixing, Casting, and Compaction of Geopolymer Concrete	26-4
26.6	Curing of Geopolymer Concrete	26-5
26.7	Design of Geopolymer Concrete Mixtures	26-6
26.8	Short-Term Properties of Geopolymer Concrete	26-8
	Behavior in Compression • Indirect Tensile Strength • Unit Weight	
26.9	Long-Term Properties of Geopolymer Concrete	26-11
	Compressive Strength • Creep and Drying Shrinkage • Sulfate Resistance • Sulfuric Acid Resistance	
26.10	Reinforced Geopolymer Concrete Beams and Columns	26-14
26.11	Economic Benefits of Geopolymer Concrete.....	26-18
26.12	Concluding Remarks.....	26-18
	References	26-19

26.1 Introduction

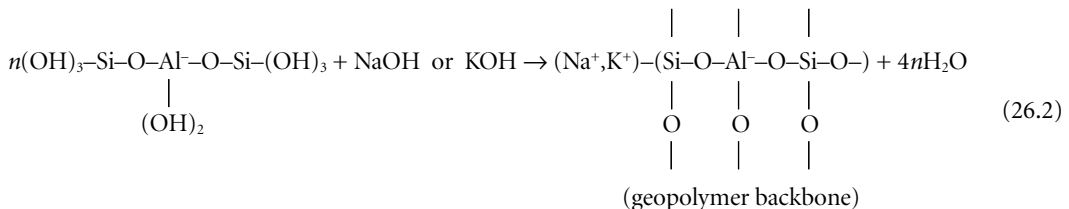
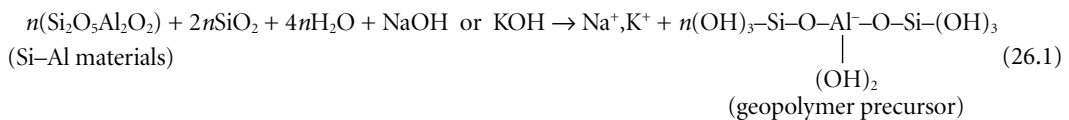
Portland cement concrete is one of the most widely used construction materials. As the demand for concrete as a construction material increases, so, too, does the demand for Portland cement. It is estimated that the production of cement will increase from about 1.5 billion tons in 1995 to 2.2 billion tons by 2010 (Malhotra, 1999). On the other hand, climate changes due to global warming have become a major concern. Global warming is caused by the emission of greenhouse gases, such as carbon dioxide (CO_2), into the atmosphere by human activities. Among the greenhouse gases, CO_2 contributes about 65% of global warming (McCaffrey, 2002). The cement industry is held responsible for some of the CO_2 emissions, because the production of 1 ton of Portland cement emits approximately 1 ton of CO_2 into

* Emeritus Professor of Civil Engineering and Past Dean, Faculty of Engineering, Curtin University of Technology, Perth, Australia; expert in concrete structural systems and high-strength materials technology.

the atmosphere (Davidovits, 1994; McCaffrey, 2002). Several efforts are in progress to reduce the use of Portland cement in concrete to address the global warming issues. These include the utilization of supplementary cementing materials such as fly ash, silica fume, granulated blast-furnace slag, rice-husk ash, and metakaolin, as well as the development of alternative binders to Portland cement. In this respect, the geopolymer technology proposed by Davidovits (1988) shows considerable promise for application in the concrete industry as an alternative binder to Portland cement. In terms of reducing global warming, the geopolymer technology could reduce CO₂ emissions to the atmosphere caused by the cement and aggregates industries by about 80% (Davidovits, 1994).

26.2 Geopolymers

Davidovits (1988, 1994) proposed that an alkaline liquid could be used to react with the silicon (Si) and the aluminum (Al) in a source material of geological origin or in by-product materials such as fly ash and rice-husk ash to produce binders. Because the chemical reaction that takes place in this case is a polymerization process, he coined the term *geopolymer* to represent these binders. Geopolymers are members of the family of inorganic polymers. The chemical composition of the geopolymer material is similar to natural zeolitic materials, but the microstructure is amorphous. The polymerization process involves a substantially fast chemical reaction under alkaline conditions on silicon–aluminum minerals that results in a three-dimensional polymeric chain and ring structure consisting of Si–O–Al–O bonds (Davidovits, 1994). To date, the exact mechanism of setting and hardening of the geopolymer material is not clear, but the formation of geopolymer materials can be described as shown in Equation 26.1 and Equation 26.2 (Davidovits, 1994; van Jaarsveld et al., 1997):



The last term in Equation 26.2 reveals that water is released during the chemical reaction that occurs during the formation of geopolymers. This water, expelled from the geopolymer matrix during the curing and further drying periods, leaves behind discontinuous nanopores in the matrix which provide benefits to the performance of geopolymers. The water in a geopolymer mixture, therefore, plays no role in the chemical reaction that takes place; it merely provides workability to the mixture during handling. This is in contrast to the chemical reaction of water in a Portland cement concrete mixture during the hydration process.

The two main constituents of geopolymers are the source materials and the alkaline liquids. The source materials for geopolymers based on alumina–silicate should be rich in silicon (Si) and aluminum (Al). These could be natural minerals such as kaolinite, clays, etc. Alternatively, by-product materials such as fly ash, silica fume, slag, rice-husk ash, red mud, etc. could be used as source materials. The choice of the source materials for making geopolymers depends on factors such as availability, cost, type of application, and specific demands of the end users. The alkaline liquids are obtained from soluble alkali metals that are usually sodium or potassium based. The most common alkaline liquid used in geopolymerization is a combination of sodium hydroxide (NaOH) or potassium hydroxide (KOH) and sodium silicate or potassium silicate.

This chapter is devoted to heat-cured, low-calcium, fly-ash-based geopolymer concrete. Low-calcium (ASTM Class F) fly ash is preferred as a source material over high-calcium (ASTM Class C) fly ash. The presence of calcium in high amounts may interfere with the polymerization process and alter the micro-structure (Gourley, 2003; Gourley and Johnson, 2005).

26.3 Constituents of Geopolymer Concrete

Geopolymer concrete can be manufactured by using the low-calcium (ASTM Class F) fly ash obtained from coal-burning power stations. The chemical composition and the particle size distribution of the fly ash must be established prior to use. An x-ray fluorescence (XRF) analysis may be used to determine the chemical composition of the fly ash. Low-calcium fly ash has been used successfully to manufacture geopolymer concrete for which the silicon and aluminum oxides constituted about 80% by mass, with a Si/Al ratio of about 2. The content of the iron oxide usually ranged from 10 to 20% by mass, whereas the calcium oxide content was less than 3% by mass. The carbon content of the fly ash, as indicated by the loss on ignition by mass, was as low as <2%. The particle size distribution tests revealed that 80% of the fly ash particles were smaller than 50 μm (Gourley, 2003; Hardjito and Rangan, 2005). Coarse and fine aggregates used by the concrete industry are suitable for the manufacture of geopolymer concrete. The grading curves currently used in concrete practice are applicable in the case of geopolymer concrete (Gourley, 2003; Hardjito and Rangan, 2005).

A combination of sodium silicate solution and sodium hydroxide (NaOH) solution can be used as the alkaline liquid. It is recommended that the alkaline liquid be prepared by mixing both of the solutions together at least one day prior to use. The sodium silicate solution is commercially available in various grades. A solution with a $\text{Na}_2\text{O}/\text{SiO}_2$ ratio by mass of approximately 2 (say, $\text{Na}_2\text{O} = 14.7\%$, $\text{SiO}_2 = 29.4\%$, and water = 55.9%) is recommended. Sodium hydroxide with 98% purity, in flake or pellet form, is commercially available. The solids must be dissolved in water to make a solution with the required concentration. The concentration of sodium hydroxide solution can vary in from 8 to 16 molar. The mass of NaOH solids in a solution varies depending on the concentration of the solution; for example, NaOH solution with a concentration of 8 molar consists of $8 \times 40 = 320$ g of NaOH solids per liter of the solution, where 40 is the molecular weight of NaOH. The mass of NaOH solids has been measured as 262 g per kg of NaOH solution with a concentration of 8 molar. Similarly, the mass of NaOH solids per kg of the solution for other concentrations has been measured as 10 molar for 314 g, 12 molar for 361 g, 14 molar for 404 g, and 16 molar for 444 g (Hardjito and Rangan, 2005). Note that the mass of NaOH solids is only a fraction of the mass of the NaOH solution, and water is the major component. To improve the workability, a high-range, water-reducer (HRWR) superplasticizer and extra water may be added to the mixture.

26.4 Mixture Proportions of Geopolymer Concrete

The primary difference between geopolymer concrete and Portland cement concrete is the binder. The silicon and aluminum oxides in the low-calcium fly ash react with the alkaline liquid to form the geopolymer paste that binds the loose coarse aggregates, fine aggregates, and other unreacted materials together to form the geopolymer concrete. As in the case of Portland cement concrete, the coarse and fine aggregates occupy about 75 to 80% of the mass of geopolymer concrete. This component of geopolymer concrete mixtures can be designed using the tools currently available for Portland cement concrete. The compressive strength and workability of geopolymer concrete are influenced by the proportions and properties of the constituent materials that make the geopolymer paste. Experimental results (Hardjito and Rangan, 2005) have shown the following:

- A higher concentration (in terms of molar) of the sodium hydroxide solution results in higher compressive strength of geopolymer concrete.
- The higher the ratio of sodium silicate solution to sodium hydroxide solution by mass, the higher the compressive strength of geopolymer concrete.

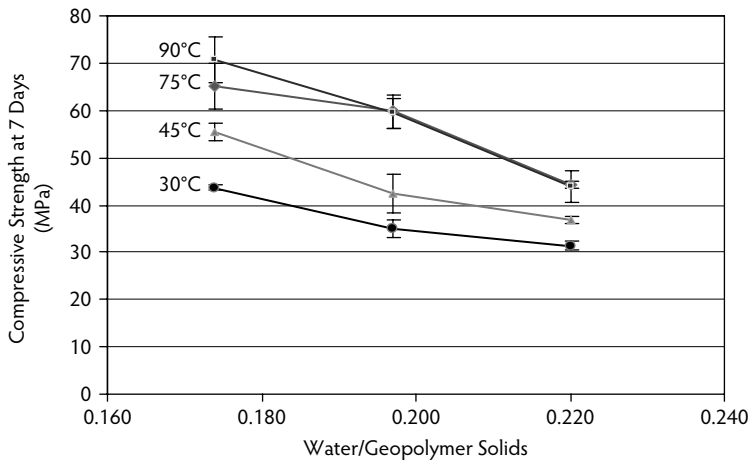


FIGURE 26.1 Effect of water-to-geopolymer solids ratio by mass on compressive strength of geopolymer concrete. (From Hardjito, D. and Rangan, B.V., *Development and Properties of Low-Calcium Fly-Ash-Based Geopolymer Concrete*, Research Report GC1, Faculty of Engineering, Curtin University of Technology, Perth, 2005.)

- The addition of naphthalene-sulfonate-based superplasticizer, up to approximately 4% of fly ash by mass, improves the workability of the fresh geopolymer concrete; however, there is a slight degradation in the compressive strength of hardened concrete when the superplasticizer dosage is greater than 2%.
- The slump value of the fresh geopolymer concrete increases when the water content of the mixture increases.
- As the $\text{H}_2\text{O}/\text{Na}_2\text{O}$ molar ratio increases, the compressive strength of geopolymer concrete decreases.
- The effect of the $\text{Na}_2\text{O}/\text{Si}_2\text{O}$ molar ratio on the compressive strength of geopolymer concrete is not significant.

As can be seen from the above, the effects of various parameters on the compressive strength and workability of geopolymer concrete are complex. To assist in the design of low-calcium, fly-ash-based geopolymer concrete mixtures, a single parameter called the **water/geopolymer solids ratio** by mass was devised. In this parameter, the total mass of water is the sum of the mass of water contained in the sodium silicate solution, the mass of water in the sodium hydroxide solution, and the mass of extra water, if any, added to the mixture. The mass of geopolymer solids is the sum of the mass of fly ash, the mass of sodium hydroxide solids, and the mass of solids in the sodium silicate solution (i.e., the mass of Na_2O and SiO_2).

Tests were performed to establish the effect of the water/geopolymer solids ratio by mass on the compressive strength and workability of geopolymer concrete. The test specimens were 100×200 -mm cylinders, heat cured in an oven at various temperatures for 24 hours. The results of these tests, plotted in Figure 26.1, show that the compressive strength of geopolymer concrete decreases as the water/geopolymer solids ratio by mass increases (Hardjito and Rangan, 2005). This test trend is analogous to the well-known effect of the water/cement ratio on the compressive strength of Portland cement concrete. Obviously, as the water/geopolymer solids ratio increases, workability increases because the mixtures contain more water.

26.5 Mixing, Casting, and Compaction of Geopolymer Concrete

Geopolymer concrete can be manufactured by adopting the conventional techniques used in the manufacture of Portland cement concrete. In the laboratory, the fly ash and the aggregates are first mixed together dry in an 80-L capacity pan mixer for about 3 minutes. The alkaline liquid is mixed with the

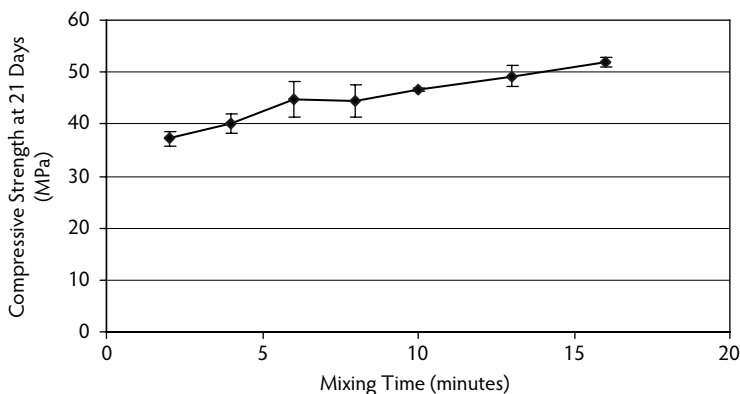


FIGURE 26.2 Effect of wet-mixing time on compressive strength of geopolymer concrete. (From Hardjito, D. and Rangan, B.V., *Development and Properties of Low-Calcium Fly-Ash-Based Geopolymer Concrete*, Research Report GC1, Faculty of Engineering, Curtin University of Technology, Perth, 2005.)

superplasticizer and extra water, if any. The liquid component of the mixture is then added to the dry materials, and the mixing continues for another 4 minutes. The fresh concrete can be handled up to 120 minutes without any sign of setting and without any degradation in the compressive strength. The fresh concrete can be cast and compacted by the usual methods for Portland cement concrete (Hardjito and Rangan, 2005; Sumajouw and Rangan, 2006; Wallah and Rangan, 2006). The compressive strength of geopolymer concrete is influenced by the wet-mixing time, as illustrated by the test data plotted in Figure 26.2. The test specimens were 100×200 -mm cylinders, steam-cured at 60°C for 24 hours, and tested in compression at an age of 21 days. Figure 26.2 shows that the compressive strength significantly increased as the wet-mixing time increased. The slump values of fresh concrete were also measured. These results showed that the slump values decreased from 240 mm for 2 minutes of wet-mixing time to 210 mm when the wet-mixing time increased to 16 minutes.

26.6 Curing of Geopolymer Concrete

Although low-calcium, fly-ash-based geopolymer concrete can be cured in ambient conditions, heat curing is generally recommended. Heat curing substantially assists the chemical reaction that occurs in the geopolymer paste. Both curing time and curing temperature influence the compressive strength of geopolymer concrete. The effect of curing time is illustrated in Figure 26.3 (Hardjito and Rangan, 2005). The test specimens were 100×200 -mm cylinders heat cured at 60°C in an oven. The curing time varied from 4 hr to 96 hr (4 days). Longer curing time improved the polymerization process, resulting in higher compressive strength. The rate of increase in strength was rapid up to 24 hr of curing time; beyond 24 hr, the gain in strength was only moderate. Thus, the heat-curing time need not be more than 24 hr in practical applications.

Figure 26.4 shows the effect of curing temperature on the compressive strength of geopolymer concrete (Hardjito and Rangan, 2005). The test specimens were 100×200 -mm cylinders heat cured in an oven for 24 hr. Higher curing temperatures resulted in greater compressive strength, although an increase in the curing temperature beyond 60°C did not increase the compressive strength substantially. The effect of curing temperature on the compressive strength is also indicated by the test data shown in Figure 26.1. Based on these test trends, a curing temperature of about 60°C is recommended.

Heat curing can be achieved by either steam curing or dry curing. Test data show that the compressive strength of dry-cured geopolymer concrete is approximately 15% larger than that of steam-cured geopolymer concrete (Hardjito and Rangan, 2005). The required heat-curing regime can be manipulated to fit the needs of practical applications. In laboratory trials, precast products were manufactured using geopolymer concrete; the design specifications required steam curing at 60°C for 24 hours. To optimize

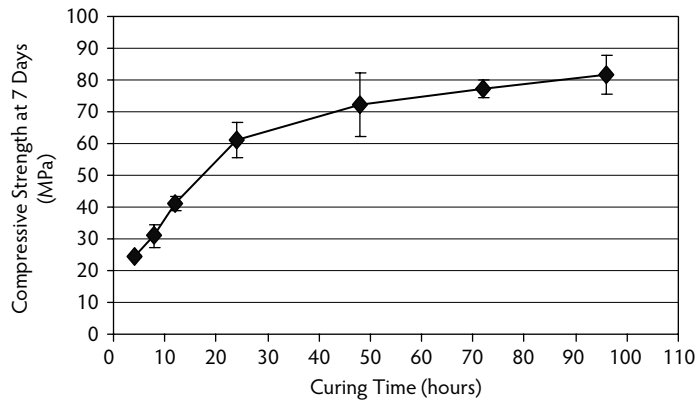


FIGURE 26.3 Effect of curing time on compressive strength of geopolymer concrete. (From Hardjito, D. and Rangan, B.V., *Development and Properties of Low-Calcium Fly-Ash-Based Geopolymer Concrete*, Research Report GC1, Faculty of Engineering, Curtin University of Technology, Perth, 2005.)

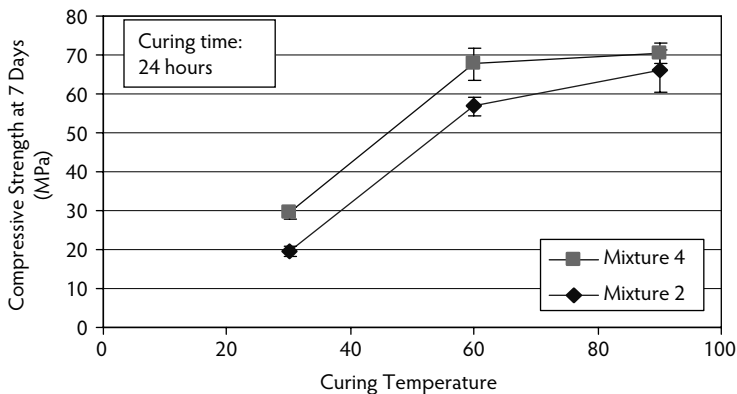


FIGURE 26.4 Effect of curing temperature on compressive strength of geopolymer concrete. (From Hardjito, D. and Rangan, B.V., *Development and Properties of Low-Calcium Fly-Ash-Based Geopolymer Concrete*, Research Report GC1, Faculty of Engineering, Curtin University of Technology, Perth, 2005.)

the usage of formwork, the products were cast and steam cured initially for about 4 hr. The steam curing was then stopped for some time to allow release of the products from the formwork. The steam curing of the products then continued for another 21 hr. This two-stage steam-curing regime did not produce any degradation in the strength of the products. The initiation of heat curing geopolymer concrete can be delayed for several days. Tests have shown that a delay in the start of heat curing up to 5 days did not produce any degradation in the compressive strength. In fact, such a delay in the start of heat curing substantially increased the compressive strength of geopolymer concrete (Hardjito and Rangan, 2005). These flexibilities in the heat-curing regime of geopolymer concrete can be exploited in practical applications.

26.7 Design of Geopolymer Concrete Mixtures

The concrete mixture design process is vast and generally based on performance criteria. Based on the information given in the previous three sections, some simple guidelines for the design of heat-cured, low-calcium, fly-ash-based geopolymer concrete are proposed here. The role and the influence of aggregates are considered to be the same as in the case of Portland cement concrete. The mass of combined aggregates may be taken to be between 75 and 80% of the mass of geopolymer concrete. The performance criteria of a geopolymer concrete mixture depend on the application. For simplicity, the compressive

TABLE 26.1 Data for the Design of Low-Calcium, Fly-Ash-Based Geopolymer Concrete Mixtures

Water/Geopolymer Solids Ratio (by mass)	Workability	Design Compressive Strength (Wet-Mixing Time of 4 Minutes, Steam Curing at 60°C for 24 Hours after Casting)
		(MPa)
0.16	Very stiff	60
0.18	Stiff	50
0.20	Moderate	40
0.22	High	35
0.24	High	30

Note: The fineness modulus of combined aggregates is taken to be in the range of 4.5 to 5.0. When cured in dry heat, the compressive strength may be about 15% larger than the values given above. When the wet-mixing time is increased from 4 minutes to 16 minutes, these compressive strength values may increase by about 30%. The standard deviation of compressive strength is about 10% of the values given above.

strength of hardened concrete and the workability of fresh concrete are selected as the performance criteria. To meet these performance criteria, the alkaline liquid/fly ash ratio by mass, water/geopolymer solids ratio (see Section 26.4 for definition) by mass, the wet-mixing time, the heat-curing temperature, and the heat-curing time are selected as parameters.

With regard to the alkaline liquid/fly ash ratio by mass, values in the range of 0.30 to 0.45 are recommended. Based on results obtained from numerous mixtures made in the laboratory over a period of 4 years, the data given in Table 26.1 are proposed for the design of low-calcium, fly-ash-based geopolymer concrete. Note that a wet-mixing time of 4 minutes and steam curing at 60°C for 24 hr after casting are proposed. The data given in Figure 26.3 and Figure 26.4 may be used as guides to choose other curing temperatures and curing times.

Sodium silicate solution is less expensive than sodium hydroxide solids. Commercially available sodium silicate solution A53 with a $\text{Na}_2\text{O}/\text{SiO}_2$ ratio by mass of approximately 2 (say, $\text{Na}_2\text{O} = 14.7\%$, $\text{SiO}_2 = 29.4\%$, and water = 55.9% by mass) and sodium hydroxide solids (NaOH) with 97 to 98% purity are recommended. Laboratory experience suggests that the ratio of sodium silicate solution to sodium hydroxide solution by mass may be taken as approximately 2.5 (Hardjito and Rangan, 2005).

The mixture design process is illustrated by the following example. A mixture proportion of heat-cured, low-calcium, fly-ash-based geopolymer concrete with a design compressive strength of 45 MPa is required for precast concrete products. Assume that normal-density aggregates are to be used and the unit weight of concrete is 2400 kg/m³. Take the mass of the combined aggregates as 77% of the mass of concrete (i.e., $0.77 \times 2400 = 1848$ kg/m³). The combined aggregates may be selected to match the standard grading curves used in the design of Portland cement concrete mixtures; for example, the aggregates may be comprised of 277 kg/m³ (15%) of 20-mm aggregates, 370 kg/m³ (20%) of 14-mm aggregates, 647 kg/m³ (35%) of 7-mm aggregates, and 554 kg/m³ (30%) of fine sand to meet the requirements of standard grading curves. The fineness modulus of the combined aggregates is approximately 5.0.

The mass of low-calcium fly ash and the alkaline liquid = $2400 - 1848 = 552$ kg/m³. Taking the alkaline liquid/fly ash ratio by mass as 0.35, the mass of fly ash = $552/(1 + 0.35) = 408$ kg/m³ and the mass of alkaline liquid = $552 - 408 = 144$ kg/m³. Taking the ratio of sodium silicate solution to sodium hydroxide solution by mass as 2.5, the mass of sodium hydroxide solution = $144/(1 + 2.5) = 41$ kg/m³ and the mass of the sodium silicate solution = $144 - 41 = 103$ kg/m³. Therefore, the trial mixture proportion is as follows: combined aggregates = 1848 kg/m³, low-calcium fly ash = 408 kg/m³, sodium silicate solution = 103 kg/m³, and sodium hydroxide solution = 41 kg/m³.

To manufacture the geopolymer concrete mixture, commercially available sodium silicate solution A53 with a $\text{Na}_2\text{O}/\text{SiO}_2$ ratio by mass of approximately 2 (say, $\text{Na}_2\text{O} = 14.7\%$, $\text{SiO}_2 = 29.4\%$, and water = 55.9% by mass) is selected. Sodium hydroxide solids (NaOH) with 97 to 98% purity are purchased from commercial sources and mixed with water to make a solution with a concentration of 8 molar. This solution is comprised of 26.2% of NaOH solids and 73.8% water by mass (see Section 26.3).

For the trial mixture, the water/geopolymer solids ratio by mass is calculated as follows. In sodium silicate solution, water = $0.559 \times 103 = 58$ kg and solids = $103 - 58 = 45$ kg. In sodium hydroxide solution, solids = $0.262 \times 41 = 11$ kg and water = $41 - 11 = 30$ kg. Therefore, the total mass of water = $58 + 30 = 88$ kg, and the mass of geopolymer solids = 408 (i.e., mass of fly ash) + $45 + 11 = 464$ kg; hence, the water/geopolymer solids ratio by mass = $88/464 = 0.19$. Using the data given in Table 26.1 for a water/geopolymer solids ratio by mass of 0.19, the design compressive strength is approximately 45 MPa, as required. The geopolymer concrete mixture proportion is therefore as follows:

20-mm aggregates = 277 kg/m^3 .

14-mm aggregates = 370 kg/m^3 .

7-mm aggregates = 647 kg/m^3 .

Fine sand = 554 kg/m^3 .

Low-calcium fly ash (ASTM Class F) = 408 kg/m^3 .

Sodium silicate solution A53 ($\text{Na}_2\text{O} = 14.7\%$, $\text{SiO}_2 = 29.4\%$, and water = 55.9% by mass) = 103 kg/m^3 .

Sodium hydroxide solution (8 molar) = 41 kg/m^3 .

Note that the 8-molar sodium hydroxide solution is made by mixing 11 kg of sodium hydroxide solids with 97 to 98% purity in 30 kg of water. The aggregates are assumed to be in saturated-surface-dry condition. The geopolymer concrete must be wet mixed at least for 4 minutes and steam cured at 60°C for 24 hr after casting. The workability of fresh geopolymer concrete is expected to be moderate. If necessary, a commercially available superplasticizer of about 1.5% of mass of fly ash (i.e., $408 \times 1.5/100 = 6 \text{ kg/m}^3$) may be added to the mixture to facilitate ease of placement of fresh concrete.

Numerous batches of this example geopolymer concrete mixture have been manufactured and tested in the laboratory over a period of 4 years. These test results have shown that the mean 7th-day compressive strength was 56 MPa with a standard deviation of 3 MPa (see Mixture 1 in Table 26.4 and Table 26.5). The mean slump of the fresh geopolymer concrete was about 100 mm. This example is used to illustrate the effects of the alkaline liquid/fly ash ratio by mass on the compressive strength and workability of geopolymer concrete. The example can be reworked using different values of the alkaline liquid/fly ash ratio by mass, and, based on the data given in Table 26.1, the following results are obtained:

Alkaline Liquid/ Fly Ash by Mass	Water/Geopolymer Solids by Mass	Workability	Compressive Strength (MPa)
0.30	0.165	Stiff	58
0.35	0.190	Moderate	45
0.40	0.210	Moderate	37
0.45	0.230	High	32

26.8 Short-Term Properties of Geopolymer Concrete

26.8.1 Behavior in Compression

The behavior and failure modes of fly-ash-based geopolymer concrete in compression are similar to those of Portland cement concrete. Figure 26.5 shows a typical stress–strain curve of geopolymer concrete. Test data show that the strain at peak stress is in the range of 0.0024 to 0.0026 (Hardjito and Rangan, 2005). Collins et al. (1993) proposed that the stress–strain relation of Portland cement concrete in compression can be predicted using the following expression:

$$\sigma_c = f_{cm} \frac{\epsilon_c}{\epsilon_{cm}} \frac{n}{n-1 + \left(\epsilon_c / \epsilon_{cm} \right)^{nk}} \quad (26.3)$$

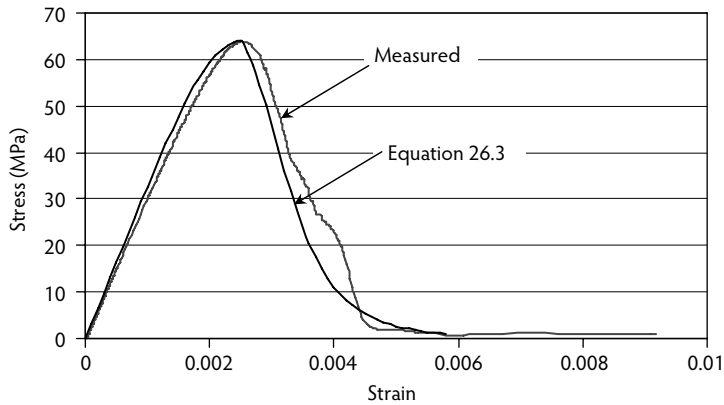


FIGURE 26.5 Stress–strain relation of geopolymer concrete in compression. (From Hardjito, D. and Rangan, B.V., *Development and Properties of Low-Calcium Fly-Ash-Based Geopolymer Concrete*, Research Report GC1, Faculty of Engineering, Curtin University of Technology, Perth, 2005.)

where f_{cm} = peak stress, ϵ_{cm} = strain at peak stress, $n = 0.8 + (f_{cm}/17)$, and $k = 0.67 + (f_{cm}/62)$ when $\epsilon_c/\epsilon_{cm} > 1$ or equal to 1.0 when $\epsilon_c/\epsilon_{cm} \leq 1$. Figure 26.5 shows that the measured stress–strain curve correlates well with that calculated using Equation 26.3.

Table 26.2 gives the measured values of the modulus of elasticity (E_c) of geopolymer concrete in compression. As expected, the modulus of elasticity increases as the compressive strength of geopolymer concrete increases (Hardjito and Rangan, 2005). For Portland cement concrete, the draft Australian Standard AS 3600 (Committee BD-002, 2005) recommends the following expression to calculate the value of the modulus of elasticity within an error of $\pm 20\%$:

$$E_c = \rho^{1.5} (0.024\sqrt{f_{cm}} + 0.12) \quad (\text{MPa}) \quad (26.4)$$

where ρ is the unit weight of concrete in kg/m^3 , and f_{cm} is the mean compressive strength in MPa.

The American Concrete Institute (ACI) Committee 363 (1992) recommended the following expression to calculate the modulus of elasticity:

$$E_c = 3320\sqrt{f_{cm}} + 6900 \quad (\text{MPa}) \quad (26.5)$$

The average unit weight of the fly-ash-based geopolymer concrete was 2350 kg/m^3 . Table 26.2 provides a comparison between the measured values of the modulus of elasticity of fly-ash-based geopolymer concrete with the values calculated using Equation 26.4 and Equation 26.5. It can be seen from Table 26.2 that the measured values were consistently lower than the values calculated using Equation 26.4 and Equation 26.5. This is due to the type of coarse aggregates used in the manufacture

TABLE 26.2 Modulus of Elasticity of Geopolymer Concrete in Compression

f_{cm}	E_c (Measured) (GPa)	E_c (Equation 26.4) (GPa)	E_c (Equation 26.5) (GPa)
89	30.8	39.5 ± 7.9	38.2
68	27.3	36.2 ± 7.2	34.3
55	26.1	33.9 ± 6.8	31.5
44	23.0	31.8 ± 6.4	28.9

TABLE 26.3 Indirect Tensile Splitting Strength of Geopolymer Concrete

Mean Compressive Strength (MPa)	Mean Indirect Tensile Strength (MPa)	Characteristic Principal Tensile Strength (Equation 26.6) (MPa)	Splitting Strength (Equation 26.7) (MPa)
89	7.43	3.77	5.98
68	5.52	3.30	5.00
55	5.45	3.00	4.34
44	4.43	2.65	3.74

of geopolymer concrete. The type of the coarse aggregate used in the test program was of a granite type. Even in the case of specimens made of mixture with $f_{cm} = 44$ MPa, the failure surface of test cylinders cut across the coarse aggregates, thus resulting in a smooth failure surface. This indicates that the coarse aggregates were weaker than the geopolymer matrix and the matrix–aggregate interface (Hardjito and Rangan, 2005). For Portland cement concrete using a granite-type coarse aggregate, Aitcin and Mehta (1990) reported modulus of elasticity values of 31.7 and 33.8 GPa when f_{cm} was equal to 84.8 and 88.6 MPa, respectively. These values are similar to those measured for geopolymer concrete given in Table 26.2. The Poisson's ratio of fly-ash-based geopolymer concrete with compressive strength in the range of 40 to 90 MPa falls between 0.12 and 0.16. These values are similar to those of Portland cement concrete.

26.8.2 Indirect Tensile Strength

The tensile strength of fly-ash-based geopolymer concrete was measured by performing the cylinder splitting test on 150 × 300-mm concrete cylinders (Hardjito and Rangan, 2005). The test results are given in Table 26.3. These test results show that the tensile splitting strength of geopolymer concrete is only a fraction of the compressive strength, as in the case of Portland cement concrete. The draft Australian Standards for Concrete Structures AS 3600 (Committee BD-002, 2005) recommends the following design expression to determine the characteristic principal tensile strength (f_{ct}) of Portland cement concrete:

$$f_{ct} = 0.4\sqrt{f_{cm}} \quad (\text{MPa}) \quad (26.6)$$

Neville (2000) suggested that the relation between the tensile splitting strength and the compressive strength of Portland cement concrete may be expressed as:

$$f_{ct} = 0.3(f_{cm})^{2/3} \quad (\text{MPa}) \quad (26.7)$$

The calculated values of f_{ct} using Equation 26.6 and Equation 26.7 are also given in Table 26.3, which shows that the indirect tensile strength of fly-ash-based geopolymer concrete is larger than the values recommended by the draft Australian Standard AS 3600 (Committee BD-002, 2005) and Neville (2000) for Portland cement concrete.

26.8.3 Unit Weight

The unit weight of concrete primarily depends on the unit mass of aggregates used in the mixture. Tests show that the unit weight of the low-calcium, fly-ash-based geopolymer concrete is similar to that of Portland cement concrete. When granite-type coarse aggregates were used, the unit weight varied between 2330 and 2430 kg/m³ (Hardjito and Rangan, 2005).

TABLE 26.4 Geopolymer Concrete Mixture Proportions

Materials	Mass (kg/m ³)	
	Mixture 1	Mixture 2
Coarse aggregates:		
20 mm	277	277
14 mm	370	370
7 mm	647	647
Fine sand	554	554
Fly ash (low-calcium ASTM Class F)	408	408
Sodium silicate solution A53 (SiO ₂ /Na ₂ O=2)	103	103
Sodium hydroxide solution	41	41
	(8 molar)	(14 molar)
Superplasticizer	6	6
Extra water	None	22.5

TABLE 26.5 Mean Compressive Strength and Unit Weight of Geopolymer Concrete

Mixture	Curing Type	7th-Day Compressive Strength (Heat Curing at 60°C for 24 Hours) (MPa)		Unit Weight (kg/m ³)	
		Mean	Standard Deviation	Mean	Standard Deviation
Mixture 1	Dry curing (oven)	58	6	2379	17
	Steam curing	56	3	2388	15
Mixture 2	Dry curing (oven)	45	7	2302	52
	Steam curing	36	8	2302	49

26.9 Long-Term Properties of Geopolymer Concrete

26.9.1 Compressive Strength

Geopolymer concrete mixture proportions used in laboratory studies are given in Table 26.4 (Wallah and Rangan, 2006). Numerous batches of these mixtures were manufactured over a period of 4 years. For each batch of geopolymer concrete made, 100 × 200-mm cylinders specimens were prepared. At least three of these cylinders were tested for compressive strength at an age of 7 days after casting. The unit weight of specimens was also determined at the same time. Table 26.5 presents the average results for the numerous specimens made from Mixture 1 and Mixture 2 and heat cured at 60°C for 24 hours after casting (Wallah and Rangan, 2006).

To observe the effect of age on the compressive strength of heat-cured geopolymer concrete, 100 × 200-mm cylinders were made from several batches of Mixture 1 (see Table 26.4). The specimens were heat cured in the oven for 24 hours at 60°C. Figure 26.6 presents the ratio of the compressive strength of specimens at a particular age as compared to the compressive strength of specimens from the same batch of geopolymer concrete tested on the 7th day after casting (Wallah and Rangan, 2006). These test data show that the compressive strength increased with age on the order of 10 to 20% when compared to the 7th-day compressive strength. The test data shown in Table 26.5 and Figure 26.6 demonstrate the consistent quality, reproducibility, and long-term stability of low-calcium, fly-ash-based geopolymer concrete.

To study the effect of age on the compressive strength of fly-ash-based geopolymer concrete cured in laboratory ambient conditions, three batches of geopolymer concrete were made using Mixture 1 (see Table 26.4). The test specimens were 100 × 200-mm cylinders. The first batch (May 05) was cast in May 2005, a second batch (July 05) was cast in July 2005, and a third batch (Sept 05) was cast in September 2005. The ambient temperature in May 2005 during the first week after casting the concrete ranged from

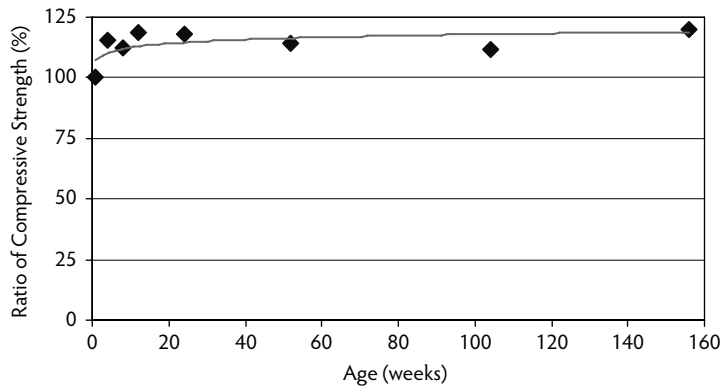


FIGURE 26.6 Change in compressive strength of heat-cured geopolymer concrete with age. (From Wallah, S.E. and Rangan, B.V., *Low-Calcium Fly-Ash-Based Geopolymer Concrete: Long-Term Properties*, Research Report GC2, Faculty of Engineering, Curtin University of Technology, Perth, 2006.)

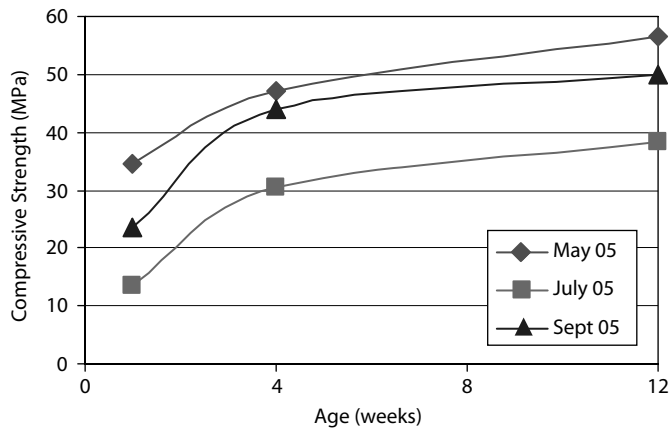


FIGURE 26.7 Compressive strength of geopolymer concrete cured in ambient condition. (From Wallah, S.E. and Rangan, B.V., *Low-Calcium Fly-Ash-Based Geopolymer Concrete: Long-Term Properties*, Research Report GC2, Faculty of Engineering, Curtin University of Technology, Perth, 2006.)

about 18°C to 25°C; this temperature varied from 8°C to 18°C in July 2005 and from 12°C to 22°C in September 2005. The average humidity in the laboratory during those months was between 40 and 60%. The test cylinders were removed from the molds one day after casting and left in laboratory ambient conditions until the day of test. The test results plotted in Figure 26.7 show that the compressive strength of ambient-cured geopolymer concrete significantly increased with age (Wallah and Rangan, 2006). This test trend is in contrast to the effect of age on the compressive strength of heat-cured geopolymer concrete as shown in Figure 26.6.

26.9.2 Creep and Drying Shrinkage

The creep and drying shrinkage behavior of heat-cured, low-calcium, fly-ash-based geopolymer concrete was studied for a period of 1 year (Wallah and Rangan, 2006). The geopolymer concrete mixture proportions used in that study were Mixture 1 and Mixture 2 (see Table 26.4). The test specimens were 150 × 300-mm cylinders, heat cured at 60°C for 24 hours. The creep tests commenced on the 7th day after casting the test specimens, and the sustained stress was 40% of the compressive strength on that day. The test results obtained for specimens made using Mixture 1 and heat cured in an oven are shown in Figure 26.8. The test trends were similar for both Mixture 1 and Mixture 2, heat cured in an oven or

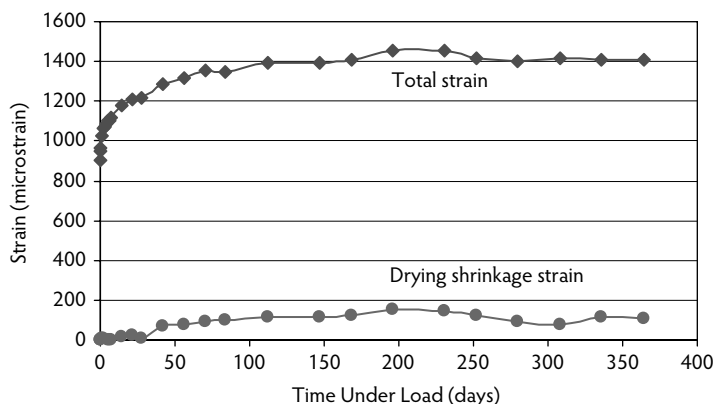


FIGURE 26.8 Total strain and drying shrinkage strain of heat-cured geopolymer concrete. (From Wallah, S.E. and Rangan, B.V., *Low-Calcium Fly-Ash-Based Geopolymer Concrete: Long-Term Properties*, Research Report GC2, Faculty of Engineering, Curtin University of Technology, Perth, 2006.)

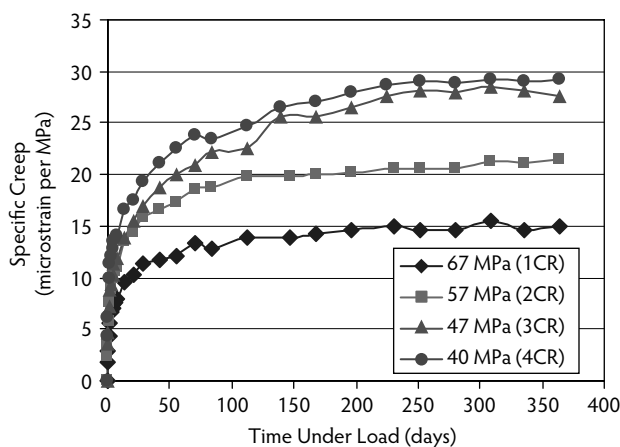


FIGURE 26.9 Effect of compressive strength on creep of heat-cured geopolymer concrete. (From Wallah, S.E. and Rangan, B.V., *Low-Calcium Fly-Ash-Based Geopolymer Concrete: Long-Term Properties*, Research Report GC2, Faculty of Engineering, Curtin University of Technology, Perth, 2006.)

steam cured. Test results show that heat-cured, fly-ash-based geopolymer concrete undergoes very little drying shrinkage, on the order of about 100 microstrains, after 1 year. This value is significantly smaller than the range of values of 500 to 800 microstrains experienced by Portland cement concrete.

The creep coefficient, defined as the ratio of creep strain to elastic strain, after 1 year of loading for heat-cured geopolymer concrete with compressive strengths of 40, 47, and 57 MPa is between 0.6 and 0.7; for geopolymer concrete with a compressive strength of 67 MPa, this value is between 0.4 and 0.5. Data for the specific creep, defined as the creep strain per unit of sustained stress, are shown in Figure 26.9; the specific creep values after 1 year of loading are given in Table 26.6 (Wallah and Rangan, 2006). These values are about 50% of the values recommended by the draft Australian Standard AS 3600 for Portland cement concrete.

The drying shrinkage strains of geopolymer concrete cured in ambient conditions are many folds larger than those experienced by the heat-cured specimens (Figure 26.10). As indicated by Equation 26.2, water is released during the chemical reaction process of geopolymers. In the specimens cured in ambient conditions, this water may evaporate over a period of time and cause significantly large drying shrinkage strains, especially in the first 2 weeks, as can be seen in Figure 26.10 (Wallah and Rangan, 2006).

TABLE 26.6 Specific Creep of Heat-Cured Geopolymer Concrete

Designation	Compressive Strength (MPa)	Specific Creep after 1 Year Loading ($\times 10^{-6}/\text{MPa}$)
1CR	67	15
2CR	57	22
3CR	47	28
4CR	40	29

26.9.3 Sulfate Resistance

Tests were performed to study the sulfate resistance of heat-cured, low-calcium, fly-ash-based geopolymer concrete (Wallah and Rangan, 2006). The test specimens were made using Mixture 1 (see Table 26.4) and were heat cured at 60°C for 24 hours after casting; they were immersed in a 5% sodium sulfate solution for various periods of exposure up to 1 year. The sulfate resistance was evaluated based on the change in mass, change in length, and change in compressive strength of the specimens after sulfate exposure. The test specimens were 100 × 200-mm cylinders for change-in-mass and change-in-compressive strength tests and 75 × 75 × 285-mm prisms for change-in-length tests. Test results suggest that heat-cured, low-calcium, fly-ash-based geopolymer concrete has an excellent resistance to sulfate attack. No damage to the surface of test specimens was observed after exposure to sodium sulfate solution up to 1 year, and no significant changes in the mass and the compressive strength of test specimens were observed after various periods of exposure up to one year. The change in length was extremely small and less than 0.015%. The deterioration of Portland cement concrete due to sulfate attack is attributed to the formation of expansive gypsum and ettringite which causes expansion, cracking, and spalling in the concrete. Low-calcium, fly-ash-based geopolymer concrete undergoes a different mechanism from that of Portland cement concrete, and the geopolymerization products are also different from hydration products. The main product of geopolymerization, as given by Equation 26.2, is not susceptible to sulfate attack as are the hydration products. Because of the lack of gypsum or ettringite formation in the main products of geopolymerization, there is no mechanism of sulfate attack in heat-cured, low-calcium, fly-ash-based geopolymer concrete. However, the presence of high calcium either in the fly ash or in the aggregates could cause the formation of gypsum and ettringite in geopolymer concrete.

26.9.4 Sulfuric Acid Resistance

Tests were performed to study the sulfuric acid resistance of heat-cured, low-calcium, fly-ash-based geopolymer concrete (Wallah and Rangan, 2006). The concentrations of the sulfuric acid solution were 2%, 1%, and 0.5%. The sulfuric acid resistance of geopolymer concrete was evaluated based on the mass loss and the residual compressive strength of the test specimens after acid exposure up to one year. The test specimens, 100 × 200-mm cylinders, were made using Mixture 1 (see Table 26.4) and were heat cured at 60°C for 24 hours after casting. The visual appearance of specimens after exposure to sulfuric acid solution showed that acid attack slightly damaged the surface of the specimens. The maximum mass loss of test specimens of about 3% after 1 year of exposure is relatively small compared to that for Portland cement concrete as reported in other studies. As shown in Figure 26.11, exposure to sulfuric acid caused degradation in the compressive strength; the extent of degradation depended on the concentration of the acid solution and the period of exposure.

26.10 Reinforced Geopolymer Concrete Beams and Columns

To demonstrate the application of heat-cured, low-calcium, fly-ash-based geopolymer concrete, 12 reinforced columns and 12 reinforced beams were manufactured and tested (Sumajouw and Rangan, 2006). In the column test program, the primary parameters were longitudinal reinforcement ratio, load eccentricity, and compressive strength of geopolymer concrete. The longitudinal reinforcement ratio was 1.47% and 2.95%. The column cross-section was 175-mm square. The average yield strength of the longitudinal

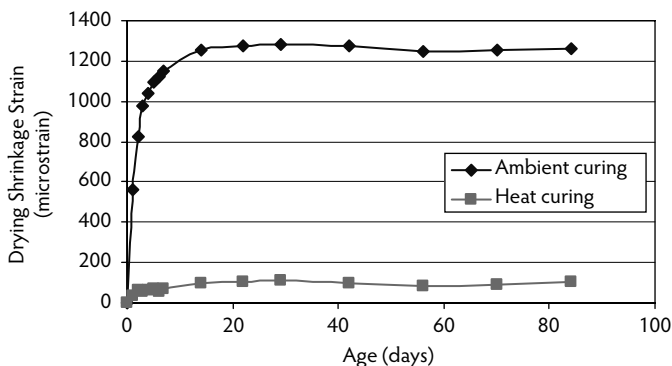


FIGURE 26.10 Drying shrinkage of heat-cured and ambient-cured geopolymer concrete. (From Wallah, S.E. and Rangan, B.V., *Low-Calcium Fly-Ash-Based Geopolymer Concrete: Long-Term Properties*, Research Report GC2, Faculty of Engineering, Curtin University of Technology, Perth, 2006.)

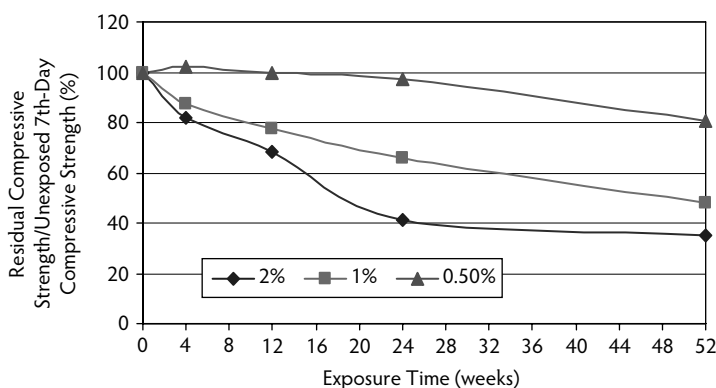


FIGURE 26.11 Acid resistance of heat-cured geopolymer concrete. (From Wallah, S.E. and Rangan, B.V., *Low-Calcium Fly-Ash-Based Geopolymer Concrete: Long-Term Properties*, Research Report GC2, Faculty of Engineering, Curtin University of Technology, Perth, 2006.)

steel was 519 MPa. Closed ties made of 6-mm-diameter hard-drawn wires at 100-mm spacing were used as lateral reinforcement. The concrete cover was 15 mm. The columns were subjected to eccentric compression and bent in single curvature bending. The columns were pin ended with an effective length of 1684 mm.

The mixture proportions of geopolymer concrete used in the manufacture of the column specimens are given in Table 26.7. The average slump of fresh concrete varied between 210 and 240 mm. The nominal compressive strength of geopolymer concrete was 40 MPa for the GCI and GCII series and 60 MPa for the GCIII and GCIV series. These target compressive strengths were achieved by using the mixtures given in Table 26.7 and by exploiting the flexibilities of the heat-curing regime of geopolymer concrete (see Section 26.6). Accordingly, for the GCI and GCII column series, the test specimens were steam cured at a temperature of 60°C for 24 hours after casting; in contrast, the GCIII and GCIV specimens were kept in laboratory ambient conditions for 3 days and then steam cured at a temperature of 60°C for 24 hours.

The mixture proportions of geopolymer concrete used in the manufacture of the beam specimens are also given in Table 26.7. The average slump of the fresh concrete varied from 175 mm for the GBIII series to 255 mm for the GBI series. The target compressive strength of the geopolymer concrete was 40 MPa for the GBI series, 50 MPa for the GBII series, and 70 MPa for the GBIII series. The specimens were kept in laboratory ambient conditions for 3 days after casting and then steam cured at 60°C for 24 hours to achieve the target strengths. The beam cross-section was 200 mm wide by 300 mm deep by 3300 mm in

TABLE 26.7 Geopolymer Concrete Mixture Proportions for Reinforced Columns and Beams

Materials	Mass (kg/m ³)		
	Columns		Beams
10-mm aggregates	555	550	550
7-mm aggregates	647	640	640
Fine sand	647	640	640
Fly ash	408	404	404
Sodium hydroxide solution	41	41	41
	(16 molar)	(14 molar)	(14 molar)
Sodium silicate solution A53	103	102	102
Superplasticizer	6	6	6
Extra added water	26	16.5	25.5 (GBI)
	(GCI and GCII)	(GCIII and GCIV)	17.0 (GBII)
			13.5 (GBIII)

length. The test parameters were concrete compressive strength and longitudinal tensile reinforcement ratio. All beams contained two 12-mm-diameter deformed bars as compression reinforcement and two-legged vertical stirrups made of 12-mm-diameter deformed bars at 150-mm spacing as shear reinforcement. The longitudinal tensile reinforcement ratios were 0.64, 1.18, 1.84, and 2.69%. The average yield strength of tensile steel bars varied between 550 and 560 MPa. The concrete cover was 25 mm. The beams were simply supported over a span of 3000 mm and were subjected to two concentrated loads placed symmetrically on the span. The distance between the loads was 1000 mm.

The behavior and failure modes of the reinforced geopolymer concrete columns were similar to those observed in the case of reinforced Portland cement concrete columns. Typical failure modes of geopolymer concrete columns are shown in Figure 26.12 (Sumajouw and Rangan, 2006). As expected, the load capacity of the columns was influenced by the load eccentricity, the concrete compressive strength, and the longitudinal reinforcement ratio. When the load eccentricity decreased, the load capacity of the columns increased. The load capacity also increased when the compressive strength of the concrete and the longitudinal reinforcement ratio increased.

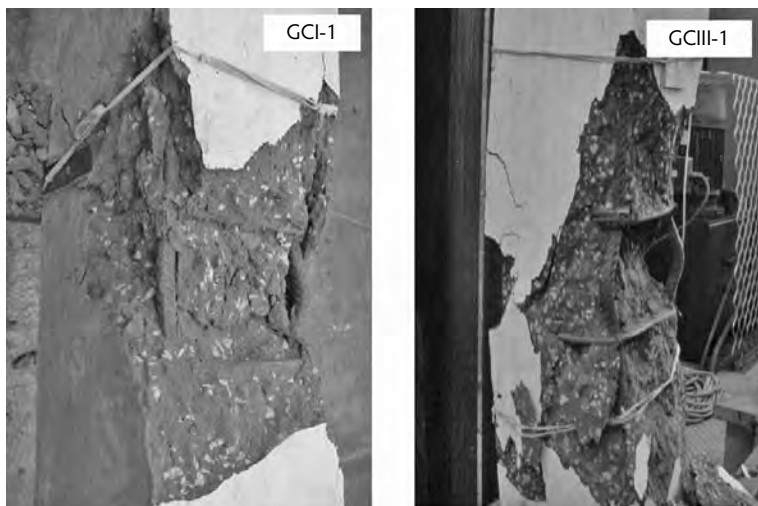


FIGURE 26.12 Failure mode of reinforced geopolymer concrete columns. (From Sumajouw, M.D.J. and Rangan, B.V., *Low-Calcium Fly-Ash-Based Geopolymer Concrete: Reinforced Beams and Columns*, Research Report GC3, Faculty of Engineering, Curtin University of Technology, Perth, 2006.)

TABLE 26.8 Correlation of Test and Calculated Failure Loads of Reinforced Geopolymer Concrete Columns

Column	f'_c (MPa)	e (mm)	p (%)	Test Failure Load (kN)	Calculated Failure Load (kN)			Failure Load Ratio ^a		
					Rangan	AS 3600	ACI 318	1	2	3
GCI-1	42	15	1.47	940	988	962	926	0.95	0.98	1.01
GCI-2	42	35	1.47	674	752	719	678	0.90	0.94	0.99
GCI-3	42	50	1.47	555	588	573	541	0.94	0.97	1.03
GCII-1	43	15	2.95	1237	1149	1120	1050	1.08	1.10	1.18
GCII-2	43	35	2.95	852	866	832	758	0.98	1.02	1.12
GCII-3	43	50	2.95	666	673	665	604	0.99	1.00	1.10
GCIII-1	66	15	1.47	1455	1336	1352	1272	1.09	1.08	1.14
GCIII-2	66	35	1.47	1030	1025	1010	917	1.00	1.02	1.12
GCIII-3	66	50	1.47	827	773	760	738	1.07	1.09	1.12
GCIV-1	59	15	2.95	1559	1395	1372	1267	1.11	1.14	1.23
GCIV-2	59	35	2.95	1057	1064	1021	911	0.99	1.04	1.16
GCIV-3	59	50	2.95	810	815	800	723	0.99	1.01	1.12
Mean								1.01	1.03	1.11
Standard deviation								0.07	0.06	0.08

^a 1 = test/Rangan; 2 = test/AS 3600; 3 = test/ACI 318.

Note: f'_c = concrete compressive strength, e = load eccentricity, and p = longitudinal reinforcement ratio.

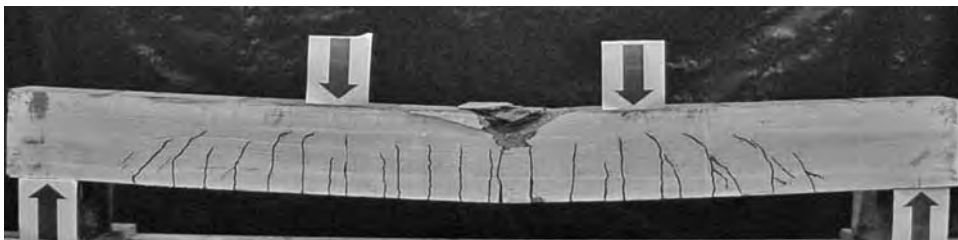


FIGURE 26.13 Crack pattern and failure mode of reinforced geopolymer concrete beam. (From Sumajouw, M.D.J. and Rangan, B.V., *Low-Calcium Fly-Ash-Based Geopolymer Concrete: Reinforced Beams and Columns*, Research Report GC3, Faculty of Engineering, Curtin University of Technology, Perth, 2006.)

The load-carrying capacity of reinforced geopolymer concrete columns was calculated using both a simplified stability analysis proposed by Rangan (1990) and the moment-magnifier method incorporated in the Draft Australian Standard for Concrete Structures AS 3600 (Committee BD-002, 2005) and ACI 318 (ACI Committee 318, 2005). As shown in Table 26.8, the calculated failure loads correlate well with the test values. These results demonstrate that the methods of calculations used in the case of reinforced Portland cement concrete columns are applicable for reinforced geopolymer concrete columns. The behavior and failure modes of the reinforced geopolymer concrete beams were similar to those observed in the case of reinforced Portland cement concrete beams. Figure 26.13 shows the crack pattern and failure mode of a reinforced geopolymer concrete beam. The flexural capacity of the beams was influenced by the concrete compressive strength and the tensile reinforcement ratio. The flexural strength of the reinforced geopolymer concrete beams was calculated using the conventional flexural strength theory of reinforced concrete beams as described in standards and building codes such as the Draft Australian Standard AS 3600 and the ACI 318. The results are given in Table 26.9 (Sumajouw and Rangan, 2006). For beams with tensile reinforcement ratios of 1.18%, 1.84%, and 2.69%, the test and calculated values agreed well. In the case of beams with a tensile steel ratio of 0.64%, the calculated values were conservative, as expected, due to the neglect of the effect of strain hardening of tensile steel bars on the ultimate bending moment.

Mid-span deflection at the service load of the reinforced geopolymer concrete beams was calculated using the elastic bending theory and the serviceability design provisions given in the Draft Australian Standard AS 3600. According to AS 3600, the calculation of short-term deflection of reinforced concrete

TABLE 26.9 Correlation of Test and Calculated Ultimate Moment of Reinforced Geopolymer Concrete Beams

Beam	Tensile Reinforcement Ratio (%)	Concrete Compressive Strength (MPa)	Mid-Span Deflection at Failure Load (mm)	Ultimate Moment (kNm)		Test/Calculated Ratio
				Test	Calculated	
GBI-1	0.64	37	56.63	56.30	45.17	1.24
GBI-2	1.18	42	46.01	87.65	80.56	1.09
GBI-3	1.84	42	27.87	116.85	119.81	0.98
GBI-4	2.69	37	29.22	160.50	155.31	1.03
GBII-1	0.64	46	54.27	58.35	42.40	1.28
GBII-2	1.18	53	47.20	90.55	81.50	1.11
GBII-3	1.84	53	30.01	119.0	122.40	0.97
GBII-4	2.69	46	27.47	168.7	162.31	1.04
GBIII-1	0.64	76	69.75	64.90	45.69	1.42
GBIII-2	1.18	72	40.69	92.90	82.05	1.13
GBIII-3	1.84	72	34.02	126.80	124.17	1.02
GBIII-4	2.69	76	35.85	179.95	170.59	1.05
Average						1.11
Standard deviation						0.14

beams should include the effects of cracking, tension stiffening, and shrinkage properties of the concrete. In these calculations, the service load was taken as the test failure load divided by 1.5; measured values of the modulus of elasticity and drying shrinkage strain of geopolymer concrete were used. Good correlation of test and calculated deflections at service load can be seen in Table 26.10 (Sumajouw and Rangan, 2006). In all, the results given in Table 26.8, Table 26.9, and Table 26.10 demonstrate that reinforced low-calcium (ASTM Class F), fly-ash-based geopolymer concrete structural members can be designed using the design provisions currently used for reinforced Portland cement concrete members.

26.11 Economic Benefits of Geopolymer Concrete

Heat-cured, low-calcium, fly-ash-based geopolymer concrete offers several economic benefits over Portland cement concrete. The price of a ton of fly ash is only a small fraction of the price of a ton of Portland cement; therefore, after allowing for the price of the alkaline liquids required to make the geopolymer concrete, the price of fly-ash-based geopolymer concrete is estimated to be about 10 to 30% less than that of Portland cement concrete. In addition, the appropriate usage of a ton of fly ash earns approximately one carbon credit, which has a redemption value of about 10 to 20 Euros. Based on the information given in this chapter, a ton of low-calcium fly ash can be utilized to manufacture approximately 2.5 m³ of high-quality, fly-ash-based geopolymer concrete and hence can earn monetary benefits through carbon-credit trade. Furthermore, the very little drying shrinkage, low creep, excellent resistance to sulfate attack, and good acid resistance offered by the heat-cured, low-calcium, fly-ash-based geopolymer concrete may yield additional economic benefits when it is utilized in infrastructure applications.

26.12 Concluding Remarks

This chapter presented information on heat-cured, fly-ash-based geopolymer concrete. Low-calcium fly ash (ASTM Class F) is used as the source material instead of the Portland cement to make concrete. Low-calcium, fly-ash-based geopolymer concrete has excellent compressive strength and is suitable for structural applications. The salient factors that influence the properties of the fresh concrete and the hardened concrete have been identified. Data regarding mixture proportions are included and illustrated by an example. The elastic properties of hardened geopolymer concrete and the behavior and strength of reinforced geopolymer concrete structural members are similar to those observed for Portland cement concrete; therefore, the design provisions contained in the current standards and codes can be used to

TABLE 26.10 Correlation of Test and Calculated Service Load Deflections of Reinforced Geopolymer Concrete Beams

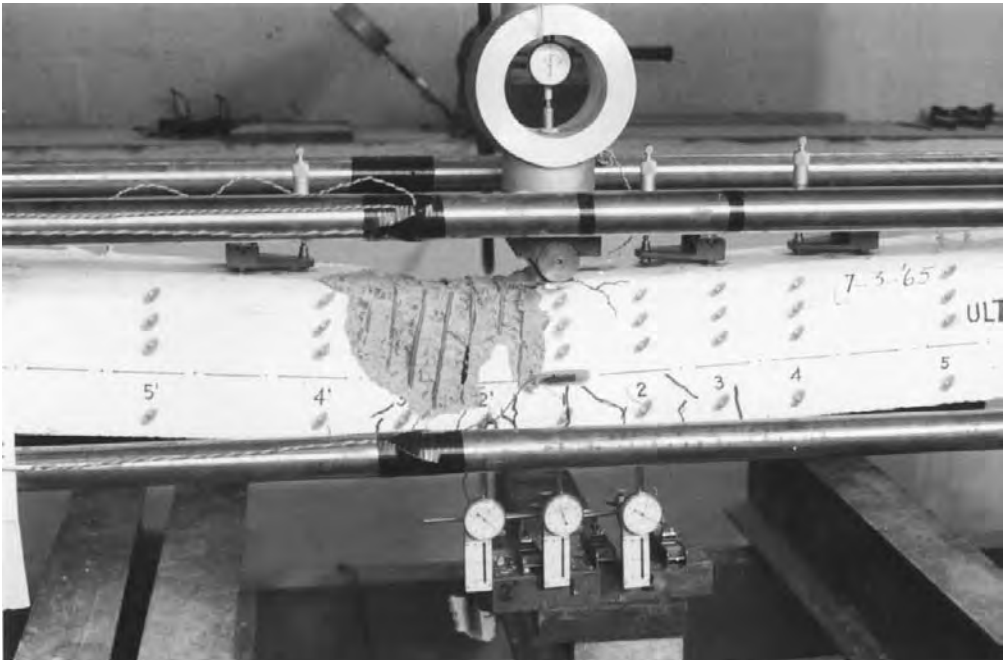
Beam	Service Load (kN)	Deflection (Test) (mm)	Deflection (Calculated) (mm)	Test/Calculated Ratio
GBI-1	75	13.49	11.88	1.17
GBI-2	117	15.27	12.49	1.25
GBI-3	156	13.71	12.41	1.14
GBI-4	217	15.60	14.21	1.14
GBII-1	78	14.25	11.91	1.21
GBII-2	121	14.38	12.58	1.20
GBII-3	159	13.33	12.36	1.14
GBII-4	225	16.16	14.18	1.17
GBIII-1	87	14.10	12.07	1.21
GBIII-2	124	12.55	12.41	1.08
GBIII-3	169	12.38	12.59	1.05
GBIII-4	240	14.88	14.16	1.10
Mean				1.15
Standard deviation				0.06

design reinforced low-calcium, fly-ash-based geopolymer concrete structural members. Heat-cured, low-calcium, fly-ash-based geopolymer concrete also shows excellent resistance to sulfate attack and good acid resistance, undergoes low creep, and suffers very little drying shrinkage. This chapter has also identified several economic benefits of using geopolymer concrete.

References

- ACI Committee 318. 2005. *Building Code Requirements for Structural Concrete*, ACI 318/318R. American Concrete Institute, Farmington Hills, MI.
- ACI Committee 363. 1992. *State-of-the-Art Report on High-Strength Concrete*, ACI 363R. American Concrete Institute, Farmington Hills, MI.
- Aitcin, P.C. and Mehta, P.K. 1990. Effect of coarse-aggregate characteristics on mechanical properties of high-strength concrete. *ACI Mater. J.*, 87(2), 103–107.
- Collins, M.P., Mitchell, D., and MacGregor, J.G. 1993. Structural design considerations for high strength concrete. *ACI Concrete Int.*, 15(5), 27–34.
- Committee BD-002. 2005. *Concrete Structures: Draft Australian Standard AS 3600-200x*. Standards Australia, Sydney.
- Davidovits, J. 1988. Soft mineralogy and geopolymers. In *Proceedings of Geopolymer 88: First European Conference on Soft Mineralogy*, June 1–3, Université de Technologie, Compiègne, France.
- Davidovits, J. 1994. High-alkali cements for 21st century concretes. In *Concrete Technology, Past, Present and Future*, Metha, P.K., Ed., pp. 383–397. American Concrete Institute, Farmington Hills, MI.
- Gourley, J.T. 2003. Geopolymers; Opportunities for Environmentally Friendly Construction Materials, paper presented at Materials 2003: Adaptive Materials for a Modern Society, October 1–3, Sydney, Australia.
- Gourley, J.T. and Johnson, G.B. 2005. Developments in Geopolymer Precast Concrete, paper presented at GCC 2005: International Workshop on Geopolymers and Geopolymer Concrete, September 28–29, Perth, Australia.
- Hardjito, D. and Rangan, B.V. 2005. *Development and Properties of Low-Calcium Fly-Ash-Based Geopolymer Concrete*, Research Report GC1. Faculty of Engineering, Curtin University of Technology, Perth (espace@curtin or www.geopolymer.org).
- Malhotra, V.M. 1999. Making concrete ‘greener’ with fly ash. *ACI Concrete Int.*, 21, 61–66.

- McCaffrey, R. 2002. Climate change and the cement industry. *Global Cement Lime Mag.*, Environmental Special Issue, pp. 15–19.
- Neville, A. M. 2000. *Properties of Concrete*. Prentice Hall, Upper Saddle River, NJ.
- Rangan, B.V. 1990. Strength of reinforced concrete slender columns. *ACI Struct. J.*, 87(1), 32–38.
- Sumajouw, M.D.J. and Rangan, B.V. 2006. *Low-Calcium Fly-Ash-Based Geopolymer Concrete: Reinforced Beams and Columns*, Research Report GC3. Faculty of Engineering, Curtin University of Technology, Perth (espace@curtin or www.geopolymer.org).
- van Jaarsveld, J.G.S., van Deventer, J.S.J., and Lorenzen, L. 1997. The potential use of geopolymeric materials to immobilise toxic metals. Part I. Theory and applications. *Minerals Eng.*, 10(7), 659–669.
- Wallah, S.E. and Rangan, B.V. 2006. *Low-Calcium Fly-Ash-Based Geopolymer Concrete: Long-Term Properties*, Research Report GC2. Faculty of Engineering, Curtin University of Technology, Perth (espace@curtin or www.geopolymer.org).



Instrumentation for biaxial loading of beam. (Photograph courtesy of Edward G. Nawy, Rutgers University.)

27

Performance Evaluation of Structures

Richard A. Miller, Ph.D., P.E.*

27.1	Introduction	27-1
27.2	ACI 318-08 Provisions on Strength Evaluation of Existing Structures.....	27-2
27.3	Pretest Planning for Reliable Structural Evaluation	27-4
27.4	Nondestructive Testing for Material and Structural Assessment.....	27-6
	Ultrasonic Testing • Infrared Thermographic Testing • Modal Testing	
27.5	Static/Quasi-Static Load Testing	27-9
	Use of Dead Loads • Vehicle Testing • Testing Using Servohydraulic Cylinders	
27.6	A Discussion of Instrumentation and Data Acquisition	27-13
	Important Issues in Instrumentation Selection • Types of Instrumentation	
27.7	Case Studies in Performance Evaluation of Concrete Structures	27-21
	Testing of a Three-Span Slab Bridge • Truck Load Testing of Damaged Concrete Bridges: Testing for Continuity • Testing of Shear-Key Cracking in Adjacent Box-Girder Bridges • Testing of a High-Rise Building after Collapse • Testing of Concrete Panels on a Steel Stringer Bridge	
	References	27-31

27.1 Introduction

Concrete structures are difficult to evaluate using theoretical models. These models require precise definitions of material properties, support conditions, and the stiffness of individual members. All of these are difficult to define for concrete structures. Other than compressive strength, test data on material properties are often not available, and when such data are available, they are likely to exhibit considerable scatter. Support conditions are not easily defined, and the stiffness of a cracked concrete member can be difficult to determine with any precision. For most structures, the fact that theoretical models cannot predict structural exact behavior is not a problem. The use of proper safety factors and years of experience

* Professor of Civil Engineering, University of Cincinnati, Cincinnati, Ohio; expert in nondestructive testing and evaluation of existing bridges.

in designing and building concrete structures have led to safe and economical designs; however, for certain structures, theoretical evaluation is inadequate. Structures with suspected design or construction flaws, damaged or deteriorated structures, or with unusual design features require a performance evaluation.

Performance evaluation can be defined as the destructive, partially destructive, or nondestructive physical test of a structure, structural system, or structural subsystem for determining critical responses under one or more loading conditions. Performance testing is used for evaluating service load behavior, determining cracking load or ultimate load capacity, determining stiffness or flexibility, detecting damage or deterioration, and evaluating the effects of the damage or deterioration, the effects of support conditions, fatigue or cyclic load behavior, and response to impact or vibrational loads. Performance tests can be divided into two groups: tests for quality control (including verification of load capacity) and tests to assess structural performance when existing theories are inadequate or nonexistent.

When most people think of performance evaluation, they usually think of strength evaluation—specifically, the method described in the American Concrete Institute's *Building Code Requirements for Structural Concrete* (ACI Committee 318, 2005). This method, discussed in Chapter 20 of the ACI Code, is intended to evaluate structures where there is some doubt that the structure meets the safety requirements of the Code. ACI 437R-03, *Strength Evaluation of Existing Concrete Buildings* (ACI Committee 437, 2003), presents a more in-depth discussion of structural strength evaluation. The report defines several cases where the strength-evaluation techniques discussed in the report may be useful:

- Distressed structures that show signs of damage due to overload, fire, vibration, etc.
- Deteriorated structures that show signs of damage through material degradation such as corrosion, excessive cracking of the concrete, spalling, etc.
- Structures suspected of containing understrength materials or to be substandard in design or construction
- Structures where the capacity to hold loads applied in the future is in doubt because the original design or construction data are not available
- Structures for which a change in usage would apply loads in excess of the original design loads
- Assessment of structures undergoing repair, retrofit, or strengthening
- Structures that require testing by order of a building official

The committee recognizes other areas where performance testing may be valuable but does not recommend using the strength-evaluation method presented in the report for these areas:

- Structures with unusual design concepts
- Product development testing used for approval or quality control for mass-produced elements
- Evaluation of foundations or soil conditions
- Structural research

Other possible areas, not mentioned in the report, where strength or performance testing may be useful include:

- To assess the condition of a structure, especially when hidden damage or deterioration is suspected
- To verify the results of analytical modeling

This chapter attempts to present performance testing in the broadest possible terms.

27.2 ACI 318-08 Provisions on Strength Evaluation of Existing Structures

The method described in Chapter 20 of the ACI Code (ACI Committee 318, 2008) is the one most commonly used for performance evaluation of concrete structures. It makes sense to begin any discussion of performance evaluation with this method. Provisions on the strength evaluation of existing structures

are intended to evaluate the safety of a structure for which the load-carrying capacity is in doubt (Section 20.1). If the effects of the strength deficiency are well understood and the structural dimensions and material strengths are easily verified, analytical evaluation of the structure is permitted (Section 20.1.2); otherwise, load testing is required (Section 20.1.3). If the structural safety is suspect due to deterioration, Section 20.1.4 seems to imply that load testing is also required, as it says that deteriorated structures meeting the load test requirements may remain in service. Section 20.1.4 allows the engineer to require periodic reevaluation if deemed necessary.

If load testing is to be undertaken, Section 20.3 requires the structure to be loaded such that any suspect areas are subjected to maximum stress and deflection. In some cases, a single load placement may not simultaneously maximize all of the critical responses and multiple load placements must be used to demonstrate the adequacy of the structure. The ACI 318-08 Code stipulates that the total load test including dead load already in place should not be less than the larger of the U value determined by Equation 27.1:

$$U = 1.15D + 1.5L + 0.4(L_r \text{ or } S \text{ or } R) \quad (27.1a)$$

$$U = 1.15D + 0.9L + 1.5(L_r \text{ or } S \text{ or } R) \quad (27.1b)$$

$$U = 1.3D \quad (27.1c)$$

where D = dead load, L = live load, L_r = roof live load, S = snow load, and R = rain load. The load factor on live load in Equation 27.1b can be reduced to 0.45 for garages, areas occupied as places of public assembly, and all areas where L is greater than 100 lb/ft².

When conducting a load test, the testing sequence is as follows:

- An initial measurement is taken of the important structural responses: deflections, strains, crack patterns, crack openings, rotations, etc. Of all these responses, only deflection and cracking are used for acceptance, but the provisions recognize that other responses, although not required, may be of interest. These responses must be measured not less than 1 hour before the test.
- The load is applied in four equal increments. Between each increment, structural response is measured. Section 20.4.4 requires the structural responses to be measured after each load increment is applied, and the Commentary (R20.4.2) suggests inspecting the structure after each load increment is applied. No maximum or minimum time limit between applications of the load increments is specified. Section 20.4.3 requires that uniform loads be applied in such a way that a uniform load distribution is obtained. In some cases, loads may be applied incorrectly, resulting in an uneven load distribution. The most common case, cited in the Commentary, is when concrete blocks are used for loading. As the structure deflects, the blocks may rotate and touch at the top, creating an arch. Subsequent loads are carried by these arches, and nonuniform load distributions result.
- When the total load is in place, it is left for 24 hr. Structural response measurements are taken at the beginning and end of this period.
- After the 24-hr period, all structural responses are measured, and the load is immediately removed. The structure is left for 24 hr, and the structural responses are measured at the end of the 24-hr period.

The tested area cannot show any signs of failure. Crushing of the concrete is considered failure.

After removal of the load, the structure must recover at least 75% of the maximum deflection:

$$\Delta_r = \frac{\Delta_1}{4} \quad (27.2)$$

where Δ_r is the deflection 24 hr after removing the load, and Δ_1 is the deflection under load after the load is in place for 24 hr. Because very stiff structures have small deflections, it may be difficult to accurately measure deflection recovery, so the code also accepts a structure if:

$$\Delta_{\max} \leq \frac{l_t^2}{20,000h} \quad (27.3)$$

where l_t is the span of the member (taken as the smaller of center to center of supports or clear span + h) and h is the member thickness. For two-way slabs, l_t is the shortest span.

Structures that fail the deflection part of the test may be retested after 72 hr and accepted if:

$$\Delta_r = \frac{\Delta_2}{5} \quad (27.4)$$

where Δ_2 is the maximum deflection during the second test.

The structure cannot exhibit excessive cracking, spalling, or crushing, which may indicate failure. The structure fails if inclined cracks appear, which may indicate a shear failure. Any inclined cracks in areas of a member without transverse reinforcement must be evaluated if the crack is longer than the depth of the member. For members with a variable depth, the depth at the midpoint of the crack is used. In anchorage zones or in areas where there are lap splices, short inclined cracks or horizontal cracks must be investigated, as these may be signs of a bond or anchorage splitting failure.

It is clear that ACI 318 requirements are narrowly tailored to evaluate structural safety against failure. If other structural responses are desired, such as performance and serviceability under working load, changes in structural response due to damage or deterioration, etc., then broader performance-testing techniques are necessary.

27.3 Pretest Planning for Reliable Structural Evaluation

The most critical phase of performance evaluation is the pretest planning. In this phase, a detailed plan or critical path should be established not only to ensure that the tests are performed correctly but also to be sure that all critical responses are measured. Pretest planning can be broken down into several distinct general tasks:

- *Determine the specific purpose of the test and desired final product.* This is probably the most overlooked part of pretest planning. Prior to beginning the test, the following items should be evaluated:
 - Determine the specific desired outcome. Possible outcomes could be service load behavior, proof of ultimate load levels, or behaviors that may indicate the presence of damage, deterioration, possible deficiencies in materials, or construction flaws. Before beginning any test, it is important to have a clear picture of the final outcome as this determines the choice of test method, load levels, and instrumentation.
 - Determine the test method that best meets the goal. When evaluating a structure, engineers often choose load testing as a first, or only, alternative. In fact, there are many ways to evaluate a structure other than just load testing (e.g., modal testing).
 - If load testing is chosen, be sure the loading method is realistic for the structure. Uniform loads are appropriate for a general structure but are not a good choice for testing bridges as traffic loads tend to be point loads. Be sure the loading method will produce the desired results; for example, due to the difficulty of applying a moving load for many cycles, stationary cyclic loads are often used to simulate repeated traffic loads, although stationary, cyclic loads may not produce the same response as an actual moving load (Petrou et al., 1994).
 - Determine the type of data required to accurately assess the structure. In many performance tests, only deflection is measured, which may not provide sufficient data. Often strains, rotations, differential movements, temperature changes, or accelerations may also have to be measured. Instrumentation should be properly chosen to provide the necessary data.

- *Gather all available design and construction information.* When the purpose of the test has been established, the next step is to gather all available design and construction information to provide a basic background of the structure and a baseline for comparing actual material test results and actual dimensions. Necessary information on design loads, material specification and strengths, design drawings, construction records, as-built drawings, and records of any modifications to the structure must be assembled and carefully examined to form a complete picture of the structure.
- It is important to obtain as much information as possible about the as-built condition of the structure as variations and deviations from the original plans are not infrequent. Obtaining as-built drawings and copies of inspection records is highly recommended.
- Reports on actual material strength are also of great importance, especially in destructive or partially destructive tests. It should be kept in mind that material specifications are usually minimum or maximum properties (as applicable), and the actual materials may have substantially greater or lower properties than required. For example, ASTM A 36 steel has a minimum yield strength of 36 ksi, but in reality the yield strength can be much higher, with values of 50 ksi not being unusual.
- *Conduct a pretest inspection of the structure and material sampling.* For many structures, the construction records may be inadequate. The records have been lost or destroyed or the inspections may have been insufficient, so detailed inspection and construction records do not exist. In such cases, a pretest inspection of the structure is necessary.
- The structure should first be checked to verify all dimensions. Several measurements of member sizes should be taken at critical sections. Where possible, member support conditions should be checked. At this time, a detailed survey of surface and visible defects should be made. ACI 201.1R-97, *Guide for Making a Condition Survey of Concrete in Service* (ACI Committee 201, 1997), provides a good method for making such a survey.
- Reinforcing bar size, spacing, and cover should be documented. Three common nondestructive methods for measuring the reinforcing bar size, cover, and spacing are magnetic, radiographic, and radar (ACI Committee 437, 2003; Malhotra and Carino, 2004). Bar size and location can also be found by removing the cover in isolated areas. This last method is often used to calibrate nondestructive testing (NDT) methods. Where practical, bar samples should be removed for further evaluation, including strength tests and assessment of the degree of corrosion, if present.
- Concrete strengths are normally determined by coring (ASTM, 2004a), as this seems to be the only accurate method for determining in-place concrete strength. Guidance on using cores to determine in-place strength is found in ACI 214.4R-03 (ACI Committee 214, 2003). Nondestructive tests for determining concrete compressive strength include the rebound hammer or probe penetration, but these methods do not directly measure strength, and they show a high degree of variability, especially when different types of concrete are being tested. As a result, the methods require calibration with drilled cores for each type of concrete being tested, and even then they are of questionable accuracy. Tensile strengths can be found by performing the split cylinder test (ASTM, 2004b) on cores or by use of sawed beams (ASTM, 2004a), if practical.
- In addition to cores removed for strength testing, cores should also be taken for petrographic (ASTM, 2004c) or chemical testing. Petrographic and chemical testing can reveal potential weaknesses in the concrete due to alkali-silica reaction (ASR), inhomogeneity, bleed, or segregation; poor air-void systems that allow freeze-thaw damage (ASTM, 2006); reinforcing steel corrosion; abrasion; fire; D-cracking of aggregates; and weathering. It is also necessary to sample and test auxiliary materials such as overlays, bearing pads, material in attached structures, etc. This is especially necessary when such materials may affect loading, boundary conditions, and structural or material behaviors.
- When sampling the material, the question arises as to how many samples are necessary to yield reliable results. The answer to this question is based on the practicality of sampling the material and the amount of error that can be tolerated. In general, the number of samples is affected by the following: (1) The amount of possible damage that would occur when samples are

removed; the attraction of nondestructive testing is that any number of samples can be taken without damaging the structure. (2) The cost, in money and time, to perform the test; often testing must be limited due to time and budget constraints. (3) The importance of the data; for example, the flexural strength of reinforced concrete is only slightly affected by the compressive strength so less accuracy can be tolerated in determining the compressive strength of a flexural member. On the other hand, the strength of axial members is greatly influenced by compressive strength, so a more accurate determination of compressive strength is necessary. To determine the number of samples required, any of a number of statistical techniques can be applied. ASTM C 823 provides information on developing a program for material sampling (ASTM, 2000).

- *Perform a pretest analytical investigation.* The data collected from records and inspection can be used to create an analytical model of the structure. This model will provide necessary information for designing the test. In the case of load tests, the model will provide information on probable cracking, yield, and ultimate load capacities. The model can also be used to pinpoint critical responses so the instrumentation can be properly placed to record these responses during the actual test. In the case of dynamic tests, frequencies, accelerations, magnification (impact) factors, and vibrational mode shapes can be estimated from the model.
- *Design the testing and instrumentation system.* The test can be designed using the results from the model. In the case of load testing, it is necessary to choose the type of load, load levels, load position, and method of loading (e.g., trucks, blocks, hydraulic). Load-reaction frames for hydraulic-loading cylinders also have to be designed at this point.
- *Lay out instrumentation grids based on the analytical results so the instruments are in place to capture critical responses.* The model results are also used to estimate the magnitude of the response so an instrument with a proper range and accuracy is chosen (see Section 27.6). The data acquisition systems should be chosen at this time.
- *Perform the test and evaluate the results.* With a properly designed test, performance of the test becomes a relatively simple task. Time spent up front in planning will greatly reduce the chance of problems occurring during the test and will lead to a successful outcome.

Unfortunately, evaluation of the results is not an easy task. Even in tests that have excellent pretest planning, ambiguities in the data often must be reconciled. In such cases, it is useful to create post-test models to assist in data evaluation.

27.4 Nondestructive Testing for Material and Structural Assessment

In pretest evaluation, it is necessary to carefully evaluate the condition of the material and the structure. Some of the previously stated methods are partially destructive or inspect only a small portion of the structure. For large-scale detection of flaws, other methods are needed. Of the many nondestructive methods for evaluation of concrete structures, only a few are presented here. A complete treatment of NDT methods can be found in Malhotra and Carino (2004).

27.4.1 Ultrasonic Testing

Sound waves have been used for testing concrete for many years. Many states still employ the *chain-drag* method for concrete bridge decks. A large metal chain is dragged across the concrete surface, subjecting the surface to small impacts, and delaminations in the concrete are found when a hollow sound is heard during the dragging of the chain. The limitations of this method are obvious: It only detects flaws near the surface, an experienced person who can differentiate the sounds is needed, and it cannot provide numerical data on the size and depth of the flaws. More modern methods of testing concrete utilize

ultrasonic waves transmitted through the concrete. A simple ultrasonic test, the *pulse-velocity test*, consists of creating an ultrasonic pulse, detecting the same pulse at a remote receiver, and measuring the time it takes for the pulse to travel the distance. Changes in the pulse transmission time can represent changes in the properties of the concrete; for example, as young concrete gains stiffness, the pulse transmission time decreases. Increases in pulse transmission time often indicate the presence of damage, as the pulse cannot transmit through a crack and instead must take a longer path around the damaged area. The *impact-echo* technique provides a more quantitative measurement of flaws in the concrete (Carino and Sansalone, 1992; Carino et al., 1986). In this method, a small impactor is used to create a wave in the concrete. When the wave hits an interface, either a free surface or a crack, it is reflected back to a receiver. By processing the returned signal, the depth and size of flaws can be determined (Carino and Sansalone, 1992).

27.4.2 Infrared Thermographic Testing

Infrared thermographic testing works on the principle that flaws in concrete will affect the way in which heat flows through the concrete. This, in turn, affects the surface temperature distribution. The concrete is either heated up or cooled down, and surface is photographed using a camera that is sensitive to infrared radiation. Damage to the concrete is seen as cooler or hotter areas (Delahaza, 1996; Weil, 1993). Often, simply allowing a concrete structure to heat up during the day due to sunlight or to cool down at night produces sufficient temperature variations to make infrared thermographic techniques usable. One advantage to the thermographic method is that it can be used in a moving system to examine pavements without having to stop or detour traffic. Several case studies outlining the use of thermographic testing for pavements are given by Weil (Malhotra and Carino, 2003).

27.4.3 Modal Testing

When evaluating a concrete structure, it is beneficial to have information about the actual stiffness or flexibility of the structure. Changes in flexibility over time can be used as a measure of global deterioration, and local changes in flexibility can be used to pinpoint local damage. For modeling purposes, the accuracy of a model can be determined by comparing the actual flexibility of the structure with the flexibility obtained from the model. One method of determining the actual flexibility of a structure is polyreference modal testing. Modal testing can be used by itself as a nondestructive method of structural evaluation. It can also be used as a pretest evaluation procedure for planning a load test of a structure, as modal testing can identify damaged, deteriorated, or suspect areas of the structure (Aktan et al., 1992). After the load test, the flexibility matrix obtained from modal testing can be used to verify the results of the load test and to calibrate finite-element models.

In the modal-testing method, structural vibrations are produced by an impact (Aktan et al., 1992; Allbright et al., 1994). (Forced vibrations have also been used, but this method is more complex so only the impact method will be discussed here.) The structural vibrations resulting from the impact are then measured by seismic accelerometers. By knowing the time histories of the impact (measured with a load cell) and the corresponding accelerations distributed through the structure, the modal frequencies, modal vectors, and damping can be calculated. Modal testing offers the advantage of not having to calculate the mass and stiffness of the member; instead, vibrational characteristics are measured and used directly. From the magnitude and frequency of the vibrations, the natural mode shapes and frequencies can be determined, and these can be used further to calculate a flexibility matrix.

Prior to conducting a modal test, an approximate theoretical or finite-element analysis should be made to provide a clear understanding of the structure for the purpose of establishing impact points and accelerometer (reference) points. The results of approximate theoretical or finite-element analysis are used so the accelerometers are not placed at grid points that would correspond to the nodes of the first few significant modes. The analysis is also used to establish the bandwidth of expected frequencies, which is necessary so the dynamic data acquisition system will read only within the band of frequencies of interest.

In theory, the test can be performed with a single accelerometer, but in practice a minimum of three noncolinear reference points are used, although more reference points will often provide better data (Aktan et al., 1992; Allbright et al., 1994). Impact to the structure is supplied either by a sledgehammer or a falling weight. In both cases, the impactor must be instrumented with a load cell so the exact impact load time history is known. Instrumented hammers are commercially available. Each grid point (including the reference points) undergoes impact, and the resulting vibrations are measured by the accelerometers. The impactor load cell and the accelerometers are read using a dynamic analyzer (these are also commercially available). A fast Fourier transform (FFT) is used to transform both the input (impactor) data and the output (accelerometer) data from the time domain into the frequency domain. The frequency response function (FRF), which is basically the ratio of the output FFT to the input FFT, is then calculated. The calculation of the FFT and FRF will normally be performed by the dynamic analyzer, although the operator should have some degree of expertise to ensure the quality of the final data.

When impacts are applied to the structure, care must be taken to ensure that the impactor does not bounce and create multiple impacts while the acceleration data are being taken, as this would corrupt the acceleration data. Also, in some cases, the impact is too hard or too soft and the resulting data are outside the range of the data acquisition system. Such tests should be discarded and redone. This is why it is essential to use a dynamic analyzer capable of processing the results in real time.

Each time a point is struck and acceleration data are taken, a single dataset is created for that point; however, one dataset per impact point is not enough to yield reliable results, so each point is tested several times to collect multiple datasets, the results of which are then averaged. In general, it is necessary to have at least five good datasets per point. When the dynamic data have been obtained for all impact points, they can be transferred to a commercial program that will then calculate the modal frequencies, modal vectors (mode shapes), and damping. Anomalies in the frequencies or mode shapes can sometime be used to identify damage (Allbright et al., 1994), but the flexibility matrix is usually required for an accurate evaluation:

$$[F] = [\psi] \left[\frac{1}{\omega^2} \right] [\psi]^T \quad (27.5)$$

where:

$[F]$ = flexibility matrix.

$[\psi]$ = unit-mass scaled modal vectors.

$[1/\omega^2]$ = diagonal matrix of ascending natural frequencies.

A method for calculating the flexibility matrix from mass-scaled modal vectors can be found in Catbas et al. (1997).

Modal testing does not provide an exact flexibility matrix, as an infinite number of modes would be required to calculate the exact flexibility; however, if a sufficient number of modes can be detected, the modal flexibility matrix can be close enough to the actual flexibility to provide highly accurate results. When the modal flexibility matrix has been obtained, it can be used to evaluate the structure:

$$[P][F] = [\delta] \quad (27.6)$$

where:

$[P]$ = vector of point loads placed at impact points.

$[F]$ = modal flexibility matrix.

$[\delta]$ = vector of displacements at impact points.

Any loading pattern can then be simulated by placing point loads at the corresponding impact points. (A uniform load is simulated by placing point loads at all impact points.) This shows one of the advantages of modal testing. Often, damage to a structure is localized and can only be detected through load testing if the load combination and load placements are ideal to reveal the damage. In a real load-test situation,

this would require an unrealistic number of load cases; however, with the modal flexibility matrix, a large number of loading patterns can be efficiently checked to see if any damage is detected. For damage detection, it is best to have a baseline modal flexibility matrix of the undamaged structure. Damage can then be detected by comparing deflections from subsequent modal flexibility matrices to deflections found from the baseline matrix. If a baseline matrix is not available, deflections found from the modal flexibility matrix can be compared to deflection generated from an idealized model of the undamaged structure (e.g., finite-element model), but this comparison is less accurate. Finally, the modal flexibility matrix can be used to fine-tune the stiffnesses and boundary conditions of a finite-element model. Here, the deflections generated from the model are compared to those generated from the modal flexibility matrix, and the model is adjusted to obtain the best comparison for several load cases. The tuned model can then be used for analysis of the structure.

27.5 Static/Quasi-Static Load Testing

Static/quasi-static load testing is the most common form of structural testing. Because many structural loads are static in nature, a static or monotonic quasi-static load test can provide valuable information on stress, strain, load distribution, and deflection under normal loading conditions. Quasi-static cyclic loading is often used to assess fatigue behavior. For moving or dynamic loads, cyclic quasi-static load testing is sometimes used as a simpler or less expensive alternative to using actual moving or dynamic loads; however, the validity of using cyclic quasi-static loading to evaluate moving or dynamic loads is questionable (Chung and Shah, 1989; Petrou et al., 1994).

27.5.1 Use of Dead Loads

One method of conducting static-load test consists of placing a dead load on the structure. Typical dead loads are concrete blocks, bricks, sandbags, or containers of gravel, sand, or water. The advantages of using dead loads are as follows:

- They can easily simulate a uniform load on a structure. A single layer of 200-mm (8-in.) hollow-core concrete blocks with 25-mm (1-in.) gaps in between to prevent arching can provide a uniform load of 1.4 kN/m² (29 psf).
- The loading materials are relatively inexpensive. In many cases, bricks, blocks, crushed stone, or sand can be borrowed from building supply yards or quarries.

The disadvantages of this type of testing are numerous and often relate to safety:

- Except for exposed structures such as roofs or bridges, the dead load often cannot be placed remotely (as by crane) and must be placed by hand. This presents a danger to workers should the structure fail while load is being applied.
- Should the structure begin to crack or collapse, the loads cannot be removed quickly or safely enough to prevent additional damage or complete collapse.
- Should the structure completely or partially collapse, the load may fall freely and perhaps injure workers or unintentionally damage other parts of the structure.
- The actual load on the structure can only be assessed through the cumbersome process of weighing the individual loading blocks or containers, and there is no easy way to record the load on modern data acquisition systems.
- This method cannot be used to simulate moving or fatigue loads.

For safety reasons, dead load testing should be limited to service load tests well below damage or collapse limit states. ACI 437R-03 (ACI Committee 437, 2003) allows the use of dead load testing but, because of safety issues, does not recommend it. When using dead loads, several practices should be observed. All loading blocks or containers should be of the same weight; ACI Committee 437 allows a

±5% variation between individual units. The loads should be placed with gaps between the individual loading blocks or containers. This is because the structure will deflect under load, and if the loading blocks or containers are too close together they may touch and form an arch. The arch formations make the actual loading pattern uncertain. Loose material (sand, gravel, water) should not be used for load testing as it may gather in low areas of the structure and pond, again creating an uncertain loading pattern. Any loose material used for loading should be placed in containers and the full containers used to apply the load.

27.5.2 Vehicle Testing

Vehicle testing is preferred for service load testing of structures such as bridges or parking decks where vehicle loads are the predominant live loads. Vehicles can be empty or loaded with sand or gravel; thus, loaded dump trucks are very effective for applying loads (Aktan, et al., 1993; Dimmerling et al., 2005; Shahrooz et al., 1994a,b). Vehicle axle or single wheel weights can be obtained using truck scales such as those found at concrete plants, building supply yards, or highway department weigh stations. Many state highway patrols have portable scales that can be used. Vehicular load testing has several advantages:

- It is the type of load that would exist on bridges, parking decks, garage floors, etc. in service load conditions.
- Because trucks can often be supplied by highway departments or local contractors and the sand or gravel to load them can be borrowed from concrete plants or building supply yards, vehicular loading is a relatively inexpensive testing method.
- Vehicular loading can be used to apply static, moving, or impact loads to a structure.

The disadvantages include:

- As with dead loads, vehicle loading requires workers (drivers, in this case) to actually place the load on the structure. Although movable, vehicular loads usually cannot be removed quickly enough to prevent injury to the drivers in the event of sudden cracking or collapse.
- Dump trucks are often used for vehicle loadings as they are usually available from contractors or state departments of transportation. Most structures designed to carry vehicles are usually designed to carry vehicles much heavier than a typical dump truck. In many cases, even a large number of fully loaded dump trucks may not be heavy enough to cause large structural responses. It may be necessary to use large trucks loaded with very heavy loads (such as concrete blocks) to obtain a large enough response to be meaningful (Issa et al., 1996).
- It is very difficult to apply the load in increments, as this would require slowly adding load to the vehicle.
- Due to possible clearance problems, it may be difficult to place the loads close together or near barriers.
- If multiple vehicles are used, it is extremely difficult to attain the same axle loads on all of the trucks, even if similar trucks are used. In addition, the loads tend to shift during testing, affecting the axle loads.
- Unless the vehicles are turned off, engine vibrations will affect the test results.
- The load cannot be recorded electronically.

27.5.3 Testing Using Servohydraulic Cylinders

Hydraulic testing consists of applying load through one or more hydraulic cylinders or actuators. This type of loading is preferred (ACI Committee 437, 2003), as it is the safest method. Hydraulic loading can be as simple as using jacks controlled through hand-operated pumps or as complicated as using sophisticated electronic, servohydraulic systems that use electric pumps and computerized controls. The advantages of hydraulic loading include:

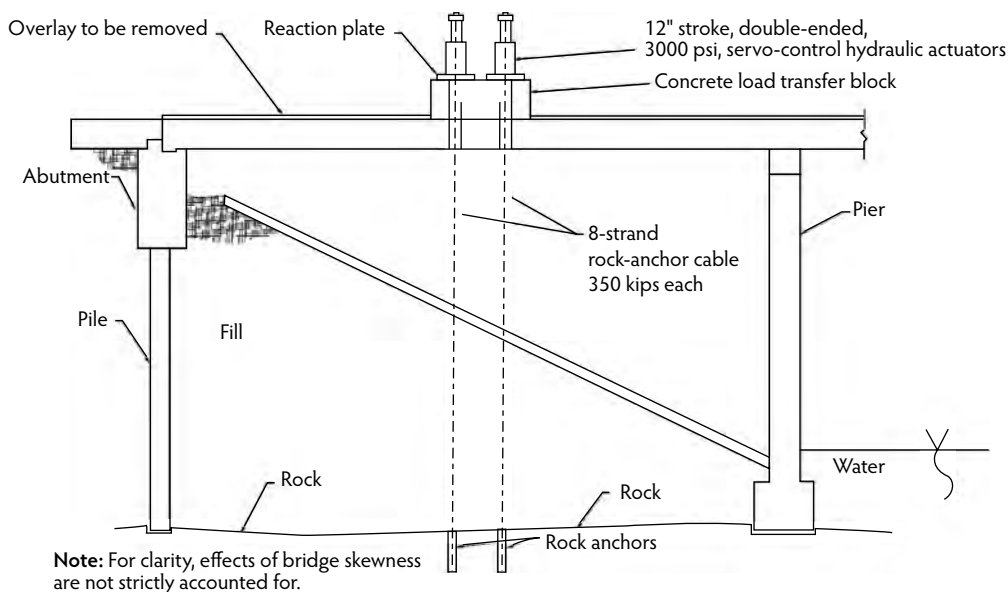


FIGURE 27.1 Use of post-tensioning tendons as a loading system.

- Hydraulic tests are safer. Loads can be placed on the structure via a remote-control mechanism, thus keeping workers safe should the structure collapse. Also, electronic hydraulic systems can be equipped with fast unloading circuits and safety shutdowns that will quickly remove all loads at the first signs of collapse.
- In a load-control test where a structure is subjected to predetermined increasing or decreasing increments of loads, a hydraulic-loading system can precisely control load increment, total load, and rate of load application.
- Use of servohydraulic, closed-loop control allows the use of displacement or strain-controlled tests, which are more stable than load-control tests and less likely to result in sudden collapse. This type of testing will often allow post-peak behaviors to be obtained.
- Hydraulic testing is the most efficient way to apply cyclic or fatigue loads.

The disadvantages of hydraulic testing include:

- Hydraulic systems apply point loads. Application of a line load or a uniform load over a small area can only be done using loading blocks or a spreader device (Azizinamini et al., 1992; Miller et al., 1994). Hydraulic systems usually cannot be easily adapted to apply a uniform load over a large area.
- Computer-controlled servohydraulic systems and the associated control systems are expensive to purchase, maintain, operate, and transport.
- Skilled technical people are often required to handle the hydraulics and electrical work to assemble the system.
- A reaction mechanism is necessary for the hydraulic system to push or pull against.

The need for a reaction mechanism is the biggest drawback of hydraulic systems. In some cases, another part of the structure can be used as a reaction frame, but doing so introduces the possibility of unintentional damage to other structural members. In many cases, a reaction frame tied to a foundation or a self-equilibrating testing frame can be built (Azizinamini et al., 1992). Another approach, shown in Figure 27.1, is to use post-tensioning tendons grouted into the soil or rock below the structure (Miller et al., 1994).

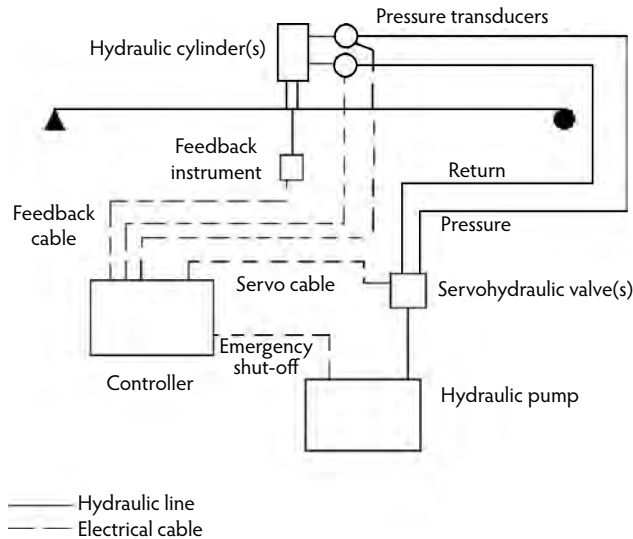


FIGURE 27.2 Closed-loop system.

Hydraulic-loading systems can be precisely controlled through the use of servohydraulic, closed-loop testing. In closed-loop testing, the structure is loaded such that some specific parameter (e.g., load, deflection, strain) increases or decreases at a set rate. To understand the usefulness of the closed-loop servohydraulic system and its limitations, it is first necessary to understand how such a system works. A schematic of a typical closed-loop system is shown in Figure 27.2.

The system consists of five parts: a pump, a servohydraulic valve, a hydraulic actuator, a feedback instrument, and a controller. The pump supplies hydraulic fluid at a set pressure up to a maximum flow rate. The rate of flow of the hydraulic fluid is controlled by a servoelectronic (“servo”) valve, which is a high-speed, proportional valve capable of quickly and precisely varying the flow of hydraulic fluid through the system. The flow rate through the valve is directly proportional to the current input to the valve by the controller.

The hydraulic actuator is a hollow cylinder fitted with a piston and rod. To apply load, hydraulic fluid is pumped into a chamber behind the piston. Some actuators are dual action, meaning fluid can be pumped into a chamber on either side of the piston so the actuator can exert force in either direction. It is important to note that actuator capacities are based on the area of the piston and the maximum pressure supplied by the pump. Quoted actuator capacities are usually based on a 21-MPa (3000-psi) pump pressure. If the pump being used in the test has a maximum pressure different than that given in the actuator manufacturer’s specifications, the quoted capacity will be different. Also, because one side of the piston has the rod attached (thus reducing the area), actuator capacities are different in each direction.

During operation, fluid is pumped into the chamber on one side of the piston. If the actuator is dual action, the chamber on the other side of the piston is opened to allow fluid to flow out. If the rod is attached to a flexible structure, pumping fluid into the chamber produces a combination of pressure in the chamber (which translates to load on the structure) and movement of the piston, which translates to deflection of the structure. Unloading is accomplished by releasing fluid and pressure from the active chamber and pumping fluid into the other chamber.

The load applied by the actuator can be accurately measured by measuring the hydraulic fluid pressure and multiplying by the piston area. This method can often be more accurate and less cumbersome than placing a load cell between the actuator and the structure. Pressure can be measured by pressure transducers that can be directly linked into a computer data acquisition system. In dual-action actuators, there is fluid on both sides of the piston, and both chambers have pressure; therefore, when attempting to calculate load, the differential pressure between the two chambers must be used.

The feedback instrument is any electronic instrument that can read the desired structural response (e.g., deflection) and translate it into a voltage. The controller uses the signal from the feedback instrument to regulate flow through the servovalve. Normally, the controller is set to regulate two things: the rate of the structural response and the maximum value of that response.

For the sake of example, assume that the system shown in Figure 27.2 is set to be a displacement-controlled test of a beam; that is, the system will control the load such that the beam deflects at a set rate up to some predetermined maximum deflection. Initially, the controller is used to pump some fluid into the actuator, and a small load is applied to the beam. An electronic instrument on the beam reads the deflection and converts it to a voltage that is transmitted to the servohydraulic controller. The controller, which is programmed to convert the voltage back to displacement, checks the rate of deflection against the target rate. If the rate of deflection is too slow, the controller will attempt to increase the flow to the hydraulic actuator to increase the loading rate and therefore the deflection rate. If the deflection rate is too fast, the controller will attempt to decrease or, if necessary, reverse the flow to the hydraulic actuator to slow the deflection rate.

When the beam reaches the target maximum deflection, the controller stops the flow to the actuator; however, the system always has some electrical and mechanical noise, so a servohydraulic system will not hold at the specified target but will oscillate about it. This oscillation will introduce noise in the response of the instruments attached to the structure, often giving the responses a sawtooth appearance. Oscillations of the system can also be caused by backlash in the control instrumentation. Backlash is a measure of the change in response necessary to elicit a change the instrument reading when the response is reversed (see Section 27.6). Noise in the system will usually cause the controller to slightly overshoot the intended target response (e.g., deflection, strain), so the controller will unload slightly to correct this condition; however, if the instrument has significant backlash, the response under unloading may not be detected immediately. The controller will miss the target and then attempt to correct by reloading. Thus, instruments with significant backlash will cause large oscillations in the system and should be avoided.

Servohydraulic systems provide an excellent means of conducting a controlled test of structures or elements. These systems, however, are extremely complicated, and a high level of expertise is required to design, build, and operate such systems; therefore competent control engineers should be retained to design and operate servohydraulic systems.

27.6 A Discussion of Instrumentation and Data Acquisition

The importance of instrumentation in a structural test is often overlooked. There is a tendency to assume that the instruments and any associated equipment for data acquisition are transparent; that is, the data coming from the instruments are not affected by the instrumentation itself or the data acquisition system. This is not true. Each instrument, whether a simple mechanical dial gauge or a sophisticated electronic device, has its own particular characteristics that can affect the test results. It is only when the test is complete and the data are found to be faulty that any problems with instrumentation are even considered.

27.6.1 Important Issues in Instrumentation Selection

When selecting instrumentation for a performance test, several issues must be addressed.

27.6.1.1 Range

It is useful to speak of the range of the instrument in terms of *total range* and *working range*. Total range is the maximum and minimum values of input that the instrument can read. Working range is the anticipated maximum and minimum values of response which will be measured during the test. It is normally desirable for the working range to be about 50% of the total range. If the working range is too close to the total range, any error in estimating the maximum or minimum responses may cause the instrument capacity to be exceeded. Some instruments exhibit nonlinearities or other errors near the limits of the range, so measurements near these limits should be avoided. Having a working range that

is very much smaller than the total range is also undesirable. Because the precision of the instrument is normally a function of the total range, trying to make small measurements with an instrument with a large range will usually provide imprecise results.

27.6.1.2 Precision

Precision is a measure of how reproducible a measurement is. Note that precision is an absolute number. A measurement can be precise, but incorrect (or inaccurate). If an instrument has the same error in each measurement, the results may all be within a narrow band, and therefore precise; however, if the average value is not close to the true value, the measurement is precise but inaccurate.

27.6.1.3 Accuracy

Accuracy can be defined as the difference between the instrument reading and the true quantity being measured. Determination of the accuracy of an instrument is a complex and difficult process that requires careful calibration of the instrument. The instrument accuracy is actually the sum of several instrument effects and errors. In general, the response of any instrument can be separated into five components, although for a given instrument some of these responses may not be present. The components are given by:

$$X_{\text{total}} = X_1 + X_2 + X_3 + X_4 + X_5 \quad (27.7)$$

where:

- X_{total} = total instrument response.
- X_1 = response due to the load.
- X_2 = response due to non-load effects on the structure.
- X_3 = instrument error.
- X_4 = error due to external effects on the instrument.
- X_5 = error due to effects of instrument mounting.

In most cases, the total response of the instrument is assumed to be only the caused load, and the other responses are ignored. This can be a grievous error. It is necessary to remove, minimize, or at least account for the other responses of the instrument. The response due to non-load effects (X_2) includes such things as changes in strain and deflection due to temperature. These effects can be significant, as previous research has shown that changes in load distribution, strains, and deflections of an exposed structure due to temperature can be greater than the response due to load (Miller et al., 2004). It is possible to correct for non-load effects by analytical estimation of the values of these effects, by placing additional instrumentation designed to specifically measure non-load related effects, or by performing tests under no applied load to specifically measure these effects.

Every instrument has a certain amount of error associated with its measurements, given by the X_3 term in the previous equation. The data acquisition system itself can cause additional sources of error. When considering the sources of error due to the instrumentation and data acquisition system, it is necessary to consider the following:

- **Resolution**—Resolution is what most people are referring to when they speak of accuracy, but it is only one component of the total accuracy of the instrument. Resolution is the smallest value of a response that can be registered by the instrument. For mechanical gauges, this is the smallest value, a single tick mark. It is possible to interpolate between two marks, but this not objective as it depends on the person reading the gauge. For gauges with digital displays, the resolution is the smallest value on the display. Resolutions of analog electrical instruments are more difficult to determine. In theory, these instruments have infinite resolution but in practice the resolution is limited by the resolution of the digital data acquisition system, electrical noise, and the behavior of the mechanical components within the gauge. Thus, for analog electrical instruments the resolution is the smallest response that provides a reliable reading from the gauge.

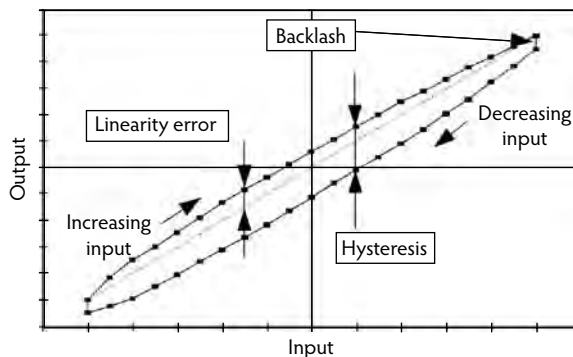


FIGURE 27.3 Definition of sensitivity, linearity, hysteresis, and backlash.

- **Sensitivity**—Sensitivity is the output of an instrument for a given input and is expressed as the ratio of output to input (Figure 27.3). Usually, sensitivity is determined by a best-fit straight line. For electrical instrumentation, the output is often influenced by the excitation applied to the instrument, so this is included in the sensitivity. As an example, consider an instrument that measures displacement and output voltage and is excited by a voltage. The sensitivity may be expressed as X volts/volt/mm. This means that a movement of 1 mm will cause the instrument to output X volts if a 1-volt excitation is used. If a 10-volt excitation is used, a 1-mm movement would output $10X$ volts. Sensitivity does not affect accuracy through the instrument itself, but rather through the data acquisition system. If an instrument has a small sensitivity, the output will be small, and the data acquisition system may not be able to read small quantities accurately. Also, small outputs in electrical instruments are often affected by noise.
- **Linearity**—Many instruments (although not all) are assumed to be linear; the output of the instrument has a linear relationship with the response. The linearity error is the measure of how far the data deviate from the best-fit line (Figure 27.2).
- **Repeatability**—Repeatability is the ability of the device to output the same value for the same response over a number of trials when the response is always increasing or decreasing (e.g., always extending the instrument, always heating the instrument) (Figure 27.3).
- **Hysteresis and backlash**—Hysteresis is the difference in a reading at a given point depending on whether the reading was obtained by an increase or decrease in response (e.g., the difference in response when a given point is reached by extending an instrument as compared to the response at the same point reached by contracting the instrument). Backlash is related to hysteresis and is a measure of the change in response required to elicit a change the instrument reading when the response is reversed (e.g., extension to retraction, load to unload, heating to cooling) (Figure 27.3).

Accuracy problems related to resolution and sensitivity can be avoided by proper selection of instruments based on reasonable estimates of the quantities to be measured. Again, this points to the need to perform proper pretest planning. The remaining errors—linearity, hysteresis/backlash, and repeatability—determine the maximum total error of the instrument. Linearity is found by providing a series of inputs over the range and plotting the input against the output (Figure 27.3). For best results, inputs should be made in both directions (e.g., extension and retraction, loading and unloading). At least three trials in each direction should be made and the results plotted on a single graph. The maximum distance from a best-fit straight line to any data point is the maximum total linearity error. Hysteresis/backlash is found by providing input to the instrument through the range in one direction and then providing input through the same range in the reverse direction. The maximum hysteresis/backlash error is the maximum distance between any two points, one in each direction, corresponding to the same input (Figure 27.2). Again, at least three trials should be used. To assess repeatability, input is provided to the instrument through the range but always in the same direction. Maximum repeatability

error is the maximum distance between any two points corresponding to the same input but on two different trials (Figure 27.3).

The X_4 term relates to error in the system introduced by external forces. Two major sources of these errors are drift and noise. Drift is the condition where the instrument reading changes even though the response being measured does not. Drift is often caused by temperature. Noise is a random fluctuation in the instrument output. In electrical instrumentation, noise is typically caused by external electromagnetic sources, such as power lines or electric lights.

The final term, X_5 , is the error associated with the instrument mounting. These errors include misalignment, random environmental vibration of the mounts, creep of the epoxy or glue used to hold the mounting bracket, slip of mechanical mounting, etc. Most of these errors can be eliminated by careful choice of mounting hardware, proper installation, and shielding the instruments from wind and vibrations.

27.6.2 Types of Instrumentation

A large number of different instruments can be used for measuring structural responses. These range from surveying instruments used to measure large deflections to strain gauges accurate to 1×10^{-6} . Each type of instrument has particular uses, accuracy, and limitations. Clearly, it is not possible in the limited space available here to cover all of the possible types of instruments that can be used. A more comprehensive coverage of instruments can be found in Dunnicliff (1993). Although Dunnicliff's work is aimed at geotechnical applications, many of the instruments listed are usable for concrete applications. What follows is a description of some instruments commonly used for concrete.

27.6.2.1 Mechanical Gauges

Mechanical gauges provide an easy, reliable, and inexpensive method for measuring displacement and strain or distortion; however, the use of these gauges is extremely labor intensive and error prone because the gauges must be read manually. This exposes the workers to hazards, leads to possible errors in recording the data, and requires a large workforce or a large amount of time to read all of the gauges. Among the many types of mechanical gauges, the two most common are the dial gauge and the portable strain/distortion gauge (Figure 27.4). Dial gauges consist of a rod attached to a dial by a gearing system. As the rod moves, the movement is registered on the dial. These gauges have various ranges and accuracies. The accuracy of the dial gauge is somewhat difficult to assess. They can be reliably read to the nearest tick mark on the analog dial, but users frequently attempt to interpolate between marks. This adds a degree of subjectivity to the data. Also, the analog gauges are easy to misread, leading to error. Some more modern dial gauges replace the mechanical dial with a digital display, thus reducing these errors. Finally, even the best jeweled movement in the gearing system will exhibit some stick (backlash), making small measurements difficult. Although a dial gauge may respond to dynamic motions, it is impossible to read accurately under these conditions. It is therefore usable only under static or low-frequency cyclic testing. The main advantages of these instruments is that they are easy to use, easy to read, and require no auxiliary equipment (data acquisition systems). They are also inexpensive, especially if the gauges are purchased through a machinery supply house rather than from a scientific supplier.

The portable distortion/strain gauge consists of a metal bar, two points, and a dial gauge (Figure 27.4). One point is fixed; the other point is attached to the dial gauge and is movable. Two targets, pieces of metal with drilled holes, are attached to or embedded in the concrete at the basic length of the gauge. A zero reading is obtained by placing the points of the gauge into the holes in the targets and reading the dial gauge. Subsequent measurements are taken in the same way and the differential movement is found by subtracting the zero reading. This instrument is particularly useful for measuring over large gauge lengths. For smaller gauge lengths, Vernier calipers or micrometers can be used. The portable distortion/strain gauge is also useful in cases where a permanently mounted gauge is impractical. This method is often used to measure strains when conducting long-term creep tests (ASTM, 2002). Bodocsi et al. (1993) used this type of gauge to measure seasonal movements of pavement joints. The portable distortion/strain gauge has the same problems as the dial gauge, but also has the additional problem that the accuracy

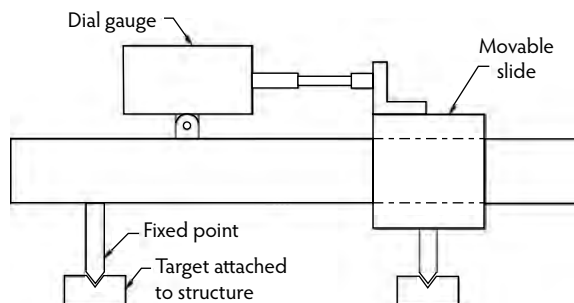


FIGURE 27.4 Portable strain gauge.

is dependent on how well the points sit in the holes in the targets. In general, there is always some play in the interface so the measurements are often not repeatable. For this gauge, it is best to take several measurements and average them. Because the gauge must be manually placed to take measurements, it is only usable for static or quasi-static tests.

27.6.2.2 Electrical Instrumentation

Electrical instrumentation has greatly improved the ability of the engineer to safely and accurately monitor structural response. These instruments have the advantage that they can be remotely monitored such that the workers never have to enter the structure during the test. This also allows engineers who cannot be present during the test to monitor the test results in real time from distant locations. Electrical instruments also have the advantage of directly sending all data to computer files, thus reducing data transcription time and errors. Many data acquisition programs allow the instrument responses or mathematical permutations of these responses to be plotted in real time so load–deflection, load–strain, or stress–strain graphs can be plotted while the test is being conducted. One major disadvantage of electrical instrumentation is that these instruments tend to cost much more than similar mechanical instruments. They also require expensive auxiliary equipment, such as data acquisition systems and cables. The biggest drawback, however, is the need for electrical power, which is not always available at remote sites. Where power is not available, it is necessary to use a generator. Generators tend to emit a large amount of electrical noise, which affects instrument accuracy, and they are prone to power surges that can damage sensitive equipment. As with mechanical instruments, it is not possible to cover all the possible instruments here, but a few common instruments will be discussed.

27.6.2.2.1 Linear Variable Differential Transformers

Linear variable differential transformers (LVDTs) (Figure 27.5) are used to measure displacements. Typical LVDTs will have ranges from 2 to 150 mm (0.1 to 6 in.). The instrument consists of a primary coil, two secondary coils, and a magnetic core. An AC voltage excites the primary coil, which in turn induces voltage in the secondary coils. The amount of voltage in each of the secondary coils depends on the position of the magnetic core. The secondary coils are connected series opposing so only the differential voltage is output. This differential voltage is linear with respect to core position. When using long lead wires, DC is preferred. Many LVDTs contain circuitry so a DC voltage can be input and a DC voltage is output. This is done by converting the input DC voltage to AC and output AC voltage back to DC. Such LVDTs are frequently referred to as DCLVDTs or DCDTs. The main error in an LVDT is linearity error, especially near the ends of the range or in the middle when the LVDT passes the null point where the differential voltage changes sign (Hrinko et al., 1994). Dunncliff (1993) reported that these instruments have no hysteresis, but hysteresis, backlash, and repeatability errors have been found in careful calibration (Hrinko et al., 1994). The LVDT, theoretically, has infinite resolution, but the actual resolution is limited by cable noise and the resolution of the data acquisition system. The instrument responds fast enough to use in any type of testing, including dynamic testing; however, LVDTs have some drift which makes them less than ideal for long-term monitoring.

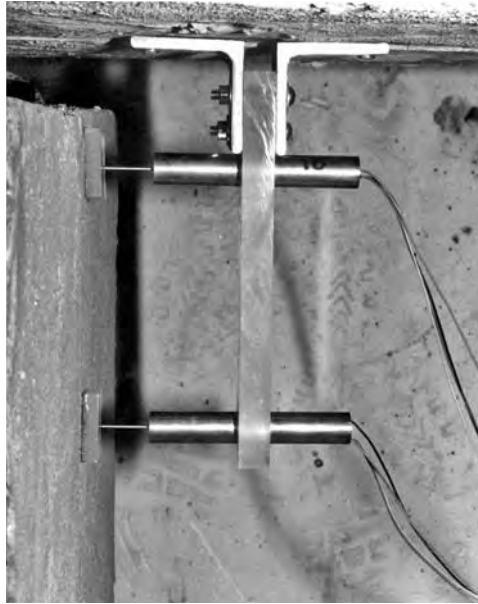


FIGURE 27.5 Linear variable differential transformer (DC type).

27.6.2.2.2 Wire Potentiometers

Wire potentiometers (Figure 27.6) are also used to measure displacement but have much bigger ranges than the LVDT. Typical ranges for a wire potentiometer are 125 to 900 mm (5 to 30 in.). The potentiometer is a contact that moves along a resistor. The resistance in the circuit changes as the contact moves, and this causes a change in voltage in the circuit. The voltage change is directly proportional to the movement of the contact. In the wire potentiometer, a wire is wound around the spindle of a spring-loaded rotational potentiometer. As the wire is pulled, the potentiometer moves and registers a voltage change proportional to the wire movement. Spring loading keeps the wire taut at all times. As with the LVDT, the wire potentiometer itself has infinite resolution, with the actual resolution limited by the data acquisition system and electrical noise. Wire potentiometers have higher error rates than do LVDTs, but they also have larger ranges, so the error, as a percentage of the range, is about the same as for an LVDT (Hrinko et al., 1994). The main errors in a wire potentiometer are backlash and hysteresis (Hrinko, et al., 1994), which introduce noise in the loading if the wire potentiometer is used as the control instrument in a closed-loop test. The backlash and hysteresis errors also make the instrument unusable for dynamic testing and of marginal use for high-frequency cyclic tests.

27.6.2.2.3 Electrical Resistance Strain Gauges

The electrical resistance consists of several loops of wire bonded to the structure such that the loops are parallel to the direction of strain. Strain in the structure causes strain in the wires which is directly proportional to change in the wire resistance. The change in resistance is read by a wheatstone bridge circuit, which is well known and can be found in most standard physics or electric circuit texts. An excellent discussion of the bridge circuit as it relates to strain gauges can be found in Dunncliff (1993). Resistance gauges come in several types:

- *Bonded foil gauges* consist of a grid of thin metal foil bonded to a plastic backing which in turn is bonded to the structure. These gauges are not particularly useful for concrete. Surface preparation is critical, but it is often difficult to obtain a smooth, clean surface on concrete, especially in the field. The foil gauges are not very robust, so the gauges must be well protected. Even then, though, the gauges will sometimes fail under extreme field conditions or when embedded.



FIGURE 27.6 Wire potentiometer.

- *Weldable gauges* have the wire loops attached to a metal backing which can then be welded to the structure. In concrete structures, these gauges are useful only for attachment to rebar or to metal embedments. As for foil gauges, protection of the gauge is of primary importance.
- *Embedment gauges* are specifically meant to be embedded in concrete. The wire loops are encased in a sheathing that protects the gauge during the casting process.

Levi (unpublished data) found that resistance strain gauges were prone to drift, making them unsuitable for long-term monitoring. He also found that, although modern resistance strain gauges are made to compensate for temperature effects, the strain readings could be influenced by temperature effects in the rest of the system—specifically, the lead wires and bridge completion circuit. Thus, resistance strain gauges are recommended only for short-term or dynamic monitoring, and it is recommended that baseline zero readings be taken before the start of each test. The electrical resistance gauge presents another problem when used with electronic data acquisition, as the gauge requires a completion circuit. It is possible to complete the circuit externally (using three more unstrained strain gauges or three resistors) and then attach the entire circuit to a channel in the data acquisition system, which reads the voltage; however, making and using the external completion bridge can often be difficult and time consuming. To avoid this complication, many data acquisition system manufacturers make special boards with the strain gauge completion bridge already wired in. This allows the strain gauge to be directly attached to the data system. Unfortunately, these boards often have eight, or multiples of eight, channels so some multiple of eight channels must be dedicated to only strain gauges. With the total number of channels in a given system limited, dedicating all these channels to strain gauges may be wasteful if only a few gauges are used. This again illustrates the need for careful planning of the instrumentation system.

27.6.2.2.4 Clip Gauge (Omega Strain Gauge)

The clip gauge (or omega strain gauge) consists of a metal arch attached to two feet such that the resulting structure resembles the capital Greek letter omega (Ω) (Figure 27.7). The arch is instrumented with four resistance strain gauges wired in a full bridge. The feet of the gauge are attached to the structure, usually by gluing metal targets to the structure and then attaching the gauge to the target with bolts. As the targets move with the structure, strain that is directly proportional to the movement of the targets (and the strain in the structure) is induced in the arch. This strain is read by the strain gauges. Use of the arch desensitizes the strain gauges, and the clip gauge can read much larger strains than the strain gauges alone; however, the clip gauge is less accurate than the strain gauge. Clip gauges are easy to install and read and are most useful for measuring fairly large strains (>100 microstrain) over short periods of time under laboratory or otherwise controlled environments. The gauges do exhibit considerable drift and noise and are not suitable for long-term field use.



FIGURE 27.7 Omega or clip gauge.

27.6.2.2.5 Vibrating Wire Strain Gauges

The vibrating wire strain gauge (VWG) is an excellent means of measuring strain in concrete under static or quasi-static conditions. The gauges are accurate to 1 microstrain and are not subject to drift, as are bonded gauges. This means that it is possible to come back to installed VWG years after installation and still obtain accurate strain values; thus, these gauges are well suited to long-term monitoring. VWGs consist of a steel wire, threaded through a tube and attached to two rigid end blocks. These blocks seal the tube but are free to move. The end blocks are either embedded into the concrete or are attached to the concrete surface. When installed, the wire is under an initial tension. An electromagnet is placed around the outside of the tube. On command from the data system, the electromagnet pulses, sweeping various frequencies. One of these frequencies will be the natural frequency of the wire. After sweeping the frequencies, the magnet remains on, and the vibrating wire cuts the magnetic field, creating electrical pulses with the same frequency as the wire vibration. The data system measures these pulses and determines the frequency of vibration. From the frequency, the tension of the wire can be found. This in turn can be used to determine the elongation and the strain in the wire. Because the end blocks are attached to or embedded in the concrete, the change in strain in the wire is the change in strain in the concrete. Although calculation of the strain from the frequency is quite simple, it is also not necessary as most data systems will do the calculations and provide direct strain readings if the gauge calibration factor (supplied by the manufacturer) is input to the data system software.

The main drawback to the VWG is that the process of reading the frequency can take a few seconds, so the gauges are not useful for dynamic situations. The module that excites and reads the wire vibration is expensive, so it is impractical to have a vibrating wire excitation module for each gauge. Normally, multiple gauges are read using a multiplexing unit that allows a single-channel data system to read multiple channels by reading one channel at a time. This allows a large number of VWGs to be read using a single excitation unit. Reading the gauges one at a time does take some time, given the slow response of individual gauges; for example, a 16-channel multiplexing unit reading all 16 gauges may take 15 to 20 seconds. Because the gauges are only used in static or quasi-static tests, this is not a limitation. VWGs also require temperature correction if the gauge is attached to or embedded in something with a coefficient of thermal expansion different from steel. The problem here is that under a temperature change, the wire may expand or contract more than the material to which it is attached, giving a false strain reading. This temperature can be easily corrected with a simple calculation if the calibration temperature (provided by the manufacturer) and the actual temperature are known. Most VWGs have built-in temperature sensors that measure the gauge temperature so the correction can be made. This makes VWGs particularly useful when they are embedded in concrete, as the temperature sensors can measure the heat of hydration and internal curing temperatures. After initial curing, these sensors can measure temperature profiles through the concrete, allowing for calculation of temperature effects in the structure.

In cases where the gauge is used on a steel structure, the wire expands or contracts at approximately the same rate as the structure; thus, the gauge is self-correcting for temperature strains. If the gauge is attached to concrete, the output should be corrected for the difference in the coefficient of thermal expansion between the two materials. Because the coefficient of thermal expansion of concrete varies and is usually not known, the accuracy of any temperature correction is questionable. The coefficient of thermal expansion for concrete is very close to that of steel, so any error in uncorrected data is likely to be small. The vibrating wire gauges are extremely stable and rugged, making them ideal for long-term field measurements.

27.6.2.3 Optical Fiber Strain Gauges

Fiberoptic sensors represent a different method of measuring strain in concrete structures. Unlike electrical sensors, strain is measured by changes in light waves transmitted through the fibers. One such sensor is the Fabry–Perot (Measures, 1995), which consists of two mirrors, separated by a distance (gauge length) set perpendicular to the axis of the fiber. The mirrors can be internal to the fiber or at the ends of two fibers, separated by a gap and joined in a coupler. This device works by sending a coherent (single-wavelength) light beam down the fiber. Some of the light is reflected off of the first mirror, which is only partially reflective. This forms a reference wave. The remaining light passes through the partially reflective mirror, reflects off the second mirror, and passes back through the partially reflective mirror. This second wave is now out of phase with the reference wave because it has traveled a longer distance. When the two waves are combined, an interference pattern results. As the fiber is strained, the distance between the two mirrors changes. This changes the path length of the second wave and therefore the interference pattern. Because the interference fringe pattern is dependent on the wavelength of the light (constant) and the path length, strain can be measured by determining the change in the interference pattern and converting this to a change in path length. A second type of sensor uses a high birefringent optical fiber (Ansari et al., 1996). Here, a circularly polarized light wave is divided into two modes along the principal axes of the fiber. External deformation causes interference of the two modes, and the output has a sinusoidal variation, the period of which is a fringe. The change in length is related to the number of fringes formed. A third type of sensor uses a Bragg grating (Chen and Nawy, 1994; Nawy and Chen, 1996; Measures, 1995). The Bragg grating is imprinted on the fiber lead, making a longitudinal, periodic variation in the refractive index of the fiber core. As light passes through the grating, a portion of the light is reflected, but the reflected light has a spectral shift in wavelength. As the grating is strained, the reflected wavelength changes, and this change in wavelength can be directly related to strain (Figure 27.8). This sensor has the unique capability of pinpointing the strain at precise locations in the structure rather than detecting average strain in a stressed zone. It was originally developed and used in concrete structural research and proved to be effective for online remote-control sensing of the deformation and cracking of structural elements at their critical locations of high stress, using sensors mounted either internally on the reinforcement or externally on the concrete surface.

27.7 Case Studies in Performance Evaluation of Concrete Structures

In surveying the recent literature on performance evaluation, it was found that the great majority of studies concern bridges. This is not to imply that buildings are not evaluated, only that such evaluations are rarely reported. One reason for this may be that bridges are subjected to more severe loading and environmental conditions and are often required by law to have periodic inspections. As a result, performance evaluation of bridge structures may be more frequent. The more probable reason for the lack of published material on building structures, however, may be that buildings tend to be privately held structures whose owners may, for legal reasons, be hesitant to publish information on building deficiencies. Although the material presented here is heavily weighted toward bridge structures, the information is applicable to almost any type of concrete structure.

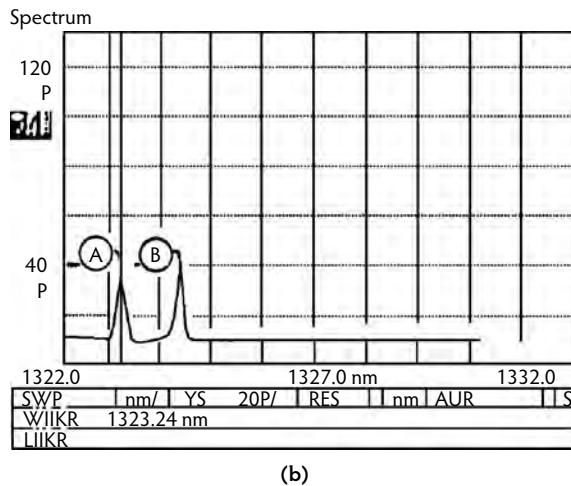
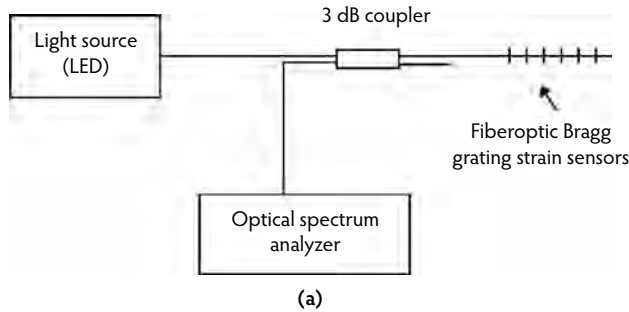


FIGURE 27.8 Fiber optic Bragg grating (FOBG) sensor system. (From Nawy, E.G. and Chen, B., *Fiber optic Sensing the Behavior of Prestressed Prism-Reinforced Continuous Composite Concrete Beams for Bridge Deck Applications*, Transportation Research Board, Washington, D.C., 1997.)

27.7.1 Testing of a Three-Span Slab Bridge

Extensive performance evaluations of a deteriorated, three-span concrete bridge were conducted by Aktan and his team at the University of Cincinnati (Aktan et al., 1992, 1993; Miller et al., 1994). The bridge, shown in Figure 27.9, had extensive deterioration along the shoulders and sides of the slab. The deterioration was so severe that the top mat rebar on the shoulders was completely exposed. The testing of this bridge had three main objectives: (1) to determine how severe deterioration affected the elastic response of the bridge, (2) to determine the effect of deterioration on the load capacity and failure mode of the bridge, and (3) to evaluate the effectiveness of nondestructive testing techniques in bridge evaluation.

The first step in the evaluation of this structure was to determine the cause and extent of the damage. Attempts were made to remove core samples from the shoulder area, but the deterioration was so severe that cores could not be removed intact and came out in layers. Some of these samples were used for material evaluation. Petrographic examination showed that the aggregate had extensively D-cracked. This type of cracking occurs when large pieces of semiporous aggregate are saturated and then permitted to freeze. Some of the aggregate was also reactive, and signs of alkali-silica reaction were found. It is believed that the aggregate cracked and the expansion of the aggregate cracked the surrounding cement paste. This provided a path for water to enter the slab, which then drove the alkali-silica reaction. There were also signs of carbonation, which lowers the pH of the cement paste and creates an environment where corrosion can occur. Chloride testing revealed that the cracked shoulder areas had high chloride contents

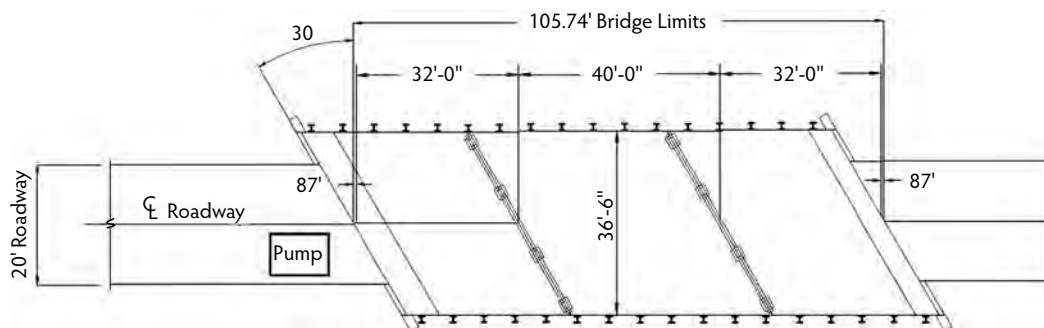


FIGURE 27.9 Three-span concrete slab bridge.

from road salt. The chloride, along with the air and water entering the slab through the cracks, caused the steel to corrode, further cracking and damaging the shoulder areas.

It is believed that the deterioration was limited to the shoulder areas because chloride-laden ice and snow would have been pushed to the shoulders by traffic and plows. Here, the snow melted and either ran over the slab edge (no other drainage was provided) or soaked into the porous asphalt layer and was trapped in between the asphalt and the slab. This would have saturated the shoulder area and provided an environment for the deterioration to occur. It is also of interest to note that chloride intrusion and milder signs of corrosion were found over the piers. It is probable that the chlorides entered through flexural cracking. Due to the short span of the bridge (the end span was only 30 ft long), it was found that only one axle would actually be at a critical point in the span as a truck passed (Figure 27.10). This rear tandem axle was duplicated by the use of two loading blocks fitted with hydraulic cylinders. The loading blocks were placed in one lane, as this provided a realistic loading pattern and the researchers felt this would also reveal any effect of nonsymmetrical loading on the slab. Estimates of bridge capacity and performance were obtained by running several finite-element analyses (Shahrooz et al., 1994a).

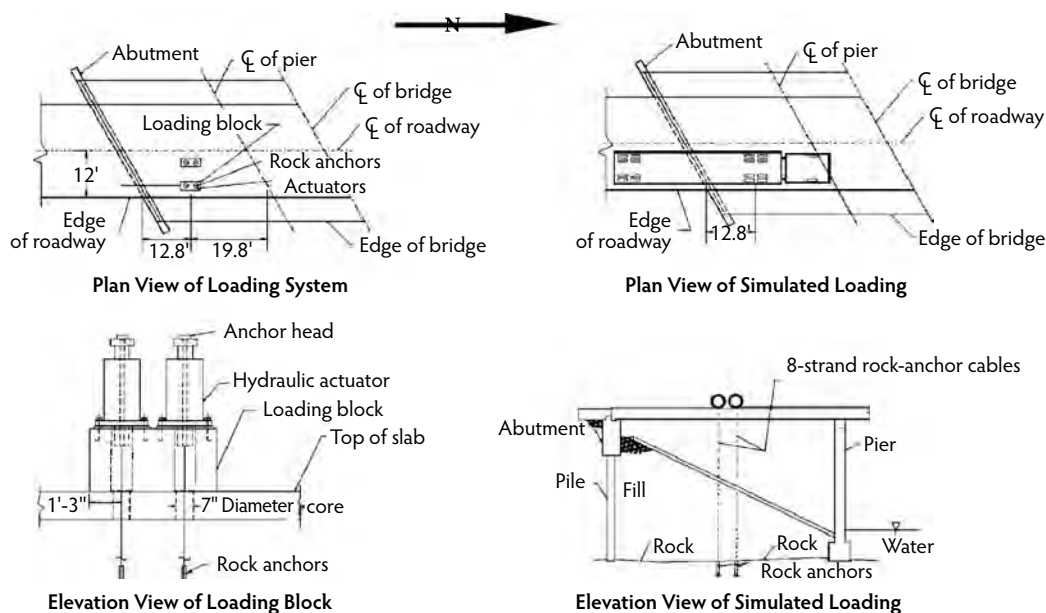


FIGURE 27.10 Load placement to simulate an HS20-44.

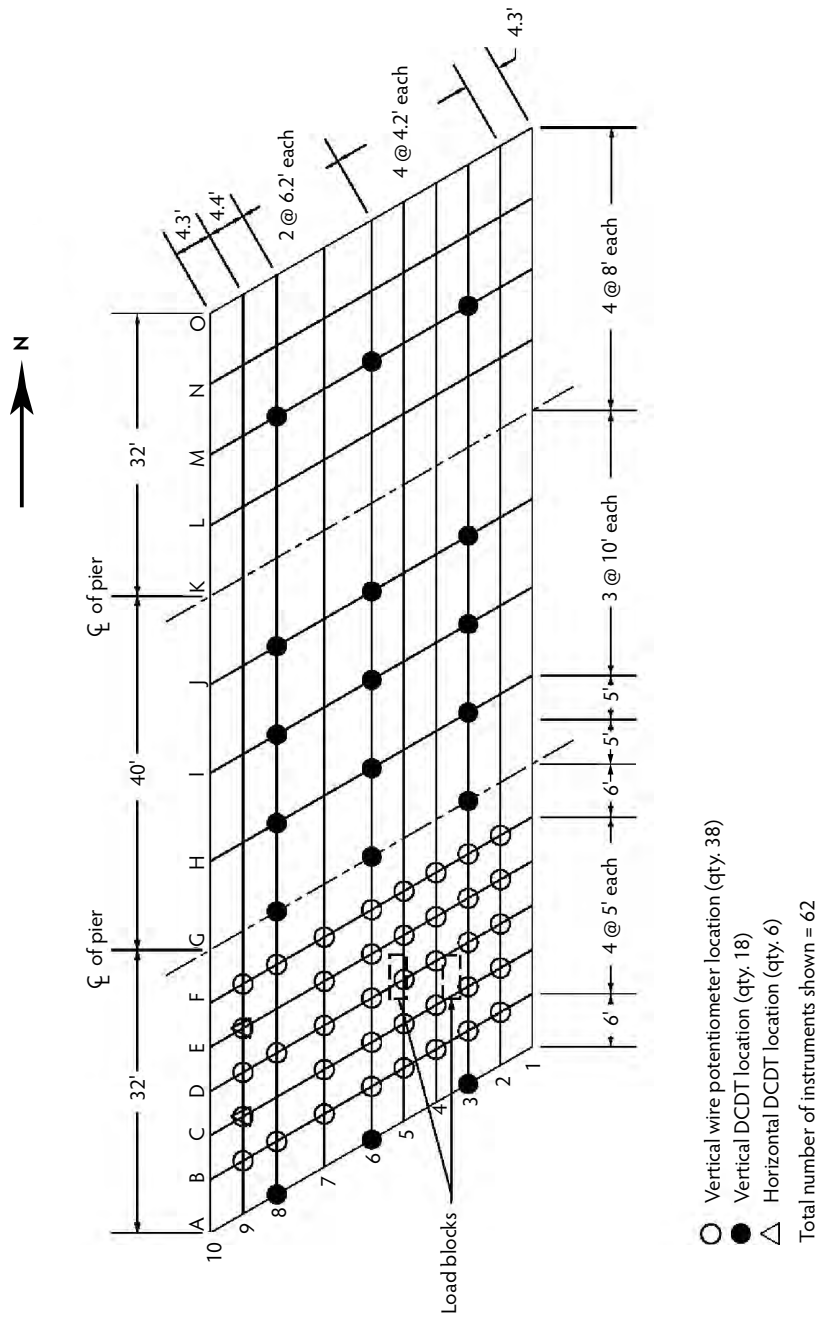


FIGURE 27.11 Instrumentation grid for the slab bridge.

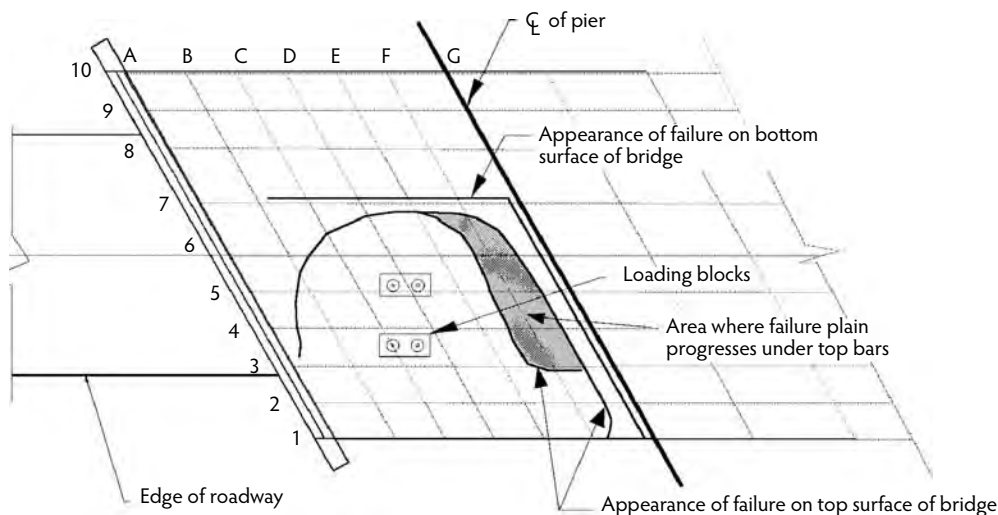


FIGURE 27.12 Final failure of the bridge.

After the finite-element analyses were completed, an extensive instrumentation was instituted (Figure 27.11) for 38 grid points. Two types of instruments were available for measuring deflection: 2-in.-range DCDTs and 10-in.-range wire potentiometers. The points in the loaded span were instrumented with the 10-in.-range wire potentiometers because preliminary finite-element analysis indicated that deflections in excess of 2 in. would be expected. Strains in the reinforcing bars were measured at 11 points on the bottom steel (clustered around the loading blocks) and at 8 points in the top steel (4 over the piers near the loading blocks and 4 at midspan near the loading blocks). Bonded resistance gauges were used in these applications. Concrete strains were measured using DCDTs that were attached between two angles glued 6 in. apart on the slab. After the truck load tests, which measured deflections, the bridge was tested to failure.

Using rock anchors (Figure 27.10), 7-in.-diameter holes were cored at four points in the deck. A 6-in. auger was then passed through the core hole and was used to drill a hole 45 ft into a rock layer beneath the bridge. A cable made of several seven-wire prestressing strands was then grouted into the rock. Two concrete loading blocks were then cast on the bridge deck over the core holes. Four 350-kip-capacity hydraulic cylinders were then placed into holes cast into the loading block. The shafts of cylinders were hollow and the rock anchor cables were passed through the shafts and tied off into button heads.

The loading cylinders were controlled by an electronic controller. This controller was linked to one of the wire potentiometers monitoring deflection below the loading blocks. The bridge was initially loaded to 64 kips (16 kips/cylinder) and then unloaded. Additional load and unload cycles were made to 112 kips and 124 kips. In each case, the bridge remained linear, although some slight hysteresis was observed on unloading. The bridge was reloaded after several days to 700 kips and then unloaded. It showed some nonlinear behavior, and flexural cracking was observed. The bridge failed at a load of 720 kips when it was reloaded the next day. Failure occurred as a circular arc around the loading blocks, resembling a punching-shear type of failure (Figure 27.12).

Subsequent analysis of the data revealed several interesting conclusions for the destructive test (Miller et al., 1994). Initially, the bridge carried the load in a direction parallel to the traffic lanes. When a rotational restraint at the abutment was overcome, the bridge began to carry load perpendicular to the skew. At about 700 kips of total load, the longitudinal reinforcing began to yield, and the load path again shifted to parallel to the traffic lanes. This shifted load back to the damaged corner (as evidenced by a sudden increase in top rebar strain at this location). The load was apparently too much for the damaged shoulder, and it failed in shear with the failure propagating throughout the entire slab. It is also of interest to note that the top steel in the shoulder areas was completely exposed and corroded; however, it was still possible to yield these bars before the failure pulled them out.

A final objective of this test was to determine the effectiveness of multireference modal testing for real structures. As noted in the Section 27.4.3 on modal testing, the test is performed by using an instrumented hammer to create impacts at various locations on the structure and reading the subsequent vibrations with accelerometers. The grid for the impacts was exactly the same as that used for the instrumentation (see Figure 27.11), except that all points shown on the grid were subject to impact, not just those points that were instrumented for the destructive test. A 12-lb sledgehammer, fitted with a load cell, was used for impact. Accelerometers were placed at points B4, C9, D6, D8, H3, I6, J3, L6, L8, M3, and N7 (Figure 27.11). Modal testing successfully located both visible and hidden damage.

The conclusion that can be drawn from the testing program is that concrete-slab bridges are extremely strong, even when damaged. This particular bridge held the equivalent of 22 HS20-44 trucks before failure. Although the damage did not prevent the bridge from safely holding normal traffic loads, it did affect bridge performance, as the final failure probably started in the damaged area.

27.7.2 Truck Load Testing of Damaged Concrete Bridges: Testing for Continuity

In the past, continuous concrete slab bridges were a popular choice for highway spans under 100 ft. Although much of this market has now gone to prestressed concrete, many continuous concrete slab bridges still exist, and many are still being built, especially in rural areas where labor is less expensive and the cost of shipping precast members may be high. The top of the slab bridge tends to deteriorate due to a combination of traffic and road salt. Often the deterioration partially or completely exposes the top reinforcing bars that provide the continuity over the pier supports. When this damage is repaired, deteriorated concrete is removed from the deck and the bars over the piers are further exposed. It is important to determine if the removal of the concrete from around the top bars over the piers could cause a loss of continuity, in effect causing the adjacent spans to behave as simple rather than continuous spans under dead load. In such a case, the dead-load stresses at the midspan of the slabs would increase, decreasing their usefulness.

To test for loss of continuity, three slab bridges were tested before, during, and after repair (Shahrooz et al., 1994b). The bridges were selected so one had minor damage (Bridge 1), one had moderate damage (Bridge 2), and one had severe damage over the piers (Bridge 3). All of the bridges were three-span, continuous-slab bridges. Spans ranged between 20 and 40 ft. The bridges were repaired in the following manner, were tested prior to repair to establish a base, and were retested after repair with truck loading:

- The asphalt layer was removed, along with 1/4 in. of the top of the concrete deck in two of the bridges.
- Three feet of the deteriorated shoulder was removed and replaced.
- All delaminated concrete from the deck was removed, and the deck was patched with microsilica concrete.
- A 1.25-in.-thick microsilica concrete wearing surface was placed on the deck.

To assess continuity, it was necessary to place the loads on the bridges in three load cases: maximum deflection in the middle span, maximum deflection in the end span, and maximum moment over the piers. Test results showed the following:

- For Bridge 1, there was little change in deflection or strains during repair, but an increase in stiffness was found after repair. Due to the low level of damage, this result was expected.
- For Bridge 2, there was little change in stiffness when the damaged shoulder was removed, indicating that the shoulder was so badly damaged that it did not participate in load resistance. After the shoulder was restored, the stiffness of the bridge increased. After the deck was repaired, a further increase in stiffness was noted, showing that the repair was very effective.
- For Bridge 3, there was a large loss of stiffness when the shoulder was removed and a large redistribution of moment. The moment transfer was estimated to increase the dead load positive moment by as much as 50%. It was also found that the stiffness after repair was only slightly greater than the before-repair stiffness, indicating that the repair was only marginally effective.

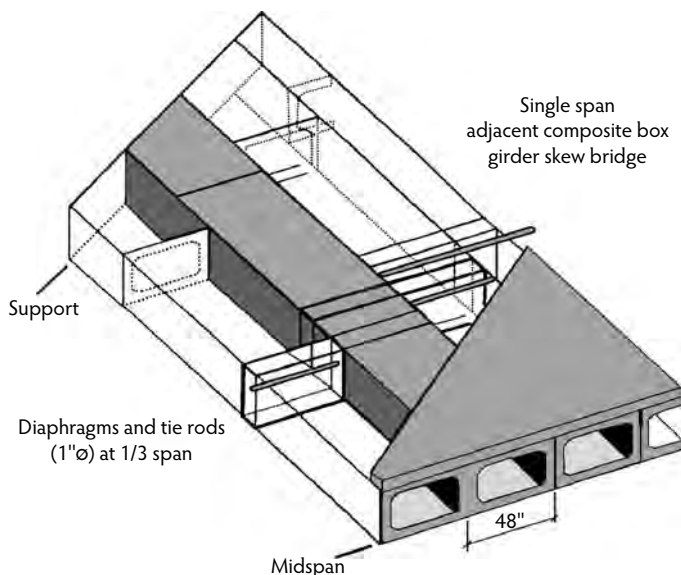


FIGURE 27.13 Adjacent box-girder bridge.

27.7.3 Testing of Shear-Key Cracking in Adjacent Box-Girder Bridges

The adjacent, precast box-girder bridge is used in over 30 states for short-span bridges (under 100 ft). In this type of bridge, precast box girders are placed side by side to form both the superstructure and the deck of the bridge (Figure 27.13). Often, the boxes are held together by transverse post-tensioning, but the method of post-tensioning varies widely between states. At one extreme, some states use threaded rods, tightened by hand using a turn-of-the-nut method. The rods are often placed only at the quarter points and midspan. At the other extreme, some states use transverse post-tensioning strands that are placed only a few feet apart. Many other intermediate combinations of post-tensioning methods are also used. Load transfer between adjacent boxes is mostly accomplished through the use of a shear key (Figure 27.14). These keys run the length of the box beam and are usually grouted after the transverse post-tensioning is applied. Many states use a nonshrink grout, but this material has often proved unsatisfactory. Some states have switched to magnesium phosphate cements or epoxies.

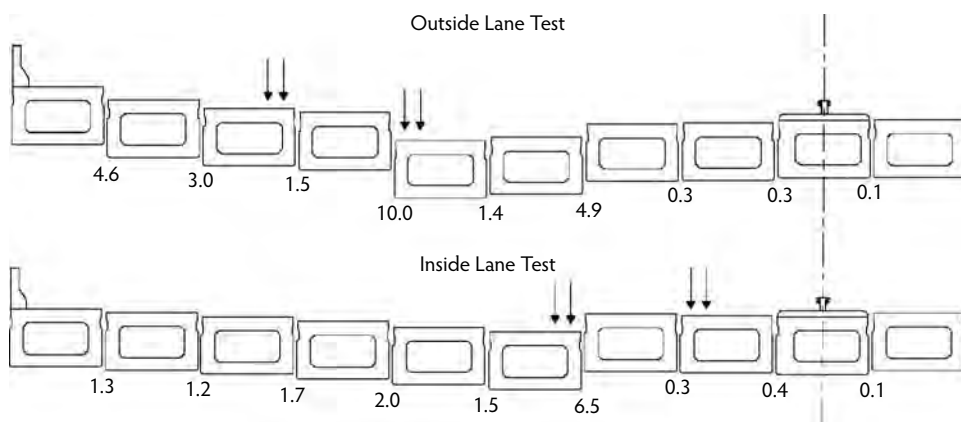


FIGURE 27.14 Relative displacement between adjacent box girders. (Figure courtesy of A. Hucklebridge, Case Western Reserve University.)

In this case study, deflectometers developed by El-Esnawi (Hucklebridge et al., 1995) were used to determine the extent of cracking and the load transfer in the shear keys. When one end of the deflectometer is displaced relative to the other, the thin element acts like a fixed beam subject to support displacement. This displacement causes moments at the ends of the beam, and the resulting strain from these moments is measured by the strain gauges. Tests conducted in this case study showed that the shear keys had cracked extensively, allowing large relative displacements of the beams (Figure 27.14). This cracking was found even in relatively new or recently repaired bridges; however, measured strains in girders indicated that some load transfer still occurred.

27.7.4 Testing of a High-Rise Building after Collapse

One common reason for testing concrete structures is to ensure structural safety if the materials of construction or the construction techniques are suspected of being faulty. One such case involved the Skyline Plaza Project at Bailey's Crossroads, Virginia (Dixon and Smith, 1980). The Skyline Plaza North Project consisted of an office building, apartments, condominiums, and parking structures. In March 1973, a section of one structure, A-4, collapsed. This collapse occurred shortly after concrete had been placed on the 24th floor of what was to be a 26-story structure. The collapse of this floor started a progressive collapse of the lower floors, resulting in the deaths of 14 workers and injury to 30 more. A study was made of the material properties, slab cracking, and cause of the collapse (Schousboe, 1976), but of interest here is the load testing that was used to determine the safety and salvageability of the uncollapsed part of the structure. The A-4 structure was a flat-plate structure, 76 ft wide and 389 ft long, with irregularly spaced columns. An expansion joint was located 171 ft from the west end of the building. The collapsed area was east of the expansion joint. The investigation of material strengths and slab cracking located 14 areas that were suspect. ACI 318, Chapter 20, was used to determine the test load. The slab self-weight was 77 psf, and an additional 19 psf was calculated as the remaining dead load that would be applied to the structure. The design live load was 40 psf; thus, the total load was $TL = 0.85[1.4(77 + 19) + 1.7(40)] = 172$ psf.

One interesting aspect of this test was the method of load application. The uniform load was applied by flooding the structure. It should be noted that ACI Committee 437 allows for the use of water as a loading method but recommends that the water be confined to tanks or containers. The use of flooding is discouraged, as the water height may vary due to variations in the level of the floor and an uncertain load distribution may be created; however, the flooding method was chosen because a large number of areas had to be tested, and this method could be easily and quickly applied.

Before testing began, all mechanical elements (pipes, ducts, etc.) that might interfere with the test were removed, and holes in slabs for these elements were sealed. A built-up roofing material was placed over the slab to act as waterproofing. This material was not actually attached to the concrete so it could be easily removed after the test to allow post-test inspection of the concrete. Bulkheads were built around the area to be tested. As required by the ACI 318, the acceptance criterion for the slabs was that deflections must be under allowable limits. Due to safety concerns, workers would not be allowed in the building during testing, so remote monitoring of deflections was needed. This was accomplished by using LVDTs mounted on wooden stands that measured the deflection of the slab from underneath.

The first load applied was 3.5 in. of water (approximately 19 psf), which represented the dead load not present on the slab. According to the version of ACI 318 in effect at the time of the test, this load had to be in place for 48 hr before any further testing was done. (A later version, ACI 318-95, did not have this requirement.) At the end of 48 hr, the deflection was measured. The remaining load was then added in three increments (so the total number of increments was 4, as required by the code), with 1 hr elapsing between increments. During the hour wait, deflections were monitored. The total load consisted of 18.5 in. of water: 3.5 in. for the dead load and 15 in. for the live load. This load was left for 24 hr, after which time deflections were measured. The water was then drained so only 3.5 in. of water, representing the increment of dead load, remained. This was left for 24 hr, and deflections were measured again.

Of the original 14 areas tested, 4 did not meet the requirements of ACI 318, which allows for retesting parts of a structure that do not pass a load test, and this was done. After retesting, two of the areas still failed and one showed an increase in slab cracking. The three areas that did not pass the test were strengthened, but the method of strengthening was not reported.

Another interesting part of this evaluation concerned punching-shear tests around the columns. As previously noted, the Skyline Plaza North building was a flat slab. Flat slabs are always at risk for punching-shear failures. Two columns on the tenth floor in an area of the building scheduled to be demolished were subjected to punching-shear tests. The slabs around the columns were shored from the bottom of the tenth floor to the sixth floor. A portion of the slab around the columns was then cut free. (Although the reference does not give the size of the cut-out portions, they appear from diagrams and pictures to be about 30 in. from each face of the column.) Eight holes were cored in the 10th- and 9th-floor slabs, two on each side of the column. A rectangular testing frame made of back-to-back channels was placed over the holes on the 10th floor. Threaded rods were passed between the channels, through the holes, and attached to post-tensioning jacks anchored to the column two floors below the testing frame. The loading sequence was as follows:

- Load all jacks to 3 kips (24 kips total load) and wait 10 minutes.
- Add 5 kips per jack (40 kips total) and wait 10 minutes.
- Add 5 more kips per jack (40 kips total) and wait 10 minutes.
- Add 3 kips per jack (24 kips total).

One slab failed in shear before all the load was applied, at a total load of 120 kips. The other slab was loaded at 1.25 kips/jack/minute until it failed in shear at 128 kips total load. Inclined cracks developed from flexural cracks at approximately 60% of the ultimate load. These cracks propagated upward until only a small compression area remained before failure. The shear loads were less than those anticipated, and shearheads were added at many column locations. As a result of the load-testing program, many parts of the existing structure were strengthened and the building was completed. The authors of the study noted that the completed building now performs well and shows no sign of the collapse.

27.7.5 Testing of Concrete Panels on a Steel Stringer Bridge

In an effort to increase the speed of bridge construction, the Ohio Department of Transportation (ODOT) used precast/prestressed concrete deck panels on a steel stringer bridge. Because this was the first use of that type of panel in Ohio, ODOT had the panels monitored during the construction phase, and they load tested the bridge after construction was complete. Complete details can be found in Dimmerling et al., (2005). The bridge was a 170-ft-long, single-span, steel stringer bridge over I-75 in Findlay, Ohio. The 10-ft by 3-in.-wide deck panels were cast as reinforced elements and then longitudinally post-tensioned prior to shipment (Figure 27.15 and Figure 27.16). The panels were placed with their longitudinal axis perpendicular to traffic. After being shipped to the site, the panels were erected in one evening. Vibrating wire strain gauges were placed in the joints between the panels. After grouting the joints, the panels were laterally post-tensioned together (this post-tensioned the panels in the direction of traffic). Post-tensioning was done before the panels were made composite with the girders. A total of 15 vibrating wire gauges were placed in 5 of 15 joints. The joints chosen were the first joint on each end, the joints at the quarter point of the bridge, and the joint at midspan. Each joint was instrumented with 3 gauges (Figure 27.17 and Figure 27.18). One of reasons for installing the gauges was to determine if the post-tensioning forces were being equally distributed through the joints. There was some concern that, due to friction, the center joints might not receive the complete post-tensioning force. Another concern was how evenly the post-tensioning was applied along the joint.

Table 27.1 shows the strain in the gauges after the post-tensioning was applied. Although there is some variation, the results show a reasonably even distribution of strain after post-tensioning. The post-tensioning would have applied a stress of approximately 400 psi. Assuming a modulus for the grout of 3,000,000 psi, the predicted strain post-tensioning strain would be 137 microstrain, which was consistent

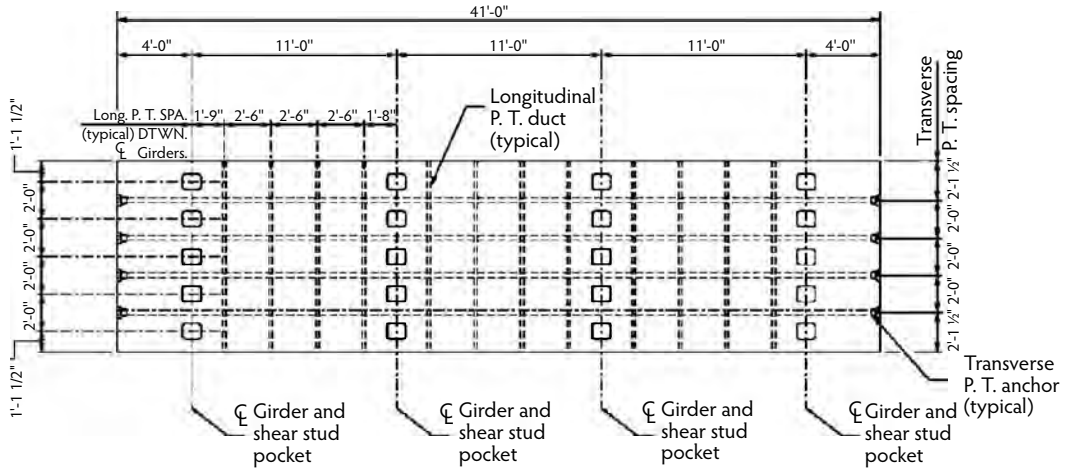


FIGURE 27.15 Plan view of the deck panels.

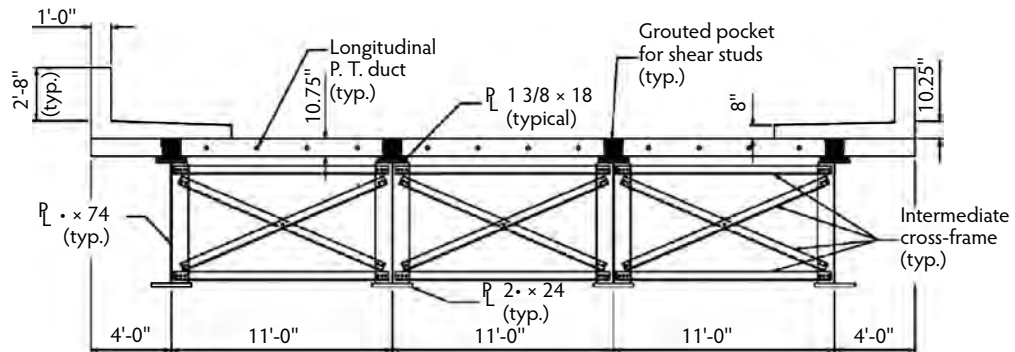


FIGURE 27.16 Cross-sectional view of the deck panels.

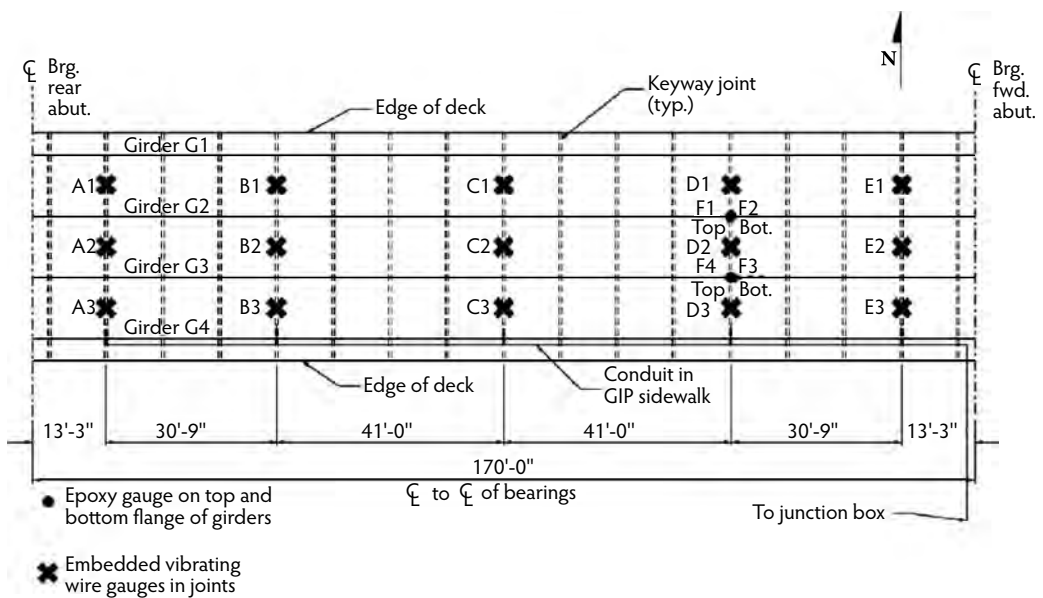


FIGURE 27.17 Instrument placement.

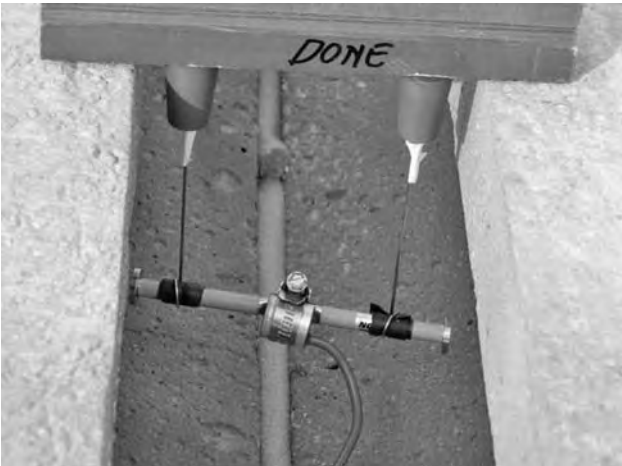


FIGURE 27.18 Vibrating wire gauge.

TABLE 27.1 Total Strain Developed by Post-Tensioning (microstrain)

	Gauge																
	A1	A2	A3	B1	B2	B3	C1	C2	C3	D1	D2	D3	E1	E2	E3		
Reading before post-tensioning	2560	2634	2691	2605	2619	2690	2458	2503	2692	2503	2584	2611	2531	2640	2532		
Reading after post-tensioning	2415	2461	2544	2481	2482	2549	2348	2332	2551	2378	2471	2474	2395	2485	2434		
Difference	145	170	147	124	136	141	110	172	141	125	113	137	136	154	98		
	West End			West Quarter Point				Center			East Quarter Point			East End			
Average	154			134				141			125			129			
Average								137									

with the average measured strain of 134 microstrain. When the data from the vibrating wire gauges were analyzed, it was not consistent with the post-tensioning sequence shown on the plans. From the data, the research team was able to reconstruct a post-tensioning sequence, and it was later confirmed that the reconstructed sequence was the one actually used. Grout pockets were left in the panels for the purpose of making the panels composite with the girders. After post-tensioning was complete, studs were welded to the girders in the grout pockets, and the pockets were grouted. Strains measured in the joints in subsequent truck load testing showed that the panels behaved as composite with the steel girders.

References

ACI Committee 201. 1997. *Guide for Making a Condition Survey of Concrete in Service*, ACI 201R1-97. American Concrete Institute, Farmington Hills, MI.

ACI Committee 214. 2003. *Guide for Obtaining Cores and Interpreting Compressive Strength Results*, 214.4R-03. American Concrete Institute, Farmington Hills, MI.

ACI Committee 318. 2008. *Building Code Requirements for Structural Concrete*, ACI 318-08. American Concrete Institute, Farmington Hills, MI.

ACI Committee 437. 2003. *Strength Evaluation of Existing Concrete Buildings*, ACI 437R-03. American Concrete Institute, Farmington Hills, MI.

- Aktan, A.E., Miller, R.A., Shahrooz, B.M., Zwick, M., Heckenmueller, M., Ho, I., Hrinko, W., and Toksoy, T. 1992. *Nondestructive and Destructive Testing of a Reinforced Concrete Slab Bridge and Associated Analytical Studies*, FHWA/OH-93/017. Federal Highway Administration, Washington, D.C.
- Aktan, A.E., Zwick, M., Miller, R.A., and Shahrooz, B.M. 1993. Nondestructive and destructive testing of a decommissioned RC highway slab bridge and related studies. *Transport. Res. Rec.*, 1371, 142–153.
- Allbright, K., Parekh, K., Miller, R., and Baseheart, T.M. 1994. Modal verification of a destructive test of a damaged prestressed concrete beam. *Exp. Mech.*, 34(4), 389–396.
- Ansari, F., Libo, Y., Lee, I., and Ding, H. 1996. A fiberoptic embedded crack opening displacement sensor for cementitious composites. In *Proceedings of the 2nd International Conference on Nondestructive Testing of Concrete in the Infrastructure*, pp. 268–277. Society for Experimental Mechanics, Bethel, CT.
- ASTM. 2000. *Standard Practice for Examination and Sampling of Hardened Concrete in Constructions*, ASTM C 823-00. American Society for Testing and Materials, West Conshohocken, PA.
- ASTM. 2002. *Standard Test Method for Creep of Concrete in Compression*, ASTM C 512-02. American Society for Testing and Materials, West Conshohocken, PA.
- ASTM. 2004a. *Standard Test Method for Obtaining and Testing Drilled Cores and Sawed Beams of Concrete*, ASTM C 42/C 42M-04. American Society for Testing and Materials, West Conshohocken, PA.
- ASTM. 2004b. *Standard Test Method for Splitting Tensile Strength of Cylindrical Concrete Specimens*, ASTM C 496/C 496M-04. American Society for Testing and Materials, West Conshohocken, PA.
- ASTM. 2004c. *Standard Practice for Petrographic Examination of Hardened Concrete*, ASTM C 856-04. American Society for Testing and Materials, West Conshohocken, PA.
- ASTM. 2006. *Standard Test Method for Microscopical Determination of Parameters of the Air-Void System in Hardened Concrete*, ASTM C 457-06. American Society for Testing and Materials, West Conshohocken, PA.
- Azizinamini, A., Shekar, Y., Boothby, T.E., and Branhill, G. 1992. Load-carrying capacity of old concrete slab bridges. In *Proc. Third NSF Workshop on Bridge Engineering Research in Progress*, pp. 113–116. National Science Foundation, Washington, D.C.
- Bodocsi, A., Minkarah, I., and Arudi, R. 1993. Analysis of horizontal movements of joints and cracks in Portland cement concrete pavements. *Transport. Res. Rec.*, 1392, 43–52.
- Carino, N. and Sansalone, M. 1992. Detection of voids in grouted ducts using the impact echo method. *ACI Mater. J.*, 89(3), 296–303.
- Carino, N., Sansalone, M., and Hsu, N. 1986. Technique for flaw detection in concrete. *J. ACI*, 83(3), 199–208.
- Catbas, F.N., Lenett, M., Brown, D.L., Doebling, S.W., Farrar, C.R., and Turer, A. 1997. Modal analysis of multi-reference impact test data for steel stringer bridges. In *Proceedings of the 15th International Modal Analysis Conference*, pp. 381–391. Society for Experimental Mechanics, Bethel, CT.
- Chen, B. and Nawy, E.G. 1994. Structural behavior evaluation of high strength concrete beams reinforced with prestressed prisms using fiber optic sensors. *ACI Struct. J.*, 91(6), 708–717.
- Chung, L. and Shah, S.P. 1989. Effect of loading rate on anchorage bond and beam column joints. *ACI Struct. J.*, 86(2), 132–143.
- Delahaza, A. 1996. Nondestructive testing of the concrete roof shell at the Kingdome in Seattle, Washington. In *Proceedings of the 2nd International Conference on Nondestructive Testing of Concrete in the Infrastructure*, pp. 256–267. Society for Experimental Mechanics, Bethel, CT.
- Dimmerling, A., Miller, R., Barker, J., Ismael, K., and Engel, R. 2005. Monitoring precast deck panels for load and environmental effects. In *Proceedings of the PCI National Bridge Conference*. Precast/Prestressed Concrete Institute, Chicago, IL.
- Dixon, D.E. and Smith, J.R. 1980. Skyline Plaza North (Building A-4): a case study. In *Full-Scale Load Testing of Structures*, W.R. Schriever, Ed., STP 702, pp. 182–199. American Society for Testing and Materials, West Conshohocken, PA.
- Dunnicliff, J. 1993. *Geotechnical Instrumentation for Monitoring Field Performance*. John Wiley & Sons, New York.

- Hrinko, W., Miller, R., Young, C., Shahrooz, B., and Aktan, A.E. 1994. Understanding errors and accuracies in DCDTs and wire potentiometers for field testing applications. *Exp. Technol.*, 18(2), 29–33.
- Hucklebridge, A., El-Esnawi, H., and Moses, F. 1995. Shear key performance in multibeam box girder bridges. *J. Perform. Construct. Factors*, 9(4), 271–285.
- Issa, M., Robinson, E. and Shahawy, M., 1996. *On-Site Evaluation of Bridge Deck Joints*. Florida Department of Transportation Structures Research Center, Tallahassee, FL.
- Malhotra, V.M and Carino, N.J., 2004. *Handbook on Nondestructive Testing of Concrete*, 2nd ed. CRC Press, Boca Raton, FL.
- Measures, R.M. 1995. Fiber optic strain sensing. In *Fiber Optic Smart Structures*, Udd, E., Ed., pp. 171–247. John Wiley & Sons, New York.
- Miller, R.A., Aktan, A.E., and Shahrooz, B.M. 1994. Destructive testing of a decommissioned concrete slab bridge. *ASCE J. Struct.*, 120(7), 2176–2198.
- Miller, R. A., Castrodale, R., Mirmiran, A., and Hastak, M., 2004. *Connection of Prestressed Concrete Girders for Continuity*, NCHRP Report 519. National Cooperative Highway Research Program, Transportation Research Board, Washington, D.C.
- Nawy, E. and Chen, B. 1996. Bragg grating fiber optic sensing the structural behavior of continuous composite concrete beams reinforced with prestressed prisms. In *Proceedings of the 2nd International Conference on Nondestructive Testing of Concrete in the Infrastructure*, pp. 1–10. Society for Experimental Mechanics, Bethel, CT.
- Nawy, E.G. and Chen, B. 1997. *Fiber optic Sensing the Behavior of Prestressed Prism-Reinforced Continuous Composite Concrete Beams for Bridge Deck Application*. Transportation Research Board, Washington, D.C.
- Petrou, M.F., Perdikaris, P.C., and Wang, A. 1994. Fatigue behavior of noncomposite reinforced concrete bridge deck models. *Transport. Res. Rec.*, 1460, 73–80.
- Schousboe, I. 1976. Bailey's Crossroads collapse reviewed. *ASCE J. Const. Div.*, 102(2), 365–378.
- Shahrooz, B.M., Ho, I.K., Aktan, A.E., deBorst, R., Blaauwendraad, J., Van der Veen, C., Iding, R.H., and Miller, R.A. 1994a. Nonlinear finite element analysis of a deteriorated RC slab bridge. *ASCE J. Struct. Eng.*, 120(2), 422–440.
- Shahrooz, B.M., Miller, R.A., Saraf, V.K., and Godbole, B. 1994b. Behavior of reinforced concrete slab bridges during and after repair. *Transport. Res. Rec.*, 1442, 128–135.
- Weil, G.J. 1993. Nondestructive testing of bridge, highway and airport pavements. In *Proceedings of the International Conference on Nondestructive Testing of Concrete in the Infrastructure*, pp. 93–105. Society for Experimental Mechanics, Bethel, CT.



Concrete masonry wall under construction. (Photograph courtesy of the National Concrete Masonry Association and Jason J. Thompson.)

28

Masonry Design and Construction

Jason J. Thompson*

28.1	Introduction	28-1
28.2	Masonry Design and Construction Codes and Standards.....	28-2
28.3	Definitions	28-2
28.4	Materials.....	28-4
	Mortar • Grout • Concrete Masonry Units • Clay Masonry Units • Reinforcement • Admixtures	
28.5	Construction.....	28-15
	Modular Layout • Mortar • Grout Placement • Bracing of Masonry • Environmental Construction Factors • Cleaning • Construction Tolerances and Workmanship	
28.6	Testing and Inspection.....	28-27
	Quality Assurance Levels • Mortar Testing • Grout Testing • Masonry Unit Testing • Verifying Compliance with f'_m	
28.7	General Detailing	28-38
	Movement Control and Control/Expansion Joints • Moisture Migration and Detailing	
28.8	Project Specifications	28-39
28.9	Structural Design	28-40
	Design Methodologies • Prescriptive Seismic Detailing • Empirical Design of Masonry • Allowable Stress Design of Masonry • Strength Design of Masonry	
28.10	Summary.....	28-68
	Acknowledgment	28-68
	References	28-68

28.1 Introduction

Masonry is our oldest permanent construction material. Its has been employed in the construction of castles, forts, majestic cathedrals reaching to the heavens, and simple home shelters for thousands of years. Historically, the design and construction of masonry structures evolved through trial-and-error methods whereby successful designs were repeated and expanded upon. Only during the past century have we begun

* Director of Engineering, National Concrete Masonry Association, Herndon, Virginia; member of codes and standards development committees, including ACI 530/ASCE 5/TMS 402 (*Building Code Requirements for Masonry Structures*) and ACI 530.1/ASCE 6/TMS 602 (*Specification for Masonry Structures*).

to apply in earnest engineering design philosophies and concepts to provide a rational design approach rather than empirical assessment. Despite its long tradition and widespread use, however, masonry remains the least understood of our major construction materials. As with design practices, the physical properties and methods of manufacturing the constituent masonry materials continue to evolve to meet ever-expanding uses and aesthetic demands. The primary purpose of this chapter is to describe and clarify the use of masonry as a construction material in a way that is applicable to modern applications, in addition to, where appropriate, reviewing the historical context from which contemporary masonry design stems. The conventional subjects of constituent masonry materials and construction practices, their governing codes and standards, and the role each component fills in the final masonry assembly are reviewed. As with any construction material, the practice of designing and constructing with masonry materials continuously revises and builds upon previous knowledge. When fitting, design resources and tools will be cited to provide the reader with alternative means of meeting the evolving demands of today's masonry projects.

28.2 Masonry Design and Construction Codes and Standards

By necessity, the long history of masonry construction is only briefly reviewed. Ancient masonry began with sun-dried mud brick, followed by fired clay units, which were used to create stone forts for security and stone cathedrals for spiritual inspiration. With the industrial revolution, many new materials and manufacturing methods were developed that facilitated the use of masonry construction for all types of uses and occupancies. As the use of masonry expanded, so did the need for establishing consistency in material properties, design methods, and construction procedures. Beginning in the early 20th century, the American Society for Testing and Materials (ASTM) published the first standard specifications for masonry units and masonry mortar. These standards supplemented concurrent efforts to codify design and construction practices for masonry structures. Toward the latter half of the 20th century, the use of masonry in the United States was governed primarily by three different model building codes: the Uniform Building Code (UBC), the Standard Building Code (SBC), and the National Building Code (NBC), which in turn drew heavily upon the content of ACI 530/ASCE 5/TMS 402 (*Building Code Requirements for Masonry Structures*) and ACI 530.1/ASCE 6/TMS 602 (*Specification for Masonry Structures*) for masonry design and construction. Today, these three model building codes have merged together under the International Building Code (IBC). Within the context of the discussion presented in this chapter, the requirements of the 2006 IBC, and by reference within the IBC, the collective provisions of the 2005 ACI 530/ASCE 5/TMS 402 *Building Code Requirements for Masonry Structures* (MSJC Code) and 2005 ACI 530.1/ASCE 6/TMS 602 *Specification for Masonry Structures* (MSJC Specification) form the basis for the design and construction requirements reviewed herein. The provisions of ACI 530/ASCE 5/TMS 402 and ACI 530.1/ASCE 6/TMS 602 are developed and maintained by the Masonry Standards Joint Committee (MSJC), a committee jointly sponsored by the American Concrete Institute (ACI), the Structural Engineering Institute of the American Society of Civil Engineers (SEI-ASCE), and The Masonry Society (TMS). These two documents are more commonly (and succinctly) referred to as the MSJC Code and MSJC Specification, respectively. The MSJC Code addresses the minimum structural design requirements for concrete masonry, clay masonry, and aerated autoclaved concrete masonry construction. The MSJC Specification complements the MSJC Code by addressing the minimum requirements for materials, construction, and workmanship. Each document is under continuous review and revision, and a new edition is published every 3 years along with a companion commentary. Additional information on the activities of the MSJC can be found at www.masonrystandards.org.

28.3 Definitions

Many terms have developed over the ages of masonry use that have specific meanings and special connotations as applied to masonry construction. Many such terms and definitions have been formalized by various codes, standards, and industry publications (ACI Committee 530, 2005; ACI Committee

530.1, 2005; ASTM, 2003a,b,c, 2006b; BIA, 2005; NCMA, 2004b). Commonly used terms are provided in the following discussion for ease of reference:

- **Area**—**Mortar bedded area** is the area of the surface of a masonry unit that is in contact with mortar; more commonly refers to a horizontal bed joint but may also apply to a vertical head joint. **Gross area** is the total cross-sectional area of a specified section delineated by the entire out-to-out dimensions of the member. **Net area** is the gross cross-sectional area minus the area of ungrouted cores, notches, cells, and unbedded mortar areas; it is the actual surface area of a cross-section of masonry. **Transformed area** is the equivalent area of one material to a second, based on the ratio of the modulus of elasticity of the first material to the second.
- **Backing**—Backing is a wall or other approved surface to which a veneer assembly is attached.
- **Bond beam**—A bond beam is a horizontal grouted element within an assembly of masonry that contains reinforcement.
- **Cavity**—A cavity is a continuous space, with or without insulation, between wythes of masonry or between masonry and its backup system. A cavity is typically greater than 2 in. (51 mm) in thickness. Conversely, a collar joint is typically less than 2 in. (51 mm) in thickness.
- **Cell**—A cell is a void space within a hollow masonry unit. Also called a *core*.
- **Cleanout**—A cleanout is an opening to the bottom of a grout pour of sufficient size and spacing to allow the removal of debris. Cleanouts are required for high-lift grouting unless it can be shown through the use of a grout demonstration panel that adequate placement and consolidation of grout can be achieved without the use of cleanouts.
- **Collar joint**—The collar joint is a plane between wythes of masonry or between masonry wythe and backup construction, usually filled with mortar or grout. Collar joints are typically less than 2 in. (51 mm) in thickness, whereas a cavity generally refers to a void plane greater than 2 in. (51 mm) in thickness.
- **Column**—For the purposes of masonry design, a column is a reinforced, isolated vertical member whose horizontal dimension measured at right angles to the thickness does not exceed 3 times its thickness and whose height is greater than 4 times its thickness. Columns support loads that act primarily in the direction of the longitudinal axis.
- **Dimensions**—**Actual dimension** is the measured size of a masonry unit or assembly. Nominal dimension is the specified dimension plus an allowance for mortar joints, typically $\frac{3}{8}$ in. (9.5 mm). **Nominal dimensions** are usually stated in whole numbers. Width (thickness) is given first, followed by height and then length. **Specified dimensions** are the dimensions specified for the manufacture or construction of a unit, joint, member, or element. Unless otherwise stated, all calculations are based on specified dimensions. Actual dimensions may vary from specified dimensions by permissible variations defined either by the MSJC Specification or the project documents.
- **Grout lift**—Grout lift is an increment of grout placed at one time within the total grout pour.
- **Grout pour**—Grout pour is the total height of a masonry wall to be grouted prior to the erection of additional masonry, generally in a continuous sequence. A grout pour consists of one or more grout lifts.
- **Joints**—A **bed joint** is the horizontal mortar joint within a masonry assembly. A **head joint** is the vertical mortar joint within a masonry assembly.
- **Masonry unit**—A masonry unit is clay brick, tile, stone, glass block, or concrete block or brick conforming to the requirements specified in the applicable standards. A **hollow masonry unit** is a masonry unit whose net cross-sectional area in every plane parallel to the bearing surface is less than 75% of the gross cross-sectional area in the same plane. A **solid masonry unit** is a masonry unit whose net cross-sectional area in every plane parallel to the bearing surface is 75% or more of the gross cross-sectional area in the same plane.
- **Pier**—A pier is an isolated vertical member whose horizontal dimension measured at right angles to its thickness is not less than 3 times its thickness nor greater than 6 times its thickness and whose height is less than 5 times its length.

- *Prism*—A prism is an assemblage of masonry units and mortar, with or without grout, that is used as a test specimen for determining or verifying the compressive strength of a masonry assemblage.
- *Reinforced masonry*—Reinforced masonry is a form of masonry construction in which reinforcement is embedded in the mortar joints or grouted cells to resist applied loads. For the determination of design strength, the tensile resistance of the masonry is neglected.
- *Unreinforced masonry*—Unreinforced masonry is masonry in which the tensile resistance of the masonry is taken into consideration during design and the resistance of reinforcement, if present, is neglected; also referred to as **plain masonry**.
- *Veneer*—Veneer is a nonstructural facing of brick, concrete, stone, tile, or other approved material attached to a backing for the purpose of ornamentation, protection, or insulation. For design, veneer is assumed to add no strength the structure or element to which it is applied. **Adhered veneer** is a veneer secured and supported through adhesion of an approved bonding material applied over an approved backing. **Anchored veneer** is veneer applied to and supported by approved connectors to an approved backing.
- *Wall*—A wall is a vertical element with a horizontal length-to-thickness ratio greater than 3.
- *Wall tie*—A wall tie is a mechanical metal fastener that connects wythes of masonry to each other or to other materials; also referred to as an **anchor**.
- *Wythe*—A wythe is the portion of a masonry element that is one masonry unit in thickness. Collar joints and cavities are not considered wythes.

28.4 Materials

The quality of materials used in masonry is specified within applicable ASTM standards and the MSJC Specification. When a given material is not covered by specific ASTM or building code requirements, quality shall be based on generally accepted good practice, subject to the approval of the building official. Reclaimed or previously used units shall meet the same applicable requirements for the intended use as for new units of the same material. An overview of masonry materials and their constituent components is provided below. Subsequent sections provide a more detailed review of the primary construction materials, their properties, and methods of evaluation.

- Aggregate
 - ASTM C 144, *Aggregates for Masonry Mortar*
 - ASTM C 404, *Aggregates for Grout*
- Cementitious materials
 - ASTM C 5, *Quicklime*
 - ASTM C 91, *Masonry Cement*
 - ASTM C 150, *Portland Cement*
 - ASTM C 207, *Hydrated Lime*
 - ASTM C 595, *Blended Hydraulic Cements and Slag Cements*
 - ASTM C 618, *Fly Ash and Raw or Calcined Natural Pozzolans*
 - ASTM C 989, *Ground Granulated Blast-Furnace Slag*
 - ASTM C 1157, *Hydraulic Cement*
 - ASTM C 1329, *Mortar Cement*
 - ASTM C 1489, *Lime Putty*
- Masonry units of clay or shale
 - ASTM C 34, *Structural Clay Loadbearing Wall Tile*
 - ASTM C 56, *Structural Clay Nonloadbearing Wall Tile*
 - ASTM C 62, *Solid Clay or Shale Building Brick*
 - ASTM C 126, *Ceramic Glazed Structural Clay Facing Tile and Brick*
 - ASTM C 212, *Structural Clay Facing Tile*

- ASTM C 216, *Solid Clay or Shale Facing Brick*
- ASTM C 652, *Hollow Clay or Shale Brick*
- ASTM C 1088, *Thin Clay or Shale Veneer Brick*
- ANSI A 137.1, *Ceramic Tile*
- Masonry units of concrete
 - ASTM C 55, *Concrete Brick*
 - ASTM C 73, *Calcium Silicate (Sand-Lime) Brick*
 - ASTM C 90, *Loadbearing Concrete Masonry Units*
 - ASTM C 129, *Nonloadbearing Concrete Masonry Units*
 - ASTM C 744, *Prefaced Concrete and Calcium Silicate Units*
 - ASTM C 1386, *Autoclaved Aerated Concrete Masonry Units*
- Masonry units of stone
 - ASTM C 503, *Marble Dimension Stone*
 - ASTM C 568, *Limestone Dimension Stone*
 - ASTM C 615, *Granite Dimension Stone*
 - ASTM C 616, *Quartz-Based Dimension Stone*
 - ASTM C 629, *Slate Dimension Stone*
- Masonry units of glass—Minimum physical properties of glass unit masonry are not covered by ASTM specifications but instead are detailed within *Specification for Masonry Structures* (ACI Committee 530.1, 2005).
- Anchors, ties, and connectors
 - ASTM A 36/A 36M, *Plate and Bent-Bar Anchors*
 - ASTM A 82, *Wire Ties and Anchors*
 - ASTM A 185, *Wire Mesh Ties*
 - ASTM A 307, *Grade A, Anchor Bolts*
 - ASTM A 480 and A 666, *Stainless Steel Plate and Bent-Bar Anchors*
 - ASTM A 480 and A 240, *Stainless Steel Sheet-Metal Anchors and Ties*
 - ASTM A 580, *Stainless Steel Wire Ties and Anchors*
 - ASTM A 1008/A 1008M, *Sheet-Metal Anchors and Ties*
 - Panel anchors for glass unit masonry are not covered by ASTM specifications, but instead are covered within *Specification for Masonry Structures* (ACI Committee 530.1, 2005).
- Mortar
 - ASTM C 270, *Mortar for Unit Masonry*
- Grout
 - ASTM C 476, *Grout for Masonry*
- Reinforcement
 - ASTM A 185, *Plain Welded Wire Fabric*
 - ASTM A 416/A 416M, *Strand Prestressing Tendons*
 - ASTM A 421, *Wire Prestressing Tendons*
 - ASTM A 496, *Deformed Reinforcing Wire*
 - ASTM A 497, *Deformed Welded Wire Fabric*
 - ASTM A 580, *Stainless Steel Joint Reinforcement*
 - ASTM A 615/A 615M, A 706/A 706M, A 767/A 767M, A 775/A 775M, and A 996/A 996M, *Reinforcing Steel*
 - ASTM A 722/A 722M, *Bar Prestressing Tendons*
 - ASTM A 951, *Joint Reinforcement*

28.4.1 Mortar

Mortar has evolved dramatically since its first introduction. The original purpose of mortar was to fill in the spaces between irregular rock or cut stones, but it subsequently evolved into a productivity-

enhancing tool by providing a way to lay masonry units more rapidly and accurately with better stress distribution and alignment. Some of the early exotic mortar mixtures included egg whites, clay, urine, and ox blood. The initial breakthrough in the evolution of masonry mortars was the addition of lime to sand to produce a product that was both workable in the plastic state and durable once cured. Later, Portland cement was added to sand–lime mortars for greater plasticity, higher early strength, and increased bond strength. The result is the cement–lime masonry mortar in use today.

The primary purposes of mortar are to enhance the strength and the homogeneous character of the masonry, to facilitate the workability and laying of units, to improve resistance to moisture penetration, and to provide desired unit alignment. In unreinforced masonry, mortar plays an important structural role by bonding units together and providing flexural tensile resistance. Reinforced masonry, conversely, relies upon the reinforcement to resist tension stresses, thus neglecting any contribution from the mortar–unit bond strength. Although the design of reinforced masonry does not take into account the mortar bond strength, this property is still present in the final assembly and may have to be considered when determining the stiffness and deflection of a masonry member.

28.4.1.1 Mortar Materials

Masonry mortars are a simple mixture of cementitious materials, aggregate, water, and possibly one or more admixtures discreetly combined to achieve a complex set of physical mortar properties. The relative proportions of each of these constituent materials are selected to ensure that both the plastic and hardened mortar properties meet the desired goal. In the plastic state, mortar must have:

- Good workability to facilitate construction and the complete filling of all mortar head and bed joints
- Long board life and water retention to allow the mason sufficient time to spread the mortar before initial set occurs
- Sufficient stiffness to prevent the mortar from squeezing out from the bed joints as subsequent courses of units are laid

Conversely, the hardened mortar must have:

- Good bond strength to the masonry units to prevent the penetration of water or air and, in the case of unreinforced masonry, to provide a minimum level structural bond strength
- Sufficient compressive strength to resist the applied loads
- Long-term durability to meet the exposure conditions in which it will be used

Masonry mortar is specified to meet the requirements of ASTM C 270, *Specification for Mortar for Unit Masonry* (ASTM, 2005d) using either the proportion requirements or property requirements of that standard. When using the proportion requirements of ASTM C 270, the relative quantities of each constituent material are batched to meet the specified mortar type in accordance with Table 28.1. When specifying masonry mortar by property, the physical properties of a laboratory-prepared mortar must meet the properties summarized in Table 28.2. When neither method is specified, the proportion requirements govern.

Despite its long history and worldwide use, mortar remains today one of the less understood and most commonly misapplied construction materials. The largest confusion stems around the minimum compressive strength requirements for field- vs. laboratory-prepared mortars—specifically, the incorrect application of the minimum compressive strength requirements shown in Table 28.2 to mortar prepared in the field. Note 4 of ASTM C 270 includes an extensive discussion detailing the reasons why the mortar properties in Table 28.2 should not be applied to mortar prepared in the field:

The required properties of the mortar in Table [28.2] are for laboratory-prepared mortar mixed with a quantity of water to produce a flow of $110 \pm 5\%$. This quantity of water is not sufficient to produce a mortar with a workable consistency suitable for laying masonry units in the field. Mortar for use in the field must be mixed with the maximum amount of water, consistent with workability,

TABLE 28.1 Masonry Mortar Proportion Requirements

Proportions by Volume (Cementitious Materials)										
Mortar	Type	Portland Cement or Blended Cement	Mortar Cement			Masonry Cement			Hydrated Lime or Lime Putty	Aggregate Ratio (Measured in Damp, Loose Conditions)
			M	S	N	M	S	N		
Cement-lime	M	1	—	—	—	—	—	—	1/4	Over 1/4 to 1/2 Over 1/2 to 1-1/4 Over 1-1/4 to 2-1/2
	S	1	—	—	—	—	—	—		
	N	1	—	—	—	—	—	—		
	O	1	—	—	—	—	—	—		
Mortar cement	M	1	—	—	1	—	—	—	—	Not less than 2-1/4 and not more than 3 times the sum of the separate volumes of cementitious materials
	M	—	1	—	—	—	—	—	—	
	S	1/2	—	—	1	—	—	—	—	
	S	—	—	1	—	—	—	—	—	
	N	—	—	—	1	—	—	—	—	
	O	—	—	—	1	—	—	—	—	
Masonry cement	M	1	—	—	—	—	—	1	—	
	M	—	—	—	—	1	—	—	—	
	S	1/2	—	—	—	—	—	1	—	
	S	—	—	—	—	—	1	—	—	
	N	—	—	—	—	—	—	1	—	
	O	—	—	—	—	—	—	1	—	

TABLE 28.2 Property Requirements of Laboratory-Prepared Mortar

Mortar	Type	Average Compressive Strength at 28 Days (min.), psi (MPa)	Water Retention (min.) (%)	Air Content (max.) (%)	Aggregate Ratio (Measured in Damp, Loose Conditions)
Cement-lime	M	2500 (17.2)	75	12	Not less than 2-1/4 and not more than 3-1/2 the sum of the separate volumes of cementitious materials
	S	1800 (12.4)	75	12	
	N	750 (5.2)	75	14 ^a	
	O	350 (2.4)	75	14 ^a	
Mortar cement	M	2500 (17.2)	75	12	
	S	1800 (12.4)	75	12	
	N	750 (5.2)	75	14 ^a	
	O	350 (2.4)	75	14 ^a	
Masonry cement	M	2500 (17.2)	75	18	
	S	1800 (12.4)	75	18	
	N	750 (5.2)	75	20 ^b	
	O	350 (2.4)	75	20 ^b	

^a When structural reinforcement is incorporated in cement-lime or mortar cement mortar, the maximum air content shall be 12%.

^b When structural reinforcement is incorporated in masonry cement mortar, the maximum air content shall be 18%.

in order to provide sufficient water to satisfy the initial rate of absorption (suction) of the masonry units. The properties of laboratory-prepared mortar at a flow of 110 ± 5 , as required by this specification, are intended to approximate the flow and properties of field-prepared mortar after it has been placed in use and the suction of the masonry units has been satisfied. The properties of field-prepared mortar mixed with the greater quantity of water, prior to being placed in contact with the masonry units, will differ from the property requirements in Table [28.2]. Therefore, the property requirements in Table [28.2] cannot be used as requirements for quality control of field-prepared mortar. Test Method C 780 may be used for this purpose.

The question naturally arises that, if the property requirements (including compressive strength) of ASTM C 270 are not to be used to verify compliance with a field-prepared mortar, which properties should be used when, for example, mortar compression cube samples are obtained in the field? While it may defy initial logic, ASTM does not stipulate minimum requirements for the physical properties of field-prepared mortars. In effect, the net resulting compressive strength of a masonry mortar properly batched using quality materials inherently complies with the necessary physical properties.

As stated within ASTM C 270, the default method of complying with the requirements of a given project's specification is through proportioning the constituent mortar materials consistent with the requirements of ASTM C 270 as shown in Table 28.1. When the individual constituent materials (cement, lime, and sand) comply with their respective standards and are batched together in accordance with the proportioning requirements of C 270, the resulting mortar will exhibit the necessary properties for satisfactory, long-term performance. Alternatively, when one of the constituent materials does not comply with the respective standardized requirements (for example, the gradation of a masonry sand, as the properties of sand can have considerable impact on the workability as well as the strength of a mortar) or when a nonstandard material is added to the mortar (such as an admixture used to enhance one or more properties of the mortar), the resulting physical properties of the mortar must be documented. When nonstandardized materials are used within a mortar, each of the constituent materials is batched together in a laboratory in accordance with ASTM C 270. The physical properties of this mortar are then compared to the minimum requirements stipulated by ASTM C 270 as shown in Table 28.2.

If it is desirable to monitor the physical properties of the mortar in the field, then a second batch of mortar is mixed using the same materials, means, and methods to be employed in the field. The evaluated properties of the field mortar are in turn compared to the laboratory mortar. The properties of these two sets of mortar are not expected to be consistent, as discussed in Note 4 of ASTM C 270, above, but this procedure does allow for a direct comparison between the two sets of mortar for future reference. By establishing a correlation between the field and laboratory mortars, samples (often compression cubes) can be obtained during construction and the properties of the sampled mortar compared back to the field mortar prepared in the laboratory. This concept is reviewed in more detail in Section 28.6.

In addition to the base materials of cement, sand, and water, admixtures are also used in masonry mortars to enhance one or more of the characteristics of the material. In accordance with ASTM C 270, admixtures should not be used without the explicit specification and consent of the designer, as some admixtures are not appropriate in some applications or compatible with other admixtures or materials. Admixtures that are commonly used in masonry mortars include coloring pigments, bond strength enhancers, workability enhancers, set retarders or accelerators, water-repellent agents, or any number of other admixtures targeted at altering either the plastic or hardened property of the mortar. Although not required by ASTM C 270, when admixtures are used in masonry mortars it is good practice to ensure that their intended application complies with the requirements of ASTM C 1384, *Standard Specification for Admixtures for Masonry Mortars* (ASTM, 2006a). ASTM C 1384 outlines specific requirements that the physical properties of modified mortar must meet for use in general masonry construction.

Unlike conventional masonry construction, autoclaved aerated concrete (AAC) masonry uses a specially manufactured thin-bed mortar for construction of AAC masonry assemblies. This proprietary mortar is specifically manufactured for use in AAC masonry construction. Because it is preblended, on-site proportioning of thin-bed AAC masonry mortar does not apply. Likewise, testing of thin-bed AAC masonry mortar typically employs third-party manufacturing verification as opposed to jobsite quality control.

28.4.1.2 Selecting a Mortar Type

Masonry mortars are classified by cement—Portland cement, masonry cement, or mortar cement—and further designated by type: Type M, S, N, or O mortar. With one exception, the choice of mortar type is left to the discretion of the designer or specifier. In accordance with the requirements of the MSJC

Code, the single exception applies to the design of elements that are part of the seismic-force-resisting system in Seismic Design Categories D, E, and F, when the mortar must be a Type M or S mortar cement or Portland cement mortar. Because of the vast number of mortar combinations available, the appropriate pairing of a mortar type to a specific application may not always be obvious. As a general rule of thumb, Type N mortars are appropriate in the majority of applications. Exceptions to this guide include high-strength masonry, masonry exposed to severe weathering environments, or where building codes specifically prohibit the use of Type N mortar. In such cases, a Type S or possibly Type M mortar may be warranted or required. The key concept to remember when specifying a mortar type is that overspecifying will likely result in reduced performance and aesthetics; that is, a mortar with an unnecessarily high compressive strength (as indicated by the relative proportion of cement content) in general will not perform as well as its lower strength counterpart. This is due, in part, to the plastic properties of the higher cement content mortar, which tends to be less workable than the same mortar with less cement. This reduction in workability can potentially lead to more voids in the mortar joint, which in turn allows more water to penetrate the assembly; likewise, higher cement content mortars tend to shrink more as they cure. When excessive shrinkage persists, cracking can develop in the mortar joints. In extreme cases, the shrinking mortar may also cause the masonry units to crack as well. Whereas cracking of this nature is typically more aesthetic than structural, it could potentially degrade the strength of a masonry system by allowing water to penetrate the assembly and corrode reinforcement, if present.

In addition to the mortar type designations, three basic cements are used in mortar, each with inherent advantages and limitations:

- *Portland cement–lime mortar* is generally characterized as the mortar with the highest compressive strength, bond strength, and durability but the lowest workability.
- *Masonry cement mortar* has excellent workability but relatively lower compressive strength and bond strength compared to Portland cement–lime mortars.
- *Mortar cement mortar* exhibits good workability analogous to masonry cement mortars, but it is distinguished by retaining the hardened physical properties similar to Portland cement–lime mortars.

Regional practices and preferences, in combination with the local availability of specific masonry cement mortar types, may drive to a large extent the use of each cement type on specific projects. Local suppliers should be consulted when a specific cement type is desired. As reviewed earlier, both the plastic and hardened properties of a masonry mortar must be taken into consideration when specifying a mortar for a particular project. The appendix to ASTM C 270 contains a comprehensive discussion on the selection and use of various masonry mortars for specific applications. Table 28.3 provides a summary list of recommended mortar types for a wide variety of common masonry applications.

28.4.2 Grout

Masonry grout serves several basic functions in masonry construction: (1) it bonds the wythes of multi-wythe construction together into a composite element, (2) it bonds the reinforcement to the masonry so the two materials will act as a homogeneous material in resisting loads, and (3) it increases the masonry volume for bearing, sound abatement, and fire resistance. Despite the widespread belief that masonry grout is concrete, it is not. Grout is produced using the same basic materials as concrete but with a few key differences. Compared to concrete, masonry grout is much more fluid so the grout can flow into and fill all intended cells, cores, and voids within the masonry assembly without segregation. Grout is also intentionally produced with a higher water-to-cement ratio than concrete. The excess water is absorbed by the masonry units as the plastic grout is placed in the masonry assembly. Further, to facilitate its consolidation and minimize the potential for voids to form within the grout, the aggregate size or gradation used in grout production is smaller than that commonly used for concrete. Likewise, grout is not mortar. While both are cementitious materials, grout and mortar exhibit very different physical properties and attributes necessary for their intended application.

TABLE 28.3 Guide for the Selection of Masonry Mortars^a

Location or Application	Building Component	Mortar Type	
		Recommended	Alternative
Exterior, above grade	Loadbearing wall	N	S or M
	Nonloadbearing wall	O ^b	N or S
	Parapet wall	N	S
Exterior, at or below grade	Foundation wall, retaining wall, manholes, sewers, pavements, walks, and patios	S ^c	M or N ^c
Interior	Loadbearing wall	N	S or M
	Nonloadbearing partitions	O	N

^a This table does not provide for many specialized mortar uses, such as chimney, reinforced masonry, restoration, and acid-resistance mortars.

^b Type O mortar is recommended for use where the masonry is unlikely to be frozen when saturated or is unlikely to be subjected to high winds or other significant lateral loads. Type N or S mortar should be used in other cases.

^c Masonry exposed to weather in a normally horizontal surface is extremely vulnerable to weathering. Mortar for such masonry should be selected with due caution.

28.4.2.1 Grout Materials

In accordance with ASTM C 476, *Standard Specification for Grout for Masonry* (ASTM, 2002), the two types of masonry grout are:

- *Fine grout* is characterized by the use of a very fine-grained aggregate similar to that used for masonry mortar.
- *Coarse grout* uses a coarser aggregate with a maximum particle size of just under 0.5 in. (12.7 mm); it is often referred to as *pea gravel*.

The vast majority of grout used today is coarse grout, due in part to its common availability as well as its slightly reduced cost relative to fine grouts. Fine grout is primarily used in clay masonry construction (when grouted) or when cell size or other congestion requires the use of a smaller aggregate to ensure adequate placement and consolidation of the grout.

As with masonry mortar, masonry grout is specified by either proportion or property. When the proportion requirements of ASTM C 476 are used, the individual constituent materials are batched together in accordance with Table 28.4. Although permitted by ASTM C 476, lime is rarely used in masonry grout. Alternatively, any proportion of materials can be used when a minimum grout compressive strength is specified. In accordance with ASTM C 476, the minimum compressive strength of such grouts is 2000 psi (14 MPa) when tested in accordance with ASTM C 1019 (ASTM, 2005f) at a slump of 8 to 11 in. (200 to 280 mm). For ease, as well as having the ability to establish and verify minimum grout compressive strengths in the field, masonry grouts are typically specified by compressive strength instead of proportion.

In addition to conventional masonry grout, self-consolidating grout (SCG) is beginning to see more application throughout the country. One of the primary advantages of SCG is that it is not necessary to mechanically consolidate and reconsolidate after initial water loss, which can translate to significant labor savings. SCG, however, is still in its infancy, and standardized testing, evaluation, and quality control measures are still under development. It is anticipated that the 2008 edition of the MSJC Specification will likely include SCG as an alternative to conventional masonry grout. To ensure that a quality SCG is being used, the following minimum criteria for SCG should be met:

- The visual stability index (VSI), as defined in ASTM C 1611 (ASTM, 2005g), should be less than or equal to 1.
- The slump flow, as determined in accordance with ASTM C 1611, should be 24 to 30 in. (610 to 762 mm).
- Unlike conventional masonry grout, SCG should not be mixed in the field due in part to the difficulty in ensuring consistent and uniform quality.

TABLE 28.4 Masonry Grout Proportion Requirements

Type	Parts by Volume of Portland Cement or Blended Cement	Parts by Volume of Hydrated Lime or Lime Putty	Aggregate (Measured in a Damp, Loose Condition)	
			Fine	Coarse
Fine	1	0–0.1	2.25–3 times the sum of the volumes of the cementitious materials	—
Coarse	1	0–0.1	2.25–3 times the sum of the volumes of the cementitious materials	1–2 times the sum of the volumes of the cementitious materials

- The masonry should be allowed to cure to at least 4 hours prior to placing SCG to minimize blowout potential.
- The minimum compressive strength of SCG should be 2000 psi (13.79 MPa) when tested in accordance with ASTM C 1019.

28.4.3 Concrete Masonry Units

Concrete masonry units come in a nearly infinite array of shapes, sizes, densities, colors, and textures to meet the demands of ever-expanding applications. Due to the wide variation in available products, local availability should be verified prior to specifying a specific product. The most commonly specified and used concrete masonry unit is a hollow, loadbearing concrete masonry unit complying with the requirements of ASTM C 90 (ASTM, 2006c). The types of concrete masonry units permitted by the MSJC Specification include:

- ASTM C 55, *Concrete Brick*
- ASTM C 73, *Calcium Silicate (Sand-Lime) Brick*
- ASTM C 90, *Loadbearing Concrete Masonry Units*
- ASTM C 129, *Nonloadbearing Concrete Masonry Units*
- ASTM C 744, *Prefaced Concrete and Calcium Silicate Units*
- ASTM C 1386, *Autoclaved Aerated Concrete Masonry Units*

Several common concrete masonry unit shapes and sizes are illustrated in Figure 28.1. A comprehensive review of the available options and physical properties of concrete masonry units (see Table 28.5) is provided in *ASTM Specifications for Concrete Masonry Units* (NCMA, 2006a), *Typical Sizes and Shapes of Concrete Masonry Units* (NCMA, 2002b), *Architectural Concrete Masonry Units* (NCMA, 2001a), and the *Concrete Masonry Shapes and Sizes Manual* (NCMA, 2000a).

28.4.4 Clay Masonry Units

The majority of clay masonry units manufactured today are used in nonstructural veneer assemblies; however, many loadbearing, hollow clay tile and brick units options are also available. Hollow brick offers the same advantages as hollow concrete masonry units by allowing the assemblies to be reinforced and grouted. Specialty clay masonry units can also be manufactured, but local availability should be verified prior to specifying. The types of clay masonry units permitted by the MSJC Specification include:

- ASTM C 34, *Structural Clay Loadbearing Wall Tile*
- ASTM C 56, *Structural Clay Nonloadbearing Wall Tile*
- ASTM C 62, *Solid Clay or Shale Building Brick*
- ASTM C 126, *Ceramic Glazed Structural Clay Facing Tile and Brick*
- ASTM C 212, *Structural Clay Facing Tile*
- ASTM C 216, *Solid Clay or Shale Facing Brick*

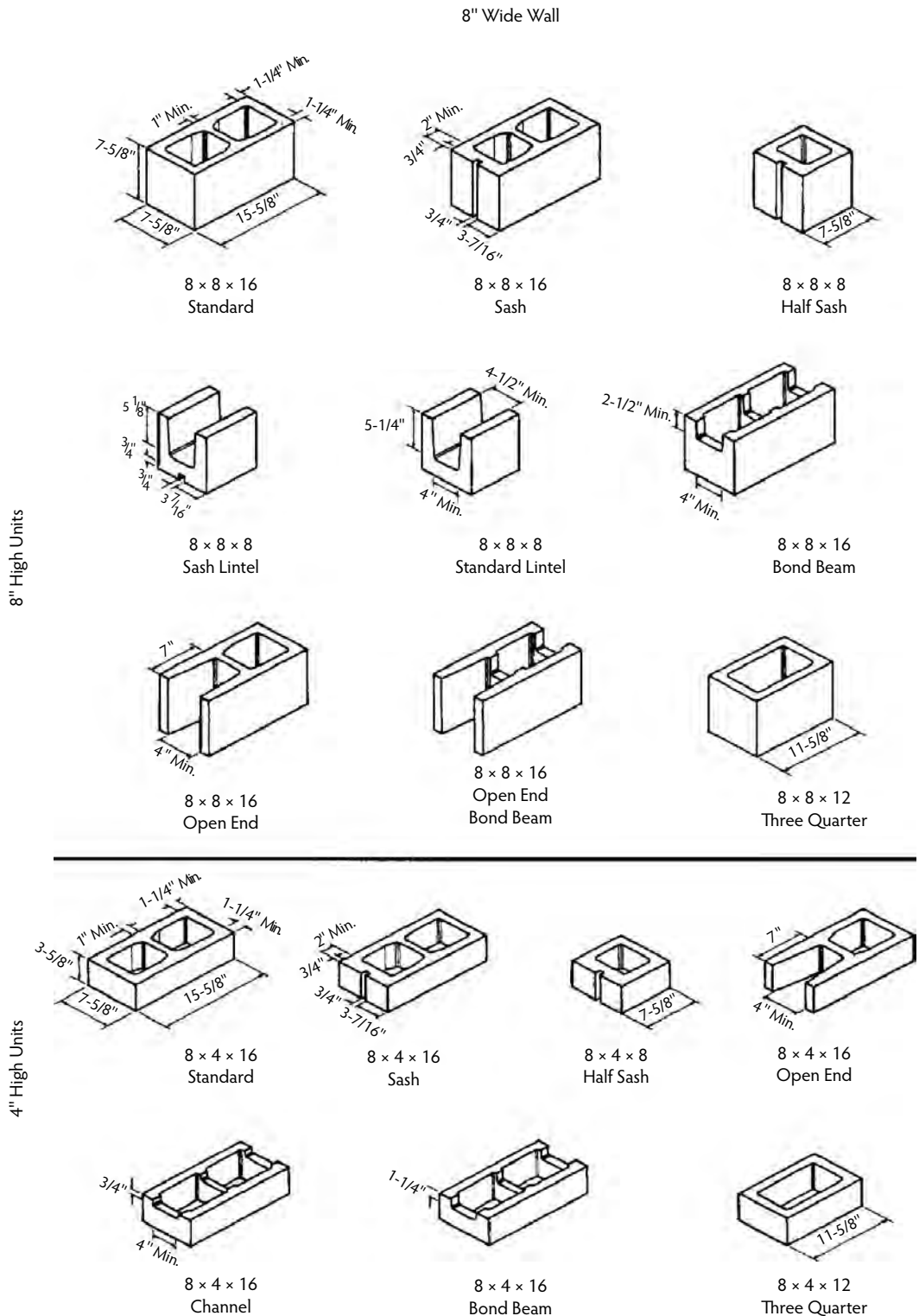


FIGURE 28.1 Shapes and sizes of concrete masonry units.

TABLE 28.5 Concrete Masonry Unit Physical Properties

Unit Type	Minimum Average Compressive Strength, lb/in. ² (MPa)	Maximum Linear Drying Shrinkage (%)	Maximum Water Absorption, lb/ft ³ (kg/m ³)		
			Weight Classification		
			Lightweight, Less than 105 lb/ft ³ (1680 kg/m ³)	Medium Weight, Less than 105 to 125 lb/ft ³ (1680 to 2000 kg/m ³)	Normal Weight, 125 lb/ft ³ (2000 kg/m ³) or More
C 55					
Grade N ^a	3500 (24.1) ^c	0.065	15 (240)	13 (208)	10 (160)
Grade S ^b	2500 (17.3) ^c	0.065	18 (288)	15 (240)	13 (208)
C 73					
Grade SW ^d	5500 (37.9) ^c	—		15 (240)	
Grade MW ^e	3500 (34.1) ^c	—		18 (288)	
C 90	1900 (13.1)	0.065	18(288)	15 (240)	13 (240)
C 129	600 (4.1)	0.065	—	—	—
C 744	— ^f	— ^f	— ^f	— ^f	— ^f
C 1386					
Class 2	360 (2.5)	0.02	— ^g	— ^g	— ^g
Class 4	725 (5.0)	0.02			
Class 6	1090 (7.5)	0.02			

^a For use where high strength and resistance to moisture penetration and severe frost action are desired.

^b For general use where moderate strength and resistance to frost action and moisture penetration are required.

^c The compressive strength of C 55 concrete brick and C 73 calcium silicate brick are based on the gross cross-sectional area of the unit.

^d Brick intended for use where exposed to temperatures below freezing in the presence of moisture.

^e Brick intended for use where exposed to temperature below freezing but unlikely to be saturated with water.

^f The concrete masonry units on which the prefaced surface is molded are required to meet the minimum physical properties of C 55, C 73, C 90, or C 129 as specified.

^g Aerated autoclaved concrete masonry units do not limit the maximum water absorption or designate density classes; instead, each unit strength class contains an array of nominal densities ranging from 25 to 50 lb/ft³ (400 to 800 kg/m³).

- ASTM C 652, *Hollow Clay or Shale Brick*
- ASTM C 1088, *Thin Clay or Shale Veneer Brick*
- ANSI A 137.1, *Ceramic Tile*

Several common clay masonry unit shapes and sizes are shown in Figure 28.2.

28.4.5 Reinforcement

To increase the structural resistance to applied loads or to decrease the potential for shrinkage cracks, reinforcement is added to masonry assemblies. Although not immediately apparent, the terms *reinforced* and *unreinforced masonry* refer to the method used to design the masonry structure as opposed to the presence of reinforcing steel; hence, it is possible to have a masonry assembly that contains reinforcement but is designed as unreinforced masonry. In such cases, the masonry is assumed to carry all the applied loads. Conversely, it is not possible to design a masonry structure as reinforced without the inclusion of reinforcement. The majority of reinforcement used in masonry construction falls into one of three categories: (1) conventional mild reinforcement placed in the cells of hollow unit masonry and then grouted, (2) cold-drawn wire reinforcement placed within the horizontal mortar bed joints at the time the units are laid, or (3) prestressing rods or tendons placed within the cells of hollow units, which may then be grouted or ungrouted. A typical reinforced masonry cross-section is shown in Figure 28.3. For design, the MSJC Code limits the specified yield strength of mild reinforcement at 60,000 psi (414 MPa). Material limits for bed joint reinforcement and prestressing reinforcement is limited only by their respective material standards. A comprehensive review of reinforcement options for masonry construction is provided in *Joint Reinforcement for Concrete Masonry* (NCMA, 2005c) and *Steel Reinforcement for Concrete Masonry* (NCMA, 2006b).

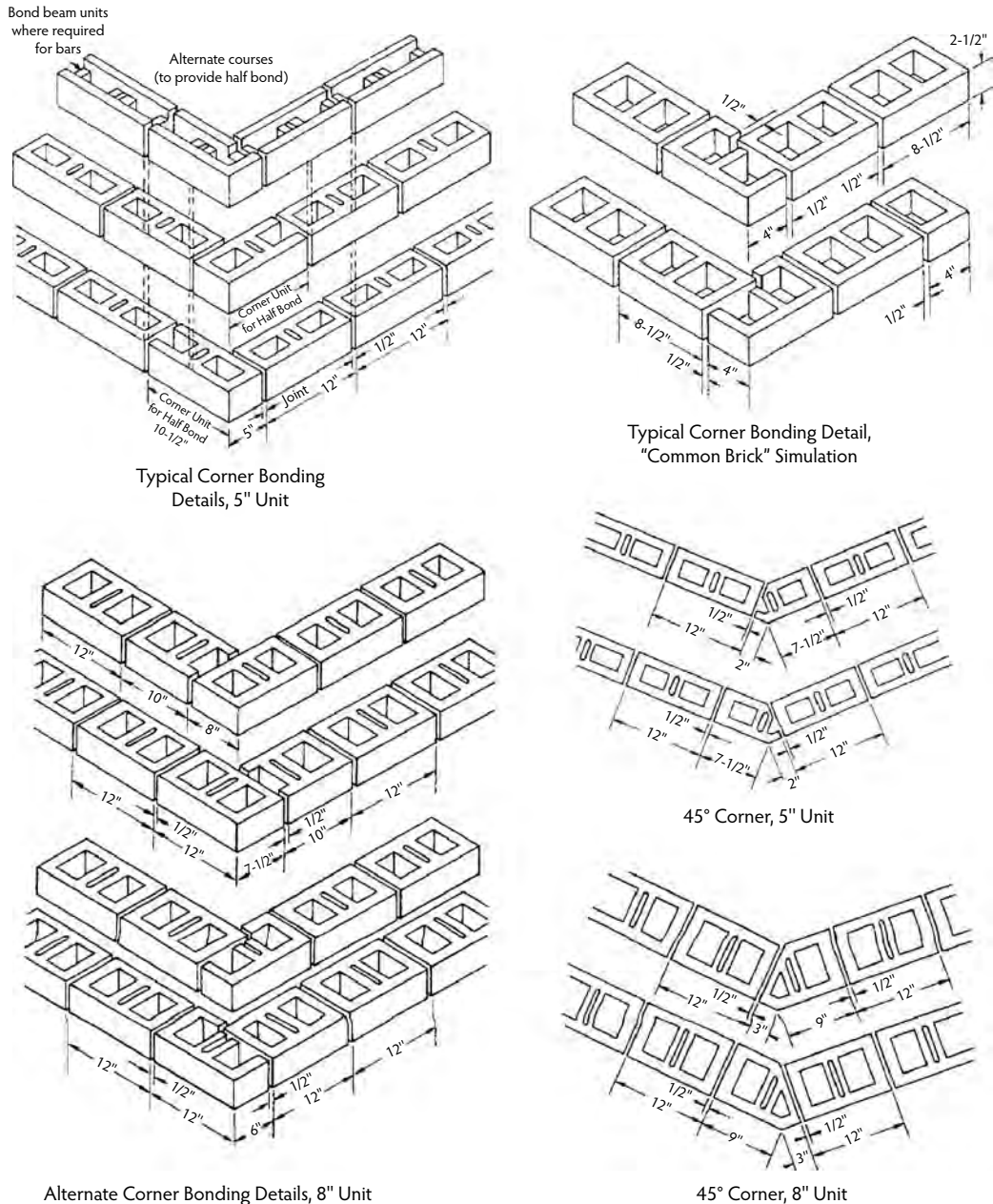


FIGURE 28.2 Shapes and sizes of clay masonry units.

28.4.6 Admixtures

Admixtures are available for use in masonry units, mortar, and grout to enhance one or more of the properties or characteristics of the material. In general, admixtures should not be used without the explicit specification and consent of the designer, as some admixtures are not appropriate in some applications or compatible with other admixtures or materials. The most commonly used admixtures are integral water repellents used in the manufacturing of concrete masonry units to increase their resistance to water penetration or to reduce the potential for the formation of efflorescence on the surface of the units. Admixtures are also commonly used in masonry mortars to increase bond strength, enhance workability,

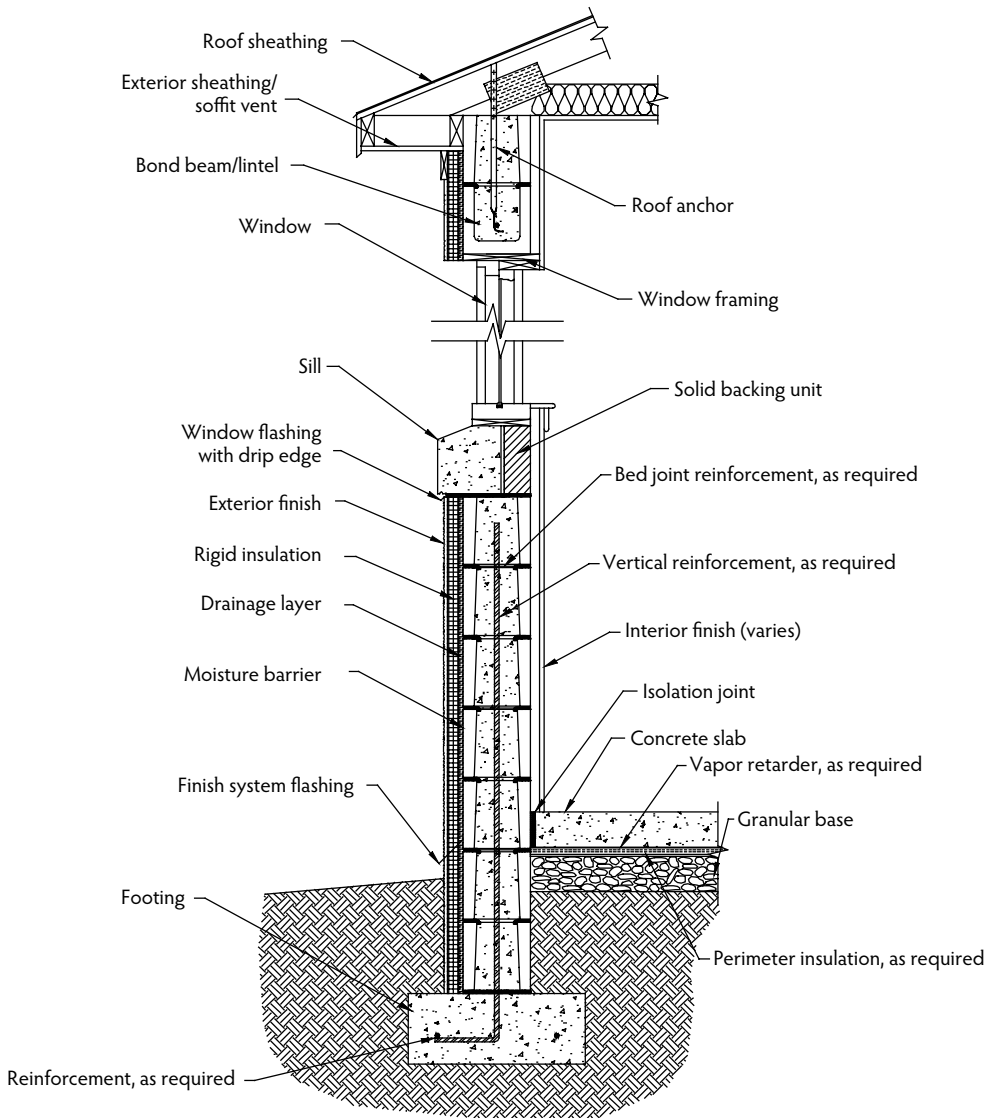


FIGURE 28.3 Reinforced masonry construction. (Courtesy of the National Concrete Masonry Association, Herndon, VA.)

retard or accelerate set times, or alter any number of other plastic or hardened mortar property. When admixtures are used in masonry mortars, they should comply with the requirements of ASTM C 1384, *Standard Specification for Admixtures for Masonry Mortars* (ASTM, 2006a). Although ASTM C 270 (ASTM, 2005d) does not currently require compliance with ASTM C 1384, separately specifying compliance to this standard helps to ensure that the admixtures used in the masonry mortar are not detrimental to the overall performance of the material or system.

28.5 Construction

The limitless combinations of masonry unit shapes, sizes, and physical properties; mortar types and mortar joint profiles; grout placement options; reinforcement details and schedules; and structural configurations permit boundless versatility in masonry construction, but this design flexibility can also

result in confusion during implementation, particularly among design personnel not familiar with the details of masonry construction. Although some construction practices are mandated by the MSJC Specification, many are simply standards of care that have developed over the long history of masonry construction. Where not covered by national codes or standards, regional differences in construction practices and preferences do surface and should be accounted for during the initial design phase.

28.5.1 Modular Layout

Masonry structures can be constructed using virtually any layout dimension. For maximum construction efficiency and economy, however, masonry elements should be designed and constructed using a modular layout of the structure and its openings. Modular coordination is the practice of laying out and dimensioning structures and elements to standard lengths and heights to accommodate modular-sized building materials. On occasion, modular coordination issues are not considered during the design phase. As a result, jobsite decisions must be made—often in haste and at a cost. When a project does require a non-modular layout, further design and construction considerations must be addressed, including:

- *Placement of vertical reinforcement*—In construction containing vertical reinforcing steel, the laying of units in other than running (half) bond or stack bond interrupts the vertical alignment of individual confined cells. As a result, the placement of reinforcement and adequate consolidation of grout becomes difficult, if not impossible.
- *Interruption of bond pattern*—In addition to the aesthetic impact that a change in the bond pattern can create, building codes often contain different design assumptions for masonry constructed in running bond vs. other bond patterns. Walls incorporating more than a single bond pattern may present a unique design situation.
- *Locating control joints*—In running bond construction, the incorporation of control joints can be accomplished using only full- and half-size units. Similarly, stack bond construction only requires full-size units when control joints are properly spaced and detailed. With other bond patterns, however, the cutting of units may become necessary if specially dimensioned units are not used or are not available.

Standard concrete masonry modules are typically 8 in. (203 mm) vertically and horizontally, but may also include 4-in. (102-mm) modules for some applications. These modules provide overall design flexibility and coordination with other building products such as windows, doors, and other similar elements. The impact of non-modular openings is illustrated in Figure 28.4.

In addition to wall elevations, sections, and openings, the overall plan dimensions of a structure must also be considered, especially when using units having nominal widths other than 8 in. (203 mm). Consider, for example, a square building with outside nominal dimensions of 360 in. (30 feet) (9144 mm), which is evenly divisible by 8 and therefore modular. Using 8-in. (203-mm) units and a running bond pattern, the walls can be constructed without cutting the units. If units 12-in. (305-mm) wide were used instead of the 8-in. (203-mm) units, however, at least one block must be cut shorter to accommodate the increased thickness of the end unit oriented perpendicular to the length of the wall, as shown in Figure 28.5. To minimize the need for cutting units, building plan dimensions should be evenly divisible by 8 in. (203 mm) plus the nominal thickness of the units used in construction. As an alternative to cutting, specially configured corner units may be available in some regions for turning corners.

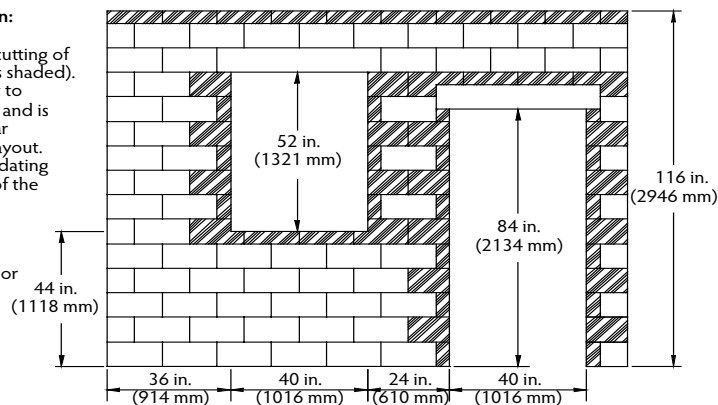
28.5.1.1 Masonry Bond Patterns

The term *bond* can generally refer to two different topics within masonry design and construction; the adhesive or mechanical interlock between mortar and units or the arrangement of units to achieve a desired pattern. This section addresses the latter. Figure 28.6 illustrates a few of the many different masonry bond pattern options available. Masonry bond patterns can be created by varying the unit heights or lengths, varying the length the units overlap from one course to the next, varying the orientation of the units, or by using units of different configurations in the same wall. Implementing one or

Not recommended construction:

Utilizing nonmodular layouts or openings results in unnecessary cutting of the masonry units (shown here as shaded). The end product is more difficult to construct, produces more waste, and is more costly compared to a similar structure employing a modular layout. Additionally, placing and consolidating grout in the reduced-size cores of the saw-cut units may prove difficult.

 = Nonstandard or field-cut units



In this example, it is obvious the aesthetic impact that nonmodular layouts have on the final appearance of a structure. Not so obvious is the additional cost of construction. To further illustrate this concept, consider the following comparison of the modular and nonmodular layouts shown here:

Total area of nonmodular layout = 122.4 ft² (11.38 m²)

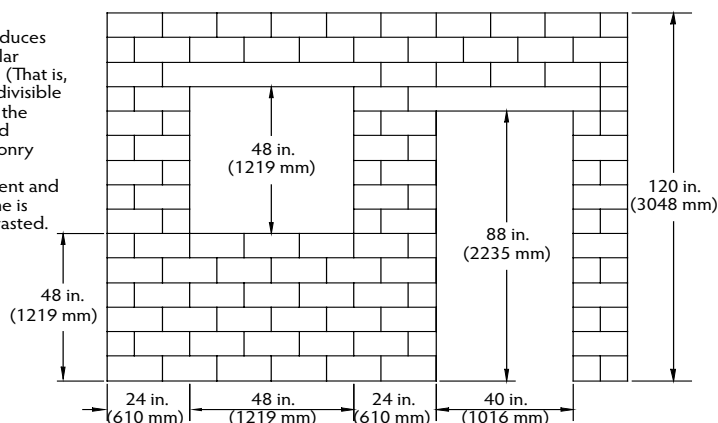
Total area of modular layout = 126.7 ft² (11.77 m²)

Number of units used in nonmodular layout = 112

Number of units used in modular layout = 106

Recommended construction:

The wall elevation shown here reduces cutting of units by utilizing modular openings and opening locations. (That is, each dimension shown is evenly divisible by 8 inches [203 mm].) Through the coordination of opening sizes and locations, the cells of hollow masonry units align (which facilitates the placement of vertical reinforcement and consolidation of grout), labor time is reduced, and materials are not wasted.



Ç

FIGURE 28.4 Modular masonry layout. (Courtesy of the National Concrete Masonry Association, Herndon, VA.)

more of these alternatives can subtly or dramatically alter the appearance of a finished masonry assembly. The aesthetic impact created by a specific bond pattern can be even more dramatic when combined with units of varying color, texture, or material.

The evolution of various masonry bond patterns has continued for centuries. As such, regional differences in terminology or construction practices have developed. The designer should be cautioned against specifying unique or complex bond patterns without thoroughly communicating the intent to the mason contractor. When specifying a unique bond pattern, elevation drawings for a particular project should clearly illustrate the intended final appearance of the structure. Also, when specifying a bond pattern that incorporates unique or nonstandard unit sizes, the availability of such units should first be verified with local manufacturers.

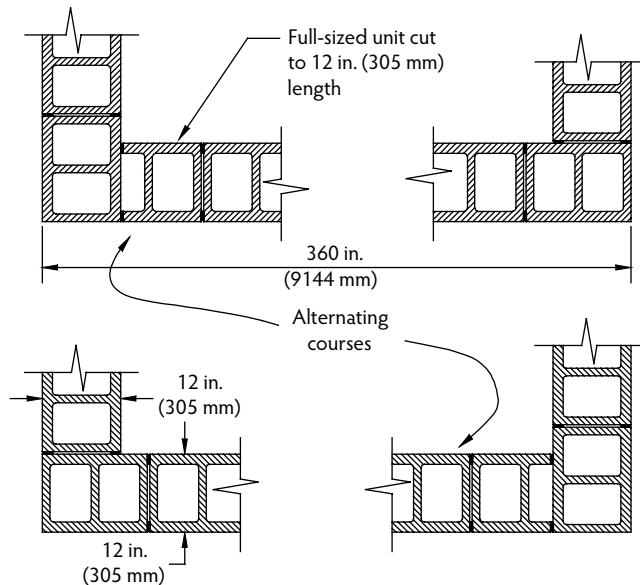


FIGURE 28.5 Nonmodular layout of masonry corners. (Courtesy of the National Concrete Masonry Association, Herndon, VA.)

The most common bond pattern in masonry construction is running bond, typically where vertical head joints of successive courses are offset by one-half the unit length. Building code design provisions (ACI Committee 530, 2005) are based primarily on structural research of wall panels laid in running bond construction. As such, the MSJC Specification (ACI Committee 530.1, 2005) requires the use of running bond unless otherwise specified. When a different bond pattern is used, the designer should consider its impact on the performance and structural capacity of the masonry element.

28.5.1.2 Metric Coordination

One additional consideration for some projects is the incorporation of standard-sized (inch-pound) units in a metric project. Similar to inch-pound units, masonry units produced to metric dimensions are 10 mm (0.39 in.) less than the nominal dimensions to accommodate the thickness of the mortar joints. Thus, the nominal metric equivalent of an $8 \times 8 \times 16$ -in. unit is $200 \times 200 \times 400$ mm ($190 \times 190 \times 390$ mm specified dimensions for a 10-mm mortar joint thickness). Because inch-pound dimensioned concrete masonry units are approximately 2% larger than hard metric units, complications can arise if they are incorporated into a structure designed according to the 100-mm (3.9-in.) metric module or *vice versa*. Additional recommendations are provided in *Metric Design Guidelines for Concrete Masonry Construction* (NCMA, 2000b) for the incorporation of soft metric units (standard inch-pound units) into a hard metric design project.

28.5.2 Mortar

Although mortar comprises only approximately 7% of the wall surface in typical concrete masonry construction, it can have a significant impact on the aesthetics and performance of the constructed masonry assembly. Head and bed joints are typically $3/8$ in. (9.5 mm) thick, except for the initial bed joint at foundations, which can range from $1/4$ to $3/4$ in. (6.4 to 19 mm) to accommodate surface irregularities in the foundation. Mortar should extend fully across the thickness of the face shells of hollow units so both head and bed joints will be completely filled. Solid units are required to be fully bedded in mortar. To perform properly, all voids in mortar joints (except weep holes) should be filled with mortar. Although it is important to provide sufficient mortar to properly bed masonry units, mortar should not extend excessively into drainage cavities or into cores to be grouted. For grouted masonry,

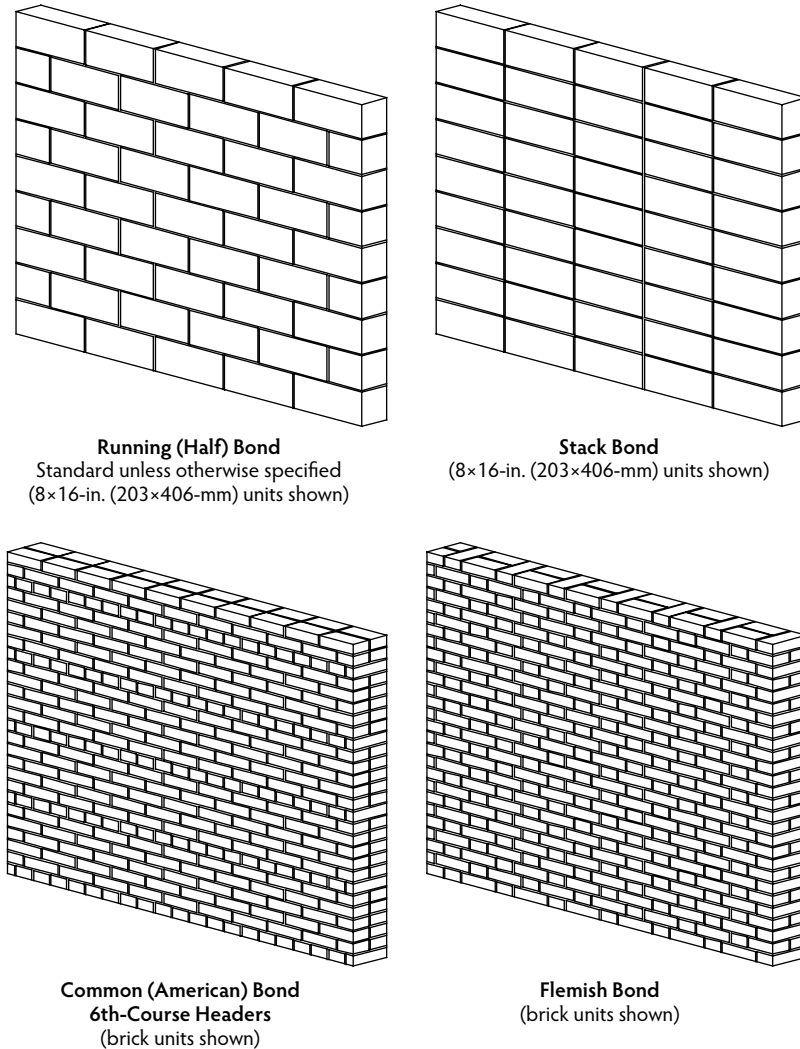
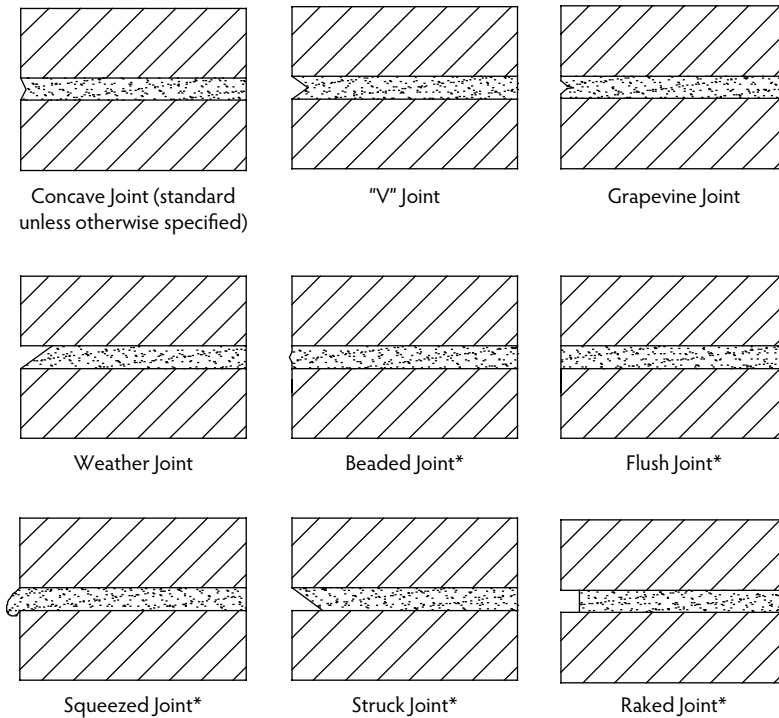


FIGURE 28.6 Masonry bond patterns. (Courtesy of the National Concrete Masonry Association, Herndon, VA.)

mortar protruding more than 1/2 in. (13 mm) into the cells or cavities to be grouted is not permitted (ACI Committee 530.1, 2005). Mortar joints should be tooled when thumbprint hard. For walls exposed to weather, concave or V-shaped joints improve water penetration resistance by directing water away from the wall surface and by compacting the mortar against the masonry unit to seal the joint. Tooling mortar joints also helps to seal the outer surface of the joint. Raked, flush, struck, beaded, or extruded joints are not recommended for exterior construction as they generally do not provide as tight a seal and may create ledges that can hold water near the wall face. For walls not exposed to weather, the selection of the joint profile can be based on aesthetics rather than functionality. Several different mortar joint profiles are illustrated in Figure 28.7.

28.5.3 Grout Placement

The versatility of grout allows it to be either mixed in the field or transported to the jobsite in a ready-mixed condition. Once mixed, grout is placed by hand or, on larger projects, is placed by pump or other mechanical delivery method. Over time, an empirical set of guidelines has been established for the



*Potentially poor weathering joints, not recommended for exterior construction.

FIGURE 28.7 Mortar joint profiles. (Courtesy of the National Concrete Masonry Association, Herndon, VA.)

successful placement and consolidation of masonry grout based on the size of opening to be grouted and the type of grout used. These practices for the placement of grout have been standardized by the MSJC Specification as detailed in Table 28.6.

At the time of placement, grout is required to have a slump of 8 to 11 in. (203 to 279 mm) for grout lifts up to 5 ft (1.52 m). For grout lifts between 5 and 12.67 ft (1.52 and 3.86 m), the grout slump is limited to 10 to 11 in. (254 to 279 mm). The high water content of masonry grout is necessary to ensure that the cells and cavities intended to be grouted are completely filled and void free while maintaining a sufficient amount of water in the plastic grout mix for hydration of the cement following the absorption of the free water of the grout by the masonry units. AAC masonry assemblies, however, unlike clay and concrete masonry assemblies, are required to be thoroughly wetted prior to placement of the grout due to the relatively high absorptive nature of AAC masonry units. Because of the relatively high water content of masonry grout, care is required when handling, placing, and consolidating grout, as too much water or excessive consolidation can result in segregation and voids in the final product.

In addition to the grout pour height limits of Table 28.6, grout must be placed in lifts not exceeding 5 ft (1.52 m), regardless of the total grout pour height. The MSJC Specification offers an exception to this requirement in that it allows grout lifts up to 12.67 ft (3.86 m) when the following conditions are met:

- The masonry has cured for at least 4 hours.
- The grout slump is maintained between 10 and 11 in. (254 and 279 mm).
- No intermediate reinforced bond beams are placed between the top and bottom of the pour height.

If any of these conditions is not met, the maximum grout lift height defaults to 5 ft (1.52 m).

After each grout lift is placed, the grout is consolidated by mechanical vibration and then reconsolidated a short time later after the excess water in the grout is absorbed by the masonry units. Consolidation of

TABLE 28.6 Grout Placement Requirements

Grout Type	Maximum Grout Pour Height, ft (m)	Minimum Width of Grout Space, ^{a,b} in. (mm)	Minimum Grout Space Dimensions for Grouting Cells of Hollow Units, ^{b-d} in. × in. (mm × mm)
Fine	1 (0.30)	0.75 (19)	1.5 × 2 (38 × 51)
Fine	5 (1.52)	2 (51)	2 × 3 (51 × 76)
Fine	12 (3.66)	2.5 (64)	2.5 × 3 (64 × 76)
Fine	24 (7.32)	3 (76)	3 × 3 (76 × 76)
Coarse	1 (0.30)	1.5 (38)	1.5 × 3 (38 × 76)
Coarse	5 (1.52)	2 (51)	2.5 × 3 (64 × 76)
Coarse	12 (3.66)	2.5 (64)	3 × 3 (76 × 76)
Coarse	24 (7.32)	3 (76)	3 × 4 (76 × 102)

^a For grouting between masonry wythes.

^b Grout space dimension is the clear dimension between any masonry protrusion and shall be increased by the diameters of the horizontal bars within the cross-section of the grout space.

^c Area of vertical reinforcement shall not exceed 6% of the area of the grout space.

^d Minimum grout space dimension for AAC masonry units shall be 3 × 3 in. (76 × 76 mm) or a 3-in. (76-mm)-diameter cell.

the grout by puddling using either the vertical reinforcing bars or by other means is permitted only when the total grout pour height is 12 in. (305 mm) or less (ACI Committee 530.1, 2005). When the grout pour height exceeds 5 ft (1.52 m), cleanouts are required at the base of the cells or cavities to be grouted to remove mortar droppings and other debris as shown in Figure 28.8. For solid grouted masonry construction, the



FIGURE 28.8 Cleanouts. (Courtesy of the National Concrete Masonry Association, Herndon, VA.)

maximum spacing between cleanouts is 32 in. (813 mm). Cleanouts are required to be of sufficient size to permit the removal of mortar droppings but not less than 3 in. (76 mm) in any dimension. To preclude the need for constructing and subsequently sealing cleanouts, some masons opt to employ low-lift grouting techniques whereby no more than 5 ft (1.52 m) of masonry is constructed at one time before the grout is placed. When the grout has been placed, construction of the masonry assembly and placement of the grout continues in increments not exceeding 5 ft (1.52 m) until the full assembly height is achieved. Alternatively, the entire height of the masonry assembly permitted by Table 28.6 is constructed in a single stage prior to grout placement. This construction technique is generally referred to as *high-lift grouting*. A detailed review of grouting of masonry is provided in *Grouting Concrete Masonry Walls* (NCMA, 2005b).

28.5.3.1 Alternative Grouting Techniques

Adherence to the above requirements for the placement of grout ensures that the masonry assembly will be free of unintended grout voids and that the structure will perform as designed. In some circumstances, however, deviating from these practices may be warranted or alternative grout placement techniques may be desired. Such instances may include higher grout lifts or pours, smaller cavity widths or cells sizes, unique consolidation methods, or altered grout slumps or materials. In recognition of the need to deviate from these standardized grout placement procedures, the MSJC Code and MSJC Specification include an option for the construction of a grout demonstration panel to verify that the alternative grout materials or grouting techniques results in the adequate placement and consolidation of the grout. Although the MSJC is silent on recommended procedures for ensuring the successful placement and consolidation of the grout, common verification methods include both nondestructive evaluation, such as infrared photography, and destructive evaluation, such as the removal of samples from the masonry assembly for testing or visual inspection. If the alternative grouting techniques are shown to be successful, those procedures then become the minimum acceptable standard of care for the project. Although not commonly employed, it is permitted to use a portion of the actual construction as the grout demonstration panel, recognizing that an unsuccessful grout placement alternative may require the removal of the affected portion of construction.

28.5.4 Bracing of Masonry

In accordance with the MSJC Specification, the need to provide, design, and install bracing to ensure the stability of the masonry assembly during construction is left to the mason contractor to implement unless unique construction loads are expected, in which case the designer may opt to provide bracing requirements. Placing this responsibility on the mason contractor recognizes both the need to remain flexible in the field when constructing masonry as well as the variable construction schedule and sequence that may not be anticipated by the designer, thus inhibiting the effective implementation of a bracing strategy. To aid the mason contractor in providing a safe and economical bracing procedure, the MSJC Specification recommends following the guidelines established in *Standard Practice for Bracing Masonry Walls Under Construction* (NCMA, 2001b). This guide contains a series of bracing triggers based on wall age, thickness, height, and weight over a range of wind speeds. As an alternative to providing bracing, which may be impractical in certain instances and loading conditions, procedures are also outlined whereby the assembly and the area around it are evacuated at prescribed wind speeds. Under this alternative, the assembly is considered sacrificial, and the protection of life is the primary concern.

28.5.5 Environmental Construction Factors

In some regions, construction of masonry structures during cold, hot, or wet weather is unavoidable. The ability to continue masonry construction in adverse weather conditions requires consideration of how environmental conditions may affect the quality of the finished masonry. When cold or hot weather is anticipated, the MSJC Specification includes a set of required construction procedures to ensure that the masonry work is not adversely affected. One of the prerequisites of successful all-weather construction is an advance knowledge of local weather conditions. Work stoppage may be justified for a short period

TABLE 28.7 Cold-Weather Construction

Ambient Temperature	Construction Requirements
32 to 40°F (0 to 4.4°C)	Do not lay units having a temperature below 20°F (−6.7°C). Remove visible ice and snow from units, foundation, and masonry to receive new construction. Heat foundation and existing masonry construction to receive new units above freezing. Heat sand or mixing water to produce a mortar temperature of 40–120°F (4.4–48.9°C) at the time of mixing. Heat grout materials to a minimum of 32°F (0°C). Do not heat mixing water or aggregates above 140°F (60°C).
25 to 32°F (−3.9 to 0°C)	In addition to above, maintain mortar temperature above freezing until used. Heat materials for grout to produce a temperature from 70–120°F (21.1–48.9°C). Maintain grout temperature above 70°F (21.1°C) when placed. Heat AAC unit to a minimum temperature of 40°F (4.4°C) before applying mortar.
20 to 25°F (−6.7 to −3.9°C)	In addition to above, heat masonry under construction to 40°F (4.4°C) and use wind breaks or enclosures when the wind velocity exceeds 15 mph (24 kph).
20°F (−6.7°C) and below	In addition to above, provide an enclosure and auxiliary heat to maintain air temperature above 32°F (0°C) within the enclosure.
Mean/Minimum Daily Temperature for UngROUTED/Grouted Masonry	Protection Requirements
25 to 40°F (−3.9 to 4.4°C)	Cover newly constructed masonry with weather-resistive membrane for 24 hours after completion.
20 to 25°F (−6.7 to −3.9°C)	Extend above time period to 48 hours for grouted masonry, unless the only cement in the grout is Type III Portland cement.
20°F (−6.7°C) and below	In addition to above, maintain newly construction masonry temperature above 32°F (0°C) for at least 24 hours after completion. Extend to 48 hours for grouted masonry unless the only cement in the grout is Type III Portland cement.

if very cold, very hot, or extreme weather is anticipated. Several sources for this type of information are available, including the National Weather Service of the U.S. Environmental Science Services Administration (ESSA), which can be accessed at their website (<http://www.ncdc.noaa.gov>). In the following discussion, *ambient temperature* refers to the surrounding jobsite temperature when construction is in progress. The *mean daily temperature* is the average of the hourly temperatures forecast by the local weather bureau over a 24-hour period following the onset of construction. Likewise, the *minimum daily temperature* is the lowest temperature forecast over this 24-hour period. Temperatures between 40 and 90°F (4.4 and 32.2°C) are considered normal temperatures for masonry construction and therefore do not require special procedures or protection protocols.

28.5.5.1 Cold-Weather Construction

Hydration and strength development in mortar and grout generally occur at temperatures above 40°F (4.4°C) and only when sufficient water is available. Masonry construction may proceed, however, when temperatures are below 40°F (4.4°C), provided cold-weather construction and protection requirements of the MSJC Specification are followed as summarized in Table 28.7. The initial water content of mortar can be a significant contributing factor to the resulting properties and performance of mortar, affecting workability, bond, compressive strength, and susceptibility to freezing. Research has demonstrated a detrimental expansion effect on the cement–aggregate matrix when fresh mortars with water contents in excess of 8% mortar are frozen (Korhonen et al., 1997). This disruptive effect increases as the water content increases; therefore, mortar should not be allowed to freeze until the mortar water content is reduced from the initial range of 11 to 16% to a value below 6%. Dry masonry units have a demonstrated capacity to achieve this moisture reduction in a relatively short time. It is for this reason that the MSJC

TABLE 28.8 Hot-Weather Construction

Ambient Temperature	Construction Requirements
Above 100°F (37.8°C), or above 90°F (32.2°C) with a wind speed greater than 8 mph (12.9 kph)	Maintain sand piles in a damp, loose condition. Maintain mortar and grout temperature below 120°F (48.9°C). Flush tools and equipment with cool water before they come into contact with mortar. Maintain mortar consistency by retempering with cool water. Use mortar within 2 hours of initial mixing. Spread thin-bed mortar for AAC masonry no more than 4 ft (1.22 m) at a time, and place AAC masonry units within 1 minute after placing thin-bed mortar.
Above 115°F (46.1°C), or above 105°F (40.6°C) with a wind speed greater than 8 mph (12.9 kph)	In addition to above, shade materials and mixing equipment from direct sunlight. Use cool mixing water for mortar and grout. Ice is permitted in mixing water as long as it is completely melted when added to the other mortar or grout materials.
Mean Daily Temperature	Protection Requirements
Above 100°F (37.8°C), or above 90°F (32.2°C) with a wind speed greater than 8 mph (12.9 kph)	Fog spray newly constructed masonry until damp, at least 3 times per day until the masonry is 3 days old.

Specification requires protection from freezing of mortar for only the first 24 hours. Like mortar, the freezing of a plastic grout can reduce bond and strength development, reducing overall performance of the structure. During cold weather, however, more attention must be directed toward the protection of grout because of the higher water content and resulting expansion that can occur from freezing of that water. Grouted masonry, therefore, generally must be protected for longer periods to allow the water content to be dissipated and the grout to cure.

28.5.5.2 Hot-Weather Construction

High temperatures, solar radiation, and ambient relative humidity influence the absorption characteristics of the masonry units and the setting time and drying rate for mortar. When mortar or grout gets too hot or when mortar or grout is placed in contact with excessively hot masonry units, they may lose water so rapidly that the cement does not fully hydrate. Early surface drying of the mortar results in decreased bond strength and less durable mortar. The hot-weather construction procedures of the MSJC Specification as summarized in Table 28.8 involve keeping masonry materials as cool as possible and preventing excessive water loss.

28.5.5.3 Wet-Weather Construction

When the moisture content of a masonry unit is elevated to excessive levels due to wetting by rain or other sources, several deleterious consequences can result, including decreased mason productivity, decreased mortar–unit bond strength, and, in the case of concrete masonry, increased shrinkage potential and possible cracking. Although reinforced masonry construction does not rely on mortar–unit bond for structural capacity, this is a design consideration with unreinforced masonry. As a means of determining if a concrete masonry unit has acceptable moisture content at the time of installation, the following industry guidance is recommended (NCMA, 2002a). This simple field procedure can quickly ascertain whether a concrete masonry unit has acceptable moisture content at the time of installation.

A concrete masonry unit for which 50% or more of the surface area is observed to be wet is considered to have an unacceptable moisture content for placement. If less than 50% of the surface area is wet, the unit is acceptable for placement. Damp surfaces are not considered wet surfaces. For this application, a surface would be considered damp if some moisture is observed, but the surface darkens when additional free water is applied. Conversely, a surface would be considered wet if moisture is observed and the surface does not darken when free water is applied. These limitations on maximum permissible moisture content are not intended to apply to intermittent masonry units that are wet cut as needed for special fit.

The relative moisture content of clay masonry units at the time of installation is evaluated through the initial rate of absorption (IRA), which is a measure of how much water the brick absorbs during the first 60 seconds after contact with fresh mortar. The value of the initial rate of absorption can influence the bond that can develop between the unit and mortar. When the IRA exceeds 30 g/min/30 in. (30 g/min/194 cm²), the unit may be too dry and a solid, watertight joint may not be achieved (ACI Committee 530.1, 2005). High IRA brick should be wetted 3 to 24 hr prior to laying to reduce the suction and to allow the surface of the brick to dry. Conversely, very low IRA brick should be covered and kept dry on the jobsite prior to use. Guidelines do not exist for the moisture content of AAC masonry units at the time of installation, due in part to the unique properties of the thin-bed mortar used in AAC masonry construction. AAC masonry is required to be thoroughly wetted, however, prior to the placement of grout.

28.5.6 Cleaning

During construction, it is often difficult to prevent the accumulation of mortar and grout smears on the surface of the masonry assembly. Recognizing this, many masonry project specifications include provisions for cleaning the completed masonry assembly following construction. Several commercially available products are available for cleaning the surface of newly constructed masonry. Cleaning products and procedures should be selected with due care, as overly aggressive techniques can damage the masonry units or mortar. Cleaning should begin in a small, nondescript location of the structure to verify that the proposed procedures and solutions are not detrimental to the masonry substrate. For years, acids were used to clean masonry following construction, occasionally with detrimental results. Today, acids and other aggressive chemical are only recommended as a last option for cleaning, and even then should be used with caution. Before applying an acid, the masonry should be thoroughly wetted to prevent the acid from being absorbed into the masonry substrate. Failure to do so can cause acid burn when the cementitious paste between the aggregates is washed away, thus altering the appearance of the surface finish.

28.5.7 Construction Tolerances and Workmanship

Although the manufacturing of masonry units has evolved considerably over the past 100 years, the construction of masonry assemblies remains today a hand-crafted art that has been practiced over centuries. The charm and beauty inherent to masonry construction are its primary aesthetic draws. To ensure that the masonry performs as intended, the MSJC Specification has established tolerance and placement requirements. Workmanship, however, can be a much more subjective value to quantify. For this reason, when aesthetics are a primary concern, the construction of a sample panel is recommended for all projects.

28.5.7.1 Construction Sample Panels

When masonry construction is governed by either quality assurance Level B (see Table 28.10) or Level C (see Table 28.11) as required by the MSJC Specification, a sample panel measuring a minimum of 4 × 4 ft (1.22 × 1.22 m) is required to be constructed, although sample panels can also be used on projects incorporating unique or complicated details or procedures. The purpose of a masonry sample panel is to help ensure that the final envisioned product is directly communicated to all affected parties, particularly in the case of aesthetics and minimum quality of workmanship, which can be difficult to stipulate in contract documents. The sample panel should incorporate all possible products, materials, and procedures specified to be part of the final construction, including the full range of masonry unit color and texture; mortar color and joint profile; flashing details; tie, anchor, and reinforcement placement; cleaning procedures; and coating application, as applicable. The sample panel should be retained on the project site until all masonry work has received final acceptance. If appropriate and acceptable to all parties, a portion of the masonry structure can be used as the sample panel for the project.

28.5.7.2 Construction Tolerances

Virtually all construction materials are manufactured to a specified tolerance; likewise, nearly all structures incorporating such building components are required to be constructed to a specified tolerance. Masonry structures and the materials used in their construction are no different. Because masonry is often used as an exposed construction material, it can be subjected to tighter tolerances than typically associated with other structural systems that are normally hidden when construction is complete. Unless otherwise specified in the contract documents, the tolerances for the placement of masonry elements are outlined in the MSJC Specification. Although the intent of the construction and placement tolerances contained within the MSJC Specification is to safeguard structural performance and not achieve any aesthetic criterion, the stipulated values are often regarded as more than adequate for common aesthetic purposes. Tighter tolerances may be required in the project documents to ensure that the final overall appearance of the masonry is acceptable. It should be cautioned, however, that using more stringent construction tolerances could significantly complicate the job and increase the cost of construction. Maintaining tight construction tolerances may be aesthetically desirable, but it must be recognized that factors such as the condition of previous construction and modular coordination of the project may require the mason to vary the masonry construction slightly from the intended plans or specifications. The details of this section outline the tolerance requirements contained within the MSJC Specification for mortar joints, alignment, location of elements, and placement of reinforcement. Further information on construction tolerances can be found in *Testing and Inspection of Concrete Masonry Construction* (NCMA, 2006c).

28.5.7.2.1 Mortar Joint Tolerances

Although primarily an aesthetic issue, significant variations in mortar joint thicknesses can result in poor structural performance. The following tolerances imposed by the MSJC Specification are intended, in part, to ensure structural performance is not compromised. These tolerances are illustrated in Figure 28.9. Mortar bed joints, typically 3/8 in. (9.5 mm) thick for most masonry construction, are permitted to vary by $\pm 1/8$ in. (3.2 mm) in thickness. The exception to this is with the initial bed joint between the top of the footing and the first course of masonry, which may vary in thickness from 1/4 to 3/4 in. (6.4 to 19 mm) to accommodate variations in the top of the footing. Head joint thickness may vary by $-1/4$ in. (6.4 mm) to $+3/8$ in. (9.5 mm); thus, for a specified joint thickness of 3/8 in. (9.5 mm), the head joint thickness may vary from a minimum thickness of 1/8 in. (3.2 mm) to a maximum thickness of 3/4 in. (19 mm). Although bed joints should be constructed level, they are permitted to vary by $\pm 1/2$ in. (13 mm) maximum from level, provided the joint does not slope more than $\pm 1/4$ in. (6.4 mm) in 10 ft (3048 mm). This requirement also applies to the top surface of bearing walls.

28.5.7.2.2 Plumb and Alignment Tolerances

The alignment and out-of-plumb tolerances required by the MSJC Specification are intended to ensure structural performance. In these cases, the intention is to limit the eccentricity of applied loads and thereby not reduce the load-carrying capacity of a given element. These tolerances are shown in Figure 28.10. Walls, columns, and other masonry building elements are required to be constructed to within $-1/4$ in. (6.4 mm) or $+1/2$ in. (13 mm) from the specified dimensions in cross-section and elevation. Masonry walls, columns, and other building elements may not vary from plumb by more than $\pm 1/2$ in. (13 mm) maximum while maintaining a slope of less than $\pm 1/4$ in. (6.4 mm) in 10 ft (3048 mm) and $\pm 3/8$ in. (9.5 mm) in 20 ft (6096 mm). Masonry building elements should also stay true to a line within these same tolerances. Columns and walls continuing from one story to another may vary in alignment by $\pm 3/4$ in. (19 mm) for nonloadbearing walls or columns and by $\pm 1/2$ in. (13 mm) for bearing walls or columns.

28.5.7.2.3 Location of Elements

For continuity of construction and to facilitate the connection of discrete elements, the MSJC Specification requires masonry members to be located within a maximum distance of $\pm 3/4$ in. (19 mm), not exceeding $\pm 1/2$ in. (13 mm) in 20 feet (6096 mm), from their intended location in plan as shown in

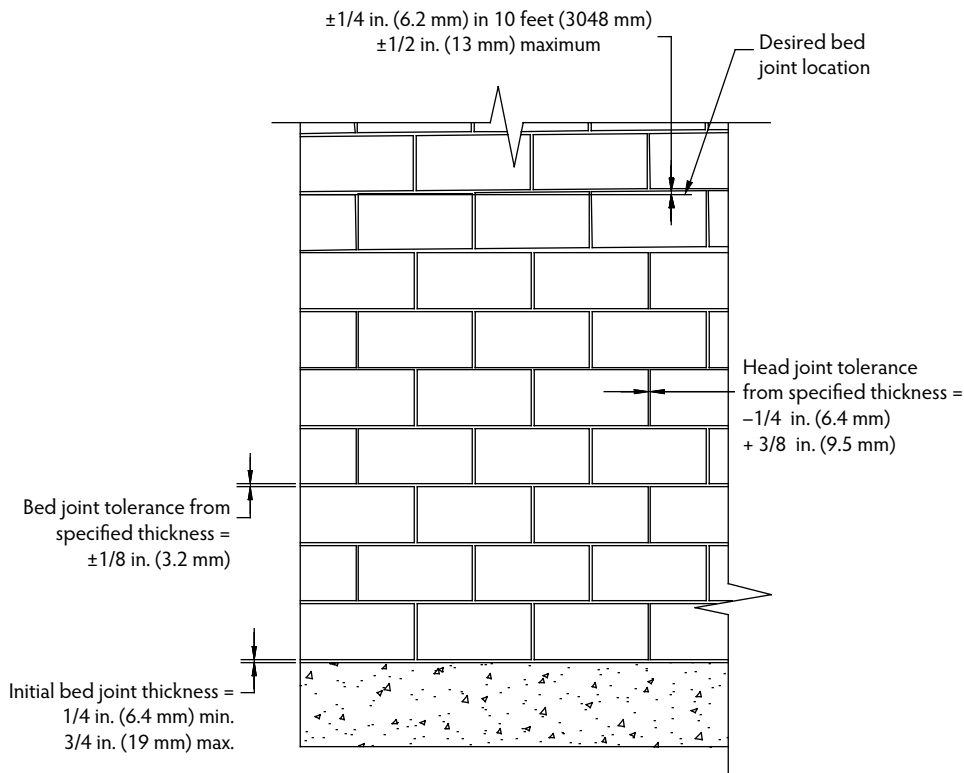


FIGURE 28.9 Mortar joint tolerances. (Courtesy of the National Concrete Masonry Association, Herndon, VA.)

Figure 28.11. Such tolerances also minimize unanticipated eccentricity of axial loads. Masonry building elements must also be located within $\pm 1/4$ in. (6.4 mm) per story height without exceeding the $\pm 3/4$ -in. (19-mm) maximum. This requirement would apply not only to the top of walls or other vertical assemblies but also to discrete elements within an assembly, such as lintels and bond beams.

28.5.7.2.4 Placement Tolerances for Reinforcement

In accordance with the MSJC Specification, the tolerance for the placement of reinforcement in walls and other flexural elements is $\pm 1/2$ in. (13 mm) when the specified effective depth (d), measured from the centerline of the reinforcement to the opposite compression face of the masonry, is 8 in. (203 mm) or less. The tolerance increases to ± 1 in. (25 mm) for d equal to 24 in. (610 mm) or less but greater than 8 in. (203 mm). For d greater than 24 in. (610 mm), the tolerance for the placement of reinforcement is $\pm 1-1/4$ in. (32 mm), as shown in Figure 28.12. Vertical bars must be placed within 2 in. (51 mm) of their specified location measured parallel to the length of the wall for all applications. The placement tolerances for such reinforcement are larger because slight deviations from specified locations have a negligible impact on the out-of-plane structural performance of an assemblage. Although not required by the MSJC Specification, to facilitate the placement of reinforcement and achieve the required placement tolerances reinforcing bar positioners may be used for both horizontal and vertical reinforcement, although bar positioners may hinder high-lift grouting procedures.

28.6 Testing and Inspection

Design of masonry, as with other construction materials, does not warrant great precision in its analysis and application. A thorough understanding of the materials, their compatibility, and proper detailing is just as important as design precision for the successful performance of the masonry system. The various

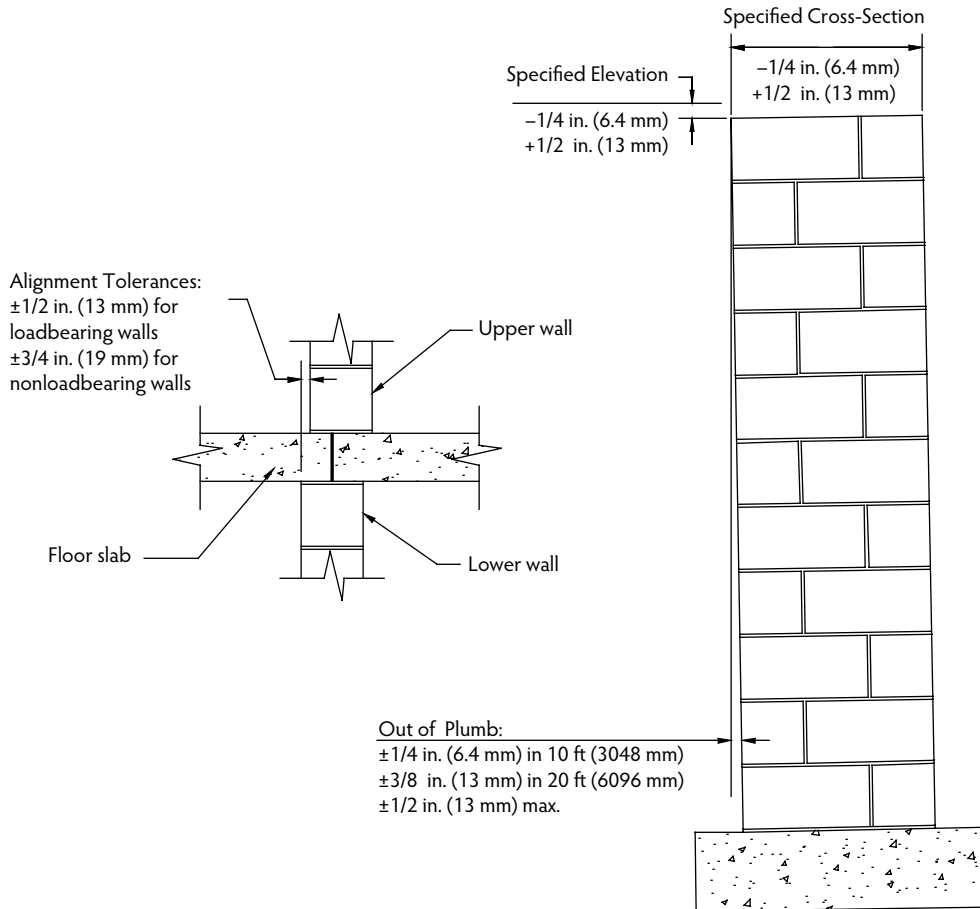


FIGURE 28.10 Alignment tolerances. (Courtesy of the National Concrete Masonry Association, Herndon, VA.)

combination of units, mortar, grout, and reinforcement, environmental conditions at the project site, and variations in workmanship are factors that will influence the end result in sometimes unpredictable and uncontrollable ways. To account for the multiple combinations of these variables and the effects they can have on the resulting construction, the design factors of safety in the past were more conservative than permitted for other construction materials. More recently, however, quality control and quality assurance programs have been established by codes and standards to provide a minimum level of confidence in the properties of the final construction. Correspondingly, when such testing and inspection programs are put into use the design of masonry structures becomes more economical. The evaluation of masonry materials generally falls into one of two categories:

- In-plant quality control as required by product standards and individual manufacturer's procedures
- Testing and inspection in the field as governed by building codes and standards

The following discussion focuses on the latter of these evaluation programs as related to verifying material properties, inspecting the masonry system, and implementing a construction quality assurance program in the field.

In the past, masonry testing and inspection could be waived at the option of the designer when the allowable design stresses were reduced by a factor of two, commonly referred to as *half-stress design* or

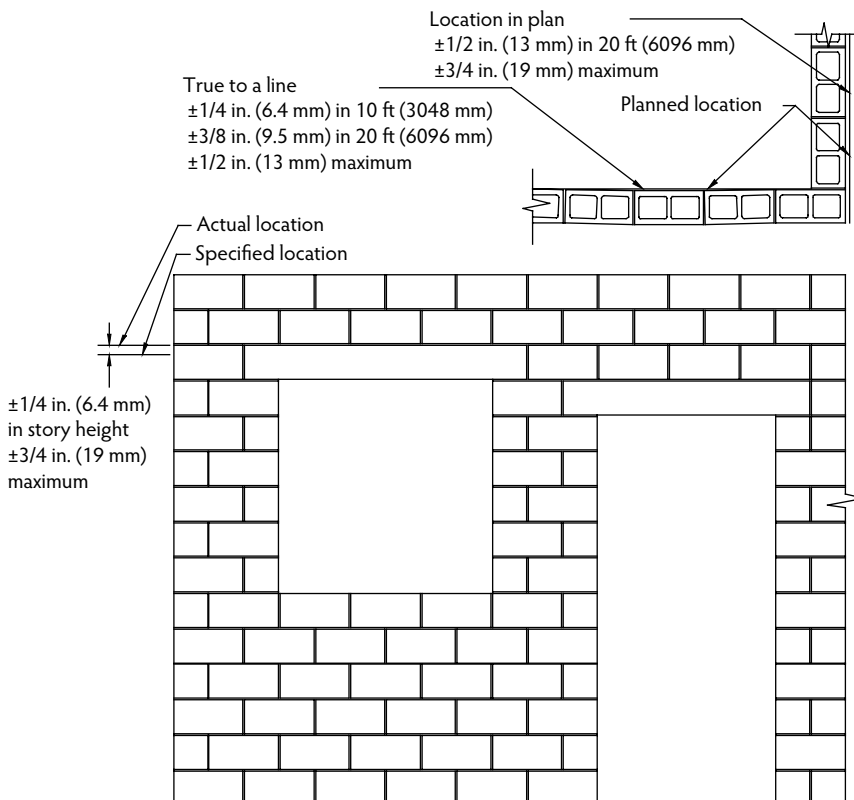


FIGURE 28.11 Tolerances for locating elements. (Courtesy of the National Concrete Masonry Association, Herndon, VA.)

un-inspected design. Within contemporary design standards for masonry this option is no longer available. As a minimum, the MSJC Code and MSJC Specification require certificates of compliance for the materials used in construction. Further, for engineered masonry structures, the MSJC requires as a minimum periodic field inspection to verify that the materials and construction are in compliance with the project specifications. Evaluation of individual masonry materials is covered by applicable ASTM standards, while acceptable workmanship and construction tolerances are addressed by the MSJC Specification. The following sections provide a general overview of the procedures used for testing various materials used in masonry construction and the required inspection procedures to verify acceptable workmanship. Further discussion related to the quality assurance and inspection of masonry is offered in *Testing and Inspection of Concrete Masonry Construction* (NCMA, 2006c).

28.6.1 Quality Assurance Levels

The MSJC Specification outlines three levels of quality assurance, each triggered by the design method used and importance of the structure, to ensure a minimum level of quality and safety. These inspection and testing programs are in turn incorporated into the IBC, although they are designated differently. The three levels of quality assurance include:

- *Level A (IBC Basic)*—These requirements are composed of the minimum quality assurance provisions as summarized in Table 28.9 and are only applicable to empirically design masonry, glass unit masonry, and masonry veneer used in the construction of structures designated as nonessential by the building code.

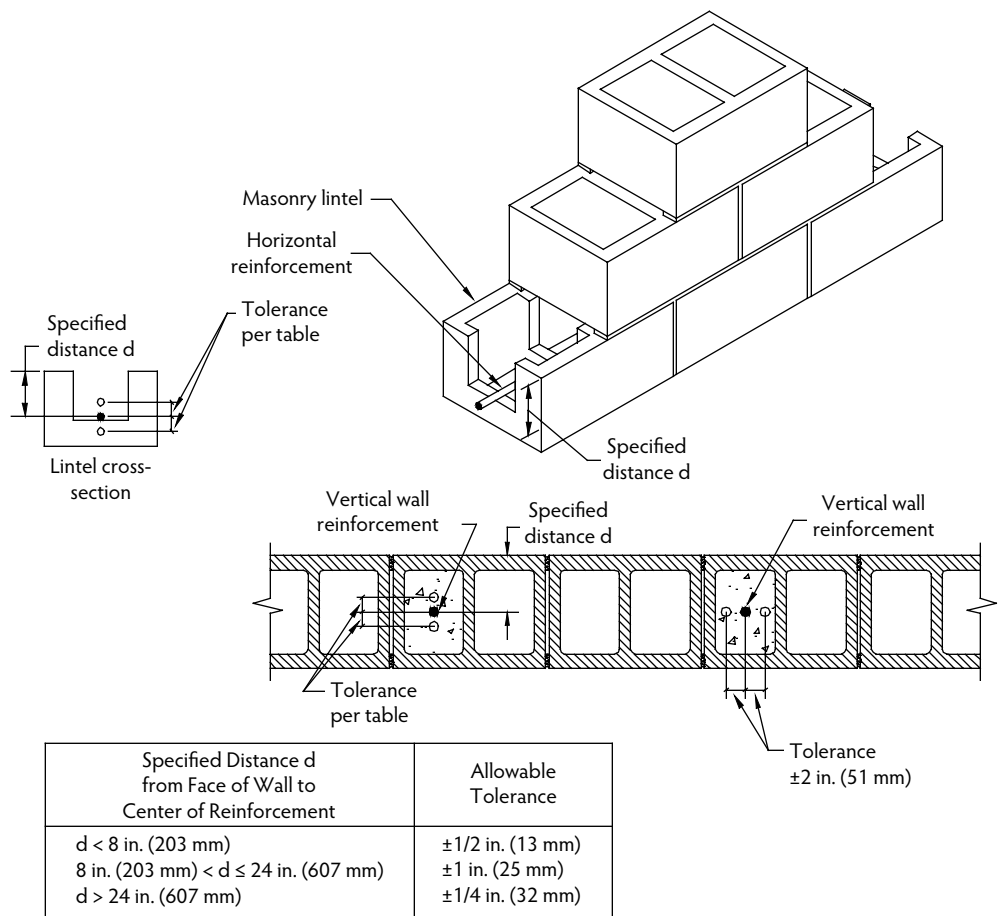


FIGURE 28.12 Placement tolerances for reinforcement. (Courtesy of the National Concrete Masonry Association, Herndon, VA.)

- *Level B (IBC Level 1)*—These requirements provide a periodic-type inspection for engineered masonry used in nonessential facilities (as defined in the building code) and for empirically designed masonry, glass unit masonry, and masonry veneer used in essential facilities as summarized in Table 28.10.
- *Level C (IBC Level 2)*—These comprehensive inspection procedures are required for essential facilities (as defined in the building code) that are designed by engineered design methods (allowable stress or strength design) as summarized in Table 28.11. Items inspected under a Level C quality assurance program are similar to those of Level B, with the added requirement that inspection must be continuous during all phases of masonry construction.

These inspection levels are minimum criteria and may be increased when deemed necessary by the owner or designer due to the relative importance or potential hazard of unique structures. In this case, the contract documents must indicate the inspection level and tests that are required to ensure that the masonry work conforms with the project requirements.

In the context of the MSJC requirements, inspection, in combination with material testing, comprises the quality assurance program as established by the administrative and procedural requirements of the contract documents. Current code provisions, however, are vague regarding the minimum qualifications for masonry inspectors conducting routine inspection tasks. Some equate qualification with a nationally recognized certification, while others have allowed a noncertified individual with sufficient experience

TABLE 28.9 Level A Quality Assurance

Minimum Tests and Submittals	Minimum Inspection
Certificates for materials used in masonry construction indicating compliance with the contract documents.	Verify compliance with the approved submittals.

TABLE 28.10 Level B Quality Assurance

Minimum Tests and Submittals	Minimum Inspection
Certificates for materials used in masonry construction indicating compliance with the contract documents	As masonry construction begins, verify that the following are in compliance: Proportions of site-prepared mortar Construction of mortar joints Location of reinforcement, connectors, and prestressing tendons and anchorages Prestressing technique
Verification of f'_m or f'_{AAC} prior to construction, except when specifically excepted by the MSJC (including masonry veneer and glass block construction)	Prior to grouting, verify that the following are in compliance: Grout space Grade and size of reinforcement; prestressing tendons and anchorages Placement of reinforcement, connectors, and prestressing tendons and anchorages Proportions of site-prepared grout and prestressing grout for bonded tendons Construction of mortar joints Verify that the placement of grout and prestressing grout for bonded tendons is in compliance. Observe preparation of grout specimens, mortar specimens, and prisms. Verify compliance with the required inspection provisions of the contract documents and the approved submittals.

TABLE 28.11 Level C Quality Assurance

Minimum Tests and Submittals	Minimum Inspection
Certificates for materials used in masonry construction indicating compliance with the contract documents	<i>From the beginning of masonry construction and continuously during construction of masonry:</i>
Verification of f'_m or f'_{AAC} prior to construction and every 5000 ft ² (464.5 m ²) during construction	Verify that the following are in compliance: Proportions of site-mixed mortar, grout, and prestressing grout for bonded tendons Grade and size of reinforcement; prestressing tendons and anchorages Placement of masonry units and construction of mortar joints Placement of reinforcement, connectors, and prestressing tendons and anchorages Grout space prior to grouting Placement of grout and prestressing grout for bonded tendons
Verification of proportions of materials in premixed or preblended mortar, grout, and prestressing grout as delivered to the site	Observe preparation of grout specimens, mortar specimens, and/or prisms. Verify compliance with the required inspection provisions of the contract documents and the approved submittals.

to serve as an inspector. As a minimum, however, a masonry inspector must be familiar with masonry materials and construction and be able to read plans and specifications effectively to judge whether or not the construction is in conformance with the contract documents. The following sections provide a brief review of the basic masonry knowledge necessary to effectively implement a testing and inspection program.

28.6.2 Mortar Testing

Reviewed earlier in this chapter were the requirements for mortar materials and their properties, as well as guidelines for selecting mortar types for specific projects. The following discussion addresses the physical testing and assessment of masonry mortars based on standardized tests as outlined in ASTM C 780, *Standard Test Method for Preconstruction and Construction Evaluation of Mortars for Plain and Reinforced Unit Masonry* (ASTM, 2006e). The quality assurance testing of masonry mortars remains one of the most commonly misinterpreted construction procedures. When mortar testing is required for a specific project, it is essential that all parties involved possess a thorough knowledge of the mortar specifications, test methods, and standard practices prior to the start of construction. Misinterpretations of these standards can result in improper testing and confusion regarding compliance with specifications.

The two methods of specifying masonry mortars in accordance with ASTM C 270, *Standard Specification for Mortar for Unit Masonry* (ASTM, 2005d), are the *proportion specification* and the *property specification*. These two compliance options are completely independent and cannot be used in conjunction with one another. Due to its ease of implementation, and because it is the default compliance method in ASTM C 270, the proportion specification is much more commonplace. Although field testing of the mortar is not required to demonstrate compliance with the proportion specification, proportion-batched mortar may be visually documented in the field or sampled and physically evaluated to verify its consistency throughout the job. Although compressive strength testing is the most common physical evaluation technique, several other testing options exist. The most important aspect of mortar quality control, however, is ensuring its consistency throughout the construction project, not the absolute value of a particular property.

The test methods outlined in ASTM C 780 are solely intended to evaluate mortar consistency, which in turn may be compared to baseline preconstruction physical properties of laboratory-prepared mortars but cannot be compared to the values required by the ASTM C 270 property specification. Further, without preconstruction baseline evaluation of mortar properties comparing laboratory-prepared mortar to field-prepared mortar, quantitative acceptance criteria for field mortars cannot be established, as ASTM does not publish minimum physical properties for field-prepared mortar. ASTM C 780 outlines several tests for the field evaluation of masonry mortars, including consistency by cone penetration, consistency retention by cone penetration, consistency by modified concrete penetrometer, aggregate ratio, water content, air content, compressive strength, and splitting tensile strength (see Figure 28.13). Due to its



FIGURE 28.13 Masonry mortar cubes. (Courtesy of the National Concrete Masonry Association, Herndon, VA.)

common use, however, the compressive strength evaluation of masonry mortars is reviewed in detail here. Additional guidance on the evaluation of field mortars is provided in ASTM C 1586, *Standard Guide for Quality Assurance of Mortars* (ASTM, 2005a), for those interested in applying alternative quality control techniques.

One of the most universally recognized properties of masonry is compressive strength. Although this property may not be the most important property for masonry mortar, it is often perceived as such in part because compressive strength values are generally understood and are relatively easy to determine. Confusion and misinterpretation sometimes exist, however, when interpreting project specification requirements and field testing results for mortar strength because ASTM standards do not include minimum requirements for field-prepared mortars. One primary reason for the necessary absence of minimum properties of field mortars is that, when fresh mortar is placed on masonry units during construction, its characteristics immediately begin to change due to water absorption by the masonry unit which lowers its water-to-cement ratio and increases its net compressive strength. Because ASTM C 780 tests are performed on mortars that have not been exposed to such absorption conditions, the resulting tested properties are expected to differ significantly from mortar in contact with masonry units. Conversely, ASTM C 270 test methods attempt to simulate this reduced water-to-cement ratio by reducing the amount of water added to the laboratory-prepared mix. The resulting laboratory-prepared mortar would be virtually unusable from a mason's perspective due to its lack of workability.

Because conditions of the units and environment can vary greatly from job to job, the properties of the plastic mortar may have to vary as well to ensure quality construction. It is for this reason that no standardized pass/fail criteria exist for field tests of mortar as well as no standardized correlation between field- and laboratory-prepared mortars. Thus, the mortar compressive strength determined in a laboratory is not directly indicative of the strength of the mortar in the wall, the mortar strength evaluated in accordance with ASTM C 780, or of the masonry assembly strength. Instead, compressive strength sampling of field mortars for quality control is a quantitative measurement of the consistency of the mortar on a project.

Although the physical process of sampling and testing masonry mortar compression specimens is understood well enough, the discussion above highlights some of the common interpretations with their use. As an alternative to mortar compression testing, the mortar aggregate ratio test of ASTM C 780, which determines the approximate relative amounts of cementitious materials to aggregate in the mortar mix, can be a very effective tool for determining the batch-to-batch mortar consistency throughout a project. The added benefit of the aggregate ratio test is that results can be obtained the same day, instead of the days or weeks that may be necessary for compression testing, thus allowing for potential problems to be identified early.

28.6.3 Grout Testing

Quality control of masonry grout typically involves:

- Conducting slump tests on the plastic grout prior to placement to ensure proper consistency and flowability
- Collecting samples to mold specimens for compression testing

The slump test can be used to give an indication of the consistency, water-to-cement ratio, and fluidity of the grout batch. As with concrete, slump testing of masonry grout is conducted in accordance with ASTM C 143, *Standard Test Method for Slump of Hydraulic-Cement Concrete* (ASTM, 2005h). When the grout lift height exceeds 5 ft (1.52 m), but is not greater than 12.67 ft (3.9 m), the grout slump must be maintained between 10 and 11 in. (254 and 279 mm). For grout lift heights of 5 ft (1.52 m) or less, the slump is permitted to vary between 8 and 11 in. (203 and 279 mm). The MSJC recognizes the need to vary grout slump from one project to another based on specific circumstances and as such permits this relatively wide range of grout slumps.

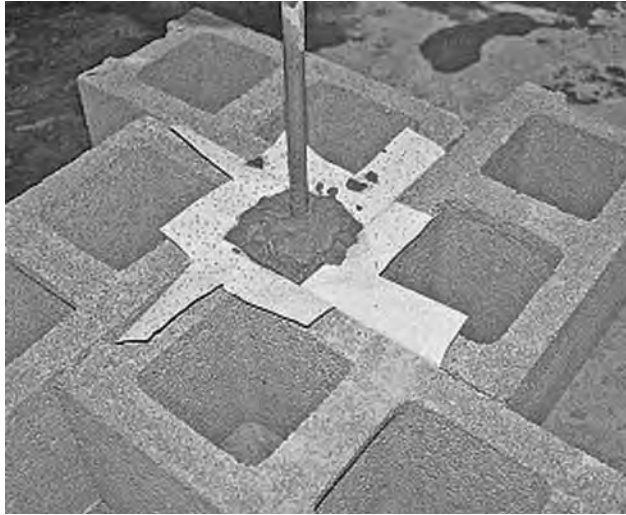


FIGURE 28.14 Molding of grout compression specimen. (Courtesy of the National Concrete Masonry Association, Herndon, VA.)

Selecting an appropriate slump for the placement of grout is more art than science. In general, when the rate of water loss from the grout is high, such as when temperatures are elevated or when the masonry units are highly absorptive, slumps in the upper part of the range (i.e., more fluid) may be desirable, although care should be taken that the grout does not segregate because it contains too much water. High-slump grouts are also advantageous when grout spaces are small or highly congested; conversely, when placing grout during relatively cold or wet weather, grouts in the lower slump range are a good choice, as excessive free water is not lost to the masonry units. When grout compressive strength testing is required, the procedures of ASTM C 1019, *Standard Test Method for Sampling and Testing Grout* (ASTM, 2005f), are used. ASTM C 1019 contains procedures for both field and laboratory grout compression testing and can be used either to help select grout proportions during preconstruction or as a quality control test for grout compressive strength during construction.

When used as part of a quality assurance program, the frequency of sampling grout specimens should be specified before the start of construction. Grout specimens are formed in molds made from masonry units with the same absorption and moisture content characteristics as those being used on the job, as shown in Figure 28.14. The purpose of the absorptive mold is to subject the plastic grout to water-loss conditions similar to those in the masonry assembly. Using plastic cylinders or other nonabsorbent means of molding grout compression specimens keeps the water-to-cement ratio in the grout artificially high, resulting in reduced compressive strength measurements. Per ASTM C 476, *Standard Specification for Grout for Masonry* (ASTM, 2002), the minimum compressive strength of masonry grout is 2000 psi (13.79 MPa); however, project requirements may require higher strengths. For example, when the unit strength method is used to determine the specified compressive strength of the masonry (f'_m), the MSJC Specification requires the compressive strength of the grout to equal or exceed f'_m but not be less than 2000 psi (13.79 MPa). As an economic rule of thumb, unless structural criteria dictate otherwise, it is best to balance the specified grout strength with the specified concrete masonry assembly strength so one element of the system is not considerably stronger than the other, resulting in material overstrength and design conservatism. As a final note, when using the strength design provisions of the MSJC Code (not the allowable stress design provisions), a maximum specified grout compressive strength of 5000 psi (34.47 MPa) for concrete masonry construction is applied. This limitation is based solely on the specified compressive strength of grout and does not limit the actual field-tested grout compressive strength. Additional discussion on the sampling and testing of masonry grouts is provided in *Testing and Inspection of Concrete Masonry Construction* (NCMA, 2006c).

28.6.4 Masonry Unit Testing

The physical properties of concrete, clay, and autoclaved aerated concrete masonry units are each evaluated under their own unique standards; ASTM C 140 (ASTM, 2006f), ASTM C 67 (ASTM, 2007b), and ASTM C 1386 (ASTM, 1998), respectively. In addition to these testing standards, some masonry units may require additional evaluation as required by ASTM C 476 (ASTM, 2002) for linear drying shrinkage potential or ASTM C 744 (ASTM, 2005e) for prefaced concrete masonry units. Each standard contains procedures specific to the type of masonry unit being evaluated. Tests addressed by the standards include frequency and methods of sampling, measurement of dimensions, absorption and density calculations, and determination of compressive strength. Each physical property, in turn, must comply with the associated ASTM specification for the unit being evaluated; for example, conventional loadbearing concrete masonry units tested in accordance with ASTM C 140 must meet the minimum specified requirements of ASTM C 90 (ASTM, 2006c). These requirements may be in addition to project-specific requirements. As shown in the three quality assurance programs outlined in Table 28.9, Table 28.10, and Table 28.11, jobsite sampling of masonry units for physical evaluation is not a default requirement unless the unit strength method of verifying the specified compressive strength of masonry as outlined in Section 28.6.5 is used.

28.6.5 Verifying Compliance with f'_m

Structural performance of masonry is largely dependent upon three key criteria:

- The engineering rationale incorporated into the design of the structure
- The physical characteristics of the materials used in the construction of the structure (i.e., the masonry units, grout, mortar, and reinforcement)
- The quality of the construction used in assembling these components

In proportioning, configuring, and reinforcing a masonry element for a prescribed set of loads, a designer bases these parameters on the minimum specified compressive strength of masonry (f'_m). This minimum value is used throughout the design in accordance with the appropriate masonry code to establish allowable stresses and design strengths for masonry elements. It should be stressed that the specified compressive strength of the masonry is related to but *not* equal to the tested compressive strength of the masonry, which conversely must equal or exceed the specified compressive strength of the masonry. Because masonry construction is a composite assemblage of mortar, units, and grout, testing these materials independently does not provide a direct indication of the compressive strength of the final construction. Instead, quality assurance efforts to document the compressive strength of an assembly are based on representative samples combining each individual material either through direct evaluation or through an established correlation. As such, compliance with the specified compressive strength is verified by one of two methods, the *unit strength method* or the *prism test method*, as required by the MSJC Specification.

28.6.5.1 Unit Strength Method

The unit strength method is often considered to be less expensive and more convenient than constructing and testing masonry prisms; however, the unit strength method also yields more conservative results when compared to the prism test method, especially at the higher range of masonry unit strengths. Further, the unit strength method cannot be used for verifying the compressive strength of AAC masonry assemblies, which is based on the strength of the AAC masonry unit alone. Compliance with f'_m by the unit strength method is based on the net area compressive strength of the concrete or clay masonry units and the type of mortar used. The compressive strength of the masonry assemblage is then established in accordance with Table 28.12 and Table 28.13 for concrete and clay masonry, respectively. Each of these tables is based on established correlations from the MSJC Specification. To use the unit strength method, the following conditions must be met:

TABLE 28.12 Compressive Strength of Concrete Masonry Based on the Compressive Strength of Concrete Masonry Units and Type of Mortar Used in Construction

Net Area Compressive Strength of Concrete Masonry Units, psi (MPa)		Net Area Compressive Strength of Masonry, psi (MPa) ^a
Type M or S Mortar	Type N Mortar	
1250 (8.62)	1300 (8.96)	1000 (6.90)
1900 (13.10)	2150 (14.82)	1500 (10.34)
2800 (19.31)	3050 (21.03)	2000 (13.79)
3750 (25.86)	4050 (27.92)	2500 (17.24)
4800 (33.10)	5250 (36.20)	3000 (20.69)

^a For units of less than 4 in. (102 mm) in height, use 85% of the values listed.

TABLE 28.13 Compressive Strength of Clay Masonry Based on the Compressive Strength of Clay Masonry Units and Type of Mortar Used in Construction

Net Area Compressive Strength of Clay Masonry Units, psi (MPa)		Net Area Compressive Strength of Masonry, psi (MPa) ^a
Type M or S Mortar	Type N Mortar	
1700 (11.72)	2100 (14.48)	1000 (6.90)
3350 (23.10)	4150 (28.61)	1500 (10.34)
4950 (34.13)	6200 (42.75)	2000 (13.79)
6600 (45.51)	8250 (56.88)	2500 (17.24)
8250 (56.88)	10,300 (71.02)	3000 (20.69)
9900 (68.26)	NP ^b	3500 (24.13)
13,200 (91.01)	NP ^b	4000 (27.58)

^a For units of less than 4 in. (102 mm) in height, use 85% of the values listed.

^b NP, not permitted.

- Masonry units must comply with ASTM C 55 or ASTM C 90 for concrete masonry or ASTM C 62, ASTM C 216, or ASTM C 652 for clay masonry.
- The thickness of the mortar bed joints cannot exceed 5/8 in. (15.9 mm).
- Mortar must comply with the requirements of ASTM C 270.
- For grouted masonry construction, the grout must meet either the requirements of ASTM C 476 or have a compressive strength equal to or greater than f'_m but not less than 2000 psi (13.79 MPa).

Although the unit strength method offers an easy-to-implement alternative to prism construction, as noted earlier, it can be conservative, particularly for higher material strengths. Table 28.12, for example, would permit an f'_m value of 3000 psi (20.69 MPa) for a 4800-psi (33.10-MPa) concrete masonry unit laid in Type S mortar. If this combination of unit compressive strength and mortar were to be used to construct and test a masonry prism, the actual measured compressive strength would be expected to be in the range of 3800 to 4000 psi (26.20 to 27.58 MPa), considerably higher than the permitted 3000 psi (20.69 MPa).

28.6.5.2 Prism Test Method

The second method for verifying the compressive strength of masonry per the MSJC Specification is the prism test method, which directly measures the compressive strength of a masonry prism constructed using the actual materials used in construction. Masonry prisms are constructed and tested in accordance with ASTM C 1314, *Standard Test Method for Compressive Strength of Masonry Prisms* (ASTM, 2003b), which outlines standardized procedures to construct, cure, transport, and test masonry prisms in compression. At the prescribed frequency as dictated by the MSJC Specification or the project specifications, one set of prisms (each set contains three individual prisms) is constructed for each combination of materials and each testing age for which the compressive strength is to be determined. Units are laid in



FIGURE 28.15 Masonry prism construction. (Courtesy of the National Concrete Masonry Association, Herndon, VA.)

stack bond (even if the corresponding construction is in running bond) on a full mortar bed using mortar representative of that used in the corresponding construction. All units used in the prisms must be of the same configuration and oriented in the same manner so webs and face shells are properly aligned. Mortar joints are cut flush regardless of the type of tooling used in construction. These specific construction techniques help to standardize the resulting compressive strength measurements. Once constructed, the prisms are cured in sealed plastic bags to ensure uniform hydration of the mortar and, if used, the grout. Under actual field conditions, longer periods may be required for hydration and the corresponding strengths to be achieved; however, curing prisms in sealed plastic bags results in measured strengths that are representative of those exhibited by the masonry throughout the life of the structure. As with the standardized construction procedures, bag curing also provides uniform and repeatable results. Where the corresponding construction is to be grouted solid, grout solid each prism using grout and consolidation techniques representative of that being used in the corresponding construction. Conversely, if the corresponding construction is to be partially grouted, two sets of prisms are constructed; one set is grouted, and the other is left ungrouted. The average measured compressive strengths of both the ungrouted and grouted prisms are required to meet the specified compressive strength of masonry f'_m per the MSJC Specification.

As an alternative to constructing prisms using full-size units, ASTM C 1314 permits reduced-size units to be used in prism construction, as shown in Figure 28.15. The only criteria for constructing prisms out of reduced-sized units is that hollow units must contain fully closed cells, the cross-section should be as symmetrical as possible, and the final length of the prism should not be less than 4 in. (102 mm). The use of reduced-size prisms, particularly in grouted masonry construction, can significantly reduce the weight of the specimens, which in turn facilitates transporting, handling, and testing the prisms accurately and without damage.

When documenting compliance with f'_m , prisms are typically tested at an age of 28 days, but a different testing age may be designated depending on the requirements of each project. When earlier compressive strength results are desired, a correlation between the 28-day compressive strength and earlier compressive

TABLE 28.14 Masonry Prism Correction Factors

Height/thickness	1.3	1.5	2.0	2.5	3.0	4.0	5.0
Correction factor	0.75	0.86	1.0	1.04	1.07	1.15	1.22

strengths can be established for each project, provided the materials and construction techniques do not change. Because masonry units are available in a wide array of shapes and sizes, the resulting size and configuration of the masonry prism also changes. To provide a standardized means of accounting for the influence that varying prism configurations can have on measured compressive strengths, ASTM C 1314 requires that the measured compressive strength be multiplied by a correction factor as shown in Table 28.14. These correction factors are applied to the measured prism compressive strength prior to reporting.

Unlike clay and concrete masonry, AAC masonry does not employ prism testing. Because the compressive strength of the AAC masonry unit is the lowest compressive strength material in the masonry assemblage, the specified compressive strength of masonry (f'_{AAC}) is simply taken as being equal to or less than the compressive strength of the AAC masonry unit.

28.7 General Detailing

The proper function of a masonry structure resides in the practice and implementation of good detailing and construction. This topic in and of itself can fill volumes; however, a few key detailing considerations are covered here. For a full review of proper detailing of masonry structures, see NCMA (2003a).

28.7.1 Movement Control and Control/Expansion Joints

Cracking in masonry construction can result from many sources. Effective abatement of cracking, from both structural and nonstructural causes, requires a comprehensive understanding of the materials, how they age, and how they respond to movement. The primary sources of cracking in masonry construction include:

- Drying shrinkage of concrete masonry
- Fluctuations in temperature
- Carbonation of cementitious materials
- Differential movement between materials
- Excessive deflection
- Structural overload
- Settlement
- Expansion of clay masonry units

To accommodate small amounts of anticipated movement, control joints or expansion joints are incorporated into masonry construction to relieve built-up stresses (Figure 28.16). For concrete masonry construction, which over an extended period of time will have a net reduction in volume as it shrinks, control joints are placed at regular intervals and at locations of stress concentration to allow the assembly to move without cracking. Clay masonry, conversely, will slowly expand over time as the units absorb water from the environment. As such, clay masonry assemblies incorporate expansion joints to allow the masonry to expand freely without cracking. A comprehensive review of expansion and control joints is provided in BIA (2005) and NCMA (2005a).

28.7.2 Moisture Migration and Detailing

Either as a result of improper detailing or poor construction quality, the water-penetration resistance of masonry structures continues to concern far too many building occupants, despite long-standing recommendations for the proper design, construction, and care of masonry assemblies. Moisture most often

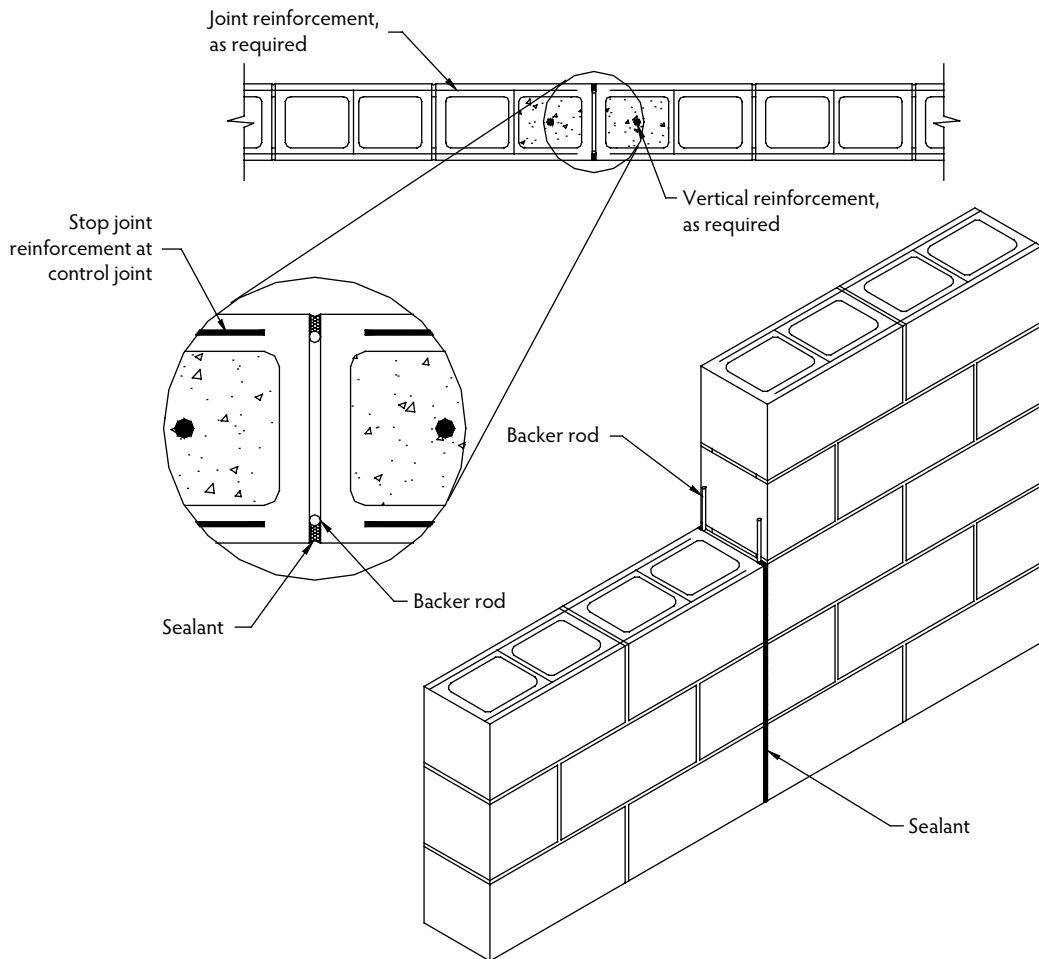


FIGURE 28.16 Concrete masonry control joint. (Courtesy of the National Concrete Masonry Association, Herndon, VA.)

enters into a masonry assembly via wind-driven rain or improperly detailed joints and connections, but it can also present itself through capillary suction and water vapor transmission. To ensure proper performance and comfort for the occupants, masonry walls must be detailed to allow water that does enter into the assembly to exit again in a controlled manner. For hollow unit construction and cavity wall construction, this means incorporating flashing at each horizontal discontinuity to collect the water and drain it to the exterior of the wall, as shown in Figure 28.17. In addition to flashing strategies, the use of surface coatings or sealants on the exterior of a masonry assembly offers a second line of defense against water migrating through the surface of the masonry. Sealants, however, do not protect against water entering through improperly designed or built joints or connections and therefore should not be solely relied upon for water penetration resistance. A comprehensive review of effective water mitigation techniques is offered in NCMA (2004a, 2006d) and BIA (2005).

28.8 Project Specifications

Specifications for masonry have the same requirement for clarity and specifics as other construction materials. Standard specifications, such as those published by ASTM, may be used for materials, but the specification for masonry construction must be addressed through project-specific requirements uniquely

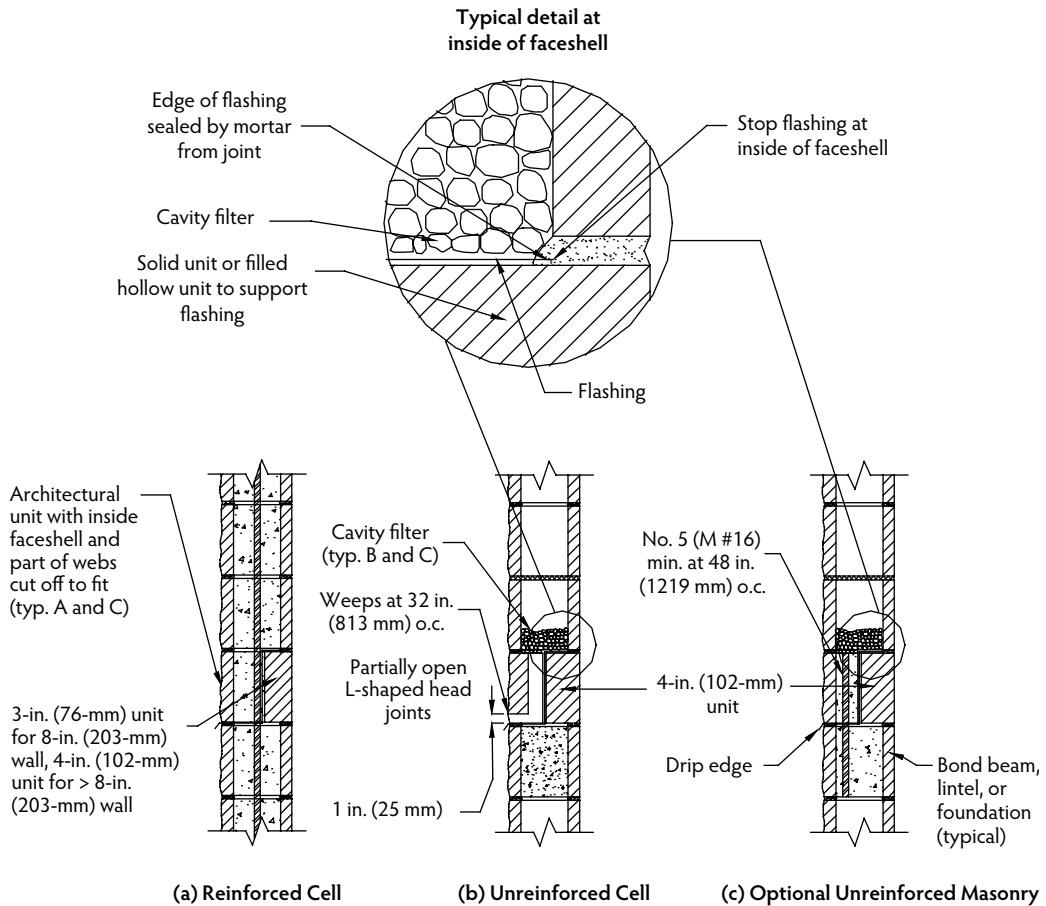


FIGURE 28.17 Flashing strategies for masonry. (Courtesy of the National Concrete Masonry Association, Herndon, VA.)

adapted to each project. Specifications must be thorough and at a minimum cover the materials, work, testing and inspection, coordination, and methods selected for each project. One of the most comprehensive generic masonry specifications is the *Annotated Guide to Masonry Specification* (TMS, 2000). This document provides a comprehensive, generic specification for masonry construction along with additional discussion and commentary to guide the user in the selection of project-specific requirements.

28.9 Structural Design

28.9.1 Design Methodologies

The structural design of masonry structures in the United States is governed by the provisions of *Building Code Requirements for Masonry Structures* (ACI Committee 530, 2005) in combination with the requirements of the locally adopted building code. The MSJC Code further stipulates that when the locally adopted building code does not contain the appropriate loading criteria for design the provisions of ASCE 7, *Minimum Design Loads for Buildings and Other Structures* (ASCE, 2005), should be used. In the context of today's structural design environment, in which the majority of the United States has adopted and enforced the International Building Code (ICC, 2006a), the structural design of masonry is governed by the MSJC Code as augmented by the IBC and ASCE 7. The following summary focuses on the requirements of the 2005 MSJC Code. The user is cautioned to review the provisions of the locally adopted building code for any applicable modifications to these provisions.

The structural design methods address by the MSJC Code include:

- *Empirical design* is also referred to as *non-engineered design* because it does not explicitly take into account applied design loads on the structure. The roots of empirical design extend back several centuries, when successful forms of construction were used as a model for subsequent projects. The contemporary practice of empirical design limits, design spans, and member sizes is based in large part on the successful use of these rules-of-thumb guidelines developed over several centuries. Because the empirical design method does not explicitly take into consideration modern design loads, its use is not permitted in areas of anticipated high wind or seismic events. Further, because of its historical basis, empirical design is limited to only conventional concrete and clay masonry materials.
- *Allowable stress design* is also referred to as *working stress design* because the stresses in the masonry are limited to the allowable, or working, level of serviceability stresses by code-imposed factors of safety. Allowable stress design is the most commonly used engineered design method for masonry today due in part to its relative ease in application and also because, although the design provisions are under constant maintenance to reflect the latest state-of-the-art design, the basic methodology has remained unchanged for many decades. As of the 2005 edition of the MSJC Code, the allowable stress design provisions applied only to conventional concrete and clay masonry construction.
- *Strength design* is very similar in concept and application to the strength design method used for reinforced concrete. Although various strength design provisions for masonry have been in existence for several decades, it was first introduced into the MSJC Code in 2002. The 2005 MSJC strength design provisions apply to conventional concrete and clay masonry, prestressed masonry, and AAC masonry materials.
- *Prescriptive detailing* (or *deemed-to-comply design*), in addition to the empirical and engineered design methods outlined in the MSJC Code, is addressed in the MSJC. As of the 2005 edition of the MSJC Code, the prescriptive design requirements are predominately limited only to masonry veneers, although several prescriptive good practices are still included in each of the engineered design methods. Several prescriptive design requirements for the structural design of residential masonry construction are contained in the International Residential Code (ICC, 2006b). Where appropriate, the code-required prescriptive design and detailing requirements are reviewed.

Both the allowable stress and strength design provisions address unreinforced and reinforced masonry construction. The distinction between unreinforced and reinforced masonry design is not the presence of reinforcement, as unreinforced masonry may actually have reinforcement present; instead, the design model for unreinforced masonry takes into consideration the flexural resistance of the masonry, neglecting the presence of any reinforcement present. Conversely, reinforced masonry design assumes that the reinforcement carries all tension stresses and assumes that the masonry is cracked. Each of these design methodologies is briefly reviewed in this section. Several comprehensive design guides are available covering the allowable stress and strength design provisions of the MSJC Code, including *Masonry Structures, Behavior and Design* (Drysdale et al., 1999) and the *Masonry Designer's Guide* (TMS, 2007), which reviews each section of the MSJC Code in detail while providing design examples and interpretation guidance. As such, the information presented here only briefly reviews these structural design provisions as they apply to masonry.

28.9.2 Prescriptive Seismic Detailing

Unlike other common design loads, including wind, soil, and live and dead loads, the design of masonry for earthquake loads assumes an inelastic response of the masonry structure during the seismic event. The one exception to this is for unreinforced masonry, which must remain uncracked for all loading conditions. To provide a minimum level of performance during an earthquake, the MSJC Code outlines minimum prescriptive design and detailing requirements for masonry as a function of the assumed seismic risk and expected level of structural ductility assumed during design. The minimum design and

TABLE 28.15 Seismic Detailing Requirements for Masonry Shear Wall Systems

Shear Wall Designation	MSJC Section Reference Design Method	Reinforcement Requirements	Use Permitted in Seismic Design Category
Empirical masonry shear walls	Section 5.3	None	A
Ordinary plain (unreinforced) masonry shear walls	Section 2.2, Section 3.2, or Chapter 4	None	A and B
Detailed plain (unreinforced) masonry shear walls	Section 2.2 or Section 3.2	Section 1.14.2.2.2	A and B
Ordinary reinforced masonry shear walls	Section 2.3 or Section 3.3	Section 1.14.2.2.3	A, B, and C
Intermediate reinforced masonry shear walls	Section 2.3 or Section 3.3	Section 1.14.2.2.4	A, B, and C
Special reinforced masonry shear walls	Section 2.3 or Section 3.3	Section 1.14.2.2.5	A, B, C, D, E, and F
Ordinary plain (unreinforced) AAC masonry shear walls	Section A.2	Section 1.14.2.2.6	A and B
Detailed plain (unreinforced) AAC masonry shear walls	Section A.2	Section 1.14.2.2.7	A and B
Ordinary reinforced AAC masonry shear walls	Section A.3	Section 1.14.2.2.8	A, B, C, D, E, and F

detailing requirements for masonry in low- to high-seismic-risk areas are triggered based on the assigned Seismic Design Category of the project. Likewise, some design methods or systems of limited ductility are restricted to projects of lower seismic risk, as shown in Table 28.15. The use of empirical design for sizing members of the lateral-force-resisting system is limited to Seismic Design Category A because the seismic loads are not directly accounted for in the design. Empirical design, however, can be used for designing nonloadbearing partitions up to and including Seismic Design Category C. Likewise, because of the limited ductility offered by unreinforced masonry members, the MSJC Code limits its use in the design of shear walls to Seismic Design Categories A and B only; hence, for projects of moderate to high seismic hazard, reinforced masonry is required for the design of elements that are part of the lateral-force-resisting system. The follow sections provide a general overview of the prescriptive seismic detailing requirements of the MSJC Code for both loadbearing and nonloadbearing masonry elements. It should be stressed that the prescriptive seismic reinforcement are minimums and may be less than that required to resist earthquake-induced loads.

28.9.2.1 Seismic Detailing Requirements for Nonloadbearing Elements

When incorporated into structures assigned to Seismic Design Category C, D, E, or F, masonry partition walls and other nonloadbearing masonry elements that are not designed to resist loads (other than those induced by their own mass) are required to be isolated from the lateral-force-resisting system. This helps to ensure that forces are not inadvertently transferred between the structural system and the nonstructural system. In addition, the nonstructural elements such as partition walls assigned to Seismic Design Category C and above must be reinforced in *either* the horizontal or vertical direction in accordance with the following and as illustrated in Figure 28.18:

- *Horizontal reinforcement*—Horizontal joint reinforcement is required to consist of at least two longitudinal W1.7 (MW 11) wires for walls having a thickness greater than 4 in. (102 mm). For walls 4 in. (102 mm) thick and less, only one W1.7 (MW 11) wire is required. The spacing of the joint reinforcement is not to exceed 16 in. (406 mm) for either case. Alternatively, bond beams incorporating at least one No. 4 bar (M #13) and spaced no farther apart than 48 in. (1219 mm) may be used instead of bed joint reinforcement. When used, the horizontal reinforcement is to be located within 16 in. (406 mm) of the top and bottom of these masonry walls.
- *Vertical reinforcement*—Vertical reinforcement is required to consist of at least one No. 4 (M #13) bar spaced no more than 48 in. (1219 mm) on-center. Vertical reinforcement must be located within 16 in. (406 mm) of the ends of the masonry wall.

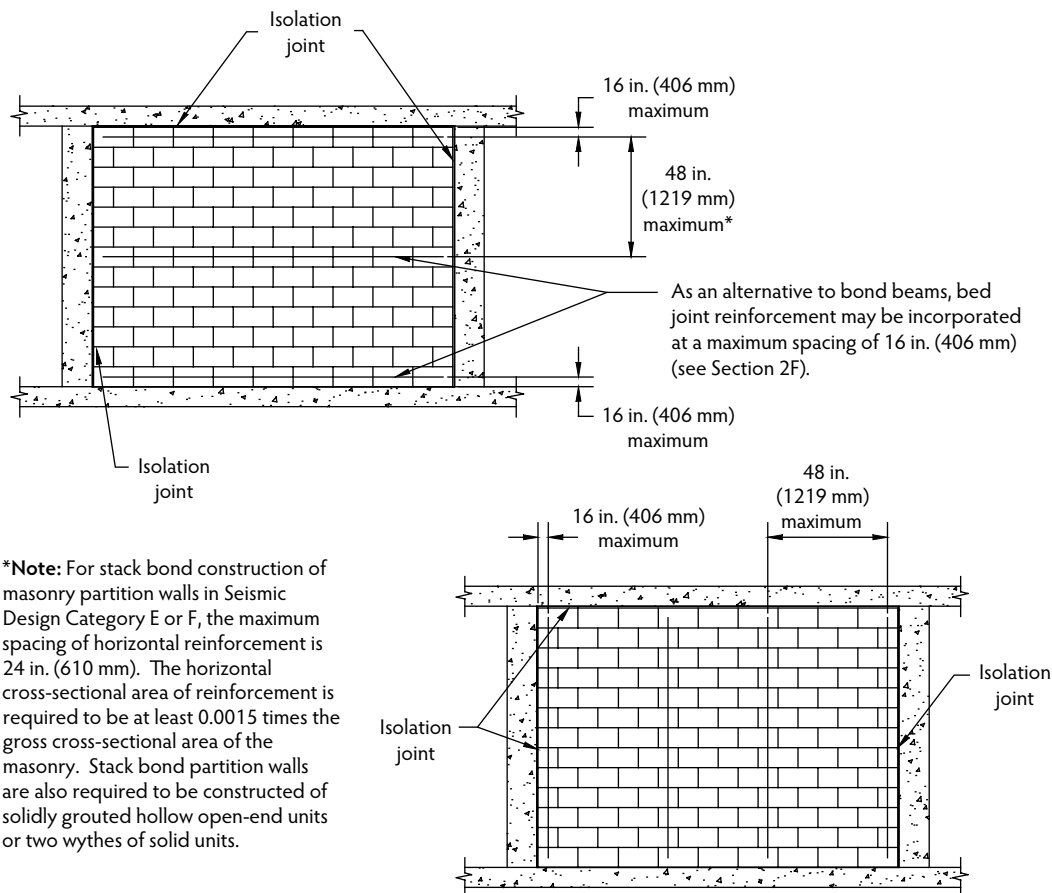


FIGURE 28.18 Minimum prescriptive seismic reinforcement for nonloadbearing masonry elements. (Courtesy of the National Concrete Masonry Association, Herndon, VA.)

28.9.2.2 Seismic Detailing Requirements for Detailed Plain (Unreinforced) and Ordinary Reinforced Masonry Shear Walls

Despite their two different names and underlying design methodology, detailed plain (unreinforced) and ordinary reinforced masonry shear walls share the same minimum prescriptive seismic detailing requirements. Detailed plain (unreinforced) masonry shear walls, which are designed as unreinforced elements of a structure, rely entirely upon the masonry to carry and distribute anticipated loads. To ensure a minimum level of performance during a design level earthquake, however, some prescriptive reinforcement is mandated by the MSJC Code for these shear wall types. Similarly, ordinary reinforced masonry shear walls, which are designed in accordance with reinforced masonry procedures, rely upon the reinforcement to carry and distribute anticipated tensile stresses while the masonry carries the compressive stresses. Although ordinary reinforced masonry shear walls contain some reinforcement, to ensure a minimum level of performance during a design-level earthquake, a minimum amount of prescriptive reinforcement is also mandated by the MSJC Code. With very few exceptions, the amount of reinforcement prescriptively required is less than that required by design. Because the reinforcement required by design may also serve as the minimum prescriptive reinforcement, compliance with the minimum prescriptive reinforcement requirements is relatively easy to achieve.

The minimum prescriptive seismic reinforcement for detailed plain (unreinforced) and ordinary reinforced masonry shear walls is summarized in the following and illustrated in Figure 28.19; neither horizontal nor vertical prescriptive reinforcement is required for openings smaller than 16 in. (406

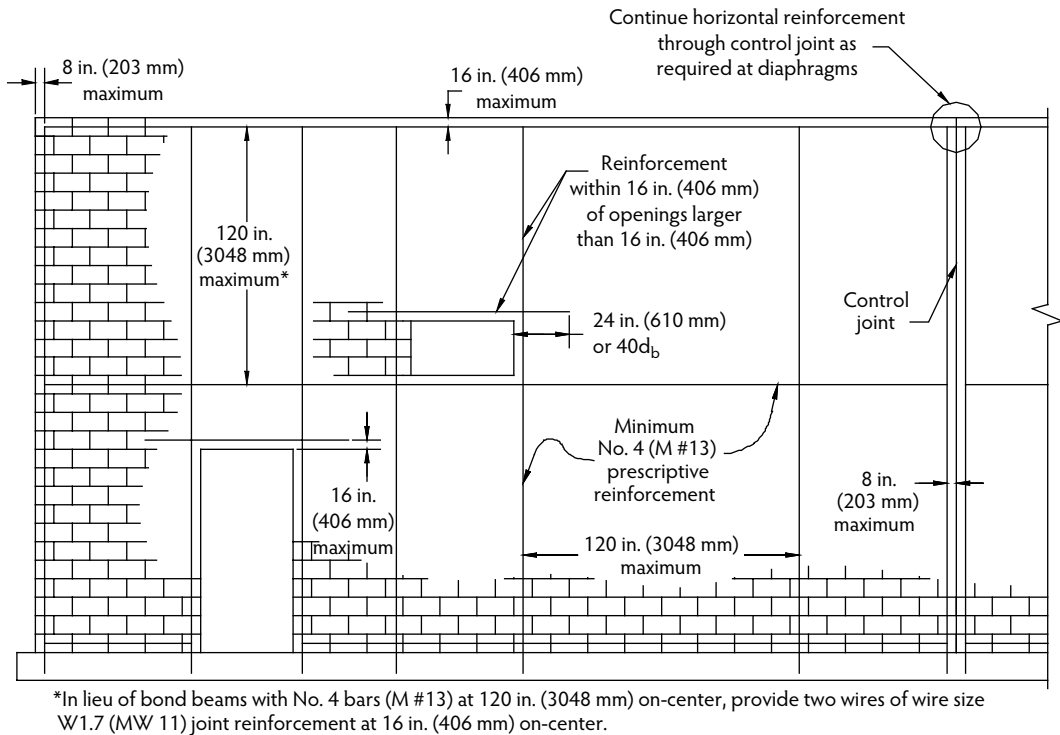


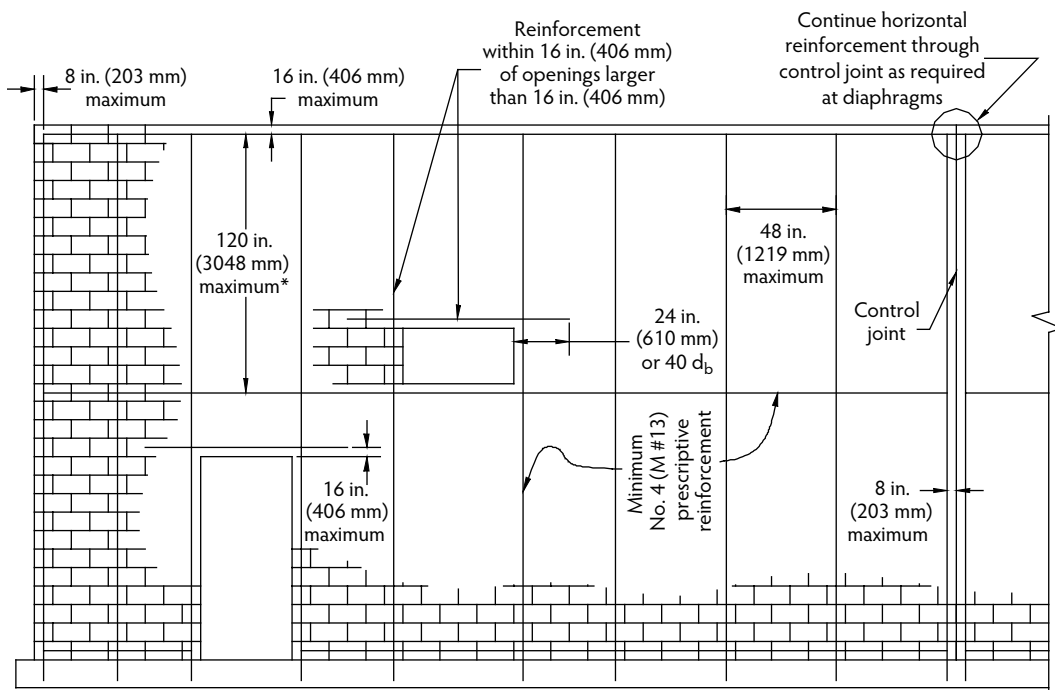
FIGURE 28.19 Minimum prescriptive seismic reinforcement for detailed plain (unreinforced) and ordinary reinforced masonry shear walls. (Courtesy of the National Concrete Masonry Association, Herndon, VA.)

mm) in either the horizontal or vertical direction, unless the required prescriptive reinforcement is interrupted by such openings:

- *Vertical reinforcement*—The prescriptive vertical reinforcement is required to consist of at least one No. 4 bar (M #13) at each corner, within 16 in. (406 mm) of each side of openings, within 8 in. (203 mm) of each side of control joints, within 8 in. (203 mm) of the ends of walls, and at a maximum spacing of 120 in. (3048 mm).
- *Horizontal reinforcement*—The minimum prescriptive horizontal reinforcement consists of at least two wires of wire size W1.7 (MW 11), with joint reinforcement spaced not more than 16 in. (406 mm) on-center or bond beams containing no less than one No. 4 (M #13) bar spaced not more than 120 in. (3048 mm) apart. Horizontal reinforcement is also required at the bottom and top of wall openings. Such reinforcement must extend at least 24 in. (610 mm) or 40 bar diameters, whichever is greater, past the opening. Structural reinforcement located at roof and floor levels is required to be continuous. The horizontal reinforcing bar located closest to the top of the wall must be placed within 16 in. (406 mm) of the top of the wall.

28.9.2.3 Seismic Detailing Requirements for Intermediate Reinforced Masonry Shear Walls

Like ordinary reinforced masonry shear walls, intermediate reinforced masonry shear walls are designed in accordance with the reinforced masonry design procedures and contain a minimum amount of reinforcement to ensure a minimum level of performance and ductility during a design-level earthquake. As shown in Figure 28.20, the prescriptive reinforcement for intermediate reinforced masonry shear walls is the same as for ordinary reinforced masonry shear walls, except that the maximum spacing of the vertical reinforcement is reduced to 48 in. (1219 mm).



*In lieu of bond beams with No. 4 bars (M #13) at 120 in. (3048 mm) on-center, provide two wires of wire size W1.7 (MW 11) joint reinforcement at 16 in. (406 mm) on-center.

FIGURE 28.20 Minimum prescriptive seismic reinforcement for intermediate reinforced masonry shear walls. (Courtesy of the National Concrete Masonry Association, Herndon, VA.)

28.9.2.4 Seismic Detailing Requirements for Special Reinforced Masonry Shear Walls

Special reinforced masonry shear walls provide the most assumed ductility of all the various shear wall types and concurrently contain the most prescriptive reinforcement of all the various masonry shear-wall types. As such, special reinforced masonry shear walls are permitted in any seismic design category. Due to the large quantities of prescriptive horizontal reinforcement, control joints are typically not necessary for special reinforced masonry shear walls. As shown in Figure 28.21, the prescriptive reinforcement for special reinforced masonry shear walls is required to comply with the requirements for intermediate reinforced masonry shear walls and the following:

- The sum of the cross-sectional area of horizontal and vertical reinforcement shall be at least 0.002 times the gross cross-sectional area of the wall, and the minimum cross-sectional area in each direction shall be not less than 0.0007 times the gross cross-sectional area of the wall. The maximum spacing of vertical and horizontal reinforcement shall be the smallest of one third the length of the shear wall, one third the height of the shear wall, or 48 in. (1219 mm) and shall be uniformly distributed. The minimum cross-sectional area of vertical reinforcement shall be one third of the required horizontal reinforcement. All horizontal reinforcement shall be anchored around the vertical reinforcement with a standard hook.
- Stack bond masonry shear walls assigned to Seismic Design Category D, E, or F are required to be constructed of fully grouted open-end units, fully grouted hollow units laid with full head joints, or solid units. The maximum spacing of reinforcement for stack bond masonry shear walls assigned to Seismic Design Category D is 24 in. (610 mm). Stack bond masonry shear walls assigned to Seismic Design Category E or F are required to have a horizontal cross-sectional area of reinforcement of at least 0.0025 times the gross cross-sectional area of the masonry at a maximum spacing of 16 in. (406 mm).

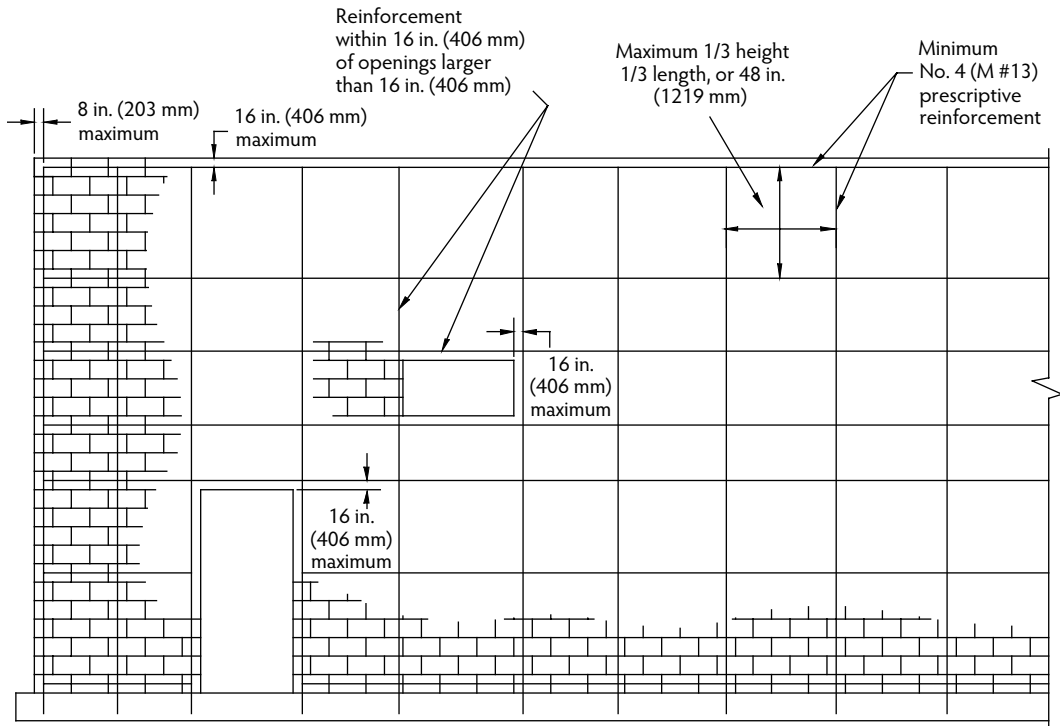


FIGURE 28.21 Minimum prescriptive seismic reinforcement for special reinforced masonry shear walls. (Courtesy of the National Concrete Masonry Association, Herndon, VA.)

28.9.3 Empirical Design of Masonry

28.9.3.1 Limitations

As previously reviewed, the use of empirical design for sizing and proportioning structural members is limited to regions of relatively low seismic risk and design wind speeds because the procedures do not directly account for design loads. Instead, the provisions are based on successful construction practices developed over a long period of time in various applications. For seismic design, the empirical requirements are not permitted to be used to design any portion of a structure assigned to Seismic Design Category D or higher. The procedure can be used to design nonloadbearing members that are not part of the lateral-force-resisting structure in Seismic Design Categories B and C. Only in Seismic Design Category A can empirical design be used to design members that are part of the lateral-force-resisting structure. The limits on the use of the empirical design procedures for resisting wind loads is slightly more complex, as it is a function of the building height, exposure conditions, type of masonry element, and basic design wind speed, as shown in Table 28.16.

28.9.3.2 Empirically Designed Shear Walls

The minimum nominal thickness of empirically designed masonry shear walls is required to be no less than 8 in. (203 mm). Shear walls must be provided in two separate planes in each principle axis of the building. The minimum cumulative length of the shear walls in each principle direction must be at least 40% of the longest building dimension in plan. Portions of a masonry wall containing openings or members whose length is less than one half its height are not permitted to be included in the cumulative shear-wall length. As an example, a building measuring 80 × 60 ft (24 × 18 m) in plan must provide 32 ft (9.8 m) of cumulative shear-wall length in each principle direction. The maximum spacing between shear walls is determined based on the type of diaphragm system used in the structure. Shear walls

TABLE 28.16 Wind Speed Limits for Empirical Design

Elements	Building Height, ft (m)	Basic Wind Speed, mph (kph)			
		≤90 (145)	90–100 (145–161)	100–110 (161–177)	>110 (177)
All masonry elements that are part of the lateral-force-resisting system and other exterior masonry elements located 35 ft (11 m) or less above ground	≤35 (11)	Permitted	Permitted	Permitted	Not permitted
Interior masonry elements that are not part of the lateral-force-resisting system in buildings other than enclosed as defined by ASCE 7	>180 (55)	Not permitted	Not permitted	Not permitted	Not permitted
	60–180 (18–55)	Permitted	Permitted	Not permitted	Not permitted
	35–60 (11–18)	Permitted	Permitted	Not permitted	Not permitted
	≤35 (11)	Permitted	Permitted	Permitted	Not permitted
Exterior masonry elements that are not part of the lateral-force-resisting system that are more than 35 ft (11 m) above ground	>180 (55)	Not permitted	Not permitted	Not permitted	Not permitted
	60–180 (18–55)	Permitted	Not permitted	Not permitted	Not permitted
	35–60 (11–18)	Permitted	Permitted	Not permitted	Not permitted

TABLE 28.17 Empirically Designed Shear Wall Spacing Limits

Diaphragm Construction	Maximum Length-to-Width Ratio of Diaphragm
Cast-in-place concrete	5:1
Precast concrete	4:1
Metal deck with concrete fill	3:1
Metal deck with no fill	2:1
Wood	2:1

supporting more rigid diaphragms are permitted to be spaced farther apart than shear walls supporting relatively less rigid diaphragms, as shown in Table 28.17. When the diaphragm is part of a roof supported by empirically designed shear walls, the roof construction is required to be provided with ties or other means so out-of-plane thrust is not imparted to the walls under roof gravity loads.

28.9.3.3 Axial Compression

Contrary to the engineered design procedures for masonry, axial compressive stresses in empirical design are based on the specified gross cross-sectional area of masonry instead of the net cross-sectional area. Further, because of the inherent limits imposed on the use of empirically designed masonry in regions of moderate to high wind and seismic risk, the axial compressive loads are calculated based solely on dead and live loads. The MSJC Code provides allowable compressive stresses for empirically designed masonry based on masonry unit type (concrete, clay, or stone), mortar type, and construction type (single- or multiple-wythe construction). Table 28.18 outlines the allowable gross area compressive stresses for solid and hollow concrete masonry units. For values of masonry strengths between those listed, the MSJC Code does permit linear interpolation of allowable compressive stresses. In addition to the allowable compressive stresses, the empirical design procedures also require that bearing walls of one-story buildings have a minimum nominal thickness of 6 in. (152 mm), whereas bearing walls supporting more than one story have a nominal thickness of not less than 8 in. (203 mm). Because the empirical design provisions for masonry assume that no reinforcement is present, axial tension is not permitted to be carried by empirically

TABLE 28.18 Allowable Compressive Stresses for Empirical Design of Single Wythe Concrete Masonry

Construction and Compressive Strength of Masonry Unit (Gross Area), psi (MPa)	Allowable Compressive Stresses Based on Gross Cross-Sectional Area, psi (MPa)	
	Type M or S Mortar	Type N Mortar
Solid masonry of solid concrete masonry unit:		
3000 (20.69) or greater	225 (1.55)	200 (1.38)
2000 (13.79)	160 (1.10)	140 (0.97)
1200 (8.27)	115 (0.79)	100 (0.69)
Masonry of hollow loadbearing units:		
2000 (13.79) or greater	140 (0.97)	120 (0.83)
1500 (10.34)	115 (0.79)	100 (0.69)
1000 (6.90)	75 (0.52)	70 (0.48)
700 (4.83)	60 (0.41)	55 (0.38)

TABLE 28.19 Lateral Support Requirements for Empirically
Designed Masonry

Construction	Maximum Length-to-Thickness or Height-to-Thickness
<i>Bearing walls</i>	
Solid units or fully grouted	20
All other	18
<i>Nonbearing walls</i>	
Exterior	18
Interior	36

designed masonry elements. (The MSJC Code does not permit unreinforced masonry elements to carry axial tension but does permit unreinforced masonry elements to carry flexural tension.) When axial tension exists in the masonry, alternative means must be provided to carry these loads.

28.9.3.4 Lateral Support

The lateral support of simply-supported masonry walls in either the horizontal or vertical direction is limited to the ratios summarized in Table 28.19. When the masonry is assumed to be spanning horizontally, the lateral support is required to be provided by cross walls, pilasters, buttresses, or structural framing members. When the masonry is spanning vertically, the lateral support is to be provided by floors, diaphragm roofs, or structural framing members. When computing the ratio for multi-wythe walls, the following thicknesses are used:

- The nominal wall thickness for solid and hollow walls meeting the bonding requirements of the MSJC Code for composite action
- The sum of the nominal thicknesses of each wythe meeting the tie requirements of the MSJC Code for noncomposite action

28.9.3.5 Foundation Walls

The design of foundation walls in accordance with the empirical design procedures are based on the unbalanced backfill height, nominal wall thickness, and construction type as shown in Table 28.20. The use of the empirical design procedures for foundation walls is dependent on the following:

- The wall height does not exceed 8 ft (2.44 m) between lateral supports.
- The terrain around the foundation wall is graded to drain surface water away from the foundation.
- A granular, free-draining backfill is used to prevent hydrostatic pressures.
- The top of the foundation wall is laterally supported prior to backfilling.

TABLE 28.20 Empirically Designed Foundation Walls

Wall Construction	Nominal Wall Thickness, in. (mm)	Maximum Depth of Unbalanced Backfill, ft (m)
Hollow unit masonry	8 (203)	5 (1.52)
	10 (254)	6 (1.83)
	12 (305)	7 (2.13)
Solid unit masonry	8 (203)	5 (1.52)
	10 (254)	7 (2.13)
	12 (305)	7 (2.13)
Fully grouted masonry	8 (203)	7 (2.13)
	10 (254)	8 (2.44)
	12 (305)	8 (2.44)

- The length of the foundation wall between supporting cross walls or pilasters is not greater than 3 times the wall height.
- The masonry is laid in running bond using Type M or S mortar.

28.9.3.6 Miscellaneous Empirical Design Requirements

In addition to the design requirements for shear walls, axial compression, lateral support, and foundation walls, the empirical design requirements address several other topics, including cantilevered and parapet walls, multi-wythe construction, bonding of intersecting walls, anchorage requirements for floors and roofs, and chases and recesses. The reader is referred to the MSJC Code (ACI Committee 530, 2005) for information on these other design topics using the empirical design provisions.

28.9.4 Allowable Stress Design of Masonry

The most widely used structural design method for masonry structures is the allowable stress design procedure, also historically referred to as the *working stress design method*. The following discussion highlights several common aspects of allowable stress design as required by the MSJC Code. The basic premise of the allowable stress design method is that code-prescribed design loads cannot exceed code-prescribed allowable loads. The procedure itself is based on the following assumptions and compliance with standard structural engineering mechanics:

- Within the range of allowable stresses, masonry elements satisfy applicable conditions of equilibrium and compatibility of strains.
- Plane sections before bending remain plane after bending; therefore, masonry strain is directly proportional to the distance from the neutral axis.
- Stress is linearly proportional to strain within the allowable stress range.
- For reinforced masonry design, all tensile stresses are resisted by the steel reinforcement; the contribution of the masonry to the tensile strength of the element is ignored.
- The units, mortar, grout, and reinforcement, if present, act compositely to resist applied loads.

Using allowable stress design, masonry elements are sized and proportioned such that the anticipated service level loads can be safely and economically resisted using the specified material strengths. The specified strength of masonry and reinforcement are in turn reduced by appropriate safety factors to allowable stress levels. For load combinations that include wind or seismic loads, the MSJC Code permits these allowable stresses to be increased by one third.

28.9.4.1 Anchorage

The allowable stress design procedures in the MSJC Code contain design provisions for plate, headed, and bent-bar anchor bolts embedded in masonry. When alternative anchor types are used, or when

higher design values are desired, testing in accordance with ASTM E 488 (ASTM, 1996) is required. The design equations for the allowable stress design of anchor bolts embedded in masonry are based on standard breakout models assuming a 45° failure plane. All masonry materials (units, mortar, and grout) are considered effective in resisting the applied loads. For these design equations to provide a reasonable prediction of anchor performance, the MSJC Code requires that all bolts be embedded at least 4 bolt diameters but not less than 2 in. (51 mm). For headed and plate anchors, the embedment length is measured from the surface of the masonry (which includes the thickness of the masonry unit, if applicable) to the bearing surface of the plate or head of the anchor bolt. Similarly, the effective embedment length of bent-bar anchors is measured from the surface of the masonry to the bearing surface of the bent end minus one anchor bolt diameter.

The allowable tension load on masonry anchors is taken as the lesser of Equation 28.1 (masonry-controlled breakout failure) and Equation 28.2 (anchor-controlled failure).

$$B_a = 0.5A_p\sqrt{f'_m} \quad (28.1)$$

$$B_a = 0.2A_b f_y \quad (28.2)$$

where:

B_a = allowable axial force on a headed, plate, or bent-bar anchor (lb, N).

A_p = projected area of failure surface (in.², mm²).

f'_m = specified compressive strength of masonry (psi, MPa).

A_b = cross-sectional area of the anchor bolt (in.², mm²).

f_y = specified yield strength of the anchor bolt (psi, MPa).

For use in Equation 28.1, the projected area on the masonry surface (A_p) is calculated by the lesser of Equation 28.3 or Equation 28.4. In cases when the projected surfaces of adjacent anchor bolts overlap, the MSJC Code requires that the projected area of each bolt be reduced by one half of the overlapping area. This requirement, however, assumes that the projected area of no more than two anchor bolts would intersect. Although rare in masonry construction, where the projected areas of more than two anchor bolts overlap the overlapping areas should be reduced in linear proportion to the number of anchors overlapping a common surface. In all cases, the portion of the projected area falling within an open cell, hollow cavity, or outside of the masonry element should be deducted from A_p :

$$A_p = \pi l_b^2 \quad (28.3)$$

$$A_p = \pi l_{be}^2 \quad (28.4)$$

where:

l_b = effective embedment length of the anchor bolt (in., mm).

l_{be} = anchor bolt edge distance, measured in the direction of load, from the edge of the masonry to the center of the cross-section of the anchor bolt (in., mm).

For headed, plate, or bent-bar anchors having an edge distance greater than or equal to 12 bolt diameters, the allowable shear strength (B_v) is governed by the lesser of Equation 24.5 (masonry-controlled failure) or Equation 24.6 (anchor-controlled failure). Where the anchor bolt edge distance is less than 12 bolt diameters, the allowable shear load is required to be reduced by linear interpolation to a value of zero at an edge distance of 1 in. (25 mm):

$$B_v = 350\sqrt{f'_m A_b} \quad (28.5)$$

$$B_v = 0.12A_b f_y \quad (28.6)$$

Where anchor bolts are subjected to combined tension and shear, the MSJC Code requires the such anchors also be designed to satisfy Equation 28.7. This linear interaction model is recognized as being relatively conservative for anchor bolt design:

$$\frac{b_a}{B_a} + \frac{b_v}{B_v} \leq 1 \quad (28.7)$$

where:

b_a/B_a = ratio of applied to allowable axial force on the anchor bolt.

b_v/B_v = ratio of applied to allowable shear force on the anchor bolt.

28.9.4.2 Development and Splicing

The minimum development lengths for wires and reinforcing bars embedded in masonry are calculated by Equation 28.8 and Equation 28.9, respectively. Equation 28.8 applies to wires in tension only, whereas Equation 28.9 applies to reinforcing bars in tension or compression. In no case is the minimum development length to be less than 6 in. (152 mm) for wires and 12 in. (305 mm) for reinforcing bars:

$$l_d = 0.0015d_b F_s \quad (28.8)$$

$$l_d = \frac{0.13d_b^2 f_y \gamma}{K \sqrt{f'_m}} \quad (28.9)$$

where:

l_d = development length or lap length of reinforcing bar or wire (in., mm).

d_b = diameter of reinforcing bar or wire (in., mm).

F_s = allowable tensile or compressive stress in reinforcement (psi, MPa).

f_y = specified yield strength of reinforcing bar or wire (psi, MPa).

K = lesser of the masonry clear cover to the reinforcement, the clear spacing between adjacent reinforcement (not spliced reinforcing bars), or $5d_b$.

γ = 1.0 for No. 3 (M #10) through No. 5 (M #16) reinforcing bars; 1.3 for No. 6 (M #19) and No. 7 (M #22) reinforcing bars; and 1.5 for No. 8 (M #25) through No. 11 (M #36) reinforcing bars.

Where epoxy-coated wire or reinforcing bars are used, the development length calculated by Equation 28.8 or Equation 28.9 is increased by 50%.

Splicing of reinforcing bars is accomplished by lapping, welding, or mechanically connecting reinforcement. The minimum length for lap-spliced reinforcement is calculated in accordance with Equation 28.9. When welding or providing mechanical couplers, the splice is required to develop no less than 125% of the nominal yield strength of the spliced reinforcement. Although not overtly apparent upon initial inspection, lap splice lengths detailed to comply with Equation 28.9 also meet this minimum yield strength requirement.

28.9.4.3 Unreinforced Masonry Design

For unreinforced masonry, the masonry assembly (units, mortar, and grout if used) is designed to carry all applied stresses. The additional capacity from the inclusion of reinforcing steel, such as reinforcement added for the control of shrinkage cracking or prescriptively required by the code, is neglected. Because the masonry is intended to resist both tension and compression stresses resulting from applied loads, the masonry must be designed to remain uncracked.

28.9.4.3.1 Axial Compression and Flexure

Although unreinforced masonry can be designed to resist flexural tension stresses due to applied loads, unreinforced masonry may not be subjected to net axial tension, such as that due to wind uplift on a roof connected to a masonry wall or due to the overturning effects of lateral loads. Compressive stresses

from dead loads can be used to offset tensile stresses, but where the wall is subject to a net axial tension reinforcement must be incorporated to resist the resulting tensile forces. When masonry walls are subjected to compressive axial loads only, the calculated compressive stress due to the applied load (f_a) must not exceed the allowable compressive stress (F_a) as given by Equation 28.10 or Equation 28.11, as appropriate. For masonry elements with h/r not greater than 99:

$$f_a \leq F_a = \frac{1}{4} f'_m \left[1 - \left(\frac{h}{140r} \right)^2 \right] \quad (28.10)$$

For masonry elements with h/r greater than 99:

$$f_a \leq F_a = \frac{1}{4} f'_m \left(\frac{70r}{h} \right)^2 \quad (28.11)$$

where:

f_a = applied compressive stress in masonry due to axial load only (psi, MPa).

F_a = allowable compressive stress in masonry due to axial load only (psi, MPa).

f'_m = specified compressive strength of masonry (psi, MPa).

h = effective height of masonry element (in., mm).

r = radius of gyration of masonry element (in., mm).

Average and net cross-sectional properties such as radius of gyration, moment of inertia, section modulus, and area are available through various industry publications, including *Section Properties of Concrete Masonry Walls* (NCMA, 2003b).

A further check for stability is also required per Equation 28.12, whereby the axial compressive load (P) is limited to one fourth the buckling load (P_e). The eccentricity of the applied load (e) used to determine P_e in Equation 28.12 is the actual eccentricity of the applied axial load, not an equivalent eccentricity due to an applied bending moment:

$$P \leq \frac{1}{4} P_e = \frac{1}{4} \left[\frac{\pi^2 E_m I_n}{h^2} \left(1 - 0.577 \frac{e}{r} \right)^3 \right] \quad (28.12)$$

where:

P = applied axial load (lb, N).

P_e = Euler buckling load (lb, N).

E_m = modulus of elasticity of masonry (psi, MPa).

I_n = moment of inertia of net cross-sectional area of masonry (in.⁴, mm⁴).

h = effective height of masonry element (in., mm).

e = eccentricity of applied axial load (in., mm).

r = radius of gyration of masonry element (in., mm).

For unreinforced masonry elements subjected to flexural tension, the allowable flexural tension values are prescribed by the MSJC Code, and vary with the direction of span, mortar type, bond pattern, and percentage of grouting, as shown in Table 28.21. For walls spanning horizontally between supports, the code conservatively assumes that masonry constructed in stack bond cannot reliably transfer flexural tension stresses across the head joints. As such, the allowable flexural tension values parallel to the bed joints (perpendicular to the head joints) for stack bond construction are assumed to be zero for design purposes.

TABLE 28.21 Allowable Flexure Tension Stresses, psi (kPa)

Direction of Flexural Tensile Stress and Masonry Type	Mortar Types			
	Portland Cement–Lime or Mortar Cement		Masonry Cement or Air-Entrained Portland Cement–Lime	
	M or S	N	M or S	N
<i>Normal to bed joints</i>				
Solid units	40 (276)	30 (207)	24 (166)	15 (103)
Hollow units: ^a				
UngROUTED	25 (172)	19 (131)	15 (103)	9 (62)
Fully grouted	65 (448)	63 (434)	61 (420)	58 (400)
<i>Parallel to bed joints in running bond</i>				
Solid units	80 (552)	60 (414)	48 (331)	30 (207)
Hollow units:				
UngROUTED and partially grouted	50 (345)	38 (262)	30 (207)	19 (131)
Fully grouted	80 (552)	60 (414)	48 (331)	30 (207)
<i>Parallel to bed joints in stack bond</i>	0 (0)	0 (0)	0 (0)	0 (0)

^a For partially grouted masonry, allowable stresses shall be determined on the basis of linear interpolation between fully grouted hollow units and ungrouted hollow units based on amount (percentage) of grouting.

Because the compressive strength of masonry is much larger than its tensile strength (or mortar–unit bond strength), the strength of unreinforced masonry subjected to net flexural stresses is almost always controlled by the flexural tension values of Table 28.21. For masonry elements subjected to a bending moment (M) and a compressive axial force (P), the resulting flexural bending stress is determined using Equation 28.13:

$$f_b = \frac{Mt}{2I_n} - \frac{P}{A_n} \quad (28.13)$$

where:

f_b = applied stresses due to bending (psi, MPa).

M = applied bending moment (in.-lb, N-mm).

t = specified thickness of masonry element (in., mm).

I_n = moment of inertia of net cross-sectional area of masonry (in.⁴, mm⁴).

P = applied compressive axial load (lb, N).

A_n = net cross-sectional area of masonry element (in.², mm²).

If the value of the bending stress (f_b) given by Equation 28.13 is positive, then the masonry section is controlled by tension and the limiting values of Table 28.21 must be satisfied. Conversely, if f_b as given by Equation 28.13 is negative, the masonry section is in compression and the compressive stress limitation of Equation 28.14 must be met:

$$f_b \leq F_b = \frac{1}{3}f'_m \quad (28.14)$$

When unreinforced masonry elements are subjected to a combination of axial load and flexural bending, a unity equation is used to proportion the available allowable stresses to the applied loads per Equation 28.15:

$$\frac{f_a}{F_a} + \frac{f_b}{F_b} \leq 1 \quad (28.15)$$

28.9.4.3.2 Shear

Shear stresses on unreinforced masonry elements are calculated based on the net cross-sectional properties of the masonry in the direction of the applied shear force using Equation 28.16:

$$f_v = \frac{VQ}{I_n b} \quad (28.16)$$

where:

- f_v = applied shear stress in masonry element (psi, MPa).
- V = applied shear force (lb, N).
- Q = first moment of inertia (in.³, mm³).
- I_n = moment of inertia of net cross-sectional area of masonry (in.⁴, mm⁴).
- b = width of masonry section (in., mm).

Equation 28.16 is applicable to the determination of both in-plane and out-of-plane shear stresses. Because unreinforced masonry is designed to remain uncracked, it is not necessary to perform a cracked section analysis to determine the net cross-sectional area of the masonry.

The calculated shear stress due to applied loads (f_v) as given by Equation 28.16 is taken as the smaller of the following code-prescribed allowable shear stress values (F_v), as applicable:

$$1.5(f'_m)^{0.5}$$

120 psi (827 kPa)

For running bond masonry not grouted solid, $37 + 0.45N_v/A_n$

For stack bond masonry with open end units and grouted solid, $37 + 0.45N_v/A_n$

For running bond masonry grouted solid, $60 + 0.45N_v/A_n$

For stack bond masonry other than open end units grouted solid, 15 psi (103 kPa)

where:

- N_v = compressive force acting normal to the shear plane (lb, N).
- A_n = net cross-sectional area of masonry element (in.², mm²).

Although the MSJC Code designates these allowable shear stress values as being applicable to in-plane shear stresses only, no allowable shear stresses are provided for out-of-plane loads. In light of the absence of out-of-plane allowable shear stress values, the MSJC Code Commentary recommends using the in-plane allowable shear stress values for out-of-plane shear design.

28.9.4.4 Reinforced Masonry Design

The design of reinforced masonry in accordance with the MSJC Code neglects the tensile resistance provided by the masonry units, mortar, and grout in determining the strength of the masonry assemblage and assumes that all tension stresses are resisted by the reinforcement. Thus, for design purposes, the portion of masonry subjected to net tensile stresses is assumed to have cracked. Although the determination of the strength of a reinforced masonry element conservatively assumes the portion of the masonry subjected to net tensile stresses has cracked, this should be verified when establishing the stiffness and deflection of a reinforced masonry element.

28.9.4.4.1 Reinforcement

The tensile stress in the reinforcement due to the applied load (f_s) is calculated as the product of the strain in the steel (which increases linearly in proportion to the distance from the neutral axis) multiplied by its modulus of elasticity (E_s). The modulus of elasticity of mild steel reinforcement (E_s) is assumed to be 29,000,000 psi (200 GPa). The code-prescribed allowable steel stresses are as follows:

- For Grade 60 reinforcement in tension, $F_s = 24,000$ psi (165.5 MPa).
- For Grade 40 and 50 reinforcement in tension, $F_s = 20,000$ psi (137.9 MPa).

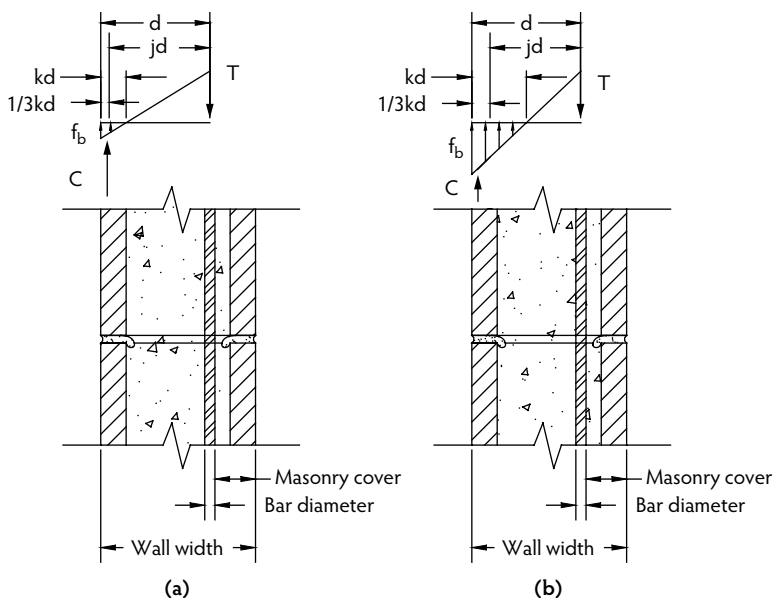


FIGURE 28.22 Allowable stress design model for reinforced masonry.

- For wire reinforcement in tension, $F_s = 30,000$ psi (206.9 MPa).
- For all reinforcement in compression, $F_s = 24,000$ psi (165.5 MPa) or $0.4f_y$, whichever is less.

Unless ties or stirrups laterally confine the reinforcement as prescribed by the MSJC Code, the reinforcement is assumed to contribute no compressive resistance to axially loaded elements. For design purposes, the effective width of the compression zone per bar is limited to the smallest of:

- Six times the wall thickness
- The center-to-center spacing of the reinforcement
- 72 in. (1829 mm)

This requirement applies to masonry constructed in running bond and to masonry constructed in stack bond containing bond beams spaced no farther than 48 in. (1219 mm) on-center. Where the center-to-center spacing of the reinforcement does not control the effective width of the compression zone, the resulting resisting moment or resisting shear is proportioned over the width corresponding to the actual reinforcement spacing.

28.9.4.4.2 Axial Compression and Flexure

As with unreinforced masonry, the allowable compressive stress in masonry (F_b) due to flexure or due to a combination of flexure and axial load is limited by Equation 28.14. When axial loads are not present or are conservatively neglected, as may be appropriate in some cases, several circumstances must be considered when determining the flexural capacity of reinforced masonry walls. For a fully grouted element, a cracked transformed section approach is used wherein the reinforcement area is transformed to an equivalent area of masonry using the modular ratio. Partially grouted walls are analyzed in the same way but with the additional consideration of the ungrouted cores. For partially grouted masonry, two types of behavior to consider are:

- When the neutral axis (the location of zero stress) lies within the compression face shell, as shown in Figure 28.22a, the wall is analyzed and designed as if the element were fully grouted.
- When the neutral axis lies within the core area, rather than the compression face shell, as shown in Figure 28.22b, the portion of the ungrouted cells (in partially grouted masonry) must be deducted from the area of masonry capable of carrying compression stresses.

The location of the neutral axis depends on the relative moduli of elasticity of the masonry and steel (n), as well as the reinforcement ratio (ρ) and the distance between the reinforcement and the extreme compression fiber (d). When analyzing partially grouted walls, it is typically assumed that the neutral axis lies within the compression face shell, as the analysis is more straightforward. Based on this assumption, the resulting value of k and the location of the neutral axis (kd) is calculated. If it is determined that the neutral axis lies outside the compression face shell, the more rigorous tee beam analysis is performed; otherwise, the rectangular beam analysis is carried out.

For fully grouted masonry elements and for partially grouted masonry elements with the neutral axis in the compression face shell, the resisting flexural capacity (M_r) is taken as the lesser of M_m (masonry controlled flexural strength) and M_s (reinforcing-steel-controlled flexural strength) calculated as follows:

$$n = \frac{E_s}{E_m} \quad (28.17)$$

$$\rho = \frac{A_s}{bd} \quad (28.18)$$

$$k = \sqrt{2\rho n + (\rho n)^2} - \rho n \quad (28.19)$$

$$j = 1 - \frac{k}{3} \quad (28.20)$$

$$M_m = \frac{1}{2} F_b k j b d^2 \quad (28.21)$$

$$M_s = A_s F_s j d \quad (28.22)$$

where:

n = modular ratio.

E_s = modulus of elasticity of reinforcing steel (psi, MPa).

E_m = modulus of elasticity of masonry (psi, MPa).

ρ = reinforcement ratio.

A_s = cross-sectional area of reinforcement (in.², mm²).

b = width of masonry element (in., mm).

d = effective depth to center of reinforcement (in., mm).

k = ratio of distance between compression face of masonry element and neutral axis to the effective depth (d).

j = ratio of distance between centroid of flexural compressive forces and centroid of tensile forces to depth (d).

M_m = flexural strength (resisting moment) when masonry controls (in.-lb, N-m).

M_s = flexural strength (resisting moment) when reinforcement controls (in.-lb, N-m).

For partially grouted masonry walls where the neutral axis is located within the cores, the resisting flexural capacity (M_r) is calculated using the neutral axis coefficient (k) given by Equation 28.23 and either Case A or Case B as follows:

$$k = \frac{-A_s n - t_{fs}(b - b_w)}{db_w} \quad (28.23)$$

where:

t_{fs} = thickness of face shell of masonry unit (in., mm).

b_w = for partially grouted walls, width of grouted cell plus each web thickness within the compression zone (in., mm).

Case A. For cases where the masonry strength controls the design:

$$f_s = nF_b \left(\frac{1-k}{k} \right) \quad (28.24)$$

where f_s is the calculated stress in reinforcement (psi, MPa). If f_s as determined using Equation 28.24 is greater than the allowable steel stress (F_s), then the strength of the section is controlled by the reinforcement and the masonry element is designed using the procedures outlined for Case B, below. Otherwise, the internal compression force (C) and tension force (T) are computed as follows:

$$C = \frac{1}{2} F_b b k d \quad (28.25)$$

$$T = A_s f_s = A_s n F_b \left(\frac{1-k}{k} \right) \quad (28.26)$$

Case B. For cases where the reinforcement strength controls the design:

$$f_b = \frac{F_s}{n} \left(\frac{k}{1-k} \right) \quad (28.27)$$

$$C = \frac{1}{2} f_b b k d = \frac{1}{2} b k d \left(\frac{F_s}{n} \left(\frac{k}{1-k} \right) \right) \quad (28.28)$$

$$T = A_s F_s \quad (28.29)$$

The resisting bending moment is then calculated by Equation 28.30 as follows:

$$M_r = C \left(\frac{2t_{f_s}}{3} \right) - T \left(d - \frac{k d}{3} - \frac{2t_{f_s}}{3} \right) \quad (28.30)$$

Axial compressive loads acting through the axis of a member are distributed over the net cross-sectional area of masonry supporting the load. The allowable axial compressive force is based on the compressive strength of masonry and the slenderness ratio of the element in accordance with Equation 28.31 or Equation 28.32, as appropriate. Axial tensile loads, conversely, are carried entirely by the reinforcement. For elements with h/r not greater than 99, the allowable compressive force (P_a) is:

$$P_a = \left(0.25 f'_m A_n + 0.65 A_{st} F_s \right) \left[1 - \left(\frac{h}{140r} \right)^2 \right] \quad (28.31)$$

For elements with h/r greater than 99, the allowable compressive force (P_a) is:

$$P_a = \left(0.25 f'_m A_n + 0.65 A_{st} F_s \right) \left(\frac{70r}{h} \right)^2 \quad (28.32)$$

where:

P_a = allowable axial compressive force (lb, N).

A_{st} = total area of laterally tied reinforcement (in.², mm²).

Often, loading conditions result in both axial load and flexure on a wall. Superimposing the stresses resulting from axial compression and flexural compression produces the combined stress. Members are proportioned so this maximum combined stress does not exceed the allowable stress limitations outlined above.

28.9.4.4.3 Shear

Shear acting on masonry flexural members and shear walls is resisted entirely either by the masonry (units, mortar and grout) or by shear reinforcement. This design approach is contrasted by that used for the strength design of reinforcement masonry, which allows the masonry and shear reinforcement to act together in resisting applied shear forces. For masonry members that are not subjected to flexural tension, the allowable shear stresses for unreinforced masonry apply. For masonry elements that are subjected to flexural tension, the applied shear stress is calculated as follows:

$$f_v = \frac{V}{bd} \quad (28.33)$$

Where reinforcement is not provided to resist the entire calculated shear stress, f_v , the allowable shear stress, F_v , is determined in accordance with the following:

For flexural members, $F_v = \sqrt{f'_m} \leq 50$ psi (345 kPa)

For shear walls where $M/Vd < 1$, $F_v = \frac{1}{3} [4 - (M/Vd)] \sqrt{f'_m} \leq 80 - 45(M/Vd)$

For shear walls where $M/Vd \geq 1$, $F_v = \sqrt{f'_m} \leq 35$ psi (241 kPa)

When shear reinforcement is provided to resist the entire shear force, the minimum amount of shear reinforcement is determined by Equation 28.34. Shear reinforcement provided in accordance with Equation 28.34 must also comply with the following:

- Shear reinforcement is oriented parallel to the direction of the shear force.
- Shear reinforcement spacing must not exceed the lesser of $d/2$ or 48 in. (1219 mm).

Reinforcement must also be provided perpendicular to the shear reinforcement. This prescriptive reinforcement must have an area of at least one third A_v as given by Equation 28.34 and may not be spaced farther apart than 8 ft (2438 mm):

$$A_v = \frac{Vs}{F_s d} \quad (28.34)$$

where:

A_v = cross-sectional area of shear reinforcement (in.², mm²).

s = spacing of shear reinforcement (in., mm).

Where reinforcement is provided to resist the entire calculated shear stress, f_v , the allowable shear stress, F_v , is determined in accordance with the following:

For flexural members, $F_v = 3.0 \sqrt{f'_m} \leq 150$ psi (1034 kPa)

For shear walls where $M/Vd < 1$, $F_v = \frac{1}{2} [4 - (M/Vd)] \sqrt{f'_m} \leq 120 - 45(M/Vd)$

For shear walls where $M/Vd \geq 1$, $F_v = 1.5 \sqrt{f'_m} \leq 75$ psi (517 kPa)

In each of the above equations, the ratio of M/Vd must be taken as a positive value.

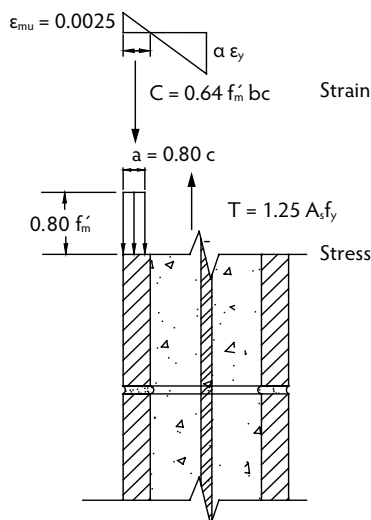


FIGURE 28.23 Strength design model for reinforced masonry.

28.9.5 Strength Design of Masonry

The following discussion provides a basic overview of design criteria and requirements for masonry structures designed using the strength design provisions contained in Chapter 3 of the MSJC Code. Strength design is based on the following design assumptions in conjunction with basic principles of engineering mechanics:

- Plane sections before bending remain plane after bending; therefore, strain in the masonry and in reinforcement, if present, is directly proportional to the distance from the neutral axis.
- For unreinforced masonry, the flexural stresses in the masonry are assumed to be directly proportional to strain. For reinforced masonry, the tensile strength of the masonry is neglected when calculating flexural strength but considered when calculating deflection.
- The units, mortar, grout, and reinforcement for reinforced masonry act compositely to resist applied loads.
- The nominal strength of masonry cross-sections for combined flexure and axial load is based on applicable conditions of equilibrium.
- The maximum masonry compressive stress is $0.8f'_m$ for both reinforced and unreinforced masonry.
- The maximum usable strain (ϵ_{mu}) at the extreme compression fiber is 0.002 for concrete masonry and 0.0035 for clay masonry.
- For reinforced masonry, reinforcement stresses below the specified yield strength (f_y) are taken equal to the modulus of elasticity of the reinforcement (E_s) times the steel strain (ϵ_s). For strains greater than that corresponding to f_y , stress in the reinforcement is taken equal to f_y .
- For reinforced masonry, the compressive stress is rectangular and uniformly distributed over an equivalent compression zone, bounded by the compression face of the masonry with a depth of $a = 0.80c$.

Based on the assumed design model outlined above, the internal distribution of stresses and strains is illustrated in Figure 28.23 for a reinforced masonry element. Using strength design, the design strength of an element is compared to the factored strength, which includes code-prescribed load factors. The design strength of masonry is the nominal strength multiplied by an appropriate strength reduction factor (ϕ). The design is acceptable when the design strength equals or exceeds the factored strength (i.e., when $\phi M_n \geq M_u$).

28.9.5.1 Strength Reduction Factors

To account for uncertainties in construction, material properties, calculated vs. actual strength and anticipated failure modes, the nominal strength of a masonry element is multiplied by an appropriate strength reduction factor (ϕ). The strength reduction factors are used in conjunction with the load factors applied to the design loads. The values of the strength reduction factors for various types of loading conditions are as follows:

- For reinforced masonry elements subjected to flexure or axial loads, $\phi = 0.90$.
- For unreinforced masonry elements subjected to flexure or axial compressive loads, $\phi = 0.60$.
- For masonry elements subjected to shear loads, $\phi = 0.80$.
- For bearing on masonry elements, $\phi = 0.60$.
- For anchor bolts:
 - Where the nominal strength of the anchor bolt is governed by masonry breakout, $\phi = 0.50$.
 - Where the nominal strength of the anchor bolt is governed by the anchor steel, $\phi = 0.90$.
 - Where the nominal strength of the anchor bolt is governed by anchor pullout, $\phi = 0.65$.

28.9.5.2 Anchorage

The strength design of anchors embedded in masonry is similar in concept to that for allowable stress design, with several key differences in the prescriptive detailing and nominal strengths. Unlike allowable stress design, the MSJC strength design provisions require embedded anchor bolts to have at least 1/2 in. (13 mm) of grout between the bolt and the masonry, except that 1/4-in. (6.4-mm)-diameter anchor bolts are permitted to be placed in mortared bed joints at least 1/2 in. (13 mm) thick. Nominal strengths of headed and bent-bar anchor bolts are determined using the equations outlined in this section. The strength design provisions do not explicitly address plate anchors embedded in masonry construction. Further, when anchor bolts penetrate the face shell of a masonry unit and are designed by the strength design method, the opening in the face shell is required to provide at least 1/2 in. (13 mm) of grout cover around the perimeter of the bolt. This prescriptive detailing requirement is intended to provide a means of inspection to ensure the adequate placement of grout around the anchor bolt and does not influence the design strength of the connection.

The nominal axial tensile strength of headed anchor bolts embedded in masonry (B_{an}) is taken as the smaller of Equation 28.35 (masonry-controlled breakout failure) and Equation 28.36 (anchor-controlled failure). The nominal axial tensile strength of bent-bar anchor bolts embedded in masonry, (B_{an}) is taken as the smallest value of Equation 28.35, Equation 28.36, and Equation 28.37 (anchor pullout failure). The second term in Equation 28.37, which accounts for frictional resistance along the shank of the anchor, is only included in the nominal axial strength calculation if jobsite inspection verifies that the shanks of the bent-bar anchors are free of oil, grease, or other debris that would decrease the bond between the anchor bolt and grout.

$$B_{an} = 4A_{pt}\sqrt{f'_m} \quad (28.35)$$

$$B_{an} = A_b f_y \quad (28.36)$$

$$B_{an} 1.5f'_m e_b d_b + \left[300\pi(l_b + e_b + d_b)d_b \right] \quad (28.37)$$

where:

B_{an} = nominal axial strength of anchor bolt (lb, N).

A_{pt} = projected area of failure surface (in.², mm²).

f'_m = specified compressive strength of masonry (psi, MPa).

A_b = cross-sectional area of the anchor bolt (in.², mm²).

f_y = specified yield strength of the anchor bolt (psi, MPa).

e_b = projected leg extension of the bent-bar anchor, measured from the inside edge of the anchor at bend to farthest point of anchor in the plane of the hook (in., mm).

d_b = diameter of the anchor bolt (in., mm).

l_b = effective embedment length of the anchor bolt, not to be less than 4 bolt diameters or 2 in. (51 mm), whichever is less (in., mm).

For use in Equation 28.35, the projected area on the masonry surface of a right circular breakout cone (A_{pt}) is calculated using Equation 28.38. In cases when the projected surfaces of adjacent anchor bolts overlap, the MSJC Code requires that the projected area of each bolt be reduced by one half of the overlapping area. This requirement, however, assumes that the projected areas of no more than two anchor bolts would intersect. Although rare in masonry construction, where the projected areas of more than two anchor bolts overlap, the overlapping areas should be reduced in linear proportion to the number of anchors overlapping a common surface. In all cases, the portion of the projected area falling within an open cell, hollow cavity, or outside of the masonry element should be deducted from A_{pt} :

$$A_{pt} = \pi l_b^2 \quad (28.38)$$

The nominal shear strength of headed and bent-bar anchor bolts (B_{vn}) is governed by the smaller of Equation 28.39 (masonry-controlled breakout failure) or Equation 28.40 (anchor-controlled failure):

$$B_{vn} = 4A_{pv}\sqrt{f'_m} \quad (28.39)$$

$$B_{vn} \leq 0.6A_b f_y \quad (28.40)$$

Where the projected area on a masonry surface of one half of a right circular cone, A_{pv} is calculated in accordance with Equation 28.41 as follows:

$$A_{pv} = \frac{\pi l_{be}^2}{2} \quad (28.41)$$

Where anchor bolts are subjected to combined tension and shear, the MSJC Code requires that such anchors also be designed to satisfy Equation 28.42; this linear interaction model is recognized as being relatively conservative for anchor bolt design:

$$\frac{b_{af}}{\phi B_{an}} + \frac{b_{vf}}{\phi B_{vn}} \leq 1 \quad (28.42)$$

where:

b_{af} = factored axial force in anchor bolt (lb, N).

b_{vf} = factored shear force in anchor bolt (lb, N).

ϕB_{an} = governing design axial strength of anchor bolt (lb, N).

ϕB_{av} = governing design shear strength of anchor bolt (lb, N).

28.9.5.3 Development and Splicing

Minimum development and lap splice lengths for strength design are nearly identical to those outlined in Section 28.9.4.2 for allowable stress design, with a couple of notable exceptions. The strength design provisions do not explicitly address requirements for the development or splicing of wire reinforcement. Further, the strength design provisions limits the maximum size of reinforcement to No. 9 (M #29) reinforcing bars. With these exceptions, minimum lap splice and development length are calculated in accordance with Equation 28.9.

28.9.5.4 Unreinforced Masonry Design

For unreinforced masonry, the masonry assembly (units, mortar, and grout, if used) is designed to carry all applied stresses. The additional capacity from the inclusion of reinforcing steel, such as reinforcement

added for the control of shrinkage cracking or prescriptively required by the code, is neglected. Because the masonry is intended to resist both tension and compression stresses resulting from applied loads, the masonry must be designed to remain uncracked.

28.9.5.4.1 Axial Compression and Flexure

As with the allowable stress design of masonry, unreinforced masonry designed by the strength design procedures can be used to resist flexural tension stresses due to applied loads; however, unreinforced masonry may not be subjected to net axial tension, such as that due to wind uplift on a roof connected to a masonry wall or due to the overturning effects of lateral loads. Although compressive stresses from dead loads can be used to offset tensile stresses, where the wall is subject to a net axial tension reinforcement must be incorporated to resist the resulting tensile forces. When masonry walls are subjected to compressive axial loads only, the nominal axial strength (P_a) is calculated in accordance with Equation 28.43 or Equation 28.44, as appropriate. For masonry elements with h/r not greater than 99:

$$P_a = 0.8 \left\{ 0.8 A_n f'_m \left[1 - \left(\frac{h}{140r} \right)^2 \right] \right\} \quad (28.43)$$

For masonry elements with h/r greater than 99:

$$P_a = 0.8 \left\{ 0.84 A_n f'_m \left(\frac{70r}{h} \right)^2 \right\} \quad (28.44)$$

where:

- P_a = nominal axial strength of the masonry element (lb, N).
- A_n = net cross-sectional area of the masonry element (in.², mm²).
- f'_m = specified compressive strength of the masonry (psi, MPa).
- h = effective height of the masonry element (in., mm).
- r = radius of gyration of the masonry element (in., mm).

For unreinforced masonry elements subjected to flexural tension, the modulus of rupture values are prescribed by the MSJC Code and vary with the direction of span, mortar type, bond pattern, and percentage of grouting, as shown in Table 28.22. For walls spanning horizontally between supports, the code conservatively assumes that masonry constructed in stack bond cannot reliably transfer flexural tension stresses across the head joints. As such, the allowable flexural tension values parallel to the bed joints (perpendicular to the head joints) for stack bond construction are assumed to be zero for design purposes.

For masonry elements subjected to a factored bending moment (M_u) and a factored axial force (P_u), the resulting flexural bending stress is determined using Equation 28.45. If the value of the bending stress (F_u) given by Equation 28.45 is positive, then the masonry section is controlled by tension, and the modulus of rupture values of Table 28.22, reduced by the appropriate strength reduction factor, must be satisfied. Conversely, if F_u as given by Equation 28.45 is negative, then the masonry section is in compression and the design compressive stress of $0.80f'_m$ applies. When using axial compressive loads to offset flexural bending stresses, only dead loads or other permanent loads should be included in P_u :

$$F_u = \frac{M_u t}{2I_n} - \frac{P_u}{A_n} \quad (28.45)$$

where:

- F_u = factored flexural stresses due to bending (psi, MPa).
- M_u = factored bending moment (in.-lb, N-mm).
- t = specified thickness of masonry element (in., mm).

TABLE 28.22 Modulus of Rupture Values, psi (kPa)

Direction of Flexural Tensile Stress and Masonry Type	Mortar Types			
	Portland Cement–Lime or Mortar Cement		Masonry Cement of Air-Entrained Portland Cement–Lime	
	M or S	N	M or S	N
<i>Normal to bed joints</i>				
Solid units	100 (689)	75 (517)	60 (413)	38 (262)
Hollow units: ^a				
UngROUTed	63 (431)	48 (331)	38 (262)	23 (158)
Fully grouted	163 (1124)	158 (1089)	153 (1055)	145 (1000)
<i>Parallel to bed joints in running bond</i>				
Solid units	200 (1379)	150 (1033)	120 (827)	75 (517)
Hollow units:				
UngROUTed and partially grouted	125 (862)	95 (655)	75 (517)	48 (331)
Fully grouted	200 (1379)	150 (1033)	120 (827)	75 (517)
<i>Parallel to bed joints in stack bond</i>	0 (0)	0 (0)	0 (0)	0 (0)

^a For partially grouted masonry, allowable stresses shall be determined on the basis of linear interpolation between fully grouted hollow units and ungrouted hollow units based on amount (percentage) of grouting.

I_n = moment of inertia of net cross-sectional area of masonry (in.⁴, mm⁴).

P_u = factored axial load (lb, N).

A_n = net cross-sectional area of masonry element (in.², mm²).

28.9.5.4.2 Shear

In-plane and out-of-plane shear stresses on unreinforced masonry elements are calculated based on the net cross-sectional properties of the masonry in the direction of the applied shear force. Because unreinforced masonry is designed to remain uncracked, it is not necessary to perform a cracked section analysis to determine the net cross-sectional area of the masonry. The nominal shear strength is taken as the smallest of the following conditions, as applicable:

$$3.8A_n(f'_m)^{0.5}$$

$$300A_n$$

For running bond masonry not grouted solid, $56A_n + 0.45N_u$

For stack bond masonry with open end units and grouted solid, $56A_n + 0.45N_u$

For running bond masonry grouted solid, $90A_n + 0.45N_u$

For stack bond masonry other than open end units grouted solid, $23A_n$

where:

N_u = factored compressive force acting normal to the shear plane that is associated with the V_u loading combination under consideration (lb, N).

A_n = net cross-sectional area of masonry element (in.², mm²).

28.9.5.5 Reinforced Masonry Design

The design of reinforced masonry in accordance with the strength design procedures of the MSJC Code neglects the tensile resistance provided by the masonry units, mortar, and grout in determining the strength of the masonry assemblage. Thus, for design purposes, the portion of masonry subject to net tensile stress is assumed to have cracked, transferring all tensile forces to the reinforcement. Strength design of reinforced masonry is based on the specified yield strength of reinforcement (f_y), which is limited to 60,000 psi (413.7 MPa). The actual yield strength of the reinforcement is limited to 1.3 times the specified yield strength. The compressive resistance of steel reinforcement is not permitted to be used unless lateral reinforcement is provided. Using strength design, reinforcing bars used in masonry are not permitted to be larger than No. 9 (M #29). Further, the nominal bar diameter is not permitted to exceed

one eighth of the nominal member thickness or one quarter of the least clear dimension of the cell, course, or collar joint in which it is placed. The area of reinforcing bars placed in a cell or in a course of hollow unit construction is not permitted to exceed 4% of the cell area.

28.9.5.5.1 Maximum Reinforcement Ratio

To provide for a prescribed level of ductility in the event of failure, the amount of reinforcement permitted in reinforced masonry construction is limited. The maximum reinforcement ratio (ρ_{\max}) is limited in accordance with Equation 28.46 or Equation 28.47, as appropriate. Equation 28.46 applies to masonry cross-sections that are fully grouted or where the neutral axis falls within the face shell of the masonry units in partially grouted construction. When the neutral axis falls within the cores of partially grouted construction, Equation 28.47 is used:

$$\rho_{\max} = \frac{0.64f'_m \left(\frac{\epsilon_{mu}}{\epsilon_{mu} + \alpha\epsilon_y} \right) - \frac{P'}{bd}}{f_y - \min \left\{ \epsilon_{mu} - \frac{d'}{d}(\epsilon_{mu} + \alpha\epsilon_y), \epsilon_y \right\} E_s} \quad (28.46)$$

$$\rho_{\max} = \frac{0.64f'_m \left(\frac{\epsilon_{mu}}{\epsilon_{mu} + \alpha\epsilon_y} \right) \left(\frac{b_w}{b} \right) + 0.8f'_m t_{fs} \left(\frac{b-b_w}{bd} \right) - \frac{P'}{bd}}{f_y} \quad (28.47)$$

where:

ρ_{\max} = maximum tensile reinforcement ratio.

ϵ_{mu} = maximum usable masonry compressive strain.

α = tension reinforcement yield strain coefficient.

ϵ_y = reinforcement strain at yield stress.

P' = axial force corresponding to load combination $D + 0.75L + 0.525Q_E$.

b = width of masonry section (in., mm).

b_w = width of the compression section minus the sum of the length of ungrouted cells (in., mm).

d = effective depth to tension reinforcement (in., mm).

d' = distance from the extreme compression fiber to the centroid of the compression reinforcement (in., mm).

f_y = nominal yield strength of reinforcement (psi, MPa).

E_s = modulus of elasticity of reinforcement (psi, MPa).

f'_m = specified compressive strength of masonry (psi, MPa).

t_{fs} = thickness of masonry face shells (in., mm).

The tension reinforcement yield strain coefficient (α) is taken as equal to 1.5 except for the following conditions:

For intermediate reinforced shear walls, $\alpha = 3.0$.

For special reinforced shear walls, $\alpha = 4.0$.

The bracketed portion of the denominator of Equation 28.46 applies when compression reinforcement is present; otherwise, this part of the expression is zero, and the denominator simply reduces to f_y . Unlike calculating nominal strengths, the compression reinforcement does not have to be laterally tied for use in Equation 28.46. This is permitted because the masonry compressive strain will always be less than the maximum permitted value. For conditions where $M_u/V_u d \leq 1$ and the masonry element is designed using a seismic response factor (R) less than or equal to 1.5, the MSJC Code does not impose an upper limit on the maximum reinforcement ratio. Similarly, when masonry shear walls are checked against the boundary element design provisions of the MSJC Code, the maximum reinforcement requirements may not apply.

28.9.5.5.2 Axial Compression and Flexure

The nominal axial strength (P_n) of masonry elements, modified to account for the effects of slenderness, is determined using Equation 28.48 or Equation 28.49, as appropriate. For masonry elements with h/r not greater than 99:

$$P_a = 0.8 \left\{ \left[0.8f'_m(A_n - A_s) + f_y A_s \right] \left[1 - \left(\frac{h}{140r} \right)^2 \right] \right\} \quad (28.48)$$

For masonry elements with h/r greater than 99:

$$P_a = 0.8 \left\{ \left[0.8f'_m(A_n - A_s) + f_y A_s \right] \left(\frac{70r}{h} \right)^2 \right\} \quad (28.49)$$

where:

- P_a = nominal axial strength of the masonry element (lb, N).
- A_n = net cross-sectional area of the masonry element (in.², mm²).
- f'_m = specified compressive strength of the masonry (psi, MPa).
- A_s = cross-sectional area of laterally tied reinforcement (in.², mm²).
- f_y = nominal yield strength of reinforcement (psi, MPa).
- h = effective height of the masonry element (in., mm).
- r = radius of gyration of the masonry element (in., mm).

The strength design method places a prescriptive cap on the axial load in accordance with Equation 28.50. Further, when the slenderness ratio (h/t) exceeds 30, the factored axial stress is limited to 5% of the specified compressive strength of the masonry ($0.05f'_m$):

$$\frac{P_u}{A_g} \leq 0.20f'_m \quad (28.50)$$

where:

- P_u = factored axial load on the masonry element (lb, N).
- A_g = gross cross-sectional area of masonry element (in.², mm²).

The nominal flexural strength (M_n) of a masonry element is determined in accordance with the following requirements. In addition, the nominal flexural strength at any section along a member shall not be less than one fourth of the maximum nominal flexural strength at the critical section. When axial loads are not present or are conservatively neglected, as may be appropriate in some cases, several circumstances must be considered when determining the nominal flexural strength of reinforced masonry walls. For a fully grouted element, the internal moment arm between the resulting compressive and tensile forces is resolved to determine the resisting capacity of the section. Partially grouted walls are analyzed in the same way but with the additional consideration of the ungrouted cores. For partially grouted masonry, two types of behavior should be considered:

- When the neutral axis (the location of zero stress) lies within the compression face shell, the wall is analyzed and designed using the procedures for a fully grouted wall.
- When the neutral axis lies within the core area, rather than the compression face shell, the portion of the ungrouted cells must be deducted from the area of masonry capable of carrying compression stresses.

The location of the neutral axis depends on the spacing of the reinforcing steel as well as the reinforcement ratio (ρ) and the distance between the reinforcement and the extreme compression fiber (d). When analyzing partially grouted walls, it is typically assumed that the neutral axis lies within the compression

face shell, as the analysis is more straightforward. Based on this assumption, the neutral axis depth (c) is calculated, where $c = 1.25a$ as determined by Equation 28.52. If it is determined that the neutral axis lies outside the compression face shell, then the more rigorous tee beam analysis is performed; otherwise, the rectangular beam analysis is carried out.

For fully grouted masonry elements and for partially grouted masonry elements with the neutral axis in the compression face shell, the nominal flexural strength (M_n) is calculated using Equation 28.51 and Equation 28.52 as follows:

$$M_n = (A_s f_y + P_u) \left(d - \frac{a}{2} \right) \quad (28.51)$$

$$a = \frac{P_u + A_s f_y}{0.8 f'_m b} \quad (28.52)$$

where:

M_n = nominal moment strength of the masonry element (in.-lb, N-mm).

A_s = cross-sectional area of tension reinforcement (in.², mm²).

f_y = nominal yield strength of tension reinforcement (psi, MPa).

P_u = factored axial load on the masonry element (lb, N).

d = effective depth to tension reinforcement (in., mm).

a = depth of equivalent compression zone (in., mm).

f'_m = specified compressive strength of the masonry (psi, MPa).

b = width of the masonry section under consideration (in., mm).

Conversely, for partially grouted masonry walls where the neutral axis is located within the cores, the nominal flexural strength (M_n) is calculated using Equation 28.53, Equation 28.54, and Equation 28.55 as follows:

$$M_n = (A_s f_y + P_u)(d - X) \quad (28.53)$$

$$X = \frac{\frac{b(t_{fs}^2)}{2} + b_w(a - t_{fs}) \left(t_{fs} + \frac{a - t_{fs}}{2} \right)}{b t_{fs} + b_w(a - t_{fs})} \quad (28.54)$$

$$a = \frac{P_u + A_s f_y}{0.8 f'_m b_w} - t_{fs} \left(\frac{b}{b_w} - 1 \right) \quad (28.55)$$

where:

b_w = width of the compression section minus the sum of the length of ungrouted cells (in., mm).

t_{fs} = thickness of the masonry face shells (in., mm).

To account for deflection resulting from the application of out-of-plane loads and the additional bending moment due to eccentrically applied axial loads, the factored bending moment at the mid-height of a simply supported wall under uniform loading is required to be determined by Equation 28.56. When other support or loading conditions exist, appropriate design models should be used instead of Equation 28.56. The deflection due to factored loads (δ_u) is determined using Equation 28.58 or Equation 28.59 by replacing M_{ser} with M_u :

$$M_u = \frac{w_u h^2}{8} + P_{uf} \frac{e_u}{2} + P_u \delta_u \quad (28.56)$$

where:

M_u = factored bending moment (in.-lb, N-mm).

w_u = factored out-of-plane uniformly distributed load (lb/in., N/mm).

- h = effective height of the masonry element (in., mm).
 e_u = eccentricity of P_{uf} (in., mm).
 δ_u = deflection due to factored loads (in., mm).
 $P_u = P_{uw} + P_{uf}$.
 P_{uf} = factored load from tributary floor or roof areas (lb, N).
 P_{uw} = factored weight of masonry element area tributary to section under consideration (lb, N).

The strength design method also includes a deflection check using unfactored service loads to satisfy Equation 28.57:

$$\delta_s = 0.007h \quad (28.57)$$

The mid-height deflection of a simply supported masonry element can be calculated using either Equation 28.58 or Equation 28.59, as appropriate. P-delta effects should be included in the deflection calculation. The cracking moment strength of the element (M_{cr}) is determined using the modulus of rupture values in Table 28.22:

Where $M_{ser} < M_{cr}$:

$$\delta_s = \frac{5M_{ser}h^2}{48E_mI_g} \quad (28.58)$$

Where $M_{cr} < M_{ser} < M_n$:

$$\delta_s = \frac{5M_{cr}h^2}{48E_mI_g} + \frac{5(M_{ser} - M_{cr})h^2}{48E_mI_{cr}} \quad (28.59)$$

where:

- δ_s = deflection at mid-height under service level loads (in., mm).
 h = effective height of the masonry element (in., mm).
 M_{ser} = mid-height bending moment including P-delta effects under service level loads (in.-lb, N-mm).
 M_{cr} = nominal cracking moment strength (in.-lb, N-mm).
 E_m = modulus of elasticity of masonry (psi, MPa).
 I_g = moment of inertia of gross cross-sectional area of masonry element (in.⁴, mm⁴).
 I_{cr} = moment of inertia of cracked cross-sectional area of masonry element (in.⁴, mm⁴).

28.9.5.5.3 Shear

Unlike allowable stress design, shear acting on reinforced masonry members design by the strength design method is resisted by the masonry and shear reinforcement, if provided, in accordance with Equation 28.60:

$$V_n = V_m + V_s \quad (28.60)$$

where V_n is not permitted to exceed the value calculated using either Equation 28.61 or Equation 28.62, as appropriate. For values of $M_u/V_u d_v$ between 0.25 and 1.0, the maximum value of V_n is permitted to be linearly interpolated.

Where $M_u/V_u d_v \leq 0.25$:

$$V_n \leq 6A_n \sqrt{f'_m} \quad (28.61)$$

Where $M_u/V_u d_v \geq 1.0$:

$$V_n \leq 4A_n \sqrt{f'_m} \quad (28.62)$$

The nominal shear strength provided by the masonry (V_m) in Equation 28.63 is determined in accordance with Equation 28.62:

$$V_m = \left[4.0 - 1.75 \left(\frac{M_u}{V_u d_v} \right) \right] A_N \sqrt{f'_m} + 0.25 P_u \quad (28.63)$$

The value of $M_u/V_u d_v$ in Equation 28.63 need not be taken greater than 1.0 but is required be taken as a positive number.

The nominal shear strength provided by the shear reinforcement (V_s) is determined by Equation 28.64:

$$V_s = 0.5 \left(\frac{A_v}{s} \right) f_y d_v \quad (28.64)$$

where:

- V_n = nominal shear strength (lb, N).
- V_m = nominal shear strength provided by the masonry (lb, N).
- V_s = nominal shear strength provided by shear reinforcement (lb, N).
- A_n = net cross-sectional area of the shear plane (in.², mm²).
- f'_m = specified compressive strength of the masonry (psi, MPa).
- M_u = factored bending moment (in.-lb, N-mm).
- V_u = factored shear force (lb, N).
- d_v = depth of masonry in the direction of the shear force (in., mm).
- P_u = factored axial load on the masonry element (lb, N).
- A_v = cross-sectional area of shear reinforcement (in.², mm²).
- s = spacing of shear reinforcement (in., mm).
- f_y = nominal yield strength of shear reinforcement (psi, MPa).

28.10 Summary

Although versatile in its application, the limitless array of possibilities offered by masonry construction also presents unique challenges that, when not properly accounted for in design and construction, can lead to problematic circumstances in the future. Throughout this chapter, emphasis has been given to some of the aspects not usually covered in conventional design and construction handbooks. When these practices and recommendations are combined with standardized design and construction provisions for masonry, however, the successful use of masonry in future projects is ensured. The discussion presented in this chapter is intended to provide the user with a general overview of the basic considerations related to masonry materials, their construction, and their governing design requirements. The references listed at the end of the chapter provide a more detailed discussion and review of this topic and should be referred to as necessary.

Acknowledgment

The author would like to acknowledge with thanks the extensive contributions of the late Walter L. Dickey for his groundbreaking advances in the art and science of masonry design and construction as well as his admirable work in writing with M. J. Dickey the earlier edition of this chapter.

References

- ACI Committee 530. 2005. *MSJC Code: Building Code Requirements for Masonry Structures*, ACI 530-05/ASCE 5-05/TMS 402-05. Reported by the Masonry Standards Joint Committee, Boulder, CO.
- ACI Committee 530.1. 2005. *MSJC Specification: Specification for Masonry Structures*, ACI 530.1-05/ASCE 6-05/TMS 602-05. Reported by the Masonry Standards Joint Committee, Boulder, CO.

- ASCE. 2005. *Minimum Design Loads for Buildings and Other Structures*, ASCE 7-05. American Society of Civil Engineers, Reston, VA, 2005.
- ASTM. 1996. *Standard Test Methods for Strength of Anchors in Concrete and Masonry Elements*, ASTM E 488. ASTM International, West Conshohocken, PA.
- ASTM. 1998. *Standard Specification for Precast Autoclaved Aerated Concrete (PAAC) Wall Construction Units*, ASTM C 1386. ASTM International, West Conshohocken, PA.
- ASTM. 2002. *Standard Specification for Grout for Masonry*, ASTM C 476. ASTM International, West Conshohocken, PA.
- ASTM. 2003a. *ASTM Standard Terminology of Mortar and Grout for Unit Masonry*, ASTM C 1180. ASTM International, West Conshohocken, PA.
- ASTM. 2003b. *Standard Test Method for Compressive Strength of Masonry Prisms*, ASTM C 1314. ASTM International, West Conshohocken, PA.
- ASTM. 2005a. *Standard Guide for Quality Assurance of Mortars*, ASTM C 1586. ASTM International, West Conshohocken, PA.
- ASTM. 2005b. *Standard Specification for Building Brick (Solid Masonry Units Made from Clay or Shale)*, ASTM C 62. ASTM International, West Conshohocken, PA.
- ASTM. 2005c. *Standard Specification for Hollow Brick (Solid Masonry Units Made from Clay or Shale)*, ASTM C 652. ASTM International, West Conshohocken, PA.
- ASTM. 2005d. *Standard Specification for Mortar for Unit Masonry*. ASTM C 270, ASTM International, West Conshohocken, PA.
- ASTM. 2005e. *Standard Specification for Prefaced Concrete and Calcium Silicate Masonry Units*, ASTM C 744. ASTM International, West Conshohocken, PA.
- ASTM. 2005f. *Standard Test Method for Sampling and Testing Grout*, ASTM C 1019. ASTM International, West Conshohocken, PA.
- ASTM. 2005g. *Standard Test Method for Slump Flow of Self-Consolidating Concrete*, ASTM C 1611/C 1611M. ASTM International, West Conshohocken, PA.
- ASTM. 2005h. *Standard Test Method for Slump of Hydraulic-Cement Concrete*, ASTM C 143/C 143M. ASTM International, West Conshohocken, PA.
- ASTM. 2005i. *Standard Terminology of Concrete Masonry Units and Related Units*, ASTM C 1209. ASTM International, West Conshohocken, PA.
- ASTM. 2005j. *Standard Terminology of Masonry*, ASTM C 1232. ASTM International, West Conshohocken, PA.
- ASTM. 2006a. *Standard Specification for Admixtures for Masonry Mortars*, ASTM C 1384. ASTM International, West Conshohocken, PA.
- ASTM. 2006b. *Standard Specification for Concrete Building Brick*, ASTM C 55. ASTM International, West Conshohocken, PA.
- ASTM. 2006c. *Standard Specification for Loadbearing Concrete Masonry Units*. ASTM C 90, ASTM International, West Conshohocken, PA.
- ASTM. 2006d. *Standard Test Method for Linear Drying Shrinkage of Concrete Masonry Units*, ASTM C 426. ASTM International, West Conshohocken, PA.
- ASTM. 2006e. *Standard Test Method for Preconstruction and Construction Evaluation of Mortars for Plain and Reinforced Unit Masonry*, ASTM C 780. ASTM International, West Conshohocken, PA.
- ASTM. 2006f. *Standard Test Methods for Sampling and Testing Concrete Masonry Units and Related Units*, ASTM C 140. ASTM International, West Conshohocken, PA.
- ASTM. 2007a. *Standard Specification for Facing Brick (Solid Masonry Units Made from Clay or Shale)*, ASTM C 216. ASTM International, West Conshohocken, PA.
- ASTM. 2007b. *Standard Test Methods for Sampling and Testing Brick and Structural Clay Tile*. ASTM C 67, ASTM International, West Conshohocken, PA.
- ASTM. 2007c. *Standard Terminology of Structural Clay Products*, ASTM C 43. ASTM International, West Conshohocken, PA.
- Beall, C. 2004. *Masonry Design and Detailing*, 5th ed. McGraw-Hill, New York.

- BIA. 1999. *Glossary of Terms Relating to Brick Masonry*, Technical Notes 2. Brick Industry Association, Reston, VA.
- BIA. 2005. *Water Penetration Resistance: Design and Detailing*, Technical Notes 7. Brick Industry Association, Reston, VA.
- BIA. 2006. *Volume Changes: Analysis and Effects of Movement*, Technical Notes 18. Brick Industry Association, Reston, VA.
- Drysdale, R.G., Hamid, A.A., and Baker, L.R. 1999. *Masonry Structures, Behavior and Design*. The Masonry Society, Boulder, CO.
- ICC. 2006a. *International Building Code*. International Code Council, Falls Church, VA.
- ICC. 2006b. *International Residential Code*. International Code Council, Falls Church, VA.
- Korhonen, C., Thomas, R., and Edel, C., 1997. *Increasing Cold-Weather Masonry Construction Productivity*, Construction Productivity Advancement Research (CPAR) Program, U.S. Army Corps of Engineers, Washington, D.C.
- NCMA. 2000a. *Concrete Masonry Shapes and Sizes Manual*. National Concrete Masonry Association, Herndon, VA.
- NCMA. 2000b. *Metric Design Guidelines for Concrete Masonry Construction*, TR-172. National Concrete Masonry Association, Herndon, VA, 2000.
- NCMA. 2001a. *Architectural Concrete Masonry Units*, TEK 2-3A. National Concrete Masonry Association, Herndon, VA.
- NCMA. 2001b. *Standard Practice for Bracing Masonry Walls Under Construction*, National Concrete Masonry Association, Herndon, VA.
- NCMA. 2002a. *All-Weather Concrete Masonry Construction*, TEK 3-1C. National Concrete Masonry Association, Herndon, VA.
- NCMA. 2002b. *Typical Sizes and Shapes of Concrete Masonry Units*, TEK 2-1A. National Concrete Masonry Association, Herndon, VA.
- NCMA. 2003a. *Annotated Design and Construction Details for Concrete Masonry*, TR-90. National Concrete Masonry Association, Herndon, VA.
- NCMA. 2003b. *Section Properties of Concrete Masonry Walls*, TEK 14-1A. National Concrete Masonry Association, Herndon, VA.
- NCMA. 2004a. *Design for Dry Single-Wythe Concrete Masonry Walls*, TEK 19-2A. National Concrete Masonry Association, Herndon, VA.
- NCMA. 2004b. *Glossary of Concrete Masonry Terms*, TEK 1-4. National Concrete Masonry Association, Herndon, VA.
- NCMA. 2005a. *Control Joints for Concrete Masonry Walls: Empirical Method*, TEK 10-2B. National Concrete Masonry Association, Herndon, VA.
- NCMA. 2005b. *Grouting Concrete Masonry Walls*, TEK 3-2A. National Concrete Masonry Association, Herndon, VA.
- NCMA. 2005c. *Joint Reinforcement for Concrete Masonry*, TEK 12-2B. National Concrete Masonry Association, Herndon, VA.
- NCMA. 2006a. *ASTM Specifications for Concrete Masonry Units*, TEK 1-1D. National Concrete Masonry Association, Herndon, VA.
- NCMA. 2006b. *Steel Reinforcement for Concrete Masonry*, TEK 12-4D. National Concrete Masonry Association, Herndon, VA.
- NCMA. 2006c. *Testing and Inspection of Concrete Masonry Construction*, TR-156A. National Concrete Masonry Association, Herndon, VA, 2006.
- NCMA. 2006d. *Water Repellents for Concrete Masonry Walls*, TEK 19-1. National Concrete Masonry Association, Herndon, VA.
- TMS. 2000. *Annotated Guide to Masonry Specification*. The Masonry Society, Boulder, CO.
- TMS. 2007. *Masonry Designer's Guide*, 5th ed. The Masonry Society, Boulder, CO.



I-280 Veterans' Glass City Skyway Bridge in Toledo, Ohio. Designed by FIGG for the Ohio Department of Transportation. This signature cable-stayed bridge features a pylon with four sides of glass and LED lighting.

29

Aesthetics in the Construction and Design of Long-Span Prestressed Concrete Bridges

Linda Figg*

29.1	Aesthetics in Concrete Bridges.....	29-1
	Introduction • Bridge Aesthetics • Signature Design • Definition of Design Principles	
29.2	Conceptual Design	29-4
	Alignment • Span Length • Structural Depth • Span-to-Depth Ratio	
29.3	Environmental Sensitivity.....	29-9
	Protecting the Natural Environment • Context-Sensitive Design	
29.4	Construction Methods.....	29-11
	Span-by-Span • Cable-Stayed Bridges • Urban Environments	
29.5	Concrete Bridge Shapes for Construction.....	29-17
	Superstructure Shape • Pier Shape • Underside Appearance • Creating Shadows	
29.6	Concrete Aesthetic Features	29-23
	Introduction to Color and Texture • Overall Bridge Color and Texture • Opportunities for Aesthetic Treatments • Use of Native Materials	
29.7	Design Details.....	29-28
	Concrete Barriers/New Vistas • Drainage • Utilities • Aesthetic Lighting • Landscaping • Innovative Technologies • Artistic Details	
29.8	Summary.....	29-31

29.1 Aesthetics in Concrete Bridges

29.1.1 Introduction

Many important factors collectively contribute to the aesthetic appeal of a bridge. Both the design and construction play key roles in achieving aesthetic qualities. This chapter explores various topics regarding the development of aesthetically pleasing, long-span prestressed concrete bridges. The focus for long

* President/Director of Bridge Art, FIGG, Tallahassee, Florida; expert in aesthetic design and construction of concrete segmental bridges.

spans is on the use of concrete segmental box girders to achieve sizeable spans and versatility of form. Bridge design and construction represent more than simply providing a transportation link between two points. Communities want bridges that are visually pleasing, reflective of their place, and sensitive to the environment. Additionally, the public wants construction projects to be completed quickly and to minimize disturbance to the already congested traffic. These increased expectations are combined with public agencies' need for economical construction due to limited funding. Designers and builders are responding to these needs and desires by becoming more innovative in their approach to bridge design and construction. Aesthetics, economy, environmental sensitivity, and sustainability are being combined with function and constructability to provide new bridges that satisfy these expectations.

29.1.2 Bridge Aesthetics

Bridge aesthetics are born out of design efficiency and sensitivity to visually pleasing details. Bridges are created with a sizeable investment of funds with the idea that a new landmark bridge will stand the test of time physically as well as visually. The bridge leaves an impression, and that impression remains for as long as the bridge remains, so bridge designers owe it to the community to create something that is beautiful. The first step is to solve the technical challenges. Many important decisions are involved in creating an economical solution, and the initial decisions form the framework of structural efficiency that ultimately leads to the final aesthetic opportunity, with the remainder of the details building upon the initial functional solution. With a concentrated effort on efficient design and construction, the bridge aesthetics can be achieved within the context of the expected construction costs and often at a cost savings.

29.1.3 Signature Design

By approaching bridge design as creating a work of art, a signature design is born. The value of bridge aesthetics is found in the iconographic power that translates into economic development and sustainability within the landscape and context of the site. Each bridge site is unique. Similar design approaches may be utilized, but to create a landmark everything unique to that location must be explored and embraced to create a one-of-a kind signature design that becomes a community landmark.

29.1.4 Definition of Design Principles

Aesthetically pleasing bridge design has four basic requirements:

- It must be functional.
- It must be economical.
- It must be culturally satisfying to the community.
- It must exist in harmony with the environment.

Design principles that guide a designer's attempts to satisfy these requirements include establishing a theme, blending shapes, creating shadows, using appropriate textures and colors, and incorporating native materials and feature lighting. Establishing a theme reflective of the local community is a unifying element for all bridge components. The bridge alignment and shapes combine to form the overall aesthetic appeal of a bridge. The shape and contours of the bridge create shadows that provide depth and varying expressions as the natural light evolves throughout the day. Color, texture, and the use of native materials further enhance the visual interest of the bridge structure. A nighttime signature may be created through the use of aesthetic lighting. Other design details, such as appropriate landscaping, can create a seamless connection between the bridge and the site.

Examples of bridges that have achieved exceptional aesthetics, as judged by numerous award juries, are the I-275 Bob Graham Sunshine Skyway Bridge in Tampa, Florida (Figure 29.1); the Natchez Trace Parkway Arches near Nashville, Tennessee (Figure 29.2); and the Blue Ridge Parkway Viaduct around Grandfather Mountain, North Carolina (Figure 29.3). All three were selected by the National Endowment for the Arts to receive the coveted Presidential Design Award.



FIGURE 29.1 Bob Graham Sunshine Skyway Bridge has a 1200-ft main span and carries I-275 across Tampa Bay, Florida; the bridge was the recipient of the 1988 Presidential Design Award.



FIGURE 29.2 Natchez Trace Parkway Arches has a 582-ft main span and is located outside of Nashville near Franklin, Tennessee; the bridge was awarded the 1995 Presidential Design Award.



FIGURE 29.3 The Blue Ridge Parkway Viaduct has 180-ft spans and wraps around Grandfather Mountain in North Carolina; the viaduct was the recipient of the 1984 Presidential Design Award.



FIGURE 29.4 The Natchez Trace Parkway Arches bridge demonstrates efficient design resulting in economical construction.

29.2 Conceptual Design

The conceptual design phase of a bridge project provides the necessary groundwork for the best aesthetic opportunity. The overall alignment and geometry are established at this time, in addition to determining span lengths and the structural depth and dimensioning of superstructure and substructure elements. These project elements are determined based on an analysis of the site and determination of the most appropriate bridge type to create both a functional and a visually pleasing bridge. The conceptual design must call on engineering judgment and an understanding of how to best optimize construction to properly balance economy, functionality, and lasting visual quality. Experience has shown that superior bridge aesthetics can be achieved at reasonable construction costs, and, in fact, efficient designs can result in costs savings. Aesthetic form follows well-designed function. An example of this is the Natchez Trace Parkway Arches project (Figure 29.4), which was completed for \$11.3 million in 1993. The functional requirement of spanning the valley resulted in a long-span arch structure with a 582-ft span. To develop a modern and open design, the vertical spandrels typically seen in traditional arches were removed, resulting in the superstructure load being translated to the arch at one expanded platform at the top. Traditional methods of precast balanced cantilever construction were used for the superstructure. The arch itself was comprised of precast segments built in a cantilever fashion from the foundations using cable supporting technology until the arch was connected in the center. By addressing components of the bridge separately and yet together, a total system can be developed founded on known methods of construction and creating a unique design (Figure 29.5).

Efficiency, as well as pleasing aesthetics, may be achieved through consistency in design elements and shapes. A uniform appearance among the bridge elements is important and may be accomplished through consistency in form, line, and pattern. The lines of a structure draw a viewer's eye from one form to another which, when done well, creates visual continuity. One way to achieve this is by using the same superstructure cross-section for the full length of the bridge. Two primary benefits emerge: a more aesthetically pleasing appearance and increased efficiency during construction due to the repetition of form. An example of this approach is the Chesapeake and Delaware Canal Bridge near St. Georges, Delaware (Figure 29.6). The superstructure was designed such that the same cross-section shape could



FIGURE 29.5 During construction, proven construction techniques combine to create a unique design.

be used for the 150-ft approach spans as well as the 750-ft cable-stayed main span. To create the cable-stayed main span, a precast delta frame was introduced to tie the two superstructure box girders together and house the cable stay anchorages below the deck level. The economical benefits were demonstrated by the low bid of \$59 million that was within budget and \$6 million less than the alternative design.

29.2.1 Alignment

Generally, bridge alignments are influenced by existing roadway networks, although some opportunities arise when new transportation corridors are created. Whether the bridge is a replacement structure, parallel structure, or new structure, it must fit within the roadway system. The specific alignment



FIGURE 29.6 The Chesapeake and Delaware Canal Bridge in Delaware uses repetition of form and construction.

determined for the bridge will consider grades and elevations of existing and proposed roads, the terrain it will traverse, and what features the structure crosses, such as bodies of water, roadways, railroads, or other existing and proposed site constraints. Bridge alignment has the first and most profound effect on the overall approach to the bridge design and aesthetics. The length of the structure, especially the length of the visually dominant main span, will dictate the type of structure and method of construction that are most suitable. Alignment and location of the bridge will affect many aspects of construction such as how materials are delivered, whether erection will take place over traffic or over an active navigational channel, or if environmentally sensitive areas will require another level of special care. These and all aspects of construction must be considered during alignment determination.

29.2.2 Span Length

In addition to the overall bridge length, the individual span lengths of a bridge are based on the alignment, existing site constraints, and potential construction methods. Span lengths are determined after the overall length and alignment have been established and existing site constraints identified. Unit configurations are also established to create a continuous structure of several spans to reduce the number of expansion joints. The various combinations of construction methods, span lengths, and unit configurations are evaluated to determine the most feasible alternative; for example, when establishing span lengths for concrete balanced-cantilever construction, side span lengths should be set at 60% of the main span length. The Smart Road Bridge (Figure 29.7) near Blacksburg, Virginia, is a 1984-ft-long bridge of one continuous unit that consists of three interior spans of 472 ft each with side spans of 284 ft. The goal in establishing the span length is to determine the optimal span length and consistently utilize this length throughout the project, as much as possible. This will increase the efficiency of the project by introducing repetition into the construction operations, resulting in economical construction costs. The balanced and repetitive span lengths also provide continuity in appearance, resulting in visually appealing structures. Span length, in concert with structure depth, is the single most important aspect of establishing the aesthetic quality of a bridge; it sets the stage for the overall appearance of the structure and how it flows into its visual environment.



FIGURE 29.7 The long spans of Virginia's Smart Road Bridge provide for open views of the valley; the bridge was built via balanced cantilever construction.



FIGURE 29.8 Four Bears Bridge in rural North Dakota has a variable depth superstructure for 316-ft spans following a uniform pattern for construction efficiency.

29.2.3 Structural Depth

Many variables go into determining structural depth. Typically, maintaining a constant box girder depth, as well as a constant cross-section, will greatly simplify casting and erection operations, thus reducing construction costs. To determine the appropriate structure depth, the bridge engineer must evaluate all spans and units to determine the governing conditions and minimum structural depth required. This is accomplished in combination with addressing the required vertical clearances. For longer span bridges, however, it is often more economical to vary the depth of the superstructure instead of maintaining a constant depth. A deeper box girder section is required to resist the higher forces closer to the piers, while at midspan a shallower section is adequate to resist the lower forces. The structural depth, therefore, is often gradually decreased over the length of the span to minimize quantities and to reduce the weight of the structure. This can be achieved with graceful, sweeping curves that will enhance the visual appeal of the structure by making it appear more slender and elegant. An example of this is the Four Bears Bridge (Figure 29.8) near New Town, North Dakota, which has 316-ft spans and a variable superstructure depth ranging from 16 ft, 7 in. at the piers to 7 ft, 7 in. at midspan.

29.2.4 Span-to-Depth Ratio

Determining an ideal span-to-depth ratio is an essential factor in the overall aesthetic appearance of the structure. It influences the visual impact of the structure within the surrounding landscape. Many options exist that can optimize the structural efficiency of the superstructure box girder cross-section while creating an elegant structure. Creating the most aesthetically pleasing combination of span length and superstructure depth is often an iterative process. Based on experience, span-to-depth ratios ranging from 20 to 30 will result in superior aesthetics. A span-to-depth ratio of 15 on uniform spans is also considered visually appealing, but less than 15 is not preferable. The Victory Bridge (Figure 29.9) in New Jersey incorporates a 440-ft precast segmental main span with a variable-depth superstructure. The span depth varies from 21 ft at the main piers to 10 ft at the center span, resulting in a span-to-depth ratio of 22. The 150-ft



FIGURE 29.9 A high span-to-depth ratio results in structures that have elegant proportions. The Victory Bridge (440-ft main span) over the Raritan River in New Jersey serves as an excellent example.

approach spans have a constant depth of 9 ft, resulting in a span-to-depth ratio of 15. Long-span girder bridges present interesting opportunities. As noted in Section 29.2.3, as the span increases, the magnitude of the forces near the piers normally requires variation in structural height. When clearance requirements allow, a circular variation in structure depth is more aesthetically pleasing than a linearly varying structure depth. An example of such an approach is the Wabasha Freedom Bridge (Figure 29.10) in St. Paul, Minnesota. This bridge has a 400-ft span with a 20-ft-deep section at the pier and an 8-ft-deep section at midspan, resulting in a span-to-depth ration of 20 and a gradually varying, long sweeping curve.



FIGURE 29.10 The Wabasha Freedom Bridge in St. Paul, Minnesota, achieves a span-to-depth ratio of 20 and demonstrates that varying the depth of the superstructure creates pleasing shapes.



FIGURE 29.11 North Carolina's Blue Ridge Parkway Viaduct was built from the top to protect the sensitive environment so the mountain's owner would allow construction of this important link.

29.3 Environmental Sensitivity

29.3.1 Protecting the Natural Environment

Innovative methods of construction have been developed to protect the natural environment while providing necessary transportation infrastructure. A section of the Blue Ridge Parkway around Grandfather Mountain in North Carolina (Figure 29.11) challenged engineers for years due to the environmentally sensitive ecology of the area. This obstacle was overcome by erecting a precast concrete segmental bridge utilizing top-down construction. Starting at the abutment, the eight-span continuous viaduct was built in a unidirectional progressive cantilever (Figure 29.12). The segments were delivered by truck over



FIGURE 29.12 A progressive unidirectional cantilever, from above, protected the mountain during construction.



FIGURE 29.13 Protecting Glenwood Canyon in Colorado was a top priority during the design and construction of its first five bridges.

the completed structure as it advanced and was progressively post-tensioned in place. Other challenges that had to be overcome included the rugged terrain, being 4400 ft above sea level, and the unusually complex alignment geometry with tight horizontal curves that reverse direction. The piers were also constructed from the top down by constructing the cantilever toward the next pier and then reaching out and down to construct the pier with precast segments. The precast pier segments were then delivered across the completed deck to the edge of the cantilever span, lowered into position, and vertically post-tensioned in place.

The Glenwood Canyon Bridges (Figure 29.13) along Interstate 70 west of Denver, Colorado, are other examples of structures built in an environmentally sensitive area. Five bridges demanded an innovative approach in design and construction to meet the environmental restrictions in the terrain of the canyon. With the Colorado River on one side and mountain cliffs on the other, the construction was confined. A precast concrete segmental bridge was designed for the location, with the precast box girders being trucked to the erection site and delivered over the completed bridge deck. Temporary erection trusses were used to support the segments in each span during construction until the longitudinal post-tensioning could be stressed to make the spans self-supporting. The trusses were temporarily supported from the permanent piers, thus eliminating the need for falsework, which would have damaged the existing landscape. Once a span was completed, the trusses were launched forward to the next span location from above, avoiding impact to the sensitive ground below. These two projects are examples of what may be accomplished with existing, proven construction techniques. Preserving the environment and enhancing the natural landscape are outcomes of thoughtfully evaluating the bridge design and construction methods during the conceptual design stage.

29.3.2 Context-Sensitive Design

Construction of a bridge should preserve and protect the existing environment and visually complement the site. Designing bridges that reflect the environment and the spirit of the communities they serve generates community pride and results in a bridge that becomes a timeless landmark and a legacy left to future generations. The Four Bears Bridge near New Town, North Dakota, spans Lake Sakakawea on the Fort Berthold Indian Reservation. This award-winning bridge was designed using the Federal Highway Administration's (FHWA) Context-Sensitive Design (CSD) process, defined as "a collaborative, interdisciplinary approach that involves all stakeholders to develop a transportation facility that fits its physical setting and preserves scenic, aesthetic, historic, and environmental resources, while maintaining safety and mobility. CSD is an approach that considers the total context within which a transportation improvement

project will exist.” For the Four Bears Bridge, CSD was accomplished through regular meetings between the North Dakota Department of Transportation (NDDOT), the design team, the Three Affiliated Tribes (TAT), and the six communities that comprise the Fort Berthold Indian Reservation. Details of the project were presented to members of the TAT, and volunteers were solicited to form a Cultural Advisory Committee (CAC) to bring Native American guidance to the CSD process. The initial purpose of the CAC was to develop a project theme. Other project components were determined through a 2-day FIGG Bridge Design Charette™ (public workshop) to further implement CSD. The design charette provided stakeholders with a formal decision-making process that considered their preferences and allowed prioritization of the following bridge elements: roadway lighting, aesthetic lighting, pier shapes, traffic railing, pedestrian railing, bridge profiles, sidewalk linear library, bridge end treatments, and bridge color and textures. The result is a celebrated, aesthetically pleasing structure that is in context with its environment and a source of pride for the surrounding communities.

29.4 Construction Methods

Concrete segmental bridges for long spans are typically erected using the span-by-span or balanced cantilever construction methods. Determining the method of construction and bridge type requires taking into consideration the required span length and the existing site constraints, such as environmental restrictions, existing traffic, bodies of water, or limited right of way. The owner’s required schedule may also dictate one method over the other, while the contractor’s equipment or the size of project may also be determining factors. The advantages and disadvantages of various approaches must be analyzed early in the conceptual design phase to determine the best one. For particularly large or complex projects, both span-by-span and balanced cantilever methods may be utilized. This may speed construction by allowing the simultaneous erection of spans at different locations of the project. Construction of the Victory Bridge in northern New Jersey, for example, was accomplished by erecting the approach spans with span-by-span construction while simultaneously erecting the main span using balanced cantilever construction (Figure 29.14). This expedited the construction schedule, which was a major goal of the



FIGURE 29.14 Span-by-span erection of the approach spans expedited completion of New Jersey’s Victory Bridge.



FIGURE 29.15 AirTrain JFK, the light rail system around New York's JFK Airport, was erected utilizing both span-by-span and balanced cantilever construction methods to achieve an aggressive schedule.

New Jersey Department of Transportation. For the superstructure of AirTrain JFK (Figure 29.15), both methods were employed. Span-by-span was used primarily to speed up the process, and balanced cantilever construction was applied to a small number of longer spans and spans with tight horizontal curvature. Both the span-by-span and balanced cantilever construction methods have been used successfully in the industry and are customary; however, advances in technology and equipment continue to be made. For all projects, a contractor may opt to use unique means and methods that may differ from the assumptions made by the design engineer during the design phase. In these circumstances, further construction analysis is required to verify the design under the revised construction loadings. A description of span-by-span construction follows. A detailed description of balanced cantilever construction, for both cast-in-place and precast concrete, can be found elsewhere in this book.

29.4.1 Span-by-Span

The span-by-span method of construction was developed to construct long bridges with repetitive span lengths, with construction taking place at deck level without the use of extensive falsework. It is typically accomplished using a truss or pair of trusses supported by the bridge piers. Segments are delivered to the site and placed on the erection truss. A winch brings the segments to their final location. When all segments are in place, temporary blocking is placed across the closure joints, and a nominal prestress force is applied to ensure tight fit of all the precast segments. Closure joint concrete is poured, longitudinal duct work secured, and post-tensioning tendons threaded and stressed. The construction cycle is completed when the assembly trusses are advanced to the next span. This is a quick and efficient method of construction for precast concrete segmental bridges and is ideal for straight or curved bridges. It requires less prestressing steel than balanced cantilever construction because no cantilever stresses occur during construction.

Precasting offers the advantage of the simultaneous casting of segments off-site, while the foundations and piers are constructed on-site. A casting yard may be established in close proximity or where land and easy access for segment delivery are available. Segments are cast in controlled, factory-like conditions that produce high-quality products and consistent results for material strength, geometry control, and rebar placement. When the concrete has been satisfactorily cured and ready for erection, segments may

be delivered from the casting yard to the project site by barge, truck, or segment haulers, depending on the contractor's equipment and the proximity of the casting yard to the project site. Pier segments can also be precast and delivered in the same manner. Depending on site constraints (limited right of way, traffic maintenance, or environmental restrictions) and contractor equipment, segment delivery and placement on the truss may be accomplished in several different ways. If construction is limited to top down, trucks can deliver segments over the newly completed structure that are then placed on the truss with a crane that moves along the progressively completed superstructure. Where at-grade access is permitted, a ground-based crane can pick segments from delivery at-grade and place them on the truss. Barge-mounted cranes may be utilized if the bridge is over navigable water.

29.4.2 Cable-Stayed Bridges

Long spans may be accomplished economically with a cable-stayed bridge design and may be either precast or cast in place. The length and depth of the span determine the number and size of pylons and cables, as well as the geometric configuration of the cables and segment lengths. In this type of construction, the preferred length of the back spans is half the length of the main span. In some situations, however, this is not possible due to existing conditions, geometry, or other site constraints. This results in asymmetrical designs that require compensation for the unequal span lengths by providing additional superstructure weight to balance the spans or by using other creative engineering solutions.

Precast segmental cable-stayed construction is a special subset of precast cantilever construction. The Chesapeake and Delaware Canal Bridge in Delaware has a 750-ft main span that was built via unidirectional cantilever using permanent cable stays and precast delta frames (Figure 29.16). The single plane



FIGURE 29.16 Precast delta frames between the parallel box girders transfer forces from the superstructure to the cable stays.

of 16 cable stays at each pylon supports the main span, creating a graceful appearance that blends the structure into the landscape. The pylons were cast in place in 10-ft lifts with cable stays initiating at the third lift above the roadway. The saddle cable stay pipe that runs through the pylon transfers the forces from the stays down through the pylon and into the main pier foundation. The cable stays anchor in the precast delta frames at the deck level spaced at 20-ft intervals. The delta frames transfer loads from the roadway segments to the cable stay system, allowing the same cross-sectional shape of the box girders to be used in both the approach spans and the main span. The delta frames also connect the twin parallel trapezoidal box girders of the main span into a single rigid cross-section. The approach spans were built using span-by-span construction prior to erection of the main span which allowed the delivery of main-span segments over the newly constructed back spans. This, in conjunction with the use of crawler cranes on both sides of the canal, allowed erection of the center span from above, with minimal disruption to the navigational traffic in the canal. The main span was erected in cycles: erection of four precast segments, erection of a precast delta frame, installation and stressing of a cable stay.

The Penobscot Narrows Bridge and Observatory (Figure 29.17) is the first cable-stayed bridge in Maine and was built using the balanced cantilever method with cast-in-place form travelers. Form travelers are forms that advance by a rail assembly that is affixed to the deck during construction. In this case, from



FIGURE 29.17 Form travelers on the cantilever tips were used to cast the superstructure in place for Maine's Penobscot Narrows Bridge and Observatory.

each of the pylons a back-span segment was cast, then a main-span segment, following a typical construction cycle of launching the traveler into position; prealigning the formwork; placing post-tensioning hardware, reinforcement, and precast struts; performing final alignment of formwork; casting the segment; performing a morning as-cast survey to verify geometry; stressing applicable post-tensioning; stripping formwork; and launching the traveler into position to cast the next segment. Traditionally, cable-stay strands have been stressed with large jacks that tension all strands simultaneously. On this bridge a different approach was used to stress the cable stays. To work within the interior of the cast-in-place box, monostrand stressing was used, where the strands were stressed one at a time. This requires a significantly smaller and more portable jack and an analysis of the different strand patterns to determine the appropriate sequence for strand stressing.

29.4.3 Urban Environments

Meeting the transportation demands of providing greater roadway capacities within restricted urban corridors requires specially tailored solutions. Some of the most challenging expansion situations may be solved by building up within the existing right of way, instead of out with more lanes at-grade. Building within the existing medians and shoulders eliminates the high expense and difficult task of obtaining new right of ways from major commercial and residential properties to expand facilities at-grade. The use of concrete segmental box girders allows for slender pier shapes and a small groundline footprint, thus maximizing the available space within the existing corridor. Another benefit of this solution is that when additional capacity is added over existing at-grade traffic signalized intersections are maintained and traffic above moves uninterrupted. This removes through traffic from the at-grade facility, reducing congestion and allowing the local at-grade traffic to reach their destinations more easily.

One example of this approach is the elevated toll road that was constructed within the median of the existing Lee Roy Selmon Crosstown Expressway (also known as State Road 618) in Tampa, Florida (Figure 29.18). To add the necessary capacity to the existing four-lane, divided, limited-access toll road without expanding the footprint of the highway, the Tampa–Hillsborough Expressway Authority developed an



FIGURE 29.18 Utilizing the existing median for an elevated structure solved commuter congestion in Tampa, Florida. Piers use 6 ft of space in the median to carry three lanes of traffic above.



FIGURE 29.19 Span-by-span erection was completed in the median of the Van Wyck Expressway, where over 160,000 vehicles pass each day.

innovative vision of an elevated structure to carry reversible express lanes. Traffic congestion is highly directional, as 80% of the morning traffic is westbound into Tampa, and 75% of the evening traffic is eastbound, headed out of the city. Reversible lanes were seen as an efficient means of providing the additional capacity when and where it was needed most. This innovative structure provides the capacity of six vehicle lanes within the 6-ft footprint of the piers. This structure was constructed while existing traffic remained in operation and was accomplished within the existing right of way.

A 2.3-mile section of the AirTrain JFK, the light-rail system for the JFK Airport, was built in the existing median of New York City's Van Wyck Expressway, an extremely congested six-lane highway closely bordered by residential and commercial properties (Figure 29.19). The erection methods and four erection trusses allowed construction to proceed with minimal disruption to traffic. An average of 2.5 spans 125 ft long were completed weekly within the median. At 7 ft, 8 in., the bases of the piers creatively utilize the space provided by the 10-ft median.

Interstate 110 in Biloxi, Mississippi, incorporated both span-by-span and balanced cantilever construction for its bridges so it could thread its way through the urban environment and over traffic (Figure 29.20). The interstate runs through a developed urban area, wraps around existing buildings, and maintains the integrity of established neighborhoods. This was accomplished by utilizing construction



FIGURE 29.20 Interstate 110 runs through downtown Biloxi, Mississippi, on an elevated structure.

systems that did not interfere with day-to-day traffic flow to provide aesthetically pleasing bridges. Using precast concrete segmental construction and slim piers, the bridges were built in existing or limited rights of way and over U.S. 90, a major tourist route that follows the Gulf Coast shoreline.

29.5 Concrete Bridge Shapes for Construction

When designed appropriately, the overall bridge form, superstructure, and substructure shapes connect seamlessly. They are in harmony with each other, and the eye flows naturally across the structure and its landscape. When forming the final sculptured shapes of bridge elements, it is important to fully consider how the shapes will integrate into the overall visual experience by taking into account the following: how light will interact with the structure, whether or not aesthetic lighting is going to be included in the project, the appropriate use of color and texture for the location, who will view the bridge, and from what vantage points the bridge be seen. Determining the final aesthetic details in the shaping of the superstructure and piers will create lines, patterns, and shadowing effects that can more completely convey the theme of the structure and be a sustainable design for the context of the site.

29.5.1 Superstructure Shape

The basic overall dimensions of the superstructure are based on structural requirements. For the 17th Street Bridge in Fort Lauderdale, Florida (Figure 29.21), the precast concrete segmental approaches to the bascule main span consist of a closed box shape with sloping vertical webs. The shaping of a closed box girder was selected for its inherent visual appeal, derived from the smooth surfaces of continuous flat planes, while the cantilever wings at the top of the box section provide openness underneath and pleasing shadow effects. There are long spans over land on both sides of the river connecting to the main span crossing the Intracoastal Waterway. Additional landscaping, aesthetic lighting, and hardscape elements beneath these land spans have created new public gathering places. The sculptural shapes of the bridge and the smooth underside enhance these new parks and green spaces. Angular lines comprise the superstructure cross-section of the Interstate 76 Susquehanna River Bridge near Harrisburg, Pennsylvania (see Figure 29.25). The simple, crisp lines add to the overall aesthetic appeal of the structure. At night, web-wall wash lighting, seemingly hidden within the lobe beneath the barrier rail, enhances the smooth web walls. The superstructure cross-section of the Lee Roy Selmon Crosstown Expressway Expansion in Tampa, Florida (Figure 29.22), contains curves in the webs and on the bottom soffit of the box that contribute to its distinctive appearance. The curves and long cantilever wings in combination with the height of the piers give the superstructure a slender appearance with shadowing. The curved lobes at the



FIGURE 29.21 Clean lines and smooth undersides of the box girder superstructure enhance Fort Lauderdale's 17th Street Bridge approaches, which largely cross over land.



FIGURE 29.22 The unique box shape of Tampa's Lee Roy Selmon Crosstown Expressway Expansion was an economical answer to achieving aesthetic goals.



FIGURE 29.23 Subtly shaped piers carry Interstates 10 and 35 in San Antonio, Texas.

corners of the soffit hide the bearings so the superstructure appears to have a seamless connection with the piers. This unique shaping creates an elegant, sculpted structure. From a constructability perspective, the overall cross-section shape remains the same throughout the bridge length to maximize the repetition of casting and to allow the casting cells to be constant. Variable bridge deck widths were accommodated by lengthening the cantilever wings as the bridge deck widens. This focus on constructability allowed the bridge to be economically constructed with a special one-of-a-kind superstructure shape.

29.5.2 Pier Shape

The pier shape is another opportunity for a designer to distinguish the aesthetics and visual appeal of the structure. The shape of the piers and their transition into the superstructure are key design features that create interesting lines and shadows. Slender piers that have a relatively high height-to-width ratio and taper at the top provide a graceful connection with the superstructure. An example is the pier shape used on the San Antonio “Y” bridges that carry Interstates 10 and 35 in downtown San Antonio, Texas (Figure 29.23).

In addition to satisfying the project design criteria, the overall cross-sectional shape of the pier should be considered in light of how the pier relates to the superstructure shape and size, the context of its environment, and the theme of the project. Simple shapes, such as an elliptical shape (Figure 29.24), can provide a classic look. An elliptical shape, while visually pleasing, also provides the benefit of reducing the drag coefficient of hurricane wind conditions such as in the case of the Bob Graham Sunshine Skyway Bridge that carries Interstate 275 across Tampa Bay, Florida (see Figure 29.1). The twin elliptically shaped piers used for the main span contribute to the overall aesthetic appeal of the bridge, but the shape was primarily chosen because it best fulfills the design requirements for the bridge to be able to sustain hurricane-force winds.

Main piers for long-span designs built in balanced cantilever are designed to provide structural stability of the cantilevers during construction, as well as providing structural capacity under final service loads. Often, unbalanced construction loads and wind loads, including hurricane winds, can require sizable main piers; however, a functional and aesthetic solution can be developed with the use of twin walls. Twin-wall, cast-in-place piers on the Wabasha Freedom Bridge in St. Paul, Minnesota (see Figure 29.10), not only provide visual appeal but also were designed to help counter the unbalanced loads on the foundations during balanced cantilever construction. The piers provided longitudinal flexibility combined with stability for cantilever erection. The piers are integrated into the superstructure with reliefs that reflect an Art Deco architectural style. The reliefs cast into the pier and the detailing at the super-



FIGURE 29.24 Elliptical pier shapes add aesthetics while reducing wind drag, an important consideration in hurricane-prone areas (I-275 Bob Graham Sunshine Skyway Bridge).

structure hide the bearings at the interface. This style was also adopted for the details of stairways, overlooks, walls, paths, and other features in the landscaped park areas to tie the entire project together.

In those situations where it is possible to eliminate bearings, a monolithic connection between the pier and the superstructure may add to the aesthetics of the bridge. At the Smart Road Bridge near Blacksburg, Virginia (see Figure 29.7), the pier faces continue vertically to intersect with the superstructure web wall, creating a fixed or monolithic connection between the piers and the superstructure. This approach eliminated the need for bearings at the piers and adds an aesthetic feature to the elevation of the bridge. In rugged environments, angular shapes blend in naturally with the mountainous terrain. An octagonal-shaped pier was used to blend the Blue Ridge Parkway Viaduct into the rocky outcroppings of Grandfather Mountain, North Carolina (see Figure 29.3 and Figure 29.11).

Visual interest may be created by the use of simple-cross sectional shapes in a cost-efficient manner. Vertical articulations may be cast into a pier recess, producing a slender appearance through shadows. Vertical lines created by casting a pier inset or by the cross-sectional shape itself may visually add to the height of a shorter pier and create visual interest for those viewing the piers from below. At the Interstate 76 Susquehanna River Bridge (Figure 29.25), a stone pattern provides texture on the piers, reflecting the stone on the nearby Pennsylvania Turnpike Commission building.



FIGURE 29.25 A stone pattern texture was used on the piers of Pennsylvania’s Susquehanna River Bridge to create a linear accent.

29.5.3 Underside Appearance

When designing a structure, it is important to consider all visual vantage points: pedestrians, passengers in a boat passing beneath the structure, and passengers in vehicles driving underneath or beside the bridge. All have unique views of the bridge and can appreciate different aesthetic features. One example of specific aesthetic treatments that were used to enhance the visual appeal of the underside of a bridge is for the piers of the Broadway Bridge (Figure 29.26), which crosses the Intracoastal Waterway in the heart of downtown Daytona Beach, Florida. The bridge is viewed by boaters and pedestrians in the park along the water, so particular attention was paid to the vantage point from these perspectives. Building on the “Timeless Ecology” theme selected by the community, the elliptical piers are wrapped with a 10-ft-tall glass mosaic tile mural of manatees and dolphins. The mural is rotated by 10° on each subsequent pier, imparting a sense of movement to those who view the piers. Properly executed aesthetic lighting enhances the pier shape and lights the murals in the evenings.



FIGURE 29.26 Mosaic tile patterns on the piers provide visual interest for boaters under Florida's Broadway Bridge.

29.5.4 Creating Shadows

Shadows created by light interacting with the bridge features will vary with changing lighting conditions. Unique effects will be experienced as the light source moves and the shadows it casts change; therefore, features exposed to natural light will appear different at various times of the day as the sun moves across the bridge site. When evaluating shadowing effects due to the contour and shape of the bridge components, artificial nighttime lighting should also be evaluated, including both aesthetic lighting and roadway safety lighting. Elements should not be considered independently, as the overall bridge shape and individual superstructure and substructure shapes interact with each other to create ever-changing shadows. The prominent component of shadowing for a bridge is the superstructure. Minimizing shadows for elevated roadways may be accomplished with tall, slim piers to create a more open space for travelers underneath and beside it. The view from underneath may be enhanced with longitudinal lines or patterns cast into the superstructure that will produce an appealing shadowing effect. Changes in the superstructure cross-section through changes in the slope of the vertical web walls will also affect how shadows



FIGURE 29.27 Octagonal-shaped piers with concave surfaces help the piers of the Blue Ridge Parkway Viaduct blend with the mountain.

create the illusion of depth. Piers provide a great canvas for the creation of shadows. The use of vertical lines on piers through recesses or curved or chamfered edges will make the pier appear slimmer and more graceful or help the pier blend in with its environment. The pier cross-section of the Blue Ridge Parkway Viaduct (Figure 29.27) around Grandfather Mountain has an octagonal shape, which was enhanced with concave faces to create an effect of shadows, regardless of the direction of the sun.

29.6 Concrete Aesthetic Features

When the primary structural form has been determined for a bridge, specific details can be considered to further enhance the aesthetics and develop the overall theme. The use of color, texture, native materials, and other details of the aesthetic design can add greatly to the beauty of the structure, make it unique to its community, and provide continuity between bridge elements. In some cases, it is these details that define the structure.



FIGURE 29.28 Consistent concrete color was achieved on New York's AirTrain JFK, despite three mixing locations.

29.6.1 Introduction to Color and Texture

Advancements have been made in the aesthetic surface treatment of concrete in the last 10 to 15 years. Today, enhancing the appearance of concrete with color and texture is more economical and feasible from a constructability perspective than ever before. With foresight, strong specifications, and attention to construction operations, the color and texture of concrete can be lasting, low-maintenance features that contribute to the aesthetics of a bridge. Color and texture can be achieved in several different ways. The size and scale of the bridge or project area receiving color and texture may dictate which method or product is best suited for that application based on location, access, intricacy of the details, colors selected, availability of materials, and level of maintenance. It is important to note that when color and texture are added to the design careful consideration should be made as to how they will complement the overall shape of the bridge and bridge elements, lighting, shadowing effects, and patterns.

29.6.2 Overall Bridge Color and Texture

A seamless and unified look may be achieved through application of a uniform color or colorization of an entire bridge. How color is applied is based largely on the desired color, cost of labor and materials, and access. Each method has advantages and disadvantages, and each should be explored in light of the owner's project goals. The natural gray color of concrete can be visually appealing. This color is most attractive if consistency is maintained throughout via the use of single-source suppliers for aggregates, sand, and cement. An example of where this was achieved is the elevated structures of the AirTrain JFK in and around JFK Airport in New York (Figure 29.28). Specifications were developed to achieve a uniform concrete color, despite three concrete mixing locations. The superstructure segments were precast off-site in Virginia, the substructure elements were cast in place using concrete mixed off-site, and the superstructure closure joints were cast in place using concrete mixed by hand on the bridge deck. All of these elements have the same uniform color because specified materials and sources were used. If a lighter shade of gray or white is desired, white cement may be used. The use of single-source materials and white cement can potentially increase costs; however, it is a lifelong, maintenance-free method to achieve consistency in color and enhance the visual appeal of the structure.



FIGURE 29.29 Patterns and colors important to the local Native American culture were used on the pedestrian walkway of North Dakota's Four Bears Bridge.

Bridge coatings have been used extensively in the United States and can be manufactured in a wide variety of custom colors. They are favored by some bridge owners not only for the aesthetic value in achieving a uniform color and texture but also for their potential protective properties, as the coating serves as a sealant in addition to providing a uniform color. The colored coating is applied when the structure is nearly complete, much like paint.

Using colors similar to the surroundings of a bridge will help it blend in with the natural landscape. A natural color and slight roughened texture were achieved by using black iron oxide in the concrete mix which created a marbled appearance and helped the Blue Ridge Parkway Viaduct blend in with the rocky terrain of Grandfather Mountain in North Carolina (see Figure 29.27). Color achieved through the application of a coating can also be used to convey the theme of a project or help link the structure visually with local architecture. The Wabasha Freedom Bridge located in downtown St. Paul, Minnesota, was coated to blend with the cliff sides of the Mississippi River, adjacent to the bridge (see Figure 29.10). Another example of the use of color is the pedestrian walkway of the Four Bears Bridge in North Dakota (Figure 29.29). This primary transportation link to the Fort Berthold Indian Reservation has a wide pedestrian walkway that showcases images important to each of the tribes in the Three Affiliated Tribes who live on the reservation. Color patterns unique to each of the tribes are used in separate sections of the walkway surface, and a unifying pattern was added between these unique sections.

Where vertical recesses are cast into the pier, the use of color, especially a contrasting color, can highlight this area. The Lee Roy Selmon Crosstown Expressway Expansion in Tampa, Florida (Figure 29.30), has a smooth sculptured superstructure complemented by slim, tapering piers that have a vertical recess that follows the curved shape of the pier. Contrasting colors, achieved with a bridge coat, were selected for the pier inset and for the exterior of the pier and superstructure. The project consists of two separate structures: one in the more urban downtown Tampa area, surrounded by existing commercial properties, and the suburban end of the project, which traverses water features and vegetation. For the urban area, a light blue hue was selected for the exterior of the pier and superstructure and a contrasting off-white color for the pier recess. In the suburban section, a bolder, metallic blue was selected for the pier recess and the same off-white color was applied to the exterior of the pier and superstructure. The bolder, metallic hue of blue was customized by the manufacturer to achieve a mirrored or glassy look. Natural sunlight enhances this effect from different angles at various times of the day.



FIGURE 29.30 Contrasting blue inserts in the center of the piers for the suburban section of the Lee Roy Selmon Crosstown Expressway Expansion are appropriate in this Tampa neighborhood.

Another method to consider in achieving overall color is concrete stain. If a soft tone is desired and an irregular but overall color is ideal, then this is a viable method. Color achieved with this method penetrates the concrete to a depth of approximately 1/8 to 1/4 in. The stain does not conceal surface imperfections in the concrete; instead, it provides an overall tint to the surface. An example is the Interstate 70 Hanging Lake Viaduct (Figure 29.31), west of Denver, Colorado, where a light brown stain was used to blend the structure with the canyon walls.

29.6.3 Opportunities for Aesthetic Treatments

When the structural form and overall bridge color and texture have been defined, opportunities for localized aesthetic color and texture treatments can be explored. Some common areas for these types of local applications include piers, pylons, and pedestrian walkways. These surfaces provide a canvas for artistic expression and further development of the aesthetic theme of the bridge project. The Penobscot Narrows Bridge and Observatory (Figure 29.32) has a theme of “Granite—Simple & Elegant,” which is reflected in its obelisk-shaped pylons. Aesthetic details of the pylons include a 4-in. horizontal recess or articulation at alternating 5- and 10-ft spacing. The pylons were cast in place with 15-ft lifts; thus, the concrete was formed with articulations at construction lift lines that replicate the size of large blocks. These recesses were also used to hide the construction joints, and they blend well with the actual granite placed at the pylon base and observatory entrance, where the bridge is experienced on a human scale. The corners of the obelisk are chamfered to create simple, clean lines. Below the deck, the chamfer is 12 in. and above the deck, the chamfer is 8 in., thus maintaining the scale of the pylon dimensions.

29.6.4 Use of Native Materials

The use of native materials can be explored as an opportunity to blend a structure with its natural environment, convey an environmental or earthen theme, or develop community pride. An example of this is the Smart Road Bridge in Blacksburg, Virginia (Figure 29.33), which contains Hokie Stone in the pier recesses. Hokie Stone is acquired from a quarry owned by nearby Virginia Tech and is a stone that



FIGURE 29.31 A stain was used to blend the Hanging Lake Viaduct into Glenwood Canyon, Colorado.



FIGURE 29.32 The pylons of Maine's Penobscot Narrows Bridge and Observatory are obelisk shaped and include articulations that replicate large blocks of granite.



FIGURE 29.33 The pier recesses of the Smart Road Bridge are faced with Hokie Stone.

is prominently used throughout the Virginia Tech campus. Use of the stone on the bridge provides a visual link among the Virginia Tech Transportation Institute, the operators of Smart Road, and the Virginia Tech campus, while adding visual interest by utilizing materials in the bridge that are consistent with the mountainous environment.

29.7 Design Details

Bridge barrier rails, aesthetic lighting, landscaping, and other artistic details can increase the visual appeal of a bridge. Additionally, functional project components such as the location of drainage appurtenances and utilities should be considered for their visual impact.

29.7.1 Concrete Barriers/New Vistas

Crash-tested traffic barriers are required on bridges, and 32-ft-tall standard concrete barriers are typically installed. Bridges frequently offer unique vantage points for the driver, opening new vistas when a new crossing is higher than any existing site or offers a unique view. In situations such as these, where drivers might appreciate a better view from the bridge, open railings that meet the required safety standards as well as the typical solid concrete barrier have been utilized. As an example, the open railing on the Blue Ridge Parkway Viaduct provides uninterrupted views of the surroundings.

29.7.2 Drainage

When bridge deck drainage must be captured and not allowed to freefall onto the ground below, the water is collected at deck level and piped to an appropriate discharge location. These piping systems, although functional, often significantly detract from the appearance of a bridge; however, some inherent aesthetic benefits may be derived from a closed box girder with regard to drainage. Stormwater runoff may be collected on the bridge deck with curb inlets. Drainage piping from these inlets can be cast into the wings of the box girder, concealing the piping within the concrete, to convey the water to an internal stormwater piping system. This piping system can be designed integral to the pier and linked to an underground drainage system, at-grade swale, or other stormwater treatment facility. Unsightly drainage piping attached to the outside of the bridge structure can then be completely avoided. Pretreatment of the stormwater by oil/water separators in the inlets and outfall into a natural filtration system, such as a grassed swale, should be given great consideration not only to meet local, state, and federal requirements but also to develop a project that is environmentally sensitive. The Lee Roy Selmon Crosstown Expressway Expansion in Tampa, Florida, incorporated this type of a closed drainage system, eliminating unsightly exterior pipes while efficiently draining the roadway.

29.7.3 Utilities

Utilities are often carried along bridges. A closed box girder offers advantages by allowing the utility conduits to be carried within the internal core, hidden from view. Another benefit is that the utilities are protected from the elements and easily accessible if repair or modifications are required. The primary utility for any bridge project is electricity, which may be required for roadway lighting, interior box lighting, or exterior aesthetic lighting. Electric conduits can be placed inside the box, either cast into the concrete itself or attached to the underside of the top slab with utility hangers. Other utilities may also be installed inside the box girders. This can be an advantageous approach to crossing a body of water for a utility company vs. installing utility poles to cross overhead or tunneling underneath the body of water. When incorporating utilities into the bridge design, loading and attachment to the inside of the box must be considered, in addition to the pipe material, curvature of the pipe as it follows the geometry of the bridge, potential high voltage (heat), and installation of fiber telecommunication lines. When determining the feasibility of carrying a utility inside a bridge, the bridge engineer must determine what might happen if the utility fails, such as the rupture of a high-pressure water line. In this case, the bridge engineer must address how this water can be removed quickly and safely. The following should be required if utilities are installed within the box girder: regular inspection of the utility pipelines and appurtenances, installation of devices that will alert the appropriate utility company of leaks or other failures, and establishment of emergency response plans. Installing utilities inside a bridge requires a great deal of communication with the utility companies and their engineers, and the design of the bridge must accommodate these utilities. Concealing these utilities rather than attaching them to the outside of the structure or having them cross overhead adjacent to the structure will greatly enhance the visual aesthetics.

29.7.4 Aesthetic Lighting

Lighting can set a bridge apart from other structures in a city's skyline by creating a unique nighttime signature. Lighting can greatly enhance the beauty of a bridge and improve vehicular safety. A good example of aesthetic lighting is the Chesapeake and Delaware Canal Bridge near St. Georges, Delaware (Figure 29.34). Subtle lighting on the pylons and cable stays illuminates the bridge shapes, making the pylons quite distinct at night. Blue uplighting on the angularly shaped pylons of the Leonard P. Zakim Bunker Hill Bridge in Boston, Massachusetts, enhances the beauty of this structure and highlights the various planes of the cable stays at night. Property values near the bridge have increased since construction was completed, and the skyline is enhanced by this signature bridge. Decorative roadway lighting fixtures can also be used to enhance the experience of pedestrians and passengers using a bridge; for example, poles on the Broadway Bridge in Daytona Beach, Florida, display banners promoting city events.



FIGURE 29.34 The Chesapeake and Delaware Canal Bridge has aesthetic lighting suitable to its less populated location.

29.7.5 Landscaping

When a bridge is designed with minimal disturbance to its surroundings, the natural landscape is preserved. When a structure is constructed in an area without landscaping, adding green spaces can greatly enhance the areas surrounding the bridge. Landscaping and a gazebo fill the spaces beneath the 17th Street Bridge in Ft. Lauderdale, Florida. These new spaces invite the public to the riverfront and provide a connection among the surrounding venues. Consideration of the landscape and creating greater green space is important to sustainable design.

29.7.6 Innovative Technologies

New technologies have arisen out of the desire for economy, aesthetics, and efficiency. An example is the Veterans' Glass City Skyway Bridge in Toledo, Ohio, where the community wanted to showcase their glass industry heritage. This state-of-the-art, cable-stayed bridge has a single, slender pylon, the top portion of which features four sides of glass. To achieve the desired slender pylon shape and to simplify the construction and maintenance of the cable-stay system, a new cradle system was developed that allows the cable stays to pass continuously through the top of the pylon, eliminating the need for anchorages (Figure 29.35). This system reduced the size of the pylon, resulting in lower costs and an ability to accommodate the glass aesthetic feature. The cradle system also facilitates inspection and maintenance by permitting removal and replacement of the strands to monitor their condition throughout the life of the bridge. This new development resulted in a low-maintenance, efficient solution while addressing the community's aesthetic desires.

29.7.7 Artistic Details

The artistic expressions in a bridge can celebrate its sense of place. Broadway Bridge in Daytona Beach, Florida (Figure 29.36), conveys the theme of "Timeless Ecology" throughout the project, but perhaps the most enjoyed element of the design is a permanent art gallery on display along the bridge sidewalks.



FIGURE 29.35 The new cradle system simplifies design and long-term maintenance while allowing for greater flexibility in pylon shape (shown is a cradle pipe that runs through the pylon).



FIGURE 29.36 Broadway Bridge in Daytona Beach provides pedestrians with an art gallery of glass tile mosaics along the walkways.

Both sidewalks showcase 18 precast concrete panels containing glass mosaic tile murals of various species indigenous to the Atlantic coast. The murals may be seen by pedestrians and motorists using the bridge. The back of the panels, as seen from the water, contain identical cast relief shells on a sea blue background of glass mosaic tile. The connection of finer details can create the uniformity of artistic expression of the form of the bridge and the message the bridge conveys.

29.8 Summary

Bridges are both structure and symbol. Their functionality serves the public good by connecting people and places to enhance the quality of life. As important infrastructures on the landscape, they should merge sustainable design and aesthetic beauty. Proper alignment, geometry, span arrangements, superstructure, and substructure shapes and the application of aesthetic design principles must be considered from the viewpoint of both good design and efficient construction. The future of modern concrete bridges recognizes the inherent qualities of redundancy and the advanced knowledge that can be gained from “smart bridge” technology. Sensors and high-tech monitoring devices can smartly guide future opportunities to streamline the final designs of bridges. Advanced concrete materials with improved strengths,

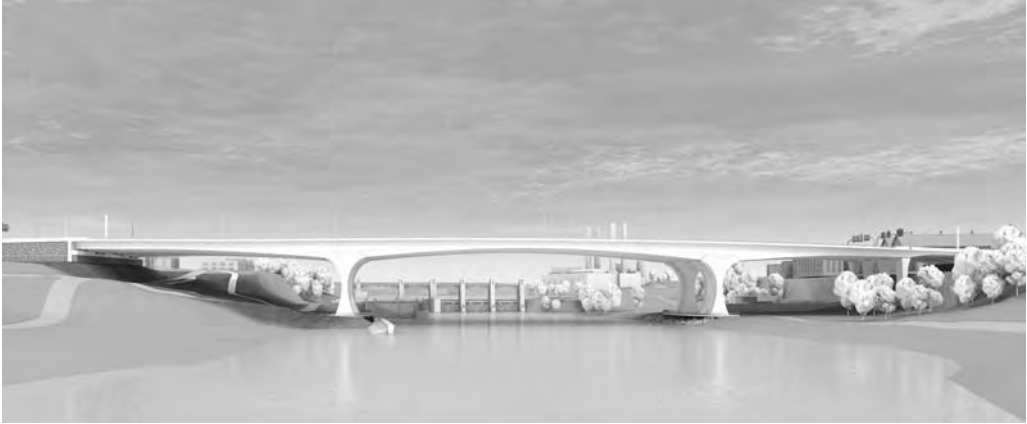


FIGURE 29.37 A functional sculptural bridge (I-35W, St. Anthony Falls Bridge in Minnesota) reflects a series of modern arch forms softly set in the context of the site to maximize openness, light, green space, and a focus on the river.



FIGURE 29.38 The pier shape creates a reflection of curved forms with continuous movement into the bridge superstructure (I-35W, St. Anthony Falls Bridge in Minnesota). Two main piers feature observation platforms along the edge of the river. The appearance underneath creates a visually clean and quiet space.

density, and placement flexibility are being used today to the benefit of functional, yet sculptural bridges. The St. Anthony Falls Bridge (I-35W) in Minneapolis, Minnesota, utilizes long, variable-depth, concrete box girder prestressed spans (504 ft over the Mississippi River), as well as sculptural curved pier shapes (70 ft tall), an open greenscape, lighting, and aesthetic features that highlight a modern concrete bridge focused on simple elegance (Figure 29.37 and Figure 29.38). Future bridges will blend shapes and maximize the repetition of form for redundancy of strength and efficiency of construction. Designers of concrete bridges should remain ever mindful of their responsibility to current and future generations to create bridges that celebrate the technology of the time and the community's sense of place.



“Reflections”—precast, high-strength polymer concrete artwork by the Civil Engineering Class of 1982 with Profs. R.H. Karol and E.G. Nawy, Rutgers University. Each slice was cast separately; the slices were assembled and epoxied together to form the thinking lady statue. (Photograph courtesy of Edward G. Nawy.)

30

Architectural Concrete

Allan R. Kenney, P.E.*

Sidney Freedman**

Updated by **James M. Shilstone, Jr., FACI*****

30.1	History of Architectural Cast-in-Place Concrete.....	30-2
	The Beginning (Prior to 1965) • Prime Years (1965–1990) •	
	Current and Future	
30.2	History of Architectural Precast Concrete	30-4
	The Beginning • Current Practice	
30.3	Applications	30-5
	Cast-in-Place • Precast • Decorative Floors	
30.4	Planning	30-6
	Budget • Drawings • Specifications • Quality Control	
	and Quality Assurance • Prebid Conference •	
	Preconstruction Conference • Mock-Up Construction	
30.5	Materials–Mixture Design	30-12
	Cement • Aggregates • Water • Admixtures • Mixture Design •	
	Wood Sealers • Release Agents	
30.6	Color and Texture	30-19
	Color • Texture: Cast-in-Place and Precast • Texture: Precast	
	Only • Combination Textures	
30.7	Construction: Cast-in-Place Concrete	30-32
	Forming • Reinforcement • Concrete Placement •	
	Concrete Consolidation • Curing • Protection •	
30.8	Production and Installation of Precast Elements	30-60
	Production • Coordination • Field Verification and Layout •	
	Delivery • Connection Considerations • Installation •	
	Tolerances • Protection of Work • Sealants	
30.9	Finish Cleanup	30-68
	Tie-Hole Repairs • Repairs • Cracks • Cleaning	
30.10	Acceptability of Appearance	30-72
30.11	Innovations	30-72
30.12	Defining Terms	30-73
	References	30-74

* President, Precast Systems Consultants, Inc., Venice, Florida; expert on architectural concrete and coeditor of *Architectural Precast Concrete* (PCI, 1989).

** Director of Architectural Precast Concrete Services, Precast/Prestressed Concrete Institute, Chicago; expert in architectural precast concrete and coeditor of *Architectural Precast Concrete* (PCI, 1989).

*** President of The Shilstone Companies, Inc., Dallas, Texas; expert on architectural concrete and member of ACI Committee 303 on architectural concrete.

30.1 History of Architectural Cast-in-Place Concrete

30.1.1 The Beginning (Prior to 1965)

Le Corbusier's Carpenter Center at Harvard University is one of the first recognized uses of architectural concrete in the United States. This daring project, along with several others in Europe, triggered a marked interest and excitement among designers in the United States. As using concrete as an architectural medium became an identifiable trend, the architectural concrete industry evolved with the speed of a fad and left an enduring impression on the construction industry. If there was a specific turning point in the acceptance and use of architectural concrete in the United States, it seems to have come with I.M. Pei's Kips Bay apartment complex in New York City, although a number of other projects were in the planning and building stages at about the same time. Outstanding achievements can be attributed to I.M. Pei; Eero Saarinen; Minoru Yamasaki; Sert, Jackson, and Gourley; Paul Rudolph; Skidmore, Owings, and Merrill (SOM); Pier Luigi Nervi; Phillip Johnson; The Architects Collaborative (TAC); and many others. Of special importance is the fact that the designs created by the architects listed have no common approach. Each is distinctive. Most of our finest examples of architectural concrete take advantage of the free-form plasticity of the material but show complete recognition of the intense discipline it requires. Where this discipline and attention to detail have not been given proper consideration in other projects, the results have been disappointing. Unfortunately, the designers frequently attribute this deficiency to the contractor's lack of knowledge. Although this may be part of the problem, it cannot account for some of the early failures.

30.1.2 Prime Years (1965–1990)

From 1965 to 1990, the use of architectural concrete bloomed. Sculpturing of the forms, better quality form liners, innovative concrete mix designs, and improved placement and consolidation procedures dramatically improved color uniformity and texture. During this period, architects such as I.M. Pei and Partners; SOM; Hellmuth, Obata, and Kassabaum (HOK); Roy P. Harrover; Greiner Engineering; Sikes, Jennings, and Kelly (Figure 30.1); Newhouse and Taylor; Rex Whittiker and Allen; Welton Becket; and others led the way.

30.1.3 Current and Future

Architectural design has gone through cycles, but architectural concrete began making a comeback in the late 1990s, when Polshek and Partners completed the Inventors Hall of Fame in Akron, Ohio, using architectural cast-in-place concrete. I.M. Pei and Partners completed the Rock and Roll Hall of Fame in Cleveland, Ohio; the National Airlines Terminal at JFK International Airport in New York; and the U.S. Holocaust Memorial Museum in Washington, D.C. Tadao Ando and Santiago Calatrava are the new stars of architectural concrete design. Ando's Pulitzer Art Museum in St. Louis and his Museum of Modern Art in Fort Worth (Figure 30.2) reflect the ruggedness and versatility that are inherent in architectural concrete. Calatrava's almost miraculous displays of concrete demonstrate a grace seldom seen in earlier concrete projects. Projects in Mexico, Europe, and Southeast Asia, where concrete is a widely available material, have eclipsed those in the United States. In spite of the many successes in both commercial and monumental types of construction, architectural concrete has experienced periods of very flat or declining growth, perhaps due to marginal aesthetic results caused by a lack of understanding by designers and contractors regarding the architectural concrete process. High labor costs, difficulties in obtaining a reliable finished product, and possible delays in project completion all work against selection of architectural cast-in-place concrete. Early construction planning can reduce all of these negative factors. Contractors have stated that every dollar spent in planning has saved \$4 to \$6 in construction costs. Early planning or a prebid conference that includes the approved contractors, ready-mix suppliers, architect, and owner is essential to familiarize everyone with the drawing details, specifications, sample mock-ups, and quality of concrete work anticipated for the project. Proper budget estimates must be prepared. Architects and contractors must be willing to produce the structure with a minimum amount of mistakes



FIGURE 30.1 First United Tower, Fort Worth, Texas; architect, Sikes, Jennings & Kelly, Houston; medium, sandblast texture.



FIGURE 30.2 Museum of Modern Art, Fort Worth, Texas; architect, Tadao Ando, Osaka, Japan. (Photograph courtesy of David Woo Photography, Dallas, TX.)

and surface blemishes. No matter how good the conceptual design, a building can be ruined by dark lines, pour lines, blotchiness, discoloration, or variations in texture. Architects in recent years have taken a cautious approach to the use of architectural cast-in-place concrete due to the potential pitfalls that can result in owner dissatisfaction.

30.2 History of Architectural Precast Concrete

30.2.1 The Beginning

The first documented modern use of architectural precast concrete was by Auguste Perret in 1923 for the Cathedral Notre Dame Du Haut in Raincy, France, although it was used only as screen walls and infill in an otherwise cast-in-place concrete structure. The depression years followed soon after and then the cataclysm of World War II. Not until World War II ended did the architectural use of precast concrete begin to flourish. Surface finishing techniques for architectural precast concrete, such as water washing and brushing, bushhammering, sandblasting, and acid etching, were initially developed for cast-in-place concrete, as was obtaining colored surfaces by means of pigments and special colored aggregates. These techniques were also well established within the cast stone industry by the 1930s.

In 1932, John J. Earley and his associates at Earley Studio in Rosslyn, Virginia, began work on producing exposed-aggregate ornamental elements for the Baha'i Temple in Wilmette, Illinois (1920–1953), one of the most beautiful and delicately detailed architectural precast concrete projects in the United States. The panels are white concrete with exposed quartz aggregate. Lack of funds postponed completion of the exterior precast concrete until 11 years after the building was begun. Another early notable use of large precast panels was for the White Horse Barn (1937), constructed for the Minnesota State Fair. This structure had panels 15 ft long, 7 ft high, and 6 in. thick. Cast with a smooth finish and cured for 7 days in steam-filled rooms, these panels were attached by the structural concrete around the edges of the panels.

A pivotal development occurred in 1938, when administration buildings at the David W. Taylor Model Testing Basin were built near Washington, D.C. Panels 2-1/2 in. thick and up to 10 ft by 8 ft were used as permanent forms for cast-in-place walls. The project was significant as the first use of the Mo-Sai manufacturing technique, with units produced by John Earley in collaboration with the Dextone Company of New Haven, Connecticut. It was also the first project in which large-area exposed-aggregate panels were adapted to serve as both the exterior form and preinspected facing for reinforced concrete building construction. Earley had patented the idea of using step (gap)-graded aggregate to achieve uniformity and color control for exposed-aggregate work. Working from this background, the Dextone Company refined and obtained patents and copyrights in 1940 for the methods under which Mo-Sai Associates (later Mo-Sai Institute, Inc.) operated. The Mo-Sai Institute grew to include a number of licensed manufacturing firms in various parts of the United States. Its public relations and advertising activities, highlighting technical achievements, were a major factor underlying general acceptance of architectural precast concrete. The surface finishes produced by the Mo-Sai process were dense, closely packed mineral aggregate with a minimum of cement/fines matrices that resembled mosaic, from which the name Mo-Sai was derived.

In 1958, a new panel-casting method was introduced in the United States under the name of Schok-beton (shocked concrete), and a number of franchised plants were established. The machinery used in this method was patented in Holland in 1932. The process is primarily a means of consolidating a no-slump concrete mixture by raising and dropping the form about 5/16 in. some 250 times per minute. This contrasts with conventional methods of consolidation using high-frequency and low-amplitude vibration. Although the production of large precast panels by this method was relatively new, small concrete units had been produced in the past on so-called drop tables, which followed the same technique without the refinement of modern machinery. Depending on the cement content, the shocking technique produces compressive strengths of 3000 to 4000 psi after 24 hours and up to 10,000 psi at 28 days.

Architectural precast concrete usage initially was complicated by the lack of mobile cranes and other efficient material-handling equipment. Because of this lack of equipment and because of competition from metal and glass curtain-walling, precast concrete was comparatively slow to develop, and the record of its eventual rise to parity, even its dominance in places, is properly that of the 1960s. Reasons for this expanding usage were improved methods of production, better handling and erecting equipment, and the realization that precast panels provided a pleasing variety of surface textures, patterns, and exterior designs that generally could not be accomplished as economically in other materials. A number of

pioneering early postwar uses of precast concrete in architecture were otherwise of limited significance. These included dormitory units at the University of Connecticut (1948) based on load-bearing wall panels; an eight-story office building in Columbia, South Carolina (1949), with window-wall cladding panels (erected by hand winch); and a six-story office building in Miami (1951) where 4-in.-thick precast panels were suspended from the soffit of a cantilevered cast-in-place floor slab.

The Hilton Hotel in Denver was completed in 1958/59 and was one of the early significant uses of window-wall panels fixed to a structural frame. The Police Administration Building in Philadelphia, completed in 1962, made history as one of the first major buildings to utilize the inherent structural characteristics of architectural precast concrete. Its exterior panels, 5 ft wide by 35 ft high (three stories), carry two upper floors and a roof. This structure was an early model for the blending of multiple systems (precasting and post-tensioning) for one building.

30.2.2 Current Practice

Architectural precast concrete can be provided in almost any color, form, or texture, making it an eminently practical and aesthetically pleasing building material. It is difficult to imagine an architectural style that cannot be expressed with precast concrete. By providing the designer complete control of the ultimate form of the facade, the precast concrete industry has experienced steady growth since the explosive 1960s, particularly in the ever-widening range of precast concrete applications. The widespread availability of architectural precast concrete, the nearly universal geographic distribution of the necessary raw materials, and the high construction efficiency of prefabricated components all add to the appeal of architectural precast concrete construction. Established precasters have a high level of craftsmanship and ingenuity along with a thorough knowledge of the material and its potential for converting the designer's vision into a finished structure.

30.3 Applications

30.3.1 Cast-in-Place

Architectural cast-in-place concrete has been used in many colleges; libraries; airport terminals; office buildings; museums; public buildings for city, state, and federal government; hospitals; sound-barrier walls; industrial warehouses; and all types of landscaping products.

30.3.2 Precast

The use of nonload-bearing precast concrete cladding has been the most common application of architectural precast concrete. Cladding panels are those precast elements that resist and transfer negligible load from other elements in the structure. Generally, they are normally used only to enclose space and are designed to resist wind, seismic forces generated from their self-weight, and forces required to transfer the weight of the panel to the support. Cladding units include wall panels, window-wall units, spandrels, mullions, and column covers. Their larger dimension may be vertical or horizontal.

Often the most economical application of precast concrete is as a loadbearing element, which resists and transfers loads applied from other elements. With very few modifications, many cladding panels may function as loadbearing members. The steel reinforcement required to physically handle and erect a unit is often more than that necessary for in-place loads. The slight increase in the load-bearing wall-panel costs (due to erection and connection requirements) can be offset by the elimination of separate structural framing (beams and columns) from exterior walls or the reduction of interior shearwalls. This savings is most apparent in buildings with a large ratio of wall to floor area.

In many structures, it is economical to take advantage of the inherent strength and rigidity of exterior precast concrete wall panels and design them to serve as the lateral-load-resisting system (shearwalls) when combined with the diaphragm action of the floor construction. A current trend is toward the use of precast concrete units as forms for cast-in-place concrete. This system is especially suitable for

combining architectural (surface aesthetics) and structural functions in load-bearing facades or for improving ductility in locations of high seismic risk. Because the cost of formwork is a significant part of the overall concrete cost in a structure, substantial savings can usually be achieved by using precast concrete units as formwork. In addition to functioning as exterior and interior wall units, precast concrete finds expression in a wide variety of aesthetic and functional uses, including: (1) art and sculpture; (2) lighting standards and fountains; (3) planters, curbs, and paving slabs; (4) balconies; (5) screen sound barriers and retaining walls; (6) screens, fences, and handrails; (7) street furniture; and (8) ornamental work.

30.3.3 Decorative Floors

Concrete floors have not traditionally fallen into the category of *architectural concrete*; however, since 1990, there has been a dramatic rise in the artistry and variety of decorative concrete floors. Concrete floors embossed with stamped patterns, pigmented with integral pigments, or treated with applied stains have become extremely popular. Polished concrete floors have become common in big-box retail stores, which have discovered that exposed concrete floors are a lower cost alternative to resilient flooring or carpet. Although decorative floors can be considered as architectural concrete, they require a different scope of expertise than formed concrete and are not addressed in this chapter.

30.4 Planning

30.4.1 Budget

Regardless of the type of building or its intended use, the architect and owner must begin with a budget estimate. Although forming, placement, concrete, and finishing costs will undoubtedly be more for an architectural concrete job, the end cost of the completed building might well be less than the total cost of a structural concrete job when rental income, maintenance costs, additional finishes, architectural treatments, and repair costs are factored into the equation. Life-cycle costs are what interest the owner. Architectural concrete projects must have an adequate budget to achieve the desired visual impact while maintaining the integrity of the structure. When the design architect has determined the image and scope of the project, an initial meeting should be held that includes the architect, architectural concrete consultant, structural engineer, and landscape architect, if one is associated with the project.

At this time, shape vs. structural requirements and precast vs. cast-in-place are evaluated. The capability of local precast facilities and availability of knowledgeable concrete contractors often determine the most economical approach to achieve the finish appearance required. The designer must decide at this time whether to follow the possibility of form and continuity inherent in cast-in-place concrete or the building-block logic, time savings, and precise quality control of precast. Relative costs can vary with time and place. Repetition is essential to maximize economy for precast concrete components. Careful planning is necessary to achieve good repetition without sacrificing design freedom.

The type of finish selected can have a large impact on budget. The architect must provide sufficient funds in the budget to allow the special finish and quality workmanship required for the method selected and must determine whether specialized construction techniques are routinely accepted and executed by local contractors. Casting structural concrete against a form liner or sandblasting the surface does not necessarily produce acceptable architectural concrete. A contractor that assumes this is about to learn an expensive, time-consuming lesson and will probably have an unhappy client who is not receptive to scheduling future projects with the firm. The secret to successful architectural concrete is early and detailed planning. Final costs and execution do not end with the building designer, but with the contractor. The general contractor must know how to carry out the designer's intentions without increasing the contractor's or owner's costs. The contractor must have knowledgeable workmen, especially for the forming and concrete superintendents. Current bidding practices often result in late award of the precast subcontract. In practice, this means that additional molds must be built to meet the project deadline. The necessity for extra molds increases costs and partially offsets the use of high repetition.



FIGURE 30.3 Waviness in the concrete surface due to lack of form rigidity during concrete consolidation.

The secret to good architectural concrete is in the forming. Forms must be strong enough to accomplish concrete placement within specified form joints and rustications without honeycomb, cold joints, or pour lines. A superintendent who has placed many thousands of yards of structural concrete where strength and a lack of honeycomb have been the criteria could be in trouble when visual excellence is required if strict attention is not paid to details.

30.4.2 Drawings

Eventually, the conceptual design must be detailed and working drawings completed. Construction elements such as control joints, construction joints, form-tie locations, concrete shrinkage, reinforcement location, reinforcement coverage, special form requirements, mix design, concrete access points, and type of finish must be considered. The contractor should pay special attention to closure technique or concealed joints in formwork. Articulated lines or rustications should be drawn at the control and construction joints. The closer the architectural concrete construction follows the natural construction sequence, the more economical the costs. In addition to the formwork items discussed below in Section 30.7.1, the contractor must consider form rigidity. Architectural concrete often includes high columns and walls. Forms must be sufficiently reinforced to eliminate wave action or pulsating action as well as form movement during the use of high-frequency vibrators (Figure 30.3). Form height is a function of drawing details involving rustication details and form-tie locations. Repetitive items in design will increase form usage and allow higher quality forms (such as steel or fiberglass) to be used economically.

The contractor needs to ensure that the drawing details work. Although the architectural concept of the drawings may be excellent, if the details do not work then the building has the potential to be a failure. Good design considers the construction needs as well as the architectural and structural criteria. The drawings set the conditions under which the contractor must work. A wall designed to be 8 in. thick, including a double curtain of reinforcing, will not allow proper concrete placement and consolidation because the space is simply too tight. If the wall has rustications and minimum cover requirements on the outside face, space requirements for vibrator placement get even tighter. Allowing for acceptable tolerances on the placement of reinforcing steel will place even tighter access for the vibrator.

Cast-in-place architectural concrete and precast elements may be successfully combined but require detailed effort on the part of the architect and an understanding of the construction process for each system on the part of the contractor. More time will be required for the selection of materials, mix



FIGURE 30.4 Matching architectural cast-in-place and precast concrete at King Saud University in Riyadh, Saudi Arabia; architects, HOK, St. Louis, MO.

designs, and finishes than if only one system were used. Realistically, large mock-ups and knowledgeable workmen must be part of the contractor's production process.

The architect has a great deal of freedom of expression in working with architectural concrete. An architect may select thin members or sculptured shapes in precast concrete and combine them with the massiveness and structural strength of cast-in-place concrete to create the curtain wall (Figure 30.4). Today, when costs for different types of facades are compared, precast or cast-in-place concrete can be competitive and compare very favorably with glass and metal facades. Design can provide either matching or contrasting colors between architectural precast and cast-in-place concrete.

The precaster's shop drawings (erection and production drawings) should be prepared in general conformance to the *PCI Drafting Handbook* (PCI, 1990). Generally shop (erection) drawings are submitted to the general contractor who, after checking them and making notations, submits them to the architect/engineer for checking and review. Timely review and approval of shop drawings and other pertinent information submitted by the precaster are essential, as fabrication should not commence until final approval or an approved-as-noted has been received.

The architect reviews the precaster's erection drawings primarily for conformance to the specifications, then passes them along to the structural engineer so he can check for conformance to the specified loads and connection locations. This allows the engineer to confirm his own understanding of the forces for the structure at the connection points and the precaster's understanding of the project requirements. Design details, connection locations, and specified loads should not be left to the discretion of the precaster. This is especially important in cladding panels, where the weight of the unit and its torsion and shear must be supported by the frame. Steel frames are more sensitive to the eccentricity of a panel unit causing deformation of the structure and may require bracing.

30.4.3 Specifications

Specifications can be a trap for the unwary contractor. Reference may be made to architectural concrete requirements in the general concrete specifications. When projects, including several monumental buildings, have had high budget estimates, the separate section for architectural cast-in-place concrete has sometimes been removed from the specification. All concrete has been covered under the general concrete section. A short added paragraph may read something like this: "The final finish surface should be a

uniform light sandblast and match the approved sample panel in Architect's office." A short paragraph near the end of the concrete section may state: "No patching or repairs will be permitted without the express permission of the Architect. Only patching of minor blemishes will be permitted." These short paragraphs added to a general concrete specification can be deadly to the contractor. No mention is made of special mix requirements, mock-ups, form or form-tie locations, placing consolidation, and finish requirements. Architectural cast-in-place concrete specifications should be used and clearly separated from those for general concrete, and the contractor should always prepare a mock-up for approval whether or not one is specifically called for in the specification. The mock-up can consist of a segment that will be incorporated in the finished structure.

Specifications can be both the friend and ally of the owner, architect, and contractor. Architectural concrete is not structural concrete with only a surface finish applied. It is a material that requires a special process leading to the final finish required. Both architectural cast-in-place and precast concrete must be clearly specified, closely supervised, and produced throughout the full construction process by knowledgeable workers who care. Architectural precast should always have a separate section in the contract specifications, as should architectural cast-in-place concrete.

The two basic types of specifications are *performance* and *prescriptive*. A pure performance specification is one that references a physical sample of concrete. It essentially says: "Produce concrete that looks like the referenced sample and meets all other concrete requirements as contained in the general concrete section." Such a specification assumes that this type of concrete finish is not new and has been satisfactorily produced before by all parties concerned. On the other hand, a prescriptive specification is necessary when the bidding list must be left open or when the finish is a new type developed by the designer. This type of specification relies on the detailed investigation of materials, mix designs, formwork, concrete placement procedures, and methods of finishing. It then gives explicit instructions on what procedures to follow. Even though instructions may be clear, a prescriptive specification requires constant supervision to keep everything rolling smoothly (Bell, 1996).

The performance type of specification is the most practical. It can be used when (1) a physical example of the concrete finish is available, (2) the contract is negotiated or only prequalified bidders are selected, or (3) craftsmen are available to produce the required performance (Bainbridge and Abberger, 1994). Too often a contractor is asked to comply not only with standards from the American Society for Testing and Materials (ASTM), American Concrete Institute (ACI), Precast/Prestressed Concrete Institute (PCI), and others, but also with references, guides, or practices published by the above because they are incorporated by reference in other documents mentioned in the contract even though no copies or details are furnished. To clarify this issue, in 1978 the American Concrete Institute published the following policy that is used today on all appropriate documents: "ACI Committee Reports, Guides, Standard Practices, and Commentaries are intended for designing, planning, executing, or inspecting construction and in preparing specifications. Reference to these documents shall not be made in the Project Documents. If items found in these documents are desired to be part of the project documents, they should be incorporated directly into the project documents."

30.4.4 Quality Control and Quality Assurance

In theory, for commercial-grade concrete construction, the contractor simply hires a testing laboratory approved by the owner or architect and sees that the reports are distributed to the responsible parties. The contractor should review ready-mix concrete facilities and local precast manufacturers for service history; reserve capacity; availability of modern trucks; plant silo, bin, and storage capacity; and availability of knowledgeable and cooperative personnel. Owners are looking for contractors to spend more time and money in construction reviews and in planning to develop more innovative ways to meet schedules and improve quality. More monumental work is being negotiated or has a very limited bid list. Contractors with prior experience in architectural concrete who can meet budget performance, maintain good safety records, and control the project processes will be in high demand (Bainbridge and Abberger, 1994).

The basic purpose of quality-control programs is to ensure that the requirements of the contract documents are met in every step of the process, from selection of materials to curing of the concrete. Written records are required to substantiate that fact. Top management personnel in construction companies need to educate their talented field people with regard to the benefits of quality control (QC) and quality assurance (QA). The contractor works for the owner and is responsible for constructing the project as designed and specified. He must ensure that the quality of construction measures up to or exceeds the standards of material and workmanship required by the contract documents. This is the contractor's primary responsibility, but the contractor must also emphasize to employees, material suppliers, and subcontractors the importance of searching for errors in design or specification and selection of inappropriate materials. Although design review is not part of the contractor's responsibility, it may be good insurance to seek a second opinion on soils engineering, structural engineering, exterior-facade details, etc. Replacing or redoing problem construction is time consuming, frustrating, and always expensive.

The contractor cannot cite lack of skilled workers, irresponsible subcontractors, or rushed or incomplete drawings as an excuse for poor quality. In today's construction environment, the contractor must live with tight budgets, low construction time, drawings that are completed as construction progresses, and lack of skilled workers. What better reason could there be to cry for improved quality control and quality assurance programs? Quality control is directed toward after-the-fact inspection and testing. Quality assurance is a broader concept that involves planning and a program that incorporates feedback from site problems, inspection, and testing. Quality assurance programs incorporate both feed-forward and feedback controls for each segment of the construction process. Quality assurance is when the contractor:

- Makes sure the field supervisors and subcontractors recognize the obligations of the contract documents
- Thinks *quality* in every decision made
- Identifies project risks and relates them to quality factors as well as time and costs
- Coordinates and communicates with the architect/engineer and owner with overall quality in mind
- Encourages all of the workers to concern themselves with the quality of construction
- Uses knowledgeable consultants to assist in planning and on-site review
- Anticipates problems and tries to alleviate them early
- Learns to listen
- Minimizes reworking or rebuilding

The most profitable projects are those that prevent defects in the first place through planning, communication, and ongoing QA programs.

An architectural precast concrete manufacturing plant should be certified by the PCI Plant Certification Program at the time of bidding. Certification should be in product group A1 (architectural concrete). The certification of a producing plant by PCI indicates that the plant has in place a system of quality, starting with management. Further, the quality system extends to all areas of plant operations including a thorough and well-documented quality control program. Certification indicates that plant practices are in conformance with time-tested industry standards. It means that the plant regularly demonstrates its ability to produce quality products. All plants are audited at least twice each year. Audits are unannounced and are usually of 2 days' duration. Audits and grading are based on the *PCI Manual for Quality Control for Plants and Production of Architectural Precast Concrete Products* (PCI, 1996). The audit covers all aspects of production and quality control as well as engineering and general plant practices. The product evaluations performed by in-house quality control personnel are also reviewed to determine if routine monitoring is correct and accurate.

30.4.5 Prebid Conference

A prebid conference should be held at least 3 weeks prior to bid. This conference should involve all of the professionals in the design team, preselected general contractors, and anticipated precast manufacturers. In addition it may include interested formwork, reinforcing steel, and concrete producer subcontractors.

Precast manufacturers should have submitted their samples, company brochures, technical literature, and proposed materials prior to the meeting. Plans for how the work is to be accomplished in accordance with the requirements of the contract documents would be available at this meeting. The architect should have the building model and any samples showing anticipated color and texture. On exceptionally large projects, an extra mock-up may be constructed, under a special contract, to be available at the prebid conference. This mock-up would help determine the feasibility of various materials, treatments, and construction procedures prior to writing the particular architectural specifications for bid. Contractors would be told what is expected in the way of workmanship, timing, and results. Samples would be discussed and material sources and adequacy of reserves reviewed. Precast production schedules, plant facilities, and personnel would also be discussed. At this meeting, potential problems would be addressed and the final architectural finishes clearly spelled out. Generally, one prebid conference is held for all anticipated contractors, subcontractors, and precast manufacturers.

30.4.6 Preconstruction Conference

Following award of the contract, the architect should schedule a preconstruction conference with the contractor at a time and place that are mutually agreeable to discuss the architectural concrete system. This allows the design team to meet with the contractor, the contractor's key personnel, the ready-mix concrete supplier, the form supplier, reinforcing and placement subcontractors, the testing laboratory, and the precast supplier (if applicable). Brochures or literature should accompany any alternative construction proposals. Patented form systems may be suggested at this conference. The contractor should be sure such systems not only meet structural needs but are also appropriate for architectural purposes. Butt joints or form-tie locations may be a problem with certain form systems. When precast and cast-in-place construction are to match, the precast manufacturer should match the cast-in-place construction. The precaster has more flexibility in matching color and texture than the cast-in-place contractor, who does not have as many options and specialty techniques available. The preconstruction conference is a good place to set ground rules and begin planning quality assurance programs. At this meeting, the design team should be responsive to suggestions and requests for approvals and additional information by the contractor. The architect should be responsive to alternative plans submitted by the contractor and make recommendations for the contractor's consideration. The contractor must be ready with a plan of construction, timing, and schedule of items that involve the design team such as mock-up timing, shop-drawing approvals, and any remaining questions as to color or texture.

30.4.7 Mock-Up Construction

Mock-up construction is where the contractor demonstrates the intended results. Materials, equipment, and construction methods used are those intended for the actual work. The mock-up should be a full-scale mock-up and contain a full complement of reinforcing steel and blockouts. The mock-up is a proving ground to test the design details, shape, construction-joint locations, gasket procedures, and finishes required under the contract documents. In the case of alternative proposals, the mock-up helps ensure that the intent of the designer is understood. For the contractor's own protection, every architectural concrete project should include a mock-up or mock-ups. This is true whether or not one is specified.

A cast-in-place concrete project may have only one large mock-up showing a column, beam, or wall section that is full scale in size and uses the design reinforcing, forming system, concrete mix, placement procedures, and consolidation methods to be used in the actual work. After completion and approval of the construction, the mock-up is used to demonstrate cleaning, repair techniques, sealers (if specified), and protection. An architectural precast project might require three mock-up samples of a size sufficient to demonstrate actual planned production conditions. Any mock-up or combination of mock-ups must be able to establish the range of acceptability with respect to color and texture variations, surface blemishes, uniformity of corners or returns, frequency and size of air-void distribution, and overall appearance. Mock-ups also test the planning and training abilities of the contractor. Mock-up usage should shorten the learning process and set the standards necessary to achieve the designer's objective.

The mock-up should be prepared or erected at the job site and be approved before the majority of the formwork for the architectural concrete construction is built or purchased. When forms are to be site made, the mock-up must be finished at least 45 days before the architectural concrete is scheduled to be cast. On larger cast-in-place projects where custom-built forms are to be used, the mock-up should be finished 90 to 120 days before forms are needed for construction. This will allow time to revise the forms or the construction methods used in the construction of the mock-up. This long lead time can be necessary. Do not let the project be delayed by inadequate planning and lead times. Construct as many full-size mock-ups as necessary to meet the approval of the architect. When a mock-up is not called for in the specifications and the concrete called for appears to be structural concrete with only a light texture finish, a contractor would be wise to go through a sample and mock-up procedure at his own expense prior to final decisions on mix design and formwork purchase. The samples and mock-up for cast-in-place concrete may have to be scaled down due to the cost factor but should not be eliminated from the early phase of the construction process. Sometimes future architectural cast-in-place concrete may use part of the early structural concrete as a testing ground for forming and concrete placement. Areas hidden from view such as basement walls or elevator shafts could be used. Some type of mock-up construction will minimize any confusion on the part of all parties involved in the project design and construction.

Approval of any mock-up should be based on the full mock-up or, in the case of precast, of at least three precast full-scale (not necessarily full size) samples. Realistically, all architectural concrete surfaces will have blemishes, irregular surfaces, and differences in color and texture. Samples and mock-ups should be used to establish the range of acceptability prior to the beginning of actual construction. Mock-ups should remain on the job site or at the plant where they are readily available for inspection and comparisons until completion of the work (Figure 30.5). Mock-ups can be most effectively assessed when presented in their final orientation: horizontal, vertical, or sloping. Details should be viewed from a distance typical for viewing the architectural concrete on the building but that is not less than 20 ft. Reference to another project or an adjacent building should never be the basis of the architectural color and texture demanded for a project. Mock-ups should be required for each project. A different building facade may have been produced under special conditions involving different specifications, use of materials no longer available, or more stringent supervision requirements.

30.5 Materials–Mixture Design

Certain variations, mix proportions, and procedures are specific to architectural concrete. A change in aggregate proportions, color, or gradation will affect the uniformity of the finish, particularly where the aggregate is exposed. In smooth concrete, the color of the cement (plus pigment) is dominant. A matte finish will result in a different color than a smooth finish. If the concrete surface is progressively removed by sandblasting, acid, tooling, retarders, or other means, the color becomes increasingly dependent on the fine and coarse aggregate. Darker and more colorful fine aggregates have more influence when used with lighter colored cements and especially with white cement. When there is a significant difference in contrast between the paste color and the aggregate color, variations in finishing will be more apparent. When the paste color is similar to the aggregate color, variations in finishing will be less apparent.

30.5.1 Cement

White Portland cement is made of selected raw materials containing negligible amounts of iron and manganese oxides, as these materials project a gray color. White cements have inherent color and strength-development characteristics depending on their source; some have a buff or cream undertone, and others have a blue or green undertone. Cement of the same type and brand and from the same mill should be used throughout the entire job to minimize color variations. Color variations in a gray cement matrix are generally greater than those in matrices made with white cement. A gray color may be projected by using white cement with a black pigment or a blend of white and gray cement. Uniformity normally increases with increased percentages of white cement. Gray cement is dominant and will have much



FIGURE 30.5 Mock-up panels for USAA regional office in Tampa, Florida; architect, Spillis Candela & Partners, Inc., Coral Gables, Florida.

greater color variation than white cement with an added black pigment. Plastic or stainless steel trowels should be used for finishing architectural concrete to minimize the danger of staining or darkening the concrete. Trowel marks or surface burns can be minimized by troweling while the concrete surface is moist or by keeping the trowel wet during finish operations (Freedman, 1968, 1969).

30.5.2 Aggregates

The choice of aggregates can have a considerable effect on the finish color of white, buff, or light-toned concrete. The choice of fine and coarse aggregate should be based on a visual inspection of the samples and the mock-up. These samples would have the proper matrix and be finished in the same manner as planned for construction. The method used to expose the aggregate in the final product influences the final appearance. Sandblast textures will generally dull the appearance of the coarse aggregate. All coarse and fine aggregates should be from the same source for the entire project. Normally, aggregates will be selected for exposed architectural purposes and specified in the contract documents as to source, size, and color. Aggregates should have proper durability and be free of staining or deleterious materials. They should be nonreactive with cement, have a proven service record or satisfactory results from laboratory testing, and have the particle shapes (rounded rather than slivers) required for good concrete and appearance. When angular aggregates, such as small-size granites, are specified, the contractor should inform the architect and owner that they will produce greater color variations, some pour lines, and increased surface blemishes such as bug holes.

Where the color depends primarily on the fine aggregates, gradation control is required. For fine aggregates purchased in bulk, the percentage of fine particles passing the No. 100 sieve should be limited to no more than 5%. This may require double washing and a secondary screening, but the premium for this can be justified by the increased uniformity of color. With a light to medium exposure, a uniform color appearance may be obtained by using crushed sand of the same material as the coarse aggregate; however, for reasons of workability, a percentage of natural sand is always desired in a concrete mix. When maximum whiteness is desired, a natural or manufactured opaque white or light yellow sand should be used. Most naturally occurring sands lack the required whiteness, and the contractor or precaster must look to the various manufactured aggregates for the white base desired. Generally, these consist of crushed limestone (dolomite, calcite) or quartz and quartzite sands.

Coarse aggregates are selected on the basis of color, hardness, size, shape, gradation, method of surface exposure, durability, cost, and availability. Colors of natural coarse aggregate vary considerably according to location and geological classifications. Coarse aggregates should be reasonably uniform in color. Light and dark coarse aggregates require caution in blending for good distribution and color uniformity in adjacent concrete. Extreme color differences between fine and coarse aggregate or between the aggregates and matrix should be avoided. Often a pigment can be added to the matrix to more closely match the color of the aggregates. Extreme color differences between the aggregates and matrix will create uniformity problems and possibly lead to aggregate transparency. The use of closely graded fine and coarse aggregate in a gap-graded combination often results in less segregation and produces a more uniform finish. While gap grading is an established and well-proven practice, it should not be carried to extremes. Extreme gap grading may lead to separation of the paste and aggregates and thus create uniformity problems. This can be particularly true when dense, hard surface forms are used in combination with high-frequency

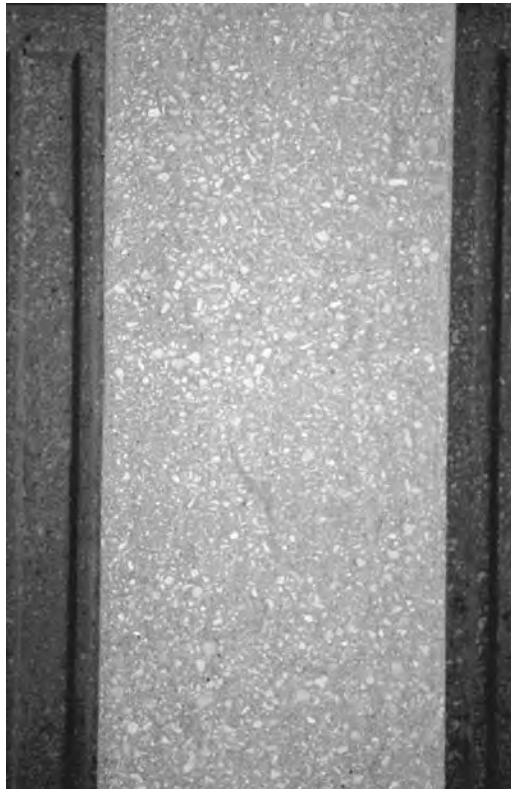


FIGURE 30.6 Separation of the paste and aggregates when using high-density forms and high-frequency vibrators. Dark paste lines are evident after sandblasting.



FIGURE 30.7 Pour lines on interior beams where the concrete was placed during hot weather. Higher dosages of admixtures could have been used to minimize the possibility of early set leading to pour lines.

vibration (Figure 30.6). The amount of fines, cement, and water should be minimized to ensure that shrinkage remains within acceptable limits and that surface absorption will be low enough to maintain good weathering qualities. The durability of the concrete would normally not be affected by any degree of gap grading as long as proper concrete cover is maintained over the reinforcement.

30.5.3 Water

Mixing water should be clean and free from oil, acid, iron or rust (which may cause staining), and injurious amounts of vegetable matter, alkalis, or other salts. Almost any natural water that is drinkable and has no pronounced taste or odor is satisfactory. Warm water may tend to cause false set or shorten the working time of the mix. Chilled water or use of ice may retard the set or make mixing more difficult.

30.5.4 Admixtures

Water-reducing and set-controlling admixtures have been found to be effective with respect to water reduction and strength increases when used with Portland cements of low tricalcium aluminate (C_3A) and alkali content. Architectural concrete dosages are in excess of those generally used for structural concrete and may require up to 50% more than the usual recommended minimum. Admixtures are important in architectural concrete for workability, to assist in placement, and to minimize the possibility of pour lines occurring in warm weather due to early set (Figure 30.7). An increase in cement fineness or a decrease in cement alkali content generally increases the amount of air-entraining admixture required for a given air content. High-range water-reducing admixtures (HRWRAs) may alter the air-void system of air-entrained concrete. Typically, the void-spacing factors are higher than in normal air-entrained concrete. This void spacing is caused by an increase in the average bubble size and a decrease in the specific surface compared to an air-entrained concrete without an HRWRA. In such cases, the dosage of the air-entraining agent would be adjusted to compensate for this effect. In some cases, a complete loss of air may occur when using HRWRA. It may be necessary to change to another HRWRA or use a different air-entraining agent. Certain air-entrained admixtures may be more effective with certain HRWRAs, in the production of adequate air entertainment. When HRWRA are used, there can be an increased tendency for segregation in the concrete mix, particularly when gap-graded aggregates are used. All admixtures should be tested to ensure their compatibility. The use of calcium chloride as an admixture may contribute to the corrosion of metals and darkening, mottling, and discoloration of the concrete surface. Its use is not recommended for architectural concrete. In spite of the use of such terms as “chloride

free,” no truly chloride-free admixture exists, as admixtures often are made with water that contains small but measurable amounts of chloride ions. If, when using the available information on the admixture and the proposed dosage rate, it is calculated that the chloride ion limitation will be exceeded, alternative admixtures or procedures should be considered. When coloring pigments are added to the concrete mixture, the amount should be less than 5% of the weight of the cement. Amounts in excess of 5% seldom produce further color intensity, while amounts greater than 10% may be harmful to the concrete quality. For any coloring agent, it is important to have tests or performance records that indicate color stability in concrete.

30.5.5 Mixture Design

Architectural concrete should provide both proper workability required for consolidation and adequate strength for the given type of concrete. The architect should specify the parameters of concrete performance requirements. A design strength for concrete should be determined by the engineer, based on in-service requirements, while not forgetting construction and, in the case of precast, handling and erection considerations. A concrete mix designed for purely structural reasons or for light acid-etched or very light sandblast texture is normally fully (continuously) graded, which means that it contains all the sizes of aggregates (below a given maximum) in amounts that ensure an optimum density of the mix.

Gradation standards for gap-graded mixes vary widely. The use of one sieve size or narrow size range for coarse aggregate, with a small percentage of concrete or masonry sand for workability, results in a more uniform distribution of exposed aggregate when texture is desirable. Gap-graded aggregates in which the coarser particles of sand and finer particles of coarse aggregate are omitted can produce a surface with greatly reduced bug holes provided proper consolidation is used. Lower sand content can result in greater color variations and aggregate transparency when dark-colored coarse aggregates are used. Good concrete mix design aims to produce uniformity of color, avoid segregation, and minimize other surface blemishes. This type of mix is not necessarily the same as that used in standard structural concrete. When a contractor accepts the concrete mix design for architectural concrete, whether it be from the architect or a local laboratory, the contractor implies that he is capable of using that mix proportion of specific materials to produce concrete with good workability and of adequate strength that will also produce concrete surfaces with an absolute minimum of surface blemishes. This is a big responsibility and should not be assumed by the contractor until after mock-ups are completed and approved.

The ratio of fine aggregate to coarse aggregate by weight should be 1:2:5 to 1:3:5 in gap-graded mixes. The fine aggregate is usually masonry sand. With high cement content concretes, coarsely graded sands may be satisfactory because the cement helps provide the needed fines for workability. With low cement contents (under 564 lb/yd³), the fine aggregate particles are necessary for good workable mixtures. Mixtures with higher cement contents can generate substantial heat. It is sometimes necessary to place thermal curing blankets around the forms to prevent rapid cooling of the exterior of the concrete and induce thermal cracks in the concrete due to temperature differentials.

Self-consolidating concrete (SCC) is becoming increasingly viable in the concrete market, particularly in precast plants. Although SCC requires increased emphasis on quality control and improved materials, the benefits derived from a reduction in air bubbles, decreased need for skilled placing labor, and improved product consistency can more than outweigh the increased cost of the mix and process. Not all locations can successfully produce SCC on a consistent basis, however. Selection of SCC as part of the process must be based on locally available materials, quality control capabilities, environmental constraints, and a proven track record on the part of the concrete producer.

30.5.5.1 Smooth Texture

For adequate consolidation of continuously graded concrete, the desirable amount of air, water, cement, and fine aggregate (i.e., the mortar fraction) is about 50 to 65% by absolute volume (45 to 60% by weight). Rounded aggregates, such as gravel, require slightly lower values, and crushed aggregate requires slightly

higher values. Fine aggregate content is usually 35 to 45% by weight or volume of the total aggregate content. Aggregate fines below a No. 50 (3-mm) screen should not be in excess of 5%. If suitable form materials, release agents, and placing techniques are used, air voids on a surface can be reduced in size and number to an acceptable level.

30.5.5.2 Very Light to Light Texture

An acid wash or very light sandblast texture often uses a maximum coarse aggregate size of 3/8 in. (9.5 mm). The very light texture is sometimes referred to as an *Indiana limestone finish*. Aggregates may be continuous or gap graded.

30.5.5.3 Medium Texture

During the process of removing the cement/sand matrix from the exposed surfaces, coarse aggregate in the middle size range may not be able to adhere to the remaining concrete surface, particularly if the particle shape is elongated, sharp, or flat. If these sizes are not eliminated from the mix, the percentage of the surface covered by the matrix (sand and cement) may be too large and the aggregate distribution too uneven to provide a good surface appearance. The maximum size aggregate in gap-graded mixes should be 1 in. (25 mm), as mixes with larger sizes of aggregate are extremely difficult to place. This is because the larger particles seldom move from their original position even with heavy vibrator effort, and they are more prone to segregation.

30.5.5.4 Heavy Texture

For a heavy exposed-aggregate finish using an aggregate of 3/4-in. (19-mm) maximum size, the No. 4 to 3/8-in. (4.75- to 9.5-mm) particles could be omitted without making the concrete unduly harsh or liable to segregation. To achieve a gap between the 1/3-in. (8-mm) size and the No. 8 (2.36-mm) size, it is advisable to limit the amount of material passing the 3/8-in. (9.5-mm) sieve to between 0 and 10%. A typical fine aggregate should have 100% passing the No. 8 (2.36-mm) sieve and from 0 to 10% passing the No. 100 (150-µm) sieve. Although a sand gradation typical for concrete can usually be used, in heavy exposed-aggregate mixes, it is advantageous in some cases to use a masonry or industrial sand for the fine aggregate where most of the particles pass a No. 8 (2.36-mm) sieve. The sand should have a fineness modulus of 2.4 or less. A greater explanation of mix requirements for different textures may be found in reference material, such as the *PCI Manual for Quality Control for Plants and Production of Architectural Precast Concrete Products* (PCI, 1996). Concrete mixtures for heavy exposed-aggregate finishes usually contain more coarse aggregate than typical concrete mixtures. These mixes must usually be placed at under a 5-in. (125-mm) slump.

30.5.6 Wood Sealers

With wood forms, release agents should generally be used over a sealed form surface. Sealers can minimize nonuniformity in surface finishes and extend the number of uses of the wood forms. Types of wood sealers are lacquer, epoxy, polyester, and polyurethane. Wood sealers help maintain a uniform color in the concrete. The lower the water/cement ratio, the darker the concrete surface, so if the absorption of the form is not uniform the concrete will vary in color uniformity. Sealed, nonabsorbent forms prevent moisture loss and result in finishes that are uniform in color but lighter than those cast in absorbent forms. Formwork surfaces must be dry and free from dirt, grease, or other impurities before form sealers are applied. The sealers should be applied to wood when it is new and unoiled. Before it can be sealed, the surface must be sanded to remove all raised grain and rough areas, and all holes or imperfections must be filled with a waterproof filler. For some sealers, minimum temperatures are stated below which they must not be applied. An appropriate drying or curing time should be allowed. The manufacturer's instructions regarding application of the sealer must be followed, and the work should be done by a skilled worker.

30.5.7 Release Agents

Release agent selection should include investigation of the following factors (ACI Committee 303, 1974):

- Compatibility of the agent with the form material, form sealer, and admixtures in the concrete mix (because of the rapid loss of slump, most superplasticized concrete requires a smooth, frictionless surface along which the concrete can easily move)
- Possible interference with the later application of sealants, sealers, or paints to the form contact face
- Discoloration and staining of the concrete face
- Amount of time allowed between application and concrete placement and the minimum and maximum time limit for forms to stay in place before stripping (release agents may require a curing period before being used; if the concrete is too fresh when the agent is applied, some of the release agent will become embedded in the concrete)
- Effect of weather and curing conditions on ease of stripping
- Uniformity of performance
- Conformance to local environmental regulations regarding the use of a volatile organic compound (VOC)-compliant form release agent

Release agents or form oils are still probably the leading cause of discoloration on architectural concrete. Today, many suppliers can offer a 100% nonstaining type if the contractor or precast manufacturer requests it. The safest approach is to evaluate the three or four products being considered by casting small-scale trial batches of concrete in forms treated with the various products. Release agents improperly applied will cause as much color variation as any other factor known. Generally, the thinner the amount of the coating, the better the surface finish. Applying too much of the release agent can cause excessive surface dusting on the finished concrete. Discoloration may be caused by excessive use or uneven application of the release agent. Bug holes can be expected where release agents are allowed to puddle on the form or mold or allowed to collect in the many nooks and crannies of a mold. Great care should be taken to see that the equipment used for applying the coating is clean (PCI, 1996).

Coating thickness can be controlled by removing excess amounts with a clean cloth. A good rule of thumb is that, if rubbing a finger across the surface results in a deposit of the freshly applied release agent, then too much is present. One brand or batch of form-release agents should be used throughout a project. Information should also be obtained from the release agent manufacturer as to the kind of form surface for which the product is intended as well as the rate of spread and the proper method of application.

Generally, water-based or emulsion-type release agents cannot be used in very cold weather because they might freeze. Even at temperatures slightly above freezing, some water-based products thicken enough to produce more bug holes and reduce performance. Also, a form face coated with a water-based agent should be protected from rain; otherwise, some of the agent can wash off and it may be necessary to apply a second coat to a dry surface before placing concrete. For steel forms, release agents should contain a rust inhibitor and be free of water. Rough surfaces on steel forms may be conditioned against sticking by rubbing on a liquid solution of paraffin in kerosene, or the molds may be cleaned and oiled with a nondrying oil, then exposed to sunlight for a day or two (PCI, 1996).

To reduce color changes, a suitable release agent should be applied for the first and all subsequent uses of glass-fiber-reinforced plastic molds or plastic form liners. An oil-based emulsion or high-quality household wax containing carnauba wax are preferable. Unsaturated oils, ketones, esters, acids, toluol, toluenes, xylenes, or halogenated solvents should be checked for compatibility with the plastic materials. If curing requires high temperatures, a silicone release agent should be used. Concrete molds will require a release agent consisting of light-colored petroleum oils or oil emulsions. The concrete surfaces may be coated with one or two coats of epoxy resin and then waxed. A saponifiable oil should not be used as a release agent.

Rubber or elastomeric liners may be coated with a thin film of castor oil, vegetable oil, lanolin, or water-emulsion wax. Mineral oil, oil-solvent-based release agents, or paraffin wax should not be used on rubber or elastomeric liners as the hydrocarbon solvent will soften the rubber. The rubber or elastomeric

supplier's recommendation should be carefully followed. Plastic foam molds are generally lightly sprayed with castor oil, petroleum jelly thinned with kerosene, or paraffin oil. As the concrete surface texture increases, the influence of the release agent becomes less important. It is desirable that the brushes or spray equipment be clean and that no laitance or build-up of concrete is on the form surface before the release agent is applied.

30.6 Color and Texture

30.6.1 Color

Architectural concrete can be cast in almost any form or texture to meet the aesthetic and practical requirements of modern architecture. Combining color with texture accentuates the natural beauty of the aggregates. Aggregate colors range from white to pastel to red, black, and green. Natural gravels provide a wide range of rich earth colors, as well as shades of gray. Color selection should be made under lighting conditions similar to those under which the architectural concrete will be viewed. Muted colors look best in subdued northern light. In climates with strong sunlight, much harder and brighter colors can be used with success. The water/cement (w/c) ratio affects the color; the more water (higher w/c ratio), the lighter the color even with the same cements. Richer mixes are darker than lean mixes. The common slump test is the usual measure of concrete consistency. Poor concrete mix control and wide variations in slump will produce different shades of color in any project. Variations in aggregate gradation can cause slump variations even when the w/c ratio remains constant. Color differential will follow variations in the w/c ratio regardless of slump. Good field control involves both aggregate gradation and slump control. Superplasticizers can change workability without adding extra water. If superplasticizers are used on one concrete placement, they should be used on all.

Color and color tone represent relative values. They are not absolute and constant but are affected by light, shadows, density, time, and other surrounding or nearby colors; for example, a concrete surface with deeply exposed opaque white quartz appears slightly gray. This is due to the fact that the shadows between the particles "mix" with the actual color of the aggregate and produce the graying effect. These shadows in turn affect the apparent color tone of the matrix. Similarly, a smooth concrete surface will change in tone when striated. A white precast concrete window unit with deep mullions will appear to change tone when bronze-colored glass is installed. A change in color tone is constantly going on as the sun travels through the day. A clear sky or one that is overcast will make a difference, as will landscaping and time. And last, but by no means least, in large city and industrial environments, air pollution can cause the tone to change. This is particularly noticeable when additions are planned to existing buildings built 10 or more years previously (Figure 30.8). The ease of obtaining uniformity in color is directly related to the ingredients supplying the color. Whenever possible, the basic color should be established using colored fine or coarse aggregates (depending on depth of exposure) and pigments to blend the aggregates and matrix. Extreme color differences between aggregates and matrix should be avoided. In all cases, color should be judged from a full-sized sample that has the proper matrix and has been finished in accordance with planned production techniques. The sample should be assessed for appearance during both wet and dry weather. The difference in tone between wet and dry concrete is normally less when white cement is used. In climates with intermittent dry and wet conditions, drying out periods often produce blotchy appearances on all-gray surfaces. On the other hand, dirt (weathering) will normally be less objectionable on gray concrete. These comparisons are based on similar water absorption or density of white and gray concrete.

30.6.2 Texture: Cast-in-Place and Precast

Textures allow the natural attributes of the concrete ingredients to be expressed, provide some scale to the mass, express the plasticity of the concrete, and normally improve its weathering characteristics (PCI, 1989). A wide variety of textures is possible, ranging from smooth or polished to a deeply exposed tooled



FIGURE 30.8 Precast addition over 15 years later using the same cement, aggregates, and mix design.

or bushhammered finish. As a general rule, a textured surface is aesthetically more satisfactory than a smooth surface because to a very large extent the texture of the surface camouflages subtle differences in texture and color of the concrete. Exposed-aggregate surfaces may be achieved by removing surrounding paste through chemical processes (retarders or acid etching) or mechanically (abrasive blasting, honing and polishing, or tooling). Each method will uniquely influence the appearance of the exposed surface. Different degrees of exposure by any of these methods are defined as follows:

- *Light exposure.* Only the surface skin of cement and some sand are removed to expose the sand and the edges of the closest coarse aggregate. Matrix color will greatly influence the overall panel color.
- *Medium exposure.* Further removal of cement and sand has caused the coarse aggregate to appear visually to be approximately equal in area to the matrix.
- *Deep exposure.* Cement and fine aggregate have been removed from the surface so the coarse aggregate becomes the major surface feature.

A currently popular but very difficult texture is one that is much lighter than the above-referenced light exposure. This texture could be referred to as a brush exposure or a texture similar to Indiana limestone. Indiana limestone results can be best obtained by blending yellow and black sands in the concrete mix design to give a veining effect. This very light texture is difficult to obtain with either acid wash (must use a very diluted solution) or a single-pass sandblast (must use a reduced nozzle pressure of 50 to 60 psi). Brush-blast exposure will expose the surface skin of the cement and part of the sand surface. No coarse aggregate is exposed.

30.6.2.1 Smooth

The smooth or as-cast texture is accepted the way it appears when the forms are removed or when the precast unit is stripped from the mold. Construction of any smooth as-cast surfaces should be approached with caution by the contractor. Even the East Building National Gallery of Art in Washington, D.C., designed by I.M. Pei and Partners, was not purely a smooth as-cast texture. The contractor, Chas H. Tompkins Co., scrubbed the exposed concrete surface with a weak acid solution to remove construction stains and environmental grime. This gave a slightly weathered look to the basically as-cast concrete surfaces.

A smooth off-the-form finish may often seem to be the most economical, but it is perhaps the most difficult finish to do well, as the color uniformity of gray, buff, or pigmented surfaces is extremely difficult to achieve. The cement exerts the primary color influence on a smooth finish because it coats the exposed surface. In some instances, the sand may also have some effect. Initially, this is unlikely to be significant

unless the sand contains a high percentage of fines or is itself highly colored. As the surface weathers, the sand will become more exposed, causing its color to become more pronounced. The color of the coarse aggregate should not be significant, as it normally is not exposed to view unless the particular unit requires extremely heavy consolidation. Under this circumstance, some aggregate transparency may occur, causing a blotchy, nonuniform appearance (PCI, 1996).

Although a uniform graded concrete mix can be used with an as-cast finish, its w/c ratio should be controlled. Concrete slumps should be held in the range of $3 \pm 1/2$ in. and never over 4 in. Good consolidation techniques and thorough blending of lifts are extremely important. Although the use of concrete pumps is sometimes possible with this type of finish, the mix should not be oversanded or given additional water to facilitate the use of a pump. Oversanding greatly increases the possibility of segregation, resulting in noticeable surface variations. Aggregate transparency, or *shadowing*, is a condition in which a light-colored, formed concrete surface is marked by dark areas similar in size and shape to particles of dark or deeply colored coarse aggregate in the concrete mix. When encountered, it usually appears on smooth surfaces (Shilstone, 1972b).

The formwork for smooth-surfaced concrete is perhaps the most critical and the most difficult to control of any type of formwork encountered for cast-in-place or precast concrete, particularly where large single-plane surface areas are involved. Any imperfection in the surface of the form or any misalignment is immediately apparent and becomes the predominant factor in the character of the surface. Impervious surfaces such as plastic liners, steel, overlaid plywood, or fiberglass-surfaced plywood will usually result in a lighter color and more uniform appearance if joints have been properly prepared to eliminate leakage. In general, the joints of the materials used to construct the casting surfaces are difficult to hide unless rustications are used.

The smooth cement film on the concrete may be susceptible to surface crazing (fine and random hairline cracks) when exposed to wetting and drying cycles. This is, in most cases, a surface phenomenon and will not affect structural properties or durability. In some environments, crazing will be accentuated by dirt collecting in the minute cracks. This will be more apparent in white than gray finishes and in horizontal more than vertical surfaces. When air voids of a reasonable size, 1/8 to 1/4 in. (3 to 6 mm), are encountered on return surfaces, it may be desirable to retain them rather than filling and sack rubbing them. Color variations can occur when sacking is performed. If smooth surfaces are "to be produced without additional surface treatment after stripping, except for possible washing and cleaning," the following precautions should be considered:

- Pay attention to detailing with provisions for ample draft, proper edges and corners, rustications at form edges, and suitable water drips and other weathering details.
- Construct forms or molds so imperfections will not be mirrored in the units. The use of plastic molds or liners with a matte finish or fiberglass-overlaid plywood, which is smooth but not glossy, will help reduce crazing tendencies.
- Use the same mold release agent throughout construction, and apply it under as nearly identical conditions as possible each time. (Some release agents help reduce the crazing tendency by breaking the contact with the glossy surface of the form.)
- Use concrete mix designs that combine a minimum cement content and a constant, low w/c ratio with high density to minimize crazing, entrapped air voids, and color variations. The mix should be fully graded with no more than 5% aggregate fines passing a No. 50 (300-mm) sieve.
- Use proper consolidation and curing to minimize nonuniformity of color, which shows easily on smooth concrete surfaces, particularly with gray concrete mixes. Uniform curing with minimum loss of moisture from the smooth surface will help minimize crazing tendencies.
- Minimize chipping or other damage because smooth finish repairs are difficult to perform in terms of texture and color match.

Many of the aesthetic limitations of smooth concrete may be minimized by the shadowing and depth provided by profiled surfaces (fluted, sculptured, board finishes, etc.) that subdivide the panel into smaller surface areas by means of vertical and horizontal rustications, or by the use of white cement.

30.6.2.2 Sand or Abrasive Blast

Sand or abrasive blasting of surfaces can provide all three degrees of exposure: light, medium, or deep (PCI, 1996). Generally, the technique is used when a light exposure is desired, because sandblasting costs increase with the depth of exposure. Sand or abrasive blasting of surfaces is suitable for exposure of either large or small aggregates. Uniformity of depth of exposure between panels and within panels is essential in abrasive blasting, as in all other exposed-aggregate processes, and is a function of the skill and experience of the operator. As much as possible, the sandblasting crew and equipment used should remain the same throughout the job. Different shadings and, to some extent, color tone will vary with depth of exposure.

The degree of uniformity obtainable in a sandblasted finish is generally in direct proportion to the depth of sandblasting. A light sandblasting may look acceptable on a small sample, but uniformity is rather difficult to achieve in a full-size wall or precast unit. A light sandblast will emphasize visible defects, particularly bug holes, and reveal defects previously hidden by the surface skin of the concrete. The lighter the sandblasting, the more critical the skill of the operator, particularly if the units are sculptured. Small variances in concrete strength at the time of blasting may further complicate results. Sculptured units will have air voids on the returns that might show strongly in a light-sandblasted texture. If such air holes are of a reasonable size, 1/8 to 1/4 in. (3 to 6 mm), it is strongly recommended that they be accepted as part of the texture because filling and sack rubbing may cause color variations. Blasting will cause some etching of the face of the aggregate, and the softer aggregates will be etched to a greater extent with heavier exposures. Sandblasted aggregates lose their sharp edges. Blasting of the aggregate surface is more noticeable on dark-colored aggregates that have a glossy surface texture. Sandblasting dark-colored aggregates will produce a muted or frosted effect, which tends to lighten the color and subdue the luster of the aggregate (Figure 30.9). The depth of sandblasting should also be adjusted to suit the aggregate hardness; for example, soft aggregates might be eroded at the same rate as the mortar.

For medium or deep exposure with a sandblasted finish, retarders may be used initially and the matrix removed by sandblasting to obtain a matte finish. The selected retarder strength should only give 50 to 75% of the expected reveal. This approach reduces blasting time and lessens the abrasion of softer aggregates. Using sandblasting to achieve the final texture allows for correction of any variations in exposure, so this method can result in a very uniform surface. Care should be taken to avoid nonuniform exposure that may be caused by the presence of soft and hard spots on the retarded surface. This is especially true and more noticeable on large, flat surfaces. Small, flat areas or surfaces that are divided by means of rustications will tend to call less attention to these texture variations. Because some aggregates change color after sandblasting, trials on sample panels using different abrasive materials are desirable to check the texture and color tone. As an additional step toward uniformity, the cement and sand color should be chosen to blend with the slightly bruised color of the sandblasted coarse aggregate, as the cement-sand matrix color will predominate when a light sandblast finish is desired. With a light sandblasting, only some of the coarse aggregates near the surface will be exposed, so a reasonable uniform distribution of such aggregates is not controllable.

The concrete mix used and the matrix strength at the time of blasting will affect the final exposure, as will the gradation and hardness of the abrasive. A good general rule in selecting an abrasive is that the particle size of the abrasive will attack a similar size particle in the concrete surface. Larger abrasive particles usually result in a rougher, more uniform matte appearance. Smaller abrasive particles typically result in a more variable luster finish. For a more uniform texture, spherical or nearly round abrasives with a close gradation should be used. Materials used in the blasting operation are washed silica sand, certain hard angular sands, aluminum carbide, blasting grit such as power plant boiler slag, carbonized hydrocarbon, crushed chat (a waste material from lead mining), and various organic grits such as ground shells, corn cobs, and rice hulls. For cleaning or light blasting of a surface, any of these abrasives will be adequate. For deep cutting, an abrasive grit should be used because of its speed of attack and cleaner surface appearance. Some types of colored abrasives impart color to the surface of the concrete. With certain gradation combinations, pressures, and volumes, impregnation of the abrasive into the surface can occur. If this happens, an abrasive of similar color to the matrix should be used. Impregnation of



FIGURE 30.9 Heavy abrasive, blasted, cast-in-place, gap-graded concrete texture on the Tennessee State Office Building in Memphis, Tennessee; architect, Roy Harover.

abrasive can be minimized by a change in the volume of material, its gradation, or the pressure being applied. Sandblasting may be done with dry abrasive in a stream of compressed air or water rings may be used to introduce water into the compressed air-sand stream at the nozzle. Sand also may be introduced into a high-pressure water washer. When using wet sandblasting, the abraded mortar should be continually washed off already sandblasted areas to prevent staining.

The inside diameter of the hose should be no less than 1-1/4 in. (32 mm) or four to six times the diameter of the nozzle orifice to keep the sand in continuous suspension while it travels through the hose. Too large a hose would reduce the velocity of media and air and would eventually plug the hose. Smaller diameter whip lines may be used for operator ease of handling. The nozzle at the end of the system is the most important element. The diameter of the nozzle and nozzle pressure should be determined by experimentation. A Venturi-type nozzle should be used to obtain a uniform blast pattern. Carbide or nitride nozzles should be selected for durability. Nozzle life depends on abrasive hardness and volume as well as the pressure and generally varies from 2 to 4 months.

The time when sandblasting should take place is determined by scheduling, economics, visual appearance desired, and hardness of the aggregate. The timing of blasting is not as critical as for other finish methods. The concrete matrix will be easier to cut in the first 72 hours after casting, but variable early concrete strengths may result in a more variable etch. As the concrete cures and gains strength, it becomes more difficult to blast to any appreciable depth, thus increasing the cost of the operation. Softer aggregates tend to abrade more when concrete strengths are high and the surface will have a duller appearance. In some cases, the higher costs of deferred blasting may be justified to avoid scheduling problems; however, all surfaces should be blasted at approximately the same age or compressive strength for uniformity of appearance.

When blasting, the operator should hold the nozzle perpendicular to the surface being blasted. Some operators will deviate slightly from this position as it seems to provide a better view of the work. The maximum deviation should be less than 15°, as too much deviation from the 90° angle will result in undercutting the coarse aggregate particles. Best results are obtained with the nozzle positioned from about 2 to 6 ft (0.6 to 1.8 m) from the element surface. The exact distance depends on the pressure used, the hardness of the concrete matrix, and the cutting ability of the abrasive. An experienced operator can quickly determine the nozzle position to produce the specified surface finish. Using a circular motion during blasting will minimize pattern marking.

30.6.2.3 Acid Etch

Acid etching of concrete surfaces can result in a pleasing fine sandy texture and retention of detail if the concrete mix and its consolidation have produced a uniform distribution of aggregate particles and cement paste at the exposed surface. The contractor should approach this finish very carefully. Vertical cast-in-place concrete exposed with acid can be an environmental problem. New equipment that uses high-pressure pumps and a controlled combination of acid and hot water has minimized the application problems. When using this equipment, runoff water is close to neutralized. Some local codes or concerned citizens may require complete containment of the acid residue runoff even though the acid parts per million are insignificant. This may involve construction of earth dams and a holding pond for the water prior to treatment. It has become increasingly difficult to perform any work requiring acid at job sites due to potential liabilities and environmental concerns. All personnel working with or near the acid application area will need protective gear and clothing to prevent injury from the spray. Prior to acid etching, all exposed glass and metal surfaces should be protected with acid-resistant coatings. These include vinyl chlorides, chlorinated rubber, styrene butadiene, rubber (not latex), bituminous paints or enamel, and polyester coatings. Architectural surfaces should be thoroughly flushed with large quantities of clean water immediately prior to the application of acid. Acid etching is most commonly used for light or medium exposure. Acid etching of concrete surfaces will result in a fine, sandy-textured distribution of aggregates and cement paste at the exposed surfaces. Concentrations of cement paste and under-and-over etching of different parts of a concrete surface or variations in sand color or content may cause some uniformity problems, particularly when the acid etching is light or used for large, plain surfaces. Carbonate aggregates (e.g., limestones, dolomites, and marbles) may discolor or dissolve due to their high calcium content. With lighter textures, the color compatibility of the cement and the aggregates becomes more important for avoiding blotchy effects. White or light colors are forgiving to the eye and increase the likelihood of a better color match from unit to unit. Gray is the worst color to select for uniformity. An acid-etch finish is more difficult to patch than many of the deeper texture finishes; however, minor air voids are fairly easy to grout and refinish. There is a minimum depth of etch that is required to obtain a uniform surface. To attempt to go any lighter than this will result in a blotchy panel finish. A minimum depth of etch will expose the sand and the very tip of the coarse aggregate approximately 1/16 in. (1 mm). It is difficult to achieve a totally uniform, very light exposure on a panel that is highly sculptured. This is due to the acid spray being deflected to other areas of the panel, particularly at the inside corners. This may be acceptable if the sculpturing creates differential shadowing. Prewetting the concrete with water fills the pores and capillaries and prevents the acid from etching too deeply, in addition to allowing all of the acid to be flushed after etching. Older dried concretes are likely to be more carbonated. Although the reactions of carbonates with the acid might not be much faster than those with other cement compounds, they cause greater efflorescence so the reaction is far more obvious and seems to go faster. Acid solutions lose their strength quickly once they come into contact with cement paste or mortar; however, even weak, residual solutions can be harmful to concrete due to the possible penetration of chlorides. Failure to completely rinse the acid solution off the surface may result in efflorescence or corrosion.

30.6.2.4 Retarders

Chemical surface retarders applied to formwork or sprayed on the top of horizontal concrete provide a nonabrasive process that is very effective in bringing out the full color, texture, and natural beauty of the

coarse aggregate. The aggregate is not damaged or changed by this exposure method. If exposing the bright, natural colors of the aggregate is the prime goal, exposing aggregate from retarded surfaces is one of the best ways to achieve this result. Surface retarders that are to be used to expose the aggregate should be thoroughly evaluated prior to use. A sample panel should be made to determine the effects created by the form or mold and concrete materials. This involves using the particular type of cement, aggregate (proportion determined by specified mix design), and selected release agent. Prolonged exposure of the forms coated with the retarder prior to placing the concrete should be avoided. Water should not contact the retarder on the form surface before the concrete is placed to prevent activation of the retarder. When using a retarder, the manufacturer's recommendations should be followed. Surface retarders can be applied by roller, brush, or spray, and care must be taken to ensure uniform application to the form surface.

The performance of the retarder will be influenced by chemistry of the individual cement, mix characteristics, temperature of the concrete, humidity, ambient temperature, characteristics of absorption of the forming material, and total water content of the concrete mix. It is important to consider protecting the treated form surfaces from weathering and ultraviolet rays before casting the concrete. Retarders function by delaying, not preventing, the set of a given amount of cement paste so the aggregate can be easily exposed. This concept will help in analyzing various mix designs for depth of retardation. If more sand or coarse aggregate is added to a mix with proper consolidation, there will be less cement paste per volume of material at the surface and thus a deeper exposure. Some retarders are effective for long periods of time, while others are active for only a few hours. Water contacting the retarder before the concrete is placed activates the action of the retarder prematurely and may result in a nonuniform surface.

The retarded concrete should be removed the same day that the forms are stripped using a high-pressure water blast through a fan nozzle. Any delay in removing the matrix will result in a lighter, less uniform texture. The stripping schedule must be coordinated with that of the work force responsible for form removal so there will not be long periods between form removal and concrete finishing. For a large project, preliminary tests should be performed before planning the casting to determine the most suitable finishing time. The timing of the surface finishing operation should be consistent each day, as some retarders cease to delay the hardening process as the product cures.

30.6.2.5 Tooled or Bushhammered Finish

A tooled or bushhammered finish is usually achieved by casting concrete against smooth or specially textured or patterned formwork. After removal from the form, the hardened concrete is treated mechanically to create the desired effect. Concrete made with most aggregates can be tool finished, but materials that can be cut or bruised without shattering, such as calcareous limestone and igneous rocks, give results that find the widest acceptance. Aggregate particles of 3/8 in. and smaller are more important for scaled and tooled surfaces. The coarser aggregate particles are more important for jackhammered surfaces. Some jackhammered surfaces, where considerable depth of finish is desired, may only require forming practices similar to a good structural concrete. Mechanically fractured surfaces are prepared by one of four methods: scaling, bushhammering, jackhammering, or tooling, which includes reeding. These types of surface textures are described as *fractured* because the surface is prepared by striking the concrete with a tool, thereby mechanically removing part of the surface. Concrete may be mechanically spalled or chipped with a variety of hand and power tools to produce an exposed-aggregate texture. Pneumatic or electric tools may be fitted with a comb chisel, crandall, or multiple pointed attachments. The type of tool will be determined by the surface effect desired. Hand tools may be used for small areas, corners, and restricted locations where a power tool cannot reach. Basically, all methods of tooling remove a layer of hardened concrete matrix while fracturing the larger aggregates at the surface. Surfaces attained can vary from a light scaling to a bold, deep texture achieved by jackhammering with a single pointed chisel.

Orientation of the equipment and direction of movement should be kept uniform throughout the tooling process as tooling produces a definite pattern on the surface. Variations caused by more than one person working on the surface may occur with this type of finish. Care should be exercised to avoid exerting excessive pressure on the tool, especially when starting, so as not to remove more material than either necessary or desirable.



FIGURE 30.10 Heavy jackhammer surface on Southern Bell Tower in Atlanta, Georgia; architect, Skidmore, Owings, and Merrill, Chicago.

Bushhammering at outside corners may cause jagged edges. If sharp corners are desired, bushhammering should be held back from the corner. It is quite feasible to execute tooling along specific lines. If areas near corners are to be tooled, this must normally be done by hand as power tools will not reach into inside corners. Chamfered corners are preferred with tooled surfaces. With care, a 1-in. (25-mm) chamfer may be tooled. Scaling is the lightest texture in bushhammered finishes. It is achieved by passing a triple-pronged scaler (originally developed to remove scale from steel prior to pointing) singly or in gangs over the surface to remove only a thin skin. A single-head scaler is lightweight and can be readily manipulated by one person. No texture as such is brought out by this technique, although some aggregate is exposed and fractured in the process. Under certain conditions, almost the same result can be achieved by light abrasive blasting.

Jackhammering should be done when the matrix has reached a strength approximating that of the coarse aggregate to fracture both the mortar and the coarse aggregate. If hammering is initiated too soon, the tool merely removes the matrix and the coarse aggregate does not fracture. Sometimes the coarse particles are knocked out, leaving blank spaces. If jackhammering is to be performed at a time when the matrix is softer than the coarse aggregate, a chisel-type tool should be used. This tool has a tendency to fracture across the aggregate, while a pointed tool has a tendency to dig into the matrix and not fracture the coarse aggregate. On the other hand, when a concrete becomes very hard the pointed tool does a superior job. Because jackhammering accentuates the presence of coarse aggregate, a higher than normal coarse aggregate content may be desirable (Figure 30.10) (PCI, 1996).

Although a dense, fully graded concrete mix is desirable, bushhammering may be successfully applied to gap-graded concrete. Natural gravels are inclined to shatter, leading to bond failure and loss of aggregate particles when bushhammered. Aggregates such as granite and quartz are difficult to bushhammer uniformly because of their hardness and may fracture into rather than across the concrete surface. Aggregates such as dolomite, marble, calcite, and limestone are softer and more suitable for bushhammered surfaces.

To prevent loosening of the aggregate, a compressive strength of 4000 psi (28 MPa) is recommended. In many cases, better uniformity may be obtained when the concrete is allowed to age for 14 to 21 days and the surface is dry. Exposing the aggregate by tooling requires trained operators to produce a uniformly textured surface, especially when large areas are to be textured. A hammered rib (or fractured fin) finish may be produced by casting ribs on the surface of the unit and then using a hammer or bushhammer

tool to break the ribs and expose the aggregate. The ribs may be hammered from alternative sides, in bands to obtain uniformity of cleavage, or randomly, depending on the effect required. There should be a definite plan, even with a so-called random pattern, because an uneven shading effect may be produced unless care is exercised. Tooling and bushhammering remove a certain thickness of material, 3/16 in. (5 mm) on average, from the surface of the concrete and may fracture particles of aggregate, causing moisture to penetrate the depth of the aggregate particle. For this reason, the minimum cover for the reinforcement should be somewhat greater than normally required. It is recommended that 2 in. (50 mm) of concrete cover be specified (prior to tooling). As a cutting head becomes worn, it should be replaced. Because the texture varies with the condition of the cutting surface, a new head should not be worked next to an area tooled with an old one. Small irregularities in the finished surface can be worked out with further tooling.

30.6.2.6 High-Pressure Water Jet Blasting

Blasting with high-pressure water instead of sand has received limited use in architectural concrete, particularly with precast concrete. Restrictions on sandblasting in many areas of the country are sure to increase the spread of this method of exposing aggregates at the surface. It uses only water, no harsh chemicals, so there is no pollution or health risk from burns or fume inhalation. Under special situations or where environmental restrictions exist, the water spray can be mixed in the nozzle with a fine spray of sand. Units are available with more than 10,000 psi of pressure, although usually 5000 psi is sufficient for aggregate exposure. Considerable splatter can develop, which requires that adjacent surfaces be protected. High-pressure water jets are used in combination with air to expose aggregates. The proper time of application must be determined for each concrete and its curing condition to obtain the desired amount of reveal without loosening the aggregate. The strength of concrete for high-pressure water washing is usually 1500 psi. It is important for the strength of concrete to be approximately the same when exposing the aggregate on different concrete placements. This method can be used with or without surface retarders (ACI Committee 303, 2004). Regardless of whether or not retarders are used, exposure should begin immediately after forms are stripped. Each equipment operator should be trained on a sample test area. All operators should be protected by rubber wet suits and goggles. They should wear rubber steel-tipped boots with clamp-on instep guards. These are required because the jet has enough force to cut through rubber into the flesh. A dead-man trigger on the gun automatically shuts off the water jet if the gun is accidentally dropped.

30.6.2.7 Form Liners

An almost unlimited variety of attractive patterns, shapes, and surface textures can be achieved by casting concrete against wood, steel, plaster, elastomeric, plastic, or foam plastic form liners. These form liners can be attached to or incorporated into the form itself. Most form liners can be used with any forming system. They are particularly useful in large heavy-duty gang form sections because the joints can be permanently aligned and sealed. Architects specify patterned concrete surfaces for the aesthetic interest generated by the play of light and shadow or to economically simulate the traditional patterns of brick, stone, and wood. Adding texture with a patterned form liner helps hide color variations and makes bug holes and other surface blemishes less noticeable. Defects due to leakage at form joints and poorly consolidated concrete also are less noticeable in patterned concrete (Hurd, 1993).

Material selection of the form liner should depend on the amount of usage and whether or not the pattern has undercut (negative drafts). The choice of liner materials may depend on whether the work is cast-in-place or precast. Thin sheets that serve well on horizontal forms may wrinkle and sag in vertical forms unless they are carefully attached. Thicker layers of liner material are more suitable for vertical surfaces. Vertical liners also must withstand the lateral pressure of concrete. This may call for control of concrete placing rates and added support for a contoured liner. The method of attaching form liners should be studied for the resulting visual effect. Form liners should be secured in forms by gluing or stapling, rather than by methods that permit impressions from nail heads, screw heads, rivets, or the like to be imparted to the surface of the concrete, unless desired. Where staples are used, they should be driven by a power stapler to ensure sufficient driving force. Staples should be aligned in a direction

consistent with the pattern to be imparted to the concrete. Staples should be spaced close enough to hold the liner securely in place. Where adhesives are used, particular attention should be given to following manufacturer's recommendations regarding adhesive cure period, ambient temperature, and moisture (Ford, 1982). Protection from the weather is essential. Attempts should be made to camouflage inequalities to within the pattern of the texture. The construction cycle, the probable number of reuses of the lined form, and the cost per use are other concerns in selecting a liner material. Trials should be made to determine the best time for stripping so the surface remains intact and liner reuse can be maximized.

Wood liners, whether used as boards, plywood panels, or nailed-on inserts, work well. Wood liner surfaces should be sealed to minimize discoloration of the concrete caused by differential absorption of mix water by the liner. The liner should then be lightly coated with a release agent prior to casting. Sandblasted wood, textured plywood, and rough-sawn lumber are often used for board-surface-textured finishes where concrete color variations and rough edges are acceptable. To prevent bowing of the boards, all sides should be coated with wood sealer by painting or immersion. Even with a sealer, some types of lumber may absorb moisture from the concrete. In other cases, natural sugars found in lumber such as pine may penetrate the sealer coating when the concrete is cast against the mold, retard the set of the cement at the surface, and cause a dusty, dark, blotchy effect. Fir is a preferred choice for board surface finishes due to its low sugar content. An effective method of sealing wood to eliminate any moisture transfer is to spray a few light coats of surface resin or urethane onto the wood. Care should be taken not to apply the sealer too thickly or the wood grain pattern will be lost. For molds with long casting durations, this process may have to be repeated. The weathering of the lumber can also affect the outcome of the concrete finish. If rough-sawn lumber is being used, it is important to produce samples to determine the effect the lumber will produce. The lumber selected should be purchased all at one time from one source to minimize the possibility of variations. Moisture leakage between pieces of lumber should be prevented, or a dark line will result from the change in w/c ratio. The joints may be sealed by using tongue-and-groove lumber. Closed-cell gasket material should be used at edges of the mold to prevent leakage. Wood liners may also be set or embedded in resin, which will eliminate the need for connectors that show as well as seal the edges against leakage (PCI, 1996).

Some experts believe porous or absorbent form liners offer a better chance to control bug holes than do impervious plastic liners, but the absorbency that provides this advantage can also pose problems. The more absorptive the form face, the darker the color of the concrete; however, as wood forms are reused and reoiled, their absorbency decreases. If patching or adjusting a much-used panel is required, the location of the new board or plywood will show up as a color difference that takes years to weather away (Figure 30.11). To avoid this problem with wood liners, up to one or two extra panels or gang forms should be made and kept in form rotation, then if one form panel or gang form is damaged it can be replaced with a form section already seasoned with use.

Elastomerics such as urethane and hot-melt vinyl are used to make liners flexible enough to permit vertical sides or some undercut areas. Elastomeric liners greatly facilitate removal from finished concrete surfaces in cases where other materials would be virtually impossible to strip. The design possibilities are almost limitless. Standard sheets are typically 4×8 to 4×12 ft, (1.2×2.5 to 1.2×3.7 m), but sizes up to 12×36 ft (3.7×11 m) can be special ordered to help minimize horizontal butt joints. Elastomeric materials should have a Shore A-2 hardness of 50 to 60 durometer and a minimum ultimate tensile strength of 600 psi (4.14 MPa). Elastomeric and rubber liners display gasketing characteristics and therefore achieve weep-free seamless joints. They also eliminate the need to cover the small slits cut in the liner for the fasteners. Elastomeric form liners may ripple unless there is a good bond to the base form. Edges of liners should be sealed to each other or to divider strips to prevent bleeding of cement paste. The sealant used should not stain the surface. Liners should not be butt-jointed without a demarcation feature to eliminate nonalignment of the texture. Liner size and module should be coordinated with panel joints, rustication strips, and blockout size.

Tough, wear-resistant elastomeric liners are relatively heavy and require good vertical support. They are usually attached to the form sheathing with adhesive, but some manufacturers supply these liners prebonded to plywood sheets. Elastomeric liners are sensitive to temperature change and may deform



FIGURE 30.11 Wood forms having varying degrees of absorbance as new sections have been added to gang forms.

significantly when exposed to surface temperatures above 140°F (60°C). Direct sunlight and the heat of hydration of the concrete can generate this level of temperature. Shade and temperature control of concrete during curing may be necessary. The liner should be checked for resistance to deterioration caused by oils commonly used as release agents and have rigidity sufficient to resist wrinkling. Solvent-based surface retarders should be checked to be sure they will not degrade the liner; if necessary, water-based or carried retarders should be used.

Several rigid liner materials such as ABS and polyvinyl chloride (PVC) come in sheets stiff enough to be considered self-supporting. High-impact polystyrene is also used to make rigid form liners. Readily available in 4 × 8-ft or 4 × 12-ft (1.2 × 2.5-m or 1.2 × 3.7-m) sheets, they can also be special ordered in lengths up to 30 ft (9.2 m) or more. Some manufacturers will supply interlocking joints at the edges of the panels that help hide vertical form joints. Rigid liners are well suited to ribbed patterns, but a detailed closure is required where the plastic flutes are cut at horizontal joints or openings. Some makers supply prefabricated closure pieces to solve this problem (Hurd, 1993). This material does not lend itself to intricate patterns, particularly with sharp corners, vertical sides, or undercuts (negative drafts). Basically, the material itself is inflexible. If it is broken, it is difficult to repair at the job site. Sheet plastics may require appropriate backup to resist movement, particularly for wide portions of liners with deep indentations. Movement can occur due to temperature changes caused by direct sunlight or the mechanical action of concrete placement. It is good policy to maintain a 10° draft on all indentation sides to prevent chipping and spalling during stripping operations. Keep all edges and corners rounded or chamfered. Relief may be more than 1 in. (25 mm) deep if the depressed area is sufficiently wide.

Foamed polystyrene or polyurethane liners create deeply revealed designs or blockouts. The preformed foam planks are easily cut to size and readily attached to the form. It is necessary to use a low-solvent contact glue that should dry before contact with the foam plastic is made or the solvent will dissolve the plastic. Liners made of polystyrene foam are used in large sheets like other liners or in smaller interlocking

modules designed to fit together with concealed joints. They typically are single use, as they are usually destroyed by the stripping process. Because of the one-time use factor, they are not cost efficient for large areas with a repetitive pattern. Repetitive form use requires a different type of liner. Rigid plastic forms can be molded to create complex liners with overall patterns or original works of art. Molded patterns have a surface skin that can be coated with a release agent. Strip the foam by hand or with air or water jets. If some of the plastic foam bonds to the concrete, it may be necessary to wirebrush or sandblast at reduced nozzle pressure to remove it.

Metal liners are available in various textures that can be combined with different types of fasteners to achieve an architectural effect. Liner joints should be at rustication strips or mold edges because leakage is difficult to prevent at butt joints. Combination finishes involving the use of more than one finishing method are almost infinite. One common example is the ribbed form liner and sandblasted finish.

30.6.2.8 Applied Coatings

Whenever concrete is to be coated or stained, only form-release agents compatible with the coating should be permitted, unless surface preparation is required to ensure good adhesion between the coating and the concrete. Coatings applied to exterior surfaces should be breathable (permeable to water vapor). The coating manufacturer's instructions regarding mixing, thinning, tinting, and application should be strictly followed. Whenever concrete is so smooth that it makes adhesion of the coating difficult to obtain, the surface should be lightly sandblasted, acid etched, or ground with silicon carbon stones to provide a slightly roughened, more bondable surface. Because of the vast differences in coating and stain types, brands, prices, and performances, knowledge of coating composition and performance standards is necessary for obtaining a satisfactory concrete coating or stain. To select proper coatings, the architect should consult with manufacturers supplying products of known durability and obtain from them, if possible, technical data explaining the chemical composition and types of coatings suitable for the job at hand. For high-performance coatings, proprietary brand-name specifications are recommended. The interior surface of exterior walls should have a vapor barrier (coating or other materials) to prevent water vapor inside the building from entering the wall.

30.6.3 Texture: Precast Only

30.6.3.1 Sand Embedment

Bold, massive, rocklike architectural qualities may be achieved by hand-placing 1 to 8-in. (25 to 200-mm)-diameter stones (cobbles or boulders), fieldstone, or flagstone into a sand bed or other special bedding material. The depth of the bedding material should keep the backup concrete 25 to 35% of the diameter of the stone away from the face. Extreme care should be taken to ensure that the aggregate is distributed evenly and densely on all surfaces, particularly around corners, edges, and openings. To achieve uniform distribution and exposure, all aggregate should be of one size gradation. Where facing materials are of mixed colors, their placement in molds should be carefully checked for the formation of unintended patterns or a local high incidence of a particular color. If the intention is to expose a particular facet of the stone, placing should be carefully checked with this in mind before the backup concrete is placed. The sand-embedment technique reveals the facing material and produces the appearance of a mortar joint on the finished panel. If a white or colored mortar joint is desired, a mortar consisting of one part white cement (plus pigment) to 2-1/2 parts well-graded white or light-colored sand with sufficient water to make a creamy mixture may be placed over the aggregate. If a mortar facing mix is used, the backup mix should be of a low slump with a maximum of 1 in. (25 mm) to absorb excess water from the facing mix; otherwise, the backup mix should be a standard structural concrete with a slump of 2 to 4 in. (50 to 100 mm). The mortar mix or part of the backup concrete should be carefully shoveled onto the stones and further spread and lightly tamped with trowels to ensure that it is worked around all the individual stones, then it should be screeded to a flat surface before the steel is placed. Care should be taken not to dislodge any of the face stones when placing the first layer of mortar or concrete. Also, care should be exercised during vibration so as not to disturb the sand or large stones, which could cause uneven stone

distribution. Upon stripping the precast concrete units, they should be raised, and any clinging sand should be removed by brushing, air blasting, or high-pressure water washing. Some sand bonds to the concrete; therefore, the color of the bedding sand should be carefully chosen to harmonize with the exposed stones.

30.6.3.2 Veneer Facing Materials

When natural stone veneer is used, it is recommended that the purchaser of the stone engage someone qualified to be responsible for coordination, which includes delivery, scheduling, and ensuring color uniformity. In evaluating properties of stone, it should be recognized that some natural stones exhibit different properties in different orientations. Also, there may be considerable variation in a given direction of grain for different samples of the same stone. The thin sections of stone are generally more sensitive than thicker sections to strength decreases due to imperfections and inclusions of minerals. Also, a stone that has a crystalline structure with dimensions large enough to approach the thickness of the slab itself will be substantially weakened. In addition, the surface finish, freezing and thawing, and large temperature fluctuations will affect the strength and in turn influence the anchorage system. Non-acid-based masking or plastic tape may be used to keep concrete out of the stone joints so as to avoid limiting stone movement (PCI, 1996).

Color control or blending for uniformity should be done in the stone fabricator's plant because ranges of color and shade, finishes, and markings such as veining, seams, and intrusions are easily seen during the finishing stages. A qualified representative of the owner, who understands the aesthetic appearance requested, or the owner or architect should perform this color control. Acceptable color should be judged for an entire building elevation rather than for individual panels. All testing to determine the physical properties of the stone veneer should be conducted by the owner prior to the award of the contract. This will reduce the need for potentially costly repairs or replacement should deficiencies in the stone veneer be found after start of fabrication. When purchasing the stone, the contractor should be sure to order an additional 5% to cover breakage and incorrect sizing by the supplier.

A complete bond breaker between the natural stone veneer and concrete should be used. Connecting the veneer to the concrete should be done with mechanical anchors that can accommodate some relative movement. When using epoxy in anchor holes, 1/2-in.-long compressible rubber or elastomeric grommets or sleeves should be used on the anchor at the back surface of the stone. Thin brick (1/2 to 1 in. thick) rather than whole bricks are generally used in precasting because adequately grouting the thin joints with whole bricks is difficult and results in the use of mechanical anchors. Some bricks are too dimensionally inaccurate for precast concrete applications. They may conform to an ASTM specification for site laid-up application, but they are not manufactured accurately enough to permit their use in the preformed grids that are used to position brick for a precast concrete unit. When both site-laid brick and brick precast units are to be used on the same project, the contractor has to be sure the precast tolerance requirements govern. Because variations in brick or tile color will occur, the clay product supplier should preblend any color variations and provide units that fall within the color range selected by the architect. Ceramic glaze units, where required for exterior use, may craze from freeze-thaw cycles or the bond may fail on exposure; therefore, the manufacturer should be consulted for suitable materials and test data.

30.6.3.3 Honed or Polished Surface

Grinding concrete produces smooth, exposed-aggregate surfaces. The grinding is called *honing* or *polishing*, depending on the degree of smoothness of the finish. Polished exposed-aggregate concrete finishes compare favorably with polished natural stone facades, allowing the architect great freedom of design. Honed and polished finishes have gained acceptance because of their appearance and excellent weathering characteristics, which makes them ideal for high traffic areas and polluted environments. To produce a good ground or polished finish, it is first necessary to produce a good plain finish. The compressive strength of the concrete should be 5000 psi before the start of any honing or polishing operations. All patches and the fill material on any bug or blow holes or other surface blemishes must also be allowed

to reach approximately 5000 psi. It is preferable that the mortar strength of the concrete mix approach the compressive strength of the aggregates, or the surface may not grind evenly or polish smoothly and aggregate particles may be dislodged. Because aggregates will polish better than the matrix, it is essential to have a minimal matrix area. A continuous graded concrete mix heavy in coarse aggregate is preferred, one that is carefully designed to provide maximum aggregate density on the surface to be polished. In choosing aggregates, special attention should be given to maximum size and hardness. Softer aggregates such as marble or onyx are much easier to grind than either granite or quartz. This will be strongly reflected in the cost of such finishes.

30.6.4 Combination Textures

The combination of a polished or honed surface and acid etching provides a surface on the precast unit that exposes a very high percentage of stone. After the grinding process, the acid removes the cement matrix and fines between the larger aggregate particles. This surface is highly resistant to weathering and is self-cleaning to a high degree. The color of the aggregates predominates in the combined polished acid-etch surface texture. A polished/sandblast finish on a precast unit provides contrast between the smooth polished aggregate and the sandblasted matrix of the concrete. The architect must ensure that the overall design concept includes suitable demarcation between the two textures, as sandblasting overflow will dull the polished surface. In many cases, stone veneer is used as an accent or feature strip on either precast units or cast-in-place concrete. When a stone veneer is applied in combination with other finishes, a 1/2-in. (12-mm) space is left between the edge of the stone and the adjacent concrete to allow for differential movements of the materials. This space is then caulked as if it were a conventional joint.

Combination finishes involving the use of one or more basic finishes together with form liners are almost infinite. Liners can be used in combination with smooth sandblast, acid, retarded, or tooled textures for either cast-in-place or precast concrete. Care in developing details must be taken to include suitable demarcation between the different textures. Some of the usual combinations include:

- Heavy abrasive blast/light abrasive blast/smooth
- Striated/abrasive blast/irregular pattern form liner
- Acid etch/abrasive blast/smooth
- Ribs or vertical rustication/acid or abrasive blast
- Tooled/hammered/form liner
- Tooled/hammered/abrasive blast
- Tooled/chiseled/smooth

30.7 Construction: Cast-in-Place Concrete

30.7.1 Forming

30.7.1.1 General

The selection of forms and forming materials to accomplish a given task is usually limited by the parameters established by the architect in the drawings, specifications, and samples and by the contractor's mock-up. Specified forms and surface treatments become vitally important to a successful project when used for architectural purposes. Any material that can contain plastic concrete without deformation is a potential concrete form. Forms must withstand the loads due to both liquid head and compactive effort. This means that the forms must support a full liquid head. With the use of concrete pumps, the concrete can be placed rapidly with a minimum of lift lines. If the forms are not able to fully support the liquid head, bottom movement will occur, resulting in concrete spillage or actual movement of the upper form from the plane of the form below (Figure 30.12). Lightweight form systems are designed for concrete placement at 6 to 8 ft (1.8 to 2.5 m) per hour. This may be insufficient. The most common forms are made of wood, plywood, concrete, steel, plastic-reinforced and nonreinforced, plaster, or a combination



FIGURE 30.12 Movement of upper form from the plane of the form below during placement and consolidation of the concrete.

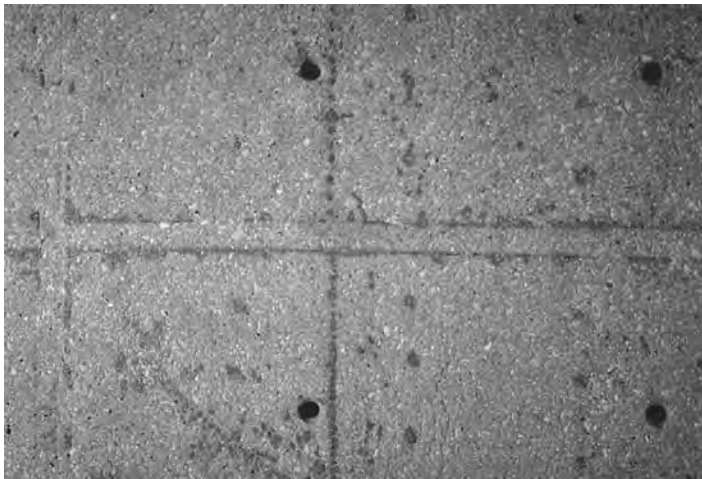


FIGURE 30.13 Moisture leakage at nail holes and at the edges of duct tape used at form butt joints reduce the w/c ratio at the point of migration, resulting in dark areas in the concrete surface.

of these materials. For complicated details, forms of plaster, elastomeric rubber, foam plastic, or sculptured sand may be used. These forms are often combined or reinforced with wood or steel depending on the size and complexity of the unit to be produced.

Forms are molds, and the cast concrete surfaces will reflect the finest details of the contact surface: wood grain, nail heads, dents, bulges, and the tile smootheners of plastic. All of these can be reproduced with startling—and sometimes distressing—fidelity. This should be remembered when choosing the forming material. Moisture leakage at nail holes and at the edges of the duct tape used at form butt joints reduce the w/c ratio at the point of migration, resulting in dark areas in the concrete surface (Figure 30.13). Overuse of forms can result in wear in areas with variable absorption. Forms that are to be reused should be carefully inspected after each use to ensure that they have not become distorted or damaged and to determine if they have any surface deterioration that may affect their ability to perform. Dark blemishes of this nature may penetrate as much as 1 in. (25 mm) into the concrete (Figure 30.14 and



FIGURE 30.14 Poor-quality form surface where the dense plywood and its surface coating have been worn through repetitive usage.

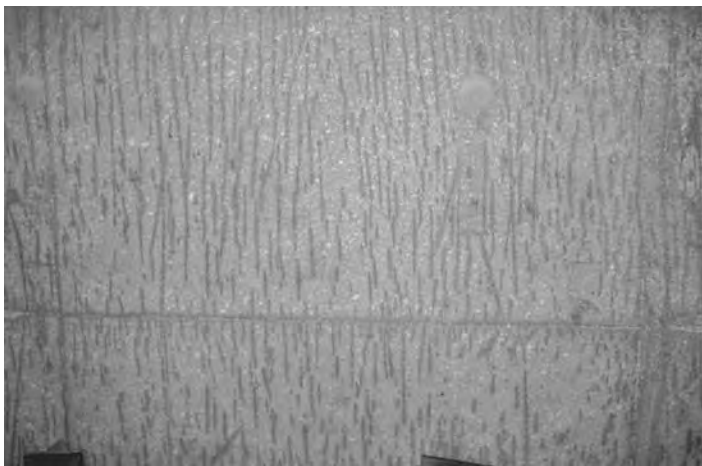


FIGURE 30.15 Result of form with vertical wear marks reflected in the finished concrete surface. Sandblasting made the surface blemishes more apparent.

Figure 30.15). Once they occur, they cannot be concealed by sandblasting or bushhammering. In fact, due to its low w/c ratio, this dark concrete is actually harder than the adjoining unaffected areas and there will be less erosion from sandblasting, which will tend to accentuate the blemishes. Regardless of the number of reuses, all forms should produce concrete surfaces matching the approved mock-up.

30.7.1.2 Materials

The selection of form materials is the responsibility of the contractor, although the architect may specify certain liners or materials to achieve a particular surface or texture. Selection of materials used for forming must consider the type of surface effect desired, which includes color impact, texture, quality, deflection, and ease of stripping. Economy is of major concern to the contractor and is a function of cost first and then the number of possible reuses while still meeting the criteria of the mock-up.

Deflection, rather than bending or horizontal shear stresses, generally governs the design of the formwork. Forms must be able to support their own weight, the weight of the plastic concrete, and the pressure of the forces from consolidating the concrete. Deflections in the contact surfaces of the formwork

reflect directly in the finished concrete surfaces. Forms for architectural concrete must be designed to minimize deflection. The deflection factor as well as the layout of tie-cone holes will affect the number of studs and wales or the number of studs and size of wales in the case of wooden forms. Limiting deflections may be only 1/16 in. (1.5 mm) in 4 ft (1.2 m), which is only half the normally acceptable 1/360 of the span for structural concrete. This limiting deflection is the one that is most restrictive yet still practical. Generally, prefabricated wooden form panels are not suitable for use in architectural concrete due to difficulties encountered in making them tight against leakage; therefore, wooden forms for walls are generally built in place. Particular care must be given to alignment, perfection of corners, quality of contact surface, and tightness of joints. Minor defects in any of these items, which may not be objectionable in structural concrete, are not acceptable for architectural concrete.

In any architectural project, the formwork must be superior to that used for structural concrete. Grade B-B plywood is often used for structural concrete construction but generally is not acceptable for architectural concrete. This plywood absorbs moisture from the concrete and will cause discoloration unless two to three coats of a urethane sealer are applied prior to use. High-density plywood can be used 10 times or more. Today, plywood can be purchased with plant-applied surface treatments that provide a nearly impervious and smooth surface. Birch plywood with a plastic coating is a plant-produced product that is higher in cost, but its high rate of reuse and its availability in sizes larger than 4×10 ft (1.2×3.1 m) may offset the cost by reducing the number of butt joints. If grain raise is to be transferred to the concrete, impervious coatings should be avoided. Sandblasting the plywood surface will impart a rough grain texture to the concrete.

Steel forms are generally used where high reuse factors or full liquid head construction is required. Steel surfaces are impervious and can provide uniform color to the concrete. The concrete may have some texture or color variation if the steel is rolled in different mills. An epoxy coating on the steel faces can combat the possibility of rust. The steel skin should be thick enough to support the load between its support members and keep deflections within acceptable limits. Quality steel forms should be well braced and manufactured of a heavy enough gauge steel to prevent twisting, buckling, and bending during erection and under the most severe usage. Formwork should incorporate adequate ribbing or channeling to provide rigidity, and, when welded to the parent member, the welded areas must exceed 6 in. (150 mm) in length to prevent tearing or popping. Skip-welding should be used instead of continuous welding to keep heat out of the plates. If continuous welding must be done on a finish surface, it is recommended that a test section be produced at the joint to determine whether or not the joint area produces an acceptable product without distortion in the concrete. The welds should be ground smooth and coated with epoxy or similar material to hide the joint. Steel plate should come from the same mill as the steel may be rolled in a variety of ways. Variations in the rolling technique can cause differences in the appearance of the concrete cast against metal from two mills. The steel skin should be pickled to remove mill scale. Bluing over welded material has been beneficial for avoiding staining from different surface characteristics. For flat horizontal surfaces and surfaces to be honed or polished, the form skin should be 3/8 in. (10 mm) thick to maintain local flatness after repeated use. Higher plate inertia also imparts a more uniform vibration pattern across the concrete surface during form vibration.

Steel is the preferred forming material for external vibration because it has good structural strength and fatigue properties. Steel forms are well suited for the attachment of vibrators and, when properly reinforced, provide good uniform transmission of vibration. Welding at the corners of vibrator-mounted members or brackets should be avoided, as this promotes angular crack propagation. Galvanized steel forms may cause concrete to stick and should be avoided. Aluminum and magnesium alloys may be used successfully if they are compatible with concrete. There is no standard test to measure compatibility. Past history of use with the same concrete mixture, forms, and curing conditions is the best known indicator of compatibility.

Fiberglass-reinforced plastic is an excellent solution when it is possible to use one form face piece for two or more adjacent surfaces. Examples are a beam face and soffit or the front and two sides of a column. In this way, the support members required in a fiberglass-reinforced form can be integral with the finish face. Such forms can ensure that there will be no leakage at the completely enclosed corners, thus minimizing one of the most objectionable surface blemishes (leakage) in architectural concrete

construction. Designers may not like the slightly rounded corners, but no one prefers leakage lines. Fiberglass-reinforced forms must have adequate horizontal and vertical ribs to properly provide rigidity and resistance to deflection.

An appropriate resin must be used on the surface face to ensure good performance through a reasonable number of reuses, usually over 100. Maintenance of the resin plastic is mandatory for surface uniformity. This can be accomplished by careful cleaning, use of release agents, and occasional touch-up of the face surface. Surface conditions, joints, and gel-coat material should be visually inspected prior to each use. Plastic molds should not be used with accelerated curing if concrete temperatures above 140°F (60°C) are anticipated. The susceptibility of the plastic form to attack by the proposed release agent should be determined prior to use. Unreinforced plastics are normally used only as liners for a form system designed to meet all of the structural requirements of concrete containment. Unreinforced plastic is only used to change the characteristics of the surface.

Plaster waste forms are used for custom designs of a sophisticated and detailed nature. The concrete is cast against the mold and the plaster is then broken away from the finished surface. Loose plaster can be removed with high-pressure water washing. Forms are almost always made with ornamental plasters, the methods used being similar to those employed in fibrous plaster work. Plaster forms must be made in sections that can be handled easily; individual pieces should not weigh over 150 lb (68.2 kg). Plaster forms are usually given two coats of white shellac to make them waterproof and nonabsorbent. If this is not done, it is quite certain that there will be a difference in the color of the concrete as compared with adjacent areas. Obviously, one-use forms are relatively expensive and should only be used for nonrepetitive forming or where intricate shapes cannot be formed by more conventional methods. An effective release agent must be used with plaster waste molds.

30.7.1.3 Joints

A surface blemish will result when water is allowed to leak from the form. Leaks of any type in forms will result in honeycomb (an aggregate-rich surface inconsistent with the normal, dense, adjacent surfaces accompanied by a color change or streaking), mottling, or a dark discoloration surrounding the point of leakage. The darker surface color is a result of less water being available for hydration. Moisture, paste, or grout can never be replaced except by repair of the concrete surface. It is therefore very important to prevent leakage. Different methods have been advanced to prevent leakage at form joints; none has proved completely successful, especially those attempting to seal the joints flush with one another. Any amount of moisture or grout will create blemishes in exposed surfaces that are difficult and that may even be impossible to remove. For this reason, many designers prefer to acknowledge the joints and mask them with reveals formed by rustication strips. It is good practice to provide rustications at the casting limit atop the preceding cast to define straight level and plumb working lines (Figure 30.16) for construction joints (Shilstone, 1973a).

When concrete is placed for the lift above or for an adjoining wall section, the forms will have a tendency to bulge under the hydrostatic head of the wet concrete and vibratory loads, causing a spill or overpour on the concrete already in place (Figure 30.17). Unless the concrete is to be bushhammered, tooled, or heavily sandblasted, which in the process remove the spill, such an overpour should be prevented. This is best accomplished by attaching a compressible gasket that is set into the reveal at the top of the previous casting and provides a watertight seal beneath the reveal. Tying the form into the previous concrete placement after the gasket is in place helps prevent form deflection. Vertical joints can be handled in a similar manner (Shilstone, 1973a).

Control joints may be defined as planes of weakness created by thin sections, encouraging the concrete to crack at predetermined locations. Stresses that cause cracking result from shrinkage, thermal effects, and differential settlement; shrinkage is generally the stress of greatest magnitude. If joints cannot be tolerated, the reinforcement design can attempt to distribute shrinkage and thermal stresses into many small hairline cracks, but it is generally better to weaken the concrete and ensure a controlled crack that can be sealed against water penetration. At times, it is desirable to cut 50% of the temperature steel at the control joint to further weaken the section.

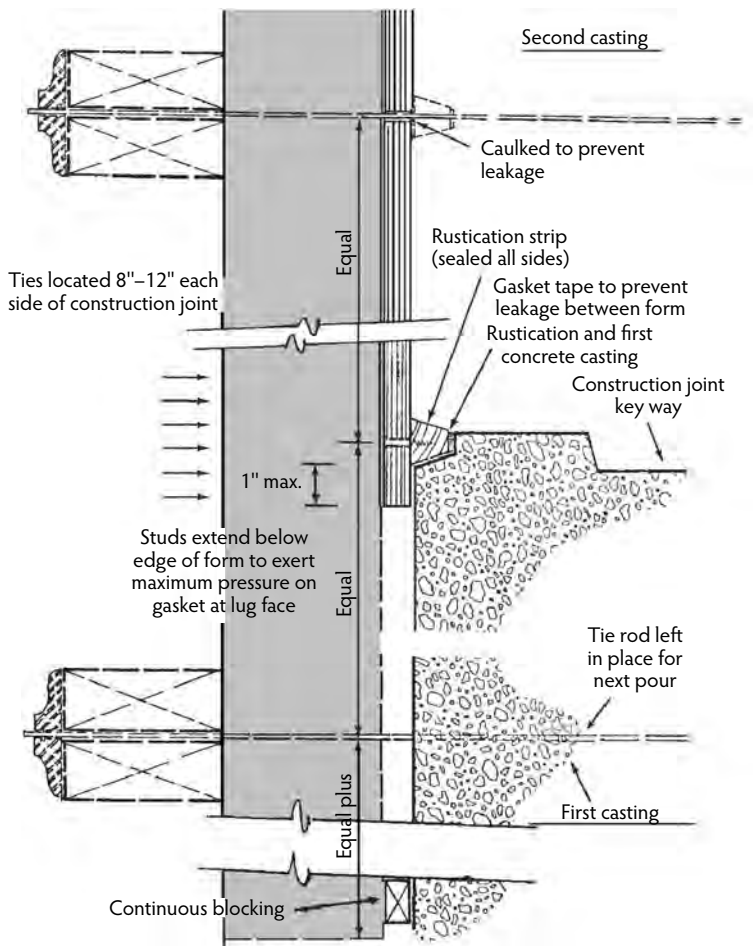


FIGURE 30.16 Typical construction joint; horizontal or vertical—no scale. (From Shilstone, J.M., *Architect. Rec.*, 161–164, 1973. With permission.)

The location of control joints should not be determined until a careful study has been made of the geometry of the structure, its elastic qualities, and the steel-reinforcement design. It is an inescapable fact that a large mass of concrete will crack. This must be anticipated in the structural and architectural design. Perhaps the surest way to plan construction joints, and one that reduces their number, is to have them correspond to locations where control joints are required. The relatively weak bond between castings will ensure that cracks develop at those points.

On many occasions, chamfers have been used at corners in an attempt to minimize leakage. If the chamfers themselves are not caulked or gasketed, moisture or paste leakage can occur at two points rather than one. It is recommended that all corners, form joints, horizontal and vertical construction joints (sometimes known as cold or pour joints), and control joints be caulked or gasketed to provide positive protection against leakage. Gaskets should be a closed-cell compressible neoprene with adhesive on one side that can be attached to the form. Plastic pressure-sensitive tape (never duct tape) has sometimes been used on the inside of the forms at butt joints when significant texturing of the surface skin is planned. To withstand the stress when the form is filled with concrete, the tape should be flexible and highly adhesive. Tape should be applied prior to the application of a release agent. Care must be taken to prevent displacement of the tape or gaskets during concrete placement. Brush-applied gum adhesive over tape has been used successfully to stabilize the tape or gasket against movement. All joints should



FIGURE 30.17 Spill or overpour at construction joint during placement and consolidation. Tying the form into the previous concrete placement and installing a compressible gasket in the reveal would have prevented this leakage.

be inspected prior to casting to be sure the tape or gaskets have not moved. When tape cannot be used because tape deformation will be visible on the fine texture concrete surface, great care must be given to locating the butt joints. It is recommended that the contractor erect the exposed form face first to allow a visual check of all joints and joint treatments to minimize potential leakage.

Other ways to seal plywood butt joints include chamfering form edges and filling them with epoxy, gasketing, and using plywood sheets that have spliced or tongue-and-groove edges that are caulked or glued. Such joints must be backed up and supported with 2×4 s (50×100 mm). The architect may designate the location of control joints, but the location of construction joints is often left to the contractor. In architectural concrete, it is best if the contractor receives input from the architect as to where construction joints will be located.

30.7.1.4 Form Ties

Except for small columns and beams, the lateral forces created by the hydraulic pressure of plastic concrete must be resisted by horizontal ties that hold the forms together and maintain their position. Ties may incorporate a spreader device that correctly spaces the distance between forms and acts as a means of removing metal parts to a sufficient depth from the surface, 1-1/2 in. (38 mm), to facilitate patching with mortar and prevent corrosion. Form ties significantly influence the visual effect of architectural concrete. They are placed in the forms in a pattern that should be consistent with the type of form design (Shilstone, 1973b). A 4-ft (1.2-m) pattern can be used with a variety of plywood sizes in a gang form. There is a tendency for many contractors to use cone snap ties. The installation of these must be done very carefully. All form-tie systems should incorporate a positive leakage-prevention detail. Bulls-eyes around tie holes are not considered attractive. Leakage can occur around form ties if they are not perfectly seated and sealed (Figure 30.18).



FIGURE 30.18 Dark leakage areas around form tie holes where moisture has migrated, resulting in localized concrete with a lower w/c ratio.

Tie-hole design and spacing are as much architectural considerations as a structural requirement for the contractor. Ties for architectural concrete should be planned so they are symmetrical with the member formed, and, wherever possible, ties should be located at rustication marks, control joints construction joints, or other points where the visual effect will be minimized. In this way, repair of tie holes will not fall in the flat panel areas. Successfully patching tie holes is not easy because it is difficult to match the finished color of the adjacent concrete surfaces. Often, patches tend to accent rather than conceal tie holes. Heavier forms with steel backing and large-diameter tapered bolts at a minimum number of locations offer a better approach to architectural concrete than using multiple snap ties. Adjustable, high-strength bolt ties facilitate the installation of subsequent forms by holding them tightly to the concrete of the previous casting, helping prevent leakage.

Ties or bolts that are to be pulled from the form must be coated with nonstaining bond breaker or encased in oiled paper sleeves to facilitate removal. Ties for architectural concrete should have the same safety factor as structural concrete. Form-tie assemblies for architectural concrete should be adjustable so as to permit tightening of the forms. Form-tie assemblies fall into one of the following groups:

- Continuous, single-member ties for specific wall thicknesses and positive breakback characteristics
- She-bolt ties, where an inner male threaded unit is left in the wall concrete and the outer fastening devices are removed and reused
- He-bolt ties, where the outer fastening devices are reused and an expendable female threaded unit is left in the wall
- Through-bolts placed through PVC pipe with removable plastic cones at the ends
- Tapered high-strength through-bolts, which can be completely removed from the concrete

The last type of bolt has a separate outer unit for proper adjustment. When using these bolts, the contractor should place the small-diameter side of the tapered bolt on the exposed face to avoid spalling when the form is stripped. Removable ties should be of a design that does not leave holes in the concrete greater than 7/8 in. (22 mm). Bolts should be tight fitting or holes should be filled with a sealant to prevent leakage at the holes in the form. All of these ties leave round and relatively clean holes, providing proper sealing procedures have been used (ACI Committee 303, 2004). These holes may be left alone, patched flush, or patched with a slight recess for an architectural shadow effect. Snap ties are not suitable for architectural concrete unless a rustic crude look is desired.

30.7.1.5 Form-Tie Removal

Ties should be removed as soon as possible after the formwork has been removed. After forms are removed, uncoated ties or ties that possess staining tendencies should be snapped and the ends should be treated to prevent rust stains. Stainless-steel snap ties, when used, present the least trouble with staining, but still should be broken off at least 1 in. (25 mm) behind the finished surface. Plastic-coated ties should be snapped and the ends treated to prevent rust staining. Holding forms together with twisted wire ties or band iron should not be allowed, as it is nearly impossible to obtain a long-term, stain-free surface without cutting into the concrete surface and cutting back the tie or band iron ends before repairing a rather large nonuniform area. Externally braced forms may be used instead of any of the above-mentioned form-tie methods to avoid objectionable blemishes in the finished surface. This is an expensive alternative unless a high degree of repetitive form use is possible.

30.7.1.6 Form Removal

Assuming that the necessary planning, care, and workmanship have been exercised in producing the quality of work desired, form removal must maintain the results already achieved. Forms should not be removed until the concrete has sufficiently hardened to permit form removal without damaging the concrete surface. Prying against the face of the concrete should not be attempted. When necessary, wooden wedges (not metal), should be used to assist in form removal. Many surfaces are marred by the use of metal wedges to loosen forming. Rough removal of forms may damage them beyond reuse. Elastomeric liners become difficult to remove if the forms are not stripped within 5 to 7 days. Easy removal of forms will reduce labor costs. More importantly, forms that can be stripped easily prevent unnecessary damage to exposed architectural surfaces. Spalled edges require expensive restoration by knowledgeable craftsmen. Sharp corners require a considerable amount of special attention in forming and form removal technique. Sharp edge lines and corners are very vulnerable to chipping or spalls at early ages. Damaged corners require costly repair work.

If forms are removed before the specified curing period is completed, measures must be taken immediately to apply and maintain satisfactory curing. In hot, dry climates, wood forms remaining in place should not be considered to be adequate curing. Forms should be removed or loosened so the concrete surfaces can be kept moist, or they should be coated with a curing agent. In cold weather, architectural concrete should not be allowed to cool more than 40°F (4.4°C) per 24 hours following the cessation of heat application. The removal of formwork may have to be deferred, or formwork that is removed should be replaced with insulated blankets to avoid thermal shock and consequent crazing of the concrete surface.

One has to be careful of small projections such as drip lines. Abrupt stripping may crack or break off the projecting tip, making the area vulnerable to moisture and subsequent corrosion of reinforcement. With embedded items such as windows or forms for openings, braces should be stripped first to allow the edge forms to be stripped without spalling the concrete. Intricate details will require a delay in stripping time to allow the concrete to gain sufficient strength and to shrink from drying (Dobrowolski, 1989). The best procedure calls for stripping to begin away from the intricate area and proceed toward it. If the edges of rustications are to be crisp after sandblasting, they must remain in the face of the concrete. Many reuses call for rustication strips to remain with the forms and new strips to be reinserted prior to sandblasting. Fastening can be by gluing with mucilage or nailing into the form.

Once formwork is removed, the concrete must be protected to prevent damage from any means including subsequent construction operations and weather. Runoff water from rain or on-site construction should be prevented from running over iron or other materials that can cause staining and then running over finished faces of architectural concrete. Surfaces must be protected from stains, graffiti, and impact damage. Differentiating concrete color hues may be expected between two surfaces where adjacent formwork is stripped at different ages. It is best to strip all adjacent form surfaces at about the same age for greatest uniformity. All forms, regardless of material selected, must be stacked level and horizontal to prevent warping. Even steel forms will warp if stored at an angle against the side of a building.



FIGURE 30.19 Electrical conduit blocking access for placement and consolidation of concrete.

30.7.2 Reinforcement

30.7.2.1 Reinforcing Steel

Reinforcing steel must be planned in advance so concrete placement can be carried out without reinforcement, thus reducing the work space required for consolidation of the concrete. Mechanical, electrical, ductwork, piping, conduit, or other embedments must also be planned as to location (Figure 30.19). If the size of a particular member does not provide adequate work space or otherwise presents difficulties for the contractor, an alternative method of detailing or construction should be considered. Often the suggested solution for a congested member is to use a smaller vibrator. This can be a problem, as the smaller vibrator may not be able to perform the compactive work necessary to produce the high quality essential for architectural concrete.

Occasionally, special vibrators have been made, such as vibrators with rigid shafts and only a 3-in. (76.0-mm) flexible joint. Even special vibrators cannot overcome lack of space. Because the amount of reinforcing required in a member is dependent on the size of the member, it may be necessary to increase the size of the member. Members cannot always be slim enough to meet the architect's design concept. Concrete members must be of sufficient size to avoid excessive amounts of reinforcing steel. Visualizing the patterns of reinforcing is important at the early stages of design—particularly at member intersections (Figure 30.20). The situation in Figure 30.20 allows little room for placement and consolidation of concrete. Honeycomb and other surface blemishes are a certainty; for example, beams should be wider than columns that have to go through the floor to avoid the familiar solid maze of vertical and horizontal

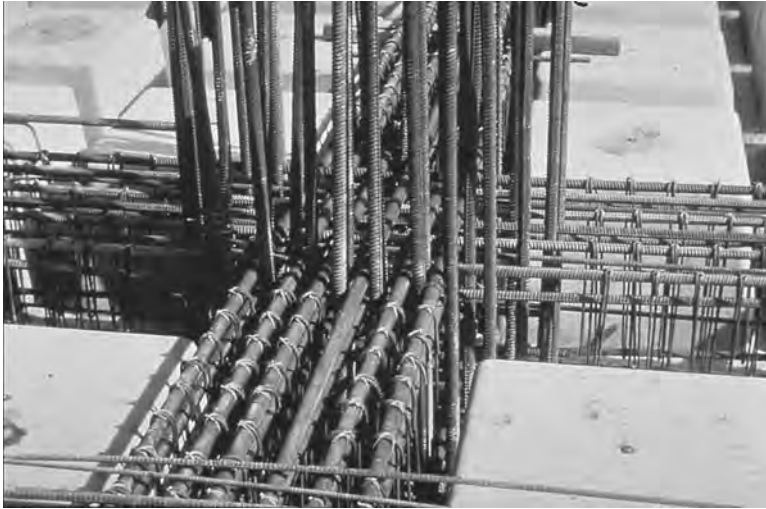


FIGURE 30.20 Intersection of reinforcing steel allowing little access for placement and consolidation of concrete.

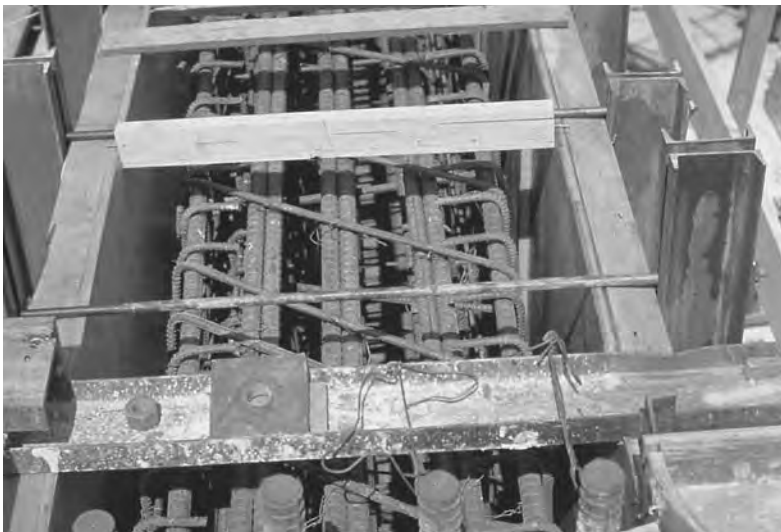


FIGURE 30.21 Bundling of reinforcing bars to allow more working space for vibration.

reinforcing. In other members, bundling bars may provide a solution to afford clear working space for vibration (Figure 30.21).

The assumption that reinforcing steel must be uniformly distributed as detailed on the structural drawings is not always accurate. In many designs, the steel bars can be bundled or otherwise spaced to allow the contractor some space to actually place and consolidate the concrete. Horizontal space available after bundling will allow entry of the vibrating equipment. Full tension welds, cadwelds, or tension splices can be employed where required to eliminate congestion caused by lapping of bars (Figure 30.22). Locating the lapping of bars throughout the beam can reduce the congestion at any one point.

Reinforcing steel for architectural concrete must be accurately positioned and held in place in such a way as to minimize movement during placement and consolidation of the concrete. Wall or beam reinforcement cover can be maintained by the use of bolsters or chairs on the inside face of the form to lessen the chance of rust stains or spalling of the concrete. When reviewing the reinforcing steel design, the contractor should consider the following:



FIGURE 30.22 Lapping of bars all occurring at one location causing congestion that can lead to honeycombing.

- For design purposes, the cover on reinforcing steel for concrete exposed to the weather should be at least 2 in. Because the ACI Code allows reinforcing metal to move $\pm 1/2$ in. from the design location, this sets a minimum of 1-1/2 in. of cover over the reinforcement.
- Horizontal bars in walls should be placed toward the outside face of the wall to allow a larger casting space between curtains of reinforcement (Figure 30.23). Single-curtain reinforcement should be positioned at the center of the wall, but with the horizontal bars closest to the architectural face.
- A minimum clear working space of 5 in. (design) is necessary to facilitate proper placement and consolidation of low-slump concrete mixes.
- When computing the space occupied by the reinforcing steel to determine the amount of space available for the worker in the field to do the work, maximum bar diameters should be used instead of the nominal diameters. The effective space occupied by the bars due to deformations is over 10% larger. Actual space is measured to the outside of the deformations on the rebar surface. These maximum deformations become significant when thin or slender concrete sections are to be cast.
- Tie wires should be a soft stainless steel specified to be tucked behind the joints and not left dangling adjacent to the exposed face.
- Chairs should not be used to space reinforcing steel from vertical surfaces. Where it is necessary to support steel in beams, the reinforcing steel should be hung from the forms with stainless steel tie wire, and any chairs should be plastic tipped with sufficient plastic cover to ensure that the metal will not rust. If reinforcing steel is hung from the forms, the forms and supporting member must be designed to take what is often very heavy weight. This method is generally only practical when steel forms are used. If the surface is to be abrasive blasted, consideration should be given to the material that will resist the abrasive blast. In most cases where there is heavy reinforcement of beams, it may be necessary to use precast concrete blocks of the same concrete used in the construction to support the metal.

Some design codes require the use of reinforcement in such quantities that constructability is markedly reduced. When such conditions are found, the fact that the amount of metal required is within the code is not an acceptable excuse for producing a design that defies proper construction. Double-check reinforcing steel details to make sure that casting space is available. For the project manager, this can be the difference between a reasonable project or an impossible task.

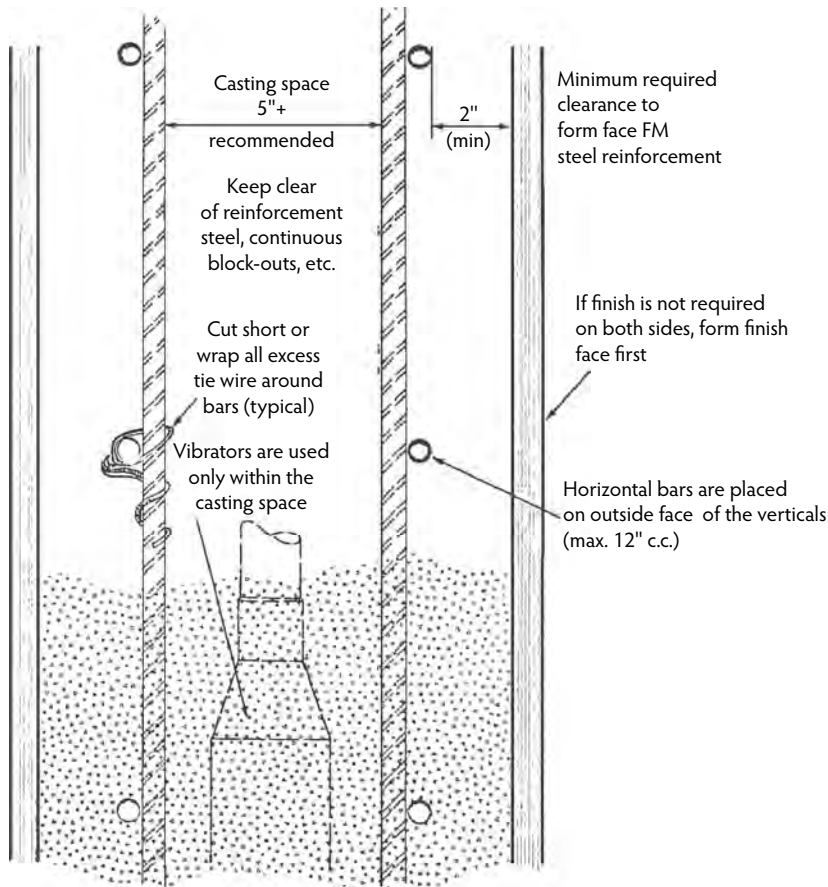


FIGURE 30.23 Double steel curtain wall: may be finished both sides; 12 in. usually minimum (not to scale).

30.7.2.2 Placing Accessories

Supporting chairs, spacers, and bolsters should be manufactured of plastic or stainless steel to prevent surface rust staining, particularly where the concrete member is to be sandblasted. Plastic colors should match the finish surface. Many steel accessory suppliers will custom color their products. Current practices in detailing are considered inadequate to achieve total concealment of accessory feet. The reinforcing steel specification should indicate the need to increase the number of chairs to compensate for steel loads that cannot be tolerated by the plastic-covered chairs, the plastic tips of the chairs, or the form materials used to support the reinforcing cages. Insufficient chairs may cause form indentation. Upon removal of the forms, these plastic or stainless steel tips will project below the ceiling or from the bottom of cast-in-place beams. Any plastic coating tips should be investigated for durability if they will be exposed to weather or sunlight. Any wire for tying reinforcement should be of soft stainless steel to minimize staining of exposed surfaces. Some stainless steel ties may rust slightly when sandblasted or exposed to severe weather conditions. For this reason, all tie wire should be cut as close as possible to the bars and bent back away from form surfaces. Tie-wire clippings must be removed from any horizontal surfaces (such as beam soffits or ceiling areas) that will be exposed to view.

30.7.2.3 Galvanized Reinforcement

Galvanizing reinforcing steel is not recommended for architectural concrete. Adequate minimum cover of well-compacted concrete is the best protection for reinforcing steel. Where galvanizing of reinforcing bars is required, galvanizing is usually performed after fabrication. This may mean several rehandlings

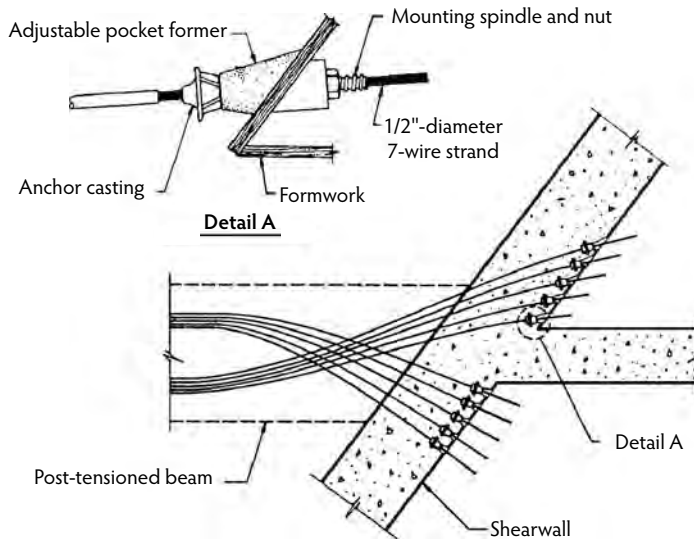


FIGURE 30.24 Plan view of typical interior shearwall anchorage. Pocket formers can be field adjusted for proper tendon alignment.

for individual bars or partially assembled cages. ASTM A 767/A 767M (ASTM, 2005) prescribes minimum finished bend diameters for bars that are fabricated before galvanizing. Smaller finished bend diameters are permitted if the bars are stress relieved. Supplementary requirement S1 requires sheared ends of bars to be coated with a zinc-rich paint formulation. When galvanized reinforcing steel is placed close to nongalvanized metal forms, the concrete may have a tendency to stick to the forms. This may also happen if nongalvanized reinforcement is used close to galvanized forms or form liners. A 2% solution of sodium dichromate or a 5% solution of chromic acid (chromium trioxide) solution applied as a wash to the galvanized surface has satisfactorily reduced the galvanic action of the metal to prevent reaction between the zinc and the alkaline fresh concrete. The addition of chromates to the concrete cannot be recommended, as their effect on concrete performance is not yet fully known. Galvanizing of reinforcement is only recommended when minimum cover requirements cannot be achieved. In these cases, the use of galvanizing should be specifically called for in the contract documents and shown in the shop drawings.

30.7.2.4 Post-Tensioning

Long-span, post-tensioned-beam framing systems have been used in combination with architectural concrete to produce unusual buildings in both the United States and the Middle East. A post-tensioned-beam framing system offers the advantages of both a higher span/depth ratio and a reduction in material quantities. With an architectural cast-in-place facade, considerable planning is required to allow for stressing of the post-tensioned structure without leaving visible signs in the exterior architectural finish. This means using exterior precast concrete panels as covers for exterior stressing pockets or providing interior stressing pockets, buttresses, and blockouts.

The contractor must be very careful in his placement of anchor pocket formers in the formwork. Improper placement of formed stressing pockets can result in misalignment of jacking equipment and application of an incidental biaxial force to the tendon, which could cause shearing of the tendon at the anchor. Preformed pocket formers can be used and field adjusted to obtain the proper alignment of typical interior shearwall anchorage, as shown in Figure 30.24. An interior girder detail at the core stressing anchorage and at the exterior wall key are shown in Figure 30.25. The 60-ft (18.3-m) single-span beams in the low-rise structure are stressed through to pockets at each end of the beam. A typical top pocket anchor detail is shown in Figure 30.26. The above three details were used at 1515 Poydras in New Orleans. Chicago-based Skidmore, Owings, and Merrill provided the architectural and engineering

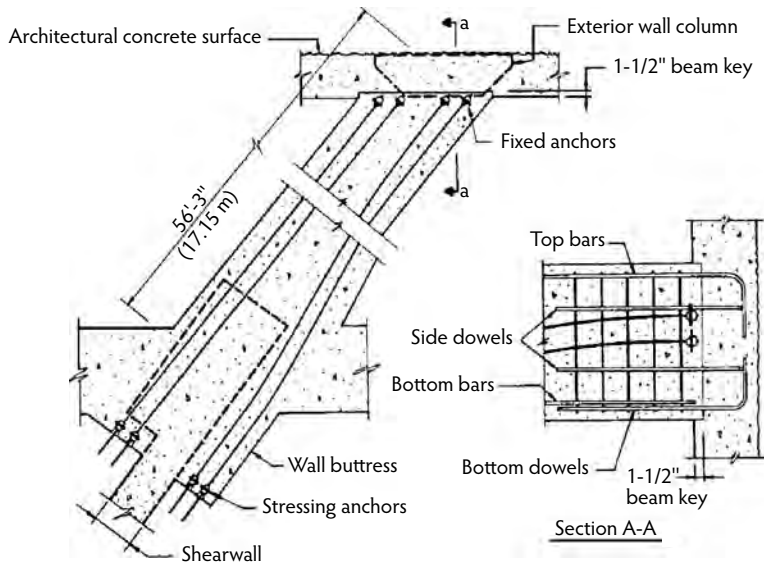


FIGURE 30.25 Interior girder detail at core stressing anchorage and at exterior wall key.

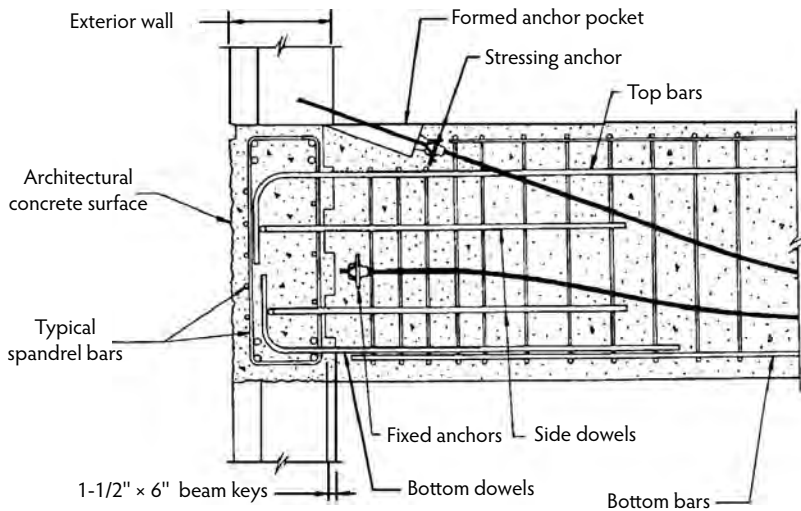


FIGURE 30.26 Typical top pocket anchor detail.

design. The unusual number of unique post-tensioned-beam anchorage configurations required intense review and quality control at the onset of construction. Considerable planning went into materials, formwork sequencing, and special falsework for the doweled reinforcement support. This is a striking example of the integration of structure and form. The exterior concrete finishes range from a heavy hammered texture to a light sandblast. Attention to detailing, finishes, and execution have allowed the architectural design of this building to be accurately expressed through cast-in-place and precast structural elements (Clark and Zils, 1984).

The original design of the post-tensioned channel beams at the roof level of the 800-ft (244-m)-long Physical Education building in Saudi Arabia called for massive 4.0-ft (1.2-m)-wide by 8.0-ft (2.4-m)-deep by 141.6-ft (42.9-m)-long cast-in-place concrete beams spanning 120 ft (36.3 m) between cast-in-place lateral supports. Each beam would have a total mass of 170 t (154 Mg) and an architectural surface area of 4670 ft² (432 m²). These channel beams were located 56 ft (17 m) above ground level and spaced

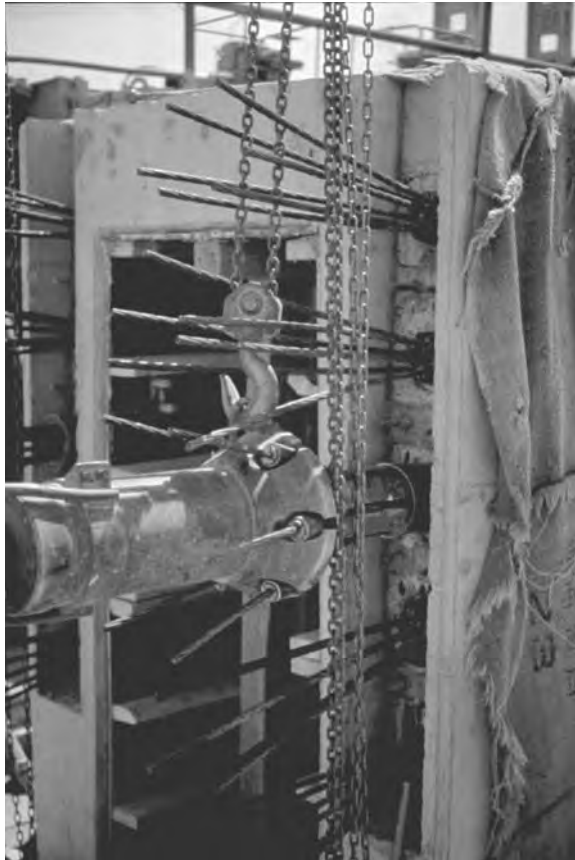


FIGURE 30.27 After all seven-wire strands were stressed and anchored, the ends were cut off inside the stressing pocket recess.

16.3 ft (4.95 m) on-center. The 47 beams were of architectural concrete with a light to medium sandblast finish. Due to severe schedule restrictions, shoring problems, and interference with work at other levels and zones of the building, it was decided to precast and post-tension the channel beams rather than cast them in place. The precasting would take place at one location at the 56-ft (17-m) level. Caudill Rowlett & Scott (CRS) in Houston, Texas, approved the design modification. This change in construction method reduced shoring and forming costs and resulted in a large reduction in labor. The channel beams were cast on a construction platform on a 6-day cycle, including 3 days of curing on top of temporary rails set on the cast-in-place lateral support beams. Seven-wire strand was threaded through sheathing to ensure minimum friction losses. After 6 days, the strands were tensioned following a computer program that determined the required gauge pressure and elongation for each strand group. When all of the strands had been properly stressed and anchored, the ends were cut inside the stressing pocket recess (Figure 30.27). Strands were then grouted in the sheathing, and the recess was filled with architectural concrete patch mix, covered with wet burlap, and protected with a wood cover (Figure 30.28). Each channel beam was moved to its final position along the rail using two hydraulic rams. After the beams reached their final position, the hydraulic ram jacking system and rails were removed and the beams were set on thick neoprene bearing pads. This was all done without the use of a crane; only hydraulic jacks were used (Kenney, 1988).

A prestressing strand is required to conform to ASTM A 416 (ASTM, 2006), Grade 250 (1725) or Grade 270 (1860). The most commonly used grade of steel is 270,000 psi (1862 MPa). This strand is 0.5 or 0.6 in. (12.7 or 15.2 mm) in diameter and is of low-relaxation type. Unbonded single-strand tendons



FIGURE 30.28 After cutting, the strands were grouted in the sheathing, and the recess was filled with architectural concrete patch mix, covered with wet burlap, and protected with a wood cover.

are composed of steel strand with anchors affixed to each end by toothed wedges coated with corrosion-resistant lubricant and encased in plastic sheathing. For wedge-type anchorages, the wedge grippers should be designed to preclude premature failure of the prestressing steel due to notch or pinching effects under static test load conditions.

Post-tensioning tendons subject to exposure or condensation and that are not to be grouted should be permanently protected against corrosion by plastic sheathing formed over the coated (greased) strand or by other appropriate means of protection. The sheathing should not be reactive with the concrete, coating, or steel. The material should be watertight and have sufficient strength and durability to resist damage and deterioration during fabrication, transport, storage, installation, concreting, and tensioning. Sheaths should be continuous over the unbonded length of the tendons and should prevent the intrusion of water or cement paste and escape of the coating material.

30.7.3 Concrete Placement

The placement of architectural concrete requires the utmost care on the part of the contractor. Consistent preplanning of each day's concrete placement should be done. The period between the truck and the forms is the most critical time in the life of architectural concrete. The ready-mix truck must transport and mix the concrete to a homogeneous state in spite of low slumps and high coarse-aggregate contents. With some architectural concrete mixes, it may be necessary to load trucks to only two thirds of their rated mixing volume. The contractor must verify that the ready-mix trucks assigned to deliver architectural concrete are clean and free of hardened buildup and have less than 20% blade wear. Trucks meeting this criteria should have their numbers recorded, or some other means of identification should be used so only approved trucks will be used for architectural concrete. Trucks should be scheduled so they arrive at the project site just before the concrete is required, thus avoiding excessive mixing while trucks are waiting or delays in placing successive lifts of concrete. Delays cause nonuniformity of pour line or appearance.

A major decision for the contractor is choosing the method for placing the concrete. Placement can make or break the quality of architectural concrete. The characteristics of certain lay-down buckets or pumps may prevent their use for placing the necessary concrete mix. When this happens, other methods or equipment may be required. Steep-sided buckets (Figure 30.29), may be required, conveyors may be used (Figure 30.30), or a different concrete pump may be selected (Figure 30.31). Change the equipment or pump, but do not adjust the concrete mix design.



FIGURE 30.29 Steep-sided bucket with easily movable chute to aid in placement of concrete.



FIGURE 30.30 Conveyors in use at construction site.



FIGURE 30.31 Several concrete pumps in use at construction site.



FIGURE 30.32 Tremie being placed in position for use.

High-quality architectural concrete can be obtained when placing concrete with trucks, tremies (Figure 30.32), buckets, or even wheelbarrows, provided proper procedures are followed. When concrete is placed directly from trucks or through tremies, the free fall should be limited to less than 5 ft (1.5 m). Tremies can be made of either sheet metal or reinforced plastic with a rectangular cross-section. Minimum inside dimensions would be 4×16 in. (100×400 mm). There must be sufficient space between reinforcing bars if a tremie is to be used. The flow of concrete from a truck or tremie must be directed within the reinforcing cage to ensure minimal bounce or deflection of the concrete off steel, conduit, or other obstructions that cause splatter or segregation of the mix. Splatter on the formwork above the level of plastic concrete can harden and cause a surface blemish that is difficult to remove. This is especially serious in finishes having a light or smooth texture.



FIGURE 30.33 Concrete pumped from the bottom up to minimize consolidation problems and bug holes. This hospital building was designed by Bertram Goldberg of Chicago.

Conveyors are useful when a low-slump concrete mix with a high coarse-aggregate proportion—2000 lb (900 kg) of coarse aggregate or more—is required. They are most often used when large floor (ceiling) and beam composite construction is required. Care should be taken with any conveying equipment to prevent contamination by nonarchitectural mixes and to prevent segregation of the mix being transported. If methods of conveyance are varied during the overall construction of architectural concrete, the uniformity of the finish surface color may be affected. When conveyors are used, they should have a high speed and have a discharge end that is easily movable to permit proper concrete mix distribution.

Concrete pumps must be rated on their ability to move concrete having a low w/c ratio that meets the architectural requirements of the project. Several pumps today have 5- or 6-in. (125- or 150-mm) lines that can handle most architectural concrete mixes. To prevent concrete consolidation problems in the walls and minimize bug holes, one contractor elected to pump walls from the bottom up. Pumping ports were installed in the wall forms 12 in. (302 mm) from the bottom and on 4-ft (1.2-m) centers along the steel forms. A superplasticizer was used to allow for 8- to 10-in. slumps (Figure 30.33). These serpentine architectural cast-in-place walls later had a white coating applied to their surface. In addition to cast-in-place concrete, battery and other vertical forms for precast products have been pumped from the bottom up. Use of a superplasticizer admixture can help the concrete to be pumped while maintaining the required w/c ratio. Variations in w/c ratio will change the color of the exposed architectural surface. When using a concrete pump, the first 1/4 yd³ (0.2 m³) should be wasted or utilized elsewhere, not in the architectural forms. It takes a certain amount of cement paste to coat the inside of the pump and hoses leading to the placement location. An alternative would be to initially charge the pump with a



FIGURE 30.34 Adjacent concrete walls from two separate days' placement showing the impact of pumping concrete directly without wasting first 1/4 yd³ (0.2 m³) to coat the pump and hoses.

high-cement grout mix prior to placing the regular concrete. Failure to do one or the other will result in a higher w/c ratio at the point of initial discharge and unsightly discoloration (Figure 30.34). The more uniform the w/c ratio, the greater the uniformity of the color and texture.

The depth of the layers of concrete placed and consolidated depends on the width of the forms, the amount of reinforcing present, the concrete placement method, and the timing required. Each new concrete lift should cover the previously placed concrete within 20 minutes. Substantial lift or pour lines may result when a 45-minute delay in placement of fresh concrete occurs. Fresh concrete is usually placed in lifts of no less than 18 in. (450 mm) and no more than 30 in. (750 mm). The surface of each lift should be fairly level so the vibrator does not have to move the concrete laterally. Lateral movement can cause segregation, leading to honeycomb or other surface blemishes. Concrete should be placed continuously at close intervals. A vibrator should be operated at the point of deposit during all concrete placement.

30.7.4 Concrete Consolidation

30.7.4.1 General

The most important single skill in architectural concrete involves the selection and operation of the vibrator. In Europe, vibration operation is recognized as being all important to good concrete work, and skilled vibrator operators are the highest paid workers on concrete crews. All too frequently in the United States, the vibrator operator is one of the most unskilled and untrained members of the concrete crew, often being picked for having a strong back rather than knowledge of concrete consolidation. A vibrator not only consolidates the concrete for maximum density but also internally blends the different lifts of concrete together into a single solid mass with few bug holes and no lift lines on the finished exposed surfaces.

30.7.4.2 Equipment

All too often vibrators are selected on the basis of their price or maintenance records. Instead, selection should be based on the following vibrator qualities (ACI Committee 309, 2005; Shilstone, 1972c):

- *Frequency* is the ability to fluidify the mix based on the number of times per minute the head moves from side to side.
- *Amplitude* is the ability to kick the mix into place. Amplitude is the measured distance of the head when it goes from side to side as measured from its neutral axis. An increase in amplitude results in an increase in the effective radius of action.

- *Power* is the ability to maintain vibration under load.
- *Size* is the ability to overcome the resistance of the concrete mix particles to movement. Use the largest diameter head permitted by the form dimensions and the spacing between reinforcement.

The high frequency of the vibrator alone will not work. If the power is constant and the frequency is increased, the amplitude decreases because the head does not have the time to travel as far as it did at lower frequency. If the power source is increased, the head has a greater amplitude, provided the frequency is not simultaneously increased. Larger vibrators provide more mass in the head. The larger mass head is necessary to provide the impulse to drive the concrete effectively into the intricacies of the form. A high-frequency, high-amplitude, high-powered vibrator moves to such a degree that it creates a churning action within the concrete mass. This is the type of vibrator necessary to combine two lifts of concrete into one. Achievement of void-free surfaces favors a higher-frequency vibrator.

Internal vibrators are generally referred to as *immersion*, *poker*, or *spud vibrators*. One of the most commonly used types is the flexible-shaft type, where the electric motor is outside the vibrator. A flexible shaft leads from the motor into the vibrator head, where it turns the eccentric weight. A universal 120-volt, single-phase, 60-Hz (cycles per second) motor is used, and the frequency of this vibrator when operating in air is quite high—in the range of 12,000 to 17,000 vibrations per minute (200 to 283 Hz) (the higher values are for smaller head sizes). Because of this high speed and the heat developed, the vibrator may burn up if operated carelessly outside the concrete; however, when the vibrator is operating in the concrete, the motor is under load and the frequency is generally reduced by about one fifth.

The electric motor-in-head vibrator type has the motor in the vibrator head, as the name implies. Most motor-in-head vibrators are high-cycle units. This means that a 180 high-cycle current is required for their operation instead of the usual 60-cycle commercial power. These vibrators use induction motors and operate at a frequency in concrete of about 10,000 vibrations per minute (vpm); this is only about 5% less than their free speed (speed in air). The high-cycle current is obtained by passing commercial power through a frequency converter or through the use of a special generator. Motor-in-head vibrators operating on a 60-cycle current with a universal motor are also available, but they have less capability than high-cycle units. The electric motor-in-head vibrators are generally at least 2 in. (50 mm) in diameter. When using electric vibrators, all power cables and connectors should be kept in good condition. Vibrators should not be lifted or carried by the electric cables. Sharp bends should be avoided in the shafts of flexible-shaft vibrators. When vibration is finished for the day, vibrators should be cleaned and concrete spills removed. It may be desirable to cover form vibrators to keep concrete from dropping on them, but not in such a way as to interfere with air cooling. Whether the consolidation equipment provides internal or external vibration, or a combination of both, its frequency and amplitude should be designed, tested, and proven for the volume, configuration, and placing technique of the product and the proportioning and consistency of the concrete for that product.

Because internal vibrators are used in wet (conductive) locations, all electric units should be grounded to the power source. Generator sets supplying power should also be grounded to maintain continuity of the grounding system. Units operating at less than 50 V or that are protected by an approved double-insulation system are excepted from the grounding system. In the United States, electric vibrators are subject to the National Electric Code, Article 250-45. External vibrators may be divided into form vibrators, surface vibrators, and vibrating tables. Form vibrators are external vibrators attached to the outside of the form or mold. They vibrate the form, which in turn transmits the vibration to the concrete. Extremely rugged forms are required where high-amplitude vibration is used. The effective penetration of the vibrations into the concrete ranges from 8 to 24 in. (200 to 600 mm). It may be necessary to supplement a form vibrator with internal vibration for sections thicker than 12 in. (300 mm) or higher than 4 ft (1.2 m). Rotary-type vibrators are preferred because reciprocating types are very hard on molds. Rotary-type vibrators may be operated pneumatically, electrically, or hydraulically. In the reciprocating type, a pneumatically driven piston is accelerated in one direction, stopped (by striking against a steel plate), and then accelerated in the opposite direction. These vibrators produce impulses acting perpendicular to the mold with frequencies usually in the range of 1000 to 5000 vpm (20 to 80 Hz).

In the pneumatically and hydraulically driven rotary-type models, centrifugal force is developed by a rotating cylinder or revolving eccentric weight. These vibrators generally work at frequencies of 6000 to 12,000 vpm (100 to 200 Hz). The frequency may be varied by changing the air pressure, usually by adjusting the air-supply valve or the fluid pressure on the hydraulic models. The amplitude and centrifugal force may be varied by changing the eccentric weight. The hydraulic models are driven by a hydraulic motor that turns an eccentric weight on a shaft. The advantage of this type of vibrator is the combination of an extremely low noise level, similar to an electric motor, with an infinitely variable speed. The unit can be locked into a specific frequency by use of a flow control. The wise contractor also has a spare for each type of vibrator available at the site in case of breakdown. If 180-cycle generators are used to power the vibrators, then two generators should be available at the site.

30.7.4.3 Internal Vibration

Internal vibration is recommended for all standard member cross-sections. The vibrator should be inserted vertically at uniform spacing over the entire area. The vibrator operator should be trained never to force the vibrator into a lift, as doing so produces voids in the earlier lift. Let the vibrator sink rapidly into the concrete to the bottom of the lift, but not less than 6 in. (150 mm) into the preceding lift, if there is one. With rapid penetration, the concrete is moved upward and outward, which drives the air and water ahead of the concrete and facilitates its escape to the top of the form surface. Because compaction does not occur below the tip of the vibrator, it is imperative for the operator to allow the vibrator to sink rapidly by its own weight into the preceding lift. If the first lift has partially set before the second is placed, it is practically impossible to blend the two layers. Unattractive lift lines and possible honeycomb will result.

The vibrator should be withdrawn slowly upward at the rate of about 2 in./sec in a slow churning (up-and-down) motion. Vibrator surge is always upward and generally at a 30° angle from the horizontal. The distance between vibrator insertions should generally be about 18 in. (depending on the properties of the mix and vibrator being used); the area visibly affected by the vibrator should overlap the adjacent just-vibrated area by a few inches. Vibrator insertions should be no farther apart than twice the radius of influence. Even the largest head vibrators have a radius of influence of 10 in. or less.

For architectural concrete, it is best to have two vibrators and two operators consolidating the concrete. The first operator is stationed at the point of deposit, where that vibrator is operated continuously. The second vibrator is used to slowly blend concrete, eliminate lift lines, and send entrapped air and water up along the form face and out of the concrete mix (Figure 30.35). When the vibrator head begins to emerge from the concrete, be sure the operator understands that it must be removed from the concrete quickly or else air will be drawn down between the concrete and the form. At no time should the head of the vibrator be half in and half out of the concrete. When that happens, immediately fully extract the vibrator from the concrete. Movement of the vibrator should not cease or pause while it is in the concrete. Constant manipulation is necessary to prevent the possible formation of harmonic motion, which could distort or deflect the form or cause failure in the form. The very least that can happen under these circumstances is paste leakage, honeycombing, or entrapping air on the form face.

Sometimes it is practical to insert a small vibrator between the reinforcement and the form face. In such cases, the vibrator should be rubber tipped; even so, any contact with the form should be avoided if at all possible because this might mar the form, disfigure the surface, and result in a darker color or leave vibrator paste marks in an exposed-aggregate surface (Figure 30.36). This entire procedure is dangerous. Actually, at no time should the head of an internal vibrator come in contact with the forms. The vibrator should be kept just within the steel reinforcing and be inserted no closer than 3 in. (75 mm) from the form on the side of the steel away from the form face.

For dry mixes, where the hole around the vibrator does not close during withdrawal, reinserting the vibrator a few inches away may solve the problem. While stiff mixes are to be encouraged, overly dry mixes may result in poor consolidation (honeycomb or excessive entrapped air) and should be avoided. Where air voids in formed surfaces are excessive, the distance between vibrator insertions should be reduced to about 12 to 15 in. (300 to 375 mm).



FIGURE 30.35 First operator is vibrating concrete at point of deposit; second operator is blending concrete to eliminate lift lines and minimize bug holes.



FIGURE 30.36 Grout lines on exposed face of architectural concrete due to an internal vibrator touching the side of the form during concrete consolidation.

Form liners have more surface area than flat forms, and they require greater internal vibration. Architectural concrete will normally require at least twice and maybe three times as much vibration and compaction effect as regular structural concrete. Sometimes very harsh mixes, such as those with gap



FIGURE 30.37 Concrete wall placed with a superplasticizer in the mixture and no internal or external vibration; settlement lines occurred at all horizontal reinforcing locations.

grading, are used to produce special architectural effects. These also require more powerful vibrators and longer vibration times. The contractor should be sure to choose a sufficiently large vibrator and see that vibration insertions are placed closely enough to consolidate all concrete. The vibration should be terminated when the mortar level reaches the top of the aggregate to minimize mortar lenses between lifts.

Superplasticized admixtures have changed the vibration techniques used in architectural concrete mixes. Superplasticized mixes require less vibration than standard mixes that do not include a superplasticizer admixture. When superplasticizers were first introduced, the literature stated that no vibration was required. This was a mistake, and several contractors unfortunately believed the technical data. Neither internal nor external vibration was used in placing the concrete. The results were disastrous; settlement cracks occurred at all horizontal reinforcing steel locations (Figure 30.37). It is virtually impossible to overvibrate a well-designed mix; however, it is possible to overvibrate a concrete mix containing a superplasticizer admixture. Overvibration of mixes containing superplasticizers may cause segregation, and the excess mixing action may entrap air or water, which will result in bug holes.

Lightweight concrete behaves differently from hard-rock concrete. Because of its lack of particle weight, it presents great problems for compaction and has a tendency to float. Considerably more surface blow holes should be expected with lightweight concrete; where these are not acceptable, lightweight concrete should not be used.

30.7.4.4 Form Vibration

Form vibration is recommended in areas inaccessible to internal vibration or where full floor height steel or reinforced plastic forms are used. External vibrators loosen joints in wood forms, causing grout leakage and honeycomb and therefore are not recommended for this use. Forms for external vibration must stand up under the repeated, reversing stresses induced by vibrators attached to the form. External vibration of forms improves surface quality, but the additional stressing of forms and liners can shorten their life. Form vibrators must be capable of transmitting the vibration more or less uniformly over a considerable area.

The form should have adequate skin thickness and suitable stiffeners. The vibrators should be rigidly attached to the form. Special attention should be given to form tightness to prevent grout leakage. Trials should be made with form vibrators prior to their large-scale use. These trials should simulate the forming conditions to be encountered on the structure. The size and spacing of form vibrators should be such that the proper intensity of vibration is distributed over the desired area of form. The spacing is a function of the type and shape of the form, depth and thickness of the concrete, force output per vibrator,

workability of the mix, and vibrating time. Current knowledge is inadequate to provide an exact solution to this complex problem (ACI Committee 309, 2005).

The recommended approach is to start with a spacing generally in the range of 4 to 8 ft (1.2 to 2.4 m). If this pattern does not produce adequate and uniform vibration, the vibrators should be relocated as necessary until proper results are obtained. Achieving the optimum spacing requires knowledge of the distribution of frequency and amplitude over the form and an understanding of the workability and compactibility of the mix. The frequency can readily be determined by a vibrating reed tachometer; however, the small amplitudes associated with form vibration have been difficult to measure in the past. Inadequate amplitudes mean poor consolidation, while excessive local amplitudes are not only wasteful of vibrator power but can in some cases also cause the concrete to roll and tumble so it does not consolidate properly. Moving one's hand over the form will locate areas of very strong or weak vibration (high or low amplitude) and dead spots.

Concrete compacted by form vibration should be deposited in layers usually 10 to 15 in. (250 to 400 mm) thick. Each layer should be vibrated separately. Vibration times are considerably longer than for internal vibration, frequently as much as 2 minutes, and possibly as much as 30 minutes or more in some deep sections. It is desirable to be able to vary the frequency and amplitude of the vibrators. On electrically driven external vibrators, amplitudes can be adjusted to different fixed values quite readily. On air-driven external vibrators, the frequency can be adjusted by varying the air pressure, and the amplitude can be changed by changing the eccentric weight. Because most of the movement imparted by form vibrators is perpendicular to the plane of the form, the form tends to act as a vibrating membrane, with an "oil-can" effect. This is particularly true if the vibration is of the high-amplitude type and the plate is too thin or lacks adequate stiffeners. This in-and-out movement can cause the forms to pump air into the concrete, especially in the top few feet (50 to 100 cm) of a wall or column lift, creating a gap between the concrete and the form. Here, there are no subsequent layers of concrete to assist in closing the gap. It is therefore often advisable to use an internal vibrator in this region. Form vibration during stripping is sometimes of benefit. The minute movement of the entire surface of the form helps to loosen it from the concrete and permits easy removal without damage to the concrete surface.

30.7.4.5 Revibration

The lift should be revibrated after initial consolidation with slow withdrawal of the vibrator head to draw out as many of the air bubbles as possible. The vibrator used to remove air bubbles from the top lift can be of lesser power or a smaller size than that used to initially consolidate the concrete. The usual high-energy vibrators have a tendency to churn air into the top lift of the concrete. This is the area where air and water pockets are most prevalent. If the architectural concrete mix is a properly designed low-slump mix, do not worry about overvibration. Revibration, after bleeding is substantially complete but before initial set, can be used to further densify the concrete and reduce air and water pockets against the form and exposed concrete face. Revibration can be accomplished any time the running vibrator will sink of its own weight into the concrete and liquefy it momentarily. It will accomplish most if it is done as late in the process as possible. Revibration generally results in improved compressive and bond strength, release of water trapped under horizontal reinforcing bars, minimized leakage under form bolts, and the removal of additional air voids. The greatest benefits are obtained for wetter concrete mixtures. Revibration should not be used where harsh gap-graded mixtures have been used to produce exposed-aggregate surfaces.

30.7.4.6 Spading

Spading may be employed in conjunction with internal or external vibration to improve finish surfaces. A flat, spade-like tool or a large plastic sail batten is repeatedly inserted through the top two lifts of concrete and withdrawn from the concrete adjacent to the form. This forces the coarse aggregate particles away from the form face and assists the air bubbles in their upward movement toward the top surface (ACI Committee 303, 2004). The spade, regardless of type, must be inserted often enough to cover the entire area of the form surface. Sometimes a wooden 1 × 4-in. (25 × 100-mm) or 1 × 6-in. (25 × 150-mm) board with a pointed chisel end is used, but better results have been obtained with a plastic sail batten.

Spading is usually done in conjunction with revibration by internal or external vibrators. The top lift must be quickly revibrated to close any gaps left by the spading. Although it is a laborious operation, the results can be worthwhile if spading is properly utilized. In addition to spading and revibration, pounding the outside of the forms with wooden mallets or a steel plate attached to an impact hammer, working from the bottom of the form upward, can release air bubbles and improve the concrete surface.

30.7.5 Curing

30.7.5.1 General

The method and period of curing should be consistent to produce a uniform concrete surface without stains, discoloration, drying, or plastic shrinkage cracks. Curing materials or methods should not allow one section of architectural concrete to cure or dry out faster than other sections, as this may produce color variations in the finish surface. Proposed methods should be tried on the site-cast mock-up to determine any adverse effects. Curing involves maintaining a satisfactory moisture content and temperature in the architectural concrete to produce the final qualities desired for both texture and durability of the surface. Unless early stripping is necessary to achieve a specific texture, concrete strength for removal of the forms is usually 2000 psi (13.8 MPa). The stripping strength is generally set by the design structural engineer. Freshly deposited and consolidated concrete should be protected from premature drying and extremes of temperature. The curing period of concrete that is of significant interest is during the early stages of strength development, from initial set until the concrete has reached the design strength appropriate for stripping of the forms. It is not necessary to wait for the mix water to finish bleeding to the surface before initiating the curing and protection of finish surfaces.

30.7.5.2 Curing in the Forms

Nearly all beams, columns, and undersides of slabs receive their curing by being left in the forms. To prevent staining caused by the type of form material, seal the forms with a liquid sealer prior to use, following the manufacturer's instructions. For vertical surfaces, the easiest thing is to leave the forms in place and keep them supplied with additional moisture through soaker hoses or other methods. Early removal of forms and application of curing compounds is generally unsuccessful for architectural concrete, although it is standard procedure for structural concrete. Curing compounds will usually stain the surface; for example, polyethylene stains the concrete a whitish color. Concrete in the form should be maintained at a temperature of not less than 50°F (10°C) during the curing period. In cold climates, the contractor may be required to use insulated forms to utilize the heat of cement hydration to maintain the temperature necessary during curing. The contractor may also have to provide heat (if necessary to maintain minimum temperatures and to minimize loss of moisture).

30.7.5.3 Moist Curing

Flat surfaces can be cured by ponding with the use of perimeter barriers and continuously operated sprinklers; however, the runoff water may create other problems at the project. Curing water should be checked for staining materials such as iron, which may cause rust stains, and the water should be uniformly applied to achieve uniformity of color. Flat surfaces can also be cured with the forms left on and the top surface covered with paper, polyethylene, or clean flannel. Burlap is dirty, can leave residual stains, and is generally not kept continuously wet. It may be necessary to erect wind breaks out of properly supported plastic sheets or temporary plywood walls. For vertical and other formed surfaces, after the concrete has hardened and while the forms are still in place, water should be applied so it runs down the inside of the form if necessary to keep the concrete uniformly wet. Immediately following form removal, the surface should be kept continuously wet with water spray or water-saturated fabric for a period of 5 days. Extending the curing period beyond 7 days does not produce additional beneficial effects, except in areas of very low humidity. Water curing has been found to reduce the possibility of cracks forming, to lighten dark blotchiness, and to create better uniformity of color. Uniformity of water application is important to obtain uniformity of color. If surface retarding agents are to be used,

water curing should be delayed until after the surface treatment has been accomplished. Rapid surface drying can lead to color variations. The contractor must have an adequate crew and all the required equipment prepared so placement, finishing, and curing can proceed without interruption and as rapidly as possible.

30.7.5.4 Membrane Curing

Liquid curing compounds may cause discoloration or staining and prevent the bond of any repairs or permanent coatings that may be needed. Curing compounds should only be used on the back of walls where the surface is not exposed or where the surface is to be removed by acid etching, sandblasting, or tooling. Manufacturers should be consulted as to the rate of coverage and the effect that their compound has in the above respects. This type of cure should be thoroughly evaluated on the preconstruction mock-up (ACI Committee 303, 2004). When used, membrane-curing compound should cover the entire surface to be cured with a uniform film that will remain in place without gaps or omissions. Areas with incomplete coating cover should be recoated. If a curing membrane is to be used, it is preferable to use an inorganic material such as sodium silicate. Organic curing compounds discolor after prolonged exposure to sunlight. The briefer the interval between stripping the form and applying the curing compound, the better, but the interval should be kept uniform from form to form to minimize color variation in the concrete. Curing compounds should be applied to the top of a wall as soon as floating is completed. Sodium silicates are especially useful for curing tops of walls because they do not break the bond between concrete and steel if sprayed on reinforcement and they do not interfere with subsequently applied cementitious toppings. Also, the sodium silicates fill the gap at the top of a wall where lower pressure compresses the plastic liner less and results in a slightly thinner wall section. In addition, sodium silicates consume free lime, greatly reducing the potential for efflorescence.

30.7.5.5 Hot-Weather Curing

The time between placing architectural concrete and initiation of curing is most critical in hot, dry, or windy weather. To minimize variations in color due to nonuniform drying and to prevent plastic shrinkage cracking, curing should commence as soon as practical (ACI Committee 303, 2004). To minimize drying shrinkage, it may be necessary to erect wind breaks out of properly supported plastic sheets or temporary plywood walls.

30.7.5.6 Cold-Weather Curing

Thermal curing is important during cold weather. If concrete forms are removed during cold weather while the concrete is still warm, rapid cooling of the concrete surface can result in crazing cracks. If steel forms are used, thermal cracking can occur without removing the forms. The problem is compounded if the concrete is to receive a sandblasted finish, which further opens the cracks. To minimize thermal cracking and crazing, leave forms in place until the concrete has cooled enough and gained sufficient strength to reduce thermal shock. If steel forms are used or if mass concrete is involved, use insulating blankets on the forms to slow heat loss. Do not use insulating blankets directly on the concrete as this can result in blotchiness where the blankets touch the concrete.

30.7.6 Protection

All freshly placed concrete should be protected from the elements and from any defacement due to subsequent building operations. One of the most common problems is rain or construction runoff water moving across rebar or other stored materials and then flowing down the face of the exposed architectural concrete. Another cause of rust staining is the use of steel scaffolding. On all architectural concrete contracts, nonferrous scaffolding should be used. If steel scaffolding is necessary, it should be maintained with all surfaces painted. Stain removal is discussed in the Portland Cement Association's publication *Removing Stains and Cleaning Concrete Surfaces* (PCA, 1988). Corners, edges, and other surfaces vulnerable to damage should be protected with suitable guards or barricades until the project is complete.

30.8 Production and Installation of Precast Elements

30.8.1 Production

Production of architectural precast has progressed from reliance on individual craftsmanship to a well-controlled and coordinated production-line method with corresponding economic and physical improvements. The contract documents should make reference to PCI's *Manual for Quality Control for Plants and Production of Architectural Precast Concrete Products* (PCI, 1996) as the industry guideline for production. The general objective of this standard is to define the required minimum practices for production and for a program of quality control to monitor the production; therefore, a performance specification based on this publication will ensure a quality product.

30.8.2 Coordination

Even if the quality of the precast concrete components delivered to the job site is good, the success of the entire project is dependent on the quality of workmanship of the erector. A poor erection job can detract not only from the performance of the structure but also from the appearance of even the best designed precast concrete project. The erector should assist the general contractor/construction manager (GC/CM) in taking the lead on a construction site to help solve problems before they occur by coordinating efforts with other participants on the project. The responsibility for the erection of precast concrete may vary as follows:

- The precast concrete manufacturer supplies the product already erected, either by in-house labor or by an independent erector.
- The manufacturer is responsible only for supplying the product, free-on-board plant or jobsite. Erection is done either by the general contractor or by an independent erector under a separate agreement with the general contractor and/or owner.
- The products are purchased by an independent erector, who has a contract with the general contractor or owner to furnish the complete precast concrete package.

On projects where the precast concrete manufacturer does not have the contractual obligation for the erection, it is extremely desirable for the manufacturer to assign a representative to observe and report on planned erection methods. Regardless of contractual obligations, it is recommended that the precast concrete manufacturer maintain adequate contact with the firms responsible for both transportation and erection to ensure that the precast concrete units are properly handled and erected according to the design and project specifications.

The GC/CM is normally responsible for the project schedule and dimensions and coordination with all other construction trades. Relative to erection of precast concrete the GC/CM, in conjunction with the precaster, should:

- Be responsible for coordinating all information necessary to produce the precast concrete erection drawings. A prejob conference should be held as soon as possible after award of the precast concrete contracts. This meeting should consider erection sequencing, weight and size limitations, special rigging, and guy and bracing scheme information. This information should be communicated to the precaster's design engineer. Upon receipt of this information, the design engineer should, if necessary, develop a bracing sequence to maintain stability of the structure during erection in conjunction with the erector and engineer of record. Limitations may state, for example, that loading of the structure should be balanced, requiring that no elevation be erected more than a stated number of floors ahead of the remaining elevations, or limitations may involve the rigidity of the structure, requiring that walls should not be erected prior to the completion of floors designed to carry the lateral loads. In steel frames, it should be determined how far in advance final frame connections must be completed prior to panel erection. Particular consideration should

be given to deflection and rotation of the supporting structure due to the precast and other superimposed loads. For concrete frames, what strength of concrete is required should be determined prior to imposing loads of the precast concrete panels. The frame designer should also recognize that connections between panel and frame impose concentrated loads on the frame and that these loads may require supplementary local reinforcing. In the case of multistory concrete frames, consideration should be given to the effects of frame shortening due to shrinkage and creep.

- Review and approve or obtain approval for all erection drawings and design.
- Be responsible for the coordination of dimensional interfacing of precast concrete with other trades.
- See that proper tolerances are maintained to guarantee accurate fit and overall conformity with precast erection drawings.
- Be responsible for providing and maintaining clear, level, well-drained unloading areas and road access around and into the structure to such a degree that the hauling and erection equipment for the precast concrete units is able to operate under their own power. Erection equipment should be able to handle units directly from the transportation equipment.

Sequencing is of the utmost importance for facilitating erection of the structure. Prior to the manufacture of precast members, the erection and job sequence should be mutually agreed upon by the GC/CM, precaster, and erector. To avoid excessive erection costs, efforts should be made to allow a unit to be handled in one motion from unloading to positioning. When a sequence has been agreed upon, it should be strictly adhered to unless severe unforeseen problems dictate a sequence change.

30.8.3 Field Verification and Layout

Surveys should be required before, during, and after erection:

- Before, so the starting point is clearly established and any potential difficulties with the support structure are determined early
- During, to maintain alignment
- After, to ensure that the products have been erected within tolerances

The benefits of surveying and laying out the support location prior to erection include: (1) when an error is found it can be corrected prior to starting erection; (2) costly erection delays for crane and crew are avoided if everything fits; and (3) layout crews may find errors on the shop drawings, which, if caught in time, can reduce costly corrections and minimize delays. It is the responsibility of the GC/CM to establish and maintain, at convenient locations, control points, benchmarks, and lines in an undisturbed condition for the erector's use until final completion and acceptance of a project. If the building frame is not precast concrete, then the benchmarks and building lines should be provided by the GC/CM at each floor level. Work points should also be provided for angled and curved building elevations. The erector should be advised by the GC/CM of any known discrepancies in field location, line, or grade and be provided with suitable work areas for layout.

Prior to beginning erection and the scheduling of delivery and handling equipment, a field check of the project should be made by the erector to ensure that foundations, walls, and structural frames are suitably constructed to accept the precast concrete units. This should include a field check of the work affecting the erection contract, including the location, line and grade of bearing surfaces, notches, blockouts, anchor bolts, cast-in-place or contractor's hardware (miscellaneous iron), a check on dimensional tolerances, and a check of all overhead electrical lines. The objective of this survey is to ensure that the areas to receive the precast concrete are ready and accessible to the erector and that the precast units will fit.

Survey notes should be kept of all discrepancies that exceed specified tolerances. Any discrepancies between site conditions and the architectural, structural, and erection drawings that may cause problems during erection, such as structural steel out of alignment, anchor bolts or dowels improperly installed,

errors in bearing elevation or location, and obstructions caused by other trades, should be noted in writing and sent to the precast concrete manufacturer and GC/CM. Erection should not proceed until discrepancies are corrected by the GC/CM, or until erection requirements are modified and reviewed by the design engineer. Verification of remedial work should be the responsibility of the GC/CM. The erector should return to the site for a final survey after all necessary corrections of site conditions have been made by the GC/CM and before any erection is started.

Working from the control points, benchmarks, and lines established by the GC/CM, the erector should establish offset lines and elevation marks as required for use at each floor level. Precast concrete members must be installed to accurate lines and grades to ensure both proper performance and correct relationships with adjoining work. It is the layout crew's duty to mark the locations to receive the precast concrete units so the erector can place them with a minimum of measuring or moving to get them into final position. The erector should establish joint locations prior to actual product installation. This will keep the differential variation in joint width to a minimum, as well as identify problems caused by the building frame, columns, or beams being out of dimensional or alignment tolerance. The layout crew should be kept well ahead of erection so if corrections are required there is adequate time for the design, approval, fabrication, and installation of repairs so as not to hinder the process of erection.

30.8.4 Delivery

Factors to be considered when delivering precast members from the plant to the job site are type, size, shape, and weight of the member; type of finish; weather; road conditions; method of transportation; type of vehicle; routing; distance to the job; and job-site conditions. The shipper, not necessarily the precast concrete manufacturer or erector, is responsible for safe delivery of precast members. The precast concrete manufacturer, shipper, and erector should develop clearly defined acceptance procedures to avoid later disagreement concerning damage. The precast concrete manufacturer or erector should advise the shipper of any special situations along possible routes and at the job site to:

- Ensure safe transportation.
- Meet various governmental transportation regulations.
- Prevent or minimize in-transit damage with proper supports, frames, blocking, cushioning, and tie-downs. These materials are normally supplied by the precast concrete manufacturer and returned for repeat usage by the shipper. All blocking, packing, and protective materials must be of a type that will not cause damage, staining, or other disfigurement of the units. The blocking points and orientation of the units on the shipping equipment should be as designated on the shop drawings.
- Permit their removal from the load in proper sequence and orientation to minimize handling and possible damage to the product.
- Ensure that the product is oriented and loaded on the trailers so it can be erected without unnecessary offloading and rehandling; unloading of product on the ground is usually costly, creates site access problems for everybody, and often results in damage to the product.
- Ensure that sufficient product is delivered to the site in the prescheduled sequence to allow for orderly, efficient installation in the structure.

30.8.5 Connection Considerations

A certain amount of field adjustment at the connections is normal. Product tolerances make the possibility of a perfect fit in the field impossible. This is true when the precast concrete pieces join to each other and is even more true when the precast units must interface with other materials. Each industry has its own recommended erection tolerances that apply when its products are used exclusively. Hardware design for connections should take into account the tolerances for both the precast concrete components and the structure. These considerations may require clip angles and plates with slots or oversized holes to compensate for dimensional variation, field welding, or sufficient shim spaces to allow for elevation

variations. Sufficient minimum clearance between precast units and the structure must be provided to allow for product and erection tolerances. Hardware should be designed to compensate for additional stress at the maximum anticipated clearance. Hardware should also be designed to allow for movement in the building. Welded connections should only be used at one end of a panel; at the other end, slotted, bolted connections or other connection types that allow for movement should be used.

Field adjustments or changes in connections that could create additional stresses in the products or connections should not be permitted without approval by the architect or engineer. Particular care should be taken to prevent damage to the precast concrete unit when adjustments are being made to bring the unit into final position. Whenever possible, the connections should be completed in such a manner to permit operations to take place on the top side of erected members rather than from below where ladders or scaffolds are required, especially for welding. The type of equipment necessary to perform operations such as welding, post-tensioning, or pressure grouting should be considered. Operations that require working under a deck in an overhead position should be avoided, especially for welding. Alternatives to any erection techniques that require temporary scaffolding should be considered. Room to place wrenches on nuts and turn them through a large arc should be provided for bolted connections. Foundation piers should extend above grade so the anchor bolts can be adjusted during erection and the base plate need not be grouted in a hole, which can fill with water and debris. Properly drypacking column or wall-panel bases in a narrow excavation is difficult.

It is desirable to have connections that are designed so the erector can safely secure the member to the structure in a minimum amount of time without totally completing the connections. If necessary, temporary bracing or connections should be used with final adjustment and alignment in all directions relative to the structure and adjacent components completed independently of crane support. This allows the hoisting device to begin placing the next unit while connections on the first are being completed. The temporary connections should not interfere with or delay the placement of subsequent members. The temporary connections may have to be relieved or cut loose prior to completion of the permanent connections.

Connection details should allow erection to proceed independently of ambient temperatures and without temporary protective measures. Materials such as grout, drypack, cast-in-place concrete, and epoxies require protection or other special provisions when placed in cold weather. Also, welding is slower when the ambient temperature is low. If the connections are designed so these processes must be completed before erection can continue, the cost of erection is increased and delays may result.

The supply of erection hardware—that is, the loose hardware required in the field for final connection of precast members—should normally be the responsibility of the precast concrete manufacturer. The responsibility for the supply of contractor's hardware to be placed on or in the structure to receive the precast concrete units depends on the type of structure and varies with local practice but in any case should be clearly defined in the contract documents. Hardware should be incorporated in the structure within the specified tolerances according to a predetermined and agreed-upon schedule to avoid delays or interference with the precast erection. Hardware should be maintained and suitably protected (such as capping of inserts and protection of threads) until used by the precast erector. At times, it may be necessary to modify connections in the field to accommodate unforeseen clearance problems or the work of other trades. The GC/CM should clear any modifications through both the precast concrete manufacturer and the designer to ensure proper performance of the connections.

30.8.6 Installation

Hoisting the precast pieces is usually the most expensive and time-critical erection process. Connections should be designed so each unit can be lifted, set, connected, and unhooked in the shortest possible time. Before the hoist can be unhooked, the precast piece must be stable and in its final position. Preplanning for the fewest, quickest, and safest possible operations that must be performed before releasing the crane will greatly facilitate erection. Bearing pads, shims, or other devices upon which the piece is to be set should be placed ahead of hoisting. Loose hardware that is required for the connection should be immediately available for quick attachment. In some cases, it may be necessary to provide temporary

fasteners or leveling devices, with the permanent connection being made after the crane is released; for example, if the permanent connection requires field welding, grouting, drypacking, or cast-in-place concrete, the use of erection bolts, C-clamps, guy lines, pins, or shims should be considered. These temporary devices must be given careful attention to ensure that they will hold the piece in its proper position during the placement of all other pieces erected before the final connection is made.

Shims are often used as spacers or as means of leveling or aligning adjacent components. They serve an interim or temporary load-transferring function. Unless such temporary loading of units has been specifically incorporated or allowed in the contract documents, the erector should be responsible for this temporary loading of the units. High-density plastic and steel shims are commonly used to attain the specified joint dimension. Shims should be placed away from the face of the unit to prevent spalling in case of excessive loading. Also, they should be recessed out of view as they can be unsightly and difficult to remove if exposed to view. Shims should be removed from joints of non-load-bearing units after connections are completed and before applying sealant, unless the shim material itself is readily deformable. If left in place, shims should be noncorrosive or protected so staining will not occur. For load-bearing units, the use of nonmetallic shims or bearing pads such as neoprene or plastic may be used where bearing pressures do not exceed the allowable concrete stresses and the potential risk of damage to concrete edges is negligible.

The indiscriminate use of shims, particularly steel shims, can sometimes lead to undesirable consequences; for example, steel shims have been used in conjunction with grouted joints in multistory bearing-wall construction. Even with well-compacted grout or drypack, the compressive modulus of the steel shim is six times that of the drypack; consequently, the grout will deform (compress) more readily than the shim. The principal load-transfer path will remain concentrated through the steel shim rather than distributed along the grout bed. High load concentrations at shims can cause spalling at panel surfaces or crack panels vertically.

Precast concrete units should be erected at locations shown on the erection drawings, within the allowable tolerances. They should be positioned so cumulative dimensional errors do not exceed allowable tolerances. Horizontal and vertical joints should be correctly aligned and uniform joint width maintained as erection progresses. The installation or prewelding of miscellaneous iron hardware should be performed prior to the start of erection, whenever possible, to minimize the cost of crew and equipment standby. All inserts for lifting and bracing should be filled immediately after units are erected to prevent staining from corrosion-sensitive inserts or water freezing in them. Wall panels should be rigged and hoisted on the structure near the final location and held in place until safely secured. Final alignment and final connections may be made at once or later by follow-up crew, depending on the type of connection.

The connections should allow for easy adjustment in all directions. Panels should be installed on a floor-by-floor basis, where feasible, to keep loading equal on the structure, or the designer of the structural frame should determine the degree of imbalanced loading permitted (the sequence should be shown on the erection drawings). Limitations may state, for example, that loading of the structure must be balanced, requiring that no elevation be erected more than a stated number of floors ahead of the remaining elevations, or limitations may involve the rigidity of the structure, requiring that walls not be erected prior to completion of the floors designed to carry lateral loads. Panels should be aligned to predetermined offset lines established for each floor level. This is important because of the drift of a high-rise structure caused by sun, wind, and eccentric loads and forces due to construction activity being performed by others. It should be determined how far in advance of precast concrete erection that final connections in steel structures must be completed and what the minimum concrete strength should be for cast-in-place structures prior to loading them with precast concrete units.

Consideration should be given to the number of floors the erector wants to erect in a structure on temporary connections before making final connections. This is especially important for grouted connections and cold-weather conditions. Precast spandrels usually extend from column line to column line at the building perimeter. They connect either at the columns or directly to the perimeter beams. Precautions should be taken against torsional rotation, due to eccentric loadings on perimeter beams, until final connections are made. Shoring may be required to assist in erection until connections are made.

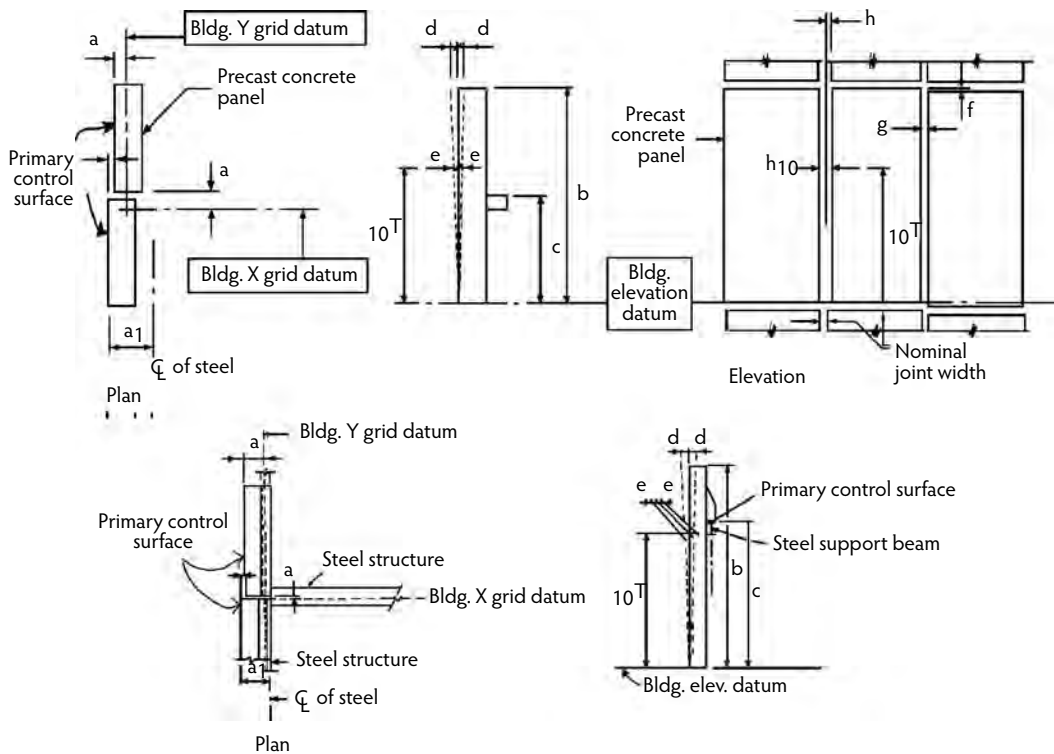


FIGURE 30.38 Erection tolerances for architectural precast concrete wall panels.

Alignment and all connections should be made or the spandrels should be safely secured prior to releasing the load and disconnecting the rigging. On long spandrels, care should be taken to ensure that the spandrel is tied back at the center either through a temporary connection until a slab tie connection is made or with a permanent connection. Spandrels should be installed on a floor-by-floor basis, where feasible, to keep equal loading on the structure. Spandrels should be aligned to predetermined offset lines established for each floor level. Vertical dimensions between spandrels should be checked to ensure that the opening size is within allowable tolerance. When spandrel panels or column covers and mullions are interspaced with strips of windows to create a layered effect of glazing, precast, and glazing, the general contractor should work closely with the designer to arrive at interface details that can be built within the sequence of construction and that embody all the elements required of the exterior wall design.

30.8.7 Tolerances

Architectural precast concrete product tolerances should comply with the industry tolerances published in PCI MNL-117 (PCI, 1996). The recommended erection tolerances are shown in Figure 30.38. During wall-panel installation, priority is generally given to aligning the exterior face of the units to meet aesthetic requirements. This may result in the interior unit faces not being in a true plane. A liberal joint width should be allowed if variations in overall building dimensions are to be absorbed in the joints. This may be coupled with a closer tolerance for variations from one joint to the next for appearance purposes. The individual joint-width tolerance should relate to the number of joints over a given building dimension. For example, to accommodate reasonable variations in actual site dimensions, a 3/4-in. (19-mm) joint may be specified with tolerances of $\pm 1/4$ in. (± 6 mm) but with only a 3/16-in. (5-mm) differential variation allowed between joint widths on any one floor or between adjacent floors. Alternatively, a jog in the alignment of an edge may be specified. The performance characteristics of the joint sealant should also be taken into account when selecting a joint size.

Variations from true length or width dimensions of the overall structure are normally accommodated in the joints or, where this is not feasible or desirable, at the corner units, in expansion joints, or in joints adjacent to other wall materials. In a situation where a joint has to match an architectural feature (such as a false joint), a large deviation from the theoretical joint width may not be acceptable, and tolerance for building lengths will have to be accommodated at the corner units. Erection tolerances are of necessity largely determined by the actual alignment and dimensional accuracy of the building foundation, and frame. The general contractor is responsible for the plumbness, level, and alignment of the cast-in-place concrete foundation and structural frame (except for precast frames) including the location of all bearing surfaces and anchorage points for the precast concrete units. If the precast concrete units are to be installed reasonably “plumb, level, square, and true,” the actual location of all surfaces affecting their alignment, including levels of floor slabs and beams, the vertical alignment of floor slab edges, and the plumbness of columns or walls, must be known before erection begins.

The architect or engineer should clearly define in the specifications the maximum tolerances permissible in the foundation and building frame alignment and then should see that the general contractor frequently checks to verify that these tolerances are being held. In addition, the architect or engineer should ensure that the details in the contract documents allow for the specified tolerances. Lack of attention to these matters often necessitates changes and adjustments in the field, not only delaying the work but also usually resulting in unnecessary extra costs and sometimes impairing the appearance of the units and the completed structure.

With reasonable tolerances for the building frame established, it is equally important for the designer to provide adequate clearances (purposely provided space between adjacent members)—for example, between the theoretical face of the structure and the back face of a precast concrete panel—when detailing the panel and its relationship to the building structure. If clearances are realistically assessed, they will enable the erector to complete the final assembly without field altering the physical dimensions of the precast units.

A good rule of thumb is that at least 3/4-in. (19-mm) clearance should be required between precast members, except for flange-to-flange connections and connection of wall panels to precast members, where 1/2-in. (13-mm) clearance should be required with a 1-in. (25-mm) clearance preferred; 1 in. (25 mm) is the minimum clearance between precast members and cast-in-place concrete, and 2 in. (50 mm) is preferred. For steel structures, 1 in. (25 mm) is the minimum clearance between the back of the member and the surface of the fireproofing, and 1-1/2 in. (38 mm) is preferred. If no fireproofing is required on the steel, then a 1-in. (25-mm) minimum clearance should be maintained. At least a 1-1/2 to 2 in. (38 to 50 mm) of clearance should be allowed in tall structures regardless of the structural framing materials. The minimum clearance between column covers and columns should be 1-1/2 in. (38 mm), with 3 in. (75 mm) being preferred because of the possibility of columns being out of plumb or a column dimension interfering with completion of the connection. If clearances are realistically assessed, they will solve many tolerance problems. Where large tolerances have been allowed for the supporting structure, or where no tolerances for the structure are given, the clearance must be increased.

All connections should be provided with the maximum adjustability in all directions that is structurally or architecturally feasible. Where a 1-in. (25-mm) clearance is required but a 2-in. (50-mm) clearance creates no structural or architectural problem, the 2-in. (50-mm) clearance should be selected. Closer tolerances are required for bolted connections than for grouted connections. To accommodate any misalignment of the building frame, connections should provide for vertical, horizontal, and lateral adjustments of at least 1 in. (25 mm).

Location of hardware items cast into or fastened to the structure by the general contractor, steel fabricator, or other trades should be ± 1 in. (± 25 mm) in all directions (vertical and horizontal), plus a slope deviation of no more than $\pm 1/4$ in. (± 6 mm) in 12 in. (0.3 m) for the level of critical bearing surfaces. All bearing surfaces are not always level. These tolerances give an acceptable deviation. Connection details should consider the possibility of bearing surfaces being misaligned or warped from the desired plane. Adjustments can be provided with the use of drypack concrete, nonshrink grout, shims, or elastomeric pads if the misalignment from horizontal plane exceeds 1/4 in. (6 mm).

30.8.8 Protection of Work

All precast concrete should be furnished to the job site in a clean and acceptable condition and kept in such condition. The erector is normally responsible for any chipping, spalling, cracking, or other damage to the units after they are delivered to the job site and until they are erected and connected. The erector should take necessary precautions to protect the erected precast concrete and the work and materials of other trades from damage during erection. After the final erection of any portion of precast work to acceptable alignment and appearance, including completion of all connections and joints, the general contractor should assume responsibility for protection of the work. Any cleaning or repair of precast concrete work subsequent to installation or acceptance should be done by the erector or precaster, but under the responsibility of the general contractor. Specifications should state this responsibility clearly. It is impractical for the precaster or erector to police the work against damage by others after it is put in place. A carefully established and implemented program of protection and later cleaning should be in place for each job that is under the responsibility of the general contractor, who alone can control all the potential sources of damage.

At the end of each working day, measures may have to be taken to protect the installation from damage; for example, adequate temporary protection must be provided where precast units in partially completed buildings could be damaged by weather, such as water freezing in holes, pipe sleeves, and inserts. The GC/CM should provide and maintain temporary protection to prevent damage or staining of exposed precast concrete during construction operations after it has been installed. Rainwater or water from hoses used during the construction of the building can cause discoloration of the precast concrete units by first washing across other building materials (such as steel, concrete, or wood) and then across the precast units. Particular care should be taken to avoid allowing jobsite water to wash the units. Dirt, mortar, and debris from concrete placing should not be allowed to remain on the precast concrete and should be washed off immediately with clean water. The erector should protect adjacent materials, such as glass and aluminum, from damage from field welding or torch cutting operations; therefore, sequencing the work of other trades should be taken into consideration by the GC/CM to prevent such damage.

30.8.9 Sealants

Sealant life and performance are greatly influenced by joint design. For optimum performance and maximum life, the recommendations of the joint-sealant manufacturer should be followed. Joints between precast units must be wide enough to accommodate anticipated wall movements, and particular care must be given to joint tolerance in order for the joint sealant system to perform within its design capabilities. If units cannot be adjusted to allow for proper joint size, saw cutting may be necessary. When joints are too narrow, bond or tensile failure of the joint sealant will occur and adjacent units may come in contact with and be subjected to unanticipated loading, distortion, cracking, and local crushing (spalling). A good general rule is to erect precast units in such a manner as to provide 1/2-in. joints between units up to 15 ft long and a minimum of 3/4-in. joints for longer units. (Joint width should equal two to four times anticipated movement, depending on the properties of the specified sealant.) Corner joints should be 1 in. wide to accommodate the extra movement and bowing often experienced at corners. Sealants should not be installed in joints smaller than 3/8 in. wide by 3/8 in. deep. The required sealant depth is dependent on the sealant width at the time of application. The optimum sealant width-to-depth relationships are best determined by the sealant manufacturer. For a comprehensive discussion of joint sealants used between wall panels, refer to ASTM C 962 (ASTM, 1996). Sealants used for specific purposes are often installed by different subcontractors; for example, the window subcontractor normally installs sealants around windows, whereas a second subcontractor typically installs sealants around panels. The designer must select and coordinate all of the sealants used on a project for chemical compatibility and adhesion to each other. In general, contact between different sealant types should be minimized. The recommendations of the sealant manufacturer should always be followed regarding mixing, surface preparation, priming, application life, and application procedure. Good workmanship by qualified sealant applicators is the most important factor for satisfactory performance.

30.9 Finish Cleanup

30.9.1 Tie-Hole Repairs

Tie holes should be plugged to prevent corrosion of the tie and possible staining of the surface, except where stainless steel form ties are used (ACI Committee 303, 2004). The holes left in the surface of the concrete as the result of the form tie may be either small or large, depending on the type of tie used. In a rough-textured surface, small holes can be plugged flush with the surface and concealed. With smooth-surface concrete, the tie holes will be more apparent, and it is better to only partially fill the holes, leaving the holes as a part of the planned appearance. Care must be exercised to avoid smearing the fill material on the surface of the concrete. Materials used for plugging tie holes include Portland cement mortar, epoxy mortar, plastic plugs, precast mortar plugs, and lead plugs. The method should be carefully selected from among those that have shown no staining or discoloration tendencies in actual use. Mortar materials of a dry-tamp consistency and densely tamped into the hole will be less likely to smear on the surface than those of wet consistency. When Portland cement mortar is used, the tie hole should first be prewet with clean water, and then a neat cement slurry bond coat should be applied to the hole surfaces before they are filled with mortar. If epoxy mortar is used, it should be applied in accordance with the manufacturer's instructions, and a caulking gun should be used to inject it into the tie hole to prevent smearing it on the surface. Cleaning or removal of any fill material is difficult and will usually leave a stain on the surface. Plastic inserts provided by cone tie manufacturers can be wedged into the tie hole, leaving a standard predetermined recess. Lead plugs can be wedged into the hole by hammering. Sometimes the removable cone becomes embedded in the concrete due to form movement or leakage around the cone. It can be removed to produce a neat appearance by drilling out the cone with a diamond bit tool that conforms to the hole size. It may be economical to remove all cones in this manner to ensure neat, uniform holes. When tie holes have to be concealed rather than visible as part of the planned appearance, the repair procedure is similar to that required for blemish repair.

30.9.2 Repairs

A certain amount of repair of architectural concrete surfaces is to be expected (Ford, 1982). Blemishes that are beyond the limits established by the quality of the preconstruction mock-up must be repaired. Major repairs of cracks or honeycomb surfaces should not be attempted until an engineering evaluation is made to determine if a sound repair can be made or if concrete removal is required. The repair work should proceed as soon as possible after form removal using the materials and methods already accepted on the approved mock-up. The repair and the surrounding concrete will then age together, and the chance of color or texture variation will be minimized.

Prior to beginning any repair, the surface blemishes must be evaluated to determine if repairs should be attempted at all. Do not make surface blemishes worse. Too often, indiscriminate repair of architectural concrete surfaces results in accenting blemishes rather than improving them. Much of the skill in repair of surface defects lies in knowing what not to attempt. Repair work should be kept to a minimum. Small repairs can be treated by hand tooling or chemical treatment using bleaches, acids, or toners. Hand tooling refers to the use of needle scalers, chisels, bushhammers, or grinders. These tools are useful for eliminating or minimizing hard spots and discolored areas such as the dark lines associated with form-leakage points. Tools can also be effective in blending offsets and cold joints in combination with grout repairs. The importance of establishing a repair method before the need arises cannot be overstressed. Once proven acceptable on the mock-up, immediate repairs can be made without delay and with confidence in the final outcome.

Repair work for architectural concrete requires expert craftsmanship and careful selection and mixing of materials if the end result is to be structurally sound, durable, and aesthetically pleasing. Where adjacent acid-etching, sandblasting, tooled, or bushhammering treatments must be matched, experimentation should be performed on unimportant areas. Ingenuity may sometimes be required to establish methods and techniques that are as satisfactory as those in standard use. Excessive deviations in color and texture

of repairs from the surrounding surfaces may result in the architectural concrete or precast concrete not being approved until the variation is minimized. Light honeycomb areas, bug holes, pour lines, or cold joints when sufficient rock is in place can receive a grout patch mix without a cutting and drypack requirement. All that is necessary is to pre-wet the area to be repaired, along with the adjacent concrete, keeping it wet for at least an hour. Then, using a dense sponge float, scrub the predetermined grout mix into the voids between the coarse aggregate. It may be necessary to scrub in a second grout patch mix application to obtain a true flush surface. When the finish has exposed aggregate, just prior to initial set wash the concrete surface with a soft sponge or bristle brush, exposing the aggregate texture desired. Begin curing procedures immediately to ensure that the repair does not dry out too quickly and develop shrinkage cracks. Cure the repair a minimum of 3 to 7 days before attempting final texturing.

Where the surface blemish cannot be repaired by mechanical, chemical, or grout treatment, the area should be cut out using a pneumatic or hand-held chipping hammer. Edges of the cut area should be square and perpendicular or undercut to the face of the sound adjacent concrete to avoid any feather-edge repairs. In an exposed-aggregate area, cut irregularly to conceal the repair. In finishes involving a liner, cut along the texture lines. The procedure for repairs is as follows:

- After all adjacent finish texture and chipping is complete, remove loose particles and brush or blow all dust from the repair surface.
- Proportion the patch mix by weight according to the same proportions used in the concrete mix but substitute 5 to 50% of the gray or buff cement with white cement. The actual amount is based on tests to determine what is required to match the finish surface. A pigment or toner is sometimes used for a closer color match or when only white cement was used in the original mix design.
- Apply a 50% diluted coat of bonding material to the root of the repair area, being careful to avoid brushing or dripping it on any concrete surface to be exposed. This prevents loss of moisture from the patch mix while also improving bond.
- Use a wood or plastic trowel to fill the repair area with patch mix in layers 1/2 in. (12 mm) thick. Vibrate or tamp the patch mix manually to approximately the density of the existing concrete. Strike the area level; if, after initial set, the finish has exposed aggregate, brush the surface to match the surrounding area.
- Begin curing procedures immediately.
- Clean the area adjacent to the repair to remove laitance and to restore the original color and texture.
- After 3 to 7 days, add the final texture and thoroughly clean the repair area.
- After 28 days, the repair can be evaluated for acceptance when the finished surface is dry. Any repair should match adjacent surfaces in color and texture when viewed at a distance of 20 ft (6 m).

It is preferable that repairs not be made when direct sunlight is on the repair area. Temporary sunshades should be provided, especially during hot weather. Heat lamps or a small heated enclosure may be necessary to maintain a minimum 50°F (10°C) for curing repairs in cold weather. Repair and patching of precast concrete is an art requiring expert craftsmanship if the end result is to be structurally sound, durable, and pleasing in appearance. Responsibility for repair work is normally resolved between the precaster and the erector. Repairs should be done immediately following occurrence of damage; however, deciding when to perform the repairs should be left to the precaster, who should be responsible for satisfactory final appearance. Because the techniques and materials for repairing precast concrete are affected by a variety of factors including mix ingredients, final finish, size and location of damaged area, temperature conditions, age of member, surface texture, etc., precise methods for repair cannot be detailed here. See PCI MNL-117-96 (PCI, 1996) for guidance on repair techniques and materials.

Repairs should be done only when conditions exist that ensure that the repaired area will conform to the balance of the work with respect to appearance, structural adequacy, and durability. Slight color variations can be expected between the repaired area and the original surface due to the different age and curing conditions of the repair. Time will tend to blend the repair into the rest of the member so it will become less noticeable. After all repairs have been completed, the repairs should be coated with a silane or dilute (2 or 3% solids) solution of an acrylic sealer to minimize moisture migration into the

repair concrete. The acrylic sealer should not stain the concrete or leave a shiny surface. Even with proper consolidation, the repaired area is more porous than the original hardened concrete and will require this dilute sealer application.

30.9.3 Cracks

Small cracks, under 0.010 in. (0.25 mm), may not require repair unless failure to do so will cause corrosion of reinforcement. If repair is required to restore structural integrity for cracks that range in width from 0.003 to 0.015 in., they should be repaired with epoxy injection. Proper preparation of the crack area is very important. Form-release agents, efflorescence, grease, oil, dirt, or fine particles of concrete prevent epoxy penetration and bonding. Preferably, contamination should be removed by vacuuming or clean water flushing or a specially effective solvent, determined by prior experience or testing. The solvent is then blown out using compressed air or adequate time is provided for air drying. Cracks may be pressure injected through entry ports with a low-viscosity, high-modulus, 100% solid, two-component epoxy that will bond to a moist surface. It is usually impossible to completely remove moisture in a crack. Care should be taken to select an epoxy color (amber, white, or gray) that most closely matches the color of the concrete. Toners can be added to the epoxy mixture to more closely match color surfaces for cracks in the exposed face of the architectural concrete. When mixing the low-viscosity epoxy resin, the epoxy hardener, and color toner, do not shake or mix too vigorously, as this can infuse air into the epoxy, which would result in the formation of undesirable voids in the hardened epoxy. Cracks wider than 0.25 in. (6 mm) should be repaired with a gel-type resin system incorporating a mineral filler or a long pot-life material. Some cracks in precast products extending downward from nearly horizontal surfaces may be filled by gravity flow. The minimum width of a crack that can be filled by gravity is a function of the viscosity of the material. If a spalled piece of concrete is available and surfaces still mate, the easiest repair is to simply glue the piece back in place using non-sag epoxy or bonding agents. Broken surfaces on both the original surface and spalled piece should be painted with the epoxy adhesive. Enough epoxy should be applied to the surface that some squeezes out of the joint when mated pieces are bound together. An epoxy with a thick enough consistency should be selected so it does not sag or run on a vertical surface. Self-leveling formulations should not be used. In some cases, it may be better to secure the repair by inserting pins into epoxy-filled holes drilled in the loose piece and the original surface.

30.9.4 Cleaning

Dirt, mortar, plastic, grout, fireproofing, or debris from concrete placement should not be permitted to remain on the concrete and should be brushed or washed off immediately with clean water. Final cleaning should be performed after caulking is completed and no earlier than 3 days after any repairs have been completed. If at all possible, concrete cleaning should be done when the temperature and humidity allow rapid drying. Slow drying increases the possibility of recurring efflorescence and discoloration. Before cleaning, a small (at least 1 yd², or 0.8 m²) inconspicuous area should be cleaned and checked to be certain there is no adverse effect on the concrete surface finish or adjacent materials. The effectiveness of the method should not be judged until the surface has dried for at least a week. Materials such as glass, metal, wood, stone, or concrete adjacent to the area to be cleaned should be adequately protected, as they can be damaged by contact with some stain removers or by physical cleaning methods. A strip-off plastic that is sprayed on can be used to protect glass and aluminum frames. The following is a suggested order for testing appropriate procedures for the removal of dirt, stains, and efflorescence (beginning with the least damaging):

- Dry scrubbing with a stiff fiber (nylon) brush is particularly effective if the surface is brushed shortly after the appearance of efflorescence.
- Abrasive blasting with industrial baking soda will remove efflorescence without otherwise affecting the concrete surface. Water must not be used to remove any residue on the surface, as salts will

be dissolved and carried into the concrete, causing additional efflorescence. Residues should be blown, vacuumed, or brushed from the surface.

- Wet scrubbing may also be effective in removing efflorescence. This procedure involves wetting the surface with water, vigorously scrubbing the finish with a stiff fiber brush, and thoroughly rinsing the surface with clean water. Low-pressure water spraying (water misting), high-pressure water jet sprayers, and steam cleaning are alternative methods of wet scrubbing.
- Chemical cleaning compounds such as detergents, muriatic or phosphoric acid, or other chemical cleaners should be in accordance with the manufacturer's recommendations. If possible, a technical representative of the product manufacturer should be present for the initial test application to ensure it is properly used. Areas to be chemically cleaned should be thoroughly saturated with clean water prior to application of the cleaning material to prevent the chemicals from being absorbed deeply into the surface of the concrete. Surfaces should also be thoroughly rinsed with clean water after application so no traces of acid remain in the surface layers of the concrete. Cleaning solutions should not be allowed to dry on the concrete finish. Residual salts can flake or spall the surface or leave difficult stains. Misapplication of hydrochloric acid can lead to corrosion of embedded metals with shallow cover. Care should be taken to use dilute solutions of acid to prevent surface etching that may reveal the aggregate and slightly change the surface color and texture. The entire unit should be treated to avoid a mottled effect. Any of several diluted solutions of acids are effective ways to remove efflorescence:

One part hydrochloric (muriatic) acid in 9 to 19 parts water

One part phosphoric acid in 9 parts water

One part phosphoric acid plus 1 part acetic acid in 19 parts water

One part acetic acid (vinegar) in 5 parts water

Hydrochloric (muriatic) acid may leave a yellow stain on white concrete; therefore, phosphoric or acetic acid should be used to clean white concrete. Workers using cleaning compounds or acid solutions should be thoroughly trained in their use. The use of proper protective wear should be strictly enforced. Rubber gloves, glasses, and other protective clothing must be worn by workmen using acid solutions or strong detergents. Materials used in chemical cleaning can be highly corrosive and are frequently toxic. All precautions on labels should be observed because these cleaning agents can affect eyes, skin, and breathing. Materials that can produce noxious or flammable fumes should not be used in confined spaces unless adequate ventilation can be provided.

- Dry or wet abrasive blasting, using sand, ferrous aluminum silicate, or other abrasives, may be considered if this method was originally used in exposing the surface of the unit. An experienced subcontractor should be engaged for sandblasting.
- Stone-veneer-faced precast concrete units should be cleaned with stiff fiber or stainless-steel or bronze wire brushes, a mild soap powder or detergent, and clean water using high pressure, if necessary. No acid or other strong chemicals that might damage or stain the veneer should be used. Information should be obtained from stone suppliers on methods for cleaning oil, rust, and dirt stains on the stone.
- Mortar stains may be removed from brick panels by thoroughly wetting the panel and scrubbing with a stiff fiber brush and a masonry-cleaning solution. A prepared cleaning compound is recommended; however, on red brick, a weak solution of muriatic acid and water (not to exceed a 10% muriatic acid solution) may be used. Acid should be flushed off the panel with large amounts of clean water within 5 to 10 minutes of application. Buff, gray, or brown brick should be cleaned in accordance with the brick manufacturer's recommendations, using proprietary cleaners rather than acid to prevent green or yellow vanadium stains and brown manganese stains. Following the application of the cleaning solution, the panel should be rinsed thoroughly with clean water. High-pressure-water cleaning techniques, with a 1000 to 2000 psi (6.9 to 13.8 MPa) washer, may also be used to remove mortar stains. Unglazed tile or terra cotta surfaces should be cleaned with a 5% solution of sulfamic acid for gray or white joints, and a more dilute (2%) solution should be

used for colored joints. The surface should be thoroughly rinsed with clean water both before and after cleaning. Glazed tile manufacturers generally do not recommend the use of acid for cleaning purposes.

For information on removing specific stains from concrete, refer to *Removing Stains and Cleaning Concrete Surfaces* (PCI, 1988).

30.10 Acceptability of Appearance

At the time the visual mock-ups or initial precast production units are approved, the acceptable range in color, texture, and uniformity should be determined. If the procedures determined by the approved mock-up were continued throughout the project, final acceptance should not be a problem. Due to the inevitable nonuniformity of construction practices, some repairs will normally be required. Their final acceptability will depend on the blending capability and skill of the contractor's or precast manufacturer's restoration personnel. The final product is exposed to view, and faulty work anywhere in the construction process can be easily seen. Acceptance lies with the value judgment of the owner, architect, and consultant. For that reason, periodic review during construction and partial acceptance creates good will and confidence for all concerned. Uniformity of texture, intensity of color, and contrast range will determine whether an architectural concrete surface is acceptable. Acceptability will vary with the characteristics of the architecture and the average viewing distance. Finish texture, color, contrast, aggregate size, and shape all affect appearance. To establish a basic criteria for both architectural cast-in-place and precast concrete, a definitive rule for acceptability is as follows:

The finish face surface shall have no obvious imperfections other than minimal color and texture variations from the approved samples or evidence of repairs when viewed in good typical daylight illuminated with the unaided naked eye at a 20-ft (6-m) viewing distance. Appearance of the surface shall not be evaluated when sunlight is illuminating the surface from an extreme angle, as this tends to accentuate minor surface irregularities.

After final acceptance, the inspector's records should be completed and filed. If later additions are made or adjoining buildings constructed, these records will be necessary for construction.

30.11 Innovations

Today, more and more building contracts are negotiated or have a limited bid list. This will accelerate in the future with significant increases in value engineering. This incentive increases the team members' willingness to offer, approve, and implement ideas quickly. Project control systems will continue to be streamlined and productivity improved as more common systematic problems of information flow are corrected. Involvement of subcontractors and suppliers as equal partners will improve the flow of ideas and total job performance. We forecast that the use of architectural facades in combination with interior structural concrete will compete with other building systems. New materials or expanded uses include superplasticizers and 15,000-psi concrete. Improved concrete pumps are able to move concrete mixes with a high aggregate content. Tower cranes will be able to handle heavier loads at a greater reach. Fiberglass and steel forms designed to handle external form vibrators and full liquid head concrete have already begun to be used. Specialty vibrators are currently used to meet specific job performance requirements. Improved sealers, sealants, and specialty coatings are already available. Architectural precast concrete is combining textures, colors, and embedded materials such as clay products or natural stone. The industry is constantly striving to develop improved methods of production, better handling and erection, and new finishing techniques and ways of combining materials. The ability to customize the color, form, and texture of concrete allows limitless design possibilities.

30.12 Defining Terms

Abrasive blasting—A process in which sand or other materials are used to texture the surface of hardened concrete. The degree of blasting may vary from a light cleaning operation to one that exposes aggregate to a depth of 3/4 in. (19 mm) or more.

Admixture—A material other than water, aggregates, or cement used as an ingredient in concrete, mortar, or grout to impart special characteristics.

Aggregate—Granular material, such as sand, gravel, and crushed stone, used with a cementing medium to form a hydraulic-cement concrete or mortar.

Architectural concrete—Any concrete with one or more surfaces to be permanently exposed to view and where the appearance of these surfaces is important from an architectural standpoint; a precast product with a specified standard of uniform appearance, surface details, color, and texture.

Backup mix—The concrete mix cast into the mold after the face mix has been placed and consolidated.

Bond breaker—A substance placed on a material to prevent it from bonding to the concrete or between a face material such as natural stone and the concrete backup.

Bonding agent—A substance used to increase the bond between an existing piece of concrete and a subsequent application of concrete such as a patch.

Bug holes—Small holes on formed concrete surfaces formed by air or water bubbles, sometimes referred to as *blow holes*.

Bushhammering—A process in which pneumatic or hand hammers are used to remove mortar and fracture aggregate at the surface of hardened concrete to produce an attractive varicolored and textured surface.

Coarse aggregate—Aggregate predominately retained on the U.S. Standard No. 4 (4.75-mm) sieve or that portion of an aggregate retained on the No. 4 (4.75-mm) sieve.

Crazing—A network of visible, fine hairline cracks in random directions breaking the exposed face of a panel into areas from 1/4 to 3 in. (6 to 75 mm) across.

Exposed-aggregate concrete—Concrete manufactured so the aggregate on the face is left protruding.

Exposed concrete—Any concrete with one or more surfaces to be permanently and regularly revealed to public view but where the appearance of the concrete surface is not important from an architectural standpoint.

Face mix—The concrete at the exposed face of a concrete unit used for specific appearance purposes.

Fine aggregate—Aggregate passing the 3/8-in. (9.5-mm) sieve and almost entirely passing the No. 4 (4.75-mm) sieve and predominately retained on the No. 200 (75- μ m) sieve, or that portion of an aggregate passing the No. 4 (4.75-mm) sieve and predominately retained on the No. 200 (75- μ m) sieve.

Form-release agent—A substance applied to the mold for the purpose of preventing bond between the mold and the concrete cast in it.

Gap-graded concrete—A mix with one or a range of normal aggregate sizes eliminated or with a heavier concentration of certain aggregate sizes over and above standard gradation limits; used to obtain a specific exposed-aggregate finish.

Matrix—The portion of the concrete mix containing only the cement and fine aggregates (sand).

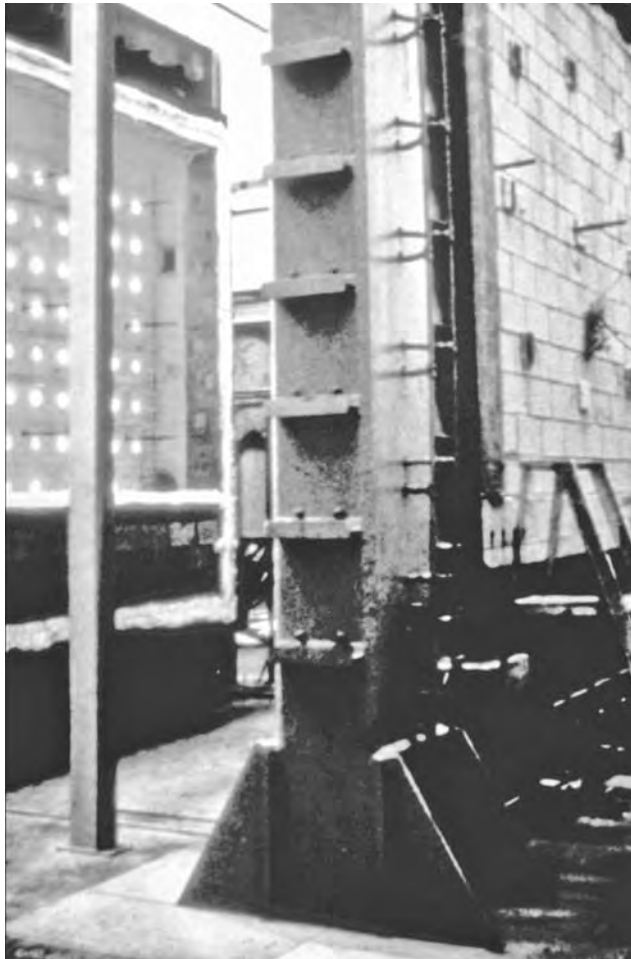
Quality—The appearance, strength, and durability that are appropriate for a specific product, its particular application, and its expected performance requirements; the totality of features and characteristics of a product that bear on its ability to satisfy stated or implied needs.

Quality assurance (QA)—All those planned or systematic actions necessary to ensure that the final product or service will satisfy given requirements for quality and perform intended function.

Quality control (QC)—Those actions related to the physical characteristics of the materials, processes, and services that provide a means to measure and control the characteristics to predetermined quantitative criteria.

References

- ACI Committee 303. 2004. *Guide to Cast-in-Place Architectural Concrete Practice*, ACI 303R. American Concrete Institute, Farmington Hills, MI.
- ACI Committee 309. 2005. *Guide for Consolidation of Concrete*, ACI 309R. American Concrete Institute, Farmington Hills, MI.
- ACI Committee 533. 1993. *Guide for Precast Concrete Wall Panels*, ACI 533R. American Concrete Institute, Farmington Hills, MI.
- ASTM. 1996. *Standard Guide for Use of Elastomeric Joint Sealants*, ASTM C 962 (discontinued 1992). American Society for Testing and Materials, Philadelphia, PA.
- ASTM. 2005. *Standard Specification for Zinc-Coated (Galvanized) Steel Bars for Concrete Reinforcement*, ASTM A 767/A 767M. American Society for Testing and Materials, Philadelphia, PA.
- ASTM. 2006. *Standard Specification for Steel Strand, Uncoated Seven-Wire for Prestressed Concrete*, ASTM A 416/A 416M. American Society for Testing and Materials, Philadelphia, PA.
- Bainbridge, L.R. and Abberger, W.A. 1994. The trend is towards cost-effective design and construction. *PCI J.*, May/June, 96–97.
- Bell, L.W. 1996. Writing specifications for architectural concrete. *Concrete Int.*, 18(6), 63–66.
- Clark, R.S. and Zils J. 1984. Long spans in post-tensioned architectural concrete. *Concrete Int.*, 6(9), 7–12.
- Dobrowolski, J.A. 1989. Formwork removal and architectural concrete. *Concrete Int.*, 11(1), 35–39.
- Ford, J.H. 1982. Reusage of plastic form liners. *ACI J.*, 51–57.
- Freedman, S. 1968. White concrete, part I. *Modern Concrete*, 30–34.
- Freedman, S. 1969. White concrete, part II. *Modern Concrete*, 30–35.
- Friedman, E.L. and Rice, B.P. 1965. Finishes for cast-in-place concrete. *Architect. Eng. News*, 26–35.
- Heun, R.C. 1985. Imagine the possibilities. *Concrete Int.*, 7(11), 16–20.
- Hurd, M.K. 1993. Patterned from liners for architectural concrete. *Concrete Const.*, 331–336.
- Kenney, A.R. 1984. Problems and surface blemishes in architectural cast-in-place concrete. *Concrete Int.*, 50–55.
- Kenney, A.R. 1988. Post-tensioning alternative reduces construction time. *Concrete Int.*, 10(2), 48–52.
- PCA. 1988. *Removing Stains and Cleaning Concrete Surfaces*, IS214. Portland Cement Association, Skokie, IL.
- PCI. 1985. *Recommended Practice for Erection of Precast Concrete*, MNL-127-85. Precast/Prestressed Concrete Institute, Chicago, IL.
- PCI. 1989. *Architectural Precast Concrete*, 2nd ed., MNL-122-89. Precast/Prestressed Concrete Institute, Chicago, IL.
- PCI. 1990. *PCI Drafting Handbook*, MNL-119-90. Precast/Prestressed Concrete Institute, Chicago, IL.
- PCI. 1995. *Erectors Safety Manual for Precast and Prestressed Concrete*, MNL-132-95. Precast/Prestressed Concrete Institute, Chicago, IL.
- PCI. 1996. *Manual for Quality Control for Plants and Production of Architectural Precast Concrete Products*, MNL 117-96. Precast/Prestressed Concrete Institute, Chicago, IL.
- Shilstone, J.M. 1972a. Ways with architectural concrete. *ACI J.*, 17–26.
- Shilstone, J.M. 1972b. The many faces of architectural concrete: a study of finishes. *Concrete Const.*, 526–530.
- Shilstone, J.M. 1972c. The fine art and hard work of placing and compacting architectural concrete. *Concrete Const.*, 536–538.
- Shilstone, J.M. 1973a. Achieving high-quality architectural concrete by understanding details of the construction process. *Architect. Rec.*, 161–164.
- Shilstone, J.M. 1973b. How to obtain predictable architectural concrete. *Concrete Const.*, 363–413.



Fire test of concrete panel. (Photograph courtesy of National Concrete Masonry Association, Herndon, VA.)

31

Fire Resistance and Protection of Structures

Mark B. Hogan, P.E.*
Jason J. Thompson**

31.1	Introduction	31-1
	Balanced Design for Fire Safety and Property Protection • Design, Construction, and Material Requirements	
31.2	Fire-Resistance Ratings	31-5
	Heat Transmission in Slabs • Fire-Resistance Ratings of Single-Wythe Masonry Walls • Single-Layer Concrete Walls, Floors, and Roofs • Multiple-Layer Walls, Floors, and Roofs	
31.3	Fire Protection of Joints	31-9
	Masonry Elements • Precast Concrete Wall Panels and Slabs	
31.4	Finish Treatments.....	31-11
31.5	Fire Resistance of Columns.....	31-11
	Reinforced Masonry Columns • Reinforced-Concrete Columns	
31.6	Steel Columns Protected by Masonry	31-13
31.7	Fire Resistance of Lintels	31-14
	References	31-14

31.1 Introduction

Life safety and property protection are critical functions of all structures, particularly as they relate to fire safety. Further, the functionality of these structures is influenced by their design, construction, and maintenance. Key elements of the design, which have an impact on both the life safety and property protection functions, include the principles of balanced design that incorporate compartmentation to limit the spread of fire, early detection to alert occupants when a fire occurs, and automatic suppression to control a fire until it can be extinguished. Concrete and masonry materials are inherently fire resistant, noncombustible, and durable and maintain structural integrity under fire conditions. These features are used in the design of compartments to contain fire and in the design of structural elements to maintain

* Vice President of Engineering, National Concrete Masonry Association, Herndon, Virginia; active member of committees in several professional societies, including ACI/TMS Committee 216 on Fire Resistance and Fire Protection of Structures.

** Director of Engineering, National Concrete Masonry Association, Herndon, Virginia; active member of several professional societies and codes and standards development committees, including ACI 530/ASCE 5/TMS 402, *Building Code Requirements for Masonry Structures*, and ACI 530.1/ASCE 6/TMS 602, *Specification for Masonry Structures*.

structural integrity during a fire. The durability and permanence of concrete and masonry can be relied on for life safety and property protection throughout the life of the structure, with minimal investment in maintenance or repair. This chapter presents criteria for the design of concrete and masonry elements to ensure both property protection and life safety functions during fire conditions.

31.1.1 Balanced Design for Fire Safety and Property Protection

Fire safety requires an awareness and understanding of the hazards so both the potential for fire occurrence and the threat to life and property during a fire are minimized. Death and injury from fire are caused by asphyxiation from toxic smoke and fumes, burns from direct exposure to the fire, heart attacks caused by stress and exertion, and impact due to structural collapse, explosions, and falls. Life safety and property protection are influenced by the design of the building, its fire-protection features, and the quality of construction materials, building contents, and maintenance. Balanced design relies on three complementary systems to reduce the risk of death and the threat to property due to fire:

- A detection system to warn occupants of the fire
- A containment system to limit the extent of the fire
- An automatic suppression system to control the fire until it can be extinguished

Each of these essential systems contributes to lowering the risk of death and injury from fire as well as to protecting property. The three balanced-design components complement each other by providing fire protection features that are not provided by the other components. Some features of each balanced-design component are intended to be redundant so if one system is breached or fails to perform, then the other components continue to provide safety. Although not a tangible element in fire protection, a strong education and training program should be an integral part of any good fire-protection plan in addition to the physical components of a balanced-design system.

31.1.1.1 Automatic Detection

Accurate early warning is the first line of defense against slow smoldering fires with low heat release rates that do not activate sprinkler heads. Detectors that respond to light smoke are important from a life-safety standpoint because they alert occupants near the origin of the fire to evacuate. Other detection or alarm systems may be used to notify the fire department, thus decreasing response time, expediting rescue operations, and limiting the resulting fire spread and property damage. Detectors wired to a central alarm and installed in corridors and common areas notify all building occupants, allow timely and orderly evacuation, and decrease the potential for injury and death. The most common detector installed is the smoke-sensing fire detector. Ideally, detectors should be wired into a continuous power supply and be provided with a battery backup in the event of a power failure. Their location is determined by judgment and in accordance with the requirements of the general building code. Each dwelling unit in residential construction should be equipped with detectors in all sleeping rooms, in areas adjacent to all sleeping rooms, and on each level of the building, including the basement. The amount of air movement, obstructions within the space, number of stories, and other factors will guide the proper selection of detector locations. The performance of detectors is vulnerable to many unpredictable malfunctions, among which are those due to acts of sabotage, lack of maintenance due to human error and neglect, and faulty power supply. Young children, the incapacitated, or the elderly may not be able to respond to alarms. All smoke detectors require regularly scheduled maintenance and, in some cases, periodic replacement.

31.1.1.2 Automatic Suppression

The function of automatic sprinkler systems is to control a fire at the point of origin. Although not designed to extinguish a fire, residential sprinklers have been shown to be reliable and effective in controlling a fire in the room of origin until it can be extinguished. Automatic sprinklers reduce the likelihood of *flashover*, the near instantaneous ignition of volatile gasses within a confined space which can be a particularly hazardous event. Suppression of a fire allows access to the building to permit rescue

and fire suppression efforts to proceed. Through the years, sprinklers have been credited with preventing hundreds, possibly thousands, of injuries and deaths.

The National Fire Protection Association (NFPA) maintains minimum standards for the design and installation of sprinkler systems. Sprinkler systems for general application are covered by NFPA 13, *Standard for the Installation of Sprinkler Systems* (NFPA, 2007a), whereas NFPA 13R, *Standard for the Installation of Sprinkler Systems in Residential Occupancies up to and Including Four Stories in Height* (NFPA, 2007b), specifically address residential applications. Ideally, when the interior construction or building contents contain a large amount of combustibles, sprinkler systems should meet the requirements of NFPA 13, regardless of height, to ensure protection in attics, closets, and other concealed spaces built with combustible materials and to provide additional suppression in all areas due to the higher fuel loadings.

The NFPA standards cover the design, installation, testing, and maintenance of sprinkler systems. Obviously, to be effective, automatic sprinklers require an adequate water supply and piping system to deliver sufficient water to the sprinkler head. Sprinkler head requirements ensure proper water coverage based on the room dimensions, area to be covered, and fuel loading. The standards also list exceptions for specific spaces that are not required to be sprinklered. When installation is complete, the standards require inspection and acceptance of the piping valves, pumps, and tanks of the system. Testing also includes verification of adequate water flow to the sprinkler heads. Finally, after the sprinkler system is in use, it must be maintained; however, specific maintenance requirements and frequency of maintenance are not specified by the standards.

Performance of automatic sprinklers can be vulnerable to system failures due to inadequate maintenance and inspection or inadequate water supply. Sprinklers are not intended to control electrical and mechanical equipment fires or fires of external origin, such as fires from adjacent buildings and brush fires. Fires in concealed spaces, including some attics, closets, flues, shafts, ducts, and other spaces where sprinkler heads are not required to be installed, can compromise life safety due to the spread of toxic fumes and smoke. An inadequate water supply can result from low pressure in the municipal water system, broken pipes due to earthquakes or excavation equipment, explosions, freezing temperatures, closed valves due to human error, arson or vandalism, corrosion of valves, pump failure due to electrical outage, and lack of system maintenance.

31.1.1.3 Compartmentation

Compartmentation limits the extent of fire by dividing a building into fire compartments enclosed by fire walls or fire separation wall assemblies and by fire-rated floors and ceilings. Compartments also minimize the spread of toxic fumes and smoke to adjacent areas of a building. Conflagrations beyond the fire compartment are prevented by limiting the total fuel load contributing to the fire. Compartmentation provides safe areas of refuge for handicapped, young, elderly, incapacitated, and other occupants who may not be capable of unassisted evacuation. Compartmentation also provides safe areas of refuge for extended periods when evacuation is precluded due to smoke-filled exit ways or blocked exits. Compartmented construction provides protection for fire and rescue operations. Highly hazardous areas, such as mechanical, electrical, or storage rooms, can be isolated from other occupied areas of a building by fire walls. Fire separation walls and floor and ceiling assemblies between dwelling units in multifamily housing afford protection from fires caused by the carelessness of other occupants. Refuge areas within a building provide protection for occupants by allowing fire fighters to concentrate on extinguishing the fire rather than on rescue efforts.

Compartmentation serves to contain a fire until it can be brought under control by firefighters. Each concrete or masonry element forming the boundary of a compartment should have a fire-resistance rating as defined by the general building code and should be capable of preserving the structural integrity of the building throughout the duration of the fire. In multifamily housing, each dwelling unit should form a separate compartment. In addition, interior exit ways, as well as storage, electrical, and mechanical rooms, should be separate compartments. Exterior walls should be fire rated to form a barrier to the penetration of exterior fires and to contain interior fires.

TABLE 31.1 Fire-Safety Functions of Balanced Design

Function	Automatic Detection	Compartmentation	Automatic Suppression
Controls fire/limits fire growth	○	●	●
Provides smoke, toxic-fume barrier	○	●	○
Provides fire barrier	○	●	○
Limits generation of smoke/toxic fumes	○	■	●
Allows safe egress	■	●	■
Provides refuge	○	●	○
Assists fire-fighting efforts	○	■	■
Reduces response time	●	○	○
Difficult to vandalize or arson	○	●	○
Performance requires little maintenance	○	●	○
<i>Property protection functions and costs of balanced design component</i>			
Limits the extent of contents damage	■	■	■
Limits the extent of structure damage	■	●	■
Low installation costs	●	■	○
Low maintenance costs	■	●	○
Limits repair time due to fire damage	■	●	●

Note: ●, Considered to be effective; ■, considered to be partially effective; ○, considered to be ineffective or only slightly effective.

The value of compartmentation may be reduced when joints between floors and walls, typically exterior curtain walls, or between walls and ceilings are not properly fire-stopped. As such, openings through compartment boundaries should be protected to prevent the migration of smoke and fire. Damage caused by equipment, abuse, or the installation of utilities that are not properly sealed can allow the passage of smoke and gas. Unsealed openings around penetrations can also allow the spread of smoke. Self-closing mechanisms on doors in compartment walls may fail if not maintained or if blocked open.

31.1.1.4 Property Protection

The initial cost of providing fire safety can be significant; however, balanced design offers advantages that offset costs. The higher level of protection for both the structure and its contents limits the potential loss due to fire. Immediate and long-term savings will be reflected in lower insurance rates for both the building and its furnishings. Balanced design limits both fire and smoke damage to the contents of the building to the compartment of fire origin. Noncombustible compartment boundaries limit damage to the structure itself and reduce repair time following a fire. Repair is generally nonstructural but may include the replacement of doors and windows; electrical outlets, switches, and wiring; heating ducts and registers; and floor, wall, and ceiling coverings.

31.1.1.5 State of the Art in Designing for Fire Safety

Fire-protection engineering is as much an art as it is a science. The number of unknowns and potential fire propagation scenarios are numerous. Fire protection is therefore generally based more on risk assessment than on precise calculation. Currently, building code prescriptive criteria, along with an understanding of the science of fire protection, guide the designer in addressing fire safety (ACI Committee 216, 1997, 2001; ICC, 2006; NIST, 1993). Some of the more significant fire safety issues requiring consideration are listed in Table 31.1, along with a relative ranking of the effectiveness of each component in contributing to balanced design. As shown by the table, more than one component may be considered effective in mitigating a particular hazard. Because none of the components is fail safe, overlapping functions are required to provide a necessary level of safety. In addition, some functions listed in the table are addressed by only one component of balanced design. There is general agreement among the fire safety and regulatory communities that computer modeling will serve to continue improving fire safety in the built environment. Widespread access to complex analytical models and computing equipment is giving fire safety engineers new and ever-evolving tools to bolster fire safety requirements in buildings.

31.1.2 Design, Construction, and Material Requirements

The fire-resistance ratings of concrete and masonry assemblies assume that the design and construction of these elements comply with the provisions of the *Building Code Requirements for Masonry Structures* (ACI Committee 530, 2005) and the *Building Code Requirements for Structural Concrete* (ACI Committee 318, 2005) for masonry and concrete elements, respectively. These codes stipulate material requirements by reference to ASTM standards and establish quality assurance provisions for the construction of these elements.

31.2 Fire-Resistance Ratings

Two major factors have to be considered in ratings: fire endurance and fire resistance. The definitions of these two terms, per ACI 216, are as follows:

- *Fire endurance*—A measure of the elapsed time during which a material or assembly continues to exhibit fire resistance under specified conditions of test and performance; as applied to elements of buildings, it shall be measured by the methods and to the criteria defined in ASTM E 119.
- *Fire resistance*—The property of a material or assembly to withstand fire or to give protection from it; as applied to elements of buildings, it is characterized by the ability to confine a fire or to continue to perform a given structural function, or both.

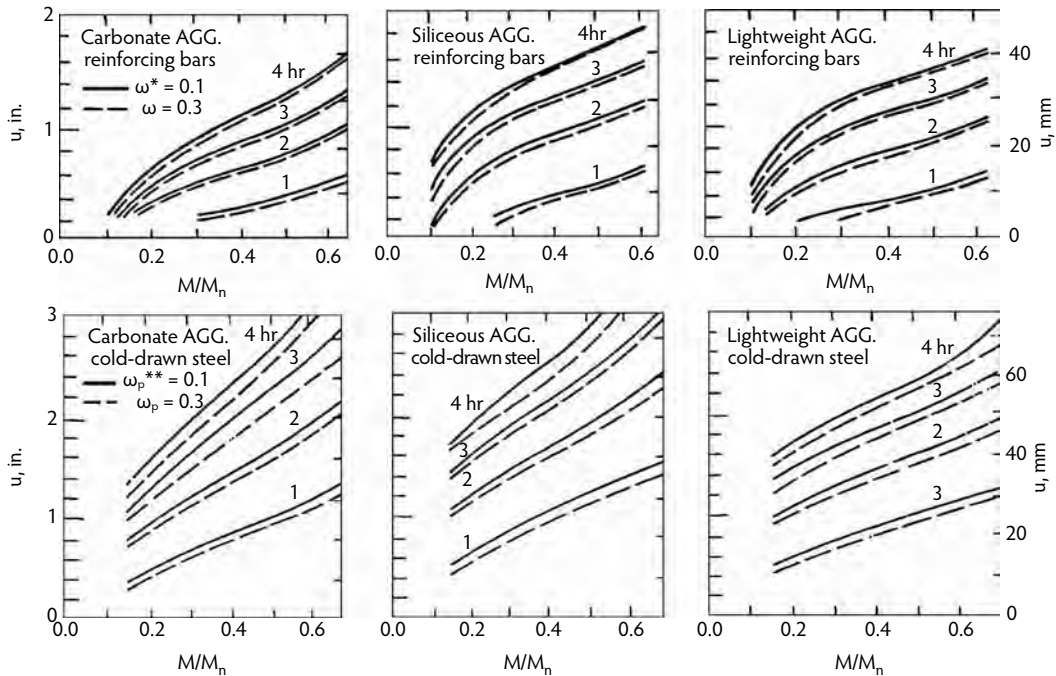
Building codes establish the minimum level of required fire resistance for specific elements within the structure based on the type of occupancy of the building, the function of the element, the importance of the structure, its contents, and other fire-protection considerations. When the required fire-resistance rating of a concrete or masonry element has been established, this chapter can assist the designer in meeting that requirement.

The fire-resistance rating criteria presented here are based on the provisions of the ACI 216.1/TMS 0216, *Standard Method for Determining Fire Resistance of Concrete and Masonry Construction Assemblies* (ACI Committee 216, 1997). This consensus standard, which is referenced by model building codes, is based on current practice in determining the fire ratings of concrete and masonry elements. The standard covers two methods of determining the fire-resistance rating of an element. The most common method for determining the fire-resistance rating is based on a calculation procedure that has established a correlation between the physical properties of the concrete or masonry member and the measured fire endurance as determined through testing in accordance with ASTM E 119, *Standard Test Methods for Fire Tests of Building Construction and Materials* (ASTM, 2005b). The second method allows for direct measurement of the fire resistance of an element or assembly through testing in accordance with ASTM E 119. A third option, which is not explicitly covered by existing codes and standards, is to establish the fire-resistance rating through a listing service, such as Underwriters Laboratory.

Fire testing of wall assemblies in accordance with ASTM E 119 defines four performance criteria that must be met:

- Resistance to the transmission of heat through the wall assembly
- Resistance to the passage of hot gases or flame through the assembly sufficient to ignite cotton waste on the non-exposed side
- Loss of load-carrying capacity of load-bearing walls
- Resistance to the impact, erosion, and cooling effects of a hose stream on the assembly after exposure to fire

The fire-resistance ratings of concrete and masonry elements are typically governed by the transmission of heat through the assembly, which is measured by temperature rise on the non-fire-exposed side of the wall. This consistent mode of failure allows for a standardized calculation procedure to be derived as described below. Conversely, the fire-resistance rating of other construction assemblies, particularly those consisting of combustible materials, is often governed by one of the other performance criteria.



* Reinforcement index for concrete beams reinforced with mild reinforcement: $\omega = A_s f_s / b d f_c$

** Reinforcement index for concrete beams reinforced with prestressing steel: $\omega_p = A_{sp} f_{sp} / b d f_c$

FIGURE 31.1 Fire resistance of concrete slabs. (From ACI Committee 216, *Guide for Determining the Fire Endurance of Concrete Elements*, ACI 216R, American Concrete Institute, Farmington Hills, MI, 2001.)

31.2.1 Heat Transmission in Slabs

The structural fire endurance of simply supported concrete slabs as affected by the constituent materials can be interpolated from Figure 31.1 by an effective concrete cover parameter (u) as a function of the moment ratio M/M_n , where M is the design moment and M_n is the nominal moment strength. In the usual case of continuous slabs and beams, a shift in the moment distribution develops, thereby increasing the stresses in the negative reinforcement resulting from the increase in the bending moments at the supports. During a fire, however, the negative reinforcement remains cooler than the positive reinforcement as it is often farther from the source of the fire. This in turn allows for an increase in the negative moment that can be accommodated (ACI Committee 216, 1997). Although the moment redistribution that results can be sufficient to result in yielding of the negative reinforcement, the resulting decrease in the positive moment in effect permits the beam or slab span to endure higher temperatures. The negative moment reinforcing bars must be long enough to accommodate the complete redistributed moments and the change of the location of the inflection points. At least 20% of the maximum negative moment reinforcement must be extended throughout the span (CEB/FIP, 1990). The fire-resistance rating of concrete slabs can also be increased through the use of undercoating, as described in ACI 216.1/TMS 0216 (ACI Committee 216, 1997).

31.2.2 Fire-Resistance Ratings of Single-Wythe Masonry Walls

The fire-resistance rating of masonry walls, including single-wythe walls, multi-wythe walls, and walls with finish treatments, is based on the following criteria, which includes the effect of grouting and the effect of filling the cores of hollow units with recognized loose fill materials.

TABLE 31.2 Fire-Resistance Rating Period of Concrete Masonry Assemblies

Aggregate Type in the Concrete Masonry Unit ^b	Minimum Required Equivalent Thickness (in.) for Fire-Resistance Rating ^a						
	4 hr	3 hr	2 hr	1.5 hr	1 hr	0.75 hr	0.5 hr
Calcareous or siliceous gravel	6.2	5.3	4.2	3.6	2.8	2.4	2.0
Limestone, cinders, or slag	5.9	5.0	4.0	3.4	2.7	2.3	1.9
Expanded clay, shale, or slate	5.1	4.4	3.6	3.3	2.6	2.2	1.8
Expanded slag or pumice	4.7	4.0	3.2	2.7	2.1	1.9	1.5

^a Fire-resistance ratings between the hourly fire-resistance rating periods listed are determined by linear interpolation based on the equivalent thickness value of the concrete masonry wall assembly.

^b Minimum required equivalent thickness corresponding to the hourly fire-resistance rating for units made with a combination of aggregates is determined by linear interpolation based on the percent by volume of each aggregate used in the manufacturing of the unit.

TABLE 31.3 Fire-Resistance Rating of Clay Masonry Assemblies

Material Type	Minimum Required Equivalent Thickness (in.) for Fire-Resistance Rating ^{a,b}			
	1 hr	2 hr	3 hr	4 hr
Solid brick of clay or shale ^c	2.7	3.8	4.9	6.0
Hollow brick or tile of clay or shale, unfilled	2.3	3.4	4.3	5.0
Hollow brick or tile of clay or shale, grouted or filled with perlite, vermiculite, or expanded shale aggregate	3.0	4.4	5.5	6.6

^a Fire-resistance ratings between the hourly fire-resistance rating periods listed should be determined by linear interpolation.

^b Where combustible members are framed into the wall, the thickness of solid material between the end of each member and the opposite face of the wall or between members set in from opposite sides should not be less than 93% of the thickness shown.

^c For units in which the net cross-sectional area of cored brick in any plane parallel to the surface containing the cores should be at least 75% of the gross cross-sectional area measured in the same plane.

31.2.2.1 Single-Wythe Concrete Masonry Walls

The calculated fire-resistance rating of single-wythe concrete masonry assemblies is determined in accordance with Table 31.2. These calculated fire-resistance ratings are derived from the requirements of ACI 216.1/TMS 0216. The equivalent thickness (T_{ea}) of concrete masonry assemblies is based on the equivalent thickness of the masonry unit (T_e) plus the equivalent thickness of any recognized finish materials (T_{ef}) as follows:

$$T_{ea} = T_e + T_{ef} \quad (31.1)$$

The equivalent thickness (T_e) of a concrete masonry unit is the net volume of the unit divided by the face area of the unit (length times height). The equivalent thickness (T_e) of solid grouted masonry walls is the actual thickness of the unit. The equivalent thickness (T_e) of hollow masonry unit walls that are completely filled with loose fill is the actual thickness of the unit when the loose fill materials are sand, pea gravel, crushed stone, or slag that meet ASTM C 33 (ASTM, 2003) requirements; pumice, scoria, expanded shale, expanded clay, expanded slate, expanded slag, expanded fly ash, or cinders that comply with ASTM C 331 (ASTM, 2005a); or perlite or vermiculite meeting the requirements of ASTM C 549 and ASTM C 516, respectively (ASTM, 2002, 2006).

31.2.2.2 Single-Wythe Clay Masonry Walls

The calculated fire-resistance rating of single-wythe clay masonry assemblies is determined in accordance with Table 31.3. The equivalent thickness (T_e) of clay masonry assemblies is determined as follows:

$$T_e = V_n / LH \quad (31.2)$$

As with concrete masonry assemblies, when solid grouted or when completely filled with approved loose fill materials, the equivalent thickness (T_e) of a clay masonry assembly is the actual thickness of the unit.

TABLE 31.4 Fire-Resistance Rating of Single-Layer Concrete Walls, Floors, and Roofs

Aggregate Type	Minimum Equivalent Thickness (in.) for Fire-Resistance Rating				
	1 hr	1.5 hr	2 hr	3 hr	4 hr
Siliceous	3.5	4.3	5.0	6.2	7.0
Carbonate	3.2	4.0	4.6	5.7	6.6
Semi-lightweight	2.7	3.3	3.8	4.6	5.4
Lightweight	2.5	3.1	3.6	4.4	5.1

31.2.3 Single-Layer Concrete Walls, Floors, and Roofs

The fire-resistance rating of plain and reinforced concrete walls, floors, and roofs that are a single layer in thickness are determined in accordance with Table 31.4 and are based on the equivalent thickness of the element. The equivalent thickness of solid concrete elements with flat surfaces is the actual thickness of the element. The equivalent thickness of hollow-core panels with a constant cross-section throughout their length is determined by dividing the net cross-sectional area by the panel width. The equivalent thickness of elements in which all of the core spaces are filled with grout or loose fill material, such as perlite, vermiculite, sand or expanded clay, shale, slag, or slate, should be the same as that of a solid wall or slab of the same type of concrete. The equivalent thickness for flanged elements in which the flanges taper is determined at the location of the lesser distance of two times the minimum thickness, or 6 in. from the point of the minimum thickness of the flange. The equivalent thickness of elements with ribbed or undulating surfaces is determined as follows:

- Where the center-to-center spacing of ribs or undulations is not less than four times the minimum thickness, the equivalent thickness is the minimum thickness of the panel.
- Where the spacing of ribs or undulations is equal to or less than two times the minimum thickness, calculate the equivalent thickness by dividing the net cross-sectional area by the panel width. The maximum thickness used to calculate the net cross-sectional area should not exceed two times the minimum thickness.
- Where the spacing of ribs or undulations exceeds two times the minimum thickness, but is less than four times the minimum thickness, calculate the equivalent thickness as follows:

$$\text{Equivalent thickness} = t + \left[\left(4t / s \right) - 1 \right] (t_e - t) \quad (31.3)$$

where:

- s = spacing of ribs or undulations (in.).
- t = minimum thickness (in.).
- t_e = equivalent thickness calculated in accordance with Equation 31.2.

31.2.4 Multiple-Layer Walls, Floors, and Roofs

ACI 216.1/TMS 0216 (ACI Committee 216, 1997) offers several alternatives to calculating the fire-resistance rating of multi-wythe and multi-layer walls, floors, and roofs using graphical, analytical, and numerical solutions. Each alternative considers various possible combinations of normal weight, semi-lightweight, and lightweight concretes; sandwich panels and insulation systems; and the use of concrete and clay masonry assemblies as part of a veneer or multi-wythe system. In addition to the material properties, the resulting fire-resistance rating is influenced by the use of finish materials, exposure conditions, and reinforcement cover distances. The user is referred to ACI 216.1/TMS 0216 for additional information on determination of the fire-resistance properties of multiple-layer concrete and masonry systems.

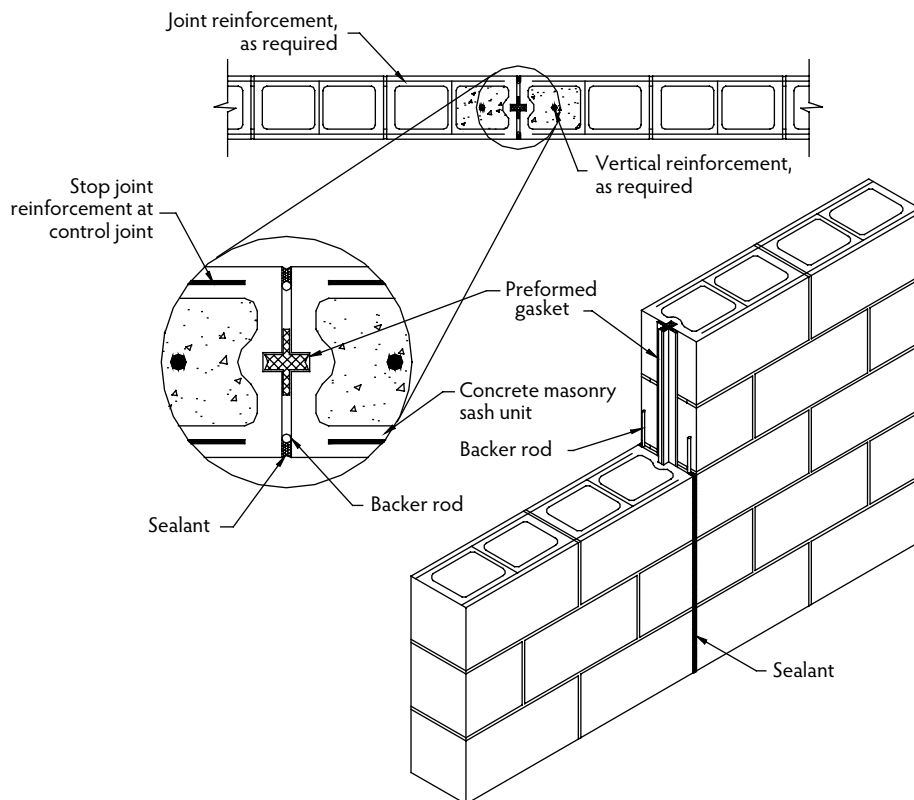


FIGURE 31.2 Two-hour control joint.

31.3 Fire Protection of Joints

31.3.1 Masonry Elements

Expansion or contraction joints in fire-rated concrete masonry wall assemblies and in clay brick wall assemblies are shown in Figure 31.2, Figure 31.3, and Figure 31.4. Figure 31.2 illustrates a standard control joint detail for a 2-hour fire-resistance rating, and Figure 32.3 and Figure 32.4 offer alternatives for 4-hour fire-resistance ratings.

31.3.2 Precast Concrete Wall Panels and Slabs

In wall panels where openings are not permitted or where it is required that openings be protected, joints must be insulated. Joints between panels that are not insulated are considered unprotected openings. Where the percentage of unprotected openings is limited in exterior walls, the area of uninsulated joints is added to the area of other unprotected openings to determine the total area of unprotected openings. Protected joints between precast concrete wall panels are filled with ceramic fiber blankets, the minimum thickness of which is calculated in accordance with ACI 216.1/TMS 0216 (ACI Committee 216, 1997). Other approved joint treatment systems that maintain the required fire-resistance rating are also used. Alternatively, joints between adjacent precast concrete slabs may be ignored when calculating the equivalent slab thickness, provided that a concrete topping not less than 1 in. thick is used. Where a concrete topping is not used, joints should be grouted to a depth of at least one third the slab thickness at the joint, but not less than 1 in., or the fire-resistance rating of the floor or roof must be maintained by other approved methods.

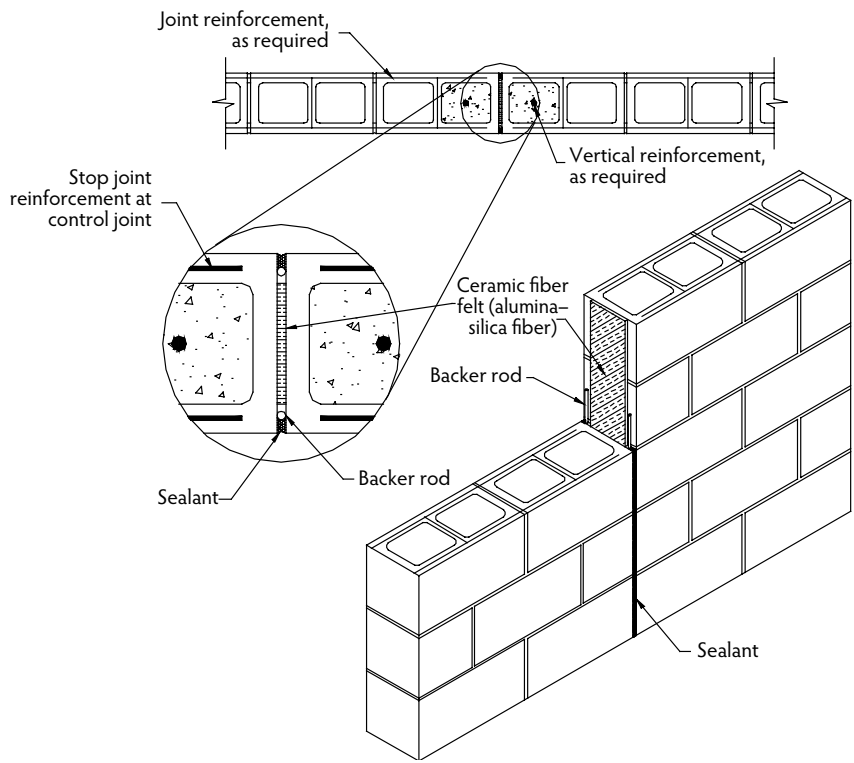


FIGURE 31.3 Four-hour control joint.

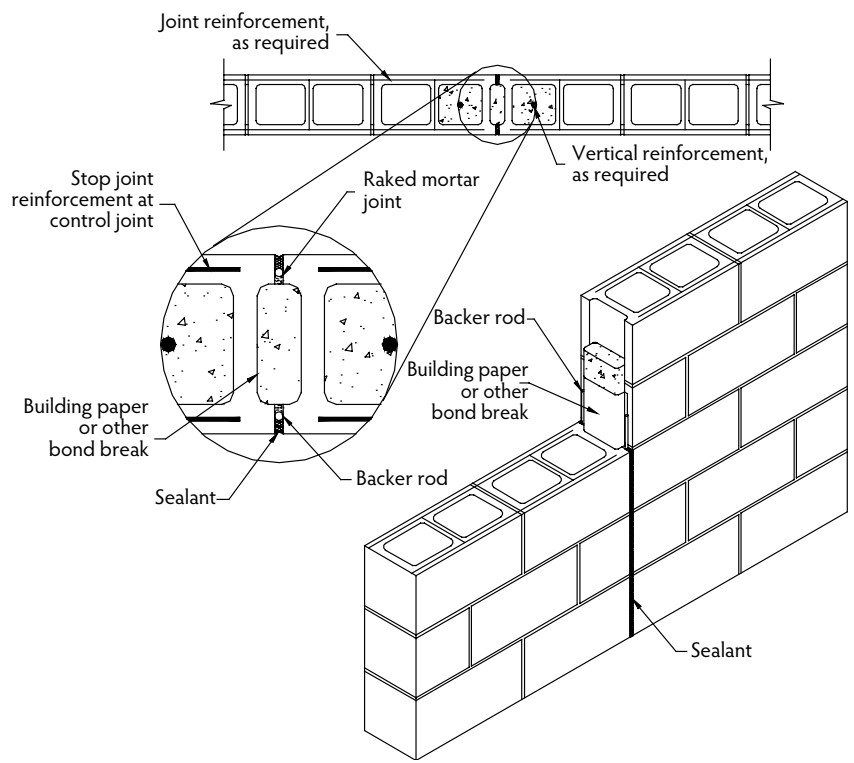


FIGURE 31.4 Four-hour control joint.

TABLE 31.5 Multiplying Factors for Finishes on the Non-Fire-Exposed Side of Concrete Slabs and Concrete and Masonry Walls

Type of Finish Applied to Slab or Wall	Type of Material Used in Slab or Wall		
	Siliceous or Carbonate Aggregate Concrete or Concrete Masonry Unit; Solid Clay Brick Masonry	Semi-Lightweight Concrete; Hollow Clay Brick; Clay Tile	Lightweight Concrete; Concrete Masonry Units of Expanded Shale, Expanded Clay, Expanded Slag, or Pumice Less Than 20% Sand
Portland cement–sand plaster ^a or terrazzo	1.00	0.75	0.75
Gypsum–sand plaster	1.25	1.00	1.00
Gypsum–vermiculite or perlite plaster	1.75	1.50	1.25
Gypsum wallboard	3.00	2.25	2.25

^a For Portland cement–sand plaster 5/8 in. or less in thickness and applied directly to concrete or masonry on the non-fire-exposed side of the wall, the multiplying factor is 1.0.

31.4 Finish Treatments

Finish treatments on concrete and masonry elements include gypsum drywall, terrazzo, or plaster. These treatments increase the fire-resistance rating of the element by delaying the temperature rise within or through the element when exposed to fire. The effect of this increase is based on whether the finish is applied to the side of the element being exposed to the fire or to the side that is not exposed to the fire. The fire-resistance rating of elements that may be exposed to fire from either side is determined based on the lower rating determined from assuming that the fire exposure is from one side or the other. The fire-resistance rating of the element including the effect of finish treatments is limited to twice the fire rating of the element excluding the effect of finish treatments. Further, the effect of finish treatments from the non-fire-exposed side of the wall is limited to one half the fire-resistance rating of the element excluding the effect of finish treatments. Finishes that are assumed to contribute to the total fire-resistance rating of an assembly must meet the minimum installation requirements as prescribed in ACI 216.1/TMS 0216.

Some finishes deteriorate more rapidly when exposed to fire than when installed on the non-exposed side of an assembly. For this reason, ACI 216.1/TMS 0216 requires two separate calculations assuming, first, that the fire exposure is on one side of the wall and then again assuming that the fire is on the other side of the wall. Table 31.5 applies to finishes on the non-fire-exposed side of the wall, while Table 31.6 applies to finishes on the fire-exposed side. The resulting fire rating of the wall assembly is the smaller of the two calculated ratings. Note that in some situations the fire is assumed to occur only on one side of the wall. For finishes on the non-fire-exposed side of the wall, the finish is converted to equivalent thickness of concrete or masonry by multiplying the thickness of the finish by the factor given in Table 31.5. This is then added to the base equivalent thickness per Equation 31.1. For finishes on the fire-exposed side of the wall, a time is assigned to the finish per Table 31.6, which is added to the fire-resistance rating determined for the base wall and non-fire-side finish. The additional times listed in Table 31.6 are essentially the length of time the various finishes will remain intact when directly exposed to fire.

31.5 Fire Resistance of Columns

31.5.1 Reinforced Masonry Columns

The fire-resistance rating of reinforced concrete and clay masonry columns is based on the least plan dimension of the column in accordance with the requirements of Table 31.7. The minimum cover for longitudinal reinforcement, measured from the outside surface of the reinforcement to the nearest outside surface of the masonry, is not permitted to be less than 2 in.

TABLE 31.6 Time Assigned to Finish Materials on Fire-Exposed Side of Concrete and Masonry Walls

Finish Description	Time (minutes)
<i>Gypsum wallboard</i>	
3/8-in.	10
1/2-in.	15
5/8-in.	20
Two 3/8-in. layers	25
One 3/8-in. layer and one 1/2-in. layer	35
Two 1/2-in. layers	40
<i>Type X gypsum wallboard</i>	
1/2-in.	25
5/8-in.	40
Direct applied Portland cement–sand plaster	— ^a
<i>Portland cement–sand plaster on metal lath</i>	
3/4-in.	20
7/8-in.	25
1-in.	30
<i>Gypsum–sand plaster on 3/8-in. gypsum lath</i>	
1/2-in.	35
5/8-in.	40
3/4-in.	50
<i>Gypsum–sand plaster on metal lath</i>	
3/4-in.	50
7/8-in.	60
1-in.	80

^a The fire-resistance rating of elements with Portland cement–sand plaster finish treatment is determined by adding the actual thickness of the plaster or 5/8 in., whichever is smaller, to the equivalent thickness of the element.

TABLE 31.7 Reinforced Masonry Columns

	Fire Resistance (hr)			
	1	2	3	4
Minimum column dimension (in.)	8	10	12	14

TABLE 31.8 Minimum Concrete Column Size

Aggregate Type	Minimum Column Dimension for Fire-Resistance Rating (in.)				
	1 hr	1.5 hr	2 hr	3 hr	4 hr
Carbonate	8	9	10	11	12
Siliceous	8	9	10	12	14
Semi-lightweight	8	8.5	9	10.5	12

31.5.2 Reinforced-Concrete Columns

The fire-resistance ratings of reinforced-concrete columns, both circular and rectangular, are determined in accordance with the requirements of Table 31.8. When a concrete column is exposed to fire on two parallel sides, additional requirements as prescribed in ACI 216.1/TMS 0216 (ACI Committee 216, 1997) must be met. The minimum thickness of concrete cover to the longitudinal reinforcement in concrete columns should not be less than 1 in. times the number of hours of required fire resistance, or 2 in., whichever is less.

31.6 Steel Columns Protected by Masonry

Because of its inherent fire-resistant properties, masonry is often used as a nonstructural fire-protection covering for structural steel members. The fire endurance of steel column protection is determined as the period of time for the average temperature of the steel to exceed 1000°F or for the temperature at any measured point to exceed 1200°F (ASTM, 2005b). These criteria depend on the thermal properties of the column cover and of the steel column. Accurate predictions of the fire endurance of protected steel columns are made possible by a numerical technique based on heat-flow analyses and research information on the thermal and rheological properties of masonry and steel at elevated temperatures (Lie and Harmathy, 1972). Using this technique, an empirical formula was developed to predict the fire endurance of masonry-protected steel columns in accordance with ACI 216.1/TMS 0216 (ACI Committee 216, 1997). The fire-resistance rating of structural steel columns protected by masonry is determined as follows:

$$R = 0.401(A_{st}/p_s)^{0.7} + \left[0.285(T_{ea}^{1.6}/k_{cm}^{0.2}) \right] \left[1.0 + 42.7 \left\{ (A_{st}/DT_{ea}) / (0.25p + T_{ea}) \right\}^{0.8} \right] \quad (31.4)$$

where:

R = fire-resistance rating of the protected column assembly (hr).

A_{st} = cross-sectional area of the structural steel column (in.²).

D = density of the masonry protection (lb/ft³).

p = inner perimeter of the masonry protection (in.).

p_s = heated perimeter of steel column (in.), per Equations 31.5, 31.6, or 31.7.

T_{ea} = equivalent thickness of the concrete masonry protection assembly (in.)

k = thermal conductivity of the masonry protection (BTU/hr·ft·°F).

For a W-section steel column, the heated perimeter (p_s) is determined as follows:

$$p_s = 2(b_f + d_{st}) + 2(b_f - t_w) \quad (31.5)$$

For a pipe-section steel column, the heated perimeter (p_s) is determined as follows:

$$p_s = \pi d_{st} \quad (31.6)$$

For a square-tube steel column, the heated perimeter (p_s) is determined as follows:

$$p_s = 4d_{st} \quad (31.7)$$

where:

b_f = width of flange (in.).

d_{st} = column depth (in.).

t_w = thickness of web of W-section (in.).

For use in Equation 31.4, the thermal conductivity of concrete masonry is:

$$k = 0.0417_e^{0.02D} \quad (31.8)$$

Likewise, the thermal conductivities of clay masonry are equal to:

$k = 1.25$ BTU/hr·ft·°F for a density of 120 lb/ft³.

$k = 2.25$ BTU/hr·ft·°F for a density of 130 lb/ft³.

Steel Column Fire Protection (NCMA, 2003) contains a comprehensive list of fire-resistance ratings for a wide variety of structural steel sections.

TABLE 31.9 Reinforced Masonry Lintels

Nominal Lintel Width (in.)	Minimum Longitudinal Reinforcement Cover for Fire-Resistance Rating (in.)			
	1 hr	2 hr	3 hr	4 hr
6	1.5	2	Not permitted	Not permitted
8	1.5	1.5	1.75	3
10 or more	1.5	1.5	1.5	1.75

31.7 Fire Resistance of Lintels

The fire-resistance rating of masonry lintels (beams spanning openings) is based on the nominal thickness of the lintel and the minimum provided cover for the longitudinal reinforcement as shown in Table 31.9. The cover is measured from the outside surface of the reinforcement to the nearest outside surface of masonry, which may consist of masonry units, grout, or mortar.

References

- ACI Committee 216. 1997. *Standard Method for Determining Fire Resistance of Concrete and Masonry Construction Assemblies*, ACI 216.1/TMS 0216. American Concrete Institute, Farmington Hills, MI.
- ACI Committee 216. 2001. *Guide for Determining the Fire Endurance of Concrete Elements*, ACI 216R. American Concrete Institute, Farmington Hills, MI.
- ACI Committee 318. 2005. *Building Code Requirements for Structural Concrete*, ACI 318. American Concrete Institute, Farmington Hills, MI.
- ACI Committee 530. 2005. *Building Code Requirements for Masonry Structures*, ACI 530/ASCE 5/TMS 402. The Masonry Society, Boulder, CO.
- ASTM. 2002. *Standard Specification for Vermiculite Loose Fill Thermal Insulation*, ASTM C 516. ASTM International, West Conshohocken, PA.
- ASTM. 2003. *Standard Specification for Concrete Aggregates*, ASTM C 33. American Society for Testing and Materials, West Conshohocken, PA.
- ASTM. 2005a. *Standard Specification for Lightweight Aggregates for Concrete Masonry Units*, ASTM C 331. American Society for Testing and Materials, West Conshohocken, PA.
- ASTM. 2005b. *Standard Test Methods for Fire Tests of Building Construction and Materials*, ASTM E 119. American Society for Testing and Materials, West Conshohocken, PA.
- ASTM. 2006. *Standard Specification for Perlite Loose Fill Insulation*, ASTM C 549. American Society for Testing and Materials, West Conshohocken, PA.
- CEB-FIP. 1990. *Model Code for Concrete Structures*. Comité Euro-International du Béton-Fédération Internationale de Précontrainte, Paris.
- ICC. 2006. *International Fire Code (IFC)*. International Code Council, Falls Church, VA.
- Lie, T.T. and Harmathy, T.Z. 1972. *A Numeral Procedure to Calculate the Temperature of Protected Steel Columns Exposed to Fire*. National Research Council of Canada, Division of Building Research, Ottawa, Ontario.
- NCMA. 2003. *Steel Column Fire Protection*, NCMA-TEK 7-6. National Concrete Masonry Association, Herndon, VA.
- NIST. 1993. *HAZARD I—Fire Hazard Assessment Method*, NIST Handbook 146. National Institute of Standards and Technology, Gaithersburg, MD.
- NFPA. 2007a. *Standard for the Installation of Sprinkler Systems*, NFPA 13. National Fire Protection Association, Quincy, MA.
- NFPA. 2007b. *Standard for the Installation of Sprinkler Systems in Residential Occupancies Up to and Including Four Stories in Height*, NFPA 13R. National Fire Protection Association, Quincy, MA.



(a)



(b)



(c)

(a) The CSU Northridge parking structure suffered no damage in the 1994 Northridge, California, earthquake, but others in the area suffered heavy damage. (Photograph courtesy of BFL Owen & Associates, Irvine, CA.) (b) Kaiser Venice Clinic after the earthquake. (Photograph courtesy of FBA, Inc., Hayward, CA.) (c) Sherman Oaks Fashion Square parking structure after earthquake. (Photograph courtesy of FBA, Inc., Hayward, CA.)

32

Seismic-Resisting Construction

Walid M. Naja, S.E.*

Christopher T. Bane, S.E.**

32.1	Fundamentals of Earthquake Ground Motion	32-2
	Introduction • Recorded Ground Motion • Characteristics of Earthquake Ground Motion • Factors Influencing Ground Motion • Evaluating Seismic Risk at a Site • Estimating Ground Motion	
32.2	International Building Code (IBC 2006).....	32-7
	IBC Design Criteria • Design Requirements for Seismic Design Category A • Design Requirements for Seismic Design Categories B, C, D, E, and F • Equivalent Lateral Force Procedure • Modal Response Spectrum Analysis • Seismic Load Combinations • Diaphragms, Chords, and Collectors • Building Separation • Anchorage of Concrete or Masonry Walls • Material-Specific Design and Detailing Requirements • Foundation Design	
32.3	Design and Construction of Concrete and Masonry Buildings.....	32-29
	Preface • Concrete Buildings • Design of Masonry Buildings • Shear-Wall Foundation Analysis and Design • Nomenclature	
32.4	Seismic Retrofit of Existing Buildings	32-42
	Introduction • Structure Weakness • Creation of Adequate Load Path • Establish Deformation Compatibility • Establish Adequate Lateral-Load-Resisting System	
32.5	Seismic Analysis and Design of Bridge Structures	32-48
	Seismic Analysis of Bridge Structures • Seismic Design of Bridge Structures •	
32.6	Retrofit of Earthquake-Damaged Bridges	32-56
	Introduction • Background • Seismic Analysis Approach • Design Approaches	
32.7	Defining Terms	32-62
	References	32-62

* Principal, FBA, Inc., Structural Engineers, Hayward, California; expert in the design and construction of concrete structures in seismically active regions, particularly low- to mid-rise buildings.

** Senior Project Engineer, FBA, Inc., Structural Engineers, Hayward, California; expert in the design of post-tensioned concrete structures and the design and retrofit of buildings in seismic regions.

32.1 Fundamentals of Earthquake Ground Motion

32.1.1 Introduction

When transmitted through a structure, ground acceleration, velocity, and displacements (referred to as *ground motion*) are in most cases amplified. The amplified motion can produce forces and displacements that may exceed those the structure can sustain. Many factors influence ground motion and its amplification. An understanding of how these factors influence the response of structures and equipment is essential for a safe and economical design. Earthquake ground motion is usually measured by a strong-motion accelerograph that records the acceleration of the ground at a particular location. Record accelerograms, after they are corrected for instrument errors and adjusted for baseline, are integrated to obtain velocity and displacement-time histories. The maximum values of the ground motion (peak ground acceleration, peak ground velocity, and peak ground displacement) are of interest for seismic analysis and design. These parameters, however, do not by themselves describe the intensity of shaking that structures or equipment experience. Other factors, such as the earthquake magnitude, distance from fault or epicenter, duration of strong shaking, soil condition of the site, and frequency content of the motion, also influence the response of a structure. Some of these effects, such as the amplitude of motion, duration of strong shaking, frequency content, and local soil conditions, are best represented through the response spectrum (1.1 to 1.4), which describes the maximum response of a damped, single-degree-of-freedom oscillator to various frequencies or periods. The response spectra from a number of records are often averaged and smoothed to obtain design spectra, which also represent the amplification of ground motion at various frequencies or periods of the structure. This section discusses earthquake ground motion. The influence of earthquake parameters such as earthquake magnitude, duration of strong motion, soil condition, and epicentral distance on ground motion is presented and discussed.

32.1.2 Recorded Ground Motion

Ground motion during an earthquake is measured by a strong-motion accelerograph that records the acceleration of the ground at a particular location. Three orthogonal components of the motion, two in the horizontal direction and one in the vertical, are recorded by the instrument. The instruments may be located in a free field or mounted in structures. Accelerograms are generally recorded on photographic paper or film. The records are digitized for engineering applications, and during the digitization process errors associated with instruments and digitization are removed. The digitization, correction, and processing of accelerograms have been carried out by the Earthquake Engineering Research Laboratory of the California Institute of Technology in the past and are now carried out by the U.S. Geological Survey.

32.1.3 Characteristics of Earthquake Ground Motion

Characteristics of earthquake ground motion that are important in earthquake engineering applications include:

- Peak ground motion (peak ground acceleration, peak ground velocity, and peak ground displacement)
- Duration of strong motion
- Frequency content

Each of these parameters influences the response of a structure. Peak ground motion primarily influences the vibration amplitudes. Duration of strong motion has a pronounced effect on the severity of shaking. A ground motion with a moderate peak acceleration and long duration may cause more damage than a ground motion with a larger acceleration and a shorter duration. Frequency content and spectral shapes relate to frequencies or periods of vibration of a structure. In a structure, ground motion is most amplified when the frequency content of the motion and the vibration frequencies of the structure are close to each other. Each of these characteristics is briefly discussed below.

32.1.3.1 Peak Ground Acceleration

Peak ground acceleration has been widely used to scale earthquake design spectra and acceleration-time histories. As will be discussed later, recent studies recommend that in addition to peak ground acceleration, peak ground velocity, and displacement should be used for scaling purposes.

32.1.3.2 Duration of Strong Motion

Several investigators have proposed procedures for computing the strong-motion duration of an accelerogram. Page et al. (1972) and Bolt (1969) proposed the **bracketed duration**, which is the time interval between the first and the last acceleration peaks greater than a specified value (usually 0.05 g). Trifunac and Brady (1985) defined the duration of the strong motion as the time interval in which a significant contribution to the integral of the square of the acceleration ($\int a^2 dt$, referred to as the *accelerogram intensity*) takes place. They selected the time interval between the 5% and the 95% contributions as the duration of strong motion. The noted procedures usually result in different values for the duration of strong motion. This is to be expected, as the procedures are based on different criteria. Because there is no standard definition of strong-motion duration, the selection of a procedure for computing it for a study depends on the purpose of the study. The bracketed duration proposed in Page et al. (1972) and Bolt (1969) may be more appropriate when computing elastic and inelastic response.

32.1.3.3 Frequency Content

The frequency content of ground motion can be examined by transforming the motion from time domain to frequency domain through a Fourier transform. The Fourier amplitude spectrum and power spectral density, which are based on this transformation, may be used to characterize the frequency content. For further discussion regarding frequency content, the reader is encouraged to consult *The Seismic Design Handbook* (Naeim, 1989). When the power spectral density of ground motion at a site is established, random-vibration methods may be used to formulate probabilistic procedures for computing the response of structures.

32.1.4 Factors Influencing Ground Motion

Earthquake ground motion and its duration at a particular location are influenced by a number of factors, the most important being: (1) earthquake magnitude, (2) distance of the source of energy release (epicentral distance or distance from causative fault), (3) local soil conditions, (4) variation in geology and propagation of velocity along the travel path, and (5) earthquake-source conditions and mechanism (fault type, stress conditions, stress drop). Past earthquake records have been used to study some of these influences. Although the effect of some of these parameters, such as local soil conditions and distance from source of energy release, are fairly well understood and documented, the influence of the source mechanism and the variation of geology along the travel path are more complex and difficult to quantify. Several of these influences are interrelated; consequently, it is difficult to discuss them individually without incorporating the others. Some of these influences are discussed below.

32.1.4.1 Distance

The variation of ground motion with distance to the source of energy release has been studied by many investigators. In most studies, peak ground motion (usually peak ground acceleration) is plotted as a function of distance. A smooth curve based on a regression analysis is fitted to the data, and the curve or its equation is used to predict the expected ground motion as a function of distance. These relationships, referred to as *motion attenuation*, are sometimes plotted independently of the earthquake magnitude. This was the case in earlier studies because of the lack of sufficient numbers of earthquake records; however, with the availability of a large number of records, particularly during the 1971 San Fernando earthquake and subsequent seismic events, the database for attenuation studies was increased and a number of investigators reexamined their earlier studies, modified their proposed relationships for estimating peak accelerations, and included earthquake magnitude as a parameter. Donovan (1973)

TABLE 32.1 Typical Attenuation Relationships

Data Source	Relationships	Ref.
1 San Fernando earthquake, February 9, 1971	$a = 190/R^{1.83}$	Donovan (1973)
2 California earthquake	$a = \frac{y_0}{1 + (R'/h)^2}$ where $\log y_0 = -(\bar{b} + 3) + 0.81m - 0.027m^2$, where \bar{b} is a site factor	Blume et al. (1992)
3 California and Japanese earthquakes	$a = \frac{0.0051}{\sqrt{T_G}} 10^{0.61m - P \log R + Q}$ where $Q = 0.167 - 1.83/R$; T_G = fundamental period of site	Yamabe and Kanai (1988)
4 Cloud (1963)	$a = \frac{0.0069e^{1.64m}}{1.1e^{1.1m} + R^2}$	Milne and Davenport (1969)
5 Cloud (1963)	$a = 1.24e^{0.67m}/(R + 25)^2$	Esteva (1969)
6 USC and USGS	$\log a = \frac{6.5 - 2 \log(R' + 80)}{981}$	Cloud and Perez (1967)
7 303 instrumental values	$a = 1.325e^{0.67m}/(R + 25)^{1.6}$	Donovan (1973)
8 Western U.S. records	$a = 0.093e^{0.8m}/(R + 400)$	Donovan (1973)
9 U.S., Japan, etc.	$a = 1.35e^{0.58m}/(R + 25)^{1.52}$	Donovan (1973)
10 Western U.S. records, USSR, Iran	$\ln a = 3.99 + 1.28m - 1.75 \ln [R + 0.147e^{0.732m}]$	Campbell (1997)
11 Western U.S. records, worldwide	$\log a = -1.02 + 0.249m - \log (R^2 + 7.3^2)^{1/2} - 0.00255(R^2 + 7.3^2)^{1/2}$	Idriss (1993)
12 Western U.S. records	$\ln a = \ln \alpha(m) - \beta(m) \ln(R + 20)$ where m = surface-wave magnitude, $m \geq 6$; local magnitude, $m < 6$; R = smallest distance to source, $m \geq 6$; hypocentral distance, $m < 6$; $\alpha(m)$ and $\beta(m)$ are magnitude-dependent coefficients	Seed and Idriss (1982)
13 Italian records	$\log a = -1.562 + 0.306m - \log(R^2 + 5.8^2)^{1/2} + 0.169S$ where $S = 1.0$ for soft sites and 0 for rock	Sabetta and Pugliese (1987, 1996)

Note: Acceleration a is in g; distance to causative fault R is in kilometers; epicentral distance R' is in miles; local depth h is in miles.

compiled a database of more than 500 recorded accelerations from seismic events in the United States, Japan, and elsewhere, and later increased it to more than 650. A plot of peak ground acceleration vs. fault distance for different earthquake magnitudes from his database shows that, for a good portion of the data, the peak acceleration decreases as the distance from the source of energy release increases. It has been reported by Housner (1965), Donovan (1973), and Seed and Idriss (1982) that at distances away from the fault or the source of energy release (far field), the earthquake magnitude influences the attenuation, whereas at distances close to the fault (near field) the attenuation is affected by smaller earthquake magnitudes and not by the larger ones. The majority of attenuation studies and the relationships presented in Table 32.1 are mainly from data in the western United States. It is believed by several seismologists that ground acceleration attenuates more slowly in the eastern United States and eastern Canada. The variation of peak ground velocity with distance from the source of energy release (velocity attenuation) has also been studied by several investigators. Velocity attenuation curves have similar shapes and follow similar trends to the acceleration attenuation; however, velocity attenuates somewhat faster than acceleration, and, unlike acceleration attenuation, velocity attenuation depends on soil condition.

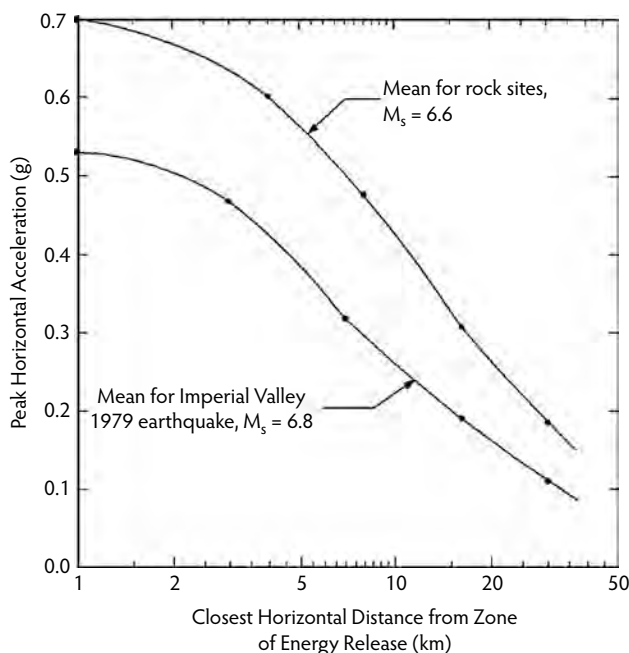


FIGURE 32.1 Comparison of attenuation curves for rock sites and the Imperial Valley earthquake of 1979. (Adapted from Seed, H.B. and Idris, I.M., *Ground Motions and Soil Liquefaction during Earthquakes*, Earthquake Engineering Research Institute, Berkeley, CA, 1982.)

Distance also influences the duration of strong motion. Correlation of the duration of strong motion with epicentral distance has been studied by Page et al. (1972), Trifunac and Brady (1975), Krinitzsky and Chang, and others. Page et al. (1972), using the bracketed duration, concluded that for a given magnitude the duration decreases with an increase in the distance from the source.

32.1.4.2 Site Geology

Soil conditions influence ground motion and its attenuation. Several investigators, such as Boore et al. (1978, 1980) and Seed and Idriss (1982), have presented attenuation curves for soil and rock. According to Boore et al., the peak horizontal acceleration is not appreciably affected by soil condition (it is nearly the same for rock and for soil). Seed and Idriss compared the acceleration attenuation for rock from earthquakes with Richter magnitudes of approximately 6.6 with that for alluvium from the 1979 Imperial Valley earthquake (Richter magnitude, 6.8). Their comparison, shown in Figure 32.1, indicates that, at a given distance from the source of energy release, peak accelerations on rock are somewhat greater than those on alluvium. The effect of soil condition on peak acceleration is illustrated in Figure 32.2. According to this figure, the difference in acceleration in rock and in stiff soil is practically negligible. There seems to be general agreement among various investigators that soil condition has a pronounced influence on velocities and displacements. Larger peak horizontal velocities are more likely to be expected in soil than in rock.

32.1.4.3 Magnitude

As expected, at a given distance from the source of energy release, larger earthquake magnitudes result in larger peak ground accelerations, velocities, and displacements. Because of the lack of adequate data for earthquake magnitudes greater than approximately 7.5, the effect of magnitude on peak ground motion and duration is generally determined through extrapolation of data from earthquake magnitudes smaller than 7.5.

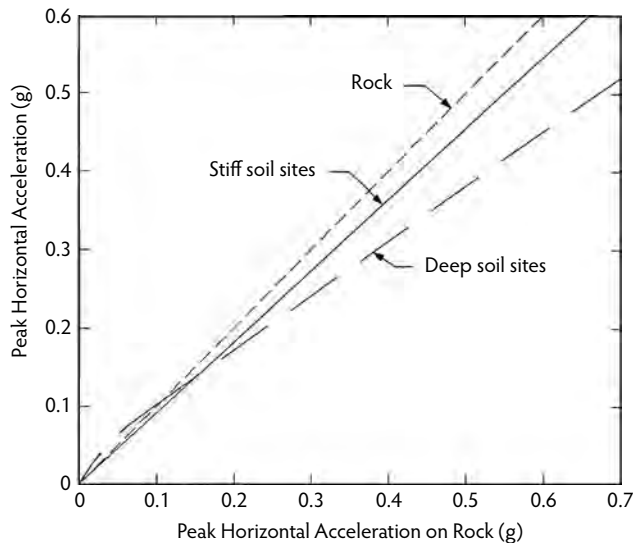


FIGURE 32.2 Relationship between peak accelerations of rock and soil. (Adapted from Seed, H.B. and Idriss, I.M., *Ground Motions and Soil Liquefaction during Earthquakes*, Earthquake Engineering Research Institute, Berkeley, CA, 1982.)

32.1.5 Evaluating Seismic Risk at a Site

Seismic-risk evaluation is based on information from three sources: (1) the recorded ground motion, (2) the history of seismic activity in the vicinity of the site, and (3) the geological data and fault activities of the region. For most regions of the world this information, particularly that from the first source, is very limited and may not be sufficient to predict the size and recurrence intervals of future earthquakes. Nevertheless, earthquake engineers have relied on this limited information to establish some acceptable levels of risk. Seismic-risk analysis usually begins with developing mathematical models that are used to estimate the recurrence intervals of future earthquakes with certain magnitudes and/or intensities. These models, together with the appropriate attenuation relationships, are commonly utilized to estimate ground-motion parameters such as the peak acceleration and velocity corresponding to a specified probability and return period. The provisions of the International Building Code (IBC) use the spectral accelerations determined from maximum considered earthquake ground motion maps prepared by the U.S. Geological Survey (USGS). The ground motion accelerations are modified for specific site characteristics to determine actual design-level accelerations. The USGS maps are extremely detailed and may be referenced in ASCE 7-05 or on the USGS website. For a discussion regarding the use of such mapped accelerations, refer to Section 32.2.1.1.

32.1.6 Estimating Ground Motion

Seismic-risk procedures and attenuation relationships are primarily developed for estimating the expected peak horizontal acceleration at the site. A statistical summary of the peak ground acceleration ratios for all four soil categories (rock, 30 ft of alluvium underlain by rock, 30 to 200 ft of alluvium underlain by rock, alluvium) is presented in Table 32.2. The table includes the ratio of the smaller to the larger of the two peak horizontal accelerations and the ratio of the vertical to the larger of the two peak horizontal accelerations. In each column, the ratios are generally close to each other, indicating that the soil condition does not influence the acceleration ratios. The 2/3 ratio of the vertical to horizontal acceleration, which has been recommended by Newmark and has been employed in seismic design, is closer to the 84.1 percentile than to the 50 percentile ratio. Although the 2/3 ratio is conservative, its use has been justified as taking into account variations greater than the median and uncertainties in the ground motion in the vertical direction.

TABLE 32.2 Summary of Peak Ground Acceleration Ratios (Lognormal Distribution)

Soil Category	a_s/a_l			a_v/a_l		
	Percentile		Mean	Percentile		Mean
	50	84.1		50	84.1	
Rock	0.81	0.99	0.82	0.48	0.69	0.52
<30 ft of alluvium underlain by rock	0.89	0.98	0.89	0.47	0.62	0.46
30–200 ft of alluvium underlain by rock	0.82	0.96	0.83	0.40	0.66	0.46
Alluvium	0.75	0.96	0.79	0.42	0.61	0.45

Note: a_s is the smaller of the two horizontal components; a_l is the larger peak acceleration of the two horizontal components; a_v is the peak acceleration of the vertical component.

32.2 International Building Code (IBC 2006)

32.2.1 IBC Design Criteria

The International Building Code (ICC, 2006) references the provisions of ASCE 7-05 (ASCE, 2005) for lateral seismic loads. The ASCE 7-05 seismic design criteria are in turn based on the *NEHRP Recommended Provisions for Seismic Regulations for New Buildings and Other Structures* (FEMA, 2003). The provisions and commentary may be found at www.bassconline.org. The basic guideline of the IBC provisions is that a minor seismic event should cause little or no damage, and a major seismic event should not result in the collapse of the structure. Accordingly, the building is expected to behave elastically when subjected to frequently occurring earthquakes and exhibit inelastic behavior when influenced only by infrequent strong earthquakes. Most low-rise concrete buildings fall into the regular structure type of the International Building Code and accordingly are designed for a loading condition resulting from equivalent static lateral force. This static load depends on the site geology and soil characteristics, the building occupancy, the building configuration and height, and the structural system being used to support the lateral load. It is important to note that code static loads are no more than one quarter to one third of the expected earthquake action. This can be justified in concrete structures where the anticipated cracking results in increased energy absorption only where ductility in each resisting member and between all the resisting members can be maintained.

32.2.1.1 Mapped Acceleration Parameters

Chapter 22 of ASCE 7-05 contains the mapped maximum considered earthquake (MCE) ground motion parameters S_s and S_1 . Both S_s and S_1 are spectral response acceleration parameters with 5% damping; S_s is determined from a 0.2-second response acceleration, and S_1 is determined from a 1-second response acceleration. Chapter 22 provides detailed maps developed by the U.S. Geological Survey (USGS), but it is not practical to determine site parameters from the maps provided. The recommended method of obtaining these parameters is to use the Ground Motion Parameter Calculator, provided on the USGS website (<http://earthquake.usgs.gov/research/hazmaps/>), which allows for the input of a Zip Code or a latitude and longitude to obtain the response parameters. It is recommended that the latitude and longitude for the specific site be used, as the response parameters can vary significantly over the region of an entire Zip Code. Websites such as <http://terraserwer.microsoft.com/> may be used to obtain latitude and longitude information for a particular address.

32.2.1.2 Site Class

Site class has replaced the term *soil profile type*, which was used in past codes such as the 1997 Uniform Building Code. Because the soil type on which a structure is founded has a great impact on the ground motion at the site, different soil types are assigned values, depending on their stiffness, from Site Class A for rocklike material to Site Class F for a soil profile that requires a site-specific analysis. Table 32.3 lists the site coefficients for different soil types. Site class should not be confused with *seismic design*

TABLE 32.3 Site Classification

Site Class		v_s (ft/sec)	N or N_{ch}	S_u (psf)
A	Hard rock	>5,000	NA	NA
B	Rock	2500 to 5000	NA	NA
C	Very dense soil and soft rock	1200 to 2500	>50	>2000 psf
D	Stiff soil	600 to 1200	15–50	1000–2000 psf
E	Soft clay soil	<600	<15	<1000 psf
		Any profile with more than 10 ft of soil having the following characteristics:		
		-Plasticity index $PI > 20$,		
		-Moisture content $w \geq 40\%$, and		
		-Undrained shear strength $s_u < 500$ psf		
F	Soils requiring site response analysis in accordance with Section 21.1 of ASCE 7-05	See Section 20.3.1 of ASCE 7-05.		

Note: For SI units, 1 ft/sec = 0.3048 m/sec; 1 lb/ft² = 0.0479 kN/m².

Source: ASCE, *Minimum Design Loads for Buildings and Other Structures*, ASCE 7-05, American Society of Civil Engineers, Reston, VA, 2005. With permission.

category, as both use the letters A through F to define different soil types or seismic design categories. Site class is one of the elements used to determine the seismic design category. When not enough information is available to determine the site class, Site Class D shall be used except when the authority having jurisdiction determines that Site Class E or Site Class F is appropriate.

32.2.1.3 Site Coefficients and Adjusted Maximum Considered Earthquake Spectral Response Acceleration Parameters

The mapped acceleration parameters contained in Chapter 22 of ASCE 7-05 are based on Site Class B. When the actual site class varies from Site Class B, the acceleration parameters must be modified based on the actual site class; for example, S_s must be multiplied by an adjustment factor (F_a) to determine S_{MS} , the maximum considered earthquake (MCE) spectral response acceleration at short periods adjusted for site class effects. The same holds true for the MCE spectral acceleration at a period of 1 second; S_1 is multiplied by F_v to determine S_{M1} . Refer to Table 32.4 and Table 32.5 for the site coefficients F_a and F_v , respectively.

32.2.1.4 Design Spectral Acceleration Parameters

The design earthquake spectral response acceleration parameters are determined by multiplying the modified MCE spectral response acceleration parameters by 2/3:

$$S_{DS} = \frac{2}{3}S_{MS}, \quad S_{D1} = \frac{2}{3}S_{M1}$$

32.2.1.5 Design Response Spectrum

When required by ASCE 7-05 and the IBC, the design response spectrum shall be developed as shown in Figure 32.3.

32.2.1.6 Importance Factor and Occupancy Category

The importance factor (I) depends on the occupancy category of a given structure. The International Building Code and ASCE 7-05 distinguish between four different categories:

- Buildings and other structures that represent a low hazard to human life in the event of failure
- All other structures besides those listed in Occupancy Categories I, III, and IV
- Buildings and structures that represent a substantial hazard to human life in the event of failure
- Essential facilities and structures containing highly toxic substances

TABLE 32.4 Site Coefficient F_a

Site Class	Mapped Maximum Considered Earthquake Spectral Response Acceleration Parameter at a Short Period				
	$S_s \leq 0.25$	$S_s = 0.5$	$S_s = 0.75$	$S_s = 1.0$	$S_s \geq 1.25$
A	0.8	0.8	0.8	0.8	0.8
B	1.0	1.0	1.0	1.0	1.0
C	1.2	1.2	1.1	1.0	1.0
D	1.6	1.4	1.2	1.1	1.0
E	2.5	1.7	1.2	0.9	0.9
F	See Section 11.4.7 of ASCE 7-05.				

Note: Use straight-line interpolation for intermediate values of S_s .
Source: ASCE, *Minimum Design Loads for Buildings and Other Structures*, ASCE 7-05, American Society of Civil Engineers, Reston, VA, 2005. With permission.

TABLE 32.5 Site Coefficient F_v

Site Class	Mapped Maximum Considered Earthquake Spectral Response Acceleration Parameter at 1-Second Period				
	$S_1 \leq 0.1$	$S_1 = 0.2$	$S_1 = 0.3$	$S_1 = 0.4$	$S_1 \geq 0.5$
A	0.8	0.8	0.8	0.8	0.8
B	1.0	1.0	1.0	1.0	1.0
C	1.7	1.6	1.5	1.4	1.3
D	2.4	2.0	1.8	1.6	1.5
E	3.5	3.2	2.8	2.4	2.4
F	See Section 11.4.7 of ASCE 7-05.				

Note: Use straight-line interpolation for intermediate value of S_1 .
Source: ASCE, *Minimum Design Loads for Buildings and Other Structures*, ASCE 7-05, American Society of Civil Engineers, Reston, VA, 2005. With permission.

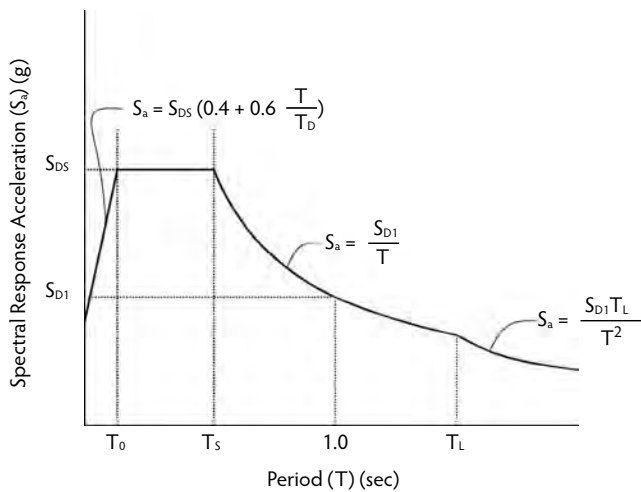


FIGURE 32.3 Design response spectrum. (From ASCE, *Minimum Design Loads for Buildings and Other Structures*, ASCE 7-05, American Society of Civil Engineers, Reston, VA, 2005, Figure 11.4-1. With permission.)

Essential facilities, in addition to having an importance factor of 1.5, require special construction review, inspection, and observation procedures. It is argued that the additional measures can improve performance more effectively than solely relying on increased design force levels. Refer to Table 32.6 for the detailed description of the various occupancy categories. Refer to Table 32.7 for importance factor I based on the occupancy category.

TABLE 32.6 Occupancy Category of Buildings and Other Structures for Flood, Wind, Snow, Earthquake, and Ice Loads

Nature of Occupancy	Occupancy Category
Buildings and other structures that represent a low hazard to human life in the event of failure, including, but not limited to: Agricultural facilities Certain temporary facilities Minor storage facilities	I
All buildings and other structures except those listed in Occupancy Categories I, III, and IV	II
Buildings and other structures that represent a substantial hazard to human life in the event of failure, including, but not limited to: Buildings and other structures where more than 300 people congregate in one area Buildings and other structures with daycare facilities with a capacity greater than 150 Buildings and other structures with elementary school or secondary school facilities with a capacity greater than 250 Buildings and other structures with a capacity greater than 500 for colleges or adult education facilities Healthcare facilities with a capacity of 50 or more resident patients but not having surgery or emergency treatment facilities Jail and detention facilities	III
Buildings and other structures, not included in Occupancy Category IV, with potential to cause a substantial economic impact and/or mass disruption of day-to-day civilian life in the event of failure, including, but not limited to: Power-generating stations ^a Water-treatment facilities Sewage treatment facilities Telecommunication centers	
Buildings and other structures not included in Occupancy Category IV (including, but not limited to, facilities that manufacture, process, handle, store, use, or dispose of such substances as hazardous fuels, hazardous chemicals, hazardous waste, or explosives) containing sufficient quantities of toxic or explosive substances to be dangerous to the public if released	
Buildings and other structures containing toxic or explosive substances shall be eligible for classification as Occupancy Category II structures if it can be demonstrated to the satisfaction of the authority having jurisdiction by a hazard assessment as described in Section 1.5.2 that a release of the toxic or explosive substances does not pose a threat to the public.	
Buildings and other structures designated as essential facilities, including, but not limited to: Hospitals and other healthcare facilities having surgery or emergency treatment facilities Fire, rescue, ambulance, police station and emergency vehicle garages Designated earthquake, hurricane, or other emergency shelters Designated emergency preparedness, communication, and operation centers and other facilities required for emergency response Power generating stations and other public utility facilities required in and emergency	IV
Ancillary structures (including, but not limited to, communication towers, fuel storage tanks, cooling towers, electrical substation structures, fire water storage tanks or other structures housing or supporting water or other fire-suppression material or equipment) required for operation of Occupancy Category IV Structures during an emergency	
Aviation control towers, air traffic control centers, and emergency aircraft hangars	
Water-storage facilities and pump structures required to maintain water pressure for fire suppression	
Buildings and other structures having critical national defense functions	
Buildings and other structures (including, but not limited to, facilities that manufacture, process, handle, store, use, or dispose of such substances as hazardous fuels, hazardous chemicals, or hazardous waste) containing highly toxic substances where the quantity of the material exceeds a threshold quantity established by the authority having jurisdiction	
Buildings and other structures containing highly toxic substances shall be eligible for classification as Occupancy Category II structures if it can be demonstrated to the satisfaction of the authority having jurisdiction by a hazard assessment as described in Section 1.5.2 that a release of the highly toxic substances does not pose a threat to the public. This reduced classification shall not be permitted if the buildings or other structures also function as essential facilities.	

^a Cogeneration power plants that do not supply power on the national grid shall be designated Occupancy Category II.

Source: ASCE, *Minimum Design Loads for Buildings and Other Structures*, ASCE 7-05, American Society of Civil Engineers, Reston, VA, 2005. With permission.

TABLE 32.7 Importance Factors

Occupancy Category	I
I or II	1.0
III	1.25
IV	1.5

Source: ASCE, *Minimum Design Loads for Buildings and Other Structures*, ASCE 7-05, American Society of Civil Engineers, Reston, VA, 2005. With permission.

TABLE 32.8 Seismic Design Category Based on Short Period Response Acceleration Parameter

Value of S_{DS}	Occupancy Category		
	I or II	III	IV
$S_{DS} < 0.167$	A	A	A
$0.167 \leq S_{DS} < 0.33$	B	B	C
$0.33 \leq S_{DS} < 0.50$	C	C	D
$0.50 \leq S_{DS}$	D	D	D

Source: ASCE, *Minimum Design Loads for Buildings and Other Structures*, ASCE 7-05, American Society of Civil Engineers, Reston, VA, 2005. With permission.

TABLE 32.9 Seismic Design Category Based on 1-Second Period Response Acceleration Parameter

Value of S_{D1}	Occupancy Category		
	I or II	III	IV
$S_{D1} < 0.067$	A	A	A
$0.067 \leq S_{D1} < 0.133$	B	B	C
$0.133 \leq S_{D1} < 0.20$	C	C	D
$0.20 \leq S_{D1}$	D	D	D

Source: ASCE, *Minimum Design Loads for Buildings and Other Structures*, ASCE 7-05, American Society of Civil Engineers, Reston, VA, 2005. With permission.

32.2.1.7 Seismic Design Category

Structures shall be assigned the more severe seismic design category as determined from Table 32.8 or Table 32.9 regardless of the period of vibration of the structure. In addition, when the mapped spectral response acceleration parameter at the 1-second period (S_1) is greater than or equal to 0.75, then the structures in Occupancy Categories I, II, or III shall be assigned to Seismic Design Category E, and structures in Occupancy Category IV shall be assigned to Seismic Design Category F. There are exceptions that allow for the seismic design category to be determined from Table 32.8 alone. To use this exception, S_1 must be less than 0.75, and all of the following requirements must be met:

- The approximate fundamental period of vibration (T_a), as determined by Equation 32.4 in each of the two orthogonal directions, is less than $0.8T_s$, where $T_s = S_{D1}/S_{DS}$.
- The fundamental period of the structure that is used to calculate the story drift in the two orthogonal directions is less than T_s .
- The seismic response coefficient (C_s) is determined by Equation 32.2.
- The diaphragms are rigid or, where diaphragms are considered flexible, the spacing between vertical elements of the lateral-force-resisting system does not exceed 40 feet.

32.2.2 Design Requirements for Seismic Design Category A

Structures designated to Seismic Design Category A are designed for minimal seismic forces. A lateral force of 1% of the dead load of each level shall be applied in each of two orthogonal directions independently. Load path connections must be designed to transfer the lateral forces induced by the elements being connected. Smaller portions of a structure are required to be tied to the remainder of the structure with a strength of at least 5% of the weight of the smaller portion. Connections to supporting elements require a positive connection to resist a horizontal force acting parallel to the member being connected. This positive connection may be obtained by connecting an element to slabs designed to act as diaphragms, but the supporting element must then be connected to the diaphragm with a connection strength of 5% of the dead plus live load reaction. Concrete and masonry walls are required to be anchored to all floors and the roof, as well as members that provide lateral support for the wall or that are supported by the wall.

32.2.3 Design Requirements for Seismic Design Categories B, C, D, E, and F

Similar to Seismic Design Category A, Seismic Design Categories B through F have some minimum requirements with respect to member design, connection design, and load path. These requirements may be found at the beginning of Chapter 12 of ASCE 7-05. The design of building structures assigned to Seismic Design Categories B through F requires the following steps:

- Determine the structural system or systems (may include a combination of systems in different directions, in the same direction, or vertical combinations).
- Determine if any structural irregularities exist.
- Determine redundancy factor ρ if the structure is assigned to Seismic Design Categories D through F.
- Determine the appropriate analytical procedure (i.e., equivalent lateral force analysis, modal response spectrum analysis, or seismic response history procedure).
- Apply the appropriate seismic load combinations to determine member design forces.
- Determine the diaphragm, chord, and collector design requirements.
- Check allowable story drift and determine building separation requirements, if necessary.
- Check deformation compatibility of members not included in the seismic-force-resisting system.
- Address foundation design requirements.
- Address material specific seismic design and detailing requirements of the structural system.

32.2.3.1 Structural System Selection

The maximum elastic response acceleration of a structure during a severe earthquake can be several times the magnitude of the maximum ground acceleration and depends on the mass and stiffness of the structure and the amplitude of the damping. Because it is unnecessary to design a structure to respond in the elastic range to the maximum seismic inertia forces, it is of the utmost importance that a well-designed structure be able to dissipate seismic energy by inelastic deformations in certain localized regions of the lateral-force-resisting system. This translates into accomplishing flexural yielding of the members and avoiding all forms of brittle failure. The code-specified design seismic force recognizes such inelastic behavior and damping and scales down the inertia forces corresponding to a fully elastic response based on the structural system used. This is accounted for in the response modification factor (R). The structural systems for buildings and the corresponding R values are listed in Table 32.10 and are defined as follows:

- *Bearing wall system*—A structural system without a complete vertical-load-carrying frame. Bearing walls provide support for all or most gravity loads. Resistance to lateral load is provided by shear walls or light-frame walls with flat-strap bracing. In Seismic Design Categories D, E, and F, concrete and masonry shear walls must be specially detailed to satisfy IBC requirements. These special reinforced-concrete or masonry shear walls are limited to a height of 160 feet in Seismic Design Categories D and E, while they are limited to a height of 100 feet in Seismic Design Category F.

- *Building frame system*—A structural system with an essentially complete frame providing support for gravity loads. Resistance to lateral load is provided by shear walls or braced frames. Shear walls in Seismic Design Categories D, E, and F are required to be specially designed and detailed to satisfy the IBC requirements. In addition, other structural elements not designated part of the lateral-load-resisting system must be able to sustain their gravity load-carrying capacity at a lateral displacement equal to a multiple times the computed elastic displacement of the lateral-force-resisting system under code-specified design seismic forces. The IBC restricts the building frame system to a maximum height of 160 feet for Seismic Design Categories D and E but lowers the limit to 100 feet for Seismic Design Category F.
- *Moment-resisting frame system*—A structural system with an essentially complete frame providing support for gravity loads. Moment-resisting frames provide resistance to lateral loads primarily by flexural action of members. In Seismic Design Category B, the moment-resisting frames can be ordinary moment-resisting frames (OMRFs) proportioned to satisfy the IBC requirements. In Seismic Design Category C, reinforced-concrete frames resisting forces induced by earthquake motions at minimum must be intermediate moment-resisting frames (IMRFs). In Seismic Design Categories D, E, and F, reinforced-concrete frames resisting forces induced by earthquake motions must be special moment-resisting frames (SMRFs).
- *Dual system*—Structural system with the following features: (1) an essentially complete frame that provides support for gravity loads; (2) resistance to lateral load provided by shear walls or braced frames and moment-resisting frames (SMRFs and IMRFs), with the moment-resisting frames designed to independently resist at least 25% of the design base shear; and (3) designed to resist total design base shear in proportion to relative rigidities considering the interaction of the dual system at all levels.
- *Shear wall-frame interactive system*—A structural system with ordinary reinforced-concrete moment frames and ordinary reinforced-concrete shear walls. This system is permitted only in Seismic Design Category B.
- *Cantilevered column system*—A structural system consisting of cantilevered column elements detailed to conform to the requirements of various moment frame systems.

32.2.3.2 Combinations of Framing Systems in Different Directions

Any combination of moment-resisting frame systems, dual systems, building frame systems, or bearing wall systems may be used to resist seismic forces in each of the two orthogonal directions of the structure. Where different systems are used, the respective R , C_d , and Ω_o coefficients shall apply to each system, including the limitations on system use contained in Table 32.10.

32.2.3.3 Combination of Framing Systems in the Same Direction

Where different seismic-force-resisting systems are used in the same direction but do not meet the requirements of a dual system, the more stringent response modification factor, deflection amplification factor, and overstrength factor shall be used in the analysis and design. Resisting elements are permitted to be designed for the least value of R for the different structural systems found in each independent line of resistance if the following three conditions are met:

- Occupancy Category I or II building
- Two stories or less in height
- Use of light-frame construction or flexible diaphragms

32.2.3.4 Vertical Combinations

The International Building Code requires that the value of the response modification factor (R) used in the design of any story be less than or equal to the value of R used in the given direction for the story above. The deflection amplification factor (C_d) and the system overstrength factor (Ω_o) used for the design of any story shall not be less than the largest value of these factors used in the given direction for the story above. Exceptions to these requirements include:

TABLE 32.10 Design Coefficients and Factors for Seismic-Force-Resisting Systems

Seismic-Force-Resisting System		ASCE 7 Section Specifying Detailing Requirements	Response Modification Coefficient (R) ^a	System Overstrength Factor (Ω_o) ^g	Deflection Amplification Factor (C_d) ^b	Structural System Limitations and Building Height (ft) Limit ^c			
						Seismic Design Category			
						B	C	D ^d	E ^d
A Bearing Wall Systems									
1	Special reinforced-concrete shear walls	14.2, 14.2.3.6	5	2-1/2	5	NL	NL	160	100
2	Ordinary reinforced-concrete shear walls	14.2, 14.2.3.4	4	2-1/2	4	NL	NL	NP	NP
3	Detailed plain concrete shear walls	14.2, 14.2.3.2	2	2-1/2	2	NL	NP	NP	NP
4	Ordinary Plain concrete shear walls	14.2, 14.2.3.1	1-1/2	2-1/2	1-1/2	NL	NP	NP	NP
5	Intermediate precast shear walls	14.2, 14.2.3.5	4	2-1/2	4	NL	NL	40 ^k	40 ^k
6	Ordinary precast shear walls	14.2, 14.2.3.3	3	2-1/2	3	NL	NP	NP	NP
7	Special reinforced masonry shear walls	14.4, 14.4.3	5	2-1/2	3-1/2	NL	NL	160	100
8	Intermediate reinforced masonry shear walls	14.4, 14.4.3	3-1/2	2-1/2	2-1/2	NL	NL	NP	NP
9	Ordinary reinforced masonry shear walls	14.4	2	2-1/2	1-1/2	NL	160	NP	NP
10	Detailed plain masonry shear walls	14.4	2	2-1/2	1-1/2	NL	NP	NP	NP
11	Ordinary plain masonry shear walls	14.4	1-1/2	2-1/2	1-1/2	NL	NP	NP	NP
12	Prestressed masonry shear walls	14.4	1-1/2	2-1/2	1-1/2	NL	NP	NP	NP
13	Light-framed walls sheathed with wood structural panels rated for shear resistance or steel sheets	14.1, 14.1.4.2, 14.5	6-1/2	3	4	NL	NL	65	65
14	Light-framed walls sheathed with shear panels of all other materials	14.1, 14.1.4.2, 14.5	2	2-1/2	2	NL	NL	35	NP
15	Light -framed wall systems using flat strap bracing	14.1, 14.1.4.2, 14.5	4	2	3-1/2	NL	NL	65	65
B Building Frame Systems									
1	Steel eccentrically braced frames, moment-resisting, connections at columns away from links	14.1	8	2	4	NL	NL	160	100
2	Steel eccentrically braced frames, non-moment- resisting, connections at columns away from links	14.1	7	2	4	NL	NL	160	100
3	Special steel concentrically braced frames	14.1	6	2	5	NL	NL	160	100
4	Ordinary steel concentrically braced frames	14.1	3 1/4	2	3-1/2	NL	NL	35 ^j	NP ^j
5	Special reinforced-concrete shear walls	14.2, 14.2.3.6	6	2-1/2	5	NL	NL	160	100
6	Ordinary reinforced-concrete shear walls	14.2, 14.2.3.4	5	2-1/2	4-1/2	NL	NL	NP	NP
7	Detailed plain concrete shear walls	14.2, 14.2.3.2	2	2-1/2	2	NL	NP	NP	NP
8	Ordinary plain concrete shear walls	14.2, 14.2.3.1	1-1/2	2-1/2	1-1/2	NL	NP	NP	NP
9	Intermediate precast shear walls	14.2, 14.2.3.5	5	2-1/2	4-1/2	NL	NL	40 ^k	40 ^k
10	Ordinary precast shear walls	14.2, 14.2.3.3	4	2-1/2	4	NL	NP	NP	NP

11	Composite steel and concrete eccentrically braced frames	14.3	8	2-1/2	4	NL	NL	160	160	100
12	Composite steel and concrete concentrically braced frames	14.3	5	2	4-1/2	NL	NL	160	160	100
13	Ordinary composite steel and concrete braced frames	14.3	3	2	3	NL	NL	NP	NP	NP
14	Composite steel plate shear walls	14.3	6-1/2	2-1/2	5-1/2	NL	NL	160	160	100
15	Special composite reinforce concrete shear walls with steel elements	14.3	6	2-1/2	5	NL	NL	160	160	100
16	Ordinary composite reinforced-concrete shear walls with steel elements	14.3	5	2-1/2	4-1/2	NL	NL	NP	NP	NP
17	Special reinforced masonry shear walls	14.4	5-1/2	2-1/2	4	NL	NL	160	160	100
18	Intermediate reinforced masonry shear	14.4	4	2-1/2	4	NL	NL	NP	NP	NP
19	Ordinary reinforce masonry shear walls	14.4	2	2-1/2	2	NL	160	NP	NP	NP
20	Detailed plain masonry shear walls	14.4	2	2-1/2	2	NL	NP	NP	NP	NP
21	Ordinary plain masonry shear walls	14.4	1-1/2	2-1/2	1-1/2	NL	NP	NP	NP	NP
22	Prestressed masonry shear walls	14.4	1-1/2	2-1/2	1-1/2	NL	NP	NP	NP	NP
23	Light-framed walls sheathed with wood structural panels rated for shear resistance or steel sheets	14.4, 14.1, 4.2, 14.5	7	2-1/2	4-1/2	NL	NL	65	65	65
24	Light-framed walls with shear panels of all other materials	14.1, 14.1, 4.2, 14.5	2-1/2	2-1/2	2-1/2	NL	NL	35	NP	NP
25	Buckling-restrained braced frames, non-moment-resisting beam-column connections	14.1	7	2	5-1/2	NL	NL	160	160	100
26	Buckling-restrained braced frames, moment-resisting beam-column connection	14.1	8	2-1/2	5	NL	NL	160	160	100
27	Special steel plate shear wall	14.1	7	2	6	NL	NL	160	160	100
C	Moment-Resisting Frame Systems									
1	Special steel moment frames	14.1, 12.2.5.5	8	3	5-1/2	NL	NL	NL	NL	NL
2	Special steel truss moment frames	14.1	7	3	5-1/2	NL	NL	160	100	NP
3	Intermediate steel moment frames	12.2.5.6, 12.2.5.7, 12.2.5.8, 12.2.5.9, 14.1	4.5	3	4	NL	NL	35 ^h	NP ^h	NP ⁱ
4	Ordinary steel moment frames	12.2.5.6, 12.2.5.7, 12.2.5.8, 14.1	3.5	3	3	NL	NL	NP ^h	NP ^h	NP ⁱ
5	Special reinforced-concrete moment	12.2.5.5, 14.2	8	3	5-1/2	NL	NL	NL	NL	NL
6	Intermediate reinforced-concrete moment frames	14.2	5	3	4-1/2	NL	NL	NP	NP	NP
7	Ordinary reinforced-concrete moment frames	14.2	3	3	2-1/2	NL	NP	NP	NP	NP
8	Special composite steel and concrete moment frames	12.2.5.5, 14.3	8	3	5-1/2	NL	NL	NL	NL	NL
9	Intermediate composite moment frames	14.3	5	3	4-1/2	NL	NL	NP	NP	NP

(continued)

TABLE 32.10 (cont.) Design Coefficients and Factors for Seismic-Force-Resisting Systems

Seismic-Force-Resisting System	ASCE 7 Section Specifying Detailing Requirements	Response Modification Coefficient (R) ^a	System Overstrength Factor (Ω_o) ^g	Deflection Amplification Factor (C_d) ^b	Structural System Limitations and Building Height (ft) Limit ^c			
					Seismic Design Category			
					B	C	D ^d	E ^d
10 Composite partially restrained moment frames	14.3	6	3	5-1/2	160	160	100	NP
11 Ordinary composite moment frames	14.3	3	3	2-1/2	NL	NP	NP	NP
D Dual Systems with Special Moment Frames Capable of Resisting at Least 25% of Prescribed Seismic Forces	12.2.5.1	—	—	—	—	—	—	—
1 Steel eccentrically braced frames	14.1	8	2-1/2	4	NL	NL	NL	NL
2 Special steel concentrically braced frames	14.1	7	2-1/2	5-1/2	NL	NL	NL	NL
3 Special reinforced-concrete shear walls	14.2	7	2-1/2	5-1/2	NL	NL	NL	NL
4 Ordinary reinforced-concrete shear walls	14.2	6	2-1/2	5	NL	NL	NP	NP
5 Composite steel and concrete eccentrically braced frames	14.3	8	2-1/2	4	NL	NL	NL	NL
6 Composite steel and concrete concentrically braced frames	14.3	6	2-1/2	5	NL	NL	NL	NL
7 Composite steel plate shear walls	14.3	7-1/2	2-1/2	6	NL	NL	NL	NL
8 Special composite reinforced-concrete shear walls with steel elements	14.3	7	2-1/2	6	NL	NL	NL	NL
9 Ordinary composite reinforced shear walls with steel elements	14.3	6	2-1/2	5	NL	NL	NP	NP
10 Special reinforced masonry shear walls	14.4	5-1/2	3	5	NL	NL	NL	NL
11 Intermediate reinforced masonry shear walls	14.4	4	3	3-1/2	NL	NL	NP	NP
12 Buckling-restrained braced frame	14.1	8	2-1/2	5	NL	NL	NL	NL
13 Special steel plate shear walls	14.1	8	2-1/2	6-1/2	NL	NL	NL	NL
E Dual Systems with Intermediate Moment Frames Capable of Resisting at Least 25% of Prescribed Seismic Forces	12.2.5.1	—	—	—	—	—	—	—
1 Special steel concentrically braced frames ^f	14.1	6	2-1/2	5	NL	NL	35	NP
2 Special reinforced-concrete shear walls	14.2	6-1/2	2-1/2	5	NL	NL	160	100

3	Ordinary reinforced masonry shear walls	14.4	3	2-1/2	NL	NP	NP
4	Intermediate reinforced masonry shear walls	14.4	3-1/2	3	NL	NP	NP
5	Composite steel and concrete concentrically braced frames	14.3	5-1/2	2-1/2	NL	160	NP
6	Ordinary composite braced frames	14.3	3-1/2	3	NL	NP	NP
7	Ordinary composite reinforced-concrete shear walls with steel elements	14.3	5	4-1/2	NL	NP	NP
8	Ordinary reinforced-concrete shear walls	14.2	5-1/2	2-1/2	NL	NP	NP
F	Shear Wall-Frame Interactive System with Ordinary Reinforced Concrete Moment Frames and Ordinary Reinforced Concrete Shear Walls	12.2.5.10, 14.2	4-1/2	2-1/2	NL	NP	NP

^a Response modification coefficient (R) for use throughout the standard. Note that R reduces forces to a strength level, not an allowable stress level.

^b Deflection amplification factor (C_d) for use in ASCE 7-05, Sections 12.8.6, 12.8.7, and 12.9.2

^c NL = not limited and NP = not permitted. For metric units, use 30.5 m for 100 ft and use 48.8 m for 160 ft. Heights are measured from the base of the structure as defined in ASCE 7-05, Section 11.2.

^d See ASCE 7-05, Section 12.2.5.4, for description of building systems limited to buildings with a height of 240 ft (73.2 m) or less.

^e See ASCE 7-05, Section 12.2.5.4, for building systems limited to buildings with a height of 160 ft (48.8m) or less.

^f Ordinary moment frame is permitted to be used in lieu of intermediate moment frame for Seismic Design Categories B or C.

^g The tabulated value of the overstrength factor (Ω_o) is permitted to be reduced by subtracting one half for structures with flexible diaphragms but shall not be taken as less than 2.0 for any structure.

^h See ASCE 7-05, Sections 12.2.5.6 and 12.2.5.7, for limitations for steel OMFs and IMFs in structures assigned to Seismic Design Category D or E.

ⁱ See ASCE 7-05, Sections 12.2.5.8 and 12.2.5.9, for limitations for steel OMFs and IMFs in structures assigned to Seismic Design Category F.

^j Steel ordinary concentrically braced frames are permitted in single-story storage building up to height of 60 ft (18.3 m) where the dead load of the roof does not exceed 20 psf (0.96kN/m²) and in penthouse structures.

^k Increase in height to 45 ft (13.7 m) is permitted for single story storage warehouse facilities.

Source: Adapted from ASCE, *Minimum Design Loads for Buildings and Other Structures*, ASCE 7-05, American Society of Civil Engineers, Reston, VA, 2005, Table 12.2-1. With permission.

- Rooftop structures not exceeding two stories in height and 10% of the weight of the entire structure
- Other supported structural systems with a weight equal to or less than 10% of the weight of the entire structure
- Detached one- and two-family dwellings of light-frame construction

A two-stage equivalent lateral force procedure is permitted to be used for structures having a flexible upper portion supported by a rigid lower portion, provided that the design of the structure complies with the following:

- The stiffness of the lower portion must be at least 10 times the stiffness of the upper portion.
- The period of the entire structure shall not be greater than 1.1 times the period of the upper portion considered as a separate structure fixed at the base.
- The flexible upper portion shall be designed as a separate structure using the appropriate values of R and ρ .
- The rigid lower portion shall be designed as a separate structure using the appropriate values of R and ρ . The reactions from the upper portion shall be those determined from analysis of the upper portion amplified by the ratio of the R/ρ of the upper portion over R/ρ of the lower portion. This ratio shall not be less than 1.0.

32.2.3.5 Combination Framing Detailing Requirements

Structural components that are common to different framing systems used to resist seismic motions in any direction shall be detailed in accordance with the requirements of ASCE 7-05, Chapter 12, for the highest response modification factor (R) of the connected framing systems. More stringent detailing is required with the higher response modification factor.

32.2.3.6 System-Specific Requirements

A series of system-specific requirements either imposes additional limitations on system use or notes exceptions to system use in particular seismic design categories. These requirements are included in ASCE 7-05, Section 12.2.5.

32.2.3.7 Diaphragm Flexibility

The relative stiffness of the diaphragms of a structure shall be considered in the analysis unless the diaphragms can be idealized as rigid or flexible. Certain types of construction may be idealized as either flexible or rigid diaphragms. When the diaphragm cannot be idealized as flexible or rigid, the structural analysis performed shall explicitly include the stiffness of the diaphragm. The inclusion of the diaphragm stiffness in the analysis is often referred to as *semirigid modeling*, which is often available as an option in commercially available structural analysis software. Concrete slabs and concrete-filled metal deck slabs with span-to-depth ratios of 3 or less in structures with no horizontal irregularities are allowed to be idealized as rigid diaphragms.

32.2.3.8 Structural Irregularities

The IBC and ASCE 7-05 require that a structure be designated as *regular* or *irregular*. Regular structures have no significant physical discontinuities in plan or vertical configurations or in their lateral-force-resisting systems. Two assumptions apply for regular structures. First, the equivalent static force distribution provides a conservative envelope of the forces and deformations due to the actual dynamic response. Second, the cyclic inelastic deformation demands during a major level of seismic ground motion will be reasonably uniform in all elements. Irregular structures are those with irregular features as described in Table 32.11 and Table 32.12. Vertical irregularities are defined as a distribution of mass, stiffness, or strength that results in lateral forces or deformations, over the height of the structure, that are significantly different from the linearly varying distribution obtained from an equivalent lateral force analysis. Plan irregularities are encountered where diaphragm characteristics create significant diaphragm deformations or stress concentrations. As will be seen in the next section, only structures with certain types of irregularities require a dynamic analysis.

TABLE 32.11 Horizontal Structural Irregularities

Irregularity Type and Description		ASCE 7-05 Reference Section	Seismic Design Category Application
1a	<i>Torsional irregularity</i> is defined to exist where the maximum story drift, computed including accidental torsion, at one end of the structure transverse to an axis is more than 1.2 times the average of the story drifts at the two ends of the structure. Torsional irregularity requirements in the reference sections apply only to structures in which the diaphragms are rigid or semirigid.	12.3.3.4 12.8.4.3 12.7.3 12.12.1 Table 12.6-1 16.2.2	D, E, and F C, D, E, and F B, C, D, E, and F C, D, E, and F B, C, D, E, and F
1b	<i>Extreme torsional irregularity</i> is defined to exist where the maximum story drift, computed including accidental torsion, at one ends of the structure transverse to an axis is more than 1.4 times the average of the story drifts at the two ends of the structure. Extreme torsional irregularity requirements in the reference sections apply only to structures in which the diaphragms are rigid or semirigid.	12.3.3.1 12.3.3.4 12.7.3 12.8.4.3 12.12.1 Table 12.6-1 16.2.2	E and F D B, C, and D C and D D B, C, and D
2	<i>Reentrant corner irregularity</i> is defined to exist where both plan projections of the structure beyond a reentrant corner are greater than 15% of the plan dimension of the structure in the given direction.	12.3.3.4 Table 12.6-1	D, E, and F D, E, and F
3	<i>Diaphragm discontinuity irregularity</i> is defined to exist where there are diaphragms with abrupt discontinuities or variations in stiffness, including those having cutout or open areas greater than 50% of the gross enclosed diaphragm area, or changes in effective diaphragm stiffness of more than 50% from one story to the next.	12.3.3.4 Table 12.6-1	D, E, and F D, E, and F
4	<i>Out-of-plane offsets irregularity</i> is defined to exist where there are discontinuities in a lateral force-resistance path, such as out -of-plan offsets of the vertical elements.	12.3.3.4 12.3.3.3 12.7.3 Table 12.6-1 16.2.2	D, E, and F B, C, D, E, and F B, C, D, E, and F D, E, and F B, CD, E, and F
5	<i>Nonparallel systems irregularity</i> is defined to exist where the vertical lateral-force-resisting elements are not parallel to or symmetric about the major orthogonal axes of the seismic-force-resisting system.	12.5.3 12.7.3 Table 12.6-1 16.2.2	C,D, E and F B, C, D, E, and F D, E, and F B, C, D, E, and F

Source: ASCE, *Minimum Design Loads for Buildings and Other Structures*, ASCE 7-05, American Society of Civil Engineers, Reston, VA, 2005. With permission.

In Seismic Design Categories E and F, structures with horizontal irregularity Type 1b or vertical irregularities Type 1b, Type 5a, and Type 5b are not permitted. Structures having vertical irregularity Type 5b in Seismic Design Category D are not permitted. Structures with a Type 5b vertical irregularity are not permitted to exceed 2 stories or 30 feet in height except when the weak story is designed to resist the forces determined by the special seismic load combinations including Ω_O . Overturning moments on discontinuous shear-resisting elements are to be carried as loads to the foundation. In Seismic Design Categories B through F, columns, beams, trusses, or slabs supporting the overturning forces of discontinuous shear walls or frames of structures are to be designed to resist the axial forces resulting from the special seismic load combinations including Ω_O . The columns carrying these factored loads may be designed considering the maximum force that can be transferred from the supported element above and must meet special detailing requirements to ensure their ductile behavior under cyclic loading.

32.2.3.9 Analysis Procedure Selection

The IBC and ASCE 7-05 recognize three different analysis procedures for the determination of seismic effects on structures. Refer to Table 32.13 for the applicability of each of the three analysis options. The equivalent lateral force analysis procedure is allowed when certain criteria of building period, occupancy, and regularity are met; the modal response spectrum analysis (dynamic analysis) procedure is always permissible for design. The third analysis option is the seismic response history procedure, which is

TABLE 32.12 Vertical Structural Irregularities

Irregularity Type and Description		ASCE 7-05 Reference Section	Seismic Design Category Application
1a	<i>Stiffness-soft story irregularity</i> is defined to exist where there is a story in which the lateral stiffness is less than 70% of that in the story above or less than 80% of the average stiffness of the three stories above.	Table 12.6-1	D,E, and F
1b	<i>Stiffness-extreme soft story irregularity</i> is defined to exist where there is a story in which the lateral stiffness is less than 60% of that in the story above or less than 70% of the average stiffness of the three stories above.	12.3.3.1 Table 12.6-1	E and F D, E, and F
2	<i>Weight (mass) irregularity</i> is defined to exist where the effective mass of any story is more than 150% of the effective mass of an adjacent story. A roof that is lighter than the floor below need not be considered.	Table 12.6-1	D, E, and F
3	<i>Vertical geometric irregularity</i> is defined to exist where the horizontal dimension of the seismic-force-resisting system in any story is more than 130% of that in an adjacent story.	Table 12.6-1	D, E, and F
4	<i>In-plane discontinuity in vertical lateral-force-resisting element irregularity</i> is defined to exist where an in-plane offset of the lateral-force-resisting element is greater than the length of those elements or there exists a reduction in stiffness of the resisting element in the story below.	12.3.3.3 12.3.3.4 Table 12.6-1	B, C, D, E, and F D, E, and F D, E, and F
5a	<i>Discontinuity in lateral strength-weak story irregularity</i> is defined to exist where the story lateral strength is less than 80% of that in the story above. The story lateral strength is the total lateral strength of all seismic resisting elements sharing the story shear for the direction under consideration.	12.3.3.1 Table 12.6-1	E and F D, E, and F
5b	<i>Discontinuity in lateral strength-extreme weak story irregularity</i> is defined to exist where the story lateral strength is less than 65% of that in the story above. The story strength is the total strength of all seismic resisting elements sharing the story shear for the direction under consideration.	12.3.3.1 12.3.3.2 Table 12.6-1	D, E, and F B and C D, E, and F

Source: ASCE, *Minimum Design Loads for Buildings and Other Structures*, ASCE 7-05, American Society of Civil Engineers, Reston, VA, 2005. With permission.

beyond the scope of this chapter. The scope of this chapter is primarily dedicated to the equivalent lateral force analysis procedure, but modal response spectrum analysis is briefly touched upon. Equivalent lateral force analysis is acceptable for use with all structures, regular or irregular, in Seismic Design Categories B and C. Equivalent lateral force analysis may be used for regular and irregular structures in Seismic Design Categories D, E, and F with a fundamental period of vibration, in each of the two orthogonal directions, less than $3.5T_s$, except when a Type 1a or Type 1b horizontal irregularity or Type 1a, Type 1b, Type 2 or Type 3 vertical irregularity exists. Additional structural characteristics that allow the use of the equivalent lateral force analysis procedure are noted in Table 32.13.

32.2.3.10 Redundancy

A redundancy factor (ρ) shall be assigned to the seismic-force-resisting system in each of two orthogonal directions for all structures. Redundancy factor ρ is permitted to equal 1.0 for the following:

- Structures assigned to Seismic Design Categories B or C
- Drift calculations and P-delta effects
- Design of nonbuilding structures that are not similar to buildings
- Design of collector elements, splices, and their connections for which the load combinations including the overstrength factor Ω_o are used
- Design of members or connections where the load combinations including the overstrength factor Ω_o are required for design

TABLE 32.13 Permitted Analytical Procedures

Seismic Design Category	Structural Characteristics	Equivalent Lateral Force Analysis (Section 32.2.4)	Modal Response Spectrum Analysis (Section 32.2.5)	Seismic Response History Procedures (ASCE 7-05, Chapter 16)
B, C	Occupancy Category I or II buildings of light-framed construction not exceeding 3 stories in height	P	P	P
	Other Occupancy Category I or II buildings not exceeding 2 stories in height	P	P	P
	All other structures	P	P	P
D, E, F	Occupancy Category I or II buildings of light-framed construction not exceeding 3 stories in height	P	P	P
	Other Occupancy Category I or II buildings not exceeding 2 stories in height	P	P	P
	Regular structures with $T < 3.5T_s$ and all structures of light-framed construction	P	P	P
	Irregular structures with $T < 3.5T_s$ and having only horizontal irregularities Type 2, 3, 4, or 5 of Table 32.11 or vertical irregularities Type 4, 5a, or 5b of Table 32.12	P	P	P
	All other structures	NP	P	P

Note: P, permitted; NP, no permitted.

Source: ASCE, *Minimum Design Loads for Buildings and Other Structures*, ASCE 7-05, American Society of Civil Engineers, Reston, VA, 2005.

- Diaphragm loads determined using Equation 32.18
- Structures with damping systems designed in accordance with ASCE 7-05, Chapter 18.

The redundancy factor (ρ) shall equal 1.3 for structures assigned to Seismic Design Categories D, E, or F, unless one of the following conditions is met, whereby ρ is permitted to be taken as 1.0:

- Each story resisting more than 35% of the base shear in the direction of interest shall comply with Table 32.14.
- Structures are regular in plan at all levels, provided that the seismic-force-resisting systems consist of at least two bays of seismic-force-resisting perimeter framing on each side of the structure in each orthogonal direction at each story resisting more than 35% of the base shear. The number of bays for a shear wall shall be calculated as the length of the shear wall divided by the story height or two times the length of the shear wall divided by the story height for light-frame construction.

32.2.4 Equivalent Lateral Force Procedure

The International Building Code and ASCE 7-05 require that structures be designed for seismic forces in each of the two orthogonal directions. Such forces may be assumed to act nonconcurrently in the direction of each principal axis of the structure except for structures with certain plan irregularities. Even though not all structures are permitted to be designed using the equivalent lateral force analysis procedure, the procedure is often used to help determine those structures that require more exhaustive analysis. When a dynamic analysis is to be preformed, an equivalent lateral force analysis generally has to be the first step of the process.

TABLE 32.14 Requirements for Each Story Resisting More Than 35% of the Base Shear

Lateral-Force-Resisting Element	Requirement
Braced frames	Removal of an individual brace, or connection thereto, would not result in more than a 33% reduction in story strength nor does the resulting system have an extreme torsional irregularity (horizontal structural irregularity Type 1b).
Moment frames	Loss of moment resistance at the beam-to-column connections at both ends of a single beam would not result in more than a 33% reduction in story strength nor does the resulting system have an extreme torsional irregularity (horizontal structural irregularity Type 1b).
Shear walls or wall pier with a height-to-length ratio greater than 1.0	Removal of a shear wall or wall pier with a height-to-length ratio greater than 1.0 within any story, or collector connections thereto, would not result in more than 33% reduction in story strength nor does the resulting system have an extreme torsional irregularity (horizontal structural irregularity Type 1b).
Cantilever columns	Loss of moment resistance at the base connections of any single cantilever column would not result in more than 33% reduction in story strength nor does the resulting system have an extreme torsional irregularity (horizontal structural irregularity Type 1b).
Other	No requirements.

Source: ASCE, *Minimum Design Loads for Buildings and Other Structures*, ASCE 7-05, American Society of Civil Engineers, Reston, VA, 2005. With permission.

32.2.4.1 Effective Seismic Weight (W)

The effective seismic weight of a building (W) is the total dead load and applicable portions of other loads:

- In occupancies where partition loads are used in the floor design, a load of not less than 10 psf shall be included.
- In occupancies such as storage and warehouses, a minimum of 25% of the floor live load shall be included.
- In areas subjected to flat roof snow loading greater than 30 psf, 20% of the snow load shall be included in the design regardless of actual roof slope.
- In buildings with permanent equipment, the weight of such equipment shall be included as part of the total dead load (W).

32.2.4.2 Seismic Base Shear

The International Building Code equation for calculating the total design lateral force at the base of a building in a given direction is as follows:

$$V = C_s W \quad (32.1)$$

The seismic response coefficient (C_s) is determined by:

$$C_s = \frac{S_{DS}}{\left(\frac{R}{I}\right)} \quad (32.2)$$

The value of C_s need not exceed the following:

$$C_s = \frac{S_{D1}}{T \left(\frac{R}{I}\right)} \text{ for } T \leq T_L \quad (32.3a)$$

$$C_s = \frac{S_{D1} T_L}{T^2 \left(\frac{R}{I}\right)} \text{ for } T > T_L \quad (32.3b)$$

TABLE 32.15 Values of Approximate Period Parameters C_t and x

Structure Type	C_t^a	x
Moment-resisting frame systems in which the frames resist 100% of the required seismic force and are not enclosed or adjoined by components that are more rigid and will prevent the frames from deflecting where subjected to seismic forces:		
Steel moment-resisting frames	0.028 (0.0724)	0.8
Concrete moment-resisting frames	0.016 (0.0466)	0.9
Eccentrically braced steel frames	0.03 (0.0731)	0.75
All other structural systems	0.02 (0.0488)	0.75

^a Metric equivalents are shown in parentheses.

Source: ASCE, *Minimum Design Loads for Buildings and Other Structures*, ASCE 7-05, American Society of Civil Engineers, Reston, VA, 2005. With permission.

In addition, for structures located where S_1 is greater than or equal to 0.6g, C_s shall not be less than:

$$C_s = \frac{0.5S_1}{\left(\frac{R}{I}\right)} \quad (32.3c)$$

where:

C_s = seismic response coefficient.

W = total seismic dead load of the system.

I = importance factor in Table 32.7.

R = response modification coefficient per Table 32.10.

T = fundamental period of vibration of the building.

T_L = long-period transition point.

V = total design lateral force or shear at the base.

S_{DS} = design, 5% damped, spectral response acceleration at short periods of vibration.

S_{D1} = design, 5% damped, spectral response acceleration at a period of 1 second.

S_1 = mapped MCE, 5% damped, spectral response acceleration at a period of 1 second.

The fundamental period of the structure (T) shall be determined using the structural properties and deformation characteristics of the resisting elements in a properly substantiated analysis. As an alternative to performing an analysis to determine the fundamental period (T), it is permitted to use the approximate building period (T_a). For all buildings, the value T_a may be approximated from the following formula:

$$T_a = C_t h_n^x \quad (32.4)$$

where h_n is the height in feet above the base to the highest level of the structure, and the numerical coefficients C_t and x are determined from Table 32.15.

The fundamental period (T) calculated by methods other than the approximate method shall not exceed an upper limit as determined from:

$$T \leq C_u T_a \quad (32.5)$$

where C_u is determined from Table 32.16.

Alternatively, the approximate period may be determined from the following equations when the structure does not exceed 12 stories in height and consists entirely of concrete or steel moment resisting frames with a story height of at least 10 feet:

$$T_a = 0.1N \quad (32.6)$$

where N = number of stories.

TABLE 32.16 Coefficient for Upper Limit on Calculated Period

Design Spectral Response Acceleration Parameter at 1 Second (S_{D1})	Coefficient C_u
0.4	1.4
0.3	1.4
0.2	1.5
0.15	1.6
≤ 0.1	1.7

Source: ASCE, *Minimum Design Loads for Buildings and Other Structures*, ASCE 7-05, American Society of Civil Engineers, Reston, VA, 2005. With permission.

For concrete or masonry shear-wall structures, the approximate period (T_a) may be determined from the following formula:

$$T_a = \frac{0.0019}{\sqrt{C_w}} h_n \quad (32.7)$$

where h_n is defined in the proceeding text, and C_w is calculated from the following formula:

$$C_w = \frac{100}{A_B} \sum_{i=1}^x \left(\frac{h_n}{h_i} \right)^2 \left[\frac{A_i}{1 + 0.83 \left(\frac{h_i}{D_i} \right)^2} \right] \quad (32.8)$$

where:

A_B = area of base of structure (ft²).

A_i = web area of shear wall i (ft²).

D_i = length of shear wall i (ft).

h_i = height of shear wall i (ft).

x = number of shear walls in the building effective in resisting lateral forces in the direction under consideration.

32.2.4.3 Vertical Distribution of Force

The total seismic force shall be distributed to each level of the structure in accordance with the following:

$$F_x = C_{vx} V \quad (32.9)$$

and

$$C_{vx} = \frac{w_x h_x^k}{\sum_{i=1}^n w_i h_i^k} \quad (32.10)$$

where:

C_{vx} = vertical distribution factor.

V = total design lateral force at the base of the structure (kips or kN).

w_p, w_x = the portion of the total effective seismic weight (W) located or assigned to level i or x .

h_p, h_x = the height (ft or m) from the base of the structure to level i or x .

k = an exponent related to the structure period as follows: (1) when $T < 0.5$ seconds, $k = 1$, and (2) when $T \geq 2.5$ seconds, $k = 2$; for structures having a period between 0.5 and 2.5 sec, k shall be taken equal to 2 or shall be determined by linear interpolation between 1 and 2.

TABLE 32.17 Allowable Story Drift (Δ_a)

Structure	Occupancy Category		
	I or II	III	IV
Structures, other than masonry shear walls structures, 4 stories or less with interior walls, partitions, ceilings and exterior wall systems that have been designed to accommodate the story drifts.	$0.25h_{sx}^a$	$0.020h_{sx}$	$0.015h_{sx}$
Masonry cantilever shear wall structures ^b	$0.010h_{sx}$	$0.010h_{sx}$	$0.010h_{sx}$
Other masonry shear wall structures	$0.007h_{sx}$	$0.007h_{sx}$	$0.007h_{sx}$
All other structures	$0.020h_{sx}$	$0.015h_{sx}$	$0.010h_{sx}$

^a There shall be no drift limit for single-story structures with interior walls, partitions, ceilings, and exterior wall systems that have been designed to accommodate the story drifts. The structure separation requirement of ASCE 7-05 Section 12.12.3 is not waived.

^b Structure in which the basic structural system consists of masonry shear walls designed as vertical elements cantilevered from their base or foundation support which are so constructed that moment transfer between shear walls (coupling) is negligible.

Note: h_{sx} is the story height below level x . For seismic-force-resisting systems comprised solely of moment frames in Seismic Design Categories D, E, and F, the allowable story drift shall comply with the requirements of ASCE 7-05, Section 12.12.1.1.

Source: ASCE, *Minimum Design Loads for Buildings and Other Structures*, ASCE 7-05, American Society of Civil Engineers, Reston, VA, 2005. With permission.

32.2.4.4 Horizontal Distribution of Shear and Horizontal Torsional Moments

The seismic design story shear (V_x , the sum of the forces F_i above that story) in any story shall be distributed to the various elements of the vertical lateral-force-resisting system in proportion to their rigidities, considering the rigidity of the diaphragm. Furthermore, the IBC and ASCE 7-05 require that provisions be made for the increased shears resulting from horizontal torsion where diaphragms are not flexible. To account for the uncertainties in load locations, the IBC and ASCE 7-05 further require that the mass at each level be assumed to be displaced from the calculated center of mass in each direction a distance equal to 5% of the building dimension at that level perpendicular to the direction of the force under consideration. This is often referred to as the *accidental torsion*. The torsional design moment at a given story is the moment resulting from the combination of this accidental torsional moment and the inherent torsional moment between the applied design lateral forces and the center of rigidity of the vertical lateral-force-resisting elements in that story (see Figure 32.5). When seismic forces are applied concurrently in two orthogonal directions, the required 5% displacement of the center of mass need not be applied in both orthogonal directions at the same time but shall be applied in the direction that produces the greater effect.

32.2.4.5 Story Drift Determination and Limitation

The IBC and ASCE 7-05 define *story drift* as the relative displacement between adjacent stories (above or below) due to the design lateral forces. The design story drift is computed as the difference of the deflections at the center of mass at the top and bottom of the story under consideration. ASCE 7-05 further expands on the requirements for calculating story drift by stating that, for structures with significant torsional deflections, the maximum story drift must include torsional effects. For structures assigned to Seismic Design Categories C, D, E, or F having horizontal irregularities of Type 1a or Type 1b, the design story drift (Δ) shall be computed as the largest difference of the deflections along any of the edges of the structure at the top and bottom of the story under consideration. The design story drift (Δ) shall not exceed the allowable story drift (Δ_a) determined from Table 32.17.

The deflections used to determine the design story drift shall be determined from the following equation:

$$\delta_x = \frac{C_d \delta_{xe}}{I} \quad (32.11)$$

where:

C_d = the deflection amplification factor in Table 32.10.

δ_{xe} = the deflection determined by elastic analysis without the upper limit on the fundamental period ($C_u T_a$).

I = the importance factor determined from Table 32.7.

Past codes, such as the Uniform Building Code, did not elaborate on how story drift is determined from analysis results. As a result, it was often assumed that the drift should be calculated at the structure extremities as is now required by ASCE 7-05 only in certain seismic design categories and when torsional irregularities exist. This can have a liberalizing effect on drift requirements of moment frame structures that are often governed by drift. Whereas these requirements seem to loosen drift requirements that would impact moment frame structures, a limitation has been put into place on the allowable story drift requiring that the design story drift not exceed Δ_u/ρ for structures assigned to Seismic Design Categories D, E, or F.

32.2.4.6 P-Delta Effects

P-delta effects on story shears and moments, the resulting member forces and moments, and the story drifts induced by these effects are not required to be considered where the stability coefficient θ , as determined by the following equation, is less than or equal to 0.10:

$$\theta = \frac{P_x \Delta}{V_x h_{sx} C_d} \quad (32.12)$$

where:

P_x = total vertical design load at and above level x (kips or kN); when computing P_x , no individual load factor need exceed 1.0.

Δ = design story drift occurring simultaneously with V_x (in. or mm).

V_x = seismic shear force acting between levels x and $x - 1$ (kips or kN).

h_{sx} = story height below level x (in. or mm).

C_d = deflection amplification factor in Table 32.10.

The stability coefficient θ shall not exceed θ_{\max} determined as follows:

$$\theta_{\max} = \frac{0.5}{\beta C_d} \leq 0.25 \quad (32.13)$$

where β is the ratio of shear demand to shear capacity for the story between levels x and $x - 1$. This ratio may conservatively be taken equal to 1.0.

When $0.10 < \theta \leq \theta_{\max}$, the incremental factor related to P-delta effects on displacement and member forces shall be determined by rational analysis. As an alternative, it is permitted to multiply displacements and member forces by $1.0/(1 - \theta)$. When $\theta > \theta_{\max}$, the structure is potentially unstable and shall be redesigned. Where P-delta effects are included in an automated analysis, Equation 32.13 will still be satisfied; however, the value of θ computed from Equation 32.12 using the results of the P-delta analysis is permitted to be divided by $(1 + \theta)$ before checking Equation 32.13.

32.2.4.7 Deformation Compatibility

For structures assigned to Seismic Design Categories D, E, or F, all framing elements not required by design to be part of the lateral-force-resisting system must be investigated and shown to be adequate for vertical-load-carrying capacity when subjected to the design story drift (Δ) resulting from the required design lateral force. Reinforced concrete frame members not designed as part of the lateral-force-resisting system shall comply with Section 21.9 of ACI 318.

32.2.5 Modal Response Spectrum Analysis

ASCE 7-05 sets some rather general requirements regarding modal response spectrum analysis (dynamic analysis). The following is a summary of the requirements:

- The analysis shall include a sufficient number of natural modes of vibration for the structure such that the modal mass participation in each direction is at least 90% of the actual mass.
- The design forces shall be determined using the properties of each mode and the response spectrum defined in either Section 32.2.1.5 or Section 21.2 of ASCE 7-05 divided by R/I . When calculating displacement and drift, values shall be multiplied by C_d/I .
- The value for each response parameter shall be combined using either the square root sum of the squares (SRSS) method or the complete quadratic combination (CQC) method, in accordance with ASCE 4.
- A base shear shall be calculated in each of the two orthogonal directions using the equivalent lateral force procedure of Section 32.2.4. When the fundamental period of vibration exceeds the cap $C_u T_a$, then $C_u T_a$ shall be used in lieu of T in that direction.
- Where the combined response for the modal base shear (V_l) is less than 85% of the calculated base shear (V) using the equivalent lateral force procedure, the forces, but not the drifts, shall be multiplied by $0.85V/V_l$.
- The horizontal distribution of shear shall be in accordance with the horizontal distribution requirements of the equivalent lateral force procedure except that the amplification of the torsional effects required when a horizontal irregularity Type 1a or Type 1b exists is not required when accidental torsional effects are included in the dynamic analysis model.
- P-delta effects are determined in accordance with the same requirements as the equivalent lateral force procedure, as well as the story shears and story drifts.
- A soil structure interaction reduction is permitted where determined using ASCE 7-05, Chapter 19.

As can be seen from the above requirements, even though a separate method of analysis is being employed, the requirements of the equivalent lateral force procedure still play a large role in the modal response spectrum analysis.

32.2.6 Seismic Load Combinations

The basic load combinations for strength design are as follows:

$$(1.2 + 0.2S_{DS})D + \rho Q_E + L + 0.2S \quad (32.14)$$

$$(0.9 - 0.2S_{DS})D + \rho Q_E + 1.6H \quad (32.15)$$

The basic load combinations for strength design with the overstrength factor (Ω_O) are as follows:

$$(1.2 + 0.2S_{DS})D + \Omega_O Q_E + L + 0.2S \quad (32.16)$$

$$(0.9 - 0.2S_{DS})D + \Omega_O Q_E + 1.6H \quad (32.17)$$

where:

D = dead loads or related internal moments and forces.

L = live loads or related internal moments and forces.

Q_E = effects of horizontal seismic forces from V or F_p .

ρ = redundancy factor from Section 32.2.3.10.

S_{DS} = design spectral acceleration parameter defined in Section 32.2.1.4.

H = load due to earth pressure, ground water pressure, or pressure of bulk materials.

S = snow load.

Ω_O = overstrength factor.

The load factor applied to the live load in the above load combinations is permitted to equal 0.5 for all occupancies where the live load is less than or equal to 100 psf with the exception of garages or areas of public assembly. The load factor on H in the above load combinations shall be set equal to zero if the structural action due to H counteracts that due to E . Where lateral earth pressure provides resistance to structural actions other than seismic, it shall not be included in H but shall be included in the design resistance. When utilizing the load combinations including the overstrength factor, the required design strength for an element need not exceed the maximum force that can be developed in the element as determined by rational, plastic mechanism analysis, or nonlinear response analysis utilizing realistic expected values of material strengths.

32.2.7 Diaphragms, Chords, and Collectors

Floor and roof diaphragms are required to be designed to resist the forces determined in the following formula:

$$F_{px} = \frac{\sum_{i=x}^n F_i}{\sum_{i=x}^n w_i} w_{px} \quad (32.18)$$

The force (F_{px}) determined in the above formula need not exceed $0.4S_{DS}Iw_{px}$ but shall not be less than $0.2S_{DS}Iw_{px}$. For structures assigned to Seismic Design Categories D, E, and F, redundancy factor ρ shall be used in the diaphragm design. For inertial forces calculated in accordance with Equation 32.18, the redundancy factor shall equal 1.0. For transfer forces, the redundancy factor shall be the same as that used for the structure. For structures assigned to Seismic Design Categories D, E, or F and having a horizontal structural irregularity of Types 1a, 1b, 2, 3, or 4 from Table 32.11 or a vertical irregularity of Type 4 from Table 32.12, the design forces determined from Section 32.2.2.2 shall be increased 25% for connections of diaphragms to vertical elements and to collectors. Collectors and their connections shall be designed for these increased forces unless they are designed for the load combinations that include the overstrength factor.

32.2.8 Building Separation

All structures have to be separated from adjoining structures a distance sufficient to avoid damaging contact under total deflection δ_x . ASCE 7-05 does not further expand on what is considered a sufficient distance; however, past codes allowed the separation to be based on the square root sum of the squares of the estimated maximum seismic displacement due to code-specified seismic forces of the two structures. The separation was calculated as $\delta_s = \sqrt{\delta_{x1}^2 + \delta_{x2}^2}$, where δ_{x1} and δ_{x2} are the displacement of adjacent buildings and δ_s is the calculated required building separation.

32.2.9 Anchorage of Concrete or Masonry Walls

Concrete or masonry walls shall be provided with a positive direct connection to all floors and roofs that provide them lateral support. Such connections shall be capable of resisting the horizontal forces induced by the seismic excitement and as specified in the code. ASCE 7-05, Section 12.11, should be consulted for further information.

32.2.10 Material-Specific Design and Detailing Requirements

The IBC and ASCE 7-05 make a series of modifications to ACI 318. The IBC in turn makes a series of modifications to both ASCE 7-05 and ACI 318 in Chapters 16 and 19. ASCE 7-05 lists the required modification as part of Chapter 14.

32.2.11 Foundation Design

The foundation shall be designed to resist the forces developed and accommodate the movements imparted to the structure by the design ground motions. Importantly, overturning effects at the soil–foundation interface are permitted to be reduced by 25% for foundations of structures that are designed in accordance with the equivalent lateral force analysis procedure provided the structure is not an inverted pendulum or cantilevered column type structure. Overturning effects at the soil–foundation interface are permitted to be reduced by 10% for foundation of structures designed in accordance with the modal response spectrum analysis procedure. Refer to ASCE 7-05, Section 12.13, for additional foundation design requirements.

32.3 Design and Construction of Concrete and Masonry Buildings

32.3.1 Preface

This section is intended to serve as a guide to engineers in the design of reinforced-concrete and masonry buildings to resist earthquake forces in conformance with the 2006 IBC and ASCE 7-05 (refer to Section 32.2). The lateral-load-resisting system, including horizontal diaphragms, is addressed. Please note that term definitions, notations, and symbols used in this chapter are provided in the 2006 IBC and ASCE 7-05.

32.3.2 Concrete Buildings

32.3.2.1 Introduction

As discussed in Section 32.2, reinforced-concrete buildings in general are designed to have adequate strength to resist the equivalent static lateral load and appropriate ductility to allow the structure to displace as a result of dynamic earthquake excitement. The building strength is achieved by selecting the appropriate member sizes, concrete strength, proper placement, and adequate size of reinforcing steel so the nominal capacity decreased by a reduction factor of each member meets or exceeds the ultimate demands. Ductility is achieved by providing confinement to the concrete section at critical locations by introducing closely spaced and appropriately anchored bars transversely to the longitudinal reinforcement in beams, columns, and boundary members such as at the ends of a shear wall (see Figure 32.9).

When designing a building to resist the seismic forces obtained in Section 32.2, the engineer would go through selection of the lateral-force-resisting system. This section addresses shear walls and special moment-resisting frames, as they are primarily used in Seismic Design Categories D, E, and F. The decision of whether to choose shear walls or moment frames or a combination of the two depends on the architectural layout of the structure. The structural engineer's role in most cases is limited to locating and sizing the lateral resisting elements. The following steps are then followed in the lateral design of the structure:

- Select the lateral-force-resisting system.
- Calculate the building weight and base shear (see Section 32.2).
- Distribute lateral load to each floor and calculate the story shear (see Section 32.2).
- Distribute story shear to the various lateral-force-resisting elements at each floor based on member stiffness (see Section 32.2.4.4).
- Design and detail lateral-force-resisting components (shear wall or moment frame) for the applied forces.
- Design and detail diaphragms to transfer story shear into shear walls or moment frames.

32.3.2.2 Horizontal Distribution of Shear and Torsional Moments

The following discussion addresses the distribution of shear and torsional moments on the basis that the lateral-force-resisting system consists of shear walls. The same discussion also applies to buildings

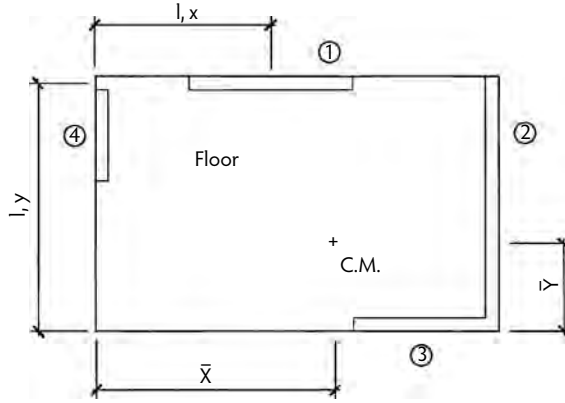


FIGURE 32.4 Schematic center of mass in shear wall.

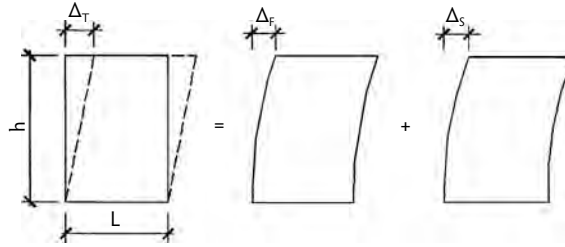


FIGURE 32.5 Cantilever shear-wall deflection.

with moment frames or combination of shear walls and moment frames. The center of mass of the floor is first calculated as follows:

$$X_m = \frac{\sum wx}{\sum w} \quad (32.19)$$

$$Y_m = \frac{\sum wy}{\sum w} \quad (32.20)$$

Figure 32.4 serves as a good illustration for the above formulas. Next, the rigidity of each wall is calculated. The deflection at the top of the wall is calculated based on the following formula:

$$\Delta_T = \Delta_F + \Delta_S = \frac{Ph^3}{3E_G I} + \frac{1.2Ph}{AE_G} \quad (32.21)$$

where r is the rigidity or stiffness of the wall panel equal to $1/\text{deflection}$ (see Figure 32.4, Figure 32.5, and Figure 32.6). The center of rigidity of the floor is then calculated as follows:

$$\bar{x}_r = \frac{\sum r_x x}{\sum r_y} \quad (32.22)$$

$$\bar{y}_r = \frac{\sum r_x y}{\sum r_x} \quad (32.23)$$

Refer to Figure 32.7 for the shear distribution formulation.

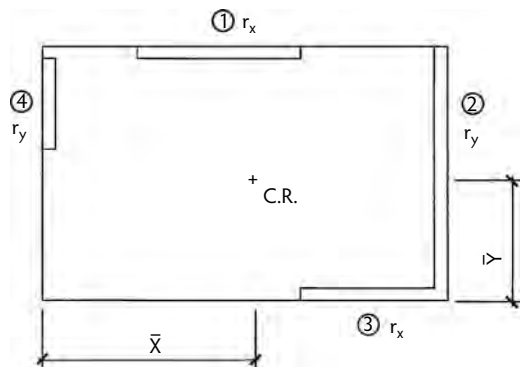


FIGURE 32.6 Schematic center of rigidity in a shear wall.

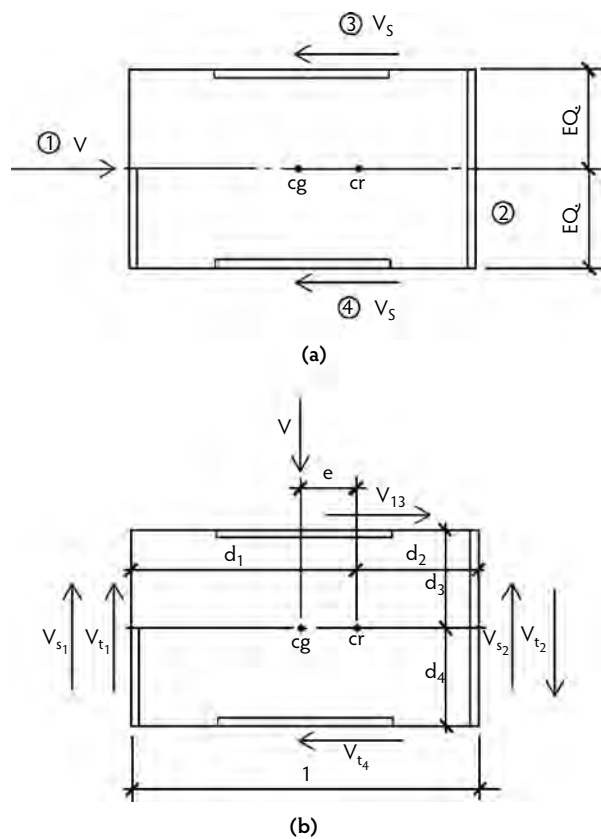


FIGURE 32.7 Shear distribution formulation.

32.3.2.3 Design of Vertical Lateral-Force-Resisting Elements

This section illustrates the design and reinforcement requirements for shear walls and moment-resisting frames through practical examples.

Example 32.1. Shear-Wall Design and Reinforcement Requirements

(See Figure 32.8.) The given values are as follows:

- $f'_c = 4000$ psi.
- t (wall thickness) = 12 in.

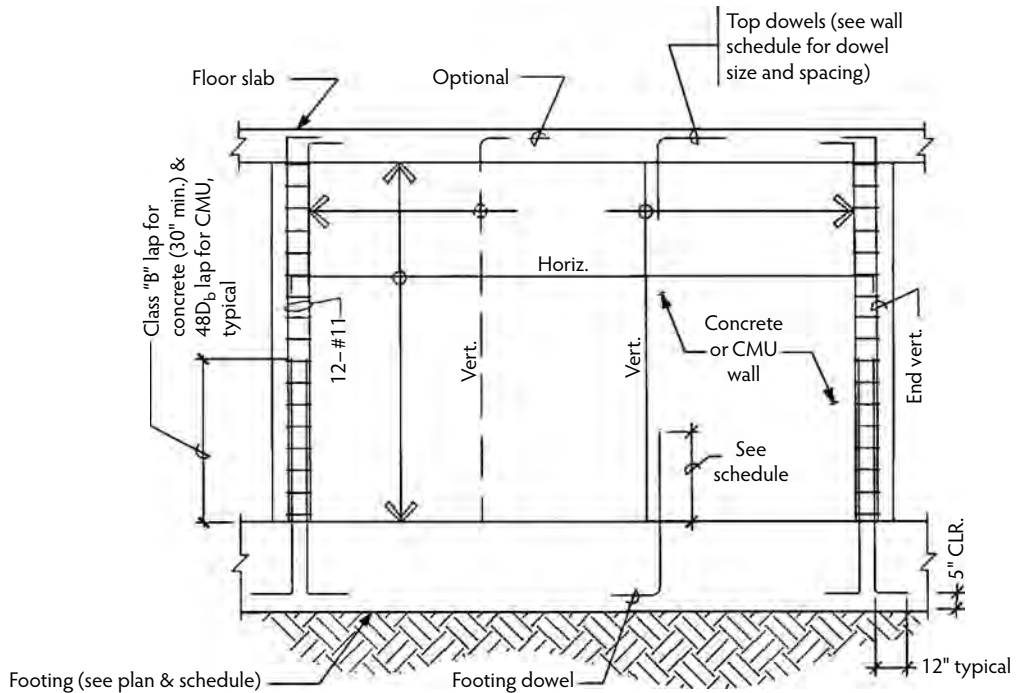


FIGURE 32.8 Typical shear wall elevation.

$V_u = 980$ kips = shear force.

$M_u = 73,500$ kip-ft = overturning moment.

$P_u = 2800$ kips = total load on wall, includes wall weight.

$S_{DS} = 1.1$ (site class D).

$L = 53$ ft.

$H = 75$ ft.

Note that walls with a height-to-width ratio (H/W) greater than 2.0 behave primarily as bending members, whereas walls with H/W below 2.0 resist lateral forces in a predominantly truss-type behavior. The maximum shear stress in walls is limited to $2\sqrt{f'_c}$.

- The vertical steel in the wall is required to equal the horizontal steel.
- At least two curtains of reinforcement shall be used in a wall if the in-plane factored shear force assigned to the wall exceeds $2A_{cv}\sqrt{f'_c}$. A_{cv} is the cross-sectional area bounded by the wall length parallel to the direction of the shear force and the wall thickness.

Check number of curtains required:

$$2A_{cv}\sqrt{f'_c} = \left(2 \times 12 \times (53 \times 12) \sqrt{4000}\right) / 1000 = 965.4 \text{ kips}$$

$$V_u = 980 \text{ kips}$$

$$V_u > 2A_{cv}\sqrt{f'_c} \therefore \text{two curtains of reinforcement are required}$$

- Required vertical and horizontal wall reinforcement:

$$\text{Minimum rebar ratio, } \rho_v = 0.0025$$

$$\text{Area of steel in each, } \rho_v A_{cv} = 0.0025 \times 12 \text{ in.} \times 12 \text{ in.} = 0.36 \text{ in.}^2/\text{ft}$$

- Try #5 bars in each direction at each face at 18 in. on-center $\leq S_{\max} = 18$ in.

$$A_m = 2 \times 0.31 \times 12 / 18 = 0.413 \text{ in.}^2$$

$$h_w / l_w = 75 \text{ ft} / 53 \text{ ft.} = 1.42 < 2$$

$$V_n = A_{cv} (\alpha_c \sqrt{f'_c} + \rho_n f_y)$$

$$A_{cv} = 12 \times (53 \times 12) = 7632 \text{ in.}^2$$

$$\alpha_c = 3.0 \quad (\alpha_c \text{ varies linearly from 3.0 for } h_w / l_w = 1.5 \text{ to 2.0 for } h_w / l_w = 2.0)$$

$$\rho_n = 2 \times 0.31 / (12 \times 18) = 0.0029$$

$$\phi = 0.6$$

- Check:

$$V_n \leq 10 A_{cv} \sqrt{f'_c}.$$

$$V_n = \frac{7632}{1000} (3 \sqrt{4000} + 0.0029 \times 60,000) = 2776 \text{ kips}$$

$$10 A_{cv} \sqrt{f'_c} = 10 \times 7632 \times \sqrt{4000} / 1000 = 4827 \text{ kips} \quad \therefore V_n < 10 A_{cv} \sqrt{f'_c} \quad (\text{OK})$$

Boundary member requirement: Boundary members shall be provided where the maximum compressive and extreme-fiber stress under factored forces exceeds $0.2f'_c$.

- Gross section properties:

$$l = 53 \text{ ft, } t = 12 \text{ in.}$$

$$A_{cv} = 53 \times 12 \times 12 = 7632 \text{ in.}^2$$

$$I_y = 12 \times (53 \times 12)^3 / 12 = 257,259,456 \text{ in.}^4$$

$$f_c = P_u / A_g + M_u (l_w / 2) / I_y$$

$$P_u = 2800 \text{ kips}$$

$$M_u = 73,500 \text{ kip-ft}$$

$$f_c = \frac{2800}{7632} + \frac{73,500 \times 12 \times 53 \times 12 / 2}{257,259,456} = 1.46 \text{ ksi}$$

$$0.2f_c = 0.2 \times 4 = 0.8 \text{ ksi} < 1.46 \text{ ksi} \quad \therefore \text{provide boundary member}$$

- Check axial capacity of 36×36 -in. boundary member with 12 #11:

$$A_y = 36 \times 36 = 1296 \text{ in.}^2$$

$$A_{st} = 12 \times 1.56 = 18.72 \text{ in.}^2$$

$$\rho_g = 18.72 / 1296 = 0.0144$$

$$\rho_{\min} = 0.01 < \rho_g < \rho_{\max} = 0.06 \quad (\text{OK})$$

$$P_u = \phi P_n = 0.6 [0.85 f'_c (A_y - A_{st}) + f_y A_{st}] = 3279 \text{ kips} > P_u \quad (\text{OK})$$

- Use 36×36 -in. boundary members with 12 #11.

- Check boundary reinforcement for tension load for load combination:

$$T_u = (0.9 - 0.2S_{DS})D \pm E$$

$$P_D = 1400 \text{ kips}$$

$$T_u = 73,500 / (53 - 3) - (0.9 - 0.2 \times 1.1) \times 1400 \times 0.5 = 994 \text{ kips}$$

$$A_s = T_u / \phi f_y = 994 / (0.9 \times 60) = 18.41 \text{ in.}^2 \quad (\text{OK})$$

Other requirements: (1) Required cross-sectional area of confinement reinforcement should be in accordance with ACI 318-05; see Nawy (2008) for a detailed example. (2) All continuous reinforcement in shear walls must be anchored or spliced as required by IBC and ACI.

32.3.3 Design of Masonry Buildings

32.3.3.1 Introduction

The majority of construction in the masonry industry involves smaller buildings, and these are often designed with the code-equivalent static loads. It is the intent of this section to briefly demonstrate how the building must be designed to resist these equivalent static lateral forces. Again, for computational convenience, the effects of ground motion are considered as if the motion acts only in one direction parallel to the perpendicular axes of the building. Several different types of structural systems are used to resist the static lateral forces and carry them into the foundation. Such systems include shear walls, braced frames, and moment-resisting space frames. Because it has not been possible, so far, to feasibly construct masonry moment-resisting frames, this chapter is limited to the discussion of concrete masonry shear walls.

32.3.3.2 General Behavior of Box Buildings

A box system does not have an independent vertical-load-carrying frame but rather depends on the walls not only to carry the vertical loads but also to provide the necessary lateral stability. Walls that are perpendicular to the assumed direction of the ground motion must span vertically between the floor diaphragms. The inertial effect of one half the wall height, both above and below the floor level in question, is considered to be transferred to that floor diaphragm. In addition, the inertial effect of the diaphragm dead load itself must be taken by the diaphragm. The diaphragm essentially behaves as a horizontal plate girder, wherein the diaphragm boundary members serve as the girder flanges and the floor functions as the web. The diaphragm therefore spans between the supporting shear walls. Through the diaphragm-to-wall connection, the total horizontal shear is transferred directly to the shear wall. Depending on the rigidity of the diaphragm, this lateral shear transfer to any shear wall may be based on the adjacent tributary area or the relative rigidities of the various shear walls. Where rigid diaphragms such as reinforced or post-tensioned concrete floor slabs are used, each wall experiences a torsional shear in addition to the direct shear when the building center of gravity and the center of rigidity of the vertical lateral-force-resisting elements do not coincide. The total direct lateral shear and the torsional shear are combined so the sum becomes the total UBC-design force imposed upon the shear wall. Figure 32.7 provides an illustration of the total shear force, lateral load combination.

32.3.3.3 Shear Walls

32.3.3.3.1 Shear-Wall Design

Roof and floor seismic forces may be carried down to the building foundation by the strength and rigidity of the building walls in a bearing wall system or building frame system. Such walls are called *shear walls*. In tall buildings, design of the shear walls is generally governed by flexure, whereas in low buildings shear is often the governing criteria. The shear wall is basically a cantilever member with the shear force resisted by the combined shear strength of the masonry and the horizontal rebar in the wall, while the vertical

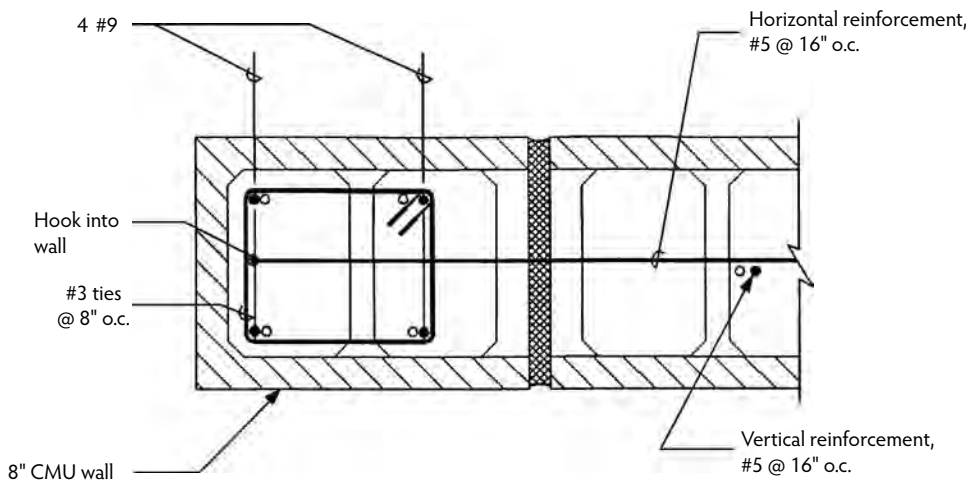


FIGURE 32.9 Typical placement of reinforcement in masonry shear wall.

boundaries (end reinforcement) provide the capacity to resist tension and compression caused by the bending moment and axial forces on the wall. A shear wall by definition is a wall resisting in-plane horizontal shear forces. In addition to horizontal force, the wall is investigated for the effects of the vertical loads it is subjected to. Example 32.2 provides a good illustration for the design of a concrete masonry wall subjected to both gravity and seismic forces.

32.3.3.3.2 Shear-Wall Detailing

For a masonry wall to function properly as a shear wall, it must be capable of resisting the diagonal tensile forces imposed by the design shear forces and the vertical compressive or tensile stresses caused by the overturning moment due the same design shear forces. A typical detail for placing reinforcing steel in a masonry wall is shown in Figure 32.9. The horizontal rebar is anchored with a 90° standard hook to ensure that the bar can be fully developed in tension. Also shown in Figure 32.9 is the end reinforcement for a four-bar condition to resist tensile forces. Figure 32.8 shows an elevation of the same wall with the wall-to-floor and wall-to-footing connections properly shown. It is important to note that the designer must take into account the limited amount of space in the cells when specifying the bar size and spacing so the placement of reinforcement does not become impossible.

Example 32.2. Masonry Shear-Wall Design

The given values are as follows:

Masonry, CMU $f'_m = 1500$ psi

Grout, type M, 2000 psi

Steel, Gr 60

Special inspection required

Wall length, 31 ft

Wall thickness, 12 in

Wall height, 12 ft

Shear force, 203.45 kips

Moment, 3051.7 kip-ft

Axial loading, 95.00 kips

The following items are required:

Stress check

Reinforcement requirements

The following calculations are necessary (calculations are based on design UBC 1991):

$$E_m = 750 \times 1500 = 1125 \text{ ksi.}$$

$$E_s = 29,000 \text{ ksi.}$$

$$\text{Ratio of moduli} = 29,000/1125 = 25.78.$$

$$\text{Allowable steel stress } (F_s) = 24,000 \text{ psi.}$$

$$\text{Increase for seismic design } (1.33F_s) = 1.33 \times 24,000 = 31,920 \text{ psi.}$$

$$\text{Allowable bending stress } (F_b) = 0.33f'_m = 0.33 \times 1500 = 495 \text{ psi.}$$

$$\text{Increase for seismic design } (1.33F_b) = 658.35 \text{ psi.}$$

$$\text{Allowable axial stress } (F_a/R) = 0.2f'_m = 0.2 \times 1500 = 300 \text{ psi.}$$

$$\text{Increase for seismic design} = 399 \text{ psi.}$$

The design for bending and axial load is as follows:

$$R = \left[1 - \left(h / 42t \right)^3 \right]$$

$$h = 12 \times 12 = 144 \text{ in.}$$

$$t = 11.625 \text{ for 12 in./in. CMU}$$

$$R = 1 - \left(\frac{144}{42 \times 11.625} \right)^3 = 0.97$$

$$f_a = \frac{P}{A} = \frac{95 \times 1000}{31 \times 12 \times 11.625} \cong 22 \text{ psi}$$

$$\text{Allowable axial stress } (F_a) = 399 \times 0.97 = 387 \text{ psi.}$$

$$\text{Axial stress ratio } (f_a/F_a) = 21.97/387 = 0.057.$$

$$\frac{f_a}{F_a} + \frac{f_b}{F_b} = 1$$

$$\text{Hence, } f_b/F_b = 1 - 0.057 = 0.943.$$

Assume that masonry stress governs and check for steel stress. If steel stress as calculated exceeds its allowable stress, then discard the assumption and proceed by assuming steel reaches its maximum allowable value first.

(I) Masonry stress governs.

$$f_b = 0.943 \times 658.35 = 621 \text{ psi}$$

$$jk = \frac{2M}{f_b b d^2} = \frac{2 \times 3051.70 \times 12,000}{620.98 \times 11.625 \times 354^2} = 0.081$$

where $d = 12 \times 3 \text{ ft} - 18 \text{ in.} = 354 \text{ in.}$

$$k^2 - 3k + 3jk = 0$$

$$k^2 - 3k + 3 \times 0.081 = 0$$

$$k = 0.0833$$

$$f_s n f_b \left(\frac{1-k}{k} \right) = 25.78 \times 620.98 \left(\frac{1-0.0833}{0.0833} \right) = 176,128 \text{ psi} > 31,920 \text{ psi} \therefore \text{N.G.}$$

(II) Steel stress governs.

$$A_s = \frac{M}{f_s j d} = \frac{3051 \times 12,000}{31,920 \times 0.972 \times 354} = 3.33 \text{ in.}^2 = \text{area of jamb reinforcement}$$

where $j = jk/k = 0.81/0.0833 = 0.972$.

Check compressive stress in the masonry:

$$\rho = A_s / bd = 3.33 / 11.625 \times 354 = 8.09 \times 10^{-4}$$

$$k = \sqrt{2\rho n + (\rho n^2)} - \rho n = \sqrt{2 \times 8.09 \times 10^{-4} \times 25.78 + (25.78 \times 8.09 \times 10^{-4})^2} - 8.09 \times 10^{-4} \times 25.78 = 0.23$$

$$j = 1 - k / 3 = 1 - 0.23 / 3 = 0.923$$

$$f_b = \frac{2M}{j k b d^2} = \frac{2 \times 3051.70 \times 12,000}{0.923 \times 0.162 \times 11.625 \times 354^2} = 336 \text{ psi} < 658.35 \text{ psi} \quad \therefore \text{OK}$$

The bending stress ratio is:

$$\frac{f_b}{F_b} = \frac{336}{658.35} = 0.51 \quad \therefore \text{OK}$$

The combined bending and axial stress ratio is:

$$\frac{f_a}{F_a} + \frac{f_b}{F_b} = 0.06 + 0.51 = 0.57 < 1 \quad \therefore \text{OK}$$

Check shear stresses:

$$\frac{M}{Vd} = \frac{3051.7}{203.45 \times (0.8 \times 31)} = 0.6 < 1 \quad \therefore \text{OK}$$

where $d \cong 0.8 \times 31$.

$$\text{for } M/Vd = 1, F_v = 1.33 \times 1.5 \sqrt{1500} = 77.27 \text{ psi} < 1.33 \times 75 \text{ psi} \quad \therefore \text{OK}$$

$$\text{for } M/Vd = 0, F_v = 1.33 \times 2 \sqrt{1500} = 103.02 \text{ psi} < 1.33 \times 120 \text{ psi} \quad \therefore \text{OK}$$

The allowable ranges for design with rebar are:

$$F_v = 77.27 + (1 - 0.6)(103.02 - 77.27) = 87.33 \text{ psi}$$

Hence, the design stress is $F_v = 77.27 + (1 - 0.6)(103.02 - 77.27) = 87.33 \text{ psi}$, and the governing stress value is $F_v = 87.33 \text{ psi}$.

The actual stress value is:

$$F_v = \frac{V_u}{b j d} = \frac{1.5 \times 203.45 \times 1000}{11.625 \times 0.923 \times 354} = 80.34 \text{ psi}$$

The shear stress ratio is:

$$\frac{f_v}{F_v} = 80.34 / 87.33 = 0.92 \quad \therefore \text{OK}$$

Calculate the shear reinforcement:

$$\text{Horizontal, } A_s = \frac{V_u s}{f_s j d} = \frac{1.5 \times 203.45 \times 1000 \times 12}{31,920 \times 0.923 \times 345} = 0.351 \text{ in.}^2$$

$$\text{Minimum, } A_s = 0.0007 \times 11.625 \times 12 = 0.1 \text{ in.}^2 < 0.351 \text{ in.}^2 \therefore \text{OK}$$

$$\rho_n = 0.351 / 11.625 \times 12 = 0.00252 > 0.002$$

Hence, minimum ρ_u governs: $A_v = 0.0007 \times 11.625 \times 12 = 0.1 \text{ in.}^2/\text{ft.}$

32.3.4 Shear-Wall Foundation Analysis and Design

32.3.4.1 Background

The analysis and design presented herein pertain to the sizing of the shear-wall foundations and determination of their structural adequacy. The algorithm adopted is aimed at obtaining economical foundation dimensions with due consideration of all the major parameters such as the actions from the shear wall, the permissible soil pressure, concrete strength, the shear-wall foundation, and grade beam dimensions. The analysis and design are directed toward the seismic-loading case only. The adequacy of the foundation under gravity loading is to be established separately. Under normal conditions, however, the size and reinforcement of a shear-wall foundation is governed by the seismic case. The gravity case check will be conducted for unusual cases and dimensions. The analysis is based on the limit design concept. A probable failure mechanism is assumed (refer to the free body diagrams in Figure 32.10). By satisfying the requirements of statics, the actions (shears and moments) at critical sections are determined, and the cross-sectional area and reinforcement at such sections are evaluated. The failure mechanism selected may not be the optimum for all cases, but it is consistently conservative.

The soil pressure is checked by determining the soil stress ratio (SSR). This is the ratio of the calculated unfactored soil pressure to the permissible soil pressure. SSR is to be kept less than 1. The analysis assumes that the foundation is tied to the remainder of the structure through grade beams. If the foundation by itself can resist the applied loading without need for grade beams, the calculated shear transfer (parameter G) between the foundation and the grade beam will become zero or negative. If a shear transfer between the foundation and the assumed grade beams results, the analysis and design must be followed by a grade beam design to ensure that the resulting shear (G) is satisfactorily dissipated into the grade beam and the other structural elements.

The applied vertical loading (P), the seismic moment (M), and the shear (V) from the shear wall are calculated elsewhere and are entered herein (see Example 32.3) as input. They act at midlength of the shear wall at the top of the foundation. This design considers the vertical loading and the moment components of the shear wall. The shear component (V) is resisted through friction at the bottom of the foundation, axial loading in the adjoining grade beams, and the connection of the foundation to the slab on grade, as well as by any passive soil pressure that may develop. In common cases, foundation and grade beam sizes, through other considerations, prove to be adequate for V ; however, for isolated foundations this may not be the case. If required, this design section is followed by a check for the shear component V .

One type of typical interior foundation is treated in Example 32.3. Numerous variations are possible depending on the existence of and location at which a grade beam ties into the foundation. The relationships developed embrace most of the common cases. If a foundation geometry does not fall within the scope of this work and cannot be modeled conservatively through the method treated herein, special analysis and design are required. In nonsymmetrical cases, different values for the shear transfer force (G) result, depending on the direction of the applied seismic-bending moment. In such conditions, the value yielding the larger shear transfer is calculated and given.

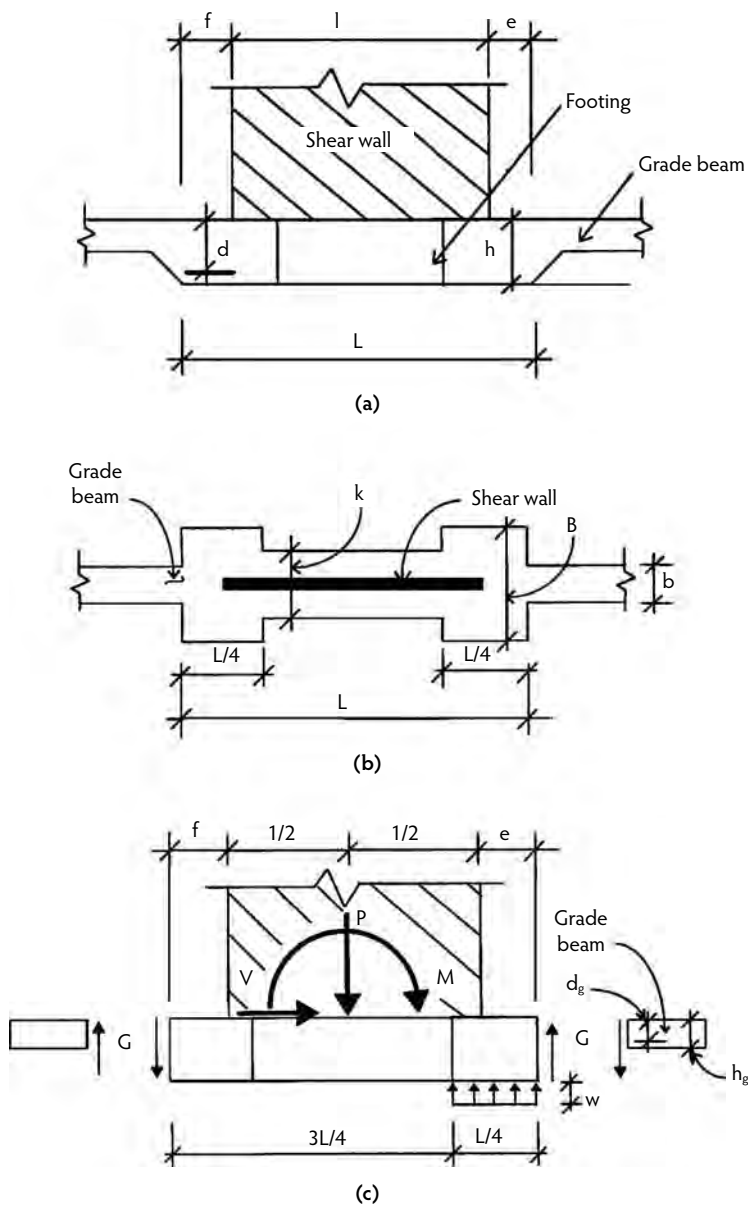


FIGURE 32.10 Shear wall foundation: (a) elevation, shear wall and footing; (b) plan; (c) free body diagram of the structural system at limit state.

32.3.4.2 Geotechnical Relationships

32.3.4.2.1 Soil Pressure

The soil pressure is:

$$s = \frac{P_d}{0.25LB} \leq 1.33SBP \quad (32.24)$$

where P_d is the total $(DL + LL)$.

32.3.4.2.2 Soil Pressure Ratio

The soil stress ratio is:

$$SSR = \frac{s}{1.33SBP} \leq 1 \quad (32.25)$$

32.3.4.2.3 Shear Transfer to Grade Beam (G)

(See Figure 32.10.) Based on the structural model adopted at the limit state, shear transfer (G) to the grade beams occurs if the shear-wall footing is not capable, through its geometry and the existing gravity loadings, to resist the overturning moment (M). The magnitude of the shear G depends also on the direction of bending moment M . The larger of the two values is considered for design:

$$G = \frac{1}{L} \left[M - 0.375PL + |0.5(e - f)| \right] \quad (32.26)$$

$$\text{Factored average soil bearing } (W) = 4P/BL \quad (32.27)$$

32.3.5 Nomenclature

- b = width of grade beam.
- B = width of foundation pad and its tips.
- d = design depth of footing.
- d_g = design depth of grade beam.
- e = distance from tip of shear wall to tip of footing at bearing end.
- f = distance from tip of shear wall to tip of footing at uplift end.
- g = distance from tip of shear wall to point of action of shear force G .
- G = factored shear force developed between the grade beam and foundation.
- h = dimensional depth of footing.
- h_g = dimensional depth of grade beam.
- j = distance from tip of shear wall to point of action of shear force G .
- k = width of footing at midlength of shear wall.
- l = length of shear wall.
- L = effective length of foundation (equal to $l + e + f$).
- M = factored moment at midlength of shear wall (equal to $M_s/0.7$).
- M_s = unfactored applied seismic moment.
- P = factored gravity load equal to $(0.9 - 0.2S_{DS})P_d$.
- P_a = unfactored gravity loading from the shear wall.
- P_d = total axial load on footing (equal to $P_a + P_f$).
- P_f = total weight of footing.
- P_L = unfactored live load from shear wall
- s = unfactored calculated soil pressure.
- SBP = allowable soil bearing pressure.
- SSR = soil stress ratio (equal to calculated/allowable).
- V = factored applied seismic shear.
- V_s = unfactored applied seismic shear.
- W = factored calculated soil pressure on soil.

Example 32.3. Shear-Wall Footing Design

(Refer to Figure 32.10 and Figure 32.11). From the soils report, $SBP = 3.0$ kips/ft². From lateral analysis, $M_s = 9800$ kip-ft, $P_a = 100$ kips, $P_L = 0$ kips, $V_s = 300$ kips, and $SDS = 1.0$. The properties are (calculations based on design IBC 2006):

$$\begin{aligned} f'_c &= 3000 \text{ psi.} \\ f_y &= 60 \text{ psi.} \end{aligned}$$

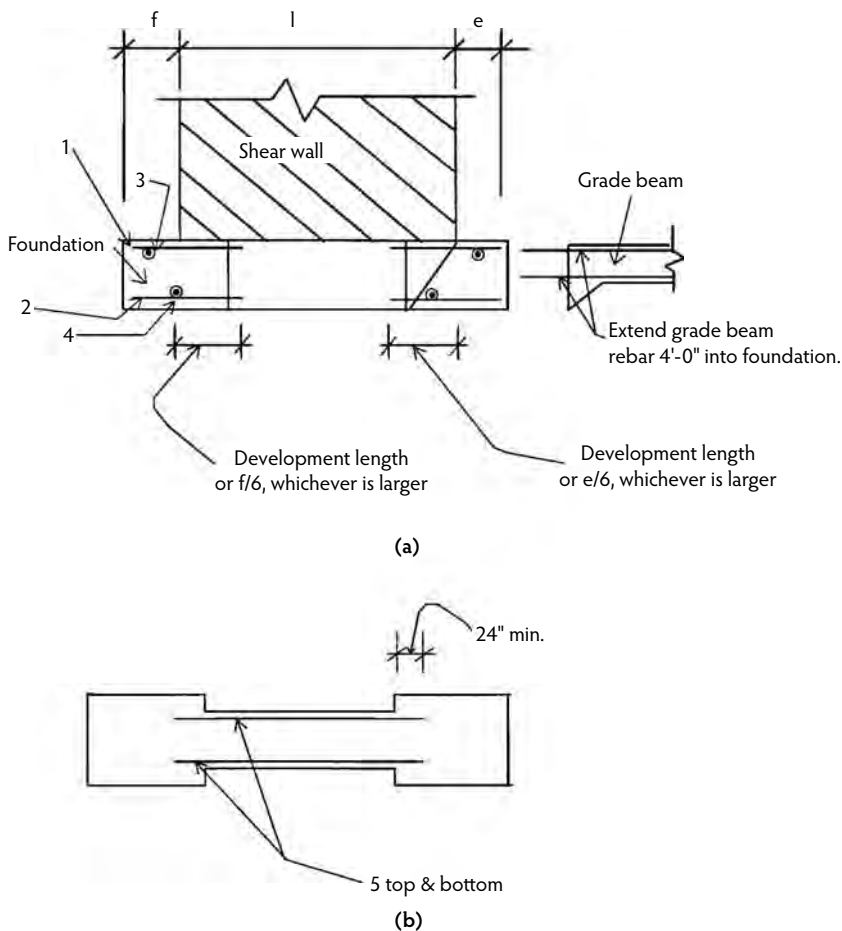


FIGURE 32.11 Reinforcement designation: (a) elevation, and (b) plan. Note: The connection between the grade beam and the foundation is modeled as hinged in the analysis. It is not necessary to design for a moment across this section.

$$e = 6 \text{ ft.}$$

$$f = 6 \text{ ft.}$$

$$l = 36 \text{ ft.}$$

$$L = l + e + f = 48 \text{ ft.}$$

The estimated weight of the footing is:

$$P_f = 60 \text{ kips}$$

$$P_d = P_a + P_f = 100 \text{ kips} + 60 \text{ kips} = 160 \text{ kips}$$

$$P = (0.9 - 0.2)(P_d - P_L)(160 \text{ kips}) = 112 \text{ kips}$$

$$M = \frac{M_s}{0.7} = \frac{9800 \text{ kip-ft}}{0.7} = 14,000 \text{ kip-ft}$$

From Equation 32.24:

$$B_{\min} = \frac{P_d}{0.25L(1.33SBP)} = \frac{160 \text{ kips}}{0.25(48 \text{ ft})(1.33 \times 3.0)} = 40.1 \text{ in.}$$

Assume $B = 48$ in.:

$$s = \frac{P_d}{0.25LB} = \frac{160 \text{ kips}}{0.25(48 \text{ ft})(4 \text{ ft})} = 3.33 \text{ kips/ft}^2$$

$$SSR = \frac{s}{1.33SBP} = \frac{3.33 \text{ kips/ft}^2}{1.33(3.0 \text{ kips/ft}^2)} = 0.833 < 1.0 \quad (\text{OK})$$

Assume $d_g = 26.5$ in.; $h_g = d_g + 3.5$ in. = 26.5 in. + 3.5 in.; therefore, $h_g = 30$ in.

From Equation 32.27:

$$W = \frac{4P}{BL} = \frac{4(112)}{(4 \text{ ft})(48 \text{ ft})} = 2.33 \text{ kips/ft}^2$$

Reinforcement requirements of foundation:

$$G = \frac{1}{L} \left[M - 0.375PL + |0.5P(e - f)| \right]$$

$$G = \frac{1}{48 \text{ ft}} \left[14,000 \text{ kip-ft} - 0.375(112 \text{ kips})(48 \text{ ft}) + 0 \right]$$

$$G = 249.67 \text{ kips}$$

See Figure 32.11a, rebar 2D 1:

$$M_u = Gf + \frac{Bfh}{12^3} \times 0.15 \frac{f}{2} = (249.67 \text{ kips})(6 \text{ ft}) + (4 \text{ ft})(6 \text{ ft})(3 \text{ ft}) \times 0.15 \text{ kcf} \times \frac{6 \text{ ft}}{2}$$

$$M_u = 1530.4 \text{ kip-ft}$$

$$A_{SREQ} = 11.68 \text{ in.}^2$$

32.4 Seismic Retrofit of Existing Buildings

32.4.1 Introduction

Historically, the seismic retrofit of existing concrete structures has been executed by introducing concrete shear walls, new steel, or concrete bracing elements or by strengthening existing lateral-force-resisting members. Recently, new methods such as base isolation and wrapping columns using steel jackets or fiber fabric with epoxy resin have been introduced. The method and the economy of the seismic retrofit depend on the characteristics of the structure. The most critical stage in the retrofit of a concrete structure is the preliminary work for the development of the retrofit scheme. During this phase, the structural components of the structure, the economy, the various retrofit schemes, the timing of the work, and the possibility of loss of occupancy are all investigated so the appropriate seismic retrofit option may be chosen.

32.4.2 Structure Weakness

Concrete structures observed to suffer the most in the aftermath of major seismic events have exhibited one or more of the following deficiencies:

- Suspect load path or, as is occasionally the case, interrupted load path
- Lack of compatibility between the vertical elements in the structure
- An inadequate lateral-load-resisting system

For a structure to respond adequately to the applied seismic loads, there must exist a continuous and adequate load path from the point of application of the seismic force to the foundation of the structure. Inadequately designed or detailed connections along the load path can and will lead to local or overall failure, regardless of how well the various components of the lateral-force-resisting system are designed and detailed. The issue of deformation compatibility can be seen very clearly in a structure with flexible vertical lateral-force-resisting elements such as moment-resisting frames. Such frames experience significant horizontal displacements. It is this earthquake-imposed deformation that can cause some or all of the lateral and vertical carrying systems to fail if they do not have the ability to allow such movement. As building codes evolve on the basis of lessons learned from various seismic events worldwide, higher design loads with a more advanced level of detailing for ductile behavior (not widely practiced before) are demanded. Structures designed according to codes as late as 1967 may be inadequate, based on current standards. Efforts to retrofit such structures to meet current governing codes can be very extensive. Toward achieving our present objectives of ensuring life safety during major seismic events and minimal structural damage during frequently occurring earthquakes, the next two sections address two critical objectives in the seismic retrofit process.

32.4.3 Creation of Adequate Load Path

The structural engineer chooses the load path to support the lateral load from the point of load application to the foundation or soil. The load path or lateral-load-resisting system is then analyzed and designed for the corresponding load actions. All components of the system and their connections are verified, and adjustments are made to ensure adequate strength and ductility. In concrete structures, such load paths are achieved by adding new shear walls or by strengthening existing ones. It is not surprising, therefore, to observe that the chosen load path is different from the original system of the structure. Compatibility of the various vertical structural elements of the structure must be investigated to ensure that the selected load path can be activated.

32.4.4 Establish Deformation Compatibility

As discussed earlier, establishing deformation compatibility is essential to ensuring that all structural elements necessary for stability and load transfer have adequate ductility and the ability to redistribute loading to safely withstand the deformations imposed upon them in response to seismic loads. In parking structures where split-level frames are common, post-earthquake investigations and studies have shown that most of the distress was due to column-shear failure in short columns. Measures for the mitigation of column-shear failure vary between existing and new structures. The options introduced in the following sections may be considered for each of the construction types.

32.4.4.1 Retrofit Construction

Retrofitting the column implies one of several options. The first is removing the column and replacing it using an adequate section with close tie spacing. A second option is jacketing the column so its shear capacity can be increased; this can be accomplished by placing vertical and hoop reinforcement around the existing column and by the application of gunite. Another option is to place a two-piece steel jacket and weld it on site. The gap between the existing column and the jacket is then grouted. Epoxy resin and fiber wrapping is another method that is very effective for round or oval columns because the structural contribution of the wrapping is developed through hoop stresses in the wrapping.

32.4.4.2 New Construction

In new construction, short columns can be designed and detailed as a continuous part of the structure to withstand the higher shear forces, or they can be detailed for moment release at their connections to the beam, as shown in Figure 32.12.

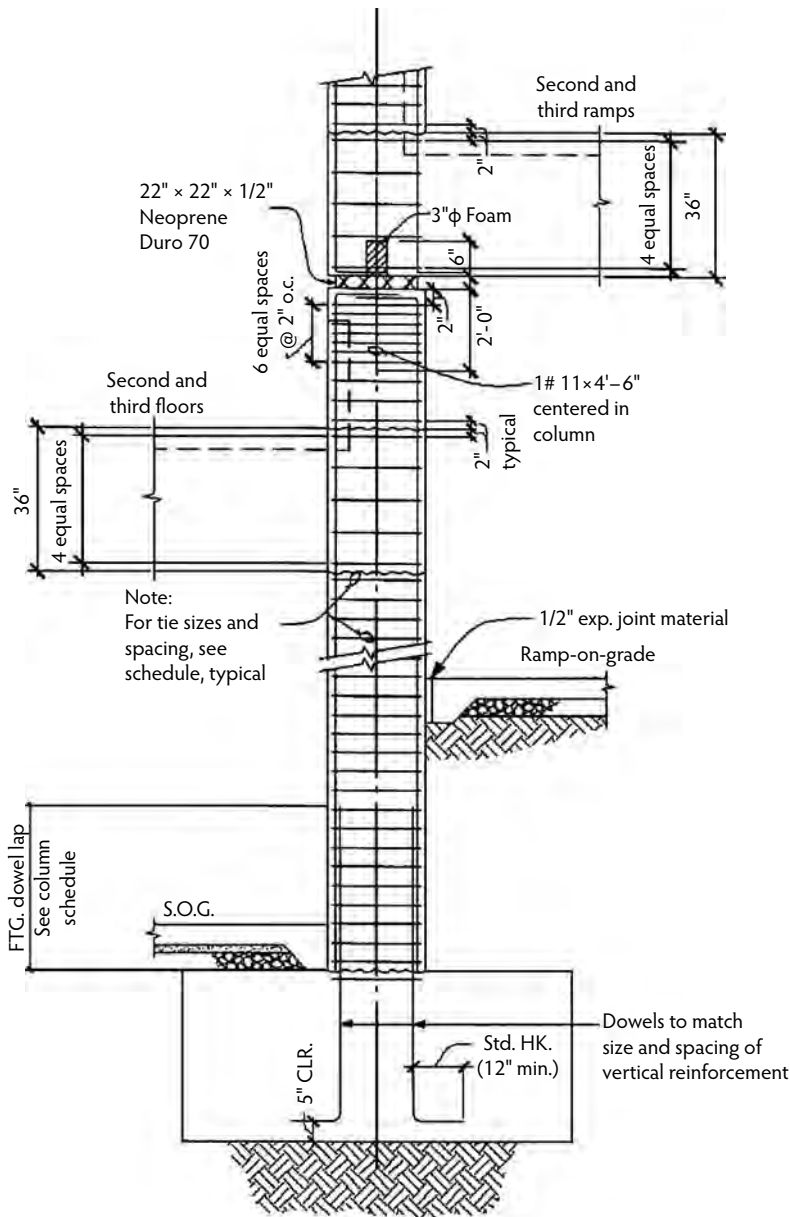


FIGURE 32.12 Slip joint at top of short columns.

32.4.5 Establish Adequate Lateral-Load-Resisting System

It is not possible to achieve our goal of ensuring life safety during major seismic events and minimal structural damage during frequently occurring earthquakes just by ensuring that the structure has an adequate vertical lateral-force-resisting system. It is imperative that the seismic force be properly collected at the roof and each floor and properly transferred into the vertical lateral-force-resisting system. Thus, the horizontal concrete diaphragms should be analyzed and strengthened as necessary so this step can be accomplished. The existing vertical resisting system is then strengthened by retrofitting the existing elements or by introducing new elements to supplement the existing capacity. Finally, the existing footing should be investigated and new footings and grade beams should be added where required.

32.4.5.1 Horizontal Diaphragms

In structures constructed prior to 1970, it is very likely that little attention was given to ensuring that the story force could be adequately transferred into the vertical lateral-force-resisting system. As part of the seismic retrofit of the building, methods of ensuring that the diaphragm does not fail should be devised. This can be achieved by introducing chord and drag elements at the floor soffit. Attaching thin steel plates onto the concrete soffit using epoxy resin is a method that can cause little disturbance to the function of the structure yet have very positive results. The connection of the diaphragm to the vertical lateral system should be closely examined. The introduction of steel angles bolted to both the floor soffit and the vertical lateral-force-resisting system is often done with satisfactory results. For diaphragms where a load path into the existing vertical lateral-force-resisting system cannot be reasonably achieved, the layout of the vertical lateral-load-resisting system should be studied. It may be imperative that new vertical members be introduced to allow the establishment of adequate load path.

32.4.5.2 Vertical Load-Resisting System

Existing concrete buildings are most likely to have one of three structural lateral systems:

- Space frame system
- Building frame system
- Bearing wall system

The level of strengthening required to achieve our goal of ensuring public safety and minimal structural damage no doubt differs from one structure to another; however, older buildings with space frames generally require more effort for establishing an adequate vertical lateral-force-resisting system. The following options are some of the available methods for strengthening the vertical lateral-force-resisting systems.

32.4.5.2.1 Introduction of New Concrete/Masonry Shear Walls

This is a method frequently used for retrofitting concrete structures. Shear-wall placement is simpler, in most cases, than adding moment-resisting frames. When the size and location of the new shear walls have been established based on the design force, new footings are placed and connected to the various floor systems by way of drilling and bonding reinforcing steel dowels to the existing slab-on-grade. Wall reinforcements are then placed. Walls can then be formed and poured in place or, as is often the case in recent years, a one-sided form can be placed and gunite applied (refer to Figure 32.13 and Figure 32.14).

32.4.5.2.2 Retrofitting of Existing Walls

In instances where the building layout or architecture offers no option for new shear wall introduction, existing walls may be thickened to the required adequate dimension (Figure 32.15). Additionally, required wall boundary elements at the end of the wall may be added if required, as shown in Figure 32.14. Existing shear walls to be thickened are properly prepared by roughening their surfaces to 0.25-in. amplitude. Appropriate dowels are then drilled and bonded into existing concrete. The required vertical and horizontal reinforcements are tied in place, and concrete is placed either conventionally by installing wall forms and pumping the concrete into place or low-slump gunite is shot in place. It is important to note that the existing footings should be verified for their ability to transfer vertical and horizontal reactions to the ground. It is often necessary to enlarge the existing footings at the thickened shear wall. Additionally, grade beams may be introduced to better defuse the lateral force into the ground.

32.4.5.2.3 Alternative Methods of Seismic Retrofit

So far, the discussion has been limited to the conventional methods for seismic retrofit of buildings where conventional lateral-load-resisting systems are engineered to support the calculated seismic forces that will be developed in a building during severe seismic activity. On the other hand, base isolation is a means by which the seismic response of the structure is significantly reduced by decoupling the building from its seismic forces by: (1) increasing the fundamental vibration period of the structure, or (2) dissipating the energy delivered to the building. Base isolation at the present time is far more expensive

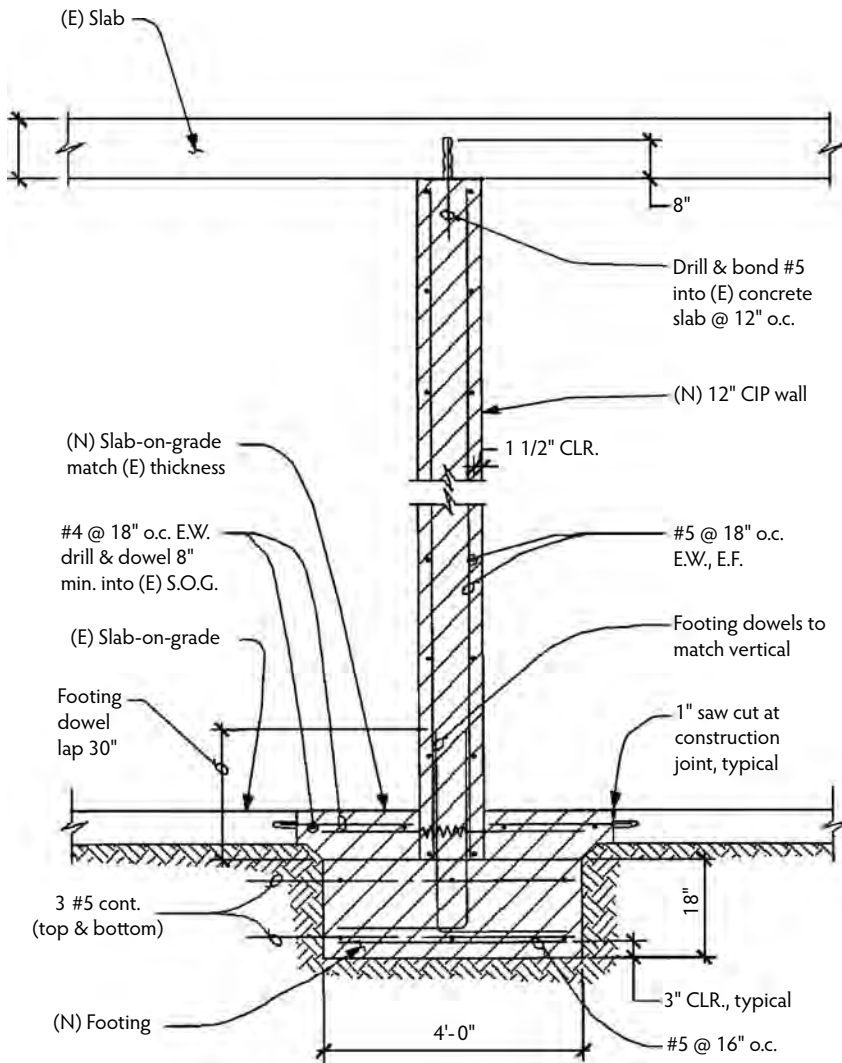


FIGURE 32.13 New concrete wall.

to implement for retrofitting existing structures than conventional methods; however, structures such as historic landmarks and vital buildings that lack an existing load path for seismic forces and have limited capacity in the existing concrete diaphragm or large penetrations in the existing concrete diaphragm that cannot be retrofitted conventionally can be successfully strengthened using base isolation. Some of the primary advantages of the base isolation system include:

- Minimum disruption of important historic features
- Minimum alteration of interior spaces
- Minimum potential damage to architectural finishes during future earthquakes
- Greater degree of life safety to building occupants
- Significantly reduced seismic response
- Significantly reduced story drift

For further information regarding base isolation, the reader is encouraged to consult Naaseh (1995).

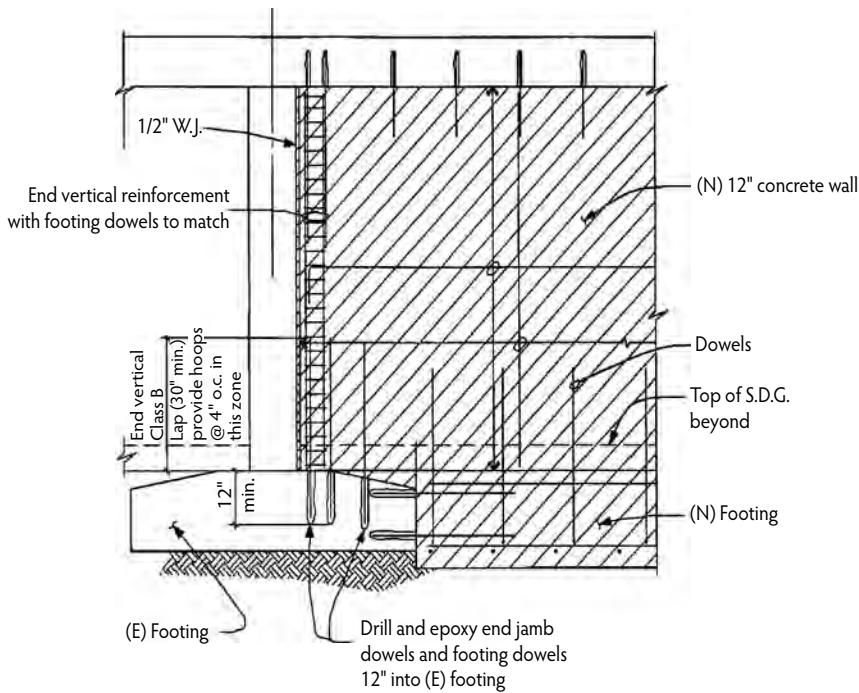


FIGURE 32.14 Wall elevation.

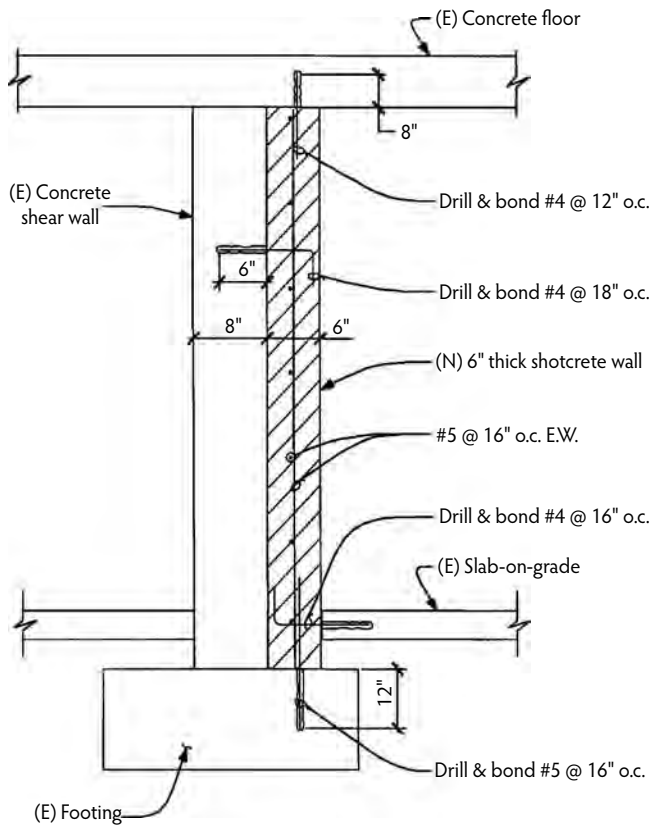


FIGURE 32.15 Retrofit of existing concrete wall.

32.5 Seismic Analysis and Design of Bridge Structures

32.5.1 Seismic Analysis of Bridge Structures

32.5.1.1 Introduction

In this section, a simple method that models a bridge as a single degree of freedom system is presented. As the bridge model becomes more complicated, however, this simple procedure becomes less accurate; thus, a multimodal dynamic analysis or time-history computer analysis is recommended. There are two basic concepts for bridge seismic analysis. The first is that there is a relationship between the mass and stiffness of a bridge and the forces and displacements that affect the structure during an earthquake; therefore, if we can calculate the mass and the stiffness for our structure, we can obtain the earthquake forces acting on it. The second concept is that bridges are designed to behave nonlinearly for large earthquakes; therefore, the engineer is required to make successive estimates of an equivalent linearized stiffness to obtain the seismic forces and displacements of the bridge.

32.5.1.2 Basics

Mass is a measure of a body's resistance to acceleration. It requires a force of 1 Newton to accelerate 1 kilogram at a rate of 1 meter per second squared. **Stiffness** is a measure of the resistance of a structure to displacement. It is the force (in Newtons) required to move a structure 1 meter. The boundary conditions for the bridge must be carefully studied to determine the stiffness of the structure. **Period** is the time (in seconds) required to complete one cycle of movement. A cycle is the trip from the point of zero displacement to completion of the farthest left and right excursions of the structure and back to the point of zero displacement. **Natural period** is the time a single degree of freedom system will vibrate at in the absence of damping or other forces. Natural period (T) has the following relationship to the mass (m) and stiffness (k) of the system:

$$T = 2\pi\sqrt{\frac{m}{k}} \quad (32.28)$$

Frequency is the inverse of period and can be measured as the number of cycles per second (f) or the number of radians per second (ω) where one cycle equals 2π radians. **Damping** (viscous damping) is a measure of a resistance of a structure to velocity. Bridges are underdamped structures. This means that the displacement of successive cycles becomes smaller. The damping coefficient (c) is the force required to move a structure at a speed of 1 meter per second. **Critical damping** (c_c) is the amount of damping that would cause a structure to stop moving after half a cycle. Bridge engineers describe damping using the damping ratio (ξ) where:

$$\xi = \frac{c}{c_c} \quad (32.29)$$

A damping ratio of 5% is used for most bridge structures.

32.5.1.3 The Force Equation

The force equation for structural dynamics can be derived from Newton's second law:

$$\sum F = ma \quad (32.30)$$

Thus, all the forces acting on a body are equal to its mass times its acceleration. When a structure is acted on by a force, Newton's second law becomes:

$$p - f_s - f_D = mu'' \quad (32.31)$$

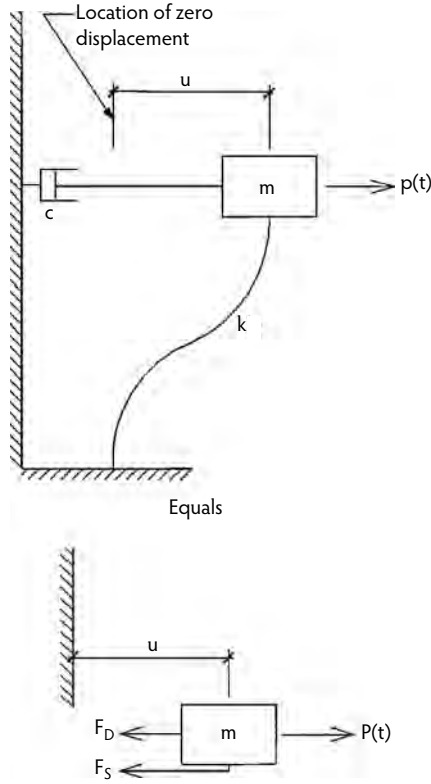


FIGURE 32.16 Forces acting on a structure according to Newton's second law.

where:

$$f_s = ku \quad (32.32)$$

is the force due to the stiffness of the structure,

$$f_D = cu' \quad (32.33)$$

is the force due to damping of the structure, and p is the external force acting on the structure (see Figure 32.16). The variables u' and u'' are the first and second derivatives of displacement u , k is the force required for a unit displacement of the structure, and c is a measure of the damping in the system.

Thus, Equation 32.31 can be rearranged as shown in Equation 32.34:

$$mu'' + cu' + ku = p(t) \quad (32.34)$$

However, for earthquakes, the force is not applied at the mass but at the ground (Figure 32.17); therefore, Equation 32.34 becomes:

$$mu'' + c(u' - z') + k(u - z) = p \quad (32.35)$$

for the relative displacement:

$$\omega = u - z \quad (32.36)$$

and the equation of motion, when there is no external force p being applied, is:

$$mu'' + c\omega' + k\omega = -mz'' \quad (32.37)$$

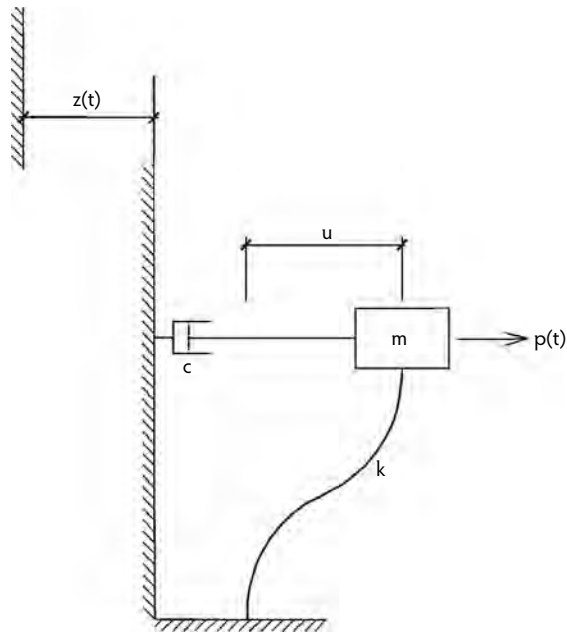


FIGURE 32.17 Earthquake-induced displacements.

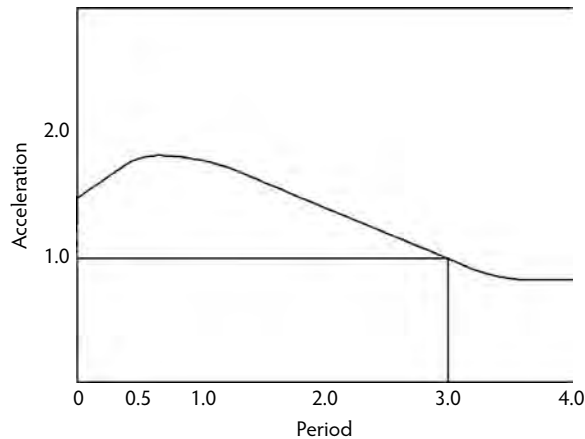


FIGURE 32.18 Example response spectra.

In Equation 32.37, mass m , damping factor c , and stiffness k are all known. The support acceleration (z'') can be obtained from accelerogram records of previous earthquakes. Equation 32.37 is a second-order differential equation that can be solved to obtain the relative displacement (u), the relative velocity (\dot{u}), and the relative acceleration (\ddot{u}) for a bridge structure due to an earthquake.

32.5.1.4 Caltrans' Response Spectra

Response spectra have been developed so engineers do not have to solve a differential equation repeatedly to capture the maximum force or displacement of their structure for a given acceleration record. Refer to Figure 32.18 for an example response spectra. Response spectra are graphs of the maximum response (displacement, velocity, or acceleration) of different single degree of freedom systems for a given earthquake record. Thus, engineers can calculate the period of the structure from its mass and stiffness and use the appropriate 5% damped spectra to obtain the response of the structure to the earthquake. The force

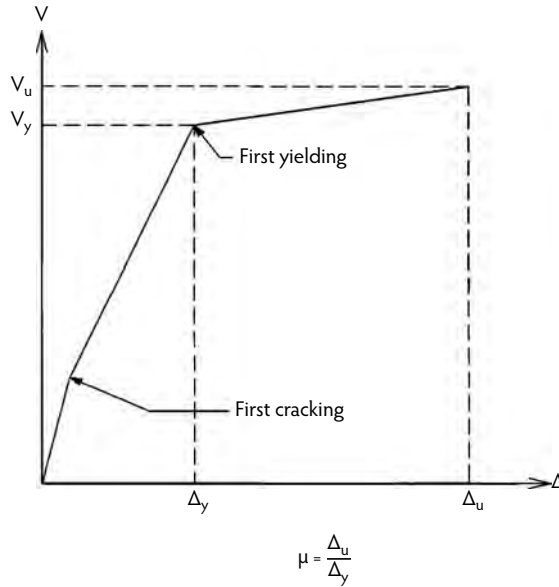


FIGURE 32.19 Nonlinear column stiffness.

equation (32.37) showed three responses that can be obtained from a dynamic analysis: displacement, velocity, and acceleration. We can also obtain these using response spectra. The spectral displacement (S_d) and velocity (S_v) can be obtained from the spectral acceleration using the following relationship:

$$Sa = \omega S_v = \omega^2 S_d \quad (32.38)$$

Therefore,

$$S_d = \frac{Sa}{\omega^2} = \frac{Sa}{(2\pi/T)^2} = \frac{T^2 Sa}{4\pi^2} \quad (32.39)$$

Caltrans developed response spectra using five large California earthquake ground motions on rock; 28 different spectra were created based on 4 soil depths and 7 peak ground accelerations (PGAs). Engineers can obtain the earthquake forces on a bridge by picking the appropriate response spectra based on the PGA and soil depth at the bridge site and calculating the natural period of their structure. These response spectra can be found in Caltrans (1995); however, Caltrans is moving toward using site-specific response spectra for many bridge sites.

32.5.1.5 Nonlinear Behavior

Bridge members change stiffness during earthquakes. The stiffness of a column is reduced when the concrete cracks in tension. It is further reduced as the steel begins to yield and plastic hinges form (Figure 32.19). The axial stiffness of a bridge changes in tension and compression as expansion joints open and close. The soil behind the abutment yields for large compressive forces and may not support tension. Engineers must consider all changes of stiffness to accurately obtain force and displacement values for a bridge. Currently, the standard is to calculate cracked stiffness for bridge columns. A value of $I_{cr} = 0.5(I_{gross})$ can be used unless a moment-curvature analysis is warranted. Also, because bridge columns are designed to yield during large earthquakes, the column force obtained from the analysis is reduced by a ductility factor, and the columns are designed for this smaller force. Caltrans is currently using a ductility factor (μ) of about 5 for designing new columns; however, a moment-curvature analysis of columns should be done when the ductility of a column is uncertain.

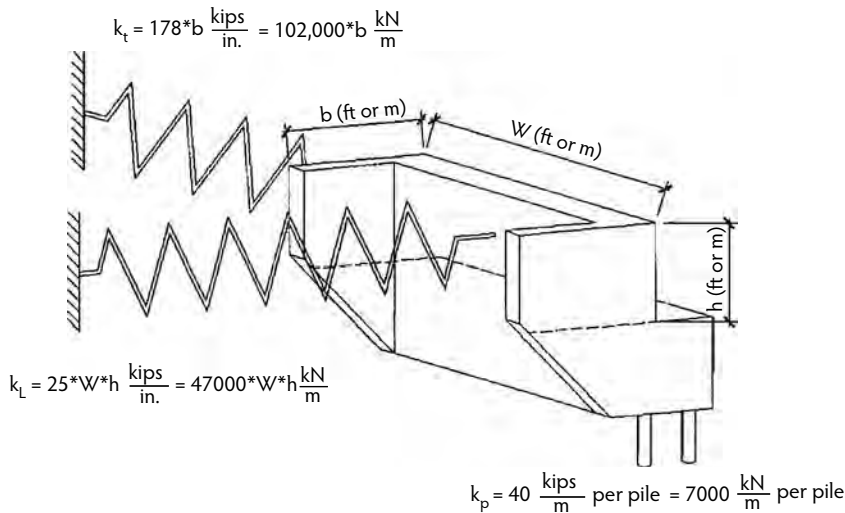


FIGURE 32.20 Abutment stiffness.

32.5.1.6 Abutment Stiffness

Longitudinally, the soil behind the back wall is assumed to have a stiffness that is related to the area of the back wall as shown in Figure 32.20:

$$k_L = (47,000)(W)(h) \text{ (kN/m)} \quad (32.40)$$

Transversely, the stiffness is considered to be two thirds effective per length of inside wing wall (assuming the wing wall is designed to take the load), and the outside wing wall is only one third effective per wing-wall length for the resultant stiffness shown in Equation 32.41:

$$k_T = (102,000)(b) \text{ (kN/m)} \quad (32.41)$$

An additional stiffness of 7000 kN/m for each pile is added in both directions; therefore, in the longitudinal direction:

$$k_T = (42,000)(W)(h) + (7000)(n) \text{ (kN/m)} \quad (32.42)$$

In the transverse direction:

$$k_T = (102,000)(b) + (7000)(n) \text{ (kN/m)} \quad (32.43)$$

More information on abutment stiffness can be obtained in Caltrans (1995). Bridge abutments are only effective in compression. A gap may have to be closed on seat-type abutments before the soil stiffness is initiated. The abutment stiffness remains linear until it reaches the ultimate strength of 370 kN/m².

32.5.1.7 Parallel and Series Systems

A simplification that allows engineers to analyze by hand many complicated and statically indeterminate structures is the concept of parallel and series structural systems. For a parallel system, all the elements share the same displacement; for a series system, they all share the same force. Also, their stiffnesses are summed differently. By assuming a rigid superstructure or by making other simplifying assumptions, bridge structures can be analyzed as combinations of parallel and series systems. This concept is particularly useful when evaluating the **longitudinal displacement** of the superstructure. Refer to Figure 32.21 and Figure 32.22.

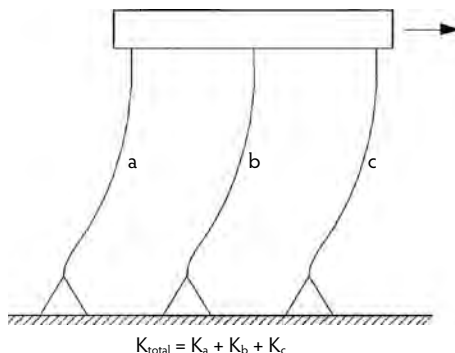


FIGURE 32.21 Parallel structural system.

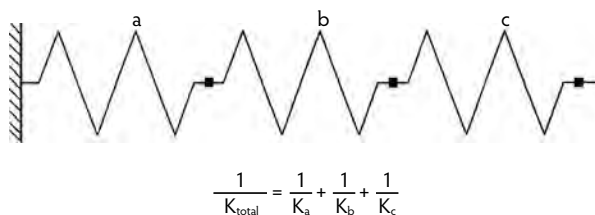


FIGURE 32.22 Series structural system.

32.5.1.8 Code Requirements

In bridge design, two load cases are considered. Case 1 is for 100% of the transverse force and 30% of the longitudinal force. Case 2 is for 100% of the longitudinal force and 30% of the transverse force. This approach takes care of uncertainty with regard to the earthquake direction and to account for curved and skewed bridges with members that take a vector component of both the longitudinal and transverse force.

32.5.2 Seismic Design of Bridge Structures

32.5.2.1 Introduction

The following collection of guidelines is intended to aid bridge engineers in producing more seismic-resistant bridge designs.

32.5.2.2 Structural System and General Plan

Seismic demands on a structure should be considered conceptually when creating the general plan. First of all, designers can control column demands on superstructures in new bridges by judiciously choosing column sizing, spacing, and flexibility. Second, column or frame stiffnesses must be carefully considered. Column types, shapes, sizes, and length are very important in the design process. Some example concepts that should be considered when establishing the general plan are as follows:

- Column stiffnesses in a frame should preferably be kept within 20% of each other.
- Isolators or sliding bearings can be used at the tops of short, stiff columns adjacent to abutments.
- End diaphragm abutments provide good seismic energy absorbers for short frames (i.e., short length end frame with stiff columns) or short bridges.
- Frames should not exceed 800 ft as a means of avoiding excessive expansion joint movements.
- Reduce joint skew angles to control loss of seat support due to frame rotation.
- Use articulated or single-span bridges in areas of suspected, but poorly defined, faulting.
- Use double columns at expansion joints.

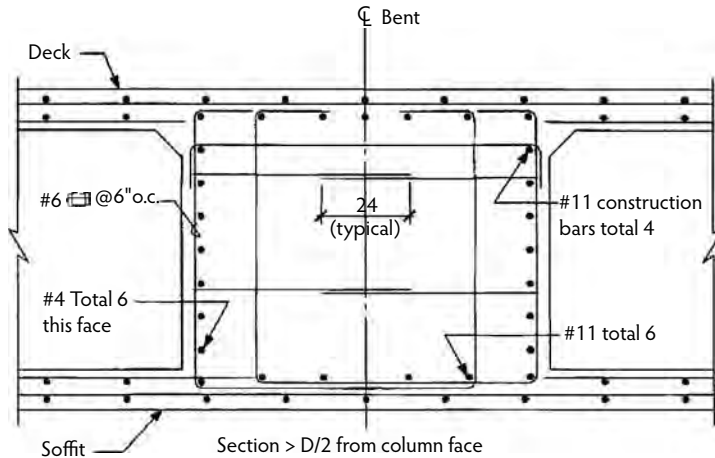


FIGURE 32.23 Example cap joint shear reinforcement skew 0° to 20° .

32.5.2.3 Superstructure Joint Shear

Below is a procedure and example details for determining joint shear reinforcement in box girder bent caps. Typical flexure and shear reinforcement in bent caps shall be supplemented in the vicinity of columns to resist joint shear. Also, the cap width and depth must be sized to limit the joint shear stress to $12 \times (f'_c)^{0.5}$. Minimum cap width shall be 2 ft greater than the column dimension in the cap width direction. The joint shear reinforcement required shall be located within the width of the cap and within a length of the cap equal to (1) two times the column width, or (2) the column width plus two times the bent cap depth, whichever is less. The effective length of cap shall be reduced appropriately for columns located near the end of the cap and closer than the column width or cap depth. Following is a procedure for determining the required reinforcement that must be provided within the specified joint shear zone; the reinforcement is uniformly distributed:

- Vertical reinforcement shall be 20% of the column steel. The quantity of vertical steel shall be a combination of cap stirrups and added bars. Added bars shall be hooked around main longitudinal cap bars. All vertical legs shall be well distributed to provide protection for both longitudinal and transverse demand or be supplemented to produce adequate coverage.
- Horizontal reinforcement shall be stitched across the cap in intermediate layers. The reinforcement shall be hairpin shaped and confine vertical bars in the hairpin bends. The hairpins shall be equivalent in area to 10% of column steel. The hairpins shall be strategically placed in two or more layers, depending on structure depth. Spacing shall be denser outside the column than that used within the column.
- Side-face reinforcement shall be 10% of the main cap reinforcement.
- Provide #4 J-bars at 6 in. on-center along longitudinal top deck bars for bent caps skewed greater than 20° . The bars shall be alternately 24 in. and 30 in. long. Locate the J-bars within a width D either side of the column centerline (D is column dimension).
- All vertical column bars shall be extended as high as practically possible without interfering with main cap bars.
- Column spiral extension into the bent cap shall be replaced by equivalent continuous hoops. This substitution facilitates placement of the various horizontal joint shear bars.

Figure 32.23 shows cap joint shear reinforcement within D distance from the column center line. Figure 32.24 shows cap joint shear reinforcement beyond a distance $D/2$ from the column face.

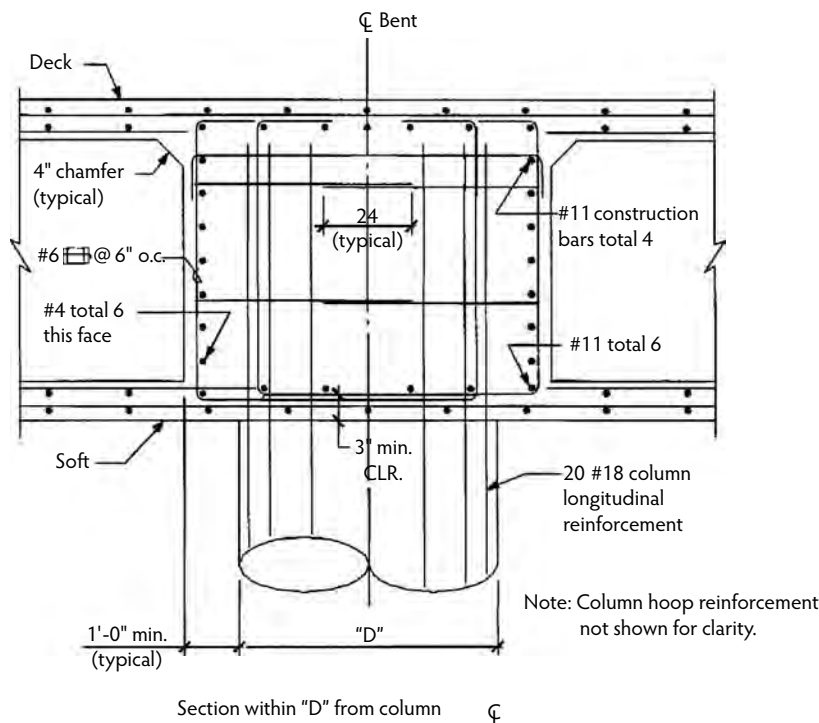


FIGURE 32.24 Example cap joint shear reinforcement skew 0° to 20° .

32.5.2.4 Superstructure Flexural Capacity

Bridge superstructures must be reinforced to resist longitudinal and transverse flexural demands produced by column plastic hinging. Conventional bar reinforcement must be provided in the slabs and bent caps in the designated zone surrounding the column to satisfy such demands. Prestressing bent caps could be an alternative solution for transverse demands and additionally can supplement joint shear capacity at the column. Pinning column tops in multiple column bents will reduce seismic demand on the superstructure but will require a more expensive fixed foundation.

32.5.2.5 Vertical Accelerations

The 1994 Northridge earthquake gave evidence of acceleration levels for vertical excitations that were higher than those recorded in the past. The flexural and joint shear reinforcement prescribed so caps and superstructures can resist column demands should be ample to provide flexural resistance to vertical acceleration demands; however, the vertical capacity of girder stirrups should be checked, and shear-friction reinforcement in the form of girder side-face reinforcement at the cap that is equal to 1.5 gravity load should be provided. Tie-downs at hinges and abutments might be required.

32.5.2.6 Column Displacement

Displacement demands will generally be determined by STRUDL analysis, although the static method is sufficient for short length bridges (one or two bents). The column displacement capacity can be determined using the push method and is dependent on combinations of vertical and horizontal reinforcement. Also, disconnecting random stiff columns from the superstructure by use of sliding bearings or isolation systems is another means of avoiding large load demands on stiff columns.

32.5.2.7 Flared Columns

Flared columns can create some unexpected demands on the superstructure, footings, and columns. Past policy has assumed that lightly reinforced flares will fuse during severe seismic activity. Superstructures, columns, and footings have been designed to resist plastic hinging demands from the column core at the top and bottom of the column; however, designers must consider alternative behavior. Developing either the full column section at the top of column or hinging at the base of flares should be investigated. Both conditions will significantly affect shear demands in the column and shear and moment demands in superstructures and footings. Flexural reinforcement for caps and superstructures must be calculated if hinging is assumed at the bases of flares.

32.5.2.8 Bent Cap Designs

The design of bent caps for nonseismic loads must be consistent with assumptions made for supports, especially with respect to column flares. If flares are expected to lose structural integrity during seismic loadings, the cap should be designed to carry all loads without benefit of the flares; however, the bridge must be analyzed for all nonseismic load cases with the stiffness and strength of the in-place flares. As in the case with flared columns, the designer must design the cap for double conditions if any type of structural damage or loss of vertical support is anticipated for other types of supports.

32.5.2.9 Footings

New footing design procedures were tested satisfactorily at the University of California, San Diego. Although only one test case was performed, results indicated that serious degradation and bridge collapse can be avoided if standard details are employed. Details included #5 at 12 in. on-center vertical ties and column bar hooks that turned outward. Designers should be cautioned that cantilevered footing sections should not exceed $L/d = 2.5$ (where L is the cantilevered footing length from the column face, and d is the effective depth of footing) in orthogonal directions and $L/d = 30$ diagonally to the footing corner with 70-t piles typically spaced at 3 ft with 1.5-ft edge distances. For higher capacity piles, the designer must ensure load paths through connections, vertical ties, development of flexural reinforcement at footing edges (e.g., hooks), etc. for both tensile and compressive demands.

32.5.2.10 Pile-Design Concepts

The designer should strive to prevent damage in foundations. Piles constructed in competent soil, in combination with passive resistance provided by cap and soil interaction and drag forces, will be sufficient to keep piles in the elastic range for flexure or shear under seismic demand. Problem areas that require guidelines include: (1) piles in soft soils or water, including P-delta effects; (2) pile head conditions, pinned (standard) or fixed (which places tremendous demands on the cap and requires more than nonstandard cap size and reinforcement); (3) pile demands for pile capacities greater than 70 t (e.g., spacing, edge distance, vertical ties that are more dense or of larger size, flexural steel hooks at footing edges); and (4) batter piles (e.g., used in dense soils; not for use in water, soft, or loose soils; capacity in combination with vertical piles). These design concepts are not intended to be a complete list of all conditions or problems or a solution to problems. They are intended to alert designers to conditions where the foundation must have the strength and displacement capacity intended under all conditions of demand.

32.6 Retrofit of Earthquake-Damaged Bridges

32.6.1 Introduction

Since the early 1970s, the California Department of Transportation (Caltrans) has undertaken a major program to ensure the seismic safety of all freeway structures. With a large portion of the work being funded in the aftermath of the Loma Prieta earthquake in 1989, analysis techniques and research to validate such techniques have progressed significantly in the past five years. Early on in the Phase 2 retrofit

program, structure overstrength analysis was the primary tool for seismic vulnerability assessment. Hinges and restrainers were always evaluated but none had been examined after a significant earthquake, so knowledge of their performance was based primarily on laboratory tests and hand calculations. Foundation-strengthening techniques had not been field tested (by real earthquakes), and design methods were based on modified service load tools and simplified assumptions. It was soon clear that these methods, although for the most part very conservative, did not always afford a true picture of the behavior or strength (resistance to collapse) of a structure and did not necessarily produce cost-effective designs. To gain a clearer picture of the performance of bridges, Caltrans engineers have been focusing on the following:

- Load path and limit-state analysis, item input ground motions
- Validity of global models
- Displacement ductility analysis
- Beam and column joint performance
- Hinges and restrainers
- Detailing ductile elements
- Foundation performance

The purpose of this section is to highlight current thinking on these items and help identify available tools to properly retrofit bridge structures.

32.6.2 Background

The goal of retrofitting is to increase the seismic resistance of a bridge to the point of preventing collapse and thereby avoiding loss of life. It is not practical or economical to retrofit all structures to meet the current seismic design performance criteria for new structures. It is, however, our responsibility to ensure that no structure collapses under the maximum credible event. Based on the no-collapse criteria, the primary goal of retrofitting bridges is to ensure that the vertical-load-carrying capacity is maintained. Traditionally, this has meant protecting the ability of the column to carry vertical loads while undergoing cyclic lateral loading. Under this kind of loading, some damage is expected to occur in plastic hinge regions of the column. With 25 years of real-life experience, since the San Fernando Earthquake in 1971, we have been provided with a good picture of where damage can be expected to occur on a concrete structure under seismic loads. These areas include:

- Column plastic hinge regions
- Column shear capacity
- Column-to-footing and column-to-superstructure connections
- Expansion joint openings and hinge restrainers
- Abutment back walls and transverse shear keys
- Pile-to-footing connections
- Pile overload

The following discussions address the seismic analysis and design approaches for retrofitting concrete bridge structures.

32.6.3 Seismic Analysis Approach

32.6.3.1 Load Path and Limit-State Analysis

Limit-state theory says, roughly, that a structure is only as good as the weakest link (or member) in the structural system. Ensuring that plastic action occurs in a predetermined location is therefore the goal. For concrete bridges, this predetermined location is typically, and preferably, in the column. Controlling the location of the plastic hinge allows the engineer to develop a rational estimate of the damage expected to a structure and its ability to resist collapse. For this to happen, all members and components of a

structure must be examined to determine whether they can actually carry the forces required to force plastic hinging to occur in the column. Testing and application of basic engineering principles to components of the structure (column superstructure joints, column–footing connections, pile cap, and pile connections) have shown that areas of analysis and design once taken for granted as adequate could be vulnerable under extreme seismic loading conditions. Rigorous analysis of the structure may determine that the capacity of a system may likely be controlled by connections to the column and not by the strength of the column itself. Current analysis techniques commonly used by engineers to estimate reinforced-concrete capacity strongly suggest that many superstructures do not have the capacity to force plastic hinging into the column. Because one objective of the retrofit is to ensure that plastic hinging does occur in the column, the superstructure strength and ductility have to be addressed in the retrofit design.

32.6.3.2 Global Behavior

Early retrofit analysis typically relied on global elastic modal models to predict moment and displacement demands. Although this is still often a valid analysis technique, in some situations global analyses are not the proper tools for seismic-demand prediction. These situations include but are not limited to:

- Short-period ($T < 0.75$ s) structures
- Very complicated structures (requiring many assumptions)

Other tools that could be used in lieu of or in conjunction with global elastic models include: (1) hand calculations with single degree-of-freedom conditions, and (2) pushover analysis to determine the order of plastic hinging in incremental collapse. Hand-calculation analysis should be limited to simple structures or structures where the number of assumptions is limited. Pushover analysis can be used for both simple and complex structures. The value of pushover analyses is that the capacity of the structural system is accounted for while the integrity of each element is determined. For example, if the two end frames of, say, a three-frame structure are designed with substantially more strength or stiffness than the interior frame, a global analysis may well conclude that the interior frame has relatively low seismic demands when in fact it is being supported, or helped, by the stronger adjacent frames. The final result could still be that the system is adequate to avoid collapse; however, it is important for the engineer to have a clear idea of where vulnerabilities and strengths exist in the system. Because the goal of retrofit is to prevent the collapse and not just prevent plastic hinging, an efficient retrofit analysis technique would explicitly estimate the system capacity at collapse and not just assume a direct correlation between plastic hinging of a single column and precollapse capacity of the system.

32.6.3.3 Displacement and Curvature Ductility Analysis

An alternative estimate of the ductility of a member (column) can be obtained using ductility analysis techniques proposed by Mander et al. (1984, 1988a,b). The implementation of this approach has been tested extensively and directed explicitly toward bridges by Priestly and Seible (1993). The predominant analysis approach until recently has been moment overload—the application of force reduction factors to loads calculated from a dynamic elastic multimodal response spectrum analysis (e.g., STRUDL or SAP90) assuming gross moments of inertia (I_g). This approach tends to underestimate system capacity. The displacement ductility approach focuses on the capacity side of the equation and directly addresses the basic premise of the *equal energy theory*—that displacements are equal for a given load whether the structure remains elastic or enters into the plastic state as long as the section has not blown apart (allowable confinement stresses have been exceeded). By directly calculating the plastic moment capacity (instead of factoring up the nominal moment capacity) and the displacement capacity of each member (instead of limiting displacement to a factor of column geometry without regard to the rotational capacity of the section itself), the engineer can make a more accurate estimate of the capacity of the system. Because the focus in this type of approach is on displacements, it is important to base the analysis on a members effective moments of inertia ($I_{eff} = I_{cr}$) instead of gross moments of inertia. Basing the dynamic

analysis on I_{cr} instead of I_g will result in larger estimated displacement demands and smaller estimated moment (force) demands. More refined analysis techniques can be employed that assess the performance of a member and estimated damage. This kind of information can be of particular interest when attempting to estimate resistance to collapse.

32.6.3.4 Foundations

Footings typically have required extensive work to increase their capacity to a level consistent with the column plastic moment. Early retrofitting techniques were often conservative (for lateral loads) by ignoring the contribution of existing piles to the capacity of the system. Large-scale testing of existing piles had not yet been done *in situ*, so nominal lateral pile capacities were often assumed when existing pile capacity was analyzed. Construction techniques for increasing the capacity of the footing relied on installing standard piles or prestressed tie-downs (tendons or rods). The technology simply had not been developed to make the leap from standard, new bridge construction to efficient, cost-effective retrofit work. Since those early days, many new technologies have come into use in the retrofit industry. Field testing of pile foundations at the Cypress structure in Oakland, and the Terminal Separation in San Francisco have shown that the actual lateral capacity of concrete piles is much greater than was originally thought (90 vs. 40 kips/pile). Note that the assumed tensile capacity of existing piles is most often 0. Pile-to-footing connections were traditionally designed to develop vertical loads in a downward direction (compression), not upward (tension). Construction techniques for installing high-capacity piles (up to 1000 kips/pile) in very confined spaces have been field tested with very promising results. Seismic modeling now takes into account soil springs and group effects instead of simply assuming that all footings are fixed, rigid members. Soil springs in a soft soil may increase the displacement estimate on the column while decreasing the moment demand at the footing. The model may also predict that a footing is moving so much that the piles must be sized to limit displacement or resist larger loads than would otherwise be expected. Liquefaction and large ground displacements along fault rupture zones continue to be items that elude easy solutions.

32.6.4 Design Approaches

32.6.4.1 Retrofit Approaches

The three primary concepts used to retrofit structures are:

- Reduce loads imposed on the system.
- Increase the capacity of the structural elements.
- Provide a new or super element.

It is not uncommon for a retrofit design to make use of more than one of these concepts. The following provides some typical details and ideas that could be used to implement these concepts:

32.6.4.1.1 Column Plastic Hinge Regions and Column Shear Capacity

Steel shells have been used extensively (and successfully throughout California and in Alaska) to add ductility and provide confinement to concrete columns (Figure 32.25). *Composite fiber wrap* provides additional confinement and ductility of concrete columns and is an idea that has been under development for several years; results are starting to yield systems that are economical and structurally equivalent to that of the steel shell (Figure 32.26). *Remove and replace portions of the substructure* is an option that has been used where performance beyond no collapse is required. *SuperBent* provides an additional support system.

32.6.4.1.2 Column-to-Footing Connections and Footings

An additional top mat on footing is a very common retrofit due to the fact that top mats of reinforcement were not used in footings until the late 1970s. The top mat adds tensile capacity to the footing (Figure 32.27). A *prestressed footing* is sometimes used for increased performance.

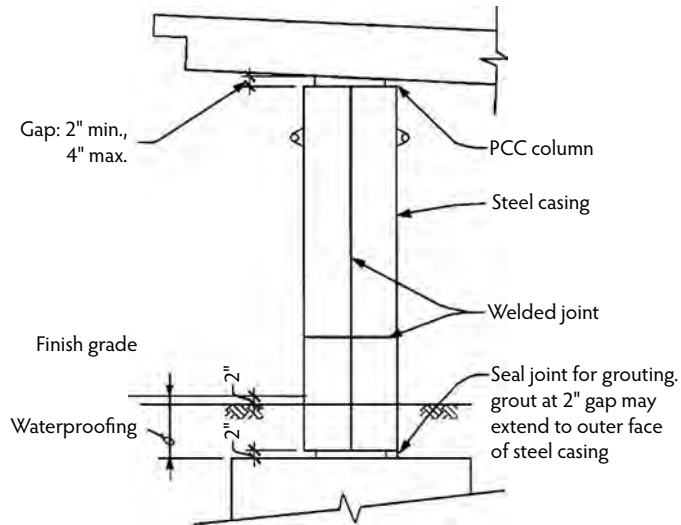


FIGURE 32.25 Steel casing of column.

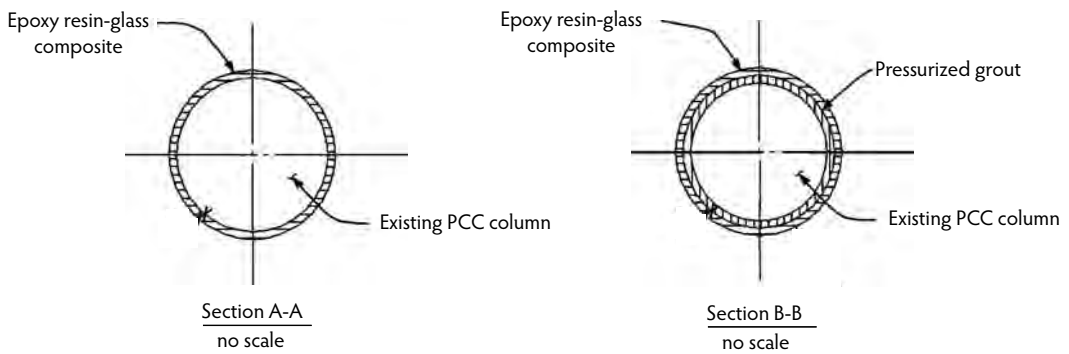


FIGURE 32.26 Composite fiber wrap.

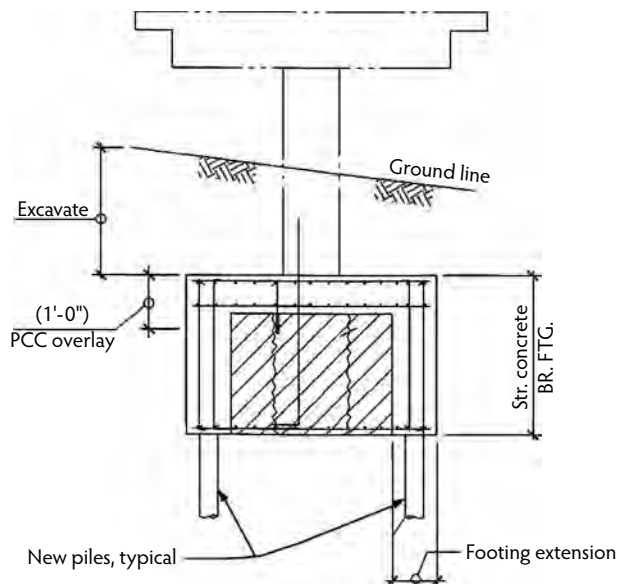


FIGURE 32.27 Footing retrofit with additional top mat.

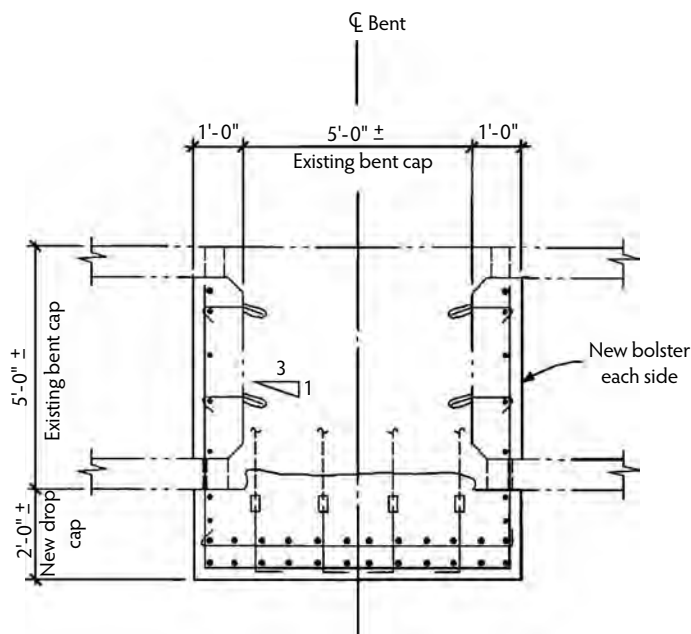


FIGURE 32.28 Bent cap bolsters.

32.6.4.1.3 Column-to-Superstructure Connections

Bent cap bolsters are used to increase the torsional capacity of the bent cap and the capacity of the column and cap joint (Figure 32.28). *Prestressed bent caps* are used to increase the torsional capacity of the bent cap and the capacity of the column and cap joint.

32.6.4.1.4 Expansion Joint Openings and Hinge Restrainers

Place additional or replace existing *restrainers*. *Seat extensions* (typically pipe) allow for displacement. Joint displacement demands are reduced by using additional restrainers.

32.6.4.1.5 Pile-to-Footing Connections

Additional piles can be used to gain greater tension and compression capacity. *Prestressed tie-downs* provide additional footing tensile (only) capacity.

32.6.4.2 Summary

Many more difficulties are encountered in retrofit construction than in standard new bridge construction; however, the field of bridge seismic analysis and retrofit has seen many developments over the past several years. Probably the most significant change in assessing the capacity of a structural system has been the adoption of **ductility analysis** and the pseudo-nonlinear analysis approach of determining a plastic hinging sequence and ultimately a systematic yield mechanism. Construction techniques are quickly adapting to the specialized demands of seismic retrofit for bridges. Materials, techniques, and equipment have been developed and integrated from other industries, such as installation of high-capacity piles (adopted from the oil industry), and new materials such as carbon fiber are being developed in laboratories. The field of seismic retrofitting has developed at a tremendous pace over the last several years. Engineers should expect additional changes as research and construction continue. The techniques used on concrete structures in California have proven to be effective, under real seismic loads (such as the 1994 Northridge earthquake). For additional information on any of the subjects addressed in this chapter, it is strongly suggested that the reader consult the references provided.

32.7 Defining Terms

Base shear—The total design lateral force at the base of a structure.

Bearing wall system—The structural system without a complete vertical-load-carrying frame.

Building frame system—An essentially complete frame that provides support for dead, live, and snow loads.

Boundary element—Special reinforcement at edges of openings, shear walls, or diaphragms.

Diaphragm—A horizontal system acting to transmit seismic forces to vertical lateral-force-resisting systems.

Dual system—A combination of shear walls or braced frames and intermediate or special moment-resisting frames proportionally designed to resist seismic forces.

Hoop—A closed tie that may be of several reinforcing elements with 135° hooks having a 6-bar diameter (3-in. minimum) extension at each end or a continuously wound tie with a 135° hook at each end with a 6-bar diameter extension (3-in. minimum) that engages the longitudinal reinforcement.

Moment-resisting frame—A frame where the frame members and joints are capable of resisting forces primarily by flexure.

Shear wall—A wall designed to resist seismic forces parallel to the plane of the wall.

Story drift—The displacement of one level relative to the level above or below.

Strength—The useable capacity of a structure or its structural members to resist lateral loads within the code-allowable deformations.

Structure base—That level in the structure at which the earthquake motions are considered to be imparted to the structure.

References

- Algermissen, S.T. and Perkins, D.M. 1972. A technique for seismic risk zoning, general considerations and parameters. In *Proceedings of International Conference on Microzonation*, November 1, Seattle, WA, pp. 865–877.
- Algermissen, S.T. and Perkins, D.M. 1976. *A Probabilistic Estimate of Maximum Acceleration in Rock in Contiguous United States*, USGS Open File Report 76–416. U.S. Geological Survey, Washington, D.C.
- ASCE. 2005. *Minimum Design Loads for Buildings and Other Structures*, ASCE 7-05. American Society of Civil Engineers, Reston, VA, pp. 3, 109–135.
- Blume, J.A., Newmark, N.M., and Corning, L.H. 1992. *Design of Multistory Reinforced Concrete Buildings for Earthquake Motions*. American Concrete Institute, Farmington Hills, MI.
- Bolt, B.A. 1969. Duration of strong motion. In *Proceedings of the Fourth World Conference on Earthquake Engineering*, January 13–18, Santiago, Chile, pp. 1304–1315.
- Boore, D.M., Joyner, W.B., Oliver, A.A., and Page, R.A. 1978. *Estimation of Ground Motion Parameters*, USGS, Circular 795. U.S. Geological Survey, Washington, D.C.
- Boore, D.M., Joyner, W.B., Oliver, A.A., and Page R.A. 1980. Peak acceleration velocity and displacement from strong motion records. *Bull. Seism. Soc. Am.*, 70(1), 305–321.
- Caltrans. 1995. *Bridge Design Aids Manual*. California Department of Transportation, Sacramento, CA.
- Campbell, K.W. 1997. Empirical near-source attenuation relationships for horizontal and vertical components of peak ground acceleration, peak ground velocity, and pseudo-absolute acceleration response spectra. *Seis. Res. Lett.*, 68, 154–179.
- Cloud, W.K. and Perez, V. 1967. Accelerograms: Parkfield earthquake. *Bull. Seism. Soc. Am.*, 57, 1179–1192.
- Conell, C.A. 1968. Engineering seismic risk analysis. *Bull. Seism. Soc. Am.*, 58(5), 1583–1606.
- Cooper, T.R. 1995. Seismic analysis procedures. In *Proceedings of the Third National Concrete and Masonry Engineering Conference*, June 15–17, San Francisco, CA.
- Donovan, N. C. 1973. *Earthquake Hazards for Buildings: Building Practices for Disaster Mitigation*. National Bureau of Standards, U.S. Department of Commerce, Washington, D.C., pp. 82–111.

- Esteva, L. 1969. Seismicity prediction: a Bayesian approach. In *Proceedings of the Fourth World Conference on Earthquake Engineering*, Santiago, Chile.
- FEMA. 2003. *NEHRP Recommended Provisions for Seismic Regulations for New Buildings and Other Structures*, FEMA 450. Federal Emergency Management Agency, Washington, D.C.
- Housner, G. W. 1965. Intensity of earthquake shaking near the causative fault. In *Proceedings of the Third World Conference on Earthquake Engineering*, January 22–February 1, Auckland, New Zealand, pp. 94–115.
- ICBO. 1994. *Uniform Building Code*, Vol. 2. International Conference of Building Officials, Whittier, CA.
- ICC. 2006. *2006 International Building Code*. International Code Council, Washington, D.C.
- Idriss, I.M. 1993. *Procedures for Selecting Earthquake Ground Motions at Rock Sites*, NIST GCR 93-625. U.S. Department of Commerce, National Institute of Standards and Technology, Gaithersburg, MD.
- Ingham, J. and Priestly, M.J.N. 1993. *Shear Strength of Knee Joints*. University of California, San Diego.
- McGuire, R.K. 1975. *Seismic Structural Response Risk Analysis, Incorporating Peak Response Progressions on Earthquake Magnitude and Distance*, Report R74-51. Massachusetts Institute of Technology, Cambridge.
- MacRae, G.A., Priestly, M.J.N., and Tao, J.R. 1993. *P-Delta Design in Seismic Regions*, SSRP No. 93/05. University of California, San Diego.
- Mander, J.B., Priestley, M.J.N., and Park, R. 1984. *Seismic Design of Bridge Piers*, Research Report 84-2. Department of Civil Engineering, University of Canterbury, Christchurch, New Zealand.
- Mander, J.B., Priestley, M.J.N., and Park, R. 1988a. Theoretical stress–strain model of confined concrete. *J. Struct. Eng.*, 114(8), 1804–1826.
- Mander, J.B., Priestley, M.J.N., and Park, R. 1988b. Observed stress–strain behavior of confined concrete. *J. Struct. Eng.*, 114(8), 1827–1849.
- Milne, W.G. and Davenport, A.G. 1969. Distribution of earthquake risk in Canada. *Bull. Seismol. Soc. Am.*, 59, 729–754.
- Moehle, J.P. and Soyer, C. 1993. *Behavior and Retrofit of Exterior RC Connections*. University of California, Berkeley.
- Naaseh, S. 1995. Seismic retrofit of San Francisco City Hall. In *Proceedings of the Third National Concrete and Masonry Engineering Conference*, June 15–17, San Francisco, CA, pp. 769–795.
- Naeim, F., Ed. 1989. *The Seismic Design Handbook*. Van Nostrand Reinhold, New York.
- Nawy, E.G. 2008. *Reinforced Concrete: A Fundamental Approach*, 6th ed. Prentice Hall, Upper Saddle River, NJ, 934 pp.
- Newmark, N.M. and Hall, W.J. 1969. Seismic design criteria for nuclear reactor facilities. In *Proceedings of the Fourth World Conference on Earthquake Engineering*, January 13–18, Santiago, Chile, pp. 37–50.
- Newmark, N.M. and Hall, W.J. 1973. *Procedures and Criteria for Earthquake Resistance Design: Building Practices for Disaster Mitigation*. National Bureau of Standards, U.S. Department of Commerce, Washington, D.C., pp. 209–236.
- Page, R.A., Boore, D.M., Joyner, W.B., and Caulter, H.W. 1972. *Ground Motion Values for Use in Seismic Design of the Trans-Alaska Pipeline System*, USGS Circular 672. U.S. Geological Survey, Washington, D.C.
- Priestly, M.J.N. and Seible, F. 1993. *Full-Scale Test on the Flexural Integrity of Cap/Column Connections with #18 Column Bars*, Report No. TR-93/01. University of California, San Diego.
- Priestly, M.J.N. and Seible, F. 1994. *Proof Test of Superstructure Capacity in Resisting Longitudinal Seismic Attack for the Terminal Separation Replacement*. University of California, San Diego.
- Priestly, M.J.N. et al. 1993. *Proof Test of Circular Column Footing Designed to Current Caltrans Retrofit Standards: Tests for Rectangular Column Also Performed*. University of California, San Diego.
- Sabetta, F. and Pugliese, A. 1987. Attenuation of peak horizontal acceleration and velocity from Italian strong-motion records. *Bull. Seism. Soc. Am.*, 77, 1491–1513.
- Sabetta, F. and Pugliese, A. 1996. Estimation of response spectra and simulation of nonstationary earthquake ground motions. *Bull. Seism. Soc. Am.*, 86, 337–352.

- SEAOC. 1996. *Recommended Lateral Force Requirements and Commentary*. Seismology Committee, Structural Engineers Association of California, Sacramento.
- Seed, H.B. and Idris, I.M. 1982. *Ground Motions and Soil Liquefaction during Earthquakes*. Earthquake Engineering Research Institute, Berkeley, CA.
- Seyed, M. 1993. *Ductility Analysis for Seismic Retrofit of Multi-Column Bridge Structures: Santa Monica Viaduct*. ASCE Publications, Reston, VA.
- Thewalt, C.R. and Stojadinovic, B. 1993. *Behavior of Bridge Outriggers: Summary of Test Results*. University of California, Berkeley.
- Trifunac, M.D. and Brady, A.G. 1975. A study of the duration of strong earthquake ground motion. *Bull. Seism. Soc. Am.*, 65, 581–626.
- Yamabe, K. and Kanai, K. 1988. An empirical formula on the attenuation of the maximum acceleration of earthquake motions. In *Proceedings of the Ninth World Conference on Earthquake Engineering*, Vol. II, pp. 337–342.

Further Information

For further information, consult California Department of Transportation (Caltrans), *Bridge Design Practice Manual*, Section 8, 1995, and Zelinski, R., *Seismic Design Memo*, Caltrans Seismic Technical Section, California Department of Transportation, Sacramento, 1995.



(a)



(b)



(c)

(a) Sunshine Skyway Bridge in Tampa, Florida. (Photograph courtesy of Portland Cement Association, Skokie, IL.)
 (b) Prefabricated bridge element. (Photograph courtesy of Portland Cement Association, Skokie, IL.) (c) Coronado Bridge in San Diego, California, which is 11,720 feet in length and 50 to 200 feet in height; girders are prestressed lightweight concrete. (Photograph courtesy of Steven Simpson, Inc., San Diego, CA.)

33

Prefabricated Bridge Elements and Systems

Michael M. Sprinkel, P.E.*

33.1	Practical Applications.....	33-1
33.2	Types of Elements	33-3
	Precast and Prestressed Slab Spans • Multi-Stemmed Beam • Prestressed Double-Tee and Channel • Prestressed Inverted Channel • Prestressed Single-Tee • Prestressed I-Beams • Prestressed Box Beams • Prestressed Bulb-Tee • Segmental Construction • Prestressed Subdeck Panels • Precast and Prestressed Deck Slabs • Precast Parapet • Substructure Elements • Precast Culverts	
33.3	Construction Considerations	33-15
33.4	Looking Ahead	33-16
	References	33-16

33.1 Practical Applications

A prefabricated concrete bridge element is defined as part of a bridge that is precast away from its final position (Sprinkel, 1985). A system is a combination of elements. Prefabricated concrete bridge elements and systems are used to construct new bridges and to rehabilitate or replace old ones. Prefabricated elements can reduce design effort, enhance quality, simplify and expedite construction, lessen inconvenience to the traveling public, improve safety for workers and the traveling public, and minimize cost. Design effort can be reduced when the same design is used on multiple bridge projects. Historically, bridge-design engineers have customized bridge designs for each site, making the prefabrication of elements impractical except for use on major multiple-span bridge projects. Recent efforts have involved making more adjustments to the site to accommodate a standard design and have developed designs that are more versatile. Fabricating elements in the controlled environment of a precast or prestressed concrete plant enhances quality. Plants are typically certified and well established, although temporary on-site plants are constructed to produce elements for a major bridge project. Plants can use high-quality reusable forms; temperature, relative humidity, and wind can be controlled; the concrete can be batched at the plant; and labor is more efficient because tasks are repeated.

Prefabricated elements, set in place at the bridge site, simplify and expedite construction by minimizing forming, form removal, and placing and curing concrete in a difficult-to-control environment. In addition, prefabricating the bridge element away from its final location minimizes traffic safety issues for both the

* Associate Director, Virginia Transportation Research Council, Charlottesville, Virginia, and Section Head, Transportation Research Board; expert in materials and construction, particularly public works.

traveling public and the worker and minimizes delays and inconvenience for the motorist. Lanes can be open during peak travel periods and closed during off-peak periods for the rapid replacement of bridge sections. Once in place, the fully cured element is ready to receive traffic. Polymer concrete and high-early-strength patching materials now make the rapid connection of prefabricated elements easier. The most significant reasons to use prefabricated elements include the economy realized from the repeated use of forms, the reduction in on-site construction time, and improved safety because of the rapid construction. Initial construction costs can be lower, depending on the costs for cast-in-place concrete construction. Life-cycle costs will likely be lower because of the higher quality and longer life of the structure. When the costs of delays and inconvenience to the motorist are considered, prefabricated elements that can be assembled and put into use during off-peak traffic periods will almost always be economical. Prefabricated elements are increasingly popular as highway funds are used to rehabilitate and replace deteriorating bridges. Bridges with high volumes of traffic can usually only be replaced during off-peak traffic periods (at night or on weekends), and prefabricated elements provide an attractive solution. Mass-produced, easily assembled elements are just as practical for replacing bridges on low-volume roads.

Prefabricated elements, however, are not the best solution for every bridge construction and replacement project. The demand for a particular shape may be too low to justify an investment in forms. Shipping costs may be too high because the nearest plant is hundreds of miles away. Connection details may cause maintenance problems that result in a higher life-cycle cost. An advantage of concrete is that it can be formed into almost any shape; thus, the architectural and site requirements for a bridge may be so complicated that custom on-site forming is required and the prefabrication of elements is not practical. A decision-making tool can be used to decide whether or not a prefabricated bridge is effective for a specific location (Rawls, 2006).

A 1984 survey indicated that the use of prefabricated bridge elements was increasing and that the structures were economical in many situations (Hill and Shirole, 1984). Earlier applications included precast and prestressed slabs and I-beams for simple spans. Later, use expanded to include subdeck panels, deck slabs, parapets, and substructure elements. Currently, all elements in a bridge can be economically constructed or replaced with prefabricated ones. Entire spans and bridges can be moved into place with a brief road closure.

In the past, cranes were typically used to move large bridge elements into place. Recent developments with bridge-moving systems have facilitated the rapid replacement of entire bridges or bridge spans (FHWA, 2004). The new systems include self-propelled modular trailers that are multi-axle, computer-controlled vehicles that can move in any horizontal direction without damaging or deforming the element. Other systems include special load frames, modular jacking systems, horizontally skidding or sliding systems, incremental launching systems, floating barges, and vertically lifting systems.

High-performance concrete mixtures containing pozzolans and admixtures have led to the fabrication of elements with concrete compressive strengths in excess of 10,000 psi (68.9 MPa). The higher quality concretes allow smaller cross-sections, longer spans, greater girder spacings, and longer service. A variety of deck wearing and protection systems can be placed on the prefabricated elements to provide a smooth-riding, skid-resistant surface that retards the penetration of chlorides and water. Wearing and protection systems that have been used include a thin bonded hydraulic cement concrete overlay, waterproof membrane overlaid with asphalt, thin bonded epoxy concrete overlay, additional monolithically cast concrete on the precast element, and low-permeability concrete in the precast element (Sprinkel, 2004).

Already in the new millennium, many publications have supported the use of prefabricated bridge elements and systems. In response to public demand for minimized traffic disruption, the Texas Department of Transportation has been a leader in the use of prefabricated bridge elements in bridge design and construction (Pruski et al., 2002). Prefabricated bridges are meeting growing market demands for fast and efficient structures (Johnson, 2002). New girder designs, strand technologies, and concrete mixes are making precast prestressed concrete bridges more popular (Dick, 2002). New guidelines and load and resistance factor design (LRFD) specifications for full-depth, precast-concrete bridge deck panel systems with no overlays or post-tensioning are now available (Badie et al., 2006). According to the Federal Highway Administration (FHWA), the use of prefabricated elements can improve construction

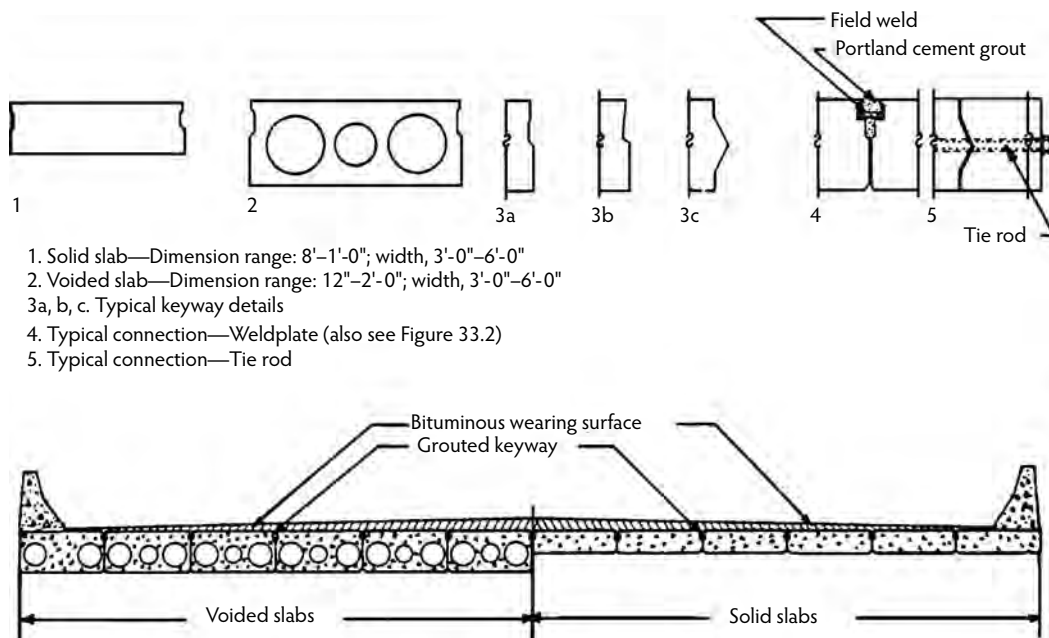


FIGURE 33.1 Slab span. (From Sprinkel, M.M., *Prefabricated Bridge Elements and Systems*, NCHRP Synthesis 119, Transportation Research Board, Washington, D.C., 1985.)

zone safety, minimize the traffic impacts, and improve constructability (FHWA, 2002). A brochure provides descriptions of 15 bridge projects that solved site-specific challenges using prefabricated bridge elements and systems (AASHTO, 2002). Implementation efforts by the Federal Highway Administration and the American Association of State Highway and Transportation Officials (AASHTO) have significantly increased the acceptance and use of prefabricated bridge elements and systems (AASHTO, 2004; FHWA, 2003; FHWA/AASHTO, 2004).

33.2 Types of Elements

The most frequently used prefabricated concrete elements and systems are the prestressed I-beam, prestressed box beam, prestressed channel, and slab span (Sprinkel, 1985). The prestressed subdeck panel was frequently used in the late 1970s and 1980s, but such use has declined in recent years because of reflective cracking in the site-cast overlay concrete. Precast parapets have been used on occasion, but problems with leakage under the parapet have curtailed acceptance. Recent years have seen increased interest in post-tensioned segmental construction for economy in medium and long spans, substructure elements to reduce the environmental impact of construction, and full-depth deck replacement slabs to facilitate the rapid replacement of decks during off-peak traffic periods. Longitudinal, partial-depth, or full-depth deck slabs that are precast on one or more concrete or steel beams have also been successfully used (FHWA, 2004).

33.2.1 Precast and Prestressed Slab Spans

Slab span elements (Figure 33.1) may be cast in various widths, depths, and lengths to accommodate spans up to 50 ft (15 m) (Table 33.1). Shorter slabs may be conventionally reinforced and fabricated at simple precast plants. Longer slabs are typically voided and prestressed or post-tensioned (PCI, 1975; VTRC, 1980). Slabs are easy to fabricate, transport, and erect. Department of Transportation (DOT) bridge crews have precast slabs (Sprinkel, 1976).

TABLE 33.1 Typical Span Lengths for Elements

Element	Length (ft)	Length (m)
Precast slab span	10–30	3–9
Prestressed slab span	20–50	6–15
Multi-stemmed beam	25–50	8–15
Prestressed double-tee and channel	20–60	6–18
Prestressed inverted channel	30–80	9–24
Prestressed single-tee	30–80	9–24
Prestressed I-beam	40–100	12–30
Prestressed box beam	50–100	15–30
Prestressed bulb-tee	60–80	18–24
Post-tensioned segmental	50–400	15–122

33.2.2 Multi-Stemmed Beam

Multi-stemmed beams (Figure 33.2) may be cast in various lengths and increments of width to accommodate short spans. Weld plates and grouted keyways provide shear transfer between beams.

33.2.3 Prestressed Double-Tee and Channel

Most prestressed concrete producers have forms for fabricating double-tees and channels for use in building construction. Additional prestressing, wider webs, and thicker flanges are typically required for bridge loadings (Figure 33.3) (Tokerud, 1975). Forms have been modified and new forms fabricated to produce members for highway applications when there has been sufficient support provided by a DOT to justify the investment in forms (Sprinkel and Alcock, 1977). Channel beams and double-tees are typically used for medium-length spans, and shear transfer between beams is typically provided by grouted keyways or weld plates. Site-cast concrete is usually placed as an overlay, but channel and double-tee members have been overlaid with asphalt (PCI, 1975).

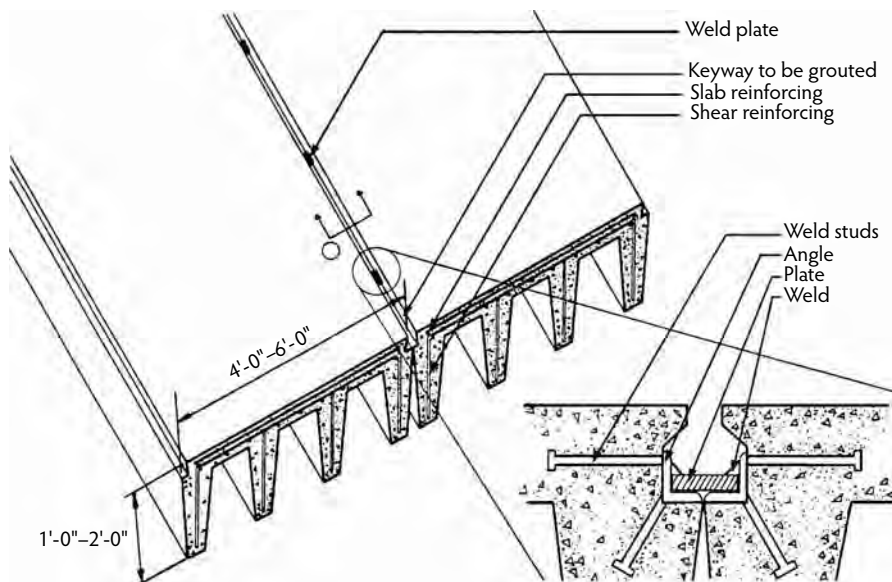


FIGURE 33.2 Multi-stemmed beam. (From Sprinkel, M.M., *Prefabricated Bridge Elements and Systems*, NCHRP Synthesis 119, Transportation Research Board, Washington, D.C., 1985.)

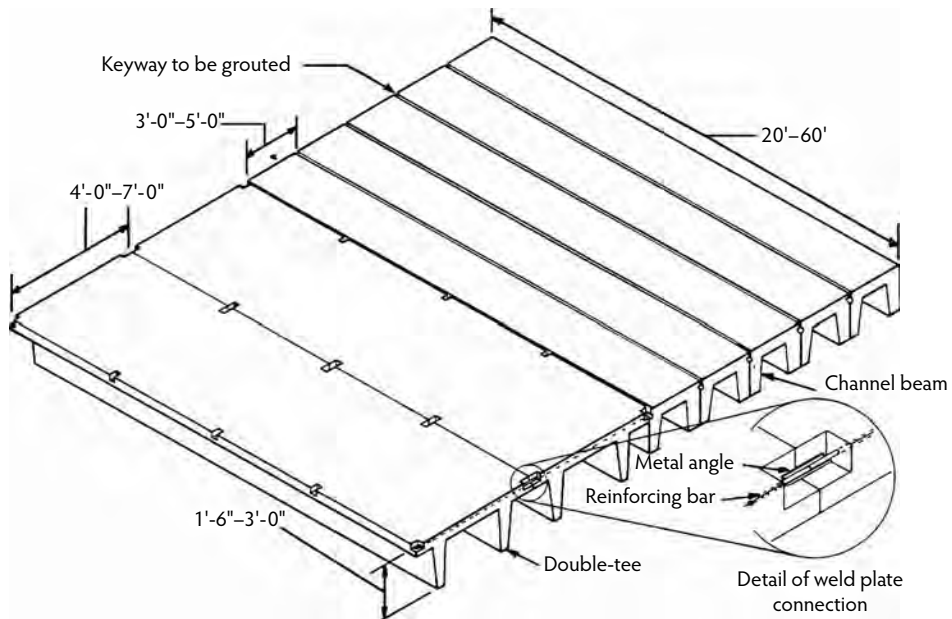


FIGURE 33.3 Double-tee and channel. (From Sprinkel, M.M., *Prefabricated Bridge Elements and Systems*, NCHRP Synthesis 119, Transportation Research Board, Washington, D.C., 1985.)

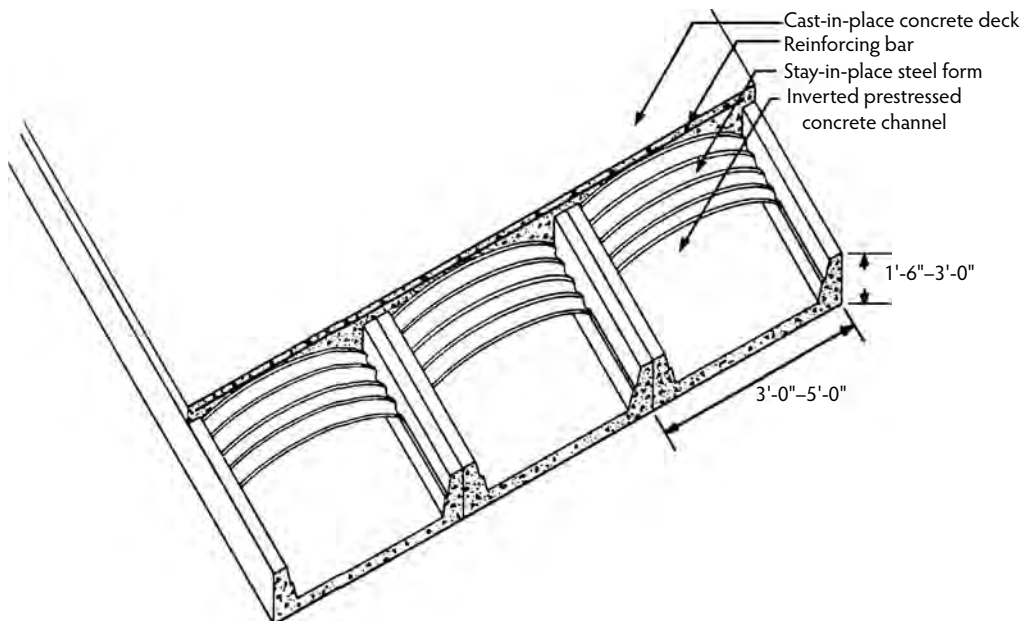


FIGURE 33.4 Prestressed inverted channel. (From Sprinkel, M.M. 1985. *Prefabricated Bridge Elements and Systems*, NCHRP Synthesis 119, Transportation Research Board, Washington, D.C.)

33.2.4 Prestressed Inverted Channel

The inverted channel (Figure 33.4) may be cast in the inverted position or cast in conventional channel forms and inverted before erection at the bridge site. Longer spans can be achieved in the inverted position because more prestressing can be placed in the bottom of the beam. The Missouri Department of Transportation used the inverted channel on many bridges (Salmons, 1971). Site-cast concrete must be

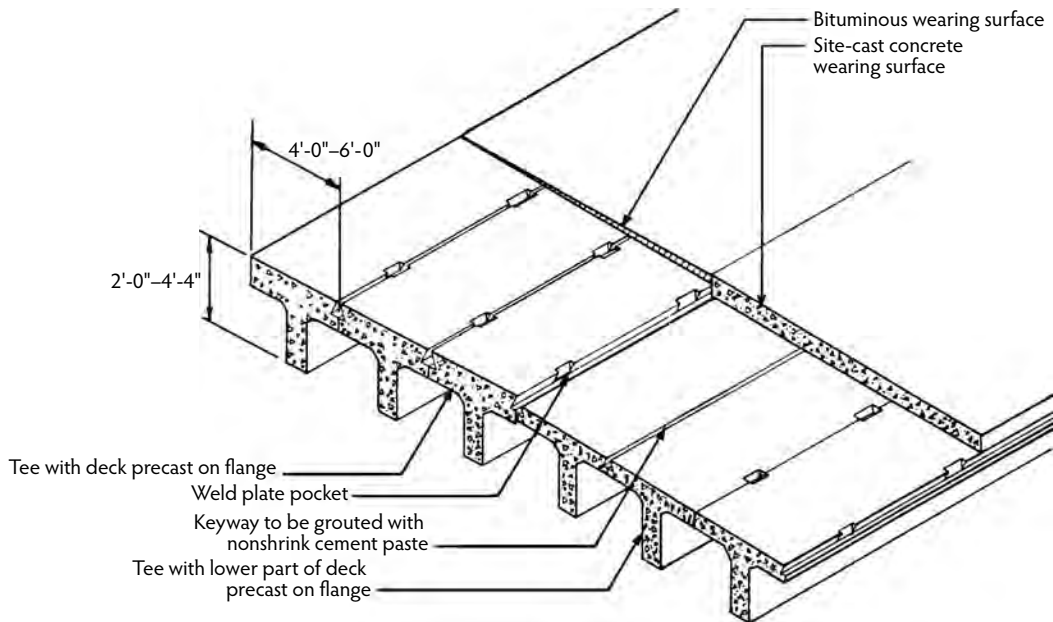


FIGURE 33.5 Prestressed single-tee. (From Sprinkel, M.M., *Prefabricated Bridge Elements and Systems*, NCHRP Synthesis 119, Transportation Research Board, Washington, D.C., 1985.)

placed to connect the channels and provide a deck surface. An alternative to the channel is inverted T-beams placed adjacent to each other and then made composite with cast-in-place concrete placed between the webs of the tees and over the tops of the stems to form a solid member (see FHWA, 2004).

33.2.5 Prestressed Single-Tee

Prestressed single-tee beams are used in building construction. Prestressed concrete plants can sometimes fabricate the beams for shorter spans using the same forms as used in building construction with additional prestressing strands to accommodate the heavier loading. With adequate support from a DOT, a precast producer can invest in new forms to produce longer span beams (Figure 33.5) suitable for highway loadings (Sprinkel and Alcock, 1977). The single-tee is unstable by design and must be supported at the bridge site to prevent overturning until the diaphragms can be cast and the keyways grouted. Site-cast concrete is usually placed to connect the tees and to provide a deck (Sprinkel, 1978). An asphalt wearing surface can be used when the flange of the tee is thick enough to accommodate shear loads.

33.2.6 Prestressed I-Beams

The prestressed I-beam (Figure 33.6) is the prefabricated element most used by DOTs (Sprinkel, 1985). Many prestressed concrete producers invested in forms during the construction of the interstate system. The standard AASHTO cross-sections simplify design and provide for mass production (Panak, 1982). The beams, cast in a variety of widths and depths, are economical for spans of 40 to 100 ft (12 to 30 m). Spans up to 140 ft (43 m) have been constructed (Anderson, 1972; PCI, 1975). Longer spans can be achieved by field-connecting the beams end to end and post-tensioning them (Fadl et al., 1977; Oesterle et al., 1989). The prestressed beams can be positioned more rapidly than a site-cast concrete beam can be constructed. For convenience, other elements are typically constructed with site-cast concrete, limiting the economy of mass production and rapid assembly to the beams. Prestressed concrete subdeck panels have been used, and a National Cooperative Highway Research Program (NCHRP) publication, *Rapid Replacement of Bridge Decks*, addresses the development of designs for prestressed full-depth deck panels

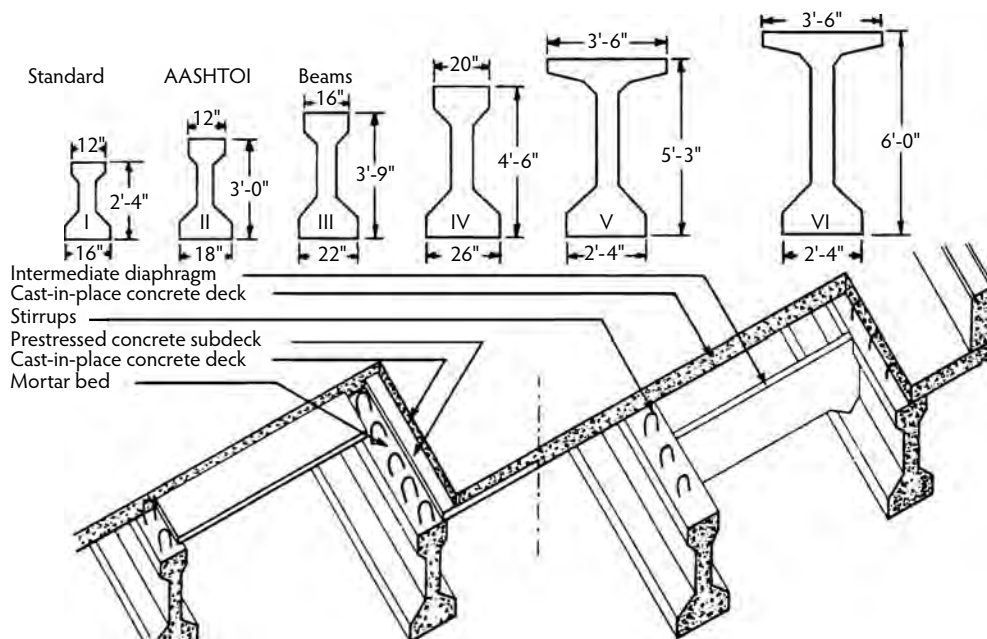


FIGURE 33.6 Prestressed I-beam. (From Sprinkel, M.M., *Prefabricated Bridge Elements and Systems*, NCHRP Synthesis 119, Transportation Research Board, Washington, D.C., 1985.)

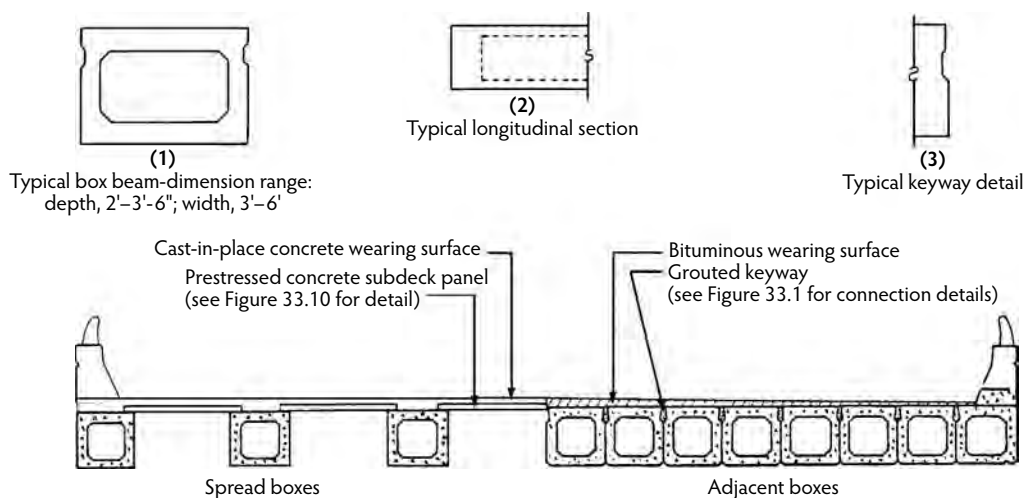


FIGURE 33.7 Prestressed box beam. (From Sprinkel, M.M., *Prefabricated Bridge Elements and Systems*, NCHRP Synthesis 119, Transportation Research Board, Washington, D.C., 1985.)

to be used with the beams (Tadros and Baishya, 1998). A recently completed NCHRP project, *Full-Depth, Precast-Concrete Bridge Deck Panel Systems*, includes designs for full-depth, precast deck panels without post-tensioning and overlays (Badie et al., 2006).

33.2.7 Prestressed Box Beams

The box beam (Figure 33.7) may be precast in a range of widths, depths, and lengths to accommodate spans of approximately 50 to 100 ft (15 to 30 m) (PCI, 1975). Boxes placed next to each other are typically tensioned in the transverse direction and covered with a wearing surface of asphalt. Boxes spaced apart

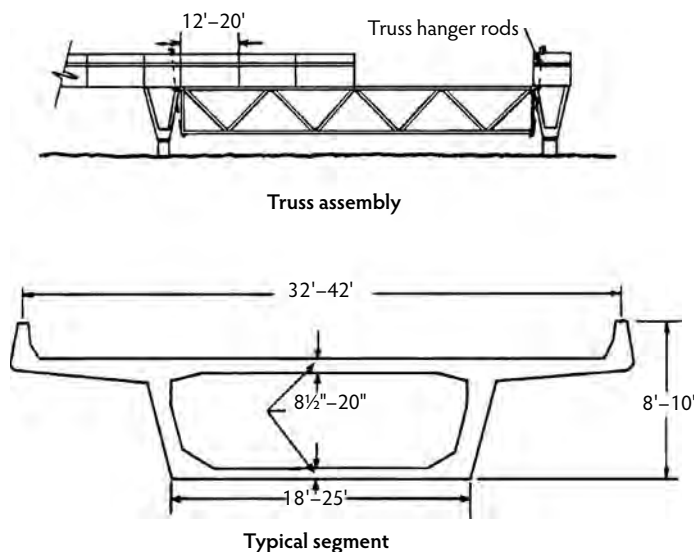


FIGURE 33.9 Post-tensioned segmental construction. (From Sprinkel, M.M., *Prefabricated Bridge Elements and Systems*, NCHRP Synthesis 119, Transportation Research Board, Washington, D.C., 1985.)

33.2.9 Segmental Construction

Elements (Figure 33.9) are typically full width, match cast, prestressed in the transverse direction, and post-tensioned in the longitudinal direction (VTRC, 1981). The elements are suitable for use on a wide range of span lengths. For shorter spans, the elements are usually erected on false work or assembled on a truss supported from pier to pier. For longer spans, the elements are erected by balanced cantilever, incremental launching, or progressive placing (Sprinkel, 1985). A patented segmental concrete overpass system economical for spans of 50 to 115 ft (15 to 35 m) provides at least 2 to 3 ft (0.6 to 0.9 m) of increased under-clearance and halves the on-site construction time for a two-span structure (Freyermuth, 1996). A procedure for the economical replacement of the top slab of a precast post-tensioned segmental bridge has recently been developed, so deck deterioration will not require the replacement of the superstructure (Stelmack and Trapani, 1991).

33.2.10 Prestressed Subdeck Panels

Prestressed subdeck panels are cast in a variety of lengths and widths, typically 4 to 8 ft (1.2 to 2.4 m). The length is a function of the spacing of the supporting beams. The panels are typically 3.5 in. (89 mm) thick and are set in a bed of grout about 0.5 in. (13 mm) thick. Site-cast concrete is placed over the panels to provide a reinforced deck (Figure 33.10). The panels are easily installed with a small crane and several laborers and do not require temporary forms or platforms to work from. Cracks usually occur in the site-cast concrete directly above the joints between the panels; consequently, many DOTs have discontinued or restricted the use of the panels. Cracking is less pronounced when the panels are placed on prestressed girders with short spans. Precast concrete subdeck panels can provide an economical and rapidly constructed deck (PCI, 1987).

33.2.11 Precast and Prestressed Deck Slabs

The deck is usually the first element in a bridge to deteriorate and to require funds for rehabilitation. In situations where traffic volumes are high, it is often necessary to rehabilitate or replace the deck in sections during off-peak periods. Because of the time required for site-cast concrete to cure, a number

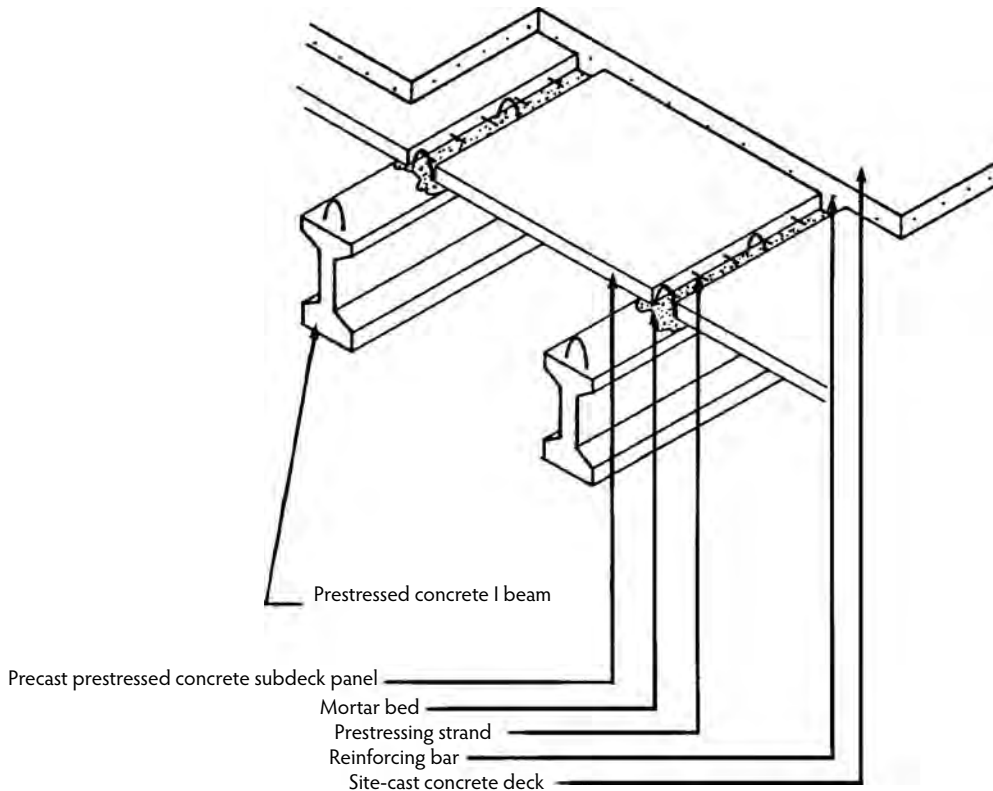


FIGURE 33.10 Prestressed subdeck panels. (From Sprinkel, M.M., *Prefabricated Bridge Elements and Systems*, NCHRP Synthesis 119, Transportation Research Board, Washington, D.C., 1985.)

of replacement strategies have been developed using prefabricated deck slabs (Issa et al., 1995a,b). Most of the systems involve a transverse segment (Figure 33.11) connected to the supporting beams with a rapid-curing polymer or hydraulic cement concrete. Shear transfer between adjacent slabs is achieved through the use of grouted keyways, site-cast concrete, and post-tensioning. Composite action is achieved through the use of studs on steel beams that extend into voided areas in the slabs that are then filled with polymer or hydraulic cement concrete.

Precast slabs can behave in a full-composite manner when connected to steel stringers with studs and epoxy mortar and when keyways are grouted with epoxy mortar (Osegueda et al., 1989). An earlier study identified some suitable connection details and concluded that the deck slabs are more economical than site-cast concrete because of the structural efficiency provided by post-tensioning and prestressing and because of the reduced construction time (Berger, 1983). Improved connection details for the use of panels on steel beams and prestressed concrete beams have been developed (Tadros and Baishya, 1998). More recently, a special loop bar reinforcement detail has been developed to provide live load distribution across transverse and longitudinal joints (see FHWA, 2004). A new full-depth precast prestressed concrete bridge deck slab system has been developed that includes stemmed slabs, transverse grouted joints, longitudinal post-tensioning, and welded threaded and headless studs (Tadros and Baishya, 1998). The deck slabs are thinner and lighter than a conventional deck and can be constructed faster.

Prestressed deck slabs typically have been used on major bridge deck replacement projects (Figure 33.12) such as the Woodrow Wilson Bridge (Lutz and Scalia, 1984). Also, most replacements have involved the use of transverse slabs. The decks on the George Washington Memorial Parkway were replaced using precast longitudinally post-tensioned transverse deck slabs (Jakovich and Alvarez, 2002). A latex-modified

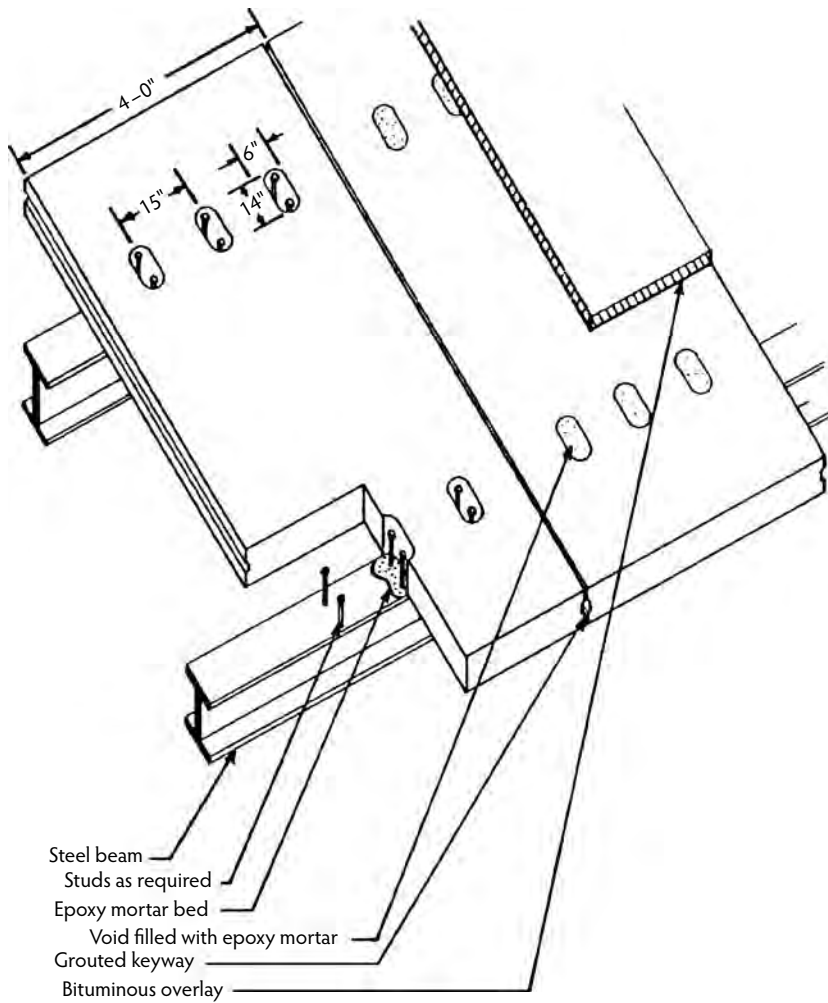


FIGURE 33.11 Prestressed deck slabs. (From Sprinkel, M.M., *Prefabricated Bridge Elements and Systems*, NCHRP Synthesis 119, Transportation Research Board, Washington, D.C., 1985.)

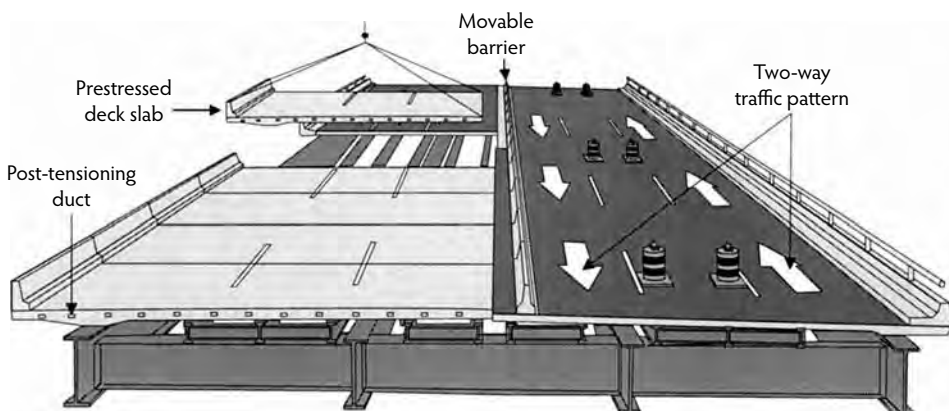


FIGURE 33.12 Prestressed post-tensioned deck slabs were installed at night to replace the deck of the Woodrow Wilson Bridge.

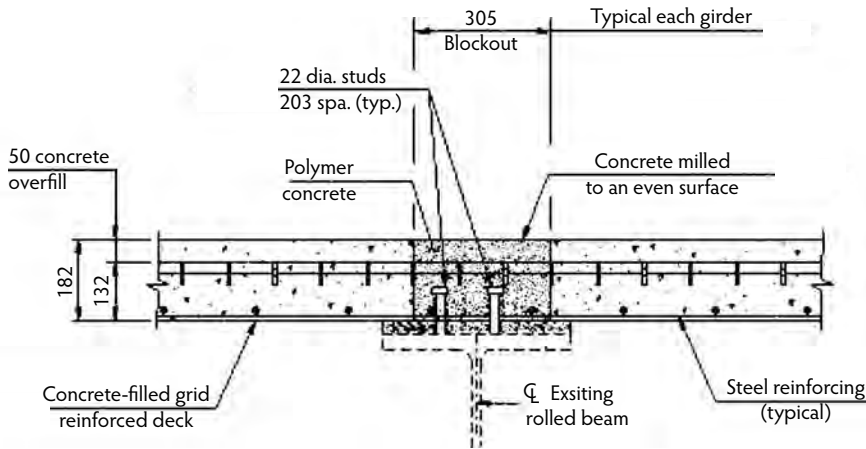


FIGURE 33.13 Special loop bar connection detail for deck slabs. (From FHA, *Prefabricated Bridge Elements and Systems in Japan and Europe*, Summary Report, International Technology Exchange Programs, Federal Highway Administration, Washington, D.C., 2004; <http://www.fhwa.dot.gov/bridge/prefab/pbesscan.htm>.)

concrete overlay was placed over the slabs. The truss spans of the deck on I-95 in Richmond, Virginia, were recently replaced with night lane closures using the full-depth transverse deck slabs (Figure 33.13). The slabs were also used to replace the deck on Route 50 in Fairfax County, Virginia (Babaei et al., 2001). The Virginia Department of Transportation first used transverse precast deck slabs to replace a deck on Route 235 over Dogue Creek in Fairfax County in 1981 (Sprinkel, 1982). Longitudinal slabs were successfully used to rehabilitate the Freemont Street Bridge (Smyers, 1984), and a new bridge was built in Thailand (Zeyher, 2003).

Longitudinal, partial-depth, or full-depth deck slabs that are precast on one or more concrete or steel beams have also been used successfully (FHWA, 2004). The superstructure elements are set next to each other and are typically connected by transverse post-tensioning in the deck and diaphragms between the beams. Keyways in the deck are grouted. The deck on I-95 in Richmond, Virginia, was recently replaced with night lane closures using the full-depth deck slabs on steel beam superstructure elements. When partial depth deck superstructure elements are set next to each other, reinforced site-cast concrete facilitates the connection of the elements.

33.2.12 Precast Parapet

The precast parapet (Figure 33.14) lends itself to prefabrication because it has a standard shape and can be easily mass produced. Several connection details have been developed to anchor the parapet. The parapet has been used in a number of states, but acceptance has been slow because of problems with water and chloride solutions leaking between the base of the parapet and the top of the deck.

33.2.13 Substructure Elements

More time is usually required to construct the substructure than the superstructure, and major reductions in construction time can be achieved by prefabricating the elements of the substructure. Most substructure elements have been prefabricated. Examples include pilings, piers, pier caps, abutments, and wing walls. Figure 33.15 shows abutment and wing-wall panels placed on temporary pads and anchored with weld plates and a site-cast concrete footing (PCI, 1975). To simplify erection, abutment and wing-wall elements have been precast with the footing and set on a site-cast footing (Sprinkel, 1985). Prestressed piling has been used for years, but pile caps are usually site cast. Bridges with prefabricated piers, pier caps, abutments, and wing walls are limited in number but use is increasing, particularly by the Texas Department of Transportation (Billington et al., 1999; Matsumoto et al., 2001, 2002). A bridge with a

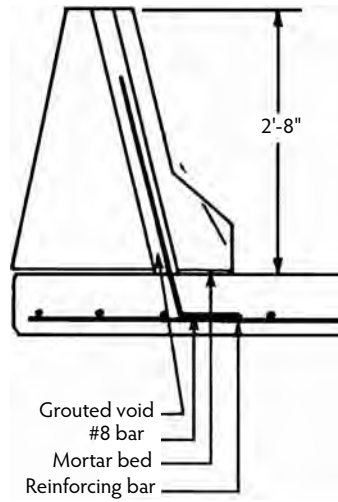


FIGURE 33.14 Precast parapet. (From Sprinkel, M.M., *Prefabricated Bridge Elements and Systems*, NCHRP Synthesis 119, Transportation Research Board, Washington, D.C., 1985.)

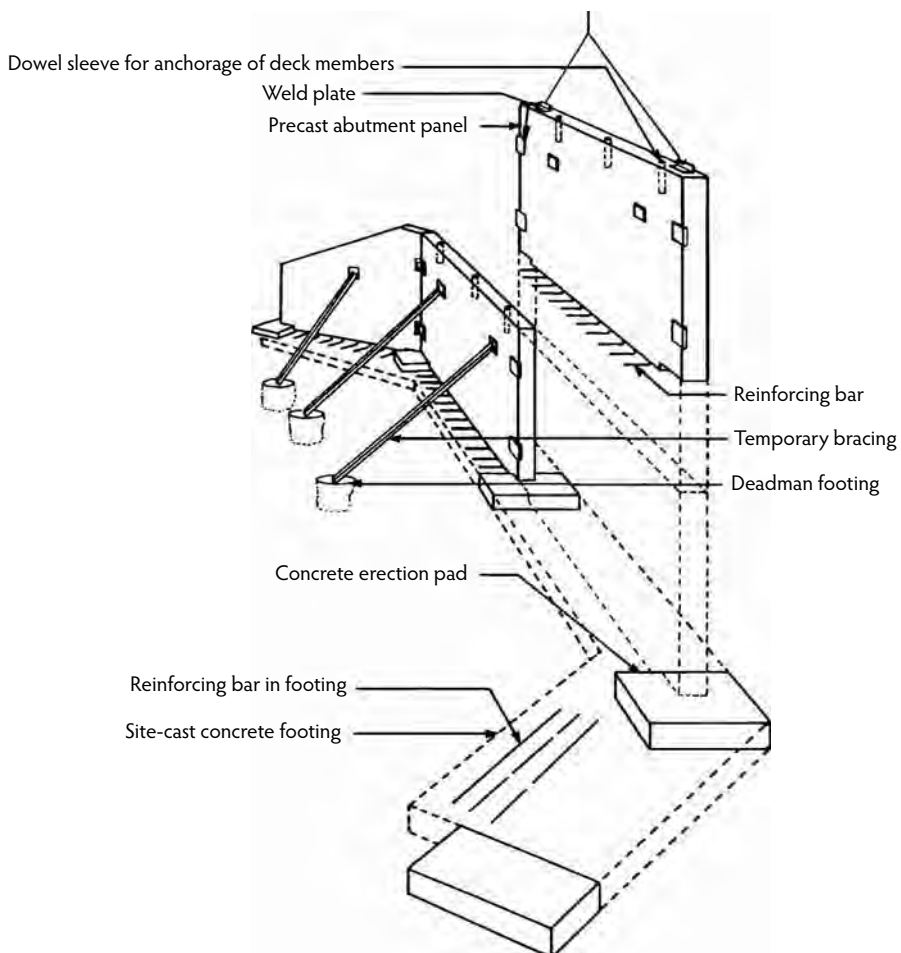


FIGURE 33.15 Precast abutment and wing wall. (From Sprinkel, M.M., *Prefabricated Bridge Elements and Systems*, NCHRP Synthesis 119, Transportation Research Board, Washington, D.C., 1985.)

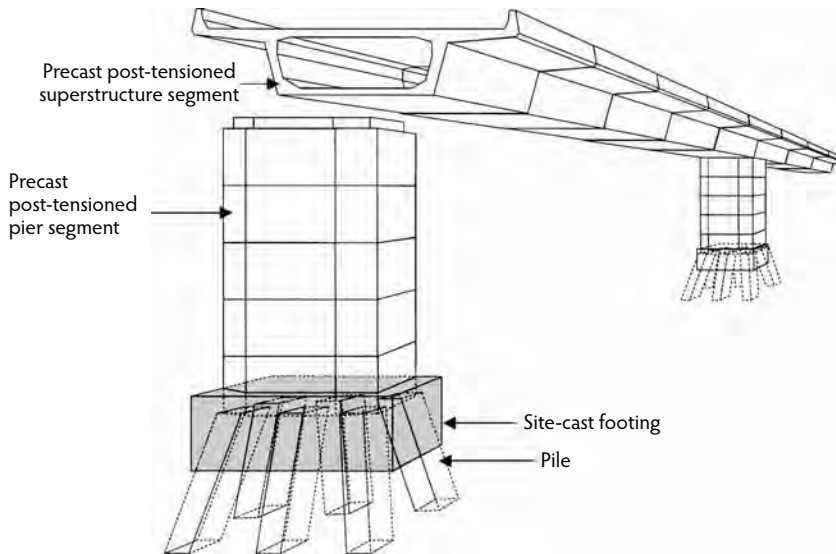


FIGURE 33.16 Prefabricated pier segments.



FIGURE 33.17 Precast concrete pier bent. (Figure courtesy of the Texas Department of Transportation, Dallas.)

precast abutment was recently constructed in Pennsylvania (Scanlon et al., 2002). It is difficult to standardize the elements because of differences between bridge sites and between piers at the same site that involve soil characteristics, location of bedrock, and the depth at which acceptable bearing can be obtained (Ganga Rao, 1978). A well-known example of the use of prefabricated piers is the Linn Cove Viaduct (Anon., 1984). The entire bridge was prefabricated to minimize environmental impact. Precast segmental superstructure segments were progressively placed and post-tensioned until a pier location was reached. Working from the cantilevered superstructure, holes were drilled into the ground. Prestressed piles were placed in the holes, and precast pier segments were placed and post-tensioned together. Site-cast concrete was placed around the bottom segment (Figure 33.16). The SPER system is a method of rapid construction of piers using precast concrete panels as both structural elements and formwork for cast-in-place concrete (see FHWA, 2004). The Texas Department of Transportation has developed and used a precast pier bent (Figure 33.17). The bent is placed on piers, and the voids in the bent around the reinforcement that extends from the piers are filled with grout.

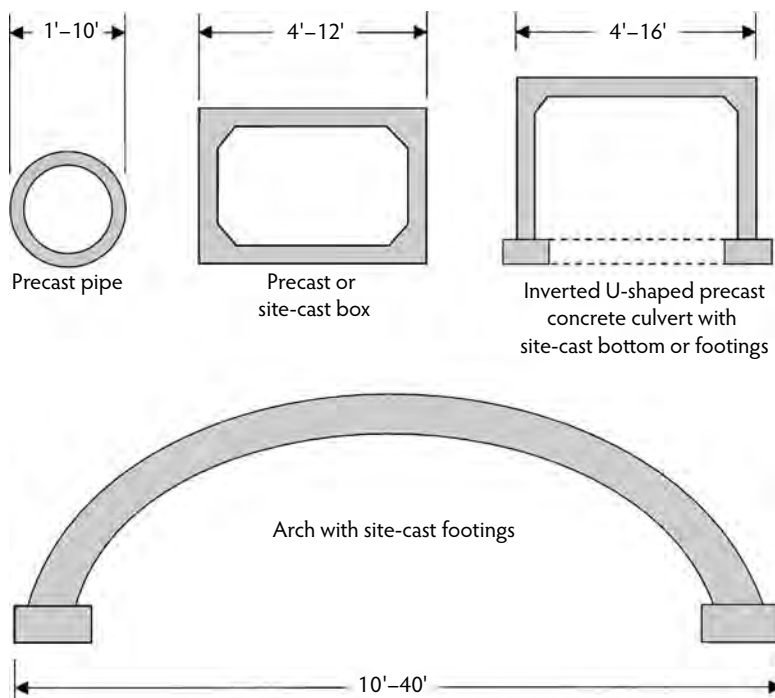


FIGURE 33.18 Precast culverts.

33.2.14 Precast Culverts

Culverts can be used instead of bridges in situations where the cross-section will not restrict flow. Culverts are easy to install, do not have a deck to deteriorate, and seldom require extensive plans. Culverts cannot be used on navigable streams. Precast culvert designs (Figure 33.18) include the pipe, box, inverted U, and arch. Site-cast footings and end walls are typically used with the inverted U and the arch. Concrete pipe is used for spans of 1 to 10 ft (0.3 to 3 m), and concrete boxes are used for spans of 4 to 12 ft (1.2 to 3.7 m) (Concrete Pipe and Products Company, 1993). Precast U-shaped culverts have been used for spans up to 16 ft (4.9 m), and the arch shape has been used for 40-ft (12-m) spans (Conspan Bridge Systems, Inc., 1995; Lambert, 1982).

33.3 Construction Considerations

On-site construction time is typically reduced when prefabricated elements are used because the concrete forming, casting, and curing occur at a precast plant. Quality elements are typically produced under controlled conditions. Elements are typically inspected at the plant and approved for shipment. Elements should fit together at the site when they are fabricated to the tolerances prescribed by the Prestressed Concrete Institute (PCI, 1977, 1978). Precasting operations should be organized to minimize the number of times an element must be moved. Excessive handling is costly and time consuming and increases the chances for damage (Waddell, 1974). The contractor should have an approved erection plan. Proper communication between the fabricator and contractor is essential. Elements should be delivered in the order in which they are to be assembled. Each element should be checked for damage that might have occurred during delivery and the plant stamp of approval should be verified. The hardware, rigging, and equipment required for handling the elements and the lifting locations should be preapproved before lifting an element. Handling and erection stresses can be greater than in-service stresses. Care should be taken to keep the stresses to a minimum. When feasible, elements should be supported during erection

as they are during delivery and storage. When lifting equipment is to be placed on the structure, the design should be checked and approved to ensure that the structure is not overstressed. Lifting equipment should be large enough to handle the elements. It is better to have equipment that is too large than too small.

Before placing elements, bearing areas should be properly prepared. Elements that fit properly can be assembled in a few minutes. Additional time is required to make corrections for improperly fitting elements. The advantage of match casting elements is a good fit. Several mortars and grouts for hydraulic cement and polymer concrete have been developed to facilitate the erection and connection of prefabricated elements (Gulyas et al., 1995). Temporary shims may be used. High-early-strength mortars and grouts can anchor the elements in a short time. When the elements have been assembled, a wearing and protection surface is usually installed. Asphalt is popular because of its low cost, but it should be used in connection with a properly installed membrane to prevent the infiltration of water and chloride ions into the prefabricated elements. Hydraulic cement concrete overlays can be installed to provide the final wearing surface. Bonded hydraulic cement concrete overlays can have a life of 30 years or more; however, these overlays are not easy to install, and construction should be done according to recommended practice. The recent failures of a number of bonded concrete overlays on major bridges before opening them to traffic or shortly thereafter illustrate the difficulties associated with constructing a successful overlay. Thin epoxy overlays have been used successfully as a wearing and protection system. Finally, deck elements can be precast with the final wearing surface, and irregularities can be removed by shot blasting or grinding the surface to provide good ride quality (Sprinkel, 2004).

33.4 Looking Ahead

The use of prefabricated bridge elements and systems will continue to increase for many reasons. With prefabrication, the work force can be more productive and can produce a better product in the controlled environment of a precast plant, compared to forming and placing reinforcement and concrete outdoors. The enhanced productivity and quality promote economy. The need to replace bridges and bridge elements is growing as our transportation system ages. The number of structures subjected to high volumes of traffic also continues to increase. Element replacement during off-peak traffic periods is becoming a necessity, and replacement with prefabricated elements is one of the few feasible options. Reducing delays for the traveling public is an additional economic incentive to use prefabricated elements. In recent years, the connection details that have caused maintenance problems and reduced the service life of elements have been improved. Better designs, enhanced materials, and more post-tensioning are allowing the construction of bridges with prefabricated elements that are more economical on a life-cycle basis than bridges constructed with site-cast concrete. There will always be a place for site-cast concrete, because concrete can take the shape of any form in which it is placed. This flexibility and versatility are necessary to satisfy many construction needs. It would be foolish to try to prefabricate concrete for every situation. Even so, the outlook for prefabricated bridge elements and systems has never been better. The use of prefabricated bridge elements and systems has increased significantly since the first edition of this *Handbook* was published. Universities, state DOTs, the FHWA, and the bridge industry have taken leadership roles in the new developments. The FHWA Summary of Prefabricated Bridge Elements and Systems website provides abstracts and contact information for recent publications on the subject (FHWA, 2004). Use will continue to increase as our roadways become more congested.

References

- AASHTO. 2002. *Prefabricated Bridges*. Technical Implementation Group, American Association of State Highway and Transportation Officials, Washington, D.C. (www.fhwa.dot.gov/download/brochure.pdf).
- AASHTO. 2004. *Prefabricated Bridge Elements and Systems Fact Sheet*. Technical Implementation Group, American Association of State Highway and Transportation Officials, Washington, D.C. (www.fhwa.dot.gov/download/facts.pdf).

- Anderson, A.R. 1972. *Systems Concepts for Precast and Prestressed Concrete Bridge Construction*, HRB Special Report 132: Systems Building for Bridges. Transportation Research Board, Washington, D.C.
- Anon. 1984. Concrete today: markets, materials, and methods. *Eng. News Rec.*, pp. 6, 8, 19, 20.
- Babaei, K., Fouladgar, A., and Nicholson, R. 2001. Nighttime Bridge deck replacement with full-depth precast concrete panels at Route 7 over Route 50, Fairfax County, Virginia. In *Proceedings of the Transportation Research Board Meeting*, January 7–11, Washington, D.C.
- Badie, S., Tadros, M., and Girgis, A. 2006. *Full-Depth, Precast-Concrete Bridge Deck Panel Systems*, NCHRP Report 12-65. National Cooperative Highway Research Program, Transportation Research Board, Washington, D.C.
- Berger, R.H. 1983. *Full-Depth Modular Precast, Prestressed Bridge Decks*. Transportation Research Board, Washington, D.C., pp. 52–59.
- Billington, J.E., Barnes, S., and Breen, R. 1999. *A Precast Substructure Design for Standard Bridge Systems*. Center for Transportation Research, University of Texas, Austin.
- Concrete Pipe and Products Company, Inc. 1993. *Pipe Design Concepts*. Vienna, VA.
- Conspan Bridge Systems, Inc. 1995. Dayton, OH.
- Dick, J.S. 2002. Precast technology and bridge design. *Struct. Eng. News, Views, Indust. Trends*, 3(4), 24–29.
- El-Ramaily, A., Tadros, M.K., Yamane, T., and Krause, G. 1996. Transverse design of adjacent precast prestressed concrete box girder bridges. *PCI J.*, 41(4), 96–113.
- Fadl, A.I., Gamble, W.L., and Mohraz, B. 1977. *Tests of a Precast Post-Tensioned Composite Bridge Girder Having Two Spans of 124 Feet*, Structural Research Series No. 439. University of Illinois, Chicago.
- FHA. 2002. *Prefabricated Bridge Elements and Systems: A Winning Idea*. Federal Highway Administration, Washington, D.C. (<http://www.tfhrc.gov/focus/may02/prefab.htm>).
- FHWA. 2003. *Prefabricated Bridge Technology: Get In, Get Out, and Stay Out*. Federal Highway Administration, Washington, D.C. (<http://www.tfhrc.gov/focus/april03/04.htm>).
- FHWA. 2004. *Prefabricated Bridge Elements and Systems in Japan and Europe*, Summary Report, International Technology Exchange Programs. Federal Highway Administration, Washington, D.C. (<http://www.fhwa.dot.gov/bridge/prefab/pbesscan.htm>).
- FHWA/AASHTO. 2004. *Prefabricated Bridges 2004*. FHWA and AASHTO Technical Implementation Group, Washington, D.C. (<http://www.fhwa.dot.gov/bridge/prefab/2004best.htm>).
- Freyermuth, C.L. 1996. *Evaluation Findings: The Segmental Concrete Channel Bridge System*, CERF Report HITEC 96-01. Civil Engineering Research Foundation, Washington, D.C.
- Ganga Rao, H.V.S. 1978. Conceptual substructure systems for short-span bridges. *Transport. Eng. J.*, 104(1).
- Gulyas, R.J., Wirthlin, G.J., and Champa, J.T. 1995. Evaluation of keyway grout test methods for precast concrete bridges. *PCI J.*, 40(1), 44–57.
- Hill, J.J. and Shirole, A.M. 1984. *Economic and Performance Considerations for Short-Span Bridge Replacement Structures*, TRR 950. Transportation Research Board, Washington, D.C., pp. 33–38.
- Issa, M.A., Idriss, A., Kaspar, I.I., and Khayyat, S.Y. 1995a. Full depth precast and precast, prestressed concrete bridge deck panels. *PCI J.*, 40(1), 59–80.
- Issa, M.A., Yousif, A.A., and Issa, M.A. 1995b. Construction procedures for rapid replacement of bridge decks. *Concrete Int.*, 17(2), 49–52.
- Jakovich, G. and Alvarez, J. 2002. The bridges that good planning and execution rebuilt. *Public Roads*, 66(2), 6–9.
- Johnson, J. 2002. Prefabricated bridges. *Bridge Builder*, 5(2), 10–14.
- Lambert, A.V. 1982. Instant arches: European style. *Concrete Int.*, 4(1), 44–47.
- Lutz, J.G. and Scalia, D.J. 1984. Deck widening and replacement of Woodrow Wilson Memorial Bridge. *PCI J.*, 29(3), 74–93.
- Matsumoto E.E., Waggoner M.C., Sumen G. Kreger M.E., Wood S.L., and Breen J.E. 2001. *Development of a Precast Bent Cap System*. Center for Transportation Research, University of Texas, Austin; U.S. Department of Transportation, Washington, D.C.; Texas Department of Transportation, Austin.

- Matsumoto, E.E., Kreger, M.E., Waggoner, M.C., and Sumen, G. 2002. *Grouted Connection Tests in Development of Precast Bent Cap System*. Transportation Research Board, Washington, D.C., pp. 55–64.
- Oesterle, R.G., Glikin, J.D., and Larson, S.C. 1989. *Design of Precast Prestressed Girders Made Continuous*, NCHRP Report 322. National Cooperative Highway Research Program, Transportation Research Board, Washington, D.C.
- Osegueda, R.A., Noel, J.S., and Panak, J.J. 1989. *Verification of Composite Behavior of a Precast Decked Simple Span*, TRR 1211. Transportation Research Board, Washington, D.C., pp. 72–83.
- Panak, J.J. 1982. *Economical Precast Concrete Bridges*, Research Report 226-1F. Texas State Department of Highways and Public Transportation, Austin, pp. 1, 12–18, 27–32.
- PCI. 1972. Modern concepts in prestressed concrete bridge design. *PCI Bridge Bull.*, Second Quarter.
- PCI. 1975. *Short Span Bridges*. Prestressed Concrete Institute, Chicago, IL.
- PCI. 1977. *Manual for Quality Control for Plants and Production of Precast Prestressed Concrete Products*. Prestressed Concrete Institute, Chicago, IL.
- PCI. 1978. Precast prestressed concrete industry code of standard practice for precast concrete. *PCI J.*, 23(1), 14–31.
- PCI. 1987. Precast prestressed concrete bridge deck panels. *PCI J.*, 32(2), 26–45.
- Pruski, K.R., Medlock, R.D., and Ralls, M.L. 2002. *Prefabrication Minimizes Traffic Disruptions*, HPC Bridge Views No. 21. Federal Highway Administration, Washington, D.C.; National Concrete Bridge Council, Skokie, IL (<http://www.portcement.org/br/newsletters.asp>).
- Rabbat, B.G., Takayanagi, T., and Russell, H.G. 1982. *Optimized Sections for Major Prestressed Concrete Bridge Girders*, Report No. FHWA/RD-82/005. Federal Highway Administration, Washington, D.C.
- Rawls, M. L. 2006. *Framework for Prefabricated Bridge Elements and Systems Decision Making*. Federal Highway Administration, Washington, D.C. (<http://www.fhwa.dot.gov/bridge/prefab/framework.cfm>).
- Salmons, J.R. 1971. Structural performance of the composite U-beam bridge superstructure. *PCI J.*, 16(4), 21–23.
- Scanlon, A., Aswad, A., and Stellar, J. 2002. *Precast Posttensioned Abutment System and Precast Superstructure for Rapid On-Site Construction*. Transportation Research Board, Washington, D.C., pp. 65–71.
- Smyers, W.L. 1984. Rehabilitation of the Fremont Street bridge. *PCI J.*, 29(5), 34–51.
- Sprinkel, M.M. 1976. *In-House Fabrication of Precast Concrete Bridge Slabs*, VHTRC 77-R33. Virginia Highway and Transportation Research Council, Charlottesville.
- Sprinkel, M.M. 1978. Systems construction techniques for short span concrete bridges. *Transport. Res. Rec. 665 Bridge Eng.*, 2, 222–227.
- Sprinkel, M.M. 1982. *Precast Concrete Replacement Slabs for Bridge Decks*, VHTRC 83-R2. Virginia Highway and Transportation Research Council, Charlottesville.
- Sprinkel, M.M. 1985. *Prefabricated Bridge Elements and Systems*, NCHRP Synthesis of Highway Practice 119. National Cooperative Highway Research Program, Transportation Research Board, Washington, D.C.
- Sprinkel, M.M. 2004. Deck protection systems for precast prestressed bridge deck panels. In *Proceedings of the PCI/FHWA International Symposium on High-Performance Concrete*, October 17–20, Atlanta, GA.
- Sprinkel, M.M. and Alcock, W.H. 1977. *Systems Bridge Construction in Virginia*. American Road and Transportation Builders Association, Washington, D.C., pp. 11–13.
- Stelmack, T.W. and Trapani, R.J. 1991. *Design Provisions for a Replaceable Segmental Bridge Deck*, Vol. 1, TRR 1290. Transportation Research Board, Washington, D.C., pp. 77–92.
- Tadros, M.K. and Baishya, M.C. 1998. *Rapid Replacement of Bridge Decks*, NCHRP Report 407. National Cooperative Highway Research Program, Transportation Research Board, Washington, D.C.
- Tokerud, R. 1975. Economical structures for low-volume roads. In *Low-Volume Roads*, Special Report 160. Transportation Research Board, Washington, D.C., pp. 273–277.

- Virginia Transportation Research Council (VTRC). 1980. *Bridges on Secondary Highways and Local Roads, Rehabilitation and Replacement*, NCHRP Report 222. National Cooperative Highway Research Program, Transportation Research Board, Washington, D.C.
- Virginia Transportation Research Council (VTRC). 1981. *Rehabilitation and Replacement of Bridges on Secondary Highways and Local Roads*, NCHRP Report 243. National Cooperative Highway Research Program, Transportation Research Board, Washington, D.C.
- Waddell, J.J. 1974. *Precast Concrete: Handling and Erection*. American Concrete Institute, Farmington Hills, MI.
- Zeyher, A. 2003. Soaring on the feet of an elephant. *Roads Bridges*, 41(8).



(a)



(b)

(a) Test specimen, University of California, San Diego; (b) precast seismic bracing elements, Paramount Building in San Francisco, California.

34

Design of Precast Concrete Seismic Bracing Systems

Robert E. Englekirk, Ph.D., S.E.*

34.1	Introduction	34-1
34.2	Basic Concepts.....	34-2
	The Development of a Strength Criterion • Creating an Effective Moment Transfer • Creating an Effective Shear Transfer	
34.3	Precast Concrete Seismic Moment-Resisting Ductile Frame Systems.....	34-7
	Bolted Assemblages • Post-Tensioned Assemblages • Interior Beam–Column Joints	
34.4	The Conceptual Design Process.....	34-18
	Bolted Systems • Post-Tensioned Systems	
34.5	Concluding Remarks.....	34-24
	References	34-24

34.1 Introduction

The precasting of concrete offers a wide variety of fabrication and assembly options. Economical seismic solutions are, to a large extent, dependent on the fabricator's capabilities and the contractor's comfort with the manner in which a particular precast component or system is integrated into the building. As a consequence, innovation is the key to creating a successful solution because the options are many. From a design perspective, options can be placed in two categories: those that emulate cast-in-place concrete construction and those that provide connections between components that are capable of sustaining post-yield deformations. We will refer to these design alternatives as *emulative* and *yielding*, respectively. The term *jointed precast* is also used to identify precast concrete elements designed to yield at the precast interface (Ghosh and Hawkins, 2001). These two approaches are shown in Figure 34.1. Systems a, b, and d of Figure 34.1 are emulative, for post-yield rotations are expected to occur in the concrete beam away from the point at which precast members are connected. Yielding systems similar to that described in Figure 34.1c are the exclusive focus of this chapter.

* Chairman Emeritus of Englekirk Companies and Adjunct Professor of Structural Engineering at the University of California, San Diego, where he actively participates in structural engineering research and teaches graduate courses in reinforced and prestressed concrete design.

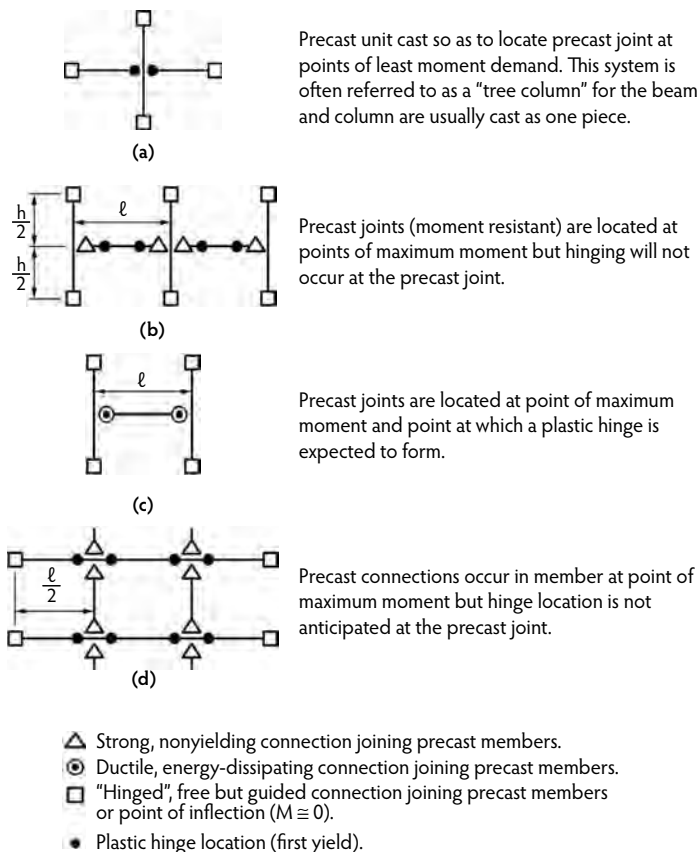


FIGURE 34.1 Classification of precast ductile frames according to component connector location. (From Englekirk, R.E., *Reinforced and Precast Concrete Buildings*, John Wiley & Sons, New York, 2003. Reprinted with permission of John Wiley & Sons, Inc.)

34.2 Basic Concepts

The cost-effective development of a yielding connector requires a simple yet effective mechanism for transferring both shear and moment as well as a suitable means of developing a strength-based loading criterion. Accordingly, these basic design and load transfer mechanisms are discussed before we explore the design of component and building systems.

34.2.1 The Development of a Strength Criterion

The introduction of a yield limit state at the point where the demand is expected to be a maximum (Figure 34.1) suggests that limit-state design procedures should be used to develop objective levels of system strength. Further, adjusting the level of provided strength is much more difficult in precast assemblies where the transfer mechanisms have established capacities that are large and do not allow modest changes in provided strength. Accordingly, a mechanism approach should be used to define the strength limit state for a precast concrete system. The mechanism approach should have as its primary objective entirely discounting the impact of dead and live loads on seismic bracing programs. The mechanism approach was introduced as *plastic design* in the 1950s and then was exclusively applied to indeterminate steel systems. The mechanism approach recognizes that system strength is based on the load required to produce a mechanism in the system and that first yield, as a limit state, does not produce consistent factors of safety.

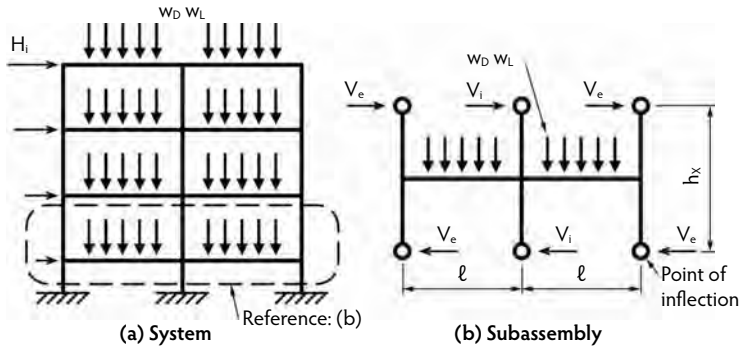


FIGURE 34.2 Frame elevation. (From Englekirk, R.E., *Reinforced and Precast Concrete Buildings*, John Wiley & Sons, New York, 2003. Reprinted with permission of John Wiley & Sons, Inc.)

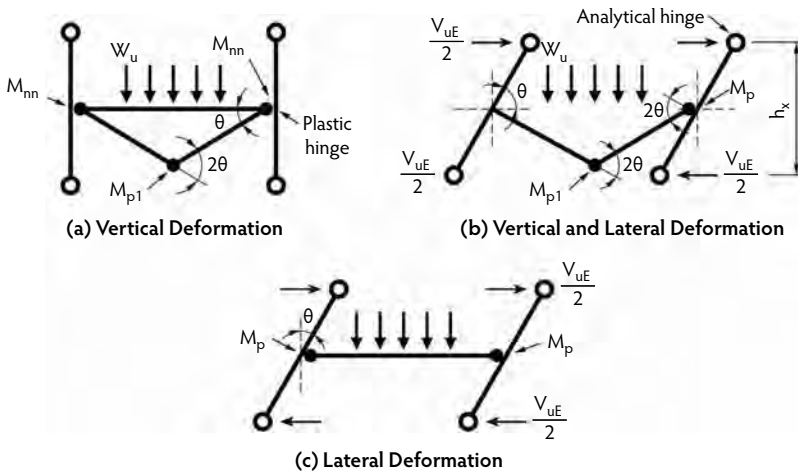


FIGURE 34.3 Subassembly mechanisms. (From Englekirk, R.E., *Reinforced and Precast Concrete Buildings*, John Wiley & Sons, New York, 2003. Reprinted with permission of John Wiley & Sons, Inc.)

Consider the frame and extracted subassembly described in Figure 34.2. The strength limit state is defined by one of the mechanisms shown in Figure 34.3. Observe that dead and live loads only impact mechanisms of Figure 34.3a and Figure 34.3b because, in the mechanism of Figure 34.3c, dead and live loads create no external work. Our seismic design objective should be to ensure that the mechanism described in Figure 34.3c precedes that described in Figure 34.3b. This objective is accomplished by comparing the lateral loads required to create the two mechanisms described in Figures 34.3b and 34.3c:

Mechanism of Figure 34.3c

$$\begin{aligned} \text{External Work} &= \text{Internal Work} \\ V_{uE} h_x \theta &= 2M_p \theta \end{aligned} \quad (34.1)$$

where M_p is assumed to be the nominal strength of the connecting assembly.

Mechanism of Figure 34.3b

$$\begin{aligned} \text{External Work} &= \text{Internal Work} \\ V_{uE} h_x \theta + 2(w_{uD} + w_{uL}) \left(\frac{\ell}{2} \right) \left(\frac{\ell}{4} \right) \theta &= 2M_p \theta + 2M_{p1} \theta \end{aligned} \quad (34.2)$$

where M_{p1} is the internal strength of the beam, assumed to be critical at midspan.

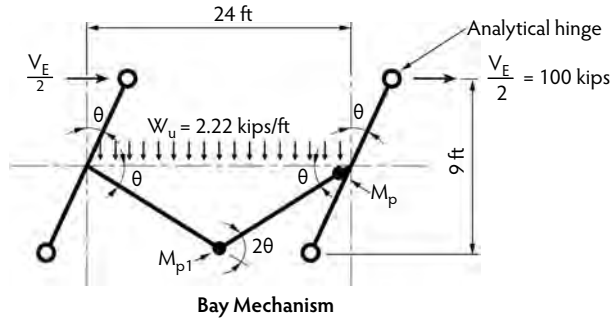


FIGURE 34.4 Internal mechanism. (From Englekirk, R.E., *Reinforced and Precast Concrete Buildings*, John Wiley & Sons, New York, 2003. Reprinted with permission of John Wiley & Sons, Inc.)

The design objective is to determine the strength relationship between the internally provided flexural strength (M_{p1}) and that provided at the ends of the beam (M_p) that would cause the mechanism of Figure 34.3c to be critical. If we define A as:

$$A = \frac{M_{p1}}{M_p} \quad (34.3)$$

then M_{p1} , the strength provided in the interior of the beam, must be greater than AM_p to attain our objective—the dominance of the side-sway mechanism (Figure 34.3c). Accordingly,

$$(A = 1)M_p > (w_{uD} + w_{uL})\frac{\ell^2}{8} + \frac{V_{uE}h_x}{2} \quad (34.4)$$

Thus, if the strength of the internal plastic hinge (AM_p) exceeds $(w_{uD} + w_{uL})\ell^2/8$ and the provided moment capacity at the support is equivalent to or larger than M_p as developed by the mechanism of Figure 34.3c ($([V_{uE}h_x]/2)$), the impact of vertical loads on the design strength provided in the yielding connector may be neglected.

Example

The 24-foot internal bay of the frame of Figure 34.2 is shown in Figure 34.4:

$$\begin{aligned} \text{External Work} &= \text{Internal Work} \\ 2\frac{V_E}{2}h_x\theta + 2w_u\left(\frac{\ell}{2}\right)\frac{\ell}{4}\theta &= 2M_p\theta + 2M_{p1}\theta \end{aligned} \quad (34.5)$$

Use Equation 34.5 to solve for the minimum value of M_{p1} if M_p is 825 ft-kips:

$$\begin{aligned} 200(9) + \frac{2.22(24)^2}{4} &= 2(825) + 2M_{p1}, \quad M_{p1} > 235 \text{ ft-kips} \\ A = \frac{M_{p1}}{M_p} &= \frac{235}{825} = 0.28 \end{aligned}$$

Observe that the design objective can be obtained by the direct application of Equation 34.2 because it is understood that Equation 34.1 must be satisfied.

Conclusion: The side-sway mechanism described in Figure 34.3b can be avoided if the strength of the beam (M_{p1}) is enough to satisfy the demand suggested by unconstrained support rotations.

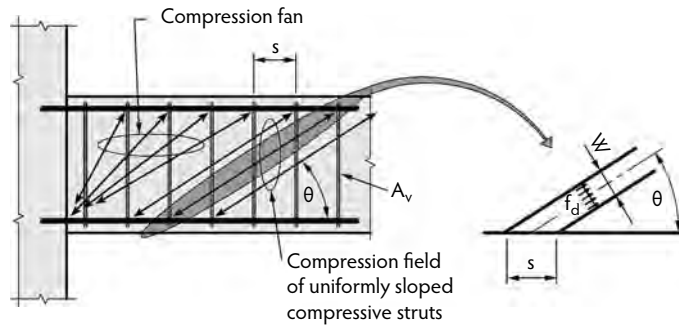


FIGURE 34.7 Shear transfer mechanisms at the beam–column interface. (From Englekirk, R.E., *Reinforced and Precast Concrete Buildings*, John Wiley & Sons, New York, 2003. Reprinted with permission of John Wiley & Sons, Inc.)

34.2.3 Creating an Effective Shear Transfer

Shear transfer in cast-in-place concrete regions of discontinuity, such as the beam–column interface described in Figure 34.7, relies on the toe region of the beam to transfer both compression and shear. This shear transfer mechanism is often referred to as *shear friction*. Essentially, the yielding of the flexural tension reinforcing of the beam is assumed to create a frictional resistance by its equilibrating compressive counterpart. The basic shear transfer strength as developed in design standards implies a shear friction factor (μ) of 0.6 to 1.4. This large range of codified friction factors is attributed to the condition of the interface where shear must be transferred. Figure 34.8 describes the interface when applied shear acts in one direction. Seismic cyclings cause the actions to reverse, and tension cracks in the top of the beam described in Figure 34.8 will close and be subjected to shear. The deterioration described in Figure 34.5, exacerbated by the buckling of the bars, will occur and create a deformation limit state. Accordingly, the shear transfer limit state is not, given a cyclic deformation, a function of the initial interface surface but rather the propensity of the interface to deteriorate. Yielding precast systems will rely on friction to transfer shear and endeavor to minimize cyclic deterioration. Yielding precast joints will often rely on a steel-to-steel or a steel-to-concrete interface, for they are also capable of transferring shear forces when the frictional demand is reasonable. The steel-to-concrete friction factor is on the order of 0.7; structural steel design procedures allow a steel-to-steel friction factor of 0.35 for clean mill-surfaced finishes based on a factor safety of between 1.4 and 1.5.



FIGURE 34.8 Compression fan at interior support of the beam, monotonic loading. (From McGregor, J., *Reinforced Concrete: Mechanics and Design*, 3rd ed., Pearson Education, Upper Saddle River, NJ, 1997. With permission.)

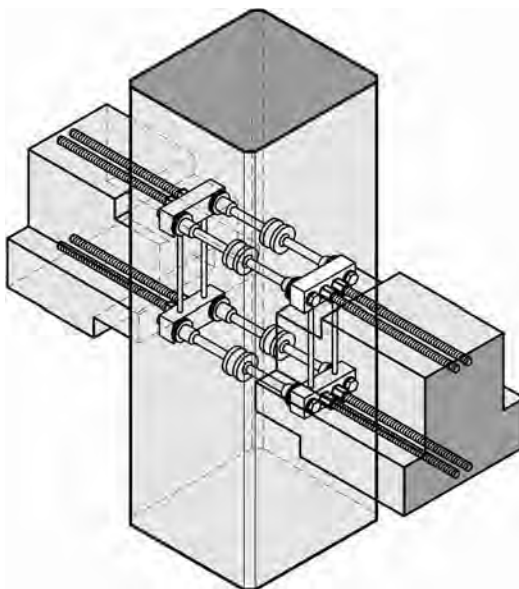


FIGURE 34.9 Isometric view of the Dywidag Ductile Connector (DDC[®]) system. (From Englekirk, R.E., *Reinforced and Precast Concrete Buildings*, John Wiley & Sons, New York, 2003. Reprinted with permission of John Wiley & Sons, Inc.)

Conclusion: The use of a nominal friction coefficient of 0.5 for steel-to-steel and 1.0 for concrete-to-concrete regardless of the type of surface finish seems reasonable. A strength reduction factor of 0.85 is often recommended but probably excessive in this case, for the compressive force is passively activated and always proportional to shear demand. This constant relationship between moment and shear obviates the need to consider overstrength factors.

34.3 Precast Concrete Seismic Moment-Resisting Ductile Frame Systems

Two basic systems are developed in this section. They have both been used successfully to construct major buildings in regions of high seismicity and represent two approaches to creating precast concrete buildings that will perform well when subjected to seismic excitations. The described approaches differ primarily in the means by which the frame beam and column are connected. They are categorized herein as *bolted* and *post-tensioned*, but it is important to realize that the concepts developed are not limiting in their potential application, for variants have been and will continue to be produced.

34.3.1 Bolted Assemblages

The development of the assemblage described in Figure 34.9 was motivated by a desire to improve post-yield behavior of concrete ductile frames, because the ultimate post-yield rotation capability of the subassembly is increased by 50%. The adaptation of the ductile connection concept to precast concrete is logical, because it allows post-yield deformations to be accommodated where members are joined (Figure 34.1c). Direct-thread alternatives have been used in both cast-in-place systems and composite precast concrete systems. The desired behavior is accomplished through a merging of steel technology with the basic objectives of seismic-load-limiting principles essential to the development of ductile behavior in structural systems that must survive earthquakes. The basic component is the *ductile rod* (Figure 34.10), which is capable of attaining strain states in excess of 30%. The assemblage described in Figure 34.9 allows tolerance in all directions and ensures proper seating of the connecting high-strength

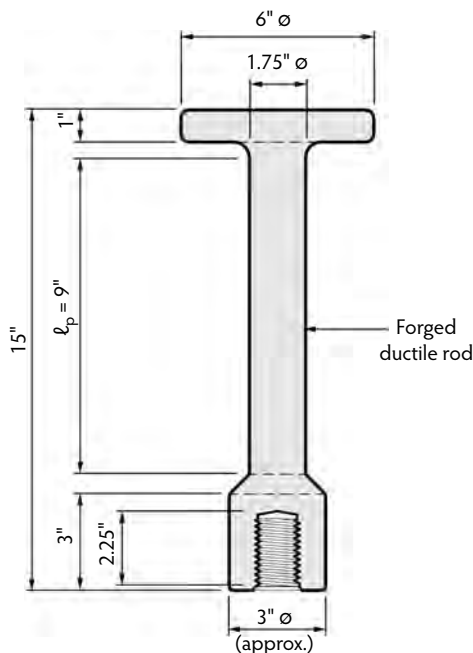


FIGURE 34.10 Prototypical forged ductile rod. (From Englekirk, R.E., *Reinforced and Precast Concrete Buildings*, John Wiley & Sons, New York, 2003. Reprinted with permission of John Wiley & Sons, Inc.)

bolts. The manufacture and distribution of the system is controlled by Dywidag Systems International under the name of Dywidag Ductile Connector (DDC®). System capacity is developed directly from accepted load transfer mechanisms and conditions of equilibrium. The strength reduction factors and overstrength factors are consistent with values used in the design of concrete ductile frames. The key element in the assembly described in Figure 34.9 is the ductile rod (Figure 34.10). This ductile rod is the yielding element. The function of the ductile rod is to accommodate post-yield system deformations.

Our analytic understanding of system behavior, then, logically starts from the ductile rod and moves first to the beam and then into the column. When a moment couple is developed between two sets of N rods separated by a distance $d - d'$ (Figure 34.11), the nominal moment capacity (M_n) developed is:

$$M_n = NT_y(d - d') \quad (34.6)$$

where T_y is the nominal tensile strength of one ductile rod. The nominal capacity of the set of ductile rods must be developed in the beam. Because the adopted design objective for the rest of the system is elastic behavior, an overstrength factor (λ_o) must be introduced.

The first load transfer point proceeding toward the beam is the beam–column interface, where the appropriate level of shear and moment must be transferred. High-strength (1-1/2-in. ϕ -A490SC) bolts are used to accomplish this transfer. The nominal tensile strength provided by this bolt is on the order of 210 kips, which exceeds the nominal tension strength of the ductile rod by more than 25%:

$$T_{bn} = \lambda_o \frac{M_n}{(d - d')}$$

$$NA_B = \frac{T_{bn}}{\phi F_t}$$

The shear load (V_{nE}) induced by the ductile rod mechanism at the beam-to-column interface is:

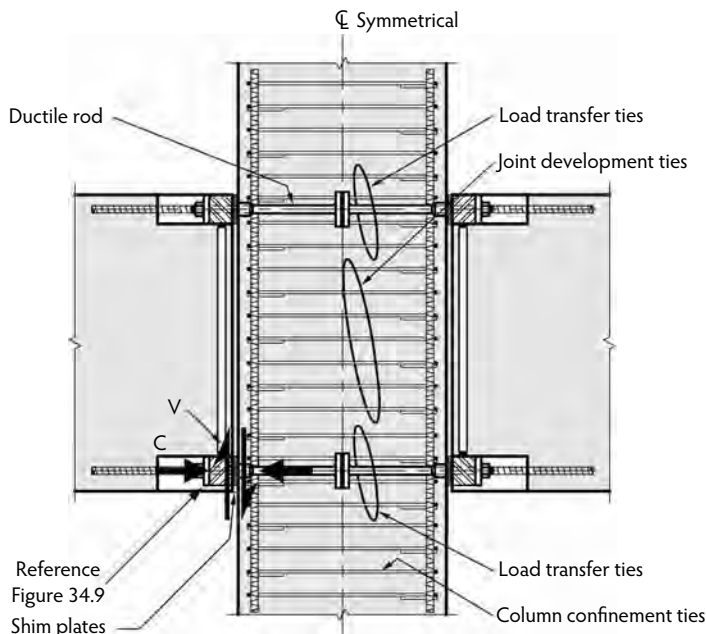


FIGURE 34.11 DDC® connection, shear transfer mechanism (friction: steel to steel). (From Englekirk, R.E., *Reinforced and Precast Concrete Buildings*, John Wiley & Sons, New York, 2003. Reprinted with permission of John Wiley & Sons, Inc.)

$$V_{nE} = \frac{2\lambda_o M_n}{\ell_c}$$

where ℓ_c is the clear span of the beam. The nominal shear capacity required of the connector is:

$$V = V_{nE} + V_D + V_L \quad (34.7)$$

Comment: Because the design objective is code compliance, factored dead and live loads are appropriately used. Concerns relative to attaining shear transfer in the plastic hinge region of a cast-in-place frame beam ($V_c = 0$) do not apply because the plastic hinge region is no longer in the beam.

The shear transfer mechanism between beam and column is friction. The load proceeds from the face of the ductile rod to the beam transfer block (see Figure 34.11) through a set of shim plates that provide longitudinal tolerance. The normal load that activates this friction load path is the larger of the bolt pretension (T_p) or flexurally induced compression ($M/d - d'$). The ability of the connector described in Figure 34.11 to transfer load will depend on the level of pretensioning ($2NT_p$) and applied moment (M). The level of applied moment (M) must at some instant be zero. At this instant, both the upper and lower connections will participate in the transfer of shear. Accordingly,

$$V_D + V_L < 2NT_p f \quad (34.8)$$

where f is the friction factor allowed by the load and resistance factor design (LRFD) specifications.

As moment is applied to the connection, the effective level of pretensioning on the tensile bolt group will be relieved. Observe that the force applied to the ductile rods is unaffected by the level of bolt preload, for the bolts serve only to clamp the beam transfer block to the ductile rod. When the preload (NT_p) has been relieved, however, the ability of the compression face connector to transfer shear will continue to increase, for the compression (C) crossing the surface described in Figure 34.11 will now be entirely a function of the level of moment imposed on the connection. Hence, C will be the larger

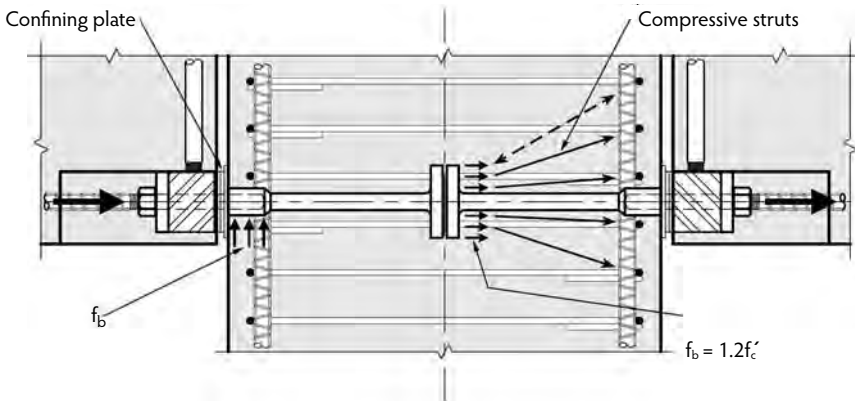


FIGURE 34.12 DDC® connection, shear transfer mechanism (concrete bearing: confined region). (From Englekirk, R.E., *Reinforced and Precast Concrete Buildings*, John Wiley & Sons, New York, 2003. Reprinted with permission of John Wiley & Sons, Inc.)

of NT_p or $(M/d - d')$. Accordingly, the nominal capacity of the shear transfer mechanism is the larger of these values:

$$V_n = \left(\frac{M}{(d - d')} \text{ or } NT_p \right) f \quad (34.9)$$

where f , the friction factor used, should be 0.35 when dead and live loads are the concern (Equation 34.8) or 0.5 when seismic limit state shears are considered (Equation 34.7) because a shear slip will not result in a system failure. Beam component design should logically proceed based on the adoption of a variable overstrength factor (λ_o). The required capacity of each element should be modified ($\lambda_o \phi$) to approximately account for uncertainties associated with each of the considered load transfer mechanisms.

The yield strength of Threadbars® (high-strength threaded bars manufactured by Dywidag) that extend into the beam (Figure 34.9) is guaranteed. The assembly has been tested to ensure that yielding does in fact occur exclusively in the ductile rod (Figure 34.10). Alternatives for connecting the Threadbars® in the beam include reverse threads in the transfer block, couplers, or splice bars. Shear reinforcement is developed from Equation 34.7, and high-strength shear reinforcement ($f_y = 75$ ksi) may also be used here because post-yield behavior in the stirrups is guarded against by the use of a capacity-based design. The load path from the ductile rod to the column is by bearing (Figure 34.12). Shear loads are equilibrated by bearing stresses under the compression side rod ends at the face of the column. The bearing stress allowed for confined concrete may appropriately be used because the shear load is only transferred through the compressed zone of the frame beam, and the shim plates provide a significant normal or confining pressure in this part of the column.

The internal bearing at the rod end when two rods abut (Figure 34.12) is subjected to a tensile load from the ductile rod on one side and a compressive load from the rod on the opposite side, at least until the post-yield strain imposed on the ductile rod has been recovered. The tensile load will at some point exceed T_{yi} , and the yield strength of the rod is accordingly factored to account for probable overstrength. The worst-case bearing load imposed on the anchor end of a ductile rod is $2\lambda_o T_{yi}$, but this will not be realized because any overstrength compression side demand will be resisted by bearing on the face of the column. The concrete within the core of the column that resists this load is well confined, and the supporting surface is wider than the bearing area on all sides. The design bearing stress may conservatively be presumed to be $0.85\phi(2)f'_c$, according to ACI 318-05, Section 10.17.1 (ACI Committee 318, 2005), and this is $1.2f'_c$.

A set of compressive struts distributes bearing stresses imposed on the rod ends to joint reinforcement located above, below, and alongside the ductile rod assembly (Figure 34.12). The internal load transfer



FIGURE 34.13 Precast concrete bracing tower. (Photograph courtesy of Englekirk Partners, Los Angeles, CA.)

mechanism within the joint itself, with the exception of the load transfer ties, is much the same as that which occurs in the panel zone of a concrete ductile frame. It is discussed in considerably more detail in Section 34.4. The bracing tower of Figure 34.13 was built using the DDC® system.

34.3.2 Post-Tensioned Assemblages

Post-tensioned assemblages consisting of precast beams and columns were first tested in the early 1970s. Early rejections of the concept were based on the fact that no energy was dissipated by the system and a concern that anchorage systems would fail. In the 1990s, these problems were overcome with the development of what is now referred to as the *hybrid system* (Cheok and Lew, 1993; Englekirk, 2003). The system was then used to construct the building shown in Figure 34.14. A comprehensive test program in support of the design of this building was conducted by Professor Stanton at the University of Washington. The exterior subassembly shown in Figure 34.15 describes the post-yield behavior of the beam for the capacity of the column, and the joint in the subassembly significantly exceeds the demand imposed on them by the beam. The fact that post-yield deformation occurred almost exclusively in the beam was confirmed by the test program.

Flexural strength in the hybrid beam (Figure 34.16) is provided by a combination of unbonded post-tensioning strands and bonded mild steel. Nine 1/2-in. 270-ksi strands stressed to 162 ksi were used in the system described in Figure 34.15 to provide an effective concentric post-tensioning force of 223.1 kips. Three #6 (GR60) reinforcing bars were placed in the top and bottom of the beam in tubes that were subsequently grouted with high-strength grout. These bars provide energy dissipation, an attribute not provided by the unbonded post-tensioning. The strength provided by the 16 × 21-in.-deep beam is defined by the size of the grout pad, which for this test was 16 × 20 in.

The design of the exterior subassembly of Figure 34.15 assumed that the stress in the mild steel compression reinforcement reached yield. Accordingly, the flexural strength provided by the mild steel (M_{ns}) was:

$$M_{ns} = T_{ns}(d - d') = 3(0.44)(60)(16.5) = 1307 \text{ in.-kips} \quad (34.10)$$

The flexural strength provided by the unbonded post-tensioning (M_{nps}) is developed as follows (see Figure 34.16):



FIGURE 34.14 Paramount Apartments, San Francisco, CA. (Photograph courtesy of David Wakely Photography, San Francisco, CA.)

$$T_{nps} = A_{ps} f_{pse}$$

$$T_{nps} = 9(0.153)(162) = 223.1 \text{ kips} \quad (34.11a)$$

$$a = \frac{T_{nps}}{0.85 f'_c b} = \frac{223.1}{0.85(5)(16)} = 3.3 \text{ in.}$$

$$M_{nps} = T_{nps} \left(\frac{h}{2} - \frac{a}{2} \right) = 223.1(10 - 1.65) = 1865 \text{ in.-kips} \quad (34.11b)$$

The nominal moment capacity of the hybrid frame beam of Figure 34.15 is:

$$M_n = M_{ns} + M_{nps} = 1307 + 1865 = 3172 \text{ in.-kips} \quad (34.12)$$

This corresponds to a beam load or shear of:

$$V_{nb} = \frac{M_n}{\ell_c} = \frac{3172}{62} = 51.2 \text{ kips}$$

The associated column shear or applied test frame force (F_{col}) is:

$$V_c = F_{col} = V_{nb} \left(\frac{\ell}{h_x} \right) = 51.2 \left(\frac{72}{117.5} \right) = 31.4 \text{ kips}$$

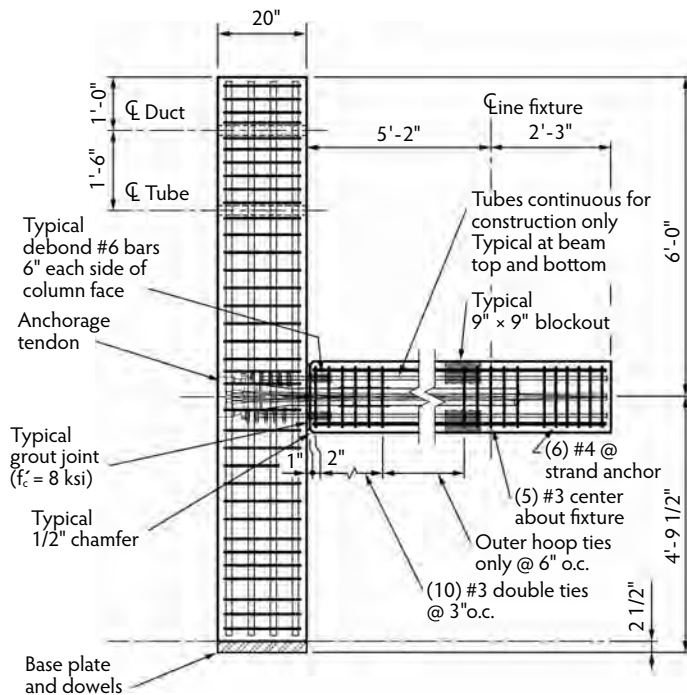


FIGURE 34.15 Exterior subassembly. (From Englekirk, R.E., *Reinforced and Precast Concrete Buildings*, John Wiley & Sons, New York, 2003. Reprinted with permission of John Wiley & Sons, Inc.)

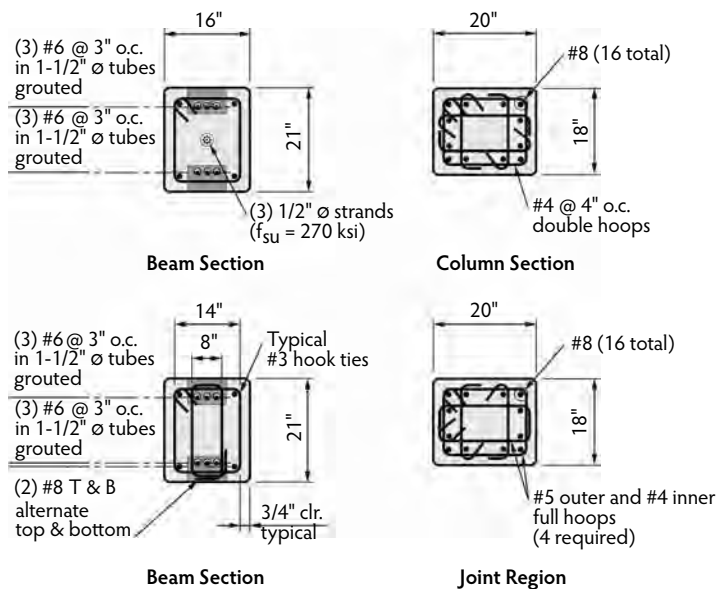
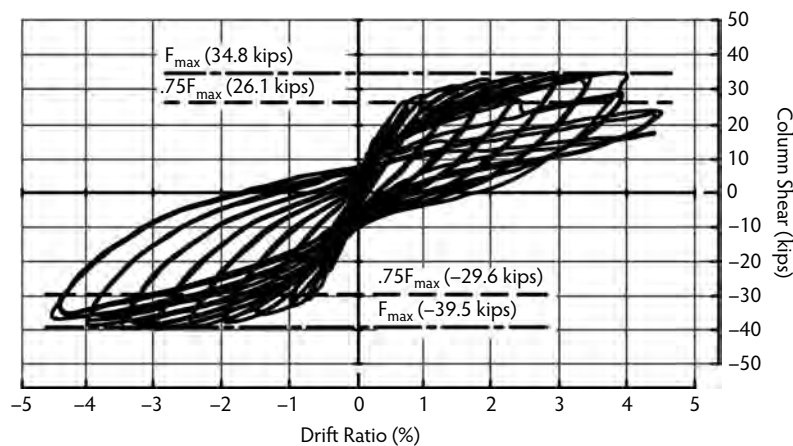


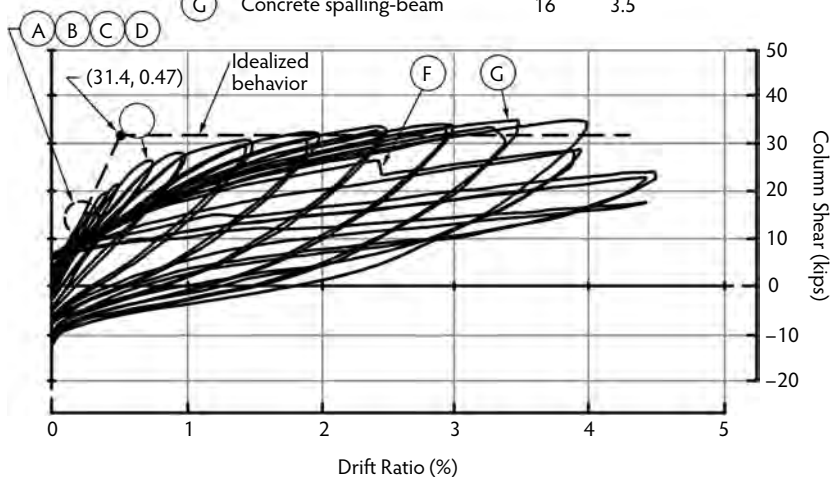
FIGURE 34.16 Beam and column cross-sections, hybrid subassembly test program. (From Englekirk, R.E., *Reinforced and Precast Concrete Buildings*, John Wiley & Sons, New York, 2003. Reprinted with permission of John Wiley & Sons, Inc.)

Figure 34.17a describes the behavior of the test specimen. Figure 34.17b identifies critical behavior milestones. The stresses imposed on the post-tensioning strands are shown in Figure 34.18, where they are related to test specimen drift. Observe that the predicted nominal strength of 31.4 kips (V_c) is not



(a) Full Hysteretic Behavior

Mark	Event	Set	Drift Ratio
A	Grout cracking interface	4	0.10
B	Grout lift-off interface	5	0.15
C	Surface cracking joint	5	0.15
D	Surface cracking beam	6	0.20
E	Bar yield, continuity bar	10	0.75
F	Bar fracture, continuity bar	17	4.0
G	Concrete spalling-beam	16	3.5



(b) Critical Behavior Milestones

FIGURE 34.17 Test specimen behavior. (From Englekirk, R.E., *Reinforced and Precast Concrete Buildings*, John Wiley & Sons, New York, 2003. Reprinted with permission of John Wiley & Sons, Inc.)

reached until a drift ratio of almost 2% is attained (Figure 34.17b). This is at least in part explained by the fact that the initially delivered post-tensioning force was only 216 kips, or 4% less than the specified 223.1 kips. A story drift of 1% was required to develop the assumed design force in the post-tensioning ($T_{nps} = 223.1$ kips).

Subassembly stiffness as predicted by idealized member stiffness is developed as follows (Englekirk, 2003):

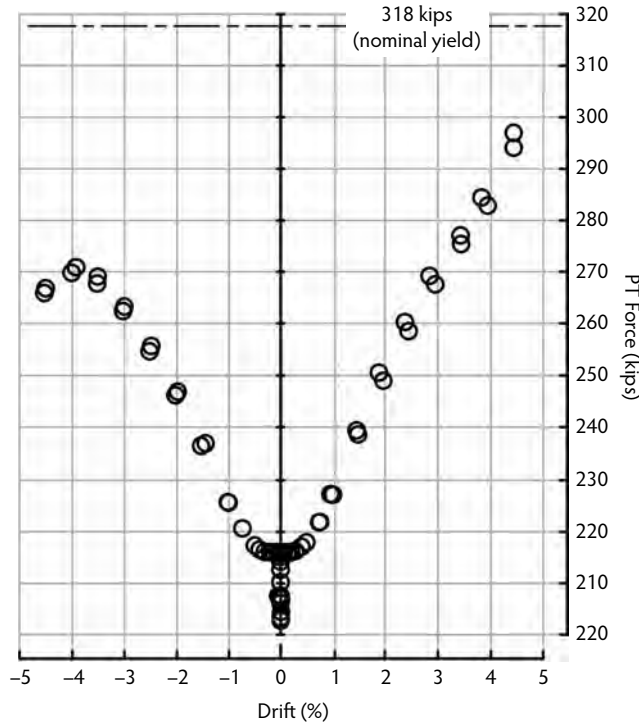


FIGURE 34.18 Post-tensioning (PT) force vs. drift relationship. (From Englekirk, R.E., *Reinforced and Precast Concrete Buildings*, John Wiley & Sons, New York, 2003. Reprinted with permission of John Wiley & Sons, Inc.)

$$\Delta_x = \frac{V_c h_x^2}{6E} \left(\frac{\ell}{I_b} + \frac{h_x}{2I_c} \right)$$

$$h_x = 117.5 \text{ in.}$$

$$\ell = 72 \text{ in.}$$

$$I_{ce} = 0.71 I_g = \frac{0.7(18)(20)^3}{12} = 8400 \text{ in.}^4$$

$$I_{be} = 0.35 I_g = \frac{0.35(16)(21)^3}{12} = 4322 \text{ in.}^4$$

$$\Delta_x = \frac{31.4(117.5)^2}{6(4000)} \left[\frac{72}{4322} + \frac{117.5}{8400} \right] = 0.55 \text{ in.}$$

The associated drift ratio (Δ/h_x) is 0.47%. This drift ratio might be accepted as an idealized representation of stiffness to a column shear of about 50% of the nominal column shear (31.4 kips) but not as a good idealization for the behavior described in Figure 34.17. The hybrid subassembly appears to be considerably softer than a cast-in-place system (Englekirk, 2003).

Probable flexural strength and ultimate strain states should be predicted during the system analysis phase, as opposed to the conceptual design phase of the project. The process begins by estimating the strain states in the reinforcing at a selected level of drift. Consider a 4% post-yield drift ratio (θ_p), our objective drift, and realize that any elastic component of story drift will be small (Figure 34.17). The plastic hinge length (ℓ_p) initially will be the debonded length of the mild steel, in this case 6 in.:

$$\theta_y = \phi_y \ell_p = \left(\frac{0.002}{h-c} \right) (6) = \left(\frac{0.002}{20-4} \right) (6) \cong 0.00075 \text{ radian}$$

Further, assume that all of the post-yield rotation will occur at the beam–column interface (Figure 34.6). The elongations of the tensile reinforcement components, (δ_p and δ_s) are best made using an iterative process, for the stress levels in the reinforcement will dictate the location of the neutral axis. Begin the iterative process by assuming a neutral axis depth (c) of 6 in.:

$$c = 6 \text{ in.}$$

$$\delta_s = (d-c)\theta_p = (18.25-6)(0.04) = 0.49 \text{ in.}$$

The intentional mild steel debond length (Figure 34.15) was 6 in. but can reasonably be expanded to include some adjacent debonding. Hence, the effective debond length (ℓ_d) is on the order of:

$$\ell_d = 6 + 2(d_b) = 7.5 \text{ in.}$$

and the post-yield strain state in the debond region (ϵ_{sp}) is:

$$\epsilon_{sp} = \frac{\delta_s}{\ell_d} = \frac{0.49}{7.5} = 0.065 \text{ in./in.}$$

This corresponds to a stress in the bar of (Englekirk, 2003):

$$\lambda_o f_y \cong 86 \text{ ksi}$$

The elongation of the post-tensioning strand (δ_{psp}) is:

$$\delta_{psp} = \left(\frac{h}{2} - c \right) \theta_p = (10-6)0.04 = 0.16 \text{ in.}$$

The overall length of the strand (Figure 34.15) is on the order of 100 in.; hence,

$$\Delta \epsilon_{psp} = \frac{0.16}{100} = 0.0016 \text{ in./in.}$$

$$\Delta f_{ps} = \Delta \epsilon_{psp} E_{ps} = 0.0016(28,000) = 45 \text{ ksi}$$

$$f_{ps} = f_{se} + \Delta f_{psp} = 162 + 45 = 207 \text{ ksi} < f_{py} \cong 230 \text{ ksi}$$

The total tensile force in the post-tensioning steel at a joint rotation (θ_p) of 0.04 radian is (theoretical):

$$\Delta T_{ps} = A_{sp} \Delta f_{psp} = 9(0.153)45 = 61.7 \text{ kips}$$

$$T_{ps} = 223.1 + 61.7 = 286 \text{ kips}$$

Comment: Observe that the projected force in the post-tensioning is consistent with that measured (on the positive cycle) at a drift angle of 4% (Figure 34.18).

The tensile force provided by the mild reinforcing is:

$$T_s = 3(0.44)(86) = 114 \text{ kips}$$

The depth to the neutral axis may now be estimated:

$$T_{ps} + T_s - C_{sy} = 286 + 114 - 79 = 320 \text{ kips}$$

$$a = \frac{320}{0.85(5)(16)} = 4.7 \text{ in.}$$

$$c = \frac{a}{0.8} = 5.9 \text{ in.}$$

Conclusion: A neutral axis depth of 6 in. was reasonably presumed.

Strain levels in the concrete are quite high. If we assume a plastic hinge length (ℓ_p) equivalent to the debond length (ℓ_d):

$$\phi_p = \frac{\theta_p - \theta_y}{\ell_p} = \frac{0.0392}{7.5} = 0.0052 \text{ rad./in.}$$

$$\epsilon_c = \phi_p c = 0.0052(6) = 0.031 \text{ in./in.} \quad (34.13)$$

$$\epsilon_s = \phi_p (d - c) = 0.0052(12.25) = 0.064 \text{ in./in.}$$

It was for this reason that the developers of the hybrid system armored beam corners with angles during the NIST tests (Cheok and Lew, 1993). The University of Washington test specimens were not armored. Beam corners did exhibit surface cracking early, but beam strength did not begin to deteriorate until drifts exceeded 4% (see Figure 34.17b). The plasticity of high-strength grout probably absorbs a disproportionate amount of the post-yield concrete strain because these grouts are usually quite ductile.

Comment: The fact that one of the mild steel bars fractured at a drift angle of 2.5% is disconcerting because the apparent strain in this bar is below that normally associated with fracture. Seven identical beams were tested, and this bar was the only one that fractured. A conservative selection of the debond length based on a fracture strain of 5% is suggested.

The probable moment capacity (M_{pr}) at a drift angle of 4% discounting the ruptured #6 bar is:

$$\begin{aligned} M_{pr} &= T_{ns} \left(d - d' \right) + T_{ps} \left(\frac{h}{2} - \frac{a}{2} \right) + (T_s - T_{ns}) \left(d - \frac{a}{2} \right) \\ &= 52.8(16.5) + 286(10 - 2.35) + 35(18.25 - 2.35) = 871 + 2188 + 373 = 3432 \text{ in.-kips} \end{aligned} \quad (34.14)$$

This corresponds to a column shear force of:

$$V_{c,pr} = M_{pr} \left(\frac{\ell}{\ell_c} \right) \left(\frac{1}{h} \right) = 3432 \left(\frac{72}{62} \right) \left(\frac{1}{117.5} \right) = 34.7 \text{ kips}$$

This predicted column shear force is consistent with the test results (Figure 34.17).

34.3.3 Interior Beam–Column Joints

34.3.3.1 Post-Tensioned Assemblies (Hybrid System)

Joint shear stress analysis procedures are developed as they are for conventionally reinforced cast-in-place concrete beam–column joints. The shear imposed on the beam–column joint ($V_{jh,prob}$) is shown in Figure 34.19:

$$V_{jh,prob} = \lambda_o T_{nps} + 2\lambda_o T_s - V_c$$

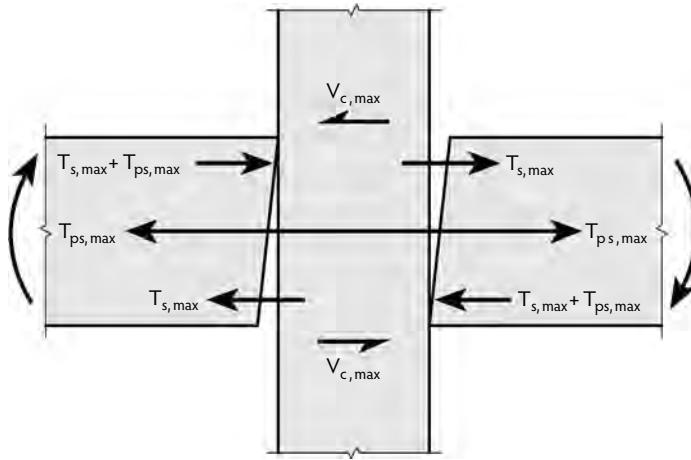


FIGURE 34.19 Forces acting on a hybrid beam–column joint. (From Englekirk, R.E., *Reinforced and Precast Concrete Buildings*, John Wiley & Sons, New York, 2003. Reprinted with permission of John Wiley & Sons, Inc.)

And the shear stress imposed on the joint ($v_{jh,prob}$) is:

$$v_{jh,prob} = \frac{V_{jh,prob}}{A_j}$$

where A_j is the gross area of the column. The allowable joint shear stress ($v_{jh,allow}$) is:

$$v_{jh,allow} = 15\phi\sqrt{f'_c}$$

34.3.3.2 Bolted Assemblies (DDC®)

Joint shear stress analysis follows those procedures adopted for cast-in-place concrete (Figure 34.20). The discontinuity between ductile rods may be handled in a variety of ways, as it increases the ability of the joint to transfer loads (Englekirk, 2003). The test specimen followed the load flow described in Figure 34.20 where the tension rod (DR1) activates the proximate tie sets, which then deliver it to the compression node. Alternatively, an interior node may be presumed at the rod heads. Given this alternative, an ℓ_c secondary strut and tie transfer will be developed, and this undoubtedly accounts for the superior performance of the DDC® beam–column joint (to drift ratios of 6%). Joint shear stress analysis procedures are conservatively developed, as they are for conventionally reinforced cast-in-place concrete beam–column joints.

34.4 The Conceptual Design Process

The process described herein is intended to provide the development team with enough data to make an informed decision regarding the appropriateness of alternative systems. The design process, in conjunction with the constructor, must create alternative solutions using these generic approaches as points of departure.

34.4.1 Bolted Systems

The approach described specifically utilizes the Dywidag Ductile Connector (DDC®) system, which is controlled by patents. This control of product is important because many subtle quality-control design issues are dealt with in the product provided; these include a fail-proof bolt setting length as well as system tolerances and ductility. The design process begins with development of the seismic-induced shear loads that the bracing system must sustain. The major system constraint lies in the fact that one assembly (two ductile rods) has a relatively high yield strength, and this strength cannot be fine tuned. This

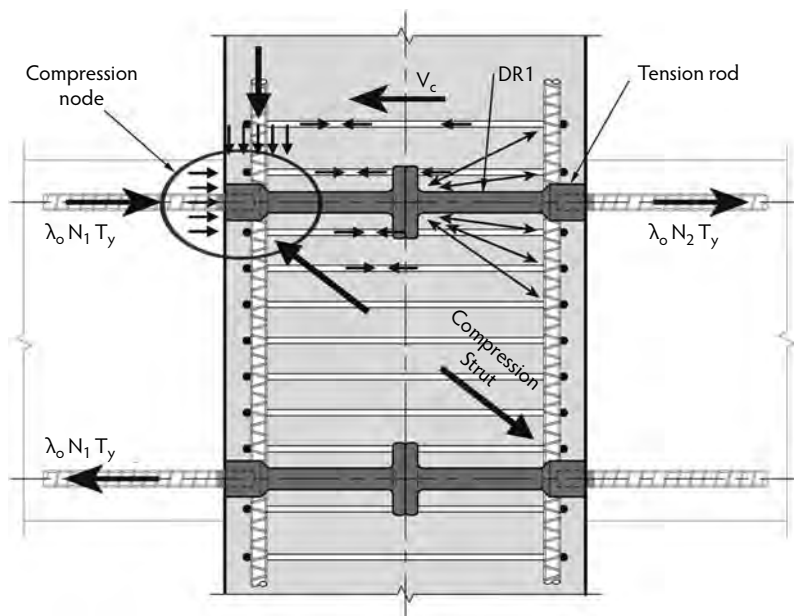


FIGURE 34.20 Load flow within a DDC® beam-column joint. (From Englekirk, R.E., *Reinforced and Precast Concrete Buildings*, John Wiley & Sons, New York, 2003. Reprinted with permission of John Wiley & Sons, Inc.)

constraint must be considered very early in the design process and the bracing program modified to accommodate system and functional objectives. The assembly described in Figure 34.9 contains two ductile rods, which establish its yield strength at about 300 kips (T_n), and this sets the strength increments.

The basic geometry of the building bracing program has been established: column spacing and story height; thus, given a story shear, the first question to be addressed is the number of frame bays required. The process must be reduced to its simplest form, and this means discounting compensating factors; for example, building torsion will increase the demand on some components, while using center-line dimensions will understate the capacity of a subassembly (they usually counterbalance each other). Hence,

$$V = \frac{2nM_u}{h_x} \quad (34.15)$$

where V is the objective base shear for the building (kips); n is the number of frame bays; M_u is the factored moment capacity of the frame beam (ft-kips); and h_x is the story height (ft).

• *Step 1: Determine the number of frames required.*

$$V = 2000 \text{ kips}$$

$$h_x = 11 \text{ ft}$$

$$M_u = 900 \text{ ft-kips (1-DDC; } d - d' = 3.33 \text{ ft)}$$

$$n = \frac{2000(11)}{900} = 24$$

Conclusions: 24 assemblies of the type described in Figure 34.9 are required. Two assemblies per beam seems most logical. System proposed should be 12 frame bays in each direction, two DDC®s per beam.

Comment: The number of required frame bays may be significantly reduced by combining the bolted and hybrid systems.

- *Step 2: Size and detail the beam.*

$$b = 30 \text{ in.}, h = 46 \text{ in.}, 2 \text{ DDC}^{\circledR} \text{ assemblies per beam (see Figure 34.9)}$$

- *Step 3: Check beam–column joint shear.*

Use procedures adopted by ACI, replacing $\lambda_o f_y A_s$ and $\lambda_o f_y A'_s$ with $\lambda_o n T_y$, where n is the number of DDC[®] assemblies, and T_y is the yield strength of one assembly (two rods \cong 300 kips).

- *Step 4: Proceed to develop the system load path as appropriate for a cast-in-place system using a capacity-based design approach.*

34.4.2 Post-Tensioned Systems

Given that the capacity of a hybrid system can be changed quite readily, the number of frames required is usually more closely related to building geometry, constructability, and function. The size of the beams and their grouping will tend to control the design process. When the objective beam size has been established, the developable strength is established and from this the bracing program for the building created.

- *Step 1: Determine a trial reinforcing program.*

It is advisable to maintain a reasonable level of restoring force, for this is clearly a very positive attribute of post-tensioning. Accordingly, a design objective should be to provide at least 50% of the moment capacity with the post-tensioning. Begin by selecting the appropriate level of mild steel reinforcing:

$$M_{us} \cong 0.4M_u$$

$$A_s = \frac{0.4M_u}{\phi f_y (d - d')}$$

Then determine the amount of post-tensioning steel required to satisfy the strength objectives:

$$M_{ups} = M_u - 0.9f_y (d - d') A_s \quad (34.16)$$

$$A_{ps} = \frac{M_{ups}}{\phi f_{ps} \left(\frac{h}{2} - \frac{a}{2} \right)} \quad (34.17)$$

where f_{ps} may be conservatively assumed to be the effective level of prestress, usually 162 ksi.

Comment: A nominal strength projection based on an effective prestress of 162 ksi will result in a strength equivalent to about 95% of its nominal strength, but this seems reasonable given the softness of the system (Figure 34.17).

- *Step 2: Determine the minimum size of the beam–column joint.*

The analysis procedure for the hybrid beam system is developed in Section 34.3.3. An approximate relationship between the area of the beam–column joint and the amount of beam reinforcing is developed in Englekirk (2003):

$$A_j = 62(A_s + A'_s) + 210A_{ps} \quad (34.18)$$

- *Step 3: Check the feasibility of placing the reinforcement suggested by the trial design.*
- *Step 4: Check to ensure that the provided level of post-tensioning is reasonable, on the order of 1000 psi.*

Comment: The hybrid beam will become an integral part of the floor system. Large stress differentials may cause undesirable cracking in unstressed floors. Accordingly, it is best to use 1000 psi as an objective prestress limit.

• *Step 5: Check the shear capacity/demand ratio to ensure that objective shear stress limit states have not been exceeded:*

$$V_b = \frac{2\lambda_o(M_{ns} + M_{nps})}{\ell_c} + V_D + V_L \quad (34.19)$$

where V_D and V_L are the dead and live load shears, respectively, and ℓ_c is the clear span of the beam.

Comment: Sufficient accuracy for design purposes may be attained through the use of an overstrength factor (λ_o) of 1.25:

$$bd \geq \frac{V_b}{5\sqrt{f'_c}}$$

Remember that, in this case, because the adopted limit state ($5\sqrt{f'_c}$) is less than that proposed in most codes, V_D and V_L should be realistically selected, not the factored loads used in a code-compliance analysis. This limit state is perhaps somewhat conservatively applied to the hybrid system because the hinge deformation tends to accumulate at the joining of the beam and the column (see Figure 34.6) and the plastic hinge region is prestressed.

• *Step 6: Check column shear if the beam is deep and the column short.*

For an exterior subassembly (Figure 34.15) this is:

$$b_c h_c \geq \frac{\lambda_o(M_{ns} + M_{nps})}{5\sqrt{f'_c} h_x} \geq \frac{3.6(M_{ns} + M_{nps})}{h_x}$$

Design Example

Design a 20 × 32-in. hybrid interior beam for the described subassembly:

$$V_{cu} = 200 \text{ kips (column shear)}$$

$$\ell_1 = 24 \text{ ft}; \ell_{c1} = 21 \text{ ft}$$

$$\ell_2 = 16 \text{ ft}; \ell_{c2} = 13 \text{ ft}$$

$$h_x = 9 \text{ ft}$$

• *Step 1: Select a trial beam reinforcement program.*

$$V_c h_x = M_{bu} \left(\frac{\ell_1}{\ell_{c1}} + \frac{\ell_2}{\ell_{c2}} \right)$$

For an interior column and an objective column shear of 200 kips,

$$M_{bu} = \frac{V_c h_x}{\left(\frac{\ell_1}{\ell_{c1}} + \frac{\ell_2}{\ell_{c2}} \right)} = \frac{200(9)}{1.14 + 1.23} = 760 \text{ ft-kips}$$

Select a mild steel reinforcing program:

$$M_{us} = 0.4M_{bu} = 0.4(760) = 304 \text{ ft-kips}$$

$$A_s = \frac{M_{us}}{\phi f_y (d - d')} = \frac{304(12)}{0.9(60)(29 - 3)} = 2.6 \text{ in.}^2$$

Try three #9 bars. Select the post-tensioning reinforcement:

$$M_{us} = A_s \phi f_y (d - d') = 3.0(0.9)(60)(29 - 3) = 4212 \text{ in.-kips} \quad (M_{ns} = 4680 \text{ in.-kips})$$

$$\phi M_{nps} = M_{bu} - M_{us} = 760(12) - 4212 = 4908 \text{ in.-kips} > 4212 \text{ in.-kips} \quad (\text{OK})$$

Accordingly, the flexural strength provided by the post-tensioning exceeds that provided by the mild steel, and this was identified as a design objective. For design purposes the nominal strength of unbonded strands (f_{pn}) is assumed to be its effective strength:

$$f_{pn} = f_{pse}$$

Comment: The development of f_{pn} in ACI 318-05 (f_{ps} , Equation 18-5) is based on a correlation between test data and analysis. Observe that a similar relationship ($f_{pse} + 10,000$) between effective and nominal strength is not appropriate for the hybrid system. The tensile force in the tendon corresponding to a strand stress of 162 ksi in the test described in Figure 34.18 would be 223 kips, and this force is not developed until the drift reaches 1.5%. Accordingly, the use of f_{pse} to define the nominal strength of a hybrid beam is viewed as being appropriate:

$$A_{ps} = \frac{\phi M_{nps}}{\phi f_{pse} \left(\frac{h}{2} - \frac{a}{2} \right)} = \frac{4908}{0.9(162)(16 - 3)}$$

where the depth of the compressive stress block (a) is presumed to be about 6 in.

$$A_{ps} = 2.59 \text{ in.}^2$$

Use 0.6-in. \emptyset strands ($A = 0.217 \text{ in.}^2$).

Comment: 0.6-in. \emptyset strand hardware is most common in the United States but local availability should be confirmed.

$$\text{Number of strands required} = 2.59/0.217 = 11.9$$

Check the level of prestress provided by 12 strands:

$$f_c = \frac{12(0.217)(162)}{20(32)} = 0.660 \text{ ksi} \quad (\text{OK})$$

Conclusion: The trial reinforcing program will consist of 12 0.6-in.-diameter strands and 3 #9 (GR 60) reinforcing bars, top and bottom. The nominal strength of this beam is:

$$M_n = M_{nps} + M_{ns}$$

$$a = \frac{T_{ps}}{0.85 f'_c b} = \frac{12(0.217)}{0.85(5)(20)} = 5 \text{ in.}$$

$$M_{nps} = T_{nps} \left(\frac{h}{2} - \frac{a}{2} \right) = 422(16 - 2.5) = 5697 \text{ in.-kips}$$

$$\phi M_n = 9340 \text{ in.-kips} > 9310 \text{ in.-kips} \quad (\text{OK})$$

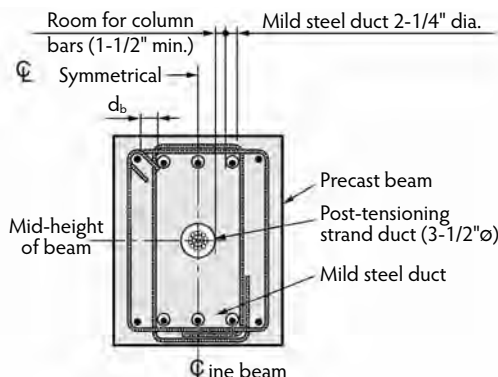


FIGURE 34.21 Hybrid beam reinforcement program. (From Englekirk, R.E., *Reinforced and Precast Concrete Buildings*, John Wiley & Sons, New York, 2003. Reprinted with permission of John Wiley & Sons, Inc.)

- *Step 2: Determine minimum size of the beam–column joint.*

$$A_i = 62(A_s + A'_s) + 210A_{ps} = 62(6) + 210(12)(0.217) = 919 \text{ in}^2$$

Conclusion: Column size should be at least 30×32 in.

- *Step 3: Develop the beam and column reinforcing program.*

The mild steel must be placed in ducts and grouted. The post-tensioning strands will also be placed in a duct and stressed using a multistrand jack. Mild steel tubes should have a diameter of at least $2d_s$. The post-tensioning duct will be of the size suggested by the supplier. Column bars will have to be placed in this central region, and they must pass the post-tensioning duct and yet be inside the outer mild steel duct (see Figure 34.21). Beam bars cast in the corners of the precast beam are also required if for no other reason than to reinforce an otherwise unreinforced region. Minimum flexural reinforcing requirements are usually satisfied by the post-tensioning, so the basis for the sizing of these bars depends on the designer's convictions relative to splicing concerns. ACI 318-05, Section 18.9, requires a minimum amount of bonded reinforcement in all flexural members with unbonded prestressing tendons:

$$A_{s,min} = 0.004A_{ct}$$

where A_{ci} is the area between the tension face and the center of gravity of the gross section. The beam-sizing process must then allow for the flexural reinforcing provided in the precast beam as well as the space that may be required to pass the column bars (see Figure 34.21). The minimum beam width becomes:

One post-tensioning duct	3.50 in.
Two #11 column bars	2.75 in.
Two mild steel ducts	4.50 in.
Two corner bar diameters	2.00 in.
Two corner bars	2.00 in.
#5 hoop ties	1.25 in.
Fire cover	3.00 in.
Total	19.00 in.

Conclusion: The minimum beam width should be 20 in.

The minimum bonded reinforcement (ACI 318-05, Equation 18-6) is:

$$A_{s,\min} = 0.004b \frac{h}{2} = 0.004(20)16 = 1.28 \text{ in.}^2$$

Conclusion: The beam should be 20 in. wide. At least one #8 bar should be provided in each corner.

Comment: This mild steel may have to be increased to reduce concrete cracking during transportation, but this will be the concern of the fabricator.

34.5 Concluding Remarks

The design of precast systems does not require special knowledge, for it follows principles used by structural engineers to design ductile moment resisting frame systems. A more detailed development of both cast-in-place and precast systems is contained in *Seismic Design of Reinforced and Precast Concrete Buildings* (Englekirk, 2003). The designer of precast frame systems is encouraged to be creative in the development of systems. The combining of the DDC® system with the hybrid system is but one example. The design–build delivery system lends itself to creative solutions, but both the hybrid and DDC systems have been constructed using the traditional design–bid–build delivery system.

References

- ACI Committee 318. 2005. *Building Code Requirements for Structural Concrete and Commentary*, ACI 318-05/318R-05. American Concrete Institute, Farmington Hills, MI.
- Cheok, G.S. and Lew, H.S. 1993. Model precast concrete beam-to-column connections subject to cyclic loading. *PCI J.*, 38(4), 80–92.
- Englekirk, R.E. 2003. *Seismic Design of Reinforced and Precast Concrete Buildings*. John Wiley & Sons, New York.
- Ghosh, S.K. and Hawkins, N.M. 2001. Seismic design provisions for precast concrete structures in ACI 318. *PCI J.*, 46(1), 28–32.
- Priestley, M.J.N. 1991. Overview of PRESSS research program, *PCI J.*, 36(1), 50–57.



Flexural cracking at ultimate load of post-tensioned prestressed beams. (Photograph courtesy of Edward G. Nawy.)

35

Cracking Mitigation and Maintenance Considerations

Florian G. Barth, P.E.*

35.1	Overview of Crack Mitigation	35-1
35.2	Member Selection.....	35-2
35.3	Crack Causes and Types	35-2
	Slab Cracks • Column Cracks • Wall Cracks	
35.4	Crack Mitigation Measures	35-7
	Planning the Layout of Restraining Members • Structural Separation • Closure Strips, Joints, and Favorable Pour Sequencing • Released Connections • Addition or Improved Layout of Mild Reinforcement • Addition or Improved Layout of Tendons	
35.5	Crack Evaluation Summary.....	35-12
35.6	Maintenance	35-13
	Structural and Preventative Maintenance • Operational and Aesthetics Maintenance • Checklist for Structural Inspection	
	References	35-18

35.1 Overview of Crack Mitigation

When selecting the concrete configuration and reinforcement layout for a concrete building, the engineer typically considers strength requirements and then addresses serviceability concerns. During the serviceability check, attention is directed to deflection and durability, but many times detailing for serviceability to mitigate cracking is overlooked. Cracking in reinforced concrete buildings can be addressed early in the design process through judicious consideration of building layout, selection of appropriate connections, and use of appropriate reinforcement detailing. It is advisable to evaluate during the member design stage those members within a structure that may be subject to various types of cracks. Predicting possible crack behavior or crack development among members within a building typically allows application of appropriate mitigating detailing. Whether cracking is caused by restrained shortening of concrete or cross-sectional action, effective detailing of concrete members can significantly impact the long-term performance and durability of the concrete structure.

* President, American Concrete Institute, and Principal Consultant, FBA, Inc., Hayward, California; expert in analysis, design, evaluation, and retrofit of post-tensioned concrete structures.

The intent of this chapter is to provide a basic understanding of crack development as well as design detailing recommendations to mitigate cracking in concrete members. It specifically excludes the review of concrete member cracking due to unique or special materials used or the preparation (mix properties/proportions), placing, and conditioning of poured concrete. The design details presented herein are limited to building structures; special structures and non-building structures are not part of this review. This chapter is limited to cast-in-place concrete frames only; precast concrete and masonry elements are excluded. Post-tensioned concrete floor systems have become the predominate choice for concrete floor systems using cast-in-place construction. For this reason, examples within this chapter focus on post-tensioned concrete floor systems when evaluating crack mitigation, as such slabs have an added elastic shortening component and concrete creep to address due to the precompressed concrete cross-section.

Many publications offer a summary of standard details for the construction of concrete structures; however, it is a challenge to find documentation of appropriate or standard detailing to aid the designer in addressing concrete cracking. This chapter, however, aims to address the overall nature of a structure and how members may experience tensile stresses due to the restraint or other cross-sectional actions resulting in tension beyond the concrete modulus of rupture.

The first objective is to capture framing conditions where the crack development of a concrete member is directly or indirectly affected by the behavior of the neighboring elements or the overall framing system and to suggest detailing to avoid or minimize such cracking. Much of the information presented has been adapted from the work by Aalami and Barth (1988).

35.2 Member Selection

Member shape and frame compatibility are the basic foundations of a performing structure. An example of framing incompatibility would be found in a structure where concrete member sizes or strength requirements are simply out of scale. This can be the case when oversized architectural columns are used to support a thin slab. The restraining effects of oversized members on the surrounding members can be significant. For this reason, it is advisable to maintain compatible member sizes and connections to mitigate restraint cracking during concrete shortening. If geometry or architectural considerations dictate such incompatibility, special consideration should be given to incompatible member connections. Alternatively, incompatible framing geometry can also be addressed using built-up foam sections after the concrete frame is completed to achieve the architectural shapes desired. Frequently, new materials are introduced, whether as composite construction or simply performance-enhancing additives to the concrete mix. The resulting alteration in shortening effects must be understood. For composite construction, such as pan-filled metal decks, construction layout and long-term shortening effects should be evaluated. An important serviceability aspect of concrete material and mixture proportions selection is the resulting shortening behavior for the particular application and geometry.

35.3 Crack Causes and Types

Several factors, when combined, can lead to restraint cracks in two-way reinforced-concrete slabs. Concrete slabs tend to shorten, and structurally stiff elements such as walls, elevator and stairwell cores, and columns can restrain the slab. When the tensile stress exceeds the tensile strength of the concrete, a restraint crack occurs (ACI Committee 224, 1997). Depending on many factors, including the stiffness of the restraining elements and the length of the slab spans, multiple restraint shrinkage cracks may form. The specific factors that cause shortening of concrete slabs include:

- Shrinkage of concrete
- Creep of concrete due to sustained loads (including precompression)
- Elastic shortening (prestressed slabs only)
- Fall in temperature

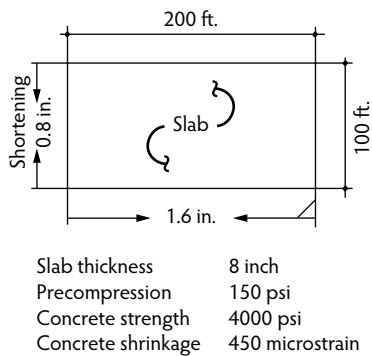


FIGURE 35.1 Factors contributing to slab shortening.

TABLE 35.1 Contribution of Various Factors to Typical Slab Shortening for Parking Structure in California

Factor	Percentage
Shrinkage	66
Creep	11
Elastic Shortening	7
Temperature	16
Total	100

For a typical parking structure in Southern California with 70% ambient humidity and a moderate temperature variation of 40°F, the contributions of the above factors to slab shortening are as given in Figure 35.1 and Table 35.1. It is noteworthy that two thirds of slab shortening is typically due to concrete shrinkage. Axial creep and elastic shortening, which are the only direct consequences of post-tensioning, contribute about one sixth of the total shortening.

To appreciate the magnitude of shortenings that are likely to occur in a post-tensioned slab, consider the example shown in Figure 35.2. For the 200 × 100-ft slab shown, the shortenings (if free to take place) are estimated to be 0.8 in. per 100 ft of slab length. Obviously, this shortening cannot materialize in most cases, because the slabs are commonly tied to supporting structural elements. The interaction of the slab with its restraining structural elements is the crucial factor in the formation of cracks. Referring to the breakdown of shortenings in Figure 35.2, only 18% of the calculated shortening is due to post-tensioning. The balance is common to nonprestressed as well as post-tensioned slabs. This shows that little difference exists between post-tensioned and nonprestressed slabs as far as crack initiation is concerned; however, crack propagation is fundamentally different between the two types of slabs.

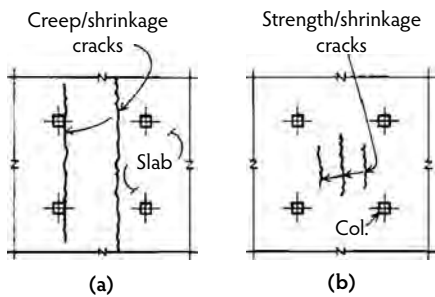


FIGURE 35.2 Reflected ceiling view of slabs: (a) post-tensioned slab; (b) reinforced concrete slab.

Prominent characteristics of cracks in unbonded post-tensioned slabs as compared to regular reinforced concrete are the following:

- Cracks are fewer in number; instead of a multitude of hairline cracks, fewer cracks form.
- Cracks are generally wider; they are spaced farther apart and generally extend deeper into the slab. In regular reinforced concrete, the spacing between cracks is of the order of slab depth, whereas in post-tensioned slabs it is more related to the span length and the overall dimensions of the slabs. In most cases, crack spacing is more than one quarter of the shorter slab span.
- Cracks are normally longer and continuous, and continuous cracks may extend over one span and beyond. In nonprestressed concrete, cracks are generally shorter in length.
- Cracks commonly do not coincide with locations of maximum moments. Restraining cracks do not necessarily develop at the bottom of midspan or the top of supports where the bending moments are maximum.
- Cracks occur at axially weak locations. Axially weak regions are typically found at construction joints, pour strips, cold joints, paths with reduced discontinuities in slab, and, finally, where precompression is reduced either due to termination of tendons or friction losses in tendons. Figure 35.2 compares typical crack patterns on the soffit of an interior panel of a two-way slab construction. For the regular reinforced-concrete structure, the shrinkage cracks are shown coinciding with the locations of maximum tension.

Unbonded post-tensioned slabs generally exhibit poorer cracking performance as a result of lesser bonded reinforcement, which mobilizes the concrete in the immediate vicinity of a crack. Hence, a series of large slab segments separated by wide cracks rather than well-distributed small cracks is produced unless either the unbonded post-tensioning is accompanied by a sufficient nonprestressed reinforcement or in-plane restraining actions are present that result in a similar improvement of the crack distribution. Examples of common cracks in slabs, columns, and walls due to restrained movement are illustrated below.

Due to the variety of member types and geometry and the array of crack initiation factors, it is imperative that each concrete member be reviewed individually and as part of the overall framing system during the design detailing process. Concentrated load application and vulnerable member joint conditions may require a very localized review of concrete detailing. On the other hand, the overall framing layout may cause indirect load transfer due to geometry or member incompatibility, resulting in concrete cracking based on overall behavior of the framing system. This chapter allows for a localized and overall performance review.

35.3.1 Slab Cracks

With regard to the overall crack behavior of a two-way slab, Figure 35.3 shows the crack formation in one of many similar slab conditions investigated by the authors. The example is representative of many slabs having similar crack patterns. The slab is post-tensioned in both directions and designed as a two-way system according to Chapter 18 of ACI 318 (ACI Committee 318, 2005). The precompression provided by the tendons in the longitudinal direction is dissipated into the supporting walls, as the primary transverse cracks extend across the entire width of the slab and through its thickness. The layout in Figure 35.3 demonstrates that the prime cause of cracks is the restraining effect of the perimeter walls. In a slab that is free to move, such as that illustrated in Figure 35.4a, the tendon force (F) is balanced by the precompression developed in the slab. If the slab movement (shortening) is restrained through stiff walls or columns, such as the walls in Figure 35.4b, a part of tendon force F is diverted to the supporting elements. One other major source of overall slab cracks is irregularities in slab geometry. Typical examples of irregularities occurring in slabs are shown in Figure 35.5. If not properly detailed, the discontinuities at the reentrant corners invariably lead to cracks that may extend as far as one quarter to one third of the shorter width at the location of crack. Figure 35.6 shows examples of localized cracks in post-tensioned slabs. The illustrated cracks normally initiate within the first few days after concrete is placed and before the application of post-tensioning.

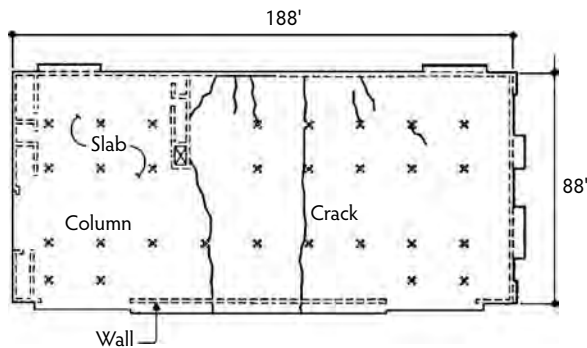


FIGURE 35.3 View of reflected ceiling showing cracks in post-tensioned slab (Village Serramonte, California).

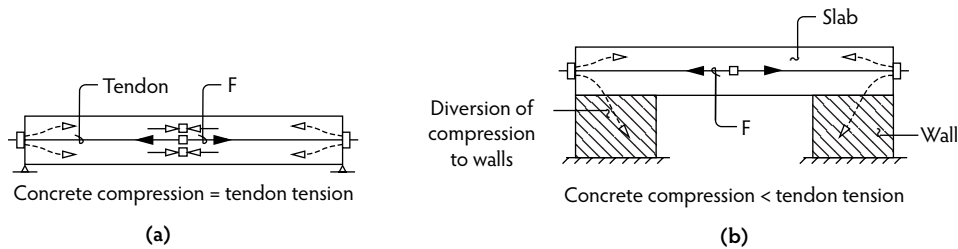


FIGURE 35.4 Diversion of post-tensioning force to walls: (a) slab free to move; (b) slab restrained against movement.

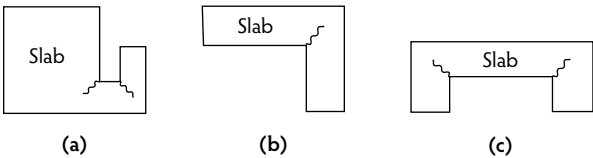


FIGURE 35.5 Irregular slab plans showing crack formation.

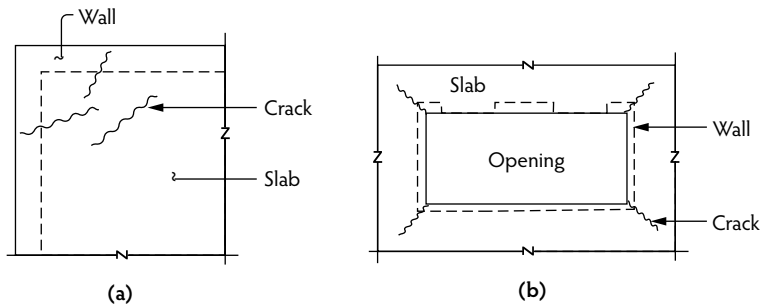


FIGURE 35.6 (a) Cracks at slab corners tied to corner walls; (b) crack formation at corners of interior openings.

35.3.2 Column Cracks

Short columns at split levels in parking structures, as illustrated in Figure 35.7, can develop severe cracks and spalling of concrete due to shortening of the parking decks immediately above and below. The same figure shows a release detail with a central dowel for prevention of such cracks. For simplicity, the stirrups in the short column are not shown. Columns tied to half-height walls, as shown in Figure 35.8a, develop cracks similar to those in the short columns described in Figure 35.7. The crack formation is especially severe in beam–slab floor constructions. Provisions of full-height or half-height joints between the walls

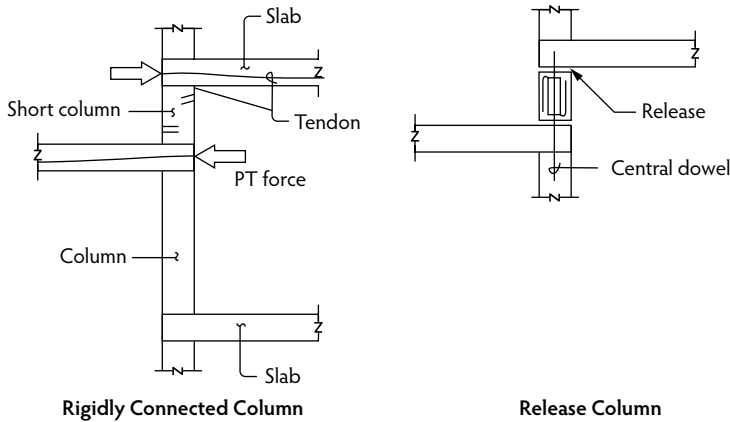


FIGURE 35.7 Cracking in short column at split level of parking structure.

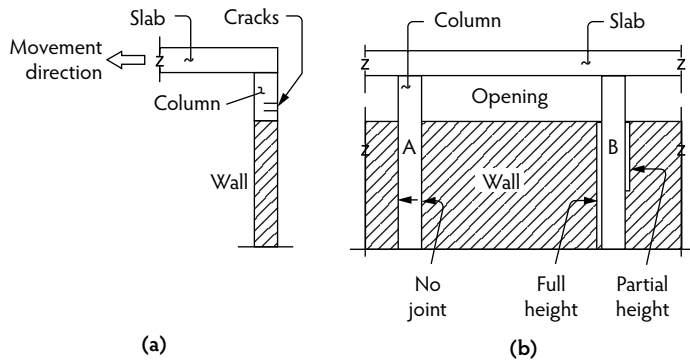


FIGURE 35.8 Wall-column release: (a) side view of column tied to wall; (b) front view.

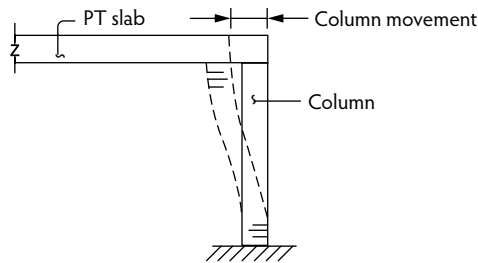


FIGURE 35.9 Cracks in end columns of long buildings.

and the columns, illustrated in Figure 35.8, are effective methods of mitigating such cracks. End columns of slabs 150 ft or more in length are particularly susceptible to cracks of the type illustrated in Figure 35.9. The moment generated in the column due to this displacement should be accounted for in the design of such columns.

35.3.3 Wall Cracks

Figure 35.10 illustrates the most common crack formation due to the overall behavior of walls tied to post-tensioned slabs. The diagonal tension cracks shown form at the ends of the walls due to the movement of the slab and extend over a region having a length of approximately one to two wall heights from the wall end. Such cracks can be reduced or eliminated by design.

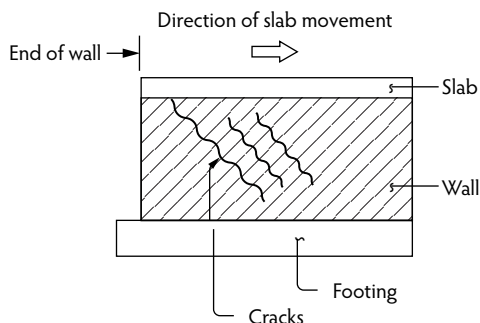


FIGURE 35.10 Cracks in wall due to slab movement.

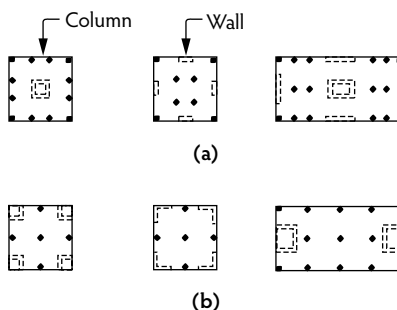


FIGURE 35.11 Planning in layout of shear walls to mitigate slab crack: (a) favorable arrangement of restraining walls; (b) unfavorable arrangement of restraining walls.

35.4 Crack Mitigation Measures

The principle techniques of crack mitigation are described in the following sections.

35.4.1 Planning the Layout of Restraining Members

The most effective method of restraint-crack prevention is the good selection of wall and column locations during the architectural planning of the building. Equal numbers and lengths of walls may be positioned so as to reduce the tendency of crack formation by allowing the slab to move freely toward a planned point of zero movement (Figure 35.11a). Figure 35.11b shows examples of unfavorably arranged walls and layouts in which the walls impede the free movement, thus creating conditions conducive to crack formation.

35.4.2 Structural Separation

Slabs of irregular geometry are particularly susceptible to cracking. Figure 35.12a shows a small slab area appended to a larger rectangular-shaped region. The structural separation shown in the figure between the two post-tensioned slabs consists of a physical gap between the slabs equal to 0.5 to 1 in. For the particular example shown, it is advisable to continue the slab separation through the supporting walls. The major difference between such structural separations and expansion joints is that the structural separation discussed herein loses its significance after a period of 2 to 3 months, during which time the bulk of the slab shortening takes place. The structural separation does not have to be designed to remain serviceable during the lifetime of the structure. An expansion joint that has been designed to accommodate temperature-induced movements must be detailed to remain operational during the in-service life of the structure. Smaller areas separated by openings or irregular slab geometries, such as the appendix shown in the top right corner of Figure 35.12b, cannot generally follow the overall pattern of shortening

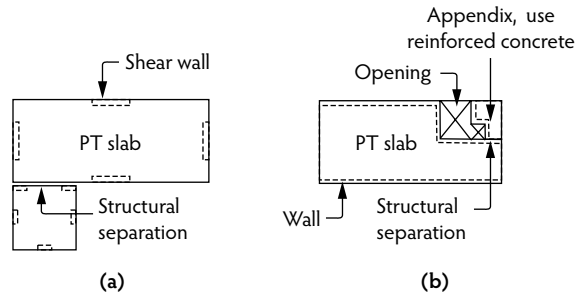


FIGURE 35.12 (a) Separation between large areas forming an irregular shape; (b) separation between a large area and a small appendix.

of the entire slab area. Their connection to the main slab is primarily over short lengths. Stairwells, elevator shafts, and other walls impart substantial restraint against free movement of small slab areas. Moreover, in most cases, it is neither economical nor practical to effectively post-tension small slab areas less than 20 ft in length. The author's practice has been to provide a separation between the two slab areas and construct the detached smaller region as a nonprestressed slab. The structural separation for such conditions need not extend through the supporting walls. Typically, the separation is achieved by placing Styrofoam™ sheets, 0.5 to 0.75 in. thick, vertically between the two slabs.

35.4.3 Closure Strips, Joints, and Favorable Pour Sequencing

A closure strip, also referred to as a *pour strip*, is a temporary separation of approximately 30 to 36 in. between two regions of slab that will be constructed and post-tensioned separately. Each region is allowed to independently undergo shortening. After a period of typically 30 to 60 days, the gap between the two post-tensioned slab regions (i.e., the closure strip) is closed by placing and consolidating nonshrink concrete. The reinforcement that extends from the concrete slab on each side into the closure strip provides the continuity of the slab over the strip.

The width of a closure strip is determined by the net distance required to position a stressing jack between the two sides of the strip and conclude the stressing operation. The reinforcement across the closure strip is designed on the basis of actions (moments and shears) occurring at the location of the strip when the entire slab is combined in a continuum. Between two adjacent supports, the preferred location of a closure strip is, for regular conditions, at a quarter span where the moments are typically small. Other considerations, however, may dictate the location of a closure strip. The position of the closure strip in relation to the entire slab is discussed at the end of this section. For corrosion protection, it is emphasized that, as a good practice, the stressing ends of the tendons terminating in the closure strip should be cut, sealed, and grouted in the same manner as at the free edges.

The time necessary to keep a closure strip open is determined by the extent of shortening deemed necessary before the two slab regions are tied together. Some engineers specializing in the design of post-tensioned slabs use an empirical value of 0.25 in. as the hypothetical displacement that can be accommodated in a post-tensioned member without apparent impairment of its serviceability. On this premise, a closure concrete should be placed when the calculated balance of shortening on each side of the closure strip is 0.25 in. or less. The shortenings are calculated using standard procedures in which concrete is assumed to be free to move. Obviously, when the closure strip has been poured and the two slab regions have been tied together, the balance of computed shortening referred to cannot take place. This empirical procedure is backed by the satisfactory performance of closure strips in place. It generally leads to closure-strip concreting between 14 to 120 days.

Construction joints are joints at predetermined locations in the slab between two concrete placements. The joints provide a planned temporary break between two slab regions for the purpose of crack control and construction operations. They are also used to subdivide a larger slab area into manageable sizes

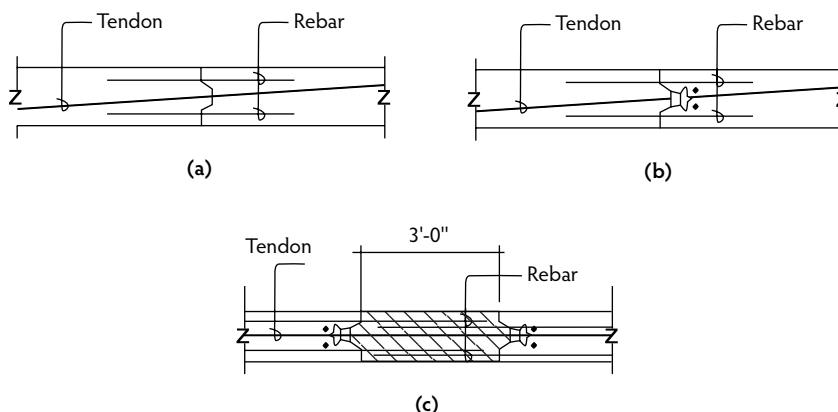


FIGURE 35.13 Details of slab joints: (a) construction joint with no stressing; (b) construction joint with intermediate stressing; (c) closure strip.

from a construction point of view. A construction joint as shown in Figure 35.13 differs from a cold joint in that (1) its location is determined by design as opposed to the location at which a concrete batch is finished, and (2) a gap of 3 to 7 days commonly occurs between the placement of first pour and the second pour; this time gap is applicable to joints that are designed for crack control. Construction joints may or may not have intermediate stressing. Intermediate stressing of tendons is carried out for long tendons where friction losses are appreciable.

From the performance experience of post-tensioned slabs, the following guidelines for the provision of closure strips or structural separations may be considered:

- If the slab length is less than 250 ft, no closure strip or structural separations are necessary, unless the supporting walls are unfavorably placed.
- If the slab length is longer than 250 ft but less than 375 ft, provide one centrally located closure strip.
- If the slab length is longer than 375 ft, provide a structural separation.

35.4.4 Released Connections

Released connections are effective means of crack mitigation when a favorable layout of supporting structural elements or provision of construction separations and closure strips cannot be fully implemented. Released connections are those in which a joint is detailed and constructed so as to permit a limited movement of the slab relative to its support. Released connections may be used in conjunction with closure strips and structural joints. Released connections with successful results are now common practice for post-tensioned slab construction in California. Released connections are grouped into wall/slab release, slab joints, and wall joints.

35.4.4.1 Wall/Slab Release

Figure 35.14 shows several types of commonly used wall/slab connections. To facilitate slippage, a slip material is normally provided at the interface of wall and slab. For simplicity in presentation, the connections shown are for the end walls and a terminating roof slab, but they are equally applicable, with appropriate modifications, to interior walls and intermediate slabs. The connection type with no ties between the slab and its supporting wall (Figure 35.14a) is the most effective release joint, but its application is restricted by the fact that, in many cases, walls must be designed to transfer shear forces, in addition to gravity loading, at their interface with the slabs. Moreover, the stability of the walls due to lateral loads may become a governing consideration. Such releases, where possible, are employed at the corners of the slab areas. It is recommended that the maximum length of a no-tie release be limited

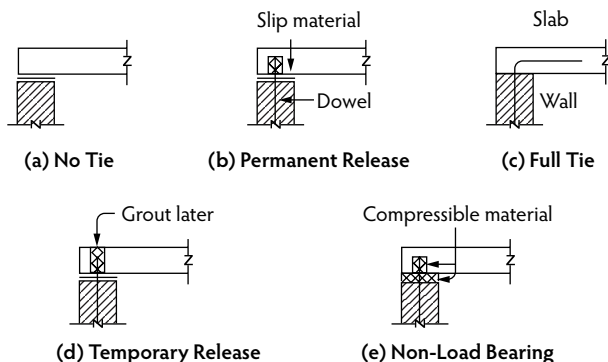


FIGURE 35.14 Typical details of different wall-slab connection types.

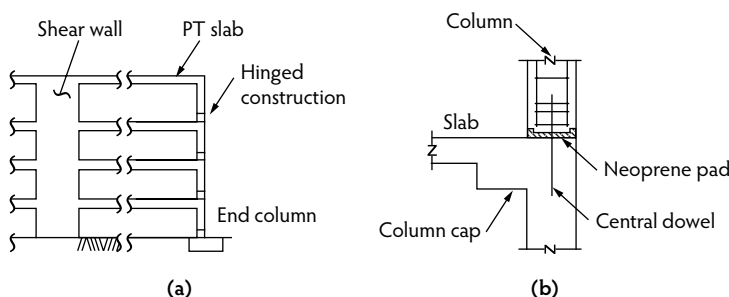


FIGURE 35.15 Hinged construction at base of end columns: (a) elevation; (b) detail of hinge construction.

to the height of the respective wall. A permanent release with a dowel encased in a compressible material is shown in Figure 35.14b. The dowel is provided to impede catastrophic movements of the wall, as in the event of an earthquake. This permanent release detail is used more frequently than the no-tie connection; however, it is more costly and requires greater care during construction. A temporary release as shown in Figure 35.14d is one where the slab is initially constructed released from the wall. After the shortening of the slab has taken place, to the extent that the balance is considered acceptable, the joint is fixed by grouting the pockets.

35.4.4.2 Slab–Column Release

Columns may be designed to withstand the anticipated forces conducive to lateral displacements between their ends without signs of distress or may be released to accommodate relative displacements of slab to column at the joints. The latter option, where applicable, leads to superior slab performance. Several items must be reviewed in arriving at a satisfactory solution. Maximum displacements are typically at the end columns, as shown in Figure 35.15. A detail providing rotational release at the base of the column, as shown in the same figure, may prove adequate. Where columns are excessively bulky, as may be required for architectural reasons, it becomes necessary to provide a detail that accommodates displacements in addition to rotation.

35.4.4.3 Wall Joints

Wall joints are vertical separations between adjacent walls that enable the walls to accommodate displacements of slabs or beams supported by walls. Wall joints are very effective in mitigating cracks in slabs or beams, as well as cracks in the supporting walls themselves. Figure 35.16 shows the plan of a rectangular slab resting on perimeter walls and interior columns. For clarity, the columns are not shown. The wall joints (WJ) provided at the corners of the slab extend through the entire height of the walls. They allow the end wall to move toward the center of the slab without being impeded by the longitudinal

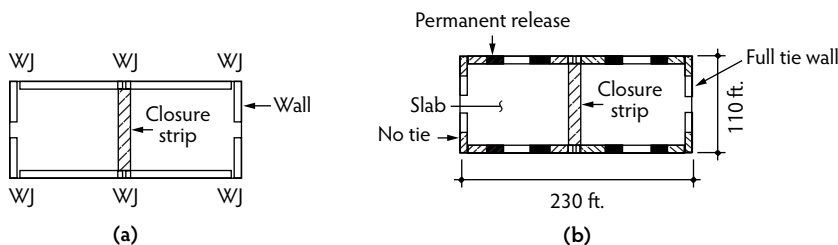


FIGURE 35.16 Wall joints: (a) plan showing wall joints (WJ) and closure strip above; (b) plan showing arrangement of various wall-slab connections.

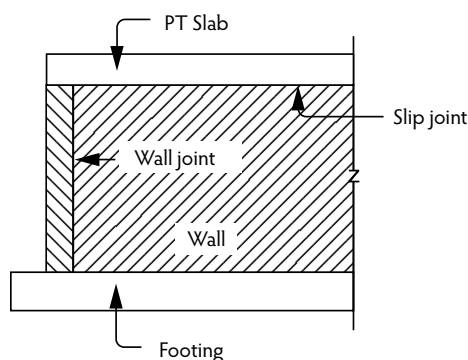


FIGURE 35.17 Elevation of corner wall showing wall joint.

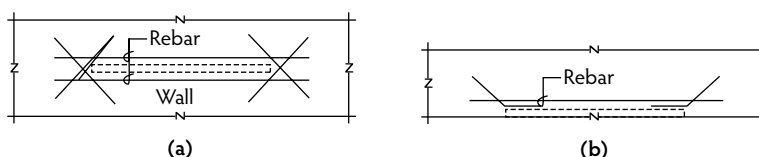


FIGURE 35.18 Crack-mitigating rebar next to shear walls: (a) interior shear wall; (b) exterior shear wall.

walls. Such wall joints perform best when accompanied by a slip joint between the slab and cross walls as shown in Figure 35.17. The detail shows joints with no ties at the corners which allows the wall shown on left to follow the movement of the slab to the right without interference from the cross wall shown in elevation. The size of the gap is estimated to be 0.75 in. per 100 ft of slab movement accommodated by the wall. Wall joints need not in all cases extend through the entire height of a wall down to the lower level.

35.4.5 Addition or Improved Layout of Mild Reinforcement

In addition to the well-planned layout of shear walls and supporting structures and provision of releases, it is necessary to place additional mild reinforcement at locations of potential distress to mitigate crack formation. Figure 35.18 and Figure 35.19 illustrate examples of typical cases. Figure 35.18 shows reinforcement added next to nonreleased exterior walls. Due to design shear-transfer requirements between a slab and its supporting wall, it might not always be feasible to provide sufficient release details to prevent all cracks. The reinforcement shown in Figure 35.18 has been found to be highly effective for such conditions. The steel is placed parallel to the wall over a width equal to approximately 10 ft normal to the wall. The steel area is determined as 0.0015 times the cross-sectional area of the slab over one third of the transverse span. The bars are spaced alternately at the top and bottom at approximately 1.5 times the slab thickness. Note that this is not a code requirement but rather a practice found to yield satisfactory results for the elimination of potential restraint cracks.

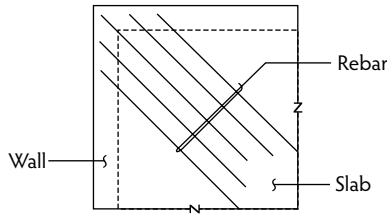


FIGURE 35.19 Reinforcement at slab corners.

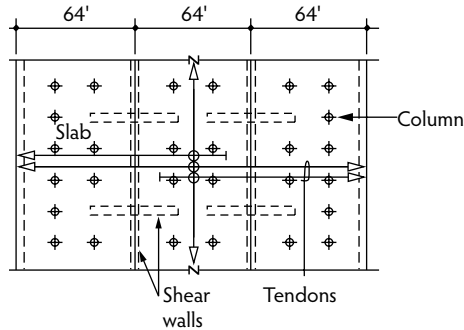


FIGURE 35.20 Tendon arrangement to compensate restraining effects of transverse walls.

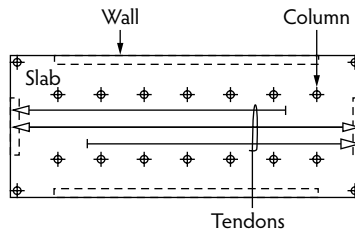


FIGURE 35.21 Tendon arrangement for mitigating cracks in central spans.

35.4.6 Addition or Improved Layout of Tendons

Figure 35.20 and Figure 35.21 show two conditions where wall restraints can lead to significant losses of precompression in the central region of the slab and consequently lead to formation of cracks. In addition to other measures, such as the releases described in the preceding sections, it is helpful to lay out the tendons so as to deposit additional compression in regions where losses are expected to be highest. Dead ending and overlapping of tendons as illustrated in Figure 35.20 and Figure 35.21 can serve this purpose. The detailing of strand layout around discontinuities and openings is also of importance. Figure 35.22 illustrates two arrangements for tendon layout at an interior opening. The detail on the right shows a common practice where the sides of the opening are pulled apart. Cracks at the corners of such openings are not uncommon. The detail on the left demonstrates an alternative tendon layout, where the opening is provided with an additional precompression ring to counteract crack-precipitating stresses at the corners.

35.5 Crack Evaluation Summary

From a study of crack formation in post-tensioned structures, a number of general conclusions have been formulated, as follows:

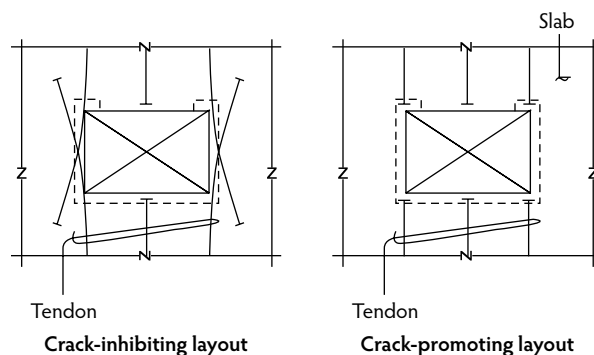


FIGURE 35.22 Arrangement of tendons at an interior opening.

- Shortening cracks (cracks due to constraint against free movement of the slab) are common in post-tensioned slabs supported on walls and stiff columns.
- Shortening cracks can be reduced significantly through crack-mitigation measures; the principal crack reduction procedures are:

Planning for layout of constraints

Structural separations

Closure strips, joints, and favorable pour sequencing

Released connections

Addition or improved layout of mild reinforcement

Addition or improved layout of tendons

With regard to implementation of crack-mitigation procedures, the following guidelines are suggested: (1) For small and simple slab geometries (10,000 ft² or less) supported on regular-size columns, design the slab to withstand the forces generated by shortening; it is not generally cost effective to implement crack-mitigation measures. (2) For slabs with substantial restraint, it is necessary to implement crack-mitigation measures.

- Most shortening cracks are not structurally significant. The most common cause of shortening of shortening cracks is the exposure of reinforcement and post-tensioning to corrosive elements; aesthetics and leakage are the next most common considerations.
- For slabs with significant support restraints, such as perimeter walls, it is often necessary to conduct a one-time maintenance routine to repair shortening cracks. In such cases, notes should be added to the structural drawings indicating the following:

Shortening cracks are likely to occur.

Shortening cracks do not normally impair the structural integrity of slabs.

Slabs should have a one-time crack maintenance operation, which consists of (1) inspecting and evaluating slabs and supporting members 2 years after construction, (2) determining cracks to be repaired, and (3) repairing cracks.

35.6 Maintenance

35.6.1 Structural and Preventative Maintenance

The most significant maintenance requirements in concrete structures are those associated with buildings having supported deck slabs and underlying structural frame members exposed to the environment such as open parking structures. Concrete is one of the most durable and low-maintenance construction materials available today; however, these attributes have led some building owners to believe that concrete structures are maintenance free. It is important for the engineer to point out to the contractor and owner that even concrete structures require continuous maintenance to retain the strength and serviceability of

the structure. One effective way to accomplish this is to add appropriate maintenance requirements in the form of general notes on the construction documents. An example of such a reference is provided below:

Maintenance:

The entire concrete frame, including elevated slabs, beams, walls, columns, slab-on-ground, and exterior concrete façade, requires continuous maintenance to remain serviceable and safe. Details of the maintenance program applicable to this project must be prepared by the owner (or designated consultant) and submitted to the facility maintenance department for execution. Failure to do so may render the structure nonserviceable or unsafe during the useful lifecycle of the structure. As a guide, the following references may be consulted as minimum requirements: Chapter 9 in *Parking Structures*, by Anthony P. Chrest and Sam Bhuyan (Routledge, 1989); *Guide for Structural Maintenance of Parking Structures* (ACI 362.2R); and *Design, Construction, and Maintenance of Cast-in-Place Post-Tensioned Concrete Parking Structures* (Post-Tensioning Institute, 2001).

When selecting a maintenance program it is necessary to address the strength and serviceability of the structural members. Structural maintenance requirements are those actions necessary to test the integrity of the material components of the structure and member configuration. Preventative maintenance requirements are those actions that improve or enhance serviceability (e.g., waterproofing, corrosion). See Table 35.2 for a summary of maintenance tasks.

TABLE 35.2 Parking Facility Structural Maintenance: Tasks and Frequencies

Task	Recommended	Minimum	Procedure
Sweep	W	M	Power sweep, vacuum, or hand sweep.
Wash down decks ^a	S	A	Hose down decks, ramps, and curbs.
Touch-up deck sealer ^b	AR	S	Reapply sealer as necessary.
Check for and evaluate cracks	AR	A	Check for leaks. Rout cracks and fill with sealant.
Check joint sealants	AR	S	Determine if cracks are structural or nonstructural.
Check isolation joint seals	AR	S	Look for leaks, adhesive or cohesive failure, tears, and adjacent concrete failures. Repair on spot basis as required.
Check traffic-bearing membrane ^b	AR	S	Review for leaks, nosing or gland damage, tears, and punctures. Repair as required.
Repaint structural steel or exposed metal	AR	A	Review wear, tear, blisters, delamination, cracks, and leaks. Repair on spot basis as required.
Check for deck surface deterioration	AR	A	Inspect for chips, peeling, and rust. Repaint on spot basis. Use special coatings, if required.
Check for water leaks	AR	S	Review for cracks, joint edge spalls, scaling, and delaminations. Repair on spot basis, as required.
Check for leakage	S	—	Consult with an engineer if deterioration is extensive.
Inspect deck drain system	M	S	Identify location and source.
Check for ponded areas	AR	A	Take corrective action as required.
Evaluate condition of previous repairs	AR	A	Drains: Remove debris and clean out drain.
Have a condition survey performed	A	AR	Drain lines: check for leaks and drainage.
			If ponding is evident, consider installing an area drain or reestablishing drainage lines.
			Evaluate condition of previous repairs; note any additional maintenance required.
			Survey should be performed periodically by a qualified structural engineer as required by conditions.

^a As weather permits.

^b This element should be maintained under warranty or service contract. Check with the manufacturer or authorized representative for terms of coverage.

Frequency: W, weekly; A = annually; AR = as required, M = monthly; S, semiannually. For items marked “As Required,” select a maintenance frequency appropriate for the particular element. Perform local repairs or replacement as needed. Special attention should be paid to areas exposed to direct sunlight or high wear, such as entries and exits, ramps, and turning aisles. Review with an engineer if uncertain about structural effects.

35.6.1.1 Concrete Slabs

The most common cause of deterioration of deck slabs and surfaces is the penetration of water and deicing chemicals into and through the slab. Preventive-maintenance measures, such as applying a protective sealer, elastomeric coating, or sealants, are most effective when applied to a new slab. On existing structures with chloride-ion contamination, the ability of a coating or sealer to suppress corrosion will depend on its ability to reduce the moisture content of the concrete. Coatings are normally more effective than sealers in reducing moisture absorption. They will not stop the corrosion completely, however, unless the chloride-ion contamination of the underlying substrate is below the corrosion threshold.

To reduce the impact of progressive deterioration and maintain serviceability, spall delaminations in the deck slab should be evaluated and patched in an appropriate manner. Temporary repairs may sometimes be required because of the time or weather constraints. Temporary repairs can be done with appropriate repair materials until long-term repairs are possible. Tar and asphaltic materials should not be used for temporary patches, however, as these will allow the migration of water and chloride ions into the concrete. Refer to ACI 546 for additional information for guidance on repair options.

Long-term repairs will require removal of all of the deteriorated concrete. Corroded reinforcement should be completely exposed, cleaned, and covered with a corrosion-inhibiting coating. Reinforcing that has lost more than 20 or 25% of its cross-sectional area may require replacement. The repair area should then be patched with an appropriate patching material. If a Portland cement-based material is used for the patches, proper curing is essential to ensure durability.

Cracking is a key cause of more serious deterioration problems in deck slabs. Fine hairline cracks can often be sealed with a low-viscosity silane sealer. Larger cracks should be routed out and sealed with a flexible, traffic-grade sealant (the rout-and-seal method). For numerous, closely spaced cracks, a traffic-bearing membrane should be installed over the area. Before the membrane is installed, the cracks should be routed and sealed or otherwise detailed in accordance with recommendations from the membrane manufacturer. If there are concerns that the cracks compromise the integrity of the structure, they should be evaluated by the engineer of record or a professional engineer with experience in structural restoration.

Ponding can also lead to significant deterioration and leakage problems. Poor finishing of the concrete can result in small areas of local ponding. Large areas of standing water are usually an indication that wither slopes to drains are not adequate or the drains do not have enough capacity. Ponding can usually be corrected by installing supplemental drains. Resurfacing to reestablish proper drainage lines may be required if the problem is widespread. Adding supplemental drains is typically the most economical approach to correct poor drainage situations, however. Refer to ACI 515.1R (ACI Committee 515, 1985) for additional information.

35.6.1.2 Beams, Columns, and Facades

Beam and column deterioration can adversely affect the structural integrity and load-carrying capacity of the structure. Deterioration of these underlying members is primarily caused by water leakage through failed joints and deck slab cracks. The vertical surfaces of columns and exterior concrete facades (spandrel railing) are also susceptible to damage from ponding water and salt splashing from moving vehicles. Beams and columns adjacent to and below expansion joints are especially susceptible to deterioration. Water leakage can contribute to freeze-thaw deterioration, corrosion of reinforcement and connections, rust staining, and leaching. Degradation can be minimized by proper maintenance of the joint sealant systems and application of a sealer or elastomeric membrane to the column bases and spandrel railing. These members are also vulnerable to user damage such as vehicle impact. They should be examined periodically for cracking and spalling. Runoff water that collects along or adjacent to interior face of exterior spandrel walls and columns can contribute to corrosion of exposed steel embedments and exposed reinforcement of these elements. This can lead to unsightly rust staining and, in extreme cases, safety concerns about the load-carrying capacity of the embedded steel. If significant ponding is present, it may be necessary to install a curb or supplemental drain to slope the concrete and move water away from the affected areas.

35.6.1.3 Stair and Elevator Towers

Leaks often occur at the joints between deck slabs and stair and elevator towers. These leaks are typically due to poor drainage around the towers. If not addressed, these leaks can cause severe deterioration of underlying elements such as metal doors, light fixtures and electrical conduits, metal stairs, exposed structural steel members, and precast connections. Drainage can be improved by providing curbs to divert the water. Frequent inspection and immediate repair of damaged isolation joints between the tower and the deck surface will also reduce the potential for deterioration. Masonry walls should typically be sealed. If a masonry wall is exposed to the weather, however, nonbreathing paints should not be used on both sides as this will tend to trap water and cause the paint to peel. Stair and elevator wall cracking should be repaired, as appropriate, to minimize moisture penetration.

35.6.1.4 Exposed Metals

An exposed concrete frame such as a parking structure may have exposed metals in the form of stairs, pedestrian railings, vehicular guardrails, precast connections, columns, or beams. Exposed metals should be visually monitored on a regular basis. Premature deterioration of metal components can be the result of atmospheric exposure, neglect, or chemical reactions between metals. Galvanic processes between two dissimilar materials such as aluminum and mild steel at a connection may cause especially severe corrosion. Treatment of metals with a proper surface preparation and appropriate paint or anticorrosion coatings will help minimize corrosion and resultant problems. Metal pan stairs with concrete infill are particularly susceptible to corrosion-related deterioration. They are not recommended in areas that use deicing salts.

35.6.2 Operational and Aesthetics Maintenance

Operational maintenance involves the regular inspection, repair, and maintenance required to keep the structure functional for its intended users. It includes housekeeping tasks such as routine cleaning, sweeping and wash-downs, snowplowing, and ice control.

35.6.2.1 Housekeeping Requirements

Routine cleaning is one of the most important aspects of good housekeeping. A clean environment makes the concrete structure more pleasant, reduces required maintenance, and extends service life. Sweeping, for example, should be done at least monthly and can be done with hand brooms, mechanized sweepers, or vacuums designed for use in parking structures. All dirt and debris should be removed from the facility. Special attention should be paid to keeping dirt and debris out of drain basins, pipes, expansion joints, and other openings. Grease buildups should be removed regularly using appropriate degreasers. In freezing climates, road salts will accumulate over the winter months. They should be removed each spring by flushing the surface with large volumes of water at low to moderate pressure. A second wash-down is recommended in the fall to remove surface debris and contaminants. Parking structures should be equipped so a 1.5-in.-diameter hose can be used to wash the deck. Areas that tend to get a higher buildup of salt such as entrances and exits and flat or ponded areas should be washed more frequently. Care should be taken not to damage joint sealants, expansion joints, or deck coating materials. Drains should be flushed carefully to avoid plugging the drainage system with sand, dirt, and debris.

35.6.2.2 Snow Removal and Ice Control

Snowplows can damage joint sealants, isolation joint seals, and concrete traffic-deck coatings. Columns, curbs, walls, and even the decks themselves can be damaged by snow removal activities. Care should be taken to use equipment that had been properly adapted to avoid direct contact with the structure. Rubber-tipped snowplow blades are one solution to this problem. All isolation joints should be marked and pointed out to the snowplow operator. Hand removal may be necessary in certain areas to avoid damage to the seals. Piling snow on the deck slab is not permissible. Packed snow can be heavy and may exceed the load capacity of the deck and contribute to cracking. Piles of snow may also create a reservoir of salt-

contaminated water that contributes to leakage and chloride buildup. Deicing chemicals are used to control ice buildup and reduce slipping and skidding hazards; however, most common chemical deicers can damage the concrete or reinforcing steel, and they should be used with caution. Calcium magnesium acetate (CMA) is considered to be less corrosive than common road salt or calcium chloride. Care should also be taken to ensure that any deicers used comply with local health and environmental codes.

35.6.2.3 Other Operational Maintenance

A parking structure has a number of operational systems. These include mechanical and electrical systems, lighting, elevators, signage, parking control equipment, security systems, graphics, and striping. Although they typically do not affect structural performance, it is sometimes cost effective to coordinate the maintenance or updating of these systems with structural maintenance. Refer to the *Parking Garage Maintenance Manual* (Parking Consultants Council, 2004) for additional information.

35.6.2.4 Aesthetics-Related Maintenance

Maintenance must address the aesthetic as well as structural and operational aspects features of a concrete structure. Aesthetics includes items such as landscaping, painting, and general appearance. Patrons appreciate a clean facility and are more inclined to treat it properly, which can ultimately reduce repair costs.

35.6.3 Checklist for Structural Inspection

A regular visual inspection of the structural and waterproofing components of the parking structure is an essential element of a preventive maintenance program. The inspection should be conducted in conjunction with a wash-down of the structure so any active leakage can be noted. The structure should be inspected systematically and the nature, location, and severity of any observed problems recorded. It is helpful to have a notebook-sized plan of each floor to use as a base sheet for taking notes during the inspection. In addition, it is helpful to develop a system of marks for use in representing various conditions while taking field notes. A digital camera or videocamera can be of great assistance in documenting developing problems. While most problems can be observed by a layperson familiar with the structure, an inspection should be performed by a qualified engineer every few years or when new or significant changes in deterioration are observed. Visual inspection of the parking structure should include the following items. (Any “Yes” answers should be followed up with action to remedy the situation.)

Deck

- Yes ☐ No ☐ Are there any cracks?
- Yes ☐ No ☐ If so, do they leak?
- Yes ☐ No ☐ Is the surface sound (or are there areas where surface scaling is present)?
- Yes ☐ No ☐ Is there any evidence of corrosion of reinforcing steel or surface spalling?
- Yes ☐ No ☐ Is there any evidence of corrosion of exposed metals?
- Yes ☐ No ☐ Is there any evidence of concrete delamination?
- Yes ☐ No ☐ Is any steel reinforcing exposed?
- Yes ☐ No ☐ Are there any signs of leakage? (Describe conditions and note location.)
- Yes ☐ No ☐ If there is a traffic-bearing membrane, are there any tears, cracks, or loss of adhesion?
- Yes ☐ No ☐ Are there low spots where ponding occurs?
- Yes ☐ No ☐ Has the concrete been tested for chloride ion content? (When was it last monitored? Are there records available?)
- _____ When was the deck last sealed?

Beams and Columns

- Yes ☐ No ☐ Are there any cracks? (If so, are they vertical or horizontal; how long and wide?)
- Yes ☐ No ☐ Are there any signs of leakage? (Describe conditions and note location.)
- Yes ☐ No ☐ Is there any concrete spalling?
- Yes ☐ No ☐ Is any steel reinforcement exposed?

Stair and Elevator Towers

- Yes ☐ No ☐ Are there any signs of a leaking roof?
 Yes ☐ No ☐ Are there any cracks in the exterior finish?
 Yes ☐ No ☐ Is any other corrective action required?

Isolation Joints

- Yes ☐ No ☐ Are there any leaks through isolation joint seals?
 Yes ☐ No ☐ If so, are they related to seal failure or failure of the adjacent concrete?
 Yes ☐ No ☐ Could the cause of these leaks be snowplows?
 _____ What type of isolation joint seal is it? Who is the manufacturer?
 Yes ☐ No ☐ Is there any isolation joint warranty in force? (Consult with the manufacturer for repair recommendations.)

Joint Sealants

- Yes ☐ No ☐ Are there any signs of leakage, loss of elastic properties, separation from adjacent substrates, or cohesive failure of the sealant?
 Yes ☐ No ☐ Are there any failures of the concrete behind the sealant (edge spalls)?

Exposed Steel

- Yes ☐ No ☐ Is there any exposed steel (structural beams, handrails, door frames, barrier cable, exposed structural connections)?
 Yes ☐ No ☐ Is rust visible on any exposed steel?
 Yes ☐ No ☐ If so, is it surface rust?
 Yes ☐ No ☐ Is there significant loss of section due to the rust?
 Yes ☐ No ☐ Is repainting required?

Drains

- Yes ☐ No ☐ Are the drains functioning properly? (When were they last cleaned out?)
 Yes ☐ No ☐ Are the drains properly located so they receive the runoff as intended?

Previous Repairs

- Yes ☐ No ☐ Are previous repairs performing satisfactorily?

References

- Aalami, B.O. 1994. *Unbonded and Bonded Post-Tensioning Systems in Building Construction*, PTI Technical Notes No. 5. Post-Tensioning Institute, Phoenix, AZ.
 Aalami, B.O. and Barth, F.B. 1988. *Restraint Cracks and Their Mitigation in Unbonded Post-Tensioned Building Structures*. Post-Tensioning Institute, Phoenix, AZ.
 ACI. 2007. *Manual of Concrete Practice*. American Concrete Institute, Farmington Hills, MI.
 ACI Committee 224. 1995. *Joints in Concrete Construction*, ACI 224.3R. American Concrete Institute, Farmington Hills, MI, 44 pp.
 ACI Committee 224. 1997. *Cracking of Concrete Members in Direct Tension*, ACI 224.2R. American Concrete Institute, Farmington Hills, MI, 12 pp.
 ACI Committee 224. 2001. *Control of Cracking in Concrete Structure*, ACI 224R. American Concrete Institute, Farmington Hills, MI, 46 pp.
 ACI Committee 318. 2005. *Building Code Requirements for Structural Concrete and Commentary*, ACI 318. American Concrete Institute, Farmington Hills, MI.
 ACI Committee 362. 2000. *Guide for Structural Maintenance of Parking Structures*, ACI 362.2R. American Concrete Institute, Farmington Hills, MI.
 ACI Committee 515. 1985. *Guide to the Use of Waterproofing, Dampproofing, Protective, and Decorative Barrier Systems for Concrete*, ACI 515.1R. American Concrete Institute, Farmington Hills, MI.

- Chrest, A.P., Smith, M.S., and Bhuyan, S. 1989. *Parking Structures, Planning, Design, Construction, Maintenance, and Repair*. Routledge, New York, chap. 9.
- Litvan, G. and Bickley, J. 1987. *Durability of Parking Structures, Analysis of Field Survey*, ACI SP 100-76. American Concrete Institute, Farmington Hills, MI.
- Nawy, E.G. 2006. *Prestressed Concrete: A Fundamental Approach*, 5th ed. Prentice-Hall, Upper Saddle River, NJ.
- Parking Consultants Council. 2004. *Parking Garage Maintenance Manual*, 4th ed. National Parking Association, Washington, D.C.
- PTI. 2001. *Design, Construction, and Maintenance of Cast-in-Place Post-Tensioned Concrete Parking Structures*. Post-Tensioning Institute, Phoenix, AZ.
- PTI. 2006. *Post-Tensioning Manual*, 6th ed. Post-Tensioning Institute, Phoenix, AZ.
- Richardson, M.G. 1987. Cracking in reinforced concrete buildings. *Concrete Int.*, 21–23.
- Suarez, M.G. and Posten, R.W. 1990. *Evaluation of the Condition of a Post-Tensioned Concrete Parking Structure after 15 Years of Service*. Post-Tensioning Institute, Phoenix, AZ.
- Walker, C.H. 1990. *Durability Systems for Concrete Parking Structures*. Carl Walker Engineers, Kalamazoo, MI.



(a)



(b)

(a) Sunshine Skyway Bridge across Tampa Bay, Florida, a 4.2-mile-long, segmented, prestressed, cable-stayed bridge that is one of the longest in the world. (b) Trump Towers in New York City, built using 12,000-psi silica fume concrete. (Photographs courtesy of the Portland Cement Association, Skokie, IL.)

36

Proportioning Concrete Structural Elements by the ACI 318-08 Code

Edward G. Nawy, D.Eng., P.E., C.Eng.*

36.1	Material Characteristics	36-2
	Modulus of Concrete • Creep of Concrete • Shrinkage of Concrete • Control of Deflection • Control of Cracking in Beams • ACI 318 Code Provisions for Control of Flexural Cracking	
36.2	Structural Design Considerations	36-5
	Axially Loaded Columns • Beams and Slabs	
36.3	Strength Design of Reinforced-Concrete Members.....	36-10
	Strain Limits Method for Analysis and Design • Flexural Strength • Shear Strength • Strut-and-Tie Theory and Design of Corbels and Deep Beams • Torsional Strength • Compression Members: Columns • Two-Way Slabs and Plates • Development of Reinforcement	
36.4	Prestressed Concrete	36-31
	General Principles • Minimum Section Modulus for Variable Tendon Eccentricity • Minimum Section Modulus for Constant Tendon Eccentricity • Maximum Allowable Stresses	
36.5	Shear and Torsion in Prestressed Elements.....	36-34
	Shear Strength: ACI Short Method When $f_{pc} > 0.40f_{pu}$ • Detailed Method • Minimum Shear Reinforcement • Torsional Strength	
36.6	Walls and Footings	36-36
	Acknowledgments.....	36-36
	References	36-36

Most structural systems constructed today are made from reinforced, prestressed, or composite concrete having a wide range of characteristics and strengths. Structural concrete, whether normal weight or lightweight, is designed to have a compressive strength in excess of 3000 psi (20 MPa) in concrete structures. When the strength exceeds 6000 psi (42 MPa) such structures are defined today as high-strength concrete structures. Concrete mixtures designed to produce 6000 to 12,000 psi in compressive strength are easily obtainable today when silica fume or other pozzolans replace a portion of the cement content, resulting in lower water/cement (w/c) and water/cementitious materials (w/cm) ratios. Concretes

* Distinguished Professor, Civil Engineering, Rutgers University, The State University of New Jersey, Piscataway, New Jersey, and ACI honorary member; expert in concrete structures, materials, and forensic engineering.

having cylinder compressive strengths of about 20,000 psi (140 MPa) have been used in several buildings in the United States. These high-strength characteristics merit qualifying such concrete as super-high-strength concrete at this time.

36.1 Material Characteristics

36.1.1 Modulus of Concrete

The ACI 318 Code (ACI Committee 318, 2008; Nawy, 2002, 2008) stipulates that the concrete modulus of elasticity (E_c) should be evaluated from:

$$E_c \text{ (psi)} = 33w^{1.5}\sqrt{f'_c} \quad (36.1a)$$

$$E_c \text{ (MPa)} = 0.043w^{1.5}\sqrt{f'_c} \quad (36.1b)$$

The expressions in Equation 36.1 are applicable to strengths up to 6000 psi (42 MPa). Available research to date for concrete compressive strength up to 12,000 psi (83 MPa) gives the following expressions (ACI Committee 435, 1995; Nawy, 2002, 2008):

$$E_c \text{ (psi)} = \left(40,000\sqrt{f'_c} + 10^6\right)\left(\frac{w_c}{145}\right)^{1.5} \quad (36.2a)$$

$$E_c \text{ (MPa)} = \left(3.32\sqrt{f'_c} + 6895\right)\left(\frac{w_c}{2320}\right)^{1.5} \quad (36.2b)$$

In Equation 36.1a and Equation 36.2a, f'_c is in units of pounds per square inch, and w_c ranges between 145 pcf for normal-density concrete and 100 pcf for structural lightweight concrete; f'_c in Equation 36.1b and Equation 36.2b is in units of megapascals and w_c ranges between 2400 kg/m³ for normal-density concrete and 1765 kg/m³ for lightweight concrete. The modulus of rupture of concrete can be taken as:

$$f_r \text{ (psi)} = 7.5\lambda\sqrt{f'_c} \quad (36.3a)$$

$$f_y \text{ (MPa)} = 0.632\lambda\sqrt{f'_c} \quad (36.3b)$$

where:

λ = 1.0 for normal-density stone aggregate concrete.

λ = 0.85 for sand lightweight concrete.

λ = 0.75 for all lightweight concrete.

36.1.2 Creep of Concrete

Concrete creeps under sustained loading due to transverse flow of the material. The creep coefficient as a function of time can be calculated from the following expression (ACI Committee 435, 1995; Nawy, 2002, 2008):

$$C_t = \left(\frac{t^{0.6}}{10 + t^{0.6}}\right)C_u \quad (36.4)$$

where time t is in days and C_u , the ultimate creep factor, is 2.35. The short-term deflection is multiplied by C_t to get the long-term deflection, which is added to the short-term (instantaneous) deflection value to obtain the total deflection.

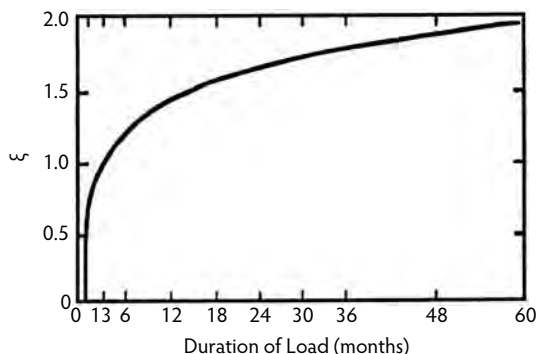


FIGURE 36.1 Long-term deflection multipliers. (From ACI Committee 318, *Building Code Requirements for Structural Concrete*, ACI 318-08; *Commentary*. ACI 318R, American Concrete Institute, Farmington Hills, MI, 2008.)

36.1.3 Shrinkage of Concrete

Concrete shrinks as the absorbed water evaporates and the chemical reaction of cement gel proceeds. For moist-cured concrete, the shrinkage strain that occurs at any time t in days 7 days after placing the concrete can be evaluated from (ACI Committee 435, 1995):

$$(\epsilon_{SH})_t = \left(\frac{t}{35+t} \right) (\epsilon_{SH})_u \quad (36.5a)$$

For steam-cured concrete, the shrinkage strain at any time t (in days) 1 to 3 days after placement of the concrete is:

$$(\epsilon_{SH})_t = \left(\frac{t}{55+t} \right) (\epsilon_{SH})_u \quad (36.5b)$$

where maximum $(\epsilon_{SH})_u$ can be taken as 780×10^{-6} in./in. (mm/mm).

Shrinkage and creep due to sustained load can also be evaluated from the ACI expression (ACI Committee 318, 2008):

$$\lambda = \left(\frac{\xi}{1+50\rho'} \right) \quad (36.5c)$$

and Figure 36.1 for the factor ξ that ranges from a value of 2.0 for 5 years or more to 1.0 for 3 months of sustained loading; $\rho' = \text{compression steel percentage} = A_s'/bd$.

36.1.4 Control of Deflection

Serviceability is a major factor in designing structures to sustain acceptable long-term behavior. Serviceability is controlled by limiting deflection and cracking in the members (ACI Committee 435, 1995). For deflection computation and control, the effective moment of inertia of a cracked section can be evaluated from the Branson equation:

$$I_e = \left(\frac{M_{cr}}{M_a} \right) I_g + \left[1 - \left(\frac{M_{cr}}{M_a} \right)^3 \right] I_{cr} \leq I_g \quad (36.6)$$

where, for reinforced-concrete beams:

- M_{cr} = cracking moment due to total load = $(f_r I_g)/y_t$.
 y_t = distance from the neutral axis to the extreme tension fibers.
 M_a = maximum service load moment at the section under consideration.
 I_g = gross moment of inertia.

In the case of prestressed concrete,

$$\left(\frac{M_{cr}}{M_a} \right) = \frac{f_{te} - f_r}{f_L} \quad (36.7)$$

where:

- M_{cr} = moment due to that portion of live load moment M_a that causes cracking.
 M_a = maximum service load (unfactored) live load moment.
 f_{te} = total calculated stress in the member.
 f_L = calculated stress due to live load.

For long-term deflection, Figure 36.1 gives the required multipliers as a function of time.

36.1.5 Control of Cracking in Beams

Control of cracking in beams and one-way slabs can be made using the expression (ACI Committee 224, 2001):

$$w_{\max} \text{ (in.)} = 0.076 \beta f_s \sqrt[3]{d_c A} \times 10^{-3} \quad (36.8a)$$

where:

- w_{\max} = crack width (in.) (25.4 mm).
 β = $(h - c)/(d - c)$.
 d_c = thickness of cover to the first layer of bars (in.).
 f_s = maximum stress in reinforcement at service load = $0.60 f_y$ (kips/in.²).
 A = area of concrete in tension divided by number of bars (in.²) = bt/γ , where γ is the number of bars at the tension side.

36.1.6 ACI 318 Code Provisions for Control of Flexural Cracking

From the author's work and briefly reported in Nawy (2002, 2005), the spacing of the reinforcement is a major parameter in limiting the crack width. As the spacing is decreased through the use of larger numbers of bars, the area of the concrete envelopes surrounding the reinforcement increases. This leads to a larger number of narrower cracks. As the crack width becomes narrow enough within the values given in Table 36.1, corrosion effects on the reinforcement are considerably reduced. The current ACI provisions on crack control deal with this problem by limiting reinforcement spacing in reinforced-concrete beams and one-way slabs to the values obtained from the following expression for maximum allowable bar spacing:

$$s = 15 \left(40,000 / f_s \right) - 2.5c_c \quad (36.8b)$$

but not greater than $12(40,000/f_s)$, where:

- f_s = calculated stress in reinforcement at service load = unfactored moment divided by the steel area and the internal arm moment; f_s is taken as $2/3 f_y$ (psi).
 c_c = clear cover from the nearest surface in tension to the flexural tension reinforcement (in.).
 s = center-to-center spacing of flexural tension reinforcement (in.) closest to the tension face of the section.

TABLE 36.1 Tolerable Crack Widths

Exposure Condition	Tolerable Crack Width	
	in.	mm
Dry air or protective membrane	0.016	0.41
Humidity, moist air or soil	0.012	0.30
Deicing chemicals	0.007	0.18
Seawater and seawater spray; wetting and drying	0.006	0.15
Water-retaining structures (excluding non-pressure pipes)	0.004	0.10

From these provisions, the maximum spacing for 60,000-psi (414-MPa) reinforcement = $12[36/(0.6 \times 60)] = 12$ in. (305 mm). The maximum spacing of 12 in. conforms with tests conducted by the author on more than 100 two-way action slabs; hence, this limitation on the distribution of flexural reinforcement in one-way slabs and wide-web reinforced-concrete beams is appropriate. In beams of normal web width in normal buildings, however, these provisions might not be as workable as controlling the crack width through the use of crack-width expressions to control the crack width within tolerable limits.

The SI expression for the value of reinforcement spacing in Equation 36.8b and f_s (MPa) is:

$$s \text{ (mm)} = 380 \left(280/f_s \right) - 2.5c_c \quad (36.8c)$$

but not to exceed $300(252/f_s)$. For the usual case of beams with grade-420 reinforcement and 50-mm clear cover to the main reinforcement and with $f_s = 252$ MPa, the maximum bar spacing is 300 mm.

It should be stressed that these provisions are applicable to reinforced-concrete beams and one-way slabs in structures subject to normal environmental conditions. For other types of structures subject to aggressive environment such as sanitary structures, refer to ACI Committee 350 (2006), Nawy (2002, 2008), and Table 36.1 for values of tolerable crack widths in reinforced-concrete structures.

36.2 Structural Design Considerations

High-strength concretes have certain characteristics and engineering properties that differ from those of lower strength concretes (ACI Committee 363, 1992). These differences seem to have larger effects as the strength increases beyond the current 6000-psi (42-MPa) plateau for normal-strength concrete. High-strength concretes are shown to be essentially linearly elastic up to failure, with a steeper declining portion of the stress–strain diagram. In comparison, the stress–strain diagram of lower strength concretes is more parabolic in nature, as seen in Figure 36.2. The stress–strain relationship of the steel reinforcement in this diagram is not to scale in its ordinate value but is intended to show the relative strain following the usual assumption of strain compatibility between the concrete and the steel reinforcement up to yield.

36.2.1 Axially Loaded Columns

Current design practice adds the contribution of the steel and the concrete to calculate the ultimate state of failure in compression members. For lower strength concretes, when the concrete reaches the nonlinearity load level at a strain of 0.001 in./in., as seen in Figure 36.2, the steel is still in the elastic range, assuming a larger share of the applied load. But, as the strain level approaches 0.002 in./in., the slope of the concrete stress–strain diagram approaches zero, while the steel reaches its yield strain that will thereafter be idealized into a constant (horizontal) plateau. The strength of the column using the addition law would then be:

$$P_n = 0.85f'_cA_c + f_yA_s \quad (36.9)$$

where:

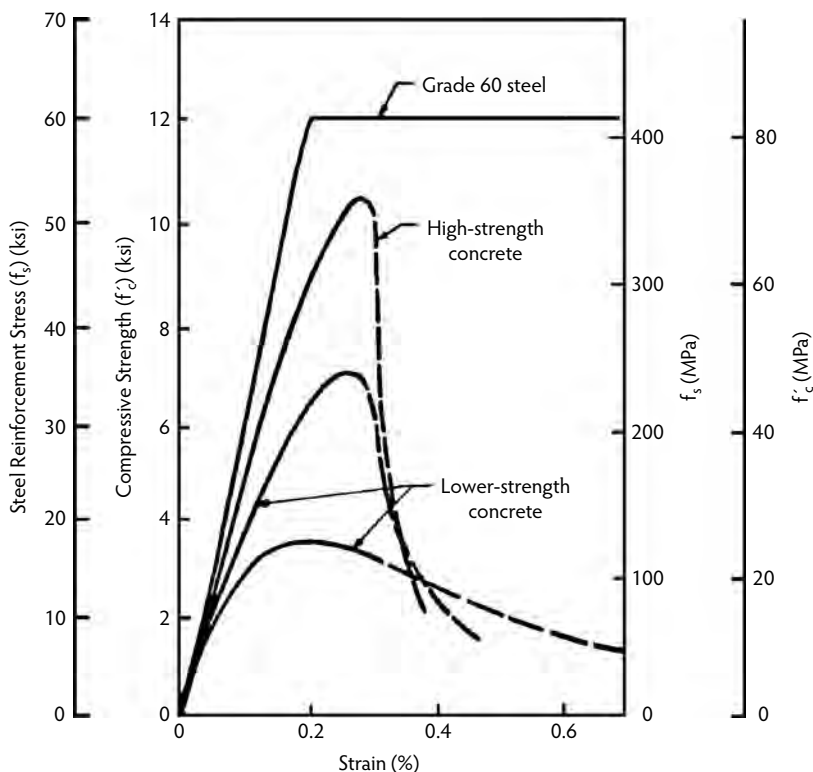


FIGURE 36.2 Concrete and steel stress–strain relationships. (From ACI Committee 363, *State-of-the-Art on High-Strength Concrete*, ACI 363R, American Concrete Institute, Farmington Hills, MI, 1992, pp. 1–55.)

f'_c = concrete cylinder compressive strength.

f_y = yield strength of the reinforcement.

A_c = gross area of the concrete section.

A_s = area of the reinforcement.

The factor 0.85 representing the adjustment in concrete strength between the cylinder test result and the actual concrete strength in the structural element has been shown by extensive testing to be sufficiently accurate for higher strength concretes (ACI Committee 363, 1992; Nawy, 2008).

Confining the concrete in compression members through the use of spirals or closely spaced ties increases its compressive capacity. The increase in concrete strength due to the confining effect of the spirals can be represented by the following expression:

$$f'_2 = \frac{1}{4} [\bar{f}_c - f''_c] \quad (36.10a)$$

where:

f'_2 = concrete confining stress due to the spiral.

\bar{f}_c = compressive strength of the confined concrete.

f''_c = compressive strength of the unconfined column concrete.

The hoop tension force in the circular spiral is:

$$2A_{sp}f_y = f'_2D'_s$$

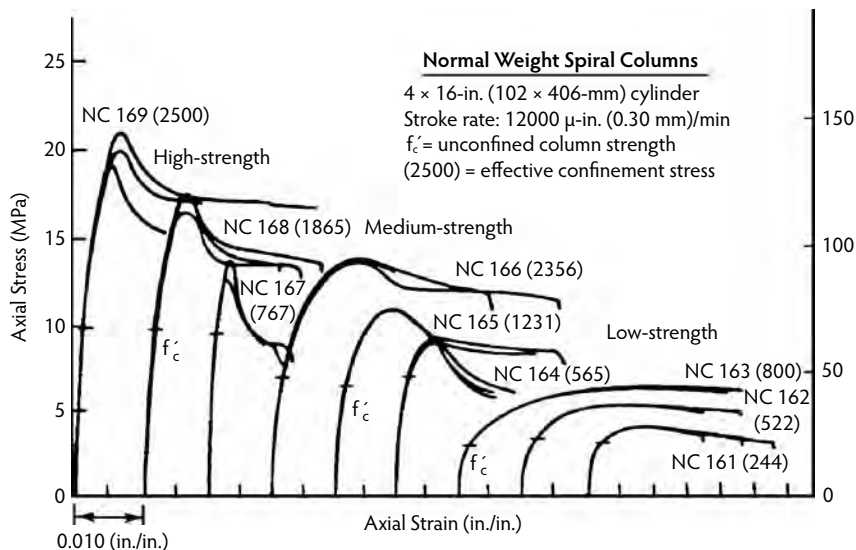


FIGURE 36.3 Stress–strain diagrams of 4 × 6-in. normal weight, spirally confined compression prisms. (From Martinez, S. et al., *ACI Struct. J.*, 81(5), 431–442, 1984.)

or

$$f'_2 = \frac{2A_{sp}f_y}{D'_s} \quad (36.10b)$$

where:

A_{sp} = cross-sectional area of the spiral.

D'_s = diameter of concrete core.

s = spiral pitch.

Equation 36.10 can be improved (ACI Committee 363, 1992; Nawy, 2002), leading to the following form for normal weight concrete:

$$(\bar{f}_c - f'_c) = 4.0f'_2(1 - s/D'_s) \quad (36.11a)$$

and for lightweight concrete:

$$(\bar{f}_c - f'_c) = 1.8f'_2(1 - s/D'_s) \quad (36.11b)$$

Figure 36.3 gives the results of peak stress comparisons vs. axial strain for spirally reinforced members for low-, medium-, and high-strength concretes. For higher strength, it shows a lower strain at peak load and a steeper decline past the peak value; however, the strength gain in concrete due to confinement seems to be well predicted for high-strength concretes in Equation 36.11.

36.2.2 Beams and Slabs

36.2.2.1 The Compressive Block

The design of concrete structural elements is based on the compressive stress distribution across the depth of the member as determined by the stress–strain diagram of the material. For high-strength concretes, the difference in the shape of the stress–strain relationship discussed in connection with Figure 36.2 results in differences in the shape of the compressive stress block. Figure 36.4 shows possible compressive blocks for use in design. Figure 36.4c could more accurately represent the stress distribution

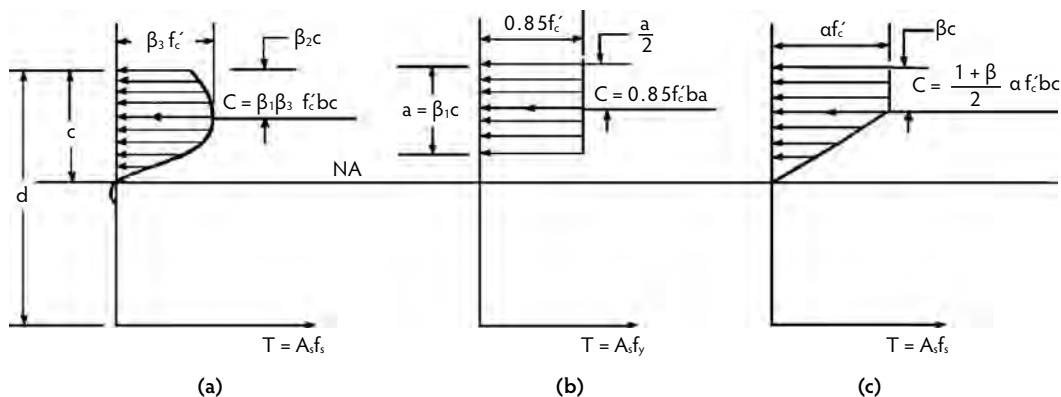


FIGURE 36.4 Concrete compressive stress block: (a) standard stress block; (b) equivalent rectangular block; and (c) modified trapezoidal block.

for higher strength concrete; however, the computed strength of beams and eccentrically loaded columns depends on the reinforcement ratio. In the ACI 318 Code provisions, which use the equivalent rectangular block, the nominal moment strength of a singly reinforced beam is calculated using the following expression:

$$M_n = A_s f_y d \left[1 - 0.59 \rho \frac{f_y}{f'_c} \right] \quad (36.12)$$

where the coefficient $0.59 = \beta_2 / \beta_1 \beta_3$. Although a detailed evaluation of the factors β_1 , β_2 , and β_3 indicates a significant difference in their separate values, depending on the concrete strength (ACI Committee 363, 1992), Figure 36.5 shows that these differences collectively balance each other and that the combined coefficient $\beta_2 / \beta_1 \beta_3$ is well represented by the 0.59 value. Consequently, for strengths up to 12,000 psi (42

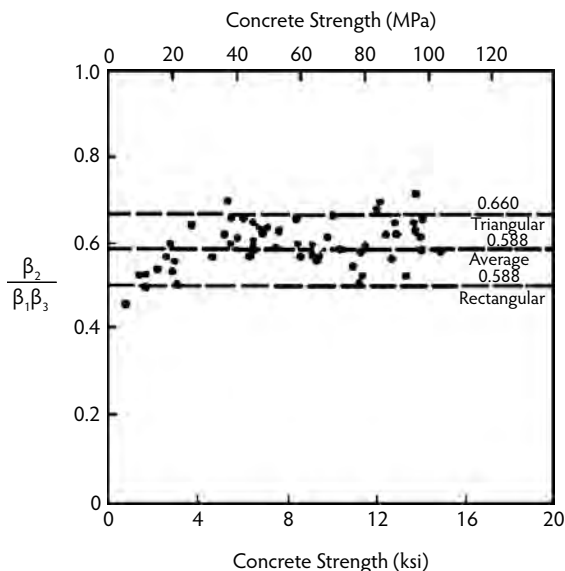


FIGURE 36.5 Stress block parameter $\beta_2 / \beta_1 \beta_3$ vs. concrete compressive strength. (From ACI Committee 363, *State-of-the-Art on High-Strength Concrete*, ACI 363R, American Concrete Institute, Farmington Hills, MI, 1992, pp. 1–55.)

TABLE 36.2 Deflection Ductility Index for Singly Reinforced Beams

Beam	f'_c		ρ/ρ_b^a	Ductility Index ($\mu = \Delta_u/\Delta_y$)
	psi	MPa		
A1	3700	26	0.51	3.54
A2	6500	45	0.52	2.84
A3	8535	59	0.29	2.53
A4	8535	59	0.64	1.75
A5	9264	64	0.87	1.14
A6(a)	8755	60	1.11	1.07

^a Ratio of tension reinforcement divided by reinforcement ratio producing balanced strain conditions.

Source: Data from Pastor, J.A. et al., *Behavior of High-Strength Concrete Beams*, Cornell University Report No. 84-3, Department of Structural Engineering, Cornell University, Ithaca, NY, 1984; Nawy, E.G., *Fundamentals of High-Performance Concrete*, 2nd ed., John Wiley & Sons, New York, 2002.

MPa), the current ACI 318 Code expressions requiring that beams be under-reinforced are equally applicable. For considerably higher strengths or for members combining compression and bending or for the over-reinforced members allowed in the codes, some differences in the value of $\beta_2/\beta_1\beta_3$ can be expected.

36.2.2.2 Compressive Limiting Strain

Although high-strength concrete achieves its peak value at a unit strain slightly higher than that of normal-strength concrete (Figure 36.2), the ultimate strain is lower for high-strength concrete unless confinement is provided. A limiting strain value allowed by the ACI 318 Code is 0.003 in./in. (mm/mm). Other codes allow a limiting strain for unconfined concrete of 0.0035 or 0.0038. The conservative ACI value of 0.003 seems to be adequate for high-strength concretes as well, although it is somewhat less conservative than that for lower strength concretes.

36.2.2.3 Confinement and Ductility

As higher strength concrete is more brittle, confinement becomes more important in order to increase its ductility. If μ is the deflection ductility index,

$$\mu = \frac{\Delta_u}{\Delta_y} \quad (36.13)$$

where:

Δ_u = beam deflection at failure load.

Δ_y = beam deflection at the load producing yield of the tensile reinforcement.

Table 36.2 shows the ductility index values of concretes in singly reinforced beams ranging in strength from 3700 to 9265 psi (25 to 64 MPa). The corresponding reduction in the ductility index ranges from 3.54 to 1.07. The addition of compressive reinforcement and confinement to geometrically similar beams seems to increase the ductility index for $f'_c = 8500$ up to a value of 5.61. Hence, the higher the concrete compressive strength, the more it becomes necessary to provide for confinement or the addition of compression steel (A_s') while using the same expression for nominal moment strength that is applicable to normal-strength concretes. It should be stated that cost would not be affected to any meaningful extent, as diagonal tension and torsion stirrups have to be used anyway, and in seismic regions closely spaced confining ties are a requirement. The maximum strain of confined concrete that can be utilized should not exceed 0.01 in./in. (mm/mm) in limit design.

36.2.2.4 Shear and Diagonal Tension

Design for shear in accordance with the ACI 318 Code is based on permitting the plain concrete in the web to assume part of the nominal shear V_n . If V_c is the shear strength resistance of the concrete, the web stirrups resist a shear force $V_s = V_n - V_c$. High-strength concrete develops a relatively brittle failure, as previously discussed, with the aggregate interlock decreasing with the increase in the compressive strength. Hence, the shear friction and diagonal tension failure capacity in beams might be unconservatively represented by the ACI 318 equations (Ahmed and Lau, 1987); however, the strength of the diagonal struts in the beam shear truss model is increased through the mobilization of more stirrups and the increased load capacity of the struts themselves. No research data are currently available to provide definitive guidelines on the minimum web steel that can prevent brittle failure. All work to date indicates no unsafe use of the current ACI 318 Code provisions for shear in the design of high-strength concrete members.

36.3 Strength Design of Reinforced-Concrete Members

36.3.1 Strain Limits Method for Analysis and Design

This approach is sometimes referred to as the *unified method*, as it is equally applicable to flexural analysis of prestressed concrete elements. The nominal flexural strength of a concrete member is reached when the net compressive strain in the extreme compression fibers reaches the ACI 318 Code strain limit of 0.003 in./in. It also stipulates that when the net tensile strain in the extreme tension steel (ϵ_t) is sufficiently large at a value equal or greater than 0.005 in./in., the behavior is fully ductile. The concrete beam section under this condition is characterized as being *tension controlled*, with ample warning of failure as denoted by excessive cracking and deflection.

If the net tensile strain at the extreme tension steel (ϵ_t) is small, such as in compression members, being equal or less than a *compression-controlled* strain limit, a brittle mode of failure is expected, with little warning of such an impending failure. Flexural members are usually tension controlled, and compression members are usually compression controlled; however, in some sections, such as those subjected to small axial loads but large bending moments, the net tensile strain (ϵ_t) in the extreme tensile reinforcement will have an intermediate or transitional value between the two strain limit states—namely, between the compression-controlled strain limit of $\epsilon_t = f_y/E_s = 60,000/29 \times 10^6 = 0.002$ in./in., and the tension-controlled strain limit $\epsilon_t = 0.005$ in./in. Figure 36.6 illustrates these three zones as well as the variation in the strength reduction factors applicable to the total range of behavior.

For the tension-controlled state, the strain limit $\epsilon_t = 0.005$ corresponds to the reinforcement ratio $\rho/\rho_b = 0.63$, where ρ_b is the reinforcement ratio for the balanced strain $\epsilon_t = 0.002$ in the extreme tensile reinforcement for 60-ksi steel. The net tensile strain $\epsilon_t = 0.005$ for a tension-controlled state is a single value that applies to all types of reinforcement, whether mild steel or prestressing steel. High reinforcement ratios that produce a net tensile strain less than 0.005 result in a ϕ -factor value lower than 0.90, resulting in less economical sections. Therefore, it is more efficient to add compression reinforcement if necessary or to deepen the section to make the strain in the extreme tension reinforcement (ϵ_t) ≥ 0.005 . Variation of the strain reduction factor ϕ as a function of strain for the range values of $\epsilon_t = 0.002$ and $\epsilon_t = 0.005$ can be linearly interpolated from the following expressions in terms of the limit strain ϵ_t :

Tied sections:

$$0.65 \leq \left[\phi = 0.65 + (\epsilon_t - 0.002) \left(\frac{250}{3} \right) \right] \leq 0.90 \quad (36.14a)$$

Spirally reinforced sections:

$$0.75 \leq \left[\phi = 0.75 + (\epsilon_t - 0.002) \left(\frac{150}{3} \right) \right] \leq 0.90 \quad (36.14b)$$

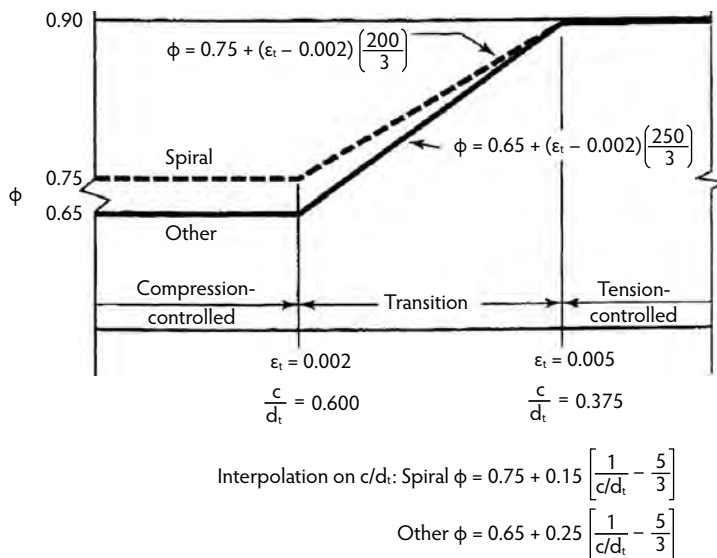


FIGURE 36.6 Strain limit zones and variation of strength reduction factor ϕ with the net tensile strain ϵ_t . (From ACI Committee 318, *Building Code Requirements for Structural Concrete*, ACI 318; *Commentary*. ACI 318R-08, American Concrete Institute, Farmington Hills, MI, 2008.)

Variation of ϕ as a function of the neutral axis depth ration c/d_t can be evaluated from the following two expressions for the limit ratios of c/d_t of 0.60 for the compression-controlled state and 0.375 for the tension-controlled state:

Tied sections:

$$0.65 \leq \left[\phi = 0.65 + 0.25 \left(\frac{1}{c/d_t} - \frac{5}{3} \right) \right] \leq 0.90 \quad (36.15a)$$

Spirally reinforced sections:

$$0.75 \leq \left[\phi = 0.75 + 0.15 \left(\frac{1}{c/d_t} - \frac{5}{3} \right) \right] \leq 0.90 \quad (36.15b)$$

36.3.2 Flexural Strength

36.3.2.1 Singly Reinforced Beams

Flexural strength is determined from the strain and stress distribution across the depth of the concrete section. Figure 36.7 shows the stress and strain distribution and forces. Taking moments of all the forces about tensile steel ($A_s' = 0$), a nominal moment strength:

$$M_n = A_s f_y \left(d - \frac{a}{2} \right) \quad (36.16)$$

$$M_n = bd^2 \omega (1 - 0.59\omega) \quad (36.17)$$

where ω = reinforcement index = $A_s/bd \times f_y/f_c'$.

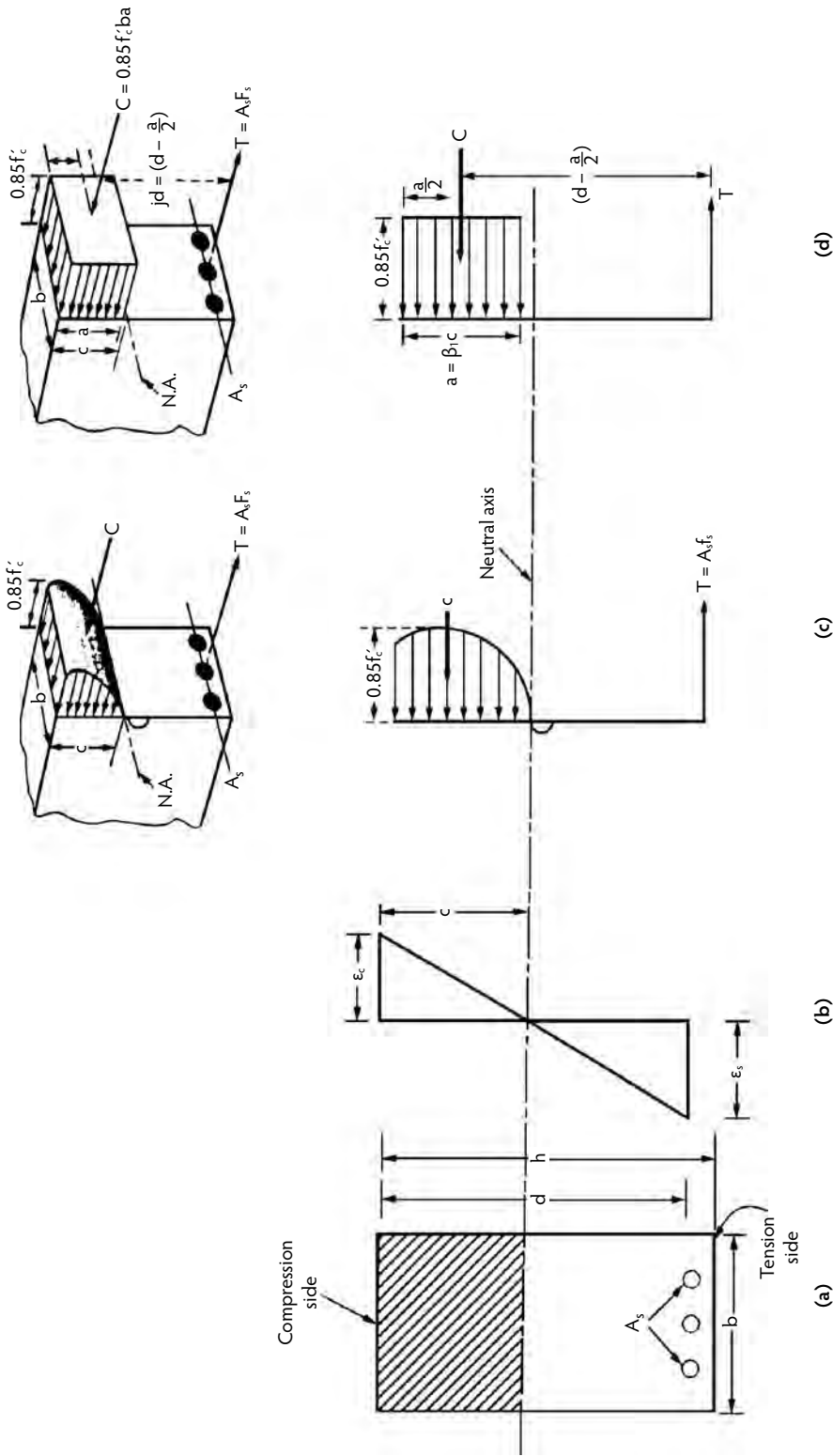


FIGURE 36.7 Stress and strain distribution across beam depth: (a) beam cross-section; (b) strain across depth; (c) actual stress block; and (d) assumed equivalent stress block.

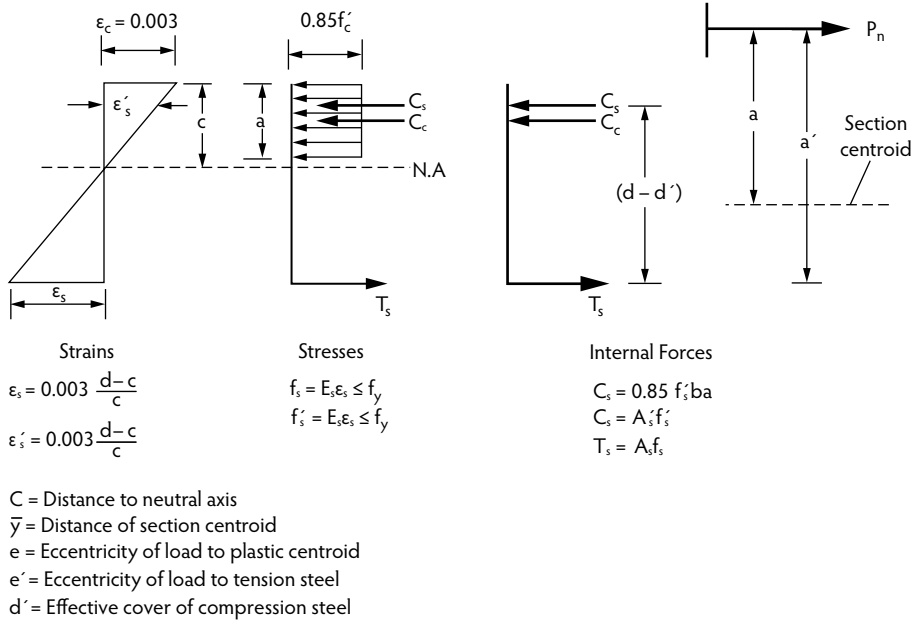


FIGURE 36.8 Stress-strain distribution across depth of compression member.

The balanced strain-state reinforcement ratio ρ_b for simultaneous yielding of the reinforcement at the tension side and crushing of the concrete at the compressions side can be obtained from the following expression:

$$\rho_b = 0.85\beta_1 \frac{f'_c}{f_y} \left(\frac{\epsilon_u}{\epsilon_u + 0.004} \right) \quad (36.18a)$$

where $\beta_1 = 0.85$ and reduces at the rate of 0.05 per 1000 psi in excess of 4000 psi, namely:

$$\beta_1 = 0.85 - 0.05 \left(\frac{f'_c - 1000}{1000} \right) \quad (36.18b)$$

with a minimum β_1 value of 0.65.

36.3.2.2 Doubly Reinforced Beams

For doubly reinforced sections that have compression steel that yielded:

$$M_n = (A_s - A'_s) f_y \left(d - \frac{a}{2} \right) + A'_s f_y (d - d') \quad (36.19)$$

If compressive reinforcement is used in a doubly reinforced section as in Figure 36.8 for compression members, the depth of the compressive block is:

$$a = \frac{A_s f_y - A'_s f'_s}{0.85 f'_c b} \quad (36.20)$$

where b is the width of the section at the compression side, and f'_s is the stress in the compression.

36.3.2.3 Flanged Sections

For flanged sections where the neutral axis falls outside the flange:

$$M_n = (A_s - A_{sf})f_y \left(d - \frac{a}{2} \right) + A_{sf}f_y \left(d - \frac{h_f}{2} \right) \quad (36.21)$$

where:

$$A_{sf} = [0.85f'_c(b - b_w)h_f]/f_y$$

b_w = web width.

h_f = flange thickness.

The depth is:

$$a = \frac{A_s f_y}{0.85 f'_c b} > h_f \quad (36.22)$$

$$\rho_f = 0.85 f'_c (b - b_w) \frac{h_f}{f_y b_w d}$$

36.3.2.4 Minimum Reinforcement

The flexural reinforcement percentage ρ has to have a minimum value of $\rho_{\min} = 3\sqrt{f'_c}/f_y$ for positive moment reinforcement, and $\rho_{\min} = 6\sqrt{f'_c}/f_y$ for negative moment reinforcement but always not less than $200/f_y$, where f_y is in units of pounds per square inch. The factored moment is:

$$M_u = \phi M_n \quad (36.23)$$

where $\phi = 0.90$ for flexure.

36.3.3 Shear Strength

External transverse load is resisted by internal shear to maintain section equilibrium. As concrete is weak in tension, the principal tensile stress in a beam cannot exceed the tensile strength of the concrete. The principal stress is composed of two components: shear stress and flexural stress. It is important that the beam web be reinforced to prevent diagonal shear cracks from opening. The resistance of the plain concrete in the web sustains part of the shear stress, and the balance has to be borne by the diagonal tension reinforcement. The shear resistance of the plain concrete is known as the *nominal shear strength*, or V_c :

$$V_c = 2.0\lambda\sqrt{f'_c}b_w d \text{ (lb)} \leq 3.5\lambda\sqrt{f'_c} \text{ (lb)} \quad (36.24a)$$

$$V_c = \left(\frac{\lambda\sqrt{f'_c}}{6} \right) b_w d \text{ (N)} \quad (36.24b)$$

or

$$V_c = \left[1.9\lambda\sqrt{f'_c} + 2500\rho_w \frac{V_u d}{M_u} \right] b_w d \text{ (lb)} \leq 3.5\lambda\sqrt{f'_c} \text{ (lb)} \quad (36.25a)$$

$$V_c = \left[\left(\lambda\sqrt{f'_c} + 120\rho_w \frac{V_u d}{M_u} \right) / 7 \right] b_w d \text{ (N)} \quad (36.25b)$$

Values for λ are given in Section 36.1.

$$\rho_w = \frac{A_s}{b_w d} \quad \text{and} \quad \frac{V_u d}{M_u} \leq 1.0$$

No web steel is needed if $V_u < 1/2 V_c$. For calculating V_n , the critical section is at a distance d from the support face. Spacing of the web stirrups is as follows:

$$s = \frac{A_v f_y d}{V_u / \phi - V_c} \quad (36.26)$$

where A_v is the cross-sectional area of web steel, and ϕ is 0.85 for shear and torsion. The transverse web steel is designed to carry the shear load $V_s = V_n - V_c$. The spacing of the stirrups is governed by the following:

$$V_s \geq 4\lambda\sqrt{f'_c} : s = \frac{d}{4}$$

$$V_s \leq 2\lambda\sqrt{f'_c} : s = \frac{d}{2}$$

$$V_s \geq 8\lambda\sqrt{f'_c} : \text{enlarge section}$$

The minimum sectional area of the stirrups is $A_{v,\min} = 50b_w s / f_y$; $s_{\max} = d/2$ where shear is to be considered; d is the effective depth to the center of the tensile reinforcement; and f_y is the yield strength of the steel (lb/in.²).

36.3.4 Strut-and-Tie Theory and Design of Corbels and Deep Beams

36.3.4.1 Strut-and-Tie Mechanism

As an alternative to the usual approach where plane sections before bending are considered to remain plane after bending, the strut-and-tie model is applied effectively in regions of discontinuity. These regions could be the support sections in a beam, the zones of load application, or the discontinuity caused by abrupt changes in section, such as brackets, beam daps, pile caps cast with column sections, portal frames, and others. Consequently, structural elements can be divided into segments called *B-regions*, where the standard beam theory applies with the assumption of linear strains, and *D-regions*, where the plane sections hypothesis is no longer applicable.

The analysis essentially follows the truss analogy approach, where parallel **inclined cracks** are assumed and expected to form in the regions of high shear. The concrete between the inclined cracks carries inclined compressive forces acting as diagonal compressive struts. The provision of transverse stirrups along the beam span results in a truss-like action where the longitudinal steel provides the tension chord of the truss as a tie, hence the “strut-and-tie” expression. Depending on the interpretation of the designer, simplifications of the paths of forces that are chosen to represent the real structure can considerably differ; consequently, this approach is more an art than an engineering science in the selection of the models, and significant over-design and serviceability checks become necessary. For equilibrium, at least three forces have to act at a joint, termed the *node*. Figure 36.9 demonstrates the simplified truss model for simply supported deep beams loaded on the top fibers, and Figure 36.10 shows a continuous beam model, as presented in the ACI 318 Code, both outlining the compression struts, the tension ties, and the nodes at the D regions which are the points of load application, discontinuity, and the support regions. Naturally, other possible alternative models can also be used, provided that they satisfy equilibrium and compatibility.

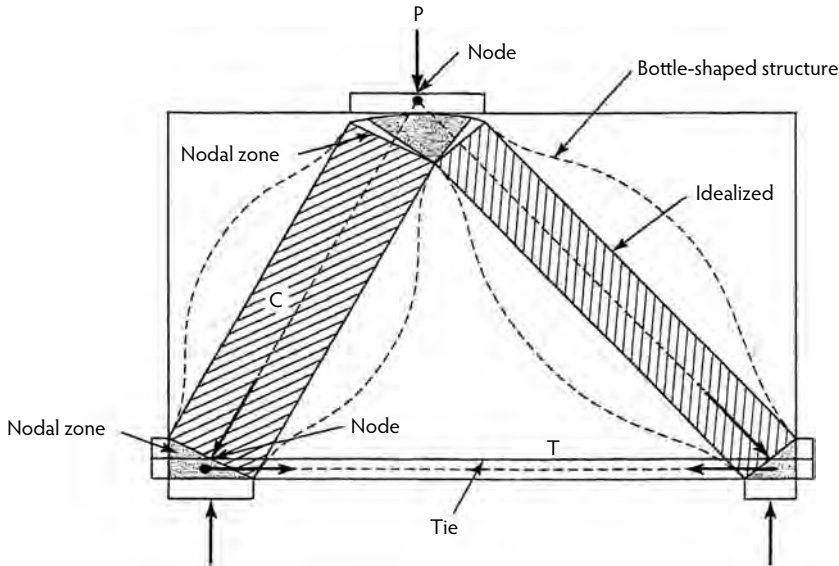


FIGURE 36.9 Strut-and-tie model of simply supported deep beam subjected to concentrated load on top. (From ACI Committee 318, *Building Code Requirements for Structural Concrete*, ACI 318; *Commentary*. ACI 318R-08, American Concrete Institute, Farmington Hills, MI, 2008.)

36.3.4.2 ACI Design Requirements by the Strut-and-Tie Method

Nodal Forces:

$$\phi F_n \geq F_u \quad (36.27)$$

where:

F_n = nominal strength of a strut, tie, or nodal zone (lb).

F_u = factored force acting on a strut, tie, bearing area, or nodal zone (lb).

ϕ = for both struts and ties (similar to the strength reduction for shear).

Strength of Struts

$$F_{ns} = f_{ce} A_{cs} \quad (36.28)$$

where:

F_{ns} = nominal strength of strut (lb).

A_{cs} = effective cross-sectional area at one end of a strut, taken perpendicular to the axis of the strut (in.²).

f_{ce} = effective compressive strength of the concrete in a strut or nodal zone (psi).

$$f_{ce} = 0.85\beta f'_c \quad (36.29)$$

where:

β = 1.0 for struts that have the same cross-sectional area of the midstrut cross-section in the case of bubble struts.

β = 0.75 for struts with reinforcement resisting transverse tensile forces.

β = 0.40 for struts in tension members or tension flanges.

β = 0.60 all other cases.

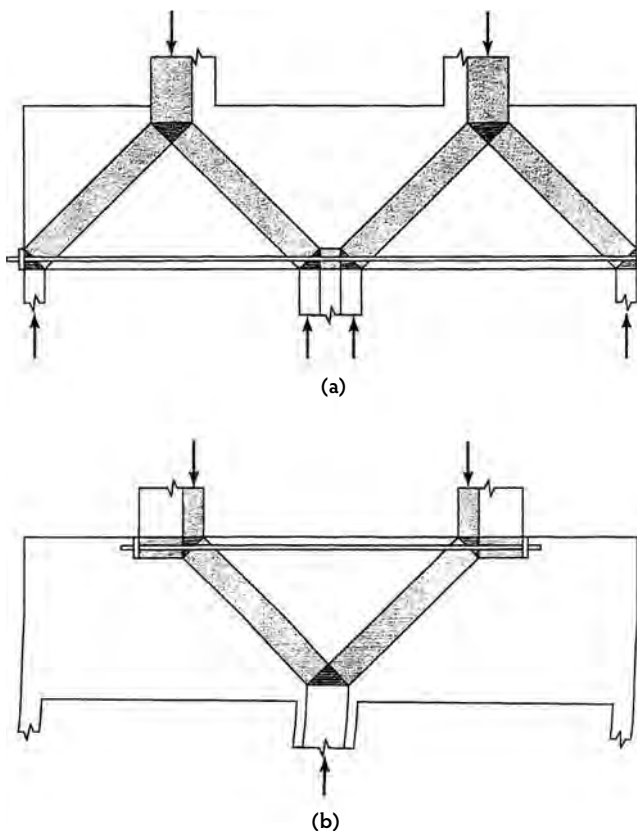


FIGURE 36.10 Typical strut-and-tie model of continuous deep beam subjected to concentrated load on top. (From ACI Committee 318, *Building Code Requirements for Structural Concrete*, ACI 318; *Commentary*. ACI 318R-08, American Concrete Institute, Farmington Hills, MI, 2008.)

Longitudinal Reinforcement

$$F_{ns} = f_{ce}A_{cs} + A'_s f'_s \quad (36.30)$$

where:

A'_s = area of compression reinforcement in a strut (in.²).

f'_c = stress in compression reinforcement (in.²).

Strength of Ties

$$F_{nt} A_{st} f_y + A_{ps} (f_{pe} + \Delta f_{ps}) \quad (36.31)$$

where:

F_{nt} = nominal strength of tie (lb).

A_{st} = area of non-prestressed reinforcement in a tie (in.²).

A_{ps} = area of prestressing reinforcement (in.²).

f_{pe} = effective stress after losses in prestressing reinforcement.

Δf_{ps} = increase in prestressing stress beyond the service load level.

$f_{pe} + \Delta f_{ps}$ should not exceed f_{py} .

When no prestressing reinforcement is used, $A_{ps} = 0$ in Equation 36.31.

$$h_{t,\max} = F_{nt} / f_{ce} \quad (36.32)$$

where $h_{t,\max}$ is the maximum effective height of concrete concentric with the tie, used to dimension the nodal zone (in.). If the bars in the tie are in one layer, the effective height of the tie can be taken as the diameter of the bars in the tie plus twice the cover to the surface of the bars. The reinforcement in the ties has to be anchored by hooks, mechanical anchorages, post-tensioning anchors, or straight bars, all with full development length.

Strength of Nodal Zones

$$F_{nm} = f_{ce} A_n \quad (36.33)$$

where:

F_{nm} = nominal strength of a face of a nodal zone (lb).

A_n = area of the face of a nodal zone or a section through a nodal zone (in.²).

It can be assumed that the principal stresses in the struts and ties act parallel to the axes of the struts and ties. Under such a condition, the stresses on faces perpendicular to these axes are principal stresses.

Confinement in the Nodal Zone

The ACI 318 Code stipulates that, unless confining reinforcement is provided within the nodal zone and its effect is supported by analysis and experimentation, the computed compressive stress on a face of a nodal zone due to the strut and tie forces should not exceed the values given by Equation 36.34:

$$f_{ce} = 0.85 \beta_n f'_c \quad (36.34)$$

where:

$\beta_n = 1.0$ in nodal zones bounded by struts or bearing stresses.

$\beta_n = 0.8$ in nodal zones anchoring one tie.

$\beta_n = 0.6$ in nodal zones anchoring two or more ties.

For detailed design examples, refer to Nawy (2008).

36.3.4.3 Design Example of a Corbel by the Strut-and-Tie Method

Design a corbel to support a factored vertical load $V_u = 80,000$ lb (160 kN) acting at a distance $a_v = 5$ in. (127 mm) from the face of the column. It has width $b = 10$ in. (254 mm), total depth $h = 18$ in. (457 mm), and an effective depth $d = 14$ in. (356 mm) (Nawy, 2008). Given:

$f'_c = 5000$ psi (34.5 MPa) for normal weight concrete.

$f_y = f_{yt} = 60,000$ psi (414 MPa).

The supporting column size is 12×14 in. Assume the corbel is to be monolithically cast with the column, and neglect the weight of the corbel in the computations.

Solution

1. Assume that the corbel is monolithically cast with the column. Total depth $h = 18$ in. and effective depth $d = 14$ in. are based on the requirement that the vertical dimension of the corbel outside the bearing area must be at least one half the column face width of 14 in. (column size, 12×14 in.). Select a simple strut-and-tie model as shown in Figure 36.11, assuming that the center of tie AB is located at a distance of 4 in. below the top extreme corbel fibers, using one layer of reinforcing bars. Also assume that horizontal tie DG lies on a horizontal line passing at the re-entrant corner C of the corbel. The solid lines in Figure 36.11 denote tension tie action (T), and the dashed lines denote compression strut action (C). The nodal points A, B, C, and D result from the selected strut-and-tie model. Note that the entire corbel is a D-region structure because of the existing statics discontinuities in the geometry of the corbel and the vertical and horizontal loads.

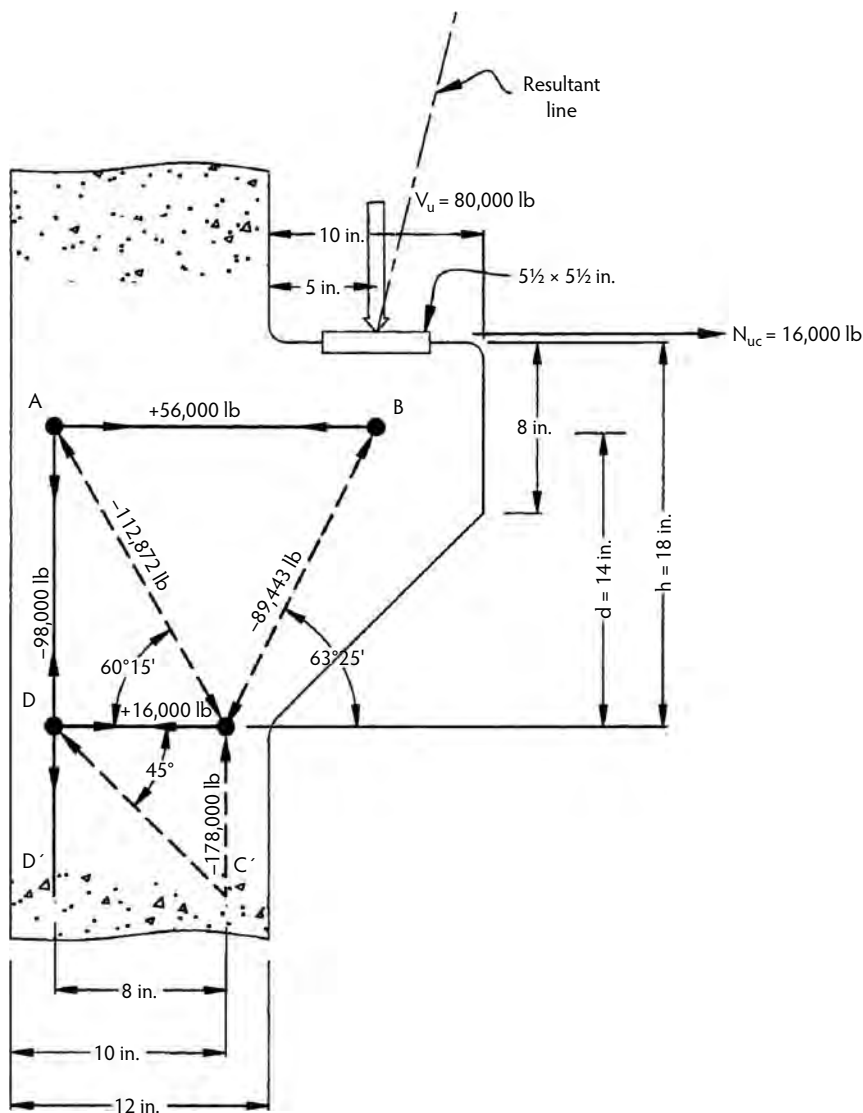


FIGURE 36.11 Strut and tie forced in corbel design example. (From Nawy, E.G., *Prestressed Concrete: A Fundamental Approach*, 5th ed., Prentice Hall, Upper Saddle River, NJ, 2006.)

- The strut and tie truss forces are $N_{uc} = 0.20$ and $V_u = 16,000$ lb. The following are the truss member forces calculated from statics in Figure 36.11.

Compression strut BC:

$$\text{Length } BC = \sqrt{(7)^2 + (14)^2} = 15.652 \text{ in.}$$

$$F_{BC} = 80,000 \times \frac{15.652}{14} = 89,443 \text{ lb}$$

Tension tie BA:

$$F_{BA} = 80,000 \times \frac{7}{14} + 16,000 = 56,000 \text{ lb}$$

Compression strut AC:

$$F_{AC} = \frac{56,000\sqrt{(8)^2 + (14)^2}}{8} = 112,872 \text{ lb}$$

Tension tie AD:

$$F_{AD} = \frac{112,872 \times 14}{\sqrt{(8)^2 + (14)^2}} = 98,000 \text{ lb}$$

Compression strut CC':

$$F_{CC'} = 80,000 + 98,000 = 178,000 \text{ lb.}$$

Tension tie CD:

$$F_{CD} = 56,000 - 40,000 = 16,000 \text{ lb}$$

Steel bearing plate design:

$f_{ce} = \phi(0.85f'_c)$, where $\phi = 0.75$ for bearing in strut-and-tie models.

$$\text{Area of plate is } A_1 = \frac{80,000}{0.75(0.85f'_c)} = \frac{80,000}{0.75 \times 0.85 \times 5000} = 25.10 \text{ in.}^2$$

Use a 5-1/2 × 5-1/2-in. plate and select a thickness to produce a rigid plate.

Tie reinforcement design:

$$A_{ts,AB} = \frac{56,000}{\phi f_y} = \frac{56,000}{0.75 \times 60,000} = 1.25 \text{ in.}^2$$

Use three #6 bars = 1.32 in.² or, conservatively, three #7 bars = 1.80 in.² These top bars in one layer have to be fully developed along the longitudinal column reinforcement:

$$A_{ts,CD} = \frac{16,000}{0.75 \times 60,000} = 0.36 \text{ in.}^2$$

Use two #6 tie bars = 0.88 in.² to form part of the cage shown in Figure 36.12.

Horizontal reinforcement A_h for crack control of shear cracks:

$$A_h = 0.50(A_{sc} - A_n)$$

where A_n is the reinforcement resisting the frictional force N_{ue} .

$$A_n = \frac{N_{ue}}{\phi f_y} = \frac{16,000}{0.75 \times 60,000} = 0.36 \text{ in.}^2$$

Hence, $A_h = 0.50(1.25 - 0.36) = 0.45 \text{ in.}^2$. Three #3 closed ties, evenly spaced vertically as shown in Figure 36.12, give $A_h = 3(2 \times 0.11) = 0.66 \text{ in.}^2 > 0.45 \text{ in.}^2$. Because $\beta_s = 0.75$ is used for calculating the effective concrete compressive strength in the struts in the following section, where $f_{cu} = 0.85\beta_s f'_c$, the minimum reinforcement provided also has to satisfy:

$$\sum \frac{A_h / \text{tie}}{bs_t} \sin \gamma_t \geq 0.003 = \frac{2(0.11)}{14 \times 3.0} \sin 60^\circ 15' = 0.0045 > 0.003$$

Hence, adopt three #3 closed ties at 3.0-in. center-to-center spacing.

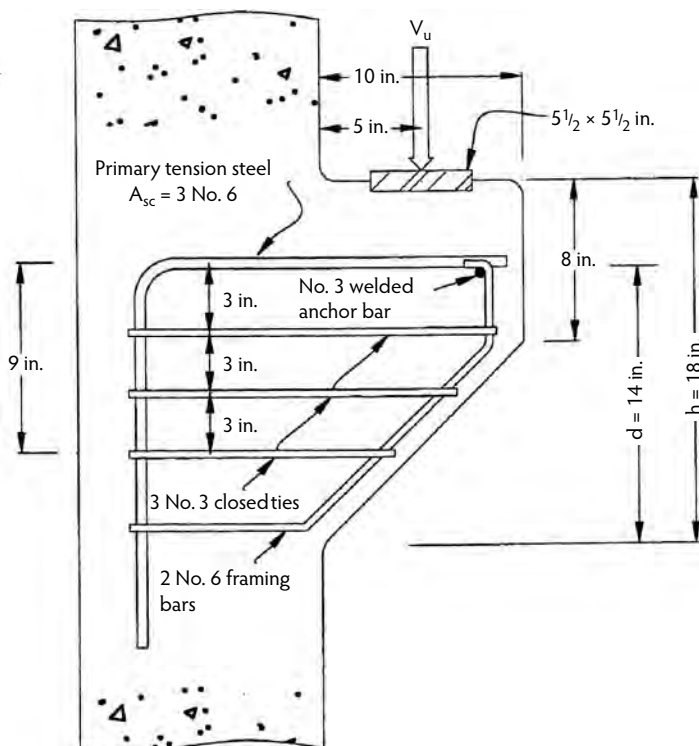


FIGURE 36.12 Corbel shear reinforcement details. (From Nawy, E.G., *Prestressed Concrete: A Fundamental Approach*, 5th ed., Prentice Hall, Upper Saddle River, NJ, 2006.)

Strut capacity evaluation:

Strut CC' —The width (w_s) of nodal zone C has to satisfy the allowable stress limit on the nodal zones, namely node B below the bearing plate and node C in the re-entrant corner to the column. Both nodes are considered unconfined.

$$F_{uCC'} \text{ for } \left(10 - \frac{w_s}{2}\right) = 80^k(5+10) + 16 \times 18 \text{ to give } \frac{w_s}{2} = 1.64 \text{ in.}$$

hence, strut width $w_s = 3.28$ in. fits within the available concrete dimension about the strut center line.

Strut BC —Nominal strength is limited to $F_{ns} = f_{ce}A_{cs}$, where $f_{ce} = 0.85\beta_s f'_c$; thus, $f_{ce} = 0.85 \times 0.75 \times 5000 = 3188$ psi = 3.188 ksi. A_{cs} is the smaller strut cross-sectional area at the two ends of the strut, namely at node C, while at node B, the node width can be assumed equal to the steel plate width of 5.50 in. A_c at node C = $14 \times 3.28 = 45.92$ in.². Available factored $F_{us,C} = \phi F_{ns,C} = 0.75 \times 3.188 \times 45.92 = 109.8$ kip, which is greater than the required $F_{BC} = 89.4$ kip.

Strut AC

$$\text{Required width } (w_s) \text{ of strut } A_c = \frac{F_{u,AC}}{\phi f_{cu} b} = \frac{112.87 \text{ kip}}{0.75 \times 3.188 \times 14} = 3.37 \text{ in.}$$

Examination of the corbel and the column depth of 12 in. suggest a minimum clear cover of 2.0 in. from the outer concrete surface; hence, the widths (w_s) of all struts fit within the corbel geometry. Adopt the design as shown in Figure 36.12.

36.3.5 Torsional Strength

The space truss analogy theory is used for the analysis and design of concrete members subjected to torsion. It is based on the shear flow in a hollow tube concept and the summation of the forces in the space truss elements (ACI Committee 318, 2008; Hsu, 1993; Nawy, 2002, 2006, 2008). ACI 318 stipulates disregarding the concrete nominal strength T_c in torsion and assigning all the torque to the longitudinal reinforcement (A_ℓ) and the transverse reinforcement (A_t), essentially assuming that the volume of the longitudinal bars is equivalent to the volume of the closed transverse hoops or stirrups. The critical section is taken at a distance d from the face of the support for the purpose of calculating torque T_u . Sections that are subjected to combined torsion and shear should be designed for torsion if the factored torsional moment (T_u) exceeds the following value for nonprestressed members:

$$T_u > \phi \lambda \sqrt{f'_c} \left(\frac{A_{cp}^2}{p_{cp}} \right) \quad (36.35)$$

where:

A_{cp} = area enclosed by the outside perimeter of the concrete cross-section.

p_{cp} = outside perimeter of the cross-section (A_{cp}) (in.).

Two types of torsion are considered: (1) *equilibrium torsion*, where no redistribution of torsional moment is possible—in this case, all the factored torsional moment is designed for; and (2) *compatibility torsion*, where redistribution of the torsional moment occurs in a continuous floor system—in this case, the maximum torsional moment to be provided for is:

$$T_u = \phi 4 \lambda \sqrt{f'_c} \left(\frac{A_{cp}^2}{p_{cp}} \right) \quad (36.36)$$

The concrete section has to be enlarged if:

$$\sqrt{\left(\frac{V_u}{b_w d} \right)^2 + \left(\frac{T_u p_h}{1.7 A_{oh}} \right)^2} \geq \phi \left(\frac{V_c}{b_w d} \right) + 8 \lambda \sqrt{f'_c} \quad (36.37)$$

where:

p_h = perimeter of centerline of outermost closed transverse torsional reinforcement (in.).

A_{oh} = area enclosed by centerline of the outermost closed transverse torsional reinforcement (in.²).

The transverse torsional reinforcement should be chosen with such size and spacing s that:

$$\frac{A_t}{2} = \frac{T_n}{2 A_o f_y \cot \theta} \quad (36.38)$$

where:

A_o = gross area enclosed by the shear path = $0.85 A_{oh}$.

θ = angle of compression diagonals (45° in reinforced concrete, 37.5° in prestressed concrete).

The longitudinal torsional reinforcement (A_ℓ) divided equally along the four faces of the beam is:

$$A_t = \frac{A_t}{s} p_h \left(\frac{f_{yv}}{f_{y\ell}} \right) \cot^2 \theta \quad (36.39)$$

$$A_{\ell, \min} = \frac{5 \sqrt{f'_c} A_{cp}}{f_{y\ell}} - \left(\frac{A_t}{s} \right) p_h \frac{f_{yv}}{f_{y\ell}} \quad (36.40)$$

where:

f_{yv} = yield strength of the transverse reinforcement.

$f_{y\ell}$ = yield strength of the longitudinal reinforcement.

The minimum area of transverse reinforcement is:

$$A_v + 2A_t \geq \frac{50b_ws}{f_y} \quad (36.41)$$

Maximum s is 12 in.

In SI units, the following are equivalent expressions:

Equation 36.35:

$$T_u = \frac{\phi\lambda\sqrt{f'_c}}{12} \left(\frac{A_{cp}^2}{P_{cp}} \right)$$

Equation 36.36:

$$T_u = \frac{\phi\lambda\sqrt{f'_c}}{3} \left(\frac{A_{cp}^2}{P_{cp}} \right)$$

For Equation 36.37, the right-hand expression is:

$$\phi \left(\frac{V_c}{b_w d} \right) + \left(\frac{8\lambda\sqrt{f'_c}}{12} \right) \text{ MPa}$$

For Equation 36.40:

$$A_{\ell, \min} = \frac{5\sqrt{f'_c}A_{cp}}{12f_{y\ell}} - \left(\frac{A_t}{s} \right) p_h \left(\frac{f_{yv}}{f_{y\ell}} \right)$$

For Equation 36.41:

$$A_v + 2A_t \geq \frac{0.35b_ws}{f_y}$$

where f_y is in megapascals. Maximum s is 300 mm.

36.3.6 Compression Members: Columns

36.3.6.1 Nonslender Columns

Columns normally fall within the *compression-controlled* zone of Figure 36.6—namely, in the strain limit condition of $\epsilon_t = 0.002$ or less at the extreme tension steel reinforcement level. The three modes of failure at the ultimate load state in columns can be summarized as follows:

- Tension-controlled state, by the initial yielding of the reinforcement at the tension side at $c/d_t = 0.375$
- Transition state denoted by the initial yielding of the reinforcement at the tension side but with a strain ϵ_t less than 0.005 but greater than the balancing strain $\epsilon_t = 0.002$ for Grade 60 steel, or $\epsilon_t = f_y/E_s$ for other reinforcement grades
- Compression-controlled state by initial crushing of the concrete at the compression face, where the *balanced strain* state occurs when failure develops simultaneously in tension and compression, a condition defined by the strain state $\epsilon_t = \epsilon_y$ at the tension reinforcement at a strain level $\epsilon_t = 0.002$ or less for Grade 60 steel

If P_{nb} is the axial load corresponding to the balanced limit strain condition—namely, when concrete at the compression face crushes simultaneously with the yielding of the extreme reinforcement at the tension face, then the modes of failure at ultimate load can also be defined as follows, where e_b is the eccentricity of the load at the balanced strain condition:

$$P_n < P_{nb}, \text{ tension failure } (e > e_b)$$

$$P_n = P_{nb}, \text{ balanced failure } (e = e_b)$$

$$P_n > P_{nb}, \text{ compression failure } (e < e_b)$$

In all of these cases, the strain-compatibility relationship must be maintained at all times through computation of the strain ϵ_s' in the compression side reinforcement on the basis of linearity of distribution of strain across the concrete section depth. It should be noted that, for each limit strain case, there are unique values of nominal thrust P_n and nominal moment M_n . Consequently, a unique eccentricity $e = M_n/P_n$ can be determined for each case. The expressions for load and moment for the balanced strain condition are:

$$P_{nb} = 0.85f_c b a_b + A_s' f_s' - A_s' f_y' \quad (36.42)$$

$$M_{nb} = P_{nb} e_b = 0.85f_c b a_b \left(y - \frac{a_b}{2} \right) + A_s' f_s' (y - d') + A_s f_y (d - y) \quad (36.43)$$

where:

$$f_s' = E_s \left[\frac{0.003(c - d')}{c} \right] \leq f_y \quad (36.44)$$

The force P_n and the moment M_n at the ultimate for any other eccentricity level are:

$$P_n = 0.85f_c b a + A_s' f_s' - A_s f_y \quad (36.45)$$

$$M_n = P_n e = 0.85f_c b a \left(\bar{y} - \frac{a}{2} \right) + A_s' f_s' (\bar{y} - d') + A_s f_y (d - \bar{y}) \quad (36.46)$$

where:

$$f_s = E_s \left[\frac{0.003(d - c)}{c} \right] \leq f_y \quad (36.47)$$

and

$\frac{c}{\bar{y}}$ = depth to the neutral axis.

\bar{y} = distance from the compression extreme fibers to the center of gravity of the section.

a = depth of the equivalent rectangular block = $\beta_1 c$, where β_1 is defined in Equation 36.18b.

The geometry of the compression member section and the forces acting on the section are shown in Figure 36.7. Equation 36.45 and Equation 36.46 are obtained from the equilibrium of forces and moments.

36.3.6.2 Slender Columns

If the compression member is slender—namely, the slenderness ratio kl_u/r exceeds 22 for unbraced members and $(34 - 12 \times M_1/M_2)$ for braced members—then failure will occur by buckling and not by material failure. In such a case, if kl_u/r is less than 100, then a first-order analysis such as the moment magnification method can be performed. If $kl_u/r > 100$, then the $P - \Delta$ effects have to be considered and a second-order analysis has to be performed. The latter is a lengthy process and is more reasonably executed using readily available computer programs.

Moment Magnification Solution ($kl_u/r < 100$)

The larger moment M_2 is magnified such that:

$$M_c = \delta_{ns} M_2 \quad (36.48)$$

where δ_{ns} is the magnification factor. The column is then designed for a moment M_c as a nonslender column. The subscript ns is non-sidesway; s is sidesway:

$$\delta_{ns} = \frac{C_m}{1 - (P_u / 0.75P_c)} \geq 1.0 \quad (36.49)$$

$$P_c = \frac{\pi^2 EI}{(k\ell_u)^2} \quad (36.50)$$

EI should be taken as:

$$EI = \frac{0.2E_c I_g + E_s I_{se}}{1 + \beta_d} \quad (36.51)$$

or

$$EI = \frac{0.4E_c I_g}{1 + \beta_d} \quad (36.52)$$

$$C_m = 0.6 + 0.4 \frac{M_1}{M_2} \geq 0.4 \quad (36.53)$$

If there is side-sway,

$$C_m = 0.6 + 0.4 \frac{M_1}{M_2} \geq 0.4 \quad (36.54a)$$

$$M_2 = M_{2ns} + \delta_s M_{2s} \quad (36.54b)$$

where:

$$\delta_s M_s = \frac{M_s}{1 - \frac{\Sigma P_u}{0.75P_c}} \geq M_s \quad (36.55a)$$

$$\delta_s M_s = \frac{M_s}{1 - Q} \geq M_s \quad (36.55b)$$

where:

$$\text{Stability index } Q = \frac{\Sigma P_u \Delta_o}{V_{us} l_c} \leq 0.05 \quad (36.55c)$$

and

Δ_o = first-order relative lateral deflection between the top and bottom of that story due to factored horizontal total shear (V_{uc}) of that story.

l_c = length of compression member.

The non-sway moment M_{2ns} is unmagnified, provided that the maximum moment is along the column height and not at its ends; otherwise, its value has to be multiplied by the non-sway magnifier δ_{ns} . If the stability index exceeds a value of 0.05, a second-order analysis becomes necessary. Effective length factor k when there is single curvature can be obtained from Figure 36.13a. For double curvature, length factor k can be obtained from Figure 36.13b. Discussion of the P-delta effect and the second-order analysis is given in Nawy, (2008).

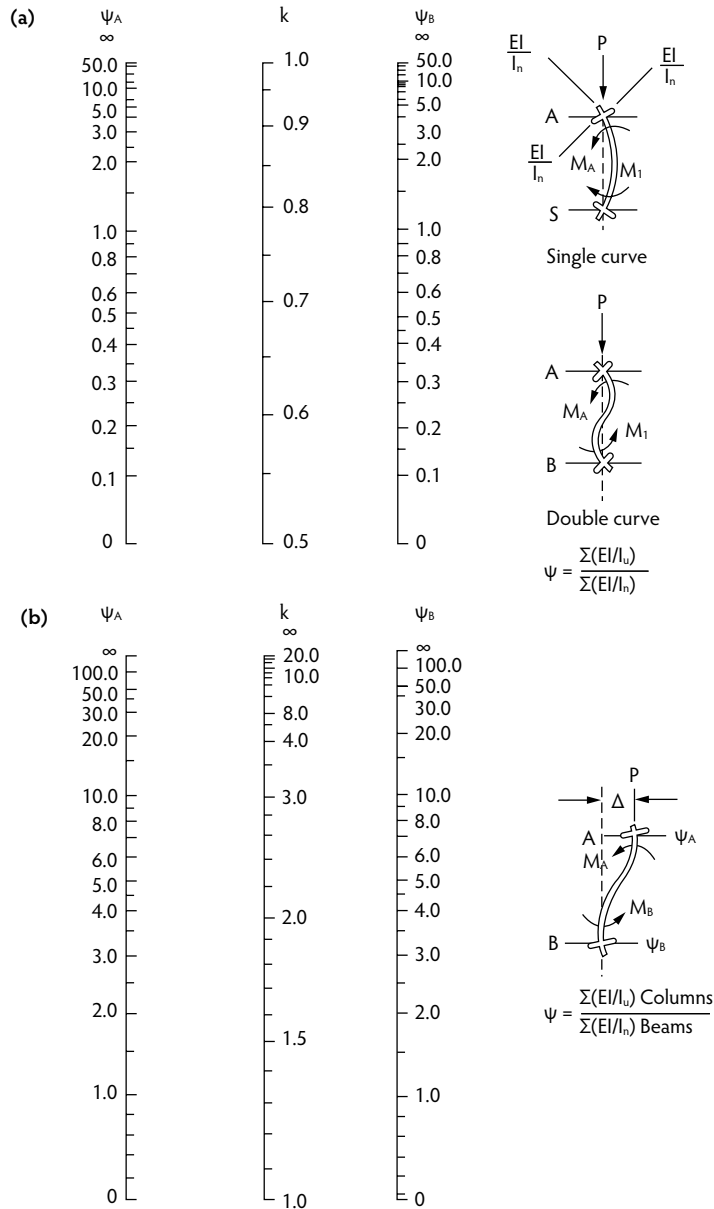


FIGURE 36.13 Slender columns end effect factor k : (a) nonsway frames; (b) sway frames. (From ACI Committee 318, *Building Code Requirements for Structural Concrete*, ACI 318-08; *Commentary*. ACI 318R-08, American Concrete Institute, Farmington Hills, MI, 2008.)

36.3.7 Two-Way Slabs and Plates

Methods for designing two-way concrete slabs and plates include:

- ACI direct design method
- ACI equivalent frame method where effects of lateral loads can be considered
- Yield line theory
- Strip method
- Elastic solutions

TABLE 36.3 Minimum Thickness of Slabs without Interior Beams, $\alpha_m = 0$

Yield Strength (f_y) (psi)	Without Drop Panels			With Drop Panels		
	Exterior Panels		Interior Panels	Exterior Panels		Interior Panels
	Without Edge Beams	With Edge Beams		Without Edge Beams	With Edge Beams	
40,000	$\ell_n/33$	$\ell_n/36$	$\ell_n/36$	$\ell_n/36$	$\ell_n/40$	$\ell_n/40$
60,000	$\ell_n/30$	$\ell_n/33$	$\ell_n/33$	$\ell_n/33$	$\ell_n/36$	$\ell_n/36$
75,000	$\ell_n/28$	$\ell_n/31$	$\ell_n/31$	$\ell_n/31$	$\ell_n/34$	$\ell_n/34$

Note: ℓ_n = effective span.

The subject is too extensive to cover in this overview; however, the important concept of serviceability as controlled by deflection and cracking limitation is briefly presented.

36.3.7.1 Deflection Control

The thickness of two-way slabs for deflection control should be determined as follows:

Flat Plate

Use Table 36.3.

Slab on Beams

If $\alpha_m \leq 0.2$, use:

$$\alpha_m > 0.2 < 2.0, \quad h \geq \frac{\ell_n (0.8 + f_y / 200,000)}{36 + 5\beta (\alpha_m - 0.2)} \quad (36.56)$$

but slab or plate thickness cannot be less than 5.0 in., so:

$$\alpha_m > 2.0, \quad \frac{(\ell_n 0.8 + f_y / 200,000)}{36 + 9\beta} \quad (36.57)$$

where:

α_m = average value of α for all beams on edges of a panel.

α = (flexural stiffness of beam section)/(flexural thickness of slab width bounded laterally by the center line of the adjacent panels on each side of the beam).

β = aspect ratio (long span/short span).

36.3.7.2 Crack Control

For crack control in two-way slabs and plates, the maximum computed weighted crack width due to flexural load (ACI Committee 224, 2001; Nawy, 2008) is as follows, where the parameter under the radical is the grid index (G_I):

$$w_{\max} \text{ (in.)} = k\beta f_s \sqrt{\frac{s_1 s_2 d_c}{d_b} \cdot \frac{8}{\pi}} \quad (36.58)$$

For w_{\max} (mm), multiply Equation 36.58 by 0.145 and use megapascals for f_s . Also,

k = fracture coefficient.

= 2.8×10^{-5} for a square uniformly loaded slab.

= 2.1×10^{-5} when the aspect ratio of short span/long span < 0.75 but > 0.5 , or for a concentrated load.

= 1.6×10^{-5} for aspect ratio less than 0.5.

β = $1.25 = (h - c)/(d - c)$, where c = depth to neutral axis.

f_s = $0.40f_y$ (kip/in²).

- h = total slab or plate thickness.
 s = spacing in direction 1 closest to the tensile extreme fibers (in.).
 s_2 = spacing in the perpendicular direction (in.).
 d_c = concrete cover to centroid of reinforcement (in.).
 d_b = diameter of the reinforcement in direction 1 closest to the concrete outer fibers (in.).

The tolerable crack widths in concrete elements are given in Table 36.1. In SI units, Equation 36.58 therefore becomes:

$$w_{\max} (\text{mm}) = 0.14k\beta f_s \sqrt{G_1}$$

where f_s is in megapascals, and s_1 , s_2 , d_c , and d_{b1} are in millimeters.

36.3.8 Development of Reinforcement

36.3.8.1 Development of Deformed Bars in Tension

The full development length (ℓ_d) for deformed bars or wires is obtained by applying multipliers to a basic theoretical development length (ℓ_{db}) in terms of the bar diameter (d_b) and other multipliers as follows:

$$\frac{\ell_d}{d_b} = \frac{3}{40} \frac{f_y}{\sqrt{f'_c}} \frac{\psi_l \psi_e \psi_s}{\left(\frac{c_b + K_{tr}}{d_b} \right)} \quad (36.59)$$

The value of $\sqrt{f'_c}$ should not exceed 100 psi (≤ 6.9 MPa) in all computations.

36.3.8.2 Modifying Multipliers of Development Length for Bars in Tension

- ψ_l = **bar location factor**. For horizontal reinforcement, when more than 12 in. of fresh concrete is below the development length or splice (top reinforcement), α is 1.3; for other reinforcement, α is 1.0.
- ψ_e = **coating factor**. For epoxy-coated bars or wires with cover less than $3d_b$ or clear spacing less than $3d_b$, β is 1.5; for all other epoxy-coated bars or wires, ψ_e is 1.2; for uncoated reinforcement ψ_e is 1.0. However, the product $\psi_l \psi_e$ should not exceed 1.7.
- ψ_s = **bar size factor**. For No. 6 and smaller bars and deformed wires (No. 20 and smaller, SI), γ is 0.8; for No. 7 and larger bars (No. 25 and larger, SI), γ is 1.0.
- c = **spacing or cover dimension** (in.). Use the smaller of either the distance from the center of the bar to the nearest concrete surface or one half the center-to-center spacing of the bars being developed.
- K_{tr} = **transverse reinforcement index**, which is equal to $(40A_{tr}/sn)$, where A_{tr} = total cross-sectional area of all transverse reinforcement within ℓ_d that crosses the potential plane of splitting adjacent to the reinforcement being developed (in.²). Also, f_{yt} = 60,000 psi is the strength value used in the development of the A_{tr} expression; s is the maximum spacing of transverse reinforcement within ℓ_d , center-to-center (in.) (mm); and n is the number of bars or wires being developed along the plane of splitting. The ACI 318 Code permits using K_{tr} as a conservative design simplification even if transverse reinforcement is present.
- λ = **lightweight-aggregate concrete factor**. When lightweight aggregate concrete is used λ is 0.75; however, when f_{ct} is specified, use $\lambda = 6.7 \sqrt{f'_c} / f_{ct}$. For all other concrete, λ is 1.0. The minimum development length in all cases is 12 in.
- λ_s = **excess reinforcement factor**. ACI 318 permits the reduction of ℓ_d if the longitudinal flexural reinforcement is in excess of that required by analysis except where anchorage or development for f_y is specifically required or the reinforcement is designed for seismic effects. The reduction multiplier $\lambda_s = (A_s \text{ required}) / (A_s \text{ provided})$ and $\lambda_{s2} = f_y / 60,000$ for cases where $f_y > 60,000$ psi. In lieu of using a refined computation for the development length of Equation 36.59, Table 36.4 can be utilized for typical construction practices by using a value of ψ_l and $\psi_e = 1.0$ and $f'_c = 4000$ psi.

TABLE 36.4a Simplified Development Length ℓ_d Equations

	#6 and Smaller Bars and Deformed Wires	#7 and Larger Bars
Clear spacing of bars being developed or spliced not less than d_b , clear cover not less than d_b , and stirrups or ties throughout ℓ_d not less than the Code minimum	$\frac{\ell_d}{d_b} = \frac{f_y \Psi_t \Psi_e}{25 \sqrt{f'_c}}$	$\frac{\ell_d}{d_b} = \frac{f_y \Psi_t \Psi_e}{20 \sqrt{f'_c}}$
or	when:	when:
Clear spacing of bars being developed or spliced not less than $2d_b$ and clear cover not less than d_b	$f'_c = 4000$ psi $\Psi_t, \Psi_e, \lambda, \lambda_s, \gamma = 1.0$ $\Psi_s = 0.8$ $\ell_d = 38d_b$	$f'_c = 4000$ psi $\Psi_t, \Psi_e, \Psi_s, \lambda, \lambda_s, \gamma = 1.0$ $\ell_d = (38/0.8)d_b = 48d_b$
Other cases	$\frac{\ell_d}{d_b} = \frac{3f_y \Psi_t \Psi_e}{50 \sqrt{f'_c}}$ $\ell_d = 57d_b$	$\frac{\ell_d}{d_b} = \frac{3f_y \Psi_t \Psi_e}{40 \sqrt{f'_c}}$ $\ell_d = 72d_b$

Note: This is a general table for usual construction conditions giving the required development length for deformed bars of sizes No. 3 to No. 18.

Source: Nawy, E.G., *Reinforced Concrete: A Fundamental Approach*, 6th ed., Prentice Hall, Upper Saddle River, NJ, 2008.

TABLE 36.4b SI Development Length Simplified Expressions

\leq No. 20	\geq No. 25
$\frac{\ell_d}{d_b} = \frac{f_y \Psi_t \Psi_e}{2 \sqrt{f'_c}}$	$\frac{\ell_d}{d_b} = \frac{5f_y \Psi_t \Psi_e}{8 \sqrt{f'_c}}$
$\frac{\ell_d}{d_b} = \frac{3f_y \Psi_t \Psi_e}{4 \sqrt{f'_c}}$	$\frac{\ell_d}{d_b} = \frac{15f_y \Psi_t \Psi_e}{16 \sqrt{f'_c}}$

Table 36.5 gives minimum development length ℓ_d (in.) in lieu of calculations using Table 36.4. In these two tables, the following assumptions are made: (1) The side cover is 1.5 in. on each side; (2) No. 3 stirrups are used for bars No. 11 or smaller; (3) No. 4 stirrups are used for bars No. 14 or No. 18; and (4) stirrups are bent around four bar diameters, so the distance from the centroid of the bar nearest the side face of the beam to the inside face of the No. 3 stirrup is taken as 0.75 in. for bars No. 11 or smaller and is equal to the longitudinal bar radius for No. 14 and No. 18 bars.

36.3.8.3 Development of Deformed Bars in Compression and the Modifying Multipliers

Bars in compression require shorter development length than bars in tension. This is due to the absence of the weakening effect of the tensile cracks; hence, the expression for the basic development length is:

$$\ell_{dc} = 0.02 \frac{d_b f_y}{\lambda_s \sqrt{f'_c}} \quad (36.60a)$$

$$\ell_{dc} = 0.0003 d_b f_y \quad (36.60b)$$

with the modifying multiplier for (1) excess reinforcement, $\lambda_s = (A_s \text{ required})/(A_s \text{ provided})$; and (2) spirally enclosed reinforcement, $\lambda_{s1} = 0.75$.

TABLE 36.5 Tension Reinforcement and Development Length

Bar Size	Cross-Sectional Area (in. ²)	Bar Diameter (in.)	Development Length (ℓ_d) ^{a,b} (in.)	
			$s \geq 2d_b$ or d_b and Clear Cover $\geq d_b$	Other
			$\leq \#6, \ell_d = 38d_b$ $\leq \#7, \ell_d = 48d_b$	$\leq \#6, \ell_d = 57d_b$ $\leq \#7, \ell_d = 72d_b$
3	0.11	0.375	15	21
4	0.20	0.500	19	29
5	0.31	0.625	24	36
6	0.44	0.750	29	43
7	0.60	0.875	42	63
8	0.79	1.000	48	72
9	1.00	1.128	54	81
10	1.27	1.270	61	92
11	1.56	1.410	68	102
14	2.25	1.693	82	122
18	4.00	2.257	108	163

^a For compression development length, ℓ_d multiplier $\times \ell_{db}$.

^b Multiply table values by $\alpha = 1.3$ for top reinforcement, $\lambda = 0.75$ for lightweight aggregate, $\psi_e = 1.5$ for epoxy-coated bars with cover less than $3d_b$ or clear spacing less than $6d_b$, and $\beta = 1.2$ for other epoxy-coated bars. Minimum ℓ_d for all cases is 12 in.

Note: For $f'_c = 4000$ psi normal weight concrete, $f_y = 60,000$ psi steel ($\psi_1, \psi_e, \lambda = 1.0$; $\gamma = 0.8$ for #6 bars or smaller and 1.0 for #7 bars and larger). For f'_c values different from 4000 psi, multiply table values by $(\sqrt{4000/f'_c})$. For $f_y = 40,000$ psi, multiply by 2/3. f' should not exceed 100.

Source: Nawy, E.G., *Reinforced Concrete: A Fundamental Approach*, 6th ed., Prentice Hall, Upper Saddle River, NJ, 2008.

36.3.8.4 Development of Bundled Bars in Tension and Compression

If bundled bars are used in tension or compression, l_d has to be increased by 20% for three-bar bundles and 33% for four-bar bundles, and f'_c should not be taken as greater than 100 psi. A unit of bundled bars is treated as a single bar of a diameter derived from the equivalent total area for the purpose of determining the modifying factors. Although the splice and development lengths of bundled bars are based on the diameter of individual bars increased by 20 or 33% as applicable, it is necessary to use an equivalent diameter of the entire bundle derived from the equivalent total area of bars when determining the factors that consider cover and clear spacing and represent the tendency of concrete to split.

36.3.8.5 SI/Metric Conversion

Where f_{yp} is in megapascals, Equation 36.59 becomes:

$$\frac{15f_y\psi_1\psi_e\psi_s}{16\sqrt{f'_c}\left(\frac{c_b + K_{tr}}{d_b}\right)} \quad \text{and} \quad K_{tr} = \frac{1.6A_{tr}}{sn}$$

36.3.8.6 Development of Welded Deformed Wire Fabric in Tension

The development length (l_d) for deformed welded wire fabric should be taken as the ℓ_d value obtained from Equation 36.59 or Table 36.4 multiplied by a fabric factor. The fabric factor, with at least one cross wire within the development length and not less than 2 in. from the point of the critical section, should be taken as the greater of the following two expressions:

$$(f_y - 35,000)/f_y \quad (36.61)$$

$$5d_b/s \quad (36.62)$$

but should not be taken as greater than 1.0. Here, s is the spacing of wire to be developed or spliced (in.).

36.4 Prestressed Concrete

36.4.1 General Principles

Reinforced concrete is weak in tension but strong in compression. To maximize the utilization of its material properties, an internal compressive force is induced on the structural element through the use of highly stressed prestressing tendons to precompress the member prior to application of the external gravity live load and superimposed dead load. A typical effect of the prestressing action shown in Figure 36.14 uses a straight tendon, as is usually the case for precast elements (Nawy, 2006). For cast-in-place elements, the tendon can be either harped, or, as is usually the case, it can be draped in a parabolic form. Figure 36.15 illustrates the stress and strain distributions across the beam depth and the forces acting on the section in a prestressed concrete beam and the compressive stress block of the section.

Stresses due to initial prestressing plus self-weight:

$$f^t = \frac{P_i}{A_c} \left(1 - \frac{ec_t}{r^2} \right) - \frac{M_D}{S^t} \quad (36.63a)$$

$$f_b = -\frac{P_i}{A_c} \left(1 + \frac{ec_b}{r^2} \right) + \frac{M_D}{S_b} \quad (36.63b)$$

Stresses at service load:

$$f^t = -\frac{P_e}{A_c} \left(1 - \frac{ec_t}{r^2} \right) - \frac{M_T}{S^t} \quad (36.64a)$$

$$f_b = -\frac{P_e}{A_c} \left(1 + \frac{ec_b}{r^2} \right) + \frac{M_T}{S_b} \quad (36.64b)$$

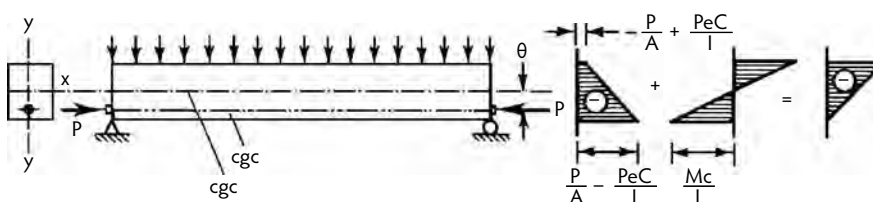


FIGURE 36.14 Stress distribution at service load in prestressed beam with constant tendon eccentricity. (From Nawy, E.G., *Prestressed Concrete: A Fundamental Approach*, 5th ed., Prentice Hall, Upper Saddle River, NJ, 2006.)

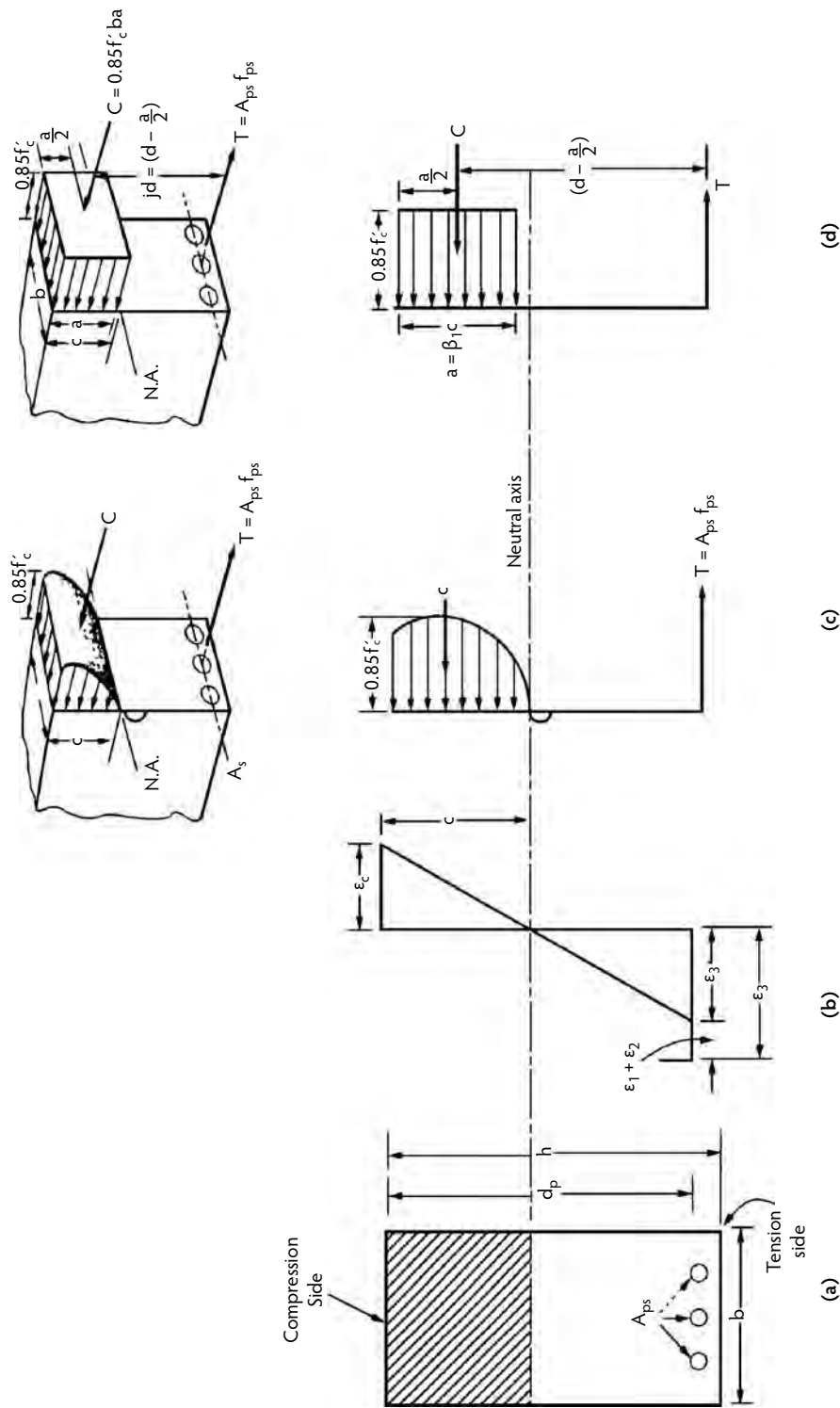


FIGURE 36.15 Stress and strain distribution across prestressed concrete beam depth: (a) beam cross-section; (b) strain across depth; (c) actual stress block; and (d) assumed equivalent block. (From Nawy, E.G., *Prestressed Concrete: A Fundamental Approach*, 5th ed., Prentice Hall, Upper Saddle River, NJ, 2006.)

36.4.2 Minimum Section Modulus for Variable Tendon Eccentricity

$$S^t \geq \frac{(1-\gamma)M_D + M_{SD} + M_L}{\gamma f_{ti} - \gamma f_c} \quad (36.65a)$$

$$S_b \geq \frac{(1-\gamma)M_D + M_{SD} + M_L}{\gamma f_t - \gamma f_{ci}} \quad (36.65b)$$

where:

- γ = percentage loss in prestress.
- M_D = self-weight moment.
- M_{SD} = superimposed dead load moment.
- M_L = live load moment.
- f_{ti} = initial tensile stress in concrete.
- f_c = service load concrete compressive strength.
- f_t = service load concrete tensile strength.
- f_{ci} = initial compressive stress in concrete.
- S^t = section modulus at top fibers (simple span).
- S_b = section modulus at bottom fibers (simple span).

36.4.3 Minimum Section Modulus for Constant Tendon Eccentricity

$$S^t \geq \frac{M_D + M_{SD} + M_L}{\gamma f_{ti} - f_c} \quad (36.66a)$$

$$S_b \geq \frac{M_D + M_{SD} + M_L}{f_t - \gamma f_{ci}} \quad (36.66b)$$

36.4.4 Maximum Allowable Stresses

36.4.4.1 ACI 318 Code Concrete Stresses

$$f'_{ci} \equiv 0.75 f'_c \text{ psi}$$

$$f_{ci} \equiv 0.60 f'_{ci} \text{ psi}$$

$$f_{ti} = \sqrt{f'_{ci}} \text{ psi on span } \left(\sqrt{f'_{ci}} / 4 \text{ MPa} \right) = \sqrt{f'_{ci}} \text{ psi on support } \left(\sqrt{f'_{ci}} / 2 \text{ MPa} \right)$$

$$f_c = 0.45 f'_c \text{ or } 0.60 f'_c \text{ where permitted by ACI 318.}$$

$$f_t = \sqrt{f'_c} \text{ psi } \left(\sqrt{f'_c} / 2 \text{ MPa} \right) = 12 \sqrt{f'_c} \text{ psi if deflection is verified } \left(\sqrt{f'_c} / 2 \text{ MPa} \right)$$

36.4.4.2 Reinforcing Tendon Stresses

Tendon jacking:

$$f_{ps} = 0.94 f_{py} \leq 0.80 f_{pu}$$

Immediately after prestress transfer:

$$f_{ps} = 0.82 f_{pj} \leq 0.74 f_{pu}$$

Post-tensioned members at anchorage immediately after tendon anchorage:

$$f_{ps} = 0.70f_{pu}$$

where:

f_{ps} = ultimate design stress allowed in tendon.

f_{py} = yield strength of tendon.

f_{pu} = ultimate strength of tendon.

A prestressed concrete section is designed for both the service load and the ultimate load. A typical distribution of stress at service load at midspan is shown in Figure 36.15. Expressions for the ultimate load evaluation are essentially similar to those of reinforced-concrete elements, taking into consideration that both prestressing tendons and mild steel bars are used. Note the similarity between Figure 36.15 and Figure 36.7. For extensive design and analysis details, refer to Nawy (2006).

36.5 Shear and Torsion in Prestressed Elements

36.5.1 Shear Strength: ACI Short Method When $f_{pe} > 0.40f_{pu}$

The nominal shear stress of the concrete in the web is:

$$V_c \text{ (lb)} = \left(0.60\lambda\sqrt{f'_c} + \frac{700V_u d}{M_u} \right) b_w d \quad (36.67a)$$

$$V_c \geq 2\lambda\sqrt{f'_c}b_w d \leq 5\lambda\sqrt{f'_c}b_w d, \quad \frac{V_u d}{M_u} \leq 1.0$$

$$V_c \text{ (Newton)} = \left(\frac{\lambda\sqrt{f'_c}}{20} + 5 \frac{V_u d}{M_u} \right) b_w d \quad (36.67b)$$

$$V_c \geq \frac{\lambda\sqrt{f'_c}}{6} b_w d \leq 0.40\lambda\sqrt{f'_c}b_w d, \quad \frac{V_u d}{M_u} \leq 1.0$$

36.5.2 Detailed Method

The smaller of the two values obtained from flexural shear (V_{ci}) or web shear (V_{cw}) in the following expressions has to be used in the design of the web reinforcement in prestressed concrete members.

36.5.2.1 Flexural Shear

$$V_{ci} \text{ (lb)} = 0.6\lambda\sqrt{f'_c}b_w d + V_d + \frac{V_i M_{cr}}{M_{\max}} \geq 1.7\lambda\sqrt{f'_c}b_w d \quad (36.68a)$$

where:

V_{ci} = flexural shear force.

$M_{cr} = M_{cr} = S_b \left(\lambda\sqrt{f'_c} + f_{ce} - f_d \right)$.

S_b = section modulus at the extreme tensile fibers.

V_d = shear force at section due to unfactored dead load.

V_i = factored shear force due to externally applied load.

f_{ce} = compressive stress in concrete due to effective prestress only at the tension face of the section.

f_d = stress due to unfactored dead load at extreme fibers in tension.

$$V_{ci} \text{ (Newton)} = \left(\frac{\lambda \sqrt{f'_c}}{20} \right) b_w d + V_d + \frac{V_i M_{cr}}{M_{\max}} \quad (36.68b)$$

36.5.2.2 Web Shear

V_{CW} = web shear force

$$V_{CW} \text{ (lb)} = \left(3.5 \lambda \sqrt{f'_c + \bar{f}_{ce}} \right) b_w d + V_p \quad (36.69)$$

$$V_{CW} \text{ (Newton)} = \left(0.3 \lambda \sqrt{f'_c + \bar{f}_{ce}} \right) b_w d + V_p$$

where:

\bar{f}_{ce} = compressive stress at center of gravity of section due to externally applied load.

V_p = vertical component of prestressing force.

The critical section for calculating V_u and T_u is taken at distance $(h/2)$ from the face of the support.

36.5.3 Minimum Shear Reinforcement

For prestressed members subjected to shear, the minimum transverse web stirrups are the smaller of:

$$A_v \text{ (in.}^2\text{)} = \frac{50 b_w s}{f_y} \quad (36.70a)$$

or

$$A_v \text{ (in.}^2\text{)} = \frac{A_{ps} f_{pu} s}{80 f_y d} \sqrt{\frac{d_p}{b_w}} \quad (36.70b)$$

where f_y is in psi and s is the web reinforcement spacing.

36.5.4 Torsional Strength

As discussed earlier, the nominal torsional strength (T_c) is disregarded, and all of the torque is assumed by longitudinal bars and the transverse closed hoops. The expressions used in the case of prestressed concrete elements are essentially the same as those for reinforced-concrete elements with the following adjustments for Equation 36.35 and Equation 36.36. Multiply the right side by:

$$\sqrt{1 + \frac{3 f_{ce}}{\sqrt{f'_c}}}$$

For hollow sections, the left side of Equation 36.37 becomes:

$$\left(\frac{V_u}{b_w d} \right) + \left(\frac{T_u p_h}{1.7 A_{oh}^2} \right)$$

The maximum spacing of the closed hoops is $1/8 p_h \leq 12$ in., and the longitudinal bar diameter is not less than $1/16s$, where s is the spacing of the hoop steel.

36.6 Walls and Footings

The design of walls and footings should be viewed in the context of designing a one-way or two-way cantilever slab in the case of footings and one-way vertical cantilevers in the case of reinforced-concrete walls. The criteria and expressions for proportioning their geometry are the same as those presented in earlier sections of this chapter. Shear V_u in one-way footings is taken at a distance d from the face of the vertical concrete wall or columns and at $d/2$ in the case of two-way footings. The nominal shear strength (capacity) V_c of the one-way slab footing is:

$$V_c = 2\lambda\sqrt{f'_c}b_wd \quad (36.71)$$

For two-way slab footings, the nominal shear strength V_c should be the smallest of:

$$V_c = 4\lambda\sqrt{f'_c}b_o d \quad (36.72a)$$

or

$$V_c = \left(2 + \frac{4}{\beta_c}\right)\lambda\sqrt{f'_c}b_o d \quad (36.72b)$$

or

$$V_c = \left(\frac{\alpha_s d}{b_o} + 2\right)\lambda\sqrt{f'_c}b_o d \quad (36.72c)$$

where b_o is the perimeter shear failure length at distance $d/2$ from all faces of columns. If the column size is $c_1 \times c_2$, then:

$b_o = 2(c_1 + d/2) + 2(c_2 + d/2)$ for an interior column.

$\beta_c =$ ratio of long side/short side of reaction area.

$\alpha_s = 40$ for interior columns, 30 for end columns, and 20 for corner columns.

The same requirement for shear in Equation 36.72 applies to the shear design of two-way action structural slabs and plates.

Acknowledgments

This chapter is based on material appearing in the previous edition of this *Handbook*; from *Fundamentals of High-Performance Concrete*, 2nd ed., by E.G. Nawy (John Wiley & Sons, 2001); from *Reinforced Concrete: A Fundamental Approach*, 6th ed., by E.G. Nawy (Prentice Hall, 2008); from *Prestressed Concrete: A Fundamental Approach*, 5th ed., by E.G. Nawy (Prentice Hall, 2006); and from various committee reports and standards of the American Concrete Institute, Farmington Hills, MI.

References

- ACI Committee 318. 2008. *Building Code Requirements for Structural Concrete*, ACI 318; *Commentary*. ACI 318R-08. American Concrete Institute, Farmington Hills, MI, 465 pp.
- ACI Committee 224. 2001. *Control of Cracking in Concrete Structures*, ACI 244R. American Concrete Institute, Farmington Hills, MI.
- ACI Committee 350. 2006. *Code Requirements for Environmental Engineering Concrete Structures and Commentary*, ACI 350 ERTA. American Concrete Institute, Farmington Hills, MI.

- ACI Committee 363. 1992. *State-of-the-Art on High-Strength Concrete*, ACI 363R. American Concrete Institute, Farmington Hills, MI, pp. 1–55.
- ACI Committee 435. 1995. *Control of Deflection in Concrete Structures*. ACI 435R. American Concrete Institute, Farmington Hills, MI, p. 7.
- Ahmed, S.H. and Lau, D.M. 1987. Flexure-shear interaction of reinforced high strength concrete beams. *Proc. ACI Struct. J.*, 84(4), 330–341.
- Hsu, T.T.C. 1993. *Unified Theory of Reinforced Concrete*. CRC Press, Boca Raton, FL.
- Martinez, S., Nilsen, A.H., and Slate, F.O. 1984. Spirally reinforced high-strength concrete columns. *ACI Struct. J.*, 81(5), 431–442.
- Nawy, E.G. 2002. *Fundamentals of High-Performance Concrete*, 2nd ed. John Wiley & Sons, New York.
- Nawy, E.G. 2006. *Prestressed Concrete: A Fundamental Approach*, 5th ed. Prentice Hall, Upper Saddle River, NJ.
- Nawy, E.G. 2008. *Reinforced Concrete: A Fundamental Approach*, 6th ed. Prentice Hall, Upper Saddle River, NJ.
- Pastor, J.A., Nilsen, A.H., and Slate, F.O. 1984. *Behavior of High-Strength Concrete Beams*, Cornell University Report No. 84-3. Department of Structural Engineering, Cornell University, Ithaca, NY.
- Yong, Y.K., Nour, M.G., and Nawy, E.G. 1988. Behavior of laterally confined high strength concrete under axial loads. *Proc. ASCE J. Struct. Eng.*, 114(2), 332–351.

Index

A

- abrasion, 2-16, 5-38, 27-5
 - losses, 20-11
 - resistance, 3-7, 3-17, 3-18, 5-17–5-20, 11-16, 13-19, 13-23, 16-12, 16-13
- abrasive blasting, 30-20, 30-22–30-24, 30-32
- absolute volume methods, for concrete
 - proportioning, 5-32
- absorption, 13-22, 13-23, 24-32
 - capacity, 1-16
- abutments, 5-15, 11-43, 14-51, 15-3, 15-23, 20-7, 20-38, 20-48, 20-49, 20-56, 20-59, 20-60, 20-62, 20-65–20-66, 20-70, 27-25, 29-9, 32-51, 32-52, 32-53, 32-55, 32-57
 - precast concrete, 33-12, 33-14
 - stiffness, 32-52
- acceleration, 32-48, 32-50, 32-51
 - parameters, 32-7, 32-8
 - spectral, 32-51
- accelerators, 3-1, 3-3, 3-4, 3-7–3-9, 3-13, 4-11, 5-30, 5-31, 5-32, 6-5, 6-7, 8-21, 8-22, 15-11, 15-17, 28-15
 - calcium chloride, 3-7
- accelerogram, 32-2, 32-3, 32-50
 - intensity, 32-3
- accelerograph, strong motion, 32-2
- accelerometers, 27-7, 27-8, 27-26
- acceptance testing, 21-26–21-27
- accidental torsion, 32-25
- accuracy, of instrumentation, 27-14–27-16
- acetylene torch, 12-40
- ACI 116R, 15-7, 15-13
- ACI 209, 4-2, 4-8, 4-12, 8-22, 8-28, 8-30, 8-31, 8-33, 9-6, 9-15
- ACI 211, 5-32, 6-18
- ACI 216.1, 31-5, 31-7, 31-8, 31-9, 31-11, 31-12, 31-13
- ACI 224, 17-8, 17-10
- ACI 228, 21-4, 21-8, 21-9, 21-12, 21-25, 21-26, 21-27, 21-28
- ACI 302.1R, 17-13
- ACI 318, 1-21, 3-8, 4-2, 4-19, 4-20, 4-24, 6-13, 8-12, 8-27, 8-28, 8-36, 8-41, 8-42, 8-43, 8-51, 8-55–8-58, 9-2, 9-3, 9-5, 9-6, 9-7, 9-13, 9-14, 9-15, 9-16, 9-17, 9-20, 10-4, 10-6, 10-8, 10-10, 10-12, 10-16, 10-17, 10-18, 10-19, 10-20, 10-21, 10-39, 16-2, 16-10, 16-18, 16-33, 16-34, 17-2, 17-5, 21-25, 21-27, 25-4, 25-8, 25-9, 25-12, 26-17, 27-2–27-4, 27-28, 27-29, 31-5, 32-26, 32-34, 34-10, 34-22, 34-23, 35-4, 36-1–36-36
- ACI 347, 7-21, 7-23, 7-24, 7-25, 7-27, 7-35, 7-43, 7-46, 8-6, 10-36
- ACI 350, 17-1, 17-5, 17-8
- ACI 357, 13-4, 13-14
- ACI 435, 4-15, 4-17, 8-52, 9-6, 9-7, 9-10, 9-14, 9-20
- ACI 437R, 27-2, 27-9
- ACI 440.1R, 25-2, 25-4, 25-6, 25-7, 25-9
- ACI 440.2R, 25-9, 25-12, 25-13, 25-14, 25-15, 25-16, 25-18, 25-19
- ACI 440.3R, 25-3, 25-12
- acid attack, 1-25–1-26
- acid etching, 30-16, 30-20, 30-24, 30-30, 30-32, 30-68
- acid wash, 30-17
- acoustic impedance, 21-32
- acrylic, in antiwashout admixtures, 15-10, 15-11
- activation energy, 21-18–21-20, 21-24
- active corrosion inhibitors, 3-9
- active vs. passive failure mechanism, 14-44
- actual dimension, masonry unit, 28-3
- actuators, 27-10–27-13
- adhesion factor, 14-60
- admixtures, 1-22, 5-2, 5-40, 6-4–6-9, 6-18, 6-30, 6-40, 9-15, 9-20, 10-25, 10-27, 11-5, 11-16, 11-41, 12-9, 20-8, 20-20, 20-40, 33-2
 - accelerating, 3-7–3-9, 5-30, 5-31, 6-5, 6-7, 15-11, 15-17, 28-15; *see also* accelerators
- acrylic, 15-10, 15-11
- activation energy, and, 21-18
- air-entraining, *see* air-entraining admixtures
- antibled, 11-19
- antifreezing, 3-12–3-13
- antiwashout, 3-13–3-14, 15-6, 15-7, 15-9–15-13
- architectural concrete, 30-15–30-16
- cellulose, 15-10, 15-11
 - chemical, 1-4, 2-20, 2-29, 3-1–3-18, 5-21, 5-30–5-31, 6-30, 6-33–6-36, 13-22, 15-2, 15-6, 15-9, 15-17, 15-20, 20-20–20-21
- chloride-containing, 5-39
- citric acid, 23-2
- corrosion-inhibiting, 1-22, 5-38, 5-39, 11-5; *see also* corrosion protection

- admixtures (cont.)
 - defined, 30-73
 - expansive, 11-23
 - fine, 6-8
 - grouting, 11-23
 - high-range water-reducing, *see* high-range water reducers
 - lateral pressure, and, 7-24
 - masonry, 28-14–28-15
 - mineral, 1-4, 1-9, 1-13, 2-1–2-42, 3-10, 3-12, 5-27, 6-5, 15-2, 15-20
 - mixing of, 6-39
 - mortar, 28-6, 28-8, 28-14–28-15
 - no-slump concrete, 6-5, 6-8
 - order of addition of, 11-6
 - polymer modifier, 3-14–3-18
 - retarding, 3-2–3-3, 5-30, 5-31, 6-23, 6-33, 7-43, 10-27, 11-5, 28-8, 28-15; *see also* retarders
 - set-controlling, 6-5, 6-8, 7-26, 10-38, 30-15
 - shrinkage-reducing, 3-14, 4-11
 - sulfate attack, and, 1-25
 - superplasticizer, *see* superplasticizers
 - thixotropic, 11-23
 - viscosity-modifying, 3-13, 3-14, 15-20
 - water-reducing, 3-3–3-4, 5-30, 5-31, 5-32, 6-5, 6-8, 6-21, 10-23, 10-27, 11-23, 15-3, 15-12, 15-13, 20-24, 30-15
 - water-repellent, 24-32, 24-33, 28-8, 28-14
 - workability-enhancing, 6-21
- advancing-slope grouting, 15-5
- aerial work platforms, 19-47, 19-48
- aesthetics, 29-1–29-32
- A-frame, crane, 19-26
- age conversion factor, 21-18, 21-19
- aggregate/cement ratio, 2-23
- aggregate/cementitious materials ratio, 15-3, 15-4
- aggregate interlock, 17-12, 17-15, 21-12, 25-17, 36-10
- aggregate modulus, 4-8
- aggregate/paste ratio, 4-8
- aggregate ratio test, 28-33
- aggregates, 1-1, 1-4, 1-13, 1-14–1-20, 2-20, 5-2, 5-6, 5-10, 5-17, 5-29–5-30, 5-34, 6-2, 6-18, 6-19, 6-22, 6-24, 6-30, 6-31, 6-36–6-38, 8-48, 9-15, 9-20, 10-27, 10-30, 11-4, 12-22, 13-19, 15-20, 17-12, 17-15, 20-2, 20-8, 20-10, 20-17, 20-45, 20-53, 21-55, 28-6
- angularity of, 5-30, 5-32, 30-13
- architectural concrete, 30-12–30-27, 30-30–30-32, 30-36, 30-48, 30-51, 30-54, 30-56, 30-57, 30-69, 30-71, 30-72, 30-73
- ASTM standards for, 28-4
- basalt, 20-10
- bridge deck, 23-10
- carbonate, 30-24
- coarse, 1-14, 1-15, 2-10, 2-20, 3-12, 4-18, 5-2, 5-17, 5-29, 5-30, 6-3, 6-8, 6-9, 6-20–6-21, 6-24, 6-29, 6-36, 6-37, 9-6, 10-24, 10-27, 11-4, 11-13, 11-16, 11-18, 11-23, 13-21, 15-2–15-6, 15-20, 15-25, 20-32, 20-46, 20-47, 22-4, 23-3, 23-13, 26-3, 26-9–26-10, 30-13, 30-14, 30-16, 30-21, 30-22, 30-24, 30-25, 30-26, 30-32, 30-48, 30-51, 30-57, 30-69, 30-73
- artificial, 6-4
- break-off test, and, 21-16
- creep strain, and, 4-7
- dry weight of, 6-24
- maximum size of, 5-32, 10-24, 23-13, 30-17
- preplacing, 15-4
- probe penetration test, and, 21-8
- crushed, 5-29
- cylinder size, and, 5-33
- defined, 30-73
- density of, 5-16, 6-4
- drying shrinkage, and, 5-21
- durability of, 1-19–1-20
- exposed, 3-2, 5-31, 10-29, 30-4, 30-12, 30-13, 30-16, 30-17, 30-19, 30-20, 30-21, 30-22, 30-25, 30-26, 30-27, 30-31, 30-54, 30-57, 30-69, 30-73
- degrees of, 30-20, 30-22
- feed rate of, 20-60
- fine, 1-14, 1-15, 2-9, 5-2, 5-29, 5-30, 6-3, 6-4, 6-8, 6-9, 6-21, 6-37, 10-27, 11-4, 11-18, 11-30, 13-22, 15-9, 15-14, 15-20, 15-25, 20-2, 20-11, 20-12, 20-13, 20-14, 20-17, 20-23–20-25, 20-30, 20-34, 20-36, 20-40, 20-58, 20-59, 22-4, 26-3, 30-13, 30-14, 30-17, 30-19, 30-20, 30-21, 30-32, 30-73
- fine/coarse ratio, 30-16
- geopolymer concrete, 26-6
- grading of, 1-15; *see also* gap grading
- hard, 21-9
- hard vs. soft, 5-17
- heavyweight, 1-14, 1-19, 6-4
- high-performance concrete, and, 11-16
- lightweight, 1-14, 1-17–1-18, 6-2–6-4, 9-15, 11-4, 11-17, 11-18, 13-21, 15-17, 23-10, 36-28
- maximum size (MSAs), 20-12, 20-26, 20-60, 20-65
- for break-off test, 21-15, 21-16
- maximum size of, in offshore structures, 13-26
- melting of, 12-40
- modulus of elasticity, and, 9-15
- moisture content of, 1-16–1-17, 5-30, 21-48
- nominal maximum size of, 15-4
- nonreactive, 30-13

- normal weight, 6-2–6-4
- nuclear-shielding, 6-4
- oven-dry, 1-16, 5-30, 20-17, 20-20
- overlay, 23-3
- placing, 15-4
- Portland cement plaster, and, 15-16
- probe penetration, and, 21-9
- pulse velocity, and, 21-7–21-8
- reactive, 5-40, 5-41, 5-42, 11-4, 15-4, 15-17, 20-11
 - cracking and, 5-39
- roller-compacted concrete, 20-11–20-12, 20-57–20-58
- saturated surface dry, 1-16, 5-30, 20-19, 20-69, 26-8
- shape of, 5-30, 15-16
- shrinkage, and, 4-11
- sieve analysis of, 5-29
- soft, 21-9
- stockpiling of, 20-57
- strength, and, 6-20–6-21
- thermal expansion coefficient of, 20-22
- transport of, 20-61
- unit weight of, 5-30, 6-4
- washed, 11-4, 20-11, 20-23, 20-24, 20-58
- wetness of, 6-27
- AHP, *see* analytic hierarchy process
- air content, 6-7, 6-8, 6-17, 6-22, 6-24, 6-29, 6-41, 9-15, 13-23, 15-3, 15-4, 15-11
 - concrete strength and, 3-10
 - roller-compacted concrete, 20-21
 - testing for, 6-42
- air-detraining agents, 3-12
- air-dry aggregates, 1-16, 5-30
- air drying, 2-35, 8-36, 30-70
- air-entrained concrete, 2-15, 2-37, 3-10, 5-35, 15-16, 20-66, 30-15
- air-entraining admixtures, 2-10, 2-20, 2-34, 2-37, 3-10–3-12, 5-28, 5-30, 5-31, 6-5, 6-7, 15-4, 15-11, 15-17, 20-23, 20-49, 23-3, 30-15
- air entrainment, 3-1, 3-2, 3-7, 3-10–3-12, 3-16, 5-32, 5-35, 6-7, 8-21, 10-2, 10-27, 11-5, 11-6, 11-7, 11-48, 13-22, 15-4, 15-9, 15-11, 15-14, 15-16, 15-17, 20-23, 23-3, 30-15
 - blast-furnace slag, and, 2-20, 2-27
 - fly ash, and, 2-10–2-11, 2-15
 - roller-compacted concrete, and, 20-20, 20-21
 - shrinkage, and, 4-11
 - silica fume, and, 2-34
- air permeability test, 5-10
- air voids, 2-10, 2-38, 5-7, 5-35, 12-22, 13-23, 20-21, 20-23, 21-31, 21-40, 27-5, 30-15, 30-17, 30-21, 30-22, 30-24, 30-54, 30-57
- AirTrain JFK, 29-12, 29-16, 29-24
- alignment tolerances, 28-26
- alkali hydroxides, 3-7, 5-39, 5-40
- alkali nitrates, 3-7
- alkali resistance, 22-19
- alkali-activated cement, 6-2
- alkali-aggregate reaction, 1-10, 1-14, 1-19–1-20, 1-23, 5-30, 8-48, 11-4, 13-23, 20-11
 - fly ash, and, 2-17
- alkali-carbonate reaction, 1-20, 2-17
- alkali-silica gel, 5-40
- alkali-silica reaction, 1-20, 2-17, 2-26–2-27, 2-38, 3-8, 3-9, 3-10, 3-18, 5-29, 5-39–5-42, 5-43, 16-3, 16-12, 23-5, 24-27, 24-36, 27-5, 27-22
- alkaline liquid/fly ash ratio, 26-7, 26-8
- alkaline liquids, geopolymer, 26-2, 26-3, 26-4–26-5, 26-7
- alkalinity, 5-11, 5-29
- alkalis, 13-20, 13-21, 15-4, 30-15
 - aluminum powder, and, 15-3
- alkyl aryl sulfonates, 3-11
- allowable design values, 7-28
- allowable stress design, 7-23, 28-41, 28-49–28-58, 28-60, 28-62
- alloys, 2-30, 11-11
 - aluminum, 30-35
 - heat-treated, 11-9
 - magnesium, 30-35
 - silicon, 2-29, 5-27, 6-9
- all-terrain cranes, 19-36, 19-39–19-40
- alluvium, 32-5
- alumina, 5-23, 5-42
- alumina-silicate, 26-2
- aluminate, 1-2, 1-3, 1-6, 1-7, 1-8, 5-25, 5-37, 6-33
- aluminosilicates, 1-2, 2-2, 2-38, 5-27, 22-24
- aluminum, 2-1, 2-24, 3-8, 26-2
- aluminum chloride, 3-7
- aluminum oxide, 2-38, 26-3
- aluminum powder, 15-3, 15-4
- aluminum sulfate, 3-13
- American Concrete Institute formwork
 - recommendations, 7-18
- American National Standards Institute formwork
 - standard, 7-21
- American Society of Civil Engineers formwork
 - standards, 7-22
- amino acid, 3-11
- ammonium ion, 3-10
- ammonium salts, 2-37
- amplitude, vibrator, 30-52, 30-53, 30-57
- analytic hierarchy process (AHP), 19-12
- anchor bolts, 7-16, 21-13, 28-49, 28-50, 28-51, 28-60, 28-61, 30-61, 30-63; *see also* bolted assemblages

- anchor plate, 11-60, 14-53
- anchorage bearing plates, installation of, 11-20
- anchorage, 11-8, 11-9, 11-11, 11-13, 11-14,
 - 11-14–11-15, 11-18, 11-21, 11-23, 11-24,
 - 11-33, 11-38, 11-41, 11-55, 11-60, 11-61, 12-2,
 - 12-3, 12-6, 12-7, 12-8, 12-10–12-11, 12-21,
 - 12-22, 12-23, 12-26, 12-42, 12-43, 13-26,
 - 16-16, 16-18, 25-4, 25-16, 25-17, 27-4,
 - 28-60–28-61, 30-45, 30-46, 32-28, 34-11,
 - 36-18, 36-28
- accessible, 11-46
- hooked-bar, 10-17
- masonry, 28-49–28-51
- removal of, 16-19
- storage of, 11-19–11-20
- wedge-type, 30-48
- anchored sheet piles, 14-53–14-55
- anchors, 7-13, 7-14, 7-35, 10-13, 11-41, 12-4, 12-7,
 - 12-9, 12-14, 12-18, 12-24, 12-28, 12-31, 12-38,
 - 12-39, 13-1, 13-2, 13-9, 13-16, 13-25, 13-29,
 - 20-49, 20-52, 28-5, 28-60, 28-61, 30-31, 30-48
- ASTM standards for, 28-5
- bent-bar, 28-60
- ground, 14-55
- in corrosive environment, 12-3
- plate, 28-50, 28-60
- post-tensioned, 11-18, 36-18
- rock, 27-25
- stressing, 16-16
- tie rod, 14-53
- wedge, 11-10, 11-25
- andesite, 5-42
- Ando, Tadao, 30-2
- anodes, 5-37, 16-26
- anodic corrosion inhibitors, 3-9; *see also* corrosion protection
- anodic reaction, 21-52
- anodic ring effect, 16-14
- anticollision systems for cranes, 19-40–19-43
- antifoaming agent, 3-16
- antifreeze admixtures, 3-12–3-13
- antiwashout admixtures, 3-13–3-14, 15-6, 15-7,
 - 15-9–15-13
- appearance, of concrete, 10-3, 30-72; *see also* color, finishes, finishing, surface finishes
 - uniform, 5-31
- applied coatings, 30-30
- aqua valves, 15-7
- aragonite, 2-26
- architectural concrete, 3-6, 20-7, 30-1–30-73
 - admixtures, 30-15–30-16
 - aggregates, *see* aggregates: architectural concrete
 - appearance, acceptability of, 30-72
 - applications, 30-5–30-6
 - cast-in-place, 30-2–30-73
 - reinforcement, 30-41–30-48
 - cleaning, 30-70–30-72
 - color, 30-19
 - consolidation, 30-52–30-58
 - construction, 30-32–30-59
 - cracks, 30-70
 - curing, 30-58–30-59
 - discoloration, 30-3, 30-15, 30-18, 30-28, 30-35,
 - 30-36, 30-52, 30-58, 30-59, 30-67, 30-68,
 - 30-70
 - finish cleanup, 30-68–30-72
 - form ties, 30-38–30-40
 - forming, 30-7, 30-32–30-40
 - innovations, 30-72
 - materials–mixture design, 30-12–30-19
 - placement, 30-48–30-52
 - planning, 30-6–30-12
 - budget, 30-6–30-7
 - drawings, 30-7–30-8
 - mock-up construction, 30-11–30-12
 - prebid conference, 30-10–30-11
 - preconstruction conference, 30-11
 - quality control, 30-9–30-10
 - specifications, 30-8–30-9
 - precast, 30-4–30-73
 - production and installation of, 30-60–30-67
 - texture, 30-30–30-32
 - tolerances, 30-65–30-66
 - protection of, 30-59
 - release agents, 30-17, 30-18–30-19, 30-21, 30-25,
 - 30-28, 30-30
 - repair of, 30-68–30-70
 - smooth surface, 30-20–30-21
 - texture, 30-16–30-17, 30-19–30-32
 - wood sealers, and, 30-17, 30-18
- architectural details, 9-19
- architectural prestressed concrete, 11-18–11-19
- architectural surface, 10-3
- architecture design/engineering/construction (A/E/C) industry, 18-12, 18-16
- argillites, 5-40
- Arrhenius equation, 21-17, 21-18–21-20, 21-24
- ArtifexPlus, 18-13, 18-16
- artificial islands, 13-15
- as-cast concrete surface, 30-20, 30-21
- as-produced silica fume, 2-29
- ASCE 7, 10-5, 32-6, 32-7–32-29
- ASD adjustment factors, 7-28–7-31
- asphalt overlays, 23-1, 23-3
- ASTM A 416, 12-3, 12-44, 30-47
- ASTM C 1019, 28-10, 28-34

ASTM C 1040, 15-25, 21-61
 ASTM C 1074, 21-17, 21-24, 21-25
 ASTM C 1150, 21-15, 21-16
 ASTM C 1157, 5-27, 5-36, 5-41
 ASTM C 1170, 15-25, 20-17
 ASTM C 1240, 5-28, 5-41
 ASTM C 1293, 5-40, 5-41
 ASTM C 1314, 28-36, 28-37, 28-38
 ASTM C 1384, 28-8, 28-15
 ASTM C 143, 5-2, 5-33, 6-9, 28-33
 ASTM C 150, 3-12, 5-23, 5-36, 5-37, 5-41, 10-3, 10-26
 ASTM C 1567, 5-40, 5-41
 ASTM C 157, 16-12, 23-4
 ASTM C 1611, 5-43, 6-35, 28-10
 ASTM C 231, 5-33, 15-3
 ASTM C 270, 28-6, 28-8, 28-9, 28-15, 28-32, 28-33, 28-36
 ASTM C 31, 5-33, 6-41
 ASTM C 33, 5-29, 10-27, 23-3, 31-7
 ASTM C 39, 6-41, 6-42
 ASTM C 476, 28-10, 28-34, 28-36
 ASTM C 494, 3-1, 3-2, 3-3, 3-4, 3-5, 3-6, 3-7, 10-23, 10-27
 ASTM C 595, 3-12, 5-27, 5-36, 5-41
 ASTM C 618, 5-28, 5-41, 6-31, 10-26
 ASTM C 642, 5-10, 24-32
 ASTM C 666, 2-27, 2-37, 24-26
 ASTM C 672, 2-39, 24-27
 ASTM C 780, 28-32, 28-33
 ASTM C 876, 21-53, 21-54
 ASTM C 90, 28-11, 28-36
 ASTM C 900, 21-12, 21-15
 ASTM C 937, 15-3, 15-4
 ASTM C 94, 6-38, 6-41
 ASTM C 989, 5-28, 5-41
 ASTM D 4580, 21-31, 21-40
 ASTM D 4748, 21-44, 21-48
 ASTM D 4788, 21-40, 21-42
 ASTM standards, 5-43–5-44
 attenuation, 21-47, 21-48, 32-3, 32-6
 acceleration, 32-3, 32-4, 32-5
 earthquake, 32-4
 foundation stress, 14-28
 ground motion, 32-5
 load, 14-67
 motion, 32-3
 radiation, 21-60
 site geology, and, 32-5
 stress, 14-68–14-69
 velocity, 32-4
 measurement, 21-8
 Atterberg limits, 14-2, 14-4–14-5
 auger, 10-14

autoclaved aerated concrete (AAC), 28-8, 28-20
 compressive strength, 28-38
 autogenous volume change, 20-22, 20-70
 automatic sprinkler systems, 31-2–31-3
 automation, 18-1–18-16
 axial capacity, 25-12, 27-6
 fiber-reinforced polymer systems, and, 25-18–25-20
 axial compression, 7-38, 7-48, 28-47–28-48, 28-49, 28-51–28-53, 28-55–28-58, 28-60, 28-62–28-63, 28-65–28-67
 axial creep, 35-3
 axial load, 10-11, 28-27, 28-52, 28-53, 28-55, 28-58, 28-59, 28-60, 28-62, 28-63, 28-65, 28-66, 28-68, 32-36, 36-5–36-7, 36-10, 36-24
 axial stress, 32-36, 32-37
 axially loaded columns, 36-5–36-7

B

backfill, 14-43–14-44, 14-45, 14-46, 14-47, 14-48, 14-50, 14-51, 20-52
 drainage of, 14-56
 backhoes, 19-2, 20-3
 backing, defined, 28-3
 backlash, 27-13, 27-15, 27-16, 27-17, 27-18
 backscatter, 21-61
 backshores, 7-14
 backup mix, 30-73
 bag houses, 2-29
 Baha'i Temple, 30-4
 balanced cantilever bridge construction, 29-11–29-12, 29-16, 29-19
 balanced strain state, 36-23
 ball and crane demolition, 12-40
 ballast, 13-25, 13-31
 bar location factor, 36-28
 bar size factor, 36-28
 barges, 11-35, 11-40, 11-43, 11-44, 11-56, 13-27, 33-2
 concrete, 13-2, 13-13–13-14
 crane, 13-4
 submersible, 13-26, 13-29
 barite, 1-19, 6-4
 base isolation, 32-45–32-46
 base shear, 32-22–32-24, 32-27, 32-29
 defined, 32-62
 batch mixers, 20-59, 20-61
 bays, column, 10-17, 10-19, 10-20
 beam daps, 36-15
 beam forms, 7-16
 beam–slab systems, one-way, 10-17–10-19
 beam-stability factor, 7-33

- beams, 9-3, 9-4, 9-7, 9-14, 9-22, 10-8, 10-9, 10-15, 10-19, 10-22, 11-29, 11-33, 12-2, 12-4, 12-8, 12-9, 12-27, 12-30, 12-31, 16-5, 18-8, 22-3, 32-19, 33-12, 36-7–36-10; *see also* joints:
 - beam–column
 - between columns, 8-16
 - bond, 28-3, 28-20, 28-42, 28-55
 - boundary, 8-7
 - box, prestressed, 33-3, 33-7–33-8
 - CAD, and, 18-8
 - cantilevered, 20-48
 - cast-in-place concrete, 30-46, 34-5, 34-6, 34-9
 - channel, 30-46, 30-47, 33-3, 33-4
 - coarse aggregates, and, 10-27
 - compression steel in, 9-17
 - compression strength, and, 8-21
 - continuous, 10-16, 36-15
 - crack control in, 36-4
 - cracked vs. uncracked, 9-7
 - cracking of, 12-28
 - dead load moments of, 9-13
 - deep, 36-15–36-21
 - demolition of, 12-40
 - displacement-controlled test of, 27-13
 - displacement of, 27-28
 - failure of, 8-27, 22-13, 36-10
 - fiberglass-reinforced, 22-19
 - fiber-reinforced polymer systems, and, 25-16
 - flexural cracking, and, 8-34, 8-36, 25-5
 - flexural strength of, 22-12, 26-17
 - grade, 32-38, 32-40, 32-45
 - high-strength concrete, 24-21
 - hybrid, 34-11, 34-12, 34-17, 34-20, 34-21
 - size of, 34-20, 34-24
 - impact-echo testing of, 21-35
 - internal strength of, 34-3, 34-4
 - maintenance of, 35-15
 - mechanized formwork for, 19-50
 - modeling of, 18-9, 18-10–18-11, 18-12
 - modulus of rupture of, 8-37
 - multi-stemmed, 33-4
 - post-tensioned, 4-28–4-29, 10-40, 30-45–30-47
 - precast, 19-4, 34-5, 34-11
 - prestressed, 10-38
 - bulb-tee, 33-8
 - inverted channel, 33-5–33-6
 - single-tee, 33-6
 - pretensioned, 10-40
 - prism-reinforced, 22-17–22-18
 - proportioning of, 10-16–10-17
 - rectangular, 9-6, 9-14
 - reinforced concrete, 24-12, 25-4, 25-6, 36-4–36-5
 - reinforced geopolymer, 26-14–26-18
 - reinforcement of, 12-11–12-12
 - retrofit of, 12-31
 - singly reinforced, 36-11
 - size of, 34-20
 - spacing of, 10-7
 - spandrel, *see* spandrels
 - steel, 33-12
 - steel/engineered cementitious composite, 24-12
 - strengthening of, 12-30
 - tension-controlled, 36-10
 - twist in, 9-9
 - with fibers, 22-8
- bearing, 7-30, 7-42, 7-45, 7-46
 - area, 7-40, 7-41, 7-42, 7-46
 - factor, 7-34
- capacity, 10-14, 14-32–14-36, 14-37, 14-58
 - estimating, 14-76–14-79
 - mat footings, 14-37–14-40
 - pile group, 14-65
- compression, 7-38
- plates, 7-9, 7-11, 11-11, 11-20
- strength, 13-22, 20-48
- stress, 4-22, 7-42, 7-46, 11-57, 20-47, 21-15, 28-53, 32-36, 32-37, 34-10, 36-18
- supports, 7-35, 7-36
- wall, 7-14, 28-26, 28-47
 - construction, 10-29
 - system, 32-12, 32-45, 32-62
- bed joints, 28-3, 28-6, 28-18, 28-26, 28-36, 28-42, 28-60, 28-62
- bedding mixtures, 20-40, 20-43, 20-44, 20-47, 20-48, 20-49, 20-51, 20-52, 20-56, 20-63
- bedrock, 14-2, 14-24, 14-28, 14-76, 14-77
- belt conveyors, 19-45; *see also* conveyors
- bendable concrete, 24-8
- bending, 7-28, 7-35, 7-36, 7-39, 7-46, 10-7, 10-8, 11-4, 11-40, 11-57, 30-34, 32-32, 36-15
 - deflection, 7-34
 - engineered cementitious composite (ECC), 24-8
 - flexural bending, 7-38, 7-40, 7-43, 7-44, 7-45, 7-46, 28-53
- load, 24-6, 32-36
- moment, 4-18, 4-25, 8-27, 8-47, 10-15, 10-18, 10-37, 11-50, 14-50, 14-57, 18-10, 18-11, 25-13, 28-52, 28-53, 28-57, 28-62, 28-67, 28-68, 31-6, 32-35, 32-38, 32-40
- stress, 4-22, 11-57, 21-15, 28-53, 32-36, 32-37
- bent cap bolsters, 32-61
- benzoates, 3-7
- berthing structures, 13-2
- Big Canopy, 18-5
- binders, 26-2, 26-3
 - engineered cementitious composite, 24-9

- Bingham fluid, 15-21
- bituminous coal, 2-2, 2-17
- bituminous fly ash, 2-13, 2-18
- black iron oxide, 29-25
- Blaine specific-surface method, 2-5, 2-6, 2-20, 2-29
- blast-furnace slag, 1-11, 1-25, 2-18–2-27, 5-27, 5-29,
 - 6-18, 11-5, 11-16; *see also* slags
 - carbonation, and, 2-27
 - creep, and, 2-23
 - durability, and, 2-24–2-27
 - expansion, and, 2-26–2-27
 - flexural strength, and, 2-23
 - granulated, 2-19, 2-20, 2-21, 2-22, 2-23, 2-24, 2-25,
 - 5-27, 5-28, 5-41, 6-33, 6-42, 15-23, 26-2
 - hardened cement, and, 2-21–2-24
 - modulus of elasticity, and, 2-23
 - permeability, and, 2-24
 - properties of, 2-20–2-21
 - proportioning, 2-20
 - shrinkage, and, 2-23
 - strength development, 2-21
 - sulfate attack, and, 2-24–2-25
- blasting mats, 11-61
- bleeding, 2-10, 2-20, 2-33, 2-34, 2-36, 3-4, 3-6, 3-7,
 - 3-14, 3-16, 4-10, 5-2–5-6, 5-28, 5-31, 5-35,
 - 6-40, 10-3, 10-17, 11-5, 11-23, 15-3, 15-4,
 - 15-11, 20-17, 27-5, 30-57, 30-58
- blended hydraulic cements, *see* cements: blended hydraulic
- blind lifts, 19-40
- blisters, 11-41, 11-55
- bloating, of raw materials, 1-17
- blockouts, 12-8, 12-14, 20-51, 30-29
- blow holes, 30-31, 30-56, 30-73; *see also* bug holes
- blowouts, 10-34, 10-36, 12-20, 12-24–12-27, 12-39,
 - 12-42, 28-11
- Blue Ridge Parkway, 29-2, 29-9–29-10, 29-20, 29-23,
 - 29-25, 29-28
- Bob Graham Sunshine Skyway Bridge, 29-2, 29-19
- Bodkin connector, 14-51
- bolsters, 11-41, 11-42
- bolt ties, 30-39
- bolted assemblages, 34-7–34-11, 34-18–34-20
- bond, 8-41, 11-18
- bond beam, 28-3, 28-20, 28-42, 28-55
- bond breaker, 10-28, 10-29, 11-39, 11-42, 12-2,
 - 16-14, 17-6, 17-15, 30-31, 30-39, 30-73
- bond failure, 16-11, 23-5, 27-4
- bond patterns, 28-16–28-18
- bond splitting, 24-12, 24-14, 24-18, 24-19, 24-21,
 - 24-22, 25-8
- bond strength, 3-16, 8-20, 8-22–8-26, 8-41, 11-26,
 - 11-56, 16-11, 23-3, 23-4–23-13
 - overlay, 23-3, 23-4–23-13
 - revibration, and, 30-57
- bond stress, 4-25
- bonded concrete overlays, 23-1–23-16, 33-2, 33-16;
 - see also* overlays
- bonded foil gauges, 27-18
- bonded post-tensioned concrete, 16-16
- bonded prestressing, 10-38
- bonding agent, 30-70, 30-73
- boom, 19-15–19-17, 19-34, 19-44, 19-45, 19-46,
 - 20-63, 21-40
 - articulated, 19-48
 - climbing, 19-3, 19-8, 19-50
 - extension, 19-38
 - knuckle, 19-43, 19-48
 - lattice, 19-35–19-36, 19-37, 19-38, 19-40
 - length of, 19-16–19-17
 - lifts, 19-48
 - luffing, 19-37
 - placing, 19-3, 19-4, 19-7, 19-8, 19-9, 19-17, 19-18
 - location of, 19-8
 - pump, 19-15, 19-17
 - rear-mounted, 19-43
 - telescopic, 19-35–19-36, 19-37, 19-43, 19-48
 - tower-mounted, 19-15, 19-17–19-19
 - trucks, 19-43–19-44
 - Z-type, 19-17
- borax, 3-2
- borescope, 21-30
- boring, 14-28, 14-29
- bottom-dump trailers, 20-64–20-65
- bottom-founded structures, 13-2–13-9, 13-24,
 - 13-25, 13-26
- boundary elements, 32-45, 32-62
- boundary members, 32-33
- boundary representation, 18-9, 18-10
- box girders, 11-43, 11-46, 27-27, 29-2, 29-5, 29-7,
 - 29-14, 29-15, 29-17, 29-29, 29-32, 32-54
- braced frames, 10-15
- bracing, 7-3, 7-9, 7-16, 7-26, 7-27, 7-34, 7-42, 10-15,
 - 10-28, 11-31
 - concrete, 13-11
 - crane, 19-28
 - cross-, 7-43
 - demolition, and, 12-40
 - design of, 7-43, 7-46–7-48
 - diagonal, 7-16, 7-42
 - excavation, 14-55–14-56
 - for precast elements, 30-60, 30-63
 - lateral, 10-15
 - pile, 13-4
 - seismic, 34-1–34-24
 - tilt-up, 11-55

- bracketed duration, 32-3
- Bragg grating, 27-21
- Branson's creep evaluation model, 4-6, 4-7, 4-9
- Brazilian split-cylinder test, 20-27, 20-28
- breakaway parapet, 20-45
- breakers, 12-40
- break-off number, 21-15, 21-16
- break-off test, 21-15–21-16, 21-26
 - failure, 21-16
- B-regions, 36-15
- brick, 8-48, 21-18–21-19, 27-9, 28-3, 28-4–28-5, 28-11, 28-13, 28-25, 30-27, 30-71, 30-31, 31-9,
- bridge coatings, 29-25
- bridge decks, 1-22, 3-14, 3-15, 5-17, 5-25, 5-38, 6-21, 7-7, 11-12, 11-34, 13-14, 15-22, 16-4, 16-5, 21-40, 21-41, 21-42, 21-45, 21-47, 21-48, 21-61, 22-3, 22-21, 22-23, 27-25; *see also* bridges
 - chain-drag testing of, 27-6
 - engineered cementitious composite (ECC), and, 24-12, 24-27, 24-31, 24-37
 - macro texture of, 23-8–23-10
 - overlays on, 23-1–23-16
 - precast concrete, 33-2, 33-3, 33-6–33-7, 33-9–33-12
- bridge piers, 7-9, 10-34, 11-15, 11-46, 11-56, 13-9, 13-14, 14-57, 15-3, 15-7, 29-7, 29-8, 29-10, 29-12, 29-13, 29-16, 29-17, 29-21, 29-22, 29-23, 29-25, 29-26
- bridges, 10-2, 10-7, 10-13, 10-26, 11-3, 11-17, 11-18, 11-20, 11-21, 11-25, 11-30, 11-33–11-46, 13-4, 13-9, 16-16, 18-9; *see also* bridge decks, bridge piers, cantilever bridge construction
 - aesthetics of, 29-1–29-32
 - color, 29-24–29-26
 - texture, 29-24–29-26
 - alignment of, 29-5–29-6
 - cable-stayed, 13-14, 29-13–29-15, 29-30
 - cable-stayed concrete segmental, 11-40
 - cast-in-place, 7-5
 - cast-in-place cantilever segmental, 11-40–11-42
 - composite reinforced concrete, 22-19
 - conceptual design of, 29-4–29-8
 - context-sensitive design of, 29-10–29-11
 - continuous concrete slab, 27-26
 - demolition of, 11-60
 - detecting delamination in, 21-40
 - drainage for, 29-29
 - earthquake-damaged, retrofit of, 32-56–32-61
 - environmental sensitivity of, 29-9–29-11
 - float-in erection, 11-43–11-44
 - floating, 13-9, 13-14, 13-26
 - in urban environments, 29-15–29-17
 - incremental launching of, 11-43
 - inspection of, 16-3
 - lift-in erection of, 11-43–11-44
 - load testing of, 27-4
 - long-span, 11-60
 - long-span prestressed, 29-1–29-32
 - construction methods for, 29-11–29-23
 - performance evaluation of, 27-21–27-28, 27-29–27-31
 - post-tensioned precast segmental, 11-38–11-40
 - precast cantilevered segmental, 11-42–11-43
 - prefabricated elements for, 33-1–33-16
 - repair of, 16-2
 - seismic analysis/design of, 32-48–32-56
 - shapes of, 29-17–29-23
 - shear-key cracking in, 27-27–27-28
 - span length of, 29-6
 - span-to-depth ratio, 29-7–29-8
 - structural depth of, 29-7
 - three-span slab, testing of, 27-22–27-26
 - truck load testing of, 27-26
 - underside appearance of, 29-21
 - utilities, and, 29-29
 - widening of, 11-60
- Brinell hardness test, 21-2
- brittleness, 20-53, 24-1, 24-2, 24-4, 24-29, 24-39, 25-3
- Broadway Bridge, 29-21, 29-29, 29-30
- bromides, 6-7
- brown coat, plaster, 15-19
- bubble-spacing factor, 2-37, 15-11
- buckets, 5-6, 8-6, 10-27, 11-6, 13-26, 15-7–15-8, 19-5, 19-6, 20-61, 20-67, 30-50
- buckling, 7-41, 7-42, 7-43, 10-15, 34-6, 36-24
 - axes, 7-34, 7-42, 7-48
 - failure, 7-34, 36-24
 - lateral, 7-39, 7-40, 7-44, 7-45
 - side-sway, 10-15
 - stiffness factor, 7-31
 - strength, 7-16
- bug holes, 30-13, 30-16, 30-18, 30-22, 30-27, 30-28, 30-31, 30-51, 30-52, 30-56, 30-69, 30-73
- building-block geometry, 18-9
- building codes, 10-4, 10-6, 10-32, 12-30, 13-18, 14-37
- building dimensions, masonry and, 28-16
- building frame system, 32-13
- building loads, *see* load
- Building Research Establishment (BRE) pullout test, 21-13, 21-15
- building separation, 32-28
- building weight, 32-18, 32-22, 32-24, 32-29
- bulb tee, 11-36

bulk density, 5-30
 bulkhead, 7-16
 bulldozers, 20-2, 20-3, 20-62, 20-66, 20-67, 20-68, 20-69
 Burgers rheological model, 4-5
 burlap, 2-34, 5-15, 8-24, 11-58, 15-25, 23-12, 30-58
 burnishing, 15-19
 bursters, 12-40
 bushhammering, 30-25–30-27, 30-32, 30-34, 30-68, 30-73
 button-head wire tendons, 12-2

C

cable-stayed bridges, 13-14, 29-13–29-15, 29-30
 caissons, 10-12, 10-13, 10-14, 13-2, 13-9, 13-15, 14-57, 14-76–14-79, 15-7, 15-8, 16-22, 16-23, 16-24, 16-26, 16-27, 16-31, 16-32, 16-38, 16-39
 drilled, 16-20
 integrity of, 21-33
 lightweight aggregate concrete, 13-15
 reinforcement of, 10-14
 Calatrava, Santiago, 30-2
 calcite, 1-3, 1-20, 30-26
 calcium, 2-1, 2-2, 26-14, 30-24; *see also* fly ash:
 low-calcium
 calcium aluminate, 1-2, 1-10, 1-11, 2-15, 2-17, 2-24, 3-2, 3-6, 3-7, 3-14
 hydrates, 5-35
 calcium aluminoferrites, 1-2, 2-17
 calcium carboaluminate hydrate, 2-26
 calcium carbonate, 1-22, 2-15, 2-26, 5-10
 calcium chloride, 2-15, 3-7, 3-8, 4-11, 5-31, 6-7, 8-21, 8-22, 8-23, 12-20, 12-27, 15-17, 16-19, 35-17
 architectural concrete, and, 30-15–30-16
 calcium formate, 3-7
 calcium hydroxide, 1-22, 2-15, 2-24, 2-25, 2-26, 2-36, 5-27, 6-31, 6-33, 11-4
 efflorescence, and, 1-25
 calcium magnesium acetate, 35-17
 calcium monosulfoaluminate, 5-42
 calcium nitrate, 3-7
 calcium nitrite, 3-8, 3-9, 5-38, 11-5
 calcium oxide, 3-14, 26-3
 calcium silicate, 1-2, 1-3, 1-4, 1-6, 1-7, 1-12, 2-15, 2-25, 3-2, 5-12, 5-23
 calcium silicate glasses, 1-17
 calcium silicate hydrate, 1-6, 2-2, 2-25, 2-32, 2-37, 5-12, 5-35, 5-42, 6-31
 calcium silicocarbonate, 2-26
 calcium sulfate, 1-10, 2-6, 2-18
 calcium sulfoaluminate, 2-25, 3-14, 23-2

calcium thiosulfate, 3-7
 calcium-alumina-silicates, 6-33
 calcium–aluminate cement, 1-10
 Calgon®, 3-7, 14-2
 Caltrans' response spectra, 32-50–32-51
 camber, 4-32, 8-49, 9-18, 9-19, 9-20, 9-21, 10-23, 11-4, 11-23, 11-32, 11-33
 cameras, for cranes, 19-40
 canopy, for high-rise construction, 18-5
 cantilever, 9-7, 9-14, 9-19, 9-20, 9-22, 11-40–11-43, 12-43
 cantilever bridge construction, 29-4, 29-6, 29-9, 29-10, 29-11, 29-12, 29-13
 cantilever retaining wall, 14-48–14-50
 cantilever sheet piles, 14-52–14-53
 cantilever suspended spans, 11-36
 cantilever wall system, 16-20, 16-28
 cantilevered column system, 32-13
 capacity-reduction factors, 16-10
 capillary pores, 1-8
 capillary suction, 24-31, 24-32–24-33
 CAPO test, 21-15
 carbohydrate esters, 3-5, 6-8
 carbohydrates, 3-3
 carbon content of fly ash, 26-3
 carbon dioxide, 1-11, 1-22, 2-15, 2-17, 2-26, 2-27, 4-12, 5-10, 5-11, 11-58, 16-13, 26-1, 26-2
 carbon-fiber fabrics, 25-11
 carbon-fiber-reinforced cement-based composites, 22-14, 22-16, 22-20–22-24
 carbon-fiber-reinforced epoxy laminates, 25-9, 25-10
 carbon-fiber-reinforced polymer (CFRP), 22-21, 22-23, 22-24, 25-2, 25-3, 25-13
 carbon-fiber sheets, 11-60, 16-15, 22-24
 tow, 25-10–25-11
 carbon–glass–polyester composites, 22-21
 carbonates, 5-10, 6-7
 carbonation, 1-22, 1-25, 5-10–5-11, 5-29, 5-37, 11-58, 16-13, 17-1, 21-4, 21-54, 24-30, 27-22, 28-38, 30-24
 blast-furnace slag, and, 2-27
 fly ash, and, 2-15, 2-18
 shrinkage, 2-15, 4-10, 4-12
 silica fume, and, 2-32, 2-36
 carbonic acid esters, 3-12
 carboxylates, 3-5, 3-10
 carboxylic acid, 3-11
 carnauba wax, 30-18
 Casagrande's liquid limit device, 14-4, 14-5
 casing, 10-13–10-14
 casing beads, 15-18
 cast-in-place concrete, *see* concrete: cast-in-place

- cast-in-place pullout test, *see* pullout test
- cathead frame, 19-26
- cathodes, 21-52
- cathodic protection, 1-22, 3-9, 5-38, 5-39, 11-59, 11-60, 16-20, 16-26–16-27, 21-60
 - impressed current, 16-20, 16-23, 16-26, 16-27, 16-38
- cathodic reaction, 21-54
- cavity, 28-3, 28-4, 28-18, 28-19, 28-20, 28-21, 28-22, 28-50, 28-61
- CEB-FIP creep model, 4-10
- CEB-FIP shrinkage model, 4-16
- cell, 28-3
- cell decompositions, 18-9
- cellulose, 15-10, 15-11
- cement grout, 11-23, 11-24
- cement paste, *see* paste, cement
- cementitious content
 - roller-compacted concrete, 20-8, 20-10–20-20, 20-22–20-28, 20-32–20-35, 20-39, 20-41, 20-44, 20-45, 20-47, 20-49, 20-53, 20-58, 20-59, 20-62, 20-65, 20-66; *see also* cementitious materials
 - permeability, and, 20-39
- cementitious materials, 11-4–11-5, 20-7–20-15, 20-22–20-29, 20-33–20-35, 20-39, 20-43, 20-60, 20-70, 28-6, 28-38; *see also* cementitious content: roller-compacted concrete
 - activation energy, and, 21-18
 - ASTM standards for, 28-4
 - permeability, and, 20-39
- cements, 1-1, 6-30, 6-31, 9-15, 9-20, 11-16, 20-8, 20-10, 20-20, 20-25, 20-40, 20-43, 20-44, 20-45, 20-60
 - air-entraining, 5-23, 5-27, 15-17
 - alkali-activated, 6-2
 - architectural concrete, 30-12–30-13
 - blended, 5-37, 5-38, 5-41, 15-17, 15-18
 - blended hydraulic, 5-10, 5-23, 5-27, 5-39
 - cracking, and, 8-48
 - densified, 6-2
 - densified small-particle, 22-14, 22-15
 - expansive, 1-10, 23-4
 - fiber-reinforced, 22-14–22-17
 - green, 1-11
 - high-alumina, 1-10–1-11, 2-24
 - high-early-age, 8-41
 - high-early-strength, 2-14, 5-27
 - hydraulic, 1-2, 1-9, 2-5, 3-14, 15-17, 5-27, 6-2, 6-4, 15-2, 15-4, 15-9, 23-2, 33-2, 33-10, 33-16
 - blended, 5-10, 5-23, 5-27, 5-39
 - overlays, 23-1–23-16
 - lateral pressure, and, 7-24
 - low-alkali, 5-39, 5-40, 5-41–5-42, 15-17
 - macrodefect-free, 6-2, 22-14
 - magnesium phosphate, 27-27
 - masonry, 15-17, 28-8, 28-9
 - mortar, 28-8, 28-9
 - performance of in concrete, 1-11–1-12
 - perlite, 6-2
 - plastic, 15-17
 - Portland, *see* Portland cement
 - rapid-hardening, 4-11
 - shrinkage in, 4-11
 - shrinkage-compensating, 17-10, 17-13
 - slag, 1-10
 - sulfate-resistant, 1-25, 2-15, 2-17, 11-4
 - superplasticizers, and, 1-4; *see also* superplasticizers
 - supersulfated, 1-10, 1-11, 2-24
 - Type K, 23-4
 - types of, 5-36, 11-4
 - white, 11-18, 29-24, 30-12, 30-19, 30-21, 30-30
- CEMROC, 1-11
- centering, 7-16
- ceramic glaze, 30-31
- chain-drag technique, 16-3, 21-40, 27-6
- chairs, 7-14, 11-9, 11-26, 12-7, 12-43, 30-42, 30-43, 30-44
- chalcedony, 5-40
- chamfer strips, 7-17
- channel beam, prestressed, 33-3, 33-4
 - inverted, 33-5–33-6
- charge-coupled device (CCD) cameras, 21-30
- checkerboard loading, 10-16
- checklist for structural inspection, 35-17–35-18
- chemical shrinkage, 21-21; *see also* shrinkage
 - silica fume, and, 2-33
- chert, 1-19, 5-30, 5-40
- Chesapeake and Delaware Canal Bridge, 29-4–29-5, 29-13–29-14, 29-29
- chloride, 5-10, 6-2, 6-7, 11-5, 11-9, 11-46, 11-58, 11-59, 12-8, 12-9, 12-22, 12-27, 13-20, 21-47, 21-54, 23-14, 23-16, 27-22, 27-23, 30-24, 33-2, 33-12
 - corrosion, and, 5-38
 - diffusion, 24-31–24-32
 - ions, 1-22, 2-14, 2-18, 2-25, 2-36, 5-29, 5-37, 11-58, 11-59, 13-23, 16-4, 16-13, 16-22, 16-25, 23-1, 23-3, 24-27, 24-30, 35-15
 - penetration, in steel reinforcement, 24-34
 - ponding test, 5-10
 - salts, 5-38
- chromates, 3-7, 30-45
- citric acid admixtures, 23-2
- city cranes, 19-24, 19-36

- cladding, 10-5, 10-6, 30-5, 30-8
- Class C fly ash, 2-2, 2-10, 2-11–2-12, 2-15, 2-16
- Class F fly ash, 2-2, 2-10, 2-11–2-12, 2-15, 2-16
- clay, 1-2, 1-3, 1-14, 1-17, 1-20, 5-30, 6-4, 14-2, 14-5, 14-10, 14-11, 14-28, 14-76, 26-2, 31-8; *see also*
 - soil: clayey
- ASTM standards for, 28-4–28-5, 28-11–28-13
- calcined, 5-28
- consolidation settlement, and, 14-18, 14-20, 14-22
- earth pressure, and, 14-55
- expansion of, 28-38
- liners, 14-26, 14-27
- sample, undisturbed, 14-29
- saturated, 14-16–14-23
- settlement in, 14-32
- ultimate bearing capacity in, 14-31
- undrained strength of, 14-12, 14-13
- cleanouts, 7-17, 28-3, 28-21, 28-22
- clearance, 11-13, 11-20, 18-13, 30-66
 - bridge, 29-7, 29-8
 - conveyor, 20-64
 - crane, 19-26, 19-37
 - material handler, 19-46
 - precast member, 30-63, 30-66
 - sawed joints, 17-5
 - under beams and joists, 7-9
- climbing boom, 19-3, 19-8, 19-50
- climbing cage, 19-8–19-9
- climbing cranes, 19-4, 19-7, 19-8, 19-9, 19-18, 19-24, 19-25, 19-28
- climbing forms, 7-13, 19-3, 19-4
- climbing passenger hoist, 19-47
- clinker, 1-3, 1-6, 1-9, 5-23
- clip gauge, 27-19
- closed-loop testing, 27-12, 27-18
- closure strips, 12-41, 35-8–35-9, 35-13
- coal, 2-1, 2-2, 2-6, 2-29, 5-27, 5-30, 6-9
- coating factor, 36-28
- coating, corrosion-preventive, 12-4; *see also*
 - corrosion: protection
- coatings, 10-13
 - architectural concrete, 30-30
 - bridge, 29-25
- codes, 8-55–8-58
- coefficient of thermal expansion, 5-21, 13-22, 16-11, 16-13, 17-6, 20-22, 20-34, 20-70, 25-3–25-4, 27-21
- cofferdams, 15-3, 15-7, 20-9
- cohesion, 14-7, 20-34, 20-35, 20-48
- coil ties, 7-11
- cold weather, 5-32–5-33, 6-40, 16-13, 20-44, 20-53, 20-61, 21-23, 28-22, 28-23–28-24, 30-18, 30-40, 30-59, 30-63, 30-64
- collapse, 7-4, 11-32
 - progressive, 8-37, 11-32, 11-33, 12-38, 13-25
- collar joint, 28-3, 28-4
- colloidal underwater concrete, 15-10
- color, 10-3, 30-19
 - accelerated concrete, 3-8
 - aggregates, and, 30-12, 30-14, 30-16, 30-19, 30-21, 30-32
 - blast-furnace slag concrete, 2-21
 - bridge, 29-24–29-26
 - silica-fume concrete, 2-32
 - uniformity, 29-24, 30-2, 30-4, 30-12, 30-13, 30-14, 30-16, 30-17, 30-18, 30-19, 30-20, 30-21, 30-22, 30-24, 30-27, 30-31, 30-35, 30-40, 30-58, 30-59, 30-68, 30-69, 30-72
 - variation, *see* color: uniformity
- coloring pigments, 30-4, 30-6, 30-12, 30-13, 30-14, 30-16
- column bay, 10-17
- column beams, fiber-reinforced polymer systems, and, 25-16
- column capitals, 10-19, 10-21, 10-22
- column cracks, 35-5–35-6
- column displacement, 32-55
- column forms, *see* forms: column
- column stability factor, 7-34, 7-42, 7-48
- column stiffness, 32-53
- column strips, 10-19, 10-20, 10-21
- column-to-footing connections, 32-59
- column-to-superstructure connections, 32-61
- columns, 6-23, 6-40, 7-43, 8-31, 8-33, 10-11, 10-12, 10-15, 10-17, 10-20, 10-21, 10-28, 10-32–10-33, 10-38, 12-4, 12-8, 12-11, 12-30, 12-31, 13-4, 13-11, 16-5, 17-10, 17-12, 32-19, 36-18–36-21, 36-23–36-25, 36-36; *see also*
 - joints: beam–column, joints: slab–column
- axially loaded, 36-5–36-7
- cantilevered, 32-13
- cast-in-place, 10-31
- composite, 10-10
- defined, 7-26, 28-3
- ductility enhancement of, 25-11
- edge, 9-15
- effective length of, 10-16
- engineered cementitious composite (ECC), 24-18–24-19
- fiber-reinforced polymer systems, and, 25-18–25-19
- fire resistance of, 31-11–31-13
- flared, 32-56
- free-standing, 10-32
- geopolymer concrete, 26-14–26-18
- impact-echo testing of, 21-35

- columns (cont.)
 - interior, 6-35, 6-40
 - lateral drift of, 10-16
 - lift-slab construction, and, 10-31
 - maintenance of, 35-15
 - mechanized formwork for, 19-50
 - modeling of, 18-9, 18-10–18-11
 - nonslender, 36-23–36-24
 - offset of, 10-20
 - one-way slabs, and, 10-19
 - Portland cement, 26-16, 26-17
 - precast, 10-31, 11-33, 34-11
 - proportioning of, 10-15–10-16
 - rectangular, 25-19, 25-20
 - reinforced concrete, 24-18–24-19
 - retrofitting, 32-43
 - seismic resistance, and, 32-53
 - site-cast, 10-28
 - size of, 10-22, 34-23
 - slender, 10-15, 10-16, 36-24–36-25
 - square, 10-22
 - steel, 10-12, 10-28, 13-4
 - protected by masonry, 31-13
 - stiffness of, 32-51
 - sway vs. nonsway, 10-16
 - unbonded post-tensioned precast, 24-21
- combined footings, 10-10, 10-11
- compact reinforced composite (CRC), 22-14, 22-15
- compact strand, 11-10; *see also* strands
- compacted silica fume, 2-29
- compaction, 6-2, 15-19, 15-20, 15-23, 20-21, 20-34, 20-49, 20-61, 20-62, 20-65, 20-66
 - architectural concrete, 30-55, 30-56
- compartmentation, for fire protection, 31-3–31-4
- compatibility torsion, 36-22
- complete quadratic combination (CQC) method, 32-27
- components and cladding, 10-5
- composite construction, 10-7–10-10
- composite fiber wrap, 32-59
- composite metal decking, 10-9
- composite steel–concrete construction, 11-18
- composites, 22-1–22-25
- compressibility
 - pile, 14-63
 - soil, 14-2, 14-5, 14-14–14-23
- compression, 2-21, 7-30, 7-43, 7-48, 13-24, 14-14–14-23, 15-15, 20-32
 - controlled strain limit, 36-10
 - cubes, 28-8
 - edge, of a beam, 7-33
 - face shell, 28-55, 28-56, 28-65, 28-66
 - members, 36-13
 - columns, 36-23–36-25
 - compression-controlled, 36-10
 - confinement of, 36-6
 - failure, 36-5
 - tensile strain in, 36-10
 - reinforcement, 4-18, 4-21–4-22, 9-4, 9-5, 9-13, 9-17, 28-64
 - splices, 11-9
 - steel, 9-17
 - stress, 7-41, 7-42, 7-48, 23-13; *see also* stress:
 - compressive
 - allowable, 7-41, 7-42, 7-48
 - strength; *see also* compressive strength
 - overlay, 23-3
 - tests, 20-60
- compressive block, 36-7–36-9, 36-13
- compressive failure, 25-5, 25-14, 36-5
- compressive force, 10-38, 28-54, 28-56, 28-57, 28-63, 32-51
 - axial, 7-48
- compressive load, 4-5, 34-10
- compressive strain, *see* strain: compressive
- compressive strength, 4-16, 4-18, 4-22, 4-29, 5-12, 5-30, 5-35, 6-8, 6-9–6-29, 6-37, 6-41, 8-20–8-27, 8-36, 8-41, 8-52, 9-15, 9-18, 10-9, 10-10, 10-23, 11-11, 11-17, 11-52, 12-8, 12-20, 12-22, 12-26, 13-19, 13-22, 14-67, 15-2, 15-13, 16-13, 16-34, 16-35, 21-18, 21-24, 21-25, 21-27, 22-3, 24-4, 24-23, 25-18, 26-9, 27-6, 36-9
 - 3-day, 5-15
 - 28-day, 4-18, 5-32
- abrasion resistance, and, 5-17
- admixtures, and, 15-11–15-12
- air entrainment, and, 3-12
- antiwashout admixtures, and, 3-14
- architectural concrete, 30-26, 30-31
- autoclaved aerated concrete, 28-8, 28-20
- average, 6-15–6-18, 6-19, 6-22, 6-25, 6-29
- blast-furnace slag, and, 2-21–2-23
- bond strength, and, 23-5
- break-off number, and, 21-16
- cement-based composite, 22-14
- clay, 14-13
- column, 24-18
- concrete, 14-77, 14-79, 36-6, 36-16, 36-33
- concrete element, 33-2
- cube, 21-2, 21-4
- cylinder, 4-16, 4-29, 6-9–6-29, 8-21, 8-24, 8-27, 8-41, 8-43, 9-20, 13-19, 25-4, 36-2, 36-6
- dam, 10-27
- engineered cementitious composite (ECC), 24-8, 24-24

- epoxy-modified concrete, 3-17
- estimating, 6-13–6-15
- fiber-reinforced concrete, 22-9–22-10
- fly ash, and, 2-12, 2-16
- geopolymer concrete, 26-3–26-4, 26-5, 26-6, 26-7, 26-8, 26-9, 26-10, 26-11–26-12, 26-13, 26-14, 26-15, 26-16, 26-17
- curing temperature, and, 26-5
- grout, 15-3, 28-10, 28-34, 28-36
- high-strength concrete, 5-2
- indentation tests, and, 21-2
- masonry, 28-35–28-38, 28-50, 28-53, 28-62, 28-64, 28-65, 28-66, 28-68
- mass concrete, 10-27
- modulus of elasticity, and, 5-16, 20-31, 36-2
- modulus of rupture, and, 21-16
- mortar, 28-6, 28-8, 28-9, 28-23, 28-32, 28-33
- normal-strength concrete, 5-2
- normal weight concrete, 36-18
- overlay, 23-3
- polymer modifier admixtures, and, 3-16
- Portland cement, 26-4, 26-10
- probe penetration, and, 21-8, 21-9
- pullout tests, and, 21-10, 21-11, 21-12
- pulse velocity, and, 21-6, 21-7
- ratio, preplaced-aggregate concrete, 15-12
- reactive powder concrete, 22-16, 22-17
- rebound number, and, 21-4
- rectangular column, 25-20
- revibration, and, 30-57
- rock, 14-79
- roller-compacted concrete, 20-23–20-27, 20-34, 20-48, 20-61
- saturated clay, 14-12
- self-consolidating grout, 28-11
- shocked concrete, 30-4
- SIFCON, 22-15
- silica fume, and, 2-34–2-35
- slab, 8-35
- specimens, 6-42
- splitting tensile strength, and, 8-26
- structural concrete, 36-1
- temperature, and, 5-15
- testing, 16-3
- time relationship, 8-43
- ultimate load, and, 21-13
- water/cement ratio, and, 5-12
- compressive stress, *see* stress: compressive
- compressive wave, 10-13
- computational errors, 9-11, 9-12
- computer-aided design (CAD), 18-6, 18-8–18-16
 - Internet, 18-12–18-13
 - object-oriented, 18-12
- computer-aided design and drafting (CADD), 18-9
- computer-aided design/computer-aided construction (CAD/CAC), 18-10
- computer-integrated construction (CIC), 18-12
- computerized engineering model, 18-11–18-16
- Concepcion Dam, 20-9, 20-10, 20-11, 20-28, 20-33, 20-41, 20-62
- concrete
 - age, loading and, 8-32–8-33
 - air-entrained, 2-15, 2-37, 3-10, 5-35, 15-16, 20-66, 30-15; *see also* air-entraining admixtures, air entrainment
 - architectural, 30-1–30-73
 - ASTM standards for, 28-5, 28-11
 - autoclaved aerated, 28-8, 28-20, 28-38
 - barriers, 29-28
 - bendable, 24-8
 - blowouts, *see* blowouts
 - buildings, seismic-force-resisting, 32-29–32-34
 - cast-in-place, 7-20, 8-57, 10-2, 10-39, 11-5, 11-6, 11-14, 11-21–11-23, 11-29, 11-32, 11-36–11-38, 19-3, 19-4, 19-33, 19-48, 33-2, 33-6, 33-14, 34-5, 34-7, 35-2, 36-31
 - architectural, 30-2–30-73
 - cantilever segmental bridge construction, 11-40–11-42
 - post-tensioned, 11-33
 - colloidal underwater, 15-10
 - components of, 11-4–11-7
 - consistency, 5-32, 20-16–20-17
 - constituent materials, 1-1–1-26, 12-22
 - containment, 10-23
 - cover, 4-22, 4-24, 4-32, 5-38, 5-39, 9-15, 9-17, 11-8, 11-54, 11-59, 12-23, 12-24, 12-27, 12-38, 13-19, 13-23, 21-10, 24-12, 24-14, 24-29, 25-7, 26-16, 30-7, 30-15, 30-27, 30-43, 31-6, 31-12, 36-4
 - thickness of, 4-24
 - deck panels, 27-29–27-31
 - dental, 20-55, 20-67
 - early-age, 5-12–5-16, 8-19–8-37
 - elastic properties of, 2-12
 - over time, 4-16–4-18
 - epoxy-modified, 3-17, 33-2
 - equivalent thickness of, 31-8, 31-11
 - expansive, 10-25
 - exposed, 30-73
 - fiber-reinforced, 22-2–22-18
 - flowing, 5-31, 11-6, 11-13, 11-27, 11-54
 - fresh, 7-2, 7-5, 7-8, 7-10, 7-23, 7-38, 7-43, 11-32, 11-36, 11-41, 11-48
 - highly reactive metakaolin, 2-38–2-39
 - lateral pressure, and, 7-24

concrete (cont.)

- plywood, and, 7-28
- silica fume, properties of, 2-32–2-34
- supplementary cementing materials, and, 5-28
- weight of, 7-14, 7-23
- geopolymer, 26-1–26-19
- hardened, 5-34, 6-20, 13-22, 13-23
 - admixtures, and, 5-28–5-29
 - blast-furnace slag, properties of, 2-21–2-24
 - effect of retarders on, 3-2–3-3
 - entrained air in, 3-12
 - ettringite in, 5-42
 - fly ash, properties of, 2-11–2-14
 - metakaolin, properties of, 2-39
 - polymer modifier admixtures, and, 3-16
 - preplaced aggregate, 15-3
 - silica fume, properties of, 2-34–2-36
- heavyweight, 5-17, 5-29, 6-2, 6-4
- high-early-strength, 6-2, 16-19
- high-performance, 6-9–6-29, 6-30–6-41, 11-5, 11-16–11-17, 11-38, 21-23, 33-2
 - testing of, 11-7
- high-strength, 1-4, 1-9, 1-11, 1-13, 1-14, 2-35, 5-1–5-44, 6-8–6-9, 6-18–6-29, 6-30–6-41, 10-2, 11-38, 13-22, 36-1, 36-5, 36-7, 36-9
 - coarse aggregate, and, 5-29
 - cracking of, 2-33
 - creep, 2-13, 4-2, 5-22
 - density of, 5-16
 - drying shrinkage of, 5-21
 - mixture proportioning for, 6-23–6-29, 6-30
 - modulus of elasticity, 4-18
 - temperature rise in, 5-33
 - testing of, 11-7
- ingredients, 5-22–5-31
- jointed precast, 34-1
- latex-modified, 2-36, 3-16, 3-17, 5-39, 11-23, 16-15, 23-2, 23-3, 33-10–33-12
- leveling, 20-56, 20-67
- lightweight, 1-17, 5-36, 6-2, 11-30, 30-56, 31-8, 36-2, 36-7
 - loads, and, 7-23
 - prestressed, 11-17
 - shrinkage in, 4-35
- low-permeability, 33-2
- low-shrinkage, 23-16
- low-slump, 17-12, 30-43, 30-51, 30-57
- masonry units, *see* masonry units
- mass, *see* mass concrete
- microsilica-containing, 10-23
- mixers, *see* mixers
- mixing, 5-6–5-10, 6-39, 6-40, 11-6
- mixtures, design of, 6-1–6-43

- modified-density, 11-18
- no-fines, 1-15
- nondispersible, 15-10, 15-12–15-13
- nonshrink, 35-8
- normal-strength, 1-13, 5-1–5-44, 6-9–6-18, 6-19, 6-30, 36-5, 36-9
 - mixture proportioning for, 6-9–6-13
- normal weight, 5-32, 5-36, 6-2, 6-9, 6-13, 6-20, 8-26, 8-27, 8-29, 12-10, 31-8, 36-7
 - density of, 5-16
 - shrinkage in, 4-35
- no-slump, 6-5, 6-8, 20-2, 20-3, 20-20, 30-4
- placement, 5-6–5-10, 6-1–6-43, 8-9, 10-14, 10-17, 10-25, 10-27, 10-28, 11-6, 11-13, 11-26–11-27, 11-41, 12-8, 15-9, 19-4, 19-15, 19-45, 19-50, 23-10, 30-48–30-52
 - underwater, 15-6
- plastic, 2-11, 5-2, 15-21
- polymer-modified, 3-14–3-18, 6-8, 33-2, 33-10, 33-16
- post-tensioned, 10-25, 10-38, 10-39–10-40, 11-12
- precast 10-2, 10-38–10-39, 11-5, 11-42–11-43, 19-3, 19-4, 20-49, 20-51, 26-7, 30-60–30-67, 33-1–33-16, 34-1–34-24, 36-32
 - architectural, 30-4–30-73
- precast pretensioned, 11-25, 11-28, 11-29–11-33
- preplaced-aggregate, 15-2–15-6, 16-13
- prestressed, *see* prestressed concrete
- pretensioned, 10-25, 10-38–10-39, 10-40, 16-16
- prism test, 5-40, 8-30, 8-52, 28-35, 28-36–28-38
- pumping distance of, 19-15
- reactive powder, 5-2, 22-14, 22-16–22-17
- ready-mix, 19-14, 19-17
- recycled, 5-29
- reinforced, *see* reinforced concrete
- removal of, 23-6
- resistivity, 21-54–21-56
- roller-compacted, *see* roller-compacted concrete
- self-consolidating, *see* self-consolidating concrete
- shocked, 30-4
- shrink-mixed, 5-6
- silica fume, *see* silica fume
- site-cast, 10-28, 30-58, 33-3, 33-4, 33-5, 33-6, 33-8, 33-9, 33-10, 33-12, 33-14, 33-15, 33-16
- slurry-infiltrated fiber, 22-14–22-15
- stain, 29-26
- structural, 10-1–10-40, 11-17
- structural elements, 36-1–36-36
- super-high-strength, 22-16
- syrene–butadiene resin, 3-16, 3-17
- transporting, 5-6–5-10, 11-6

- truck-mixed, 5-6
- underwater, 3-13, 15-6–15-13
- unit weight of, 5-29, 11-17, 13-23, 26-7, 26-9, 26-10
- unreinforced
 - creep, 8-31–8-34
 - shrinkage, 8-29–8-31
- vacuum, *see* vacuum processing
- very high-strength, 6-18
- weight of, 15-9
- concrete–air interfaces, 21-44, 21-62
- concrete-to-concrete friction coefficient, 34-7
- condensed silica fume, 5-27
- condition assessment, 16-3, 16-4
- conduits, 12-8
- cone penetration test, 14-7, 14-13–14-14, 28-32
- cone snap ties, 30-38; *see also* ties: snap
- confined compressive strain, 25-19, 25-20
- confinement, compressive strength and, 36-9
- connectors, ASTM standards for, 28-5
- consolidated drained/undrained tests, 14-8–14-11
- consolidation, 5-2–5-6, 10-27, 11-6, 12-8, 12-22, 13-18, 13-22, 13-23, 13-26, 15-13, 15-20, 19-19, 23-10, 23-11, 23-16, 30-4, 30-16, 30-21
 - architectural concrete, 30-52–30-58
 - grout, 28-20–28-21
 - mobility slope, and, 21-36
 - settlement, 14-17, 14-18, 14-20, 14-22
 - test, one-dimensional, 14-17, 14-19
- constant rate of penetration test, 14-73
- constructability, 6-30, 6-40, 10-2–10-3, 16-11, 16-18, 19-4, 25-9, 29-19, 30-43, 33-3, 34-20
- construction joints, *see* joints: construction
- construction load, *see* load: construction
- construction load factor, 8-41–8-42
- Construction Robotics Management System (CREMS), 18-7
- construction tolerances, masonry, 28-26–28-27
- construction variations, 9-15
- construction, masonry, 28-15–28-27
- constructive solid geometry (CSG), 18-9–18-10
- contact surface materials, 7-6–7-8
- contact time, impact-echo testing, 21-34
- contaminants, in water, 15-4
- Context-Sensitive Design (CSD), 29-10–29-11
- continuous beams, 4-20
- continuous footings, 10-30
- continuous members, 9-7, 9-19
- continuous mixers, 20-59, 20-60, 20-62
- continuous multiple-span bending members, 7-35, 7-38, 7-44, 7-45
- contraction, 17-6, 17-10, 20-22, 20-54
 - thermal, 20-11, 23-14
- contraction joints, *see* joints: contraction
- control joints, *see* joints: control
- control tests, 5-33
- conveyors, 5-6, 11-6, 15-8, 19-45, 20-2, 20-10, 20-54, 20-61, 20-61–20-65, 20-68, 20-70, 30-51
 - belt speed of, 20-63
 - crawler-mounted, 20-62
 - wheel-mounted, 20-62
- coolants, 10-27
- corbels, 10-39, 36-18–36-21
- coring, 16-3, 16-4, 16-16, 16-22, 16-25, 20-38, 20-67, 27-5, 27-25
- corner reinforcement, 15-18
- correlation testing, 21-27–21-28
- corrosion, 1-21–1-22, 1-23, 3-7, 3-8, 4-32, 5-10, 5-11, 6-7, 11-5, 11-9, 11-18, 11-19, 11-33, 11-34, 11-55, 11-58, 12-3, 12-4, 12-22, 12-23, 12-27, 13-19, 15-2, 16-14, 16-2, 16-17, 16-18, 16-23, 16-24, 16-25, 16-29, 16-37, 16-38, 16-39, 16-40, 17-13, 22-23, 22-24, 23-16, 24-29, 24-30, 27-2, 27-5, 27-22, 27-23, 30-15, 35-8, 35-15, 36-4
 - assessment of, 16-25
 - blast-furnace slag, and, 2-27
 - calcium chloride, and, 5-31
 - carbonation, and, 2-15, 2-27
 - chloride-induced, 16-20, 16-23
 - evaluation of, 21-52–21-60
 - fly ash, and, 2-17–2-18
 - inhibitors, 1-22, 3-8, 3-9, 5-38, 5-39, 11-5, 11-58, 11-59, 11-60, 12-4, 12-5, 16-16, 16-18
 - categories of, 3-9
 - setting times, and, 3-9
 - overlays, and, 23-3, 23-5
- pavement, 11-58
- pier, 27-23
- pile, 11-46
- potential, 21-53
- protection, 5-37–5-39, 11-2, 11-10, 11-12, 11-19, 11-23–11-24, 11-38, 11-60, 12-2, 12-4, 12-9, 12-31, 16-14, 16-15, 16-18, 16-19
- rate testing, 21-60
- reinforcing bar, 13-20
- reinforcing steel, *see* reinforcing steel: corrosion of resistance, 5-29
 - steel-reinforced engineered cementitious composite (R/ECC), 24-33–24-36
- seasonal variation in, 21-59
- steel reinforcement, 16-1, 16-2, 16-14, 16-20
 - rate of, 16-3, 24-34
- strand, 12-23
- strength, and, 16-2
- water/cement ratio, and, 5-32, 5-39

- cost analysis, life-cycle, 16-23–16-24
- cost estimates, equipment, 19-4–19-5, 19-6–19-10
- Coulomb method, 14-9, 14-10, 14-46–14-47
- Coulomb's friction principle, 14-7
- counterforts, 10-26
- counter-jib, 19-25, 19-26
- coupler, tendon, 12-20, 12-21, 12-43
- cover dimension, 36-28
- covermeters, 21-48–21-52, 21-58
- crack comparator, 21-30
- crack control, 4-30, 4-31–4-32, 4-34, 5-20–5-21, 5-33, 5-38, 17-5, 17-12, 17-13–17-14, 20-8, 22-3, 22-9, 22-17, 24-6, 24-22–24-23, 36-4–36-5, 36-27–36-28; *see also* joints
- crack evaluation, 35-12–35-13
- crack, inclined, 27-4, 36-15
- crack, moving, 16-14
- crack repair, 16-14
- crack resistance, 20-32, 20-33
- crack spacing, 4-22, 4-25–4-26, 35-4
- crack width, 4-18, 4-22–4-34, 5-21, 11-42, 12-31, 22-17, 35-4, 36-4, 36-5, 36-27, 36-28
 - architectural concrete, 30-70
 - engineered cementitious composite (ECC), 24-6, 24-9, 24-22–24-23, 24-24, 24-27, 24-32, 24-34, 24-36, 24-37
 - flexural, 4-22–4-34, 25-5, 25-7
 - maximum, 25-7
- cracked second moment, 25-8
- cracked stiffness, 9-16, 32-51
- cracking, 2-33, 2-34, 4-2, 4-11, 4-18, 4-22, 5-34, 5-40, 6-39, 6-40, 8-51, 10-6, 10-7, 10-12, 10-16, 10-17, 10-23, 10-24, 10-26, 10-30, 10-38, 10-40, 11-4, 11-7, 11-14, 11-27, 11-30, 11-50, 11-52, 11-54, 11-57, 11-58, 11-59, 11-60, 11-61, 12-22, 12-24, 12-28–12-30, 12-32, 13-22, 15-16, 17-1, 17-2, 17-6, 20-18, 26-14, 27-2, 27-4, 30-36, 30-59
 - architectural concrete, 30-70
 - causes of, 35-2–35-6
 - chloride salts, and, 5-38
 - circular prestressed concrete tank, 4-33–4-34
 - column, 35-5–35-6
 - computing, 9-4–9-5
 - corner, 11-15–11-16
 - creep loading, and, 8-51
 - dam, 21-6
 - flexural, 4-30–4-31, 8-27, 8-34–8-37, 9-3, 9-6, 9-7, 25-5, 25-7, 25-14, 27-23, 27-25, 36-4–36-5
 - flexural stiffness, and, 9-12
 - Griffith, 24-7
 - groove, 17-5
 - high-strength prestressed beam, 4-29–4-30
 - laminar, 11-41
 - load, 4-25, 8-34, 8-35, 8-36
 - masonry, 28-38
 - mass concrete, 20-31
 - mitigation, 35-1–35-13
 - modulus of rupture, and, 9-19
 - moment, 4-18–4-22, 9-4, 9-12, 9-13, 28-67, 36-4
 - mortar, 28-9
 - negative moment zone, 11-36
 - notes on structural drawings regarding, 12-6, 12-9–12-10
 - overlay, 23-2, 23-4, 23-5, 23-12, 23-13, 23-14, 23-16
 - pavement, 11-58, 17-15
 - plastic, 5-28, 5-32
 - pozzolans, and, 20-30
 - precast concrete subdeck panels, and, 33-9
 - prestressing, and, 11-18
 - pulse velocity, and, 21-8
 - repair, 12-28–12-30, 16-12
 - restraint, 35-2, 35-7, 35-13
 - roller-compacted concrete, 20-7, 20-22
 - settlement, 30-56
 - shear, 25-14
 - shear key, 27-28
 - shrinkage, 2-34, 3-14, 20-49, 20-51, 28-51, 28-62, 35-2, 35-4
 - silica fume, 2-34
 - slab, 8-4, 17-10, 17-11, 35-4
 - stress, 9-16, 14-27
 - sulfate attack, and, 5-42
 - surface, map-pattern, 5-39
 - tensile, 11-15, 36-29
 - thermal, 6-40, 13-23, 13-26, 20-10, 20-44, 20-51, 20-56, 30-16, 30-59
 - torsional, 9-8, 9-9
 - types of, 35-2–35-6
 - unbonded post-tensioned vs. reinforced-concrete slab, 35-4
 - vertical, 17-6, 17-8
 - volumetric change, 17-1, 17-2, 17-5, 17-8
 - wall, 35-6
 - wall-slab, 4-34
 - web-shear, 8-27
 - wedge, 12-21
- crane employment table, 19-5, 19-6
- crane trucks, 19-43–19-44
- cranes, 5-6, 7-5, 7-9, 7-11, 11-31, 11-34, 11-44, 11-50, 12-38, 12-39, 12-40, 13-4, 18-5, 19-1–19-12, 19-21–19-43, 20-63
 - A-frame, 19-26
 - all-terrain, 19-36, 19-39–19-40
 - anticollision systems for, 19-40–19-43

- barge-mounted, 11-40, 13-4, 29-13
- city, 19-24, 19-36
- climbing, 19-4, 19-7, 19-8, 19-9, 19-18, 19-24, 19-25, 19-28
- crawler, 11-35, 19-21, 19-37, 20-62, 20-63, 29-14
 - undercarriage, 19-35
- creter, 20-62
- cycle times for, 19-6, 19-34
- daily employment of, 19-5
- deployment of, 19-9
- dismantling of, 19-9
- fast-erecting, 19-22
- flat-top, 19-26
- hoist, 18-5
- internal climbing, 19-4, 19-27, 19-28–19-29
- lifting hook, 19-6
- loader, 19-43
- luffer, 19-26
- mobile, 19-2, 19-9, 19-21, 19-26, 19-27, 19-28, 19-32, 19-34–19-40, 30-4
 - maximum lifting capacity, 19-36
 - types of, 19-35–19-40
- pump use with, 19-15
- rough-terrain, 19-37–19-38, 19-39, 19-44, 19-47
- self-erecting, 19-22
- service, 19-43
- software for selection of, 19-40
- specialized, 19-40
- taxi, 19-43
- topless, 19-26
- tower, 10-33, 11-32, 18-5, 19-2, 19-3, 19-4, 19-8, 19-9, 19-18, 19-21–19-34, 19-37, 19-40, 30-72
 - American-type, 19-37
 - bottom-slewing, 19-22, 19-29–19-32, 19-33
 - classification of, 19-33
 - flat-top, 19-22
 - sectional, 19-24, 19-29
 - telescopic, 19-29
 - top-slewing, 19-22–19-29, 19-33
 - traveling, 19-22, 19-29
- track-mounted, 19-21
- truck, 11-30, 11-32, 11-35, 19-36, 19-39, 19-43
- truck-mounted, 19-21, 19-29, 19-32, 19-36, 19-43
- undercarriage of, 19-22–19-24
- crazing, 30-21, 30-31, 30-59, 30-73
- creep, 2-13, 2-23, 2-35, 3-8, 3-14, 4-1–4-10, 4-18, 4-21, 5-2, 5-21–5-22, 5-29, 8-48, 9-6, 9-11, 9-15, 9-18, 9-20, 11-2, 11-4, 11-17, 11-20, 11-23, 11-26, 11-30, 11-32, 11-40, 11-41, 11-42, 11-50, 12-6, 12-8, 12-10, 12-29, 12-31, 12-43, 13-22, 15-12, 16-11, 16-12, 17-1, 22-14, 23-2, 23-14, 25-7, 35-2, 36-2, 36-3
- age, and, 8-32–8-33
- axial, 35-3
- basic (true), 8-31
- CEB-FIP model for, 4-10
- coefficient, 9-6, 9-7, 9-15, 26-13, 36-2
- defined, 20-70
- deflection, and, 8-49–8-52, 9-4, 9-12, 9-17, 9-19, 10-8
- deformation, 4-2–4-6, 14-51
- drying, 4-8, 8-31, 8-32, 8-33
- effects of, 4-5
- factors affecting, 4-7–4-8
- geopolymer concrete, 26-12–26-13, 26-18
- high-range water reducers, and, 3-7
- irreversible nature of, 8-33–8-34
- leveling concrete, 20-56
- long-term, 9-6
- member size, and, 8-33
- prediction, 4-6–4-10
- prestressing, and, 11-4
- recovery, 4-4, 8-33
- relative humidity, and, 8-33
- rheological models for, 4-5–4-6
- roller-compacted concrete, 20-11, 20-22, 20-29, 20-32, 20-34, 20-53
- rupture, 25-3, 25-8, 25-13
- silica fume, 2-35
- specific, 4-6, 8-31–8-32, 26-13
- strain, 2-23, 2-35, 4-1, 4-2, 4-3, 4-6, 4-7, 4-8, 5-22, 8-49–8-51, 17-2, 26-13
- temperature, and, 9-6
- time, and, 8-33
- unreinforced concrete, 8-31–8-34
- wetting, 4-8
- creter cranes, 20-62
- cristobalite, 2-29, 5-40
- critical damping, 32-48
- critical depth ratio, 14-58
- critical fiber length, 22-5–22-6
- critical fiber spacing, 22-6–22-7
- crossing-beam method, 9-7
- cross-power spectrum, 21-38
- cruise ship docks, 13-14
- crumbling, 5-34
- crushed stone, 1-15, 5-2, 5-29, 6-3, 6-36, 11-4, 13-21, 15-6, 15-9, 15-25, 31-7
- crushing, of concrete, 10-40, 36-13, 36-23
- cryogenic liquids, 11-55
- crystalline phases, fly ash, 2-6
- cube compressive strength, 13-19, 21-2, 21-4, 28-8
- cube strength, 8-21, 8-24
- cubes, 11-7, 20-20
- culverts, precast, 33-15

cure time, antiwashout admixtures, and, 3-14
 curing, 2-26, 2-33, 5-15, 5-29, 6-2, 6-40–6-41, 8-49,
 10-3, 10-27, 10-28, 10-39, 11-6–11-7, 11-16,
 11-25, 11-27, 13-18, 13-26, 15-25, 16-14,
 16-18, 20-34, 20-51, 26-2, 30-21
 abrasion resistance, and, 2-16
 accelerated, 3-15
 air, 23-3
 architectural concrete, 30-58–30-59
 blast-furnace slag, and, 2-21
 cold-weather, 30-59
 compound, 2-34, 5-15, 20-55, 30-58
 cracking, and, 17-14
 creep, and, 9-18
 deflection, and, 9-18
 dry, 2-35, 4-35, 23-4, 26-5
 fly ash, and, 2-15
 fog, 15-16
 geopolymer concrete, 26-5–26-6
 heat, 11-27, 22-17, 26-4, 26-5–26-6, 26-7, 26-11,
 26-12, 26-13, 26-14, 26-15
 hot-weather, 30-59
 membrane, 11-6, 30-59
 methods of, 5-32
 moist, 2-12, 2-15, 2-16, 2-23, 2-35, 2-36, 4-13,
 5-10, 5-11, 5-32, 5-35, 8-20, 8-21, 8-22,
 8-29, 8-31, 15-19, 20-69, 23-3, 23-4, 23-12,
 30-58–30-59, 36-3
 overlay concrete, 23-11–23-12
 prism, 28-37
 repairs, 30-69
 roller-compacted concrete, 20-69–20-70
 shrinkage, and, 4-35, 9-18
 steam, 3-8, 4-13, 11-6, 11-15, 11-18, 11-27, 11-28,
 11-39, 21-17, 26-5, 26-6, 26-7, 26-13,
 26-15, 36-3
 temperature, 2-12, 2-15, 2-21, 2-35, 5-15,
 8-20–8-22, 8-24, 21-17, 21-18–21-24, 23-2,
 26-5, 26-7, 26-11–26-12, 26-14, 26-15,
 27-20, 30-58
 test specimen, 21-3
 time, overlays and, 23-2
 water, 2-35, 3-17, 6-40, 8-20, 15-15
 wet, 11-5, 11-6, 23-4, 24-11, 24-26
 wet burlap, 5-15, 8-24, 11-58, 15-25, 23-12
 curtain walls, 30-8, 31-4
 cushion block, 11-53, 11-54
 cut and pullout (CAPO) test, 21-15
 cyclic quasi-static loading, 27-9
 cylinder compressive strength, 4-16, 4-29, 6-9–6-29,
 8-21, 8-24, 8-27, 8-41, 8-43, 9-20, 13-19, 25-4,
 36-2, 36-6
 cylinder splitting test, 26-10

cylinders, 5-33, 8-24, 8-29, 8-32, 8-33, 8-37, 8-43,
 8-57, 11-7, 11-28, 11-32, 12-8, 13-2, 20-27,
 20-28, 20-30, 20-42, 20-43, 20-61, 21-9, 21-10,
 21-12, 21-21, 23-3, 24-11, 26-4, 26-5, 26-10,
 26-11, 26-12, 26-14, 27-6, 27-25, 28-34
 servohydraulic, 27-10–27-13

D

D'Arcy's law, 14-24
 damage tolerance, 24-22
 damping, 32-48, 32-49, 32-50
 dams, 10-27, 13-9, 14-10, 14-11, 14-24, 15-14, 15-23,
 20-22, 20-32, 20-33, 20-38, 20-39
 cementitious materials, and, 20-8
 cracking in, 21-6
 downstream slope of, 20-44
 fill and embankment, 20-7
 horizontal zones of, 20-48
 resurfacing of, 15-3
 roller-compacted concrete, 20-1–20-14,
 20-41–20-70
 width of, 20-45
 dashpots, 4-5, 4-6
 data acquisition, structural test, 27-13–27-21
 Davisson's offset limit method, 14-74, 14-75
 D-cracking, 27-5, 27-22
 De Beer's method, 14-74
 dead load, 7-14, 7-27, 8-6, 8-41, 9-7, 9-17, 10-9,
 10-10, 10-20, 10-31, 11-38, 11-40, 20-40, 27-3,
 27-26, 28-41, 36-31, 36-33, 36-34
 balancing, 9-18
 classifying, 10-4
 compressive stresses, 28-52, 28-62
 concrete, 7-23, 7-24, 9-12, 9-18
 concrete beam, 12-36
 deflection, and, 8-43, 11-36, 11-38, 25-8
 demolition, and, 12-39, 12-41
 diaphragm, 32-34
 distribution, 8-42, 11-21
 engineered cementitious composites, and, 24-4
 factor, 25-9, 25-12
 factored, 8-34, 25-13, 34-9
 formwork, 7-23, 7-38, 8-2
 gravity load, and, 10-5
 load factor for, 10-4
 moments, 9-13
 offshore structure, 13-23
 reinforcement, 7-2
 seismic, 32-12, 32-22, 32-23, 32-27, 34-2, 34-3,
 34-9, 34-10, 34-21
 slab, 7-23, 7-38, 8-13, 8-38–8-39, 11-34, 12-30,
 12-41

- spans, and, 10-16
- temporary supports, and, 11-23, 11-32
- use of for load testing, 27-9–27-10, 27-28
- deadman, 7-16, 14-53
- deaerating agent, 3-14
- debond length, 34-16, 34-17
- debonding, 34-5
 - fiber-reinforced polymer systems, 25-14, 25-16
- decentering, 7-16
- decompression load, 4-26, 4-27
- deconstruction analysis, 12-39
- decorative surface, 7-7
- deemed-to-comply design, 28-41
- deep-draft concrete floaters (DDCFs), 13-9, 13-11–13-13
- deflection, 4-5, 4-18, 4-20, 4-21, 4-32, 7-39, 7-43, 9-1–9-22, 10-17, 10-19, 10-23, 10-30, 11-30, 11-32, 11-33, 11-36, 11-41, 11-43, 11-48, 11-60, 12-28, 12-30, 12-31, 12-32, 12-38, 16-29, 20-32, 22-17, 22-21, 22-23, 25-6, 25-8, 25-14, 27-4, 28-38, 28-66, 30-61
 - allowable, 9-20–9-22
 - amplification factor, 32-13, 32-26
 - angle, engineered cementitious composite (ECC), and, 24-19
 - beam, 36-9
 - bending, 7-34
 - calculating, 28-67
 - construction techniques for, 9-18–9-19
 - control, 36-3–36-4, 36-27
 - creep, 8-49–8-52, 9-12, 9-19, 10-8, 36-2
 - dead load, 10-10, 11-38
 - design techniques for, 9-16–9-18
 - engineered cementitious composite (ECC), 24-8, 24-19
 - factors affecting, 9-10–9-15
 - flexural, 9-14, 25-13
 - formwork, 30-34–30-35
 - frame, 10-6
 - horizontal, 16-40
 - hydraulic testing, and, 27-13
 - incremental, 9-4, 9-5, 9-20, 9-21, 9-22
 - lateral, 10-15, 10-16, 36-25
 - limits, 7-39, 7-40, 7-41, 7-44, 7-46, 9-18, 9-20, 9-21
 - load testing, and, 27-3–27-4
 - long-term, 8-49–8-51, 9-4, 9-6–9-7, 9-12, 9-17
 - materials selection, and, 9-20
 - maximum, 25-7, 25-8
 - midbay, 9-7
 - mid-span, 10-8, 26-17
 - modal testing, and, 27-9
 - overlays, and, 23-15
 - pile, 14-73
 - plate, 14-31
 - reducing, 9-16–9-20
 - remote monitoring of, 27-28
 - response, 9-1, 9-2, 9-3, 9-16, 9-18
 - second-order, 16-28
 - seismic activity, and, 10-7
 - shear, 7-34
 - shrinkage, and, 8-49, 8-51, 8-52
 - slab, 4-5, 8-2, 8-11, 8-52–8-55
 - causes of, 8-48–8-49
 - control of, 8-52–8-55
 - story drift, and, 32-25–32-26
 - strand, 11-28
 - temperature, 9-9–9-10
 - torsional, 9-7–9-9, 32-25
- deflectometers, 27-28
- defoaming agents, 3-12
- deformability, 5-43
- deformability factor, engineered cementitious composite (ECC), 24-10–24-11
- deformation, 4-1–4-6, 4-18, 4-22, 5-21–5-22, 11-9, 11-36, 11-38, 11-56, 11-61, 12-31, 12-43, 13-25, 20-27, 20-30, 20-32, 22-10, 22-17, 32-12, 32-18
 - axial load, 25-3
 - column, 8-11, 8-12
 - compatibility, 32-43
 - creep, 4-2–4-6 8-34, 14-51
 - cyclic inelastic, 32-18
 - dams, 20-32
 - elastic, 11-41
 - embankment, 20-48
 - engineered cementitious composite (ECC), and, 24-2, 24-3, 24-6, 24-22, 24-24, 24-31
 - epoxy, 16-11
 - ground movement, 14-55
 - in tanks, 11-54
 - post-yield, 34-1, 34-7, 34-8, 34-11
 - remote control sensing of, 27-21
 - roller-compacted concrete, 20-17
 - shores, 8-2
 - slab, 8-2, 8-48, 17-11
 - surface, 4-31
 - temperature, and, 8-51, 12-6
 - tensile, 24-6
- deformed bars, 1-21, 8-23, 36-29
- deicers, 1-22, 2-15, 2-17, 2-37–2-38, 2-39, 3-7, 3-10, 5-10, 5-29, 5-31, 5-32, 5-34–5-35, 5-37, 5-38, 5-39, 5-40, 11-20, 11-34, 11-58, 12-5, 16-13, 23-5, 24-27, 27-23, 35-15, 35-16
- delamination, 11-8, 11-18, 11-38, 11-50, 11-55, 11-59, 12-22, 15-17, 16-6, 16-20, 16-24, 16-25, 16-27, 21-28, 21-35, 21-37, 21-40

- delamination (cont.)
 - causes of, 23-2, 23-4, 23-12, 23-13, 23-14
 - chain-drag test, and, 27-6
 - detection of, 21-31, 21-40, 21-47
 - fiber-reinforced polymer strengthening system, 25-14
 - randomly distributed, 16-30
 - spall, 35-15
 - stress, 11-8
- delayed ettringite formation (DEF), 5-42
- delta frame, 29-5, 29-13, 29-14
- demolition, 11-60–11-61, 12-36–12-42
 - ball and crane, 12-40
 - engineered vs. nonengineered, 12-39
 - explosives, and, 12-40
 - grit blast, 23-6
 - high-rise structure, 12-41
 - hydro, 23-6, 23-8
 - pressure bursting, 12-40
 - shot blast, 23-6
 - thermal lance, 12-40
 - torch, 12-40
- densification, 5-11
- densified cement, 6-2
- densified small-particle (DSP) cement, 22-14, 22-15
- Densit®, 24-12
- density, 5-16–5-17, 21-5, 21-31, 21-32, 24-9
 - maximum achievable, 20-21
 - meter, 21-60, 21-61
 - roller-compacted concrete, 20-21
 - theoretical air-free, 20-21, 20-71
- dental concrete, 20-55, 20-67
- derricks, 19-28, 19-29
- deshoring, 12-9
- design, of concrete mixtures, 6-1–6-43
- destressing, 11-61
- destructive testing, 12-23, 12-27, 12-28, 16-4
- detensioning, 12-27, 12-38, 12-41, 12-43
- detergents, synthetic, 3-11
- deterioration, 5-34, 5-38, 5-39, 12-22, 12-29, 12-30, 12-42, 13-19, 16-2, 16-3, 16-4, 16-8, 16-10, 16-11, 16-12, 16-13, 16-14, 16-15, 16-17, 16-19, 16-20, 16-22, 16-23, 16-24, 22-24, 24-29, 27-2, 35-15
 - assessment of, 16-4, 16-25
 - bridge, 27-22
 - engineered cementitious composite (ECC), 24-35
 - freeze–thaw, 20-22
 - load testing, and, 27-3
 - pavement, 17-15
 - removal of, 23-6
 - see also* repair, of concrete structures
- deviation points, 11-28, 11-29
- deviators, 11-24, 11-46
- dewatering, 15-3, 15-6
 - excavations, 14-25–14-26
- dial gauges, 27-13, 27-16
- diamond saws, 12-40
- diaphragm, 32-34, 33-6, 33-8
 - abutments, 32-53
 - defined, 32-62
 - flexible vs. rigid, 32-18
 - floor, 32-28
 - horizontal, 32-45
 - roof, 32-28
 - stiffness, 32-18
- diatomaceous earth, 5-28
- dibutylphthalate, 3-12
- dicalcium silicate, 23-2
- dielectric constants, 21-44, 21-47, 21-48
- diesel hammer, 11-52, 11-53
- differential settlement, 10-14
- diffusion coefficients, 2-14, 2-24
- diffusion constant, overlay concrete, 23-14
- digital video cameras, 21-30
- dinky, 20-61
- direct costs, equipment, 19-7
- direct-design method, 10-20
- direct-member strengthening, 12-30–12-31
- discoloration, architectural concrete, 30-3, 30-15, 30-18, 30-28, 30-35, 30-36, 30-52, 30-58, 30-59, 30-67, 30-68, 30-70
- discrete footings, 10-30
- disintegration, 6-3
- dispersion curve, 21-38, 21-39
- dispersion resistance, 15-11
- dispersion, uniform, 22-4
- displacement, 7-3, 9-19, 10-14, 10-15, 11-8, 27-28, 32-49, 32-50, 32-51, 32-52, 32-58, 32-61
 - analysis, 32-57
 - capacity, 32-58
 - column, 32-55
 - ductility analysis, 32-58–32-59
 - incremental, calculating, 16-28
 - lateral, 35-10
 - longitudinal, 32-52
 - post-tensioned member, 35-8
 - spectral, 32-51
 - strand, 11-50
- distance from energy release, ground motion and, 32-3–32-5
- dobie blocks, 11-9, 11-26
- docks, 13-4
 - floating, 13-9, 13-14
- dolomite, 1-20, 30-26
 - crushed, 5-17

- domes, 7-9
 - double-tee, 11-30, 11-36
 - prestressed, 11-29, 33-4
 - dowels, 11-60, 12-7, 17-7, 17-11, 17-12, 17-13, 17-15, 32-45, 35-5, 35-10
 - dozer, *see* bulldozers
 - drainage, bridge, 29-29
 - drainage, soil, 14-7
 - drains, 11-20
 - dam, 20-38, 20-41, 20-42, 20-47, 20-49, 20-51
 - dredged channels, 13-30, 13-31
 - D-regions, 36-15
 - drift error, 27-16, 27-17, 27-19
 - drift ratio, 34-14, 34-15, 34-18
 - drilling rigs, 13-9
 - drip screeds, 15-18
 - drop caps, 10-19, 10-21, 10-22, 10-23, 12-8, 12-30
 - drop hammer, 11-53
 - drop panels, 8-16
 - drop shoots, 5-7
 - drop tables, 30-4
 - drophead, 7-14
 - drum mixers, 20-59
 - dry docks, 13-4, 13-14, 13-15, 13-26–13-28, 13-31
 - dry mixtures, 20-16, 20-17, 20-20, 20-59, 20-68
 - dry-pipe placement, 15-8–15-9
 - dry-rodDED unit weight (DRUW), 6-24
 - dry sample boring, 14-28
 - drying
 - flexural cracking, and, 8-34–8-37
 - time required, 4-11
 - drying shrinkage, 1-10, 1-22, 3-8, 3-14, 3-15, 4-1–4-2, 4-10, 4-11, 4-12, 5-11, 5-21, 5-29, 5-31, 11-15, 11-27, 11-49, 11-55, 15-3, 15-13, 16-11, 17-1, 17-3, 17-10, 17-13, 17-14, 20-56, 22-14, 23-4, 23-12, 28-35, 28-38
 - blast-furnace slag, and, 2-23
 - fly ash, and, 2-14
 - geopolymer concrete, 26-12–26-13, 26-18
 - metakaolin, and, 2-39
 - silica fume, and, 2-35
 - drypack, 30-63, 30-64, 30-66, 30-69
 - duct, 16-16
 - Ductal®, 24-3–24-4, 24-12
 - ductile moment, 10-2
 - ductile rod, 34-7, 34-8, 34-10, 34-18, 34-19
 - ductility, 10-6, 10-14, 10-17, 10-39, 11-43, 13-25, 16-34, 16-40, 22-9, 22-16, 22-17, 24-2, 24-4, 24-5, 24-6, 24-7, 24-8, 24-21, 24-23–24-24, 24-27, 24-29, 24-37, 24-38, 25-9, 25-11, 25-18, 32-29, 32-43, 34-7–34-18, 36-9, 36-10
 - analysis, 32-57, 32-58–32-59
 - carbon fiber, 22-21
 - carbon-fiber-reinforced plastic, and, 22-23
 - enhancement of, 25-19–25-20
 - factor, 32-51
 - index, 36-9
 - ducts, 11-21, 11-23, 11-33, 11-36–11-37, 11-38, 11-39, 11-42, 11-43, 11-55, 12-2
 - installing, 11-20
 - metal, 16-16
 - plastic, 16-16
 - polyethylene, 11-46
 - post-tensioning, 11-5, 11-12–11-13
 - prestressing, 11-41
 - durability, 1-23–1-26, 2-6, 2-9, 2-11, 2-14–2-18, 2-20, 2-24–2-27, 2-36–2-38, 2-39, 3-1, 3-3, 3-4, 3-6, 3-7, 5-2, 5-6, 5-10, 5-30, 5-31, 5-38, 6-30, 10-2, 10-38, 11-2, 11-3, 11-4, 11-17, 11-61, 12-1, 12-23, 13-19, 13-22, 13-23, 16-2, 16-8, 20-70, 25-9
 - admixtures, and, 5-29
 - concrete cover, and, 11-8
 - corrosion, and, 16-2
 - gap grading, and, 30-15
 - limit state, 16-2, 16-27
 - mortar, 28-6
 - repair, 16-12–16-13
 - vacuum processing, and, 15-14
 - water/cement ratio, and, 5-32
 - duty-cycle work, 19-35
 - dynamic increase factor, 20-45
 - dynamic load, cracking, and, 22-14
 - dynamic load test, 14-73
 - Dywidag Ductile Connector (DDC®), 34-8, 34-11, 34-18, 34-19, 34-20
- ## E
- early-age concrete, 5-12–5-16, 8-19–8-37
 - earth pressures, 14-43, 14-44–14-48, 14-50, 14-52, 14-53, 14-55, 14-60, 16-34
 - lateral, 16-33
 - earthquake ground motion, *see* ground motion
 - earthquake loading, 16-29, 16-33, 16-35, 16-36, 16-37
 - earthquake magnitude, 32-3, 32-5
 - earthquakes, 10-14, 11-31, 11-54, 11-60, 13-25, 16-23, 16-24, 20-45, 22-21, 24-22, 28-41, 28-42, 28-43, 34-7, 35-10; *see also* ground motion
 - force, and, 32-49
 - ECC, *see* engineered cementitious composite
 - eddy currents, 21-48, 21-49–21-50, 21-51
 - edge form, 10-28, 12-17, 12-18, 12-20, 12-43
 - effective absorption, 1-16

- effective chloride diffusion coefficient, 24-31, 24-34
- effective length, 10-16
- effective seismic weight, 32-22
- effective stress, 14-7, 14-9–14-10, 14-16
- efflorescence, 1-25, 11-19, 28-14, 30-70, 30-70–30-71
- effluent leakage, 17-7, 17-8
- elastic calculation methods, 9-2–9-5
- elastic modulus, *see* modulus of elasticity
- elastic shortening, 4-27, 35-2, 35-3
- elastic springs, 4-5, 4-6
- elastic stiffness, 21-37
- elastic strain, 4-1, 4-2, 4-3, 4-4, 4-5, 5-21, 5-22, 17-2, 26-13
 - delayed, 4-5
 - delayed recoverable, 4-5
- electrical conductance–rapid chloride permeability test, 5-10
- electrical instrumentation, 27-17–27-21
- electrical resistance strain gauges, 27-18–27-19
- electrical resistivity, 11-5, 11-56
- electrodes, 21-57, 21-58
- electrolytes, 16-26
- electromagnetic induction, 21-48
- electromagnetic waves, 21-42
- elevator shaft, 19-4, 19-8, 19-28
- elevator, crane, 19-25
- Elk Creek Dam, 20-63, 20-66
- elongation, 12-9, 12-19, 12-20, 12-21, 12-43, 17-6
- embankments, 14-10, 14-11, 20-1, 20-17, 20-48, 20-66
- embedment depth, pile, 14-52, 14-53, 14-54, 14-55, 14-74, 14-78, 14-79
- embedment gauges, 27-19
- embedment length, anchors, 28-50, 28-61
- embedment, maximum length of, 14-77
- embedments, 11-15–11-16
- empirical design, 28-41, 28-46–28-49
- emulative systems, 34-1
- end gates, 11-49
- end-region stiffness, 9-14, 9-15
- engineered cementitious composite (ECC), 24-1–24-39; *see also* steel-reinforced
 - engineered cementitious composite (R/ECC)
 - alkali–silicate reaction resistance, 24-27
 - chloride diffusion coefficients, 24-31–24-32
 - damage tolerance, 24-22
 - deformability factor, 24-10–24-11
 - design considerations, 24-6–24-8
 - durability of, 24-24–24-37
 - green (G-ECC), 24-4
 - high-early-strength (HES-ECC), 24-4, 24-7
 - lightweight (LW-ECC), 24-4, 24-7
 - long-term performance, 24-36–24-37
 - material processing, 24-8–24-12
 - mixture proportioning, 24-8–24-12
 - physical properties of, 24-5
 - polyvinyl alcohol (PVA-ECC), 24-5, 24-7, 24-9, 24-24
 - precasting, 24-12
 - quality control, 24-8–24-12
 - self-consolidating, 24-4, 24-8
 - self-healing (SH-ECC), 24-4
 - strain capacity, 24-25–24-26
 - structural elements, behavior of, 24-12–24-24
 - tensile characteristics, 24-5–24-6
 - transport properties of, 24-30–24-33
 - tropical climate exposure, 24-26
- engineering model, computerized, 18-11–18-16
- Engineering News-Record (ENR) equation, 14-69
- enstatite, 2-29
- entringite, 11-6
- environmental reduction factor, 25-4, 25-13
- environmental sensitivity, bridges and, 29-9–29-11
- epicentral distance, 32-2, 32-3, 32-5
- epoxy, 11-12, 11-18, 11-20, 11-23, 11-39, 11-40, 11-42, 11-50, 11-54, 11-58, 11-59, 11-60, 11-61, 12-10, 12-30, 16-11, 16-14, 16-15, 16-19, 17-13, 20-56, 21-14, 21-53, 22-24, 23-14, 25-9, 25-10, 25-13, 27-27, 28-51, 30-17, 30-18, 30-31, 30-68, 30-70, 32-43, 32-45, 36-28
 - asphalt, 11-55
 - coated rebar, 1-23, 11-9
 - modified concrete, 3-17, 33-2
 - mortar, 33-10
 - overlays, 33-2, 33-16
- equal energy theory, 32-58
- equilibrium torsion, 36-22
- equipment, 19-1–19-50
 - direct costs of, 19-7
 - employment times, 19-5–19-6
 - fixed costs, 19-7
 - indirect costs, 19-7
 - production-dependent costs, 19-7
 - selection of, 19-2–19-12
 - time-dependent costs, 19-7
 - weight, 10-4
- equipotential line, 14-23
- equivalent frame method (EFM), 8-12, 8-13, 8-14, 8-18, 8-40, 10-20, 10-21
- equivalent lateral force analysis, 32-19, 32-20, 32-21–32-26, 32-27
- erection, 11-30–11-33, 11-38, 11-39, 11-42, 12-41
 - float-in, 11-43–11-44
 - gantry, 11-42
 - lift-in, 11-43–11-44

precast bridge elements, 33-5, 33-12, 33-15, 33-16
 precast elements, 30-60–30-69, 30-72
 trusses, 29-10, 29-12, 29-16
 erosion, 2-16, 14-24
 protection, 20-41, 20-48
 resistance, 3-7
 ettringite, 1-6, 1-10, 1-25, 2-25, 2-36, 5-42, 26-14
 Euler buckling load, 10-15, 28-52
 evaluation, of concrete structures, 12-22–12-23,
 16-3–16-8
 testing, 16-4–16-8
 evaporation, 2-34, 8-29, 8-30, 23-11–23-12, 23-16
 excavations, 20-44, 20-55
 braced, 14-55–14-56
 dewatering of, 14-25–14-26
 repair, 16-13, 16-18
 excess reinforcement factor, 36-28
 expansion, 6-8, 17-6, 17-10, 17-13, 20-22, 26-14
 alkali–silica reactions, and, 2-26–2-27, 2-38
 chemical attack, and, 2-36
 clay masonry, 28-38
 fly ash, and, 2-17
 grout, 15-4
 heat-induced delayed, 5-42–5-43
 joints, *see* joints: expansion
 overlay, 23-4
 seawater, and, 2-25
 expansive cement, 1-10, 23-4
 experience factor, 7-34
 explosives, 11-60, 11-61, 12-40
 exposed aggregate, *see* aggregates: exposed
 external tendons, 11-24, 11-40, 11-43, 11-46, 11-60,
 12-31
 extreme tension fibers, 4-18
 extrusion, 24-12
 sheathing, 12-3

F

Fabry–Perot sensor, 27-21
 facades, 10-6
 maintenance of, 35-15
 face, dam, 20-3, 20-7, 20-8, 20-20, 20-22, 20-38,
 20-40, 20-41, 20-42, 20-43, 20-44, 20-45,
 20-49–20-52
 face mix, 30-73
 failure, 8-19–8-20, 8-37, 16-28, 16-29, 17-2
 anchor pullout, 28-60
 anchorage splitting, 27-4
 anchor-controlled, 28-50, 28-60, 28-61
 beam, 8-27, 22-13, 36-10
 bearing-capacity, 14-32, 14-33, 14-37, 14-38
 bond, 16-11, 23-5, 27-4

brittle, 25-12, 32-12, 36-10
 buckling, 7-34, 36-24
 column, 36-23
 column-shear, 32-43
 compression, 36-23, 36-24
 compressive, 25-5, 25-14, 36-5
 crushing of concrete, 27-3, 27-4
 debonding, 25-14, 25-16
 ductile, 25-12
 engineered cementitious composite (ECC), 24-6
 fiber springs, 24-7
 flexural, 8-47, 25-6
 high-strength concrete, 36-5, 36-9, 36-10
 joint, 17-13
 limit states, and, 16-2
 loads, geopolymer concrete, 26-17, 26-18
 masonry-controlled breakout, 28-50, 28-60, 28-61
 overlay, 23-4, 23-5, 23-16
 pavement, 17-15
 premature, 8-27, 16-2
 progressive, 11-32, 11-33
 punching shear, 8-27, 8-37, 8-38, 27-25, 27-29
 repair, 16-3
 seawall, 16-20, 16-38, 16-40
 shear, 8-47, 10-22, 27-4
 splitting bond, 25-8
 strain
 design, 25-4, 25-12–25-13
 guaranteed, 25-4
 strand, 16-16, 16-18
 strength, 8-20
 structural, 8-19–8-20
 tension, 36-23, 36-24
 wedge, 14-47
 zone, probe penetration, 21-9
 false yokes, 10-35
 falsework, 7-5, 11-21–11-23, 11-36–11-38
 -supporting forms, 7-28
 fast-erecting cranes, 19-22
 fast Fourier transform, 16-5, 21-34, 27-8
 fast-load strain capacity, 20-32
 fatigue, 25-3, 25-5, 25-7, 25-8, 25-13
 behavior, 27-9
 fatigue cracking, 24-12
 fatigue resistance, 11-17
 fatigue strength, 13-22
 f'_c , *see* compressive strength
 f'_{cr} , *see* compressive strength: average
 feldspar, 2-38
 felt, waterproof, 15-18
 ferric oxide, 3-9
 ferric sulfate, 3-13
 ferrite, 1-6, 1-7

- ferrophosphorous, 1-19
- ferrosilicon alloys, 2-29
- ferry terminals, concrete, 13-15
- FeSi-50%, 2-29
- fiber efficiency factor, 22-8
- fiber–matrix interface, 1-21
- fiber orientation, 22-8
- fiber-reinforced concrete, 1-21, 9-20, 22-2–22-18, 24-1–24-2, 24-12, 24-22, 24-23
 - mechanical properties of, 22-8–22-14
- fiber-reinforced Densit® (FRD), 24-12
- fiber-reinforced polymer [plastic] (FRP), 1-21, 21-42, 25-2–25-20
 - composites, 22-18–22-25
 - material reduction factors, 25-12
 - reinforcement ratios, 25-4
 - reinforcing bars, 25-2–25-9
 - design of, 25-4–25-9
 - flexural capacity, 25-4, 25-5–25-6
 - properties of, 25-2–25-4
 - serviceability, 25-7–25-8
 - shear capacity, 25-4, 25-6–25-7
 - strengthening systems, 25-9–25-20
 - design of, 25-12–25-20
- fiber reinforcement, 1-21
- fiber saturation point, 7-33
- fiber shape, effect of, 22-11
- fiber spacing, 22-6–22-7, 22-9
- fiberglass reinforcement, 22-2, 22-3, 22-18, 22-19–22-24
- fiberoptic sensors, 27-21
- fiberscope, 21-30
- fill, dam, 20-44, 20-48
- fillet, 20-47, 20-67
- final set, 5-12
 - fly ash, and, 5-28
- fineness
 - cement, 1-5, 2-14, 2-23, 3-6
 - cementitious materials, 6-20
 - fly ash, 2-5, 2-6, 2-10, 2-13
 - sand, 6-9
 - silica fume, 2-29, 6-32
 - slag, 2-20, 2-23
- fineness modulus, 1-15, 1-15–1-16, 6-21, 6-24, 6-37
- finer, *see* aggregates: fine
- finish cleanup, architectural concrete, 30-68–30-72
- finish coat, plaster, 15-19
- finishes
 - architectural, 10-28
 - fire resistant, 31-11
- finishing, 13-23, 15-6
- finite-element modeling, 18-9, 20-53, 27-7, 27-9, 27-23, 27-25
- fir, as liner, 30-28
- fire compartments, 31-3–31-4
- fire detectors, 31-2
- fire endurance, defined, 31-5
- fire protection, 10-15, 11-11, 11-33, 12-34, 12-35, 12-36, 25-13; *see also* fire resistance, fire suppression, fireproofing
 - joint, 31-9
- fire resistance, 11-17, 12-31, 13-25, 22-24, 28-9, 31-1–31-14; *see also* fire protection, fire suppression, fireproofing
 - balanced design for, 31-2–31-4
 - column, 31-11–31-13
 - defined, 31-5
 - finishes, and, 31-11
 - floor, 31-8
 - joints, and, 31-9
 - lintel, 31-14
 - ratings, 31-5–31-8
 - single-wythe masonry walls, 31-6–31-7
- fire suppression, 31-2–31-3
- fireproofing, 10-28, 11-17, 11-60, 16-15; *see also* fire protection, fire resistance
 - clearance, and, 30-66
- first cracking load, 22-5, 22-12
- first-generation superplasticizers, 3-5
- fixed earth support, 14-53
- fixity, 9-11, 9-14–9-15, 10-30, 10-32
 - point of, 10-13
- fjords, floating concrete pontoons in, 13-14
- flanges, 9-6, 9-14, 9-16, 9-18, 10-8, 10-13, 10-31, 11-24, 11-30, 11-36, 11-38, 11-41, 11-43, 15-18, 30-66, 32-34, 33-4, 33-6, 36-14, 36-16
 - thin, 9-6
 - use of rubber gaskets with, 11-6
 - width of, 22-18
- flare towers, 13-16
- flares, column, 32-56
- flashing, 28-25, 28-39
- flashover, 31-2
- flat crack propagation, 24-7
- flat-plate construction, 8-57, 8-58, 9-3
- flat-plate floors, 7-8, 7-38
- flat-plate slabs, 7-38, 8-16
- flat-plate structures, 8-6, 8-27, 8-37, 8-38, 8-43, 8-53
- flat plates, 10-19–10-23
 - two-way, 10-31
- flat slabs, 7-8
- flat ties, 7-11
- flat-top cranes, 19-26
- flat-use factor, 7-33
- Flatkin, 18-3–18-5

- flaw detection, 21-28–21-62
- flexibility, 27-7
- flexibility matrix, 27-8, 27-9
- flexural bending, 7-38, 7-40, 7-43, 7-44, 7-45, 7-46, 28-53
 - maximum moment, 7-38, 7-40, 7-41, 7-44, 7-45, 7-46
- flexural breaks, 8-21
- flexural capacity, 25-4, 25-5, 25-6, 25-9, 25-12, 28-56
- flexural crack control, 4-30
- flexural crack width, 4-22–4-34, 25-5, 25-7
- flexural cracking, 4-30–4-31, 8-27, 8-34–8-37, 9-3, 9-6, 9-7, 25-5, 25-7, 25-14, 27-23, 27-25, 36-4–36-5
 - drying, and, 8-34–8-37
- flexural load, 28-55, 28-59, 28-60, 36-27
- flexural members, 9-13
 - cracking of, 9-3, 9-6, 9-7
 - size of, 9-1, 9-16
 - tension-controlled, 36-10
- flexural reinforcement, 16-20, 32-54, 32-55, 32-56, 34-5, 34-6, 36-28
- flexural shear, 36-34
- flexural stiffness, 8-2, 8-48, 9-4, 9-5, 9-7, 9-8, 9-11, 9-12, 9-13–9-14, 9-18, 9-19, 36-27
- flexural strength, 3-16, 5-15, 5-16, 6-9, 8-21, 8-22, 8-23–8-24, 9-6, 15-12, 16-13, 21-16, 22-12–22-13, 22-24, 24-35, 25-13, 25-14, 25-16, 26-17, 28-56, 28-59, 28-65, 28-66, 34-4, 34-11, 34-15, 34-22, 36-10, 36-11–36-14
 - antiwashout admixtures, and, 3-14
 - blast-furnace slag, and, 2-23
 - engineered cementitious composite (ECC), 24-8
 - static, 22-8
- flexural stress, 8-27, 10-13, 10-14, 10-23, 10-24, 10-30, 12-28, 28-53, 36-14
- flexural tension, 28-62, 36-4
 - strength, 8-27, 8-36
- flexure, 2-21, 2-23, 3-7, 8-41, 8-43, 8-47, 9-6, 10-21, 13-24, 17-2, 22-19, 28-51–28-53, 28-55–28-58, 28-62–28-63, 28-65–28-67, 32-56, 36-14
- flint, 1-19
- floating (troweling), 19-20
- floating bridges, 13-14
- floating structures, 13-2, 13-3, 13-4, 13-9–13-15, 13-24, 13-25, 13-26
 - prestressed, 11-56–11-57
- flooding, for load testing, 27-28
- floor-forming systems, 7-8–7-9
- floor loading ratio, 8-2, 8-4
- floor slabs, *see* slabs: floor
- floor-to-floor depth, 10-7
- floors, 30-6, 31-8
 - cast-in-place, 7-9
 - existing, examination of, 12-22–12-23
 - fire resistance of, 31-8
 - flat-plate, 7-8, 7-38
 - post-tensioned concrete, 35-2
 - strengthening of, 12-30
 - unstressed, 34-20
- flowability, 15-10, 15-12, 15-13, 15-20
 - grout, 15-4
- flowing concrete, *see* concrete: flowing
- flownets, 14-23–14-24
- fluidifiers, 15-3, 15-4
- fluorides, 3-7
- fluorosilicates, 3-7
- fly ash, 1-11, 1-20, 2-1–2-18, 3-6, 5-27, 5-28, 5-32, 5-39, 5-41, 6-7, 6-8, 6-9, 6-18, 6-20, 6-23, 6-25, 6-26, 6-27, 6-29, 6-31, 6-32, 6-33, 6-34, 6-42, 10-26, 11-4, 11-5, 11-6, 11-16, 11-19, 11-23, 13-20, 15-2, 15-20, 15-23, 20-2, 20-10, 20-23, 20-25, 20-26, 20-27, 20-29, 20-30, 20-33, 20-34, 22-4, 22-15, 23-2, 23-3, 23-14, 24-27, 24-32, 31-7
 - abrasion resistance, and, 2-16
 - air entrainment, and, 2-10–2-11
 - bituminous, 2-4, 2-5, 2-6, 2-13, 2-18
 - calcium content of, 2-5
 - Class C, 2-2, 2-10, 2-11–2-12, 2-15, 2-16
 - Class F, 2-2, 2-10, 2-11–2-12, 2-15, 2-16
 - classes of, 2-2
 - composition of, 2-6
 - effect of on carbonation, 2-15, 2-18
 - effect of on creep, 2-13
 - effect of on durability, 2-14–2-18
 - effect of on elastic properties, 2-12
 - effect of on hardened concrete, 2-11–2-14
 - effect of on permeability, 2-14
 - effect of on reinforcing steel corrosion, 2-17–2-18
 - effect of on seawater-exposed concrete, 2-18
 - effect of on volume change, 2-14
 - erosion resistance, and, 2-16
 - freeze–thaw resistance, and, 2-15–2-16
 - high-calcium, 2-6, 2-9, 2-11, 2-13, 2-17
 - low-alkali, 5-41
 - low-calcium, 2-10, 2-11, 2-17, 26-1–26-19
 - Portland cement setting time, and, 2-9–2-10
 - properties of, 2-3–2-6
 - proportioning, 2-6–2-9, 2-11
 - roller-compacted concrete, and, 20-25
 - strength development, and, 2-11–2-12
 - subbituminous, 2-4, 2-5, 2-6
 - sulfate resistance, and, 2-16–2-17
- fly jib, 19-36

- flying forms, 7-9, 8-38
- flying-truss forming system, 8-18
- fog curing, 15-16
- footings, 7-35, 10-10–10-12, 10-30, 15-23, 16-32, 16-35, 16-36, 32-56, 32-59
 - cantilevered, 32-56
 - culvert, 33-15
 - design of, 36-36
 - discrete, 10-30
 - eccentricity, and, 14-36
 - joints, and, 17-7
 - mat, 14-37–14-43
 - one-way, 36-36
 - precast concrete, 33-12
 - prestressed, 32-59
 - reinforcement for, 10-12
 - roller-compacted concrete, 20-54–20-55
 - seawall, 16-32
 - seismic retrofit of, 32-45
 - shallow, 14-32–14-37
 - bearing capacity of, 14-32–14-36, 14-58
 - shear wall, 32-35, 32-40, 32-40–32-42
 - spread, 14-37, 14-40
 - square, 20-55
 - strip, 10-10
 - thickness of, 10-12
 - two-way, 36-36
- force, 32-27, 32-28, 32-29, 32-48, 32-49, 32-50, 32-51
 - axial, 32-19, 32-35
 - compressive, 32-51
 - earthquake motion, 32-13
 - gravity, 32-35
 - inertia, 32-12, 32-28
 - lateral, 32-7, 32-11, 32-12, 32-18, 32-19, 32-20, 32-21–32-27, 32-29, 32-31–32-34, 32-42, 32-43, 32-44, 32-45
 - levels, design, 32-9
 - longitudinal, 32-53
 - restoring, 34-20
 - seismic, 32-12, 32-13, 32-20, 32-21, 32-26, 32-27, 32-28, 32-29, 32-34, 32-43, 32-44, 32-45, 32-46, 32-48
 - shear, 32-34, 32-35, 32-40, 32-43
 - shear transfer, 32-38
 - static, 32-18
 - story, 32-45
 - tensile, 22-12, 32-35, 34-22
 - transfer, 32-28
 - transverse, 32-53
- force equation, 32-48–32-51
- Ford Island Bridge, 13-14
- forklifts, 19-2
- form liners, *see* liners
- form pressures, 15-5
- form ties, 7-9, 7-11, 7-22, 7-26, 7-35, 7-42, 7-45, 30-7, 30-38–30-40, 30-68
 - design of, 7-46
 - removal of, 30-40
 - stainless steel, 30-68
- form vibrators, 30-53, 30-56–30-57, 30-72
- formed-in-place FRP strengthening systems, 25-9, 25-10, 25-10–25-11
- forming systems, 19-1, 19-2
- forms, 11-27, 11-28, 15-3, 19-10, 20-68; *see also*
 - formwork, slip-form construction
 - architectural concrete, 30-7, 30-32–30-40
 - beam, 7-16
 - bottom, 7-4
 - cast-in-place, 30-5
 - circular, 17-3
 - climbing, 7-13
 - column, 7-9, 7-11, 7-14, 7-17, 7-24, 7-26
 - concrete, 11-6, 30-32
 - construction sequence, and, 8-4
 - curing, and, 6-40
 - double tee, 11-36
 - dye-transfer, and, 12-22
 - edge, 10-28, 12-17, 12-18, 12-20, 12-43
 - elastomeric rubber, 30-33
 - end, 11-49
 - estimating cost of, 7-5
 - fiberglass, 30-7, 30-72
 - flying, 7-9, 8-38
 - foam plastic, 30-33
 - gang, 7-11
 - jump, 7-13, 11-54
 - mechanized systems for, 19-48–19-50
 - metal deck, 7-7
 - mock-ups of, 30-12
 - one-sided, 32-45
 - overuse of, 30-33
 - panel, 7-11–7-12
 - permanent, 7-7, 30-4
 - piling, 11-48
 - plaster, 30-32, 30-33
 - plastic, 30-32
 - plywood, 30-32
 - polyethylene-lined, 8-37
 - precast concrete deck, 7-7
 - prefabricated, 7-5
 - removal of, 8-53, 10-3, 19-49, 21-24, 23-13, 30-40; *see also* forms: stripping of
 - from flexural members, 8-36, 8-37
 - premature, 7-4
 - reuse of, 7-3, 7-4, 7-5, 7-14, 7-28, 8-4, 10-3, 10-37, 20-52, 30-34, 33-2

- roller-compacted concrete, and, 20-49
- sculptured sand, 30-33
- self-climbing, 19-50
- side, 7-4
- slab, design example, 7-38–7-43
- slip, 7-12, 11-54, 13-25, 13-26; *see also* slip-form construction
- steel, 10-27, 11-6, 11-26, 11-27, 11-30, 15-14, 30-7, 30-32, 30-43, 30-59, 30-72
 - release agents, and, 30-18
- stripping of, 7-4, 7-5, 7-38, 8-2, 8-4, 8-6, 8-9, 8-37, 8-42, 8-43, 10-3, 11-11, 11-26, 30-18, 30-40, 30-57; *see also* forms: removal of
- surface of, flexural cracking and, 8-37
- table, 7-9
- timber, 15-4
- tunnel, 19-49
- void, 11-48, 11-50
- wall, 7-10–7-14, 32-45
 - bracing for, 7-27
- washing aggregate in, 15-4
- weight of, 7-24
- with oiled plywood bottoms, 8-37
- wood, 30-32, 30-56
- formwork, 7-1–7-48, 9-18, 9-19, 10-15, 10-39, 12-6, 12-43, 15-20, 18-12, 19-2, 22-14, 22-15, 25-9; *see also* forms, slip-form construction
- break-off tests, and, 21-15
- chairs, and, 12-7
- cost of, 10-2, 10-2–10-3, 10-28
- defined, 7-5
- deflections, and, 8-49
- design, 7-35–7-38
- design criteria for, 7-27–7-28
- failure of, 7-3, 8-37
- geopolymer concrete, and, 26-6
- horizontal load, and, 7-27
- leak-free, 10-3
- loads, 7-23–7-27
- objectives of, 7-2
- precast concrete units as, 30-6
- pressures, 7-23–7-27
- recommended practices, 7-17–7-23
- scheduling, 7-5
- self-weight, calculation of, 7-24
- smooth-surfaced concrete, 30-21
- standards, 7-17–7-23
- suppliers, 7-22
- supports, 8-2
- textured, 30-25
- two-sided wall, 19-50
- types of, 7-5–7-17
- foundation, 6-41, 8-2, 8-3, 8-9, 8-11, 8-12, 10-3, 10-6, 10-10–10-14, 11-36, 11-46, 14-1–14-79, 20-38, 20-67, 32-43, 32-59
 - below water level, 10-14
 - clay and weathered-rock, 20-48
 - dam, 20-41
 - deep, 10-10, 10-12–10-14, 14-58
 - engineering, 14-1–14-27
 - flaw detection in, 21-33
 - ground motion, and, 32-29
 - lift-slab construction, and, 10-31
 - load transfer to, 20-47
 - mat, 10-12, 15-23
 - medium stiff clayey, 14-10
 - medium, strength of, 14-5
 - pile, 14-57–14-75
 - post placement in, 20-55
 - restraint, 20-48
 - roller-compacted concrete, 20-55, 20-56
 - roller-compacted concrete, and, 20-67–20-68
 - settlement, *see* settlement
 - shallow, 10-10–10-12
 - shear-wall, 32-38–32-40, 32-42
 - subsea, 13-25
 - underwater, 15-4–15-5, 15-7, 15-8
 - walls, 28-48–28-49
- Four Bears Bridge, 29-7, 29-10–29-11, 29-25
- fracture test, 21-3
- fractured surface texture, 30-25
- frame bays, 34-19
- frame systems, seismic moment-resisting, 34-7–34-18
- frames, 10-6
 - braced vs. unbraced, 10-15
 - modeling of, 18-9
 - ordinary moment-resisting, 32-13
 - rigid, 10-14–10-15
 - structural, 10-14–10-17
 - sway vs. nonsway, 10-15, 10-16
- free earth support, 14-53
- free-water content of aggregates, 5-30
- freeboard, 20-45
- freefall mixers, 19-14
- freeze–thaw attack, 1-19, 1-23, 2-10, 2-18, 3-2, 3-8, 3-10, 3-11, 3-12, 5-29, 5-31, 5-32, 5-34–5-35, 5-38, 6-8, 6-21, 10-23, 11-5, 11-47, 11-48, 11-55, 11-59, 13-19, 13-22, 13-23, 15-2, 15-11, 15-13, 15-14, 15-17, 15-22, 16-12, 16-13, 20-20, 20-21, 20-23, 22-14, 23-5, 24-26, 24-27, 24-29, 24-37, 27-5, 30-31, 35-15
- blast-furnace slag, and, 2-27
- fly ash, and, 2-15–2-16
- roller-compacted concrete, and, 20-22–20-23
- silica fume, and, 2-37

frequency, 10-6
 analysis, 21-33, 21-34
 content, 32-2, 32-3
 defined, 32-48
 vibrator, 30-52, 30-53, 30-57
 friction, 7-24, 11-21, 11-26, 11-27, 11-28, 11-33,
 11-50, 11-53, 11-54, 11-55, 12-2, 12-21, 14-52,
 15-20, 20-34, 20-47, 20-48
 angle, 14-14, 14-60, 14-78, 14-79, 20-35, 20-36
 coefficient, 11-43, 34-6, 34-7
 internal, 12-24, 14-7, 14-60
 ratio, 14-13
 shear, *see* shear friction
 side, 14-58
 skin, 10-12, 14-60, 14-62, 14-67, 14-70, 14-71
 wall, 14-46
 wobble, 12-44
 frictional losses, 11-21, 11-28, 12-8, 12-43, 35-9
 frictional resistance, 4-5, 28-60
 frictional slip, 1-21
 front-end loaders, 20-65, 20-67
 frost, 5-39
 frost resistance, 6-7, 15-3, 15-4
 accelerators, and, 3-7
 polymer-modified concrete, and, 3-17
 silica fume, and, 2-37-2-38
 fungus, 11-19
 fuse plug, 20-45

G

galleries, 20-7, 20-8, 20-38, 20-45-20-47, 20-70
 galvanized reinforcement, 30-44-30-45
 galvanizing, 11-10, 11-12
 galvanostatic pulse method, 21-59
 gamma ferric oxide, 2-27
 gamma rays, 15-25, 21-60, 21-61, 21-62
 gang forms, 7-11
 gantry, 11-42, 11-50
 gap grading, 1-15, 30-14, 30-15, 30-16, 30-17, 30-26,
 30-55, 30-57, 30-73
 garages, 27-3
 gas reactors, 11-55
 gaskets, neoprene, 30-37
 gates, bucket, 15-8
 gauges
 dial, 27-13, 27-16
 mechanical, 27-13, 27-14, 27-16-27-17
 strain, 27-16, 27-18-27-21
 gehlenite, 1-10
 gel, 2-27, 4-10, 6-3, 6-20, 6-31
 gel pores, 1-8
 generic primitive, 18-9

geocomposites, 14-56
 geogrid-reinforced walls, 14-51-14-52
 geomembranes, 14-26, 14-27, 14-50, 20-49
 geonets, 14-56
 Geopak®, 18-13-18-16
 geopolymer concrete, 26-1-26-19
 beams, 26-14-26-18
 casting of, 26-4-26-5
 columns, 26-14-26-18
 load-carrying capacity of, 26-17
 compaction of, 26-4-26-5
 compressive strength, 26-3-26-4, 26-5, 26-6,
 26-7, 26-8, 26-9, 26-10, 26-11-26-12,
 26-13, 26-14, 26-15, 26-16, 26-17
 curing temperature, and, 26-5
 constituents of, 26-3
 creep, 26-12-26-13, 26-18
 curing of, 26-5-26-6
 design of, 26-6-26-8
 drying shrinkage, 26-12-26-13, 26-18
 economic benefits of, 26-18
 long-term properties of, 26-11-26-14
 mixing of, 26-4-26-5
 mixture proportions, 26-3-26-4, 26-7-26-8, 26-15
 modulus of elasticity, 26-9, 26-18
 short-term properties of, 26-8-26-10
 slump, 26-8, 26-15
 sulfate resistance of, 26-14, 26-18
 sulfuric acid resistance of, 26-14
 unit weight of, 26-9, 26-10
 geopolymers, 26-2-26-3
 geosynthetics, 14-56
 geotechnical engineering, 14-1
 geotextile reinforcement, 14-52, 14-56, 22-19
 GGBFS, *see* ground granulated blast-furnace slag
 girders, 7-5, 11-13, 11-15, 11-17, 11-20, 11-25, 11-27,
 11-28, 11-29, 11-33, 11-40, 11-42, 11-46,
 12-38, 15-22, 15-23, 18-2, 18-3, 24-12, 27-27,
 27-28, 27-29, 27-31, 30-45, 32-55, 33-2, 33-8
 box, 11-43, 11-46, 27-27, 29-2, 29-5, 29-7, 29-14,
 29-15, 29-17, 29-29, 29-32, 32-54
 bridge, 11-34-11-36
 horizontal plate, 32-34
 I-beam, 11-34, 11-36
 post-tensioned, 11-36-11-38
 precast box, 27-27
 precast pretensioned, 11-34-11-36
 prestressed concrete, 7-7
 glass, 28-29
 ASTM standards for, 28-5
 glass-fiber-reinforced polymer (GFRP), 22-19,
 22-21-22-23, 22-24
 glass-fiber-reinforced vinylester bars, 25-2

- glass transition temperature, 3-17, 25-3, 25-11, 25-12
- Glenwood Canyon Bridges, 29-10
- global warming, 26-1, 26-2
- Glomar Beaufort Sea I, 13-26
- gneiss, crushed, 20-27
- go-devil, 15-8–15-9
- goethite, 1-19
- grade beams, 32-38, 32-40, 32-45
- grading curves, 1-15, 11-4, 26-3, 26-7
- grading, of aggregates, 1-15, 5-29, 5-30, 5-32, 6-2, 6-4, 11-4
- grain direction, 7-28, 7-34, 7-38, 7-41, 7-42, 7-43, 7-48
- granite, 1-19, 5-17, 5-21, 5-40, 20-11, 26-10, 30-13, 30-26, 30-32
- graphic recorder, 21-45–21-47
- gravel, 1-15, 5-2, 5-29, 5-40, 6-4, 6-36, 11-4, 13-21, 14-2, 14-14, 14-27, 14-56, 15-6, 15-25, 20-11, 20-12, 20-21, 20-68, 30-26; *see also* pea gravel
 - weight of, 6-12
- graving docks, 11-58, 13-14, 13-15, 13-26
- gravity-base structures, 13-2, 13-3, 13-15, 13-25
 - dry dock construction of, 13-28
 - skid-way construction of, 13-29
- gravity dam section, 20-44–20-45
- gravity-fill polymers, 23-14
- gravity load, *see* load: gravity
- gravity mixer, 19-14
- gravity retaining wall, 14-48
- graywacke, 1-19, 5-40
- grease, 11-11, 11-19, 11-24, 11-33, 11-38, 11-46, 11-60, 12-2, 12-3, 12-5, 12-6, 12-9, 16-16, 16-18, 16-19, 17-12, 17-15
- green cement, 1-11
- greenhouse gases, 1-11
- grid index, 4-31, 4-34, 36-27
- Griffith cracking, 24-7
- grooves, 17-5, 17-15, 23-14
- gross area, 28-3
- ground acceleration, peak, 32-2, 32-3, 32-4, 32-5, 32-6
- ground displacement, peak, 32-2, 32-5
- ground granulated blast-furnace slag (GGBFS), 1-10, 2-24, 5-27, 5-41, 6-42, 15-23, 28-4; *see also* blast-furnace slag: granulated
- ground motion, 32-2–32-6; *see also* earthquakes, seismic
 - characteristics of, 32-2–32-3
 - distance from energy release, and, 32-3–32-5
 - duration of, 32-2, 32-3
 - estimating, 32-6
 - factors influencing, 32-3–32-5
 - recorded, 32-2
- Ground Motion Parameter Calculator, 32-7
- ground-penetrating radar, 21-42–21-48
- ground velocity, peak, 32-2, 32-5
- groundwater seepage, 14-23–14-24
- groundwater table, 14-34, 14-36
- grout, 11-5, 11-12, 11-13, 11-19, 11-20, 11-23, 11-24, 11-33, 11-39, 11-43, 11-54, 11-55, 11-60, 11-61, 12-8, 12-9, 12-22, 12-27, 16-13, 20-8, 20-38, 20-47, 20-51, 20-56, 20-63, 21-14, 27-31, 28-3, 28-4, 28-9–28-11, 28-14, 28-16, 28-36, 28-49, 28-59, 30-24, 30-64, 30-66, 31-9, 31-14, 33-16
 - admixtures, 28-14
 - ASTM standards for, 28-5
 - coarse, 28-10
 - compressive strength, 15-3, 28-10, 28-34, 28-36
 - curtain, 20-47, 20-70
 - enriched roller-compacted concrete, 20-20–20-21, 20-49, 20-52
 - expansive, 20-47
 - field-mixed, 15-4
 - fine, 28-10
 - fluidifier, 15-3, 15-4
 - fluidity, 15-5
 - fly-ash, 15-2
 - freezing of, 28-24
 - high-slump, 28-34
 - high-strength, 34-11
 - injection, 15-5
 - intrusion, 15-3, 15-4, 15-6
 - lifts, 28-3, 28-20, 28-33
 - modulus, 27-29
 - pad, 34-11
 - pipes, 20-56
 - placement, 28-19–28-22
 - pour, 28-3
 - pumping of, 15-5
 - self-consolidating, 28-10–28-11
 - slump, 28-20, 28-33, 28-34
 - steel shims, and, 30-64
 - strength, 12-20
 - testing of, 28-33–28-34
 - tubes, 20-47
 - vs. concrete, 28-9
 - vs. mortar, 28-9
- grouting procedure, for preplaced-aggregate concrete, 15-5–15-6
- Grundy–Kabaila method, 8-9, 8-11, 8-12, 8-13, 8-38, 8-39, 8-41, 8-43
- gunite, 32-45
- gypsum, 1-3, 1-6, 1-7, 1-25, 2-9, 2-25, 5-23, 11-5, 26-14
 - drywall, 9-22, 31-11
- gyration, of masonry element, 28-52, 28-62, 28-65

H

HAC, *see* high-alumina cement

hairpins, 32-54

half-cell oxidation reaction, 21-52

half-cell potential method, 21-53–21-54

half-cell reduction reaction, 21-52

half-stress design, 28-28

hammer, 14-11, 14-12, 14-69, 14-71, 14-75

pneumatic, 23-6

rebound, 21-3–21-5, 21-9, 21-27, 27-5

spring-loaded, 21-3

hammerhead jib, 19-25

hand-held magnifier, 21-30

Hansen's expression for bearing capacity, 14-33, 14-35

Harbour Cay Condominiums, 8-37, 8-38–8-40

hardening, rapid, 4-11; *see also* strain: hardening

hardware, for precast concrete elements, 30-63–30-64

hazardous waste pond, 14-27

he bolts, 7-11, 30-39

head joints, 28-3, 28-6, 28-18, 28-26, 28-52, 28-62

head, water, 14-23, 14-24

headache ball, 11-60, 12-40

headers, 10-19

heat-induced delayed expansion, 5-42–5-43

heat liberation, 1-7

rate of, 1-5

heat of hydration, 1-10, 2-6, 5-23, 5-25, 5-27, 5-28, 5-42, 6-34, 6-41, 10-26, 11-5, 15-23, 16-13, 17-5, 20-33–20-34, 20-52, 20-53, 20-70, 27-20, 30-29

heat of reaction, 3-2

heat-shrink tape, 11-12, 11-36, 11-38

heat transfer, 20-53

heavy lifter, reinforced concrete, 13-17

hematite, 1-19, 2-6

hexagonal hydrates, 1-7

high-alumina cements, 1-10–1-11

high-density polyethylene (HDPE), 11-59

high-lift grouting, 28-3, 28-22

high-performance fiber-reinforced cementitious composites (HPFRCC), 24-2–24-4

high-performance, high-volume fly ash concrete, 1-11

high-pressure water blasting, 30-27

high-range water reducers, 1-4, 2-32, 3-2, 3-4, 3-5–3-7, 3-14, 5-31, 5-43, 6-8, 6-9, 6-18, 6-21, 6-23, 6-24, 6-28, 6-29, 6-30, 6-35, 6-40, 6-41, 10-23, 10-27, 11-5, 11-16, 11-41, 13-22, 13-26, 15-20, 20-51, 23-3, 24-9–24-10, 26-3, 30-15

generations of, 3-5–3-6

naphthalate-based, 6-35

high-rise building, testing after collapse of, 27-28–27-29

high-strength concrete, *see* concrete: high-strength

highly reactive metakaolin, 2-38–2-42

highway, 5-2, 5-29, 10-2, 14-40, 15-22

dividers, 10-38

slabs, 2-14

hinge line, 12-32

hinge, bridge, 11-41

hinges, plastic, 32-51, 32-55, 32-56, 32-57, 32-58, 34-4, 34-5, 34-9

length, 34-15, 34-17

order of, 32-58

hoisting speed, 19-6, 19-34

hoists, 7-5, 19-1, 19-47–19-48

Hokie Stone, 29-26–29-28

hollow-core plank, 10-39

honeycombing, 10-25, 10-27, 11-13, 11-27, 12-20, 21-28, 21-35, 30-7, 30-41, 30-52, 30-54, 30-56, 30-68, 30-69

honing, 30-31–30-32

and polishing, 30-20

Hood Canal Bridge, 13-14

Hooke's law, 8-28

hoop, 32-43, 32-54, 36-6, 36-22, 36-35 defined, 32-62

hopper, 20-64

intake, 19-15, 20-61, 20-63

horizontal flow time, nondispersible underwater concrete, 15-12–15-13

horizontal lacing, 7-16

horizontal layer grouting, 15-5

hot weather, 5-32–5-33, 6-34, 10-27, 11-5, 15-25, 16-13, 20-10, 21-23, 24-26, 28-22, 28-23, 28-24, 30-59

HRWRs, *see* high-range water reducers

hulls

barge, 11-35

concrete, 11-57, 13-2, 13-4, 13-11, 13-14

leakage into, 13-25

Hungry Horse Dam, 2-2

hurricanes, 11-31, 29-19

hybrid system, of seismic bracing, 34-11, 34-12, 34-15, 34-17, 34-20, 34-22

hydrates, hexagonal, 1-7

hydration, 1-5, 1-6–1-9, 2-25, 2-39, 3-4, 4-16, 5-10, 5-12, 5-23, 5-25, 5-27, 5-28, 5-30, 6-20, 6-41, 15-15, 15-23, 15-25, 26-2

accelerators, and, 3-1, 3-13

chemistry of, 1-6–1-7

curing, and, 2-21

degree of, 1-8, 21-20, 21-21, 21-23, 21-24

heat of, *see* heat of hydration

high-range water reducers, and, 3-5, 3-6
 kinetics, 21-21
 polymers, and, 3-15
 products, 1-6, 1-7–1-9
 retarding admixtures, and, 3-2
 water-reducing admixtures, and, 3-4
 hydraulic breakers, 12-40
 hydraulic bursters, 12-40
 hydraulic cement, *see* cements: hydraulic
 hydraulic cement concrete (HCC) overlays,
 23-1–23-16; *see also* cement: hydraulic, overlays
 hydraulic gradient, 14-24, 14-25
 hydraulic testing, 27-10–27-13
 hydraulicity, latent, 2-18
 hydrocalumite, 2-26
 hydrochloric acid, 30-71
 hydrometer analysis, soils, 14-2–14-4
 hydroxide ions, 5-38
 hydroxyethylcellulose (HEC), 3-14, 15-10
 hydroxyethylmethylcellulose (HEMC), 3-14, 15-10
 hydroxyl, 2-27
 hydroxylated carboxylic acids, 3-3
 hydroxypropylmethylcellulose (HPMC), 3-14, 15-10
 hypophosphates, 3-7
 hysteresis, 27-15, 27-17, 27-18, 27-25

I

I.M. Pei and Partners, 30-2, 30-20
 I-beam, prestressed, 33-2, 33-3, 33-6–33-7
 ice, 3-5, 10-27, 11-5, 11-55, 20-53, 30-15
 ice control, 35-16–35-17
 ICES-STRUDL II, 8-38
 ICRI molded standards, 23-9
 illmenite, 1-19
 immersion vibrator, 30-53
 impact ball, 12-39
 impact-echo testing, 16-4–16-7, 16-20, 16-22, 16-23,
 16-24, 16-24–16-25, 16-29, 16-30, 16-38,
 16-39, 16-40, 21-33, 21-34, 21-35, 21-37,
 21-44, 27-7
 impactor, 27-7, 27-8
 impedance testing, 21-35
 impermeability, 15-17
 importance factor, 32-8–32-9
 impressed current, 16-20, 16-23, 16-26, 16-27, 16-38,
 21-56
 impulse radar, 21-42
 impulse–response testing, 21-35, 21-36, 21-37
 impurities, 1-3, 1-7, 1-14
 incising factor, 7-31
 inclined cracks, 27-4, 36-15
 incremental launching, 11-43

indentation tests, 21-2, 21-3
 Indiana limestone, 30-17, 30-20
 indirect-member strengthening, 12-31
 induction stage, of hydration, 1-7
 industrial plantships, 13-9, 13-13
 influence line, 10-16
 infrared thermography, 21-39–21-42, 27-7
 infrastructure, concrete, 16-2, 21-29
 initial rate of absorption (IRA), 28-25
 initial set, 5-12
 fly ash, and, 5-28
 in-place strength, estimating, 21-2–21-28, 21-62
 inshore concrete structures, 13-1, 13-2, 13-3, 13-23,
 13-25
 inspection
 checklist, 35-17–35-18
 masonry, 28-27–28-38
 instrumentation, 27-13–27-21
 accuracy, 27-14–27-16
 electrical, 27-17–27-21
 precision, 27-14
 range, 27-13–27-14
 types of, 27-16–27-21
 intake hopper, 19-15, 20-61, 20-63
 integrity tests, *see* nondestructive testing
 interfacial zone, 1-13
 intermediate moment-resisting frames (IMRFs), 32-13
 intermediate stressing joints, 12-41
 internal fracture test, 21-13
 internal friction, 14-7
 International Building Code (IBC), 8-55, 10-4, 28-2,
 28-40, 32-6, 32-7–32-29
 inverted channel beam, 33-5–33-6
 iron, 2-1, 2-2, 2-29, 5-23, 5-27, 30-12, 30-40, 30-58
 scrap, 1-19
 iron chloride, 5-38
 iron hydroxide (FeOH), 5-38
 iron ions, 5-38
 iron oxide, 1-2, 1-22, 5-30, 5-38, 16-26, 21-52, 26-3
 black, 29-25
 irradiation, 6-8
 irregular structures, 32-18–32-19
 islands, caisson-retained, 13-15
 Isola di Porto Levante LNG terminal, 13-6
 isolation joints, 17-1, 17-2, 17-3, 17-7, 17-12–17-13,
 17-15

J

jack, 7-14, 11-28, 11-49, 11-60, 12-21, 12-43
 center-pull, 11-60
 feet, 12-21
 hang-up of, 12-19–12-20

- jack (cont.)
 - heavy lift, 11-43
 - hydraulic, 10-34, 11-25, 11-28, 11-43, 11-60, 14-73, 16-18, 12-21, 12-40, 21-15, 30-47
 - lifting, 10-31, 10-32, 10-33, 10-34
 - multistrand, 11-21, 11-24, 11-25, 11-26, 34-23
 - pneumatic, 10-34
 - post-tensioning, 27-29
 - screw, 10-34, 11-32
 - shores, 7-14
 - single-strand, 11-21, 11-25, 11-48
 - strutting, 12-2, 12-17, 35-8
 - types of, 10-34
- jack-up rigs, 13-13
- jackhammer, 16-18, 30-25, 30-26
- jacking force, 10-38, 12-43
- jacking rods, 10-34
- Java, 18-12–18-13
- jetting, 11-53, 11-54
- jib, 19-4, 19-5, 19-9
 - bottom-slewing tower crane, 19-29
 - length, 19-32, 19-33
 - luffing, 19-26, 19-29
 - top-slewing tower crane, 19-25–19-26
- jobsite control, 6-40, 6-41
- joint filler, 17-8–17-9
- joint formers, 17-3
- joint sealants, 17-13, 30-67
- joint shear reinforcement, 32-54
- jointed precast concrete, 34-1
- joints, 5-21, 10-17, 10-23, 10-24, 10-28, 12-13–12-14, 17-1–17-15, 20-8, 35-8–35-9
 - beam–column, 10-6, 10-15, 10-17, 12-11, 12-39, 24-19, 24-21, 34-5, 34-8, 34-16, 34-17–34-18, 34-20
 - size of, 34-20, 34-23
- bed, 28-3, 28-6, 28-18, 28-26, 28-36, 28-42, 28-60, 28-62
- butt, 17-2, 30-30, 30-33, 30-37, 30-38
 - architectural concrete, 30-11
 - horizontal, 30-28
- cast-in-place, 11-38, 11-50
- cold, 10-33, 15-5, 15-23, 20-47, 20-48, 30-7, 30-37, 30-69, 35-4, 35-9
- collar, 28-3, 28-4
- congestion of, 10-17
- construction, 11-36, 17-1, 17-2, 17-7, 17-14, 20-59, 20-69, 23-2, 23-12–23-13, 23-14, 23-16, 29-26, 30-37, 30-38, 35-4, 35-8–35-9
 - in seawall, 16-20, 16-22, 16-24, 16-25, 16-29, 16-39
- construction of, 15-5
 - contraction, 17-1, 17-2, 17-3–17-6, 17-8, 17-10–17-12, 17-15, 20-56, 31-9
 - effectiveness of, 17-5–17-6
 - formed, 17-3
 - joint former placement, and, 17-3
 - sawed, 17-3, 17-5
 - tooled, 17-3, 17-5
- control, 17-2, 17-3, 28-16, 28-38, 30-7, 30-36, 30-37, 30-38, 31-9
- dowelled, 17-11, 17-12
- dry, 11-38, 11-39
- expansion, 17-1, 17-2, 17-3, 17-6–17-10, 17-12–17-13, 17-15, 22-3, 23-13, 27-28, 28-38, 31-9, 32-51, 32-53, 32-57, 35-7, 35-15
 - spacing of, 17-7–17-8
 - width of, 17-6
- fire protection of, 31-9
- formed, 20-56
- full-height, 35-5–35-6
- half-height, 35-5–35-6
- head, 28-3, 28-6, 28-18, 28-26, 28-52, 28-62
- horizontal, 10-36, 20-49
- horizontal bed, 28-3, 28-13
- inside corner, 15-18
- insulated, 31-9
- isolation, 17-1, 17-2, 17-3, 17-6, 17-7, 17-12–17-13, 17-15
- keyed, 17-12, 17-15
- lift, *see* lift joints
- longitudinal, 17-15, 20-47, 20-56
- monolith, 10-17, 20-3, 20-38, 20-48, 20-54, 20-55, 20-57
- mortar, 28-9, 28-19, 28-26, 28-37
 - tolerances, 28-26
- pavement, 17-10–17-15
- pour, 30-37
- preformed, 17-12
- reinforcement of, 10-17
- release, 35-9–35-11
- sawed, 17-12
- sealing, 17-13
- seepage at, 20-40, 20-41
- seismic, 17-9–17-10
- shear, 32-54
- shore–slab, 8-9
- slab, 12-4, 17-2, 17-10–17-15
- slab–column, 8-11, 8-16, 8-37, 8-40, 8-43, 10-6, 10-17, 10-21, 10-32
- slip, 35-11
- spacing of, 10-25, 17-2, 17-5, 17-6, 17-7–17-8, 17-10, 17-11–17-12
- stiffness of, 9-14

tank, 11-55
 tongue-and-groove, 17-2, 17-3, 17-12
 tooled, 17-12
 transverse, 17-15, 20-56
 treatment of, 20-69
 tremie, 15-8, 15-9
 vertical, 11-38, 20-49, 20-51, 20-56
 vertical head, 28-3
 wall, 35-10-35-11
 wall-slab, 4-34, 17-8, 17-10
 water penetration, and, 28-39
 watertight, 20-51
 width of, 17-6, 17-8, 17-9, 30-65-30-66, 30-67
 joists, 7-8, 7-9, 7-34, 7-35, 7-38, 7-40, 7-41, 9-17
 design of, 7-39-7-40
 lateral buckling of, 7-39
 steel, 10-30
 J-ring test, 5-43
 jump forms, 7-13

K

kaolinite, 26-2
 Kevlar®, 22-21
 keys, 20-47, 20-48, 30-45
 shear, 11-38, 11-44, 11-54, 27-27-27-28, 33-8
 keyways, 17-12, 33-4, 33-6, 33-10, 33-12
 kiln, 1-2-1-3

L

laboratory, prequalification of, 6-43
 lacing, 7-16
 lagging, 7-6
 laminated veneer lumber (LVL), 7-35
 laminated strand lumber (LSL), 7-35
 landfill liners, 14-26-14-27
 landfills, 14-26
 landscaping, around bridges, 29-30
 lap splices, 11-8-11-9, 25-9, 27-4, 28-51, 28-61
 lateral displacement capacity, 25-19-25-20
 lateral-force-resisting system, 32-11, 32-12, 32-13,
 32-18, 32-25, 32-26, 32-29, 32-31-32-34,
 32-42, 32-43, 32-44-32-46, 32-62
 vertical, 32-45-32-46
 lateral forces, 7-3, 11-23, 14-43, 14-45, 14-46, 14-47,
 14-48, 28-42, 28-46, 32-7, 32-12, 32-18, 32-19,
 32-20, 32-21-32-27, 32-29
 lateral loads, 7-16, 10-5-10-7, 10-13, 10-14, 10-16,
 10-30, 10-34, 10-35, 12-39, 16-28, 16-29,
 28-62, 30-5, 32-7, 32-12, 32-13, 32-29, 32-34,
 32-43, 32-57, 32-59, 32-62, 34-3
 lateral pressure, 7-10, 7-16

latex-modified concrete (LMC), 3-16, 3-17, 16-15,
 23-2, 23-3, 23-15
 high early strength, 23-2, 23-4, 23-15
 very early strength, 23-2, 23-4, 23-12, 23-15
 laths, 15-16, 15-18, 15-19
 lay-up, 25-10
 L-box test, 5-43
 leachate, 14-26, 14-27
 ledges, 10-39
 Lee Roy Selmon Crosstown Expressway, 29-15,
 29-17, 29-25, 29-29
 length factor, 22-5-22-6
 leveling concrete, 20-56, 20-67
 life-cycle cost analysis, 16-23-16-24
 lift-joint quality index (LJQI), 20-34-20-35, 20-70
 lift joints, 20-2, 20-8, 20-10, 20-12, 20-13, 20-14,
 20-17, 20-20, 20-22, 20-34-20-37, 20-38,
 20-40, 20-41-20-42, 20-45, 20-47, 20-51,
 20-66, 20-67, 20-68, 20-69
 seepage, 20-41, 20-42, 20-49
 lift-off test, 12-21
 lift-slab construction, 10-28, 10-30-10-33, 11-29,
 11-33, 12-41
 lifting capacity, crane, 19-32, 19-33, 19-36, 19-38,
 19-40, 19-43
 lifting collars, 10-32, 10-33
 lifting height, crane, 19-32, 19-33
 lifting hook, crane, 19-6, 19-21, 19-33, 19-40
 lifting inserts, 11-50
 lifting jacks, 10-31, 10-32, 10-33, 10-34
 lifting lugs, 10-39
 lifting moment, 19-33
 lifting points, 11-51
 lifts, 19-1, 19-47-19-48, 29-26, 30-52, 30-53, 30-54,
 30-57
 grout, 28-3, 28-20, 28-33
 passenger, 19-4
 roller-compacted concrete, 20-8, 20-10, 20-14,
 20-17, 20-18, 20-21, 20-34, 20-38, 20-40,
 20-43-20-47, 20-51-20-53, 20-55, 20-57,
 20-58, 20-62, 20-64-20-70
 scissor-type, 19-2, 19-47
 thickness of, 20-67
 lighting, bridge, 29-29
 lightweight-aggregate concrete factor, 36-28
 lignin, 3-2, 3-11
 lignite, 2-2, 2-4, 2-6, 2-11, 2-17
 lignosulfonates, 3-3, 3-7, 6-8
 lime, 1-10, 2-11, 2-23, 2-32, 2-36, 2-39, 5-23, 6-8,
 28-6, 28-8, 28-10
 limestone, 1-2, 1-3, 1-19, 5-17, 5-21, 11-4, 20-25,
 30-14, 30-26
 limit-state analysis, 32-57-32-58

- limit states, 16-2–16-3, 16-27, 34-2, 34-3, 34-10
 - shear stress, 34-21
 - strain, 36-10
 - strength, mechanism approach to, 34-2, 34-3
- limonite, 1-19, 6-4
- line pump, 19-17
- linear hyperbolic function, 21-21, 21-22, 21-23
- linear kinetics, 21-21
- linear polarization, 21-56–21-60
- linear variable differential transformers (LVDTs), 27-17, 27-18, 27-25, 27-28
- linearity, of an instrument, 27-15
- liners, 20-38, 30-27–30-30, 30-32, 30-34, 30-55
 - elastomeric, 30-18–30-19, 30-28–30-29, 30-40
 - landfill, 14-26–14-27
 - metal, 30-30
 - plastic, 7-7, 30-18, 30-21, 30-28, 30-29
 - polystyrene foam, 30-29–30-30
 - polyurethane, 30-29
 - polyvinyl chloride, 30-29
 - rubber, 30-18–30-19, 30-28
 - wood, 30-28
- lintels, fire resistance of, 31-14
- liquefied natural gas (LNG), 11-3, 11-55, 13-5–13-6, 13-13, 13-14, 13-27
- liquefied petroleum gas (LPG), 13-13
- liquid-containing structures, 10-23–10-26, 16-2; *see also* liquid-retaining structures, tanks
- liquid head, 7-24
- liquid limit, 14-4–14-5, 20-12
- liquid nitrogen, 11-5, 11-55
- liquid-retaining structures, 4-34, 14-23, 17-2, 17-6, 17-7, 17-8; *see also* liquid-containing structures, tanks
- lithium compounds, 3-18
- live end, 16-16
- live load, 4-21, 7-2, 7-8, 7-10, 7-14, 7-23, 7-24, 7-38, 8-6, 8-9, 8-34, 8-41, 8-42, 8-43, 8-47, 9-7, 9-12, 10-9, 10-16, 10-20, 10-31, 10-34, 11-18, 11-36, 11-41, 24-37, 25-8, 25-9, 25-13, 27-3, 28-41, 32-12, 32-22, 32-27, 32-28, 33-10, 34-2, 34-3, 34-9, 34-10, 34-21, 36-4
 - deflection, 9-17, 9-18, 9-20
 - demolition, and, 12-39
 - design, 10-5, 27-28
 - vs. service, 9-12
 - gravity, 10-5
 - lateral, 10-5–10-7
 - factor, 10-4, 12-39
 - moments, 9-13
 - permanent, 9-12
 - repeated cycles of, 8-51
 - roof, 27-3
- load, 4-4, 4-5, 4-6, 4-7, 7-3, 7-8, 7-9, 7-12, 7-13, 7-14, 7-15, 7-16, 7-17, 7-18, 7-21, 7-22, 7-23–7-27, 7-35–7-36, 9-12, 10-3–10-7, 10-39; *see also* loading
 - accidental, offshore structure, 13-25
 - axial, 10-11, 28-27, 28-52, 28-53, 28-55, 28-58, 28-59, 28-60, 28-62, 28-63, 28-65, 28-66, 28-68, 32-36, 36-5–36-7, 36-10, 36-24
 - axial compressive, 28-52
 - bending, 24-6, 32-36
 - buckling, 10-16, 28-52
 - column, 10-11
 - compression, 7-16
 - compressive, 4-5, 34-10
 - construction, 8-1–8-19, 9-13, 9-19, 10-10, 10-33
 - serviceability consequences of, 8-47–8-55
 - strength consequences of, 8-37–8-47
 - cracking, 4-25, 8-34, 8-35, 8-36
 - dead, *see* dead load
 - decompression, 4-26, 4-27
 - deformation, offshore structure, 13-25
 - design, 8-6, 8-7, 8-19, 8-49, 9-18, 10-3, 10-31, 28-46
 - dynamic, 11-31
 - earth, 10-4, 10-5
 - environmental, offshore structure, 13-25
 - equipment, 12-38
 - Euler buckling, 10-15
 - external, 4-10, 4-18, 4-22, 4-25, 17-2
 - flexural, 28-55, 28-59, 28-60, 36-27
 - floor, 8-2
 - gravity, 8-12, 8-16, 10-5, 10-15, 10-20, 10-21, 12-30–12-31, 32-13, 32-38, 32-40
 - horizontal, 7-26, 7-27, 7-43, 10-15, 12-38, 36-18
 - horizontal brace, 7-47
 - hydrostatic, 10-4, 10-5
 - lateral, 7-16, 10-5–10-7, 10-13, 10-14, 10-16, 10-30, 10-34, 10-35, 12-39, 16-28, 16-29, 28-62, 30-5, 32-7, 32-12, 32-13, 32-29, 32-34, 32-43, 32-57, 32-59, 32-62, 34-3
 - line, 7-47
 - live, *see* live load
 - offshore structure, 13-25
 - partition, 32-22
 - permanent, offshore structure, 13-25
 - pile failure, 14-74, 14-75
 - pullout, 21-12
 - rain, 27-3
 - reshore, 8-7
 - seismic, 10-4, 10-5, 10-6, 16-23, 16-29, 32-19, 32-43, 34-7
 - combinations, 32-27–32-28

service, 9-3, 9-4, 9-12, 10-3, 10-4, 10-5, 10-6,
 10-9, 10-31, 10-39, 16-37, 16-38, 16-40,
 25-7, 25-8, 25-13, 25-16, 25-19, 26-18,
 27-10, 28-67, 36-4, 36-31, 36-33, 36-34
 shear, 10-8, 24-6, 28-50, 28-60, 34-8, 36-15
 shore, 8-7, 8-9, 8-11, 8-12, 8-13, 9-18
 slab, 8-4, 8-7, 8-9, 8-11, 8-14, 8-15, 8-18, 8-19
 snow, 10-4, 27-3, 32-22
 static, 32-7, 32-29
 stringer, 7-40
 sustained, 4-1, 4-2, 4-4, 4-8, 25-7, 36-3
 tensile, 14-5, 24-7, 34-10
 tension, 24-6
 transverse, external, 36-14
 ultimate, 10-17, 10-39, 21-12, 22-2, 22-19, 36-34
 variable functional, offshore structure, 13-25
 vertical, 7-16, 7-23–7-24, 10-11, 10-13, 10-34,
 10-35, 12-38, 32-12, 32-26, 32-34, 32-35,
 32-38, 32-57, 32-59, 32-62, 34-4, 36-18
 wind, 7-27, 10-4, 10-5, 10-6, 28-41, 28-46
 working, 7-14, 27-4
 load and resistance factor design (LRFD), 7-23, 25-4,
 25-12, 33-2, 34-9
 load-bearing capacity, presumptive, 14-37
 load cell, 8-9
 load combinations, seismic, 32-27–32-28
 load distribution, 8-7, 8-16, 14-43, 14-50, 14-65
 factors, 8-4
 load duration, 7-34
 factor, 7-31, 7-34
 load factors, 7-31, 7-34, 8-4, 10-3, 10-4, 25-9
 load path, 32-42, 32-43, 32-45, 32-46, 32-57–32-58,
 34-10, 34-20
 load ratio, 8-2–8-7
 load testing, 14-73–14-75, 16-10, 27-3–27-4, 27-6,
 27-9–27-13, 27-28, 27-29
 truck, 27-26
 vehicle, 27-10
 load transfer, 10-21, 10-30, 10-39, 14-74, 17-12,
 17-15, 19-8, 20-47, 21-13, 25-11, 27-27, 27-28,
 34-8, 34-10–34-11, 35-4
 loader crane, 19-43
 loading, 9-12–9-13; *see also* load
 checkerboard, 10-16
 concrete age, and, 8-32–8-33
 earthquake, 16-29, 16-33, 16-35, 16-36, 16-37
 hydraulic, 27-10–27-11
 in high-rise buildings, 8-1–8-58
 pattern, 9-12, 10-16
 seawall, 16-28–16-29, 16-31, 16-33–16-34
 skip live, 10-16
 loading buoys, offshore, 13-16
 lock chambers, resurfacing of, 15-3

lofting, of piles, 11-51
 Lok-Test, 21-10, 21-12, 21-15
 long-span prestressed bridges, 29-1–29-32
 longitudinal force, 32-53
 loop ties, 7-11
 low-calcium fly ash, 26-1–26-19
 luffing boom, 19-37
 luffing jib, 19-26, 19-29
 lugs, load-resisting, 10-13
 lumber, 7-27
 air-dried, 7-33
 bracing, 10-28
 failure stress of, 7-33
 form, 7-28
 laminated strand, 7-35
 laminated veneer, 7-35
 moisture content of, 7-33
 parallel-strand, 7-35
 presoaking, 10-36
 rough, 7-28
 sawn, 7-33, 7-34
 shores, 7-14
 stresses, adjustment factors for, 7-28–7-31
 structural composite, 7-35
 unit price of, 7-5

M

macrocracks, 4-22, 4-24
 macrodefect-free cement, 6-2, 22-14
 macropores, 1-8
 magnesium, 2-2
 magnesium carbonate, 1-20
 magnesium oxide, 2-29
 magnesium phosphate, 27-27
 magnesium sulfate, 2-25, 5-35
 magnetic reluctance, 21-48–21-49, 21-51
 magnetite, 1-19, 2-6, 6-4
 magnifier, hand-held, 21-30
 main wind force-resisting systems, 10-5
 maintained load test, 14-73
 maintenance, 35-13–35-18
 costs, for repaired structures, 16-20
 mandrels, 11-12, 11-20, 11-36, 11-38, 11-41, 11-42,
 11-50
 manganese oxide, 30-12
 manufactured wood products, 7-35
 mapped acceleration parameters, 32-7, 32-8
 marble, 30-26, 30-32
 Marina del Rey Seawall, 16-20–16-40
 marine environments, 10-13, 11-46
 marine structures, 13-2, 13-31
 marlstone, 20-11

- Marsh cone flow test, 24-11
- masonry, 9-22, 28-1–28-68
 - admixtures, 28-14–28-15
 - bond patterns, 28-16–28-18
 - bracing of, 28-22
 - buildings, seismic-force-resisting, 32-34–32-38
 - cement mortar, 28-9
 - clay, 31-7
 - cleaning of, 28-25
 - codes and standards, 28-2
 - compressive strength, 28-35–28-38, 28-50, 28-53, 28-62, 28-64, 28-65, 28-66, 28-68
 - construction, 28-15–28-27
 - environmental factors, 28-22–28-25
 - tolerances, 28-26–28-27
 - cracking, 28-38
 - detailing, 28-38–28-39
 - equivalent thickness of, 31-7, 31-11
 - grout, 28-3, 28-4, 28-5, 28-9–28-11, 28-14, 28-16, 28-19–28-22
 - inspection, 28-27–28-38
 - lateral support of, 28-48, 28-49
 - lintels, fire resistance of, 31-14
 - materials, 28-4–28-15
 - modular layout of, 28-16–28-18
 - moisture migration, 28-38–28-39
 - painting of, 35-16
 - partially grouted, 28-55, 28-56, 28-64, 28-65, 28-66
 - plain, 28-4
 - project specifications, 28-39–28-40
 - quality assurance levels, 28-29–28-31
 - reinforced, 28-4, 28-13, 28-24, 28-41, 28-42, 28-43–28-45, 28-54–28-58, 28-59, 28-60, 28-63–28-68
 - sample panels, 28-25
 - shear walls, 32-34–32-38
 - approximate period of, 32-24
 - seismic detailing of, 28-43–28-45, 32-35–32-38
 - structural design, 28-40–28-68
 - testing, 28-27–28-38
 - unreinforced, 28-4, 28-13, 28-41, 28-42, 28-43–28-44, 28-51–28-54, 28-59, 28-60, 28-61–28-63
 - walls, fire-resistance rating of, 31-6–31-7
- masonry units, 28-59, 31-14
 - clay, 28-11–28-13
 - concrete, 28-11
 - defined, 28-3
 - equivalent thickness of, 31-7
 - hollow, 28-3, 28-11, 28-13, 28-18, 28-37, 28-39, 28-45, 28-47, 31-7
 - solid, 28-3, 31-7
 - testing, 28-35
- mass, 32-49, 32-50
 - defined, 32-48
- mass concrete, 10-26–10-27, 15-22–15-23, 20-3, 20-11, 20-34, 20-38, 20-40, 20-42, 20-53, 20-64, 30-59
 - cracking analysis of, 20-31
 - materials for, 10-26–10-27
 - mixture design of, 10-27
 - quality control, 10-27
 - Soniscopes testing of, 21-6
- mast-climbing passenger hoist, 19-47
- masts, crane, 19-4, 19-8, 19-9, 19-19, 19-22, 19-24, 19-25, 19-26, 19-28, 19-29, 19-40
 - types of, 19-29
- mat
 - blasting, 11-61
 - timber, 11-32
 - vacuum, 15-14
- mat footings, 14-37–14-43
 - bearing capacity of, 14-37–14-40
 - flexible, design of, 14-40–14-43
- mat foundations, 10-12, 15-23
- match casting, 11-38, 11-39, 11-42
- material allowances, 12-10
- material handlers, 19-1, 19-45–19-47
- material weights, 10-5
- maturity, 8-25, 8-26, 21-17, 21-24
 - degree-hr, 20-69
- maturity index, 21-18, 21-23, 21-24
- maturity, lift-joint, 20-34, 20-36
- maturity meters, 21-26
- maturity method for estimating strength, 21-16–21-25
- maturity rule, 21-17
- maximum considered earthquake (MCE), 32-7, 32-8, 32-23
- maximum distributed pressure, 7-43
- maximum practical achievable density (MPAD), 20-21
- mechanical gauges, 27-13, 27-14, 27-16–27-17
- mechanically stabilized earth, 14-56
- mechanized form systems, 19-48–19-50
- medians, bridge construction within, 29-15
- melamine formaldehyde, 6-8
- member size
 - creep, and, 8-33
 - shrinkage and, 8-30
- membrane
 - curing, 11-6, 30-59
 - curing compounds, 11-50
 - electrometric, 35-15

- PVC, 20-49, 20-51
 - sealing compounds, 11-5
 - traffic-bearing, 35-15
 - upstream, 20-38, 20-40, 20-42, 20-44
 - waterproof, 33-2
- mesopores, 1-8
- metakaolin, 11-4, 26-2
- metakaolin, highly reactive, 2-38–2-42
 - composition of, 2-38
- metal deck forms, 7-7
- metal decking, composite, 10-9
- methacrylate, 23-14
 - surface treatment, 5-38
- methylcellulose, 3-17
- metric dimensions, of masonry units, 28-18
- microcracking, 3-15, 4-4, 4-22, 11-7, 11-16, 11-55, 22-2, 22-3
 - engineered cementitious composite (ECC), and, 24-4, 24-6, 24-7, 24-8, 24-12, 24-14–24-15, 24-21, 24-22, 24-24, 24-27, 24-31, 24-32, 24-34
- micromechanics, 24-4, 24-5, 24-6
- micrometers, 27-16
- micropores, 1-8
- microsilica, 5-27, 10-23, 11-5, 11-6, 11-16, 11-17, 11-19, 11-55; *see also* silica fume
- microwaves, 21-42
- midbay deflection, 9-7
- midspan shoring, 11-36
- midspan moment, 9-3, 10-8, 10-16
- midspan stiffness, 9-7, 9-14, 9-15
- mild steel reinforcement, 10-38, 10-39, 10-40, 11-2, 11-36, 11-42, 16-17, 22-19, 34-11, 34-15, 34-16, 34-20, 34-21, 34-22, 34-23, 35-11, 35-13, 36-34
 - locating, in concrete, 16-8
- mineral admixtures, 2-1–2-42
- minimum-thickness tables, 9-3
- mixed corrosion inhibitors, 3-9
- mixers, concrete, 19-12–19-15
 - batch, 20-59
 - continuous, 20-59, 20-60, 20-62
 - drum, 20-59
 - pugmill, 20-59, 20-60, 20-62, 20-63
 - self-propelled mobile, 19-15
- mixing concrete, 5-6–5-10, 6-39, 6-40, 11-6
- mixing water, 5-29, 5-40, 6-8, 6-21, 6-22, 6-24, 6-25, 9-6, 10-23, 10-27, 13-22, 15-14, 15-17, 15-18, 20-70
 - architectural concrete, 30-15
- mobile cranes, *see* cranes: mobile
- mobility, 21-36, 21-37
- modal response spectrum analysis, 32-19, 32-20, 32-27
- modal testing, 27-7–27-9, 27-26
- modeling
 - beams, 18-9, 18-10–18-11, 18-12
 - columns, 18-9, 18-10–18-11
 - creep, 4-5–4-6, 4-10
 - finite-element, 18-9, 20-53, 27-7, 27-9, 27-23, 27-25
 - frames, 18-9
 - rebar, 18-10, 18-11, 18-13–18-16
 - roller-compacted concrete, 20-53
 - semirigid, 32-18
 - slabs, 18-9, 18-10, 18-11
 - solid geometric, 18-9–18-11
 - trusses, 18-9
- modification coefficient, 8-11, 8-12
- modification factor, 10-16
- modified lignosulfonate (MLS), 3-5
- modulus of elasticity, 1-21, 2-12, 2-23, 2-35, 3-14, 4-10, 4-11, 4-18, 5-16, 6-9, 6-36, 7-28, 7-30, 7-34, 8-4, 8-6, 8-9, 8-26, 8-27–8-29, 8-32, 8-48, 8-49, 8-52, 9-8, 9-12, 9-13, 9-15, 9-18, 9-19, 9-20, 10-8, 10-24, 11-2, 11-17, 11-18, 11-21, 11-32, 13-22, 14-40, 15-2, 16-13, 21-5, 21-6, 21-31, 22-14, 22-16, 24-6, 25-19, 28-3, 36-2
 - accelerators, and, 3-7
 - defined, 20-71
 - engineered cementitious composite (ECC), 24-8, 24-22
 - geopolymer concrete, 26-9, 26-18
 - masonry, 28-52, 28-56, 28-67
 - mild steel reinforcement, 28-54
 - pile, 14-63, 14-74
 - Portland cement, 26-9, 26-10
 - reinforcement, 28-56, 28-59, 28-64
 - roller-compacted concrete, 20-19, 20-27, 20-29–20-31, 20-32, 20-34, 20-47, 20-61
 - self-consolidating concrete, 15-22
 - settlement, and, 14-15–14-16, 14-21
 - soil, 14-63, 14-67
 - subgrade, 14-41
 - static, 8-28, 20-29
 - sustained, 8-50, 20-71
 - temperate–time factor, and, 21-24
 - underwater concrete, 15-12, 15-13
- modulus of rupture, 4-17, 5-15, 8-22, 8-27, 8-36, 8-37, 9-6, 9-13, 9-15, 9-18, 9-19, 9-20, 10-24, 10-26, 13-22, 17-1, 17-10, 28-62, 28-67, 36-2
 - compressive strength, and, 21-16
 - engineered cementitious composite (ECC), 24-8
- Mohr circle diagram, 14-9, 14-10
- Mohs hardness, 21-8

- moisture content, 1-16–1-17, 20-23, 20-27, 20-30, 20-33, 21-48, 21-54
 - aggregate, 11-6, 20-21, 20-58, 20-59
 - dielectric constants, and, 21-44
 - optimum, 20-17, 20-19
 - pulse velocity, and, 21-8
- moisture factor, 7-33
- mold, 6-9, 6-42, 11-7
 - break-off test, 21-15
 - grout, 28-34
- moment capacity
 - nominal, 34-8, 34-12
 - probable, 34-17
- moment coefficient, 10-16
- moment distribution, 9-14, 9-15
- moment frames, 10-14
- moment-magnifier method, 10-16, 36-24, 36-25
- moment of inertia, 4-18, 4-18–4-22, 8-51, 9-3, 9-12, 9-13, 10-9, 10-10, 10-21, 28-52, 28-53, 28-54, 28-63, 28-67, 36-4
 - cracked, 9-13, 9-14, 9-15, 36-3
 - gross vs. effective, 32-58
 - uncracked, 9-14
- moment ratio, 31-6
- moment-resisting frames, 10-6, 32-13, 32-29, 32-34, 32-43, 32-45
 - defined, 32-62
 - seismic, 34-7–34-18
- moment strength, 36-8, 36-9, 36-11
- moments, 10-2, 10-12, 10-14, 10-15, 10-16, 10-17, 10-37, 10-38, 32-58, 36-24
 - antisymmetrical, 24-18
 - applied service load, 25-8
 - beam, 10-21
 - bending, 4-18, 4-25, 8-27, 8-47, 10-15, 10-18, 10-37, 11-50, 14-50, 14-57, 18-10, 18-11, 25-13, 28-52, 28-53, 28-57, 28-62, 28-67, 28-68, 31-6, 32-35, 32-38, 32-40
 - column, 10-16
 - construction load, 10-10
 - cracked second, 25-8
 - cracking, 28-67, 36-4
 - design, 10-16
 - distributed load, 14-43
 - distribution of, 10-20, 10-21
 - elastic, 10-16
 - envelopes, 10-16
 - first, 10-9
 - horizontal, 16-34, 16-36, 16-37
 - internal, 10-39
 - lifting, 19-33
 - magnified, 10-16
 - maximum, 7-38, 7-39, 7-40
 - maximum allowable, 7-43, 7-44, 7-45
 - midspan, 10-8
 - negative, 10-8, 10-16, 10-17, 10-18, 10-21, 11-36, 11-38, 11-40, 11-50, 12-11, 16-34, 16-36, 16-37, 18-11, 22-17, 31-6, 36-14
 - overturning, 32-40
 - positive, 10-16, 10-17, 10-21, 11-41, 16-36, 16-37, 18-11, 27-26, 31-6, 36-14
 - radial, 14-43
 - redistribution of, 12-23
 - release, 32-43
 - secondary bending, 10-15
 - seismic, 32-38
 - service, 9-3–9-4, 9-12, 25-7
 - shear, 14-50, 32-29–32-30
 - static, 10-21
 - superimposed load, 10-10
 - torsional, 10-21, 32-25, 32-29–32-30, 36-22
 - transfer, 10-23, 10-33, 27-26, 34-5, 34-8
 - unbalanced, 10-21
 - vertical, 16-34, 16-35, 16-36, 16-37
- monostrand tendons, *see* tendons: unbonded monostrand
- mooring, 13-2, 13-9, 13-11, 13-13, 13-14, 13-25, 13-28, 13-30
- mortar, 2-10, 2-24, 2-27, 2-36, 3-12, 3-15, 5-43, 6-7, 6-8, 6-18, 6-31, 11-12, 11-18, 11-20, 11-49, 11-50, 11-54, 11-60, 15-13, 16-13, 20-18, 20-56, 21-12, 21-16, 21-18, 21-21, 21-23, 23-13, 24-2, 24-6, 24-11, 24-31, 24-35, 28-2, 28-3, 28-4, 28-5–28-9, 28-10, 28-18–28-19, 28-36, 28-49, 28-59, 30-22, 30-30, 30-32, 30-68, 31-14
 - activation energy of, 21-18
 - aggregate ratio test, 28-33
 - ASTM standards for, 28-5
 - bars, expansion of, 2-27
 - bedded area, 28-3
 - cement–lime, 28-6
 - compressive strength, 28-6, 28-8, 28-9, 28-23, 28-32, 28-33
 - cubes, 6-31, 20-20
 - epoxy, 33-10
 - field-prepared, 28-6–28-8, 28-32, 28-33
 - for overlays, 23-10, 23-11
 - freezing of, 28-23
 - high-early-strength, 33-16
 - joints, 28-9, 28-19, 28-26, 28-37, 30-30
 - tolerances, 28-26
 - laboratory-prepared, 28-6–28-8, 28-32
 - Portland cement, 28-6, 28-8, 28-9, 30-68
 - reinforced, 24-31, 24-32, 24-35, 24-36, 24-37
 - sand–lime, 28-6

- selecting, 28-8–28-9
- stains, 30-71
- testing of, 28-32–28-33
- volume/stone volume ratio, 6-18
- Mo-Sai process, 30-4
- motion attenuation, 32-3
- motor-in-head vibrators, 30-53
- moving-counterweight system, for cranes, 19-26
- mudsills, 7-3, 7-16, 7-35
- Mueller–Breslau principle, 10-16
- mullite, 2-6
- multi-bay model, 8-13, 8-14, 8-15, 8-16, 8-39, 8-40
- multiple fine cracking fiber-reinforced cementitious composite, 24-4
- multi-stemmed beam, 33-4
- muratic acid, 30-71
- mushrooming, 6-40

N

- nanopores, 26-2
- naphthalene formaldehyde, 6-8
- Natchez Trace Parkway Arches, 29-2
- native materials, use of for bridge construction, 29-26–29-28
- natural period, 32-48, 32-51
- near-surface-mounted (NSM) strengthening rods, 25-3
- negative moment, 10-8, 10-16, 10-17, 10-18, 10-21, 11-36, 11-38, 11-40, 11-50, 12-11, 16-34, 16-36, 16-37, 18-11, 22-17, 31-6, 36-14
- neoprene bearing pads, 11-23, 11-32, 11-36, 11-54, 30-47, 30-64
- net area, 28-3
- neural network analysis, 21-35
- Newton's second law, 32-48
- nitrogen injection, 5-32
- No. 4 sieve, 1-14, 1-15, 6-4, 20-11, 30-17
- No. 8 sieve, 1-15, 30-17
- No. 16 sieve, 1-15
- No. 30 sieve, 1-15
- No. 50 sieve, 1-15, 30-17, 30-21
- No. 100 sieve, 1-14, 1-15, 5-43, 6-4, 14-2, 30-14, 30-17
- No. 200 sieve, 20-23, 20-58
- nodal zone, 36-16, 36-18, 36-21
- nodes, 36-15, 36-16
- no-fines concrete, 1-15
- noise error, 27-16, 27-18, 27-19
- nominal dimension, masonry unit, 28-3
- nominal maximum size aggregate (NMSA), 15-4, 20-60, 20-61
- nominal moment strength, 22-12, 36-24

- nominal shear strength, 36-14
- nondestructive testing, 11-32, 16-3, 16-4, 16-20, 16-24, 16-38, 16-39, 16-40, 21-1–21-63, 27-2, 27-5, 27-6–27-9
 - condition assessment, 21-28–21-62
 - flaw detection, 21-28–21-62
 - modal, 27-7
 - to estimate in-place strength, 21-2, 21-2–21-28
 - to evaluate integrity, 21-2
- nondispersible concrete, 15-10
 - horizontal flow time of, 15-12–15-13
- non-engineered design, 28-41
- nonprismatic members, 9-14
- nonsway frames, 10-15
- Norhordland Bridge, 13-14
- normal-strength concrete, *see* concrete:
 - normal-strength
- no-slump concrete, 20-2, 20-3, 20-20
- nuclear power reactors, 11-55
- nuclear reactors, 11-24
- nuclear test methods, 21-60–21-62
- Nurse–Saul maturity function, 21-17, 21-18
- nylon fibers, 22-19

O

- Objective MicroStation, 18-12, 18-13
- object-oriented CAD, 18-12
- occupancy category, 32-8–32-9, 32-11
- occupancy, changes in, 8-49
- Occupational Safety and Health Administration
 - formwork standards, 7-19–7-21
- ocean spray, 5-38
- octyl alcohol, 3-12
- Odyssey™, 18-5–18-6
- offshore structures, 11-3, 11-15, 11-17, 11-18, 11-56, 13-1–13-31, 14-50
 - construction of on barges, 13-29
 - cost of, 13-31
 - service life of, 13-19
 - steel, removal of, 13-17
 - surface of, 13-23
- oil-storage facilities, 13-13
- oil-storage tanks, subsea, 13-15
- omega strain gauge, 27-19
- one-way joist construction, 7-9
- onshore concrete structures, 13-1, 13-2, 13-3, 13-6, 13-25
 - precast, 13-26
- on-site precasting, 10-28–10-30
- onyx, 30-32
- opal, 5-40
- opaline cherts, 5-28

operator cab, crane, 19-25, 19-29, 19-36, 19-37, 19-39

optical fiber strain gauges, 27-21

ordinary least squares, 21-25

ordinary moment-resisting frames (OMRFs), 32-13

O-ring gasket, 11-39, 11-40

oscillographs, 21-45

out-of-plumb tolerances, 28-26

outriggers, 11-32, 11-35, 19-17, 19-29, 19-32, 19-36, 19-37, 19-38, 19-46

oven-dry aggregates, 1-16, 5-30, 20-17, 20-20

overburden pressure, 14-11, 14-12, 14-14, 14-16, 14-21, 14-22

overcompression, 11-34

overconsolidation ratio, 14-60

overdesign, 6-13, 6-38, 20-42–20-43

overlays, 23-1–23-16

- aggregates used in, 23-3
- bonded concrete, 23-1–23-16, 33-2, 33-16
- bond strength of, 23-4–23-13
- compressive strength of, 23-3
- cost of, 23-15
- delamination of, 23-2, 23-4, 23-12, 23-13, 23-14
- joints, and, 23-12–23-13
- material properties of, 23-2–23-4
- mixture proportions of, 23-2–23-3
- permeability of, 23-3–23-4, 23-14
- protection characteristics of, 23-14
- rapid construction of, 23-15
- service life of, 23-16
- shrinkage of, 23-4
- surface characteristics of, 23-14
- surface preparation for, 23-6–23-10
- test patches of, 23-8
- thickness of, 23-4, 23-13

over-reinforced beams, 25-4, 25-5, 25-8

overstrength factor, 32-13, 32-20, 32-27, 32-28, 34-8, 34-10, 34-21

overstress, 10-14, 11-36, 12-27, 16-35, 16-36, 16-37

overvibration, 30-56, 30-57

oxide film, 5-11, 5-37

- on steel, 1-22, 2-17

oxides, 1-3, 1-4

oxidization, 12-29

P

pachometer, 16-18

pads

- neoprene bearing, 11-23, 11-32, 11-36, 11-54, 30-47, 30-64
- vacuum, 15-14

pan joist, 7-9

panel forms, 7-11–7-12

panel thickness, 10-30

pans, 7-9

paper, waterproof, 15-18

parabolic hyperbolic model, 21-21, 21-22

parallel strand lumber (PSL), 7-35

parallel structural system, 32-52

parallel-to-grain loading, 7-28

parapets, 20-45

- precast concrete, 33-2, 33-3, 33-12

parking structures, 1-25, 4-25, 4-30, 5-10, 5-38, 9-9, 10-19, 10-23, 11-33, 11-58, 12-4, 12-31, 16-2, 16-11, 16-16, 23-1, 32-43, 35-3, 35-5, 35-16

particle grading, 1-14, 1-15–1-16, 5-30, 5-32, 20-11

particle-size distribution, 1-14, 1-15, 2-5, 2-32, 14-3, 26-3

partition, 9-22

- load, 32-22

passenger hoists/lifts, 19-4, 19-47

passivation, 2-18

passive–active corrosion inhibitors, 3-9

passive corrosion inhibitors, 3-9

passive vs. active failure mechanism, 14-44

paste, 1-6, 1-7, 1-8, 1-9, 1-13, 1-14, 1-15, 1-23, 2-10, 2-14, 2-15, 2-20, 2-21, 2-23, 2-24, 2-25, 2-26, 2-27, 2-30, 2-33, 2-34, 2-36, 2-37, 3-3, 3-4, 3-6, 3-10, 3-13, 3-14, 3-16, 4-7, 4-8, 4-11, 4-12, 5-2, 5-10, 5-16, 5-30, 5-34, 5-35, 5-40, 5-42, 10-3, 10-25, 11-50, 12-6, 15-14, 15-20, 20-35, 20-47, 20-48, 20-51, 20-58, 20-62, 20-68, 20-69, 21-55, 22-15, 22-16, 24-2, 27-22, 28-25, 30-14, 30-20, 30-24, 30-25

- color, 30-12
- defined, 20-71
- geopolymer, 26-3, 26-5
- permeability, 5-10, 5-11
- roller-compacted concrete, 20-2, 20-14, 20-18, 20-20

paste–aggregate interface, 21-31

paste/aggregate ratio, 6-18

patching, 11-59, 12-20

pavement, 17-14–17-15, 20-1, 22-3

- bonded overlays for, 23-15
- flaw detection in, 21-36
- measuring thickness of, 21-47
- overlay mixtures on, 23-3
- prestressed concrete, 11-58
- stiffness, 23-15

paving lanes, 20-66

PCI Plant Certification, 30-10

P-delta effect, 10-15, 10-16, 10-30, 28-67, 32-20, 32-26, 32-27, 32-56, 36-25

pea gravel, 11-23, 28-10, 31-7

- peak ground acceleration, 32-2, 32-3, 32-4, 32-5, 32-51
 - ratios, 32-6
- peak ground displacement, 32-2, 32-5
- peak ground velocity, 32-2, 32-5
- peak plotting, 21-46
- pedestrian walkways, 29-25, 29-26
- pelletization, 2-19, 2-22
- penetration blow count, 14-37
- penetration resistance, soil, 14-11
- penetrations, in beams or drop caps, 12-8
- Penobscot Narrows Bridge and Observatory, 29-14–29-15
- percussion tools, hand-held, 12-40
- performance evaluation, 27-1–27-31
 - bridges, 27-21–27-31
 - pretest planning, 27-4–27-6
- performance specifications, 30-9
- period, 10-6
 - defined, 32-48
 - natural, 32-48, 32-51
- perlite, 1-17, 6-2, 15-17, 31-8
- permanent forms, 7-7, 30-4
- permeability, 2-15, 2-24, 2-25, 3-2, 3-7, 3-15, 5-2, 5-10, 5-29, 5-35, 5-38, 5-39, 6-8, 10-23, 11-5, 11-7, 12-22, 13-22, 14-29, 16-12, 24-31
 - blast-furnace slag, and, 2-24
 - clay liner, 14-26
 - coefficient, 14-24, 14-26, 14-27
 - defined, 20-71
 - fly ash, and, 2-14
 - overlay, 23-3–23-4, 23-14
 - polymer-modified concrete, 3-16
 - roller-compacted concrete, 20-38–20-40
 - silica fume, and, 2-36
 - water/cement ratio, and, 5-10
- permeation, 24-31, 24-33
- petrographic testing, 5-42, 11-5, 11-7, 11-48, 16-3, 27-5, 27-22
- petroleum acid salts, 3-11
- pH, 1-22, 1-25, 2-17, 2-27, 5-11, 5-37, 15-11, 24-27, 27-22
- phase velocities, 21-38
- phases, mineral, 1-3
- phosphates, 3-7
- phyllites, 5-40
- pier bent, precast, 33-14
- pier-cap segment, 11-40–11-41
- piers, 10-10, 10-12, 10-13, 10-14
 - bridge, 7-9, 10-34, 11-15, 11-46, 11-56, 13-9, 13-14, 14-57, 15-3, 15-7, 29-7, 29-8, 29-10, 29-12, 29-13, 29-16, 29-17, 29-21, 29-22, 29-23, 29-25, 29-26
 - shape of, 29-19–29-20, 29-25
 - corrosion of, 27-23
 - defined, 28-3
 - drilled, 14-76–14-79
 - floating, 13-9, 13-14, 13-15
 - precast concrete, 33-12, 33-14
 - reinforcement of, 10-14
 - shape of, 29-11, 29-15
 - sheet piling, 15-3
- pigment, *see* coloring pigments
- pilasters, 10-10, 28-48, 28-49
- pile capacity, estimating, 14-58–14-62, 14-64, 14-65, 14-73–14-75
- pile caps, 10-12, 10-13, 14-64, 14-65, 32-58, 33-12, 36-15
 - precast concrete, 33-12
- pile-driving analyzer (PDA) method, 14-75
- pile-driving equations, 14-69
- pile failure load, 14-74, 14-75
- pile foundations, 14-57–14-75
- pile groups, 14-64–14-69, 14-73, 14-76
 - bearing capacity of, 14-65
 - efficiency of, 14-65, 14-67
 - settlement of, 14-65–14-69
- pile load tests, 14-73–14-75
- piles, 10-12, 10-13, 11-4, 11-25, 11-26, 11-58, 11-59, 13-1, 13-2, 32-61
 - anchored sheet, 14-53–14-55
 - auger cast, 10-14
 - batter, 10-13, 10-14, 11-54, 32-56
 - bearing, 11-46
 - cantilever sheet, 14-52–14-53
 - cylinder, 11-48, 11-49, 11-50, 11-54, 13-4
 - driving, 11-52, 11-53, 11-54
 - durability of, 11-46–11-48
 - fender, 11-46
 - filled with concrete, 10-13
 - hollow-core, 11-48
 - installation of, 11-51–11-54
 - integrity of, 21-33
 - length of, calculating, 21-36
 - lofting of, 11-51
 - manufacture of, 11-48–11-50
 - mobility plot for, 21-36
 - precast, 10-13, 13-26, 33-12
 - prestressed, 10-13, 11-46–11-54, 13-24
 - seismic force resisting, 32-56
 - settlement of, 14-62–14-63, 14-65
 - sheet, 11-46
 - skin-friction capacity of, 14-60
 - spud, 13-4
 - steel, 10-13, 14-57
 - stiffness of, 32-52

- piles (cont.)
 - testing of, 32-59
 - timber, 10-13, 14-57
 - types of, 14-57
- pipe delivery, of roller-compacted concrete, 20-61
- pipe strut, 11-34
- pipeline, 19-9, 19-15, 19-17–19-19
- pipng, 14-24
- pitch-catch testing, 16-25
- placement
 - architectural concrete, 30-48–30-52
 - concrete, *see* concrete: placement
 - tolerances, 28-27
 - grout, 28-19–28-22
- placing boom, 19-3, 19-4, 19-7, 19-8, 19-9, 19-17, 19-18
- plain masonry, 28-4, 28-43–28-44
- plan irregularities, 32-18
- plank, hollow-core, 10-39
- plaster, 9-22, 31-11; *see also* Portland cement: plaster
- plaster of Paris, 24-37
- plaster stops, 15-18
- plastic design, 34-2
- plastic hinges, 32-51, 32-55, 32-56, 32-57, 32-58, 34-4, 34-5, 34-9
 - length, 34-15, 34-17
 - order of, 32-58
- plastic limit, 14-4
- plastic liners, 7-7, 30-18, 30-21, 30-28, 30-29
- plastic molds, 21-15, 28-34, 30-18, 30-19, 30-21
- plastic moment capacity, 32-58
- plastic sail batten, 30-57
- plastic shims, 30-64
- plastic shrinkage, 4-10, 30-58, 30-59
- plastic strips, 17-3, 17-12
- plasticity, 6-8, 15-14, 15-21, 20-12
 - index, 14-5, 14-27, 20-12
- plasticizers, 3-2, 3-3, 5-2, 5-7, 6-8, 6-28, 15-18, 22-15
- plate compactors, 20-68
- plate load tests, 14-15, 14-31–14-32, 14-40
- plates, 1-21, 10-17–10-23, 10-40, 16-5, 21-37, 36-26–36-28
 - anchor, 14-53
 - anchorage bearing, 11-20
 - bearing, 7-9, 7-11, 11-11, 11-20
 - deflection, 14-31
 - flat, 10-19–10-23, 10-31
 - horizontal, 32-34
 - impact-echo testing of, 16-6, 21-33, 21-34, 21-35
 - impulse–response testing of, 21-36, 21-37
 - post-tensioned two-way, 10-23
 - two-way action, 4-30, 4-31, 4-33
 - washer, 7-11
- platforms, climbing, 19-50
- plinth, 20-49
- plugs, 11-18
 - for tie holes, 30-68
- plywood, 15-14, 30-21
 - cushion blocks, 11-53
 - deflection, 7-34
 - fiberglass-overlaid, 30-21
 - forms, 7-11, 7-28, 7-38, 7-43, 30-28
 - liners, 30-28
 - sheathing, 7-6, 7-7, 7-9, 7-38, 7-42, 7-44, 8-53
 - stresses, 7-34, 7-38
- pneumatic breakers, 12-40
- pneumatic jack, 10-34
- pocket former, 12-2, 12-7, 12-18, 12-19, 12-20, 12-44, 30-45
- point capacity
 - clay, 14-60
 - sand, 14-59
 - ultimate, 14-58
- point resistance, 14-62, 14-70, 14-71
 - limiting, 14-59
- Poisson's ratio, 13-22, 14-15, 14-40, 14-41, 14-63, 14-78, 14-79, 16-13, 21-5, 21-31, 21-32, 21-39, 26-10
 - defined, 20-71
 - roller-compacted concrete, 20-22
- poker vibrator, 30-53
- polarization, 21-56
 - resistance, 21-56–21-59
- polishing, 30-31–30-32
- polyacrylamide polymer, 15-10
- polycarboxylate, 3-6, 24-10
 - ethers, 5-43
 - polymers, 6-35
- polyethylene, 11-46, 11-58, 11-60, 12-2, 23-10, 23-12, 24-5
 - caps, 11-46
 - ducts, 11-12, 11-46
 - pigmented, 11-46
 - sheathing, 11-6, 11-21, 11-24, 11-33, 11-46, 12-3, 12-4
 - sleeves, 11-46, 11-59
- polymer, 5-38, 6-5, 6-8, 6-18
 - concrete, 6-8
 - overlays, 23-1
 - gravity-fill, 23-14
 - modified admixtures, 3-14–3-18
 - polycarboxylate, 6-35
 - thermosetting, 25-2, 25-4, 25-9, 25-10
- polymer/cement ratio, 3-16
- polymer/concrete ratio, 6-8
- polyoxyethylenated compounds, 3-10

- polypropylene, 24-5
 - fibers, 22-19
 - sheathing, 12-4
- polyreference modal testing, 27-7
- polystyrene liners, 30-29
- polyurethane, 3-17, 11-55, 11-58, 30-17, 30-29
- polyvinyl acetates, 3-17
- polyvinyl alcohol fiber, 24-5, 24-7, 24-9, 24-24, 24-27, 24-37
- polyvinyl chloride, 30-39
 - liners, 30-29
 - water stops, 17-8
- ponding, 35-15
- pontoons, 13-2, 13-11, 13-14
 - cast-in-place concrete, 13-14
 - precast concrete, 13-14
 - prestressed concrete, 13-14
- pop-outs, 5-30
- pore pressure, 14-7, 14-9, 14-10, 14-13, 14-14, 14-16, 14-24, 20-16, 20-18
 - settlement, and, 14-14
- pore sizes, 1-8, 1-13, 2-24, 2-25
- pores, 1-8, 1-13
- porosity, 1-8, 1-9, 1-14, 1-17, 1-19, 1-23, 1-25
 - accelerators, and, 3-7
 - strength, and, 1-12-1-13
- Portland cement, 1-2-1-10, 1-14, 2-3, 2-6, 2-10, 2-12, 2-14, 2-15, 3-1, 5-2, 5-12, 5-23-5-27, 5-28, 5-29, 5-30, 5-35, 5-37, 6-2, 6-7, 8-41, 8-42, 8-43, 10-23, 10-26, 11-4, 11-5, 17-13, 20-25, 22-14, 23-2, 23-3, 24-32, 24-37, 26-1, 26-2, 30-15
 - air entrainment of, 2-37
 - blast-furnace slag, and, 2-18, 2-20, 2-21, 2-23, 2-24, 2-25, 2-26, 2-27
 - carbonation of, 2-15, 5-10, 5-11
 - columns, 26-16, 26-17
 - greenhouse gases, and, 1-11
 - hydration of, 1-6-1-9
 - lime mortar, 28-9
 - low-alkali, 5-41
 - manufacture of, 1-2-1-5
 - marine, 13-19, 13-20
 - modified, 1-9-1-10
 - monomers, and, 3-2
 - mortar, 28-6, 28-8, 28-9, 30-68
 - ordinary, 15-20
 - patches, 35-15
 - plaster, 15-16-15-19
 - application of, 15-19
 - metal bases for, 15-18
 - mixing, 15-18
 - proportioning, 15-17-15-18
 - surface preparation, 15-19
 - technical aspects of, 15-17
 - weather barrier backing for, 15-18
- pozzolanic reaction, and, 2-32
- roller-compacted concrete, and, 20-2
- seawater, and, 2-25
- setting time, fly ash and, 2-9-2-10
- stress-strain relationship, 26-8
- surface-area measurement of, 2-5
- surface area vs. silica fume, 2-29
- surface area vs. slags, 2-20
- tensile strength, 26-10
- types of, 1-4, 5-23-5-26
- vs. geopolymer concrete, 26-2, 26-3, 26-4, 26-5, 26-6, 26-7, 26-8, 26-10, 26-13, 26-14, 26-16, 26-17, 26-18
- vs. silica fume, 2-29, 2-32, 2-33, 2-34, 2-35, 2-36, 2-38
- white, 5-27, 30-12
- positive moment, 10-16, 10-17, 10-21, 11-41, 16-36, 16-37, 18-11, 27-26, 31-6, 36-14
- post-and-beam construction, 10-14
- post-tensioned assemblages, 34-11-34-17, 34-20-34-24
- post-tensioned beams, 4-28-4-29, 10-40, 30-45-30-47
- post-tensioned cast-in-place concrete, 11-21-11-23; *see also* concrete
- post-tensioned concrete, 10-25, 10-38, 10-39-10-40, 11-12; *see also* concrete
- post-tensioned two-way plates, 10-23
- post-tensioning, 10-23, 11-12, 11-14, 11-18, 11-19-11-24, 11-29, 11-33, 11-40, 11-41, 11-42, 11-43, 11-44, 11-46, 11-60, 17-10, 17-13-17-14, 27-27
- architectural concrete, 30-45-30-48
- bonded, 16-16
- concrete pavement, 11-58
- external, 16-15
- jacks, 27-29
- longitudinal, 33-10
- precast concrete elements, 33-2, 33-9
- precasting, and, 30-5
- sequence, 27-31
- shortening, and, 35-3
- slabs, 33-3, 33-10
- strain, 27-29
- systems, 11-9
- tank, 11-55
- tendons, 11-20, 27-11
- transverse, 27-27, 33-10, 33-12
- unbonded, 12-1-12-44
 - repair of, 16-16-16-19

- potable water, 1-12, 6-38, 13-22, 23-10, 30-15
- potassium, 5-40
- potassium carbonate, 3-7
- potassium hydroxide, 26-2
- potassium oxide, 1-3
- potassium silicate, 26-2
- pour sequencing, 35-8–35-9, 35-13
- pour strip, 10-31, 35-4, 35-8
- power-driven fasteners, 12-6, 12-21–12-22
- power mixers, 19-14
- power vibrator, 30-53
- power washing, 23-6
- pozzolanic activity index, silica fume, 2-29
- pozzolanic reaction, 2-32
- pozzolans, 1-10, 1-20, 1-25, 2-2, 2-5, 2-10, 2-11, 2-17, 2-25, 2-26, 2-33, 2-36, 5-27, 5-28, 5-32, 5-38, 5-39, 5-40, 5-41, 6-7, 6-8, 6-30, 10-26, 11-4, 13-20, 15-4, 15-9, 15-20, 20-17, 20-20, 20-23, 20-27, 20-29, 20-33, 20-40, 20-45, 20-60, 20-61, 22-14, 24-27, 33-2, 36-1
 - defined, 20-71
 - permeability, and, 20-39
 - roller-compacted concrete, 20-2, 20-8, 20-10, 20-11, 20-13, 20-14
 - shrinkage, and, 4-11
- precast concrete, 10-2, 10-38–10-39, 11-5, 11-42–11-43, 19-3, 19-4, 20-49, 20-51, 26-7, 30-60–30-67, 33-1–33-16, 34-1–34-24, 36-32
 - architectural, 30-4–30-73
 - piles, 14-57
 - seismic bracing systems, 34-1–34-24
- precasting, 11-25
 - bridge segments, 29-12–29-13
 - on-site, 10-28–10-30, 11-25
 - post-tensioning, and, 30-5
- precision, of instrumentation, 27-14
- precompression, 10-13, 10-23, 10-38, 10-39, 11-61, 35-2, 35-4, 35-12
- preconstruction meetings, 6-30
- precured FRP strengthening systems, 25-9, 25-10, 25-11
- prefabricated bridge elements, 33-1–33-16
 - types of, 33-3–33-15
- preloading, 16-16
- preplaced-aggregate concrete, 15-2–15-6, 16-13
- prescriptive detailing, 28-41
 - seismic, 28-41–28-45
- prescriptive specifications, 30-9
- preshores, 7-14, 8-53
- pressure, 7-12, 7-17, 7-18, 7-22, 7-23–7-27
 - internal concrete, 7-9, 7-23, 7-26
 - lateral, 7-10, 7-16, 7-24–7-26, 7-43
 - maximum distributed, 7-43
- pressure bursting demolition, 12-40
- prestress, 34-20
 - loss of, 4-5
 - release of, 11-27–11-28
- prestressed bent caps, 32-61
- prestressed concrete, 4-15, 5-39, 10-37–10-40, 11-1–11-62, 24-2, 36-4, 36-10, 36-22, 36-31–36-34
 - architectural, 11-18–11-19
 - beams, 4-21, 4-25–4-30
 - box, 33-3, 33-7–33-8
 - bulb-tee, 33-8
 - channel, 33-3, 33-4
 - inverted channel, 33-5–33-6
 - cracking of, 4-29–4-30, 9-17–9-18
 - I-beam, 33-3
 - load balancing, and, 9-7
 - single-tee, 33-6
- bridge girders, 11-34–11-36
- buildings, 11-29–11-33
- circular tanks, 4-33–4-34
- demolition of, 11-60–11-61
- elements, 4-5, 22-17–22-18
- existing, strengthening of, 11-60
- floating structures, 11-56–11-57
- maintenance of, 11-58–11-59
- pavement, 11-58
- piles, 11-46–11-54, 14-74; *see also* piles
- pretensioned, erection of, 11-30–11-33
- prism elements, 22-17–22-18
- post-tensioned segmental bridges, 11-38–11-40
- repair of, 11-59–11-60, 16-16
- sleepers, 11-55–11-56
- special provisions for, 11-13–11-19
- tanks, 10-25, 11-54–11-55
- prestressed tie-downs, 32-61
- prestressing, 5-38, 9-7, 9-17–9-18, 10-25, 11-23, 11-40, 11-41, 13-25, 13-26, 17-14
 - bonded, 10-38
 - external, 12-30–12-31
 - for gravity-load strengthening, 12-30–12-31
 - force, 12-38, 12-39, 12-42, 12-43, 12-44
 - steel, 1-22, 11-8, 11-10, 11-18, 11-46, 11-58, 11-59, 12-1, 12-3, 12-4, 12-7, 12-9, 12-42, 12-43, 12-44
 - systems, 11-8–11-13
 - tendons, 11-9–11-10, 11-11, 11-12, 11-14, 11-18, 11-19, 11-21, 11-36, 11-58, 11-59, 25-3, 28-13, 36-31
 - corrosion protection of, 11-23–11-24
 - storing of, 11-19–11-20
 - unbonded, 12-36
- pretensioned beams, 4-27–4-28

pretensioned concrete, *see* concrete: pretensioned
 pretensioning, 11-14, 11-24–11-29, 11-46
 systems, 11-9
 primitive instancing, 18-9, 18-10
 principal stress, 20-48, 20-71
 prism
 construction of, 28-36–28-38
 curing, 28-37
 defined, 28-4
 test, 5-40, 8-30, 8-52, 28-35, 28-36–28-38
 prismatic members, 10-16, 22-17–22-18
 ProActiveM, 18-12, 18-13
 probe penetration test, 21-8–21-10
 progressive failure, 7-3, 12-38, 13-25, 16-38
 property specification, 28-32
 proportion specification, 28-32
 proportioning, 13-18
 proportioning concrete mixtures, 5-31–5-32, 5-41,
 6-2, 6-9–6-29, 13-18, 22-4–22-5, 22-15, 23-2,
 23-16, 30-12
 engineered cementitious composite (ECC),
 24-8–24-12
 geopolymer concrete, 26-3–26-4
 procedure for, 6-22–6-23
 public exposure, seawall panel, 16-38
 pugmill mixers, 20-59, 20-60, 20-62, 20-63, 20-71
 pull-off test, 21-26
 pullout, 1-21, 11-14, 11-32, 11-42, 24-7
 fiber, 22-5, 22-6, 22-13, 24-7, 24-26
 resistance, 22-9
 strength, 8-26, 21-11, 21-12, 21-24
 test, 21-3, 21-10–21-15, 21-26, 24-27
 cast-in-place, 21-10, 21-13
 coefficient of variation for, 21-12
 failure mechanism of, 21-12, 21-13
 post-installed, 21-13–21-15
 pulse-echo testing, 16-25, 21-31
 pulse velocity, 21-5–21-8, 21-27, 27-7
 pumice, 1-17, 31-7
 pumpability, 13-23
 pump-and-boom combination, 19-15–19-17
 pump-delivery system, 10-27
 pumps, 5-6, 11-6, 12-8, 13-26, 15-7, 15-8, 15-13,
 19-1, 19-2, 19-3, 19-4, 19-6, 19-9,
 19-15–19-19, 30-21, 30-32, 30-51–30-52
 boom, 19-17
 line, 19-17
 stationary, 19-9, 19-17
 trailer, 19-17
 truck-mounted, 19-17
 vacuum, 15-15
 vs. belt conveyors, 19-45
 with pipelines, 19-17–19-19

punch diameter, 8-27
 punching shear, 8-12, 8-27, 8-37, 8-38, 8-40, 8-43,
 10-22, 10-23, 11-8, 11-14, 27-25, 27-29
 failure, 8-27, 8-37, 8-38, 27-25, 27-29
 strength, 8-27, 8-37, 8-38, 8-40, 8-43
 stresses, 8-43, 8-46, 8-47
 test, 21-3
 two-way, 10-12
 PUNDIT, 21-8
 purlins, 8-53
 pushover analysis, 32-58
 P-waves, 16-4–16-7, 21-31, 21-32, 21-33, 21-34,
 21-35
 pylons, 29-13, 29-14, 29-15, 29-26

Q

quality assurance
 architectural concrete, 30-9–30-10
 defined, 30-73
 masonry, 28-29–28-31, 28-35
 quality control
 architectural concrete, 30-9–30-10
 defined, 30-73
 quartz, 1-2, 2-6, 2-29, 2-38, 5-21, 5-40, 6-9, 22-16,
 30-14, 30-26, 30-32
 quartzite, 1-19
 quasi-static load testing, 27-9–27-13, 27-17, 27-20
 quays, floating, 13-14
 quick load test, 14-73

R

R/ECC, *see* steel-reinforced engineered cementitious
 composites
 radar, ground-penetrating, 21-42–21-48, 21-63
 radiation shielding, 1-19, 5-17, 6-4
 radioactive test methods, 21-60–21-62
 radiography, 21-60, 21-61–21-62, 27-5
 radiometry, 21-60–21-61
 raft foundation, 10-12
 railroad ties, 11-55–11-56
 rain, 5-15, 7-43, 8-48, 11-20, 11-21, 11-33, 11-40,
 11-41, 14-26, 15-17, 20-34, 28-24–28-25,
 28-39, 30-40, 30-59
 load, 27-3
 release agents, and, 30-18
 roller-compacted concrete, and, 20-10, 20-17,
 20-69–20-70
 ramp loading, 7-48
 ramps, 20-56
 Rankine method, 14-44–14-45, 14-46
 rapid chloride permeability test, 11-7, 15-22, 16-3

- rapid load test, 14-73
- rapid mortar bar test, 5-40
- rate constant model, of relative strength
 - development, 21-23
- rate of reaction, 1-5, 1-7
- RCC, *see* roller-compacted concrete
- reaction frame, 27-11
- reactive powder concrete, 5-2, 22-14, 22-16–22-17
- ready-mix trucks, 11-6, 15-8, 19-4, 19-13, 19-17,
 - 23-3; *see also* truckmixers
 - architectural concrete, and, 30-48
- rebar, *see* reinforcing bars
- rebound hammer, 21-3–21-5, 21-9, 21-27, 27-5
- rebound number, 21-3, 21-4, 21-9, 21-27
- rectangle adjacency graph (RAG), 18-10–18-11
- rectangular beam analysis, 28-56, 28-66
- red mud, 26-2
- redistribution of moments, 12-23
- redundancy, 9-12
- redundancy factor ρ , 32-12, 32-18, 32-20–32-21,
 - 32-27, 32-28
- reeding, 30-25
- reference design values, lumber, 7-28
- reference temperature, 21-17
- reflection, 21-32, 21-33, 21-34, 21-44, 21-47, 24-37
- refusal, 14-69
- regular structures, 32-18–32-19, 32-21
- rehabilitation, 16-2
- reinforced concrete, 5-39, 11-60, 13-2, 16-16, 17-2,
 - 24-12, 24-14, 24-18, 24-19, 24-20, 24-22,
 - 24-23, 24-34, 25-15, 30-4, 32-29–32-34,
 - 36-4–36-5, 36-22, 36-31, 36-35; *see also*
 - reinforcement, reinforcing bars, steel
 - reinforcement
 - beams, 4-18–4-21, 4-24–4-25
 - columns, eccentricity of, 4-5
 - shrinkage of, 4-11, 5-21
 - strength design of, 36-10–36-31
- reinforced walls, 14-51–14-52
- reinforcement, 1-1, 1-21–1-23, 10-6, 10-13, 10-14,
 - 10-17, 10-19, 11-8–11-13, 13-22, 28-49, 28-59,
 - 36-28–36-31; *see also* reinforcing bars, steel
 - reinforcement
 - anchored, 9-14
 - assessment of, 16-4
 - ASTM standards for, 28-5
 - cast-in-place architectural concrete, 30-41–30-48
 - composite, 22-17–22-18
 - compression, 4-21–4-22, 9-6, 28-64, 36-9, 36-10,
 - 36-13, 36-29, 36-30
 - continuous, 22-2, 22-3
 - corner, 15-18
 - crack control, 24-22–24-23
 - deterioration of, 12-42
 - electrical/magnetic methods for evaluating,
 - 21-48–21-60
 - end-span, 9-15
 - excess, 36-28, 36-29
 - fiber, 1-21
 - flexural, 16-20, 32-54, 32-55, 32-56, 34-5, 34-6,
 - 36-28
 - footing, 14-39
 - galvanized, 30-44–30-45
 - geotextile, 14-52
 - hoop, 32-43, 32-54, 32-62, 36-6, 36-22, 36-35
 - horizontal, 4-34, 10-30, 17-2, 17-8, 28-27, 28-42,
 - 28-44, 28-45, 32-34, 32-35, 32-54, 36-20,
 - 36-28
 - geopolymer concrete, 26-14
 - joint shear, 32-54, 32-55
 - loads, and, 7-23
 - longitudinal, 10-15, 10-17, 18-10, 26-14, 26-16,
 - 27-25, 31-11, 31-12, 31-14, 36-17, 36-22,
 - 36-23, 36-28, 36-35
 - long-term, 4-34
 - masonry, 28-13, 28-67
 - mild steel, *see* mild steel reinforcement
 - negative vs. positive, 31-6
 - overlays, and, 23-5
 - passive, 11-19
 - polarization resistance of, 21-58
 - prestressed, 36-17
 - prestressing carbon fiber, 22-21
 - pulse velocity, and, 21-8
 - retaining wall, 14-50
 - shear, 10-32, 11-30, 24-21, 25-4, 25-6–25-7, 26-16,
 - 28-58, 28-67, 28-68, 32-38, 34-10, 36-35
 - shear-head, 10-22
 - shear-moment transfer, 10-19
 - shrinkage, 10-17, 17-8
 - slab, 17-10
 - solid modeling of, 18-10–18-11
 - special, 11-14–11-15
 - spiral, *see* spiral reinforcement
 - steel, *see* steel reinforcement
 - stress, 4-24, 4-31, 28-57, 28-59, 36-4
 - tank, 10-24
 - tensile, 9-6, 34-16, 36-9, 36-10
 - tensile stress in, 28-54–28-55
 - tension, 9-17, 28-52, 28-62, 28-64, 28-66, 36-10,
 - 36-14, 36-23, 36-29, 36-30
 - tie, 10-10, 11-18, 25-18; *see also* ties
 - tolerances for, 28-27
 - torsional, 36-22
 - transverse, 27-4, 36-22, 36-23, 36-35
 - index, 36-28

- transverse closed-tie, 10-17
- two-way, 20-52
- vertical, 10-24, 17-2, 28-16, 28-21, 28-27, 28-42, 28-44, 28-45, 32-54
- web, 10-12, 36-5, 36-34, 36-35
- weight of, 7-8, 7-14
- reinforcement index, 22-17, 36-11
- reinforcement ratio, 9-13, 25-18, 25-19, 25-20, 26-16, 26-17, 28-56, 28-64, 36-8, 36-10, 36-13
 - balanced, 25-15
- reinforcing bars, 7-38, 10-2, 10-10, 10-17, 11-8–11-9, 11-13, 11-15, 11-23, 11-26, 11-37, 13-19, 13-23, 16-8, 16-15, 16-25, 17-7, 18-8, 18-12, 20-51, 22-3, 26-16, 32-37, 34-11, 34-22; *see also* reinforcement, steel reinforcement
 - automated manufacturing of, 18-16
 - bent, 11-30
 - bundled, 11-8, 11-13, 30-42, 36-30
 - cathodic protection of, 1-22
 - congestion, 10-17
 - contraction joints, and, 17-5, 17-6
 - corrosion of, 13-20
 - detection of by covermeters, 21-48–21-52
 - detection of by radiometry, 21-60–21-61
 - development length, 28-51, 28-61
 - eddy currents, and, 21-49–21-50
 - epoxy-coated, 1-23, 5-38, 5-39, 11-9, 36-28
 - fiberglass, 22-19
 - fiber-reinforced polymer (FRP), 25-2–25-9
 - graphic recorders, and, 21-46–21-47
 - magnetic-reluctance meters, and, 21-48–21-49
 - modeling of, 18-11, 18-13–18-16
 - negative moment, 31-6
 - nominal moment strength, and, 22-12
 - positioners, 28-27
 - replacement of, 11-59, 35-15
 - resistivity measurements, and, 21-56
 - size, measuring, 27-5
 - space occupied by, 30-43
 - spacing of, 4-24, 4-30, 4-32, 5-32, 21-51, 21-52, 21-56, 22-9, 25-7, 27-5, 30-43, 30-50, 36-4–36-5, 36-35
 - strength design, and, 28-63–28-64
 - zone of influence, and, 21-50–21-51
- reinforcing steel, *see* steel reinforcement
- relative humidity, 2-33, 2-36, 4-8, 4-9, 4-11, 4-12, 4-15, 5-15, 5-21, 5-42, 8-20, 8-33, 9-13, 9-15, 11-20, 11-58, 23-12, 28-24
 - carbonation, and, 5-11
 - creep, and, 8-33
 - shrinkage, and, 8-29, 8-30
 - strength development, and, 8-21
- relaxation, 12-27, 12-28
- release agents, 30-18–30-19, 30-21, 30-25, 30-28, 30-30
- release joints, 35-9–35-11
- released connections, 35-9–35-11, 35-13
- reluctance, 21-48, 21-49
- repair, of concrete structures, 12-24–12-30, 13-19, 15-3, 16-1–16-41
 - case study, 16-20–16-40
 - limit states design for, 16-2–16-3
 - long-term performance of, 16-20
 - material selection for, 16-11–16-14
- repeatability, 27-15, 27-17
- repetitive-use factor, 7-34
- reshores, 7-4, 7-14, 7-15, 7-38, 8-4–8-19, 8-38, 8-42, 8-43, 8-52, 8-53, 9-12, 12-9, 12-41
- resin, inorganic, 22-24
- resistance factors, 25-4, 25-12
- resistivity, 21-54–21-56
- resolution vs. accuracy, 27-14
- response modification factor, 32-12, 32-13, 32-18
- response spectra, 32-50–32-51
 - ground motion, 32-2, 32-8
- restoration, 16-2
- restrainers, 32-61
- restraint cracks, 35-2, 35-7, 35-13
- retaining walls, 14-43–14-56
 - design of, 14-48–14-50
 - drainage, and, 14-50
 - rough, nonvertical, 14-46
- retarders, 2-29, 3-2–3-3, 3-4, 3-5, 3-6, 3-11, 5-30, 5-31, 6-33, 6-39, 6-40, 10-23, 11-5, 20-20, 20-56, 20-66, 28-8, 28-15, 30-20, 30-22
 - chemical surface, 30-24–30-25, 30-27, 30-29
- retempering, 6-41
- retrofitting, 12-22, 12-24, 12-30–12-36
 - seismic, 32-42–32-46, 32-56–32-61
- reuse, of forms, 7-3, 7-4, 7-5, 7-14, 7-28, 8-4, 10-3, 10-37, 20-52, 30-34, 33-2
- revibration, 30-57, 30-58
- rheology, concrete, 5-43, 15-21, 15-22
 - creep models, 4-5–4-6
- rhometer, 15-21
- rhyolite, 5-42
- ribs, 8-53
- rice-husk ash, 2-25, 11-5, 26-2
- Richter magnitude, 32-5
- rigid frames, 10-14–10-15
- rigidity
 - flexural, 8-47
 - foundation, 8-11, 8-12
 - of shores, 8-9
- RILEM, 2-18, 3-2, 21-7
- rip-rap, 11-54, 16-22

roads, haul, 20-65
 ROBCAD, 18-16
 robotics, 18-1–18-8
 rodding, 16-13
 rods, 11-9
 ductile, 34-7, 34-8, 34-10, 34-18, 34-19
 Roll's rheological model, 4-6
 roller-compacted concrete, 15-23–15-25,
 20-1–20-71
 adiabatic temperature rise in, 20-33–20-34, 20-53
 advantages/disadvantages, 20-7–20-10
 aggregates for, 20-11–20-12
 air content, 20-21
 autogenous volume change, 20-22, 20-70
 bulldozers, and, 20-66
 cavitation, 20-23
 cementitious content of, *see* cementitious
 content, roller-compacted concrete
 coefficient of thermal expansion, 20-22
 compaction, 20-68–20-69
 compressive strength, 20-23–20-27
 consistency of, 20-16–20-17
 construction, 20-54–20-70
 conventional concrete, and, 20-67
 costs, 20-7–20-9
 creep, 20-32
 curing, 20-69–20-70
 dams, 20-3
 delivery, 20-60–20-65
 spreading, 20-65–20-68
 density, 20-21
 design, 20-40–20-53
 design section options, 20-43–20-53
 equipment, 20-10
 erosion resistance, 20-23
 grout-enriched, 20-20–20-21, 20-49, 20-52
 history of, 20-3–20-7
 inspection, 20-69
 joint treatment, 20-69
 mixing, 20-58–20-60
 mixtures, 20-12–20-21, 20-68–20-69
 modulus of elasticity, 20-29–20-31
 permeability, 20-38–20-40
 placing, 20-65–20-68
 plants, 20-59, 20-60
 Poisson's ratio, 20-22
 scheduling, 20-9
 seepage, 20-38–20-40
 shear strength, 20-34–20-37
 tensile strain, 20-32–20-33
 tensile strength, 20-27–20-29
 thermal conductivity, 20-22
 thermal considerations, 20-52–20-53

 thermal diffusivity, 20-22
 thermal stress in, 20-34
 time limit for placing, 20-61
 watertightness, 20-38–20-40
 weather, and, 20-10
 rollers, 20-69
 selection of, 20-68
 vibratory, 20-2, 20-16, 20-67, 20-69, 23-10
 walk-behind, 20-68
 rolling shear, 7-28
 roofs, fire resistance of, 31-8
 Ross rheological model, 4-5
 rotation, 10-12, 10-14, 10-32, 11-32, 16-32, 17-8,
 27-4, 30-61, 32-53, 34-1, 34-4, 34-5, 35-10
 post-yield, 34-7, 34-16
 sheet pile, 14-53
 torsional, 30-64
 wall, 16-30
 rotors, 19-19, 19-20, 19-21
 rough lumber, 7-28
 running bond, 28-16, 28-18, 28-37, 28-49, 28-54,
 28-55, 28-63
 rupture
 fiber-reinforced polymer systems, 25-14
 tendon, 12-27–12-28
 rust, 5-38, 11-18, 12-6, 16-26, 21-52, 30-59
 rust-inhibiting paint, 12-9
 rust staining, 10-2, 10-30, 30-40, 30-42, 30-44, 30-58,
 35-15
 rustications, 30-7, 30-21, 30-22, 30-28, 30-30, 30-32,
 30-36, 30-39, 30-40
 R-waves, 21-31, 21-32, 21-33, 21-37, 21-38

S

S4S, 7-27
 saddle jib, 19-25
 saddles, 12-34
 duct, 11-20
 safety analysis, 8-41–8-47
 sag, 4-2, 7-4, 9-18, 9-19, 9-20, 11-60
 salts, 11-12
 sample panels, masonry construction, 28-25
 samples, number of, 27-5–27-6
 sampling, 6-41–6-42
 sand, 1-15, 3-6, 5-2, 5-29, 5-40, 6-4, 6-11, 6-23, 6-24,
 6-25, 6-28, 6-37, 10-24, 10-25, 10-29, 10-30,
 11-4, 11-16, 11-17, 11-18, 11-23, 11-30, 11-58,
 13-22, 14-2, 14-5, 14-14, 14-28, 14-56, 14-62,
 14-76, 15-2, 15-14, 15-17, 15-18, 15-20, 15-25,
 20-11, 20-21, 22-14, 22-15, 24-9, 24-27, 26-7,
 28-6, 28-8, 30-14, 30-16, 31-8; *see also* soil:
 sandy

- absorption, 6-27
- earth pressure, and, 14-55
- embedment, 30-30–30-31
- point resistance for, 14-62
- settlement in, 14-32
- silty, 14-5
- ultimate bearing capacity in, 14-31
- weight of, 6-12, 6-25, 6-26
- sand/binder ratio, 24-9
- sandblasting, 30-4, 30-6, 30-9, 30-12, 30-13, 30-16, 30-17, 30-20, 30-22–30-24, 30-27, 30-28, 30-30, 30-32, 30-34, 30-35, 30-36, 30-40, 30-44, 30-46, 30-47, 30-59, 30-68, 30-71
- sandstone, 1-19
- saturated surface dry aggregates, 1-16, 5-30, 20-19, 20-69, 26-8
- saturation, 5-10
 - of soils, 14-7, 14-20, 14-69
- saws, 17-5
- scaffolding, 7-14, 7-19, 8-9, 10-34, 10-36, 11-21–11-23, 12-6
- Scaffolding, Shoring, and Forming Institute guides, 7-22
- scaling, 5-31, 5-34, 5-35, 15-22, 16-14, 22-14, 30-25, 30-26
 - resistance, 2-15, 2-37, 2-39, 3-7, 3-8, 3-12, 5-29, 5-34–5-35
- scarification, 23-6
- schists, 1-19
- Schokbeton, 30-4
- scoria, 1-17, 31-7
- scrapers, 20-64–20-65
- scratch coat, plaster, 15-19
- screeds, 15-18, 18-2–18-3, 23-10, 23-14, 23-15
- screw jack, 10-34, 11-32
- sea salts, 13-21
- sealants/sealers, 5-35, 17-8, 30-17, 30-18, 30-28, 35-15
 - acrylic, 30-69–30-70
 - joint, 17-13, 30-67
 - precast concrete, 30-67
 - silane, 23-14, 35-15
 - surface, 5-38, 5-39
 - wood, 30-17, 30-18, 30-28
- seat extensions, 32-61
- seawalls, 13-9, 14-50
 - repair of, 16-20–16-40
- seawater, 1-22, 1-25, 2-14, 2-17, 2-18, 2-24, 3-7, 5-10, 5-29, 5-37, 5-38, 11-9, 11-58, 11-59, 13-2, 13-19, 13-20, 13-22, 13-25, 16-20, 16-26
 - blocking inflow of, 11-59
 - galvanizing, and, 11-10
 - resistance to, 2-25–2-26
- secant modulus, 8-28
- second-generation superplasticizers, 3-5
- section modulus, 7-39, 7-40, 7-41, 9-3
 - beam, 10-10
 - composite member, 10-10
- sectional tower crane, 19-24, 19-29
- seepage, 14-10
 - groundwater, 14-23–14-24, 14-25
 - joint, 20-40, 20-41
 - lift-joint, 20-42, 20-49
 - roller-compacted concrete, 20-7, 20-38–20-40
- segmental concrete construction, 33-9
- segregation, 5-2, 5-6, 5-31, 5-43, 6-40, 10-3, 10-27, 15-2, 15-18, 15-20, 15-25, 20-11, 20-14, 20-23, 20-34, 20-61, 20-63, 20-65, 20-66, 27-5, 30-21, 30-51, 30-52
- seismic
 - activity/events, 7-27, 10-14, 10-30, 11-17, 16-24, 16-27, 20-46
 - base shear, 32-22–32-24
 - bracing systems, 34-1–34-24
 - hybrid system of, 34-11, 34-12, 34-15, 34-17, 34-20, 34-22
 - strength criterion for, 34-2–34-4
 - design, bridges, 32-48–32-56
 - design categories, 32-7, 32-11–32-21, 32-29
 - detailing, masonry, 28-41–28-45
 - detailing, prescriptive, 28-41–28-45
 - detailing, shear walls, 28-43–28-45, 32-35–32-38
 - echo method, 21-33
 - effects, analysis of, 32-19–32-20
 - force, 32-12, 32-13, 32-20, 32-21, 32-26, 32-27, 32-28, 32-29, 32-34, 32-43, 32-44, 32-45, 32-46, 32-48
 - design, code-specified, 32-12, 32-13, 32-28
 - horizontal, 32-27
 - resisting piles, 32-56
 - resisting system, 32-12, 32-13, 32-20, 32-21, 32-29–32-34
 - vertical distribution of, 32-24
 - joints, 17-9–17-10
 - load, *see* load: seismic
 - moment-resisting frame systems, 34-7–34-18
 - regions, 11-54, 36-9
 - resistance, 16-22, 16-23, 24-39, 32-1–32-61
 - columns, 32-53
 - response history, 32-19
 - retrofit, 32-42–32-46, 32-56–32-61
 - footings, 32-45
 - risk evaluation, 32-6
 - wave, 17-10
 - weight, effective, 32-22
 - zones, 22-24

- self-consolidating concrete, 3-6, 3-14, 5-2, 5-43, 6-35, 7-26, 11-6, 11-54, 15-19–15-22, 30-16
 - applications, 15-22
 - mix design, 15-20
 - testing methods, 15-20–15-22
- self-consolidating grout, 28-10–28-11
- self-erecting cranes, 19-22
- self-propelled mobile mixer, 19-15
- semirigid modeling, 32-18
- sensitivity, of an instrument, 27-15
- sensors, embedded, 16-20
- series conveyor, 19-45
- series structural system, 32-52
- service crane, 19-43
- service load, *see* load: service
- service moments, 9-3–9-4, 9-12, 25-7
- service torsional moment, 9-8
- serviceability, 4-18–4-34, 12-23, 12-28, 12-29, 12-31, 16-2, 16-3, 16-8, 27-4, 35-14, 35-15, 36-3, 36-27
 - corrosion, and, 16-2
 - failures, 8-20
 - limit state, 16-2, 16-27
- servohydraulic cylinders, 27-10–27-13
- setting, 10-23, 10-26; *see also* setting time
 - rapid, 8-21
 - rate, 5-31, 5-32
- setting time, 3-3, 5-12, 5-33, 6-7, 6-8, 6-34, 7-26; *see also* retarders
 - admixtures, and, 5-28
 - antiwashout admixtures, and, 3-14, 15-11, 15-13
 - calcium chlorides, and, 3-7
 - corrosion inhibitors, and, 3-9
 - maturity method, and, 21-24
 - Portland cement, 2-9–2-10
 - silica fume, 2-34
 - slags, and, 2-20
- settlement, 10-14, 10-17, 11-32, 14-14–14-23, 17-10, 20-44, 28-38
 - consolidation, 14-17, 14-22, 14-62, 14-68, 14-69
 - cracks, 30-56
 - differential, 14-23, 17-6, 30-36
 - elastic, 14-74
 - immediate, 14-21–14-22, 14-68, 14-69
 - in clay, 14-32
 - in granular soils, 14-15–14-16
 - in saturated clays, 14-16–14-23
 - mat footing, 14-40
 - maximum allowable, 14-22, 14-23
 - pile, calculation of, 14-62–14-63
 - pile group, 14-65–14-69
 - secondary, 14-14
- shadowing, 30-21
- shadows, on bridges, 29-22–29-23
- shale, 1-14, 1-17, 1-19, 5-28, 5-30, 6-4, 20-11, 31-7, 31-8
 - ASTM standards for, 28-4–28-5
- shape, aggregate, 1-14, 1-15, 5-30, 6-7, 6-36, 6-37, 20-11, 21-16
- she bolts, 7-11, 30-39
- shear, 3-14, 7-30, 8-27, 8-41, 8-47, 10-7, 10-8, 10-11, 10-15, 10-16, 10-17, 10-24, 10-33, 10-37, 10-38, 11-15, 11-18, 11-32, 11-36, 11-57, 12-38, 13-24, 14-5, 16-34, 17-2, 20-43, 25-11, 28-58, 28-63, 28-67–28-68, 32-23, 32-38, 32-56, 36-10
 - base, 32-22–32-24, 32-27, 32-29, 32-62
 - beam–column joint, 34-17, 34-20
 - bond-reduction coefficient, 25-16
 - capacity, 25-4, 25-6, 25-7, 25-9, 25-12, 25-16–25-18, 32-26, 32-43
 - allowable, 10-22
 - nominal, 34-9
 - coefficient, 10-16
 - column, 34-21
 - connectors, 10-8, 10-9
 - cracks, 36-14
 - deflection, 7-34
 - demand, 32-26
 - distribution, 32-30
 - engineered cementitious composite (ECC), 24-14–24-15
 - failure, 8-47, 10-22, 27-4
 - flexural, 36-34
 - flow, 10-8
 - footings, and, 10-12
 - force, 10-9, 10-16, 10-33, 14-39, 18-10, 18-11, 28-51, 28-54, 28-58, 28-61, 28-63, 32-34, 32-35, 32-40, 32-43, 36-34
 - column, 34-17
 - maximum, 7-36, 7-39, 7-40, 7-41, 7-43, 7-44, 7-45, 7-46, 8-12, 14-50
 - modulus of rupture, and, 8-27
 - radial, 11-4
 - total, 8-16
 - friction, 13-22, 22-18, 34-6, 36-10
 - interlock, 22-9
 - heads, 10-22, 10-32
 - horizontal, 10-7, 10-8, 11-36, 11-41, 32-34, 32-35, 36-25
 - distribution of, 32-27
 - horizontal torsional moments, and, 32-25
 - joint, 32-54
 - keys, 11-38, 11-44, 11-54, 27-27–27-28
 - lag, 11-43
 - lateral, 32-34

- load, 10-8, 24-6, 28-50, 28-60, 34-8, 36-15
- mixers, 11-6
- modulus, 21-39
- moment, 14-50, 32-29–32-30
- nominal, 36-10
- perimeter, 8-27, 10-22
- plywood, 7-38
- prestressed elements, 36-34–36-35
- punching, *see* punching shear
- reinforcement, 10-32, 11-30, 24-21, 25-4, 25-6–25-7, 26-16, 28-58, 28-67, 28-68, 32-38, 32-54, 34-10, 36-35
- rolling, 7-28
- solid rectangular beam, 7-36
- story, 32-25, 32-26, 32-27, 32-29, 34-19
- strength, 5-15, 8-20, 8-41, 10-22, 11-17, 13-22, 20-34–20-37, 22-13, 22-24, 28-50, 28-61, 28-68, 36-14–36-15, 36-36
 - foundation soil, 14-7, 14-11
 - nominal, 36-14
 - pullout strength, and, 21-12
 - roller-compacted concrete, 20-34–20-37
- stress, *see* stress: shear
- torsional, 32-34
- transfer, 10-10, 10-19, 10-21, 11-18, 11-41, 32-34, 32-38, 32-40, 33-4, 33-10, 34-6, 34-8, 34-9, 34-10, 35-11
- upward, 14-39
- vertical, 10-21, 11-36
- walls, 10-6, 10-14, 10-15, 10-16, 10-34, 12-38, 15-23, 28-42, 28-58, 28-64, 30-5, 30-45, 32-12, 32-13, 32-29, 32-30, 32-31, 32-34, 32-34–32-42, 32-43, 32-45, 35-11
 - approximate period of, 32-24
 - calculating number of bays for, 32-21
 - defined, 32-62
 - deflection of, 10-6
 - discontinuous, 32-19
 - empirical design of, 28-46–28-49
 - foundation analysis/design, 32-38–32-40
 - seismic detailing requirements for, 28-43–28-45
- yield stress, 15-21
- shear span/depth ratio, 22-13
- sheathing, 7-6–7-8, 7-10, 7-11, 7-34, 7-35, 10-34, 10-36, 12-4, 12-7, 12-17, 12-22, 12-24, 12-27, 16-19
 - design of, 7-38–7-39, 7-44
 - electrically isolated, 12-3
 - minimal thickness of, 12-4
 - nailing to joists, 7-39
 - plastic, 16-16, 30-48
 - plywood, 7-6, 7-7, 7-9, 7-38, 7-42, 7-43–7-44, 8-53
 - polyethylene, 11-6, 11-21, 11-24, 11-33, 11-46, 12-3, 12-4
 - repair, 12-18
 - slippage, 12-6
 - swelling of, 10-36
- sheet pile, 14-50, 14-52–14-55
- sheeting, *see* sheathing
- Shelby tube, 14-29
- shims, 30-62, 30-63, 30-64, 30-66
 - steel, 30-64
- ships, reinforced concrete, 13-2
- shoots, 5-6
- shop drawings, 12-6, 12-10, 12-38
- shored construction, 10-9–10-10
- shores, 7-5, 7-8, 7-14–7-16, 7-34, 7-38, 8-1–8-19, 8-36, 8-52, 11-32, 11-36, 11-59, 12-9, 12-27, 12-39, 12-41, 27-29, 30-47, 30-64
 - aluminum, 7-14
 - compressible, 8-19
 - demolition, 12-38, 12-41, 12-42
 - design of, 7-41–7-42
 - floor slabs, and, 8-2, 8-7, 8-9
 - for demolition, 11-61
 - horizontal, 7-9
 - jack, 7-14
 - levels of, 8-2, 8-3, 8-4, 8-6, 8-7, 8-9, 8-13, 8-14, 8-19, 8-42, 8-43, 8-52
 - number of per bay, 8-18
 - permanent, 8-53
 - premature removal of, 7-4
 - removal of from flexural members, 8-36, 8-37
 - rigidity of, 8-9
 - temporary, 7-8
 - vertical, 7-21
- shoring and reshoring, 7-14, 8-4, 8-6, 8-7, 8-19, 8-38, 8-41, 8-42, 8-43, 8-49, 8-52, 8-53, 9-15, 9-18–9-19, 12-42
- short-pulse radar, 21-42
- shortening, 11-4, 11-14, 11-19, 11-23, 11-27, 11-32, 11-38, 11-58, 11-60, 12-6, 12-8, 12-28, 12-29, 12-43, 23-13, 35-2, 35-3, 35-4, 35-7–35-8, 35-10, 35-13
 - pile, 14-62
- shot blasting, 23-6–23-8
- shotcrete, 3-17, 11-54, 11-55, 11-60, 14-56, 16-13, 16-15, 20-56, 22-3, 24-12
- shrinkage, 2-15, 4-1–4-2, 4-6, 4-7, 4-10–4-16, 4-18, 4-27, 5-2, 5-30, 5-31, 8-48, 8-49, 8-52, 9-11, 9-13, 9-15, 9-17, 9-18, 9-20, 10-12, 10-23, 10-24, 10-25, 10-26, 11-2, 11-4, 11-15, 11-17, 11-23, 11-30, 11-33, 11-41, 11-42, 12-6, 12-8, 12-10, 12-29, 13-22, 13-25, 15-22, 22-14, 23-2, 23-14, 30-7, 30-15, 30-36, 35-2, 35-3, 36-3

shrinkage (cont.)

- antiwashout admixtures, and, 3-14
 - autogenous, 4-35, 20-22, 20-70, 23-4
 - CEB-FIP model for, 4-16
 - chemical, 21-21
 - silica fume, and, 2-33
 - cracking, 2-34, 3-14, 20-49, 20-51, 28-51, 28-62, 35-2, 35-4
 - creep, and, 8-51
 - deflection, and, 8-49, 8-51, 8-52, 9-4
 - drying, *see* drying shrinkage
 - due to carbonation, 2-15, 4-12
 - high-range water reducers, and, 3-7
 - long-term, 4-34
 - member size, and, 8-30
 - mortar, 28-9
 - overlay, 23-4, 23-12
 - plastic, 5-43, 6-40, 23-4, 23-12, 23-14, 30-58, 30-59
 - prediction, 4-12–4-15
 - reducing admixtures, 3-14
 - reinforcement, 10-17, 17-8
 - relative humidity, and, 8-30
 - slab, 17-13
 - slump, and, 4-16
 - strain, 4-2, 4-3, 4-10, 4-11, 4-13, 4-14, 4-15, 4-16, 4-35, 9-6, 17-2
 - stress, 30-36
 - strips, 17-2
 - thermal, 11-27, 11-50
 - time, and, 8-30–8-31
 - ultimate, 8-29–8-30
 - unreinforced concrete, 8-29–8-31
 - volume/surface ratio, and, 9-6
 - water, and, 4-16
 - water-reducing admixtures, and, 3-4
- side form spacers, 7-14
- side-grain loading, 7-28
- side-sway, 34-4, 36-25
- sieve analysis, of soils, 14-2
- SIFCA®, 22-14
- SIFCON, 22-15, 22-18
- signalers, 19-40
- silane, 5-39, 11-58
 - sealer, 23-14, 35-15
 - surface treatment, 5-38
- silica, 5-23
- silica fume, 1-25, 2-22, 2-23, 2-29–2-38, 3-6, 5-10, 5-27, 5-28, 5-29, 5-38, 5-39, 5-41, 6-8–6-9, 6-18, 6-20, 6-25, 6-32, 9-20, 11-4, 11-5, 11-16, 11-17, 11-23, 11-56, 13-20, 15-20, 22-14, 22-16, 22-17, 23-2, 23-3, 23-14, 23-15, 26-2, 36-1
- air entrainment, and, 2-37
- as-produced, 2-29
- bleeding of, 2-33, 2-34, 2-36
- carbonation, and, 2-32, 2-36
- characteristics of, 2-29–2-30
- chemical composition of, 2-30
- chemical resistance, 2-36–2-37
- compressive strength, and, 2-34–2-35
- condensed, 2-33, 2-37
- cracking of, 2-34
- creep, 2-35
- durability, and, 2-36–2-38
- freeze–thaw resistance, 2-37
- physicochemical mechanisms, 2-30–2-32
- production of, 2-29
- setting time, 2-34
- types of, 2-29
- water demand, 2-32–2-33, 2-34
- workability, 2-33
- silicates, 3-7, 5-27, 6-7, 6-33
- silicon, 2-1, 5-27, 11-5, 24-32, 26-2
- silicon alloys, 2-29
- silicon dioxide, 2-38, 6-9
- silicon oxide, 26-3
- silt, 1-2, 5-30, 14-2, 20-26
- siltstones, 5-40
- silty sand, 14-5
- single-bay model, 8-12, 8-13, 8-14, 8-15, 8-16, 8-39, 8-40
- single-span bending members, 7-35
- single-tee beam, 11-30
 - prestressed, 33-6
- single-wythe masonry walls, fire-resistance ratings of, 31-6–31-7
- site-cast concrete, *see* concrete: site-cast
- site class, 32-7–32-8
- site exploration, 14-27–14-32
- site geology, ground motion and, 32-5
- size factor, 7-33
- skid derricks, 11-40–11-41, 11-42, 11-43
- skid ways, 13-26, 13-29–13-30, 13-31
- skin friction, 10-12, 14-60, 14-62, 14-67, 14-70, 14-71
- skip live-loading, 10-16
- Skyline Plaza Project, Bailey's Crossroads, Virginia, 27-28–27-29
- slab, 1-21, 2-14, 4-24, 4-33, 6-40, 7-11, 9-7, 9-17, 9-18, 9-19, 9-22, 10-17–10-23, 12-9, 12-30, 12-38, 14-39, 16-5, 16-6, 19-49, 21-37, 32-19, 36-7–36-10; *see also* floors, lift-slab construction
 - advancing-slope grouting, and, 15-5
 - apron, 20-44

as rigid diaphragm, 32-18
 casting, 11-25
 cast-in-place, reinforcement of, 12-32
 –column joints, *see* joints: slab–column
 –column released connections, 35-10
 compressive strength of, 8-35
 compressive stresses in, 10-9
 conduit embedment in, 12-8
 connecting, 19-50
 contraction joints, 17-3
 control of deflections in, 8-52–8-55, 36-27
 cracking, 4-34, 8-35, 9-18, 10-17, 12-9, 17-6, 17-8, 35-4
 curling, 17-11, 17-13, 17-14
 dam, 20-49
 dead load of, 7-23
 deflection, 4-5, 8-2, 8-11, 8-52–8-55
 causes of, 8-48–8-49
 control of, 8-52–8-55
 demolition, 12-40
 diameter, 8-27
 drying, 17-11
 equivalent thickness, 31-9
 finishing of, 19-19
 flat, 7-8, 10-19–10-23, 17-10, 27-29
 flat-plate, 7-38, 8-16
 flaw detection in, 21-33, 21-34, 21-36, 21-40, 21-60
 flexural cracking, and, 8-34, 8-36
 floor, 4-10, 4-32, 7-7, 7-8, 7-38–7-43, 8-1–8-20, 8-47, 9-18, 10-28, 10-31, 11-18, 11-25, 11-29
 shores, and, 8-2, 8-9
 –forming systems, 7-14
 foundation, 4-34; *see also* foundation
 free vs. fixed edges of, 8-12
 ground-supported post-tensioned, 12-4
 heat transmission in, 31-6
 heaving, 10-29
 highway, 14-40
 hollow-core, 11-30
 irregular geometry, 35-7
 joints, 12-4, 17-2, 17-10–17-15
 load, 8-4, 8-7, 8-9, 8-11, 8-14, 8-15, 8-18, 8-19
 maintenance of, 35-15
 modeling of, 18-9, 18-10, 18-11
 negative bending moment, and, 18-11
 number of, 8-19
 on grade, 17-10–17-14, 17-15, 22-3
 one-way, 4-24, 4-25, 8-52, 9-3, 10-17–10-19, 10-40, 12-30, 18-11, 22-3, 36-4, 36-5, 36-36
 failure of, 8-27

post-tensioned, 8-48, 10-31, 10-32, 10-33, 12-6, 12-9, 12-23, 35-2, 35-3, 35-4, 35-6, 35-8, 35-9, 35-13
 precast bridge deck, 33-2, 33-3, 33-9–33-12; *see also* bridge decks
 precast prestressed, 11-36
 precast pretensioned, 11-32
 pullout tests, and, 21-11
 rectangular tank, 10-26
 reinforced-concrete, 8-12, 35-2, 35-4
 reinforcement in, 17-15
 repair of, 16-14
 retrofit of, 12-32–12-36
 ribbed, 9-6, 9-17
 robotic screeding of, 18-2–18-3
 roller-compacted concrete, 15-25
 roof, 7-7, 9-14, 10-28, 10-31, 10-32, 11-25, 11-29, 11-33
 safety analysis of, 8-42–8-47
 sawed joints, and, 17-5
 settlement of, *see* settlement
 shortening of, 35-2, 35-3, 35-7–35-8, 35-10, 35-13
 shrinkage-compensating cement, and, 17-13
 site-cast, 10-28
 spans, 8-47, 10-19
 precast and prestressed, 33-3
 steel-reinforced, 17-14
 stiffness, 8-2, 8-9, 8-16, 8-18, 8-49
 stripping time for, 8-9
 supported, 10-31–10-32
 tank, 10-24
 T-beams, and, 10-8
 temperature differentials and, 8-51, 15-23
 thickness of, 8-16, 8-27, 8-47, 8-48, 9-3, 10-9, 10-18, 10-19, 10-22, 14-40
 two-way, 4-24, 4-30–4-33, 8-47, 8-52, 9-7, 10-19, 10-20, 10-31, 10-40, 12-11, 12-30, 16-34, 18-11, 22-3, 27-4, 35-2, 35-4, 36-26–36-28, 36-36
 fiberglass-reinforced, 22-19
 post-tensioned, 12-7
 unbonded monostrand tendons, and, 12-2
 underwater, 15-7
 vacuum processing, and, 15-15
 warping of, 8-48
 weight of, 10-9
 without joints, 17-13
 slags, 1-10, 1-11, 1-14, 1-17, 1-25, 2-15, 5-27, 5-32, 5-39, 5-40, 5-41, 6-4, 6-8, 6-9, 6-20, 13-20, 15-20, 15-23, 20-40, 20-61, 23-2, 23-3, 23-14, 26-2, 31-7, 31-8; *see also* blast-furnace slag
 glassy, 2-19
 roller-compacted concrete, and, 20-2

- slate, 1-17, 31-7, 31-8
- sledgehammer, 27-8, 27-26
- sleepers, prestressed, 11-55–11-56
- sleeves, 11-9, 11-12, 11-20, 11-24, 11-36, 11-38, 11-46, 11-59, 11-60, 12-15
- slenderness effects, 10-15
- slenderness ratio, 36-24
- slewing handlers, 19-46
- slewing platform, crane, 19-29
- slewing ring, 19-25, 19-29, 19-36
- slewing speed, 19-34
- sliding, 20-35, 20-41, 20-44, 20-45, 20-47, 20-48, 20-69
- slings, 11-9, 11-34, 11-35, 11-50, 11-51
- slip-form construction, 10-33–10-37, 13-25, 13-26, 19-49–19-50, 20-51, 20-52, 20-68, 21-61, 23-15
 - materials for, 10-34–10-36
- slippage, 35-9
- slope-layer method, 20-67
- slow-load strain capacity, 20-32
- slump, 2-10, 2-16, 2-21, 2-33, 3-4, 3-5, 3-12, 5-2–5-3, 5-7, 5-28, 5-31, 6-8, 6-9, 6-17, 6-23, 6-24, 6-27, 6-28, 6-29, 6-30, 6-31, 6-35, 6-40, 6-41, 6-42, 7-25, 7-43, 9-15, 9-20, 10-14, 10-23, 10-27, 10-34, 11-5, 11-6, 15-9, 15-12, 15-18, 15-20, 15-21, 16-13, 20-16, 20-52, 24-10, 30-51; *see also* no-slump concrete
- antiwashout underwater concrete, 15-10
- as-cast concrete, 30-21
- effect on shrinkage, 4-16
- flow test, 5-43
- geopolymer concrete, 26-4, 26-5, 26-8, 26-15
- grout, 28-20, 28-33, 28-34
- high-range water reducers, and, 3-6–3-7, 6-21
- loss, 6-40
- temperature, and, 8-21
- tests, 5-2, 5-32, 5-33, 6-9
 - grout, 28-33–28-34
- variations, 30-19
- zero, 10-34, 15-23, 15-25
- slurry-infiltrated fiber concrete (SIFCON), 22-14–22-15, 24-2
- Smart Road Bridge, 29-6, 29-20, 29-26
- smooth rods, *see* tendons: single-bar
- snap ties, 7-11, 30-38, 30-39, 30-40
- snow load, 10-4, 27-3, 32-22
- snow removal, 35-16–35-17
- sodium, 5-40
- sodium bentonite, 14-27
- sodium benzoate, 3-9
- sodium chloride, 3-7
- sodium chromate, 3-9
- sodium hexametaphosphate, 14-2
- sodium hydroxide, 3-11, 26-2, 26-3, 26-4, 26-7, 26-8
- sodium nitrite, 3-9
- sodium oxide, 1-3, 2-27, 5-42, 13-20, 15-4
- sodium silicate, 14-2, 26-2, 26-3, 26-4, 26-7, 26-8
- sodium sulfate, 26-14
- sodium thiocyanate, 3-8
- soil
 - aggressive, 10-14
 - Atterberg limits, 14-2, 14-4–14-5
 - classification of, 14-2–14-5, 14-13, 14-29
 - clayey, 14-10, 14-19, 14-29, 14-31, 14-32, 14-50, 14-60, 14-62, 14-65, 14-67, 14-76; *see also* clay
 - coarse-grained, 14-2, 14-5
 - compressibility, 14-2, 14-5, 14-14–14-23
 - conditions, ground motion and, 32-3
 - dry, 14-7
 - fine-grained, 14-2, 14-4, 14-5
 - granular, 14-14, 14-15–14-16, 14-26, 14-29, 14-37, 14-58, 14-60
 - liquid, 14-4–14-5
 - mechanical analysis of, 14-2–14-4
 - nailing, 14-56
 - partly saturated, 14-7
 - plastic, 14-4
 - pores, 14-7
 - pressure, 10-11, 10-13, 32-39–32-40
 - profile type, 32-7–32-8
 - resistivity, 21-55
 - sampling, 14-29
 - sandy, 14-5, 14-9, 14-31, 14-32, 14-34, 14-35, 14-56, 14-59, 14-60, 14-76
 - saturated, 14-7, 14-20, 14-69
 - semisolid, 14-4
 - settlement, 9-19
 - shear strength, 14-7
 - springs, 32-59
 - strength, 14-5–14-14
 - stress ratio (SSR), 32-38
 - subsea, 13-25
 - suction, 14-7
 - unified soil classification system (USCS), 14-2, 14-5
 - voids, 14-7
 - wet, 14-7
- soils approach, 20-20
- solid modeling, 18-9–18-11
- solid waste, 14-26
- sonic-echo method, 21-33
- Soniscopes, 21-6, 21-7
- sorptivity index, 24-32–24-33
- sorptivity test, 24-32

- sound abatement, 28-9
- sounding, 21-31
 - devices, 15-5–15-6
- soundness, 1-19
- space factor, 22-6–22-7
- space frames, 32-45
- space truss elements, 36-22
- spacing dimension, 36-28
- spading, 30-57–30-58
- spalling, 5-38, 10-7, 11-23, 11-50, 11-54, 11-55,
 - 11-59, 11-61, 12-22, 12-29, 23-16, 24-12,
 - 24-19, 24-21, 24-22, 24-29, 24-34–24-36,
 - 26-14, 27-2, 27-4, 30-25, 30-29, 30-40, 30-42,
 - 30-64, 30-70, 30-71, 35-5, 35-15
- span-by-span bridge construction, 29-11–29-13,
 - 29-16
- span/deflection ratio, 9-20
- span/depth ratio, 9-18, 29-7–29-8, 32-18
- span length, 29-6
- spandrels, 7-4, 35-15
 - precast, 30-64, 30-65
- spans, 7-16, 7-39, 7-46, 7-48, 10-16
 - clear, 7-9
 - direction of, 7-28, 7-38
 - falsework, and, 11-40
 - float-in, 11-44
 - length of, 7-9, 10-20
 - lifted-in, 11-43
 - long, 10-17, 11-40
 - maximum, 7-43, 7-44
 - maximum allowable, 7-44, 7-45, 7-46
 - number of, 7-35, 7-36, 7-38, 7-40, 7-44
 - post-tensioned, 11-38
 - short, 11-30, 11-36
 - slab, 8-47, 10-19
 - precast and prestressed, 33-3
 - suspended, 11-36
- spar buoy platform, 13-13
- spatial occupancy enumeration (SOE), 18-9
- special moment-resisting frames (SMRFs), 32-13
- specialized applications, 15-1–15-25
- specific creep, 4-6, 8-31–8-32, 26-13
- specific gravity, 1-19, 2-5–2-6
 - aggregate, 5-30, 20-21
 - fly ash, 6-25
 - highly reactive metakaolin, 2-38
 - of slags, 2-20, 2-23
 - sand, 6-24
 - silica fume, 2-29
 - soil, 14-69
- specific surface, 2-37
 - of fly ash, 2-5, 2-6
 - of highly reactive metakaolin, 2-38
- specifications, architectural concrete, 30-8–30-9
- specified dimension, masonry unit, 28-3
- spectral acceleration, 32-51
- spectral analysis of surface waves (SASW), 21-37,
 - 21-39
- spectral displacement, 32-51
- spectral response acceleration parameters, 32-8,
 - 32-23, 32-27
- spectral velocity, 32-51
- spider, 19-19
- spillways, 20-3, 20-7, 20-8, 20-41, 20-52
- spiral reinforcement, 11-8, 11-9, 11-11, 11-12, 11-13,
 - 11-21, 11-48, 11-49, 11-54, 25-18, 25-19, 36-6,
 - 36-7, 36-10, 36-11, 36-29
- splices/splicing, 11-11, 11-12, 11-20, 11-36, 11-38,
 - 11-58, 12-20, 12-21, 12-27, 12-38, 12-39,
 - 28-51, 34-23
 - bundled bar, 36-30
 - lap, 11-8–11-9, 25-9, 27-4, 28-51, 28-61
 - tendon, 16-17, 16-18
 - tension, 30-42
- split-cylinder strength, 8-24, 8-27
 - estimating, 8-27
 - test, 27-5
- split spoon sampler, 14-11, 14-29
- splitting tensile strength, 6-8, 6-9, 8-22, 8-26,
 - 20-27–20-29
 - compressive strength, and, 8-26
 - estimating, 8-26
 - mortar, 28-32
 - temperature–time factor, and, 21-24
- splitting tension, 11-14
 - test, 21-14
- spread footings, 10-10, 10-11, 10-12
- spreader, 7-11
- spreader beam, 11-34
- sprinkler systems, 31-2–31-3
- Spruce–Pine–Fir (SPF), 7-38, 7-40
- spud piles, 13-4
- spud vibrator, 30-53
- square root sum of the squares (SRSS) method,
 - 32-27, 32-28
- stability analysis, 12-39
- stabilized maximum/minimum crack spacing, 4-25
- stabilizers, 5-43, 19-46
- stable correlation, 21-26
- stack bond, 28-16, 28-37, 28-45, 28-52, 28-54, 28-55,
 - 28-63
- stair and elevator towers, 35-16
- stairs, metal pan with concrete infill, 35-16
- stairwells, 19-8
- standard penetration test (SPT), 14-7, 14-11–14-12,
 - 14-21, 14-34, 14-38, 14-60

- standards, 8-55–8-58
- static cone penetration test, 14-7, 14-13–14-14
- static fatigue, 25-3
- static flexural strength, 22-8
- static force, 32-18
- static load, 32-7, 32-29
 - test, 14-73, 14-74, 27-9–27-13, 27-17, 27-20
- static moment, 10-21
- static pile capacity, 14-58–14-62, 14-73
- statistical methods for estimating in-place strength, 21-25–21-28
- staves, concrete, 11-54, 11-55
- steel columns, 10-12, 10-28, 13-4, 31-13
- steel–concrete construction, 10-7–10-10
- steel fibers, 22-2, 22-3, 22-4, 22-6, 22-9, 22-10, 22-11, 22-12, 22-13, 22-14–22-17, 24-1, 24-12
- steel, prestressing, 1-22, 11-8, 11-10, 11-18, 11-46, 11-58, 11-59, 12-1, 12-3, 12-4, 12-7, 12-9, 12-42, 12-43, 12-44
- steel punchings, 6-4
- steel-reinforced engineered cementitious composite (R/ECC), 24-4, 24-6, 24-12–24-24, 24-38, 24-39
 - cast-in-place, 24-39
 - corrosion resistance, 24-33–24-36
 - durability of, 24-27–24-36
 - spall resistance, 24-34–24-36
- steel reinforcement, 1-21–1-23, 4-28, 4-24, 4-27, 5-2, 5-11, 5-31, 5-32, 6-7, 8-49, 10-17, 10-18, 10-23, 10-24, 10-26, 10-35, 10-37, 11-8–11-9, 11-28, 11-38, 11-58, 11-59, 12-22, 12-40, 12-42, 13-22, 14-40, 15-2, 15-3, 15-11, 15-22, 16-1, 16-2, 16-3, 16-14, 16-34, 17-14, 19-50, 24-22, 25-3, 25-5, 25-6, 25-8, 25-9, 25-12–25-19, 30-41–30-43; *see also* reinforcement, reinforcing bars
- chloride penetration in, 24-34
- cladding panels, and, 30-5
- concrete cover for, 30-43
- contraction joints, and, 17-5
- corrosion of, 2-17–2-18, 2-27, 3-7, 3-8, 3-9, 16-14, 16-18, 16-20, 16-22, 16-23, 16-25, 16-26, 16-29, 16-31, 16-34, 16-37, 16-38, 16-40
- cracking load, and, 8-35
- ducts, and, 11-20
- engineered cementitious composite (ECC), and, 24-4, 24-6, 24-12–24-24, 24-38, 24-39
- epoxy, and, 5-38, 16-14, 16-18, 16-20, 16-25
- galvanized, 5-38
- horizontal, 16-26
- live load, and, 8-34
- loss of, 16-29, 16-30, 16-32, 16-38, 16-40
- mass loss of, 24-36
- modulus of elasticity, 28-56
- offshore structure, 13-26
- overlays, and, 23-3
- probe penetration test, and, 21-10
- pulse-echo testing, and, 21-31
- removing concrete around, 23-6
- service stress levels in, 17-8
- tensioned, 16-16
- unstressed, 11-26
- vertical, 16-20, 16-22, 16-23, 16-26, 16-29, 16-37
- vs. fiberglass reinforcement, 22-19
- steel shells, column, 32-59
- steel shims, 30-64
- steel stress, 4-24, 4-25, 4-27, 4-30, 8-51, 32-36, 32-37
- steel stringer bridge, testing of, 27-29–27-31
- steel-to-concrete friction factor, 34-6
- steel-to-steel friction factor, 34-6, 34-7
- steel yielding, 24-22, 25-3, 25-5, 25-12, 25-13, 25-14, 25-15
- Stefan–Boltzman law, 21-41
- stiffening, 15-3
 - rate of, 11-50
- stiffness, 4-18, 4-19, 4-32, 6-41, 6-42, 7-28, 9-14, 9-20, 10-6, 10-13, 11-33, 11-48, 14-40, 16-28, 20-29, 20-30, 20-33, 20-41, 20-43, 20-53, 21-4, 21-36, 21-37, 21-39, 22-3, 24-9, 24-12, 24-22, 24-27, 25-11, 25-13, 27-7, 27-9, 27-26, 32-29, 34-14–34-15, 35-2
- abutment, 32-52
- beam, 10-15, 10-20
- bridge deck, 23-15
- bridge design, and, 32-48, 32-49, 32-50, 32-51
- coefficients, 8-12, 10-21
- column, 10-15, 32-51, 32-53
- composite floor system, 10-7
- cracked, 9-16, 32-51
- defined, 32-48
- diaphragm, 32-18
- distribution of, 10-6
- end-region, 9-14, 9-15
- estimating, 9-3–9-4
- fiber-reinforced polymer systems, 25-14
- flexural, 8-2, 8-48, 9-4, 9-5, 9-7, 9-8, 9-11, 9-12, 9-13–9-14, 9-18, 9-19, 36-27
- joint, 9-14
- leveling concrete, 20-56
- member width, and, 9-17
- midspan, 9-7, 9-14, 9-15
- pavement, 23-15
- pile, 10-13
- shore, 8-12, 8-18
- shoring system, 8-15–8-18
- slab, 8-2, 8-9, 8-16, 8-18, 8-49

- torsional, 9-9, 9-14
- torsional beam, 10-21
- uncracked, 9-16
- vertical framing, 32-18
- stirrups, 9-8, 10-12, 11-8, 11-13, 11-14, 11-36, 11-41, 11-43, 18-10, 18-11, 18-12, 18-13, 22-8, 22-13, 24-19, 24-21, 25-4, 25-6, 25-7, 25-9, 26-16, 28-55, 32-54, 32-55, 34-10, 35-5, 36-9, 36-10, 36-15, 36-22, 36-29, 36-35
- Stokes' law, 14-3
- stone, ASTM standards for, 28-5
- stone, crushed, 1-15, 5-2, 5-29, 6-3, 6-36, 13-21, 15-6, 15-9, 15-25, 31-7
- story drift, 32-11, 32-12, 32-25–32-26, 32-46, 34-14
 - defined, 32-62
 - design, 32-25, 32-26
- story shear, 32-25, 32-26, 32-27, 32-29, 34-19
- strain, 4-1, 4-4, 4-8, 4-10, 4-15, 4-22, 4-24, 4-27, 4-35, 8-27, 11-15, 20-22, 20-32, 22-17, 24-2, 25-13, 25-17, 25-19, 36-23
 - anchorage zone, 11-14–11-15
 - at sharp corners, 11-15
 - balanced, 36-23, 36-24
 - compressive, 25-15, 36-10
 - confined, 25-19, 25-20
 - limiting, 36-9
 - confined concrete, 36-9
 - creep, 2-23, 2-35, 4-1, 4-2, 4-3, 4-6, 4-7, 4-8, 5-22, 8-49–8-51, 17-2, 26-13
 - elastic, 4-1, 4-2, 4-3, 4-4, 4-5, 5-21, 5-22, 17-2, 26-13
 - fiber-reinforced polymer system, 25-14–25-15, 25-17
 - gauges, 27-16–27-21
 - gradient, 4-24
 - hardening, 24-2–24-3, 24-5, 24-6, 24-9, 24-22, 24-24, 24-30
 - hardening cementitious composite (SHCC), 24-4
 - irrecoverable, 4-5
 - limit states, 36-10
 - limits, 36-10–36-11, 36-23
 - load-induced, 4-7
 - masonry, 28-49
 - maximum usable, 28-59
 - post-tensioning, 27-29
 - recoverable, 4-5
 - reduction factor, 36-10
 - shrinkage, 4-2, 4-3, 4-10, 4-11, 4-13, 4-14, 4-15, 4-16, 4-35, 9-6, 17-2
 - softening, 20-41
 - steel, 28-59
 - tempering, 12-27
 - tensile, 4-22, 4-31, 4-34, 11-15, 11-54, 20-27, 25-14, 25-15, 36-10
 - thermal, 11-55, 11-57, 11-58
 - total, 17-2
 - transverse, 11-54
 - transverse cracking, 25-18, 25-19
 - ultimate, 34-15
 - ultimate, fiber-reinforced polymer systems, 25-15
 - strands, 11-26, 11-28, 11-42, 11-46, 11-54, 11-56, 11-60, 12-21, 12-44, 33-2; *see also* tendons
 - bundled loops of, 11-50
 - burning of, 11-28
 - cable-stay, 29-15
 - compact, 11-10
 - corrosion of, 12-23
 - coupling of, 12-20
 - creased, 12-24
 - deflected, 11-28, 11-29, 11-30, 11-34
 - failure of, 16-16, 16-18
 - fatigue of, 11-52
 - installing, 11-21
 - number of per bundle, 12-7
 - pile, 11-49
 - polyethylene-sheathed, 11-33
 - post-tensioning elongation of, 34-16
 - prestressing, 5-38, 5-39, 10-13, 10-38, 11-2, 11-10, 11-12, 11-13, 11-23, 30-47–30-48
 - pretensioned, 11-18, 11-24, 11-32
 - relaxation of, 12-27, 12-28
 - rupture of, 12-27
 - seven-wire, 11-9, 11-10, 11-25, 12-2, 12-3, 12-25, 12-27, 12-44, 16-16, 16-18, 16-19, 27-25, 30-47
 - side-by-side, 11-38
 - slipping of, 12-19–12-20
 - tensioning, 10-23
 - transverse post-tensioning, 27-27
 - unbonded, 12-6
 - post-tensioning, 34-11, 34-13, 34-22
 - unsheathed, 12-17
 - Strategic Highway Research Program (SHRP), 16-3, 16-41
 - strength, 3-1, 3-2, 3-3, 3-4, 3-6, 3-10, 3-17, 5-2, 5-6, 5-31, 6-30, 6-41, 7-28, 8-20–8-27, 9-12, 10-14, 11-2, 11-4, 16-2, 16-8
 - admixtures, and, 6-4–6-9
 - age, and, 21-21, 21-22, 21-23, 21-24
 - assessment of, 16-4
 - bearing, 13-22, 20-48
 - bond, 3-16, 8-20, 8-22–8-26, 8-41, 11-26, 11-56, 16-11, 23-3, 23-4–23-13
 - overlay, 23-3, 23-4–23-13
 - revibration, and, 30-57

strength (cont.)

- break-off, 21-16
- compressive, *see* compressive strength
- compressive cylinder, 8-41, 8-43
- concrete, 8-43, 12-8, 12-20, 36-8–36-9
- construction loads, and, 8-37–8-47
- corrosion, and, 16-2
- cube, 8-21
- cylinder, 8-21, 8-24, 8-27, 9-20
- defined, 32-62
- design, 8-41, 8-42, 8-43, 9-15, 9-18, 9-19, 14-51, 20-42–20-43, 25-4, 25-12–25-13, 28-41, 28-59–28-68
 - reinforced-concrete members, 36-10–36-31
- design yield, 10-10
- ductility, and, 24-23–24-24
- early-age, 5-12–5-16, 5-25, 8-41, 21-12, 21-16
- evaluation, 27-2–27-4
 - uses for, 27-2
- failures, 8-20
- first-crack, 22-5
- flexural, *see* flexural strength
- fly ash, and, 2-11–2-12
- gain, *see* strength gain
- grout, 12-20
- guaranteed, 25-4
- in-place, 21-2, 27-5
 - estimating, 21-2–21-28
- insufficient, 8-37
- material, 24-23
- maturity, and, 21-25
- maturity index, and, 21-23
- modulus of elasticity, and, 8-29
- nondestructive testing for, *see* nondestructive testing
- offshore structure concrete, 13-2
- overdesign, 20-42–20-43
- porosity, and, 1-12–1-13
- pozzolans, and, 20-14–20-15
- pullout, 8-26, 21-11, 21-12, 21-24
- punching shear, 8-27, 8-37, 8-38, 8-40, 8-43
- reduction factors, 28-60, 28-62, 34-8
- relationship, 21-25, 21-28
 - establishing, 21-27
 - in-place testing of, 21-26
- relative, 21-23
- shear, 8-20, 8-41, 11-17, 13-22, 20-34–20-37, 28-50, 28-61, 28-68
- soil, 14-2, 14-5–14-14
- split-cylinder, 8-24, 8-27
- splitting tensile, *see* splitting tensile strength
- strut, 36-16
- tensile, *see* tensile strength

- tenth-percentile, 21-28

- test, 5-33

- time, and, 4-16–4-18

- torsional, 36-22–36-23, 36-35

- ultimate, 4-4

- ultimate, fiber-reinforced polymer systems, 25-15

- vacuum processing, and, 15-14

- water/cement ratio, and, 5-32

- yield, *see* yield strength

- strength gain, 1-7, 1-8, 1-10, 2-11, 2-12, 2-13, 2-22, 2-23, 2-35, 5-12, 5-15, 5-28, 6-9, 6-31, 7-4, 7-38, 9-6, 11-5, 11-6, 11-27, 13-19, 16-13, 20-30, 21-17, 36-7

- at anchors, 7-13

- calcium chloride, and, 5-31

- ettringite, and, 5-43

- load tests, and, 14-73

- slab, 7-15

- superplasticizers, and, 3-6

- temperature, and, 5-33, 8-25, 21-17, 21-18–21-24

- strengthening, 16-2, 16-15

- stress, 1-21, 4-2, 4-4, 4-5, 4-6, 4-8, 4-21, 4-35, 7-33, 7-44, 8-27, 9-3, 9-16, 9-22, 10-6, 10-7, 10-13, 10-24, 10-37, 11-21, 11-26, 17-2, 21-31, 25-5, 25-13, 36-4

- actual, 7-41, 7-46

- allowable, 28-41, 28-49–28-58

- allowable compression, 7-48

- axial, 32-36, 32-37

- bearing, 4-22, 7-42, 7-46, 11-57, 20-47, 21-15, 28-53, 32-36, 32-37, 34-10, 36-18

- bending, 4-22, 11-57, 21-15, 28-53, 32-36, 32-37

- bond, 4-25

- bond interface, 23-13

- bursting, 11-8

- compression, allowable, 7-41, 7-42, 7-48

- compressive, 4-21, 8-28, 8-49, 10-9, 10-38, 10-39, 11-25, 11-27, 11-60, 20-43, 20-47, 28-43, 28-47, 28-51, 28-52, 28-55, 28-59, 28-62, 32-35, 32-37, 36-13, 36-18, 36-33, 36-34, 36-35

- concrete, 10-24

- crack spacing, and, 4-28

- cracking, 9-16, 14-27

- creep, and, 5-22, 8-31

- delamination, 11-8

- design, 10-24, 28-28, 28-41

- direct, 4-22

- distribution, 10-38, 11-43

- effective soil, 14-7, 14-9–14-10, 14-16

- fiber-reinforced polymer systems, 25-15

- flexural, 8-27, 10-13, 10-14, 10-23, 10-24, 10-30, 12-28, 28-53, 36-14

- flexural bending, 28-53, 28-62
- longitudinal yield, 10-10
- lumber, ASD adjustment factors for, 7-28–7-31
- maximum allowable, 7-39, 10-25, 36-33–36-34
- maximum, in fiber-reinforced polymer bars, 25-7
- nonuniform, 8-50
- pile group, 14-69
- principal, 20-48, 20-71
- pullout tests, and, 21-12
- punching shear, 8-43, 8-46, 8-47
- radial, 11-14, 11-55
- rebar, 25-5
- reducers, 3-10
- reinforcement, 4-24, 4-31, 28-57, 28-59, 36-4
- relaxation, 11-10, 20-32, 20-53
- rust, and, 5-38
- service, 10-3, 10-39, 17-8
- shear, 8-27, 10-14, 10-18, 10-24, 10-26, 11-57, 14-78, 20-43, 21-12, 21-15, 21-31, 22-13, 23-13, 24-22, 25-14, 28-54, 28-58, 30-34, 32-32, 32-37, 34-18, 34-21, 36-14
 - beam–column joint, 34-18
 - horizontal, 30-34
 - limit states, 34-21
- shrinkage, 30-36
- soil, effective vs. total, 14-51
- steel, 4-24, 4-25, 4-27, 4-30, 8-51, 32-36, 32-37
- stripping, 10-39
- sustained, 8-50
- tendon, 12-8
- tensile, 4-18, 4-22, 4-26, 8-28, 9-3, 9-13, 9-16, 10-13, 10-24, 10-25, 10-39, 11-32, 11-52, 11-53, 12-44, 14-48, 14-52, 17-1, 17-3, 17-5, 17-10, 17-14, 20-34, 20-45, 20-47, 20-52, 21-12, 25-8, 28-52, 28-54, 28-62, 28-63, 32-35, 35-2, 36-14, 36-33
- tension, 10-18, 10-38
- thermal, 5-21, 10-24, 20-29, 20-32, 20-34, 20-43, 20-45, 20-48, 20-52, 20-53, 30-36
 - roller-compacted concrete, 20-34
- torsional, 11-57
- transfer of, 11-9, 11-25
- transport, 10-39
- ultimate, 10-3, 10-4, 10-5, 10-6
- ultimate design, 36-34
- vertical effective, 14-35
- waves, 16-6, 16-25, 21-5, 21-31–21-39, 21-43, 21-62
- working, 10-10
- stress–strain curves, 24-3, 24-5
 - geopolymer concrete, 26-8
 - Portland cement, 26-9
 - stress–strain relationship, 4-3, 4-5, 4-10, 4-18, 8-27, 8-28, 12-27, 13-22, 20-41, 22-9, 22-10, 22-15, 22-19, 25-3, 25-6, 36-5, 36-7, 36-11, 36-31
- stress/strength ratio, 2-23, 9-6, 9-15
- stress-wave propagation testing, 21-31–21-39
- stressing, 12-13, 12-21, 35-8, 35-9
 - stage, 12-44
- stringers, 7-8, 7-9, 7-14, 7-35, 7-38, 7-40, 7-41, 7-42, 8-52, 8-53
 - design of, 7-40–7-41
 - grain direction of, 7-42
 - lateral buckling of, 7-40
- strip footings, 10-10
- stripping, 7-4, 7-5, 7-38, 8-2, 8-4, 8-6, 8-9, 8-37, 8-42, 8-43, 10-3
 - stress, 10-39
- strong-backs, 7-11, 16-20, 16-22, 16-23, 16-27, 16-31–16-38, 16-40
 - spacing of, 16-37
- strong-motion accelerograph, 32-2
- strong-motion duration, 32-3, 32-5
- structural concrete, 10-1–10-40, 11-17; *see also* concrete
- structural depth, bridge, 29-7
- structural drawings, 12-6
- structural elements, proportioning of, 36-1–36-36
- structural evaluation, *see* performance evaluation
- structural failure, 8-19–8-20
- structural frames, 10-14–10-17
- structural inspection checklist, 35-17–35-18
- structural irregularities, 32-18–32-19, 32-28
- structural separation, to prevent cracks, 35-7–35-8
- structural steel, 10-2, 10-10, 10-28
- structural system, seismic-force-resisting, 32-12–32-13
- STRUDL analysis, 32-55
- strut-and-tie method, 36-15–36-21
- struts, 7-11, 7-48, 36-10
 - capacity evaluation of, 36-21
 - compressive, 34-10, 36-15
 - design of, 14-55, 14-56
 - strength of, 36-16
- stucco, 15-16, *see also* Portland cement: plaster
- studs, 7-10–7-11, 7-34, 7-35, 7-42, 7-43, 7-44, 7-45, 7-46
 - design of, 7-44
 - headed, 10-9
 - length of, 10-9
 - welded, 10-9
- styrene–butadiene latex, 23-2, 23-14
- styrene–butadiene resin concrete, 3-16, 3-17
- subbituminous coal, 2-2, 2-11, 2-17
- subdeck panels, precast, 33-2, 33-3, 33-6, 33-8, 33-9

sugars, 3-2
 sulfate, 5-25, 5-26, 5-39, 12-22, 13-20
 sulfate attack, 1-10, 1-25, 5-10, 5-42, 11-4, 13-20, 13-23, 24-29, 26-18
 Portland cement, and, 26-14
 resistance, *see* sulfate resistance
 sulfate esters, 3-10
 sulfate ions, 11-5, 11-59
 sulfate resistance, 2-16–2-17, 2-20, 2-24–2-25, 2-36, 3-7, 3-8, 3-10, 5-27, 5-29, 5-35–5-37, 16-12
 geopolymer concrete, 26-14
 Type V cement, 5-25
 water/cement ratio, and, 5-36
 sulfonated lignins, 3-6, 3-11
 sulfonated melamine formaldehyde (SMF), 3-5, 6-8
 sulfonated naphthalene formaldehyde (SNF), 3-5, 6-8
 sulfonates, 3-10, 3-11, 6-8
 sulfonic acid esters, 3-5, 6-8
 sulfuric acid resistance, geopolymer concrete SuperBent, 32-59
 superplasticizers, 1-4, 2-27, 2-29, 2-32, 2-34, 2-35, 2-38, 3-2, 3-5, 3-6, 5-30, 5-31, 5-38, 6-5, 6-8, 6-18, 6-21, 6-30, 6-31, 6-32, 6-35, 6-39, 10-23, 10-25, 10-27, 11-5, 11-6, 11-41, 13-22, 13-26, 15-20, 26-3, 26-4, 26-5, 30-19, 30-51, 30-56, 30-72
 first, second, third generations of, 3-5
 vibration, and, 30-56
 super-strength reactive powder concrete, 22-14, 22-16–22-17
 supersulfated cement, 1-10, 1-11
 surface finishes, 3-6, 5-17, 5-43, 7-3
 architectural concrete, 30-12
 robotic application of, 18-2, 18-3–18-5
 surface flatness, 20-34
 surface moisture, 1-17
 surface-penetrating radar (SPR), 16-4, 16-7–16-8
 surface sealers, 5-38, 5-39
 surface temperature, 21-39, 21-40, 21-42
 surface tightness, 20-34
 surface vibrators, 30-53
 surface waves, 21-37–21-39
 surfaced on four sides (S4S), 7-27
 surfactants, 3-10
 surficial materials, 14-1
 sustained load, 4-1, 4-2, 4-4, 4-8, 25-7, 36-3
 sustained modulus, 20-32
 sustained modulus of elasticity, 8-50
 S-waves, 16-4–16-7, 21-31, 21-32, 21-33
 sway frames, 10-15
 sweep representations, 18-9, 18-10
 swelling, 4-10

swelling-strip water stops, 20-51
 synthetic air, 20-20
 synthetic aperture focusing technique (SAFT), 21-31
 synthetic detergents, 3-11

T

table forms, 7-9
 tamping compactors, 20-68
 tanks, 11-54–11-55, 15-23, 16-16; *see also*
 liquid-containing structures, liquid-retaining structures
 aeration, 17-8
 buried, 11-55
 circular, 10-24–10-25, 11-54
 prestressed concrete, 4-33–4-34
 flaw detection in, 21-36
 oil-storage, subsea, 13-15
 rectangular, 10-26
 repair of, 11-60
 water, 17-8
 tape, 30-38
 duct, 30-33
 masking, 30-31
 plastic, 30-31, 30-37
 Tarsuit Caisson Retained Island, 13-15
 tartaric acids/salts, 3-2
 taxi crane, 19-43
 T-beam, 9-14, 10-8
 analysis, 28-56, 28-66
 bulb, 11-36
 compression steel for, 9-17
 inverted, 33-6
 section modulus of, 9-3
 uncracked, 9-16
 tee beam, *see* T-beam
 telehandlers, 19-2, 19-4, 19-15, 19-45–19-47
 telescopic tower crane, 19-29
 temperature, 4-27, 5-32–5-33, 6-39, 9-15, 9-17, 10-12, 10-26, 10-27, 10-36, 11-5, 20-17, 35-2
 aggregate stockpile, 20-53, 20-57
 alkali-silica reactivity, and, 5-42
 carbonation, and, 5-11
 changes, *see* temperature: gradient
 compressive strength, and, 2-11, 5-15
 concrete, 5-31, 7-25, 7-43
 control of, 15-23
 corrosion rate testing, 21-60
 cracking, and, 4-34
 creep, and, 4-8, 9-6
 curing, 2-12, 2-15, 2-21, 2-35, 5-15, 8-20–8-22, 8-24, 21-17, 21-18–21-24, 23-2, 26-5, 26-7, 26-11–26-12, 26-14, 26-15, 27-20, 30-58

- deflection, and, 8-51, 9-9–9-10
- deformations, 12-6
- differential, *see* temperature: gradient
- drop in, 17-3
- engineered cementitious composite (ECC), and, 24-11
- ettringite formation, and, 5-42
- factor, 7-31
- fluctuations, *see* temperature: gradient
- freezing and below, 3-12
- glass transition, 25-3
- gradient, 5-38, 8-48, 11-32, 15-23, 16-11, 17-6, 17-10, 17-11, 17-13, 17-14, 27-7, 28-38, 30-16, 35-3
- grout, and, 15-4
- history, of concrete, 21-16, 21-24
- mass concrete, and, 15-23
- maximum curing, 11-6
- polymer-modified concrete, and, 3-16
- radiant energy, and, 21-41
- reinforcement, 10-17, 17-8
- roller-compacted concrete, and, 15-25, 20-33–20-34
- sensitivity factor, 21-20
- setting time, and, 2-20, 5-12, 21-24
- shrinkage, and, 4-11
- slump, and, 3-7
- strain, and, 17-2
- strain gauges, and, 27-19, 27-20
- strength development, and, 2-11, 2-12, 8-20–8-26
- strength gain, and, 21-18–21-24
- surface, 11-7, 21-39, 21-40
- tests for, 6-42
- time factor, 21-17, 21-24, 21-25
- vacuum processing, and, 15-14
- variation, *see* temperature: gradient
- water demand, and, 5-32
- workability, and, 5-2–5-3
- working, increase in, 3-2
- templates, 7-16
- tendon anchorage zone, 12-10–12-11
- tendon ducts, voids in, 21-35
- tendon force, 35-4
- tendons, 11-36, 11-38, 11-42, 35-4; *see also* strands
 - banded, 12-9, 12-11
 - beam, 12-9
 - bonded, post-tensioning, multi-strand, 11-61
 - bundles of, 12-12
 - button-head wire, 12-2
 - carbon-fiber-reinforced plastic (CFRP), 22-24
 - continuity, 11-41
 - crack mitigation, and, 35-12
 - damaged, 11-60
 - detensioning of, 12-19, 12-20, 16-18, 16-19
 - external, 11-24, 11-40, 11-43, 11-46, 11-60, 12-31
 - harped, 12-7, 12-30, 12-34, 12-35
 - heat-sealed, 12-2, 12-3, 12-24
 - installation of, 11-25–11-26
 - internal, 11-43
 - locating, 16-18
 - low-relaxation, 12-8
 - monostrand, 12-2, 12-3, 12-4, 12-10, 12-44
 - multistrand, 12-2, 16-16
 - multiwire, 12-2
 - paper-wrapped, 12-2, 12-3
 - placement of, 12-7
 - polyethylene-sheathed, 11-33
 - post-tensioning, 11-24, 11-38, 11-41, 11-61, 27-11, 30-48
 - prestressing, 11-9–11-10, 11-11, 11-12, 11-14, 11-18, 11-19, 11-21, 11-36, 11-58, 11-59, 25-3, 28-13, 36-31
 - corrosion protection of, 11-23–11-24
 - storing of, 11-19–11-20
 - profile of, 11-28–11-29
 - push-through, 12-2, 12-3
 - repair of, 16-17, 16-18
 - retensioning, 16-19
 - rupture of, 12-27–12-28
 - short, 12-21
 - single-bar, 12-2
 - single-strand, 16-16
 - slab, 12-9
 - spacing of, 11-37, 12-7
 - splicing, 12-20–12-21
 - stress-relieved, 12-8
 - stressing of, 11-25–11-26, 12-8–12-10
 - stuffed, 12-2, 12-3
 - tank, 11-55
 - two-way slab, 12-11
 - unbonded, 11-61, 12-1–12-44
 - durability of, 12-4–12-5
 - environmental considerations for, 12-5
 - installation of, 12-7
 - prestressing, 34-23
 - single-strand, 30-47
 - uniform, 12-9, 12-11
 - variable-eccentricity, 36-33
- tensile bond strength, for overlays, 23-8
- tensile coupon test, 24-11, 24-27
- tensile cracks, 36-29
- tensile face, 4-28, 4-31, 4-32
- tensile force, 22-12, 32-35, 34-22
- tensile load, 14-5, 24-7, 34-10
- tensile rebound wave, 11-52

- tensile splitting, 21-13
 - strength, 8-24, 26-10
- tensile strain, 4-22, 4-31, 4-34, 11-54, 20-27, 25-14, 25-15
 - roller-compacted concrete, 20-32–20-33
- tensile strength, 3-15, 3-16, 4-17, 4-25, 5-15–5-16, 5-20, 5-34, 8-20, 8-22–8-26, 8-27, 8-41, 11-16, 11-17, 11-18, 11-25, 11-28, 11-54, 12-3, 12-22, 13-22, 15-12, 15-17, 16-13, 20-32, 20-40, 20-48, 20-61, 21-10, 21-13, 21-24, 22-3, 22-6, 22-9, 24-2, 24-3, 24-4, 24-9, 24-15, 24-27, 27-5, 35-2, 36-14
- bolts, high-strength, 34-8
- carbon fibers, 22-16
- elastomeric liners, 30-28
- fiber-reinforced polymer systems, 25-3, 25-14
- geopolymer concrete, 26-10
- masonry, 28-53, 28-59
- nominal axial, of headed anchor bolts, 28-60
- nominal, ductile rod, 34-8
- overlay, 23-8
- roller-compacted concrete, 20-27–20-29, 20-32, 20-33
- split, 20-27–20-29
- temperature–time factor, and, 21-24
- tensile stress, 4-18, 4-22, 4-26, 8-28, 9-3, 9-13, 9-16, 10-13, 10-24, 10-25, 10-39, 11-32, 11-52, 11-53, 12-44, 14-48, 14-52, 17-1, 17-3, 17-5, 17-10, 17-14, 20-34, 20-45, 20-47, 20-52, 21-12, 25-8, 28-52, 28-54, 28-62, 28-63, 32-35, 35-2, 36-14, 36-33
- tensile surface strength, for overlays, 23-8
- tension, 13-24
 - bars, 9-15
 - cracks, 4-18, 14-47
 - fibers, 4-19
 - leg platforms (TLPs), 13-9–13-11, 13-16, 13-29
 - members, 36-16
 - reinforcement, 9-5, 9-13, 9-17, 28-52, 28-62, 28-64, 28-66
 - ties, 7-26, 36-15
 - wave, 10-13
- terrazzo, 31-11
- Terzaghi's bearing capacity expression, 14-32
- Terzaghi's consolidation theory, 14-14, 14-18
- tests/testing, 6-41–6-43, 11-7
 - acceptance, 21-26–21-27
 - aggregate ratio, 28-33
 - air permeability, 5-10
 - Brazilian split-cylinder, 20-27, 20-28
 - break-off test, 21-15–21-16, 21-26
 - CAPO, 21-15
 - closed-loop, 27-12, 27-18
 - cone penetration, 14-7, 14-13–14-14, 28-32
 - consolidated drained/undrained, 14-8–14-11
 - constant rate of penetration, 14-73
 - control, 5-33
 - correlation, 21-27–21-28
 - cylinder splitting, 26-10
 - destructive, 12-23, 12-27, 12-28, 16-4
 - dynamic load, 14-73
 - electrical conductance–rapid chloride permeability, 5-10
 - fracture, 21-3
 - hydraulic, 27-10–27-13
 - impact-echo, 16-4–16-7, 16-20, 16-22, 16-23, 16-24, 16-24–16-25, 16-29, 16-30, 16-38, 16-39, 16-40, 21-33, 21-34, 21-35, 21-37, 21-44, 27-7
 - impedance, 21-35
 - impulse–response, 21-35, 21-36, 21-37
 - indentation, 21-2, 21-3
 - internal fracture, 21-13
 - J-ring, 5-43
 - L-box, 5-43
 - lift-off, 12-21
 - load, *see* load testing
 - maintained load, 14-73
 - Marsh cone flow, 24-11
 - masonry, 28-27–28-38
 - modal, 27-7–27-9, 27-26
 - polyreference, 27-7
 - mortar, 28-32–28-33
 - nondestructive, *see* nondestructive testing
 - petrographic, 5-42, 11-5, 11-7, 11-48, 16-3, 27-5, 27-22
 - pile load, 14-73–14-75
 - pitch-catch, 16-25
 - plate load, 14-15, 14-31–14-32, 14-40
 - probe penetration, 21-8–21-10
 - pull-off, 21-26
 - pullout, *see* pullout: test
 - pulse-echo, 16-25, 21-31
 - ultrasonic, 21-31
 - quasi-static load, 27-9–27-13, 27-17, 27-20
 - quick load, 14-73
 - rapid chloride permeability, 11-7, 15-22, 16-3
 - rapid load, 14-73
 - rapid mortar bar, 5-40
 - sorptivity, 24-32
 - standard penetration, 14-7, 14-11–14-12, 14-21, 14-34, 14-38, 14-60
 - static cone penetration, 14-7, 14-13–14-14
 - stress-wave propagation, 21-31–21-39
 - tensile coupon, 24-11, 24-27
 - transient dynamic response, 21-35

- triaxial, 14-7, 14-8–14-11
- U-box, 5-43
- ultrasonic, 21-31, 27-6–27-7
- unconsolidated undrained, 14-8–14-11, 14-36
- vehicle load, 27-10
- water permeability, 5-10
- tethers, 13-9
- thaumasite, 2-26
- theoretical air-free density, 20-21, 20-71
- thermal coefficient of expansion, 10-24
- thermal conductivity
 - masonry, 31-13
 - roller-compacted concrete, 20-22
- thermal cracking, 20-10, 20-44, 20-51, 20-56, 30-16
- thermal diffusivity
 - roller-compacted concrete, 20-22
- thermal expansion, coefficient of, 5-21
- thermal gradients, 6-40, 6-41, 13-23, 13-25
- thermal lance demolition, 12-40
- thermal stress, 5-21, 10-24, 20-29, 20-32, 20-34, 20-43, 20-45, 20-48, 20-52, 20-53, 30-36
 - roller-compacted concrete, 20-34
- thermography, infrared, 21-39–21-42
- thickness frequency, 21-33, 21-34, 21-35
- thiocyanates, 3-7
- third-generation superplasticizers, 3-5
- thixotropic agents, 11-5, 11-23
- Threadbars®, 34-10
- three-sided U-wrap, 25-16, 25-17
- three-span continuous arrangement, 7-39, 7-40, 7-44, 7-45
- through-bolts, 30-39
- tidal zone, 11-50, 13-20
- tie hole repair, 30-38, 30-39, 30-68
- tie reinforcement, 10-10, 11-18, 25-18
- tie rods, 14-53, 14-54, 14-55
- ties, 7-11, 7-43, 7-48, 11-18, 18-10, 18-11, 18-13, 19-8–19-9, 19-28, 19-47, 25-19, 28-4, 28-5, 28-55, 36-6, 36-15–36-21
 - ASTM standards for, 28-5
 - bolt, 30-39
 - closed, 26-15, 36-20
 - coil, 7-11
 - continuous, single-member, 30-39
 - crane, 19-9
 - deviator, 11-46
 - flat, 7-11
 - footing, 32-56
 - form, 7-9, 7-11, 7-22, 7-26, 7-35, 7-42, 7-46, 30-7, 30-38–30-40, 30-68
 - design of, 7-46
 - removal of, 30-40
 - stainless steel, 30-68
 - he bolt, 7-11, 30-39
 - load transfer, 34-11
 - loop, 7-11
 - railroad, 11-9, 11-25, 11-55–11-56
 - removable, 30-38
 - roof, 28-47
 - she bolt, 7-11, 30-39
 - snap, 7-11, 30-38, 30-39, 30-40
 - spacing of, 10-10, 36-6, 36-9
 - spiral, 18-13
 - steel, 11-11, 11-18, 30-44, 30-68
 - strength of, 36-17
 - tension, 7-26, 36-15
 - through-bolt, 30-39
 - vertical, 32-56
- tilt-up construction, 10-28–10-30
- timber mats, 11-32
- time
 - creep, and, 8-31, 8-33
 - domain analysis, 21-33, 21-43
 - shrinkage, and, 8-30–8-31
- titania, 2-38
- tongue-and-groove joints, 17-2, 17-3, 17-12
- tooling, 30-20, 30-25–30-27, 30-32, 30-68
- tornado, 11-31
- torque, 36-22, 36-35
- torsion, 36-15
 - accidental, 32-25
 - prestressed elements, 36-34–36-35
 - stirrups, 36-9
- torsional deflection, 9-7–9-9
- torsional moment, 9-9, 10-21, 32-25, 32-29–32-30
- torsional stiffness, 9-9, 9-14
- torsional strength, 36-22–36-23, 36-35
- total range, 27-13–27-14
- toughness, 1-21, 22-9, 22-10, 22-12, 24-23
 - index, 22-10
 - roller-compacted concrete, 20-33
- tower belt, 20-63
- tower cranes, 10-33, 19-2, 19-3, 19-4, 19-8, 19-9, 19-18, 19-21–19-34; *see also* cranes
 - American-type, 19-37
 - bottom-slewing, 19-29–19-32, 19-33
 - crawler-mounted, 19-32
 - dismantling of, 19-32
 - erection of, 19-32
 - stationary truck-mounted, 19-32
 - transport of, 19-32
- classification of, 19-33
- flat-top, 19-22
- sectional, 19-24, 19-29
- telescopic, 19-29
- top-slewing, 19-22–19-29, 19-33

tower cranes (cont.)
 dismantling of, 19-27, 19-28
 erection of, 19-27
 freestanding, 19-29
 internal climbing, 19-28–19-29
 transport of, 19-27
 traveling, 19-29
 traveling, 19-22, 19-29
 tower-mounted booms, 19-15, 19-17–19-19
 Trace Parkway Arches, 29-4
 tracking, dozer, 20-66
 traffic barriers, 29-28
 trailer pump, 19-17
 transformed area, 28-3
 transient dynamic response testing, 21-35
 translation, 16-32
 transport stress, 10-39
 transporting concrete, 5-6–5-10, 6-40
 transverse cracking strain, 25-18, 25-19
 transverse force, 32-53
 transverse reinforcement index, 36-28
 travel times, 19-5, 19-6
 traveling speed, crane, 19-34
 tremies, 3-6, 11-14, 15-6, 15-7, 15-8, 15-8–15-9, 30-50
 trial batches, 3-3, 3-4, 3-7, 3-9, 3-18, 6-16, 6-19, 6-23, 6-25, 6-27, 6-29, 6-30, 6-31
 design strength of, 6-17–6-18
 trial-wedge method, 14-47–14-48
 triaxial test, 14-7, 14-8–14-11
 tributylphosphate, 3-12
 tricalcium aluminate, 5-25, 11-4, 13-20, 30-15
 tridymite, 5-40
 triethanolamine, 6-7
 triple-tee, 11-36
 trolleying, 19-26
 speed, 19-34
 troubleshooting split anchor, 12-19, 12-20
 troweling architectural concrete, 30-13
 trowels
 power, 19-19–19-21
 robotic, 18-2–18-5
 truck cranes, 11-30, 11-32, 11-35, 19-36, 19-39, 19-43
 truck loaders, 19-43–19-44
 knuckle-boom, 19-43
 stiff-boom, 19-43
 truck pump, 19-17
 truckmixers, 5-6, 6-39, 6-40, 19-12, 19-13, 19-14, 19-15, 19-17
 front- vs. rear-discharge, 19-13
 sizes of, 19-14
 trumpets, 11-13, 11-20, 16-19

trusses, 7-9, 7-31, 8-38, 11-34, 11-38, 11-46, 32-19, 36-10, 36-15
 erection, 29-10, 29-12, 29-16
 modeling of, 18-9
 tubes, 11-20
 as column forms, 7-9
 tuffs, 1-17, 5-28
 tunnel forms, 19-49
 tunnels, underwater, 13-15
 turbine mixers, 11-6
 Twaron®, 22-21
 28-day strength, 2-12, 2-13, 2-14, 2-21, 2-22, 2-23, 2-25, 2-35, 5-15, 5-32, 6-2, 6-9, 6-13, 6-16, 6-19, 6-23, 6-29, 7-14, 8-16, 8-20, 8-21, 8-22, 8-35, 8-41, 8-42, 8-43, 8-52, 10-9, 10-27, 13-15, 21-20, 21-22, 21-23, 21-24, 24-26, 28-37
 twisting members, 9-7–9-9
 twisting, of wires/strands, 12-7
 two-sided wrap, 25-16, 25-17
 two-way joist construction, 7-9

U

U-box test, 5-43
 ultimate limit state, 16-2, 24-4, 24-6
 ultimate modulus, 20-30, 20-31, 20-71
 ultimate point capacity, 14-58
 ultrasonic pulse velocity, 21-5–21-8, 27-7
 ultrasonic testing, 27-6–27-7
 pulse-echo, 21-7, 21-31
 unbonded post-tensioning, 12-1–12-44, 24-21
 demolition, and, 12-36–12-42
 evaluation/repair of, 12-22–12-36
 external, retrofit of, 12-31–12-36
 field shortcomings of, 12-14–12-22
 general notes for, 12-6–12-10
 standard details for, 12-10–12-14
 unbraced frames, 10-15
 unconsolidated undrained tests, 14-8–14-11, 14-36
 uncracked stiffness, 9-16
 undercarriage, crane, 19-22–19-24, 19-29, 19-32, 19-37
 types of, 19-35
 undercoating, slab, 31-6
 under-reinforcement, 10-38, 25-4, 25-5, 25-6, 25-8, 36-9
 underwater concrete tunnels, 13-15
 underwater placement, 10-13, 11-5
 underwater structures, 15-3, 15-4–15-5, 15-6–15-13
 undrained strength parameters, 14-9, 14-10, 14-12
 uniaxial geogrids, 14-51
 unified method, 36-10
 unified soil classification system (USCS), 14-2, 14-5
 uniform appearance, 5-31

un-inspected design, 28-28
 unit mass, 5-30
 unit strength method, 28-35–28-36
 unit weight, tests for, 6-42
 unloading, 8-27
 unshored construction, 10-9–10-10
 uplift, 20-38, 20-40, 20-41, 20-42, 20-47, 20-49, 20-51
 Upper Stillwater Dam, 20-8, 20-14, 20-28, 20-38
 urethane, 23-14, 30-28
 utilities, carried on bridges, 29-29

V

vacuum mats, 15-14
 vacuum processing, 15-13–15-16
 Valdez, Alaska, dock, 13-14
 vapor barrier, 30-30
 variable vs. constant, 8-9
 Vebe times, 20-17, 20-66
 vehicle load testing, 27-10
 velocity, 32-48, 32-50, 32-51
 spectral, 32-51
 veneer, 28-3, 28-4, 28-11, 28-29, 31-8
 anchored, 28-4
 stone, 30-31, 30-71
 ventilating screeds, 15-18
 vents, 11-20, 11-23
 vermiculite, 1-17, 15-17, 31-8
 Vernier calipers, 27-16
 vertical irregularities, 32-18, 32-19, 32-20, 32-28
 vertical load, *see* load: vertical
 vertical plant, 19-50
 vertical tendon blowout, 12-24
 vibrating tables, 30-53
 vibrating wire strain gauge, 27-20, 27-29, 27-31
 vibration, 5-6, 5-7, 5-31, 5-43, 6-40, 7-3, 7-24, 7-25, 7-43, 10-14, 11-6, 11-7, 11-27, 11-41, 11-49, 12-8, 15-14, 15-15, 15-19, 15-23, 18-2, 22-5, 23-10, 28-20, 30-4, 30-15, 30-52–30-58
 external, 30-53
 form, 30-56–30-57
 fundamental period of, 32-23
 impact, 27-7, 27-8, 27-26
 in floors, 9-20
 internal, 30-53, 30-54–30-56, 30-57
 measurements, 12-41
 screed, 23-10
 -sensitive equipment, 9-19, 9-21
 vibrators, 11-13, 11-14, 11-20, 11-27, 11-29, 12-18, 19-19, 20-3, 23-10, 30-7, 30-41, 30-52–30-58
 external, 30-53, 30-56, 30-57, 30-58
 form, 30-53, 30-56–30-57, 30-72

 internal, 30-53, 30-54–30-56, 30-57, 30-58
 motor-in-head, 30-53
 qualities of, 30-52–30-53
 reciprocating, 30-53
 rotary-type, 30-53, 30-54
 Victory Bridge, 29-7–29-8, 29-11
 Vinsol™, 2-10, 3-10
 vinylester, 25-9, 25-10
 viscosity, 5-43, 15-21
 antiwashout underwater concrete, 15-10, 15-13
 control, 11-5
 -enhancing admixtures, 3-13, 3-14
 -modifying admixtures, 15-20
 self-consolidating concrete, 15-19
 viscous damping, 32-48
 visual inspection, 16-4, 21-29–21-31
 visual stability index (VSI), 28-10
 void ratio, 6-21
 volcanic ashes, 5-28
 volcanic glasses, 1-19, 5-40, 5-42
 voltmeter, 21-53
 volume change, 2-14, 5-20–5-21
 autogenous, 20-22, 20-70
 cracking, 17-1, 17-2, 17-5, 17-8
 effect of fly ash on, 2-14
 volume of permeable voids, 5-10
 volume/surface ratio, 8-30, 8-31, 8-33, 9-6, 9-15, 9-18
 voxels, 18-9

W

w/c, *see* water/cement ratio
 Wabasha Freedom Bridge, 29-8, 29-19, 29-25
 waffle joist, 7-9
 wales, 7-11, 7-35, 7-42, 7-43, 7-44, 7-48, 10-34, 10-36
 design of, 7-45
 spacing of, 7-48
 wall cladding, precast, 9-10
 wall cracks, 35-6
 wall footings, 10-10
 wall-forming system, 19-3, 19-4, 19-6, 19-8, 19-9–19-10
 wall forms, 7-10–7-14, 19-49
 design of, 7-43–7-48
 mechanized, 19-50
 wall joints, 35-10–35-11
 wall panels, 10-28, 10-29, 10-38, 10-39, 11-25, 11-29, 16-20, 16-22, 16-23, 16-25, 16-27, 16-28–16-38
 architectural precast, 30-5, 30-45
 engineered cementitious composite (ECC), 24-20
 installation of, 30-64

- wall/slab released connections, 35-9–35-10
- wall thicknesses, 10-10
- wall tie, 28-4
- walls, 2-14, 8-31, 10-10
 - cast-in-place, 11-54
 - defined, 7-26
 - design of, 36-36
 - fire rating of, 31-11
 - fire resistance of, 31-8
 - flaw detection in, 21-33, 21-34, 21-36
 - geotextile-reinforced, 14-52
 - half-height, 35-5
 - reinforced, 14-51–14-52
 - sheet pile, 14-52–14-55
 - thickness of, 10-26
- warping, 9-6, 9-9, 9-17, 11-39, 17-11, 17-14
- wash boring, 14-28
- washer plates, 7-11
- water
 - blasting, 30-27
 - content, 15-20, 20-17–20-19, 20-20
 - demand, 3-4, 5-32, 6-9, 6-20, 6-21, 11-4
 - roller-compacted concrete, 20-14
 - silica fume, 2-32–2-33, 2-34
 - for prestressed concrete, 11-5
 - jetting, 12-41
 - mixing, *see* mixing water
 - penetration
 - masonry, 28-38–28-39
 - permeability test, 5-10
 - preplaced-aggregate concrete, and, 15-4
 - quality, 1-12
 - reducers, 3-2, 3-3–3-4, 3-6, 3-11, 5-28, 5-30, 5-31,
 - 5-32, 6-5, 6-8, 6-21, 6-33, 15-3, 15-11,
 - 15-12, 15-13, 20-20, 20-24
 - super, 3-5
 - stops, 17-2, 17-7, 17-8–17-9, 20-40, 20-49, 20-51
 - swelling-strip, 20-51
 - weight of, 6-9, 6-12
- water-based silica fume slurry, 2-29
- water/binder ratio, 15-20
- water/cement + blast-furnace slag ratio, 2-23
- water/cement + fly ash ratio, 2-18
- water/cement ratio, 1-4, 1-8, 1-9, 1-11, 1-12–1-13,
 - 1-17, 1-23, 1-25, 6-4, 15-16
 - activation energy, and, 21-18
 - air-entraining admixtures, and, 2-20, 6-7
 - aggregates, and, 5-30
 - antiwashout admixtures, and, 3-14
 - architectural concrete, 30-21, 30-28
 - bleeding, and, 5-6
 - bond strength, and, 8-24
 - bonded concrete overlays, and, 23-2
 - carbonation, and, 2-36, 5-11
 - chemical resistance, and, 2-36
 - compressive strength, and, 5-12–5-14, 6-9, 6-13,
 - 6-16, 6-17, 8-20, 26-4, 28-33, 36-1
 - color of concrete, and, 30-17, 30-19
 - containment concrete, 10-23
 - corrosion protection, and, 5-38, 5-39
 - engineered cementitious composites, and, 24-27,
 - 24-32
 - deflection, and, 9-20
 - drying shrinkage, and, 2-23
 - durability, and, 5-32, 10-2
 - fly ash concrete, 2-9, 2-13, 2-15, 2-18
 - grout, 28-9, 28-34
 - mass concrete, 10-27
 - permeability, and, 5-10
 - Portland cement plaster, and, 15-17
 - preplaced aggregate concrete, 15-3
 - pulse velocity, and, 21-7
 - relative humidity, and, 5-42
 - repairs, and, 16-13
 - roller-compacted concrete, 15-23, 20-17–20-20,
 - 20-29
 - shrinkage, and, 4-11, 4-16
 - shrinkage-reducing admixtures, and, 3-16, 3-17
 - slag, and, 2-24, 2-27
 - slump, and, 6-41, 8-21
 - strength, and, 2-11, 5-32
 - sulfate attack, and, 5-36, 5-37
 - temperature, and, 5-32
 - tensile strength, and, 8-24
 - water demand, and, 2-32–2-33
 - water-reducing admixtures, and, 3-3, 3-4, 3-5,
 - 3-6, 5-31, 6-33, 15-12
- water/cement + silica fume ratio, 2-33, 2-34, 2-35,
 - 2-36, 2-37, 2-38
- water/cement + slag ratio, 2-20, 2-22, 2-23, 2-27
- water/cementitious materials ratio, 5-6, 5-32, 6-2,
 - 6-30
 - admixtures, and, 11-5
 - carbonation, and, 2-36
 - compressive strength, and, 6-18, 6-20, 6-22, 6-25,
 - 6-28, 36-1
 - creep, and, 2-35, 4-8
 - curing, and, 6-40
 - engineered cementitious composites, and, 24-32
 - fiber-reinforced composites, and, 22-4, 22-15
 - fly ash concrete, 1-11, 2-16, 2-18
 - high-performance, high-volume fly ash concrete,
 - 1-11
 - high-range water reducers, and, 6-9, 6-41
 - maturity method, and, 21-23
 - offshore concrete structures, 13-19

- permeability, and, 2-36
- pile durability, and, 11-47, 11-48
- plasticized concretes, and, 2-38
- prestressed concrete, 11-5
- setting time, and, 2-34
- shrinkage, and, 4-11, 4-16, 4-35
- silica fume, and, 2-38
- slag, and, 2-21
- sulfate attack, and, 5-36
- superplasticizers, and, 6-31
- vs. strength, 1-13
- Young's modulus of elasticity, and, 2-35, 20-29
- water/concrete ratio, 30-33
- water/geopolymer solids ratio, 26-4, 26-7, 26-8
- water/Portland cement ratio, 5-35
- water-treatment facilities, 17-8
- waterfall plot, 21-45
- waterproofing, 11-33, 12-8
- watertightness, 12-4, 13-26, 15-14, 20-8, 20-42, 20-44, 20-47, 20-49, 20-51, 20-52, 20-69, 24-6
 - roller-compacted concrete, 20-38–20-40
- wave equation, 14-69–14-73
- weather barrier, plaster, 15-18
- weather protection, 20-69–20-70
- weathervane, 19-26
- web shear, 36-34, 36-35
 - cracks, 8-27
- wedges, 11-10, 11-11, 11-24, 11-25, 11-28, 11-32, 12-3, 12-8, 12-9, 12-19, 12-20, 12-21, 12-27, 12-43, 12-44, 14-53
 - cracked, 12-21
- weep holes, 14-50, 28-18
- weight, of equipment, 10-4
- weight, of structure, 32-18, 32-22, 32-24, 32-29
- welan gum, 3-14
- weldable gauges, 27-19
- welded deformed wire fabric, 36-30–36-31
- wet mixtures, 20-16, 20-17, 20-19, 20-59, 20-68
- wet-pipe placement, 15-8–15-9
- wet use factor, 7-34
- wetting–drying cycles, 2-18
- wheelbarrows, 5-6, 13-26, 30-50
- wheeled undercarriage, 19-35
- white cement, *see* cements: white
- Whitney stress block, 25-5, 25-15
- Willow Creek Dam, 20-8, 20-11, 20-14, 20-22, 20-28, 20-38
- wind, 7-27, 7-46, 10-4, 12-38, 13-25, 13-30
 - force, 10-5–10-6
 - load, 7-27, 10-4, 10-5, 10-6, 28-41, 28-46
 - pressure, 7-47, 10-5
 - speed, 10-5
 - top-slewing tower cranes, and, 19-26
- Windsor probe, 21-8–21-9
- wing walls, precast concrete, 33-12
- wire, 1-21, 4-24, 8-58, 10-39, 12-7, 12-22, 12-24, 16-16, 26-15; *see also* strands, tendons
 - broken, 12-23, 16-19
 - chicken, 15-18
 - closed ties, 26-15
 - cold-drawn, 11-9
 - deformed, 36-28
 - development length, 28-51, 28-61
 - epoxy-coated, 28-51, 36-28
 - fabric reinforcement, 1-21, 10-39, 36-30
 - failure, 12-27
 - lath, 15-16, 15-18
 - mesh, 7-21, 14-56, 15-18, 16-15, 24-37
 - pinched, 12-27
 - potentiometers, 27-18, 27-25
 - prestressing, and, 10-25, 10-38, 11-2, 11-8, 11-9, 11-10, 11-12, 11-13, 11-21, 11-23, 11-24, 11-26, 11-30, 11-54
 - reinforcement, 8-52, 28-13, 28-42, 28-44, 28-55, 28-61, 30-44, 8-58, 22-2
 - rope, 12-27
 - shape, 22-2
 - screen, 15-14
 - size, in composites, 22-2
 - ties, 30-40, 30-43, 30-44
 - vibrating, strain gauge, 27-20
 - yield strength, 28-51
- wobble, 11-12
- wobble friction, 12-43, 12-44
- wood sealers, 30-17, 30-18, 30-28
- workability, 2-6, 2-9, 2-11, 2-32, 3-1, 3-4, 3-5, 3-6, 3-12, 5-2–5-6, 5-30, 5-31, 6-3, 6-20, 6-21, 6-23, 6-29, 6-30, 6-34, 6-37, 6-40, 10-25, 10-26, 11-5, 13-22, 13-23, 15-9, 15-14, 20-17, 20-43, 20-67, 20-68, 22-6, 23-3, 26-2, 28-14, 30-14, 30-16, 30-19
 - accelerators, and, 3-7
 - admixtures, and, 6-4–6-9
 - antiwashout admixtures, and, 3-14
 - fly ash, and, 2-10
 - geopolymer concrete, 26-3–26-4, 26-8
 - mortar, 28-6, 28-8, 28-9, 28-33
 - plasticizers, and, 3-3
 - polymer-modified concrete, 3-16
 - retarders, and, 3-2
 - silica fume, and, 2-33
 - slags, and, 2-23
 - superplasticizers, and, 3-5
- working platform, 10-36
- working range, 27-13–27-14
- working stress design, 28-41, 28-49

wrapped sections, 25-16–25-19
wrapping, 22-24
wrecking strips, 7-17
wythes, 28-3, 28-4, 28-9, 28-47, 28-48, 28-49,
31-6–31-7, 31-8

X

x-rays, 21-60, 21-61, 21-62

Y

yield point, 10-4, 24-5
yield strength, 11-54, 26-14, 26-16, 27-5, 28-59,
34-18
anchor bolt, 28-50, 28-60
mild reinforcement, 28-13
reinforcement, 28-51, 28-63, 28-64, 28-65, 36-6,
36-23
tension, 28-66
shear, 28-68
spliced, 28-51
steel, 1-21, 36-15

tendon, 36-34
Threadbars®, 34-10
wire, 28-51
yielding
system, 34-1
precast seismic system, 34-6
premature, 8-48
reinforcement, 36-13, 36-23, 36-24
yokes, 10-34–10-35, 10-36
Young's modulus of elasticity
defined, 8-28
blast-furnace slag, 2-23
metakaolin concrete, 2-39
silica fume, 2-35

Z

Z-booms, 19-17
zinc, 30-45
zinc anodes, 16-26
zinc bracelets, 11-59
zinc silicate, 11-59
zirconium, 22-19

Civil Engineering

Concrete is one of the most versatile materials of this century and for the next millennium. **The Concrete Construction Engineering Handbook, Second Edition**, provides in-depth coverage of concrete construction engineering and technology. It features state-of-the-art discussions on what design engineers and constructors need to know about concrete, focusing on:

- The latest advances in engineered concrete materials
- Reinforced and prestressed concrete construction
- Specialized construction techniques
- Design recommendations for high performance

In the second edition of the **Concrete Construction Engineering Handbook**, designers, constructors, educators, and field personnel will learn how to produce the best and most durably engineered constructed facilities.

- Encompasses the vital topics necessary for the engineering construction of concrete facilities as well as in-depth coverage of fiber-reinforced plastics (FRP), a new chapter on engineered cementitious composites (ECC), and an extensive new chapter on equipment for building construction
- Includes more than 1,100 tables, charts, graphs, and illustrations presenting many applications in both construction of systems and proportioning materials of construction
- Addresses problems often faced in the design office and in the field pertaining to concrete construction technology, including information on material behavior, design of concrete mixtures, long-term behavior, and high performance qualities of constructed systems
- Covers the latest requirements for structural concrete in accordance with the ACI 318-08 Building Code for flexure, shear, torsion, compression, long-term effects, long columns, and development of reinforcement, as well as the latest IBC 1997 provisions and examples on earthquake design and construction, including the design of precast concrete seismic bracing systems
- Provides in its 36 chapters indispensable information for design engineers, construction engineers, field personnel, researchers in materials, and civil engineering undergraduate and graduate students
- Supplies extensive references at the end of each chapter that direct you to further information on specialized topics

The 37 contributors are world-class leaders in research, design, and construction with a combined professional practice of more than 1,200 years. The wealth of up-to-date knowledge they provide allows you to develop concrete systems that are vastly better, more efficient, and longer enduring.



CRC Press

Taylor & Francis Group
an informa business

www.crcpress.com

6000 Broken Sound Parkway, NW
Suite 300, Boca Raton, FL 33487

270 Madison Avenue
New York, NY 10016

2 Park Square, Milton Park
Abingdon, Oxon OX14 4RN, UK

7492

ISBN: 978-0-8493-7492-0



90000

9 780849 374920

